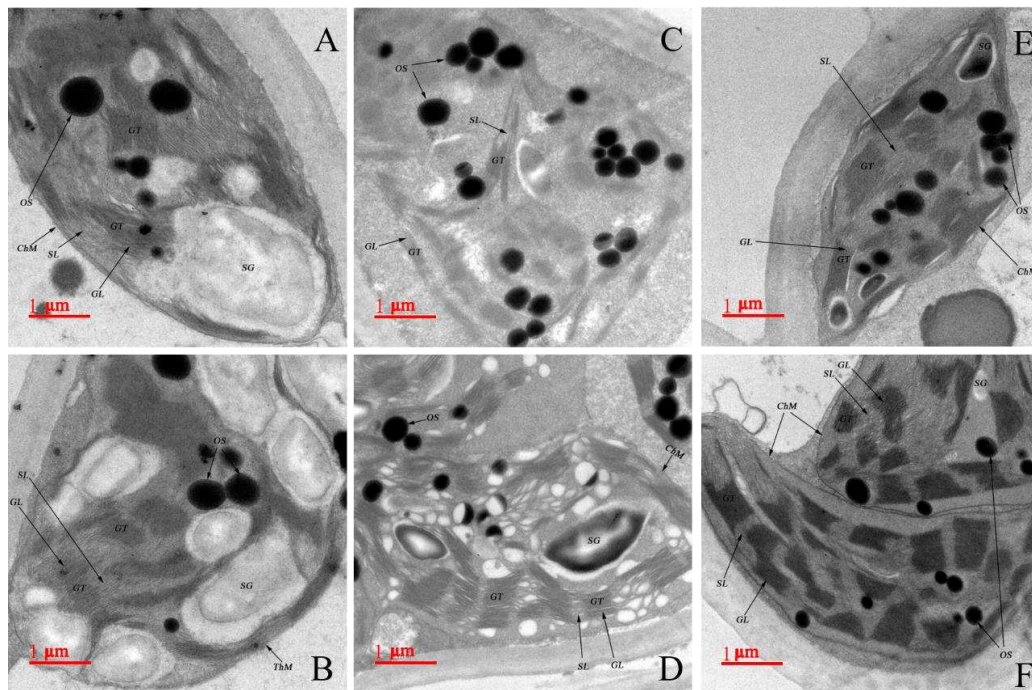


Applied Ecology and Environmental Research

International Scientific Journal



VOLUME 18 * NUMBER 3 * 2020

<http://www.aloki.hu>
ISSN 1589 1623 / ISSN 1785 0037
DOI: <http://dx.doi.org/10.15666/aecr>

EFFECTS OF SAVANNAH CONSERVATION ON THE FLORISTIC DIVERSITY AND STRUCTURE OF SPECIES CHARACTERISTICS OF THE SAVANNAS OF MANZONZI IN DEMOCRATIC REPUBLIC OF CONGO

MBANGILWA, M. M.¹ – MALOTIE, J. M.² – KASORO, R. F.³ – JIANG, L. C.^{1*}

¹*Key Laboratory of Sustainable Forest Ecosystem Management, Ministry of Education, School of Forestry, Northeast Forestry University, Harbin 150040, P.R China*

²*Post-university Regional School for Integrated Management and Management of Tropical Forests and Territories (ERAIFT), University of Kinshasa, B.P. 15.373 Kinshasa, Democratic Republic of Congo*

³*College of Resources and Environment Sciences, Jilin Agricultural University, 2888 Xincheng St, Nanguan, Changchun, Jilin, P.R. China*

**Corresponding author
e-mail: jlichun@nefu.edu.cn*

(Received 1st Aug 2019; accepted 25th Nov 2019)

Abstract. The variation of floristic diversity and the structure of the vegetation were observed in sixteen plots of one hectare each, eight of which were in the savannah set aside and eight in the one under fire. The study was limited to ligneous plants with a focus on regeneration in subplots installed in each plot. A statistical analysis and indices were employed to compare the results of the two treatments. On the floristic level, the savannah put under protection compared to that subjected to the fires is the most diversified (63 species compared to 17), and that its contact with the forest puts it in a situation of evolution. The density is higher in the defended savannah (406.3/ha) than in the burned savanna (256.3/ha) with a larger basal area (5.3m²/ha against 2.3). The analysis of similarity indicates that these two treatments are different floristically. The study also reveals that protection yields great economic, social and environmental benefits.

Keywords: *density, subplots, plot, ligneous plants, basal area*

Introduction

The structure and diversity of tropical vegetation are determined by the discontinuous distribution of several biotic and/ or abiotic factors, which act on different spatial and temporal scales (Dale, 1999; Peña-Claros et al., 2012; Arruda et al., 2015a; Rodrigues et al., 2016). However, African dry forest and woodland vegetation types are characterized by more or less continuous tree cover (70%), prolonged drought lasting more than three months per year, and by their occurrence within the savanna biome (Menaut et al., 1995; Savadogo et al., 2007). They cover approximately 13 million km², 43% of the total area of the continent, and are divided into two distinct regions, in the northern hemisphere (Sudanian region) and the southern hemisphere (Zambezi region) (Savadogo et al., 2007).

Savannahs are complex ecosystems characterized by the coexistence of herbaceous strata and one or more shrub and / or tree layers under the effect of the interaction of several environmental factors: various rainfall patterns, the role of fire and fire breeding (Jacquin, 2010) as well as the nature of the soil. It is an open grassland formation composed mainly of perennial or annual grasses (Jacquin, 2010). Its vegetation may be purely grassy or scattered

with shrubs or trees and varies with rainfall, soil and anthropogenic activity (Clément, 1982; Manlay et al., 2002). In the Democratic Republic of Congo (DRC), savannas cover 76.8 million hectares and are the second type of ecosystem after the dense forests that represent 10% of the world forests (Lubalega, 2016).

The ecology of savannas and the consequences of the fire regime of animal and plant species on the environment is one of the most important issues for conservation biology and ecological principles. Several ecological studies suggest that some species may survive in repeated fire regimes (Burrows, 2008; Guenon, 2010), however, more information is needed to better understand what kind of habitats they are associated with. The lack of in-depth studies on this issue makes it impossible to accurately assess the effect of bush fire and the management of its impacts on vegetation structure.

For a long time, ecologists have been fascinated by savannas because trees and grasses coexist, while competing mainly for the same resource, namely water, which is the main limiting factor (Walter, 1971; Scholes and Archer, 1997; Sankaran et al., 2004). Classical ecological theory, such as the competitive exclusion principle, predicts that only one vegetation type can survive in these conditions (Hutchinson, 1961; Tilman, 1982). To solve this conundrum, numerous experimental and modeling studies have explored the nature of tree–grass competition and coexistence (e.g., Walker and Noy-Meir, 1982; Scholes and Walker, 1993; Higgins et al., 2000; House et al., 2003; Sankaran et al., 2004; Bodena et al., 2015).

For this investigation, our hypothesis is that savannas kept safe from fires become more stable and tend to contain more species, and increase in diameter and density of stems. On the other hand, fire savannas would contain a low density of arboreal trees, small trees and shrubs would be more common.

The objective of the present work was to evaluate the effects of the conservation of savannas subjected to the fire regime on the floristic diversity and the structure of their vegetation. Specifically, it is a question of analyzing and comparing the floristic diversity and the structure of the savannas put in defense for six years to those of the savannas subjected to the regime of different intensity.

Materials and Methods

Study area and data

This research was conducted in a savanna patch in the villages of Manzonzi and Mao (S 5°43'45" – E 13°15'0"), a few km south of the UNESCO Man and Biosphere Reserve of Luki and approximately 30 km north of the city of Boma (Lower Congo province, Democratic Republic of the Congo, hereafter referred to as DRC). The region of Bas-Congo (currently Kongo Centrale) has a tropical climate characterized by two distinct seasons: a dry season and a rainy season. The dry season is well marked with a season that goes from May to September, as well as a small dry season of 2 or 3 weeks in February (Quinif, 1986). According to the Köppen Classification, this phytogeographical region of Congolese Mayombe forest belongs to the AW4 system (Deklerck, 2019). Average annual rainfall is between 1200 - 1400 mm (Sys, 1960). However, the current data collected in the Luki (plateau) climatological station places it in the Aw5 system, unlike Sys (1960), where the first rains are not expected until mid-October and the annual averages hardly reach 1100 mm.

The Mayombe climate of which Manzonzi is a part depends on the Atlantic Ocean, it is influenced by the cold Benguela current and the Southeast trade winds (Lubini, 1997). This cold marine current of Benguela is responsible for the small dry season rains known locally as

"masala" (Kapa et al., 1987). These so-called occult rains (De Foresta, 1990) are expected towards the end of the August month, and plays the role of compensation of soil water deficit. We meet a dry season (May-September) and a rainy season (September-May) with a small dry season of 2 or 3 weeks in February (Quinif, 1986). The dry season is characterized by a slight drop in temperature due to frequent morning fogs or mists. For this work, the meteorological data (*Figure 1*) relate to the general situation of the Luki Biosphere Reserve (RBL), as the site under study (Manzonzi) generally enjoys the same conditions.

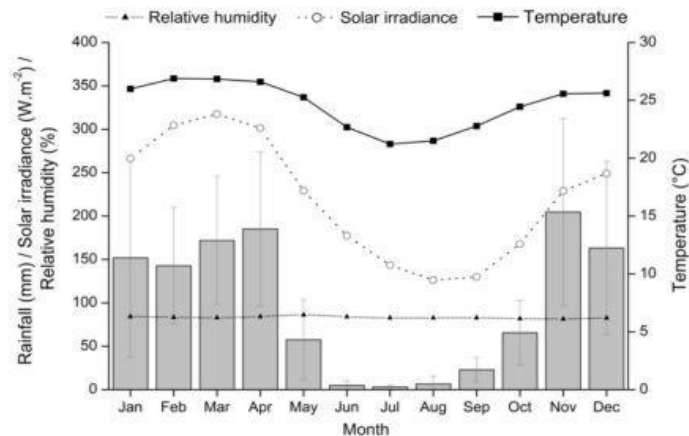


Figure 1. Climate diagram of the Luki meteorological station, Democratic Republic of Congo: monthly means of rainfall (\pm SD), temperature, air humidity (1959–2006) and solar irradiance (1959–1994) (Couralet et al., 2010b)

The Mayombe extends from Gabon through Angola (Cabinda) to the Democratic Republic of Congo (DRC). The Mayombe range has a four-storey geological structure, the most recent of which is the West-Congolian floor (Lubini, 1997). It is formed by Middle Precambrian volcanic and metamorphic rocks (Quinif, 1986). It includes schisto-sandstone and schist-limestone systems (Lubini, 1997). Thus, shales, quartzites, graphitic rocks, feldspathic sandstones, micaschists, muscovites, amphibolochists and intrusive rocks are observed. These various rocks have allowed the formation of the various types of soils encountered there. Most of the soil consists of ferrasols on undefined rocks (Sys, 1960). The rock formations are covered with a layer of surface soils of thickness ranging from 20 cm to 3 m. These eluvia or colluvium derives from the underlying or surrounding geological basement (Sys, 1960).



Figure 2. Image of Manzonzi savanna plots around the Luki Biosphère reserve in Bas-Congo (Source: Field investigation)

Data and methods

Selection of inventory sites

In 2010, WWF proceeded with the opening of the variable-length transect according to the physiognomy of the site to be used for systematic inventories to characterize the large plant formations in this Manzonzi savannah (*Figure 3*). A total of 101 plots of 80 m x 50 m each and 20 m apart from each other were placed there. This device has the advantage of capturing the heterogeneity of the ecological gradients of the environments traversed and of probing the homogeneous superimposed surfaces.

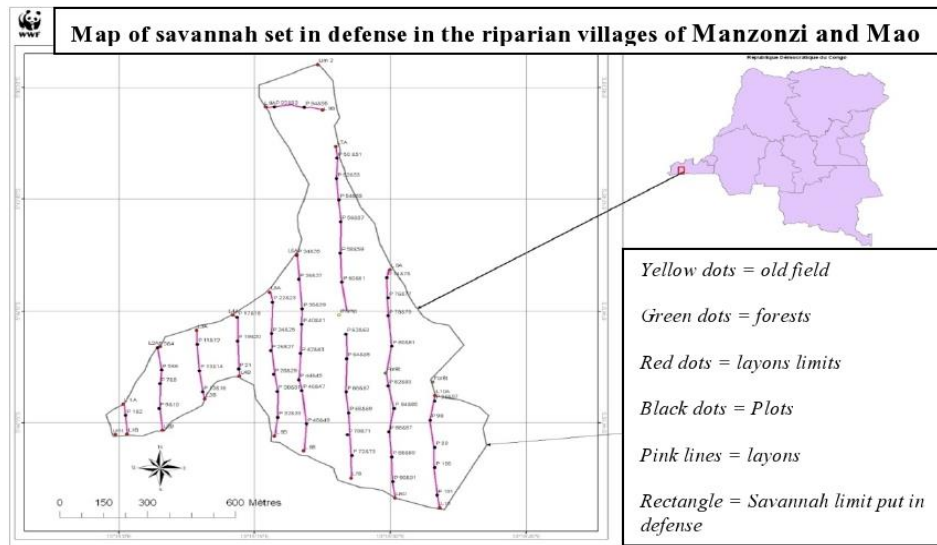


Figure 3. Systematic inventory system in the savannah of Manzonzi

For the present study conducted in June 2018, we have through this device set up a stratified sampling of plots distributed in the savannah and in the edge. The selection of firewood savanna (SRF) plots was based on annual fire passage, and populations were consulted for this choice. Plots were placed in a given orientation, indicated by the compass. Three vegetation formations have been identified: edge, savanna and grassy savannah. Each starting point of the plots is materialized by a stake bearing the number of the plots of inventory. The distance marking stakes were made from the stems of the small trees harvested on site and were placed every 50 m. Depending on the slope, a certain distance was added in order to have a real horizontal distance corresponding to the length sought for the plots (SPIAF, 2007). All plots were geo-referenced using a GPS and a tracking was done for the savannah defensive (SMD). The tracking data included in the Geographic Information System (GIS) allowed us to use the ARC GIS 9.2 software to produce the site map under study (*Figure 4*).

Botanical inventory and data collection

Eight other plots of 1 ha each were installed in the savannah set aside and another eight in the savannas under fire following the same vegetation, in order to ensure the representativeness of the plots (Devineau et al., 1984; Favrichon et al., 1998), and their

diversity (Dibi et al., 2008). The inventory concerned only ligneous plants (trees and shrubs), other plant forms (lianas, herbs...) were assessed qualitatively (Favier et al., 2004).

The location of the plots took into account the topographic features of the environment, the physiognomy of the vegetation and the fact that they significantly include ligneous plants of different heights. All species in plots were surveyed (Favier et al., 2004; Dibi et al., 2008) and all trees ≥ 20 cm measured (Duarte et al., 2006). The use of the ribbon was preferred to the forest compass because of the ease of work and the fact that the circumference gives a better estimate of the volume than that obtained by the compass (Rondeux, 1993).

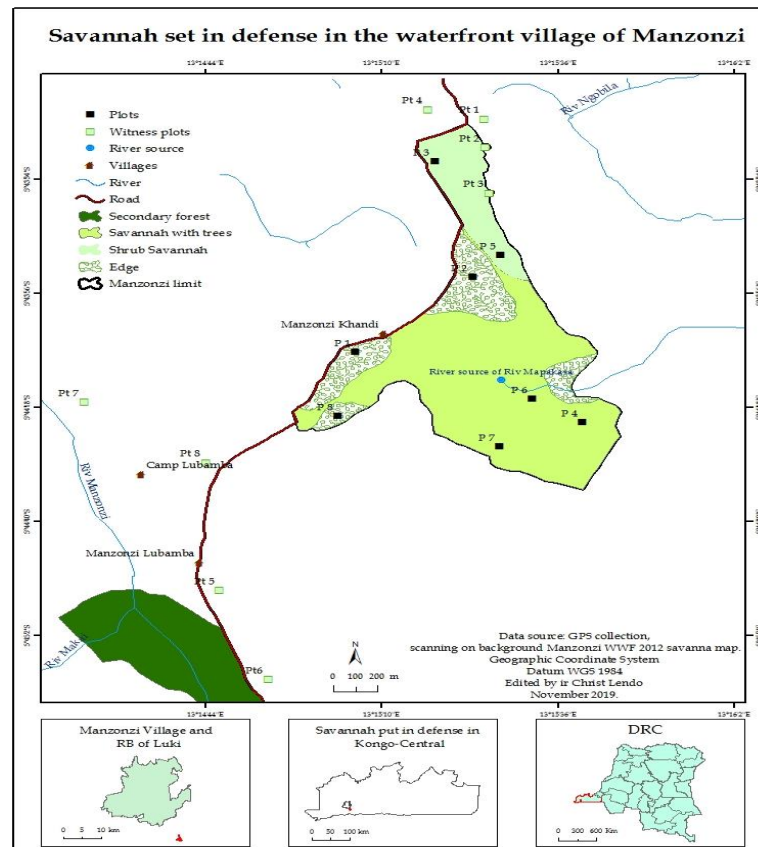


Figure 4. Layered inventory device in the savanna laid out in Manzonzi defenses

In each plot, a 10 x 10 m sub-plot was installed to assess the regeneration of woody species in the herbaceous layer. All seedlings whose total height did not exceed 30 cm were identified and counted. For seedlings exceeding 30 cm in height and with a circumference less than 20 cm, their diameter was measured using a caliper at the neck of the stem.

Analytical and statistical approaches to the data

Analysis of floristic composition and vegetation structure

The vegetation structure for these two types of treatment (SMD and SRF) was described by the calculation of non-parametric indices or structural indices, including: relative density, relative frequency, relative dominance, and value index importance of species and families (Mueller-Dombois and Ellenberg, 1974). These different indices have been calculated by the formulas below:

The relative density (DER) of the stand that is representative of the number of individuals of each species or each family:

$$DER = 100 \times \frac{\text{Number of individuals of a species or family}}{\text{Total number of individuals in the sample}} \quad (\text{Eq.1})$$

Relative dominance (DOR) that is representative of the basal area of each family or species:

$$DOR = 100 \times \frac{\sum \text{Basal area of individuals of species or families}}{\sum \text{Basal area of individuals of all species or families}} \quad (\text{Eq.2})$$

The relative frequency (FRR) that is representative of the dispersal of individuals in the field (the frequency of a species or the number of occurrences of a species, the number of plots in which the species is present.

$$FER = 100 \times \frac{\text{Number of frequencies of a species or family}}{\text{Total number of frequencies}} \quad (\text{Eq.3})$$

Relative diversity (DIR) that is representative of the number of species in a family:

$$DIR = 100 \times \frac{\text{Number of species in a family}}{\text{Total number of species}} \quad (\text{Eq.4})$$

Significance value indices:

$$IVIDOR + DER + FRR/3 \text{ (for a species)} \quad (\text{Eq.5})$$

$$VFI = DOR + DER + DIR \text{ (for a family)} \quad (\text{Eq.6})$$

The Value of Significance of Species index gives information on the number of individuals, their distribution on the survey and their importance according to the basal area they occupy. In contrast, the PFD index provides information on the floristic importance of each family by the number of individuals in the family, the number of species representing the family, and the quantitative importance of families through the family of their terrific surfaces. This index makes it possible to highlight the most important species (Mueller-Dombois and Ellenberg, 1974; Kent and Coker, 1992).

Unlike previous indexes that can range from 0 to 100, it ranges from 0 to 300 (Doucet, 2003).

For a thorough analysis of the diversity of flora in these two types of treatment, we estimated:

(a) Sorensen Coefficient of Similarity (C_s): $C_s (s) = 100[2c/(a + b)]$ (Doucet, 2003; Dibi et al., 2008). With a = number of species of medium A, b = number of species of medium B, c = number of species common to both ecological environments.

(b) The density of ligneous (D), which is expressed by the following formula: N/S where, N = number of stems in the plots of the medium considered, S = total area of the plots in ha.

(c) The basal area (A), which is calculated according to the following expression: $A = d^2(P_1/4)$ (Dibi et al., 2008) or $G = \pi D^2/4$ (Ouedraogo et al., 2008), with D = diameter at 1.30 m from the ground.

Statistical analysis

Statistical tests were based on the variance between the fire regime and the defenses. The main factor was the effect of defencion on savannas subject to the fire regime. The Fisher (ANOVA) test was the best choice because it had satisfactory results. Variables taken into account were floristic diversity and density. We used R version 2.10.1 software. (Cornillon et al., 2010) and the level of significance of the results retained is 0.05 and 0.0001 depending on the case.

Results

Floristic composition

The analyzes performed relate to density (N), relative density (DER), basal areas (G), occurrences, frequencies, relative dominance (DOR), importance value of species (IVI) and the importance value of families (VIF). The *figure 5* below shows the Specific Wealth in SMD and SRF

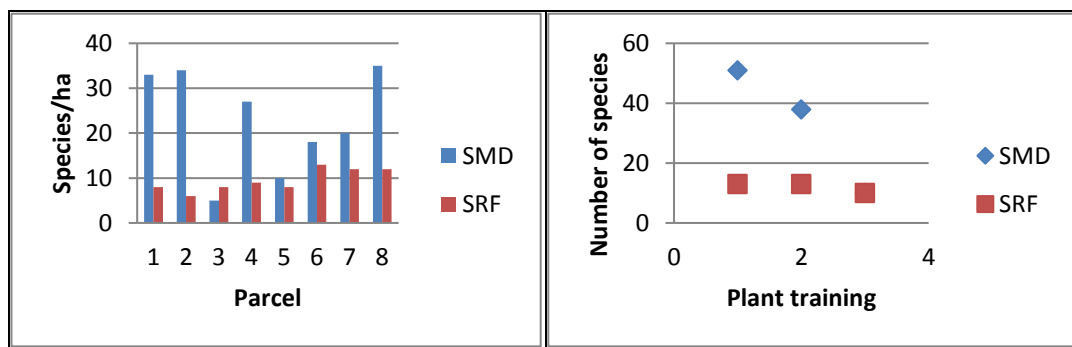


Figure 5. Specific Wealth in SMD and SRF

The following diagrams (*Figure 6*) present the results of analyzes based on species importance indices (IVI), family importance value indices (VIF) in the SMD and SRF, and relative dominance (DER) in sub-categories plots of the SMD.

The following table (*Table 1*) presents a summary of the different variables used for the analysis of the floristic composition and *Table 2* the Synthesis of the regeneration in the savanna sub-plots placed in defense.

Table 1. Summary analysis of indices in plots

Type	Variables	Oc.	FRR	DER	DOR	IVI	VIF
SMD	Average	3.19	1.78	1.75	1.75	5.26	12.00
	Stdev	2.15	1.18	4.23	3.76	8.71	25.62
	Variability (%)	67.34	66.40	241.02	214.20	165.44	213.47
SRF	Average	4.53	5.88	5.88	5.88	17.65	30.00
	Stdev	2.55	3.31	11.26	10.81	24.32	56.96
	Variability (%)	56.35	56.35	191.46	183.82	137.80	189.86

Oc = Occurrence; FRR = Relative Frequency; DER = Relative Density; DOR = Relative Dominance; IVI = Value of Significance Index; VIF = Family Importance Index

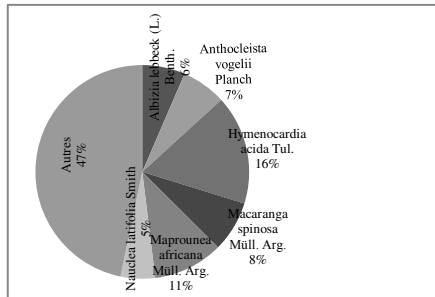


Diagram 1. Dominant Species / SMD

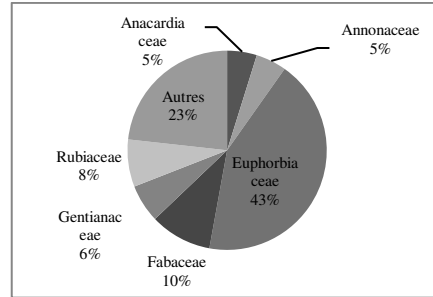


Diagram 2. Dominant Families / SMD

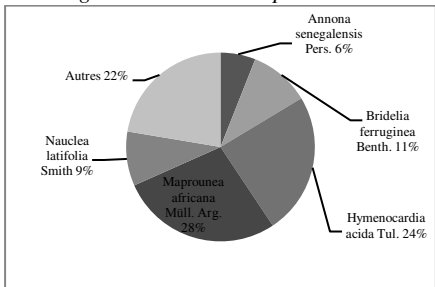


Diagram 3. Dominant species / SRF

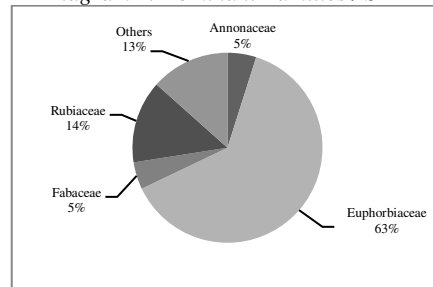


Diagram 4. Dominant families / SRF

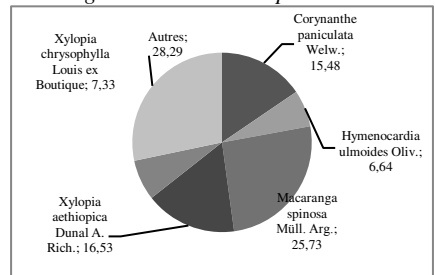


Diagram 5. Species and dominant families in the subplots

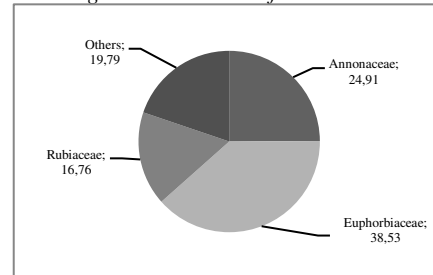


Diagram 6. Dominant families in the subplots

Figure 6. Percentage of dominant species and families in the two types of savannah (SMD and SRF) as well as in the subplots

Table 2. Synthesis of the regeneration in the subplots of the savannah put in defense

Number	Species	N.I	Oc.	FRR	DER
1	<i>Macaranga spinosa</i> Müll. Arg.	221	5	8,1	25,7
2	<i>Xylopias aethiopica</i> Dunal A. Rich.	142	4	6,5	16,5
3	<i>Corynanthe paniculata</i> Welw.	133	5	8,1	15,5
4	<i>Xylopias chrysophylla</i> Louis ex Boutique	63	3	4,8	7,3
5	<i>Hymenocardia ulmoides</i> Oliv.	57	4	6,5	6,6
6	<i>Oncoba welwitschii</i> Oliv.	42	3	4,8	4,9
7	<i>Anthocleista vogelii</i> Planch	32	4	6,5	3,7
8	<i>Albizia adianthifolia</i> (Schumach.) W. Wight	30	3	4,8	3,5
9	<i>Symphonia globulifera</i> L. f.	30	1	1,6	3,5
10	<i>Hymenocardia acida</i> Tul.	25	3	4,8	2,9
11	<i>Croton sylvaticus</i> Hochst. ex Krauss	21	3	4,8	2,4
12	<i>Vernonia conferta</i> Benth.	11	2	3,2	1,3
13	<i>Heinsia pulchella</i> (G. Don) K. Schum.	10	4	6,5	1,2
14	<i>Xylopias hypolampra</i> Mildbr.	9	3	4,8	1,0
15	<i>Tetrorchidium didymostemon</i> (Baill) Pax et K.	7	1	1,6	0,8
16	<i>Holarrhena congolensis</i> Stapf	5	1	1,6	0,6
17	<i>Albizia lebeck</i> (L.) Benth.	4	2	3,2	0,5
18	<i>Barteria nigritiana</i> Hook. f.	4	2	3,2	0,5
19	<i>Hylodendron gabunense</i> Taub.	3	1	1,6	0,3
20	<i>Zanthoxylum gillettii</i> (De Wild.) P.G. Waterman	3	2	3,2	0,3
21	<i>Markhamia sessilis</i> Sprague	2	1	1,6	0,2
22	<i>Albizia ferruginea</i> (Guill. & Perr.) Benth.	1	1	1,6	0,1
23	<i>Canthium oddonii</i> (De Wild.) C. Evrard	1	1	1,6	0,1
24	<i>Dacryodes buettneri</i> (Engl.) H. J. Lam	1	1	1,6	0,1
25	<i>Millettia versicolor</i> Welw. ex Baker	1	1	1,6	0,1
26	<i>Trichilia gilgiana</i> Harms	1	1	1,6	0,1

Oc = Occurrence; FRR = Relative Frequency; DER = Relative Density; NI = Number of individuals

Density of stand of the plots in the savannah put in defenses and the savannah under fire regime

This density is presented in *Figure 7* for the two types of savannah, namely SMD and SRF.

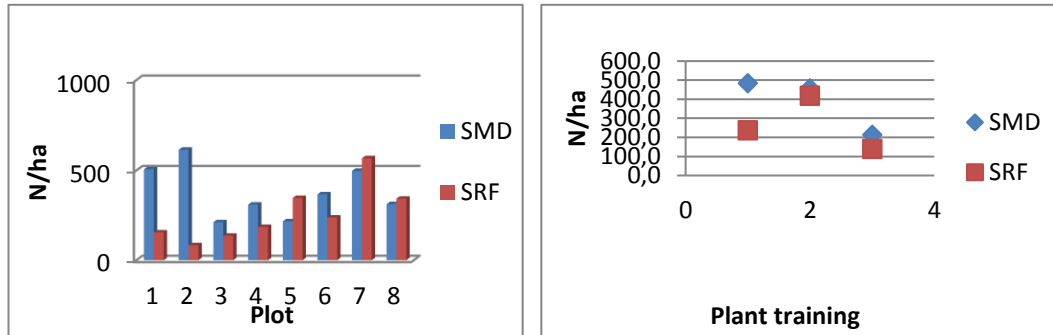


Figure 7. Density in the SMD & SRF

Structure of the planted flora in the savannah set in defense (SMD) and savannah under fire regime (SRF)

The figures from 8 to 13 show the growth of trees based on their circumferences and heights divided into classes of 10 cm and 5 m respectively. The figures 8 and 9 show the general horizontal and vertical tree structure in SMD and SRF as well as the basal area in the two savannah landscapes. Figures 10 and 11 show the horizontal and vertical structure of two characteristic species: *M. africana* Müll. Arg. and *H. acida* Tul. in SMD and SRF.

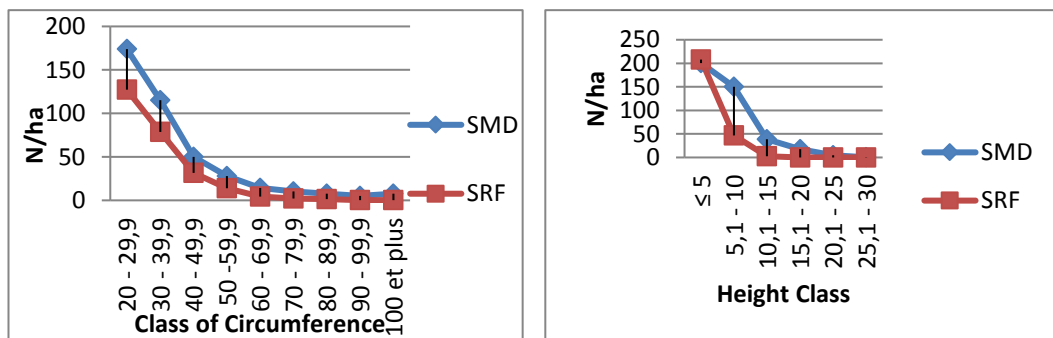


Figure 8. Horizontal and vertical tree structure in SMD and SRF

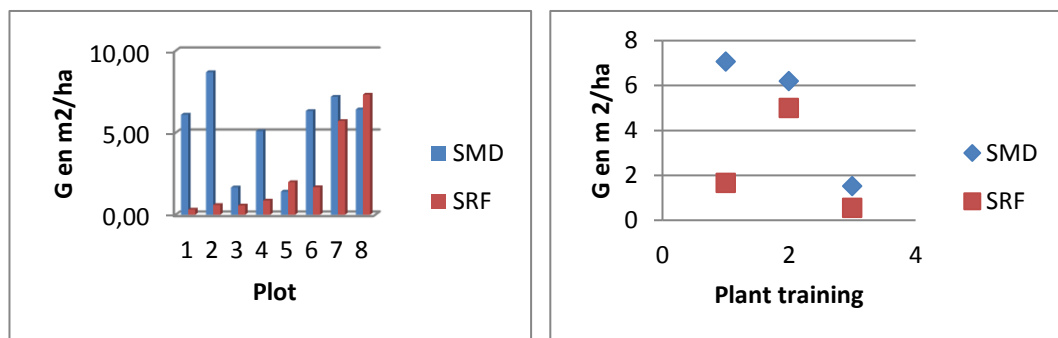


Figure 9. Basal area in SMD and SRF

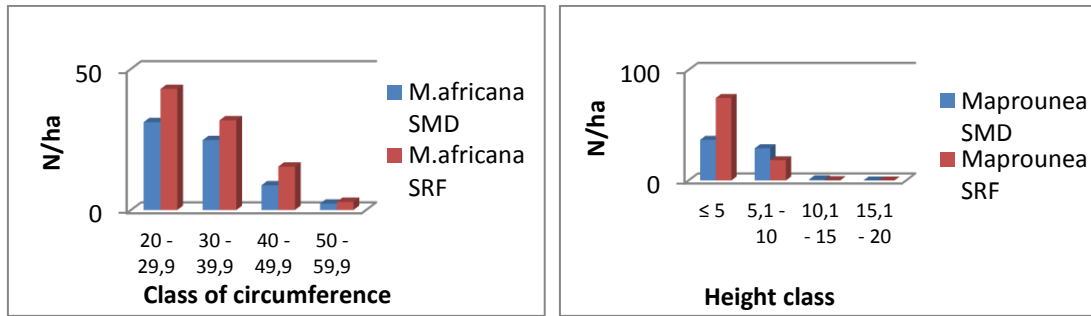


Figure 10. Horizontal and vertical structure of *M. africana* Müll. Arg. in the SMD and the SRF

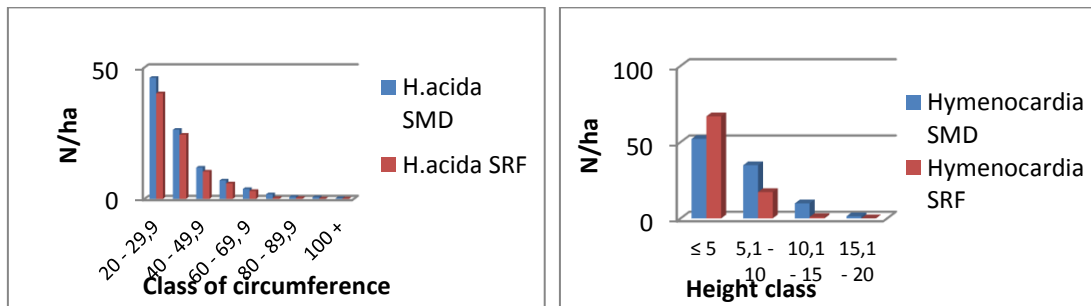


Figure 11. Horizontal and vertical structure of *H. acida* Tul. in SMD and SRF

Figures 12 and 13 show the horizontal and vertical structure of a pre-forest species (*M. spinosa* Müll. Arg.) in the SMD as well as the horizontal and vertical structure of a forest species (*X. aethiopica* Dunal A. Rich.) in the SMD and the SRF.

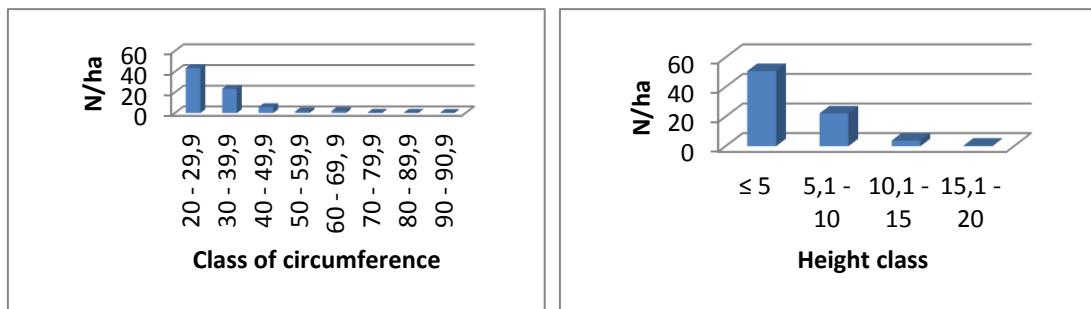


Figure 12. Horizontal and vertical structure of *M. spinosa* Müll. Arg. in the SMD

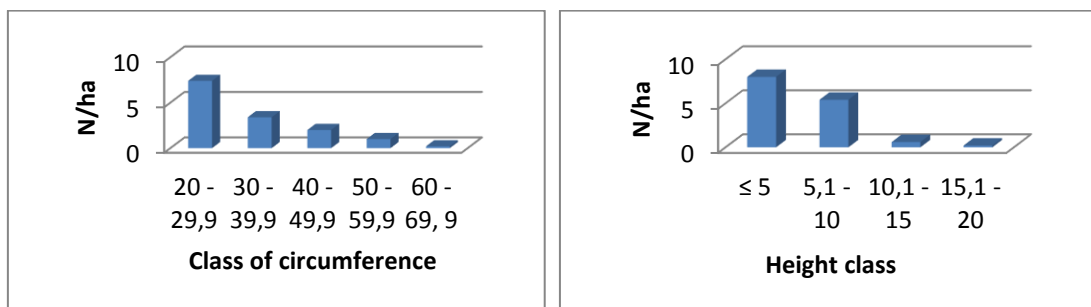


Figure 13. Horizontal and vertical structure of *X. aethiopica* Dunal A. Rich. In the SMD and the SRF

Statistical analysis

Statistical analysis presents the Specific Richness (*Figure 14*), the Density (*Figure 15*), as well as the basal area (*Figure 16*) for the SMD and SRF.

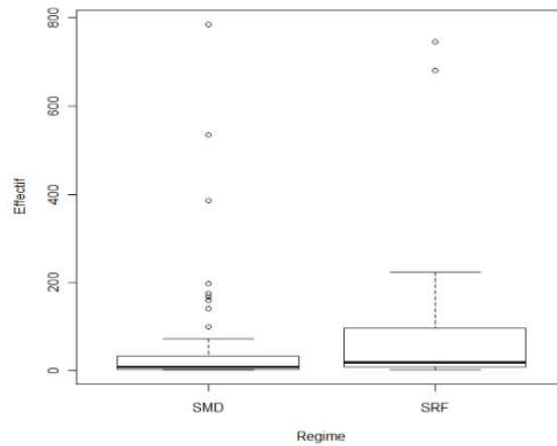


Figure 14. Dispersion of the numbers of woody species in two regimes (SMD and SRF) ($F = 2.04, P > 0.05$)

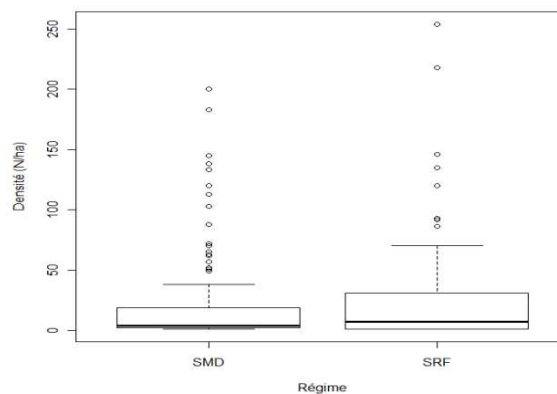


Figure 15. Density dispersion of woody species from two regimes (SMD and SRF). ($F = 3.05, P > 0.05$)

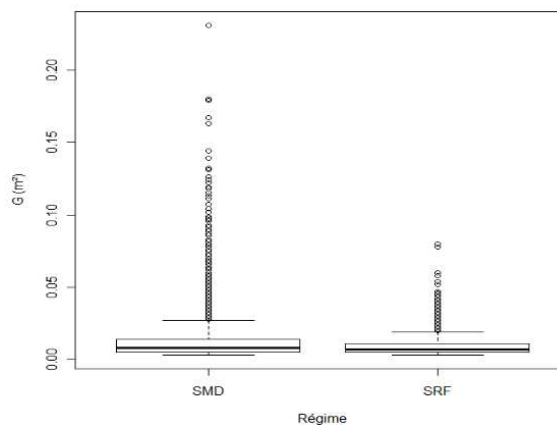


Figure 16. Basal area value dispersion for the two regimes (SMD and SRF). ($F = 108.53, P < 0.0001$)

Discussion

Floristic diversity

The results obtained in this work show that SMD includes the highest number of species (61), genera (50) and families (25). SRF has a low diversity: 17 species, 16 genera and 10 families. The overall average species is 10 species / ha for SRF and 23 species / ha for SMD. The IVI analysis shows that *Hymenocardia acida* Tul., *Maprounea africana* Müll. Arg., *Macaranga spinosa* Müll. Arg., *Anthocleista vogelii* Planch, *Albizia lebbek* (L.) Benth., *Nauclea latifolia* Smith., *Lannea welwitschii* (Hiern) Engl. and *Bridelia ferruginea* Benth. are species with a higher relative density in the savannah protected; better distributed in the SMD (50%) and are highly important depending on the basal area they occupy (*Figure 6 / Diagram 1*).

The analysis shows that the families Euphorbiaceae, Fabaceae and Rubiaceae, are the most important families (*Figure 6 / Diagram 2*). In the work of Dibi et al. (2008), carried out in forest-savanna contact zone, these families are among the most important families. In the SRF, *Maprounea africana* Müll. Arg., *Hymenocardia acida* Tul., *Bridelia ferruginea* Benth., *Nauclea latifolia* Smith, and *Annona senegalensis* Pers., are species with higher DER. Likewise, these species are best distributed and are highly important depending on the basal area they occupy (*Figure 6 / Diagram 3*).

According to the work of Devred (1956), these species are among the typical species of the Bas-Congo savannah, adapted to fires and difficult conditions. Such vegetation can be described as a pyrophyte because its destruction by fire is followed by a reconstitution phenomenon, (although slow because of edaphic conditions), but without any profound change in the type of vegetation or flora (Jaffré et al., 1998). This reflects the ability of the ecological system to respond to a disturbance by returning to the stage before it. In SRF Euphorbiaceae, Rubiaceae and Annonaceae are the most important families (*Figure 6 / Diagram 4*). Note in the SMD that *Hymenocardia acida* Tul. and *Maprounea africana* Müll. Arg. are dominant, their proportion remains low compared to the SRF, likewise for the Euphorbiaceae family. In the SRF *Maprounea africana* Müll. Arg. is more represented than *Hymenocardia acida* Tul; *Maprounea africana* Müll. Arg. withstands fire better because of its thick bark.

The sub-plots were dominated inside of the SRF and SMD by the species like: *Macaranga spinosa* Mull, *Xylopi aethiopica* Dunal, *Corynanthe paniculata* Welwich, *Xylopi chrysophylla* Louis, *Hymenocardia ulmoides* Oliv; as well as families of Euphorbiaceae, Anonaceae, Rubiaceae and others (*Figure 6 / Diagram 5*). The diversity is low in plots 3 and 5 (SMD), this is related to the nature of the substrate on which they are based. The substrate can play an important role in the non-installation of species that can not withstand these harsh conditions even though the savannah is put in defense. On poor soil, the work of Louppe et al. (1995) shows that in plots protected from fire there are 6 times fewer species, 32 times fewer individuals and a reduced basal area of nine tenths.

Parcel 6 in the SRF (Border), although subject to fire, is based on low-lying humus soil that provides favorable conditions for the establishment of other species. Plots 7 and 8 of the SRF are in a kraal and are used as pasture. These are covered by an early fire to allow livestock to have green grass during the dry season. A well-conducted early fire eliminates the risk of a second fire during the same dry season. Jacquin (2010) states that, at the intra-annual scale, early fires in the dry season favor the development of woody species by disadvantaging herbaceous species.

By analyzing the results of the parcel-by-plot inventory, it is noted that the border in the SMD, presents a highly evolved floristic composition with a high recovery rate (*Figure 7*). The presence in the edges of SMD of pre-forest and forest fallow species (*Trema orientalis* (L.) Blume, *Tetrorchidium didymonstemon* (Baill) Pax and K., *Albizia gummifera* (JF Gmel.) CA Sm., *Oncoba welwitschii* Oliv, *Harungana madagascariensis* Lam. Ex Poir, etc., and forest species (*Eriocoelum microspermum* Radlk, ex De Wild, *Deinbolia acuminata* Exell, *Microdesmis puberula* Hook, ex Planch, *Musanga cecropioides* R. Br. *Myrianthus arboreus* P. Beauv., *Pseudospondias microcarpa* (A. Rich.) Engl., Etc.), testifies to the positive effect of the setting in defense and a proof that a protected savanna, in contact with the forest can evolve towards a climactic ecosystem.

Louppe et al. (2008), states that *Albizia gummifera* (J. F. Gmel.) C. A. Sm., Occurs in the savannahs near the forest. Youta (1998) estimates that the genus *Albizia* is present in clearings and windfall; their presence outside these openings testifies to the existence of old clearing without which they could not grow normally. The setting in defense allowed certain groves to maintain, and even to extend, which would not be possible under the conditions of the fires. Jacquin (2010) states that the absence of fire pressures would promote forest regeneration.

The averages of the indices in *Table 1* give higher values in the SRF than in the SMD, which is explained by the low specific diversity observed in the SRF compared to the SMD. The more a stand is diversified; the averages of these indices are small. It is also noted that there is a great heterogeneity between the different stands in both SMD and SRF because the variability is far greater than 15% (*Table 1*). This shows that after 6 years of protection against fire, species of savannas adapted to fire and difficult conditions continue to dominate in the floristic composition of the SMD and the SRF. Statistically, there is no difference between SMD and SRF ($F = 2.04$, $P > 0.05$) (*Figure 14*).

Density of stands

Statistically, there is no difference in density between SMD and SRF ($F = 3.05$, $P > 0.05$) (*Figure 15*). Numerically, the SMD gives a higher result (403.88 ind./ha on average) than that of the SRF (256.38 ind./ha on average). The results of a study conducted by FAO in the Lubumbashi region (available at <http://www.fao.org/docrep/T0748F/t0748f07.htm>) show that after 6 years of establishment in a forest clear, the density of the plots can double. The figures obtained after inventory for our study in the SMD (403 ind./ha on average) are generally satisfactory because they are close to the figures obtained by the FAO in Lubumbashi, by Dibi et al. (2008) in the PNM in the forest zone and by Bouko et al. (2007) in Benin. These results are superior to those obtained by Dibi et al. (2008) in the PNM in savanna (203 and 56 plants / ha). The results obtained in shrubby savanna are low compared to those obtained by Devineau (1997) in Burkina Faso where the density is 1500 plants / ha.

The work of Louppe et al. (1995) shows that the number of surviving species, after 58 years of fire, is only 20 for 214 individuals per hectare. The work of Monnier (1990) shows that after 30 years of defencion savannah has 21,780 individuals against 13,227 in that which was subject to early fire and only 4,251 in that subject to late fires.

Stand structure

A good analysis of stand dynamics takes into account two variables that are important: the vertical and horizontal structure (Mitja, 1992). Mitja (1992) argues that the vertical structure offers, among other things, an interest in providing an indicator of site richness and that the horizontal structure accounts for the distribution of individuals in the horizontal plane.

The analysis of *Figures 8 and 10-13*, dealing with the distribution of stems by circumference class and height shows a decrease in the number of individuals as the circumference and height increase. Looking at *Figure 8*, we note that the overall structure of the stand is not a decreasing asymptote or an inverted J as it might be the case for a tropical dense rain forest (Dibi et al. 2008), but rather tends towards a decreasing distribution in L (Bouko et al. 2007). These could be growing populations because of the very high numbers of small trees and a very small number of trees with large circumferences. But some characteristic species of individual savannas, including *Hymenocardia acida* Tul (*Fig. 11*), offer an asymptotic structure.

There is also a fairly large gap between the SMD and the SRF curve for both circumference and height. The SRF curve drops rapidly to zero a little further than that of the SMD and shows that in the SRF there is a very small number of trees of great circumference following the action of the fire. The work of Dupuy et al. (1997) shows that there are more individuals in the 1st class of diameter in the exploited and burnt forest.

Statistically, analyzing the basal areas in the SMD and the SRF we note that the difference is very significant ($F = 108.53$, $P < 0.0001$). The box plot in *Figure 16* shows the interval in which 50% of the basal areas are grouped and the thick bar inside the box indicates the mean; the bar below indicates the minimum basal area and the bar above the box indicates the maximum basal area. The presence of individuals appearing above the upper mustache is often considered to be aberrant (Cornillon, 2010). For this study these individuals are mostly individuals of the edge whose G values deviate from the general average and this is a proof of the strong variability that characterizes all stands.

Figure 9 shows that SMD plots have higher basal areas than SRF plots. Similarly, in plant formations, the averages are higher in SMD than in SRF. In the SRF there is an increase for parcels 7 and 8, which are located in a kraal covered by an early fire. The results obtained in the SMD are low compared to those obtained by Dibi et al. (2008) in the forest-oriented PNM, but they are satisfactory compared with those obtained by Bouko et al. (2007) in Benin in the forest, wooded savannah, fallows and fields. The results obtained by Devineau (1997) in shrubby savanna are about five times higher than those obtained by our study in the SMD.

The vertical structure (*Figure 11*), which is the distribution of individuals by height class, shows that the SMD is higher than the SRF. It can also be noted that the fire often lit at critical periods (end of the dry season) does not allow ligneous trees to develop important parts (heights and trunk diameters). This difference in the vertical structure of SMD and SRF is well numerically perceptible at the level of stem densities (*Figure 9*). This difference is perceptible statistically in the basal areas (*Figure 16*). The structure of species *H. acida* Tul and *M. africana* Müll. Arg. which are dominant in the SMD and the SRF, shows that the most represented individuals are in the circumference class of 20 and 30, most of which do not exceed 5 m high (*Figures 10 and 11*). This confirms the work of Devred (1956) whose results show that these species are pyrophytes and adapted to extreme conditions.

The results showed that *M. africana* Müll. Arg is much more adapted to fires than *H. acida* Tul, attributable to its thick bark. Both species have good regeneration in both SMD but not in SRF. These assertions are made subject as long as the work of the dendrochronology does not confirm them, because we estimate that in the difficult conditions of the sites, the size of the trees can not necessarily translate the age of the trees. *M. spinosa* Müll. Arg. (Figure 12) which is a pre-forest species exhibits good behavior in SMD. Similarly, *X. aethiopica* Dunal A. Rich (Figure 13), which is a secondary forest species, also exhibits good behavior; blatant sign of the reforestation process in the SMD.

Regeneration

The purpose of this inventory was to analyze the effective regeneration of species (Mitja, 1992), the effects of bush fires and the benefits of defensive management, but also to predict the future floristic physiognomy. In the FRS, subplot inventory results indicate the complete absence of young individuals, even in plot 3 and 5 of the SMD. Clément (1982) states that in a bushfire savannah the original tree vegetation does not recover. Louppe et al. (1995) argue that adult trees of fire-resistant pyrophile species can continue to grow but fail to regenerate and that young subjects, booms and stumps are often destroyed by fire. They claim that some saplings can survive, perhaps during very rainy years that limit the intensity of fire. The low rainfall in the area of our study makes this regeneration unlikely after fire.

In the SMD, the results obtained (Table 2) in general are encouraging, although some concerns remain on the northern part of the savanna (plots 3 and 5), a situation attributed to the substrate. The hygrophilic nature of most of the savannah patches put in defense (consequence of the setting in defense) is favorable with the germination of very many seedlings. The frequencies in the sub-plots of SMD show that there is a strong presence of species that are not strongly represented in the adult state. The work of Mitja (1992) confirms these results.

This analysis allows us to predict a significant change in the floristic composition of the tree and tree layer if the fire protection of this savannah continues. The FAO report on the study of open woodlands around Lubumbashi shows that defensibility allows for considerable enrichment, especially in young people. A closer analysis shows that, in parallel with the increase in the number of individuals, there is a marked improvement in the floristic composition. The most savanna species are becoming scarce over the years, as are the indicators of degraded situations (fire or arid and poor soil). The Euphorbiaceae family remains the most dominant family as is the case in the SMD and SRF plots (Figures 7, 9 and 11).

Similarity between the savannah protected and plots under fire

The value of the Sorensen similarity coefficient between SMD and SRF is less than 50% (43.24), indicating that at the level of the floristic composition, these two entities are different from each other (Dibi et al., 2008). By analyzing this parcel ratio per parcel, the parcels of the SMD have a strong similarity between them.

Comparing the large plant formations (edge, tree savannah and shrub savannah) of the SMD, there is a strong similarity between the edges of the edge and those of the wooded savanna (71.91), while between the plots of the edge and those of the shrub savannah the similarity is less (32.78). The patches of savannah and shrub savannah also have a low similarity (41.66). This same comparison shows that there is a strong

similarity between the plant formations of the SRF. The similarity is weak between the plant formations (edge and savanna tree) of the SMD and the SRF, but it remains high between the bush savannah of the SMD and the SRF (edge, savannah and savannah shrub).

The work of Dibi et al. (2008) has shown that the different savannah formations have a similarity coefficient of less than 50% and are therefore floristically different. In the SMD, plots P3 and P5 are those which do not undergo a spectacular evolution in terms of species that the rest of the savannah plots put in defenses. The soil (ferruginous gravel, quartz pebbles) and the presence of boulders from bedrock spoilage in these patches may be the cause.

Nébié (2005) states that these harmful aspects inherent to the soil represent an obstacle to the normal development of the vegetation, since the roots have only a small thickness of exploitable soil. Soils in these areas are generally shallow (Doucet, 2003), and characterized by downward leaching of clay downward and infiltration of rainwater (Nébié, 2005). Their structure is massive, frequently compact, indurated on the surface (Devineau, 1997), their chemical wealth is low: deficiency in lime and magnesium. Devineau (1997) considers that if such soil has never been cultivated, it must be considered as a stage of degradation of the pyroclimax under the effect of grazing. But in the case of our study it is rather a highly anthropized savanna.

Conclusion

Work in the SMD and SRF identified 63 plant species across all SMD plots and 17 species in SRF. These species are divided into 51 genera and 26 families. The dominant species are *H. acida* Tul and *M. africana* Müll. Arg, and the dominant families are: Euphorbiaceae, Fabaceae and Rubiaceae. The overall average of species is 10 species per ha for SRF and 23 species per ha for SMD. The results of this study showed that SMD is more diversified than SRF but this diversity is still very low compared to the diversity observed in forest areas. Stand structure indicates that SMD has a larger basal area than SRF. Overall, trees in SMD are taller than SRF trees.

In each case study (SMD and SRF), the community or similarity coefficient is very high between plots of the same case, but comparing these two treatments the coefficient of similarity is low (43.23). Which means that at the floristic level the SMD and different from the SRF.

The results of this work showed that 6 years after the setting in defense, the vegetation of the savannah is in full evolution and that the putting in defense of the savannas constitutes one of the effective means to favor the forest regeneration around Luki. These results show that the reforestation process started well before the defensive period, and confirm that the protection of this savannah allowed this savannah to reach the current structure. These preliminary results contribute to understanding the impact of savanna conversions on climate change. This will enable decision-making in the sustainable management of savannas and the protection of the environment.

As a recommendation related to this study we suggest the following:

A. To researchers:

- Always characterize the savannas to be defended and make a floristic inventory in the first year of disposal, in case the experiment should be duplicated. This would make it possible to follow the normal evolution of the savannah put in defenses year by year.

- Conduct analytical studies of soils in different plant formations and / or plots of the SMD, to further explain the flora they display.
 - Monitor the plots and subplots installed in the SMD annually to understand the evolution of their composition and structure and determine annual increments.
 - Integrate the work of dendrochronology to estimate the age of the SMD stands, this work would make it possible to determine the speed of the progression of the forest.
 - Install plots at the savanna edge interface to assess the rate of savannah colonization by edge features.
 - Continue to support local populations by multiplying projects and income-generating activities promoting development in order to free them from the total dependence of forest products.
 - Increase awareness
- B. To the local people surrounding the savannah of Manzonzi:
- Continue to protect the protected savannah in order to safeguard its assets.

REFERENCES

- [1] Arruda, D. M., Schaefer, C. E. G. R., Correa, G. R., Rodrigues, P. M. S., Duque-Brasil, R., Ferreira-JR, W., Oliveira-Filho, A. T. (2015): Landforms and soil attributes determines the vegetation structure in the Brazilian semiarid. – *Folia Geobot* 50: 175-184.
- [2] Baudena, M., Dekker, S. C., van Bodegom, P. M., Cuesta, B., Higgins, S. I., Lehsten, V., Reick, C. H., Rietkerk, M., Scheiter, S., Yin, Z., Zavala, M. A., Brovkin, V. (2015): Forests, savannas, and grasslands: bridging the knowledge gap between ecology and Dynamic Global Vegetation Models. – *Biogeosciences* 12: 1833-1848.
- [3] Bouko, B. S., Sinsin, B., Soule, B. G. (2007): Effects of land-use dynamics on the structure and floristic diversity of open forests and savannas in Benin. – *Tropicultura* 25(4): 221-227.
- [4] Burrows, N. D. (2008): Linking fire ecology and fire management in South - West Australian forest landscapes. – *Forest ecology and management* 255: 2394-2406.
- [5] Clément, J. (1982): Estimation of volumes and productivity of mixed tropical forest and grass formations. Data on french African countries in northern Ecuador and recommendations for conducting new studies. – *Forestry and Forests of the Tropics magazine* 198(4), 24 p.
- [6] Cornillon, P. A., Guyader, A., Husson, F., Jegou, N., Josse, J., Kloareg, M., Matzner, L. E., Rouviere, L. (2010): *Statistics with R*. 2nd augmented edition. – Rennes University Presses, French statistical society, 274 p.
- [7] Dale, M. R. T. (1999): *Spatial Pattern Analysis in Plant Ecology*. – Cambridge, UK. Cambridge University Press.
- [8] De Foresta, H. (1990): Origin and evolution of intramayambian savannahs (D.R Congo). II. Contributions of forest botany. – *Quaternary Landscapes of Central Atlantic Africa*. Available at: http://horizon.documentation.ird.fr/exl-doc/pleins_textes/divers11-10/34796.pdf.
- [9] Deklerck, V., De Mil, T., Ilondea, B. A., Nsenga, L., De Caluwe, C., Van den Bulcke, J., Van Acker, J., Beeckman, H., Hubau, W. (2019): Rate of forest recovery after fire exclusion on anthropogenic savannas in the Democratic Republic of Congo. – *Biological Conservation* 233: 118-130.
- [10] Devineau, J. L., Lecordier, C., Vuattoux, R. (1984): Evolution of the specific diversity of the woody stand in a pre-forest succession of colonization of a savannah protected from

- fire (Lamto, Ivory Coast). – *Candollea* 39(1): 103-134. Available at: http://hal.archives-ouvertes.fr/docs/00/43/49/47/PDF/Devineau_et_al_1984.pdf.
- [11] Devineau, J. L. (1997): Seasonal evolution and rate of increase of basal areas of ligneous trees in some Sudanese savannah stands in western Burkina Faso. – *Ecology* 78(3): 217-232.
- [12] Devred, R. (1956): The grassy savannas of Mvuazi region (Bas Congo). – INEAC publications, Scientific Series No. 65, 122 p.
- [13] Dibi, N. H., Yao, C. Y. A., Kouakou, N. E., Kone, M., Yao, S. C. (2008): Analysis of the floristic diversity of the Marahoué National Park, Central West of Côte d'Ivoire. – *Africa science* 4(3): 552-579.
- [14] Doucet, J. L. (2003): The delicate alliance of forest management and biodiversity in the forests of central Gabon. – Original dissertation submitted for the degree of Doctor of Agricultural Sciences and Biological Engineering. University Faculty of Agricultural Sciences, Gembloux, Belgium, 390 p.
- [15] Duarte, L. Da S., Dos-Santos, M. M. G., Hartz, S. M., Pillar, V. D. (2006): Role of nurse plants in *Araucaria* Forest expansion over grassland in south Brazil. – *Austral Ecology* 31(4): 520-528.
- [16] Dupuy, B., Bertault, J. G., Doumbia, F., Diahuissie, A., Brevet, R., Miezan, K. (1997): Natural regeneration in dense Ivorian forest production. – *CIRAD-Forêt. Tropical forests and forests* 24(4): 25-38.
- [17] Favier, C., Namur, C. D., Dubois, M. A. (2004): Forest progression modes in coastal Congo, Central Atlantic Africa. – *Journal of Biogeography* 31: 1445-1461.
- [18] Favrichon, V., Gourlet-Fleury, S., Barhen, A., Dessart, H. (1998): Permanent plots in dense rainforest. Element for a data analysis methodology. – CIRAD - Forêt Campus International de Baillarquet. FORAFRI 1998 series document 14, 30432 Montpellier Cedex 1, France, 67 p.
- [19] Guenon, R. (2010): Vulnerability of Mediterranean soils to recurrent fires and restoration of their chemical and microbiological qualities by the addition of composts. – Thesis to obtain the degree of doctor of the university Paul Cézanne. Faculty of Science and Technology, 248 p. <http://www.fao.org/docrep/T0748F/t0748f07.htm>.
- [20] Higgins, S. I., Bond, W. J., Trollope, W. S. W. (2000): Fire, resprouting and variability: a recipe for grass–tree coexistence in savanna. – *J. Ecol.* 88: 213-229.
- [21] House, J. I., Archer, S., Breshears, D. D., Scholes, R. J. (2003): Conundrums in mixed woody-herbaceous plant systems. – *J. Biogeogr.* 30: 1763-1777.
- [22] Hutchinson, G. E. (1961): The paradox of the plankton. – *Am. Nat.* 95: 137-145.
- [23] Jacquin, A. (2010): Dynamics of savanna vegetation in relation to the use of fires in Madagascar. Time series analysis of remote sensing images. – Thesis in order to obtain the doctorate of the University of Toulouse, 146 p.
- [24] Jaffré, T., Rigault, F., Dagostini, G. (1998): Impact of bush fires on the ligno-herbaceous maquis of the ultramafic rocks of New Caledonia. – *FAO, AGRIS, Adansonia* 20(1).
- [25] Kapa, B., Nkiama, M., Malele, M., Ritvisay, M. (1987): Development of the Luki Biosphere Reserve. – SPIAF, 67 p.
- [26] Kent, M., Coker, P. (1992): *Vegetation Description and Analysis: A Practical Approach*. – Boca Raton: CRC Press.
- [27] Louppe, D., N'klo, O., Alasanne, C. (1995): Effect of bush fires on vegetation. – *Tropical wood and forest* 245(3), 16 p.
- [28] Louppe, D., Oteng – Amoako, A. A., Brink, M., Lemmens, R. H. M. J., Oyen, L. P. A., Cobbinah, J. H. (2008): *Plant Resources of Tropical Africa* 7(1): timbers 1. – PROTA Foundation / Blachhuys publishers / CTA. Wageningen, the Netherlands, 785 p.
- [29] Lubalega, T. (2016): Évolution naturelle des savanes mises en défens à Ibvillage, sur le plateau des Bateke, en République Démocratique du Congo. – Thèse en cotutelle Université Laval/ Québec, Canada/ Philosophiae doctor (Ph.D.).

- [30] Lubini, A. (1997): Vegetation of the Luki Biosphere Reserve in Mayombe (Zaire). – *Opera botanica Belgica* 10. National Botanical Garden of Belgium, Meise, 155 p.
- [31] Manlay, R., Peltier, R., N'toupka, M., Gautier, D. (2002): Assessment of the tree resources of a Sudanese savanna village in North Cameroon for sustainable management. – In: Jamin, J. Y., Seiny Boukar, L., Floret, C. (eds.). *African savannahs: changing spaces, actors facing new challenges*. Proceedings of the symposium, May 2002, Garoua, Cameroon. Prasac, N'Djamena, Chad - CIRAD, Montpellier, France, 17 p.
- [32] Menaut, J. C., Lepage, M., Abbadie, L. (1995): Savannas, woodlands and dry forests in Africa. – In: Bullock, S. H., Mooney, H. A., Medina, E. E. (eds.) *Seasonally dry tropical forests*. Cambridge University Press. Cambridge, England, 64-92 pp.
- [33] Mitja, D. (1992): Influence of shifting cultivation on wet savannah vegetation in Côte d'Ivoire (Booro - Borotou - Touba). – ORSTOM, Paris, 269 p.
- [34] Monnier, Y. (1968): Dust and ash. Landscapes, dynamic plant formations of societies in West Africa. – Ministry of Cooperation and Development / ACCT, Paris, 264 p.
- [35] Mueller-Dombois, L. D., Ellenberg, E. (1974): *Aims and Methods of Vegetation Ecology*. – New York: John Wiley and Sons.
- [36] Nebie, O. (2005): *Settlement Experience and Development Strategies in the Nakambe Valley Burkina Faso*. – Thesis presented at the Faculty of Arts and Humanities of the University of Neuchâtel to obtain the degree of doctor in human sciences. University of Neuchâtel Faculty of Arts and Humanities, 246 p.
- [37] Ouedraogo, O., Thiombiano, A., Hahn-Hadjali, K., Guinko, S. (2008): Diversity and structure of woody groups in Arly National Park (Eastern Burkina Faso). – *Flora and Vegetatio Sudano-Sambesica* 11: 5-16.
- [38] Peña-Claros, M., Poorter, L., Alarcón, A., Blate, G., Choque, U., Fredericksen, T. S., Justiniano, M. J., Leano, C., Licona, J. C., Pariona, W., Putz, F. E., Quevedo, L., Toledo, M. (2012): Soil effects on forest structure and diversity in a moist and a dry tropical forest. – *Biotropica* 44: 276-83.
- [39] Quinif, Y. (1986): Genesis of karts with turns in intertropical countries the example of Bas - Zaire. – *Annale of the Geological Society of Belgium* 109: 515-527.
- [40] Rodrigues, P. M. S., Gonçalves, C. E., Schaefer, R., de Oliveira Silva, J., Gomes, W., Júnior, F., Santos, R., Neri, A. V. (2016): The influence of soil on vegetation structure and plant diversity in different tropical savannic and forest habitats. – *Journal of Plant Ecology* 11(2): 226-236.
- [41] Rondeux, J. (1993): *The measurement of trees and forest stands*. – 1st edition, Gembloux, Belgium: Agronomical Press of Gembloux, 522 p.
- [42] Sankaran, M., Ratnam, J., Hanan, N. P. (2004): Tree-grass coexistence in savannas revisited - insights from an examination of assumptions and mechanisms invoked in existing models. – *Ecol. Lett.* 7: 480-490.
- [43] Savadogo, P., Tigabu, M., Sawadogo, L., Odén, P. C. (2007): Woody species composition, structure and diversity of vegetation patches of a Sudanian savanna in Burkina Faso. – *Bois et Forêts des Tropiques* 294(4).
- [44] Scholes, R. J., Walker, B. H. (1993): *An African Savanna: Synthesis of the Nylsvley Study*. – Cambridge University Press, Cambridge, UK.
- [45] Scholes, R. J., Archer, S. R. (1997): Tree-grass interactions in savannas. – *Annu. Rev. Ecol. Syst.* 28: 517-544.
- [46] SPIAF. (2007): *Forest Management Inventory Standards. Operational guide*. – Ministry of the Environment Conservation of Nature and Tourism, 33 p.
- [47] Sys, C. (1960): *Map of soils and vegetation of the Belgian Congo and Ruanda-Urundi, explanatory note of the soil map of the Belgian Congo and Ruanda-Urundi*. – Publications of the National Institute for the Agricultural Study of the Belgian Congo (INEAC), A. R. 22-12-33 and 21-12-39, Brussels, 96 p.
- [48] Tilman, D. (1982): *Resource competition and community structure*. – Princeton University Press, Princeton, New Jersey, USA.

- [49] Walker, B. H., Noy-Meir, I. (1982): Aspects of stability and resilience of savanna ecosystems. – In: Huntley, B. J., Walker, B. H. (eds.) *Tropical savannas*: 556-590. Springer-Verlag, Berlin.
- [50] Walter, H. (1971): *Natural Savannas*, in *Ecology of Tropical and Subtropical Vegetation*. – Oliver and Boyd, Edinburgh, UK.
- [51] Youta, J. H. (1998): *Trees against grasses: the slow invasion of the savannah by the forest in central Cameroon*. – Doctoral thesis. University of Paris-Sorbonne (Paris IV), France, 241 p.

ASPERGILLUS PAKISTANICUS: MICROSCOPIC AND PHYLOGENETIC ANALYSIS OF A NEW ENTOMOPATHOGENIC FUNGI ISOLATED FROM THE SOIL OF THE CHANGA MANGA FOREST, PAKISTAN

ABRAR, A.^{1*} – MUGHAL, T. A.¹ – SARWAR, S.² – ONEEB, M.³ – MALIK, K.⁴ – SAIF, S.¹ – ABBAS, M.¹

¹*Department of Environmental Science, Lahore College for Women University, Lahore, Pakistan*

²*Department of Botany, Lahore College for Women University, Lahore, Pakistan*

³*Department of Parasitology, University of Veterinary and Animal Sciences, Lahore, Pakistan*

⁴*Center for Excellence in Molecular Biology, University of The Punjab, Lahore, Pakistan*

**Corresponding author*

e-mail: amina.abrar@outlook.com

(Received 22nd Aug 2019; accepted 3rd Feb 2020)

Abstract. Changa Manga forest is a man-made forest in Pakistan. The soil properties of this forest serve an ideal habitat for a vast variety of entomopathogenic fungi. A number of entomopathogenic fungi were isolated from the soil samples collected from the Changa Manga Forest using *Galleria* bait method during this investigation. Among these isolated fungi, *Aspergillus pakistanicus* was found to be morphologically and phylogenetically different from closely related *Aspergillus* species thus described as a new species. The fungal species was identified on the basis of colony morphology; light microscopy; scanning electron microscopy and by molecular analysis. Macroscopic and microscopic comparison with other species of the respective genus along with sequencing of 18S rRNA genes confirmed its uniqueness and supports its recognition as a novel species. Its angular ornamented conidia and separate clade in the phylogenetic tree support it as a new taxa. A detailed description, microscopic images, and comparison with morphologically and phylogenetically similar species are presented.

Keywords: *ascomycetes, insect bait, Indomalaya ecozone, taxonomy, 18S rRNA*

Introduction

Fertile soil of forests and agricultural lands provide natural habitats for the entomopathogenic fungi. Soil type and geographical location are important contributory factors to mark out the occurrence of these fungi (Meyling and Eilenberg, 2007). Terrestrial planes of Punjab, Pakistan support a rich diversity of soil born entomopathogenic fungi (Wakil et al., 2014). Changa Manga forest is situated in the district of Kasur near Lahore, Pakistan with the total area of 5063 ha. According to WWF classification it is located in the Indomalaya ecozone. The fertile soil of the Changa Manga forest supports many plant species. The pH (7.7 to 8.0) and other properties of the soil in the Changa Manga forest provide ideal habitat for soil associated entomopathogenic fungi. The Changa Manga forest is the home of many mammals, birds, reptiles, amphibians and insects. Common floral biota comprise of *Morus alba*, *Dalbergia sissoo*, *Acacia nilotica*, *Populus* and *Eucalyptus* species (Ahmad, 2017).

For the recovery of entomopathogenic fungi, *Tenebrio molitor* or *Galleria mellonella* are usually added to soil samples as insect bait (Ali-Shtayeh et al., 2003; Abrar et al., 2019). Entomopathogenic fungi presents a broad array of ecologically, morphologically

and phylogenetically diverse fungal species belonging to Ascomycetes and Zygomycetes (Araujo and Hughes, 2016). *Aspergillus* species are widespread in the environment. Species of genus *Aspergillus* belong to the group having many important functions in natural ecosystems and also proved to be beneficial for human economy. These fungi are usually found associated with the plant litter and soil of many terrestrial habitats (Bennett, 2010). The genus *Aspergillus* with diverse group of species can adapt to a broad range of environmental conditions including humidity and temperature (Cray et al., 2013). Asexual conidia produced by *Aspergillus* species are stress tolerant and also produce highly persistent sexual ascospores for reproduction supporting widespread distribution of these species (Krijghsheld et al., 2013). A number of species of *Aspergillus* are strong pathogens of insects and used as biocontrol agents against many insect vectors (Nnakumusana, 1985; Lage-de-Moraes et al., 2001; Yang et al., 2015; Zhang et al., 2015; Bawin et al., 2016; Kaur et al., 2019). During the present study a new entomopathogenic *Aspergillus* species has been isolated from the Changa Manga forest of Pakistan.

Materials and methods

Fungal isolation

The local strains of entomopathogenic fungi were isolated from the soil of the Changa Manga Forest, Pakistan located 80 km south west of Lahore at 31°05'N 73°58'E in the district of Kasur (Fig. 1). The isolation was carried out after the moon soon period in September-October, 2017. The isolation of fungi was done by employing insect bait method (Meyling and Eilenberg, 2006). Forth instars of *Galleria Mellonella* were used as bait insects. PDA media was used for the mass culturing of the local fungal isolates at 25 °C for seven days to obtain fungal colonies on plates (Abreu et al., 2003).



Figure 1. Map showing sampling site Changa Manga forest, Kasur, Pakistan. (Source: www.googleearth.com accessed on 13-06-2017)

Macroscopic and microscopic examination

The fungi were identified on the basis of colony morphology, vegetative and reproductive structures using taxonomic key (Klich, 2002; Bennet, 2010; Varga et al., 2011; Afzal et al., 2013). Morphological characteristics studied for the identification of

species were color and shape of the fungal colony, margins and growth rate. Microscopic characteristics were studied under 100X magnification of Nikon E-200 Trinocular Microscope equipped with DS-Fi 1-L2 camera system (Japan). The characteristics regarding hyphae, vesicle, metula, phalides, conidiophore and conidia were observed.

Scanning electron microscopic examination

The SEM technique was carried out at the Electron Microscope Unit of the Central Research Laboratory, LCWU, Lahore by using standard protocol. Spores ornamentations were photographed.

Molecular and phylogenetic analyses

Molecular analysis was done to confirm the identification of isolated entomopathogenic fungi. DNA was extracted by following the method described by Devarajan and Kim (2018) and specific PCR assays were carried by employing primers NS1 5' (GTA GTC ATA TGC TTG TCT C) 3' and NS8 5' (TCC GCA GGT TCA CCT ACG GA) 3' (Embley et al., 1992). Ultra Clean PCR Clean-up DNA Purification kit (MoBio, USA) was used to clean the specific PCR products. The PCR purified products were directly sequenced for 18S rRNA region by the company Macrogen (Seoul, Korea).

Consensus sequence was subjected to BLAST analysis at NCBI. Sequences which showed maximum similarity were retrieved from the GenBank and aligned by Muscle Alignment Tool (Edgar, 2004). Phylogenetic analysis was carried out with maximum likelihood criterion using MEGA5 software following algorithm and Jukes and Cantor (1969) model of the sequences evolution (Tamura et al., 2011) and 1000 bootstrap values. The sequence was deposited in GenBank.

Results

Holotype

Aspergillus pakistanicus Abrar, Mughal & Sarwar sp. nov. (Fig. 2) MycoBank No.: MB 830877.

Pakistan, Punjab Province: Lahore District, Changa Manga Forest, 24 September 2017, AA100717; GenBank MK371711.

Description

Colony: dark green with yellow undersurface; Colony reverse: mustered brown; Texture: powdery; Margins: entire; Growth rate: rapid; Hyphae: branched septate; Conidiophore: smooth, 100-250 µm in length, 4-5 µm in diameter; Conidial head: compact and densely columnar; Conidia: irregular to angular, spiny, about 3 µm in diameter; Vesicles: globose to hemispherical, biseriate; Metula: long ampuliform; Phialides: long ampuliform; Thermo tolerant species with optimal growth temperature 30-40 °C.

Key features

Colony color dark green with yellow undersurface, long ampuliform metula and phalides, angular and spiny conidia.

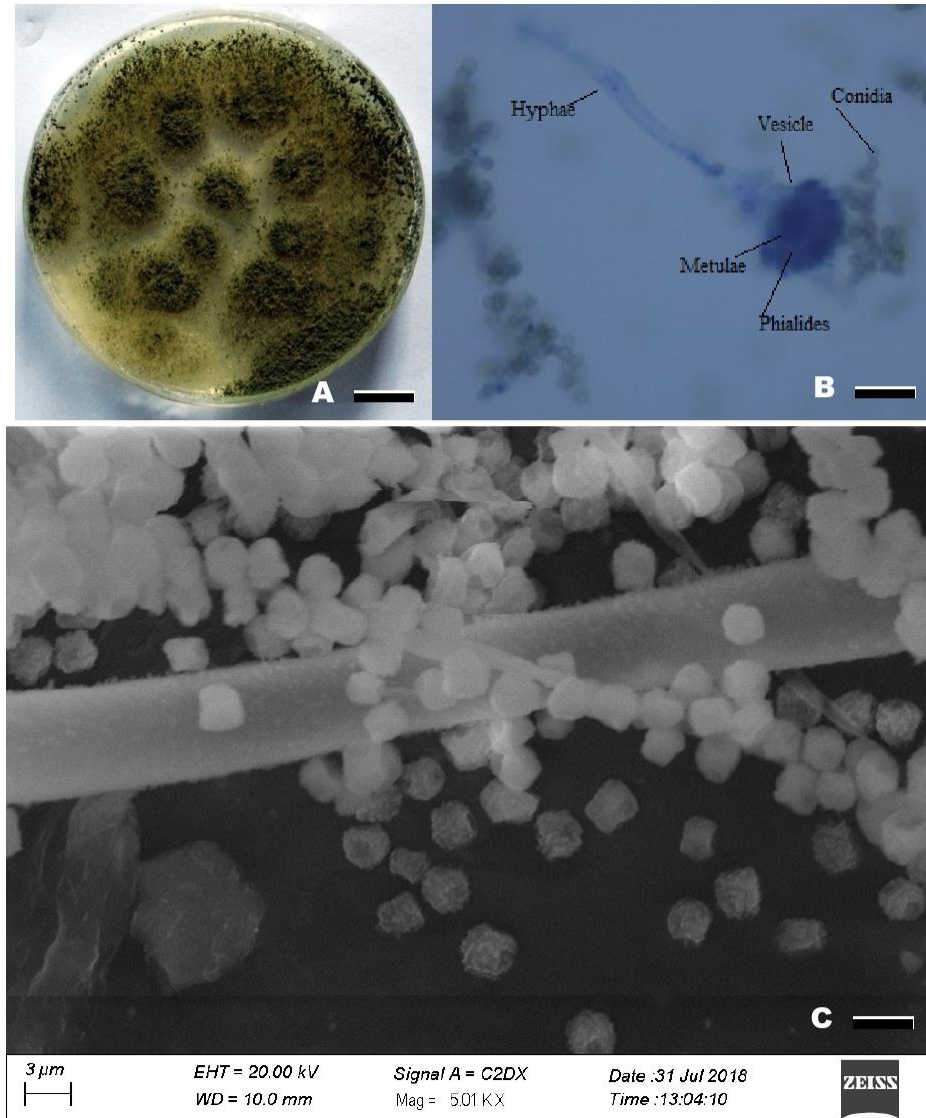


Figure 2. (A-C) *Aspergillus pakistanicus*. (A) Macroscopic features of colony; (B) Microscopic features by LM showing vesicle, conidia, conidiophore, phalides, metula and hyphae. (C) SEM micrograph of conidia highlighting their shape, ornamentation and size. Bars for A & B = 1.5 cm, for C = 2 μ m

Etymology

It was based on locality as it was isolated from a forest of Pakistan.

Distribution

It was found in the soil of the Changa Manga forest, Kasur District, Punjab Province, Pakistan.

Material examined

Aspergillus pakistanicus Abrar, Mughal & Sarwar: Pakistan, forest soil of Changa Manga, 24 September 2017, AA100717; GenBank MK371711.

Molecular phylogeny

During BLAST analysis sequences showed maximum similarity (less than cut off 97% value) with related species of genus *Aspergillus*. Phylogenetic analyses were based on data set of 31 sequences including the sequences from Pakistan. MUSCLE alignment tool was used to align all sequences. After editing and trimming, phylogenetic analysis was done by MEGA5 using maximum likelihood criterion. There were 1787 characters in final data set including 1022 conserved, 702 variable and 616 parsimony informative sites. In the resulting consensus phylogram, the sequence generated during this study form separate clade showing distinct identity (Fig. 3).

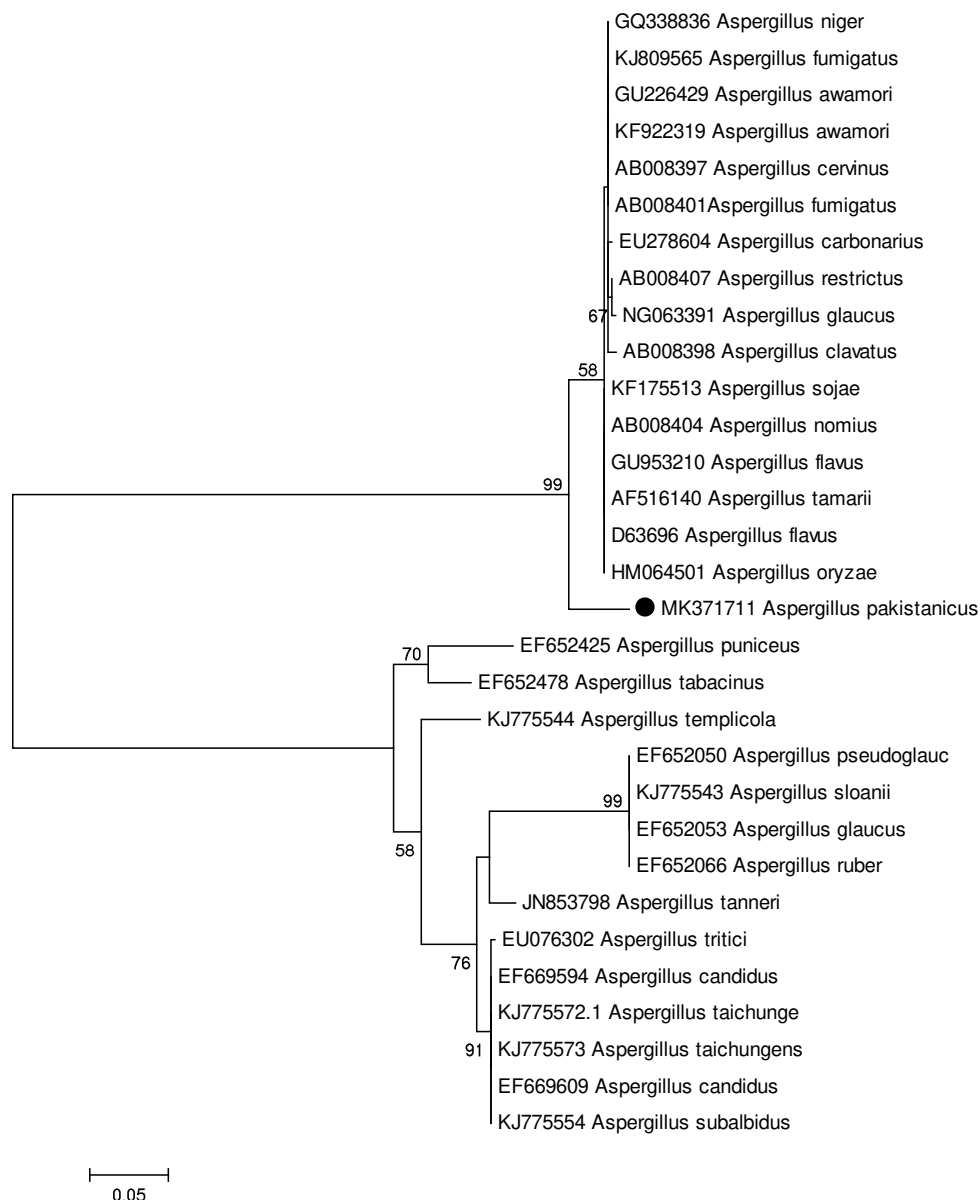


Figure 3. Phylogenetic position of *Aspergillus pakistanicus* with other *Aspergillus* spp. Tree inferred by maximum likelihood analysis. The numbers against branches indicate the percentage (>50%) at which a given branch was supported in 1000 bootstrap replications. GenBank accession number are given at the end of species names. ● indicates species reported from Pakistan

Discussion

The present research was based on the morphological and molecular identification of entomopathogenic fungus belonging to the genus *Aspergillus*. The species was isolated from the Changa Manga Forest, Pakistan. Identification of many *Aspergillus* species remain challenging because of the variability in phenotypic characteristics of genetically distinct species (Samson et al., 2006). In recent years, with the help of phylogenetic analyses, various new species belonging to the genus *Aspergillus* have been identified (Guinea et al., 2015).

A number of *Aspergillus* species were isolated during the present study including *Aspergillus terreus*, *Aspergillus parasiticus*, *Aspergillus niger*, *Aspergillus oryzae* and a novel *Aspergillus* species (Fig. 4). Morphological characteristics of various entomopathogenic *Aspergillus* species isolated during the study were observed on PDA media (Table 1).

Table 1. Macroscopic and microscopic characteristics of entomopathogenic *Aspergillus* species isolated from the Changa Manga forest, Pakistan.

Fungal isolate	Macroscopic morphology	Microscopic morphology
<i>Aspergillus parasiticus</i>	Colony color dark green, growth moderate to rapid, margins entire, texture powdery	Hyphae branched septate, conidiophore short, 400 to 500 μm in length, vesicles small averaging 30 μm in size to which the phialides are directly attached and conidia rough thick walls and spherical in shape
<i>Aspergillus terreus</i>	Colony brownish in color when observed after 3 rd day of incubation and gets darker like cinnamon-brown colony coloration observed after 7-8 days, growth rapid, margins entire, texture velvety	Hyphae branched septate, conidiophore smooth, 100-250 μm in length, 4-6 μm in diameter, vesicles globose with cylindrical metulae and phialides, conidia globose-shaped and smooth-walled and about 2 μm in diameter
<i>Aspergillus niger</i>	Colony starts with pale yellow color and gets dark brown to black quickly, growth very rapid, margins entire, texture powdery	Hyphae branched septate, conidiophore unbranched, double walled and smooth, 200 to 400 μm in length, 7 to 10 μm in diameter, vesicles globose, conidial head blackish brown, split with age, conidia round and 2.5-4 μm in diameter
<i>Aspergillus oryzae</i>	Colony color grayish green to olive green, growth moderate to rapid, margins entire, texture velvety	Hyphae branched septate, conidiophore smooth, 400 to 700 μm in length, 22 to 25 μm in diameter, vesicles globose with short metulae and elongated cylindrical phialides, conidia with smooth walls and about 4 to 6 μm in diameter
<i>Aspergillus pakistanicus</i>	Colony light yellow in color initially and then dark green with light yellow undersurface, margins entire; growth rate rapid; texture powdery	Hyphae branched septate; conidiophore smooth, 100-250 μm in length, 4-5 μm in diameter; conidial head compact and densely columnar; conidia irregular to angular, spiny, about 3 μm in diameter; vesicles globose to hemispherical, biserial; metula long ampuliform; phialides long ampuliform


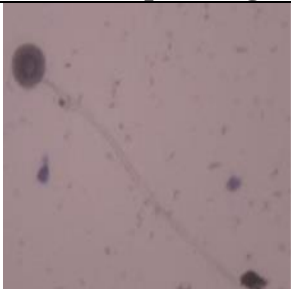

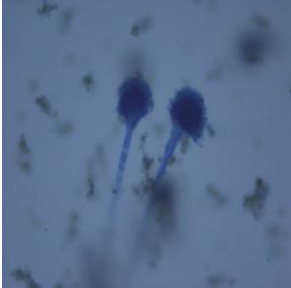

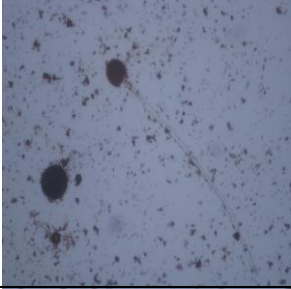
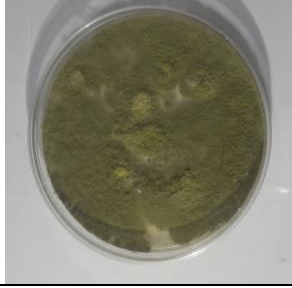
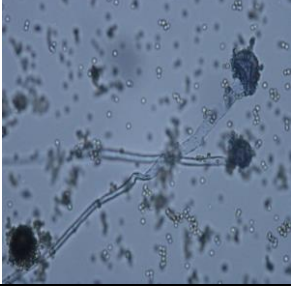


Fungal isolate	Colony morphology	Microscopic image
<i>Aspergillus parasiticus</i>		
<i>Aspergillus terreus</i>		
<i>Aspergillus niger</i>		
<i>Aspergillus oryzae</i>		
<i>Aspergillus pakistanicus</i>		

Figure 4. Colony morphology on PDA and microscopic images of entomopathogenic *Aspergillus* species isolated from Changa Manga forest, Pakistan

Detailed morphological analyses of the new species revealed that *A. pakistanicus* closely resembles *A. oryzae* but have some distinguished macroscopic and microscopic characteristics. Specifically, *A. pakistanicus* have dark green colony colour due to

pigmentation of the vegetative mycelium with light yellow undersurface and powdery texture while *A. sojae* have white to grayish green to olive green colony colour with velvety texture as reported in many studies (Matsuura and Miyazima, 1993; Haack et al., 2006; Ye et al., 2014). Both *A. pakistanicus* and *A. oryzae* have biserial vesicles and produce asexual conidia that are also known as phialidic conidia found at the end of conidiophores. Conidia of *A. oryzae* have smooth surface (Haack et al., 2006) while the new species have rough surfaced angular conidia. Genetically *A. pakistanicus* matches closely with *A. oryzae* but less matching value than standard BLAST (less than 97% identity) and well differentiated position in phylogenetic tree showed this species as new.

Conclusion

Entomopathogenic *Aspergillus pakistanicus* is regarded as novel species, based on the morphological characteristics and genetic distinction with well differentiated position in the phylogenetic tree reported during the present investigation. Further studies can be conducted to evaluate the entomopathogenic efficacy of *Aspergillus pakistanicus* against insects to explore its insecticidal potential.

REFERENCES

- [1] Abrar, A., Mughal, T. A., Oneeb, M., Tahir, E., Khalid, S., Malik, K. (2019): Persistence of local strain of entomopathogenic fungi *Aspergillus flavus* in indoor air. – International Journal of Bioscience 14(3): 133-139.
- [2] Abreu, J., Gonzalez, J., Jaqueman, F. (2003): Conservación por liofilación de diferentes especies de géneros de levaduras. – Alimentaria 40: 119-122.
- [3] Afzal, H., Shazad, S., Qamar, S., Nisa, S. Q. U. (2013): Morphological identification of *Aspergillus* species from the soil of Larkana District (Sindh, Pakistan). – Asian Journal of Agricultural Sciences 1(105): e17.
- [4] Ahmad, M. (2017): Community based ecological restoration of Changa Manga forest, Punjab, Pakistan. – Master's thesis, Norwegian University of Life Sciences, Ås.
- [5] Ali-Shtayeh, M. S., Mara'i, A. B. B., Jamous, R. M. (2003): Distribution, occurrence and characterization of entomopathogenic fungi in agricultural soil in the Palestinian area. – Mycopathologia 156(3): 235-244.
- [6] Araujo, J. P., Hughes, D. P. (2016): Diversity of entomopathogenic fungi: which groups conquered the insect body? – Advances in Genetics 94: 1-39.
- [7] Bawin, T., Seye, S., Boukraa, J. Y., Zimmer, F. N., Raharimalala, Q., Francis, F. (2016): Production of two entomopathogenic *Aspergillus* species and insecticidal activity against the mosquito *Culex quinquefasciatus* compared to *Metarhizium anisopliae*. – Biocontrol Science and Technology 26(5): 617-629.
- [8] Bennett, J. W. (2010): An overview of the genus *Aspergillus*. – Molecular Biology and Genomics 1-17.
- [9] Cray, J. A., Bell, P., Bhaganna, A. Y., Mswaka, D. J., Timsonand, J. E. (2013): The biology of habitat dominance. Can microbes behave as weeds? – Microbial Biotechnology 6: 453-492.
- [10] Devarajan, N., Kim, M. (2018): *Aspergillus terreus* (Trichocomaceae): A natural, eco-friendly mycoinsecticide for control of malaria, filariasis and dengue vectors and its toxicity assessment against an aquatic model organism *Artemia nauplii*. – Frontiers in Pharmacology 9: 1355-1357.

- [11] Edgar, R. C. (2004): MUSCLE: multiple sequence alignment with high accuracy and high throughput. – *Nucleic Acids Research* 32: 1792-1797.
- [12] Embley, T. M., Finlay, B. J., Thomas, R. H., Dyal, P. L. (1992): The use of rRNA sequences and fluorescent probes to investigate the phylogenetic positions of the anaerobic ciliate *Metopus palaeformis* and its archaeobacterial endosymbiont. – *Journal of General Microbiology* 138: 1479-1487.
- [13] Guinea, J., M., Sandoval-Denis, P. E., Pelaez, T. (2015): *Aspergillus citrinoterreus*, a new species of the section *Terrei* isolated from samples of patients with nonhematological predisposing conditions. – *Journal of Clinical Microbiology* 53: 611-617.
- [14] Haack, M. B., Olsson, L., Hansen, K., Lantz, A. E. (2006): Change in hyphal morphology of *Aspergillus oryzae* during fed-batch cultivation. – *Applied Microbiology and Biotechnology* 70(4): 482-487.
- [15] Jukes, T. H., Cantor, C. R. (1969): *Evolution of Protein Molecules*. – Academic Press, New York, pp: 21-132.
- [16] Kaur, M., Chadha, P., Kaur, S., Kaur, A., Kaur, R., Yadav, A. K., Kaur, R. (2019): Evaluation of genotoxic and cytotoxic effects of ethyl acetate extract of *Aspergillus flavus* on *Spodoptera litura*. – *Journal of Applied Microbiology* 126(3): 881-893.
- [17] Klich, M. A. (2002): *Identification of Common Aspergillus Species*. – Centraal Bureau voor Schimmelcultures, Utrecht.
- [18] Krijgsheld, P., Bleichrodt, R. V., Van Veluw, G. J., Wang, F., Muller, W. H., Dijksterhuis, J., Wosten, H. A. B (2013): *Development in Aspergillus*. – *Studies in Mycology* 74: 1-29.
- [19] Lage de Moraes, A. M., Lara da Costa, G., Ziccardi de Camargo, B. M., Lourenço de, R., Cunha de Oliveira, P. (2001): The entomopathogenic potential of *Aspergillus* spp. in mosquitoes vectors of tropical diseases. – *Journal of Basic Microbiology: An International Journal on Biochemistry, Physiology, Genetics, Morphology, and Ecology of Microorganisms* 41(1): 45-49.
- [20] Matsuura, S., Miyazima, S. (1993): Colony of the fungus *Aspergillus oryzae* and self affine fractal geometry of growth fronts. – *Fractals* 1(01): 11-19.
- [21] Meyling, N. V., Eilenberg, J. (2006): Occurrence and distribution of soil-borne entomopathogenic fungi within a single organic agroecosystem. – *Agriculture, Ecosystems and Environment* 113: 336-341.
- [22] Meyling, N. V., Eilenberg, J. (2007): Ecology of the entomopathogenic fungi *Beauveria bassiana* and *Metarhizium anisopliae* in temperate agro ecosystems: potential for conservation biological control. – *Biological Control* 43(2): 145-155.
- [23] Nnakumusana, E. S. (1985): Laboratory infection of mosquito larvae by entomopathogenic fungi with particular reference to *Aspergillus parasiticus* and its effects on fecundity and longevity of mosquitoes exposed to conidial infections in larval stages. – *Current Science* 54(23): 1221-1228.
- [24] Samson, R. A., Hong, S. B., Frisvad, J. C. (2006): Old and new concepts of species differentiation in *Aspergillus*. – *Medical Mycology* 44: S133-S148.
- [25] Nnakumusana, E. S. (1985): Laboratory infection of mosquito larvae by entomopathogenic fungi with particular reference to *Aspergillus parasiticus* and its effects on fecundity and longevity of mosquitoes exposed to conidial infections in larval stages. – *Current Science* 1221-1228.
- [26] Tamura, K., Stecher, G., Peterson, D., Filipowski, A., Kumar, S. (2011): MEGA6: molecular evolutionary genetics analysis version 6.0. – *Molecular Biology and Evolution* 30(12): 2725-2729.
- [27] Varga, J., Frisvad, J. C., Samson, R. A. (2011): Two new aflatoxin producing species and an overview of *Aspergillus* section *flavi*. – *Studies in Mycology* 69: 57-80.
- [28] Wakil, W., Ghazanfar, M. U., Yasin, M. (2014): Naturally occurring entomopathogenic fungi infecting stored grain insect species in Punjab, Pakistan. – *Journal of Insect Sciences* 14(82): 2-7.

- [29] Yang, Y., Zhang, Y., Wang, M., Li, S. S., Ma, X. Y., Xu, Z. H. (2015): Bioefficacy of entomopathogenic *Aspergillus* strains against the melon fly, *Bactrocera cucurbitae* (Diptera: Tephritidae). – *Applied Entomology and Zoology* 50(4): 443-449.
- [30] Ye, M., Lin, Y., Huang, W., Wei, J. (2014): Comparative analysis of *Aspergillus oryzae* with normal and abnormal color conidia. – *Indian Journal of Microbiology* 54(1): 108-110.
- [31] Zhang, P., You, Y., Song, Y., Wang, Y., Zhang, L. (2015): First record of *Aspergillus oryzae* (Eurotiales: Trichocomaceae) as an entomopathogenic fungus of the locust, *Locusta migratoria* (Orthoptera: Acrididae). – *Biocontrol Science and Technology* 25(11): 1285-1298.

ROLE OF INDOLE ACETIC ACID ON GROWTH AND BIOMASS PRODUCTION OF ATHEL TREE (*TAMARIX APHYLLA*) BY USING DIFFERENT CUTTING LENGTHS

RASHID, M. H. U.^{1,3,4†} – FAROOQ, T. H.^{2†} – IQBAL, W.⁴ – ASIF, M.⁴ – ISLAM, W.⁵ – LIN, D. C.^{1,3}
– AHMAD, I.⁴ – WU, P. F.^{1,3*}

¹*Forestry College, Fujian Agriculture and Forestry University, Fuzhou 350002, Fujian Province, PR China*

²*College of Life Science and Technology, National Engineering Laboratory for Applied Technology of Forestry & Ecology in South China, Central South University of Forestry and Technology, Changsha 410000, Hunan Province, PR China*

³*Fujian Provincial Colleges and University Engineering Research Center of Plantation Sustainable Management, Fujian Agriculture and Forestry University, Fuzhou 350002, Fujian Province, PR China*

⁴*Department of Forestry and Range Management, University of Agriculture, Faisalabad 38000, Punjab Province, Pakistan*

⁵*Institute of Geography, Fujian Normal University, Fuzhou 350007, Fujian Province, PR China*

[†]*These authors contributed equally to this work*

**Corresponding author*

e-mail: fjjwupengfei@126.com, fjjwupengfei@fafu.edu.cn; phone/fax: +86-591-8378-0261

(Received 6th Sep 2019; accepted 11th Feb 2020)

Abstract. Forests play a vital role in supporting life on earth. Diversification in industrialization, urbanization and overpopulation make it challenging to eliminate the impurities from the environment and to conserve our flora and fauna for basic ecological services. To enhance forest cover and growth of a plant, vegetative propagation plays a vital role. Cuttings are important plant parts that affect the growth of the plant in asexual propagation. This study aimed to observe growth response and biomass production of *Tamarix aphylla* with and without Indole-3-acetic acid (IAA) treatments at different cutting lengths. By analyzing the effect of IAA, different morphological factors were observed such as root, shoot and leaves fresh and dry weight, whole plant biomass, root and shoot length, root to shoot ratio and moisture content availability. Results showed that by increasing the cutting lengths, the growth of cuttings increased by applying IAA treatment. Overall, IAA produced a positive effect on *T. aphylla* cuttings growth as compared to IAA non-treated. According to the findings, indole acetic is a worthwhile option to get a good quality of seedling production. For that reason, understanding of this mechanism can help to make future decisions for plant growth and biomass production.

Keywords: *vegetative propagation, morphology, growth hormone application, tree production*

Introduction

Pakistan has a unique combination of ecological zones like deserts, plains, and the coastal line. Generally, Pakistan has arid subtropical weather conditions and it possesses a considerable variation of annual rainfall (Hussain et al., 2003). In recent years Pakistan is facing a severe shortage of timber and firewood, and only 10% timber requirement are

fulfilled by state forests, whereas 90% are met by the farmlands. Therefore, to supplement production from the state forests trees on-farm has been making a handsome contribution.

Moreover, agroforestry techniques are playing a crucial role to fulfill our wood requirement. *Tamarix aphylla* belongs to a genus of family *Tamaricaceae*, and largest known species of *Tamarix*. It consists of 54 native species and mainly present in the Pakistan, Iran, Afghanistan, Kazakhstan, China, some parts of Turkmenistan and Mediterranean areas. Moreover, it is spread widely throughout Europe and Africa (Orwa et al., 2009). In the form of shrub, mainly it is found at beaches, coastal areas and islands. A reasonable size of an evergreen tree of almost 18m height has resistance to sudden shock. It's hard, close grained, fibrous wood has very good mechanical properties. (Orwa et al., 2009).

Via seed germination, expected plant propagation is not possible on a sustainable basis that is the basic and potential advantage of vegetative propagation. However, due to the physiological factor like age of the parent plant, plant raised via vegetative propagation uphold a specific propagation period earlier than flowering. There is a risk that soon after flowering propagation death of a plant could occur (Banik, 1985), environmental factors that may change such status.

Several times, factors responsible for successful macro propagation of cuttings are internal or external, respectively. Many of these domestic and superficial causes are accountable for the successful propagation with cuttings, age of a parent plant (Saharia and Sen, 1990), cutting type (Singh et al., 2011), setting of propagation mode, specific concentration and type of plant growth hormones (Singh et al., 2012), season of propagation (Singh et al., 2011; Chhetri and Kumar, 2015) and material which is used in propagation (Ray and Ali, 2016, 2017) etc. With the addition of external factors like the intensity of heat present (Senyanzobe et al., 2013), balance of water, channel for rooting, intensity of light, pest and diseases attack, wind speed and humidity factors for limiting macro propagation (Banik, 1985).

Vegetative propagation practice of 1-year old cutting in different tree plants has been done, such as *Bambusa balcooa* (Gantait et al., 2018), 1.5-year old for *B. vulgaris* (Bhol and Nayak, 2012), 2-year old for *B. vulgaris* (Senyanzobe et al., 2013), *A. alpine* (Senyanzobe et al., 2013), *O. abyssinica* (Elbasheer and Raddad, 2013). Islam et al (2011), reported successful vegetative propagation of *B. vulgaris*, and found that immature cuttings are considered foremost appropriate due to the presence of extremely vigorous buds, which plays a crucial role in macro propagation (Elbasheer and Raddad, 2013). Plenty of queries have been carried out by various researchers to find out the influence of different lengths of cuttings on survival rate and growth of seedlings of various trees (Rashid et al., 2018).

The purpose of the study is to observe the response of different cutting lengths of *T. aphylla* under Indole-3-acetic acid (IAA) to check their survival and growth as well as biomass production. In this experiment, *T. aphylla* was selected because of its importance for timber, fuelwood; provide high-value forage, good salt absorption ability, and other non-tangible benefits. It can successfully grow in different areas in both tree and shrub form with diverse soil moisture contents.

Materials and methods

Site description

The proposed study was carried out in the experimental area of the Department of Forestry and Range Management, University of Agriculture Faisalabad, Punjab,

Pakistan (Fig. 1). The site was located at the latitude of 36°-26° N and longitude of 73°-06° E with an altitude of 184 m.

During the whole experimental period, weather conditions were recorded from agricultural meteorology cell, University of Agriculture, Faisalabad. Weather condition of the study site reported in Table 1, while the information about soil physical and chemical properties mentioned in Table 2. Weather data about average temperature, average rainfall, relative humidity, average sunshine and wind speed at site mentioned for six months due to the total length of experiment.

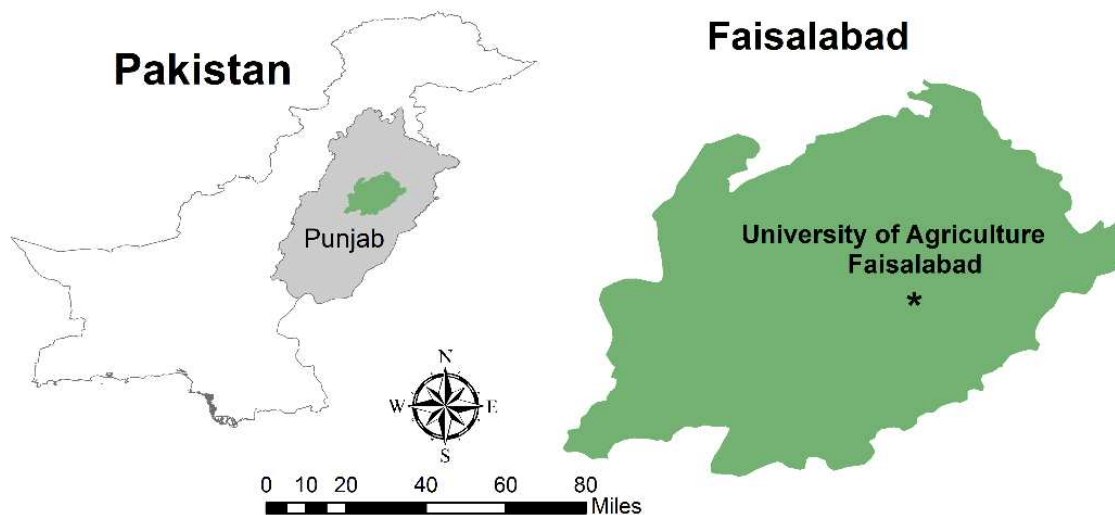


Figure 1. Location of the experimental site (University of Agriculture Faisalabad)

Table 1. Weather condition of the study site (Agromet bulletin, Agricultural meteorology cell, University of Agriculture Faisalabad). Six-month experiment conducted from February 2019 to July 2019

Month	Temperature			R.H (%)	Rainfall (mm)	Sunshine (h)	Wind speed (Km/h)
	Max (°C)	Min (°C)	Avg (°C)				
February	24.0	9.5	16.7	73.3	9.5	6.5	3.8
March	31.2	16.4	23.8	61.4	12.5	8.6	5.2
April	36.8	20.8	28.8	47.3	7.9	9.1	3.1
May	40.3	23.7	32.0	29.8	21.6	8.6	3.4
June	39.8	27.9	33.9	56.5	92.0	9.3	4.3
July	38.0	28.0	33.0	70.2	195.8	7.9	5.2

Table 2. Soil physical and chemical properties of experimental site

Parameters	Sand (%)	Silt (%)	Clay (%)	pH	EC (dSm ⁻¹)	TSS (ppm)	N (%)	P (ppm)	K (ppm)	Organic matter (%)
0-20 cm	37	42	13	8.0	1.54	1176	0.068	3.6	280	1.43
20-40 cm	66	15.5	10.5	8.1	1.21	1236	0.04	9.4	250	0.87

Experimental design

Sunken beds were prepared in the usual way by making them weed-free and loosening of soil by having a sandy clay loam texture, at the forest nursery of Department of Forestry and Range Management, University of Agriculture, Faisalabad (Fig. 2). From the mature tree of *T. aphylla*, different sizes of cuttings were prepared, from the Punjab Forestry Research Institute(PFRI), Gutwala, Faisalabad, Pakistan. Duration of this experiment was six months. IAA and non-IAA treatments with four cutting lengths were used with the ten replications for each treatment. Half number (forty) of cuttings were treated with the solution of IAA (5000 ppm) dose (Guney et al., 2016), while the other half were untreated. Overall, 80 pots (40 each for both IAA and non-IAA treatment) were used in the experiment (Fig. 2). Information about cutting lengths is given below:

1. T1 (15.24 cm cutting length of *Tamarix aphylla*)
2. T2 (22.86 cm cutting length of *Tamarix aphylla*)
3. T3 (30.48 cm cutting length of *Tamarix aphylla*)
4. T4 (38.10 cm cutting length of *Tamarix aphylla*)

The experiment was laid out in Completely Randomized Design (CRD). Daily observation was made but measurements were taken at the end of the trial. Concluding observations were taken on the 10th of July, 2019.

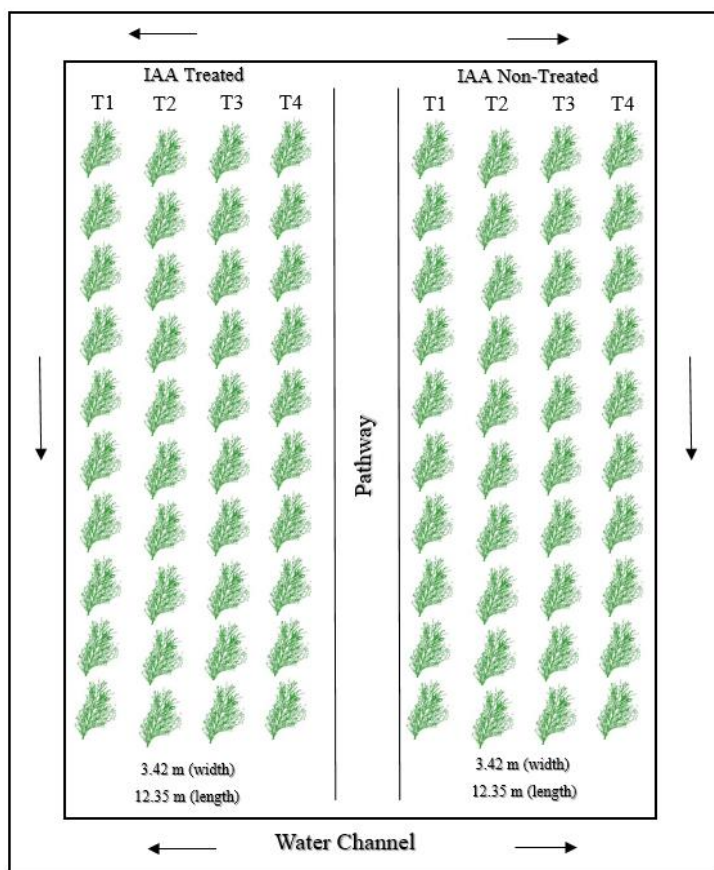


Figure 2. Layout of the experimental design (T1, T2, T3 and T4 are cutting of 15.24 cm, 22.86 cm, 30.48 cm 38.10 cm lengths, respectively)

Cutting transplanting

Planting rod was used for transplanting the cuttings of *T. aphylla* in two blocks, 1: IAA treated and 2: IAA non-treated. Cuttings planted in the mid of February 2019 to analyze the hormonal effect on the morphological characteristics of different size of cuttings. Irrigation was given immediately after planting the cuttings.

Harvesting and observed parameters

Root length and stem height, root, stem and leaves fresh and dry weight, whole plant biomass, root-shoot ratio and moisture content availability were measured. Measured plant age was almost 6 months at the time of harvesting. The sampled plants were felled and the roots were excavated by digging up to the maximum root depth. In field, the soil was removed from the roots by hand to take the fresh weight. Then the samples were brought to the laboratory for further processing. In lab, root samples were oven dried for the calculation of biomass produced. The length of shoot was measured with measuring tape while the root length was measured with a meter rod and then average was calculated to express mean length of the whole plant. For mean length, plant per block average calculated. Cuttings average were taken under each treatment for both factors with the application of IAA and without applying IAA. While recording the dry weight; material was put into the paper bags and oven dried at 75 °C for 24h and then weighed with the help of electrical balance.

Statistical analysis

Two-way ANOVA was used to observe the interaction between IAA and cutting length and showed significant differences when compared by using Tukey's test. Statistical analyses were conducted using SPSS Statistical Package (SPSS 17.0, SPSS Ins., IL, USA). Results were statistically analyzed using a $P < 0.05$ level of significance.

Results

Plant morphological growth

Cutting length had a significant effect on the morphological growth of root and shoot. Conferring to our results, highly significant ($P < 0.05$) variations among different cutting levels in both treatments were observed. Stem height was observed higher in T4 IAA treated cuttings with 42.79 ± 1.02 cm as compared to non-treated where maximum height was 37.40 ± 1.4 cm (*Fig. 3*). In comparison of hormone treatment, all the cutting treated with IAA growth showed better shoot growth in their respective lengths as compare to plants, which were un-treated. Overall, in terms of stem height, T4 cutting responded much better as compare to other cuttings in both IAA treated and non-treated cuttings.

Similarly, in root length T4 cutting responded better and it was higher with the value of 27.84 ± 1.6 cm in IAA treated cuttings and 23.12 ± 1.7 cm in non-treated plants, while in stem height the same pattern was observed. Root length and stem height consistently increased as the cutting length increased and IAA treated cutting lengths show better growth as compare to IAA non-treated plants among all cutting lengths (*Fig. 3*).

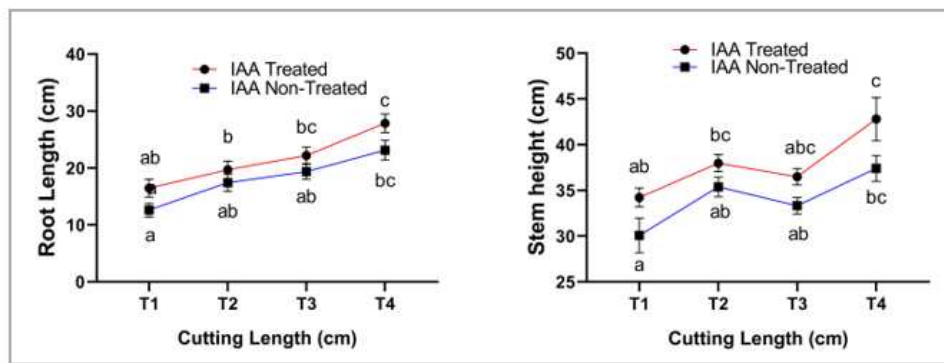


Figure 3. Average root and stem length under different sized cuttings treated with IAA hormone and non-treated cuttings. (T1, T2, T3 and T4 are cutting of 15.24 cm, 22.86 cm, and 30.48 cm 38.10 cm lengths, respectively)

Fresh biomass of plant organs

Root fresh weight increased from 8.1 ± 0.6 to 15.25 ± 1.55 gm in cutting treated with IAA and it was found highest in T4 cutting and lowest in T1 cutting. Moreover, same pattern was observed in non-treated IAA plants. In comparison of hormonal application, it was highest in IAA treated plants.

Among all treatments of cutting lengths and hormone application, stem fresh weight was also observed highest in T4 cutting treated with IAA application (37.2 ± 3.16 g), similarly, leaves fresh weight was also observed highest in T4 cutting treated with IAA application (15.5 ± 1.23 g). Overall, fresh weight of all organs like root, stem and leaves increased consistently as the cutting lengths increased both in treated and untreated plants but it was highest in the IAA treated plants (Fig. 4).

Dry biomass of plant organs

According to statistical analysis, a significant difference ($P < 0.05$) was observed in the dry biomass distribution of different plant organs among IAA treated and non-treated cuttings. Root dry biomass was observed highest in T4 and lowest in T2 in both IAA treated and non-treated cuttings. However, in hormonal application comparison it was observed highest in cutting which was treated with IAA. In cuttings lengths comparison, it consistently increased as the cutting length increased in both IAA and treated cuttings.

Stem dry biomass increased in T4 cuttings and it was observed 18.25 ± 0.7 g in the cuttings which were treated with IAA hormone as compare to un-treated cutting where it was 7.75 ± 0.7 g and it decreased to 4.25 ± 0.3 g and 6.75 ± 0.3 g, respectively in T1 cuttings. Same as stem, in leaves higher biomass value was observed in T4 cuttings (8.125 ± 0.7 g) where it was treated with IAA and as compare to non-treated cuttings (Fig. 5).

Root shoot ratio

The root-shoot ratio showed a significant difference ($P = 0.002$) among different treatments. Highest root shoot ratio in terms of biomass production was found in T1 cuttings of both IAA treated and not treated, while lowest was observed in T2 cuttings. In terms of IAA hormonal application and non-application comparison, root shoot ratio

was highest in non-treated cutting with the value of (0.6443 ± 0.08) as compare to IAA treated plants (0.6270 ± 0.01) , in T1 cuttings (Fig. 6).

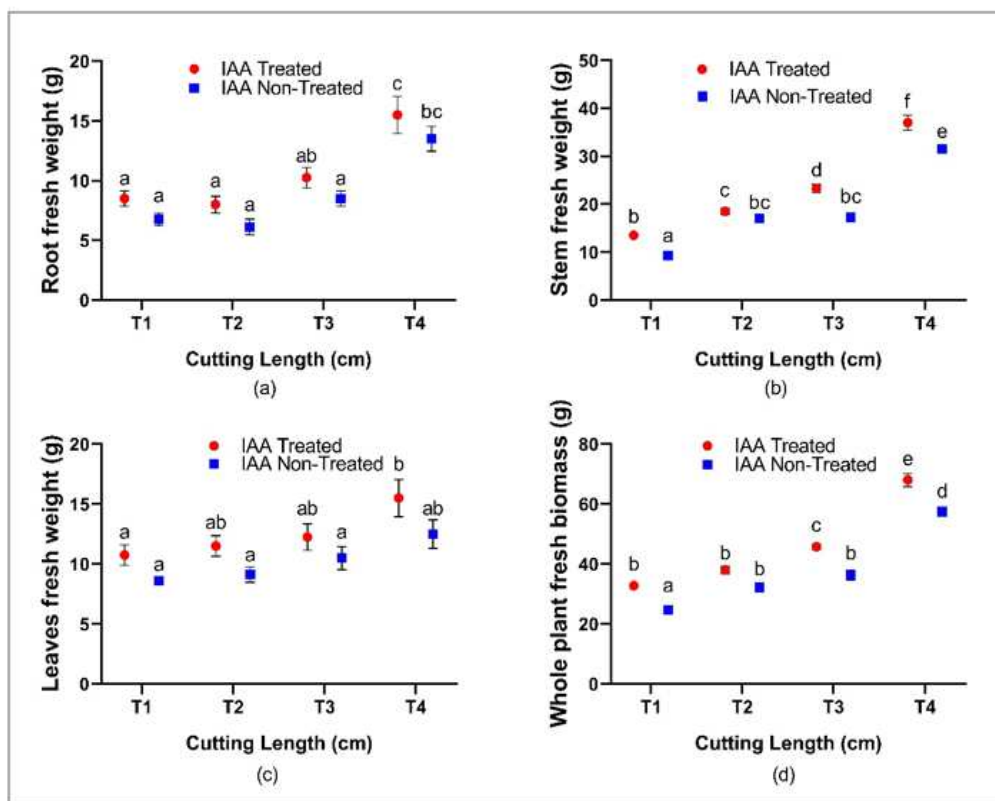


Figure 4. (a) Root fresh biomass, (b) stem fresh biomass, (c) leaves fresh biomass and (d) whole plant fresh biomass of different cutting lengths treated with IAA treated and non-treated cuttings

Moisture content availability

Moisture content availability showed non-significant results between IAA treated and non-treated cutting, same as with cutting lengths ($P = 0.352$) (Fig. 7).

Interaction between IAA and cutting length

Under two-way ANOVA analysis, the interaction between IAA and cutting length showed a non-significant behavior in our results (Table 3).

Table 3. P values of ANOVA of morphological growth parameters, biomass production and moisture content availability

Factors	df	P-value and significance level							
		Root dry weight	Stem dry weight	Leaves dry weight	Whole-plant biomass	Root shoot ratio	Root length	Stem height	Moisture content availability
IAA	1	0.005***	<0.001***	0.001***	<0.001***	<0.709NS	<0.007***	0.001***	<0.709NS
Cutting length	3	<0.001***	<0.001***	<0.001***	<0.001***	<0.042*	<0.001***	<0.001***	<0.302NS
IAA × cutting length	3	0.632NS	<0.089NS	0.899NS	<0.151NS	<0.453NS	0.841NS	0.789 NS	<0.201NS

Significance of analysis of variance factor: NS: non-significant, * $P < 0.05$, ** $P < 0.01$, *** $P < 0.001$

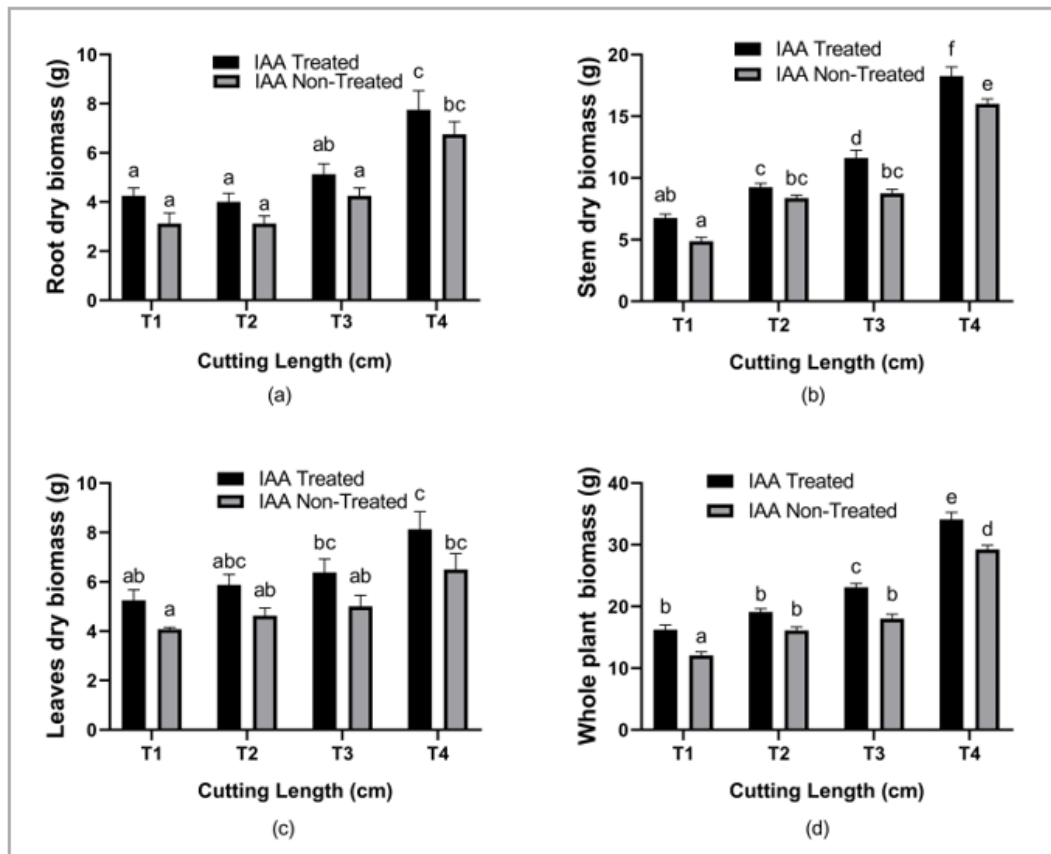


Figure 5. (a) Root dry biomass, (b) stem dry biomass, (c) leaves dry biomass, and (d) whole plant dry biomass of different cutting lengths treated with IAA treated and non-treated

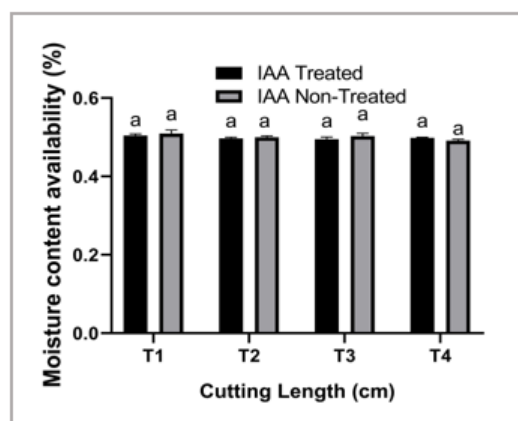


Figure 6. Root shoot ratio of different cutting length treated with IAA and non-treated cuttings

Discussion

Plant development is controlled by different environmental aspects, which directly influence plant morphological and physiological growth (Rashid et al., 2018). IAA is the main hormones in plants which play a direct role in plant growth, having an intricate pattern of active transport (Gehlot et al., 2014). In cuttings, auxins enter through the cut

surface area. Auxin helps to maintain the divergence of growth in plants and distinguish the connection of plants organs (Rahbin et al., 2012). The stimulatory effect of IAA was observed on morphological traits of *T. aphylla*. IAA showed a significant difference on T4 cuttings, which attributed in root and shoot weight, root and shoot length, and root to shoot ratio.

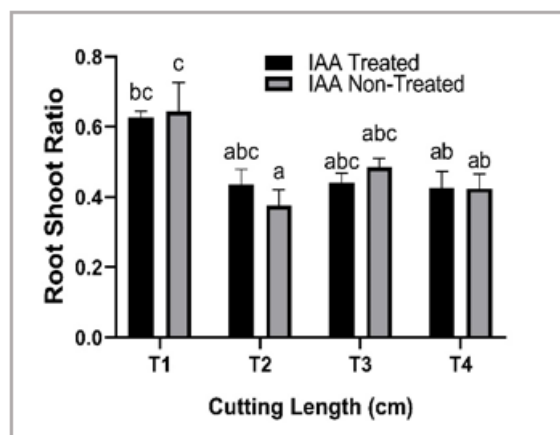


Figure 7. Moisture content availability of different cutting length treated with IAA and non-treated cuttings

IAA was suitable to stem cuttings in encouraging the morphological growth. According to our analysis of variance, results showed that IAA increased all traits significantly compared to IAA non-treated as in the work of (Singh et al., 2012; Mohana et al., 2014). The application of IAA persuades root growth on leafy cuttings is widely predictable (Husen and Pal, 2007). IAA has a direct effect on the root system, enhancing their ability to thrive for better growth (Sevik and Guney, 2013; Reena et al., 2012; Štefančič et al., 2005; Nordström et al., 1991). It indicates that IAA had a positive effect on the root development success of cuttings (Trobec et al., 2005). As also described by our results that IAA concentration significantly impacted root and shoot lengths and these were maximum in T4 cuttings of *T. aphylla*. These findings are partially agreed with the work of (Khan et al., 2006), who proved that auxins help to enhance vegetative growth of a plant. The stimulation of adventitious roots through different environmental and endogenous factors like temperature, light, sugar and IAA applications reported by (Pop et al., 2011). To achieve vigorous rooting optimum environmental conditions required, which help in the plant morphological and physiological growth (Sevik and Cetin, 2016).

Biomass production of *T. aphylla* showed a significant difference among IAA concentration in our studies, the plant showed a vigorous growth with T4 cuttings as compared to other cuttings both with IAA and IAA non-treated but was higher in IAA treated in their respective comparison which agrees with the results of (Sorin et al., 2005; Khudhur and Omer, 2015).

As IAA participates in different developmental processes of plants growth, from a cellular level to structural and eventually, the whole plant (Pandey et al., 2011) So, it was also quite clear that the growth of *T. aphylla* with T4 cutting with a cutting length of 15 was much better under the effect of IAA.

Conclusion

Plantation of *T. aphylla* is a sustainable option for good quality of timber production and is one of the fast-growing tree plants with a reasonable size having high resistance to sudden shock. Different applications of IAA had a significant effect on the morphological growth of *T. aphylla*. IAA was very beneficial to plant growth and development. Overall positive impact of IAA on different morphological traits and biomass production of *T. aphylla* was observed. It was concluded that by the optimal application of IAA, we can enhance the growth of *T. aphylla*.

Acknowledgments. This study was financially supported by the Science and Technology Major Project of Fujian Province (2018NZ0001-1) and the Special Technology Innovation Foundation of Fujian Agriculture and Forestry University (CXZX2018134). As well as we are thankful to Endowment fund, funded project (TT113/16).

Conflict of interests. Authors declare that there is no conflict of interests.

REFERENCES

- [1] Banik, R. L. (1985): Techniques of Bamboo Propagation with Special Reference to Pre-rooted and Pre-rhizomed Branch Cuttings and Tissue Culture. – In: Rao, A. N. et al. (eds.) Proc. International Bamboo Workshop, Hangzhou, China, 6–14 October 1985. IDRC, Canada, pp. 160-169.
- [2] Bhol, N., Nayak, H. (2012): Effect of planting alignment and cutting size on propagation of *Bambusa vulgaris*. – Journal of Tree Sciences 31(1-2): 69-75.
- [3] Chhetri, S., Kumar, H. (2015): Effect of planting position on rhizogenesis in Buddha belly bamboo (*Bambu saventricosa*) under nursery condition. – Journal of International Academic Research for Multidisciplinary 2(12): 283-289.
- [4] Elbasheer, Y. H. A., Raddad, E. A. Y. (2013): Vegetative propagation of (*Oxytenanthera abyssinica*) by culm cuttings. – Journal of Natural Resources and Environmental Studies 1(3): 1-5.
- [5] Gantait, S., Pramanik, B. R., Banerjee, M. (2018): Optimization of planting materials for large scale plantation of *Bambusa balcooa* Roxb.: Influence of propagation methods. – Journal of the Saudi Society of Agricultural Sciences 17(1): 79-87.
- [6] Gehlot, A., Gupta, R. K., Tripathi, A., Arya, I. D., Arya, S. (2014): Vegetative propagation of *Azadirachta indica*: effect of auxin and rooting media on adventitious root induction in mini-cuttings. – Advances in Forestry Science 1(1): 1-9.
- [7] Guney, K., Cetin, M., Sevik, H., Guney, K. B. (2016): Influence of germination percentage and morphological properties of some hormones practice on *Lilium martagon* L. seeds. – Oxidation Communications 39(1): 466-474.
- [8] Husen, A., Pal, M. (2007): Metabolic changes during adventitious root primordium development in *Tectona grandis* Linn. f.(teak) cuttings as affected by age of donor plants and auxin (IBA and NAA) treatment. – New Forests 33(3): 309-323.
- [9] Hussain, S. S., Arshad, M. K., Shahzad, A. M. (2003): Mountains of Pakistan: Protection, Potential and Prospects. – Global Change Impact Studies Centre, Islamabad, pp. 133-232.
- [10] Islam, M. S., Bhuiyan, M. K., Hossain, M. M., Hossain, M. A. (2011): Clonal propagation of *Bambusa vulgaris* by leafy branch cuttings. – Journal of Forestry Research 22(3): 387-392.
- [11] Khan, M. S., Khan, R. U., Waseem, K. A. S. H. I. F. (2006): Effect of some auxins on growth of damask rose cuttings in different growing media. – Journal of Agriculture & Social Sciences 2(1): 13-16.

- [12] Khudhur, S. A., Omer, T. J. (2015): Effect of NAA and IAA on stem cuttings of *Dalbergia sissoo* (Roxb). – Journal of Biology and Life Science 6(2): 208-220.
- [13] Mohana, M., Majd, A., Jafari, S., Kiabi, S., Paivandi, M. (2014): The effect of various concentrations of Iba and Naa on the rooting of semi hardwood cuttings of *Azalea alexander* L. – Advances in Environmental Biology 8(7): 2223-2231.
- [14] Nordström, A. C., Jacobs, F. A., Eliasson, L. (1991): Effect of exogenous indole-3-acetic acid and indole-3-butyric acid on internal levels of the respective auxins and their conjugation with aspartic acid during adventitious root formation in pea cuttings. – Plant Physiology 96(3): 856-861.
- [15] Orwa, C., Mutua, A., Kindt, R., Jamnadass, R., Simons, A. (2009): Agroforestry Database: A Tree Reference and Selection Guide. Version 4. – World Agroforestry Centre, Kenya.
- [16] Pandey, A., Tamta, S., Giri, D. (2011): Role of auxin on adventitious root formation and subsequent growth of cutting raised plantlets of *Ginkgo biloba* L. – International Journal of Biodiversity and Conservation 3(4): 142-146.
- [17] Pop, T. I., Pamfil, D., Bellini, C. (2011): Auxin control in the formation of adventitious roots. – Notulae Botanicae Horti Agrobotanici Cluj-Napoca 39(1): 307-316.
- [18] Rahbin, A., Aboutalebi, A., Hasanzadeh, H. (2012): Evaluation the effect of cultural media and IBA on rooting characters of night jessamine (*Cestrum nocturnum*) stem cutting. – Journal of Applied and Basic Sciences 3(11): 2258-2261.
- [19] Rashid, M. H. U., Asif, M., Farooq, T. H., Gautam, N. P., Nawaz, M. F., Ahmad, I., Gilani, M. M., Wu, P. (2018): Cuttings growth response of *Dalbergia sissoo* (shisham) to soil compaction stress. – Applied Ecology and Environmental Research 17(1): 1049-1059.
- [20] Ray, S. S., Ali, M. N. (2017): Factors affecting macropropagation of bamboo with special reference to culm cuttings: a review update. – New Zealand Journal of Forestry Science 47(1): 17.
- [21] Ray, S. S., Ali, M. N. (2016): Evaluation of inexpensive bedding materials for culm cutting of *Bambusa balcooa* Roxb. and its field performance. – J Biotechnol Biomater 6(227): 2.
- [22] Reena, J., Tewari, S. K., Kaushal, R., Tewari, L. (2012): Rooting behaviour of *Bambusa balcooa* Roxb. in relation to season, age and growing conditions. – Indian Forester 138(1): 79-83.
- [23] Saharia, U. K., Sen, S. K. (1990): Optimum age of bamboo culms for nodal cuttings. – Indian Forester 116(10): 780-784.
- [24] Senyanzobe, J. M. V., Rono, J., Mukanyamwasa, G., Nizeyimana, F., Mukagakwaya, G., de Dieu, R. R. J. (2013): Growth of *Bambusa vulgaris* and *Araundinaria alpina* under different nursery site conditions at the higher institute of agriculture and animal husbandry, Northern Rwanda. – Journal of Biodiversity and Environmental Sciences (JBES) 3(9): 9-14.
- [25] Sevik, H., Cetin, M. (2016): Effects of some hormone applications on germination and morphological characters of endangered plant species *Lilium artvinense* L. onion scales. – Bulgarian Chemical Communications 48(2): 256-260.
- [26] Sevik, H., Guney, K. (2013): Effects of IAA, IBA, NAA, and GA3 on rooting and morphological features of *Melissa officinalis* L. stem cuttings. – The Scientific World Journal. <https://doi.org/10.1155/2013/909507>.
- [27] Singh, B., Yadav, R., Bhatt, B. P. (2012): Vegetative propagation of *Dalbergia sissoo*: effect of growth regulators, length, position of shoot and type of cuttings on rooting potential in stem cuttings. – Forestry Studies in China 14(3): 187-192.
- [28] Singh, S., Yadav, S., Patel, P. K., Ansari, S. A. (2011): Adventitious rhizogenesis in *Bambusa nutans* and *Bambusa tulda*: influence of seasonal variation, IBA and cutting type. – Journal of Forestry Research 22(4): 693.

- [29] Sorin, C., Bussell, J. D., Camus, I., Ljung, K., Kowalczyk, M., Geiss, G., Bellini, C. (2005): Auxin and light control of adventitious rooting in *Arabidopsis* require ARGONAUTE1. – *The Plant Cell* 17(5): 1343-1359.
- [30] Štefančič, M., Štampar, F., Osterc, G. (2005): Influence of IAA and IBA on root development and quality of Prunus 'GiSelA 5' leafy cuttings. – *HortScience* 40(7): 2052-2055.
- [31] Trobec, M., Štampar, F., Veberič, R., Osterc, G. (2005): Fluctuations of different endogenous phenolic compounds and cinnamic acid in the first days of the rooting process of cherry rootstock 'GiSelA 5' leafy cuttings. – *Journal of Plant Physiology* 162(5): 589-597.

THE PROTECTION OF SAVANNAS AND ITS EFFECTS ON THE VOLUME OF WOOD, BIOMASS AND CARBON SEQUESTRATION

MBANGILWA, M. M.¹ – MALOTIE, J. M.² – MBAYU, M. F.³ – KASORO, R. F.⁴ – JIANG, L. C.^{1*}

¹*Key Laboratory of Sustainable Forest Ecosystem Management, Ministry of Education, School of Forestry, Northeast Forestry University, Harbin 150040, P.R China*

²*Post-university Regional School for Integrated Management and Management of Tropical Forests and Territories (ERAIFT), University of Kinshasa, B.P. 15.373 Kinshasa, Democratic Republic of Congo*

³*Faculty of Management of Natural and Renewable Resources (FGRNR), University of Kisangani, B.P 2012 Kisangani, Democratic Republic of Congo*

⁴*College of Resources and Environment Sciences, Jilin Agricultural University, 2888 Xincheng St, Nanguan, Changchun, Jilin, P.R. China*

**Corresponding author
e-mail: jlichun@nefu.edu.cn*

(Received 6th Sep 2019; accepted 25th Nov 2019)

Abstract. The variation in the productivity (biomass and wood volume) and sequestered carbon of savannas was monitored in Manzozi, Bas-Congo province (Kongo-central) in the Democratic Republic of Congo. Sixteen plots of one hectare each have been set up, eight of which were in the protected savannah and eight in ones subject to fires. The study was limited to ligneous trees and shrubs. The savannah put in defenses is richer in volume of wood (3.6 m³/ha against 7.8 m³/ha); biomass (29.8 t/ha vs. 8.2) and carbon (14.9 t/ha versus 4.1) than that under fire.

Keywords: *deferred grazing, shrubs, ligneous trees, Manzonzi, Bas-Congo (Kongo-central)*

Introduction

Tropical savannas and forests are important components of the land carbon sink (Pan et al., 2011; Liu et al., 2015; Ahlström et al., 2015; Trugman et al., 2018). However, their ability to continue sequestering carbon is uncertain (Malhi et al., 2008), due in part to the impact of projected increases in drought frequency and changes in the fire regime on woody carbon stocks (Brando et al., 2014; Trugman et al., 2018). Globally, tropical forests, savannas, and grasslands comprise ~60% of total terrestrial gross primary productivity (Beer et al., 2010) but are also responsible for over 65% of global carbon emissions stemming from fire and deforestation (Van der Werf et al., 2010, 2009; Trugman et al., 2018).

Savannas are one of the world's major terrestrial ecosystems, comprising between 10% and 15% of the world's land surface, depending on definition (Scholes and Hall, 1996; Shackleton and Scholes, 2010). Distributed across nearly all the continents, they occur in broad bands between the equatorial forests and mid-latitude deserts. Approximately 50% of the African continent and parts of Democratic Republic of the Congo are savannas. They are home to over 30% of the world's population (Solbrig et al., 1991), and consequently experience marked impacts from human activities. Of particular concern are deforestation and land use change activities which reduce or eliminate the biomass of trees and shrubs. This not only alters local nutrient, water and carbon cycles,

thereby affecting local livelihood options and agricultural productivity, but also adds to global CO₂ emissions (Miles and Kapos, 2008; Shackleton and Scholes, 2010).

However, we can also say that savannas are complex ecosystems marked by the coexistence of herbaceous strata and one or more layers shrub and / or tree as a result of the interaction of several environmental factors varied rainfall regimes, role of fire and the breeding (Jacquin, 2010) as well as the nature of the soil. It is also defined as an open grassland formation composed mainly of perennial or annual grasses (Jacquin, 2010). Its vegetation may be purely grassy or scattered with shrubs or trees and varies according to rainfall, soil and anthropogenic activity (Clement, 1982; Manlay et al., 2002).

The Mayombe, of which Manzonzi is a part, is a region where anthropogenic pressure (deforestation, bushfire) has played an important role in the reduction of forest areas and the conversion of the ecosystem. Bush fire has also influenced landscape physiognomy in recent decades and has become a determining factor in the maintenance of savanna vegetation. Savanna ecology and the consequences of fire regime on wood volume, biomass and carbon sequestration is one of the most important issues for savanna management. There are to date few studies dealing with the bush fire effect on productivity in the savannas. The lack of in-depth studies on this issue makes it impossible to accurately assess the effect of bush fire and the management of its impacts on vegetation. However, in many regions intensive land use is not permanent, leading to a mosaic of land use types with varying levels of woody biomass (Giannecchini et al., 2007; Eaton and Lawrence, 2009) and hence carbon sequestration potential. Consequently, carbon accounting for specific geographic regions needs to be able to accommodate such dynamic changes, benchmarked against relatively un-impacted sites.

The international concern with and modelling of carbon emissions and sequestration requires adequate coverage of locally quantified carbon stocks. However, several authors have commented on the relative dearth of quantitative estimates for dry forests and savannas relative to moist tropical forests (e.g. Salis et al., 2006; Williams et al., 2008), although with exceptions, such as work in the Thicket Biome of South Africa (Mills et al., 2005; Mills and Cowling, 2006; Powell, 2008). Whilst biomass per unit area in savannas is less than tropical forests, the high rates of disturbance through fire and land clearing and their significant global extent, makes it imperative that the carbon stocks of savannas are adequately quantified and reported (Bombelli et al., 2009). This will then provide the basis for more accurate global estimates and predictive allometric equations, thereby bringing substance to the appeal of Lal (2002), namely to facilitate mobilization of provisions of the Kyoto protocol to manage savannas for carbon sequestration benefits through maintenance of existing woody biomass or reforestation. Lal (2002) also suggests agricultural intensification and biofuel plantations as two other approaches to increase carbon pools in savannas and drylands. However, the low rainfall and competition with other land uses limit their viability in many places (Woomer et al., 2004; Shackleton and Scholes, 2010).

Whilst time-consuming work, determination of woody plant biomass relationships with any of a series of morphometric variables usually yields highly significant results, especially after transformation of one or both sides of the dependent and independent variables. The most commonly used independent variable from a variety of vegetation types is stem diameter or stem circumference (Dayton, 1978; Hofstad, 2005; Dias et al., 2006; Salis et al., 2006). Inclusion of tree height sometimes improves the relationship (Chidumayo, 1988; Brown et al., 1989), although not always (Brown et al., 1989). It is also a covariate with stem diameter. Crown diameter, area or volume have also been

used as the predictor variable by some authors (Kelly and Walker, 1977; Deshmukh, 1992), but generally yield weaker regression relationships than stem circumference, and become very variable in dense vegetation where crown size is constrained (Tietema, 1993; Powell, 2008). Combinations of diameters, height and crown dimensions may provide the best predictive capacity, but are rarely worth the extra time and effort required to measure all three (Hofstad, 2005).

Within the context of the study that we are leading here, our hypothesis is that savannas enclosure becoming more stable tend to have higher productivity and sequester more carbon. On the other hand, fire savannas would have low productivity and sequester less carbon. The objective of the present work was to evaluate the effects of the protection of savannas subject to the fire regime and the productivity of savannas (biomass and volume of wood) and sequestered carbon. Specifically, it is a question of analyzing and comparing the productivity (volume, biomass), and the carbon content of the savannah woody vegetation put in defense to that of the savannas subjected to the fire regime of different intensity. Also, it is a question of demonstrating the advantages that the conservation of the savannas in the ecological planes in relation to the climate.

Field of study

The Mayombe climate is tributary of the Atlantic Ocean, influenced by the cold Benguela current and the southeastern trade winds (Lubini, 1997). This cold marine current of Benguela is responsible for the small dry season rains known locally as "masala" (Kapa et al., 1987). These so-called occult rains (De Foresta), are expected towards the end of August, and play the role of compensation of the deficit of water of the ground. There is a dry season (May - September) and a rainy season (September - May) with a short dry season of 2 or 3 weeks in February (Quinif, 1986).

The site under study is part of the Mayombe chain stretching from Gabon through Angola (Cabinda) to the Democratic Republic of the Congo (DRC). The chain has Mayombe is a geological structure which includes four stages, the newest upstairs though the west-congo (Lubini, 1997). It is made up of volcanic and metamorphic rocks formed at the middle Precambrian (Quinif, 1986). It includes schisto-grafic and schisto-calcareous systems (Lubini, 1997). In addition, shales, quartzites, graphitic rocks, feldspathic sandstones, micaschists, muscovites, amphiboloschists and intrusive rocks are observed. These various rocks have allowed the formation of the various types of soils encountered there. The soil is mostly made up of ferralsols on undefined rocks (Sys, 1960). The rock formations are covered with a layer of surface soils of thickness ranging from 20 cm to 3 m. These eluvia or colluvium derives from the underlying or surrounding geological basement (Sys, 1960).



Figure 1. Image of Manzonzi savanna plots around the Luki Biosphère reserve in Bas-Congo
(Source: Field investigation)

Materials and Methods

Study area and data

In 2010, WWF proceeded with the opening of the variable-length layons according to the physiognomy of the site to be used for systematic inventories to characterize the large plant formations in this Manzonzi savannah. A total of 101 plots of 80 m x 50 m each and 20 m apart from each other were placed there. This device has the advantage of capturing the heterogeneity of the ecological gradients of the environments traversed and of probing the homogeneous superimposed surfaces.

For the present study conducted in April 2018, the system put in place was based on a stratified sampling of plots distributed in the savannah. The selection of firewood savanna (SRF) plots was based on annual fire passage, and populations were consulted for this choice. Plots were placed in a given orientation, indicated by the compass and had the following GPS positions: Pt1: (SMD: 13°15'24.2" North and 5°43'34.2" South), (SRF: 13°15'06.2" North and 5°44'56, 1" South); Pt2: (SMD: 13°15'24.2" North and 5°43'29.4" South), (SRF: 13°15'22.0" North and 5°43'08.2" South); Pt3: (SMD: 13°15'24.1" North and 5°43'22.3" South), (SRF: 13°15'17.0" North and 5°43'09.3" South); Pt4: (SMD: 13°15'16.0" North and 5°43'17.2" South), (SRF: 13°15'37.9" North and 5°44'45.6" South); Pt5: (SMD: 13°14'48.1" North and 5°45'15.2" South), (SRF: 13°15'25.1" North and 5°43'12.6" South); Pt6: (SMD: 13°14'54.1" North and 5°45'02.7" South), (SRF: 13°15'33.1" North and 5°44'47.1" South); Pt7: (SMD: 13°14'31.6" North and 5°44'47.1" South), (SRF: 13°15'25.2" North and 5°44'41.2" South); Pt8: (SMD: 13°14'46.0" North and 5°44'38.1" South), (SRF: 13°15'04.1" North and 5°44'46.3" South). Each starting point of the plot is materialized by a stake bearing the number of the parcel of inventory. The distance marking stakes were made from the stems of the small trees harvested on site and were placed every 50 m. Depending on the slope, a certain distance was added in order to have a real horizontal distance corresponding to the length sought for the plots (SPIAF, 2007).

All plots were geo-referenced using a GPS and a tracking was done for the savannah defensive (SMD). The tracking data included in the Geographic Information System (GIS) allowed us to use the ARC GIS 9.2 software to produce the site map under study (Figure 2).

Botanical inventory and data collection

Eight other plots (100 m × 100 m) were installed in the savannah and eight others in savannas under fire following the same vegetation. The aim was to ensure the representativeness of the plots (Favrichon et al., 1998; Devineau et al., 1984), their diversity (Dibi et al., 2008), and stratified sampling. The location of the plots took into account the topographic features of the environment, the physiognomy of the vegetation and the fact that they significantly include ligneous plants of different heights. Inside the plots, all the species have been recorded (Favier et al., 2004; Dibi et al., 2008) and all woody trees ≥ 20 cm measured (Duarte et al., 2006). The use of the ribbon was preferred to the forest compass because of the ease of work and the fact that the circumference gives a better estimate of the volume than that obtained by the compass (Rondeux, 1993).

The height was measured using a 5 m tall graduated wooden stem for shrubs and or Blum Leiss for trees. For individuals with multiple stems above 1.30 m or in tuft (case of *Nauclea latifolia* Smith), all stems are measured and differentiated by letters a, b or c as appropriate. Sea grass samples of species not directly identified in the field were

collected. The herbarium of Luki and of the Faculty of Science of the University of Kinshasa enabled the identification of our equipment. Each double of the collection has also been deposited. For botanical nomenclature, we followed the system of Angiosperms Phylogeny Group (APG), and also the nomenclature of the RMCA available on www.Metafro.be for synonymy and authors.

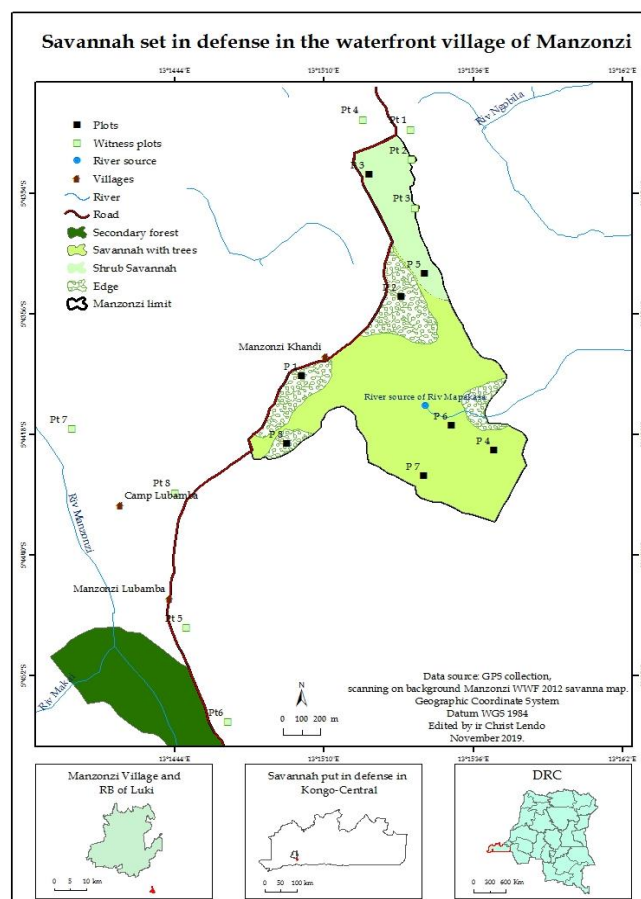


Figure 2. Layered inventory device in the savanna laid out in Manzonzi defenses

Analytical and statistical approaches to the data

Calculation of the volume of wood available

The calculation of the volume of wood is given by the formula of Rondeux (1993).

$$V = G \times H \times f \quad (\text{Eq.1})$$

Where: G: basal area in m², H: height in meter and f: form factor.

The calculation of the shape of the trees was essential to make more reliable the estimate of the volume of wood available in this savanna. This coefficient was obtained on trees taken as a model. Trees (templates) were selected to cut based on their straightness, to obtain a normal diametric decrease. Measurements of circumference were taken along the stem of the tree at intervals of 1 m, whose reference circumference was that taken at 0 m. Some trees were measured on feet without being cut, as they offered the possibility. For these model trees a series of coefficients was calculated according to the linear regression model: $1/h (x_1^2 + x_2^2 + x_3^2 + \dots + x_n^2)$, (Rondeux,

1999); with h : the height of the tree, X_1 =circumference of segment 1, X_2 = circumference of segment 2 etc. The shape coefficients thus obtained for each model tree are summed and a mean value is found for each species.

Calculation of biomass and sequestered carbon

To estimate the biomass of trees, we used the allometric equations developed by Malimbwi et al. (1994) for Miombo. This equation is described as follows:

$$B = 0.1.Dbh^{1.916}H^{0.74} \quad (\text{Eq.2})$$

Where B is biomass and Dhp is the diameter at chest height.

The Miombo are the wooded savannahs characteristic of the subtropical region of southern Africa (Ryan et al., 2011), which includes the south of the DRC biogeographically. This equation makes it possible to obtain the biomass of the stems and the roots of the trees. The results obtained in this work integrate the biomass and the carbon of the roots. Rate corresponding atoms were estimated by assuming that 50% of the biomass consists of carbon (Dupouey et al., 2002).

Statistical analysis

Statistical tests were based on the variance between the fire regime and the defenses. The main factor to be observed was the effect of defencion on savannas subject to the fire regime. The Fisher test (ANOVA) was the most appropriate because it had given satisfactory results. Variables taken into account were floristic diversity, density and volume of available wood, biomass and carbon. We used R version 2.10.1 software (Cornillon et al., 2010) and the level of significance of the results retained is 0.05 and 0.0001 as appropriate.

Results

This section presents the results in terms of the volume of available wood and the treed areas of the trees in each plot of the savannah set aside and the SRF. The figures below present, among other things, the volume of wood from the different plots and plant formations in the defensive savannahs (SMD) and the savannahs under fire regime (SRF) (Figure 3); biomass in plots and plant formations at the level of SMD and SRF (Figure 4); carbon in plots and plant formations in the SMD and SRF (Figure 5).

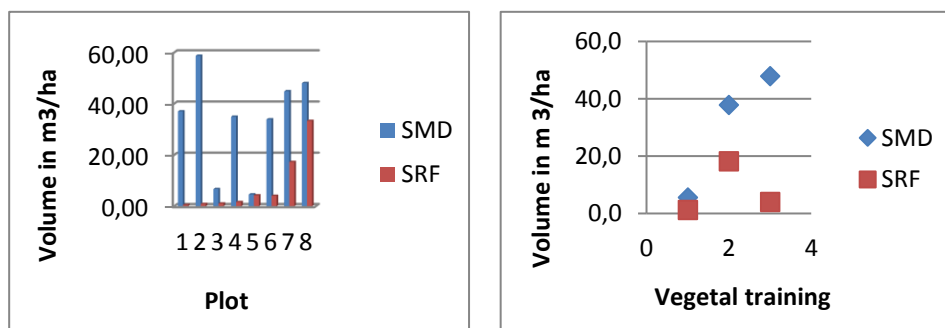


Figure 3. Wood volume of the plots and plant formations of the SMD and the SRF

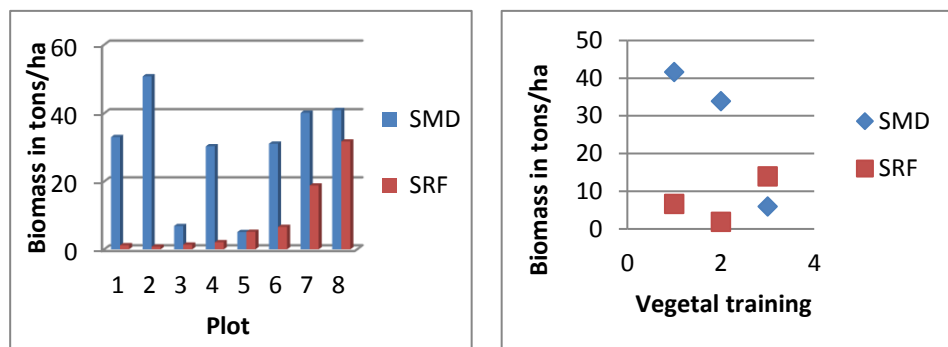


Figure 4. Biomass in the plots and plant formations of the SMD and in the SRF

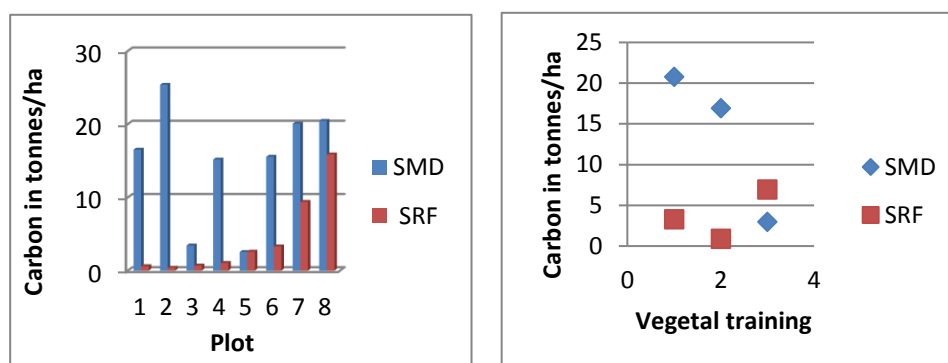


Figure 5. Sequestered carbon in the plots and plant formations of the SMD and in the SRF

Statistical analysis

The statistical analysis presents the volume of wood available, the biomass and the Carbon sequestered through the three figures below which show the dispersion of the volume values for the two landscape types including the SMD and the SRF (*Figures 6, 7 and 8*). It also presents in *Table 1* below the summary of the diversity of the species as well as the frequency of the individual species displayed plot by plot in the SMD, and in *Table 2* it summarizes the density data and certain variables related to the structure of vegetation, wood volume, biomass and sequestered carbon. In *Appendices 1 and 2*, the table summarizing the list of inventoried and defended species and the family structure of the savanna sub-plots put in defense.

Table 1. Species diversity and the frequency of the individual species displayed plot by plot in the SMD

Plots	Diversity of species by plots	Frequencies
Pt1	154	7.5%
Pt2	83	4.05%
Pt3	136	6.6%
Pt4	185	9.02%
Pt5	348	16.9%
Pt6	237	11.6%
Pt7	567	27.7%
Pt8	341	16.6%
Total	2051	

Table 2. Density of stand of the plots in the savannah put in defenses (SMD) and the savannah under fire regime (SRF)

Bloc	N.E.	N.F.	N.I.	Mean of_CHP (in cm)	Mean of_height (in m)	Mean of_G (m ²)	Mean of_Vol (m ³)	Mean of_B (tonne)	Mean of_Cs (tonne)
Plot SMD 1	33	15	506	35.24 ± 16.52	6.25 ± 3.23	0.01 ± 0.01	0.07 ± 0.21	0.065±0.152	0.032±0.075
Plot SMD 2	34	16	614	37.59 ± 19.11	6.73 ± 3.83	0.01 ± 0.01	0.09 ± 0.22	0.082±0.167	0.041±0.083
Plot SMD 3	5	2	211	30.17 ± 8.90	5.26 ± 2.10	0.007 ± 0.005	0.03 ± 0.03	0.032±0.032	0.016±0.016
Plot SMD 4	27	17	309	41.06 ± 19.70	7.44 ± 3.94	0.01 ± 0.01	0.11 ± 0.21	0.098±0.160	0.049±0.080
Plot SMD 5	10	7	216	27.97 ± 5.99	4.69 ± 1.43	0.006 ± 0.003	0.02 ± 0.02	0.023±0.018	0.011±0.009
Plot SMD 6	18	10	566	34.76 ± 13.96	6.21 ± 2.81	0.01 ± 0.01	0.05 ± 0.12	0.054±0.093	0.027±0.046
Plot SMD 7	20	10	497	38.83 ± 17.58	7.02 ± 3.52	0.01 ± 0.01	0.09 ± 0.16	0.080±0.128	0.040±0.064
Plot SMD 8	35	20	312	45.82 ± 21.51	8.49 ± 4.22	0.02 ± 0.02	0.15 ± 0.26	0.0131±0.204	0.065±0.102
Plot SRF 1	8	5	154	20.59 ± 0.45	2.58 ± 0.41	0.003 ± 0.000	0.005 ± 0.001	0.007±0.004	0.003±0.002
Plot SRF 2	6	5	83	21.78 ± 0.24	3 ± 0	0.003 ± 8.550	0.007 ± 0.000	0.009±0.0001	0.004±0.0000
Plot SRF 3	8	5	136	22.73 ± 0.45	3 ± 0.01	0.004 ± 0.000	0.007 ± 0.000	0.010±0.004	0.005±0.002
Plot SRF 4	9	6	185	24.19 ± 0.51	3 ± 0	0.004 ± 0.000	0.008 ± 0.000	0.011±0.004	0.005±0.002
Plot SRF 5	8	5	346	26.75 ± 1.00	3.32 ± 0.21	0.005 ± 0.000	0.012 ± 0.001	0.014±0.001	0.007±0.0008
Plot SRF 6	13	7	237	29.76 ± 0.81	3.91 ± 0.13	0.007 ± 0.000	0.017 ± 0.002	0.018±0.002	0.009±0.001
Plot SRF 7	12	7	567	35.46 ± 2.90	4.68 ± 0.42	0.010 ± 0.000	0.030 ± 0.007	0.033±0.007	0.016±0.003
Plot SRF 8	12	7	341	51.06 ± 9.47	6.74 ± 1.41	0.021 ± 0.009	0.098 ± 0.009	0.093±0.053	0.046±0.029

NI = Number of Individuals; NE = Number of species; NF = Number of Families; CHP = Breast Height Circumference; G = basal area; B = Biomass; C = sequestered carbon

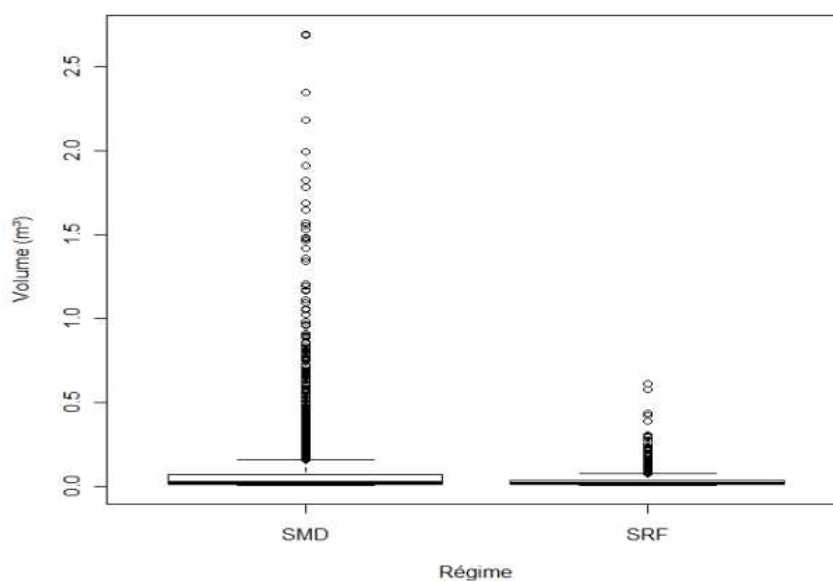


Figure 6. Dispersion of volume values for both schemes: SMD and SRF. ($F = 148.48$, $P < 0.0001$)

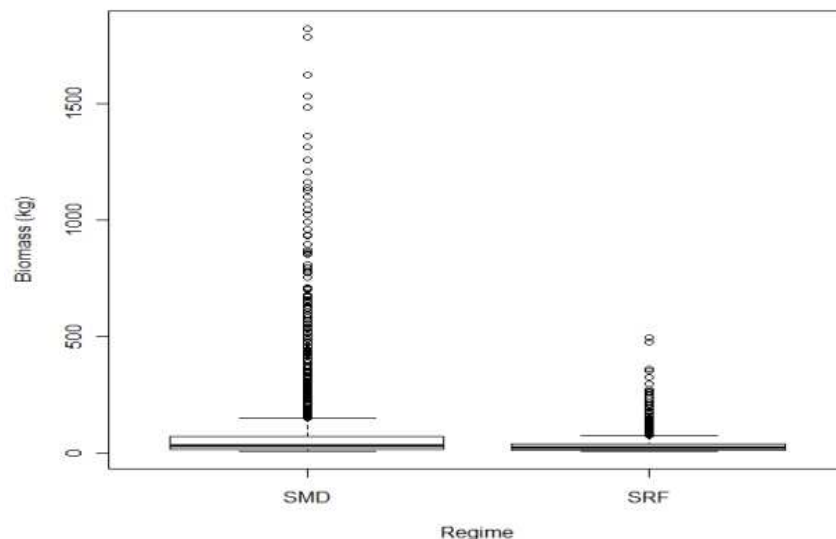


Figure 7. Dispersion of biomass for both schemes: SMD and SRF. ($F = 167.36$, $P < 0.0001$)

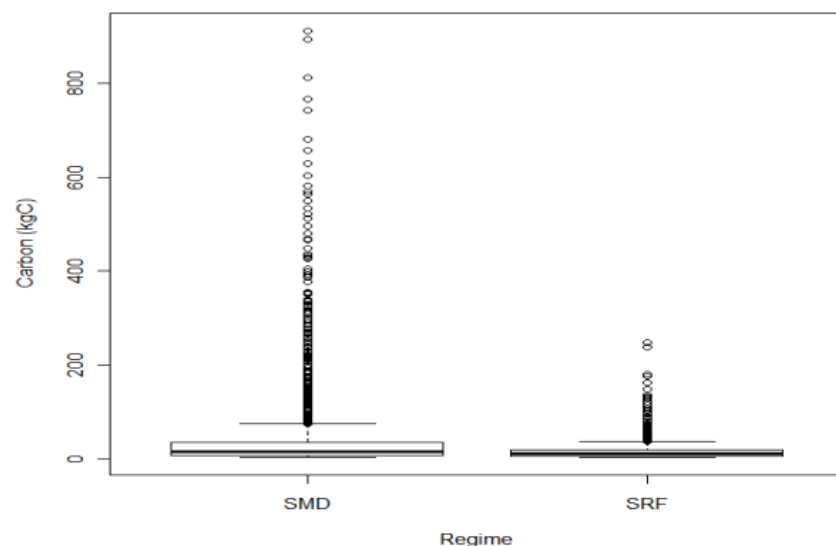


Figure 8. Dispersion of sequestered carbon for both schemes: SMD and SRF. ($F = 167.36$, $P < 0.0001$)

Discussion

In forestry, stands and their increments are usually expressed in wood volume. These volumes can be expressed by sintering or applying the cubic rate (Devineau, 1997). For our study, the volume of wood is obtained by the relation $V = G \times H \times f$ described in the methodology. The results of the study presented in *Figures 3, 4* and *5* show that it is in SMD that there is a greater volume of wood plus biomass and carbon.

Statistically, the difference between SMD and SRF on volume of timber, biomass and carbon are very significant. We denote respectively $F = 148.48$, $P < 0.0001$, 167.36 , $P < 0.0001$ and 167.36 , $P < 0.0001$. *Figures 6, 7* and *8* present the results of these analyzes and box plots represent 50% of the volume, biomass and carbon values.

Carbon is the value of the biomass divided by two or 50%, i.e. if in SMD we have 100 tons of biomass we will have 50 tons of carbon and if in SRF we have 25 tons of biomass we will have 12.5 tons of carbon. This means that the appearance of the biomass/carbon ratios will be the same (*Figures 7 and 8*). The dispersion is represented by the two mustache boxes. It is their comparison which gives the statistical result presented. Thick bars inside the boxes; bars below the volume, biomass and minimum carbon and the bar at the top of the box indicate the maximum value. It is also noted that many things are aberrant apart from mosquitoes which are actually individuals of reading, mean and great variability.

We note that the plots located in the edge (1,2 and 8) have higher volume, biomass and carbon. These values in terms of volume, biomass and carbon are generally superior to all the other plant formations present. In this plant formation, we find large trees whose circumference varies between 80 at 150 cm. Then come the plots of wooded savannah (4,6 and 7). There is an increase in plot 7 which is due to its higher density (497 individuals) compared to the other two plots (309 and 366 individuals) of its category.

Plots 3 and 5 of the savannah set in the bush savanna are the poorest in terms of wood volume, biomass and carbon. The volume results obtained in plot 3 and 5 are low compared to the results of Devineau (1997) which obtained 18.2 m³ / ha in shrub savanna in Burkina Faso. It is in these plots (3 and 5) that we notice the greatest number of shrubs and the lowest density.

In the SRF, that are the plots in the savannah which a volume of wood, biomass and carbon higher than the two other vegetation. Pt7 and 8 are located in an area of Kraal that is covered by early fires in order to provide cattle with green grass during the dry season. The control plot located in the edge (Pt6) is poor in volume of wood, biomass and carbon due to its low density.

The results of Bellier et al. work (1969) made in a savannah with palmyra show rather that a savannah close to a forest can evolve towards a forest in spite of the action of the fire. The fact that the savanna in question is a savannah included in a forest block may be decisive in their conclusions. In SRF, plots 1, 2, 3 and 4 in bushland savannas such as SMD are very low in wood volume in biomass and carbon (*Figures 3-5*). We think that in addition to the action of fire there is the nature of the substrate (ferruginous) which can play an important role in the development of trees.

Specifically, *Hymenocardia acida* Tul., *Anthocleista vogelii* Planch, *Albizia lebbek* (L.) Benth., *Maprounea Africana* Müll. Arg. are the most important species in terms of volume of wood, biomass and carbon in the SMD, while in the SRF they are *Hymenocardia acida* Tul., *Maprounea Africana* Müll. Arg and *Bridelia ferruginea* Benth, the most important species of *Hymenocardia acida* Tul. owes its place in this ranking due to its high density while *Anthocleista vogelii* Planch owes its place in this ranking following its rapid growth even though it has a low density. The results of our study showed that the savannah set in defense contains a higher volume of wood (3.6m³/ha) only in the bushfire savannah (7.8m³/ha).

In relation to biomass, SMD contains a biomass of 29.8 t/ha compared with 8.2 t/ha. The sequestered carbon amounted to 14.9 tC/ha in the SMD, compared to 4.1 tC/ha in the SRF, which seems lower compared to the result obtained by Lubalega (2016) wich, in his work on the natural evolution of the savannahs defended at Ibivillage, on the Bateke plateau, in the Democratic Republic of Congo where it obtained average values of 107.477 t / ha of total biomass, ie 51.05 megagram (Mg) C / ha in the gallery forest,

103,772 t / ha of total biomass is 49.29 Mg C / ha in the forest island, and 22,336 t / ha of total biomass is 10.60 Mg C / ha in the plantation.

The differences observed between the edge, the savannah and shrub savanna both in the SMD and in the SRF are due largely unlike their structure and their floristic composition. The averages obtained in the SMD in terms of volume, biomass and carbon are respectively 36 m³ /ha, 28.8 t/ha and 14.4 t/ha. According to Grace et al. (2006) Aboveground Carbon Stock in Savannas worldwide varies considerably depending on the extent of forest cover. It ranges from 1.8 tC/ ha where trees are absent to more than 30 tC/ha where tree cover is important. They claim that the average productivity of savannas from 1 to 12 tC/ha/year and that are lower values are mostly found in the savannas dry and semi-arid who from most vast areas of Africa.

In our study, the carbon content (limited to ligneous species) after 6 years of protection is relatively low in some plots, especially shrub savanna. The results obtained in the edge (20.7 tC/ha) of the MDS are satisfactory compared to the results obtained in other countries. For example, Ryan et al. (2011) obtained 29.7 t/ha in miombo woodland in Mozambique. Ibrahima and Abib Fanta (2008) found in Ngaoundéré (Cameroon) that the quantity total carbon is of the order of 81.48 and 118.36 tC/ ha respectively for the shrub and tree savanna. In the wooded savannah, most of the carbon is stored in the phytomass of trees (65.30 tC /ha) and in the ground (48.37 tC/ha); the contribution of shrubs (3.83 t/ha) herbaceous (0.30 t/ha), roots (1.96 tC/ha) and litters (1.88 tC/ha) is weak, less than 5% of total carbon. On the other hand, in the shrub savannah, soil is the main carbon reservoir (74.35 tC/ha). The other components namely shrubs (0.66 tC/ha), herbaceous plants (3.15 tC/ha), roots (1.98 tC/ha) and litters (1.34 tC/ha) have a very small contribution, less than 9% quantity total carbon. Mushini et al. (2010) obtained 19.2 tC/ha in their work in wooded areas of Miombo Woodlands of the Southern Highland from the Republic of Tanzania.

Conclusion and suggestions

The objective of this paper was to evaluate the effects of savanna protection under fire regime, savanna productivity (biomass and wood volume) and sequestered carbon, and to analyze and compare the productivity and carbon content of woody savannah vegetation with that of savannas subject to the fire regime of different intensity, and to demonstrate the ecological benefits of savanna conservation in relation to climate.

In terms of productivity (biomass, carbon and wood volume), this study found that SMD was more productive than SRF and that species such as, *Hymenocardia acida* Tul., *Anthocleista vogelii* Planch, *Albizia lebbek* (L.) Benth., *Maprounea africana* Müll. Arg. are the most important species in terms of the volume of available wood, biomass and carbon in the MSD, while in the SRF they are *Hymenocardia acida* Tul., *Maprounea africana* Müll. Arg. and *Bridelia ferruginea* Benth, the most important species.

One of the objectives of the defense of savannah is to restore the vegetation cover and increase the diversity in the areas considered by using fire which is a means of protecting savannah against fire over wide areas. In terms of biodiversity, we attest that the protection of savannas is an effective way to restore vegetation cover, increase productivity and biodiversity in an ecosystem. It allows the developments of organisms adapted to the ecological conditions of the environment and allow the ecosystem to evolve towards the climax, unlike reforestation with these exotic species. Muys (2007) argues that local communities often opt for fast-growing exotic trees, but in the name of restoring biodiversity, it is preferable that they replant indigenous species that carry

with them a procession of trees organizations that have coevolved. In addition, these native species have a wood often denser which compensates, at least partially, their lower growth in volume. Beyer et al., 2007 state that the average temperature increase is expected to be about 0.1 to 0.4% per decade. The protection of savannas is one of the effective means of helping to regulate the climate at the local scale because the forest cover it creates leads to a decrease in albedo (warming), but at the same time a higher evapotranspiration (cooling) and recycling of rainwater (Silver and Defries, 1990).

Tropical forests are known to play an important role in cooling the global climate by immobilizing carbon (Puig, 2001), and by their high evapotranspiration capacity. The protection of savannas can not only contribute to increasing the forest area (if successful) but also contributes effectively to the overall services provided to the environment.

Based on the above, we suggest:

- Popularize the defensive technique used in this study to help expand forest areas and promote the conversion of shrubby savannas to forest while increasing the possibilities of access to ecosystem services (climate regulation, water cycle, service supply and ecological habitat).
- Ensure the increase of the basal area thus increasing the richness and the specific diversity of two formations, thus reflecting natural reforestation.
- Take into account in the future the assessment of the biomass of grasses as well as scrubland because these are as important as the woody species in the case of this typical savannah.
- Conduct analytical studies of soils in different plant formations and / or plots of the SMD, to further explain the flora they display.
- Ensure significant forest regeneration by planting fast-growing tree species that can in the near future show an expansion of the forest that will contribute to increasing carbon storage areas and increasing the amount of carbon in different compartments or reservoirs (wells) of the savannah ecosystem (aboveground biomass, belowground biomass, in dead wood, litter and soil).
- Install plots at the savanna edge interface to assess the rate of savannah colonization by edge features.
- Continue to support local populations by multiplying projects and income-generating activities promoting development in order to free them from the total dependence of forest products.
- Increase awareness.

REFERENCES

- [1] Ahlström, A., Raupach, M. R., Schurgers, G., Smith, B., Arneeth, A., Jung, M., Reichstein, M., Canadell, J. G., Friedlingstein, P., Jain, A. K., Kato, E., Poulter, B., Sitch, S., Stocker, B. D., Viovy, N., Wang, Y. P., Wiltshire, A., Zaehle, S., Zeng, N. (2015): The dominant role of semi-arid ecosystems in the trend and variability of the land CO₂ sink. – *Science* 348: 895-899. <https://doi.org/10.1126/science.aaa1668>.
- [2] Beer, C., Reichstein, M., Tomelleri, E., Ciais, P., Jung, M., Carvalhais, N., Rodenbeck, C., Arain, M. A., Baldocchi, D., Bonan, G. B., Bondeau, A., Cescatti, A., Lasslop, G., Lindroth, A., Lomas, M., Luyssaert, S., Margolis, H., Oleson, K. W., Rouspard, O., Veenendaal, E., Viovy, N., Williams, C., Woodward, F. I., Papale, D. (2010): Terrestrial gross carbon dioxide uptake: global distribution and covariation with climate. – *Science* 329: 834-838. <https://doi.org/10.1126/science.1184984>.

- [3] Bellier, L., Gillon, D., Gillon, Y., Guillaumet, J. L., Perraud, A. (1969): Research on the origin of a savanna included in the lower Cavally forest block (Ivory Coast) by the study of soils and biocenosis. – Cahor Orstom, Sér.Biol. No.10, 30 p.
- [4] Beyer, G., Defays, M., Fisher, M., Fletcher, J., Munck, E. D., Jaeger, F. D., Riet, C. V., Vandeweghe, K., Wijnendaele Gonze, C., Guy, J. C., Coutrot, D. (2007): Fight against climate change: use the wood. – Wood in sustainable development. Brussels, Belgium, 84 p.
- [5] Bombelli, A., Henry, M., Castaldi, S., Adu-Bredu, S., Arneith, A., De Grandcourt, A., Grieco, E., Kutsch, W. L., Lehsten, V., Rasile, A., Reichstein, M., Tansey, K., Weber Valentini, R. (2009): The Sub-Saharan Africa carbon balance, an overview. – Biosciences Discussions 6: 2085-2123.
- [6] Brando, P. M., Balch, J. K., Nepstad, D. C., Morton, D. C., Putz, F. E., Coe, M. T., Silverio, D., Macedo, M. N., Davidson, E. A., Nobrega, C. C., Alencar, A., Soares-Filho, B. S. (2014): Abrupt increases in Amazonian tree mortality due to droughtfire interactions. – P. Natl. Acad. Sci. USA 111: 6347-6352.
<https://doi.org/10.1073/pnas.1305499111>.
- [7] Brown, S., Gillespie, A. J., Lugo, A. E. (1989): Biomass estimation methods for tropical forests with applications to forest inventory data. – Forest Science 35: 881-902.
- [8] Chidumayo, E. N. (1988): Estimating fuelwood production and yield in regrowth dry miombo woodland in Zambia. – Forest Ecology and Management 24: 59-66.
- [9] Clément, J. (1982): Estimation of volumes and productivity of mixed tropical forest and grass formations. Data on francophone African countries in northern Ecuador and recommendations for conducting new studies. – Magazines Tropical Woods and Forests 198 (4), 24 p.
- [10] Cornillon, P. A., Guyader, A., Husson, F., Jegou, N., Josse, J., Kloareg, M., Matzner, L. E., Rouviere, L. (2010): Stat with R. 2nd augmented edition. – Presses Universitaires de Rennes, French statistical society, 274 p.
- [11] Dayton, B. F. (1978): Standing crops of dominant Combretum species at three browsing levels in the Kruger National Park. – Koedoe 21: 67-76.
- [12] Deshmukh, I. (1992): Estimation of wood biomass in the Jubba Valley, southern Somalia, and its application to East African rangelands. – African Journal of Ecology 30: 127-136.
- [13] Devineau, J. L., Lecordier, C., Vuattoux, R. (1984): Evolution of the specific diversity of the woody stand in a pre-forest succession of colonization of a savannah protected from fire (Lamto, Ivory Coast). – Available at:
http://hal.archives-ouvertes.fr/docs/00/43/49/47/PDF/Devineau_et_al_1984.pdf.
- [14] Devineau, J. L. (1997): Seasonal evolution and rate of increase of basal areas of ligneous trees in some Sudanese savannah stands in western Burkina Faso. – Ecology 28(3): 217-232.
- [15] Dias, A. T. C., De Mattos, E. A., Vieira, S. A., Azeredo, J. V., Sacarano, F. R. (2006): Aboveground biomass stocks of native woodland on a Brazilian sandy coastal plain: estimates based on the dominant tree species. – Forest Ecology and Management 226: 364-367.
- [16] Dibi, N., Cya, Y., Ne, K., Kone, M., Yao, S. C. (2008): Analysis of the floral diversity of the Marahoué National Park, Central West of Ivory Coast. – Africa science 4(3): 552-579.
- [17] Duarte, L. da S., Dos-Santos, M. M. G., Hartz, S. M., Pillar, V. D. (2006): Role of nurse plants in Araucaria Forest expansion over grassland in south Brazil. – Austral Ecology 31(4): 520-528.
- [18] Dupouey, J. L., Pignard, G., Badge, V., Thimonier, A., Dhote, J. F., Nepveu, G., Berges, L., Augusto, L., Belkacem, S., Nys, C. (2002): Stock and carbon flux in French forests. – Proceedings of the Academy of Agriculture of France. INRA, Paris, 16 p.
- [19] Eaton, J. M., Lawrence, D. (2009): Loss of carbon sequestration potential after several decades of shifting cultivation in the southern Yucatán. – Forest Ecology and Management 258: 949-958.
- [20] Favier, C., De Namur, C., Dubois, M. A. (2004): Forest progression modes in littoral Congo, Central Atlantic Africa. – Journal of Biogeography 31: 1445-1461.

- [21] Favrichon, V., Gourlet-Fleury, S., Barhen, A., Dessart, H. (1998): Permanent plots in dense rainforest. Element for a data analysis methodology. – CIRAD - Forêt Campus International of Baillarquet. FORAFRI 1998 series document 14, 30432 Montpellier Cedex 1, France, 67 p.
- [22] Giannecchini, M., Twine, W., Vogel, C. (2007): Land-cover change and human–environment interactions in a rural cultural landscape in South Africa. – *Geographical Journal* 173: 26-42.
- [23] Grace, J., San Jose, J., Meir, P., Miranda, H. S., Montes, R. A. (2006): Productivity and carbon fluxes of tropical savannas. – *Journal of Biogeography* 33: 387-400.
- [24] Hofstad, O. (2005): Review of biomass and volume function for individual trees and shrubs in southeast Africa. – *Journal of Tropical Forest Science* 17: 151-162.
- [25] Ibrahima, A., Abib Fanta, C. (2008): Estimation of the carbon stock in the wooded and shrubby facies of the Sudano-Guinean savannahs of Ngaoundéré, Cameroon. – *Cameroon newspaper of experimental biology* 4(3): 1-11.
- [26] Jacquin, A. (2010): Dynamics of savanna vegetation in relation to the use of fires in Madagascar. Time series analysis of remote sensing images. – Thesis in order to obtain the doctorate of the University of Toulouse. 146 p.
- [27] Kapa, B., Nkiama, M., Malele, M., Ritvisay, M. (1987): Development of the Luki Biosphere Reserve. – SPIAF, 67 p.
- [28] Kelly, R. D., Walker, B. H. (1977): The effects of different forms of land use on the ecology of a semi-arid region in south-eastern Rhodesia. – *Journal of Ecology* 64: 553-576.
- [29] Lal, R. (2002): Carbon sequestration in dryland ecosystems of West Asia and North Africa. – *Land Degradation & Development* 13: 45-59.
- [30] Liu, Y. Y., van Dijk, A. I. J. M., de Jeu, R. A. M., Canadell, J. G., McCabe, M. F., Evans, J. P., Wang, G. (2015): Recent reversal in loss of global terrestrial biomass. – *Nat. Clim. Change* 5: 470-474. <https://doi.org/10.1038/nclimate.2581>.
- [31] Lubalega, T. (2016): Natural evolution of the savannahs defended at Ibivillage, on the Bateke plateau, in the Democratic Republic of Congo. – Joint thesis Université Laval / Québec, Canada / Philosophiae doctor (Ph.D.).
- [32] Lubini, A. (1997): Vegetation of the Luki Biosphere Reserve in Mayombe (Zaire). – *Opera botanica Belgica* 10. Garden Botanical National of Belgium, Meise, 155 p.
- [33] Malhi, Y., Roberts, J. T., Betts, R., Killeen, T. J., Li, W., Nobre, C. (2008): Climate Change, Deforestation, and the Fate of the Amazon. – *Science* 319: 169-172.
- [34] Malimbwi, R. E., Solberg, B., Luoga, E. (1994): Estimation of biomass and volume in miombo woodland at Kitulangalo Forest Reserve, Tanzania. – *Journal of Tropical Forest Science* 7(2): 230-242.
- [35] Manlay, R., Peltier, R., N'Toupka, M., Gautier, D. (2002): Assessment of the tree resources of a Sudanese savannah village in North Cameroon for sustainable management. – In: Jamin, J. Y., Seiny Boukar, L. (eds.) Symposium "African savannahs: changing spaces, actors facing new challenges." 27-31 May 2002. PRASAC, Garoua, Cameroon. in C.D. Rom.
- [36] Miles, L., Kapos, V. (2008): Reducing greenhouse gas emission from deforestation and forest degradation: global land-use implications. – *Science* 320: 1454-1455.
- [37] Mills, A. J., Cowling, R. M., Fey, M. V., Kerley, G. I. H., Lechmere-Oertel, R. G., Sigwela, A., Skowno, A., Rundel, P. W. (2005): Effects of goat pastoralism on ecosystem carbon storage in semi-arid thicket, Eastern Cape, South Africa. – *Austral Ecology* 30: 807-813.
- [38] Mills, A. J., Cowling, R. M. (2006): Rate of carbon sequestration at two thicket restoration sites in the Eastern Cape, South Africa. – *Restoration Ecology* 14: 38-49.
- [39] Munishi, P. K. T., Mringi, S., Shirima, D. D., Linda, S. K. (2010): The role of the Miombo Woodlands of the Southern Highlands of Tanzania as carbon sinks. – *Journal of Ecology and the Natural Environment* 2(12): 261-269.

- [40] Muys, B. (2007): The importance of tropical forests in carbon sequestration and climate management. – *Science Connection* 18: 15-18. Brussels, Belgium.
- [41] Pan, Y., Birdsey, R. A., Fang, J., Houghton, R., Kauppi, P. E., Kurz, W. A., Philipps, O. L., Shvidenko, A. Z., Lewis, S. L., Canadell, J. G., Ciais, P., Jackson, R. B., Pacala, S. W., McGuire, A. D., Piao, S., Rautiainen, A., Sitch, S., Hayes, D. (2011): A Large and Persistent Carbon Sink in the World's Forests. – *Science* 333(6045): 988-993.
- [42] Powell, M. J. (2008): Restoration of degraded subtropical thickets in the Baviaanskloof Megareserve, South Africa: the role of carbon stocks and *Portulacaria afra* survivorship. – MSc Thesis, Rhodes University, Grahamstown, 144 p.
- [43] Puig, H. (2001): The tropical rainforest. – Editions Belin, Saint-Amand-Montrond, France, ISBN 2-7011-2446-8, 447 p.
- [44] Quinif, Y. (1986): Genesis of karts in tows in intertropical countries the example of Bas - Zaire. – *Annale of the Geological Society of Belgium* 109: 515-527.
- [45] Rondeux, J. (1993): The measurement of trees and forest stands. – 1st edition, Gembloux, Belgium: Agronomic Press of Gembloux, 522 p.
- [46] Rondeux, J. (1999): The measurement of trees and forest stands. – 2nd edition, Gembloux, Belgium: Agronomic press of Gembloux, 521 p.
- [47] Ryan, C. M., Williams, M., Grace, J. (2011): Above-and Belowground Carbon Stocks in Miombo Woodland Landscape of Mozambique. – *Biotropica* 43(4): 423-432.
- [48] Salis, S. M., Assis, M. A., Mattos, P. P., Pião, A. C. S. (2006): Estimating aboveground biomass and wood volume of a savanna woodland in Brazil's Panatal wetlands based on allometric correlations. – *Forest Ecology and Management* 228: 61-68.
- [49] Scholes, R. J., Hall, D. O. (1996): The carbon budget of tropical savannas, woodlands and grasslands. – In: Breymer, A. I., Hall, D. O., Melillo, J. M., Agren, G. I. (eds.) *Global Change: Effects on Coniferous Forests and Grasslands*. John Wiley & Sons, Chichester, UK, pp. 69-99.
- [50] Shackleton, C. M., Scholes, R. J. (2010): Above ground woody community attributes, biomass and carbon stocks along a rainfall gradient in the savannas of the central lowveld, South Africa. – *South African Journal of Botany* 77(1): 184-192.
- [51] Silver, C. S., DeFries, R. (1990): A planet, a future. – National Academy of Sciences, New Horizons, Washington DC, USA, 189 p.
- [52] Solbrig, O. T., Menaut, J. C., Mentis, M., Shugart, H. H., Stott, P., Wigston, D. (1991): Savanna modelling for global change. – *Biology International* 24.
- [53] SPIAF (2007): Forest management inventory standards. Operational guide. – Ministry of Environment, Conservation of Nature and Tourism. 33 p.
- [54] Sys, C. (1960): Soil and vegetation map of the Belgian Congo and Rwanda-Urundi, explanatory note of the soil map of the Belgian Congo and Rwanda-Urundi. – Publications of the National Institute for Agronomic Study of the Belgian Congo (INEAC.) A. R. of 22-12-33 and 21-12-39, Brussels, 96 p.
- [55] Tietema, T. (1993): Biomass determination of fuelwood trees and bushes of Botswana, southern Africa. – *Forest Ecology and Management* 60: 257-269.
- [56] Trugman, A. T., Medvigy, D., Hoffmann, W. A., Pellegrini, A. F. A. (2018): Sensitivity of woody carbon stocks to bark investment strategy in Neotropical savannas and forests. – *Biogeosciences* 15(1).
- [57] van der Werf, G. R., Morton, D. R., DeFries, R. S., Olivier, J. G. J., Kasibhatla, P. S., Jackson, R. B., Randerson, J. T. (2009): CO₂ emissions from forest loss. – *Nat. Geosci.* 2: 737-738.
- [58] van der Werf, G. R., Randerson, J. T., Giglio, L., Collatz, G. J., Mu, M., Kasibhatla, P. S., Morton, D. C., DeFries, R. S., Jin, Y., van Leeuwen, T. T. (2010): Global fire emissions and the contribution of deforestation, savanna, forest, agricultural, and peat fires (1997–2009). – *Atmos. Chem. Phys.* 10: 11707-11735. <https://doi.org/10.5194/acp-10-11707-2010>.

- [59] Williams, M., Ryan, C. M., Rees, R. M., Sambane, E., Fernando, J., Grace, J. (2008): Carbon sequestration and biodiversity of re-growing miombo woodlands in Mozambique. – *Forest Ecology and Management* 254: 145-155.
- [60] Woomer, P. L., Touré, A., Sall, M. (2004): Carbon stock in Senegal's transition zone. – *Journal of Arid Environments* 59: 499-510.

APPENDIX

Appendix I. List of inventoried and defended species

Species	Number of Dhp (in cm)	Number of Chp (in cm)	Number of Height (in m)
<i>Albizia ferruginea</i> (Guill. & Perr.) Benth.	9	9	9
<i>Albizia gummifera</i> (J.F. Gmel.) C.A. Sm.	13	13	13
<i>Albizia lebbeck</i> (L.) Benth.	197	197	197
<i>Alchornea cordifolia</i> (Schumach. & Thonn.) Müll. Arg.	8	8	8
<i>Annona senegalensis</i> Pers.	48	48	48
<i>Anthocleista vogelii</i> Planch	159	159	159
<i>Antiaris toxicaria</i> Lesch.	3	3	3
<i>Barteria nigritiana</i> Hook.f.	6	6	6
<i>Blighia welwitschii</i> (Hiern) Radlk.	1	1	1
<i>Bridelia atroviridis</i> Müll. Arg.	1	1	1
<i>Bridelia ferruginea</i> Benth.	175	175	175
<i>Canarium schweinfurthii</i> Engl.	1	1	1
<i>Canthium oddonii</i> (De Wild.) C. Evrard	21	21	21
<i>Chrysophyllum africanum</i> A. DC.	2	2	2
<i>Corynanthe paniculata</i> Welw.	3	3	3
<i>Crossopteryx febrifuga</i> (Afzel. ex G. Don) Benth.	20	20	20
<i>Crossopteryx sp</i>	27	27	27
<i>Croton sylvaticus</i> Hochst. ex Krauss	10	10	10
<i>Dacryodes buettneri</i> (Engl.) H. J. Lam	7	7	7
<i>Deinbolia acuminata</i> Exell	5	5	5
<i>Dracaena mannii</i> (Willd.) Link	1	1	1
<i>Eriocoelum microspermum</i> Radlk. ex De Wild.	1	1	1
<i>Ficus mucuso</i> Welw. ex Ficalho	1	1	1
<i>Ficus recurvata</i> De Wild.	8	8	8
<i>Harungana madagascariensis</i> Lam. ex Poir.	5	5	5
<i>Holarrhena congolensis</i> Stapf	11	11	11
<i>Hymenocardia acida</i> Tul.	786	786	786
<i>Hymenocardia ulmoides</i> Oliv.	39	39	39
<i>Lannea welwitschii</i> (Hiern) Engl.	140	140	140
<i>Macaranga monandra</i> Müll. Arg.	32	32	32
<i>Macaranga spinosa</i> Müll. Arg.	386	386	386
<i>Maesopsis eminii</i> Engl.	10	10	10
<i>Maprounea africana</i> Müll. Arg.	535	535	535
<i>Markhamia sessilis</i> Sprague	21	21	21
<i>Microdesmis puberula</i> Hook. f. ex Planch.	1	1	1
<i>Millettia versicolor</i> Welw. ex Baker	61	61	61
<i>Monodora myristica</i> (Gaertn.) Dunal	6	6	6
<i>Morinda lucida</i> Benth.	1	1	1
<i>Musanga cecropioides</i> R. Br. ex Tedlie	1	1	1
<i>Myrianthus arboreus</i> P. Beauv.	1	1	1
<i>Nauclea latifolia</i> Smith	167	167	167
<i>Ochna afzelii</i> R. Br. ex Oliv.	4	4	4
<i>Oncoba welwitschii</i> Oliv.	100	100	100
<i>Piptadeniastrum africanum</i> (Hook.f.) Brenan	1	1	1
<i>Pseudospondias microcarpa</i> (A. Rich.) Engl.	7	7	7
<i>Pteleopsis hyloidendron</i> Mildbr.	7	7	7
<i>Symphonia globulifera</i> L. f.	2	2	2

Species	Number of Dhp (in cm)	Number of Chp (in cm)	Number of Height (in m)
<i>Tetrochidium didymonstemon</i> (Baill.) Pax & K. Hoffm.	40	40	40
<i>Trema orientalis</i> (L.) Blume	9	9	9
<i>Trichilia gilgiana</i> Harms	4	4	4
<i>Trilepsium madagascariense</i> Thouars ex DC.	4	4	4
<i>Vernonia conferta</i> Benth.	3	3	3
<i>Vismia affinis</i> Oliv.	2	2	2
<i>Vitex madiensis</i> Oliv.	9	9	9
<i>Xylopia aethiopica</i> Dunal A. Rich.	71	71	71
<i>Xylopia chrysophylla</i> Louis ex Boutique	20	20	20
<i>Zanthoxylum gillettii</i> (De Wild.) P.G. Waterman	18	18	18
Total général	3231	3231	3231

CHP = Breast Height Circumference

Appendix 2. Family structure in the savannah sub-parcels put in defense

Number	Families	N.E.	N.I.	DIR	DER
1	<i>Euphorbiaceae</i>	5	331	19.2	38.5
2	<i>Fabaceae</i>	5	39	19.2	4.5
3	<i>Annonaceae</i>	3	214	11.5	24.9
4	<i>Rubiaceae</i>	3	144	11.5	16.8
5	<i>Apocynaceae</i>	1	5	3.8	0.6
6	<i>Bignoniaceae</i>	1	2	3.8	0.2
7	<i>Burseraceae</i>	1	1	3.8	0.1
8	<i>Clusiaceae</i>	1	30	3.8	3.5
9	<i>Compositae</i>	1	11	3.8	1.3
10	<i>Flacourtiaceae</i>	1	42	3.8	4.9
11	<i>Gentianaceae</i>	1	32	3.8	3.7
12	<i>Meliaceae</i>	1	1	3.8	0.1
13	<i>Passifloraceae</i>	1	4	3.8	0.5
14	<i>Rutaceae</i>	1	3	3.8	0.3

NI = Number of individuals; NE = Number of species; DIR = Relative Diversity; DER = Relative density

IMPACT OF SIMULATED CLIMATE CHANGE ON SLUG GRAZING IN DESIGNED PLANT COMMUNITIES

ALIZADEH, B.* – HITCHMOUGH, J. D.

Department of Landscape Architecture, The University of Sheffield, Sheffield S10 2TN, UK

**Corresponding author
e-mail: behdadalizade@gmail.com*

(Received 8th Sep 2019; accepted 12th Feb 2020)

Abstract. Climate change is currently altering ecosystem services which are a supply of benefits that support human life and well-being provided by ecosystems to our society. Although recently, many studies have investigated effects of biodiversity on ecosystem functions, there is a considerable lack of studies on the responses of invertebrates to climate change. The grazing behavior of slugs is of critical importance in the sparse herbaceous vegetation of cool-temperate zones and also in the temperate regions with seasonally moist climates. They significantly influence the development, composition and biomass of both semi-natural and designed herbaceous vegetation. This experiment aimed to investigate how the selectivity of grazing by herbivores affected relationships between plant species in designed plant communities under 2050 UK climate change scenarios. Thirty-six species from three different ecological regions were chosen to represent a gradient from well fitted to poorly fitted to the current British climate and from palatable to unpalatable to slugs. They also were selected to share the similar morphological characteristics, regarding canopy size and flower attractiveness for urban green space users. The molluscs showed different behaviours in dry, wet, warm and ambient temperature, and this led to significant differences in the biomass and structure of the plant communities.

Keywords: *mollusc grazing, herbivory, meadow-like community, plant species fitness, urban landscape*

Introduction

Today, much attention is paid to biodiversity and the potential impact of climate change on biodiversity. Nowadays, the “quality of life”, “human well-being” and “biodiversity are three critical factors for all the landscape planner. Greenspaces are one of the most important wildlife habitats in the urban area. Urban landscape not only provide physical habitat for native and non-native fauna but also provide pollen and nectar for wild life through the plant species and vegetation (Dunnett and Hitchmough, 2004). These habitats also support large populations of slugs and snails, and these herbivores have a reciprocal impact on the vegetation itself (Hitchmough and Wagner, 2011).

Greenhouse gases, moisture availability and temperature, are three critical factors that should be considered in climate change research. Researchers in different aspects investigated impacts of water stress on plant growth in the urban landscape. In moist temperate climates slugs and snails significantly affect the “development and composition” of herbaceous vegetation (Bruehlheide and Scheidel, 1999; Wilby and Brown, 2001; Holland et al., 2007; Hitchmough and Wagner, 2011; Hitchmough et al., 2017). Mollusc herbivory is an essential element for limiting plant species distribution as it has been shown, for instance, with *Arnica montana*. Herbivory is vital because when combined with competition between plant species it acts to exaggerate competition, slow growing, shade-intolerant species that are palatable are likely to be eliminated much more quickly from the vegetation than unpalatable species of similar competitiveness. Food selection by snail and slug in plant communities has been

investigated by Grime et al. (1973, 1977, 1998, 2006), Pallant (1972), Dirzo (1980), Wardle et al. (1998), Lawrey (1983), Rathke (1985), Briner and Frank (1998), Speiser and Rowell-Rahier (1993), Jennings and Barkham (1975), Hoyle et al. (2017) and Alizadeh and Hitchmough (2019a).

In most parts of the world, plant distribution will be affected by climate change. According to the IPCC (2014), climate change is estimated to exacerbate the loss of species most, where those species have restricted climate and habitat requirements, and limited migration capabilities. Thomas et al. (2004) have estimated that climate change may lead to the extinction of 3–21% of all endemic plant species in Europe by 2050. Species composition will change in every part of Europe differently. Bakkenes et al. (2006) suggests that “The most dramatic changes will occur in Northern Europe, where more than 35% of the species composition in 2100 will be invasive, and in Southern Europe, where up to 25% of the species now present will have disappeared under the climatic circumstances forecasted for 2100” (Bakkenes et al., 2006).

On the European and other continental land masses climate change will lead to movement of species, as some existing species become less fit and current unfit species become more fitted. In the designed, culturally founded landscapes of cities reducing the climate change will need to involve parallel, but actively human-mediated processes. New plant species, from other parts of the world, which are more similar to future climate change scenarios and hence more tolerant, will become essential in designed sustainable urban landscapes (Alizadeh and Hitchmough, 2019b). Although currently in most parts of the world, alien plant species are considered as unsustainable design elements in urban landscapes (Hitchmough, 2011), in the future, these attitudes will have to change.

These incoming or alien plant species have ecological functions in the urban landscape, as do current native species. They support native invertebrates and also are attractive for people, and facilitate a range of ecosystem service functions, which are generic and not based on plant origin.

The effects of different climate change scenarios on the designed plant community in the urban area were investigated before by Alizadeh (2016). In this article, the effect of simulated climate change on slug grazing effects on three communities of varying palatability is studied. The present research appears to be the first study on food selection by slug and snail under different climate change scenarios.

Materials and methods

Planting mixes were designed as described by Ahmad and Hitchmough (2007), Sayuti and Hitchmough (2013), Alizadeh and Hitchmough (2019) to create meadow-like plant communities to test the research questions.

The undertaken criteria for plants selection in the study are as follows:

- Seed availability
- Typical fitness to UK conditions
- Canopy size, and form, morphological similarity
- Flowering period, plant height and aesthetic function of the species
- Diverse yet complementary ecological strategies
- Slug palatability
- UK 2050-2080 climate change scenarios

The sowing mix was composed of 36 grassland forbs from the three different climatic types (Western Europe with Maritime climate (well fitted to the current UK climate), Southern Europe (intermediate in fitness to the current UK climate) and Rocky Mountain/Eurasian Steppe Region (Temperate Continental climate, poorly fitted to the current UK climate). Twelve species from each climatic type were present in the seed mix to produce a gradient of species from well fitted to poorly fitted to the current British climate. The characteristics of these species are shown in *Tables 1, 2* and *3*. Selection was based on many years of prior experience working with these species both in experiments and in practice, backed up by ecological strategy models developed by Grime (1977, 1979). The communities of these 36 species were then managed and manipulated to create a biological assay to investigate climate change in the form of a multi-layer (low, medium, and tall) designed meadow community and slug grazing on designed meadow community under different climate change scenarios (*Tables 1, 2* and *3*). These layers were important in the meadow community both in aesthetic and ecological terms, with short species (unless shade tolerant), being most likely to be eliminated due to light competition where unfit, and hence species were selected and characterised as four groupings on the basis of the predominant height of their typical mature canopy: 1: < 20 cm, 2: 20-40 cm, 3: 40-80 cm, 4: > 80 cm.

The plant species were categorized based on slug or snail palatability under current UK climate scenarios as well.

Research started in spring 2012 with site and soil preparation and the construction of 48 external growth cabins at the Sheffield Botanical Garden.

During the five years of the research, the mean annual rainfall in Sheffield was 877 mm and the mean annual temperature was 10 °C. The 2050–2080 UK climate change scenarios (Theccc.org.uk, 2018) were used as the base for decisions on manipulating precipitation and temperature within the growth cabins.

Climate scenarios

The climate in the UK is maritime. The Sheffield's weather conditions of the study years (2010 to 2016) are presented in *Tables 4* and *5*.

Table 1. Temperate maritime climate (mostly western Europe) plant species

Species	Habit	Typical fitness in current UK climate	Slug palatability
<i>Arnica montana</i>	Rosette with ascending stem	Well fitted	Palatable
<i>Bupthalmum salicifolium</i>	Hummock	Well	Palatable
<i>Centaurea montana</i>	Hummock	Well	Palatable
<i>Galium verum</i>	Mat with ascending stem	Well	Unpalatable
<i>Geranium sylvaticum</i>	Hummock	Well	Unpalatable
<i>Knautia arvensis</i>	Hummock with ascending stem	Well	Unpalatable
<i>Origanum vulgare</i>	Hummock	Well	Unpalatable
<i>Phyteuma spicatum</i> var. <i>coeruleum</i>	Hummock with ascending stem	Well	Palatable
<i>Primula veris</i>	Mat with ascending stem	Well	Unpalatable
<i>Prunella vulgaris</i>	Mat with ascending stem	Well	Unpalatable
<i>Salvia pratensis</i>	Hummock with ascending stem	Well	Palatable
<i>Scabiosa caucasica</i> *	Hummock with ascending stem	Well	Palatable

*Temperate grasslands of the Caucasus

Table 2. Southern European plant species

Species	Habit	Typical fitness in current UK climate	Slug palatability
<i>Asphodelus lutea</i>	Hummock with ascending stem	Intermediate	Palatable
<i>Centaurea triumfettii</i>	Hummock with ascending stem	Intermediate	Palatable
<i>Centaurea orientalis</i>	Hummock with ascending stem	Intermediate	Palatable
<i>Dianthus carthusianorum</i>	Mat with ascending stem	Intermediate	Unpalatable
<i>Euphorbia nicaeensis</i>	Hummock	Intermediate	Unpalatable
<i>Hedysarum hedysaroides</i>	Hummock	Intermediate	Palatable
<i>Linum flavum</i>	Hummock	Intermediate	Unpalatable
<i>Linum narbonense</i>	Hummock with ascending stem	Intermediate	Unpalatable
<i>Lychnis coronaria</i>	Hummock with ascending stem	Intermediate	Unpalatable
<i>Lychnis flos-jovis</i>	Mat with ascending stem	Intermediate	Unpalatable
<i>Paradisea liliastrum</i>	Hummock with ascending stem	Intermediate	Palatable
<i>Salvia nemorosa</i>	Hummock with ascending stem	Intermediate	Palatable

Table 3. Continental climate (mostly southern Rocky Mountain Region) plant species

Species	Habit	Typical fitness in current UK climate	Slug palatability
<i>Amsonia jonesii</i>	Hummock	Poor	Unpalatable
<i>Asclepias tuberosa</i> (Colorado populations)	Hummock	Poor	Palatable
<i>Balsamorhiza sagittifolia</i>	Hummock with ascending stem	Poor	Palatable
<i>Centaurea pulcherrima</i> ¹	Hummock	Poor	Palatable
<i>Delphinium barbeyi</i>	Hummock with ascending stem	Poor	Palatable
<i>Dracocephalum grandiflorum</i> ²	Mat with ascending stem	Poor	Palatable
<i>Geum triflorum</i>	Mat with ascending stem	Poor	Unpalatable
<i>Hymenoxys grandiflora</i>	Mat with ascending stem	Poor	Palatable
<i>Penstemon strictus</i>	Mat with ascending stem	Poor	Unpalatable
<i>Salvia pachyphylla</i>	Hummock	Poor	Unpalatable
<i>Sphaeralcea coccinea</i>	Hummock	Poor	Unpalatable
<i>Zinnia grandiflorus</i>	Hummock	Poor	Unpalatable

¹Turkey

²Kazakhstan, Central Asia

Table 4. The Sheffield mean monthly average of the temperature during 2010 to 2016

MEAN MONTHLY AVERAGE TEMPERATURE

YEAR	JAN	FEB	MAR	APR	MAY	JUN	JUL	AUG	SEP	OCT	NOV	DEC
2010	1.2	1.9	5.9	9.1	10.9	15.2	16.2	14.9	13.4	9.5	4.9	0.4
2011	3.9	6.0	6.6	12.0	12.0	14.2	15.8	15.8	14.9	12.2	8.9	5.4
2012	5.1	4.5	8.6	6.7	11.6	13.4	15.5	16.2	12.7	8.8	6.1	4.2
2013	3.4	2.7	1.7	7.4	10.6	14.1	18.4	16.8	13.3	11.7	6.2	6.3
2014	5.0	5.6	7.4	10.1	12.2	15.3	17.9	14.9	14.4	11.4	7.8	5.2
2015	4.1	3.8	5.9	9.1	10.6	13.9	15.7	15.8	12.2	10.2	8.7	8.6
2016	4.8	4.2	5.5	7.0	11.8	14.6	16.6	16.6	15.4	10.2	5.4	6.3

Table 5. The Sheffield mean monthly average of rain fall during 2010 to 2016

MEAN MONTHLY RAINFALL

YEAR	JAN	FEB	MAR	APR	MAY	JUN	JUL	AUG	SEP	OCT	NOV	DEC
2010	63.7	64.4	65.0	28.7	18.1	45.9	80.6	49.4	63.5	69.3	122.4	31.9
2011	53.5	93.1	11.2	12.4	42.4	53.0	23.5	41.3	29.1	59.7	40.2	110.1
2012	82.0	26.8	30.5	196.6	47.1	182.3	118.8	96.0	102.0	64.3	116.2	155.1
2013	62.6	56.7	69.8	9.0	88.7	31.0	63.4	39.6	53.3	143.7	63.7	65.5
2014	137.5	106.4	49.0	63.0	139.5	49.8	34.3	92.8	14.4	87.8	105.4	96.1
2015	76.2	33.0	73.4	23.6	91.5	53.6	47.1	90.6	28.0	81.2	114.8	122.3
2016	99.0	64.7	95.1	60.8	64.5	112.5	31.7	64.6	38.0	35.5	107.9	30.5

The average precipitation of Sheffield during the March to September growth season during the last 50 years was used as the ambient base line during the experiments. This allowed three precipitation scenarios to be designed around the ambient value (Ambient – 50%, Ambient, Ambient + 50%) (Table 6).

Table 6. Calculation of water added to the experimental blocks (mm per month) for the rainfall scenarios based on Sheffield rainfall averages from 1955-2012

Month	Average (ambient)	Ambient + 50%	Ambient – 50%	Mean days of rainfall
March	62.9	94.35	31.45	12.3
April	60.0	90	30	10.3
May	60.69	91.03	30.34	9.6
June	67.1	100.65	33.55	9.1
July	60.6	90.9	30.3	9.2
August	67.8	101.5	33.9	9.9
September	64.3	96.45	32.15	8.9

The maximum temperature of Sheffield during the March to September growth season during the last 50 years was used as a baseline temperature upon which two temperature scenarios were designed (Temperature: Ambient and Ambient + 3 °C). In order to achieve the desired 3 °C elevation of air temperature within the growth cabins, in a calibration study prior to the main experiment with two replications, a series of different sized vents representing; 10%, 15%, 20%, 30%, 60% of the area of the wall were cut in one of the polyethylene walls of the growth cabins. The temperature in cabins with a vent and in those with none was recorded every 30 min via Tinytag recorders over a one-year period. When considered in terms of both day and night temperature, a permanently open vent of 10% of the area of the wall was found to provide on average 2.6 to 3 °C difference from the ambient during the growth season.

The combination of three precipitation and two temperature scenarios led to a research design with six climate change scenarios:

- a) 50% increase in precipitation (Ambient + 50%); no change in temperature (Ambient)
- b) 50% increase in precipitation (Ambient + 50%); 3 °C increase in temperature (Ambient + 3 °C)

- c) Ambient precipitation and ambient temperature
- d) Ambient precipitation; 3 °C increase in temperature (Ambient + 3 °C)
- e) 50% decrease in precipitation (Ambient – 50%); no change in temperature (Ambient)
- f) 50% decrease in precipitation (Ambient – 50%); 3 °C increasing in temperature (Ambient + 3 °C)

In all treatments (ambient, ambient ± 50) all growth cabins were covered with a transparent polythene (1.3 × 1.0 × 1.0 m), to exclude natural rainfall from the plots to allow the scenarios to be achieved by carefully controlled irrigation.

In the case of the ambient treatments growth cabins had a polythene cover on the roof. For example, The average precipitation in Sheffield during March over the last 50 years was 62.3 mm and the average number of rainfall days during the same time were 12, equating to a rainfall event approximately 3 times per week. Ambient precipitation treatment plots were therefore irrigated 3 times a week and each time they received 5.0 mm of water/m² during March. For the plots with other precipitation treatments (-50% or +50%), this amount of water was increased or decreased in relation to the value of 5.0 mm at each irrigation event (Table 4).

Seeds of the 36 species were sown in seedling trays in April 2012 in a greenhouse and a growth cabinet. Before seed sowing, those species which needed a period of chilling to germinate were pre-chilled in small pots of moist compost in a fridge at 2 °C for varying durations to ensure that their chilling requirements were sufficiently satisfied to achieve uniform germination in the experiment. The species with hard seed coats were scarified. After seeds had emerged and were well established, the seedling trays and pots were transferred outside of the greenhouse to harden them off. Seedlings were transplanted into the experimental plots, which were covered with 75 mm deep mulch layer of sand from June 2012. Four seedlings of each species (144 seedlings in total) were planted randomly in each 1 m × 1.30 m treatment plots (Fig. 1).

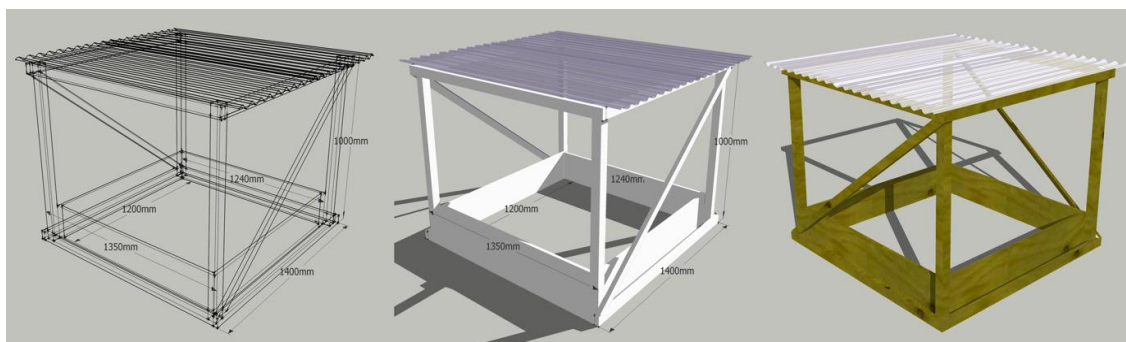


Figure 1. The dimensions of plots and climate control chambers

The purpose of the experiments was to create two areas with different densities of molluscs, low and higher. In order to achieve this aim and evaluate the above objectives, it was necessary to provide two experimental blocks. The mollusc was involved to one of the blocks and the other block was kept as free or low-density mollusc area (Fig. 2).

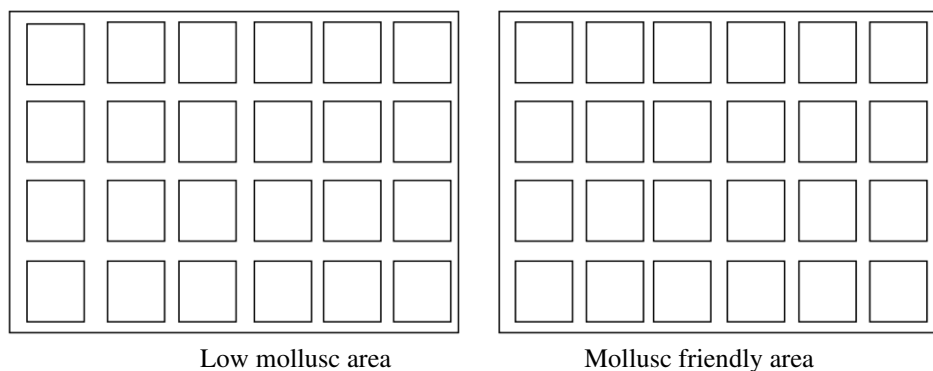


Figure 2. The layout plan of the research area and the mollusc friendly and non mollusc blocks

In mollusc friendly area, to provide a desirable place for mollusc grazing, a combination of cat food was offered to the slugs on saucers that also contained garden soil and was covered with a black film. These saucers were then used to inoculate the most intense mollusc feeding in mollusc friendly block (half of the experiment) (Figs. 3-7).



Figure 3. Adding cat food to the slug's shelter; cat food is very palatable to slugs



Figure 4. The slug shelter covered with black film and were added to the mollusc friendly area. At first next to the plots and later inside them. Slug availability was checked every day during early spring and late summer



Figure 5. *Salvia nemorosa* is palatable to slugs and snails

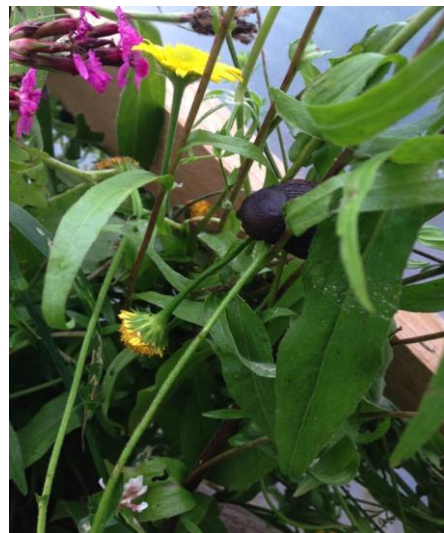


Figure 6. Slug grazing on *Bupthalmum salicifolium*



Figure 7. During the night, the slugs feeding from the species of plots and in the morning they come back to the shelter

Data collection and data analysis

The productivity of plant species within each plot was recorded from spring 2013 to autumn 2014. The number of plants of each species in each plot was counted every two-weeks to get the percentage of individual species that disappeared during the observation period. The plants were harvested in October 2013 after the first growing season. A harvesting procedure was developed to cope with highly variable biomass and species of very different sizes within an individual plot and plant groups, and also to ensure that all plant samples were available for harvest at the end of the summer. Each of the sampled plant species from all species were cut off at a ground level and the cut biomass of each individual plant placed into individual coded envelopes. Samples were dried at ambient temperatures (15- 25 °C) within a botanical garden greenhouse before being transferred to the oven at 60 °C for five days. A similar protocol was utilized in November 2014 after the second growth season.

Each of the lower and higher mollusc density blocks was subdivided into 24 subplots (48 subplots in total). The subplots represented the six treatments with four replications inside of each block. The non-completely random, directed blocking approached used in this experiment was based on statistical advice to reduce shade effects from the tree and hedges near the plots. Cumulative dry mass of the different harvests in one year was used for data analysis. The Shannon–Wiener index and Shannon evenness (Magurran, 1996) were calculated based on biomass data for the species in the first year, and based on the cover values obtained for the next years. The following equations were used:

$$\text{Shannon-Wiener index: } H' = -\sum_{i=1}^S P_i * \ln P_i$$

$$\text{Shannon evenness: } E' = H' / \ln S$$

where p is the biomass of species (first year) or cover (third year) and S is the number of species.

Statistical analysis was undertaken using SPSS and also Minitab for Mac. Data was initially explored through a variety of statistical approaches, both parametric and non-parametric. This included transformation \log_e for weight data, and arcsine square root for percentage data to improve the properties of the data sets for parametric analysis, namely distributional characterizes and homogeneity of variance (Zar, 1999).

Results

The effects of different climate scenarios on a community of three ecological groups of species in the absence of molluscs were investigated by Alizadeh (2016). In this research, the effects of mollusc grazing on plant communities, under different climate scenarios has been studied. In all the figures overlapping SE bars indicate that, the difference between the two means is not statistically significant ($P > 0.05$). In all graphs the mean of biomass is represented for the two years of the study.

Comparison of mollusc grazed and non-mollusc grazed communities

Effects of molluscs on the total biomass of the communities

The graph in *Figure 8* suggests that the overall biomass of a community of well fitted species is not greatly influenced by mollusc grazing, whereas the intermediate fitted species are much more affected, i.e. as a group are much more palatable. There is no difference for poorly fitted species (*Fig. 8*).

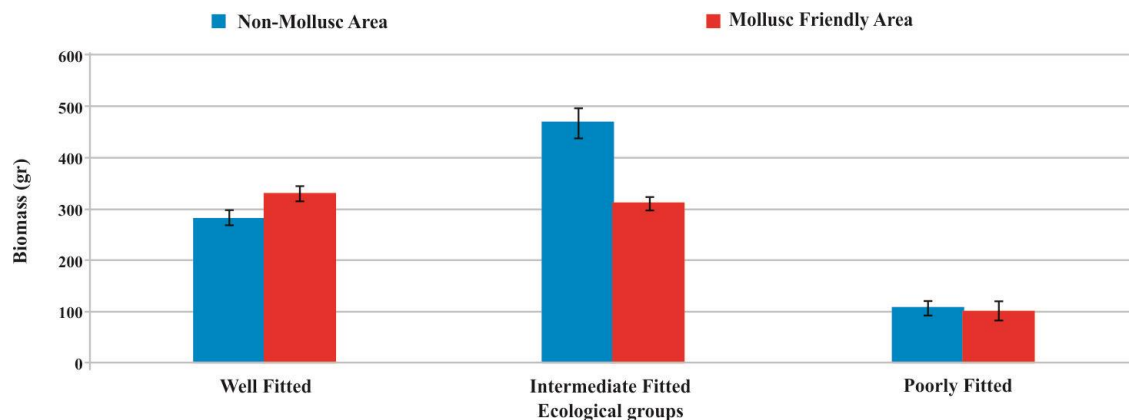


Figure 8. The effects of mollusc grazing on overall biomass production of different fitness groups

Effects of molluscs on the total biomass of the communities at different moisture regimes

The difference between -mollusc and + mollusc treatments are not very notable for the well and poorly fitted groups. For the poorly fitted group the main factor is clearly inability to tolerate elevated moisture, rather than slug grazing. Within the well fitted group there is a step wise progression in biomass as one moves from -50% to +50%. It is clear that the molluscs are not causing the biomass to decline below that of the communities with no mollusc treatment as soil moisture increases. This suggests that positive benefits of more water on biomass production are greater than the negative effects of molluscs on consuming that biomass. This is perhaps different to what might be expected: wetter conditions allow longer mollusc grazing and hypothetically greater consumption of plant biomass. The intermediate fitted group clearly shows the effects of mollusc grazing most strongly with biomass productivity of these species much higher when molluscs are excluded, and much less when present (*Fig. 9*).

Effects of molluscs on the total biomass of the communities at different temperature regimes

Increasing the temperature levels improves the biomass productivity of all the species in all ecological groups whether molluscs are present or not. In the most responsive group (the intermediate group) the molluscs do however appear to apply a break to biomass production as temperature rises, perhaps because molluscs are more active at these elevated temperatures.

In well-fitted species the biomass productivity in the mollusc area at both temperatures were more than that in the non-mollusc areas. The actual differences are

very small, reinforcing the fact that molluscs did not have a great deal of impact on these well fitted species (Fig. 10).

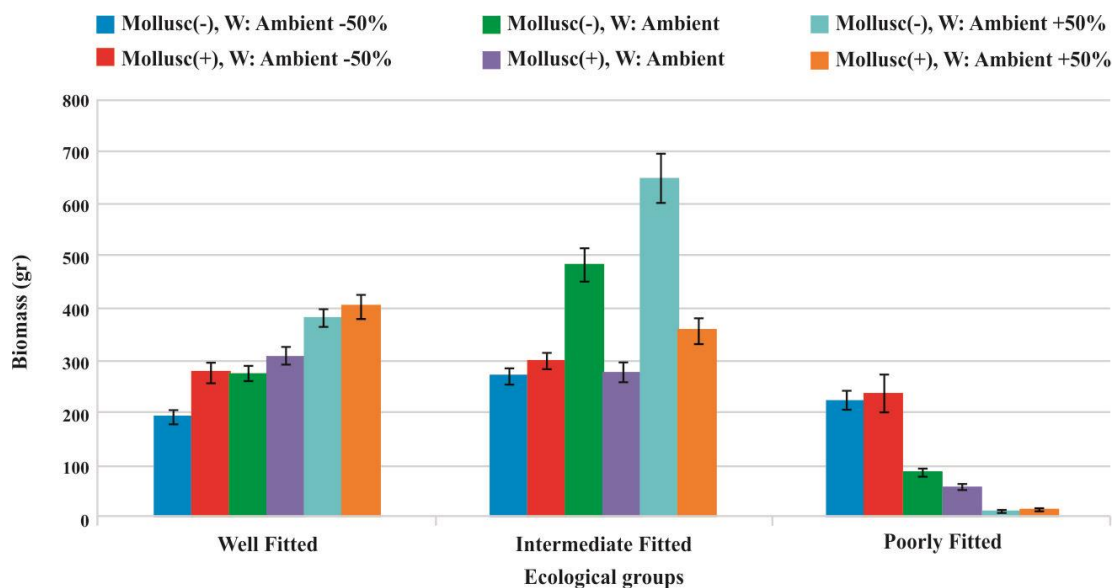


Figure 9. Comparison of mollusc grazed area and non mollusc area - the effects of mollusc grazing and moisture availability on biomass production of the studied species within the different group

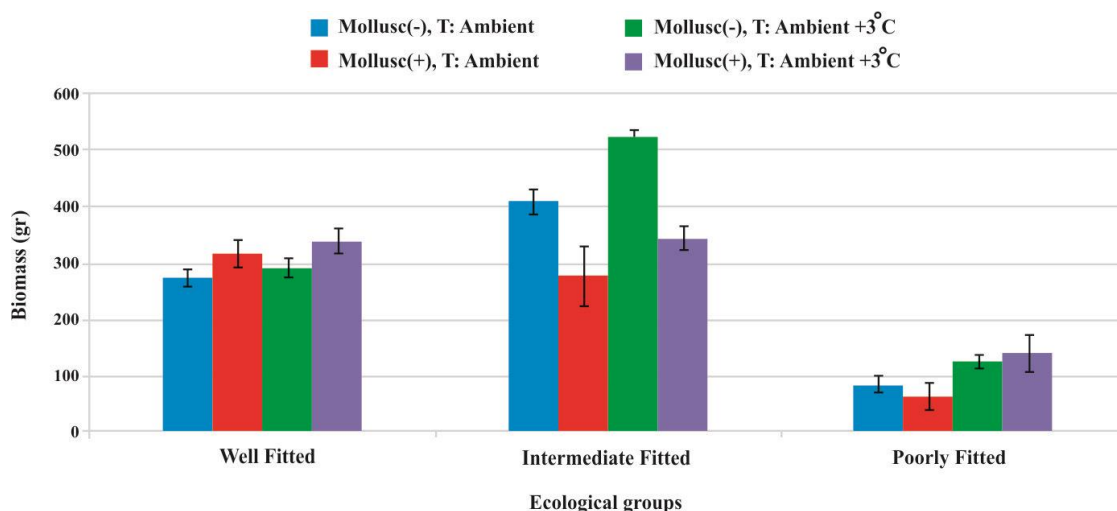


Figure 10. This figure shows how biomass production of the studied species has been affected in non-mollusc and mollusc friendly area as a result of variation in the temperature treatments

Effects of molluscs on the total biomass of the communities at different temperature and moisture regimes

The graph in Figure 11 compares how mollusc grazing can be affected by the combination of the water and temperature treatments. The overall pattern is similar to what was observed in the previous graphs. The main effects are seen in the intermediate fitted group where the presence of molluscs has a significant reduction in total biomass,

compared to when absent, and this pattern is generally repeated across all climatic comparisons. The effect of the molluscs on the fitted species is rarely significant, suggesting that the species chosen are either fundamentally less palatable to molluscs, or that the least palatable species in the mix were able to utilize the increased resources made available by damage to the more palatable species. This process does not seem to be able to operate in the intermediate species. Normally slugs and snails do not show activity at drier and warmer conditions (w: Ambient – 50%). So the mass production of species at these climate conditions is not caused by the mollusc activities. Also the results indicated that the poorly fitted species cannot survive under wetter condition (w: Ambient + 50%). In this situation biomass productivity of species in both blocks (mollusc grazed and non-mollusc area) did not show significant difference. As explained before, for the well fitted group mollusc presence reduce the competition between species (Fig. 11).

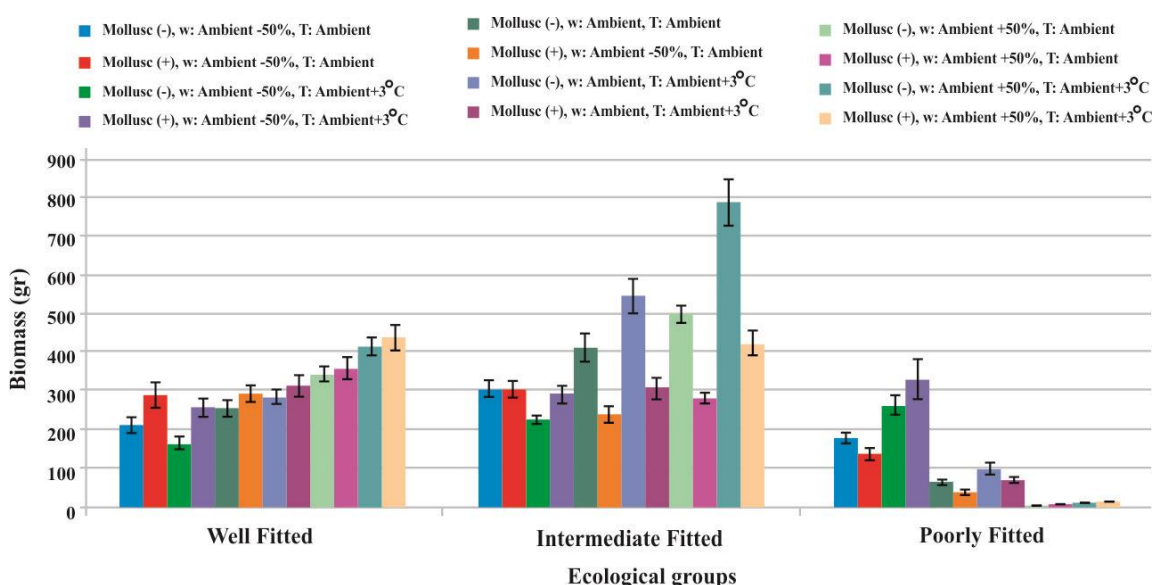


Figure 11. The effects of mollusc grazing on biomass of species under different levels of moisture and temperature

The effect of mollusc grazing on individual plant species with the well fitted and intermediate fitted species

The effects of mollusc grazing on well fitted species and intermediate fitted species are evaluated in this section. As it was not clear that palatable species in poorly fitted species disappeared as a result of mollusc grazing or the climate condition, the poorly fitted species are not compared.

Effects of molluscs on the total biomass of the well fitted species

The biomass productivity of the well-fitted species under mollusc grazing condition is compared with the mass productivity of non mollusc area and shown in the graph in Figure 12. As seen clearly, the most palatable species in these group, *Arnica montana*, *Phyteuma spicatum*, *Salvia pratense* and *Scabiosa caucasica* show much lower biomass when they are exposed to mollusc grazing. The unpalatable species, *Galium verum*, *Geranium sylvaticum*, *Knautia arvensis*, *Origanum vulgare*

and *Prunella vulgaris* on the other hand show even higher biomass production. Although *Bupthalmum salicifolium* and *Centaurea montana* were included as palatable species on the basis of experience in previous studies, at present of the other palatable species they behaved as non-palatable, in this study. The molluscs preferred to feed on others (Fig. 12).

Effects of molluscs on the total biomass of the well fitted species at different moisture regimes

The effects of mollusc grazing on the biomass productivity of the well fitted species when exposed to the moisture treatments and condition is shown in the graph in Figure 13. The general pattern here mirrors what was shown in previous graphs of total biomass. In general, biomass increases as water increases; the greater opportunities for slugs to be active does not prevent this occurring except in the most palatable species. In the case of *Arnica*, *Phyteuma*, *Salvia* and *Scabiosa*, these species disappear at ambient and ambient plus 50% water treatments.

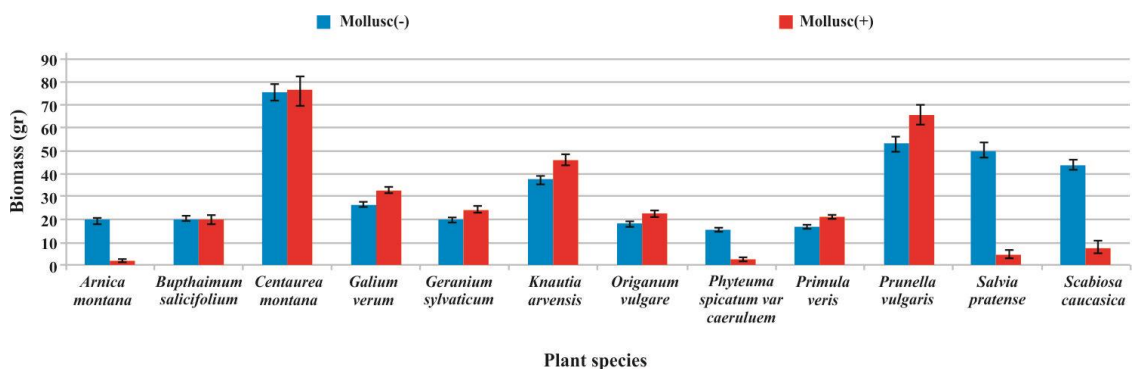


Figure 12. The effects of mollusc grazing on total biomass of well fitted species

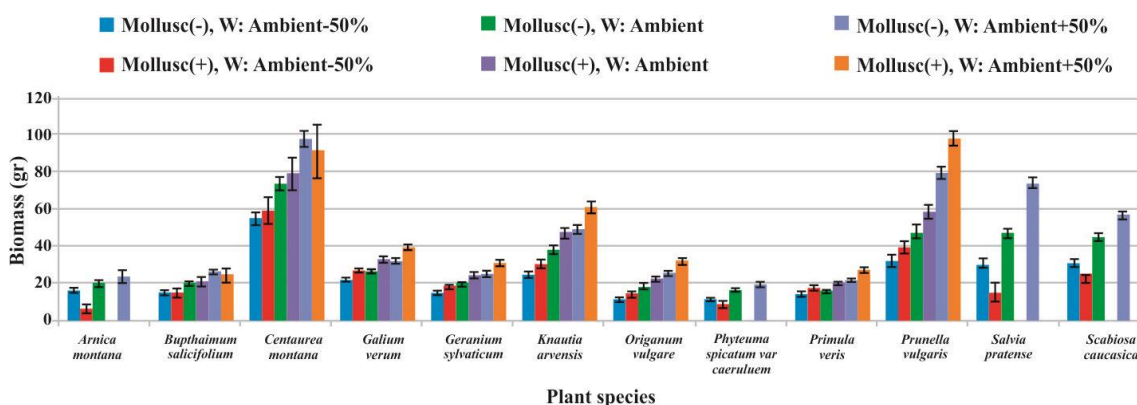


Figure 13. Comparison of mollusc grazed area and non-mollusc area- the effects of mollusc grazing on biomass productivity of well fitted species under different levels of moisture availability

It is clear that molluscs do not have activity when we have Ambient – 50% moisture level and showed their maximum at Ambient + 50%. Palatable species in these group (*Arnica montana*, *Phyteuma spicatum*, *Salvia partense* and *Scabiosa caucasica*) show

much lower biomass presence when they are exposed to mollusc grazing. In these species we see some degree of biomass presence when we have Ambient – 50% moisture level. This is due to lower activities of molluscs in drier environments. The unpalatable species; (*Bupthalmum salicifolium*, *Centaurea montana*, *Galium verum*, *Geranium sylvaticum*, *Knautia arvensis*, *Origanum vulgare* and *Prunella*) however show more biomass with increasing moisture levels (Fig. 13).

The effects of molluscs on the total biomass of the well fitted species at different temperature regimes

As the graph in Figure 14 shows clearly, increasing the temperature (3 °C) does not make a significant effect on growth and development of well-fitted species. The same patterns of reductions in the biomass of the palatable species are shown as in previous graphs, irrespective of temperature. The graph indicates that increasing the temperature has negative effects on mollusc activity and the biomass productivity of palatable species at ambient level of temperature is less than ambient + 3 °C (because of more mollusc activity) (Fig. 14).

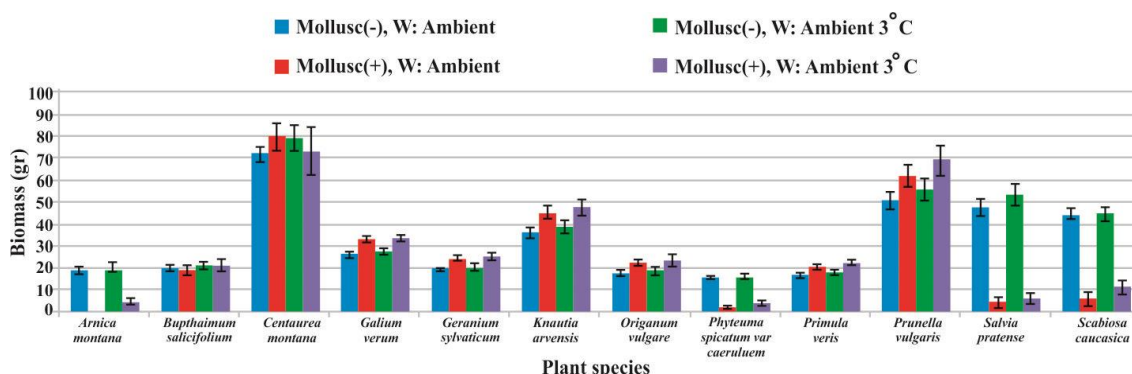


Figure 14. The effects of mollusc grazing on biomass productivity of well fitted species under different levels of temperature

Effects of molluscs on the total biomass of the well fitted species at different temperature and moisture regimes

The graph in Figure 15 shows that combined effects of higher moisture and temperature, provided more desirable environment for mollusc activity and all the palatable species disappeared in this climate (Ambient + 50% and Ambient + 3 °C), but mirrors the trends previously shown in response to temperature and moisture as individual factors. This kind of climate leads the non-palatable species to produce more biomass not only because the climate condition, but also because the mollusc activity. Some species such as *Arnica montana* are very palatable for molluscs. They disappeared even at Ambient – 50% of water regime and ambient level of temperature (Fig. 15).

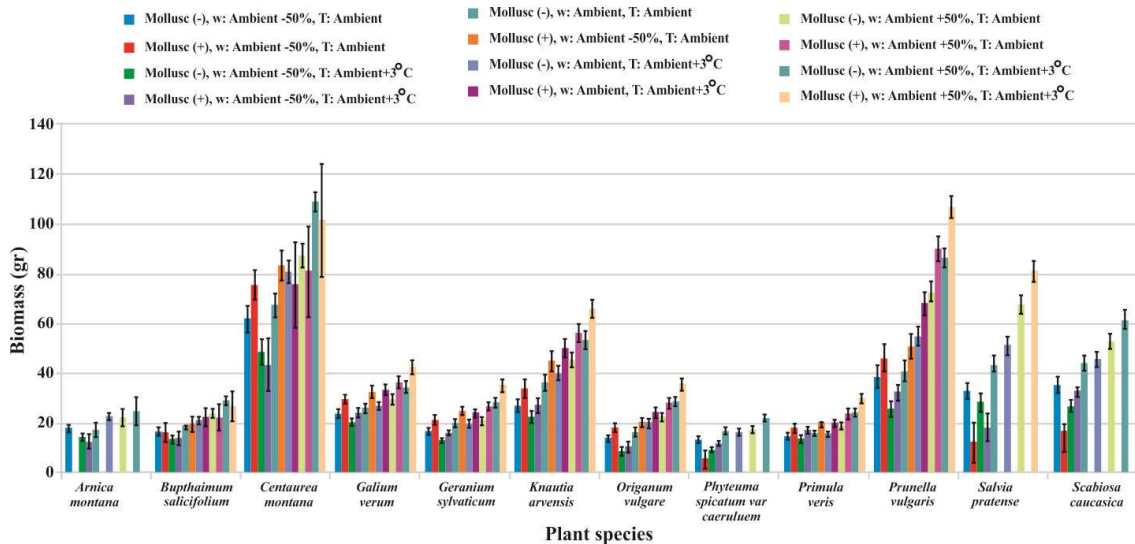


Figure 15. The effects of mollusc grazing on biomass productivity of well fitted species under different levels of moisture and temperature

Effects of molluscs on the total biomass of the intermediate fitted species

The biomass productivity of the intermediate fitted species under mollusc grazing condition is shown in the graph in Figure 16. The unpalatable species; *Dianthus carthusianorum*, *Euphorbia nicaensis*, *Linum flavum 'Compactum'*, *Linum narbonense*, *Lychnis coronaria* and *Lychnis flos-jovis* show increased biomass production, for the same reasons as previously proposed for fitted species. This can be attributed to the role of mollusc grazing. Unpalatable species show higher growth and mass productivity in mollusc friendly area. One reason can be more space for growth and reducing the competition for light, water and nutrition. The palatable species in these group *Asphodeline lutea*, *Centaurea triumfetti*, *Centaurea orientalis*, *Hedysarum hedysaroides*, *Paradisea liliastrium* and *Salvia nemorosa* show much lower biomass presence when they are exposed to mollusc grazing. Hedysarum appears to be the most palatable species on the basis of grazed biomass as a percentage of non-grazed biomass (Fig. 16).

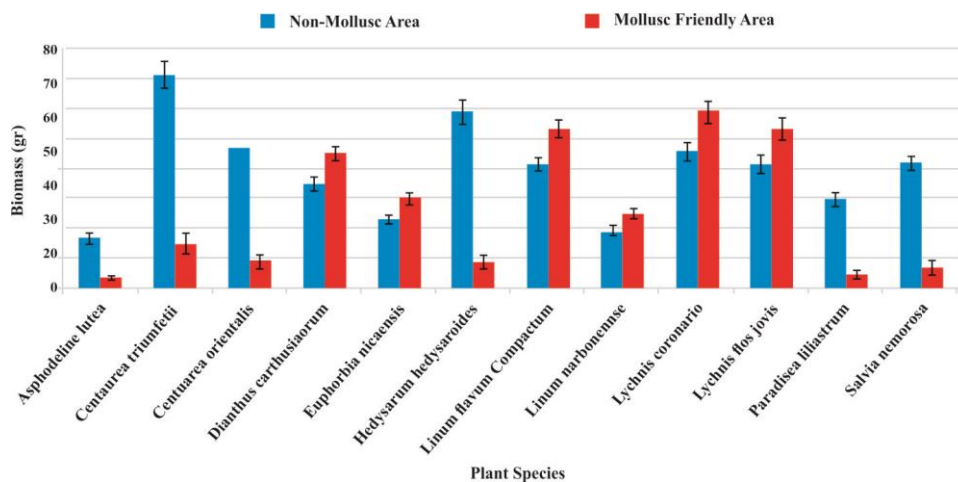


Figure 16. The effects of mollusc grazing on total biomass productivity of intermediate fitted species

Effects of molluscs on the total biomass of the intermediate fitted species at different moisture regimes

The biomass productivity of the intermediate fitted species when exposed to the moisture treatments and under mollusc grazing condition is shown in the graph in *Figure 17*. Biomass increases step wise in intermediated fitted species as water increases except in the case of palatable species which are severely damaged or eliminated at these higher moisture levels. The palatable species in these group (*Asphodeline lutea*, *Centaurea triumfetii*, *Centaurea orientali*, *Hedysarum hedysaroides*, *Paradisea liliastrum*, *Salvia nemorosa*) show much lower biomass presence when they are exposed to mollusc grazing. So due to lower activities of mollusc in drier environments the differences between mass productivity of species between non mollusc area and mollusc grazed area may refer to the other factors. The unpalatable species, *Dianthus carthusinorum*, *Euphorbia nicaensis*, *Linum flavum Compactum*, *Linum narbonennse*, *Lychnis cornonoria*, *Lychnis flos jovis*, however, show more biomass with increasing moisture levels (*Fig. 17*).

Effects of molluscs on the total biomass of the intermediate fitted species at different temperature regimes

The general pattern for biomass is to increase with an increase in temperature. Higher temperature and drier environments potentially hamper mollusc activity, however in the case of the palatable species in the graph in *Figure 18* there is no compelling evidence that higher temperature has this effect. All of the palatable species in the intermediate fitted group (*Asphodeline lutea*, *Centaurea triumfetii*, *Centaurea orientali*, *Hedysarum hedysaroides*, *Paradisea liliastrum*, *Salvia nemorosa*) have produced sharply less biomass under mollusc friendly area condition. The higher temperature treatment leads to more biomass productivity for these species under non-mollusc grazing condition. Not a notable difference is observed between the produced biomass in mollusc friendly environment between the two temperature treatments, that though the mollusc grazing is less but overall they are active enough to consume the produced biomass under the higher temperature treatment. The unpalatable species; (*Dianthus carthusinorum*, *Euphorbia nicaensis*, *Linum flavum Compactum*, *Linum narbonennse*, *Lychnis cornonoria* and *Lychnis flos jovis*) however show slightly more biomass with increasing the temperature levels (*Fig. 18*).

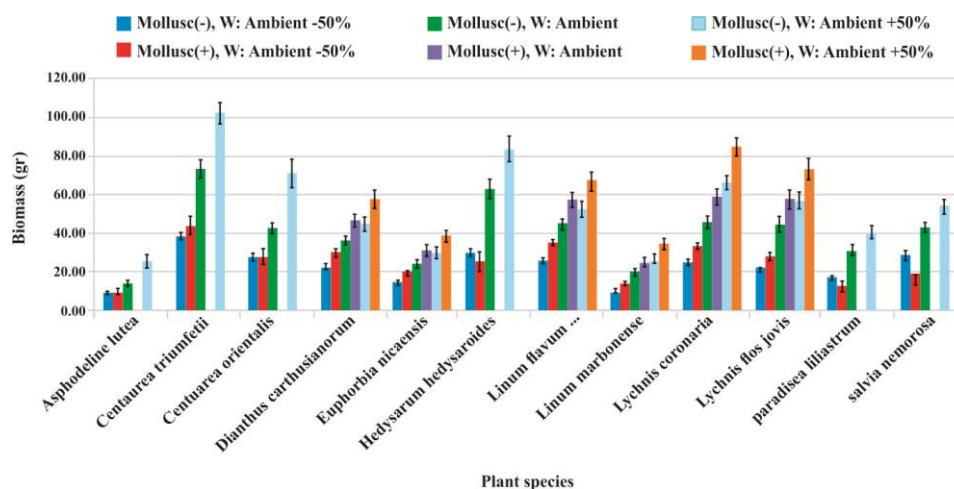


Figure 17. The effects of mollusc grazing on biomass productivity of intermediate fitted species under different levels of moisture

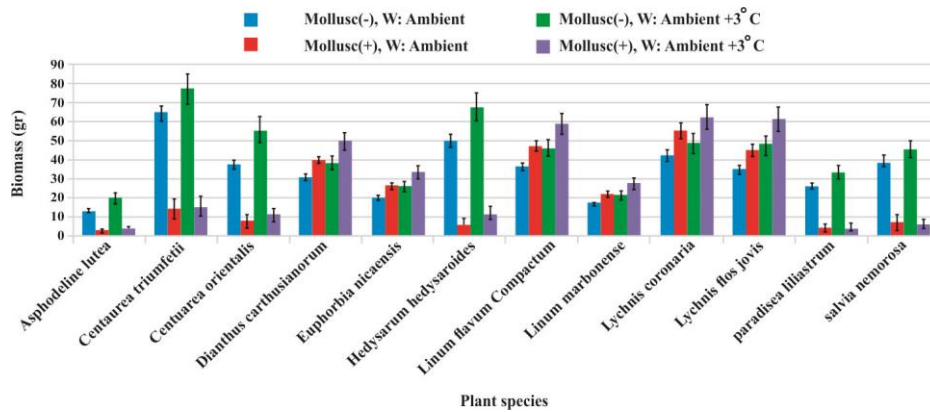


Figure 18. The effects of mollusc grazing on biomass productivity of intermediate fitted species under different levels of temperature

Effects of molluscs on the total biomass of the intermediate fitted species at different temperature and moisture regimes

The data for the different treatment combinations of water, temperature with and without mollusc grazing, follow the same patterns as the previously shown graphs, i.e. there is a net increase in biomass as temperature and water increase but this is reversed in the presence of molluscs in the case of palatable species. Increasing the temperature do not show significant effect in mollusc grazing in intermediate fitted species. Because palatable species disappeared in both levels of temperature in ambient and Ambient + 50% of moisture availability. Comparison of non mollusc area and mollusc grazed area show that in the presence of mollusc grazing, unpalatable species growth is increased more and more mass is produced. For example, *Lychnis coronaria* at in mollusc grazed area and at Ambient + 50% of moisture and Ambient + 3 °C of temperature produced 26% more biomass than the same treatment in non mollusc area (Fig. 19).

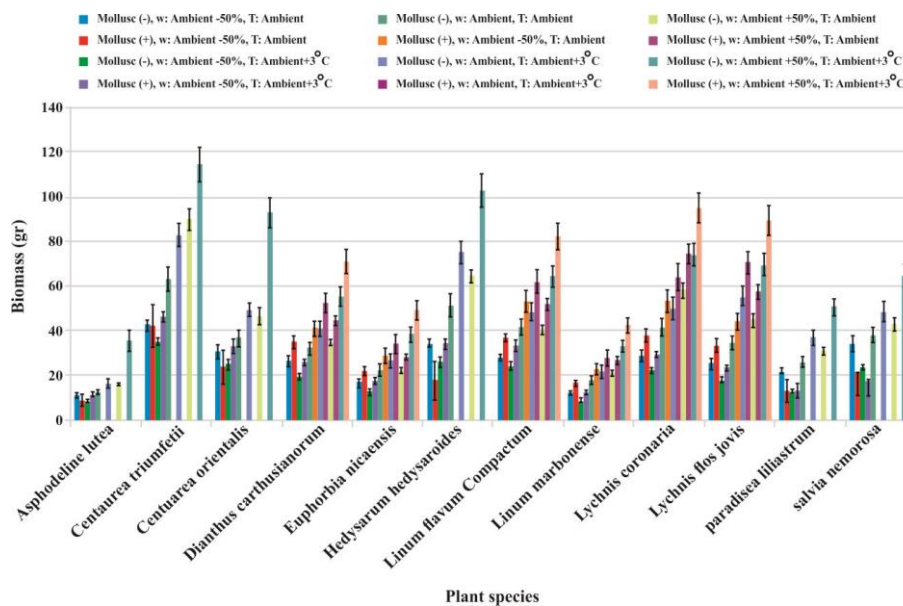


Figure 19. The effects of mollusc grazing on biomass productivity of intermediate fitted species under different levels of moisture and temperature

Discussion

Climate change affects all parts of an ecosystem. Greenspace and greenspace's biodiversity as a part of the urban ecosystem will be affected by climate change. So, in this study, the responses of slugs and snails to the different climate change scenarios in a designed plant community were investigated. This study aimed to investigate how mollusc grazing and environmental conditions (water and temperature) affect the biomass productivity among different plant species. We are aware that the majority of ecosystem services are affected by invertebrates in some ways (Prather et al., 2013), though studies that investigate the relationships between climate change-related responses by invertebrate to ecosystem services consequences are somewhat limited.

Mollusc behaviour and impacts on ecosystems under climate change scenarios are not thoroughly studied; nevertheless, previous studies provide a general understanding about climate change impacts on slug herbivory (e.g., Hitchmough and Wagner, 2011; Frank, 2003; Briner and Frank, 1998; Fenner et al., 1999; Keller et al., 1999; Scheidel and Bruelheide, 1999; Hulme, 1994). For instance, the role of moisture on mollusc grazing activities is well established. Nystrand and Granstrom (1997) showed that the activities of soft body animals are highly related to available moisture levels. When the soil moisture is reduced, and bodies of these animals face desiccation, their feeding activity is significantly hampered.

For each of the three ecological groups studied in this research, six palatable and six unpalatable plant species were exposed to mollusc activities. As mentioned earlier, when the growth conditions were favourable and adequate moisture for mollusc grazing was provided, mollusc grazing significantly reduced the level of biomass for palatable species. Interestingly, unpalatable plant species, due to low competition, showed more biomass productivity in mollusc friendly environments. This scenario may lead to the dominance of the most unpalatable and productive species. Moisture and temperature are not the only factors that affect plant consumption by molluscs. As the study of Hitchmough and Wagner (2011) suggest, the effect of mollusc grazing on palatable species also depends on the physical size and growth rate of the seedlings. For instance, palatable species with slow growth or small seedlings are typically more likely to be eliminated due to mollusc grazing. They also conclude that mollusc grazing can affect the population and community dynamics of plant species. Scheidel and Bruelheide (1999) research reveals that mollusc feeding behaviour even depends on morphological factors. For instance, epidermal cell thickness and hairiness of a plant's leaves are affected if molluscs prefer them.

Molluscan herbivory, designed plant community, individual species and climate change

The results showed that increasing moisture levels improve mollusc activities and also the plant growth and, on the other hand higher temperature reduces mollusc activity. Non-palatable species produced more dry mass in mollusc friendly area than in non mollusc area because of low competition. The graph indicates that slugs and snails select their food from palatable species. This is presumed to be because grazing is either acting as a stimulus to produce more biomass, rather like a form of light pruning, or more likely, because damage to the more palatable species is freeing up resources which they can use to increase their own biomass. Thus, reduced competition and access to

more favorable environment as a result of deleting the palatable species by mollusc grazing, is the key reason of the increasing biomass production of unpalatable species.

The results indicated that molluscan herbivory interactions with climate change affected the stability of both individual species and the plant community. The results also confirm the findings of the previous researchers, such as Vorosmarty and Sahagian (2000) and Melillo et al. (1993). Because of the slug's entirely soft-bodied, they are susceptible to reductions in rainfall. The species at different stage of their life, have different shapes, structures and the chemical compounds.

The chemical compounds, structure and the shape of the species which are affected by climate change, are very important for mollusc palatability.

During this study, the maximum activity of slugs was recorded in early spring and late summer. At this time the weather was colder and wetter. The results showed that rises in temperature reduced mollusc activity.

On the other hand, increasing precipitation enhanced slugs' activities. This study showed that all environmental factors have important effects on molluscs' behaviours, but their interaction will be more critical. At Ambient – 50% of moisture availability and Ambient + 3 °C of temperature, the slugs hardly had any activity. While at Ambient + 50% level of water and ambient temperature and also Ambient + 3 °C, they showed their maximum activities. Increasing temperature and decreasing humidity are two reasons for the appearance of small and tiny hair (in terms of size and number) on the leaves of plant species. It is the reaction of the species to drought situations which can usually, (but not always) make the species unpalatable to molluscs. Because the snails have a shell, they can better manage water loss. So they are generally able to feed better than slugs under drier conditions.

What was apparent from observing the experiment was that mollusc feedings tended to vary greatly depending on the abundance of plant species, and, in particular, the abundance of palatable species. On the other hand, a community of palatable species, providing a good situation for mollusc activity in terms of humidity and temperature helps them to select their food.

They reduce some species, allowing the other to receive more space to grow and develop as well as more light and nutrition. Therefore, mollusc grazing affected the competition between species in the plant community. As a result, the flowering development and flowering period of the species were affected by mollusc grazing as well. With adding more palatable spices to the designed plant community, we can keep our valuable species within a plant community (*Figs. 20 and 21*).



Figure 20. Snail grazing a necrotic area on a hairy leaf

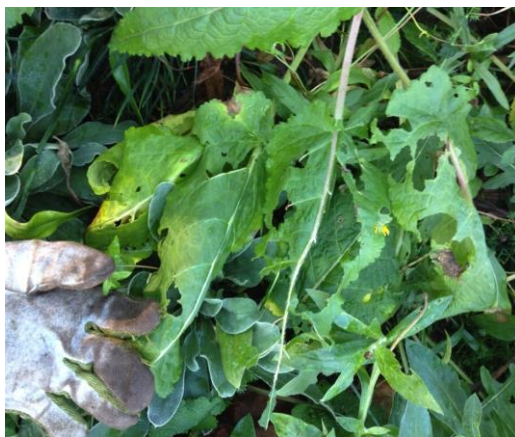


Figure 21. Effects of mollusc grazing on *Salvia nemorosa*

Comparison of mollusc and non-mollusc experimental areas

The well and poorly fitted species show overall similar (but not equal) patterns of biomass productivity when exposed to the mollusc grazing. In the well-fitted group, even the mollusc friendly environment produced slightly less biomass, which can be attributed to the contribution to the biomass of *Bupthalmum salicifolium* and *Centaurea montana*. The intermediate fitted group shows an apparent decrease in biomass production as a result of mollusc grazing. This pattern suggests that when mollusc species selectively choose palatable plants, the other less favourable or unpalatable plants have a more favourable environment to grow and face less competition in their ambient environment. It can lead to their overall better growth that compensates for the biomass lost to molluscs. Unlike the well-fitted species, the unpalatable plant species cannot produce enough biomass in the intermediate fitted group. When the studied ecological groups were exposed to combined effects of the moisture and treatment variations in mollusc friendly and non-mollusc environments, they showed that increasing moisture would increase their activity and therefore, the grazing levels. Though the plant species grow better when they are exposed to more moisture, the presence of molluscs prevents these species from reaching their full biomass productivity potential in the new growth environment. It also can be deduced that when the mollusc selectively chooses palatable species for grazing the unpalatable plants face less competition and can compensate removed biomass of palatable plants. The increased temperature when more moisture is also available does not have a tangible effect on the mollusc grazing providing adequate moisture is available. The intermediate fitted group clearly showed when the unpalatable species cannot compensate the palatable species biomass removal in mollusc friendly areas, how dramatic is the impact of mollusc grazing on biomass productivity. For instance, for this group, the biomass productivity has reduced by half in the Ambient + 50% moisture and Ambient + 3 °C Temperature when these species are exposed to mollusc grazing.

Well fitted species

The palatable species in this group (*Arnica montana*, *Bupthalmum salicifolium*, *Centaurea montana*, *Phyteuma spicatum* var. *caeruleum*, *Salvia pratense*, *Scabiosa*

caucasica) to some extent reacted differently to molluscs when exposed to different moisture levels. Although, *Bupthalmum salicifolium*, *Centaurea montana* at the outset of the experiment were considered as palatable species (based on previous experimental work) these two species proved to be unpalatable in this study. Not surprisingly all of the unpalatable species *Galium verum*, *Geranium sylvaticum*, *Knautia arvensis*, *Knautia arvensis*, *Origanum vulgare*, *Prunella vulgaris* and *Primula veris* showed better growth and more biomass productivity with increasing moisture availability. It can be because of two reasons, the first one is the positive impact of moisture on these species' growth, and the other one is less competition for light and better-growing conditions. When the palatable species are reduced and consumed due to mollusc grazing, these species have a better environment for growth. Exposure to the higher temperature, Ambient + 3 °C, supports this finding. The plant species in this group show a slight increase in biomass productivity; however, interestingly the palatable species fail to survive in higher moisture levels. Higher temperature leads to less moisture due to evaporation. Mollusc grazing is reduced when soil is less moist, and therefore we see better growth even for the palatable species. During Year 2, more biomass productivity is observed for the species in the well-fitted group. It is compatible with the findings of Hitchmough and Wagner (2011) that suggest some of the plant species that were heavily consumed by mollusc grazing in the first year when smaller and more juvenile could show considerable growth during the Year 2.

The combined effects of the moisture and temperature treatments are in line with the above findings. Apart from *Bupthalmum salicifolium* and *Centaurea montana* that produces biomass under the different combined treatment, other palatable species; *Arnica montana*, *Phyteuma spicatum* var. *caeruleum*, *Salvia pratense*, and *Scabiosa caucasica* retain their biomass only when the moisture levels are at Ambient – 50%. It indicates that grazing activities with increasing moisture levels are enough to eliminate these plants. Even for these species under the Ambient – 50% moisture level, Ambient + 3 °C temperature leads to better growth, which is due to reduced activity of mollusc species. It is assumed that increased biomass productivity of **Bupthalmum salicifolium**, **Centaurea montana** when grazing conditions are suitable, is due to the presence of alkaloids and other toxic molecules in the leaves of adult plants.

Intermediate fitted species

Among the three ecological groups in this research, the intermediate fitted group species clearly show the most significant impact of grazing on their biomass productivity. *Asphodeline lutea*, *Centaurea triumfettii*, *Centaurea orientalis*, *Hedysarum hedysaroides* and *Paradisea liliastrum* are palatable to highly palatable species that disappear with increasing moisture levels. With increasing the moisture levels leads to better biomass productivity for the *Dianthus carthusianorum*, *Euphorbia nicaensis*, *Linum flavum* 'Compactum', *Linum narbonneense*, *Lychnis coronaria*, *Lychnis flos jovis* unproductive plant species. The same growth pattern was expected for the palatable species because of the high moisture levels, but they disappeared when the temperature reaches Ambient and Ambient + 50% moisture levels. Again, this can be attributed to higher mollusc grazing due to more available moisture. Similar to the well-fitted group these plant species show a slight increase with increasing temperature to Ambient + 3 °C.

Interestingly all of the palatable species are present when the temperature increases. Higher temperature, more evaporation and less available moisture to molluscs, hampers

their grazing, which causes more biomass productivity at the higher temperature treatment. For the combined water and temperature treatment, the plants in the intermediate fitted group produce their least amount of biomass if the water treatment is at Ambient – 50% and the temperature is Ambient + 3 °C. Although many of these species naturally grow in landscapes that experience significant drought in summer, many of these species grow earlier in the year thus avoiding the most severe moisture stress. While the highest biomass production belongs to Ambient + 50% and Ambient + 3 °C. Increasing mollusc activities due to the more available moisture was neutralized by higher temperature levels. The palatable species in this group; *Asphodeline lutea*, *Centaurea triumfettii*, *Centaurea orientalis*, *Hedysarum hedysaroides*, *Paradisica liliastrum* and *Salvia nemorosa* are all naturally distributed in parts of Europe and Eurasia with prolonged dry conditions in summer. The exception to this is *Paradisica*, which occurs at moderate altitudes in the Alps at which slug populations are small or absent. These species are likely to become better fitted to Southern Britain in the future where climate change models currently predict drier spring to autumn conditions.

Poorly fitted species

The plant species disappear when the moisture availability levels reach Ambient + 50%. Some of the species show biomass productivity when the moisture is at the ambient level. These plant groups are mostly native of the continental temperate steppe grassland and cannot tolerate higher moisture levels. At lower levels of moisture in these habitats, molluscs are mostly absent, and hence these species are potentially palatable. *Balsamorhiza sagitifolius*, *Centaurea pulcherrimus*, *Delphinium barbeyi*, *Dracocephalum grandiflorum* and *Hymenoxys grandiflora* are the palatable species in this group. When the moisture levels reach Ambient and Ambient + 50% even if some of the palatable species can survive the moisture level and consequently the increased grazing of mollusc grazing make them disappear. Similar to the well and intermediate fitted group, but to a much higher degree, the plants in this category show better biomass productivity when the temperature is increased. At Ambient + 3 °C, not only all of these species show better growth but also the palatable species are present, which is because of hampered mollusc grazing due to the environmental dryness. These native US and central Asian plant species show their best biomass production when they are exposed to less water and higher temperatures. Not surprisingly the highest biomass production in these species, when exposed to the combined temperature and moisture treatments, belongs to Ambient – 50% moisture and Ambient + 3 °C temperature.

How attractive were the communities under different climate change scenarios and mollusc grazing? The design aspect of plant communities

Todorova (2004) believes that attractiveness of any meadow- like vegetation is related to the factors such as repeating patterns of species in the mix, vegetation structure, flowering colour, and flowering duration. These are very important factors in the urban landscape in the perception of people. As a result, the combination of different flowering species potentially can provide new forms of design impact. The species were used in this research as a new naturalistic design form are attractive for the visitors, and they can provide strong visual impact through flowering in spring, summer, and autumn. During the four growth seasons (2013 and 2016) the flowering period and phenology of the plant species in the community among the different climate scenarios in the presence or

absence of the molluscs were monitored. Because of parameters such as three levels for water regime, two level of temperature, three ecological groups (well fitted, intermediate fitted and poorly fitted), thirty-six species in two group in terms of mollusc attraction (palatable and unpalatable), the following discussion is based on daily observation and not on statistical data analysis. The phenological aspects of a designed meadow-like grassland community were recorded from the first year of the growing season. Results from the experiments showed the flowering phenology of species in the community was affected by temperature, moisture availability and also mollusc grazing. However, the Interaction of these environmental factors was more important. The results indicate that the temperature is imperative for flowering initiation and development. While the water regime is more critical for the flowering period. Mollusc grazing affected the flowering development and flowering period by reducing the competition between species in the plant community. They reduce some species and let the other species receive more space to growth and development, more light and nutrition. A considerable difference between the first year, the second, third and fourth years was observed, but this is normal in sown or planted meadow vegetation. The flowers of most species were observed much later in the first year compared to years 2, 3 and 4. This situation happened because of variation in size and state of development and also because some of the species were not large enough to flower until late in the second year. Almost all species from well-fitted and intermediate fitted species were flowering in the second growing season. The peak attractive flowering impact in year one was August, and in the non-mollusc area and year, two was in July in the mollusc friendly area. The visual impact of the slow-growing species is significant for designing multiple canopy layers of meadow-like communities. They need more time developing, and this, in turn, reduces the aesthetic value of a developing community in the first year. The development of species and their growth rate can also be affected by climate change; the aesthetic characteristics of a designed plant community will be affected by climate change as well (*Fig. 22*).





Figure 22. Some plant species of the plant community: *Linum flavum* ‘Compactum’, *Scabiosa caucasica*, *Centaurea orientalis*, *Salvia nemorosa*, *Knautia arvensis*, *Salvia pratense*, *Bupthalmum salicifolium*, *Lychnis coronaria*, *Euphorbia niceaensis*, *Centaurea montana*, *Lychnis flos-jovis*

Conclusions

In this study the effects of slug grazing on “designed plant communities” under different climate scenarios that closely reflected those predicted for 2050 were investigated. The species to develop a meadow- like community were selected from three different habitat types/ecological regions. Mollusc grazing was affected by different climate scenarios (from dry and warm to wet and hot). The molluscs showed different behaviours in dry, wet, warm and ambient temperature, and this led to significant differences in the biomass and structure of these communities. This study provided strong observation support that native fauna such as an insect (bees and hoverflies) and mollusc (slug and snail) were supported by non-native as well as native species of the plant community. It was clear that the flowers of many species in the community were attractive to generalist pollinators. Because of the long period of flowering time through the different species and different treatment as well, the plant community provided an excellent habitat for insect activity.

In this study, the impact of climate change and slug grazing on designed plant community (36 species) were investigated. Independent research about the impact of mollusc grazing on each species under current UK climate situation and future climate scenarios of UK is recommended.

More studies about the possibility of keeping the valuable species in the urban landscape with offering the more palatable species for the molluscs and less useful species for the greenspace are recommended as well.

REFERENCES

- [1] Ahmad, H., Hitchmough, J. D. (2007): Germination and emergence of under storey and tall canopy forbs used in naturalistic sowing mixes. A comparison of performance in vitro v the field. – *Seed Science and Technology* 35(3): 624-637.
- [2] Alizadeh, B. (2016): The impacts of climate change on designing sustainable urban landscapes. – *Doctoral Dissertation, University of Sheffield, Sheffield.*
- [3] Alizadeh, B., Hitchmough, J. (2019a): A review of urban landscape adaptation to the challenge of climate change. – *International Journal of Climate Change Strategies and Management* 11(2): 178-194.

- [4] Alizadeh, B., Hitchmough, J. D. (2019b): Designing sustainable urban landscape and meeting the challenge of climate change: a study of plant species adaptation and fitness under different climate change scenarios in public landscape of UK. – *Landscape Research* 45(2): 228-246.
- [5] Bakkenes, M., Alkemade, J. R. M., Ihle, F., Leemans, R., Latour, J. B. (2002): Assessing effects of forecasted climate change on the diversity and distribution of European higher plants for 2050. – *Global Change Biology* 8(4): 390-407.
- [6] Briner, T., Frank, T. (1998): The palatability of 78 wildflower strip plants to the slug *Arion lusitanicus*. – *Annals of Applied Biology* 133(1): 123-133.
- [7] Bruelheide, H., Scheidel, U. (1999): Slug herbivory as a limiting factor for the geographical range of *Arnica montana*. – *Journal of Ecology* 87(5): 839-848.
- [8] Dirzo, R. (1980): Experimental studies on slug-plant interactions. I. The acceptability of thirty plant species to the slug *Agriolimax caruanae*. – *Journal of Ecology* 68: 981-998.
- [9] Dunnett, N., Hitchmough, J. (2004): *The Dynamic Landscape: Design, Ecology and Management of Naturalistic Urban Planting*. – Taylor & Francis, London.
- [10] Fenner, M., Hanley, M. E., Lawrence, R. (1999): Comparison of seedling and adult palatability in annual and perennial plants. – *Functional Ecology* 13(4): 546-551.
- [11] Frank, T. (2003): Influence of slug herbivory on the vegetation development in an experimental wildflower strip. – *Basic and Applied Ecology* 4(2): 139-147.
- [12] Grime, J. P. (1973): Competitive exclusion in herbaceous vegetation. – *Nature* 242(5396): 344.
- [13] Grime, J. P. (1977): Evidence for the existence of three primary strategies in plants and its relevance to ecological and evolutionary theory. – *The American Naturalist* 111(982): 1169-1194.
- [14] Grime, J. P. (1979): *Plant Strategies and Vegetation Processes*. – Wiley, Chichester.
- [15] Grime, J. P. (1998): Benefits of plant diversity to ecosystems: immediate, filter and founder effects. – *Journal of Ecology* 86(6): 902-910.
- [16] Grime, J. P. (2006): *Plant Strategies, Vegetation Processes, and Ecosystem Properties*. 2nd Ed. – John Wiley & Sons, Chichester.
- [17] Hitchmough, J. (2011): Exotic plants and plantings in the sustainable, designed urban landscape. – *Landscape and Urban Planning* 100(4): 380-382.
- [18] Hitchmough, J., Wagner, M. (2011): Slug grazing effects on seedling and adult life stages of North American Prairie plants used in designed urban landscapes. – *Urban Ecosystems* 14(2): 279-302.
- [19] Hitchmough, J., Wagner, M., Ahmad, H. (2017): Extended flowering and high weed resistance within two layer designed perennial “prairie-meadow” vegetation. – *Urban Forestry & Urban Greening* 27: 117-126.
- [20] Holland, K. D., McDonnell, M. J., Williams, N. S. (2007): Abundance, species richness and feeding preferences of introduced molluscs in native grasslands of Victoria, Australia. – *Austral Ecology* 32(6): 626-634.
- [21] Hoyle, H., Hitchmough, J., Jorgensen, A. (2017): Attractive, climate-adapted and sustainable? Public perception of non-native planting in the designed urban landscape. – *Landscape and Urban Planning* 164: 49-63.
- [22] Hulme, P. E. (1994): Seedling herbivory in grassland: relative impact of vertebrate and invertebrate herbivores. – *Journal of Ecology* 82(4): 873-880.
- [23] Jennings, T. J., Barkham, J. P. (1975): Food of slugs in mixed deciduous woodland. – *Oikos* 26(2): 211-221.
- [24] Keller, M., Kollmann, J., Edwards, P. J. (1999): Palatability of weeds from different European origins to the slugs *Deroceras reticulatum* Müller and *Arion lusitanicus* Mabille. – *Acta Oecologica* 20(2): 109-118.
- [25] Lawrey, J. D. (1983): Lichen herbivore preference: a test of two hypotheses. – *American Journal of Botany* 70(8): 1188-1194.

- [26] Magurran, A. E. ((1996): *Ecological Diversity and its Measurement*. – Chapman & Hall, London.
- [27] Melillo, J. M., McGuire, A. D., Kicklighter, D. W., Moore, B., Vorosmarty, C. J., Schloss, A. L. (1993): Global climate change and terrestrial net primary production. – *Nature* 363(6426): 234.
- [28] Nystrand, O., Granström, A. (1997): Forest floor moisture controls predator activity on juvenile seedlings of *Pinus sylvestris*. – *Canadian Journal of Forest Research* 27(11): 1746-1752.
- [29] Pallant, D. (1972): The food of the grey field slug, *Agriolimax reticulatus* (Müller), on grassland. – *The Journal of Animal Ecology* 41(3): 761-769.
- [30] Prather, C. M., Pelini, S. L., Laws, A., Rivest, E., Woltz, M., Bloch, C. P., Del Toro, I., Ho, C. K., Kominoski, J., Newbold, T. S., Parsons, S. (2013): Invertebrates, ecosystem services and climate change. – *Biological Reviews* 88(2): 327-348.
- [31] Rathcke, B. (1985): Slugs as generalist herbivores: tests of three hypotheses on plant choices. – *Ecology* 66(3): 828-836.
- [32] Sayuti, Z., Hitchmough, J. D. (2013): Effect of sowing time on field emergence and growth of South African grassland species. – *South African Journal of Botany* 88: 28-35.
- [33] Scheidel, U., Bruelheide, H. (1999): Selective slug grazing on montane meadow plants. – *Journal of Ecology* 87(5): 828-838.
- [34] Speiser, B., Rowell-Rahier, M. (1993): Does the land snail *Arianta arbustorum* prefer sequentially mixed over pure diets? – *Functional Ecology* 7(4): 403-410.
- [35] Team, C. W., Pachauri, R. K., Meyer, L. A. (2014): IPCC, 2014: Climate Change 2014: Synthesis Report. Contribution of Working Groups I, II and III to the Fifth Assessment Report of the Intergovernmental Panel on Climate Change. – IPCC, Geneva.
- [36] The London Climate Change Partnership (2018): London's warming - the impacts of climate change on London. – https://ukcip.ouce.ox.ac.uk/wp-content/PDFs/London_tech.pdf (accessed 3 July 2018).
- [37] Thomas, C. D., Cameron, A., Green, R. E., Bakkenes, M., Beaumont, L. J., Collingham, Y. C., Erasmus, B. F., De Siqueira, M. F., Grainger, A., Hannah, L., Hughes, L. (2004): Extinction risk from climate change. – *Nature* 427(6970): 145.
- [38] Todorova, M. (2018): What Is or Is There a Balkan Culture, and Do or Should the Balkans Have a Regional Identity? – In: Todorova, M. (ed.) *Scaling the Balkans*. Brill, Leiden, pp. 221-231.
- [39] Vörösmarty, C. J., Sahagian, D. (2000): Anthropogenic disturbance of the terrestrial water cycle. – *Bioscience* 50(9): 753-765.
- [40] Wardle, D. A., Barker, G. M., Bonner, K. I., Nicholson, K. S. (1998): Can comparative approaches based on plant ecophysiological traits predict the nature of biotic interactions and individual plant species effects in ecosystems? – *Journal of Ecology* 86(3): 405-420.
- [41] Wilby, A., Brow, V. K. (2001): Herbivory, litter and soil disturbance as determinants of vegetation dynamics during early old-field succession under set-aside. – *Oecologia* 127(2): 259-265.

ANIMAL MANURE FUNCTIONS AS SOIL AMENDMENT FOR URBAN GREEN SPACE IN THE LOESS PLATEAU

ZHANG, J. W.¹ – HUANG, M. S.^{2*} – PETROPOULOS, E.³ – SONG, L.⁴ – HE, S. Y.^{5,6}

¹*State Key Laboratory of Soil and Sustainable Agriculture, Institute of Soil Science, Chinese Academy of Sciences, Nanjing, PR China*

²*Beijing Capital Co., LTD, Beijing, PR China*

³*School of Engineering, Newcastle University, Newcastle upon Tyne, NE1 7RU, UK*

⁴*Nanjing Dechuang Environmental Protection Technology Co. LTD, Nanjing, PR China*

⁵*Institute of Agricultural Resources and Environment, Jiangsu Academy of Agricultural Sciences, Nanjing, PR China*

⁶*School of Environment and Safety Engineering, Jiangsu University, Zhenjiang, PR China*

**Corresponding author*

e-mail: hms@capitalwater.cn; phone: +86-025-8688-1367; fax: +86-025-8688-1000

(Received 17th Sep 2019; accepted 8th Jan 2020)

Abstract. Urban green space could efficiently tackle surface water management issues in modern cities, especially in the Loess Plateau where the urban environment is constrained by poor soil quality as well as limited and unevenly distributed precipitation. Numerous studies based on farmland have demonstrated that organic amendments could improve soil quality and the water holding capacity by increasing soil organic matter content and aggregate stability via functions of soil microorganisms. In this case, we show that organic amendments that successfully applied in agriculture could also be served to improve the soil quality underneath the urban green space in the Loess Plateau. On the whole, organic amendments performed better than inorganic ones. Specifically, animal manure imposed the greatest beneficial effects on soil water holding capacity, soil aggregation, as well as microbial diversity and activity, followed by plant residue and mushroom residue. In contrast, polyvinyl alcohol and volcanic pumice imposed no obvious, if not negative, effect on soil properties. In conclusion, animal manure could be a good soil amendment for urban green space, especially in the arid area of the Loess Plateau or other regions with similar soil properties.

Keywords: *Sponge City, water storage and conservation, aggregate stability, soil organic matter, organic amendment*

Introduction

“Sponge City” is a novel urban operational concept that aims to make city a more livable environment, with focus on tackling urban water management issues, such as purification of surface runoff, attenuation of peak as well as water conservation (Chan et al., 2018). As core component of this concept, urban green space could efficiently tackle those problems that coming with the rapid urbanization and industrialization, such as air pollution (Chen et al., 2019), heat-island effect (Cai et al., 2019), surface-water management (Chan et al., 2018). To achieve these purposes, it is necessary to transform the traditional urban conditions accordingly, especially the soil underneath the green space. Regarding the soil amelioration in urban green space, related studies mainly focused on the soils that were contaminated by heavy metals (Khan et al., 2017) and/or organic pollutants (Gong et al., 2016), while ignored those that were unpolluted but

constrained by fragile structure and poor fertility. But soil natural quality (physical, chemical and biological properties) could also affect directly and/or indirectly the health of urban soil and the corresponding ecological functions, including the environmental livability and urban landscape (Vienneau et al., 2017).

As core component of soil physical quality, soil aggregates are groups of soil particles that bind to each other more closely than to adjacent particles (Follett et al., 2009). Often, the stability of soil aggregate can indicate the formation, stabilization and degradation of the soil structure (Verchot et al., 2011). In general, soils with an optimum level of aggregation will be more resistant to rapid water penetration and erosion (Karlen et al., 2008). Soil organic matter (SOM) is another indicator of soil quality because of its important roles including biological functions regarding the growth of beneficial soil microorganisms; chemical functions regarding the cycling and supplying essential plant nutrients; physical functions regarding the soil structure, runoff, as well as water and air transmission (Karlen et al., 2008; Zou et al., 2015; Tang et al., 2018; Zhang et al., 2018). Often, the stability and content of soil aggregates are positively correlated with soil fertility because the cohesion of aggregates is promoted mainly by organic polymer binding agents (Zhang et al., 2018). For example, Loess, an aeolian deposit, is primarily composed of silt-sized particles (<2.0 mm), and it is indeed constrained by both fragile soil structure and low soil organic matters (Guo et al., 2019). Such soil formation occurs widely around the world with the most extensive distribution in China (Sun, 2002; Hua et al., 2016). Influenced by continental monsoons and large variation in seasonal precipitation, the Loess soil often induces severe environmental disasters (Xu and Wang, 2016), i.e. the easily slaked soil aggregates lead to soil collapse in rainstorm, while cause severe drought/dust in dry season (Tisdall and Oades, 1982).

Currently, soil amelioration mainly focuses on agricultural system (Karlen et al., 2008; Zhang et al., 2011). Numerous studies have reported successful application of, both organic and inorganic, soil amendments on improving soil structure and fertility (Miao et al., 2013; Chang et al., 2019; Su et al., 2019). Organic amendments, such as typical agricultural residues - animal manure and plant straw - are widely applied to improve soil fertility mainly by introducing amount of organic carbon as well as other nutrient/resources. Soil microbial community stimulated by these increased substrate could accelerate the formation of soil organic matters (SOM), with which to increase the binding of soil particles and soil aggregation (Peregrina et al., 2012; Feng et al., 2015; Wang et al., 2018). For example, in North China Plain, after 2 - 4 years of manure application, indigenous *Bacillus asahii* becomes the predominant population, which plays a key role of increasing crop yield and soil fertility (Feng et al., 2015). There are also many synthetic organic polymers that applied in soil amelioration practice for a long time (Stefanson, 1973; Wu et al., 2010). Take polyvinyl alcohol (PVA), a type of uncharged but hydrophilic synthetic organic polymer for example. With the attachment between polymer and clay surface by hydrogen binding, PVA could efficiently defend surface soil from rainfall shock in clay soil (Stefanson, 1973; Wiśniewska, 2010), and they have already applied to improve soil aggregation, hydraulic conductivity and decrease water evaporation with quite stable performance (Bouranis et al., 2008). For inorganic amendment, volcanic pumice (VOP) is a widely-used naturally-suited soil conditioner with numerous benefit for soil properties. With its porous structure on surface and more than 70 trace minerals inside, VOA could promote soil moisture retention and nutrient availability, stimulate soil aggregation and enhance soil drainage, and it doesn't decompose, rot or blow away (Noland et al., 1992; Temiz and Cayci, 2018). However,

due to limited investigation, it is not clear whether these soil amelioration practices in the agricultural system are still effective in urban green space.

In this study, we conducted an experiment to estimate the effect of several soil amendments (organic vs. inorganic) on the physical and biological properties of the soils underneath urban green space in Guyuan, a typical small city located in the central of the Loess Plateau. More than 50% of Guyuan annual precipitation falls during summer, most of which are in heavy storms (Zhang et al., 2014), causing urban waterlogging and soil collapse, threatening the construction and maintenance of urban infrastructures (Liu et al., 2015). In contrast, the rainfall from February to March only accounts for 3% ~ 6% of the total annual precipitation, inducing spring drought, causing surface cracking and soil layer spalling (Li et al., 2019). In this case, we have two aims: 1) estimate the effect on urban green space of effective soil amendments that have already successfully applied in agriculture; 2) compare the amelioration effects of organic and inorganic amendments.

Materials and Methods

Soil selection and experiments

The soil was collected at the roadsides of Guyuan City (35°14'-35°38'N, 105°20'-106°58'E), Ningxia Hui Autonomous Region, which lies in the Loess Plateau. Located in the arid area of northern China, Guyuan has a typical continental monsoon climate with a mean annual precipitation ranging between 250-820 mm and annual evaporation ranging from 1250 to 2000 mm (Chao et al., 2017). The dominant soil type in the study area is loessal Cambisol (Xue and An, 2018) with a loamy texture (clay 20%, silt 60%, sand 20%), and its basic properties were as follows: pH 8.4, soil organic carbon (SOC) 4.7 g/kg, soil total nitrogen (TN) 0.53 g/kg, soil total phosphorus (TP) 0.45 g/kg, soil total potassium (TK) 10.9 g/kg, alkaline nitrogen (AN) 43 mg/kg, available phosphorus (AP) 7.5 mg/kg, available potassium (AK) 123 mg/kg. Before use, the soil was air-dried, homogenized and sieved <2 mm. Roots and other plant residues were carefully removed. There were 6 treatments with 3 replicates 5 soil amendments prepared in the experiment: They were soils amended with three common agricultural residues: animal manure (naturally air-dried cow manure without composting here, AM), mushroom residues (composted spent mushroom substrate, MR), plant residues (air-dried maize straw without further treatment, PR) and other two widely used inorganic amendments: synthetic polyvinyl alcohol (PVA), natural volcanic pumice (VOP). AM, PR and MR were ground to debris and sieved through 2 mm before use. PVA and VOP were powders. About 150 g air-dried soil was homogeneously mixed with the above-mentioned organic substrates and inorganic amendments at a ratio of 3% w/w. The mixed soils were immediately filled into containers (60 ml tubes, 12 cm in height). The physical mixing of the soil was performed with the unamended control soil.

A modified cutting-ring method (Lu, 2000) was adapted to evaluate the water holding capacity (WHC) of soils with a simulated precipitation and the following drainage process. Briefly, all tubes were submerged into the water for 6 hours to make a saturation. Initial weight of each tube was recorded after taking out from water and standstill for 1-hour. Maximal water-holding capacity of soils were calculated by the weight difference of water-saturated soils and air-dried soils. The samples were then positioned outside, the weight of the tubes was recorded daily to estimate the changes of soil WHC during the drainage. After two cycles of wetting-drying, the soils were collected to measure enzyme activity, aggregate stability and microbial diversity. Soil aggregate stability was measured

following the method developed by Le Bissonnais (2016) and expressed as mean weight diameter (MWD). MWD values above the threshold of 1.3 denoted stable soil structures (Le Bissonnais, 2016). Dehydrogenase and β -glucosidase activity were determined following the method of Casida et al. (1964) and Eivazi and Tabatabai (1990), respectively.

Soil bacterial community assays

Soil total genomic DNA was extracted from 0.5 gram of soil using the FastDNA Spin Kit for Soil (MP Biomedicals, Santa Ana, USA) according manufacturer's instructions. For more information on PCR procedure and sequence analysis could be referred to Feng et al. (2018).

Total 347,556 sequences of bacterial 16S rRNA gene with a range of 8,018 and 36,503 sequences per sample were obtained. Alpha diversity was calculated using 8,000 reads per sample (nearly closed to minimum number of sequences required to normalize the differences in sampling effort) with multiple indices (observed species (hereafter, Richness), Shannon-Winner index (hereafter, Shannon) and phylogenetic diversity (hereafter, PD)).

Statistical analysis

Statistical procedures were calculated using the IBM Statistical Product and Service Solutions (SPSS) Statistics for windows (Version 13). The data were expressed as the means with standard deviation (SD), and different letters indicated significant differences among different amendments. ANOVA was performed to determine the effects of amendments, followed by Tukey's HSD test. Differences of $P < 0.05$ were considered significant.

Result

Changes of soil chemical and physical properties

Important soil fertility indices such as pH and SOC, as well as soil aggregate stability were quantified (*Fig. 1*). Soil pH was slightly alkaline and not affected by the different amendments. Compared to the unamended soil (*Ctrl*), AM amendment significantly increased the SOC content, while other amendments had no significant effects on SOC content ($p < 0.05$). AM and PR amendmentssignificantly increased the soil MWD value ($p < 0.05$). The results showed that animal manure could efficiently bind soil particles together very likely due to the increased SOC content. While, two inorganic amendments PVA and VOP did not alter soil proterties, regardless of chemical (pH and SOC) and physical (MWD) features. However, MWD for all treatments was less than 1.3, close to the threshold which differentiates a stable from an unstable soil (Le Bissonnais, 2016). This indicates that improved soil structures in such soil-eroded areas are in scarcity and it would require prolonged periods of time or more amount of amendments to be formed.

Changes of soil water holding capacity

We further present the alteration of soil water holding capacity (WHC) among different amendments (*Fig. 2*), the results show very similar dynamic patterns with those observed for soil aggregate stability and SOC content (*Fig. 1*). Four amendments AM, PR, MR, and PVA had a higher WHC than *Ctrl* treatment, indicating an increased soil

water storage capacity. It is obvious that three treatments of organic amendments had strogher effects than two treatments of inorganic amendments. In contrast, VOP amendment had no effects or even negative effects on WHC (Fig. 2 and Table 1).

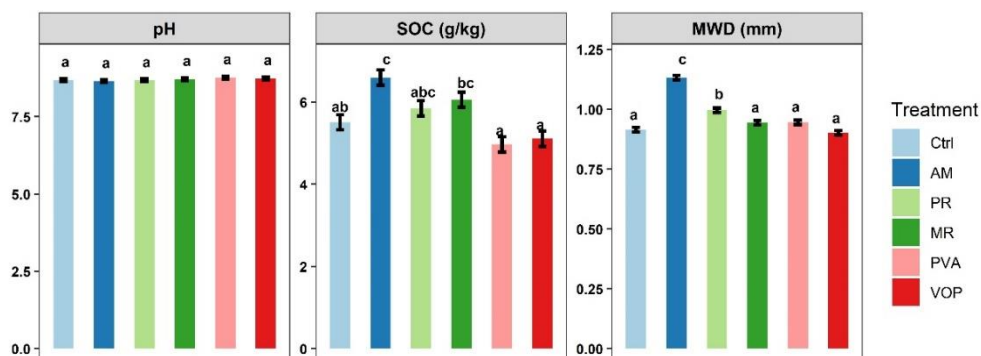


Figure 1. Soil pH, SOC content and aggregate stability (MWD, mean weight diameter) of soils amended with animal manure (AM), mushroom residue (MR), plant residue (PR), synthetic polyvinyl alcohol (PVA) and natural volcanic pumice (VOP). Different letters above bars denotes significant differences at $p < 0.05$

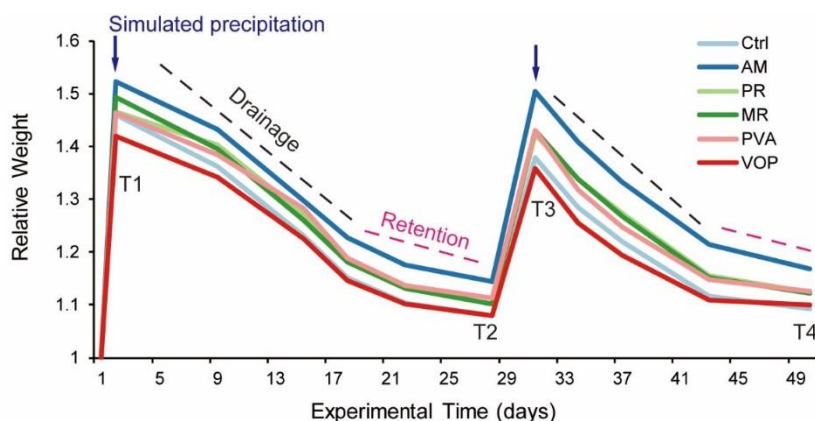


Figure 2. Changes of soil water holding capacity from soils amended with animal manure (AM), mushroom residue (MR), plant residue (PR), synthetic polyvinyl alcohol (PVA) and natural volcanic pumice (VOP). Data were means of 3 replicates. Two peaks represent simulated heavy rainfall

Table 1. Soil water holding capacity among different amendments at four timepoints (corresponding to Figure 2)

	T1	T2	T3	T4
Ctrl	1.46 ± 0.01 (b)	1.08 ± 0.01(ab)	1.38 ± 0.01 (ab)	1.09 ± 0.01 (a)
AM	1.52 ± 0.01 (d)	1.14 ± 0.01 (d)	1.5 ± 0.02 (c)	1.17 ± 0.02 (c)
PR	1.46 ± 0.01 (bc)	1.1 ± 0.01 (bc)	1.42 ± 0.01 (b)	1.12 ± 0.01 (b)
MR	1.49 ± 0.01 (cd)	1.1 ± 0.01 (bc)	1.43 ± 0.02 (b)	1.12 ± 0.01 (b)
PVA	1.46 ± 0.02 (bc)	1.11 ± 0.01 (c)	1.43 ± 0.02 (b)	1.13 ± 0.01 (b)
VOP	1.42 ± 0.02 (a)	1.08 ± 0.01 (a)	1.36 ± 0.03 (a)	1.1 ± 0.02 (ab)

Data were shown as mean±SD. Different letters in one column denote significant differences at $P < 0.05$

Across the two wetting-drainage cycles, AM consistently increased soil WHC ($P < 0.05$, Fig. 2). Specifically, compared to *Ctrl*, the soil with AM amendment could store

13%, 75%, 31% and 88% more water at T1, T2, T3 and T4, respectively (Table. 1). It indicated that AM amendment was able to increase the maximal WHC during precipitation and maintain a higher moisture during drought. MR and PVA increased soil WHC after precipitation (T1) and drainage (T3) during first wetting-drainage cycle, respectively, while VOP significantly decreased soil WHC. During second cycle, PR, MR, PVA amendments all significantly increase soil WHC at drainage stage.

Effects of soil amendments on bacterial diversity and activity

The microbial communities developed at different soil amendment conditions after nearly 60 days of two cycles of wetting-drainage process were investigated. A dataset of 347,556 quality sequences were produced from all soil samples, with almost all classified to the kingdom of bacteria. The total number of OTUs was 2,640 defined by 97% sequence similarity. Both AM and PR amendments significantly increased the bacterial Richness, Shannon values ($p < 0.05$), with AM having the largest effect among all amendments. MR imposed no significant impact on bacterial community at taxonomic level (Richness and Shannon) ($p > 0.05$), while VOP significantly decreased the bacterial diversity at both taxonomic diversities (Richness and Shannon) ($p < 0.05$) (Fig. 3).

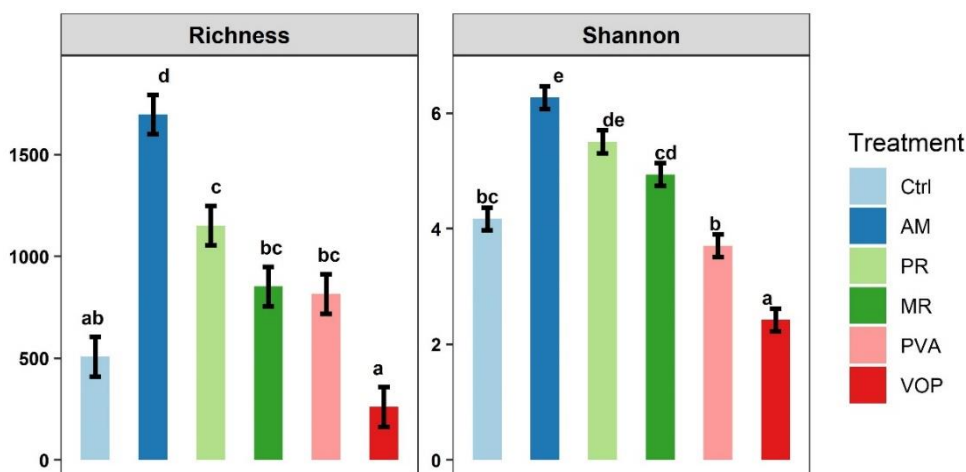


Figure 3. Bacterial community diversity of soils amended with animal manure (AM), mushroom residues (MR), plant residues (PR), synthetic polyvinyl alcohol (PVA) and natural volcanic pumice (VOP). Data are means of 3 replicates (mean \pm SD). Different letters above bars denote significant differences at $p < 0.05$

The dehydrogenase and β -glucosidase were used to estimate the influence of the amendments on soil microbial activities to indicate the degradation of organic matter as well as its nutrient turnover capacities (Schröder et al., 2014). Compared to the unamended soil, AM, MR, and PR all significantly increased the soil dehydrogenase and β -glucosidase activities ($p < 0.05$), while PVA and VOP imposed no evident impact ($p > 0.05$) (Fig. 4). AM imposed the greatest positive impact on the two important soil enzymes; this indicated that animal manure could efficiently increase soil biogeochemical activity. This observation was consistent with the significant increase in SOC content (Fig. 1).

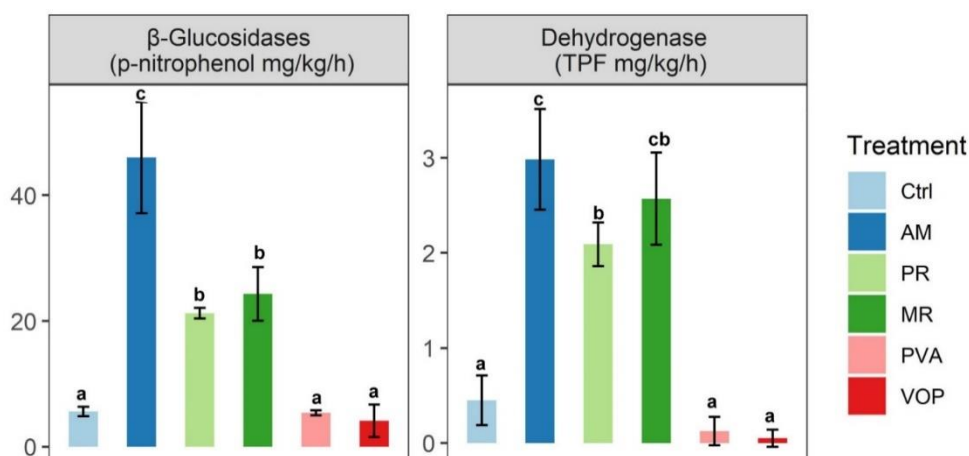


Figure 4. *β-glucosidase and dehydrogenase activity of soils amended with animal manure (AM), mushroom residues (MR), plant residues (PR), synthetic polyvinyl alcohol (PVA) and natural volcanic pumice (VOP). Data are means of 3 replicates ± 1 SD. Different letters above bars denote significant differences at threshold $p < 0.05$*

Discussion

Soil quality is strongly defined by several interactions between chemical and biological components, including soil organic matter and microbial community, which both play key roles on soil fertility (Faissal et al., 2017). As a typical place in the Loess Plateau, Guyuan is characterized with a rather poor soil quality (Fig. 1). The MWD is rather less than 1.3, the threshold that indicates a relative stable soil structure (Le Bissonnais, 2016), and its soil fertility is also quite lower than the typical infertile soil (Feng et al., 2015). In this study, overall, organic amendments significantly increased SOC content, soil aggregate stability as well as the concomitant soil water holding capacity and microbial diversity/activity in different degree, while inorganic amendments didn't impose any beneficial effect (Figs. 1-4).

Accelerating number of studies have confirmed that organic amendments (manure, straw, fermentation, etc.) could be used to improve soil structure (i.e., increase soil porosity and aggregate stability, but decrease bulk density) and fertility mainly by increased SOC (García-Orenes et al., 2005; Peregrina et al., 2012; Li et al., 2014). In this process, soil microorganisms drive the turnover of humic substances which could increase the connectivity of soil particles. In addition, they are the primary means by which nutrients in organic matter can be utilized by plants and other autotrophs (Bell et al., 2005; Verchot et al., 2011). When soil structure improves through aggregation by binding soil particles together (Fig. 1), it provides with a proper niche for soil microbial community (Chen et al., 2017). Indeed, we observed consistent dynamic patterns on the increased soil bacterial diversity (Fig. 3) and enzyme activities (Fig. 4) with organic amendments. It is acknowledged that microbial communities with relatively high biodiversity could transform carbon from organic debris into biomass at accelerated rates with higher conversion efficiency (Maeder et al., 2002; Bell et al., 2005; Patsch et al., 2018). These results were consistent with other previous studies. For example, Maeder et al. (2002) found that organic manure supports a diverse and active biotic community which could decompose more carbon than the ones present in conventional soil. In addition, manure amendments could also inhibit the pathogenic microbes in soil; thus,

reduce plant diseases (i.e. scab and wilt incidence) (Conn and Lazarovits, 1999). Taking together, with the significant effect on improving soil structure and fertility, organic amendments could strengthen the roles of urban green space to regulate and conserve surface water source in the Loess Plateau (*Fig. 2*).

Among all organic amendments in this study, we consistently observed that animal manure surpasses plant and mushroom residues on their soil amelioration effects in both physical and biochemical properties. This is likely relevant to animal-source manure's feature as it is primarily composed of labile fractions (Xing et al., 2012; Wang et al., 2019) as a result of the intestinal digestion. In comparison, plant and mushroom residues are more recalcitrant due to their higher fractions of lignin and cellulose (Bao et al., 2019; Wang et al., 2019). Easily degradable carbon substances impose an intense effect on soil quality while more recalcitrant ones, such as lignin and cellulose, usually have lower effects (Diacono and Montemurro, 2010). Mushroom substrate has been used as a soil amendment due to its high organic matter content as well as other nutrients, however, it usually takes up to 4 years to present a steady beneficial effect on soil quality due to its recalcitrant nature (Peregrina et al., 2012). Similar studies showed that amendments of organic materials from ex situ farmlands (animal manure, and other residues) could also promote soil quality more efficiently compared to in situ similar additives (Long et al., 2015). However, we should bear in mind that animal manure should be processed in harmless treatment to avoid negative effects such as the contamination of antibiotics (Peng et al., 2015) and heavy metals (Ji et al., 2012). Composted manure after batch fermentation, to a large degree, could overcome such problems (Peng et al., 2015).

As expected, inorganic amendments imposed less effect on either soil physical or biochemical properties than organic amendments (*Figs. 1-4*). PVA (polyvinyl alcohol) is a type of uncharged synthetic organic polymer used as soil conditioner (Blavia et al., 1971). With plausible interaction between the polymers and the clay surface via hydrogen binding, PVA could efficiently protect the soil from water ingress (Stefanson, 1973). Consistently, in this case we found that the water hold capability was increased by PVA amendment. However, the other soil properties were not improved. The underlying reason could be that PVA characteristics were dependent on the soil carbon content and humidity (Moayed et al., 2011), both of which are rarely available in the Loess Plateau where the poor soil quality (silt-dominated, but not clay) and limited precipitation are the two major threats. Additionally, PVA can become easily degradable, implying that it would just impose an intense but transient effect on the soil properties as well as soil microorganisms (Wiśniewska, 2010). VOP is a prospering naturally-suited, hardly degradable soil conditioner with numerous beneficial effect for the soil properties (Noland et al., 1992; Cruz-Ruíz et al., 2016). However, in this study, VOP imposed no effect on the soil's physical and/or biochemical properties when compared to other amendments. Similar phenomena were also reported by Temiz and Cayci (2018), who found that pumice had little effect on soil aggregation, compared to plant residues. Given the fact that evaporation is often larger than precipitation in the Loess Plateau (Chao et al., 2017), plausible high mineral content in VOP amendments (Cruz-Ruíz et al., 2016) could even deteriorate soil quality via increased soil salinity (de Meester, 1970). In addition, considering the main constraint in the Loess Plateau was the rather low SOM content (Guo et al., 2019), VOP could offer nothing to improve, if not worsen the status of soil functioning as a carbon sink (*Fig. 1*). Above all, VOP and PVA amendments alone could not impose long-last beneficial effects, and thus were inappropriate to improve the soil structure in arid areas.

Conclusion

Application of exogenous amendments can affect the soil structure and bacterial community in soils from the arid area of the Loess Plateau. Compared with the widely used inorganic soil amendments (i.e. polyvinyl alcohol and volcanic pumice), organic amendments (animal manure, plant residue and mushroom residue) significantly increased soil water holding capacity, aggregate stability as well as microbial diversity and activity. Overall, animal manure imposed the greatest beneficial effect to the soil properties, followed by plant residue and mushroom residue. Animal manure could function as soil amendment for urban green space in the Loess Plateau and other regions with similar soil properties.

Acknowledgements. We are grateful to Mr. Ke Tian for soil sample collection.

REFERENCES

- [1] Bao, Y., Dolfing, J., Wang, B., Chen, R., Huang, M., Li, Z., Lin, X., Feng, Y. (2019): Bacterial communities involved directly or indirectly in the anaerobic degradation of cellulose. – *Biology and Fertility of Soils* 55: 201-211.
- [2] Bell, T., Newman, J. A., Silverman, B. W., Turner, S. L., Lilley, A. K. (2005): The contribution of species richness and composition to bacterial services. – *Nature* 436: 1157-1160.
- [3] Blavia, F. J., Moldenhauer, W. C., Law, D. E. (1971): Soil and water management and conservation. – *Soil Science Society of America Journal* 35.
- [4] Bouranis, D. L., Theodoropoulos, A. G., Drossopoulos, J. B. (2008): Designing synthetic polymers as soil conditioners. – *Communications in Soil Science and Plant Analysis* 26: 1455-1480.
- [5] Cai, Y., Chen, Y., Tong, C. (2019): Spatiotemporal evolution of urban green space and its impact on the urban thermal environment based on remote sensing data: A case study of Fuzhou City, China. – *Urban Forestry and Urban Greening* 41: 333-343.
- [6] Casida, L. E. J., Klein, D. A., Santoro, T. (1964): Soil Dehydrogenase Activity. – *Soil Science* 98: 371-376.
- [7] Chan, F. K. S., Griffiths, J. A., Higgitt, D., Xu, S., Zhu, F., Tang, Y., Xu, Y., Thorne, C. R. (2018): "Sponge City" in China-A breakthrough of planning and flood risk management in the urban context. – *Land Use Policy* 76: 772-778.
- [8] Chang, R. X., Yao, Y., Cao, W. C., Wang, J., Wang, X., Chen, Q. (2019): Effects of composting and carbon-based materials on carbon and nitrogen loss in the arable land utilization of cow manure and corn stalks. – *Journal of Environmental Management* 233: 283-290.
- [9] Chao, W., Lin, Z., Bingzhen, D. (2017): Assessment of the impact of China's Sloping Land Conservation Program on regional development in a typical hilly region of the Loess plateau-A case study in Guyuan. – *Environmental Development* 21: 66-76.
- [10] Chen, Z., Wang, H., Liu, X., Zhao, X., Lu, D., Zhou, J., Li, C. (2017): Changes in soil microbial community and organic carbon fractions under short-term straw return in a rice-wheat cropping system. – *Soil and Tillage Research* 165: 121-127.
- [11] Chen, M., Dai, F., Yang, B., Zhu, S. (2019): Effects of urban green space morphological pattern on variation of PM_{2.5} concentration in the neighborhoods of five Chinese megacities. – *Building and Environment* 158: 1-15.
- [12] Conn, K. L., Lazarovits, G. (1999): Impact of animal manures on verticillium wilt, potato scab, and soil microbial populations. – *Canadian Journal of Plant Pathology* 21: 81-92.

- [13] Cruz-Ruíz, A., Cruz-Ruíz, E., Vaca, R., Del Aguila, P., Lugo, J. (2016): Effects of pumice mining on soil quality. – *Solid Earth* 7: 1-9.
- [14] de Meester, T. (1970): Soils of great Kanya Basin, Turkey. – *Agricultural Research Reports* 740, Centre for Agricultural Publishing and Documentation, Wageningen.
- [15] Diacono, M., Montemurro, F. (2010): Long-term effects of organic amendments on soil fertility. A review. – *Agronomy for Sustainable Development* 30: 401-422.
- [16] Eivazi, F., Tabatabai, M. A. (1990): Factors affecting glucosidase and galactosidase activities in soils. – *Soil Biology and Biochemistry* 22: 891-897.
- [17] Faissal, A., Ouazzani, N., Parrado, J. R., Dary, M., Manyani, H., Morgado, B. R., Barragán, M. D., Mandi, L. (2017): Impact of fertilization by natural manure on the microbial quality of soil: Molecular approach. – *Saudi journal of biological sciences* 24: 1437-1443.
- [18] Feng, Y., Chen, R., Hu, J., Zhao, F., Wang, J., Chu, H., Zhang, J., Dolfing, J., Lin, X. (2015): *Bacillus asahii* comes to the fore in organic manure fertilized alkaline soils. – *Soil Biology and Biochemistry* 81: 186-194.
- [19] Feng, Y., Chen, R., Stegen, J. C., Guo, Z., Zhang, J., Li, Z., Lin, X. (2018): Two key features influencing community assembly processes at regional scale: Initial state and degree of change in environmental conditions. – *Molecular Ecology* 27: 5238-5251.
- [20] Follett, R. F., Varvel, G. E., Kimble, J. M., Vogel, K. P. (2009): No-Till Corn after Bromegrass: Effect on Soil Carbon and Soil Aggregates. – *Agronomy Journal* 101: 261-268.
- [21] Garccía-Orenes, F., Guerrero, C., Mataix-Solera, J., Navarro-Pedreño, J., Gómez, I., Mataix-Beneyto, J. (2005): Factors controlling the aggregate stability and bulk density in two different degraded soils amended with biosolids. – *Soil and Tillage Research* 82: 65-76.
- [22] Gong, Y., Tang, J., Zhao, D. (2016): Application of iron sulfide particles for groundwater and soil remediation: A review. – *Water Research* 89: 309-320.
- [23] Guo, Z., Zhang, J., Fan, J., Yang, X., Yi, Y., Han, X., Wang, D., Zhu, P., Peng, X. (2019): Does animal manure application improve soil aggregation? Insights from nine long-term fertilization experiments. – *Science of The Total Environment* 660: 1029-1037.
- [24] Hua, L., Zhong, L., Ke, Z. (2016): Precipitation recycling and soil–precipitation interaction across the arid and semi-arid regions of China. – *International Journal of Climatology* 36: 3708-3722.
- [25] Ji, X., Shen, Q., Liu, F., Ma, J., Xu, G., Wang, Y., Wu, M. (2012): Antibiotic resistance gene abundances associated with antibiotics and heavy metals in animal manures and agricultural soils adjacent to feedlots in Shanghai; China. – *Journal of Hazardous Materials* 235-236: 178-185.
- [26] Karlen, D. L., Andrews, S. S., Wienhold, B. J., Zobeck, T. M. (2008): Soil Quality Assessment: Past, Present and Future. – *J. Integr. Biosci.* 6(1): 3-14.
- [27] Khan, M. A., Khan, S., Khan, A., Alam, M. (2017): Soil contamination with cadmium, consequences and remediation using organic amendments. – *Science of The Total Environment* 601-602: 1591-1605.
- [28] Le Bissonnais, Y. (2016): Aggregate stability and assessment of soil crustability and erodibility: I. Theory and methodology. – *European Journal of Soil Science* 67: 11-21.
- [29] Li, J., Lu, J., Li, X., Ren, T., Cong, R., Zhou, L. (2014): Dynamics of potassium release and adsorption on rice straw residue. – *PloS one* 9: e90440-e90440.
- [30] Li, Y., Xie, Z., Qin, Y., Xia, H., Zheng, Z., Zhang, L., Pan, Z., Liu, Z. (2019): Drought Under Global Warming and Climate Change: An Empirical Study of the Loess Plateau. – *Sustainability* 11: 1281-1295.
- [31] Liu, Z., Liu, F., Ma, F., Wang, M., Bai, X., Zheng, Y., Yin, H., Zhang, G. (2015): Collapsibility, composition, and microstructure of loess in China. – *Canadian Geotechnical Journal* 53: 673-686.

- [32] Long, P., Sui, P., Gao, W., Wang, B., Huang, J., Yan, P., Zou, J., Yan, L., Chen, Y. (2015): Aggregate stability and associated C and N in a silty loam soil as affected by organic material inputs. – *Journal of Integrative Agriculture* 14: 774-787.
- [33] Lu, R. (2000): Analytical methods for soil and agrochemistry. – Beijing, Chinese Agriculture Science and Technology Press. (In Chinese).
- [34] Maeder, P., Fliessbach, A., Dubois, D., Gunst, L., Fried, P., Niggli, U. (2002): Soil Fertility and Biodiversity in Organic Farming. – *Science* 296: 1694-1697.
- [35] Miao, S. J., Shi, H., Wang, G. H., Jin, J., Liu, J. D., Zhou, K. Q., Sui, Y. Y., Liu, X. B. (2013): Seven years of repeated cattle manure addition to eroded Chinese Mollisols increase low-molecular-weight organic acids in soil solution. – *Plant and Soil* 369: 577-584.
- [36] Moayedi, H., Asadi, A., Moayedi, F., Huat, B. B. K. (2011): Zeta Potential of Tropical Soil in Presence of Polyvinyl Alcohol. – *International Journal of Electrochemical Science* 6: 1294-1306.
- [37] Noland, D. A., Spomer, L. A., Williams, D. J. (1992): Evaluation of pumice as a perlite substitute for container soil physical amendment. – *Communications in Soil Science and Plant Analysis* 23: 1533-1547.
- [38] Patsch, D., van Vliet, S., Marcantini, L. G., Johnson, D. R. (2018): Generality of associations between biological richness and the rates of metabolic processes across microbial communities. – *Environmental Microbiology* 20: 4356-4368.
- [39] Peng, S., Wang, Y., Zhou, B., Lin, X. (2015): Long-term application of fresh and composted manure increases tetracycline resistance in the arable soil of eastern China. – *Science of The Total Environment* 506-507: 279-286.
- [40] Peregrina, F., Larrieta, C., Colina, M., Mariscal-Sancho, I., Martín, I., Martínez-Vidaurre, J. M., García-Escudero, E. (2012): Spent Mushroom Substrates Influence Soil Quality and Nitrogen Availability in a Semiarid Vineyard Soil. – *Soil Science Society of America Journal* 76(5): 1655-1666.
- [41] Schröder, C., Elleuche, S., Blank, S., Antranikian, G. (2014): Characterization of a heat-active archaeal β -glucosidase from a hydrothermal spring metagenome. – *Enzyme and Microbial Technology* 57: 48-54.
- [42] Stefanson, R. C. (1973): Polyvinyl alcohol as a stabilizer of surface soils. – *Soil Science* 115(6): 420-428.
- [43] Su, C. C., Ma, J. F., Chen, Y. P. (2019): Biochar can improve the soil quality of new creation farmland on the Loess Plateau. – *Environmental Science and Pollution Research* 26: 2662-2670.
- [44] Sun, J. (2002): Provenance of loess material and formation of loess deposits on the Chinese Loess Plateau. – *Earth and Planetary Science Letters* 203: 845-859.
- [45] Sun, J., Guo, X., Liang, J., Chen, G., Zhang, G., Zhou, T. (2017): Effects of mulching time on soil temperature and moisture and potato yield in the hilly area of Southern Ningxia. – *Acta Prataculturae Sinica* 26: 24-34.
- [46] Tang, H. M., Xiao, X. P., Li, C., Wang, K., Guo, L. J., Cheng, K. K., Sun, G., Pan, X. C. (2018): Impact of long-term fertilization practices on the soil aggregation and humic substances under double-cropped rice fields. – *Environmental Science and Pollution Research* 25: 11034-11044.
- [47] Temiz, C., Cayci, G. (2018): The effects of gypsum and mulch applications on reclamation parameters and physical properties of an alkali soil. – *Environmental Monitoring and Assessment* 190: 347.
- [48] Tisdall, J. M., Oades, J. M. (1982): Organic matter and water-stable aggregates in soils. – *Journal of Soil Science* 33: 141-163.
- [49] Verchot, L. V., Dutaur, L., Shepherd, K. D., Albrecht, A. (2011): Organic matter stabilization in soil aggregates: Understanding the biogeochemical mechanisms that determine the fate of carbon inputs in soils. – *Geoderma* 161: 182-193.

- [50] Vienneau, D., de Hoogh, K., Faeh, D., Kaufmann, M., Wunderli, J. M., Rössli, M. (2017): More than clean air and tranquillity: Residential green is independently associated with decreasing mortality. – *Environment International* 108: 176-184.
- [51] Wang, K., Mao, H., Li, X. (2018): Functional characteristics and influence factors of microbial community in sewage sludge composting with inorganic bulking agent. – *Bioresource Technology* 249: 527-535.
- [52] Wang, Z., Yun, S., Xu, H., Wang, C., Zhang, Y., Chen, J., Jia, B. (2019): Mesophilic anaerobic co-digestion of acorn slag waste with dairy manure in a batch digester: Focusing on mixing ratios and bio-based carbon accelerants. – *Bioresource Technology* 286: 121394.
- [53] Wiśniewska, M. (2010): The structure of electrical double layer of silica in the presence of polyvinyl alcohol (PVA) at different temperatures. – *Materials Letters* 64: 1611-1613.
- [54] Wu, S., Wu, P., Feng, H., Bu, C. (2010): Influence of amendments on soil structure and soil loss under simulated rainfall China's Loess plateau. – *African Journal of Biotechnology* 9: 6116-6121.
- [55] Xing, M., Li, X., Yang, J., Huang, Z., Lu, Y. (2012): Changes in the chemical characteristics of water-extracted organic matter from vermicomposting of sewage sludge and cow dung. – *Journal of Hazardous Materials* 205-206: 24-31.
- [56] Xu, H., Wang, X. (2016): Effects of altered precipitation regimes on plant productivity in the arid region of northern China. – *Ecological Informatics* 31: 137-146.
- [57] Xue, Z., An, S. (2018): Changes in Soil Organic Carbon and Total Nitrogen at a Small Watershed Scale as the Result of Land Use Conversion on the Loess Plateau. – *Sustainability* 10: 1-14.
- [58] Zhang, F., Cui, Z., Fan, M., Zhang, W., Chen, X., Jiang, R. (2011): Integrated Soil-Crop System Management: Reducing Environmental Risk while Increasing Crop Productivity and Improving Nutrient Use Efficiency in China. – *Journal of Environmental Quality* 40: 1051-1057.
- [59] Zhang, Y., Guo, S., Liu, Q., Jiang, J. (2014): Influence of soil moisture on litter respiration in the semiarid Loess plateau. – *PloS one* 9: e114558.
- [60] Zhang, J. Y., Sun, C. L., Liu, G. B., Xue, S. (2018): Effects of long-term fertilization on aggregates and dynamics of soil organic carbon in a semi-arid agro-ecosystem in China. – *Peerj* 6: e4758.
- [61] Zou, P., Fu, J. R., Cao, Z. H., Ye, J., Yu, Q. G. (2015): Aggregate dynamics and associated soil organic matter in topsoils of two 2,000-year paddy soil chronosequences. – *Journal of Soils and Sediments* 15: 510-522.

FOLIAR SULPHUR APPLICATION AND ITS TIMINGS IMPROVE WHEAT (*TRITICUM AESTIVUM* L.) PRODUCTIVITY IN SEMI-ARID CLIMATE

SHAH, S. A. A.^{1,2*} – MIAN, I. A.² – SHARIF, M.² – IQBAL, A.³ – SHAH, T.² – SHAH, S. A. A.⁴ – ABRAR, M. M.¹ – MUSTAFA, A.¹ – XU, M.^{1,5*}

¹*National Engineering Laboratory for Improving Quality of Arable Land, Institute of Agricultural Resources and Regional Planning, Chinese Academy of Agricultural Sciences, Beijing 100081, China*

²*Department of Soil and Environmental Sciences, The University of Agriculture, Peshawar-KPK, Pakistan*

³*State Key Laboratory of Cotton Biology, Institute of Cotton Research of CAAS, Anyang, Henan 455000, China*

⁴*Department of Vegetable Sciences, College of Horticulture, China Agriculture University, Beijing, China*

⁵*South Subtropical Crop Research Institute, Chinese Academy of Tropical Agricultural Sciences (CATAS), Zhanjiang, Guangdong 524091, China*

**Corresponding authors*

e-mail: xuminggang@caas.cn, shah_syed18@yahoo.com

(Received 21st Sep 2019; accepted 23rd Jan 2020)

Abstract. Sulphur fertilization is beneficial for improving growth, yield and yield determining components of field crops under a semiarid climate. The present field experiment was conducted to investigate the response to the foliar application of sulphur at various phenological stages of wheat. For this purpose, five treatments were explored i.e., control (no spray); water spray; 7.5 kg S ha⁻¹; 15 kg S ha⁻¹; 21 kg S ha⁻¹. The results revealed that the application of foliar sulphur at the rate of 15 kg ha⁻¹ increased the yield components (grain yield and biological yield) of wheat by 31 and 9% compared to control. The following trend (15 kg S ha⁻¹ > 21 kg S ha⁻¹ > 7.5 kg S ha⁻¹ > water spray > control) was observed for the yield components. Conversely, the application of sulphur at 21 kg ha⁻¹ increased the concentration of sulphur in soil and plant by 104 and 195% respectively, compared to control. A positive linear relationship was observed between soil sulphur and grain yield of wheat ($R^2 = 0.76$ and $P < 0.0001$). Furthermore, it was observed that the growth and yield of wheat increased significantly when foliar sulphur was applied in two equal splits (50% each at tillering and booting) compared to the full application at tillering and booting. It was inferred from this study that application of foliar sulphur at the rate of 15 kg ha⁻¹ in two equal splits (50% each at tillering and booting) improves growth and productivity of wheat in the semiarid climate.

Keywords: *foliar, sulphur, application timing, wheat, phenology*

Introduction

The ongoing globalization with the ever increasing human population are threatening the food security and environmental quality. It is estimated that the world's population may reach to 9.1 billion (34% higher than today) by 2050. These trends show that the demand for food would continue to grow to feed both the humans and animals as well (Tilman et al., 2011). The desired increase in agricultural production to meet global

food demand casts immense pressure on the sparse resources that are already on the edge to be endangered. Meanwhile, the agricultural intensification to get more production have shown certain drawbacks in the form of environmental degradation (Davidson, 2009), damages to the biodiversity (Christopher and Tilman, 2008) and degradation of land and water resources which are increasing continuously and are even stagnant in some countries (Diaz and Rosenberg, 2008; Guo et al., 2010; Mustafa et al., 2019a). Agriculture is the mainstay of Pakistan's national economy. It is a major contributor to support Pakistan's population and to food security accounting for 20.9% share to country's GDP (GOP, 2015; Chandio et al., 2016).

Wheat (*Triticum aestivum* L.) is the world's most important cereal crop. In Pakistan, wheat is also the main staple crop of the people, meeting 95% of the country's food demand (Malik et al., 2006). It also occupies a significant position due to largest area under single crop cultivation (Mustafa et al., 2019b). Its agricultural added value accounts for 10.1%, about 2.1% of the GDP reached the planting area is 9.18 million ha¹ in 2014-2015, and the average yield was 2852 kg ha⁻¹ (MNFSR, 2014-15). These figures are not satisfactory because the country's average wheat yield is lower than that of some major wheat producers in the world, such as France, Mexico, China and the United States (Kakar et al., 2015). The factors contributing to the low yields in Pakistan are the lack of education to apply appropriate doses of fertilizer at different stages of the crop and over time. As a result, smallholders are facing certain socio-economic constraints, lack of extension services, inability to obtain high-quality seeds during the growth period and increasing costs of fertilizer (Pathak et al., 2006).

Since wheat is an exhaustive crop, this means it reduces the soil fertility and productivity leading to reduced crop yields. It is very important to evaluate the soil fertility status of main wheat producing areas. In fact, due to its frequent scarcity in time and space, sulphur is of great significance all over the world. Though sulphur is required in lesser amounts for optimum wheat growth, yet its concentration is low in world soils causing potential reductions in attainable yields. Various aspects contribute to the deficiencies of S, such as the high chemical fertilizer usage without S, several types and excessive planting intensity, and the treatment, leaching and erosion from crop residues for feed and fuel (Tandon, 1984). Sulphur plays an important role in the major functions of plant growth, metabolism, and enzymatic reactions (Mengal and Kirkby, 1987). Without sulphur, the activity of sulphur-containing amino acids such as cysteine, cysteine, and methionine would not be possible. Sulphur is an ingredient particularly involved in s-glycosides, co enzyme, vitamin biotin, and thiamine (Tisdale et al., 1985).

Sulphur can also be used as a foliar application in order to ensure higher crop productivity. Leaf surface application of S have shown the potential to control mildew stage of *Erysiphe graminis* (Hussain and Leitch, 2005) at the top of the canopy in terms of disease control. Moreover, foliar application of S improved the efficiency of fungicides (Zahid and Leitch, 2005). At the best time for wheat, foliar application of S can improve grain protein content and improve the production quality of bread wheat (Zahid and Leitch, 2005). Thus, there is a great scope to be find best application methods and timings to ensure maximum wheat production per unit utilization of S fertilizer. The response of wheat bread quality to S is more general than that of grain yield. The use of S does not directly affect grain protein concentration, but increases the weight of gelatinous protein in flour and the ratio of polymeric protein (Saeed et al., 2013). Sulphur deficiency may lead to harder grains, and the dough made from these grains is usually hard and non-elastic (Ryant and Hrivna, 2004). After applying S, the

total absorption and concentration of S tended to be increased (Zahid and Leitch, 2005), hence improving the quality of wheat grains.

Foliar fertilization (provision of nutrients through aerial plant parts) has been considered an efficient technique which enhances availability of nutrients, use efficiencies and hence the subsequent crop yields (Saeed et al., 2012; Aziz et al., 2018). Studies on appropriate levels and timings of sulphur spraying in agroecological wheat growing areas in Khyber Pakhtunkhwa, Pakistan, have not been carried out earlier. In addition, little is known on how to ensure greater nutrient use efficiency via reduced nutrient losses have been remained neglected in the past especially in the area under consideration. Moreover, there is also a need to explore foliarly applied S at different growth stages of wheat in order to ensure maximum crop productivity. Therefore, present study was aimed to evaluate the response rate of foliar application of sulphur and its application timings on growth, phenology and yield of wheat which was grown as a reference crop.

Materials and methods

Experimental site characteristics

To study the effect of foliar sulphur and its application timings on yield and yield components of wheat, present field experiment was conducted at New Developmental Farm, The University of Agriculture Peshawar, Pakistan during 2013-2014 in winter season. In the mid of November, 2013, wheat seeds were sown in the field and the crop was harvested in the mid of May, 2014. The research farm is located at 34.01°N, 71.35°E, at an altitude of 350 m above sea level in the Peshawar valley. Peshawar is located about 1600 km north of the Indian ocean and has semiarid climate. The research farm is irrigated by the Warsak canal linked to Kabul river. Soil particle analysis (Gee and Bauder, 1979) revealed that the texture of soil was clay loam, alkaline (pH 8.2) in nature, calcareous, with a low organic matter content of 8.7 g kg⁻¹ (Amanullah et al., 2009), total N content of 0.07%, low concentrations of available phosphorus of 6.57 mg kg⁻¹ measured by following the method of (Watanabe and Olsen, 1965) and exchangeable potassium of 121 mg kg⁻¹ by following the method given by Simard (1993) on atomic absorption spectrophotometer. The climate of the area is semiarid where the mean annual rainfall is very low (300 to 500 mm), 60-70% of which occurs in summer, while the remaining 30-40% rainfall occurs in winter (Amanullah et al., 2016).

Experimental design and crop establishment

The experiment was laid out in randomized complete block design having three replications. Each replication was consisted of 5 treatments *viz* five foliar sulphur levels (no spray, water spray, 7.5, 15 and 21 kg S ha⁻¹) and three application times at specific wheat growth stages (tillering, booting and half at tillering + half at booting stage). Sublimed sulphur (Analar) was used as a source for S containing (200 g L⁻¹) S.

Plot size of 4 m × 3 m (10 rows, 4 m long and 30 cm apart) was used. The recommended doses of 120 kg N ha⁻¹ (as urea), 90 kg P ha⁻¹ (as ammonium phosphate) and 60 kg K ha⁻¹ (as potassium sulphate) were applied (Mustafa et al., 2019b). The required nitrogen was applied in two equal splits i.e. 50% at sowing and 50% at 30 days after sowing. Seeds of wheat verity (Atta Habib) kindly donated by Department of Agronomy, University of Agriculture, Peshawar, Pakistan were sown at the seed rate of

120 kg ha⁻¹. All other agronomic practices i.e. seed bed preparation, irrigations, hoeing and weeding were practiced uniformly to all the plots throughout the growth period for maximum yield. Good quality canal water was used for irrigation and crop protection measures were carried out as and when required throughout the experimental duration.

Plant growth, phenological and yield attribute recordings

Certain growth, yield and phenological observations were recorded as and when required on specific crop growth periods. Days to heading were recorded in each sub plot after completion of 80% heading. The number of days to heading was counted from the date of sowing to the date when 50% heading were completed in each subplot. The days to physiological maturity were recorded by counting the days from date of sowing to the date when plants become physiologically mature. Complete loss of the green color of glumes was used as indication of physiological maturity. Data on plant height were recorded by measuring randomly selected 10 plants in each subplot from base of plant to the tip of spikes excluding awns at maturity. The internode lengths of five randomly selected tillers was measured with the help of meter rod and then averaged accordingly. Data on number of tillers were recorded by counting the numbers of tillers in central three rows of each sub plot, and were converted to numbers of tillers m⁻². Data on number of spikes m⁻² was recorded by counting the number of spikes in three randomly selected rows of one-meter length and were converted into spikes m⁻². Grains from five randomly selected spikes were obtained by hand threshing and was counted and converted into average number of grains spike⁻¹. Thousand grains were counted from the grains randomly picked from each sub plot and weighed with a digital balance. Four central rows were harvested in each subplot and was sun dried and bundles were weighed. Small wheat thresher was used for threshing the biological yield taken from four central rows in each sub plot. After threshing the grains were weighed by balance and converted to kg ha⁻¹ by using the formula:

$$\text{Grain yield (kg ha}^{-1}\text{)} = \frac{\text{Grain yield in four central rows}}{\text{R} - \text{R} \times \text{No of rows} \times \text{row length}} \times 1000 \quad (\text{Eq.1})$$

Harvest index were calculated as the ratio of grain yield to the total biological yield and expressed as percentage.

The sampling of leaf was accomplished by collecting matured 10 leaves from healthy and suitable plants from each plot in the field. The central rows were selected and collect leaves for leaf sampling and these samples were than analyzed for SO₄-S in the tissues of leaf.

Soil analysis

For soil analysis a composite sample at the depth of 15 cm was randomly taken from the experimental field before sowing of crop and was analyzed to major physio-chemical properties of the soil. Post-harvest soil sample from each experimental unit was also taken and analyzed for soil and leaf sulphur content. Completely oven dried ground leaf samples up to 0.5 depth were used in a 150 ml conical flask. 15 ml concentrated HNO₃ was placed into the flask for overnight, 2 mL concentrated H₂SO₄ along with 5 mL per chloric acid was heated up eventually digested until visible massive gases as well as the gases layering inside the beaker appeared. Then the sample was cooled and 50 ml distilled water was added and heated again. The sample was

filtered by using Whatmann filter paper # 40. The filtrate was obtained in a volumetric flask then the essential volume was produced by putting distilled water (Richard, 1954). Soil sulphate form of S was determined by the method described by Rayan et al. (2001).

Statistical analyses

The data recorded for each parameter were analyzed statistically by using Statistix® 8.1 software and means were compared by using fisher protected least significance difference (LSD) test at 5% level of significance (Steel and Torrie, 1980). The analysis of correlation was performed by using sigma-stat function in sigma plot 14.0 software for windows. A simple linear regression was used to evaluate the relationship between the sulphur concentration and yield of wheat. According to the linear model based on a first-order kinetics equation ($Y = a + bx$), where a is intercept and b is slope and both are constants). We used probability level ($P < 0.01$) for considering the significant result.

Results

Influence of foliar sulphur and its timings on phenological attributes and growth of wheat

Application of foliar sulphur at higher rate of 21 and 15 kg ha⁻¹ delayed heading (121 days) and physiological maturity (161 and 160 days) compared to control, while the early heading (119 days) and maturity (156 days) was noted in control. Similarly, the application of sulphur at the time of tillering took more days to heading (120 days) and non-significant differences were found between full booting and two equal splits (50% each at tillering and booting) respectively. Furthermore, sulphur application delayed maturity (159 days) at booting followed by tillering stage, while early maturity (157 days) was observed in sulphur application at two equal splits (50% each at tillering and booting) as shown in *Table 1*.

Table 1. Days to heading, days to maturity, plant height, internode length, tiller m⁻², spike m⁻² and grains spike⁻¹ as affected by foliar sulphur and its application timing

Sulphur spray (kg ha ⁻¹)	Days to heading	Days to maturity	Plant height (cm)	Internode length (cm)	Tillers m ⁻²	Spike m ⁻²	Grains spike ⁻¹
Control	119 c	156 c	92.1 d	10.8	291 d	283 c	52 c
Water	118 c	157 b	94.3 c	10.8	309 c	307 b	53 bc
7.5	120 b	158 b	97.8 b	11.1	319 b	316 a	55 b
15	121 ab	160 ab	99.2 ab	10.7	320 b	318 a	59 a
21	123 a	161 a	100.3 a	11	323 a	309 b	54 b
LSD	1.1	1.3	2.5	ns	10	11	2.6
Application timing (AT)							
Tillering	121 a	158 b	95.3 b	10.9	322 a	315 a	53 b
Booting	120 b	159 a	96.3 b	10.9	310 b	317 a	54 b
1/2 tillering + 1/2 booting	120 b	158 b	98.7 a	10.8	295 c	288 b	56 a
LSD	0.8	1	1.9	ns	7	8	1.9
Interaction							
S × AT	**	**	ns	ns	ns	ns	ns

Means of the same category followed by different letters are significantly different from each other using LSD test ($P \leq 0.05$). ns stands for non-significant data and ** indicates that data is significant at 1% level of probability

Interaction between S × AT indicated that the maximum days to heading and maturity were recorded with the application of sulphur at the rate of 21 kg ha⁻¹ half at tillering half at booting was applied as shown in *Figures 1* and 2. Compared to control (CK) the application of sulphur at the rate of 21 kg ha⁻¹ produced taller plants (100 cm), which was followed by 15 kg ha⁻¹, while dwarf plants (92 cm) and minimum internode length were recorded in control plot. Split application of sulphur (50% each at tillering and booting) produced the tallest plants (98 cm), while lowest plant height (95 cm) was recorded in plots treated with sulphur at the time of tillering. There were generally no-significant differences among foliar sulphur and its application timing for internode length of wheat. The application of foliar sulphur at 21 kg ha⁻¹ produces maximum tillers m⁻² (323), however, the application of sulphur at 15 and 7.5 kg ha⁻¹ were statistically similar in response to tillers m⁻² (320 and 319) compared to control. The spike m⁻² and grain spike were statistically observed maximum (318 and 55) at the rate of 15 kg ha⁻¹ while lowest (283 and 52) at control respectively (*Table 1*).

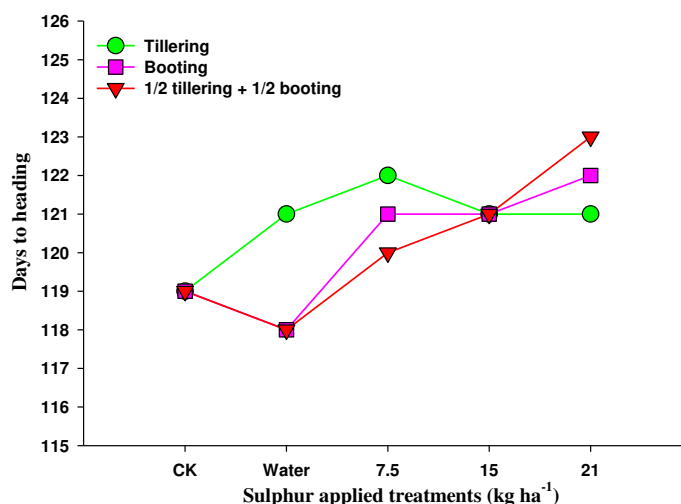


Figure 1. Response of days to heading of wheat to sulphur levels and application timing (S × AT)

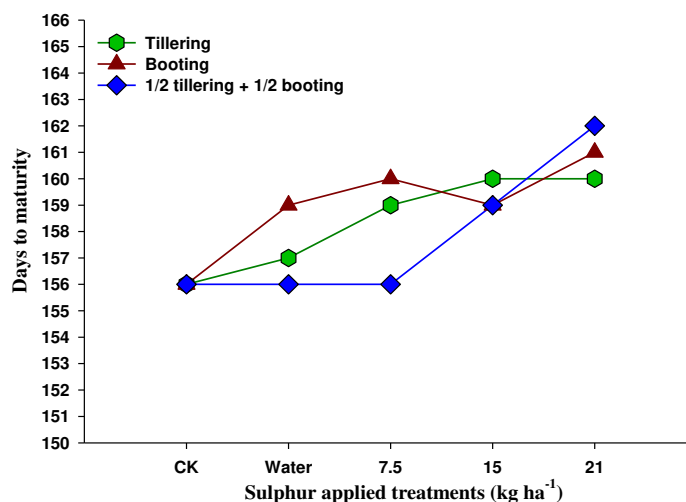


Figure 2. Response of days to maturity of wheat to sulphur levels and application timing (S × AT)

Influence of foliar sulphur and its timings on yield components of wheat

Thousand grain weight were maximum (48 g) with the application of 15 kg S ha⁻¹ compared to control. The yield components (grain yield and biological yield) of wheat were increased (31% and 9%) by the application of 15 kg ha⁻¹ compared to the control treatment. However, the following increasing trend (15 kg ha⁻¹ > 21 kg ha⁻¹ > 7.5 kg ha⁻¹ > water spray > control) was observed for the yield components of wheat as shown in Table 2, respectively. The favorable stage for increasing the yield components (grain yield and biological yield) was noted where sulphur was applied in two equal splits (50% each at tillering and booting). However, the interaction between sulphur and its application timing was found highest for thousand grains weight when sulphur was applied at the rate of 15 kg ha⁻¹ in two equal splits (Fig. 3). Analysis of correlation between soil sulphur and grain yield showed strong relationship at R² = 0.76, and P < 0.0001 (Fig. 4). The harvest index was found to be highest (41%) with the application of sulphur at the rate of 15 kg ha⁻¹ and was also highest when sulphur was applied in two equal splits (50% each at tillering and booting) stage.

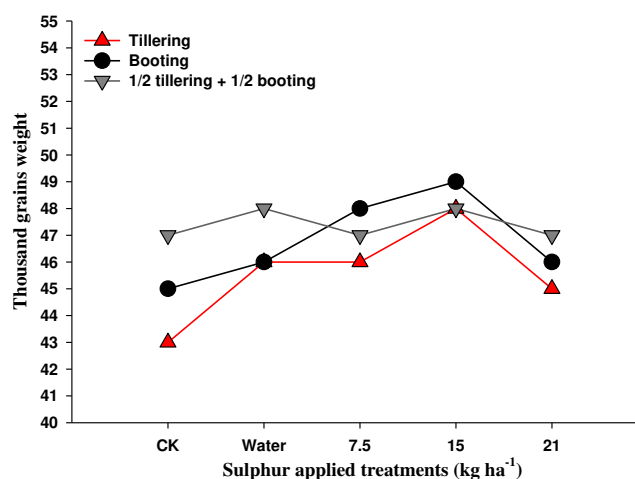


Figure 3. Response of thousand grains weight of wheat to sulphur levels and application timing (S × AT)

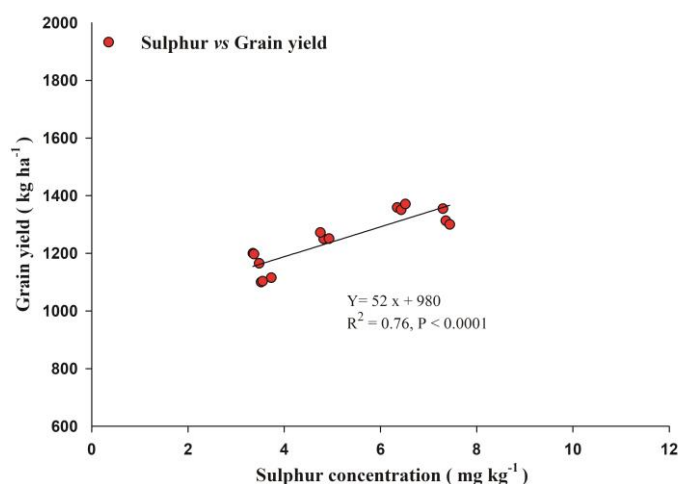


Figure 4. Correlation of sulphur with grain yield

Table 2. Thousand grains weight (g), biological yield (kg ha⁻¹), grain yield (kg ha⁻¹), harvest index (%) as affected by foliar sulphur and its application timing

Sulphur spray (kg S ha ⁻¹)	Thousand grains weight (g)	Biological yield (kg ha ⁻¹)	Grain yield (kg ha ⁻¹)	Harvest index (%)
Control	45.1 c	9347 c	3168 c	33.9 c
Water	46.7 bc	9402 c	3622 b	38.5 b
7.5	47.3 b	9769 b	3791 b	38.8 b
15	48.4 a	10187 a	4145 a	40.8 a
21	45.3 c	9928 ab	3923 ab	39.5 ab
LSD	1.14	362	213	2.4
Application timing (AT)				
Tillering	45.4 b	9526 b	3585 b	37.6
Booting	46.8 ab	9750 ab	3694 ab	37.8
1/2 tillering + 1/2 booting	47.6 a	9902 a	3910 a	39.5
LSD	0.9	280	165	ns
Interaction				
S × AT	*	ns	ns	ns

Means of the same category followed by different letters are significantly different from each other using LSD test ($P \leq 0.05$). ns stands for non-significant data and * indicates that data is significant at 5% level of probability

Influence of foliar sulphur and its timings on soil and plant sulphur concentration (mg kg⁻¹)

The influence of foliar sulphur and its timing on the soil post-harvest S (mg kg⁻¹) and plant-post harvest S is shown in *Figure 5a, b*. It was observed that application of sulphur at the rate of 21 kg ha⁻¹ increased the sulphur concentration in soil and plant (104 and 195%) which was followed by 15 kg ha⁻¹ in both the soil and plant post-harvest (78 and 166%) compared to control respectively. However, sulphur applied in two splits (50% each at tillering and booting) was the significant stage which increased the sulphur concentration in soil as well as in the plant. Furthermore, it was observed that booting stage followed the two splits stage and increased the concentration of sulphur in soil post-harvest while tillering stage followed the two split stage and increased the sulphur concentration in plant. Overall the same trend was observed for soil and plant as (21 kg ha⁻¹ > 15 kg ha⁻¹ > 7.5 kg ha⁻¹ > CK > water).

Discussion

To situate the problem addressed here it was noted that the higher dose of S delayed the phenology which might be due to more vegetative growth of plants (Hussain and Leitch et al., 2005). However, reducing the sulphur levels can delay the aging of wheat crop. These findings are in line with Lestache et al. (2004). Moreover, Nawaz et al. (1989) and Khaliq et al. (2008) have also reported that the application of macronutrients delayed the phenology of crops (Lestache et al., 2004; Fageria, 2009). The application of S in two splits at the rate of 21 kg ha⁻¹, significantly increased wheat growth. The most possible reason behind this might be the split application of S at different growth stages that matches with the nutrient requirement of the crop. These findings support the

previous results of (Togay et al., 2008), they noted that sulphur application significantly increased the plant height and growth of wheat. Foliar application of nutrients enhances nutrient availability to main crops. We found increased S concentration in wheat plants upon foliar S application. Our results are in line with those reported by Laura et al. (2011) and Marinaccio et al. (2015). Recently, Aziz et al. (2018) reported increased growth, yield and nutrients concentration of wheat under the foliarly applied micronutrients spray at various wheat growth stages.

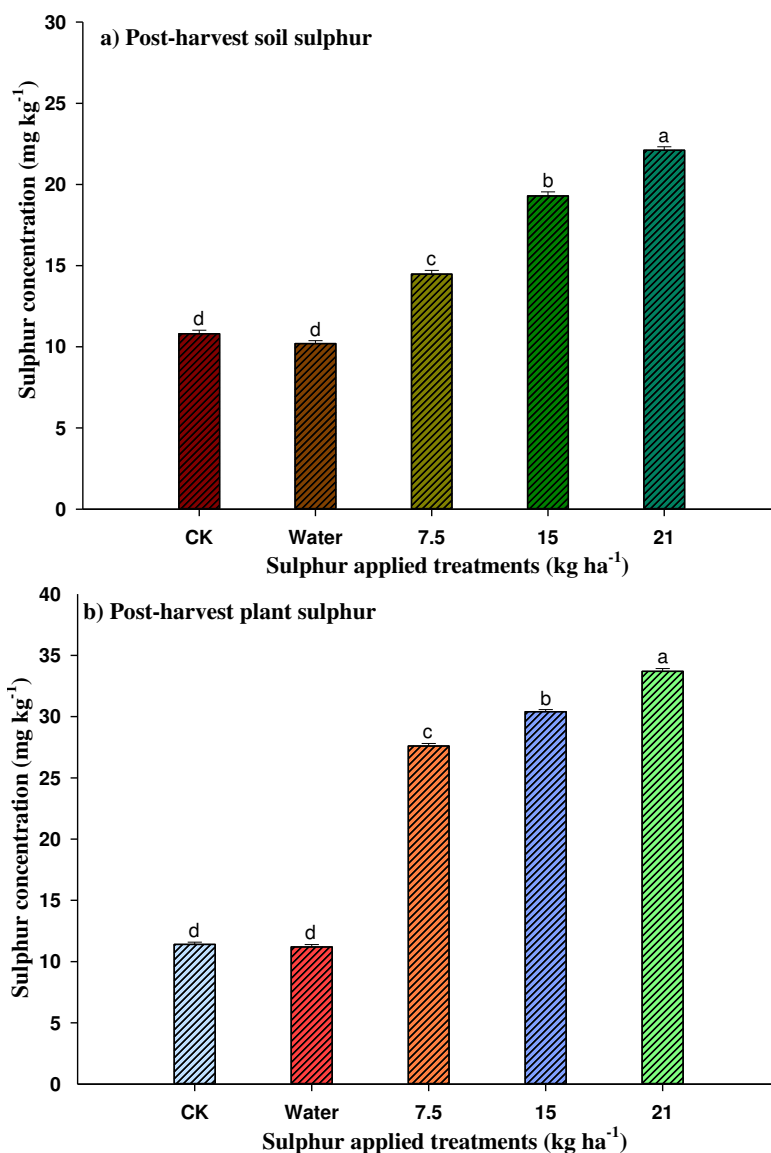


Figure 5. (a) Post-harvest soil sulphur concentration (mg kg⁻¹). (b) Post-harvest plant sulphur concentration (mg kg⁻¹)

The higher dose of sulphur, increased the number of grains per row was mainly attributed due to the increase of panicle length. These findings are similar to those reported by Mahmood (1994), Rasheed et al. (2003) and Khaliq et al. (2009). Similar results were also documented by Ali et al. (2012), who indicated that application of sulphur significantly improved the number of tillers m⁻². Pasha et al. (2006) in another

study reported that the application of sulphur increased the panicle length and thousand grains weight of wheat. Laura et al. (2011) also reported that application of sulphur at the rate of 15 kg ha⁻¹ increased the concentration of sulphur in leaves and thousand grains weight in different stages.

Sulphur application at the rate of 15 kg ha⁻¹, divided into two equal amounts (50% at tillering stage and 50% at booting stage), significantly increased grain yield, biological yield and yield index of wheat. These results are substantiated with Saeed et al. (2013). Ramos et al. (2008) emphasized that the application of S in tillering could improve grain yield. One possible reason for this might be that when the leaves absorbed sulphur, they produce methionine, a biological precursor of ethylene (Saeed et al., 2013). The beneficial effect of the number of panicles on flowering biomass was greater than that of grain yield, which indicated that the number of panicles had a strong correlation with the source vigor and was also restricted by the environment. Hussain and Leitch (2005), Khan et al. (2006) and Ercoli et al. (2011) found that the application of sulphur can significantly increase the wheat grain yield and straw yield. Dorothee et al. (2012) reported the beneficial effects of sulphur fertilizer on grain yield and protein composition of mature wheat.

Kulczycki (2010) described that maximum biological yield was observed when sulphur was applied in two equal splits half at tillering and half at booting. These findings are consistent with those given by Girma et al. (2005), who claimed that application of sulphur could increase the grain yield of wheat. In the same way, the maximum grain yield is pointed out that when sulphur application is applied in two splits and recorded the minimum yield of grain, when sulphur was applied to the crop at tillering stage at the same time Marinaccio et al. (2015) and Ercoli et al. (2012) reported that the S rate division and stem elongation before sowing were the highest in grain yield and plant absorption of S. The results showed that the harvest index value increased with the increase of S concentration. These findings are in line with those reported by (Hammad et al., 2011). Khan et al. (2006) in a similar study stated that the high dose of S will eventually improve the SO₄-S content in the soil. Bharathi and Poongothai (2008) further claimed that the application of sulphur to soil improves the current status of SO₄-S content which is ultimately linked to higher crop growth and yield responses.

Conclusions

It was concluded from the study that the foliar sulphur application improved growth, increased yield and yield components of wheat under semiarid climate of Peshawar, Pakistan. Application of S at the rate of 15 kg ha⁻¹ was found more beneficial in terms of better growth, higher yield and yield components of wheat compared to control (no spray). However, post-harvest soil and plant sulphur concentration was maximum when sulphur was applied at the rate of 21 kg ha⁻¹. Among application timings, foliar application of sulphur at two equal splits (50% each at tillering and booting) was a better time for improving growth, yield and yield components of wheat. Therefore, the application of sulphur at the rate of 15 kg ha⁻¹ is recommended as a foliar spray in two equal splits (50% each at tillering and booting) to maximize not only growth and yield but also the level of sulphur in soil which will ultimately improve wheat production in local semiarid climate.

Acknowledgements Financial support from the National Natural Science Foundation of China (41620104006 and 41571298) is gratefully acknowledged. Authors are highly grateful to the Higher Education Commission of Pakistan and University of Agriculture, Peshawar-KPK-Pakistan.

REFERENCES

- [1] Ali, A., Arshadullah, M., Hyder, S. I., Mahmood, I. A. (2012): Effect of different levels of sulfur on the productivity of wheat in a saline sodic soil. – *Soil & Environment* 31(1).
- [2] Amanullah, K. R., Khalil, S. K. (2009): Effects of plant density and N on phenology and yield of maize. – *J Plant Nutr* 32: 246-260.
- [3] Aziz, M. Z., Yaseen, M., Abbas, T., Naveed, M., Mustafa, A., Hamid, Y., Saeed, Q., Xu, M. (2018): Foliar application of micronutrients enhances crop stand, yield and the biofortification essential for human health of different wheat cultivars. – *Journal of Integrative Agriculture* 18(6): 1369-1378.
- [4] Bharathi, C., Poongothai, S. (2008): Direct and residual effect of sulphur on growth, nutrient uptake, yield and its use efficiency in maize and subsequent green gram. – *Research Journal of Agriculture and Biological Sciences* 4(5): 368-72.
- [5] Chandio, A. A., Yuansheng, J., Magsi, H. (2016): Agricultural sub-sectors performance: an analysis of sector-wise share in agriculture GDP of Pakistan. – *International Journal of Economics and Finance* 8(2): 156-162.
- [6] Clark, C. M., Tilman, D. (2008): Loss of plant species after chronic low-level nitrogen deposition to prairie grasslands. – *Nature* 451(7179): 712.
- [7] Davidson, E. A. (2009): The contribution of manure and fertilizer nitrogen to atmospheric nitrous oxide since 1860. – *Nat. Geosci.* 2: 659-662.
- [8] Diaz, R. J., Rosenberg, R. (2008): Spreading dead zones and consequences for marine ecosystems. – *Science* 321(5891): 926-929.
- [9] Ercoli, L., Lulli, L., Arduini, I., Mariotti, M., Masoni, A. (2011): Durum wheat grain yield and quality as affected by S rate under Mediterranean conditions. – *European Journal of Agronomy* 35(2): 63-70.
- [10] Fageria, N. K., Moreira, A. (2011): The role of mineral nutrition on root growth of crop plants. – *Advances in Agronomy* 110: 251-331.
- [11] Garrido-Lestache, E., López-Bellido, R. J., López-Bellido, L. (2004): Effect of N rate, timing and splitting and N type on bread-making quality in hard red spring wheat under rainfed Mediterranean conditions. – *Field Crops Research* 85(2-3): 213-236.
- [12] Gee, G. W., Bauder, J. W. (1979): Particle size analysis by hydrometer: a simplified method for routine textural analysis and a sensitivity test of measurement parameters. – *Soil Sci Soc Am J* 43: 1004-1007
- [13] Girma, K., Mosali, J., Freeman, K. W., Raun, W. R., Martin, K. L., Thomason, W. E. (2005): Forage and grain yield response to applied sulfur in winter wheat as influenced by source and rate. – *Journal of Plant Nutrition* 28(9): 1541-1553.
- [14] Government of Pakistan (GOP) (2015): Economic Survey of Pakistan. – Ministry of Food, Agriculture and Livestock, Federal Bureau of Statistics 2014-15.
- [15] Guo, J. H., Liu, X. J., Zhang, Y., Shen, J. L., Han, W. X., Zhang, W. F., Christie, P., Goulding, K. W. T., Vitousek, P. M., Zhang, F. S. (2010): Significant acidification in major Chinese croplands. – *Science* 327(5968): 1008-1010.
- [16] Győri, Z. (2005): Sulphur content of winter wheat grain in long term field experiments. – *Communications in Soil Science and Plant Analysis* 36(1-3): 373-382.
- [17] Hammad, H. M., Ahmad, A., Khaliq, T., Farhad, W., Mubeen, M. (2011): Optimizing rate of nitrogen application for higher yield and quality in maize under semiarid environment. – *Crop Environ* 2(1): 38-41.

- [18] Hussain, Z., Leitch, M. H. (2005): The effect of applied sulphur on the growth, grain yield and control of powdery mildew in spring wheat. – *Annals of Applied Biology* 147(1): 49-56.
- [19] Iqbal, A., Hidayat, Z. (2016): Potassium management for improving growth and grain yield of maize (*Zea mays* L.) under moisture stress condition. – *Scientific Reports* 6: 34627.
- [20] Kakar, K. M., Saleem, M., Iqbal, A. (2015): Effect of irrigation levels and planting methods on phenology, growth, biomass and harvest index of spring wheat under semiarid condition. – *Pure and Applied Biology* 4(3): 375.
- [21] Khaliq, T., Ahmad, A., Hussain, A., Ranjha, A. M., Ali, M. A. (2008): Impact of nitrogen rates on growth, yield, and radiation use efficiency of maize under varying environments. – *Pak. J. Agri. Sci* 45(3): 1-7.
- [22] Khaliq, T., Ahmad, A., Hussain, A., Ali, M. A. (2009): Maize hybrids response to nitrogen rates at multiple locations in semiarid environment. – *Pak. J. Bot* 41(1): 207-224.
- [23] Khan, M. J., Hafeez, M. K., Khattak, R. A., Jan, M. T. (2006): Response of maize to different levels of sulfur. – *Commun. Soil Sci. Plant Anal.* 37(1): 41-51.
- [24] Kulczycki, G. (2010): The Effect of Soil and Foliar Sulphur Application on Winter Wheat Yield and Soil Properties. – *Wroclaw University of Environmental and Life Sciences, Wroclaw.*
- [25] MacRitchie, F., Gupta, R. B. (1993): Functionality-composition relationships of wheat flour as a result of variation in sulfur availability. – *Australian Journal of Agricultural Research* 44(8): 1767-1774.
- [26] Mahmood, T. (1994): Impact of water and nutrient management on growth, yield and quality of maize (*Zea mays* L.) – *Doctoral dissertation, University of Agriculture Faisalabad Pakistan.*
- [27] Malik, M. A., Irfan, M., Ahmed, Z. I., Zahoor, F. (2006): Residual effect of summer grain legumes on yield and yield components of wheat (*Triticum aestivum* L.). – *Pakistan Journal of Agriculture, Agricultural Engineering and Veterinary Sciences* 22(1): 9-11.
- [28] Marinaccio, F., Reyneri, A., Blandino, M. (2015): Enhancing grain yield and quality of winter barley through agronomic strategies to prolong canopy greenness. – *Field Crops Research* 170: 109-118.
- [29] Mengal, S. H., Kirkby, D. S. (1987): The role of sulphur to assess crop productivity. – *J. Agric. Biol.* 773-789(7): 137-190.
- [30] Mustafa, A., Naveed, M., Saeed, Q., Ashraf, M. N., Hussain, A., Abbas, T., Kamran, M., Sun, N., Xu, M. (2019a): Application Potentials of Plant Growth Promoting Rhizobacteria and Fungi as an Alternative to Conventional Weed Control Methods. – *InTechOpen, London.*
- [31] Mustafa, A., Naveed, M., Abbas, T., Saeed, Q. (2019b): Growth response of wheat and associated weeds to plant antagonistic rhizobacteria and fungi. – *Italian Journal of Agronomy* 14(4): 191-198.
- [32] Nawaz, A. (1989): Effect of time and method of fertilizer application on the growth and yield potential of maize. – *M.Sc. Thesis, Univ. Agric. Faisalabad.*
- [33] Pasha, A., Chittapur, B. M., Patil, B. N., Hiremath, S. M. (2010): Effect of prolonged nitrogen application and sulphur nutrition on grain quality and nutrient uptake of wheat and soil available nutrient dynamics. – *Karnataka Journal of Agricultural Sciences* 20(2).
- [34] Pathak, H., Wasmann, C. R., Ladha, J. K. (2006): Stimulation of nitrogen balances in rice-wheat system of the Indo-Gangetic Plains. – *Soil Sci. Soc. Agric. J.* 70: 1612-1622.
- [35] Ramos, J. M., Garcia Del Moral, L. F., Molina-Cano, J. L., Salamanca, P., De-Togores, F. R. (2008): Effects of an early application of sulphur or Ethepon as foliar spray on the growth and yield of spring barley in a Mediterranean environment. – *J. Agron. Crop Sci.* 163(2): 129-137.

- [36] Rasheed, M., Mahmood, T., Nazir, M. S. (2003): Response of hybrid maize to different planting methods and nutrient management. – Pakistan Journal of Agricultural Sciences 40(1-2): 39-42.
- [37] Rashid, A. 1986. Mapping zinc fertility of soils using indicator plants and soil analyses. – Doctoral dissertation, University of Hawaii, Manoa.
- [38] Rayan, J., Garabet, S., Rashid, A., El-Gharous, M. (2001): Soil test celebration workshop in West Asia - North Africa. – Proc. 3rd Regional Workshop. Amman, Jordan, Sept. 3-9 1988, ICARDA, Aleppo, Syria.
- [39] Richard, L. A. (1954): Diagnostic and Improvement of Saline and Alkali Soils. – Agric. Handbook 60, USDA, Washington, DC.
- [40] Ryant, P., Hrivna, L. (2004): The effect of sulphur fertilization on yield and technological parameters of spring wheat grain. – Annales Universitatis Mariae Curie-Sklodowska Sectio E Agricultura 59(4): 1669-1678.
- [41] Saeed, B., Gul, H., Khan, A. Z., Parveen, L. (2012): Growth factors and straw yield of wheat cultivars in relation with nitrogen and sulfur fertilization. – APRN Journal of Agricultural and Biological Science 7(1).
- [42] Saeed, B., Khan, A. Z., Khalil, S. K., Rahman, H. U., Ullah, F., Gul, H., Akbar, H. (2013): Response of soil and foliar applied nitrogen and sulfur towards yield and yield attributes of wheat cultivars. – Pak. J. Bot 45(2): 435-442.
- [43] Simard, R. (1993): Ammonium Acetate-Extractable Elements. – In: Carter, M. R. (ed.) Soil Sampling and Methods of Analysis. Lewis Publisher, Boca Raton, pp. 39-42.
- [44] Singh, B. R. (2003): Sulfur and Crop Quality—Agronomical Strategies for Crop Improvement. – COST Action 829 Meetings, Braunschweig, Germany, May 15-18, 2003, pp. 15-18.
- [45] Soltanpour, P. N. (1985): Use of ammonium bicarbonate DTPA soil test to evaluate elemental availability and toxicity. – Communications in Soil Science and Plant Analysis 16(3): 323-338.
- [46] Steel, R. G., Torrie, J. H. (1980): Principles and Procedures of Statistics. A Biometrical Approach. 2nd Ed. – McGraw-Hill Kogakusha, Tokyo.
- [47] Steinfurth, D., Zörb, C., Braukmann, F., Mühling, K. H. (2012): Time-dependent distribution of sulphur, sulphate and glutathione in wheat tissues and grain as affected by three sulphur fertilization levels and late S fertilization. – Journal of Plant Physiology 169(1): 72-77.
- [48] Tandon, H. L. S. (1984): Sulphur Research and Agricultural Production in India. Technical Report. – Fertiliser Development and Consultation Organisation, New Delhi.
- [49] Tilman, D., Balzer, C., Hill, J., Befort, B. L. (2011): Global food demand and the sustainable intensification of agriculture. – Proceedings of the National Academy of Sciences 108(50): 20260-20264.
- [50] Tisdale, S. L., Nelson, W. L., Beaton, J. D. (1985): Soil Fertility and Fertilizers. – Macmillan, New York, pp. 75-79.
- [51] Togay, Y., Togay, N., Cig, F., Erman, M., Celen, A. E. (2008): The effect of sulphur applications on nutrient composition, yield and some yield components of barley (*Hordeum vulgare* L.). – African Journal of Biotechnology 7(18).
- [52] Watanabe, F. S., Olsen, S. R. (1965): Test of an ascorbic acid method for determining phosphorus in water and NaHCO₃ extracts from soil. – Soil Sci Soc Am J 291: 677-678.
- [53] Zhao, F. J., Hawkesford, M. J., McGrath, S. P. (1999): Sulphur assimilation and effects on yield and quality of wheat. – Journal of Cereal Science 30(1): 1-17.

EFFECTS OF HYDROPHILIC POLYMER ON THE SURVIVAL, GROWTH, AND FLOWERING CHARACTERISTICS OF PINEAPPLE SAGE (*SALVIA ELEGANS*) IN UNIRRIGATED GREEN ROOFS

JU, J. H.¹ – XU, H.² – YEUM, K. J.³ – YOON, Y. H.^{1*}

¹Department of Green Convergence Technology, Konkuk University, 268 Chungwondaero, Chungju, Chungcheongbuk-do 27478, South Korea

²College of Landscape Architecture, Central South University of Forestry and Technology, No. 498 Shaoshannanlu, Changsha 410004, China

³Division of Food Bioscience, College of Biomedical and Health Science, Konkuk University, 268 Chungwondaero, Chungju, Chungcheongbuk-do 27478, South Korea

*Corresponding author

e-mail: yonghan7204@kku.ac.kr; phone: +82-43-840-3538; fax: +82-43-851-4169

(Received 2nd Oct 2019; accepted 19th Mar 2020)

Abstract. This study aimed to determine the effects of different amounts of hydrophilic polymer, in three green roof substrates, on the growth of *Salvia elegans*. Coir dust and perlite were mixed in ratios of 80% to 20% (C₄P₁), 50% to 50% (C₁P₁), and 20 to 80% (C₁P₄) at a substrate depth of 20 cm. Hydrophilic polymer were added to three substrates in the amounts of 0, 0.25, 0.5, 1.0, and 2.0 kg·m⁻³. The survival rate and visual quality of *Salvia elegans* were positively associated with hydrophilic polymer content in the three substrates. Although the growth of *Salvia elegans* was the greatest under the C₄P₁ substrate when measured in June (dry season), the greatest growth under the C₁P₄ substrate was in August (rainy season). Therefore, C₄P₁ and C₁P₁ substrates with high coir dust materials is not recommended for *Salvia elegans* because the plants showed low growth and chlorophyll contents in the rainy season and poor flowering with these substrates. Thus, perlite-based C₁P₄ amended with hydrophilic polymer at a level of > 1.0 kg·m⁻³ should be considered for the optimal substrate for *Salvia elegans* during droughts as well as rainy seasons on green roofs.

Keywords: hydrogels, ornamental herb, rainwater retention, inorganic amendment, urban agriculture

Introduction

Green roofs, also known as vegetated roofs, planted roofs, eco roofs, living roofs, or roof gardens, are roofs that are partially or completely covered with vegetation and substrate (Castleton et al., 2010). Because they provide environmental benefits, and open-air amenities without additional land acquisition costs, green roofs have become popular in many cities around the world (Getter et al., 2009). However, environmental conditions on rooftops are often extreme including high temperatures, strong winds, and long-term drought. An extensive green roof with a thin layer of substrate easily result in water deficit conditions (Young et al., 2017). Thus, extensive green roofs almost exclusively use vegetation such as herbs, grasses, mosses, and drought-tolerant succulents including sedum (Getter and Row, 2006). The composition and characteristics of green roof vegetation depends on many factors, growing substrate in particular (Krawczyk et al., 2017). To a large extent, substrate depth dictates vegetation diversity and the range of possible species (Oberndorfer et al., 2007). If growth media depth is limited and there is no additional irrigation, rainfall can restrict the use of

certain species. Even though various organic components are effective in sustaining vegetation and increasing water retention (Xue and Farrell, 2020), high rates of organic matter (> 20%) can be problematic on green roofs due to rapid decomposition. It can lead to compaction, which reduces substrate depth, air supply for roots and water infiltration and retention (Handreck and Black, 2010) resulting in temporarily increased nutrient loads in stormwater runoff (Berndtsson, 2010). Therefore, to increase the use of green roofs, the utilization of inorganic amendments which can retain rainwater must be explored.

Hydrophilic polymers, also described as hydrogels or super absorbent polymers, are cross-linked crystalline forms of insoluble polyacrylamide gel that can keep water several hundred times heavier than that of theirs. The stored water in the hydrophilic polymers can be released to meet the needs of the plants. Therefore, they have been widely used to improve soil moisture in agriculture, horticulture, and forestry (Farrell et al., 2013). Many studies have demonstrated the effects of hydrophilic polymer amendment on plant growth. Barley (*Hordeum vulgare* L.), wheat (*Triticum aestivum* L.), and chickpea (*Cicer arietinum* L.) found that hydrogels delayed wilting time, improved soil water availability, and increased plant establishment (Akhter et al., 2004). Hydrogel amendment prolonged the survival of *Picea abies*, *Pinus sylvestris*, and *Fagus sylvatica* seedlings and improved their biomass under water stress (Orikiriza et al., 2013). Also, hydrogel amendment increased the survival of trees and reduced their evapotranspiration rates, *Araucaria cunninghamii*, and *Maesopsis eminii* (Hüttermann et al., 2009). Water retention gel and coarser particle size substrates can significantly improve the drought tolerance of green roof plants (Young et al., 2017). However, some studies have suggested that the volume of hydrophilic polymers has no effect on net photosynthesis, stomatal conductance, plant growth, or biomass. Meanwhile, Water retention gel and large brick substrates increased both *Festuca ovina* and *Linaria vulgaris*'s drought tolerance while a Sedum living mulch had no effect (Apostol et al., 2009), there is need to examine various substrate compositions and characteristics as a valuable component of green roofs substrates, including hydrophilic polymer.

The genus *Salvia* is the largest genus in the Lamiaceae family, and contains more than 900 species worldwide (González-Cortazar et al., 2013). Because of its brilliant red flowers and pineapple-scented leaves, *Salvia elegans* is widely used in landscaping to attract butterflies and hummingbirds (Cuevas et al., 2018). This species need regular watering because of its sensitivity to drought and perish in deep frost (Silva et al., 2018). To the best of our knowledge, no studies have assessed the use of *Salvia elegans* on green roofs due to its sensitivity to drought. Therefore, the objectives of this study were to determine the effects of different amounts of hydrophilic polymer depending on three types of substrate on the growth of *Salvia elegans* on unirrigated agricultural green roofs.

Materials and methods

Site description and experimental set up

This experiment had a factorial design with three different substrates and five hydrophilic polymer treatments used. There were three replicates for each treatment and each replicate consisted of three plants. Although *Salvia elegans* is native to Mexico and grows in temperate climates (González-Cortazar et al., 2013), it can be frozen at a

temperature lower than -5°C (Park, 2007). Therefore, it is grown as an annual plant, which blooms until the first frost date in South Korea. For this reason, experimental period has been limited from May to November.

A total of 45 square plots ($50\text{ cm [L]} \times 50\text{ cm [W]} \times 25\text{ cm [H]}$) were installed on a roof platform. From top to bottom, each square plot consisted of the following four layers: vegetation, substrate, geotextile filter, and drainage layer (Xu et al., 2014). A geotextile filter (0.8 mm thick) with good air and water permeability was used to prevent the loss of substrate particles. Drainage layer was used to support the three layers above, restrict root growths, increase insulation, and retain excess water (Papafotiou et al., 2013).

All these plots were placed on the rooftop of Konkuk University, Chungju, South Korea located at latitude $35^{\circ}49'\text{N}$ and longitude $127^{\circ}08'\text{E}$ (Fig. 1). Monthly precipitation was 24.6, 88.2, 110.6, 277.7, 122.7, 153.8, and 23.5 mm in May, June, July, August, September, October, and November, respectively (Xu et al., 2014). These results showed reduced rainfall in June resulted in a severe drought period, while frequent rainfall was observed during the summer rainy season in August on the rooftop.

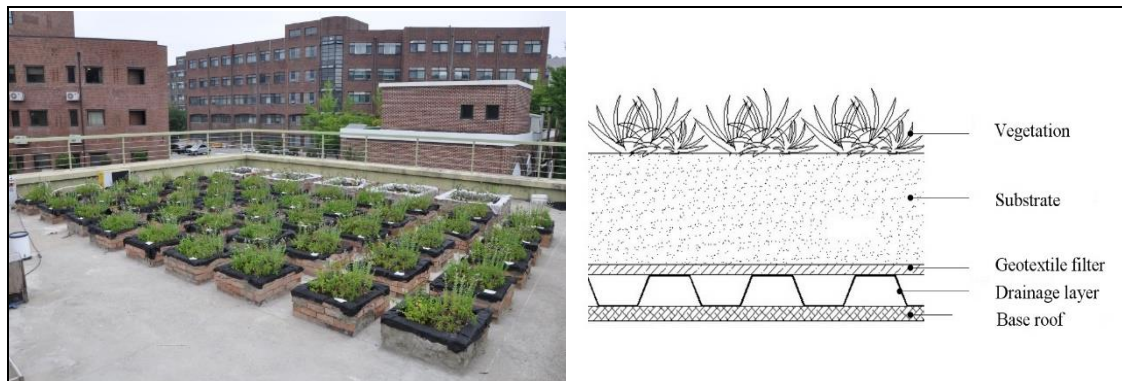


Figure 1. Field experimental study site (left) and sketch of cross section of the green roof (right)

Experimental design and data analysis

Seedlings of *Salvia elegans* were obtained from a commercial nursery. Three seedlings of *Salvia elegans* that had consistent plant height of 8 cm were transplanted into each green roof container on 14 May 2014. All plants were watered every 2 days in the first week after transplanting for seedling establishment, followed by no watering. In consideration of green roof substrate generally contains about 10-20% organic and 80-90% inorganic components (Rowe, 2011), experimental substrates were formulated with 20%, 50%, or 80% (by volume) coir dust (Fibrosoil, Jayampathi Lanka Exports (Pvt) Ltd., Sri Lanka) and 80%, 50%, or 20% (by volume) perlite (Pearl shine No.2, GFC. Co., Ltd., Korea). Coir dust and perlite were mixed in ratios of 80% to 20% (C_4P_1), 50% to 50% (C_1P_1), and 20 to 80% (C_1P_4), respectively. Hydrophilic polymer (acrylic acid-sodium acrylate copolymer > 94%) powders (K-SAM, Kolon Chemical Co., Ltd., Korea) were incorporated into substrates at densities of 0 (Control), 0.25, 0.5, 1.0, or $2.0\text{ kg}\cdot\text{m}^{-3}$ (polymer:medium [w/v], dry weight basis), with three replicates per treatment. Organic fertilizers (saudust:manure (v/v) = 70:30%, TouJjang, DooHo LandTech., Korea) were added to substrates at 5% of the total volume to ensure that the

same quantity was applied to each substrate for healthy plant growth. The depth of all substrates was 20 cm.

Survival rate was calculated by comparing the number of surviving plants versus the number of total plants in each treatment using the following formula. Plants with no green leaves, no new buds were considered to be dead (Pengzhen et al., 2019).

$$\text{Survival rate} = (\text{surviving plants} / \text{total plants}) \times 100 (\%) \quad (\text{Eq.1})$$

The growth parameters observed were plant height, leaf number, leaf length, leaf width of all the plants ($n = 9$) in June and August, respectively. Plant height (H) above the stem base, width at the widest vegetative point of the plant passing through the center (W1), and greatest width perpendicular to W1 (W2) were measured in June and August during the peak growth period. Height and width measurements were used to calculate the growth index (GI).

$$\text{Growth index (GI)} = [(W1 + W2)/2 + H]/2 \quad (\text{Eq.2})$$

The relative appearance of the plant was evaluated according to visual quality, which was categorized into five grades: grade 1, severely stressed and completely dried out; grade 2, stressed with less than 50% of the leaves retaining green pigmentation; grade 3, mildly stressed with 50% of the leaves retaining green pigmentation; grade 4, minor stress with over 50% of the leaves appearing healthy; and grade 5, unstressed with all leaves appearing healthy (Nagase and Dunnett, 2010). The chlorophyll content of the leaves was measured for 9 leaves per container using a SPAD-502 meter (Minolta Camera Co., Ltd, Osaka, Japan). The total number of flowers per plant was monitored from September to November during the blooming season.

Data were subjected to analysis of variance (ANOVA) with SAS 9.1 software package (SAS version 9.1, SAS Institute, Cary, NC). Post hoc analysis was conducted using Tukey's post-hoc test. Statistical significance was considered when p value was less than 0.05.

Results

Compared to C₄P₁ substrate, the survival rate of *Salvia elegans* was reduced to 89% and 78% in the C₁P₁ and C₁P₄ substrates, respectively, under the Control treatment in June. There were no obvious differences in plant survival rate among the three different substrate and five hydrophilic polymer treatments in August. The plant height, leaf number, and growth index of *Salvia elegans* were significantly higher in the C₄P₁ and C₁P₁ substrates than the C₁P₄ substrate in June. There were significant interactions between substrate and hydrophilic polymer, despite leaf length and leaf width (Table 1). This might have occurred because the higher coir dust-based C₄P₁ substrate and hydrophilic polymer increased the water-holding capacity available for plant growth in June, when there was less rainfall, resulting in better growth. However, the higher hydrophilic polymer treatments had little significant effect on growth of *Salvia elegans* in C₄P₁ substrate, while a higher hydrophilic polymer level (e.g., 2.0 kg·m⁻³) produced greater growth index of *Salvia elegans* under C₁P₁ or C₁P₄ substrate in August (Table 2).

Table 1. Survival rate and plant parameters (plant height, leaf number, leaf length, leaf width, and growth index) of *Salvia elegans* grown in three green roof substrates during the drought period (June)

Substrate	Polymer rate (kg·m ⁻³)	Survival rate (%)	Plant height (cm)	No. of leaves (per plant)	Leaf length (mm)	Leaf width (mm)	Growth index
C ₄ P ₁ ^y	Control ^x	100 a	17.7 a ^z	73.7 ab	55.7 b	26.0 b	17.1 a
	0.25	100 a	16.6 a	66.1 b	54.2 b	25.6 b	16.6 a
	0.50	100 a	17.6 a	86.2 a	58.0 ab	25.0 b	17.2 a
	1.00	100 a	17.2 a	82.1 a	61.6 a	27.6 a	16.9 a
	2.00	100 a	15.5 a	76.7 ab	55.4 b	25.7 b	15.9 a
C ₁ P ₁	Control	89 a	17.4 a	61.1 b	59.0 a	23.1 a	16.2 a
	0.25	100 a	15.2 a	58.2 b	53.9 a	24.5 a	14.8 a
	0.50	100 a	15.1 a	69.5 ab	54.6 a	23.0 a	15.8 a
	1.00	100 a	16.0 a	67.8 ab	59.2 a	24.4 a	15.7 a
	2.00	89 a	15.9 a	73.8 a	61.5 a	26.3 a	15.5 a
C ₁ P ₄	Control	78 a	14.5 a	73.2 a	50.3 b	20.8 b	14.5 ab
	0.25	100 a	14.1 a	70.7 a	49.6 b	25.2 ab	14.0 bc
	0.50	100 a	13.8 a	66.6 a	48.4 b	21.7 ab	13.4 b
	1.00	100 a	13.4 a	68.7 a	54.2 ab	21.4 ab	13.8 bc
	2.00	100 a	15.0 a	73.0 a	57.4 a	24.9 a	15.4 a
Significance	Substrate	NS	***	***	**	**	***
	Polymer rate	NS	NS	*	*	NS	**
	Interaction	NS	NS	*	NS	NS	***

^z Means followed by the same letters in columns are not significantly different according to Turkey's post hoc test at $p \leq 0.05$ level (n = 9). ***, **, *: $p < 0.001$, $p < 0.01$, $p < 0.05$, respectively. NS: not significant. ^y Substrate: C₄P₁: coir 80%, perlite 20%; C₁P₁: coir 50%, perlite 50%; C₁P₄: coir 20%, perlite 80% (% by volume). ^x Hydrophilic polymer rate: 0 (referred as to Control), 0.25, 0.5, 1.0, and 2.0 kg·m⁻³ [polymer: medium (w/v), dry weight basis]

Table 2. Survival rate and plant parameters (plant height, leaf number, leaf length, leaf width, and growth index) of *Salvia elegans* grown in three green roof substrates during the rainy period (August)

Substrate	Polymer rate (kg·m ⁻³)	Survival rate (%)	Plant height (cm)	No. of leaves (per plant)	Leaf length (mm)	Leaf width (mm)	Growth index
C ₄ P ₁ ^y	Control ^x	100 a	30.1 a ^z	76.9 ab	69.6 a	28.3 a	27.1 a
	0.25	100 a	27.0 a	75.0 ab	67.8 a	27.4 a	25.6 ab
	0.50	100 a	30.3 a	94.1 a	72.0 a	29.4 a	27.4 a
	1.00	100 a	28.7 a	92.9 a	71.4 a	28.4 a	26.7 a
	2.00	100 a	25.6 a	25.6 a	65.3 b	62.6 a	26.0 a
C ₁ P ₁	Control	89 a	26.8 a	65.2 c	65.7 a	27.0 a	24.1 a
	0.25	100 a	25.2 a	57.8 c	64.0 a	25.2 a	23.2 a
	0.50	100 a	24.5 a	91.0 ac	69.5 a	27.7 a	24.7 a
	1.00	100 a	27.7 a	92.2 a	73.2 a	31.0 a	26.0 a
	2.00	89 a	27.2 a	69.8 bc	74.2 a	29.7 a	24.9 a
C ₁ P ₄	Control	89 a	28.2 a	93.9 a	67.5 b	27.9 b	26.9 ab
	0.25	100 a	27.8 a	103.1 a	71.0 b	29.0 ab	26.2 ab
	0.50	100 a	26.5 a	84.1 a	72.8 ab	30.1 ab	25.5 b
	1.00	89 a	26.7 a	89.2 a	73.3 ab	30.0 ab	27.1 ab
	2.00	100 a	28.6 a	99.2 a	78.9 a	31.3 a	28.4 a
Significance	Substrate	NS	*	**	NS	NS	***
	Polymer rate	NS	NS	NS	NS	NS	NS
	Interaction	NS	NS	NS	NS	NS	*

^z Means followed by the same letters in columns are not significantly different according to Turkey's post hoc test at $p \leq 0.05$ level (n = 9). ***, **, *: $p < 0.001$, $p < 0.01$, $p < 0.05$, respectively. NS: not significant. ^y Substrate: C₄P₁: coir 80%, perlite 20%; C₁P₁: coir 50%, perlite 50%; C₁P₄: coir 20%, perlite 80% (% by volume). ^x Hydrophilic polymer rate: 0 (referred as to Control), 0.25, 0.5, 1.0, and 2.0 kg·m⁻³ [polymer: medium (w/v), dry weight basis]

In C₄P₁ and C₁P₁ substrates with 2.0 kg·m⁻³ of hydrophilic polymer, visual quality was at least 1.7-fold greater than in C₁P₄ substrates. Higher visual quality of *Salvia elegans* was associated with higher hydrophilic polymer content in the three substrates under drought stress in June, especially under the condition of 2.0 kg·m⁻³. This finding highlights the effectiveness of hydrophilic polymer as a soil conditioner that can hold water in substrates during dry periods. However, in August, the hydrophilic polymer treatment caused decreased gradually under the C₄P₁ and C₁P₁, but not in C₁P₄ substrates.

Chlorophyll contents were lower in the C₄P₁ substrate compared with other treatments, and the addition of hydrophilic polymer tended to decrease chlorophyll contents in June. There was no significant interaction observed between substrate and hydrophilic polymer rate on chlorophyll contents, while significantly higher chlorophyll contents in substrates C₁P₄ and C₁P₁ than in the C₄P₁ substrate. Overall, chlorophyll contents reduction was present in all treatments in August compared to June, which might have occurred because *Salvia elegans* experienced waterlogging in the high water content substrate (Table 3).

Table 3. Visual quality and chlorophyll contents of *Salvia elegans* grown in different green roof substrates during the drought and the rainy periods

Substrate	Polymer rate (kg·m ⁻³)	June		August	
		Visual quality (5 grade)	Chlorophyll contents (SPAD value)	Visual quality (5 grade)	Chlorophyll contents (SPAD value)
C ₄ P ₁ ^y	Control ^x	1.2 b ^x	30.02 ab	4.6 a	21.49 ab
	0.25	1.2 b	28.47 ab	4.6 a	21.90 ab
	0.50	1.7 b	31.13 ab	4.6 a	20.30 b
	1.00	1.7 b	31.83 a	4.4 ab	22.99 a
	2.00	3.4 a	27.94 b	4.0 a	23.42 a
C ₁ P ₁	Control	1.0 b	38.26 a	4.4 a	23.48 b
	0.25	1.0 b	33.39 ab	4.3 a	24.43 ab
	0.50	1.0 b	37.04 ab	4.1 a	25.48 ab
	1.00	1.6 b	36.49 ab	3.9 a	25.66 a
	2.00	2.9 a	31.72 b	4.0 a	26.18 a
C ₁ P ₄	Control	1.0 b	35.84 a	4.1 b	25.54 a
	0.25	1.0 b	36.41 a	4.9 a	23.66 a
	0.50	1.0 b	34.33 a	4.6 a	24.12 a
	1.00	1.0 b	35.96 a	5.0 a	23.80 a
	2.00	1.4 a	34.40 a	5.0 a	24.76 a
Significance	Substrate	***	***	***	***
	Polymer rate	***	*	NS	*
	Interaction	***	NS	*	*

^z Means followed by the same letters in columns are not significantly different according to Turkey's post hoc test at $p \leq 0.05$ level (n = 9). ***, **, *: $p < 0.001$, $p < 0.01$, $p < 0.05$, respectively.

NS: not significant. ^y Substrate: C₄P₁: coir 80%, perlite 20%; C₁P₁: coir 50%, perlite 50%; C₁P₄: coir 20%, perlite 80% (% by volume). ^x Hydrophilic polymer rate: 0 (referred as to Control), 0.25, 0.5, 1.0, and 2.0 kg·m⁻³ [polymer: medium (w/v), dry weight basis]

In our study, *Salvia elegans* bloomed from the middle of September through the middle of November, after first frost. The peak blooming period was from early October until the first frost. There was a significant difference in the total number of inflorescences per plant among the three substrates. The mean number of inflorescences

grown in C₁P₄ substrate was 1.78- folder higher than those grown in C₄P₁ and 1.91-fold higher than those grown in C₁P₁ substrate. Hydrophilic polymer increased the total number of inflorescences in C₁P₄ substrate, especially under the 2.0 kg·m⁻³ treatment, compared to the other hydrophilic polymer treatments or the Control treatment (Fig. 2).

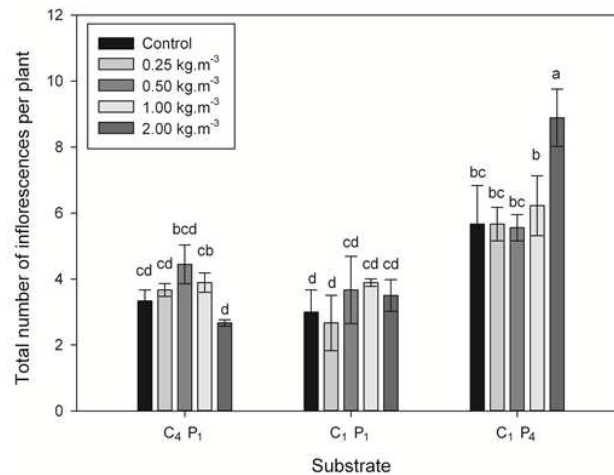


Figure 2. Total number of inflorescences of *Salvia elegans* per plant of the three different green roof substrates [C₄P₁: coir 80%, perlite 20%; C₁P₁: coir 50%, perlite 50%; C₁P₄: coir 20%, perlite 80% (% by vol.)] amended with five contents of hydrophilic polymer, including 0 (referred as Control), 0.25, 0.5, 1.0, and 2.0 kg·m⁻³ [polymer: medium (w/v), dry weight basis]. Different letters indicate significant differences by Turkey's post hoc test at $p \leq 0.05$ level. Data represent mean \pm SE ($n = 9$)

Discussion

Higher survival of *Salvia elegans* was associated with higher hydrophilic polymer content in the three substrates under drought stress. This finding is consistent with other studies, in which the addition of hydrophilic polymer prolonged the survival of seedlings compared to the Control (no hydrophilic polymer) treatment. In addition, hydrophilic polymer can be used to improve the transplant success of seedlings (Thomas, 2008). The addition of hydrogels slowed soil moisture loss and delayed the wilting time of seedlings by 4 to 5 days (Akhter et al., 2004). Greater hydrophilic polymer addition also improved the water-holding properties of substrate and delayed the permanent wilting point (Patil et al., 2011). Therefore, application of hydrophilic polymer is an important remedy for perlite-based substrate, as it assists growth by increasing water retention and availability to plant in dry periods. Meanwhile, frequent rainfall during the summer rainy season in August might have resulted in frequent wetting of the substrates, thus leading to waterlogging and reduced effectiveness of the hydrophilic polymer. For this reason, a further increase in coir dust-based substrate had no or minimal effect on growth of *Salvia elegans* in August, during the rainy season.

The higher hydrophilic polymer was inefficient for plants grown in C₄P₁ and C₁P₁ substrates in the rainy season. These results confirmed that the growth of *Salvia elegans* was affected by the composition of the substrate more than the level of hydrophilic polymer during the drought period. In addition, the substrate amended with a high amount of coir dust might have aided with water holding-capacity, thus maintaining the structural integrity of plants, as coir dust has a high surface area of 4 m²/g (Bilderback

et al., 2005). A previous study found that shoot and root growth of *Gerbera* were greater under coir-based substrate than rockwool (Cho et al., 2006). The growth of highbush blueberry (*Vaccinium* Sp.) under various amounts of substrates for container production and found that total plant dry weight was greater under higher contents of coir substrate (Kingston et al., 2017). However, another study did not recommend high level of coir dust in green roof substrate (Olle et al., 2012), and the substrate containing 10% organic matter was optimal for the growth of four herbaceous plants under dry and wet conditions on green roofs (Nagase and Dunnett, 2011). Increased organic matter, such as coir dust or peat-moss, can result in lush growth that might suffer damage under drought stress or frequent rainfall, resulting in frequent drying and wetting cycles.

The chlorophyll meter is a simple tool to measure the relative chlorophyll content or greenness; thus, it is an efficient indicator of stress in plants (Netto et al., 2005). The change in chlorophyll content of plants under water stress depends on the rate of stress and plant species (Hassanzadeh et al., 2009). In the present study, higher chlorophyll content was associated with low water content of the substrate under severe drought stress in June. This finding can be explained by reductions in relative water content and leaf water potential under mild water stress, which can change the color of the leaf to dark green compared with the color of the plant in a substrate with a higher water content (Marenco et al., 2009).

Salvia species prefers moist, well-drained, fertile loam or sandy loam soils (Silva et al., 2018). Several studies have found that drought reduces inflorescence numbers (Razmjoo et al., 2008; Beya-Marshall et al., 2018). Hydrophilic polymer supplementation increased substrate water content, and thereby prevented drought in perlite-based C₁P₄ substrate, while the intensity of rainfall in August might have caused waterlogging in C₄P₁ and C₁P₁ substrates, reducing the number of inflorescences. Hydrophilic polymer treatments were positively associated with number of inflorescences of *Salvia elegans* in the three substrates. However, C₄P₁ and C₁P₁ substrates with high coir dust matter are not recommended for *Salvia elegans* because the plants showed low growth in the rainy season and poor ornamental quality at peak flower time with these substrates. Therefore, it is feasible to use hydrophilic polymer in inorganic-based substrate to diversify the variety of plants used by increasing substrate water content on green roofs.

Conclusions

The growth of *Salvia elegans* was the greatest using 80% and 20% of coir dust and perlite in June, and 20% and 80% of coir dust and perlite in August after the rainy season. The survival rate and visual quality of *Salvia elegans* were positively associated with hydrophilic polymer content in three different substrates. However, 50-80% coir dust in substrates is not recommended for *Salvia elegans* because the plants showed low growth during the rainy season and poor ornamental quality at peak flower time with these substrates. Overall, 80% perlite-based substrate amended with a hydrophilic polymer level $> 1.0 \text{ kg} \cdot \text{m}^{-3}$ may be considered as the optimal substrate compared to the 50-80% coir dust based substrate in the dry as well as rainy season on green roofs. Therefore, it is feasible to use hydrophilic polymers in perlite-based substrates to increase substrate water content in diverse plants growing on green roofs. Further studies warrant to determine the effects of substrates with higher rates of hydrophilic polymer in various plants on green roof for a long-term.

Acknowledgements. This paper was supported by Konkuk University in 2018.

REFERENCES

- [1] Akhter, J., Mahmood, K., Malik, K. A., Mardan, A., Ahmad, M., Iqbal, M. M. (2004): Effects of hydrogel amendment on water storage of sandy loam and loam soils and seedling growth of barley, wheat and chickpea. – *Plant Soil Environ.* 50: 463-469.
- [2] Apostol, K. G., Jacobs, D. F., Dumroese, R. K. (2009): Root desiccation and drought stress responses of bareroot *Quercus rubra* seedlings treated with a hydrophilic polymer root dip. – *Plant Soil* 315: 229-240.
- [3] Berndtsson, J. C. (2010): Green roof performance towards management of runoff water quantity and quality: a review. – *Ecol. Eng.* 26: 351-360.
- [4] Beya-Marshall, V., Herra, J., Fichet, T., Trentacoste, E. R., Kremer, C. (2018): The effect of water status on productive and flowering variables in young “Arbequina” olive trees under limited irrigation water availability in a semiarid region of Chile. – *Hortic. Environ. Biote.* 59: 815-826.
- [5] Bilderback, T. E., Warren, S. L., Owen, J. S., Albano, J. P. (2005): Healthy substrates need physicals too!. – *HortTechnology* 15: 747-751.
- [6] Castleton, H. F., Stovin, V., Beck, S. B. M., Davison, J. B. (2010): Green roofs; building energy savings and the potential for retrofit. – *Energy Buildings* 42: 1582-1591.
- [7] Cho, M. S., Park, Y. Y., Jun, H. J., Chung, J. B. (2006): Growth of *Gerbera* in mixtures of coir dust and perlite. – *Hortic. Environ. Biotechnol.* 47: 211-216.
- [8] Cuevas, E., Espino, J., Marques, I., Scopece, G. (2018): Reproductive isolation between *Salvia elegans* and *S. fulgens*, two hummingbird-pollinated sympatric sages. – *Plant Biology* 20(6): 1075-1082.
- [9] Farrell, C., Ang, X. Q., Rayner, J. P. (2013): Water-retention additives increase plant available water in green roof substrates. – *Ecol. Eng.* 52: 112-118.
- [10] Getter, K. L., Rowe, D. B. (2006): The role of extensive green roofs in sustainable development. – *HortScience* 41: 1276-1285.
- [11] Getter, K. L., Rowe, D. B., Robertson, G. P., Cregg, B. M., Andresen, J. A. (2009): Carbon sequestration potential of extensive green roofs. – *Environ. Sci. Technol.* 43(19): 7564-7570.
- [12] González-Cortazar, M., Maldonado-Abarca, A. M., Jiménez-Ferrer, E., Marquina, S., Ventura-Zapata, E., Zamilpa, A., Tortoriello, J., Herrera-Ruiz, M. (2013): Isosakuranetin-5-O-rutinoside: A new flavanone with antidepressant activity isolated from *Salvia elegans* Vahl. – *Molecules* 18(11): 13260-13270.
- [13] Handreck, K. M., Black, N. D. (2010): *Growing media for ornamental plants and turf.* – 4th (ed.) University of New South Wales Press, Radwick, NSW.
- [14] Hassanzadeh, M., Ebadi, A., Panahyane, K. M., Eshghi, A. G., Jamaatiesomarin, S. H., Saeidi, M., Zabihie, M. R. (2009): Evaluation of drought stress on relative water content and chlorophyll content of *Sesamum indicum* L. genotypes at early flowering stage. – *Res. J. Environ. Sci.* 3: 345-350.
- [15] Hüttermann, A., Orikiriza, L. J., Agaba, H. (2009): Application of superabsorbent polymers for improving the ecological chemistry of degraded or polluted lands. – *Clean Soil Air Water* 37: 517-526.
- [16] Kingston, P. H., Scagel, C. F., Dryla, D. R., Strik, B. (2017): Suitability of sphagnum moss, coir, and douglas fir bark as soilless substrate for container production of highbush blueberry. – *HortScience* 52: 1692-1699.
- [17] Krawczyk, A., Domagala-Swiatkiewicz, I., Lis-Krzyscin, A., Daraz, M. (2017): Waste silica as a valuable component of extensive green-roof substrates. – *Pol. J. Environ. Stud.* 26(2): 643-653.

- [18] Marengo, R. A., Antenzana, V. S. A., Nascimento, H. C. S. (2009): Relationship between specific leaf area, leaf thickness, leaf water content and SPAD-502 readings in six Amazonian tree species. – *Photosynthetica* 47: 184-190.
- [19] Nagase, A., Dunnett, N. (2010): Drought tolerance in different vegetation types for extensive green roofs: effects of watering and diversity. – *Landscape Urban Plan.* 97: 318-327.
- [20] Nagase, A., Dunnett, N. (2011): The relationship between percentage of organic matter in substrate and plant growth in extensive green roofs. – *Landscape Urban Plan.* 103: 230-236.
- [21] Netto, A. T., Campostrini, E., Oliveira, J. G., Bressan, S. R. E. (2005): Photosynthetic pigments, nitrogen, chlorophyll a fluorescence and SPAD-502 readings in coffee leaves. – *Sci. Hortic.* 104: 199-209.
- [22] Obnerdorfer, E., Lundholm, J., Bass, B., Coffman, R. R., Doshi, H., Dunnett, N., Gaffin, S., Köhler, M., Liu, K. K. Y., Rowe, B. (2007): Green roofs as urban ecosystems: ecological structures, functions, and services. – *Bioscience* 57(10): 823-833.
- [23] Olle, M., Ngouajio, M., Siomos, A. (2012): Vegetable quality and productivity as influenced by growing medium: a review. – *Zemdirbyste* 99: 399-408.
- [24] Orikiriza, L. J. B., Agaba, H., Eilu, G., Kabasa, J. D., Worbes, M., Hüttermann, A. (2013): Effects of hydrogels on tree seedling performance in temperate soils before and after water stress. – *J. Environ. Prot.* 4(7): 713-721.
- [25] Papafotiou, M., Pergialioti, N., Tassoula, L., Massas, I., Kargas, G. (2013): Growth of native aromatic xerophytes in an extensive Mediterranean green roof as affected by substrate type and depth and irrigation frequency. – *HortScience* 48: 1327-1333.
- [26] Park, K. W. (2007): *Herb & Aromatherapy*. – Sunjinmunhwasa, Seoul.
- [27] Patil, S. V., Salunke, B. K., Patil, C. D., Salunkhe, R. B. (2011): Studies on amendment of different biopolymers in sandy loam and their effect on germination, seedling growth of *Gossypium herbaceum* L. – *Appl. Biochem. Biotechnol.* 163: 780-791.
- [28] Pengzhen, D., Stefan, K., Arndt, C. F. (2019): Is plant survival on green roofs related to their drought response, water use or climate of origin? – *Science of the Total Environment* 667: 25-32.
- [29] Razmjoo, K., Heydarizadeh, P., Sabzalian, M. R. (2008): Effect of salinity and drought stresses on growth parameters and essential oil content of *Matricaria chamomile*. – *Int. J. Agric. Biol.* 10: 451-454.
- [30] Rowe, D. B. (2011): Green roofs as a means of pollution abatement. – *Environ. Pollut.* 159: 2100-2110.
- [31] Silva, H., Arrigada, C., Campos-Saez, S., Baginsky, C., Castellaro-Galdames, G., Morales-Salina, L. (2018): Effect of sowing data and water availability on growth of plants of chia (*Salvia hispanica* L.) established in Chile. – *PLoS One* 13(9): e0203116.
- [32] Thomas, D. S. (2008): Hydrogel applied to the root plug of subtropical eucalypt seedlings halves transplant death following planting. – *Forest Ecol. Manage.* 255(3-4): 1305-1314.
- [33] Xu, H., Yoon, Y. H., Choi, E. Y., Kang, H. K., Ju, J. H. (2014): Combination effects of the use of hydrophilic polymer for green roof substrate and rainy season condition on growth and biomass partitioning of *Aster koraiensis*. – *J. Food Agric. Environ.* 12: 1177-1181.
- [34] Xue, M., Farrell, C. (2020): Use of organic wastes to create lightweight green roof substrates with increased plant-available water. – *Urban Forestry & Urban Greening* 48: 126569.
- [35] Young, T. M., Cameron, D. D., Phoenix, G. K. (2017): Increasing green roof plant drought tolerance through substrate modification and the use of water retention gels. – *Urban Water J.* 14: 551-560.

EFFECT OF SELECTED FUNGICIDES ON THE GROWTH OF ACAROPATHOGENIC FUNGI FROM THE GENUS *HIRSUTELLA*

TKACZUK, C.* – MAJCHROWSKA-SAFARYAN, A.

Siedlce University of Natural Science and Humanities
Faculty of Bioengineering and Animal Husbandry, Institute of Agriculture and Horticulture
B. Prusa 14, 08-110 Siedlce, Poland

**Corresponding author*
e-mail: cezary.tkaczuk@uph.edu.pl

(Received 29th Oct 2019; accepted 12th Feb 2020)

Abstract. The aim of the research was to study the impact of selected fungicides on the growth of a fungal colony of mite pathogens belonging to the *Hirsutella* Pat. genus. In a laboratory bioassay effects of five fungicides on the growth of selected strains of acaropathogenic fungi: *H. thompsonii* F.E. Fisher, *H. thompsonii* var. *synnematosus* Samson, C.W. McCoy and O'Donnell, *H. vandergeesti* Bałazy, Mietkiewski et Tkaczuk and *H. danubiensis* Tkaczuk, Bałazy et Wegensteiner were examined. Fungicides used in the research were as follows: sulphur, cyprodinil and fludioxonil, mancozeb, copper oxychloride and azoxystrobin. They were added to sterile SDA media in the recommended field dose as well 10 and 100 times lower doses than the recommended one. The effect of fungicides on the growth of acaropathogenic fungi varied depending on the applied substance and its concentration in the culture medium. Of all fungicides tested the fungal growth was most strongly limited by mancozeb and a mixture of cyprodinil and fludioxonil while sulphur had the weakest effect.

Keywords: mites, mite-pathogenic fungi, pesticides, toxicity, mycelial growth, inhibition

Introduction

Mites are pests commonly found on crops growing both in the field and under cover (Boczek, 1999). So far relatively few pathogens of mites have been identified, but fungi constitute the most numerous group infecting these arthropods (van der Geest et al., 2000). Fungal pathogens are a permanent component of mite natural habitats. For the most part, they represent *Ascomycota* anamorphs, grouped in the *Hirsutella* and *Lecanicillium* W. Gams and Zare genera (van der Geest et al., 2000; Bałazy et al., 2008). *Hirsutella* (Patouillard, 1892) includes over 70 species of asexually-reproducing pathogens of insects, mites, and nematodes that mainly belong to within Ophiocordycipitaceae G.H. Sung, J.M. Sung, Hywel-Jones and Spatafora (Kepler et al., 2013; Quandt et al., 2014), though the genus is usually considered to be associated with the genus *Ophiocordyceps* typified by a sexual morph (Sung et al., 2007). *Hirsutella* infects hosts by using conidia born at the tip of phialides (Lipa, 1971), and infection quickly leads to a death of the hosts (McCoy, 1981).

The greatest impact on the depletion of species composition of acaropathogenic fungi is exerted by human activity, by the intensification of agricultural production and the use of chemical plant protection products in particular. In commercial production systems, the need for chemical pesticides persist, despite many efficient introductions of biological control agents, including entomopathogenic fungi. These compounds, especially fungicides, applied against plant pathogens might also negatively affect the populations of entomopathogenic fungi, and thus reducing a pest regulation potential as a consequence (Mietkiewski et al., 1997; Hummel et al., 2002; Meyling and Eilenberg, 2007).

Research conducted in laboratories shows a negative impact of pesticides, in particular fungicides, on entomopathogenic and acaropathogenic fungi. Those products may restrict their growth, germination, and intensity with which fungi infect potential hosts (Majchrowicz and Poprawski, 1993; Miętkiewski et al., 1996; Andalo et al., 2004; Li et al., 2004; Tkaczuk and Miętkiewski, 2005; Fiedler and Sosnowska, 2007, 2017; Tkaczuk et al., 2012; Celar and Kos, 2016; Perez-González and Sánchez-Pena, 2017).

The task of modern plant protection is to provide effective methods and solutions to combat pests - with the smallest possible pressure on the environment. The biological method based on products containing entomopathogenic fungi is one of the most environment-friendly ones (Lipa, 2000; Sosnowska, 2013). Because of their properties, in integrated plant protection programs acaropathogenic fungi can be used to limit the populations of herbivorous mites.

The aim of the study was to analyse an impact of selected fungicides on the growth of a colony of *Hirsutella* fungi, in laboratory conditions.

Materials and methods

Fungal isolates

The fungal material was obtained from stock collections maintained at the Department of Plant Protection and Breeding, Siedlce University of Natural Sciences and Humanities, Siedlce, Poland. Tests were performed with four fungal species isolated from mites. The characteristics of the fungal isolates are presented in *Table 1*. Prior to treatments, isolates were applied to Petri-plates with Sabouraud dextrose agar (SDA) medium and maintained at $20 \pm 2^\circ\text{C}$ for 7 days in total darkness. The fungi isolated from mites were identified with standard keys (Hodge, 1998). Moreover, molecular studies were conducted to confirm the proper identification of the fungal isolates. The ITS marker was chosen for identification as it has been proposed as universal DNA barcode marker for fungi (Schoch et al., 2012).

Table 1. Characteristics of fungal isolates used in the experiment

Fungal species	Host mite species	Host plant
<i>Hirsutella thompsonii</i> var. <i>synnematos</i>	Pear-leaf blister mite, <i>Eriophyes piri</i> (Pgst.)	European pear, <i>Pyrus communis</i> L.
<i>Hirsutella thompsonii</i>	Two-spotted spider mite, <i>Tetranychus urticae</i> Koch.,	Raspberry, <i>Rubus idaeus</i> L.
<i>Hirsutella vandergeesti</i>	<i>Amblyseius angulatus</i> Karg	Raspberry, <i>Rubus</i> sp.
<i>Hirsutella danubiensis</i>	Raspberry spider mite, <i>Neotetranychus rubi</i> Trag.	Raspberry, <i>Rubus idaeus</i> L.

Preparation of media with fungicides

Five fungicides, that are commonly used to protect fruit crops against fungal diseases, were selected for the testing. Detailed characteristics of the fungicides are shown in *Table 2*. Fungicides were added to sterile SDA medium at about 40-50°C in the following doses:

- A – recommended field dose,
- B – dose 10 times lower than the recommended,
- C – dose 100 times lower than the recommended.

Table 2. Characteristics of fungicides used in the experiment

Brand name	Active ingredient	Recommended dose
Siarkol Extra 80 WP	sulphur - 80%	12.5 g/l
Switch 62,5 WG	cyprodinil - 375 g/l fludioxonil - 250 g/l	1.3 g/l
Dithane Neo Tec 75 WG	mancozeb - 750 g/l	6.0 g/l
Miedzian 50 WP	copper oxychloride - 50%	2.5 g/l
Amistar 250 SC	azoxystrobin - 250 g/l	1.2 ml/l

The media supplemented with fungicides were poured into 9 cm-diameter Petri dishes and inoculated with fungi after 24 hours. After inoculating the media with mycelium fragments, the dishes were incubated in an incubator at $22^{\circ}\text{C} \pm 1\text{C}^{\circ}$. Observation of colonies was carried out by measuring their diameter every 5 days until the 25th day. A fungi culture growing on SDA medium without fungicides was used as control. Every experimental combination was replicated four times. The results were presented as a colony diameter expressed as a percentage in relation to control.

Statistical analysis

The results obtained on the 25th day were statistically processed using two-factor analysis of variance for homogeneous groups ANOVA. To compare means Tukey's test was used, assuming the significance level of $\alpha = 0.05$. All the calculations were performed in STATISTICA®, version 12.0.

Results

The effect of the fungicides on the growth of tested species of acaropathogenic fungi was diverse, and their reaction was dependent on the applied product and its concentration in the culture medium. Of all tested fungicides, the growth of *Hirsutella thompsonii* var. *synnematos*a was the least inhibited by sulphur (Fig. 1).

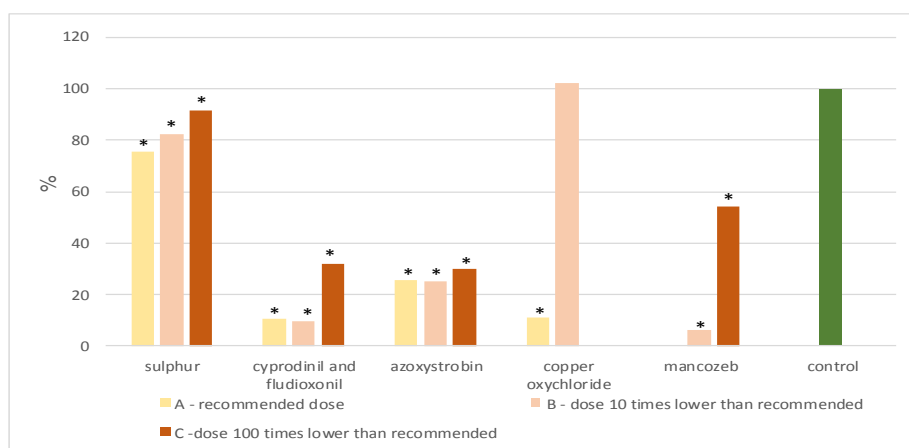


Figure 1. *Hirsutella thompsonii* var. *synnematos*a colony size on media supplemented with investigated fungicides on the 25th day of observation (expressed in % relative to control)
* - significance at the level $\alpha = 0.05$ in relation to the control

After 25 days of cultivation, colonies growing on the medium with A fungicide concentration (recommended), B (10 times lower than the recommended), and C (100 times lower than recommended) constituted 75.6%, 82.2, and 91.4% of the control culture size.

A potent inhibitor of fungal testing colony growth turned out to be azoxystrobin. Cultures growing on the media with this fungicide were smaller, irrespective of the dose, than control colonies by an average of 75%. However, the strongest growth restriction of *H. thompsonii* var. *synnematos*a was caused by mancozeb. This fungicide, when added to the medium in the recommended dose (A), completely inhibited the development of this pathogen. Cultures with B and C concentrations reached 6.2% and 54% of the control colony size, respectively.

By analyzing the growth of *Hirsutella thompsonii*, it turned out that azoxystrobin had the strongest toxic effect and when applied in all doses it completely stopped the growth of the fungus (Fig. 2). Fungicides Switch 62.5 WG with cyprodinil and fludioxonil and Dithane Neo Tec 75 with mancozeb as their active substance applied in the recommended dose (A) and 10 times less than recommended (B) completely inhibited the growth of the isolate too. Of all tested fungicides sulphur was the least effective in hindering the growth of *H. thompsonii* culture, and this growth limitation was statistically significant in relation to control.

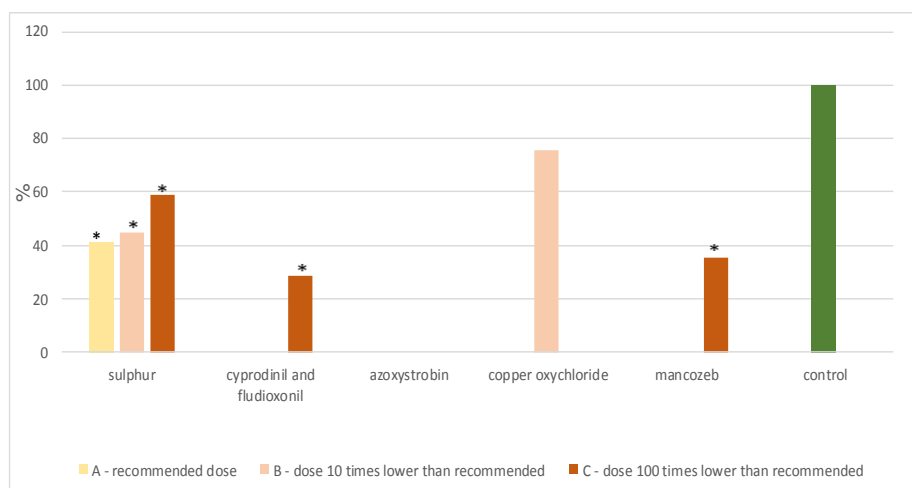


Figure 2. *Hirsutella thompsonii* colony size on media supplemented with investigated fungicides on the 25th day of observation (expressed in % relative to control)

* - significance at the level $\alpha = 0.05$ in relation to the control

The fungicides tested in this research significantly restricted the development of the colony of the *H. vandergeesti* fungal isolate (Fig. 3), with cyprodinil and fludioxonil having the most adverse effect on pathogen development. The fungicide with A (recommended) and B (10 times lower than the recommended) concentrations, completely prevented colony development. However, the culture of *H. vandergeesti* showed relatively high tolerance to sulphur. Colonies growing on media that contained the fungicide were smaller than control by 23.2% at A concentration, and 23.6 % and 13.9% at B and C concentrations. The tests showed that adding copper oxychloride and mancozeb to the medium according to the recommended dose (A) completely stopped the

growth of *H. vandergeesti*. Mancozeb had its fungicidal effect on the growth of fungal colonies also at the concentration 10 times and 100 times lower than the recommended field dose.

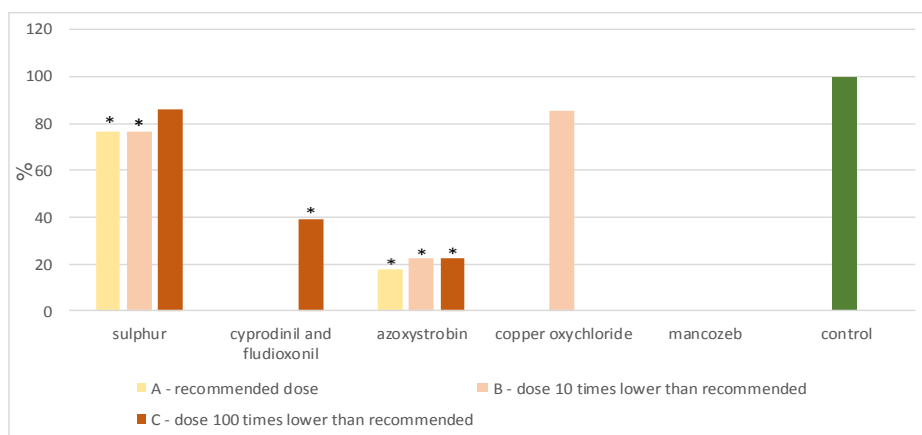


Figure 3. *Hirsutella vandergeesti* colony size on media supplemented with investigated fungicides on the 25th day of observation (expressed in % relative to control)
 * - significance at the level $\alpha = 0.05$ in relation to the control

The present studies showed that applied fungicides strongly limited the growth of the fungal colonies of *H. danubiensis* (Fig. 4).

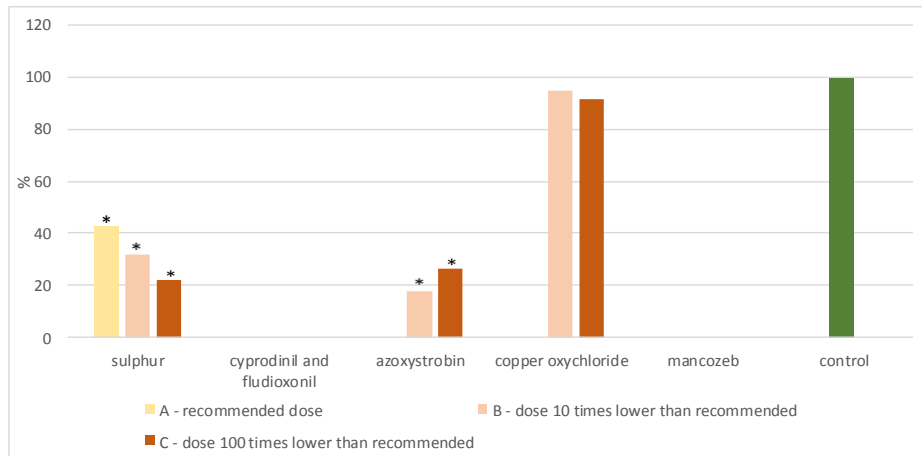


Figure 4. *Hirsutella danubiensis* colony size on media supplemented with investigated fungicides on the 25th day of observation (expressed in % relative to control)
 * - significance at the level $\alpha = 0.05$ in relation to the control

There was no growth of colonies on media containing cyprodinil and fludioxonil and mancozeb, irrespective of the dose. The other tested fungicides, except for sulphur, added to the medium at the recommended field dose (A) also prevented the development of the colonies of this fungus. Sulphur proved to be relatively little toxic to the tested strain. The size of *H. danubiensis* colonies growing on solid medium with that fungicide in A, B, and

C concentrations constituted 42.5%, 31.6% and 22.0% of the control diameter, respectively.

Discussion

Fungi that infect mites in natural conditions are constantly exposed to pesticides used to protect crops against other pests. Numerous reports (Miętkiewski et al., 1997; Tkaczuk et al., 2012; Celar and Kos, 2016; Fiedler and Sosnowska, 2017; Perez-González and Sánchez-Pena, 2017) indicate that chemical substances in pesticides may affect the natural occurrence of such fungi, their growth, sporulation, as well as their pathogenicity.

In the literature there are only a few reports on the impact of pesticides (fungicides) on the growth of fungal colony of the *Hirsutella* genus isolated from mites. They deal with species such as *H. thompsonii* (Sosa Gomez et al., 1987; Sosa Gomez, 1991), *H. nodulosa* (Tkaczuk et al., 2004, 2015), *H. kirchneri* and *H. brownorum* (Tkaczuk and Miętkiewski, 2005). Therefore, the results of tests on the effect of different types of active substances present in the fungicides carried out on the acaropathogenic species of *H. vandergeesti* and *H. danubiensis* are innovative. These species have been described relatively recently, and so far have not been subjected to this kind of laboratory tests.

The present research has shown that fungicides added to media adversely affect the growth of acaropathogenic fungi. Tkaczuk and Miętkiewski (2005) came to similar conclusions in their studies when they demonstrated that difenconazole was the most toxic to the strains of *Hirsutella* genus fungi. Exploring the effects of synthetic pesticides on *H. nodulosa* Petch, Tkaczuk et al. (2004) stated that fungicide iprodion added to the medium at the concentration 100 times lower than the recommended field dose, to a large extent reduced the growth of the fungi. Klingen and Westrum (2007) carried out an experiment to estimate the impact of pesticides on the development of the *Neozygites floridana* (J. Weiser and Muma) Remaud. and S. Keller mite-pathogenic entomophthoralean fungus. On the basis of the results they concluded that the fungicides strongly limited its survivability and potential infectiousness against the two-spotted spider mite (*T. urticae*).

Of the fungicides tested in the experiment mancozeb limited growth of the acaropathogenic fungi strains the strongest. Studies carried out by Tkaczuk and Miętkiewski (2001) found that this substance also had strong toxic effects on a strain of the *Hirsutella aphidis* Petch fungus, a pathogen of aphids. Additionally, research conducted by Tkaczuk et al. (2013) as well as by Todorova et al. (1998) and Jaros-Su et al. (1999), confirmed high toxicity of mancozeb to other species of entomopathogenic fungi.

Applied to the medium at a dose recommended by the manufacturer Miedzian 50 WP with the active substance of copper oxychloride strongly limited the growth of the isolates of investigated fungi. It was observed that this product inhibited the growth of the tested acaropathogenic fungi more at C concentration (0.01 of recommended dose) than B (0.1 of recommended dose). The colonies of the *H. thompsonii* strain growing on the medium with the dose 10 times lower than the recommended dose reached diameter bigger than control. Examining the impact of copper hydroxide, and elemental sulphur on the vegetative growth of the *Hirsutella citriformis* Speare fungus Hall et al. (2012) observed that these fungicides administered in the highest dose inhibited its growth. This suggested that such chemical control regimens may have a negative impact on biological control of *Diaphorina citri* Kuwayama (Hemiptera: Psyllidae) by the fungus in citrus orchards.

Spray oils and other chemical treatments to citrus might negate biological control by reducing infectivity and growth of *H. citriformis* as well as the longevity of mummies on leaves.

In our studies, sulphur limited the growth of the acaropathogenic fungal isolates less than other fungicides, but copper oxychloride, when added to the medium with recommended concentration, often prevented or significantly inhibited the development of the fungi. The results of this research confirm the studies of Sosa Gomez et al. (1987) and Sosa Gomez (1991), who found that copper oxychloride constrained the growth of *H. thompsonii* fungal colonies much more strongly than sulphur powder applied in the form of dust. It is worth noting that both of the above fungicides based on copper and sulphur are currently authorised for use in organic crops.

It should be, however, emphasized that the laboratory research on fungal susceptibility to fungicides do not necessarily reflect the complex situation in field, where the interactions between fungi and pesticides could be modified by a number of biotic and abiotic factors. Keller et al. (1993) suggested that the non-target effect of chemical pesticides on arthropod-pathogenic fungi applied as a microbial control agent might not be significant under practical conditions. For the use of *Beauveria brongniartii* (Sacc.) Petch in orchards, for example, the fungus is applied at a soil depth of some centimeters so that a direct contact with fungicides is avoided, thereby preventing adverse effects. In contrast to fungicides, soil herbicides penetrate several centimeters into the soil, which directly affects entomopathogenic fungi, i.e. *Beauveria bassiana* (Bals.-Criv.) Vuill.

Conclusions

The effect of fungicides on the growth of acaropathogenic fungi from the genus *Hirsutella* varied depending on the applied substance and its concentration in the culture medium. Of all fungicides tested the fungal growth was most strongly limited by mancozeb and a mixture of cyprodinil and fludioxonil. Of all the tested fungicides, sulphur showed the least adverse effect and is therefore probably compatible with fungi from the genus *Hirsutella* in the field. However, extensive field studies complemented by parallel pot experiments should consider assessing the interaction between fungicides and *Hirsutella* isolates to evaluate their ecological impact in crop environments.

Acknowledgements. The results of the research carried out under research theme No. 44/20/B were financed from the science grant granted by the Ministry of Science and Higher Education.

REFERENCES

- [1] Andalo, V., Moino, A., Santa-Cecilia, L. V. S., Souza, G. C. (2004): Compatibility of *Beauveria bassiana* with chemical pesticides for the control of the coffee root mealybug *Dysmicoccus texensis* Tinsley (Hemiptera: Pseudococcidae). – *Neotropical Entomology* 33: 463-467.
- [2] Bałazy, S., Miętkiewski, R., Tkaczuk, C., Wegensteiner, R., Wrzosek, M. (2008): Diversity of acaropathogenic fungi in Poland and other European countries. – *Experimental and Applied Acarology* 46(1-4): 53-70.
- [3] Boczek, J. (1999): *Zarys akarologii rolniczej*. – PWN Warszawa (in Polish).

- [4] Celar, F. A., Kos, K. (2016): Effects of selected herbicides and fungicides on growth, sporulation and conidial germination of entomopathogenic fungus *Beauveria bassiana*. – Pest Management Science 72: 2110-2117.
- [5] Fiedler, Ž., Sosnowska, D. (2007): Side effects of insecticides on entomopathogenic fungi. – Biological methods in integrated plant protection and production, Information Bulletin EPRS/IOBC, 36, Poznań-Pushkino, pp. 227-231.
- [6] Fiedler, Ž., Sosnowska, D. (2017): Side effects of fungicides and insecticides on entomopathogenic fungi in vitro. – Journal of Plant Protection Research 57(4): 355-360.
- [7] Hall, D. G., Hentz, M. G., Meyer, J. M., Kriss, A. B., Gottwald, R. T., Bobcias, D. G. (2012): Observations on the entomopathogenic fungus *Hirsutella citriformis* attacking adult *Diaphorina citri* (Hemiptera: Psyllidae) in a managed citrus grove. – BioControl 57: 663-675.
- [8] Hodge, K. T. (1998): Revisionary studies in *Hirsutella* (Anamorphic Hypocerales: Clavicipitaceae). – UMI Microform 9900074, Ann Arbor.
- [9] Hummel, R. L., Walgenbach, J. F., Barbercheck, M. E., Kennedy, G. G., Hoyt, G. D., Arellano, C. (2002): Effects of production practices on soil-borne entomopathogens in western North Carolina vegetable systems. – Environmental Entomology 31: 84-91.
- [10] Jaros-Su, J., Groden, E., Zhang, J. (1999): Effects of selected fungicides and timing of fungicide application on *Beauveria bassiana*-induced mortality of the Colorado potato beetle (Coleoptera: Chrysomelidae). – Biological Control 15: 259-269.
- [11] Keller, S., Parli, B., Lujan, M., Schweizer, C. (1993): Influence of fungicides on the insect pathogenic fungus *Beauveria brongniartii* (Sacc) Petch. – Anzeiger für Schädlingskunde, Pflanzen und Umweltschutz 66: 108-114.
- [12] Kepler, R. M., Ban, S., Nakagiri, A., Bischoff, J.F., Hywel-Jones, N. L., Owensby, C. A., Spatafora, J. W. (2013): The phylogenetic placement of hypocrealean insect pathogens in the genus *Polycephalomycetes*: an application of One Fungus One Name. – Fungal Biology 117: 611-622.
- [13] Klingen, I., Westrum, K. (2007): The effect of pesticides used in strawberries on the phytophagous mite *Tetranychus urticae* (Acari: Tetranychidae) and its fungal natural enemy *Neozygites floridana* (Zygomycetes: Entomophthorales). – Biological Control 43: 222-230.
- [14] Li, W., Fang, X. F., Sheng, C. F. (2004): Impact of sixteen chemical pesticides on conidial germination of two entomophthoralean fungi: *Conidiobolus thromboides* and *Pandora nouryi*. – Biocontrol Science and Technology 14: 737-741.
- [15] Lipa, J. (1971): Microbial control of mites and ticks. – In: Burges, H. D., Hussey, N. W. (eds.) Microbial Control of Insects and Mites. Academic Press, New York.
- [16] Lipa, J. (2000): Current and future place of biological and other non-chemical methods of plant protection. – Progress in Plant Protection 40(1): 62-72.
- [17] Majchrowicz, I., Poprawski, T. J. (1993): Effects in vitro of nine fungicides on growth of entomopathogenic fungi. – Biocontrol Science and Technology 3: 321-336.
- [18] McCoy, C. W. (1981): Pest control by the fungus *Hirsutella thompsonii*. – In: Burges, H. D. (ed.) Microbial Control of Pests and Plant Diseases, 1970-1980. Academic Press, London.
- [19] Meyling, N. V., Eilenberg, J. (2007): Ecology of the entomopathogenic fungi *Beauveria bassiana* and *Metarhizium anisopliae* in temperate agroecosystems: potential for conservation biological control. – Biological Control 43: 145-155.
- [20] Miętkiewski, R., Machowicz-Stefaniak, Z., Górski, R. (1996): Occurrence of entomopathogenic fungi in soil of the hop plantations and adjacent arable fields. – Roczniki Nauk Rolniczych 25(1-2): 47-51. (in Polish).
- [21] Miętkiewski, R. T., Pell, J., Clark, S. J. (1997): Influence of pesticides use on the natural occurrence of entomopathogenic fungi in arable soils in the UK. Field and laboratory comparisons. – Biocontrol Science and Technology 7: 565-575.
- [22] Patouillard, N. T. (1892): Une Clavariée entomogène. – Revue Mycologique 14: 67-70.

- [23] Perez-González, O., Sánchez-Pena, S. R. (2017): Compatibility *in vitro* and *in vivo* of the entomopathogenic fungi *Beauveria bassiana* and *Hirsutella citriformis* with selected Insecticides. – Southwestern Entomologist 42(3): 707-718.
- [24] Quandt, C. A., Kepler, R. M., Gams, W., Araujo, J. P. M., Ban, S. (2014): Phylogenetic-based nomenclatural proposals for Ophiocordycipitaceae (Hypocreales) with new combinations in *Tolypocladium*. – IMA Fungus 5: 121-134.
- [25] Schoch, C. L., Seifert, K. A., Huhndorf, S., Robert, V., Spouge, J. L., Levesquem, C. A., Chen, W. (2012): Nuclear ribosomal internal transcribed spacer (ITS) region as a universal DNA barcode marker for fungi. – Proceedings of the National Academy of Sciences of the United States of America 109: 6241-6246.
- [26] Sosa-Gomez, D. R. (1991): Production of three *Hirsutella thompsonii* varieties on semisolid media and different effects of two fungicides. – Anais da Sociedade Entomológica do Brasil 120: 155-163.
- [27] Sosa-Gomez, D. R., Manzur, J., Nasca, A. J. (1987): Influence of some pesticides on the three varieties of *Hirsutella thompsonii* Fisher (Hyphomycetes: Moniliales). – Anais da Sociedade Entomológica do Brasil 16: 399-408.
- [28] Sosnowska, D. (2013): Progress in research and the use of pathogenic fungi in integrated plant protection. – Progress in Plant Protection 53(4): 747-750.
- [29] Sung, G.-H., Hywel-Jones, N. L., Sung, J.-M., Luangsaard, J. J., Shrestha, B., Spatafora, J. W. (2007): Phylogenetic classification of *Cordyceps* and the clavicipitaceous fungi. – Studies in Mycology 57: 5-59.
- [30] Tkaczuk, C., Miętkiewski, R. (2001): The growth of *Hirsutella aphidis* Petch – less-known pathogen of aphids – on media containing pesticides. – Aphids and Other Homopterous Insects 8: 423-428.
- [31] Tkaczuk, C., Łabanowska, B. H., Miętkiewski, R. (2004): The influence of pesticides on the growth of fungus *Hirsutella nodulosa* (Petch) – entomopathogen of strawberry mite (*Phytonemus pallidus* ssp. *fragariae* Zimm.). – Journal of Fruit and Ornamental Plant Research 12: 119-126.
- [32] Tkaczuk, C., Miętkiewski, R. (2005): Effect of selected pesticides on the growth of fungi from *Hirsutella* genus isolated from phytophagous mites. – Journal of Plant Protection Research 45(3): 171-179.
- [33] Tkaczuk, C., Krzyczkowski, T., Głuszczyk, B., Król, A. (2012): The influence of selected pesticides on the colony growth and conidial germination of the entomopathogenic fungus *Beauveria bassiana* (Bals.) Vuill. – Progress in Plant Protection 52(4): 969-974.
- [34] Tkaczuk, C., Majchrowska-Safaryan, A., Zawadzka, M. (2013): The effect of spinosad and selected synthetic insecticides on the growth of entomopathogenic fungi *in vitro*. – Journal of Research and Applications in Agricultural Engineering 58(4): 194-198.
- [35] Tkaczuk, C., Harasimiuk, M., Król, A., Bereś, P. (2015): The effect of selected pesticides on growth of entomopathogenic fungi *Hirsutella nodulosa* and *Beauveria bassiana*. – Journal of Ecological Engineering 16(3): 177-183.
- [36] Todorova, S. I., Coderre, D., Duchesne, R. M., Côté, J. C. (1998): Compatibility of *Beauveria bassiana* with selected fungicides and herbicides. – Environmental Entomology 27: 427-433.
- [37] Van der Geest, L. P. S., Elliot, S. L., Breeuwer, J. A. J., Beerling, E. A. M. (2000): Diseases of mites. – Experimental and Applied Acarology 24: 497-560.

PHYTOPLANKTON COMMUNITY STRUCTURE IN AN INTEGRATED MULTI-TROPHIC AQUACULTURE SYSTEM REVEALED BY MORPHOLOGICAL ANALYSIS AND HIGH-THROUGHPUT SEQUENCING

QIAO, L.^{1,2,3} – CHANG, Z.^{2,3} – LI, J.^{2,3*} – CHEN, Z.^{2,3}

¹Key Laboratory of Sustainable Utilization of Technology Research for Fishery Resource of Zhejiang Province, Marine Fishery Institute of Zhejiang Province, Zhoushan 316012, China

²Key Laboratory of Sustainable Development of Marine Fisheries, Ministry of Agriculture and Rural Affairs; Yellow Sea Fisheries Research Institute, Chinese Academy of Fishery Sciences, Qingdao 266071, China

³Laboratory for Marine Fisheries and Food Production Processes, Pilot National Laboratory for Marine Sciences and Technology, Qingdao 266071, China

*Corresponding author

e-mail: lijian@ysfri.ac.cn; phone: +86-532-8583-0183

(Received 11th Nov 2019; accepted 30th Jan 2020)

Abstract. With increasing concern over the negative environmental impact of mariculture, integrated multi-trophic aquaculture (IMTA) has received extensive attention in recent years. To comprehensively assess the phytoplankton community structure in the late culture stage of a typical pond IMTA system, both morphological analysis and high-throughput sequencing method were used in the present study. 9 phyla of phytoplankton were identified by using the two methods, and the Bacillariophyta, Cyanophyta and Euglenophyta were the most dominant. The dominant phytoplankton of the IMTA pond system in which clams were reared in a separate pond has changed from cyanophytes to diatoms from September to October, and it has changed from diatoms and cyanophytes to euglenophytes, haptophytes and green algae in the IMTA pond with shrimp, crab and clam together. Results of direct gradient analysis revealed that the phytoplankton community structure seemed to be linked with the variables of temperature, salinity, pH, dissolved inorganic nitrogen (DIN) and dissolved silica (DSi) concentrations, DIN/dissolved inorganic phosphorus (DIP), DSi/DIN and DSi/DIP. The relationship between phytoplankton community and *Vibrio* abundance indicated that diatoms and chlorophytes might inhibit the proliferation of *Vibrio*, while cyanophytes bloom might be beneficial to the *Vibrio* growth.

Keywords: phytoplankton, water quality, *Vibrio*, mariculture, aquaculture models

Introduction

As one of the most important seafood production practices worldwide, aquaculture is facing serious environmental challenges due to the detrimental impacts of intensive farming methods (Sladonja, 2011). Integrated multi-trophic aquaculture (IMTA) has been known as an ecologically well-balanced aquaculture practice, in which co-cultures of species at various trophic levels are able to promote the recycling of aquaculture wastes as a food resource (Chopin et al., 2008). In this system, fish or shrimp are cultured in combination with other extractive species, such as filtering clam, which can prevent additional nutrient inflow into the surrounding environment, and they are desirable products with high market value as well (Troell et al., 2009). IMTA has been practiced for several decades in China, initially through land-based operations which later expanded to marine systems (Wartenberg et al., 2017). However, the IMTA is still

heavily relying on traditional and inefficient methods, and further study on developing engineered IMTA systems that are well adapted to a variety of species and environmental circumstances are needed.

Phytoplankton plays a very important role in aquaculture ecosystems. They are useful in maintaining water quality by uptake of nutrients during photosynthesis (Harrison et al., 2005), and serve as a direct or indirect food source for cultured organisms (Pulz and Gross, 2004; Martins et al., 2016). In addition, beneficial phytoplankton might inhibit the growth of pathogenic bacteria. The *Vibrio* is ubiquitous in the marine and estuarine environments (Pruzzo et al., 2005a). The genus includes some species (e.g. *Vibrio parahaemolyticus*, *V. harveyi*, *V. anguillar*, *V. alginolyticus*, *V. vulnificus*) that is pathogenic to both invertebrates and vertebrates, such as corals, clam, shrimp and fish (Pruzzo et al., 2005b). Studies showed that some phytoplankton, such as diatoms and green algae can effectively inhibit the multiplication of *Vibrio* (Lio-Po et al., 2005), while some phytoplankton (such as cyanophytes) might facilitate the proliferation of *Vibrio* in their natural environment (Eiler et al., 2007). The establishment of a healthy aquaculture environment requires a balance of algae that is beneficial to its organisms. The succession of dominant species often dominates the trend of algal facies balance, which affects the quality of water environment and the healthy development of aquaculture (Xu et al., 2015). So, monitoring and assessing the phytoplankton community structure and dominant species succession are vital in managing aquaculture systems.

In this study, the phytoplankton community structure and dominant species succession in the late stage of a typical pond IMTA system were assessed using traditional morphological analysis and high-throughput sequencing together, and its relationship with the water quality parameters were analyzed as well. Our primary objectives were to (i) clarify the phytoplankton community structure of pond IMTA system using morphological analysis and high-throughput sequencing; (ii) investigate the relationship between phytoplankton community and water quality parameters; and (iii) explore the effect of the aquaculture model on water quality and phytoplankton community.

Materials and methods

IMTA systems and sample collection

This study was performed in Rizhao Kaihang Aquatic Products Co., Ltd., located in Shandong Province in eastern China (35°19'8"N; 119°24'40"E) in September and October in 2018. Two pond IMTA models were selected in this study, One model (aquaculture model I) consists of a culture pond (pond 1), where *Fenneropenaeus chinensis* were co-cultured with *Portunus trituberculatus* and tilapia (*Oreochromis niloticus*) together, and a biological purification pond (pond 3) with clam *Meretrix meretrix* stocked was connected to pond 1 through a recirculating pipeline system (Fig. 1). The other model (aquaculture model II) is polyculture of shrimp (*F. chinensis*), crab (*P. trituberculatus*) and clam (*Mercenaria mercenaria*) together in the same pond as shown in pond 5 and 6 in Fig. 1. During the study period, Fresh baits and commercial feeds containing 38% of crude protein (Tongwei Co., Ltd., Lianyungang) were provided in pond 1, 5 and 6. Feed amount was adjusted daily according to the estimated aquatic animals consumption, mortality rate and leftover feed. No supplemental feed was provided in pond 3 during the study period.

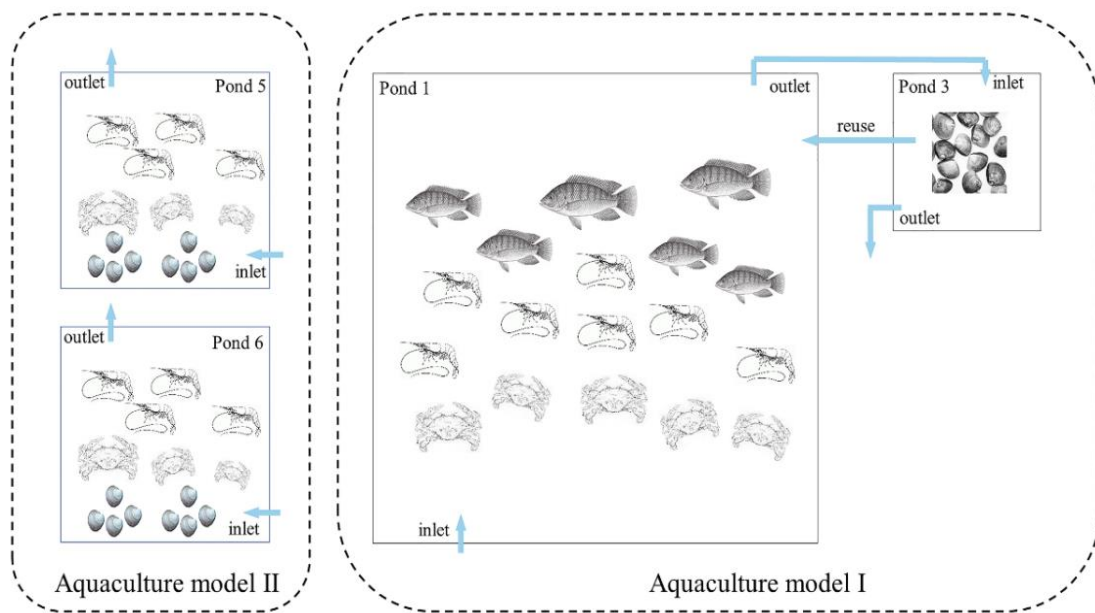


Figure 1. Schematic illustration of the simplified plan of IMTA system. Aquaculture model I consists of pond 1 where *F. chinensis* were co-cultured with *P. trituberculatus* and *O. niloticus* together and pond 3 where *M. meretrix* stocked. Aquaculture model II consists of pond 5 and 6 where *F. chinensis*, *P. trituberculatus* and *M. mercenaria* cultured together in the same pond

Samplings were conducted on September 7 and October 17, 2018. The sampling methods referred to Qiao et al. (2019). Water temperature, salinity, dissolved oxygen (DO) and pH in each pond were recorded in situ using a YSI Model Handheld Instrument (YSI Incorporated, Yellow Springs, Ohio, USA). 1 L of water were sampled from the center and four corners (including the water inlet and the water outlet) of the culture pond, respectively. 5 L of water samples were well mixed and then prefiltered through a sieve with a pore size of 200 μm to remove large suspended particles, microzooplankton, and other large cells. Then, 1 L of filtrate fixed with 5 mL of Lugol's solution for phytoplankton identification and counting, 500 mL of filtrate was further filtered with 0.22 μm Millipore membrane to collect the phytoplankton for DNA analysis, and 500 mL of filtrate was further filtered with 0.45 μm membranes to measure the ammonium (NH_4^+), nitrate (NO_3^-), nitrite (NO_2^-), phosphate (dissolved inorganic phosphorus, DIP), silicate (dissolved silica, DSi), dissolved total nitrogen (DTN) and dissolved total phosphorus (DTP) contents.

Analysis of water quality parameters

Concentrations of NH_4^+ , NO_3^- , NO_2^- , DIP, and DSi were measured using a QuAatro nutrient auto analyzer (Seal Analytical Ltd., Germany) (Parsons et al., 1984). DTN and DTP were determined with alkaline persulfate digestion (SAC, 2007) and evaluated using a QuAatro nutrient auto analyzer (Seal Analytical Ltd., Germany). The dissolved inorganic nitrogen (DIN) concentration was the sum of NH_4^+ , NO_3^- and NO_2^- concentrations. The dissolved organic nitrogen (DON) and dissolved organic phosphorus (DOP) values were calculated as the difference between DTN and DIN and between DTP and DIP, respectively.

Quantitative analysis of *Vibrio*

To quantify patterns in the whole *Vibrio* community, the primer pair Vib1-f (5'-GGCGTAAAGCGCATGCAGGT-3') and Vib2-r (5'-GAAATTCTACCCCCCTCTACAG-3') (Thompson et al., 2004; Vezzulli et al., 2012) were used to amplify 16S rRNA genes specific to the *Vibrio* genus (114 bp). All qPCR assays were carried out in triplicate using an ABI PRISM®7500 Sequence Detection System (Applied Biosystems, USA) with the SYBR Green method to determine the copy concentration of *Vibrio*. The abundance of *Vibrio* was expressed as number of cells per liter (cells/L), which was calculated by the average 16S rDNA copy number in vibrios (Acinas et al., 2004; Vezzulli et al., 2012).

Morphological analysis of phytoplankton

The water samples for morphological analysis of phytoplankton were preserved with 0.5% Lugol's solution. Each sample was concentrated to 50 mL, and then stored in darkness at 4°C until analysis. Phytoplankton species were identified and cell numbers were counted using a phytoplankton enumeration chamber under an inverted microscope (Olympus CKX41, Olympus Corporation, Tokyo, Japan).

High-throughput sequencing of phytoplankton and bioinformatic analysis

The total genomic DNA was extracted from all samples using the FastDNA spin kit for soil (MP Biomedicals, OH, USA), following the manufacturer's instructions. DNA quality and concentration were measured by gel electrophoresis and a Nanodrop spectrophotometer (NanoDrop Technologies, Wilmington, DE, USA), respectively. PCR was performed with the 23S rDNA gene primer pair p23SrV_f1 (5'-GGA CAG AAA GAC CCT ATG AA-3') and p23SrV_r1 (5'-TCA GCC TGT TAT CCC TAG AG-3') (Sherwood and Presting, 2007). The PCR products were extracted from a 2% agarose gel and further purified using the AxyPrepDNA Gel Extraction Kit (Axygen Biosciences, USA) referring to the manufacturer's instruction, and quantified using QuantiFluor™-ST (Promega, USA). Purified amplicons were pooled in equimolar and paired-end reads (PE300) on an Illumina MiSeq platform (Illumina, San Diego, USA) referring to the standard protocols by Majorbio Bio-Pharm Technology Co. Ltd (Shanghai, China). Sequence data can be retrieved from GenBank under accession number SRP185765 and SRP185766.

Sequences from the Illumina MiSeq platform were processed using the QIIME (version 1.91, <http://qiime.org/>, Caporaso et al., 2010) software package. Raw fastq files were demultiplexed, quality-filtered by Trimmomatic and merged by FLASH (version 1.2.11, <https://ccb.jhu.edu/software/FLASH/index.shtml>, Magoc and Salzberg, 2011). Operational taxonomic units (OTUs) were clustered with 97% similarity cutoff using UPARSE (version 7.1, <http://drive5.com/uparse>, Edgar, 2013). The chimeric sequences were identified and removed using UCHIME (version 7, <http://www.drive5.com/uchime>, Edgar et al., 2011). The taxonomic assignment was determined for the representative sequence of each OTU using the Basic Local Alignment Search Tool (BLAST) in the NCBI database (<http://www.ncbi.nlm.nih.gov>). Following the exclusion of bacteria (all non-cyanobacteria) and unclassified sequences, phytoplankton sequences were selected for analysis of community structure and diversity based on the taxonomic information.

Phytoplankton community analysis

Dominant species was defined as its dominance >10%. Phytoplankton community diversity was evaluated using the Shannon-Wiener diversity index.

Phytoplankton dominance:

$$Y = \frac{n_i}{N} \times f_i \quad (\text{Eq.1})$$

In *Equation 1*, n_i is the species cell abundance, N is the total cell abundance, and f_i is the frequency of the occurrence of the species in a pond.

Shannon-Wiener diversity index:

$$H = - \sum_{i=1}^S P_i \ln P_i \quad (\text{Eq.2})$$

In *Equation 2*, S is the total number of species or OTUs, and P_i is the relative abundance of species i or OTU i .

Correlations between phytoplankton community and water quality parameters were determined through direct gradient analysis using Canoco for Windows (version 4.5, Braak and Smilauer, 2002).

Results

Water quality parameters and abundance of *Vibrio*

The Water quality parameters and the abundance of *Vibrio* in the aquaculture waters of IMTA system are summarized in *Table 1*. During the whole study period, the surface seawater temperature declined from 26.32°C to 18.24°C, the average salinity, DO and pH increased from 23.01 to 26.01 g/L, 4.85 to 6.84 mg/L and 8.19 to 8.70, respectively, while the concentration of NH_4^+ , NO_3^- , NO_2^- , DIN, DON, DIP and DSi, were decreased. The average abundance of *Vibrio* in September was three orders higher than that in October (*Table 1*). The analysis of variance showed that there were significant differences in water quality between different aquaculture models ($p < 0.05$). The average concentrations of NH_4^+ , NO_3^- , NO_2^- , DIN, DON, DIP and DSi in aquaculture model I were lower than those in aquaculture II (*Table 1*). By comparing water quality parameters in pond 1 and 3, the concentrations of NH_4^+ , NO_3^- , NO_2^- , DIN, DON, DOP and DSi in pond 1 were higher than those in pond 3 in September and October, while the concentration of DIP in pond 1 was lower than those in pond 3. The abundances of *Vibrio* in pond 1 were higher than those in pond 3. The approach for judging nutrient limitation that Justić et al. (1995) proposed was used in this study. The result showed that pond 1 and 3 in October were silicon limitation ($\text{DSi} < 2 \mu\text{M}$, $\text{DSi/DIP} < 10$ and $\text{DSi/DIN} < 1$). The other ponds were no nutrient limitation.

Table 1. Water quality parameters and abundance of *Vibrio* in the aquaculture waters of IMTA system in 2018

Date	Ponds	T (°C)	S (g/L)	DO (mg/L)	pH	NH ₄ ⁺ (mg/L)	NO ₃ ⁻ (mg/L)	NO ₂ ⁻ (mg/L)	DIN (mg/L)	DON (mg/L)	DIP (mg/L)	DOP (mg/L)	DSi (mg/L)	DIN/DIP	DSi/DIN	DSi/DIP	<i>Vibrio</i> (cells/L)
September	Pond 1	25.66	22.72	6.71	8.63	0.124	0.446	0.137	0.706	0.789	0.016	0.022	1.460	99.72	1.03	103.07	2.03×10 ⁷
	Pond 3	26.20	24.28	6.59	8.60	0.108	0.233	0.008	0.348	0.059	0.022	0.009	0.909	35.49	1.31	46.34	8.60×10 ⁶
	Pond 5	26.60	22.79	3.06	7.73	1.403	0.603	0.225	2.231	0.708	0.059	0.015	0.079	84.13	0.02	1.49	5.51×10 ⁸
	Pond 6	26.80	22.24	3.06	7.81	0.674	0.943	0.149	1.766	0.598	0.163	0.003	0.354	24.03	0.10	2.41	1.56×10 ⁶
	Average	26.32	23.01	4.85	8.19	0.577	0.556	0.130	1.263	0.538	0.065	0.012	0.700	43.21	0.28	11.99	1.45×10 ⁸
October	Pond 1	17.74	26.19	8.45	8.91	0.059	0.045	0.001	0.105	0.414	0.012	0.012	0.016	20.04	0.08	1.52	9.89×10 ⁵
	Pond 3	18.40	26.27	7.27	8.91	0.045	0.016	B.D.L.	0.062	0.279	0.013	0.011	0.007	10.59	0.05	0.58	9.51×10 ⁴
	Pond 5	18.35	25.87	6.66	8.66	0.057	0.084	0.004	0.145	0.364	0.056	0.017	0.382	5.76	1.32	7.59	6.45×10 ⁵
	Pond 6	18.45	25.72	4.96	8.31	0.096	0.252	0.012	0.360	0.432	0.081	0.026	0.431	9.86	0.60	5.90	2.25×10 ⁴
	Average	18.24	26.01	6.84	8.70	0.064	0.099	0.006	0.168	0.372	0.040	0.017	0.209	9.23	0.62	5.75	4.38×10 ⁵

Note: T: temperature; S: salinity; DO: dissolved oxygen; NH₄⁺: ammonium; NO₃⁻: nitrate; NO₂⁻: nitrite; DIN: dissolved inorganic nitrogen; DON: dissolved organic nitrogen; DIP: dissolved inorganic phosphate; DOP: dissolved organic phosphate; DSi: dissolved silicate; DIN/DIP, DSi/DIN and DSi/DIP are molar ratios of DIN to DIP, DSi to DIN and DSi to DIP, respectively; B.D.L.: below detectable limit

Phytoplankton community structure revealed by morphological analysis

Phytoplankton community composition

A total of 44 taxa of phytoplankton were identified by morphological analysis in the study (Table A.1). 50.00% of the identified taxa belongs to Bacillariophyta, followed by Dinophyta, Cryptophyta, Chlorophyta and Cyanophyta with 20.45%, 11.36%, 9.09% and 6.82%, respectively. Euglenophyta was represented by only one species. Only three species, *Cyclotella* sp., *Nitzschia* sp.1 and *Gymnodinium* spp. were detected by morphological analysis at all samples.

Temporal and spatial variations of phytoplankton abundance

Phytoplankton abundance indicated by cell density in September (4.91×10^5 cells/L) was lower than those in October (8.83×10^6 cells/L). The phytoplankton average abundance in aquaculture model I was higher than that in aquaculture model II in September and October. By comparing pond 1 and 3, the phytoplankton abundance in pond 1 was lower than those in pond 3 (Fig. 2).

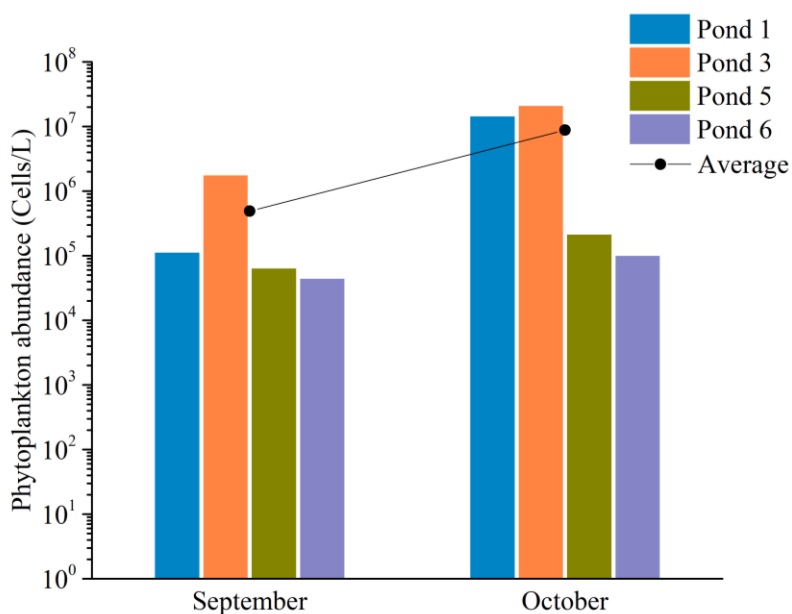


Figure 2. Temporal and spatial variations of phytoplankton abundance in the IMTA system revealed by morphological analysis. Aquaculture model I consists of pond 1 where *F. chinensis* were co-cultured with *P. trituberculatus* and *O. niloticus* together and pond 3 where *M. meretrix* stocked. Aquaculture model II consists of pond 5 and 6 where *F. chinensis*, *P. trituberculatus* and *M. mercenaria* cultured together in the same pond

In September, diatoms were the most abundant species, which accounted for 59.09-96.41% of the total phytoplankton in pond 1, 5 and 6. The relative abundances of euglenophyte and diatoms were higher than other species in pond 3 (Fig. 3). In October, diatoms were the most abundant group which contributed over 99% of the total phytoplankton in pond 1 and 3, while the abundance of euglenophyte was the highest in ponds 5 and 6 (Fig. 3).

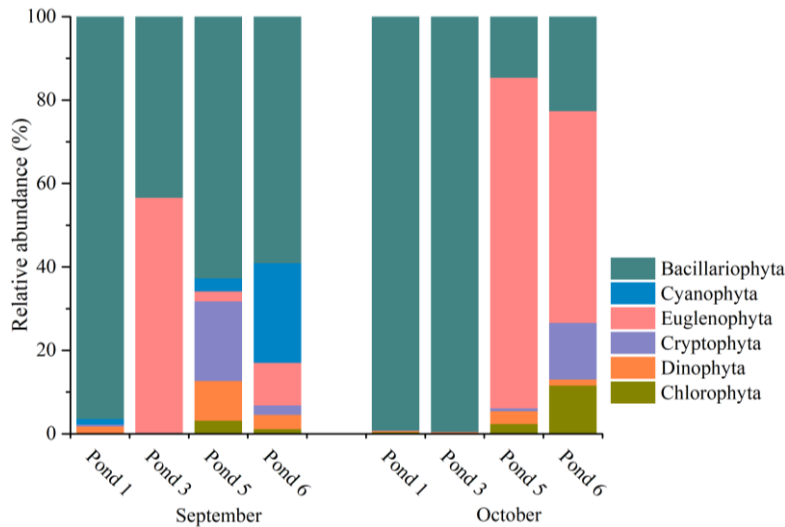


Figure 3. Temporal and spatial variations of relative abundance of phytoplankton at the phylum level in the IMTA system revealed by morphological analysis. Aquaculture model I consists of pond 1 where *F. chinensis* were co-cultured with *P. trituberculatus* and *O. niloticus* together and pond 3 where *M. meretrix* stocked. Aquaculture model II consists of pond 5 and 6 where *F. chinensis*, *P. trituberculatus* and *M. mercenaria* cultured together in the same pond

Dominant species of phytoplankton

In September, Diatoms, *Cyclotella* sp. and *Cyclotella meneghiniana* Kuetzing were the dominated species in pond 1, which accounted for 70.85% and 11.21% of the total abundance. There were three dominant species in pond 3 including *Eutreptiella* sp., *Melosira* sp. and *Cyclotella* sp., which contributed to about 97.99% of the total abundance. There were two (*Cyclotella* sp. and *Teleaulax acuta*) and four (*Mastigocoleus* sp., *Cyclotella* sp., *Surirella* sp. and *Eutreptiella* sp.) species were dominant in pond 5 and 6, respectively. *Cyclotella* sp. was one of the dominated species in all ponds in September (Table 2).

Table 2. Dominant species, cell density and dominance of phytoplankton in the IMTA system

Time	Ponds	Dominant species	Cell density (cells/L)	Dominance
September	Pond 1	<i>Cyclotella</i> sp.	7.90×10^4	0.71
		<i>Cyclotella meneghiniana</i> Kuetzing	1.25×10^4	0.11
	Pond 3	<i>Eutreptiella</i> sp.	9.81×10^5	0.56
		<i>Melosira</i> sp.	4.23×10^5	0.24
		<i>Cyclotella</i> sp.	3.06×10^5	0.18
	Pond 5	<i>Cyclotella</i> sp.	2.60×10^4	0.41
		<i>Teleaulax acuta</i>	1.05×10^4	0.17
	Pond 6	<i>Mastigocoleus</i> sp.	8.50×10^3	0.19
		<i>Cyclotella</i> sp.	8.00×10^3	0.18
		<i>Surirella</i> sp.	6.50×10^3	0.15
<i>Eutreptiella</i> sp.		4.50×10^3	0.10	
October	Pond 1	<i>Leptocylindrus danicus</i>	1.39×10^7	0.98
	Pond 3	<i>Leptocylindrus danicus</i>	2.06×10^7	0.99
	Pond 5	<i>Eutreptiella</i> sp.	1.68×10^5	0.79
	Pond 6	<i>Eutreptiella</i> sp.	5.05×10^4	0.51
		<i>Pyramimonas</i> sp.	1.05×10^4	0.11

In October, *Leptocylindrus danicus* was the only dominant species in pond 1 and 3, which reached a high cell density of 1.39×10^7 and 2.06×10^7 cells/L with 97.70% and 99.24% of the total abundance, respectively. *Eutreptiella* sp. was the only dominant species (79.25% of the total) in pond 5, with cell density at 1.68×10^5 cells/L. *Eutreptiella* sp. and *Pyramimonas* sp. dominated in pond 6 (Table 2).

Phytoplankton diversity

Shannon indices were ranged from 1.09 to 2.46 in September, and ranged from 0.06 to 1.89 in October. Phytoplankton diversity in September was higher than those in October in all ponds. The two surveys showed that phytoplankton diversity in aquaculture model I was lower than that in aquaculture model II. By comparing pond 1 and 3, the phytoplankton diversity in pond 1 was higher than that in pond 3 (Fig. 4).

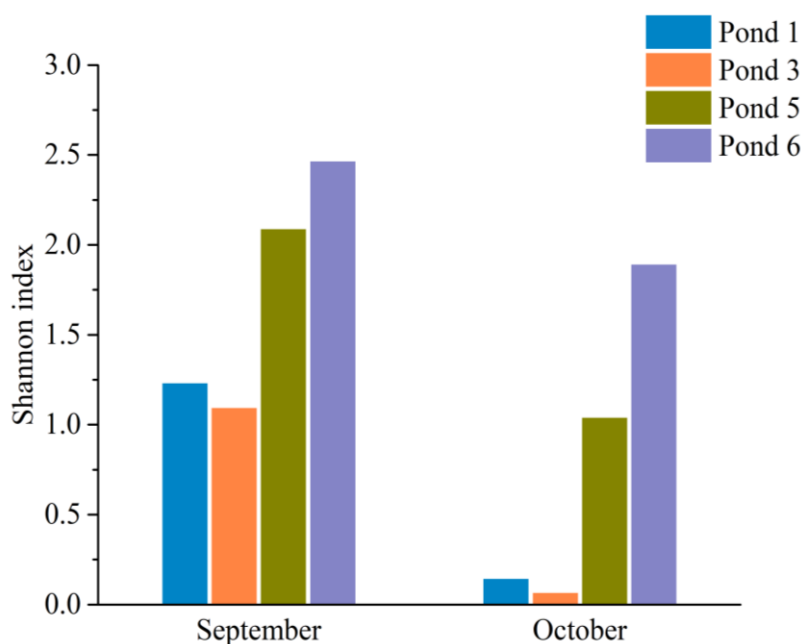


Figure 4. Phytoplankton diversity revealed by morphological analysis. Aquaculture model I consists of pond 1 where *F. chinensis* were co-cultured with *P. trituberculatus* and *O. niloticus* together and pond 3 where *M. meretrix* stocked. Aquaculture model II consists of pond 5 and 6 where *F. chinensis*, *P. trituberculatus* and *M. mercenaria* cultured together in the same pond

Phytoplankton community structure revealed by high-throughput sequencing

High-throughput sequencing data statistics

A total of 406,246 raw reads were obtained using high-throughput Illumina sequencing for all samples, and the number of reads for each sample ranged from 31,364 to 64,004. After quality and chimera checking and removal of the low-quality reads, a total of 374,428 clean reads were obtained. The average reads length was 388 nucleotides. The reads for all samples were classified into 162 OTUs, ranging from 34 to 103 OTUs, at a 97% similarity level (Table 3).

Table 3. Numbers of sequences in quality control analysis

Date	Pond Number	Raw Reads	Clean Reads	Total OTUs	Phytoplankton Reads	Phytoplankton OTUs
September	Pond 1	31,364	27,270	34	16,821	26
	Pond 3	64,004	55,587	38	35,708	28
	Pond 5	56,775	52,596	46	27,625	31
	Pond 6	49,022	47,125	103	27,489	42
October	Pond 1	54,764	51,338	66	47,083	40
	Pond 3	61,902	57,306	89	51,542	40
	Pond 5	37,164	33,930	65	23,916	30
	Pond 6	51,251	49,276	62	38,539	30
Sum		406,246	374,428	162	268,723	68

Taxa were assigned to the representative sequence of each OTU using the NCBI database. According to the taxonomic information, the sequences that were annotated as eukaryota and bacteria accounted for 63.98% and 35.57%, respectively (Fig. 5). At phylum level, Cyanobacteria sequences accounted for the greatest proportion of the total sequences (28.73%), followed by Bacillariophyta (24.04%), Chlorophyta (6.04%), Proteobacteria (6.00%), Haptophyta (5.63%), Euglenophyta (4.78%) and Cryptophyta (1.80%). The sequences of Ochrophyta, Verrucomicrobia, Bacteroidetes, Raphidophyta, Dinophyta and Firmicutes accounted for less than 1% of the total sequences. 268,723 sequences ranging from 16,821 to 51,542 were assigned to phytoplankton after the exclusion of bacteria (except cyanobacteria) and unclassified sequences (Table 3). The number of phytoplankton sequences was randomly rarefied to 16,821 per sample, which were used in further analyses of phytoplankton community structure and diversity.

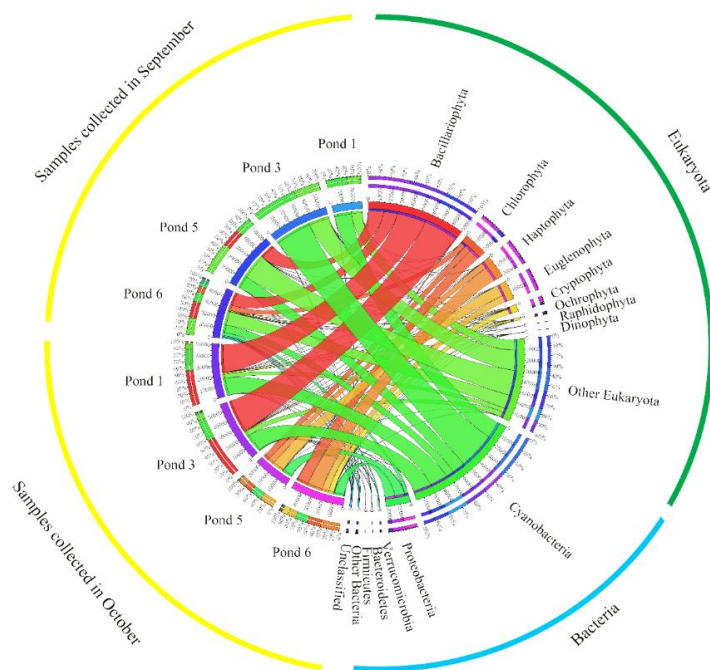


Figure 5. Circular representation of sequences assigned to eukaryota, bacteria and unclassified. Aquaculture model I consists of pond 1 where *F. chinensis* were co-cultured with *P. trituberculatus* and *O. niloticus* together and pond 3 where *M. meretrix* stocked. Aquaculture model II consists of pond 5 and 6 where *F. chinensis*, *P. trituberculatus* and *M. mercenaria* cultured together in the same pond

Phytoplankton community composition

A total of 68 OTUs assigned to phytoplankton were identified by high-throughput sequencing in the study (Table 3). The OTUs number of Cyanophyta was the highest (30.88%), followed by Chlorophyta (29.41%), Bacillariophyta (16.18%) and Dinophyta (5.88%). Cryptophyta, Ochrophyta and Haptophyta were represented by three OTUs, Euglenophyta was represented by two OTUs, and Raphidophyta was represented by only one OTU. Among these OTUs, OTU6, OTU94, OTU108, OTU148, which were affiliated with *Cyanobium gracile*, *Synechococcus* sp. WH 8020, *Nannochloropsis oculata* and *Cyclotella* sp. WC03_2, respectively, existed in all ponds (Table A.2).

Relative abundance of phytoplankton

In aquaculture mode I, Cyanophyta was the most dominant phylum in September with relative abundance > 99%, while Bacillariophyta was the dominant phylum in October with relative abundance > 59% (Fig. 6a). At genus level, *Cyanobium* was the most abundant in September, while *Leptocylindrus* was the most dominated, followed by *Cyanobium*, *Synechococcus* and *Cerataulina* in October (Fig. 6b).

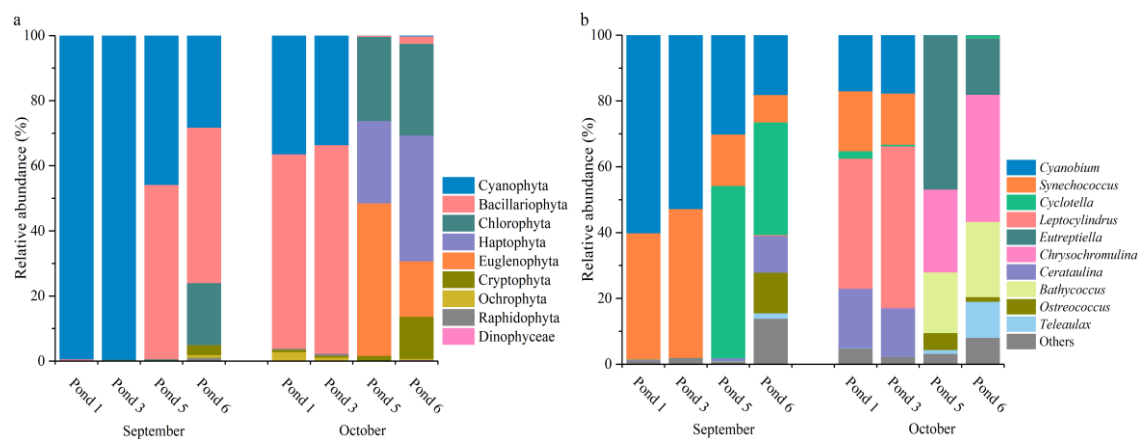


Figure 6. Relative abundance of phytoplankton at the phylum (a) and genus (b) levels.

Aquaculture model I consists of pond 1 where *F. chinensis* were co-cultured with *P. trituberculatus* and *O. niloticus* together and pond 3 where *M. meretrix* stocked. Aquaculture model II consists of pond 5 and 6 where *F. chinensis*, *P. trituberculatus* and *M. mercenaria* cultured together in the same pond

In aquaculture mode II, Bacillariophyta was the most dominant phylum, followed by Cyanophyta in September, while Euglenophyta, Haptophyta and Chlorophyta were the abundant phylum in October (Fig. 6a). At genus level, *Cyclotella* whose relative abundance was over 34%, was the most dominant genus, followed by *Cyanobium* in September, while *Eutreptiella*, *Chrysochromulina* and *Bathycoccus* were the abundant genus in October (Fig. 6b).

Phytoplankton diversity

Shannon indices were ranged from 1.72 to 2.42 in September and ranged from 1.44 to 2.06 in October. Phytoplankton diversity in September was lower than those in October in aquaculture model I, while phytoplankton diversity in September were

higher than those in October in aquaculture model II. By comparing pond 1 and 3, the phytoplankton diversity in pond 1 was higher than that in pond 3 in October (Fig. 7).

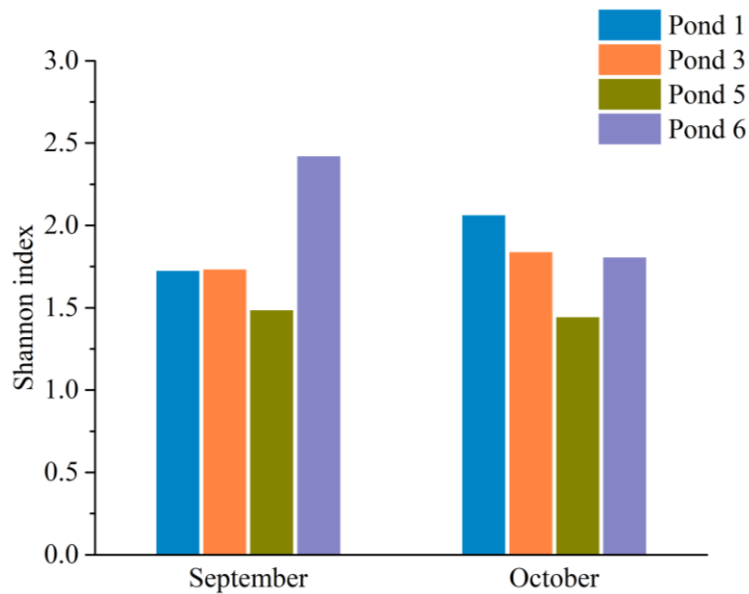


Figure 7. Phytoplankton diversity revealed by high-throughput sequencing. Aquaculture model I consists of pond 1 where *F. chinensis* were co-cultured with *P. trituberculatus* and *O. niloticus* together and pond 3 where *M. meretrix* stocked. Aquaculture model II consists of pond 5 and 6 where *F. chinensis*, *P. trituberculatus* and *M. mercenaria* cultured together in the same pond

Correlations between phytoplankton community and water quality

The relationship between the dominated species of phytoplankton revealed by morphological analysis and water quality parameters in the IMTA system were examined by direct gradient analysis using redundancy analysis (Fig. 8a). The first axis was positively correlated with the S (0.6066) and pH (0.6023), and negatively correlated with the T (-0.6595), DSi (-0.6087), DSi/DIP (-0.5620) and DSi/DIN (-0.5469). The second axis was positively correlated with DIN/DIP (0.8577), DON (0.7027), DIN (0.6518) and negatively correlated with S (-0.7241). These results showed that T, S, pH, DIN, DON, DSi, DIN/DIP, DSi/DIN and DSi/DIP greatly influenced on the phytoplankton community. The dominant species *L. danicus* was negatively correlated with the DIN, DIP, DSi, DON, DOP concentrations, DIN/DIP, DSi/DIN, DSi/DIP and *Vibrio* abundance. The euglenophyte *Eutreptiella* sp. and green algae *Pyramimonas* sp. had negative correlation with DIN, DON concentrations, DIN/DIP and *Vibrio* abundance and positive correlation with DIP, DOP concentrations, DSi/DIN and DSi/DIP. The relationships between abundant genus of phytoplankton revealed by high-throughput sequencing and water quality parameters in the IMTA system were examined by direct gradient analysis using canonical correspondence analysis (Fig. 8b). The first axis was positively correlated with the DOP (0.5697), DSi/DIN (0.5164) and negatively correlated with the DIN/DIP (-0.6759), and the second axis was positively correlated with the S (0.7849), pH (0.6670) and negatively correlated with the T (-0.8311), DIN (-0.6981), DSi (-0.6653), DIN/DIP (-0.6401) and DSi/DIP (-0.6074). These results showed that the T, S, pH, DIN, DOP, DSi, DIN/DIP, DSi/DIN and DSi/DIP had the greatest influences on the phytoplankton community. The diatom, *Leptocylindrus* was

negatively correlated with the DIN, DIP, DSi, DON, DOP concentrations, DIN/DIP, DSi/DIN, DSi/DIP and *Vibrio* abundance. The euglenophyte *Eutreptiella*, green algae *Bathycoccus* and *Ostreococcus*, and haptophyte *Chrysochromulina* showed negative correlation with DIN, DON concentrations, DIN/DIP and *Vibrio* abundance and positive correlation with DIP, DOP concentrations, DSi/DIN, while the cyanophytes, *Cyanobium* and *Synechococcus* showed positive correlations with DIN, DON concentrations, DIN/DIP and *Vibrio* abundance and negative correlation with DSi/DIN.

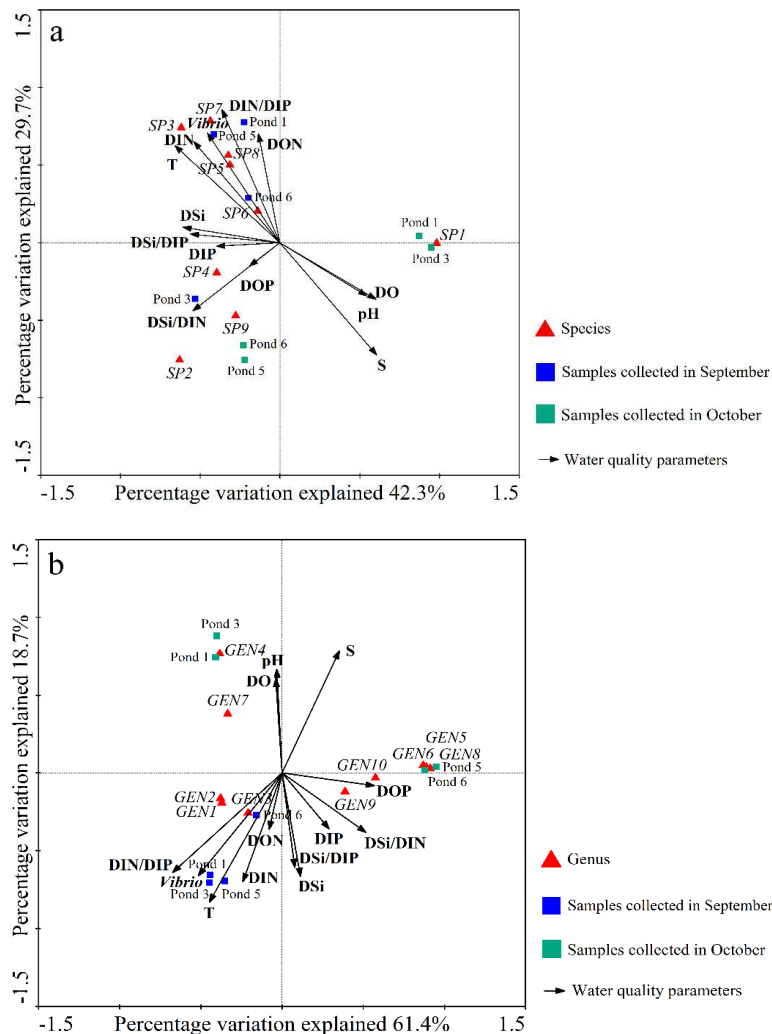


Figure 8. Direct gradient analysis of phytoplankton community revealed by morphological analysis (a) and high-throughput sequencing (b) methods and water quality parameters. The numbers with letter represent the relevant species or genus: SP1 *Leptocylindrus danicus*, SP2 *Eutreptiella* sp., SP3 *Cyclotella* sp., SP4 *Melosira* sp., SP5 *Surirella* sp., SP6 *Mastigocoleus* sp., SP7 *Cyclotella meneghiniana*, SP8 *Teleaulax acuta*, SP9 *Pyramimonas* sp., GEN1 *Cyanobium*, GEN2 *Synechococcus*, GEN3 *Cyclotella*, GEN4 *Leptocylindrus*, GEN5 *Eutreptiella*, GEN6 *Chrysochromulina*, GEN7 *Cerataulina*, GEN8 *Bathycoccus*, GEN9 *Ostreococcus*, GEN10 *Teleaulax*. Aquaculture model I consists of pond 1 where *F. chinensis* were co-cultured with *P. trituberculatus* and *O. niloticus* together and pond 3 where *M. meretrix* stocked. Aquaculture model II consists of pond 5 and 6 where *F. chinensis*, *P. trituberculatus* and *M. mercenaria* cultured together in the same pond

Discussion

Phytoplankton community structure revealed by two methods

In the late stage of aquaculture, the nutrients in the residual feeds are accumulated constantly in the pond water, leading to eutrophication and subsequently the flourishing of phytoplankton (Huang et al., 2016). Some phytoplankton groups, such as diatoms and green algae, are beneficial due to their high nutritional value and contribution to water quality (Roy and Pal, 2015; Brito et al., 2016). Other groups, such as cyanobacteria and dinoflagellates, are harmful because of their low nutritional value and toxins they produced (Sinden and Sinang, 2016; Pérez-Morales et al., 2017). Therefore, understanding the phytoplankton community is critical for good management and high yield in pond culture practice. In this study, 9 phyla of phytoplankton were identified by both 2 methods, and Bacillariophyta Cyanophyta and Euglenophyta were the dominant group. It is notable that phyla Ochrophyta, Haptophyta and Raphidophyta were only found by the high-throughput sequencing (Fig. 3, Fig. 6). A total of 60 genera were detected by both methods, but only 12 genera (*Cerataulina*, *Chaetoceros*, *Cyclotella*, *Cylindrotheca*, *Leptocylindrus*, *Nitzschia*, *Gymnodinium*, *Pyramimonas*, *Nephroselmis*, *Teleaulax*, *Chroomonas* and *Eutreptiella*) were consistent. Therefore, the combination of molecular and morphological techniques will be useful to get a comprehensive understanding of phytoplankton communities in aquatic ecosystems (Qiao et al., 2019).

In September, diatom was the dominant group in all ponds and the relative abundance of Cyanophyta was under 24% revealed by morphological analysis. While, cyanophyte of picoplanktonic cell sizes (0.2 to 2.0 μm) accounted for 28.26-99.54% of total phytoplankton abundance revealed by high-throughput sequencing, including *Cyanobium*, *Synechococcus* and *Synechocystis* (Fig. 6b), which were too small to observe by microscope. Cyanophytes had strong tolerance to pollutants, and often dominated the phytoplankton community (>88%) in shrimp ponds (Alonso-Rodriguez and Paez-Osuna, 2003). Studies have shown that the blue-green algae bloom, caused by changes in the weather, eutrophication of water, or imbalance between carbon, nitrogen and phosphorous in the water, results in deterioration of water quality and is highly detrimental to aquaculture organisms (Kong et al., 2013; Wu et al., 2013; Fu et al., 2015; Ajin et al., 2016). Furthermore, bloom-forming blue-green algae can produce a diverse array of secondary metabolites, some of which are toxic to plants, invertebrates and vertebrates including humans at naturally occurring concentrations (Smith et al., 2008; Meriluoto et al., 2017; Huisman et al., 2018). Therefore, it was necessary to take some measures (the reduction of undesirable algae via physical/chemical methods, and post-harvest treatment techniques) to control noxious algal blooms or remedy their effects (Smith et al., 2008). In October, the diatom, *L. danicus* was the most dominated species in aquaculture model I revealed by both methods, which reached a high cell density of 10^7 cells/L. *L. danicus* is 3-13 μm in diameter, 22-75 μm in pervalvar length, forming filamentous chains (Nanjappa et al., 2013). This alga has a fast growth rate and the potential to form auxospores and resting spores, which is clear advantages to survival (Ajani et al., 2016). Studies have shown that *L. danicus* is a major component of coastal phytoplankton communities (Nanjappa et al., 2013; Ajani et al., 2016). In aquaculture model II, the euglenophyte (*Eutreptiella*) was dominated revealed by both methods. Phototrophic euglenophytes have diverse roles in marine planktonic food webs: they are primary producers (Kingston, 1999); predators that feed on prey species such as eubacteria and picocyanobacteria (Yoo et al., 2018); and prey for diverse grazers such as heterotrophic dinoflagellates and ciliates (Jeong et al., 2011). In addition, some

euglenophytes could lead to dense blooms in diverse environments and produce the alkaloid toxin causing significant fish kills (Kingston, 2002; Zimba et al., 2017). Because of lacking of cell walls, euglenoids are very sensitive to environment change (Liu, 2009). In a natural environment, any action leading to a significant increase in the organic matter present will cause a marked cell deformation (Conforti, 1998), and might even cause algae dead and deterioration of water quality.

Except for the dominant species, some attention should also be paid to the toxic algae that might cause red tides. In this study, the raphidophyte, *Heterosigma akashiwo* was detected in pond 3 and 6 by high-throughput sequencing (Fig. 6a, Table A.2), but was missing in morphological analysis. This might be related to its lack of a cell wall. The addition of normal preservatives such as Lugol's solution has been shown to result in rapid cell clumping in some studies (Tyrrell et al., 2001; O'Halloran et al., 2006), making enumeration by light microscopy challenging. *H. akashiwo* has been implicated in fish killing blooms (Engesmo et al., 2016). Therefore, more attention should be paid to its potential toxicity to shrimp, crab and clam.

Relationships between water quality and phytoplankton community

During an aquaculture production cycle, feed supply in shrimp ponds increases concomitantly with the stocking biomass, which can induce an increasing eutrophication level in the pond ecosystem (Burford et al., 2003). Subsequently there is an increase in algal biomass. Phytoplankton communities are primary producers and consumers of dissolved oxygen and maintaining the stability in the stocking biomass and metabolic activity of phytoplankton communities is essential to provide a suitable environment for cultured animals. Changes in the phytoplankton community due to the increase in nutrients may result in outbreaks of harmful algal blooms (Alonso-Rodriguez and Paez-Osuna, 2003). Our results indicated that T, S, pH, DIN, DSi concentrations, DIN/DIP, DSi/DIN and DSi/DIP can affect the phytoplankton community structure inferred from both methods.

The cyanophytes (*Cyanobium* and *Synechococcus*) were dominated in September (Fig. 6a), while diatom (*Leptocylindrus*) and euglenophyte (*Eutreptiella*) were dominated in October (Fig. 3, Fig. 6a). On the one hand, the temperature in September (26°C) was suitable for the outbreak of cyanophytes (Paerl and Huisman, 2008); on the other hand, the cyanophytes could out-compete other phytoplankton organisms due to their high nutrient affinity, especially under conditions of phosphorus or nitrogen limitation (Moisander et al., 2003). Furthermore, some of the species can fix free nitrogen, making them superior competitors (González-Madina et al., 2019). In the present study, the cyanophytes showed positive correlation with DIN/DIP and negative correlation with DIP and DOP concentrations (Fig. 8). The result indicated that cyanophytes might be phosphorus limitation. Studies have shown that phosphorus availability is one of the main factors linked to the abundance of cyanobacteria, and cyanobacterial dominance increased with the increases of the total phosphorus concentration (Downing et al., 2011). Therefore, controlling internal phosphorus loading in ponds could be used to control cyanobacterial blooms that are likely to increase in frequency and intensity in response to eutrophication (Bormans et al., 2016). The cyanobacteria can fix nitrogen and use the organic nitrogen as their nitrogen resource, whose demand for inorganic nitrogen was lower than that of eukaryotes (Glibert et al., 2004). That might be the reason why the DIN concentration in September was higher than that in October (Table 1). The high DIN concentrations provided suitable nutrient conditions for the outbreak of diatom (*L. danicus*) and euglenophyte (*Eutreptiella*) in October. Studies suggested that diatom (*L. danicus*) and

euglenophyte favors nutrient-enriched seawater (Olli et al., 1996; Kingston, 2002; Zhu et al., 2009). In this study, the dominant species *L. danicus* was negatively correlated with the DIN, DIP, DSi, DON, DOP concentrations, DIN/DIP, DSi/DIN and DSi/DIP (Fig. 8). The results indicated that *L. danicus* might be able to utilize various forms of nutrients. Nutrient enrichment experiments indicated that nitrate, urea and phosphate addition promoted the growth of *L. danicus* (Zhu et al., 2009). The euglenophyte (*Eutreptiella*) showed negative correlation with DIN concentration and DIN/DIP (Fig. 8), which indicated euglenophyte could prefer to use DIN. Investigation reveals that high population of *Eutreptiella* was kept in the inner bay during the spring and summer associated with high DIN after river discharge following rainfall, suggesting that DIN supply might have triggered the increase of *Eutreptiella* population (Lee et al., 2016). The density and biomass of euglenophyte in heavily polluted areas were markedly higher than in a relatively clean area, which are used as biological indicators of the organic pollution of water (Stonik and Selina, 2001).

Statistical relationships between *Vibrio* and environmental parameters have suggested that high water temperature (Thompson et al., 2004) as well as low salinity favor the growth of *Vibrio* (Wright et al., 1996; DePaola et al., 2003). This is consistent with the results, which found positive correlation between *Vibrio* abundance and temperature and negative correlation between *Vibrio* abundance and salinity in this study (Fig. 8). In addition, *Vibrio* abundance had significant positive correlation with NH_4^+ ($p < 0.01$), suggesting that *Vibrio* was more likely to grow in the high ammonia water. Some studies indicated the importance of phytoplankton biomass, or phytoplankton community composition, for *Vibrio* growth (Turner et al., 2009). In this study, the relationship between phytoplankton community and *Vibrio* abundance were analyzed. The results showed that the diatoms and green algae were negatively correlated with *Vibrio* abundance, while the cyanophytes showed positive correlations with *Vibrio* abundance (Fig. 8). It can be inferred that diatoms and chlorophytes might inhibit the development of *Vibrio*, while cyanophytes bloom might be beneficial to the growth of *Vibrio*. Studies found that phytoplankton associated with green water, such as diatoms (*Chaetoceros calcitrans*, *Nitzschia* sp., *Skeletonema costatum*, *Phaeodactylum tricorutum*) and green algae (*Chlorella* spp., *Nannochlorum* sp., *Tetraselmis suecica*) can effectively inhibit the multiplication of *Vibrio* (Lio-Po et al., 2005; Makridis et al., 2006). On the contrary, some phytoplankton (such as cyanophytes) might facilitate the proliferation of *Vibrio* in their natural environment. Studies have shown that cyanobacterial-derived organic matter has been reported as an important growth factor for *Vibrio* (Eiler et al., 2007). In addition, it was demonstrated by both laboratory and field studies that cyanobacteria can play important roles as environmental reservoirs for *Vibrio* (Tamplin et al., 1990; Islam et al., 2004; Baffone et al., 2006). It was observed by phase-contrast, fluorescent, and immunoelectron microscopy that *Vibrio* were located within the mucilaginous sheath of cyanobacteria, and could multiply and maintain their progeny in cyanobacteria (Islam et al., 1999).

Aquaculture models influencing water quality and phytoplankton community structure

One of the key environmental concerns regarding aquaculture is the accumulation of nutrients, which can cause adverse effects in water quality deteriorations and the form of harmful algae blooms within ponds (Huang et al., 2016). Studies have shown that IMTA not only have higher nutrient use efficiency than monoculture, but also can improve aquaculture production (Wang et al., 1999; Tian et al., 2001; Hosseini Aghuzbeni et al., 2017; Li et al., 2019). However, the efficiency and ecological influence of pond aquaculture largely depends on species combination (Jena et al., 2002; Rahman and Verdegem, 2007).

In the present study, there were two aquaculture models. Aquaculture model I was consisting of a culture pond (pond 1), where shrimps were co-cultured with crab and tilapia together, and a biological purification pond (pond 3) with clam stocked. Aquaculture model II was polyculture of shrimp, crab and clam together in the same pond (*Fig. 1*). Investigations revealed that DIN (NH_4^+ , NO_3^- , NO_2^-) concentrations in pond 3 were lower than those in pond 1 (*Table 1*), which indicated that aquaculture pond attached to clam pond could be effectively purify water quality (Jones et al., 2002). In addition, the average concentrations of DIN in aquaculture model I were lower than those in aquaculture model II (*Table 1*). Therefore, the combination of aquaculture species should be reasonably selected according to different ecological niches.

Hierarchical clustering tree on OTU level showed that phytoplankton community structure in pond 1 was similar with that in pond 3, while phytoplankton community structure in pond 5 was similar with that in pond 6 (*Fig. 9*). Phytoplankton community structure in aquaculture waters is not only affected by water temperature, salinity, pH and nutrients, but also controlled by the top-down effect of aquaculture species (Hulot et al., 2018; Dantas et al., 2019).

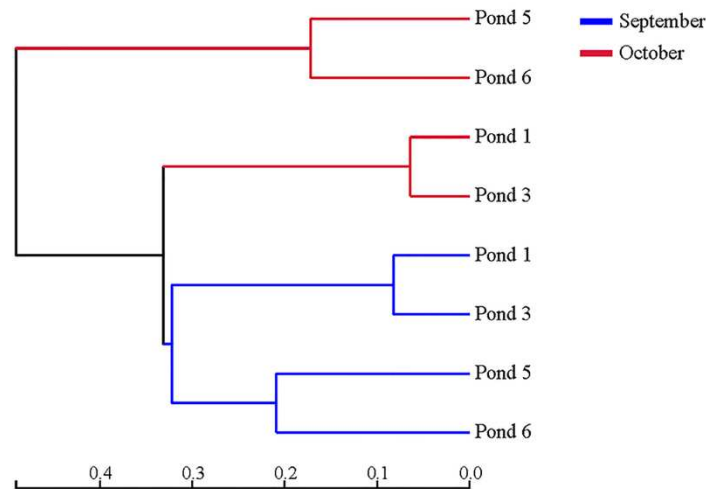


Figure 9. Hierarchical clustering tree on OTU level revealed by high-throughput sequencing. Aquaculture model I consists of pond 1 where *F. chinensis* were co-cultured with *P. trituberculatus* and *O. niloticus* together and pond 3 where *M. meretrix* stocked. Aquaculture model II consists of pond 5 and 6 where *F. chinensis*, *P. trituberculatus* and *M. mercenaria* cultured together in the same pond

Tilapia is a filter-feeding omnivorous fish that can have a negative effect on phytoplankton resources (Menezes et al., 2010; Sun et al., 2011) and their selective feeding regime can also unbalance phytoplankton constituents of the water column (Figueredo and Giani, 2005). Study has shown that tilapia feeds selectively on large algae (Figueredo and Giani, 2005). The dominant group in pond 1 in September was picocyanobacteria (*Cyanobium*, *Synechococcus* and *Synechocystis*) (*Fig. 6b*), which were too small ($< 3 \mu\text{m}$) to be ingested. In addition, feeding selectivity of tilapia changed slightly as their weight increased, resulting in a shift in phytoplankton community (Abdel-Tawwab, 2011). Investigations found that tilapia could select Cyanobacteria and Euglenophyceae at all fish weights, meanwhile Chlorophyceae and Bacillariophyceae were eaten with slight selectivity at larger weights (Abdel-Tawwab, 2011). And the strength of its effects on plankton

community should decrease with increasing plankton biomass, e.g., during an algal bloom (Vasconcelos et al., 2018). These might be the reason why diatoms dominated in aquaculture model I, while euglenophytes were abundant in aquaculture model II in October (Fig. 3).

Clams growth is highly adaptable to a wide range of temperatures and diet varieties making them a highly successful global aquaculture species well suited for IMTA (Troell et al., 2009). Clams are filter feeders that acquire energy filtering suspended particles such as phytoplankton and detritus (Reid et al., 2010; Macdonald et al., 2011; Sarà et al., 2012). Their selective feeding behavior could also affect phytoplankton community structure (Newell, 2004). In this study, some picophytoplankton including Cyanobacteria (*Cyanobium* and *Synechococcus*) and chlorophytes (*Bathycoccus* and *Ostreococcus*) were abundant revealed by high-throughput sequencing (Fig. 6). Studies have shown that larger nanoplankton cells may be preferentially removed in comparison with smaller picoplankton species that are retained less efficiently on the gill of most bivalve species (Newell, 2004), leading to the situation where picoplankton become relatively more abundant than larger species in areas with clam populations (Newell et al., 2009). Except for cell size, feeding selectivity was also dependent on nutritional value and swimming ability of phytoplankton (Bricelj et al., 1984; Zhuang et al., 2004). Cyanobacteria can produce microcystins, which have caused detrimental effects in aquatic organisms (Smith et al., 2008). Studies found that cyanobacteria could be recognized by selective filter-feeding invertebrates as nutritionally poor or toxic and the formation of colonies or elongated filaments could mechanically interfere with grazing (Smith et al., 2008). Therefore, one of the reasons cyanobacteria were dominated in September (Fig. 6) might be related to the low grazing pressure of clam. *Eutreptiella*, *Chrysochromulina* and *Teleaulax* have flagella, with which they can move freely (Edvardsen and Paasche, 1992; Rhodes and Burke, 1996; Stonik, 2007; Xing et al., 2008; Laza-Martínez et al., 2012). Their motility made them less easily ingested by clam, which might be one reason for its higher relative abundance.

Conclusions

In summary, Bacillariophyta, Cyanophyta and Euglenophyta were the dominant group in IMTA system in the late stage of aquaculture revealed by both morphological analysis and high-throughput sequencing. The dominant phytoplankton of the IMTA pond system in which clams were reared in a separate pond has changed from cyanophytes to diatoms from September to October, and it has changed from diatoms and cyanophytes to euglenophytes, haptophytes and green algae in the IMTA pond with shrimp, crab and clam together. The variables of temperature, salinity, pH, DIN, DSi concentrations, DIN/DIP, DSi/DIN and DSi/DIP were the main factors influencing the phytoplankton community structure. The relationship between phytoplankton community and *Vibrio* abundance indicated that diatoms and chlorophytes might inhibit the development of *Vibrio*, while cyanophytes bloom might be beneficial to the growth of *Vibrio*. A detailed description of the dynamics of phytoplankton community hasn't been given in this study since the samples only cover a period of 2 months. Hence there is a need to carry out successive studies to investigate the succession of the phytoplankton community within the culture ponds sampled over several years in order to fully characterize the variations both due to water quality and variability in climatic conditions. This study is useful for the future research as a foundation study towards characterization of phytoplankton community dynamics in an IMTA system.

Acknowledgements. We thank the manager and staff of the farm for providing experimental site, offering management data. This study was supported by the National Key Research and Development Program of China (2018YFD0900702-4), the Qingdao postdoctoral applied research project (JZ1920S10600), the National Natural Science Foundation of China (31873039), the China Agriculture Research System (No. CARS-48) and the Taishan Industrial Leader Talent Project of Shandong Province (No. LJNY 2015002).

REFERENCES

- [1] Abdel-Tawwab, M. (2011): Natural food selectivity changes with weights of Nile tilapia, *Oreochromis niloticus* (Linnaeus), reared in fertilized earthen ponds. – *Journal of Applied Aquaculture* 23(1): 58-66.
- [2] Acinas, S. G., Marcelino, L. A., Klepac-Ceraj, V., Polz, M. F. (2004): Divergence and redundancy of 16S rRNA sequences in genomes with multiple *rrn* operons. – *Journal of Bacteriology* 186(9): 2629-2635.
- [3] Ajani, P. A., Armbrecht, L. H., Kersten, O., Kohli, G. S., Murray, S. A. (2016): Diversity, temporal distribution and physiology of the centric diatom *Leptocyclus Cleve* (Bacillariophyta) from a southern hemisphere upwelling system. – *Diatom Research* 31(4): 351-365.
- [4] Ajin, A. M., Silvester, R., Alexander, D., Nashad, M., Abdulla, M. H. (2016): Characterization of blooming algae and bloom-associated changes in the water quality parameters of traditional pokkali cum prawn fields along the South West coast of India. – *Environmental Monitoring and Assessment* 188(3): 145.
- [5] Alonso-Rodríguez, R., Páez-Osuna, F. (2003): Nutrients, phytoplankton and harmful algal blooms in shrimp ponds: a review with special reference to the situation in the Gulf of California. – *Aquaculture* 219(1-4): 317-336.
- [6] Baffone, W., Tarsi, R., Pane, L., Campana, R., Repetto, B., Mariottini, G. L., Pruzzo, C. (2006): Detection of free-living and plankton-bound vibrios in coastal waters of the Adriatic Sea (Italy) and study of their pathogenicity-associated properties. – *Environmental Microbiology* 8(7): 1299-1305.
- [7] Bormans, M., Maršálek, B., Jančula, D. (2016): Controlling internal phosphorus loading in lakes by physical methods to reduce cyanobacterial blooms: a review. – *Aquatic Ecology* 50(3): 407-422.
- [8] Braak, C. T., Smilauer, P. (2002): *Canoco Reference Manual and User's Guide to Canoco for Windows: Software for Canonical Community Ordination (Version 4.5)*. – Microcomputer Power, New York.
- [9] Bricelj, V. M., Malouf, R. E. (1984): Influence of algal and suspended sediment concentrations on the feeding physiology of the hard clam *Mercenaria mercenaria*. – *Marine Biology* 84(2): 155-165.
- [10] Brito, L. O., dos Santos, I. G. S., de Abreu, J. L., de Araujo, M. T., Sever, W., Galvez, A. O. (2016): Effect of the addition of diatoms (*Navicula* spp.) and rotifers (*Brachionus plicatilis*) on water quality and growth of the *Litopenaeus vannamei* postlarvae reared in a biofloc system. – *Aquaculture Research* 47(12): 3990-3997.
- [11] Burford, M. A., Costanzo, S. D., Dennison, W. C., Jackson, C. J., Jones, A. B., McKinnon, A. D., Preston, N. P., Trott, L. A. (2003): A synthesis of dominant ecological processes in intensive shrimp ponds and adjacent coastal environments in NE Australia. – *Marine Pollution Bulletin* 46(11): 1456-1469.
- [12] Caporaso, J. G., Kuczynski, J., Stombaugh, J., Bittinger, K., Bushman, F. D., Costello, E. K., Fierer, N., Peña, A. G., Goodrich, J. K., Gordon, J. I., Huttley, G. A., Kelley, S. T., Knights, D., Koenig, J. E., Ley, R. E., Lozupone, C. A., McDonald, D., Muegge, B. D., Pirrung, M., Reeder, J., Sevinsky, J. R., Turnbaugh, P. J., Walters, W. A., Widmann, J.,

- Yatsunenکو, T., Zaneveld, J., Knight, R. (2010): QIIME allows analysis of high-throughput community sequencing data. – *Nature Methods* 7(5): 335-336.
- [13] Chopin, T., Robinson, S. M. C., Troell, M., Neori, A., Buschmann, A. H., Fang, J. (2008): Multitrophic Integration for Sustainable Marine Aquaculture. – In: Jorgensen, S. E., Fath, B. D. (eds.) *The Encyclopedia of Ecology, Ecological Engineering*, pp. 2463-2475.
- [14] Conforti, V. (1998): Morphological changes of Euglenophyta in response to organic enrichment. – *Springer-Interscience*, pp. 277-285.
- [15] Dantas, D. D., Rubim, P. L., de Oliveira, F. A., Da Costa, M. R., de Moura, C. G., Teixeira, L. H., Attayde, J. L. (2019): Effects of benthivorous and planktivorous fish on phosphorus cycling, phytoplankton biomass and water transparency of a tropical shallow lake. – *Hydrobiologia* 829(1): 31-41.
- [16] DePaola, A., Nordstrom, J. L., Bowers, J. C., Wells, J. G., Cook, D. W. (2003): Seasonal abundance of total and pathogenic *Vibrio parahaemolyticus* in Alabama oysters. – *Applied and Environmental Microbiology* 69(3): 1521-1526.
- [17] Downing, J. A., Watson, S. B., McCauley, E. (2001): Predicting cyanobacteria dominance in lakes. – *Canadian Journal of Fisheries and Aquatic Sciences* 58(10): 1905-1908.
- [18] Edgar, R. C. (2013): UPARSE: highly accurate OTU sequences from microbial amplicon reads. – *Nature Methods* 10(10): 996-998.
- [19] Edgar, R. C., Haas, B. J., Clemente, J. C., Quince, C., Knight, R. (2011): Uchime improves sensitivity and speed of chimera detection. – *Bioinformatics* 27(16): 2194.
- [20] Edvardsen, B., Paasche, E. (1992): Two motile stages of *Chrysochromulina polylepis* (prymnesiophyceae): morphology, growth, and toxicity. – *Journal of Phycology* 28(1): 104-114.
- [21] Eiler, A., Gonzalez-Rey, C., Allen, S., Bertilsson, S. (2007): Growth response of *Vibrio cholerae* and other *Vibrio* spp. to cyanobacterial dissolved organic matter and temperature in brackish water. – *FEMS Microbiology Ecology* 60(3): 411-418.
- [22] Engesmo, A., Eikrem, W., Seoane, S., Smith, K., Edvardsen, B., Hofgaard, A., Tomas, C. R. (2016): New insights into the morphology and phylogeny of *Heterosigma akashiwo* (Raphidophyceae): with the description of *Heterosigma minor* sp. nov. – *Phycologia* 55(3): 279-294.
- [23] Figueredo, C. C., Giani, A. (2005): Ecological interactions between Nile tilapia (*Oreochromis niloticus*, L.) and the phytoplanktonic community of the Furnas Reservoir (Brazil). – *Freshwater Biology* 50(8): 1391-1403.
- [24] Fu, K. Z., Moe, B., Li, X., Le, X. C. (2015): Cyanobacterial bloom dynamics in Lake Taihu. – *Journal of Environmental Sciences* 32: 249-251.
- [25] Glibert, P. M., Heil, C. A., Hollander, D. J., Revilla, M. I., Hoare, A., Alexander, J. A., Murasko, S. (2004): Evidence for dissolved organic nitrogen and phosphorus uptake during a cyanobacterial bloom in Florida Bay. – *Marine Ecology Progress Series* 280: 73-83.
- [26] González-Madina, L., Pacheco, J. P., Yema, L., de Tezanos, P., Levrini, P., Clemente, J., Crisci, C., Lagomarsino, J. J., Méndez, G., Fosalba, C. (2019): Drivers of cyanobacteria dominance, composition and nitrogen fixing behavior in a shallow lake with alternative regimes in time and space, Laguna del Sauce (Maldonado, Uruguay). – *Hydrobiologia* 829(1): 61-76.
- [27] Harrison, W. G., Perry, T., Li, W. K. (2005): Ecosystem indicators of water quality Part I. Plankton biomass, primary production and nutrient demand. – *Springer-Interscience*, pp. 59-82.
- [28] Hosseini Aghuzbeni, S. H., Hajirezaee, S., Matinfar, A., Khara, H., Ghobadi, M. (2017): A preliminary study on polyculture of western white shrimp (*Litopenaeus vannamei*) with mullet (*Mugil cephalus*): an assessment of water quality, growth parameters, feed intake efficiency and survival. – *Journal of Applied Animal Research* 45(1): 247-251.

- [29] Huang, S., Wu, M., Zang, C., Du, S., Domagalski, J., Gajewska, M., Gao, F., Lin, C., Guo, Y., Liu, B. (2016): Dynamics of algae growth and nutrients in experimental enclosures culturing bighead carp and common carp: Phosphorus dynamics. – *International Journal of Sediment Research* 31(2): 173-180.
- [30] Huisman, J., Codd, G. A., Paerl, H. W., Ibelings, B. W., Verspagen, J. M. H., Visser, P. M. (2018): Cyanobacterial blooms. – *Nature Reviews Microbiology* 16(8): 471-483.
- [31] Hulot, V., Saulnier, D., Lafabrie, C., Gaertner-Mazouni, N. (2018): Shrimp culture: a complex driver of planktonic communities. – *Reviews in Aquaculture*: 1-14.
- [32] Islam, M. S., Rahim, Z., Alam, M. J., Begum, S., Moniruzzaman, S. M., Umeda, A., Amako, K., Albert, M. J., Sack, R. B., Huq, A. (1999): Association of *Vibrio cholerae* O1 with the cyanobacterium, *Anabaena* sp., elucidated by polymerase chain reaction and transmission electron microscopy. – *Transactions of the Royal Society of Tropical Medicine and Hygiene* 93(1): 36-40.
- [33] Islam, M. S., Mahmuda, S., Morshed, M. G., Bakht, H. B., Khan, M. N., Sack, R. B., Sack, D. A. (2004): Role of cyanobacteria in the persistence of *Vibrio cholerae* O139 in saline microcosms. – *Canadian journal of microbiology* 50(2): 127-131.
- [34] Jena, J. K., Ayyappan, S., Aravindakshan, P. K., Dash, B., Singh, S. K., Muduli, H. K. (2002): Evaluation of production performance in carp polyculture with different stocking densities and species combinations. – *Journal of Applied Ichthyology* 18(3): 165-171.
- [35] Jeong, H. J., Kim, T. H., Yoo, Y. D., Yoon, E. Y., Kim, J. S., Seong, K. A., Kim, K. Y., Park, J. Y. (2011): Grazing impact of heterotrophic dinoflagellates and ciliates on common red-tide euglenophyte *Eutreptiella gymnastica* in Masan Bay, Korea. – *Harmful Algae* 10(6): 576-588.
- [36] Jones, A. B., Preston, N. P., Dennison, W. C. (2002): The efficiency and condition of oysters and macroalgae used as biological filters of shrimp pond effluent. – *Aquaculture Research* 33(1): 1-19.
- [37] Justić, D., Rabalais, N. N., Turner, R. E., Dortch, Q. (1995): Changes in nutrient structure of river-dominated coastal waters: stoichiometric nutrient balance and its consequences. – *Estuarine, Coastal and Shelf Science* 40(3): 339-356.
- [38] Kingston, M. B. (1999): Effect of light on vertical migration and photosynthesis of *Euglena proxima* (Euglenophyta). – *Journal of Phycology* 35(2): 245-253.
- [39] Kingston, M. B. (2002): Effect of subsurface nutrient supplies on the vertical migration of *Euglena proxima* (Euglenophyta). – *Journal of Phycology* 38(5): 872-880.
- [40] Kong, Y., Xu, X., Zhu, L., Miao, L. (2013): Control of the harmful alga *Microcystis aeruginosa* and absorption of nitrogen and phosphorus by *Candida utilis*. – *Applied Biochemistry and Biotechnology* 169(1): 88-99.
- [41] Laza-Martínez, A., Arluzea, J., Miguel, I., Orive, E. (2012): Morphological and molecular characterization of *Teleaulax gracilis* sp. nov. and *T. minuta* sp. nov. (Cryptophyceae). – *Phycologia* 36(1): 37-52.
- [42] Lee, M. J., Kim, D., Kim, Y. O., Sohn, M., Moon, C. H., Baek, S. H. (2016): Seasonal phytoplankton growth and distribution pattern by environmental factor changes in inner and outer bay of Ulsan, Korea. – *The Sea* 21(1): 24-35.
- [43] Li, Y., Qin, J., Zheng, X., Wang, Y. (2019): Production performance of largemouth bass *Micropterus salmoides* and water quality variation in monoculture, polyculture and integrated culture. – *Aquaculture Research* 50(2): 423-430.
- [44] Lio-Po, G. D., Leño, E. M., Peñaranda, M. M. D., Villa-Franco, A. U., Sombito, C. D., Guanzon Jr, N. G. (2005): Anti-luminous *Vibrio* factors associated with the 'green water' grow-out culture of the tiger shrimp *Penaeus monodon*. – *Aquaculture* 250(1-2): 1-7.
- [45] Liu, G. (2009): Characteristics, harm and regulation of Euclyorophyta bloom in aquaculture ponds. – *China Fisheries* 2: 59-60.
- [46] MacDonald, B. A., Robinson, S. M. C., Barrington, K. A. (2011): Feeding activity of mussels (*Mytilus edulis*) held in the field at an integrated multi-trophic aquaculture

- (IMTA) site (*Salmo salar*) and exposed to fish food in the laboratory. – *Aquaculture* 314(1-4): 244-251.
- [47] Magoc, T., Salzberg, S. L. (2011): Flash: fast length adjustment of short reads to improve genome assemblies. – *Bioinformatics* 27(21): 2957-2963.
- [48] Makridis, P., Costa, R. A., Dinis, M. T. (2006): Microbial conditions and antimicrobial activity in cultures of two microalgae species, *Tetraselmis chuii* and *Chlorella minutissima*, and effect on bacterial load of enriched *Artemia* metanauplii. – *Aquaculture* 255(1-4): 76-81.
- [49] Martins, T. G., Odebrecht, C., Jensen, L. V., D'Oca, M. G., Wasielesky Jr, W. (2016): The contribution of diatoms to bioflocs lipid content and the performance of juvenile *Litopenaeus vannamei* (Boone, 1931) in a BFT culture system. – *Aquaculture Research* 47(4): 1315-1326.
- [50] Menezes, R. F., Attayde, J. L., Rivera Vasconcelos, F. (2010): Effects of omnivorous filter-feeding fish and nutrient enrichment on the plankton community and water transparency of a tropical reservoir. – *Freshwater Biology* 55(4): 767-779.
- [51] Meriluoto, J., Spoof, L., Codd, G. A. (2017): Handbook of cyanobacterial monitoring and cyanotoxin analysis. – Wiley-Interscience, New York.
- [52] Moisaner, P. H., Steppe, T. F., Hall, N. S., Kuparinen, J., Paerl, H. W. (2003): Variability in nitrogen and phosphorus limitation for Baltic Sea phytoplankton during nitrogen-fixing cyanobacterial blooms. – *Marine Ecology Progress Series* 262: 81-95.
- [53] Nanjappa, D., Kooistra, W. H., Zingone, A. (2013): A reappraisal of the genus *Leptocylindrus* (Bacillariophyta): with the addition of three species and the erection of *Tenuicylindrus* gen. nov. – *Journal of Phycology* 49(5): 917-936.
- [54] Newell, R. I. E. (2004): Ecosystem influences of natural and cultivated populations of suspension-feeding bivalve molluscs: a review. – *Journal of Shellfish Research* 23(1): 51-62.
- [55] Newell, R. I. E., Tettelbach, S. T., Gobler, C. J., Kimmel, D. G. (2009): Relationships between reproduction in suspension-feeding hard clams *Mercenaria mercenaria* and phytoplankton community structure. – *Marine Ecology Progress* 387(12): 179-196.
- [56] O'Halloran, C., Silver, M. W., Holman, T. R., Scholin, C. A. (2006): *Heterosigma akashiwo* in central California waters. – *Harmful Algae* 5(2): 124-132.
- [57] Olli, K., Heiskanen, A., Seppälä, J. (1996): Development and fate of *Eutreptiella gymnastica* bloom in nutrient-enriched enclosures in the coastal Baltic Sea. – *Journal of Plankton Research* 18(9): 1587-1604.
- [58] Paerl, H. W., Huisman, J. (2008): Blooms like it hot. – *Science* 320(5872): 57-58.
- [59] Parsons, T. R., Maita, Y., Lalli, C. M. (1984): A manual of chemical and biological methods for seawater analysis. – Pergamon Press, Oxford.
- [60] Pérez-Morales, A., Band-Schmidt, C. J., Martínez-Díaz, S. F. (2017): Mortality on zoea stage of the Pacific white shrimp *Litopenaeus vannamei* caused by *Cochlodinium polykrikoides* (Dinophyceae) and *Chattonella* spp. (Raphidophyceae). – *Marine Biology* 164(3): 57.
- [61] Pruzzo, C., Huq, A., Colwell, R. R., Donelli, G. (2005a): Pathogenic *Vibrio* species in the marine and estuarine environment. – In: Belkin, S., Colwell, R. R. (eds.) *Oceans and Health: Pathogens in the Marine Environment*. Springer, Boston MA, pp. 217-252.
- [62] Pruzzo, C., Gallo, G., Canesi, L. (2005b): Persistence of vibrios in marine bivalves: the role of interactions with haemolymph components. – *Environmental Microbiology* 7(6): 761-772.
- [63] Pulz, O., Gross, W. (2004): Valuable products from biotechnology of microalgae. – *Applied Microbiology and Biotechnology* 65(6): 635-648.
- [64] Qiao, L., Chang, Z., Li, J., Chen, Z., Yang, L., Luo, Q. (2019): Phytoplankton community structure and diversity in the indoor industrial aquaculture system for *Litopenaeus vannamei* revealed by high-throughput sequencing and morphological identification. – *Aquaculture Research* 50(9): 2563-2576.

- [65] Rahman, M. M., Verdegem, M. C. (2007): Multi-species fishpond and nutrients balance. – In: van der Zijpp, A. J., Verreth, J. A. J., Le Quang Tri, van Mensvoort, M. E. F., Bosma, R. H., Beveridge, M. C. M. (eds.) *Fishponds in farming systems*. Wageningen Academic Publishers, The-Netherlands, pp. 79-88.
- [66] Reid, G. K., Liutkus, M., Bennett, A., Robinson, S. M. C., Macdonald, B., Page, F. (2010): Absorption efficiency of blue mussels (*Mytilus edulis* and *M. trossulus*) feeding on Atlantic salmon (*Salmo salar*) feed and fecal particulates: Implications for integrated multi-trophic aquaculture. – *Aquaculture* 299(1): 165-169.
- [67] Rhodes, L., Burke, B. (1996): Morphology and growth characteristics of *Chrysochromulina* species (Haptophyceae = Prymnesiophyceae) isolated from New Zealand coastal waters. – *New Zealand Journal of Marine and Freshwater Research* 30(1): 91-103.
- [68] Roy, S. S., Pal, R. (2015): Microalgae in Aquaculture: A Review with Special References to Nutritional Value and Fish Dietetics. – *Proceedings of the Zoological Society* 68(1): 1-8.
- [69] SAC (2007): The specification for marine monitoring-Part 4: Seawater analysis. – GB 17378.4-2007 Standards Press of China -Interscience, China. (in Chinese).
- [70] Sarà, G., Reid, G. K., Rinaldi, A., Palmeri, V., Troell, M., Kooijman, S. A. L. M. (2012): Growth and reproductive simulation of candidate shellfish species at fish cages in the Southern Mediterranean: Dynamic Energy Budget (DEB) modelling for integrated multi-trophic aquaculture. – *Aquaculture* 324(5): 259-266.
- [71] Sherwood, A. R., Presting, G. G. (2007): Universal primers amplify a 23S rDNA plastid marker in eukaryotic algae and cyanobacteria. – *Journal of Phycology* 43(3): 605-608.
- [72] Sinden, A., Sinang, S. C. (2016): Cyanobacteria in aquaculture systems: linking the occurrence, abundance and toxicity with rising temperatures. – *International Journal of Environmental Science and Technology* 13(12): 2855-2862.
- [73] Sladonja, B. (2011): *Aquaculture and the Environment: A Shared Destiny*. – InTech-Interscience, Croatia.
- [74] Smith, J. L., Boyer, G. L., Zimba, P. V. (2008): A review of cyanobacterial odorous and bioactive metabolites: impacts and management alternatives in aquaculture. – *Aquaculture* 280(1-4): 5-20.
- [75] Stonik, I. V. (2007): Species of the genus *Eutreptiella* (Euglenophyceae) from Russian waters of East/Japan Sea. – *Ocean Science Journal* 42(2): 81-88.
- [76] Stonik, I. V., Selina, M. S. (2001): Species composition and seasonal dynamics of density and biomass of euglenoids in Peter the Great Bay, Sea of Japan. – *Russian Journal of Marine Biology* 27(3): 174-176.
- [77] Sun, W., Dong, S., Jie, Z., Zhao, X., Zhang, H., Li, J. (2011): The impact of net-isolated polyculture of tilapia (*Oreochromis niloticus*) on plankton community in saline-alkaline pond of shrimp (*Penaeus vannamei*). – *Aquaculture International* 19(4): 779-788.
- [78] Tamplin, M. L., Gauzens, A. L., Huq, A., Sack, D. A., Colwell, R. R. (1990): Attachment of *Vibrio cholerae* serogroup O1 to zooplankton and phytoplankton of Bangladesh waters. – *Applied and Environmental Microbiology* 56(6): 1977-1980.
- [79] Thompson, J. R., Randa, M. A., Marcelino, L. A., Tomita-Mitchell, A., Lim, E., Polz, M. F. (2004): Diversity and dynamics of a North Atlantic coastal *Vibrio* community. – *Applied and Environmental Microbiology* 70(7): 4103-4110.
- [80] Tian, X., Li, D., Dong, S., Yan, X., Qi, Z., Liu, G., Lu, J. (2001): An experimental study on closed-polyculture of penaeid shrimp with tilapia and constricted tagelus. – *Aquaculture* 202(1-2): 57-71.
- [81] Troell, M., Joyce, A., Chopin, T., Neori, A., Buschmann, A. H., Fang, J. (2009): Ecological engineering in aquaculture-potential for integrated multi-trophic aquaculture (IMTA) in marine offshore systems. – *Aquaculture* 297(1-4): 1-9.

- [82] Turner, J. W., Good, B., Cole, D., Lipp, E. K. (2009): Plankton composition and environmental factors contribute to *Vibrio* seasonality. – The ISME journal 3(9): 1082-1092.
- [83] Tyrrell, J. V., Bergquist, P. R., Bergquist, P. L., Scholin, C. A. (2001): Detection and enumeration of *Heterosigma akashiwo* and *Fibrocapsa japonica* (Raphidophyceae) using rRNA-targeted oligonucleotide probes. – Phycologia 40(5): 457-467.
- [84] Vasconcelos, F. R., Menezes, R. F., Attayde, J. L. (2018): Effects of the Nile tilapia (*Oreochromis niloticus* L.) on the plankton community of a tropical reservoir during and after an algal bloom. – Hydrobiologia: 1-9.
- [85] Vezzulli, L., Brettar, I., Pezzati, E., Reid, P. C., Colwell, R. R., Höfle, M. G., Pruzzo, C. (2012): Long-term effects of ocean warming on the prokaryotic community: evidence from the vibrios. – The ISME journal 6(1): 21-30.
- [86] Wang, J., Li, D., Dong, S., Wang, K., Tian, X. (1999): Comparative studies on cultural efficiency and profits of different polycultural systems in penaeid shrimp ponds. – Journal of Fisheries of China 23(1): 45-52. (in Chinese).
- [87] Wartenberg, R., Feng, L., Wu, J. J., Mak, Y. L., Chan, L. L., Telfer, T. C., Lam, P. K. (2017): The impacts of suspended mariculture on coastal zones in China and the scope for Integrated Multi-Trophic Aquaculture. – Ecosystem Health and Sustainability 3(6): 1340268.
- [88] Wright, A. C., Hill, R. T., Johnson, J. A., Roghman, M., Colwell, R. R., Morris, J. G. (1996): Distribution of *Vibrio vulnificus* in the Chesapeake Bay. – Applied and Environmental Microbiology 62(2): 717-724.
- [89] Wu, T., Qin, B., Zhu, G., Luo, L., Ding, Y., Bian, G. (2013): Dynamics of cyanobacterial bloom formation during short-term hydrodynamic fluctuation in a large shallow, eutrophic, and wind-exposed Lake Taihu, China. – Environmental Science and Pollution Research 20(12): 8546-8556.
- [90] Xing, X., Chen, C., Gao, Y., Liang, J., Huang, H., Li, B., Ho, K., Lin, X., Qi, Y. (2008): Observations of several cryptomonad flagellates from China Sea by scanning electron microscopy. – Journal of Systematics and Evolution 46(2): 205-212.
- [91] Xu, F., Hu, L., Zhou, Z., Zhong, N., Wu, S., Cai, T., Peng, L., Zhu, S. (2015): The algae on the impact of change on aquaculture research progress. – Journal of Aquaculture 36(1): 48-52. (in Chinese).
- [92] Yoo, Y. D., Seong, K. A., Kim, H. S., Jeong, H. J., Yoon, E. Y., Park, J., Kim, J. I., Shin, W., Palenik, B. (2018): Feeding and grazing impact by the bloom-forming euglenophyte *Eutreptiella eupharyngea* on marine eubacteria and cyanobacteria. – Harmful Algae 73: 98-109.
- [93] Zhu, A. J., Huang, L. M., Lin, Q. Y., Zhan-Zhou, X. U. (2009): Influence of nitrogen and phosphorus on phytoplankton community structure in the Dapeng'ao Bay, Daya Bay: II Species composition. – Journal of Tropical Oceanography 28(6): 103-111. (in Chinese).
- [94] Zhuang, S. H., Wang, Z. Q. (2004): Influence of size, habitat and food concentration on the feeding ecology of the bivalve, *Meretrix meretrix* Linnaeus. – Aquaculture 241(1-4): 689-699.
- [95] Zimba, P. V., Huang, I., Gutierrez, D., Shin, W., Bennett, M. S., Triemer, R. E. (2017): Euglenophycin is produced in at least six species of euglenoid algae and six of seven strains of *Euglena sanguinea*. – Harmful Algae 63: 79-84.

APPENDICES

Table A.1. List of phytoplankton species from integrated multi-trophic aquaculture system revealed by morphological analysis

Phylum	Species	September				October			
		Pond 1	Pond 3	Pond 5	Pond 6	Pond 1	Pond 3	Pond 5	Pond 6
Bacillariophyta	<i>Cerataulina pelagica</i> (Cleve) Hendey							√	
	<i>Chaetoceros</i> sp.				√				√
	<i>Cyclotella meneghiniana</i> Kuetzing	√	√	√	√	√	√	√	
	<i>Cyclotella</i> sp.	√	√	√	√	√	√	√	√
	<i>Cyclotella striata</i> (Kütz.) Grunow in Cleve & Grunow	√	√	√	√	√	√	√	
	<i>Cylindrotheca closterium</i> (Ehr.) Reimann et Lewin	√	√					√	√
	<i>Dactyliosolen fragilissimus</i> (Bergon) Hasle, 1996	√							
	<i>Melosira</i> sp.	√	√						
	<i>Navicula</i> sp.	√		√	√		√	√	√
	<i>Nitzschia</i> sp.1	√	√	√	√	√	√	√	√
	<i>Nitzschia</i> sp.2	√	√	√					
	<i>Nitzschia panduriformis</i>						√	√	
	<i>Pinnularia</i> sp.	√	√	√	√		√	√	√
	<i>Pleurosigma</i> sp.	√	√				√		
	<i>Skeletonema costatum</i> (Greville) Cleve emend. Zingone et Sarno	√		√					
	<i>Surirella</i> sp.			√	√				
	<i>Amphora</i> sp.				√		√	√	√
	<i>Amphiprora alata</i> (Ehrenebrg) Kuetzings							√	√
	<i>Leptocylindrus danicus</i>				√	√	√	√	√
	<i>Pleurosigma acutum</i>				√		√	√	√
	<i>Achnanthes brevipes</i>							√	
	<i>Melosira sulcata</i>				√				
	Dinophyta	<i>Gymnodinium</i> spp.	√	√	√	√	√	√	√
<i>Gymnodinium simplex</i> (Lohmann) Kofoid & Swezy			√	√		√	√	√	√
<i>Gonyaulax verior</i> Sourmai		√							
<i>Gyrodinium spirale</i> (Bergh) Kofoid et Swezy					√	√	√	√	
<i>Prorocentrum micans</i> Ehrenberg						√	√		
<i>Protoperidinium pellucidum</i>						√	√		
<i>Protoperidinium</i> sp.						√	√	√	
<i>Azadinium</i> sp.							√		
<i>Scrippsiella trochoidea</i>						√			
Cryptophyta	<i>Chroomonas acuta</i> Uterm			√	√		√	√	√
	<i>Teleaulax acuta</i>	√	√	√					
	<i>Cryptomonas</i> sp.					√		√	√
	<i>Rhodomonas</i> sp.			√					√
	<i>Teleaulax</i> sp.						√	√	√
Chlorophyta	<i>Dunaliella salina</i> (Dunal) Teodoresco, 1905				√				
	<i>Pyramimonas</i> sp.		√	√		√	√	√	√
	<i>Nephroselmis pyriformis</i> (N. Carter) Ettl		√	√					
	<i>Scenedesmus</i> sp.								√
Cyanophyta	<i>Oscillatoria</i> sp.	√	√	√					
	<i>Chroococcus turgidus</i>				√				
	<i>Mastigocoleus</i> sp.				√				
Euglenophyta	<i>Eutreptiella</i> sp.		√	√	√	√	√	√	√

Table A.2. List of phytoplankton species from integrated multi-trophic aquaculture system revealed by high-throughput sequencing

Phylum	Species	September				October			
		Pond 1	Pond 3	Pond 5	Pond 6	Pond 1	Pond 3	Pond 5	Pond 6
Cyanophyta	OTU1	√	√	√		√	√		
	OTU2	√	√	√	√	√	√		
	OTU4	√	√		√	√	√		
	OTU5	√	√	√	√	√	√		√
	OTU6	√	√	√	√	√	√	√	√
	OTU13	√	√	√		√	√		
	OTU20								
	OTU21	√				√	√		
	OTU23				√				√
	OTU35				√				
	OTU61	√	√	√		√	√		
	OTU63	√	√	√		√	√		
	OTU64				√	√	√		
	OTU72		√			√	√		
	OTU73		√			√	√		
	OTU84	√	√	√	√	√	√		
	OTU93	√	√	√	√	√	√		
	OTU94	√	√	√	√	√	√	√	√
	OTU95	√	√	√	√	√	√	√	√
	OTU97	√	√	√	√	√	√	√	√
OTU106	√	√	√	√	√	√	√	√	
Chlorophyta	OTU3	√	√		√				
	OTU19	√	√		√				
	OTU32			√				√	√
	OTU42			√				√	
	OTU44		√	√	√			√	
	OTU50							√	
	OTU74	√	√				√	√	
	OTU88	√	√			√	√	√	√
	OTU99					√	√	√	
	OTU110							√	√
	OTU116				√			√	√
	OTU121			√				√	√
	OTU122							√	√
	OTU123	√	√			√	√	√	√
	OTU127							√	
	OTU136				√				√
	OTU145					√			√
	OTU154					√	√	√	√
OTU155			√				√	√	
OTU157					√		√	√	
Bacillariophyta	OTU10			√	√			√	
	OTU14			√	√				
	OTU26				√				
	OTU79					√	√		
	OTU96	√		√		√	√		
	OTU105	√				√	√	√	√
	OTU109	√	√	√		√	√		
	OTU128			√					
	OTU135								√
	OTU146			√		√	√	√	√
	OTU148	√	√	√		√	√	√	√
Dinophyta	OTU69			√		√	√	√	√
	OTU71					√	√		
	OTU152								√
	OTU162								√
Cryptophyta	OTU111		√	√		√	√	√	√
	OTU117			√		√	√	√	√
	OTU119			√	√	√	√	√	√

Phylum	Species	September				October			
		Pond 1	Pond 3	Pond 5	Pond 6	Pond 1	Pond 3	Pond 5	Pond 6
Ochrophyta	OTU78					√	√		
	OTU107					√	√		
	OTU108	√	√	√	√	√	√	√	√
Haptophyta	OTU75					√	√	√	
	OTU103					√	√	√	
	OTU114	√	√		√	√	√	√	√
Euglenophyta	OTU43				√				
	OTU124			√		√	√	√	√
Raphidophyta	OTU137		√		√				√

COMPOSITION AND DISTRIBUTION OF COMMON REED (*PHRAGMITES AUSTRALIS*) ALONG AN URBANIZED RIVER: A CASE FROM CENTRAL JAPAN

CAO, Y.* – NATUHARA, Y.

Graduate School of Environmental Studies, Nagoya University, Nagoya 4648601, Japan

**Corresponding author
e-mail: cao0019@outlook.com*

(Received 20th Nov 2019; accepted 23rd Mar 2020)

Abstract. As an attraction of anthropogenic activity, the impact of artificial disturbance on riparian ecosystems is an increasingly ecological question. However, how riparian species response to urbanization and human disturbance is unclear. This research aimed to study the relationship between ecological characteristics of the common reed and environmental factors along an urbanized river. The 40 sampling plots along the Shonai River that run across the urban and suburban areas of central Japan were investigated. The distribution of common reed was investigated in six plant community types with different species composition. We found that common reed with a dominant stand tends to distributed in the riparian habitats that close to the river while far from roads. Our results showed that the soil properties such as electrical conductivity, and pH were negatively related to the colonization of common reed. Among the anthropogenic factors, the percentage of impervious surface and distance to the road had a negative correlation with the coverage and biomass of common reed. These results suggested that the negative effects of anthropogenic impacts on the ecology of common reed, and appropriate management should be conducted to maintain the sustainability in riparian areas.

Keywords: *common reed, urban ecology, riparian areas, vegetation–environment interactions, land cover, soil property*

Introduction

Riparian areas are aquatic-terrestrial ecotones formed by fluvial and upland ecological process, are comprised of a series of heterogonous environments and various vegetation communities (Décamps et al., 2009). Vegetation composition and diversity within the riparian area are highly variable due to the influence of various environmental factors (e.g., flooding regime, soil condition, topography, and anthropogenic disturbances), which restrict the occurrence and colonization of riparian species (Lyon and Gross, 2005). Also, riparian areas are the most sensitive ecosystem compare with the surrounding environment, but also the most severely disturbed by human beings globally (González et al., 2017).

Urbanization and human impact driving profound changes to the natural ecosystems that remain with urbanized areas (Zipperer et al., 2012). In riparian areas, urbanization and the human impact such as land-use change, the construction of flood protection works, soil and water pollution, and human trampling would be associated with the structure and distribution patterns of riparian plant communities (Cao, 2019). However, there are few studies on the distribution pattern of riparian plant species at a local level, despite the availability of some studies referring to the correspondence with habitat conditions and distribution patterns of main component species of riparian area (Mligo, 2016). Few studies have been conducted to focus on the effect of land-use and human impact on the composition and distribution patterns of riparian plant species.

Common reed (*Phragmites australis*) is a constructive species in the riparian areas in Japan and is widely distributed from subtropical to cold zones because of its well-adapted ability to a large variety of environments (Clevering and Lissner, 1999). In Asia, the common reed is a native aquatic plant species that provide habitats and breeding sites for birds and insects, and amphibians (Packer et al., 2017), and play a crucial role in stabilization of riparian ecosystem (SijiMol et al., 2016).

In natural riparian habitats that with less human disturbance, common reed can rapidly colonize large areas, and often represent a dominant stand in areas such as wetland, and marshland, where they can form a single species community; this phenomenon has been reported in previous research (McCormick, 2009; Uddin et al., 2017). The ecology and colonization of common reed along the urbanized river where under a high level of human disturbance is still unclear. Indeed, previous studies have mainly focused on the natural environmental variables that affect the ecology of common reed (e.g., moisture and soil properties), but the impact of anthropogenic disturbance on the colonization of this species has received little attention (Burdick et al., 2001; Hudon et al., 2005; Thevs, 2007). For example, the impervious surface, transformed from natural or semi-natural riparian habitats, which in turn can alter the environmental conditions (e.g., soil properties, habitat fragmentation, resource availability), leading to degradation of riparian habitats and vegetation (Grella et al., 2018). The construction and existence of roads, as an index of accessibility to anthropogenic disturbance, have shown deleterious effects on numerous ecosystems (Liu et al., 2014). Generally, there are three main ecological influences of road. Firstly, roads can be corridors for the spread and propagation of alien species (Lázaro-Lobo and Ervin, 2019); secondly, the access of human and vehicles may alter the plant community structure and decrease habitat resilience (Daryanto et al., 2013); thirdly, roads leading the habitat loss and fragmentation, which may negatively affect the colonization and growth of native species (Haddad et al., 2015). Therefore, it limits our understanding of the ecology of common reed if we lose sight of anthropogenic factors, particularly in riparian areas along an urbanized river, which are characterized by fragmented habitats and intense artificial activities.

We studied the distribution pattern and colonization of common reed along the Shonai River, Japan. Our objective was to explore the distribution pattern of common reed and explore the relationship between the colonization of common reed and environmental factors. We hypothesize the common reed with a dominant stand tend to distribute in habitats that under less human-disturbed and, we also hypothesizing that colonization of common reed is negatively affected by anthropogenic pressure.

Methods

Study area

The Shonai River runs through the Aichi and Gifu prefecture, Japan (35°04'–35°24' N, 136°49'–137°20' E) (*Figure 1*). The Shonai River originates from Mt. Yudachi, goes through the basin of Gifu - Tohnoh District, Tamano Valley, Nobi plain, and finally out to the Ise Bay. The basin of the Shonai River covers an area of 1010 km², and the length of the mainstream is 96 km. The river basin area has a typical temperate maritime climate, the monthly maximum and minimum temperatures were 27.8°C (August) and 4.5°C (January), respectively. The average annual air temperature and precipitation in 1998-2018 was 15.8 and 1529 mm, respectively (Aichi Prefectural Government, 2019). The Shonai River is considered one of the most urbanized rivers in Japan because it has

been affected by various processes of migration and urban development. The Shonai basin has Nagoya, the fourth largest city in Japan, as well as other rapidly urbanizing cities such as Kasugai, Owari-Asahi, Seto, and Tajimi, with a population density of approximately 2400 persons/km². The land use of the Shonai River basin comprises built-up areas (55.2%), agricultural fields (10.7%), and forest (34.1%) (Ministry of Land, Infrastructure, Transport and Tourism, 2018).

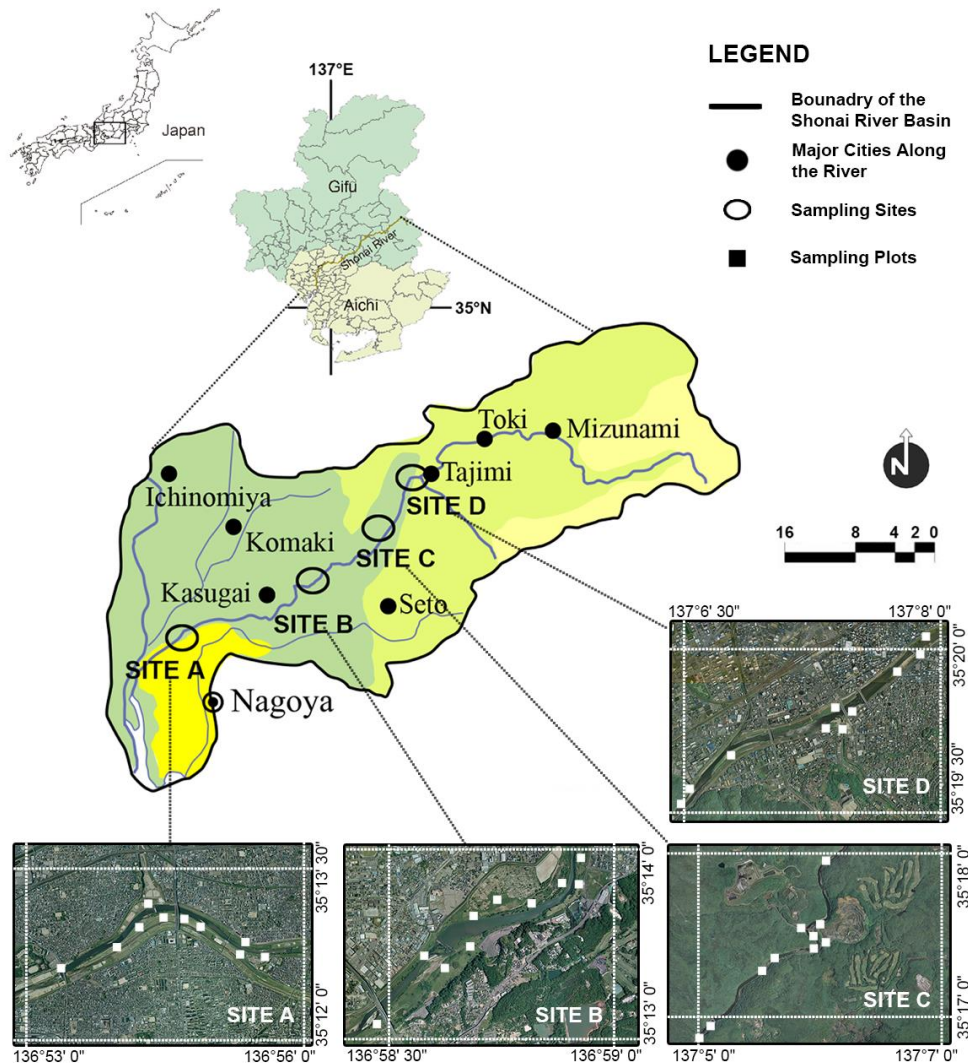






Figure 1. Locations of the study sites, sampling plots, and an overview of the Shonai River system in Japan

Sampling design

The field survey was conducted from April to July in 2018. Four sampling sites were selected from the lower to upper reaches of the Shonai River. Site A was located to the northwest of Nagoya City, in the lower reaches of the river section. This area has developed over a long period and contains a large human population and recreational spaces. Sites B and C were located outside the urban area, in the middle reaches of the river section, which is undergoing the process of city expansion and is associated with

the continued disappearance of forest and farmland. Site D was located in the upper reaches of the river system. As the central region of Tajimi City, this area is inhabited by a large number of local residents (*Table 1*).

Table 1. The description and characteristics of each sampling site

Sampling site	Plots surveyed	Sampling site description	Altitude variation(m)		Example image of surveyed habitats
			Min	Max	
Site A	10	Site A was located to the northwest of densely built metropolitan city Nagoya. The riparian area in Site A was transformed by the levee, recreational spaces, and different levels of roads.	7.4	11.3	
Site B	10	Sites B was located in the suburban region of Nagoya city. The riparian area was surrounded by a few small patches of farmland and residential areas.	16.5	20.1	
Site C	10	Site C was located in the middle reaches of the river section. The riparian area remains a semi-natural state with continuous shrub and grassland.	43.8	52.1	
Site D	10	Site D was located in the upper reaches of the river system. In order to make it easy for everyone to access the river and enjoy the scenery, the loose inclination at the lower riverbed was designed.	89.3	97.1	

In each sampling site, ten 10×10 m plots were established along the river and used for the sampling of woody and shrub species. In each plot, five 1×1 m small plots were established for the sampling of herbaceous species and nested in the center and four corners of each plot (*Figure 2*). Plots were separated by a distance > 50 m. To reduce the marginal effect, the areas within five meters from the river were excluded. The plots were selected at random and depended on the presence of common reed.

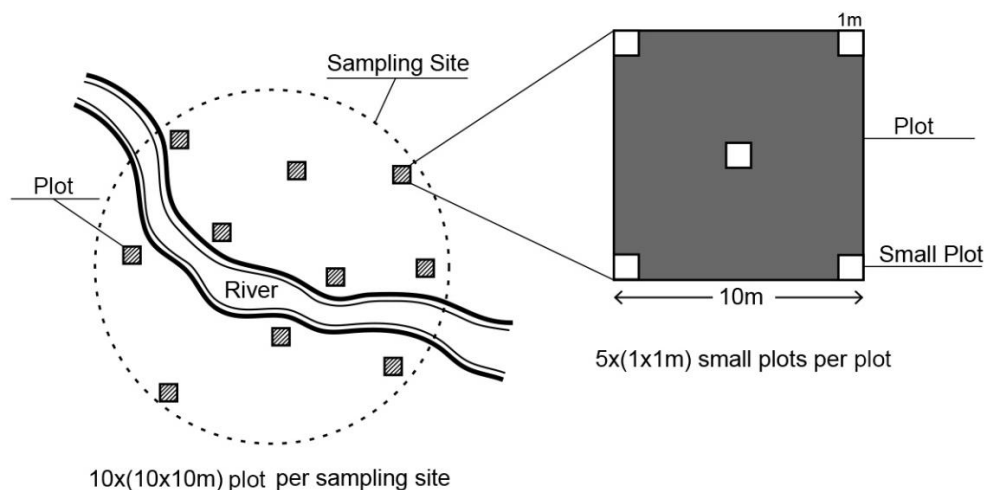


Figure 2. Example of the typical vegetation sampling strategy for each sampling site

Data collection

In each plot, we measured a series of variables describing the characteristics of common reed communities and individual: 1) scientific name, coverage, and abundance of all plant species presented in the plot; and 2) the aboveground biomass and density of common reed. The coverage of plant species was measured by visually (Damgaard, 2014); The density of common reed was measured by recording the number of this species in a 1×1 m range; The aboveground biomass was divided into leaves and stems, and dried at 70°C until constant weight (Sinacore et al., 2017). The results were showed in g dry mass m^{-2} . From each plot, soil samples were collected from the center and four corners of plots at depths 20–40 cm to analyze the soil physical and chemical properties. To measure the soil water content, each soil sample was placed in an aluminum box and weighed, and after dried in an oven at 105°C for 24 h, they were weighed again. The electrical conductivity of each soil sample was tested as follows: first, each of the soil samples was pushed through a 2 mm sieve, and the solution was conducted as soil: water as 1:5, and then an electromagnetic conductivity meter was used for testing (Mamat et al., 2016). The soil pH was determined using an electric pH meter. In addition, in each plot, the distances from the road (DRO) and river (DRI) were calculated using the Euclidean distance method in ArcGIS 9.3. The land use or land cover types in sampling sites were classified by farmland and impervious surface and were calculated based on a color aerial photo and estimated by ArcGIS 9.3. Urban facilities, such as buildings, footpaths, playgrounds, and roads, indicated the impervious surface. Agriculture fields, flower nursery, and orchards were considered as farmland in current research.

Data analysis

Cluster analysis was used to classify the common reed community types. The importance value (calculated based on the relative frequency, relative coverage, and relative density) of each species present in the 40 plots was used as the basis of cluster analysis (Ruiz and Lugo, 2012; Ross et al., 2016).

The Euclidean distances and Ward's method were used to select an optimum pruning point for the dendrogram. The cluster analysis was performed with R (version 3.5.1).

To investigate the environmental factors affecting the distribution pattern and composition of common reed communities, we use canonical correspondence analysis (CCA; in CANOCO version 4.5) to ordinate the environment variables. The Monte Carlo permutation test was conducted to examine the statistical significance of environmental variables for CCA.

We conducted two steps of the analysis to explore the relationship between the colonization of common reed and environmental variables. Firstly, we use the Tukey's HSD test in one-way analysis of variance (ANOVA) to explore the differences in the coverage, density, and biomass of common reed among the classified common reed communities; Secondly, we used a generalized linear model constructed with R to determine the environmental factors affecting the colonization of common reed. The independent environmental variables included elevation (m), precipitation (mm), distance to the river (m), the proportion of impervious surface (%), the proportion of farmland (%), distance to the road (m). The factors related to soil property such as soil water content (g/g), soil electrical conductivity ($\mu\text{S/cm}$), and pH were considered in the analysis. We calculated the model with the lowest Akaike information criterion as the best model for the colonization of common reed, using the MASS package.

Results

Floristic diversity and composition of common reed community

In riparian areas along the Shonai River, six groups of common reed communities were classified (Fig. 3). These six groups of communities mainly differed in coverage of common reed and species composition (Table 2). The characteristics of each group of community are as following.

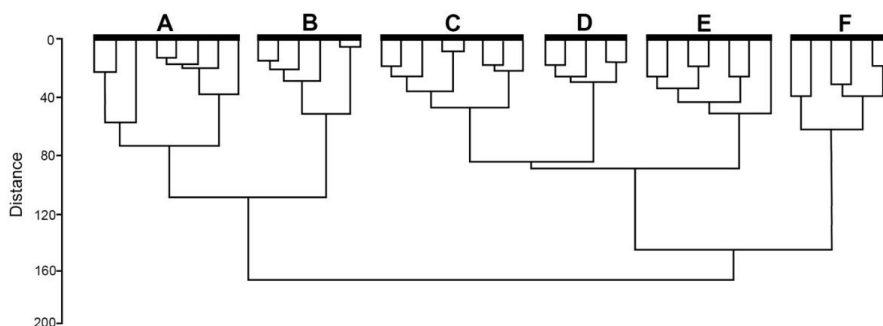


Figure 3. The result of cluster analysis (Ward's method, Euclidean distances), identified six groups of communities

Table 2. Species composition, species frequency (Fr%), and mean coverage (Co%) within the groups obtained in cluster analysis

Species	Group A		Group B		Group C		Group D		Group E		Group F	
	Fr%	Co%	Fr%	Co%	Fr%	Co%	Fr%	Co%	Fr%	Co%	Fr%	Co%
<i>Erigeron philadelphicus</i> L.*			83.4	3.9			40	3.5	28.6	2.1	16.7	3.2
<i>Festuca arundinacea</i> *	25	4.1	100	32.1			40	3.5	28.6	2.1	16.7	3.2
<i>Lolium multiflorum</i> Lam.*			16.7	2.7	87.5	5.4	80	5.7	59.1	5.8	16.7	3.7
<i>Miscanthus sacchariflorus</i>	25	6	16.7	1.9	100	31.2	100	34.5	100	62.1		
<i>Poa annua</i> L.	37.5	6.5			62.5	3.8			42.9	4.2	16.7	1.9
<i>Pueraria montana</i> var. <i>lobata</i>			16.7	2.2	50	5.9			42.9	3.9	16.7	2.8
<i>Rosa multiflora</i> Thunb.	25	2.4	50	2.8	62.5	4	40	3.4			66.7	5.2
<i>Solidago altissima</i> L.*					37.5	2.7	100	37.5	28.6	2.8	100	32.2
<i>Trifolium repens</i> L.*	25	1.9	66.7	3.3	25	2.4			42.9	3.7	16.7	1.7
<i>Erigeron annuus</i> (L.) Pers.*			50	2.3			80	2.7	42.9	2.1	33.5	1.9

The plants represent the accompanying species with common reed. We just listed the top ten species in order of importance value. Non-native species were shown with “*”, the dominant species were shown in bold.

Group A was the common reed community. The structure of Group A communities was dominated by common reed with high coverage.

Group B was the common reed – *Festuca arundinacea* community. This type of community was dominated by common reed and *F. arundinacea* in the herb layer.

Group C was the common reed–*Miscanthus sacchariflorus* community. This type of community was dominated by common reed and *M. sacchariflorus*. The herb species *Solidago altissima* was also present in this group of communities.

Group D was the *M. sacchariflorus*–*S. altissima* community. This type of community was dominated by *M. sacchariflorus*, *S. altissima* was mainly distributed under the shrub layer, which mainly comprised of *M. sacchariflorus*. Common reed was sparsely distributed in these communities, with low coverage.

Group E was the *M. sacchariflorus* community. This group of the community was dominated by *M. sacchariflorus*, with an average coverage of 62.1%. Common reed was distributed associated with *M. sacchariflorus* in the shrub layer with an average coverage of 4.3%.

Group F was the common reed–*S. altissima* community. This type of community was dominated by common reed and *S. altissima*.

Distribution and composition pattern of common reed communities

Canonical correspondence analysis (CCA) was conducted to determine the distribution pattern of the six groups of plant communities. The CCA ordination exhibited strong correlations between plant species abundance and environmental factors. The cumulative proportions for CCA1 and CCA2 were occupied nearly 72% (Table 3). Therefore, these two axes can be considered proper predictors of plant community distribution and species abundance. The Monte Carlo permutation test indicated that five environmental variables significantly affected the distribution pattern of riparian communities and dominant plant species ($P < 0.05$) (Table 4).

Table 3. Summary statistics for CCA ordinations

	CCA1	CCA2	CCA3	CCA4
Eigenvalue	0.1026	0.09177	0.03484	0.02196
Proportion explained	0.3809	0.3409	0.1294	0.08156
Cumulative proportion	0.3809	0.72185	0.85128	0.93284

Table 4. Results of the Monte Carlo permutation test to select the environmental variables for the canonical correspondence analysis (CCA), The significant variables ($p < 0.05$) were selected

Variables	R ²	P-value
Altitude	0.2421	0.018*
Distance from the river	0.2420	0.016*
Distance from the road	0.3100	0.011*
Proportion of impervious surface	0.2803	0.006**
Proportion of farmland	0.1860	0.046*

* $P \leq 0.05$, ** $P \leq 0.01$

The CCA1 axis was the best predictor of the differences in the pattern of community distribution and species composition. The correlations between the CCA axes and environmental factors are listed in Table 3. The altitude and proportion of impervious surface were strongly negatively correlated with CCA1; however, the distance from the river, distance from the road, and the proportion of farmland were positively correlated. The distance from the road was positively correlated with CCA2. The factor of the proportion of farmland was positively correlated with the CCA3. None of the environmental factors had a strong relationship with CCA4 (Table 5).

Table 5. Eigenvalues and correlation matrix of the relationship between the environmental factors and the four axes of the canonical correspondence analysis (CCA) for the six groups of communities growing in the riparian area along the Shonai River

Factor	CCA1	CCA2	CCA3	CCA4
Altitude	-0.7348**	0.16896	0.4996	0.4246
Distance from the river	0.5454*	0.51605	0.4222	0.1825
Distance from the road	0.6085*	0.71496**	0.1237	0.2010
Proportion of impervious surface	-0.8268**	-0.02352	0.1758	-0.3369
Proportion of farmland	0.6703*	-0.02179	0.5708*	-0.3018

* $P \leq 0.05$, ** $P \leq 0.01$

The CCA ordination indicates the distribution patterns of the dominant species in each riparian plant community (Figure 4). The distance from the road had an influence on the distribution pattern of community Group1 and most plant communities of Group E. The existence of several dominant species, native species such as *P. montana var. lobata*, was related to the distance from the road. The factor of altitude strongly affected the distribution pattern of Group B and portion of communities of Group A. The species of *F. arundinacea* were strongly associated with the altitude variable. The proportion of impervious surface influenced the distribution of Group B, and part of Group D; the dominant species *S. altissima* and *E. philadelphicus* was also associated with this variable. The dominant species in Group C and D, and parts of Group E and F, *M. sacchariflorus*, *L. multiflorum*, and *P. annua*, had obviously positive correlations with the distance from the river (Figure 4). The dominant species in Group A and B, common reed, and *F. arundinacea* had obviously negative correlations with the distance from the river (Figure 4). The proportion of farmland had an influence on the dominant species in Group E. Dominant species, such as *P. annua* and *T. repens*, were associated with the proportion of farmland.

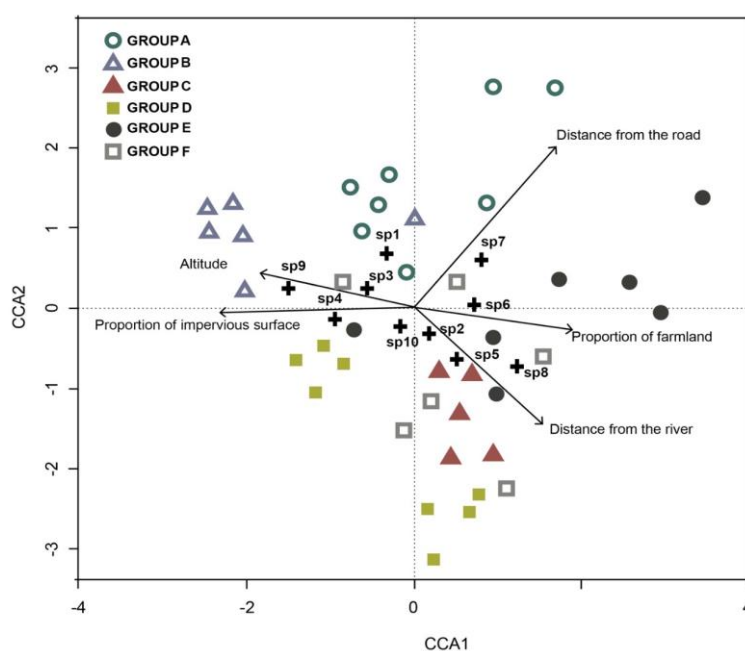


Figure 4. CCA ordination diagram between vegetation characteristics and environmental factors. SP1: common reed; SP2, *M. sacchariflorus*; SP3, *F. arundinacea*; SP4, *S. altissima*; SP5, *Lolium multiflorum* Lam., SP6, *Trifolium repens*; SP7, *Pueraria montana var. lobata*; SP8, *Poa annua* L. SP9, *Erigeron philadelphicus* L., SP10, *Rosa multiflora* Thunb

These results suggest that the Group A community was located in the area with less anthropogenic disturbance along the Shonai River (long distance to the road, short distance to the river). In contrast, Group B was mainly distributed in areas under high anthropogenic pressure (high proportion of impervious surface, higher altitude). The rural areas of the Shonai River were always associated with the location of Groups C and E (high proportion of farmland). Group D tended to be distributed through areas near the road and far away from the river. The distribution pattern of Group F showed a relatively decentralized condition, but the overall trend was located in the areas far from the river.

Variation in the characteristics of common reed

The coverage, density, and biomass common reed showed a similar variation tendency in groups A-F (Figure 5).

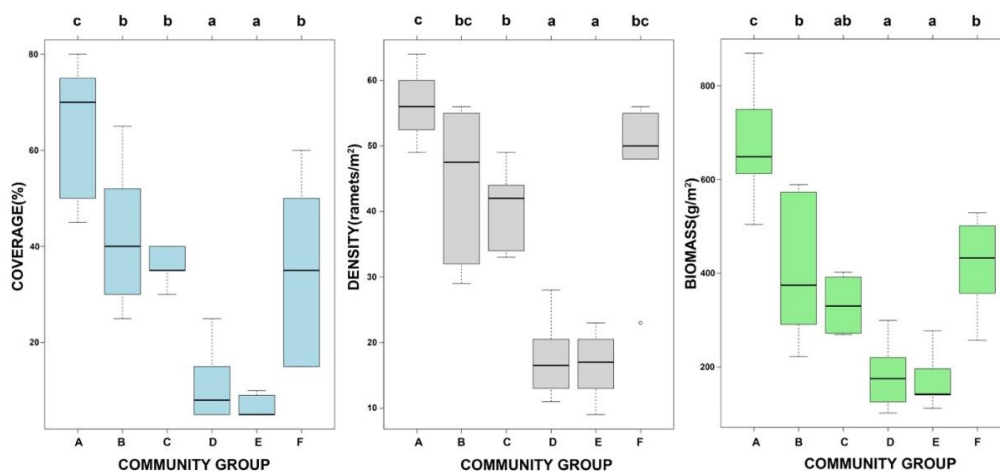


Figure 5. Differences in the coverage, density, and biomass of common reed in the six groups of the plant communities. Values with the same letter means they are not significantly different at the 0.05 significance level

The coverage of common reed showed the highest values in group A and reached its lowest value in group E ($P < 0.05$).

The density of common reed showed significantly ($P < 0.05$) higher values in group A while reached its lowest value in group D ($P < 0.05$).

The biomass of common reed reached its highest value in group A ($P < 0.05$), and showed the lowest value in group E.

Environmental factors affecting the colonization of common reed

The colonization of common reed in the riparian areas affected by numerous environmental variables in GLM analysis (Table 6). The coverage of common reed was highly influenced by soil property (positive/negative) and negatively affected by the distance from the river and the proportion of impervious surface. Besides, the coverage of common reed tends to increase with the increasing of distance from the road. The biomass of common reed was also affected by many factors and was positively correlated with soil water content, distance from the road, and the proportion of farmland. They were also negatively affected by soil electrical conductivity, distance from the river, and

proportion of impervious surface. The density of common reed was only positively affected by soil water content, but negatively affected by soil electrical conductivity, and the proportion of impervious surface.

Table 6. Generalized linear model (GLM) analysis of the relationship between the colonization of common reed with the environmental factors; electrical conductivity (EC), soil water content (SWC), distance from the river (DRI), distance from the road (DRO), the proportion of impervious surface (IMP), the proportion of farmland(FIELD), altitude (ALT)

Characteristics	Environmental factors							
	pH	EC	SWC	DRI	DRO	IMP	FIELD	ALT
Coverage	-0.176*	-0.009***	0.006***	-0.005***	0.001**	-0.009**		
Density		-0.005***	0.003***			-0.005*		
Biomass		-0.004***	0.004***	-0.003***	0.001**	-0.003**	0.006**	

The values in the cells are model regression coefficients; only significant coefficients selected for the minimum AIC value are included. *indicates a significant difference (* $P \leq 0.05$, ** $P \leq 0.01$, *** $P \leq 0.001$).

Discussion

Distribution and composition pattern of common reed communities

Regarding the Group A (common reed), a negative correlation between the community distribution and its distance from the river was detected, suggesting that the plant growth in this group depends on the relatively humid environment at the flood plain area of the Shonai River (with distance from the river ranging from 7–55.8 m) (Table 7). The major soil types in the location of Group A near the Shonai River were sandy soil and wet clay, both of which gave exclusive advantages to common reed. On the one hand, due to the unsatisfactory water retention performance of the sandy soil, common reed has a higher survival rate with its remarkable adaptability compared to other species (Rice, 2012; Legault et al., 2018). On the other hand, common reed can grow and spread rapidly in appropriate soil conditions, which makes it more competitive against other species (Ter Heerdt et al., 2017). In addition, the distribution of Group A communities was positively correlated with the distance from roads. This could be explained by the fact that a long distance from roads implies relatively fewer degrees of human disturbance, which could create a relatively stable environment suitable for the growth of vegetation. The distribution pattern of Group A communities accords with our expectation that common reed community tends to distribute in less human-disturbed habitats.

In Group B (common reed- *F. arundinacea*), it was found that the distribution was also negatively associated with the distance from the river. The suitable moisture environment was leading to high coverage of common reed (Packer et al., 2017). In addition, it was shown that the distribution of the Group B community was positively related to the proportion of impervious surface. A large proportion of impervious surface implies a link to modern management of the rivers for flood control and recreational land use (Washitani, 2001), indicating that this group was at high risk because they would be affected by anthropogenic disturbance (White and Greer, 2006). The various construction works and frequent human disturbance thought to be the major factors facilitating the invasion of alien grasses such as *F. arundinaceae* (Washitani, 2001). The riparian areas along the Shonai River, where the presence of Group B communities was always fragmented by construction measures and combined with other land-use types (e.g., residential areas,

footpaths, farmlands, golf courses, and parking lots). Consequently, in these areas, common reed was no longer the dominant species. Instead, the alien species in Japan, *F. arundinacea* (Miyawaki and Washitani, 2004), became another dominant species with a high coverage.

Table 7. Characteristics of environmental factors in the six classified common reed communities. Values represent means \pm SE

	GROUP A	GROUP B	GROUP C	GROUP D	GROUP E	GROUP F
Distribution feature						
	Near the river Far from road	Near the city	Near farmland	Near road Far from river	Near farmland	No obvious features
Potential disturbance						
	Hydrology and sediment	Human disturbance	Agriculture management	Human disturbance	Agriculture management	---
Environmental factor						
pH	5.50 \pm 0.18	6.12 \pm 0.04	6.05 \pm 0.21	6.16 \pm 0.21	6.14 \pm 0.13	5.68 \pm 0.27
EC (μS/cm)	45.52 \pm 12.84	46.22 \pm 18.87	51.51 \pm 15.34	96.70 \pm 27.05	90.36 \pm 15.25	86.99 \pm 17.95
SWC (g/g)	0.26 \pm 0.04	0.19 \pm 0.02	0.21 \pm 0.02	0.18 \pm 0.01	0.19 \pm 0.01	0.25 \pm 0.03
DRO(m)	96.86 \pm 32.79	25.21 \pm 5.83	4.56 \pm 0.88	15.30 \pm 2.95	111.29 \pm 39.48	28.40 \pm 15.73
DRI(m)	26.13 \pm 6.95	11.65 \pm 3.30	57.28 \pm 30.44	36.25 \pm 10.34	50.29 \pm 11.33	50.95 \pm 15.31
IMP (%)	3.9 \pm 1.47	25.7 \pm 7.15	8.1 \pm 4.26	17.4 \pm 6.44	6.9 \pm 4.48	13.6 \pm 8.72
FIELD (%)	0	0	31.2 \pm 14.11	4.9 \pm 2.85	19.7 \pm 8.29	8.3 \pm 5.28
ALT (m)	31.25 \pm 5.63	41.87 \pm 11.58	37.12 \pm 12.62	26.81 \pm 9.37	40.22 \pm 21.08	40.15 \pm 14.78

EC, electrical conductivity; SWC, soil water content; DRO, distance from the road; DRI, distance from the river; IMP, the proportion of impervious surface; FIELD, the proportion of farmland; ALT, altitude

The distribution of Group C (common reed – *M. sacchariflorus*) and Group E (*M. sacchariflorus*) communities were mainly positively associated with the proportion of farmland, suggesting that most of them were located in the rural area along the middle part of the Shonai River. Most of these areas were dominated by *M. sacchariflorus*, which was found along the farmland sides or in agricultural wasteland. Interspecies competition might be a possible explanation for the non-dominant of common reed in Groups C, and E. Common reed and *M. sacchariflorus* are both hydrophilic plants, and it is widely known that they have similar environmental requirements, but *M. sacchariflorus* has a broader range of adaptation (Yamasaki and Tange, 1981; Yamasaki, 1990). When common reed and *M. sacchariflorus* coexist, common reed may not be vigorous enough to occupy the dominant position. Besides, in previous studies, the soil nutrient and organic matter content in the areas surrounded by farmland was often diversified due to agricultural management (Loveland and Webb, 2003; Santos et al., 2012); the soil with a wide variation on soil nutrient and organic matter content might facilitate the colonization of *M. sacchariflorus*, which affect the growth of common reed.

The distribution of Group D (*M. sacchariflorus*- *S. altissima*) communities was positively correlated with the distance from the river. Besides, most of the communities in Group D were also found to be negatively related to the distance from the road, suggesting that the communities of Group D were under the stresses of human disturbance and a relative drought environment. As *M. sacchariflorus* and *S. altissima* are two species with impressive adaptability to a range of different environmental conditions, they became the dominant species in the areas where there were multiple disturbances (Song

et al., 2016; Szymura and Szymura, 2016). Since it relies on a moist and stable environment to grow, common reed was found to be sparsely distributed in these communities with low coverage.

Although the communities in Group F (common reed - *S. altissima*) did not demonstrate an obvious distribution pattern, a positive correlation was shown between its vegetation cover extent and the distance from the river in most of these communities, indicating that these plant communities became established in areas far away from the alluvial plain of the river.

Factors determining the colonization of common reed

The variation in the coverage, density, and biomass of common reed was a result of the interaction between the environmental factors and vegetation. In the current study, we found the soil electrical conductivity and soil water content significantly affected the colonization of common reed. Our results are consistent with those of previous studies concluded that soil moisture and soil properties are major factors that influence the characteristics of vegetation (Oztas et al., 2003; Ursino, 2005). Besides, the surrounding land-use type and the human impact also have a remarkable influence on the colonization of common reed in our research.

As a conventional standard for determining soil salinity, electrical conductivity was negatively correlated with the coverage, density, and biomass of common reed, suggesting that an increase in soil electrical conductivity can inhibit the growth of common reed. Previous studies have demonstrated that electrical conductivity is negatively correlated with the growth of common reed (Lissner and Schierup, 1997; Haraguchi, 2014). Although common reed was well known as a salt tolerance species, with the increase of soil electrical conductivity, density and biomass of common reed were decreased to adapt to the damage of stress. Especially in Groups D and E, where the plant communities were located near to the roads or with a high proportion of farmland, the electrical conductivity of the soil was relatively high among the six groups (*Table 7*) that may be affected by agricultural irrigation methods or intensive human disturbance, leading to a low coverage value of common reed (Wu et al., 2008).

Soil moisture has always been an important factor affecting the growth of common reed in riparian areas (Engloner, 2004). In our study, the soil water content and distance from the river were adopted to measure the effect of soil moisture on the growth of common reed. Consistent with the literature, this research found soil moisture positively related to the colonization of common reed. Due to the short distance from the river and the favorable water holding capacity of the soil in Group 1, the value of the soil water content was the highest in Group 1 (*Table 7*) compared to that in all the other groups, resulting in a relatively higher coverage, density, and biomass of common reed with large individuals in this group (*Figure 5*). Although locations close to the river may be subject to flood pressure, all of our sampling sites are located at least 5 meters from the river and are therefore relatively less affected by flooding.

The proportion of impervious surface was negatively associated with the coverage, density, and biomass of common reed. This result indicated that the colonization of common reed is negatively affected by anthropogenic pressure. A significant increase in impervious surfaces may degrade aquatic and terrestrial habitats by aggregating human activities and increasing surface runoff (White and Greer, 2006). Besides, the impervious surfaces tremendously influenced the soil ecosystem by impeding the exchange of water and materials between soil and the atmosphere (Hu et al., 2018). Thus, the inhibition of

the growth and colonization of common reed might be attributed to the increased impervious surface, and human disturbance enhanced the propagation and growth of wide adaptable and invasive species. Groups B and D, which surrounded by the large proportion of impervious surface, was dominated by invasive species *S. altissima*, *F. arundinacea*, and accompanied by various ubiquitous species. Also, the inhibition of the growth and colonization of common reed may be the habitat fragmentation associated with the construction of the impervious surface. Fragmentation of habitats destroys essential mechanisms such as dispersion and facilitation, which results in a reduction in the colonization of common reed (de Frutos et al., 2015).

In addition to the anthropogenic disturbance in general, roads, in particular, are important determinants of the plant community characteristics and floristic composition of plants (Root-Bernstein and Svenning, 2018). In our study, it was discovered that the distance from the roads positively affected the coverage and biomass of common reed, indicating that the communities located near the roads are easily influenced by anthropogenic disturbance. The natural riparian habitats could be changed by road, which might result in the alternation of the external environment for the colonization and growth of plants. Previous studies reported that heavy metals accumulation and soil nutrient alternation along the roadside, which might affect the vegetation adjacent to road indirectly (Pagotto et al., 2001; Truscott et al., 2005). Besides, the road can be corridors for the spread and propagation of alien species (Lázaro-Lobo and Ervin, 2019). The previous studies reported that the high species richness of alien species was observed adjacent to the road verge (Zeng et al., 2011). As such, in Group D, the short distance to the road enabled non-native species, such as *E. philadelphicus* and *L. multiflorum*, to survive.

Conclusion

Our study confirmed the importance of moisture and soil properties for the growth and colonization of common reed, which had been reported in previous studies. Meanwhile, we found the anthropogenic factors had significant effects of reduced the population and biomass of common reed. Our findings highlight the effects of land cover types and local environmental conditions on the population variation of riparian plant species. Thus, in riparian areas, management measures, such as restricting construction of public land in riverside, and establishing protective zones for common reed is recommended in future ecological restoration in urban areas. High electrical conductivity value also strongly influenced the colonization of common reed. Thus controlling urban runoff by strengthening supervision and rationally planning urban and river junction zones were suggested in this regard.

However, only 40 sampling plots were selected to determine the characteristics of common reed in this study. This is the deficiency of the sampling design in the current study. Thus, more sampling sites and replicates will be adopted in future work to explore more information about the response of common reed in the urban ecosystem. In addition, there exist many other environmental factors influencing the population of common reed, such as flooding frequency, chemical and physical water characteristics. These factors, as potential co-variates, might affect the variation of common reed in the urban ecosystem. In the future, more factors should be investigated to disentangle the effect of anthropogenic disturbance from hydrological conditions on the colonization of riparian plant species.

Acknowledgements. We thank reviewers for their suggestions which helped to improve the manuscript. We are grateful to Noelikanto Ramamonjisoa and Yamamoto Mariko for their suggestions on an early version of this manuscript. We thank Wenhui Zhang, Chuan Wu, Xiaohui Zhao and Xiaojun Zheng for the field survey. We thank Claire Oire and Rhys Nicholls for the spell check.

REFERENCES

- [1] Burdick, D. M., Buchsbaum, R., Holt, E. (2001): Variation in soil salinity associated with expansion of *Phragmites australis* in salt marshes. – *Environmental and Experimental Botany* 46(3): 247-261.
- [2] Cao, Y., Natuhara, Y. (2019): Effect of Urbanization on Vegetation in Riparian Area: Plant Communities in Artificial and Semi-Natural Habitats. – *Sustainability* 12(1): 204.
- [3] Clevering, O. A., Lissner, J. (1999): Taxonomy, chromosome numbers, clonal diversity and population dynamics of *Phragmites australis*. – *Aquatic Botany* 64(3): 185-208.
- [4] Damgaard, C. (2014): Estimating mean plant cover from different types of cover data: a coherent statistical framework. – *Ecosphere* 5(2): 1-7.
- [5] Daryanto, S., Eldridge, D. J., Wang, L. (2013): Spatial patterns of infiltration vary with disturbance in a shrub-encroached woodland. – *Geomorphology* 194: 57-64.
- [6] de Frutos, Á., Navarro, T., Pueyo, Y., Alados, C. L. (2015): Inferring resilience to fragmentation-induced changes in plant communities in a semi-arid Mediterranean ecosystem. – *PloS one* 10(3): e0118837.
- [7] Décamps, H., Naiman, R. J., McClain, M. E. (2009): Riparian Zones. – In: Likens, G. E. (ed.) *Encyclopedia of Inland Waters*. Oxford: Academic Press: 396-403.
- [8] Engloner, A. I. (2004): Annual growth dynamics and morphological differences of reed (*Phragmites australis* [Cav.] Trin. ex Steudel) in relation to water supply. – *Flora - Morphology, Distribution, Functional Ecology of Plants* 199(3): 256-262.
- [9] González, E., Felipe-Lucia, M. R., Bourgeois, B., Boz, B., Nilsson, C., Palmer, G., Sher, A. A. (2017): Integrative conservation of riparian zones. – *Biological Conservation* 211: 20-29.
- [10] Grella, C., Renshaw, A., Wright, I. A. (2018): Invasive weeds in urban riparian zones: the influence of catchment imperviousness and soil chemistry across an urbanization gradient. – *Urban Ecosystems* 21(3): 505-517.
- [11] Haddad, N. M., Brudvig, L. A., Clobert, J., Davies, K. F., Gonzalez, A., Holt, R. D., Lovejoy, T. E., Sexton, J. O., Austin, M. P., Collins, C. D., Cook, W. M., Damschen, E. I., Ewers, R. M., Foster, B. L., Jenkins, C. N., King, A. J., Laurance, W. F., Levey, D. J., Margules, C. R., Melbourne, B. A., Nicholls, A. O., Orrock, J. L., Song, D.-X., Townshend, J. R. (2015): Habitat fragmentation and its lasting impact on Earth's ecosystems. – *Science Advances* 1(2): e1500052.
- [12] Haraguchi, A. (2014): Effects of Salinity on Germination, Seedling Growth and Ecological Properties of *Phragmites australis* Communities in the Estuary of the Chikugogawa River, Southwestern Japan. – *American Journal of Plant Sciences* 5(5): 584-595.
- [13] Hu, Y. D., Li, J. Y., Li, F. (2018): Impervious Surfaces Alter Soil Bacterial Communities in Urban Areas: A Case Study in Beijing, China. – *Frontiers in Microbiology* 9: 226.
- [14] Hudon, C., Gagnon, P., Jean, M. (2005): Hydrological factors controlling the spread of common reed (*Phragmites australis*) in the St. Lawrence River (Québec, Canada). – *Écoscience* 12(3): 347-357.
- [15] Lázaro-Lobo, A., Ervin, G. N. (2019): A global examination on the differential impacts of roadsides on native vs. exotic and weedy plant species. – *Global Ecology and Conservation* 17: e00555.
- [16] Legault, R. II, Zogg, G. P., Travis, S. E. (2018): Competitive interactions between native *Spartina alterniflora* and non-native *Phragmites australis* depend on nutrient loading and temperature. – *PlosOne* 13(2): e0192234.

- [17] Lissner, J., Schierup, H.-H. (1997): Effects of salinity on the growth of *Phragmites australis*. – *Aquatic Botany* 55(4): 247-260.
- [18] Liu, S., Dong, Y., Deng, L., Liu, Q., Zhao, H., Dong, S. (2014): Forest fragmentation and landscape connectivity change associated with road network extension and city expansion: A case study in the Lancang River Valley. – *Ecological Indicators* 36: 160-168.
- [19] Loveland, P., Webb, J. (2003): Is there a critical level of organic matter in the agricultural soils of temperate regions: a review. – *Soil and Tillage Research* 70(1): 1-18.
- [20] Lyon, J., Gross, N. M. (2005): Patterns of plant diversity and plant–environmental relationships across three riparian corridors. – *Forest Ecology and Management* 204(2): 267-278.
- [21] Mamat, Z., Halik, U., Muhtar, P., Nurmamat, I., Abliz, A., Aishan, T. (2016): Influence of soil moisture and electrical conductivity on the growth of *Phragmites australis* (Cav.) in the Keriya oasis, China. – *Environmental Earth Sciences* 75(5): 423.
- [22] McCormick, M., Kettenring, K., Weiner, H., Whigham, D (2009): Extent and Reproductive Mechanisms of *Phragmites australis* Spread in Brackish Wetlands in Chesapeake Bay, Maryland (USA). – *Wetlands* 30: 67-74.
- [23] Miyawaki, S., Washitani, I. (2004): Invasive alien plant species in riparian areas of Japan: the contribution of agricultural weeds, revegetation species and aquacultural species. – *Global Environmental Research* 8(1): 89-101.
- [24] Mligo, C. (2016): Diversity and distribution pattern of riparian plant species in the Wami River system, Tanzania. – *Journal of Plant Ecology* 10(2): 259-270.
- [25] Oztas, T., Koc, A., Comakli, B. (2003): Changes in vegetation and soil properties along a slope on overgrazed and eroded rangelands. – *Journal of Arid Environments* 55(1): 93-100.
- [26] Packer, J. G., Meyerson, L. A., Skálová, H., Pyšek, P., Kueffer, C. (2017): Biological Flora of the British Isles: *Phragmites australis*. – *Journal of Ecology* 105(4): 1123-1162.
- [27] Pagotto, C., Rémy, N., Legret, M., Le Cloirec, P. (2001): Heavy Metal Pollution of Road Dust and Roadside Soil near a Major Rural Highway. – *Environmental Technology* 22(3): 307-319.
- [28] Rice, D., Rooth, J., Stevenson, J. C. (2012): Colonization and expansion of *Phragmites Australis* in upper Chesapeake Bay tidal marshes. – *Wetlands* 20: 280.
- [29] Root-Bernstein, M., Svenning, J.-C. (2018): Human paths have positive impacts on plant richness and diversity: A meta-analysis. – *Ecology and Evolution* 8(22): 11111-11121.
- [30] Ross, A. M., Johnson, G., Gibbs, J. P. (2016): Spruce grouse decline in maturing lowland boreal forests of New York. – *Forest Ecology and Management* 359: 118-125.
- [31] Ruiz, M. A., Lugo, A. E. (2012): Landscape effects on structure and species composition of tabonuco forests in Puerto Rico: Implications for conservation. – *Forest Ecology and Management* 266: 138-147.
- [32] Santos, V. B., Araújo, A. S. F., Leite, L. F. C., Nunes, L. A. P. L., Melo, W. J. (2012): Soil microbial biomass and organic matter fractions during transition from conventional to organic farming systems. – *Geoderma* 170: 227-231.
- [33] SijiMol, K., Dev, S. A., Sreekumar, V. B. (2016): A Review of the Ecological Functions of Reed Bamboo, Genus *Ochlandra* in the Western Ghats of India: Implications for Sustainable Conservation. – *Tropical Conservation Science* 9(1): 389-407.
- [34] Sinacore, K., Hall, J. S., Potvin, C., Royo, A. A., Ducey, M. J., Ashton, M. S. (2017): Unearthing the hidden world of roots: Root biomass and architecture differ among species within the same guild. – *PlosOne* 12(10): e0185934.
- [35] Song, J.-S., Lim, S.-H., Lim, Y., Nah, G., Lee, D., Kim, D.-S. (2016): Herbicide-based Weed Management in *Miscanthus sacchariflorus*. – *BioEnergy Research* 9(1): 326-334.
- [36] Szymura, M., Szymura, T. H. (2016): Interactions between alien goldenrods (*Solidago* and *Euthamia* species) and comparison with native species in Central Europe. – *Flora - Morphology, Distribution, Functional Ecology of Plants* 218: 51-61.

- [37] Ter Heerdt, G. N. J., Veen, C. G. F., Van der Putten, W. H., Bakker, J. P. (2017): Effects of temperature, moisture and soil type on seedling emergence and mortality of riparian plant species. – *Aquatic Botany* 136: 82-94.
- [38] Thevs, N., Zerbe, S., Gahlert, F., Mijit, M., Succow, M (2007): Productivity of reed (*Phragmites australis* Trin. ex Steud.) in continental-arid NW China in relation to soil, groundwater, and land-use. – *Journal of Applied Botany and Food Quality* 81(1).
- [39] Truscott, A. M., Palmer, S. C. F., McGowan, G. M., Cape, J. N., Smart, S. (2005): Vegetation composition of roadside verges in Scotland: the effects of nitrogen deposition, disturbance and management. – *Environmental Pollution* 136(1): 109-118.
- [40] Uddin, M. N., Robinson, R. W., Buultjens, A., Al Harun, M. A. Y., Shampa, S. H. (2017): Role of allelopathy of *Phragmites australis* in its invasion processes. – *Journal of Experimental Marine Biology and Ecology* 486: 237-244.
- [41] Ursino, N. (2005): The influence of soil properties on the formation of unstable vegetation patterns on hillsides of semiarid catchments. – *Advances in Water Resources* 28(9): 956-963.
- [42] Washitani, I. (2001): Plant conservation ecology for management and restoration of riparian habitats of lowland Japan. – *Population Ecology* 43(3): 189-195.
- [43] White, M. D., Greer, K. A. (2006): The effects of watershed urbanization on the stream hydrology and riparian vegetation of Los Peñasquitos Creek, California. – *Landscape and Urban Planning* 74(2): 125-138.
- [44] Wu, J., Vincent, B., Yang, J., Bouarfa, S., Vidal, A. (2008): Remote Sensing Monitoring of Changes in Soil Salinity: A Case Study in Inner Mongolia, China. – *Sensors* 8(11): 7035-7049.
- [45] Yamasaki, S., Tange, I. (1981): Growth responses of *Zizania latifolia*, *Phragmites australis* and *Miscanthus sacchariflorus* to varying inundation. – *Aquatic Botany* 10: 229-239.
- [46] Yamasaki, S. (1990): Population dynamics in overlapping zones of *Phragmites australis* and *sacchariflorus sacchariflorus*. – *Aquatic Botany* 36(4): 367-377.
- [47] Zeng, S.-L., Zhang, T.-T., Gao, Y., Ouyang, Z.-T., Chen, J.-K., Li, B., Zhao, B. (2011): Effects of road age and distance on plant biodiversity: a case study in the Yellow River Delta of China. – *Plant Ecology* 212(7): 1213-1229.
- [48] Zipperer, W. C., Foresman, T. W., Walker, S. P., Daniel, C. T. (2012): Ecological consequences of fragmentation and deforestation in an urban landscape: a case study. – *Urban Ecosystems* 15(3): 533-544.

A REVIEW ON ALUMINUM TOXICITY AND QUANTITATIVE TRAIT LOCI MAPPING IN RICE (*ORYZA SATIVA* L)

RASHEED, A.¹ – FAHAD, S.² – HASSAN, M. U.³ – TAHIR, M. M.⁴ – AAMER, M.³ – WU, Z. M.^{1*}

¹*Key Laboratory of Crop Physiology, Ecology and Genetic Breeding, Ministry of Education/Collage of Agronomy, Jiangxi Agricultural University
Nanchang 330045, PR. China*

²*Department of Agriculture, University of Swabi, Khyber Pakhtunkhwa, Pakistan*

³*Research Center on Ecological Sciences, Jiangxi Agricultural University
Nanchang 330045, PR. China*

⁴*Department of Soil and Environmental Sciences, Faculty of Agriculture, University of Poonch,
Rawalaot, Azad Jammu and Kashmir, Pakistan*

**Corresponding author
e-mail: wuzm@jxau.edu.cn*

(Received 1st Dec 2019; accepted 24th Mar 2020)

Abstract. Rice is one of the main staple foods of 50% of the world's population. Aluminum (Al) toxicity is affecting rice growth on acidic soils. We described positive and toxic effects of aluminum on rice, growth on acidic soils as well as function of mutant genes viz. *Nrat1*, *ART1*, *STAR1* and *STAR2* which require further analysis, especially regulation of *ART1*, *STAR1* at transcriptional level to unfold their role in Al tolerance. *Nrat1* gene involved in natural variations for Al tolerance and this would be a novel step in generating natural variation in rice populations. This review highlighted strong theoretical base to understand Al toxicity tolerance mechanisms in rice and we presented several quantitative trait loci e.g. *qRRE-11*, *qRRE-1* controlling Al tolerance in rice at seedling stage which could be transferred via master-assisted selection to enhance Al tolerance in rice. Preliminary screening technique using Al toxic levels is an ideal way to screen resistant seedling in hydroponic environment with the secondary method entailing alterations in soil pH. The molecular basis of Al tolerance should be under more focus, including the novel markers and genes, secondary tolerance indices, BRILs population to develop tolerant varieties in rice but physiological base tolerance mechanisms cannot be overlooked.

Keywords: *marker-assisted selection, population, preliminary screening, hydroponic solution, genes*

Introduction

Rice is (*Oryza sativa* L) one of the main staple food of almost of the world population and people are realizing its significance as dietary role. The production of rice needs to enhance on acidic soil where its growth is lower than normal lands (Tao et al., 2018; Nezames et al., 2018). Heavy metals toxicity is a major problem for crop growth globally (Aamer et al., 2018). Al is third most abundant metal in earth crust after oxygen and silicon. Al solubilizes into most phytotoxic forms such as $AlCl^{3+}$ when soil pH drops below 5 (Awasthi et al., 2017; Muhammad et al., 2018). About 40-50% of world arable lands are acidic and leading to Al phyto-toxicity (Von Uexkull and Murter, 1995; Panda et al., 2009). Al is serious growth limiting factor in rice crop grown on acidic soils (Alvim et al., 2012; Pandey et al., 2013). Root growth inhibition is main symptom of Al toxicity and it leads a typical morphological marker to assess the level of Al tolerance in crop (Chandran et al., 2008). This symptom is caused by damaging of root apex by Al which lead to the decline in grain quality and ultimately affecting the rice production (Li et al., 2013). Root

growth inhibition, damage of root apex, inhibition of nutrients uptake are the symptoms which appeared within minutes after treated with Al toxicity (Silva et al., 2012). Rice is more tolerant to Al toxicity under hydroponic condition and it is two to five folds more tolerant than other cereals (Maron et al., 2008).

Extent of Al tolerance is affected in many crops such as wheat (*Triticum aestivum* MILL) (Sasaki et al., 2004), sorghum (*Sorghum bicolor*) (Magalhaes et al., 2007) and rice (Yamaji et al., 2009). Four mutant's genes lead to Al toxicity have been identified and cloned, such as *Nrat1*, *STAR2*, *ART1* and *STAR1* (Chandran et al., 2008). Al-induced genes *STAR1* and *STAR2* encode an ATP-binding protein and a transmembrane domain protein, respectively. The *STAR1*–*STAR2* complex transports UDP-glucose, a substrate used to modify the cell wall and mask Al-binding sites (Huang et al., 2009). *Nrat1* a (natural resistance-associated macrophage protein) (*Nramp*) encodes an Al transporter (Xia et al., 2010). It was documented that, *Nrat1* gene induces Al tolerance by transferring Al into the cell and finally it reduce its concentration in cell wall (Xia et al., 2010). Only *Nrat1* is responsible for natural variation for Al toxicity tolerance in rice as reported previously (Ma et al., 2002), suggesting that these genes may be accountable for basis of Al toxicity tolerance (Huang et al., 2009; Xia et al., 2010).

QTLs mapping is a powerful tool being used to understand the genetic mechanism of complex traits in crops and it has been used widely to recognize genetic loci determining metals ion uptake and tolerance in rice (Ishikawa et al., 2009; Famoso et al., 2011). A total of 148 QTLs have been reported in rice for Al toxicity tolerance in rice via linkage mapping using bi-parental crosses and genome wide association mapping (Famoso et al., 2011; Zhang et al., 2016). Improving rice tolerance to Al toxicity is primary goal of plant breeders. Screening of the rice varieties with different Al levels would be a better strategy for sustainable agricultural development on acidic soils (Awasthi et al., 2017). Rice crop offers good point for investigating genetic as well as physiological basis of Al tolerance due to its high level of Al tolerance and genetic resources and Al tolerance in rice is quantitatively inherited trait (Famoso et al., 2011; Zhang et al., 2016). Rice has been divided into two major groups, *japonica* (highly resistant to Al) and *indica* (sensitive to Al toxicity) (Famoso et al., 2011; Zhang et al., 2016) and many QTLs have been reported in rice using different type mapping populations. Acidic soils are worldwide problem and rice production has been decreasing badly due to presence of Al toxicity. Al toxicity tolerance is quantitatively inherited trait and very complex in nature. Genetic mechanism for Al tolerance is very complex and therefore until now it is not completely unfolded. Lot of studies have been conducted but it's still unclear. Lot of space and scope is present to investigate further to unfold this mechanism. Al tolerance is mainly determined or assessed on the basis of root length trait (Tao et al., 2018). We highlighted novel QTL of latest studies and some earlier studies. We have mentioned some newly reported potent QTL and most of these QTL are novel QTL and on basis of these QTL we made our own prospective that by pyramiding of these QTL via marker-assisted selection, we can enhance Al tolerance in rice. There is an urgent need to develop rice varieties which can grow best on acidic soils to maintain the production status of rice in order to meet the global food need (Guimaraes et al., 2014). Process of soil acidification is shown in *Figure 1*. Exact Al tolerance mechanism in rice is not clear. Current review would focus to analyze different tolerance mechanism in rice, especially, quantitative traits loci conferring Al toxicity tolerance mechanism in rice and to draw a future prospective to develop Al tolerance varieties to increase rice production on acidic soils. Process of plant growth stimulation and effects of Al on plant growth are shown in *Figure 2*.

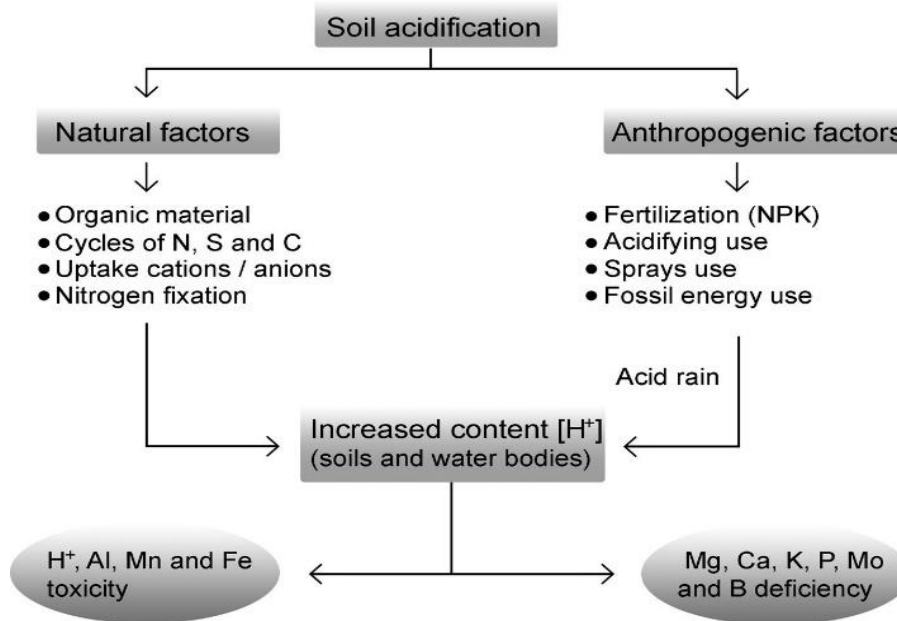


Figure 1. Showed the process of soil acidity with Al. Interaction of Al with other metals in ionic form (adopted from Bojorquez-Quintal et al., 2017)

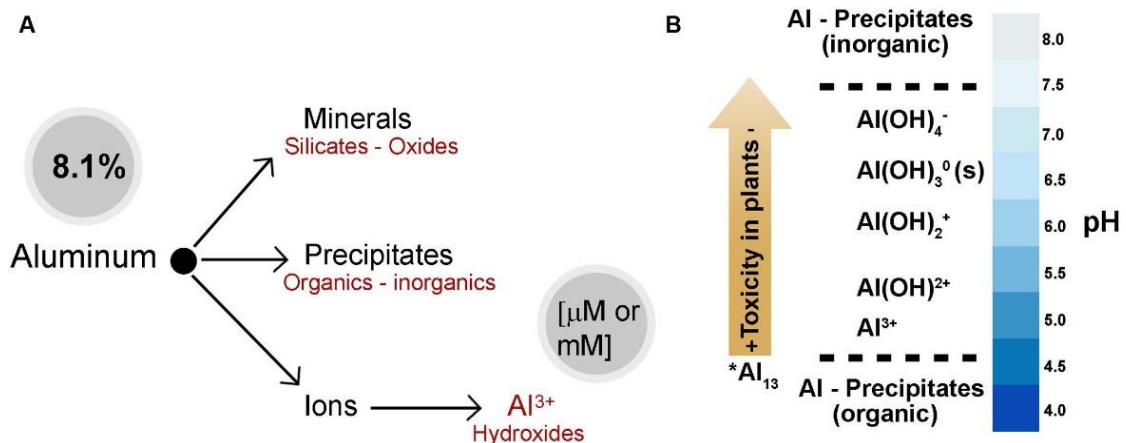


Figure 2. Various type of Al in soil & water. Al is generally originated in mineral form. Al is either in form of precipitates as well as molecular ions dependent on pH of the soil. (B) Aluminum types and their effect on plants (adopted from Bojorquez-Quintal et al., 2017)

Effects of Al on rice growth

Al toxicity

Al and other metals are usually present in paddy soils at very low concentration, but excessive use of some fertilizers increases acidity which enhanced concentration of phytotoxic ions (Bidhan and Bhadra, 2014; Awasthi et al., 2017). About 100 years ago, it was first reported that soluble Al is toxic for crop growth when its concentration rises in acidic soils (Veitch, 1904) and it result in inhibition of root growth (Kopittke et al., 2016). Al becomes more toxic when pH of the spoils falls below 5 and easily taken by roots therefore inhibiting root growth of rice (Tanaka and Navasero, 1966; Panda et al.,

2009). Rice root growth is restricted by presence of Al in rhizosphere which significantly reduces crop productivity. In many studies effects of Al toxicity on seedling root growth (RL), shoot length (SL), shoot dry weight (SDW), and root dry weight (RDW) have been investigated. Al toxicity in rice reduces shoot growth by decreasing nutrients (Ca, Mg) concentration and hormonal imbalance. Roy et al. (2014) also observed significant decrease in shoot length, root length and their dry weight. Al mostly delays and disturbs rice plant metabolism by reducing water absorption (Bidhan and Bhadra, 2014). Process of cell division at root ape is affected by Al and therefore Al increases rigidity of the cell wall and reduces the DNA replication (Zhang, 2014; Eekhout et al., 2017). The number of toxic alterations regarding cell division and nucleolus are brought by Al (Zhang et al., 2014). Al forms an alignment with phosphorous in less existing and insoluble shape in the soils and rice roots, therefore, producing phosphorous deficiency for crop growth.

Positive effects

Recently, a lot of research articles have been published which deal with role of Al role in economically significant crops, but no evidences have shown its exact role in growth. In case of rice (Famoso et al., 2011; Moreno-Alvarado et al., 2017) observed an increment in rice root growth when exposed to concentration of Al (160 and 200 μM) toxicity. In rice Al played a significant role to reduce manganese toxicity which can be related to reduce metals accumulation in shoots which result in decrease Mn contents in shoots. The decrease of manganese application in rice root was a concern of fluctuations in the membrane potential. Al also increased insoluble Mn contents and altered the functions of junction to cell wall and makes manganese less available to rice roots (Wang et al., 2015, 2017). There are also evidences that Al could significantly increase the contents of chlorophyll, sugar, amino acids and hormones in rice (Mariyama et al., 2016; Xu et al., 2016; Moreno-Alvarado et al., 2017). Al rises the soluble sugar concentration and differentially regulate the expression of NAC transcription factors that can improve rice growth and biomass (Moreno-Alvarado et al., 2017). A view of Al positive effects, its toxic effects and defense mechanism adopted by plants is given below in *Figure 3*.

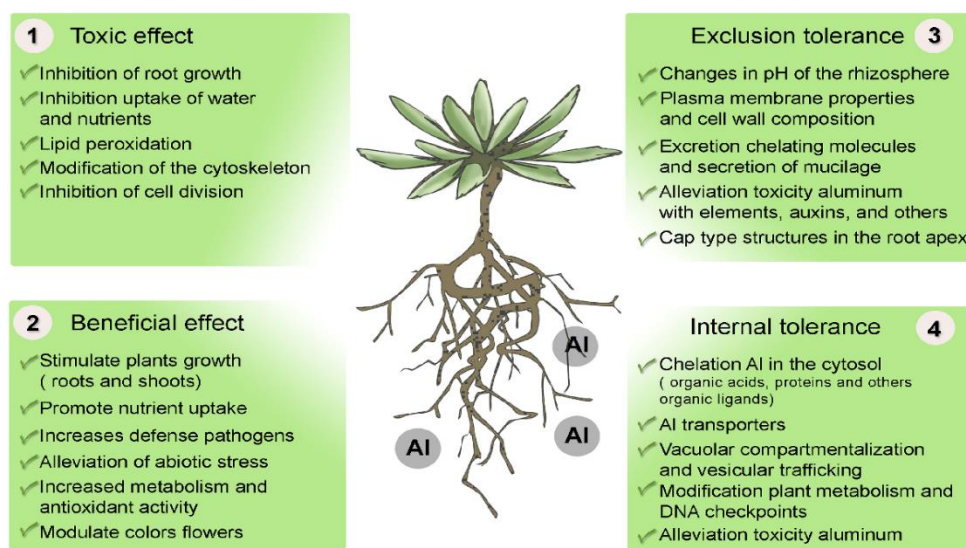


Figure 3. Al toxicity stress, its effects on plants, type of defense mechanism adopted by plants to counter Al stress (adopted from Bojorquez-Quintal et al., 2017)

Physiological basis of Al tolerance in rice

A small increase in soil pH result in reduction in solubility, activity and content of Al in soil due to secretion of several OA (organic acids) by rice plants roots (Yang et al., 2011). Many evidences regarding biochemical, molecular and physiological mechanism of defense have demonstrated that alterations in cell wall composition may reduce the Al toxicity in crops (Che et al., 2016; Muhammad et al., 2018). Rice is most tolerant to Al as compared to cereal crops (Yang et al., 2008; Famoso et al., 2010; Escobar-Sepulveda et al., 2017). Yang et al. (2008) observed significant correlation between polysaccharide contents and Al accumulation in rice and highlighted the significance of cell wall composition. The concentration of pectin and its notch of (methylation) in cell wall added to alterations in tolerance to Al (Eticha et al., 2005; Yang et al., 2011). In rice crop Maejima and Watnanabe (2014) noticed an increment in Al tolerance due to reduction in phospholipids of root cell. For some instance, sterol also played a fruitful role in tolerance to Al in rice (Hossain et al., 2009; Wagatsuma et al., 2014). Small peptide, attaching the plasma membrane, could stop Al influx in the cell wall through bonding with cations added confrontation in the rice (Xia et al., 2013). Chelating compounds mucilage in rice has been evidenced to enhance aluminum tolerance. *MATE* gene (Yang et al., 2011) *VuMATE1*, has been identified in rice to play key role in mediating citrate efflux in rice, conferring Al tolerance. Rice adopted several mechanisms to alleviate aluminum toxicity. For example, ammonium decreases the Al addition of Al in roots as a result of the (pH) modifications brought through ammonium entrance & straight cooperation of Al and ammonium for binding sites of the cell call (Wang et al., 2015).

In rice many genes played a role in internal mechanism of tolerance. *OsALSI* is an ortholog of *AtALSI* whose expression is brought quickly and specially by aluminum. Inside reclamation of Al in the rice is brought by *OsALSI* is located which is involved in compartmentalization of aluminum in vacuoles (Huang et al., 2009, 2012). In rice several alternative ways of cellular inhalation add to Al tolerance. Lou et al. (2016) advocated that accumulation is responsible in (H⁺) and Al encouraged growth of root in rice. These are all possible physiological ways through which rice can response to Al toxicity to sustain its growth on acidic soils (Eekhout et al., 2017).

Mutant's genes of Al tolerance in rice

Four mutant genes that responsible for Al sensitivity in rice have been cloned, *Nrat1* (*Nramp aluminum transporter*), *ART1* (Al rhzotoxicity1, *STAR1* (sensitive to Al rhzotoxicity1) and *STAR2* (sensitive to Al rhzotoxicity2) (Huang et al., 2009; Xia et al., 2010) (*Table 1*). Products of both of genes (*STAR1* and *STAR2*) are mostly shown in the roots and these are the components of bacterial type genes ABC transporter. These genes are activated after exposure to Al at transcription level and lose of genes function result in increase in sensitivity to Al toxicity. Arabidopsis sensitive mutants, *als1* and *als3* also encoding ABC transporters are similar to our genes *STAR1* and *STAR2* (Larsen et al., 2005, 2007). *ART1* gene is a novel (C2H2 type zinc transcription factor) which act together with the starting area of *STAR1* gene. *ART1* is reported to involve in regulation of 30 downstream genes which play a strong role in Al detoxification and increase Al tolerance in rice crop (Yamaji et al., 2009). The gene (*Nrat1*) is regulated by *ART1* and reported to be involved in Al transporter that is localized to root cells plasma membrane (Huang et al., 2009; Xia et al., 2010). *Nrat1* gene ensure Al tolerance by transferring Al into cell and decreasing Al concentration in the cell (Xia et al., 2010). Only *Nrat1* genes

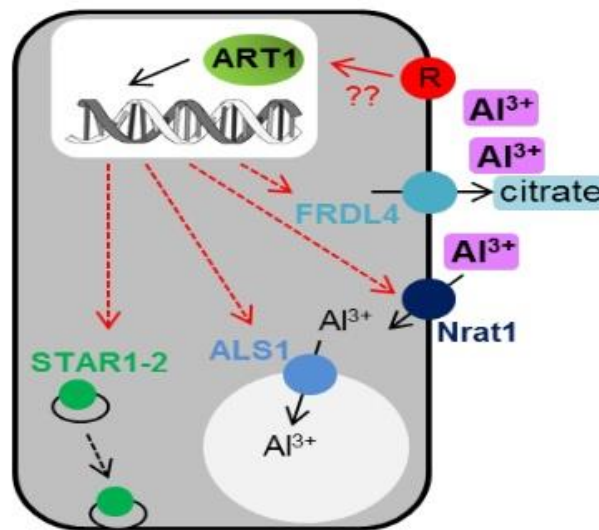
has been studied to have role in natural variations against Al tolerance, beside this other genes have no role for natural variation of Al tolerance (Ma et al., 2002) which indicating that these genes might be involved in basis of Al tolerance (Huang et al., 2009; Yamaji et al., 2009; Xia et al., 2010). More accurate and deep investigation is essential to define whether are natural variation linked with these loci which would assist to trace their evolutionary origins which confirmed their role in high level of Al tolerance observed in the rice (Figure 4, Table 1).

Table 1. Al tolerance genes and their function in rice

Sr No	Crop	Genes	Type	Function	Ref.
1	Rice	<i>STAR1</i>	ABC Transporter	Al tolerance	Larsen et al., 2007
2	Rice	<i>STAR2</i>	ABC Transporter	Al tolerance	Larsen et al., 2005
3	Rice	<i>NRAT1</i>	Al transporter	Transporting Al into the cell	Yamaji et al., 2009
4	Rice	<i>ART1</i>	Novel C2H2-type	Work together with promoter region of <i>STAR1</i>	Huang et al., 2009

Candidate Rice Al Tolerance Genes Identified via Forward Genetics Approaches

- *Art1*: Al regulated transcription factor that activates the expression of candidate tolerance genes.
- *STAR1/2*: PM ABC transporter that exports UDP-Glucose to the cell wall, possibly reducing Al binding.
- *FRL4*: MATE citrate transporter (homolog of *SbMATE*) that plays a minor role in tolerance.
- *Nrat1* & *ALS1*: Al transporters that absorb Al from cell wall (*Nrat1*) and sequester it in vacuole.
- **Ma found that none of these genes mapped to previously identified Al tolerance QTL**



Ma (2007) Syndrome of Al toxicity & diversity of Al resistance in higher plants. *Int. Rev. Cyt.* 264:225-253

Figure 4. Showed the candidate Al tolerance genes in rice (adopted from Ma, 2007, Kochian, 2013)

Putative QTLs expressed after exposure to Al stress

QTLs mapping is one of the powerful way to mark the specific gene of interest on particular chromosome. Many studies have been conducted in past, identified lot of QTLs for Al tolerance in rice using several mapping several populations. Wu et al. (2000) used hydroponic culture experiment and conducted QTL mapping by using single marker analysis method and identified a QTL *qRRL-12* for relative root length, explained 12% and 10% variation across different populations at second and 4th week of stress which suggested its prolong contribution to Al tolerance in rice. Nguyen et al. (2001) used hydroponic screening technique for Al toxicity tolerance in rice at seedling stage and conducted QTL analysis by method of interval mapping and reported QTL *QAIRr1a* on chromosome 1 which explained 25 % of phenotypic variation and contributed positively towards Al tolerance.

In another study Nguyen et al. (2002) used the hydroponic technique screening technique for Al toxicity tolerance and detected a significant genomic region *qALRR-2* on chromosome 2 by QTL mapping analysis using interval mapping method that contributed greatly to Al tolerance. This QTL indicated that Al tolerance is mainly determined by relative root length ratio of rice seedling evaluated in hydroponic conditions. A genomic region with LOD value of 8.3 with 24.9% of contribution in variance was involved in natural variation against Al tolerance and conserved across cereals suggesting the possibilities for QTLs pyramiding to boost Al toxicity tolerance in rice (Ninamango-Cardenas et al., 2003). Nguyen et al. (2003) used nutrient culture solution to sort out the seedling of rice against Al toxicity tolerance and conducted QTL analysis using interval mapping method and detected *QAIRr3.1* which provided important insights into Al tolerance in rice.

Xue et al. (2006) used hydroponic screening method for Al tolerance using 71 RIL population and conducted QTL analysis using mix linear model method. They identified a novel QTL *qRRE-11* which provided important case for isolating genes involved in varying mechanism for Al tolerance among cereals. Xue et al. (2007) evaluated rice population in hydroponic solution for screening for Al tolerance and conducted QTLs analysis using composite interval mapping method and identified putative QTLs, *qRRE-1*, *qRRE-11* which had 17.68% and 13.53% of contribution in phenotypic variations and showed positive additive effect, indicated the enhancement of Al tolerance in rice. A major QTLs *AltLRD 9.1* among the flanking markers RM257/RM160 was identified by Famoso et al. (2011) using composite interval method which was responsible for controlling longest root growth in rice RIL population. In this study they grown plants hydroponically for screening for Al tolerance. Soomro and Jian (2015) used two sets of reciprocal introgression lines in hydroponic culture and identified 14 QTLs by QTL analysis across all environments. Some of the QTLs were newly reported QTLs with larger contribution for Al tolerance (Table 2). *qAIRL1.1* an Al tolerance QTL was documented by Meng et al. (2017) using GWA analysis conducted by using mix linear model method. Five magic populations were evaluated in hydroponic solution. This region involved in rice tolerance to Al toxicity and could be exploited to develop Al tolerant lines in rice. Beside root length, shoot length is also used to determine the degree of Al tolerance in rice. Recently two QTLs *qSL-1* and *qRL-1* were identified by Tao et al. (2018) which had 5.7% and 9.6% of their contribution in variance. These QTLs greatly affected the degree of Al tolerance in rice seedling. All of these reported regions could be exploited to develop Al tolerant varieties in rice (Table 2). In this study population was

grown in hydroponic culture solution and GWA analysis was performed using mix linear model approach for mapping of QTLs for Al tolerance.

Table 2. Putative QTLs identified in rice after exposure to Al stress

Parents	Progeny	Growth stage	Traits	Markers	QTL	Chr	LOD	PVE (%)	Ref
IR1552/Azucena	150 RIL	Seedling	RRL	RFLP, AFLP	<i>qRRL-12</i>	12	4.89	0.18	Wu et al., 2000
Chiembau/Omon269-65	182F3	Seedling	RRL	RFLP	<i>QAlRr1a</i>	1	10.71	25.0	Nguyen et al., 2001
CT9993/IR62266	146 DH	Seedling	RRL	RFLP,SSR	<i>qALRR-2</i>	2	4.54	13.4	Nguyen et al., 2002
IR64/ Rufipogon	171F6	Seedling	RRL	SSR	<i>QAlRr3.1</i>	3	8.3	24.9	Nguyen et al., 2003
Asominori/IR24	71RILs	Seedling	RRE		<i>QRRE-11</i>	11	2.64	13.53	Xue et al., 2006
Asominori/IR24	66 CSSLs	Seedling	RRE	RFLP	<i>qRRE-1, qRRE-11</i>	1,11	3.60, 2.64	17.68, 13.53	Xue et al., 2007
Azucena/IR64	134RIL	Seedling	LRG	SNP	<i>AltLRD 9.1</i>	9	6.57	0.16	Famose et al., 2011
02428/Munghui	BC2F1	Seedling	RL	SNP	<i>qRRL-12</i>	12	2.52		Sommro et al., 2015
MAGIC population	=	Seedling	RL	SNP	<i>qAlRL1.1</i>	1		0.1	Meng et al., 2017
	222,211 Acc	Seedling	SL		<i>qSL-1</i>	1		5.7	Tao et al., 2018
	222,211 Acc	Seedling	RL		<i>qRL-1</i>	1		9.6	Tao et al., 2018

RRL: relative root length, RRE: relative root elongation, LRG: longest root growth, RL: root length, SL: shoot length, QTLs: quantitative trait loci, Acc: Accessions, RIL: recombinant inbred lines, BC: backcross population, DH: double Haploid, CSSL, chromosomal segment substitution lines, Al: aluminum, SNP: single nucleotide polymorphism, SSR: single sequence repeat, AFLP: amplified fragment length polymorphism, RFLP: randomly amplified length polymorphism PVE: phenotypic variance, LOD: lod of algorithm

Genome wide association study (GWAS) and bulk segregant analysis as powerful techniques

In case of QTLs mapping, it requires development of mapping population and polymorphic markers so it is time consuming and increase labor cost. To overcome this difficulty a new approach is being used by scientists called genome wide association study (GWAS) which is a powerful technique used widely for the QTLs mapping and genes identification. It is widely used for natural resources. GWAS is more accurate in identification of recombination points in genome. By using GWAS we can get large number of significant associations, which lead to fine mapping and gene discovery. GWAS application becomes limited when population size small, therefore for identification of genes, usually requires high SNP density and large population size (Tao et al., 2018). Another most powerful and fast method for identification of QTL is bulk segregant analysis–seq which includes combination of bulk segregant as well as whole

genome re-sequencing. Researchers across the world are using these methods nowadays for rapid identification of QTLs and genes for objective trait. Third, use of Model base QTL detection is also an effective and novel way of QTL detection.

QTLs mapping types

Single marker analysis, interval mapping, composite interval mapping and multi traits mapping. Use of multi traits mapping is one of the best method of QTL analysis in which we can use more than one QTL at same time.

Use of some novel techniques to screen for Al toxicity tolerance in rice

Use of preliminary screening technique, SSR markers and BRILs population

One of the best method to determine the Al tolerance in rice at seedling stage is use of preliminary screening methods. In preliminary experiment rice seedlings can be grown in modified hydroponic culture with different toxic level of Al toxicity. We have used a new modified hydroponic culture to screen for Al tolerance at seedling stage to build a hypothesis that which dose of Al toxicity could be best for Al tolerance. Experiment was comprised of different rice lines which were allowed to grow under various toxic levels (10, 30, 50, and 100uM) of Al. Genotypes showed best response at 100uM of Al toxicity. By using this method in future studies, possibilities of screening of Al tolerance rice genotypes and identification of QTLs would be more fruitful.

Secondly we used novel rice population in BRILs (backcross recombinant inbred lines) which was developed by our research group (Jiang et al., 2017) at experimental station of Jiangxi Agricultural University, Nanchang, PR. China, in our regular experiment and here we are writing some of its features, which would be ideal population to tolerate Al toxicity if grown on acidic soils. This population was screened for Al tolerance at seedling stage and we found a significant difference for Al toxicity tolerance. BRILs population has major portion of genome from its recurrent parent and therefore it's is ideal population for targeted gene cloning. Single sequence repeats are ideal markers which were used for construction of linkage map to find the position of QTLs. Use of other markers do not give ideal information when linkage distance becomes zero, therefore SSR markers would be a best choice for linkage map construction to identify the QTLs for Al toxicity tolerance in rice.

Use of secondary tolerance indices as a new way to determine the Al tolerance

Al tolerance is mainly based on the relative root length of genotypes, that's why majority of the QTLs reported here are detected for root growth traits. Here we suggest some of the secondly tolerance indices to determine the degree of Al tolerance like, shoot length, shoot fresh weight, root fresh weight, shoot dry weight and root dry weight (Jiang et al., 2017). This index was used in our early study and these morphological attributes could be a potential indicator of Al toxicity tolerance in rice.

Concluding remarks

As far as rice growth on acidic soils is concerned, rice breeders have serious concerned to minimize the constraints of Al toxicity in rice to ensure global food security (Canito et

al., 2014). Rice production especially in China is greatly influenced by Al toxicity. Many strategies have been presented to enhance rice production on acidic soils. The urgent need is to identify and screen the Al tolerance genotypes in rice using various breeding techniques. Rice has adopted both physiological and molecular mechanism of defense to cope with Al toxicity (Bojorquez-Quintal et al., 2017). Several alterations in soil rhizosphere like pH changes should be done to minimize the effect of Al toxicity. Soil amendment with various fertilizers can be a viable approach to change the toxic Al into its immobile form so it cannot be entered into roots of rice, acceleration of plant physiological defense mechanism, is an important strategy to accelerate the secretion of several organic acids from roots for chelation of $AlCl^{3+}$ (Kochian et al., 2015). Rice is major Al tolerant crops, but until now no clear mechanism has known which is possibly involve in Al tolerance in rice. Lot of QTLs described above are responsible for governing Al tolerance in rice, which should be isolated and cloned for QTLs pyramiding to develop resistant lines which can grow best on acidic soils.

The various genes such as *Nrat1* which is a novel transporter should be studied more deeply to increase natural variation for Al tolerance. Use of mutation breeding can also be used to generate the mutants in rice population. Different mapping populations such as, BRIL, RIL, IL, CSSL, NIL should be tested against different level of Al tolerance to know their potential against Al. Some novel QTLs like, qRRE-11 and qRRE-1 controlling Al tolerance should be cloned and transferred to develop resistant lines. Real mechanism behind Al tolerance in rice is still unknown. In end we suggest some novel approaches like, use of preliminary screening technique, use of effective and modified nutrient solution with various levels of Al toxicity, BRIL population, SSR markers, secondary tolerance indices, is best way to select screen Al tolerant lines at seedling stage by applying various levels of Al toxicity, effective QTLs analysis and secondly, use of novel Al phenotyping platform and transcriptional regulation of mutant genes would lead to increase in Al tolerance in rice. Change in rhizosphere pH would change the toxic form of Al into nontoxic form and moreover activation of physiological base defense mechanism can reduce Al toxicity in rice.

Acknowledgments. Authors are thankful to the Prof Wu Ziming for his financial support during entire study. Authors are also thankful to the lab fellows for their support during manuscript preparation.

Funding. The research was supported by the National Natural Science Foundation of China (31560350 and 31760350), the National Key Research and Development Program of China (2018YFD0301102), the Key Research and Development Program of Jiangxi Province (20171ACF60018 and 20192ACB60003) and the Jiangxi Agriculture Research System (JXARS-18).

REFERENCES

- [1] Aamer, M., Muhammad, U. H., Abid, A., Su, Q., Liu, Y., Adnan, R., Muhammad, A. U. K., Tahir, A. K., Huang, G. (2018): Foliar application of glycine betaine (GB) alleviates the cadmium (Cd) toxicity in spinach through reducing Cd uptake and improving the activity of antioxidant systems. – *Applied Ecology and Environment Research* 16(6): 7575-7583.
- [2] Alia, F. J., Shamshuddin, J., Fauziah, C. I., Husni, M. H. A., Panhwar, Q. A. (2015): Effects of Aluminum, iron and/or low pH on rice seedlings grown in solution culture. – *International Journal of Agriculture and Biology* 17: 702-710.
- [3] Alvim, M., Ramos, F., Oliveira, D., Isaias, R., Franca, M. (2012): Aluminum localization and toxicity symptoms related to root growth inhibition in rice (*Oryza sativa* L.) seedlings. – *Journal of Biosciences* 37: 1079-1088.
- [4] Arbelaez, J. D., Maron, L. G., Jobe, T. O., Pineros, M. A., Famoso, A. N., Rebelo, A. R., Singh, N., Ma, Q., Fei, Z., Kochian, L. V. (2017): Aluminum resistance transcription factor 1 (*ART1*) underlies a major Al resistance QTL and interacts with natural variation in the genetic background to quantitatively regulate Al resistance in rice. – *BioRxiv*: 1-17.
- [5] Awasthi, J. P., Saha, B., Regon, P., Sahoo, S., Chowra, U., Pradhan, A., Roy, A., Panda, S. K. (2017): Morpho-physiological analysis of tolerance to aluminum toxicity in rice varieties of North East India. – *PloS one* 12: e0176357.
- [6] Bidhan, R., Bhadra, S. (2014): Effects of toxic levels of aluminium on seedling parameters of rice under hydroponic culture. – *Rice Science* 21: 217-223.
- [7] Bojórquez-Quintal, E., Escalante-Magaña, C., Echevarría-Machado, I., Martínez-Estévez, M. (2017): Aluminum, a friend or foe of higher plants in acid soils. – *Frontiers in Plant Science* 8: 1-16.
- [8] Caniato, F. F., Hamblin, M. T., Guimaraes, C. T., Zhang, Z., Schaffert, R. E., Kochian, L. V., Magalhaes, J. V. (2014): Association mapping provides insights into the origin and the fine structure of the sorghum aluminum tolerance locus, *AltSB*. – *PLoS One* 9: 1-12.
- [9] Chandran, D., Sharopova, N., Ivashuta, S., Gantt, J. S., Van den Bosch, K. A., Samac, D. A. (2008): Transcriptome profiling identified novel genes associated with aluminum toxicity, resistance and tolerance in *Medicago truncatula*. – *Planta* 228: 151-166.
- [10] Che, J., Yamaji, N., Shen, R. F., Ma, J. F. (2016): An Al-inducible expansin gene, *Os EXPA10* is involved in root cell elongation of rice. – *The Plant Journal* 88: 132-142.
- [11] Eekhout, T., Larsen, P., De Veylder, L. (2017): Modification of DNA Checkpoints to Confer Aluminum Tolerance. – *Trends in Plant Science* 22: 102-105.
- [12] Escobar-Sepúlveda, H. F., Trejo-Téllez, L. I., García-Morales, S., Gómez-Merino, F. C. (2017): Expression patterns and promoter analyses of aluminum-responsive NAC genes suggest a possible growth regulation of rice mediated by aluminum, hormones and NAC transcription factors. – *PLoS One* 12: 1-25.
- [13] Eticha, D., Stass, A., Horst, W. J. (2005): Cell-wall pectin and its degree of methylation in the maize root-apex: significance for genotypic differences in aluminum resistance. – *Plant, Cell & Environment* 28: 1410-1420.
- [14] Famoso, A. N., Clark, R. T., Shaff, J. E., Craft, E., McCouch, S. R., Kochian, L. V. (2010): Development of a novel aluminum tolerance phenotyping platform used for comparisons of cereal aluminum tolerance and investigations into rice aluminum tolerance mechanisms. – *Plant Physiology* 153: 1678-1691.
- [15] Famoso, A. N., Zhao, K., Clark, R. T., Tung, C.-W., Wright, M. H., Bustamante, C., Kochian, L. V., McCouch, S. R. (2011): Genetic architecture of aluminum tolerance in rice (*Oryza sativa*) determined through genome-wide association analysis and QTL mapping. – *PLoS Genetics* 7: 1-16.
- [16] Guimaraes, C. T., Simoes, C. C., Pastina, M. M., Maron, L. G., Magalhaes, J. V., Vasconcellos, R. C., Guimaraes, L. J., Lana, U. G., Tinoco, C. F., Noda, R. W., Jardim-Belicuas, S. N., Kochian, L. V., Alves, V. M., Parentoni, S. N. (2014): Genetic dissection

- of Al tolerance QTLs in the maize genome by high density SNP scan. – *BMC Genomics* 15: 2-14.
- [17] Hossain Khan, M. S., Tawarayama, K., Sekimoto, H., Koyama, H., Kobayashi, Y., Murayama, T., Chuba, M., Kambayashi, M., Shiono, Y., Uemura, M. (2009): Relative abundance of $\Delta 5$ -sterols in plasma membrane lipids of root-tip cells correlates with aluminum tolerance of rice. – *Physiologia Plantarum* 135: 73-83.
- [18] Huang, C. F., Yamaji, N., Mitani, N., Yano, M., Nagamura, Y., Ma, J. F. (2009): A bacterial-type ABC transporter is involved in aluminum tolerance in rice. – *The Plant Cell* 21: 655-667.
- [19] Huang, C. F., Yamaji, N., Chen, Z., Ma, J. F. (2012): A tonoplast-localized half-size ABC transporter is required for internal detoxification of aluminum in rice. – *The Plant Journal* 69: 857-867.
- [20] Ishikawa, S., Abe, T., Kuramata, M., Yamaguchi, M., Ando, T., Yamamoto, T., Yano, M. (2009): A major quantitative trait locus for increasing cadmium-specific concentration in rice grain is located on the short arm of chromosome 7. – *Journal of experimental botany* 61: 923-934.
- [21] Jiang, N., Shi, S., Shi, H., Khanzada, H., Wassan, G. M., Zhu, C., Peng, X., Yu, Q., Chen, X., He, X., Fu, J., Hu, L., Xu, J., Ouyang, L., Sun, X., Zhou, D., He, H., Bian, J. (2017): Mapping QTL for seed germinability under low temperature using a new high-density genetic map of rice. – *Frontiers in Plant Science* 8: 1-9.
- [22] Kisnieriené, V., Lapeikaité, I. (2015): When chemistry meets biology: the case of aluminium- a review. – *Chemija* 26: 148-158.
- [23] Kochian, L. V., Pineros, M. A., Liu, J., Magalhaes, J. V. (2015): Plant adaptation to acid soils: the molecular basis for broop aluminum resistance. – *Annual Review of Plant Biology* 66: 571-598.
- [24] Kochian, L. GCP Project G7009.07: GRM 2013: Cloning, characterization and validation of AltSB/A1 tolerance in rice P1: Leon Kochian, USDA-ARS, Cornell University Co-P1: Susan McCouch, Department of Plant Breeding, Cornell University. – (2013): Technology.
- [25] Kopittke, P. M., Menzies, N. W., Wang, P., Blamey, F. P. (2016): Kinetics and nature of aluminium rhizotoxic effects: a review. – *Journal of Experimental Botany* 67: 4451-4467.
- [26] Larsen, P. B., Geisler, M. J., Jones, C. A., Williams, K. M., Cancel, J. D. (2005): ALS3 encodes a phloem-localized ABC transporter-like protein that is required for aluminum tolerance in Arabidopsis. – *The Plant Journal* 41: 353-363.
- [27] Larsen, P. B., Cancel, J., Rounds, M., Ochoa, V. (2007): Arabidopsis ALS1 encodes a root tip and stele localized half type ABC transporter required for root growth in an aluminum toxic environment. – *Planta* 225: 1447-14458.
- [28] Li, J. Y., Liu, J., Dong, D., Jia, X., McCouch, S. R., Kochian, L. V. (2014): Natural variation underlies alterations in *Nramp* aluminum transporter (*NRATI*) expression and function that play a key role in rice aluminum tolerance. – *Proceedings of the National Academy of Sciences* 111: 6503-6508.
- [29] Liang, Y. S., Zhan, X. D., Wang, H. M., Gao, Z. Q., Lin, Z. C., Chen, D. B., Shen, X. H., Cao, L. Y., Cheng, S. H. (2013): Locating QTLs controlling several adult root traits in an elite Chinese hybrid rice. – *Gene* 526: 331-335.
- [30] Ma, J. F., Shen, R., Zhao, Z., Wissuwa, M., Takeuchi, Y., Ebitani, T., Yano, M. (2002): Response of rice to Al stress and identification of quantitative trait loci for Al tolerance. – *Plant and Cell Physiology* 43: 652-659.
- [31] Ma, J. F. (2007): Syndrome of aluminum toxicity and diversity of aluminum resistance in higher plants. – *International Review of Cytology* 264: 225-252.
- [32] Maejima, E., Watanabe, T. (2014): Proportion of phospholipids in the plasma membrane is an important factor in Al tolerance. – *Plant Signaling & Behavior* 9: 29277.
- [33] Magalhaes, J. V., Liu, J., Guimaraes, C. T., Lana, U. G., Alves, V. M., Wang, Y. H., Schaffert, R. E., Hoekenga, O. A., Pineros, M. A., Shaff, J. E. (2007): A gene in the

- multidrug and toxic compound extrusion (*MATE*) family confers aluminum tolerance in sorghum. – *Nature Genetics* 39: 1156-61.
- [34] Maron, L. G., Kirst, M., Mao, C., Milner, M. J., Menossi, M., Kochian, L. V. (2008): Transcriptional profiling of aluminum toxicity and tolerance responses in maize roots. – *New Phytologist* 179: 116-128.
- [35] Meng, L., Wang, B., Zhao, X., Ponce, K., Qian, Q., Ye, G. (2017): Association mapping of ferrous, zinc, and aluminum tolerance at the seedling stage in indica rice using MAGIC populations. – *Frontiers in Plant Science* 8: 1-15.
- [36] Moreno-Alvarado, M., García-Morales, S., Trejo-Téllez, L. I., Hidalgo-Contreras, J. V., Gómez-Merino, F. C. (2017): Aluminum enhances growth and sugar concentration, alters macronutrient status and regulates the expression of NAC transcription factors in rice. – *Frontiers in Plant Science* 8: 1-16.
- [37] Moriyama, U., Tomioka, R., Kojima, M., Sakakibara, H., Takenaka, C. (2016): Aluminum effect on starch, soluble sugar, and phytohormone in roots of *Quercus serrata* Thunb. seedlings. – *Trees* 30: 405-413.
- [38] Muhammad, N., Zvobgo, G., Zhang, G. P. (2018): A review: the beneficial effect of aluminum on plant growth in acid soil and the possible mechanisms. – *Journal of Integrative Agriculture* 17: 60345-7.
- [39] Nezames, C. D., Ochoa, V., Larsen, P. B. (2013): Mutational loss of Arabidopsis SLOW WALKER2 results in reduced endogenous spermine concomitant with increased aluminum sensitivity. – *Functional Plant Biology* 40: 67-78.
- [40] Nguyen, V. T., Burow, M. D., Nguyen, H. T., Le, B. T., Le, T. D., Paterson, A. H. (2001): Molecular mapping of genes conferring aluminum tolerance in rice (*Oryza sativa* L.). – *Theoretical and Applied Genetics* 102: 1002-1010.
- [41] Nguyen, V., Nguyen, B., Sarkarung, S., Martinez, C., Paterson, A., Nguyen, H. (2002): Mapping of genes controlling aluminum tolerance in rice: comparison of different genetic backgrounds. – *Molecular Genetics and Genomics* 267: 772-780.
- [42] Nguyen, B. D., Brar, D. S., Bui, B. C., Nguyen, T. V., Pham, L. N., Nguyen, H. T. (2003): Identification and mapping of the QTL for aluminum tolerance introgressed from the new source, *Oryza rufipogon* Griff., into indica rice (*Oryza sativa* L.). – *Theoretical and Applied Genetics* 106: 583-593.
- [43] Ninamango-Cárdenas, F. E., Guimarães, C. T., Martins, P. R., Parentoni, S. N., Carneiro, N. P., Lopes, M. A., Moro, J. R., Paiva, E. (2003): Mapping QTLs for aluminum tolerance in maize. – *Euphytica* 130: 223-232.
- [44] Panda, S. K., Baluška, F., Matsumoto, H. (2009): Aluminum stress signaling in plants. – *Plant Signaling & Behavior* 4: 592-597.
- [45] Pandey, P., Srivastava, R. K., Dubey, R. (2013): Salicylic acid alleviates aluminum toxicity in rice seedlings better than magnesium and calcium by reducing aluminum uptake, suppressing oxidative damage and increasing antioxidative defense. – *Ecotoxicology* 22: 656-670.
- [46] Roy, R., Singh, S. K., Chauhan, L., Das, M., Tripathi, A., Dwivedi, P. D. (2014): Zinc oxide nanoparticles induce apoptosis by enhancement of autophagy via PI3K/Akt/mTOR inhibition. – *Toxicology Letters* 227: 29-40.
- [47] Sasaki, T., Yamamoto, Y., Ezaki, B., Katsuhara, M., Ahn, S. J., Ryan, P. R., Delhaize, E., Matsumoto, H. (2004): A wheat gene encoding an aluminum-activated malate transporter. – *Plant Journal* 37: 645-653.
- [48] Silva, S., Pinto, G., Dias, M. C., Correia, C. M., Moutinho-Pereira, J., Pinto-Carnide, O., Santos, C. (2012): Aluminium long-term stress differently affects photosynthesis in rye genotypes. – *Plant Physiology and Biochemistry* 54: 105-112.
- [49] Soomro, A. A., Jian, J. (2015): QTL mapping for Aluminum (Alcl3+) toxicity tolerance in two sets of Reciprocal Introgression Lines in Rice (*Oryza sativa* L.). – *International Journal of Scientific & Engineering Research* 6(7): 740-748.

- [50] Tanaka, A., Navasero, S. (1966): Aluminum toxicity of the rice plant under water culture conditions. – *Soil Science and Plant Nutrition* 12: 9-14.
- [51] Tao, Y., Niu, Y., Wang, Y., Chen, T., Naveed, S. A., Zhang, J., Xu, J., Li, Z. (2018): Genome-wide association mapping of aluminum toxicity tolerance and fine mapping of a candidate gene for *Nrat1* in rice. – *PLoS One* 13: 0198589.
- [52] Veitch, F. (1904): Comparison of methods for the estimation of soil acidity. – *Journal of the American Chemical Society* 26: 637-662.
- [53] Von Uexküll, H. R., Mutert, E. (1995): Global extent, development and economic impact of acid soils. – *Plant and Soil* 171: 1-15.
- [54] Wagatsuma, T., Khan, M. S. H., Watanabe, T., Maejima, E., Sekimoto, H., Yokota, T., Nakano, T., Toyomasu, T., Tawaraya, K., Koyama, H. (2014): Higher sterol content regulated by CYP51 with concomitant lower phospholipid content in membranes is a common strategy for aluminium tolerance in several plant species. – *Journal of Experimental Botany* 66: 907-918.
- [55] Wang, L. Q., Yang, L. T., Guo, P., Zhou, X. X., Ye, X., Chen, E. J., Chen, L. S. (2015): Leaf cDNA-AFLP analysis reveals novel mechanisms for boron-induced alleviation of aluminum-toxicity in *Citrus grandis* seedlings. – *Ecotoxicology and Environmental Safety* 120: 349-359.
- [56] Wang, Y., Li, R., Li, D., Jia, X., Zhou, D., Li, J., Lyi, S. M., Hou, S., Huang, Y., Kochian, L. V. (2017): NIP1; 2 is a plasma membrane-localized transporter mediating aluminum uptake, translocation, and tolerance in *Arabidopsis*. – *Proceedings of the National Academy of Sciences* 114: 5047-5052.
- [57] Wu, P., Liao, C., Hu, B., Yi, K., Jin, W., Ni, J., He, C. (2000): QTLs and epistasis for aluminum tolerance in rice (*Oryza sativa* L.) at different seedling stages. – *Theoretical and Applied Genetics* 100: 1295-1303.
- [58] Xia, J., Yamaji, N., Kasai, T., Ma, J. F. (2010): Plasma membrane-localized transporter for aluminum in rice. – *Proceedings of National Academy of Science U S A* 107: 18381-18385.
- [59] Xia, J., Yamaji, N., Ma, J. F. (2013): A plasma membrane-localized small peptide is involved in rice aluminum tolerance. – *The Plant Journal* 76: 345-355.
- [60] Xu, Q., Wang, Y., Ding, Z., Song, L., Li, Y., Ma, D., Wang, Y., Shen, J., Jia, S., Sun, H. (2016): Aluminum induced metabolic responses in two tea cultivars. – *Plant Physiology and Biochemistry* 101: 162-172.
- [61] Xue, Y., Wan, J., Jiang, L., Liu, L., Su, N., Zhai, H., Ma, J. F. (2006): QTL analysis of aluminum resistance in rice (*Oryza sativa* L.). – *Plant and Soil* 287: 375-383.
- [62] Xue, Y., Jiang, L., Su, N., Wang, J., Deng, P., Ma, J., Zhai, H., Wan, J. (2007): The genetic basic and fine-mapping of a stable quantitative-trait loci for aluminum tolerance in rice. – *Planta* 227: 255-262.
- [63] Yamaji, N., Huang, C. F., Nagao, S., Yano, M., Sato, Y., Nagamura, Y., Ma, J. F. (2009): A zinc finger transcription factor ART1 regulates multiple genes implicated in aluminum tolerance in rice. – *The Plant Cell* 21: 3339-3349.
- [64] Yang, J. L., Li, Y. Y., Zhang, Y. J., Zhang, S. S., Wu, Y. R., Wu, P., Zheng, S. J. (2008): Cell wall polysaccharides are specifically involved in the exclusion of aluminum from the rice root apex. – *Plant Physiology* 146: 602-611.
- [65] Yang, Y., Wang, Q., Geng, M., Guo, Z., Zhao, Z. (2011): Rhizosphere pH difference regulated by plasma membrane H⁺-ATPase is related to differential Al tolerance of two wheat cultivars. – *Plant, Soil and Environment* 57: 201-206.
- [66] Zhang, H., Jiang, Z., Qin, R., Zhang, H., Zou, J., Jiang, W., Liu, D. (2014): Accumulation and cellular toxicity of aluminum in seedling of *Pinus massoniana*. – *BMC Plant Biology* 14: 264.
- [67] Zhang, P., Zhong, K., Tong, H., Shahid, M. Q., Li, J. (2016): Association mapping for aluminum tolerance in a core collection of rice landraces. – *Frontiers in Plant Science* 7: 2-11.

EXOGENOUS APPLICATION OF INORGANIC SALTS DURING GROWTH STAGES INFLUENCES THE VEGETATIVE GROWTH, MARKETABLE YIELD AND QUALITY OF STRAWBERRY (*FRAGARIA* × *ANANASSA*) CULTIVAR ‘CHANDLER’

SHAHZAD, S.¹ – AHMAD, S.^{1*} – RASHID, M. Z.² – SHEHZAD, S.³ – SHAFQAT, W.¹ – HANIF, A.¹

¹*Institute of Horticultural Sciences, University of Agriculture, Faisalabad 38000, Pakistan*

²*Horticultural Research Institute, Ayub Agricultural Research Institute, Faisalabad 38850, Pakistan*

³*Department of Plant Pathology, University of Agriculture, Faisalabad 38000, Pakistan*

**Corresponding author*

e-mail: saeedsandhu@uaf.edu.pk, sanashahzad247@gmail.com; phone: +92-300-768-8958

(Received 9th Dec 2019; accepted 24th Mar 2020)

Abstract. In Pakistan strawberry yield and cultivation area is significantly lower as compared the major strawberry growing countries. Defective agronomic practices cause reduction in yield and quality. This experiment was conducted by using non-chemical techniques including exogenous application of inorganic salts CaCl₂ (3, 5 and 7 mM/L) and ZnSO₄ (50, 100 and 150 mg/L) during growth stages (3-4 leaves stage and after fruit setting) and their effects on marketable yield and quality of strawberry were documented. The highest number of leaves (18.25), leaf area (47 cm²) and crowns (7.50) were found with 7 mM/L CaCl₂ as compared to control plants. Minimum numbers of days (27.7) for flower anthesis were recorded with 100 mg/L ZnSO₄. Maximum marketable yield (348.5 g plant⁻¹), firmness (0.96 kg. cm⁻²), total soluble solids (8.2 °Brix), TSS:TA ratio (7.62), vitamin C (55.69 mg 100 g⁻¹), total phenolic contents (186.5 mg GAE 100 g⁻¹) and higher total antioxidants (75.5% DPPH) were observed with 7 mM/L CaCl₂ application. However, maximum superoxide dismutase activity (30.2 U mg⁻¹ protein) was examined with 100 mg/L ZnSO₄ while peroxidase activity (1.05 U mg⁻¹ protein) decreased with this concentration. Overall, the response of 7 mM/L CaCl₂ was highly effective for increasing marketable yield and quality.

Keywords: *calcium chloride, zinc sulfate, total phenolic contents, total antioxidants, marketable yield*

Introduction

Strawberry (*Fragaria* × *ananassa* Duch.) a sweet flavored small fruit belonging to the Rosaceae family (Sharma, 2002). Among berry fruits strawberry is most popular and economically important fruit crop (Santos and Chandler, 2009). Nature has blessed Pakistan with different agro climatic conditions which are suitable for production of strawberry. Strawberry plants require low chilling condition and can be planted in wide range of soil types (Asad, 1997). Strawberry is newly emerging small fruit crop in Pakistan; therefore, yield is very lower as compared to other major strawberry producing countries due to improper research techniques and defective field practices (Mabood, 1994). In Pakistan strawberry is cultivated on 179 hectares with 609 tons annual production (GOP, 2015). Strawberries are delicious low-calorie fruits with rich source of vitamins, minerals, anthocyanins and phenolics (Adda Bjarnadottir, 2012).

Rapid growth of strawberry plants (crowns, leaves and runners) can occur within 2-3 months, which depends on nutrients, light, temperature and water conditions (Li et al., 2010). Fast growth habit of strawberry plant demands sufficient supply of macro and micro nutrients synchronized with growth stages of the crop (Phillips, 2004; Medeiros

et al., 2015). Exogenous application is a supplemental application method to supply nutrients during growth stages when plants cannot uptake adequate nutrients from soil due to complex soil chemistry, leaching of nutrients, low soil temperature, immobile nutrients and low water availability which solubilize the nutrients (Anonymous, 2018; Ghani et al., 2011). In general, through foliar application essential nutrients penetrate in the cuticle or enter through the stomata of leaves more rapidly as compared to soil application (Alshaal and Ramady, 2017). Exogenous application of salts enhances the vegetative growth (plant height, crown diameter, canopy growth, runner growth and leaf area) and also improves the quality and yield of strawberry (Qureshi et al., 2013). In inorganic salts calcium chloride is important which improved the inflexibility of plant cells (Sams, 1999; Maas, 1998). Plants obtain calcium from soil solution through root system via xylem. Deficiency of calcium in root system disturbs the normal life cycle of plants and causes malformation (White, 2000).

Exogenous application of calcium considered as cultural practice for improving fruit calcium contents and it also reduced the decay problem (Bramlage et al., 1985; Elad and Volpin, 1993). Foliar applied calcium chloride before harvest delayed tissue softening, fruit ripening process and reduced grey mould disease in strawberries (Cheour et al., 1990). Zinc sulfate as inorganic salt involved in plant enzymatic reactions and regulate protein and carbohydrate metabolism (Lolaei et al., 2012). Zinc is major component of several enzymes, proteins and important metal element for normal metabolic process of plants. It increased the activity of enzyme called tryptophan which, further enhanced the production of growth hormone called indole acetic acid and acted as growth promoter (Nasiri et al., 2010). Through foliar application zinc played important role for increasing the fruit set, production and quality attributes of fruits and reduced the different physiological disorders in fruit trees (Meena et al., 2014).

In literature, very little information available but not complete answers regarding the effects of foliar application of salts for increasing the marketable yield of strawberry and for improving fruit quality. Foliar application of fungicides is largely used practice in Pakistan which causes the health issues but not focus on non-chemical techniques which reduce the health issues in humans. By keeping in view previous studies, the present study was executed to pursue the following goal: To optimize the best concentration of CaCl_2 and ZnSO_4 which increase the marketable yield and also improve the quality of strawberry.

Materials and methods

Experimental site

Field experiment was conducted at Ayub Agricultural Research Institute (AARI), Jhang Road Faisalabad, Pakistan in the fruit research area during October, 2016 to April, 2017. Raised beds were prepared after one month of soil preparation and their width was 45 cm. Black polyethylene sheet as mulching material was used to cover the beds and for controlling weeds. Plant to plant distance was 25 cm. Healthy and disease-free bare root transplants of strawberry cv. 'Chandler' were collected from Agricultural Research Institute North Mingora, Swat, Khyber Pakhtoonkhwa. Different foliar applications of salts including CaCl_2 (3, 5 and 7 mM/L) and ZnSO_4 (50, 100 and 150 mg/L) were applied on strawberry plants and these were compared with control plants. This experiment was consisted of 7 treatments replicated four times. There were 40 plants in each treatment and total 280 plants used for this experiment. First foliar

application of salts was applied after 2 weeks of runner transplantation when old leaves were dried and new sprouting occurred at 3-4 leaves stage and second was done at fruit setting stage. Same amount of salt concentration was used in two different growth stages. Each concentration was dissolved separately in one liter of water for 10 plants. For foliar spray 100 ml water was used for single strawberry plant for better absorption and penetration. The surfactant Tween-20 (0.01%) was added as wetting agent for foliar application. Foliar application was applied during morning time 6-7 am with handheld sprinkler in a very gentle way.

Vegetative parameters

Numbers of leaves were counted during growing season. At the end of season three healthy plants from each replication were pull out from beds and then each plant was cut into two halves in such way that trifoliate leaves with petioles separated and below portion crown separated. After cutting of each plant numbers of leaves and crowns were counted. Leaf area of strawberry plants was measured with leaf area meter (LI-COR, 3100C). Numbers of days required for flower anthesis and numbers of runners per plant were also counted after first foliar application (Sangha and Agehara, 2016).

Yield parameters

Strawberry harvesting was started during end of January and continued till mid-May. Yield was accounted as marketable, unmarketable and small size (g plant⁻¹). Strawberries which were 75-80% fully mature, bright red color, larger size and disease free counted as marketable yield during whole season. Strawberry fruits which were affected due to grey mould disease (*Botrytis cinerea*), anthracnose fungal disease (*Colletotrichum*), powdery mildew (*Podosphaera aphanis*), thrips attack, phyllody (abnormal development of floral parts into leafy structures caused by *phytoplasma* or virus infections) and due to environmental factors (chilling injury and frost injury) counted as unmarketable yield during season. Strawberries which were (<10 g) and bullet shaped counted as small size yield during whole season (Sangha and Agehara, 2016).

Fruit quality parameters

Firmness

Fruit firmness was measured with digital penetrometer (Humboldt H-1240D) by using 3 mm diameter probe which measure the penetration force.

Total soluble solids, titratable acidity and TSS:TA ratio

Total soluble solids (°Brix), TA (%) and TSS:TA ratio measured with digital TSS/Acid meter (Atago, Japan).

Vitamin C

For the measurement of vitamin C (mg 100 g⁻¹) contents in strawberry extract, first of all strawberry extract was filtered then (10 ml) aliquot was taken in (100 ml) volumetric flask and volume was made up to mark after addition of (0.4%) oxalic acid. For titration purpose (5 ml) aliquot was taken in beaker and titration was done with (2,

6-dichlorophenol indophenol) when pink color appeared it was indication of end point. Calculations were done with the method described by Ruck (1969).

Total phenolic contents

For the determination of TPC of strawberry extract FC method was used. It is called as Folin-Ciocalteu method. Total phenolic contents (mg GAE 100 g⁻¹) were determined by using spectrophotometer and read at 765 nm against the standard curve of Gallic acid (R² = 0.7884). Calculations were performed according to method as described by Ainsworth and Gillespie (2007).

Total antioxidants

For TA determinations take supernatant (50 µL) and methanolic solution 0.004% (5 ml) in test tube. Methanolic solution expressed in (2, 2-diphenyl-1 picrylhydrazyl radical) % DPPH. Samples were tested with the interval of 30 minutes. Changes in absorbance were measured at 517 nm by microplate reader using spectrophotometer. Calculations were performed by using method described by Brand-Williams et al. (1995).

Activities of anti-oxidative enzymes

For catalase activity hydrogen peroxide was used to initiate the reaction mixture. Enzyme extract (100 µL) was mixed in H₂O₂ (100 µL) and then activity was observed 240 nm by microplate reader. Peroxidase activity was measured by using potassium phosphate buffer (0.1 M), hydrogen peroxide (40 mM) and guaiacol (20 mM) with different ratios (8:1:1). Absorbance was noted at 470 nm by microplate reader using spectrophotometer. Calculations were performed by using method described by Liu et al. (2009). For estimation of superoxide dismutase activity nitro blue tetrazolium was used for 50% inhibition of photochemical reduction. Absorbance was noted at 560 nm by using microplate reader. The enzymatic activities were calculated in Unit (U mg⁻¹ protein) by using method described by Jimenez et al. (2003).

Survival

Diseased, damaged and dead plants were removed from field during entire season. At the end of season remaining plants were counted for plants survival percentage.

$$\text{Survival \%} = \frac{\text{Number of disease, damage and dead plants}}{\text{Total number of plants}} \times 100 \quad (\text{Eq.1})$$

Statistical analysis

Results were statistically analyzed by using (MINITAB[®]18.0 and SPSS 21 Software). Randomized Complete Block Design (RCBD) was used for this experiment. To test the overall significance of data ANOVA techniques were employed. To compare the differences among treatment means ($P \leq 0.05$) Fisher's Least Significant Difference (LSD) test was used (Meier, 2006).

Results

Vegetative parameters

Vegetative growth was significantly increased with exogenous application of salts throughout strawberry season as compared to control treatment (*Fig. 1*). Maximum number of leaves (18.25) was observed in strawberry plants those were treated with 7 mM/L CaCl_2 followed by other treatments including 100 mg/L ZnSO_4 (15.25), 150 mg/L ZnSO_4 (14.50), 5 mM/L CaCl_2 (13.50), 3 mM/L CaCl_2 (12.0) and 50 mg/L ZnSO_4 (10.75) per plant, respectively (*Table 1*). Mean values of treatments showed that leaf area (47 cm^2) was increased in all treated plants and maximum increment was observed with 7 mM/L CaCl_2 application as compared to non-treated plants. Minimum numbers of days (27.7) for flower anthesis were required when strawberry plants were treated with 100 mg/L ZnSO_4 as compared to control treatment where maximum numbers of days (42.25) were observed for flower anthesis. The response of ZnSO_4 foliar application was more for early flower initiation while all CaCl_2 treatments were statistically at par with each other. Crown growth was also increased with foliar application of salts and maximum numbers of crowns (7.50) were found with 7 mM/L CaCl_2 as compared to others. The effect of foliar application of salts for increasing runner growth of strawberry plants was found non-significant. Overall, runner growth was increased with foliar application of CaCl_2 and ZnSO_4 but statistically all treatments means were same (*Table 1*).

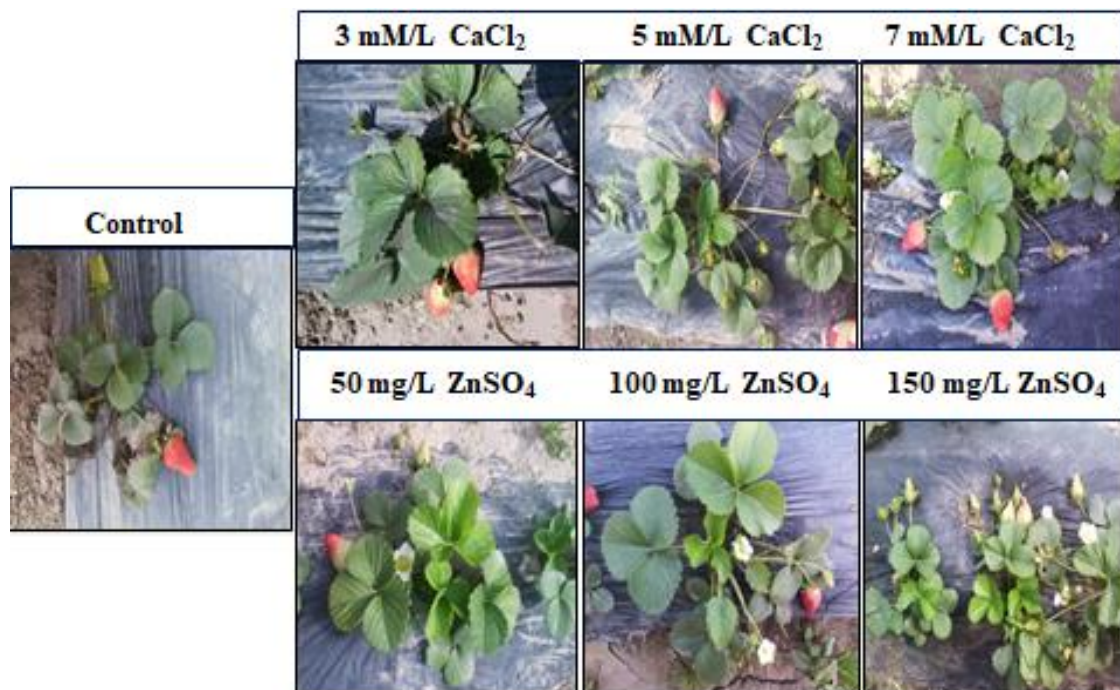


Figure 1. Canopy growth of 'Chandler' strawberry affected by exogenous application of inorganic salts. Treated strawberry plants were healthier as compared to control plants

Yield parameters

Statistical analysis regarding strawberry marketable yield demonstrated significant increased results (*Table 2*). Marketable yield was increased with exogenous application

of salts during growing season. Maximum marketable yield (348.5 g plant⁻¹) was observed from strawberry plants those were sprayed with 7 mM/L CaCl₂ followed by other treatments including 100 mg/L ZnSO₄ (319.0 g plant⁻¹), 150 mg/L ZnSO₄ (285.0 g plant⁻¹), 5 mM/L CaCl₂ (218.2 g plant⁻¹), 3 mM/L CaCl₂ (177.2 g plant⁻¹) and 50 mg/L ZnSO₄ (159.7 g plant⁻¹), respectively while minimum marketable yield (156.7 g plant⁻¹) was found with control treatment. It was noted that higher concentration of CaCl₂ (7 mM/L) and medium concentration of ZnSO₄ (100 mg/L) found more responsive for increasing marketable yield however when ZnSO₄ concentration was increased from 100 mg/L decreasing trend was observed. Unmarketable yield (40.5 g plant⁻¹) was also reduced with 7 mM/L CaCl₂ while maximum unmarketable yield (107.0 g plant⁻¹) was observed with control treatment. It was suggested that foliar application of CaCl₂ (7 mM/L) was more effective for increasing the marketable yield and to reduced unmarketable yield. Small size yield was also influenced with 7 mM/L CaCl₂ application and decreasing trend was observed in all treated strawberry plants while maximum yield of small sized strawberries (84.0 g plant⁻¹) were observed in control treatment (Table 2).

Table 1. Effect of exogenous application of inorganic salts on vegetative growth of strawberry plants cv. 'Chandler' Mean ± SE

Treatments	No. of leaves (plant ⁻¹)	Leaf area (cm ²)	Flower anthesis (days)	No. of crowns (plant ⁻¹)	No. of runners (plant ⁻¹)
Control	8.00 ± 1.08 g	27.50 ± 1.04 g	42.25 ± 0.48 a	2.50 ± 0.29 g	3.50 ± 0.29 a
3 mM/L CaCl ₂	12.00 ± 0.41 e	35.00 ± 0.41 e	41.50 ± 0.65 a	3.25 ± 0.25 f	3.75 ± 0.25 a
5 mM/L CaCl ₂	13.50 ± 0.29 d	39.50 ± 1.71 d	41.25 ± 0.63 a	4.50 ± 0.29 d	3.75 ± 0.25 a
7 mM/L CaCl ₂	18.25 ± 0.25 a	47.00 ± 1.08 a	40.00 ± 0.71 a	7.50 ± 0.29 a	3.80 ± 0.41 a
50 mg/L ZnSO ₄	10.75 ± 0.48 f	34.50 ± 0.65 f	39.75 ± 0.25 b	3.50 ± 0.29 e	3.71 ± 0.25 a
100 mg/L ZnSO ₄	15.25 ± 0.48 b	44.00 ± 0.91 b	27.75 ± 0.75 d	6.50 ± 0.00 b	3.78 ± 0.25 a
150 mg/L ZnSO ₄	14.50 ± 0.29 c	42.75 ± 1.38 c	33.50 ± 0.29 c	5.50 ± 0.29 c	3.75 ± 0.29 a
LSD (<i>P</i> ≤ 0.05)	1.25	2.32	1.69	0.79	0.79
C.V. %	6.2	4.4	2.92	11.43	19.05

Treatments means which represent same letter are statistically non-significant (*p* > 0.05)

Table 2. Effect of exogenous application of inorganic salts on yield of strawberry cv. 'Chandler' Mean ± SE

Treatments	Marketable (g plant ⁻¹)	Unmarketable (g plant ⁻¹)	Small size (g plant ⁻¹)
Control	156.7 ± 1.31 g	107.0 ± 3.49 a	84.0 ± 2.27 a
3 mM/L CaCl ₂	177.2 ± 8.33 e	92.2 ± 1.11 b	65.0 ± 1.47 b
5 mM/L CaCl ₂	218.2 ± 4.23 d	72.2 ± 1.11 d	54.2 ± 1.11 d
7 mM/L CaCl ₂	348.5 ± 7.08 a	40.5 ± 1.55 g	38.0 ± 1.29 g
50 mg/L ZnSO ₄	159.7 ± 12.97 f	90.0 ± 0.41 c	63.7 ± 0.85 c
100 mg/L ZnSO ₄	319.0 ± 15.03 b	54.7 ± 1.60 f	41.7 ± 0.48 f
150 mg/L ZnSO ₄	285.0 ± 14.30 c	65.5 ± 1.94 e	53.0 ± 0.91 e
LSD (<i>P</i> ≤ 0.05)	36.28	6.59	4.42
C.V. %	9.65	5.2	4.56

Treatments means which represent same letter are statistically non-significant (*p* > 0.05)

Fruit quality parameters

Firmness

Statistical analysis of strawberry fruit firmness affected by foliar application of salts demonstrated significant differences among different treatment means. Maximum firmness (0.96 kg. cm^{-2}) was achieved in fruits where plants were sprayed with 7 mM/L CaCl_2 followed by plants sprayed with different concentrations of CaCl_2 and ZnSO_4 while, less firmness (0.42 kg. cm^{-2}) was observed in control fruits (Fig. 2). Calcium chloride as firming agent was proved better for enhancing strawberry firmness when sprayed on plants during growth stages.

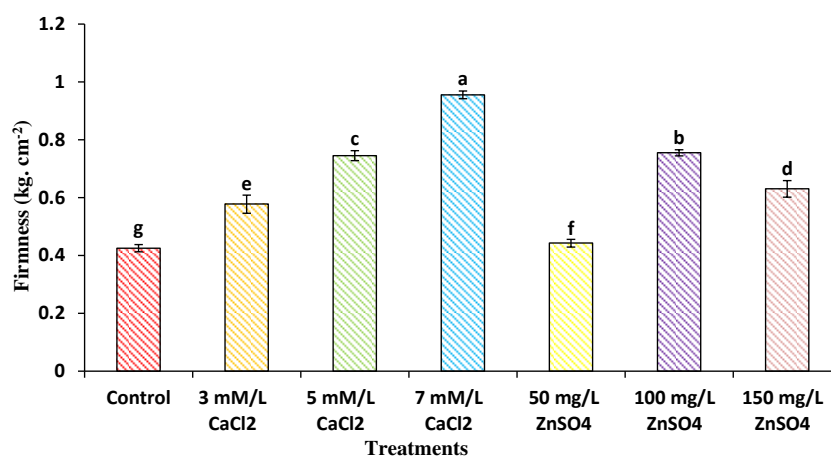


Figure 2. Effect of exogenous application of inorganic salts on firmness (kg. cm^{-2}) of strawberry fruit cv. 'Chandler'. Vertical bars represent \pm SE of means

Total soluble solids

Total soluble solids increased in those strawberry fruits where plants were treated with different concentrations of CaCl_2 and ZnSO_4 . Maximum amount of total soluble solids (8.2°Brix) were observed with 7 mM/L CaCl_2 application followed by other treatments including 100 mg/L ZnSO_4 (7.5°Brix), 5 mM/L CaCl_2 (7.1°Brix), 150 mg/L ZnSO_4 (6.8°Brix), 3 mM/L CaCl_2 (6.2°Brix) and 50 mg/L ZnSO_4 (5.9°Brix), respectively while minimum TSS contents (5.7°Brix) were observed in control treatment (Fig. 3a).

Titrateable acidity

Non-significant trend was recorded regarding effect of foliar spray of CaCl_2 and ZnSO_4 on acid contents of strawberry fruit. Quantitatively acid contents were found maximum in control treatment as compared to fruits of treated plants but statistically there was no difference between different treatment means (Fig. 3b).

TSS:TA ratio

TSS:TA ratio is major indicator of quality which determines the shelf life of fruit. Statistical analysis regarding strawberry fruit TSS:TA ratio showed significant increased trend. Maximum TSS:TA ratio (7.62) was observed in strawberry fruits where plants were treated with 7 mM/L CaCl_2 while minimum TSS:TA ratio (4.48) was

observed in control treatment (Fig. 3c). Increasing trend in TSS:TA ratio was found in treated fruits due maximum TSS contents and minimum acid contents however, in control fruits decreasing trend was found due to maximum acid contents and minimum TSS contents.

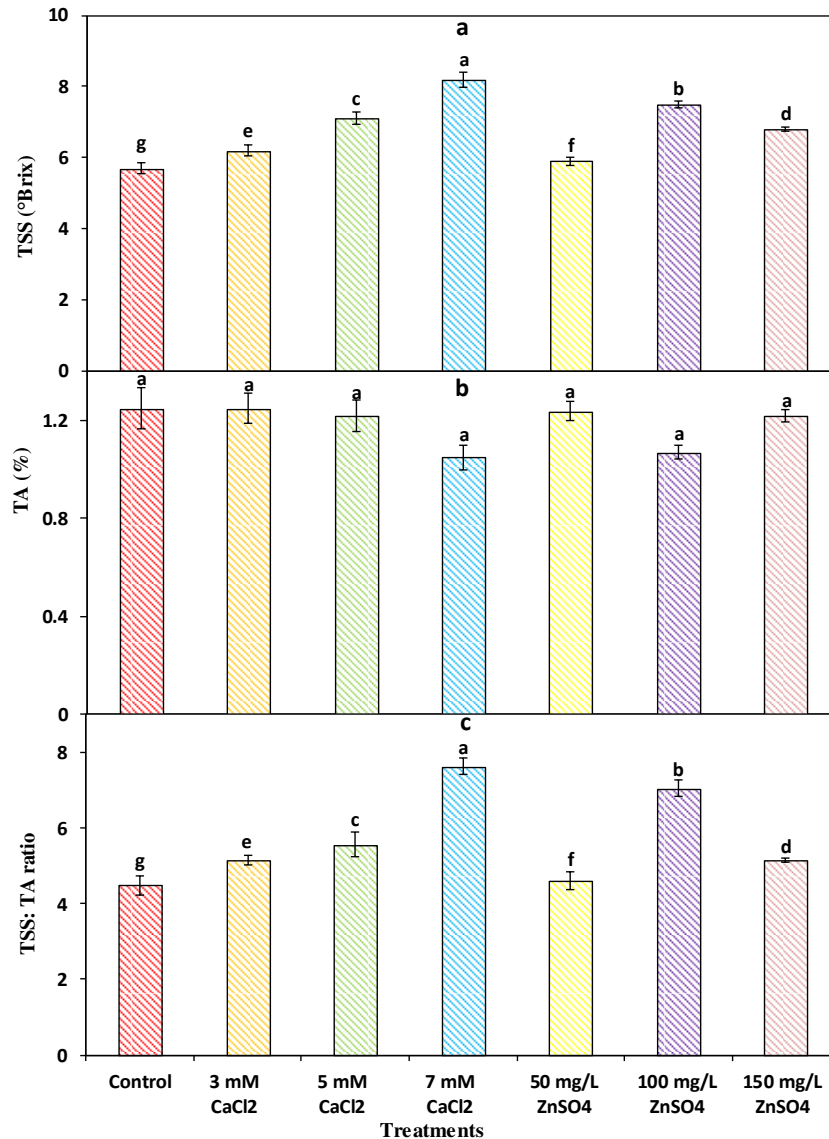


Figure 3. Effect of exogenous application of inorganic salts on (a) total soluble solids, (b) titratable acidity and (c) TSS:TA ratio of strawberry fruit cv. 'Chandler'. Vertical bars represent \pm SE of means

Vitamin C

Statistically significant increased trend was noted regarding vitamin C contents of strawberry fruit. Maximum (55.69 mg 100 g⁻¹) values were observed in strawberry fruits where plants were treated with 7 mM/L CaCl₂ followed by other treatments including 100 mg/L ZnSO₄ (53.30 mg 100 g⁻¹), 5 mM/L CaCl₂ (46.86 mg 100 g⁻¹), 150 mg/L ZnSO₄ (43.29 mg 100 g⁻¹), 3 mM/L CaCl₂ (41.16 mg 100 g⁻¹) and 50 mg/L ZnSO₄ (40.77 mg 100 g⁻¹), respectively while minimum value (35.55 mg 100 g⁻¹) was observed in control

treatment. Similar to other parameters the effect of exogenous application of salts was more effective for increasing vitamin C contents of strawberry fruit (Fig. 4a).

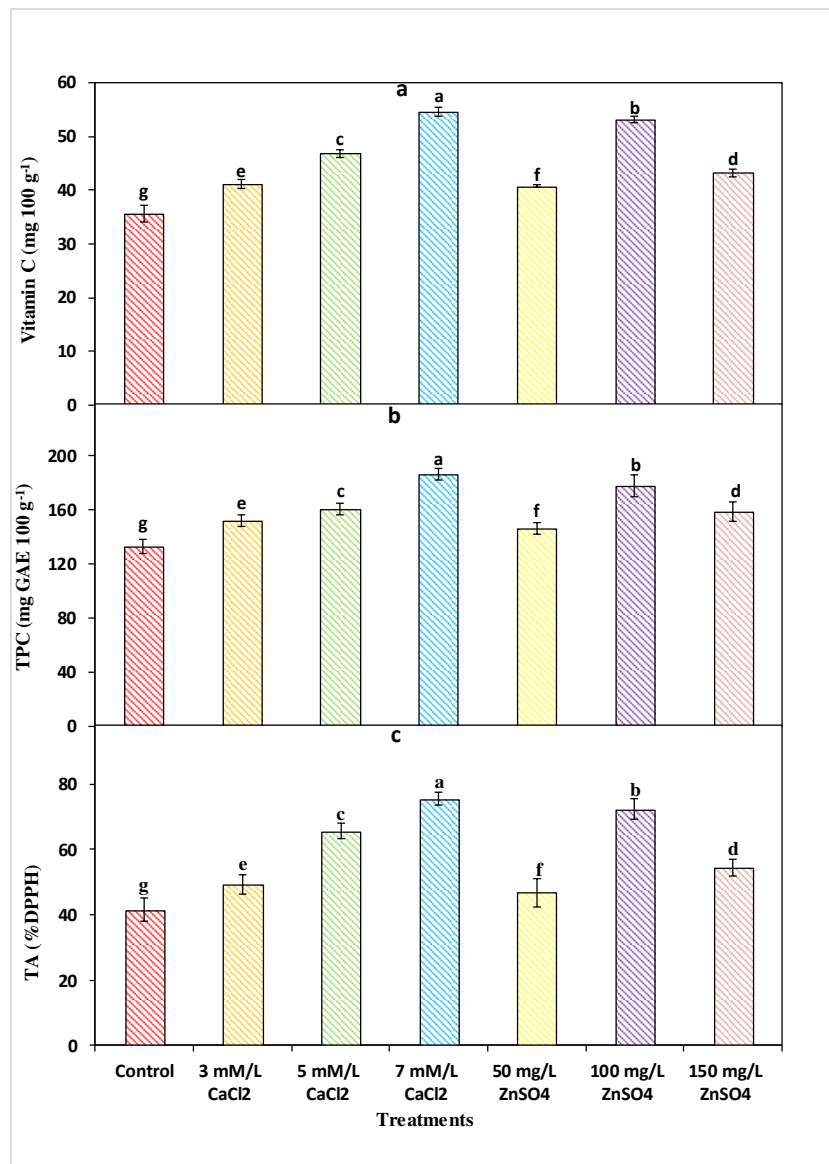


Figure 4. Effect of exogenous application of inorganic salts on (a) vitamin C contents (b) total phenolic contents and (c) total antioxidants of strawberry fruit cv. 'Chandler'. Vertical bars represent \pm SE of means

Total phenolic contents

Total phenolic contents of strawberry fruit highly influenced with application of salts during growth stages. Increasing trend was noticed with 7 mM/L CaCl₂ and showed higher TPC (186.5 mg GAE 100 g⁻¹) value followed by other treatments including 100 mg/L ZnSO₄ (177.5 mg GAE 100 g⁻¹), 5 mM/L CaCl₂ (160.5 mg GAE 100 g⁻¹), 150 mg/L ZnSO₄ (158.5 mg GAE 100 g⁻¹), 3 mM/L CaCl₂ (151.5 mg GAE 100 g⁻¹) and 50 mg/L ZnSO₄ (146.5 mg GAE 100 g⁻¹), respectively (Fig. 4b). Decreasing trend was noticed with control treatment and observed lower TPC (132.75 mg GAE 100 g⁻¹) value.

Total antioxidants

Statistical results regarding total antioxidants in strawberry fruit affected by exogenous application of salts showed significant increased trend. Higher antioxidants (75.5% DPPH) were noted in strawberry fruits where plants were treated with 7 mM/L CaCl₂ application. The response of exogenous application of CaCl₂ and ZnSO₄ was highly effective for increasing the antioxidants in strawberry fruit while minimum (41.5% DPPH) values were observed in control treatment (Fig. 4c).

Activities of anti-oxidative enzymes

Enzymatic activities were also influenced with exogenous application of salts (Table 3). While non-significant trend was found regarding catalase activity of strawberry fruit. Quantitatively higher CAT activity was observed in fruits of control treatment as compared to other treatments. Maximum SOD activity (30.2 U mg⁻¹ protein) was observed in strawberry fruits where plants were sprayed with 100 mg/L ZnSO₄ followed by other treatments including 7 mM/L CaCl₂ (26.4 U mg⁻¹ protein), 150 mg/L ZnSO₄ (24.4 U mg⁻¹ protein), 5 mM/L CaCl₂ (22.3 U mg⁻¹ protein), 50 mg/L ZnSO₄ (20.1 U mg⁻¹ protein) and 3 mM/L CaCl₂ (19.2 U mg⁻¹ protein), respectively while lower SOD activity (18.0 U mg⁻¹ protein) was noted in control treatment. It was exhibited that POD activity (1.05 U mg⁻¹ protein) was decreased with foliar application of 100 mg/L ZnSO₄ while maximum POD activity (3.89 U mg⁻¹ protein) was observed in fruits of control treatment. From results it was found that exogenous application of ZnSO₄ (100 mg/L) increased the SOD activity in strawberry fruits while POD activity was decreased with this concentration (Table 3).

Table 3. Effect of exogenous application of inorganic salts on enzymatic activities of strawberry fruit cv. 'Chandler' Mean ± SE

Treatments	CAT (U mg ⁻¹ protein)	SOD (U mg ⁻¹ protein)	POD (U mg ⁻¹ protein)
Control	12.8 ± 0.01 a	18.0 ± 0.11 g	3.89 ± 0.26 a
3 mM/L CaCl ₂	10.7 ± 0.01 a	19.2 ± 0.12 f	2.34 ± 0.03 b
5 mM/L CaCl ₂	10.8 ± 0.01 a	22.3 ± 0.22 d	2.16 ± 0.01 d
7 mM/L CaCl ₂	10.6 ± 0.01 a	26.4 ± 0.23 b	1.35 ± 0.02 f
50 mg/L ZnSO ₄	10.2 ± 0.25 a	20.1 ± 0.36 e	2.25 ± 0.02 c
100 mg/L ZnSO ₄	10.0 ± 0.24 a	30.2 ± 0.37 a	1.05 ± 0.02 g
150 mg/L ZnSO ₄	10.6 ± 0.21 a	24.4 ± 0.38 c	1.57 ± 0.02 e
LSD (<i>P</i> ≤ 0.05)	0.4	1.61	1.19
C.V. %	21.72	3.57	11

Treatments means which represent same letter are statistically non-significant (*p* > 0.05)

Survival

During whole growing season maximum survival (94.7%) was observed in those strawberry plants treated with 7 mM/L CaCl₂ followed by other treatments 100 mg/L ZnSO₄ (90.7%), 150 mg/L ZnSO₄ (83.5%), 5 mM/L CaCl₂ (80.5), 3 mM/L CaCl₂ (72.2%) and 50 mg/L ZnSO₄ (71.5%), respectively. Minimum plants survival (64.2%) was observed in control plants. It was suggested that exogenous application of salts is highly effective strategy to enhance survival (%) of strawberry plants (Fig. 5).

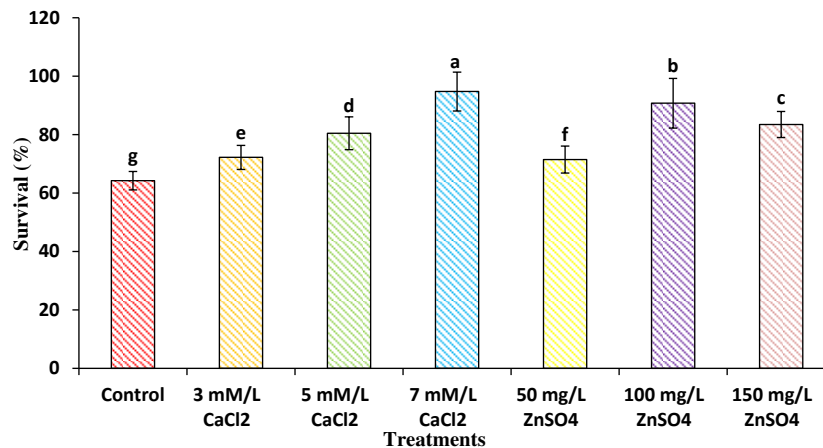


Figure 5. Effect of exogenous application of inorganic salts on survival (%) of strawberry plants cv. 'Chandler'. Vertical bars represent \pm SE of means

Discussion

Strawberry has fast growing habit which needs sufficient amount of macro and micro nutrients throughout growing season (Medeiros et al., 2015). Foliar application of salts at proper and regular intervals play major role in increasing fruit set and productivity of strawberry plants (Phillips, 2004; Abdollahi et al., 2010). For successful strawberry production calcium is classified as secondary important nutrient for strawberry plant requirement and structural part of cell walls and promotes rapid plant growth (Anonymous, 2014). Zinc is metal compound associated with many enzymes and proteins which played functional role for improving normal plant growth and developmental processes (Nasiri et al., 2010).

In current study, different concentrations of CaCl₂ and ZnSO₄ were applied through foliar application at different growth stages. Maximum number of leaves, leaf area and number of crowns were found with highest concentration of CaCl₂ (7 mM/L) as compared to other treatments (Table 1). Calcium as important secondary nutrient for strawberry plant growth enhanced the vegetative growth because it improve the inflexibility of plasma membrane of plant cells, most prominent in the apoplast, the cell wall space where it plays major role for cross-link within pectin polysaccharide matrix and contribute their stability (Lester and Grusak, 1999; Anonymous, 2014). The quantity of calcium taken up by the plants from the soil solution, most of it transferred to the leaves but very little amount goes to the fruit (Kadir, 2004). Therefore, for better growth plants need regular supply of calcium for vigorous canopy development (Del-Amor and Marcelis, 2003). Our findings regarding foliar application of CaCl₂ enhanced the vegetative growth of strawberry plants similar with previous findings where they observed that foliar spray of CaCl₂ (0.6%) increased the number of leaves, leaf area and improved plant canopy of strawberry (Bakshi et al., 2013). Our results exhibited that strawberry flowering was not affected by CaCl₂ application and these results are in line with previous findings where foliar applied 0.3% CaCl₂ not increased the cluster of flowers in tomato crop (Rab and Haq, 2012). In this study flower initiation was found earlier with 100 mg/L ZnSO₄ application as compared to other treatments and these results are in accordance with Lolaei et al. (2012) who reported that foliar application of ZnSO₄ improved the flowering in strawberry cultivar 'Camarosa'.

During whole growing season increasing trend was found regarding marketable yield and fruit setting was increased with 7 mM/L CaCl₂ as compared to other treatments (Table 2). Our results proved that CaCl₂ treatments reduced the unmarketable and small size strawberries and increased the marketable yield. The mechanism through which external application of CaCl₂ improved plant growth and marketable yield of strawberries, it is because of calcium on plant surface create electrochemical potential gradient which favors inward movement of calcium (Anonymous, 2014). Calcium sequestered into vacuole through transport across the tonoplast, binds to calcium binding proteins (calmodulin) and also with intracellular organelles such as mitochondria, nucleus, endoplasmic reticulum and chloroplast. After binding, it is transmitted to receptor proteins that elicit proper responses to the stimulus (Taiz and Zeiger, 2006). Our results exhibited that marketable yield increased with foliar spray of CaCl₂ similar with some previous findings where foliar application of 10 mM/L CaCl₂ improved the yield and qualitative characteristics of strawberry cultivar 'Pajaro' (Kazemi, 2015). The beneficial aspect of CaCl₂ for increasing fruit setting and yield was due to maximum capability of photosynthesis and CaCl₂ increased the process of hormone metabolism due to that process auxin synthesis increase in strawberry plants which is essential for yield and growth (Bakshi et al., 2013; Kazemi, 2015).

Higher strawberry firmness was achieved with 7 mM/L CaCl₂ application as compared to other treatments (Fig. 2). Firmness quality increased with foliar spray of CaCl₂ because calcium spray increased the level of pectin in fruit cells due to that cell wall rigidity increased and fruits nature was more firm (Sams, 1999; Maas, 1998). In previous findings it was confirmed that foliar application of calcium containing products improved firmness of kiwifruit cultivar 'Tsechelidis' as compared with control treatment (Koutinas et al., 2010). Maximum total soluble solids were found in those strawberries which were treated with CaCl₂ (7 mM/L) as compared to other treatments (Fig. 3a). Statistically acid contents were found non-significant but maximum were noted with control treatment (Fig. 3b). In this experiment it was noted that calcium and zinc foliar sprays decrease the acid contents which resulted in increased total soluble solids contents of fruit. Similar findings were reported by Ahlawat et al. (1985) in grapes. Maximum TSS:Acid ratio was also observed in strawberries where plants treated with 7 mM/L CaCl₂ as compared to others (Fig. 3c). The balance between TSS:Acid ratio was major indication of strawberry ripening and maturity.

Vitamin C known as ascorbic acid acted as an antioxidant which increased the nutritional value of fruit (Rapisarda et al., 2008). Higher contents of vitamin C were observed with 7 mM/L CaCl₂ application (Fig. 4a). Vitamin C increased with CaCl₂ application because calcium spray enhanced the activity of several catalytic enzymes which played major role in biosynthesis of vitamin C contents (Kadir, 2004). Over all, fruit quality was increased because calcium spray played major role in plant cell wall integrity and improved the nutritional status of fruits. Calcium deficiency in fruits showed less resistance against pathogens and increased the chances of disease occurrence in plants, so calcium spray suggested as for disease management (Ghani et al., 2011; Naradisorn, 2013). Kazemi (2014) also observed similar findings regarding foliar application of CaCl₂ (10 mM/L) enhanced the quality of strawberry. In literature it was proved that foliar spray of CaCl₂ (0.6%) increased the TSS contents, ascorbic acid contents of strawberry and lower acidity than control (Bakshi et al., 2013).

In current study, it was observed that application of CaCl₂ significantly increased the phenolic compounds and antioxidants in strawberry. Maximum phenolic contents and

antioxidants were found with 7 mM/L CaCl₂ application as compared to others (*Fig. 4b, 4c*). External application of calcium activated environmental signals against biotic and abiotic stresses (high light intensity, day length, extreme temperatures, drought, osmotic stress and attack of pathogens) in cell membranes that catalase rapid calcium influx to cytosol and enhanced cytosolic free calcium concentration which enhanced the phenolic compounds and antioxidants in plants (Taiz and Zeiger, 2006; Ali et al., 2013).

Enzymatic activities were influenced with ZnSO₄ treatments. Our results suggested that higher catalase and peroxidase activities were observed in control treatment as compared to other treatments (*Table 3*). Higher catalase activity leading towards senescence and higher peroxidase activity caused off flavor in strawberry fruits. Maximum SOD activity was noted in strawberry fruits where plants were treated with 100 mg/L ZnSO₄ while lower activity was observed in control treatment. In some previous studies it was exhibited that reactive oxygen species (ROS) produced during biochemical changes in strawberry such as hydrogen peroxide and hydroxyl radical which cause oxidative damage (Jimenez et al., 2003). These (ROS) species caused early fruit ripening and led to senescence. Activities of various antioxidant enzymes (CAT, SOD and POD) produce during different growth stages of strawberry fruit and increase the defense response against these ROS species (Anand et al., 2009). Zinc played major role in defense mechanism of plant by increasing activities of antioxidant enzymes and also the regulation process of those genes (chitinase) which required for creating resistance against environmental stresses in plants (Marschner, 1995; Cakmak, 2000).

According to our results it is clear that maximum survival was achieved with 7 mM/L CaCl₂ application while, the other treated plants also respond better for achieving maximum survival as compared to control plants (*Fig. 5*). Previous studies showed that calcium signaling played critical role in plant resistance to diseases; create defense mechanism against insects and acclimatization against non-biological stresses (Sun et al., 2009). Due to that enzymatic activities increased which enhanced the survival mechanism of strawberry plants. During whole growing season treated strawberry plants showed better response as compared with untreated plants.

Conclusion and future recommendations

Calcium as secondary important nutrient for strawberry plant plays major role in growth and development. In current study 7 mM/L CaCl₂ treatment was proved best for improving the number of leaves, leaf area and number of crowns while early flower initiation was observed with 100 mg/L ZnSO₄ application. Marketable yield, fruit quality and survival mechanism of strawberry plants maximized with 7 mM/L CaCl₂ application. However, enzymatic activities were highly influenced with 100 mg/L ZnSO₄ application. By comparison, it is concluded that exogenous application of 7 mM/L CaCl₂ during growth stages is highly effective strategy for improving marketable yield and quality.

In future combined application of CaCl₂ and ZnSO₄ should be applied for improving maximum marketable yield and quality. More work is needed on other strawberry cultivars such as Douglas, Toro, Pocahontas, Honeyo and Tufts by using salts to increase the marketable yield and to improve quality attributes.

Acknowledgments. We pay thanks to Ayub Agricultural Research Institute (AARI) for providing the research area for field experiment and special thanks to Institute of Horticultural Sciences and

Biochemistry Department of University of Agriculture Faisalabad for fruit quality analysis. This paper is extracted from the PhD dissertation of the first author. The first author thankfully acknowledges the University of Agriculture Faisalabad for providing Ph.D. fellowship scholarship for financial support.

REFERENCES

- [1] Abdollahi, M., Eshghi, S., Tafazzoli, E., Moosavi, N. (2010): Effects of paclobutrazol, boric acid and zinc sulfate on vegetative and reproductive growth of strawberry cv. Selva. – J. Agr. Sci. Tech. 14: 357-363.
- [2] Adda-Bjarnadottir, M. (2012): Strawberries. Nutrition facts and health benefits. – <https://authoritynutrition.com/foods/strawberries/>.
- [3] Ahlawat, V. P., Sharma, S., Dahia, S. S., Yamdagni, R. (1985): Effect of iron sprays on physico-chemical characteristics of grapes cv. Beauty Seedless. – Progressive Horticulture 17: 100-2.
- [4] Ainsworth, E. A., Gillespie, K. M. (2007): Estimation of total phenolic contents and other oxidation substances in plant tissue using Folin-Ciocalteu reagent. – Nature Protocols. 2: 875-877.
- [5] Ali, S., Masud, T., Abbasi, K. S., Mahmood, T., Hussain, I. (2013): Influence of CaCl₂ on biochemical composition, antioxidant and enzymatic activity of apricot at ambient storage. – Pak. J. Nutr. 12: 476-483.
- [6] Alshaal, T., El-Ramady, H. R. (2017): Foliar application: from plant nutrition to Biofortification. – Env. Biodiv. Soil Security 1: 71-83.
- [7] Anand, T., Ghaskaran, R., Raguchander, T., Samiyappan, R., Prakasan, V., Gopalakrishnan, C. (2009): Defence responses of chilli fruits to *Colletotrichum capsici* and *Alternaria alternata*. – Biol. Plant. 53: 553-559.
- [8] Anonymous (2014): Haifa. Strawberry crop guide: mineral nutrition of strawberries. – http://www.haifagroup.com/knowledge_center/crop_guides/strawberry/mineral_nutrition_of_strawberries/.
- [9] Anonymous (2018): Growing produce. Why foliar feeding? – <https://www.Growingproduce.com/sponsor/yara/why-foliar-feeding/>.
- [10] Asad, A. (1997): Strawberry production and marketing potentials. – Advisory Leaflet of MFVDP 30: 1-2.
- [11] Bakshi, P., Jasrotia, A., Wali, V. K., Sharma, A., Bakshi, M. (2013): Influence of pre-harvest application of calcium and micro-nutrients on growth, yield, quality and shelf-life of strawberry cv. Chandler. – Indian. J. Agr. Sci. 83(8): 831-835.
- [12] Bramlage, W. G., Drake, M., Weis, S. A. (1985): Comparisons of calcium chloride, calcium phosphate and a calcium chelate as foliar sprays for 'McIntosh' apple trees. – J. Am. Soc. Hortic. Sci. 110: 786-789.
- [13] Brand-Williams, W., Cuvelier, M. E., Berset, C. (1995): Use of free radical method to evaluate antioxidant activity. – Lebensm. Wiss. Technol. 28: 25-30.
- [14] Cakmak, I. (2000): Possible roles of zinc in protecting plant cells from damage by reactive oxygen species. – The New Phytologist 146(2): 185-205.
- [15] Cheour, F., Willemot, C., Arul, J., Desjardin, Y., Makhlof, J., Charest, P. M., Gosselin, A. (1990): Foliar application of calcium chloride delays postharvest ripening of strawberry. – J. Am. Soc. Hortic. Sci. 115: 789-792.
- [16] Del-Amor, F. K., Marcelis, L. F. M. (2003): Regulation of nutrient uptake, water uptake and growth under calcium starvation and recovery. – J. Hort. Sci. Biotechnol. 78: 343-349.
- [17] Elad, Y., Volpin, H. (1993): Reduced development of grey mould (*Botrytis cinerea*) in bean and tomato plants by calcium nutrition. – J. Phytopathol. 139: 146-156.

- [18] Ghani, M. A. A., Awang, Y., Sijam, K. (2011): Disease occurrence and fruit quality of pre-harvest calcium treated red flesh dragon fruit (*Hylocereus polyrhizus*). – Afr. J. Biotech. 10(9): 1550-1558.
- [19] GOP (2015): Fruits, Vegetables and Condiments Statistics of Pakistan. – Government of Pakistan, Ministry of National Food Security and Research, Islamabad.
- [20] Jimenez, A., Gomez, F. J. M., Llanos, M. R., Sevilla, F. (2003): Antioxidant systems and their relationship with the response of pepper fruits to storage at 20°C. – J. Agr. Food Chem. 51: 6293-6299.
- [21] Kadir, S. A. (2004): Fruit quality at harvest of 'Jonathan' apple treated with foliar applied calcium chloride. – J. Plant. Nut. 27: 1991-2006.
- [22] Kazemi, M. (2014): Influence of foliar application of iron, calcium and zinc sulfate on vegetative growth and reproductive characteristics of strawberry cv. 'Pajaro'. – Trakia J. Sci. 1: 21-26.
- [23] Kazemi, M. (2015): Effect of iron (Fe-EDDHA), calcium chloride and zinc sulphate on vegetative growth, yield and fruit quality of strawberry (*Fragaria* × *Ananassa* Duch. cv. Pajaro). – Jordan J. Agr. Sci. 173(3643): 1-8.
- [24] Koutinas, N., Sotiropoulos, T., Petridis, A., Almaliotis, D., Deligeorgis, E., Therios, I., Voulgarakis, N. (2010): Effects of preharvest calcium foliar sprays on several fruit quality attributes and nutritional status of the kiwifruit cultivar 'Tsechlidis'. – HortScience 45(6): 984-987.
- [25] Lester, G. E., Grusak, M. A. (1999): Postharvest application of calcium and magnesium to honeydew and netted muskmelons: effects on tissue ion concentrations, quality and senescence. – J. Amer. Soc. Hort. Sci. 124: 545-552.
- [26] Li, H., Huang, R., Li, T., Hu, K. (2010): Ability of nitrogen and phosphorus assimilation of seven strawberry cultivars in a northern Atlantic coastal soil. – World Congress of Soil Science, Soil Solutions for a Changing World (Vol. 19). 1 – 6 August 2010, Brisbane, Australia.
- [27] Liu, D., Zou, J., Meng, Q., Zou, J., Jiang, W. (2009): Uptake and accumulation and oxidative stress in garlic (*Allium sativum* L.) under lead phytotoxicity. – Ecotoxicol. 18: 134-143.
- [28] Lolaei, A., Rezaei, M. A., Khorrami, M., Kaviani, B. (2012): Effect of paclobutrazol and sulfate zinc on vegetative growth, yield and fruit quality of strawberry (*Fragaria* × *ananassa* Duch. cv. Camarosa). – Ann. Biol. Res. 3(10): 4657-4662.
- [29] Maas, J. L. (1998): Compendium of Strawberry Diseases. – APS Press, St. Paul, MN.
- [30] Mabood, M. (1994): The future prospects of strawberry production in Pakistan. – Advisory Leaflet 17: 51-52.
- [31] Marschner, H. (1995): Mineral Nutrition of Higher Plants. 2nd Ed. – Academic Press, London.
- [32] Medeiros, R. F., Pereira, W. E., Rodrigues, R. D. M., Nascimento, R. D., Suassuna, J. F., Dantas, T. A. (2015): Growth and yield of strawberry plants fertilized with nitrogen and phosphorus. – Rev. Bras. Eng. Agr. Amb. 19: 865-870.
- [33] Meena, D., Tiwari, R., Singh, O. P. (2014): Effect of nutrient spray on growth, fruit yield and quality of aonla. – Ann. Plant Soil Res. 16(3): 242-245.
- [34] Meier, U. (2006): A note on the power of Fisher's least significant difference procedure. – Pharmaceutical Statistics: J. App. Stat. 5(4): 253-263.
- [35] Naradisorn, M. (2013): Effect of calcium nutrition on fruit quality and post-harvest diseases. – Int. J. Sci. Innovations and Discoveries 3(1): 8-13.
- [36] Nasiri, Y., Zehtab-Salmasi, S., Nasrullahzadeh, S., Najafi, N., Ghassemi-Golezani, K. (2010): Effects of foliar application of micronutrients (Fe and Zn) on flower yield and essential oil of chamomile (*Matricaria chamomilla* L.). – J. Med Plant. Res. 4: 1733-1737.

- [37] Phillips, M. (2004): Economic benefit from using micronutrients for the farmer and the fertilizer producer. – IFA. International Symposium on Micronutrients, Feb 23-24, 2004, New Delhi.
- [38] Qureshi, K. M., Chughtai, S., Qureshi, U. S., Abbasi, N. A. (2013): Impact of exogenous application of salt and growth regulators on growth and yield of strawberry. – Pak. J. Bot. 45(4): 1179-1185.
- [39] Rab, A., Haq, I. U. (2012): Foliar application of calcium chloride and borax influences plant growth, yield, and quality of tomato (*Lycopersicon esculentum* Mill.) fruit. – Turk. J. Agric. For. 36(6): 695-701.
- [40] Rapisarda, P., Marisol, B., Pannuzo, P., Timpanaro, N. (2008): Effect of cold storage on vitamin C, phenolics and antioxidant activity of five orange genotype (*Citrus sinensis* L. osbeck). – Postharvest Biol. Technol. 49: 346-354.
- [41] Ruck, J. A. (1969): Chemical Methods for Analysis of Fruits and Vegetables. – Res. Stat. Dept. Agri. Can., Summerland, pp. 27-30.
- [42] Sams, C. E. (1999): Preharvest factors affecting postharvest texture. – Postharvest Biol. Technol. 15: 249-254.
- [43] Sangha, B., Agehara, S. (2016): Optimization of growth-stage specific nitrogen fertilization improves strawberry growth and yield. – Proc. Fla. State Hort. Soc. 129: 137-139.
- [44] Santos, B. M., Chandler, C. K. (2009): Influence of nitrogen fertilization rates on the performance of strawberry cultivars. – Int. J. Fruit Sci. 9: 126-135.
- [45] Sharma, R. R. (2002): Growing Strawberries. – International Book Distributing Co., Lucknow.
- [46] Sun, F., Xia, X., Yin, W. (2009): The mutual regulations between ABA and calcium signal transduction pathways under abiotic stress. – Genomics and Applied Biology 28(2): 391-397.
- [47] Taiz, L., Zeiger, E. (2006): Plant Physiology. 4th Ed. – Sinauer Associates Inc., Sunderland, MA, pp. 207-208.
- [48] White, P. J. (2000): Calcium channels in higher plants. – Biochimica et Biophysica Acta 1465: 171-189.

RESPONSES OF PHOTOSYNTHESIS, CHLOROPLAST ULTRASTRUCTURE, AND ANTIOXIDANT SYSTEM OF *MORINDA OFFICINALIS* HOW. TO EXOGENOUS 2, 4-EPIBRASSINOLIDE TREATMENTS UNDER HIGH TEMPERATURE STRESS

CAI, Y. Q.^{1,2,4} – TARIN, M. W. K.³ – FAN, L. L.¹ – XIE, D. J.¹ – RONG, J. D.¹ – HE, T. Y.³ – CHEN, L. G.¹ – ZHENG, Y. S.^{1,3*}

¹College of Forestry, Fujian Agriculture and Forestry University, Fuzhou 350002, PR China

²College of Biological Sciences and Technology, Minnan Normal University, Zhangzhou 363000, PR China

³College of Landscape and Architecture, Fujian Agriculture and Forestry University, Fuzhou 350002, PR China

⁴Fujian Provincial Key Laboratory of Garden Plants with South Fujian Characteristics, Minnan Normal University, Zhangzhou 363000, PR China

*Corresponding author
e-mail: zys1960@163.com

(Received 18th Dec 2019; accepted 27th Mar 2020)

Abstract. The present study attempts to evaluate the effects of EBR (2, 4-epibrassinolide) on photosynthetic parameters, biochemicals, antioxidant systems, and chloroplast ultrastructure in the leaves of *Morinda officinalis* under high temperature (HT). HT stress significantly reduced the net photosynthetic rate (P_N), stomatal conductance (G_s), and transpiration rate (T_r), photosynthetic pigments, and inhibited photochemical activity. Besides, the application of EBR alleviated the decrease in chlorophyll contents and the inhibition of photosynthesis induced by HT stress and improved photosystem II efficiency. Furthermore, HT stress markedly increased reactive oxygen species levels and lipid per-oxidation, while the application of 0.5-1.0 mg L⁻¹ EBR inhibited their increase and enhanced the activity of anti-oxidative enzymes. Microscopic analyses revealed that HT stress induced damages to chloroplasts and thylakoid membranes, displaying chloroplast envelopes disrupted, grana lamellae blurred and stroma lamellar disordered, while 0.5-1.0 mg L⁻¹ EBR treatment effectively protected the thylakoid membrane structure from HT stress, maintained the typical shape of chloroplasts, and promoted the formation of grana. It can be concluded that 0.5-1.0 mg L⁻¹ EBR can reduce the harmful effects of HT on *M. officinalis* seedlings by improving photosynthesis and protecting the photosynthetic membrane system from oxidative damage through up-regulating the capacity of antioxidant system.

Keywords: photosynthetic parameters, chlorophyll, photosystem II, lipid per-oxidation, thylakoid membrane

Abbreviations: BRs - brassinosteroids; EBR - 2, 4-epibrassinolide; P_N - net photosynthetic rate; G_s - stomatal conductance; T_r - transpiration rate; C_i - intercellular carbon dioxide concentration; Chl - chlorophyll; Car - carotenoids; F_0 - minimal fluorescence; F_m - the maximum fluorescence; F_v/F_m - maximal photochemical efficiency; Φ_{PSII} - actual photochemical efficiency of PSII; NPQ - non-photochemical quenching; qP - photochemical quenching; APX - ascorbate peroxidase; CAT - catalase; MDA - malondialdehyde; POD - peroxidase; SOD - superoxide dismutase; GR - glutathione reductase; GSH - reduced glutathione; ROS - reactive oxygen species; O_2^- - superoxide radical; H_2O_2 - hydrogen peroxide; EL - electrolyte leakage; ChM - chloroplast membrane; SG - starch granule; OS - osmiophilic plastoglobuli; GT - grana thylakoid; SL - stroma lamellae; GL - grana lamellae; control - normal temperature with distilled water; HT - high temperature with distilled water; HB1 - high temperature with spraying 0.10 mg L⁻¹ EBR; HB2 - high temperature with spraying 0.50 mg L⁻¹ EBR; HB3 - high temperature with spraying 1.00 mg L⁻¹ EBR

Introduction

Temperature is the most important environmental factor affecting plant growth and development. Excessive temperature is considered to be one of the most severe abiotic stresses restricting plant distribution, growth, and productivity (Jin, 2011; Niu and Wan, 2008). This stress often leads to molecular, biochemical, and physiological modifications which negatively affect the metabolism, reducing the growth and development of plants (Chen et al., 2017; Zhou et al., 2019; Tarin et al., 2020a). Photosynthesis is a key plant physiological process most sensitive to HT stress (Mathur et al., 2014). The thylakoid lamellae of photochemical reaction sites and chloroplast matrix of carbon metabolism sites are the main sites of damage under HT stress (Wise et al., 2010). Photosystem II (PSII) is the most sensitive link to HT during photosynthesis (Crafts-Brandner and Law, 2000). HT not only causes the significant changes in the number, morphology, and structure of organelles such as chloroplasts and mitochondria in plant leaves (Havaux and Tardy, 1996), it also changes the photosynthetic rate by changing the stomatal structure of plant leaves (Zheng et al., 2013), reducing chlorophyll content (Habap et al., 2014) and affecting the electron transfer process of PSII (He et al., 2017; Zushi et al., 2012). Furthermore, HT stress often destroys the balance of reactive oxygen species (ROS) metabolism in plant leaves, causes the accumulation of ROS free radicals, causes membrane lipid peroxidation, protein degeneration, cell membrane damage, resulting the increase of cell membrane permeability or even disintegration, and hindrance in normal metabolism of cells (Khanna-Chopra, 2012; Sedigheh et al., 2011; Silva and Asaeda, 2017). Simultaneously, it also promotes the activities of antioxidant enzymes such as SOD, POD, CAT, APX and the contents of non-antioxidant enzymes such as ASA and GSH to scavenge reactive oxygen species and alleviate the damage of HT stress to plants (Djanaguiraman et al., 2010; Gupta et al., 2013; Wu et al., 2014). In recent past, rise in temperature globally (Hansen et al., 2010; Virginia and Ebi, 2012), many provinces and regions in China have been experiencing prolonged summer with HT (Liu et al., 2015; Peng, 2014), particularly in the vast areas of southern China, which have experienced severe heat waves (Liu et al., 2017; Peng, 2014; Zuo et al., 2016).

Morinda officinalis How. is a vine shrub of Rubiaceae family, mainly grows in tropical and subtropical mountainous areas and forests and is distributed in Fujian, Guangdong, Guangxi, Hainan, and other southern provinces of China (Chen and Taylor, 2011). More than 100 compounds have been isolated from the flesh roots of *M. officinalis*, including anthraquinones, iridoid glycosides, phytosterols, polysaccharides, and oligosaccharides (Chen and Xue, 1987). The compounds extracted from the root of this plant can be used to relieving a wide spectrum of diseases, such as impotence (Wu et al., 2015), osteoporosis (Zhu et al., 2008), depression (Li et al., 2004), rheumatoid arthritis (Shin et al., 2013), dermatitis (Zhang et al., 2013a), and many other diseases. Furthermore, the roots of this plant have long been used as a tonic for kidney and yang, strengthening muscles and bones, eliminating rheumatism, and improving immunity, which has become one of the most common traditional medicines in China and even in Northeast Asia (Zhang et al., 2018). The suitable growth temperature of *M. officinalis* is 20-25 °C, in which the wild growth environment is a shrub or sparse forest edge on a hillside at an altitude of about 300 m approximately. An increase in the market demand for wood has put enormous pressure on the natural plantation *M. officinalis*. Recently, efforts have been made on the artificial plantation of *M. officinalis* by expanding the planting area in Fujian and Guangdong provinces covering almost 5000 ha in total (Zhang et al., 2016). *M. officinalis* is normally planted for 5-6 years before the final harvest. Most of the planting areas are low mountains

and hills with an altitude of 300-700 m and a slope of 20-40 degrees. Previous reports have shown that *M. officinalis* is susceptible to destruction in stem rot resulted from HT stress in summer (Ding and Xu, 2003; Huang, 1982). HT in summer has seriously affected the normal growth and quality of *M. officinalis*. Therefore, there is a need to explore, how to improve the heat tolerance of *M. officinalis* which has become a serious problem in cultivation.

The application of exogenous phytohormones is the most effective and commonly used method to improve plant tolerance under abiotic stress. Brassinosteroids (BRs) are a class of natural products widely existing in plants, which are similar to animal and insect steroids, which have been identified as the sixth major plant hormone regulating plant growth and development (Clouse and Sasse, 1998). Brassinolide is the first BR isolated and identified (Grove et al., 1979). BRs can regulate plant growth (Que et al., 2018), stimulate different plant metabolic processes (Sasse, 2003), reduce oxidative stress, alleviate photosynthesis inhibition, improve plant resistance and yield under adverse conditions, such as drought stress (Lima and Lobato, 2017), high and low-temperature stress (Qu et al., 2011; Zhang et al., 2013b), heavy metal stress (Ramakrishna and Rao, 2013), salt stress (Karlidag et al., 2011), and other biotic or abiotic stresses. 2, 4-epibrassinolide (EBR) is a synthetic high-activity analogue of brassinolide. It has been widely used in production because of its good stability and low cost (Bajguz and Hayat, 2009). Zhang et al. (2014) reported that exogenous 2, 4-EBR ($0.5-1.5 \text{ mg L}^{-1}$) alleviated the growth inhibition induced by HT stress. 1.0 mg L^{-1} 2, 4-EBR could increase the antioxidant enzyme activity, soluble protein and free proline content of melon under HT stress, and reduce the content of malondialdehyde. Spraying $0.05-0.2 \text{ mg L}^{-1}$ EBR could improve photosynthetic efficiency and antioxidant enzyme system of eggplant seedlings under HT stress, and inhibit the accumulation of reactive oxygen species and lipid peroxidation (Wu et al., 2014). Pretreatment of *Robinia pseudoacacia* seeds with $1.04 \mu\text{M}$ 2, 4-EBR improved the stability of chloroplast cell membrane and thylakoid membrane, decreased the concentration of sodium ion in leaves, significantly reduced photosynthesis inhibition, and maintained a higher net photosynthetic rate (Yue et al., 2019).

However, BRs-mediated stress response occurs in different tissues, and the mechanism of BRs-induced tolerance is not fully understood. There are few reports about the effect of BRs on heat tolerance of woody plants (Li et al., 2018). Therefore, this study aims to investigate the impact of exogenous 2, 4-EBR on chloroplast ultrastructure, gas exchange, chlorophyll fluorescence, and antioxidant system of *M. officinalis* seedlings exposed to HT stress, and to reveal how EBR acting to alleviate HT stress on *M. officinalis* seedlings.

Materials and methods

Description of the study area, plant material, and treatments

The present experiment was started from April to September 2018 in Fujian Agriculture and Forestry University ($26^{\circ}08'N$, $119^{\circ}24'E$), Fujian Province, China. Five-month-old healthy cutting seedlings of *M. officinalis* of uniform size (height: 20 cm) were obtained from Nanjing County, Hexi Town, Zhangzhou City, Fujian Province, China. The well-growing seedlings of *M. officinalis* were grown in plastic containers (17 cm in height and 15 cm in diameter) in a completely randomized design (Fig. A1 in the Appendix), with a mixture of red soil and peat (9:1 volume ratio). Two plants per container were placed in Greenhouse with 60% to 70% relative humidity at $28/22^{\circ}\text{C}$ (day/night) for 8 weeks. The pre-culturing of cutting seedlings of *M. officinalis* were carried out in the plant incubator

(60 cm × 60 cm × 50 cm) under the following controlled conditions; a 12-h photoperiod, the temperature of 28/22 °C (day/night), the photosynthetic photon flux density 600 μmol m⁻² s⁻¹ with 60 to 70% relative humidity. All plants were irrigated every two days and NPK nutrients solution containing 1.0 mM Ca (NO₃)₂, 9.0 mM KNO₃, 0.5 mM KH₂PO₄ was applied once a week.

The 2, 4-epibrassinolide (EBR, sigma, USA) was dissolved in a minimum volume of ethanol and made to be a storage solution with distilled water, stored at 4 °C. Then the storage solution was diluted into the concentrations required for the test with distilled water, and adding tween 20 with a volume ratio of 0.5% as the surfactant. The EBR and HT treatment started after ten days of pre-culturing. Plants were divided into two groups; normal temperature (28 °C/22 °C) and HT (38 °C/30 °C), before exposure to the HT treatment under the similar condition of a 12 h photoperiod and 600 μmol m⁻² s⁻¹ photosynthetic photon flux density. Five different treatment combinations were made; (1) normal temperature + distilled water as control, (2) HT + distilled water as HT, (3) HT + spraying 0.10 mg L⁻¹ EBR as HB1, (4) HT + 0.50 mg L⁻¹ EBR as HB2, and (5) HT + 1.00 mg L⁻¹ EBR as HB3 (Wu et. al., 2014). The pots were arranged in a completely randomized design with three replicates for each treatment (96 plants) with 480 plants in total for all five treatments. All the plants were sprayed with 25 ml of distilled water or EBR once in every two days. On the third day after spraying (the 10th day under HT stress), leaves from the middle part of plant for each replicate were selected for the measurement of photosynthetic parameters and the third leaf of plant for each replicate from the five treatment were sampled for chloroplast ultrastructure observation, then the others were sampled for determination of chlorophyll contents, ROS and antioxidant systems as described under.

Measurement of gas exchange parameters

The net photosynthetic rate (P_N), transpiration rate (T_r), stomatal conductance (G_s) and intercellular CO₂ concentration (C_i) of the third or fourth fully expanded leaf from the top were measured by using an infrared gas analyzer portable photosynthesis system (LI-6400 XT, LI-COR Inc., Lincoln, NE, USA) from 09:00 to 11:30 h local time as described by Tarin et al. (2019b). During the measurements, the photosynthetic photon flux density was set to 800 μmol m⁻² s⁻¹, the air relative humidity was from 60 to 70%, the leaf temperature was maintained at 25 °C and the ambient CO₂ concentration was about 400 μmol mol⁻¹. Photosynthesis measurement was made once for each leaf and five leaves from different plants per treatment and repeated three times in each treatment.

Determination of chlorophyll fluorescence

Chlorophyll fluorescence parameters were measured by using a portable pulse-modulated fluorometer (PAM-2500, Walz, Effeltrich, Germany). The data were taken once on the fourth fully expanded leaf of each plant, and six leaves of each treatment were chosen and numbered basipetally. The minimum fluorescence (F_0) and the maximum fluorescence (F_m) induced by a saturation pulse under a weak modulated light were determined after 30 min of dark adaption. Then the minimum fluorescence (F_0') and the maximum fluorescence (F_m') induced by a second saturation pulse in the light-adapted state, and the steady-state fluorescence (F_s) were recorded after light adaption at actinic light of 600 μmol m⁻² s⁻¹. The maximum photochemical quantum yield of PSII (F_v/F_m), the effective photochemical quantum yield of PSII (Φ_{PSII}), non-photochemical quenching (NPQ), and

photochemical quenching (qP) were calculated as the following formula, respectively (Genty et al., 1989; Roháček, 2002).

$$F_v/F_m = \frac{F_m - F_0}{F_m} \quad (\text{Eq.1})$$

$$\text{NPQ} = \frac{F_m}{F_m'} - 1 \quad (\text{Eq.2})$$

$$\Phi_{\text{PSII}} = \frac{F_m' - F_s}{F_m'} \quad (\text{Eq.3})$$

$$qP = \frac{F_m' - F_s}{F_m' - F_0'} \quad (\text{Eq.4})$$

Estimation of photosynthetic pigment determination

The photosynthetic pigment concentrations were extracted from 0.2 g leaves with 80% acetone (v/v) in the dark. The absorbance of the extracts was recorded by spectrophotometric measurements at 645, 663, and 470 nm, and the contents of chlorophyll a, chlorophyll b, total chlorophyll, and carotenoids, respectively were calculated according to the methodology of Lichtenthaler (1987).

Determination of ROS production and lipid peroxidation

The contents of hydrogen peroxide (H₂O₂) were determined by the absorbance of the peroxide-titanium complex at 410 nm as described by Patterson et al. (1984). The determination of the superoxide radical (O₂⁻) production rate was based on the method of Elstner and Heupel (1976). The content of superoxide radical (O₂⁻) was calculated from the standard curve of nitrite formed from the chemical reaction of hydroxylamine and superoxide radical (O₂⁻).

The contents of malondialdehyde (MDA) were measured as described by Guo et al. (2006a) by monitoring the thiobarbituric acid reactive products. Electrolyte leakage was determined by the method of Gong et al. (1998). The electrical conductance value (EC₁) was measured by inserting the electrode of the conduct meter into the exosmosis solution of leaves samples, then heating at 95 °C for 20 min to release the electrolytes. After cooling, the electrical conductance value (EC₂) was measured again. The percentage of electrolyte leakage was calculated by the following the formula:

$$\text{Electrolyte leakage (\%)} = \frac{\text{electrical conductance value of fresh sample}}{\text{electrical conductance value of sample cooked}} \times 100 \quad (\text{Eq.5})$$

Determination of antioxidant enzyme activity and reduced glutathione (GSH) content

The activity of superoxide dismutase (SOD) was analyzed by the NBT method of Giannopolitis et al. (1977). One unit of SOD activity is the amount of enzyme required to inhibit the photochemical reduction of nitro blue tetrazolium (NBT) by 50% at 560 nm. Catalase (CAT) activity was measured according to Havir and Mchale (1987).

The activity of catalase was defined as the decrease in the absorbance at 240 nm for 1 min following the consumption of H₂O₂.

The activity of ascorbate peroxidase (APX) was determined according to the method of Nakano and Asada (1987) by monitoring the decrease of ascorbate peroxidase and measuring the change in absorbance at 290 nm for 1 min. Peroxidase activity (POD) was estimated by using the method of Kochba et al. (1977) by following the rate of guaiacol oxidation at 470 nm. The content of reduced glutathione (GSH) and the production rate of glutathione reductase (GR) both were determined by the method given by Foyer and Halliwell (1976).

Determination of free proline and soluble proteins content

Free proline contents were determined according to the method of Bates et al. (1973) by monitoring the ninhydrin colorimetric reaction. The contents of the total soluble proteins were determined by using the method of Bradford (1976). The absorbance was measured at 595 nm using bovine serum albumin as a standard.

Observation of chloroplast ultrastructure

Samples were collected from the middle of the main vein of the third leaf below the apical bud, cut into pieces of 1~2 mm². The cut leaves were immediately fixed in a solution containing 3% (v/v) glutaraldehyde in a 0.1 mol L⁻¹ phosphate buffer (pH 7.2, 4 °C) for 2 h followed by 2% (w/v) osmium tetroxide in the same buffer for 2 h. After dehydration in a gradient series of ethanol and embedding in Epon 812, ultrathin sections (50~60 nm thick) were made with using an ultramicrotome, then stained with uranium acetate and lead citrate according to the method of Sun et al. (2011), and examined under a Tecnai G2 Spirit Bio Twin transmission electron microscopy (TECNAI, American) at an accelerating voltage of 120 KV.

Statistical analysis

Three replicates were chosen for all biochemical analyses, the data were expressed as the mean ± standard deviation (SD) with a minimum of three replicates. Statistical analysis was performed by one-way ANOVA with SPSS 17.0 (SPSS, Chicago, USA), the significant differences between the means were determined by using Duncan's multiple range comparison tests at 0.05 level of significance.

Results

Effects of 2, 4-EBR on the gas exchange parameters under HT stress

Compared to control treatment, HT stress significantly decreased P_N (Fig. 1A), T_r (Fig. 1C) and G_s (Fig. 1D) by 58.54%, 21.60%, and 50.96% respectively and significantly increased C_i (Fig. 1B) by 50.42% ($P < 0.05$). The application of 0.5-1.0mgL⁻¹ EBR during stress significantly increased P_N (Fig. 1A), G_s (Fig. 1C) and T_r (Fig. 1D), and significantly decreased C_i (Fig. 1B) ($P < 0.05$) compared to HT treatment. The 0.1 mg L⁻¹ EBR also significantly increased P_N , T_r , and decreased C_i ($P < 0.05$), but the increase in G_s was not significant. The highest P_N (3.37 μmol CO₂ m⁻² s⁻¹), G_s (0.03 mol H₂O m⁻² s⁻¹) and T_r (1.02 mmol H₂O m⁻² s⁻¹), and lowest C_i (239.5 μmol CO₂ mol⁻¹) were observed in HB2 treatment, which were 135.73%,

62.57%, 61.03% higher ($P < 0.05$), and 31.20% ($P < 0.05$) lower than HT treatment, respectively. Whereas the P_N and C_i under HB2 treatment, no significant difference as compared to control treatment (Fig. 1).

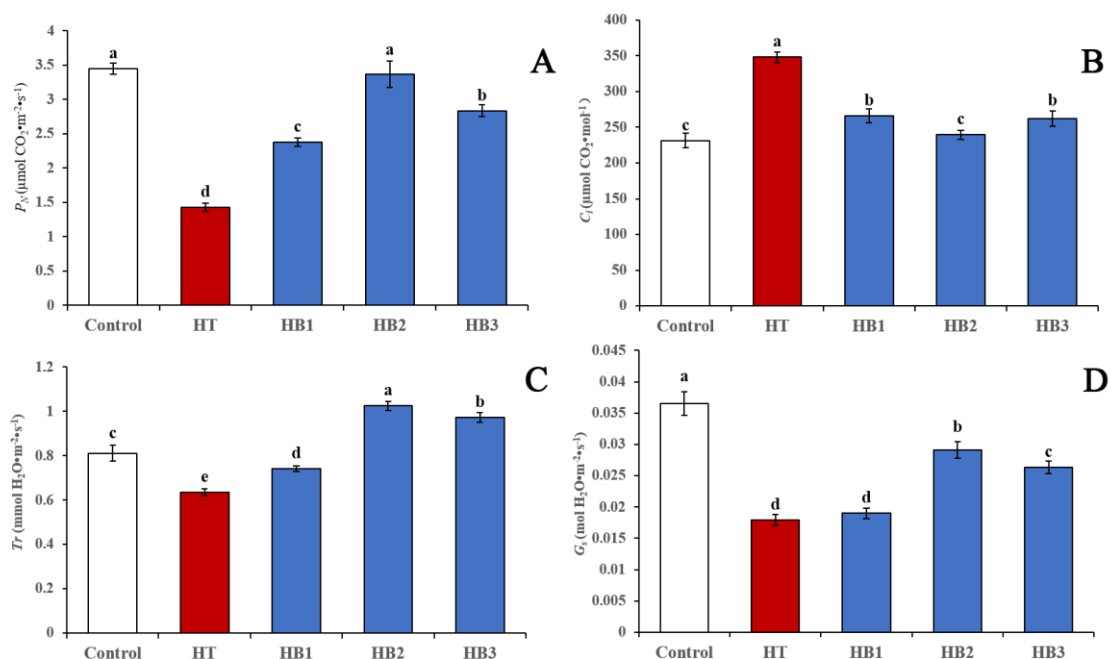


Figure 1. Effects of EBR on gas exchange parameters in leaves of *M. officinalis* under HT stress. (A) P_N : Net photosynthetic rate, (B) C_i : Intercellular carbon dioxide concentration, (C) T_r : Transpiration rate, (D) G_s : Stomatal conductance. Treatments include: Control; Normal temperature with distilled water, HT; High temperature with distilled water, HB1; High temperature with spraying 0.10 mg L^{-1} EBR, HB2; High temperature with spraying 0.50 mg L^{-1} EBR, HB3; High temperature with spraying 1.00 mg L^{-1} EBR. Different letters indicate significant differences ($P < 0.05$) among various treatments with vertical bars as standard deviations

Effects of 2, 4-EBR on chlorophyll fluorescence parameters under HT stress

Compared to control treatment, the F_m (Fig. 2B), F_v/F_m (Fig. 2C), Φ_{PSII} (Fig. 2D) and qP (Fig. 2E) of *M. officinalis* seedlings were significantly decreased by 25.48%, 18.68%, 34.86% and 20.23% ($P < 0.05$), whereas F_0 (Fig. 2A) and NPQ (Fig. 2F) were increased by 25.59% and 81.35% respectively ($P < 0.05$) under HT. The application of $0.1\text{-}1.0 \text{ mg L}^{-1}$ EBR treatments significantly increased F_m , F_v/F_m , Φ_{PSII} and qP (Fig. 2B-E), and decreased F_0 (Fig. 2A) and NPQ (Fig. 2F) compared with HT treatment, and HB2 treatment caused the largest increase in F_m , F_v/F_m , Φ_{PSII} and qP by 21.09%, 20.56%, 42.50% and 18.85% ($P < 0.05$) respectively, while the biggest decrease in F_0 and NPQ by 18.59% and 43.98% ($P < 0.05$) than that of HT treatment (Fig. 2).

Effects of 2, 4-EBR on photosynthetic pigments under HT stress

The contents of chlorophyll a, chlorophyll b, total chlorophyll, and carotenoids in leaves of *M. officinalis* seedlings under HT stress were significantly lower than that of control treatment by 40.78%, 38.99%, 40.33%, and 33.98%, respectively ($P < 0.05$;

Table 1). Application of EBR at 0.1~1.0 mg L⁻¹ significantly increased the contents of chlorophyll a and chlorophyll b under HT stress ($P < 0.05$). The effect of different concentrations of EBR treatment on the contents of photosynthetic pigments was different. As compared to the HT treatment, HB2 treatment had the best effect on increasing the contents of chlorophyll a, chlorophyll b, total chlorophyll, and carotenoids by 58.49%, 57.62%, 58.27%, and 45.30%, respectively ($P < 0.05$; Table 1).

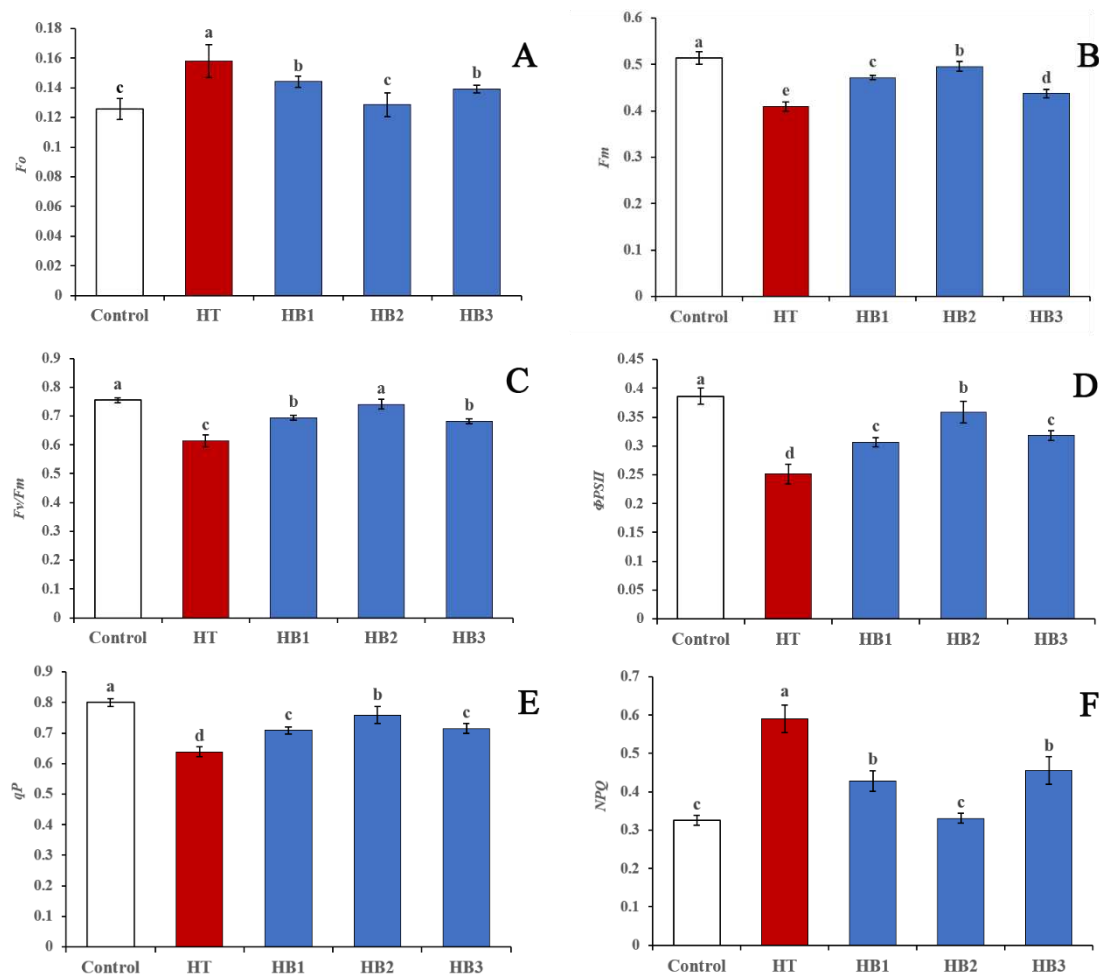


Figure 2. Effects of EBR on chlorophyll fluorescence parameters in leaves of *M. officinalis* under HT stress. (A) F_0 : Minimal fluorescence, (B) F_m : The maximum fluorescence, (C) F_v/F_m : Maximal photochemical, (D) Φ_{PSII} : Actual photochemical efficiency of PSII efficiency, (E) qP : Photochemical quenching, (F) NPQ: Non-photochemical. Treatments include: Control; Normal temperature with distilled water, HT; High temperature with distilled water, HB1; High temperature with spraying 0.10 mg L⁻¹ EBR, HB2; High temperature with spraying 0.50 mg L⁻¹ EBR, HB3; High temperature with spraying 1.00 mg L⁻¹ EBR. Different letters indicate significant differences ($P < 0.05$) among various treatments with vertical bars as standard deviations

Effects of 2, 4-EBR on the producing rate of O₂, contents of MDA and H₂O₂, electrolyte leakage under HT stress

HT stress caused a remarkable increase in the content of H₂O₂ and the rate of O₂⁻ production of *M. officinalis* seedlings by 2.03 and 3.46 times, respectively ($P < 0.05$)

(Fig. 3A, B), as compared to the control treatment. While the application of 0.1-1.0 mg L⁻¹ EBR significantly reduced the levels of H₂O₂ content and O₂⁻ producing rate of *M. officinalis* leaves in the HT stress, and the content of H₂O₂ and the rate of O₂⁻ production both contributed u-shaped curves with the increase of EBR concentration (Fig. 3A, B). The lowest levels of H₂O₂ content and O₂⁻ production rate were observed in HB2 treatment, which was lower than that of HT treatment by 50.49% and 53.65%, respectively (*P* < 0.05).

Table 1. Photosynthetic pigments in *M. officinalis* seedlings sprayed with EBR under HT stress

Treatment	<i>Chl. a</i> (mg g ⁻¹ FW)	<i>Chl. b</i> (mg g ⁻¹ FW)	<i>Total Chl</i> (mg g ⁻¹ FW)	<i>Car.</i> (mg g ⁻¹ FW)
Control	2.04 ± 0.037 a	0.68 ± 0.017 a	2.72 ± 0.022 a	0.49 ± 0.011 a
HT	1.21 ± 0.017 e	0.42 ± 0.026 c	1.62 ± 0.039 d	0.33 ± 0.007 c
HB1	1.87 ± 0.022 c	0.64 ± 0.011 a	2.51 ± 0.028 b	0.43 ± 0.010 b
HB2	1.92 ± 0.010 b	0.65 ± 0.029 a	2.57 ± 0.032 b	0.47 ± 0.007 a
HB3	1.76 ± 0.015 d	0.52 ± 0.035 b	2.28 ± 0.021 c	0.45 ± 0.013 b

Chl a: Chlorophyll a, *Chl b*: Chlorophyll b, *Total Chl*: Total Chlorophyll, *Car*: Carotenoids. Treatments include: Control; Normal temperature with distilled water, HT; High temperature with distilled water, HB1; High temperature with spraying 0.10 mg L⁻¹ EBR, HB2; High temperature with spraying 0.50 mg L⁻¹ EBR, HB3; High temperature with spraying 1.00 mg L⁻¹ EBR. Different letters indicate significant differences (*P* < 0.05) among various treatments with ± as standard deviations

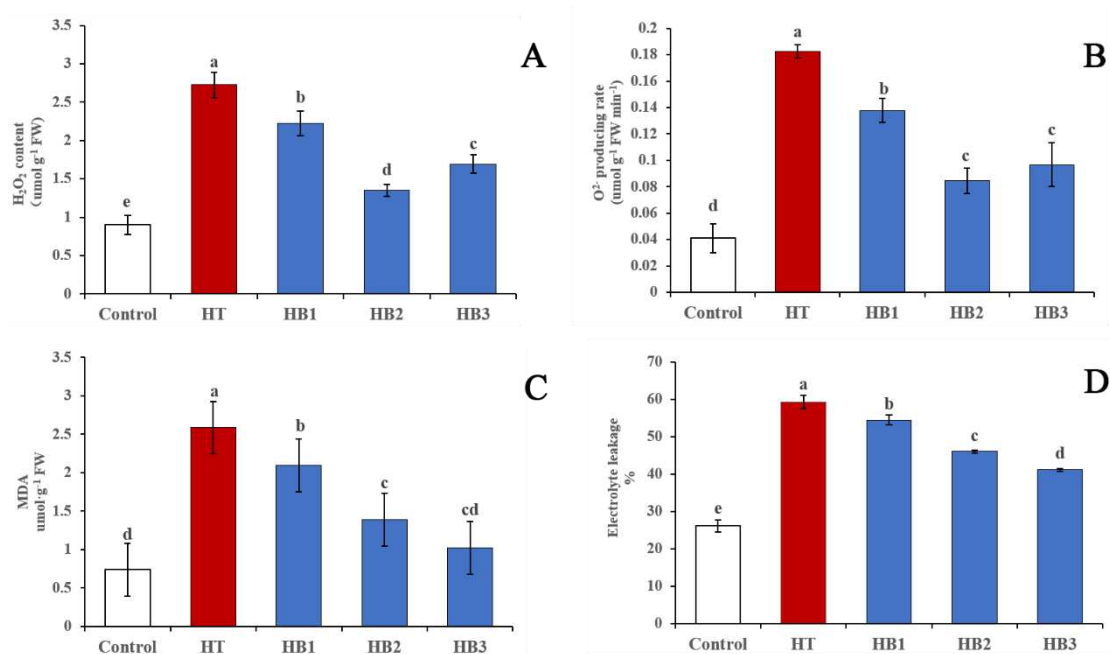


Figure 3. Effects of EBR on (A) Hydrogen peroxide (H₂O₂) content, (B) Superoxide anion (O₂⁻) producing rate, (C) Malondialdehyde (MDA) content, (D) Electrolyte leakage in leaves of *M. officinalis* under HT stress. Treatments include: Control; Normal temperature with distilled water, HT; High temperature with distilled water, HB1; High temperature with spraying 0.10 mg L⁻¹ EBR, HB2; High temperature with spraying 0.50 mg L⁻¹ EBR, HB3; High temperature with spraying 1.00 mg L⁻¹ EBR. Different letters indicate significant differences (*P* < 0.05) among various treatments with vertical bars as standard deviations

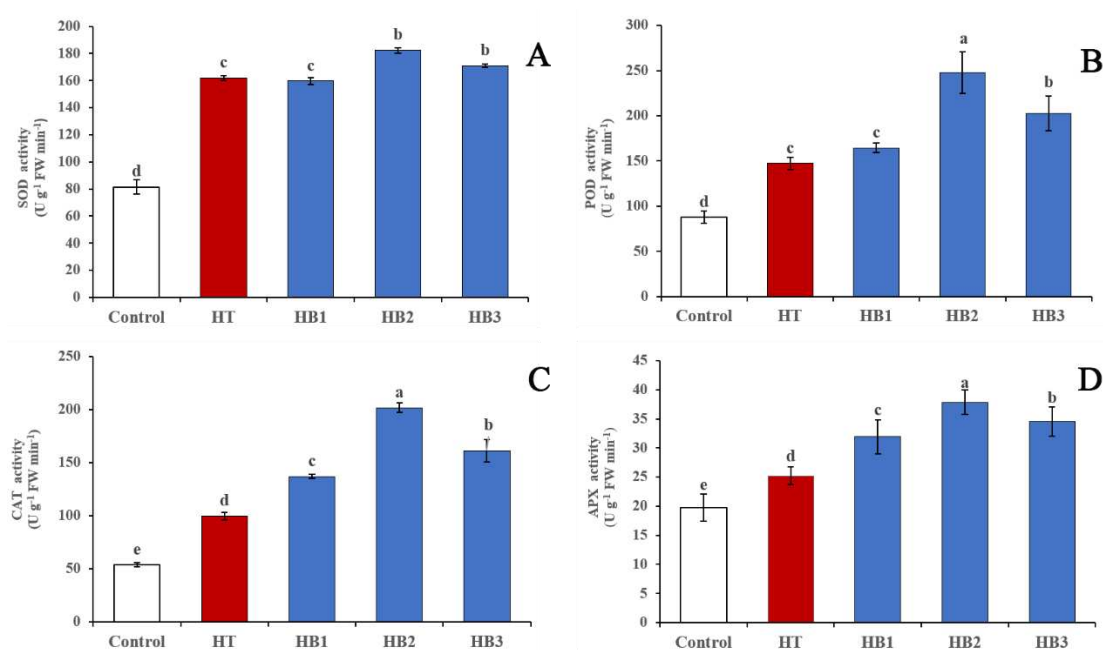
Compared with control treatment, HT stress resulted in a significant increase in the MDA content and electrolyte leakage of seedlings by 2.50 and 1.27 times ($P < 0.05$) (Fig. 3C, D), respectively. However, the application of EBR decreased the MDA content and electrolyte leakage of seedlings under stress gradually with the increase of EBR concentration in comparison with HT treatment (Fig. 3C, D). HB3 treatment significantly decreased the MDA content and the electrolyte leakage by 60.46% and 30.62% ($P < 0.05$), respectively as compared to HT treatment. Moreover, for MDA contents, no significant difference was observed between HB3, HB2, and control treatment, respectively.

Effects of 2, 4-EBR on the activities of the antioxidant enzyme under HT stress

HT stress significantly induced the activities of SOD, CAT, POD, APX, and GR by 98.82%, 85.70%, 67.61%, 27.72%, and 89.32% higher, respectively than that of the control treatment ($P < 0.05$) (Fig. 4A-E). Compared with HT treatment, 0.5-1.0 mg L⁻¹ EBR remarkably enhanced the five enzyme activities during stress, while 0.1 mg L⁻¹ EBR treatment significantly increased the activities of CAT, APX, and GR during stress, and had no significant difference on the activities of SOD and POD under HT treatment (Fig. 4A-E). HB2 treatment was found most effective for increasing the activities of SOD, CAT, POD, APX, and GR by 12.56%, 102.41%, 68.14%, 50.01%, and 116.09% respectively ($P < 0.05$), as compared to those under HT.

Effects of 2, 4-EBR on reduced glutathione content under HT stress

The GSH content in leaves of *M. officinalis* under HT stress increased remarkably by 1.11 times in comparison to control treatment ($P < 0.05$; Fig. 4F). Compared with HT treatment, the application of 0.5-1.0 mg L⁻¹ EBR significantly increased the GSH content under stress, while HB1 treatment showed no influence on the GSH content (Fig. 4F). Moreover, HB2 treatment exhibited the highest increase in the contents of GSH by 99.65% ($P < 0.05$) higher than that of HT treatment (0.85 mg·g⁻¹ FW), with no significant difference over HB3 treatment.



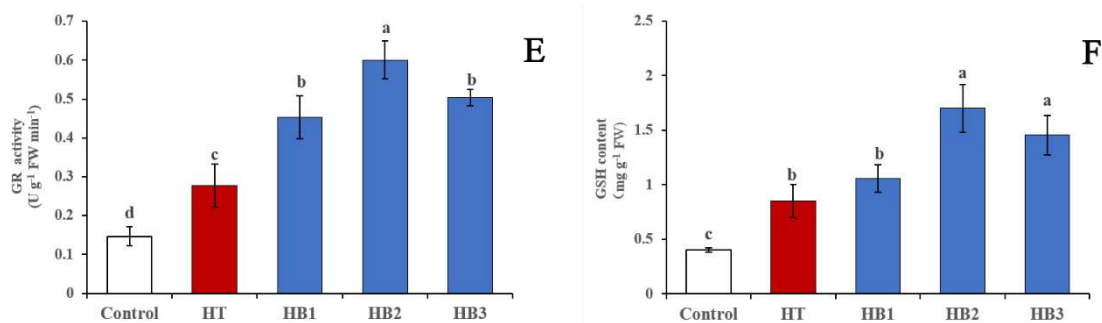


Figure 4. Effects of EBR on activities of (A) Superoxide dismutase (SOD), (B) Peroxidase (POD), (C) Catalase (CAT), (D) Ascorbate peroxidase (APX), (E) Glutathione reductase (GR), and (F) Contents of reduced glutathione (GSH) in the leaves of *M. officinalis* under HT stress. Treatments include: Control; Normal temperature with distilled water, HT; High temperature with distilled water, HB1; High temperature with spraying 0.10 mg L⁻¹ EBR, HB2; High temperature with spraying 0.50 mg L⁻¹ EBR, HB3; High temperature with spraying 1.00 mg L⁻¹ EBR. Different letters indicate significant differences ($P < 0.05$) among various treatments with vertical bars as standard deviations

Effects of 2, 4-EBR on the content of proline and soluble protein under HT stress

Soluble protein content in leaves of *M. officinalis* under HT stress decreased significantly by 22.24% as compared with the control treatment (208.41 $\mu\text{g g}^{-1}$ FW) ($P < 0.05$; Table 2). EBR treatment increased the content of soluble protein under HT stress, but there was no significant difference between EBR treatments for soluble protein contents (Table 2). The soluble protein content at HB2 treatment did not show a more significant difference than that of the control treatment (close to the control level; Table 2). While the proline contents under HT increased 1.24 times in comparison to the control treatment (30.25 $\mu\text{g g}^{-1}$ FW) ($P < 0.05$). Compared with HT treatment, EBR treatment remarkably enhanced the proline content under stress, and with the increase in EBR concentration, the content of proline showed an increasing trend first and then decreased. The maximum accumulation of proline at HB2 treatment (108.39 $\mu\text{g g}^{-1}$ FW) was observed 59.89% ($P < 0.05$) higher than that of HT treatment (67.79 $\mu\text{g g}^{-1}$ FW).

Effects of 2, 4-EBR on the ultrastructural changes of chloroplasts and thylakoids under HT stress

The ultrastructure of chloroplast showed thylakoids with grana under control treatment in (Fig. 5A, B). HT stress caused remarkable changes in the ultrastructure of chloroplasts and thylakoids (Fig. 5C, D). Compared with the control, the chloroplasts of high-temperature stress were swollen with increasing the number of plastoglobuli, and chloroplast envelopes partly were destroyed as becoming indistinct. Furthermore, the number of grana lamellae decreased in some chloroplast under stress in comparison to the control, and the thylakoid matrix was swelling with distorted and loosened grana lamellae (Fig. 5C, D). Under HT stress, the chloroplast in mesophyll cells showed no significant swelling, the chloroplast envelope was intact and the fabric of thylakoid lamellar was maintained by applying the EBR (Fig. 5E, F). The chloroplast ultrastructure had no noticeable change under HT by the application of 0.5-1.0 mg L⁻¹ EBR as compared with the control, and the obvious decreased number of plastoglobuli

and the stacked tightly grana lamellae was observed, as granum were well-arranged and had the smooth thylakoid membranes (Fig. 5F). Most of the chloroplasts maintained the typical shape at 0.1 mg L⁻¹ EBR treatment under stress, while few thylakoid grana lamellae were slightly swollen and the number of plastoglobuli were much more than that of the control (Fig. 5E).

Table 2. Content of proline and soluble protein in *M. officinalis* seedlings splayed with EBR under HT stress

Treatment	Proline content μg g ⁻¹ FW	Soluble protein content μg g ⁻¹ FW
Control	30.25 ± 1.44 d	208.41 ± 10.83 a
HT	67.79 ± 4.22 c	162.05 ± 9.33 c
HB1	80.22 ± 5.85 b	173.62 ± 14.92 bc
HB2	108.39 ± 9.24 a	191.74 ± 5.15 ab
HB3	89.81 ± 7.49 b	183.49 ± 6.97 b

Treatments include: Control; Normal temperature with distilled water, HT; High temperature with distilled water, HB1; High temperature with spraying 0.10 mg L⁻¹ EBR, HB2; High temperature with spraying 0.50 mg L⁻¹ EBR, HB3; High temperature with spraying 1.00 mg L⁻¹ EBR. Different letters indicate significant differences ($P < 0.05$) among various treatments with ± as standard deviations

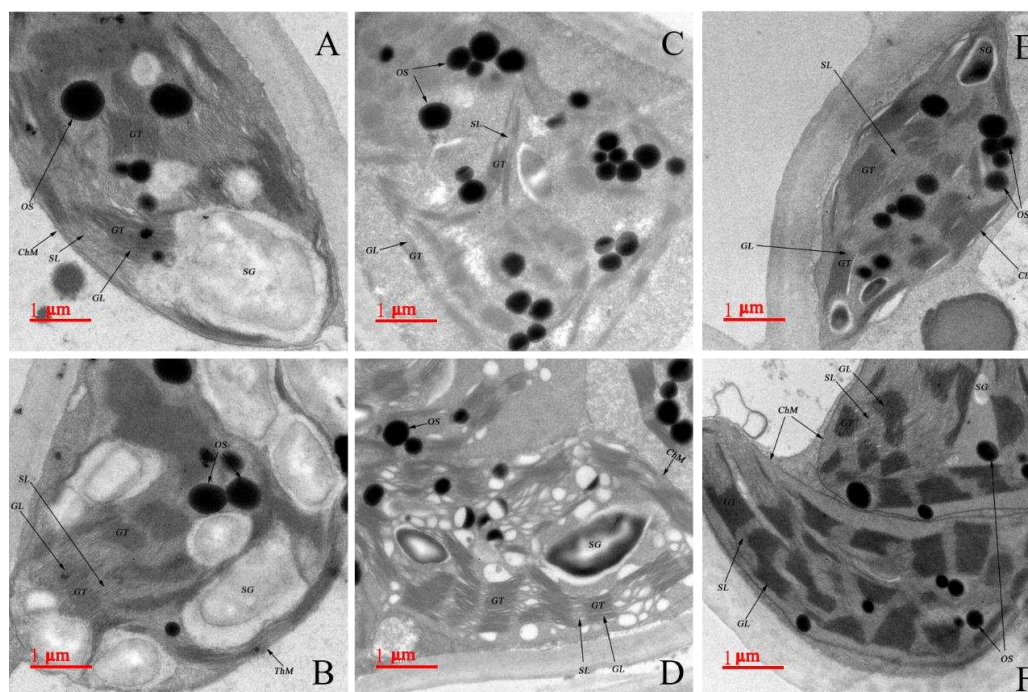


Figure 5. Effects of HT on the ultrastructure of chloroplasts and thylakoids in the leaves of *M. officinalis* with or without EBR treatment. (A, B) The ultrastructure of chloroplasts and thylakoids under control treatment, (C, D) The ultrastructure of chloroplasts and thylakoids under high temperature treatment, (E) The ultrastructure of chloroplasts and thylakoids under high temperature with spraying 0.10 mg·L⁻¹ EBR, (F) The ultrastructure of chloroplasts and thylakoids under high temperature with spraying 0.50mg·L⁻¹ EBR, ChM: Chloroplast membrane, SG: Starch granule, OS: Osmiophilic plastoglobuli, GT: Grana thylakoid, SL: Stroma lamellae, GL: Grana lamellae

Discussion

Numerous studies have shown that the application of exogenous 2, 4-EBR can regulate various physiological metabolic processes in plants and improve the stress resistance including abiotic stresses such as drought stress (Lima and Lobato, 2017), salt stress (Yue et al., 2019), flood stress (Wang et al., 2015), high or low-temperature stress (El-Bassiony et al., 2012; Shu et al., 2016). However, reports that contain the effects of 2, 4-EBR on the woody plant are scant. Wang et al. (2015) pointed out that the application of exogenous EBR protected the photosynthetic organelles of grape leaves from the adverse effects of water stress, and increased chlorophyll content, and reduced the limitation of stomatal and non-stomatal photosynthesis. Whereas Yue et al. (2019) observed that pretreatment of locust seeds and seedlings with exogenous 2, 4-EBR enhanced the activity of antioxidant system in leaves of locust seedlings under salt stress, stabilized chloroplast and thylakoid membrane ultrastructure, and related effects on sodium ion concentration and photosynthetic gas exchange parameters in leaves. In our study, it was found that appropriate concentration of exogenous EBR effectively enhanced the photosynthetic characteristics of *M. officinalis* leaves, reduce oxidative damage and protect the chloroplast ultrastructure of mesophyll in plants when subjected to HT stress.

HT stress inhibits the photosynthesis process by decreasing the photosynthetic rate and reducing light energy conversion efficiency. According to Farquhar et al. (1982), the decrease of photosynthetic rate may be contributed to stomatal or non-stomatal limitation, when the decrease of P_N is mainly caused by stomatal limitation, G_s and C_i decrease simultaneously, when the decrease of P_N is mainly caused by non-stomatal limitation, C_i increases or remains constant accompanied with a decrease in G_s . In this study, HT stress reduced P_N of plants without EBR treatment in parallel with decreased G_s and increased C_i , suggesting that HT stress affected non-stomatal limitation (Fig. 1A-D). While EBR treatment alleviated the decline of P_N and G_s in plants under HT stress and promoted the decrease of C_i and the increase of T_r at the same time (Fig. 1A-D), which is consistent with the results of Thussagunpanit et al. (2015b) and Zhang et al. (2014). It is possible that EBR treatment can mitigate the non-stomatal limitation to photosynthesis, increase the activity of Rubisco (Xia et al., 2009), and the absorption capacity of CO_2 in the Calvin cycle (Zhao et al., 2017) under HT. Meanwhile, the increase of G_s and T_r in EBR-treated plants may decrease the leaf temperature (Singh and Shono, 2005), which helps to reduce the damage from HT stress and maintain a high photosynthetic rate.

Studies have shown that HT stress accelerated the degradation of chlorophyll and inhibited the biosynthesis of chlorophyll, resulted in the reduction of chlorophyll content (Aien et al., 2011). In our study, HT stress significantly reduced chlorophyll a, chlorophyll b, total chlorophyll content and carotenoid content in leaves, while EBR treatment increased photosynthetic pigments content of *M. officinalis* seedlings (Table 1), which is similar to the previous studies (Thussagunpanit et al., 2015a; Zhang et al., 2013b). The possible reason is that EBR enhances the antioxidant enzyme system, effectively eliminates the accumulation of reactive oxygen species, and reduces the damage of membrane lipid peroxidation products (MDA) to chloroplast membrane (Lima and Lobato, 2017), promotes the biosynthesis of chlorophyll (Eriko et al., 2014). This indicated that EBR with appropriate concentration could alleviate the damage of HT to the chloroplast of plants, enhance the ability of light capture, lessen the non-stomatal limitation of HT on net photosynthetic rate, and improve photosynthesis effectively, which is in the line with studies of *Cucumis sativus* (Fariduddin et al.,

2013). Carotenoids are considered to be used as antioxidants to resist lipid peroxidation, reduce the fluidity of thylakoid membranes, and increase the stability of membranes (Tang et al., 2007). Besides, the increase of the carotenoids contents helps to eliminate the accumulation of excess excitation energy, thus playing the role of photoprotection (Calatayud and Barreno, 2004).

Chlorophyll fluorescence is a subtle reflection of the primary response of photosynthesis. It is widely used to study the effect of environmental stress on photosynthesis (Sayed, 2003). In our study, the maximum photochemical efficiency of PSII as F_v/F_m , the effective photochemical quantum yield of PSII as Φ_{PSII} , and photochemical quenching of PSII as qP in *M. officinalis* leaves significantly decreased in response to HT stress (Fig. 2C-E). However, EBR-treated plants showed the less decrease in F_v/F_m ratio under HT (Fig. 2C), suggesting that exogenous EBR can alleviate the damage of HT to PSII reaction center, which may be because of exogenous EBR which improves the conversion efficiency of PSII primary light energy and reduces photosynthesis inhibition (Maxwell and Johnson, 2000; Zhang et al., 2014). Correspondingly, the changes pattern of Φ_{PSII} and qP are similar to those of F_v/F_m (Fig. 2C-E). Under HT, EBR treatment induced the increase of Φ_{PSII} (Fig. 2D), indicating that exogenous EBR promotes an enhancement of the carboxylation efficiency caused by downstream regulation mechanism (Zhang et al., 2014). The increase in qP suggested that an improvement in the rate of reductant consumption and ATP formation by noncyclic electron transport relative to the excitation rate of the open PSII reaction center (Nogués and Baker, 2000). Whereas, the increase in qP is conducive to the separation of electron charges in the reaction center to obtain a higher photochemical quantum yield of PSII and electron transfer rate (Guo et al., 2006b). NPQ is photochemical quenching of PSII, representing the energy absorbed by PSII antenna pigments which could not be used for energy dissipation of electron transfer in photochemistry (Vasil'Ev et al., 1998). The increase of NPQ in EBR treated plants with varying degrees under HT was smaller than that of untreated plants under HT stress (Fig. 2F), suggesting that the application of EBR protected the PSII reaction center, with accelerating the rate of photosynthetic electron transfer and reducing heat dissipation of excitation energy in PSII antenna under HT (Zhang et al., 2013b). Similar findings were observed by Ogwenó et al. (2008) and Janeczko et al. (2011) both that EBR treatment could protect PSII against over-excitation and from the damage of thylakoid membrane induced by HT.

HT stress affects the utilization and transformation of light energy in plant leaves. Surplus light energy is converted to the excitation energy of Mehler reaction, and the improvement of the reaction of photosynthetic electron transfer in branch with molecular oxygen as its receptor, which accelerates the production of reactive oxygen species and destroys the dynamic balance between reactive oxygen species accumulation and antioxidant defense system in plants, and leads to the accumulation of reactive oxygen species (Grennan and Ort, 2007). Accumulation of reactive oxygen species (ROS) causes lipid peroxidation and electrolyte leakage, affecting the normal physiological function of cells. MDA is one of the end products of membrane lipid peroxidation which binds with proteins and enzymes on the membrane, resulting in the destruction of membrane integrity and loss of selective permeability, and increase of conductivity (Anjum et al., 2016). It has been further explained that exogenous EBR could induce the expression of related regulatory genes involved in defense and antioxidant response, thus increasing the tolerance of plants to oxidative stress and

alleviating the damage of stress to cells (Wu et al., 2014). In our study, HT caused a significant increase of O_2^- production rate and H_2O_2 content in *M. officinalis* leaves (Fig. 3A, B), accelerated the accumulation of membrane lipid peroxide MDA and led to an increase in MDA content and electrolyte leakage (Fig. 3C, D), which indicates that HT had induced oxidative stress to *M. officinalis*.

An active oxygen scavenging system plays an important role in protecting cells from photooxidation damage (Mittler, 2002). In our study, HT increased the activities of SOD, POD, APX, CAT, and GR in *M. officinalis* leaves (Fig. 4A-E), and EBR treatment further enhanced the activities of these five enzymes and also reduced the production rate of O_2^- and H_2O_2 content, MDA content and electrolyte leakage in the leaves of *M. officinalis* seedlings under HT stress (Fig. 3A-D). Recently, many studies have shown that EBR plays an important role in activating antioxidant defense system and scavenging reactive oxygen species under abiotic stresses. Lima1 et al. (2017) reported that EBR treatment significantly reduced the MDA content and electrolyte leakage in cowpea plants under drought stress, which could be attributed to the application of EBR to increase SOD, POD, APX and CAT activities under stress, and to reduce the rate of O_2^- production and H_2O_2 content. Arora et al. (2010) also showed that MDA contents in mustard leaves treated with EBR decreased significantly under zinc stress, while the activities of antioxidant enzymes (SOD, CAT, POD, APX, GR, MDhar and Dhar) increased significantly. The increase in activities of antioxidant enzymes after EBR treatment might be due to BR induces de novo synthesis or activate the enzymes mediated through transcription or translation of specific genes (Bajguz, 2000).

GSH is one of the important non-enzymatic antioxidants in the ASA-GSH cycle, which plays an important role in protecting plants from ROS damage (Yuan et al., 2013). EBR regulates the activities of antioxidant enzymes (APX, GR) involved in the ASA-GSH cycle, improves the circulation ability of ASA-GSH, and reduces oxidative stress damage (Yuan et al., 2013). Wu et al. (2014) described that exogenous EBR increased the content of non-enzymatic antioxidants ASA and GSH in the leaves of eggplant plants under the HT stress, and inhibited the production of free radicals and membrane lipid peroxidation, thereby enhancing the tolerance of plants to HT stress. In this study, 0.5 mg L^{-1} EBR significantly enhanced GR and APX activities in the leaves of *M. officinalis* under HT stress, increased GSH content, and enhanced the ability of scavenging ROS (Fig. 4F). Our results indicated that the application of EBR could eliminate ROS in time by increasing the activity of antioxidant enzymes and the content of non-enzymatic antioxidants, reduction in the damage of reactive oxygen species to the membrane, maintained the integrity and stability of the membrane structure and improved the resistance of *M. officinalis* seedling to HT oxidative stress.

Under abiotic stress, proline largely accumulates in plants as an important membrane stabilizer and scavenger of harmful free radicals, which plays an important role in protecting cell membranes, stabilizing protein structure, and improving cell water retention (Shamsul et al., 2012). However, abiotic stress has a negative impact on the protein biosynthesis of plants (Wahid et al., 2007). In our study, seedlings subjected to HT stress showed increased proline content and decreased protein content (Table 2) which was also reported in *Cucumis melo* under HT stress by Zhang et al. (2014). Moreover, $0.5\text{-}1.0 \text{ mg L}^{-1}$ EBR treatment further increased proline contents and enhanced the accumulation of soluble protein of the leaves under HT stress (Table 2). Wu et al. (2014) indicated that the application of $0.05\text{-}0.2 \text{ }\mu\text{M}$ EBR significantly increased the contents of proline and soluble protein in eggplant under HT stress. EBR

application enhances the accumulation of proline may be attributed to stimulate the activity of delta-pyrrolidine-5-carboxylate synthase (a key enzyme in proline biosynthesis pathway) or inhibit the activity of proline dehydrogenase, thus promoting the biosynthesis of proline or enhancing the accumulation of proline. The increase in soluble protein contents in the present study might be due to EBR inducing or activating de novo polypeptide synthesis (Ramakrishna and Rao, 2012). Kulaeva et al. (1991) had earlier proposed that EBR activated the synthesis of protein in wheat leaves under HT stress, also improved the anti-stress ability of the protein synthesis system and the characteristics of the cell membrane. It seems to believe that EBR can induce plants to increase the accumulation of different compatible solutes to protect plants from oxidative damage caused by HT stress.

Chloroplasts are not only the main sites of photosynthesis, energy flow in plants, but also one of the most sensitive organelles to stress (Stoyanova and Yordanov, 2000). Studies have shown that oxidative stress induced by stress often leads to oxidative damage of organelles (Djanaguiraman et al., 2018). Austin et al. (2006) reported that the numbers of osmiophilic granules in chloroplasts were in dynamic equilibrium at normal temperature, lipids accumulated in thylakoid membranes, and released into plastoglobuli with the increase of temperature. Almeida et al. (2005) also indicated that the number of osmiophilic precipitates increased in chloroplasts of plants treated with hydrogen oxide. Yue et al. (2019) found that salt stress not only induced oxidative stress to *Robinia pseudoacacia* seedlings but also resulted in swelling of chloroplast and rupture of the thylakoid membrane in leaves. In this study, microscopic analysis showed that HT stress led to the chloroplast swelling, and some thylakoid grana lamellae became swollen and loosened as the number of osmiophilic granules increased (Fig. 5C, D), suggesting that HT stress had destroyed chloroplasts and thylakoids, which is consistent with the results of Djanaguiraman et al. (2018) in response to HT stress in wheat. Zhang et al. (2010) demonstrated that the oxidation of membrane lipids in chloroplasts or thylakoids induced by ROS resulted in the formation of osmiophilic granules, the size and number of them involved in the degree of membrane lipid peroxidation in chloroplasts.

The thylakoid membrane is the place of light-dependent reaction in photosynthesis, where chlorophyll is mainly located (Mathur et al., 2014). It is more sensitive to HT than chloroplast membrane or other organelles (Sayed et al., 1989), as the damage of HT stress occurring would lead to the degradation of chlorophyll and the decrease of photosynthetic rate (Jumrani et al., 2017). Almeida et al. (2005) reported that exogenous homobrassinolide increased the activities of antioxidant enzymes in potato plants under the condition of 100 mM H₂O₂ treatment, and significantly lowered the negative effects of H₂O₂ on mesophyll subcellular structure of the plants, with restoring the affected cell structure and reducing the symptoms of leaf injury. Our results showed that exogenous EBR alleviated the degradation of chloroplast subjected to HT (Fig. 5E, F). In particular, under HT stress the application of 0.5 mg L⁻¹ EBR was beneficial to keep the integrity of chloroplast ultrastructure and normalize the overall morphology of thylakoids in chloroplasts (Fig. 5F), as promoting the synthesis of chlorophyll and maintaining the structural integrity and relative stability of photosynthetic membrane system (Dobrikova et al., 2014; Yue et al., 2019). This could be explained by the fact that exogenous EBR protected the photosynthetic membrane system from oxidative damage caused by HT stress through improving the antioxidant system and reducing lipid peroxidation. Simultaneously, it was confirmed with the decrease in H₂O₂ and MDA contents in *M. officinalis* plants treated EBR under HT stress.

Conclusion

In conclusion, exogenous EBR reduced the inhibition of photosynthesis of *M. officinalis* seedlings under HT stress, enhanced antioxidant system and the content of photosynthetic pigments, decreased the accumulation of reactive oxygen species and the degree of membrane lipid peroxidation, stabilized the membrane's structure of chloroplast and thylakoid, and alleviated the oxidative damage of heat stress to the photosynthetic apparatus. EBR also had a dose-effect on alleviating the adverse effects of HT stress on *M. officinalis* seedlings, and EBR at 0.5 mg L⁻¹ was the best concentration. However, further research is needed to focus on the elucidation of EBR-induced thermotolerance on molecular levels of plants that how EBR enhances the accumulation of heat-shock proteins and affects the transcriptional level of heat-shock proteins genes.

Acknowledgments. This work was funded by Young and Middle-aged Teacher Education Research Foundation of Fujian Education Department (JAT170359), Modern Seed Industry Development Foundation of Zhang Zhou city in Fujian Province (201842), The Science and Technology Innovation Foundation of Fujian Agriculture and Forestry University (CXZX2017497), and Fujian Provincial Key Laboratory of Garden Plants with South Fujian Characteristics Construction Funds in Fujian Province, China.

REFERENCES

- [1] Aien, A., Khetarpal, S., Pal, M. (2011): Photosynthetic characteristics of potato cultivars grown under HT. – *American-Eurasian J Agric & Environ Sci* 11: 633-639.
- [2] Almeida, J. M., Fidalgo, F., Confraria, A., Santos, A., Pires, H., Santos, I. (2005): Effect of hydrogen peroxide on catalase gene expression, isoform activities and levels in leaves of potato sprayed with homobrassinolide and ultrastructural changes in mesophyll cells. – *Functional Plant Biology* 32: 707-720.
- [3] Anjum, S. A., Tanveer, M., Hussain, S., Shahzad, B., Ashraf, U., Fahad, S., Hassan, W., Jan, S., Khan, I., Saleem, M. F. (2016): Osmoregulation and antioxidant production in maize under combined cadmium and arsenic stress. – *Environmental Science & Pollution Research* 23: 11864-11875.
- [4] Arora, P., Bhardwaj, R., Kanwar, M. K. (2010): 24-epibrassinolide induced antioxidative defense system of *Brassica juncea* L. under Zn metal stress. – *Physiology & Molecular Biology of Plants* 16: 285-293.
- [5] Austin, J., Frost, E., Vidi, P., Kessler, F., Staehelin, L. (2006): Plastoglobules are lipoprotein subcompartments of the chloroplast that are permanently coupled to thylakoid membranes and contain biosynthetic enzymes. – *Plant Cell* 18: 1693-1703.
- [6] Bajguz, A. (2000): Effect of brassinosteroids on nucleic acids and protein content in cultured cells of *Chlorella vulgaris*. – *Plant Physiology & Biochemistry* 38: 209-215.
- [7] Bajguz, A., Hayat, S. (2009): Effects of brassinosteroids on the plant responses to environmental stresses. – *Plant Physiol Biochem* 47: 1-8.
- [8] Bates, L. S., Waldren, R. P., Teare, I. D. (1973): Rapid determination of free proline for water-stress studies. – *Plant & Soil* 39: 205-207.
- [9] Bradford, M. M. (1976): A rapid and sensitive method for the quantitation of microgram quantities of protein utilizing the principle of protein-dye binding. – *Analytical Biochemistry* 72: 248-254.

- [10] Calatayud, A., Barreno, E. (2004): Response to ozone in two lettuce varieties on chlorophyll fluorescence, photosynthetic pigments and lipid peroxidation. – *Plant Physiology & Biochemistry* Ppb 42: 549-555.
- [11] Chen, T., Taylor, C. M. (2011): *Flora of China*. – Science Press, Beijing, pp. 226-227.
- [12] Chen, Y. E., Zhang, C. M., Su, Y. Q., Ma, J., Zhang, Z. W., Yuan, M., Zhang, H. Y., Yuan, S. (2017): Responses of photosystem II and antioxidative systems to high light and HT co-stress in wheat. – *Environmental & Experimental Botany* 135: 45-55.
- [13] Chen, Y. W., Xue, Z. (1987): Chemical constituents of *M. officinalis* How. – *Bulletin of Traditional Chinese Medicine* 12: 39-40.
- [14] Clouse, S. D., Sasse, J. M. (1998): Brassinosteroids: essential regulators of plant growth and development. – *Annual Review of Plant Physiology & Plant Molecular Biology* 49: 427.
- [15] Crafts-Brandner, S. J., Law, R. D. (2000): Effect of heat stress on the inhibition and recovery of the ribulose-1,5-bisphosphate carboxylase/oxygenase activation state. – *Planta* 212: 67-74.
- [16] Ding, P., Xu, H. (2003): Effects of cultivation conditions on active ingredients of *M. officinalis*. – *Journal of Chinese Medicinal Materials* 26: 621-622.
- [17] Djanaguiraman, M., Prasad, P. V. V., Seppanen, M. (2010): Selenium protects sorghum leaves from oxidative damage under HT stress by enhancing antioxidant defense system. – *Plant Physiology & Biochemistry* 48: 999-1007.
- [18] Djanaguiraman, M., Boyle, D. L., Welti, R., Jagadish, S. V. K., Prasad, P. V. V. (2018): Decreased photosynthetic rate under HT in wheat is due to lipid desaturation, oxidation, acylation, and damage of organelles. – *BMC Plant Biology* 18: 55.
- [19] Dobrikova, A. G., Vladkova, R. S., Rashkov, G. D., Todinova, S. J., Krumova, S. B., Apostolova, E. L. (2014): Effects of exogenous 24-epibrassinolide on the photosynthetic membranes under non-stress conditions. – *Plant Physiology & Biochemistry* Ppb 80: 75-82.
- [20] El-Bassiony, A. M., Ghoname, A. A., El-Awadi, M. E., Fawzy, Z. F., Gruda, N. (2012): Ameliorative effects of brassinosteroids on growth and productivity of snap beans grown under HT. – *Gesunde Pflanzen* 64: 175-182.
- [21] Elstner, E. F., Heupel, A. (1976): Inhibition of nitrite formation from hydroxylammoniumchloride: a simple assay for superoxide dismutase. – *Analytical Biochemistry* 70: 616-620.
- [22] Eriko, Y., Mai, K., Ayumi, Y., Mieko, H. T., Minami, M., Yusuke, K., Yukihisa, S., Masaaki, S., Hiroyuki, O., Tadao, A. (2014): BPG3 is a novel chloroplast protein that involves the greening of leaves and related to brassinosteroid signaling. – *Bioscience Biotechnology & Biochemistry* 78: 420-429.
- [23] Fariduddin, Q., Khalil, R. R. A. E., Mir, B. A., Yusuf, M., Ahmad, A. (2013): 24-Epibrassinolide regulates photosynthesis, antioxidant enzyme activities and proline content of *Cucumis sativus* under salt and/or copper stress. – *Environmental Monitoring & Assessment* 185: 7845-7856.
- [24] Farquhar, G. D., Sharkey, T. D. (1982): Stomatal conductance and photosynthesis. – *Annual Review of Plant Physiology* 33: 317-346.
- [25] Foyer, C. H., Halliwell, B. (1976): The presence of glutathione and glutathione reductase in chloroplasts: a proposed role in ascorbic acid metabolism. – *Planta* 133: 21-25.
- [26] Genty, B., Briantais, J. M., Baker, N. R. (1989): The relationship between the quantum yield of photosynthetic electron transport and quenching of chlorophyll fluorescence. – *BBA - General Subjects* 990: 87-92.
- [27] Giannopolitis, C. N., Ries, S. K. (1977): Superoxide dismutases: II. Purification and quantitative relationship with water-soluble protein in seedlings. – *Plant Physiology* 59: 315-318.

- [28] Gong, M., Li, Y. J., Chen, S. Z. (1998): Abscisic acid-induced thermotolerance in maize seedlings is mediated by calcium and associated with antioxidant systems. – *J Plant Physiol* 153: 488-496.
- [29] Grennan, A. K., Ort, D. R. (2007): Cool temperatures interfere with D1 synthesis in tomato by causing ribosomal pausing. – *Photosynthesis Research* 94: 375-385.
- [30] Grove, M. D., Spencer, G. F., Rohwedder, W. K., Mandava, N., Worley, J. F., Warthen, J. D., Steffens, G. L., Flippen-Anderson, J. L., Cook, J. C. (1979): Brassinolide, a plant growth-promoting steroid isolated from *Brassica napus* pollen. – *Nature* 28: 216-217.
- [31] Guo, F. X., Zhang, M. X., Chen, Y., Zhang, W. H., Xu, S. J., Wang, J. H., An, L. Z. (2006a): Relation of several antioxidant enzymes to rapid freezing resistance in suspension cultured cells from alpine. – *Cryobiology* 52: 241-250.
- [32] Guo, H. X., Liu, W. Q., Shi, Y. C. (2006b): Effects of different nitrogen forms on photosynthetic rate and the chlorophyll fluorescence induction kinetics of flue-cured tobacco. – *Photosynthetica* 44: 140-142.
- [33] Gupta, N. K., Agarwal, V. P., Nathawat, N. S., Gupta, S. (2013): Effect of short-term heat stress on growth, physiology and antioxidative defence system in wheat seedlings. – *Acta Physiologiae Plantarum* 35: 1837-1842.
- [34] Habap, D. L., Matal, D. L., Molina, E., Agüera, E. (2014): HT promotes early senescence in primary leaves of sunflo. – *Revue Canadienne De Phytotechnie* 94: 659-669.
- [35] Hansen, J. R., Ruedy, R., Sato, M., Lo, K. (2010): Global Surface Temperature Change. – *Reviews of Geophysics* 48: 103-110.
- [36] Havaux, M., Tardy, F. (1996): Temperature-dependent adjustment of the thermal stability of photosystem II in vivo: possible involvement of xanthophyll-cycle pigments. – *Planta* 198: 324-333.
- [37] Havir, E. A., Mchale, N. A. (1987): Biochemical and developmental characterization of multiple forms of catalase in tobacco leaves. – *Plant Physiology* 84: 450-455.
- [38] He, B., Guo, T., Huang, H., Xi, W., Chen, X. (2017): Physiological responses of *Scaevola aemula* seedlings under HT stress. – *South African Journal of Botany* 112: 203-209.
- [39] Huang, Z. (1982): The astrobological characteristics and cultivation techniques of *M. officinalis*. – *Subtropical Plant Science* 11: 4-14.
- [40] Janeczko, A., Oklešťková, J., Pocięcha, E., Kościelniak, J., Mirek, M. (2011): Physiological effects and transport of 24-epibrassinolide in heat-stressed barley. – *Acta Physiologiae Plantarum* 33: 1249-1259.
- [41] Jin, B. (2011): The effect of experimental warming on leaf functional traits, leaf structure and leaf biochemistry in *Arabidopsis thaliana*. – *Bmc Plant Biology* 11: 35.
- [42] Jumrani, K., Bhatia, V. S., Pandey, G. P. (2017): Impact of elevated temperatures on specific leaf weight, stomatal density, photosynthesis and chlorophyll fluorescence in soybean. – *Photosynthesis Research* 131: 1-18.
- [43] Karlidag, H., Yildirim, E., Turan, M. (2011): Role of 24-epibrassinolide in mitigating the adverse effects of salt stress on stomatal conductance, membrane permeability, and leaf water content, ionic composition in salt stressed strawberry (*Fragaria ananassa*). – *Scientia Horticulturae* 130.
- [44] Khanna-Chopra, R. (2012): Leaf senescence and abiotic stresses share reactive oxygen species-mediated chloroplast degradation. – *Protoplasma* 249: 469-481.
- [45] Kochba, J., Lavee, S., Spiegelroy, P. (1977): Differences in peroxidase activity and isoenzymes in embryogenic and non-embryogenic 'Shamouti' orange ovular callus lines. – *Plant & Cell Physiology* 18: 463-467.
- [46] Kulaeva, O. N., Burkhanova, E. A., Fedina, A. B., Khokhlova, V. A., Adam, G. (1991): Effect of Brassinosteroids on Protein Synthesis and Plant-Cell Ultrastructure under Stress Conditions. – In: Cutler, H. G. et al. (eds.) *Brassinosteroids. Chemistry, Bioactivity, and Applications*. ACS Symposium Series. ACS, Washington, DC, pp. 141-155.
- [47] Li, X., Wei, J. P., Ahammed, G. J., Zhang, L., Li, Y., Yan, P., Zhang, L. P., Han, W. Y. (2018): Brassinosteroids attenuate moderate HT-caused decline in tea quality by

- enhancing theanine biosynthesis in *Camellia sinensis* L. – *Frontiers in Plant Science* 9: 1016.
- [48] Li, Y. F., Liu, Y. Q., Yang, M., Wang, H. L., Huang, W. C., Zhao, Y. M., Luo, Z. P. (2004): The cytoprotective effect of inulin-type hexasaccharide extracted from *Morinda officinalis* on PC12 cells against the lesion induced by corticosterone. – *Life Sciences* 75: 1531-1538.
- [49] Lichtenthaler, H. K. (1987): Chlorophylls and carotenoids: pigments of photosynthetic biomembranes. – *Methods in Enzymology* 148C: 350-382.
- [50] Lima, J. V., Lobato, A. K. S. (2017): Brassinosteroids improve photosystem II efficiency, gas exchange, antioxidant enzymes and growth of cowpea plants exposed to water deficit. – *Physiol Mol Biol Plants* 23: 59-72.
- [51] Liu, G., Wu, R., Sun, S., Wang, H. (2015): Synergistic contribution of precipitation anomalies over northwestern India and the South China Sea to HT over the Yangtze River Valley. – *Advances in Atmospheric Sciences* 32: 1255-1265.
- [52] Liu, G., Wu, R., Wang, H., Ji, L. (2017): Effect of tropical Indian Ocean thermal condition during preceding winter on summer HT anomalies over the southern Yangtze River valley. – *International Journal of Climatology* 37: 3478-3490.
- [53] Mathur, S., Agrawal, D., Jajoo, A. (2014): Photosynthesis: response to HT stress. – *Journal of Photochemistry & Photobiology B Biology* 137: 116-126.
- [54] Maxwell, K., Johnson, G. N. (2000): Chlorophyll fluorescence - a practical guide. – *Journal of Experimental Botany* 51: 659-668.
- [55] Mittler, R. (2002): Oxidative stress, antioxidants and stress tolerance. – *Trends in Plant Science* 7: 405-410.
- [56] Nakano, Y., Asada, K. (1987): Purification of ascorbate peroxidase in spinach chloroplasts; its inactivation in ascorbate-depleted medium and reactivation by monodehydroascorbate radical. – *Plant & Cell Physiology* 28: 131-140.
- [57] Niu, S., Wan, S. (2008): Warming changes plant competitive hierarchy in a temperate steppe in northern China. – *Journal of Plant Ecology* 1: 103-110.
- [58] Nogués, S., Baker, N. R. (2000): Effects of drought on photosynthesis in Mediterranean plants grown under enhanced UV-B radiation. – *Journal of Experimental Botany* 51: 1309-1317.
- [59] Ogwen, J. O., Xing, S. S., Kai, S., Wen, H. H., Wei, H. M., Yan, H. Z., Jing, Q. Y., Nogués, S. (2008): Brassinosteroids alleviate heat-induced inhibition of photosynthesis by increasing carboxylation efficiency and enhancing antioxidant systems in *Lycopersicon esculentum*. – *Journal of Plant Growth Regulation* 27: 49-57.
- [60] Patterson, B. D., MacRae, E. A., Ferguson, I. B. (1984): Estimation of hydrogen peroxide in plant extracts using titanium(IV). – *Analytical Biochemistry* 139: 487-492.
- [61] Peng, J. B. (2014): An Investigation of the formation of the heat wave in southern China in summer 2013 and the relevant abnormal subtropical high activities. – *Atmospheric & Oceanic Science Letters* 7: 286-290.
- [62] Qu, T., Liu, R., Wang, W., An, L., Chen, T., Liu, G., Zhao, Z. (2011): Brassinosteroids regulate pectin methylesterase activity and AtPME41 expression in *Arabidopsis* under chilling stress. – *Cryobiology* 63: 111-117.
- [63] Que, F., Khadr, A., Wang, G. L., Li, T., Wang, Y. H., Xu, Z. S., Xiong, A. S. (2018): Exogenous brassinosteroids altered cell length, gibberellin content, and cellulose deposition in promoting carrot petiole elongation. – *Plant Sci* 277: 110-120.
- [64] Ramakrishna, B., Rao, S. S. R. (2012): 24-Epibrassinolide alleviated zinc-induced oxidative stress in radish (*Raphanus sativus* L.) seedlings by enhancing antioxidative system. – *Plant Growth Regulation* 68: 249-259.
- [65] Ramakrishna, B., Rao, S. S. R. (2013): 24-Epibrassinolide maintains elevated redox state of AsA and GSH in radish (*Raphanus sativus* L.) seedlings under zinc stress. – *Acta Physiologiae Plantarum* 35: 1291-1320.

- [66] Roháček, K. (2002): Chlorophyll Fluorescence parameters: the definitions, photosynthetic meaning, and mutual relationships. – *Photosynthetica* 40: 13-29.
- [67] Sasse, J. M. (2003): Physiological actions of brassinosteroids: an update. – *Journal of Plant Growth Regulation* 22: 276-288.
- [68] Sayed, O. H. (2003): Chlorophyll fluorescence as a tool in cereal crop research. – *Photosynthetica* 41: 321-330.
- [69] Sayed, O. H., Earnshaw, M. J., Emes, M. J. (1989): Photosynthetic responses of different varieties of wheat to HTII. – *Journal of Experimental Botany* 40: 633-638.
- [70] Sedigheh, H. G., Mortazavian, M., Norouzian, D., Atyabi, M., Akbarzadeh, A., Hasanpoor, K., Ghorbani, M. (2011): Oxidative stress and leaf senescence. – *Bmc Research Notes* 4: 477-477.
- [71] Shamsul, H., Qaiser, H., Mohammed Nasser, A., Arif Shafi, W., John, P., Aqil, A. (2012): Role of proline under changing environments: a review. – *Plant Signal Behav* 7: 1456-1466.
- [72] Shin, J. S., Yun, K. J., Chung, K. S., Seo, K. H., Park, H. J., Cho, Y. W., Baek, N. I., Jang, D. S., Lee, K. T. (2013): Monotropine isolated from the roots of *M. officinalis* ameliorates proinflammatory mediators in RAW 264.7 macrophages and dextran sulfate sodium (DSS)-induced colitis via NF- κ B inactivation. – *Food & Chemical Toxicology* 53: 263-271.
- [73] Shu, S., Tang, Y., Yuan, Y., Sun, J., Zhong, M., Guo, S. (2016): The role of 24-epibrassinolide in the regulation of photosynthetic characteristics and nitrogen metabolism of tomato seedlings under a combined low temperature and weak light stress. – *Plant Physiology & Biochemistry* 107: 344-353.
- [74] Silva, H. C. C. D., Asaeda, T. (2017): Effects of heat stress on growth, photosynthetic pigments, oxidative damage and competitive capacity of three submerged macrophytes. – *Journal of Plant Interactions* 12: 228-236.
- [75] Singh, I., Shono, M. (2005): Physiological and molecular effects of 24-epibrassinolide, a brassinosteroid on thermotolerance of tomato. – *Plant Growth Regulation* 47: 111-119.
- [76] Stoyanova, D., Yordanov, I. (2000): Influence of drought, HT, and carbamide cytokinin 4-PU-30 on photosynthetic activity of plants. 2. Chloroplast ultrastructure of primary bean leaves. – *Photosynthetica* 37: 621-625.
- [77] Sun, Z., P., Li, T., L., Liu, Y., L. (2011): Effects of elevated CO₂ applied to potato roots on the anatomy and ultrastructure of leaves. – *Biologia Plantarum* 55: 675.
- [78] Tang, Y., Wen, X., Lu, Q., Yang, Z., Cheng, Z., Lu, C. (2007): Heat stress induces an aggregation of the light-harvesting complex of photosystem II in spinach plants. – *Plant Physiology* 143: 629-638.
- [79] Tarin, M. W. K., Fan, L., Shen, L., Lai, J., Li, J., Deng, Z., Chen, L., He, T., Rong, J., Zheng, Y. (2020a): Rice straw biochar impact on physiological and biochemical attributes of *Fokienia hodginsii* in acidic soil. – *Scand. J. For. Res.* 35(1-2): 59-68.
- [80] Tarin, M. W. K., Fan, L., Tayyab, M., Sarfraz, R., Chen, L., He, T., Rong, J., Chen, L., Zheng, Y. (2019b): Effects of bamboo biochar amendment on the growth and physiological characteristics of *Fokienia hodginsii*. – *Appl Ecol Environ Res* 16: 8055-8074. https://doi.org/10.15666/aeer/1606_80558074.
- [81] Thussagunpanit, J., Jutamane, K., Kaveeta, L., Chai-Arree, W., Pankean, P., Homvisasevongsa, S., Suksamrarn, A. (2015a): Comparative effects of brassinosteroid and brassinosteroid mimic on improving photosynthesis, lipid peroxidation, and rice seed set under heat stress. – *Journal of Plant Growth Regulation* 34: 320-331.
- [82] Thussagunpanit, J., Jutamane, K., Sonjaroon, W., Kaveeta, L., Chai-Arree, W., Pankean, P., Suksamrarn, A. (2015b): Effects of brassinosteroid and brassinosteroid mimic on photosynthetic efficiency and rice yield under heat stress. – *Photosynthetica* 53: 312-320.
- [83] Vasil'Ev, S., Wiebe, S., Bruce, D. (1998): Non-photochemical quenching of chlorophyll fluorescence in photosynthesis. 5-hydroxy-1,4-naphthoquinone in spinach thylakoids as a

- model for antenna based quenching mechanisms. – *Biochim Biophys Acta* 1363: 147-156.
- [84] Virginia, M., Ebi, K. L. (2012): IPCC special report on managing the risks of extreme events and disasters to advance climate change adaptation (SREX). – *Journal of Epidemiology & Community Health* 66: 759.
- [85] Wahid, A., Gelani, S., Ashraf, M., Foolad, M. R. (2007): Heat tolerance in plants: an overview. – *Environmental & Experimental Botany* 61: 199-223.
- [86] Wang, Z., Zheng, P., Meng, J., Xi, Z. (2015): Effect of exogenous 24-epibrassinolide on chlorophyll fluorescence, leaf surface morphology and cellular ultrastructure of grape seedlings (*Vitis vinifera* L.) under water stress. – *Acta Physiologiae Plantarum* 37: 1729.
- [87] Wise, R. R., Olson, A. J., Schrader, S. M., Sharkey, T. D. (2010): Electron transport is the functional limitation of photosynthesis in field-grown Pima cotton plants at HT. – *Plant Cell & Environment* 27: 717-724.
- [88] Wu, X., Yao, X., Chen, J., Zhu, Z., Zhang, H., Zha, D. (2014): Brassinosteroids protect photosynthesis and antioxidant system of eggplant seedlings from high-temperature stress. – *Acta Physiologiae Plantarum* 36: 251-261.
- [89] Wu, Z. Q., Chen, D. L., Lin, F. H., Lin, L., Shuai, O., Wang, J. Y., Qi, L. K., Zhang, P. (2015): Effect of bajijiasu isolated from *Morinda officinalis* F. C. how on sexual function in male mice and its antioxidant protection of human sperm. – *Journal of Ethnopharmacology* 164: 283-292.
- [90] Xia, X., Huang, L., Zhou, Y., Mao, W., Shi, K., Wu, J., Tadao, A., Chen, Z., Yu, J. (2009): Brassinosteroids promote photosynthesis and growth by enhancing activation of Rubisco and expression of photosynthetic genes in *Cucumis sativus*. – *Planta* 230: 1185-1196.
- [91] Yuan, L. Y., Du, J., Yuan, Y. H., Shu, S., Sun, J., Guo, S. R. (2013): Effects of 24-epibrassinolide on ascorbate–glutathione cycle and polyamine levels in cucumber roots under Ca(NO₃)₂ stress. – *Acta Physiologiae Plantarum* 35: 253-262.
- [92] Yue, J., You, Y., Zhang, L., Fu, Z., Wang, J., Zhang, J., Guy, R. D. (2019): Exogenous 24-epibrassinolide alleviates effects of salt stress on chloroplasts and photosynthesis in *Robinia pseudoacacia* L. seedlings. – *Journal of Plant Growth Regulation* 38: 669-682.
- [93] Zhang, H., Li, J., Xia, J., Lin, S. (2013a): Antioxidant activity and physicochemical properties of an acidic polysaccharide from *M. officinalis*. – *International Journal of Biological Macromolecules* 58: 7-12.
- [94] Zhang, J. H., Xin, H. L., Xu, Y. M., Shen, Y., He, Y. Q., Hsien-Yeh, Lin, B., Song, H. T., Juan-Liu, Yang, H. Y. (2018): *M. officinalis* How. - a comprehensive review of traditional uses, phytochemistry and pharmacology. – *Journal of Ethnopharmacology* 213: 230-255.
- [95] Zhang, R., Wise, R. R., Struck, K. R., Sharkey, T. D. (2010): Moderate heat stress of *Arabidopsis thaliana* leaves causes chloroplast swelling and plastoglobule formation. – *Photosynthesis Research* 105: 123-134.
- [96] Zhang, R., Li, Q., Qu, M., Gao, J., Ma, W., Liu, W., Sun, T., Ding, P. (2016): Investigation on germplasm resources of *Morinda officinalis*. – *Modern Chinese Medicine* 18: 482-487.
- [97] Zhang, Y. P., Zhu, X. H., Ding, H. D., Yang, S. J., Chen, Y. Y. (2013b): Foliar application of 24-epibrassinolide alleviates high-temperature-induced inhibition of photosynthesis in seedlings of two melon cultivars. – *Photosynthetica* 51: 341-349.
- [98] Zhang, Y. P., He, J., Yang, S. J., Chen, Y. Y. (2014): Exogenous 24-epibrassinolide ameliorates HT-induced inhibition of growth and photosynthesis in *Cucumis melo*. – *Biologia Plantarum* 58: 311-318.
- [99] Zhao, G., Xu, H., Zhang, P., Su, X., Zhao, H. (2017): Effects of 2,4-epibrassinolide on photosynthesis and Rubisco activase gene expression in *Triticum aestivum* L. seedlings under a combination of drought and heat stress. – *Plant Growth Regulation* 81: 377-384.

- [100] Zheng, Y., Xu, M., Hou, R., Shen, R., Qiu, S., Ouyang, Z. (2013): Effects of experimental warming on stomatal traits in leaves of maize (*Zea may* L.). – *Ecology & Evolution* 3: 3095-3111.
- [101] Zhou, H. W., Zhang, H. Y., Wang, Z. H., He, C., You, L. L., Fu, D. H., Song, J. B., Huang, Y. J., Liao, J. L. (2019): Discovery of unique single nucleotide polymorphisms in rice in response to high nighttime temperature stress using a hybrid sequencing strategy. – *Environmental and Experimental Botany* 162: 48-57.
- [102] Zhu, M., Wang, C., Zhang, H., Pei, X. (2008): Protective effect of polysaccharides from *M. officinalis* on bone loss in ovariectomized rats. – *International Journal of Biological Macromolecules* 43: 276-278.
- [103] Zuo, J. Q., Ren, H. L., Li, W. J., Wang, L. (2016): Interdecadal variations in the relationship between the winter North Atlantic oscillation and temperature in South-Central China. – *Journal of Climate* 29: 7477-7493.
- [104] Zushi, K., Kajiwara, S., Matsuzoe, N. (2012): Chlorophyll a fluorescence OJIP transient as a tool to characterize and evaluate response to heat and chilling stress in tomato leaf and fruit. – *Scientia Horticulturae* 148: 39-46.

APPENDIX



Figure A1. View of seedlings showing different stages of *M. officinalis* How., arranged in completely randomized design

ROLE OF GENETIC FACTORS IN REGULATING CADMIUM UPTAKE, TRANSPORT AND ACCUMULATION MECHANISMS AND QUANTITATIVE TRAIT LOCI MAPPING IN RICE. A REVIEW

RASHEED, A.¹ – FAHAD, S.² – AAMER, M.³ – HASSAN, M. U.³ – TAHIR, M. M.⁴ – WU, Z. M.^{1*}

¹Key Laboratory of Crop Physiology, Ecology and Genetic Breeding, Ministry of Education/Collage of Agronomy, Jiangxi Agriculture University, Nanchang 330045, PR. China

²Department of Agriculture, University of Swabi, Khyber Pakhtunkhwa, Pakistan

³Research Center on Ecological Sciences, Jiangxi Agricultural University, Nanchang 330045, PR. China

⁴Department of Soil and Environmental Sciences, Faculty of Agriculture, University of Poonch, Rawalaot, Azad Jammu and Kashmir, Pakistan

*Corresponding author
e-mail: wuzm@jxau.edu.cn

(Received 21st Dec 2019; accepted 24th Mar 2020)

Abstract. Rice is an imperative staple food globally; however, it is a major source of cadmium (Cd) intake for humans. Cd is a heavy metal and it has no biological functions in plant and, thus it causes adverse effects in plant and humans. Thus, it is of the utmost importance to minimize the Cd content in rice to protect humans from its drastic effects. In this review, we discussed the mechanisms related to the uptake and translocation of Cd in rice. *OsNramp5*, *OsHMA3* *OsHMA2* are the genes responsible for Cd uptake, translocation, and sequestration in the vacuole, so modification of these genes function result in no uptake of Cd, and leading to reduction in risk of Cd toxicity in rice. The different genetic factors involved in Cd stress and accumulation are shown here and put into several categories according to their function. The identification of novel QTLs (*qSH6*, *qSH7* and *qLR3*) detected for morphological traits could be cloned and transferred to develop Cd resistant rice lines. Use of mapping population and some putative quantitative traits loci related to uptake and transport could provide strong base to develop the Cd tolerant genotypes. In addition, use of different agronomic practices may be more fruitful to minimize Cd in rice.

Keywords: *cd*, *master assisted selection*, *QTLs*, *agronomic practices*, *toxicity*

Background

Cd is heavy metal and has no biological role in plants, therefore, it has a high rate of mobility in living things, especially in humans (Song et al., 2015). Heavy metals and mineral oil are the major pollutants causing the soil contamination globally. Globally, it has been reported that about 820 metric tons per year Cd released into the environment through the weathering of soils, volcanic eruptions (Cook and Morrow, 1995; Hayat et al., 2019). Additionally, human activities also responsible for the addition of more than 8000-10,000 mt Cd per year in our environment (WHO, 1992). The chief sources of Cd entry into our environment includes, chemical fertilizers, sewage sludge and effluents, Cd manufacturing, and run-offs of agriculture (Xue et al., 2014). Cadmium is of great concern, because it enters in the plant leaves in higher quantity and therefore can easy enter in the food chains is (Zu et al., 2005). The excess of Cd cause severe implications in humans, including the dys-functioning of kidneys and lungs. Additionally, Cd also cause

kidney cancer, breast cancer, failure of heart, hypertensions, proteinuria, eyes cataract, emphysema and renalin sufficiency (Nawrao et al., 2006; Godt et al., 2016). The WHO, has suggested the tolerable weekly intake for the Cd is 7 µg/kg of body weight. This tolerable weekly intake accounts for 60 µg and 70 µg for an average 60 kg and 70 kg man and woman per day (WHO, 1992). Additionally, the concentration of cd in different food stuff has been given in the *Table 1*.

Table 1. Concentration of Cd in different food stuff

Food stuff	Cd concentration (µg/kg)
Sunflower	375
Spinach	117
Potato chips	93
French fries	44
Roasted peanuts	45
Wheat Cereal	51
Peanut butter	53
Leaf lettuce	62

Spungen, 2019

In China about 2.786×10^9 m² of agricultural land is contaminated by Cd (Liu et al., 2014). Third major pollutant of supreme hazard to the environment after mercury and lead is Cd and is considered as the only metal that has health threats to humans and animals at the concentration that is usually not phytotoxic (Ismael et al., 2019). Cd due to its non-essential nature and it causes several deleterious changes in, physiology, biochemistry and morphology of plants even at low concentrations (Song et al., 2015). Reduction in plant growth, development, chlorosis and finally plants death are the most critical symptoms observed under Cd toxicity (Ashraf et al., 2015).

In China, heavy doses of nitrogen resulted in more acidic and Cd contaminated soils. Cadmium is released from industrial wastes, and sewage irrigation (John et al., 2007; Pandey et al., 2007). Globally, more than 50% world's population consumes rice as a daily diet (Li et al., 2012b; Song et al., 2015). Therefore, Cd simply moved from soil to rice grains and entered into the human body (Aziz et al., 2015; Xie et al., 2015) and causing several deadly diseases including cancer, heart failure, hypertension and eye cataract formation. Cadmium was responsible for the occurrence of Itai-Itai disease in Japan in 1950s, via consumption of Cd contaminated rice (Horiguchi et al., 1994). Moreover, from 1990-2015, the normal consumption of Cd in diet in the Chinese population was more than double (Song et al., 2017; Chen et al., 2018). Schematic display of Cd uptake in soil is shown below in *Figure 1*.

In order to prevent human health from Cd toxicity, reliable steps should be taken to reduce Cd from rice gains, including agronomic practices, like water management, tillage management and fertilizer management. One of the most powerful techniques to decrease the bioavailable Cd in rice is in situ immobilization of Cd (Homa et al., 2016). Absorption, cation exchange and surface complexation are primary mechanisms of Cd immobilization mediated by agronomic practices (Shaheen and Rinklebe, 2016). Efforts have been made to introduce a novel and cost-effective approaches. In recent studies conducted by Shaheen and Rinklebe (2016) and Li et al. (2017) revealed that lime stone and sugar beet industry meaningfully reduced the cadmium solubility because of higher contents of total calcium carbonate and alkalinity.

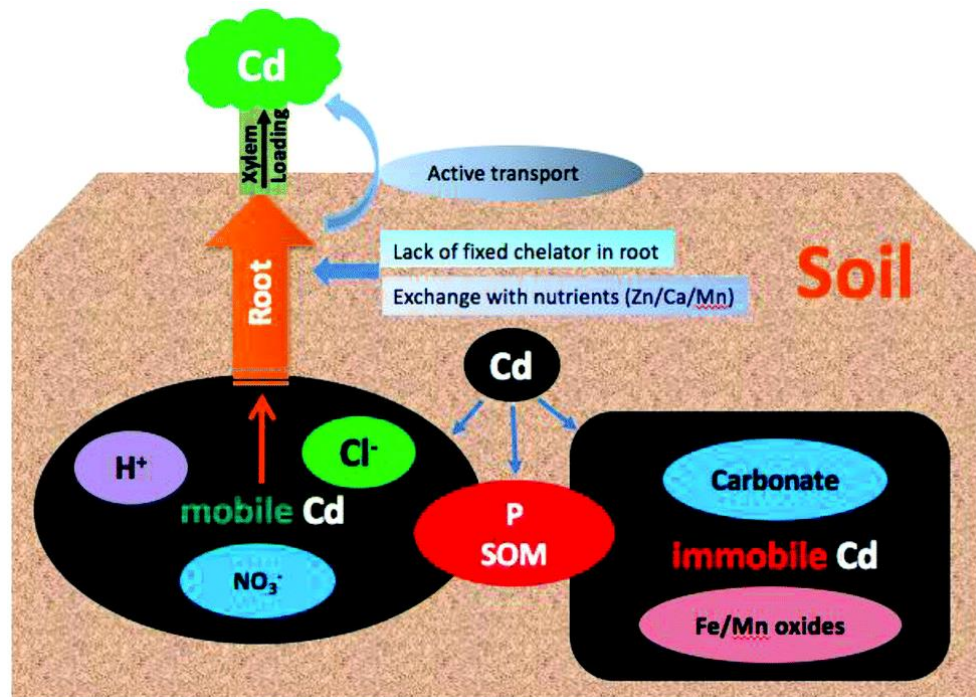


Figure 1. Factors affecting the Cd uptake from the soil (adopted from Huang et al., 2017)

Biochar application decreased the concentration of Cd as studied by Rinklebe et al. (2016). Use of fertilizers can also alter the soil characteristics like, surface charge, pH, but sometime it directly interacts with soils Cd. Use of fertilizers of phosphate, MPP (potassium phosphate monobasic), TCP (calcium phosphate tribasic), DAP (diammonium phosphate) and SSP (calcium super phosphate on) decreased the bioavailable Cd in soil as evidenced by Yan et al. (2015) and Li et al. (2017). Thirdly, water management had a key part in reducing the Cd availability in soil by changing (redox potential) and pH of soil (Li et al., 2015; Homa et al., 2016). Some of the recent findings of experiments (pot and field) presented that use of flooding before & after the heading significantly decreased cadmium concentration in rice, while Cd concentration enhanced under aerobic condition (Hu et al., 2015). Hence, stage of heading in rice stage is a crucial time for lowering Cd entrance. Use of water managing technique would be a cheapest & cost-effective plan to reduce Cd assimilation in rice. Crops rotations, intercropping and tillage managing changed the soil, physical, chemical, and biological properties and therefore can reduce Cd uptake in rice as reported by Liu et al. (2016), Li et al. (2017) and Chen et al. (2019). High concentration of organic matter in reduced tillage soil, produced due to deposit of previously grown crops, could increase the adsorption & complexation of Cd. Guo et al. (2010) reported a decrease in Cd in rice by application of reduced tillage management practice because of the decrease of microbial activity. Bioremediation is environmental friendly and cost-effective technique to eliminate the heavy metals from a contaminated environment, which involve the use of certain microorganisms to treat the contaminated soils to retain to its healthy state (Gaur et al., 2014). Phyto-extraction is most cost effective and novel technique for elimination of heavy metals and metalloids from polluted oils and water. Cd tolerant plant species that can absorb high concentration of Cd can be used for this strategy (He et al., 2015). Some of the indica rice cultivars have the capability to accumulate the Cd up to the

concentration of 3.9 mg kg⁻¹ in grains by using phyto extraction technique. Indica rice variety, Chokoukoku tested for two years and showed a reduction of 883 g Cd ha⁻¹, and reduced Cd in japonica rice grown later with reduced yield (Murakami et al., 2009). It is therefore more viable strategy to use rice cultivars with high contents of cadmium for remediation of contaminated paddy fields. Soil microorganism have strong interaction with plants and can influence plant growth and nutrients mobility, therefore understanding the complex interaction between soil microorganisms and plant is necessary for best results of phyto-remediation (Muehe et al., 2015; Li et al., 2017). Liu et al. (2015) showed that use of plant growth promoting rhizobacteria (PGPR) can improve plant tolerance to heavy metals. They used roots of cadmium accumulating plants, and isolated 9 strains of cadmium tolerant plant growth promoting rhizobacteria and discovered that cadmium hyper-accumulator (*S. plumbizincicola*) treated with *Rhodococcus erythropolis NSX2* and *Cedecea davisae LCRI* showed better growth and more cadmium accumulation in shoots. Together all of these agronomic practices are highly recommended to reduce Cd in rice for decreasing human health risk and to sustain rice production on Cd effected soils.

QTLs mapping is one of the most powerful technique to locate the gene of interest on chromosomes. Use of different mapping population is an economically sustainable approach to enhance rice production under cadmium stress conditions (Xue et al., 2009). To screen cadmium tolerant genotypes at seedling stage by using different levels of Cd stress in hydroponic condition is more viable way. Cd toxicity tolerance in rice at morphological, physiological and biochemical has been widely investigated. Use of agronomic practices is an important strategy to minimize Cd in rice (Li et al., 2017). Genetic factors regulating cadmium uptake and transport should need to understand to minimize cadmium contents in grains (Chen et al., 2019). The present review focused on understanding the genetic basis of Cd stress, uptake, accumulation and transportation in rice and to suggest the ways to improve rice tolerance against the Cd toxicity. There are several QTLs reported being responsible for Cd accumulation and for breeding Cd free rice cultivars. We need to transfer these QTLs via markers-assisted selection (MAS selection) along with the alleles with novel functions to accumulate low Cd in rice. The development of Cd resistant rice lines and identification of unknown transporters would be more useful to grow rice on Cd affected soils to maintain production to ensure the food security.

Survey methodology

The papers reviewed in this review paper were obtained from the diverse databases and the professional websites. We conducted a survey in the Google scholar, web of science, science direct, PubMed, CAB abstracts, Springer, Taylor and Francis using different keywords including rice, cadmium, genes, QTLs, Cd transport, Cd accumulation, mass selection, Cd stress, Putative QTLs, efflux protein and molecular mechanism to obtain any relevant information regarding, toxic effects of Cd, and genetic factors in regulating the cadmium uptake, transport and accumulation mechanisms in rice.

Rice growth under Cd stress

Cd toxicity is worldwide problem for crop growth and environmental safety (Aamer et al., 2018). Rice germination and growth is badly affected by Cd stress (He et al., 2006; Liu et al., 2014, 2019a), and exposure of rice seeds to Cd for a long time resulted in lower

germination (Ahsan et al., 2007), and it also leads to chlorosis and necrosis in rice (Ishimaru et al., 2006). Moreover, Cd stress also caused different physiological as well as physical changes in rice including the reduction in seedling length, number of roots and shoots (Kanu et al., 2017). Cadmium stress affects the stomatal conductance in rice (Li et al., 2012b), absorption and transport of important nutrients in rice crop (Li et al., 2012a, 2012b), and thereby results in severe reduction in final production and grain nutrient contents (Mahmood et al., 2006; Abin and Prasad, 2014; Kanu et al., 2017). Rice cope with Cd toxicity by possessing numerous strategies at molecular and physiological levels (Zhang et al., 2018; Islam et al., 2019).

Plants have mechanisms including the accumulation of Cd in cell wall and vacuole of root cell, which enable them to stop the transportation of Cd from root to shoots and thus leads to reduction in the corresponding effects of Cd on other cells (Fu et al., 2011; Qiu et al., 2011). Many ATP binding-cassette (ABC) protein facilitates the vacuolar spreading of Cd-glutathione in *Arabidopsis thaliana* (Kim et al., 2007). Rice genes (*OsPDR5/ABCG43*) are responsible to hold ABC-type proteins, which favors the Cd extrusion from the cell cytoplasm (Oda et al., 2011). Cadmium transporter (*OsHMA3*) in membranes of the vacuole in rice roots can enhance rice tolerance to Cd and lessen the accumulation of Cd in rice grains (Ueno et al., 2010a; Ke et al., 2015). The vacuoles inside the plants are targeted by detoxification of metal due to chelated toxic metals (Hall, 2002; Haydon and Cobbett, 2007). Organic acids including malate and citrate are accountable for uptake and long-distance transportation of metals into plant vacuoles (Verbruggen et al., 2009; Revathi and Venugopal, 2013). Chelators played a key role in forming a barrier against Cd accumulation (Nocito et al., 2011). Plants boost the antioxidant defense system to improve tolerance against Cd stress (Hassan et al., 2005; Zhao et al., 2013). The concentration of various substances including, glutathione, salicylic acid, jasmonic acids and nitric oxide considerably increased on exposure to Cd stress (Wang et al., 2011; Asgher et al., 2015). Mitogen-activated protein kinase *OsWJUMK1*, *OsMSRMK2* regulates auxin signal fluctuations which result in disruption of rice root growth exposed to Cd stress (Agrawal et al., 2003; Zhao et al., 2013). Cadmium stress response and root development are associated with auxin transporter *OsAUX1* in rice (Yu et al., 2015). Cadmium accumulation and uptake are reduced by the application of iron, zinc and silicon (Hermans et al., 2013; Chen et al., 2018). Cadmium pathway from roots towards shoots shown in *Figure 2*.

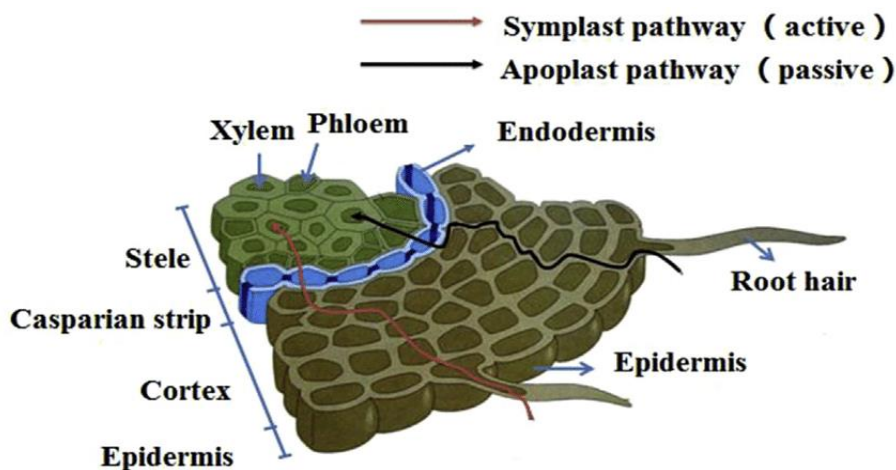


Figure 2. Cd pathway from roots towards shoots (adopted from Li et al., 2017)

Some important Cd tolerance genes are shown below (Table 2, Figure 3). *OsHMA9* is an important copper (Cu) efflux protein, present in the plant plasma membranes; this protein favors the efflux of Cd from the plant roots, therefore, leads to a substantial reduction in the Cd accumulation in rice grains (Lee et al., 2007). Knockout of a low Cd gene (LCD) decreased Cd accumulation and therefore improves the rice growth in Cd stressed conditions, and low Cd gene is a protein linked with Cd equilibrium (Shimo et al., 2011). Arabidopsis thaliana plant growth under Cd stress enhanced by *OsCDT1* owing to fact; cysteine rich peptide encoded by *OsCDT1* improved the rice tolerance against the Cd stress (Kuramata et al., 2008). *OsCLT1* probably responsible for normalizing the transfer of glutamylcysteine and glutathione plastids to cytoplasm, which therefore, effects Cd reclamation in rice (Islam et al., 2019). A schematic display of cadmium transport from soil towards rice grains is shown in Figure 4.

Table 2. Putative genes expressed in rice in response to Cd stress

Gene	Chr	Location	Genotype	Screening	Gene name	Role	References
<i>OsIRT2</i>	3	26276301–26277206	Rice	Hydroponic	Iron-regulated transporter	Cd and Fe transporter	(Nakanishi et al., 2006)
<i>OsIRT1</i>	3	26286156–26292023	Rice	Hydroponic	Iron-regulated transporter	Cd and Fe transporter	(Lee and An, 2009)
<i>OsNramp5</i>	7	8871436–8878905	Rice	Hydroponic	Natural Resistance associated Macrophage protein	Cd, Mn and Fe Transporters	(Ishimaru et al., 2012)
<i>OsNramp1</i>	7	8966025–8970882	Rice	Hydroponic	Natural resistance-associated macrophage protein	Cd and Fe transporters	(Takahashi et al., 2011)
<i>OsZIP1</i>	1	42905566–42907474	Rice	Hydroponic	Zinc- and iron-regulated transporter	Cd and Zn transporter	(Ramesh et al., 2003)
<i>OsHMA3</i>	7	7405745–7409553	Rice		P-Type Heavy Metal ATPase	Sequester Cd in the plant roots	(Ueno et al., 2010b)
<i>OsHMA2</i>	6	29477949–29480905	Rice	Hydroponic	P-Type Heavy Metal ATPase	Cd and Zn translocations	(Takahashi et al., 2012)
<i>OsZIP7</i>	5	6090801–6094068	Rice	HS/field screening	Zinc- and iron-regulated transporter	Cd and Zn accumulation	(Tan et al., 2019)
<i>OsLCT1</i>	6	22566775–22571982	Rice		Low affinity cation transporter	Cd transporter in phloem	(Uraguchi et al., 2011)
<i>OsMTP1</i>	5	1675488–1679056	Rice		Metal tolerance protein gen	Cd translocation	(Yuan et al., 2012)
<i>OsZIP6</i>	5	3807974–3810752	Rice	Hydroponic	Zinc- and iron-regulated transporter	Cd transport	(Kavitha et al., 2015)
<i>PEZ1</i>	3	20793053–20799805	Rice		Phenol efflux protein	Cd accumulation	(Ishimaru et al., 2011)
<i>OsCDT4</i>	2	6078179–6079111	Rice	Hydroponic	Encoding a Cys-rich peptide	Cd uptake inhibitor	(Kuramata et al., 2008)
<i>OsMSRMK3</i>	6	29398191–29402466	Rice	Invitro/vivo	Mitogen-activated protein kinase	Cd signal	(Agrawal et al., 2003)
<i>OsABCG43</i>	7	20214025–20218702	Rice		ATP-binding cassette transporter	Cd compartmentalization	(Oda et al., 2011)
<i>OsCLT1</i>	1	42086484–42095424	Rice	Hydroponic	CRT-like transporter 1	Cd tolerance	(Yang et al., 2016b)

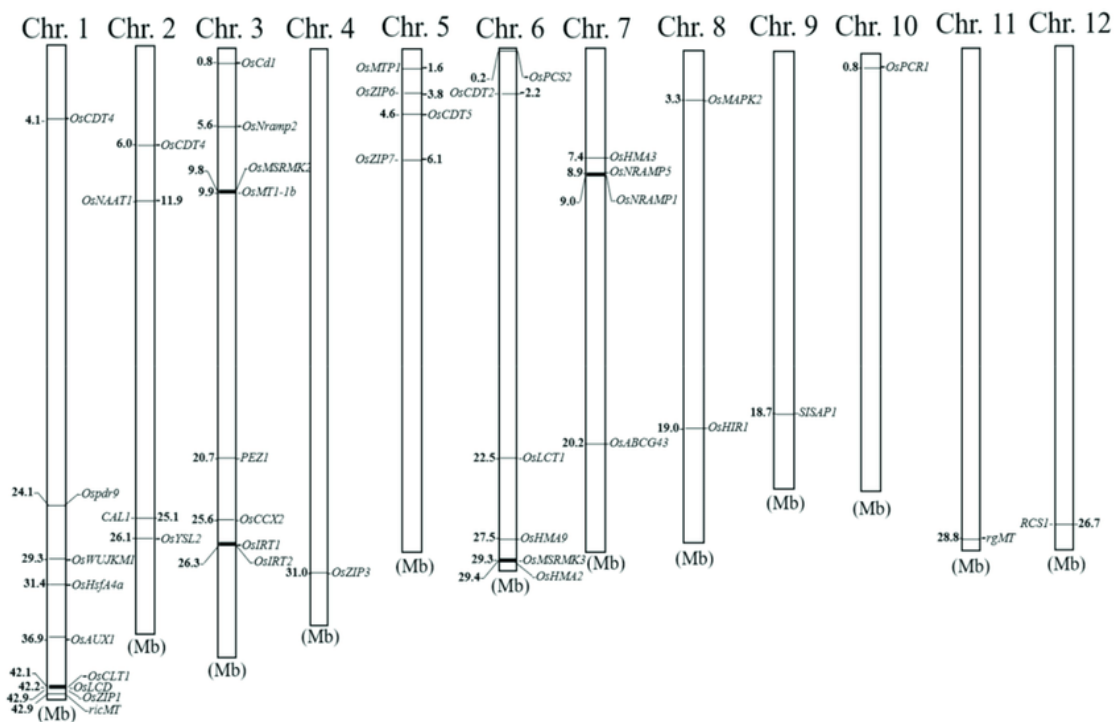


Figure 3. Physical location of genes related to Cd toxicity tolerance in rice (adopted from Chen et al., 2019)

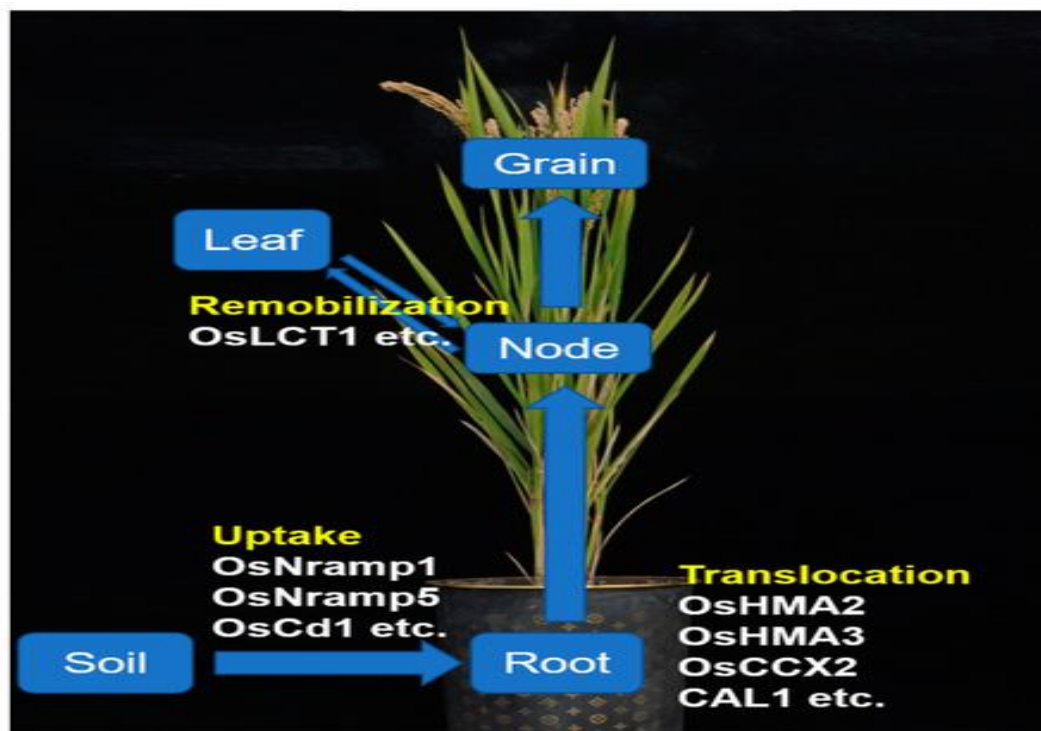


Figure 4. Shows how Cd moves from soil to roots. First cadmium moves from soil to root and grains and this process is mediated by the genes (*OsNramp1*, *OsNramp5*, and *OsCd1*) (adopted from Chen et al., 2019)

Cd uptake and transport mechanism in rice

Cd uptake and transport pathway in rice plant include these four steps: (i) uptake via roots; (ii) transportation to shoots via xylem tissues (iii) circulation and transport by the plant nodes (iv) Cd passage to grains from leaf blades by the phloem as shown in *Figure 4* (Chen et al., 2019). The *Figure 4* shows, how Cd moves from soil to roots. First cadmium moves from soil to root and grains and this process is mediated by the genes (*OsNramp1*, *OsNramp5*, and *OsCd1*) as shown in *Figure 4* (Chen et al., 2019).

Cd tolerance genes in rice

Mechanisms of uptake of some important elements (Mn, Zn, and Fe) which are responsible for Cd entrance into rice plants is described by (Abin and Prasad, 2014; Islam et al., 2019). Cadmium efflux activity in yeast is shown by iron transporters (*OsIRT1* and *OsIRT2*) which shows that *OsIRT1* and *OsIRT2* may have a role in the uptake of Cd in the root system (Nakanishi et al., 2006; Abin and Prasad, 2014). Expression of *OsIRT1* considerably improved the Cd in roots and shoots in MS medium presented by Murashige and Skoog with surplus Cd but no noticeable phenotype was detected under field conditions, proposing that *OsIRT1* may be responsible for Cd uptake in rice but environment had enormous effects on its contribution (Lee et al., 2007; Lee and An, 2009). Cadmium uptake in rice roots owing to natural resistance associated with macrophage protein 5 *OsNramp5* which is accountable for the transport of Cd from soil solution to root cells (Ishimaru et al., 2012; Sasaki et al., 2012). A researcher recently identified the main quantitative traits loci (*qGMN7.1*) for Cd tolerance (Liu et al., 2017). New most effective lines of rice with less Cd accumulation have been developed by bumping out the metal transporters (*OsNramp5*). Using (CRISPR/CAS9) system, a chain of *indica* rice lines having the capability of accumulating low Cd were developed. *OsNRAMP1* genes located on the plasma membrane participated in Cd transport activity in roots cells (Takahashi et al., 2011; Islam et al., 2019). Yeast sensitivity to Cd is increased by the function of *OsZIP1*; a zinc-regulated/iron-regulated transporter-like protein (Ramesh et al., 2003), and Cd uptake in *Xenopus* leaves oocytes could be enhanced by *OsZIP6* overexpression (Kavitha et al., 2015).

The key factor defining the Cd accumulation in shoots is xylem-mediated Cd translocation (Uraguchi and Fujiwara, 2012), and *OsHMA2* and *OsHMA3* (Yamaji et al., 2013; Kavitha et al., 2015). Transport of Cd from roots to shoots is controlled by *OsHMA2* and it has important role in regulating the spread of Cd via phloem to developing tissues (Takahashi et al., 2012). *OsHMA3* has the main part in vacuolar requisition of Cd in cells of the root, the over-expression of *OsHMA3* decreases the Cd burden in the xylem and Cd accretion in the plant shoot. Moreover, the *OsHMA3* deficiency leads to higher Cd concentration both in plant roots and shoots (Ueno et al., 2010a). *OsZIP7* has substantial role in the xylem loadings in the roots, and to bring the Cd and Zn in the upper parts of rice (Tan et al., 2019). Cadmium transfer from xylem to phloem by the plant nodes has imperative part in the Cd transportation to grains (Fujimaki et al., 2010). *OsLCT1* is a Cd efflux carrier located on plasma membrane and accountable for phloem Cd transportation (Uraguchi et al., 2011). *OsLCT1* expression was found to be higher in nodes and leaf blades during the propagative period, particularly in node I. The Cd concentration in the rice grains, as well as the exudates of phloem in RNAi plants were appreciably decreased compared with wild plants, however, the Cd concentration in the xylem sap remained same in both plants. The current outcomes indicated that *OsLCT1*

genes in the leaf blade of plants help in re-mobilization of Cd by the phloem. Moreover, in node I, *OsLCT1* has an important part in the intra-vascular Cd translocation, which involves in translocation of Cd from a larger vascular bundle to diffused ones attached with the panicle (Uraguchi et al., 2011). *Figure 3* and *Table 2* showed positions of cloned cadmium stress-related genes in rice chromosomes.

Molecular mechanism behind Cd accumulation

The major transporter for Cd in rice roots is *OsNramp5* family (Sasaki et al., 2012), which is the transporter of divalent cations like, Fe and Cd (Supek et al., 1996), while one *OsNramp1* transfer toxic aluminum in rice (Xia et al., 2010). *OsNramp5* is also controlled Mn uptake in rice (Sasaki et al., 2012). The knockout of this gene results in complete loss of Cd uptake which showed that this gene is responsible for Cd uptake. *OsIRT1* and *OsIRT2* are also responsible for Cd uptake in rice (Nakanishi et al., 2006). Ample NO₃ enriched Cd efflux in the elongation zone of rice roots by enhancing *OsIRT1* expression causes more uptake and accumulation of Cd in rice grains (Yang et al., 2016a). The second important step is vacuolar sequestration of Cd in rice roots. *OsHMA3* a major member of heavy metals family involved in this process. This gene was isolated from large QTLs located on the short arm of chromosome 7 resulting from the cross a cross among *indica* cultivar (Anjana Dhan) which contains more Cd contents in grain, and second japonica cultivar (Nipponbare) with lower contents of cadmium (Ueno et al., 2009). *OsHMA3* is mostly expressed in the roots, and its expression is not affected by Cd exposure. A recent study showed that the novel function of *OsHMA3* named as zinc carrier (Sasaki et al., 2014).

The third step is root to shoot translocation of Cd. *OsHMA3* was studied to be accountable for translocation from root to shoot in rice (Yamaji et al., 2013). This gene is localized in the plasma membrane and pericycle of roots. The knockout in the activity of this gene caused a decrease in Cd accumulation in yeast. The final stage of this mechanism is Cd accumulation in rice grains. *OsHMA2* is responsible for Cd distribution in rice grains, more importantly, its functions appeared to be stronger at the reproductive stage in node 1; *OsHMA2* is present at the phloem of enlarged and diffuse vascular bundles in node 1 (Yamaji et al., 2013). The knockout of *OsHMA2* resulted in the reduction in the concentration of Zn and Cd in upper nodes and reproductive organs compared with wild-type rice. *OsLCT1* (*Oryza sativa*) low-affinity cation transporter 1 involved in the intravascular transfer of Cd. *OsLCT1* is localized in the plasma membrane and represents efflux carrying activity for Cd and K, and not for the Fe and Na (Uraguchi et al., 2011). The knockdown of *OsLCT1* resulted in a reduction in Cd concentration in phloem and grains (Uraguchi et al., 2011). Expression of *OsLCT1* in the nodes was only observed at the ripening stage as compared to *OsHMA2* which expressed in nodes throughout the reproductive stage.

Putative QTLs in response to Cd stress in rice

Rice genotypes have significant genetic diversity regarding their ability to Cd accumulation and tolerance which stated the scope of selection (Liu et al., 2003; He et al., 2006). Genetic factors controlling Cd assimilation in rice have scanty described. *OsHMA3* encodes a Cd transporter found in the membrane of vacuoles, which favors the Cd segregation in the vacuole (Liu et al., 2019a). The reduction in *OsHMA3* functioning frequently enhanced Cd transfer in shoots and grains of rice (Abe et al., 2013; Liu et al., 2019a). *OsHMA3* improves Cd tolerance in the rice plant and reduces the Cd accretion in

the rice kernels (Ueno et al., 2010a; Sasaki et al., 2014). A gene *OsCdl* from major facilitator superfamily was identified by Yan et al. (2019) through genome-wide association analysis (GWAS) which has an association with the variation for Cd assimilation in rice. Two quantitative traits loci governing the Cd application in brown rice stated by Sato et al. (2011) *qLCdG11* contributed to 9.4–12.9% phenotypic variance and *qLCdG3* contributed 8.3–14% phenotypic alterations. Yan et al. (2013) made a RIL population of F₇ to recognize Cd cadmium assimilation and dispersal. Abe et al. (2013) studied population containing 46 CSSL (chromosome segment substitution lines) and detected 8 quantitative traits loci correlated with Cd contents in grain by single-label analysis of variance). Additional different genes QTLs expressed in the rice exposed to Cd stress are given in Table 3.

Table 3. Putative QTLs express during the rice exposure to the Cd stress

Parents	Population	Stage	Traits	QTLs	Marker	Chr	Ref
Nipponbare/Anjana Dhan	965 F2	Seedling stage	Cd concentration in shoot	<i>OsHMA3</i>	SSR	7	(Ueno et al., 2010b)
SNU-SG1/Suwon490	91 RIL	Seedling stage	Cd concentration in shoot	<i>scc10</i>	124 SSR	10	(Yan et al., 2013)
Koshihikari/LAC23 46 CSSLs	46 CSSLs	Seedling stage	Cd concentration in shoots	<i>glGCd3</i>	345 SNP	3	(Abe et al., 2013)
Anjana Dhan/Nipponbare	177 F2	Seedling stage	Root-to-shoot Cd translocation	<i>qCdT7</i>	SSR	7	(Ueno et al., 2009)
Tainan1/Chunjiang06	119DH,3651 BC3F3	Seedling stage	Cd accumulation in leaves	<i>CAL1</i>	RFLP	1	(Luo et al., 2018)
JX17/ZYQ8	127 rice cultivars	Maturing stage	Cd accumulation in grains	<i>OsCdl</i>	GWAS	3	(Yan et al., 2019)
Sasanishiki/Habataki	85 BIL	Maturing stage	Cd accumulation in grains	<i>qGCd7</i>	SSR	2,7	(Ishikawa et al., 2009)
Fukuhibiki/LAC23	126 RIL	Maturing stage	Cd accumulation in grains	<i>gLCdG3</i> , <i>gLCdG1</i>	454 SNP	3,11	(Sato et al., 2011)
SNU-SG1/Suwon490 91 RIL	91 RIL	Maturing stage	Cd accumulation in grains	<i>gcc3</i> , <i>sgr5</i>	124 SSR	3,5	(Yan et al., 2013)
Xiang 743/Katy	115 RIL,	Maturing Stage	Cd accumulation in grains	<i>qCd-2</i> , <i>qCd-7</i>	SSR GWA	2,7	(Liu et al., 2019b)
JX17/ZYQ8	378 rice cultivars	Maturing Stage	Cd accumulation in grains	<i>qCd3</i> , <i>qCd5</i> .	GWAS (Statistical approach)	3,5	(Hosseini et al., 2012)

Chr: chromosomes, Ref: references, RIL: recombinant inbred lines, DH: double haploid, BIL: backcross inbred lines population, CSSL: chromosomal segment substitution lines, SSR: single sequence repeat, RFLP: restriction fragment length polymorphism, SNP: single nucleotide polymorphism, GWAS: genome wide association study

Identification of QTLs is response to Cd toxicity in rice at seedling stage

Use of mapping population in to identify the putative QTLs in rice regarding Cd toxicity tolerance, has been a fruitful way to screen resistant rice genotypes. Significant difference among the rice genotypes in Cd tolerance at seedling stage has been widely studied (Cheng et al., 2006; Yu et al., 2006; Xue et al., 2009; Ding et al., 2018). Recently lots of genetic factors have been identified controlling Cd tolerance in rice at seedling stage. Evaluation of rice genotypes in hydroponic condition using different levels of Cd

stress is an economically sustainable approach to increase rice production (Ding et al., 2018).

Xue et al., (2009) conducted a hydroponic experiment and reported some of the functional QTLs (*qSH6*, *qSH7*, *qRL1*, *qCDS7*) in rice explaining 9.11%, 14.36%, 8.11% and 0.12% of the phenotypic variance. Positive additive effect was shown by the QTLs for shoot height and allele was contributed by donor parent. These results suggested their novel role in increasing cadmium tolerance at seedling stage. A QTL *qCD7* was involved in reducing CD concentration in rice. Wang et al. (2018) identified a cadmium tolerance QTL *qGLR3* for leaf rolling in rice and concluded that this region had novel contribution in response to cadmium stress in rice. Additionally, another major QTL *qLR1* was responsible for controlling leaf rolling in DH population of rice at seedling stage. Defection of QTLs for cadmium toxicity tolerance for morphological traits are rarely reported in rice, however use of high-resolution mapping population, and use of different levels of Cd in hydroponic condition would be an effective method to identify the putative QTLs controlling Cd tolerance at seedling stage. Hence Cd tolerance could be increased using an effecting nutrient solution and secondly genetically divergent parents to construct progeny to be evaluated in cultural solution *Table 4*.

Table 4. Some of the novel QTLs identified in rice for morphological traits in hydroponic environment

Parents	Progeny	Indexes	QTLs	Stage	Markers	Chr	Ref
ZYQ8/JY17	127DH	SH	<i>qSH6</i>	seedling	160RFLP	6	Xue et al., 2009
ZYQ8/JY17	127DH	SH	<i>qSH7</i>	seedling	160RFLP	7	Xue et al., 2009
ZYQ8/JY17	127DH	RL	<i>qRL1</i>	seedling	160RFLP	1	Xue et al., 2009
ZYQ8/JY17	127DH	CDS	<i>qCDS7</i>	seedling	160RFLP	7	Xue et al., 2009
ZYQ8/JY17	27DH	LR	<i>qGLR3</i>	seedling	83SSR/160RFLP	3	Wang et al., 2018
ZYQ8/JY17	27DH	LR	<i>qLR1</i>	seedling	83SSR/160RFLP	1	Wang et al., 2018
ZYQ8/JY17	27DH	GLR	<i>qLR9</i>	seedling	83SSR/160RFLP	9	Wang et al., 2018

DH: double haploid, QTLs: quantitative traits loci, Chr: chromosomes, Ref: references, RFLP: restriction fragment length polymorphism, SSR: single nucleotide polymorphism, SH: shoot height, LR: leaf rolling, GLR: green leaf ratio, CDS: cadmium concentration

Conclusion and future research direction

Globally, Cd toxicity is a serious threat to living organisms especially humans (Aziz et al., 2015). The different agronomic practices like tillage, nutrients management, water management, use of fertilizers could be adopted to minimize Cd uptake in rice (Li et al., 2012b; Kanu et al., 2019). Many genetic factors involved in Cd uptake and accumulation have been identified and fruitful progress has been made in this aspect. The factors affecting uptake and accumulation of Cd needs to be understand to make strategies for reducing Cd toxicity. The identification of more unknown transporter and molecules is an urgent need to understand the way through which Cd is accumulated in rice grains. The use of biotechnological tools is important for this and genes (*OsNramp5*) mutation (*OsNramp5*) result in a noticeable reduction in the accumulation of Cd in rice grains (Ishimaru et al., 2012). Many transporters need to be recognized in future studies by using different techniques. Cd efflux transporters in rice roots exodermis and endodermis cells are accountable for xylem unloading and phloem loading of Cd, however, these was not still studied. There is no specific transporter involved in Cd accumulation but these are the transporters belong to other metals, like Mn (*OsNramp5*) and Fe (*OsHMA2*). We

cannot use these genes for developing new rice varieties but there is a need to screen new alleles with new functions to develop resistant varieties to Cd toxicity.

A hybrid cultivar of rice was developed which has low contents of Cd in rice grain (Tang et al., 2017). The accumulation and translocation of Cd were reduced by overexpression of functional *OsHMA3* (Ueno et al., 2009). Three rice mutants were made by (Ishikawa et al., 2012) using carbon ion-beam irradiation and in these mutants, Cd was not recognized when grown on the Cd stress conditions, additionally, and there was no pronounced difference among the wild and mutants. The use of markers assisted selection is one of the best strategies to identify the locus governing Cd accumulation in rice. Transfer of QTLs from a low Cd cultivar to a cultivar with higher contents of Cd could be a significant approach (Uraguchi and Fujiwara, 2012). Few genetic factors regarding Cd accumulation have been recognized and cloned (Ueno et al., 2010a) but natural variation in alleles of Cd grain accumulation among the varieties has not fully understood.

The present review suggested to do more investigation on the identification of QTLs controlling Cd accumulation in grain essential to clone further QTLs governing grain Cd accumulation and use of the theoretical base for MAS (markers assisted selection) to develop rice varieties with low Cd contents. Secondly, identification of unknown transporters is a fruitful approach to find the novel function and built a barricade against Cd uptake and accumulation in rice grains. Some of the novel QTLs (*qSH6*, *qSH7* and *qLR3*) reported for morphological traits should be transferred to develop Cd resistant lines in rice. Hence use of mapping population and screening of genotypes at seedling stage in hydroponic environment would be a powerful way to reduce Cd toxicity in rice. There are a lot of QTLs reported being responsible for Cd accumulation and for breeding Cd free rice cultivars we need to transfer these QTLs via MAS selection. For instance, Identification of quantitative traits loci from a low cadmium accumulating cultivar and then transfer this QTL to high Cd cultivar may be a more feasible way to decrease Cd accumulation in rice. Additionally, specific farms practices should be adopted to prevent the entry of Cd in soils. Futuristic studies should be aimed to understand the Cd uptake and translocation in diverse soils and its interference with Fe and Zn pathways. Moreover, develop the scrutiny system Cd in crops and reduce the allowable Cd in the fertilizers. Moreover, understand the bio-available fractions of Cd from the different food stuffs and factors influencing the Cd absorption in human body.

Acknowledgements. The authors would like to thanks the supervisor, Professor Wu Ziming for his valuable suggestions in the preparation of this draft. The authors would like to thank Dr. Saif Ali for English editing and anonymous reviewers; they helped to improve the quality of the paper.

Funding. The research was supported by the National Natural Science Foundation of China (31560350 and 31760350), the National Key Research and Development Program of China (2018YFD0301102), the Key Research and Development Program of Jiangxi Province (20171ACF60018 and 20192ACB60003) and the Jiangxi Agriculture Research System (JXARS-18).

Competing Interests. All authors declare that there are no competing interests.

REFERENCES

- [1] Aamer, M., Muhammad, U. H., Abid, A., Su, Q., Liu, Y., Adnan, R., Muhammad, A. U. K., Tahir, A. K., Huang, G. (2018): Foliar application of glycinebetaine (GB) alleviates the cadmium (Cd) toxicity in spinach through reducing Cd uptake and improving the activity of antioxidant systems. – *Applied Ecology and Environment Research* 16(6): 7575-7583.
- [2] Abe, T., Nonoue, Y., Ono, N., Omoteno, M., Kuramata, M., Fukuoka, S., Yamamoto, T., Yano, M., Ishikawa, S. (2013): Detection of QTLs to reduce cadmium content in rice grains using LAC23/Koshihikari chromosome segment substitution lines. – *Breeding Sci* 63: 284-291.
- [3] Abin, S., Prasad, M. (2014): Cadmium minimization in rice. A review. – *Agronomy for Sustainable Development* 34(1): 155-173.
- [4] Agrawal, G. K., Agrawal, S. K., Shibato, J., Iwahashi, H., Rakwal, R. (2003): Novel rice MAP kinases OsMSRMK3 and OsWJUMK1 involved in encountering diverse environmental stresses and developmental regulation. – *Biochemical and Biophysical Research Communications* 300: 775-783.
- [5] Ahsan, N., Lee, S.-H., Lee, D.-G., Lee, H., Lee, S. W., Bahk, J. D., Lee, B.-H. (2007): Physiological and protein profiles alternation of germinating rice seedlings exposed to acute cadmium toxicity. – *Comptes Rendus Biologies* 330: 735-746.
- [6] Asgher, M., Khan, M. I. R., Anjum, N. A., Khan, N. A. (2015): Minimising toxicity of cadmium in plants—role of plant growth regulators. – *Protoplasma* 252: 399-413.
- [7] Ashraf, U., Kanu, A. S., Mo, Z., Hussain, S., Anjum, S. A., Khan, I., Abbas, R. N., Tang, X. (2015): Lead toxicity in rice: effects, mechanisms, and mitigation strategies—a mini review. – *Environmental Science and Pollution Research* 22(23): 18318-18332.
- [8] Aziz, R., Rafiq, M. T., Li, T., Liu, D., He, Z., Stoffella, P., Sun, K., Xiaoe, Y. (2015): Uptake of cadmium by rice grown on contaminated soils and its bioavailability/toxicity in human cell lines (Caco-2/HL-7702). – *Journal of Agricultural and Food Chemistry* 63(13): 3599-3608.
- [9] Chen, H., Yang, X., Wang, P., Wang, Z., Li, M., Zhao, F.-J. (2018): Dietary cadmium intake from rice and vegetables and potential health risk: a case study in Xiangtan, southern China. – *Science of the Total Environment* 639: 271-277.
- [10] Chen, J., Zou, W., Meng, L., Fan, X., Xu, G., Ye, G. (2019): Advances in the uptake and transport mechanisms and QTLs mapping of cadmium in rice. – *International Journal of Molecular Sciences* 20: 1-17.
- [11] Cheng, W. D., Zhang, G. P., Yao, H. G., Wu, W., Xu, M. (2006): Genotypic and environmental variation in cadmium, chromium, arsenic, nickel and lead concentrations in rice grains. – *Journal of the Zhejiang University Science* 7: 565-571.
- [12] Cook, M. E., Morrow, H. (1995): Anthropogenic sources of cadmium in Canada. – In: *National Workshop on Cadmium Transport into Plants; Canadian Network of Toxicology Centres: Ottawa, ON, Canada.*
- [13] Fu, X., Dou, C., Chen, Y., Chen, X., Shi, J., Yu, M., Xu, J. (2011): Subcellular distribution and chemical forms of cadmium in *Phytolacca americana* L. – *Journal of Hazardous Materials* 186: 103-107.
- [14] Fujimaki, S., Suzui, N., Ishioka, N. S., Kawachi, N., Ito, S., Chino, M., Nakamura, S. I. (2010): Tracing cadmium from culture to spikelet: noninvasive imaging and quantitative characterization of absorption, transport, and accumulation of cadmium in an intact rice plant. – *Plant Physiology* 152: 1796-1806.
- [15] Gaur, N., Flora, G., Yadav, M., Tiwari, A. (2014): A review with recent advancements on bioremediation-based abolition of heavy metals. – *Environmental Science Processes and Impact* 16: 180-193.
- [16] Godt, J., Scheidig, F., Grosse-Siestrup, C., Esche, V., Brandenburg, P., Reich, A., Groneberg, D. A. (2016): The toxicity of cadmium and resulting hazards for human health. – *Journal of Occupational Medicine and Toxicology* 1: 1-22.

- [17] Guo, J., Liu, X. J., Yong, Z., Shen, J. L., Han, W. X., Zhang, W. F., Christie, P., Goulding, K. W. T., Vitousek, P. M., Zhang, F. S. (2010): Significant acidification in major Chinese crop lands. – *Science* 327: 1008-1010.
- [18] Hall, J. (2002): Cellular mechanisms for heavy metal detoxification and tolerance. – *Journal of Experimental Botany* 53: 1-11.
- [19] Hassan, M. J., Shao, G., Zhang, G. (2005): Influence of cadmium toxicity on growth and antioxidant enzyme activity in rice cultivars with different grain cadmium accumulation. – *Journal of Plant Nutrition* 28: 1259-1270.
- [20] Hayat, M. T., Nauman, M., Nazir, N., Ali, S., Bangash, N. (2019): Environmental hazards of cadmium: Past, present, and future. – In: Hasanuzzaman, M., Prasad, M. N. V., Fujita, M. (eds.) *Cadmium Toxicity and Tolerance in Plants. From Physiology to Remediation*. Academic Press: London, UK, pp. 163-183.
- [21] Haydon, M. J., Cobbett, C. S. (2007): Transporters of ligands for essential metal ions in plants. – *New Phytologist* 174: 499-506.
- [22] He, J., Zhu, C., Ren, Y., Yan, Y., Jiang, D. (2006): Genotypic variation in grain cadmium concentration of lowland rice. – *Journal of Plant Nutrition and Soil Science* 169: 711-716.
- [23] He, S. Y., He, Z. L., Yang, X. E., Stoffella, P. J., Baligar, V. C. (2015): Soil biogeochemistry, plant physiology, and phytoremediation of cadmium-contaminated soils. – *Advances in Agronomy* 134: 134-225.
- [24] Hermans, C., Conn, S. J., Chen, J., Xiao, Q., Verbruggen, N. (2013): An update on magnesium homeostasis mechanisms in plants. – *Metallomics* 5: 1170-1183.
- [25] Honma, T., Ohba, H., Kaneko-Kadokura, A., Makino, T., Nakamura, K., Katou, H. (2016): Optimal soil Eh, pH, and water management for simultaneously minimizing arsenic and cadmium concentrations in rice grains. – *Environmental Science and Technology* 50: 4178-4185.
- [26] Horiguchi, H., Teranishi, H., Niiya, K., Aoshima, K., Katoh, T., Sakuragawa, N., Kasuya, M. (1994): Hypoproduction of erythropoietin contributes to anemia in chronic cadmium intoxication: clinical study on Itai-itai disease in Japan. – *Archives of Toxicology* 68: 632-636.
- [27] Hosseini, M., Houshmand, S., Mohamadi, S., Tarang, A., Khodambashi, M., Rahimsorouh, H. (2012): Detection of QTLs with main, epistatic and QTL× environment interaction effects for rice grain appearance quality traits using two populations of backcross inbred lines (BILs). – *Field Crops Research* 135: 97-106.
- [28] Hu, P. J., Ouyang, Y. N., Wu, L. H., Shen, L. B., Luo, Y. M., Christie, P. (2015): Effects of water management on arsenic and cadmium speciation and accumulation in an upland rice cultivar. – *Journal of Environmental Science* 27: 225-231.
- [29] Huang, Y., He, C., Shen, C., Guo, J., Mubeen, S., Yuan, J., Yang, Z. (2017): Toxicity of cadmium and its health risks from leafy vegetable consumption. – *Food and Function* 8: 1-29.
- [30] Ishikawa, S., Abe, T., Kuramata, M., Yamaguchi, M., Ando, T., Yamamoto, T., Yano, M. (2009): A major quantitative trait locus for increasing cadmium-specific concentration in rice grain is located on the short arm of chromosome 7. – *Journal of Experimental Botany* 61: 923-934.
- [31] Ishikawa, S., Ishimaru, Y., Igura, M., Kuramata, M., Abe, T., Senoura, T., Hase, Y., Arao, T., Nishizawa, N. K., Nakanishi, H. (2012): Ion-beam irradiation, gene identification, and marker-assisted breeding in the development of low-cadmium rice. – *Proceedings of the National Academy of Sciences* 109: 19166-19171.
- [32] Ishimaru, Y., Suzuki, M., Tsukamoto, T., Suzuki, K., Nakazono, M., Kobayashi, T., Wada, Y., Watanabe, S., Matsushashi, S., Takahashi, M. (2006): Rice plants take up iron as an Fe³⁺-phytosiderophore and as Fe²⁺. – *The Plant Journal* 45: 335-346.
- [33] Ishimaru, Y., Kakei, Y., Shimo, H., Bashir, K., Sato, Y., Sato, Y., Uozumi, N., Nakanishi, H., Nishizawa, N. K. (2011): A rice phenolic efflux transporter is essential for solubilizing

- precipitated apoplasmic iron in the plant stele. – *Journal of Biological Chemistry* 286: 24649-24655.
- [34] Ishimaru, Y., Takahashi, R., Bashir, K., Shimo, H., Senoura, T., Sugimoto, K., Ono, K., Yano, M., Ishikawa, S., Arao, T. (2012): Characterizing the role of rice NRAMP5 in manganese, iron and cadmium transport. – *Scientific Reports* 2: 1-8.
- [35] Islam, F., Wang, J., Farooq, M. A., Yang, C., Jan, M., Mwamba, T. M., Hannan, F., Xu, L., Zhou, W. (2019): Rice responses and tolerance to salt stress: Deciphering the physiological and molecular mechanisms of salinity adaptation. – In: Hasanuzzaman, M., Fujita, M., Nahar, K., Biswas, J. K. (eds.) *Advances in Rice Research for Abiotic Stress Tolerance*, pp. 791-819.
- [36] John, R., Ahmad, P., Gadgil, K., Sharma, S. (2007): Antioxidative response of *Lemna polyrrhiza* L. to cadmium stress. – *Journal of Environmental Biology* 28: 583-589.
- [37] Kanu, A. S., Ashraf, U., Bangura, A., Yang, D., Ngaujah, A. S., Tang, X. (2017): Cadmium (Cd) stress in rice; phyto-availability, toxic effects, and mitigation measures-a critical review. – *IOSR Journal of Environmental Science, Toxicology and Food Technology* 11: 7-23.
- [38] Kanu, A. S., Ashraf, U., Bangura, A., Yang, D. M., Ngaujah, A. S., Tang, X. (2019): Cadmium (Cd) Stress in rice; phyto-availability, toxic effects, and mitigation measures-a critical review. – *IOSR Journal of Environmental Science, Toxicology and Food Technology* 11: 55-61.
- [39] Kavitha, P. G., Kuruvilla, S., Mathew, M. K. (2015): Functional characterization of a transition metal ion transporter, OsZIP6 from rice (*Oryza sativa* L.). – *Plant Physiology and Biochemistry* 97: 165-174.
- [40] Ke, S., Cheng, X.-Y., Zhang, N., Hu, H.-G., Yan, Q., Hou, L.-L., Sun, X., Chen, Z.-N. (2015): Cadmium contamination of rice from various polluted areas of China and its potential risks to human health. – *Environmental Monitoring and Assessment* 187: 1-11.
- [41] Kim, D. Y., Bovet, L., Maeshima, M., Martinoia, E., Lee, Y. (2007): The ABC transporter AtPDR8 is a cadmium extrusion pump conferring heavy metal resistance. – *The Plant Journal* 50: 106-117.
- [42] Kuramata, M., Shuichi, M., Yoshihiro, T., Etsuko, K., Chihiro, I., Satoru, I., Shohab, Y., Tomonobu, K. (2008): Novel cysteine-rich peptides from *Digitaria ciliaris* and *Oryza sativa* enhance tolerance to cadmium by limiting its cellular accumulation. – *Plant Cell and Physiology* 50: 106-117.
- [43] Lee, S., Kim, Y.-Y., Lee, Y., An, G. (2007): Rice PIB-type heavy-metal ATPase, OsHMA9, is a metal efflux protein. – *Plant Physiology* 145: 831-842.
- [44] Lee, S., An, G. (2009): Over-expression of OsIRT1 leads to increased iron and zinc accumulations in rice. – *Plant, Cell & Environment* 32: 408-416.
- [45] Li, B., Wang, X., Qi, X., Huang, L., Ye, Z. (2012a): Identification of rice cultivars with low brown rice mixed cadmium and lead contents and their interactions with the micronutrients iron, zinc, nickel and manganese. – *Journal of Environmental Sciences* 24: 1790-1798.
- [46] Li, S., Yu, J., Zhu, M., Zhao, F., Luan, S. (2012b): Cadmium impairs ion homeostasis by altering K⁺ and Ca²⁺ channel activities in rice root hair cells. – *Plant, Cell & Environment* 35: 1998-2013.
- [47] Li, Z., Wu, L. H., Zhang, H., Luo, Y. M., Christie, P. (2015): Effects of soil drying and wetting-drying cycles on the availability of heavy metals and their relationship to dissolved organic matter. – *Journal of Soil Sediment* 15: 1510-1519.
- [48] Li, H., Luo, N., Li, Y. W., Cai, Q. Y., Li, H. Y., Mo, C. H., Wong, M. H. (2017): Cadmium in rice: transport mechanisms, influencing factors, and minimizing measures. – *Environmental Pollution* 224: 622-630.
- [49] Liu, J., Li, K., Xu, J., Liang, J., Lu, X., Yang, J., Zhu, Q. (2003): Interaction of Cd and five mineral nutrients for uptake and accumulation in different rice cultivars and genotypes. – *Field Crops Research* 83: 271-281.

- [50] Liu, L., Sun, H., Chen, J., Zhang, Y., Li, D., Li, C. (2014): Effects of cadmium (Cd) on seedling growth traits and photosynthesis parameters in cotton (*Gossypium hirsutum* L.). – *Plant Omics* 7(4): 284-290.
- [51] Liu, F., Liu, X., Ding, C., Wu, L. (2015): The dynamic simulation of rice growth parameters under cadmium stress with the assimilation of multi-period spectral indices and crop model. – *Field Crops Research* 183: 225-234
- [52] Liu, Y., Liu, K., Li, Y., Yang, W. Q., Wu, F. Z., Zhu, P., Zhang, J., Chen, L. H., Gao, S., Zhang, L. (2016): Cadmium contamination of soil and crops is affected by intercropping and rotation systems in the lower reaches of the Minjiang River in south-western China. – *Environmental Geochemistry and Health* 38: 811-820.
- [53] Liu, C., Chen, G., Li, Y., Peng, Y., Zhang, A., Hong, K., Jiang, H., Ruan, B., Zhang, B., Yang, S., Gao, Z., Qian, Q. (2017): Characterization of a major QTL for manganese accumulation in rice grain. – *Scientific Reports* 7: 17704.
- [54] Liu, W., Pan, X., Li, Y., Duan, Y., Min, J., Liu, S., Liu, L., Sheng, X., Li, X. (2019a): Identification of QTLs and Validation of qCd-2 Associated with Grain Cadmium Concentrations in Rice. – *Rice Science* 26: 42-49.
- [55] Liu, X., Chen, S., Chen, M., Zheng, G., Peng, Y., Shi, X., Qin, P., Xu, X., Teng, S. (2019b): Association study reveals genetic loci responsible for arsenic, cadmium and lead accumulation in rice grain in contaminated farmlands. – *Frontiers in Plant Science* 10: 61.
- [56] Luo, J.-S., Huang, J., Zeng, D.-L., Peng, J.-S., Zhang, G.-B., Ma, H.-L., Guan, Y., Yi, H.-Y., Fu, Y.-L., Han, B. (2018): A defensin-like protein drives cadmium efflux and allocation in rice. – *Nature Communications* 9: 1-9.
- [57] Mahmood, Q., Hassan, M., Zhu, Z., Ahmad, B. (2006): Influence of cadmium toxicity on rice genotypes as affected by zinc, sulfur and nitrogen fertilizers. – *Caspian Journal of Environmental Sciences* 4: 1-8.
- [58] Muehe, E. M., Weigold, P., Adaktylou, I. J., Planer-Friedrich, B., Kraemer, U., Kappler, A., Behrens, S. (2015): Rhizosphere microbial community composition affects cadmium and zinc uptake by the metal-hyperaccumulating plant *Arabidopsis halleri*. – *Applied Environmental Microbiology* 81: 2173-2181.
- [59] Murakami, M., Nakagawa, F., Ae, N., Ito, M., Arao, T. (2009): Phytoextraction by rice capable of accumulating Cd at high levels: reduction of Cd content of rice grain. – *Environmental Science and Technology* 43: 5878-5883.
- [60] Nakanishi, H., Ogawa, I., Ishimaru, Y., Mori, S., Nishizawa, N. K. (2006): Iron deficiency enhances cadmium uptake and translocation mediated by the Fe²⁺ transporters OsIRT1 and OsIRT2 in rice. – *Soil Science & Plant Nutrition* 52: 464-469.
- [61] Nawrot, T., Plusquin, M., Hogervorst, J., Roels, H. A., Celis, H., Thijs, L., Vangronsveld, J., Van Hecke, E., Staessen, J. A. (2006): Environmental exposure to cadmium and risk of cancer: A prospective populationbased study. – *Lancet Oncol* 7: 119-126.
- [62] Nocito, F. F., Lancilli, C., Dendena, B., Lucchini, G., Sacchi, G. A. (2011): Cadmium retention in rice roots is influenced by cadmium availability, chelation and translocation. – *Plant, Cell & Environment* 34: 994-1008.
- [63] Oda, K., Otani, M., Uruguchi, S., Akihiro, T., Fujiwara, T. (2011): Rice ABCG43 is Cd inducible and confers Cd tolerance on yeast. – *Bioscience, Biotechnology, and Biochemistry* 75: 1211-1213.
- [64] Pandey, S., Gupta, K., Mukherjee, A. (2007): Impact of cadmium and lead on *Catharanthus roseus*-A phytoremediation study. – *Journal of Environmental Biology* 28: 655-662.
- [65] Qiu, Q., Wang, Y., Yang, Z., Yuan, J. (2011): Effects of phosphorus supplied in soil on subcellular distribution and chemical forms of cadmium in two Chinese flowering cabbage (*Brassica parachinensis* L.) cultivars differing in cadmium accumulation. – *Food and Chemical Toxicology* 49: 2260-2267.
- [66] Ramesh, S. A., Shin, R., Eide, D. J., Schachtman, D. P. (2003): Differential metal selectivity and gene expression of two zinc transporters from rice. – *Plant Physiology* 133: 126-134.

- [67] Revathi, S., Venugopal, S. (2013): Physiological and biochemical mechanisms of heavy metal tolerance. – *International Journal of Environmental Sciences* 3(5): 1339-1354.
- [68] Rinklebe, J., Shaheen, S. M., Frohne, T. (2016): Amendment of biochar reduces the release of toxic elements under dynamic redox conditions in a contaminated floodplain soil. – *Chemosphere* 142: 41-47.
- [69] Sasaki, A., Yamaji, N., Yokosho, K., Ma, J. F. (2012): Nramp5 is a major transporter responsible for manganese and cadmium uptake in rice. – *The Plant Cell* 24: 2155-2167.
- [70] Sasaki, A., Yamaji, N., Ma, J. F. (2014): Overexpression of OsHMA3 enhances Cd tolerance and expression of Zn transporter genes in rice. – *Journal of Experimental Botany* 65: 6013-6021.
- [71] Sato, H., Shirasawa, S., Maeda, H., Nakagomi, K., Kaji, R., Ohta, H., Yamaguchi, M., Nishio, T. (2011): Analysis of QTL for lowering cadmium concentration in rice grains from 'LAC23'. – *Breeding Science* 61: 196-200.
- [72] Shaheen, S. M., Rinklebe, J. (2016): Impact of different soil amendments on the mobilization and phytoavailability of toxic metals in a contaminated flood plain soil. – *International Conference on Heavy Metals in the Environment* pp 1-2.
- [73] Shimo, H., Ishimaru, Y., An, G., Yamakawa, T., Nakanishi, H., Nishizawa, N. K. (2011): Low cadmium (LCD), a novel gene related to cadmium tolerance and accumulation in rice. – *Journal of Experimental Botany* 62: 5727-5734.
- [74] Song, W. E., Chen, S. B., Liu, J. F., Li, C., Song, N. N., Ning, L., Bin, L. (2015): Variation of Cd concentration in various rice cultivars and derivation of cadmium toxicity thresholds for paddy soil by species-sensitivity distribution. – *Journal of Integrative Agriculture* 14: 1845-1854.
- [75] Song, Y., Wang, Y., Mao, W., Sui, H., Yong, L., Yang, D., Jiang, D., Zhang, L., Gong, Y. (2017): Dietary cadmium exposure assessment among the Chinese population. – *PLoS One* 12(5): e0177978.
- [76] Spungen, J. (2019): Children's exposures to lead and cadmium: FDA total diet study 2014–16. – *Food Additives and Contaminants, Part A* 36(6): 893-903.
- [77] Supek, F., Supekova, L., Nelson, H., Nelson, N. (1996): A yeast manganese transporter related to the macrophage protein involved in conferring resistance to mycobacteria. – *Proceedings of the National Academy of Sciences* 93: 5105-5110.
- [78] Takahashi, R., Ishimaru, Y., Senoura, T., Shimo, H., Ishikawa, S., Arao, T., Nakanishi, H., Nishizawa, N. K. (2011): The OsNRAMP1 iron transporter is involved in Cd accumulation in rice. – *Journal of Experimental Botany* 62: 4843-4850.
- [79] Takahashi, R., Ishimaru, Y., Shimo, H., Ogo, Y., Senoura, T., Nishizawa, N. K., Nakanishi, H. (2012): The OsHMA2 transporter is involved in root-to-shoot translocation of Zn and Cd in rice. – *Plant, Cell & Environment* 35: 1948-1957.
- [80] Tan, L., Zhu, Y., Fan, T., Peng, C., Wang, J., Sun, L., Chen, C. (2019): OsZIP7 functions in xylem loading in roots and inter-vascular transfer in nodes to deliver Zn/Cd to grain in rice. – *Biochemical and Biophysical Research Communications* 512: 112-118.
- [81] Tang, L., Mao, B., Li, Y., Lv, Q., Zhang, L., Chen, C., He, H., Wang, W., Zeng, X., Shao, Y. (2017): Knockout of OsNramp5 using the CRISPR/Cas9 system produces low Cd-accumulating indica rice without compromising yield. – *Scientific Reports* 7: 1-12.
- [82] Ueno, D., Emi, K., Izumi, K., Tsuyu, A., Masahiro, Y., Feng, M. J. (2009): Identification of a novel major quantitative trait locus controlling distribution of Cd between roots and shoots in rice. – *Plant and Cell Physiology* 50: 2223-2233.
- [83] Ueno, D., Koyama, E., Yamaji, N., Ma, J. F. (2010a): Physiological, genetic, and molecular characterization of a high-Cd-accumulating rice cultivar, Jarjan. – *Journal of Experimental Botany* 62: 2265-2272.
- [84] Ueno, D., Yamaji, N., Kono, I., Huang, C. F., Ando, T., Yano, M., Ma, J. F. (2010b): Gene limiting cadmium accumulation in rice. – *Proceedings of the National Academy of Sciences* 107: 16500-16505.

- [85] Uraguchi, S., Kamiya, T., Sakamoto, T., Kasai, K., Sato, Y., Nagamura, Y., Yoshida, A., Kyojuka, J., Ishikawa, S., Fujiwara, T. (2011): Low-affinity cation transporter (OsLCT1) regulates cadmium transport into rice grains. – *Proceedings of the National Academy of Sciences* 108: 20959-20964.
- [86] Uraguchi, S., Fujiwara, T. (2012): Cadmium transport and tolerance in rice: perspectives for reducing grain cadmium accumulation. – *Rice* 5(1): 5.
- [87] Verbruggen, N., Hermans, C., Schat, H. (2009): Molecular mechanisms of metal hyperaccumulation in plants. – *New Phytologist* 181: 759-776.
- [88] Wang, B., Zhu, C., Liu, X., Wang, W., Ding, H., Jiang, M., Li, G., Liu, W., Yao, F. (2011): Fine mapping of qHD4-1, a QTL controlling the heading date, to a 20.7-kb DNA fragment in rice (*Oryza sativa* L.). – *Plant Molecular Biology Reporter* 29: 702-713.
- [89] Wang, J., Fang, Y., Tian, B., Zhang, X., Zeng, D., Guo, L., Hu, J., Xue, D. (2018): New QTLs identified for leaf correlative traits in rice seedlings under cadmium stress. – *Plant Growth Regulation* 85: 329-335
- [90] World Health Organisation (WHO). (1992): Environmental Health Criteria 134 - Cadmium International Programme on Chemical Safety (IPCS) Monograph. – World Health Organization: Geneva, Switzerland.
- [91] Xia, J., Naoki, Y., Tomonari, K., Feng, M. J. (2010): Plasma membrane-localized transporter for aluminum in rice. – *Proceedings of the National Academy of Sciences* 107: 18381-18385.
- [92] Xie, P. P., Deng, J. W., Zhang, H. M., Ma, Y. H., Cao, D. J., Ma, R. X., Liu, R. J., Liu, C., Liang, Y. G. (2015): Effects of cadmium on bioaccumulation and biochemical stress response in rice (*Oryza sativa* L.). – *Ecotoxicology and Environmental Safety* 122: 392-398.
- [93] Xue, D., Chen, M., Zhang, G. (2009): Mapping of QTLs associated with cadmium tolerance and accumulation during seedling stage in rice (*Oryza sativa* L.). – *Euphytica* 165: 587-596.
- [94] Xue, D. W., Jiang, H., Deng, X. X., Zhang, X. Q., Wang, H., Xu, X. B., Hu, J., Zeng, D., Guo, L., Qian, Q. (2014): Comparative proteomic analysis provides new insights into cadmium accumulation in rice grain under cadmium stress. – *Journal of Hazardous Material* 280: 269-278.
- [95] Yamaji, N., Xia, J., Mitani-Ueno, N., Yokosho, K., Ma, J. F. (2013): Preferential delivery of zinc to developing tissues in rice is mediated by P-type heavy metal ATPase OsHMA2. – *Plant Physiology* 162: 927-939.
- [96] Yan, Y. F., Lestari, P., Lee, K. J., Kim, M. Y., Lee, S. H., Lee, B. W. (2013): Identification of quantitative trait loci for cadmium accumulation and distribution in rice (*Oryza sativa* L.). – *Genome* 56: 227-232.
- [97] Yan, Y., Zhou, Y. Q., Liang, C. H. (2015): Evaluation of phosphate fertilizers for the immobilization of Cd in contaminated soils. – *PLOS One* 10: e0124022.
- [98] Yan, H., Xu, W., Xie, J., Gao, Y., Wu, L., Sun, L., Feng, L., Chen, X., Zhang, T., Dai, C. (2019): Variation of a major facilitator superfamily gene contributes to differential cadmium accumulation between rice subspecies. – *Nature communications* 10: 2562.
- [99] Yang, J., Gao, M. X., Hu, H., Ding, X. M., Lin, H. W., Wang, L., Xu, J. M., Mao, C. Z., Zhao, F. J., Wu, Z. C. (2016a): OsCLT1, a CRT-like transporter 1, is required for glutathione homeostasis and arsenic tolerance in rice. – *New Phytologist* 211: 658-670.
- [100] Yang, Y., Xiong, J., Chen, R., Fu, G., Chen, T., Tao, L. (2016b): Excessive nitrate enhances cadmium (Cd) uptake by up-regulating the expression of OsIRT1 in rice (*Oryza sativa*). – *Environmental and Experimental Botany* 122: 141-149.
- [101] Yu, H., Wang, J., Fang, W., Yuan, J., Yang, Z. (2006): Cadmium accumulation in diverse rice cultivars and screening for pollution-safe cultivars of rice. – *Science of the Total Environment* 370: 302-309.
- [102] Yu, C., Sun, C., Shen, C., Wang, S., Liu, F., Liu, Y., Chen, Y., Li, C., Qian, Q., Aryal, B. (2015): The auxin transporter, Os AUX 1, is involved in primary root and root hair

- elongation and in Cd stress responses in rice (*Oryza sativa* L.). – *The Plant Journal* 83: 818-830.
- [103] Yuan, L., Yang, S., Liu, B., Zhang, M., Wu, K. (2012): Molecular characterization of a rice metal tolerance protein, OsMTP1. – *Plant Cell reports* 31: 67-79.
- [104] Zhang, X., Wu, H., Chen, L., Liu, L., Wan, X. (2018): Maintenance of mesophyll potassium and regulation of plasma membrane H⁺-ATPase are associated with physiological responses of tea plants to drought and subsequent rehydration. – *The Crop Journal* 6: 611-620.
- [105] Zhao, F. Y., Hu, F., Zhang, S. Y., Wang, K., Zhang, C. R., Liu, T. (2013): MAPKs regulate root growth by influencing auxin signaling and cell cycle-related gene expression in cadmium-stressed rice. – *Environmental Science and Pollution Research* 20: 5449-5460.
- [106] Zu, Y., Li, Y., Chen, J., Chen, H. Y., Li, Q., Schratz, C. (2005): Hyper accumulation of Pb, Zn and Cd in herbaceous grown on lead-zinc mining area in Yunnan, China. – *Environmental International* 31(5): 755-762.

SOIL PROPERTIES, LEAF NUTRIENTS AND FRUIT QUALITY RESPONSE TO SUBSTITUTING CHEMICAL FERTILIZER WITH ORGANIC MANURE IN A MANGO ORCHARD

FENG, H. D.^{1†} – CHEN, H. Y.^{2†} – DANG, ZH. G.¹ – NI, B.³ – HE, C. C.¹ – WEI, ZH. Y.¹ – CHEN, Y. Y.^{1*}

¹*Tropical Crops Genetic Resources Institute, CATAS, Haikou, Hainan 570211, China*

²*Rubber Research Institute, CATAS, Haikou 571101, China*

³*Modern Agricultural Inspection Testing Control Center of Hainan Province, Haikou 571101, China*

**Corresponding author*

e-mail: chenyy1962@126.com; phone: +86-138-0758-2106

[†]*These authors contributed equally to this study.*

(Received 22nd Dec 2019; accepted 23rd Mar 2020)

Abstract. It is highly significant to reduce the amount of chemical fertilizer application in mango orchards and substituting it with organic manure. The field location method was applied to examine the effects of substituting chemical fertilizer with organic manure on soil physical and chemical properties, leaf nutrients, fruit yield and quality in a mango orchard, it can provide a foundation for reducing chemical fertilizer application in mango orchards. Results indicated that, compared to conventional fertilization, treatments substituting chemical fertilizer with organic manure at different concentrations can reduce the volume weight of different levels of orchard soil and improve soil porosity. The decrease of volume weight and the increase of total porosity in the 0-20cm soil layer were greater than those in the 20-40cm soil layer. Substituting chemical fertilizer with organic manure can improve soil pH and organic matter content in the different soil layers. Although alkali-hydrolysable nitrogen declined compared with conventional fertilization, it did not attain a significant difference. The concentrations of available phosphorus, potassium calcium and magnesium in soils increased compared with the control. All the treatments improved mango yield, however, there was a non-significant effect on single fruit weight. Soluble solid, vitamin C and solidity-acid ratio in fruits all increased, and the titratable acid content decreased compared with the control. Comprehensive comparison indicated that a 30% substitution of organic manure is the most effective treatment to improve soil fertility and fruit quality.

Keywords: *mango, organic manure, soil physical and chemical properties, yield, fruit quality*

Introduction

Mango (*Mangifera indica* L.), also called the “King of Tropical Fruits” is widely distributed in tropical and subtropical regions from 30°S to 30°N. Mango was introduced to China from India during the Tang Dynasty, having a cultivation period longer than 1300years (Hu et al., 2015). In China, mango is mainly distributed in the provinces of Hainan, Guangxi, Yunnan, Sichuan, Guangdong, Guizhou and Fujian in the tropical and subtropical regions. In 2017, the total planting area in China was 3.868 million Mu with a yield of 2.053 million tons, making China the fourth largest producer in the world (MADOSATC, 2018).

Soil fertility provides a comprehensive reflection of the different soil properties, and it has an important effect on crop growth. Investigations using different practices and methods into improving soil fertility are important for improving crop yield and fertilizer use. The use of organic fertilizers increases soil basic fertility by applying

organic materials to the soil in order to improve the fertilization capacity of the soil (Chen, 2015). Suitable soil fertilization is not the only key to improving soil quality, and it is also a core problem for guaranteeing the sustainable utilization of agricultural resources (Liu et al., 2006). Current research indicates that the most effective fertilization method for arable soil is by adding organic materials, namely soil organic fertilizers (Wang, 2014). Li et al. (2014) showed that the long-term application of organic manure could significantly improve the organic matter content in a soil, especially active organic matter. Results by Zeng et al. (2008) indicated that long-term application of organic manure could significantly improve the organic carbon content in the 0-30cm soil layer. Moharana et al. (2012) considered that the application of organic manure was conducive to the sustainable development of agricultural production and soil quality improvement. Previously scientists indicated that the yields of tomato and potato can increase significantly after the application of organic manure (Valšíková-Frey et al., 2018; Sukri, 2018; Tamad, 2019). Findings by Zang et al. (2015) indicated that soil available nutrients and mango fruit quality were higher when chemical fertilizers were substituted with organic manure, while the suitable substitutional proportions for chemical fertilizer with organic manure still unclear.

Recently, with an improvement in mango cultivation techniques, the economic benefits of mango cultivation have significantly improved. With a change of mango cropping patterns, ahead florescence and shortened growth period, the requirements of soil nutrients have correspondingly increased. Current practices suggest mango is planted in loam and sandy loam soil, with a pH value around 6.5. It is also recommended that plants have good ventilation and medium soil fertility (Xu et al., 2012). However, the main mango production area in Hainan Island is located on hillsides on low mountains, having a relatively barren soil with low organic matter, available nitrogen, available phosphorus, calcium and magnesium contents were deficit (Liao et al., 2008). The application of organic manure has non-substitutable effects on improving soil structure, fertilization and nutrients (Fu et al., 2013). Findings by Han et al. (2004) showed that the application of organic manure in successive years could effectively improve soil physical properties, reduce soil volume weight, increase the effective porosity in fields and increase the water storage and retention capacity of the soil, resulting in well-developed aggregates. The practice of substituting chemical fertilizer with organic manure have mainly focused on fruit trees including tangerine, pear and apple; few studies have studies effects on mango trees (Fu et al., 2013; Moharana et al., 2012; Wang, 2014). The purpose of this study is to analyze the effects of different substitution levels of chemical fertilizer with organic manure on soil quality, fruit yield and quality in a mango orchard. The results can provide a foundation for improving soil quality, fertilization, fruit yield and quality in a mango orchard.

Materials and Methods

Site location and characteristics

The experimental field was located at Fruit Island Base in Tianya District, Sanya, Hainan province. The site was located on a hilly slope having a typical tropical insular monsoon climate with an annual average temperature of 22°C-27°C and annual precipitation of 1500-2000 mm. The site has favorable light and heat conditions, and the parent soil was mainly granite weathered products. Guifei mango, which was introduced

into Hainan Province in 1997 from Taiwan and is currently one of the main cultivars in tropical area of China, was the mango variety examined in this study which has been field planting for 12 years. Basic soil physical and chemical properties in the experimental field are shown in *Table 1*.

Table 1. Basic physical and chemical soil properties

Layer cm	pH	OM g/kg	Available N mg/kg	Available P mg/kg	Available k mg/kg	Available Ca mg/kg	Available Mg mg/kg
0-20	5.69	11.2	120.3	23.61	70.54	154.22	64.50
20-40	5.47	9.9	103.5	23.17	58.40	143.16	55.42

Experiment design

The experiment was initiated in June, 2017, after the fruit harvest season, which was April to May, and completed in June, 2018. A gradient design of different substitutional proportions for chemical fertilizer with organic manure was applied, and plants with consistent growth were selected as the test objects. Four treatments were established: (1) Conventional fertilization (CK); (2) 10% nitrogen reduction of chemical fertilizer with organic fertilizer fermented by sheep manure (organic fertilizer fermented by sheep manure with the nutrient contents in dry basis of 2.23% nitrogen, 1.78% P₂O₅ and 3.91% K₂O); (3) 30% nitrogen reduction of chemical fertilizer; (4) 50% nitrogen reduction of chemical fertilizer (*Table 2*). Nine trees were selected in each treatment, with three replicas. According to the results of He et al. (2013) and Zeng et al. (2003), 0.6kg N, P₂O₅ 0.3kg P₂O₅ and 0.6 kg K₂O were applied to each mango tree every year, and all fertilizers were applied at the same time.

Table 2. The experiment design of this study

Treat	N kg		P ₂ O ₅ kg		K ₂ O kg	
	Organic	Chemical	Organic	Chemical	Organic	Chemical
CK	0	0.60	0	0.30	0	0.60
T1	0.06	0.54	0.05	0.25	0.11	0.49
T2	0.18	0.42	0.14	0.16	0.32	0.28
T3	0.30	0.30	0.24	0.06	0.53	0.07

Treat	Organic manure kg	Urea kg	Calcium magnesium phosphate kg	Potassium chloride kg
CK	0	1.3	1.7	1.0
T1	2.7	1.2	1.4	0.8
T2	8.0	0.9	0.9	0.5
T3	13.5	0.7	0.3	0.1

Sample collection and analysis

Soil and mango leaf samples were collected in May, 2018. Mango leaf samples were collected from fruit bearing shoots at the top and middle of the crown. Samples east,

south, west and north of each tree were also collected and mixed. All samples were blanched at 105°C for 30 min, dried at 75°C for 120 hours, ground using a plant mill and passed through a 0.149 mm nylon sieve. The total nitrogen was determined by H₂SO₄-H₂O₂-indophenol blue colorimetry, total phosphorus was determined by vanadium molybdenum yellow colorimetry, and total potassium was determined by flame photometry (Gao, 2006). The concentrations of calcium and magnesium were determined by dry ashing-dilute hydrochloric acid dissolution method (Gao, 2006).

Soil samples were collected on the drip line of mango tree, and different layers (0-20 cm and 20-40 cm) soil sampled separately in sample points. Four sample points for one mango tree, and soil samples from three trees were combined to make a composite sample. The samples were air dried, passed through a 2 mm sieve and stored in sealed plastic sealing bags. Before the arrangement of the experiments, mixed soil samples from the experimental field were collected and a mixed sample of the soil plough layers for each treatment was collected separately after the fruit harvest. The soil pH was measured using glass electrode, at 1:5 (W/V) ratio of soil: water (Lu, 2000). After oxidized by K₂Cr₂O₇, the content of organic matter in soil was measured by the titration method (Lu, 2000). Alkali-hydrolysable nitrogen concentrations in soil was measured by diffusion method (Lu, 2000). Available phosphorus in soil was determined by hydrochloric acid-ammonium fluoride method (Lu, 2000). Available potassium concentration in soil was measured by ammonium acetate extraction method, and the contents of available calcium and magnesium in soil were determined by ammonium acetate exchange-EDTA complexometric titration method (Lu, 2000).

Mango yield and fruit quality was determined by field observations. Twelve uniform fruits with 80% maturity from four directions from mango tree were collected for quality determination. Plot yield was determined according to the yields of each mango plants. The soluble solid was determined using MASTER-53T electronic refractometer, vitamin C was determined using the 2, 6-dichloroindophenol titration method, and titrable acid was determined using standard acid-base titration (Gao, 2006).

Data analysis

Descriptive statistics analysis and least significant difference analysis were undertaken using SAS9.0 software.

Results

The effects of different concentrations of organic manure on soil physical properties

Soil volume weight and porosity under the different treatments (*Table 3*) recorded a decreasing trend. Treatments T2 and T3 in the 0-20 cm soil layer decreased by 2.1% and 2.9% compared with the control, respectively, recording a significant difference with the control and T1. Volume weights in treatments T2 and T3 in the 20-40 cm soil layer decreased by 1.4% and 2.1% compared to the control, respectively, having a significant difference with the control and T1. Although a decrease in total porosity at the different soil layers was noticeable, these results were not significant. As soil depth increased, total porosity decreased; total porosity at the 20-40 cm soil layer was smaller than it at the 0-20 cm surface soil layer, indicating that the root aeration status at the 20-40 cm soil layer was weaker than that at the surface soil layer.

Table 3. The effects of different concentrations of organic manure on soil physical properties^{†‡}

Treatment	Soil layer cm	Volume weight g/cm ³	Total porosity %
CK	0-20	1.38±0.01a	46.74±0.15a
	20-40	1.46±0.01a	45.31±0.20a
T1	0-20	1.37±0.01a	45.08±0.22a
	20-40	1.45±0.01a	45.12±0.22a
T2	0-20	1.35±0.01b	44.94±0.19a
	20-40	1.44±0.01b	45.02±0.30a
T3	0-20	1.34±0.01c	44.90±0.34a
	20-40	1.43±0.00c	45.01±0.19a

[†]mean ± standard deviation

[‡]a, b and c represent significant differences between treatments (P<0.05)

The effects of different concentrations of organic manure on soil chemical properties

pH and organic matter content in the treatments recorded an increase as the proportion of organic manure increased; T2 and T3 in the 0-20 cm soil layer recorded significant differences compared to the control and T1. Compared with conventional methods, organic matter content in T2 and T3 increased by 27.6 % and 33.6 % in the 0-20 cm soil layer and by 28.9 % and 32.3 % in the 20-40 cm soil layer, respectively (Table 4). Compared with the control, alkali-hydrolysable nitrogen in the different soil layers decreased as the concentration of organic manure increased, results however did not record a significant difference. The contents of available phosphorus, available potassium, available calcium and magnesium increased compared with the control, and significant differences were recorded for available potassium and available magnesium in treatments T2 and T3 in the 0-20 cm soil layer compared with conventional fertilization and T1. No significant differences were recorded between T3 and T2. A comprehensive comparison between the concentration of organic manure indicated that T2 had a better effect on soil fertility than T3.

Table 4. The effects of different concentrations of organic manure on soil chemical properties^{†‡}

Treatments	Soil layer cm	pH	OM g/kg	Available N mg/kg	Available P mg/kg	Available K mg/kg	Available Ca mg/kg	Available Mg mg/kg
CK	0-20	5.68±0.04a	9.30±1.99a	70.66±2.15a	20.61±0.44a	217.45±0.47a	433.24±1.13a	48.43±0.49a
	20-40	5.51±0.02a	8.10±1.34a	66.43±1.72a	21.82±0.76a	235.41±1.02a	441.63±1.27a	44.05±0.41a
T1	0-20	5.71±0.02a	9.50±2.43a	65.43±1.95a	21.47±0.42a	225.20±1.48a	439.35±3.58a	46.25±0.33a
	20-40	5.66±0.03a	8.86±1.79a	62.45±1.43a	17.46±0.45a	223.19±1.26a	410.47±2.54a	43.11±0.47a
T2	0-20	5.74±0.10b	11.87±2.54b	62.1±0.68a	28.50±0.35b	241.2±2.24b	443.8±4.61a	57.54±0.57b
	20-40	5.69±0.11a	10.44±1.93b	59.43±0.77a	18.73±0.41a	198.48±0.52a	401.76±2.49a	54.81±1.12a
T3	0-20	6.12±0.02c	12.43±2.91c	59.47±2.44a	28.76±0.64b	293.31±2.15b	446.29±3.44a	59.48±1.07b
	20-40	5.84±0.06b	10.72±1.18b	59.26±2.01a	19.64±0.55a	195.72±1.99a	386.28±3.02a	55.79±0.88a

[†]mean ± standard deviation

[‡]a, b and c represent significant differences between treatments (P<0.05)

The effects of different concentrations of organic manure on leaf mineral nutrients

Mineral element content results in mango leaves under different treatments (*Table 5*) recorded a reduction of total nitrogen content and an increase of total phosphorus, total potassium, calcium and magnesium compared to the control. However, results did not record a significant difference, indicating that there were non-significant effects of the substitution of chemical fertilizer with organic manure on the absorption of nutrients in mango leaves.

Table 5. *The concentrations of mineral nutrients in mango leaves^{†‡}*

Treatments	Total N %	Total P %	Total K %	Ca %	Mg %
CK	1.78±0.04a	0.12±0.10a	0.46±0.02a	1.74±0.03a	0.21±0.04a
T1	1.79±0.02a	0.12±0.01a	0.47±0.02a	1.75±0.13a	0.21±0.11a
T2	1.78±0.07a	0.12±0.11a	0.47±0.02a	1.78±0.09a	0.21±0.09a
T3	1.77±0.01a	0.12±0.02a	0.47±0.01a	1.76±0.07a	0.22±0.05a

[†]mean ± standard deviation

[‡]a, b and c represent significant differences between treatments (P<0.05)

The effects of different concentrations of organic manure on fruit yield and quality

Compared with conventional fertilization, there were non-significant effects for treatments with different concentrations of organic manure on crop yield (*Table 6*) or single fruit weight. However, soluble solid, Vc and solidity-acid ratio in fruits all increased, with the proportions in T2 increasing by 23.7%, 6.4% and 16.34% compared to the control, respectively. Although the soluble solid content in treatment T1 did not reach a significant difference compared to the control, it did record a significant difference compared with T2 and T3. The titratable acid contents in fruits under different treatments decreased compared to the control, recording a significant difference. Non-significant differences between vitamin C and titratable acid in T2 and T3 were also recorded.

Table 6. *The results of mango fruit yield and quality^{†‡}*

Treatment	Yield kg/plant	Single fruit weight kg	Soluble solid %	vitamin C mg/100g	Titratable acids %	Solidity-acid ratio %
CK	45.7±0.4a	0.22±0.21a	10.04±0.24a	2.03±0.17a	0.253±0.022c	35.73±0.94a
T1	45.2±0.5a	0.25±0.09a	11.18±0.22a	1.75±0.26a	0.247±0.014b	37.17±0.85a
T2	45.9±0.7a	0.24±0.16a	12.42±0.08b	2.16±0.09a	0.241±0.016a	41.57±1.02b
T3	46.3±0.6a	0.23±0.20a	12.81±0.21c	2.17±0.12a	0.240±0.031a	42.37±1.34c

[†]mean ± standard deviation

[‡]a, b and c represent significant differences between treatments (P<0.05)

Discussion

The effects on soil physical properties

In mango orchard, the application of organic manure could effectively improve the soil environment, reduce soil volume weight, and increase total porosity. And this is consistent with the results of Ge (2018). Ma et al. (2010) also indicated that the application of organic manure, as well as the combined application of chemical fertilizer and organic manure, could effectively improve soil physical properties, decrease soil volume weight, and increase total porosity and effective porosity.

Effects on soil fertility improvement

Soil pH and contents of organic matters in mango orchard increased under treatments T2 and T3 in the 0-20cm and 20-40cm soil layers. Organic matter attained a significant level, similar to the results of Zang et al. (2015). By substituting chemical fertilizer with organic manure, soil pH increased, however non-significant differences were recorded between each treatment. Soil mineral nutrition was the direct nutrient resource for fruit tree growth and fruit development (Chen et al., 2018). In our study, alkali-hydrolysable nitrogen decreased, and available phosphorus, available potassium, available calcium and magnesium increased to a certain extent compared to the control. Our findings indicated that T2 recorded the best enhancement effects on soil nutrients. In each treatment, the contents of available calcium and magnesium increased to a certain extent, a finding that may be related to an increase in cation content in the soil due to a certain amount of ash elements, including calcium and magnesium, contained in the organic manure (Zhu et al., 2012). Under the hot and humid soil conditions in southern China, soil acidification in orchards is the result of long-term and large-scale application of chemical fertilizers, as well as lack of organic manure in the orchard soil. The addition of organic manure can improve the soil quality by not only increasing soil pH, but also by improving soil fertility, thus improving fruit quality and guaranteeing the sustainable production and development of fruit trees (Zhao, 2013). Therefore, the combined application of chemical fertilizer with organic manure is not only conducive to the improvement and fertility of the soil, it also increases the capacity for supplying and preserving fertilizers in the orchard soil (Zang et al., 2016).

Effects on fruit yield and quality

Due to the effects of field condition and the growth cycle of mango trees, all of the treatments improved fruit yield to a certain extent, however they did not attain significant differences. After the application of organic manure, there were certain effects on the contents of soluble solid, vitamin C and titrable acid in the fruits. Soluble solid, vitamin C and solidity-acid ratio all recorded an increasing trend; when the substitution proportion of chemical fertilizer with organic manure was 30%, soluble solid, vitamin C and the solidity-acid ratio increased by 23.7%, 6.4% and 16.34% compared to the control, respectively. Titrable acid slightly decreased, this being similar to previous findings (Lai et al., 2011; Wan et al., 2012; Zhang et al., 2018).

Conclusions

In mango orchard, substituting chemical fertilizer with organic manure can decrease soil volume weight, improve total porosity, and significantly increased the soil pH and organic matter content. Available nutrients concentrations in soil increased compared to the control. Substituting chemical fertilizer with organic manure improved mango yields and increased soluble solids, vitamin C content and the solidity-acid ratio. Comprehensive comparison indicated that a 30% substitution of organic manure is an economic and effective treatment to improve soil fertility and fruit quality.

Acknowledgments. This research was supported by The National Key Research and Development Program of China (2017YFD0202100), Key Research and Development Program of Hainan Province Hainan Province (ZDYF2018065), Major Science and Technology Program of Hainan Province (ZDKJ2017003) and the Central Public-interest Scientific Institution Basal Research Fund for Chinese Academy of Tropical Agricultural Sciences (1630032017042).

REFERENCES

- [1] Chen, C. (2015): Effects of different manures and their mixed application on soil microbiological properties and corn yield. – Jilin Agriculture University.
- [2] Chen, R. Z., Li, J., Fan, J. H., Lin, D. (2018): Effects of different fertilizer ratio on soil nutrient, microbial quantity. – Chinese Journal of Tropical Crops 39: 1055-1060.
- [3] Fu, C. Y., Zhang, X. F., Wang, Y. J., Wang, S. X., Cui, S. M. (2013): Effects of organic fertilizer and sulfur application on the growth of *Nanfeng* tangerine and chemical properties of calcareous soil under greenhouse. – Soil and Fertilizer Sciences in China 2: 17-21.
- [4] Gao, J. F. (2006): Guidance of plant physiology experiments. – Higher Education Press, Beijing 74-77.
- [5] Ge, X. W. (2018): Effects of different organic fertilizers on soil quality and wine grape quality in orchard. – Ningxia University.
- [6] Han, B. J., Chen, Y., Qiao, Y. F., Han, X. Z., Meng, K. (2004): Effect of long-term application organic fertilizer on soil physiochemical properties. System. – Sciences and Comprehensive Studies in Agriculture 20: 294-296.
- [7] He, L. J. (2013): The impact of different fertilization levels and methods on yield of mango in northern mountain area of Tianyang County. – Journal of Guangxi Agriculture 28:21-23.
- [8] Hu, Y., Zhang, D. S., Liu, K. D. (2015): Developing history and influence factors of the mango industry in China. – Chinese Journal of Agricultural Resources and Regional Planning 36: 53-59.
- [9] Lai, Y., Tong, Y. A., Chen, L. L., Gao, Y. M., Yang, J. F. (2011): Effect of fertilization on Kiwifruit yield and quality. – Journal of Northwest A & F University(Natural Science Edition) 39: 171-176.
- [10] Li, J., Yang, X. Y., Sun, B. H., Zhang, S. L. (2014): Effects of soil management practices on stability and distribution of aggregates in Lou soil. – Journal of Plant Nutrition and Fertilizer 20: 346-354.
- [11] Liao, X. J., Tang, S. M., Wu, D., Feng, Y. S., Xia, C. J. (2008): Effect of the soil environment of mango plantation on mango quality in Hainan province. – Ecology and Environment 17: 727-733.
- [12] Liu, Z. F., Fu, B. J., Liu, G. H., Zhu, Y.G. (2006): Soil quality: concept, indicators and its assessment. – Acta EcologicaSinica 26: 901-913.

- [13] Lu, R. K. (2000): Soil Agricultural Chemistry Analysis. – China Agriculture Science & Technology Press.
- [14] Ma, J. Y., Cao, C. Y., Zheng, C. L., Li, K. J., Ren, T. S. (2010): Effect of Long-term application of chemical fertilizers and organic manure on soil organic carbon and bulk density. – Soil and Fertilizer Sciences in China 6: 38-42.
- [15] Ministry of Agriculture Development Office of South Asia Tropical Crops (MADOSATC). (2018): Crop production in tropical and subtropical regions of China. – Ministry of Agriculture Development Office of South Asia Tropical Crops, Beijing China.
- [16] Moharana, P. C., Sharma, B. M., Biswas, D. R., Dwivedi, B. S., Singh, R. V. (2012): Long-term effect of nutrient management on soil fertility and soil organic carbon pools under a 6 years old pearl millet-wheat cropping system in an inceptisol of subtropical India. – Field Crops Research 136: 32-41.
- [17] Sukri, M. Z., Sari, V. K., Firgiyanto, R. (2018): Improving soil fertilizer through application of organic fertilizer humic acid and mikoriza in supporting growth and production of chilli plants in sand land. – Earth and Environ Sciences 207: 1-6.
- [18] Tamad, Soesanto, L., Rostaman, R., Agustin, P. E., Khoiriyah, N. (2019): Enhancing potato (*Solanum tuberosum* L.) yield by using biological organic fertilizers and soil conservation practices on the slope andisol. – Earth and Environ Sciences 250:012098.
- [19] Valšíková-Frey, M., Sopková, D., Rehuš, M., Komár, P. (2018): Impact of Organic Fertilizers on Morphological and Phenological Properties and Yield of Tomatoes. – Acta Horti et Regiotechnurae 21: 48-53.
- [20] Wan, S. X., Li, F., Jiang, G. Y., Wang, W. J., Zhu, H. B. (2012): Effects of different organic fertilizer rates on soil microbe and quality and yield of cabbage. – Soil and Fertilizer Sciences in China 6: 74-76.
- [21] Wang, F. (2014): Effects of organic amendments on soil fertility and plant growth. – Northwest A & F University.
- [22] Xu, L. B., Gao, A. P., Pu, J. J., Wu, Y. L., Zhu, M., Huang, J. F. (2012): Technical guidelines for safety production of banana and mango. – China Agriculture Publishing Press, Beijing, China 11-22.
- [23] Zang, X. P., Lin, X. E., Zhou, Z. X., Tan, L., Ge, Y., Dai, M. J., Ma, W. H. (2015): Effects of different fertilization treatments on quality of mango fruit and soil fertility. – Subtropical Plant Science 44: 146-149.
- [24] Zang, X. P., Zhou, Z. X., Lin, Y. E., Dai, M. J., Ge, Y., Liu, Y. X., Ma, W. H. (2016): Effects of different organic manure application rate on mango fruit quality and soil fertility. – Soil and Fertilizer Sciences in China 1: 98-101.
- [25] Zeng, F. Z., Cao, H. L., Huang, J. Q., Wu, G. Y., Zhang, D. Q. (2003): Soil Characteristics and Fertility Regulation of Mango Orchard in Laterite Red Soil. – Agricultural Sciences Guangdong Province 25-27.
- [26] Zeng, J., Guo, T. W., Bao, X. G., Wang, Z., Sun, J. H. (2008): Effections of soil organic carbon and soil inorganic carbon under long- term fertilization. – Soil and Fertilizer Sciences in China 2: 11-14.
- [27] Zhang, M., Yao, Y. L., Tian, Y. H., Ceng, K., Zhao, M., Zhao, M., Yin, B. (2018): Increasing yield and N use efficiency with organic fertilizer in Chinese intensive rice cropping systems. – Field Crops Research 227: 102-109.
- [28] Zhao, L., Liu, C. T. (2013): Effects of different organic materials on soil fertility and aggregates stability. – Journal of Northwest A & F University(Natural Science Edition) 41: 130-136, 144.
- [29] Zhu, C. B., Wu, S. H., Zhang, X. Y., Zhou, D. P., Fan, J. Q., Jiang, Z. F. (2012): Effects of application of manure and microbial fertilizer on soil fertility and leaf nutrient. – Chinese Agricultural Science Bulletin 28: 201-205.

THE COMPREHENSIVE AND INTERACTION EFFECT OF EIGHT CULTIVATION METHODS ON WATER CONSUMPTION, WATER USE EFFICIENCY, AND MAIZE (*ZEA MAYS* L.) YIELDS IN THE ARID REGION OF NORTHERN CHINA

LIU, H. T.^{1,2,3} – ZHENG, X. Q.^{2*} – CHEN, J. F.² – HUANG, X. F.^{1,3} – HUANG, M. J.^{1,3} – WANG, J. L.¹

¹*Shanxi Academy of Agricultural Sciences Arid Farming Research Center
Taiyuan, Shanxi 030031, China
(phone: +86-351-7125-695; fax: +86-351-7135-600)*

²*College of Water Resources and Engineering, Taiyuan University of Technology
Taiyuan, Shanxi 030024, China*

³*Organic Dry Farming of Shanxi Province Key Laboratory
Taiyuan, Shanxi 030031, China*

**Corresponding author
e-mail: zhengxiuqing@tyut.edu.cn*

(Received 22nd Dec 2019; accepted 23rd Mar 2020)

Abstract. Water resource crises have become the main factor limiting agricultural development in the arid and semi-arid regions of northern China. Accordingly, water saving agriculture has been a focus of researchers to improve the comprehensive use efficiency of limited water resources. The present study used the Uniform Design and examined the comprehensive and interaction effect of eight cultivation methods, including irrigation amount (IA), growth stages of irrigation (GI), sowing date (SD), planting density (PD), base nitrogen (BN), base phosphorus (BPS), base potassium (BPM), and nitrogen topdressing (NT) on water consumption (WC), water use efficiency (WUE), and maize (*Zea mays* L.) yields. Three key results were observed. (1) WC showed a significant positive correlation with IA, and the interaction effect of IA and GI on WC was significant and had the strongest effect. (2) WUE showed a significant positive correlation with PD, and the interaction effect of BPS and GI on WUE was significant. (3) An optimizing statistical model was used to maximize yield based on cultivation methods as a reference for agricultural practices. Overall, this research indicated that efforts to optimize cultivation methods to increase yield should first focus on optimizing IA and GI, with optimized irrigation management occurring secondarily. The present findings provide the foundation for improving both comprehensive water resource use efficiency and maize production.

Keywords: *water resource, irrigation, planting density, agricultural factors, Uniform Design*

Introduction

Agricultural production in the arid and semiarid regions of northern China has been limited by current water resource crises. Arid and semi-arid regions now account for 52.5% of the total landmass in China, and these regions play critical roles in grain production (Yang et al., 2016). However, increasing demand on global food supplies (Zeng et al., 2018) and water shortages are the primary problems occurring in arid agricultural regions (Zhang et al., 2018). Agriculture is a major consumer of water in such areas, and efficient agricultural water use is critical for sustaining and maximizing the benefits of limited water resources. Agricultural water resources will continue to be reduced by drought associated with climate change, non-sustainable groundwater use, and increasing competition from municipal, environmental, and industrial water needs (Han et al., 2016). Consequently, to achieve a delicate balance between

water use and crop yield, increased crop water use efficiency, i.e., making less water produce higher yields, is a key objective in improving the productivity of agriculture in arid regions (Feng et al., 2019).

Water consumption, water use efficiency, and maize (*Zea mays* L.) yields are not only impacted by climate factors, but also have close relationships with agricultural methods, including tillage methods, mulch application, irrigation techniques, and planting density. Previous studies have revealed several relevant findings: deep plowing techniques can improve the water storage ability of soil and promote maize root to better absorb deep soil water, thus improving water use efficiency (Liu et al., 2013; Zhao et al., 2014); the negative influence of no-tillage becomes noticeable after 3 years, leading to significantly lower yield compared to plow tillage in northeastern Germany (Huynh et al., 2019); conservation agriculture can improve soil water content by reducing evaporation compared to conventional tillage (Ahadi et al., 2013); minimum tillage with optimum irrigation is evaluated as the best options for continuous maize cultivation in the red brown terrace soil without any yield penalty in Bangladesh (Sayed et al., 2019). Residue mulch decreased maximum soil temperature by 3.5–8.5°C resulting in better root growth in north-west India (Rajbir and Arora, 2019); plastic mulch can reduce wasteful crop water evaporation, thereby accelerating plant growth and maize maturation, ultimately increasing WUE and yield (Fan et al., 2017; Dong et al., 2018; Yang et al., 2018). Yet, maize characteristics often exhibit a parabolic relationship with field water consumption (Pereira et al., 2012; Zhang et al., 2014). In southern Italy, suitable irrigation strategies should be adopted in relation to the crop, soil characteristics and rainfall regime (Cucci et al., 2019); Irrigation and rainfall type can also impact field water evapotranspiration and yield, with water consumption increasing as irrigation volumes are added for a given irrigation frequency (Dong et al., 2014); when water is scarce, a 60% lower limit for relative soil moisture was recommended for use with conventional furrow irrigation (Wang et al., 2015). Different planting methods also lead to differences in the canopy structure. The intensity and degree of the available light in the canopy will induce changes in the structure and physiological characteristics of maize leaves (Liu et al., 2012). High planting density increased water use efficiency (by 13%) under irrigation but decreased water use efficiency (by 17%) under rainfed conditions in semi-arid Kenya (Ogola et al., 2007); with the increase of planting density in arid regions in China, the plant height of maize was a little different at the jointing stage and significant decreased at heading stage in normal years; and in wet year, the plant height of maize showed a rising tendency at jointing stage or heading stage (Zhang et al., 2014). Sowing date and planting density had significant interaction on the number and depth of deflated grains, but it had little effect on the number of grains and bald tip. Early sowing can delay the growth process of maize and prolong the growth period. With the delay of sowing date, the growth process was accelerated (Yu et al., 2013).

Above all, most studies focused on single or double cultivation factors effect on maize growth and production, However, few studies have focused on the comprehensive and interaction effects of multiple cultivation factors on water consumption, water resource utilization, and maize yields in the northern arid region of China, and due to heavy workload, the practice of multiple cultivation factors experiment was very difficult.

Thus, this study used a Uniform Design that combined eight cultivation methods: irrigation amount (IA), growth stages of irrigation (GI), sowing date (SD), planting density (PD), base nitrogen (BN), base phosphorus (BPS), base potassium (BPM), and nitrogen topdressing (NT) at the experimental field, and was undertaken at a Jinzhong Basin study site in Shanxi, which is a representative arid area of northern China. We assessed the effects of

these eight cultivation methods on water consumption (WC), water use efficiency (WUE), and maize yield using correlation analyses. In addition to characterizing correlations, we also assessed interaction effects. This research forms the basis for improving both comprehensive water resource utilization and maize production efficiency in the arid regions of northern China.

Materials and Methods

Experimental site

The field experiment was conducted in 2016 at a site in Dongyang township, Yuci district, Jinzhong City, Shanxi Province, China. This region is located in the Xiao River alluvial plain within the Jinzhong Basin (42°37'N, 112°40'E), a traditional area of grain and vegetable production. The climate conditions are continental monsoon type in a temperate zone, with four distinct seasons throughout the year, i.e., hot and rainy summers, cold and dry winters, and short spring and autumn seasons. The mean annual sunshine duration and mean annual air temperature are 2639 h and 9.8°C, respectively. The mean temperatures in January and July are -6.1°C and 23.5°C, respectively. The mean annual precipitation is 430.2 mm, with the highest annual precipitation being 624.9 mm. The mean annual frost-free season was 154 days (Shanxi Statistical Yearbook, 2016). The soil type is moist soil with a pH of 8.0, and the basic soil physical properties are summarized in *Table 1*. The amounts of organic matter, total nitrogen, available nitrogen, available phosphorus, and available potassium were 17.4 g•kg⁻¹, 1.95 g•kg⁻¹, 119.5 mg•kg⁻¹, 11.6 mg•kg⁻¹, 241.9 mg•kg⁻¹, respectively.

Table 1. Basic physical soil properties of the experimental site

Soil depth (cm)	Soil texture	Bulk density (g/cm ³)	Field capacity (V%)	Wilting point (V%)
0–20	clay soil	1.22	32.7	11.6
20–40	clay soil	1.47	30.9	14.0
40–60	sandy clay	1.39	31.6	11.9
60–80	sandy loam	1.37	32.9	7.1
80–100	clay sandy	1.42	35.9	10.3
100–120	clay sandy	1.41	33.4	11.9
120–140	clay soil	1.41	33.3	13.3
140–160	clay soil	1.41	33.3	13.3
160–180	clay soil	1.41	33.3	13.3
180–200	clay soil	1.41	33.3	13.3

During maize growing season of experiment from April to October, the mean daily air temperature ranged from 7.9°C (April) to 27.8°C (August), the mean daily relative humidity ranged from 14% (May) to 89% (September), the average daily wind velocity ranged from 0.4 m/s (October) to 4.8 m/s (April), the amount of precipitation was 382 mm, and monthly precipitation were 63.4 mm (April), 17.6 mm (May), 103.8 mm (June), 23.9 mm (July), 45.2 mm (August), 56.7 mm (September), 17.4 mm (October), respectively.

Experimental design

The study used a Uniform Design that combined eight cultivation methods (IA, PD, BN, BPS, BPM, NT, SD, GI), and each cultivation methods had five different levels. A conventional management plan and optimizing water saving plan were established as

contrasting treatments (CK1 and CK2), bringing the total number of treatments to 27 (Table 2).

Table 2. Experimental design

Treatments	SD (date/month)	PD (plants·ha ⁻¹)	BN (N) (kg·ha ⁻¹)	BPS (P ₂ O ₅) (kg·ha ⁻¹)	BPM (K ₂ O) (kg·ha ⁻¹)	IA (m ³ ·ha ⁻¹)	NT (kg·ha ⁻¹)	GI (leaf expansion)
1	16 April	45,000	150	225	300	60	600	18th
2	16 April	54,000	0	75	300	120	1200	15th
3	16 April	63,000	225	300	300	180	300	12th
4	16 April	72,000	75	150	300	240	900	9th
5	16 April	72,000	225	0	225	0	0	6th
6	23 April	81,000	75	300	225	120	900	6th
7	23 April	45,000	300	150	225	180	0	18th
8	23 April	54,000	150	0	225	240	600	15th
9	23 April	63,000	0	225	225	0	1200	12th
10	23 April	63,000	150	75	150	60	300	9th
11	29 April	72,000	0	0	150	180	1200	9th
12	29 April	81,000	225	225	150	240	300	6th
13	29 April	45,000	75	75	150	0	900	18th
14	29 April	54,000	300	300	150	60	0	15th
15	29 April	54,000	75	150	75	120	600	12th
16	6 May	63,000	300	75	75	240	0	12th
17	6 May	72,000	150	300	75	0	600	9th
18	6 May	81,000	0	150	75	60	1200	6th
19	6 May	45,000	225	0	75	120	300	18th
20	6 May	45,000	0	225	0	180	900	15th
21	13 May	54,000	225	150	0	0	300	15th
22	13 May	63,000	75	0	0	60	900	12th
23	13 May	72,000	300	225	0	120	0	9th
24	13 May	81,000	150	75	0	180	600	6th
25	13 May	81,000	300	300	300	240	1200	18th
CK1	29 April	72,000	375	180	150	0	1200	11th
CK2	29 April	72,000	225	180	150	150	600/750	9th/11th

Note: sowing date (SD), planting density (PD), base nitrogen (BN), base phosphorus (BPS), base potassium (BPM), irrigation amount (IA), topdressing (NT), growth stages of irrigation (GI)

The Uniform Design was a new experimental design method, it was found by Chinese scholars Fang K and Wang Y and won the second prize of State Natural Science Award in 2008. The advantage of it was the factors levels can be increased largely, but the treatments were decreased. At present the total number of citations recognized by SCI is more than 700, and it would be more and more widely used in practices (Jia et al., 2011; Maria et al., 2016; Zhou et al., 2019).

The plot area was 30 m² (60 cm × 50 cm), and plants were grown in rows spaced 60 cm apart. There was a 1-m space between plots in order to minimize irrigation water spreading among treatments, and irrigation was controlled by raised ridges between the plots. Across the maize growth stages, cultivation methods were applied to all plots in accordance with the design, and conventional field management methods, including intertillage, weed, pest, and disease controls, and suitable harvest times, were used to regulate growth (Figure 1).



Figure 1. Irrigation and plots of the field experiment

The applied maize variety name was ‘Dafeng 30’, which was the main cultivar in this district in recent years. The tillage methods was crushed maize straw and returned to the field after harvest in autumn of last year and made preparations for plough and sowing in spring. The seeds had been coated to prevent pest and disease and herbicides were applied after sowing for plant protection.

Experimental measurements

Subheading Soil water content

The soil water content of 20-cm-deep cores from depths ranging from 0 to 200 cm were measured using the oven-drying method at maize stages corresponding to the expansion of the 6th, 9th, 12th, and 15th leaf, silking, 15 and 30 days after silking, and harvest, respectively. Each sample was taken by soil auger, and after being weighed, soil samples were dried for 24 h at 105°C. Oven-dried weight was then determined, followed by the calculation of gravimetric soil water content, which is [(wet soil weight) - (dry soil weight)] / (dry soil weight). Volumetric soil water content was then determined by multiplying the gravimetric soil water content by the respective bulk density at each sample depth, as shown in *Table 1*. The water content of each layer was converted to mm and summed to obtain the soil water content of the 0–200-cm-deep soil profile.

Water consumption

Water consumption (WC) was determined using the following field water balance equation:

$$WC = \Delta W_x + I + P + G \quad (\text{Eq.1})$$

Here, *WC* is the water consumption (mm), *I* is the irrigation amount (mm), *P* is the effective precipitation, ΔW_x is the difference in soil water content of the 0–200-cm soil depth between the beginning and end of maize growing season, *G* is the groundwater

supplementary amount, which can be considered as negligible because of the deep water table level (80 m).

Water use efficiency

Water use efficiency (WUE) was calculated using the following equation:

$$WUE = Y / WC \quad (\text{Eq.2})$$

Here, Y is the grain yield (kg/ha), and WC is again the water consumption over the whole growing season (mm).

Maize yield

Ears were harvested from the two central rows of each plot, dried, and shelled. Unshelled ear samples were also taken from experimental plots, and the ear length, ear diameter, number of kernel rows, kernels per row, and hundred-kernel-weight per ear were recorded, respectively; each ear sample was composed of 10 healthy ears from the central rows of each plot. The total yield was then extrapolated based on these results.

Statistical analysis

Data were analyzed using Excel 2007 (Microsoft Corp., Redmond, WA, USA) and SPSS statistical analysis software (IBM Corp., Armonk, NY, USA). Correlation analysis and regression were used to determine the effects of cultivation on WC and WUE, respectively. Statistical significance was assessed at probability thresholds of $p < 0.05$ and $p < 0.01$.

Results

Effects of treatments on WC and WUE

As shown in *Table 3*, WC and WUE differed among treatments, with respective maximum ranges of 141.8 mm between treatments 4 and 1 and of $7.7 \text{ kg} \cdot \text{ha}^{-1} \cdot \text{mm}^{-1}$ between treatments 24 and 8. While WC was higher for the CK group than for all others, WUE for the CK group was lower than that for all other groups. Accordingly, WC and WUE under each treatment were analyzed to determine a superior irrigation plan for this region.

Analysis of correlations and interaction effects of cultivation methods on WC

IA had positive and significant ($p < 0.01$) correlations with WC (*Table 4*), the index of correlation (IC) values reached 0.74, demonstrating that WC increase with IA in this region (*Figure 2*), likely because water absorbed and used by maize was efficiently increased by irrigation. And by analyzing the correlations between yield and WC (*Figure 2*), water was apparently mainly used for maize transpiration, with little field evaporation; thus, WC and yield increased together.

Table 3. Water consumption (WC) and water use efficiency (WUE) of treatments

Treatments	WC (mm)	WUE (kg·ha ⁻¹ ·mm ⁻¹)	Treatments	WC (mm)	WUE (kg·ha ⁻¹ ·mm ⁻¹)	Treatments	WC (mm)	WUE (kg·ha ⁻¹ ·mm ⁻¹)
1	428.2	25.8	10	474.7	27.0	19	475.2	24.8
2	555.1	24.8	11	466.4	26.3	20	479.5	23.2
3	548.3	24.3	12	503.7	27.3	21	542.9	23.2
4	570.8	25.8	13	433.8	25.7	22	487.8	26.3
5	490.0	25.8	14	457.8	27.4	23	500.9	25.7
6	512.3	27.2	15	470.7	27.4	24	446.4	30.1
7	488.9	26.6	16	523.7	25.3	25	489.6	26.9
8	537.1	22.4	17	467.9	28.6	CK1	535.2	26.9
9	479.6	29.7	18	513.7	24.7	CK2	573.8	24.9

Table 4. Analyze of correlation between water consumption (WC) and cultivation methods

IC	SD (date/month)	PD (plants·ha ⁻¹)	BN (N) (kg·ha ⁻¹)	BPS (P ₂ O ₅) (kg·ha ⁻¹)	BPM (K ₂ O) (kg·ha ⁻¹)	NT (kg·ha ⁻¹)	IA (m ³ ·ha ⁻¹)	GI (leaf expansion)	Yield
WC	-0.22	0.2	0.01	0	0.25	0.05	0.74**	-0.27	0.53**

Note: * $p < 0.05$, ** $p < 0.01$, index of correlation (IC), sowing date (SD), planting density (PD), base nitrogen (BN), base phosphorus (BPS), base potassium (BPM), irrigation amount (IA), topdressing (NT), growth stages of irrigation (GI)

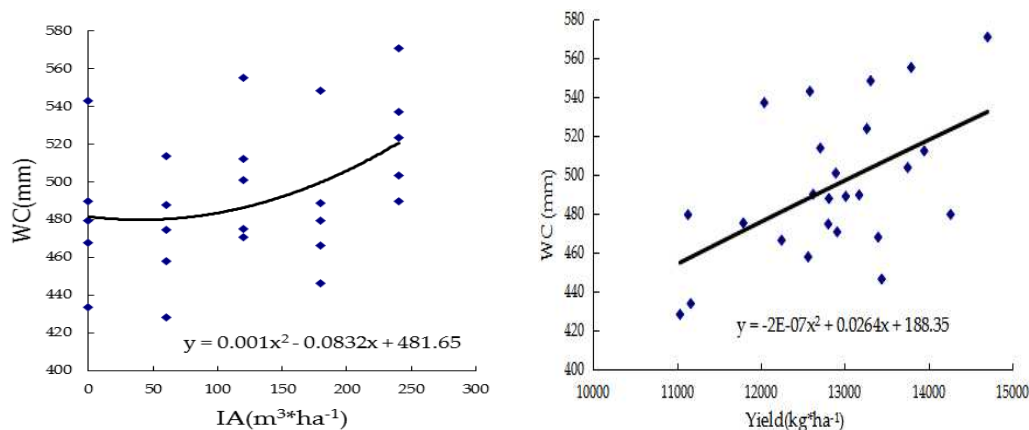


Figure 2. Correlation analysis for water consumption (WC) and yield with irrigation amount (IA)

Quadratic polynomial stepwise regression analysis (Table 5) revealed that IA and GI as well as BN and BPM had positive and significant interaction effects on yield, respectively ($p < 0.01$). Through further assessment with path analysis and comparisons of direct path coefficients, we found that the interaction effect of IA and GI was highest, with a direct path coefficient (DPC) of 0.69, and interaction effects of the other interaction effects, PD × BN and BN × BPM, had DPC values of 0.46 and 0.27, respectively, indicating little effect on WC. Accordingly, growth stage should be considered when developing irrigation plans in this region in order to optimize irrigation.

Table 5. Test results and path analysis of water consumption (WC) model regression index

Agricultural factors	Partial correlation	t-test value	p-value	Direct path analysis
IA	0.8699	7.8878	0.0001	1.3889
PD × BN	0.4104	2.0125	0.0572	0.2787
BN × BPM	-0.5864	3.2378	0.0039	-0.4555
IA × GI	-0.6618	3.9481	0.0007	-0.6872

Note: planting density (PD), base nitrogen (BN), base potassium (BPM), irrigation amount (IA), growth stages of irrigation (GI)

Analysis of correlations and interaction effects of cultivation methods on WUE

WUE improvement is a key focus of maize research. As shown in Table 6, PD had a positive significant correlation with WUE; the IC value was 0.42; and further analysis found that WUE had a negative significant correlation with WC (Figure 3). This demonstrated that PD increases could increase WUE significantly in this region, likely because field evaporation can be reduced by increased PD during maize seedling stage; furthermore, the limited water resource use efficiency was improved.

Table 6. Correlation analysis for water use efficiency (WUE) and cultivation methods

IC	SD (date/month)	PD (plants·ha ⁻¹)	BN (N) (kg·ha ⁻¹)	BPS (P ₂ O ₅) (kg·ha ⁻¹)	BPM (K ₂ O) (kg·ha ⁻¹)	NT (kg·ha ⁻¹)	IA (m ³ ·ha ⁻¹)	GI (leaf expansion)	Yield	WC
WUE	0.08	0.42*	-0.01	0.26	-0.02	0.01	-0.26	0.22	0.47*	-0.50**

Note: * $p < 0.05$, ** $p < 0.01$, water consumption (WC), index of correlation (IC), sowing date (SD), planting density (PD), base nitrogen (BN), base phosphorus (BPS), base potassium (BPM), irrigation amount (IA), topdressing (NT), growth stages of irrigation (GI)

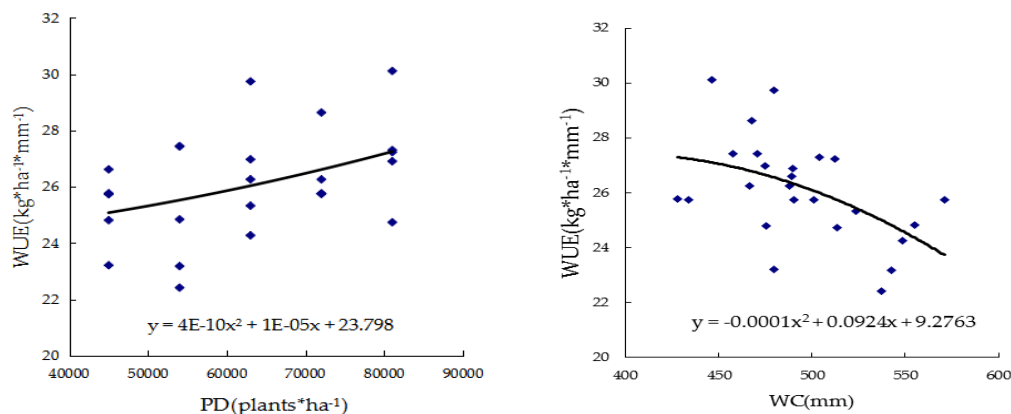


Figure 3. Correlation analysis for water use efficiency (WUE) with planting density (PD) and water consumption (WC)

The effect of agricultural factors on WUE summarized in Table 7 is based on quadratic polynomial stepwise regression analysis, with only BPS and GI having positive and significant interaction effects on WUE ($p < 0.05$). Path analysis and a comparison of direct path coefficients revealed that the interaction effect of BPS and GI was higher than that of the others, with a DPC of 0.37. The interaction effect of SD and IA was lower than that of BPS and GI, with a DPC of only 0.29; this was possibly

explained by maize root growth not being improved by increased BPS, and thus deep soil water could not be absorbed. Meanwhile, when GI was conducted at the critical demand stage, WUE was improved effectively.

Table 7. Test results and path analysis for water use efficiency (WUE) model regression index

Agricultural factors	Partial correlation	t-test value	p-value	Direct path analysis
PD × PD	0.4659	2.4126	0.0246	0.4204
SD × IA	-0.3399	1.656	0.1119	-0.2902
BPS × GI	0.4192	2.116	0.0459	0.3703

Note: planting density (PD), sowing date (SD), base phosphorus (BPS), irrigation amount (IA), growth stages of irrigation (GI)

Optimizing statistical model of yield

The yields of different treatments are shown in Table 8. Quadratic polynomial stepwise regression analysis revealed the following statistical model describing the relationship between the cultivation methods and yield:

$$Y = -96.82 + 5.37PD - 0.00054PD * PD + 0.44IA * IA - 0.0067PD * IA - 2.88BN * NT + 3.19BPS * NT + 2.13IA * GI \quad (\text{Eq.3})$$

Table 8. Yields and yield characters of different treatments

Treatments	Ear length (cm)	Ear diameter (mm)	Number of kernel rows (rows)	Kernels per row (kernels)	Hundred kernel weight per ear (g)	Planting density (number of plant ha ⁻¹)	Yield (kg·ha ⁻¹)
1	20.5	5.05	17	39	37.43	45000	11035.5
2	20.5	5.00	16	40	39.11	54000	13792.5
3	20.6	4.98	17	34	38.09	63000	13309.5
4	18.0	4.77	15	37	35.69	72000	14704.5
5	17.0	6.56	15	33	35.14	72000	12624.0
6	16.8	4.73	17	30	34.58	81000	13948.5
7	20.8	5.01	16	47	38.86	45000	13012.5
8	20.3	4.87	16	38	36.87	54000	12040.5
9	20.3	4.87	15	39	38.45	63000	14263.5
10	18.9	4.72	16	38	33.59	63000	12804.0
11	17.7	4.82	16	33	32.08	72000	12247.5
12	19.0	4.85	16	29	36.18	81000	13752.0
13	20.2	7.27	16	43	35.83	45000	11164.5
14	20.5	4.94	16	39	38.04	54000	12564.0
15	20.4	4.87	17	40	36.14	54000	12910.5
16	19.7	5.00	17	36	34.82	63000	13264.5
17	20.0	5.02	16	35	33.09	72000	13399.5
18	16.7	4.46	17	31	30.73	81000	12709.5
19	22.0	5.18	17	39	40.15	45000	11791.5
20	20.8	5.14	17	40	37.43	45000	11131.5
21	20.3	5.03	17	38	36.09	54000	12585.0
22	18.9	4.87	17	37	32.49	63000	12811.5
23	17.7	4.78	16	35	32.00	72000	12894.0
24	16.2	4.79	16	31	32.70	81000	13441.5
25	18.1	4.84	17	31	31.30	81000	13173.0
CK1	18.3	4.74	16	36	34.15	72000	14415.0
CK2	19.2	4.63	17	35	34.17	72000	14313.0

The optimizing results showed when the SD was 16 April, PD was 72000 plants·ha⁻¹, BN was 0 kg·ha⁻¹, BPS was 300 kg·ha⁻¹, BPM was 250 kg·ha⁻¹, NT was 240 kg·ha⁻¹, IA was 1200 m³·ha⁻¹, and GI was maize at the 18th leaf expansion stage, the highest theoretical value of 15,458.75 kg·ha⁻¹ was reached.

While most scholars recognized that increased N fertilizer can be very useful for improving maize yields, in this study, the optimizing model revealed that BN was not needed. This may be explained by the soil base N being sufficient for maize seedling growth, perhaps demonstrating that excess N fertilizer had been used on the field previously; alternatively, N might have leached into the field from polluted groundwater. Accordingly, groundwater pollution should be considered, and less fertilizer N should be used compared with that often considered necessary for maximum maize yields.

Discussion

Water consumption is a research focus in water-limited regions, and it is affected by many cultivation factors. Generally, WC can be equal to crop evapotranspiration in agricultural fields. Many studies have confirmed that irrigation has substantial effects on evapotranspiration. For example, in Kirklareli, Turkey, seasonal evapotranspiration of maize ranges from 762 mm under full irrigation to 265 mm in unirrigated fields (Cakir, 2004). Similarly, in Aydin, Turkey, seasonal evapotranspiration of closed-end furrow irrigated maize ranged from 558 mm under full irrigation to 174 mm in unirrigated fields (Dagdelen et al., 2006). In Nebraska, USA, seasonal evapotranspiration in maize varied between 625 mm and 366 mm depending on different irrigation treatments (Payero et al., 2006). In our study, WC under different treatments ranged from 570.8 mm to 428.2 mm, and effective irrigation management was useful in decreasing crop water consumption through selecting proper IA and GI. Identifying the most sensitive growth stage of irrigation was also an important way to enhance crop productivity while keeping WC low. Additionally, linear relationships between maize yield and evapotranspiration, which was the same as WC in our study, have been reported by Payero and Djaman, akin to our results (Payero et al., 2009; Djaman and Irmak, 2013).

In arid regions, an understanding of WUE is essential for evaluating crops when water resources are a limiting factor. Many studies have indicated that low irrigation is one way to maximize water use efficiency for higher yields per unit of irrigation water applied in arid and semiarid regions (Bekele and Tilahun, 2007). However, under water limitation, other cultivation factors (e.g., soil fertility, tillage, and soil composition) have a significant role in enhancing crop water productivity (Molden et al., 2009). For example, amending soil with biochar under limited water supply might be a novel approach for enhancing maize yield and water use efficiencies by minimizing the negative impact of drought stress (Faloye et al., 2019). In our study, WUE values were improved by increasing PD, while yield was also increased, but was negatively correlated with WC. Additionally, proper BPS and GI selection can improve maize WUE, achieving an ideal root type for improved water and P-uptake in maize, as has been reported (Lynch, 2013). Accordingly, this would be an appropriate direction for future research as a means of improving water resource utilization.

Increasing maize yields has long been an important research topic. The present study examined eight cultivation methods, with each measure consisting of five levels. Using

a traditional design method, such field tests can be very complicated and difficult to realize, but by adopting a uniform design and dynamic adjustment method, this situation can be examined effectively with the impact of each measure accurately evaluated. Finally, through processing experimental data and regression analysis, effective cultivation methods were established, which suggest conditions for optimal maize yields.

Conclusions

In eight different cultivation methods of our study, Firstly, IA had a significant impact on WC, and the interaction effect of IA and GI could significantly affect WC; Secondary, PD had the greatest impact on WUE, and BPS and GI had the obviously interaction effect on WUE; thus, we should reduce WC while increasing WUE in maize production, and need to focus on IA and PD and GI and BPS; Finally, we found that when the SD was 16 April, PD was 72000 plants•ha⁻¹, BN was 0 kg•ha⁻¹, BPS was 300 kg•ha⁻¹, BPM was 250 kg•ha⁻¹, NT was 240 kg•ha⁻¹, IA was 1200 m³•ha⁻¹, and GI was maize at the 18th leaf expansion stage, the maize yield could reached 15,458.75 kg•ha⁻¹, but it was the theoretical value, and need to test in practices in future.

While maize yield has been continuously improved in China, agricultural water consumption has also increased. Consequently, the groundwater level has been continuously falling, and water overexploitation has become a serious issue. Accordingly, discovering approaches to balancing water resource used and yield production in northern arid regions of China has become important. As growth and metabolism processes consume more water, drought stress-sensitive stages and optimized irrigation schedules should be consider specially when planning irrigation. The present research can be refined through more years of experimentation at the site in order to validate the suitability of this model to different environmental conditions.

Acknowledgements. This research was financially supported by the National Natural Science Foundation of China (41572239), the National Public Project of China Ministry of Agricultural (201503124), the Shanxi Key Research and Development Projects (201703D211002), the Shanxi Academy of Agricultural Sciences Foundation (YGG1639), Organic Dry Farming of Shanxi Province Key Laboratory (201805D111015). We would also like to thank all the staff for technical assistance in carrying out the field experiments.

REFERENCES

- [1] Ahadi, R., Samani, Z., Skaggs, R. (2013): Evaluating on-farm irrigation efficiency across the watershed: a case study of New Mexico's Lower Rio Grande Basin. – *Agricultural Water Management* 124: 52-57.
- [2] Bekele, S., Tilahun, K. (2007): Regulated deficit irrigation scheduling of onion in a semiarid region of Ethiopia. – *Agricultural Water Management* 98: 148-152.
- [3] Cakir, R. (2004): Effect of water stress at different development stages on vegetative and reproductive growth of corn. – *Field Crop Research* 89(1): 1-16.
- [4] Cucci, G., Lacolla, G., Boari, F., Mastro, M. A., Cantore, V. (2019): Effect of water salinity and irrigation regime on maize (*Zea mays* L.) cultivated on clay loam soil and irrigated by furrow in Southern Italy. – *Agricultural Water Management* 222: 118-124.

- [5] Dagdelen, N., Yilmaz, E., Sezgin, F., Talih, G. (2005): Water-yield relation and water use efficiency of cotton and second crop corn in western Turkey. – *Agricultural Water Management* 82(1): 63-85.
- [6] Djaman, K., Irmak, S. (2013): Actual crop evapotranspiration and alfalfa and grass-reference crop coefficients of maize under full and limited irrigation and rainfed conditions. – *Journal of Irrigation & Drainage Engineering* 139: 433-446.
- [7] Dong, Y. Y., Wang, B. C., Jia, L. H., Mu, H. W., Fei, L. J. (2014): Study on the water consumption characteristics and efficiency of summer corn under film hole water production irrigation. – *Agricultural Research of Arid Areas* 32: 7-12.
- [8] Dong, Q. G., Yang, Y., Yu, K., Feng, H. (2018): Effects of straw mulching and plastic film mulching on improving soil organic carbon and nitrogen fractions, crop yield and water use efficiency in the Loess Plateau, China. – *Agricultural Water Management* 201: 133-143.
- [9] Faloye, O. T., Alatise, M. O., Ajayi, A. E., Ewulo, B. S. (2019): Effects of biochar and inorganic fertilizer application on growth, yield and water use efficiency of maize under deficit irrigation. – *Agricultural Water Management* 217: 165-178.
- [10] Fan, Y. Q., Ding, R. S., Kang, S. Z., Hao, X. M., Du, T. S., Tong, L., Li, S. E. (2017): Plastic mulch decreases available energy and evapotranspiration and improves yield and water use efficiency in an irrigated maize cropland. – *Agricultural Water Management* 179: 122-131.
- [11] Feng, Y., Hao, W. P., Gao, L. L., Li, H. R., Gong, D. Z., Cui, N. B. (2019): Comparison of maize water consumption at different scales between mulched and non-mulched croplands. – *Agricultural Water Management* 216: 315-324.
- [12] Han, M., Zhang, H. H., Kendall, C. D., Louise, H. C., Thomas, J. T. (2016): Estimating maize water stress by standard deviation of canopy temperature in thermal imagery. – *Agricultural Water Management* 177: 400-409.
- [13] Huynh, H. T., Hufnagel, J., Wurbs, A., Bellingrath-Kimura, S. D. (2019): Influences of soil tillage, irrigation and crop rotation on maize biomass yield in a 9-year field study in Müncheberg, Germany. – *Field Crop Research* 241: 107565.
- [14] Jia, L. P., Wang, Y. P., Fan, L. (2011): Uniform Design Based Hybrid Genetic Algorithm for Multiobjective Bilevel Convex Programming. – *Computational Intelligence and Security (CIS), Seventh International Conference*.
- [15] Liu, T. D., Song, F. B., Liu, S. Q., Zhu, X. C. (2012): Light interception and radiation use efficiency response to narrow-wide row planting patterns in maize. – *Australian Journal of Crop Science* 6(3): 506-513.
- [16] Liu, Y., Gao, M. S., Wu, W., Sikander, K. T., Wen, X. X., Liao, Y. C. (2013): The effects of conservation tillage practices on the soil water-holding capacity of a non-irrigated apple orchard in the Loess Plateau, China. – *Soil Tillage Research* 130: 7-12.
- [17] Lynch, J. P. (2013): Steep, cheap and deep: an ideotype to optimize water and N acquisition by maize root systems. – *Annals of Botany* 112: 347-357.
- [18] Molden, D., Oweis, T., Steduto, P., Bindraban, P., Hanjra, M. A., Kijne, J. (2009): Improving agricultural water productivity: between optimism and caution. – *Agricultural Water Management* 97(4): 528-535.
- [19] Ogola, J. B. O., Wheeler, T. R., Harris, P. M. (2007): Predicting the effects of nitrogen and planting density on maize water use in semi-arid Kenya. – *South African Journal of Plant and Soil* 24(1): 51-57.
- [20] Payero, J. O., Melvin, S. R., Irmak, S., Tarkalson, D. (2006): Yield response of corn to deficit irrigation in a semiarid climate. – *Agricultural Water Management* 84(1): 101-112.
- [21] Payero, J. O., Tarkalson, D. D., Irmak, S., Davison, D., Petersen, J. L. (2009): Effect of timing of a deficit-irrigation allocation on corn evapotranspiration, yield, water use efficiency and dry mass. – *Agricultural Water Management* 96(10): 1387-1397.

- [22] Pereira, L. S., Cordery, I., Iacovides, I. (2012): Improved indicators of water use performance and productivity for sustainable water conservation and saving. – *Agricultural Water Management* 108: 39-51.
- [23] Rajbir, K., Arora, V. K. (2019): Deep tillage and residue mulch effects on productivity and water and nitrogen economy of spring maize in north-west India. – *Agricultural Water Management* 213: 724-731.
- [24] Sayed, A., Sarker, A., Kim, J.-E., Rahman, M., Mahmud, G. A. (2019): Environmental sustainability and water productivity on conservation tillage of irrigated maize in red brown terrace soil of Bangladesh. – *Journal of the Saudi Society of Agricultural Sciences* 03: 002.
- [25] Shanxi Provincial Bureau of Statistics & Survey Office of the National Bureau of Statistics in Shanxi. (2016): *Shanxi Statistical Yearbook*. – China Statistics Press, Beijing 34.
- [26] Takahashi, M. B., Rocha, J. C., Núñez, E. G. F. (2016): Optimization of artificial neural network by genetic algorithm for describing viral production from uniform design data. – *Process Biochemistry* 51(3): 422-430.
- [27] Wang, S. S., Liu, D. X., Wang, K. S., Meng, P. T. (2015): Fuzzy comprehensive evaluation on water consumption characteristics and yield of summer corn under different furrow irrigation patterns. – *Transactions of the Chinese Society of Agricultural Engineering* 31(24): 89-94.
- [28] Yang, L., Yang, Y. Z., Feng, Z. M., Zheng, Y. N. (2016): Effect of maize sowing area changes on agricultural water consumption from 2000 to 2010 in the West Liaohe Plain, China. – *Journal of Integrative Agriculture* 15(6): 1407-1416.
- [29] Yang, J., Mao, X. M., Wang, K., Yang, W. C. (2018): The coupled impact of plastic film mulching and deficit irrigation on soil water/heat transfer and water use efficiency of spring wheat in Northwest China. – *Agricultural Water Management* 201: 232-245.
- [30] Yu, J. L., Nie, L. X., Zheng, H. B., Zhang, W. J., Song, Z. W., Tang, J. H., Lin, Z. Q., Qi, H. (2013): Effect of matter production and yield formation on sowing date and density in maize. – *Journal of Maize Sciences* 21(5): 76-80.
- [31] Zeng, Z., Gower, D. B., Wood, E. F. (2018): Accelerating forest loss in Southeast Asian Massif in the 21st century: a case study in Nan Province, Thailand. – *Global Change Biology* 24(10): 4682-4695.
- [32] Zhang, D. M., Zhang, W., Chen, Q., Huang, X. F., Jiang, C. X., Han, Y. L., Liu, E. K., Chi, B. L. (2014): Effects of planting density on plant traits and water consumption characteristics of dryland maize. – *Journal of Maize Sciences* 22: 102-108.
- [33] Zhang, F., Zhang, W. J., Qi, J. G., Li, F. M. (2018): A regional evaluation of plastic film mulching for improving crop yields on the Loess Plateau of China. – *Agricultural and Forest Meteorology* 248: 458-468.
- [34] Zhao, Y. L., Xue, Z. W., Guo, H. B., Mu, X. Y., Li, C. H. (2014): Effects of tillage and straw returning on water consumption characteristics and water use efficiency in the winter wheat and summer maize rotation system. – *Scientia Agricultura Sinica* 47(17): 3359-3371.
- [35] Zhou, Y., Wang, J. Y., Gao, X. J., Wang, K., Wang, W. W., Wang, Q., Yan, P. S. (2019): Isolation of a novel deep-sea *Bacillus circulans* strain and uniform design for optimization of its anti-aflatoxicogenic bioactive metabolites production. – *Bioengineered* 10(1): 13-22.

SELENIUM BIOFORTIFICATION ENHANCES SOYBEAN SEMET AND COQ10 CONTENT

YANG, Y. L.^{1*} – LIU, Y. Y.² – JIANG, L. Z.³

¹*Department of Applied Chemistry, Northeast Agricultural University, Harbin 150030, China*

²*College of Resources and Environment, Northeast Agricultural University, Harbin 150030, China*

³*College of Food Science, Northeast Agricultural University, Harbin 150030, China*

**Corresponding author*

e-mail: yangyuling@neau.edu.cn

(Received 22nd Dec 2019; accepted 23rd Mar 2020)

Abstract. As a further study of the effect of selenomethionine content (SeMet) and coenzyme Q content in plants, Se-enriched soybeans were obtained by cultivating the soybeans in the presence of different concentrations of Se. The content of SeMet and coenzyme Q were determined in soybeans. The results show a positive correlation was found between the selenium concentration of Se-enriched soybeans and both the content of SeMet and the content of coenzyme Q₁₀, which suggests that the inorganic selenium is absorbed by soybeans and converted into organic Se species with high bioavailability. The effect of SeMet on the content of coenzyme Q₁₀ in soybeans was studied as well. The content of coenzyme Q₁₀ increased in the Se-enriched soybeans compared to the control. There is a linear relationship between the content of coenzyme Q₁₀ and SeMet. In conclusion, a Se-enriched treatment can raise the content of coenzyme Q₁₀ and SeMet in soybeans, which could be used as potential functional food additives for improving soybean nutrition values subsequently human health.

Keywords: *selenium, selenium fertilization, soybean, selenomethionine, coenzyme Q₁₀*

Introduction

Selenium (Se) is an essential trace element for animals and humans (Fang et al., 2017). Low Se intake can have serious consequences on health. Animal studies have indicated that a low Se diet directly correlates with the incidence of various types of cancer (Li et al., 2008; Ding et al., 2014). Generally speaking, selenium content in most soils was low and thus plants grown on that soils contain low amount of Se (Pilon-Smits et al., 2009; Nothstein et al., 2016). Therefore, biofortification with Se had emerged as an effective strategy to increase Se content in plant-based food products. Coenzyme Q₁₀ (CoQ₁₀, *Fig. 1*) was a lipid-soluble quinone that was widely distributed in plants and animals. CoQ₁₀ has many important physiological functions, including transferring electrons in the respiratory chain (Lenaz et al., 2007). CoQ₁₀ was a natural antioxidant and can boost the immune system (Tawfik, 2015; Ozer et al., 2017). Animal experiments had shown that Se was a component of glutathione peroxidase and can protect tissues from oxidative damage, thereby maintain the ability of cells to synthesize reduced CoQ₁₀ and prevent the degradation of CoQ₁₀. Selenium can promote the synthesis of CoQ₁₀ in animals, and the content of Se was positively related to the CoQ content (Vadhanavikit et al., 1994); however, research on the relationship between Se and CoQ in plants was limited (Liu et al., 2003). Therefore, the bullet points of this study included the following two aspects: the first was biofortification of selenium in Soybean; the second was whether selenium-enriched soybeans (plants) affect CoQ₁₀ content.

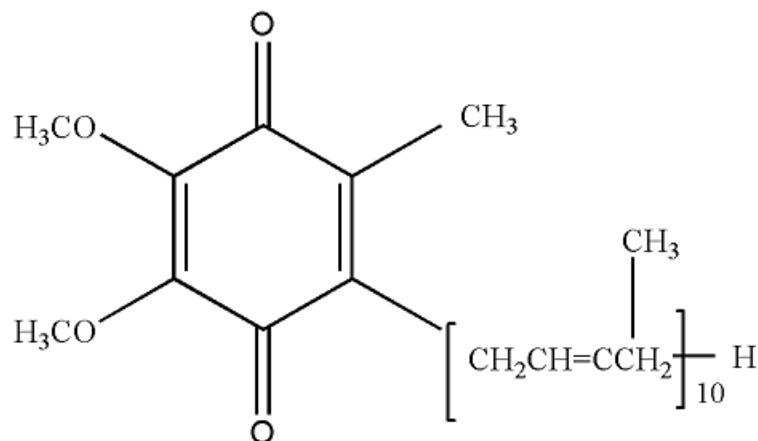


Figure 1. The structure of coenzyme Q_{10}

Materials and Methods

Instruments and reagents

The following instruments were used: Agilent 1200 High Performance Liquid Chromatography, DAD diode array UV detector from USA Agilent Technologies Ltd.; Z36 High-speed refrigerated centrifuge from German Hermle company; JY92-II D ultrasonic cell disrupter from Ningbo Xinzhi Bio-Technology Co., Ltd.; OSB-2100 rotary evaporator from Japan Eyela company; AFS-930 dual channel atomic fluorescence spectrometer from Beijing Titan Instruments Co., Ltd; and KXL-1010 type temperature digestion furnace from Beijing Reborn Industrial Co., Ltd.

The following reagents were used: CoQ₁₀ standard (99.9%): Sigma Company; Methanol, ethanol, and isopropanol chromatography from Merck Company; Nitric acid, hydrochloric acid, and perchloric acid are of pure class; Mixed acid (nitric and perchloric acid volume ratio of 4:1), potassium cyanoborohydride, sodium hydroxide, selenium standard solution (1000 $\mu\text{g}\cdot\text{ml}^{-1}$ medium is 10% hydrochloric acid), Argon, and deionized water.

Experimental Details and Treatments

Experimental material

The experiment was started on May 10, 2012 in Xiangfang experimental station (east longitude 125°42', north latitude 44°04') of Northeast Agricultural University in Harbin city, Heilongjiang Province of P.R. China. Specific permissions were not required for these experiments as they were carried out at the Northeast Agricultural University. The experiments did not involve endangered or protected species.

Treatments

The soybean variety utilized in these studies was Dongnong 52 (one of the typical local varieties). The fertilizer application rates in the field experiment were as following: N 27 $\text{kg}\cdot\text{hm}^{-2}$, P₂O₅ 69 $\text{kg}\cdot\text{hm}^{-2}$, and K₂O 50 $\text{kg}\cdot\text{hm}^{-2}$. The field experiment included the following 4 treatments: Ck as a control, no Se addition; Se1, Se2 and Se3 based on different amounts of Na₂SeO₃. Based on our previous study experience (Yang

et al., 2014), the contents of sodium selenite were 0, 10 g·ha⁻¹, 20 g·ha⁻¹, 30 g·ha⁻¹ (in pure selenium meter), and the control was sprayed with distilled water only. Previous experiments have shown that higher selenium application (over 30 g·ha⁻¹) may lead to plant visibility damage. Three replicates in the experiment were arranged randomly in the area of 300 m² (Repetition is to avoid environmental impact on experimental results). Selenite was applied via foliar during seed filling stage. The grains were hand harvested on September 24, 2012. The experimental soil was black soil, and the water soluble selenium content of soil tillage layer was 0.014 mg·kg⁻¹, soil pH value was 7.07, soil total N 0.105%, total phosphorus 0.046%, available phosphorus 25.60 mg·kg⁻¹, available potassium 155.65 mg·kg⁻¹.

Methods

Determination of total selenium

Extraction of total selenium

The sample (0.5000 g) was weighed in 50-mL Erlenmeyer flasks. Ten milliliters of thick nitric acid were added for the digestion, then, 5 mL of mixed acid (HNO₃:HClO₄=4:1) were added. The digestion liquid was heated and maintained at 40°C until a white smoke arose. Five milliliters of 6 mol·L⁻¹ thick hydrochloric acid were added until white fumes were generated. The samples were diluted to 10 mL with 5% hydrochloric acid. The Se content was determined by HG-AFS. The standard solutions were prepared in the same acidic media as the samples.

Determination of total selenium content

After preheating for 30 min, the selenium standard solution (50 µg·mL⁻¹) was poured into an autosampler, with a set gradient of different concentrations of standard solutions including 0.0, 5.0, 10.0, 20.0, 30.0, 50.0 µg·mL⁻¹ selenium. The instrument automatically diluted the injections and drew the standard curve. The fluorescence values of each solution were determined. The selenium content in the sample was calculated using the external standard. All measurements were taken in parallel three times, the same below.

Method for the determination of CoQ10

Sample pretreatment

The soybean flour (2.00 g) was weighed in a 50-mL centrifuge tube, added to 30 mL of 70% methanol, mixed by oscillation for 30 min, and centrifuged for 10 min at 8000 r·min⁻¹; the supernatant was discarded. Thirty milliliters of isopropyl alcohol were added to the defatted soybean flour, and extracts were prepared by cell disruption (400 w, 2s/1s, 50). The extracts were washed, combined and concentrated with isopropanol to a volume of 2 mL, filtered using a 0.25 µm microporous membrane, and refrigerated in the dark (He et al., 2010).

Chromatographic Conditions

A ZORBAX SB-C18 chromatographic column (4.6×250 mm, 5 µm, Agilent) was utilized with a mobile phase that consisted of 50% ethanol:50% methanol at a flow rate of 2.0 mL·min⁻¹. The column temperature was 30°C, the detection wavelength was 275 nm, and the injection volume was 10 µL.

Statistical Analysis

All data were subjected to Analysis of Variance (ANOVA), and differences between the means were evaluated by Duncan's Multiple Range Test (Steel et al., 1996). SPSS statistic program (Version 18.0) was used for the data analysis. The significance of statistical analysis was to use scientific methods to get the difference between different treatments.

Results

Total selenium content in Se-enriched soybean

The determination of the total selenium contents in soybeans was shown in Fig. 2. In contrast to the control group, the total selenium contents increased significantly in the selenite-enriched soybeans. Additionally, the total Se contents in the soybeans increased as the application concentration of sodium selenite increased, which was closely related to Se of foliar application. These results indicated that the differences between the different treatments were consistent with other Se-enriched plants (Cankur et al., 2006). Eating Se-enriched soybeans might promote extra nutritional value to the human body. There was no visual plant damage during the growth of the Se-enriched soybeans.

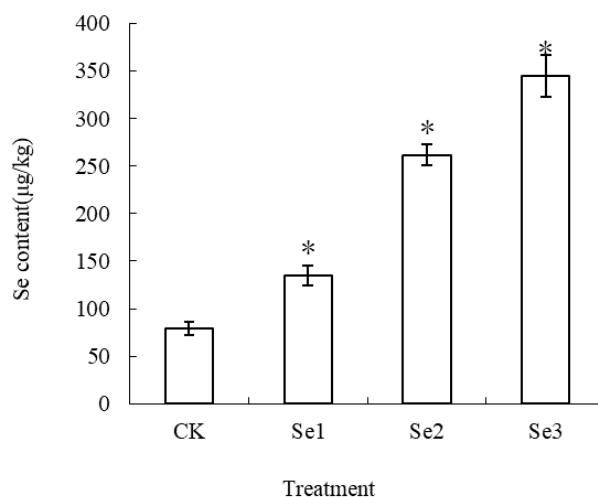


Figure 2. Se content in soybean seeds treated by different Se concentration. Data are the mean \pm SEM. * $P < 0.05$ versus control (control means soybean were sprayed with equal amount of distilled water), $n = 3$ (repetitions, same below)

Effects of different selenium concentrations on selenomethionine content in soybeans

Fig. 3A showed a chromatogram from the HPLC-HG-AFS analysis of the Se(Cys)₂, Se (IV) and SeMet standard. The sample was separated on a Hamilton PRP-100 anion exchange column, with a 40 mmol·L⁻¹ (NH₄)₂HPO₄ solution as the mobile phase (pH 6.0) and a flow rate of 0.5 mL·min⁻¹.

Determination of SeMet in the soybean extracts was carried out according to the above optimized conditions. An overlay chromatogram of SeMet in the soybean extract and standard curve was shown in Fig. 3B. Using retention time matching, SeMet content in the soybean extract can be determined.

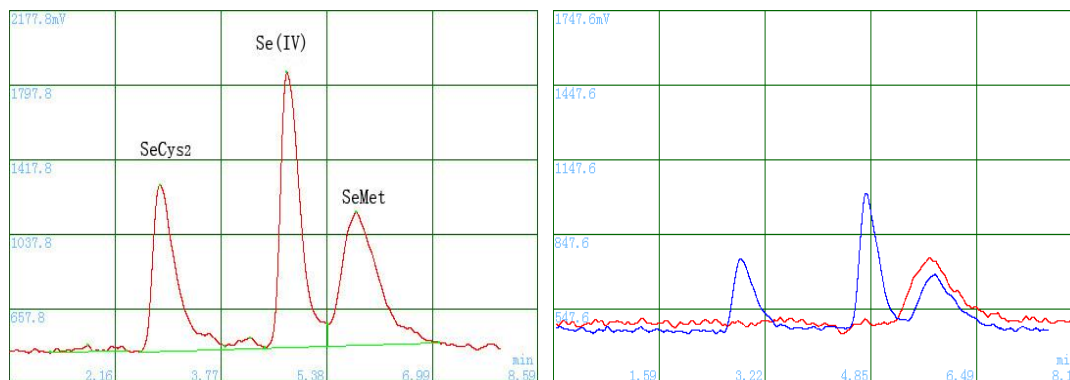


Figure 3. Chromatogram of $Se(Cys)_2$, $Se(IV)$ and $SeMet$: A Standard chromatogram of $Se(Cys)_2$, $Se(IV)$ and $SeMet$; B Overlay chromatogram of $SeMet$ in the soybean extract and standard curve

The content of $SeMet$ in the selenite-enriched soybeans was indicated in Fig. 4. Compared with the control, the content of $SeMet$ in the selenized soybeans was increased, and increased as the application concentration of sodium selenite increased. There were significant differences between the treatments. The $SeMet$ contents of Se1, Se2 and Se3 treatment were 5.85 times, 11.06 times and 18.06 times higher than that of CK.

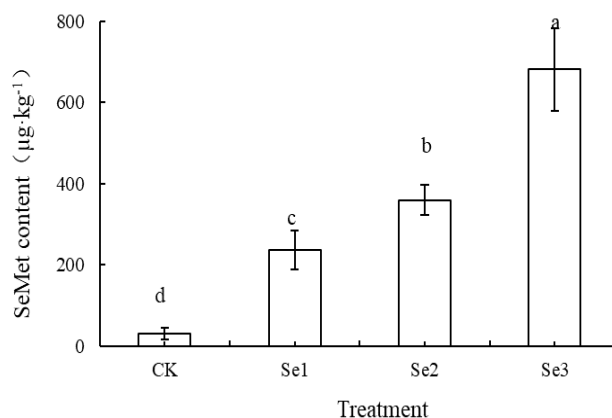


Figure 4. Effects of the Se rates on the selenomethionine content in soybean seeds. Data are the mean \pm SEM. a,b,c,d, $P < 0.05$ versus control (control means soybean were sprayed with equal amount of distilled water), $n = 3$

Effects of different selenium concentrations on CoQ10 content in soybeans

CoQ₁₀ analysis using HPLC-UV. Fig. 5A showed a chromatogram from the HPLC-UV analysis of the CoQ₁₀ standard. Fig. 5B shows an overlay chromatogram of CoQ₁₀ in the soybean extract. The method resulted in excellent resolution of CoQ₁₀ from the other lipophilic components of the 2-propanol extract with the CoQ₁₀ observed at a retention time of 12.5 min. By retention time matching, we can see that the absorption peak marked 1 was the CoQ₁₀ standard and the absorption peak marked 2 was the CoQ₁₀ in the soybean extract.

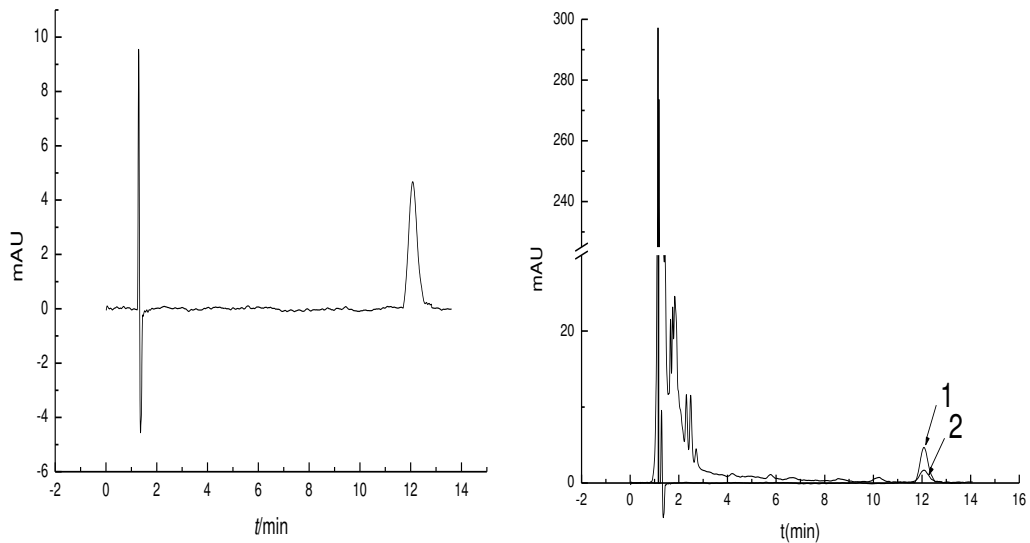


Figure 5. Chromatogram of the CoQ₁₀: A Chromatogram of the CoQ₁₀ standard; B Overlay chromatogram of CoQ₁₀ in the soybean extract (1. CoQ₁₀ standard; 2. CoQ₁₀ in soybean extract)

The contents of CoQ₁₀ in the soybean samples were indicated in Fig. 6. Compared with the control, the content of CoQ₁₀ in the selenized soybeans was increased, which resulted an increased application concentration of sodium selenite. The CoQ₁₀ levels in Se1, Se2 and Se3 increased by 0.51-2.27 times compared to those of the control.

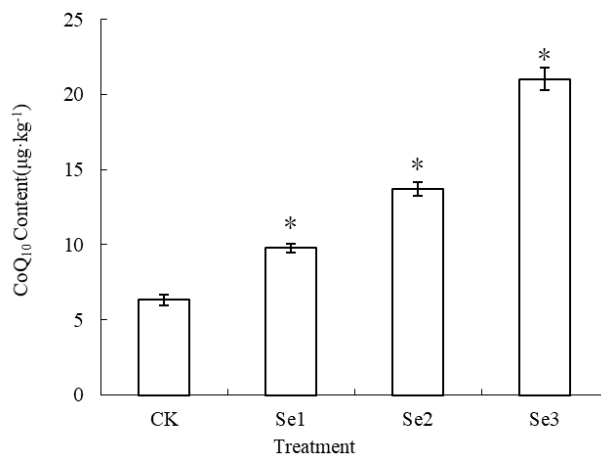


Figure 6. Content of CoQ₁₀ in soybean seeds. Data are the mean \pm SEM. * $P < 0.05$ versus control (control means soybean were sprayed with equal amount of distilled water), $n = 3$

As seen in Fig. 7, the soybean seeds showed a good linear relationship between the content of CoQ₁₀ and the SeMet content under different contents of selenium fertilizer in the test, using the linear equation: $y = 0.0256x + 5.4321$. This result was likely because selenium can promote the synthesis of CoQ₁₀, which increased the CoQ₁₀ content in the soybean seeds.

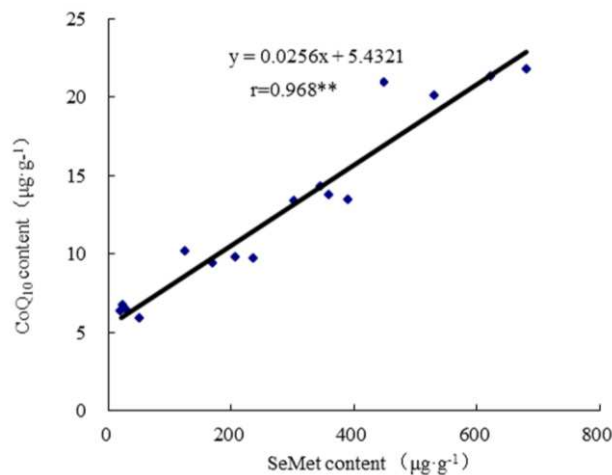


Figure 7. The relationship between the content of CoQ₁₀ and SeMet in soybeans. Data are the mean ± SEM. ** $P < 0.01$ versus control (control means soybean were sprayed with equal amount of distilled water), $n = 3$

Repeatability and recovery test

Four soybean flour, one blank, the remaining three were added 200, 300, 400 µL of the standard 100 µg/mL, the reproducibility and recovery rate of the solution were tested. Repeat two times to take the average as a result. The CoQ₁₀ content of blank samples was deducted and the recovery rate was calculated. The results showed that the recovery rate was 81.29%-87.64%. The recovery and reproducibility were good.

Discussion

Plants have the capability to convert inorganic Se into organic Se such as Se-Cys and thus plant metabolism can be beneficially exploited for obtaining Se-rich crop, commonly known as biofortification (Pilon-Smits et al., 2009; D'Amato et al., 2018). Se was considered as a useful element, but not an essential element for higher plants. Se improves photosynthetic rate, growth and biomass accumulation in a range of plant species (Pilon-Smits et al., 2009). Previous research has shown that SeMet was the primary selenium compound in the bean (Chan et al., 2010). According to the reports of Gao et al. (1999), methionine (Met) can significantly improve CoQ₁₀ content in tobacco. Li et al. (2009) found that certain concentration of Met had a good effect on the growth of tobacco cells and the synthesis of CoQ₁₀ in tobacco experiments. Met was a methyl donor that can enrich the sources of raw materials for the synthesis of CoQ₁₀ and increase the CoQ₁₀ content. Possible mechanism for catalytic body by adenosyltransferase, Met reacted with ATP to form the active S-adenosylmethionine (SAM). The active methyl can be transferred to various methyl acceptors to form methyl compounds. Under different methyl transferase enzymes, three methyls of CoQ₁₀ were provided by S-adenosine methionine (Fofana et al., 2014) and selenium can promote the synthesis of Met. Therefore, an increase in the amount of selenium can improve the content of the methyl donor precursor of Met for the synthesis of CoQ₁₀, thereby increased the CoQ₁₀ levels (Yu, 2001; Fofana et al., 2014).

Early studies have found that selenium has affected on the content of CoQ₁₀ in animals. Therefore, we were interested in the content of CoQ₁₀ in Soybean after selenium fertilization. Vadhanavikit et al. (1994) studied the effect of long-term (18 months) selenium deficiency on the levels of liver coenzyme Q in the rat. The results showed that level of coenzyme Q₁₀ in the liver of selenium-deficient rats were 67% of the levels in selenium-adequate animals. According to Pedersen et al. (1999) survey, CoQ₁₀ in the Eskimos living in Greenland was significantly higher than that in other regions population, and it was significantly positively related to the intake of selenium in the diet. This was attributed to the marine animal diet, and the selenium content of marine animal was generally high. Animal experiments had also confirmed that adding selenium to animal feed can increase the level of CoQ₁₀ in the heart. The results of this experiment are of great significance to the study of the effect of selenium on coenzyme Q₁₀ content in plants.

Conclusion

The effect of the content of SeMet on CoQ₁₀ in soybeans was reported for the first time. In this study, the content of SeMet and CoQ₁₀ was determined in soybeans. The application of increased selenium concentrations can significantly improve the CoQ₁₀ in soybean seeds.

Acknowledgements. The study was funded by the Heilongjiang postdoctoral fund (China, Grant no.LBH-Z16016).

REFERENCES

- [1] Cankur, O., Yathavakilla, S. K. V., Caruso, J. A. (2006): Selenium speciation in dill (*Anethum graveolens* L.) by ion pairing reversed phase and cation exchange HPLC with ICP-MS detection. – *Talanta* 70: 784-790.
- [2] Chan, Q., Afton, S. E., Caruso, J. A. (2010): Selenium speciation profiles in selenite-enriched soybean (*Glycine Max*) by HPLC-ICPMS and ESI-ITMS. – *Metallomics* 2: 147-53.
- [3] D'Amato, R., Fontanella, M. C., Falcinelli, B., Beone, G. M., Bravi, E., Marconi, O. (2018): Selenium biofortification in Rice (*Oryza sativa* L.) sprouting: effects on se yield and nutritional traits with focus on phenolic acid profile. – *Journal of Agricultural and Food Chemistry* 66: 4082-4090.
- [4] Ding, G. B., Nie, R. H., Lv, L. H., Wei, G. Q., Zhao, L. Q. (2014): Preparation and biological evaluation of a novel selenium-containing exopolysaccharide from *Rhizobium* sp.N613. – *Carbohydrate Research* 109: 28-34.
- [5] Fang, Y., Chen, X., Luo, P. Z., Pei, F., Kimatu, B. M., Liu, K. L., Du, M. J., Qiu, W. F., Hu, Q. H. (2017): The Correlation Between In Vitro Antioxidant Activity and Immunomodulatory Activity of Enzymatic Hydrolysates from Selenium-Enriched Rice Protein. – *Journal of Food Science* 82: 517-522.
- [6] Fofana, B., Main, D., Ghose, K. (2014): Selenomethionine and Total Methionine Ratio is Conserved in Seed Proteins of Selenium-Treated and Nontreated Soybean, Flax, and Potato. – *Crop Science* 54: 2551-2561.
- [7] Gao, X. Y., Kang, Q. L., Mu, H. (1999): Effects of a few Organic Substances on the Formation of Coenzyme Q10 in Tobacco (*Nicotiana tobacum* L.) Cells in Suspension Culture. – *Chinese Journal of South China Agricultural University* 20: 51-56.

- [8] He, Q., Lu, L. B., Zheng, X. H. (2010): Qualitative and quantitative analysis of coenzyme Q10 from Soybean. – *J. Chin. Cereals and Oils Association* 25: 126-128.
- [9] Lenaz, G., Fato, R., Formiggini, G., Genova, M. L. (2007): The role of Coenzyme Q in mitochondrial electron transport. – *Mitochondrion* 7S: S8-S33.
- [10] Li, G. X., Lee, H. J., Wang, Z. (2008): Superior in vivo inhibitory efficacy of methylseleninic acid against human prostate cancer over selenomethionine or selenite. – *Carcinogenesis* 29: 1005-1012.
- [11] Li, Y. H., Lv, C. M., Fan, H. Y. (2009): The effect of precursor substances on the synthesis of coenzyme Q (10) in tobacco cells. – *Tobacco Science and Technology* 263: 51-55.
- [12] Liu, Y., Yu, Y., Lou, S. G., Peng, X., Jiang, B. (2003): Effects of selenium on CoQ10 content and ultrastructure of mitochondria and chloroplast in Soybean Leaves under continuous cropping stress. – *The Tenth National Congress and the fifth Cross Strait Academic Symposium on Soil and fertilizer China Soil Society*: 136-138.
- [13] Nothstein, A. K., Eiche, E., Riemann, M., Nick, P., Winkel, L. H. E., Göttlicher, J., Steininger, R., Brendel, R., von Brasch, M., Konrad, G., Neumann, T. (2016): Tracking Se assimilation and speciation through the rice plant - nutrient competition, toxicity and distribution. – *Plos One* 11: e0152081.
- [14] Ozer, E. K., Goktas, M. T., Kilinc, I., Pehlivan, S., Bariskaner, H., Ugurluoglu, C., Iskit, A. B. (2017): Coenzyme Q10 improves the survival, mesenteric perfusion, organs and vessel functions in septic rats. – *Biomedicine & Pharmacotherapy* 91: 912-919.
- [15] Pedersen, H. S., Mortensen, S. A., Rohde, M. (1999): High serum coenzyme Q10, positively correlated with age, selenium and cholesterol, in Inuit of Greenland. – *Biofactor* 9: 319-323.
- [16] Pilon-Smits, E. A., Quinn, C. F., Tapken, W., Malagoli, M., Schiavon, M. (2009): Physiological functions of beneficial elements. – *Current Opinion in Plant Biology* 12: 267-274.
- [17] Steel, R. G., Dickey, D. A., Torrie, J. H. (1996): Principles and procedures of statistics: A biometrical approach. – *McGraw-Hill College* 672.
- [18] Tawfik, M. K. (2015): Combination of coenzyme Q10 with methotrexate suppresses Freund's complete adjuvant-induced synovial inflammation with reduced hepatotoxicity in rats: effect on oxidative stress and inflammation. – *International Immunopharmacology* 24: 80-87.
- [19] Vadhanavikit, S., Ganther, H. E. (1994): Selenium Deficiency and Decreased Coenzyme Q Levels. – *Molecular Aspects of Medicine* 15: s103-s107.
- [20] Yang, Y. L., Liu, Y. Y. (2014): Distribution of selenium in selenite-enriched soybean. – *Journal of Chemical and Pharmaceutical Research* 6(4): 318-321.
- [21] Yu, Y. (2001): Effects of Selenium on CoQ10 and Membrane Lipid Peroxidation of soybean under Salt and Continuous Cropping Stress. – *Northeast Agriculture University, Harbin*.

INVESTIGATION OF FACTORS AFFECTING THE ORGANIC AGRICULTURAL PRODUCTION AMOUNT IN TURKEY: A PANEL DATA ANALYSIS

BAHSI, N.

Osmaniye Korkut Ata University, Kadirli School of Applied Sciences, Department of Organic Farming Management Business Kadirli Campus, 80750 Osmaniye, Turkey
e-mail: nerminbahsi@osmaniye.edu.tr; phone: +90-328-888-0090; fax: +90-328-888-0091
ORCID ID: 0000-0003-1630-7720

(Received 31st Dec 2019; accepted 23rd Mar 2020)

Abstract. As a result of the fact that materials and practices used to increase productivity in agricultural production all over the world are harming the environment in different ways due to increasing concerns about the environment and health, organic agriculture has come to the forefront. These concerns lead to an increase in the demand for organic products by consumers, and lead to an increase in production. The purpose of this study, organic farming production which is expected to ensure the protection of the environment and human health is to examine the factors that influence. By using panel data analysis method, the relations between organic agriculture production amount and organic agriculture production area and number of farmers were examined. To this end, in Turkey the 2003-2018 period was included in a research conducted on the production of 43 provinces on a regular basis. There results indicated that in all panel data models, the total organic agricultural production across the country was between 66.01% and 67.79%, the number of farmers and the explanatory power of the production area and the organic agricultural production value between 34% and 35% depended on other factors. Panel data shows that the impact of the cultivation area is greater than the number of farmers.

Keywords: *organic production, organic farm field, number of organic farmers, Pooled OLS, fixed effects, random effects*

Introduction

Although there is an expansive consensus in literature on the topic of agricultural sustainability, sustainable agriculture is defined in different manners. But with its widest use, it can be defined as “the maintenance of agricultural operations in the future”. Just as Marsh (1997), Ambroise et al. (1998), Legg and Viatte (2001), and Gafsi et al. (2006) specified in their studies, the growing interest in sustainable agriculture is relevant because of the negative impacts of conventional agriculture on environmental quality and the wealth of resources, deterioration in human health, and the clear effects of the desertification of rural areas, especially in developed countries. In the focus of attention on sustainable agriculture is not just the avoidance of influences that are harmful to the environment and the health of living beings but also ensuring the ability of the maintenance of agricultural operations as they exist around the world by preserving the quality and wealth of soil and water. Sustainable agricultural operations carry economic value and are a driving force in the development of countries.

The growing phenomenon of agricultural sustainability can be descriptive of the improvements in the sustenance conditions for the rural segment, may provide for a relative decrease in food production, and may contribute to other important functions. Along with creating a significant impact over local and regional food security with mainstays for people in rural segments should these approaches be commonly adopted, the benefits that improvements that contribute to food security and natural, social, and

humane capital provide with open support through means of international, national, and local policy reforms can spread to numerous farmers and rural areas in the coming years (Pretty et al., 2003). Especially in recent years, the provision of the expansion of the sector has become an important topic in terms of sustainable agriculture by regaining for the sector people who ended their operations due to rising costs and falling profit margins and with people who will be newly added.

While there exist different approaches on the topic of ensuring and maintaining agricultural sustainability, sustainability must ensure an increase in yield as well as food security and must materialize in a manner cleansed of elements that threaten human and environmental health. This is because the phenomenon of sustainability is a comprehensive and important concept that increases in yield alone cannot explain.

Similar important emphasis is on taking the measures necessary to reduce the intensity of the use of inorganic fertilizers and insecticides, to control the deterioration of agricultural fields, and to increase the profit margins of farmers by reducing the costs of production. Farmers also must encourage the use of organic fertilizers and integrated insect-management technologies to control pests. These types of inputs produce the possibility of reducing the intensity of use and thus increasing the profit margin of farmers without sacrificing the yield of the goods. The effective implementation of these types of policies requires the repeated guidance of the sector, which has thus far focused on the promotion of traditional agriculture (Zulfiqar and Thapa, 2016, 2017). Along with sustainable agriculture and other natural resources, another important element that will execute agriculture are farmers. The people who will realize agricultural production operations must be made aware on the topic of sustainability and be included in the process. This is because farmers are the most important stake holder of sustainable agriculture.

Organic agriculture has come to the fore around the world due to the observance that materials used and practices performed to increase yield in agricultural production harm the environment in different ways and due to the increase in environmental concerns. Organic agriculture is among the systems of sustainable agriculture. Earth and water resources are not unlimited, and breakdowns that occur in the environment cannot be easily resolved. In this regard, the sustainability of agricultural capacity and the healthy use of natural resources are an important issue. In a system of sustainable agriculture, the deterioration of the environment is reduced, yield is attempted to be preserved, short- and long-term economic vibrancy is encouraged, and living standards are aimed to be increased by preventing migration in the rural segment (Turhan, 2005). Agricultural practices that may be environmentally harmful must be withdrawn and environmental and agricultural sustainability must be shown in an integrated manner in terms of ensuring the sustainability of environmental quality in relation to the problems that have been on the agenda in recent years especially. In this regard, organic agriculture carries importance on the topic of environmental sustainability.

Organic agriculture is a topic that came to the fore in the 1920s around the world based on the idea that it was necessary to turn to forms of natural production to prevent the harm caused to the environment by agricultural production. It has exhibited clear developments in different regions. However, especially in the 1970-80 period, societies' increased sensitivity to the environment and their shift toward foods and products not harmful to health in turn increased demand for organic agricultural products while also increasing the market volume. It is striking that developed countries began to reach the position of consumer while developing countries reached the position of producer

(Kızılaslan and Olgun, 2012). The national and international standards on the topic of organic agriculture were created after 1980. However, it does not appear possible to meet the food needs of the global population with products acquired from organic agriculture in small areas. Organic agricultural practices in Turkey began not to meet domestic need but to be implemented for exports upon the demand of countries purchasing agricultural products from us. The provision of the expansion of demand in domestic markets together with foreign markets causes an increase in the volume of organic agriculture and will provide benefit in terms of sustainable agriculture.

Although it is low, the people who demand organic products around the world comprise high-income people who want to pay in excess for these. Behind the higher payments for organic products are the roles of factors like environmentally friendly methods of production, low levels of pesticides in foods, products cultivated by small family farms, agricultural workers being subjected to fewer insecticides, and there existing greater flavor or nutritional content among the others (Thompson, 2000).

Demand for and production of organic food products is quickly rising today because of growing concerns for food security. Organic production also is an environmentally friendly system of agriculture that aims for high-quality products and agricultural practices that don't harm the environment or people. However, insufficient market supply, traceability, lack of consumer knowledge about market position, and the high price that emerges when compared with other traditional foods are the main factors that influence the purchase behaviors of people (Narmilan and Sugirtharan, 2015). Although there are various reasons in the tendencies toward organic products, the most important factors are income and price effect. By providing for an increase in production and a decrease in prices due to the spread of organic agriculture over a wide area, the consumption of organic products by more people and the spread of the benefits that arise in relation to this to all shareholders must be ensured.

The increase in demand leads to an increase in the volume of trade in organic agricultural products worldwide and countries are making efforts to increase the production of organic agricultural products in order to gain more shares from this market. The increase in agricultural production depends on the quantity and quality of the inputs (land, labor, seed, fertilizer, medicine, etc.) used in production. In addition, product prices in the market and subsidies provided by the government are among the factors that direct producers to produce more agricultural production. However, the effect of each factor on the amount of production is different. On the other hand, consensus has been reached on minimizing the amount of agricultural inputs such as pharmaceuticals and fertilizers which are thought to have a negative impact on the environment and health in organic agriculture. Therefore, it is thought that other factors will have more effect on the increase in organic production. It is necessary to investigate how the desired rate of increase can be achieved and to determine which factors influence the amount of production. When determined how rate of which factor is effective, the measures to be taken to increase the amount of organic production to the desired level can be determined more clearly.

In the literature, there are studies (Isin et al., 2007; Toma and Mathijs, 2007; Alexopoulos et al., 2010; Kafle, 2011; Lapple and Rensburg, 2011; Jierwiryapant et al., 2012; Rana et al., 2012; Asadollahpour et al., 2014; Shams, 2017; Bostan et al., 2019) investigating the factors affecting the adoption of organic agriculture. In addition, there are studies (Hepelwa et al., 2013; Brenes-Munoz et al., 2016; Gupta et al., 2019) investigating the factors affecting the expansion of the land, which is an important factor

in the increase of agricultural production. No studies investigating the factors affecting organic agricultural production and the effects of these factors on production have been evaluated.

The purpose of this study, organic farming production which is expected to ensure the protection of the environment and human health is to examine the factors that influence.

Organic Agriculture Around the World

Although organic agriculture has existed as a concept for about 100 years, it gained significant interest from consumers, environmentalists, farmers, and, finally, political structures around the world only since the 1980s. Growing concerns on the topic of the negative environmental impacts that the industrialization of the agricultural sector after this turning point, World War II, brought were influential (Varini and Andrighetto, 2019).

One of the topics that has come to the agenda in recent years with globalization is the concept of sustainability. Organic agriculture has assumed a key role when considering the tendencies in agriculture regarding globalization and sustainability. In recent years, organic agriculture has quickly spread both in Turkey and around the world and has captured the attention of consumers and producers. In this context, the organic food market is gradually growing in a global sense, and those who wish to receive a share of this market increase the levels of competition with the new tendencies (Deviren and Çelik, 2017). Growing economic and political instability in European countries (migration issues, Brexit, referendum in Catalan, etc.) contributed to the instability of currency exchange rates and to the general drop in the growth of the consumer market (including organic food markets) (Nechaev et al., 2018).

Along with the developments experienced in various countries in recent years, organic agriculture has actually been a popular and striking topic for years. To look at the primary indicators regarding organic agriculture in the report (2019) that the Research Institute of Organic Agriculture (FIBL) and the International Federation of Organic Agriculture Movements (IFOAM) prepared:

Organic agricultural operations have taken place in 181 countries around the world since 2017. However, there are nine countries that have organic regulations around the world. The total organic agriculture space comprises 69.8 million hectares, and the countries with the largest organic agricultural space are Australia (35.6 million hectares), Argentina (3.4 million hectares), and China (3 million hectares). In 1999, when organic agricultural operations began to become popular, the global organic agricultural space comprised a total 11 million hectares. The share within the total agricultural space for organic agricultural space was 1.4% in 2017.

The regions that have the largest organic agricultural spaces are Oceania (35.9 million hectares, half of the world's organic agricultural fields), Europe (14.6 million hectares, 21%), Latin America (8 million hectares, 11%), Asia (6.1 million hectares, 9%), and North America (3.2 million hectares, 5%). However, nearly one in four (16.8 million hectares) of organic agricultural space in the world and more than 87% (2.4 million) producers are found in developing countries and developing markets (Willer et al., 2019). Liechtenstein receives the greatest share of organic agriculture area within the total agricultural area by country (37.9%). Following this are Samoa (37.6%) and Austria (24%).

The wild collection spaces and other non-agricultural spaces around the world (e.g. apicultural operations) are 42.4 million hectares. These areas are the greatest in Finland (11.6 million hectares), Zambia (6 million hectares), and Tanzania (2.4 million hectares). The wild collection spaces and other non-agricultural spaces around the world were 4.1 million hectares in 1999.

The number of people who perform organic agricultural operations around the world is 2.9 million, considering the numbers of producers. The countries in which there are the most organic agricultural producers are India (835,000 people), Uganda (20,352), and Mexico (20,000). The total number of people who were performing organic agricultural operations around the world in 1999 was 200,000.

The global organic market was at a level of \$17.9 billion in 2000, but this figure reached \$97 billion (about €90 million) in 2017. The countries with the greatest share within the organic market are the United States (\$45.2 billion), Germany (\$11.3 billion), and France (\$8.9 billion). Switzerland ranks first in the world in the consumption of organic products per capita (\$325). Apart from this, Denmark (\$315) and Sweden (\$268) top the list in consumption of organic products per capita. The global average consumption of organic products per capita is \$12.8. To evaluate the organic market by region, North America is in a leading position (\$46.35 billion), and behind it are Europe (\$40.21 billion) and Asia (\$10.35 billion) (Lernoud and Willer, 2019). The ranking of the countries with the greatest share in the global organic market and the greatest consumption per capita show us the effect of income in the demand for organic products. This is because the national income per capita for the countries in the rankings materialize much higher than the global average.

The organic food market continues to develop, with global sales reaching \$97 billion in 2017. Organic products are produced in almost every country anymore, but demand is gradually increasing. North America and Europe acquire almost 90 percent of the global revenue in the organic market, but these two markets constitute just one-fourth of the organic area. No matter how much domestic markets develop, most organic products cultivated in Asia, Africa, and Latin America are targeted at export markets (Sahota, 2019). In addition to this, Asia has the third largest market for organic products. Historically, the most important consumer markets are Japan and South Korea, and increases in demand are experienced in especially the Chinese and Indian markets in Asia with the driving force of food scandals and health scares (Sahota, 2019).

Organic Agriculture Around Turkey

Although organic agriculture came to the fore in the 1920s around the world based on the idea that it was necessary to turn to forms of natural production to prevent the harm caused to the environment by agricultural production, it began not based on domestic demand in Turkey but based on exports in the 1980s, in line with the demand coming from European countries. Exports initially began with traditional products like dried grapes, apricots, and figs and continue with production of eight products from 1985-1986 up to the 1990s. The first serious attempt at organic agriculture took place with the opening of organic product stores by a civil society organization between the years of 1998-2000 (Merdan, 2018). In Turkey, just as around the world, organic agriculture markets are constantly expanding for reasons such as the propagation of environmental awareness, agricultural sustainability, and health concerns. The change of consumer preferences ensured an increase in the diversity of organic products.

According to 2017 data in IFOAM and FIBL (2019), Turkey ranks 17th in the world in terms of organic agricultural space. It is seventh in terms of the number of organic producers. It is eighth in terms of organic agricultural spaces in Europe and first in terms of number of producers with a 19% share.

Data related to the development of organic production in Turkey were collected from Ministry of Agriculture statistics about organic farming (2019). In 2002, approximately 12,428 producers produced 310,125 tons of organic products on 89,827 hectares of land, while as of 2018, 791,663 producers produced 2,371,612 tons of organic products on 626,885 hectares of land. Although the number of products and areas of organic production vary in years, the number of farmers engaged in organic production and production amounts generally tend to increase continuously. The average annual increase in organic agriculture in Turkey between the years 2002-2018 are as follows: the number of products 2.2%, number of producers 12.3%, production area 12.9%, produce amount 13.6%. Despite the continuous development of areas for organic agriculture in Turkey, the share in total agricultural land is only 1.4%, according to data from 2017. While 64% of the total production areas were farming areas in 2002, 86% of the total organic production areas were farming areas in 2018. In 2018, 86.7% of the total organic production (transition process excluded) was made up of farming products, while 13.3% is collected from nature. In 2018, 27.7% of the production and 27.1% of the production areas were made up of transition process production. Inclusion of organic agricultural production in support since 2005 also has an impact on the developments of organic agriculture sector in Turkey.

In addition to external demand, domestic demand has been continuously increasing in recent years due to health concerns and environmental awareness. In 2018 a total of 213 kinds of organic products are produced in Turkey. These products are not only products grown by manufacturers, but also include products such as blackberries, rosehip, thyme, centaury, hawthorn, a blend of powdered thyme grass and raspberries that grow spontaneously in nature. In addition, some cultivated products are grown wild in nature and are considered as organic products collected from nature. Turkey has an important potential at the point of collection and evaluation of these products as organic. 9.6% of the total production in Turkey is composed of organic wild collection products.

In 2018, with the maximum amount of production in organic agriculture in Turkey Aydın province (352 639 tonnes), Manisa (220 293 tonnes) and Van (166 784 tonnes). The provinces with the highest organic production area in terms of production area were Aydın (73933 hectares), Van (61293 hectares) and Kayseri (53889 hectares). The provinces with the highest number of organic farmers were Aydın (14388 people), Rize (10711 people) and Van (4595 people). The most produced organic products in 2018 were olives (213369 tons), wheat (195131 tons) and apples (98136 tons). The ratios of these products in total organic production were listed as olives (11.4%), wheat (10.8%) and apples (10.4%).

The development of organic animal products not increased like crop production in Turkey. All entries must be organic to organic farming, the plant must be suitable for the welfare of animals, organic reasons such as lack of meadows and pastures organic farming makes it difficult and costly in Turkey (Dalbeyler and Işın, 2017). The number of farmers engaged in organic animal farming was reached 5,177 in 2018. The number of farmers engaged in beekeeping increased from 256 to 455. In 2018, approximately 68% of the farmers engaged in organic farming produce broiler and ovary chickens, while 20% of them are bovine and about 12% of them are sheep.

Although red meat production varies each year. Total organic milk production was 12,884 tons in 2018. Production of organic cheese, yogurt, butter and cream is not produced regularly but in 2018, 15 tons of cheese, 1 ton of butter and 7 tons of cream were produced. There is no production of organic yogurt.

To increase organic agriculture, direct income support for crop production has started in 2005, in Turkey. Later, the scope was expanded to include livestock, aquaculture and beekeeping. Organic livestock subsidies started in 2011. Producers engaged in organic farming has to registered to the Farmer Registration System and Organic Agriculture Information System to get benefit from support payments in crop production. Government support given to organic farmers in Turkey area-based payments, contract manufacturing, leasing of organic farming for treasure land, low-interest investments and business loans, support for the protection of the environment for agricultural land, state can be listed as supports for the rustic arrangements.

Entrepreneurs who produce organic agricultural products and inputs have been given the opportunity to use operating and investment loans within the scope of the low interest agricultural loan application since 2004. In addition, the Ministry of Agriculture and Forestry signed a grant agreement to farmers who participated in the Environmental Protection of Agricultural Land (ÇATAK) Program in order to take necessary cultural measures to protect soil and water quality in agricultural lands, sustainability of renewable natural resources and mitigate the negative effects of intensive agricultural activities. support payments are made. Within this scope, 240.2\$ / ha (The average exchange rate of the relevant years has been taken into consideration in the conversion of the local currency into foreign currency) is paid for 3rd category environmentally friendly agricultural techniques and cultural practices (Ministry of Agriculture and Forestry, 2019).

In 2018, organic farming supports were organized into 4 categories. Scope of support; The first category (Fruit-Vegetable and Medicinal-Itri Plants) products found in 221.2\$ / ha (The average exchange rate of the relevant years has been taken into consideration in the conversion of the local currency into foreign currency), the second category products (Pistachio and Olives) 154.87\$ / ha, the third category (field crops with high economic value) 66.37\$ / ha products, the fourth category (Other products and fallow) products are 22.12\$ / ha. In addition, organic beekeeping support is provided as 2.21\$ per bee hive.

Materials and Methods

In the study, organic agricultural production data of 43 provinces in Turkey between 2003 and 2018 were used. According to data from the Ministry of Agriculture and Forestry in all provinces (81 provinces) have organic agricultural production. All provinces data were collected, and provinces having data not suitable for panel data analysis were excluded. Provinces without regular organic production in the period included in the analysis were excluded from the analysis. In other words, 43 provinces in total were subjected to the research between 2003 and 2018. Provinces (painted in yellow) used in the panel data analysis were given in the *Figure 1*.

The increase in agricultural production depends on the increase in the quantity and quality of the inputs to be used in production. However, in organic agriculture, it is aimed to protect the environment and human health by reducing the use of inputs such as drugs and fertilizers in order to ensure sustainability in agriculture rather than

increase productivity. For this reason, it is considered that the most important factor in order to increase the production in organic agriculture is to increase the agricultural areas. In the research, the variables of the amount of organic agricultural production of the provinces and the production area and number of farmers were used for the analysis of the factors affecting the amount of organic agricultural production.



Figure 1. Provinces included in panel data analysis

StataMP 14 (64 Bit) was used for data analysis. In this study, panel data analysis was used to examine the relationships between variables. There are some advantages of using panel data models: increasing the sample size; capturing the heterogeneity involved both in cross-section units and time dimensions; testing hypotheses about the presence of heteroscedasticity or autocorrelation, or both; and, finally, they are better suited to study the dynamics of change and complex behavioral models (Gil-Garcia and Puron-Cid, 2013). Panel data model is estimated by using one of the Pooled Least Squares (HEKK - Pooled OLS, Classic Model), Fixed Effects and Random Effects approaches (Onder, 2017). In the panel data analysis, total organic agriculture production values were examined separately for each Pooled OLS, Entity Fixed Effects Model, Random Effects Model and Entity and Time Fixed Effects Model. As with all time series analysis, in panel data analysis that performs both time and horizontal section analysis together, variables should be stationary in order not to cause false relationships between variables (Baytar, 2012). In study, Levin-Lin-Chu (2002) and Pesaran's (2006) CADF tests were used for unit root tests.

Results

General tendencies of the variables included in the analysis for the period 2003-2018 were shown in the *Figure 2*, *Figure 3* and *Figure 4*.

According to *Figure 2*, the change in production areas is generally constant trend and there is an irregular change in provinces 10, 12, 16, 21, 24, 25, 27 and 34. An increase was observed in 12 and 28 provinces by years.

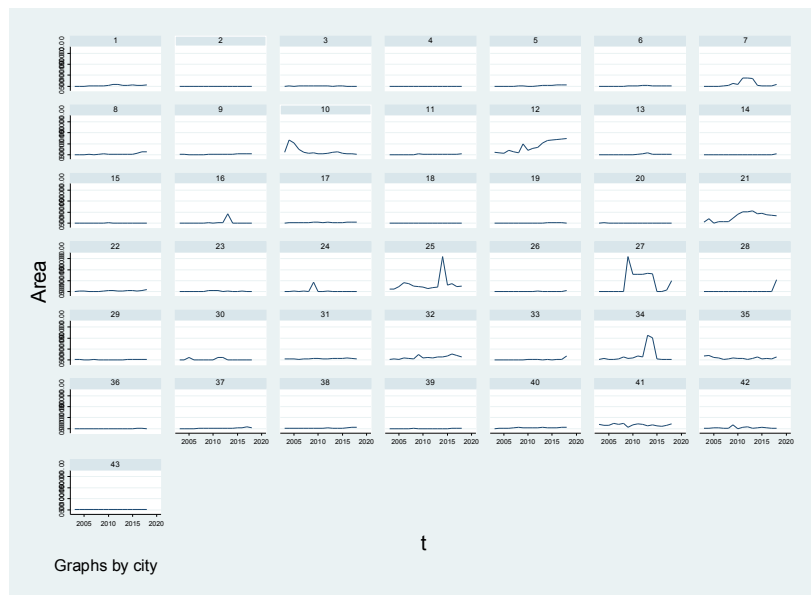


Figure 2. Distribution of area values for each province by years

According to *Figure 3*, although 8, 9, 12, 21, 25, 27, 29, 31, 32, 37 and 41 provinces have increased year by year, there is a very limited increase over the whole time period (2003-2018). The increase in provinces 12, 21 and 32 has a significant upward trend over the period of time.



Figure 3. Distribution of total production value for each province by years

In general, the number of farmers in the provinces has a stable series structure compared to the years and a significant increase trend has been observed in the 5 and 12 provinces over time (*Figure 4*).



Figure 4. Distribution of the number of farmers by year for each province

Descriptive statistics of the parameters used in the study are given in *Table 1*.

Table 1. Descriptive statistics of the parameters used in the research

	Mean	Std. Deviation	Range
Total organic production	19007.54	41463.68	0-360228.2
Total organic farm area	6795.354	15918.99	0.85-160273.5
Number of farmers	720.5029	1650.205	0-14388

In order for econometric analysis to yield reliable results, it is necessary to determine whether the variables have a unit root. Levin-Lin-Chu (LLC) and Pesaran's CADF analysis results for unit root test of the parameters used in the research are given in *Table 2*.

Table 2. Levin-Lin-Chu and Pesaran's CADF unit root tests for research parameters

LLC Unit Root Test						
	ADF regression lags average	Barlett kernel lags average	Unadjusted t	Adjusted t	p	
Total organic production	1.23	8.00	-8.2010	-1.2061	0.1139	
Total organic farm area	0.79	8.00	-10.3415	-3.7440	0.0001	
Number of farmers	1.28	8.00	-6.3889	1.1193	0.8685	
Pesaran's CADF Unit Root Test						
	t-bar	CV10	CV5	CV1	Z	p
Total organic production	-1.955	-2.540	-2.620	-2.760	2.176	0.985
Total organic farm area	-2.067	-2.540	-2.620	-2.760	1.449	0.926
Number of farmers	-1.325	-2.540	-2.620	-2.760	6.262	1.000

Since different panel data models (Pooled OLS, Entity Fixed Effects Model, Random Effects Model and Entity and Time Fixed Effects Model) will be compared, both I.st and II.nd generation unite root tests were used together. II.nd generation unit root tests also show horizontal dependency. Since models used in panel data include Vector Error Correction Model (VECM), cointegration was not analyzed. According to LLC unit root test results, whereas area does not contain unit root ($p < 0.05$), Quantity and Number of Farmers data contain unit root ($p > 0.05$). According to Pesaran's CADF test, all variables contain unit root ($p > 0.05$). Therefore, logarithmic transformations of variables were included in the analysis.

In panel data analysis, four models (Pooled OLS, Entity Fixed Effects Model, Random Effects Model and Entity and Time Fixed Effects Model) were used in order to compare fitness level of given models. Panel data analysis results for total organic farm production amount, organic farm area and number of farmers were given in the *Table 3*.

Table 3. Panel data analysis results for total organic farm production amount, organic farm area and number of farmers

	Pooled OLS	Entity Fixed Effects Model	Random Effects Model	Entity and Time Fixed Effects Model
Constant	2.677613*	3.145068*	3.059708*	3.000439*
Log (Farmer)	0.3291965*	0.4895464*	0.4695072*	0.4841949*
Log (Area)	0.5580943*	0.3783911*	0.4041707*	0.369698*
R ²	0.6779	0.6601	0.6649	0.6705
F-statistics for Hausmann Test	721.81 (2,683)	500.25 (2,641)	236.33 (Wald X ²)	65.12 (17,626)

According to the panel data analysis, explanation power of total organic agriculture production amount was 67.79% in OLS model, 66.01% in Entity Fixed Effects model, 66.49% in Random Effects model and 67.05% in Entity and Time Fixed model. These results indicated that in all panel data models, the total organic agricultural production across the country was between 66.01% and 67.79%, the number of farmers and the explanatory power of the production area and the organic agricultural production value between 34% and 35% depends on other factors.

According to regression coefficients of the parameters, it was found that the contribution of production area parameter to total organic production (0.5580943) was higher than the contribution of the number of farmers to total organic production (0.3291965) in OLS regression with the highest explanatory power. The ratio between these two parameters was $(0.3291965 / 0.5580943 \approx 59)$ is 59%. In other words, the contribution of the total production area was more important than the number of farmers. In this study, an evaluation was made in terms of agricultural area and number of farmers which are thought to be effective in increasing the amount of organic agricultural production. In the literature (Bor and Bayaner, 2009), it is pointed out that the area of the land to be cultivated is limited and other factors are more effective in increasing production. Although it is not possible to increase the area in conventional agriculture, the amount of production will be increased by increasing the area in terms of organic agriculture which has a very small share in total agricultural areas. In addition, the projection of minimizing the use of inputs such as pharmaceuticals and fertilizers in organic agriculture shows that the most important factor in the increase in production will be the increase in agricultural land. The results of this study confirm this.

It is seen that the amount of land and the number of farmers are important factors in increasing the amount of organic agricultural production. As the rate of adoption of organic agriculture increases, the number of farmers and the amount of land will increase accordingly. Brenes-Munoz et al. (2016) states that increases in organic area are affected by organic farming subsidies. Apart from this, other factors that are effective in the adoption of organic agriculture may also indirectly lead to an increase in the organic field. The most important of these factors are education (Gardebroek, 2002; Isin et al., 2007; Kafle, 2011), income (Jierwiryapant et al., 2012; Asadollahpour et al., 2014; Shams, 2017) and environmental factors (Toma and Mathijs, 2007; Alexopoulos et al., 2010; Lapple and Rensburg, 2011; Asadollahpour et al., 2014).

Conclusions

In today's world, agriculture maintains its importance in order to provide self-sufficiency and income for the survival of the societies and this importance reaches an even higher level. From this point of view, agricultural activities should be sustainable. However, from the past to the present day in order to ensure world nutrition, inputs used to increase productivity have threatened human health and the environment, as well as endangering food safety. Loss of biodiversity, erosion and degradation of soil structure, pollution and depletion of water resources and increasing greenhouse gas emissions are just some of the negative consequences of the current agricultural and food system (Çelik et al., 2017). Due to these negative results, the sustainability of agriculture has been suspected.

In order to ensure sustainability in agriculture, different methods and practices have been introduced over time. It was understood that agricultural inputs such as pesticides and fertilizers used to increase productivity caused great damage to productivity over time and consensus was reached on minimizing the amount of such production inputs within the framework of both good agricultural practices and organic farming practices.

On the basis of organic agriculture and good agricultural practices, however, it is more important to maintain living and environmental health, but also to optimize and conserve natural resource use, while at the same time ensuring agricultural sustainability. With an average of 2.9 million producers and a market size of 97 billion dollars, organic agriculture has grown by 102.6% and 105.3% in terms of organic agriculture, especially in the last decade when sustainability is on the agenda. Turkey's climate and soil characteristics, is an advantageous position for organic farming in terms of biodiversity. However, organic agricultural products are mainly made for export in our country. Turkey number of items in over a 16-year period from 2002-2018, 42%, manufacturer number of about 540%, production area is about 598%, the total amount of organic production was increased approximately 665%. Organic farming, despite the fact that the world has shown significant improvements in the overall share of organic farming in the total agricultural land is only 1.4% in the world and Turkey.

In order to Expansion of organic farming activities within the framework of sustainable agriculture and get an increasing share of the agricultural sector which has an important economic value in the world, it is necessary to increase the product range and production amounts.

Panel data show that the impact of the cultivation area is greater than the number of farmers. From this point of view, it can be said that in organic production, larger scale farmers or enterprises with more areas increased in years. In addition, it is beneficial to

open more areas to organic agriculture in the supports to be given. The contribution of the agricultural area and the number of farmers, which are the most basic data of organic agriculture production, to the total production is around 67% and a serious ratio of 33% points to other factors. For this reason, research should be carried out to determine the effect of these factors by including other factors which are effective on organic agricultural production in future studies. In addition, it should be investigated whether the factors affecting organic farming production have the same effect for different countries. According to the years, only two of the 43 provinces which regularly made production in Turkey has been seen increase in production area. Therefore, the increase in the area needs to be supported to increase the potential.

REFERENCES

- [1] Alexopoulos, G., Koutsouris, A., Tzouramani, I. (2010): Should I stay or should I go? Factors affecting farmers' decision to convert to organic farming as well as to abandon it. – In 9th European IFSA Symposium, Vienna (Austria): 1083-1093.
- [2] Ambroise, R., Barnaud, M., Manchon, O., Vedel, G. (1998): Bilan de l'expérience des plans de développement durable du point de vue de la relation agriculture-environnement. – *Courrier de l'environnement de l'INRA* 34: 5-9.
- [3] Asadollahpour, A., Omidinajafabadi, M., Jamalhosseini, S. (2014): Factors affecting the conversion to organic farming in Iran: A case study of Mazandaran rice producers. – *Science International (Lahore)* 26(4): 1844-1860.
- [4] Baytar, R. A. (2012): Türkiye ve BRIC ülkeleri arasındaki ticaret hacminin belirleyicileri: Panel çekim modeli analizi. – *İstanbul Ticaret Üniversitesi Sosyal Bilimler Dergisi* 11(21): 403-424.
- [5] Bor, Ö., Bayaner, A. (2009): How Responsive is the Crop Yield to producer prices? A panel data approach for the case of Turkey. – *New Medit N.* 4: 28-33.
- [6] Bostan, I., Onofrei, M., Gavriluta, A. F., Toderaşcu, C., Lazar, C. M. (2019): An integrated approach to current trends in organic food in the EU. – *Foods* 8(5): 144.
- [7] Brenes-Munoz, T., Lakner, S., Brümmer, B. (2016): What influences the growth of organic farms? Evidence from a panel of organic farms in Germany. – *German Journal of Agricultural Economics* 65(1): 1-15.
- [8] Çelik, Z., Erdal, Ü., Etöz, M. (2017): Economic dimension of ecological agriculture in Turkey and impact on climate change. – *I. Uluslararası Organik Tarım ve Biyoçeşitlilik Sempozyumu*, 27-29 Eylül Bayburt.
- [9] Dalbeyler, D., Işın, F. (2017): Organic agriculture in Turkey and its future. – *Turkish Journal of Agricultural Economics* 23(2): 215-222.
- [10] Deviren, N. V., Çelik, N. (2017): Evaluation of economic aspects of organic agriculture in the World and Turkey. – *The Journal of International Social Research* 10(48): 66-678.
- [11] FIBL and IFOAM (2019): The World of Organic Agriculture, Statistics & Emerging Trends 2019. – Willer, H., Lernoud, J. (eds.) Research Institute of Organic Agriculture (FIBL), Frick, and IFOAM - Organics International, Bonn.
- [12] Gafsi, M., Legagneux, B., Nguyen, G., Robin, P. (2006): Towards sustainable farming systems: Effectiveness and deficiency of the French procedure of sustainable agriculture. – *Agricultural Systems* 90: 226-242.
- [13] Gardebroek, C. (2002): Farm-specific factors affecting the choice between conventional and organic dairy farming. – Xth EAAE Congress 'Exploring Diversity in the European Agri -Food System', Zaragoza (Spain), 28-31 August 2002: 1-9.
- [14] Gil-Garcia, J. R., Puron-Cid, G. (2014): Using panel data techniques for social science research: an illustrative case and some guidelines. – *CIENCIA ergo-sum, Revista Científica Multidisciplinaria de Prospectiva* 21(3): 203-216.

- [15] Gupta, G., Rathore, T., Arora, G., Anand, S. (2019): Socioeconomic and biophysical drivers of agricultural intensification in India: A dynamic panel analysis using remotely-sensed data and administrative surveys (An economic characterization of india's land use change). – BTP report submitted in partial fulfillment of the requirements for the Degree of B. Tech. in Computer Science & Engineering, Indraprastha Institute of Information Technology, New Delhi, India.
- [16] Hepelwa, A. S., Selejio, O., Mduma, J. K. (2013): The Voucher System and the Agricultural Production in Tanzania: Is the model adopted effective? Evidence from the Panel Data analysis. – Environment for. Develop. Initiatives. Available from: <http://www.efdiinitiative.org/news/events/voucher-system-and-agricultural-production-tanzania-model-adopted-effective-evidence> (Date accessed: November 2019).
- [17] Isin, F., Cukur, T., Armagan, G. (2007): Factors affecting the adoption of the organic dried fig agriculture system in Turkey. – *Journal of Applied Sciences* 7(5): 748-754.
- [18] Jierwiryapant, P., Liangphansakul, O. A., Chulaphun, W., Pichaya-Satrapongs, T. (2012): Factors affecting organic rice production adoption of farmers in Northern Thailand. – *CMU. J. Nat. Sci. Special Issue on Agricultural & Natural Resources* 11(1): 327-333.
- [19] Kafle, B. (2011): Factors affecting adoption of organic vegetable farming in Chitwan District, Nepal. – *World Journal of Agricultural Sciences* 7(5): 604-606.
- [20] Kızılaslan, H., Olgun, A. (2012): Organic agriculture and supports given to organic agriculture in Turkey. – *GOÜ, Ziraat Fakültesi Dergisi* 29(1): 1-12.
- [21] Lapple, D., Van Rensburg, T. (2011): Adoption of organic farming: Are there differences between early and late adoption? – *Ecological Economics* 70(7): 1406-1414.
- [22] Legg, W., Viatte, G. (2001): Farming systems for sustainable agriculture. – *OECD Observer* 226-227: 21-24.
- [23] Lernoud, J., Willer, H. (2019): Current statistics on organic agriculture worldwide: area, operators, and market. – *The World of Organic Agriculture Statistics & Emerging Trends 2019*: 36-128.
- [24] Levin, A., Lin, C. F., Chu, C. S. J. (2002): Unit root tests in panel data: Asymptotic and finite-sample properties. – *Journal of Econometrics* 108(1): 1-24.
- [25] Marsh, J. S. (1997): The policy approach to sustainable farming systems in the EU. – *Agriculture, Ecosystems and Environment* 64: 103-114.
- [26] Merdan, K. (2018): Current state of organic agriculture in Turkey and evaluation of its potential development by means of swot analysis. – *Social Sciences Studies Journal* 4(14): 523-536.
- [27] Ministry of Agriculture and Forestry (2019): Bitkisel üretim - organik tarım. – <https://www.tarimorman.gov.tr/Konular/Bitkisel-Uretim/Organik-Tarim>. (Date accessed: July 2019).
- [28] Narmilan, A., Sugirtharan, A. (2015): Demand for Organic food Products in the urban areas of the Batticaloa District, Sri Lanka. – *Research Journal of Agriculture and Forestry Sciences* 3(11): 21-26.
- [29] Nechaev, V., Mikhailushkin, P., Alieva, A. (2018): Trends in demand on the organic food market in the European countries. – *MATEC Web of Conferences* 212, 07008, ICRE 2018, 1-10.
- [30] Onder, K. (2017): Pamuk arzını etkileyen faktörlerin panel veri ile analizi: 2000-2015. – *Eskişehir Osmangazi Üniversitesi İİBF Dergisi* 12(1): 83-98.
- [31] Pesaran, H. (2006): A simple panel unit root test in the presence of cross section dependence. – Cambridge University, Working Paper No:0346.
- [32] Pretty, J. N., Morison, J. I. L., Hine, R. E. (2003): Reducing food poverty by increasing agricultural sustainability in developing countries. – *Agriculture, Ecosystems and Environment* 95: 217-234.
- [33] Rana, S., Parvathi, P., Waibel, H. (2012): Factors affecting the adoption of organic pepper farming in India. – Poster presented at Tropentag.

- [34] Sahota, A. (2019): The global market for organic food & drink. – *The World of Organic Agriculture Statistics & Emerging Trends 2019*: 146-150.
- [35] Shams, A., Fard, Z. H. M. (2017): Factors affecting wheat farmers' attitudes toward organic farming. – *Polish Journal of Environmental Studies* 26(5): 2207-2214.
- [36] Thompson, G. (2000): International consumer demand for organic foods. – *Horl Technology* 10(4): 663-674.
- [37] Toma, L., Mathijs, E. (2007): Environmental risk perception, environmental concern and propensity to participate in organic farming programmes. – *Journal of Environmental Management* 83(2): 145-157.
- [38] Turhan, Ş. (2005): Sustainability in agriculture and organic farming. – *Turkish Journal of Agricultural Economics* 11(1): 13-24.
- [39] Varini, F., Andrighetto, J. K. (2019): Policies supporting the organic sector. – *The World of Organic Agriculture Statistics & Emerging Trends 2019*: 167-171.
- [40] Willer, H., Lernoud, J., Kemper, L. (2019): The world of organic agriculture 2019: Summary. – *The World of Organic Agriculture Statistics & Emerging Trends 2019*: 25-34.
- [41] Zulfiqar, F., Thapa, G. B. (2016): Is 'better cotton' better than conventional cotton in terms of input use efficiency and financial performance? – *Land Use Policy* 52: 136-143.
- [42] Zulfiqar, F., Thapa, G. B. (2017): Agricultural sustainability assessment at provincial level in Pakistan. – *Land Use Policy* 68: 492-502.

EFFECTS OF SUPER ABSORBENT POLYMER ON THE PHYSIOLOGICAL CHARACTERISTICS AND DROUGHT RESISTANCE OF BERMUDAGRASS [*CYNODON DACTYLON* (L.) PERS.] SEEDLINGS

CAO, Y.^{1,2*} – XIE, Q.^{1*} – WANG, J.¹ – YANG, J.¹ – XIE, Z.^{1,2}

¹College of Geography and Environment, Jiangxi Normal University, Nanchang 330022, PR China

²Key Laboratory of Poyang Lake Wetland and Watershed Research, Ministry of Education, Jiangxi Normal University, Nanchang 330022, PR China

*Corresponding authors

e-mail: yun.cao@163.com, 2829364804@qq.com

(Received 6th Jan 2020; accepted 24th Mar 2020)

Abstract. *Cynodon dactylon* (L.) Pers. seedlings was used as test material and applied five SAP concentrations: 0.00%, 0.10%, 0.20%, 0.30%, and 0.40%. The effects of the five SAP treatments on the physiological characteristics of *C. dactylon* seedlings under two water supply conditions were studied and a comprehensive drought resistance evaluation method was used to analyze and evaluate the drought resistance of *C. dactylon*. Results: (1) the concentrations of photosynthetic pigments, including Chlorophyll a, Chlorophyll b, and Chlorophyll a+b were all higher than those in the CK group when the SAP concentration was 0.10%–0.30%; (2) The malondialdehyde, superoxide dismutase, peroxidase, and catalase activities in the leaves of *C. dactylon* treated with SAP were all altered, and the concentrations of MDA were higher than those in the CK group, indicating that applying SAP could minimize the environmental stress experienced by *C. dactylon*. (3) The addition of SAP could improve the drought resistance of *C. dactylon* seedlings. Under adequate water conditions, the order of drought resistance of *C. dactylon* under the five SAP concentrations would be 0.30% > 0.10% > 0.20% > 0.40% > 0.00%, and under limited water conditions, the order would be 0.20% > 0.30% > 0.40% > 0.10% > 0.00%.

Keywords: super absorbent polymer concentrations, *Cynodon dactylon*, (L.) Pers, physiological ecological characteristics, evaluation of drought resistance, under adequate and limited water supply

Abbreviations: SAP: super absorbent polymer; *C. dactylon*: *Cynodon dactylon*, (L.) Pers; SOD: superoxide dismutase ($\text{U}\cdot\text{g}^{-1}$); POD: peroxidase ($\text{U}\cdot(\text{g}\cdot\text{min}^{-1})$); CAT: catalase ($\text{U}\cdot\text{g}^{-1}$); MDA: malondialdehyde ($\text{nmol}\cdot\text{g}^{-1}$); Chl-a: chlorophyll a ($\text{mg}\cdot\text{g}^{-1}$); Chl-b: chlorophyll b ($\text{mg}\cdot\text{g}^{-1}$); Chl a+b: the total chlorophyll content ($\text{mg}\cdot\text{g}^{-1}$); Chla/b: chlorophyll a/b ($\text{mg}\cdot\text{g}^{-1}$); Car: carotenoid ($\text{mg}\cdot\text{g}^{-1}$)

Introduction

Cynodon dactylon (L.) Pers., which is widely distributed globally but occurs predominantly in tropical and warm temperate regions (Zeng and Li, 2019; Hameed et al., 2008), is a perennial herb in the genus *Eragrostoideae* Pilger (Jayanthi et al., 2016). Because of its low height, strong breeding capacity, and drought, salinity, and heavy metal resistance (Archer and Caldwell, 2004; Kim et al., 2009; Hameed et al., 2008; Xie et al., 2016), it is widely used in soil and water conservation (Srivastava and Singh, 2012), ecological restoration, and green building (Singh et al., 2013; Leung et al., 2015). In China, *C. dactylon* is distributed in areas with varying rainfall from the north to the south. Moisture conditions influence plant survival and growth, and excessive water or drought would affect plant morphology and physiology (Hu et al., 2014).

Super absorbent polymer (SAP) is a safe and harmless polymer compound (Suresh et al., 2018). It can absorb and hold water weighing more than a hundred or even a thousand times its own weight (Zohuriaan-Mehr and Kabiri, 2008). Therefore, it could be used to improve soil structure, enhance soil water retention, reduce soil moisture loss, improve the emergence rates of plants and drought tolerance (Arbona et al., 2005; Yang et al., 2014), and promote aboveground and belowground growth (Islam, et al., 2011). Appropriate SAP concentration selection is very critical. A too low dosage would not achieve the desired effects, while a too high dosage would affect soil permeability severely (Li et al., 2019), which would, in turn, result in respiration challenges or even root rot.

In recent years, numerous studies have explored the effects of SAP on agricultural applications, soil properties, plant growth and physiology, and its influence on plant production (Fernando et al., 2017; Tongo et al., 2014; Karimi et al., 2009; Wu et al., 2018). However, studies on the physiological characteristics of *C. dactylon* under different SAP concentrations and moisture conditions have not been conducted. And whether the application of SAP to *C. dactylon* can also promote the development of aboveground part and root system is less studied. Therefore, the present study, five SAP concentrations (0.00%, 0.10%, 0.20%, 0.30%, and 0.40%) were applied to soil under two moisture conditions (adequate and limited water supply) to investigate the effects of SAP on the physiological characteristics and drought resistance of *C. dactylon* seedlings under different water availability. In addition, we explore the optimal SAP concentrations for the growth of *C. dactylon*, which could offer a theoretical basis for the application of SAP in the production and exploitation of *C. dactylon*.

Materials and methods

Experimental design

The experiments used SAP manufactured by Henan God biological science and technology, which exhibits the highest water holding capacity, at 300–500 times the SAP weight. The experimental matrices were mixed at a 1:1:1 volume ratio, and the soil, sand, and straw ash in their natural states were mixed in an experimental basin with a height of 13 cm, a length of 35 cm, and a width of 26 cm, and the weight of each substrate was 8 ± 0.5 kg. The concentration of SAP was mixed with the test substrate based on mass ratios of 0.00% (the CK group), 0.10%, 0.20%, 0.30%, and 0.40%. Before planting *C. dactylon* stolons, they were processed into 1–3 cm (2 buds) segments, placed in a basin filled with distilled water, soaked for 0.5 h, seeded by layering every pot planting 30 segment, covering 1 cm, dealing with repeated 3 times in each group. The experiments were carried out from March to May 2016 in a sun culture room at the Key Laboratory of Poyang Lake Wetland and Watershed Research, Ministry of Education, Nanchang, Jiangxi, China, lasted for 60 days. Water treatments were divided into a limited water supply group and an adequate water supply group. In the limited water supply group, the plants were watered with 150 ml every 20 days, while in the adequate water supply group, the plants were watered with 150 ml every 4 days. The soil moisture concentrations in the two treatment groups were measured using a HH2 soil moisture meter (Delta-T, Burwell, Cambridge, UK) every 3 days. The average soil moisture concentrations in the two groups were $28.5 \pm 3\%$ and $10.5 \pm 5\%$.

Determination of physiological indices of seedlings

At the end of the experiments, the seedlings were harvested from the pots, washed with distilled water, and dried. The fresh plant leaves were collected to measure the physiological indices of the seedlings. The physiological indices were determined according to Wang (2006). Chlorophyll concentrations and Carotenoid (Car) concentrations were determined following extraction with 95% ethanol and spectrophotometry. Superoxide dismutase (SOD) concentrations were determined using the nitrogen blue tetrazolium method, while peroxidase (POD) concentrations was determined by measuring guaiacol peroxidase activity using guaiacol. Catalase (CAT) concentrations were determined using the potassium permanganate titration method, and malondialdehyde (MDA) concentrations were measured using the thiobarbituric acid method (Wang., 2006).

Comprehensive evaluation of drought resistance

Analysis of drought resistance in *C. dactylon* was based on the measured physiological indicators. Principal component analysis was adopted for performing dimensionality reductions on the original indices, and Equation 3 was used to determine the percentages of each factor. Subsequently, Equations 1, 2, and 4 were used for the evaluation of each synthetic index of drought resistance, in addition to SOD, POD, and MDA in the anti-subordinate function analysis, the remaining indexes using the method of subordinate function. Eventually let every comprehensive index can represent the difference basically between the original.

(1) Membership function analysis (Wang et al., 2013):

Membership function values:

$$R(X_i) = (X_i - X_{\min}) / (X_{\max} - X_{\min}) \quad (\text{Eq.1})$$

Anti-membership function values:

$$R(X_i) = 1 - (X_i - X_{\min}) / (X_{\max} - X_{\min}) \quad (\text{Eq.2})$$

Where X_i is the index value, and X_{\min} and X_{\max} are the minimum and maximum values of any indices of the test materials.

(2) Weight calculation:

$$W_i = \frac{P_i}{\sum_{i=1}^n P_i} \quad i = 1, 2, \dots, n \quad (\text{Eq.3})$$

Where W_i is the important degree of the i th comprehensive index in all indices, and P_i is the contribution rate of the i th comprehensive index.

(3) Evaluation of drought resistance:

$$D = \sum_{i=1}^n [R(X_i) \times W_i] \quad i = 1, 2, \dots, n \quad (\text{Eq.4})$$

Where D value is the comprehensive evaluation value of plant drought resistance calculated at the concentration of different super absorbent polymer concentrations.

Statistics analysis

Data analysis was completed by MS Excel 2010 (Microsoft Corp., Redmond, WA, USA) and IBM SPSS Statistics 21.0 (IBM Corp., Armonk, NY, USA). The effects of different SAP treatments on physiological ecological characteristics of *C. dactylon* seedlings were analyzed using one-way analysis of variance, and the differences between indices in different groups were tested using the least significant difference test.

Results

Effects of different SAP concentrations on chlorophyll concentration in *C. dactylon* leaves

The concentrations of chlorophyll a (Chl-a), chlorophyll b (Chl-b), chlorophyll a+b (Chl a+b), and carotenoid (Car) increased significantly after the application of reasonable concentrations of SAP under the two water conditions. Under the adequate water supply condition, the concentrations of Chl-a ($10.646 \sim 11.704 \text{ mg}\cdot\text{g}^{-1}$) and Chl-b ($4.192 \sim 4.811 \text{ mg}\cdot\text{g}^{-1}$) were significantly lower in the leaves of *C. dactylon* treated with different SAP concentrations, which were higher than the concentrations in the CK group and were the highest at the 0.30% SAP concentration. Chl-a, Chl-b, and Chl a+b concentrations increased by 22.41%, 22.09%, and 23.74%, respectively. In addition, the Car concentration at the 0.40% SAP concentration ($1.767 \text{ mg}\cdot\text{g}^{-1}$) was the highest increased compared to the CK group ($0.990 \text{ mg}\cdot\text{g}^{-1}$), which represented a 43.95% increase. Under limited water conditions, the concentrations of Chl-a, Chl-b, Chl a+b, and Car first increased and then decreased with an increase in SAP concentration. When the SAP concentrations were 0.20%–0.30%, the concentrations of all the indices were higher than in the CK group. The concentrations of Chl-a, Chl-b, and Chl a+b were the highest at the 0.20% SAP concentration, which represented 15.53%, 10.31%, and 14.08% increases, respectively. However, the Car concentrations in all the treatment groups were the highest at the 0.30% SAP concentration ($2.001 \text{ mg}\cdot\text{g}^{-1}$), compared with the CK group ($1.567 \text{ mg}\cdot\text{g}^{-1}$), which represented a 21.71% increase compared to the CK group.

Under the adequate water supply and the limited water supply conditions, the chlorophyll a/b concentrations between the treatment groups treated with SAP varied minimally. However, with an increase in SAP concentration, chlorophyll a/b content of sufficient water supply ($2.449 \sim 2.593 \text{ mg}\cdot\text{g}^{-1}$) and limited water supply ($2.497 \sim 2.649 \text{ mg}\cdot\text{g}^{-1}$) are both higher than CK group (2.360 and $2.451 \text{ mg}\cdot\text{g}^{-1}$). Compared to the CK group, the chlorophyll a/b concentrations in the adequate water supply treatment group increased by 3.63%, 7.06%, 2.98%, and 8.96%, under the 0.10%, 0.20%, 0.30%, and 0.40% SAP concentrations, respectively. The greatest increase was an increase of 8.96%, under the 0.4% SAP concentration. In the limited water supply treatment groups, chlorophyll a/b concentrations increased by 1.81%, 5.82%, 7.44% and 5.25%, under the 0.10%, 0.20%, 0.30%, and 0.40% SAP concentrations, respectively, with the maximum increase observed under the 0.30% SAP concentration, which was 7.44%. According to the results, the increase of the chlorophyll a/b concentrations in the leaves of the seedlings was not obvious by applying SAP under the two moisture conditions (Table 1).

Table 1. Effects of SAP on chlorophyll concentration in *C. dactylon* leaves ($\text{mg}\cdot\text{g}^{-1}$)

Treatment (%)	Sufficient water supply					Limited water supply				
	Chl-a	Chl-b	Chl a+b	Car	Chl a/b	Chl-a	Chl-b	Chl a+b	Car	Chl a/b
CK	8.847a	3.748a	12.595a	0.990a	2.360a	11.767a	4.799a	16.566a	1.567a	2.451a
0.10	11.487b	4.690b	16.177b	1.376b	2.449a	13.153b	5.268b	18.421b	1.920b	2.497a
0.20	10.646c	4.192c	14.838c	1.526b	2.539a	13.930c	5.351b	19.281c	1.923b	2.603a
0.30	11.704b	4.811b	16.515d	1.415b	2.433a	12.991b	4.904c	17.895d	2.001b	2.649a
0.40	10.904c	4.206c	15.110e	1.767c	2.593a	11.388d	4.401d	15.788e	1.749ab	2.588a

The letters represent the differences within the group. The same letters represent no differences. The different letters represent differences ($p < 0.05$)

Effects of different SAP concentrations on *C. dactylon* leaf enzyme activity

The concentrations of SOD and POD in the leaves of *C. dactylon* were significantly lower than those in the CK group, and CAT concentrations were higher than those in the CK group under the two moisture conditions. There were differences in the change range of each enzyme activity index. Under the adequate water supply condition, the concentrations of SOD in each group were relatively low, ranging from 146.48 to 156.72 $\text{U}\cdot\text{g}^{-1}$, and the lowest value was observed at the 0.30% SAP concentration treatment, which was a 16.67% decrease compared to the CK. In addition, the concentrations of POD in the leaves of *C. dactylon* varied considerably, and the values in each group ranged between 20.67 and 53.34 $\text{U}\cdot(\text{g}\cdot\text{min}^{-1})$. In the treatment group with the 0.30% SAP concentration, the POD concentration was 75.60% lower than the concentration in the CK group. In addition, CAT activity was higher than in the CK group, with the highest value observed under the 0.30% SAP concentration, which was a 67.42% increase compared to the value in the CK group.

Under the limited water supply condition, the concentrations of SOD and POD decreased with an increase of the concentration of SAP, and the lowest values were observed under the 0.40% SAP concentration, which were 21.36% and 46.61% lower, respectively, than the concentration in the CK group. CAT activity was higher than in the CK group, with the highest value observed under the 0.40% SAP concentration, which a 78.55% increase compared to the value was observed in the CK group (Fig. 1).

Effects of different SAP concentrations on MDA content in *C. dactylon* leaves

Under water stress conditions, plants will increase MDA concentrations, which could have toxic effects on cell membranes. Under both moisture conditions, the changes in MDA concentrations in each group were lower than the changes in the CK group under the different SAP concentrations. Under adequate water supply, with an increase in the concentrations of the water-absorbing agent, MDA concentrations decreased by 25.77%, 29.36%, 11.67%, and 8.69%, under 0.10%, 0.20%, 0.30%, and 0.40% SAP concentrations, respectively, compared to those in the CK group. The lowest value was observed under the 0.20% SAP concentration.

Under the limited water supply conditions, the MDA concentrations in the 0.10%, 0.20%, 0.30%, and 0.40% treatments decreased by 8.84%, 12.34%, 9.05% and 27.96%, respectively, compared to the CK group. In addition, the lowest MDA concentration was observed under the 0.40% SAP concentration. According to the results, the application of SAP could reduce the degree of stress on *C. dactylon* to minimize the accumulation of MDA, and, in turn, minimize potential cell membrane damage (Fig. 2).

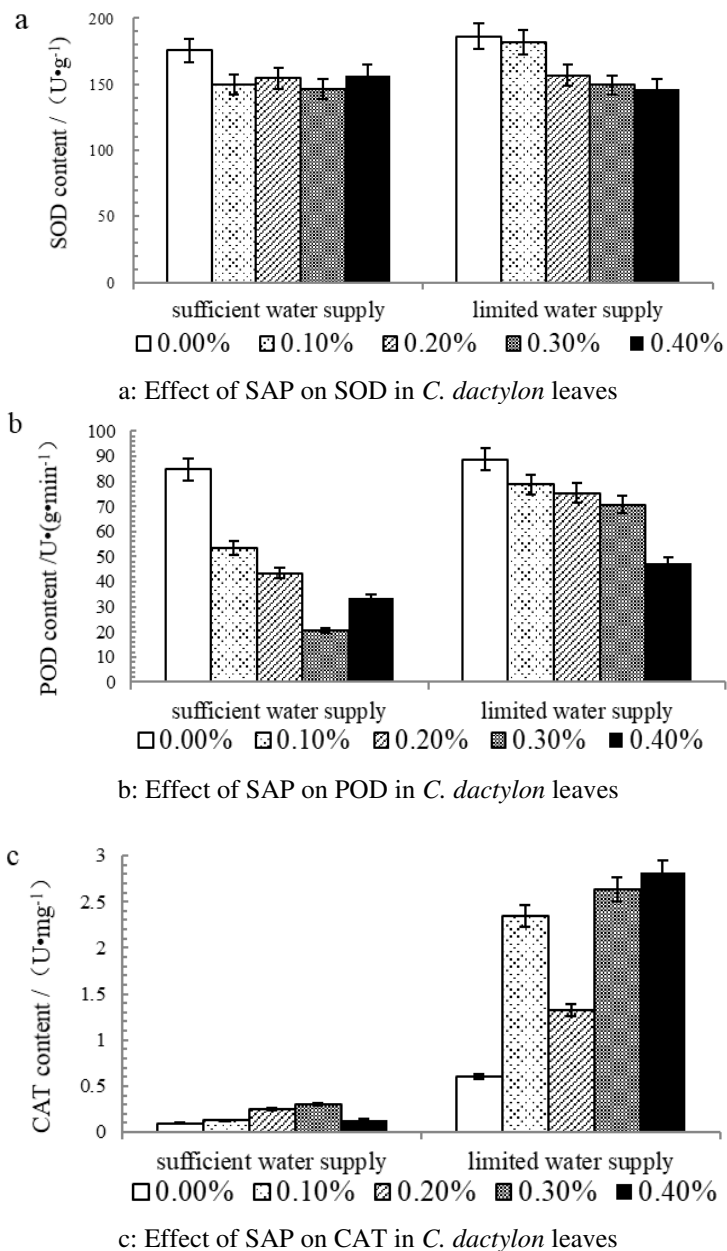


Figure 1. Effects of different SAP concentrations on *C. dactylon* leaf enzyme activity

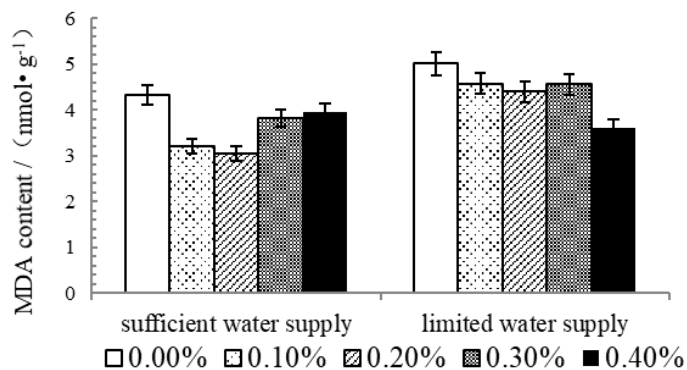


Figure 2. Effect of different SAP concentrations on MDA in *C. dactylon* leaves

Effects of different SAP concentrations on drought resistance of C. dactylon seedlings

Under water stress conditions, different concentrations of SAP will influence plant morphology and physiology variably, in addition to the effects of interactions and influence of various indices. The fuzzy membership function method could simplify the interrelationships among various indices, reveal the linkages among the indices of drought resistance, avoid the one-sidedness associated with the single index, and evaluate the drought resistance of plants more comprehensively (Wang et al., 2013). The analysis of fuzzy membership function of drought resistance of *C. dactylon* was based on the analysis of 9 indices, including Chl-a, Chl-b, Chl a+b, Car, Chl a/b, SOD, POD, CAT, and MDA. To evaluate the drought resistance of *C. dactylon* under the different SAP concentrations, the comprehensive evaluation value was calculated. According to the results, adding SAP could improve the drought resistance of *C. dactylon* seedlings. In addition, under adequate water conditions, the optimal SAP concentrations for the growth of *C. dactylon* based on their impacts on drought resistance in the species would be in the order of 0.30% > 0.10% > 0.20% > 0.40% > 0.00%. Conversely, under limited water conditions, the order would be 0.20% > 0.30% > 0.40% > 0.10% > 0.00% (Table 2& 3).

Table 2. The membership function and comprehensive evaluation of drought tolerance index for sufficient water supply of *C. dactylon* seedlings

Determination index	Treatment					Weight
	CK	0.10%	0.20%	0.30%	0.40%	
Chl-a	0.000	0.924	0.630	1.000	0.720	0.356
Chl-b	0.000	0.886	0.418	1.000	0.431	0.356
Chl a+b	0.000	0.914	0.572	1.000	0.642	0.356
SOD	0.000	0.877	0.726	1.000	0.651	0.356
POD	0.000	0.49	0.646	1.000	0.802	0.356
Car	0.000	0.496	0.690	0.547	1.000	0.291
Chl a/b	0.000	0.382	0.771	0.312	1.000	0.291
CAT	0.000	0.146	0.790	1.000	0.185	0.199
MDA	0.024	0.462	1.000	0.209	0.000	0.154
Comprehensive evaluation value	0.004	1.812	1.802	2.261	1.774	
Order	5	2	3	1	4	

Discussion

Response of photosynthetic pigments of C. dactylon seedlings to different SAP concentrations

When plants are under water stress, the cell membrane system will be impaired, which would lead to the damage of the chloroplast ultrastructure and chlorophyll degradation, in addition to a decrease in chlorophyll concentration (Manuchehri and Salehi, 2014). According to the results of the present study, the concentrations of photosynthetic pigments in *C. dactylon* seedlings, including Chl-a, Chl-b, and Chl a+b, were all higher than the concentrations in the CK when the SAPs with 0.10%–0.30% concentrations were applied under the two moisture conditions. The results indicated that in the process of SAP regulating soil water, and in turn plant growth, soil water content was not lower than

the plant stress threshold, so that the chlorophyll concentration was not affected, and over time, SAP could enhance plant chlorophyll concentration indirectly to ensure that plants exploit the available light energy efficiently (Khadem et al., 2010). Similarly, the present study revealed that applying SAP could improve the concentrations of Car and chlorophyll a/b in *C. dactylon*. The increase in Car concentrations in could facilitate *C. dactylon* to tolerate stress induced by the production of lipid peroxides by membrane lipids (Jia et al., 2009). Zhang and Tan (2001) also suggested that drought resistance in species could be assessed based on a decrease in the Chl a/b ratio (Zhang and Tan, 2001). In the present study, the Chl a/b ratio in each SAP group was higher than in the CK group, and the variations were relatively low, which indicated that SAP application could promote *C. dactylon* seedling growth.

Table 3. The membership function and comprehensive evaluation of drought tolerance index for limited water supply of *C. dactylon* seedlings

Determination index	Treatment					Weight
	CK	0.10%	0.20%	0.30%	0.40%	
Chl a/b	0.000	0.23	0.768	1.000	0.69	0.364
MDA	0.000	0.316	0.441	0.324	1.000	0.364
SOD	0.000	0.110	0.746	0.929	1.000	0.364
POD	0.000	0.242	0.323	0.435	1.000	0.364
Chl-a	0.149	0.695	1.000	0.631	0.000	0.282
Chl-b	0.42	0.912	1.000	0.53	0.000	0.282
Chl a+b	0.223	0.754	1.000	0.603	0.000	0.282
Car	0.000	0.812	0.819	1.000	0.419	0.282
CAT	0.000	0.787	0.328	0.918	1.000	0.163
Comprehensive evaluation value	0.022	0.151	0.205	0.195	0.191	
Order	5	4	1	2	3	

Responses of *C. dactylon* antioxidant enzymes to different SAP concentrations

Under normal conditions, plants can eliminate the generated free radicals (O_2^-) through their free radical-clearing systems, so that the production and elimination of reactive oxygen species in tissues are maintained at equilibrium states (Peng et al., 2002). When the equilibrium is lost, excess free radicals could trigger membrane lipid peroxidation and cause cell membrane system damage (Porcel et al., 2003). In the present study, the activities of membrane lipid peroxidation products, MDA, and protective enzymes, SOD, POD, and CAT, in *C. dactylon*, all changed following treatment with SAP under the two moisture conditions. The results showed that the SOD and POD activities in *C. dactylon* leaves treated with the SAP were lower than those in the CK, while CAT activity was higher than that in the CK. In addition, the MDA concentrations were also lower than in the CK. The reasons for the changes above could be as follows. Under the limited water supply condition, the SAP could reduce soil drought by regulating soil moisture availability, which is beneficial to the synergistic effects of SOD, POD, and CAT in *C. dactylon* leaves, to ensure that the free radicals are maintained at low levels to minimize the damage to the plant leaf membrane systems, similar to the production of lipid peroxidation product (MDA) to minimize the damage caused by drought on plants (Dacosta and Huang, 2007; Reddy et al., 2008). However, under adequate water conditions, sufficient water also led to shifts in the protective enzyme activities of

seedlings, potentially due to the ability of SAP to absorb water and decrease the rate of evaporation of soil moisture, in turn, increasing the soil moisture concentrations under the adequate water supply condition, leading to a reduction in soil permeability, a decrease in nutrient-supply capacity, an increase in osmotic adjustment in leaves of seedlings, and eventually an increase in the concentrations of osmoregulation substances, and changes in protective enzyme activity and the lipid peroxidation products of leaves of seedlings leaves, as reported by Yang (2017).

***C. dactylon* drought resistance under different SAP concentrations**

Under water stress, different SAP concentrations will influence plant morphology and physiology differently. This is consistent with the research on Wheat (*Triticum aestivum* L.) seedling conducted by Guan and Wu (2010). In addition, the indicators would interact and influence each other. A single drought resistance index may not comprehensively reflect the capacity of a plant to adapt to drought conditions (Wang et al., 2011). However, the values obtained from membership function analysis are average values, which could address the shortcomings of evaluations based on a few indicators. In addition, since the averages are whole numbers, the drought resistance indices become comparable. In the present study, under adequate water conditions, the five SAP concentrations were appropriate for *C. dactylon* seedlings in the order of 0.30% > 0.10% > 0.20% > 0.40% > 0.00%. Conversely, under limited water availability conditions, the order was 0.20% > 0.30% > 0.40% > 0.10% > 0.00%. The findings demonstrate that adding SAP could improve *C. dactylon* seedling drought resistance and are consistent with the results of previous studies where the addition of SAP to soil enhanced plant drought resistance (Qados, 2015; Yang et al., 2017).

Conclusion

In summary, the addition of SAP under different water conditions could improve the drought resistance of *C. dactylon* seedlings. The optimal SAP concentration was 0.30% under the adequate water conditions, and 0.20% under the limited water conditions. Therefore, in different areas where *C. dactylon* is adopted for greening, water conservation efforts should consider the 0.20-0.30% SAP concentration range for SAPs, which is conducive for the establishment of lawn and would extend the lawn irrigation time. In the present study, we investigated the effects of SAP on the physiological characteristics and drought resistance of *C. dactylon* seedlings under different water availability status. The effect of SAP on the entire life cycle of *C. dactylon* requires further investigation.

Acknowledgements. This research was supported by the Natural Scientific Foundation of China (41361017), the Natural Scientific Foundation of Jiangxi Province (20181BAB203021).

REFERENCES

- [1] Qados, A. M. S. A. (2015): Effects of super absorbent polymer and *Azotobacter vinelandii* on growth and survival of *Ficus benjamina* L. seedlings under drought stress conditions. – International Research Journal of Agricultural Science and Soil Science 5(2): 45-57.

- [2] Arbona, V., Iglesias, D. J., Jacas, J., Primo-Millo, E., Talon, M. (2005): Hydrogel substrate amendment alleviates drought effects on young citrus plants. – *Plant and Soil* 270(1): 73-82.
- [3] Archer, M. J. G., Caldwell, R. A. (2004): Response of Six Australian Plant Species to Heavy Metal Contamination at An Abandoned Mine Site. – *Water Air Soil Pollution* 157: 257-267.
- [4] Dacosta, M., Huang, B. (2007): Changes in Antioxidant Enzyme Activities and Lipid Peroxidation for Bentgrass Species in Response to Drought Stress – *Journal of the American Society for Horticultural Science* 132(3): 319-326.
- [5] Fernando, T. N., Ariaduraai, S. A., Disanayaka, C. K., Kulathunge, S., Aruggoda, A. G. B. (2017): Development of radiation grafted super absorbent polymers for agricultural applications. – *Energy Procedia* 127: 163-177.
- [6] Guan, X. J., Wu, J. C. (2010): Effect of super absorbent polymers on physiological characteristics of wheat seedling under different soil moisture level. – *Journal of Henan Agricultural Sciences* 39(08): 28-32.
- [7] Hameed, M., Ashraf, M. (2008): Physiological and biochemical adaptations of *Cynodon dactylon* (L.) Pers. from the Salt Range (Pakistan) to salinity stress. – *Flora* 203(8): 683-694.
- [8] Hu, H., Cao, Y., Yang, Y. (2014): Effects of soil moisture content on stolons germination and seedling growth of *Cynodon dactylon*. – *Research of Soil and Water Conservation* 21(3): 284-287 + 292.
- [9] Islam, M. R., Hu, Y. G., Mao, S. S., Mao, J. Z., Eneji, A. E., Xue, X. Z. (2011): Effectiveness of a water-saving super-absorbent polymer in soil water conservation for corn (*Zea mays* L.) based on eco-physiological parameters. – *Journal of the Science of Food and Agriculture* 11: 1998-2005.
- [10] Jayanthi, J., Jalal, J. S., Lakshminarasimhan, P. (2016): Wild grasses and legumes of the Great Indian Bustard Wildlife Sanctuary, Maharashtra. – *Ela Journal of Forestry and Wildlife* 5(2): 183-191.
- [11] Jia, G. M., Zhang, H. Y., Han, J. C., Huang, Y. P. (2009): Effects of soil water contents on the ecophysiological characteristics of Bermuda grass leaves. – *Research of Soil and Water Conservation* 16(05): 199-202.
- [12] Karimi, A., Noshadi, M., Ahmadzadeh, M. (2009): Effects of Super Absorbent Polymer (Igeta) on Crop, Soil Water and Irrigation Interval. – *Journal of Science and Technology of Agriculture and Natural Resources* 12(46), 403-414.
- [13] Khadem, S. A., Galavi, M., Ramrodi, M., Mousavi, S. R., Roustaa, M. J., Parviz, R. M. (2010): Effect of animal manure and superabsorbent polymer on corn leaf relative water content, cell membrane stability and leaf chlorophyll content under dry condition. – *Australian Journal of Crop Science* 4(08): 642-647.
- [14] Kim, C., Lemke, C., Paterson, A. H. (2009): Functional dissection of drought-responsive gene expression patterns in *Cynodon dactylon* L. – *Plant Molecular Biology* 70: 1-16.
- [15] Leung, A. K., Garg, A., Coe, J. L., Ng, C. W. W., Hau, B. C. H. (2015): Effects of the roots of *Cynodon dactylon* and *Schefflera heptaphylla* on water infiltration rate and soil hydraulic conductivity. – *Hydrological Processes* 29(15): 3342-3354.
- [16] Li, L. B., Zhang, H. M., Zhou, X. M., Chen, M. X., Lu, L. C., Cheng, X. (2019): Effects of super absorbent polymer on scouring resistance and water retention performance of soil for growing plants in ecological concrete. – *Ecological Engineering* 138: 237-247.
- [17] Manuchehri, R., Salehi, H. (2014): Physiological and biochemical changes of common bermudagrass (*Cynodon dactylon*, [L.] Pers.) under combined salinity and deficit irrigation stresses. – *South African Journal of Botany* 92: 83-88.
- [18] Peng, L. X., Li, D. Q., Shu, H. R. (2002): Progress in water stress physiology and drought tolerance mechanism of horticultural plant. – *Acta Botanica Boreali-Occidentalia Sinica* 22(05): 1275-1281.

- [19] Porcel, R., Barea, J. M., Ruiz-Lozano, J. M. (2003): Antioxidant activities in mycorrhizal soybean plants under drought stress and their possible relationship to the process of nodule senescence. – *New Phytologist* 157: 135-143.
- [20] Reddy, P. C. O., Sairanganayakulu, G., Thippeswamy, M., Thippeswamy, M., Sudhakar Reddy, P., Reddy, M. K., Chinta, S. (2008): Identification of stress-induced genes from the drought tolerant semi-arid legume crop horsegram (*Macrotyloma uniflorum*, (Lam.) Verdc.) through analysis of subtracted expressed sequence tags. – *Plant Science* 175(3): 372-384.
- [21] Singh, K., Pande, V. C., Singh, R. P. (2013): *Cynodon dactylon*: An efficient perennial grass to revegetate sodic lands. – *Ecological Engineering* 54: 32-38.
- [22] Srivastava, P., Singh, S. (2012): Conservation of soil, water and nutrients in surface runoff using riparian plant species. – *Journal of Environmental Biology* 33(1): 43-49.
- [23] Suresh, R., Prasher, S. O., Patel, R. M., Qi, Z., Elsayed, E., Schwinghamer, T., Ehsan, A. M. (2018): Super Absorbent Polymer and Irrigation Regime Effects on Growth and Water Use Efficiency of Container-Grown Cherry Tomatoes. – *the American Society of Agricultural and Biological Engineers* 61(2): 523-531.
- [24] Tongo, A., Mahdavi, A., Sayad, E. (2014): Effect of superabsorbent polymer Aquasorb on chlorophyll, antioxidant enzymes and some growth characteristics of *Acacia victoria* seedlings under drought stress. – *Ecopersia* 2(2): 571-583.
- [25] Wang, T., Song, X., Yang, C. Z., Li, S., Xie, J. L. (2011): Remote sensing analysis on aeolian desertification trends in northern China during 1975–2010. – *Journal of Desert Research* 31(6): 1351-1356.
- [26] Wang, X. K. (2006): *Experimental Principles and Techniques of Plant Physiology and Biochemistry*. – Higher Education Press, Beijing.
- [27] Wang, Z. T., Ma, R., Ma, Y. J., Li, Y. (2013): The drought resistance of 5 species of *Lespedeza*. – *Journal of Arid Land Resources and Environment* 27(09): 119-123.
- [28] Wu, Y., Sun, B. P., Zhang, J. F., Song, S. S., Shen, H. J., Chen, C., He, Y. (2018): Effects of water-retaining agent in different dosage on the growth and root morphology of 4 woody plants. – *Science of Soil and Water Conservation* 16(01): 96-102.
- [29] Xie, Y., Fan, J. B., Zhu, W. X., Amombo, E., Lou, Y. H., Chen, L., Fu, J. M. (2016): Effect of heavy metals pollution on soil microbial diversity and bermudagrass genetic variation. – *Frontiers in Plant Science* 7: 755. <https://doi.org/10.3389/fpls.2016.00755>.
- [30] Yang, J., Cao, Y., Wang, X. W., Huang, J. C., Li, S. (2017): Effect of super absorbent polymer on germination and physiological characteristics of *Festuca arundinacea*. – *Research of Soil and Water Conservation* 24(1): 351-356.
- [31] Yang, L. X., Yang, Y., Chen, Z., Guo, C. X., Li, S. C. (2014): Influence of super absorbent polymer on soil water retention, seed germination and plant survivals for rocky slope eco-engineering. – *Ecological Engineering* 62: 27-32.
- [32] Zeng, L. S., Li, P. Y. (2019): Evaluation on drought resistance of 10 bermudagrass (*Cynodon dactylon*) germplasms from Xinjiang. – *Chinese Journal of Grassland* (03): 22-29.
- [33] Zhang, M. S., Tan, F. (2001): Relationship between ratio of chlorophyll a and b under water stress and drought resistance of different sweet potato varieties. – *Seed* 21(04): 23-25.
- [34] Zohuriaan-Mehr, M. J. A. D., Kabiri, K. (2008): Superabsorbent polymer materials: a review. – *Iranian Polymer Journal* 17(6): 451-477.

DETECTION OF PLANT WATER STRESS USING UAV THERMAL IMAGES FOR PRECISION FARMING APPLICATION

AWAIS, M. – LI, W. * – YANG, Y. F. – JI, L. L.

Research Center of Fluid Machinery Engineering & Technology, Jiangsu University, China

**Corresponding author*

e-mail: lwjiangda@ujs.edu.cn; phone: +86-186-5285-0503

(Received 18th Jan 2020; accepted 24th Mar 2020)

Abstract. Adequate and real-time monitoring of water stress is critical to enhance productivity, crop quality, as well as water use efficiency. This study contributes to the new approach of precise and rapid estimation of real-time water stress using thermal images taken with an Unmanned aerial vehicle. Different physiological parameters stomatal conductance (gs), leaf area, and ground reality parameter (Tc) were calculated between 11.30 and 13.30 (Chinese standard time) on sampling day. The volumetric water content (θ , $\text{m}^3 \text{m}^{-3}$) of the soil at different depths of (20, 40, and 60 cm) was measured. Data processing steps were implemented in MATLAB for thermal images to calculate the canopy temperature T_1 . Empirical (CWSI_e) and statistical (CWSI_s) methods of CWSI were applied for model calibration. Results showed that different spectral indices (TCARI, NDVI, OSAVI TCARI/OSAVI) had a high correlation with stomatal conductance (gs) ($R^2 = 0.590$) and transpiration rate (tr) ($R^2 = 0.602$) as compared to CWSI_e and CWSI_s. Volumetric water content (θ) and CWSI_s have a high correlation coefficient (0.872). However, the transpiration rate shows a weak correlation with spectral indices (TCARI, NDVI, OSAVI, and TCARI/OSAVI) as compared with CWSI. The plotted high-resolution map shows the distribution of water stress in different irrigation treatments and potentially applied in precision irrigation management.

Keywords: *stomatal conductance, precision agriculture, PIX4D software, unmanned aerial vehicles, remote sensing*

Introduction

Uses of water in sustainable agriculture has become a precarious issue in all developing countries, because of climate and water scarcity changes, so accurate irrigation water management strategies are required. In general terms, agriculture consumes most of the world water resources (Jiang et al., 2013). At the same time, other industries are trying to consume more and more water, and thus people are competing with food production. Globally 46% of the food supply is produced from the agricultural land, which covers only 18% of the cultivated land (Döll and Siebert, 2002). So, it is essential to manage irrigation with the optimal use of water. Worldwide, farmers are facing many problems, particularly in semi-arid areas, related to agriculture water resources (Gonzalez-Dugo et al., 2010; Jin et al., 2018). Plant transpiration and climate change affect the crop productivity, quality and soil water balance significantly.

Using thermal information for identifying plant water stress at ground level with thermal sensors become popular in the 1960s (Tanner, 1963). Crop water stress index (CWSI) has been familiarized for indicating water stress of crop based on the difference between air temperature and greenery of the crop (Jackson et al., 1981; Jones, 2013; Idso et al., 1981) which is most commonly used as the indicator of plant water status derived from canopy temperature. Jones (1999) developed a new reformulated CWSI by the difference between threshold temperature and canopy temperature (T_{Canopy}), which is normalized by the difference in temperature between T_{wet} (full transpiring temperature)

and T_{dry} (non-transpiring temperature) as upper and lower reference temperature (Jones, 1999). In order to calculate crop water stress index (CWSI) (Jackson et al., 1981) proposed a method to calculate the theoretical CWSI with the theory of crop energy balance, but this approach needs too many metrological data. For obtaining the design parameter of empirical CWSI_e, the secure method is to analyze the normalized temperature of the canopy (Jones, 1999; Jones et al., 2002) over calculating wet reference (T_{wet}) temperature and dry reference (T_{dry}) temperature. However, the location of reference leaf and metrological factors are easily distributed; these essential reference surfaces and CWSI may not be the same in a different region. Another feasible method for calculating (T_{wet}) from the temperature histogram of the average of the lowest 5% and (T_{dry}) temperature is supposed to be the same as (T_{air}) air temperature +50 °C (Cohen et al., 2005, 2017; Rud et al., 2014; Agam et al., 2014). In the agricultural sector, one of the most generally oppressed in remote sensing is optical or visual (RS) remote sensing. It uses different bands, i.e., SWIR (short wave infrared) and NIR (near-infrared) sensors, to get pictures from ground surfaces by reflecting phenomena from the target area surface (Prasad and Bruce, 2011). Satellite images are collected by using visible, NIR, traditional aircraft and Unmanned Aerial Vehicles (UAVs). Numerous studies (Hatfield and Prueger, 2010; Jordan, 1969) have monitored crop conditions in the agriculture sector.

In contrast, thermal sensors were used to detect surface temperature, and it was found to be a very quick response variable for monitoring crop health and crop stress (Anderson et al., 2013; Stark et al., 2014). Thermal remote sensing is a process that measures the radiation that is discharged from a surface body and transforming into temperature values without producing any interaction with an object. All surface object emits radiation with a temperature above 0 K or -273 °C (Khanal et al., 2017). The intensity of radiation of each object depends on the temperature, the higher the temperature the greater the intensity of the radiation is. Thermal remote sensing provides us with significant fluxes of temperature and energy from the earth's surface which are necessary to converse the landscape's processes and responses (Quattrochi and Luvall, 1999; De-Cai et al., 2012).

CWSI estimation with TIR imagery is a practical approach that was introduced to eliminate the VIS imagery with the co-registration method (Meron et al., 2010). Many studies on assessing CWSI approaches through remote sensing have concentrated on image processing techniques from the nearby ground platform, to detect the stress level at different crop levels (Möller et al., 2006). Statically modeling techniques were used to calculate the lower reference temperature and canopy related temperature in TIR imagery. Recently detection of water stress from (UAVs) has been used worldwide with a higher spatial resolution with a potential of providing new ideas for farmers to observe the water stress at field level (Berni et al., 2009; Poblete-Echeverría et al., 2014; Espinoza et al., 2017). It is necessary to develop a new approach for measuring CWSI by using temperature histogram from UAV thermal Images and analyze water stress of crop and improve the irrigation efficiency. Overall objectives of this research are to (1) exclude soil background pixels to get the pure canopy pixel using different edge detection method and series of UAV thermal imagery; (2) estimate the values of (T_{wet}), (T_{dry}) and (T_{canopy}) from the histogram of canopy temperature which is simply recognized from UAV thermal images; (3) determine and optimize correlation to successfully identify the water stress from field condition by comparing different parameters of CWSI and spectral indices.

Materials and methods

Experimental design

This study was conducted in a cultivated land of 1.13-ha research field in a tea garden located at the (right) bank of the Yangtze River in Jiangsu Province, PR China (32°1'00"N, 119°4'00"E), with an elevation of 18.5 m above sea level. The tea plant was four-year-old Anji white tea, with a plant row spacing of 1.5 m and plant spacing with the row of 1 m. This research field was divided and completely randomized with four irrigation treatments with three replicates. Site area soil is silty-loam texture. The climate in this area is semi-arid, and the annual rainfall and ET_0 respectively are 360 mm and 1094 mm, for the year 2019. There were four randomized irrigation treatments with three replications and a total of 12 experimental plots, and each plot was designed to be 4 m wide (7 rows) and 5 m long. The four treatments were (T_4) severe water stress, (T_3) moderate water stress, (T_2) mild water stress, and (T_1) full irrigation. These twelve plots were selected randomly, and different treatment was irrigated to keep up the volumetric water content on a different level of the field capacity, respectively. In order to maintain the difference in irrigation, the four treatment plots were watered to maintain the volumetric soil water content at 90-100%, 75%, 60%, and 50% of the field capacity, respectively. Drip irrigation controller system was installed to irrigate the land, and an individual solenoid valve was opened and closed, which corresponding to each irrigation sector with one line per row had a stream rate of 1.5 Lh^{-1} and were spaced 0.85 m apart. In each plot, three sites for data gathering were selected for ground truth data. For post-processing image calibration, Pix-4D mapper was used in this research for obtaining thermal infrared mosaic images (*Fig. 1*). FLIR Tools software was also used for temperature calibration parameters, i.e., relative humidity, target distance, background temperature, and emissivity.

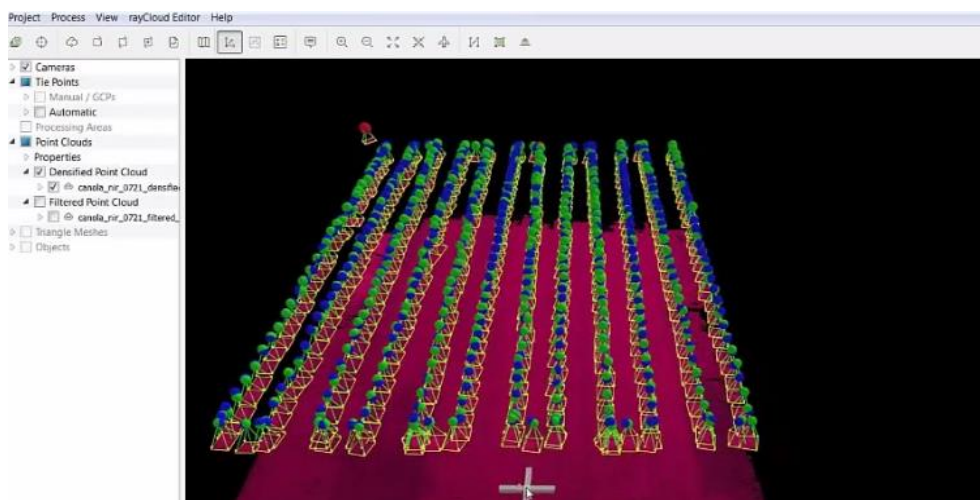


Figure 1. Post-processing calibration in Pix4d software

Aerial image acquisition and software solutions

Figure 2 shows the main procedure of acquisition and pre-treatment of UAV imageries. A multi-rotor UAV drone manufactured by DJI (S900) equipped with RGB and thermal cameras (Zemuse XT, FLIR System, Inc., USA) was used to measure the

canopy temperature. Temperature and spectral range of thermal cameras are 7.5-13 μm , with a resolution of 640×512 pixels, thermal sensitivity < 0.05 $^{\circ}\text{C}$ at $+ 30$ $^{\circ}\text{C}$ and focal length of 25 mm. Due to its high matrices and multi-rotor function, they have a capability for a stable and safe flight with a long battery. The flying speed of UAV is 2.5 ms^{-1} with a high elevation of 80 m beyond the earth's surface with a sample space distance of 6.12 cm and has sufficient overlap for photogrammetric processing. The most significant uncertainty occurring in thermal mapping is sensor calibration. In our case, there is automatic sensor calibration while obtaining thermos MAP. Evaposensors (Skye Instruments, Llandrindod Wells, UK) were used to acquire the canopy reference temperature indices T_{wet} and T_{dry} for supporting the segmentation of the thermal image.

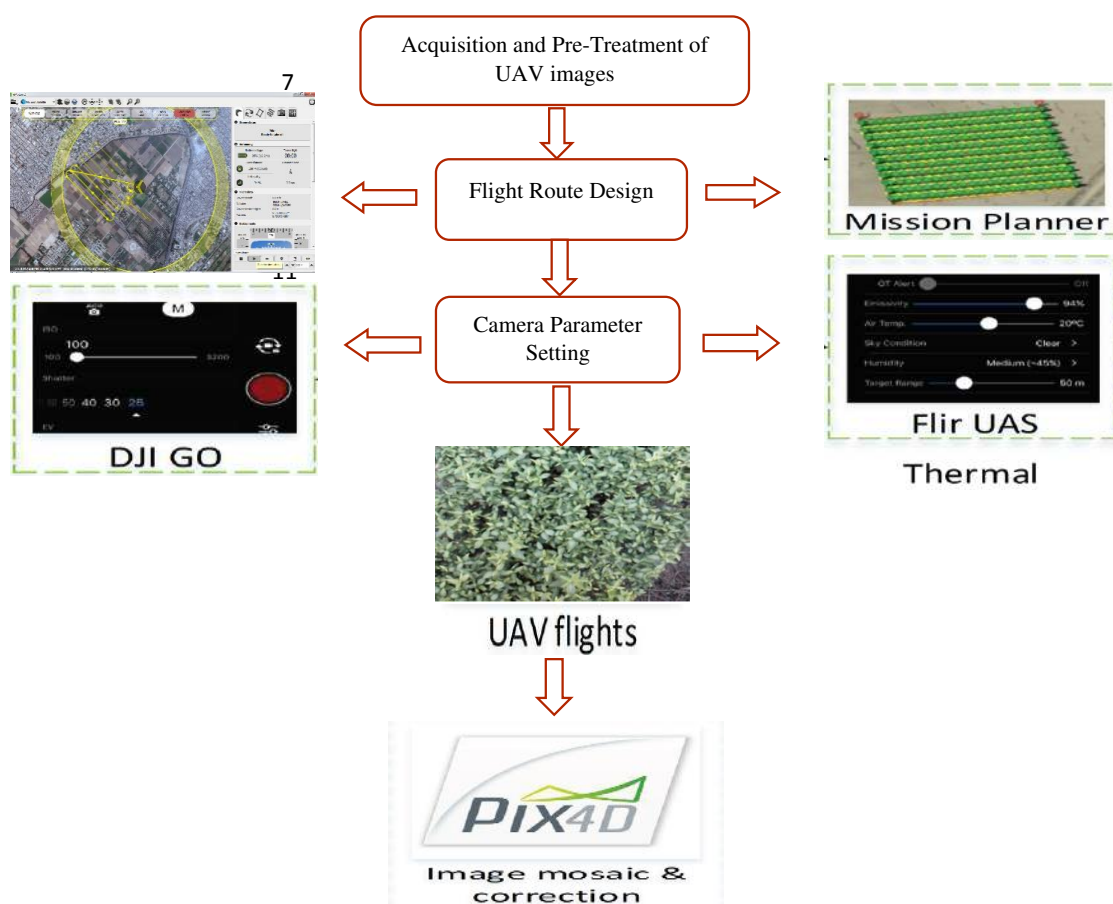


Figure 2. Flow chart of image acquisition and pre-treatment of an unmanned aerial vehicle

Physiological data collection

Leaves temperature for thermal image calibration was calculated regarding five sunny leaves and five sheltered leaves using a portable infrared thermometer (TN410LCE, ZyTemp, Radiant Innovation Inc.) at the same time with UAV image acquisition. Different physiological parameter stomata conductance (Ahrenfeldt et al., 2013), ground truth T_c , soil water content, and leaf area was calculated around 11.30 and 13.30 (Chinese standard time) on sampling day. Transpiration rate (t_r , $\text{mmol m}^{-2} \text{ s}^{-1}$) and the stomatal conductance (g_s , $\text{mol m}^{-2} \text{ s}^{-1}$) of the leaves were calculated using a portable photosynthesis system (LI-6400, LI-COR Inc. USA). The leaf was the fourth

from the upper part of the tea canopy and fully exposed to the sun, and three leaves per plot were measured. LAI was measured 2 h earlier before sunset just to avoid the effect of direct sunlight. The 'soil volumetric' water content (θ , $\text{m}^3 \text{m}^{-3}$) at different depths (20, 40, and 60 cm) was measured using soil moisture sensors (Decagon EM50 data logger, ECH20 sensor), when thermal infrared images were collected. Ground-truth T_c was measured by a handheld infrared thermometer (RAYTEK, ST60+, Raytek Inc., Santa Cruz, USA) with a temperature range of 32-600 °C and a spectral range of 8-12 μm .

Data processing

Data processing steps were implemented in MATLAB R2016b (Math works Inc., Matick, MA, USA) for thermal images to calculate the T_1 . Mapping of CWSI and extraction of canopy pixels from soil and other non-leaf material must be required. Calculation of T_1 must require transparent canopy pixel from thermal images to show the higher temperature during midday periods. Edge recognition methods were used to exclude soil background pixels to get the transparent canopy pixel using Matlab. These edge detection methods are designed in the vertical and horizontal direction to identify gradient changes extremely to boundaries (Maini and Aggarwal, 2008). In this stage, two other edge detection methods Roberts and Prewitt, can also be applied to check the changes in gradient and edges of images. The mixed pixel was intensified for more conservative elimination, which is further dispersed up to more six pixels along and across the edge direction of the thermal gradient.

CWSI calculation

This study was suggested by (Jones, 2013) to estimate the CWSI algorithm, which can be represented as follows:

$$CWSI = \frac{K_{Conopy} - T_{wet}}{K_{Dry} - T_{wet}} \quad (\text{Eq.1})$$

where T_{canopy} is the temperature that is acquired by aerial TIR images, T_{wet} is the lower reference temperature or entirely transpirence leaf, and T_{dry} is the non-transpiring leaf temperature, which is also called an upper reference. The CWSI was acquired using simplified, statistical, and empirical approaches based on T_{dry} and T_{wet} values. The temperature of fully transpiring plants leaves was measured using a spray of water on both sides of leaf (T_{wet}), and petroleum jelly was used to calculate the temperature of non-transpiring leaves covered with jelly (T_{dry}). In this approach, individually, numerical analysis is performed to measure the threshold values of T_{wet} and T_{dry} , which is dependent on sub-regions. Initially, TIR images were used to generate the temperature histogram for each region. Different studies assume that T_{wet} from the histogram is derived from the coldest part, and further, T_{dry} is derived from the highest part of the histogram (Rud et al., 2014). Different spectral indices were also calculated using spectral reflectance of the canopy, i.e., transformed chlorophyll absorption for reflectance index (TCARI), Normalize Difference Vegetation Index (NDVI), optimize soil adjusted vegetation index (OSAVI).

$$TCARI = 3 * [(R700 - R670) - 0.2 * (R700 - R550) * (R700 / R670)] \quad (\text{Eq.2})$$

$$OSAVI = (1 + 0.16) * (R800 - R670) / (R800 + R670 + 0.16) \quad (\text{Eq.3})$$

$$NDVI = \frac{R800 - R680}{R800 + R680} \quad (\text{Eq.4})$$

Adaptive T_{wet} and T_{dry}

A static approach is proposed to estimate the threshold values of T_{wet} , and T_{dry} which depends on the regions. The histogram temperature was acquired as shown in the flow chart (Fig. 3). The average density distribution and distinctive bimodal are the histogram feature which is used to represent the soil pixels and vegetated pixels. In this study, Gaussian mixture modeling (GMM) was used to estimate the typical values of T_{wet} and T_{dry} for canopy by fitting temperature distribution to cluster soil/canopy pixel. In the Gaussian distribution component, higher temperature representing the non-canopy pixel of soil background affects Gaussian distribution.

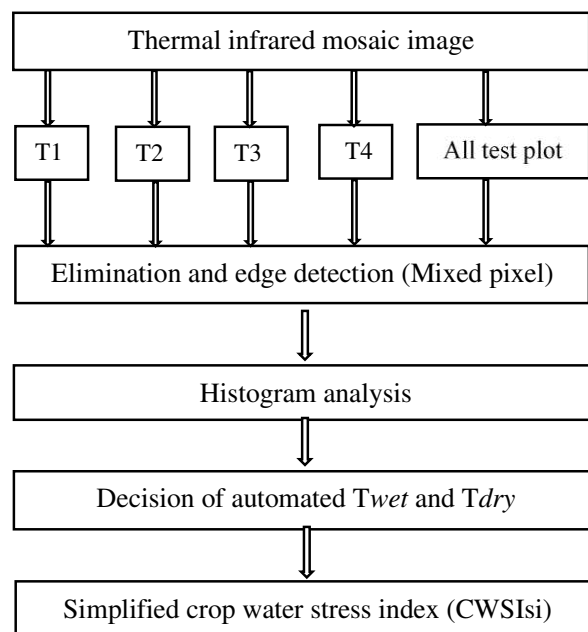


Figure 3. Flow chart of detection (CWSI) using temperature histogram approach

Results

Feature extraction

CWSI mapping required feature extraction of canopy pixel from the soil background images, which must have excluded non-leaf material and soil from the UAV images. Different canopy edge detection was used to show the transparent canopy pixel of higher temperature during midday of periods and compared these methods to indicate the raster image between copy and soil background pixel. *Figure 4* shows a vibrant edge detection of the canopy plant by using edge detection algorithm in the raster image, and the mixture of crop canopy and pixel of different edges were screened out from orthomosaic images. White pixels show the temperature of clear canopy that was acquired.

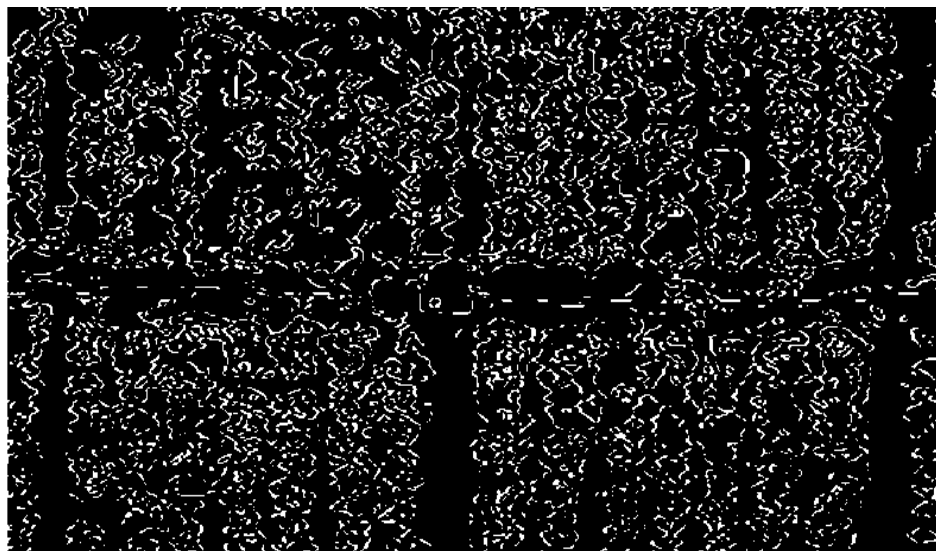


Figure 4. Example of the orthomosaic image with Edge detection methods

Canopy temperature histogram and calculation of CWSI

Images from UAV thermal cameras were used to obtain the canopy temperature histogram based on the irrigation treatment of entire experiment plants. T_{wet} and T_{dry} values were attained from the average of the highest and the lowest values of 0.5% from canopy temperature histogram, respectively. *Figure 5* shows the surface temperature distribution of soil and canopy pixels from each experimental plot, which was bimodal (*Fig. 5a*). This soil and canopy temperature histogram represent the mixture of bare and dry soil, whereas it shows transpiring and actively growing canopies. This histogram's bimodal distribution featured representing soil and vegetation background in between 23 and 43 °C due to the difference of apparent temperature up to 34 °C. To remove the accuracy of CWSI, removal of soil background is very crucial, so after soil background was removed, the temperature distribution was Gaussian (*Fig. 5b*).

T_{wet} values of different methods for CWSI was 25.8 °C, 28.9 °C, and 28.5 °C. Canopy and soil background temperature for selected plots are shown in *Figure 5*. Therefore, experimental results of temperature histogram stated that the temperature of canopy pixel is worse than that of soil pixel. The air temperature was measured from the entire experiment plots, and it was 38.3 °C. From this temperature, a considerable gap difference shows, which represents the undefined error in the measured values of T_{wet} and T_{air} . So T_{wet} values of CWSIs and simplified CWSI (CWSIsi) methods were approximately similar. Furthermore, the T_{dry} values of CWSIsi, CWSIs, and CWSIe were 39.4 °C, 43.8 °C, and 44.2 °C. T_i values of four different irrigation treatment plants were derived and analyzed the apparent difference from canopy temperature histogram. Soil and canopy temperature distribution of these four different treatments are shown in *Figure 6*. Results showed that plot 4 (T_4) has the highest temperature value of T_i (35.6 °C) than T_2 , T_3 , and T_1 . These four treatments plot show higher difference among the values of T_i that is obtained from the histogram approach, so canopy edged detection approach is an acceptable method to calculate the canopy temperature.

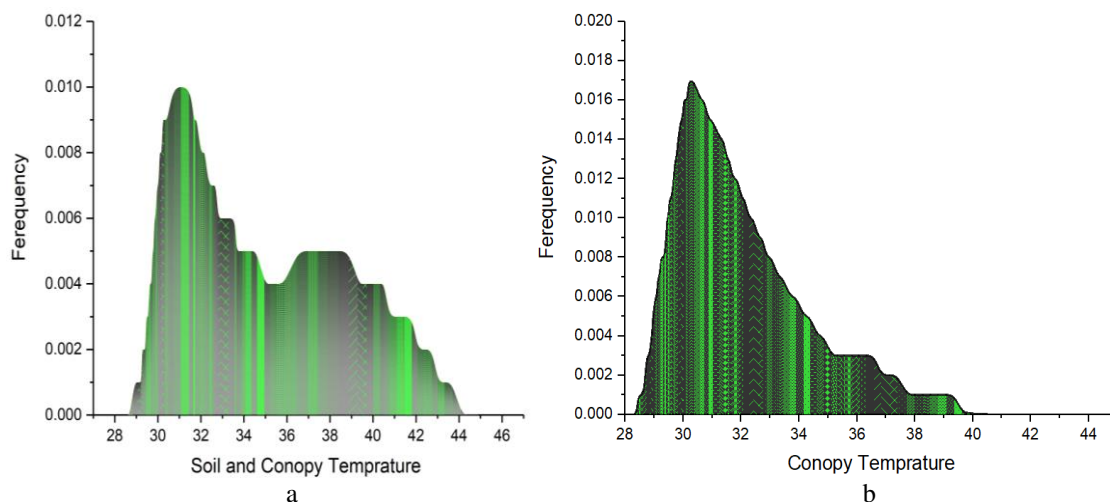
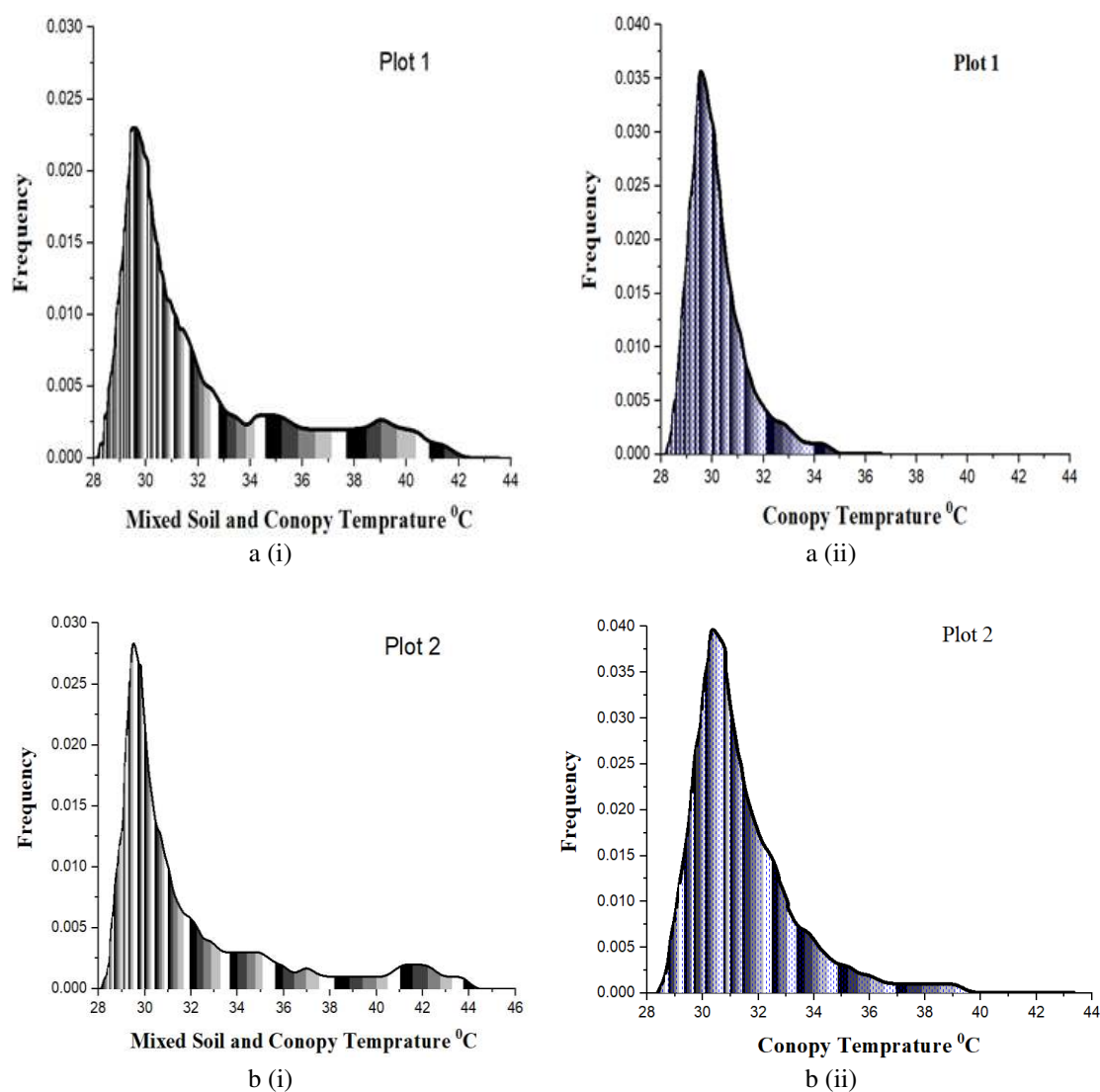


Figure 5. Histogram (canopy and soil pixels) of temperatures of the entire experimental plot (a), Histogram (canopy pixels) of canopy temperatures of the entire experimental plot (b). Note: dark black lines of histogram represent null temperature values



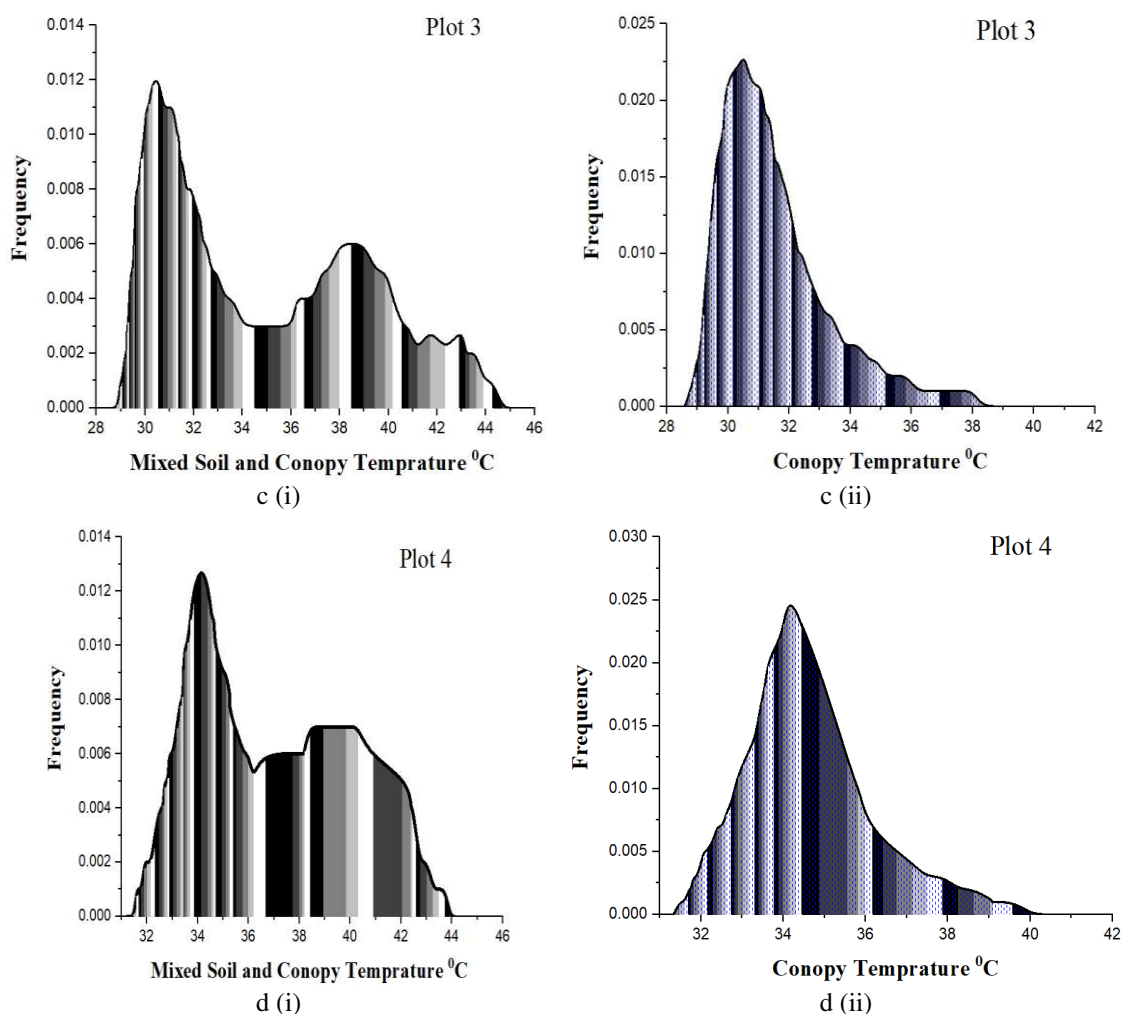


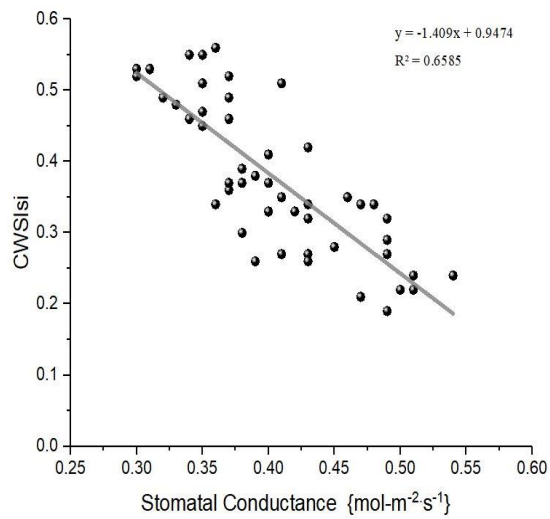
Figure 6. Temperature histograms of soil pixel and canopy pixels for each experimental plot (a–d). (i) Mixed canopy and soil pixels, ii) canopy pixel

Relationship of CWSI and physiological indicators

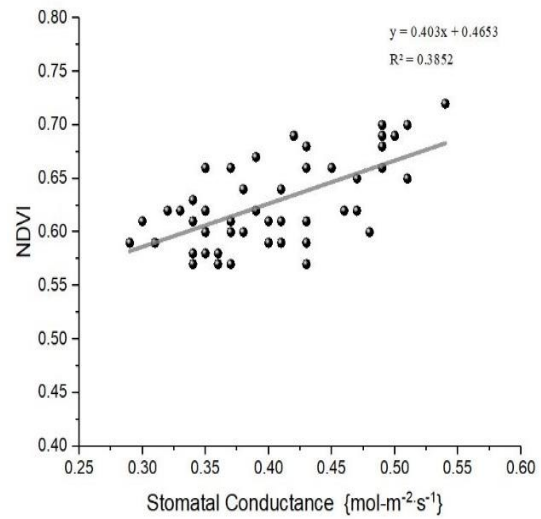
Many researchers (Gago et al., 2013; Jones, 1999; Pallavi et al., 2017) have proved that values of CWSI and stomatal conductance have a high correlation. *Figure 7* shows the relationship of stomatal conductance with different CWSI values from the UAV thermal camera images. Stomatal and transpiration rates were calculated to identify the accurateness of CWSI by different parameters. Results revealed that stomatal conductance (gs) shows a negative correlation with three different models of calculating CWSI, and the value of R^2 (coefficient of determination) is different.

While taking thermal images on the same day transpiration rate was also considered at midday. The result stated that (*Fig. 8*) there is a negative correlation between transpiration rate and simplified, statistical, and experimental values with CWSI and R^2 values remained 0.519, 0.501, and 0.5696 individually. CWSI from the histogram approach highly correlated with the measured transpiration rate, which reflects the water stress of crop (*Fig. 8a-c*). Experimental results suggest that water stress from the histogram approach is highly accepted and accurately shows the water stress condition. Besides, it can be observed (*Fig. 8d-g*) that transpiration rate has a

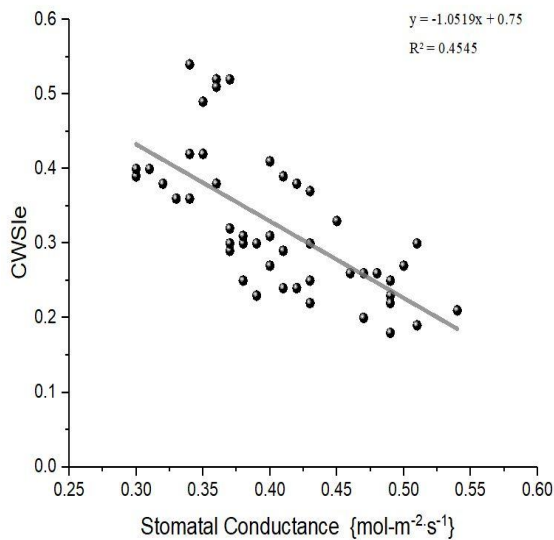
week correlation of spectral indices (TCARI, NDVI, OSAVI TCARI/OSAVI) as compared with CWSI.



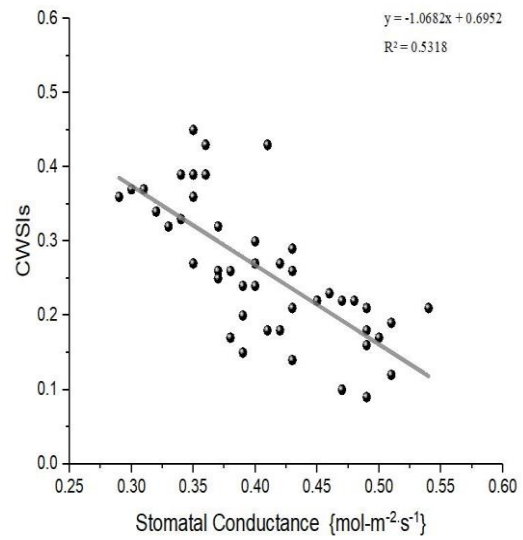
a



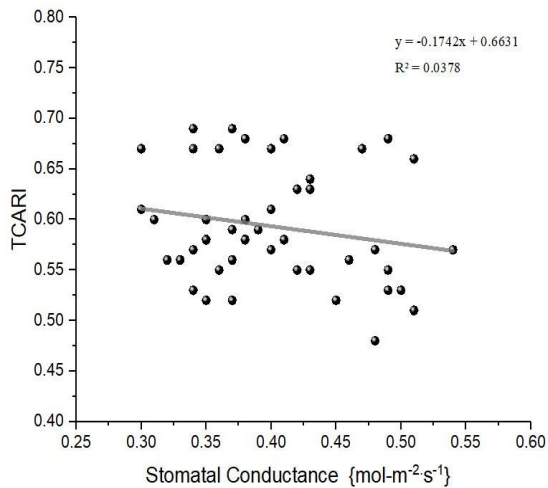
b



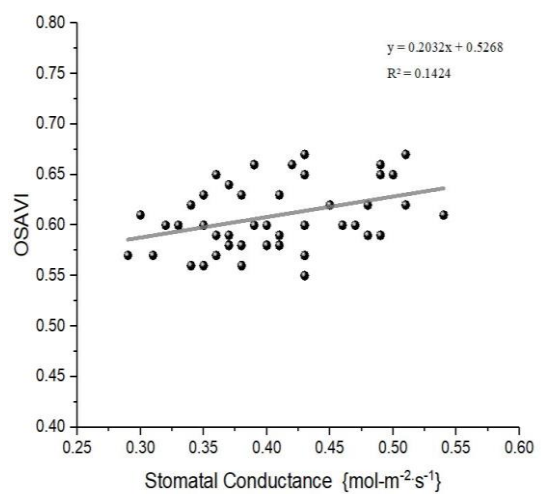
c



d



e



f

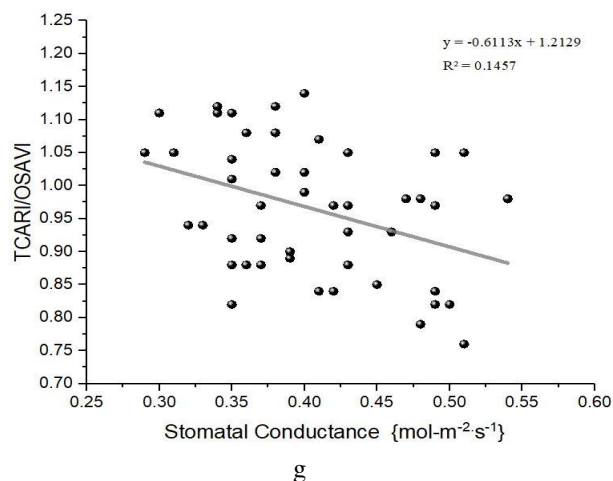
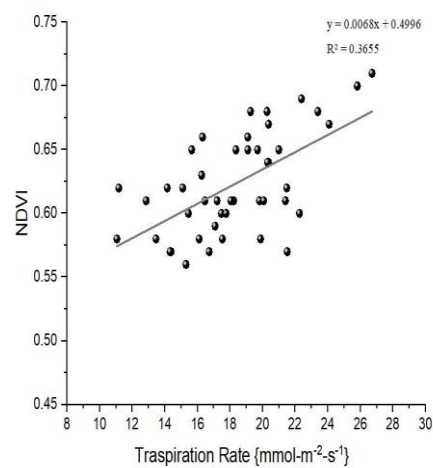
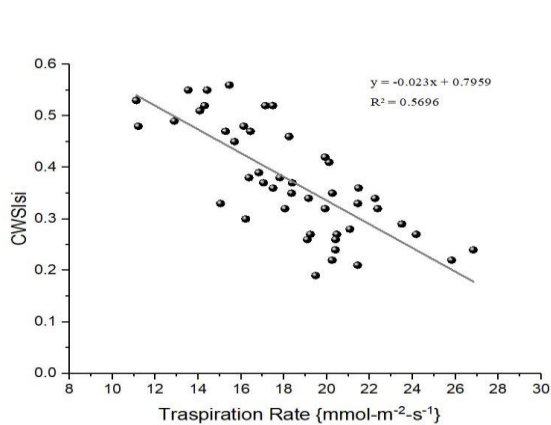
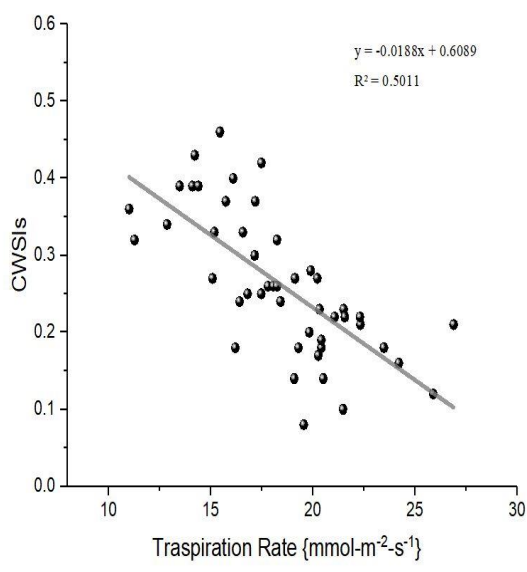
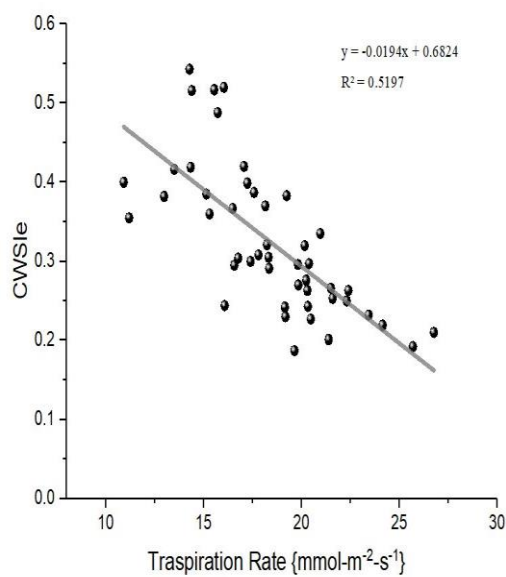


Figure 7. Stomatal conductance relationship with and (a) empirical (b) statistical (c) simplified CWSI (d) (NDVI), (e) (TCARI), (f) (OSAVI), (g) TCARI/OSAVI



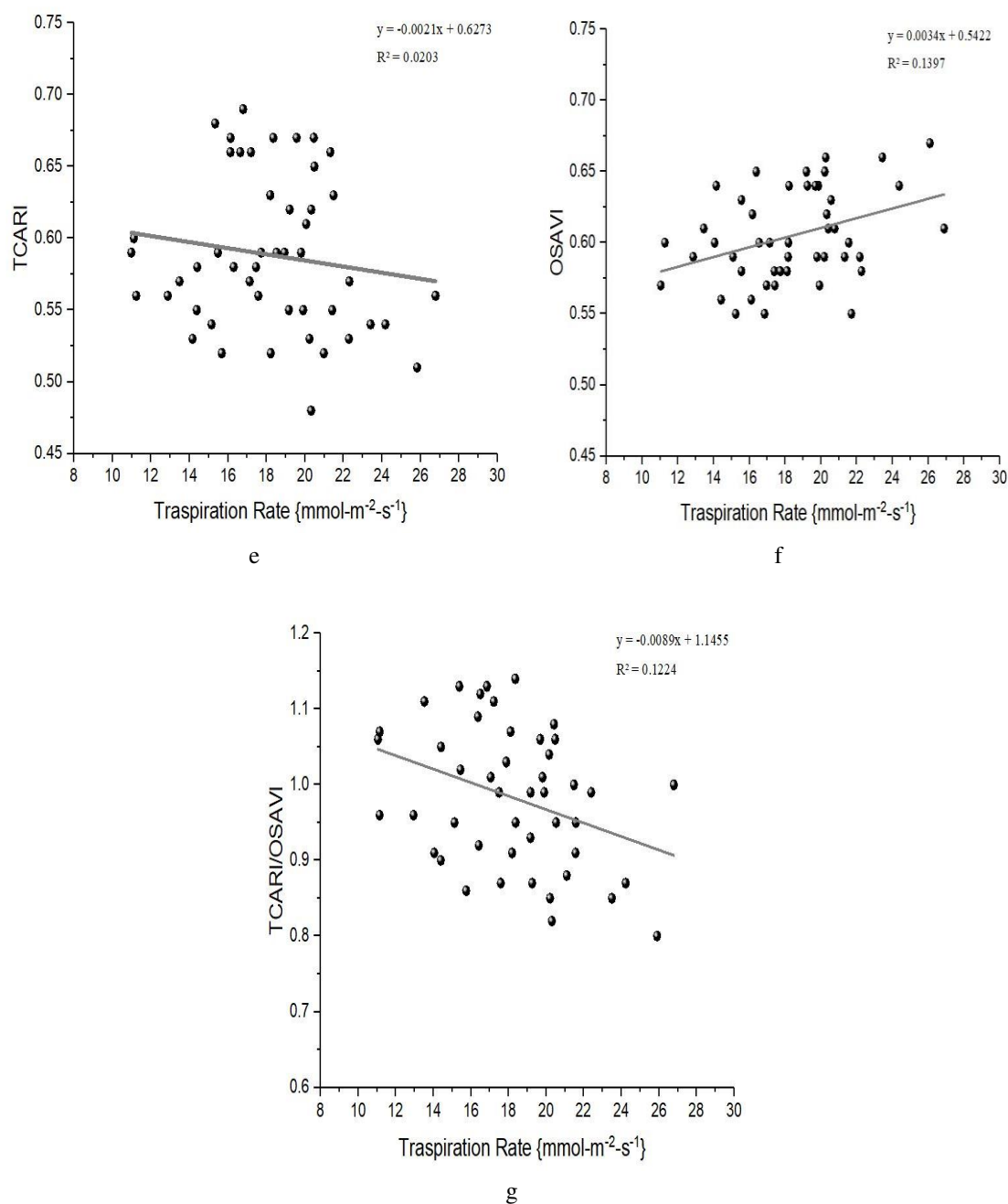


Figure 8. Transpiration rate relationship with (a) empirical (b) statistical (c) simplified CWSI (d) (NDVI), (e) (TCARI), (f) (OSAVI), (g) TCARI/OSAVI.

Adaptive CWSI mapping

Figure 9 shows the high-resolution predictable map of the CWSI index, which is based on the values of T_{wet} and T_{dry} in four different experimental plots for agriculture water management. Detailed values of CWSIs of water deficit are in between 0.100 to 0.810, and the exact mean values of water stress index of four plots remained 0.161, 0.362, 0.521, and 0.692 individually. This water stress map shows a stable relationship between the water stress condition of plots and CWSIs.

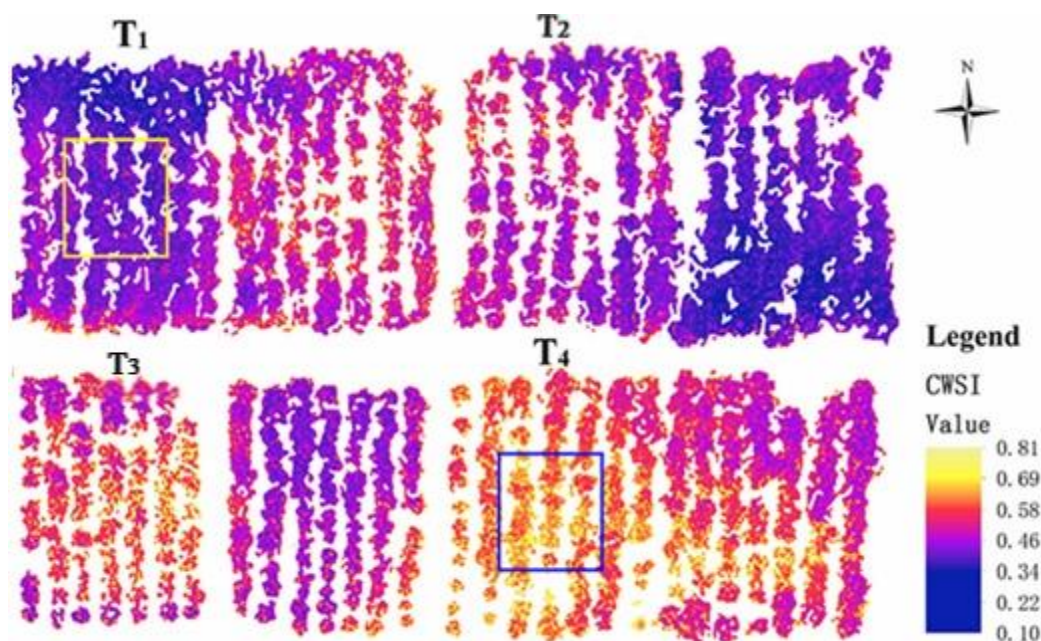


Figure 9. Example of Adaptive CWSI mapping

Discussion

In this study, the ability of UAV technology with thermal camera images was used to determine the crop water status at the canopy scale. However, CWSI provides a critical piece of information for irrigation water management. Furthermore, soil background pixel was eliminated to get the transparent canopy pixel using different edge detection methods, and series of UAV thermal imagery and canopy temperature histogram approach was employed to calculate the CWSI_{si} parameter (T_1 , T_{wet} , and T_{dry}). CWSI is a handy parameter for assessing the water stress condition of the crop. Many previous studies (Pallavi et al., 2017; Davcev et al., 2018) stated that there is a perfect relationship between stomatal conductance, transpiration rate, and CWSI, respectively. The proposed methods were based on the assumption that there exists a water stress level in the field for representing canopy temperature values for stress and non-stress plants, and no metrological data is essential for the calculation of CWSI_{si}. To calculate the CWSI from the canopy temperature, soil background pixels should be removed from the UAV thermal camera images. In this work, ArcGIS and Pix4D software were used to pre-process the UAV thermal images (Fig. 4). The average canopy temperature of different four plots which is carried out by edge detection algorithm is T_4 (35.6 °C), T_3 (31.9 °C), T_2 (31.2 °C), and T_1 (30.1 °C) respectively. This temperature difference results have been proved with previous research (García-Tejero et al., 2016; Testi et al., 2008). T_{dry} values can be calculated by different methods, and values of simplified, statistical, and empirical water stress was 39.4 °C, 43.8 °C, and 44.2 °C. Previous studies also suggested the reasonable values of T_{dry} temperature are 39.2 °C (Khorsandi et al., 2018). A bimodal histogram was obtained before the removal of soil background pixels, this histogram approach not only explained the temperature difference but also showed us the partially overlapping temperature.

Besides, this approach for estimating CWSI is not a direct method for the measurement of actual water stress since its mean values can fluctuate with

environmental factors and moisture conditions. Crop physiological indicator and water stress induce relationship were compared and observed that values of R^2 of stomatal conductance and TCARI, NDVI, OSAVI, TCARI/OSAVI are 0.037, 0.385, 0.142, and 0.145. The R^2 value of CWSI_{si} calculated from the histogram approach (0.658) is higher than other CWSIs statistical (0.531) and CWSI_e empirical (0.454), respectively. Some previous studies also suggested the low correlation between stomatal and these spectral indices TCARI, NDVI, OSAVI, TCARI/OSAVI (Gago et al., 2013; Baluja et al., 2012). The values of empirical and statistical water stress range from 0.14 to 0.53 and 0.04 to 0.49, while the values of simplified water stress are 0.14 to 0.55, respectively. These values are expected from the different approaches for estimated values of T_{wet} and T_{dry} temperature, which was measured from the average values of the highest and the lowest 0.5% from canopy temperature histogram approach. The temperature of fully transpiring plants leaves was measured using a spray of water on both sides of leaf (T_{wet}), and petroleum jelly was used to calculate the temperature of non-transpiring leaf covered with jelly (T_{dry}). Furthermore, wet and dry temperature values of simplified water stress are stable and easy to calculate. This study is carried out in one flight of UAV, and our finding suggested that CWSI may be applied for precision irrigation management.

Conclusion

This study proposed new techniques for the calculation of adaptive water stress index using a different approach: 1) canopy pixel extraction from different detection algorithm and statistical analysis approach for surface temperature distribution and histogram method is a very operational tool for the judgment of crop water stress: 2) adaptive CWSI_{si} and efficient determination of (wet) and (dry) references, and T_l is the more vigorous parameter for CWSI_e, CWSI_s, TCARI, NDVI, OSAVI, TCARI/OSAVI. T_{wet} and T_{dry} values were attained from the average of the highest and the lowest values of 0.5% from canopy temperature histogram, respectively. A strong linear relationship between adaptive CWSI_{si} and stomatal conductance was obtained. The current approach exists hypothetically and provides us a practical method for plant water stress calculation with a high spatial resolution at the field scale and plant for automated irrigation purposes. As for future work, further research will consider the effects of different vintages, and various phenotypic phases will be examined and applied to these methods for the control system of highly efficient, intelligent irrigation systems.

Acknowledgments. The authors would like to acknowledge the Jiangsu University, China, for their support in providing experiment station and filed. The work was sponsored by the synergistic innovation, center of Jiangsu modern agriculture equipment, and technology (No. 4091600014).

Conflict of interests. The authors reported no potential conflict of interests.

REFERENCES

- [1] Agam, N., Segal, E., Peeters, A., Levi, A., Dag, A., Yermiyahu, U., Ben-Gal, A. (2014): Spatial distribution of water status in irrigated olive orchards by thermal imaging. – Precision Agriculture 15: 346-359.

- [2] Ahrenfeldt, J., Egsgaard, H., Stelte, W., Thomsen, T., Henriksen, U. B. (2013): The influence of partial oxidation mechanisms on tar destruction in two-stage biomass gasification. – *Fuel* 112: 662-680.
- [3] Anderson, M. C., Hain, C., Otkin, J., Zhan, X., Mo, K., Svoboda, M., Wardlow, B., Pimstein, A. (2013): An intercomparison of drought indicators based on thermal remote sensing and NLDAS-2 simulations with us drought monitor classifications. – *Journal of Hydrometeorology* 14: 1035-1056.
- [4] Baluja, J., Diago, M. P., Balda, P., Zorer, R., Meggio, F., Morales, F., Tardaguila, J. (2012): Assessment of vineyard water status variability by thermal and multispectral imagery using an unmanned aerial vehicle (UAV). – *Irrigation Science* 30: 511-522.
- [5] Berni, J., Zarco-Tejada, P., Sepulcre-Cant, G., Fereres, E., Villalobos, F. (2009): Mapping canopy conductance and CWSI in olive orchards using high resolution thermal remote sensing imagery. – *Remote Sensing of Environment* 113: 2380-2388.
- [6] Cohen, Y., Alchanatis, V., Meron, M., Saranga, Y., Tsipris, J. (2005): Estimation of leaf water potential by thermal imagery and spatial analysis. – *Journal of Experimental Botany* 56: 1843-1852.
- [7] Cohen, Y., Alchanatis, V., Saranga, Y., Rosenberg, O., Sela, E., Bosak, A. (2017): Mapping water status based on aerial thermal imagery: comparison of methodologies for upscaling from a single leaf to commercial fields. – *Precision Agriculture* 18: 801-822.
- [8] Davcev, D., Mitreski, K., Trajkovic, S., Nikolovski, V., Koteli, N. (2018): IOT agriculture system based on Lorawan. – 14th IEEE International Workshop on Factory Communication Systems (WFCS), 2018, IEEE 1-4.
- [9] De-Cai, W., Zhang, G.-L., Xian-Zhang, P., Yu-Guo, Z., Ming-Song, Z., Gai-Fen, W. (2012): Mapping soil texture of a plain area using fuzzy-c-means clustering method based on land surface diurnal temperature difference. – *Pedosphere* 22: 394-403.
- [10] Döll, P., Siebert, S. (2002): Global modeling of irrigation water requirements. – *Water Resources Research* 38: 8-1-8-10.
- [11] Espinoza, C. Z., Khot, L. R., Sankaran, S., Jacoby, P. W. (2017): High resolution multispectral and thermal remote sensing-based water stress assessment in subsurface irrigated grapevines. – *Remote Sensing* 9: 961.
- [12] Gago, J., Martorell, S., Tom, S. M., Pou, A., Mill, N. B., Ram, N. J., Ruiz, M. S., Nchez, R., Galm, S. J., Conesa, M. (2013): High-resolution aerial thermal imagery for plant water status assessment in vineyards using a multicopter-RPAS. – First Conference of the International Society for Atmospheric Research Using Remotely-Piloted Aircraft, Palma de Mallorca, Spain.
- [13] Garc A-Tejero, I., Costa, J., Egipto, R., Dur N-Zuazo, V., Lima, R., Lopes, C., Chaves, M. (2016): Thermal data to monitor crop-water status in irrigated Mediterranean viticulture. – *Agricultural Water Management* 176: 80-90.
- [14] Gonzalez-Dugo, V., Durand, J.-L., Gastal, F. (2010): Water deficit and nitrogen nutrition of crops. A review. – *Agronomy for Sustainable Development* 30: 529-544.
- [15] Hatfield, J. L., Prueger, J. H. (2010): Value of using different vegetative indices to quantify agricultural crop characteristics at different growth stages under varying management practices. – *Remote Sensing* 2: 562-578.
- [16] Idso, S., Jackson, R., Pinter Jr, P., Reginato, R., Hatfield, J. (1981): Normalizing the stress-degree-day parameter for environmental variability. – *Agricultural Meteorology* 24: 45-55.
- [17] Jackson, R. D., Idso, S., Reginato, R., Pinter Jr, P. (1981): Canopy temperature as a crop water stress indicator. – *Water Resources Research* 17: 1133-1138.
- [18] Jiang, Z.-Y., Li, X.-Y., Ma, Y.-J. (2013): Water and energy conservation of rainwater harvesting system in the Loess Plateau of China. – *Journal of Integrative Agriculture* 12: 1389-1395.

- [19] Jin, N., Ren, W., Tao, B., He, L., Ren, Q., Li, S., Yu, Q. (2018): Effects of water stress on water use efficiency of irrigated and rainfed wheat in the Loess Plateau, China. – *Science of the Total Environment* 642: 1-11.
- [20] Jones, H. G. (1999): Use of infrared thermometry for estimation of stomatal conductance as a possible aid to irrigation scheduling. – *Agricultural and Forest Meteorology* 95: 139-149.
- [21] Jones, H. G. (2013): *Plants and Microclimate: A Quantitative Approach to Environmental Plant Physiology*. – Cambridge University Press, Cambridge.
- [22] Jones, H. G., Stoll, M., Santos, T., Sousa, C. D., Chaves, M. M., Grant, O. M. (2002): Use of infrared thermography for monitoring stomatal closure in the field: application to grapevine. – *Journal of Experimental Botany* 53: 2249-2260.
- [23] Jordan, C. F. (1969): Derivation of leaf-area index from quality of light on the forest floor. – *Ecology* 50: 663-666.
- [24] Khanal, S., Fulton, J., Shearer, S. (2017): An overview of current and potential applications of thermal remote sensing in precision agriculture. – *Computers and Electronics In Agriculture* 139: 22-32.
- [25] Khorsandi, A., Hemmat, A., Mireei, S. A., Amirfattahi, R., Ehsanzadeh, P. (2018): Plant temperature-based indices using infrared thermography for detecting water status in sesame under greenhouse conditions. – *Agricultural Water Management* 204: 222-233.
- [26] Maini, R., Aggarwal, H. (2008): Study and comparison of various image edge detection techniques. – *International Journal of Image Processing (IJIP)* 3(1).
- [27] Meron, M., Tsipris, J., Orlov, V., Alchanatis, V., Cohen, Y. (2010): Crop water stress mapping for site-specific irrigation by thermal imagery and artificial reference surfaces. – *Precision Agriculture* 11: 148-162.
- [28] Möller, M., Alchanatis, V., Cohen, Y., Meron, M., Tsipris, J., Naor, A., Ostrovsky, V., Sprintsin, M., Cohen, S. (2006): Use of thermal and visible imagery for estimating crop water status of irrigated grapevine. – *Journal of Experimental Botany* 58: 827-838.
- [29] Pallavi, S., Mallapur, J. D., Bendigeri, K. Y. (2017): Remote sensing and controlling of greenhouse agriculture parameters based on IOT. – *International Conference on Big Data, IOT and Data Science (BIGD)*, 2017, IEEE, 44-48.
- [30] Poblete-Echeverr A, C., Sepulveda-Reyes, D., Ortega-Farias, S., Zu Iga, M., Fuentes, S. (2014): Plant water stress detection based on aerial and terrestrial infrared thermography: a study case from vineyard and olive orchard. – *XXIX International Horticultural Congress on Horticulture: Sustaining Lives, Livelihoods and Landscapes (IHC2014)* 1112: 141-146.
- [31] Prasad, S., Bruce, L. M. (2011): *A Divide-and-Conquer Paradigm for Hyperspectral Classification and Target Recognition*. – In: Prasad, S. et al. (eds.) *Optical Remote Sensing*. Springer, Berlin.
- [32] Quattrochi, D. A., Luvall, J. C. (1999): Thermal infrared remote sensing for analysis of landscape ecological processes: methods and applications. – *Landscape Ecology* 14: 577-598.
- [33] Rud, R., Cohen, Y., Alchanatis, V., Levi, A., Brikman, R., Shenderoy, C., Heuer, B., Markovitch, T., Dar, Z., Rosen, C. (2014): Crop water stress index derived from multi-year ground and aerial thermal images as an indicator of potato water status. – *Precision Agriculture* 15: 273-289.
- [34] Stark, B., Smith, B., Chen, Y. (2014): Survey of thermal infrared remote sensing for unmanned aerial systems. – *International Conference on Unmanned Aircraft Systems (ICUAS)*, 2014, IEEE 1294-1299.
- [35] Tanner, C. (1963): Plant temperatures 1. – *Agronomy Journal* 55: 210-211.
- [36] Testi, L., Goldhamer, D., Iniesta, F., Salinas, M. (2008): Crop water stress index is a sensitive water stress indicator in pistachio trees. – *Irrigation Science* 26: 395-405.

PURIFICATION AND CHARACTERIZATION OF LIPASE FROM PSYCHROPHILIC BACTERIA *PSEUDOMONAS MANDELII* HTB2 FROM BATURA GLACIER, PAKISTAN

SHAHEEN, M.^{1,2} – ULLAH, I.¹ – RAFIQ, M.^{1,3} – MAQSOOD UR REHMAN, M.¹ – SHAH, A. A.¹ – HASAN, F.^{1*}

¹*Department of Microbiology, Quaid-i-Azam University, Islamabad, Pakistan*

²*Department of Zoology, GC University, Faisalabad, Pakistan*

³*Department of Microbiology, Balochistan University of Information Technology, Engineering and Management Sciences, Quetta, Pakistan*

*Corresponding author
e-mail: farihahasan@yahoo.com

(Received 28th Jul 2018; accepted 4th Feb 2019)

Abstract. Lipases are fat splitting enzymes. Psychrotrophic enzymes including lipases possess huge potential for many industries due to their high activity at low temperatures. Lipase produced by the psychrophilic bacteria HTB2 identified as *Pseudomonas mandelii*, by using different molecular techniques, isolated from Batura glacier, Hunza Valley, Pakistan, was partially purified through acetone precipitation and gel permeation chromatography. During purification studies two types of peaks were observed in spectrophotometric analysis which indicated the presence of two different sizes of lipases produced by *Pseudomonas mandelii* HTB2. The purified enzyme from *P. mandelii* HTB2 showed best activity at 45°C, however, maximum lipase activity was attained at pH 10. It is a unique finding that an enzyme from a psychrophilic bacterium was active at thermophilic range and extreme alkaline condition. This is the first report of purification of lipase from psychrophilic bacteria from Batura glacier, and it holds promise for potential industrial applications.

Keywords: enzyme, alkaline, thermophilic range, low temperature, industrial applications

Introduction

A large part of the earth consists of cold environment and covered by glaciers, oceans, polar and alpine regions, high mountains, deep seas and cold soils. All of these environments are permanently cold but despite the extreme environmental conditions diverse groups of microorganisms colonize this habitat by developing adaptation strategies to survive or to be highly successful like true psychrophiles (Åqvist et al., 2017). In an efficiently adapted organism the metabolic fluxes become comparatively same to those living at moderate temperature which needs suitable reaction rates. As we know, enzymes are mostly involved in catalysis of many metabolic reactions, so the enzymes produced by these organisms are also cold adapted. This is because of their molecular structure that they work efficiently in cold environment (Pulicherla et al., 2011).

Enzymes are basically proteins generated by living organisms and functioning as specialized catalysts for biochemical reactions. Mostly enzymes are produced from bio-based materials by the process of fermentation (Renge et al., 2012; Smaniotto et al., 2014). Mostly, biomass present in different parts of earth, consists of lipids, and lipolytic enzymes have an important role in the breakdown, and transfer and

mobilization of (water-insoluble) compounds (Ray, 2012). Formerly, it was found that there are many microorganisms that yields chemical that act as biosurfactants and are involved in solubilization of lipids (Pulicherla et al., 2011).

The specific advantages that are provided by enzymes are specificity for substrates, mild conditions and also reduce waste. By choosing the precise enzyme it may be possible to control which products are produced and unwanted side reactions are reduced via enzyme specificity that involve in the waste stream. The increase in the BOD of water in waste stream due to enzyme is negligible (Szilveszter et al., 2009).

Lipases have appeared one of the leading enzyme and captured more interest for last few years because of great range of applications in many industries. Large numbers of lipases have been screened for its involvement in medicines, food, cosmetics and laundry detergents etc. In animal feed industry lipid hydrolyzing enzymes can be used an additive to enhance energy gain from feed in the animal feed industry. The enzyme supplement is particularly necessary for young and new born animals (Ravindran, 2013).

The microbes producing lipase can be found in diverse habitat like industrial wastes, vegetable oil processing factories, oil contaminated soil, oil seeds and hot springs. Lipase producing microbes constitute bacteria, fungi, yeast, and actinomyces (Wang et al., 2009). Lipase produced by bacteria with various properties and specificities have been studied and characterized. Lipase can be isolated from different bacterial species like *Bacillus*, *Pseudomonas* (Kiran et al., 2008; Wang et al., 2009).

Cold active lipases are those lipolytic enzymes which are isolated from microorganisms dwelling in cold habitats. Cold-adapted enzymes function efficiently at cold temperature with high catalytic activity as compared to mesophilic or thermophilic lipases. The cold active or psychrophilic lipases adapted structural characteristics that show a high level of flexibility, especially around the active site are translated into low activation enthalpy, low-substrate affinity and higher specific activity at low temperature range. The research work on cold active lipases is increasing at a rapid and exciting rate (Joseph et al., 2011).

Microorganism's tolerating low temperatures (near 5°C) are the sources of cold active lipases. As a lot of number of lipase producing sources are existed, only a few bacteria and yeast were exploited for the generation of cold active lipolytic enzymes. From time to time many research studies have been done to check and isolate lipids from those microbes possessing high activity at low temperature. Deep-sea bacteria is another excellent source of cold active lipases, *Aeromonas hydrophila* is another marine bacterium proliferating at temperature range between 4 and 37°C can also produce cold active lipases (Kavitha, 2016).

Lipolytic enzymes are mostly consumed in lipids and oils processing. It is also used in detergents and degreasing formulations, food processing, the synthesis of fine chemicals and pharmaceuticals, paper industry, and cosmetic manufacture (Rasmey et al., 2017). It can also be used to speed up the breakdown of fatty waste and polyurethane (Andualema and Gessesse, 2012). Low temperature microorganisms can be utilized for bioremediation of polluted cold soils and wastewaters and their enzymes can have application in molecular biology, medical research, food or feed industries, detergents or cosmetics (Margesin and Feller, 2010). Based on their efficient catalytic activity at low temperature and low thermos-stability and uncommon specificity of cold active lipases suggest new opportunities for biotechnological exploitation. They are used as additional supplements in detergents, food industries, bioremediation and molecular biology applications (Cavicchioli et al., 2011; Rasmey et al., 2017).

Currently lipases from psychrophiles are attracting enormous attention because of the reason that they have tremendous biotechnological and industrial application potential. Most of the lipolytic enzymes used in industry are of microbial origin (Singh et al., 2016). There is an increasing desire to produce feasible ways and search out optimized conditions to produce psychrophilic enzymes because they are used in detergents. It can become feasible to develop laundry applications that can be performed at lower temperature with such enzymes. For achieving such purposes psychrophilic lipases have great commercial importance.

The enzymes of produced by cold adapted microorganisms are cold active which are economically beneficial because of saving energy, minimize the need for expensive heating step, work efficiently in cold medium and during the winter season, produce enough reaction yields, accommodate a high stereospecificity, reduces unwanted chemical reactions that usually occurs at high temperature. They are also thermal labile which exhibit the property of rapid and easy inactivation when it is required (Kumar et al., 2011). The heat inactivation capabilities of cold active enzymes have special concern to the food industry where it is used to avoid any modification of heat sensitive components of food (Ray and Rosell, 2017).

On basis of rapid developments in biotechnology and industries, there is a need for new lipases with novel characteristics (Ugras and Umez, 2016). Searching for more microorganisms to produce more lipolytic enzymes will provide new ways to answer different environmental problems and to execute many synthetic reactions. The increase in interest about bacterial lipases is due the facts that they are more stable in severe conditions as compared to those isolated from other organisms. The increasing attention towards psychrophilic enzymes enables us to screen bacteria and optimize culture conditions for efficient enzymes production. Therefore, present study aims to isolate bacteria from cold habitat and its screening for lipase production, purification, characterization and phylogenetic analysis.

Materials and methods

Lipase produced by the psychrophilic bacteria *Pseudomonas mandelii* HTB2 isolated from Batura glacier, Hunza Valley, Pakistan, was used for the study.

Qualitative and quantitative test

Production of lipase was detected by using the mehtod, mentioned by Sierra (1957). Tween 80 (Sorbitan Monooleate) was used as a substrate. The medium used for screening purpose contained (g/l); peptone 10.0, NaCl 5.0, CaCl₂·2H₂O 0.1 and agar 20.0. pH of this medium was 7.

Tween 80 was sterilized separately by autoclaving for 20 min at 15 Ibs pressure. About 1 ml of Tween 80 was added per 100 ml of sterilized medium and pouring was done. After solidification of media, four different cultures were inoculated. The appearance of the clear zones around the colonies indicated lipolytic activity, due to degradation of the substrate. The bacterial cultures that showed clear zones were used for further studies.

Rhodamine B assay

Rhodamine B and olive oil containing medium was also used for screening of lipase producing bacteria. Medium was composed of (ml/l or g/l); sucrose 1.0, yeast extract 1.0,

peptone 2.0, NH₄SO₄ 1.0, K₂HPO₄ 1.0, MgSO₄.7H₂O 0.1, FeSO₄.7H₂O 0.01, Olive oil 3 ml and Rhodamine B solution (0.1% w/v) 3 ml.

Olive oil and Rhodamine B dye containing medium was used for the screening of lipolytic enzyme. The appearance of clear zone around the culture streak indicated lipase production. The lipase positive colonies were visualized by the help of trans illuminator. For quantitative test, above mentioned liquid medium with lipase substrates was used. To analysed the activity of lipase, enzyme assay (for lipase), and estimation of protein was performed.

Production and purification of lipase

The bacterial isolate HTB2 was grown in above mentioned production media in shaking incubator for 72 hours by keeping all the optimized condition (pH 9) at 10°C, temperature, in the presence of Tween-80, for maximum production of lipase, for further purification purpose. Optimisation results have already been reported in early part of research work (Shaheen et al., 2018). The culture was centrifuged and following steps were done for lipase purification.

- Separation of bacterial cells from fermentation medium.
- Precipitation (Acetone precipitation and Ammonium sulphate precipitation).
- Column chromatography.

Separation of bacterial cells from fermentation medium

The bacterial cells separation from fermentation medium was facilitated by centrifugation process. The enzyme production medium was centrifuged (Kokusan, Japan) for 25 minutes at 10000 rpm at 4°C temperature. The supernatant obtained was stored and its lipolytic activity was determined and recorded.

Acetone precipitation

Organic solvents brought out precipitation of proteins mainly by changing the solvation of proteins with water. This reaction was carried out at low temperature to avoid denaturation due to the heat of mixing when the organic solvent is added to water. Acetone was used as solvent for precipitating proteins. The optimum amount of acetone to precipitate proteins was optimized by adding varying amount of acetone. Protein estimation and lipase assay were done with each batch of precipitation. Chilled acetone was added slowly drop wise to avoid the formation of locally high concentration of organic solvent. The solvent temperature was kept below 0°C. The mixture was allowed to stand overnight and then centrifuged. The supernatant was decanted carefully. Residues of organic solvent can be removed from solvent by vacuum. The pellet was dissolved in minimum amount of sulphate buffer having pH 8.0 and stored at -20°C temperature and used for analytical studies.

Ammonium sulphate precipitation

Solid ammonium sulphate was added to the crude enzymes at a concentration of 60%. Precipitates were collected by centrifuging the solution at 10000 rpm for 25 minutes. The supernatant lipolytic activity was checked. If there was lipolytic activity in supernatant then again, the solution is treated with 60% ammonium sulphate for further precipitation.

Column chromatography (Sephadex G-75)

Sephadex G-75 was used as a medium for column chromatography. It was prepared by adding 3 g Sephadex G-75 in 200 ml phosphate buffer along with 0.02% sodium azide and fluconazole and incubated for 48 hours at 45°C. Sodium azide and fluconazole were used as antimicrobial agents while incubation was required to attain the final size. Before addition to column, gel and buffers were sonicated for 1 hour. Column was cleaned by thoroughly washing with distilled water and observed for leakage. Column was filled in such a way that bubbles were not formed. The column was allowed overnight at room temperature for proper packing. Partially purified enzymes were added to the column with a flow rate of 0.30 ml/min. About 3 ml of sample was passed with the help of continuous addition of buffer and total 24 fractions were collected. Each fraction was analyzed for protein estimation by taking O.D at 280 nm. Lipase positive fractions were combined and stored at 4°C for further alipase activity analysis.

Lipase assay

Activity of lipase was determined by using the following method (Lesuisse et al., 1993). A chromogenic substrate (*p*NPL), *p*- nitrophenyl laurate was used. Lipase acted on *p*NPL and break it into lauric acid and *p*-nitrophenol. Activity (in terms of unit), is defined as the quantity of enzyme that can hydrolyze 1 µl / mole substrate in one minute.

Protein estimation

For calculating protein estimation, Lowry method (Lowry et al., 1951) was performed using BSA (bovine serum albumin) as standard.

Characterization of purified lipases

Purified lipases were further characterized and analyzed for factors that are known to affect their activity. Relative activity (%) was calculated by taking the highest value as 100%.

Effect of temperature on lipase activity

Purified lipase activity was observed by incubating the purified lipase at various temperatures (25, 30, 35, 40, 45 and 50°C) and determining the residual activity.

Effect of pH on lipase activity

The activity of purified lipase was observed at various pH; 3.0, 4.0, 5.0, 6.0, 7.0, 8.0, 9.0, 10 and pH 11 and determining the residual activity.

Molecular identification

DNA extraction, PCR amplification and sequencing

Thermoscientific DNA extraction kit was used to extract the DNA of HTB2 isolate. The extraction protocol was used as given by Thermoscientific company. 16S rRNA gene was amplified by using a set of universal primers i.e. 27F (5'- AGA GTT TGA TYM TGG CTC AG-3') and 1492R (5'-TAC CTT GTT AYG ACT T-3'). Optimized conditions of PCR were as; initial denaturing at 94°C for 5 min followed by 35 cycles, each cycle consisted of denaturing for 30 seconds at 94°C, primers annealing for 30 seconds at 54°C,

extension for 30 seconds at 72°C, followed by final extension of 10 minutes at 72°C. These steps were followed by infinite hold at 4°C until PCR product was collected. PCR product was run along with DNA ladder sequence on agarose gel to confirm the size of our PCR product. Amplified PCR product was sent to Macrogen Inc. Korea for sequencing purpose. The quality of obtained sequence was analyzed by using BioEdit and Chromas elite software. The good quality sequences were selected for BLAST search, homology and phylogenetic analysis.

Identification and phylogenetic analysis

The selected sequences were used for homology search in National Centre for Biotechnology (NCBI) data base to find out the identity of the study isolates. For phylogenetic analysis sequences were obtained from NCBI. MEGA 6 software was used to construct the phylogenetic tree.

Overall the study deals with the partial purification of lipase produced by a psychrophilic bacteria *Pseudomonas mandelii* HTB2 by acetone precipitation and gel permeation chromatography, and checked its activity at varying temperatures and pH values. The experiments were run in triplicates. All the standard methodologies were followed for analysis and enzyme assays.

Results

Qualitative tests

Based on qualitative analysis, the HTB2 isolate was found effective producer of lipase among the four isolates. The formation of zone around the colonies indicated the lipases production (*Fig. 1*).

Rhodamine B plate assay

The lipase production from HTB2 isolate was further verified by using both (Rhodamine B), and (olive oil), in agar media. Transilluminator was used to visualize HTB2 and the fluorescence indicated the lipase activity (*Fig. 1*).

Previously reported (Shaheen et al., 2018) optimum growth conditions for the production of lipase (7.6 and 25.9 U/mg) by the same strain HTB2 at 10°C, after 72 hours of incubation, respectively, and Tween 80 was best among different substrates, for lipase production (20.8 U/mg), in liquid medium with pH 9, at 10°C. Glucose (19.4 U/mg) and casein (15.5 U/mg), were found good additional sources (carbon and nitrogen), in the enhancement of production of lipase. These conditions were applied here for production of lipase and then subjected to purification.

Purification of lipase

Acetone precipitation

Different concentrations of Acetone were added to already centrifuge fermentation medium or cell free supernatant which highly affected the precipitation. The concentration of precipitated lipase enhanced until 90% of acetone. Any further addition of acetone caused decrease in the concentration of enzyme.

Ammonium sulphate precipitation

The result of ammonium sulphate precipitation showed poor yield of lipase.

Column chromatography

The precipitated enzymes were subjected to column chromatography using Sephadex G 75-120. Maximum activity was found among fractions 5 - 7 and 12 - 16, while highest specific activity was observed in fractions 7 and 15 with activity of 9.11 and 9.77 U/ml, respectively (Fig. 2).

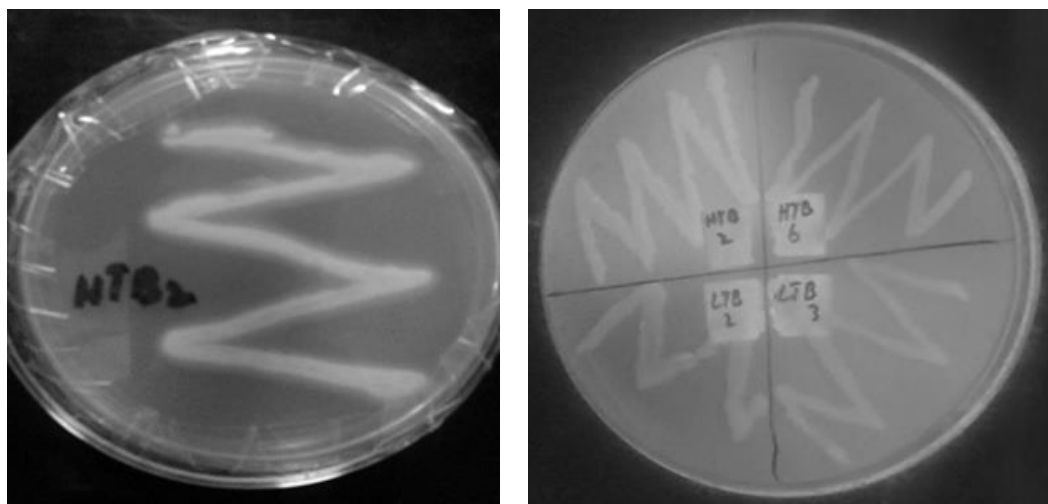


Figure 1. Rhodamine B plate assay of isolate HTB2 at 10°C after 72 hours of incubation

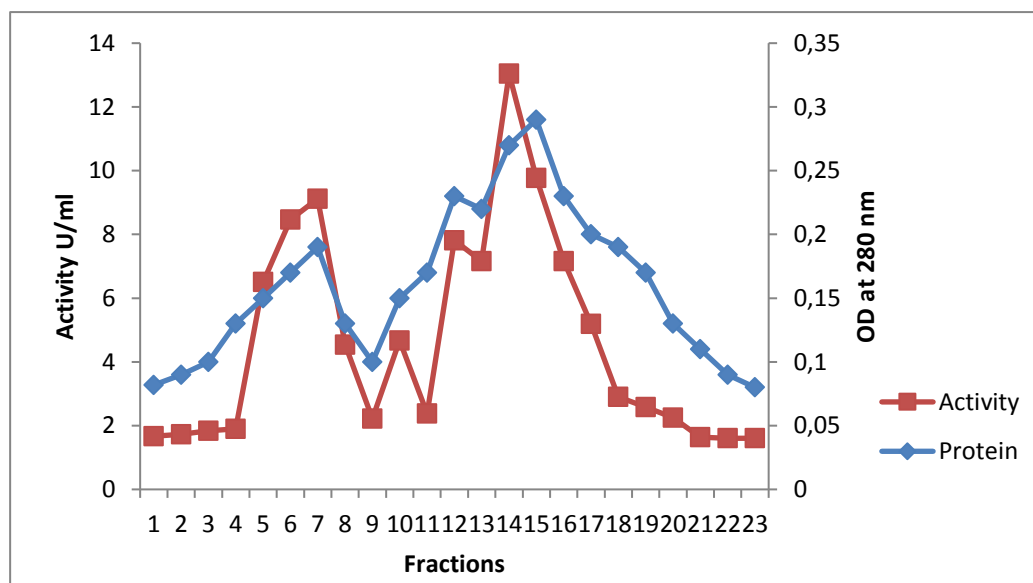


Figure 2. Profile of lipases from *Pseudomonas mandelii* HTB2 after filtration of Sephadex G 75-120 chromatography. The two peaks of lipase activity in the graph indicated multiple forms of enzyme

Characterization of lipases

Effect of temperature on the purified lipases

The activity of lipase after purification was also analyzed at various temperatures, ranges from 25 – 50°C and maximum specific activity was found at 45°C (Fig. 3). The lipases showed 80% and 50% initial activity at 50 and 35°C, respectively.

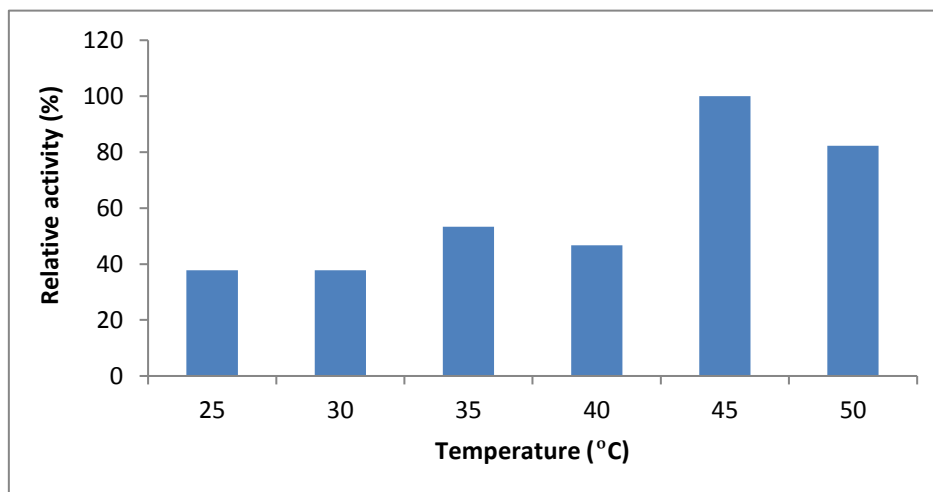


Figure 3. Effect of temperature on purified lipase activity

Effect of pH on purified lipases

The activity of purified lipases was evaluated at various pH on optimum temperature (45°C). The lipases were highly active at pH 10 while showed activity at a wide pH range (Fig. 4). More than 75% activity was found at pH 9.0 and 11.0.

Molecular identification and phylogenetic analysis

Sequencing of DNA product showed that HTB 2 belonged to different taxonomic groups. Similarity index of HTB 2 with other isolates is shown in Table 1. Evolutionary relationship of HTB 2 is shown in Fig. 5.

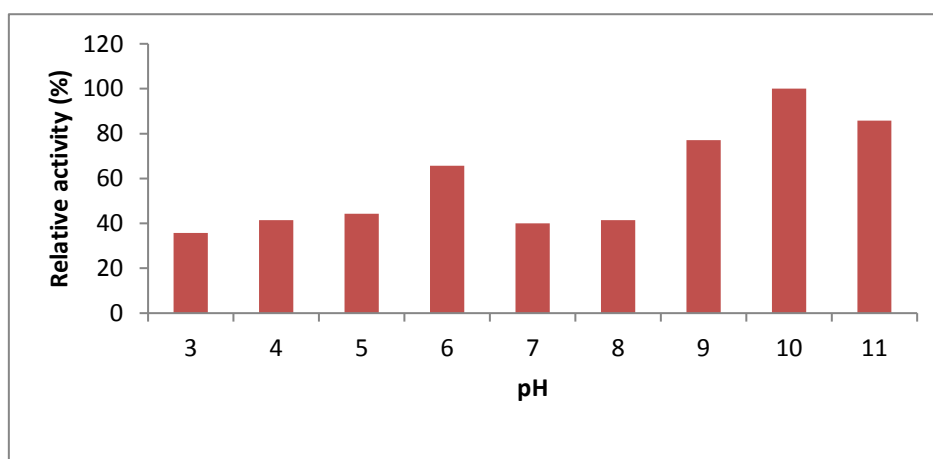


Figure 4. Effect of pH on purified lipase activity

Table 1. Phylogenetic analysis of HTB 2

Isolate	Homologous sp.	Identity (%)
HTB 2	<i>Pseudomonas mandelii</i>	100
	<i>Shewanella</i> sp.	97
	<i>Halomonas</i> sp.	97
	<i>Pectobacterium carotovorum</i>	97

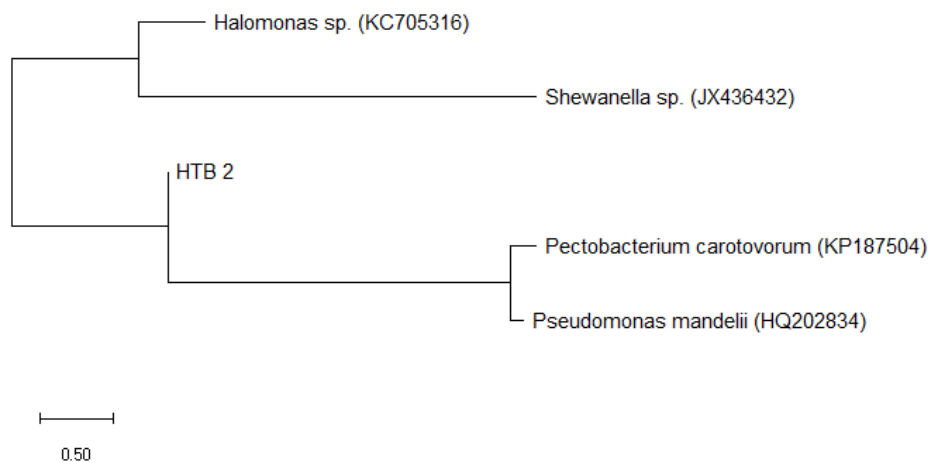


Figure 5. Phylogenetic relation of the HTB 2 with the isolates obtained from NCBI

Discussion

Microorganisms thrive in cold environment. Psychrophilic and psychrotrophic microbes have the ability to generate cold active enzymes that have potential application in industries. Furthermore, high enzymatic activity at reduced temperature and thermal stability are the important factors which make these enzymes ‘cold adapted’. By virtue of these unique characteristics, lipases are key products of rapidly growing biotechnology industry (Kavitha, 2016). Moreover, understanding the whole structure of proteins is necessarily required to point out the link between the structure and function of proteins (Singh et al., 2016).

In the past decades the attention towards microbial cold active enzymes has been increased. This is due to the reason that they are highly specific and economically advantageous without any ecological impact. Use of these enzymes instead of harsh conditions and harsh chemicals, is helpful to conserve energy and avoid pollution. As these enzymes are substrate specific thus prevent production of unwanted byproducts so avoiding extensive downstream processing. When immobilized, these enzymes can be reused several times (Robinson, 2015).

Many potential producers including bacteria, yeast and fungi have been studied for lipase production through techniques of fermentation. Extracellular lipase was isolated from various bacterial species like *Pseudomonas* (Ertuğrul et al., 2007; Kiran et al., 2008; Wang et al., 2009).

Bacterial isolate HTB2, previously recovered from Batura glacier (Pakistan) in Applied Environmental and Geomicrobiology Laboratory, Department of Microbiology, Quaid-i-Azam University Islamabad, is identified in the current study as *Pseudomonas mandelii* HTB2. Very few researchers have reported this species from low temperature

environment. *Pseudomonas* is generally of very diverse nature and ubiquitous in nature and are also known to produce a number of metabolites and produce biofilm as well. *Pseudomonas mandelii* is a fluorescent, Gram negative, rod-shaped bacterium reported to occur in natural mineral waters (Jang et al., 2012) and agricultural fields (Dandie et al., 2007). *P. mandelii* is nonhalophilic and thrives at low temperatures and produces extracellular enzymes (Gratia et al., 2009).

Li et al. (2013) have reported a novel facultative psychrotroph *Pseudomonas mandelii* strain CBS-1 from soil of Changbai Mountain, China, that accumulated poly- β -hydroxybutyrate (PHB). Another novel strain of *Pseudomonas mandelii* isolated from Antarctica was found to produce high concentrations of alginate (Vásquez-Ponce et al., 2017). Psychrotolerant *Pseudomonas mandelii* SR1 synthesized the small sized silver nanoparticles (AgNPs) at 12°C, and showed larvicidal activity, against *Anopheles subpictus* and *Culex tritaeniorhynchus* larvae, thus can be used control of larvae in waters in cold environments (Mageswari et al., 2015).

Lipase produced by *Pseudomonas mandelii* HTB2 was purified and characterized on basis of activity at different pH and temperature. The purified lipase showed optimum activity at 45°C. Every enzyme has a specific pH at which works most efficiently called optimum pH. This phenomenon is due to the exact arrangement of the active site of an enzyme occupied by hydrogen and ionic bond to some extent (between $-\text{NH}_2$ and $-\text{COOH}$ groups). Even small amount of change in pH alter this bonding which causes conformational changes in the active site which then become unable to attach with the substrate. The *Pseudomonas mandelii* HTB2 showed maximum residual activity at pH 10. On basis of these unique properties of enzyme from *P. mandelii* HTB2 showing activity at higher temperature and alkaline pH, can have a number of applications in industry as well as environment. Residual activity of psychrotrophic lipase from *Acinetobacter* sp. O16 to be optimum at 40°C, while optimal activity was observed at 35°C and pH 7.5 (Sahay and Chouhan, 2018), while that from *Acinetobacter* sp. SY-01 lipolytic activity was optimum at 50°C and pH 10 (Han et al., 2003) with potential application in detergent industry (Wang et al., 2012). In another study performed by Yuan et al. (2010), lipase retained 80.7% of its activity at 40°C. *Acinetobacter* sp. XMZ-26 was isolated from soil samples obtained from glaciers in Xinjiang Province, China. Maximal lipase activity was observed at 15°C and pH 10. Purified lipase was active between 5°C and 35°C (Zheng et al., 2011). Most of the lipases isolated from *Burkholderia* origin showed residual activity in the range pH 3 to 10.5 (Yuan et al., 2010). The lipases from psychrotrophic *Serratia marcescens* was characterized, the optimum pH was between 8 and 9 (Abdou, 2003).

Conclusions

This study investigated the lipase screening qualitatively and quantitatively from cold adapted *Pseudomonas mandelii* HTB2, lipase purification was carried out by using acetone and ammonium sulphate precipitation and column chromatography methods. Stability of semi-purified lipase was analysed at various range of temperature and pH, in the presence of different substrates. We conclude that further characterization related to combined effect of different factors is needed with respect to lipase production and its stability. Present study would provide basis for investigation of other industrially important enzyme producing bacteria from this habitat.

REFERENCES

- [1] Andualema, B., Gessesse, A. (2012): Microbial lipases and their industrial applications. – *Biotechnology* 11: 100-118.
- [2] Åqvist, J., Isaksen, G. V., Brandsdal, B. O. (2017): Computation of enzyme cold adaptation. – *Nature Reviews Chemistry* 1: 0051.
- [3] Cavicchioli, R., Charlton, T., Ertan, H., Omar, S. M., Siddiqui, K. S., Williams, T. J. (2011): Biotechnological uses of enzymes from psychrophiles. – *Microbial Biotechnology* 4: 449-460.
- [4] Dandie, C. E., Burton, D. L., Zebarth, B. J., Trevors, J. T., Goyer, C. (2007): Analysis of denitrification genes and comparison of nosZ, cnorB and 16S rDNA from culturable denitrifying bacteria in potato cropping systems. – *Systematic and applied microbiology* 30: 128-138.
- [5] Ertuğrul, S., Dönmez, G., Takaç, S. (2007): Isolation of lipase producing *Bacillus* sp. from olive mill wastewater and improving its enzyme activity. – *Journal of Hazardous Materials* 149: 720-724.
- [6] Gratia, E., Weekers, F., Margesin, R., D'Amico, S., Thonart, P., Feller, G. (2009): Selection of a cold-adapted bacterium for bioremediation of wastewater at low temperatures. – *Extremophiles* 13: 763-768.
- [7] Han, S. J., Back, J. H., Yoon, M. Y., Shin, P. K., Cheong, C. S., Sung, M. H., Hong, S. P., Chung, I. Y., Han, Y. S. (2003): Expression and characterization of a novel enantioselective lipase from *Acinetobacter* species SY-01. – *Biochimie* 85: 501-510.
- [8] Jang, S. H., Kim, J., Kim, J., Hong, S., Lee, C. (2012): Genome sequence of cold-adapted *Pseudomonas mandelii* strain JR-1. – *Journal of bacteriology* 194: 3263-3263.
- [9] Joseph, B., Upadhyaya, S., Ramteke, P. (2011): Production of cold-active bacterial lipases through semisolid state fermentation using oil cakes. – *Enzyme Research*, 2011.
- [10] Kavitha, M. (2016): Cold active lipases—an update. – *Frontiers in Life Science* 9: 226-238.
- [11] Kiran, G. S., Shanmughapriya, S., Jayalakshmi, J., Selvin, J., Gandhimathi, R., Sivaramakrishnan, S., Arunkumar, M., Thangavelu, T., Natarajaseenivasan, K. (2008): Optimization of extracellular psychrophilic alkaline lipase produced by marine *Pseudomonas* sp.(MSI057). – *Bioprocess and Biosystems Engineering* 31: 483-492.
- [12] Kumar, L., Awasthi, G., Singh, B. (2011): Extremophiles: a novel source of industrially important enzymes. – *Biotechnology* 10: 121-135.
- [13] Lesuisse, E., Schanck, K., Colson, C. (1993): Purification and preliminary characterization of the extracellular lipase of *Bacillus subtilis* 168, an extremely basic pH-tolerant enzyme. – *European Journal of Biochemistry* 216: 155-160.
- [14] Mageswari, A., Subramanian, P., Ravindran, V., Yesodharan, S., Bagavan, A., Rahuman, A. A., Karthikeyan, S., Gothandam, K. M. (2015): Synthesis and larvicidal activity of low-temperature stable silver nanoparticles from psychrotolerant *Pseudomonas mandelii*. – *Environmental Science and Pollution Research* 22: 5383-5394.
- [15] Margesin, R., Feller, G. (2010): Biotechnological applications of psychrophiles. – *Environmental Technology* 31: 835-844.
- [16] Pulicherla, K. K., Ghosh, M., Kumar, P. S., Sambasiva Rao, K. R. S. (2011): Psychrozymes-the next generation industrial enzymes. – *Journal of Marine Science: Research and Development* 1: 1-7.
- [17] Rasmey, A. H. M., Aboseidah, A. A., Gaber, S., Mahran, F. (2017): Characterization and optimization of lipase activity produced by *Pseudomonas monteilli* 2403-KY120354 isolated from ground beef. – *African Journal of Biotechnology* 16: 96-105.
- [18] Ravindran, V. (2013): Feed enzymes: The science, practice, and metabolic realities. – *Journal of Applied Poultry Research* 22: 628-636.
- [19] Ray, A. (2012): Application of lipase in industry. – *Asian Journal of Pharmacy and Technology* 2: 33-37.

- [20] Ray, R. C., Rosell, C. M. (2017): Lipase: Properties, Functions and Food Applications. – Microbial Enzyme Technology in Food Applications (pp. 228-254). CRC Press.
- [21] Renge, V. C., Khedkar, S. V., Nandurkar, N. R. (2012): Enzyme synthesis by fermentation method: a review. – Chemical Society Reviews 2: 585e90.
- [22] Robinson, P. K. (2015): Enzymes: principles and biotechnological applications. – Essays in Biochemistry 59: 1-41.
- [23] Sahay, H., Babu, B. K., Singh, S., Kaushik, R., Saxena, A. K., Arora, D. K. (2013): Cold-active hydrolases producing bacteria from two different sub-glacial Himalayan lakes. – Journal of Basic Microbiology 53: 703-714.
- [24] Shaheen, M., Ullah, I., Rafiq, M., Rehman, M. M., Hasan, F. (2018): Influence of physicochemical conditions on the production of lipase by Psychrophilic Bacteria Isolated from Batura Glacier, Hunza Valley, Pakistan. – International Journal of Biosciences 12: 1-11.
- [25] Sierra, G. (1957): A simple method for the detection of lipolytic activity of microorganisms and some observations on the influence of the contact between cells and fatty substrates. – Antonie van Leeuwenhoek 23: 15-22.
- [26] Singh, R., Kumar, M., Mittal, A., Mehta, P. K. (2016): Microbial enzymes: industrial progress in 21st century. – 3 Biotechnology 6: 174.
- [27] Smaniotto, A., Skovronski, A., Rigo, E., Tsai, S. M., Durrer, A., Foltran, L. L., Paroul, N., Luccio, M. D., Oliveira, J. V., Oliveira, D. D., Treichel, H. (2014): Concentration, characterization and application of lipases from *Sporidiobolus pararoseus* strain. – Brazilian Journal of Microbiology 45: 294-301.
- [28] Szilveszter, Sz., Raduly, B., Miklóssy, I., Ábrahám, B., Lanyi, Sz., Nicolae, D. R. (2009): Enzymatic activity studies of biological wastewater treatment. – Universitatis Babeş-Bolyai, p.113.
- [29] Ugras, S., Uzmez, S. (2016): Characterization of a newly identified lipase from a lipase-producing bacterium. – Frontiers in Biology 11: 323-330.
- [30] Vasquez-Ponce, F., Higuera-Llantén, S., Pavlov, M. S., Ramírez-Orellana, R., Marshall, S. H., Olivares-Pacheco, J. (2017): Alginate overproduction and biofilm formation by psychrotolerant *Pseudomonas mandelii* depend on temperature in Antarctic marine sediments. – Electronic Journal of Biotechnology 28: 27-34.
- [31] Wang, S. L., Lin, Y. T., Liang, T. W., Chio, S. H., Ming, L. J., Wu, P. C. (2009): Purification and characterization of extracellular lipases from *Pseudomonas monteilii* TKU009 by the use of soybeans as the substrate. – Journal of Industrial Microbiology and Biotechnology 36: 65-73.
- [32] Wang, H., Zhong, S., Ma, H., Zhang, J., Qi, W. (2012): Screening and characterization of a novel alkaline lipase from *Acinetobacter calcoaceticus* 1-7 isolated from Bohai bay in China for detergent formulation. – Brazilian Journal of Microbiology 43: 148-156.
- [33] Yuan, B., Cai, Y., Liao, X., Yun, L., Zhang, F., Zhang, D. (2010): Isolation and identification of a cold-adapted lipase producing strain from decayed seeds of *Ginkgo biloba* L. and characterization of the lipase. – African Journal of Biotechnology 9: 2661-2667.
- [34] Zheng, X., Chu, X., Zhang, W., Wu, N., Fan, Y. (2011): A novel cold-adapted lipase from *Acinetobacter* sp. XMZ-26: Gene cloning and characterisation. – Applied Microbiology and Biotechnology 90: 971-980.

SENSITIVITY OF ODONATE NYMPHS TO DIFFERENT CLASSES OF AGRICULTURAL INSECTICIDES, FREQUENTLY APPLIED IN SWAT VALLEY PAKISTAN

ILAH, I.^{*1} – YOUSAFZAI, A. M.² – RAHIM, A.¹ – HAQ, T. U.³ – WAHAB, S.¹ – ALI, H.¹ – HALIMULLAH¹ – FAROOQ, M.¹ – MUHAMMAD, H.¹ – ULLAH, F.¹ – AHMAD, B.¹ – ULLAH, S.⁴ – HUSSAIN, S.¹

¹Department of Zoology, University of Malakand
Chakdara, Dir Lower, Khyber Pakhtunkhwa, Pakistan

²Department of Zoology, Islamia College Peshawar
Peshawar, Khyber Pakhtunkhwa, Pakistan

³Department of Biotechnology, University of Malakand
Chakdara, Dir Lower, Khyber Pakhtunkhwa, Pakistan

⁴Department of Botany, University of Malakand
Chakdara, Dir Lower, Khyber Pakhtunkhwa, Pakistan

*Corresponding author
e-mail: ikramilahi@uom.edu.pk

(Received 7th Feb 2019; accepted 1st May 2019)

Abstract. The sensitivity of blue-tailed damselfly (*Ischnura elegans*) and crimson marsh glider dragonfly (*Trithemis aurora*) nymphs to six different insecticides were studied during 48-hour exposure in the laboratory conditions. Lambda cyhalothrin was found to be the most toxic. Chlorpyrifos was found least toxic. The highest concentrations of deltamethrin, cypermethrin, lambda cyhalothrin, chlorpyrifos, dichlorvos and acetamiprid that caused no mortality of *I. elegans* were 0.0078, 0.0039, 0.00048, 0.0078, 0.0039 and 0.00195 ppm, respectively. The highest concentrations of deltamethrin, cypermethrin, lambda cyhalothrin, chlorpyrifos, dichlorvos and acetamiprid that caused no mortality of *T. aurora* were 0.0039, 0.00195, 0.00048, 0.0156, 0.0078 and 0.000975 ppm, respectively. The lowest concentrations of deltamethrin, cypermethrin, lambda cyhalothrin, chlorpyrifos, dichlorvos and acetamiprid that caused 100% mortality of *I. elegans* were 0.5, 0.5, 0.0156, 1.0, 0.5 and 0.25 ppm, respectively. The lowest concentrations of deltamethrin, cypermethrin, lambda cyhalothrin, chlorpyrifos, dichlorvos and acetamiprid that caused 100% mortality of *T. aurora* were 0.25, 0.25, 0.0312, 2, 1 and 0.125 ppm, respectively. Significantly ($P < 0.05$) lowest LC₉₀ values were observed for lambda cyhalothrin (LC₉₀ against *I. elegans* = 0.01 ppm, LC₉₀ against *T. aurora* = 0.018 ppm). Next to the lambda cyhalothrin, significantly ($P < 0.05$) lowest LC₉₀ values were observed for acetamiprid (LC₉₀ against *I. elegans* = 0.122 ppm, LC₉₀ against *T. aurora* = 0.093 ppm). From the findings of the present study, it was concluded that *I. elegans* and *T. aurora* nymphs are highly sensitive to lambda cyhalothrin and acetamiprid.

Keywords: deltamethrin, cypermethrin, lambda cyhalothrin, chlorpyrifos, dichlorvos, acetamiprid

Introduction

Damselfly (order Odonata, sub order Zygoptera) and dragonfly (order Odonata, sub order Anisoptera) nymphs are well known predators of mosquito larvae that play important role in the natural regulation of mosquito population (Boyd, 2005; Din et al., 2013). Odonate nymphs are very useful biological control agent against mosquitoes (Mitra, 2006). Odonate nymphs face environmental pressure due to increasing pollutants in their habitats. Aquatic habitats are contaminated with agricultural insecticides as a result of spray drift or runoff (Armbrust and Peeler, 2002; Hilz and Vermeer, 2012). Aquatic insects are very sensitive to insecticides (Mokry and Hoagland, 1990; Mian and Mulla, 1992).

Insecticides are the agents applied for the control of insect pests. They are generally called adulticides, ovicides, pupicides and larvicides. Insecticides may be synthetic chemicals or derived from plants. Insecticides which are derived from plants are also called botanical insecticides. Alkaloids, pyrethrins, rotenone, rotenoids and neem are the known botanical insecticides. Some synthetic chemical insecticides have been modeled after natural botanical insecticides. For example nicotinoids or neonicotinoids such as imidacloprid, acetamiprid etc. are the synthetic chemical insecticides modeled on plant nicotine, while pyrethroids such as deltamethrin, lambda cyhalothrin, cypermethrin etc. have been modeled on plant pyrethrins (Gullan and Cranston, 2005). Carbamates (e.g. carbofuran, carbaryl etc.), organochlorines (DDT, endosulfan, aldrin, dieldrin etc.) and organophosphates (e.g. dichlorvos, chlorpyrifos, malathion etc.) are the synthetic chemical insecticides which are not modeled on botanical insecticides (Gullan and Cranston, 2005).

Organochlorine insecticides are highly toxic, bioaccumulative and persistent (Jayaraj et al., 2016). The vast application of organochlorines destroy both, pests and non-target organisms (Zacharia, 2011). After the application of organophosphates on target organisms, they can reach to the target pests, or reach surface water bodies and ground water; they can also contaminate the atmosphere or they can be ingested by non-target organisms. The chemical and physical characteristics, application methods and conditions of sites influence the destiny and effect of organophosphates (Lourencetti et al., 2008). Due to the frequent and excessive application of organophosphate pesticides and their slow decomposition rates, they accumulate in the soils and subsequently contaminate surface water bodies (Sirotkina et al., 2012). Chlorpyrifos which is an organophosphate, has been detected in arctic sea water and air (Vorkamp and Rig  t, 2014). Some carbamates have also been detected in aquatic habitats (Tien et al., 2013). Herbicides compounds are also persistent in the soil from where they reach to the ground water and surface water bodies (Cai et al., 2004). It has been reported that the degradation of organochlorine herbicide compounds occur in soil due to light effect and microbial action (Fenoll et al., 2014). The presence of some of these herbicide compounds and their breakdown products have been detected in ground water and surface water bodies (Osano et al., 2002). Among the organochlorines, DDT (Dichloro diphenyltrichloroethane) played effective role in eradication of insect pests but on the other hand it has also damaged wild life and human health due to its persistence in the environment and bioaccumulation (Turusov et al., 2002; Jayaraj et al., 2016). Organophosphates, inhibitors of acetylcholinesterase, rapidly degrade by hydrolysis when exposed to water, soil, air and light, however their small amount have been detected in water and food (Jayaraj et al., 2016). They have been reported for their adverse effect on non-target aquatic organisms (Stenersen, 2004; Huynh and Nugegoda, 2012; Rubach et al., 2012). The insecticides of class pyrethroids are very effective against insect pests and they kill insect pests at low dose and are less bioavailable in the natural environment due to their strong absorptive characteristic and low water solubility (Davies, 1985). Pyrethroids inhibit ATPase enzymes that result in the disturbance of ionic balance which is the main toxic effect of pyrethroids (Coats et al., 1989). Pyrethroids are highly toxic for aquatic insects, aquatic crustaceans and fish (Mian and Mulla, 1992; Werner and Moran, 2008). Neonicotinoid cause toxic effects on insects by acting directly on the nicotinic acetylcholine receptors (nAChRs) (Nishiwaki et al., 2003; Casida and Durkin, 2013). There is emerging evidence about the adverse effect of neonicotinoids on non-target organisms (Malev et al., 2012; Anderson et al., 2015; Morrissey et al., 2015).

To the author knowledge, very limited studies have been reported about the insecticides toxicity with odonate nymphs. For example, Beketov (2002) studied the comparative sensitivity of larvae of damselfly, dragonfly, mayfly and *Daphnia magna* to deltamethrin and

esfenvalerate. They reported the deltamethrin 48-hour LC50 values of 0.0145 µg/l and 0.0760 µg/l against nymphs of *Lestes sponsa* (damselfly) and *Cordulia aenea* (dragonfly), respectively. The LC50 values of deltamethrin against larvae of two species of mayflies, *Cloeon dipterum* and *Caenis miliaria* and larvae of *Daphnia* were 0.005 µg/l, 0.0091 µg/l and 0.0293 µg/l, respectively.

In Swat valley, Pakistan, insecticides are regularly applied in agricultural fields on peach orchards, vegetables and cereal crops for many years (Nafees et al., 2008; Nafees and Jan, 2009). The watershed of River Swat in Malakand Division, Pakistan, is called Swat Valley, which comprises of Swat, Malakand (Swat Ranizai Tehsil), and Chakdara (Adenzai Tehsil). Keeping in view, the impact of frequent application of insecticides on non-target organisms in the area, a laboratory study was conducted for the assessment of toxicity of agricultural insecticides to non-target aquatic insects, specifically native odonate nymphs, which are the predators of mosquito larvae.

Materials and methods

Selection of insecticides for sensitivity study

During the present study, the farmers who were cultivating vegetables and growing peach orchards in Swat, Pakistan, were interviewed about the type and brand of pesticides they apply on vegetables and fruit trees. Questionnaires were arranged for interview, in which the type, brand and frequency of application of pesticides were asked. The pesticide dealers at Matta bazar, Khwazakhela bazar, Mingora city, Shamoza bazar and Barikot bazar were also interviewed about the type and brand of pesticides they provide to the farmers. Six hundred farmers in Swat, Pakistan, were interviewed. The farmers were applying insecticide spray on tomato crops, three times from seedling to fruit ripening. They were applying insecticide spray on peach orchards, four times from before flowering to fruit ripening. Peaches are grown throughout Swat Valley (*Figure 1*). According to the information obtained during interview, the main insecticides that the farmers apply are deltamethrin, cypermethrin, lambda cyhalothrin, chlorpyrifos, dichlorvos and acetamiprid. The details of manufacturer of these insecticides were also inquired. The farmers apply deltamethrin (25% w/w) of HERANBA Industries Limited India, cypermethrin (10% w/v) of M/S Halex (M) SDN (BDH) Malaysia, lambda cyhalothrin (2.5% w/v) of Jiangsu Fengshan Group Co. Ltd China, chlorpyrifos (40% w/v) of M/S Halex (M) SDN (BDH) Malaysia, dichlorvos (100% w/v) of Insecticides India Limited and acetamiprid (20% w/w) of Jiangsu Fengshan Group Co. Ltd China. The reason of choice of insecticides of the above manufacturers by the farmers when inquired was the lower price. *Table 1* shows the outcome of questionnaires.

Collection of odonate nymphs

Damselfly and dragonfly nymphs of 6 to 8 instars were collected from slow moving water on the bank of River Swat near the Chirchil picquit at Chakdara, Dir Lower, Khyber Pakhtunkhwa, Pakistan. A rectangular plastic dipper (38 cm length, 28 cm width and 6.5 cm height) was used as dipper during collection. The nymphs were brought to the laboratory in large plastic bottles along with water of collection site to the laboratory at University of Malakand, Khyber Pakhtunkhwa, Pakistan. In laboratory, the nymphs were maintained in small fish aquarium (45 cm length, 40 cm width and 40 cm height) in water of collection site. The laboratory was well ventilated and receiving sunlight through windows. Before starting experiment provided mosquito larvae as food. Proper literature was used for the identification of

specimens (Yousuf et al., 1996; Anjum, 1997; Mitra, 2002; Din et al., 2013). One species of blue-tailed damselfly, *Ischnura elegans* (Vander Linden, 1820) and one species of crimson marsh glider dragonfly namely, *Trithemis aurora* (Burmeister, 1839) were found in sufficient number; therefore, experiments were conducted on nymphs of these two species. The sensitivity of nymphs to the three classes of insecticides i.e., pyrethroids, organophosphates and neonicotinoids was studied in different times during May-September 2017. The maximum laboratory temperature was 29-33°C during experiments.



Figure 1. Figure derived from Google map showing watershed of River Swat in Malakand Division, Pakistan, where pesticides are applied on peach orchards. Latitude and Longitude: 34° 49' 19" North, 72° 29' 20" East. Blue line represents River Swat

Table 1. Types of insecticides applied on vegetables and peach orchards in Tehsil Matta District Swat

Insecticides	Manufacturer	Number of Farmers	Farmers %
Deltamethrin	HERANBA Industries Ltd, India	60	10
Cypermethrin	M/S Halex (M) SDN (BDH), Malaysia	90	15
Lambda cyhalothrin	Jiangsu Fengshan Group Co. Ltd, China	120	20
Chlorpyrifos	M/S Halex (M) SDN (BDH), Malaysia	120	20
Dichlorvos	Insecticides India Limited	90	15
Acetamiprid	Jiangsu Fengshan Group Co. Ltd, China	120	20
Total	-----	600	100

Sensitivity of Odonate nymphs to pyrethroids

The sensitivity of odonate (damselfly and dragonfly) nymphs to pyrethroids i.e., deltamethrin, cypermethrin and lambda cyhalothrin were studied during May-June 2017 (max temperature 29-33°C). Initially range finding bioassay was conducted for finding

concentration range of each pyrethroids for each odonate species, to be used for determining lethal concentrations (LC₅₀ and LC₉₀ values) in definitive test. The ecological effects test guidelines of Environmental Protection Agency, USA (US EPA, 1996) for aquatic invertebrate acute toxicity test were followed for determining the concentration range. The following are the details.

Solutions preparation

Deltamethrin (25% w/w) of HERANBA Industries Limited, India, cypermethrin (10% w/v) of M/S Halex (M) SDN (BDH), Malaysia and lambda cyhalothrin (2.5% w/v) of Jiangsu Fengshan Group Co. Ltd, China, were used. A 500 ml stock solution of 100 ppm of each insecticide was prepared in non-chlorinated tap water. Based on dilution equation ($C_1V_1=C_2V_2$), 600 ml test solution of 2 ppm of each pyrethroid was prepared from the respective stock solution (of 100 ppm). The 2 ppm solution of each pyrethroid was serially diluted by a factor of 2 and thus several dilutions of reducing concentrations were prepared in polyethylene containers (400 ml each). The detail of serial dilution of each pyrethroid was as under: From 600 ml initial solution of 2 ppm, 300 ml solution was taken and put into 1000 ml volumetric flask in which 300 ml tap water was already added to make a 600 ml solution of 1 ppm (1/2 dilution). Again, from this solution, 300 ml was taken and put into 1000 ml volumetric flask in which 300 ml tap water was already added to make a 600 ml solution of 0.5 ppm (1/4 dilution). Again, from this solution, 300 ml was taken and put into 1000 ml volumetric flask in which 300 ml tap water was already added to make a 600 ml solution of 0.25 ppm (1/8 dilution). This serial dilution was continued till obtaining solution of 0.00195 ppm (1/1024-fold). At each step, there was a 2-fold dilution in concentration, however volume of each dilution remained constant i.e. 300 ml. From the last dilution, 300 ml solution was discarded so as to keep 300 ml volume as in the previous dilutions. A total of 11 solutions of each pyrethroid were arranged. The 11 solutions were of the following concentrations: 2 ppm, 1 ppm, 0.5 ppm, 0.25 ppm, 0.125 ppm, 0.0625 ppm, 0.03125 ppm, 0.015625 ppm, 0.0078125, 0.003906 and 0.00195 ppm. The schematic for stock solutions preparation and serial dilution of pyrethroids is shown in *Figure 2*.

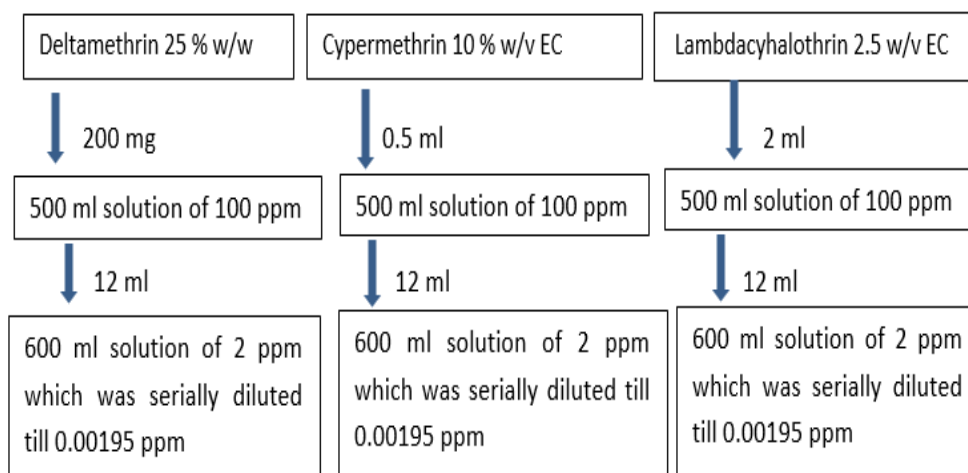


Figure 2. Schematic of stock solutions preparation and serial dilution of pyrethroids for toxicity study in odonate nymphs

Exposure of nymphs to pyrethroids for range finding

The detail of procedure of range finding bioassay for each pyrethroid was as under: Eleven test solutions of 2, 1, 0.5, 0.25, 0.125, 0.0625, 0.0315, 0.0156, 0.0078, 0.0039 and 0.00195 ppm concentrations of each pyrethroid were separately tested against nymphs of each odonate species in 400 ml polyethylene containers. To each concentration of each pyrethroid, five nymphs of *I. elegans* were individually exposed in five polyethylene containers. To avoid cannibalism, nymphs were individually exposed to test solutions. The volume of test solution in each container was 250 ml. In addition, five nymphs were placed in five 400 ml polyethylene control containers, each containing 250 ml non-chlorinated tap water. In short, for testing each pyrethroid against *I. elegans*, 60 polyethylene cups (55 containers for 11 concentrations and 5 control containers) containing 60 nymphs were arranged. At the same time, the nymphs of *T. aurora* were also exposed to each pyrethroid. The detail of the exposure was the same as for *I. elegans*.

The period of exposure was 48 hours. Following standard toxicity protocols, the nymphs were not fed during the 48-hour exposure period (ASTM standard E47, 2008). After 48 hours of exposure period, the number of dead nymphs was noted. The criterion for death was lack of response to prodding. In case of lambda cyhalothrin, mortality was higher therefore further dilutions were made (diluted up to 0.00048 ppm) and tested.

The highest concentration of each pyrethroid that caused no mortality was noted for each odonate species. The concentration of each pyrethroid that caused lowest mortality was determined for each odonate species. Similarly, the lowest concentration of each pyrethroid that caused 100 % mortality was also determined for each species. The schematic for range finding bioassay is shown in *Figure 3*.

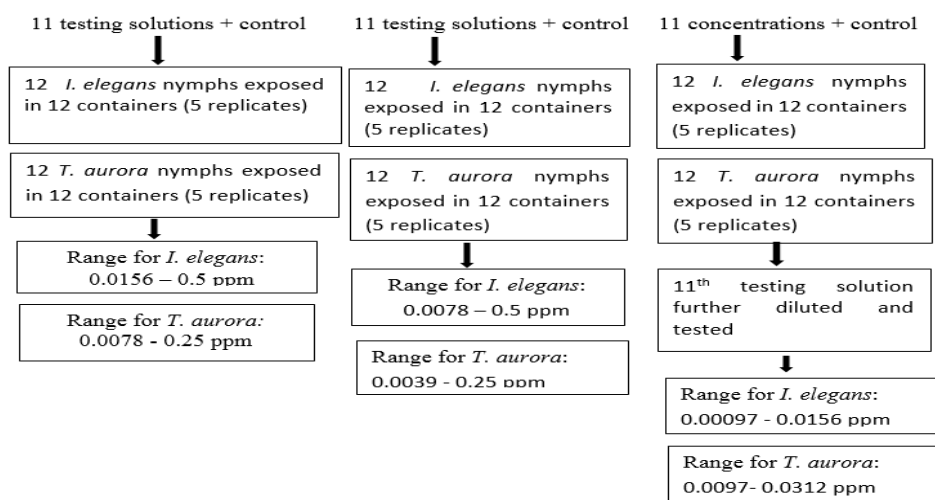


Figure 3. Schematic of range finding bioassay for determining the concentration ranges of pyrethroids during toxicity study in odonate nymphs

Definitive test for determination of lethal concentrations of pyrethroids

LC₅₀ also called median lethal concentration is a measure of the lethal concentration of a toxin that kill 50 % of the test population after exposure for a specified period. Lower LC₅₀ values indicate higher toxicity of a toxin. During definitive test, LC₅₀ value of each pyrethroid against nymphs of each odonate species was determined. For

determination of LC₅₀ values, nymphs of each odonate species were separately exposed to various concentrations of each pyrethroid within the concentration range determined during range finding bioassay. The schematic for definitive bioassay is shown in Figure 4. The following are the details.

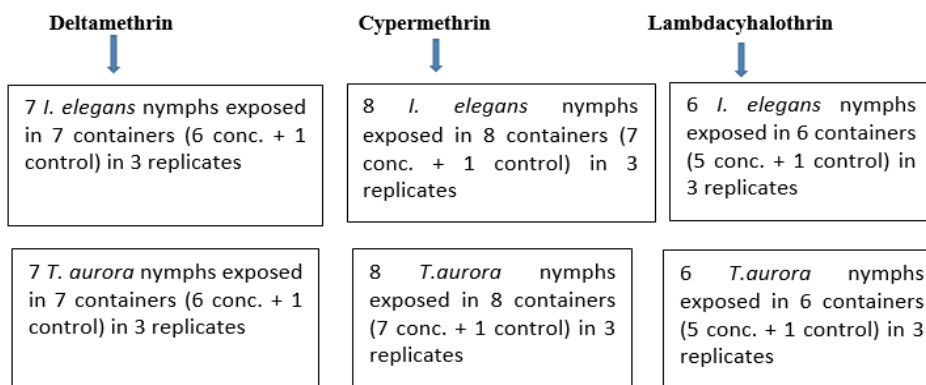


Figure 4. Schematic of experiment for determining LC₅₀ and LC₉₀ values of three pyrethroids against odonate nymphs

Exposure to deltamethrin for determining LC₅₀

The concentrations of deltamethrin used against *I. elegans* were 0.0156, 0.03125, 0.0625, 0.125, 0.25 and 0.5 ppm. Thus seven intact last instar nymphs of *I. elegans* were placed in seven polyethylene containers (six concentrations and one control). Similarly, the concentrations of deltamethrin used against *T. aurora* were 0.0078, 0.0156, 0.03125, 0.0625, 0.125 and 0.25 ppm. In this case, seven intact last instar nymphs of *T. aurora* were placed in seven polyethylene containers (six concentrations and one control). The volume of each container was 400 ml and testing solution was 250 ml. The control container was containing only 250 non-chlorinated tap water.

Exposure to cypermethrin for determining LC₅₀

The concentrations of cypermethrin used against *I. elegans* were 0.0078, 0.0156, 0.03125, 0.0625, 0.125, 0.25 and 0.5 ppm. Thus eight intact last instar nymphs of *I. elegans* were placed in eight polyethylene containers (seven concentrations and one control). The concentrations of cypermethrin used against *T. aurora* were 0.0039, 0.0078, 0.0156, 0.03125, 0.0625, 0.125 and 0.25 ppm. Thus eight intact last instar nymphs of *T. aurora* were placed in seven polyethylene containers (seven concentrations and one control).

Exposure to lambda cyhalothrin for determining LC₅₀

The concentrations of lambda cyhalothrin used against *I. elegans* were 0.00097, 0.00195, 0.0039, 0.0078 and 0.0156 ppm. Thus six intact last instar nymphs of *I. elegans* were placed in six polyethylene containers (five concentrations and one control). Similarly, the concentrations of lambda cyhalothrin used against *T. aurora* were 0.0097, 0.00195, 0.0039, 0.0078, 0.0156 and 0.0312 ppm. Thus seven intact last instar nymphs of *T. aurora* were placed in seven polyethylene containers (six concentrations and one control).

Sensitivity of odonate nymphs to Organophosphates

The sensitivity of odonate (damselfly and dragonfly) nymphs to organophosphates i.e., chlorpyrifos and dichlorvos was studied during July-August 2017 (max temperature 28-32°C). Chlorpyrifos (40% w/v) of M/S Halex (M) SDN (BDH), Malaysia and dichlorvos (100% w/v) of Insecticides India Limited were used.

Solutions preparation

The detail of preparation of solutions of each organophosphate was the same as described for pyrethroid.

Exposure of nymphs to organophosphates for range finding

The procedure of bioassay for finding concentration ranges of two organophosphates (chlorpyrifos and dichlorvos) against odonate nymphs was the same as described for pyrethroids.

Definitive test for determination of lethal concentrations of organophosphates

During definitive test, LC₅₀ and LC₉₀ values of each organophosphate against each odonate nymph was determined. For determination of LC₅₀ and LC₉₀ values, nymphs of each odonate species were separately exposed to various concentrations of each organophosphate within the concentration range determined during range finding bioassay. The following are the details.

Exposure to chlorpyrifos for determining LC₅₀

The concentrations of chlorpyrifos used against *I. elegans* were 0.0156, 0.03125, 0.0625, 0.125, 0.25, 0.5 and 1 ppm. Thus eight intact last instar nymphs of *T. aurora* were placed in eight polyethylene containers (seven concentrations and one control). Similarly, the concentrations of chlorpyrifos used against *T. aurora* were 0.03125, 0.0625, 0.125, 0.25, 0.5, 1 and 2 ppm. Thus eight intact last instar nymphs of *T. aurora* were placed in eight polyethylene containers (seven concentrations and one control). The procedure of bioassay was the same as described for pyrethroids.

Exposure to dichlorvos for determining LC₅₀

The concentrations of dichlorvos used against *I. elegans* were 0.0078, 0.0156, 0.03125, 0.0625, 0.125, 0.25 and 0.5 ppm. Thus eight intact last instar nymphs of *T. aurora* were placed in seven polyethylene containers (seven concentrations and one control). Similarly, the concentrations of dichlorvos used against *T. aurora* were 0.0156, 0.03125, 0.0625, 0.125, 0.25, 0.5 and 1 ppm. Thus eight intact last instar nymphs of *T. aurora* were placed in seven polyethylene containers (seven concentrations and one control). The procedure of bioassay was the same as described for pyrethroids.

Sensitivity of odonate nymphs to neonicotinoid

The sensitivity of odonate (damselfly and dragonfly) nymphs to neonicotinoid i.e., acetamiprid was studied during September 2017 (max temperature 29-33°C). Acetamiprid (20% w/w) of Jiangsu Fengshan Group Co. Ltd, China was used.

Solutions preparation

The detail of preparation of solutions of neonicotinoid (acetamiprid) was the same as described for pyrethroid.

Exposure of nymphs to neonicotinoid (acetamiprid) for range finding

The detail of bioassay for finding concentration range of neonicotinoid (acetamiprid) against odonate nymphs was the same as described for pyrethroids.

Definitive test for determination of lethal concentrations of neonicotinoid (acetamiprid)

During definitive test, LC₅₀ and LC₉₀ values of neonicotinoid (acetamiprid) against each odonate nymph was determined. For determination of LC₅₀ and LC₉₀ values, nymphs of each odonate species were separately exposed to various concentrations of neonicotinoid (acetamiprid) within the concentration range determined during range finding bioassay. The following are the details:

The concentrations of acetamiprid used against *I. elegans* were 0.0039, 0.0078, 0.0156, 0.03125, 0.0625, 0.125 and 0.25 ppm. Thus eight intact last instar nymphs of *T. aurora* were placed in seven polyethylene containers (seven concentrations and one control). Similarly, the concentrations of acetamiprid used against *T. aurora* were as 0.00195, 0.0039, 0.0078, 0.0156, 0.03125, 0.0625, and 0.125 ppm. Thus eight intact last instar nymphs of *T. aurora* were placed in seven polyethylene containers (seven concentrations and one control). The procedure of bioassay was the same as described for pyrethroids.

Period of exposure and observations

The period of exposure for each insecticide was 48 hours. Following standard toxicity protocols, the nymphs were not fed during the 48-hour exposure period (ASTM standard E47, 2008). After 48 hours of exposure period, the number of dead nymphs was noted. The criterion for death was lack of response to prodding. Experiment for each insecticide was run in triplicate. Several trips were conducted for collection of nymphs and experiments were repeated continuously till the number of nymphs in each replica of each concentration of each insecticide reached 20. In total 20 independent experiments were conducted for each insecticide (*Figure 5*). There occurred the death of only two nymphs in control containers during the whole experiments, indicating that conditions during each experiment were suitable and the nymphs were healthy.



Figure 5. Picture of polyethylene jars arranged for range finding test

Analysis of data

The percent mortality of nymphs in each replica of each concentration of each insecticide against each odonate species was calculated from cumulative total of 20 nymphs after 20 independent experiments (single nymph exposed to each concentration during each experiment). The average percent mortality data were subjected to log probit analysis (Finney, 1971) for calculating LC₅₀ and LC₉₀ values, using SPSS 16 software. The LC₅₀ values were compared by 95% confidence limits overlap method of Wheeler et al. (2006).

Results

Sensitivity of damselfly and dragonfly nymphs to pyrethroids

The sensitivity of odonate nymphs of damselfly (*I. elegans*) and dragonfly (*T. aurora*) were studied during exposure to three pyrethroids (deltamethrin, cypermethrin and lambda cyhalothrin) for 48 hours in laboratory conditions. Table 2 shows the 48-hour mortality data for three pyrethroids (deltamethrin, cypermethrin and lambda cyhalothrin) against the 7th to 8th instar nymphs of *I. elegans*. The highest concentrations of deltamethrin, cypermethrin and lambda cyhalothrin that caused no mortality of *I. elegans* were 0.0078 ppm, 0.0039 ppm and 0.00048 ppm, respectively. The lowest concentrations of deltamethrin, cypermethrin and lambda cyhalothrin that caused 100% mortality of *I. elegans* were 0.5 ppm, 0.5 ppm and 0.0156 ppm, respectively. Table 3 shows the 48-hour mortality data for three pyrethroids against the 7th to 8th nymphs of *T. aurora*. The highest concentrations of deltamethrin, cypermethrin and lambda cyhalothrin that caused no mortality of *T. aurora* were 0.0039 ppm, 0.00195 ppm and 0.00048 ppm, respectively. The lowest concentrations of deltamethrin, cypermethrin and lambda cyhalothrin that caused 100% mortality of *T. aurora* were 0.25 ppm, 0.25 ppm and 0.0312 ppm, respectively.

Table 2. 48-hour percent mortality data for three pyrethroids against *I. elegans* nymph

Pyrethroids	Concentrations	Mortality (Mean ± SE) %
Deltamethrin	0.0078	0
	0.0156	3.3±1.6
	0.03125	6.6±1.6
	0.0625	15±2.8
	0.125	50±11.5
	0.25	76.6±3.3
	0.5	100±0
Cypermethrin	0.0039	0
	0.0078	3.3±1.6
	0.0156	8.3± 1.6
	0.03125	16.6±3.3
	0.0625	30±5.8
	0.125	46.6±8.8
	0.25	70±5.8
0.5	100±0	
Lambda cyhalothrin	0.000485	0
	0.00097	10±2.8
	0.00195	23.3±6
	0.0039	51.6±4.4
	0.0078	75±5.8
	0.0156	100±0

Table 3. 48-hour percent mortality data for three pyrethroids against *T. aurora* nymph

Pyrethroids used	Concentration (ppm)	Mortality (Mean ± SEM) %
Deltamethrin	0.0039	0
	0.0078	3.3±1.6
	0.0156	6.6±1.6
	0.03125	18.3±6.01
	0.0625	46.6±8.8
	0.125	70±5.8
	0.25	100±0
Cypermethrin	0.00195	0
	0.0039	1.6±1.6
	0.0078	6.6±1.6
	0.0156	15±2.8
	0.03125	45±8.6
	0.0625	66.6±8.8
	0.125	86.6±3.3
	0.25	100±0
Lambdacyhalothrin	0.000485	0
	0.00097	6.6±1.6
	0.00195	15±2.8
	0.0039	35±2.8
	0.0078	61.6±4.4
	0.0156	85±2.8
	0.0312	100±0

LC₅₀ values of pyrethroids against damselfly and dragonfly nymphs

Columns of the *Table 4* show the comparison of LC₅₀ values of three pyrethroids against nymph of each odonate species. During the study of *I. elegans*, significantly lower LC₅₀ value (48-hour LC₅₀= 0.004 ppm) was recorded for lambdacyhalothrin when compared with the LC₅₀ values of deltamethrin and cypermethrin. Similarly, during the study of *T. aurora*, lowest LC₅₀ value was recorded for lambdacyhalothrin (LC₅₀= 0.005 ppm) followed by cypermethrin (LC₅₀= 0.038) and deltamethrin (LC₅₀= 0.064). The LC₅₀ values of all the three pyrethroids against *T. aurora* were significantly different from each other when compared through 95% confidence overlap method.

Table 4. 48-hour LC₅₀ values of three pyrethroids against *I. elegans* and *T. aurora* nymphs

Pyrethroids	<i>I. elegans</i>	<i>T. aurora</i>
Deltamethrin	0.112 (0.061-0.22) b	0.064 (0.045-0.054) c
Cypermethrin	0.111 (0.073-0.161) b	0.038 (0.033-0.043) b
Lambda cyhalothrin	0.004 (0.002-0.005) a	0.005 (0.005-0.006) a

The alphabetical order in column is according to increasing LC₅₀ values. LC₅₀ values sharing no letter are significantly different at P<0.05 significance level

Susceptibility of damselfly and dragonfly nymphs to organophosphates

Table 5 shows the 48-hour mortality data for two organophosphates i.e., chlorpyrifos and dichlorvos against 7th to 8th instars nymphs of *I. elegans*. The highest concentrations of chlorpyrifos and dichlorvos that caused no mortality of *I. elegans* were 0.0078 ppm and 0.0039 ppm, respectively. The lowest concentrations of chlorpyrifos and

dichlorvos that caused 100% mortality of *I. elegans* were 1.0 ppm and 0.5 ppm, respectively. Table 6 shows the 48-hour mortality data for two organophosphates i.e., chlorpyrifos and dichlorvos against 7th to 8th instars nymphs of *T. aurora*. The highest concentrations of chlorpyrifos and dichlorvos that caused no mortality of *T. aurora* were 0.0156 ppm and 0.0078 ppm, respectively. The lowest concentrations of chlorpyrifos and dichlorvos that caused 100% mortality of *T. aurora* were 2.0 ppm and 1.0 ppm, respectively.

Table 5. 48-hour percent mortality data for two organophosphates against last instar nymph of *I. elegans*

Organophosphates	Concentration (ppm)	Mean ± SE %
Chlorpyrifos	0.0078	0
	0.0156	6.6±1.6
	0.03125	8.3±1.6
	0.0625	23.3±6.1
	0.125	46.6±8.8
	0.25	61.6±10.1
	0.5	83.3±6.6
	1	100±0
Dichlorvos	0.0039	0
	0.0078	3.3±1.6
	0.0156	6.6±1.6
	0.03125	10±2.8
	0.0625	18.3±6.01
	0.125	45±5.8
	0.25	66.6±8.8
	0.5	100±0

Table 6. 48-hour mortality data for two organophosphates against last instar nymphs of *T. aurora*

Organophosphates	Concentration (ppm)	Mean ± SEM %
Chlorpyrifos	0.0156	0
	0.03125	3.3±1.6
	0.0625	15±2.8
	0.125	35±8.6
	0.25	46.6±12.01
	0.5	63.3±12.01
	1	81.6±4.4
	2	100±0
Dichlorvos	0.0078	0
	0.0156	1.6±1.6
	0.03125	8.3±1.6
	0.0625	23.3±8.8
	0.125	53.3±14.5
	0.25	80±5.8
	0.5	93.3±3.3
	1	100±0

LC₅₀ values of organophosphates against damselfly and dragonfly nymphs

Figure 6 shows the LC₅₀ values of chlorpyrifos and dichlorvos against *I. elegans*. The LC₅₀ values of chlorpyrifos and dichlorvos against *I. elegans* were 0.142 ppm

and 0.125 ppm, respectively. Based on 95% confidence interval overlap method, there was no significant difference in the LC₅₀ values of dichlorvos and chlorpyrifos against *I. elegans*. Figure 7 shows the LC₅₀ values of chlorpyrifos and dichlorvos against *T. aurora*. The LC₅₀ values of chlorpyrifos and dichlorvos against *T. aurora* were 0.257 ppm and 0.119 ppm, respectively. Based on 95% confidence interval overlap method, the LC₅₀ value of dichlorvos against *T. aurora* was significantly lower when compared to the LC₅₀ value chlorpyrifos against *T. aurora*.

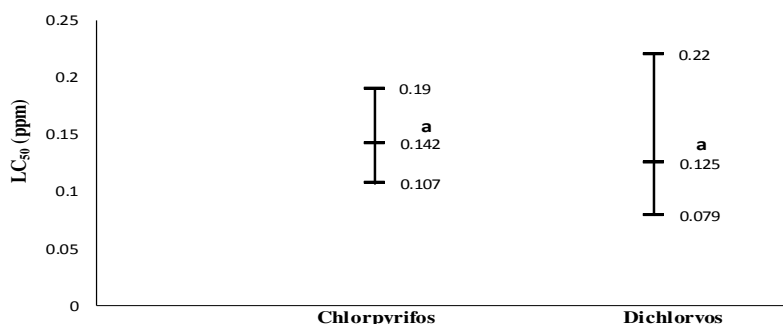


Figure 6. Comparison of LC₅₀ values of chlorpyrifos and dichlorvos against *I. elegans*. Error bars represent 95 % confidence limits. Similar letter represents that LC₅₀ values are not different significantly at $P < 0.05$ significance level

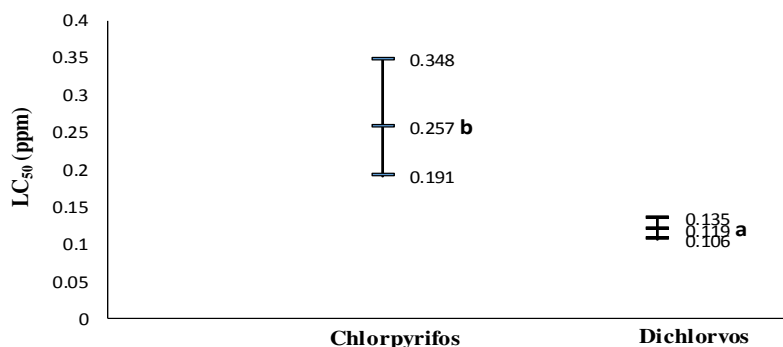


Figure 7. Comparison of LC₅₀ values of chlorpyrifos and dichlorvos against *T. aurora*. Error bars represent 95 % confidence limits. Different letters represent that LC₅₀ values are significantly different at $P < 0.05$ significance level

Figure 8 shows the comparisons of chlorpyrifos LC₅₀ values for *I. elegans* and *T. aurora*. The LC₅₀ value of chlorpyrifos for *I. elegans* (0.142 ppm) was significantly lower than its LC₅₀ value for *T. aurora* (0.3 ppm). Figure 9 shows the comparison of dichlorvos LC₅₀ values for *I. elegans* (0.125 ppm) and *T. aurora* (0.12 ppm). There was no significant difference in the LC₅₀ values of dichlorvos for *I. elegans* and *T. aurora*.

Sensitivity of damselfly and dragonfly nymphs to neonicotinoid

Table 7 shows the 48-hour mortality data of acetamiprid against the nymphs (7th to 8th instar) of *I. elegans* and *T. aurora*. The highest concentrations of acetamiprid that caused no mortality of *I. elegans* was 0.00195 ppm. The highest concentration of acetamiprid that caused no mortality of *T. aurora* was 0.000975 ppm. The lowest

concentrations of acetamiprid that caused 100% mortality of *I. elegans* and *T. aurora* were 0.25 ppm and 0.125 ppm, respectively.

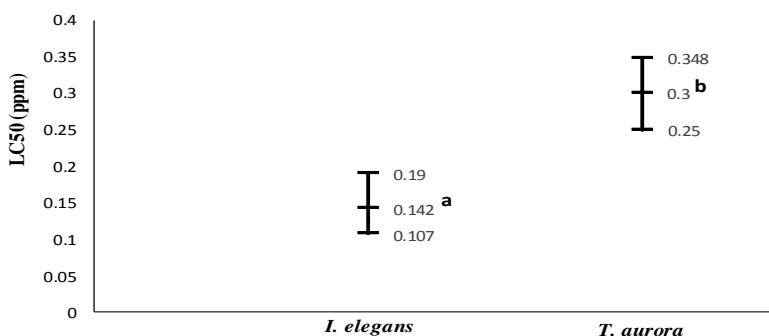


Figure 8. Comparison of chlorpyrifos LC₅₀ values for *I. elegans* and *T. aurora*. Error bars represent 95 % confidence limits. Different letters represent that LC₅₀ values are significantly different at P<0.05 significance level

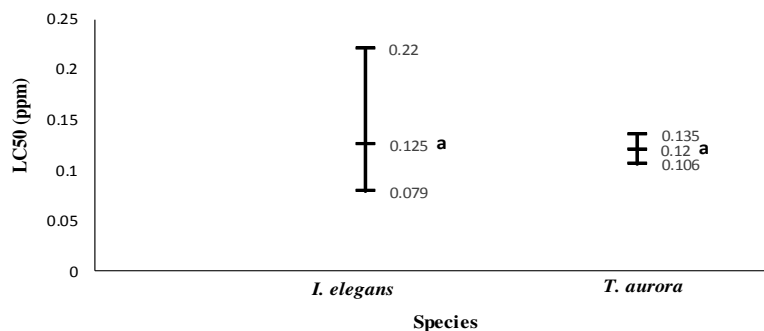


Figure 9. Comparison of dichlorvos LC₅₀ values for *I. elegans* and *T. aurora*. Error bars represent 95 % confidence limits. Similar letter represents that LC₅₀ values are not different significantly at P<0.05 significance level

Table 7. 48-hour percent mortality data for a neonicotinoid, acetamiprid against damselfly and dragonfly nymphs nymphs

Odonate species	Concentration (ppm)	Mean ± SEM %
<i>I. elegans</i>	0.00195	0
	0.0039	3.3±1.6
	0.0078	10±2.8
	0.0156	18.3±4.4
	0.03125	46.6±8.8
	0.0625	56.6±8.8
	0.125	85±2.8
	0.25	100±0
<i>T. aurora</i>	0.000975	0
	0.00195	3.3±1.6
	0.0039	6.6±1.6
	0.0078	16.6±7.3
	0.0156	30±11.5
	0.03125	56.6±8.8
	0.0625	80±5.8
	0.125	100±0

LC₅₀ values of neonicotinoid against damselfly and dragonfly nymphs

Figure 10 shows the LC₅₀ values of a neonicotinoid, acetamiprid against predator of mosquito larvae i.e., *I. elegans* and *T. aurora*. The LC₅₀ values of acetamiprid against *I. elegans* and *T. aurora* were 0.038 ppm and 0.023 ppm, respectively. Based on 95% confidence interval overlap method, the LC₅₀ value of acetamiprid for *T. aurora* was significantly lower than its LC₅₀ value for *I. elegans*.

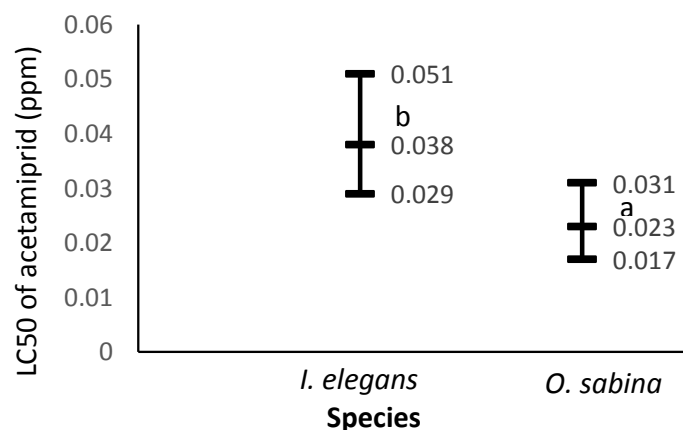


Figure 10. LC₅₀ values of acetamiprid against *I. elegans* and *T. aurora*. Error bars represent 95% confidence limits. Different letters represent that LC₅₀ values are significantly different at $P < 0.05$ significance level

LC₉₀ values of six insecticides against damselfly and dragonfly nymphs

Table 8 shows the LC₉₀ values of six insecticides for *I. elegans*. Minimum LC₉₀ values was observed for lambda cyhalothrin (0.01 ppm). The LC₉₀ value of lambda cyhalothrin was significantly different from the LC₉₀ values of the remaining insecticides. Next to the lambda cyhalothrin, acetamiprid showed lowest LC₉₀ value (0.122 ppm) which was significantly different from the LC₉₀ values of the remaining insecticides. Maximum LC₉₀ value was observed for chlorpyrifos (0.655 ppm) and dichlorvos (0.535 ppm). The difference in LC₉₀ values against *I. elegans* among chlorpyrifos, dichlorvos, cypermethrin and deltamethrin were not significant.

Table 8. 48-hour LC₉₀ values of six insecticides against *I. elegans* nymph

Insecticides	LC ₉₀ (95% confidence limits)
Deltamethrin	0.351 (0.188-2.19) c
Cypermethrin	0.504 (0.291-1.35) c
Lambda cyhalothrin	0.01 (0.007-0.027) a
Chlorpyrifos	0.655(0.436-1.214) c
Dichlorvos	0.535 (0.283-2.108) c
Acetamiprid	0.122 (0.086-0.204) b

The alphabetical order in columns is according to increasing LC₉₀ values. LC₉₀ values sharing no letter are significantly different

Table 9 shows the LC₉₀ values of six insecticides for *T. aurora*. Minimum LC₉₀ value was observed for lambda cyhalothrin (0.018n ppm). The LC₉₀ value of Lambda cyhalothrin was significantly different from the LC₉₀ values of the remaining insecticides. The second most toxic insecticide was acetamiprid which showed LC₉₀ value of 0.093 ppm. Maximum LC₉₀ value was observed for chlorpyrifos (1.306 ppm). The second least toxic insecticide was dichlorvos with LC₉₀ value of 0.404 ppm. The LC₉₀ value of chlorpyrifos was significantly different from the LC₉₀ values of other insecticides. The LC₉₀ value of dichlorvos was insignificantly higher than the LC₉₀ value of deltamethrin however it was significantly higher than the LC₉₀ value of cypermethrin.

Table 9. 48-hour LC₉₀ values of six insecticides against of *T. aurora* nymph

Insecticides	LC ₉₀ (95 % confidence limits)
Deltamethrin	0.205(0.13-0.49) d
Cypermethrin	0.132 (0.11-0.165) c
Lambda cyhalothrin	0.018 (0.015-0.023) a
Chlorpyrifos	1.306(0.852-2.526) e
Dichlorvos	0.404 (0.34-0.498) d
Acetamiprid	0.093(0.062-0.174) b

The alphabetical order in columns is according to increasing LC₉₀ values. LC₉₀ values sharing no letter are significantly different

Discussion

During the study of susceptibility of predators of mosquito larvae (*I. elegans* and *T. aurora*) to pyrethroids, the predators were found more susceptible to lambda cyhalothrin than to deltamethrin and cypermethrin (Tables 2-3). The 48-hour LC₅₀ values of lambda cyhalothrin against nymphs of *I. elegans* and *T. aurora* were significantly lower when compared to the 48-hour LC₅₀ values of deltamethrin and cypermethrin against these nymphs (Table 4). Aquatic insects appear highly susceptible to synthetic pyrethroids, even very low concentration (< 1 µg/L) of pyrethroid can create toxic effects (Mian and Mulla, 1992). The high sensitivity of aquatic insects to synthetic pyrethroid may be attributed to disruption of ionic balance in aquatic insects (Coats et al., 1989). During the present study, *I. elegans* showed similar sensitivity to both, deltamethrin and cypermethrin (LC₅₀ of deltamethrin = 0.112 ppm, LC₅₀ of cypermethrin = 0.111 ppm) (Table 4). Such trend has been also observed in the reported work of Beketov (2004), where *Daphnia magna* showed similar susceptibility to two different synthetic pyrethroids, deltamethrin and esfenvalerate. Their 96-hour LC₅₀ values of deltamethrin and esfenvalerate were 0.00003 ppm and 0.00003 ppm, respectively. During the present study, *T. aurora* appeared more susceptible to cypermethrin (LC₅₀= 0.038 ppm) than deltamethrin (LC₅₀= 0.064 ppm) (Table 4). It has been reported that a given insect species may not be equally susceptible to different insecticides of the same class (Boiteau and Noronha, 2007; Nielsen et al., 2008).

During the present study, the susceptibility of nymphs of *I. elegans* and *T. aurora* to a particular pyrethroids was not the same. During lambda cyhalothrin toxicity study, nymphs of *I. elegans* were more susceptible than nymphs of *T. aurora*. On the other hand, during deltamethrin and cypermethrin toxicity study, nymphs of *T. aurora* were found more susceptible than nymphs of *I. elegans* (Table 4). It has been shown that different insect species may respond differently to an insecticide (Banks et al., 2017).

The differential tolerance of different insect species to an insecticide is due to differences in size, behavior, insecticide penetration, target sensitivity, excretion and metabolism (Wen et al., 2011). The enzymes P450 catalyse the oxidation of toxic compounds in the presence of NADPH cytochrome P450-reductase and or cytochrome b5 which are obligatory electron donor (Murataliev et al., 2008). The resistance of insects to insecticides is due to the presence of P450 enzymes (Karunker et al., 2009). Deltamethrin, cypermethrin and lambda-cyhalothrin that were studied for their toxicity with odonate nymphs during the present research, belong to type II pyrethroids. These pyrethroids cause hyperactivity, incoordination, convulsions and writhing. These type II pyrethroids produce stimulus-dependent nerve depolarization and blockage (Ecobichon, 1996).

The toxicity of deltamethrin with aquatic invertebrates has been reported. For example, Beketov (2002), studied the comparative sensitivity of larvae of damselfly, dragonfly, mayfly and *Daphnia magna* to deltamethrin and esfenvalerate. They reported the deltamethrin 48-hour LC₅₀ values of 0.0000145 ppm and 0.000076 ppm against nymphs of one damselfly species, *Lestes sponsa* and one dragonfly species such as *Cordulia aenea*, respectively. During the present research, the LC₅₀ values of deltamethrin against odonate nymphs were well above than the LC₅₀ values of deltamethrin reported by Beketov (2002). This difference might be explained by differences in species, brand of insecticides and experimental design. Deltamethrin toxicity with other invertebrates has also been reported. For example, de Castro et al. (2013) exposed the major lepidopteran pest of soybean, *Anticarsia gemmatilis* and its predators *Podisus nigrispinus* and *Supputius cincticeps* (Heteroptera: Pentatomidae) to deltamethrin, methamidophos, spinosad and chlorantraniliprole. The LC₅₀ values of deltamethrin against *Anticarsia gemmatilis*, *Podisus nigrispinus* and *Supputius cincticeps* were 2.76 ppm, 1.83 ppm and 1.83 ppm, respectively.

Lambdacyhalothrin toxicity to aquatic invertebrates has been reported. For example, in laboratory tests, the 48-hour EC₅₀ value of lambdacyhalothrin against nymph of *I. elegans* was 0.00013 ppm (Maund et al., 1998). Schroer et al. (2004) studied the toxicity of the pyrethroid insecticide λ-cyhalothrin to freshwater invertebrates in laboratory, in situ bioassays and in field microcosms. In laboratory tests, the 48-hour LC₅₀ value against *Erythromma viridulum* (Zygoptera, dragonflies) was 0.001583 ppm, *Asellus aquaticus* (Crustacea, Isopoda) 0.00014 ppm, *Gammarus pulex* (Crustacea, Amphipoda) 0.0000314 ppm, *Cloeon dipterum* (Ephemeroptera, mayflies) 0.000122 ppm, *Sigara striata* (Hemiptera, true bugs) 0.0000492 ppm and *Daphnia galeata* (Crustacea, Cladocera) was 0.397 ppm. The 48-hour LC₅₀ values of lambdacyhalothrin against *I. elegans* and *T. aurora* observed during the present research are far below than the lambdacyhalothrin 48-hour LC₅₀ values reported by Maund et al. (1998) and Schroer et al. (2004).

Organophosphate insecticides cause toxicity through inhibition of acetylcholinesterase, which is responsible for the degradation of the excitatory neurotransmitter, acetylcholine, thereby terminating transmission of nerve impulses at cholinergic synapses (Fukuto, 1990). Inhibition of this enzyme prolongs the residence time of acetylcholine at synapses resulting in hyper-excitation and eventual death (Fukuto, 1990). During the present study, *I. elegans* was found more susceptible to dichlorvos than to chlorpyrifos (Table 5). The lowest concentration of dichlorvos that caused 100% mortality of *I. elegans* nymphs was lower than the lowest concentration of chlorpyrifos that caused 100% mortality of *I. elegans* nymphs. The 48-hour LC₅₀ value

of dichlorvos for *I. elegans* nymphs was significantly lower than the 48-hour LC value of chlorpyrifos for *I. elegans* nymphs (Figure 6). Similar trend was observed during the study of susceptibility of *T. aurora* to chlorpyrifos and dichlorvos (Table 6, Figure 7). The findings of the present research showed that nymphs of *I. elegans* and *T. aurora* are more susceptible to dichlorvos than to chlorpyrifos. Similar trend was also reported by Ahmed and Irfanullah (2004). They studied the toxicity of dichlorvos and chlorpyrifos against house fly, *Musca domestica*. They reported dichlorvos as the most effective insecticide. Gupta et al. (2007) reported dichlorvos more deleterious than chlorpyrifos against fly. Chlorpyrifos toxicity with aquatic stages of invertebrates has been reported. For example, Rubach et al. (2010) reported the toxicokinetic variation in 15 freshwater arthropod species exposed to the insecticide chlorpyrifos. The 48-hour LC₅₀ values of larvae of *Anax imperator* (Anisoptera, dragonflies), *Chaoborus obscuripes* (Diptera), *Cloeon dipterum* (Ephemeroptera, mayflies) and *Sialis lutaria* (Megaloptera) were 0.00313 ppm, 0.000438 ppm, 0.000763 ppm and 0.00155 ppm, respectively. During the present research, the 48-hour LC₅₀ value of chlorpyrifos for *I. elegans* and *T. aurora* were 0.142 ppm and 0.3 ppm, respectively (Figure 8). These LC₅₀ values are far above than the LC₅₀ values reported by and Rubach et al. (2010) for chlorpyrifos against aquatic stages of Odonates or other insect species. To the author knowledge there are no reports about the toxicity of dichlorvos with the nymphs of *I. elegans* and *T. aurora*. However, there are reports about dichlorvos toxicity with fish (Kumar and Gautam, 2014; Patar et al., 2015), birds (Ezeji and Onwurah, 2017), mammals (WHO, 1989) and other aquatic organisms (McHenry et al., 1996). US EPA Ecotox database was searched for the LC₅₀ values of dichlorvos against damselfly and dragonfly nymphs. In the database, 24-hour LC₅₀ values of dichlorvos against the damselfly nymphs of *Agriocnemis sp.*, *Copera sp.* and *Ceriagrion sp.* were 4.57 ppm, 0.91 ppm and 0.63 ppm, respectively. The experimental medium was fresh water and the experiments were conducted in laboratory. The 24-hour LC₅₀ value of dichlorvos for the nymphs of *Agriocnemis sp.* is far above than the 48-hour dichlorvos LC₅₀ values for the *I. elegans* and *T. aurora* nymphs during the present research. The 24-hour LC₅₀ value of dichlorvos for the nymphs of *Copera sp.* and *Ceriagrion sp.* were closer to the 48-hour LC₅₀ value of dichlorvos against *I. elegans* and *T. aurora* during the present study.

The nymphs of *I. elegans* and *T. aurora*, showed different susceptibility against chlorpyrifos. For example, during exposure to chlorpyrifos, *I. elegans* was found more susceptible than *T. aurora* (Figure 8). All insecticides are not equally toxic to a given insect species, neither is a given insecticide equally effective against all insect species (Boiteau and Noronha, 2007; Nielsen et al., 2008). It has been shown that different insect species may respond differently to different insecticides (Banks et al., 2017). Differences among insect species in their capacity for P450-mediated detoxification of insecticides are an important factor responsible for differential tolerance among insect species to insecticides (Wen et al., 2011). During the present research, the susceptibility of *I. elegans* and *T. aurora* to acetamiprid (a neonicotinoid) were studied (Table 7). The nymphs of *T. aurora* was more susceptible than *I. elegans* nymphs. The 48-hour LC₅₀ value of acetamiprid for *T. aurora* (LC₅₀= 0.023 ppm) was significantly lower than its LC₅₀ value for *I. elegans* (LC₅₀= 0.038 ppm) (Figure 10). Thus *T. aurora* was found more sensitive to acetamiprid than *I. elegans*. It has been already reported that different insect species respond differently to an insecticide (Banks et al., 2017). Neonicotinoids act as agonists on nicotinic acetylcholine receptors (nAChRs) opening cation channels (Casida and Durkin, 2013). At the same time, voltage-gated calcium channels are also

involved (Jepson et al., 2006). This agonistic action results in continuous excitation of neuronal membrane, production of discharge that lead to paralysis and exhaustion of cell energy that leads to the death of insects. Thus, the channel opening of nAChRs induced by the binding of neonicotinoids to receptors leads to insecticidal activity (Nishiwaki et al., 2003). To the author knowledge, there are no reports about the LC₅₀ values of acetamiprid with dragonflies or damselflies nymphs. However, acetamiprid toxicity with other terrestrial and aquatic invertebrates has been reported. For example, the acetamiprid 48 hours LC₅₀ value of 49.8 ppm against *Daphnia magna* in static fresh water condition has been reported (Mineau and Palmer, 2013). Wang et al. (2012) studied the comparative acute toxicity of 24 insecticides against earthworm, *Eisenia fetida*. The LC₅₀ values of 0.0088 µg/cm² and 1.52 mg/kg were observed for acetamiprid against *Eisenia fetida* during contact filter paper test and contact artificial soil test, respectively.

During the present study, the LC₉₀ values of different insecticides for the nymphs of *I. elegans* and *T. aurora* were compared (Tables 8-9). Based on the comparison of LC₉₀ values, *I. elegans* and *T. aurora* were found more susceptible to lambda cyhalothrin and acetamiprid. They were found least susceptible to chlorpyrifos and dichlorvos. These results are in accordance with the early reports about the toxicity of different classes of insecticides to the aquatic insects and other invertebrates. According to Poirier and Surgeoner (1988), organophosphates insecticides and carbamates insecticides are less toxic to insect larvae but very toxic to some species. According to Anderson (1989), the most toxic group of insecticides is the pyrethroids which have broad spectrum of activity and kill most species.

Conclusion and recommendation

From the findings of the present study, it was concluded that damselfly i.e., *Ischnura elegans* and dragonfly i.e., *Trithemis aurora* nymphs are highly sensitive to a pyrethroid, lambda cyhalothrin and a neonicotinoid, acetamiprid. Synthetic chemical insecticides are highly toxic to damselfly and dragonfly nymphs even at very low concentrations. The application of synthetic chemical insecticides should be minimized and safe application in the areas adjacent to aquatic habitats must be ensured. Application of other methods of insect pest control such as integrated pest management should be encouraged. Further research is recommended for determining the effect of environmentally realistic high concentrations of agricultural insecticides in water bodies of agricultural areas on the predator avoidance behavior, development and predatory ability of odonate nymphs.

REFERENCES

- [1] Ahmed, S., Irfanullah, M. (2004): Toxicity of dichlorvos 50ec and chlorpyrifos 40ec against house fly, *Musca domestica* L. – Pak J Agri Sci 41(1): 65-71.
- [2] Anderson, R. L. (1989): Toxicity of synthetic pyrethroids to fresh water invertebrates. – Environ Toxicol Chem 8(5): 4003-4010.
- [3] Anderson, J. C., Dubetz, C., Palace, V. P. (2015): Neonicotinoids in the Canadian aquatic environment: a literature review on current use products with a focus on fate, exposure, and biological effects. – Sci Total Environ 505: 409-22.

- [4] Anjum, S. A. (1997): Biosystematics of odonate naiads of the Punjab by rearing techniques. – M.Sc. thesis, Department of Agriculture Entomology University of Agriculture Faisalabad, Pakistan.
- [5] Armbrust, K. L., Peeler, H. B. (2002): Effects of formulation on the run-off of imidacloprid from turf. – *Pest Manag Sci* 58(7): 702-706.
- [6] ASTM- American Society for Testing and Materials (2008): Guide for Conducting Acute Toxicity Tests on Aqueous Ambient Samples and Effluents with Fishes, Macroinvertebrates, and Amphibians. – ASTM International.
- [7] Banks, J. E., Vargas, R. I., Ackleh, A. S., Stark, J. D. (2017): Sublethal Effects in Pest Management: A Surrogate Species Perspective on Fruit Fly Control. – *Insects* 8: 78.
- [8] Beketov, M. A. (2002): Ammonia toxicity to larvae of *Erythromma najas* (Hansemann), *Lestes sponsa* (Hansemann) and *Sympetrum flaveolum* (Linnaeus) (Zygoptera: Coenagrionidae, Lestidae; Anisoptera: Libellulidae). – *Odonatologica* 31(3): 297-304.
- [9] Boiteau, G., Noronha, C. (2007): Topical, residual and ovicidal contact toxicity of three reduced-risk insecticides against the European corn borer, *Ostrinia nubilalis* (Lepidoptera: Crambidae), on potato. – *Pest Manag Sci* 63: 1230-1238.
- [10] Boyd, S. (2005): Damselflies and dragonflies. Scientific Illustration Major. – University of Georgia, Athens. <http://www.discoverlife.org/nh/tx/Insecta/Odonata/>.
- [11] Cai, Z., Wang, D., Ma, W. T. (2004): Gas chromatography/ion trap mass spectrometry applied for the analysis of triazine herbicides in environmental waters by an isotope dilution technique. – *Analytica Chimica Acta* 503: 263-270.
- [12] Casida, J. E., Durkin, K. A. (2013): Neuroactive insecticides: targets, selectivity, resistance, and secondary effects. – *Annu Rev Entomol* 58: 99-117.
- [13] Coats, J. R., Symonik, D. M., Bradbury, S. P., Dyer, S. D., Timson, L. K., Atchison, G. J. (1989): Toxicology of synthetic pyrethroids in aquatic organisms: An overview. – *Environ Toxicol Chem* 8: 671-679.
- [14] Davies, J. H. (1985): The pyrethroids: an historical introduction. – In: Leahey, J. P. (ed.) *The Pyrethroid Insecticides*. Taylor and Francis, Philadelphia, pp. 1-40.
- [15] de Castro, A. A., Corrêa, A. S., Legaspi, J. I., Guedes, R. N. C., Serrão, J. E., Zanuncio, J. C. (2013): Survival and behavior of the insecticide-exposed predators *Podisus nigrispinus* and *Supputius cincticeps* (Heteroptera: Pentatomidae). – *Chemosphere* 93(6): 1043-1050.
- [16] Din, A. U., Zia, A., Bhatti, A. R., Khan, M. N. (2013): Odonata naiads of Potohar Plateau, Punjab, Pakistan. – *Pakistan J Zool* 45: 695-700.
- [17] Ecobichon, D. J. (1996): Toxic effects of pesticides. – In: Klaassen, C. D., Amdur, M. O., Doull, J. (eds.) *Casarett & Doull's Toxicology: The Basic Science of Poisons*. McGraw-Hill, Health Professions Division. New York, NY. pp. 643-690.
- [18] Ezeji, E. U., Onwurah, I. N. E. (2017): Biochemical Effects of Dichlorvos Pesticide on the Liver of Poultry Birds (*Gallus domestica*). – *American Journal of Biochemistry* 7(2): 23-26.
- [19] Fenoll, J., Vela, N., Garrido, I., Pérez-Lucas, G., Navarro, S. (2014): Abatement of spinosad and indoxacarb residues in pure water by photocatalytic treatment using binary and ternary oxides of Zn and Ti. – *Environ Sci Pollut Res* 21(21): 12143-12153.
- [20] Finney, D. J. (1971): Probit analysis. – Cambridge University Press, London, pp. 68-78.
- [21] Fukuto, T. R. (1990): Mechanism of Action of Organophosphorus and Carbamate Insecticides. – *Environmental Health Perspectives* 87: 245-254.
- [22] Gullan, P. J., Cranston, P. S. (2005): *The Insects: An Outline of Entomology*, 3rd Edition. – Blackwell Publishing Ltd.
- [23] Gupta, S. C., Siddique, H. R., Mathur, N., Vishwakarma, A. L., Mishra, R. K., Saxena, D. K., Chowdhuri, D. K. (2007): Induction of hsp70, alterations in oxidative stress markers and apoptosis against dichlorvos exposure in transgenic *Drosophila melanogaster*: modulation by reactive oxygen species. – *Biochim Biophys Acta* 1770(9): 1382-1394.
- [24] Hilz, B. E., Vermeer, A. W. P. (2012): Effects of formulation on spray drift: a case study for commercial imidacloprid products. – *Asp Appl Biol* 114: 445-450.

- [25] Huynh, H., Nuggeoda, D. (2012): Effects of chlorpyrifos on growth and food utilization in Australian catfish, *Tandanus tandanus*. – Bull Environ Contam Toxicol 88: 25-29.
- [26] Jayaraj, R., Megha, P., Sreedev, P. (2016): Organochlorine pesticides, their toxic effects on living organisms and their fate in the environment. – Interdiscip Toxicol 9(3-4): 90-100.
- [27] Jepson, J. E. C., Brown, L. A., Sattelle, D. B. (2006): The actions of the neonicotinoid imidacloprid on cholinergic neurons of *Drosophila melanogaster*. – Invert Neurosci 6: 33-40.
- [28] Karunker, I., Morou, E., Nikou, D., Nauen, R., Sertchook, R., Stevenson, B. J., Paine, M. J., Morin, S., Vontas, J. (2009): Structural model and functional characterization of the Bemisia tabaci CYP6CM1vQ, a cytochrome P450 associated with high levels of imidacloprid resistance. – Insect Biochem Mol Biol 39: 697-706.
- [29] Kumar, S., Gautam, R. K. (2014): Study of biochemical toxicity of nuvan in *Channa punctatus* (Bloch.). – Adv Res Agri Veter Sci 1(1): 31-34.
- [30] Lourencetti, C., Marchi, M. R. R., Ribeiro, M. L. (2008): Determination of sugar cane herbicides in soil and soil treated with sugar cane vinasse by solid-phase extraction and HPLC UV. – Talanta 77: 701-709.
- [31] Malev, O., Klobucar, R. S., Fabbretti, E., Trebse, P. (2012): Comparative toxicity of imidacloprid and its transformation product 6-chloronicotinic acid to non-target aquatic organisms: microalgae *Desmodesmus subspicatus* and amphipod *Gammarus fossarum*. – Pestic Biochem Phys 104(3): 178-86.
- [32] Maund, S. J., Hamer, M. J., Warinton, J. S., Kedwards, T. J. (1998): Aquatic ecotoxicology of the pyrethroid insecticide lambda-cyhalothrin: Considerations for higher-tier aquatic risk assessment. – Pestic Sci 54: 408-417.
- [33] McHenry, J. G., Francis, C., Davies, I. M. (1996): Threshold toxicity and repeated exposure studies of dichlorvos to the larvae of the common lobster (*Homarus gammarus* L.). – Aquat Toxicol 34(3): 237-251.
- [34] Mian, L., Mulla, M. (1992): Effects of pyrethroid insecticides on non-target invertebrates in aquatic ecosystems. – J Agric Entomol 9: 73-98.
- [35] Mineau, P., Palmer, C. (2013): Neonicotinoid insecticides and birds: the impact of the nation's most widely used insecticides on birds. – American Bird Conservancy.
- [36] Mitra, T. R. (2002): Geographical distribution of Odonate (Insecta) of Eastern India (Memoirs Zool Survey India). – Zoological Survey of India, 203p.
- [37] Mitra, A. (2006): Current status of the Odonata of Bhutan: A checklist with four new records. – Bhu JRNR 2(1): 136-143.
- [38] Mokry, L. E., Hoagland, K. D. (1990): Acute toxicities of five synthetic pyrethroid insecticides to *Daphnia magna* and *Ceriodaphnia dubia*. – Environ Toxicol Chem 9: 1045-1051.
- [39] Morrissey, C. A., Mineau, P., Devries, J. H., Sanchez-Bayo, F., Liess, M., Cavallaro, M. C., Liber, K. (2015): Neonicotinoid contamination of global surface waters and associated risk to aquatic invertebrates: a review. – Environ Int 74: 291-303.
- [40] Murataliev, M. B., Guzov, V. M., Walker, F. A., Feyereisen, R. (2008): P450 reeducates and cytochrome b5 interactions with cytochrome P450: effects on house fly CYP6A1 catalysis. – Insect Biochem Mol Biol 38: 1008-1015.
- [41] Nafees, M., Jan, M. R., Khan, H. (2008): Pesticide Use in Swat Valley, Pakistan. – Mt Res Dev 28(3): 201-204.
- [42] Nafees, M., Jan, M. R. (2009): Residues of cypermethrin and endosulfan in soils of Swat valley. – Soil & Environ 28(2): 113-118.
- [43] Nielsen, A. L., Shearer, P. W., Hamilton, G. C. (2008): Toxicity of insecticides to *Halyomorpha halys* (Hemiptera: Pentatomidae) using glass-vial bioassays. – J Econ Entomol 101: 1439-1442.
- [44] Nishiwaki, H., Nakagawa, Y., Kuwamura, M., Sato, K., Akamatsu, M., Matsuda, K., Komai, K., Miyagawa, H. (2003): Correlations of the electrophysiological activity of neonicotinoids with their binding and insecticidal activities. – Pest Manag Sci 59: 1023-1030.

- [45] Osano, O., Admiraal, W., Klamerc, H. J. C., Pastor, D., Bleeker, E. A. J. (2002): Comparative toxic and genotoxic effects of chloroacetanilides, formamidines and their degradation products on *Vibrio fischeri* and *Chironomus riparius*. – *Environ Pollut* 119: 195-202.
- [46] Patar, A. A., Hassan, W. R. M., Hashim, N., Yusof, F. Z. M. (2015): Toxicity Effects of Malathion, Dichlorvos and Temephos on acetylcholinesterase in climbing perch (*Anabas testudineus*). – *Adv Env Biol* 9(21): 81-86.
- [47] Poirier, D. G., Surgeoner, G. A. (1988): Evaluation of a field bioassay technique to predict the impact of aerial applications of forestry insecticides on stream invertebrates. – *Can Entomol* 120: 627-637.
- [48] Rubach, M. N., Ashauer, R., Maund, S. J., Baird, D. J., van den Brink, P. J. (2010): Toxicokinetic variation in 15 freshwater arthropod species exposed to the insecticide chlorpyrifos. – *Environ Toxicol Chem* 29(10): 2225-2234.
- [49] Rubach, M. N., Baird, D. J., Boerwinkel, M.-C., Maund, S. J., Roessink, I., van den Brink, P. J. (2012): Species traits as predictors for intrinsic sensitivity of aquatic invertebrates to the insecticide chlorpyrifos. – *Ecotoxicology* 21: 2088-2101.
- [50] Schroer, A. F. W., Belgers, J. D. M., Brock, T. C. M., Matser, M., Maund, S. J., van den Brink, P. J. (2004): Comparison of Laboratory Single Species and Field Population-Level Effects of the Pyrethroid Insecticide λ -Cyhalothrin on Freshwater Invertebrates. – *Arch Environ Contam Toxicol* 46: 324-335.
- [51] Sirotkina, M., Lyagin, I., Efremenko, E. (2012): Hydrolysis of organophosphorus pesticides in soil: New opportunities with eco-compatible immobilized His6-OPH. – *Int Biodeter & Biodegr* 68: 18-23.
- [52] Stenersen, J. (2004): Chemical pesticides: mode of action and toxicology. – CRC Press, Boca Raton, Florida.
- [53] Tien, C. J., Lin, M. C., Chiu, W. H., Chen, C. S. (2013): Biodegradation of carbamate pesticides by natural river biofilms in different seasons and their effects on biofilm community structure. – *Environ Pollut* 179: 95-104.
- [54] Turusov, V., Rakitsky, V., Tomatis, L. (2002): Dichlorodiphenyltrichloroethane (DDT): Ubiquity, persistence, and risks. – *Environ Health Perspec* 110(2): 125-128.
- [55] US EPA. (1996): Ecological Effects Test Guidelines: Aquatic Invertebrate Acute Toxicity Test, Freshwater Daphnids. – EPA 712-C-96-114.
- [56] Vorkamp, K., Rigét, F. F. (2014): A review of new and current-use contaminants in the Arctic environment: Evidence of long-range transport and indications of bioaccumulation. – *Chemosphere* 111: 379-395.
- [57] Wang, Y., Cang, T., Zhao, Z., Yu, R., Chen, L., Wu, C., Wang, Q. (2012): Comparative acute toxicity of twenty-four insecticides to earthworm, *Eisenia fetida*. – *Ecotoxicol Environ Saf* 79: 122-128.
- [58] Wen, Z., Zhang, X., Zhang, Y. (2011): P450-mediated Insecticide Detoxification and Its Implication in Insecticide Efficacy. – In: Liu, T., Kang, L. (eds.) *Recent Advances in Entomological Research: From Molecular Biology to Pest Management*. Springer Heidelberg Dordrecht London New York, pp. 229-244.
- [59] Werner, I., Moran, K. (2008): Effects of Pyrethroid Insecticides on Aquatic Organisms. – *Synthetic Pyrethroids*, Chapter 14, pp. 310-334.
- [60] Wheeler, M. W., Park, R. M., Bailer, A. J. (2006): Comparing median lethal concentration values using confidence interval overlap or ratio tests. – *Environ Toxicol Chem* 25: 1441-1444.
- [61] WHO. (1989): Dichlorvos. *Environmental Health Criteria* 79. – World Health Organisation, Geneva, Switzerland.
- [62] Yousuf, M., Khan, M. J., Khaliq, A. (1996): Description of some final instar naiads (*Libellulidae*: *Odonata*) from Punjab and Sindh. – *Pak Entomol* 18(1-2): 17-23.
- [63] Zacharia, J. T. (2011): Ecological Effects of Pesticides. – In: Stoytcheva, M. (ed.) *Pesticides in the Modern World - Risks and Benefits*. ISBN: 978-953-307-458-0.

THE ANTHROPOCENE AND GREAT ACCELERATION AS CONTROVERSIAL EPOCH OF HUMAN-INDUCED ACTIVITIES: CASE STUDY OF THE HALK EL MENJEL WETLAND, EASTERN TUNISIA

GHARSALLI, N.^{1,2*} – ESSEFI, E.^{3,4} – BAYDOUN, R.⁵ – YAICH, C.^{1,2}

¹*RU: Sedimentary Dynamics and Environment (DSE) (Code 03/UR/10-03), National Engineering School of Sfax, University of Sfax, Sfax, Tunisia*

²*GEOGLOB Laboratory, Faculty of Science of Sfax, University of Sfax, Sfax, Tunisia*

³*Higher Institute of Applied Sciences and Technology of Gabes, University of Gabes, Gabes, Tunisia*

⁴*Unité de Recherche Electrochimie, Matériaux et Environnement UREME (UR17ES45), Faculté des Sciences de Gabes, Université de Gabes, Gabes, Tunisia*

⁵*Lebanese Atomic Energy Commission, National Council for Scientific Research, P.O. Box11-8281, Riad El Solh, Beirut, Lebanon*

**Corresponding author
e-mail: garsalli_najoua@yahoo.fr*

(Received 1st Mar 2019; accepted 19th Mar 2020)

Abstract. The Anthropocene covers the recentest period of globally widespread climate and environmental changes during which polluting human activities represent major risks for populations and their resources. The aim of this study is to investigate the drastic change in the sedimentary record of the sebkha Halk El Menjel, located in Tunisia, along a 10-cm long core to discuss the possible onset and limits of the Anthropocene and the Great Acceleration in this wetland. Sampling was carried out each 2 mm. According to the age-depth model and the increasing pattern of heavy metals content, we propose that the Anthropocene onset is located at ~300 yr BP. The increasing heavy metals content may be correlated to natural and/or anthropogenic sources such as volcanic eruptions and mining activities respectively. Also, the evolution of grain size percentages shows an increasing sediment flux during the Anthropocene and accentuated during the Great Acceleration. The principal component analysis shows three main groups of variables related to pollution, climate change and eustatism, indicating the combined effect of the natural and human induced activities during the Anthropocene. The evolution of microfauna shows that some microorganisms were influenced by the Anthropocene conditions whereas others remain indifferent.

Keywords: *Anthropocene, industrial revolution period, heavy metal pollution, western Mediterranean*

Introduction

Determining the full stretch of natural and anthropogenic pollution (and its causal link with climate variability) on spatial and temporal scales relevant to ecosystems functioning and human wellbeing is of utmost importance to anticipate the impact of, and improve the preparedness of communities to, future climate change. Most of coastal regions in Tunisia have been affected by different sources of pollution, which is well documented through the investigation of recent surface sediments (Gargouri, 2001; Ghannem et al., 2011, 2014; Wali et al., 2015; Zaaboub et al., 2015; Ennouri et al., 2016). Worldwide, this pollution dates back to the setting of mining and industrial activities during the Anthropocene and the subsequent Great Acceleration (GA) periods (Waters et al., 2014, 2016, 2018), which are, also, marked by drastic changes in climatic conditions (Hébert et al., 2017). Currently, the

Anthropocene is an under discussion geologic epoch dating back to the setting of noticeable human impact on terrestrial environments and the subsequent biotic conditions (Yusoff, 2013; Young et al., 2016). It has recently occupied the heart of earth sciences (Crutzen et al., 2006). In spite of the existence of signs of micropaleontological biomarkers characterizing this epoch (Wilkinson et al., 2014), until August 2016, neither the International Commission of Stratigraphy (ICS) nor the International Union of Geological Sciences (IUGS) have yet officially approved the term “Anthropocene” as a standalone subdivision of the geological timescale (Castree, 2017). Different Anthropocene bases (“beginnings”) were controversially proposed, because of the various disciplinary perspectives and criteria. First proposed by Crutzen and Stoermer (2000), the term “Anthropocene” covers the second half of the 20th century overlying therefore the Holocene in term of stratigraphy and geochronology. During this period, the global effect of human activities was clearly noticeable. The increasing release of the greenhouse gasses (GHGs) associated to the onset of the Industrial Revolution (IR) as a beginning of the Anthropocene was later rejected (Certini and Scalenghe, 2011). Instead, the pedosphere was considered as the best recorder of such human-induced modifications of the total environment. Based on the study of the anthropogenic soils (Certini and Scalenghe, 2011), the beginning of the Anthropocene was attributed to ~2000 cal yr BP. After reviewing the onset of the Anthropocene, (Smith et al., 2013) has considered the Anthropocene to be coeval with the Holocene controversially with Waters et al. (2016). This “Anthropocene onset” controversy is mainly due to its regionally depending limits which are not worldwide. Yet, some common features can be found concerning the setting of the Anthropocene: polluted environments and climate change.

In the aftermath of the Anthropocene settings, the term “GA” has emerged as a new concept which documents and describes the increasing impact of human societies on the Earth systems (Steffen et al., 2015). Since 1950, the dramatic increase in most Earth’s systems parameters was attributed to the growing impact of human societies on the ecosystems, and was used to demark the initiation of the Anthropocene (Zalasiewicz et al., 2012) has been later rejected. Regarding this controversy, the Anthropocene Working Group (AWG), a working group of the Subcommission on Quaternary Stratigraphy (SQS) of the International Commission on Stratigraphy (ICS) has been spurring scientists to define the beginning of the Anthropocene in the Geologic Timescale.

The aim of this work is twofold; On the one hand, the content of heavy metal and the magnetic susceptibility measurements were combined to identify the onset of the Anthropocene and the individualization of the GA in Eastern Tunisia in terms of environmental pollution. On the other hand, other geochemical (Ca, Na and K), micropaleontological (ostracods, foraminifera, charophytes and gastropods) and sedimentary (clay, silt and sand percentages) proxies were used to provide further information about the sedimentary dynamic environmental changes related to the Anthropocene settings.

Study area

Geographic location

Coastal regions and estuaries (wetlands) are sensitive environments to record the setting of the Anthropocene (Leorri and Cearreta, 2009; Emeis et al., 2015; Irabien et al., 2015; Waters et al., 2018), unlike mountains which are remote far from the impact of human induced activities (Gabriel and Barbante, 2014). The sebkha-lagoon Halk El Menjel is a 17

km² coastal are located 1 km westward of Hergla harbor (35°58'28"N, 10°31'27"E to 36°00'38"N, 10°27'29"E) (Fig. 1c). It has been considered as a “recipient” of various pollutants (APAL, 2002) notably the heavy metals, resulted of an accelerated industrialization and urbanization of the surrounding vicinities.

Bioclimatic and rainfall setting

In the western part of the Mediterranean Sea (Fig. 1a), Tunisia extends on different climatic stages ranging from: (1) humid to sub-humid zones, (2) semi-arid to arid zones in central Tunisia and (3) arid to saharian zones in southern Tunisia with sub-desert to desert vegetation (Lebreton et al., 2015) (Fig. 1d). Plains and foothills of the study area region are approximately located in the semi-arid bioclimatic zone, between the 200 mm and 400 mm isohyets (Fig. 1d). A long drought summer occurs from March to August, and three aridity gradients are observed: (1) from the sea shore to the Tunisian-Algerian frontier (a longitudinal one), (2) from the North to the South, a (latitudinal one) and (3) along the elevation, an altitudinal one (Lebreton et al., 2015) (Fig. 1). The mean annual temperature is around 19 °C, with mean summer temperature 27.1 °C and mean winter temperature 12 °C (APAL, 2002) while the mean annual rainfall is about 350 mm, ranging from 100 to 680 mm (APAL, 2003). The sebkha-lagoon Halk El Menjel is surrounded by a complex hydrographic network. It collects fresh waters and sediments mainly from sebkha Kalbia through the Menfas and As-sod wadis (APAL, 2002). The sebkha Kalbia itself is fed by hydraulic sedimentation through main wadis of Merguellil, Nebhana and Zroud (Khdheri et al., 2011; Duplay et al., 2013; Kchouk et al., 2015) which incised the southern slope of the Dorsal Mountains (Jbel Trozza, Jbel Serj and Jbel Bargou) (Fincoa et al., 2018; Figs. 1b, c).

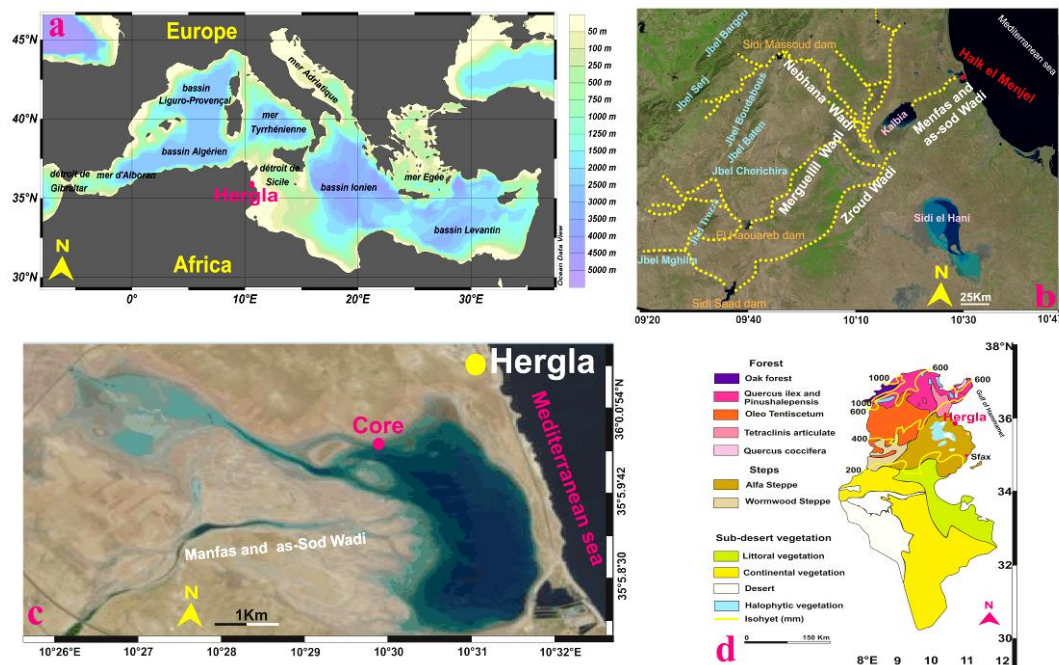


Figure 1. Location of the Halk El Menejl sebkha-lagoon delta system. (a) Connection of Hergla coastal harbour with the Mediterranean Sea. (b) Satellite image (<https://earthexplorer.usgs.gov/>) marked the connection of Halk El Menjel sebkha-lagoon with hydrogeological systems's sebkha endoreic Kalbia. (c) Satellite image (<https://earthexplorer.usgs.gov/>) of sebkha-lagoon Halk el Menjel showing the coring location. (d) Bioclimatic map of Tunisia (modified after Lebreton et al., 2015)

Anthropogenic setting

As for anthropogenic activities, since the Neolithic, the vicinities of the study area have been occupied by primitive to recent human populations (Mulazzani et al., 2010; Belhouchet et al., 2014; Essefi et al., 2014). Moreover, the majority of the coastal areas of Tunisia are threatened by an increasing pollution (Ennouri et al., 2016; Pradel et al., 2016). Also, the climate witnessed an increasing aridity recorded in the micropaleontological (Zaibi, 2011), sedimentary and mineralogical contents (Gargouri, 2011). Connected with the Mediterranean Sea, the wetland of Halk El Menjel is marked by a well-shaped delta system related to a temporary river without a dam (*Fig. 1c*). This type of delta had potentially recorded the variability of sediment flux during the Anthropocene (James and Kettner, 2011).

Methods and materials

Sampling and chronological framework

During the field expedition, a 10-cm long core (HK3) was recovered in the sebkha-lagoon of Halk El Menjel (36°00'01"N, 10°30'08"E) next to the core of (Lebreton et al., 2015), merely few meters of lateral distance. In laboratory, the sediment of the core was sampled each 2 mm to collect 50 samples. Since our core is located exactly next to the core of (Lebreton et al., 2015), we relied on its age-depth model already carried out based on eight dated samples. The mean sediment accumulation rate is ~0.16 mm/yr for the past 3000 yr (*Table 1*), giving, therefore, a total duration of 628 yr for the 10 cm core. Our mean sediment accumulation rate found in sebkha-lagoon of Halk el Menjel is comparable to other sedimentation rates found in different western Mediterranean areas.

Table 1. 14C AMS radiocarbon ages of the studied core (Lebreton et al., 2015)

Laboratory	Lab reference	Depth (m, a.s.l.)	Conventional age (14C yr BP)	Calibrated age (2σ) (calyr BP)	Mean cal age (calyr BP)
Beta Analytic	Beta-290411	-0.58	3410 ± 40	3731–3562	3646 ± 85

Petromagnetic and geochemical analysis

Low and high frequency (LF and HF) magnetic susceptibility (MS) and grain size parameters were measured using Bartington MS2B probe and FRITSCH laser granulometer, respectively. The resulted MS measurements were expressed as mass susceptibility χ_{lf} and χ_{hf} , and the corresponding frequency dependence of magnetic susceptibility (FD) was calculated as follows:

$$FD(\%) = \frac{(\chi_{lf} - \chi_{hf})}{\chi_{lf}} \times 100 \quad (\text{Eq.1})$$

Then, percentages of clay, silt and sand were calculated using/based on the cumulative curves.

Geochemistry is a more relevant tool to assess the Anthropocene environmental changes (Gałuszka et al., 2014). After three concentrated acids (Nitric, perchloric,

chloridric) attack of each sample, the amounts of heavy metals (Cr, Ni, Cu, Zn, and Fe) were measured by atomic adsorption to calculate the geo-accumulation index (Igeo). Igeo is considered as a relevant criterion to determine the degree of sediments metal contamination by comparing current concentrations with pre-industrial levels (Müller, 1981). It can be calculated using the following equation:

$$I_{geo} = \log_2 \left[\frac{C_n}{1.5 \times C_{Bn}} \right] \quad (\text{Eq.2})$$

where C_n is the measured concentration of the examined metal (n) in the sediment, B_n is the background concentration of the metal (n), and 1.5 is the background matrix correction factor due to lithogenic effect. According to the scale of (Müller, 1981), the calculated Igeo related to the studied samples showed different levels of contamination for the analyzed metals (*Table 2*).

Table 2. Sediment classes according to Müller (1981)

Geo Index value	Class	Quality of sediment
Less than 0	0	Unpolluted
0-1	1	From unpolluted to moderately polluted
1-2	2	Moderately polluted
2-3	3	From moderately to strongly polluted
3-4	4	Strongly polluted
4-5	5	From strongly to extremely polluted
More than 5	6	Extremely polluted

In addition, Ca^{++} , K^+ , and Na^+ contents were measured, following two methods: attacked and bulk sediment. These analyses were carried out using Flame Photometer in Geochemistry Laboratory in the National Engineering School of Sfax (Tunisia). In saline systems, the measurement of Ca^{++} , K^+ , and Na^+ by the acids attacked, includes both those due to past climatic change and those due to present groundwater feeding, whereas measurement on bulk shows the cations related to groundwater feeding. Hence, the subtraction result highlights the climatic signal (Essefi et al., 2015) recorded in the studied wetland.

Paleobiological analysis

The fauna within samples was studied to find out the defaunation at the onset of the Anthropocene. Each sample was disaggregated with diluted hydrogen peroxide for 4 to 5 h and washed into 250 μm and 63 μm sieves. The residues were dried under 50 °C then the density of foraminifera, ostracods, charophytes and gastropods was calculated (in individual/kg).

Principal component analysis (PCA)

To understand the relationship between various parameters related to the Anthropocene and GA, or other possible sources of production, the Principal

Component Analysis (PCA) of the, χ_{lf} , χ_{hf} , FD, heavy metals (Fe, Zn, Cu, Cr, and Ni contents), clay, silt and sand percentages was computed and plotted on the PCA diagram.

Results

The 10 cm of the studied core HK3 represents the fifth pollen zone PZ-5 (Fig. 2) at the top of the core of (Lebreton et al., 2015) reflecting the modern local and regional semi-arid vegetation. At the middle of this biofacies, an abrupt appearance of the Oleaster wild olive species (*Olea europaea* subsp. *Europaea* var. *sylvestris*) can be noticed (Lebreton et al., 2015). It is worth noting that the Oleaster is relevant to the Mediterranean regions and belongs to the thermophilous Mediterranean vegetation, indicating arid conditions probably related to the setting of the Anthropocene. The latter age and the subsequent GA might be also recorded through chemical (heavy metals), sedimentological (clay, silt, and sand percentages), and paleontological (foraminifera, ostracods, charophytes, gastropods) proxies.

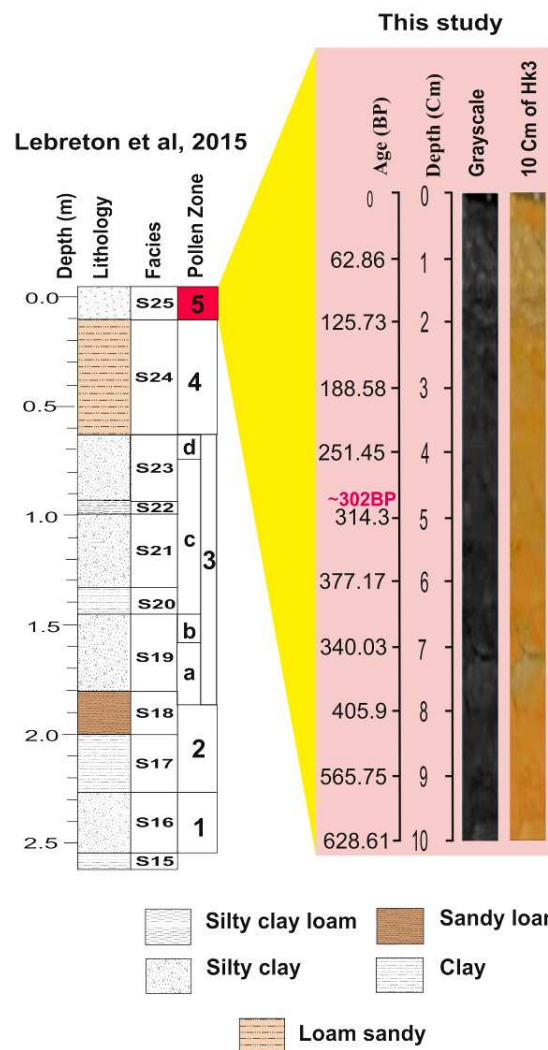


Figure 2. Relationship between Lebreton core and the 10 Cm of HK3 core from the sebkhalagoon of Halk El Menjel

Heavy metals content during the Anthropocene-Holocene transition and the Great Acceleration

The evolution of the heavy metals content (Fig. 3) shows an upward increasing pollution related to the setting of the Anthropocene. According to the age-depth model (Fig. 2), the polluted period may have started at ~300 yr BP, and henceforth, all heavy metals contents have increased indicating an important source of pollution. Worldwide, the Anthropocene is marked by a dramatic increase of heavy metals content in the exceptionally damaged wetlands due to natural and/or anthropogenic origins (Álvarez-Vázquez et al., 2016). In fact, multiphase heavy metals geochemical processes interfere in the atmosphere-biosphere interface, influencing the climatic conditions during the Anthropocene (Pöschl and Shiraiwa, 2015). Nonetheless, due to their natural and anthropic origins, absolute values of heavy metals contents relevant to the Anthropocene still are ambiguous and cannot serve as a pacemaker for the setting of its limits. In the case of the Halk El Menjel wetland/sebkha-lagoon, this proxy may only show the existence of an increasing pollution. To get over this limitation, we need to compute the Igeo to determine the degree of contamination. Moreover, the increasing trend of some heavy metals contents such as Zn is more pronounced at the top of the core due to their anthropogenic impact during the GA. However, heavy metals having natural origin such as iron do not show an obvious increase. Cr, Cu and Ni indicate a rapid setting rate of the Anthropocene dating back to ~300 yr. The content of all heavy metals does not show an obvious individualization of the GA.

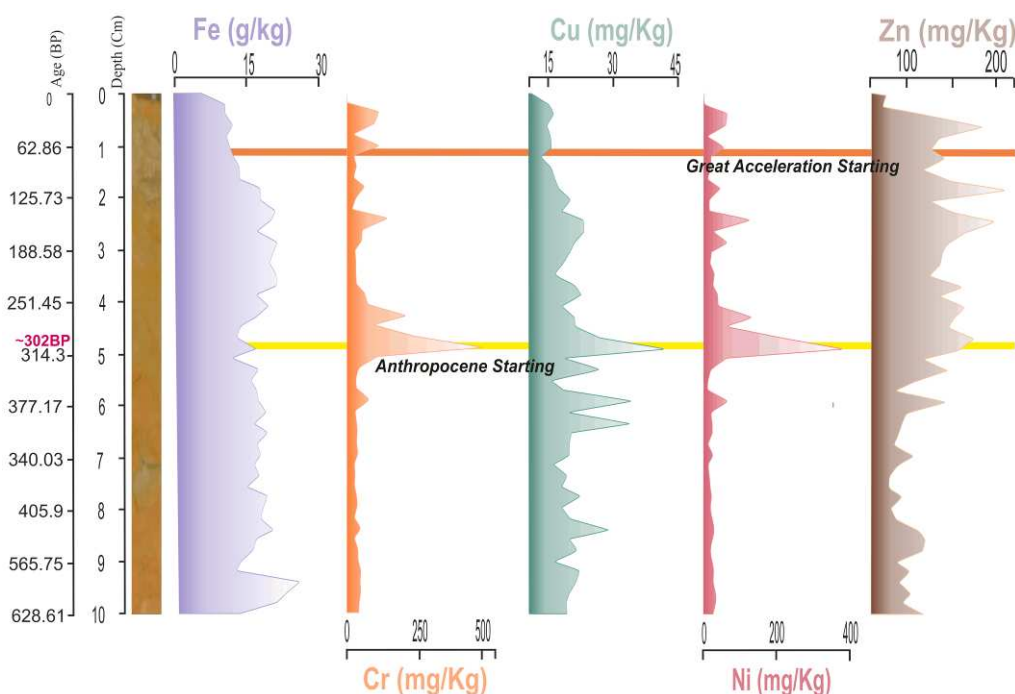


Figure 3. Evolution of the heavy metals content along the 10 cm core from the sebkha of Halk El Menjel

Due to the overlap of the natural and anthropogenic factors in wetlands, the onset the Anthropocene and the GA based on heavy metals is not straightforward. This led us to calculate and plot the Igeo against the core (Fig. 4), which enhanced more the

visualization of the Anthropocene limit already identified through the bulk content of heavy metals. In fact, the study had experienced the succession of many civilizations who had used fire and old traditional tools (Lebreton et al., 2015). The Igeo of Zn, Cr, Ni and Cu along the core may also points to the setting of Anthropocene at ~300 yr PB, whereas the GA is well pronounced through the Igeo of Ni and Cr. The Igeo varies from strong to extreme polluted for Cr and Ni and is moderately polluted for Zn, Cu and Fe, which allowed us inferring that the sebkha sediments are contaminated by heavy metals the same way as many Tunisian coastal regions (Gargouri, 2001; Ghannem et al., 2011, 2014; Wali et al., 2015).

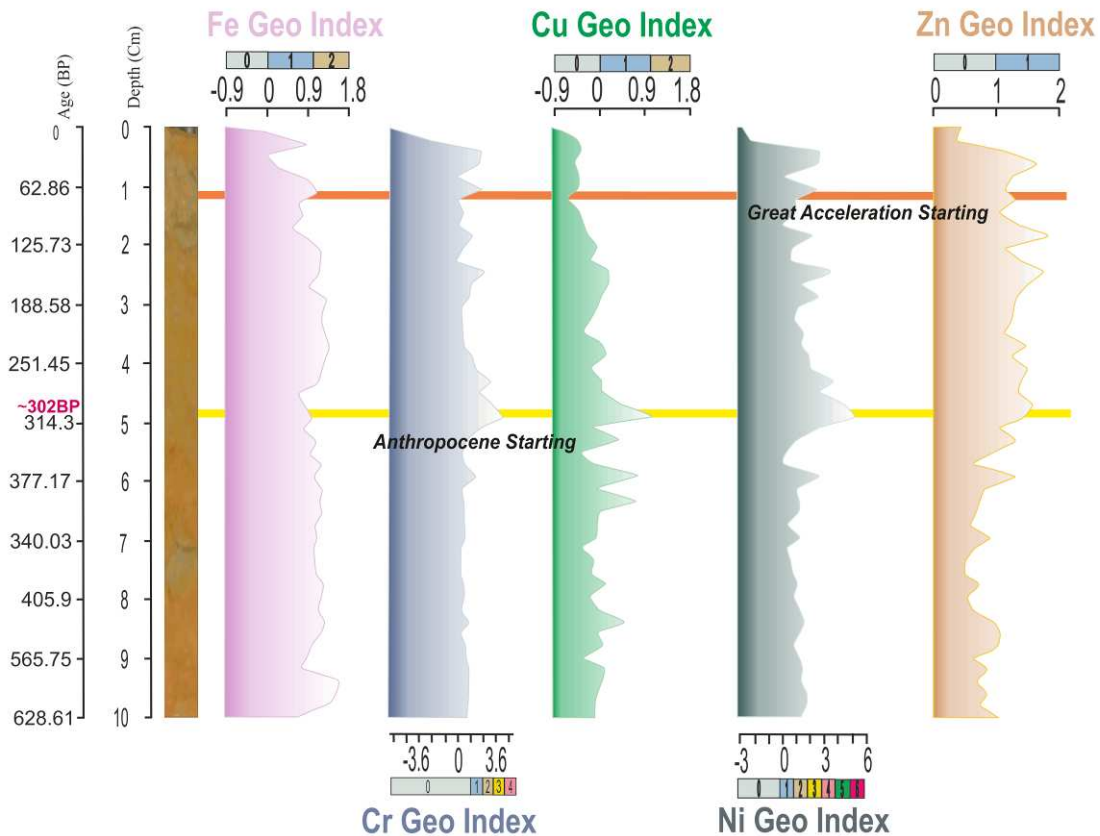


Figure 4. Evolution of Geo-accumulation Index along the 10 cm core from the sebkha of Halk El Menjel

Grain size variability during the Great Acceleration and the Anthropocene-Holocene transition: the sedimentary flux

The variability of clay, silt and sand percentages (Fig. 5) is related to sedimentary flux which has increased considerably indicating a dramatic climate change particularly during the GA (James and Kettner, 2011). Actually, scientists (Ribot, 2014) are still debating concerning the realistic scenarios of the climate change during the Anthropocene because of the overlap of the natural and the anthropogenic causes. Grain size parameters (Fig. 5) show an upward tendency toward a decrease of clay percentage unlike silt and sand percentages which increase considerably along the last 5 cm of the core HK3. This may indicate an increase of the hydraulic sediment flux, which is

related to some human induced activities worldwide taking place during the Anthropocene and GA (James and Kettner, 2011): (1) soil erosion related to deforestation, slope failure and downstream sedimentation; (2) agricultural activities in the Eastern Tunisian coastal region consist of tillage, irrigation systems, terracing, and subsurface water pumping, leading, respectively, to an increased soil erosion, creep, siltation and subsidence. The coastal management takes place along the wetland shoreline through groynes, jetties, seawalls, breakwaters and harbours, causing unnatural coastal erosion or sedimentation, as well as wetland, mangrove and dune alterations; (3) the waterway construction, including reservoirs and dams, diversions, channel levees, discharge focusing, channel deepening and ultimately coastline erosion.

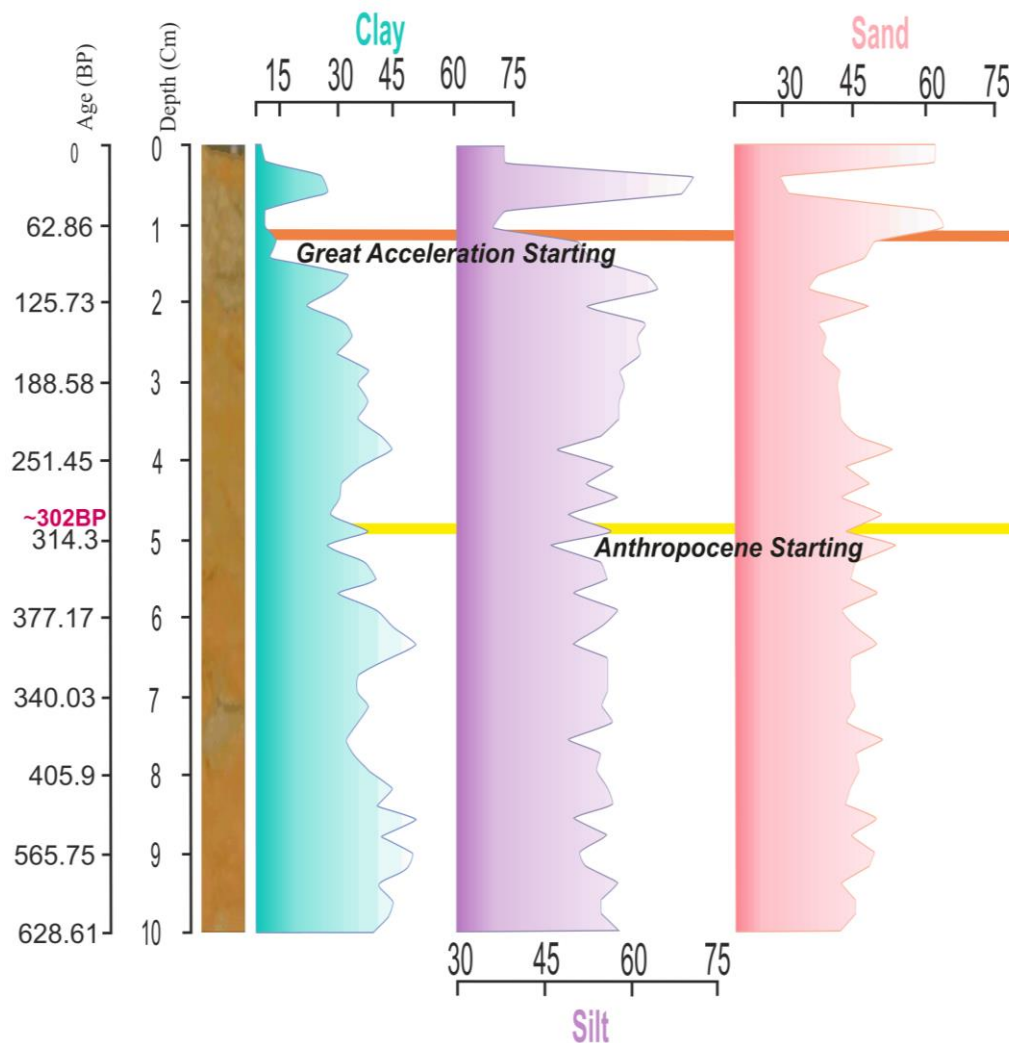


Figure 5. Evolution of grain size parameters along the 10 cm core from the sebkha-lagoon of Halk El Menjel indicating an increasing sediment flux

Geochemical proxies' evolution during the Great Acceleration and the Anthropocene-Holocene transition

Climate conditions and sea-level change may have a direct impact on the geochemistry of the sedimentary record. These changes deal also with aeolian erosion

and perturbation of the surface geochemistry characteristics during the Anthropocene (Marx et al., 2014). Toward the inland, Anthropocene conditions change the response of the main Wadis feeding the studied sebkha (Meybeck, 2001; James and Kettner, 2011). The increase of Ca^{++} , Na^{++} and K^{+} contents is a direct indicator of an increasing aridity and/or sea level fall. The vertical evolution of these ions contents (*Fig. 6*) does not indicate a systematic variability relevant to the Anthropocene settings. Compared to other stratigraphic changes described in longer geologic periods, the climate and sea-level signals of the Anthropocene are not strongly expressed, because they reflect, somehow, the combined effects of fast and slow climate feedback mechanisms.

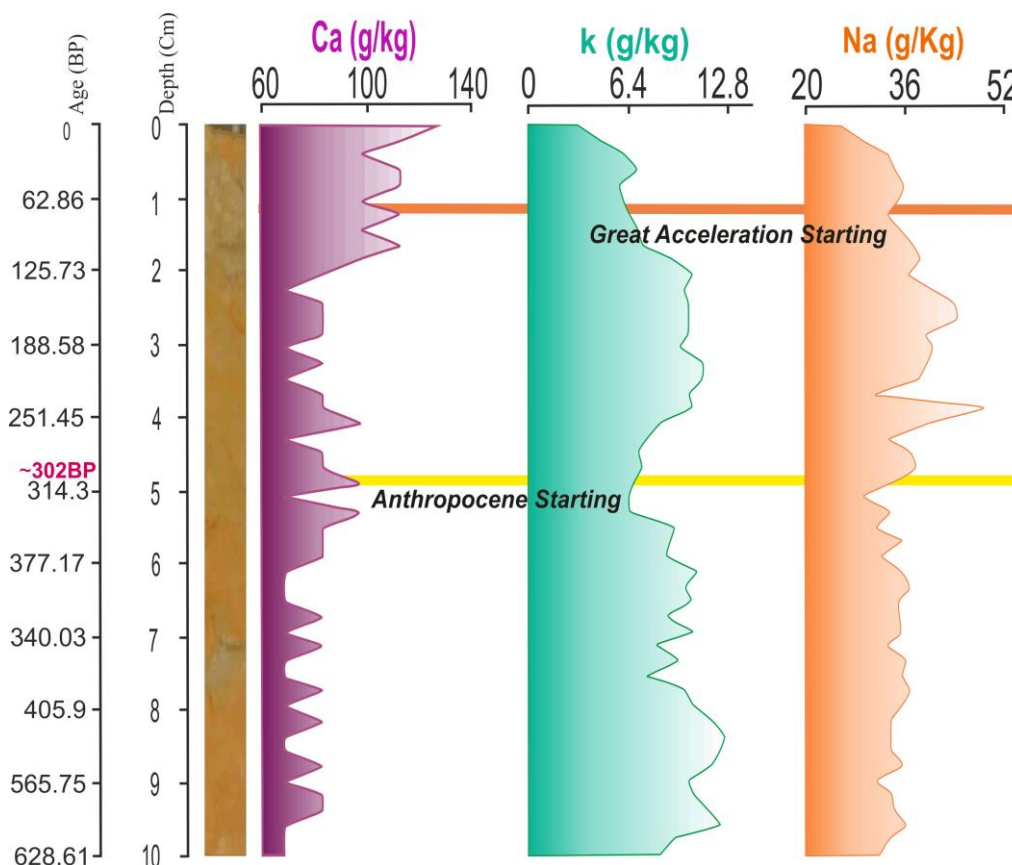


Figure 6. Evolution of Ca, Na and K contents along the 10 cm core from the sebkha of Halk El Menjel

Magnetic susceptibility evolution during the Great Acceleration and the Anthropocene-Holocene transition

The convolution of the geochemical data of attacked and non-attacked sediments plotted against the magnetic susceptibility (*Fig. 7*) does not match well the setting of the Anthropocene. Instead, its cyclic pattern may be related to astronomic and/or oceanographic forcing. The magnetic susceptibility variations may go in line with the heavy metals content (Dearing et al., 1996, 2001). Also, the setting of a new microbiologic response related to the Anthropocene may be the origin of the development of magnetobacteria (Gillings and Paulsen, 2014), which are responsible for the increasing pattern of the magnetic susceptibility variations. The use of

petromagnetic measurements in wetland sediments as a marker for the start of the Anthropocene has been widely adopted recently. Indeed, the starting of the Anthropocene is worldwide marked by an increase of the magnetic susceptibility in recent sediments (Olfield, 2001).

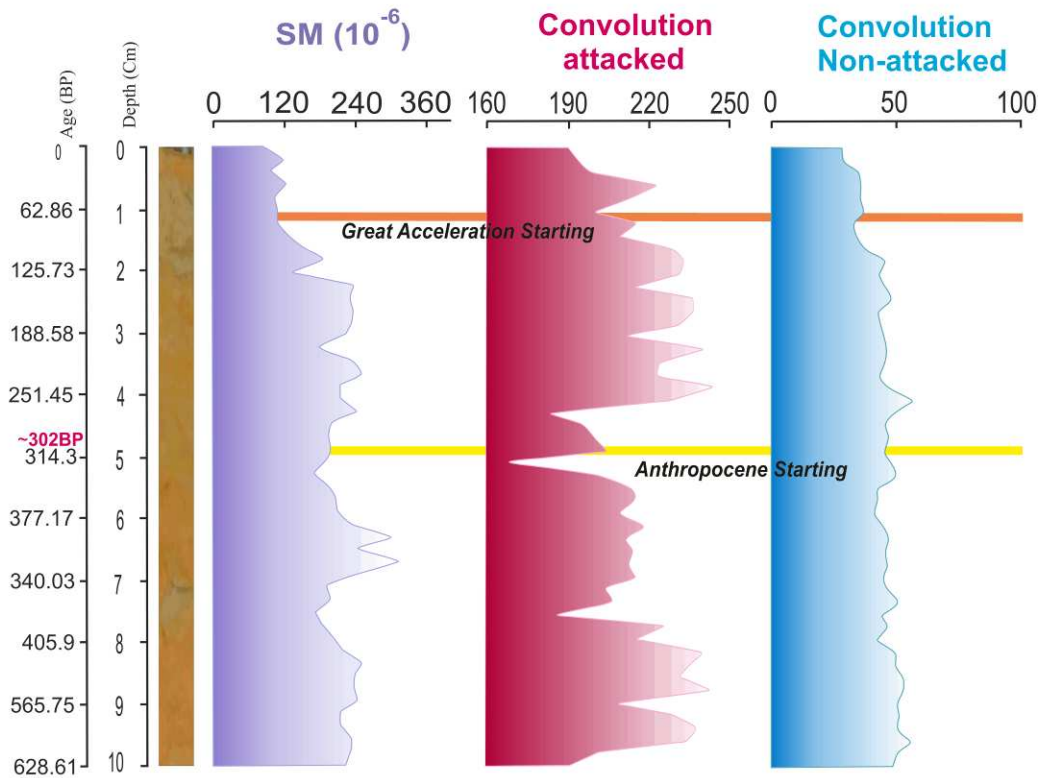


Figure 7. Evolution of the magnetic susceptibility and the convolution of geochemical elements (Ca, Na, K) for the attacked and non-attacked sediment along the 10 cm core from the sebkha of Halk El Menjel

Principal Component Analysis: an overview on the behavior of the proxies and these agents of control during the Anthropocene-Holocene transition

The Principal Component Analysis PCA of all variables (Fig. 8) shows the individualization of three different groups. The first one is made up of χ_{lf} , χ_{hf} , Clay percentage and Iron related to wetter climatic conditions and/or sea level fall which triggered a sediment flux during Anthropocene. The second group is made up of the heavy metals Cu, Cr, Zn and Ni. As it is indicated by the Igeo values, it is related to an environmental pollution. During the Anthropocene, heavy metals pollution had been caused by natural and anthropogenic factors. Although that various anthropogenic sources contribute to heavy metals pollution in the environment, the most important source remains the mining activities that lead to a global dispersal through oceanic and atmospheric dissemination. The third group is made up of FD, silt and sand percentages. It is related to sea level rise and/or and increasing erodability. The PCA shows the overlap of natural and human induced effects during the Anthropocene. The pollution and climate change combined together had generated the Anthropocene conditions.

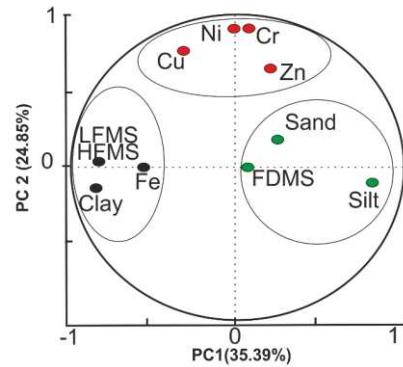


Figure 8. Principal Component Analysis of geophysical (LFMS, HFMS and FDMS), geochemical (Fe, Zn, Cu, Cr, and Ni contents) and sedimentological proxies (clay, silt and sand percentages)

Defaunation during the Anthropocene

One of the most interesting targets of the Anthropocene definition is the search for a wider understanding of how human activities have modified and disturbed the Earth's ecosystems and biological resources. In terms of paleontological content, marine foraminifera show an obvious defaunation due to the setting of stressful conditions related to coastal pollution starting since the Anthropocene onset and accentuated during the GA. The defaunation of continental charophytes is probably due to the synergetic effects between human activities eutrophication and climatic conditions disrupting their intensity of the population density (Fig. 9). Ostracods are not obviously influenced during the Anthropocene and began to increase dramatically during the GA. Likewise, gastropods remain not obviously influenced during both periods. The anthropic acceleration of fauna and flora extinctions during the Anthropocene and the GA due to pollution or climate change have been noticed for many species (Braje and Erlandson, 2013). In fact, anthropogenic climate change is playing an important role; the primary operator of modern extinctions seems to be habitat loss, introduced species and human predation (Briggs, 2011).

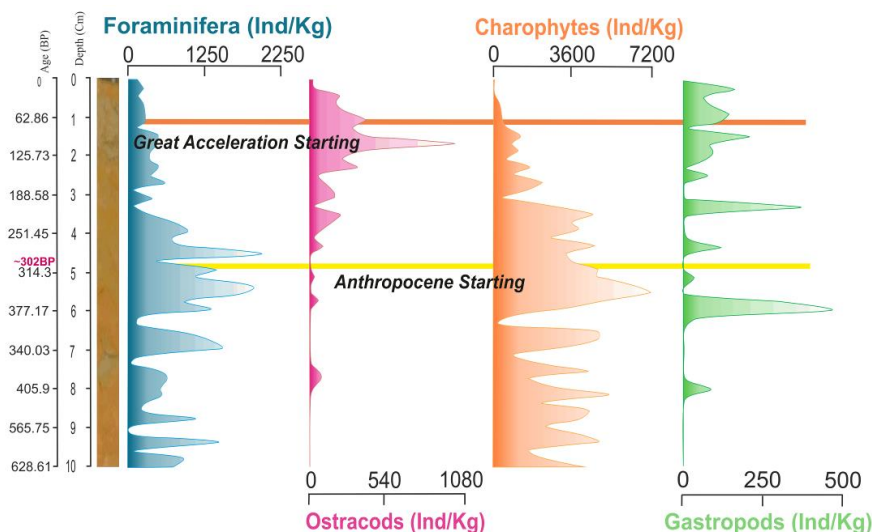


Figure 9. Evolution of fauna density (individuals per kg) along the 10 cm core from the sebkha of Halk El Menjel

Discussion

Early to middle Little Ice Age (LIA) (AD 1400- 1712)

In this work, we consider this interval as a pre-Anthropocene period. It is marked by a lower fluctuation of pollutants; weak rate of Cr and Ni and moderate rate in Cu and Zn (Figs. 3, 4 and 10). This fluctuation may be related to atmospheric metal deposition which have had a causal link to a natural source due to two major volcanic eruptions of Kuwae (Vanuatu, Southern Pacific) and St. Helens at AD 1452-1453 and 1480-1482 respectively (Yamaguchi, 1983; Gao, 2006). For example, the particular Kuwae volcano emitted to the atmosphere some of the broadest aerosol fluxes in the past 700 years (Buat-Menard and Arnold, 1978). Indeed, many heavy metals have been found at an increased concentration in volcanic emissions; metals (Fe, Cr, Cu, Mn, Ni, Pb, and Zn among others) and polluted gases (CO₂, sulfur and chlorine compounds) (Buat-Menard and Arnold, 1978; Favalli et al., 2004; Andronico et al., 2009). In addition, the volcanic eruptions during this period are the major natural source of many heavy metals such as gaseous mercury (Hg) emissions to the atmosphere which may include more than 1000 mg of Hg per event (Nriagu, 1990; Nriagu and Becker, 2003; Pyle and Mather, 2003), 40-50% of the global flux of Cd (Nriagu, 1990; Pyle and Mather, 2003), and 20-40% of other volatile metals (As, Cu, Ni, Pb and Sb) (Nriagu, 1990).

Mediterranean basin was marked by the development of mining activities during the early LIA (Corella et al., 2017) especially, in Spain (Rio Tinto mining, Mines of Parzán and Almadén mining) and Slovenia (Idrija mine) (Corella et al., 2017). Nevertheless, anthropogenic emissions have greatly overpassed natural release to the atmosphere over historical times (Allan et al., 2013; Beal et al., 2015; Corella et al., 2017; Erykh et al., 2017). Most of heavy metal contents show a slight (Fe and Cr) to significant (Ni and Zn) increase after the Anthropocene onset (Fig. 4) which could be explain by the double impact of natural and anthropogenic pollution sources.

This period represented the early to middle LIA which this last framed within the Medieval Climatic Anomaly (MCA) and post-LIA warming recorded during the second half of 19th century. LIA is a one of the coldest periods over the Northern Hemisphere during the Holocene (Grove, 2004; Wanner et al., 2011), it was characterized by cold periods with regionally variable magnitude controlling by a various mechanisms associated to external forcing mechanisms (Hunt, 2006) where the main processes was attributed to the increasing volcanic activity (Crowley, 2000; Hegerl et al., 2011) and radiative forcing (Solar Irradiation) (Dorado-Liñán et al., 2016) represented by two major grand solar activity minima; the Spörer minimum (1460-1550) and the Maunder minimum (MM) (1645-1715) (Eddy, 1976). This external forcing, especially volcanic aerosols have been initiated to multidecadal changes in internal climate system mechanism (ocean heat content (OHC), Arctic sea ice extent, the Atlantic Meridional Overturning Circulation (AMOC), and Sea Surface Temperatures (SSTs)) through a series of climate feedbacks. (Broecker, 2000; Church et al., 2005; Hegerl et al., 2011; Iwi et al., 2012; Schleussner and Feulner, 2013; McGregor et al., 2015). The multi-decadal timescales mechanisms caused a succession of warm and cold 'sub-periods' with an irregular annual and seasonal precipitation bring about to both floods and droughts (Machado et al., 2011). This climate fluctuation may explain the particular trend of our measured data in Figure 5 (%sand, %silt and %clay). In fact, the grain size parameter measured along the HK3 core show a particular pattern which goes in line with the pre- and the post-climate setting of the Anthropocene. The latter, which is

characterized by long negative NAO phases (Baker et al., 2015) (*Fig. 10.13*) leading to wetter conditions (Benito et al., 2003, 2015) and more pronounced flooding events, shows higher coarse fractions (silt and sand) (*Fig. 5*) during the early to middle LIA comparing to finer particles (clay) which decrease obviously after the proposed Anthropocene onset (*Fig. 5*).

Late LIA: the Anthropocene onset (AD (1712-1850)

This transition is marked by a dramatic increase of heavy metal contents (*Fig. 3*) and Igeo values (particularly the Ni and Cr) (*Figs. 4, 10.1, 10.2, 10.3 and 10.4*) increasing records which can be attributed to natural and anthropogenic sources. Firstly, the natural one is related to volcanic eruptions which are frequent in Mediterranean Sea; series of explosive volcanic eruptions causes an increase in the levels of atmospheric metals such as (1) Vesuvius explosive eruption (Italy, Tyrrhenian Sea) in AD 1631 (Barberi et al., 1995), (2) the most violent phase of explosive eruption of Kolumbo (Greece, Aegean Sea) marked at AD 1650 (Fouqué, 1879; Ulvrova et al., 2016), (3) AD 1669 represented the largest historic eruption during the last 400 years of Etna (Eastern Sicily, Ionian Sea) (Tanguy et al., 2007; Branca et al., 2013) and (4) Santorini volcanic eruption from AD 1707-1711 (Greece, Aegean Sea) (Gorée, 1710; Tarillon, 1715; Watts et al., 2015). Aerosols injected into the atmosphere during explosive eruptions consist of mixtures of varying particles such as gases, soot, ash, secondary organic aerosols, metals and mineral dust (Pyle and Mather, 2003; Seinfeld et al., 2006). Aerosols can be transported by turbulent mixing and convection atmospheric circulations to remote higher altitudes or other continents before they are eliminated from the atmosphere by dry and/or wet deposition. Secondly, the mining activity is considered as the most important source of the anthropogenic emissions and pollution before the Industrial Period (IP) in Western Mediterranean region (Cortizas et al., 1999, 2002; Allan et al., 2013). It has largely overpassed the natural sources of pollution since the Anthropocene onset henceforth. Southern Spain is known as a historical mining area; the Almadén mining district (since 2500 yr BP) (Cortizas et al., 1999) and the Bielsa-Parzán mining district (since pre-Roman times) (Calvo, 2008). Moreover, the border of the 'Massif Central' (Southern France) has been known as an important mining area of non-ferrous (Pb-Zn-Ag-Au) metals since at least the medieval period (Poulichette et al., 2017). Consequently, a growth stock of metal deposit (Kaye, 2005; Poulichette et al., 2017) is concentrated in the mining areas which represented a potential environmental risk in the Mediterranean basin during contemporaneous storms and flooding events (Salomons and Förstner, 1984; Blais et al., 2015).

The accumulation of pollutants coincided with transition period under particular climatic conditions marked by the transit from the MM period to relatively higher δ TSI (Herrera et al., 2015) (transit phase from a very cold period to warmer period) (*Fig. 10.16*). This change in TSI had controlled the contemporaneous NAO pattern (*Fig. 10.13*), which is in turn, controlled the main climate variability in the Mediterranean region during the last 500 years (Luterbacher et al., 2002; Hurrell et al., 2003). Negative NAO phase triggered the precipitation and the river runoff which caused frequent floods in the Western and Central Mediterranean region (Benito et al., 2015). When the NAO is positive, dry conditions develop over North Africa and southern Europe (Nieto-Moreno et al., 2015).

Moreover, Dezileau et al. (2011) have reported that the late LIA was a period of superstorm activity in the Western Mediterranean region with high fluvial activity and

major historical flooding events which might lead to an increasing detrital flux into the Mediterranean basin and high sand level which has been shown by our data (*Figs. 5 and 10.7*). Several authors have documented a major periods of high flood frequency occurring in Western Mediterranean region during the late 17th and beginning of 18th century; (Degeai et al., 2017) shows a flood event in Southern French coastal region between 1660 and 1780, (Barriendos and Fernando, 2006) described Large Catastrophic Events in northeastern Spain during 1651 (Segura River basins), 1663 and 1678 (Coastal basins of Catalonia). These extreme climatic conditions coincided with progressive increase in atmospheric pollutants and huge quantities of hazardous mine wastes from polymetallic ores for the production of Pb, Zn, Ag, As, Hg, Ti, Sb, Cd, Au, Cu... (have been heavily worked in Mediterranean regions since pre-Roman times) due to mining processing and smelting activities which had been transported to the Mediterranean basin (Poulichette et al., 2017). Spanish and French rivers discharging to Mediterranean basin are able to transport mining contaminants, during the flooding events and remote from their sources (Puig et al., 1999; Baudrimonta et al., 2005; Poulichette et al., 2017) even though the mines are abandoned (Pyatt et al., 2000; Audry et al., 2004; Baron et al., 2005, 2006). Spanish rivers play a very important role through its evacuation point which is the Alboran Sea. In terms of oceanography, the Alboran Sea is considered as master piece of the thermohaline circulation; it is the place of mixture by Alboran Gyre of the incoming Atlantic waters (AW) through Gibraltar Strait (Jordà et al., 2017; Testor et al., 2018) with the previously mentioned polluted water of main Spanish rivers. AW are rapidly becoming Modified Atlantic Waters (MAW) (La Violette, 1987; Tintore et al., 1988; Arnone et al., 1990) and progress eastward up to Eastern Mediterranean. Most of French rivers (The Herault river basin and The Gardon river basin which is the tributary of the Rhone River) evacuated polluted waters in the Gulf of Lion (GoL). This leads to consider that no water mass in the Mediterranean Sea can escape the anthropogenic metal inputs including the Tunisian coastal regions, and hence, our study area of Sebkh-lagoon of Halk El Menjel. Therefore, the origin of the second group shown by the PCA (Cu, Cr, Zn and Ni) (*Fig. 8*) may be linked to this kind of transport and their Igeo values to these sources of contamination (*Figs. 4, 10.1, 10.2, 10.3 and 10.4*).

At the end of 17th century and the dawn of the 18th century, the synergetic effects between human activities and climate change in Tunisian regions were particularly intense and have been accentuated further with demographic development in coastal areas and around the rivers' vicinities (Ghazali, 2003; Chaldeos, 2016; Cherni et al., 2016). This situation, associated with human-induced soil erosion (Lacarra, 1972), had led to the so-called anthropogenic land cover change (ALCC). This had been spurred further by the use of fire for the creation of pastureland and cropland, and the use of coal in factories which was significantly intensified (Houghton et al., 1996; Ruddiman, 2007) at the end of the 18th century. Our dataset (grain size parameters) support this fact as we notice a remarkable increase of % clay, % silt and % sand during this period (*Fig. 5*). The increasing of population affecting the environment (Smith and Zeder, 2013) particularly the marine ecosystems caused an eutrophication (Lotze et al., 2011) which was triggered by a huge discharge of suspended matter, nutrients and trace elements (Degobbis et al., 2000; Zonneveld et al., 2012; Salvi et al., 2015). Consequently, a defaunation occurred marked by a noticeable falling in the intensity of the population density of marine organisms (including foraminifera, gastropods and ostracods) (*Figs. 9, 10.10, 10.11, and 10.12*). However, increasing heavy metals seems

to be affectless on charophytes population density; no significant influence of Cu, Co and Ni has been evidenced on charophytes occurrence (*Figs. 10.2, 10.3, and 10.9*) (Lamber and Davy, 2010) on their population density. Yet, a slight decrease is noticed around the Anthropocene onset. Actually, charophytes are known as a sensitive indicator of water clarity. The occurrence of most charophytes is limited to clear water columns with alkaline pH and low nutrient amount (Phillips et al., 2005) which seems to be perturbed by increasing detrital inputs triggered by major flooding events during this period.

Industrial period

This period is known as the first acceleration phase during which anthropogenic heavy metal environmental pollution begun with mining activities, the domestication of fire and later the Industrial Revolution (IR). The IR yielded a higher demand for metals, excessive burning of fossil fuels and an exponential increase in the intensity of heavy metal pollution (Nriagu, 1996). Consequently, an increasing level of aerosol particles in the atmosphere as well as the increase in GHGs caused an unprecedented sunlight reflection, and triggered, thus, the global warming (Owens et al., 2017). As a result, a potential contamination might be globally widespread into the environment (air, water, soils, sediments) including Tunisian coastal zones. Our data show an important Igeo value for Cr, Ni and Zn (*Figs. 4, 10.1, 10.3 and 10.4*) which may represent the aftermath of this contamination. The industrialization was associated with a decrease of average ocean surface waters pH by ~0.1 (induced by deposition of acidifying pollutants or microbial oxidation of sulphides and ammonia to form sulphuric and nitric acids (Feely et al., 2009; Rice and Herman, 2012)) and an abrupt increase in CH₄ presumably caused by increased fossil fuel emissions (Houweling et al., 2008; Mischler et al., 2009; Sapart et al., 2012). The combination of both the environmental acidification phenomena (Rice and Herman, 2012) and the eutrophication had yielded the damage of marine communities and had reduced species diversity (de Faveri et al., 2015); foraminifera (industrial period is characterized by an increase of warm water species (Margaritelli et al., 2016)) and charophytes which are known as sensitive indicators of indirect consequences of eutrophication (water quality, lack of light, water clarity and sediment accumulation (Phillips et al., 2005)). Some other species can also show a tolerant response to anthropogenic stress (Suárez-Álvarez et al., 2012; Sarker et al., 2013), such as gastropods and ostracods were found predominantly during the following the IR which dose match very well our fauna data in *Figure 9*.

Modern Warming Period (MWP)

This period started with the so-called “GA” in 1950. The GA marked the transition between the IP and the Modern Warming Period (MWP) which is characterized by globally-widespread anthropogenic impact on planet Earth (McNeill, 2000; Steffen et al., 2004). The abrupt increasing in human activities resulting from the rising of world population density (*Fig. 10.9*) from 3 to 6 billion in only 50 years (Steffen et al., 2011) is the main cause of global warming (IPCC, 2007). The level of CO₂ emissions had risen sharply to 379 ppm according to the 2005 measurements (Altava-Ortiz et al., 2011). This increase has been caused by the burning of fossil fuels and the changes in land use which make up the largest share of the GHG emissions. Furthermore, other non-CO₂ greenhouse gases such as nitrous oxide (N₂O) and methane (CH₄) also

contribute substantially to the overall warming GHG. Atmospheric CH₄ had increased from ~900 ppb in 1900 to ~1800 ppb in 2010 (Ghosh et al., 2015). The combined effect of these factors with the Total Solar Irradiance (TSI) (*Fig. 10.16*) caused an increase in the Sea Surface Temperature (SST) since the 1950s. This increase of the SST has affected the global rainfall (Bozkurt and Sen, 2011) particularly in the Mediterranean basin (Turuncoglu, 2015) which caused an important ingredient for the onset and the intensification of Heavy Precipitation Events (HPE), especially in its western part (Miglietta et al., 2011; Pastor et al., 2015, 2018), Central Europe (Volosciuk et al., 2016) and the coastal regions of Tunisia (Rowell, 2003). Moreover, Marcos et al. (2009) noticed a significant correlation between the storm events in the Western and Central Mediterranean and the NAO pattern.

Two peaks are obviously distinguished in the heavy metals Igeo during the second half of the 20th century which might be correlated to the Western Mediterranean HPE (WMHPE) especially Tunisian flooding events (*Figs. 10.1, 10.2, 10.3, and 10.4*). The first peak coincides with positive NAO phase (*Fig. 10.13*). Yet, HPE was documented over Western Mediterranean basin during the 1960s (Valencia flooding on October 1957 in Barcelona in September 1962 (Olcina et al., 2016)) which may be due to positive AMO phase (Gray et al., 2004) (*Fig. 10.14*). Tunisia was affected by an exceptional flooding event in 1969 with a return period estimated at 150 years (Besbes et al., 2019). The Oued Zeroud flooding on 27 September 1969, had a maximum flow of 17,000 m³/s, seven times higher than the historic flooding of 1910 in Paris (2400 m³/s) with a five-times smaller watershed (Besbes et al., 2019) and the Merguellil wadi flow exceeded 3000 m³/s (grain size parameters). A second peak occurred during the 1980s, coinciding with an increase in the global SST (IPCC, 2013) and the transition to a positive NAO (Pastor et al., 2018) phase (*Fig. 10.13*). Yet, some floods episodes occurring since 1980 in the Western Mediterranean (Olcina, 2009; Cortesi et al., 2012). That decade began with possibly the flooding of 1982; October's flooding in Valencia, November's flooding in Andorra and the Catalan Pyrenees and the flooding of August 1983 in the Basque Country (1982-1990) (Olcina, 2009). Likewise, Tunisia experienced such remarkable flooding events during the same period (Ellouze and Abida, 2008; Daoud, 2013; Fehri et al., 2014) which goes in line with our Igeo dataset in *Figures 10.1, 10.2, 10.3 and 10.4*. During flooding events, the capability of a fluvial system to lift and carry on detrital influx (*Figs. 10.7, and 10.8*), including heavy metals, far from their origin increases significantly which is the case for Zeroud, Merguellil and Nebhana wadis (Hollis and Kallel, 1986) (*Fig. 1b*). The Zeroud wadi incised the surrounding catchments of the Jebel Trozza ancient mine (active between 1907 and 1937) which is considered as an important pollution source (Duplay et al., 2013; Elmayel et al., 2019). A third remarkable peak occurred during the dawn of 21st century but concerns only the %sand. It may be related to the flooding events that affected North Africa during this period. Indeed, the decade began with the catastrophic flash floods that affected Algeria (10 November 2001) (Tripoli et al., 2005) and Tunisia (2003) (Kadomura, 2005). Nevertheless, heavy metal contents show a very low response to such events which may be related to the construction of the Sidi Saâd dam (1982) (Bel Hadj Salem et al., 2012) and the Houareb dam (1989) (Leduc et al., 2009) upon the Zeroud wadi and Merguellil wadi respectively. These wadis surround the ancient mine of Jebel Trozza and are responsible for the main transport of heavy metal pollution in this area. Consequently, the hydraulic exchange between the Kalbia and Halk El Menjel wetlands (*Fig. 1b*) had been reduced dramatically and affected the heavy metal pollution in the study area.

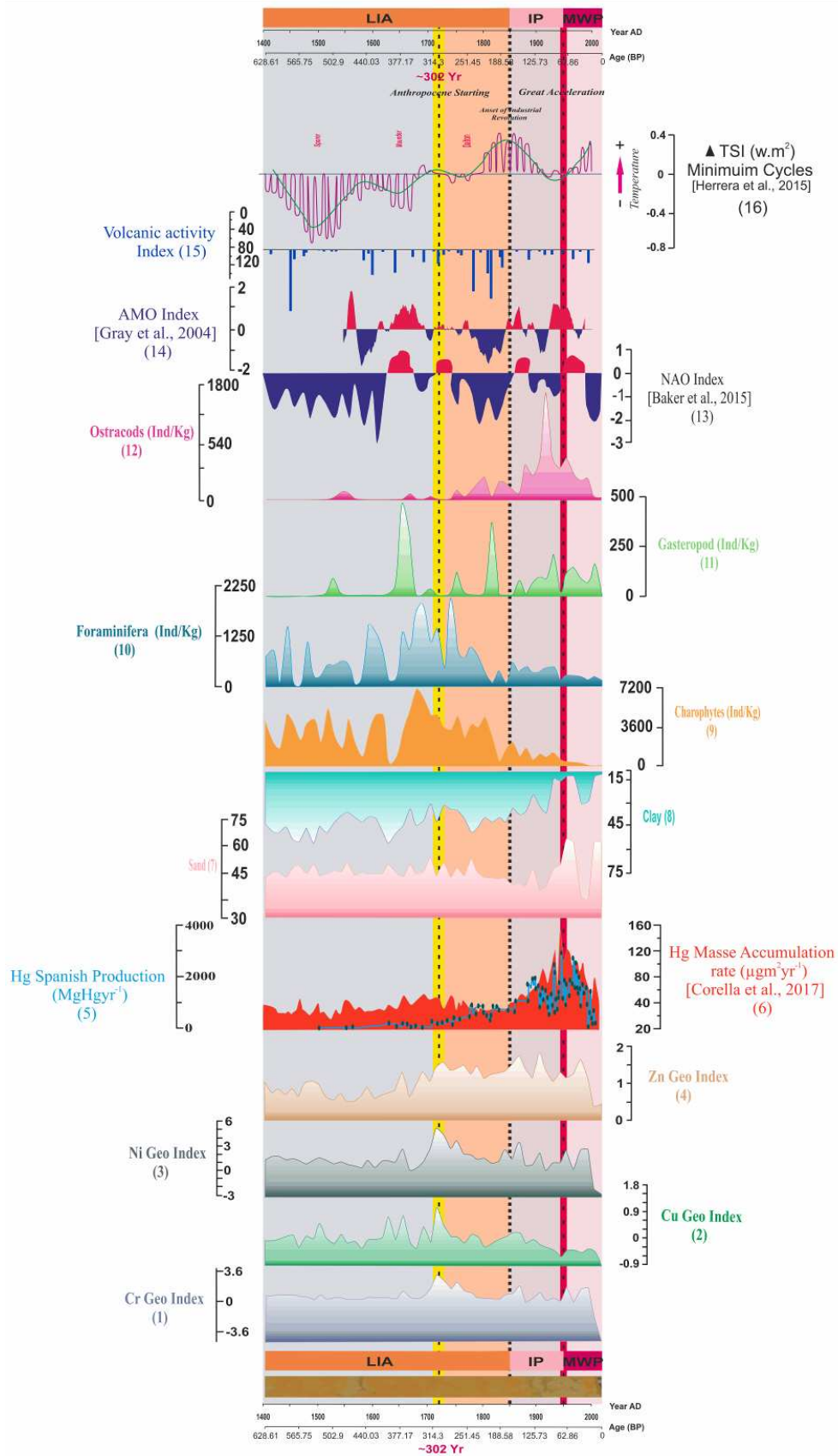


Figure 10. Synergy of anthropogenic, natural and climatic factors to understand Anthropocene phenomena and the Great Acceleration

Continued global warming, in combination with other human-caused stresses and anthropogenic factors would have important consequences for the changing in physical, biological, and chemical processes in soils and water (McNeill and Engelke, 2016). The expected increasing of atmospheric CO₂ cause a reduce of oceanic pH and carbonate ion concentrations (Bates et al., 2008; Waldbusser and Salisbury, 2013): the current pH of the surface ocean of about 8.1 (Feely et al., 2009) has already decreased by 0.1 units since the end of the pre-industrial period (Solomon et al., 2007; Gattuso and Lavigne, 2009) and the acidity of the ocean surface has increased by 30% (Dupont and Pörtner, 2013). Coastal areas were the most sensitive regions where the acidification and the warming of the sea water columns can interact synergistically in decreasing the calcification (Bates et al., 2008) which caused a weakening population density for many calcifying marine organisms (Fabry et al., 2008) such as charophytes (*Fig. 10.9*) cold-water corals, coralline algae, sea urchins and plankton (Reynaud et al., 2003; Anthony et al., 2011; Andersson and Mackenzie, 2011; Kroeker et al., 2013). Besides, the density of foraminifera community had been affected by oceanic acidification which shown an abundance fall (Hall-Spencer et al., 2008; Martin et al., 2008) (*Fig. 10.10*), and also shifts from one majority dominated by calcareous forms to one minority dominated by agglutinated taxa (Hall-Spencer et al., 2008; Dias et al., 2010; Pettit et al., 2015).

Gazeau et al. (2013) have reported that the decrease of pH below 0.4 unit compared to the current value seems to be without any effect on gastropods due to their ability to regulate their internal acid-base equilibrium, shell mineralogy and also their environmental conditions which explain their resistance to intolerant conditions. However, our dataset (*Fig. 10.11*) shows that gastropods density decreased during the MWP. This could be explained by the decrease of influx of dissolved oxygen (DO₂). The latter parameter depends on the input of organic matter and nutrient (Diaz and Rosenberg, 2008; Levin et al., 2009) from coastal watersheds during wet period which causes the increase of the biological oxygen demand by aerobic microbial communities. This environmental change seems to be the major factors influencing the densities of many species such as gastropods and ostracods (*Figs. 10.11 and 10.12*), (Levin and Gage, 1998; Rabalais et al., 2010).

Conclusion

This work implements a multidisciplinary approach to set the limit of the Anthropocene and the subsequent GA in eastern Tunisia. Based on previous published age-depth model and analyses of heavy metals (Cu, Cr, Ni, and Zn), the Anthropocene-Holocene boundary is likely located at 300 yr BP. At this age, the Igeo indices increased significantly indicating hence more pronounced polluting activities. Igeo (particularly the Ni and Cr) shows also several positive peaks indicating, thus, remarkable polluting activities since the GA and hence forward. In term of sedimentologic features, the onset of the Anthropocene is marked by an increasing sedimentary flux indicated by the dominance of the coarse fraction comparing to finer sediments. In addition, the marine fauna was affected by a sharp defaunation during the Anthropocene period related to the setting of stressful environmental conditions. The eutrophication of the sebkha-lagoon Halk El Menjel had been triggered by a huge discharge of suspended matter, nutrients and trace elements during flooding events which caused a falling in the intensity of the population density of marine organisms (including foraminifera, gastropods and ostracods and charophytes). During the MWP, the acidification and the warming of the

sea water columns caused a weakening calcification phenomenon and decrease in population density for many calcifying marine organisms such as charophytes. The decrease of the gastropods and ostracods density seems to be affected by the decrease of the dissolved oxygen (DO₂) during remarkable flooding events.

The Principal Component Analysis found out three groups; two of them are related to natural change of environmental conditions. One group is related to the impact of polluting activities. The human induced activities on the natural environments have dual effect: pollution and climate change.

REFERENCES

- [1] Allan, M., Le Roux, G., Sonke, J. E., Piotrowska, N., Streel, M., Fagel, N. (2013): Reconstructing historical atmospheric mercury deposition in Western Europe using: Misten peat bog cores, Belgium. – *Science of the Total Environment* 442: 290-301.
- [2] Altava-Ortiz, V., Llasat, M-C., Ferrari, E., Atencia, A. Sirangelo, B. (2011): Monthly rainfall changes in Central and Western Mediterranean basins, at the end of the 20th and beginning of the 21st centuries. – *International Journal of Climatology* 31: 1943-1958.
- [3] Álvarez-Vázquez, M. A., Caetano, M., Álvarez-Iglesias, P., Pedrosa-García, M. C., Calvo, S., De Uña-Álvarez, E., Quintana, B., Vale, C., Prego, R. (2016): Natural and Anthropocene fluxes of trace elements in estuarine sediments of Galician Rias. – *Estuarine, Coastal and Shelf Science* 95-120.
- [4] Andersson, A. J. Mackenzie, F. T. (2011): Ocean acidification: setting the record straight. – *Biogeosciences Discuss* 8: 6161-6190.
- [5] Andronico, D., Spinetti, C., Cristaldi, A., Buongiorno, M. F. (2009): Observations of Mt. Etna volcanic ash plumes in 2006: an integrated approach from ground-based and polar satellite NOAAVHRR monitoring system. – *Journal of Volcanology and Geothermal Research* 180: 135-147.
- [6] Anthony, K. R. N., Maynard, J. A., Diaz-Pulido, G., Mumby, P. J., Marshall, P. A., Cao, L. (2011): Ocean acidification and warming will lower coral reef resilience. – *Global Change Biology* 17(5): 1798-1808.
- [7] APAL, Coastal Protection and Planning Agency of Tunisia (2002): Management Study of the Sensitive Area of Sebkh-Lagoon Halk el Menjel; Phase I: Characterization of the Natural Environment. – APAL, Tunisia (in French).
- [8] APAL, Coastal Protection and Planning Agency of Tunisia (2003): Management Study of the Sensitive Area of Sebkh-Lagoon Halk el Menjel; Phase II: Detailed Management Scheme. – APAL, Tunisia (in French).
- [9] Arnone, R. A., Wiesenburg, D. A., Saunders, K. D. (1990): The origin and characteristics of the Algerian Current. – *Journal of Geophysical Research* 95: 1587-1598.
- [10] Audry, S., Schäfer, J., Blanc, G., Jouanneau, J. M. (2004): Fifty-year sedimentary record of heavy metal pollution (Cd, Zn, Cu, Pb) in the Lot River reservoirs (France). – *Environmental Pollution* 132: 413-426.
- [11] Baker, A., Hellstrom, J. C., Kelly, B. F. J., Mariethoz, G., Trouet, V. (2015): A composite annual-resolution stalagmite record of North Atlantic climate over the last three millennia. – *Nature* 5(10307).
- [12] Barberi, F., Principe, C., Rosi, M., Santacroce, R. (1995): Scenario eruttivo al Vesuvio nel caso di riattivazione a medio-breve termine. Aggiornamento al 20 gennaio 1995. – Internal Report National Group for Volcanology, Italian. National Researches Council (GNV) 14.
- [13] Baron, S., Carignan, J., Ploquin, A. (2006): Dispersion of heavy metals (metalloids) in soils from 800-year-old pollution (Mont-Lozère, France). – *Environmental Science & Technology* 40: 5319-5326.

- [14] Baron, S., Lavoie, M., Ploquin, A., Carignan, J., Pulido, M., De Beaulieu, J-L. (2005): Record of metal workshops in peat deposits: history and environmental impact on the Mont Lozère Massif, France. – *Environmental Science & Technology* 39: 5131-5140.
- [15] Barriendos, M., Fernando, R. S. (2006): Study of historical flood events on Spanish rivers using documentary data. – *Hydrological Sciences Journal* 51(5) 765-783.
- [16] Bates, B., Kundzewicz, Z. W., Wu, S., Palutikof, J. (2008): *Climate Change and Water*. – IPCC Working Group II, Geneva.
- [17] Baudrimonta, M., Schäfer, J., Marie, V., Maury-Brachet, R., Bossy, C., Boudou, A., Blanc, G. (2005): Geochemical survey and metal bioaccumulation of three bivalve species (*Crassostrea gigas*, *Cerasto dermaedule* and *Ruditapes philippinarum*) in the Nord Médoc salt marshes (Gironde estuary, France). – *Science of the Total Environment* 337: 265-280.
- [18] Beal, S. A., Erich, C. O., Zdanowicz, C. M., Fisher, D. A. (2015): An ice core perspective on mercury pollution during the past 600 years. – *Environ. Sci. Technol.* 49: 7641-7647.
- [19] Bel Hadj, S. S., Chkir, N., Zouari, K., Cognard-Planc, A. L., Valles, V., Marc, V. (2012): Natural and artificial recharge investigation in the Zéroud Basin, Central Tunisia: impact of Sidi Saad Dam storage. – *Environmental Earth Sciences* 66: 1099-1110.
- [20] Belhouchet, L., Mulazzani, S., Pelegrin, J. (2014): Evolution of a 9th–8th mill. cal BP Upper Capsian site: the techno-typological study of bladelet production at SHM-1 (Hergla, Tunisia). – *Quaternary International* 320: 28-42.
- [21] Benito, G., Díez-Herrero, A., Fernández de Vilalta, M. (2003): Magnitude and frequency of flooding in the Tagus Basin (central Spain) over the last millennium. – *Climatic Change* 58: 171-192.
- [22] Benito, G., Macklin, M. G., Zielhofer, C., Jones, A. F., Machado, M. J. (2015): Holocene flooding and climate change in the Mediterranean. – *Catena* 130: 13-33.
- [23] Besbes, M. M., Chahed, J., Hamdane, A. (2019): *National Water Security*. Chap. 1: The World Water Issues. – Springer, Cham, pp. 1-29.
- [24] Blais, E. L., Clark, S., Dow, K., Rannie, B., Stadnyk, T., Wazney, L. (2015): Background to flood control measures in the Red and Assiniboine River Basins. – *Canadian Water Resources Journal* 41(1-2): 31-44.
- [25] Bozkurt, D., Sen, O. L. (2011): Precipitation in the Anatolian Peninsula: sensitivity to increased SSTs in the surrounding seas. – *Climate Dynamics* 36: 711-726.
- [26] Braje, T. J., Erlandson, J. M. (2013): Human acceleration of animal and plant extinctions: a Late Pleistocene, Holocene, and Anthropocene continuum. – *Anthropocene* 4: 14-23.
- [27] Branca, S., De, Beni, E., Proietti, C. (2013): The large and destructive 1669 AD Etna eruption: reconstruction of the lava flow field evolution and effusion rate trend. – *Bulletin of Volcanology* 75(694): 2-16.
- [28] Briggs, J. C. (2011): Marine extinctions and conservation. – *Mar. Biol.* 158: 485-488.
- [29] Broecker, W. S. (2000): Was a change in thermohaline circulation responsible for the Little Ice Age? – *Proceeding of National Academy Science of the USA* 97(4): 1339-1342.
- [30] Buat-Menard, P. and Arnold, M. (1978): The heavy metal chemistry of atmospheric particulate matter emitted by Mount Etna volcano. – *Geophysical Research Letters* 5: 245-248.
- [31] Calvo, M. (2008): *Minerales de Aragón*. – Prames, Zaragoza.
- [32] Castree, N. (2017): Anthropocene: social science misconstrued. – *Nature* 541: 289.
- [33] Certini, G., Scalenghe, R. (2011): Anthropogenic soils are the golden spikes for the Anthropocene. – *The Holocene* 21(8): 1269-1274.
- [34] Chaldeos, A. (2016): The Greek community of Tunis (XVI-XVIII cent.): aspects of its formation and commercial enterprise. – *Proceedings Ekklesiastikos Pharos* 2014(1): 57 - 67
- [35] Cherni, L., Pakstis, A. J., Boussetta, S., Elkamel, S., Frigi, S., Khodjet-El-Khil, H., Barton, A., Haigh, E., Speed, W. C., Elgaaiied, A. B. A., Kidd, J. R., Kidd, K. K. (2016):

- Genetic variation in Tunisia in the context of human diversity worldwide. – *American Journal of Physical Anthropology* 161: 62-71.
- [36] Church, J. A., White, N. J., Arblaster, J. M. (2005): Significant decadal-scale impact of volcanic eruptions on sea level and ocean heat content. – *Nature* 438: 74-77.
- [37] Corella, J. P., Valero-Garcés, B. L., Wang, F., Martínez-Cortizas, A., Cuevas, C. A., Saiz-Lopez, A. (2017): 700 years reconstruction of mercury and lead atmospheric deposition in the Pyrenees (NE Spain). – *Atmospheric Environment* 155: 97-107.
- [38] Cortesi, N., González-Hidalgo, J. C., Brunetti, M., Martin-Vide, J. (2012): Daily precipitation concentration across Europe 1971-2010. – *Natural Hazards and Earth System Science* 12(9): 2799-2810.
- [39] Cortizas, M. A., Pontevedra-Pombal, X., García-Rodeja, E., NóvoaMuñoz, J. C., Shotyk, W. (1999): Mercury in a Spanish peat bog: archive of climate change and atmospheric metal deposition. – *American Association for the Advancement of Science* 284(5416): 939-942.
- [40] Cortizas, M. A., García-Rodeja, E., Pontevedra Pombal, X., Nóvoa Muñoz, J. C., Weiss, D., Cheburkin, A. (2002): Atmospheric Pb deposition in Spain during the last 4600 years recorded by two ombrotrophic peat bogs and implications for the use of peat as archive. – *Science of the Total Environment* 292(1-2): 33-44.
- [41] Crowley, T. J. (2000): Causes of climate change over the past 1000 years. – *Science* 289: 270-277.
- [42] Crutzen, P. J. (2006): The “Anthropocene”. – In: Ehlers E., Krafft T. (eds.) *Earth System Science in the Anthropocene*. Springer, Berlin, pp. 13-18.
- [43] Crutzen, P. J., Stoermer, E. F. (2000): *Anthropocene Global Change Newsletter*. – *International Geosphere, Biosphere Programme* 41: 17-18.
- [44] Daoud, A. (2013): Feedback on flooding in the city of Sfax (southern Tunisia) from 1982 to 2009: from prevention to the territorialization of risk. – *Revue Géographique de l'Est*. 53: 1-2.
- [45] De Faveri, C., Schmidt, E. C., Simioni, C., Martins, C. D. L., Bonomi-Barufi, J., Horta, P. A., Bouzon, Z. L. (2015): Effects of eutrophic seawater and temperature on the physiology and morphology of *Hypneamusciformis* J. V. Lamouroux (Gigartinales, Rhodophyta). – *Ecotoxicology* 24(5): 1040-1052.
- [46] Dearing, J. A., Hay, K. L., Baban, S. M. J., Huddleston, A. S., Wellington, E. M. H., Loveland, P. J. (1996): Magnetic susceptibility of soil: an evaluation of conflicting theories using a national data set. – *Geophysical Journal International* 127: 728-734.
- [47] Dearing, J. A., Hannam, J. A., Anderson, A. S., Wellington, E. M. H. (2001): Magnetic, geochemical and DNA properties of highly magnetic soils in England. – *Geophysical Journal International* 144: 183-196.
- [48] Degeai, J. P., Devillers, B., Blanchemanche, P., Dezileau, L., Oueslati, H., Tillier, M., Bohbot, H. (2017): Fluvial response to the last Holocene rapid climate change in the Northwestern Mediterranean coastlands. – *Global and Planetary Change* 152: 176-186.
- [49] Degobbi, D., Precali, R., Ivancic, I., Smodlaka, N., Fuks, D., Kveder, S. (2000): Long-term changes in the northern Adriatic ecosystem related to anthropogenic eutrophication. – *International Journal of Environmental Pollution* 13: 495-533.
- [50] Dezileau, L., Sabatier, P., Blanchemanche, P., Joly, B., Swingedouw, D., Cassou, C., Castaings, J., Martinez, P., Grafenstein, Von, U. (2011): Intense storm activity during the Little Ice Age on the French Mediterranean coast. – *Palaeogeography, Palaeoclimatology, Palaeoecology* 299: 289-297.
- [51] Dias, B. B., Hart, M. B., Smart, C. W., Hall-Spencer, J. M. (2010): Modern seawater acidification: the response of foraminifera to high-CO₂ conditions in the Mediterranean Sea. – *Journal of the Geological Society* 167: 843-846.
- [52] Diaz, R. J., Rosenberg, R. (2008): Spreading dead zones and consequences for marine ecosystems. – *Science* 321: 926-929.

- [53] Dorado-Liñán, I., Sanchez-Lorenzo, A., Gutiérrez Merino, E., Planells, O., Heinrich, I., Helle, G., Zorita, E. (2016): Changes in surface solar radiation in Northeastern Spain over the past six centuries recorded by tree-ring $\delta^{13}\text{C}$. – *Climate Dynamics* 47: 937-950.
- [54] Duplay, J., Khedhiriz, S., Semhiy, K., Darragiz, F. (2013): Water quality in a protected natural wetland: sebkhet El Kelbia, Tunisia. – *International Journal of Environmental Studies* 70(1): 33-48.
- [55] Dupont, S., Pörtner, H. (2013): Get ready for ocean acidification. – *Nature* 498: 429.
- [56] Eddy, J. A. (1976): The Maunder minimum. – *Science* 192: 1189-1202.
- [57] Ellouze, M., Abida, H. (2008): Regional flood frequency analysis in Tunisia: identification of regional distributions. – *Water Resources Management* 22: 943-957.
- [58] Elmayel, I., Higuera, P. L., Bouzid, J., Noguero, E. M. G., Elouae, Z. (2019): Heavy Metals Distribution in Soils of an Agricultural Area Impacted by Former Mining Activities: Case of Trozza Mine, Tunisia. – In: Kallel A. et al. (eds.) *Recent Advances in Geo-Environmental Engineering, Geomechanics and Geotechnics, and Geohazards. CAJG 2018. Advances in Science, Technology & Innovation (IEREK Interdisciplinary Series for Sustainable Development)*. Springer, Cham.
- [59] Emeis, K. C., Van Beusekom, J., Callie, U., Ebinghaus, R., Kannen, A., Kraus, G., Möllmann, C. (2015): The North Sea - a shelf sea in the Anthropocene. – *Journal of Marine Systems* 141: 18-33.
- [60] Ennouri, R., Zaaboub, N., Fertouna-Bellakhal, M., Chouba, L., Aleya, L. (2016): Assessing trace metal pollution through high spatial resolution of surface sediments along the Tunis Gulf coast (southwestern Mediterranean). – *Environmental Science and Pollution Research* 23: 5322-5334.
- [61] Essefi, E. (2013): Wet aeolian sedimentology and sequence stratigraphy in Eastern Tunisia: implications for wet aeolian sedimentology and sequence stratigraphy on mars. – Ph. D. Thesis, National Engineering School of Sfax.
- [62] Essefi, E., Tagorti, M. A., Touir, J., Yaich, C. (2014): Past human life in the vicinities of saline systems in Tunisia: the geoarcheological approach to link paleoclimatology, paleoepidemiology, and populations dynamics. – *Arabian Journal of Earth Sciences*.
- [63] Essefi, E., Gharsalli, N., Yaich, C. (2015): Geophysical and geochemical study of the silico- evaporitic sedimentary filling of Boujmal wetland, eastern Tunisia: inferring the climatic signal within groundwater noise. – *Journal of Basic and Applied Research International* 2(1): 14-25.
- [64] Eyrikh, S., Eichler, A., Tobler, L., Malygina, L., Papina, T., and Schwikowski, M. (2017): A 320-year ice-core record of atmospheric Hg pollution in the Altai, Central Asia. – *Environmental Science & Technology* 51(20): 11597-11606.
- [65] Fabry, V. J., Seibel, B. A., Feely, R. A., Orr, J. C. (2008): Impacts of ocean acidification on marine fauna and ecosystem processes. International Council for the Exploration of the Sea ICES. – *Journal of Marine Science* 65(3): 414-432.
- [66] Favalli, M., Mazzarini, F., Pareschi, M. T., Boschi, E. (2004): Role of local wind circulation in plume monitoring at Mt. Etna volcano (Sicily) insight from a mesoscale numerical model. – *Geophysical Research Letters* 31: L09105.
- [67] Feely, I. A., Doney, S. C., Sarah, C. R. (2009): Ocean acidification: present conditions and future changes in a high- CO_2 world. – *Oceanography* 22(4): 36-47.
- [68] Fehri, N. (2014): L'aggravation du risque d'inondation en Tunisie. *Éléments De Réflexion*. – *Géographie Physique et Environnement* 8. <https://doi.org/10.4000/physio-geo.3953>.
- [69] Fincoa, C., Pontoreau, C., Schampera, C., Massuel, S., Hovhannissian, G., Rejib, F. (2018): Time-domain electromagnetic imaging of a clayey confining bed in a brackish environment: a case study in the Kairouan Plain Aquifer (Kelbia salt lake, Tunisia). – *Hydrological Processes*. 32: 3954-3965.
- [70] Fouque, F. (1879): *Santorini and Its Eruptions* (translated and annotated by A. R. McBirney, 1998). – John Hopkins University Press, Baltimore, Maryland, pp. 13-21.

- [71] Gabrieli, J., Barbante, C. (2014): The Alps in the age of the Anthropocene: the impact of human activities on the cryosphere recorded in the Colle Gnifetti glacier. – *Rend. Fis. Acc. Lincei* 25: 71-83.
- [72] Gałuszka, A., Migaszewski, Z. M., Zalasiewicz, J. (2014): Assessing the Anthropocene with geochemical methods. – *Geological Society, London, Special Publications* 395(1): 221-238.
- [73] Gao, C., Robock, A., Self, S., Witter, J. B., Steffenson, J. P. (2006): The 1452 or 1453 A. D. Kuwae eruption signal derived from multiple ice core records: greatest volcanic sulfate event of the past 700 years. – *Journal of Geophysical Research* 111: D12107.
- [74] Gargouri, Z. (2011): Sedimentological and radiochronological study of the deposits of the paralic domain in the golf of Gabes (Sebkha El-Guettiate - Sebkha Dreiaa) (in French). – PhD Thesis, Faculty of Sciences of Sfax.
- [75] Gattuso, J. P., Lavigne, H. (2009): Perturbation experiments to investigate the impact of ocean acidification: approaches and software tools. – *Biogeosciences Discuss* 6: 4413-4439.
- [76] Gazeau, F., Parker, L. M., Comeau, S., Gattuso, J. P., O'Connor, W. A., Martin, S., Portner, H. O., Ross, P. M. (2013): Impacts of ocean acidification on marine shelled molluscs. – *Marine Biology* 160: 2207-2245.
- [77] Ghannem, N., Azri, C., Sarbeji, M., Yaich, C. (2011): Spatial distribution of heavy metals in the coastal zone of "Sfax-Kerkennah" plateau, Tunisia. – *Environmental Progress & Sustainable Energy* 30(2): 221-233.
- [78] Ghannem, N., Gargouri, D., Sarbeji, M. M., Yaich, C., Azri, C. (2014): Metal contamination of surface sediments of the Sfax–Chebba coastal line, Tunisia. – *Environmental Earth Sciences* 72(9): 3419-3427.
- [79] Ghazali, M. (2003): Le cosmopolitisme dans la régence de Tunis à la fin du XVIIIe siècle à travers le témoignage des espagnols. – *Cahiers de la Méditerranée. Du cosmopolitisme en Méditerranée* 67: 85-110.
- [80] Ghosh, A., Patra, P. K., Ishijima, K., Umezawa, T., Ito, A., Etheridge, D. M., Sugawara, S., Kawamura, K., Miller, J. B., Dlugokencky, E. J., Krummel, P. B., Fraser, P. J., Steele, L. P., Langenfelds, R. L., Trudinger, C. M., White, J. W. C., Vaughn, B., Saeki, T., Aoki, S., Nakazawa, T. (2015): Variations in global methane sources and sinks during 1910-2010. – *Atmospheric Chemistry and Physics* 15: 2595-2612.
- [81] Gillings, M. R., Paulsen, I. T. (2014): Microbiology of the Anthropocene. – *Anthropocene* 5: 1-8.
- [82] Gorée, F. (1710): A relation of a new island, which was raised up from the bottom of the sea on the 23rd of May 1707, in the Bay of Santorin, in the Archipelago. – *Philosophical Transactions of the Royal Society* 27: 354-375.
- [83] Gray, S. T., Graumlich, L. J., Betancourt, J. L., and Pederson, G. T. (2004): A tree-ring based reconstruction of the Atlantic Multidecadal Oscillation since 1567 A.D. – *Geophysical Research Letters* 31: L12205.
- [84] Grove, J. M. (2004): *Little Ice Ages: Ancient and Modern*. – Routledge, London.
- [85] Hall-Spencer, J. M., Rodolfo-Metalpa, R., Martin, S., Ransome, E., Fine, M., Turner, S. M., Rowley, S. J., Tedesco, D., Buia, M-C. (2008): Volcanic carbon dioxide vents show ecosystem effects of ocean acidification. – *Nature Research* 454: 96-99.
- [86] Hébert, R., Lovejoy, S. (2017): A scaling model for the Anthropocene climate variability with projections to 2100. – *Geophysical Research Abstracts* 19: 9943.
- [87] Hegerl, G., Luterbacher, J., González-Rouco, F., Tett, S. F. B., Crowley, T., Xoplaki, E. (2011): Influence of human and natural forcing on European seasonal temperatures. – *Nature Geoscience* 4: 99-103.
- [88] Herrera, V. M. V., Mendoza, B., Herrera, G. V. (2015): Reconstruction and prediction of the total solar irradiance: from the Medieval Warm Period to the 21st century. – *New Astronomy* 34: 221-233.

- [89] Hollis, G. E., Kallel, M. R. (1986): Modelling natural and man-induced hydrological changes on Sebkhet Kelbia, Tunisia. – *The Royal Geographical Society* 11(1): 86-104.
- [90] Houghton, J. T., Meiro, Filho, L. G., Callander, B. A., Harris, N., Kattenburg, A., Maskell, K. (1996): *Climate Change 1995: The Science of Climate Change: Contribution of Working Group I to the Second Assessment Report of the Intergovernmental Panel on Climate Change*. – Cambridge University Press.
- [91] Houweling, S., Van der Werf, G. R., Goldewijk, K. K., Röckmann, T., Aben, I. (2008): Early anthropogenic CH₄ emissions and the variation of CH₄ and 13CH₄ over the last millennium. – *Glob. Biogeochem. Cycles* 22(1): GB1002.
- [92] Hunt, B. G. (2006): The Medieval Warm Period, the Little Ice Age and simulated climatic variability. – *Climate Dynamics* 27: 677-694.
- [93] Hurrell, J. W., Kushnir, Y., Visbeck, M., Ottersen, G. (2003): Atlantic Oscillation. – In: Hurrell, J. W., Kushnir, Y., Ottersen, G., Visbeck, M. (eds.) *The North Atlantic Oscillation: Climate Significance and Environmental Impact*. Geophysical Monograph Series 134. AGU, Washington, DC, pp. 1-35.
- [94] IPCC (2007): *Climate Change 2007: The Physical Science Basis*. – In: Solomon, S., Qin, D., Manning, M., Chen, Z., Marquis, M., Averyt, K. B., Tignor, M., Miller, H. L. (eds.) *Contribution of Working Group I to the Fourth Assessment Report of the Intergovernmental Panel on Climate Change*. Cambridge University Press. Cambridge.
- [95] IPCC (2013): *Climate Change 2013: The physical science basis*. – In: Stocker, T. F., Qin, D., Plattner, G.-K., Tignor, M., Allen, S. K., Boschung, J. et al. (eds.) *Contribution of Working Group I to the Fifth Assessment Report of the Intergovernmental Panel on Climate Change*. – Cambridge University Press, New York.
- [96] Irabien, M. J., García-Artola, A., Cearreta, A., Leorri, E. (2015): Chemostratigraphic and lithostratigraphic signatures of the Anthropocene in estuarine areas from the eastern Cantabrian coast (N. Spain). – *Quaternary International* 364: 196-205.
- [97] Iwi, A. M., Hermanson, L., Haines, K., Sutton, R. T. (2012): Mechanisms linking volcanic aerosols to the Atlantic meridional overturning circulation. – *Journal of Climate* 25: 3039-3051.
- [98] James, P. M. S., Kettner, A. (2011): Sediment flux and the Anthropocene. – *Philosophical Transactions of the Royal Society* 369: 957-975.
- [99] Jordà, G., Sánchez-Román, A., Gomis, D. (2017): Reconstruction of transports through the strait of gibraltar from limited observations. – *Climate Dynamics* 48(3): 851-865.
- [100] Kadomura, H. (2005): climate anomalies and extreme events in Africa in 2003, including heavy rains and floods that occurred during northern hemisphere summer. – *African Study Monographs* 30: 165-181.
- [101] Kaye, A. (2005): The effects of mine drainage water from Carrock Mine on the water quality and benthic macroinvertebrate communities of Grainsgill Beck: a preliminary study. – *Earth & Environment* 1: 120-154.
- [102] Kchouk, S., Braiki, H., Habaieb, H., Burte, J. (2015): The lowlands of the Kairouan plain: from marginalized land to places for agricultural experimentation (in French). – *Cahiers Agricultures* 24: 404-411.
- [103] Khedhiri, S., Semhi, K., Duplay, J., Darragi, F. (2011): Comparison of sequential extraction and principal component analysis for determination of heavy metal partitioning in sediments: the case of protected Lagoon El Kelbia (Tunisia). – *Environmental Earth Sciences* 62: 1013-1025.
- [104] Kroeker, K. J., Kordas, R. L., Crim, R., Hendriks, I. E., Ramajo, L., Singh, G. S., Duarte, C. M., Gattuso, J. P. (2013): Impacts of ocean acidification on marine organisms: quantifying sensitivities and interaction with warming. – *Global Change Biology* 19(6): 1884-1896.
- [105] La Violette, P. E. (1987): Portion of Western Mediterranean Circulation Experiment completed. – *EOS* 68(9): 123-124.
- [106] Lacarra, J. M. (1972): *Aragon en el pasado*. – Espasa-Calpe, Madrid.

- [107] Lambert, S. J., Davy, A. J. (2010): Water quality as a threat to aquatic plants: discriminating between the effects of nitrate, phosphate, boron and heavy metals on charophytes. – *New Phytologist* 189: 1051-1059.
- [108] Lebreton, V., Jaouadi, S., Mulazzani, S., Boujelben, A., Belhouchet, L., Gammar, A. M., Fouache, E. (2015): Early oleiculture or native wild *Olea* in eastern Maghreb: new pollen data from the sebkha-lagoon Halk el Menjel (Hergla, Central Tunisia). – *Environmental Archaeology* 20(3): 265-273.
- [109] Leduc, C., Ben Ammar, S., Favreau, G., Beji, R., Virrion, R., Lacombe, G., Tarhouni, J., Aouadi, C., Zenati Chelli, B., Jebnoun, N., Oi, M., Michelot, J. L., Zouari, K. (2009): Impacts of hydrological changes in the Mediterranean zone: environmental modifications and rural development in the Merguellil catchment, central Tunisia/Un exemple d'évolution hydrologique en Méditerranée: impacts des modifications environnementales et du développement agricole dans le bassin-versant du Merguellil (Tunisie centrale). – *Hydrological Sciences Journal* 52(6): 1162-1178.
- [110] Leorri, E., Cearreta, A. (2009): Anthropocene versus Holocene relative sea-level rise rates in the southern Bay of Biscay. – *Geogaceta* 46: 127-130.
- [111] Levin, L. A., Gage, J. D. (1998): Relationships between oxygen, organic matter and the diversity of bathyal macrofauna. – *Deep Sea Research II: Topical Studies in Oceanography* 45: 129-163.
- [112] Levin, L. A., Ekau, W., Gooday, A. J., Jorissen, F., Middelburg, J. J., Naqvi, S. W. A., Neira, C., Rabalais, N. N., Zhang, J. (2009): Effects of natural and human-induced hypoxia on coastal benthos. – *Biogeosciences* 6: 2063-2098.
- [113] Lotze, H. K., Coll, M., Dunne, J. (2011): Historical changes in marine resources, food-web structure and ecosystem functioning in the Adriatic Sea. – *Ecosystems* 14: 198-222.
- [114] Luterbacher, J., Xoplaki, E., Detrich, D., Jones, P. D., Davies, T. D., Portis, D., GonzalezRouco, J. F., Von Storch, H., Gyalistras, D., Casty, C., Wanner, H. (2002): Extending North Atlantic Oscillation reconstructions back to 1500. – *Atmospheric Science Letters*.
- [115] Machado, M. J., Benito, G., Barriendos, M., Rodrigo, F. S. (2011): 500 Years of rainfall variability and extreme hydrological events in southeastern Spain dry lands. – *Journal of Arid Environments* 75: 1244-1253.
- [116] Marcos, M., Tsimplis, M. N., Shaw, A. G. P. (2009): Sea level extremes in southern Europe. – *Journal of Geophysical Research: Oceans* 114. <https://doi.org/10.1029/2008JC004912>.
- [117] Margaritelli, G., Vallefucio, M., Rita, F. D., Capotondi, L., Bellucci, L. G., Insinga, D. D., Petrosino, P., Bonomo, S., Cacho, I., Cascella, A., Ferraro, L., Florindo, F., Lubritto, C., Lurcock, P. C., Magri, D., Pelosi, N., Rettori, R., Lirer, F. (2016): Marine response to climate changes during the last five millennia in the central Mediterranean Sea. – *Global and Planetary Change* 142: 53-72.
- [118] Martin, S., Rodolfo-Metalpa, R., Ransome, E., Rowley, S., Buia, M. C., Gattuso, J. P., Hall-Spencer, J. (2008): Effects of naturally acidified seawater on seagrass calcareous epibionts. – *Biology Letters* 4: 689-692.
- [119] Marx, S. K., Mc. Gowan, H. A., Kamber, B. S., Knight, J. M., Denholm, J., Zawadzki, A. (2014): Unprecedented wind erosion and perturbation of surface geochemistry marks the Anthropocene in Australia. – *Journal of Geophysical Research: Earth Surface* 119(1): 45-61.
- [120] McGregor, H., Coauthors, V. (2015): Robust global ocean cooling trend for the pre-industrial Common Era. – *Nature Geoscience* 8: 671-677.
- [121] McNeill, J. R. (2000): *Something New under the Sun*. – W. H. Norton and Company, New York-London.
- [122] McNeill, J. R., Engelke, P. (2016): *The Great Acceleration: An Environmental History of the Anthropocene Since 1945*. – Belknap Press, Cambridge, MA.

- [123] Meybeck, M. (2001): River Basins under Anthropocene Conditions. – In: Bodungen, B. von, Turner, R. K. (eds.) *Science and Integrated Basin Management*. Dahlem University Press, Dahlem, pp. 275-294.
- [124] Miglietta, M. M., Moscatello, A., Conte, D., Mannarini, G., Lacorata, G., Rotunno, R. (2011): Numerical analysis of a Mediterranean “hurricane” over south-eastern Italy: sensitivity experiments to sea surface temperature. – *Atmospheric Research* 101: 412-426.
- [125] Mischler, J. A., Sowers, T. A., Alley, R. B., Battle, M., McConnell, J. R., Mitchell, L., Popp, T., Sofen, E., Spencer, M. K. (2009): Carbon and hydrogen isotopic composition of methane over the last 1000 years. – *Global Biogeochemical Cycles* 23: GB4024.
- [126] Mulazzani, S., Le Bourdonnec, F. X., Belhouchet, L., Poupeau, G., Zoughlami, J., Dubernet, S., Khedhaier, R. (2010): Obsidian from the Epipalaeolithic and Neolithic eastern Maghreb. A view from the Hergla context (Tunisia). – *Journal of Archaeological Science* 37(10): 2529-2537.
- [127] Müller, G. (1981): The heavy metal pollution of the sediments of the Neckar and its tributaries: an inventory, chemistry in our time. (Die Schwermetallbelastung der Sedimente des Neckars und seiner Nebenflüsse: Eine Bestandsaufnahme.) – *Chemie in unserer Zeit* 105: 157-164 (in German).
- [128] Nieto-Moreno, V., Martínez-Ruiz, F., Gallego-Torres, D., Giralt, S., García-Orellana, J., Masqué, P., Sinninghe Damsté, J. S., Ortega-Huertas, M. (2015): Palaeoclimate and palaeoceanographic conditions in the westernmost Mediterranean over the last millennium: an integrated organic and inorganic approach. – *Holocene Climate Change* 172: 264-271.
- [129] Nriagu, J. O. (1990): Global metal pollution; poisoning the biosphere. – *Environment: Science and Policy for Sustainable Development* 32(7): 7-33.
- [130] Nriagu, J. O. (1996): A history of global metal pollution. – *Science* 272(5259): 223.
- [131] Nriagu, J., Becker, C. (2003): Volcanic emissions of mercury to the atmosphere: global and regional inventories. – *Science of the Total Environment*. 304(1-3): 3-12.
- [132] Olcina, J. (2009): “Cambioclimático y riesgosclimáticos en España”. – *Investigaciones Geográficas* 49: 197-220.
- [133] Olcina, J., Saur, D., Hernández, M., Ribas, A. (2016): Flood policy in Spain: a review for the period 1983-2013. – *Disaster Prevention and Management* 25(1): 1-20.
- [134] Oldfield, F. (2001): Can the magnetic signatures from inorganic fly ash be used to mark the onset of the Anthropocene? – *The Anthropocene Review* 2(1): 3-13.
- [135] Owens, M. J., Lockwood, M., Hawkins, E., Usoskin, I., Jones, G. S., Barnard, L., Schurer, A., Fasullo, J. (2017): The Maunder minimum and the Little Ice Age: an update from recent reconstructions and climate simulations. – *Space Weather and Space Climate* 7(A33).
- [136] Pastor, F., Valiente, J. A., Estrela, M. J. (2015): Sea surface temperature and torrential rains in the Valencia region: modelling the role of recharge areas. – *Natural Hazards and Earth System Sciences* 15(7): 1677-1693.
- [137] Pastor, F., Valiente, J. A., Palau, J. L. (2018): Sea surface temperature in the Mediterranean: trends and spatial patterns (1982-2016). – *Pure and Applied Geophysics* 175: 4017-4029.
- [138] Pettit, L. R., Smart, C. W., Hart, M. B., Milazzo, M. (2015): Seaweed fails to prevent ocean acidification impact on foraminifera along a shallow-water CO₂ gradient. – *Ecology and Evolution* 5(9): 1784-1793.
- [139] Phillips, G., Kelly, A., Pitt, J. A., Sanderson, R., Taylor, E. (2005): The recovery of a very shallow eutrophic lake, 20 years after the control of effluent derived phosphorus. – *Freshwater Biology* 50: 1628-1638.
- [140] Pöschl, U., Shiraiwa, M. (2015): Multiphase chemistry at the atmosphere-biosphere interface influencing climate and public health in the anthropocene. – *Chemical reviews* 115(10): 4440-4475.

- [141] Poulichet, E. F., Resongles, E., Bancon-Montigny, C., Delpoux, S., Freydier, R., Casiot, C. (2017): The environmental legacy of historic Pb-Zn-Ag-Au mining in river basins of the southern edge of the Massif Central (France). – *Environmental Science and Pollution Research* 24: 20725-20735.
- [142] Pradel, N., Cayol, J. L., Fardeau, M. L., Karray, F., Sayadi, S., Alazard, D., Ollivier, B. (2016): Analysis of a population of magnetotactic bacteria of the Gulf of Gabès, Tunisia. – *Environmental Science and Pollution Research* 23(5): 4046-4053.
- [143] Puig, P., Palanques, A., Sanchez-Cabeza, J., Masque, P. (1999): Heavy metals in particulate matter and sediments in the southern Barcelona sedimentation system (North Western Mediterranean). – *Marine Chemistry* 63: 311-329.
- [144] Pyatt, F. B., Gilmore, G., Grattan, J. P., Hunt, C. O., McLaren, S. (2000): An imperial legacy? An exploration of the environmental impact of ancient metal mining and smelting in Southern Jordan. – *Archaeological Science* 27: 771-778.
- [145] Pyle, D. M., Mather, T. A. (2003): The importance of volcanic emissions for the global atmospheric mercury cycle. – *Atmospheric Environment* 37(36): 5115-5124.
- [146] Rabalais, N. N., D'iaz, R. J., Levin, L. A., Turner, R. E., Gilbert, D., Zhang, J. (2010): Dynamics and distribution of natural and human-caused hypoxia. – *Biogeosciences* 7: 585-619.
- [147] Reynaud, S., Leclercq, N., Romaine-Lioud, S., Ferrier-Page, S. C., Jaubert, J., Gattus, J.-P. (2003): Interacting effects of CO₂ partial pressure and temperature on photosynthesis and calcification in a Scleractinian coral. – *Global Change Biology* 9: 1660-1668.
- [148] Ribot, J. (2014): Cause and response: vulnerability and climate in the Anthropocene. – *Journal of Peasant Studies* 41(5): 667-705.
- [149] Rice, K. C., Herman, J. S. (2012): Acidification of Earth: an assessment across mechanisms and scales. – *Applied Geochemistry* 27(1): 1-14.
- [150] Rowell, D. P. (2003): The impact of Mediterranean SSTs on the Sahelian rainfall season. – *Journal of Climate* 16: 849-862.
- [151] Ruddiman, W. F. (2007): The early Anthropogenic hypothesis: challenge and responses. – *Reviews of Geophysics* 45: RG4001.
- [152] Salomons, V., Förstner, U. (1984): *Metals in the Hydrocycle*. – Springer-Verlag, Berlin.
- [153] Salvi, G., Buosi, C., Arbulla, D., Cherchi, A., Giudici, G. D., Ibbà, A., Muro, S., De (2015): Ostracoda and foraminifera response to a contaminated environment: the case of the Ex-Military Arsenal of the La Maddalena Harbour (Sardinia, Italy). – *Micropaleontology* 61(1/2): 115-133.
- [154] Sapart, C. J., Monteil, G., Prokopiou, M., van de Wal, R. S. W., Kaplan, J. O., Sperlich, P., Krumhardt, K. M., van der Veen, C., Houweling, S., Krol, M. C., Blunier, T., Sowers, T., Martinerie, P., Witrant, E., Dahl-Jensen, D., Röckmann, T. (2012): Natural and anthropogenic variations in methane sources during the past two millennia. – *Nature* 490(85).
- [155] Sarkar, A., Ravindran, G., Krishnamurthy, V. (2013): A brief review on the effect of cadmium toxicity: from cellular to organ level. – *International Journal of Bio-Technology and Research* 3(1): 17-36.
- [156] Schleussner, C. F., Feulner, G. (2013): A volcanically triggered regime shift in the subpolar North Atlantic Ocean as a possible origin of the Little Ice Age. – *Climate Past* 9: 1321-1330.
- [157] Seinfeld, J. H., Pandis, S. N. (2006): *Atmospheric Chemistry and Physics: From Air Pollution to Climate Change*. – Wiley, Hoboken.
- [158] Smith, B. D., Zeder, M. A. (2013): The onset of the Anthropocene. – *Anthropocene* 4: 8-13.
- [159] Solomon, S., Quinn, D., Manning, M., Chen, Z., Marquis, M., Averyt, K. B., Tignor, M., Miller, H. (eds.) (2007): *Climate Change 2007: The Physical Science Basis. Contribution of Working Group I to the Fourth Assessment Report of the Intergovernmental Panel on Climate Change*. – Cambridge University Press, New York.

- [160] Steffen, W., Sanderson, R. A., Tyson, P. D., Jäger, J., Matson, P. A., Moore III, B., Oldfield, F., Richardson, K., Schellnhuber, H. J., Turner, B. L., Wasson, R. J. (2004): Global change and the earth system: a planet under pressure. – *Global Change and the Earth System* 332: 258.
- [161] Steffen, W., Grinevald, J., Crutzen, P., McNeill, J. (2011): The Anthropocene: conceptual and historical perspectives. – *Philosophical Transactions of the Royal Society* 369(1938): 842-867.
- [162] Steffen, W., Broadgate, W., Deutsch, L., Gaffney, O., Ludwig, C. (2015): The trajectory of the Anthropocene: the Great Acceleration. – *The Anthropocene Review* 2: 81-98.
- [163] Suárez-Álvarez, S., Gómez-Pinchetti, J. L., García-Reina, G. (2012): Effects of increased CO₂ levels on growth, photosynthesis, ammonium uptake and cell composition in the macroalga *Hypneaspinnella* (Gigartinales, Rhodophyta). – *Journal of Applied Phycology* 24(4): 815-823.
- [164] Tanguy, J. C., Condomines, M., Le Goff, M., Chillemi, V., La Delfa, S., Patané, G. (2007): Mount Etna eruptions of the last 2,750 years: revised chronology and location through archeomagnetic and 226Ra-230Th dating. – *Bulletin of Volcanology* 70: 55-83.
- [165] Tarillon (1715): Relation en forme de journal de la nouvelle isle sortie de la mer dans le Golfe du Santorin. – In: Fleurian D'Armenonville, T. C. (ed.) *Nouveaux memoires des missions de la compagnie de Jesus, dans le Levant*. Nicolas Le Clerc, Paris, pp. 126-161 (in French).
- [166] Testor, P., Bosse, A., Houpert, L., Margirier, F., Mortier, L., Legoff, H., et al. (2018): Multiscale observations of deep convection in the northwestern Mediterranean Sea during winter 2012-2013 using multiple platforms. – *Journal of Geophysical Research: Oceans* 123: 1745-1776.
- [167] Tintore, J., Gomis, D., Alonso, S., Wang, D. P. (1988): A theoretical study of large sea level oscillations in the Western Mediterranean. – *Journal of Geophysical Research* C9: 10797-10803.
- [168] Tripoli, G. J., Medaglia, C. M., Dietrich, S., Mugnai, A., Panegrossi, G., Pinori, S., Smith, E. A. (2005): The 9-10 November 2001 Algerian flood: a numerical study. – *Bulletin of the American Mathematical Society* 86: 1229-1235.
- [169] Turuncoglu, U. U. (2015): Identifying the sensitivity of precipitation of Anatolian peninsula to Mediterranean and Black Sea surface temperature. – *Climate Dynamics* 44(7-8): 1993-2015.
- [170] Ulvrova, M., Paris, R., Nomikou, P., Kelfoun, K., Leibrandt, S., Tappin, D. R., McCoy, F. W. (2016): Source of the tsunami generated by the 1650 AD eruption of Kolumbo submarine volcano (Aegean Sea, Greece). – *Journal of Volcanology and Geothermal Research*. DOI: 10.1016/j.jvolgeores.2016.04.034.
- [171] Volosciuk, C., Maraun, D., Semenov, V., A., Tilinina, N., Gulev, S. K., Latif, M. (2016): Rising Mediterranean Sea surface temperatures amplify extreme summer precipitation in Central Europe. – *Scientific Reports* 6(3245).
- [172] Waldbusser, G. G., Salisbury, J. E. (2013): Ocean acidification in the coastal zone from an organism's perspective: multiple system parameters, frequency domains, and habitats. – *Annual Review of Marine Science* 6: 221-247.
- [173] Wali, A., Kawachi, A., Seddik, M., Bougi, M., Ben Dhia, H., Isoda, H., Tsujimura, M., Ksibi, M. (2015): Effects of metal pollution on sediments in a highly saline aquatic ecosystem: case of the Moknine Continental Sebkh (Eastern Tunisia). – *Bulletin of Environmental Contamination and Toxicology* 94: 511-518.
- [174] Wanner, H., Solomina, O., Grosjean, M., Ritz, S. P., Jetel, M. (2011): Structure and origin of Holocene cold events. – *Quaternary Science Reviews* 30(21-22): 3109-3123.
- [175] Waters, C. N., Zalasiewicz, J. A., Williams, M., Ellis, M. A., Snelling, A. M. (2014): A stratigraphical basis for the Anthropocene? – *Geological Society, London, Special Publications* 395(1): 1-21.

- [176] Waters, C. N., Zalasiewicz, J., Summerhayes, C., Barnosky, A. D., Poirier, C., Gałuszka, A., Jeandel, C. (2016): The Anthropocene is functionally and stratigraphically distinct from the Holocene. – *Science* 351(6269): 26-22.
- [177] Waters, C. N., Zalasiewicz, J., Summerhayes, C., Fairchild, I. J., Rose, N. L., Loader, N. J., Shoty, W., Cearrea, A., Head, M. J., James, P. M., Syvitski, J. M. P., Williams, M., Wapre, M., Barnosky, A. D., Zhisheng, A., Leinfelder, R., Jeandel, C., Gałuszka, A., Ivar do Sul, J. A., Gradstein, F., Steffen, W., McNeill, J. R., Wing, S., Poirier, C., Edgeworth, M. (2018): Global Boundary Stratotype Section and Point (GSSP) for the Anthropocene Series: where and how to look for potential candidates. – *Earth-Science Reviews* 178: 379-429.
- [178] Watts, A. B., Nomikou, P., Moore, J. D. P., Parks, M. M., Alexandri, M. (2015): Historical bathymetric charts and the evolution of Santorini submarine volcano, Greece. – *Geochemistry, Geophysics, Geosystems* 16: 847-869.
- [179] Wilkinson, I. P., Poirier, C., Head, M. J., Sayer, C. D., Tibby, J. (2014): Microbiotic signatures of the Anthropocene in marginal marine and freshwater palaeoenvironments. – *Geological Society* 395(1): 185-219.
- [180] Yamaguchi, David, K. (1983): New tree-ring dates for recent eruptions of Mount St. Helens. – *Quaternary Research* 20(2): 246-250.
- [181] Young, H. S., McCauley, D. J., Galetti, M., Dirzo, R. (2016): Patterns, causes, and consequences of anthropocene defaunation. – *Annu. Rev. Ecol. Evol. Syst* 47: 333-58.
- [182] Yusoff, K. (2013): Geologic life: prehistory, climate, futures in the Anthropocene. – *Environment and Planning D: Society and Space* 31(5): 779-795.
- [183] Zaaboub, N., Virgini, M., Martins, A., Dhib, A., Bejaoui, B., Galgani, F., El Bour, M., Aleya, L. (2015): Accumulation of trace metals in sediments in a Mediterranean Lagoon: usefulness of metal sediment fractionation and elutriate toxicity assessment. – *Environmental Pollution* 207: 226-237.
- [184] Zaïbi, C. (2011): Paleoenvironments Forcing and associated extreme events at the location of the south coast of Skhira during the Holocene: contribution of ostracodes and foraminifera. – PhD Thesis, Faculty of Sciences of Sfax (in French).
- [185] Zalasiewicz, J., Cearreta, A., Crutzen, P., Ellis, E., Ellis, M., Grinevald, J., McNeill, J., Poirier, C., Price, S., Scholes, M., Steffen, W., Vidas, D., Waters, C., Williams, M., Wolfe, A. P. (2012): Response to Autin and Holbrook on “Is the Anthropocene an issue of stratigraphy or pop culture?” – *Comments & Replies* 22: 21. DOI: 10.1130/GSATG162C.
- [186] Zonneveld, K. A. F., Chena, L., Elshanawanya, R., Fischerb, H. W., Hoina, M., Ibrahimc, M. I., Pittauerova, D., Versteegha, G. J. M. (2012): The use of dinoflagellate cysts to separate human-induced from natural variability in the trophic state of the Po River discharge plume over the last two centuries. – *Marine Pollution Bulletin* 64(1): 114-132.

INFLUENCE OF ECOLOGICAL PARAMETERS ON GROWTH OF BUSH TEA (*ATHRIXIA PHYLOCOIDES* DC.) IN LIMPOPO PROVINCE, SOUTH AFRICA

TSHIKHUDO, P. P.^{1*} – NTUSHELO, K.¹ – KANU, S. A.¹ – MUDAU, F. N.^{1,2}

¹University of South Africa, College of Agriculture and Environmental Sciences, Department of Agriculture and Animal Health, Private Bag X6, Science Campus, Florida 1710, South Africa

²School of Agricultural, Earth and Environmental Sciences, University of KwaZulu-Natal, Private Bag X01, Scottsville 3209, Pietermaritzburg, South Africa

*Corresponding author
e-mail: tshikhudopp@gmail.com

(Received 23rd Apr 2019; accepted 11th Jul 2019)

Abstract. The influence of ecological factors on the growth of bush tea was studied at Haenertsburg, Witvlag, and two sites at Khalavha in the Limpopo Province of South Africa in three consecutive years viz., 2014, 2016 and 2017, respectively. In each site, a hundred meter transect divided into one square meter quadrats five meters apart was laid. In each quadrat, bush tea plants were counted manually. Plant height and stem diameter were measured and leaves were counted for each plant. Bush tea density, frequency, abundance, ground cover and species richness were also recorded. Higher bush tea density, frequency, abundance, species richness and ground cover were positively correlated with the plant height, stem diameter and number of leaves per plant within the plant community. Bush tea density, frequency and abundance had the highest influence on the number of leaves and plant height. Plant ground cover and species richness influenced plant height, stem diameter and number of leaves the most. This study provided understanding on effect of ecological parameters on growth of bush tea individuals in a plant community in order to establish large scale bush tea plantations.

Keywords: abundance, density, frequency, ground cover, species richness

Introduction

Bush tea (*Athrixia phylocoides* DC.) is a shrub with high potential currently being utilized as a traditional medicine for cleansing blood, treating ailments such as boils, headaches, infested wounds and coughing. Biochemical profiling of bush tea has shown that it possesses significant compounds such as 5-hydroxyl - 6,7,8,3',4',5'-hexamethoxy flavon- 3- ol (Mashimbye et al., 2006; Mavundza et al., 2010), 3-O-demethyldigicitrin, 5,6,7,8,3',4'-hexamethoxyflavone and quecetin, total polyphenols (Mudau et al., 2007a,b), tannins (Mudau et al., 2007b) and total antioxidants (Mogotlane et al., 2007).

However, as a member of a plant community bush tea interacts with other plant species and the environment. These interactions determine the growth of bush tea. In areas of favourable conditions bush tea plants are likely to produce more biomass and in marginal areas growth is likely to be stifled. The intention of plant community ecologists is to understand these dynamics and the occurrence and abundance of certain species in space and time (Loreau et al., 2001; Rehfeldt et al., 2006).

For various plant species, it is known how ecological dynamics influence the growth of the plant such as in the studies of Tilman (1988), Weiner (1988) and Bardgett et al. (2005), which recorded various aspects of plant species interactions. Bush tea height, stem diameter and number of leaves per plant significantly ($p < 0.01$) increased with

average daily rainfall (39.85 mm), average relative humidity (63.83%) and average temperature (29.21°C) in Limpopo Province, South Africa (Tshikhudo et al., 2019). However, knowledge on the influence of bush tea density, bush tea frequency, bush tea abundance, species richness and ground cover on growth of bush tea has not been generated. The goal of the present study was to test whether relationships exist between density, frequency, abundance, species richness and ground cover that influence growth of bush tea.

Materials and methods

Study area, measurement of plant growth and plant community parameters

Four roadside and easily accessible areas in Haenertsburg (23°56'21"S, 29°53'27"E), Khalavha Site 1 (22°55'43"S, 30°77'37"E), Khalavha Site 2 (22°55'41"S, 30°17'20"E), and Witvlag (22°58'44"S, 29°57'07"E), all situated in the Limpopo Province of South Africa were selected for the current study (*Figure 1*). Three site visits were conducted on 14 November 2014, 12 January 2016 and on 09 January 2017.

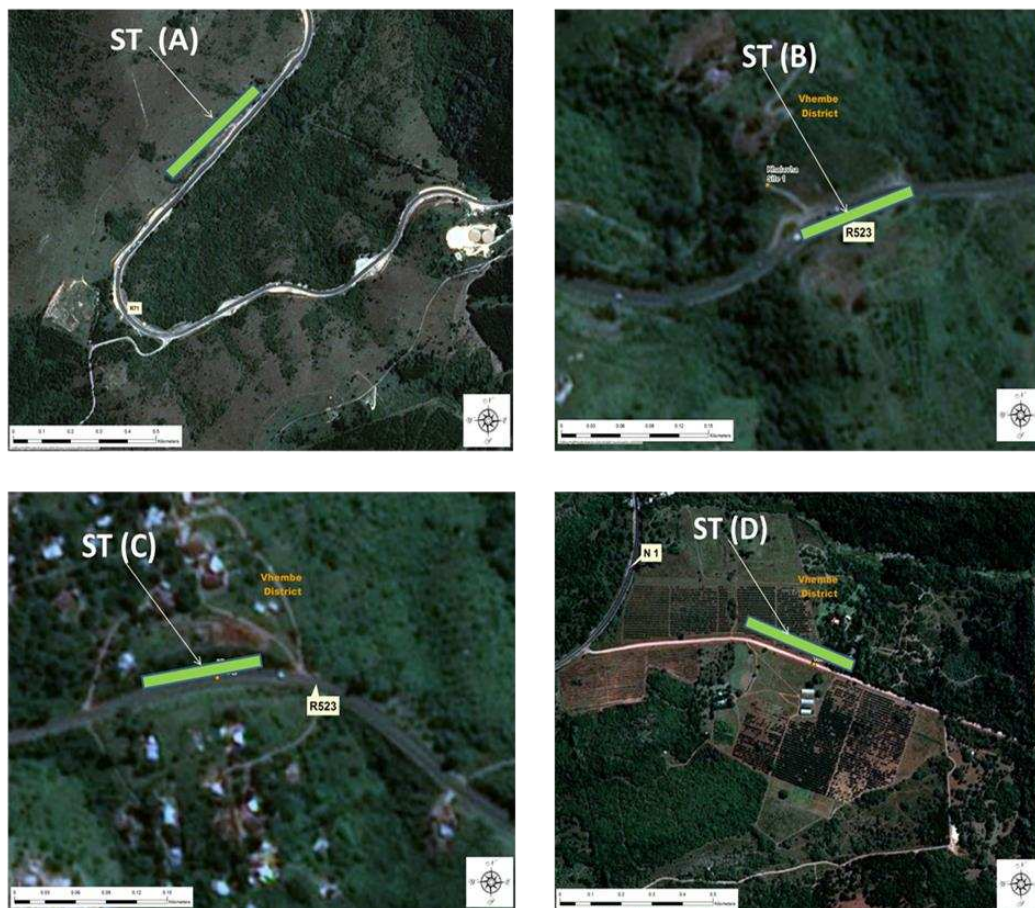


Figure 1. Sampling locations for bush tea (*Athrixia phylcooides* DC.) in the study sites (Haenertsburg (A), Khalavha Site 1 (B), Khalavha Site 2 (C) and Witvlag (D)) in Limpopo Province. A 100 metre site transect (ST) was used for sampling 1 m² quadrats at each sampling site

In each of the four selected sites, a hundred meter transect divided into one square meter quadrats five meters (i.e 20 quadrats per transect) apart was laid. In each quadrat, bush tea plants were counted. Plant height and stem diameter were measured using tape measure and vernier caliper. The leaves were counted for each plant. Bush tea density, frequency, and abundance were calculated with reference to the methods performed by Curtis and Melntoch (1950); and Mueller-Dombois and Ellenberg (1974) as shown in *Equations 1–3*:

$$BT_{density} = \left(\frac{\text{Total number of BT in all quadrats on a transect}}{\text{Total number of quadrats studied on a transect}} \right) \quad (\text{Eq.1})$$

$$BT_{frequency} = \left(\frac{\text{Total number of BT in all quadrats on a transect}}{\text{Total number of quadrats studied on a transect}} \right) \times 100 \quad (\text{Eq.2})$$

$$BT_{abundance} = \left(\frac{\text{Total number of BT in all quadrats on a transect}}{\text{Total total number of quadrats in which BT occurred on a transect}} \right) \quad (\text{Eq.3})$$

where, $BT_{density}$ (BT_d) refers to an expression of the numerical strength of a bush tea plant where the total number of bush tea individuals in all the quadrats is divided by the total number of quadrats studied, $BT_{frequency}$ (BT_f) is the degree of dispersion of bush tea plants in an area and usually expressed in terms of percentage occurrence, $BT_{abundance}$ (BT_a) is the number of individuals of different species in the community per unit area, and BT stands for bush tea individuals studied.

Number of each plant species was calculated in each quadrat to determine species richness. Plant ground cover (vegetation litter, plant debris and living plants) was estimated based on field observations.

Data analysis

The data on bush tea growth parameters were correlated with ecological parameters using Pearson correlations in Statistica, Version 2010 (StatSoft Inc., Tulsa, OK, USA). A plant community with high correlation coefficient with any plant growth parameter was assumed to have had the biggest influence on that particular parameter.

Results

The current study revealed that increased bush tea density, frequency, abundance, species richness and ground cover were positively correlated with the plant height, stem diameter and numbers of leaves per plant within the plant community. Bush tea density, frequency and abundance had the highest influence on the number of leaves and plant height.

Bush tea community analysis and growth parameters

In all sampling periods (three consecutive years viz., 2014, 2016 and 2017, respectively), 855 bush tea individuals were assessed for their abundance, density, frequency, ground cover they occupy and number of plant species co-existing with bush tea (*Table 1*). Plant height and stem diameter measurements, leaf counts per plant during all survey periods in all sampling sites are also appearing in *Table 1*. In terms of abundance, bush tea individuals ranged from 8.5 to 10.3 on 1 m² quadrat along 100 m transect during all sampling periods in all study sites. Density of bush tea individuals

ranged from 2.9 to 3.9 plants per quadrat with a frequency of 32.5-38.7% during all survey periods in all sampling times. Number of different plant species recorded in all areas during all survey periods ranged from 3.5-9.1 mixed with vegetation litter and debris covered about 30.2-83.2% of ground. On average, bush tea plant height ranged from 126.3 to 509.5 mm, with a stem diameter ranging from 1.3-4.7 mm, and 100.8-494 leaves per plant (*Table 1*).

Table 1. Bush tea density, frequency and abundance values at Haenertsburg, Khalavha Site 1, Khalavha Site 2 and Witvlag during all survey periods. Plants sampled on the different sampling dates. The count of plants is for the entire 100 m transect laid during the survey in all the three survey dates growth parameters of naturally growing bush tea

Sampling date	Parameter	Haenertsburg	Khalavha Site 1	Khalavha Site 2	Witvlag	Average
14 November 2014	n	114	23	110	48	73.7
	BT _d	2.8	1.1	5.4	2.3	2.9
	BT _f (%)	30.0	25.0	50.0	25.0	32.5
	BT _a	9.3	4.4	10.9	9.4	8.5
	SP	3.5	4.0	3.1	3.5	3.5
	PGC (%)	35.1	29.5	11.3	45.0	30.2
	Pant height (mm)	128.6	121.1	135.1	120.7	126.3
	Stem diameter (mm)	1.3	1.4	1.5	1.2	1.3
	Number of leaves per plant	136.0	84.5	97.6	85.4	100.8
15 January 2016	n	32	35	113	60	60.0
	BT _d	3.2	1.7	5.6	2.9	3.3
	BT _f (%)	30.0	35.0	55.0	30.0	37.5
	BT _a	10.6	5.0	10.1	11.8	9.3
	SP	6.4	6.3	6.8	6.6	6.5
	PGC (%)	5.7	42.7	56.5	64.6	42.3
	Pant height (mm)	256.8	416.8	468.5	410.3	388.1
	Stem diameter (mm)	2.4	3.9	3.8	3.8	3.4
	Number of leaves per plant	222.3	402.6	390.5	402.8	354.5
12 January 2017	n	82	41	113	84	80.0
	BT _d	4.0	2.0	5.7	4.2	3.9
	BT _f (%)	35.0	35.0	55.0	30.0	38.7
	BT _a	11.5	5.7	10.3	14.0	10.3
	SP	9.4	9.5	7.8	9.8	9.1
	PGC (%)	85	82.8	83.4	81.8	83.2
	Pant height (mm)	472.6	538.6	496.4	530.7	509.5
	Stem diameter (mm)	4.2	5.1	4.3	5.5	4.7
	Number of leaves per plant	464.3	521.1	467.5	523.1	494.0

BT_d = Bush tea density, BT_f = Bush tea frequency, BT_a = Bush tea abundance, SR = Species richness, PGC = Plant ground cover, n = Number of bush tea individuals present and assessed) (N=855)

Relationship between plant community and bush tea growth

Plant community parameters correlated strongly with the growth of bush tea in all sites (Haenertsburg, Witvlag, Khalavha Site 1 and Khalavha Site 2 in the Limpopo Province. Increased plant height, stem diameter and the number of leaves per plant were associated with increased ground cover, species richness, bush tea density, frequency and bush tea abundance across all the four study (*Table 2*).

Table 2. Correlation between bush tea density, bush tea frequency, bush tea abundance, species richness and plant ground cover with the growth of bush tea at Haenertsburg (A), Khalavha Site 1 (B), Khalavha Site 2 (C) and Witvlag (D) during all survey times

Ecological parameters	Plant height (mm)				Stem diameter (mm)				Number of leaves per plant			
	A	B	C	D	A	B	C	D	A	B	C	D
BT _d	0.87 (p=0.000)	0.87 (p=0.000)	0.80 (p=0.000)	0.92 (p=0.000)	0.64 (p=0.000)	0.89 (p=0.000)	0.86 (p=0.000)	0.88 (p=0.000)	0.86 (p=0.000)	0.94 (p=0.000)	0.80 (p=0.000)	0.90 (p=0.000)
BT _f	0.87 (p=0.000)	0.87 (p=0.000)	0.80 (p=0.000)	0.92 (p=0.000)	0.64 (p=0.000)	0.89 (p=0.000)	0.86 (p=0.000)	0.88 (p=0.000)	0.86 (p=0.000)	0.94 (p=0.000)	0.80 (p=0.000)	0.90 (p=0.000)
BT _a	0.87 (p=0.000)	0.87 (p=0.000)	0.80 (p=0.000)	0.92 (p=0.000)	0.64 (p=0.000)	0.89 (p=0.000)	0.86 (p=0.000)	0.88 (p=0.000)	0.86 (p=0.000)	0.94 (p=0.000)	0.80 (p=0.000)	0.90 (p=0.000)
SP	0.73 (p=0.000)	0.49 (p=0.000)	0.61 (p=0.000)	0.76 (p=0.000)	0.61 (p=0.000)	0.51 (p=0.000)	0.74 (p=0.000)	0.72 (p=0.000)	0.72 (p=0.000)	0.51 (p=0.000)	0.62 (p=0.000)	0.74 (p=0.000)
PGC	0.58 (p=0.000)	0.42 (p=0.000)	0.75 (p=0.000)	0.92 (p=0.000)	0.45 (p=0.000)	0.40 (p=0.000)	0.80 (p=0.000)	0.88 (p=0.000)	0.55 (p=0.000)	0.44 (p=0.000)	0.76 (p=0.000)	0.89 (p=0.000)

Correlations between variables were assessed using Pearson rank correlation test. R² values are considered significant at P ≤ 0.05. BT_d = Bush tea density, BT_f = Bush tea frequency, BT_a = Bush tea abundance, SR = Species richness, PGC = Plant ground cover

In all four study sites at Haenetsburg, Khalavha 1, Khalavha 2 and Witvlag, bush tea density, frequency and abundance positively and strongly correlated ($R^2 > 0.86$; $p < 0.01$) with plant heights of bush tea across all the four study sites (*Table 2*). Results of the current study showed that bush tea density, density and abundance positively and strongly correlated ($R^2 > 0.81$; $p < 0.01$) with stem diameter of bush tea in all four study sites (*Table 2*). Similarly, bush tea density, density and abundance positively and strongly correlated ($R^2 > 0.87$; $p < 0.01$) with bush tea's number of leaves per plant across all four study sites (*Table 2*).

In the current survey of plant community analysis, species richness strongly correlated ($0.61 \leq R^2 \leq 0.68$; $p < 0.01$) with growth of bush tea in terms of plant height in all four sites (*Table 2*). Species richness also had a strong relationship ($0.61 \leq R^2 \leq 0.68$; $p < 0.01$) with the bush tea stem diameter across all four sites (*Table 2*).

There was a strong relationship between species richness and bush tea number of leaves per plant in all four areas ($R^2 > 0.64$; $p < 0.01$; *Table 2*). During the current study it was evident that in sites where the species richness was high the bush tea plant outgrew other plant species within the community.

The results presented in *Table 2* indicate that there was a strong influence of plant ground cover on growth of bush tea plant in terms of bush tea plant height ($0.58 \leq R^2 \leq 0.75$; $p < 0.01$) in all four sites. Plant ground cover also had a positive and significant relationship with bush tea stem diameter ($0.60 \leq R^2 \leq 0.75$; $p < 0.01$; *Table 2*) across all four sites. The number of leaves per bush tea plant had a positive and significant correlation with ground cover ($0.60 \leq R^2 \leq 0.72$; $p < 0.01$; *Table 2*) in all four selected sites.

Bush tea density, frequency and abundance had the highest influence on number of leaves and plant height. Plant ground cover and species richness influenced plant height, stem diameter and number of leaves the most (*Table 2* and *Table 3*). Ranking of the ecological factors' influence on bush tea growth parameters seems to indicate that bush tea density, bush tea frequency, and bush tea abundance ranked higher than species richness and plant ground cover in all selected study sites (*Table 3*).

Table 3. Ranking of the level of influence of ecological factors on the plant growth parameters

Rank	Plant height (mm)				Stem diameter (mm)				No of leaves per plant			
	A	B	C	D	A	B	C	D	A	B	C	D
Rank 1	BT _d ,	BT _d ,	BT _d ,	BT _d ,	BT _d ,	BT _d ,	BT _d ,	BT _d ,	BT _d ,	BT _d ,	BT _d ,	BT _d ,
	BT _f ,	BT _f ,	BT _f ,	BT _f ,	BT _f ,	BT _f ,	BT _f ,	BT _f ,	BT _f ,	BT _f ,	BT _f ,	BT _f ,
	BT _a	BT _a	BT _a	BT _a	BT _a	BT _a	BT _a	BT _a	BT _a	BT _a	BT _a	BT _a
Rank 2	SR	SR	PGC	SR	SR	SR	PGC	SR	SR	SR	PGC	PGC
Rank 3	PGC	PGC	SR		PGC	PGC	SR		PGC	PGC	SR	SR

A = Haenetsburg, B = Khalavha Site 1, C = Khalavha Site 2, D = Witvlag, BT_d = Bush tea density, BT_f = Bush tea frequency, BT_a = Bush tea abundance, SR = Species richness, PGC = Plant ground cover

Discussion

Understanding the relationship between ecological parameters and growth of plant is crucial to assess species adaptation in a particular area. The current study has revealed how plant density, frequency, abundance, species richness and ground cover can influence the vegetative growth of wild bush tea (*Athrixia phylicoides*). Bush tea density, frequency, abundance, species richness and ground cover at Haenertsburg, Khalavha Site 1, Khalavha Site 2 and Witvlag in the Limpopo Province positively correlated with plant height, stem diameter and number of leaves of *A. phylicoides*. It was evident in the study sites that bush tea plant height, stem diameter and number of leaves were all higher at all study sites that had higher bush tea density, frequency, abundance, species richness and ground cover (*Table 1*).

Looking at the fact that associations of ecological factors and vegetative growth of plant are often complex, densities of individual species and the overall plant species diversity are often inversely related in natural communities and interact to affect plant populations (Bach and Hruska, 1981). Densities and individual plant weights together determine yield per unit area. Net primary production (NPP) is the rate of change in yield per unit area. Increases in biomass from growth, decreases from mortality, and tissue-nutrient concentrations provide the necessary information for evaluation of changing nutrient pools (Clark, 1990). The results of the current study may be associated with the density-plant-weight relationships and Michaelis-Menten uptake dynamics for light and below-ground resources that influence the individual plant's growth and population mortality on the timing of NPP. This may also influence the relationship between NPP and rate of individual plant weight gain, resource limitation, and below-ground resource pool size (Clark, 1990).

Plant density is an important ecological parameter that manipulates micro environment and affects growth, development and yield formation of plants (Rahman et al., 2011; Turbin et al., 2014). Plant height and number of branches per plant influence the canopy closure and therefore, they contribute to light interception by the plant. Species that are restricted in their geographic distribution tend to be scarce whereas widespread species are likely to occur at high densities (Verberk, 2011). In the current study, bush tea abundance was estimated by recording species presence in 100 m² transects in the study sites. The abundance and distribution of each species are limited by the combination of physical and biotic environmental variables that determines the multidimensional niche (Brown, 1984). This was probably the situation in the four study sites visited in this field study where bush tea plants were found mostly abundant in the wild along roadsides (*Table 1*).

The relationship between species richness and productivity is an example where different patterns have been found at different scales, and hence different models were used to explain variation in species richness at different scales (Waide et al., 1999; Grytnes, 2000). Increased resources available to plant may lead to greater productivity leading to greater cover and height of shrubs (Harper et al., 2018). Inter-specific competition among plant species during early stages of plant establishment can influence individual plant growth and determine subsequent development patterns of plant community (Boyden et al., 2009). Competitive interactions in young plants are positively related to photosynthetic capacity and relative growth rates that have strong positive correlations with plant traits such as specific leaf area and leaf area ratio (Boyden et al., 2009). As seen in all the study sites in the Limpopo Province, bush tea grows together with about 6 to 9 species of broad-leaved annual plants and graminoids.

Ground cover is another useful variable in soil protection and evapotranspiration estimations (Mullan and Reynolds, 2010). Percent ground cover analysis is typically used to estimate abundance of ground vegetation (Mueller-Dombois and Ellenberg, 1974; Chiarucci et al., 1999). In the current study, the percentage ground cover had a strong positive correlation with growth of bush tea plant in terms of height, stem diameter and number of leaves per plant (*Table 2*). From the study conducted by Harper et al. (2018) to determine the patterns of shrub abundance and relationships with other plant types within the forest–tundra ecotone in northern Canada, it was found that in the ecotone there were positive correlations of short and medium-tall shrubs with graminoids, forbs, and sphagnum, and negative correlations with lichens, other moss, and trees (only with trees for medium-tall shrubs) at very fine scales.

On the other hand, the tundra, shrub richness was negatively correlated with the cover of graminoids, forbs, and non-sphagnum moss, but positively correlated with lichens. The relationships between biomass and percentage cover can be used in ecosystem and carbon-cycle modelling for estimation of the aboveground biomass of plants (Naeem et al., 1994; Tilman et al., 2001; Muukkonen et al., 2006). Since bush tea is grown in open herbaceous vegetation, plant growth may be limited by the availability of below ground resources in unproductive habitats - or by the maximum growth rates of species - early phase of vegetation regeneration after disturbance in productive habitats.

He et al. (2018) determined whether shrubs facilitate or have negative effects on neighbouring herbaceous vegetation, and such effects vary with herb growth stage and with shrub orientation relative to herbs, and found that species number of herb-layer plants tended to increase from beneath the canopy to the opening, but plant density, cover and plant height decreased with distance away from shrub base. It was found that the presence of *Reaumuria soongorica* had positive effects on density, cover, and plant height, and negative on the number of herbaceous species during the entire growing season. Furthermore, Gatti et al. (2017) determined the relationship between vascular plant species richness and average forest canopy height and discovered a significant strong correlation between species richness and plant height. In agreement with findings in the current study, a strong positive correlation was found between species richness and bush tea plant height in three of the study sites (Haenertsburg (73%); Khalavha Site 2 (61%) and Witvlag (73%)), however, in Khalavha Site 1, the correlation was relatively weak (49%) (*Table 2*).

The species composition of total woody plants and their seedlings can be similar in various habitats, including both closed and open canopies (Sharma et al., 2016). In the current study, bush tea plants and their seedlings were noted to occur in plant communities that were composed other broad-leaved and grass species. However, the assessment of density, frequency and density was only focused on bush tea individuals. Species with fast growth rate have greater potential of making a higher ground cover percentage over a shorter period of time. All the surveyed sites were dominated by both shrubs and grasses during all survey times.

It is important to take into consideration that other key factors such as climatic factors, soil fertility and plant characteristics play a role in the growth of plants in the wild. Previous studies on climatic conditions demonstrated that rainfall, relative humidity and temperature determined plant height, stem diameter and leaf number in wild bush tea in the Limpopo Province (Tshikhudo et al., 2019). In terms of soil fertility fertilizer combinations of 300 N, 300 P and 200 K (kg ha^{-1}), an increased fresh and dry

shoot mass, number and area of leaves, as well as the concentrations of total polyphenols in bush tea plant were reported, regardless of the season (Mudau et al., 2007a).

Conclusion

From this study, in general, based on the different growth stages of bush tea plant, its distribution along road sides at Haenertsburg, Witvlag, Khalavha Site 1 and Khalavha Site 2 was common in plant communities with other plant species. Bush tea plants showed optimum values of density, frequency and abundance in most plant communities in all study sites. Bush tea plants seem to have a good competitive ability to actively grow in the wild, together with other plant species. The bush tea plant height, stem diameter and number of leaves per plant significantly increased as the survey seasons progressed. In all study sites, the bush tea growth parameters (height, stem diameter and number of leaves) positively correlated with ground cover, species richness, bush tea density, frequency and bush tea abundance. This study has provided an understanding of the influence of ecological factors on bush tea's growth in a plant community. Effect of ecological parameters such as ground cover, species richness, density, frequency and abundance should not be neglected when determining competitive ability of bush tea during commercial cultivation. However, future studies should be conducted to investigate the phyto-sociological survey on weed species together with bush tea plants.

Acknowledgements. We greatly appreciate the assistance we received from our colleagues, Dr Ronald Nnzeru, Mr Livhuwani Nemutandani, Mr Khathutshelo Maedza and Mr Mpho Nematswerani. This study was funded partially by the National Research Foundation (NRF) grant (TTK 1206051038).

Conflicts of Interests. The authors declare that they have no conflicts of interests.

REFERENCES

- [1] Bach, C. E., Hruska, A. J. (1981): Effects of Plant Density on the Growth, Reproduction and Survivorship of Cucumbers in Monocultures and Polycultures. – *Journal of Applied Ecology* 18(3): 929-943.
- [2] Bardgett, R. D., Bowman, W. D., Kaufmann, R., Schmidt, S. K. (2005): A temporal approach to linking aboveground and belowground ecology. – *Trends in ecology & evolution* 20(11): 634-641.
- [3] Boyden, S. B., Reich, P. B., Puettmann, K. J., Baker, T. R. (2009): Effects of density and ontogeny on size and growth ranks of three competing tree species. – *Journal of Ecology* 97: 277-288.
- [4] Brown, J. H. (1984): On the relationship between abundance and distribution of species. – *The American Naturalist* 124(2): 255-279.
- [5] Chiarucci, A., Wilson, J. B., Anderson, B. J., De Dominicis, V. (1999): Cover versus biomass as an estimate of species abundance: does it make a difference to the conclusions? – *Journal of Vegetation Science* 10(1): 35-42.
- [6] Clark, J. S. (1990): Integration of Ecological Levels: Individual Plant Growth, Population Mortality and Ecosystem Processes. – *Journal of Ecology* 78(2): 275-299.
- [7] Curtis, J. T., McIntosh, R. P. (1950): An upland forest continuum in the prairie-forest border region of Wisconsin. – *Ecology* 32: 476-496.

- [8] Gatti, R. C., Di Paola, A., Bombelli, A., Noce, S., Valentini, R. (2017): Exploring the relationship between canopy height and terrestrial plant diversity. – *Plant Ecology* 218(7): 899-908.
- [9] Grytnes, J. A. (2000): Fine-scale vascular plant species richness in different alpine vegetation types: relationships with biomass and cover. – *Journal of Vegetation Science* 11(1): 87-92.
- [10] Harper, K. A., Lavalley, A. A., Dodonov, P. (2018): Patterns of shrub abundance and relationships with other plant types within the forest–tundra ecotone in northern Canada. – *Arctic Science* 4: 691-709.
- [11] He, Y., Liu, X., Xie, Z. (2014): Shrub Effects on Herbaceous Vegetation Vary with Growth Stages and Herb Relative Location. – *Polish Journal of Ecology* 62(3): 421-429.
- [12] Loreau, M., Naeem, S., Inchausti, P., Bengtsson, J., Grime, J. P., Hector, A., Hooper, D. U., Huston, M. A., Raffaelli, D. (2001): Biodiversity and Ecosystem Functioning: Current Knowledge and Future Challenges. – *Science Compass* 294: 804-808.
- [13] Mashimbye, M. J., Mudau, F. N., Soundy, P., van Ree, T. (2006): A new flavonol from *Athrixia phylloides* (Bush Tea). – *South African Journal of Chemistry* 59: 1-2.
- [14] Mavundza, E. J., Tshikalange, T. E., Lall, N., Hussein, A. A., Mudau, F. N., Meyer, J. J. M. (2010): Antioxidant activity and cytotoxicity effect of flavonoids isolated from *Athrixia phylloides*. – *Journal of Medicinal Plants Research* 4(23): 2584-2587.
- [15] Mogotlane, I. D., Mudau, F. N., Mashela, P. W., Soundy, P. (2007): Seasonal responses of total antioxidant contents in cultivated bush tea (*Athrixia phylloides* D.C.) leaves to fertilizer rates. – *Journal of Medicinal and Aromatic Plant Science and Biotechnology* 1: 77-79.
- [16] Mudau, F. N., Soundy, P., du Toit, E. S. (2007a): Nitrogen, phosphorus and potassium increases on growth and chemical analyses of bush tea (*Athrixia phylloides* L.) as influenced by seasons in a shaded nursery environment. – *HortTechnology* 17(1): 107-110.
- [17] Mudau, F. N., Ngele, A., Mashele, P. W., Soundy, P. (2007b): Seasonal variation of tannin contents in wild bush tea. – *Journal of Medicinal and Aromatic Plant Science and Biotechnology* 1: 74-76.
- [18] Mueller-Dombois, D., Ellenberg, H. (1974): Aims and methods of vegetation ecology. – New York: J. Wiley.
- [19] Mullan, D. J., Reynolds, M. P. (2010): Quantifying genetic effects of ground cover on soil water evaporation using digital imaging. – *Functional Plant Biology* 37: 703-712.
- [20] Muukkonen, P., Mäkipää, R., Laiho, R., Minkkinen, K., Vasander, H., Finér, L. (2006): Relationship between biomass and percentage cover in understorey vegetation of boreal coniferous forests. – *Silva Fennica* 40(2): 231-245.
- [21] Naeem, S., Thompson, L. J., Lawler, S. P., Lawton, J. H., Woodfin, R. M. (1994): Declining biodiversity can alter the performance of ecosystems. – *Nature* 368: 734-737.
- [22] Rahman, M., Hossain, M., Bell, R. W. (2011): Plant density effects on growth, yield and yield components of two soybean varieties under equidistant planting arrangement. – *Asian Journal of Plant Sciences* 10(5): 278-286.
- [23] Rehfeldt, G. E., Crookston, N. L., Warwell, M. V., Evans, J. S. (2006): Empirical Analyses of Plant-Climatic Relationships for the Western United States. – *International Journal of Plant Sciences* 167(6): 1123-1150.
- [24] Sharma, L. N., Grytnes, J. A., Måren, I. E., Vetaas, O. R. (2016): Do composition and richness of woody plants vary between gaps and closed canopy patches in subtropical forests? – *Journal of Vegetation Science* 27(6): 1129-1139.
- [25] Tilman, D. (1988): Plant strategies and the dynamics and structure of plant communities. – Princeton University Press.
- [26] Tilman, D., Reich, P. B., Knops, J., Wedin, D., Mielke, T., Lehman, C. (2001): Diversity and productivity in a long-term grassland experiment. – *Science* 294: 843-845.

- [27] Tshikhudo, P. P., Ntushelo, K., Kanu, S. A., Mudau, F. N. (2019): Growth response of bush tea (*Athrixia phylocooides* DC.) to climatic conditions in Limpopo Province, South Africa. – South African Journal of Botany 121: 500-504.
- [28] Turbin, V. A., Sokolov, A. S., Kosterna, E., Rosa, R. (2014): Effect of plant density on the growth, development and yield of brussels sprouts (*Brassica oleracea* L. var. *gemmifera* L.). – Acta Agrobotanica 67(4): 51-58.
- [29] Verberk, W. (2011): Explaining General Patterns in Species Abundance and Distributions. – Nature Education Knowledge 3(10):38.
- [30] Waide, R. B., Willig, M. R., Steiner, C. F., Mittelbach, G., Gough, L., Dodson, S. I., Juday, G. P., Parmenter, R. (1999): The relationship between productivity and species richness. – Annual review of Ecology and Systematics 30(1): 257-300.
- [31] Weiner, J. (1988): The influence of competition on plant reproduction. – In: Doust, J. L., Doust, L. L. (eds.) Plant Reproductive Ecology: patterns and strategies. pp. 228-245.

THE EFFECTS OF IRRIGATION REGIMES ON SOIL MOISTURE DYNAMICS, YIELD AND QUALITY OF LUCERNE UNDER SUBSURFACE DRIP IRRIGATION

WANG, Y. D.¹ – KOU, D.² – MUNEER, M. A.¹ – FANG, G. J.¹ – SU, D, R.^{1*}

¹College of Grassland Science, Beijing Forestry University, Beijing 100083, China

²State Key Laboratory of Vegetation and Environmental Change, Institute of Botany, Chinese Academy of Sciences, Beijing 100093, China

*Corresponding author

e-mail: suderong@bjfu.edu.cn; phone: +86-10-6233-6284

(Received 17th Sep 2019; accepted 21st Jan 2020)

Abstract. Lucerne (*Medicago sativa* L.), as a grass legume is mowed many times in the Hexi Corridor, PR of China, which holds a vital position in the crop-pasture and animal husbandry. Cultivating high-quality lucerne under such extreme water shortage conditions is a necessary approach to develop regulated deficit irrigation (RDI). However, applications of Regulated Deficit Drip Irrigation (RDDI) needs to be explored further in order to increase both the yield and quality of lucerne. Therefore, the main objective of this study was to investigate the effect of different regulated deficit irrigation on soil moisture (SM) dynamics, yield and quality of lucerne. A field experiment was designed with four deficit irrigation treatments in the year of 2013 and 2017. The lucerne was harvested three times per year. Our results showed that with deficit drip irrigation increasing, the yield was decreased for lucerne crop, crude protein (CP), and relative feed value (RFV), while, the content of CP and RFV was increased. SM was directly proportional to the amount of irrigation volume except high water deficit (HWD). Deep SM showed that annual lucerne SM was greater in HWD than in low water deficit (LWD). The biennial lucerne SM was greater in HWD than in each treatment in most cases. Considering the influence factors of yield, qualities and water use efficiency (WUEs (Including WUE, WUE_{CP} and WUE_{RFV})), it is more appropriate that annual lucerne should not be treated with deficit irrigation. In the following year, the LWD reduced the forage yield, but more or less increased the yield of CP (CP_{yield}) and RFV (RFV_{yield}) to compensate the loss of forage yield.

Keywords: *Medicago sativa* L., regulated deficit irrigation, crude protein, relative feed value, water use efficiency

Introduction

Lucerne (*Medicago sativa* L.), is known as “Queen of Forages” because of its high yield, extraordinary protein quality, and best nutritive value as a forage, plays an important role in crop-pasture and animal husbandry systems all over the world (Bouton, 2012). In the United States, lucerne is the fourth largest crop after maize, wheat and soybean, with an area of over 10 million hectares, accounting for about one third of the world's total cultivated area (Hanson, 2007). In contrast, lucerne planting industry in China is lagging behind and accounts for only 4.5% of the world's total planting area (industry compare to plants area, should be considered further). In addition, lucerne production in China is low and of poor quality. Because the crude protein content of lucerne products varies 16%-20%, which falls between level 2 and 3, (the quality standards issued by the state), and some products have even lower than 16% (Kou et al., 2014). As a resultant, China has become the largest importer of lucerne in the world (www.mofcom.gov.cn/). So, there is an urgent need to increase the large-scale cultivation of lucerne to develop high-yielding and high-quality lucerne industry in China.

Hexi Corridor is located in arid and semi-arid area of Northwest China, where rainfall is scarce and atmospheric evaporative demand is very large, as a resultant limited available water resources have posed a serious threat to the sustainable and stable development of local agriculture and animal husbandry (Kou et al., 2014; Xiao et al., 2015). Therefore, the development of ecological water conservation must be required to improve the water use efficiency of crops in these areas, so that agricultural production can be increased. In this arid and semiarid region, due to water scarcity, it is very difficult to apply the full water requirement of the crop to get maximum growth and yield (Romero et al., 2004). So, it's important to find strategic ways and means to maintain crop yield and growth under water deficit conditions.

Firstly, the subsurface drip irrigation (SDI) is considered as more efficiency method of irrigation for perennial pasture and lucerne (Palacios-Díaz et al., 2009; Kandelous et al., 2012; Lamm et al., 2012; Ismail and Almarshadi, 2013; Montazar et al., 2016). SDI not only reduces the evaporation but also transport the water effectively in the root zone, and as resultant reduce/eliminate the surface runoff and deep seepage (Lamm et al., 2012). Moreover, SDI is considered as the best method because it increases the water use efficiency of lucerne about 20% compared to furrow irrigation (Hutmacher et al., 2001). The lucerne yield is increased about 20% with 40% less irrigation water compared to flood irrigation (Godoy et al., 2003), 7% more yield with 22% less irrigation water than sprinkler irrigation (Alam et al., 2002), while compared with border irrigation, subsurface drip irrigation can increase yield by 30% and water use efficiency by 53% (Trejo et al., 2010).

Secondly, regulated deficit irrigation (RDI), as a kind of artificial water control, which allows plants to suffer a certain water deficit condition, while maintaining or increasing the crop growth and yield (Fereris and Soriano, 2006; Nunes et al., 2008; Geerts and Raes, 2009; Chen et al., 2014). For pasture, especially lucerne, the study of RDI are scarce and mostly focused on the influence of yield under dry irrigation in the midsummer (Hanson et al., 2007), yield under drought and re-watering during the next period (Kou et al., 2014; Liu et al., 2018), and the impact of seasonal drought on yield (Rogers et al., 2016). A study conducted by Hanson (2007) showed that although the re-watered plants could resume their growth in midsummer under deficit irrigation, no irrigation in July and August resulted in lucerne yield reduction about 4.68-6.47 Mg ha⁻¹. Kou (2014) reported that although moderate water deficit reduced lucerne yield, late rehydration could compensate part of the yield, it was still lower than non-deficit treatment. Rogers et al. (2016) suggested that the lucerne stand is able to fully recover once a full irrigation regime is resumed during seasonal drought.

So far, the both methods SDI and RDI have been extensively applied separately, in this study we combined both methods to increase the water use efficiency and forage production, and named it regulated deficit drip irrigation (RDDI). The aim of this study was to determine the effects of different regulated deficit irrigation volume under SDI conditions on soil moisture dynamics, yield and quality of lucerne. At the same time, the results of this experiment were compared with the results of the experiment in 2013.

Materials and methods

Site description

A field experiment with Lucerne (*Medicago sativa* L.) was conducted at the Shiyanghe Experimental Station of China Agricultural University at Wuwei, Gansu Province of

Northwest China (N37°52'20", E102°50'50", altitude 1581 m) (*Figure 1A*). The site has a typical continental temperate climate with mean sunshine duration of 3000 h, mean annual precipitation of 164.4 mm, pan evaporation of 2000 mm, frost-free period of 150 d and mean annual temperature of 8.8°C. Growing-season precipitation and mean temperature daily in 2013 and 2017 are presented in *Figure 2*. The groundwater table is consistently below 25 m (Kandelous et al., 2012). The experimental site has a sandy loam soil with average field capacity of 0.29 cm³ cm⁻³, soil bulk density of 1.50 g cm⁻³ and a permanent wilting point of 0.12 cm³ cm⁻³ in the upper 1 m of the soil profile.

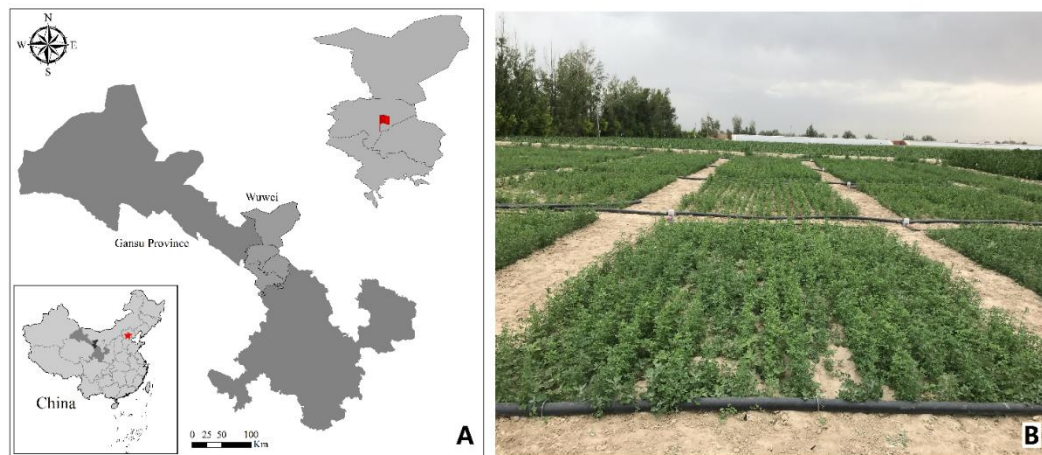


Figure 1. The location of the experimental site (A) and photo of the study site (B)

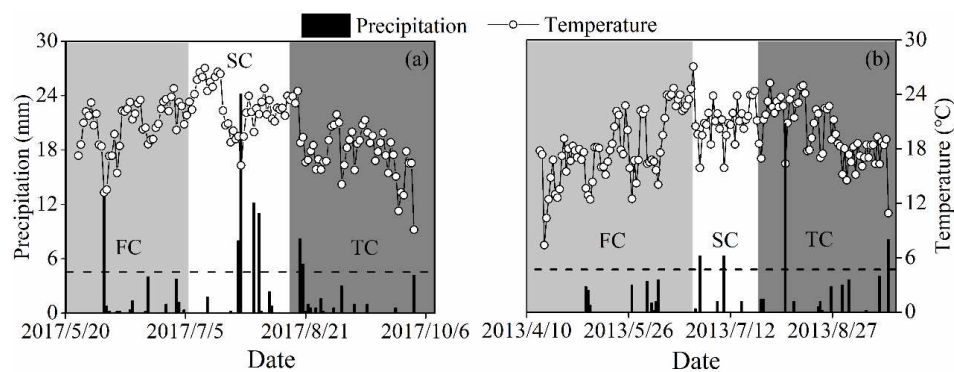


Figure 2. Daily mean temperature and precipitation at the experimental site in 2017 (a) and 2013 (b) at Shiyanghe Experimental Station for Water-saving Agriculture Ecology, China Agricultural University, Wuwei, Gansu Province, China

Experimental design

In 2013, we conducted the experiment of regulating deficit irrigation for lucerne under SDI in this experimental station, with 30 cm buried depth of the drip tube, variety Crown, and 22.5 cm row spacing. The experiment in 2017 adjusted the burying depth of drip irrigation pipe to 20 cm, the spacing between lucerne rows to 20 cm and the variety of lucerne to 4020, so as to be closer to the local lucerne production practice. In 2013, the experimental area was 16.2 m² (6 m × 2.7 m), and the test area was 24 m² (6 m × 4 m) in 2017 (*Figure 1B*). The plant density was about 600 no. m⁻² in the experiment.

The pressure-compensating emitters with delivery rate at 3L h⁻¹ were spaced at 0.3 m. The irrigation pipes were spaced at 0.9 m and 0.8 m in 2012 and 2017. Each irrigation system had their own pond, filtration system (sand and screen mesh), and pipeline network (Dayu water saving group co., ltd., Gansu, China). One drip line controls four rows of lucerne. Four irrigation levels were used with no water deficit (NWD), low water deficit (LWD), medium water deficit (MWD) and high water deficit (HWD), shown in *Table 1* and *Table 2*. The irrigation frequency was fixed to 7 days.

Table 1. Irrigation level and harvest time in the crop management

Stands	Abbreviations	Designed water levels (mm)	1 st . cutting (FC)	2 nd . cutting (SC)	3 rd . cutting (TC)	Irrigation time
annual	NWD	390	2017/7/6	2017/8/17	2017/10/2	13
	LWD	260				
	MWD	130				
	HWD	0				
biennial	NWD	390	2013/6/25	2013/7/25	2013/9/5	10
	LWD	260				
	MWD	130				
	HWD	0				

Table 2. Irrigation time and actual irrigation amount in no water deficit (NWD), low water deficit (LWD), medium water deficit (MWD) and high water deficit (HWD) in the experiment

Irrigation number	Irrigation time	NWD	LWD	MWD	HWD
1	2017/6/17	30	20	10	0
2	2017/6/24	30	20	10	0
3	2017/7/1	30	20	10	0
4	2017/7/8	30	20	10	0
5	2017/7/15	30	20	10	0
6	2017/7/22	30	20	10	0
7	2017/8/5	30	20	10	0
8	2017/8/12	30	20	10	0
9	2017/8/27	30	20	10	0
10	2017/9/3	30	20	10	0
11	2017/9/10	30	20	10	0
12	2017/9/16	30	20	10	0
13	2017/9/23	30	20	10	0
Actual irrigation amount (2017)		390	260	130	0
1	2013/5/15	15.24	11.20	6.00	0
2	2013/5/22	17.55	12.25	9.24	0
3	2013/5/29	90.66	60.14	28.32	0
4	2013/6/25	82.89	52.57	23.89	0
5	2013/7/7	39.70	23.88	11.05	0
6	2013/7/17	50.33	31.18	14.67	0
7	2013/7/27	9.18	6.08	2.70	0
8	2013/8/14	24.40	15.56	7.08	0
9	2013/8/14	28.35	18.29	8.44	0
10	2013/8/19	31.05	20.32	9.71	0
Actual irrigation amount (2013)		389.36	251.47	121.09	0

Sampling and measurements

Forage yield

Three lucerne stubbles were harvested 5 cm above the ground level; 1st cutting (FC), 2nd cutting (SC), and 3rd cutting (TC) at different times interval in the year 2013 and 2017,

in the early flowering period (*Table 1*). At each harvest, the forage biomass was cut at ground level from three representative sample quadrats (1 m×1 m) in each plot. After the quadrats had been removed, the rest of the plot was cut at the same height as in the quadrats and all the forage samples were oven-dried at 105°C for 1 h and then kept 70°C until a constant weight was reached.

Forage qualities

Dry plant samples were crushed into fine powder and then sieved through 0.5 mm mesh, and used for the determination of quality attributes like crude protein (CP), acid detergent fibre (ADF) and neutral detergent fibre (NDF). CP (%) tested by FOSS Kjeltec™ 8400, then ADF (%) and NDF (%) were tested by ANKOM2000 Automated Fiber Analyzer in the bag suspender.

The index of relative feed value (RFV) was calculated by integrating the formulae of (Zhang et al., 2018), to access the forage nutritive value using the forage quality attributes measured by *Eq. 1*:

$$RFV(\%) = \left[88.9 - (0.779 \times ADF(\%)) \right] \times 120 / NDF(\%) \times 0.775 \quad (\text{Eq.1})$$

In order to compare the relative nutrition yields amongst the forages accounting for both biomass and forage quality attributes, crude protein yield (CP_{yield}) and relative feed value yield (RFV_{yield}) were calculated as the product of biomass and CP concentration and RFV on each sampling occasion by *Eq. 2 and 3*.

$$CP_{\text{yield}} (\text{kg} \cdot \text{ha}^{-1}) = DM (\text{kg} \cdot \text{ha}^{-1}) \times CP(\%) \quad (\text{Eq.2})$$

$$RFV_{\text{yield}} (\text{kg} \cdot \text{ha}^{-1}) = DM (\text{kg} \cdot \text{ha}^{-1}) \times RFV(\%) \quad (\text{Eq.3})$$

Soil moisture, actual crop evapotranspiration and water use efficiency

Soil moisture measurement in every plot was made at 0.1 m intervals with maximal soil depth of 1.0 m at every 3–5 days or before and after irrigation using portable soil moisture monitoring system (Diviner 2000, Sentek Pty. Ltd., Australia). The arrangement of PVC access tubes used for the measurements of soil moisture content were specifically described by (Chen et al., 2014). Calibration was conducted before using the data obtained from Diviner 2000. Soil samples near every tube were acquired at 0.1 m intervals with maximal soil depth of 1.0 m, and the moisture content of the samples was determined using the gravimetric method (oven dry basis). The ratios of the soil moisture values measured by the gravimetric method to those by Diviner 2000 were used to calibrate the measurements by Diviner 2000. The unit of soil moisture is $\text{cm}^3 \text{cm}^{-3}$. The calculation of soil moisture in shallow and deep layers is the average accumulated value of 0-0.4 m and 0.5-1 m layer. The calibration curves of the relative frequency readings during the two-year experiment are as follows *Equation 4*:

$$(F_A - F_S) / (F_A - F_W) = 0.2869 \times \theta_v^{0.3356} \quad (\text{Eq.4})$$

where F_A is capacitance frequency reading of probe passing through PVC tube in air, F_S capacitance frequency reading corresponding to a depth of the probe passing through a PVC tube in soil, F_W is the capacitance frequency reading of the probe passes through the PVC tube placed in the water and inputs it before calibration of the instrument, θ_v is soil volumetric moisture.

The actual crop evapotranspiration was estimated with the soil water balance method (Chen et al., 2014). The soil moisture changes in 0–100 cm soil layer by subsurface drip irrigation over a period time were used to estimate actual crop evapotranspiration with the following Equation 5.

$$\Delta W = P + I + S - (ET_a + D) \quad (\text{Eq.5})$$

where ΔW is the change in soil water storage (mm); P is precipitation (mm), automatic weather station HOBO recorded; I is irrigation water volumes (mm); S is supplement of ground water (mm); ET_a is actual crop evapotranspiration (mm) and D is deep percolation (mm). In the experiment site, the contribution of groundwater was negligible because groundwater table is deeper than 25 m, so $S = 0$. The subsurface drip system arranged by control irrigation volume in this experiment, so $D = 0$. Thus by Eq. 6 can be simplified as follows:

$$ET_a = P + I - \Delta W \quad (\text{Eq.6})$$

where irrigation water volume was measured using water meters; ΔW was obtained from soil moisture observations in the 0-1 m soil layer at the beginning and end of the period. Calculation of ET_a at end of each cutting.

Water-use efficiency (kg mm^{-1} evapotranspiration (ET_a)) was calculated for biomass (WUE ; (Eq. 7)), crude protein yield (WUE_{CP} ; (Eq.8)), and relative feed value yield (WUE_{RFV} ; (Eq. 9)) (Zhang et al., 2018):

$$WUE = DM / ET_a \quad (\text{Eq.7})$$

$$WUE_{CP} = CP_{yield} / ET_a \quad (\text{Eq.8})$$

$$WUE_{RFV} = RFV_{yield} / ET_a \quad (\text{Eq.9})$$

Statistical analysis

Analysis of variance (ANOVA) was performed using the general linear model-univariate procedure from IBM SPSS Statistics 20 software (IBM Corp, AMONG, NY, USA). ANOVAs were done with irrigation volumes and stands years as the main effects and their interaction. Differences for all tests were assessed for significance at $P \leq 0.05$, $P \leq 0.01$ and $P \leq 0.001$; significant differences ($P \leq 0.05$) between means were identified using the least significant difference (LSD) test. Correlation analyses were used to evaluate the interrelationships among the measured variables. All determinations reported were the means of three replicates. All figures are done using OriginPro 2016 (Originlab Corp, Northampton, Massachusetts, USA) software.

Results

Soil moisture dynamics in two years

Generally speaking, the drying rate near the soil surface is faster and larger than that in the deep soil. In 2017, the variation of soil moisture in the layer of 0-40 cm was large, because the depth of the burial zone of the drip irrigation tape was 20 cm to the shallow soil moisture (SM) disturbance (Figure 3a,b,c,d). Meanwhile, the SM increased with higher trend of irrigation treatment, but it was not obvious in the 1st cutting (FC) (Figure 3a,b,c,d). At the depth of 40 cm, the SM were slightly higher to the irrigation treatment of medium water deficit (MWD) as compared to the high water deficit (HWD) (Figure 3d). While at the depth of 50-60 cm, the SM in HWD were lower than MWD treatment (Figure 3e). We also observed that with the increase in irrigation volume, SM also increased at the depth of 60 cm (Figure 3f). In contrast, at the depth of 70-100 cm, the HWD had higher SM than the MWD treatment (Figure 3g,h,i,j,l). Moderate rain (10-25 mm day⁻¹) occurred on July 27, 2017, with a precipitation of 24.2 mm. It can be seen that the water content of shallow soil increased rapidly the next day, especially in the surface layer of soil (Figure 3a,b,c,k). In the annual FC of rain-fed (HWD) lucerne soil moisture compensation only occurred on July 27, 2017.

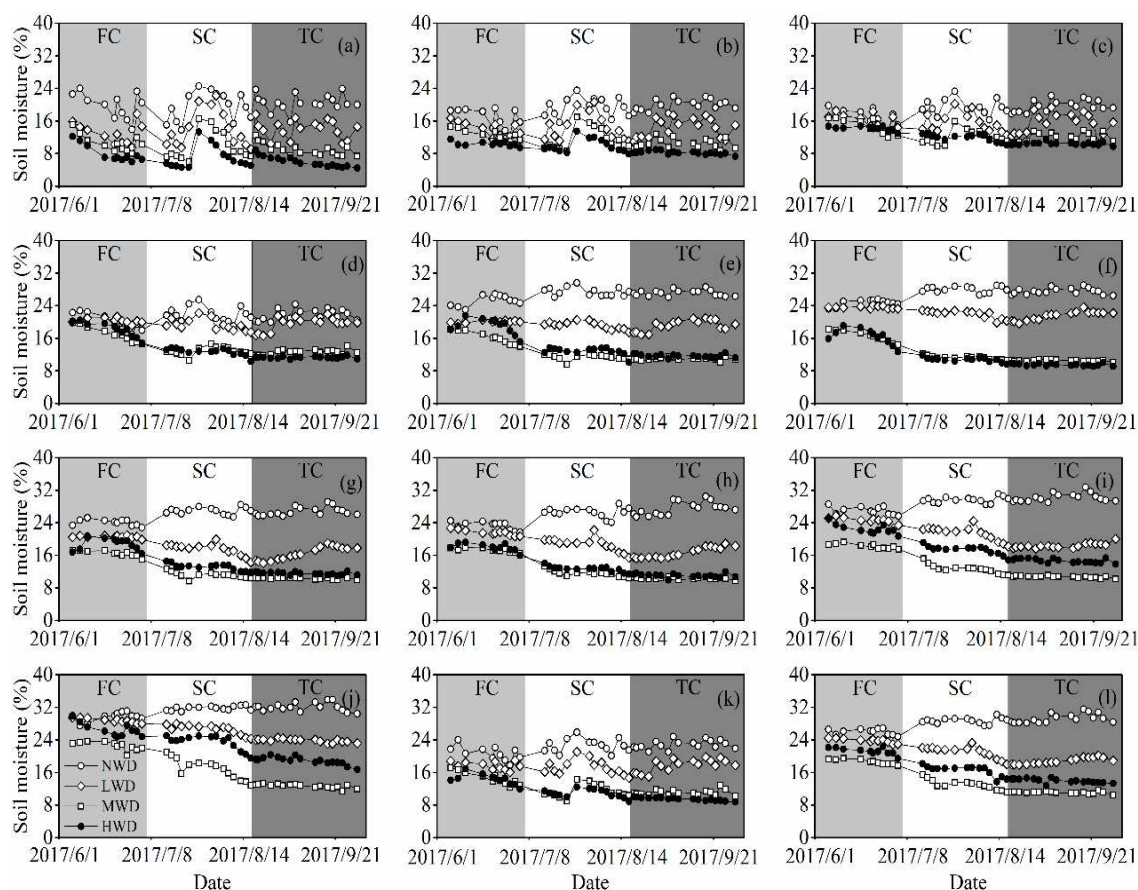


Figure 3. Soil moisture dynamics in the 0-10 cm (a), 10-20 cm (b), 20-30 cm (c), 30-40 cm (d), 40-50 cm (e), 50-60 cm (f), 60-70 cm (g), 70-80 cm (h), 80-90 cm (i), 90-100 cm (j), 0-60 cm (k) and 70-100 cm (l) soil layers in annual lucerne. The light gray area represents the dynamics of soil moisture in the FC, the white area represents the dynamics of soil moisture in the SC, and the dark gray area represents the dynamics of soil moisture in the TC

Compared with the SM of annual lucerne (2017), the SM of the biennial lucerne (2013) also showed dramatic changes in the shallow soil depth 10-40 cm (Figure 4a,b,c,d,k). Meanwhile, the SM decreased while increasing water deficit conditions in the shallow soil depth 10-50 cm (Figure 4a,b,c,d,e,k). In 60-90 cm depth, HWD had more SM in the FC and 3rd cutting (TC) than that of any treatments (Figure 4f,g,h,i,l). In the 2nd cutting (SC), SM of 50-60 cm was negatively correlated with increasing water deficit (Figure 4f); at 60-70 cm, the SM of HWD were higher than low water deficit (LWD) and medium water deficit (MWD) (Figure 4g); while at 70-90 cm soil layer, HWD had higher SM than MWD (Figure 4h,i,l).

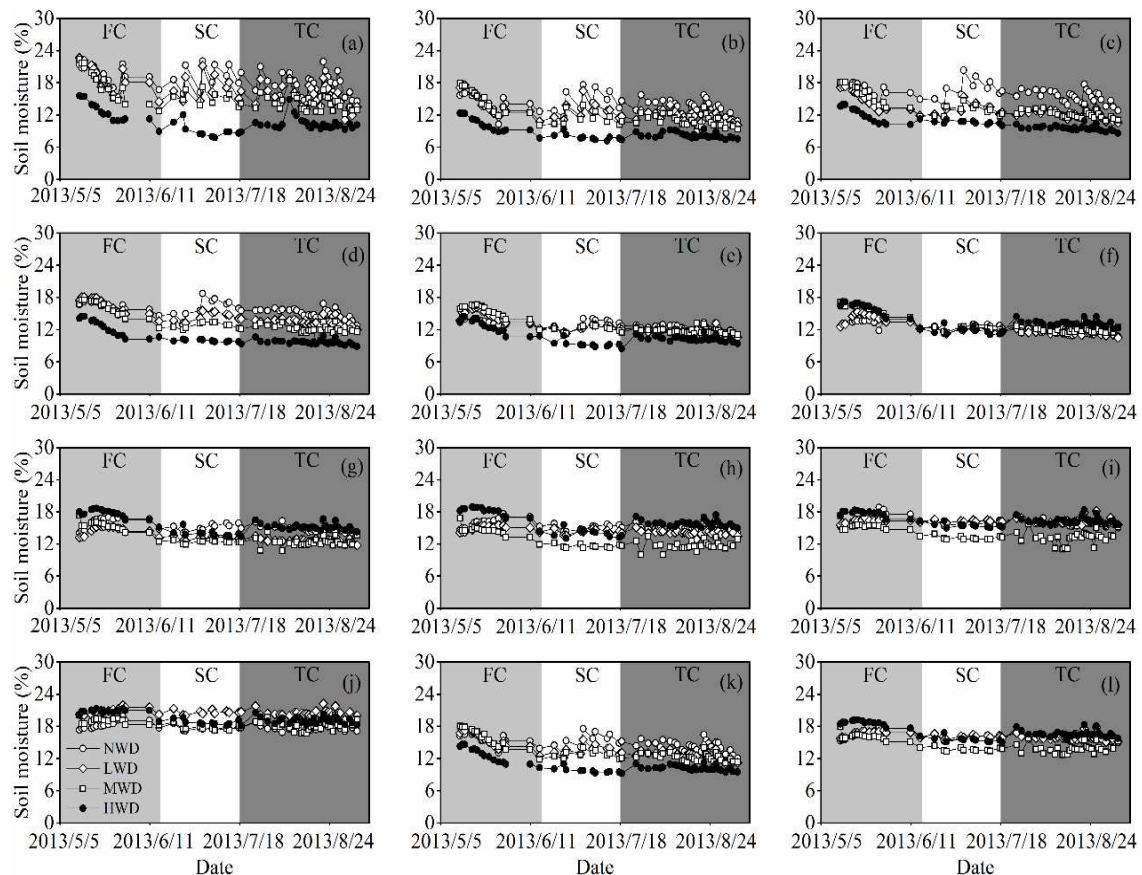


Figure 4. Soil moisture dynamics in the 0-10 cm (a), 10-20 cm (b), 20-30 cm (c), 30-40 cm (d), 40-50 cm (e), 50-60 cm (f), 60-70 cm (g), 70-80 cm (h), 80-90 cm (i), 90-100 cm (j), 0-60 cm (k) and 70-100 cm (l) soil layers in biennial lucerne. The light gray area represents the dynamics of soil moisture in the FC, the white area represents the dynamics of soil moisture in the SC, and the dark gray area represents the dynamics of soil moisture in the TC

Forage yield

The highest mean annual forage yield (12930 kg ha⁻¹) was recorded with NWD treatment in 2017, and it was higher than biennial lucerne of 2013 (12165 kg ha⁻¹), shown in Table 3. Increasing water deficit conditions significantly decreased the forage yield in 2013 and 2017. The forage yield of all treatments was well-fitted ($R^2 = 0.533$, $P < 0.001$) by Pearson's correlation (Table 4).

Table 3. Forage yield (kg ha^{-1}) of annual and biennial lucerne stand age (S) and irrigation volumes (I) at 1st. cutting (FC), 2nd. cutting (SC) and 3rd. cutting (TC)

Stands	Treatment	Forage yield (kg ha^{-1})			
		FC	SC	TC	Annual
annual	HWD	2752d	2256d	1556d	6565d
	MWD	3384c	2594cd	2696c	8674c
	LWD	4425b	3021bc	3082b	10529b
	NWD	5904a	3517ab	3509a	12930a
biennial	HWD	3948b	3236	2361c	9545d
	MWD	4782a	3456	2612bc	10850c
	LWD	5420a	3719	2862bc	12000bc
	NWD	5466a	3570	3129ab	12165ab
Statistical significance					
Stand(S)		**	***	NS	***
Irrigation volumes(I)		***	**	***	***
S*I		NS	NS	**	**

Statistical significance: NS = not significant, *, **, and *** represent $P < 0.05$, <0.01 and <0.001 , respectively. The lowercase letters indicate significant differences between different irrigation volumes at each year ($P = 0.05$). The same as below

Table 4. Correlation analysis of lucerne forage yield and qualities with irrigation volumes, ET_a and WUEs

	forage yield	CP (%)	NDF (%)	ADF (%)	RFV	CP _{yield}	RFV _{yield}
I	0.533***	-0.461***	-	0.653***	-0.311**	0.417***	0.256*
ET_a	0.518***	-0.256*	0.417***	0.733***	-0.556***	0.539***	-
WUE	-	-	-0.308**	-0.5***	0.333**	-	-
WUE _{CP}	-	-	-0.426***	-0.461***	0.499***	-	-
WUE _{RFV}	-0.263*	-	-0.522***	-0.609***	0.643***	-0.312**	-

We also found that there was significant difference between the biennial forage yield at HWD and NWD treatments. FC forage yield was highest at each treatment in both annual and biennial lucerne. No significant differences were observed in different treatments of water deficit for the forage yield of SC in 2013, while significant differences were found for TC forage yield at NWD and HWD treatments of biennial lucerne (Table 3).

Lucerne quality

Crude protein concentration (CP) in forage dry matter was determined and expressed as percentage of crude protein (%CP) (Table 5). It was found that in biennial lucerne, CP was decreased with increase in water deficit except FC, while in annual lucerne, CP was highest at LWD for all cuttings (23.6, 23.6, and 24.29%) (Table 5). CP was significantly influenced by the lucerne stand age (annual and biennial lucerne) ($P < 0.05$) (Table 5).

In case of Crude protein yield (CP_{yield}), the biennial lucerne showed non-significant difference between FC and SC, while TC showed significant difference between HWD and NWD ($P < 0.05$) (Table 5). The annual lucerne showed significant differences among different treatments for CP_{yield}, while HWD had the highest CP_{yield} (2721 kg ha^{-1}). The Pearson correlation coefficient between the irrigation treatments and CP_{yield} was 0.417 ($P < 0.001$) (Figure 5a, Table 4).

Table 5. Crude protein content (%) and Crude protein yield (kg ha^{-1}) of annual and biennial lucerne at 1st. cutting (FC), 2nd. cutting (SC) and 3rd. cutting (TC)

Stands	Treatment	CP (%)			CP _{yield} (kg ha^{-1})			
		FC	SC	TC	FC	SC	TC	Annual
annual	HWD	21.92b	21.92b	22.68	841c	550c	354d	1745d
	MWD	23.6a	23.6a	24.29	835c	523c	654bc	2011c
	LWD	21.32c	21.32c	21.9	954b	596bc	675bc	2224b
	NWD	19.32d	19.32d	24.73	1151a	703ab	868a	2721a
biennial	HWD	21.41	21.31a	23.11ab	823b	647	539b	2009c
	MWD	19.75	19.26b	22.6ab	944a	665	582ab	2191bc
	LWD	18.68	19.18b	21.92bc	1012a	707	620ab	2339ab
	NWD	18.51	18.61b	21.25c	1012a	694	666a	2371ab

Statistical significance							
S	***	***	*	NS	**	NS	NS
I	***	***	NS	**	NS	***	***
S*I	***	***	NS	NS	NS	***	**

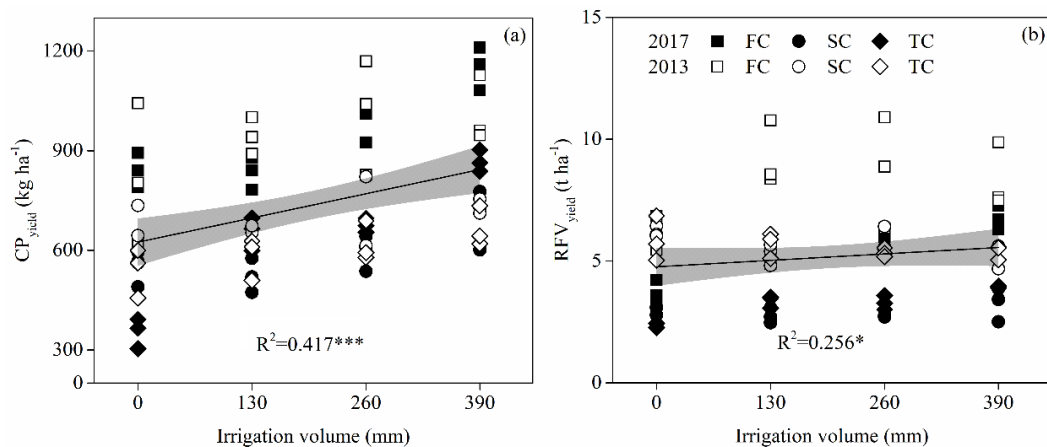


Figure 5. The relationships between (a) irrigation volumes (mm) and CP_{yield} (kg ha^{-1}), (b) irrigation volumes (mm) and $\text{RFV}_{\text{yield}}$ (t ha^{-1}) under four irrigation volumes (0 mm, 130 mm, 260 mm, 390 mm). The significant linear regression equations are shown, * $P < 0.05$, ** $P < 0.01$, *** $P < 0.001$

Acid detergent fibre (ADF %) and neutral detergent fibre (NDF %) were significantly influenced by the lucerne stands age (annual and biennial lucerne) ($P < 0.05$) and irrigation volumes (I) ($P < 0.001$) (Table 6). These were increased with the increase in water deficit except for ADF in TC and NDF in FC of annual lucerne. The lower ADF and NDF, the better the forage digestibility, thus, water deficit might improve forage digestibility by reducing ADF and NDF.

The trend in relative feed value (RFV) was directly correlated with the lucerne stand age (S) and irrigation volume (I) ($P < 0.001$) (Table 4). Lucerne stands with NWD showed lower RFV, compared with other irrigation treatments except at LWD of TC of annual lucerne (Table 7). There was no significant difference between SC of annual lucerne and TC of biennial lucerne in the relative feed value yield ($\text{RFV}_{\text{yield}}$) (Table 7), but the annual lucerne $\text{RFV}_{\text{yield}}$ was significantly positively correlated to irrigation volumes ($P < 0.01$) (Figure 5b). The annual $\text{RFV}_{\text{yield}}$ was increased by 35.9% and 4.14% at HWD compared with NWD in annual and biennial lucerne respectively (Table 7).

Table 6. ADF (%) and NDF (%) of annual and biennial lucerne at 1st. cutting (FC), 2nd. cutting (SC) and 3rd. cutting (TC)

Stands	Treatment	ADF (%)			NDF (%)		
		FC	SC	TC	FC	SC	TC
annual	HWD	27.91d	20.8d	22.52c	46.14ab	51.57	43.34b
	MWD	28.79cd	32.12bc	25.09b	43.22b	56.1	52.01a
	LWD	31.13bc	34.07bc	31.45a	46.03ab	62.27	56.37a
	NWD	33.7ab	35.42ab	29.68a	48.58a	62.32	54.53a
biennial	HWD	24.44	24.69c	19.9d	34.14	33.8d	27.65c
	MWD	27.98	28.39b	22.97c	35.4	38.35c	29.45c
	LWD	28.9	29.5b	25.46b	39	39.99bc	32.96b
	NWD	30.75	32.33a	29.17a	39.7	41.69ab	37.07a
Statistical significance							
S		**	*	***	***	***	***
I		***	***	***	**	**	***
S*I		NS	**	***	NS	NS	**

Table 7. RFV (%) and RFV_{yield} (t ha⁻¹) of annual and biennial lucerne at 1st. cutting (FC), 2nd. cutting (SC) and 3rd. cutting (TC)

Stands	Treatment	RFV			RFV _{yield} (t ha ⁻¹)			
		FC	SC	TC	FC	SC	TC	Annual
annual	HWD	135.39ab	132.66a	153.29a	3.73c	2.94	2.39c	8.89c
	MWD	143.45a	106.44ab	124.36a	5.3b	2.76	3.35b	11.39b
	LWD	130.89ab	93.22abc	106.5b	5.63ab	2.82	3.29b	11.71b
	NWD	120.42b	92.67c	112.25c	6.76a	3.26	3.94a	13.87a
biennial	HWD	190.36a	192.48a	248.14a	5.95b	6.19a	5.86	18.29b
	MWD	182.84ab	162.17bc	224.27b	9.24a	5.29b	5.7	20.59a
	LWD	158.85bc	153.76cd	195.79c	8.7ab	5.8ab	5.35	20.23ab
	NWD	151.65cd	142.32d	166.27d	8.32ab	5.3b	5.38	19.08ab
Statistical significance								
S		***	***	***	***	***	***	***
I		***	***	***	**	NS	NS	**
S*I		NS	NS	**	NS	NS	**	*

Correlations among forage yield and qualities with irrigation volume, ET_a and WUEs

The forage yield, CP_{yield} and RFV_{yield} were positively correlated with the irrigation volume (I), and the correlation coefficients were 0.533 ($P < 0.001$), 0.417 ($P < 0.001$) and 0.235 ($P < 0.05$), respectively (Table 4). The forage yield and CP_{yield} showed significant positive correlation with actual crop evapotranspiration (ET_a), but significant negative correlation with WUE_{RFV} (Table 4, Figure 6).

There was no correlation between NDF and irrigation volume (I), CP and WUEs (Including WUE, WUE_{CP} and WUE_{RFV}). We found some interesting information in Table 7. First, CP has a negative correlation with I and ET_a, and the correlation coefficients were -0.461 ($P < 0.001$) and -0.256 ($P < 0.05$), respectively. Secondly, not only NDF positive correlation with ET_a, it also had significant negative correlation with WUEs. Third, ADF had a positive correlation with I and ET_a, but it was also negatively correlated with WUEs. Last, RFV, in contrast to NDF and ADF, showed a negative correlation with I and ET_a, but significantly and positively correlated with WUEs.

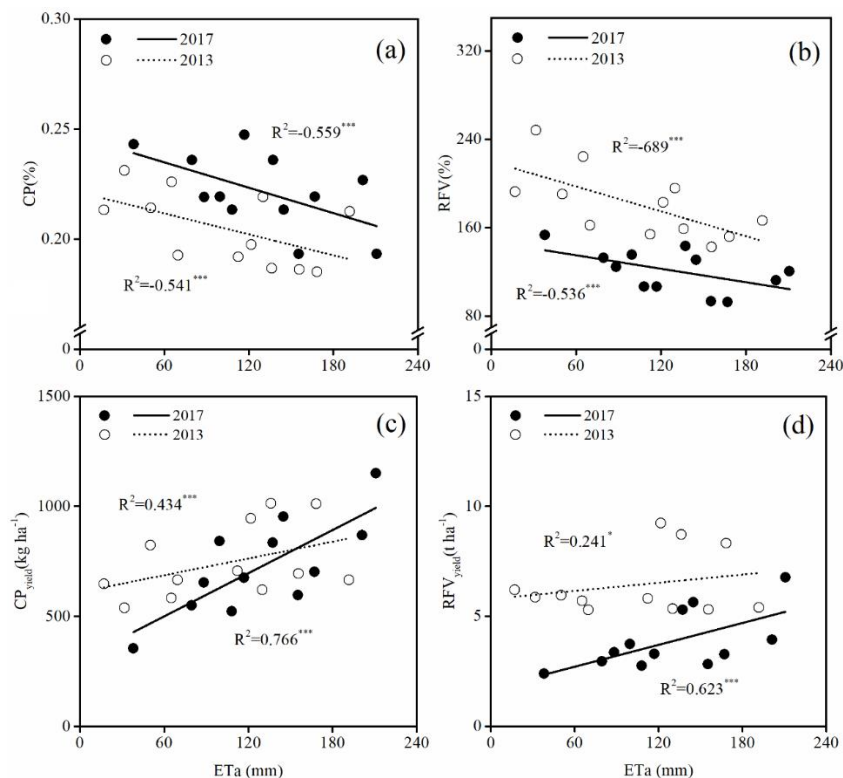


Figure 6. The relationships between (a) ET_a (mm) and CP (%), (b) ET_a (mm) and RFV (%), (c) ET_a (mm) and CP_{yield} ($kg\ ha^{-1}$), (d) ET_a (mm) and RFV_{yield} ($t\ ha^{-1}$). The significant linear regression equations are shown, * $P < 0.05$, ** $P < 0.01$, *** $P < 0.001$

Discussion

The Hexi Corridor has been characterized by extreme water shortage, and thus water availability is insufficient to satisfy crop water consumption. So many water-saving methods were proposed to improve the local crop water utilization efficiency, such as drip irrigation under plastic film mulch, regulated deficit irrigation (RDI), partial root-zone irrigation and subsurface drip irrigation. These technologies play an important role in water-saving irrigation cultivation in Hexi Corridor. Subsurface drip irrigation has been proven to improve water use efficiency of pasture (Kandelous et al., 2012), and be able to obtain greater investment return on lucerne (Heard et al., 2012). The possible reason is the water absorption layer of the root system is distributed in the shallow region (Bai and Li, 2003; Ayars et al., 2009; Kandelous et al., 2012). The subsurface drip irrigation system transports water around the main absorbent roots of lucerne to ensure greater water use efficiency. So that soil moisture in the soil layer of 0-40 cm changed greatly (Figure 3a,b,c,d and Figure 4a,b,c,d). Although surface evaporation can also reduce soil moisture, at this time, because lucerne almost completely covers the ground, ground evaporation almost not be considered. Therefore, the variation of shallow soil moisture is mainly caused by root water absorption (Bai and Li, 2003). In addition, irrigation water is supplied to lucerne shallow root-zone by capillary movement from the bottom. Infiltration movement induces plant hardening or internal physiological regulations caused by mild water stress (Chai et al., 2016). This perennial pasture, which can be mowed many times in one year, is in good agreement with the properties of SDI system.

On the other hand, RDI is often applied to pasture as an irrigation strategy in arid areas (Hanson et al., 2007; Geerts and Raes, 2009; Neal et al., 2012; Liu et al., 2018), it usually shows a certain compensation effect after rehydration (Geerts and Raes, 2009; Liu et al., 2018). It is also possible to induce a super compensation effect in the time of water insensitivity (Zhou et al., 2011; Albasha et al., 2015). The results of this experiment showed that RDI decreased the yield of lucerne (*Table 3*), but increased the quality of lucerne (*Tables 5 and 6*). The annual lucerne yield was 6565-12930 kg ha⁻¹ and 9545-12165 kg ha⁻¹ in the biennial lucerne, is in the high range of reported from semiarid areas (Bai and Li, 2003; Li and Huang, 2008; Lamm et al., 2012; Ismail et al., 2013; Klonie et al., 2013; Xiao et al., 2015; Holman et al., 2016; Rogers et al., 2016; Anower et al., 2017; Cavero et al., 2017; Li and Su, 2017; Huang et al., 2018; Liu et al., 2018). Different from many other studies of lucerne yield, the yield of annual lucerne is almost the same as that of biennial lucerne. The reason for this may be that we harvested three cuttings in the second year of our experiment as well as in the first year. Unlike other crops, lucerne is harvested as a nutrient, while the general field crops harvest seeds or fruit production (Kang et al., 2000; Chen et al., 2014; Du et al., 2016; Yang et al., 2017). The redundant growth of crops can be reduced more or less by RDI on those crops (Kang et al., 2000; Du et al., 2016; Yang et al., 2017). But lucerne harvest is aboveground biomass, the more vigorous the plant growth, the higher the yield we get. There is a positive correlation between the volume of irrigation and the forage yield (*Figure 2*), which is consistent with the study of many predecessors (Bai and Li, 2003; Klonie et al., 2013; Holman et al., 2016), except for excessive irrigation research (Xiao et al., 2015; Cavero et al., 2017).

There is a positive correlation between irrigation and evapotranspiration of lucerne (Saeed and El-Nadi, 1997; Klocke et al., 2013; Li and Su, 2017), while photosynthetic assimilates accumulated more to yield (Mouradi et al., 2016; Anower et al., 2017). This paper also showed a positive correlation between forage evapotranspiration and forage yield ($P < 0.001$) (*Table 4*). Studies in this region also suggest that lucerne evapotranspiration is around 400 mm (Li and Su, 2017), and the maximum volume of water set in this experiment is 390 mm.

In our experiment, especially CP yield and RFV yield are positively correlated with irrigation volume. Though irrigation volume negative correlation with RFV, RFV_{yield} value is the product of RFV and yield of lucerne, which largely offset the negative correlation of RFV. In addition to NDF (%), there was a significant correlation between the quality indexes and the irrigation volumes (*Figure 5, Table 4*). In particular, the second-year stand forage CP (%) has a negative correlation with the volume of irrigation, which can be explained as the water deficit increase the pasture CP (%). The results showed that RFV has a negative correlation with the volumes of irrigation, and it can also be consistent with the previous conclusion (Harmony et al., 2013; Holman et al., 2016).

CP (%) and RFV were not the decisive factors for forage quality. Quality yield depends on the forage yield, forming two important quality indexes, namely, CP_{yield} and RFV_{yield}. In this study, the correlation coefficient between irrigation volume and CP_{yield}, RFV_{yield} was 0.417 ($P < 0.001$) and 0.256 ($P < 0.05$), respectively (*Figure 5 and Table 4*). Therefore, with the increase of the volume of irrigation, CP_{yield} and RFV_{yield} tend to increase. The reason is largely because the contribution of the irrigation volumes to the yield is greater than that of the quality. That is to say, the regulated deficit irrigation can improve the quality of lucerne, but it is based on the decline of yield (Holman et al., 2016). In the irrigation treatment MWD (260 mm), the output of the first year and second years

decreased by 18.57% and 1.37% compared with the irrigation treatment of NWD (390 mm) (Table 2). It shows that the influence of irrigation volume on yield decreases with the increase of year. The CP_{yield} decreased by 18.27% in the same case for the first year, and 1.35% in second years. RFV_{yield} decreased by 15.57% in the first year with the same treatment, while second years showed an increase of 6.03%. We could know that pasture is sensitive to water in the first year, so it can be fully irrigated, while moderate deficit in second years is more conducive to the formation of forage RFV_{yield} . Another study in Gansu showed that forage in this area CP_{yield} swung between 360-1200 kg ha⁻¹ and RFV_{yield} was between 1-9.5 t ha⁻¹ (Zhang et al., 2018). In this experiment, the CP_{yield} of annual forage under no irrigation is 1,745 kg, and the next year's CP_{yield} is higher than that of annual pasture (Table 5). Under the same conditions, the first year of RFV_{yield} was 8.89 t ha⁻¹, 18.29 t ha⁻¹ for the biennial forage (Table 7). The CP_{yield} was much higher than the other pasture although the annual RFV_{yield} was lower than the highest RFV_{yield} of maize. Thus, lucerne is undoubtedly the most valuable pasture, whether it is the development of grassland agriculture, or the development of cultivated forage.

Conclusion

The drying rate near the soil surface is faster and larger than that in the deep soil. The water content of deep soil is higher than that of shallow soil. 60 cm of subsurface drip-irrigated lucerne can be considered as the diagnostic layer of water deficit. This study showed that regulated deficit drip irrigation reduced forage yield, but increased quality content and water use efficiency of lucerne. Recommends no deficit in the first year, and moderate water deficit in second year in the practical cultivation and irrigation of lucerne.

Acknowledgments. This research was supported by National Key Research and Development Program of China (2016YFC0400306). The authors thank for Liliang Han's help, staff member of Shiyanghe Experimental Station Liang Zhang and Quan Lu for help of the field trial in 2013 and 2017.

REFERENCES

- [1] Alam, M., Trooien, T. P., Rogers, D. H., Dumler, T. J. (2002): Using subsurface drip irrigation for alfalfa. – Journal of the American Water Resources Association 38: 1715-1721.
- [2] Albasha, R., Mailhol, J., Cheviron, B. (2015): Compensatory uptake functions in empirical macroscopic root water uptake models – Experimental and numerical analysis. – Agricultural Water Management 155: 22-39.
- [3] Anower, M. R., Boe, A., Auger, D., Mott, I. W., Peel, M. D., Xu, L., Kanchupati, P., Wu, Y. (2017): Comparative drought response in eleven diverse alfalfa accessions. – Journal of Agronomy and Crop Science 203: 1-13.
- [4] Ayars, J. E., Shouse, P., Lesch, S. M. (2009): In situ use of groundwater by alfalfa. – Agricultural Water Management 96: 1579-1586.
- [5] Bai, W., Li, L. (2003): Effect of irrigation methods and quota on root water uptake and biomass of alfalfa in the Wulanbuhe sandy region of China. – Agricultural Water Management 62: 139-148.
- [6] Bouton, J. H. (2012): An overview of the role of lucerne (*Medicago sativa* L.) in pastoral agriculture. – Crop and Pasture Science 63: 734-738.

- [7] Cavero, J., Faci, J. M., Medina, E. T., Martínez-Cob, A. (2017): Alfalfa forage production under solid-set sprinkler irrigation in a semiarid climate. – *Agricultural Water Management* 191: 184-192.
- [8] Chai, Q., Gan, Y., Zhao, C., Xu, H., Waskom, R. M., Niu, Y., Kadambot, H. M. (2016): Regulated deficit irrigation for crop production under drought stress. A review. – *Agronomy for Sustainable Development* 36: 3.
- [9] Chen, J., Kang, S., Du, T., Guo, P., Qiu, R., Chen, R., Gu, F. (2014): Modeling relations of tomato yield and fruit quality with water deficit at different growth stages under greenhouse condition. – *Agricultural Water Management* 146: 131-148.
- [10] Du, S., Kang, S., Li, F., Du, T. (2016): Water use efficiency is improved by alternate partial root-zone irrigation of apple in arid northwest China. – *Agricultural Water Management* 179: 184-192.
- [11] Fereres, E., Soriano, M. A. (2006): Deficit irrigation for reducing agricultural water use. – *Journal of Experimental Botany* 58: 147-159.
- [12] Geerts, S., Raes, D. (2009): Deficit irrigation as an on-farm strategy to maximize crop water productivity in dry areas. – *Agricultural Water Management* 96: 1275-1284.
- [13] Godoy, A. C., Pérez, G. A., Torres, E. C. A., Hermosillo, L. J., Reyes, J. (2003): Water use, forage production and water relations in alfalfa with subsurface drip irrigation. – *Agrociencia-Mexico* 37: 107-115.
- [14] Hanson, B., Putnam, D., Snyder, R. (2007): Deficit irrigation of alfalfa as a strategy for providing water for water-short areas. – *Agricultural Water Management* 93: 73-80.
- [15] Harmony, K. R., Lamm, F. R., Johnson, S. K., Aboukheira, A. A. (2013): Reducing water inputs with subsurface drip irrigation may improve alfalfa nutritive value. – *Forage and Grazinglands* 11(1): 1-8.
- [16] Heard, J. W., Porker, M. J., Armstrong, D. P., Finger, L., Ho, C. K. M., Wales, W. J., Malcolm, B. (2012): The economics of subsurface drip irrigation on perennial pastures and fodder production in Australia. – *Agricultural Water Management* 111: 68-78.
- [17] Holman, J., Min, D., Klönie, N., Kisekka, I., Currie, R. (2016): Effects of irrigation amount and timing on alfalfa nutritive value. – *Transactions of the ASABE* 59: 849-860.
- [18] Huang, Z., Liu, Y., Cui, Z., Fang, Y., He, H., Liu, B., Wu, G. (2018): Soil water storage deficit of alfalfa (*Medicago sativa*) grasslands along ages in arid area (China). – *Field Crops Research* 221: 1-6.
- [19] Hutmacher, R. B., Phene, C. J., Mead, R. M., Jobs, J. (2001): Subsurface drip and furrow irrigation comparison with alfalfa in the Imperial Valley, California. – *Alfalfa & Forage Symposium*, Modesto, CA.
- [20] Ismail, S., Almarshadi, M. (2013): Maximizing productivity and water use efficiency of alfalfa under precise subsurface drip irrigation in arid regions. – *Irrigation and Drainage* 62: 57-66.
- [21] Kandelous, M. M., Kamai, T., Vrugt, J. A., Šimůnek, J., Hanson, B., Hopmans, J. W. (2012): Evaluation of subsurface drip irrigation design and management parameters for alfalfa. – *Agricultural Water Management* 109: 81-93.
- [22] Kang, S., Shi, W., Zhang, J. (2000): An improved water-use efficiency for maize grown under regulated deficit irrigation. – *Field Crops Research* 67: 207-214.
- [23] Klocke, N. L., Currie, R. S., Holman, J. D. (2013): Alfalfa response to irrigation from limited water supplies. – *Transactions of the ASABE* 56: 1759-1768.
- [24] Kou, D., Su, D., Wu, D., Li, Y. (2014): Effects of regulated deficit irrigation on water consumption, hay yield and quality of alfalfa under subsurface drip irrigation. – *Transactions of the Chinese Society of Agricultural Engineering* 30: 116-123. (in Chinese with English abstract).
- [25] Lamm, F. R., Harmony, K. R., Aboukheira, A. A., Johnson, S. K. (2012): Alfalfa production with subsurface drip irrigation in the Central Great Plains. – *Transactions of the ASABE* 55: 1203-1212.

- [26] Li, Y., Huang, M. (2008): Pasture yield and soil water depletion of continuous growing alfalfa in the Loess Plateau of China. – *Agriculture, Ecosystems & Environment* 124: 24-32.
- [27] Li, Y., Su, D. (2017): Alfalfa Water Use and Yield under Different Sprinkler Irrigation Regimes in North Arid Regions of China. – *Sustainability-Basel* 9: 1380.
- [28] Lin, H., Li, R., Liu, Y., Zhang, J., Ren, J. (2017): Allocation of grassland, livestock and arable based on the spatial and temporal analysis for food demand in China. – *Front. of Agric. Sci. and Eng* 4: 69-80.
- [29] Liu, Y., Wu, Q., Ge, G., Han, G., Jia, Y. (2018): Influence of drought stress on alfalfa yields and nutritional composition. – *BMC Plant Biology* 18: 13.
- [30] Montazar, A., Zaccaria, D., Bali, K., Putnam, D. (2016): A model to assess the economic viability of alfalfa production under subsurface drip irrigation in California. – *Irrigation and Drainage* 66(1): 90-102.
- [31] Mouradi, M., Farissi, M., Bouzigaren, A., Makoudi, B., Kabbadj, A. (2016): Effects of water deficit on growth nodulation and physiological and biochemical processes in *Medicago sativa* rhizobia symbiotic association. – *Arid Land Research & Management* 30: 193-208.
- [32] Neal, J. S., Murphy, S. R., Harden, S., Fulkerson, W. J. (2012): Differences in soil water content between perennial and annual forages and crops grown under deficit irrigation and used by the dairy industry. – *Field Crops Research* 137: 148-162.
- [33] Nunes, C., de Sousa Araújo, S., Da Silva, J. M., Feveiro, M. P. S., da Silva, A. B. (2008): Physiological responses of the legume model *Medicago truncatula* cv. Jemalong to water deficit. – *Environmental and Experimental Botany* 63: 289-296.
- [34] Palacios-Díaz, M. P., Mendoza-Grimón, V., Fernández-Vera, J. R., Rodríguez-Rodríguez, F., Tejedor-Junco, M. T., Hernández-Moreno, J. M. (2009): Subsurface drip irrigation and reclaimed water quality effects on phosphorus and salinity distribution and forage production. – *Agricultural Water Management* 96: 1659-1666.
- [35] Rogers, M. E., Lawson, A. R., Kelly, K. B. (2016): Lucerne yield, water productivity and persistence under variable and restricted irrigation strategies. – *Crop and Pasture Science* 67: 563-573.
- [36] Romero, P., Botia, P., Garcia, F. (2004): Effects of regulated deficit irrigation under subsurface drip irrigation conditions on water relations of mature almond trees. – *Plant and Soil* 260: 155-168.
- [37] Trejo, M., Aguilu, A., Ramirez, O., Lopez, R., Gonzalez, R., Rangel, P., Trejo, M., Castruita, S., Vidal, O., Coronado, Y. (2010): Uso del agua en la alfalfa (*Medicago sativa*) con riego por goteo subsuperficial. – *Revista Mexicana de ciencias pecuarias* 1(2): 145-156.
- [38] Xiao, Y., Zhang, J., Jia, T. T., Pang, X. P., Guo, Z. G. (2015): Effects of alternate furrow irrigation on the biomass and quality of alfalfa (*Medicago sativa*). – *Agricultural Water Management* 161: 147-154.
- [39] Xu, R., Ren, J., Nan, Z., Huang, J., Deng, X., Lin, H., Qiu, H. (2016): Strategies and policies for the ecological and food security of China's grassland. – *Engineering Science* 18: 8-16. (in Chinese with English abstract).
- [40] Yang, H., Du, T., Qiu, R., Chen, J., Wang, F., Li, Y., Wang, C., Gao, L., Kang, S. (2017): Improved water use efficiency and fruit quality of greenhouse crops under regulated deficit irrigation in northwest China. – *Agricultural Water Management* 179: 193-204.
- [41] Zhang, Q., Bell, L. W., Shen, Y., Whish, J. P. M. (2018): Indices of forage nutritional yield and water use efficiency amongst spring-sown annual forage crops in north-west China. – *European Journal of Agronomy* 93: 1-10.
- [42] Zhou, L., Gan, Y., Ou, X., Wang, G. (2011): Progress in molecular and physiological mechanisms of water-saving by compensation for water deficit of crop and how they relate to crop production. – *Chinese Journal of Eco-Agriculture* 19: 217-225. (in Chinese with English abstract).

THE EFFECTS OF OXYTETRACYCLINE CHRONIC TOXICITY ON THE POPULATION DYNAMICS OF *D. MAGNA* IN THE PRESENCE OF UV-B

LINARES GONZÁLEZ, Y.¹ – LINARES FLEITES, G.² – GARCÍA VARGAS, S.³ –
MARTÍNEZ CONTRERAS, R.⁴ – PEÑA MORENO, R.³ – MORALES, L. L.^{5*}

¹*Posgrado en Ciencias Ambientales, Instituto de Ciencias, Benemérita Universidad Autónoma de Puebla, Edificio IC 6, Ciudad Universitaria, C. P. 72570 Puebla, México*

²*Departamento de Investigación en Ciencias Agrícolas, Instituto de Ciencias, Benemérita Universidad Autónoma de Puebla, Av. 4 Sur 104, C. P. 72000 Puebla, México*

³*Centro de Química, Instituto de Ciencias, Benemérita Universidad Autónoma de Puebla, Av. 4 Sur 104, C. P. 72000 Puebla, México*

⁴*Laboratorio de Ecología Molecular Microbiana, Centro de Investigaciones en Ciencias Microbiológicas, Instituto de Ciencias, Benemérita Universidad Autónoma de Puebla, Av. 4 Sur 104, C. P. 72000 Puebla, México*

⁵*Facultad de Ciencias Químicas, Benemérita Universidad Autónoma de Puebla, Av. 4 Sur 104, C. P. 72000 Puebla, México*

*Corresponding author
e-mail: laura.morales@correo.buap.mx

(Received 20th Sep 2019; accepted 8th Jan 2020)

Abstract. Oxytetracycline is a broad-spectrum antibiotic which is mainly used to improve the health of aquaculture and livestock animals, which is the reason why it is released into water bodies through the discharges of these industries potentially causing an imbalance in the freshwater ecosystems. Additionally, the depletion of stratospheric ozone has caused an increase in the levels of ultraviolet radiation, which can increase the toxicity of the drug, due to the interaction between oxytetracycline and the UV-B region of the electromagnetic spectrum in particular, thus deteriorating the conditions necessary for the survival of aquatic species. This work analyzes the toxicity of oxytetracycline in presence of UV-B radiation using model organism *Daphnia magna* and the impact of these stressors on the population development, and expands the subject with a mathematical model that explores its effects on freshwater ecosystems. A chronic test was performed by combined exposures of oxytetracycline and UV-B radiation. Results showed that the effect of the stressors significantly decreased the growth rate coinciding with the alterations identified in the reproduction, thus modifying the population dynamics. This was simulated with mathematical modeling which shows that both oxytetracycline and UV-B radiation are factors that reduce survival and modify the reproductive cycle of the model organism.

Keywords: *mathematical model, population structure, reproductive effects, carrying capacity, model organism*

Introduction

Uncontrolled consumption of pharmaceutical products for human and veterinary uses has caused a raise in pollution levels within freshwater ecosystems (Heckmann et al., 2007) and represents an environmental risk for species that are sensible to biologically active substances. There has been much research focusing on antibiotics, given that their presence in water contributes to the propagation of microbial resistance

(Segura et al., 2015), and that their interactions with other environmental factors causes a raise in toxicity. Such is the case of Tetracycline (TC), an antibiotic that is used regularly as a therapeutic agent and promoter of animal growth. The cyclic structure of these antibiotics allows them to absorb light from the ultraviolet region, thus making them photolabile (Chen et al., 2011; Liu et al., 2018).

Oxytetracycline (OTC) is an antibiotic in the TC group, it has been detected frequently in water bodies and sediments from several countries (Zhao et al., 2013), due to its low absorption level in organisms, especially in animals, its active form is released to the environment through urine and feces. It is estimated that approximately 1900 Kg of OTC can reach surface water bodies yearly (Daghrir et al., 2013) with an average residence time of about 9 days in these ecosystems and without any alteration in its structure (Jeffrey et al., 2006; Leal et al., 2019). However, when OTC interacts with the ultraviolet region of solar light, especially with the UV-B portion (i.e. 320 – 280 nm), it fosters an increase in its toxicity, affecting aquatic organisms by lowering their productivity and reproduction, and it affects species such as phytoplankton, zooplankton, macroalgae, fish eggs, and larvae particularly (Häder et al., 2015).

Freshwater zooplankton is composed mainly by three taxonomic groups: Rotifer, Cladocera and Copepod. *Daphnia magna* (*D. magna*) is an herbivorous cladoceran, that is largely used as a model organism to assess the impact of environmental changes due to its key position within the trophic chain as a link between primary producers (phytoplankton) and higher-level consumers (fish). *D. magna* serves as an indicator for water quality given that there is a close relation between environmental factors and these organisms sensitivity to changes in their surroundings, may they be either chemical or physical (Nevesa et al., 2015).

This research focused on exploring the OTC toxicity when interacting with UV-B radiation through a chronic test on the model organism *D. magna* and the impact these factors would have in the population development of the aforementioned species. By using a mathematical model that considers the organisms life cycle, as well as survival and fertility rates, it was possible to predict the changes that can happen to the structure and functioning of the population within freshwater ecosystems (Nevesa et al., 2015).

Materials and methods

Test organisms

The organism employed for this study was *D. magna*, obtained from the Laboratory of Ecology and Restoration of Aquatic Systems in the Autonomous University of Puebla, in Puebla, Pue., Mexico. Daphnid cultures were started with 10 female neonates out of a batch of reproducers of known age. Groups composed by 20 daphnids were maintained in 1 L of reconstituted hard water (i.e. total hardness of 250 mg/L of CaCO₃) with pH between 7 – 9. The water was renewed twice per week. For the purposes of this study, 9 batches were implemented for asexual reproduction, and the offspring was in subsequent tests. The cultures were kept at room temperature with a 16:8 photoperiod (light:darkness) and fed every third day with a mix of Spirulina and yeast (TetraVeggieTM) in a 25,000 cells/mL concentration (Kim et al., 2009; Hall et al., 2012).

Experimental design

OTC toxicity test

OTC is commercially available in several formulations that can be presented as pre-mixed food, injectables, soluble powder and tablets for animal use. The OTC used in this study was obtained as an injectable solution (C₂₂H₂₄N₂O₉) from NorVet (SAGARPA Q-7827-047, batch: 174140). In principle, OTC is soluble in water (100 g/L) at 20°C either in acid or basic solutions (Baguer et al., 2000), it can also behave as a strong chelating agent by forming complexes with metallic ions such as Ca²⁺ and Mg²⁺ (Jeffrey et al., 2006).

The ideal OTC concentration for this work was selected from acute and chronic toxicity tests. At first, the acute test method established in the literature (Gallina et al., 2008) was used to determine the OTC toxicity in daphnids cultured in the laboratory. The estimated EC₅₀ for OTC at 48 hours was 0.2 mg/mL (Gallina et al., 2008). Subsequently, for a period of 28 days the populations were exposed to concentrations lower than the EC₅₀ (i.e. 0.025 mg/mL, 0.010 mg/mL and 0.004 mg/mL) with manual counting and medium replacement every third day; this was done to find a suitable sublethal concentration for monitoring individuals in subsequent experiments. This pilot study showed impacts on the daphnid reproduction, especially for the group subjected to the 0.025 mg/mL concentration, which is why it was selected to carry out further tests.

UV-B irradiation toxicity test

A pilot test was carried out to select the UV-B radiation intensity, period of irradiation and the age at which daphnids should be irradiated. Survival tests were performed with a UV-B lamp (model UVB-313, INSTRULAMP). The containers enclosed 10 individuals of different ages (i.e. 48 hours, 4 days and 7 days) in 120 mL of reconstituted hard water in triplicate. They were placed at two different heights under the UV-B lamp (i.e. 10 and 20 cm). The exposures were recorded several times, which included irradiation times of 10 and 20 minutes followed by monitoring after 24, 48, 72 and 96 hours had passed until the immobilization of less than 50% of the organisms was observed, and to allow subsequent follow-up. The UV intensity was measured during the exposure periods, using a specific radio device that was placed under the lamp to obtain information on the intensity provided in W/m².

On the other hand, to achieve a biologically relevant dose of UV radiation, a weighting factor was used according to the reference action spectrum of the International Commission on Illumination (ICI) for erythema on human skin (Eq. 1).

$$E_{erythema} (J/m^2) = I (W/m^2) \times \varepsilon \times t (s) \quad (\text{Eq. 1})$$

where:

$E_{erythema}$ stands for erythematic irradiation; I stands for the spectral radiation from the source (UV lamp, model UVB-313 INSTRULAMP) in W/m²; ε stands for the erythematic coefficient; and t stands for time in seconds (Azevedo et al., 2016).

By using this equation, an effective dose of 75.57 J/m² was determined. In this way, when the spectrum of erythematic action of the ICI is used, the effective dose can also be expressed as the erythemal standard dose (ESD) with a numerical value of 100 J/m². For this work, an ESD of 0.75 was used.

OTC chronic test and UV-B radiation

The chronic test considered four groups in triplicate, each group contained twenty neonatal individuals within 120 mL of medium and were exposed to different conditions: one group was subjected to an OTC constant concentration of 0.025 mg/mL; another one to UV-B radiation (2.2 W/m²). The tests were delayed until the daphnids reached an age of seven days to ensure a larger survival rate. The containers were placed at 20 centimeters from the lamp (UVB-313 INSTRULAMP) for 10 minutes, they were then moved under different lamps (WCAM 207229) to provide them with a normal photoperiod. The same conditions were adopted for the group that considered the interaction between OTC and UV-B radiation. Lastly, there was a control group that was kept under standard conditions. These populations were observed over 20 days and monitored every third day by manual counting.

Statistical methods

All treatments were performed in triplicate and the results were reported as mean ± standard deviation. Statistical analyzes were performed by generalized linear model adjustment with Poisson distribution using logarithms as a link function, then the Tukey test was carried out as a post-hoc test to determine the effects on the population parameters evaluated.

Mathematical model

To describe the population dynamics of *D. magna*, matrix population models were used. They project the population growth from time t to time $t + 1$ in terms of the vital rates during each life stage, focusing especially on the reproduction and survival (Webb et al., 2011), in this way a projection matrix (Eq. 2) is constructed:

$$An_t = n_{t+1} \quad (\text{Eq.2})$$

where:

n is a vector $q \times 1$ that describes the distribution of the population for each the life stage at time t ; q is the number of stages; and A is the population projection matrix, constructed from the decomposition of the life cycle of *D. magna* in categories (Fig. 1) to achieve a transition structure (Eq. 3) (Takada et al., 1992).

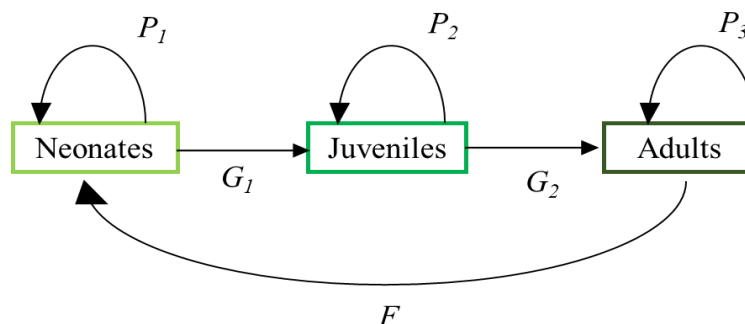


Figure 1. Life cycle of *D. magna* in which the population was classified in three stages: neonates, juveniles and adults. P_i is the probability of surviving and staying in the same stage; G_i is the probability of surviving and growing onto the next stage; and F is the fertility, calculated by observation period

$$A = \begin{matrix} P_1 & 0 & F \\ G_1 & P_2 & 0 \\ 0 & G_2 & P_3 \end{matrix} \quad (\text{Eq.3})$$

where, P is the probability of surviving and staying in Stage i , G , is the probability of surviving and growing into the next stage, and F , is the fertility per female per period. In addition, each of the elements of the equation were calculated from the population monitoring with the consequent elaboration of the life tables and considering the vital rates value (Eqs. 4 and 5).

$$G_{ij} = s_j g_{ij} \quad (\text{Eq.4})$$

$$P_{ij} = s_j(1 - g_{ij}) \quad (\text{Eq.5})$$

where:

s_j : survival rate

f_j : fertility rate

g_{ij} : “growth” rate (phase transition).

Additionally, the observation of the populations supports the definition of fertility as a parameter that depends on the carrying capacity of the system (K) as well as on the percentage of individuals of reproductive age.

The simulation and manipulation of the mathematical model was done with a computational program designed using the Visual Studio compiler (2017) in C++ language (Tokachi et al., 2019).

Results

Chronic effect of OTC over reproduction

The most significant effects in the OTC pilot study were observed in reproduction, given that the time to reach sexual maturity (i.e. the day of first reproduction) for the three exposed groups was delayed with respect to control group ($P < 0.05$). The group that was subjected to 0.025 mg/mL was the one with the most notable difference ($P = 0.016$). Moreover, a decrease in the number of released neonates per female was identified. These results are shown in *Table 1*.

Table 1. *Reproduction and survival of D. magna after being exposed to OTC for 28 days*

Assessed parameter	Control	0.01 mg OTC/mL	0.004 mg OTC/mL	0.025 mg OTC/mL
Time to reach sexual maturity (d)	8.60 ± 0.57 ^a	10.60 ± 0.57 ^b	9.60 ± 0.50 ^{ab}	12.60 ± 0.57 ^c
Number of females (Adults)	73 ± 2.83 ^a	72 ± 8.80 ^{ac}	65 ± 5.00 ^d	83 ± 1.52 ^c
Number of neonates	286 ± 4.24 ^a	125 ± 2.10 ^c	225 ± 1.41 ^b	116 ± 2.12 ^c
Number of juveniles	142 ± 0.73 ^a	115 ± 141 ^b	132 ± 2.12 ^c	96 ± 2.83 ^a
Number of dead	14 ± 1.41 ^a	12.50 ± 0.70 ^a	13 ± 1.41 ^a	16.50 ± 0.73 ^b

The table reports mean values ± standard deviation. The letters indicate significant differences ($P < 0.05$)

UV-B radiation preliminary test

The results for the pilot testing (Fig. 2) correspond to the variation between distance and exposure times to which the individuals of different ages were subjected, while keeping light intensity constant (2.2 W/m^2). Higher mortality rates were recorded in the younger groups, neonates and juveniles ($P < 0.05$), thus demonstrating the vulnerability of these organisms to the minimum exposure time.

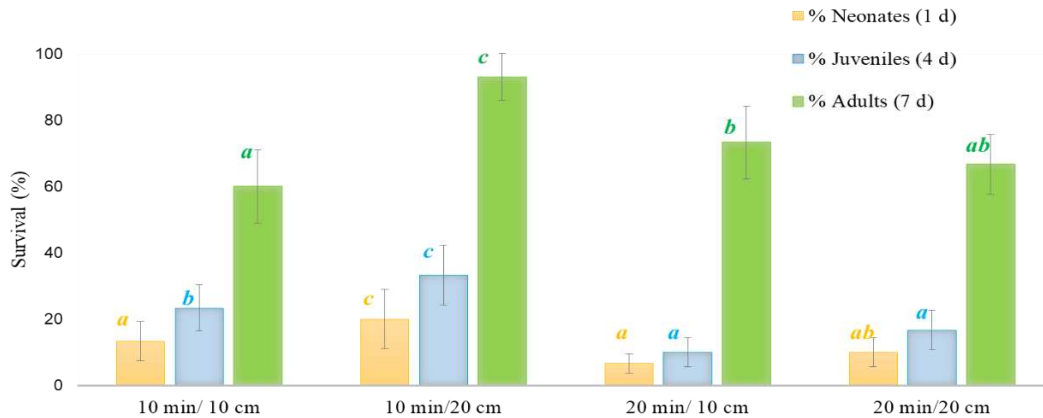


Figure 2. Toxicity test for *D. magna* subjected to UV-B radiation for different time periods and distances. Each bar represents the survival percentage for each age group, depending on the conditions to which they were subjected. The letters indicate significant differences ($P < 0.05$)

Similarly, the statistical analysis allowed to rule out the influence of the type of treatment on survival. However, given the obtained data, the highest survival percentage for the three age groups was registered for individuals exposed at 20 cm separation from the lamp for 10 minutes. Thus, these conditions were chosen, despite not having registered significant differences ($P = 0.06$).

Population dynamic alterations due to OTC and UV-B

One of the objectives of this study was to identify the toxicity of OTC in interaction with UV-B radiation by means of a chronic test that evidences the impact on the population development of *D. magna* by using survival and fertility rates as parameters that describe the population behavior. In the case of reproduction (Table 2) one of the most significant effects was the delay of the first laying ($P < 0.05$) for the three treatments compared to the control group; however, this delay was more evident in the groups subjected to OTC ($P = 0.0012$) and both stressors ($P = 0.0037$). This result, however, does not depend on the interaction between the antibiotic and UV-B irradiation; for the treatment that included both, OTC and UV-B, the first reproduction happened before (i.e. day 12) than in the treatment that had OTC only (i.e. day 13).

Total reproduction (i.e. total number of births over 21 days) was assessed, resulting in a negative relationship depending on the type of treatment, showing a decrease in the number of neonates for each group according to the type of stressor (Table 2). Similarly, when compared to the control group all the treatments present significant differences ($P < 0.05$). However, the largest impact is seen in the group subjected to constant concentration of OTC (0.025 mg/mL) where the total number of neonates is 70% lower

compared to the control group, coinciding with the decrease in fertility observed in the trials. All in all, the average number of neonates that a female had throughout her life was significantly reduced in all treatments, when compared to the control group ($P < 0.05$).

Table 2. Reproduction and survival rates for *D. magna* after 21 days

Assessed parameter	Conditions of the experiment			
	Control	0.025 mg OTC/mL	UV-B	0.025 mg OTC/mL and UV-B
Time to reach sexual maturity (d)	8.6 ± 0.57 ^a	13 ± 0 ^b	11.60 ± 1.15 ^b	12.30 ± 1.15 ^b
Total reproduction (Total number of neonates)	380.60 ± 46.90 ^a	105 ± 19.92 ^b	285.31 ± 10.01 ^c	179.60 ± 18.14 ^d
Neonates per female	5.60 ± 0.57 ^a	3.14 ± 0.16 ^{cb}	4 ± 0.14 ^{ba}	2.80 ± 0.25 ^c
Number of molts	266.30 ± 4.72 ^a	169 ± 9.84 ^c	193.60 ± 9.45 ^b	181 ± 10.14 ^{cb}

The table reports mean values ± standard deviation. The letters indicate significant differences ($P < 0.05$)

On the other hand, individuals were classified in three stages of development (i.e. neonates, juveniles and adults) to assess alterations in the population structure induced by the physicochemical factors that were being studied (Fig. 3). The results show the impact of both stressors on the populations by registering high percentages of adults for all the treatments compared to the control group. In the OTC and UV-B group the relative percentage of adults doubled, a fact that in conjunction with the decrease in fertility, can risk the survival of the population over time.

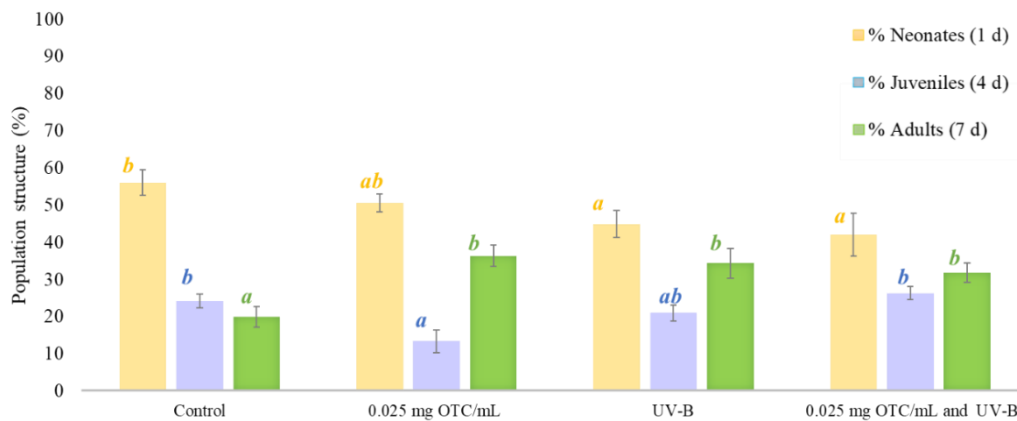


Figure 3. Distribution of *D. magna* populations in three age groups after 20 days of treatment (mean value ± standard deviation). Different letters indicate significant differences ($P < 0.05$)

Projection of the population dynamics through mathematic modeling

The population projection for *D. magna* in a simulated control group ($K = 600$ individuals) indicates an average monthly growth of 13% and a mortality of 3.5% (Floydand et al., 1988; Lo et al., 1995; Coll et al., 2019) with a net reproductive rate (R_0) of 6.2, and a generation time (T) of 3 days (Meyer et al., 1986). The age distribution,

which corresponds to the population structure, is similar to the one observed in the control groups, with a population composed mostly by neonates and juveniles, maintaining a stable reproduction rate and ensuring the survival of the population over time (Fig. 4).

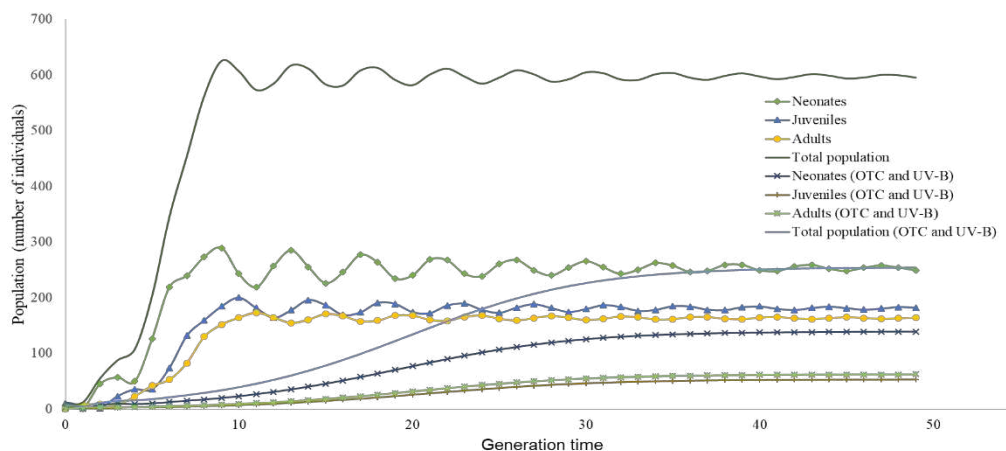


Figure 4. Simulation of the population dynamics of *D. magna* for the control group and the group subjected to OTC and UV-B

Conversely, the population projection for organisms subjected to chronic exposure of oxytetracycline in the presence of UV-B, while keeping the population size ($K = 600$ individuals), presents a monthly average growth of 7.3% and a mortality of 4.5% (Floydand et al., 1988; Lo et al., 1995; Coll et al., 2019). The value of R_0 was 2.8 with T of 3 days, therefore, the average number of neonates per gravid female that integrate into the population every third day was diminished by 54% with respect to the control group, thus altering the population structure because of the relative increase in the number of adults, in comparison with the quantities of juveniles and neonates due to a decline in reproduction rates (Fig. 4) (Meyer et al., 1986; Bernhardt et al., 2018). The registered changes on the finite population growth rate show negative values, which can account for the decline in a population that might as well be facing extinction (Heckmann et al., 2007).

Discussion

The results of this study show the consequences over *D. magna* populations when exposed to OTC concentrations of environmental relevance for a certain time period, specific effects were observed on parameters associated with reproduction: the population structure was altered as a consequence of delays in sexual maturity and the reduction in the number of neonates per female, which also decreased the number of juveniles.

This reproductive effect is supported by the "Principle of allocation" according to which the energy obtained by an individual is divided among the different requirements for maintenance, growth and reproduction. Any extra energy spent in any one of the aforementioned requirements will result in less available energy for the other two. Therefore, the decrease in reproduction would allow for some energy to be invested in the maintenance and survival of organisms (Mollet et al., 2002; Heckmann et al., 2007). This effect has been reported in various ecotoxicological studies, such as Koivisto et al.

(1995) and Eluk et al. (2017), which agree on the importance of assessing not only mortality as an alert parameter but also the reproductive effects, like important bioindicators in order to infer possible damage to aquatic communities in water bodies receiving residual discharges (Rautiainen et al., 2004).

It should be noted that no synergism was observed among the assessed stressors, because the effect of UV-B radiation is covered by the presence of OTC. Some studies have revealed that TC can cause a higher production of melanin and other complexes (Rok et al., 2015), a phenomenon that might explain the fact that daphnids treated with UV-B and OTC are, apparently, less damaged (*Table 2*) than the groups that were treated with any of the stressors individually; given that melanin is a compound that grants protection against adverse environmental conditions, such as UV radiation. However, it is important to highlight the chronic changes in the population structure (*Fig. 3*) caused by the presence of UV-B and OTC, which cause late reproduction and the reduction in the number of neonates per female, which in turn also decreases the number of juveniles and causes a decline in the population due to the inability to reproduce (Heckmann et al., 2007).

In contrast, the observations of the different treatments admit the incorporation of K as a parameter that, along with the percentage of individuals of reproductive age, define fertility and therefore the number of neonates that are integrated into the population. By considering these factors together, the simulations of population dynamics of *D. magna* become more realistic than models that are solely based on the population structure and their vital rates as demonstrated by Lo et al. (1995). It is also worth to mention that the incorporation of changes in somatic duration within the matrix model achieves more realistic projections, when comparing them to models that suppose a fixed duration for the various growth stages.

These results show the importance of adding convenient variables to the matrix models in order to get better explanations to evaluate chronic toxicity of the studied phenomenon. In this study the simulations were compared with monitored groups, which showed an exponential growth that tended to stabilize; however, for the group of interacting OTC and UV-B said stabilization occurred abruptly and without reaching the K value, mainly because of failures in reproductive events (Metcalf et al., 2015) that resulted in an $R_0 = 2.8$, with a 54% decrease in the total number of neonates, when compared to the control group. Therefore, the population is far from an equilibrium since the birth rate cannot reach the mortality rate (4.5%), thus destabilizing the population structure (*Fig. 4*).

Conclusions

This study has demonstrated that anthropogenic pollutants of the TC type, and OTC in particular, can have negative effects on the reproduction of *D. magna*, a species that is sensitive to physical and chemical alterations caused by their presence in fresh water. Some of these effects include delays in the sexual maturity of daphnids, as well as a reduction in birth rates, decreasing the number of neonates that integrate into the population and altering population dynamics. This scenario was verified through simulations supported by mathematical modeling, that showed that both OTC and UV-B radiation are limiting factors to the population growth and that they reduce the survival rates and modify the reproductive cycle of the organism.

In contrast, with the introduction of parameters that define the population dynamics into matrix models, it is possible to obtain detailed simulations of the population behavior

of *D. magna* under realistic environmental conditions that represent a useful tool for the interpretation of later empirical studies. In future researches it will be necessary the development of chronic studies which allow the evaluation of population dynamics, through mathematical models which incorporate another variables of aquatic ecosystems such as pH, hardness, temperature, dissolved oxygen, which could lead to increased toxicity induced by physicochemical factors OTC and UVB, in order to achieve a better understanding and evaluation of the environmental risk of these pollutants.

REFERENCES

- [1] Azevedo, S. L., Ribeiro, F., Jurkschat, K., Soares, A. M., Loureiro, S. (2016): Co-exposure of ZnO nanoparticles and UV radiation to *Daphnia magna* and *Danio rerio*: Combined effects rather than protection. – *Environmental Toxicology and Chemistry* 35(2): 458-67.
- [2] Baguer, A. J., Jensen, J., Henning, K. P. (2000): Effects of the antibiotics oxytetracycline and tylosin on soil fauna. – *Chemosphere* 40(7): 751-757.
- [3] Bernhardt, J. R., Sunday, J. M., Thompson, P. L., O'Connor, M. I. (2018): Nonlinear averaging of thermal experience predicts population growth rates in a thermally variable environment. – *The royal society publishing* 285(1886): 1-10.
- [4] Chen, Y., Li, H., Wang, Z., Tao, T., Hu, C. (2011): Photoproducts of tetracycline and oxytetracycline involving self-sensitized oxidation in aqueous solutions: Effects of Ca^{2+} and Mg^{2+} . – *International Journal of Environmental Science and Technology* 23(10): 1634-1639.
- [5] Coll, C., Sánchez, E. (2019): Parameter identification and estimation for stage-structured population models. – *International Journal of Applied Mathematics and Computer* 29(2): 327-336.
- [6] Daghrir, R., Drogui, P. (2013): Tetracycline antibiotics in the environment: a review. – *Environmental Chemistry Letters* 11(13): 209-227.
- [7] Eluk, D., Althaus, R., Nagel, O., Reno, U., Gagnetten, A. M. (2017): Uso de *Daphnia magna* -organismo no target- para evaluar el impacto ambiental de quinolonas. – V Jornada de difusión de la investigación y extensión.
- [8] Floydand, S. K., Ranker, T. A. (1998): Analysis of a transition matrix model for *Gaura neomexicana* ssp. *coloradensis* (Onagraceae) reveals spatial and temporal demographic variability. – *International Journal of Plant Sciences* 159(5): 853-863.
- [9] Gallina, G., Poltronieri, C., Merlanti, R., De Liguoro, M. (2008): Acute toxicity evaluation of four antibacterials with *Daphnia magna*. – *Veterinary Research Communications* 32: 287-290.
- [10] Hall, M. D., Ebert, D. (2012): Disentangling the influence of parasite genotype, host genotype and maternal environment on different stages of bacterial infection in *Daphnia magna*. – *Proc Biol Sci* 279(1741): 3176-83.
- [11] Häder, D. P., Kumar, H. D., Smith, R. C., Worrest, R. C. (2015): Effects of UV radiation on aquatic ecosystems and interactions with other environmental factors. – *Photochemical & Photobiological Sciences* 14: 108-106.
- [12] Heckmann, L. H., Callaghan, A., Hooper, H. L., Connon, R., Hutchinson, T. H., Maund, S. J., Sibly, R. M. (2007): Chronic toxicity of ibuprofen to *Daphnia magna*: Effects on life history traits and population dynamics. – *Toxicology Letters* 172(3): 137-145.
- [13] Jeffrey, J., Werner, J. J., William, A. A., McNeill, K. (2006): Water Hardness as a Photochemical Parameter: Tetracycline Photolysis as a Function of Calcium Concentration, Magnesium Concentration, and pH. – *Environmental Science & Technology* 40(23): 7236-7241.

- [14] Kim, J., Lee, M., Oh, S., Ku, J. L., Kim, K. H., Choi, K. (2009): Acclimation to ultraviolet irradiation affects UV-B sensitivity of *Daphnia magna* to several environmental toxicants. – *Chemosphere* 77(11): 1600-1608.
- [15] Koivisto, S. (1995): Is *Daphnia magna* an ecologically representative zooplankton species in toxicity tests? – *Environmental Pollution* 90(2): 263-267.
- [16] Leal, J. F., Esteves, V. I., Santos, E. B. H. (2019): Solar photodegradation of oxytetracycline in brackish aquaculture water: New insights about effects of Ca²⁺ and Mg. – *Journal of Photochemistry & Photobiology A: Chemistry* 372: 218-225.
- [17] Liu, X., Lu, S., Guo, W., Xi, B., Wang, W. (2018): Antibiotics in the aquatic environments: A review of lakes, China. – *Science of the Total Environment* 627: 1195-1208.
- [18] Lo, N., Smith, P., Butler, J. (1995): Population growth of northern anchovy and Pacific sardine using stage-specific matrix models. – *Marine Ecology Progress Series* 127(1): 15-26.
- [19] Metcalf, C. J. E., Ellner, S. P., Childs, D. Z., Gomez, R. S., Merow, C., McMahon, S. M., Jongejans, E., Rees, M. (2015): Statistical modelling of annual variation for inference on stochastic population dynamics using Integral Projection Models. – *Methods in Ecology and Evolution* 6: 1007-1017.
- [20] Meyer, J. S., Ingersoll, C. G., McDonald, L. L., Boyce, M. S. (1986): Estimating Uncertainty in Population Growth Rates: Jackknife vs. Bootstrap Techniques. – *Ecology* 67(5): 1156-1166.
- [21] Mollet, H. F., Cailliet, G. M. (2002): Comparative population demography of elasmobranchs using life history tables, Leslie matrices and stage-based matrix models. – *Marine and Freshwater Research* 53: 503-516.
- [22] Nevesa, M., Castroa, B. B., Vidala, T. T., Marques, J. C., Coutinho, J. A. P., Goncalves, F., Goncalves, A. M. M. (2015): Biochemical and populational responses of an aquatic bioindicator species, *Daphnia longispina*, to a commercial formulation of a herbicide (Primextra® Gold TZ) and its active ingredient (S-metolachlor). – *Ecological Indicators* 53: 220-230.
- [23] Rautiainen, P., Laine, A. L., Aikio, S., Aspi, J., Siira, J., Hyvärinen, M. (2004): Seashore Disturbance and Management of the Clonal *Arctophila fulva*: Modelling Patch Dynamics. – *Applied Vegetation Science* 7(2): 221-228.
- [24] Rok, J., Buszman, E., Delijewski, M., Otręba, M., Beberok, A., Wrześniok, D. (2015): Effect of tetracycline and UV radiation on melanization and antioxidant status of melanocytes. – *Journal of Photochemistry and Photobiology B: Biology* 148: 168-173.
- [25] Segura, P. A., Takada, H., Correa, J. A., El Saadi, K., Koike, T., Agyeman, S. O., Ofosu-Anime, J., Sabi, E. B., Wasonga, O. V., Mghalu, J. M., Dos Santos Junior, A. M., Newman, B., Weerts, S., Yargeau, V. (2015): Global occurrence of anti-infectives in contaminated surface waters: Impact of income inequality between countries. – *Environment International* 80: 89-97.
- [26] Takada, T., Nakajima, H. (1992): An analysis of life history evolution in terms of the density-dependent Lefkovich matrix model. – *Mathematical Biosciences* 112(1): 155-176.
- [27] Tokachil, M. N., Yahya, A. (2019): The Lefkovich Matrix of *Aedes Aegypti* with Rainfall Dependent Model for Eggs Hatching. – *Journal of Physics* 1366: 1-8.
- [28] Webb, A. R., Slaper, H., Koepke, P., Schmalwieser, A. W. (2011): Know your standard: clarifying the CIE erythema action spectrum. – *Photochemistry and Photobiology* 87(2): 483-486.
- [29] Zhaoa, C., Pelaez, M., Duan, X., Denga, H., O'Shea, K., Fatta-Kassinos, D., Dionysiou, D. D. (2013): Role of pH on photolytic and photocatalytic degradation of antibiotic oxytetracycline in aqueous solution under visible/solar light: Kinetics and mechanism studies. – *Applied Catalysis B: Environmental* 134: 83-92.

THE EFFECT OF SINGLE AND COMPOSITE ADDITIVES ON CD AND PB MOBILITY, SPECIATION AND ACCUMULATION IN LATE RICE (*ORYZA SATIVA* L.) GROWN ON CONTAMINATED SOIL

TONG, W.^{1#} – HAMID, Y.^{2##} – HUSSAIN, B.² – USMAN, M.³ – SHER, A.^{4,5} – LIU, L.¹ – YANG, X.^{2*}

¹*Qiujiang Agricultural and Rural Bureau, Quzhou District, Zhejiang Province, China*

²*Ministry of Education (MOE) Key Lab of Environ. Remediation and Ecol. Health, College of Environmental and Resources Science, Zhejiang University, Hangzhou 310058, China*

³*PEIE Research Chair for the Development of Industrial Estates and Free Zones, Center for Environmental Studies and Research, Sultan Qaboos University, Al-Khoud 123, Muscat, Oman*

⁴*School of Agronomy, Anhui Agricultural University, Hefei, Anhui, China*

⁵*Key Laboratory of Crop Chemical Regulation and Chemical Weed Control, College of Agronomy, Shanxi Agricultural University, Taigu, Shanxi, China*

#These authors contributed equally to this work.

**Corresponding authors*

e-mail: yasirses2007@gmail.com; xeyang@zju.edu.cn

(Received 29th Oct 2019; accepted 30th Jan 2020)

Abstract. This field trial investigated the cadmium (Cd) and lead (Pb) immobilization in contaminated paddy soil. Five stabilizing agents including lime, biochar, phosphatic fertilizer (PF) and two composites (S1, S2) were investigated (1% w/w) for metals immobilization by growing late rice as a test crop. The results revealed the improved pH and decreased metal availability in lime, S1, biochar and S2 treated plots. The Cd and Pb speciation results depicted a decrease in exchangeable Cd content to less mobile forms (29 and 30%) with addition of biochar and S1 in harvest stage samples. The exchangeable fraction of Pb was significantly reduced to 29, 29 and 36% with S1, S2 and biochar, respectively. Moreover, Cd and Pb accumulation in rice grains was lowest in composite stabilizers and biochar treatments. Our results showed a significant increase in leaf photosynthetic rate, transpiration rate, biomass and grains yield in S1 amended plot. These lessening effects are owed to the conversion of available metal contents to the least mobile forms. Our results confirmed the effectiveness of organic additives alone and in mixture with inorganics in reducing metal mobility, improving immobilization, enhancing growth and decreasing accumulation in food parts and showed a great prospect in safer food production.

Keywords: *metals immobilization, lime, biochar, phosphatic fertilizer, rice uptake*

Introduction

Trace metals especially cadmium (Cd) and lead (Pb) have a strong toxic effect on animals and humans which exerts health concerns worldwide (Chen et al., 2018). Cd and Pb contamination are often reported in agricultural soils due to natural and anthropogenic activities but their entry into the soil environment is mostly associated with agricultural inputs and mining or smelting effluents (Hamid et al., 2018). Cd and Pb are among the most toxic metals due to their high accumulation in edible parts of plants hence posing a high risk of contamination to the food chain (Liang et al., 2016; Igalavithana et al., 2019). Therefore, it is of utmost importance to remediate metals

polluted soils without influencing the crop yield (Xiong et al., 2019). Moreover, it is important to unveil the metals availability and related processes for the development of innovative techniques to improve metals stability in soil and reduced accumulation in plants.

In recent years, the sorption of metals with low cost and environment-friendly stabilizers has been emerged as an innovative approach to remove contaminants from polluted sites. Various inorganic or organic stabilizers have been reported for their effectiveness in immobilizing the metals in different soil types (Hamid et al., 2019b). Stabilizers reduce metals availability owing to adsorption/stabilization/precipitation/ion exchange attributes. However, many adsorbents show disadvantages due to their less stability, adsorption capacity and success in multi metals contaminated soils (Hu et al., 2017). Moreover, in some cases single additive show effectiveness for one metal and did not present significant difference for other elements. So, composite addition of additives may be more efficient in reducing metal contamination in co-contaminated soil (Lahori et al., 2017). Our earlier reports (Hamid et al., 2019a) also confirmed the effectiveness of composite amendments on metals stability in co-contaminated soils.

Immobilization is a process of remediating the contaminants by transforming their high mobile fraction to less available form. Lime is regarded as one of the most effective immobilizer for metallic compounds (Bade et al., 2012). Liming the polluted region points to reduced metal availability by increasing soil pH and the production of hydroxyl ions due to hydrolysis of CaCO_3 (Wu et al., 2016). Liming induces metals availability by making carbonate-metal precipitates which reduces the exchangeable fraction of metals (Singh and Kalamdhad, 2013). In a field experiment, Rehman et al. (2017a) reported a decrease in available Cd contents with a combined addition of lime and biochar. Recently, in-situ stabilization of metal contaminated soils with phosphatic fertilizer has gained keen attention as an alternative remediation technique. Phosphate induced stabilization comprises of metals precipitation with inorganic phosphate or metals adsorption (Hong et al., 2008, 2010). Phosphatic fertilizers addition can alleviate soil characteristics such as pH, available phosphate contents, soil surface charge or directly interacts with metal ions in the soil. These changes can induce a swing in the metal available form to a more stable form (Zhao et al., 2014; Yan et al., 2015).

Biochar is an organic material pyrolyzed at different temperatures under low oxygenic conditions (Leng et al., 2019) by combustion of wood, plant residues etc. Biochar is a stable compound mainly used in the restoration of metal contaminated sites. Biochar has ability to retain metals owing to complexation, adsorption or ion exchange mechanisms (El-Naggar et al., 2018). Biochar addition improved the plant growth by increasing nutrients availability and reducing leaching in soil (Cornelissen et al., 2018; Li et al., 2019). Meanwhile, metals adsorption on the surface of biochar depends upon raw material, metal concentration and pyrolysis temperature. An improved stability of biochar with high combustion temperature is reported in literature (Song et al., 2012; Bashir et al., 2018).

To date, different inorganic and organic additives have been adopted in stabilization of metal but most of the studies focused on single contaminant and rarely on multi-metal contamination. Therefore, there is a shortage of studies focusing on stabilization of multi -metal contamination with composite treatments and the comparison of effectiveness with their commercial competitors. Moreover, this study was established

on improved Cd and Pb immobilization with the incorporation of single and composite additives by increasing soil pH and CEC. The objective of our study was (a) to check the efficacy of inorganic and organic amendments alone and their novel mixtures on improved rice biomass and grains yield, (b) to examine the availability of Cd and Pb and subsequent uptake or accumulation by late rice, (c) to gain the insights of immobilization mechanisms by speciation method, (d) to identify the most favorable soil amendment for safer food production on Cd-Pb co-contaminated site.

Materials and methods

Study site, additives collection and application

This field experiment was conducted in a contaminated red paddy field situated in Qujiang County (E 119.01, N 29.05), Zhejiang province, China having annually mean temperature (17 °C) and precipitation (1,723 mm). Cd and Pb contents of studied soil ranged to 0.54 mg kg⁻¹ and 95.42 mg kg⁻¹ respectively (Cao et al., 2019). Late rice cultivar (Yong You 9) was cultured in mid-July (15-07-2017) and three-week (07-08-2017) old seedlings were shifted to the field. This late rice cultivar is been widely used in this specific area due to its high grains production and improved biomass. Lime, biochar, PF (phosphatic fertilizer), organic manure, wood powder, sepiolite, and zeolite were collected from different commercial sources. Biochar used in this experiment was pyrolyzed from coconut shell at 350 °C. Six treatments including control, lime, biochar, PF, S1 and S2 were investigated for their effectiveness as immobilizers. S1 and S2 were cycled by mixing various organic and inorganic additives with clay minerals at different ratios. S1 was derived by mixing biochar with lime, sepiolite and zeolite while S2 was composited by manual mixing of manure with lime and sepiolite. Amendments were applied in triplicates and were arrayed according to RCBD (randomized complete block design) with each plot having area 64 m². Each treatment block was separated with ridges and includes separate inlet and outlet for watering and drainage. All the treatments were applied at 1% (w/w) before 20 days (18-07-2017) of seedling transplantation and were mixed mechanically on the upper layer of soil. Fertilization was completed by adding N (130 kg ha⁻¹), P₂O₅ (50 kg ha⁻¹) and K₂O (150 kg ha⁻¹) in shape of urea, di-ammonium phosphate and muriate of potash before start of experiment. Additional phosphatic fertilizer was not added in the treatment of PF due to its use as a stabilizing agent. Photosynthetic rate (Pn) and transpiration rate (Tr) were measured using an IRGA (infrared gas analyzer) after 70 days of crop growth.

Soil and plant sampling

Soil samples were collected from experimental site for pH, organic carbon, and total metal concentration in soil (*Table 1*). Furthermore, for available metal contents soil sampling was done after the addition of soil additives. Samples were taken 1 day before nursery transplantation (zero month) in the field and at harvest (2017-11-10).

Meanwhile, plants were harvested at maturity and plant height, biomass and grains yield were measured. From each plot, plants were harvested (1 m²) and weighed for biological yield. Harvested fifteen plants were sampled and brought to the lab for metal analysis. Plants were cut into pieces (roots, shoots and grains), washed with tap water, and then rinsed with ultra-pure water. Plants were oven dried until constant weight, grinded and analyzed for metal accumulation in different parts.

Table 1. Physico-chemical properties of soil and applied additives

No.	Treatment/soil	pH	Organic carbon (g kg ⁻¹)	Total Pb (mg kg ⁻¹)	Total Cd (mg kg ⁻¹)
1	Soil	5.71	54.76	95.42	0.54
2	Lime	11.12	nd	0.624	0.20
3	Biochar	8.06	387	1.656	0.05
4	PF	7.21	nd	2.57	0.35
5	S1	11.12	74.68	4.800	0.20
6	S2	11.34	32.11	3.895	0.15

Soil with silty clay texture (Sand 15%, Silt 32.10%, Clay 52.90%) PF: Phosphatic fertilizer, S1 and S2 (stabilizers)

Amendments, soil and plant analysis

Basic physicochemical properties of soil and amendments were measured with standard methods proposed by (Li, 2000; Bao, 2008). Amendments and soil pH were measured by shaking material and water at ratio 1: 2.5 using a PB-10, Sartorius, Germany pH meter (Table 1). Total metal concentration in additives and soil was measured by digesting the material with a solution of HNO₃-HF-HClO₄ for 12 h. DTPA extraction was performed to analyze available Cd and Pb concentration in treated soil. Soil (20 g) was shaken with a DTPA-TEA mixture (50 mL) for 2 h at room temperature. Suspension was then filtered from 0.45-µm filter and bio-available Cd and Pb concentration in solution was calculated using ICP-MS (Agilent, 7500a, USA) (Li, 2000; Bao, 2008).

Cd and Pb fractionation in treated and untreated soil at harvest were estimated by the sequential extraction method (Table 2) proposed by (Tessier et al., 1979).

Dried and grounded plant samples were digested for accumulated Cd and Pb concentration in different parts. Cd and Pb concentration were measured by digesting 0.20 g of desired plant sample with an acidic solution of HClO₄ and HNO₃ at 170 °C for 4 h. Metals concentration in the digested solution was measured with ICP-MS (Bao, 2008).

Table 2. The sequential extraction procedure for Cd and Pb

Fraction	Procedure
F1: Exchangeable	1 g soil (treated/untreated) shaken with 8 ml of 1 M MgCl ₂ solution (pH = 7)
F2: Carbonate bound	F1 residues extracted with NaOAc (1 M), pH: 5 for 5 h
F3: Fe-Mn oxide bound	Residues of F2 were mined with 20 mL (0.04 M) NH ₂ OH•HCl in 25% CH ₃ COOH for 6 h at 96 °C
F4: Organic matter bound	Firstly, F3 residues shaken with 5 mL of H ₂ O ₂ (30%) for 3 h (at 85 °C) and then with 3.2 M ammonium acetate for half an hour and mixture was collected and mixed to make one solution
F5: Residual	Remaining residues were digested with HNO ₃ - HF-HClO ₄ and diluted

Cadmium and Pb translocation factor (TF) from roots to shoot was calculated with the following formula (Eq. 1):

$$TF (\%) = \text{Cd, Pb concentration in shoots} / \text{Cd, Pb concentration in roots} * 100 \quad (\text{Eq.1})$$

Statistical analyses

All the used chemicals and reagents in this experiment were of analytic grade. The digestion tubes were washed with distilled water, put overnight in acidic solution and again washed with distilled water followed by rinsing with ultra-pure water before each use. Data presented are means of three replicates \pm S.E which was estimated with MS Excel 2007. Statistical analysis (LSD test) was performed with SPSS 20.0 and graphical illustration was done with Origin Pro 8.0.

Results

Effect of applied passivators on soil pH and DTPA extractable Cd and Pb at different time intervals

The effect of applied additives on soil pH at zero month and harvest is presented in *Figure 1*. Zero month samples were taken around 20 days of amendments. There was a quick elevation in soil pH with lime and S2 treatment at zero month. Lime and S2 treatment showed an increase of 1.68 and 0.93 units in soil pH as compared to control. Meanwhile, a significant increase in soil pH with lime, S2, biochar and S1 was also observed at harvest samples. These treatments improved soil pH to a significant level with values of 7.56, 6.84, 6.71 and 6.53 respectively as compared to respective control (5.8). It was noteworthy; that addition of PF did not improve the soil pH at both sampling stages and showed slightly acidic behavior. Cd availability (DTPA extractable) was reduced with biochar and composite mixtures (S1 and S2) (*Fig. 2*). Composite treatment (S2) showed a significant reduction in Cd availability at zero month while, S1 and biochar were effective in reducing metal availability in harvest stage samples. Maximum Cd was extracted in control treatment at both sampling stages (0.374 and 0.357 mg kg⁻¹). When compared with the control, S1 treatment and biochar significantly ($p < 0.05$) reduced the DTPA extractable Cd by 63 and 60% respectively in the second sampling stage. Application of treatments reduced the DTPA extractable Cd in following order S1 \approx biochar > S2 \approx lime > PF > control.

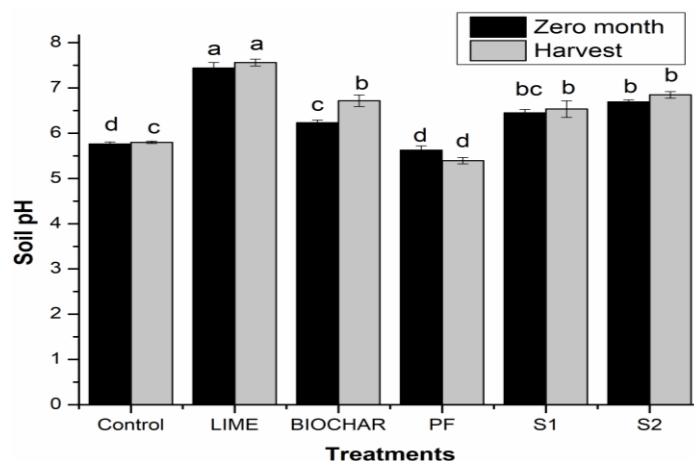


Figure 1. Effect of soil amendments on soil pH at different time intervals. Control, lime, biochar, PF, S1 and S2 were employed in triplicates (1% w/w). Error bars with different letters show significance at different sampling time

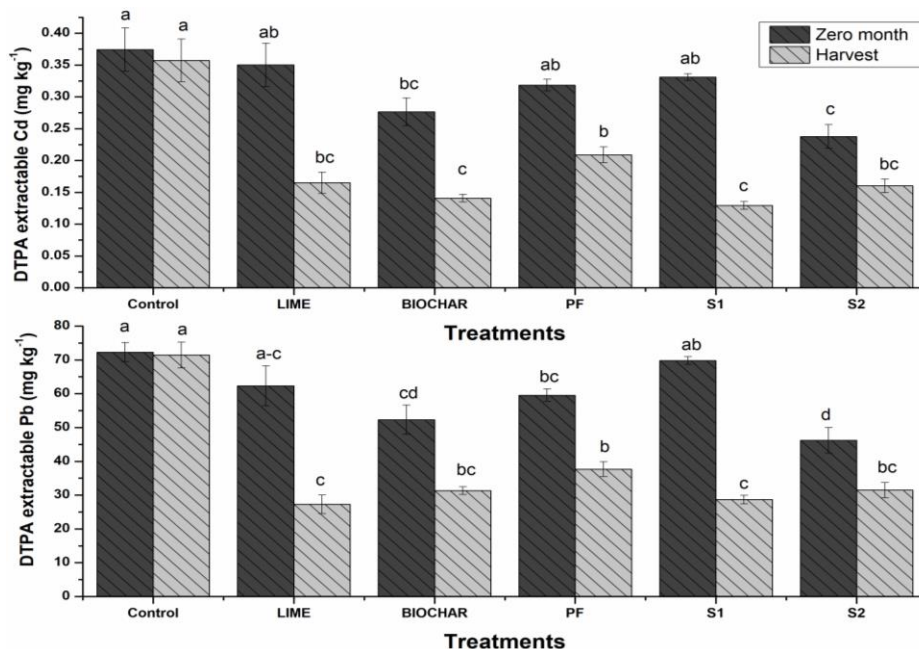


Figure 2. Effect of soil additives on available Cd and Pb contents of contaminated soil. Control, lime, biochar, PF, S1 and S2 were employed in triplicates (1% w/w). Error bars with different letters show significance at different sampling time

Meanwhile, alone lime and its combination with organic and clay additives (S1) reduced the Pb extractability by 61 and 59% as compared to respective control in harvesting stage soil samples. Biochar treatment also signifies the reduction in Pb extraction in comparison with control by decreasing Pb availability by 56%. Generally, all the applied treatments significantly improved the metals immobilization by decreasing metal mobility and extraction at end of experiment. Pb availability with applied treatments reduced in subsequent order S1≈lime > S2≈ biochar > PF > as compared to control.

Correlation between soil pH and DTPA extractable Cd and Pb at different time intervals

A negative linear correlation was found between soil pH and DTPA extractable Cd and Pb at zero month and harvesting stage samples (*Fig. 3*). Correlation between available Cd and soil pH at both sampling stages showed negative behavior ($R^2 = 0.0027$, $p = 0.837$ and $R^2 = 0.0182$, $p = 0.594$). Meanwhile, amendments addition resulted in a significant negative correlation between soil pH and available Pb contents in zero month and harvest samples ($R^2 = 0.2851$, $p = 0.022$ and $R^2 = 0.3147$, $p = 0.015$).

Cd and Pb species distribution with applied additives

The chemical speciation of Cd and Pb in zero month and harvest soil samples is summarized in *Figure 4*. The applied treatments showed little difference for Cd portioning at zero month soil samples with maximum exchangeable Cd in control treatments (58%) and lowest in biochar treated blocks (41%). During the experiment, Cd quantities for different species varied with amendments. In general, exchangeable Cd content decreased with an increase in carbonate, oxide, organic bound and residual

fractions. Biochar treatments reduced the Cd exchangeability to 29% followed by S1 (30%), PF (32%), S2 (33%) and lime (37%) as compared to control (50%). The effect of treatments on Pb mobility and partitioning showed the effectiveness of composite treatments and biochar at the experiment end. Pb exchangeable fraction was decreased to 29% each for S2 and S1 followed by biochar (36%), PF (38%) and lime (40%) in comparison with control (63%).

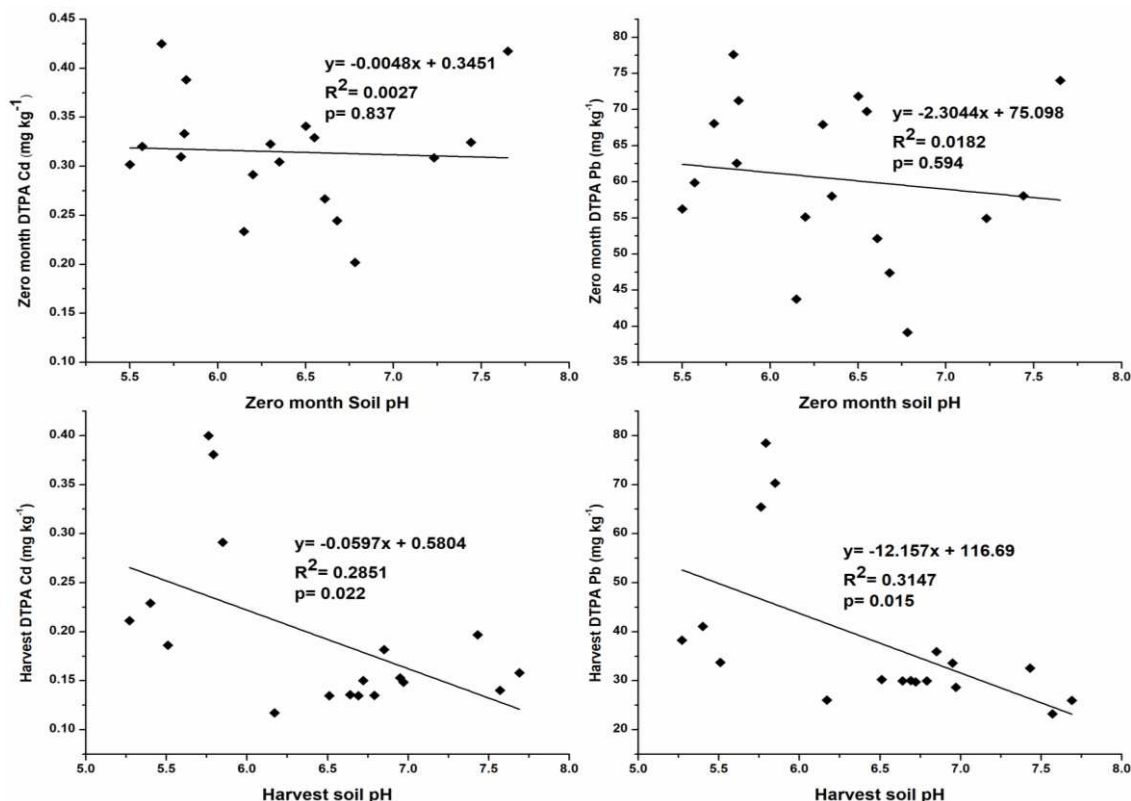


Figure 3. Correlation between soil pH and available Cd and Pb contents of contaminated soil

Effect of applied additives on gaseous exchange

All the applied treatments significantly increased the photosynthetic rate (Pn) of rice (Fig. 5). Photosynthetic rate increased in S2 followed by S1 which increased up to 112 and 102% as compared to control. Biochar, PF and lime also showed significant increase in photosynthetic rate by 85, 82 and 75% respectively as compared to the control. Maximum increase in transpiration rate (Tr) was witnessed in S2 and S1 treated plots which was 162% and 152% higher than control (Fig. 5). On the other side, biochar, PF and lime also significantly improved the Tr by 124, 118 and 93% respectively, compared to control.

Cd and Pb accumulation in plant parts

Uptake and accumulation of Cd and Pb in rice were significantly affected by treatments (Table 3). At maturity all the applied treatments significantly reduced Cd contents in rice roots compared to the control but there was no significant difference among applied additives for Cd accumulation in roots. Adding S2 and biochar

significantly reduced the shoots Cd concentration by reducing uptake to 0.216 and 0.227 mg kg⁻¹ as compared to the control (0.322 mg kg⁻¹). Moreover, Cd content in rice grains was reduced to 0.049 and 0.056 mg kg⁻¹ in S2 and biochar treatments with the highest in control (0.231 mg kg⁻¹). On the other hand, Pb accumulation in rice grains was significantly reduced with S2, S1 and biochar treatment (0.070, 0.101 and 0.126 mg kg⁻¹) respectively which was much less than control (1.818 mg kg⁻¹). Lime and PF treatments also significantly reduced Pb accumulation in rice grains with values of 0.395 and 0.922 mg kg⁻¹.

Translocation of Cd and Pb from roots to shoots is presented in *Figure 6*. There was no significant difference for roots to shoots Cd translocation among the treatments with minimum translocation in S1 (62%) followed by lime (65%). While, Pb translocation in shoots was significantly reduced with biochar and S2 treatments (20% and 29%), as compared to control.

Table 3. Effect of soil additives on metal contents of late rice

Treatments	Cd concentration (mg kg ⁻¹)			Pb concentration (mg kg ⁻¹)		
	Roots	Shoots	Grains	Roots	Shoots	Grains
Control	0.462 ± 0.038a	0.322 ± 0.022a	0.231 ± 0.011a	61.10 ± 2.61a	45.26 ± 0.590a	1.818 ± 0.045a
Lime	0.362 ± 0.023b	0.238 ± 0.012bc	0.115 ± 0.015c	45.59 ± 0.807bc	20.80 ± 1.732b	0.395 ± 0.108c
Biochar	0.328 ± 0.008b	0.227 ± 0.007c	0.056 ± 0.018d	40.34 ± 1.277c	8.20 ± 0.508d	0.126 ± 0.019d
PF	0.366 ± 0.041b	0.276 ± 0.012b	0.177 ± 0.011b	48.02 ± 1.001b	21.50 ± 0.699b	0.922 ± 0.026b
S1	0.369 ± 0.015b	0.231 ± 0.016bc	0.119 ± 0.010c	40.97 ± 2.21c	18.35 ± 0.629b	0.101 ± 0.013d
S2	0.314 ± 0.002b	0.216 ± 0.007d	0.049 ± 0.011d	45.19 ± 1.06bc	13.40 ± 1.386c	0.070 ± 0.028d

Control, lime, biochar, PF, S1 and S2 were employed in triplicates (1% w/w). Different letters indicates significantly different values at 5% significance level. All treatments including control receive recommended dose of N, P and K except treatment PF in which phosphorus was not applied. PF: phosphatic fertilizer, S1 and S2 (stabilizers)

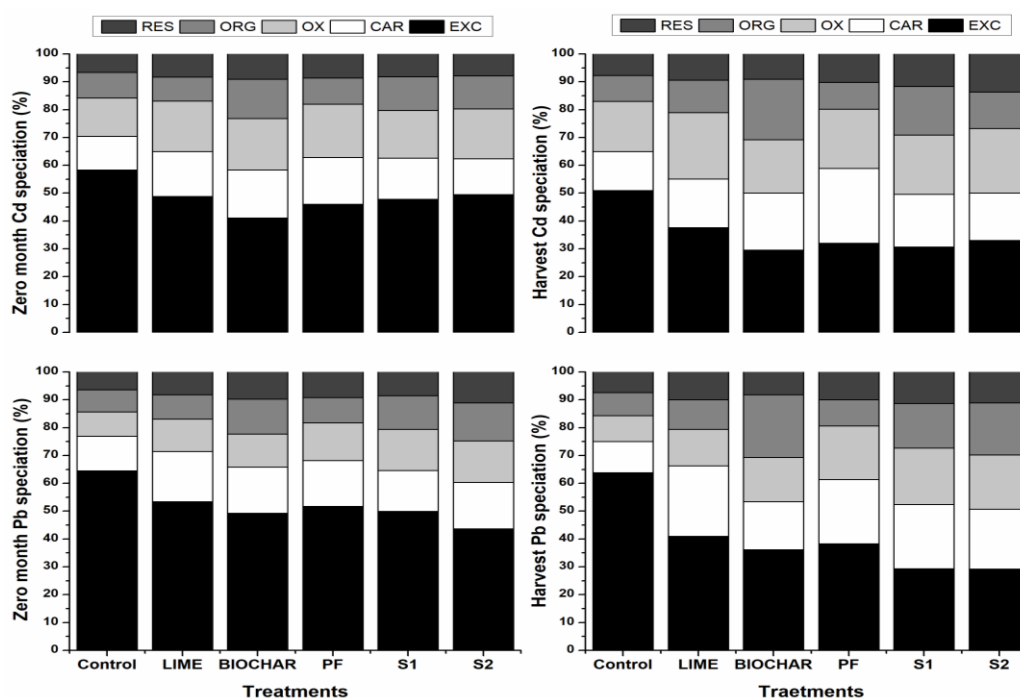


Figure 4. Effect of soil additives on Cd and Pb speciation of contaminated soil

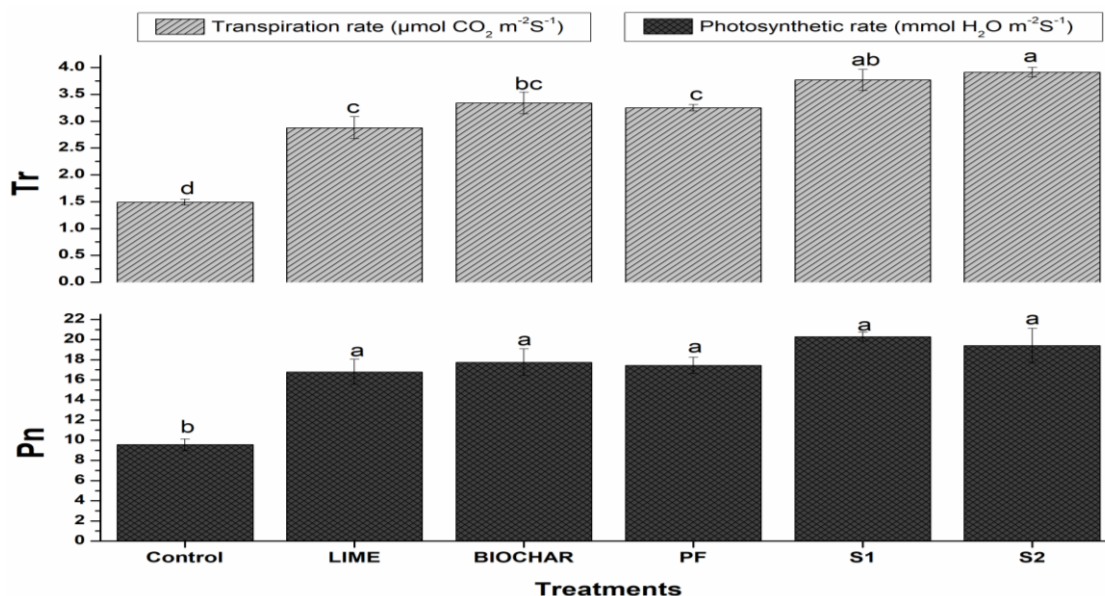


Figure 5. Effect of soil additives on leaf photosynthesis and yield parameters of late rice. Control, lime, biochar, PF, S1 and S2 were employed in triplicates (1% w/w). Error bars with different letters show significance at different sampling time

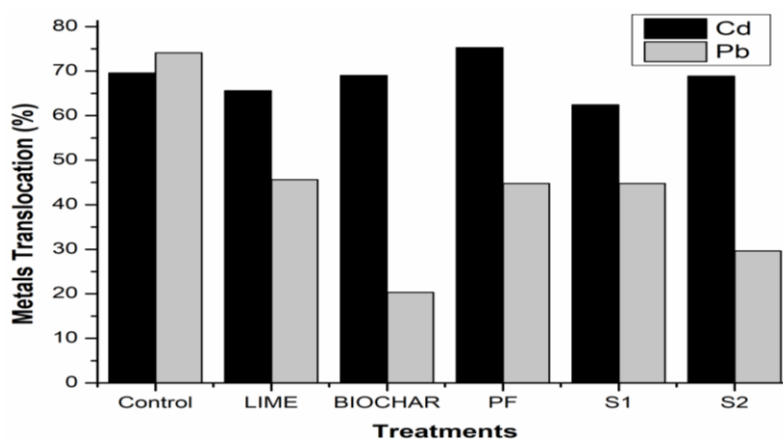


Figure 6. Effect of soil additives on metals translocation from roots to shoots. Control, lime, biochar, PF, S1 and S2 were employed in triplicates (1% w/w)

Effect of additives on the growth of late rice

Rice biomass was determined at harvest and results revealed that all the additives significantly improved rice biological yield (Table 4). But there was no significant difference for biomass yield among the additives. Maximum rice biomass was found in S1 followed by PF, S2, biochar and lime (18342, 18000, 17931, 17903, 17600, 14666 kg ha⁻¹). All the treatments significantly increased grains yield but maximum per hectare grains yield was observed in S1 (7530 kg ha⁻¹) followed by S2 and biochar (7129 and 7026 kg ha⁻¹) which was a significant increase as compared to control. A similar pattern was observed in plant height where all applied treatments significantly improved plant height but with no obvious difference among the additives.

Table 4. Effect of soil additives on growth of late rice

Treatments	Biomass (Kg ha ⁻¹)	Grains yield (Kg ha ⁻¹)	Plant height (cm)
Control	14666 ± 240b	6040 ± 247c	93 ± 1.453b
Lime	17600 ± 351a	6741 ± 274b	102 ± 2.185a
Biochar	17903 ± 250a	7026 ± 241ab	104 ± 2.081a
PF	18000 ± 568a	7022 ± 98ab	106 ± 2.962a
S1	18342 ± 218a	7530 ± 132a	103 ± 1.763a
S2	17931 ± 470a	7129 ± 82ab	104 ± 1.701a

Control, lime, biochar, PF, S1 and S2 were employed in triplicates (1% w/w). Different letters indicates significantly different values at 5% significance level. All treatments including control receive recommended dose of N, P and K except treatment PF in which phosphorus was not applied. PF: Phosphatic fertilizer, S1 and S2 (stabilizers)

Discussion

In this field experiment, the effect of several soil additives on metal translocation and accumulation was trialed out by growing paddy rice. Amendments application showed a linear increase in soil pH. Our results found that maximum increase in soil pH was obtained with lime application. Previously, studies have reported an increased soil pH with the lime treatment (Shaha et al., 2012). Liming in the contaminated soil increased soil pH through release of hydroxyl group by hydrolysis mechanism. Our results are in line with Shi et al. (2019) that increase in lime application increased soil pH even under flooded conditions. Effect of lime treatment in increased soil pH was also reported which may cause metals precipitation or adsorption on soil, leading to decreased mobility (Mahar et al., 2015; Yan-bing et al., 2017).

Biochar, lime and their composites reduced the metal availability at both stages. Amending the contaminated soils with biochar can reduce metals availability by matter-metal complex (Shen et al., 2017). Recent experiments have shown the potential of biochar in reducing metal bioavailability because of porous structure, high pH and CEC and dynamic functional groups (Sui et al., 2018; Qiu et al., 2018). Biochar addition alters soil pH resulting in metals precipitation and adsorption on biochar surface. Ability of biochar to bind metals is attributed to different chemical or physical binding or direct sorption on biochar surface (Cornelissen et al., 2018; Schweizer et al., 2018). A low-cost amendment (lime) can retain metals in contaminated soil by reducing their availability. An increase in soil pH with lime treatment may cause an elevation in soil pH further reducing metal extractability due to adsorption or complexing processes (Chen et al., 2016b). Lime addition can improve carbonate and Fe or Mn oxide bound metals that decreased the metal contents in plant tissues (Zhu et al., 2010). The Addition of CaCO₃ as liming material considerably reduced the acidic effect and favored the metal precipitation (Simón et al., 2010). Meanwhile, a decrease in metal availability with the addition of Ca(OH)₂ in contaminated soil was also reported in the literature. Composite of lime with organic materials increased soil pH, reduced EC and improved the metals immobilization in contaminated soils (Hamid et al., 2018). Meanwhile, a good correlation was observed between available metals and soil pH at both stages. This correlation may be ascribed to the change in soil pH with applied amendments which is an important factor in regulating the availability of metals (Ma et al., 2010).

Moreover, application of soil amendments reduced the highly exchangeable fraction to least available form. It has been stated that biochar due to high surface area, CEC,

high pH and active functional groups can interact with metals in reducing metals bioavailability to field crops. Stable biochar-metal complexes result in reduced metals availability in soil. A decreased Cd bioavailability with biochar application was reported by Li et al. (2009). Moreover, Park et al. (2011) investigated the enhanced Cd immobilization and reduced availability with chicken manure and green waste biochar. Biochar addition tends to improved oxide bound and organic bound metals by formation of precipitates and complexes (Méndez et al., 2013; Wang et al., 2014).

Photosynthetic and transpiration rate were higher in amended blocks as compared to control treatment. Our findings are in line with Tian et al. (2011), who reported that metals toxicity negatively affected plant photosynthesis. The reduced photosynthetic activity in control may be attributed to adverse effects of metals toxicity on plants (Rehman et al., 2017b; Hamid et al., 2019c).

Changes in physical or chemical properties e.g. soil pH and metals availability with additives results in reduced metals accumulation and uptake by plants. In our study organic amendments in composite (S2) or alone (biochar) reduced metals accumulation in rice especially grains. Organic manure changes soil pH and cation exchange capacity of soil which results in improved immobilization (Dourado et al., 2013). Organic wastes have active functional groups that actively form organic-metal complexes. This complexation process might restrict metals mobility in soil and plant (Liu et al., 2015). Combined treatment of additives may increase soil pH and metal accumulation in plant parts. Addition of lime with sepiolite was reported for improved pH and reduced metal contents in the plant (Shirvani et al., 2006). Various studies have confirmed the enriched soil pH with biochar addition (Sun et al., 2014; Chen et al., 2016a). Generally, biochar induced metal stabilization includes metal-phosphate precipitates, metals adsorption, biochar-metal electro static interaction, activated functional groups and chelation (Rodríguez-Vila et al., 2015; Ok et al., 2015; Wiszniewska et al., 2016; Khan et al., 2018). These processes might have favored the reduced accumulation of metals in rice grains. This decreased translocation might be due to improved immobilization with applied additives (Hamid et al., 2018). Biochar and organic source addition helps in improved organic matter contents of soil which further improve nutrients availability and reduces metals activity by enhanced immobilization (Chen et al., 2016a; Khan et al., 2018). It is intended that findings of this field experiment can be used for in-situ metal stabilization but further studies regarding effective dose and long-term stability are still needed.

Conclusion

Amendments application increased the soil pH and reduced metals availability in contaminated soil. Composite treatment S1 and biochar were effective in reducing Cd and Pb extraction while lime application elevated the soil pH to a significant level. This improved metal immobilization with applied treatments is attributed to complexing, adsorption, ion exchange, and/or precipitation processes. Briefly the results of this study indicated the changes in exchangeable Cd fraction to more stable form with biochar application. Meanwhile, composite treatments were effective in reducing exchangeable Pb contents at harvest stage samples. Moreover, composite treatment S2 and biochar not only reduced the metals bio-availability but also assisted in reduced grains Cd and Pb concentration in rice grown on contaminated soil. The results of our experiment pointed out the stability of amendments in improved immobilization of toxic metals in

contaminated soil but their effective dose rate and their effectiveness in different soil types needs to be addressed in later studies. Moreover, future trials regarding amendments' effect on the microbial community, enzymatic activity, long term metals immobilization and their effect under different moisture regimes can be elucidated.

Acknowledgments. This research was financially supported by the key project from Zhejiang Provincial Science and Technology Bureau (#2018C02029; Ministry of Science and Technology of China (#2016YFD0800805), and Sub-projects from Zhejiang Provincial Science and Technology Bureau (#2015C02011-3; #2015C03020-2), and the fundamental Research Funds for the Central Universities of China.

Conflict of interests. The authors declare that they have no conflict of interests.

REFERENCES

- [1] Bade, R., Sanghwa, O., Won, S. S. (2012): Assessment of metal bioavailability in smelter-contaminated soil before and after lime amendment. – *Ecotox. Environ. Safe.* 80: 299-307.
- [2] Bao, S. D. (2008): *Soil Agricultural Chemistry Analysis Method*. Third Ed. – China Agriculture Press, Beijing (in Chinese).
- [3] Bashir, S., Muhammad, S., Qaiser, H., Sajid, M., Jun, Z., Qingling, F., Omar, A., Hongqing, H. (2018): Influence of organic and inorganic passivators on Cd and Pb stabilization and microbial biomass in a contaminated paddy soil. – *J. Soils Sediments* 18: 2948-2959. <https://doi.org/10.1007/s11368-018-1981-8>.
- [4] Cao, X., Wang, X., Tong, W., Gurajala, H. K., Lu, M., Hamid, Y., Feng, Y., He, Z., Yang, X. (2019): Distribution, availability and translocation of heavy metals in soil oilseed rape (*Brassica napus* L.) system related to soil properties. – *Environ. Pollut.* 252: 733-741.
- [5] Chen, D., Guo, H., Li, R., Li, L., Pan, G., Chang, A., Joseph, S. (2016a): Low uptake affinity cultivars with biochar to tackle Cd-tainted rice—a field study over four rice seasons in Hunan, China. – *Sci. Total Environ.* 541: 1489-1498.
- [6] Chen, H. P., Yang, X. P., Wang, P., Wang, Z. X., Li, M., Zhao, F. J. (2018): Dietary cadmium intake from rice and vegetables and potential health risk: a case study in Xiangtan, southern China. – *Sci. Total Environ.* 639: 271-277.
- [7] Chen, Y. C., Tuanhui, X., Qiaofeng, L., Mengjiao, L., Mingliu, Z., Mingkuang, W., Guo, W. (2016b): Effectiveness of lime and peat applications on cadmium availability in a paddy soil under various moisture regimes. – *Environ. Sci. Pollut. Res.* 23: 7757-7766. <https://doi.org/10.1007/s11356-015-5930-4>.
- [8] Cornelissen, G., Jubaedah., Nurida, N. L., Hale, S. E., Martinsen, V., Silvani, L., Mulder, J. (2018): Fading positive effect of biochar on crop yield and soil acidity during five growth seasons in an Indonesian Ultisol. – *Sci. Total Environ.* 634: 561-568.
- [9] Dourado, M. N., Martins, P. F., Quecine, M. C., Piotto, F. A., Souza, L. A., Franco, M. R., Tezotto, T., Azevedo, R. A. (2013): *Burkholderia* sp. SCMS54 reduces cadmium toxicity and promotes growth in tomato. – *Ann. Appl. Biol.* 163: 494-507.
- [10] El-Naggar, A., Shaheen, S. M., Ok, Y. S., Rinklebe, J. (2018): Biochar affects the dissolved and colloidal concentrations of Cd, Cu, Ni, and Zn and their phytoavailability and potential mobility in a mining soil under dynamic redox-conditions. – *Sci. Total Environ.* 624: 1059-1071.
- [11] Hamid, Y., Lin, T., Wang, X., Bilal, H., Muhammad, Y., Muhammad, Z. A., Xiaoe, Y. (2018): Immobilization of cadmium and lead in contaminated paddy field using inorganic and organic additives. – *Scientific Reports* 8: 17839. DOI: 10.1038/s41598-018-35881-8.

- [12] Hamid, Y., Tang, L., Yaseen, M., Hussain, B., Zehra, A., Aziz, M. A., He, Z. L., Yang, X. (2019a): Comparative efficacy of organic and inorganic amendments for cadmium and lead immobilization in contaminated soil under rice-wheat cropping system. – *Chemosphere* 214: 259-268.
- [13] Hamid, Y., Tang, L., Muhammad, I. S., Xuerui, C., Hussain, B., Aziz, M. A., Muhammad, U., He, Z. L., Yang, X. (2019b): An explanation of soil amendments to reduce cadmium phytoavailability and transfer to food chain. – *Sci. Total Environ.* 660: 80-96.
- [14] Hamid, Y., Tang, L., Lu, M., Bilal, H., Afsheen, Z., Muhammad, B. K., Zhenli, H., Hanumanth, K. G., Xiaoe, Y. (2019c): Assessing the immobilization efficiency of organic and inorganic amendments for cadmium phytoavailability to wheat. – *J. Soils Sed.* <https://doi.org/10.1007/s11368-019-02344-0>.
- [15] Hong, C. O., Lee, D. K., Kim, P. J. (2008): Feasibility of phosphate fertilizer to immobilize cadmium in a field. – *Chemosphere* 70: 2009-2015. DOI: 10.1016/j.chemosphere.2007.09.025.
- [16] Hong, C. O., Doug, Y. C., Do, K. L., Pil, J. K. (2010): Comparison of phosphate materials for immobilizing cadmium in soil. – *Arch. Environ. Contam. Toxicol.* 58: 268-274. DOI: 10.1007/s00244-009-9363-2.
- [17] Hu, W., Zhang, Y., Huang, B., Teng, Y. (2017): Soil environmental quality in greenhouse vegetable production systems in eastern China: current status and management strategies. – *Chemosphere* 170: 183-195.
- [18] Igalavithana, A. D., Eilhann, E. K., Meththika, V., Jörg, R., Deok, H.M., Erik, M., Daniel, C. W. T., Yong, S. O. (2019): Soil lead immobilization by biochars in short-term laboratory incubation studies. – *Environ. Internation.* 127: 190-198.
- [19] Khan, M. A., Khan, S., Ding, X., Khan, A., Alam, M. (2018): The effects of biochar and rice husk on adsorption and desorption of cadmium on to soils with different water conditions (upland and saturated). – *Chemosphere* 193: 1120-1126.
- [20] Lahori, A. H., Zhang, Z. Q., Guo, Z. Y., Mahar, A., Li, R. H., Awasthi, M. K., Sial, T. A., Kumbhar, F., Wang, P., Shen, F., Zhao, J. C., Huang, H. (2017): Potential use of lime combined with additives on (im)mobilization and phytoavailability of heavy metals from Pb/Zn smelter contaminated soils. – *Ecotox. Environ. Saf.* 145: 313-323.
- [21] Leng, L. J., Xu, X. W., Wei, L., Fan, L. L., Huang, H. J., Li, J. A., Lu, Q., Li, J., Zhou, W. G. (2019): Biochar stability assessment by incubation and modelling: methods, drawbacks and recommendations. – *Sci. Total Environ* 664: 11-23.
- [22] Li, H., Shi, W. Y., Shao, H. B., Shao, M. A. (2009): The remediation of the lead polluted garden soil by natural zeolite. – *J. Hazard. Mater.* 169: 1106-1111.
- [23] Li, H. S. (2000): Principle and Technology of Plant Physiological and Biochemical Experiment. – Higher Education Press, Beijing (in Chinese).
- [24] Li, Y. L., Cheng, J. Z., Lee, X., Chen, Y., Gao, W. C., Pan, W. J., Tang, Y. (2019): Effects of biocharbased fertilizers on nutrient leaching in a tobacco-planting soil. – *Acta Geochimica* 38: 1-7.
- [25] Liang, X., Yi, X., Yingming, X., Pengchao, W., Lin, W., Yuebing, S., Qingqing, H., Rong, H. (2016): Two-year stability of immobilization effect of sepiolite on Cd contaminants in paddy soil. – *Environ. Sci. Pollut. Res.* 23: 12922-12931. <https://doi.org/10.1007/s11356-016-6466-y>.
- [26] Liu, K., Lv, J., He, W., Zhang, H., Cao, Y., Dai, Y. (2015): Major factors influencing cadmium uptake from the soil into wheat plants. – *Ecotoxicol. Environ. Saf.* 113: 207-213.
- [27] Ma, L., Xu, R., Jiang, J. (2010): Adsorption and desorption of Cu (II) and Pb (II) in paddy soils cultivated for various years in the subtropical China. – *Environ Sci.* 22: 689-695.

- [28] Mahar, A., Wang, P., Li, R., Zhang, Z. (2015): Immobilization of lead and cadmium in contaminated soil using amendments: a review. – *Pedosphere* 25: 555-568. [http://dx.doi.org/10.1016/S1002-0160\(15\)30036-9](http://dx.doi.org/10.1016/S1002-0160(15)30036-9).
- [29] Méndez, A., Terradillos, M., Gascó, G. (2013): Physicochemical and agronomic properties of biochar from sewage sludge pyrolysed at different temperatures. – *J. Anal. Appl. Pyrolysis*. 102: 124-130.
- [30] Ok, Y. S., Chang, S. X., Gao, B., Chung, H. J. (2015): SMART biochar technology—a shifting paradigm towards advanced materials and healthcare research. – *Environ. Technol. Innov.* 4: 206-209.
- [31] Park, J. H., Lamb, D., Paneerselvam, P., Choppala, G., Bolan, N., Chung, J. W. (2011): Role of organic amendments on enhanced bioremediation of heavy metal (loid) contaminated soils. – *J. Hazard. Mater.* 185: 549-574.
- [32] Qiu, Z., Chen, J., Tang, J., Zhang, Q. (2018): A study of cadmium remediation and mechanisms: improvements in the stability of walnut shell-derived biochar. – *Sci. Total Environ* 636: 80-84. <https://doi.org/10.1016/j.scitotenv.2018.04.215>.
- [33] Rehman, M. Z., Hinnan, K., Fatima, A., Shafaqat, A., Muhammad, R., Muhammad, F. Q., Muhammad, I., Muhammad, U. K., Muhammad, A. (2017a): Effect of limestone, lignite and biochar applied alone and combined on cadmium uptake in wheat and rice under rotation in an effluent irrigated field. – *Environ. Pollut.* 227: 560-568.
- [34] Rehman, M. Z., Muhammad, R., Shafaqat, A., Muhammad, S., Muhammad, I. S. (2017b): Contrasting effects of organic and inorganic amendments on reducing lead toxicity in wheat. – *Bull. Environ. Contam. Toxicol.* 99: 642-647. DOI: 10.1007/s00128-017-2177-4.
- [35] Rodríguez-Vila, A., Asensio, V., Forjánand, R., Covelo, E. F. (2015): Chemical fractionation of Cu, Ni, Pb and Zn in a mine soil amended with compost and biochar and vegetated with *Brassica juncea* L. – *J. Geochem. Explor.* 158: 74-81.
- [36] Schweizer, S. A., Seitz, B., van der Heijden, M. G. A., Schulin, R., Tandy, S. (2018): Impact of organic and conventional farming systems on wheat grain uptake and soil bioavailability of zinc and cadmium. – *Sci. Total Environ.* 639: 608-616.
- [37] Shaha, S. C., Abul, M. K., Osman, T. K. (2012): Effect of lime and farmyard manure on the concentration of cadmium in water spinach (*Ipomoea aquatica*). – *ISRN Agronomy* 6. DOI: 10.5402/2012/719432 (2012).
- [38] Shen, Z. T., Zhang, Y. Y., Jin, F., McMillan, O., Al-Tabbaa, A. (2017): Qualitative and quantitative characterisation of adsorption mechanisms of lead on four biochars. – *Sci. Total Environ.* 609: 1401-1410.
- [39] Shi, L., Zhaohui, G., Fang, L., Xiyuan, X., Chi, P., Peng, Z., Wenli, F., Hongzhen, R. (2019): Effect of liming with various water regimes on both immobilization of cadmium and improvement of bacterial communities in contaminated paddy: a field experiment. – *Int. J. Environ. Res. Public Health* 16: 498. DOI: 10.3390/ijerph16030498.
- [40] Shirvani, M., Shariatmadari, H., Kalbasi, M., Nourbakhsh, F., Najaf, B. (2006): Sorption of cadmium on palygorskite, sepiolite and calcite: equilibria and organic ligand affected kinetics. – *Colloids and Surfaces A: Physicochem. Engin. Aspects* 287: 182-190.
- [41] Simón, M., Diez, M., González, V., García, I., Martín, F., de Haro, S. (2010): Use of liming in the remediation of soils polluted by sulphide oxidation: a leaching-column study. – *J. Hazard. Mater.* 180: 241-246.
- [42] Singh, J., Kalamdhad, A. S. (2013): Effects of lime on bioavailability and leachability of heavy metals during agitated pile composting of water hyacinth. – *Bioresour. Technol.* 13: 148-155.
- [43] Song, W., Guo, M. (2012): Quality variations of poultry litter biochar generated at different pyrolysis temperatures. – *J. Anal. Appl. Pyrolysis* 94: 138-145.
- [44] Sui, F., Zuo, J., Chen, D., Li, L., Pan, G., Crowley, D. E. (2018): Biochar effects on uptake of cadmium and lead by wheat in relation to annual precipitation: a 3-year field

- study. – Environ. Sci. Pollut. Res. 25: 3368-3377. <https://doi.org/10.1007/s11356-017-0652-4>.
- [45] Sun, J., Lian, F., Liu, Z., Zhu, L., Song, Z. (2014): Biochars derived from various crop straws: characterization and Cd(II) removal potential. – Ecotoxicol. Environ. Saf. 106: 226-231.
- [46] Tessier, A., Campbell, P. G. C., Bisson, M. (1979): Sequential extraction procedure for the speciation of particulate trace metals. – Anal Chem. 51: 844-851.
- [47] Tian, T., Ali, B., Qin, Y., Malik, Z., Gill, R. A., Ali, S., Zhou, W. (2011): Alleviation of lead toxicity by 5-aminolevulinic acid is related to elevated growth, photosynthesis, and suppressed ultrastructural damages in oilseed rape. – Biomed. Res. Int. 1-11.
- [48] Wang, Y., Fang, Z. Q., Liang, B., Tsang, E. P. (2014): Remediation of hexavalent chromium contaminated soil by stabilized nanoscale zero-valent iron prepared from steel pickling waste liquor. – Chem. Eng. J. 247: 283-290.
- [49] Wiszniewska, A., Hanus-Fajerska, E., Muszyńska, E., Ciarkowska, K. (2016): Natural organic amendments for improved phytoremediation of polluted soils: a review of recent progress. – Pedosphere 26: 1-12.
- [50] Wu, Y. J., Zhou, H., Zou, Z. J., Zhu, W., Yang, W. T., Peng, P. Q., Zeng, M., Liao, B. H. (2016): A three-year in-situ study on the persistence of a combined amendment (limestone sepiolite) for remedying paddy soil polluted with heavy metals. – Ecotoxicol Environ. Saf. 130: 163-170.
- [51] Xiong, Z., Junqing, Z., Peng, C., Wenli, C., Qiaoyun, H. (2019): Bio-organic stabilizing agent shows promising prospect for the stabilization of cadmium in contaminated farmland soil. – Environ. Sci. Pollut. Res. <https://doi.org/10.1007/s11356-019-05619-8>.
- [52] Yan, Y., Yi, Q. Z., Cheng, H. L. (2015): Evaluation of phosphate fertilizers for the immobilization of Cd in contaminated soils. – PLoS ONE 10: e0124022. DOI: 10.1371/journal.pone.0124022.
- [53] Yan-bing, H., Huang, D. Y., Zhu, Q. H., Wang, S., Liu, S. L., He, H. B., Zhu, H. H., Xu, C. (2017): A three-season field study on the in-situ remediation of Cd-contaminated paddy soil using lime, two industrial by-products, and a low-Cd accumulation rice cultivar. – Ecotoxicol. Environ. Saf. 136: 135-141.
- [54] Zhao, Z., Jiang, G., Mao, R. (2014): Effects of particle sizes of rock phosphate on immobilizing heavy metals in lead zinc mine soils. – J. Soil Sci. Plant Nutrition 14: 258-266.
- [55] Zhu, Q. H., Huang, D. Y., Zhu, G. X., Ge, T. D., Liu, G. S., Zhu, H. H., Liu, S. L., Zhang, X. N. (2010): Sepiolite is recommended for the remediation of Cd-contaminated paddy soil. – Acta Agric. Scand. B. 60: 110-116.

SEGETAL SPECIES IN PLANT COMMUNITIES OF ENVIRONMENTAL ISLANDS IN AN AGRICULTURAL LANDSCAPE IN GREATER POLAND

KLARZYŃSKA, A.^{1*} – KRYSZAK, A.¹ – MAĆKOWIAK, Ł.²

¹*Department of Grasslands and Natural Landscape, Poznan University of Life Sciences, Poznan, Poland
(e-mail: anna.kryszak@up.poznan.pl)*

²*Department of Nature Conservation and Natura 2000 Areas, Regional Directorate for Environmental Protection in Poznan, Poznan, Poland
(e-mail: lukasz.mackowiak.poznan@rdos.gov.pl)*

**Corresponding author
e-mail: agnieszka.klarzynska@up.poznan.pl*

(Received 8th Nov 2019; accepted 12th Feb 2020)

Abstract. The aim of the research conducted in the years 2013-2018 in the Greater Poland region of Poland was to acquire knowledge about segetal plants representing the *Stellarietea mediae* class, which appears in the agricultural landscape of environmental islands, and also to determine the reason for its variability both in terms of habitat and connected with the type of agricultural utilization in neighbouring areas. In the areas from 5 to 50 m², 116 phytosociological releves were taken using the classic Braun-Blanquet's method, and these were then subjected to multilateral analysis. Species from *Stellarietea mediae* definitely dominate in the phytocenoses of inter-field balks (37 taxons), where they reach high stages of constancy. They were encountered less often among inter-field afforestations. In inter-field balks and inter-field waterhole banks species from *Centauretalia cyani* dominate among grain tillage, whereas ones from *Polygono-Chenopodietalia* are predominant in cornfields. Where live form structure is concerned, inter-fields balks are dominated by annual plants, whereas on the banks on inter-field waterholes and afforestations, the dominant forms are hemicryptophytes. In balks and afforestations almost 100% of species are synanthropic (mainly aphytes and archaeophytes) and inter-field waterhole banks are dominated by native flora. The results show that variability in the species structure of marginal habitats in the agricultural landscape depends strictly on the type of tillage and utilization of neighbouring areas, as well as on soil and ecological conditions.

Keywords: *biodiversity, segetal species, agriculture areas, balks, slopes of inter-field waterholes, inter-field afforestations*

Introduction

The significance of agricultural terrains in the protection of biodiversity is noticed more and more often (Symonides, 2010; Bjelajac et al., 2014; Dias Tavares et al., 2019). Observing the results of the deformation of the natural environment in agricultural areas caused by human activities aimed at obtaining food for people and fodder for animals, attention has been drawn to the surfaces of the elements of natural landscape structure – the so-called ‘ecological margins’ – still characterized by high biodiversity (Banaszak and Cierzeniak, 2002; Chappell and LaValle, 2011; Jacot et al., 2006; Karg, 2003; Loster, 1991; Ożgo, 2010). Such parts are microecosystems of the agricultural environment, i.e. inter-field afforestations, waterholes and balks. They function as environmental islands. These environmental islands are themselves act as support for biodiversity. They also help sustain the durability of the surrounding agroecosystems by being both a barrier to pollution and ecological corridors, and

support for animals (Knapp and Řezáč, 2015; Morelli, 2013; Duelli and Obrist, 2003; Tschardt et al., 2002). They are covered with typical flora, the retention of which is increasingly difficult, as it is endangered by agrotechnical pressure (Barrios et al., 2018; Fisher and Lindenmayer, 2007). A visible aspect which is a threat to their floral diversity is the simplification of agricultural landscape structure as a result of monoculturalization of tillage and the implementation of modern agrotechnical solutions (Kleps, 2009). On one hand, this leads to the extinction of groups of narrowly specialized organisms, and on the other, to the proliferation of organisms of which are often expansive and of a wide ecological scale (Afranowicz-Cieślak, 2011; Batáry et al., 2011; Kapeluszny and Haliniarz, 2010; Tokarska-Guzik et al., 2011). Owing to this, the appearance of common weeds, along with the simultaneous impoverishing of their population composition (Dąbrowska-Prot, 1984), is observed more and more often in phytocenoses formed in balks, inter-field afforestations, on the banks of inter-field waterholes.

The aim of the research was to identify flora covering what are termed 'environmental islands of the agricultural landscape' with a special analysis of segetal plants representing the *Stellarietea mediae* class. Furthermore, the reasons for the diversification of phytocenoses of ecological margins – both of the habitat and that which is dependent on the type of agricultural tillage of the directly adjacent areas – were defined.

Materials and methods

Floristic research was conducted in Greater Poland region (Poland) (Fig. 1) in vegetative seasons (May, June and the beginning of July) from 2013 to 2018 (Figs. A1-3 in the Appendix).

In areas ranging from 5 to 50 m², 116 phytosociological relevés were taken using the Braun-Blanquet method (Table 1.).



Figure 1. Location of the research

Table 1. Research areas

Agrocoenoses adjacent with surfaces of studied of environmental islands		Number of phytosociological relevés
Balks		
1	Between tillages of maize and rape	7
2	Between tillages of maize and cereals	13
3	Between tillages of root crops and grain	13
4	Between tillages of cereals	16
Slopes of inter-field waterholes		
5	Among tillage of cereals	18
6	Among tillages of maize	15
Inter-field afforestations		
7	Bordering the tillage of cereals	12
8	Bordering the tillage of maize	11
9	Bordering the tillage of rape	11

Phytosociological relevés were saved in a database of the TURBOVEG program (Hennekens and Schaminée, 2001) and subsequently imported to the JUICE program (Tichý, 2002), with the assistance of which the initial hierarchical TWINSpan classification analysis (Hill, 1979) was conducted. This analysis enabled them to be divided and gave an initial insight into the similarities and differences between the photos. The collection of 116 phytosociological relevés was also analyzed by means of the CANOCO 5.0 program (Braak and Šmilauer, 2014). First, NMDS (non-metric multidimensional scaling) analysis was conducted, which showed Euclidean distances between each releve. These distances are the ecological distance and corresponds with the differences in species composition between the samples (Kindt and Coe, 2005). Next, in order to obtain environmental gradients explained with floral data, PCA analysis results were presented.

Phytosociological structure (Matuszkiewicz, 2012) and botanical diversity were analyzed using classical methods, diversity was marked with Shannon-Wiener – H' rate (Magurran, 1996); the structure of life forms (Zarzycki et al., 2002), and the origin of flora (Jackowiak, 1990) were also marked and the stability of segetal species entering these habitats was defined.

Diversification of habitat conditions was defined with the phytoindication method (Ellenberg and Leuschner, 2010). Indicators such as: L - light conditions, F - habitat moisture, R - soil reaction, N - nitrogen content were considered.

Results

Among the environmental islands of the agricultural landscape analyzed, phytocenoses formed on the banks of inter-field waterholes are the richest in plant species. 127 plant species were found on their surfaces, whereas the fewest species among all the analyzed areas were found on the balks – 74 taxons.

However, what influences the species richness of environmental islands in the agricultural landscape is not only their type but also the neighborhood of the agrocoenoses. According to both the total number of species and the average number of species in the phytosociological relevé, more plant species were found in the phytocenoses bordering cereal tillage. On each environmental island in the areas bordering those tillages, an average of 15 species was observed in the phytosociological relevé. Slightly fewer species were found in the areas bordering corn tillage, whereas

significantly fewer species were observed in the phytosociological relevés taken on environmental islands adjacent to rape and root crop tillages (Table 2).

Table 2. Floral diversification of environmental islands

Type of the environmental island	Type of tillage	Number of research plots	Number of species	Number of segetal species with <i>Stellarietea mediae</i> class	Number of species - general	Average in phytosociological relevé	H'
Balks	Cereals - cereals	16	47	27	74	14.9	1.70
	Maize - cereals	13	48	25		10.8	1.48
	Root crops - cereals	13	35	16		8.0	1.16
	Maize - rape	7	13	8		6.6	1.52
Slopes of inter-field waterholes	Cereals	18	98	14	127	14.7	1.72
	Maize	15	85	9		13.0	1.56
Inter-field afforestations	Cereals	12	73 + 12 (tree)	22	101 (herbaceous layer) + 19 (trees layer)	14.6	1.92
	Maize	11	68 + 10 (tree)	21		14.4	1.98
	Rape	11	52 + 11 (tree)	19		11.7	1.66

The analysis of segetal species in the phytocenoses of environmental islands carried out on the basis of phytosociological structure showed their highest percentage on inter-field balks (45-59%) and a lower one in inter-field afforestations (29-39%). Nevertheless, what draws attention on the banks of inter-field waterholes is the highest proportion of species characteristic of *Molinio-Arrhenatheretea* class (c. 40%) with a very low proportion of species from the *Stellarietea mediae* class (Fig. 2). Moreover, on balks as well as on the banks of inter-field waterholes and afforestations, in general, the highest proportion in the total number of species is for taxons characteristic of the *Stellarietea mediae* class in the areas bordering grain tillage, while far fewer of these species were observed in the phytocenoses of environmental islands bordering corn and rape tillages.

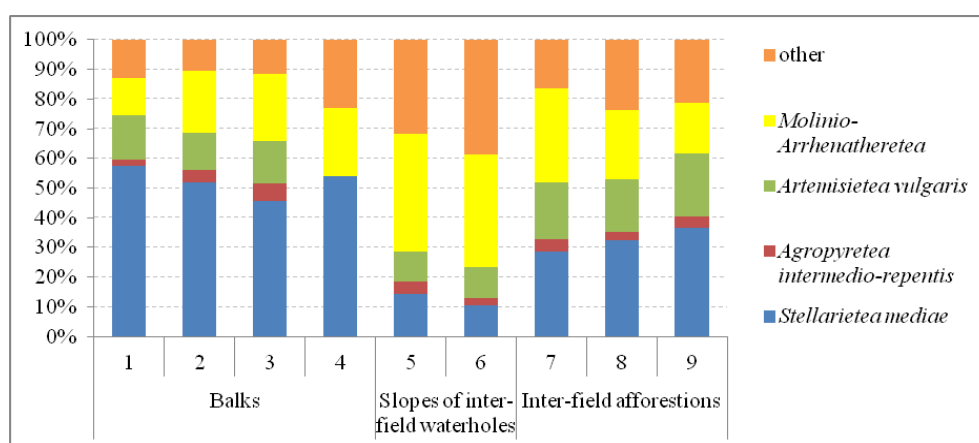


Figure 2. Phytosociological diversification of ecological margin flora. Explanations: Balks 1 - between tillages of maize and rape; 2 - between tillages of maize and cereals; 3 - between tillages of root crops and grain; 4 - between tillages of cereals; Slopes of inter-field waterholes 5 - among tillage of cereals; 6 - among tillages of maize; Inter-field afforestations 7 - bordering the tillage of cereals; 8 - bordering the tillage of maize; 9 - bordering the tillage of rape

What is particularly notable when analyzing the syntaxonomical diversification of the *Stellarietea mediae* class species is the high proportion of species characteristic of phytocenoses adjacent to cereal and flax tillages from *Centauretalia cyani*. Their particularly significant level was observed in balk phytocenoses (39-49%). The growing influence of adjacent agrocenoses on the species composition of the phytocenoses of environmental islands is also proved by the highest degree of species characteristic of phytocenoses accompanying root species from *Polygono-Chenopodietalia* cultivated in fertile and semi-fertile soils when these areas were adjacent to rape tillage. By contrast, the species composition of afforestation undergrowth is often random, therefore the appearance of numerous species of annuals and biennials of ruderal areas in the first stadium of *Sisymbrietalia* succession was observed in the areas analyzed (Fig. 3).

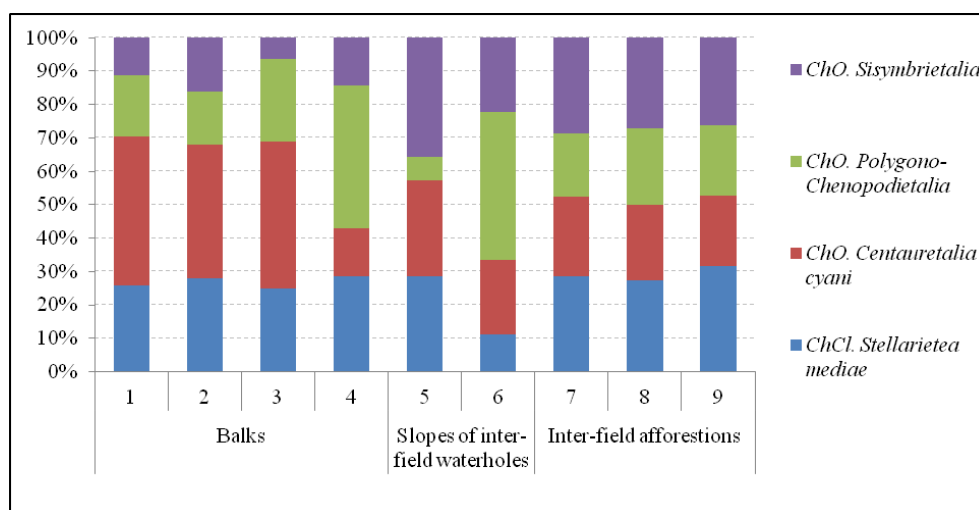


Figure 3. Diversification of *Stellarietea mediae* class. Explanations: Balks 1 - between tillages of maize and rape; 2 - between tillages of maize and cereals; 3 - between tillages of root crops and grain; 4 - between tillages of cereals; Slopes of inter-field waterholes 5 - among tillage of cereals; 6 - among tillages of maize; Inter-field afforestations 7 - bordering the tillage of cereals; 8 - bordering the tillage of maize; 9 - bordering the tillage of rape

Multidimensional scaling showed mainly that the value of the species cover coefficient from the *Stellarietea mediae* class determine the floral diversification of environmental islands (Fig. 4). Having taken into consideration axis X (59.97% defined changeability), balk phytocenoses showed the highest coefficient of the coverage with the species, whereas on axis Y (20.83% defined changeability), releves diffused due to the domination of taxons characteristic of those from the *Stellarietea mediae* class in floral composition.

Environmental islands undergo a strong influence from their surroundings and therefore do not develop stable abiotic and biotic conditions, which results in a high proportion of short-term species (terophytes) and synanthropic ones, among which species from the *Stellarietea mediae* class clearly predominate (from almost 80% to 100%). The biggest share of terophytes was observed in balk phytocenoses (from more than 57% to 66%). In the structure of species' live forms existing in inter-field afforestation and on waterholes' banks, the domination of hemicryptophytes was observed, yet terophytes were the second biggest group of plants in terms of number (from more than 17% to more than 42%) (Table 3).

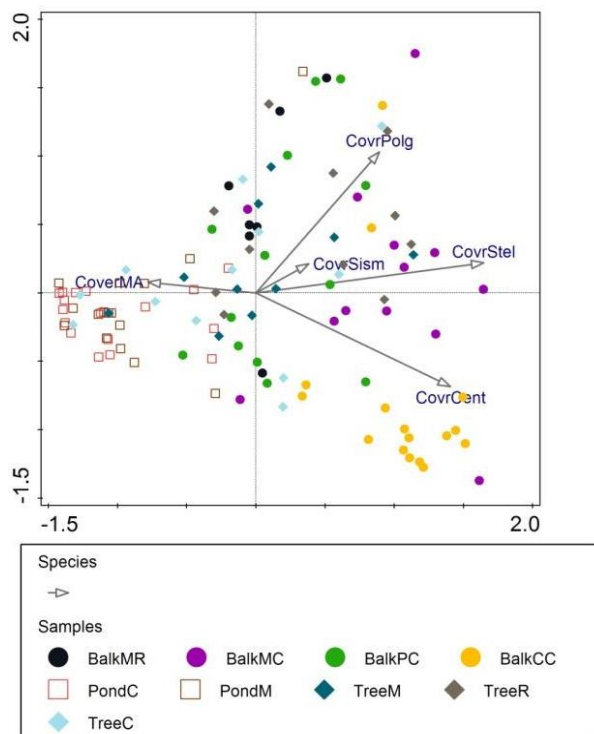


Figure 4. NMSD diagram of Euclidean distances between samples. Explanations: CoverMA - cover by species from Mollinio-Arrhenatheretea Class; CoverStel - cover by species from Stellarietea mediae Class; CoverPolg - cover by species from Polygono-Chenopodietalia Order; CoverSism - cover by species from Sisymbrietalia Order; CoverCent - cover by species from Centauretalia cyani Order; BalkMR - balks between tillages of maize and rape; BalkMC - balks between tillages of maize and cereals; BalkPC - balks between tillages of root crops and grain; BalkCC - balks between tillages of cereals; PondC - slopes of inter-field waterholes among tillage of cereals; PondM - slopes of inter-field waterholes among tillages of maize; TreeM - inter-field afforestations bordering the tillage of maize; TreeR - inter-field afforestations bordering the tillage of rape; TreeC - inter-field afforestations bordering the tillage of cereals

In the general flora of the areas examined, the biggest proportion was represented by native species (from more than 50% to almost 90%) and among them synanthropic plants – apophytes. A particularly large number of native species, both apophytes and spontaneophytes, was found in the phytocenoses of inter-field waterhole banks. The majority of anthropophytes were archaeophytes – from more than 7% to almost 45% – and the dominant group comprised species from the *Stellarietea mediae* class. A comparative analysis of archaeophytes appearing on the surfaces of environmental islands proved that they play the most important role in the phytocenoses of balks, especially those separating cereal tillages. However, the areas most resistant to the development of anthropophytes are the areas of waterhole banks (Table 3).

When analyzing the frequency of appearance of species characteristic of the *Stellarietea mediae* class in the phytocenoses of environmental islands, what draws attention is that the highest – 5th and 6th level of constancy in balks and inter-field afforestations was observed in *Apera spica-venti*, *Chenopodium album* and *Viola arvensis*. However, what was also identified on balks was very the frequent appearance of *Centaurea jacea*, *Chamomilla recutita*, *Conyza canadensis*, *Viola arvensis*, and

frequent of *Anchusa arvensis*, *Consolida regalis*, *Myosotis arvensis*, *Centaurea cyanus*, *Echinochloa crus-gali*. However, no segetal species at the 5th or 6th level were noted on the phytocenoses of inter-field waterhole banks. Most of the segetal species on the banks are taxons rarely seen in phytosociological photos and therefore only reaching the 1st or 2nd level of constancy. Such a structure of constancy levels of waterhole banks species may prove the low constancy of developed phytocenoses which may be endangered by the appearance of common species and sometimes invasive ones from neighbouring phytocenoses. Furthermore, their instability may be associated with high moisture in the banks, which depends on the ground water level, and it often changes throughout the vegetation season. Segetal species present in the undergrowth of banks cannot cope with such fluctuations in moisture and therefore disappear, to be replaced by species with high adaptability to their surroundings and biological traits (Table 4). Among the segetal species observed, some are not harmful newcomers which take on the status of domesticated invasive plants and contribute to the loss of environmental islands' naturalness. These include *Conyza canadensis*, *Echinochloa crus-gali* and *Veronica persica*.

Table 3. Spectrum of live forms and geographic and historical ones of phytocenoses of the environmental islands analyzed

Type of use		Balks				Slopes of inter-field waterholes		Inter-field afforestations		
		Cereals - cereals	Maize - cereals	Root crops - cereals	Maize - rape	Cereals	Maize	Cereals	Maize	Rape
Life form of species [%]										
Ch	Total	8.5	4.2	2.9	7.7	6.1	3.5	2.7	5.9	3.8
G	Total	10.6	12.5	17.1	7.7	13.3	16.5	12.3	11.8	11.5
	<i>Stel. med.</i>	3.7	0.0	0.0	0.0	7.1	0.0	4.8	0.0	5.3
H	Total	14.9	25.0	20.0	23.1	48.0	44.7	46.6	42.6	34.6
	<i>Stel. med.</i>	3.7	12.0	0.0	12.5	14.3	0.0	4.8	9.1	10.5
Hy	Total	0.0	0.0	0.0	0.0	8.2	10.6	0.0	0.0	0.0
F	Total	0.0	0.0	2.9	0.0	7.1	4.7	4.1	4.4	7.7
T	Total	66.0	58.3	57.1	61.5	17.3	20.0	34.2	35.3	42.3
	<i>Stel. med.</i>	92.6	88.0	100.0	87.5	78.6	100.0	90.5	90.9	84.2
Sum		100	100	100	100	100	100	100	100	100
Geographical-historical spectrum of flora [%]										
Ap	Total	48.9	54.2	57.1	53.8	68.4	71.8	71.2	63.2	61.5
	<i>Stel. med.</i>	29.6	32.0	25.0	37.5	35.7	11.1	19.0	18.2	26.3
Arch	Total	44.7	33.3	34.3	30.8	11.2	7.1	23.3	25.0	30.8
	<i>Stel. med.</i>	66.7	52.0	62.5	37.5	57.1	55.6	71.4	68.2	68.4
Ee	Total	0.0	2.1	0.0	0.0	1.0	1.2	0.0	2.9	1.9
	<i>Stel. med.</i>	0.0	4.0	0.0	0.0	0.0	11.1	0.0	9.1	5.3
Ken	Total	4.3	8.3	5.7	15.4	2.0	2.4	4.1	4.4	5.8
	<i>Stel. med.</i>	3.7	12.0	12.5	25.0	7.1	22.2	9.5	4.5	0.0
Sp	Total	2.1	2.1	2.9	0.0	17.3	17.6	1.4	4.4	0.0
Sum		100	100	100	100	100	100	100	100	100

Ch – Chamephytes; G – Geophytes; H – Hemikryptophytes; F – Fanerophytes; T – Terophytes; Ap – Apophytes; Arch – Archeophytes; Ee – Epekophytes; Ken – Kenophytes; Sp – Spontaneophytes

The species composition of environmental island phytocenoses, including the appearance of segetal species, is strictly connected with habitat conditions. The most homogenous habitat conditions assessed with ecological coefficients in terms of light and moisture are balks, whereas the highest ecological amplitudes in terms of light are found in inter-field afforestation phytocenoses, and in terms of moisture and trophism,

in inter-field waterhole banks. It may be assumed that a small number of species, including a major percentage of terophytes and species characteristic of cereal tillage phytocenoses from *Centauretalia cyani* observed on balks, may be connected with moisture conditions that show drying (the average value of F coefficient – c. 5) and quite high firmness of the herbal layer, which creates the conditions for half-shadow (the average value of the L coefficient – c. 6.5). In the low and firm undergrowth of inter-field waterhole banks, light interception is better (the average value of light L coefficient – c. 6) in plants, at mild moisture (the average value of F coefficient – almost 7) and habitat trophism (the average value of N coefficient – c. 7). These are favorable conditions for the appearance of a high number of plant species, a higher share of hemicryptophytes and species characteristic for phytocenoses accompanying roots cultivated in fertile and semifertile soils, representing *Polygono-Chenopodietalia*. The species composition of inter-field afforestations mostly influences the shadowing of the herbal layer of undergrowth (the average value of L coefficient – c. 6), when compound with moisture (the average value of F coefficient – more than 7) and high richness of soils in nitrogen (the average value of N coefficient – more than 6.6). Out of all the phytocenoses of environmental islands, it is characterized by the biggest proportion of *Sisymbrietalia* species (Fig. 5).

Table 4. Distribution of constancy levels of species observed in the phytocenoses of environmental islands

Environmental islands	Type of tillage	Constancy		
		V	IV	III
Balks	Cereals - cereals	<i>Agropyron repens</i> , <i>Apera spica-venti</i> , <i>Centaurea jacea</i> , <i>Chamomilla recutita</i> , <i>Conyza canadensis</i> , <i>Viola arvensis</i>	<i>Anchusa arvensis</i> , <i>Chenopodium album</i> , <i>Consolida regalis</i> , <i>Myosotis arvensis</i>	<i>Convolvulus arvensis</i> , <i>Fallopia convolvulus</i> , <i>Papaver dubium</i> , <i>Stellaria media</i>
	Maize - cereals	<i>Apera spica-venti</i>	<i>Agropyron repens</i> , <i>Centaurea cyanus</i> , <i>Echinochloa crus-galli</i>	<i>Anthoxanthum aristatum</i> , <i>Galeopsis tetrachit</i> , <i>Polygonum lapatifolium</i> , <i>Viola arvensis</i>
	Root crops - cereals	<i>Agropyron repens</i>	<i>Chenopodium album</i> , <i>Viola arvensis</i>	<i>Centaurea cyanus</i> , <i>Chamomilla recutita</i> , <i>Echinochloa crus-galli</i>
	Maize - rape	<i>Agropyron repens</i> , <i>Artemisia campestris</i> , <i>Chenopodium album</i>		<i>Galinsoga ciliata</i> , <i>Viola arvensis</i>
Slopes of inter-field waterholes	Cereals			<i>Cirsium arvense</i> , <i>Galium aparine</i> , <i>Galium palustre</i> , <i>Lyschmachia nummularia</i> , <i>Urtica dioica</i> ,
	Maize			<i>Lychnis flos-cuculi</i> , <i>Holcus lanatus</i> , <i>Poa pratensis</i>
Inter-field afforestations	Cereals	<i>Sambucus nigra</i> , <i>Urtica dioica</i>	<i>Galium aparine</i>	<i>Achillea millefolium</i> , <i>Agropyron repens</i> , <i>Anthoxanthum aristatum</i> , <i>Arrhenatherum elatius</i> , <i>Chenopodium album</i> , <i>Cirsium arvense</i> , <i>Convolvulus arvensis</i> , <i>Dactylis glomerata</i> , <i>Poa trivialis</i>
	Maize		<i>Bromus tectorum</i> , <i>Chenopodium album</i> , <i>Sambucus nigra</i> , <i>Urtica dioica</i>	<i>Agropyron repens</i> , <i>Anthriscus sylvestris</i> , <i>Arrhenatherum elatius</i> , <i>Cirsium arvense</i> , <i>Dactylis glomerata</i> , <i>Galium aparine</i>
	Rape	<i>Chenopodium album</i>	<i>Agropyron repens</i> , <i>Urtica dioica</i> , <i>Viola arvensis</i>	<i>Arrhenatherum elatius</i> , <i>Galium aparine</i> , <i>Sambucus nigra</i>

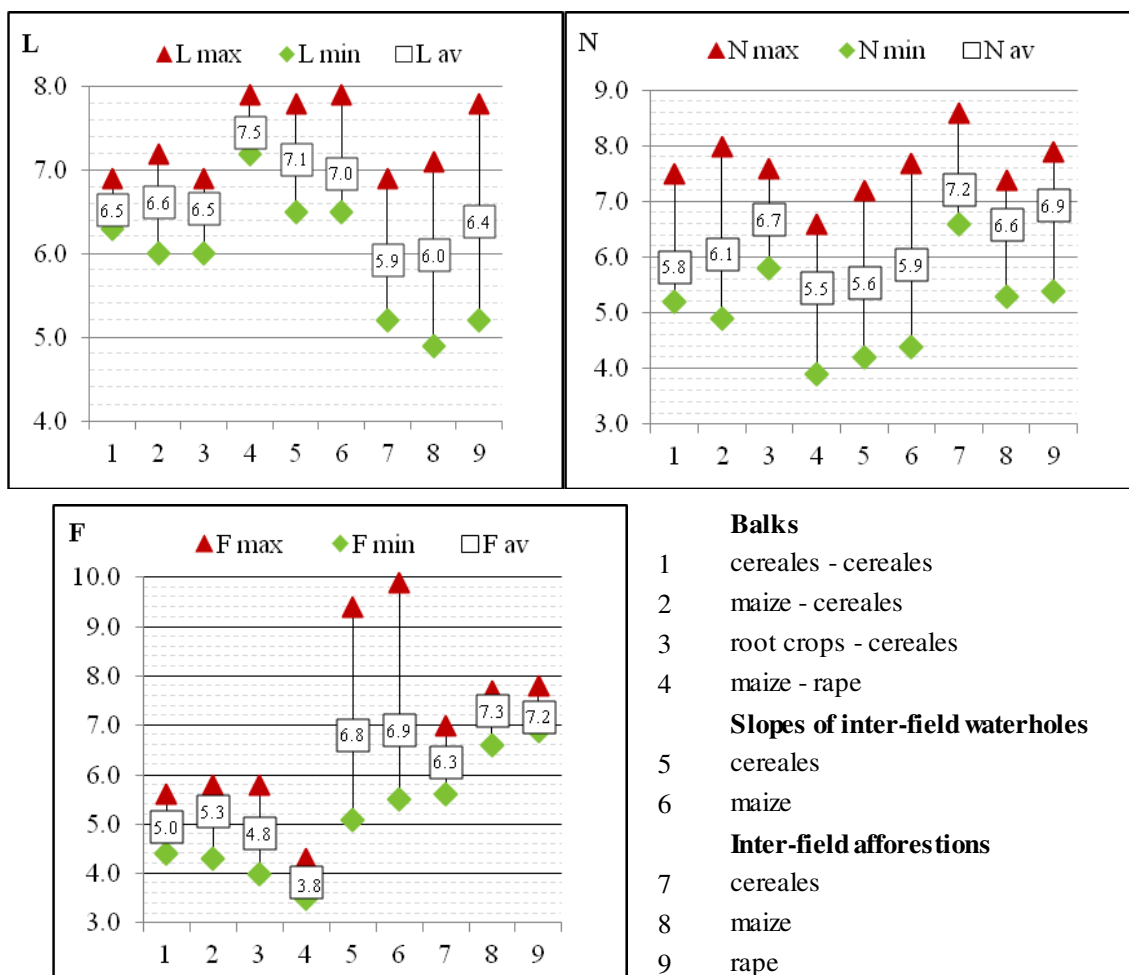


Figure 5. Averages and scopes of phytoindicative coefficients: L - light, F - moisture, N - richness of soil in nitrogen for the analyzed phytocenoses of environmental islands

Therefore, moisture was a crucial factor in differentiating the islands that were analyzed. It was most visible on the inter-field waterhole banks and least visible in the phytocenoses of inter-field balks (Fig. 6). Moreover, almost half of the variables on the chart may be explained with the gradients of trophism and insolation i.e. the habitats with high nitrogen content in soil are characteristic of afforestations and balks at root and corn tillages (the result of fertilization and/or a high amount of organic matter, which dissolutes quickly) and the N coefficients' values of balk habitats between cereals and of inter-field waterhole banks are lower than at a simultaneously far stronger insolation.

To sum up, habitat conditions characterizing moisture, light, trophism shape the phytosociological structure of environmental islands where species from the *Stellarietea mediae* class are concerned, i.e.:

- Balks among cereal tillages with a high proportion of *Cenaturetalia* species and low moisture.
- Inter-field waterhole banks among cereals and corn tillages, where not many segetal species were observed, were more moisturized and shadowed.
- Balks at roots and corn tillages with a greater proportion of *Polygono-Chenopodietalia* species from and higher trophism of soil (Fig. 7).

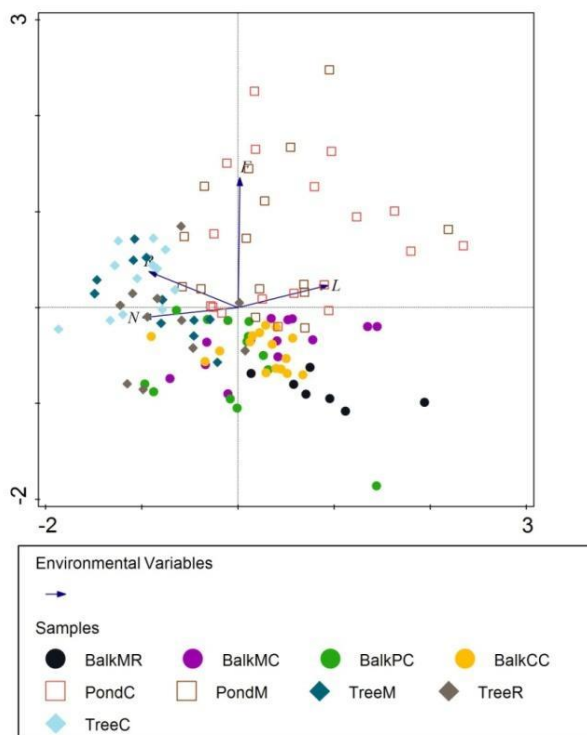


Figure 6. PCA chart of Ellenberg's phytosociological coefficients variability within the phytosociological relevés analyzed. Explanations: L - Light; F - Moisture; R - Soil Reaction; N - Nutrient Content; BalkMR - balks between tillages of maize and rape; BalkMC - balks between tillages of maize and cereals; BalkPC - balks between tillages of root crops and grain; BalkCC - balks between tillages of cereals; PondC - slopes of inter-field waterholes among tillage of cereals; PondM - slopes of inter-field waterholes among tillages of maize; TreeM - inter-field afforestations bordering the tillage of maize; TreeR - inter-field afforestations bordering the tillage of rape; TreeC - inter-field afforestations bordering the tillage of cereals

Discussion

Arable areas are terrain affected by dynamic processes and changes connected with human activity, which endangers biodiversity, including segetal and ruderal phytocenoses (Lososová and Simonová, 2008; Kleps, 2009; Meyer et al., 2010). One of the means to retain this is landscape diversification and maintenance of the highest possible fragments of natural and half-natural flora (Božetka, 2007; Loster, 1991; Nicholas and Altieri, 2013). Erissman et al. (2016) stresses that agriculture can contribute to the increase in and conservation of biodiversity, for example, by smarter management of marginal land, but also by managing fertile areas. Floral phytocenoses formed on these special environmental islands are characterized by a large number of species whose biological spectrum are not distorted by arable cultivation conducted on the neighbouring agrocenoses. However, phytocenoses of these areas differ both in terms of the total number of species and the presence of segetal species represented by the *Stellarietea mediae* class. The results obtained here show that phytocenoses formed in the habitats of well moisturized inter-field waterhole banks and brushwood are the richest in floral species. Myśliwy et al. (2007) also draw attention to the fact that inter-field brushwood contains numerous species, which is the result of the appearance of all the floral layers.

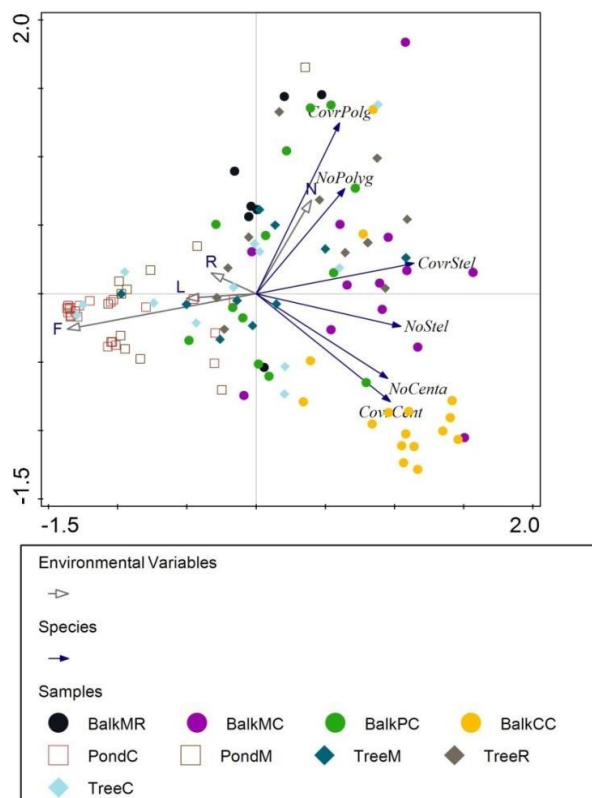


Figure 7. Ordination area representing the spread of photos between phytosociological data and habitat coefficients. Explanations: L - Light; F - Moisture; R - Soil Reaction; N - Nutrient Content; CoverPolg - cover by species from Polygono-Chenopodietalia Order; NoPolyg - Number of species from Polygono-Chenopodietalia Order; CoverSism - cover by species from Sisymbrietalia Order; NoSism - Number of species from Sisymbrietalia Order; CoverCent - cover by species from Centauretalia cyani Order; NoCent - Number of species from Centauretalia cyani Order; BalkMR - balks between tillages of maize and rape; BalkMC - balks between tillages of maize and cereals; BalkPC - balks between tillages of root crops and grain; BalkCC - balks between tillages of cereals; PondC - slopes of inter-field waterholes among tillage of cereals; PondM - slopes of inter-field waterholes among tillages of maize; TreeM - inter-field afforestations bordering the tillage of maize; TreeR - inter-field afforestations bordering the tillage of rape; TreeC - inter-field afforestations bordering the tillage of cereals

Reichholf (1998) and Özgo (2010) claim that good light flow in changing moisturization is beneficial for fast succession processes and the colonization of banks by species from the neighbouring phytocenoses, which shapes their rich floral composition. The dependencies presented here may prove that the difference in the total number of species between the phytocenoses of environmental islands may be connected with their origin and type of habitat (Leinert, 2004).

A thorough analysis of the results, including the statistical analysis conducted with PCA and NMDS ordination methods, allows us to explain the number of segetal species from the *Stellarietea mediae* class observed in the phytocenoses of environmental islands from the cultivations carried out in the neighbouring fields. The type of tillage is strictly connected with soil conditions and the intensity of the agrotechnics that are conducted, which also influence the development of the accompanying species – weeds (Aoncioaie, 2012; Batáry et al., 2012; Kutyna and Malinowska, 2011). Therefore, the presence of

fields with grain tillage positively influenced the appearance of a large proportion of species from *Centauretalia cyani* in the area examined, whereas in the areas attached to the root or rape tillage conducted on wheat complexes, more *Polygono-Cheniopodietalia* species were observed, which was also proved the results of the assessment of habitat conditions conducted using the phytoidentification method. According to these results, habitats of environmental islands neighbouring intensive root, corn or rape tillages reached higher values of the N coefficient at high moisturization. Moreover, Symonides (2010) and Andrzejewski (2002) highlight the particular abiotic conditions of environmental islands, which, in their opinion, may be caused by their small areas and, consequently, the impossibility of normal ecosystem processes.

The dependency between the number of segetal species on balks and the intensity of tillage was investigated by Karg (2003). According to his study, in the East of Poland, where agricultural is mostly ecological, almost 400 plant species were observed on balks and neighbouring parts of fields, whereas on balks at intensively cultivated fields in Wielkopolska, a lower number of species was found (c. 150) (Krasicka-Korczyńska and Borzych, 2002). In comparison to this data, the number of 70 plant species on the balks analyzed (including 8-27 taxons from the *Stellarietea mediae* class) may be considered very low and proof that the adjacent fields are intensively cultivated, especially in terms of 'weed control'. The influence of the neighborhood on the species composition of inter-field afforestations was also observed, especially in the undergrowth (Pykälä et al., 2005). Jones and Haggar (1999), French and Cummins (2001) and Honnay et al. (2005) claim that the herbal layer of inter-field brushwood is often influenced by the intensity of cultivation in the adjacent areas, especially in the range of nitrogen and natural fertilization. Furthermore, Stulichowa (1979) emphasizes the impact of brushwood origins on their species composition. They may be the remains of forests or develop spontaneously. Their spontaneous development usually happens on balks, and in such conditions, in the undergrowth, segetal species from the *Stellarietea mediae* class are found. The results of floristic research concerning phytosociological structure of inter-field brushwood phytocenoses prove their spontaneous growth on balks. The lack of occasional mowing led to their gradual bushing and the growth of trees.

Analysis of the results concerning the spectrum of live forms from the geographical-historical forms confirms that the phytocenoses of environmental islands are characterized by minor constancy (Myśliwy et al., 2007; Skrzyczyńska et al., 2014). Their species composition depends on the cultivation intensity of the neighbouring arable lands, which may endanger the floral variability of balks dominated by short-term species and archaeophytes (Dobrzański and Adamczewski, 2009). In turn, the assessment of constancy levels of species observed in the research areas shows that in the arable land, flora, especially of small water tanks and their banks, is endangered. In the waterhole habitats, no species of the 5th or 6th constancy level was found. The great threat to the flora of small water tanks in the arable landscape is explained by Myśliwy et al. (2007) with their disappearance as a result of amelioration, among other factors.

In the era of intensity of agriculture, environmental islands have become the only place of survival to the segetal flora and especially for short-term species (Peterken and Francis, 1999). They are vulnerable due to the agrotechnical measures conducted in the adjacent agroecosystems. Nevertheless, one needs to remember that these areas are some of only very few places in the agricultural landscape where half-natural flora grows, and therefore play an important role in the maintenance of biodiversity. As a consequent, more and more programs are being launched in order to protect segetal flora (Meyer et al., 2010).

Conclusions

1. Ecological margins are characterized by large floral diversity, which stems from:
 - *Cultivation of adjacent areas* - the biggest species diversity was observed on environmental islands adjacent to grain tillages; it was also where the largest average number of species in the phytosociological photo was found.
 - *Habitat variability* - the total largest species richness was observed on the inter-field waterhole banks, which was characterized by a wide spectrum of moisturization and trophism.
2. Segetal species from the *Stellarietea mediae* class usually expand to inter-field balks, where they reach high levels of constancy. They are also found among inter-field afforestations, albeit less frequently.
3. Inter-field balks and inter-field waterhole banks are clearly dominated by species from *Centauretalia cyani* among grain tillages, whereas species from *Polygono-Chenopodietalia* predominate among corn fields.
4. In the structure of live forms, annual terophytes dominate on inter-field balks, whereas inter-field waterhole banks and inter-field afforestations are dominated by hemicryptophytes.
5. On balks and in afforestations, almost 100% of the species are synanthropic ones (mainly aphytes and archaeophytes), and inter-field waterhole banks are dominated by native flora with a 10% share of non-synanthropic spontaneophytes.
6. Further research on the conservation of species diversity in agricultural areas is extremely important as it allows for the selection of appropriate management tools for these areas in order to protect biodiversity as effectively as possible.

REFERENCES

- [1] Afranowicz-Cieślak, R. (2011): Udział i rola antropofitów we florze zadrzewień w rolniczym krajobrazie Żuław Wiślanych. W: Kącki Z., Stefanek-Krzaczek E. [red.] Synantropizacja w dobie zmian różnorodności biologicznej. – Acta Botanica Silesiana 6: 157-170.
- [2] Andrzejewski, R. (2002): Wyspy środowiskowe - kilka pojęć i zagadnień. – In: Banaszak, J. (ed.) Wyspy środowiskowe. Bioróżnorodność i próby typologii. Wydawnictwo Akademii Bydgoskiej, Bydgoszcz, pp. 291-302.
- [3] Aoncioaie, C. (2012): Changes in the situation of segetal associations from the agrocoenosis of a previously well studied region of Romania. – Romanian Agricultural Research INCDA Fundulea 29: 379-388.
- [4] Banaszak, J., Cierzeniak, T. (2002): Wyspy środowiskowe krajobrazu rolniczego. – In: Banaszak, J. (ed.) Wyspy środowiskowe. Bioróżnorodność i próby typologii. Pr. zbior. Wydaw. Ak. Bydg., Bydgoszcz, pp. 25-34.
- [5] Barrios, E., Valencia, V., Jonsson, M., Brauman, A., Hairiah, K., Mortimer, P. E., Okubo, S. (2018): Contribution of trees to the conservation of biodiversity and ecosystem services in agricultural landscapes. – International Journal of Biodiversity Science, Ecosystem Services & Management 14(1): 1-16. DOI: 10.1080/21513732.2017.1399167.
- [6] Batáry, P., Fischer, J., Báldi, A., Crist, T. O., Tschardtke, T. (2011): Does habitat heterogeneity increase farmland biodiversity? – Front Ecol Environ. 9: 152-153.
- [7] Batáry, P., Holzschuh, A., Orci, K. M., Samu, F., Tschardtke, T. (2012): Responses of plant, insect and spider biodiversity to local and landscape scale management intensity in cereal crops and grasslands. – Agriculture, Ecosystems & Environment 146(1): 130-136.

- [8] Bjelajac, Z., Mijatovic, M. D., Fatic, M. Z., Dukanovic, D. (2014): Liability for biodiversity protection with special focus on wild flora and fauna conservation. – *Journal of Environmental Protection and Ecology* 15(1): 194-203.
- [9] Bożętka, B. (2007): Wybrane problemy waloryzacji zadrzewień i zakrzaczeń obszarów rolnych. – In: Kistowski, M., Korwel-Lejkowska, B. (eds.) *Waloryzacja środowiska przyrodniczego w planowaniu przestrzennym*. Fundacja Rozwoju Uniwersytetu Gdańskiego, Gdańsk, pp. 117-127.
- [10] Braak, C. J. F., Šmilauer, P. (2002): *Canoco Reference Manual and User's Guide: Software for Ordination (Version 5.0)*. – Microcomputer Power, Ithaca.
- [11] Chappell, M. J., LaValle, L. A. (2011): Food security and biodiversity: can we have both? An agroecological analysis. – *Agriculture and Human Values* 28(1): 3-26.
- [12] Dąbrowska-Prot, E. (1984): Biocoenoses in an industrial landscape. – *Polish Ecological Studies* 10: 3-230.
- [13] Dias Tavares, P., Camardelli Uzeda, M., Santos Pires, A. (2019): Biodiversity conservation in agricultural landscapes: the importance of the matrix. – *Floresta Ambient.* 26(4). DOI: 10.1590/2179-8087.066417.
- [14] Dobrzański, A., Adamczewski, K. (2009): Wpływ walki z chwastami na bioróżnorodność agrofitycenozy. – *Progress in Plant Protection* 49(3): 982-995.
- [15] Duelli, P., Obrist, M. K. (2003): Regional biodiversity in an agricultural landscape: the contribution of seminatural habitat islands. – *Basic and Applied Ecology* 4: 129-138.
- [16] Ellenberg, H., Leuschner, C. (2010): *Vegetation Mitteleuropas mit den Alpen in ökologischer, dynamischer und historischer Sicht*. 6. Aufl. – Eugen Ulmer, Stuttgart.
- [17] Erisman, J. W., Eekeren, N., Wit, J., Koopmans, C., Cuijpers, W., Oerlemans, N., Koks, B. J. (2016): Agriculture and biodiversity: a better balance benefits both. – *AIMS Agriculture and Food* 1(2): 157-174 DOI: 10.3934/agrfood.2016.2.157.
- [18] Fisher, J., Lindenmayer, D. B. (2007): Landscape modification and habitat fragmentation: synthesis. – *Global Ecology and Biogeography* 16: 265-280.
- [19] French, D. D., Cummins, R. P. (2001): Classification, composition, richness and diversity of British hedgerows. – *Appl. Veg. Sci.* 4: 213-228.
- [20] Hill, M. O. (1979): *TWINSPAN - a FORTRAN Program for Arranging Multivariate Data in an Ordered Two-Way Table by Classification of the Individuals and Attributes*. – Section of Ecology and Systematics, Cornell University, New York.
- [21] Hennekens, S. M., Schaminée, J. H. J. (2001): TURBOVEG, a comprehensive data base management system for vegetation data. – *Journal of Vegetation Science* 12: 589-591.
- [22] Honnay, O., Jacquemyn, H., Bossuyt, B., Hermy, M. (2005): Forest fragmentation effects on patch occupancy and population viability of herbaceous plant species (Tansley review). – *New Phytologist* 165(5): 1-14.
- [23] Jackowiak, W. (1990): Antropogeniczne przemiany flory roślin naczyniowych Poznania. – *Wyd. Nauk. UAM* 42: 1-242.
- [24] Jacot, K., Eggenschwiler, L., Junge, X., Luka, H., Bosshard, A. (2006): Improved field margins for a higher biodiversity in agricultural landscape. – *Aspects Appl Biol.* 81: 1-277.
- [25] Jones, D., Haggard, R. J. (1999): Impact of nitrogen and organic manures on yield botanical composition and herbage quality of two contrasting field margins. – *Biol. Agric. Hort.* 14: 107-123.
- [26] Kapeluszny, J., Haliniarz, M. (2010): Ekspansywne i zagrożone gatunki flory segetalnej w środkowo-wschodniej Polsce. – *Annales Universitatis Mariae Curie-Skłodowska Lublin-Polonia, Sectio E* 65(1): 26-33.
- [27] Karg, J. (2003): *Zadrzewienia śródpolne, strefy buforowe i miedze*. – Biblioteczka Krajowego Programu Rolnośrodowiskowego, MRiRW, Warszawa.
- [28] Kindt, R., Coe, R. (2005): *Three Diversity Analysis. A Manual and Software for Common Statistical Methods for Ecological and Biodiversity Studies*. – World Agroforestry Centre (ICRAF), Nairobi.

- [29] Kleps, C. (2009): Sustainable agriculture - the sole alternative for the present environmental and climatic constrains. – *Journal of Environmental Protection and Ecology* 10(4): 1187-1193.
- [30] Knapp M., Řezáč M (2015): Even the smallest non-crop habitat islands could be beneficial: distribution of carabid beetles and spiders in agricultural landscape. – *PLoS ONE* 10(4): e0123052. <https://doi.org/10.1371/journal.pone.0123052>.
- [31] Krasicka-Korczyńska, E., Borzych, W. (2002): Rośliny lecznicze wysp środowiskowych w krajobrazie rolniczym na przykładzie gminy Kcynia. – In: Banaszak, L. J. (ed.) *Wyspy środowiskowe. Bioróżnorodność i próby typologii*. Wyd. ABydg., Bydgoszcz, pp. 25-34.
- [32] Kutyna, I., Malinowska, K. (2011): Struktura geograficzno-historyczna flory zbiorowisk upraw zbóż ozimych i kilkunastoletnich odłogów. *Folia Pomeranae Universitatis Technologiae Stetinensis. – Agricultura, Alimentaria, Piscaria et Zootechnica* 17: 31-39.
- [33] Lienert, J. (2004): Habitat fragmentation effects on fitness of plant populations - a review. – *Journal for Nature Conservation* 12: 53-72.
- [34] Lososová, Z., Simonová, D. (2008): Changes during the 20th century in species composition of synanthropic vegetation in Moravia (Czech Republic). – *Preslia* 80: 291-305.
- [35] Loster, S. (1991): Różnorodność florystyczna w krajobrazie rolniczym i znaczenie dla niej naturalnych i półnaturalnych zbiorowisk wyspowych. – *Fragm. Flor. Geobot.* 36(2): 427-457.
- [36] Magurran, A. (1996): *Ecological Diversity and Its Measurement*. – Blackwell Publishing, Malden.
- [37] Matuszkiewicz, W. (2012): *Przewodnik do oznaczania zbiorowisk roślinnych Polski*. – Wyd. naukowe PWN, Warsaw.
- [38] Meyer, S., Wesche, K., Leuschner C., van Elsen, T., Metzner, J. (2010): A new conservation strategy for arable plant vegetation in Germany - the project “100 fields for biodiversity”. – *Plant Breeding and Seed Science* 61: 25-34.
- [39] Morelli, F. (2013): Relative importance of marginal vegetation (shrubs, hedgerows, isolated trees) surrogate of HNV farmland for bird species distribution in Central Italy. – *Ecol. Eng.* 57: 261-266.
- [40] Myśliwy, M., Ciaciura, M., Umiastowska, M. (2007): Siedlsika marginalne źródłiskowego odcinka doliny Płoni ostoją chronionych, rzadkich i zagrożonych gatunków roślin naczyniowych. *Zeszyty Naukowe Uniwersytetu Szczecińskiego. – Acta Biologica* 14: 163-183.
- [41] Nicholls, C. I., Altieri, M. A. (2013): Plant biodiversity enhances bees and other insect pollinators in agroecosystems. A review. – *Agronomy for Sustainable Development* 33(2): 257-274.
- [42] Ożgo, M. (2010): Rola małych zbiorników wodnych w ochronie bioróżnorodności. – *Parki Narodowe i Rezerwaty Przyrody* 29(3): 117-124.
- [43] Pykälä, J., Luoto, M., Heikkinen, R., Kontula, T. (2005): Plant species richness and persistence of rare plants in abandoned semi-natural grasslands in northern Europe. – *Basic Appl. Ecol.* 6: 25-33.
- [44] Peterken, G. F., Francis, J. L. (1999): Open spacer as habitats for vascular Grodnu flora species in the woods of central Lincolnshire, UK. – *Biol. Conserv.* 91: 55-72.
- [45] Reichholf, J. (1998): *Tereny wilgotne (leksykon przyrodniczy)*. – GeoCenter, Warszawa.
- [46] Skrzyczyńska, J., Stachowicz, P., Rzymowska, Z., Skrajna, T. (2014): Floristic variation in communities of fallow lands of the Podlaski Przełom Bugu mesoregion depending on the time of removal of fields from cultivation. – *Acta Agrobotanica* 67(1): 99-108.
- [47] Stulichowa, B. (1979): Roślinność miedz i zadrzewień śródpolnych pasma Policy w Karpatach Zachodnich. – *Fragm. Flor. et Geobot.* 25(1): 113-122.
- [48] Symonides, E. (2010): Znaczenie powiązań ekologicznych w krajobrazie rolniczym. – *Woda-Środowisko-Obszary Wiejskie* 10(4): 249-263.

- [49] Tschardtke, T., Steffan-Dewenter, I., Kruess, A., Thies, C. (2002): Contribution of small habitat fragments to conservation of insect communities of grassland–cropland landscapes. – *Ecological Applications* 12(2): 354-363.
- [50] Tichy, L. (2002): JUICE, software for vegetation classification. – *Journal of Vegetation Science* 13: 451-453.
- [51] Tokarska-Guzik, B., Dajdok, Z., Zając, M., Urbisz, A., Danielewicz, W. (2011): Identyfikacja i kategoryzacja roślin obcego pochodzenia jako podstawa działań praktycznych. W: Kącki, Z., Stefańska-Krzaczek, E. [red], *Synantropizacja w dobie zmian różnorodności biologicznej*. – *Acta Botanica Silesiaca* 6: 23-53.
- [52] Zarzycki, K., Trzczińska-Tacik, H., Różański, W., Szelał, W., Wołek, J., Korzeniak, U. (2002): *Ecological Indicator Values of Vascular Plants of Poland (Ekologiczne liczby wskaźnikowe roślin naczyniowych Polski)*. – Wyd. PAN, Kraków.

APPENDIX

Figure A1. Balks





Figure A2. Slopes of inter-field waterholes



Figure A3. *Inter-field afforestations*



ASSESSING INTER-SEASONAL VARIATIONS OF VEGETATION COVER AND LAND SURFACE TEMPERATURE IN THE NCR USING MODIS DATA

MALLICK, J.^{1*} – HANG, T. H.² – RAHMAN, A.² – HASAN, M. A.¹ – IBRAHIM, F.¹ – AHMED, M.¹

¹*Department of Civil Engineering, College of Engineering, King Khalid University, Abha, Saudi Arabia*

²*Urban Environmental & Remote Sensing Division, Faculty of Natural Sciences, Jamia Millia Islamia, New Delhi, India*

**Corresponding author*

e-mail: jmallick@kku.edu.sa; phone: +966-17-241-8171; fax: +966-17-241-8816

(Received 22nd Nov 2019; accepted 24th Mar 2020)

Abstract. Complex land use/land cover (LULC) patterns were investigated in the National Capital Region, India (NCR). India have a major impact on prevailing surface temperature circumstances. Various studies have been undertaken to establish the relationship between Normalized Difference Vegetation Index (NDVI) and land surface temperature (LST) in various geographic regions and ecosystems over the past two decades. However, studies aiming to understand the seasonal variation of environmental conditions, especially the thermal environment at the regional level are missing in NCR. This study employs MODIS satellite imagery to assess the temporal relationship between land surface temperature mechanics for LULC and vegetation cover in the NCR over five seasons. Results showed that concerning the scrubland/fallow land areas and agricultural land, the difference between the maximum and minimum temperature is the highest for all seasons, largely corresponding to NCR Cities' peripheral areas. The LST plays a significant role in NDVI related to vegetation vigour and growth in the NCR. The study shows that the seasonal distribution of LST needs to be overcome with high vegetation cover and some other appropriate mitigation measures.

Keywords: *thermal environment, LULC, NDVI, urban heat islands, Delhi*

Introduction

Urbanisation has led to large scale changes on the Earth's surface, and land surface temperature is one of them. Owing to the transformation of vegetation and agricultural lands into built-up areas, rural and suburban areas are converted into impermeable surfaces, thereby altering both the surface temperature and the atmospheric temperature. With increasing concretization and associated changes in land use/land cover (LU/LC) in urban areas, land temperature patterns have changed which lead to the development of different microclimates in cities and towns (Singh et al., 2012). Motor vehicles, industries, air conditioning and other city lifestyle activities add additional heat to nearby areas (Valsson and Bharat, 2009). Therefore, high-temperature islands develop in some urban areas called urban heat islands (UHIs), whereas relatively cool suburbs are noticed. Reducing the green cover and increasing the built-up area (impervious surface) contribute to the increase of urban heat island (UHI) phenomenon in the cities which leads to the deterioration of the quality of environment in the urban area (Tongliga et al., 2016). According to the 2011 Census of India, 833 million (68.84%) of the 1.21 billion Indians live in rural areas, while 377 million (31.16%) live in urban areas. In India, urbanization rose from 27.81% in 2001 to 31.16% in 2011. Further, 42.6% urban populations live in 53 metropolitan cities of

India. The four largest cities of India, i.e. Mumbai, Kolkata, Delhi and Chennai together account for about 15.4% of India's urban population. In the NCR (sub-region Haryana, UP, Rajasthan and NCT-Delhi) the urban population increased from 50.2% in 1991 to 62.5% in 2011, although the NCR rural population decreased from 49.8% (1991) to 37.5% (2011).

The data of urban population shows that there is an increasing trend in the urban population. So, to accommodate these people in urban areas, the city needs more housing and other related activities, such as educational, commercial and recreation, etc. This leads to an increase in the built-up areas and with this the land surface temperature (LST) is bound to increase which is the indicator of the thermal environment of urban areas. An urban area's LST is influenced by many factors such as season, daytime, topography, clouds, wind, rural environment, location, land use, city-building materials and geometry (Valsson and Bharat, 2009). The LST has an indirect but significant impact on air temperatures, in particular, the canopy layer near to the ground. (Mallick et al., 2008). The vegetated areas act as the city's lungs and contribute to temperature control (Owen et al., 1998). In contrast water, soil and vegetation are replaced by impermeable asphalt, concrete and hard rock surfaces in urban areas, which has environmental consequences, including a decrease in evapotranspiration, high rainfall-runoff and increased surface temperatures, which leads to a deterioration of the general urban and thermal environment (Owen et al., 1998).

Because of their importance to regional climate, quality of life, urban air quality, land use/land cover (LULC) transition and urban carbon emission situation have been studied extensively in the last two decades worldwide namely, Houston (Streutker, 2003), Salt lake valley (Gluch et al., 2006), Lahore (Ali and Nitivattananon, 2012), Wisconsin (Deng and Wu, 2013), Faisalabad (Shabana et al., 2015), Baotou (Tongliga et al., 2016), Bangkok (Ali et al., 2017), the NCR, India (Hang et al., 2018). Research on the urban thermal environment has gained importance in the Indian scenario over the last decade (Mallick et al., 2008; Pandey et al., 2012; Chakraborty et al., 2013; Mallick et al., 2013; Mathew et al., 2016; Hang et al., 2018; Kumari et al., 2018).

The land surface temperature also varies with the changing seasons over different LU/LC (Deng et al., 2013). The land surface temperature magnitude varies with the seasons due to changes in ground cover, sun intensity, and weather conditions. Due to this variation, the terrestrial surface temperature is typically higher in the summer than in winter (Oke, 1982). Research on the seasonal comparison of the urban thermal environment has been carried out by various scholars, e.g. Pandey et al. (2009) examined UHI for day-night conditions in Delhi during the summer, Li et al. (2012) studied Shanghai's seasonal changes in UHI. Mallick et al. (2013) investigated the spatial and temporal variation in land surface temperature strongly associated with the impermeable surface area (ISA) to study the effects of urbanization on the spring season of the NCT-Delhi and Weng and Yang (2004) examined the adverse thermal effects of urban development in Guangzhou, China, during the summer and winter seasons. While Streutker (2003) studied the land surface temperature for Houston seasonal UHI analysis, Zhang et al. (2013) used Landsat data. Nevertheless, studies to understand the seasonal variation of environmental conditions, especially regarding the thermal environment at regional level lacks in India.

Normalized Difference Vegetation Index (NDVI) and LST are crucial to understand the relationships between terrestrial ecosystems and the climate system in

an environmentally sensitive area. Research on the relationship between LST and NDVI (Zhang et al., 2013) helps to understand the factors that cause environmental deterioration, significant changes in the carbon cycle of the land-based environment and highlights the mechanisms that control land carbon storage response to climate variability (Braswell et al., 1997). Several studies have undertaken to establish the relationship between NDVI and LST in various ecosystems and geographic regions over the past two decades. However, vegetation response mechanisms to temperature are still unclear (Weng, 2003). Some of these studies relates explicitly to the change in NDVI and LST as factors or examined their spatial changes during the growing season (Schultz and Halpert, 1995; Pottar and Brooks, 1998). However, there are no studies in the NCR region that focus on NDVI and LST in different seasons. It is therefore essential to study the variation in the vegetation cover and the relationship between NDVI and LST in the area.

With this background of the factual issue and lack of research into inter-seasonal variations in the thermal environment, in particular in the NCR, India, this study is extremely important. The objective of this paper is, therefore, to analyse the temporal relationship between land surface temperature mechanics for land use/land cover and vegetation cover (NDVI) in the National Capital Region (NCR) over five seasons.

Materials and methods

The details of data sets from different sources used in this study related to the NCR, India are given below:

(a) Moderate Resolution Imaging Spectroradiometer (MODIS) NDVI 16-day composite raster data L3 product (MOD13Q1) with the spatial resolution of 250 m (4800 rows \times 4800 columns) in HDF format was acquired from the NASA Earth Observation System (EOS) data gateway (<https://earthexplorer.usgs.gov/>) for January 2016 to December 2016. MODIS is the main instrument onboard the Aqua and Terra satellites, which view the entire surface of the Earth every 1 to 2 days and collect data from 0.4 μ m to 14.4 μ m in 36 discrete spectral bands. This information has improved our knowledge of global dynamics in land, oceans and the lower atmosphere (Ren et al., 2008). MODIS has the potential of spectral and spatial resolutions higher than NOAA/AVHRR and spectral and temporal resolutions higher than SPOT or Landsat TM. Since MODIS data are collected in a narrow spectrum, the effect of water vapour absorption in the NIR band is minimized the red band data is much more sensitive to chlorophyll, thus improving the quality of NDVI data (Huete et al., 2002; Van et al., 1999). Consequently, MODIS NDVI was widely used in vegetation classification (Wardlow et al., 2007), vegetation phenology (Beck et al., 2006), LULC change (Lunetta et al., 2006) and crop mapping (Xiao et al., 2005) etc.

(b) MODIS LST level-3 data (MOD11A2 L3) with 1000 m spatial resolution available in every eight days in HDF format with 1200 rows \times 1200 columns were downloaded from the NASA Earth Observation System (EOS) data gateway (<https://earthexplorer.usgs.gov/>) from January 2016 to December 2016.

(c) Field visit and Google Earth data were used in the study area to analyze, validate and monitor land use.

The detail of the methodological procedure for the analysis of various data set has been discussed below.

(a) Creation of base layers

Base layers such as the NCR sub-regions, India, district boundaries, roads, water bodies etc. were created at a scale of 1:50000 from SOI toposheets.

In this study, in the NCR region the year is divided up into five seasons: winter, spring, summer, monsoon, and autumn. Each season lasts 2-3 months with summer being the warmest season, winter being the coldest, monsoon being the rainiest, and spring and autumn lie in between of winter and summer. Winter season is in December and January, spring season is in February and March, summer season is in April, May, June, monsoon season is in July, August and September and autumn season is in October and November

(b) MODIS NDVI data georeferencing

MODIS NDVI data were projected to UTM WGS84 and resampled to a 250 m grid cell, followed by layer stack and subsetting of the region of interest (ROI).

(c) MODIS LST data georeferencing

MODIS LST data were projected to UTM WGS84, followed by subsetting of the study area. These MODIS data of 1000 m bands were resampled to a 250 m grid in accordance with MODIS NDVI bands using the nearest neighbourhood technique. NDVI layer is a 16-bit signed integer with a fill value of -3000 and a valid range of -2000 to 1000. However, there is a 0.0001 or 1/10000 scale factor. This explains that a value of 10,000 in the raster should be multiplied by 0.0001 to reach the real data value.

(d) Computation of LST from MODIS LST bands

MODIS Land Surface Temperature/Land Surface Emissivity (LST/LSE) data were multiplied by a scale factor of 0.02 or 2/100. This means that an LST value in the raster should be multiplied by 0.02 to reach the actual data value.

(e) Computation of monthly and seasonal NDVI

Daily images have been composed in semi-monthly span (two per month, from the first day of the month to the fifteenth and from the sixteenth to the end of the month) using the NDVI of maximum value recorded. Instead of the average semi-monthly periods, maximum NDVI values were used to ensure the minimum effect on our data of any remaining cloud coverage. Whereas seasonal NDVI was obtained using mean NDVI for a specific seasonal period.

(f) LULC map

LULC map was generated using LANDSAT-8 and resampled to a 250 m grid in accordance with MODIS NDVI bands using the nearest neighbourhood technique. The eight LULC classes were made based on the NRSC classification scheme of 1996 agricultural cropland, built-up land, water bodies, scrubland and fallow land, bare soil and exposed rocks and vegetation. An extensive field survey was carried out to collect the information of land cover during the months of April to May 2016 (cloud-free date). The locations of the samples were recorded using a handheld global positioning system (GPS) with an accuracy of less than 5 m.

(g) Analysis of seasonal pattern/trend

The statistics of surface temperature and NDVI by LU/LC types were obtained by overlaying LU/LC map with LST, and NDVI. In order to evaluate their distribution in different seasons (autumn, summer, monsoon, spring and winter), NDVI and LST data from the LU/LC class were analyzed.

(h) Statistical analysis

Statistical analysis is performed to evaluate the seasonal relationship between NDVI, LST and LULC data.

Results and discussion

MODIS NDVI and LST data have been used to produce monthly NDVI and monthly LST maps. Detailed literature of the MODIS NDVI composite process and the Science Data Sets for Quality Assessment (QASDS) can be found on the MODIS website of NASA (MODIS, 1999) and the same has been used in the analysis. Similarly, the guide for the generation of data, data attributes and quality assurance details could be found in MODIS LST products user and is used in the chapter. The LST maps have been calibrated and validated from previous NOAA data records (<http://gis.ncdc.noaa.gov/map/viewer>).

Monthly and seasonal vegetation density (NDVI) analysis

The rural-agricultural area of the NCR is getting urbanized and industrialized, with which the vegetation cover is significantly changing and also leads to an increase in pollution in the region. The NDVI is an important parameter that provides information on the vigour and growth of vegetation in any area or region. It is one of the land's greenery representations that also provides information on the type of vegetation, growth rate and water demand and also helps to study the environmental condition of regions. The NDVI is a sensitive parameter that provides information on vegetation growth and helps predict environmental change in any region. Singh et al. (2003) regarded NDVI as an important parameter in the assessment of the impact of drought. In order to better understand the dynamic nature of NDVI, seasonal variability of NDVI and its effect on meteorological parameters in NCR has been studied in this paper.

Season-wise vegetation density (NDVI) analysis using MODIS NDVI

In this part of the thesis seasonal changes in spatial pattern of NDVI are examined in relation to general pattern of LU/LC using NDVI maps (*Fig. 1*) extracted for the five seasons (i.e. winter season, spring season, summer season, monsoon season and autumn season) from the MODIS NDVI (MOD13Q1). The overall understanding of LU/LC information was derived from the Landsat-8, Google Earth and field survey done during January to February 2016.

The seasonal spatial distribution of NDVI shows that the lowest mean NDVI values (0.284) were recorded in the summer season (*Fig. 1*) i.e. in April, May, June. The climatic factors such as precipitation, solar radiation and land without crops are some of the limiting factors for low NDVI value (*Fig. 1*).

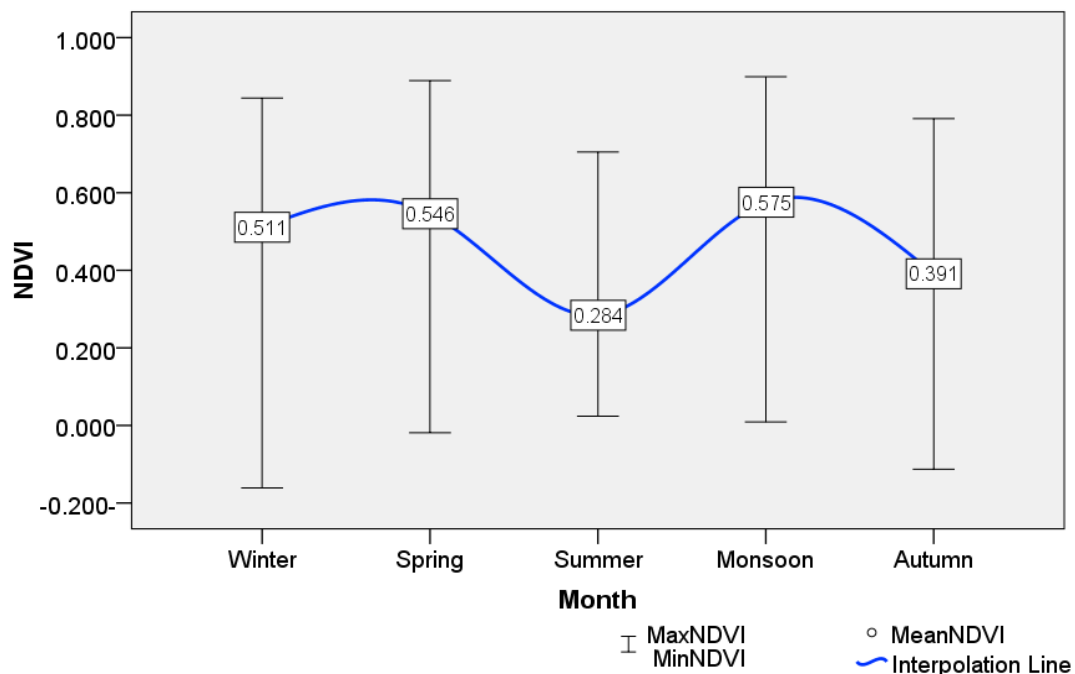


Figure 1. The seasonal variation of NDVI during 2016

Lower NDVI values (<0.2) were observed in the maximum areas of NCR except in the Ganga-Yamuna river basin areas (Eastern and north-eastern part of NCR) and patched with ridge forest area that could be observed in Delhi-NCT, southern NCR near Alwar. During summer the shortage of water, agricultural cropland and high thermal intensity are responsible for the lower NDVI values across the NCR. The lowest NDVI values of the summer season are observed in the bare soil and exposed rocks (BSER), the values range between 0.177 and 0.288 with a mean NDVI of 0.258 and a standard deviation (STD) of 0.056 (Table 1). The highest NDVI values are notified in the vegetation (VEG) ranging from 0.223 to 0.689 with a mean NDVI of 0.384 and an STD of 0.097. The highest standard deviation is found over water bodies due to the pixel mixed with vegetated areas (as a limitation of MODIS data because of too low spatial resolution).

The seasonal variation of NDVI suggests that the lowest mean NDVI values (0.391) were recorded in the autumn season (Fig. 3), i.e. October and November, which is the beginning of the winter season. This is due to the stop of photosynthesis when autumn arrives, the leaves lose chlorophyll, change colour and eventually fall. The variation of NDVI during the autumn season is shown in Figure 3.

The lower NDVI values were observed in the central, north-western parts of the study area, which are mainly covered by built-up land, fallow land and bare soil (Fig. 2). The eastern and north-eastern part of NCR, i.e. Ganga-Yamuna Basin areas and the rocky ridge of Aravali hills in Delhi-NCT and southern NCR region (near Alwar) with linear stretch from south to northeast directions show the highest NDVI values. The lowest NDVI was found over the build-up land with a mean of 0.208 and standard deviation of 0.049 whereas, the highest NDVI is observed over vegetation located toward the southern part of NCR, i.e. in the ridge forest.

December and January are the coldest months of the year, and in these months the highest and lowest NDVI values are -0.161 and 0.844 with the mean of 0.511. The

lowest NDVI values were noticed in the central parts of the study area, primarily covered by urban and rural built-up areas. In the north, west and south-east part of the study area, high NDVI values were notified. This is due to the cultivation of “Ravi” agricultural crops in these areas. *Table 1* shows the statistics of NDVI of the winter season. The higher NDVI values found over the agricultural cropland of the mean value of 0.624, whereas the lower NDVI values could be seen over the built-up areas. Moderate NDVI value was found over the vegetated land due to topical deciduous characterizes.

In the entire study area, overall high NDVI were recorded in the spring season compared to winters (*Fig. 2*). The NDVI value pattern, however, is similar to the winter season except for the ridge forest areas. During, spring season the highest and lowest NDVI values were -0.19 and 0.889 with the mean of 0.546. Lower NDVI values are recorded in the central and south-western parts of NCR, which are dominated by built-up and bare soil/exposed rocks. There is a moderate value of NDVI found over the surrounding of Delhi-NCT which corresponds to fallow land. There were also few patches to the southern part of the NCR. During the spring season, the NDVI over different LULC is shown in *Table 1*. The maximum NDVI value is shown in agricultural cropland with an average NDVI value of 0.523 and a STD of 0.062. The minimum NDVI found over built-up land with a mean NDVI of 0.206 and a STD of 0.073.

Table 1. Statistics of NDVI over different LULC during different seasons in 2016

Seasons	Properties	AGRI	BL	WB	SLAF	BSER	VEG
Winter season	Minimum NDVI	0.500	0.040	0.198	0.324	0.268	0.220
	Maximum NDVI	0.753	0.445	0.488	0.548	0.608	0.674
	Mean NDVI	0.624	0.183	0.350	0.340	0.321	0.398
	Standard deviation	0.062	0.065	0.098	0.075	0.069	0.800
Spring season	Minimum NDVI	0.368	0.076	0.189	0.234	0.205	0.203
	Maximum NDVI	0.630	0.595	0.516	0.405	0.426	0.683
	Mean NDVI	0.523	0.206	0.357	0.357	0.309	0.478
	Standard deviation	0.062	0.073	0.105	0.036	0.041	0.101
Summer season	Minimum NDVI	0.380	0.090	0.139	0.146	0.177	0.223
	Maximum NDVI	0.541	0.440	0.503	0.354	0.288	0.689
	Mean NDVI	0.438	0.211	0.320	0.297	0.258	0.384
	Standard deviation	0.043	0.058	0.135	0.047	0.056	0.097
Monsoon season	Minimum NDVI	0.507	0.123	0.094	0.307	0.242	0.411
	Maximum NDVI	0.755	0.422	0.567	0.675	0.478	0.847
	Mean NDVI	0.621	0.287	0.376	0.488	0.408	0.625
	Standard deviation	0.049	0.100	0.183	0.056	0.036	0.082
Autumn season	Minimum NDVI	0.383	0.082	0.117	0.213	0.346	0.282
	Maximum NDVI	0.542	0.297	0.407	0.476	0.478	0.698
	Mean NDVI	0.475	0.208	0.303	0.376	0.421	0.473
	Standard deviation	0.036	0.049	0.107	0.046	0.033	0.081

AGRI = agricultural cropland; BL = builtup land; WB = waterboides; SLFL = scrubland and fallowland; BSER = bare soil and exposed rocks; VEG = vegetation

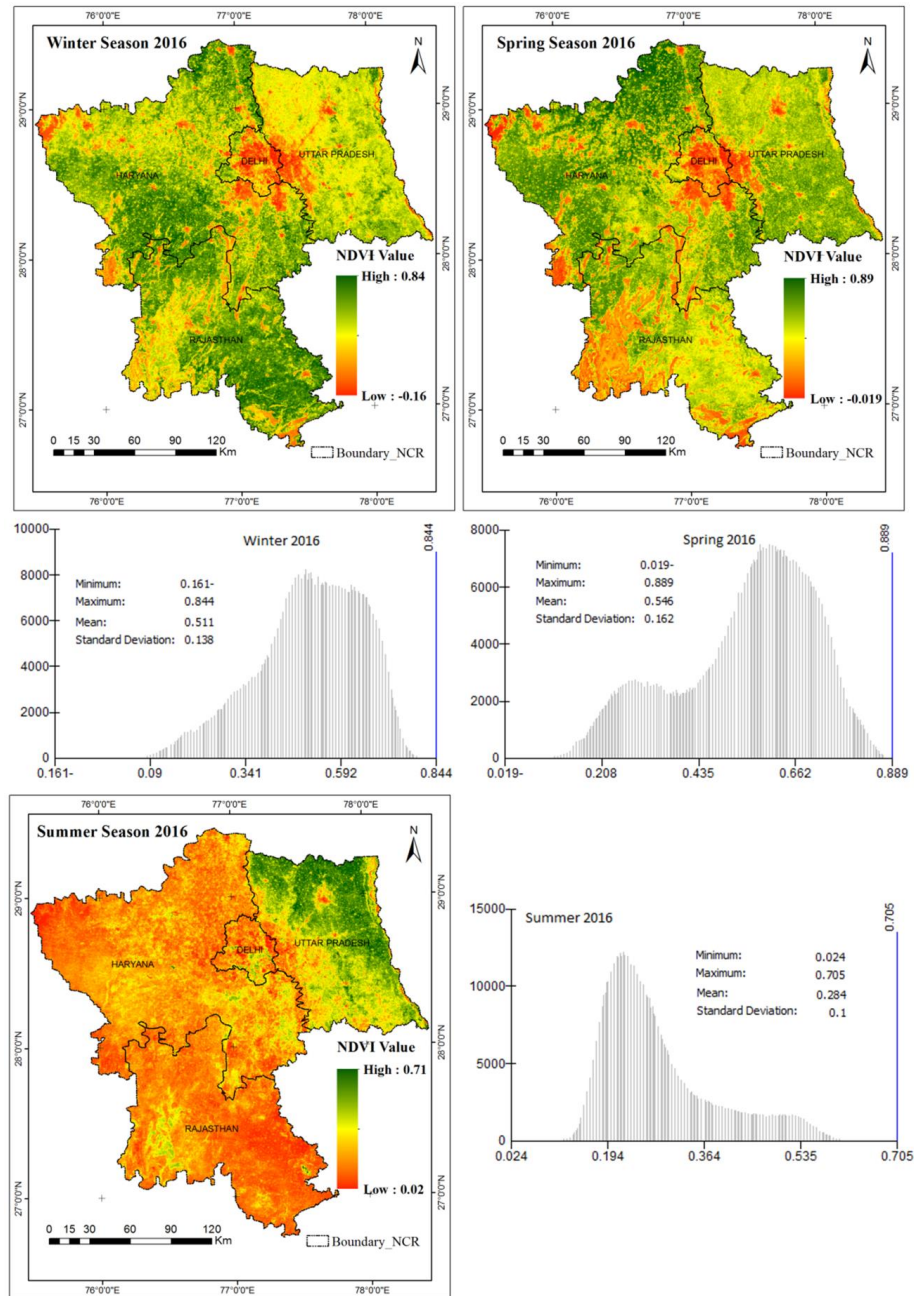


Figure 2. Spatial distribution of seasonal average NDVI during winter, spring and summer with their histogram (frequency) in 2016

The monsoon season (July, August and September) is dominated by rainfall, higher temperature and high humidity and because of this, the highest NDVI value (0.575) is recorded in this season. However, low NDVI values are spatially limited to areas built up throughout the city (Delhi, Ghaziabad, Gurgaon, Meerut, Rewari, etc.). Due to built-up areas are concrete and asphalt-dominated surfaces that do not maintain long-term moisture this minimized the NDVI value. During monsoons when most part of the cities has plenty of moisture, the impermeable areas are still largely free of moisture and such surfaces emerge as low NDVI areas. In monsoon and post-monsoon season, temperatures fall sharply and the pattern of NDVI distribution changes significantly.

The land cover ridge forests (i.e. near Delhi, near Alwar) and other forest patches show higher NDVI. The north-western, western, central and south-eastern parts of the NCR, which are predominantly scrubland/fallow land, built-up and barren land, have the lowest NDVI values (*Fig. 3*). It is important to note that in the summer season, areas with the lowest NDVI value experienced the high NDVI in monsoon due to increased greenness. During the monsoon season, the NDVI over different LULC is shown in *Table 1*. Low NDVI values were shown in built-up land with an average NDVI of 0.287 and high NDVI values were found over the vegetated surfaces, ranging between 0.411 to 0.847 with the mean value of 0.625 and a STD of 0.082. The vegetated and agricultural cropland (Kharif crops) that dominates the eastern, north and surrounding the urban peripheries show high NDVI values.

Season-wise surface temperature analysis using MODIS LST

Agricultural cropland cultivated in the NCR is approximately 1271.5 km², which is concentrated mainly in Yamuna, Hindon, Kali and Ganga rivers forming Ganga-Yamuna basin areas. The agricultural land (fallow land) is left barren during the summer months, while different crop varieties are grown depending on the season during the rest of the year. Agriculture is also practiced along the Yamuna, Hindon, Kali and Ganga rivers etc. because of this, it divides the study area into two parts, the east (Ganga-Yamuna basin areas) and west semi and Arid land. Between these two areas, there was a buffer zone which could be clearly seen in the summer season on LST maps (*Fig. 4*). The water bodies (i.e. rivers, lakes, ponds and water tanks) can be observed in the north, east and central part in the NCR and cover a very small area, i.e. 257 km². Healthy forests and tree cover is mostly located in the central and eastern part of the NCR. The forest types are the dry deciduous forests and the predominant trees as per Forest Survey of India (FSI, 2000) are Teak, Sal, Rosewood, Satinwood, Bel, Khair, kiker, Dhok, Asan, Bamboo, Bahera, Raunj, Salar, Ber, Jhigan, and Thor etc. According to the Forest Survey of India (FSI) estimates (2011), forest and tree cover account for approximately 7.6% of the total area of the NCR. As per our LULC map 2016, the dense vegetation and sparse vegetation covers approximately 10% of the total area of the NCR.

The seasonal variation of LST shows that the lowest surface temperature was recorded in the winter season (*Fig. 5*), i.e. in December and January, which are the coldest months of the year. In winters (December-January), LST ranges between 19.28 °C and 31.35 °C with a mean of 23.87 °C. The distribution of the lowest temperature ranges between 19.28 to 23.49 °C, which could be observed in the central, north-eastern, eastern, central-southern and some pockets towards the southern parts of the study area, mainly covered by agricultural land (under the Rabi crop), sparse and dense vegetation, and rural development. The water bodies, including lakes and ponds, are well distributed in the study area, mainly the Yamuna river stretches, and Ganga river stretches, dominate the peripheral areas where very low land surface temperature range is recorded (19.28-22.5 °C). The rocky ridge of Aravali hills in southern NCR with linear stretch from south to north and east directions with some forest patches also shows the lowest land surface temperature range (23-26 °C). The highest temperature of the winter season is observed on the bare soil and exposed rocks which range between 23.74 and 27.33 °C with a mean land surface temperature of 25.19 °C and a STD of 0.800 (*Table 2*). LST of more than 27 °C could be observed towards the western side of Bhiwani, Narnaul, and Alwar, some land patches which were under construction and development activities in Gurgaon, Faridabad and Ghaziabad (24-27 °C). The urban

land which is mainly in the central-eastern parts of cities shows moderate temperature conditions ranging between 23 to 25 °C. The built-up rural land is similar to the built-up urban land but having lower land surface temperature compared to the big urban area, which may be due to the densely built-up land in the areas (Fig. 4).

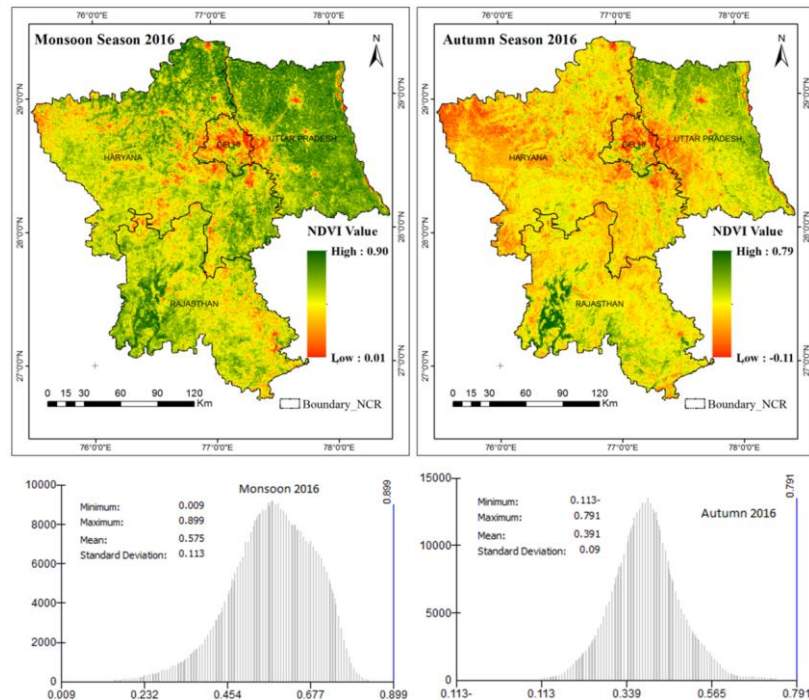


Figure 3. Spatial distribution of seasonal average NDVI during monsoon and autumn with their histogram (frequency) in 2016

In all parts of the study area, the high temperature was recorded in the spring season compared to winter (Fig. 5). The LST pattern, however, is similar to the winter season. During the spring season, LST ranges between 25.8 and 42.91 °C with a mean of 32.62 °C. The spatial distribution of lower temperature ranges between 26 to 32 °C which could be observed in north, northeast and eastern parts of the NCR. These are the vegetated areas, dominated by agriculture, in Ganga-Yamuna. In the spring season, the temperature of the water bodies is higher than in the winter season (27-33 °C). There is a moderate temperature (31-35 °C) in urban land that dominates central, patches in Ganga-Yamuna river basin areas and eastern NCR. The agricultural fallow lands, bare soils, open areas and parts of built-up urban land in Gurgaon, southeast: south Delhi and airport's open area of NCT-Delhi record this season's highest temperatures (Fig. 4). During the spring season, the LST over different LULC is shown in Table 2. The maximum LST is shown in scrubland and agricultural fallow land with an average land surface temperature of 36.05 °C and a STD of 1.082 and minimum over water bodies between 27.41 and 33.54 °C with a mean land surface temperature of 30.68 °C and a STD of 2.280. During the daytime, due to its high thermal inertia and convection and turbulence (e.g. wave action), water tended to warm up slowly. Moreover, characteristics of rivers, canals, ponds and suspended particulates mixed in water bodies, their soil temperature values vary, resulting in a high standard deviation value of 2.280 over water bodies.

Table 2. Land surface temperature over different LULC during different seasons in 2016

Seasons	Properties	AGRI*	BL*	WB*	SLFL*	BSER*	VEG*
Winter season	Minimum temp °C	21.56	21.80	19.69	22.12	23.74	20.75
	Maximum temp °C	22.88	26.00	22.80	30.48	27.33	24.61
	Mean temp °C	22.02	23.30	21.22	24.04	25.19	22.82
	Standard deviation	0.381	0.769	1.323	1.238	0.689	0.800
Spring season	Minimum temp °C	29.62	30.91	27.41	32.86	31.26	27.78
	Maximum temp °C	33.08	36.94	33.54	38.27	38.03	35.45
	Mean temp °C	31.38	33.38	30.68	36.05	34.62	32.41
	Standard deviation	0.772	0.787	2.280	1.082	1.176	1.815
Summer season	Minimum temp °C	35.27	38.19	34.33	46.06	40.15	33.82
	Maximum temp °C	39.49	44.14	42.18	51.77	48.06	42.91
	Mean temp °C	37.29	40.50	38.20	49.86	43.28	38.90
	Standard deviation	0.924	1.051	3.234	1.237	1.521	1.831
Monsoon season	Minimum temp °C	30.56	32.49	28.97	34.70	27.40	29.60
	Maximum temp °C	33.00	37.44	32.09	39.75	34.99	35.09
	Mean temp °C	31.79	34.69	30.64	36.80	30.50	31.49
	Standard deviation	0.488	0.809	1.182	0.892	1.299	1.232
Autumn season	Minimum temp °C	28.46	29.98	26.45	35.66	27.62	26.93
	Maximum temp °C	31.86	33.63	30.35	38.98	35.40	33.03
	Mean temp °C	30.58	31.34	28.23	37.58	32.11	29.92
	Standard deviation	0.883	0.571	1.597	0.735	1.494	0.987

AGRI = agricultural cropland; BL = builtup land; WB = waterbodies; SLFL = scrubland and fallowland; BSER = bare soil and exposed rocks; VEG = vegetation

The present study shows that during the summer season, the temperature rises sharply and the pattern of variation of surface temperatures significantly changes. Only water bodies (drains, river Ganga, river Yamuna and lakes), ridge forests and other forest patches record lower temperatures (34-41 °C). The vegetation cover serves as sinks for heat and plays a significant role in mitigating the local and neighbouring environment, thus regulating the extreme heating of the areas concerned as also reported by Yuan and Bauer (2009) and Singh et al. (2014). The south-eastern, north-western and eastern and parts of the NCR, which are predominantly scrubland/fallow land, built-up and barren land, have the highest land surface temperature which ranges between 45 and 52 °C). It is important to note that areas with the highest summer temperature experienced the lowest winter temperature. There is also intense heating in the over open and barren land of NCT-Delhi nearby the IGI airport where about some time 48 °C temperature is recorded. More than 44 °C LST is observed in the open areas of NCT-Delhi airport and also in some patches which were under construction and development activities. The land surface temperature magnitude varies with the seasons (winter to summer) due to changes in ground cover, sun intensity, and weather conditions. Due to this variation, the terrestrial surface temperature is typically higher in the summer than in the winter (Oke, 1982). During the summer season, the highest and lowest temperatures were

33.66 °C and 51.93 °C with the mean of 44.35 °C (*Fig. 4*). *Table 2* provides details of the highest and lowest temperature associated with each type of land use/land cover.

The monsoon season (July, August and September 1st half) is dominated by rainfall and high air humidity. The third highest land surface temperature has been observed during the monsoon season (13.8 °C). This is because the monsoon season has the highest rainfall. However, high land surface temperature values are spatially limited to build up areas almost in every city (Delhi, Ghaziabad, Gurgaon, Meerut, Rewari, etc.). This is due to the incoming short-wave incident at the rural site, which is higher during the monsoon (*Fig. 6*), perhaps because the urban area is a continuous source of high anthropogenic emissions of aerosols and low urban albedo. This is also because built-up areas are concrete and asphalt-dominated surfaces that do not maintain moisture for long term. During monsoons, when most of the land surfaces have plenty of moisture, the impermeable areas are still largely free of moisture, and such surfaces emerge as high land surface temperature areas with high intensity. In monsoon and post-monsoon season, temperatures fall sharply and the pattern of spatial temperature distribution changes significantly. The land cover, the water bodies, river basin areas, ridge forests (i.e. near Delhi, near Alwar) and other forest patches record a lower range of land surface temperature (19-31 °C). The north-western (western side of Bhiwani and Charki Dadri), western (western side of Rewari), central and south-eastern parts of the NCR, which are predominantly scrubland/fallow land, built-up and barren land, have the highest range of LST (35-42 °C). It is important to mention that areas with the highest summer temperature experienced the lowest monsoon temperature and therefore, the lowest temperature range compared to the summer season due to increased greenness leads to decreased surface albedo, resulting in high-level cooling. During monsoon season, the LST over different LULC is showed in *Table 1*. The maximum LST is shown in scrubland and agricultural fallow land with an average land surface temperature of 36.80 °C and minimum over water bodies with a mean land surface temperature of 30.64 °C. The vegetated and agricultural cropland (Kharif crops cropped during south-west monsoon season) that dominates the eastern, north and surrounding the urban peripheries show moderate temperature conditions (31-35 °C).

In all parts of the study area, overall high temperature was recorded in the autumn season compared to the monsoon season (*Fig. 5*). The land surface temperature pattern, however, is similar to the summer season; however, the temperature was low compared to the summer season. The high land surface temperature pattern of the autumn season is similar to that of the summer season, as high land surface temperature dominance is seen in the outskirts of the city. However, the high land surface temperature areas in the autumn season are relatively smaller than in the summer. During, autumn season the highest and lowest temperature ranges between 26.45 and 38.93 °C with the mean of 32.96 °C. In autumn, western portions also bear elevated temperature, with the maximum reaches in south-eastern parts of the NCR. Central, northern and eastern NCR are relatively cooler (*Fig. 6*). Mallick et al. (2012) revealed similar results for LST in the autumn season over Delhi using a Landsat TM image of October 25, 2009. The 10-12 °C cooler areas were observed around the ridge forests and river basin areas. Because of the prevalence of fallow lands towards the western and south-eastern, the land surface temperature is high, but the incoming radiation is comparatively less compared to the summer season. Scrubland and fallow lands drag the average LST to a higher side (compare to monsoon season), but lower land surface temperature areas tend to be high during the autumn season due to lower heating of other land surfaces.

NDVI and LST are crucial to understanding the relationships between terrestrial ecosystems and the climate system in an environmentally sensitive area. This research inferred that the relationship between LST and NDVI could help to understand the factors that cause environmental deterioration, significant changes in the carbon cycle of the land-based environment and highlights the mechanisms that control land carbon storage response to climate variability (Zhang et al., 2013; Braswell et al., 1997).

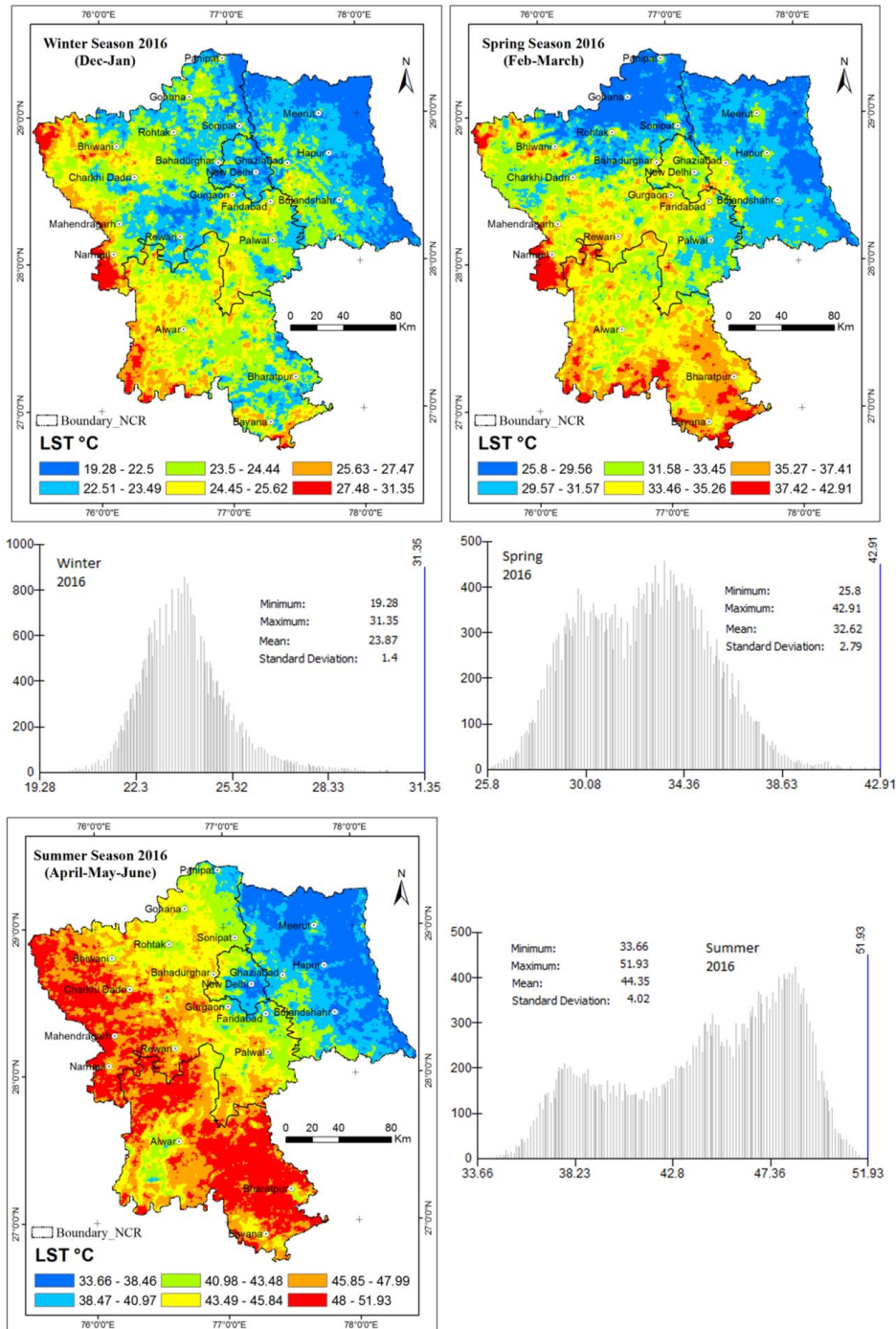


Figure 4. Spatial distribution of seasonal average LST during monsoon and autumn with their histogram (frequency) in 2016

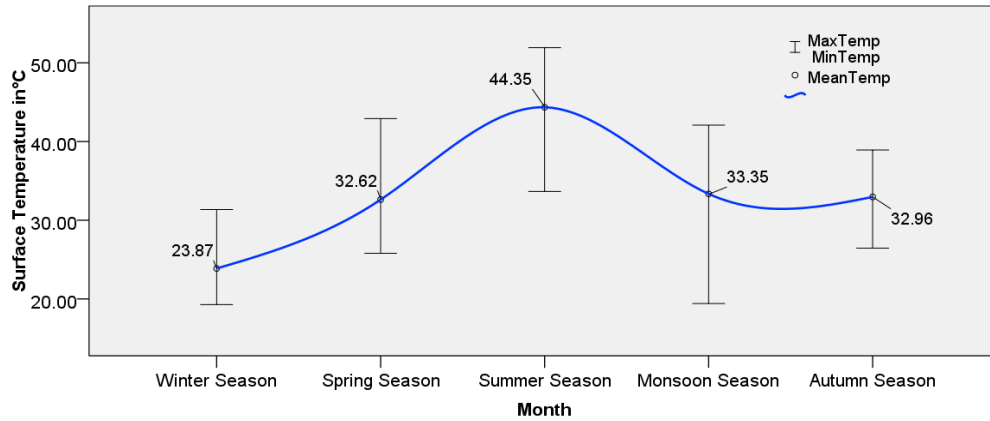


Figure 5. Graphical representation of minimum, maximum and mean LST with different seasons in 2016

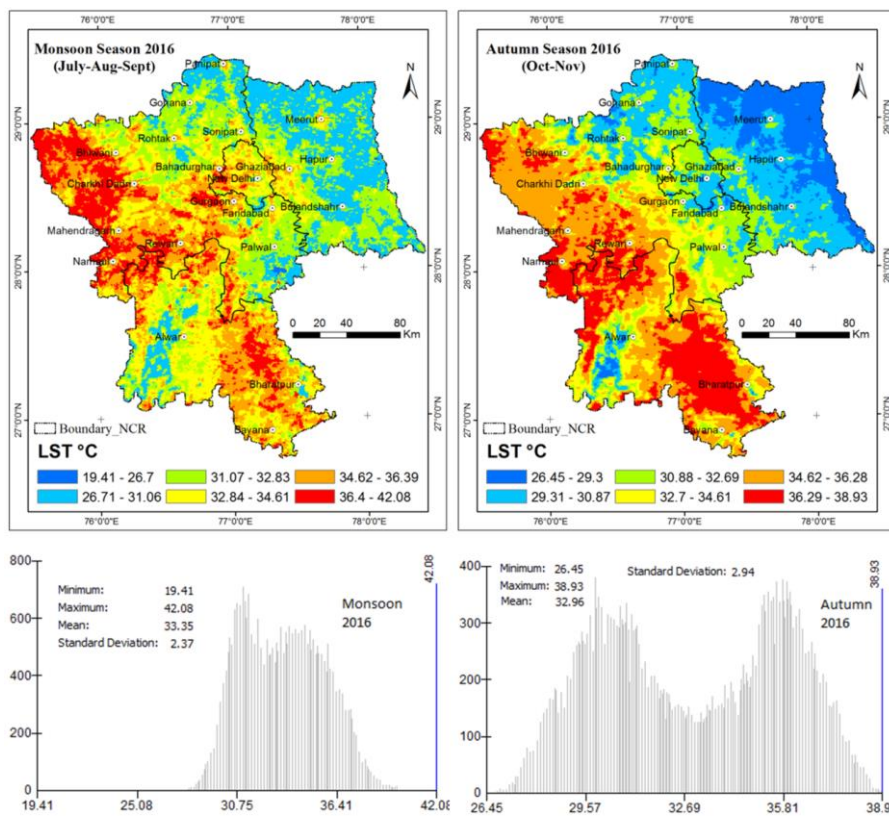


Figure 6. Spatial distribution of seasonal average LST during monsoon and autumn with their histogram (frequency) in 2016

Limitations of research

In this study, the temporal relationship between land surface temperature mechanics for land use/land cover and vegetation cover (NDVI) were analysed in the National Capital Region (NCR) over the five seasons. The analysis was based on data obtained from January 2016 to December 2016 (short timeframe). However, the short time frame (1-year datasets) may not account satisfactory for the long-term horizon dynamic

environmental conditions. Moreover, the results are satisfactory for status quo but still can be improved if temporal long-term datasets are considered. Given the importance of long term dynamic environmental factors, future studies need to integrate the long-term data sets to analyze the effects of land surface temperature mechanics for land use/land cover and vegetation cover (NDVI) in the National Capital Region (NCR).

Conclusions

The studies to understand the seasonal variation of environmental conditions, especially the thermal environment at a regional level lack in India specially in the NCR. Herein, the analysis of the temporal relationship between land surface temperature mechanics for land use/land cover and vegetation cover (NDVI) in the National Capital Region (NCR) over the five seasons has been carried out. The results inferred that the temporal and spatial pattern of LST distribution in the NCR is significantly diverse. The coldest month shows lower LST over all types of land use/land cover, but the highest temperature is accounted for the summer month. For scrubland/fallow land areas and agricultural land, the difference between the maximum and minimum temperature is the highest for all seasons, mainly corresponding to NCR Cities' peripheral areas. This difference is the lowest due to albedo factor for water bodies and vegetation cover. The presence of a perennial river (Ganga river, Yamuna river etc.) flowing through the eastern parts of the NCR has a significant influence to reduce the thermal effects. However, dense built-up area influences rather lead to the increase of the thermal effects. The analysis shows that LST plays a significant role in NDVI related to vegetation vigour and growth in the NCR. The results over the NCR region clearly show NDVI values ranging from 0.229 (April) to 0.627 (August) for all land cover categories, whereas the maximum NDVI value could be seen during Monsoon. The vegetation covers over the NCR region as the mean NDVI values range from 0.398 (Winter) to 0.625 (Monsoon). The study shows that the seasonal distribution of LST needs to be overcome with the high vegetation cover and some other appropriate mitigation measures. One way of mitigating such seasonal peripheral thermal effects could be to adopt better cropping practices in order to minimize the agricultural fallow period and to promote green roofing concepts in urban areas and using porous concrete for construction which might help to mitigate impacts of high LST in urban areas of the NCR.

Future research will concentrate on integrating the long-term data sets to analyze the effects of land surface temperature mechanics for land use/land cover and vegetation cover (NDVI) in the National Capital Region (NCR), India and also to analyze the thermal environment of different NCR Indian cities and comparing their urban thermal behaviour.

Acknowledgements. The authors extend their appreciation to the Deanship of Scientific Research at King Khalid University for funding this work through General Research Project under grant number (R.G.P2/92/41). NASA-USGS personnel at the land DAAC who provided the satellite image are also much appreciated.

REFERENCES

- [1] Ali, G., Pumijumng, N., Cui, S. (2017): Valuation and validation of carbon sources and sinks through land cover/use change analysis: the case of Bangkok metropolitan area. – *Land Use Policy* 70: 471-478.
- [2] Ali, G., Nitivattananon, V., Mehmood, H., Sabir, M., Sheikh, S. R., Abbas, S. (2012): A synthesis approach to investigate and validate carbon sources and sinks of a mega city of developing country. – *Environ. Dev.* 4: 54-72.
- [3] Beck, P. S. A., Atzberger, C., Hogda, K. A. (2006): Improved monitoring of vegetation dynamics at very high latitudes, a new method using MODIS NDVI. – *Remote Sensing of Environment* 100: 321-336.
- [4] Braswell, B. H., Schimel, D. S., Linder, E., Moore, B. (1997): The response of global terrestrial ecosystems to interannual temperature variability. – *Science* 238: 870-872.
- [5] Chakraborty, S. D., Kant, Y., Mitra, D. (2013): Assessment of land surface temperature and heat fluxes over Delhi using remote sensing data. – *J. Environ. Manag.* 148: 143-152.
- [6] Deng, C., Wu, C. (2013): Examining the impacts of urban biophysical compositions on surface urban heat island: a spectral unmixing and thermal mixing approach. – *Remote Sensing of Environment* 131: 262-274.
- [7] Deng, X. Z., Huang, J. K., Lin, Y. Z., Shi, Q. L. (2013): Interactions between climate, socio-economics, and land dynamics in Qinghai Province, China: a LUCD model-based numerical experiment. – *Adv. Meteorol.* DOI: 10.1155/2013/297926.
- [8] FSI (Forest Survey of India) (2000): The State of Forest Report 1999. – FSI, Government of India, Dehradun.
- [9] Gluch, R. Q., Saaroni, D. A., Luvall, J. C. (2006): A multi-scale approach to urban thermal analysis. – *Remote Sens. Environ.* 104(2): 123-132. <http://dx.doi.org/10.1016/j.rse.2006.01.025>.
- [10] Hang, H. T., Rahman, A. (2018): Characterization of thermal environment over heterogeneous surface of National Capital Region (NCR), India using LANDSAT-8 sensor for regional planning studies. – *Urban Climate* 24: 1-18. DOI: 10.1016/j.uclim.2018.01.001.
- [11] Huete, A. R., Didan, K., Miura, T., Rodriguez, E. P., Gao, X., Ferreira, L. G. (2002): Overview of the radiometric and biophysical performance of the MODIS vegetation indices. – *Remote Sensing Environment* 83(1-2): 195-213.
- [12] Kumari, B., Tayyab, M., Shahfahad, Salman, Mallick, J., Khan, M. F., Rahman, A. (2018): Satellite-driven land surface temperature (LST) using Landsat 5, 7 (TM/ETM+SLC) and Landsat 8 (OLI/TIRS) data and its association with built-up and green cover over urban Delhi, India. – *Remote Sensing in Earth Systems Sciences*. DOI: 10.1007/s41976-018-0004-2.
- [13] Li, Y. Y., Zhang, H., Kainz, W. (2012): Monitoring patterns of urban heat islands of the fast-growing Shanghai metropolis, China: using time-series of Landsat TM/ETM+ data. – *Int. J. Appl. Earth Obs. Geoinf.* 19: 127-138.
- [14] Lunetta, R. S., Knight, J. F., Ediriwickrema, J., Lyon, J. G., Worthy, L. D. (2006): Land-cover change detection using multi-temporal MODIS NDVI data. – *Remote Sensing of Environment* 105(2): 142-154.
- [15] Mallick, J., Kant, Y., Bharath, B. D. (2008): Estimation of land surface temperature over Delhi using Landsat ETM+. – *Journal of Indian Geophysical Union* 12(3): 131-140.
- [16] Mallick, J., Singh, C. K., Shashtri, S., Rahman, A., Mukherjee, S. (2012): Land surface emissivity retrieval based on moisture index from Landsat TM satellite data over heterogeneous surfaces of Delhi city. – *Int. J. Appl. Earth Obs. Geoinf.* 19: 348-358.
- [17] Mallick, J., Rahman, A., Singh, C. K. (2013): Modeling urban heat islands in heterogeneous land surface and its correlation with impervious surface area by using night-time ASTER satellite data in highly urbanizing city, Delhi-India. – *Adv. Space Res.* 52: 639-655.

- [18] Mathew, A., Sreekumar, S., Khandelwal, S., Kaul, N., Kumar, R. (2016): Prediction of surface temperatures for the assessment of urban heat island effect over Ahmedabad city using linear time series model. – *Energ. Buildings* 128: 605-616.
- [19] MODIS (1999): MODIS Vegetation Index (MOD 13): Algorithm Theoretical Basis (version 3). – http://modis.gsfc.nasa.gov/data/atbd/atbd_mod13.pdf.
- [20] Oke, T. R. (1982): The energetic basis of the urban heat island. – *Q. J. R. Meteorol. Soc.* 108: 1-24.
- [21] Owen, T. W., Carlson, T. N., Gillies, R. R. (1998): An assessment of satellite remotely-sensed land cover parameters in quantitatively describing the climatic effect of urbanization. – *International Journal of Remote Sensing*. DOI: 10.1080/014311698215171.
- [22] Pandey, P., Kumar, D., Prakash, A., Kumar, K., Jain, V. K. (2009): A study of the summertime urban heat island over Delhi. – *Int. J. Sustain. Sci. Stud.* 1: 27-34.
- [23] Pandey, P., Kumar, D., Prakash, A., Masih, J., Singh, M., Kumar, S., Jain, V. K., Kumar, K. (2012): A study of urban heat island and its association with particulate matter during winter months over Delhi. – *Sci. Total Environ.* 414: 494-507.
- [24] Potter, C. S., Brooks, V. (1998): Global analysis of empirical relations between annual climate and seasonality of NDVI. – *International Journal of Remote Sensing* 15: 2921-2948.
- [25] Ren, J., Chen, Z., Zhou, Q., Tang, H. (2008): Regional yield estimation for winter wheat with MODIS-NDVI data in Shandong, China. – *International Journal of Applied Earth Observation and Geoinformation* 10: 403-413.
- [26] Schultz, P. A., Halpert, M. S. (1995): Global correlation of temperature, NDVI and precipitation. – *Advance in Space Research* 13: 277-280.
- [27] Shabana, Ali, G., Bashir, M. K., Ali, H. (2015): Housing valuation of different towns using the hedonic model: a case of Faisalabad City, Pakistan. – *Habitat Int.* 50: 240-249.
- [28] Singh, R. B., Kumar, D. (2012): Remote sensing and GIS for land use/cover mapping and integrated land management: case from the middle Ganga plain. – *Front. Earth Sci.* 6: 167-176.
- [29] Singh, R. B., Grover, A., Zhan, J. (2014): Inter-seasonal variations of surface temperature in the urbanized environment of Delhi using LANDSAT thermal data. – *Energies*. DOI: 10.3390/en7031811.
- [30] Singh, R. P., Roy, S., Kogan, F. (2003): Vegetation and temperature condition indices from NOAA AVHRR data for drought monitoring over India. – *Int. J. Remote Sens.* 24: 4393-4402.
- [31] Streutker, D. R. (2003): Satellite-measured growth of the urban heat island of Houston, Texas. – *Remote Sens. Environ.* 85: 282-289.
- [32] Tongliga, B., Xueming, L., Jing, Z., Yingjia, Z., Shenzhen, T. (2016): Assessing the distribution of urban green spaces and its anisotropic cooling distance on urban heat island pattern in Baotou, China. – *Int J Geo-Inform* 5(2): 12.
- [33] Valsson, S., Bharat, A. (2009): Urban heat island: cause for microclimate variations. – *Architecture - Time Space & People* 2009(April): 21-25.
- [34] Wardlow, B. D., Egbert, S. L., Kastens, J. H. (2007): Analysis of timeseries MODIS 250 m vegetation index data for crop classification in the U. S. Central Great Plains. – *Remote Sensing Environment* 108(3): 290-310.
- [35] Weng, Q., Yang, S. (2004): Managing the adverse thermal effects of urban development in a densely populated Chinese city. – *J. Environ. Manag.* 70: 145-156.
- [36] Weng, Q. H. (2003): Fractal analysis of satellite-detected urban heat island effect. – *Photogrammetric Engineering and Remote Sensing* 69(5): 555-566.
- [37] Xiao, X., Boles, S., Liu, J., Zhuang, D., Frohling, S., Li, C., Salas, W., Moore, B. J. (2005): Mapping paddy rice agriculture in southern China using multi-temporal MODIS images. – *Remote Sensing Environment* 95(4): 480-492.

- [38] Yuan, F., Bauer, M. E. (2007): Comparison of impervious surface area and normalized difference vegetation index as indicators of surface urban heat island effects in Landsat imagery. – *Remote Sens. Environ.* 106: 375-386.
- [39] Zhang, H., Qi, Z. F., Ye, X. Y., Cai, Y. B., Ma, W. C. (2013): Analysis of land use/land cover change, population shift, and their effects on spatiotemporal patterns of urban heat islands in metropolitan Shanghai, China. – *Appl. Geogr.* 44: 121-133.

LAGGED EFFECTS OF WINTER CATCH CROPS FOLLOWED BY SWEET CORN (*ZEA MAYS* L. VAR. *SACCHARATA* KORN.) AND SUBSEQUENTLY SPRING BROCCOLI (*BRASSICA OLERACEA* L. VAR. *ITALICA* PLENCK)

ROSA, R.* – FRAN CZUK, J. – ZANIEWICZ-BAJKOWSKA, A.

*Siedlce University of Natural Sciences and Humanities, Faculty of Agrobioengineering and Animal Husbandry, Prusa 14 Street, 08-110 Siedlce, Poland
(e-mail: warzywa@uph.edu.pl)*

*Corresponding author

e-mail: robert.rosa@uph.edu.pl; ORCID ID: 0000-0001-6344-538X

(Received 27th Nov 2019; accepted 23rd Mar 2020)

Abstract. This paper deals with lagged effects of winter catch crops on the growth, yield, and quality of spring broccoli. In the first year of the experiment (2008-2010), hairy vetch (VV), white clover (TR), winter rye (SC), and Italian ryegrass (LM) were sown as winter catch crops. In the next spring (2009-2011) they were ploughed into the soil, and sweet corn was grown on plots with incorporated catch crops. To other sweet corn plots farmyard manure was applied at a dose of 30 t·ha⁻¹. Finally, sweet corn was followed by the Loreto F₁ and Milady F₁ varieties of broccoli in 2010-2012. The effect of the catch crops was compared with the control plants (with no organic fertilizer) and that of the effect of manure. Manure application resulted in the highest broccoli yield. However, a statistically similar marketable yield of curds was also recorded on plots with the incorporated catch crops of hairy vetch, white clover, and winter rye. Grown in the second year after the incorporation of SC, VV, and manure they were richer in protein, and those grown after VV and TR contained more total sugars than the control plants. The largest concentration of P was found in broccoli grown after VV and TR as catch crops, K in plants following VV and manure, and Mg in those following VV. It was found that hairy vetch, white clover, and winter rye could be used as organic fertilizers, alternatives for manure. Their growth promoting effect extends to the second year after their incorporation.

Keywords: *FYM, green manure, nutritional value, organic fertilisation, yield*

Introduction

Broccoli (*Brassica oleracea* var. *italica*) is an important vegetable grown worldwide. The plant originates from the Mediterranean region and belongs to the *Brassicaceae* family. Considered to be a valuable source of vitamins, antioxidants, glucosinolates, and other compounds with proven anticancer activity, it is tasty and more nutritious than any other vegetable of the same kind (Parente et al., 2013). Today, the broccoli market is growing steadily all over the world since consumers find its curds an important component of a healthy diet. Over the last 35 years, the consumption of fresh broccoli has increased so much that now it is the 11th most consumed fresh vegetable.

The worldwide production of broccoli (and cauliflower) is 26.5 million tonnes. The main producer is China, with a 40% share in the volume of global production. The top 10 countries producing fresh broccoli are China, India, USA, Spain, Mexico, Italy, France, Poland, Bangladesh and Turkey (FAOSTAT, 2019). In Poland approx. 15% the total European broccoli is produced, but the largest producer in Europe is Spain, with a share of 37%. Due to the of growing demand for high-quality products and an increase in environmental awareness, agricultural producers use more environmentally friendly production methods. One of the priorities is enriching the soil with organic matter, which

restores soil fertility and increases its buffer properties. The production of fertilisers of animal origin across Europe is insufficient, and, therefore, increasing attention is paid again to green fertilisers of plant origin (Talgre et al., 2012; Fekete and Pepó, 2018; Thavarajah et al., 2019). Green manure should become a permanent element of improving soil fertility in the integrated and organic farming systems. It is a factor that alleviates the negative effect of farming intensification, excessive soil compaction, and one-sided mineral fertilization (Kristensen and Thorup-Kristensen, 2004; Rogers et al., 2004; Choi et al., 2014). Catch crops also have a many-sided effect on biological, physical and chemical soil properties. They reduce erosion, build soil organic matter, and positively influence soil organisms (Snapp et al., 2005; Reddy, 2016). Catch crops protect the forms of nutrients easily available for plants from leaching into deeper layers of the soil profile and into groundwater. During the process of catch crop mineralization, biomass N is gradually released and becomes available for the subsequent plants (Vos and van der Putten, 2001; Reddy, 2016; Iivonen et al., 2017).

Some studies have shown that the use of green fertilizers allows not only the achievement satisfactory yields of subsequent vegetable plants, but also improves their quality and nutritional value (Jabłońska-Ceglarek and Rosa, 2003; Adamczewska-Sowińska and Kołota, 2008; Zhang et al., 2010).

The purpose of this research was to determine the effect of winter catch crops on the size and quality of the broccoli yield.

Material and Methods

Experimental site

A field experiment was carried out from 2008 to 2012 at the Experimental Farm of the Siedlce University of Natural Sciences and Humanities, located in central eastern Poland (52°03'N, 22°33'E) (*Figure 1*). The soil was classified as Luvisol (IUSS, 2015), with the average organic carbon content of 0.99%, the humus layer reaching a depth of 30–40 cm, and pH_{KCl} of 6.2. Total macronutrient content in air dried matter amounted to 61 mg of N (NO₃ + NH₄), 63 mg of P, 73 mg of K, 31 mg of Mg, and 255 mg of Ca per 1 dm³.

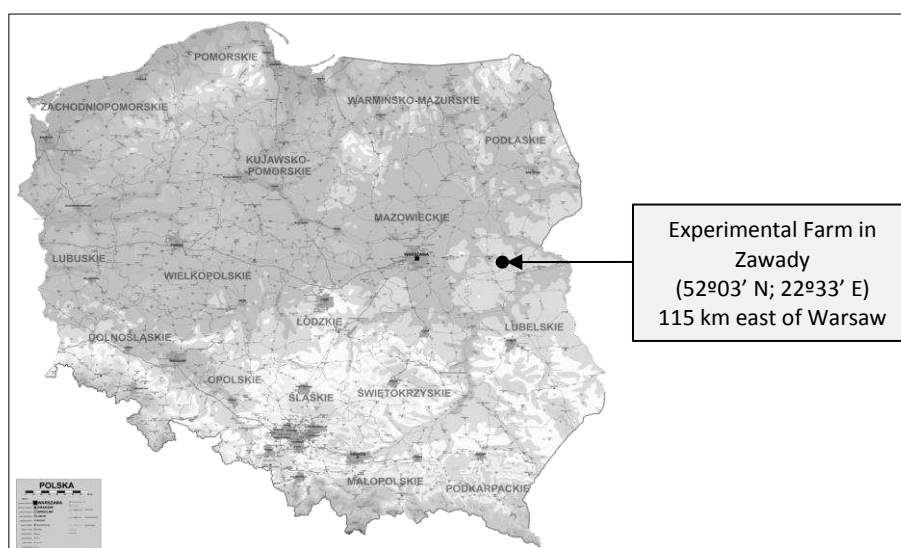


Figure 1. Location of the Experimental Farm

Experimental design

The experiment was established in a split-block design with three replicates, and it included two factors: factor I – broccoli cultivar, factor II – organic manure (*Table 1*). In the autumn each year between 2008 and 2010 catch crops were sown. They were incorporated each spring between 2009 and 2011 and followed by sweet corn. At the same time, farmyard manure at a dose of 30 t·ha⁻¹ was applied prior to planting sweet corn on other plots. Broccoli was grown between 2010 and 2012, each time in the second year after the incorporation of winter catch crops and manure. Detailed dates and succession of crops are listed in *Table 2*. The content of minerals in the catch crops and in the farmyard manure is presented in *Table 3*. The direct impact of the incorporated green fertilizers on the growth, yields and nutritional value of sweet corn has been described in previous publications (Rosa, 2014, 2015).

Table 1. Factors of the experiment

Broccoli cultivars:		
Factor I	Loreto F ₁	This cultivar is grown for summer and autumn harvests, with the first fully grown curds after 65 days. The plant is tall, strong, with leaves erected, producing large curds with a mass reaching 750 g. It is highly resistant to downy mildew and wet rot. Seminis Vegetable Seeds, Bayer Group.
	Milady F ₁	This cultivar is especially recommended for early-spring cultivation. Curds are ready for harvesting about 60 days after seedling planting. It produces curds of similar sizes, weighing more than 400 g. Plants do not form hollowed stems, and they are resistant to downy mildew and wet rot. Seminis Vegetable Seeds, Bayer Group.
Organic fertilizer:		
Factor II	Control	Without organic fertilizer.
	FYM	Farmyard manure applied at a rate of 30 t·ha ⁻¹ , incorporated in early May 2009-2011.
	VV	Hairy vetch (<i>Vicia villosa</i> Roth.) winter catch crop – seeds sown in early September at a rate of 70 kg·ha ⁻¹ , incorporated in early May 2009-2011.
	TR	White clover (<i>Trifolium repens</i> L.) winter catch crop – seeds sown in early September at a rate of 20 kg·ha ⁻¹ , incorporated in early May 2009-2011.
	SC	Winter rye (<i>Secale cereale</i> L.) winter catch crop – seeds sown in early September at a rate of 180 kg·ha ⁻¹ , incorporated in early May 2009-2011.
	LM	Italian ryegrass (<i>Lolium multiflorum</i> L.) winter catch crops – seeds sown in early September at a rate of 35 kg·ha ⁻¹ , incorporated in early May 2009-2011.

Table 2. Chronology of field operations

Winter catch crops (2008-2011)	Catch crops sowing	8 September 2008, 10 September 2009, 9 September 2010
↓	Catch crops incorporated (Farmyard manure incorporated)	7 May 2009, 11 May 2010, 5 May 2011
Sweet corn (2009-2011)	Sweet corn sowing	14 May 2009, 24 May 2010, 11 May 2011
↓	Sweet corn harvest	8 September 2009, 23 August 2010, 3 September 2011
Broccoli (2010-2012)	Broccoli sowing	15 March 2010, 17 March 2011, 14 March 2012
	Broccoli planting	19 April 2010, 15 April 2011, 20 April 2012
	Broccoli harvest	14 June 2010, 16 June 2011, 11 June 2012

Table 3. The quantity of fresh and dry matter and the amount of macronutrients incorporated with farmyard manure and catch crops

Kind of organic manure / catch crops	Year of incorporation	Fresh matter (t·ha ⁻¹)	Dry matter (t·ha ⁻¹)	N	P	K	Ca	Mg
				Accumulation (kg·ha ⁻¹)				
Farmyard manure (FYM)	2009	30.0 ^a	7.1 ^a	90.8 ^a	46.3 ^a	126.4 ^a	58.1 ^a	32.8 ^a
	2010	30.0 ^a	7.6 ^a	106.4 ^a	49.7 ^a	140.0 ^a	70.1 ^a	39.1 ^a
	2011	30.0 ^a	8.1 ^a	120.7 ^a	53.1 ^a	133.2 ^a	64.1 ^a	45.4 ^a
	Mean	30.0 ^{CD}	7.6 ^B	106.0 ^B	49.7 ^B	133.2 ^B	64.1 ^B	39.1 ^C
Hairy vetch (VV)	2009	18.5 ^a	2.9 ^a	105.4 ^a	11.4 ^a	38.7 ^a	26.4 ^a	5.6 ^a
	2010	15.7 ^a	2.6 ^a	92.9 ^a	8.9 ^a	36.7 ^a	23.8 ^a	6.1 ^a
	2011	20.0 ^a	3.4 ^a	127.7 ^a	14.3 ^a	46.0 ^a	29.0 ^a	6.8 ^a
	Mean	18.1 ^B	3.0 ^A	108.7 ^B	11.5 ^A	40.5 ^A	26.4 ^A	6.2 ^A
White clover (TR)	2009	11.8 ^a	2.1 ^a	56.0 ^a	9.9 ^a	52.7 ^a	22.0 ^a	6.0 ^a
	2010	12.4 ^a	2.4 ^a	84.8 ^a	10.4 ^a	62.7 ^a	25.1 ^a	7.4 ^a
	2011	10.6 ^a	1.9 ^a	52.1 ^a	8.6 ^a	47.2 ^a	20.0 ^a	5.3 ^a
	Mean	11.6 ^A	2.1 ^A	64.3 ^A	9.6 ^A	54.2 ^A	22.4 ^A	6.2 ^A
Winter rye (SC)	2009	36.0 ^a	8.7 ^a	167.5 ^b	60.5 ^a	182.6 ^a	61.3 ^a	30.6 ^a
	2010	35.1 ^a	6.9 ^a	120.7 ^{ab}	54.4 ^a	150.7 ^a	55.2 ^a	25.2 ^a
	2011	35.3 ^a	6.4 ^a	115.9 ^a	50.1 ^a	128.7 ^a	49.9 ^a	23.7 ^a
	Mean	35.5 ^D	7.3 ^B	134.7 ^C	55.0 ^B	154.0 ^B	55.5 ^B	26.5 ^B
Italian ryegrass (LM)	2009	17.8 ^a	4.2 ^b	72.5 ^a	20.5 ^a	165.5 ^b	24.1 ^a	13.3 ^a
	2010	9.5 ^a	1.9 ^a	31.2 ^a	10.9 ^a	99.4 ^a	11.7 ^a	7.2 ^a
	2011	12.4 ^a	2.5 ^{ab}	43.8 ^a	13.5 ^a	128.7 ^{ab}	18.4 ^a	7.9 ^a
	Mean	13.2 ^{AB}	2.9 ^A	49.2 ^A	15.0 ^A	131.2 ^B	18.1 ^A	9.5 ^A

Means followed by different lowercase and uppercase letters in columns differ significantly at $p \leq 0.05$

Seedling preparation

Broccoli seedlings were grown in a non-heated greenhouse. Seeds were sown in the successive growing seasons on 15, 17 and 14 March to multi-trays with a size of 400 × 600 mm and 54 cells with a diameter of 54 mm. The Aura substrate produced by Hollas - Greenyard Horticulture Poland Ltd. was used for the production of seedlings. It was made of de-acidified ‘highmoor’ peat with 5.5-6.5 pH and salinity not greater than 2 g of NaCl per litre. The substrate was enriched with mineral fertilisers (NPK: 14-16-18%) and Mg (5%). On average nutrient content in the substrate was as follows (mg·dm⁻³): 238 NO₃-N, 18 NH₄-N, 70 P, 207 K, 1016 Ca, and 158 Mg.

Field work

The crop preceding broccoli was sweet corn (*Zea mays* L. var. *Saccharata*), to which organic treatment was applied (organic fertilisers in the form of winter crops and farm manure according to the doses in *Table 1*) with mineral fertilisers (pre-sowing treatment: 60 kg N, 50 kg P₂O₅, 180 kg K₂O per 1 ha + top dressing of 60 kg N·ha⁻¹). After harvesting the cobs, sweet corn plants were cut down and removed from the field. In the autumn the field was ploughed, and in the spring, two weeks before planting seedlings, disc harrowing was used. After that, mineral fertilizers were applied up to the optimal level for broccoli: 205 kg N, 145 kg P₂O₅, 275 kg K₂O per ha. Plants were planted in the successive study years on the 19, 15 and 20 of April, at a spacing of 50 × 50 cm. The area of a plot (unit) was 8 m² (2 m × 4 m), with 32 plants in each. The area of the whole field together with paths between experimental combinations and replicates was 750 m². After broccoli were planting, they were covered with the polypropylene fibre Pegas Agro 17UV (Rybnik, Poland). The cover was removed after three weeks. Then 50 kg of N per hectare was applied (top dressing).

Sample collection and laboratory analysis

Broccoli was harvested by hand on 14 June in 2010, 16 June in 2011, and 11 June in 2012. The area of each plot to be harvested was 6 m² (12 plants). The marketable yield, weight of the marketable curd, length of the curd arc, and the stalk diameter were determined after the harvest. From each plot a curd sample was collected (four randomly selected curds) for chemical analysis to determine: dry matter content by drying to the constant weight at 105°C (Polish Standard PN-EN 12145, 2001); protein content with the Kjeldahl method, using the 6.25 factor (AOAC, 1984); L-ascorbic acid content with the Tillmans method (PN-A-04019, 1998); total sugars content with the Luff-Schoorl method (EU, 2009). In 2011 and 2012, the content of macronutrients (P, K, Ca and Mg) in broccoli was also determined. P content was measured by colorimetry with the SPEKOL 221 spectrophotometer (Carl Zeiss AG, Germany). The content of K and Ca was determined with the FLAPHO 41 flame photometer (Carl Zeiss AG, Germany). The content of Mg was determined with the SOLAR 929 absorption spectrophotometer (ATI Unicam Ltd., UK). In 2009-2011, the quantity of fresh and dry matter of catch crops and the content of accumulated macronutrients were determined.

Statistical analysis

The results were statistically processed with ANOVA for the split-block design. The significance of differences was determined with Tukey's test at the significance level of $P \leq 0.05$. All the calculations were performed with the Statistica software (version 10, Statsoft, USA).

Weather conditions

The basic weather conditions of the experimental area in individual growing seasons are presented in *Table 4*. Years 2010 and 2012 were characterized by similar average temperatures during the growing period and favourable precipitation distribution for the growth and development of broccoli. The least favourable conditions were in 2011, with higher mean air temperatures than in the other growing seasons, but with insufficient quantity of precipitation.

Table 4. Weather condition in the experiment area, 2010–2012 (Zawady Meteorological Station, Poland)

Month	2010		2011		2012	
	T (°C)	P (mm)	T (°C)	P (mm)	T (°C)	P (mm)
April	8.9	10.7	10.1	31.0	8.9	29.9
May	14.0	93.2	13.4	36.1	14.6	53.4
June	17.4	62.6	18.1	39.1	16.3	76.2
Mean	13.4	-	13.9	-	13.3	-
Total	-	166.5	-	106.2	-	159.5

T – average temperature, P – sum of precipitation

Results and Discussion

The quantity of incorporated fresh and dry matter and macronutrient content in catch crops varied across the years of research (*Table 3*). On average, between 2009 and 2011, the highest yields of fresh matter were recorded for winter rye (35.5 t·ha⁻¹), and the lowest

for white clover and Italian ryegrass. The amount of dry matter (DM) in incorporated winter rye ($7.3 \text{ t}\cdot\text{ha}^{-1}$) was similar to the amount of DM in the incorporated farmyard manure (FYM) with an average of $7.6 \text{ t}\cdot\text{ha}^{-1}$ DM. The least DM was produced by white clover (TR). O'Reilly et al. (2011) and Dolijanovic et al. (2012) report that the biomass produced by the catch crops of rye and hairy vetch can correspond even to $30 \text{ t}\cdot\text{ha}^{-1}$ FYM.

The highest amount of N was in incorporated winter rye (SC). Its amounts accumulated by hairy vetch (VV) catch crops were similar, whereas in TR and LM the content of this macronutrient was significantly lower than in FYM. The quantity of P in SC was similar to that of FYM. Non-leguminous catch crops and FYM contained significantly more K than leguminous catch crops. SC accumulated significantly more Ca and Mg than VV, TR, and LM. Incorporated FYM introduced the most Ca and Mg into the soil. The total amount of macronutrients accumulated by the catch crops constituted 40-122% of the quantity introduced with $30 \text{ t}\cdot\text{ha}^{-1}$ FYM. Thorup-Kristensen (2001) and Kramberger et al. (2009) reported that rye was one of the most effective catch crop plants recovering nutrients from deeper soil strata. The quantity of macronutrients in catch crops depends on a number of factors, including plant species, soil type, climatic conditions, and timing of cultivation. N is the element which exerts the greatest effect on the yield. The amounts of N in hairy vetch may range from 52 to $227 \text{ kg}\cdot\text{ha}^{-1}$ (Caporali et al., 2004; Franczuk, 2006; Salmerón et al., 2011). White clover leave soil in good condition, fixing from 100 to $240 \text{ N}\cdot\text{ha}^{-1}$ (Kärner and Kärner, 1996; Kramberger et al., 2014). In turn, rye may enrich the soil with $40\text{-}143 \text{ kg}\cdot\text{ha}^{-1}$ (Thorup-Kristensen, 2001; Franczuk, 2006).

Weather conditions in the successive growing seasons had a significant influence on the marketable yield of broccoli curds, mass of the marketable curd, and biological parameters (Tables 5–6). The highest marketable yield ($26.3 \text{ t}\cdot\text{ha}^{-1}$) and the highest weight of the curd (696.3 g) was in 2010, the most favourable for broccoli growth (Table 5). Both broccoli cultivars tested in the experiment produced similar yields, but the Loreto F₁ cultivar developed slightly bigger curds than Milady F₁. Statistical analysis of the results showed a significant effect of the types of organic fertilizer on broccoli yields. On average, across the growing seasons the largest marketable yield of curds ($27.9 \text{ t}\cdot\text{ha}^{-1}$) was on plots where in the previous year manure (FYM) was applied to sweet corn. A similar yield of curds was recorded in plants grown after incorporated hairy vetch (VV), white clover (TR), and winter rye (SC). Compared with control plants the commercial yield of broccoli from the FYM and VV plots was greater by 64% and 42%, respectively, with these differences being statistically significant. An increase in the yield of broccoli grown after the other catch crops was 8-34% greater than in the control plot, but the results were not statistically significant.

The largest broccoli curds (725.9 g) were harvested on plots where manure was applied to sweet corn (Table 5) in the previous year. A weight similar to the above, with a borderline statistical significant difference, was recorded for broccoli plants grown after VV, TR, and SC incorporation. In addition, broccoli preceded by FYM, VV, TR, and SC in crop rotation developed curds of a substantially greater weight than the control plants. de Freitas et al. (2011), using green manure (GM) of legume plants at doses of 5.0 and $2.5 \text{ t}\cdot\text{ha}^{-1}$ DM before planting broccoli, obtained curds with a mass greater by 180 and 120% than those in the control plot (without fertilization). However, production effects of green manure were worse than those obtained on plots with intensive mineral fertilizer treatment. An increase in the production of broccoli after GM was also recorded by Diniz et al. (2015), who observed that the yield of curds increased with an increase in a dose of GM biomass. Peralta-Antonio et al. (2019) suggest that on soils with average fertility,

GM used on its own is insufficient to significantly affect the growth and yield of broccoli. Combined use of mineral fertilizer and GM is necessary, which is a viable option to reduce the amounts of the former. Production results of such combined application are similar to those obtained with high doses of mineral fertilizers.

Table 5. Effect of winter catch crop on the yield of broccoli and the weight of curds

Organic manure	Year			Broccoli cultivar		Mean
	2010	2011	2012	Loreto F ₁	Milady F ₁	
Marketable yield (t·ha ⁻¹)						
Control	17.5	18.4	15.0	16.5	17.5	17.0 ^a
FYM	31.4	25.8	26.5	27.2	28.7	27.9 ^c
VV	30.1	19.2	23.1	26.8	21.5	24.1 ^{bc}
TR	30.9	16.9	20.7	22.6	23.1	22.8 ^{abc}
SC	26.9	20.0	19.0	22.9	20.9	21.9 ^{abc}
LM	21.0	18.0	16.1	18.8	17.9	18.4 ^{ab}
Mean	26.3 ^B	19.7 ^A	20.1 ^A	22.4	21.6	22.0
<i>HSD</i> _{0.05} : year = 3.8, broccoli cultivar = NS, organic manuring = 6.8, interactions = NS						
Weight of marketable curd (g)						
Control	481.1	512.0	470.3	464.0 ^a	511.5 ^a	487.8 ^a
FYM	795.3	678.6	703.8	694.6 ^{cd}	757.3 ^b	725.9 ^c
VV	796.3	550.9	639.2	742.7 ^d	581.6 ^a	662.2 ^{bc}
TR	813.8	523.1	564.9	638.7 ^{bcd}	629.2 ^a	633.9 ^{bc}
SC	698.2	622.3	503.9	626.0 ^{bc}	590.2 ^a	608.1 ^{abc}
LM	592.9	543.6	470.7	551.8 ^{ab}	519.6 ^a	535.7 ^{ab}
Mean	696.3 ^B	571.7 ^A	558.8 ^A	619.6	598.2	608.9
<i>HSD</i> _{0.05} : year = 69.8, broccoli cultivar = NS, organic manuring = 136.4, broccoli cultivar × organic manuring = 17.7, other interactions = NS						

Means followed by different lowercase letters in columns and different uppercase letters in rows differ significantly at $p \leq 0.05$; FYM – farmyard manure, VV – hairy vetch, TR – white clover, SC – winter rye, LM – Italian ryegrass; NS – not significant

In the present experiment significant interaction of broccoli cultivars with organic fertilisers was recorded. The Loreto F₁ cultivar grown after VV (742.7 g) produced the biggest curds, with similar results recorded when it followed incorporated FYM or when it followed TR and SC. However, when it was grown after FYM incorporation, the Milady F₁ cultivar produced significantly the largest curds (757.3 g).

Hairy vetch, white clover and winter rye cultivated as winter catch crops may successfully replace farmyard manure. Many researchers point to their short-term and long-term effects on the yields of subsequent crops (Salmerón et al., 2011; Choi et al., 2014; Zandvakili et al., 2017; Makarewicz et al., 2018; Thavarajah et al., 2019). However, the yield is not the only reason why catch crops should be included into crop rotation. They should be planted due to ecological reasons, such as reduction of weed infestation and herbicide use, limitation of soil erosion, recovery of nutrients from deeper soil strata and protection against them being leached out into groundwater, an increase in the amount of organic matter, as well as a positive reaction of micro and mesofauna in the soil (Hartwig and Ammon, 2002; Snapp et al., 2005; Reddy, 2016).

In 2010 broccoli plants had stems with a larger diameter than those grown in 2012. Plants grown in 2010 and 2012 had a longer curd arc than in 2011 (Table 6). Organic

fertilisers also differentiated the biometric parameters of broccoli curds. Across the growing seasons, the largest stem diameter and the longest curd arc were recorded in broccoli grown on plots with manure applied to sweet corn the previous year (4.02 cm and 33.7 cm, respectively). Similar values were also found in plants grown after VV. As an average for all treatments the Loreto F₁ cultivar developed longer curd arcs than the Milady F₁ cultivar.

Table 6. Effect of winter catch crop on broccoli curd biological parameters

Organic manure	Year			Broccoli cultivar		Mean
	2010	2011	2012	Loreto F ₁	Milady F ₁	
Stalk diameter (cm)						
Control	3.68 ^{ab}	3.85 ^{bc}	3.19	3.49 ^a	3.65 ^c	3.57 ^a
FYM	4.14 ^b	4.31 ^c	3.60	3.98 ^c	4.06 ^d	4.02 ^b
VV	3.86 ^{ab}	3.68 ^{abc}	3.56	3.88 ^{bc}	3.52 ^{abc}	3.70 ^{ab}
TR	3.43 ^a	3.09 ^a	3.45	3.45 ^a	3.19 ^a	3.32 ^a
SC	3.44 ^a	3.18 ^a	3.44	3.43 ^a	3.28 ^{ab}	3.35 ^a
LM	3.61 ^{ab}	3.57 ^{ab}	3.57	3.56 ^{ab}	3.61 ^{bc}	3.58 ^a
Mean	3.69 ^B	3.61 ^{AB}	3.47 ^A	3.63	3.55	3.59
<i>HSD</i> _{0.05} : year = 0.17, broccoli cultivar = NS, organic manuring = 0.39, year × organic manuring = 0.66, broccoli cultivar × organic manuring = 0.35, other interactions = NS						
Curd circumference length (cm)						
Control	34.05	24.77	31.07	31.01	28.91	29.96 ^a
FYM	38.15	28.88	34.03	35.69	31.69	33.69 ^b
VV	37.32	25.95	36.78	36.06	30.63	33.34 ^b
TR	32.40	22.68	33.13	30.98	27.83	29.40 ^a
SC	31.95	21.05	32.22	29.63	27.18	28.41 ^a
LM	32.17	22.18	32.25	29.29	28.44	28.87 ^a
Mean	34.34 ^B	24.25 ^A	33.25 ^B	32.11 ^B	29.11 ^A	30.61
<i>HSD</i> _{0.05} : year = 1.20, broccoli cultivar = 0.78, organic manuring = 2.77, interactions = NS						

Means followed by different lowercase letters in columns and different uppercase letters in rows differ significantly at $p \leq 0.05$; FYM – farmyard manure, VV – hairy vetch, TR – white clover, SC – winter rye, LM – Italian ryegrass; NS – not significant

The average content of dry matter in broccoli curds was 8.51%, with protein constituting 4.17% FM (fresh matter), ascorbic acid 71.76 mg·100g⁻¹ FM, and total sugars 2.78 g·100g⁻¹ FM (Table 7). Chemical composition of vegetables is genetically determined, but it is modified by factors affecting the plant during its growth (Lee and Kadar, 2000). In the present studies, the effects of weather conditions and organic fertilizers on the content of minerals and nutrients in broccoli were significant. The plants produced the driest matter and total sugars in 2012, protein in 2011, and ascorbic acid in 2011 and 2012. The smallest amounts of dry matter and ascorbic acid were in broccoli grown in 2010, protein in 2012, and total sugars in 2011.

Broccoli plants grown after sweet corn treated with incorporated SC, VV, and manure were significantly richer in protein than those grown in control. The difference was 0.24-0.32%. Broccoli grown after SC contained more protein than after TR and LM. The highest amounts of total N (Table 3) were recorded in plants grown after manure (FYM), winter rye (SC), and hairy vetch (VV). After the mineralization of organic matter, taking place in the first and second years after catch crop incorporation, N became available to

broccoli. Plants used it for tissue building and protein synthesis. In addition, broccoli plants grown on plots with incorporated TR and VV contained significantly more total sugars than those grown in control, respectively, by 0.21 and 0.19 g·100g⁻¹ FM. According to Worthington (2001) and Talgre et al. (2012), an increase in available N content stimulates protein production, which may explain increased protein content in plants following legume catch crops, those additional sources of available N living in symbiosis with N-fixing bacteria. Increased content of protein and vitamin C was earlier recorded by Jabłońska-Ceglarek and Rosa (2003), who used spring-incorporated green manures.

Table 7. The content of selected components of nutritive value of broccoli

Treatment	Dry matter (%)	Protein (% FM)	Ascorbic acid (mg·100g ⁻¹ FM)	Total sugars (g·100g ⁻¹ FM)
Years				
2010	7.58 ^a	4.15 ^a	69.81 ^a	2.81 ^b
2011	8.56 ^b	4.30 ^b	72.40 ^b	2.62 ^a
2012	9.39 ^c	4.05 ^a	73.08 ^b	2.92 ^c
Broccoli cultivar				
Loreto F ₁	8.45	4.13 ^a	72.44 ^b	2.84 ^b
Milady F ₁	8.57	4.21 ^b	71.08 ^a	2.72 ^a
Organic manure				
Control	8.28	4.00 ^a	71.79	2.66 ^a
FYM	8.64	4.24 ^{bc}	73.02	2.80 ^{ab}
VV	8.58	4.24 ^{bc}	73.19	2.85 ^b
TR	8.53	4.10 ^{ab}	70.22	2.87 ^b
SC	8.69	4.32 ^c	70.68	2.79 ^{ab}
LM	8.32	4.10 ^{ab}	71.66	2.73 ^{ab}
Mean	8.51	4.17	71.76	2.78

*HSD*_{0.05} for dry matter: years = 0.79, broccoli cultivar = NS, organic manure = NS;

*HSD*_{0.05} for protein: years = 0.11, broccoli cultivar = 0.07, organic manure = 0.16;

*HSD*_{0.05} for ascorbic acid: years = 2.02, broccoli cultivar = 1.32, organic manure = NS;

*HSD*_{0.05} for total sugars: years = 0.10, broccoli cultivar = 0.07, organic manure = 0.17.

Means followed by different letters in columns differ significantly at $p \leq 0.05$; FYM – farmyard manure, VV – hairy vetch, TR – white clover, SC – winter rye, LM – Italian ryegrass; FM – fresh matter; NS – not significant

The content of the nutrients was also dependent on the broccoli cultivar. The Loreto F₁ cultivar contained more ascorbic acid and total sugars, but less protein than Milady F₁.

Between 2011 and 2012 concentrations of P, K, Ca, and Mg were determined in broccoli curds. In 2011 plants contained significantly less P and Ca, but significantly more Mg than in 2012 (Table 8). Both varieties contained similar amounts of P, K, and Ca, while the Loreto F₁ cultivar contained significantly more Mg. The catch crops and manure, both incorporated before sweet corn, had a significant impact on the concentrations of P, K and Mg in broccoli. The most P was recorded in broccoli grown after VV and TR as winter catch crops, significantly more than in control plants and more than plants on plots preceded by FYM and LM. Significantly the most K was recorded in broccoli grown after FYM and VV. Broccoli plants grown after VV were also the richest in Mg. The approximate amount of this element was recorded in broccoli grown after incorporated manure and TR.

Table 8. Concentrations of macronutrients in broccoli

Treatment	P	K	Ca	Mg
	(g·kg ⁻¹ DM)			
Years				
2011	4.53 ^a	23.0	3.33 ^a	2.16 ^b
2012	5.23 ^b	22.8	3.37 ^b	2.01 ^a
Broccoli cultivar				
Loreto F ₁	4.89	22.9	3.34	2.11 ^b
Milady F ₁	4.87	22.8	3.36	2.06 ^a
Organic manure				
Control	4.36 ^a	22.4 ^a	3.29	1.99 ^a
FYM	4.62 ^{ab}	23.5 ^b	3.38	2.15 ^{bc}
VV	5.39 ^c	23.4 ^b	3.37	2.20 ^c
TR	5.25 ^c	22.8 ^a	3.36	2.13 ^{bc}
SC	4.91 ^{bc}	22.5 ^a	3.32	2.06 ^{ab}
LM	4.76 ^{ab}	22.6 ^a	3.38	1.99 ^a
Mean	4.88	22.9	3.35	2.09

*HSD*_{0.05} for P: years = 0.08, broccoli cultivar = NS, organic manure = 0.49;

*HSD*_{0.05} for K: years = NS, broccoli cultivar = NS, organic manure = 0.5;

*HSD*_{0.05} for Ca: years = 0.02, broccoli cultivar = NS, organic manure = NS;

*HSD*_{0.05} for Mg: years = 0.04, broccoli cultivar = 0.04, organic manure = 0.09.

Means followed by different letters in columns differ significantly at $p \leq 0.05$; FYM – farmyard manure, VV – hairy vetch, TR – white clover, SC – winter rye, LM – Italian ryegrass; DM – dry matter; NS – not significant

Conclusions

1. The effect of winter catch crops ploughed into the soil, like *Vicia villosa* Roth., *Trifolium repens* L. and *Secale cereale* L. on the broccoli yield was statistically similar to that of manure applied at a dose of 30 t·ha⁻¹. Among the above catch crops, hairy vetch affected the yield of subsequent crops the most.
2. Organic fertilisers applied to the crops preceding broccoli affected its content of protein and sugars. A significant increase in protein content in relation to control was observed in broccoli plants grown after farmyard manure and incorporated hairy vetch and winter rye treatments, and in total sugars after hairy vetch and white clover.
3. The largest P concentration was in broccoli grown after hairy vetch and white clover, while the largest amounts of K was after farmyard manure application and after hairy vetch incorporation, and Mg when broccoli was grown after hairy vetch.
4. Broccoli varieties produced similar yields. The Loreto F₁ cultivar contained more ascorbic acid, total sugars and Mg, but less protein than the Milady F₁ cv.
5. It was found that in horticulture, winter catch crops like hairy vetch, white clover and winter rye can be an alternative for manure, an organic fertiliser increasingly more difficult to obtain. The beneficial effect of those crops, similar to the effect of manure, on the yield of following crops was also evident in the second year. They can be successfully used in the following sequence: winter catch crops – sweet corn – broccoli.
6. The results of the research allowed to issue practical recommendations to farmers on the use of these catch crops in the cultivation of sweet corn and broccoli.
7. Research on other plants and their mixtures is still necessary to replace FYM and to reduce mineral fertilisation in vegetable cultivation.

Acknowledgements. The research carried out under the theme No. 226/06/S was financed by the science grant of the Ministry of Science and Higher Education.

REFERENCES

- [1] Adamczewska-Sowińska, K., Kołota, E. (2008): The effect of living mulches on yield and quality of tomato fruits. – *Vegetable Crops Research Bulletin* 69(1): 31-38. DOI: 10.2478/v10032-008-0018-z.
- [2] AOAC (1984): Association of Official Analytical Chemists. Official methods of analysis. 14th ed. Assn. – Official Analytical Chemists, Arlington, Va. sec. 14.067.
- [3] Caporali, F., Campiglia, E., Mancinelli, R., Paolini, R. (2004): Maize performances as influenced by winter cover crop green manure. – *Italian Journal of Agronomy* 8(1): 37-45.
- [4] Choi, B., Lim, J. E., Sung, J. K., Jeon, W. T., Lee, S. S., Oh, S.-E., Yang, J. E., Ok, Y. S. (2014): Effect of Rapeseed green manure amendment on soil properties and rice productivity. – *Communications in Soil Science and Plant Analysis* 45(6): 751-764. DOI: 10.1080/00103624.2013.858728.
- [5] de Freitas, G. B., Rocha, M. S., Santos, R. H. S., Monteiro da Silva Freitas, L., de Almeida Resende, L. (2011): Broccoli yield in response to top-dressing fertilization with green manure and biofertilizer. – *Revista Ceres* 58(5): 645-650. DOI: 10.1590/s0034-737x2011000500016.
- [6] Diniz, E. R., de Oliveira Vargas, T., Santos, R. H. S., de Almeida, A. R., de Mattos, U. B. M. (2015): Crescimento e produção de brócolis adubado com doses de mucuna-cinza em casa de vegetação. – *Semina: Ciências Agrárias* 36(3): 1277-1286. DOI: 10.5433/1679-0359.2015v36n3p1277.
- [7] Dolijanovic, Z., Momirovic, N., Mihajlovic, V., Simic, M., Oljaca, S., Kovacevic, D., Kaitovic, Z. (2012): Cover crops effects on the yield of sweet corn. – *Third International Scientific Sympozjum “Agrosym Jahorina 2012”*: 104-110.
- [8] EU (2009): Commission Regulation No. 152/2009. – *Official Journal of the European Union* L54: 1-130.
- [9] FAOSTAT (2018): Broccoli (and cauliflower) production in 2018, Crops/Regions/World list/Production Quantity (pick lists). – UN Food and Agriculture Organization, Corporate Statistical Database. Retrieved 9 March 2020.
- [10] Fekete, Á., Pepó, P. (2018): The role of green manure crops in Hungarian plant production. – *Acta Agraria Debreceniensis* 74: 49-53. DOI: 10.34101/actaagrar/74/1663.
- [11] Franczuk, J. (2006): Efekty stosowania nawozów zielonych w postaci międzyplonów ozimych oraz słomy żytniej w uprawie warzyw. (The effects of the use of green manure in the form of winter catch crops and rye straw in the cultivation of vegetables). – *Wydawnictwo Akademii Podlaskiej w Siedlcach, Rozprawa Nauk* 84: 122 p. (in Polish).
- [12] Hartwig, N., Ammon, H. (2002): Cover crops and living mulches. – *Weed Sciences* 50(6): 688-699.
- [13] Iivonen, S., Kivijärvi, P., Suojala-Ahlfors, T. (2017): Characteristics of various catch crops in the organic vegetable production in northern climate conditions – Results from an on-farm study. Reports 165. – University of Helsinki, Ruralia Institute, <http://hdl.handle.net/10138/229443>.
- [14] IUSS Working Group WRB (2015): World Reference Base for Soil Resources 2014 (update 2015). – *International Soil Classification System for Naming Soils and Creating Legends for Soil Maps, World Soil Resources Reports No. 106*. Rome, FAO.
- [15] Jabłońska-Ceglarek, R., Rosa, R. (2003): Influence of green manures on the quantity and quality of the yield of red beet. – *Acta Scientiarum Polonorum, Hortorum Cultus* 2(1): 21-30. (in Polish with English summary).
- [16] Kärner, M., Kärner, E. (1996): White clover as a source of N on Estonian grassland on acid soils poor in humus. – *REUR Technical Series* 42: 104-106.

- [17] Kramberger, B., Gselman, A., Janzekovic, M., Kaligarić, M., Bracko, B. (2009): Effects of cover crops on soil mineral N and on the yield and N content of maize. – *European Journal of Agronomy* 31(2): 103-109. DOI: 10.1016/j.eja.2009.05.006.
- [18] Kramberger, B., Gselman, A., Kristl, J., Lešnik, M., Šuštar, V., Muršec, M., Podvršnik, M. (2014): Winter cover crop: the effects of grass–clover mixture proportion and biomass management on maize and the apparent residual N in the soil. – *European Journal of Agronomy* 55: 63-71. DOI: 10.1016/j.eja.2014.01.001.
- [19] Kristensen, H., Thorup-Kristensen, K. (2004): Root growth and nitrate uptake of three different catch crops in deep soil layers. – *Soil Science Society of America Journal* 68(2): 529-537. DOI: 10.2136/sssaj2004.5290.
- [20] Lee, S. K., Kader, A. A. (2000): Preharvest and postharvest factors influencing vitamin C content of horticultural crops. – *Postharvest Biology and Technology* 20(3): 207-220. DOI: 10.1016/S0925-5214(00)00133-2.
- [21] Makarewicz, A., Płaza, A., Gąsiorowska, B., Rosa, R., Cybulska, A., Górski, R., Rzażewska, E. (2018): Effect of manure with undersown catch crops and production system on the potato tuber content of macroelements. – *Journal of Elementology* 23(1): 7-19. DOI: 10.5601/jelem.2017.22.1.1398.
- [22] O'Reilly, K. A., Robinson, D. E., Vyn, R. J., van Eerd, L. L. (2011): Weed populations, sweet corn yield, and economics following fall cover crops. – *Weed Technology* 25(3): 374-384. DOI: 10.1614/WT-D-10-00051.1.
- [23] Parente, C. P., Reis Lima, M. J., Teixeira-Lemos, E., Moreira, M. M., Barros, A. A., Guido, L. F. (2013): Phenolic content and antioxidant activity determination in broccoli and lamb's lettuce. – *International Journal of Agricultural and Biosystems Engineering* 7: 70-73.
- [24] Peralta-Antonio, N., Watthier, M., Santos, R. H. S., Martinez, H. E. P., Vergütz, L. (2019): Broccoli nutrition and changes of soil solution with green manure and mineral fertilization. – *Journal of Soil Science and Plant Nutrition* 19(4): 816-829. DOI: 10.1007/s42729-019-00081-4.
- [25] PN-A-04019 (1998): Polish Standard. Food products – Determination of vitamin C content. – Polish Committee for Standardization, Warsaw, Poland. (in Polish).
- [26] Polish Standard PN-EN 12145 (2001): Fruit and vegetable juices – Determination of total dry matter – Gravimetric method with loss of mass on drying. – Polish Committee for Standardization, Warsaw, Poland. (in Polish).
- [27] Reddy, P. P. (2016): Cover/Green Manure Crops. – *Sustainable Intensification of Crop Production*: 55-67. DOI: 10.1007/978-981-10-2702-4_4.
- [28] Rogers, G. S., Little, S. A., Silcock, S. J., Williams, L. F. (2004): No-till vegetable production using organic mulches. – *Acta Horticulturae* 638: 215-223. DOI: 10.17660/actahortic.2004.638.28.
- [29] Rosa, R. (2014): The structure and yield level of sweet corn depending on the type of winter catch crops and weed control method. – *Journal of Ecological Engineering* 15(4): 118-130. DOI: 10.12911/22998993.1125466.
- [30] Rosa, R. (2015): Quality of sweet corn yield depending on winter catch crops and weed control method. – *Acta Scientiarum Polonorum, Hortorum Cultus* 14(2): 59-74.
- [31] Salmerón, M., Isla, R., Caveró, J. (2011): Effect of winter cover crop species and planting methods on maize yield and N availability under irrigated Mediterranean conditions. – *Field Crops Research* 123(2): 89-99. DOI: 10.1016/j.fcr.2011.05.006.
- [32] Snapp, S. S., Swinton, S. M., Labarta, R., Mutch, D., Black, J. R., Leep, R., Nyiraneza, J., O'Neil, K. (2005): Evaluating cover crops for benefits, costs and performance within cropping system niches. – *Agronomy Journal* 97: 322-332. DOI: 10.2134/agronj2005.0322.
- [33] Talgre, L., Lauringson, E., Roostalu, H., Astover, A., Makke, A. (2012): Green manure as a nutrient source for succeeding crops. – *Plant, Soil and Environment* 58(6): 275-281. DOI: 10.17221/22/2012-pse.

- [34] Thavarajah, D., Siva, N., Johnson, N., McGee, R., Thavarajah, P. (2019): Effect of cover crops on the yield and nutrient concentration of organic kale (*Brassica oleracea* L. var. *acephala*). – Scientific Reports 9: 10374. DOI: 10.1038/s41598-019-46847-9.
- [35] Thorup-Kristensen, K. (2001): Are differences in root growth of N catch crops important for their ability to reduce soil nitrate-N content, and how can this be measured? – Plant and Soil 230: 185-195.
- [36] Vos, J., van der Putten, P. E. L. (2001): Field observations on N catch crops. III. Transfer of N to the succeeding main crop. – Plant and Soil 236: 263-273.
- [37] Worthington, V. (2001): Nutritional quality of organic versus conventional fruits, vegetables and grains. – The Journal of Alternative and Complementary Medicine 7(2): 161-173.
- [38] Zandvakili, O. R., Ebrahimi, E., Hashemi, M., Barker, A. V., Akbari, P. (2017): The potential of green manure mixtures to provide nutrients to a subsequent lettuce crop. – Communications in Soil Science and Plant Analysis 48(19): 2246-2255. DOI: 10.1080/00103624.2017.1408819.
- [39] Zhang, Y., Gao, L., Zhou, W., Li, Z. (2010): Effects of intercropping clover on yield, quality of sweet corn and soil mineral N in field. – Acta Agriculturae Boreali-Sinica S1: 236-238.

EFFECTS OF ANIMAL MANURES ON YIELD QUALITY AND NUTRIENT CONTENT IN ORGANIC BROCCOLI (*BRASSICA OLERACEA* L. VAR. *ITALICA*)

YOLDAS, F.^{1*} – CEYLAN, S.¹ – ELMACI, O. L.²

¹*Odemis Technical Training College, Ege University, Izmir, Turkey*

²*Soil Science Department, Faculty of Agriculture, Ege University, Izmir, Turkey*

**Corresponding author*

e-mail: funda.yoldas@ege.edu.tr; phone: +90-542-322-53-85; fax: +90-232-544-43-56

(Received 29th Nov 2019; accepted 24th Mar 2020)

Abstract. This study was conducted to determine the animal manures on yield, quality, and nutrient content of broccoli heads. Treatments consisted of 0, 30 and 60 t ha⁻¹ of sheep and cattle manure and organic commercial fertilizer (B5A). Manure rates significantly increased yield, average weight of main and secondary heads, and the diameter in broccoli compared to control. The highest total yield (27.74 t ha⁻¹) was obtained using sheep manure (30 t ha⁻¹). At harvest, the highest amount of the total N in broccoli heads was measured at organic commercial fertilizer application. Potassium (K), sodium (Na), iron (Fe) and manganese (Mn) content increased with higher doses but, phosphorus (P), calcium (Ca), copper (Cu) and zinc (Zn) contents were not influenced. Additionally, the highest nutrient removal for broccoli heads was obtained at 30 t ha⁻¹ sheep manure application rate.

Keywords: *nutrients contents, yield, quality, removed nutrient, sheep manure, cattle manure*

Introduction

Broccoli (*Brassica oleracea* L. var. *italica*) belongs to the Brassicaceae family is a perennial plant widespread in the west and northwest part of Turkey. Broccoli production in Turkey has increased considerably in recent years. The production reached 69592 tons in 2019 (Anonymous, 2019a). Broccoli is high in nutritional value and is found in the most efficient group of vegetables from the standpoint of food production. Also, Broccoli has been shown to be very useful for human health in terms of its ingredients and to provide protection against certain types of cancer (Yoldas, 2003; Yoldas and Eşiyok, 2004; Yoldas et al., 2008, 2009, 2019; Anonymous, 2019b; Vanduchova, 2019). Broccoli is not a very selective vegetable in terms of soil requirements. Soils rich in organic matter are suitable for broccoli cultivation.

Fertilization is very important for increasing yield and quality in crop production. Plant nutrition is one of the most important factors that increase plant production (Ninou et al., 2017). However, fertilizer needs vary according to varieties, soil properties, organic matter content and ecology. One of the most important problems in plant production is the accumulation of nitrate. Farmer's unconscious and excessive use of fertilizer plants may cause nitrate accumulation and environmental pollution (Mordoğan et al., 2001; Yoldas et al., 2017). Intensive fertilizer and pesticide use often leads to occurring of significant hazards for humans and their environment (Atılgan et al., 2007). The use of organic and plant-based organic substances in agriculture as an alternative to chemical fertilizer or as a way of reducing their amount is becoming widespread (Yoldas et al., 2009). Comparisons of conventional and organic farms compared to soil type indicated that organic practices improved soil quality (Liebig and Doran, 1999).

Healthy life and environmental awareness are important today. This case it caused to increase on naturel human nutrition. Using of chemical fertilizer was decreased and natural production became important. Increasing the productivity of our soil resources by natural manure will be appropriate. Soil organic matter improves physical, chemical, biological properties of soil and is also affect the availability of nutrient (Sezen, 1995; Chaterjee et al., 2005; Kandil and Gad, 2009). In sustainable agriculture, organic fertilizers not only supply plant nutrients but also improve soil organic matter contents (Yaldiz et al., 2017). The importance of organic fertilizers in soil fertility and the fact that the soils of the region are poor organic matter in sandy texture reveals the need for organic fertilizers (Yoldas and Ceylan, 2010).

The objectives of this study were to (i) evaluate broccoli yield and yield components according to different organic manure doses, (ii) to find effects of organic manure doses on nutrient content in heads, and (iii) to determine amounts of nutrients removed by broccoli heads.

Materials and methods

This research was conducted during the winter growing season at Odemis Technical Training College of Ege University (altitude 123 m and 38° 13' 8.4216" North and 27° 58' 18.3432" east). Ironmen variety was used as a test crop (the head that reaches the harvest maturity -80-85 days after transplanting- has the feature of waiting like the main head without spoiling its quality). The experiment was designed in a randomized block with three replications (in October). The experimental design included unfertilized control plots. Seeds were sown in pots which had included 105 ml torf. They were transplanted 50 cm apart between plants and 70 cm apart in rows (Yoldas, 2003), when they became optimum size for planting. The experimental area was dripped with discharrow. Each plot area was 3.5 m² and contained 10 plants. Marketable parts of broccoli were collected (Yoldas, 2003). Fertilizer treatments included control (no fertilizer treatment) four rates of organic manures (30, 60 t ha⁻¹ sheep manure and 30, 60 t ha⁻¹ cattle manure), organic commercial fertilizer (B5A-production by BMR Agriculture) were mixed with the soil before planting. In experiment, weeds are cleaned by hand during the plant development period and irrigation was conducted regularly (Vural et al., 2000).

Broccoli heads of marketable size were harvested (in February - for 1.5 months) from each plot: total yield (t ha⁻¹), main head yield (t ha⁻¹), secondary head of yield (t ha⁻¹), average weight of main head (g), average weight of secondary head (g), diameter of head (cm), and length of head (cm) of broccoli were determined.

Soil samples were taken from depths of 0-30 cm and 30-60 cm of the experiment area. Samples were air dried, ground and passed through 2 mm sieve for the determination of chemical parameters (Kacar, 1984). Some physical and chemical characteristics of experimental soils, determined by standard analytical methods specified in Klute (1986) and Page et al. (1982).

Available K, Ca, Na flame photometer (Eppendorf) and Mg, Fe, Zn, Mn and Cu were determined by atomic absorption spectrophotometer (AAS; Varian AA 240 FS) (Lindsay and Norvell, 1978; Atalay et al., 1986) some physical and chemical properties of soils before applications are given in *Table 1*.

When *Table 1* is examined, the soil of the trial area is neutral at 30 cm depth. Total N at 0-30 cm depth low, 30-60 cm depth medium, available K and Ca content poor (Güneş

et al., 2000), the available P content is sufficient when evaluated according to Chapman and Pratt (1982). Mg content is in good condition at both depths. Micronutrients Fe, Cu, Mn, Zn were found to be good and adequate (Güneş et al., 2000).

Table 1. Some physical and chemical properties of soil

Properties	Unit	0-30 cm	30-60 cm
pH		6.60	7.24
Total salt	(%)	0.030	0.001
Lime	(%)	0.737	0.395
Sand	(%)	66.8	74.8
Clay	(%)	7.6	7.6
Silt	(%)	25.6	17.6
Texture		Sandy loam	Sandy loam
Organic matter	(%)	1.17	1.34
Total N	(%)	0.09	0.04
Available P	mg kg ⁻¹	44	30
Available K	mg kg ⁻¹	79	44
Available Ca	mg kg ⁻¹	720	641
Available Mg	mg kg ⁻¹	181	172
Available Fe	mg kg ⁻¹	13	12
Available Cu	mg kg ⁻¹	1.0	0.07
Available Zn	mg kg ⁻¹	0.7	0.2
Available Mn	mg kg ⁻¹	14	6

In the experiment, organic manures fermented for 6 months were used. Organic sheep and cattle manure samples were also analyzed with methods used in plant samples. The manure and broccoli heads samples were wet digested [(nitric (HNO₃): perchloric acid (HClO₄); 4:1] for P, K, Ca, Mg, Na, Fe, Cu, Zn and Mn analyses. Following the digestions, Quantifications were made for phosphorus colorimetric method, for K, Ca and Na by flame photometer for Mg, Fe, Cu, Zn and Mn by AAS (Moore, 1992; Campbell and Plank, 1992). Total nitrogen in plant samples was analyzed according to the modified Kjeldahl method (Baker and Thompson, 1992). The results of the analysis of organic manures are given in *Table 2*.

Data were analyzed using the SPSS 25.0 statistical package programme and findings were determined based on differences between the mean LSD multivariate analyses (SPSS, 2017).

Yield and yield components

Yield and some yield characteristics are presented in *Table 3*. Organic manure and organic commercial fertilizer (B5A) application significantly increased the total yield, yield of main and secondary heads ($p < 0.01$). The highest total and secondary head yield was obtained from 30 t ha⁻¹ doses of sheep manure (27.74 t ha⁻¹ and 10.35 t ha⁻¹, respectively) (*Fig.1*). Also, the highest yield of main head was obtained from 30 t ha⁻¹ doses of sheep manure. The yield of main head, secondary head, and total yield were increased by treatments compared with control (64%, 45% and 13%, respectively). But,

total yield decreased with excessive sheep manure (60 t ha⁻¹) applications. Similar results were obtained by Zebarth et al. (1995), Babic and Elkner (2000), Belec et al. (2001).

Table 2. Results of analysis of organic manures

Properties	Unit	Cattle manure	Sheep manure
pH		7.75	8.04
Total salt	(%)	2.73	3.26
Dry matter	(%)	90.29	58.71
Organic matter	(%)	33.55	52.75
C/N		22.67	31.29
Total N	(%)	0.86	0.98
P	(%)	0.59	0.46
K	(%)	1.55	1.03
Ca	(%)	2.03	2.20
Mg	(%)	0.92	0.40
Na	(%)	0.10	0.07
Fe	mg kg ⁻¹	3.19	1.28
Cu	mg kg ⁻¹	28	16
Zn	mg kg ⁻¹	536	202
Mn	mg kg ⁻¹	221	111

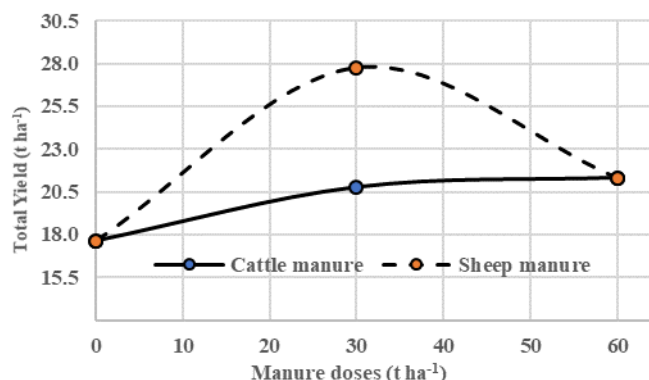


Figure 1. Effect of manure doses on total yield (t ha⁻¹)

But, Castellanos et al. (1999) has reported the highest marketable yield of broccoli was obtained from 400 kg N ha⁻¹. Our findings, in regards to yield, are in agreement with observations made by many researchers (Yoldas, 2003, 14.6–18.6 t ha⁻¹; Rekowska, 2000, 18.8–19.3 t ha⁻¹; Mihov and Antonova, 2000, 15–19.4 t ha⁻¹; Kunicki et al., 1999, 16.6 t ha⁻¹; Albarracin et al., 1995, 20 t ha⁻¹).

Ceylan et al. (2000) determined that the amounts of N, P, K, Ca, Mg, Fe, Cu, Zn and Mn in lettuce leaves increased significantly with organic fertilizer application.

Ceylan et al. (2006) found that, the maximum yield determined by using cattle manure at doses 60 t ha⁻¹. When the results compared to the control, application the yield increased 21%.

Average weight of main and secondary head, weight of secondary head and diameter of head, which are the important quality criterion, were significantly increased by organic manure rates ($p < 0.01$). The highest weight of head and length of head values were determined for 30 t ha^{-1} (608 g, 16.4 cm, respectively) (Table 3). Similar results have been reported by Dellacecca et al. (1994). However, Griffith and Carling (1991), Kunicki et al. (1999), Callens et al. (2000) and Yoldas et al. (2008) found smaller head diameters than ours. Head diameter was found 16.2-16.3 cm by Albarracin et al. (1995).

Secondary head's weight was changed by an increase of manure doses (Table 3). Increasing manure rates significantly increased head diameter compared to the control. The highest value was recorded from sheep manure (30 t ha^{-1}). It again decreased with increasing doses. There was not significant effect of treatments on length of head.

Table 3. The effects of treatments on yield and yield components (total yield (TY, t ha^{-1}), main head yield (Mhy, t ha^{-1}), secondary head of yield (Shy, t ha^{-1}), average weight of main head (Awh, g), average weight of secondary head (Awsh, g), diameter of head (Dh, cm), length of head (Lh, cm) of broccoli

	TY	Mhy	Shy	Awh	Awsh	Dh	Lh
Rates	t ha^{-1}	t ha^{-1}	t ha^{-1}	(g)	(g)	(cm)	(cm)
Control	17.63 c	13.05 c	4.58 b	457 c	160 b	14.5	13.7
Organic commercial fertilizer (B5A)	19.06 bc	13.91 bc	5.14 b	487 bc	180 b	13.9	14.6
Cattle manure 30 t ha^{-1}	20.76 b	14.46 bc	6.30 b	506 bc	221 b	14.8	14.2
Cattle manure 60 t ha^{-1}	21.31 b	15.73 ab	5.58 b	550 ab	195 b	14.0	13.8
Sheep manure 30 t ha^{-1}	27.74 a	17.39 a	10.35 a	608 a	362 a	15.2	16.4
Sheep manure 60 t ha^{-1}	21.29 b	14.35 bc	6.94 b	502 bc	243 b	15.6	15.3
Minimum	17.63	13.05	4.58	457	160	13.9	13.7
Maximum	27.74	17.39	10.35	608	243	15.6	16.4
LSD	2.904**	2.473**	3.107**	86.979**	108.99**	ns	ns

a, b, c, d: average which is shown with different letters in the same column, is between differences are significant

**The difference is significant at the $P < 0.01$ level. ns: No significant difference

Mineral contents of broccoli head

Mineral contents of broccoli head are given in Table 4. K, Na, Fe and Mn contents in broccoli head were significantly affected by sheep and cattle manure treatments ($p < 0.01$). Highest K and Fe content in broccoli were determined in the parcels which the cheap manure was applied as 60 t ha^{-1} . The effect of organic manure on Fe-uptake at these doses, could be due to the reason that organic carbon acts as a source of energy for soil microorganism, which upon mineralization releases organic acids that decreased soil pH and improves availability of makes Fe (Bokhtiar and Sakurai, 2005). However highest Na content in the heads were obtained in the parcels which the animal manure was applied compared to the control and organic commercial fertilizer parcels.

Nitrogen is the most recognized in plants for its presence in the structure of the protein molecule (Ninou et al., 2017). In this study, it was determined that maximum N content in the heads were obtained by organic commercial fertilizer applied. However, significant effect of the applications has not been determined statistically on the nitrogen content of broccoli. This result may be due to low nitrogen content of soils before planting and slow release of organic fertilizers and their effects on the

subsequent products. P, K, Ca and Zn contents were reached maximum at 60 t ha⁻¹ sheep manure. But, N, P, Ca, Mg, Cu and Zn in head were not significantly affected by applications.

Table 4. The effects of treatments on macro and micro element contents in head of broccoli

Rates	%					mg kg ⁻¹				
	N	P	K	Ca	Mg	Na	Fe	Cu	Mn	Zn
Control	5.80	0.22	3.36 b	1.12	0.36	583 b	74.33 ab	4.90	23 b	77.00
Organic commercial fertilizer (B5A)	6.33	0.21	3.44 b	1.06	0.40	598 b	63.67 b	5.00	31 a	75.00
Cattle manure 30 t ha ⁻¹	5.70	0.21	3.25 b	1.03	0.36	771 a	63.33 b	5.03	22.33 b	73.66
Cattle manure 60 t ha ⁻¹	6.17	0.22	3.71 ab	1.13	0.31	788 a	74.67 ab	5.90	25.67 b	74.67
Sheep manure 30 t ha ⁻¹	5.90	0.21	3.88 ab	1.12	0.34	665 ab	90.33 a	4.87	23 b	74.67
Sheep manure 60 t ha ⁻¹	6.03	0.22	4.31 a	1.13	0.33	759 a	57.67 b	5.30	22.33 b	79.67
Minimum	5.70	0.21	3.25	1.03	0.31	583	57.67	4.87	22.33	73.66
Maximum	6.33	0.22	4.31	1.13	0.40	788	90.33	5.90	25.67	79.67
LSD	ns	ns	0.691**	ns	ns	157.15**	17.769**	ns	5.036**	ns

a, b, c, d: average which is shown with different letters in the same column, is between differences are significant
**The difference is significant at the P < 0.01 level. ns: No significant difference

Removed minerals by yield (broccoli head)

Amount of removed minerals by broccoli head were increased by treatments compared with control generally (Table 5). These increases were statistically significant for P, K, Mg, Fe and Mn (p < 0.05).

Table 5. The effects of treatments on removed nutrients amount by heads

Rates	%					mg kg ⁻¹				
	N	P	K	Ca	Mg	Na	Fe	Cu	Mn	Zn
Control	0.09	15.3 b	220.6 c	896	93.00 c	34.33	6.83 ab	1.08	4.17 a	1.59
Organic commercial fertilizer (B5A)	0.10	16.3 b	230.3 c	1024	109.66 b	35.00	6.07 b	1.09	4.33 a	1.51
Cattle manure 30 t ha ⁻¹	0.10	25.3 ab	287.6 bc	1152	182.66 ab	45.33	8.38 a	1.17	4.33 a	1.76
Cattle manure 60 t ha ⁻¹	0.11	26.7 a	397.3 a	1166	231.66 a	39.66	5.61 b	0.81	2.51 b	1.62
Sheep manure 30 t ha ⁻¹	0.11	18.3 ab	317.0 b	1056	167.00 abc	35.00	6.15 b	0.92	2.75 b	1.64
Sheep manure 60 t ha ⁻¹	0.11	27.3 a	334.ab	1152	181.66 ab	36.00	7.39 ab	1.18	4.49 a	1.95
Minimum	0.09	15.3	220.6	896	93.00	34.33	5.61	0.81	2.51	1.51
Maximum	0.11	27.3	397.3	1166	231.66	45.33	8.38	1.18	4.49	1.95
LSD	ns	7.882*	77.092**	ns	86.908**	ns	1.986*	ns	1.381**	ns

a, b, c, d: average which is shown with different letters in the same column, is between differences are significant
*The difference is significant at the P < 0.05 level. ns: No significant difference

The highest amount of P, K, Mg, Fe and Mn removed was achieved at the rate of 60 t ha⁻¹ sheep manure, 60 t ha⁻¹ cattle manure, 60 t ha⁻¹ cattle manure, 30 t ha⁻¹ cattle manure and 60 t ha⁻¹ sheep manure doses, respectively.

Rincon et al. (1999) have shown that removed total quantity of N, P, K, Ca and Mg by crop were 243.9, 28.7, 240.9, 221.3, and 23.0 kg ha⁻¹, respectively.

It was determined that the amount of removed minerals by broccoli head were highest at the 60 t ha⁻¹ sheep manure and 60 t ha⁻¹ cattle manure doses, at which maximum total yield was also obtained.

Conclusions

Increasing health problems is also noteworthy the use of friendly organic fertilizers. Slow release organic fertilizers are beneficial for production with these properties. However, environmental pollution can be prevented by conscious use.

According to the results, increasing the application dose of organic manure increased the yield. The highest yield was obtained from supplying 30 t ha⁻¹ sheep manure. Therefore, 30 t ha⁻¹ sheep manure application can be recommended for broccoli under these conditions. In broccoli head, K, Na, Fe, and Mn contents, which are the important for healthy nutrition, increased with increases in organic manure doses.

Acknowledgements. This research is a work supported by Scientific Research Project Commission of Ege University; Contact no: 2010/OMYO/002.

REFERENCES

- [1] Albarracin, M., Berbin, C., Machado, W. (1995): Agronomic evaluation of broccoli (*Brassica oleracea* var. *italica*) cultivars. – Revista de la Facultad de Agronomia, Universidad Central de Venezuela, Caracas, Venezuela 21(1-2): 71-83.
- [2] Anonymous (2019a): Agricultural Statistics. TUIK 2018 Data. (Tarım İstatistikleri. TUIK 2018 yılı verileri). – Turkish Statistical Institute, Ankara.
- [3] Anonymous (2019b): The amazing health benefits of broccoli. – [http://organicjar.com/2009/2001/The Amazing Health Benefits of Broccoli](http://organicjar.com/2009/2001/The%20Amazing%20Health%20Benefits%20of%20Broccoli), 2019.
- [4] Atalay, İ. Z., Kılıç, R., Anaç, D., Yokaş, İ. (1986): Potassium status of rendzina soils in Gediz Basin and methods to be used in determining the amount of potassium that can be taken in these soils. (Gediz havzası rendzina topraklarının potasyum durumu ve bu topraklarda alınabilir potasyum miktarının tayininde kullanılacak yöntemler.) – Bilge Printing, Izmir.
- [5] Atılğan, A., Coskan, A., Saltuk, B., Erkani, M. (2007): The level of chemical and organic fertilizer usage and potential environmental impacts in greenhouses in Antalya region. – Ekoloji 15: 37-47.
- [6] Babic, I., Elkner, K. (2000): The effect of nitrogen fertilization and irrigation on yield and quality of broccoli. – Acta Horticulturae 571: 33-43
- [7] Baker, W. H., Thompson, T. L. (1992): Determination of Total Nitrogen in Plant Samples by Kjeldahl. – In: Plank, C. O. (ed.) Plant Analysis Reference Procedures for the Southern Region of the United States, Southern Cooperative Series Bulletin 368. North Carolina Agricultural Research Service, Raleigh, NC, pp. 13-16.
- [8] Belec, C., Villeneuve, S., Coulombe, J., Tremblay, N. (2001): Influence of nitrogen fertilization on yield, hollow stem incidence and sap nitrate concentration in broccoli. – Can. J. Plant Sci. 81: 765-772.
- [9] Bokhtiar, S. M., Sakurai, K. (2005): Integrated use of organic manure and chemical fertilizer on growth, yield and quality of sugarcanes in high Ganges River floodplain soils of Bangladesh. – Soil Sci. Plant Analysis 36: 1823-37.
- [10] Callens, D., Reycke, L' de., Reycke, D., Rooster, L. (2000): Cultivar trial for early cultivation of broccoli planting date determines cultivar choice. – Proeftuinnieuws 10(1): 40-41.
- [11] Campbell, R. C., Plank, C. O. (1992): Sample Preparation. – In: In: Plank, C. O. (ed.) Plant Analysis Reference Procedures for the Southern Region of the United States, Southern Cooperative Series Bulletin 368. North Carolina Agricultural Research Service, Raleigh, NC, pp. 5-7.

- [12] Castellanos, J. Z., Lazcano, I., Sosa-Balbidia, A., Badillo, V., Villalobos, S. (1999): Nitrogen fertilization and plant nutrient status monitoring-the basis for high yields and quality of broccoli in potassium-rich vertisols of central Mexico. – *Better Crops International* 13(2): 25-27.
- [13] Ceylan, Ş., Yoldas, F. (2010): Compost, Green fertilizer and animal fertilizers in organic agriculture. (Organik Tarımda Kompost, Yeşil Gübre ve Hayvansal Gübrelerin Kullanımı.) – IV. Organic Agriculture Symp., 28 June - 1 July, 2010, Erzurum, Turkey, pp. 646-649.
- [14] Ceylan, Ş., Yoldas, F., Mordoğan, N., Çakıcı, H. (2000): Effect of different cattle fertilizers on yield and quality in tomato cultivation. (Domates Yetiştiriciliğinde Farklı Sığır Gübrelerin Verim ve Kaliteye Etkisi.) – III. Symposium on Vegetable Agriculture, September 11-13, 2000, Isparta, pp. 51-55.
- [15] Ceylan, S., Mordogan, N., Akdemir, H., Cakici, H. (2006): Effect of organic fertilizers on some agronomic and chemical properties of potato (*Solanum tuberosum* L.). – *Asian J. Chem.* 18(2): 1223-1230.
- [16] Chapman, H. D., Pratt, P. F. (1982): *Methods of Analysis for Soils Plants and Waters.* – University of California, Division of Agricultural Sciences, USA.
- [17] Chatterjee, B., Ghanti, P., Thapa, U., Tripathy, P. (2005): Effect of organic nutrition in sprout broccoli (*Brassica oleracea* var.). – *Vegetable Science* 33(1): 51-54.
- [18] Dellacecca, V., Dias, J. S., Crute, I., Monteiro, A. A. (1994): New agro techniques to promote broccoli picking. – International Symposium on Brassicas. Ninth Crucifer Genetics Workshop, 15-18 Nov. 1994, Lisbon, Portugal. *Acta Horticulturae* 407: 347-351.
- [19] Elkner, F., Peschke, H., Köhn, W., Chmielewski, F., Baumecker, M. (2000): Tillage and fertilizing effects on sandy soils. – *J. Plant Nut. Soil. Sci.* 163: 267-272.
- [20] Griffith, M., Carling, D. D. (1991): Effects of plant spacing on broccoli yield and hollow stem in Alaska. – *Can. J. Plant Sci.* 71: 579-585.
- [21] Güneş, A., Alpaslan, M., İnal, A. (2000): *Plant Nutrition and Fertilization.* (Bitki Besleme ve Gübreleme.) – Ankara University, Faculty of Agriculture, Publication No: 1514, Ankara.
- [22] Kacar, B. (1984): *Plant Nutrition Application Guide.* (Bitki besleme uygulama kılavuzu.) – Ankara University Faculty of Agriculture, Ankara.
- [23] Kandil, H., Gad, N. (2009): Effects of inorganic and organic fertilizers on growth and production of broccoli (*Brassica oleracea* L.). – *Factori și Procese Pedogenetice din Zona Temperată 8(S. nouă)*: 61-69.
- [24] Klute, A. (ed.) (1986): *Methods of Soil Analysis. Part 1. Physical and Mineralogical Methods.* 2nd Ed. Agron. Monogr. 9. – ASA and SSSA, Madison, WI.
- [25] Kunicki, E., Capecka, E., Siwek, P., Kalisz, A. (1999): The effect of plant spacing on the yield and quality for three broccoli cultivars in autumn growing. – *Folia Horticulturae* 11: 69-79.
- [26] Liebig, M. A., Doran, J. W. (1999): Impact of organic production practices on soil quality indicators. – *J. Environ. Qual.* 28: 1601-1609.
- [27] Lindsay, W. L., Norvell, W. A. (1978): Development of a DTPA soil test for zinc, iron, manganese and copper. – *Soil Science Society of American J.* (42): 421-428.
- [28] Mihov, K., Antonova, G. (2000): Assessment of broccoli (*Brassica oleracea* var. *italica* Pl.) hybrids for late field production. – *Cruciferae Newsletter* 22: 85-86.
- [29] Moore, K. P. (1992): Determination of phosphorus in plant tissue by colorimetry. – In: Plank, C. O. (ed.) *Plant Analysis Reference Procedures for the Southern Region of the United States*, Southern Cooperative Series Bulletin 368. North Carolina Agricultural Research Service, Raleigh, NC, pp. 29-31.
- [30] Mordoğan, N., Ceylan, Ş., Çakıcı, H., Yoldas, F. (2001): The effect of nitrogen fertilization on nitrogen accumulation in lettuce. (Azotlu Gübrelemenin Marul Bitkisindeki Azot Birikimine Etkisi.) – *Ege Univ. Zir Fak. Bull.* 38(1): 85-92.

- [31] Ninou, E. G., Paschalidis, K. A., Mylonas, I. G., Vasilikiotis, C., Mavromatis, A. G. (2017): The effect of genetic variation and nitrogen fertilization on productive characters of Greek oregano. – *Acta Agriculture Scandinavia, Section B-Soil & Plant Science* 67(4): 372-9.
- [32] Page, A. L., Miller, R. H., Keeney, D. R. (eds.) (1982): *Methods of Soil Analysis. Part 2. Chemical and Microbiological Properties*. 2nd Ed. Agron. Monogr. 9. – ASA and SSSA, Madison, WI.
- [33] Rekowska, E. (2000): Effect of cultivars and sowing date on the yielding of broccoli. – *Biologiczne i Agrotechniczne Czynniki Plonowania i Jakosci Warzyw*, Lublin, Polska, 15-16 Czerwca 2000. *Annals Universitatis Mariae Curie Sklodowska, Sectio EEE, Horticultura* 8(Suppl.): 61-66.
- [34] Rincon, L., Saez, J., Perez-Crespo, J. A., Gomez Lopez, M. D., Pellicer, C. (1999): Growth and nutrient absorption of broccoli. – *Investigacion Egraria Proccion y Proccion Vegetables* 14(1-2): 225-236.
- [35] Sezen, Y. (1995): *Soil Chemistry Edition of Atatürk University No: 790*. – Erzurum Atatürk Univ. Faculty of Agriculture. No: 322. Series of Lesson Book, 71.
- [36] SPSS (2017): *IBM SPSS Statistics Base 25*. – IBM, New York.
- [37] Vanduchova, A., Anzenbacher, P., Anzenbacherova, E. (2019): Isothiocyanate from broccoli, sulforaphane, and its properties. – *Journal of Medicinal Food* 22(2). <https://doi.org/10.1089/jmf.2018.0024>.
- [38] Vural, H., Esiyok, D., Duman, I. (2000): *Vegetable Production*. – Aegean University Press, Bornova, Izmir.
- [39] Yaldız, A., Arıcı, Y. K., Yılmaz, G. (2017): Phytochemical analysis, antioxidant and antibacterial activities of four Lamiaceae species cultivated in barnyard manure. – *Journal of Agricultural Sciences*. 2017(23): 95-108.
- [40] Yoldas, F. (2003): Effects of temperature different plant spacing sowing and planted dates on plant growth and yield of broccoli cultivars. – PhD Thesis, Ege University, Graduate School of Natural and Applied Sciences, Izmir.
- [41] Yoldas, F., Ceylan, Ş. (2010): Determinants of organic agriculture in Turkey; production areas and product designs. (Türkiye’de Organik Tarımı Belirleyen Faktörler, Üretim Alanları ve Ürün Desenleri.) – Turkey IV. Organic Agriculture Symposium, June 28 - July 1, 2010, Erzurum, Turkey, pp. 732-735.
- [42] Yoldas, F., Eşiyok, D. (2004): Effects of planting frequency, sowing and planting times on yield and quality parameters in broccoli. (Dikim Sıklığı, Ekim ve Dikim Zamanlarının Brokolide Verim ve Kalite Parametreleri Üzerine Etkileri.) – *Ege Univ. Faculty of Agriculture Bull.* 41(2): 37-48.
- [43] Yoldas, F., Ceylan, S., Yagmur, B., Mordogan, N. (2008): Effects of nitrogen fertilizer on yield quality and nutrient content in broccoli. – *Journal of Plant Nutrition* 31(7): 1333-1343. DOI: 10.1080/019041608 02135118.
- [44] Yoldas, F., Ceylan, Ş., Elmaci, Ö. L. (2009): The influence of organic and inorganic fertilizer on yield, quality and nutrient content in processing tomato. – *Ege Üniv. Zir. Fak. Derg.* 46(3): 191-197.
- [45] Yoldas, F., Ceylan, S., Mordogan, N., Ongun, A. R. (2017): Effects of organic chicken manure on nitrate accumulation and nutrient element content of broccoli. – *Acta Biologica Turcica* 30(4): 169-173.
- [46] Yoldas, F., Ceylan, S., Mordogan, N. (2019): Residue effect of chicken manure on yield and yield criteria of onion (*Allium cepa* L.) as second crop. – *Applied Ecology and Environmental Research* 17(5): 12639-12647.
- [47] Zebarth, B. J., Bowen, P. A., Toivonen, P. M. A. (1995): Influence of nitrogen fertilization on broccoli yield, nitrogen accumulation and apparent fertilizer-nitrogen recovery. – *Can. J. Plant Sci.* 75: 717-725.

BIODIVERSITY CONSERVATION IN AGRICULTURAL LANDSCAPES: AN ECOLOGICAL OPPORTUNITY FOR COAL MINING SUBSIDENCE AREAS

ZHANG, G. X.^{1,2,3} – YUAN, X. Z.^{1,2,3*} – WANG, K. H.^{1,2,3} – ZHANG, M. J.^{1,2,3} – ZHOU, L. L.^{1,2,3} – ZHANG, Q. Y.¹ – HU, Y. X.²

¹*State Key Laboratory of Coal Mine Disaster Dynamics and Control, Chongqing, China*

²*Faculty of Architecture and Urban planning, Chongqing University, Chongqing, China*

³*Key Laboratory of the Three Gorges Reservoir Region's Eco-Environment, Chongqing, China*

**Corresponding author*

e-mail: 1072000659@qq.com; phone: +86-138-9603-9266

(Received 3rd Dec 2019; accepted 6th May 2020)

Abstract. Rapid population growth and economic development increase energy and grain demands. However, in the high-groundwater coal basins where coal seams and agricultural production overlap, mining subsidence destroys much arable land, causing a series of environmental and social issues. This study investigated plants, beetles, spiders and birds in typical intensive farmlands and farmlands containing mining subsidence mosaics (i.e., mosaic farmlands) in North China. The species composition of these four taxonomic groups differed significantly between the intensive farmlands and mosaic farmlands, with 271 plant, 17 spider, 49 beetle and 138 bird species in the mosaic farmlands and 76, 12, 35 and 30 such species in the intensive farmlands, respectively. The mosaic farmlands hosted more and different species than the intensive farmlands. Additionally, these four taxonomic groups, especially plants and birds, showed a higher abundance and diversity in mosaic farmlands than in intensive ones. These mosaics thus have increased biodiversity conservation value. We emphasize that attention should be paid not only to the environmental damage and human property loss caused by coal mining subsidence but also to the ecological opportunities from the formation of such new habitats. These post-mining habitats represent a new ecological landscape that should be a part of natural conservation.

Keywords: *landscape mosaic, plant, bird, beetle, spider*

Introduction

Natural and semi-natural habitats are considered the main source of biodiversity in agricultural landscapes (Duflo et al., 2015). While there is growing recognition of the need for their conservation, natural and semi-natural habitats continue to be lost throughout the world (Myers et al., 2000; He et al., 2014). Furthermore, rapid population growth and economic development worldwide have resulted in an increased demand for grain and energy. This further requires people to expand the scale of arable land and mining. In this context, agriculture has started to transform from traditional agriculture to intensive agriculture, and mining activities have also become more intense (Li, 2006; Meng et al., 2009). More than 92% of the total coal supply comes from underground mining, which often leads to serious surface subsidence (Xiao et al., 2018).

Most high-groundwater coal basins overlap with coal seams and agricultural production areas commonly have multiple and thick coal seams, a high groundwater table and flat terrain (Xiao et al., 2018). Underground mining compromises the stability of overlying rock, causing surface distortion, subsidence and eventually the formation

of water patches of various sizes (Hu et al., 2012). In China, subsidence areas are expected to increase by 2,104 ha annually (Hu and Xiao, 2013), and coal mining poses challenges that threaten the environment and human property (destruction of roads, farmland, buildings, etc.) (Xie et al., 2013; Xu et al., 2014; Xiao et al., 2018) and is traditionally perceived as a form of secondary geological disaster (Bell et al., 2000; Ju and Xu, 2015; Zhang et al., 2019b). Thus, coal mining subsidence is one of the most prominent environmental and social issues (Xu et al., 2014).

At present, most studies have reported the negative effects of coal mining subsidence. Many countries and regions recommend that measures such as reclamation and restoration must be adopted to address coal mining subsidence (Lokhande et al., 2005; Xu et al., 2014; Rola et al., 2015). However, recent studies have shown that after a period of development, mining subsidence sites can demonstrate typical features of a wetland ecosystem, such as a submerged environment, soil gleying and typical wetland vegetation (Harabiš et al., 2013; Harabiš, 2016; Zhang et al., 2019a), and some post-mining sites provide high biodiversity (Lewin et al., 2015; De Lucca et al., 2018; Moradi et al., 2018b; Błońska et al., 2019). This seems to indicate that a new ecological landscape is emerging and that some of the most degraded lands could be designed and used as ecologically very valuable habitats.

The characteristics and influencing factors of biodiversity in these newly formed landscapes have not been sufficiently studied. Therefore, assessing the ecological significance of mining subsidence sites from the perspective of biodiversity would not only shed light on the impact of mining subsidence on local biodiversity but also provide a basis for biodiversity management, utilization, protection and restoration. This study focuses on plant, beetle, spider and bird communities in typical intensive farmlands and farmlands containing mining subsidence mosaics in North China (a typical area in which agricultural activity overlaps with coal mining). We tested whether and how differences in the species composition, abundance and diversity of these four taxonomic groups occurred between these two types of landscapes.

Materials and methods

Study area

The Yanzhou coalfield (116°50'–116°55'E, 35°30'–35°25'N) is one of the most important coal production regions in China, where coal mining has been practised for more than 40 years (Xiao et al., 2018). The study area is located in the eastern part of the North China Plain and belongs to the temperate monsoon climate zone. This area has a long history of agriculture and the annual double-crop rotation system, wheat and corn, is the most popular planting pattern. Mining led to a noticeable shrinking of arable land from 18,652.84 ha in 1985 to 12,042.67 ha in 2015, a decrease of 6,610.17 ha; however, the area of water bodies increased from 474.47 ha in 1985 to 1,471.23 ha in 2015 (Xiao et al., 2018). The area of the mining subsidence is expected to reach 30,000 ha by 2020.

The main type of land use in this area was dry farmland in the pre-mining stage. However, once mining subsidence took place, the surface began to show different habitat types due to different historical subsidence features, such as abandoned agricultural fields, puddles, swales, and ponds. In this context, typical “mining subsidence wetlands” with soaked soils and hydrophilic plants were formed under waterlogging conditions. These wetlands were isolated in the agricultural landscape, as

they are characterized by a short formation history and no hydrological connections with other water bodies. Most of these water bodies are abandoned. They are disturbed to a very small degree and have a near-natural development process.

Sampling procedure

The study was conducted in 2 types of landscape. One (intensive farmland) is a typical intensive agricultural landscape and has few non-cropped elements (*Table 1*). The other (mosaic farmland) exhibited a newly formed agricultural landscape that included landscape mosaics (including features such as abandoned agricultural fields, puddles, swales, and ponds) formed by coal mining subsidence and dry farmland. Each type of agricultural landscape has 6 sites (*Fig. 1*). The area of each site was 0.5 km², and they were spaced at least 500 m apart. The crops in these 12 sites were planted almost simultaneously, with corn (*Zea mays*) from May to October and wheat (*Triticum aestivum*) in the rest of the year.

The plants, spiders, beetles and birds at these 12 sites were sampled during April, July and October 2017. An additional survey of birds in January 2018 was performed, as this area was located on the migration route of East Asian-Australian migratory birds. Samples from 9 herbaceous quadrats (1 m × 1 m) (Fang et al., 2009), 6 beetle and spider pitfall traps (Brown and Matthews, 2016), and 5 bird sites (Marsden, 1999) were collected randomly at each site. A qualitative survey of these four taxonomic groups was conducted based on spot investigation. A total of 324 plant samples, 216 beetle and spider samples, and 240 bird samples were obtained over the course of the study. Beetles and spiders were identified to the lowest possible classification unit using a binocular stereomicroscope in the laboratory.

Table 1. Main environmental characteristics of the mosaic farmlands and intensive farmlands

Characteristic		Mosaic farmlands	Intensive farmlands
Environmental conditions	Slope (°)	5.61-29.80	0.02-1.00
	Subsidence history (year)	3-20	-
	Water area (ha)	0.003-15	-
	Water depth (m)	0.10-1.30	-
	Water temperature (°C)	18.66-31.73	-
	Soil temperature (°C)	25.54-33.58	26.92-33.89
	Soil moisture (g kg ⁻¹)	0.15 -0.97	0.08-0.26
	Air temperature (°C)	26.31-34.2	26.70-33.9
	Air humidity (%)	58-77	53-73

Data analysis

The richness, rarefied richness, abundance and Shannon diversity of plants, spiders, beetles and birds in mosaic farmlands and intensive farmlands were calculated by using Estimate S (Colwell, 2005). Nonmetric multidimensional scaling (NMDS) was performed in CANOCO 5.0 to visualize the variation in community composition between mosaic farmlands and intensive farmlands based on the Bray-Curtis

dissimilarity index, which was calculated from the log (x + 1)-transformed abundance data for beetle, spider, and bird communities and data averaged by the relative height, abundance and coverage of plant communities (Ter Braak and Smilauer, 2001). Primer 5.0 was used to analyse the Bray-Curtis similarity of the species composition of these four groups between sites (Clarke and Gorley, 2001). Rarefaction was used in Estimate S to compare cumulative species richness between mosaic farmlands and intensive farmlands over the sampling periods (Colwell, 2005). One-way analysis of variance (ANOVA) performed in IBM SPSS 20.0 was used to test for differences in species richness, rarefied richness, abundance, and the diversity index of these four taxonomic groups between mosaic farmlands and intensive farmlands. The data from all samples from each site were averaged by season.

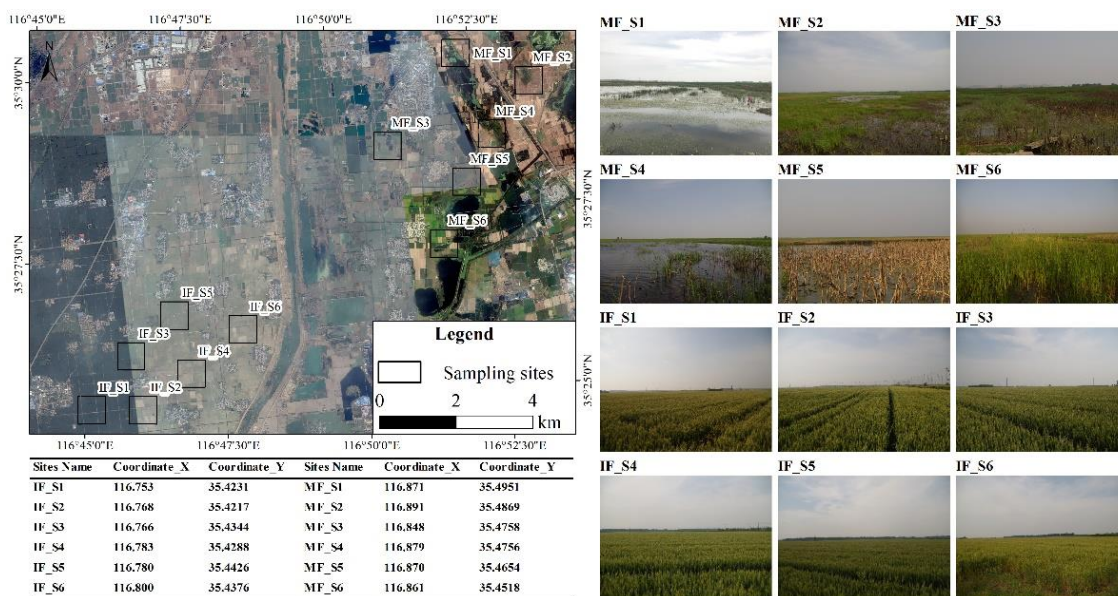


Figure 1. Location of mosaic farmland (MF) sites and intensive farmland (IF) sites

Results

Species composition of plant, spider, beetle and bird communities

A total of 271 species of plants, 17 species of spiders, 49 species of beetles and 138 species of birds were collected in mosaic farmlands, and 76 plant, 12 spider, 35 beetle and 30 bird species were collected in intensive farmlands (*Appendix*).

The results of PERMANOVA showed that most samples from mosaic farmlands were separated from those of intensive farmlands, indicating significant differences in plant, spider, beetle and bird species composition between these two types of landscape ($R^2 = 0.2025$, $p = 0.01$; $R^2 = 0.1249$, $p = 0.01$; $R^2 = 0.2752$, $p = 0.01$; and $R^2 = 0.2734$, $p = 0.01$, respectively; *Fig. 2*). The result of Bray-Curtis similarity analysis showed differences in the species composition of these four groups between sites (*Tables 2–5*), especially in plants, beetles, and birds. From an overall perspective, the lowest similarity was between mosaic farmland sites and intensive farmland sites, followed by the change between mosaic farmland sites, and the most similar were between intensive farmland sites.

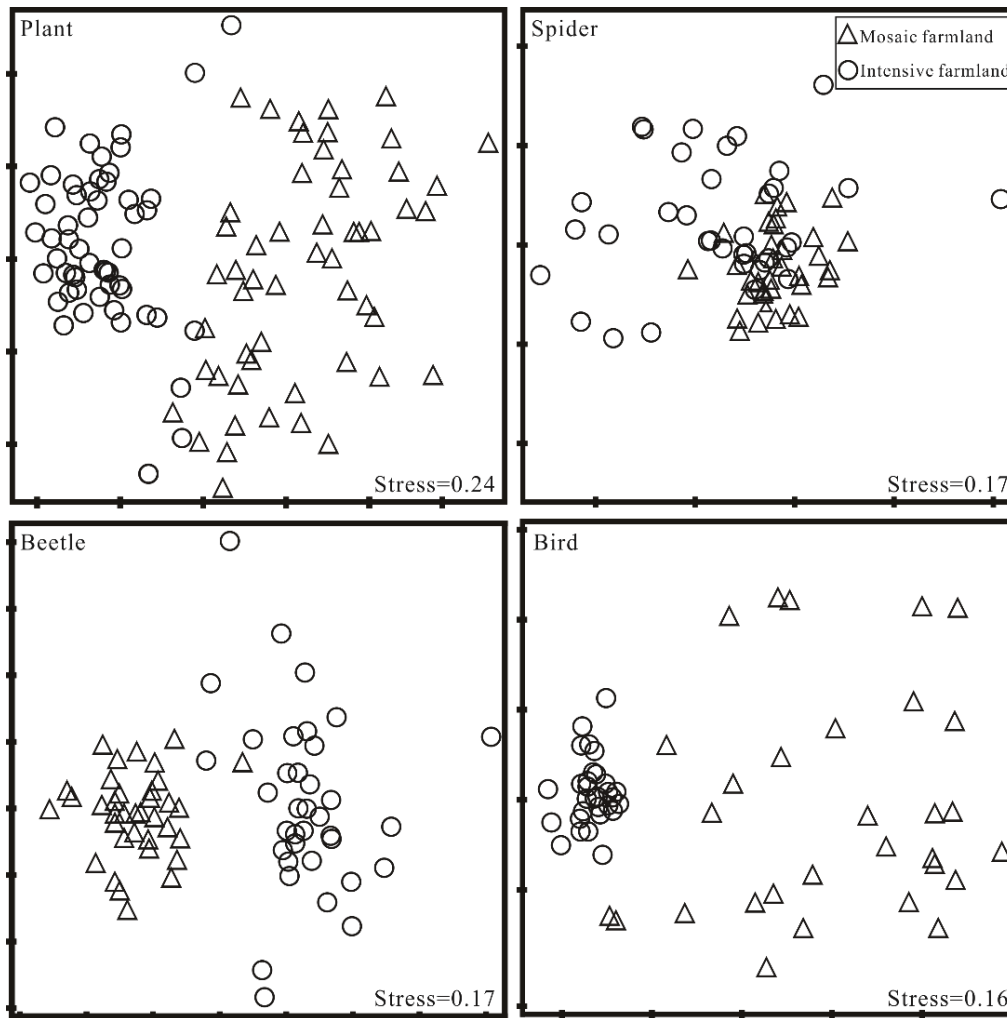


Figure 2. Nonmetric multidimensional scaling ordination of variation in the community composition of plant, spider, beetle and bird species between mosaic farmlands and intensive farmlands based on Bray-Curtis dissimilarities

Table 2. Bray-Curtis similarity analysis of species composition of plant communities in mosaic farmland sites (MS) and intensive farmland sites (IS)

	MS1	MS2	MS3	MS4	MS5	MS6	IS1	IS2	IS3	IS4	IS5	IS6
MS1	1											
MS2	0.51	1										
MS3	0.52	0.46	1									
MS4	0.39	0.47	0.45	1								
MS5	0.45	0.41	0.57	0.51	1							
MS6	0.50	0.40	0.50	0.50	0.57	1						
IS1	0.26	0.27	0.25	0.20	0.19	0.23	1					
IS2	0.33	0.32	0.31	0.22	0.21	0.26	0.60	1				
IS3	0.31	0.31	0.30	0.21	0.28	0.34	0.39	0.47	1			
IS4	0.28	0.25	0.31	0.17	0.28	0.25	0.57	0.50	0.48	1		
IS5	0.38	0.34	0.36	0.26	0.30	0.34	0.55	0.57	0.51	0.72	1	
IS6	0.29	0.29	0.30	0.20	0.23	0.24	0.61	0.56	0.43	0.66	0.73	1

Table 3. Bray-Curtis similarity analysis of species composition of beetle communities in mosaic farmland sites (MS) and intensive farmland sites (IS)

	MS1	MS2	MS3	MS4	MS5	MS6	IS1	IS2	IS3	IS4	IS5	IS6
MS1	1											
MS2	0.62	1										
MS3	0.77	0.49	1									
MS4	0.74	0.46	0.90	1								
MS5	0.55	0.79	0.44	0.41	1							
MS6	0.53	0.76	0.44	0.43	0.79	1						
IS1	0.10	0.17	0.09	0.07	0.14	0.10	1					
IS2	0.11	0.24	0.10	0.09	0.19	0.17	0.33	1				
IS3	0.10	0.21	0.09	0.08	0.17	0.12	0.73	0.55	1			
IS4	0.12	0.27	0.11	0.09	0.22	0.15	0.36	0.57	0.40	1		
IS5	0.09	0.20	0.10	0.07	0.17	0.12	0.52	0.68	0.74	0.48	1	
IS6	0.09	0.20	0.09	0.07	0.15	0.12	0.54	0.62	0.75	0.46	0.81	1

Table 4. Bray-Curtis similarity analysis of species composition of spider communities in mosaic farmland sites (MS) and intensive farmland sites (IS)

	MS1	MS2	MS3	MS4	MS5	MS6	IS1	IS2	IS3	IS4	IS5	IS6
MS1	1											
MS2	0.77	1										
MS3	0.65	0.63	1									
MS4	0.80	0.85	0.71	1								
MS5	0.58	0.68	0.63	0.72	1							
MS6	0.66	0.72	0.77	0.78	0.78	1						
IS1	0.16	0.21	0.15	0.20	0.27	0.25	1					
IS2	0.50	0.60	0.59	0.62	0.63	0.65	0.30	1				
IS3	0.46	0.56	0.64	0.54	0.58	0.70	0.28	0.78	1			
IS4	0.26	0.31	0.24	0.30	0.33	0.32	0.42	0.38	0.38	1		
IS5	0.38	0.49	0.41	0.46	0.51	0.47	0.35	0.69	0.56	0.49	1	
IS6	0.50	0.60	0.65	0.61	0.69	0.74	0.29	0.84	0.77	0.34	0.63	1

Table 5. Bray-Curtis similarity analysis of species composition of bird communities in mosaic farmland sites (MS) and intensive farmland sites (IS)

	MS1	MS2	MS3	MS4	MS5	MS6	IS1	IS2	IS3	IS4	IS5	IS6
MS1	1											
MS2	0.56	1										
MS3	0.69	0.51	1									
MS4	0.67	0.55	0.57	1								
MS5	0.35	0.49	0.20	0.37	1							
MS6	0.53	0.59	0.41	0.52	0.51	1						
IS1	0.15	0.23	0.09	0.28	0.33	0.29	1					
IS2	0.13	0.20	0.09	0.27	0.36	0.28	0.79	1				
IS3	0.15	0.22	0.08	0.26	0.35	0.30	0.71	0.72	1			
IS4	0.14	0.21	0.10	0.28	0.35	0.30	0.71	0.72	0.71	1		
IS5	0.18	0.23	0.09	0.27	0.34	0.36	0.73	0.74	0.68	0.71	1	
IS6	0.14	0.19	0.08	0.25	0.32	0.27	0.66	0.69	0.81	0.71	0.61	1

The dominant species of plants in the mosaic farmlands were *Phragmites australis*, *Digitaria sanguinalis* and *Bromus japonicus*, while *Aegilops tauschii*, *Galium aparine* and *Descurainia sophia* were the dominant plant species in the intensive farmlands. In the mosaic farmlands, the dominant species of beetles were *Pheropsophus jessoensis* (73.37%, relative abundance), *Chlaenius micans* (4.52%) and *Phacophallus japonicus* (3.58%), but *Chlaenius micans* (54.30%), *Atholus depistor* (24.89%) and *Atomaria lewisi* (3.62%) were the dominant beetle species in the intensive farmlands. Furthermore, the dominant species of spiders in the mosaic farmlands were *Pardosa astrigera* (42.10%), *Pardosa* sp. (17.77%) and *Trochosa ruricola* (13.58%), while *Erigone prominens* (26.11%), *Pardosa astrigera* (24.18%) and *Trochosa ruricola* (15.47%) were the dominant spider species in the intensive farmlands. The dominant species of birds in the mosaic farmlands were *Fulica atra* (21.58%), *Anas crecca* (7.95%) and *Tachybaptus ruficollis* (7.92%), while *Passer montanus* (42.70%), *Pica pica* (21.66%) and *Hirundo rustica* (14.36%) were the dominant bird species in the intensive farmlands.

Species accumulation curves showed that the mosaic farmlands supported more species than the intensive farmlands (Fig. 3). A total of 196 species of plants (such as *Rumex dentatus*) (Table 6; Appendix), 5 species of spiders (such as *Asianellus* sp.), 23 species of beetles (such as *Harpalus pallidipennis*) and 109 species of birds (such as *Himantopus himantopus*) were exclusively found in the mosaic farmlands, while *Veronica persica*, 9 species of beetles (such as *Oenopia conglobata*) and *Corvus corone* were exclusively found in the intensive farmlands.

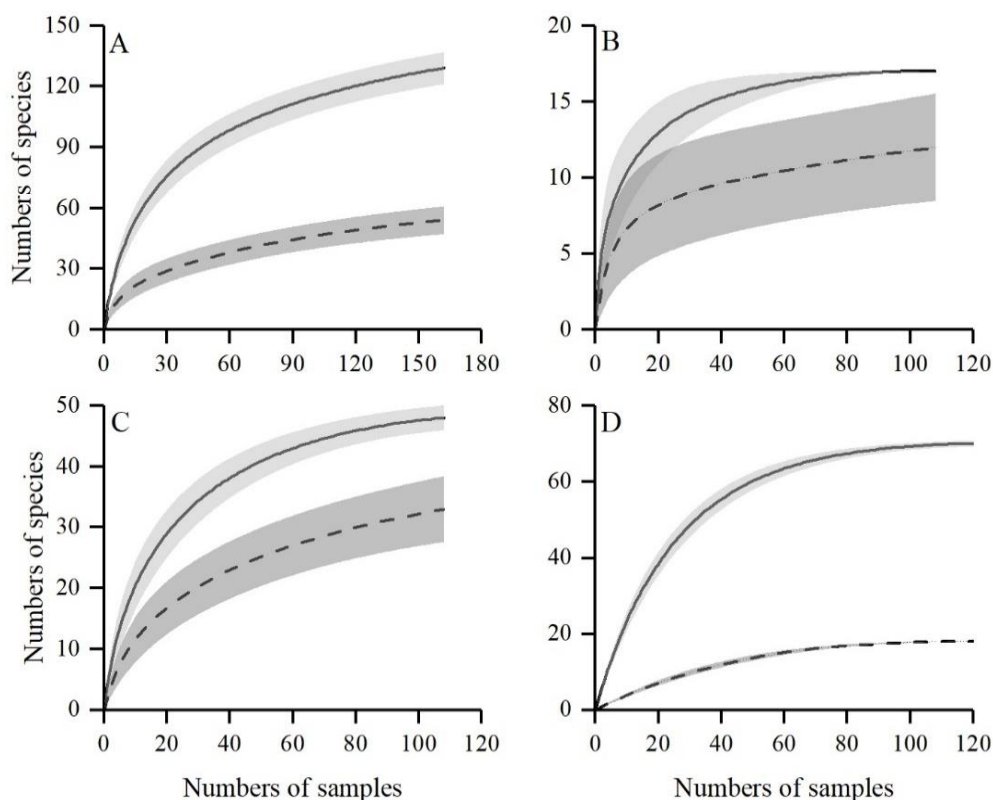


Figure 3. Species accumulation curves for plants (A), spiders (B), beetles (C) and birds (D). The solid line represents the mosaic farmlands, and the dotted line represents the intensive farmlands. Shading indicates the 95% confidence interval

Table 6. Comparison of the species compositions of plant, spider, beetle and bird communities between mosaic farmlands and intensive farmlands

Taxonomic group	Mosaic farmlands		Intensive farmlands		Mutual species
	Total species	Unique species	Total species	Unique species	
Plant	271	196	76	1	75
Spider	17	5	12	0	12
Beetle	49	23	35	9	26
Bird	138	109	30	1	29

Furthermore, most of the unique species of plants in the mosaic farmlands were hydrophytic (52 species) and aquatic plants (28), while only 5 hydrophytic species were recorded in the intensive farmlands (*Appendix*). Similarly, 59 species of waterfowl and 23 species of beetles were found in only the mosaic farmlands (*Appendix*).

Notably, 134 species of birds were on the International Union for Conservation of Nature (IUCN) Red List (*Appendix*). Six bird species are near-threatened (such as *Emberiza yessoensis*, *Paradoxornis heudei*, *Anas falcata* and *Coturnix japonica*), and *Aythya baeri* is critically endangered, all of which were observed in only mosaic farmlands.

These observations indicated that compared to the intensive farmlands, the mosaic farmlands hosted more and different species.

Community structure of plants, spiders, beetles and birds

ANOVA showed that the richness and abundance of plants, spiders, beetles and birds in the mosaic farmlands were significantly higher than those in intensive farmlands ($p < 0.05$) (*Fig. 4; Appendix*). Similarly, the rarefied species richness and Shannon diversity of plants and birds in mosaic farmlands were significantly higher than those in intensive farmlands ($p < 0.05$). Despite none of the other comparisons being significant ($p > 0.05$), the indexes increased in mosaic farmlands. These observations indicate that the abundance and diversity of these taxonomic groups in mosaic farmlands were higher than those in intensive farmlands, especially for plants and birds.

Discussion

Understanding patterns of biodiversity during landscape change is one of the central pursuits of community ecology and relevant for improved conservation theory (Soykan et al., 2012). The mosaic farmlands showed higher biodiversity than the intensive farmlands, suggesting that such mosaics represent important supplements to the agricultural landscape. Studies have shown that natural and semi-natural habitats in agricultural landscapes can provide valuable habitats for communities in China (Liu et al., 2010; De-Jun et al., 2011; Toral et al., 2011; Zhao and Zhou, 2018) and in other regions such as Japan (Amano et al., 2008; Katayama et al., 2015), Europe (Ma, 2008; Frenzel et al., 2016; Lewis-Phillips et al., 2019) and North America (Elphick, 2000).

Biodiversity in mosaic farmlands and intensive farmlands

The communities of plants, spiders, beetles and birds exhibited significant differences in species composition between the mosaic farmlands and intensive

farmlands (Fig. 2). The mosaic farmlands hosted more and different species than the intensive farmlands (Table 6). Furthermore, the mosaic farmlands showed a higher abundance and diversity of these taxonomic groups than the intensive farmlands did, while the rarefied richness and Shannon diversity of beetles and spiders did not show a similar pattern (Fig. 3). These results are consistent with those of other studies (Duelli and Obrist, 2003; Ma, 2008; Nagy et al., 2017; Lee and Goodale, 2018; Li et al., 2018; Šálek et al., 2018), especially for plants (Bratli et al., 2006; Ma, 2008), beetles (Gioria et al., 2010; Li et al., 2018), spiders (Knapp and Řezáč, 2015) and birds (Giralt et al., 2008; Wuczyński et al., 2014; Morelli, 2018). Studies have shown that the impact of habitats and landscape features on beetles and spiders is limited (Jeanneret et al., 2003). However, a direct positive effect of mosaic farmlands was found for waterfowl and migratory birds, suggesting that the mosaic farmlands supply food or breeding facilities not provided by intensive farmlands (Appendix). These resources could be provided because these newly formed mosaics differ from traditional intensive farmlands, as they do not experience crop rotation and agricultural practices such as mowing, fertilization and oversowing with seeds of desirable plants. These practices are known to affect plants and birds (Gaujour et al., 2012; Frenzel et al., 2016; Nagy et al., 2017) and probably also affect arthropods, including carabids and spiders (Cerezo et al., 2011; Knapp and Řezáč, 2015). In other respects, the hydrological conditions of the newly formed mosaics can provide many species with adequate moisture and moist soil (Mathias and Moyle, 1992; Duelli, 1997; Bornette and Puijalón, 2011; Xu et al., 2019). Studies have reported that coal mining subsidence can be characterized as an intermediate disturbance to plant communities in semi-arid areas: changes in the functioning of local ecosystems and the number of plant species are limited after coal mining subsidence (Czaja et al., 2014; He et al., 2017). However, our results indicate that in high-groundwater coal basins, mining subsidence mosaics increase the plant diversity of the local landscape. The appearance of some unique species may be promoted by an increase in subsidence cracks, which trap seeds transported by the wind and participate in increasing plant richness (He et al., 2017). It is also possible that the surface upheavals and cracks caused by coal mining subsidence offer conditions for the germination of seeds, especially those with seeds buried in the soil for a long time. A soil seed bank is considered a potential contributor to plant diversity, as it can take part in the renewal and succession of the surface vegetation (De Villiers et al., 2001; Szarek-Lukaszewska et al., 2007; Liu et al., 2016), especially after natural or human intervention (Bell et al., 1993). Furthermore, the higher plant diversity may also be due to the dispersal mechanism of plant propagules (Moran et al., 2004; Cramer et al., 2007; Brudvig et al., 2009); with the assistance of the wind and animals (especially birds), some plant propagules were introduced into the coal mining subsidence area, further enriching the regional species pool.

In stark contrast to the formation processes that occur in valuable habitats such as natural habitats, mining subsidence was the main driver of the mosaic farmlands, and it often changes the original landscape patterns, imposing great pressure on environmental recovery; in addition, land use transformations have usually been fast, with uncertain consequences (Zhang et al., 2019a). There is a temporal component of this study obtained by comparing current mosaic farmlands and intensive farmlands. The hypothesis was that the biodiversity changed and increased after these mosaics formed. Similar to the results above, in limestone quarries in the Bohemian Karst, Czech Republic, 153 species of vascular plants were found (Tropek et al., 2010); likewise, in

post-mining sites in the Sokolov district, western Czech Republic, 380 species of arthropods were found (Moradi et al., 2018a). These studies suggest that the high diversity in post-mining areas is not random but may be caused by their particular origin and subsequent environmental changes. Therefore, in our study, the environmental changes that occurred after these mosaics formed must be considered to explain the change in the diversity of plants, beetles, spiders and birds.

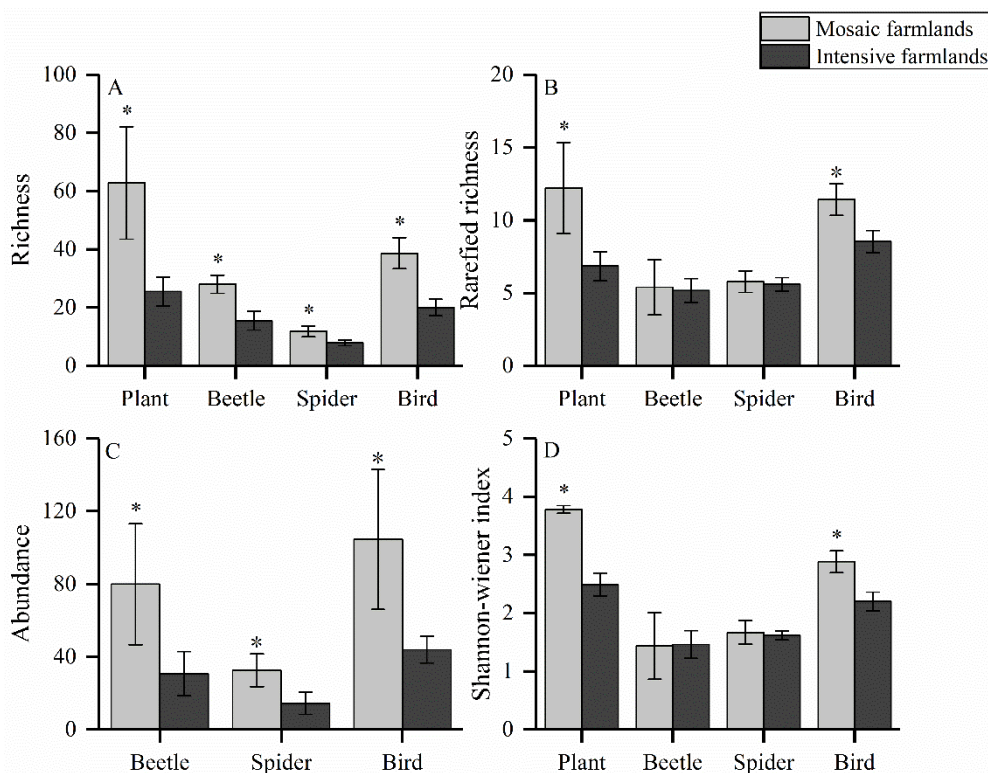


Figure 4. Mean species richness, rarefied richness, abundance, and Shannon diversity of plants, spiders, beetles and birds in mosaic farmlands and intensive farmlands. * means $p < 0.05$. Standard error is represented by the vertical bars

Generally, landscape modification can not only directly impact local biodiversity (Cerezo et al., 2011) but also indirectly affect local biodiversity by changing environmental conditions (Dolný and Harabiš, 2012; Li et al., 2019), such as water, soil and the microclimate (Mantyka-Pringle et al., 2012; Růžicka et al., 2012; Huang et al., 2019; Oishi, 2019). Studies have reported that environmental conditions significantly affect plants and arthropods in certain cases (Lindenmayer et al., 1999; Lundholm and Larson, 2003; Joern and Laws, 2013), while site-level conditions may be more important for highly mobile species such as birds (Lindenmayer et al., 2010). A previous study in the same area confirmed the positive effect of the newly formed mosaics on local landscape heterogeneity: compared to the mosaics, the surrounding landscapes were almost homogeneous habitats, while the mosaics were the more diverse habitats (Xiao et al., 2018). Due to differences in subsidence history, newly formed mosaics with different shapes, sizes and water depths were created, including features such as puddles, swales, ponds, and even shallow lakes, which are different from the surrounding landscapes and increase the local water area and heterogeneity of water

characteristics such as its area, depth and temperature (*Table 1*) but are capable of providing important habitats for more and different species than homogeneous landscapes (Frouz et al., 2018). Non-cropped elements (such as the mosaics in this study) represent high-quality habitats for various taxa, and their positive impact on biodiversity in agricultural landscapes has been previously documented in studies on plants and animals (Chiron et al., 2010; Ma and Herzon, 2014; Kirk and Lindsay, 2017). In accordance with traditional gradient theories (Austin, 1999; Gaston, 2000; Reynolds, 2002; Telesh et al., 2013), an increase in water heterogeneity will create additional ecological niches and allow the coexistence of an increased number of species, especially wetland specialists (Pollock et al., 1998). For example, 59 waterfowl species were found in the mosaic farmlands but not in the intensive farmlands (*Appendix*). Similarly, 28 species of aquatic plants were collected in only the mosaic farmlands, including submerged plants such as *Potamogeton crispus* and *Ceratophyllum demersum*, floating-leaved plants such as *Euryale ferox* and *Nymphoides peltata*, and emergent plants such as *Phragmites australis* and *Typha angustifolia*.

Studies have shown that mining subsidence can change local soil conditions (Quadros et al., 2016; Hu et al., 2017; Willscher et al., 2017) such as moisture, temperature and nutrient levels. Plants and animals are sensitive to soil conditions; for example, in temporary wetlands in agricultural landscapes in northeastern Germany, an increase in soil moisture increased the diversity of arthropods (Brose, 2001, 2003a, b). An increase in soil moisture can also help improve habitat quality and subsequently improve the survival rate of eggs and larvae (Huk and Kühne, 1999). In our study, 94 xerophytic, 92 mesophytic, 56 hygrophytic and 28 aquatic species of plants were found in the mosaic farmlands (*Appendix*), while only 28 xerophytic, 42 mesophytic and 5 hygrophytic species were found in the intensive farmlands. Moreover, *Pheropsophus jessoensis* (73.37% relative abundance in mosaic farmlands), which prefers high soil moisture (Frank et al., 2009; Sugiura, 2018), was found in the mosaic farmlands but not in the intensive farmlands. Furthermore, changes in soil temperature, soil quality and soil nutrient conditions can also impact the biotic community (Iannone Iii and Galatowitsch, 2008; Sutton-Grier et al., 2011; Altenfelder et al., 2016; Hong et al., 2017).

Landscape change, such as the transformation from intensive farmlands to mosaic farmlands, can also influence aspects of the local microclimate (Bai et al., 2013; Mclaughlin and Cohen, 2013) such as air temperature and air humidity (*Table 1*). The temperature and insolation of microenvironments are important factors affecting nest site choice by Anatidae species because stable microclimatic conditions can improve the efficiency of heat transfer to eggs (Shutler et al., 1998). Research has reported that carabids are sensitive to ambient temperature changes (Niemelä, 2001; Allen, 2016). In our study, 19 Anatidae species and 18 carabid species were collected in the mosaic farmlands, while only 9 of these carabid species were collected in the intensive farmlands (*Appendix*). This difference may be because mosaic farmlands provide better microclimatic conditions for these species.

Increases or decreases in diversity within a trophic level are highly relevant for the rest of the community because of an ecosystem's balance between ecological niche complementarity effects and community trophic cascades (Ives et al., 2005; Finke and Snyder, 2008; Schneider et al., 2016). For example, research has revealed that differences in vegetation among systems may lead to disparities in other communities (Davidowitz and Rosenzweig, 1998). Plants also provide food and habitats for arthropods and birds (Zimmer et al., 2000; Gucel et al., 2012), and high heterogeneity of

microhabitats is reciprocally related to the diversity of plants (Bogusch et al., 2016). Thus, in our study, the increase in plant diversity must also impact beetles, spiders and birds. In contrast, changes in animals can have effects on plants (Schemske et al., 2009; Stam et al., 2014). For example, *Podiceps cristatus* and *Fulica atra* build nests with branches of *Potamogeton crispus* or *Phragmites australis*, and the “floating nests” of these two bird species can be formed only with the support of the stems of emergent plants. Moreover, common bird species, such as *Acrocephalus orientalis* and *Cisticola juncidis*, are reported to inhabit both *Phragmites australis* and *Typha angustifolia* communities (Ueda, 1993; Katayama et al., 2015). Some waterfowl such as *Aythya baeri* and *Fulica atra* feed on the roots, stems, leaves and seeds of submerged plants (e.g., *Potamogeton crispus*). The structure of vegetation is also an important factor, affecting, for example, the presence and abundance of oviposition sites and potential predator–prey interactions of arthropods (Katayama et al., 2015; Li et al., 2018).

Implication for conservation

Many studies of biodiversity differences between landscapes generally focus on one taxonomic group, while we compared the biodiversity of mosaic farmlands with that of intensive farmlands from the perspective of four taxonomic groups, which makes our results more accurate. Our important result is that these newly formed mosaic farmlands can support higher biodiversity than the traditional intensive farmlands and host many unique species that are not present within the intensive farmlands, especially some endangered species, such as *Aythya baeri* (Appendix), of which fewer than 1,000 individuals remain worldwide (Wang et al., 2012). In fact, some species have difficulties migrating to newly emerging habitats, and there will always be a group of rare and threatened organisms with low migration ability or very specific habitat requirements, which can hardly be provided by newly formed habitats. However, for disturbance-dependent species, the mosaics (such as these post-mining sites) are nearly ideal. Importantly, the newly formed mosaics have been shown to be important intermediate stops on the migration route of East Asian–Australian migratory birds because the bird community contains a large number of migratory bird species that travel along the route, such as *Calidris ferruginea*, *Numenius arquata*, *Aythya nyroca*, *Aythya baeri* and *Vanellus vanellus*. These findings indicate that these mosaics are valuable habitats for plants and animals and can contribute to regional biodiversity conservation.

The traditional understanding of coal mining subsidence mainly involves its damage to the environment and human property (Bell et al., 2000; Bell and Genske, 2001; Yao and Gui, 2008; Hu et al., 2016; Yu et al., 2018). However, these newly formed mosaics are important supplements to the agricultural landscape and could help dampen the effects of intensive farming activities and landscape fragmentation because they provide additional refuges and overwintering habitats, hence enhancing the overall diversity in agricultural landscapes (Schmidt et al., 2005; Li et al., 2018). Importantly, with economic development and human population growth, natural habitats will continue to decrease due to intensification and urbanization (Erwin, 2008; Verburg et al., 2010; Mao et al., 2018). Intuitively, however, farmers are not willing to sacrifice large areas of arable land to create non-crop habitats. Although studies have shown the importance of non-crop habitats for the conservation of beneficial arthropod diversity in agricultural landscapes (Knapp and Řezáč, 2015; Li et al., 2018), the positive impact of the presence of non-crop habitats on pest control services cannot be replicated by crop rotation management (Rusch et al., 2013).

However, these newly formed ecosystems are unstable, and their occurrence, development and succession are prone to external influences due to their short period of development and immaturity. Although we do not know how the biodiversity of mosaic farmlands will change with succession in the future, our study can facilitate understanding and aid in biodiversity conservation in this area. We emphasize that attention should be paid not only to the environmental damage and human property loss caused by coal mining subsidence but also to the ecological opportunities brought about by the formation of such new habitats.

Conclusions

Mining subsidence mosaics situated inside arable land are important supplements to the agricultural landscape and host many unique species that are not present within surrounding arable land. These newly formed landscape mosaics have been strengthened due to the decreasing natural habitats and provide important habitats for plants and animals at different times of the year. We presume that the high diversity in mosaic farmlands is not coincidental and that these habitats comprise an important component from a nature conservation perspective. This paper demonstrates a path forward from some of the most destructive land uses. Please note that the paper is not encouraging mining but rather offers a potential utilization idea after mines have closed or moved to another location. Future studies should investigate (i) whether and how the species respond to subsidence, and (ii) a variety of habitats in agricultural landscape, including mining subsidence habitats (puddles, swales, and ponds), intensified and abandoned fields, to assess the value of these habitats and propose appropriate ‘win-win’ solutions for agricultural development and biodiversity conservation in agricultural landscape.

Acknowledgements. This study was funded by the Foundation of the State Key Laboratory of Coal Mine Disaster Dynamics and Control, Chongqing University (2011DA105287—ZD201402).

REFERENCES

- [1] Allen, D. C. (2016): Microclimate modification by riparian vegetation affects the structure and resource limitation of arthropod communities. – *Ecosphere* 7: e01200.
- [2] Altenfelder, S., Schmitz, M., Poschlod, P., Kollmann, J., Albrecht, H. (2016): Managing plant species diversity under fluctuating wetland conditions: the case of temporarily flooded depressions. – *Wetlands Ecology and Management* 24: 597-608.
- [3] Amano, T., Kusumoto, Y., Tokuoka, Y., Yamada, S., Kim, E.-Y., Yamamoto, S. (2008): Spatial and temporal variations in the use of rice-paddy dominated landscapes by birds in Japan. – *Biological Conservation* 141: 1704-1716.
- [4] Austin, M. P. (1999): The potential contribution of vegetation ecology to biodiversity research. – *Ecography* 22: 465-484.
- [5] Bai, J., Lu, Q., Zhao, Q., Wang, J., Ouyang, H. (2013): Effects of alpine wetland landscapes on regional climate on the Zoige Plateau of China. – *Advances in Meteorology* 2013: 7.
- [6] Bell, D. T., Plummer, J. A., Taylor, S. K. (1993): Seed germination ecology in southwestern Western Australia. – *The Botanical Review* 59: 24-73.
- [7] Bell, F. G., Genske, D. D. (2001): The influence of subsidence attributable to coal mining on the environment, development and restoration: some examples from western Europe and south Africa. – *Environmental, Engineering Geoscience* 7: 81-99.

- [8] Bell, F. G., Stacey, T. R., Genske, D. D. (2000): Mining subsidence and its effect on the environment: some differing examples. – *Environmental Geology* 40: 135-152.
- [9] Błońska, A., Kompała-Bąba, A., Sierka, E., Bierza, W., Magurno, F., Besenyi, L., Ryś, K., Woźniak, G. (2019): Diversity of vegetation dominated by selected grass species on coal-mine spoil heaps in terms of reclamation of post-industrial areas. – *Journal of Ecological Engineering* 20: 209-217.
- [10] Bogusch, P., Macek, J., Janšta, P., Kubík, Š., Řezáč, M., Holý, K., Malenovský, I., Baňaf, P., Mikát, M., Astapenková, A., Heneberg, P. (2016): Industrial and post-industrial habitats serve as critical refugia for pioneer species of newly identified arthropod assemblages associated with reed galls. – *Biodiversity and Conservation* 25: 827-863.
- [11] Bornette, G., Puijalón, S. (2011): Response of aquatic plants to abiotic factors: a review. – *Aquatic Sciences* 73: 1-14.
- [12] Bratli, H., Økland, T., Økland, R. H., Dramstad, W. E., Elven, R., Engan, G., Fjellstad, W., Heegaard, E., Pedersen, O., Solstad, H. (2006): Patterns of variation in vascular plant species richness and composition in SE Norwegian agricultural landscapes. – *Agriculture, Ecosystems & Environment* 114: 270-286.
- [13] Brose, U. (2001): Relative importance of isolation, area and habitat heterogeneity for vascular plant species richness of temporary wetlands in east-German farmland. – *Ecography* 24: 722-730.
- [14] Brose, U. (2003a): Bottom-up control of carabid beetle communities in early successional wetlands: mediated by vegetation structure or plant diversity? – *Oecologia* 135: 407-413.
- [15] Brose, U. (2003b): Regional diversity of temporary wetland carabid beetle communities: a matter of landscape features or cultivation intensity? – *Agriculture Ecosystems & Environment* 98: 163-167.
- [16] Brown, G. R., Matthews, I. M. (2016): A review of extensive variation in the design of pitfall traps and a proposal for a standard pitfall trap design for monitoring ground-active arthropod biodiversity. – *Ecology and Evolution* 6: 3953-3964.
- [17] Brudvig, L. A., Damschen, E. I., Tewksbury, J. J., Haddad, N. M., Levey, D. J. (2009): Landscape connectivity promotes plant biodiversity spillover into non-target habitats. – *Proceedings of the National Academy of Sciences of the United States of America* 106: 9328-9332.
- [18] Cerezo, A., Conde, M. C., Poggio, S. L. (2011): Pasture area and landscape heterogeneity are key determinants of bird diversity in intensively managed farmland. – *Biodiversity and Conservation* 20: 2649.
- [19] Chiron, F., Filippi-Codaccioni, O., Jiguet, F., Devictor, V. (2010): Effects of non-cropped landscape diversity on spatial dynamics of farmland birds in intensive farming systems. – *Biological Conservation* 143: 2609-2616.
- [20] Clarke, K., Gorley, R. (2001): Primer E-v5: User Manual/Tutorial. – Primer-E, Plymouth.
- [21] Colwell, R. (2005): EstimateS: Statistical Estimation of Species Richness and Shared Species from Samples. Software and User's Guide. – viceroy.eeb.uconn.edu/estimateS.
- [22] Cramer, J. M., Mesquita, R. C. G., Williamson, G. B. (2007): Forest fragmentation differentially affects seed dispersal of large and small-seeded tropical trees. – *Biological Conservation* 137: 415-423.
- [23] Czaja, S., Rahmonov, O., Wach, J., Gajos, M. (2014): Ecohydrological Monitoring in Assessing the Mining Impact on Riverside Ecosystems. – *Polish Journal of Environmental Studies* 23: 629-637.
- [24] Davidowitz, G., Rosenzweig, M. L. (1998): The latitudinal gradient of species diversity among North American grasshoppers (Acrididae) within a single habitat: a test of the spatial heterogeneity hypothesis. – *Journal of Biogeography* 25: 553-560.
- [25] De-Jun, K., Xiao-Jun, Y., Qiang, L., Xing-Yao, Z., Jun-Xing, Y. (2011): Winter habitat selection by the Vulnerable black-necked crane *Grus nigricollis* in Yunnan, China: implications for determining effective conservation actions. – *Oryx* 45: 258-264.

- [26] De Lucca, G. S., Barros, F. A. P., Oliveira, J. V., Dal Magro, J., Lucas, E. M. (2018): The role of environmental factors in the composition of anuran species in several ponds under the influence of coal mining in southern Brazil. – *Wetlands Ecology and Management* 26: 285-297.
- [27] De Villiers, A. J., Van Rooyen, M. W., Theron, G. K. (2001): Seedbank phytosociology of the Strandveld Succulent Karoo, South Africa: a pre-mining benchmark survey for rehabilitation. – *Land Degradation & Development* 12: 119-130.
- [28] Dolný, A., Harabiš, F. (2012): Underground mining can contribute to freshwater biodiversity conservation: allogenic succession forms suitable habitats for dragonflies. – *Biological Conservation* 145: 109-117.
- [29] Duelli, P. (1997): Biodiversity evaluation in agricultural landscapes: an approach at two different scales. – *Agriculture, Ecosystems & Environment* 62: 81-91.
- [30] Duelli, P., Obrist, M. K. (2003): Regional biodiversity in an agricultural landscape: the contribution of seminatural habitat islands. – *Basic and Applied Ecology* 4: 129-138.
- [31] Dufлот, R., Aviron, S., Ernoult, A., Fahrig, L., Burel, F. (2015): Reconsidering the role of 'semi-natural habitat' in agricultural landscape biodiversity: a case study. – *Ecological Research* 30: 75-83.
- [32] Elphick, C. S. (2000): Functional equivalency between rice fields and seminatural wetland habitats. – *Conservation Biology* 14: 181-191.
- [33] Erwin, K. L. (2008): Wetlands and global climate change: the role of wetland restoration in a changing world. – *Wetlands Ecology and Management* 17: 71.
- [34] Fang, J., Wang, X., Shen, Z., Tang, Z., He, J., Yu, D., Jiang, Y., Wang, Z., Zheng, C., Zhu, J., Guo, Z. (2009): Methods and protocols for plant community inventory. – *Biodiversity Science* 17: 533-548.
- [35] Finke, D. L., Snyder, W. E. (2008): Niche partitioning increases resource exploitation by diverse communities. – *Science* 321: 1488.
- [36] Frank, H., Erwin, T. L., Hemenway, R. C. (2009): Economically beneficial ground beetles. The specialized predators *Pheropsophus aequinoctialis* (L.) and *Stenaptinus jessoensis* (Morawitz): their laboratory behavior and descriptions of immature stages (Coleoptera: Carabidae: Brachininae). – *ZooKeys* 14: 1-36.
- [37] Frenzel, M., Everaars, J., Schweiger, O. (2016): Bird communities in agricultural landscapes: What are the current drivers of temporal trends? – *Ecological Indicators* 65: 113-121.
- [38] Frouz, J., Mudrak, O., Reitschmiedova, E., Walmsley, A., Vachova, P., Simackova, H., Albrechtova, J., Moradi, J., Kutcera, J. (2018): Rough wave-like heaped overburden promotes establishment of woody vegetation while leveling promotes grasses during unassisted post mining site development. – *Journal of Environmental Management* 205: 50-58.
- [39] Gaston, K. J. (2000): Global patterns in biodiversity. – *Nature* 405: 220-227.
- [40] Gaujour, E., Amiaud, B., Mignolet, C., Plantureux, S. (2012): Factors and processes affecting plant biodiversity in permanent grasslands. A review. – *Agronomy for Sustainable Development* 32: 133-160.
- [41] Gioria, M., Schaffers, A., Bacaro, G., Feehan, J. (2010): The conservation value of farmland ponds: predicting water beetle assemblages using vascular plants as a surrogate group. – *Biological Conservation* 143: 1125-1133.
- [42] Giralt, D., Brotons, L., Valera, F., Krištín, A. (2008): The role of natural habitats in agricultural systems for bird conservation: the case of the threatened Lesser Grey Shrike. – *Biodiversity and Conservation* 17: 1997-2012.
- [43] Gucel, S., Kadis, C., Ozden, O., Charalambidou, I., Linstead, C., Fuller, W., Kounnamas, C., Ozturk, M. (2012): Assessment of biodiversity differences between natural and artificial Wetlands in Cyprus. – *Pakistan Journal of Botany* 44: 213-224.

- [44] Harabiš, F. (2016): High diversity of odonates in post-mining areas: meta-analysis uncovers potential pitfalls associated with the formation and management of valuable habitats. – *Ecological Engineering* 90: 438-446.
- [45] Harabiš, F., Tichanek, F., Tropek, R. (2013): Dragonflies of freshwater pools in lignite spoil heaps: restoration management, habitat structure and conservation value. – *Ecological Engineering* 55: 51-61.
- [46] He, C., Liu, Z., Tian, J., Ma, Q. (2014): Urban expansion dynamics and natural habitat loss in China: a multiscale landscape perspective. – *Global Change Biology* 20: 2886-2902.
- [47] He, Y., He, X., Liu, Z., Zhao, S., Bao, L., Li, Q., Yan, L. (2017): Coal mine subsidence has limited impact on plant assemblages in an arid and semi-arid region of northwestern China. – *Écoscience* 24: 91-103.
- [48] Hong, M. G., Nam, B. E., Kim, J. G. (2017): Effects of soil fertility on early development of wetland vegetation from soil seed bank: focusing on biomass production and plant species diversity. – *Journal of Plant Biology* 60: 241-248.
- [49] Hu, Y., Dong, Z., Liu, G. (2017): Distribution and potential ecological risk of heavy metals accumulated in subsidence lakes formed in the Huainan Coalfield, China. – *Environmental Forensics* 18: 251-257.
- [50] Hu, Z., Xiao, W. (2013): Optimization of concurrent mining and reclamation plans for single coal seam: a case study in northern Anhui, China. – *Environmental Earth Sciences* 68: 1247-1254.
- [51] Hu, Z., Xu, X., Zhao, Y. (2012): Dynamic monitoring of land subsidence in mining area from multi-source remote-sensing data - a case study at Yanzhou, China. – *International Journal of Remote Sensing* 33: 5528-5545.
- [52] Hu, Z., Zhang, R., Chugh, Y. P., Jia, J. (2016): Mitigating mine subsidence dynamically to minimise impacts on farmland and water resources: a case study. – *International Journal of Environment and Pollution* 59: 169-186.
- [53] Huang, C., Zhou, Z., Peng, C., Teng, M., Wang, P. (2019): How is biodiversity changing in response to ecological restoration in terrestrial ecosystems? A meta-analysis in China. – *Science of The Total Environment* 650: 1-9.
- [54] Huk, T., Kühne, B. (1999): Substrate selection by *Carabus clatratus* (Coleoptera, Carabidae) and its consequences for offspring development. – *Oecologia* 121: 348-354.
- [55] Iannone Iii, B. V., Galatowitsch, S. M. (2008): Altering light and soil N to limit *Phalaris arundinacea* reinvasion in sedge meadow restorations. – *Restoration Ecology* 16: 689-701.
- [56] Ives, A. R., Cardinale, B. J., Snyder, W. E. (2005): A synthesis of subdisciplines: predator-prey interactions, and biodiversity and ecosystem functioning. – *Ecology Letters* 8: 102-116.
- [57] Jeanneret, P., Schüpbach, B., Pfiffner, L., Walter, T. (2003): Arthropod reaction to landscape and habitat features in agricultural landscapes. – *Landscape Ecology* 18: 253-263.
- [58] Joern, A., Laws, A. N. (2013): Ecological mechanisms underlying arthropod species diversity in grasslands. – *Annual Review of Entomology* 58: 19-36.
- [59] Ju, J., Xu, J. (2015): Surface stepped subsidence related to top-coal caving longwall mining of extremely thick coal seam under shallow cover. – *International Journal of Rock Mechanics and Mining Sciences* 78: 27-35.
- [60] Katayama, N., Osawa, T., Amano, T., Kusumoto, Y. (2015): Are both agricultural intensification and farmland abandonment threats to biodiversity? A test with bird communities in paddy-dominated landscapes. – *Agriculture, Ecosystems & Environment* 214: 21-30.
- [61] Kirk, D. A., Lindsay, K. E. F. (2017): Subtle differences in birds detected between organic and nonorganic farms in Saskatchewan Prairie Parklands by farm pair and bird functional group. – *Agriculture, Ecosystems & Environment* 246: 184-201.

- [62] Knapp, M., Řezáč, M. (2015): Even the smallest non-crop habitat islands could be beneficial: distribution of carabid beetles and spiders in agricultural landscape. – *PLoS One* 10: e0123052.
- [63] Lee, M.-B., Goodale, E. (2018): Crop heterogeneity and non-crop vegetation can enhance avian diversity in a tropical agricultural landscape in southern China. – *Agriculture, Ecosystems & Environment* 265: 254-263.
- [64] Lewin, I., Spyra, A., Krodkiewska, M., Strzelec, M. (2015): The importance of the mining subsidence reservoirs located along the trans-regional highway in the conservation of the biodiversity of freshwater molluscs in industrial areas (Upper Silesia, Poland). – *Water, Air, & Soil Pollution* 226: 189.
- [65] Lewis-Phillips, J., Brooks, S., Sayer, C. D., Mccrea, R., Siriwardena, G., Axmacher, J. C. (2019): Pond management enhances the local abundance and species richness of farmland bird communities. – *Agriculture, Ecosystems & Environment* 273: 130-140.
- [66] Li, C., Yang, S., Zha, D., Zhang, Y., De Boer, W. F. (2019): Waterbird communities in subsidence wetlands created by underground coal mining in China: effects of multi-scale environmental and anthropogenic variables. – *Environmental Conservation* 46: 67-75.
- [67] Li, M. S. (2006): Ecological restoration of mineland with particular reference to the metalliferous mine wasteland in China: a review of research and practice. – *Science of The Total Environment* 357: 38-53.
- [68] Li, X., Liu, Y., Duan, M., Yu, Z., Axmacher, J. C. (2018): Different response patterns of epigaeic spiders and carabid beetles to varying environmental conditions in fields and semi-natural habitats of an intensively cultivated agricultural landscape. – *Agriculture, Ecosystems & Environment* 264: 54-62.
- [69] Lindenmayer, D. B., Cunningham, R. B., Pope, M. L., Donnelly, C. F. (1999): The response of arboreal marsupials to landscape context: a large-scale fragmentation study. – *Ecological Applications* 9: 594-611.
- [70] Lindenmayer, D. B., Knight, E. J., Crane, M. J., Montague-Drake, R., Michael, D. R., Macgregor, C. I. (2010): What makes an effective restoration planting for woodland birds? – *Biological Conservation* 143: 289-301.
- [71] Liu, Q., Yang, J., Yang, X., Zhao, J., Yu, H. (2010): Foraging habitats and utilization distributions of Black-necked Cranes wintering at the Napahai Wetland, China. – *Journal of Field Ornithology* 81: 21-30.
- [72] Liu, X., Zhou, W., Bai, Z. (2016): Vegetation coverage change and stability in large open-pit coal mine dumps in China during 1990-2015. – *Ecological Engineering* 95: 447-451.
- [73] Lokhande, R. D., Prakash, A., Singh, K. B., Singh, K. K. K. (2005): Subsidence control measures in coalmines: a review. – *Journal of Scientific & Industrial Research* 64: 323-332.
- [74] Lundholm, J. T., Larson, D. W. (2003): Relationships between spatial environmental heterogeneity and plant species diversity on a limestone pavement. – *Ecography* 26: 715-722.
- [75] Ma, M. (2008): Multi-scale responses of plant species diversity in semi-natural buffer strips to agricultural landscapes. – *Applied Vegetation Science* 11: 269-278.
- [76] Ma, M., Herzon, I. (2014): Plant functional diversity in agricultural margins and fallow fields varies with landscape complexity level: conservation implications. – *Journal for Nature Conservation* 22: 525-531.
- [77] Mantyka-Pringle, C. S., Martin, T. G., Rhodes, J. R. (2012): Interactions between climate and habitat loss effects on biodiversity: a systematic review and meta-analysis. – *Global Change Biology* 18: 1239-1252.
- [78] Mao, D., Wang, Z., Wu, J., Wu, B., Zeng, Y., Song, K., Yi, K., Luo, L. (2018): China's wetlands loss to urban expansion. – *Land Degradation & Development* 29: 2644-2657.
- [79] Marsden, S. J. (1999): Estimation of parrot and hornbill densities using a point count distance sampling method. – *Ibis* 141: 327-390.

- [80] Mathias, M. E., Moyle, P. (1992): Wetland and aquatic habitats. – *Agriculture, Ecosystems & Environment* 42: 165-176.
- [81] Mclaughlin, D. L., Cohen, M. J. (2013): Realizing ecosystem services: wetland hydrologic function along a gradient of ecosystem condition. – *Ecological Applications* 23: 1619-1631.
- [82] Meng, L., Feng, Q.-Y., Zhou, L., Lu, P., Meng, Q.-J. (2009): Environmental cumulative effects of coal underground mining. – *Procedia Earth and Planetary Science* 1: 1280-1284.
- [83] Moradi, J., Potocký, P., Kočárek, P., Bartuška, M., Tajovský, K., Tichánek, F., Frouz, J., Tropek, R. (2018a): Influence of surface flattening on biodiversity of terrestrial arthropods during early stages of brown coal spoil heap restoration. – *Journal of Environmental Management* 220: 1-7.
- [84] Moradi, J., Vicentini, F., Šimáčková, H., Pižl, V., Tajovský, K., Stary, J., Frouz, J. (2018b): An investigation into the long-term effect of soil transplant in bare spoil heaps on survival and migration of soil meso and macrofauna. – *Ecological Engineering* 110: 158-164.
- [85] Moran, C., Catterall, C. P., Green, R. J., Olsen, M. F. (2004): Functional variation among frugivorous birds: implications for rainforest seed dispersal in a fragmented subtropical landscape. – *Oecologia* 141: 584-595.
- [86] Morelli, F. (2018): High nature value farmland increases taxonomic diversity, functional richness and evolutionary uniqueness of bird communities. – *Ecological Indicators* 90: 540-546.
- [87] Myers, N., Mittermeier, R. A., Mittermeier, C. G., Da Fonseca, G. A. B., Kent, J. (2000): Biodiversity hotspots for conservation priorities. – *Nature* 403: 853-858.
- [88] Nagy, G. G., Ladányi, M., Arany, I., Aszalós, R., Czúcz, B. (2017): Birds and plants: comparing biodiversity indicators in eight lowland agricultural mosaic landscapes in Hungary. – *Ecological Indicators* 73: 566-573.
- [89] Niemelä, J. (2001): Carabid beetles (Coleoptera: Carabidae) and habitat fragmentation: a review. – *EJE* 98: 127-132.
- [90] Oishi, Y. (2019): The influence of microclimate on bryophyte diversity in an urban Japanese garden landscape. – *Landscape and Ecological Engineering* 15: 167-176.
- [91] Pollock, M. M., Naiman, R. J., Hanley, T. A. (1998): Plant species richness in riparian wetlands. A test of biodiversity theory. – *Ecology* 79: 94-105.
- [92] Quadros, P. D. d., Zhalnina, K., Davis-Richardson, A. G., Drew, J. C., Menezes, F. B., Camargo, F. A. d. O., Triplett, E. W. (2016): Coal mining practices reduce the microbial biomass, richness and diversity of soil. – *Applied Soil Ecology* 98: 195-203.
- [93] Reynolds, C. S. (2002): Ecological pattern and ecosystem theory. – *Ecological Modelling* 158: 181-200.
- [94] Rola, K., Osyczka, P., Nobis, M., Drozd, P. (2015): How do soil factors determine vegetation structure and species richness in post-smelting dumps? – *Ecological Engineering* 75: 332-342.
- [95] Rusch, A., Bommarco, R., Jonsson, M., Smith, H. G., Ekbom, B. (2013): Flow and stability of natural pest control services depend on complexity and crop rotation at the landscape scale. – *Journal of Applied Ecology* 50: 345-354.
- [96] Růžička, V., Zacharda, M., Němcová, L., Šmilauer, P., Nekola, J. C. (2012): Periglacial microclimate in low-altitude scree slopes supports relict biodiversity. – *Journal of Natural History* 46: 2145-2157.
- [97] Šálek, M., Hula, V., Kipson, M., Daňková, R., Niedobová, J., Gamero, A. (2018): Bringing diversity back to agriculture: smaller fields and non-crop elements enhance biodiversity in intensively managed arable farmlands. – *Ecological Indicators* 90: 65-73.
- [98] Schemske, D. W., Mittelbach, G. G., Cornell, H. V., Sobel, J. M., Roy, K. (2009): Is there a latitudinal gradient in the importance of biotic interactions? – *Annual Review of Ecology, Evolution, and Systematics* 40: 245-269.

- [99] Schmidt, M. H., Roschewitz, I., Thies, C., Tschardtke, T. (2005): Differential effects of landscape and management on diversity and density of ground-dwelling farmland spiders. – *Journal of Applied Ecology* 42: 281-287.
- [100] Schneider, F. D., Brose, U., Rall, B. C., Guill, C. (2016): Animal diversity and ecosystem functioning in dynamic food webs. – *Nature Communications* 7: 12718.
- [101] Shutler, D., Gloutney, M. L., Clark, R. G. (1998): Body mass, energetic constraints, and duck nesting ecology. – *Canadian Journal of Zoology* 76: 1805-1814.
- [102] Soykan, C. U., Brand, L. A., Ries, L., Stromberg, J. C., Hass, C., Simmons, D. A., Jr., Patterson, W. J. D., Sabo, J. L. (2012): Multitaxonomic diversity patterns along a desert riparian–upland gradient. – *PLoS One* 7: e28235.
- [103] Stam, J. M., Kroes, A., Li, Y., Gols, R., Loon, J. J. A. v., Poelman, E. H., Dicke, M. (2014): Plant interactions with multiple insect herbivores: from community to genes. – *Annual Review of Plant Biology* 65: 689-713.
- [104] Sugiura, S. (2018): Anti-predator defences of a bombardier beetle: is bombing essential for successful escape from frogs? – *PeerJ* 6: e5942.
- [105] Sutton-Grier, A. E., Wright, J. P., McGill, B. M., Richardson, C. (2011): Environmental conditions influence the plant functional diversity effect on potential denitrification. – *PLoS One* 6: e16584.
- [106] Szarek-Lukaszewska, G., Grodzinska, K., Grodzinska, K. (2007): Vegetation of a post-mining open pit (Zn/Pb ores): three-year study of colonization. – *Polish Journal of Ecology* 55: 261-282.
- [107] Telesh, I., Schubert, H., Skarlato, S. (2013): Life in the salinity gradient: discovering mechanisms behind a new biodiversity pattern. – *Estuarine, Coastal and Shelf Science* 135: 317-327.
- [108] Ter Braak, C., Smilauer, P. N. (2001): *Canoco Reference Manual and CanoDraw for Windows User's Guide: Software for Canonical Community Ordination*. – Microcomputer Power, Houston, TX.
- [109] Toral, G. M., Aragonés, D., Bustamante, J., Figuerola, J. (2011): Using Landsat images to map habitat availability for waterbirds in rice fields. – *Ibis* 153: 684-694.
- [110] Tropek, R., Kadlec, T., Karesova, P., Spitzer, L., Kocarek, P., Malenovsky, I., Banar, P., Tuf, I. H., Hejda, M., Konvicka, M. (2010): Spontaneous succession in limestone quarries as an effective restoration tool for endangered arthropods and plants. – *Journal of Applied Ecology* 47: 139-147.
- [111] Ueda, K. (1993): Effects of neighbours: costs of polyterritoriality in the Fan-tailed Warbler *Cisticola juncidis*. – *Ethology Ecology & Evolution* 5: 177-180.
- [112] Verburg, P. H., Van Berkel, D. B., Van Doorn, A. M., Van Eupen, M., Van Den Heiligenberg, H. A. R. M. (2010): Trajectories of land use change in Europe: a model-based exploration of rural futures. – *Landscape Ecology* 25: 217-232.
- [113] Wang, X., Barter, M., Cao, L., Lei, J., Fox, A. D. (2012): Serious contractions in wintering distribution and decline in abundance of Baer's Pochard *Aythya baeri*. – *Bird Conservation International* 22: 121-127.
- [114] Willscher, S., Schaum, M., Goldammer, J., Franke, M., Kuehn, D., Ihling, H., Schaarschmidt, T. (2017): Environmental biogeochemical characterization of a lignite coal spoil and overburden site in Central Germany. – *Hydrometallurgy* 173: 170-177.
- [115] Wuczyński, A., Dajdok, Z., Wierzcholska, S., Kujawa, K. (2014): Applying red lists to the evaluation of agricultural habitat: regular occurrence of threatened birds, vascular plants, and bryophytes in field margins of Poland. – *Biodiversity and Conservation* 23: 999-1017.
- [116] Xiao, W., Fu, Y., Wang, T., Lv, X. (2018): Effects of land use transitions due to underground coal mining on ecosystem services in high groundwater table areas: a case study in the Yanzhou coalfield. – *Land Use Policy* 71: 213-221.

- [117] Xie, K., Zhang, Y., Yi, Q., Yan, J. (2013): Optimal resource utilization and ecological restoration of aquatic zones in the coal mining subsidence areas of the Huaibei Plain in Anhui Province, China. – *Desalination and Water Treatment* 51: 4019-4027.
- [118] Xu, T., Weng, B., Yan, D., Wang, K., Li, X., Bi, W., Li, M., Cheng, X., Liu, Y. (2019): Wetlands of international importance: status, threats, and future protection. – *International Journal of Environmental Research and Public Health* 16: 1818.
- [119] Xu, X., Zhao, Y., Hu, Z., Yu, Y., Shao, F. (2014): Boundary demarcation of the damaged cultivated land caused by coal mining subsidence. – *Bulletin of Engineering Geology and the Environment* 73: 621-633.
- [120] Yao, E.-Q., Gui, H.-R. (2008): Four trace elements contents of water environment of mining subsidence in the Huainan diggings, China. – *Environmental Monitoring and Assessment* 146: 203-210.
- [121] Yu, Y., Chen, S.-E., Deng, K.-Z., Wang, P., Fan, H.-D. (2018): Subsidence mechanism and stability assessment methods for partial extraction mines for sustainable development of mining cities - a review. – *Sustainability* 10: 113.
- [122] Zhang, G., Yuan, X., Wang, K. (2019a): Biodiversity and temporal patterns of macrozoobenthos in a coal mining subsidence area in North China. – *PeerJ* 7: e6456.
- [123] Zhang, M., Yuan, X., Guan, D., Liu, H., Zhang, G., Wang, K., Zhou, L., Wu, S., Sun, K. (2019b): Eco-exergy evaluation of new wetlands in the Yanzhou coalfield subsidence areas using structural-dynamic modelling. – *Mine Water and the Environment* 38: 746-756.
- [124] Zhao, J.-M., Zhou, L.-Z. (2018): Area, isolation, disturbance and age effects on species richness of summer waterbirds in post-mining subsidence lakes, Anhui, China. – *Avian Research* 9: 8.
- [125] Zimmer, K. D., Hanson, M. A., Butler, M. G. (2000): Factors influencing invertebrate communities in prairie wetlands: a multivariate approach. – *Canadian Journal of Fisheries and Aquatic Sciences* 57: 76-85.

APPENDIX

Descriptive statistics of the community structure of plants, spiders, beetles and birds between mosaic farmlands and intensive farmlands

Taxonomic group	Variable	Mosaic farmlands (mean ± SD)	Intensive farmlands (mean ± SD)	F	p
Plant	Richness	62.83 ± 19.29	25.50 ± 5.01	21.051	0.001
	Rarefied richness	12.21 ± 3.13	6.85 ± 0.98	16.058	0.002
	Shannon diversity	3.78 ± 0.07	2.49 ± 0.20	223.093	0.000
Beetle	Richness	28.00 ± 3.16	15.50 ± 3.21	46.182	0.000
	Rarefied richness	5.39 ± 1.90	5.16 ± 0.82	0.000	0.996
	Abundance	78.89 ± 33.29	30.69 ± 12.07	14.24	0.004
	Shannon diversity	1.43 ± 0.57	1.46 ± 0.24	0.184	0.677
Spider	Richness	11.83 ± 1.83	7.83 ± 0.98	22.154	0.001
	Rarefied richness	5.78 ± 0.74	5.61 ± 0.45	0.252	0.627
	Abundance	32.53 ± 9.05	14.36 ± 6.10	16.631	0.002
	Shannon diversity	1.67 ± 0.20	1.62 ± 0.08	0.249	0.629
Bird	Richness	38.67 ± 5.32	20.00 ± 2.90	57.018	0.000
	Rarefied richness	11.42 ± 1.09	8.52 ± 0.76	28.491	0.000
	Abundance	104.47 ± 38.39	43.93 ± 7.31	24.002	0.001
	Shannon diversity	2.88 ± 0.19	2.20 ± 0.16	45.938	0.000

The species list of plants of mosaics farmlands (MF) and intensive farmlands (IF)

Species list of plants				Species list of birds				
Species	MFS	IF	WE	Species	MF	IF	ICUN	Migration
Salviniaceae				Phasianidae				
1. <i>Salvinia natans</i>	+		A	1. <i>Coturnix japonica</i>	+		NT	P
Equisetaceae				2. <i>Phasianus colchicus</i>	+	+	LC	R
2. <i>Equisetum ramosissimum</i>	+		M	Anatidae				
Marsileaceae				3. <i>Anser fabalis</i>	+		LC	W
3. <i>Marsilea quadrifolia</i>	+		A	4. <i>Anser anser</i>	+		LC	P
Azollaceae				5. <i>Anser albifrons</i>	+		LC	P
4. <i>Azolla imbricata</i>	+		A	6. <i>Cygnus columbianus</i>	+		LC	W
Nymphaeaceae				7. <i>Tadorna ferruginea</i>	+		LC	R
5. <i>Nelumbo nucifera</i>	+		A	8. <i>Aix galericulata</i>	+		LC	P
6. <i>Euryale ferox</i>	+		A	9. <i>Anas strepera</i>	+		LC	P
Ceratophyllaceae				10. <i>Anas falcata</i>	+		NT	W
7. <i>Ceratophyllum demersum</i>	+		A	11. <i>Anas crecca</i>	+		LC	P
8. <i>Ceratophyllum oryzetorum</i>	+		A	12. <i>Anas platyrhynchos</i>	+		LC	W
9. <i>Ceratophyllum</i> sp.	+		A	13. <i>Anas clypeata</i>	+		LC	P
Ranunculaceae				14. <i>Anas querquedula</i>	+		LC	W
10. <i>Ranunculus chinensis</i>	+		H	15. <i>Anas formosa</i>	+		LC	P
11. <i>Ranunculus sceleratus</i>	+		H	16. <i>Anas zonorhyncha</i>	+		LC	R
12. <i>Ranunculus japonicus</i>	+		H	17. <i>Aythya ferina</i>	+		LC	P
13. <i>Semiaquilegia adoxoides</i>	+		M	18. <i>Aythya baeri</i>	+		CR	W
Papaveraceae				19. <i>Aythya nyroca</i>	+		NT	W
14. <i>Dicranostigma leptopodum</i>	+		X	20. <i>Aythya fuligula</i>	+		LC	W
Moraceae				21. <i>Mergellus albellus</i>	+		LC	W
15. <i>Humulus scandens</i>	+	+	M	22. <i>Mergus squamatus</i>	+		LC	P
Rubiaceae				Podicipedidae				
16. <i>Galium aparine</i>	+	+	M	23. <i>Tachybaptus ruficollis</i>	+		LC	R
17. <i>Galium bungei</i>	+		M	24. <i>Podiceps cristatus</i>	+		LC	R
18. <i>Rubia cordifolia</i>	+		M	Ardeidae				
Chenopodiaceae				25. <i>Nycticorax nycticorax</i>	+		LC	S
19. <i>Chenopodium album</i>	+	+	M	26. <i>Ardeola bacchus</i>	+		LC	R
20. <i>Chenopodium serotinum</i>	+	+	M	27. <i>Ardea cinerea</i>	+		LC	R
21. <i>Chenopodium ambrosioides</i>	+		H	28. <i>Ardea purpurea</i>	+		LC	S
22. <i>Chenopodium glaucum</i>	+		M	29. <i>Ardea alba</i>	+		LC	R
23. <i>Kochia scoparia</i>	+		M	30. <i>Egretta garzetta</i>	+		LC	S
24. <i>Salsola collina</i>	+	+	X	31. <i>Botaurus stellaris</i>	+		LC	S
Amaranthaceae				32. <i>Ixobrychus sinensis</i>	+		LC	S
25. <i>Alternanthera philoxeroides</i>	+		H	33. <i>Platalea leucorodia</i>	+		LC	S
26. <i>Alternanthera sessilis</i>	+		H	Phalacrocoracidae				
27. <i>Amaranthus hybridus</i>	+		M	34. <i>Phalacrocorax carbo</i>	+		LC	P
28. <i>Amaranthus paniculatus</i>	+		X	Pandionidae				
29. <i>Amaranthus caudatus</i>	+		M	35. <i>Pandion haliaetus</i>	+		LC	P
30. <i>Amaranthus polygonoides</i>	+		M	Accipitridae				
31. <i>Amaranthus retroflexus</i>	+	+	M	36. <i>Elanus caeruleus</i>	+	+	LC	P
32. <i>Amaranthus spinosus</i>	+	+	M	37. <i>Circus cyaneus</i>	+		LC	P
33. <i>Amaranthus viridis</i>	+	+	M	38. <i>Circus spilonotus</i>	+		LC	W
34. <i>Amaranthus lividus</i>	+		M	39. <i>Buteo japonicus</i>	+		LC	P
Polygonaceae				40. <i>Accipiter nisus</i>	+		LC	P
35. <i>Rumex dentatus</i>	+		H	Falconidae				
36. <i>Rumex maritimus</i>	+		H	41. <i>Falco tinnunculus</i>	+		LC	R
37. <i>Rumex amurensis</i>	+		H	42. <i>Falco subbuteo</i>	+		LC	P
38. <i>Rumex patientia</i>	+		H	43. <i>Falco amurensis</i>	+		LC	P
39. <i>Fallopia multiflora</i>	+		H	44. <i>Falco peregrinus</i>	+		LC	P
40. <i>Polygonum aviculare</i>	+	+	M	Strigidae				
41. <i>Polygonum perfoliatum</i>	+		H	45. <i>Athene noctua</i>	+	+	LC	R
42. <i>Polygonum longisetum</i>	+		H	Rallidae				
43. <i>Polygonum hydropiper</i>	+		H	46. <i>Amaurornis phoenicurus</i>	+		LC	S
44. <i>Polygonum lapathifolium</i>	+	+	M	47. <i>Gallinula chloropus</i>	+		LC	S

45. <i>Polygonum plebeium</i>	+		H	48. <i>Fulica atra</i>	+		LC	R
Caryophyllaceae				49. <i>Rallus indicus</i>	+		LC	P
46. <i>Dianthus chinensis</i>	+		X	50. <i>Porzana pusilla</i>	+		LC	P
47. <i>Dianthus superbus</i>	+		X	Recurvirostridae				
48. <i>Silene firma</i>	+		X	51. <i>Himantopus himantopus</i>	+		LC	R
49. <i>Silene aprica</i>	+		X	Charadriidae				
50. <i>Stellaria apetala</i>	+		M	52. <i>Vanellus cinereus</i>	+		LC	S
51. <i>Myosoton aquaticum</i>	+	+	M	53. <i>Vanellus vanellus</i>	+		LC	P
52. <i>Arenaria serpyllifolia</i>	+	+	M	54. <i>Charadrius dubius</i>	+		LC	S
53. <i>Cerastium glomeratum</i>	+		M	55. <i>Charadrius alexandrinus</i>	+		LC	S
Phytolaccaceae				56. <i>Pluvialis fulva</i>	+		LC	P
54. <i>Phytolacca americana</i>	+		M	57. <i>Charadrius veredus</i>	+		LC	P
Malvaceae				Scolopacidae				
55. <i>Abutilon theophrasti</i>	+	+	M	58. <i>Calidris ferruginea</i>	+		LC	P
56. <i>Corchorus aestuans</i>	+		M	59. <i>Calidris temminckii</i>	+		LC	P
57. <i>Hibiscus trionum</i>	+		X	60. <i>Gallinago gallinago</i>	+		LC	P
58. <i>Sida acuta</i>	+		X	61. <i>Gallinago stenura</i>	+		LC	P
Violaceae				62. <i>Numenius arquata</i>	+		NT	P
59. <i>Viola philippica</i>	+	+	X	63. <i>Tringa erythropus</i>	+		LC	P
60. <i>Viola prionantha</i>	+		X	64. <i>Tringa nebularia</i>	+		LC	P
Umbelliferae				65. <i>Tringa stagnatilis</i>	+		LC	P
61. <i>Ligusticum jeholense</i>	+		M	66. <i>Tringa ochropus</i>	+		LC	P
62. <i>Daucus carota</i>	+		M	67. <i>Actitis hypoleucos</i>	+		LC	S
63. <i>Torilis scabra</i>	+		M	68. <i>Scolopax rusticola</i>	+		LC	P
64. <i>Cnidium monnieri</i>	+		M	Glareolidae				
65. <i>Oenanthe javanica</i>	+		H	69. <i>Glareola maldivarum</i>	+		LC	S
Cruciferae				Laridae				
66. <i>Lepidium virginicum</i>	+		X	70. <i>Chroicocephalus ridibundus</i>	+		LC	W
67. <i>Rorippa dubia</i>	+		H	71. <i>Chlidonias hybrida</i>	+		LC	S
68. <i>Rorippa islandica</i>	+		H	72. <i>Sterna hirundo</i>	+		LC	S
69. <i>Rorippa indica</i>	+		H	Jacaniidae				
70. <i>Rorippa cantoniensis</i>	+		H	73. <i>Hydrophasianus chirurgus</i>	+		LC	S
71. <i>Capsella bursa-pastoris</i>	+	+	M	Columbidae				
72. <i>Erysimum cheiranthoides</i>	+	+	X	74. <i>Streptopelia orientalis</i>	+	+	LC	R
73. <i>Descurainia sophia</i>	+	+	M	75. <i>Spilopelia chinensis</i>	+	+	LC	R
74. <i>Draba nemorosa</i>	+		H	76. <i>Streptopelia tranquebarica</i>	+		LC	S
75. <i>Cardamine hirsuta</i>	+		M	Cuculidae				
76. <i>Cardamine flexuosa</i>	+		M	77. <i>Cuculus canorus</i>	+		LC	S
77. <i>Nasturtium officinale</i>	+		M	Alcedinidae				
Primulaceae				78. <i>Ceryle rudis</i>	+		LC	S
78. <i>Lysimachia candida</i>	+		H	79. <i>Alcedo atthis</i>	+		LC	R
79. <i>Androsace umbellata</i>	+		M	Upupidae				
Crassulaceae				80. <i>Upupa epops</i>	+	+	LC	S
80. <i>Sedum aizoon</i>	+		X	Picidae				
Rosaceae				81. <i>Dendrocopos canicapillus</i>	+	+	LC	R
81. <i>Duchesnea indica</i>	+	+	M	82. <i>Dendrocopos major</i>	+		LC	R
82. <i>Potentilla supina</i>	+		M	83. <i>Picus canus</i>	+		LC	R
Leguminosae				Laniidae				
83. <i>Glycine soja</i>	+		H	84. <i>Lanius schach</i>	+	+	LC	R
84. <i>Gueldenstaedtia multiflora</i>	+		X	85. <i>Lanius sphenocercus</i>	+		LC	W
85. <i>Gueldenstaedtia maritima</i>	+		X	86. <i>Lanius cristatus</i>	+		LC	P
86. <i>Kummerowia stipulacea</i>	+	+	X	Dicruridae				
87. <i>Lespedeza juncea</i>	+		X	87. <i>Dicrurus macrocercus</i>	+		LC	S
88. <i>Melilotus officinalis</i>	+		M	Corvidae				
89. <i>Vicia tetrasperma</i>	+		X	88. <i>Pica pica</i>	+	+	LC	R
90. <i>Vicia hirsuta</i>	+		X	89. <i>Cyanopica cyanus</i>	+		LC	R
91. <i>Vicia bungei</i>	+		X	90. <i>Corvus corone</i>		+	LC	P
92. <i>Vicia sativa</i>	+		X	Paridae				
93. <i>Vicia kioshanica</i>	+		X	91. <i>Parus major</i>	+	+	-	R
94. <i>Vicia angustifolia</i>	+	+	X	92. <i>Parus minor</i>	+	+	LC	R
95. <i>Vigna minima</i>	+		X	Remizidae				

96. <i>Medicago lupulina</i>	+		X	93. <i>Remiz consobrinus</i>	+		LC	R
Haloragidaceae				Alaudidae				
97. <i>Myriophyllum spicatum</i>	+		A	94. <i>Alauda arvensis</i>	+	+	LC	P
98. <i>Myriophyllum verticillatum</i>	+		A	95. <i>Alauda gulgula</i>	+	+	LC	R
Lythraceae				Pycnonotidae				
99. <i>Ammannia multiflora</i>	+		H	96. <i>Pycnonotus sinensis</i>	+	+	LC	R
Trapaceae				Hirundinidae				
100. <i>Trapa bicornis</i>	+		A	97. <i>Hirundo rustica</i>	+	+	LC	S
101. <i>Trapa bispinosa</i>	+		A	98. <i>Cecropis daurica</i>	+	+	LC	S
Onagraceae				Aegithalidae				
102. <i>Gaura parviflora</i>	+		M	99. <i>Aegithalos glaucogularis</i>	+		LC	R
103. <i>Ludwigia prostrata</i>	+		H	Phylloscopidae				
Euphorbiaceae				100. <i>Phylloscopus fuscatus</i>	+		LC	P
104. <i>Acalypha australis</i>	+	+	M	101. <i>Phylloscopus proregulus</i>	+		LC	P
105. <i>Euphorbia esula</i>	+	+	X	102. <i>Phylloscopus inornatus</i>	+		LC	P
106. <i>Euphorbia helioscopia</i>	+	+	M	103. <i>Phylloscopus coronatus</i>	+		LC	S
107. <i>Euphorbia humifusa</i>	+		X	Acrocephalidae				
108. <i>Euphorbia maculata</i>	+	+	X	104. <i>Acrocephalus orientalis</i>	+		-	S
109. <i>Phyllanthus ussuriensis</i>	+		X	105. <i>Acrocephalus arundinaceus</i>	+		LC	S
Oxalidaceae				Cisticolidae				
110. <i>Oxalis bowiei</i>	+		M	106. <i>Cisticola juncidis</i>	+	+	LC	P
111. <i>Oxalis corniculata</i>	+		X	Sylviidae				
Geraniaceae				107. <i>Paradoxornis heudei</i>	+		NT	R
112. <i>Erodium stephanianum</i>	+		X	108. <i>Sinosuthora webbiana</i>	+	+	LC	R
113. <i>Geranium carolinianum</i>	+	+	X	Sturnidae				
Vitaceae				109. <i>Spodiopsar cineraceus</i>	+		LC	R
114. <i>Cayratia japonica</i>	+	+	M	110. <i>Spodiopsar sericeus</i>	+		LC	P
Asclepiadaceae				Turdidae				
115. <i>Metaplexis japonica</i>	+	+	X	111. <i>Turdus eunomus</i>	+		-	P
116. <i>Euphorbia esula</i>	+	+	X	112. <i>Turdus merula</i>	+	+	LC	R
117. <i>Cynanchum thesioides</i>	+		X	Muscicapidae				
118. <i>Cynanchum chinense</i>	+		X	113. <i>Tarsiger cyanurus</i>	+		LC	P
Solanaceae				114. <i>Phoenicurus auroreus</i>	+	+	LC	R
119. <i>Solanum nigrum</i>	+		M	115. <i>Saxicola maurus</i>	+	+	-	P
120. <i>Nicandra physalodes</i>	+		M	116. <i>Ficedula parva</i>	+		LC	P
121. <i>Datura stramonium</i>	+		X	117. <i>Copsychus saularis</i>	+	+	LC	R
122. <i>Physalis minima</i>	+		M	118. <i>Rhyacornis fuliginosa</i>	+		LC	P
Convolvulaceae				Passeridae				
123. <i>Pharbitis purpurea</i>	+	+	M	119. <i>Passer montanus</i>	+	+	LC	R
124. <i>Calystegia hederacea</i>	+		X	Motacillidae				
125. <i>Calystegia sepium</i>	+	+	X	120. <i>Motacilla tschutschensis</i>	+		LC	P
126. <i>Calystegia pellita</i>	+		X	121. <i>Motacilla alba</i>	+	+	LC	S
127. <i>Convolvulus arvensis</i>	+	+	X	122. <i>Motacilla tschutschensis</i>	+		LC	P
128. <i>Pharbitis hederacea</i>	+	+	M	123. <i>Dendronanthus indicus</i>	+		LC	S
129. <i>Pharbitis nil</i>	+	+	M	124. <i>Anthus spinoletta</i>	+		LC	P
130. <i>Cuscuta chinensis</i>	+		X	125. <i>Anthus hodgsoni</i>	+	+	LC	P
Gentianaceae				126. <i>Anthus cervinus</i>	+		LC	W
131. <i>Nymphoides peltata</i>	+		A	Fringillidae				
Boraginaceae				127. <i>Carduelis sinica</i>	+	+	LC	R
132. <i>Lithospermum arvense</i>	+		X	128. <i>Fringilla montifringilla</i>	+		LC	W
133. <i>Lithospermum erythrorhizon</i>	+		X	129. <i>Eophona migratoria</i>	+		LC	P
134. <i>Trigonotis peduncularis</i>	+	+	X	130. <i>Fringilla montifringilla</i>	+		LC	W
135. <i>Bothriospermum tenellum</i>	+		X	Emberizidae				
136. <i>Bothriospermum secundum</i>	+		X	131. <i>Emberiza cioides</i>	+		LC	R
137. <i>Thyrocarpus glochidiatus</i>	+		X	132. <i>Emberiza pusilla</i>	+	+	LC	W
138. <i>Lappula myosotis</i>	+		X	133. <i>Emberiza chrysophrys</i>	+	+	LC	P
Portulacaceae				134. <i>Emberiza elegans</i>	+		LC	P
139. <i>Portulaca oleracea</i>	+		M	135. <i>Emberiza rustica</i>	+		LC	W
140. <i>Portulaca grandiflora</i>	+		M	136. <i>Emberiza fucata</i>	+		LC	P
Labiatae				137. <i>Emberiza spodocephala</i>	+	+	LC	P
141. <i>Lagopsis supina</i>	+	+	X	138. <i>Emberiza pallasi</i>	+		LC	S

142. <i>Leonurus artemisia</i>	+	+	X	139. <i>Emberiza yessoensis</i>	+		NT	P
143. <i>Mentha haplocalyx</i>	+	+	M	Species list of beetles				
144. <i>Scutellaria barbata</i>	+		H	Species	MS	IS		
145. <i>Glechoma longituba</i>	+		H	Coccinellidae				
146. <i>Lamium amplexicaule</i>	+		M	1. <i>Propylaea japonica</i>	+			
147. <i>Salvia plebeia</i>	+	+	M	2. <i>Oenopia conglobata</i>			+	
Plantaginaceae				3. <i>propylaea</i> sp.			+	
148. <i>Plantago asiatica</i>	+	+	M	4. <i>illeis</i> sp.			+	
149. <i>Plantago depressa</i>	+		M	5. <i>Calvia</i> sp.			+	
150. <i>Veronica persica</i>		+	X	6. <i>Anisosticta kobensis</i>	+			
Scrophulariaceae				Scarabaeidae				
151. <i>Mazus japonicus</i>	+		M	7. <i>Gymnopleurus</i> sp.				
152. <i>Lindernia procumbens</i>	+		H	8. <i>Copris ochus</i>				
153. <i>Rehmannia glutinosa</i>	+		X	9. <i>Brahmina faldermanni</i>	+			
154. <i>Veronica anagallis-aquatica</i>	+		H	Cryptophagidae				
155. <i>Veronica peregrina</i>	+		M	10. <i>Atomaria lewisi</i>	+			
156. <i>Veronica didyma</i>	+	+	M	11. <i>Haptoncus</i> sp.	+			
Acanthaceae				12. <i>Cryptophagidae</i> sp.	+			
157. <i>Rostellularia procumbens</i>	+		M	Carabidae				
Lentibulariaceae				13. <i>Cicindela raleea</i>	+			
158. <i>Utricularia vulgaris</i>	+		M	14. <i>Carabus brandti</i>	+			
Cucurbitaceae				15. <i>Pheropsophus jessoensis</i>	+			
159. <i>Actinostemma tenerum</i>	+		M	16. <i>Chlaenius micans</i>	+			
160. <i>Cucumis bisexualis</i>	+		X	17. <i>Chlaenius</i> sp.	+			
Compositae				18. <i>Chlaenius spoliatus</i>	+			
161. <i>Artemisia carvifolia</i>	+		X	19. <i>Chlaenius naeviger</i>	+			
162. <i>Artemisia annua</i>	+		X	20. <i>Carabus granulatus</i>	+			
163. <i>Artemisia selengensis</i>	+		X	21. <i>Harpalus pallidipennis</i>	+			
164. <i>Artemisia argyi</i>	+		X	22. <i>Harpalus</i> sp.	+			
165. <i>Artemisia lavandulaefolia</i>	+		X	23. <i>Tachys</i> sp1.	+			
166. <i>Artemisia capillaris</i>	+		X	24. <i>Tachys</i> sp2.	+			
167. <i>Artemisia rubripes</i>	+		X	25. <i>Dolichus</i> sp.	+			
168. <i>Erigeron annuus</i>	+	+	X	26. <i>Dischissus</i> sp.	+			
169. <i>Aster subulatus</i>	+	+	M	27. <i>Calosoma chinense</i>	+			
170. <i>Bidens frondosa</i>	+	+	M	28. <i>Scarites</i> sp.	+			
171. <i>Bidens bipinnata</i>	+	+	X	<i>Carabus smaragdinus</i>	+			
172. <i>Bidens biternata</i>	+	+	M	29. <i>Calosoma lugens</i>	+			
173. <i>Bidens pilosa</i>	+		H	Curculionidae				
174. <i>Carpesium abrotanoides</i>	+		X	30. <i>Sympiezomias</i> sp.	+			
175. <i>Cirsium setosum</i>	+	+	M	31. <i>Phytoscaphus gossypii</i>				
176. <i>Conyza canadensis</i>	+	+	X	32. <i>Orchestes</i> sp.	+			
177. <i>Conyza bonariensis</i>	+	+	X	Chrysomelidae				
178. <i>Dendranthema lavandulifolium</i>	+		X	33. <i>Medythia nigrobilineata</i>	+			
179. <i>Eclipta prostrata</i>	+	+	H	34. <i>Psylliodes</i> sp.	+			
180. <i>Hemistepta lyrata</i>	+	+	M	35. <i>Chrysochus chinensis</i>	+			
181. <i>Inula japonica</i>	+	+	M	Dryopidae				
182. <i>Inula britannica</i>	+		M	36. <i>Praehelichus sericatus</i>	+			
183. <i>Kalimeris integrifolia</i>	+		M	Elateridae				
184. <i>Siegesbeckia orientalis</i>	+		M	37. <i>Pleonomus</i> sp.	+			
185. <i>Tripolium vulgare</i>	+		M	Anthicidae				
186. <i>Xanthium sibiricum</i>	+	+	M	38. <i>Stricticollis tobias</i>	+			
187. <i>Xanthium mongolicum</i>	+		M	Nitidulidae				
188. <i>Centipeda minima</i>	+		M	39. <i>Urophorus</i> sp.	+			
189. <i>Gnaphalium affine</i>	+		M	Lucanidae				
190. <i>Carduus crispus</i>	+		M	40. <i>Dorcus</i> sp.	+			
191. <i>Olgaea tangutica</i>	+		X	Scolytidae				
Cichorioideae				41. <i>Ips</i> sp.				
192. <i>Ixeridium chinense</i>	+	+	X	Histeridae				
193. <i>Ixeridium sonchifolium</i>	+		X	42. <i>Atholus depistor</i>	+			
194. <i>Ixeris polycephala</i>	+		X	43. <i>Atholus pirithous</i>	+			
195. <i>Mulgedium tataricum</i>	+		M	Mycetophagidae				

196. <i>Pterocypsela laciniata</i>	+	+	M	44. <i>Mycetophagus</i> sp.		+
197. <i>Pterocypsela formosana</i>	+		M	Staphylinidae		
198. <i>Sonchus oleraceus</i>	+	+	M	45. <i>Paederus fuscipes</i>	+	+
199. <i>Sonchus asper</i>	+		X	46. <i>Paederinae</i> sp1.	+	+
200. <i>Taraxacum mongolicum</i>	+	+	X	47. <i>Paederinae</i> sp2.	+	
201. <i>Youngia japonica</i>	+	+	M	48. <i>Stenus</i> sp.	+	
202. <i>Lactuca seriola</i>	+		M	49. <i>Steninae</i> sp.	+	+
Butomaceae				50. <i>Aleochara curtula</i>	+	+
203. <i>Butomus umbellatus</i>	+		A	51. <i>Phacophallus japonicus</i>	+	+
Hydrocharitaceae				52. <i>Anotylus latiusculus</i>	+	+
204. <i>Hydrocharis dubia</i>	+		A	53. <i>Staphylininae</i> sp1.	+	
205. <i>Hydrilla verticillata</i>	+		A	54. <i>Staphylininae</i> sp2.	+	+
Potamogetonaceae				55. <i>Scaphidinae</i> sp.	+	+
206. <i>Potamogeton crispus</i>	+		A	56. <i>Aleochara bilineata</i>	+	
207. <i>Potamogeton lucens</i>	+		A	57. <i>Aleocharinae</i> sp.	+	+
208. <i>Potamogeton malaianus</i>	+		A	Species list of spiders		
209. <i>Potamogeton pectinatus</i>	+		A	Species	MS	IS
Najadaceae				Lycosidae		
210. <i>Najas marina</i>	+		A	1. <i>Pardosa astrigera</i>	+	+
Araceae				2. <i>Pardosa</i> sp.	+	+
211. <i>Acorus calamus</i>	+		H	3. <i>Trochosa ruricola</i>	+	+
Lemnaceae				Linyphiidae		
212. <i>Spirodela polyrrhiza</i>	+		A	4. <i>Erigone prominens</i>	+	+
213. <i>Lemna minor</i>	+		A	5. <i>Ummeliata feminea</i>	+	+
Commelinaceae				6. Linyphiidae sp.	+	
214. <i>Commelina communis</i>	+		M	Araneidae		
215. <i>Commelina bengalensis</i>	+	+	M	7. <i>Araneus</i> sp.	+	+
Juncaceae				8. <i>Larinioides cornuta</i>	+	+
216. <i>Juncus taonanensis</i>	+		H	Gnaphosidae		
Cyperaceae				9. <i>Gnaphosa kansuensis</i>	+	+
217. <i>Carex raddei</i>	+		H	10. <i>Drassodes</i> sp.	+	+
218. <i>Carex neurocarpa</i>	+		H	11. Gnaphosidae sp.	+	
219. <i>Cyperus rotundus</i>	+	+	H	Clubionidae		
220. <i>Cyperus glomeratus</i>	+		A	12. <i>Clubiona</i> sp.	+	+
221. <i>Cyperus exaltatus</i>	+		H	Philodromidae		
222. <i>Cyperus microiria</i>	+	+	H	13. <i>Thanatus</i> sp.	+	
223. <i>Cyperus amuricus</i>	+		H	Thomisidae		
224. <i>Cyperus fuscus</i>	+		H	14. <i>Xysticus</i> sp.	+	+
225. <i>Cyperus nipponicus</i>	+		H	15. <i>Xysticus eohippiatus</i>	+	+
226. <i>Cyperus difformis</i>	+		H	Salticidae		
227. <i>Cyperus michelianus</i>	+		H	16. <i>Asianellus</i> sp.	+	
228. <i>Fimbristylis bisumbellata</i>	+		H	17. <i>Evarcha</i> sp.	+	
229. <i>Juncellus serotinus</i>	+		H			
230. <i>Pycreus sanguinolentus</i>	+		H			
231. <i>Pycreus globosus</i>	+		H			
232. <i>Scirpus planiculmis</i>	+		A			
233. <i>Scirpus triqueter</i>	+		A			
234. <i>Scirpus ehrenbergii</i>	+		A			
235. <i>Scirpus validus</i>	+		H			
Gramineae						
236. <i>Arthraxon hispidus</i>	+		X			
237. <i>Beckmannia syzigachne</i>	+		H			
238. <i>Bromus inermis</i>	+		X			
239. <i>Bromus japonicus</i>	+	+	M			
240. <i>Bothriochloa ischaemum</i>	+		X			
241. <i>Chloris virgata</i>	+		X			
242. <i>Cleistogenes chinensis</i>	+		X			
243. <i>Cynodon dactylon</i>	+	+	M			
244. <i>Digitaria sanguinalis</i>	+	+	X			
245. <i>Digitaria ischaemum</i>	+		X			
246. <i>Diplachne fusca</i>	+		H			

247. <i>Echinochloa crusgalli</i>	+	+	H		
248. <i>Echinochloa caudata</i>	+		H		
249. <i>Eleusine indica</i>	+	+	X		
250. <i>Eragrostis cilianensis</i>	+		X		
251. <i>Eragrostis Pilosa</i>	+		X		
252. <i>Eragrostis autumnalis</i>	+		X		
253. <i>Eriochloa villosa</i>	+		X		
254. <i>Hemarthria altissima</i>	+	+	M		
255. <i>Imperata cylindrica</i>	+	+	X		
256. <i>Leersia japonica</i>	+		H		
257. <i>Leptochloa panicea</i>	+		X		
258. <i>Leptochloa chinensis</i>	+		X		
259. <i>Paspalum paspaloides</i>	+		H		
260. <i>Phragmites australis</i>	+	+	H		
261. <i>Polypogon fugax</i>	+		H		
262. <i>Poa sphondylodes</i>	+		X		
263. <i>Setaria faberii</i>	+	+	X		
264. <i>Setaria viridis</i>	+	+	X		
265. <i>Themeda japonica</i>	+		X		
266. <i>Triarrhena sacchariflora</i>	+	+	X		
267. <i>Avena fatua</i>	+	+	X		
268. <i>Alopecurus aequalis</i>	+	+	M		
269. <i>Aegilops tauschii</i>	+	+	M		
270. <i>Roegneria japonensis</i>	+	+	M		
Typhaceae					
271. <i>Typha angustifolia</i>	+		A		
Dioscoreaceae					
272. <i>Dioscorea opposita</i>	+		M		

Abbreviations: WE, Water ecotypes (H, hygrophytic plant; A, aquatic plant; X, xerophytic plant; M, mesophytic plant); IUCN, IUCN Red List of Birds (EN, endangered; VU, vulnerable; NT, near threatened; LC, least concern; -, no assessment); Migration (R, resident bird; P, passing migrant birds; S, summer migratory bird; W, winter migratory bird)

ESTIMATION OF HERITABILITY AND GENETIC ADVANCE TO DEVELOP DROUGHT TOLERANCE IN COTTON (*GOSSYPIMUM HIRSUTUM* L.)

YAR, M. M.^{1*} – IQBAL, M.¹ – MEHMOOD, A.² – NAEEM, M.¹

¹Department of Plant Breeding & Genetics, University College of Agriculture & Environmental Sciences, The Islamia University of Bahawalpur, Bahawalpur, Pakistan

²Ayub Agricultural Research Institute, Faisalabad, Pakistan

*Corresponding author

e-mail: majidabbasi1998@gmail.com

(Received 3rd Dec 2019; accepted 22nd May 2020)

Abstract. Water scarcity is a major constraint to sustainable cotton production worldwide. Therefore, development of drought tolerant cotton varieties is the main objective of the cotton breeding program. A reduction has been observed in seed cotton yield in cotton plants under drought condition. To evaluate the genetic material under normal and drought conditions, three generations (18F₂, 18BC₁ and 18 BC₂), and two parents (6P₁ and 3P₂) were studied for heritability and genetic advance estimation. F₂, BC₁ and BC₂ populations were derived through cross combinations of nine parental varieties of upland cotton (*Gossypium hirsutum* L.). Data were recorded for plant height, number of monopodial branches per plant, number of sympodial branches per plant, number of bolls per plant, boll weight, seed cotton yield per plant, lint percentage and seed index. Heritability estimates ranged from low to high for all traits. Results represent that all studied traits can be improved easily due to high heritability values and phenotypic variations. IUB-09 × FH-1000 and BH-160 × MNH-129 had maximum broad sense, narrow sense heritability and genetic advance for various characters under drought conditions. These two crosses may further increase until later generation to develop drought tolerant cotton cultivars.

Keywords: broad sense heritability, narrow sense heritability, water deficit, seed cotton yield

Introduction

Cotton is the most important cash and fiber crop of global importance (Anderson and Rajasekaran, 2016), cultivated in tropical and subtropical areas of more than 60 different countries (Feng et al., 2017). Cotton crop has 0.8% share in GDP and gives 4.5% in value addition of agriculture. Better cotton genotypes are desirable to progress the cotton business although cotton yield, high ginning out turn (GOT) and fine fiber quality are these parameters affect cotton fiber price in the world market (Anonymous 2018-19).

Drought stress reduced the total plant stature up to 35%, decreased leaf area index caused 8% reduction in solar radiation interception (Pettigrew, 2004). Saranga et al. (1991) observed that the change in water potential explains 87% change in plant height. The whole phenomenon of drought stress and growth reduction affects total yield of the crop (Pettigrew, 2004; Babar et al., 2009). Boll development is the most critical stage in cotton which is affected by drought stress (Radin et al., 1992). Krieg (2000) mentioned the most critical period for drought stress, in terms of final yield, is from square initiation to first flower. Drought tolerance in cotton is a quantitatively genetically controlled trait (Ahmad et al., 2009). Cotton cultivars display variable genetic response for physiological and morphological parameters under water deficit environments (Hinze et al., 2012; Patil et al., 2017).

Heritability values provide information about extent of transmission of traits to subsequent generation and response to selection. High heritability represents greater selection response. Heritability estimates will help for effective selection, therefore traits selection on the base of high heritability makes the improvement easier. If environmental influence is small as compare to genetic differences, the selection will be more effective (Khan, 2001). Statistical parameters like mean, variance, genetic advance and heritability support in measuring genetic potential, genetic diversity and stability of any variety (Firouzian, 2003; Ali et al., 2008). Various cotton breeders studied heritability and genetic advance to evaluate hybrid population (Ahsan et al., 2015; Jarwar et al., 2018; Gnanasekaran et al., 2018; Nawaz et al., 2019; Riaz et al., 2019).

The aim of current study is to estimate variability and genetic parameters for yield and other agronomic traits and to investigate new sources of drought tolerance among the segregating populations. These estimates will help in effective selection for improvement of studied traits.

Materials and methods

The experimental work was conducted during the year 2018, at research area of Department of Plant Breeding & Genetics, University College Agriculture and Environmental Sciences, The Islamia University of Bahawalpur, Pakistan. Eighty (80) cotton genotypes were evaluated under drought stress at seedling stage by using root and shoot traits. From screening study, six drought tolerant (IUB-09, B-557, 149-F, BH-160, BH-118 and FH-900) and three drought susceptible (MNH-129, FH-1000 and FH-901) cotton genotypes were selected.

Next year, six drought tolerant (IUB-09, B-557, 149-F, BH-160, BH-118 and FH-900) and three drought susceptible (MNH-129, FH-1000 and FH-901) cotton genotypes were crossed in line \times tester (Kempthorne, 1957) scheme to develop 18 cross combinations. Total 27 experimental entries comprising of 9 parents (six lines and three testers) and their 18F₁ hybrids were sown. The experiment was performed in RCBD with 3 replications under normal and drought stress conditions.

Development of F₂, BC₁ and BC₂ generations

At maturity F₁ plants of eighteen crosses were selfed. These selfed seeds were picked individually as a source of F₂ generation. F₁ plants were crossed with 1st parent (P₁) of a specific cross to produce BC₁; in the same way they were also crossed with 2nd parent (P₂) male parent to produce BC₂ generations.

Evaluation of F₂, BC₁ and BC₂ generation

The seed of nine parents, 18 F₂, 18 BC₁ and 18 BC₂ were planted in field under split plot design. There were two factors i.e. generations and parents and water stress levels. Drought stress was developed after 30 days of sowing. During crop season, drought stress was imposed by supplying 50% less irrigations till crop maturity in the drought treatment (Kirda et al., 2005). The total irrigation water applied to well water and water-deficit condition was 24 acre inches and 12 acre inches respectively. The amount of rainfall, maximum and minimum temperature during the crop duration are given in *Table 1*. The normally irrigated plot was watered when required. For drought stressed plot, irrigation water was applied at critical growth stages of cotton plant i.e.

germination and emergence, seedling establishment, canopy development, flowering and boll setting. Water stress levels were applied to the main plots while parents and generations were allocated to the sub plots. Each entry was planted in row to row distance 75 cm whereas plant to plant distances were 30 cm.

Table 1. Monthly average temperature along with total rainfall at experimental site

Month	Tmax (°C)	Tmin (°C)	Rainfall (mm)
April	37	22.4	3.05
May	39.3	26.1	8.13
June	39.8	29	18.8
July	38.3	28.9	56.9
August	37.2	28.4	10.93
September	36.2	25.8	0
October	33.6	19.6	0
November	27.5	14	0

Tmax = average maximum temperature; Tmin = average minimum temperature

All the cultural practices were adopted according to routine production technology except drought experiment. Data were recorded on individual plant basis for parents, BC₁, BC₂ and F₂ generations. For the parents and F₁, data were recorded on 10 randomly selected plants in each replication for each trait. For F₂ and backcross generations, data were recorded from 50 and 30 randomly selected plants respectively in each replication.

Data were recorded for Plant height (cm), Number of monopodial branches per plant, Number of sympodial branches per plant, Number of Bolls per Plant, Boll Weight (g), Seed cotton yield per plant (g), Lint Percentage, Seed index.

The obtained lint from each sample was weighed and lint percentage was calculated by using following formula:

$$\text{Lint percentage (\%)} = \frac{\text{Weight of lint}}{\text{weight of seed cotton}} \times 100 \quad (\text{Eq.1})$$

To calculate the seed index, 100 seeds were taken at random for each sample and weighed in gram.

Statistical analysis

Heritability and genetic advance

Broad sense heritability was computed as described by Mahmud and Kramer (1951).

$$H^2_{(BS)} = \frac{VF_2 - \sqrt{VP_1 \times VP_2}}{VF_2} \times 100 \quad (\text{Eq.2})$$

where: H^2_{BS} = broad sense heritability; VF_2 = variance of F₂ population; VP_1 = variance of Parent 1; VP_2 = variance of parent 2.

Heritability in narrow sense were computed using the following formula suggested by warner (1952).

$$H^2_{(n.s)} = \frac{2VF_2 - (VBC_1 + VBC_2)}{VF_2} \times 100 \quad (\text{Eq.3})$$

where: $H^2_{(n.s)}$ = heritability in narrow sense; VF_2 = variance of F_2 population, VBC_1 = variance of back cross-I population, VBC_2 = variance of back cross-II population.

Genetic advance was calculated by following formula suggested by Allard (1960).

$$G.A = \sigma \rho \times h^2 \times I \quad (\text{Eq.4})$$

where: GA = genetic advance; $\sigma \rho$ = phenotypic standard deviation of F_2 population; h^2 = estimation of broad sense heritability in fraction, I = constant value that reflects the selection intensity. The value of I = 1.755 in this study the selection pressure is 10%.

Results

Heritability and genetic advance

Heritability and genetic advance are remarkable selection parameters. Heritability and genetic advance predict the genetic gain for selection (Johanson et al., 1955). Heritability and genetic advance for different yield traits are as follows.

Plant height

Under normal condition, broad sense heritability estimates were ranged from 45.77% (BH-118 × MNH-129) to 93.13% (IUB-09 × FH-1000). Heritability values in narrow sense were ranged from 20.79% (FH-900 × FH-1000) to 73.45% (IUB-09 × FH-1000). Genetic advance values were ranged from 2.13 (BH-118 × FH-901) to 11.25 (IUB-09 × FH-1000). Under drought condition, broad sense heritability values were ranged from 35.59% (BH-118 × FH-901) to 94.06% (IUB-09 × FH-1000). Heritability values in narrow sense were ranged from 17.82% (149F × MNH-129) to 68.51% (IUB-09 × FH-1000). Genetic advance values were ranged from 1.08 (BH-118 × FH-901) to 9.24 (IUB-09 × FH-1000) (Table 2).

Table 2. Heritability (broad and narrow sense) and genetic advance for plant height under normal and drought conditions

Crosses	Normal condition			Drought condition		
	H^2_{bs}	H^2_{ns}	G.A.	H^2_{bs}	H^2_{ns}	G.A.
B-557 × MNH-129	65.58	37.05	4.02	66.75	40.34	3.05
B-557 × FH-1000	64.88	38.16	3.74	58.82	39.61	2.45
B-557 × FH-901	54.23	41.40	2.57	60.44	21.04	2.46
149F × MNH-129	50.52	45.34	2.62	72.35	17.82	3.34
149F × FH-1000	53.28	48.85	2.70	63.37	48.14	2.57
149F × FH-901	69.03	23.75	4.04	72.81	54.24	3.30
BH-160 × MNH-129	64.57	38.97	3.42	76.53	25.35	3.50
BH-160 × FH-1000	63.76	39.69	3.17	75.68	25.75	3.44
BH-160 × FH-901	92.34	61.69	9.40	93.71	62.05	8.06
IUB-09 × MNH-129	68.03	34.64	4.01	76.30	24.78	3.71

IUB-09 × FH-1000	93.13	73.45	11.25	94.06	68.51	9.24
IUB-09 × FH-901	59.15	39.74	2.75	65.66	36.08	2.58
BH-118 × MNH-129	45.77	45.34	2.27	68.04	25.09	3.01
BH-118 × FH-1000	51.88	33.57	2.60	49.01	29.74	1.74
BH-118 × FH-901	47.31	36.30	2.13	35.59	27.66	1.08
FH-900 × MNH-129	66.54	48.14	3.99	52.07	31.00	1.93
FH-900 × FH-1000	52.16	20.79	2.48	49.71	43.00	1.82
FH-900 × FH-901	60.24	22.28	2.96	54.65	41.59	2.03

Var = variance, H^2_{bs} = broad sense heritability, H^2_{ns} = narrow sense heritability, G.A. = genetic advance

Number of monopodial branches per plant

Broad sense heritability estimates were ranged from 42.09% (B-557 × MNH-129) to 77% (IUB-09 × FH-1000). Heritability values in narrow sense were ranged from 18.10% (FH-900 × MNH-129) to 73.80% (IUB-09 × FH-1000). The genetic advance values were ranged from 0.43 (BH-160 × FH-1000) to 1.10 (FH-900 × FH-1000) under normal condition. Under drought condition, broad sense heritability estimates were ranged from 49.58% (BH-160 × FH-901) to 78.12% (IUB-09 × FH-1000). Heritability values in narrow sense were ranged from 13.56% (B-557 × FH-1000) to 74.25% (IUB-09 × FH-1000). The genetic advance values were ranged from 0.50 (FH-900 × FH-1000) to 1.15 (IUB-09 × FH-1000) (Table 3).

Table 3. Heritability (broad and narrow sense) and genetic advance for monopodial branches per plant under normal and drought conditions

Crosses	Normal condition			Drought condition		
	H^2_{bs}	H^2_{ns}	G.A.	H^2_{bs}	H^2_{ns}	G.A.
B-557 × MNH-129	42.09	30.73	0.48	59.84	31.42	0.67
B-557 × FH-1000	50.55	29.17	0.54	60.98	13.56	0.73
B-557 × FH-901	51.54	38.13	0.58	54.84	26.29	0.72
149F × MNH-129	58.10	37.42	0.72	60.24	35.73	0.65
149F × FH-1000	57.03	34.37	0.60	64.29	20.04	0.77
149F × FH-901	50.28	36.25	0.52	56.54	25.11	0.72
BH-160 × MNH-129	55.27	28.28	0.59	68.18	21.97	0.85
BH-160 × FH-1000	49.76	38.00	0.43	65.80	24.62	0.83
BH-160 × FH-901	64.76	27.14	0.70	49.58	25.39	0.61
IUB-09 × MNH-129	66.87	64.67	0.92	73.15	66.94	0.92
IUB-09 × FH-1000	77.00	73.80	1.10	78.12	74.25	1.15
IUB-09 × FH-901	57.00	34.02	0.63	51.17	14.23	0.59
BH-118 × MNH-129	54.10	28.74	0.67	65.87	15.16	0.75
BH-118 × FH-1000	57.96	31.97	0.65	61.95	28.34	0.71
BH-118 × FH-901	45.15	36.09	0.46	59.94	20.89	0.79
FH-900 × MNH-129	48.78	18.10	0.60	67.67	27.86	0.72
FH-900 × FH-1000	66.05	27.65	0.86	53.58	15.50	0.50
FH-900 × FH-901	60.51	26.44	0.76	63.02	16.56	0.78

H^2_{bs} = broad sense heritability, H^2_{ns} = narrow sense heritability, G.A. = genetic advance

Number of sympodial branches per plant

Under normal condition, broad sense heritability estimates were ranged from 46.26% (149F × FH-1000) to 90.49% (IUB-09 × FH-1000). Heritability values in narrow sense were ranged from 10.29% (B-557 × FH-1000) to 78.36% (BH-118 × FH-1000). The genetic advance values were ranged from 1.77 (149F × FH-1000) to 8.89 (IUB-09 × FH-1000). Under drought condition, broad sense heritability estimates were ranged from 49.36% (FH-900 × FH-901) to 86.81% (IUB-09 × FH-1000). Heritability values in narrow sense were ranged from 12.70 (BH-160 × FH-1000) to 81.52% (IUB-09 × FH-1000). The genetic advance values were ranged from 1.89 (FH-900 × FH-901) to 6.64 (IUB-09 × FH-1000) (Table 4).

Table 4. Heritability (broad and narrow sense) and genetic advance for number of sympodial branches per plant under normal and drought conditions

Crosses	Normal condition			Drought condition		
	H ² _{bs}	H ² _{ns}	G.A.	H ² _{bs}	H ² _{ns}	G.A.
B-557 × MNH-129	65.16	14.49	3.14	68.13	18.27	3.18
B-557 × FH-1000	57.31	10.29	2.56	64.27	29.79	3.32
B-557 × FH-901	61.79	16.71	2.67	57.44	20.35	2.32
149F × MNH-129	54.92	13.11	2.24	64.35	13.59	3.21
149F × FH-1000	46.26	24.24	1.77	59.97	19.37	3.31
149F × FH-901	55.24	25.27	2.12	62.63	22.61	3.05
BH-160 × MNH-129	61.07	23.61	3.25	71.86	22.51	3.25
BH-160 × FH-1000	46.44	20.78	2.16	58.18	12.70	2.53
BH-160 × FH-901	57.58	15.69	2.76	62.46	26.96	2.45
IUB-09 × MNH-129	52.64	24.25	2.26	66.40	24.48	2.71
IUB-09 × FH-1000	90.49	67.09	8.89	86.81	81.52	6.64
IUB-09 × FH-901	49.53	18.52	1.94	69.25	22.46	2.96
BH-118 × MNH-129	54.36	31.63	2.37	60.70	21.20	2.50
BH-118 × FH-1000	89.58	78.36	8.35	82.92	71.08	6.08
BH-118 × FH-901	65.19	24.95	3.05	62.78	15.68	2.66
FH-900 × MNH-129	74.04	20.88	4.82	53.47	21.66	2.14
FH-900 × FH-1000	52.48	25.98	2.59	58.93	20.31	2.95
FH-900 × FH-901	48.52	24.25	2.11	49.36	19.65	1.89

H²_{bs} = broad sense heritability, H²_{ns} = narrow sense heritability, G.A. = genetic advance

Number of bolls per plant

Under normal condition, broad sense heritability values were ranged from 43.53% (BH-118 × MNH-129) to 82.68% (IUB-09 × FH-1000). Heritability values in narrow sense were ranged from 10.59% (FH-900 × FH-1000) to 75.23% (IUB-09 × FH-1000). The genetic advance values were ranged from 4.57 (BH-160 × FH-1000) to 12.76 (IUB-09 × FH-1000). Under drought condition, broad sense heritability values were ranged from 49.53% (FH-900 × FH-1000) to 81.12% (IUB-09 × FH-1000). Heritability values in narrow sense were ranged from 11.96% (FH-900 × FH-901) to 82.03% (IUB-09 × FH-1000). The genetic advance values were ranged from 3.54 (FH-900 × FH-1000) to 11.23 (IUB-09 × FH-1000) (Table 5).

Table 5. Heritability (broad and narrow sense) and genetic advance for number of bolls per plant under normal and drought conditions

Crosses	Normal condition			Drought condition		
	H ² _{bs}	H ² _{ns}	G.A.	H ² _{bs}	H ² _{ns}	G.A.
B-557 × MNH-129	60.69	14.11	7.54	77.54	19.58	7.56
B-557 × FH-1000	66.23	17.65	8.03	64.35	12.00	5.48
B-557 × FH-901	62.69	42.93	6.60	66.28	30.79	5.66
149F × MNH-129	58.99	11.30	7.29	63.60	25.70	5.35
149F × FH-1000	46.86	13.32	4.60	51.55	24.56	4.14
149F × FH-901	53.63	48.12	5.15	50.63	15.40	3.93
BH-160 × MNH-129	72.67	63.63	9.82	73.40	60.87	6.54
BH-160 × FH-1000	50.42	15.56	4.57	65.16	20.38	5.58
BH-160 × FH-901	55.29	11.48	4.82	57.43	23.33	4.34
IUB-09 × MNH-129	52.07	21.28	5.34	59.56	29.61	5.12
IUB-09 × FH-1000	82.68	75.23	12.76	81.12	82.03	11.23
IUB-09 × FH-901	58.62	12.32	5.34	56.94	24.26	5.09
BH-118 × MNH-129	43.53	29.34	4.98	55.36	19.75	4.19
BH-118 × FH-1000	66.97	23.66	9.06	62.18	30.28	5.62
BH-118 × FH-901	55.17	41.88	5.85	50.55	12.08	3.90
FH-900 × MNH-129	52.43	16.20	6.64	66.44	14.79	5.30
FH-900 × FH-1000	48.45	10.59	5.33	49.53	17.38	3.54
FH-900 × FH-901	55.63	20.58	6.02	56.02	11.96	4.19

H²_{bs} = broad sense heritability, H²_{ns} = narrow sense heritability, G.A. = genetic advance

Boll weight

Under normal condition, the heritability values in broad sense were ranged from 45.59% (149F × FH-1000) to 78.11% (BH-160 × FH-901). Heritability values in narrow sense were ranged from 9.67% (FH-900 × FH-901) to 64.04% (IUB-09 × FH-1000). The genetic advance values were ranged from 0.55 (BH-118 × MNH-129) to 1.61 (IUB-09 × FH-1000). Under drought condition, broad sense heritability values were ranged from 28.26% (FH-900 × FH-1000) to 71.97% (B-557 × MNH-129). Under drought condition, heritability values in narrow sense were ranged from 10.12% (IUB-09 × FH-901) to 65.75% (B-557 × MNH-129). The genetic advance values were ranged from 0.37 (FH-900 × FH-1000) to 1.50 (B-557 × MNH-129) (Table 6).

Seed index

Under normal condition, broad sense heritability values were ranged from 44.06% (149F × FH-1000) to 79.32% (IUB-09 × FH-1000). Heritability values in narrow sense were ranged from 10.24% (FH-900 × MNH-129) to 72.14% (IUB-09 × FH-1000). The genetic advance values were ranged from 0.96 (BH-118 × FH-1000) to 2.86 (IUB-09 × FH-1000). Under drought condition, broad sense heritability values were ranged from 51.90% (B-557 × MNH-129) to 81.15% (IUB-09 × FH-1000). Heritability values in narrow sense were ranged from 10.15% (IUB-09 × FH-901) to 75.30% (IUB-09 × FH-1000). The genetic advance values were ranged from 0.67 (B-557 × FH-1000) to 2.23 (IUB-09 × FH-1000) (Table 7).

Table 6. Heritability (broad and narrow sense) and genetic advance for boll weight under normal and drought conditions

Crosses	Normal condition			Drought condition		
	H ² _{bs}	H ² _{ns}	G.A.	H ² _{bs}	H ² _{ns}	G.A.
B-557 × MNH-129	76.07	61.02	1.47	71.97	65.75	1.50
B-557 × FH-1000	49.69	14.38	0.78	51.62	16.68	0.88
B-557 × FH-901	53.22	25.38	0.58	50.61	16.53	0.80
149F × MNH-129	55.35	31.13	0.97	52.73	21.39	0.80
149F × FH-1000	45.59	25.33	0.85	58.07	10.80	1.01
149F × FH-901	55.90	34.54	0.77	55.98	12.68	0.88
BH-160 × MNH-129	48.13	14.59	0.56	54.21	16.99	0.76
BH-160 × FH-1000	59.53	15.62	0.93	52.72	17.24	0.78
BH-160 × FH-901	78.11	34.02	1.10	55.07	43.11	0.78
IUB-09 × MNH-129	49.00	41.00	0.67	52.96	20.31	0.82
IUB-09 × FH-1000	72.84	64.04	1.61	69.06	60.07	1.42
IUB-09 × FH-901	52.96	25.09	0.59	50.70	10.12	0.77
BH-118 × MNH-129	46.96	14.11	0.55	51.11	10.94	0.81
BH-118 × FH-1000	55.21	29.11	0.83	52.23	11.75	0.90
BH-118 × FH-901	67.22	15.88	0.78	51.41	11.85	0.82
FH-900 × MNH-129	51.62	12.86	0.62	51.74	19.42	0.76
FH-900 × FH-1000	48.50	11.20	0.67	28.26	11.09	0.37
FH-900 × FH-901	67.54	9.67	0.78	49.81	10.48	0.72

H²_{bs} = broad sense heritability, H²_{ns} = narrow sense heritability, G.A. = genetic advance

Table 7. Heritability (broad and narrow sense) and genetic advance for seed index under normal and drought conditions

Crosses	Normal condition			Drought condition		
	H ² _{bs}	H ² _{ns}	G.A.	H ² _{bs}	H ² _{ns}	G.A.
B-557 × MNH-129	61.73	15.16	1.46	51.90	18.79	0.69
B-557 × FH-1000	52.47	13.54	1.11	53.04	11.51	0.67
B-557 × FH-901	51.36	15.85	1.15	56.64	18.79	0.68
149F × MNH-129	50.62	11.10	1.27	54.92	14.76	0.85
149F × FH-1000	44.06	12.78	1.04	62.78	12.99	0.99
149F × FH-901	49.86	14.36	1.32	57.76	16.35	0.79
BH-160 × MNH-129	51.77	11.38	1.29	67.76	13.50	1.16
BH-160 × FH-1000	50.07	17.68	1.22	77.39	70.81	1.47
BH-160 × FH-901	49.09	14.33	1.27	75.24	10.66	1.26
IUB-09 × MNH-129	54.33	12.14	1.32	55.95	17.49	1.08
IUB-09 × FH-1000	79.32	72.14	2.86	81.15	75.30	2.23
IUB-09 × FH-901	66.96	60.51	2.04	62.71	10.15	1.13
BH-118 × MNH-129	50.97	26.37	1.11	55.41	10.23	0.77
BH-118 × FH-1000	46.19	15.12	0.96	66.90	18.97	1.01
BH-118 × FH-901	48.52	18.31	1.10	58.21	22.61	0.72
FH-900 × MNH-129	47.21	10.24	1.11	54.93	19.33	0.86
FH-900 × FH-1000	50.66	19.13	1.23	59.42	21.49	0.91
FH-900 × FH-901	45.61	11.80	1.12	72.42	16.51	1.24

H²_{bs} = broad sense heritability, H²_{ns} = narrow sense heritability, G.A. = genetic advance

Seed cotton yield per plant

Under normal condition, broad sense heritability values were ranged from 56.54% (BH-160 × MNH-129) to 76.07% (IUB-09 × FH-1000). Heritability values in narrow sense were ranged from 11.10% (B-557 × FH-1000) to 62.21% (IUB-09 × FH-1000). Genetic advance values were ranged from 10.38 (BH-160 × MNH-129) to 18.79 (IUB-09 × FH-1000). Under drought stress condition, broad sense heritability values were ranged from 54.70% (B-557 × MNH-129) to 80.33% (IUB-09 × FH-1000). Heritability values in narrow sense were ranged from 11.34% (BH-118 × MNH-129) to 77.24% (IUB-09 × FH-1000). Genetic advance values were ranged from 8.73 (BH-118 × FH-901) to 19.34 (IUB-09 × FH-1000) (Table 8).

Table 8. Heritability (broad and narrow sense) and genetic advance for seed cotton yield per plant under normal and drought conditions

Crosses	Normal condition			Drought condition		
	H ² _{bs}	H ² _{ns}	G.A.	H ² _{bs}	H ² _{ns}	G.A.
B-557 × MNH-129	60.02	21.43	11.07	54.70	22.20	9.03
B-557 × FH-1000	56.91	11.10	10.41	61.80	18.47	10.74
B-557 × FH-901	61.75	13.61	11.57	70.59	24.22	13.88
149F × MNH-129	58.72	16.52	11.56	65.38	26.10	12.23
149F × FH-1000	60.95	16.82	12.70	69.73	20.49	13.49
149F × FH-901	64.07	17.88	13.43	72.87	23.52	14.78
BH-160 × MNH-129	56.54	18.20	10.38	75.69	15.64	15.63
BH-160 × FH-1000	68.11	61.36	15.02	77.97	70.19	16.35
BH-160 × FH-901	67.59	18.23	14.27	64.81	16.43	10.68
IUB-09 × MNH-129	65.90	18.67	13.25	64.89	14.80	12.10
IUB-09 × FH-1000	76.07	62.21	18.79	80.33	77.24	19.34
IUB-09 × FH-901	68.30	58.91	14.14	73.82	69.61	15.29
BH-118 × MNH-129	57.57	18.20	11.42	66.35	11.34	12.26
BH-118 × FH-1000	56.65	11.54	11.45	62.05	26.19	10.44
BH-118 × FH-901	59.32	28.61	11.94	56.16	19.71	8.73
FH-900 × MNH-129	66.49	17.58	11.67	63.09	13.68	12.05
FH-900 × FH-1000	68.12	13.28	12.62	61.49	13.27	11.11
FH-900 × FH-901	64.23	15.18	10.84	57.73	19.73	9.89

H²_{bs} = broad sense heritability, H²_{ns} = narrow sense heritability, G.A. = genetic advance

Lint percentage

Under normal condition, broad sense heritability values were ranged from 35.91% (BH-160 × FH-901) to 72.85% (BH-160 × MNH-129). Heritability values in narrow sense were ranged from 10.06% (BH-160 × FH-1000) to 66.50% (IUB-09 × FH-1000). Genetic advance values were ranged from 0.84 (BH-160 × FH-901) to 2.90 (IUB-09 × FH-1000). Under drought condition, broad sense heritability values were ranged from 47.71% (IUB-09 × MNH-129) to 86.54% (BH-160 × MNH-129). Heritability values in narrow sense were ranged from 10.49% (BH-118 × MNH-129) to 82.07% (BH-160 × MNH-129). The genetic advance was ranged from 1.11 (BH-160 × FH-1000) to 3.55 (IUB-09 × FH-1000) (Table 9).

Table 9. Heritability (broad and narrow sense) and genetic advance for lint percentage under normal and drought conditions

Crosses	Normal condition			Drought condition		
	H ² _{bs}	H ² _{ns}	G.A.	H ² _{bs}	H ² _{ns}	G.A.
B-557 × MNH-129	59.19	11.54	1.81	66.38	11.85	2.01
B-557 × FH-1000	49.54	14.58	1.65	58.95	16.31	1.58
B-557 × FH-901	52.74	30.10	1.58	48.70	12.00	1.32
149F × MNH-129	53.07	17.43	1.51	58.85	13.10	1.89
149F × FH-1000	60.43	11.49	2.26	64.92	17.57	2.20
149F × FH-901	54.41	16.43	1.66	61.17	11.35	2.24
BH-160 × MNH-129	72.85	64.87	2.47	86.54	82.07	3.33
BH-160 × FH-1000	47.18	10.06	1.38	54.41	34.00	1.11
BH-160 × FH-901	35.91	15.19	0.84	64.65	13.52	1.70
IUB-09 × MNH-129	63.18	14.30	1.84	47.71	13.14	1.29
IUB-09 × FH-1000	71.93	66.50	2.90	80.89	69.04	3.55
IUB-09 × FH-901	58.64	14.41	1.70	63.60	11.29	2.29
BH-118 × MNH-129	59.50	14.22	1.95	67.47	10.49	1.81
BH-118 × FH-1000	54.36	10.87	2.03	69.68	15.03	1.89
BH-118 × FH-901	57.38	13.89	1.94	71.85	62.93	2.29
FH-900 × MNH-129	53.23	11.28	1.53	62.09	14.16	1.65
FH-900 × FH-1000	61.49	10.96	2.36	64.92	18.67	1.75
FH-900 × FH-901	62.76	14.91	2.14	57.03	28.35	1.57

H²_{bs} = broad sense heritability, H²_{ns} = narrow sense heritability, G.A. = genetic advance

Discussion

Drought is the most significant abiotic stress manipulating the performance of crop plants. Therefore, screening for identification or development of tolerant varieties is of high importance for enhancing cotton production (Dahab et al., 2012). In order to achieve such evidence in *G. hirsutum*, 18 hybrids were assessed for growth and productivity characters under normal and drought conditions.

Genetic variation is valuable for permanent genetic improvement (Singh, 2000). Most of the crosses of plant height revealed high magnitude of broad sense heritability under normal and drought conditions. Generally moderate to high values of broad and narrow sense heritability exhibited that genetic effects were greater than influence of the environment and characters can be improved by selection (Bnejdi and Gazzah, 2008) while selection on the base of low heritability may be misleading due to more effect of environment on the genetic makeup (Nadarajan and Gunasekaran, 2005). Estimated narrow sense heritability and genetic advance differed for various hybrids under both conditions. Various crosses of plant height exhibited low to moderate narrow sense heritability in both conditions. Crosses with moderate heritability values are indicative of smaller environmental effects which recommends that improvement of the said traits can be easily improved through simple selection procedures (Noor et al., 2017). Batool et al. (2013) and Khan and Hassan (2011) also reported high and moderate heritability for plant height. Under both conditions, IUB-09 × FH-1000 and BH-160 × FH-901 exhibited maximum high broad sense heritability as well as high narrow sense

heritability and higher genetic advance for plant height showed that these crosses are controlled by additive genes and selection for these crosses would be valuable.

Most of the crosses of monopodial branches per plant revealed high magnitude of the broad sense heritability under normal and drought conditions. Estimated narrow sense heritability and genetic advance varied for various hybrids in both conditions. Ahmed et al. (2006) and Khan and Hassan (2011) reported high and moderate heritability for number of monopodial branches per plant. Under both conditions, IUB-09 × FH-1000 and IUB-09 × MNH-129 exhibited maximum high broad sense heritability as well as high narrow sense heritability and appreciable genetic advance for monopodial branches per plant, suggested that these crosses are controlled by additive genes and thus could lead to development of new genotype by the use of efficient selection techniques.

Most of the crosses of sympodial branches per plant exhibited moderate to higher broad sense heritability estimates. Various crosses exhibited low to moderate narrow sense heritability in both conditions. Low narrow sense heritability may be caused by low additive effects and high dominance gene action (Falconer and Mackay, 1996). Soomro et al. (2010) and Khan and Hassan (2011) reported high and moderate heritability values for sympodial branches per plant. Under both conditions, IUB-09 × FH-1000 and BH-118 × FH-1000 exhibited maximum high broad and narrow sense heritability and appreciable genetic advance for sympodial branches per plant showed that this cross is controlled by additive genes and selection for these crosses would be effective.

Most of the crosses for bolls per plant revealed high broad sense heritability under normal and drought conditions. Genetic advance and narrow sense heritability estimates varied for different crosses under both conditions. High heritability values with high genetic advance are highly effective in predicting gains under selection in the development of genotypes (Khan et al., 2015). Dhivya et al. (2014) and Ahsan et al. (2015) stated high and moderate heritability values for bolls per plant. Under both conditions, IUB-09 × FH-1000 and BH-160 × MNH-129 exhibited maximum high broad sense heritability as well as high narrow sense heritability and appreciable genetic advance for number of bolls per plant showed that these crosses are controlled by additive gene action and selection for these crosses would be valuable.

The low narrow sense heritability might be due to large epistatic effects (Hakizimana et al., 2004). The value of heritability alone does not provide any indication the amount of genetic progress that may lead to selection of best individual, but heritability with genetic advance are more useful (Mishra et al., 2015; Joshi and Patil, 2018). Genetic advance is also of great significance as it shows magnitude of the expected genetic gain from single cycle of selection (Hamdi et al., 2003). Most crosses of boll weight revealed high magnitude of the broad sense heritability under both conditions. Estimated genetic advance and narrow sense heritability differed for different hybrids under both conditions. Jarwar et al. (2018), Gnanasekaran et al. (2018) and Riaz et al. (2019) reported high and moderate heritability values for boll weight. Under both conditions, IUB-09 × FH-1000 and B-557 × MNH-129 exhibited maximum high broad sense heritability with high narrow sense heritability and higher genetic advance for boll weight showed that these crosses are controlled by additive gene action and selection for these crosses would be valuable.

Most of the crosses of seed index revealed high magnitude of broad sense heritability under normal and drought conditions. Estimated genetic advance and narrow sense heritability differed for different hybrids under both conditions. Shakeel et al. (2015),

Shao et al. (2016) and Jarwar et al. (2018) stated high and moderate heritability estimates for seed index. Under normal condition, IUB-09 × FH-1000 and IUB-09 × FH-901 whereas under drought condition, IUB-09 × FH-1000 and BH-160 × FH-1000 exhibited maximum high broad sense heritability with high narrow sense heritability and higher genetic advance for seed index showed that these crosses are controlled by additive gene action and selection for these crosses would be valuable.

Seed cotton yield per plant is determined from two basic traits i.e. boll number and boll weight. When drought stress occurs during the flowering stage, seed cotton yield decreases due to shedding of squares and young bolls (Cook and El-Zik, 1992). Higher estimates of heritability are not only useful in predicting gain under selection but also indicative of additive gene effects (Farooq et al., 2018). Various crosses of seed cotton yield per plant revealed high magnitude of broad sense heritability under both conditions. Genetic advance and narrow sense heritability differed for different hybrids under both conditions. Riaz et al. (2019) and Nawaz et al. (2019) reported high and moderate heritability estimates for seed cotton yield per plant. Under both conditions, IUB-09 × FH-1000, BH-160 × FH-1000 and IUB-09 × FH-901 exhibited maximum high broad sense heritability with high narrow sense heritability and higher genetic advance for seed cotton yield showed that these crosses are controlled by additive gene action and selection for these crosses would be valuable.

Most of the crosses of lint percentage revealed high magnitude of the broad sense heritability under both conditions. Estimated genetic advance and narrow sense heritability differed for each hybrid under both conditions. Most of the crosses of lint percentage exhibited low to moderate narrow sense heritability in both conditions. Dhamayanthi et al. (2018) and Nawaz et al. (2019) reported high and moderate heritability estimates for lint percentage. Under normal condition, IUB-09 × FH-1000 and BH-160 × MNH-129 whereas under drought condition, IUB-09 × FH-1000, BH-118 × FH-901 and BH-160 × MNH-129 exhibited maximum high broad sense heritability with high narrow sense heritability and higher genetic advance for lint percentage showed that these crosses are controlled by additive gene action and selection for these crosses would be valuable.

Conclusions

From heritability estimates, it is manifest that crosses i.e. IUB-09 × FH-1000 and BH-160 × MNH-129 exhibited high heritability ($H^2_{b,s}$) with high genetic advance for plant height, monopodial branches per plant, sympodial branches per plant, bolls per plant, boll weight, seed cotton yield per plant, lint percentage and seed index. It is therefore recommended that varieties involved in these promising hybrids should be given due consideration in further breeding program and selection for these traits could be practiced with due care to achieve desirable level of yield potential in cotton and the highest values of saving water at the same time. Furthermore, the progenies of these crosses may be raised till later generation to develop cotton drought tolerance cultivars.

REFERENCES

- [1] Ahmad, R. T., Malik, T. A., Khan, I. A., Jaskani, M. J. (2009): Genetic analysis of some morpho-physiological traits related to drought stress in cotton (*Gossypium hirsutum*). – International Journal of Agriculture and Biology 1: 235-240.

- [2] Ahmed, H. M., Kandhro, M. M., Laghari, S., Abro, S. (2006): Heritability and genetic advance as selection indicators for improvement in cotton (*Gossypium hirsutum* L.). – Journal of Biological Sciences 6: 96-99.
- [3] Ahsan, M. Z., Majidano, M. S., Bhutto, H., Soomro, A. W., Panhwar, F. H., Channa, A. R., Sial, K. B. (2015): Genetic variability, coefficient of variance, heritability and genetic advance of some *Gossypium hirsutum* L. accessions. – Journal of Agricultural Science 7(2): 147-151.
- [4] Ali, Y., Atta, B. M., Akhtar, J., Monneveux, P., Lateef, Z. (2008): Genetic variability, association and diversity studies in wheat (*Triticum aestivum* L.) germplasm. – Pakistan Journal of Botany 40(5): 2087-2097.
- [5] Allard, R. W. (1960): Principles of Plant Breeding. – John Wiley and Sons, Inc., New York.
- [6] Anderson, D. M., Rajasekaran, K. (2016): The Global Importance of Transgenic Cotton. – In: Ramawat, K. G., Ahuja, M. R. (eds.) Fiber Plants: Biology, Biotechnology and Applications. Springer International Publishing, Cham, pp. 17-33.
- [7] Anonymous (2018-19): Agricultural Statistics of Pakistan. – Government of Pakistan, Ministry of Food, Agriculture and Live Stock, Economic Wing, Islamabad.
- [8] Babar, M., Saranga, Y., Iqbal, Z., Arif, M., Zafar, Y., Lubbers, E., Chee, P. (2009): Identification of QTLs and impact of selection from various environments (dry vs irrigated) on the genetic relationships among the selected cotton lines from F6 population using a phylogenetic approach. – African Journal of Biotechnology 8: 4802-4810.
- [9] Batool, S., Khan, N. U., Gull, S., Baloch, M. J., Turi, N. A., Taran, S. A., Saeed, M. (2013): Genetic analysis for yield and yield contributing variables in upland cotton. – Journal of Food, Agriculture and Environment 11: 624-630.
- [10] Bnejdi, F., Gazzah, M. E. I. (2008): Inheritance of resistance to yellowberry in durum wheat. – Euphytica 163: 225-230.
- [11] Cook, C. G., El-Zik, K. M. (1992): Cotton seedling and first-bloom plant characteristics: relationships with drought-influenced boll abscission and lint yield. – Crop Science 32: 1464-1467.
- [12] Dahab, A. H. A., Mohamed, B. B., Husnain, T., Saeed, M. (2012): Variability for drought tolerance in cotton (*Gossypium hirsutum* L.) for growth and productivity traits using selection index. – African Journal of Agricultural Research 7(35): 4934-4942.
- [13] Dhamayanthi, K. P. M., Manivannan, A., Saravanan, M. (2018): Evaluation of new germplasm of Egyptian cotton (*G. barbadense*) through multivariate genetic component analysis. – Electronic Journal of Plant Breeding 9(4): 1348-1354.
- [14] Dhivya, R., Amalabalu, P., Pushpa, R., Kavithamani, D. (2014): Variability, heritability and genetic advance in upland cotton (*Gossypium hirsutum* L.). – African Journal of Plant Science 8(1): 1-5.
- [15] Falconer, D. S., Mackay, T. F. C. (1996): Introduction to Quantitative Genetics. 4th Ed. – Longman Group Limited, England.
- [16] Farooq, J., Rizwan, M., Saleem, S., Sharif, I., Chohan, S. M., Riaz, M., Ilhai, F., Kainth, R. A. (2018): Determination of genetic variation for earliness, yield and fiber traits in advance lines of cotton (*Gossypium hirsutum*). – Advances in Agricultural Science 6(2): 59-74.
- [17] Feng, L., Dai, J., Tian, L., Zhang, H., Li, W., Dong, H. (2017): Review of the technology for high yielding and efficient cotton cultivation in the northwest inland cotton-growing region of China. – Field Crops Research 208: 18-26.
- [18] Firouzian, A. (2003): Heritability and genetic advance of grain yield and its related traits in wheat. – Pakistan Journal of Biological Sciences 4(24): 2020-2023.
- [19] Gnanasekaran, M., Thiyagu, K., Gunasekaran, M. (2018): Genetic variability heritability and genetic advance studies in cotton (*Gossypium hirsutum* L.). – Electronic Journal of Plant Breeding 9(1): 377-382.

- [20] Hakizimana, F., Ibrahim, M. H., Langham, A. C., Rudd, C. J., Haley, D. S. (2004): Generation mean analysis of wheat streak mosaic virus resistance in winter wheat. – *Euphytica* 139: 133-139.
- [21] Hamdi, A., El-Ghareib, A. A., Shafey, S. A., Ibrahim, M. A. M. (2003): Genetic variability, heritability and expected genetic advance for earliness and seed yield from selection in lentil. – *Egyptian Journal of Agricultural Research* 81: 125-137.
- [22] Hinze, L. L., Dever, J. K., Percy, R. G. (2012): Molecular Variation among and within improved cultivars in the U.S. cotton germplasm collection. – *Crop Science* 52: 222-230.
- [23] Jarwar, A. H., Wang, X., Wang, L., Ma, Q., Fan, S. (2018): Genetic advancement, variability and heritability in upland cotton (*Gossypium hirsutum* L.). – *Journal of Environmental and Agricultural Sciences* 16: 24-31.
- [24] Johanson, H. W., Robinson, H. F., Comstock, R. E. (1955): Estimation of genetic and environmental variability in soybean. – *Agronomy Journal* 47: 314-318.
- [25] Joshi, V., Patil, B. R. (2018): Genetic variability and heritability study in F2 population for yield, yield attributes and fibre quality traits in cotton (*Gossypium hirsutum* L.). – *Journal of Pharmacognosy and Phytochemistry* 7(4): 2816-2818.
- [26] Kempthorne, O. (1957): *An Introduction to Genetic Statistics*. – John Wiley and Sons, Inc., New York.
- [27] Khan, M. A. (2001): Experimental design and analysis heritability estimation. – 2: 210-211.
- [28] Khan, N., Ullah, F., Khalil, I. H., Naheed, H., Abid, S. (2015): Heritability and genetic advance studies for biochemical traits in F2-3 introgressed families of brassica. – *Pakistan Journal of Botany* 47(3): 883-888.
- [29] Khan, N. U., Hassan, G. (2011): Genetic effects on morphological and yield traits in cotton (*Gossypium hirsutum* L.). – *Spanish Journal of Agricultural Research* 9(2): 460-472.
- [30] Kirda, C., Topeu, S., Kaman, H., Ulger, A. C., Yazici, A., Cetin, M., Derici, M. R. (2005): Grain yield response and nitrogen fertilizer recovery of maize under deficit irrigation. – *Photosynthetica* 19: 312-319.
- [31] Krieg, D. R. (2000): Cotton Water Relations. Special Report – In: Oosterhuis, D. M. (ed.) *Proc. Cotton Research Meeting and Summaries of Cotton Research*. Arkansas Agric. Exp. Sta., Fayetteville, AR.
- [32] Mahmud, I., Kramer, H. H. (1951): Segregation for yield, height and maturity following a soybean cross. – *Agronomy Journal* 43: 605-609.
- [33] Mishra, P. K., Ram, R. B., Kumar, N. (2015): Genetic variability, heritability, and genetic advance in strawberry (*Fragaria* × *ananassa* Duch.). – *Turkish Journal of Agriculture and Forestry* 39: 451-458.
- [34] Nadarajan, N., Gunasekaran, M. (2005): *Quantitative Genetics and Biometrical Techniques in Plant Breeding*. – Kalyani Publ., New Delhi.
- [35] Nawaz, B., Sattar, S., Malik, T. A. (2019): Genetic analysis of yield components and fiber quality parameters in upland cotton. – *International Multidisciplinary Research Journal* 9: 13-19.
- [36] Noor, M., Rahman, H. U., Iqbal, M. (2017): Heritability estimates for maturity and plant characteristics in popcorn. – *Sarhad Journal of Agriculture* 33(2): 276-281.
- [37] Patil, N. P., Salve, A. N., Adsare, A. D. (2017): Combining ability studies over environments for sucking pest and yield in upland cotton. – *Journal of Global Biosciences* 6(4): 4918-4934.
- [38] Pettigrew, W. T. (2004): Physiological consequences of moisture deficit stress in cotton. – *Crop Science* 44: 1265-1272.
- [39] Radin, J. W., Mauney, J. R., Reaves, L. L., French, O. F. (1992): Yield enhancement by frequent irrigation during fruiting. – *Agronomy Journal* 84: 551-557.

- [40] Riaz, B., Saeed, A., Fiaz, S., Riaz, A. (2019): Genetic diversity among Bt cotton (*Gossypium hirsutum* L.) germplasm assessed through morphological and within boll yield attributes. – Journal of Animal and Plant Sciences 29(1): 226-231.
- [41] Saranga, Y., Rudich, J., Marani, A. (1991): The relations between leaf water potential of cotton plants and environmental and plant factors. – Field Crops Research 28: 39-46.
- [42] Shakeel, A., Talib, I., Rashid, M., Saeed, A., Ziaf, K., Saleem, M. F. (2015): Genetic diversity among upland cotton genotypes for quality and yield related traits. – Pakistan Journal of Agricultural Sciences 52(1): 73-77.
- [43] Shao, D., Wang, T., Zhang, H., Zhu, J., Tang, F. (2016): Variation, heritability and association of yield, fiber and morphological traits in a near long staple upland cotton population. – Pakistan Journal of Botany 48(5): 1945-1949.
- [44] Singh, B. D. (2000): Plant Breeding: Principles and Methods. – Kalyani Publishers, New Delhi.
- [45] Soomro, Z. A., Kumbhar, M. B., Larik, A. S., Imran, M., Brohi, S. A. (2010): Heritability and selection response in segregating generations of upland cotton. – Pakistan Journal of Agricultural Research 23(1): 25-30.
- [46] Warner, J. N. (1952): A method for estimating heritability. – Agronomy Journal 44: 427-430.

LEAFCUTTER ANT REFUSE (*ATTA MEXICANA*) AS AN EXCELLENT COMPOST FOR TOMATO PRODUCTION

QUEVEDO-MARTÍNEZ, E. A. – ALCÁNTARA-MONDRAGÓN, E. – MEJÍA-UGALDE, M. – MEJÍA-UGALDE, I. – ÁVILA-JUÁREZ, L.*

Biosystems Laboratory Group, Division of Graduate Studies, Faculty of Engineering, Autonomous University of Querétaro, C.U. Cerro de las Campanas S/N, Colonia Las Campanas, 9 C.P. 76010, Santiago de Querétaro, Querétaro, México

*Corresponding author

e-mail: luciano.avila@uaq.mx; phone: +52-442-192-1200; fax: +52-442-192-1200 (ext. 6006)

(Received 5th Dec 2019; accepted 6th May 2020)

Abstract. For hundreds of years, leafcutter ants (*Atta spp.*) have been cultivating the fungus *Leucoagaricus gongylophorus*, which grows on foraged plant biomass and subsequently serves as food for the ants. Once the biomass nutrients are depleted, mainly due to enzymatic attack by the fungus, the ants discard what we label as leafcutter ant compost (LCAC). Here, we tested whether the LCAC behaved as a compost that is capable of releasing nutrients to grow greenhouse tomato plants. Our results indicate that *Atta spp.* together with *Leucoagaricus gongylophorus* produce a mature and stable compost with a high nutrient content that is able to nourish tomato crops at a dose of 32.5 t ha⁻¹. The LCAC significantly increased the organic matter content and permeability of the soil and provided soluble essential nutrients for the tomato plant, producing a yield that was not statistically different from that obtained with soluble inorganic salts without compromising the nutraceutical quality of the fruit. Our results suggest that LCAC resembles a stable compost, which immediately releases its nutrients to plants. *Atta spp.* play an important ecological role as they transport biomass across great distances, compost it and return it to the environment for use by neighbouring plants.

Keywords: ant compost, soluble nutrients, *Leucoagaricus gongylophorus*, biomass degradation, fungus garden

Introduction

Over millions of years, the ants of the genus *Atta* have developed a mutualistic relationship with the basidiomycete *Leucoagaricus gongylophorus* (Pagnocca et al., 2001; Silva-Pinhati et al., 2004), which is cultivated primarily on the leaves, stems and flowers of plant material that is located in specialized underground chambers of the ant nest (Sternberg et al., 2007). In these chambers, the basidiomycete is grown and subsequently develops hyphae that are harvested by the ants as food for themselves and their larvae (Mueller et al., 2001, 2005). Through a strict cleaning system, the workers produce symbiotic glandular and bacterial secretions to provide an aseptic environment that prevents the proliferation of parasitic fungi and unwanted microorganisms (Hölldobler and Wilson, 1990; Little et al., 2006). Through a complex process of plant material degradation, the fungus *Leucoagaricus gongylophorus* produces enzymes capable of degrading proteins, starch and the polysaccharides of the cell wall (Moller et al., 2011). In fact, metaproteomic analyses have identified 145 lignocellulosic enzymes, including pectinases, amylases and cellulases (Aylward et al., 2013). Once the process of decomposition and depletion of the plant material has elapsed, the worker ants dispose of it, depending on the genus, either in specialized internal waste chambers underground in the nest or, as in the genus *Atta*, by bringing the already decomposed material to the surface and piling it outside of the nest entrance. To obtain its food from

the plant material, *Leucoagaricus gongylophorus* penetrates the leaf with its hyphae, which causes the release of nutrients such as N, Ca, Mg and K (Moutinho et al., 2003; Saha et al., 2012), among others; this process may be derived from the decomposition of organic matter. Farji-Brener and Ghermandi (2008) analysed the waste from nests of *Acromyrmex lobicornis*, a species of foraging ant, and found acceptable levels of organic matter, N, P, K, Ca and Mg; the values were very similar to those of commercial compost. This finding is to be expected because the leaves are one of the largest reservoirs of nutrients in the plant.

Within the underground waste chamber where plant matter decomposes in the nest, at a certain humidity and temperature that is currently unknown, the process of aerobic decomposition is very similar to the process known as “composting”. The ants use these chambers as continuous bioreactors of plant matter, as they feed new substrate to the bioreactor (the “fungal garden”) in the upper part of the chamber where the fresh plant material is found, and they remove the digested plant material that is commonly found in the stratum below the fungal garden. This has been confirmed by studies of enzymatic activity of the waste from above, in the middle of and at the bottom of a fungal garden (Bot et al., 2001; Hart, 2002; Moller et al., 2011; Schiøtt et al., 2008). Similar to the composting process, the ants take on average of two or three months to discard the plant material that is no longer used in the bioreactor. This has been confirmed using N:¹⁵N isotope ratios in the leaves collected from *A. colombica* (Sternberg et al., 2007). However, there are reports showing that the degraded plant material not used for the fungal garden takes four to six weeks to be removed (Aylward et al., 2013).

As in the fungal garden bioreactor, the composting process is the controlled aerobic decomposition of organic wastes through the involvement of mesophilic and thermophilic organisms, which generate a waste residue that can be used as an organic amendment (Körner et al., 2003). However, unlike the well-characterized microorganisms in compost, the contribution of many of the microorganisms that break down plant biomass in the fungal garden bioreactor is not clear, except for the basidiomycete *Leucoagaricus gongylophorus* (Pagnocca et al., 2001; Silva-Pinhati et al., 2004). The working hypothesis is that the plant material collected by the foraging ants is composted and initially attacked by the arsenal of enzymes of the fungus *Leucoagaricus gongylophorus*, which confers the capacity to release nutrients that satisfy the demands of a plant. The objective of this work was to determine the effect of *Atta mexicana* ant waste on the growth of tomato plants and on the soil characteristics under greenhouse conditions.

Materials and methods

Collection and physical and chemical characterization of ant compost

Leafcutter ant compost (LCAC) from *Atta mexicana* was collected in May 2017 in the vicinity of their nests (20°22'54.9"N, 100°04'46.7"W) and then held in plastic bags until use (Fig. 1A). An LCAC sample was analysed to make the following determinations: total nitrogen (N) was measured using the Dumas method; and potassium (K₂O), calcium (Ca), magnesium (Mg), sodium (Na), iron (Fe), copper (Cu), manganese (Mn), phosphorus (P₂O₅), boron (B) and zinc (Zn) were analysed by spectrometry (Model ICP-iCAP 7000; Thermo Scientific, Massachusetts, USA) following wet digestion (Model Mars 6; CEM, North Carolina, USA) of the material.

Sulfur (S) was determined by wet digestion (Model Mars 6; CEM, North Carolina, USA) with the turbidimetric method. The electrical conductivity (EC) and pH were determined following the Mexican Standard NMX-FF-109-SCFI-2007 using a pH meter (Model; PC18, Conductronic, Puebla, Mexico). The moisture content was evaluated using the gravimetric method. The ash and organic content were measured after calcination. The organic carbon content was calculated as a percentage of the original material, whereas the C/N ratio was determined on a dry weight basis.



Figure 1. Ant compost (LCAC) application. A) Leaf-cutting ants and their refuse deposits, B) LCAC application at different doses, C) plants growing in the greenhouse

Plant material, cultivation conditions and treatments

The experiment was conducted in a greenhouse with lateral and zenithal ventilation at temperatures of 15 to 27 °C, a relative humidity of 45 to 90% and a maximum of 933 W m⁻². The study was carried out in Queretaro, Mexico (20°35'28"N, 100°24'36"W). The LCAC was mixed homogeneously into the soil at a working depth of 30 cm (Fig. 1B). The dose used was calculated based on the nitrogen content contained in the LCAC and the N requirement of a tomato plant. Thus, for the first treatment, 15.04 g of N per plant was added, which is equivalent to 0.792 kg of LCAC (Tlow); for the second treatment, 24.70 g of N was mixed per plant, which is equivalent to 1.3 kg of LCAC (Tmed); and for the third treatment, 34.96 g of N (1.84 kg of LCAC) was added per plant (Thigh). A fourth treatment without LCAC was used as a control, but a universal nutrient solution (Steiner, 1984) was used to nourish the plants (Tcontrol). The universal solution contained the following components (mg L⁻¹): N (167), P (31), K (277), Mg (49), Ca (183), S (111), Fe (1.33), Mn (0.62), B (0.44), Cu (0.02), Zn (0.11) and Mo (0.048). The pH was adjusted to 5.8 using a pH meter (Model; PC18, Conductronic, Puebla, Mexico). The EC was managed according to the phenological stage of the crop using the method of Ávila-Juárez et al. (2015) using a conductivity meter (Model; PC18, Conductronic, Puebla, Mexico). Tomato seeds (*Solanum lycopersicum* L. cv. Cid) from Harris Moran were planted in polystyrene germination trays with 200 cavities with peat moss and placed in a germination chamber (80% RH, 25 °C) until germination. After the plants sprouted, they were transplanted to a density of 2.5 plants m⁻² in soil with the characteristics listed in Table 2 ("soil before"). The amount of water supplied to the plants was activated by a tensiometer at

20 centibars placed in each treatment. The experimental design was completely randomized with four treatments, six replicates and an experimental unit of three plants.

Determinations in plants and soil

Plant growth (16 plants per treatment: *Fig. 1C*) was measured at 25 (flowering phase), 57, 95 (fruiting phase) and 123 (senescence phase) days after transplant (DAT). The total yield was also measured. Once the experiment was completed, the degree of soil compaction (in kPa) at 0.08, 0.15 and 0.30 m was determined with a soil penetrometer (Spectrum Inc., USA). Samples were taken from 0 to 0.30 m in depth to determine the following physical properties: saturation (SAT), field capacity (FC), wilting point (WP), hydraulic conductivity (HC), bulk density (BD), cation exchange capacity (CEC) and EC (Model; PC18, Conductronic, Puebla, Mexico). In addition, the following chemical properties were determined: organic matter (OM), inorganic nitrogen (IN), total P, K, Ca, Mg, Na, Fe, Zn, Mn, Cu, B, S and pH. The IN was measured using the Dumas method. The EC and pH values (Model; PC18, Conductronic, Puebla, Mexico) were determined following the Mexican Standard NMX-FF-109-SCFI-2007. The resulting elements K, Ca, Mg, Na, Fe, Cu, Mn, P, B and Zn were analysed by spectrometry (Model ICP-iCAP 7000; Thermo Scientific, Massachusetts, USA) after wet digestion (Model Mars 6; CEM, North Carolina, USA) of the material.

Quantification of total phenols and flavonoids in tomato fruit

The tomato samples (16 fruits from 16 plants per treatment) were homogenized with a dispersing instrument (Ultra Turrax) for 1 min and protected from light with aluminium foil. The homogenized sample (100 mg) was extracted with 2 ml of a methanol:water:formic acid 80:18:2 v/v solution, and the solution was then vortexed for 30 s. The sample was sonicated for 30 s before being centrifuged at 14,000 rpm for 15 min at 4 °C. The supernatant was recovered and filtered with a 0.20 µm filter and held in the dark at -20 °C until analysis. The phenols were extracted using the Folin-Ciocalteu colorimetric method according to Dewanto et al. (2002). Briefly, the tomato extracts (30 µL) were diluted with 460 µL of distilled water. Then, 150 µL of Folin-Ciocalteu solution was added to each sample. Subsequently, samples were mixed and allowed to stand for 10 min before adding 120 µL of a 20% sodium carbonate aqueous solution. Afterwards, the samples were left to stand for 120 min in complete darkness at room temperature. The samples were read at 765 nm against a blank using a MULTISKAN GO microplate spectrophotometer (Model 51119300; Thermo Scientific, Vantaa, Finland) and compared with the standard. A standard with a known concentration of gallic acid was used for calibration of the curve (0.0-600 µL). All values were expressed as the average of three replicates in milligrams of gallic acid equivalents (GAE) per gram of tomato (fresh weight).

The method for the determination of the flavonoid content was modified from Oomah et al. (2005) for use with microplates. Briefly, 100 µL of the methanolic extract was mixed with 30 µL of 5% NaNO₂ at time zero. After 5 min, 30 µL of 10% AlCl₃ was added. At 6 min, 200 µL of 1 N NaOH was added. Subsequently, timing was stopped, and 240 µL of distilled water was added to each sample and stirred gently until the solutions were homogenized. The samples were read at 510 nm against a blank using a MULTISKAN GO microplate spectrophotometer (Model 51119300) and compared

with the standard. A standard with a known concentration of catechin hydrate was used for calibration of the curve (0-1000 μL). All values were expressed as the mean of three replicates in milligrams of catechin hydrate (CH) equivalents per gram of tomato (fresh weight).

Determination of antioxidant activity in tomato fruit

The radical elimination capacity (antioxidant activity) for tomato extract was determined by the 2,2-diphenyl-1-picrylhydrazyl (DPPH) method modified from Oomah et al. (2005) for use in microplates. Briefly, a solution of 2,2-diphenyl-1-picrylhydrazyl (DPPH) (150 μM) was prepared in 80% aqueous methanol. The samples or the standard (20 μL) were added to a 96-well flat-bottom visible-light plate containing 200 μL of the DPPH solution. The plate was covered and left in the dark at room temperature. After 120 min, the absorbance was measured at 480 nm in a MULTISKAN GO microplate spectrophotometer (Model 51119300) at 30, 60, 90 and 120 min. For each sample or standard, a solution (20 μL) of 100 μM butyl hydroxytoluene (BHT) was added to each well of the plate containing 200 μL of the DPPH solution. Subsequently, the Trolox (6-hydroxy-[2,5,7,8]-tetramethylchroman-[2]-carboxylic acid) water-soluble analogue was used to prepare the standard curve (range 0-200 μL). The activity was reported in milligrams of Trolox equivalent antioxidant capacity (TEAC) per gram of tomato sample. To determine the antioxidant capacity of Trolox by the FRAP method (ferric reducing antioxidant power assay), the tomato extract was prepared in the same manner as for the DPPH method. Then, 20 μL of the sample (in triplicate) were mixed with 280 μL of the FRAP reagent that was previously prepared with 7.808 mg tripyridyl-s-triazine (TPTZ), 2.5 ml of 40 mM hydrochloric acid, 25 ml of acetate buffer (1.8 g of anhydrous sodium acetate, 3.1 g of sodium acetate trihydrate and 16 ml of glacial acetic acid, adjusted to 1 L) and 2.5 ml of FeCl_3 . The previously made mixture was allowed to rest for 120 min and was completely protected from light. The samples were then read at 630 nm against a blank using a MULTISKAN GO microplate spectrophotometer (Model 51119300; Thermo Scientific, Vantaa, Finland) and compared with the standard. A standard with a known concentration of Trolox was used for calibration of the curve (0-200 μL). All values are expressed as the mean of three replicates in milligrams of Trolox equivalents (TE) per gram of tomato.

Statistical analysis

The data were analysed using an analysis of variance (ANOVA). When significant differences were detected, the means were compared using Tukey's test (with $P < 0.05$) in the Origin Pro 8.0 software (Origin Lab, USA).

Results

The composition of the LCAC was compared with the previously published composition of three other composts from different production sources, and the results are presented in *Table 1*. The N content of the LCAC was similar to the published composition of other composts. The K content was 75% higher in the LCAC compared with conventional compost (composted cow manure) and 6.78 times higher than in municipal waste compost (MWC). The LCAC showed lower values of Zn, Cu and Mn

than composted cow manure. In general, the nutrient content of the LCAC was as acceptable for supplying crops with nutrients as conventional compost (composted cow manure) and had a C/N ratio of 14.4, which indicates acceptable maturation of the material that ants compost in their nests (*Table 1*).

Table 1. Comparison between ant compost and compost from different processing sources

	LCAC	Cow compost ^a	Wood compost ^b	MWC compost ^c
Chemical properties				
pH	6.34	7.26	5.19	6.9
EC (dS m ⁻¹)	6.3	3.5	5.73	12
N total (%)	1.9	1.49	1.16	1.25
P (P ₂ O ₅) (%)	0.11	0.63	0.052	0.081
K (K ₂ O) (%)	1.56	0.89	0.16	0.23
Ca (%)	0.89	0.96	3.8	0.06
Mg (%)	0.22	0.3	3.33	0.03
Na (%)	0.95	0.62	-	0.12
S (%)	0.22	0.34	-	0.09
Fe (%)	0.92	0.85	0.05	0.41
Cu (ppm)	17.6	41.3	0.82	230
Mn (ppm)	533	855	14.59	240
Zn (ppm)	57.2	334	10.38	349
B (ppm)	22.9	18.8	-	-
OM (%)	47.3	51.3	-	18.9
Organic C (%)	27.4	29.8	33.54	-
Ratio C/N	14.4	20	-	15

LCAC: leafcutter ant compost, MWC: municipal waste compost

^aÁvila-Juárez et al. (2015)

^bMladenov (2018)

^cRajaie and Tavakoly (2016)

As can be seen in *Table 2*, the physical properties of the soil improved as the dose of LCAC increased. The OM of the soil at any dose of LCAC was statistically higher than the OM content of the initial soil and the control, reaching 4.1 times more OM in the soil with respect to the control at the highest dose of LCAC per plant (*Fig. 2*), which helped to improve the HC; at this high dose of LCAC, the HC was suitable for the soil (0.8 cm h⁻¹). The tomato plants showed no deficiencies at any phenological stage, which indicates that the release of the nutrients contained in the LCAC was rapid and timely, even leaving residual acceptable levels in the soil (*Table 2*). In contrast, at the end of the experiment, the application of chemical fertilizers left unused ions that can be leached or accumulate over time and be harmful to the subsequent crop. For example, the control treatment left 2.8 times more NO₃⁻ and 4.84 times more S in the soil compared with the high dose of LCAC (*Table 2*). These ions are noted here because the soil cannot retain them given their negative charge, which easily leads to leaching and contamination of groundwater.

Table 2. Physicochemical properties of the soil before and after adding ant compost to a tomato crop (in kg of LCAC per plant: $T_{low} = 0.792$; $T_{med} = 1.3$; $T_{high} = 1.84$)

	Soil before	Soil after			
		T_{low}	T_{med}	T_{high}	$T_{control}$
Physical properties					
SAT (%)	54.0	53.1	57.5	63.3	53.8
FC (%)	28.9	28.3	30.8	33.9	28.8
WP (%)	17.2	16.8	18.3	20.2	17.1
HC (cm h ⁻¹)	4.1	2.3	1.6	0.8	2.3
BD (g cm ⁻³)	1.0	0.9	0.8	0.8	0.9
EC (dS m ⁻¹)	0.1	0.4	1.1	1.1	1.4
CEC (meq 100 g ⁻¹)	11.1	10.3	13.1	13.8	9.6
Chemical properties					
pH (1:2 water)	6.7	6.0	6.3	6.2	5.8
IN (ppm)	3.5	21.0	33.7	37.2	106.7
P-Bray (ppm)	0.6	42.1	51.3	58.0	34.4
K (ppm)	173.0	290.0	605.3	638.3	385.0
Ca (ppm)	1557.0	1331.0	1604.0	1700.7	1184.0
Mg (ppm)	340.0	326.0	402.7	418.3	309.7
Na (ppm)	15.0	40.2	46.4	49.7	42.5
Fe (ppm)	7.3	5.2	7.5	9.6	4.8
Zn (ppm)	0.3	0.8	2.0	1.6	0.9
Mn (ppm)	20.8	18.6	32.7	44.0	7.2
Cu (ppm)	0.2	0.3	0.4	0.5	0.2
B (ppm)	0.1	0.3	0.3	0.4	0.4
S (ppm)	6.1	12.6	20.8	21.3	103.2

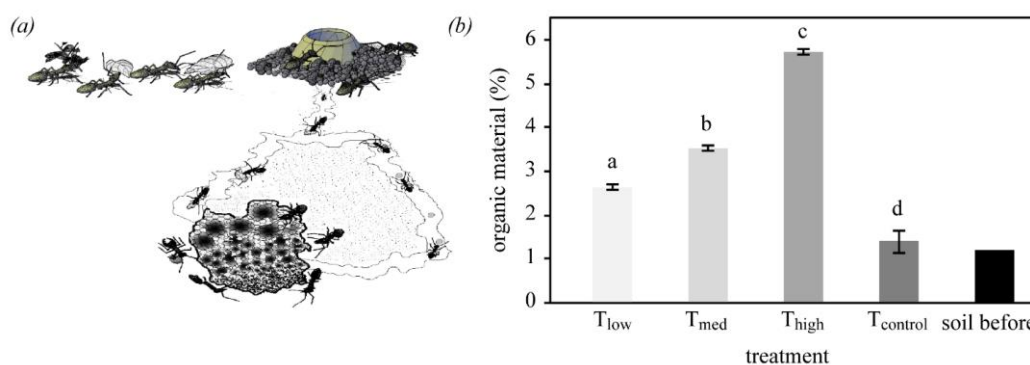


Figure 2. Ant compost increases the OM content of the soil. (a) Production of ant compost by *Atta mexicana*. (b) Increase in OM in the soil by the application of ant compost. Doses of LCAC in kg per plant: $T_{low} = 0.792$; $T_{med} = 1.3$; $T_{high} = 1.84$. Mean \pm standard error, $p < 0.001$ with Tukey's test

In general, in all treatments where the LCAC was applied, the compaction was well below the level considered moderate (more than 200 kPa). In fact, on average, these treatments showed 18% less soil compaction than the initial soil. In the control treatment,

conditions similar to the initial soil were observed with only a 1.8% increase in compaction (*Fig. 3*). The treatment that reduced compaction to the greatest degree was the dose administered at 0.792 kg of LCAC per plant, which is equivalent to 19.8 t ha⁻¹.

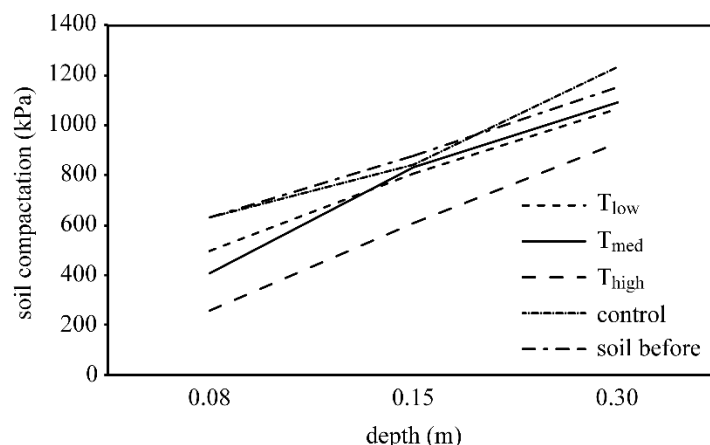


Figure 3. Soil compaction at different depths as a result of ant compost before and after the experiment (doses of LCAC in kg per plant: *T_{low}* = 0.792; *T_{med}* = 1.3; *T_{high}* = 1.84)

In general, plant height was similar in the treatments with the medium (1.3 kg) and high dose (1.84 kg) of LCAC with respect to the control. There was only one taller plant at 57 DAT for the aforementioned treatments compared with the control (*Fig. 4*). The total daily growth in the high LCAC treatment was 2.24 cm, which was not statistically different from the control. We only found differences in plant height between the *T_{low}* and *T_{high}* treatments, which have the lowest and highest doses of LCAC, respectively, and therefore the lowest and highest nutrient contents. This finding may suggest that high doses of LCAC provided sufficient levels of nutrients such as NPK that are necessary to form plant biomass.

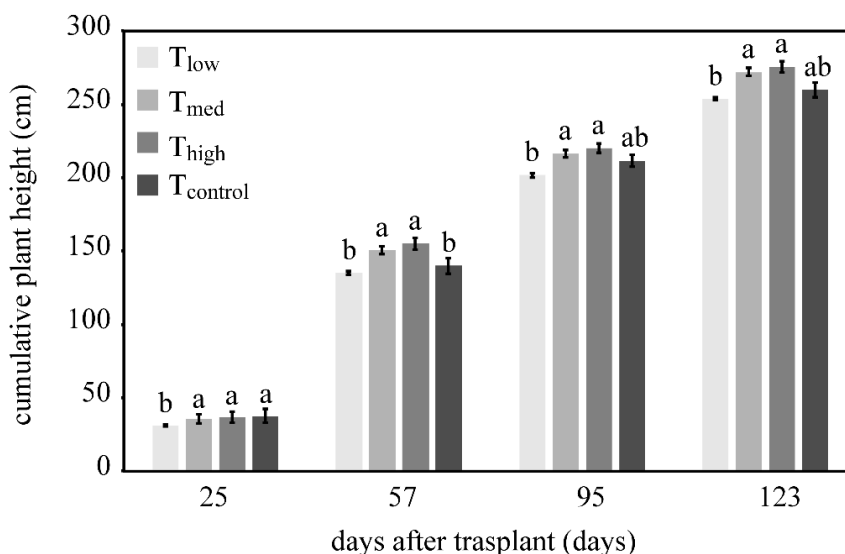


Figure 4. Effect of the application of ant compost on plant height at different days after transplant. Doses of LCAC in kg per plant: *T_{low}* = 0.792; *T_{med}* = 1.3; *T_{high}* = 1.84. Mean \pm standard error, $p < 0.05$ with Tukey's test

According to our results, the application of LCAC at 19.8 t ha⁻¹ (T_{low}) or 46 t ha⁻¹ (T_{high}) at a density of 2.5 plants m⁻² in a greenhouse tomato crop produced the same yield ($p < 0.05$) as the application of chemical fertilizers. This finding indicates that ant compost has a high nutrient content that is readily available to the plant (the LCAC was applied one week before transplanting) (Fig. 5). For example, the high dose of LCAC provided 19 kg of N for each ton applied, which is higher than composted cow manure that provided 35 g of N per plant, whereas chemical fertilization provided 20.54 g of N per plant (167 ppm NL⁻¹ for 153 days).

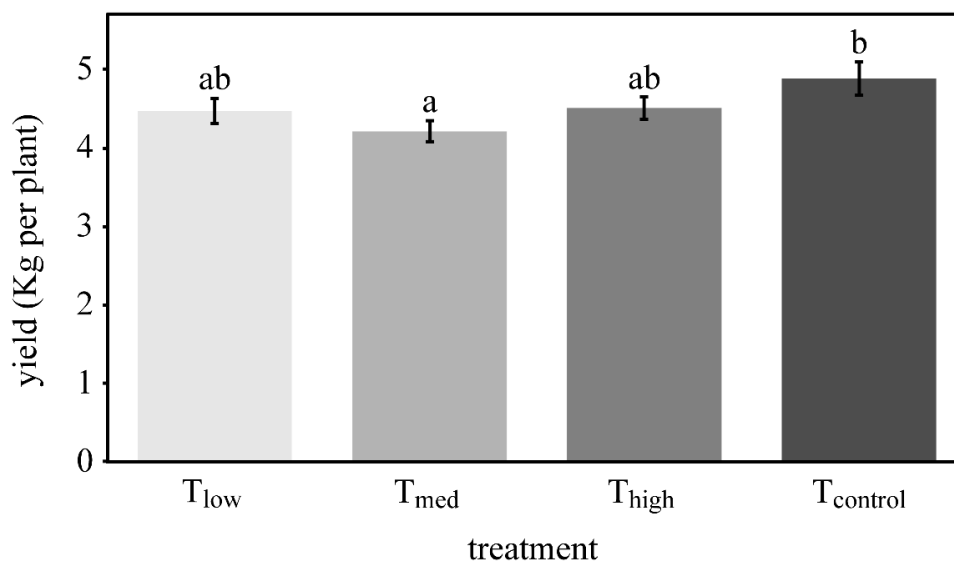


Figure 5. Tomato plant yield for different applications of ant compost. Doses of LCAC in kg per plant: T_{low} = 0.792; T_{med} = 1.3; T_{high} = 1.84. Mean \pm standard error, $p < 0.05$ with Tukey's test

There were no significant differences ($p < 0.05$) in the content of total phenols, flavonoids or antioxidant capacity in the LCAC treatments compared with the control. The level of nutrients in the LCAC was sufficient, in terms of quantity and availability, to avoid biochemical damage to the plant that could lead to a loss of nutraceutical properties (Fig. 6).

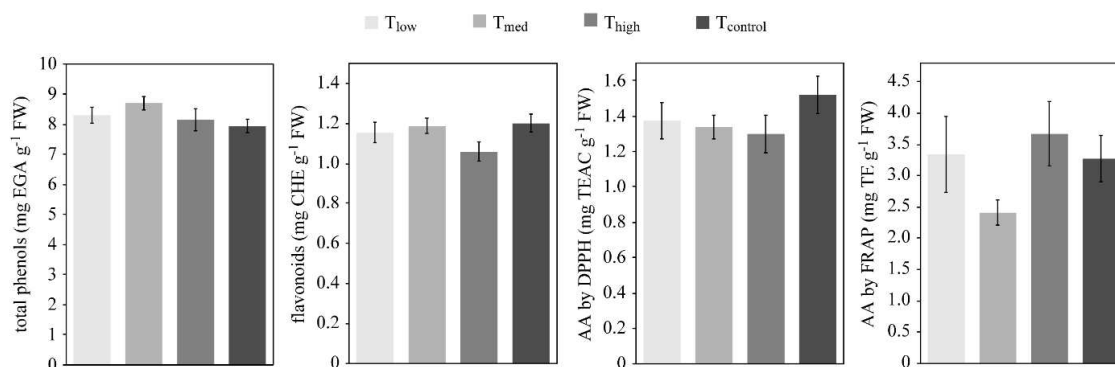


Figure 6. Effect of different doses of ant compost on the biochemical properties of tomato fruit. Doses of LCAC in kg per plant: T_{low} = 0.792; T_{med} = 1.3; T_{high} = 1.84. Mean and standard error ($n = 18$ or more), $p < 0.05$ with Tukey's test

Discussion

The cell wall of plants is composed of cellulose, hemicellulose and pectin, which represents 70% of plant biomass (Jørgensen et al., 2007), as well as macro and microelements (Bolan et al., 2010) and some trace elements (Faridullah et al., 2014). The fungus *L. gongylophorus* has developed the ability to produce lignocellulases, pectinases, amylases and cellulases that disintegrate plant matter (Aylward et al., 2013) into more soluble compounds (Huang et al., 2014), simultaneously lysing the cell by the penetration of their hyphae and releasing the nutritional content of the leaves, including N, P, K and Ca. This finding suggests that the LCAC contains the necessary nutrients to meet the nutritional demands of a tomato plant. In terms of yield, the treatments with LCAC at low and high doses were not significantly different from the control treatment (with soluble fertilizers). Given the need to take advantage of agricultural waste, various treatment techniques have been developed such as vermicomposting, anaerobic digestion and various composting strategies (Altuntas et al., 2018; Irshad et al., 2013; Nayak and Kalamdhad, 2014; Yardimci, 2013). In the case of LCAC, composting is performed as part of the symbiotic relationship between the ants of the genus *Atta*, among other genera, and the fungus *L. gongylophorus*. Although it is not clear when this symbiotic relationship developed, we are certain that it was hundreds of years ago. The production of the ant waste we refer to as “ant compost” is very similar to a solid state reactor because the fungal garden produces not only biomass as a raw material but also a series of microbial secretions, enzymes and hydrolysis products; the ants prepare the plant substrate to feed the system, and the cellular mass is continuously reinoculated, naturally producing waste material (ant compost) (Somera et al., 2015). One of the sterilization phases in the composting process is the thermophilic phase, in which a large quantity and variety of microorganisms that can damage the plant die. However, in this high-temperature phase (above 40 °C) (Chen et al., 2011), it is common for some of the nitrogen to volatilize in the form of ammonia, particularly when the pH is close to 7 (Tam and Tiquia, 1999). In the LCAC, the pH was 6.34. The higher N content (27% more than composted cow manure) may explain the good pH regulation maintained by the ants in their nests (by an as yet unknown process). The ratio of C/N at the end of the composting process is one of the most frequently measured indicators of stability. In general, the C/N ratio decreases as the compost matures due to the loss of carbon in the form of carbon dioxide (Raj and Antil, 2011; Wichuk and McCartney, 2010). A C/N ratio below 20 is adequate for a mature compost; however, a C/N ratio lower than 15 is more desirable (Raj and Antil, 2011). The LCAC had a C/N ratio of 14.4 before being applied, whereas composted cow manure has a ratio of approximately 20 (Ávila-Juárez et al., 2015). The low C/N ratio of ant compost, together with the decrease in OM, explains the higher degree of maturity in the LCAC because when the OM is lost, the dry weight is reduced and the proportion of C/N decreases (Bernal et al., 2009). Although the C/N of any compost depends on the input used, in the case of the ants, this ratio depends fundamentally on the type of forage harvested by the ants (Huang et al., 2014). The levels of N and C in the LCAC suggest that there is little loss of these two elements, possibly because the composting process occurs in partially closed underground chambers. EC has been proposed as an indicator of compost stability, and its lower limit should be 3 mS m⁻¹ (Gao et al., 2010) with a maximum of 4 mS m⁻¹ (Chowdhury et al., 2013). The EC of ant compost was 6.3 mS m⁻¹, which is 80% higher than composted cow manure and 52.5% less than the MWC. Because EC is the content of soluble salts in the compost (Gao et al., 2010), the ant

compost had a higher content of available nutrients for the plant compared with composted cow manure, which is reflected in the similarity of yields found in the treatments with medium and high doses and compared with the control, in which soluble chemical fertilization was applied. We believe that the limits of EC that have been established to indicate whether a compost is mature and stable should be a function of the quality and quantity of its components (nutrients) and not the EC of the compost because there are elements such as Na that elevate the EC without being essential or beneficial for the plant. In fact, the fewer trace elements or Na that a compost contains and the higher the proportions of essential elements, the greater the EC of a compost, which translates into less application to the soil needed to meet nutritional demands.

Compost has been used for many years as a fertilizer due to its ability to increase soil health (Arslan et al., 2008; Canali et al., 2011); promote the increase in aggregates, structure and fertility of the soil; increase the population of beneficial microorganisms; and increase the water-holding capacity and cation exchange (Angelova et al., 2013; Arslan et al., 2008). The HC serves as an indicator of the movement of water and solutes in the soil. If the HC is below 0.5 cm h^{-1} , drainage can be compromised causing possible root problems (Saunders et al., 1978). However, there are problems with water retention and the loss of nutrients to the subsoil. The HC was decreased in treatments with compost, up to 0.8 cm h^{-1} for the high dose, as has been found with the use of conventional compost (Angelova et al., 2013; Arslan et al., 2008). This finding is mainly because the treatment with the high dose contained four times more OM than the control, which caused an 80% reduction in the HC and improved water retention as evidenced by the FC, which had increased by 17.3% at the end of the experiment. Our results confirm that the OM in the soil has an impact on the percolation of water through the soil and increases the water-holding capacity (Uzoma et al., 2011). In contrast, the absence of OM in the soil causes, in addition to salt accumulation, a decrease in SAT as observed in the control and the treatment with a low dose of compost. Similar patterns were observed for FC and the WP, possibly as a result of a very high HC (2.3 cm h^{-1}), which was derived from an absence of OM in the soil.

A common practice among farmers is to add compost one month before transplanting so that the soil microorganisms can help release/solubilize the nutrients present in the compost and make them available for the development of the plant. In the case of the LCAC, it was not necessary to allow a significant period of time before transplanting (it was added one week before), because it possessed a high EC. As mentioned previously, the EC measures the amount of soluble salts present in the sample. It has been observed that when compost is added to the soil, there is a high level of N in the form of NH_4^+ , and through the process of nitrification, H^+ ions are released, which causes a decrease in the pH of the medium (Shen et al., 2011). The pH of the LCAC was 6.34, and at the end of the experiment, the pH of the soil was 6 to 6.3 at the different doses used, which was well above the control treatment. It is possible that in the *Atta mexicana* fungal garden, the nitrification process is operating because the plants in our experiment showed no N deficiencies or toxicity. The concentration of P in the LCAC was almost six times lower than that reported for compost (Ávila-Juárez et al., 2015). However, at the end of the experiment, the treatments with LCAC had more P than the control, which indicates that the P present was sufficient for plant growth and was immediately available because the P of a compost recently applied to the soil is typically immobilized by soil microorganisms, which leads to low availability to plants (Barral et al., 2011). This

finding confirms that when the LCAC was applied, there was no need for nutrient transformation from a poorly soluble state to a more soluble state by soil microorganisms, as is the case with conventional composts. However, the high availability of P for the tomato crop was the result of the adequate pH of the LCAC, because pH values below 6 and above 7.5 directly affect the availability of P (Fuentes et al., 2006). The increase in Ca in the soil increases with the dose of the compost (Ch'ng et al., 2014), which was reflected in the treatments with LCAC. The highest Ca content in the soil at the end of the experiment was observed in the high-dose LCAC treatment (46 t ha⁻¹). This result can be attributed to the relatively high concentration of Ca in the compost before being applied to the soil and to the relatively high initial concentration that the soil possessed before the experiment (1557 ppm). The high concentration of K in the soil, which was also dose-dependent, was a product of the high concentration of K in the compost (1.56%) and its release during the decomposition of the OM in the “fungal garden”. The highest concentration of K in the soil (638 ppm) was obtained with a dose of 46 t ha⁻¹ of LCAC, which is 1.65 times more than with chemical fertilization, suggesting that there is residual K available for the next crop and that less LCAC could be used for the next cycle. The increase in Mg, Fe, Zn, Mn and Cu in the soil can be attributed to the release of these elements during the decomposition/mineralization of the compost in the “fungal garden”. Similar results for the content of OM, C, N, P, Ca, K and Mg have been reported (Farji-Brener and Ghermandi, 2008). This increase is to be expected because the leaves collected by the ants are important stores of nutrients that plants take up from the soil. These nutrients, derived from the enzymatic processes mentioned above, are released into more soluble forms and concentrated in the nests of the ants and are derived from the reduction in the biomass collected.

For millennia, compost has been used for soil remediation and as an amendment to add nutrients for crops (Indriyati, 2014). Our results show that there was no significant difference in the plant height between the LCAC treatments and the control at the end of the experiment (123 DAT). However, the content of major nutrients such as NPK with an LCAC dose of 19.8 t ha⁻¹ (Tlow) was not sufficient to meet the nutrient demands of the tomato crop because there was a significant difference in yield (410 g plant⁻¹) with respect to the control. This result was confirmed by the yields of the tomato fruit (fresh weight) from the high and medium dose treatments of LCAC, which were not statistically different from the control. The quantity (kg) of fertilizer supplied by the nutrient solution (Steiner, 1984) during the experiment for the tomato crop were N:770, P:143, K:1278, whereas for the high LCAC dose (46 t ha⁻¹), they were N:874, P:50.6, K:718. The P level in the nutrient solution was 2.8 times higher than the P level of the high-dose LCAC; however, P did not limit the yield from tomato cultivation. In contrast, the contribution of OM from the LCAC may have reduced the HC, resulting in less leaching of nutrients such as P and K, because after the experiment the residual P and K in the soil was higher than in the soil with the nutrient solution. Our results suggest that a) the variety and quantity of nutrients present in the LCAC are sufficient (at Tlow and Thigh) to grow a tomato crop without the need for inorganic fertilizers and b) the nutrients present in the LCAC are highly soluble and can be immediately taken up by the plant once the tomato root has contact with the LCAC. Our results concur with other previously published studies on the growth surrounding *Acromyrmex* ant nests, which are very similar to those of *Atta mexicana*, which concluded that the nutrient content of the ant waste is high enough to satisfy the demands of a plant (Farji-

Brener and Werenkraut, 2017; Farji-Brener and Ghermandi, 2008; Saha et al., 2012). However, we found no significant differences in total phenols, flavonoids or antioxidant activity via DPPH or FRAP in any of the compost treatments compared with the control. This finding indicates that the dose of LCAC used does not modify the secondary metabolism of the tomato plant.

Conclusions

In summary, we discovered that the symbiotic relationship between the ant *Atta mexicana* and the fungus *L. gongylophorus* produces a product very similar to the conventional composted cow manure produced by humans. Given the nutritional characteristics and other indicators such as the C/N ratio found in ant waste, it is inferred that the ants facilitate a process similar to that of the composting activities that have been performed by humans for many years. In fact, the LCAC was able to satisfy the nutritional demands, in terms of quality and quantity of nutrients, of a tomato crop without the need for inorganic fertilizers. The LCAC increased the amount of OM and provided nutrients to the soil as does a conventional compost. *Atta* spp. are excellent nutrient recyclers and maintain an ecological balance in the environment by producing a high-quality compost that is available to plants. For future research, we recommend analyzing the effect of LCAC on the soil for a longer period of time, such as 3 years, as it may, according to our results, positively modify the soil by supporting the recovery of eroded soils without the use of physical structures or plant-based nutrient contents.

Acknowledgements. The authors acknowledge support from the Autonomous University of Queretaro, Queretaro, Mexico. Additionally, they acknowledge FOVIN-UAQ (SUV-DVT-2018-031) and FOFI-UAQ (FIN-2018-24) for partial support of this research.

REFERENCES

- [1] Altuntas, O., Durak, A., Kucuk, R. (2018): Optimization and comparison of the effects of vermicompost and conventional fertilization on spinach (*Spinacia oleracea* L.) growth. – *Applied Ecology and Environmental Research* 16: 7001-7016.
- [2] Angelova, V., Akova, V., Artinova, N., Ivanov, K. (2013): The effect of organic amendments on soil chemical characteristics. – *Bulgarian Journal of Agricultural Science* 19: 958-971.
- [3] Arslan, E., Obek, E., Kirbag, S., Ipek, U., Topal, M. (2008): Determination of the effect of compost on soil microorganisms. – *International Journal of Science & Technology* 3: 151-159.
- [4] Ávila-Juárez, L., Rodríguez González, A., Rodríguez Piña, N., Guevara González, R. G., Torres Pacheco, I., Ocampo Velázquez, R. V., Moustapha, B. (2015): Vermicompost leachate as a supplement to increase tomato fruit quality. – *Journal of Soil Science and Plant Nutrition* 15: 46-59.
- [5] Aylward, F. O., Burnum-Johnson, K. E., Tringe, S. G., Teiling, C., Tremmel, D. M., Moeller, J. A., Scott, J. J., Barry, K. W., Piehowski, P. D., Nicora, C. D., Malfatti, S. A., Monroe, M. E., Purvine, S. O., Goodwin, L. A., Smith, R. D., Weinstock, G. M., Gerardo, N. M., Suen, G., Lipton, M. S., Currie, C. R. (2013): *Leucoagaricus gongylophorus* produces diverse enzymes for the degradation of recalcitrant plant polymers in leaf-cutter ant fungus gardens. – *Applied and Environmental Microbiology* 79(12): 3770-3778.

- [6] Barral, M. T., Paradelo, R., Domínguez, M., Díaz-Fierros, F. (2011): Nutrient release dynamics in soils amended with municipal solid waste compost in laboratory incubations. – *Compost Science & Utilization* 19(4): 235-243.
- [7] Bernal, M. P., Albuquerque, J. A., Moral, R. (2009): Composting of animal manures and chemical criteria for compost maturity assessment. A review. – *Bioresource Technology* 100(22): 5444-5453.
- [8] Bolan, N. S., Szogi, A. A., Chuasavathi, T., Seshadri, B., Rothrock, M. J., Panneerselvam, P. (2010): Uses and management of poultry litter. – *World's Poultry Science Journal* 66(4): 673-698.
- [9] Bot, A. N. M., Currie, C. R., Hart, A. G., Boomsma, J. J. (2001): Waste management in leaf-cutting ants. – *Ethology Ecology & Evolution* 13(3): 225-237.
- [10] Canali, S., Di Bartolomeo, E., Tittarelli, F., F., M., Verrastro, V., Ferri, D. (2011): Comparison of different laboratory incubation procedures to evaluate nitrogen mineralization in soils amended with aerobic and anaerobic stabilized organic materials. – *Journal of Food Agriculture and Environment* 9(2): 540-546.
- [11] Ch'ng, H. Y., Ahmed, O. H., Majid, N. M. A. (2014): Improving phosphorus availability in an acid soil using organic amendments produced from agroindustrial wastes. – *The Scientific World Journal* 2014: 506356.
- [12] Chen, L., Marti, M. D. H., Moore, A., Falen, C. (2011): *The Composting Process*. – The University of Idaho, Moscow.
- [13] Chowdhury, A. K. M. M. B., Akrotos, C. S., Vayenas, D. V., Pavlou, S. (2013): Olive mill waste composting: a review. – *International Biodeterioration & Biodegradation* 85: 108-119.
- [14] Dewanto, V., Wu, X., Adom, K. K., Liu, R. H. (2002): Thermal processing enhances the nutritional value of tomatoes by increasing total antioxidant activity. – *Journal of Agricultural and Food Chemistry* 50(10): 3010-3014.
- [15] Faridullah, P. A., Irshad, M., Alam, A., Mahmood, Q., Ashraf, M. (2014): Trace elements characterization in fresh and composted livestock manures. – *Austin Journal of Hydrology* 1: 1-16.
- [16] Farji-Brener, A. G., Ghermandi, L. (2008): Leaf-cutting ant nests near roads increase fitness of exotic plant species in natural protected areas. – *Proceedings of the Royal Society B: Biological Sciences* 275(1641): 1431-1440.
- [17] Farji-Brener, A. G., Werenkraut, V. (2017): The effects of ant nests on soil fertility and plant performance: a meta-analysis. – *Journal of Animal Ecology* 86(4): 866-877.
- [18] Fuentes, B., Bolan, N., Naidu, R., Mora, M. D. L. L. (2006): Phosphorus in organic waste-soil systems. – *Revista de la Ciencia del Suelo y Nutrición Vegetal* 6(2): 64-83.
- [19] Gao, M., Liang, F., Yu, A., Li, B., Yang, L. (2010): Evaluation of stability and maturity during forced-aeration composting of chicken manure and sawdust at different C/N ratios. – *Chemosphere* 78(5): 614-619.
- [20] Hart, A. G. (2002): Waste management in the leaf-cutting ant *Atta colombica*. – *Behavioral Ecology* 13(2): 224-231.
- [21] Hölldobler, B., Wilson, E. O. (1990): *The Ants*. – Harvard University Press, Cambridge, MA.
- [22] Huang, E. L., Aylward, F. O., Kim, Y.-M., Webb-Robertson, B.-J. M., Nicora, C. D., Hu, Z., Metz, T. O., Lipton, M. S., Smith, R. D., Currie, C. R., Burnum-Johnson, K. E. (2014): The fungus gardens of leaf-cutter ants undergo a distinct physiological transition during biomass degradation. – *Environmental Microbiology Reports* 6(4): 389-395.
- [23] Indriyati, L. T. (2014): Chicken manure composts as nitrogen sources and their effect on the growth and quality of *Komatsuna* (*Brassica rapa* L.). – *Journal of the International Society for Southeast Asian Agricultural Sciences* 20(1): 52-63.
- [24] Irshad, M., Eneji, A. E., Hussain, Z., Ashraf, M. (2013): Chemical characterization of fresh and composted livestock manures. – *Journal of Soil Science and Plant Nutrition* 13: 115-121.

- [25] Jørgensen, H., Vibe-Pedersen, J., Larsen, J., Felby, C. (2007): Liquefaction of lignocellulose at high-solids concentrations. – *Biotechnology and Bioengineering* 96(5): 862-870.
- [26] Körner, I., Braukmeier, J., Herrenklage, J., Leikam, K., Ritzkowski, M., Schlegelmilch, M., Stegmann, R. (2003): Investigation and optimization of composting processes—test systems and practical examples. – *Waste Management* 23(1): 17-26.
- [27] Little, A. E. F., Murakami, T., Mueller, U. G., Currie, C. R. (2006): Defending against parasites: fungus-growing ants combine specialized behaviours and microbial symbionts to protect their fungus gardens. – *Biology Letters* 2(1): 12-16.
- [28] Mladenov, M. (2018): Chemical composition of different types of compost. – *Journal of Chemical Technology and Metallurgy* 53: 712-716.
- [29] Moller, I. E., De Fine Licht, H. H., Harholt, J., Willats, W. G. T., Boomsma, J. J. (2011): The dynamics of plant cell-wall polysaccharide decomposition in leaf-cutting ant fungus gardens. – *PLoS ONE* 6(3): e17506.
- [30] Moutinho, P., Nepstad, D. C., Davidson, E. A. (2003): Influence of leaf-cutting ant nests on secondary forest growth and soil properties in Amazonia. – *Ecology* 84(5): 1265-1276.
- [31] Mueller, U. G., Schultz, T. R., Currie, C. R., Malloch, D. (2001): The origin of the attine ant-fungus mutualism. – *The Quarterly Review of Biology* 76(2): 169-197.
- [32] Mueller, U. G., Gerardo, N. M., Aanen, D. K., Six, D. L., Schultz, T. R. (2005): The evolution of agriculture in insects. – *Annual Review of Ecology, Evolution, and Systematics* 36(1): 563-595.
- [33] Nayak, A. K., Kalamdhad, A. S. (2014): Feasibility of composting combinations of sewage sludge, cattle manure, and sawdust in a rotary drum reactor. – *Environmental Engineering Research* 19(1): 47-57.
- [34] Oomah, B. D., Cardador-Martínez, A., Loarca-Piña, G. (2005): Phenolics and antioxidative activities in common beans (*Phaseolus vulgaris* L.). – *Journal of the Science of Food and Agriculture* 85(6): 935-942.
- [35] Pagnocca, F. C., Bacci, M., Fungaro, M. H., Bueno, O. C., Hebling, M. J., Sant'anna, A., Capelari, M. (2001): RAPD analysis of the sexual state and sterile mycelium of the fungus cultivated by the leaf-cutting ant *Acromyrmex hispidus fallax*. – *Mycological Research* 105(2): 173-176.
- [36] Raj, D., Antil, R. S. (2011): Evaluation of maturity and stability parameters of composts prepared from agro-industrial wastes. – *Bioresource Technology* 102(3): 2868-2873.
- [37] Rajaie, M., Tavakoly, A. R. (2016): Effects of municipal waste compost and nitrogen fertilizer on growth and mineral composition of tomato. – *International Journal of Recycling of Organic Waste in Agriculture* 5(4): 339-347.
- [38] Saha, A. K., Carvalho, K. S., Sternberg, L. d. S. L., Moutinho, P. (2012): Effect of leaf-cutting ant nests on plant growth in an oligotrophic Amazon rain forest. – *Journal of Tropical Ecology* 28(3): 263-270.
- [39] Saunders, L., Libardi, P., Reichardt, K. (1978): Condutividade hidráulica da terra roxa estruturada em condições de campo. – *Revista Brasileira de Ciencia do Solo* 2: 164-167.
- [40] Schiøtt, M., De Fine Licht, H. H., Lange, L., Boomsma, J. J. (2008): Towards a molecular understanding of symbiont function: identification of a fungal gene for the degradation of xylan in the fungus gardens of leaf-cutting ants. – *BMC Microbiology* 8(1): 40.
- [41] Shen, Y., Ren, L., Li, G., Chen, T., Guo, R. (2011): Influence of aeration on CH₄, N₂O and NH₃ emissions during aerobic composting of a chicken manure and high C/N waste mixture. – *Waste Management* 31(1): 33-38.
- [42] Silva-Pinhati, A. C. O., Bacci Jr, M., Hinkle, G., Sogin, M. L., Pagnocca, F. C., Martins, V. G., Bueno, O. C., Hebling, M. J. A. (2004): Low variation in ribosomal DNA and internal transcribed spacers of the symbiotic fungi of leaf-cutting ants (Attini: Formicidae). – *Brazilian Journal of Medical and Biological Research* 37(10): 1463-1472.
- [43] Somera, A. F., Lima, A. M., dos Santos-Neto, Á. J., Lanças, F. M., Bacci, M. (2015): Leaf-cutter ant fungus gardens are biphasic mixed microbial bioreactors that convert plant

- biomass to polyols with biotechnological applications. – Applied and Environmental Microbiology 81(13): 4525-4535.
- [44] Steiner, A. A. (1984): The Universal Nutrient Solution. – Proceedings of IWOSC 1984 6th International Congress on Soilless Culture, Wageningen.
- [45] Sternberg, L. D. S. L., Pinzon, M. C., Moreira, M. Z., Moutinho, P., Rojas, E. I., Herre, E. A. (2007): Plants use macronutrients accumulated in leaf-cutting ant nests. – Proceedings of the Royal Society B: Biological Sciences 274(1608): 315-321.
- [46] Tam, N. F. Y., Tiquia, S. M. (1999): Nitrogen transformation during co-composting of spent pig manure, sawdust litter and sludge under forced-aerated system. – Environmental Technology 20(3): 259-267.
- [47] Uzoma, K., Inoue, M., Andry, H., Zahoor, A., Nishihara, E. (2011): Influence of biochar application on sandy soil hydraulic properties and nutrient retention. – Journal of Food, Agriculture and Environment 9: 1137-1143.
- [48] Wichuk, K. M., McCartney, D. (2010): Compost stability and maturity evaluation—a literature review. – Canadian Journal of Civil Engineering 37(11): 1505-1523.
- [49] Yardimci, M. (2013): Waste to wealth strategies: recycling poultry manure. – Kocatepe Veterinary Journal 6(1): 69-72.

POST-HARVEST RESIDUES OF NARROW-LEAVED LUPIN (*Lupinus angustifolius* L.) / SPRING RYE (*Secale cereal* L.) MIXTURES AS A SOURCE OF BIOLOGICAL NITROGEN FOR WINTER TRITICALE (*Triticosecale* Wittm. ex A. Camus)

PLAZA, A. – GAŚSIOROWSKA, B. – RZAŻEWSKA, E.*

*Siedlce University of Natural Sciences and Humanities, Faculty of Agrobioengineering and
Animal Husbandry, Institute of Agriculture and Horticulture, Siedlce, Poland*

*Corresponding author

e-mail: emilia.rzazewska@uph.edu.pl

(Received 3rd Dec 2019; accepted 24th Mar 2020)

Abstract. Field research was conducted in 2010-2012 to determine the manuring value of the post-harvest residues of narrow-leaved lupin (*Lupinus angustifolius* L.)/spring rye (*Secale cereal* L.) mixtures. The following two experimental factors were investigated: I. forecrop – mixtures: narrow-leaved lupin – pure stand 100%, spring rye – pure stand 100%, narrow-leaved lupin 75% + spring rye 25%, narrow-leaved lupin 50% + spring rye 50%, narrow-leaved lupin 25% + spring rye 75%; II. forecrop harvest date: narrow-leaved lupin flowering stage, flat green pod stage. It was inferred, based on the obtained results, that the greatest quantity of post-harvest residues was supplied by spring rye as well as narrow-leaved lupin/spring rye mixtures containing 25 + 75% and 50 + 50% of the respective components, harvested at the stage of flat green pod of narrow-leaved lupin, the greatest nitrogen amount being supplied by narrow-leaved lupin harvested at the aforementioned development stage. The highest grain yield was produced by winter triticale (*Triticosecale* Wittm. ex A. Camus) following an incorporation of the post-harvest residues of narrow-leaved lupin/spring rye mixture containing 50 + 50% of the respective components and harvested at the stage of narrow-leaved lupin flat green pod.

Keywords: forecrop, 1000 grain weight, yield, total nitrogen content

Introduction

Legume/cereal mixtures are valuable green fodder crops fed to cattle, their post-harvest residues being a source of biological nitrogen for following crop plants, cereals in particular. Also, they are more environmentally friendly than mineral nitrogen fertilisers (Jensen and Hauggard-Nielsen, 2003; Herridge et al., 2008). Compared to legume post-harvest residues, such biomass has a broader C:N ratio, which results in its mineralisation process being slowed down. As reported by Mayer et al. (2003), Tripolskaja and Šidlauskas (2010) as well as Nemeikšiene et al. (2010), an application of legume post-harvest residues preceding winter wheat results in mineral nitrogen leaching into deeper soil strata during the autumn-winter-spring period, which is caused by rapid mineralization of such biomass. As far as the post-harvest residues of legume/cereal mixtures are concerned, the biological nitrogen is gradually released to be used by the following plant throughout the whole growing season, which prevents its leaching and protects the soil environment (Arlauskiene and Maiksteniene, 2008; Nemeikšiene et al., 2010).

Triticale is a species which has been recently introduced for cultivation purposes. A paucity of literature has been noticed pertaining to the manuring value of legume/cereal post-harvest residues for this crop plant.

It has been assumed that an incorporation of the crop residues of narrow-leaved lupine/spring rye mixtures at the stage of narrow-leaved lupin flowering and flat green pod will make it possible to determine differences in yield performance and amount of nitrogen accumulated in winter triticale grain, and indicate which mixtures have the most beneficial effect on grain yield and amount of nitrogen accumulated in winter triticale grain.

The objective of the study was to determine the manuring value of post-harvest residues of narrow-leaved lupin/spring rye mixtures harvested at the stage of narrow-leaved lupin flowering and flat green pod, expressed in terms of grain yield and amount of biological nitrogen accumulated in winter triticale grain.

Materials and Methods

Field research was conducted in 2010-2012 at the Zawady Experimental Farm (52°03'39"N, 22°33'80"E) of Siedlce University of Natural Sciences and Humanities in Poland. The soil on which the experiment was set up was Stagnic Luvisol, its reaction was neutral and it contained average amounts of available phosphorus, potassium and magnesium. Humus content was 1.40%. The experiment was a split-block arrangement with three replicates. The following two factors were examined: I. forecrop – mixtures: narrow-leaved lupin, pure stand 100%, spring rye, pure stand 100%, narrow-leaved lupin 75% + spring rye 25%, narrow-leaved lupin 50% + spring rye 50%, narrow-leaved lupin 25% + spring rye 75%; II. harvest date: the stage of narrow-leaved lupin flowering, the stage of narrow-leaved lupin flat green pod. The following seeding rates were used: narrow-leaved lupin 260 seeds m⁻², spring rye 217 grains m⁻², narrow-leaved lupin 195 seeds m⁻² + spring rye 54 grains m⁻², narrow-leaved lupin 130 seeds m⁻² + spring rye 109 grains m⁻², narrow-leaved lupin 65 seeds m⁻² + spring rye 163 grains m⁻². In all the study years, the mixtures were preceded by oats. The agrotechnics of mixtures narrow-leaved lupin + spring rye are presented in the *Table 1*. Narrow-leaved lupin (cv. Zeus) and spring rye (cv. Bojko) seeds were planted in early April as described for factor I. The plants were harvested in late June (stage of narrow-leaved lupin flowering) and early July (stage of narrow-leaved lupin flat green pod). Following forecrop harvest, post-harvest residues of narrow-leaved lupin/oat mixtures were collected from an area of 1 m² and to the depth of 30 cm in each plot in order to determine their dry matter yield. The residue dry matter was used to determine total nitrogen content (by means of Kjeldahl method).

Winter triticale cv. Borwo was sown in mid-September at the rate of 239 grains m⁻². Pre-plant phosphorus and potassium applications were made at the rates adjusted to soil availability, that is 70 kg ha⁻¹ P and 99 kg ha⁻¹ K. Nitrogen fertiliser was split into two rates of 40 and 60 kg ha⁻¹ applied, respectively, after the cereal resumed growth in the spring, and at the stage of stem elongation. Winter triticale was harvested in late July. Grain yield was determined in each plot and its average samples were taken to determine total nitrogen by Kjeldahl method (AOAC, 2006). Additionally, 1000 grain weight was recorded.

Analysis of variance (split-block) was performed on the data for each experimental characteristic. Means were compared using Tukey's test, at the significance level of P ≤ 0.05, when significant sources of variation had been confirmed. All the statistical calculations were performed using the authors' algorithms in MS Excel 7.0.

Table 1. The agrotechnics of mixtures narrow-leaved lupin + spring rye in experiment 2010-2012

Forecrop – mixtures	Fertilization			Plant protection
	Before sowing		BBCH 31-32	
	in autumn	in spring		
Narrow-leaved lupine – pure stand 100%	35.2 kg⊙ha ⁻¹ P 99.6 kg⊙ha ⁻¹ K	-	-	mechanical weed control (harrow)
Spring rye – pure stand 100%	35.2 kg⊙ha ⁻¹ P 99.6 kg⊙ha ⁻¹ K	30 kg⊙ha ⁻¹ N	50 kg⊙ha ⁻¹ N	mechanical weed control (harrow)
Narrow-leaved lupine 75% + spring rye 25%	35.2 kg⊙ha ⁻¹ P 99.6 kg⊙ha ⁻¹ K	30 kg⊙ha ⁻¹ N	30 kg⊙ha ⁻¹ N	mechanical weed control (harrow)
Narrow-leaved lupine 50% + spring rye 50%	35.2 kg⊙ha ⁻¹ P 99.6 kg⊙ha ⁻¹ K	30 kg⊙ha ⁻¹ N	30 kg⊙ha ⁻¹ N	mechanical weed control (harrow)
Narrow-leaved lupine 25% + spring rye 75%	35.2 kg⊙ha ⁻¹ P 99.6 kg⊙ha ⁻¹ K	30 kg⊙ha ⁻¹ N	30 kg⊙ha ⁻¹ N	mechanical weed control (harrow)

Results

Dry matter yield of the post-harvest residues of narrow-leaved lupin/spring rye mixtures

The dry matter yield of the post-harvest residues of narrow-leaved lupin/spring rye mixtures was significantly affected by the experimental factors and their interaction (Table 2).

Table 2. Dry matter quantity of forecrop post-harvest residues (averaged across 2010-2011), t⊙ha⁻¹

Forecrop – mixtures (I)	Forecrop harvest date (II)		Means
	Stage of narrow-leaved lupine flowering	Stage of narrow-leaved lupine flat green pod	
Narrow-leaved lupine – pure stand 100%	4.86a*	5.78a	5.32A
Spring rye – pure stand 100%	5.12a	6.84b	5.98B
Narrow-leaved lupine 75% + spring rye 25%	4.93a	5.87a	5.40AB
Narrow-leaved lupine 50% + spring rye 50%	5.03a	6.42ab	5.73AB
Narrow-leaved lupine 25% + spring rye 75%	5.09a	6.69b	5.89AB
Means	5.01A	6.32B	-
<i>ANOVA</i>	P-value		HSD _{0.05}
Forecrop – mixtures (I)	<0.001		0.61
Forecrop harvest date (II)	<0.001		0.28
Interaction: IxII	<0.001		0.74

*Values in columns followed by the same small letter and values in rows followed by the same capital letter do not differ significantly at P < 0.05

The greatest post-harvest residue biomass was supplied by spring rye cultivated in pure stand and mixed with narrow-leaved lupin. The lowest biomass of post-harvest residues was introduced to the soil by narrow-leaved lupin grown in pure stand. Harvest date had a significant influence on the quantity of dry matter of post-harvest residues of narrow-leaved lupin mixed with spring rye, it being higher for mixtures harvested at the stage of narrow-leaved lupin flat green pod compared with the flowering stage. An interaction of the experimental factors resulted in the highest biomass of post-harvest residues being supplied by spring rye and its mixtures with narrow-leaved lupine when they contained 25 + 75% and 50 + 50% of the respective components.

Nitrogen amount supplied to the soil by incorporating the biomass of post-harvest residues

Statistical analysis revealed a significant impact of the experimental factors and their interaction on the amount of nitrogen introduced into the soil with the incorporated biomass of the post-harvest residues of narrow-leaved lupin and spring rye (Table 3).

Table 3. Nitrogen amount introduced into soil with incorporated biomass of post-harvest residues (averaged across 2010-2011), kg ha⁻¹

Forecrop – mixtures (I)	Forecrop harvest date (II)		Means
	Stage of narrow-leaved lupine flowering	Stage of narrow-leaved lupine flat green pod	
Narrow-leaved lupine – pure stand 100%	114.7d*	135.2d	124.9D
Spring rye – pure stand 100%	68.4a	79.8a	74.1A
Narrow-leaved lupine 75% + spring rye 25%	98.9c	121.4dc	110.2C
Narrow-leaved lupine 50% + spring rye 50%	92.6b	109.7b	101.2C
Narrow-leaved lupine 25% + spring rye 75%	81.5b	91.6b	86.6B
Means	91.2A	107.6B	-
<i>ANOVA</i>	P-value		HSD _{0.05}
Forecrop – mixtures (I)	<0.001		10.2
Forecrop harvest date (II)	<0.001		3.8
Interaction: IxII	<0.001		12.4

*Values in columns followed by the same small letter and values in rows followed by the same capital letter do not differ significantly at P < 0.05

The highest nitrogen amount was associated with an incorporation of narrow-leaved lupine post-harvest residues, the quantity of nitrogen accumulated by legume/cereal post-harvest residues being lower. Of the legume/cereal mixtures, the 75 + 25% and 50 + 50% mixtures were the greatest nitrogen contributors. The mixture containing 25 + 75% of narrow-leaved lupin and spring rye, respectively, supplied less nitrogen accumulated in its post-harvest residues, it being the lowest in spring rye-post harvest residues. Forecrop harvest date had a significant effect on nitrogen amount introduced into the soil due to an application of post-harvest residues. More nitrogen was supplied

by the post-harvest residues of narrow-leaved lupin/spring rye mixtures harvested at the stage of narrow-leaved lupin green pod stage, compared with the flowering stage. An interaction between experimental factors was confirmed. Narrow-leaved lupin grown in pure stand and harvested at the flat green pod stage provided more nitrogen in its post-harvest residues. Of the mixtures, the post-harvest residues of narrow-leaved lupin/spring rye mixtures containing 75 + 25% and 50 + 50% of the respective components harvested at the stage of narrow-leaved lupin flat green pod introduced more nitrogen into the soil than the 25 + 75% mixture harvested at the same development stage. The post-harvest residues of spring rye harvested at the stage of narrow-leaved lupin flowering and flat green pod were the poorest nitrogen sources.

Winter triticale grain yield

Winter wheat grain yield was significantly affected by the experimental factors and their interaction (Table 4).

Table 4. Winter triticale grain yield (averaged across 2011-2012), $t\circ ha^{-1}$

Forecrop – mixtures (I)	Forecrop harvest date (II)		Means
	Stage of narrow-leaved lupine flowering	Stage of narrow-leaved lupine flat green pod	
Narrow-leaved lupine – pure stand 100%	9.02cd*	9.83c	9.43CD
Spring rye – pure stand 100%	6.37a	7.08a	6.73A
Narrow-leaved lupine 75% + spring rye 25%	8.78c	9.74c	9.26C
Narrow-leaved lupine 50% + spring rye 50%	9.47d	10.18c	9.83D
Narrow-leaved lupine 25% + spring rye 75%	7.19b	8.76b	7.98B
Means	8.17A	9.12B	-
<i>ANOVA</i>	P-value		HSD _{0.05}
Forecrop – mixtures (I)	<0.001		0.48
Forecrop harvest date (II)	<0.001		0.24
Interaction: IxII	<0.001		0.55

*Values in columns followed by the same small letter and values in rows followed by the same capital letter do not differ significantly at $P < 0.05$

The highest winter triticale grain yield was obtained following an incorporation of the pos-harvest residues of narrow-leaved lupin grown in pure stand and mixed with spring rye, the respective components being 50 + 50%. In the remaining plots, grain yield was significantly lower, it being the lowest following an incorporation of spring rye post-harvest residues. Harvest date significantly affected winter triticale grain yield. The yield was higher when narrow-leaved lupin/spring rye mixtures had been harvested at the stage of narrow-leaved lupin flat green pod rather than the flowering stage. An interaction between the experimental factors was confirmed. The highest winter triticale grain yield was produced after the cereal followed an incorporation of the post-harvest residues of narrow-leaved lupin/spring rye mixture harvested at the stage of narrow-

leafed lupin flat green pod, and pure-stand narrow-leaved lupin harvested at the aforementioned stage. The lowest yield was produced by cereal following the post-harvest residues of spring rye harvested at the stage of narrow-leaved lupin flowering.

1000 grain weight of winter triticale

1000 grain weight of winter triticale was significantly affected by the experimental factors and their interaction (Table 5).

Table 5. Winter triticale 1000 grain weight (averaged across 2011-2012), g

Forecrop – mixtures (I)	Forecrop harvest date (II)		Means
	Stage of narrow-leaved lupine flowering	Stage of narrow-leaved lupine flat green pod	
Narrow-leaved lupine – pure stand 100%	46.7c*	47.9c	47.3C
Spring rye – pure stand 100%	43.5a	44.9a	44.2A
Narrow-leaved lupine 75% + spring rye 25%	46.8cd	47.2c	47.0C
Narrow-leaved lupine 50% + spring rye 50%	47.5d	48.9d	48.2D
Narrow-leaved lupine 25% + spring rye 75%	45.3b	46.0b	45.7B
Means	46.0A	47.0B	-
<i>ANOVA</i>	P-value		HSD _{0.05}
Forecrop – mixtures (I)	<0.001		0.5
Forecrop harvest date (II)	<0.001		0.2
Interaction: IxII	<0.001		0.7

*Values in columns followed by the same small letter and values in rows followed by the same capital letter do not differ significantly at P < 0.05

The highest 1000 grain weight was recorded for winter triticale following an incorporation of the post-harvest residues of narrow-leaved lupin/spring rye mixture containing 50 + 50% of the respective components. 1000 weight of winter triticale following an incorporation of the post-harvest residues of 75 + 25% mixture of narrow-leaved lupine and spring rye was similar but lower than the value recorded for the best experimental unit. In the remaining plots, significantly lower values were recorded, in particular after an incorporation of spring rye post-harvest residues. Harvest date had a significant influence on 1000 grain weight, it being higher after winter triticale followed narrow-leaved lupin/spring rye mixtures harvested at the stage of narrow-leaved lupine flat green pod stage rather than the legume flowering stage. An interaction was confirmed: the highest 1000 grain weight of winter triticale was recorded after an incorporation of the post-harvest residues of the 50 + 50% mixture of narrow-leaved lupine and spring rye harvested at the stage of narrow-leaved lupine flat green pod. 1000 grain weight of winter triticale following an incorporation of the post-harvest residues of narrow-leaved lupin grown in pure stand and the 75 + 25% mixture of narrow-leaved lupin and spring rye harvested at the stage of narrow-leaved lupin flat

green pod, although significantly lower, remained at a beneficial level. The lowest 1000 grain weight of winter triticale was recorded after an incorporation of the post-harvest residues of spring rye, regardless of the harvest date.

Total nitrogen amount accumulated in winter triticale grain

Statistical analysis demonstrated a significant effect of the experimental factors and their interaction of the total nitrogen amount accumulated in winter triticale grain (Table 6).

Table 6. Total nitrogen amount accumulated in winter triticale grain (averaged across 2011-2012), kg ha⁻¹

Forecrop – mixtures (I)	Forecrop harvest date (II)		Means
	Stage of narrow-leaved lupine flowering	Stage of narrow-leaved lupine flat green pod	
Narrow-leaved lupine – pure stand 100%	168.6c*	181.7bc	175.2B
Spring rye – pure stand 100%	128.9a	139.5a	134.2A
Narrow-leaved lupine 75% + spring rye 25%	169.5c	179.3b	174.4B
Narrow-leaved lupine 50% + spring rye 50%	180.6c	196.7c	188.7B
Narrow-leaved lupine 25% + spring rye 75%	142.4b	148.1a	145.3A
Means	158.0A	169.1B	-
<i>ANOVA</i>	P-value		HSD _{0.05}
Forecrop – mixtures (I)	<0.001		14.5
Forecrop harvest date (II)	<0.001		9.0
Interaction: IxII	<0.001		16.2

*Values in columns followed by the same small letter and values in rows followed by the same capital letter do not differ significantly at P < 0.05

The highest total nitrogen amount was accumulated in the grain of winter triticale following the post-harvest residues of narrow-leaved lupin/spring rye mixture containing 50 + 50% of the respective components, and narrow-leaved lupin grown in pure stand. In the remaining units, total nitrogen amount accumulated in winter triticale grain was significantly lower after an incorporation of the post-harvest residues of narrow-leaved lupin/spring rye mixtures, it being the lowest following an incorporation of spring rye post-harvest residues. Harvest date had a significant impact on the amount of total nitrogen accumulated in winter triticale grain. More nitrogen was accumulated in the grain of winter triticale grown after an incorporation of the post-harvest residues of narrow-leaved lupin mixed with spring rye harvested at the stage of narrow-leaved lupin flat green pod rather than the flowering stage. An interaction of the experimental factors was confirmed it indicating that total nitrogen accumulation in grain was the highest when winter triticale was cultivated after the ploughing down of the post-harvest residues of 50 + 50% mixture of narrow-leaved lupin and spring rye, and pure-stand narrow-leaved lupin harvested at the stage of flat green pod. The lowest total nitrogen

amount was accumulated in the grain of winter triticale following an incorporation of the post-harvest residues of spring rye harvested at the stage of narrow-leaved lupin flowering and flat green pod.

Discussion

The research reported in this work demonstrated that the post-harvest residues of narrow-leaved lupin and its mixtures with spring rye are a valuable source of biological nitrogen for winter triticale. Modern agriculture strives for reducing mineral nitrogen application and replacing it with biological nitrogen which does not pose a threat to the environment (Bergvist, 2003; Hauggard-Nielsen et al., 2012). Also Thorsed et al. (2006) and Arlauskienė and Maikstienė (2008) reported that, following biological transformation, incorporated biomass becomes a source of nitrogen for the crop plants in the subsequent year. In the experiment reported here, the highest amount of post-harvest residues was supplied by spring rye and narrow-leaved lupin/spring rye mixtures containing 25 + 75% and 50 + 50% of the respective components. Buraczyńska et al. (2011), who cultivated field pea, spring wheat and their mixtures for seed production purposes, found that highest amounts of post-harvest residues were supplied by spring triticale grown in pure stand and mixed with field pea, the respective components being 25 + 75%. High biomass production by grasses and cereals was also confirmed by Watson et al. (2002), Arlauskienė and Maikstienė (2008), Nemeikšienė et al. (2010) and Sarunaite et al. (2013). In the present study, the post-harvest residues of narrow-leaved lupin grown in pure stand introduced the lowest biomass amount into the soil. Also research by Bergvist (2003) and Panagiotis (2015) confirmed that, compared with cereals or grasses, leguminous plants supply less biomass, which is due to the fact that their rooting system is not as well developed as that of grasses although narrow-leaved lupin forms a tap root system. In the present experiment, harvest date had a significant effect on the amount of dry matter supplied by the post-harvest residues of narrow-leaved lupin/spring rye mixtures. A significantly higher amount of post-harvest biomass was supplied by the legume/cereal mixtures harvested at the stage of narrow-leaved lupine flat green pod compared with the flowering stage. It can be explained by the fact that plants harvested at a more advanced growth stage develop more root matter, which translates into a higher amount of biomass supplied with post-harvest residues.

Post-harvest residues of leguminous plants and their mixtures with cereals are a valuable source of biological nitrogen for the following crops (Buraczyńska et al., 2011). In the present study, the highest nitrogen quantity was supplied to the soil with the post-harvest residues of narrow-leaved lupin, which corresponds with findings reported by Bergvist (2003), Thorsed et al. (2006), Sarunaite et al. (2013) and Panagiotis (2015). It should be stressed that the post-harvest residues of legume/cereal mixtures supply large nitrogen amounts for the following crop (Lemola et al., 2000; Känkänen and Eriksson, 2007; Kramberger et al., 2009; Buraczyńska et al., 2011). In the study discussed here, the highest nitrogen supply was associated with the 75 + 25% and 50 + 50% mixtures of narrow-leaved lupin and spring rye, it being the lowest for spring rye crop residues, which is due to the fact that non-legumes contain less nitrogen and, as a result, are poorer sources of this element for the following plant. The research by Känkänen and Eriksson (2007) confirms this finding as the authors demonstrated that grasses provided less nitrogen for the crop that followed. In the study reported here, harvest date had a significant influence on the amount of nitrogen introduced into the

soil with post-harvest residues. More nitrogen was supplied by residues of narrow-leaved lupin mixed with spring rye and harvested at the stage of narrow-leaved lupin flat green pod compared with the flowering stage, which can be explained by the fact that plants harvested at an earlier development stage contained more nitrogen but their supply of this element is lower because they develop less biomass in the form of post-harvest residues than plants harvested later in the season, the finding corresponding with results reported by Mechri et al. (2016).

Studies by Smagacz (2004), Piekarczyk (2010), Prusiński et al. (2016) and Faligowska et al. (2019) demonstrated that the grain yield of winter cereals following leguminous crops was higher compared with cereal forecrops. Triticale is a species which has been recently introduced for cultivation. As a result, there is a paucity of research into the effect of agrotechnological factors, including forecrop, on triticale yield (Noworolnik and Jaśkiewicz, 2018). In the present study, the highest grain yield of winter triticale was recorded after the cereal followed the narrow-leaved lupin/spring rye mixture containing 50 + 50% of the respective components, and after pure-stand narrow-leaved lupin. High grain yield was also recorded after an incorporation of the 75 + 25% mixture of narrow-leaved lupin and spring rye harvested at the stage of narrow-leaved lupin flat green pod. Research by Buraczyńska et al. (2011) revealed that the highest winter wheat grain yield was associated with an incorporation of the post-harvest residues and straw of spring triticale/field pea mixture containing 25 + 75% of the respective components, as well as field pea post-harvest residues and straw. Also Pszczołkowska et al. (2018) reported a high increase in spring wheat grain yield following leguminous plants. In turn, Känkänen et al. (2001), Känkänen and Erikssen (2007) as well as Nemeikšien et al. (2010) reported that undersown legumes positively affected cereal grain yield. In the experiment reported here, winter triticale grain yield was the lowest following an incorporation of spring rye post-harvest residues. Piekarczyk (2010) and Buraczyńska et al. (2011) demonstrated that post-harvest residues of cereals grown for grain contributed to a decline in cereal grain yield compared with leguminous residues. Känkänen and Erikssen (2007) as well as Nemeikšien et al. (2010) reported a decline in grain yield when cereal had followed undersown grasses. It may have been due to the fact that leguminous plants and their mixtures with cereals or grasses have a narrower C:N ratio compared with cereals or grasses. It contributed to a more rapid decomposition of the incorporated biomass and release of more nitrogen to be used by the following crop which was able to produce a higher yield. In the present study, harvest date of narrow-leaved lupin/spring rye mixtures significantly affected winter triticale grain yield. The yield was higher following an incorporation of the post-harvest residues of narrow-leaved lupine mixed with spring rye and harvested at the stage of flat green pod compared with the flowering stage. This finding can be explained by the fact that post-harvest residues of narrow-leaved lupin/spring rye mixtures ploughed down at an earlier development stage undergo more rapid mineralization, and the following crop cannot fully utilize the nitrogen provided in this way. The element is leached into deeper soil layers and pollutes the soil environment. Better results may be obtained after an incorporation of post-harvest residues of narrow-leaved lupin/spring rye mixtures at a later development stage, that is the stage of narrow-leaved lupine flat green pod.

In the present study, the highest 1000 grain weight of winter triticale was recorded after the cereal followed the 50 +50% mixture of narrow-leaved lupin and spring rye. Good results were also obtained for winter triticale grown after an incorporation of the

narrow-leaved lupin/spring mixture containing 75 + 25% of the respective components. Also research by Buraczyńska et al. (2011) demonstrated that the highest 1000 grain weight of winter wheat, in addition to the greatest grain yield, was produced when the crop had followed a spring triticale/field pea mixture containing 25 + 75% of the respective components. It may be explained by the fact that winter cereal growing in good, biological nitrogen-rich soil performs well in terms of grain yield and fill.

In the experiment reported here, winter triticale grain accumulated different amounts of total nitrogen depending on the forecrop. The highest total nitrogen quantity was determined in the grain of winter triticale following the narrow-leaved lupin/spring rye mixture containing 50 + 50% of the respective components as well as narrow-leaved lupin grown in pure stand, which corresponds with findings reported by Buraczyńska et al. (2011). These authors obtained the highest nitrogen amounts in the grain of winter wheat following field pea grown for grain, and after spring triticale/field pea mixture containing 25 + 75% of the respective components. A positive effect of leguminous plants on nitrogen accumulation in cereal grain has also been reported by Känkänen and Eriksson (2007), Herridge et al. (2008), Nemeikšien et al. (2010) and Hauggard-Nielsen et al. (2012), which was due to the fact that the post-harvest residues of legumes leave a large quantity of nitrogen compared with non-legumes, a great share of this nitrogen being available for the following plant after mineralization. The work reported here demonstrated that the narrow-leaved lupin/spring rye mixture containing 75 + 25% of the respective components positively affected nitrogen accumulation in winter triticale grain. The amount of total nitrogen was higher when winter triticale had followed narrow-leaved lupin mixed with spring rye and harvested at the flat green pod stage compared with the flowering stage. The possible explanation is that the post-harvest residues of narrow-leaved lupin/spring rye mixtures accumulated more nitrogen at the legume flat green pod stage than the flowering stage. As a result, the cereal retrieved the nitrogen fixed from the air by legumes thus reducing the risk of nitrogen leaching (Nykänen et al., 2009; Nemeikšiene et al., 2010). Taking the above into account, it seems necessary to continue research on the forecrop effect of post-harvest residues of other legume/cereal mixture combinations in winter cereal production.

Mixture of narrow-leaved lupine with spring rye with 50% + 50% components collected in the flat green pod stage is a good forecrop for winter triticale.

Conclusions

- 1) The greatest quantity of post-harvest residues was supplied by spring rye and narrow-leaved /spring rye mixtures containing 25 + 75% and 50 + 50% of the respective components harvested at the stage of narrow-leaved lupin flat green pod, the nitrogen supply being the highest for narrow-leaved lupin harvested at the aforementioned development stage.
- 2) The highest grain yield was produced by winter triticale cultivated after an incorporation of the post-harvest residues of narrow-leaved lupin/spring rye mixture containing 50 + 50% of the respective components and harvested at the stage of legume flat green pod.
- 3) Grain of winter triticale following an incorporation of the post-harvest residues of narrow-leaved lupin/spring rye mixtures had the highest 1000 grain weight and the greatest nitrogen accumulation, regardless of the date on which the mixtures were harvested.

- 4) It is recommended to continue research on the subsequent impact of legumes and cereals on the yield of winter cereals or winter oilseed rape.

REFERENCES

- [1] AOAC (2006): Official methods of analysis of AOAC International. – 18th edition, Horwitz, W., Latimer Jr., G. (eds.), Publisher: Gaihersburg.
- [2] Arlauskienė, A., Maikstienė, S. (2008): The effects of cover crops and straw on soil mineral nitrogen dynamics and losses from arable land. – *Agronomijas Vēstis* 11: 195-201.
- [3] Bergvist, G. (2003): Effect of white clover and nitrogen availability on the grain yield of winter wheat in a three-season intercropping system. – *Soil Plant Science* 53: 97-109.
- [4] Buraczyńska, D., Ceglarek, F., Gąsiorowska, B., Zaniewicz-Bajkowska, A., Płaza, A. (2011): Cultivation of wheat following pea and triticale/pea mixtures increases yields and nitrogen content. – *Acta Agric. Scan. Ser. B, Soil and Plant Sci.* 61: 622-632.
- [5] Faligowska, A., Szymańska, G., Panasiewicz, K., Szukala, J., Koziara, W., Ratajczak, K., (2019): The long-term effect of legumes as forecrops on the productivity of rotation (winter rape-winter wheat-winter wheat) with nitrogen fertilization. – *Plant, Soil and Env.* 65(3): 138-144.
- [6] Hauggard-Nielsen, H., Mundus, S., Jensen, E.S. (2012): Grass-clover undersowing affects nitrogen dynamics in a grain legume-cereal arable cropping system. – *Field Crops Research* 136: 23-31.
- [7] Herridge, D.F., Peoples, M.B., Boddey, R.M. (2008): Global inputs of biological nitrogen fixation in agricultural system. – *Plant and Soil* 311: 1-18.
- [8] Jensen, E.S., Hauggaard-Nielsen, H. (2003): How can increased use of biological N₂ fixation in agriculture benefit the environment? – *Plant and Soil* 252: 177-186.
- [9] Känkänen, H., Eriksson, C., Rökköläinen, M., Vuorinen, M. (2001): Effect of annually repeated undersowing on cereal grain yields. – *Agricultural and Food Science in Finland* 10: 197-208.
- [10] Känkänen, H., Eriksson, C. (2007): Effects of undersown crops on soil mineral N and grain yield of spring barley. – *European Journal of Agronomy* 27: 25-34.
- [11] Kramberger, B., Gselman, A., Janzekovic, M., Kaligarić, M., Bracko, B. (2009): Effects of cover crops on soil mineral nitrogen and on yield and nitrogen content of maize. – *European Journal of Agronomy* 31: 103-109.
- [12] Lemola, R., Turtola, E., Eriksson, C. (2000): Undersowing Italian ryegrass diminishes nitrogen leaching from spring barley. – *Agric. Food Sci. Finland* 9: 201-215.
- [13] Mayer, J., Buegger, F., Jensen, E.S. (2003): Residual nitrogen contribution from grain legumes to succeeding wheat and rape and related microbial process. – *Plant and Soil* 255(2): 541-554.
- [14] Mechri, M., Patil, S.B., Saidi, W., Hajri, R., Jarrahi, T., Gharbi, A., Jedidi, N. (2016): Soil organic carbon and nitrogen status under fallow and cereal-legume species in a Tunisian semi-arid conditions. – *European Journal of Earth and Environment* 3(1): 1-13.
- [15] Nemeikšienė, D., Arlauskienė, A., Šlepetienė, A. (2010): Mineral nitrogen content in the soil and winter wheat productivity as influenced by the pre-crop grass species and their management. – *Žemdirbyste=Agriculture* 97(4): 23-36.
- [16] Noworolnik, K., Jaśkiewicz, B. (2018): Wpływ zróżnicowanych warunków glebowych na plonowanie odmian pszenżyta ozimego. – *Frag. Agron.* 35(1): 62-71.
- [17] Nykänen, A., Salo, T., Granstedt, A. (2009): Simulated cereal nitrogen uptake and soil mineral nitrogen after clover-grass leys. – *Nutrient Cycling in Agroecosystems* 85: 1-15.
- [18] Panagiotis, D. (2015): Grain legume effects on soil nitrogen mineralization potential and wheat productivity in Mediterranean environment. – *Archives of Agronomy and Soil Science* 61(4): 461-473.

- [19] Piekarczyk, M.(2010): Effect of forecrops and nitrogen fertilization on the yield and grain technological quality of winter wheat grown on light soil. – Acta Sci. Pol. Agric. 9(2): 25-33.
- [20] Prusiński, J., Borowska, M., Kaszkowiak, E., Olszak, G. (2016): The after-effect of chosen Fabaceae forecrops on the yield of grain and protein in winter triticales (*Triticosecale* sp. Wittmack ex A. Camus 1027) fertilized with mineral nitrogen. – Plant, Soil and Environ. 62(12): 571-576.
- [21] Pszczółkowska, A., Okorski, A., Olszewski, J., Fordoński, G. (2018): Effects of pre-preceding leguminous crops on yield and chemical composition of winter wheat grain. – Plant, Soil and Env. 64(12):592-596.
- [22] Sarunaite, L., Kadziuline, Z., Deveikyte, I., Kadziulis, L. (2013): Effect of legume biological nitrogen on cereals yield and soil nitrogen budget in double-cropping system. – Journal of Food Agriculture and Environment 11(1): 528-533.
- [23] Smagacz, J. (2004): Reakcja wybranych odmian pszenicy ozimej na przedplon. – Biul. IHAR 231: 65-71.
- [24] Thorsted, M.D., Olesen, J.E., Weiner, J. (2006): Mechanical control of clover improves nitrogen supply and growth of wheat in winter wheat/white clover intercropping. – European Journal of Agronomy 24: 149-155.
- [25] Tripolskaja, L., Šidlauskas, G. (2010): The influence of catch crops for green manure and straw on the infiltration of atmospheric precipitation and nitrogen leaching. – Žemdirbyste=Agriculture 97(1): 83-92.
- [26] Watson, C.A., Atkinson, D., Gosling, P. (2002): Managing soil fertility in organic farming systems. – Soil Use and Management 18: 239-247.

BIOCHEMICAL RESPONSES AND SALT REMOVAL POTENTIAL OF *PEGANUM HARMALA* L. (WILD RUE) UNDER DIFFERENT NaCl CONDITIONS

KARAKAS, S.

*Harran University, Faculty of Agriculture, Department of Soil Science and Plant Nutrition,
63300 Sanliurfa, Turkey
(e-mail: skarakas@harran.edu.tr)*

(Received 6th Dec 2019; accepted 6th May 2020)

Abstract. In this study, biochemical and molecular responses of *Peganum harmala* L. (wild rue) were investigated following NaCl treatment (0, control-, 150- and 300 mmol L⁻¹) under growth room conditions. *P. harmala* seeds were placed in pots to germinate the seeds. NaCl application to the seedlings was done at the 4th week of seedling growth. The plants were then respectively irrigated with NaCl solution for a period of 5-week. Following harvest, it was noted that fresh and dry weights of *P. harmala* increased with salinity levels. Chlorophyll-*a* and *b*, proline, and malondialdehyde and hydrogen peroxide contents as well as the activity of antioxidant enzymes such as catalase and peroxidase significantly increased as a result of treatments at concentrations between 150 and 300 mmol L⁻¹ NaCl when compared to those of control plants ($P \leq 0.05$). The highest Na⁺ and Cl⁻ ions were 78.8 and 68.1 mg g⁻¹ DW at 300 mmol L⁻¹ NaCl, respectively. On the other hand, ion contents such as K⁺, Ca⁺⁺ and Mg⁺⁺ decreased under 150-300 mmol L⁻¹ NaCl when compared to the control plants ($P \leq 0.05$). Removal of Na⁺ as the adjusted removal capacity per hectare under field conditions were 304.6 and 404.2 kg at 150- and 300 mmol L⁻¹ NaCl concentrations. DNA damage measurement showed that DNA integrity of the halophyte preserved its uniform shape at 150- and 300 mmol L⁻¹ NaCl according to measurements of the results of the comet assay. This study showed that *P. harmala* could well used to clean-up highly saline soils to regain them for agricultural purposes.

Keywords: *phytoremediation, salt stress, ameliorate, comet assay, DNA damage*

Introduction

Salt stress in soil layers or in irrigation waters is a major threat to modern agriculture via causing inhibition and impairment of plant growth and productivity, especially in arid and semi-arid regions of the world (Hussain et al., 2009; Isayenkov and Maathuis, 2019). More than 20% of cultivated land worldwide, which is about 45 million hectares is affected by salt stress and the amount is increasing day by day (Gupta and Huang, 2014; Shrivastava et al., 2015). A soil is considered to be saline when the electric conductivity (EC) of the soil solution reaches 4 dS m⁻¹ (equivalent to approximately 40 mmol L⁻¹ NaCl) and it generates an osmotic pressure of about -0.2 MPa. Under these circumstances, yields of most of the crops are significantly reduced. As a consequence, ion toxicity lead to chlorosis and necrosis mainly due to Na⁺ accumulation that interferes with many physiological processes in plants (Munns and Tester, 2008; Roupheal et al., 2018). Under saline conditions, plants have to activate different physiological and biochemical mechanisms in order to cope with the resulting stress. Such mechanisms include changes in toxic ion uptake, ion compartmentation and/or exclusion, osmotic regulation, photosynthesis, chlorophyll content, toxic ion distribution, homeostasis, reactive oxygen species (ROS), and antioxidant metabolites and enzymes (Ashraf and Haris, 2013; Acosta-Motos et al., 2017; Carillo, 2019).

Plants on the basis of adaptive evolution can be classified as either glycophytes or halophytes (Gupta and Huang, 2014; Cheeseman, 2015). Glycophytes are not

salt-tolerant plants, which include most of the crop plants. The survival of these plants is seriously retarded after 100-200 mmol L⁻¹ NaCl concentrations (Zakharin and Panichkin, 2009; Carillo et al., 2011). Halophytic plants are known to accumulate excess salts in tissues, they remove salt from the immediate environment (Simpson et al., 2018). They are naturally adapted to live in soil characterized by high salt concentrations. They do not have problems with salinity exceeding 300-400 mmol L⁻¹ NaCl. They have developed better salt resistance mechanisms as described above (Stuart et al., 2012; Cheeseman, 2015).

P. harmala belongs to Zygophyllaceae family, which is a perennial plant growing spontaneously in semi-arid conditions, stepp areas and sandy soils. It is native to eastern Mediterranean region. It is a shrub, 0.3-0.8 m tall with short creeping roots, white flowers and round seed capsules carrying more than 50 seeds. The plant is widely distributed and used as a medicinal plant in Central Asia, North Africa and Middle East (Frison et al., 2008; Wanntorp and Ronse De Craene, 2011). In this study, we aimed to determine the performance of *P. harmala* in terms of biochemical responses and Na⁺ ion removal capacity under different NaCl conditions (0, control-, 150- and 300 mmol L⁻¹) for phytoremediation purposes.

Material and Methods

Experimental set up and plant growth

Experiment was conducted at the University of Harran, Sanliurfa, Turkey. The halophyte species of *P. harmala* seeds were initially sterilized with 70% ethanol for 30 s and then with 0.1% (w/v) HgCl₂ for five min following three washes with sterile distilled water. Trials were performed in a randomized block design with three replicates. Air-dry soil was passed through 4-mm sieve for the pot experiment and 2-mm sieve for the analysis of physicochemical properties. Soil saturated paste was prepared and electrical conductivity (EC), pH were measured (Richards, 1954). Texture (clay, silt and sand) was determined by using Bouyoucos hydrometer method (Bouyoucos, 1953). Physicochemical properties are reported in *Table 1*. The seeds at batches of 10 were sown into the 1.5 L plastic pots containing 1 kg of air-dry in a growth room at 35/25°C of day/night temperature. After germination, the seedlings were irrigated with full pot capacity during this period; salt treatments were started with the irrigation water containing various concentrations of NaCl (0 (control)-, 150- and 300 mmol L⁻¹) solutions (*Fig. 1*). The treatment continued for further 5 weeks, then the plants were harvested for the evaluation of salinity responses. For this, the harvested leaves of *P. harmala* were stored at -22°C until analyses.

Table 1. *Physicochemical properties of the soil*

<i>Soil parameter</i>	<i>Values</i>
EC (dS m ⁻¹)	1.2
pH	7.8
Clay (%)	56.7
Silt (%)	32.5
Sand (%)	10.8

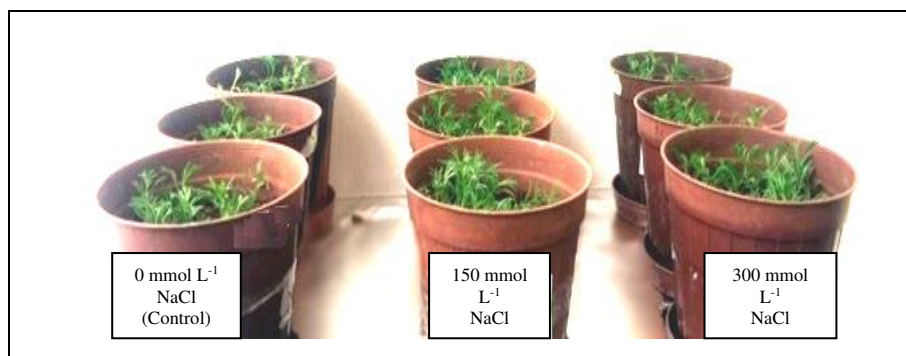


Figure 1. Growth of *P. harmala* at different NaCl conditions

Growth parameters

For the growth analysis, the fresh weight (FW) was determined right after the harvest. The dry weight (DW) of plants was determined after drying of samples at 70°C until they reached a constant weight.

Determination of biochemical responses

Chlorophyll (Chl-*a* and Chl-*b*) contents of *P. harmala* were determined based on the method of Arnon (1949) with slight modifications (Dikilitas, 2003). Leaf samples (0.5 g) were homogenized in a 10 mL acetone:water (80:20, v:v) mixture and filtered through Whatman No.2 filter paper then placed in dark tubes. Chl-*a* and Chl-*b* of the plant samples were read at a UV microplate spectrophotometer (Epoch, SN: 1611187, made in USA) at 663-645 nm respectively against 80% acetone blank. The results were calculated as mg L⁻¹ and expressed as mg g⁻¹ fresh weight.

The proline (pro) measurement was conducted according to the method of Bates et al. (1973) with slight modifications (Karakas et al., 2019a). Leaf material (0.5 g) was homogenized in 3% w/v sulphosalicylic acid using a mortar and a pestle. The homogenate was filtered through Whatman No. 2 filter paper. Then, 2 mL of filtrate was mixed in a test tube with 2 mL of acid-ninhydrin reagent (1.25 g of ninhydrin in 30 mL of glacial acetic acid and 20 mL of 6 M phosphoric acid) and boiled at 100°C for one hour. The reaction was terminated in an ice bath. The reaction mixture was then extracted using 5 mL of toluene. The tubes were thoroughly shaken for 15-20 seconds and left for 20 min at room temperature in order to achieve separation for two layers. The chromophore containing toluene was removed and allowed to warm to room temperature, and the absorbance of the solution was measured at 515 nm using a toluene blank. Proline concentration was determined using calibration curve made with L-proline (Sigma-Aldrich 81202-06-4) as µmol g⁻¹ fresh tissue.

The malondialdehyde (MDA) content was determined according to the method of Sairam and Saxena (2000) with slight modifications (Karakas et al., 2019a). Leaf material (0.5 g) was homogenized in 10 ml of 0.1% (w/v) TCA solution. The homogenate was centrifuged at 10,000g for five minutes. Four mL of 20% v/v TCA containing 0.5% v/v thiobarbituric acid (TBA) was added to one milliliter of the supernatant. The mixture was incubated in boiling water for 30 min, and the reaction was stopped by placing the reaction tubes in an ice bath. The mixture was centrifuged again at 10,000g for 5 min and the absorbance of the supernatant was read at 532 and 600 nm. Here, the MDA content of leaves is expressed as nmol g⁻¹ fresh tissue (*Eq. 1*).

$$MDA (nmol g^{-1}) = \frac{\text{Extract volume (ml)} \times [(A_{532} - A_{600}) / (155 mM^{-1} cm^{-1})]}{\text{Sample amount (g)}} \times 10^3 \quad (\text{Eq.1})$$

Catalase enzyme activity (CAT, E.C. 1.11.1.6) was determined by monitoring the decomposition of H₂O₂ according to the method of Milosevic and Slusarenko (1996) with slight modifications (Karakas et al., 2019a). Fresh leaf tissue (0.5 g) was homogenized in 10 mL of 50 mmol L⁻¹ Na-phosphate buffer solution, then 50 µL of plant extract was added to a 2.95 mL (10 mmol L⁻¹ H₂O₂, 50 mmol L⁻¹ Na-phosphate buffer and 4 mmol L⁻¹ Na₂EDTA) reaction mixture and measured for 30 seconds at 240 nm with a UV microplate spectrophotometer (Epoch, SN: 1611187, made in USA). One CAT activity unit (U) is defined as a change of 0.1 absorbance unit per minute. Activity is expressed as enzyme units per gram FW.

Peroxidase enzyme activity (E.C.1.11.1.7) was determined according to the method by Cvikrova et al. (1994) with slight modifications (Karakas et al., 2019a). For the analysis, 100 µL of extract (obtained as above) was added to 3 mL of the reaction mixture (13 mmol L⁻¹ guaiacol, 5 mmol L⁻¹ H₂O₂, and 50 mmol L⁻¹ Na-phosphate, pH 6.5). The reaction was initiated with a H₂O₂ addition and was measured at 470 nm using a UV microplate spectrophotometer (Epoch, SN: 1611187, made in USA) at one-minute interval until 3rd minute. One unit of POX activity was defined as a change of 0.1 absorbance unit per minute at 470 nm. Activity is expressed as enzyme units per gram of FW.

Hydrogen peroxide levels (H₂O₂) were determined according to Sergiev et al. (1997) with slight modifications (Karakas et al., 2019a). Fresh plant tissue (0.5 g) was homogenized in an ice bath with 5 ml 0.1% (w:v) trichloroacetic acid (TCA). The homogenate was centrifuged at 12,000g for 15 min at 4°C and 0.5 mL of the supernatant were added to 0.5 ml 10 mmol L⁻¹ potassium phosphate buffer (pH 7.0) and 1 mL 1 M potassium iodide. The absorbance was read at 390 nm using a UV microplate spectrophotometer (Epoch, SN: 1611187, made in USA). The H₂O₂ content was calculated as µmol g⁻¹ FW.

Determination of ion contents

The ion contents (Na⁺, K⁺, Ca²⁺, Mg²⁺) of leaves were determined according to the procedure of Chapman and Pratt (1961) with slight modifications (Karakas, 2013). Samples burned at 500°C were homogenized in 5 mL of a 2N HCl. The homogenate obtained following filtration was analyzed by Inductively Coupled Plasma (ICP, Perkin Elmer). Chloride was determined by ion chromatography (IC) after the filtration through filter paper.

Determination of Sodium ion Removal

The concentration of Na⁺ ion removed by harvested *P. harmala* was calculated according to the equation made by Qadir et al. (2003) with slight modifications (Karakas et al., 2017) (Eq. 2).

$$S_{Na-removal} = [(S_{Na-conc})(S_{DW}) / (10^3)] / (MW_{Na}) \quad (\text{Eq.2})$$

where $S_{\text{Na-removal}}$ is the Na^+ removal through harvest (mmol pot^{-1}), $S_{\text{Na-conc}}$ is the ion concentration in the harvested plant (mg kg^{-1}), S_{DW} is the plant dry weight (g pot^{-1}), and MW_{Na} is the molecular weight of Na^+ .

Determination of DNA damage

Assessment of DNA damage caused by NaCl was made via the comet assay method developed for plants (Gichner et al., 2004; Pourrut et al., 2015). *P. harmala* leaves were placed in a 60-mm Petri dish kept on ice and spread with 250 μl of cold 400 mmol L^{-1} Tris buffer, pH 7.5. The plate was kept tilted on ice so that the isolated leaves nuclei would collect in the buffer. Frosted-end microscope slides were dipped into a solution of 1% NMP agarose prepared with water at 50°C, dried overnight at room temperature and kept dry in slide boxes until use. Onto each slide, nuclear suspension (50 μl) and 1% low melting point (LMP) agarose (50 μl) prepared with phosphate-buffered saline (PBS) were added at 40°C. The nuclei and the LMP agarose were gently mixed and 80 μL aliquots were placed on microscope slides which were pre-coated with 1% normal melting point (NMP) agarose. The drops were then covered with a coverslip and the slides were placed on ice for 5 min. Then, the coverslips were removed and the slides were placed in a horizontal gel electrophoresis tank containing freshly prepared cold electrophoresis buffer (1 mmol L^{-1} Na_2 EDTA and 300 mmol L^{-1} NaOH, pH > 13). The nuclei were incubated for 15 min to allow the DNA to unwind prior to electrophoresis at 0.72 V/cm (26V, 300 mA) for 5 min at 4°C. DNA damage was examined after the assay protocol in both control and NaCl-exposed groups. The damaged DNA resembled comets when checked under a fluorescence microscopy. The intensity of the comet tail relative to the head reflected the number of DNA breaks (Collins, 2004). Tail length was assessed using a software called comet assay software program (CASP) (Konca et al., 2003).

Data analysis

Data were statistically analyzed by one-way analysis of variance (ANOVA) using the SPSS software program (Version 22.0). To separate treatment means for each measured parameter, Duncan's Multiple Range Test was performed at a significance level of $P \leq 0.05$.

Results

Soil properties

Soil physicochemical properties were measured before the start the experiment. The soil properties were shown in *Table 1*. According to our findings, soil electrical conductivity of soil paste extract (EC) and pH were 1.2 dS m^{-1} and 7.8, respectively. The soil texture was determined as clay.

With this table, we observed that the soil was suitable to accumulate excess ions due to its "clay" structure. Therefore, any improvements on this soil through phytoremediation of *P. harmala* would be a promising approach to clean up such soils. Since EC level of the soil was 1.2 dS m^{-1} , which is quite suitable for agricultural purposes, it is important to determine build up toxic salt ions and their salt level is reduced.

Plant growth of *P. harmala* under high NaCl stress

Growth parameters were determined as shoot FW and DW. At control, 0 mmol L⁻¹ NaCl conditions, shoot FW and DW of the plants significantly decreased while at 150- and 300 mmol L⁻¹ NaCl conditions, shoot FW and DW of the plants significantly increased. *P. harmala* produced almost twice as much shoot DW yield as that of 0 mmol L⁻¹ NaCl (control) condition (Fig. 2A and 2B, Table 2).

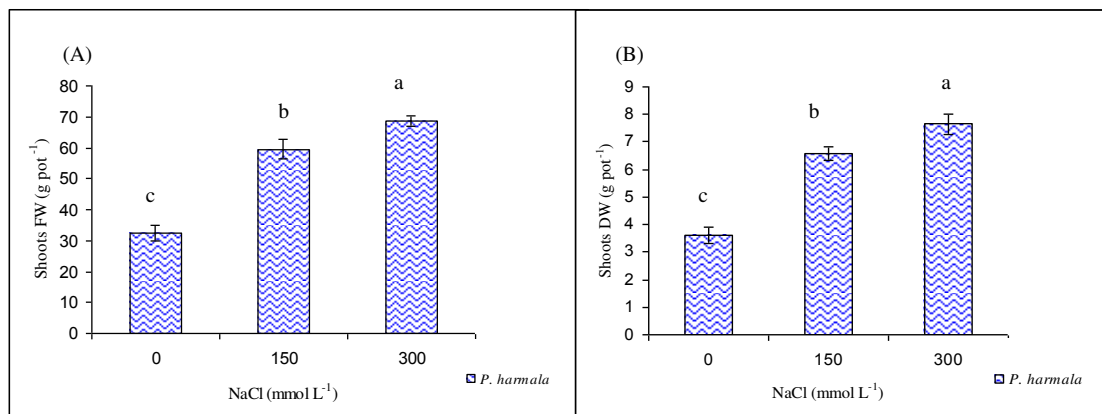


Figure 2. A) Shoots FW; B) Shoots DW of *P. harmala* plants at different NaCl concentrations. Bars indicate the means of threes replicates ± standard error. Bars with different letters indicate the significant differences from one another according to Duncan's Multiple Range Test at $P \leq 0.05$

Determination of biochemical responses of *P. harmala* under high NaCl stress

To determine the biochemical responses of *P. harmala*, measured from the leaves of sampled plants in terms of some parameters were of chlorophyll contents (Chl-*a*, Chl-*b*), proline, MDA, CAT, POX and H₂O₂ levels.

Chlorophyll contents (Chl-*a* and Chl-*b*) were twice as much under 150-300 mmol L⁻¹ NaCl as the control plants growing in no salt conditions (Fig. 3A, 3B, Table 2).

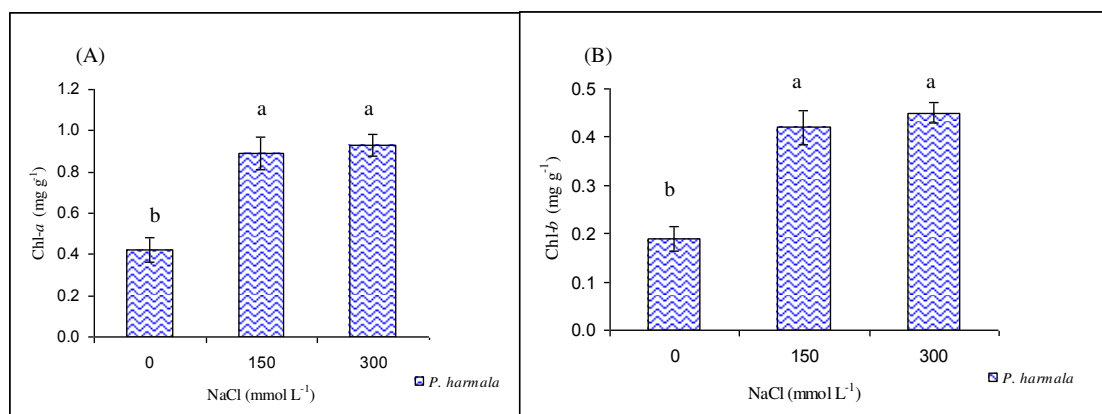


Figure 3. A) Chl-*a*; B) Chl-*b* of *P. harmala* plants at different NaCl concentrations. Bars indicate the means of threes replicates ± standard error. Bars with different letters indicate significant differences from one another according to Duncan's Multiple Range Test at $P \leq 0.05$

Table 2. Analyses of plant parameters using ANOVA

Plant parameters	Salt levels	n	Mean±S.E	F	Sig.
FW	0	3	32.45±2.54	54.33	0.00
	150	3	59.51±3.19		
	300	3	68.21±1.67		
	Total	9	53.50±5.56		
DW	0	3	3.62±0.30	43.17	0.00
	150	3	6.60±0.25		
	300	3	7.65±0.39		
	Total	9	5.95±0.62		
Chl- <i>a</i>	0	3	0.42±0.07	16.10	0.00
	150	3	0.89±0.09		
	300	3	0.93±0.05		
	Total	9	0.75±0.09		
Chl- <i>b</i>	0	3	0.19±0.03	26.56	0.00
	150	3	0.42±0.04		
	300	3	0.45±0.02		
	Total	9	0.35±0.04		
pro	0	3	1.29±0.13	24.24	0.00
	150	3	3.66±0.31		
	300	3	4.25±0.44		
	Total	9	3.07±0.48		
MDA	0	3	6.58±0.79	10.36	0.01
	150	3	14.23±1.86		
	300	3	16.72±2.00		
	Total	9	12.51±1.73		
CAT	0	3	0.67±0.08	5.70	0.04
	150	3	1.14±0.10		
	300	3	1.13±0.14		
	Total	9	0.98±0.10		
POX	0	3	2.39±0.24	9.89	0.01
	150	3	4.38±0.37		
	300	3	3.71±0.34		
	Total	9	3.49±0.33		
H ₂ O ₂	0	3	3.37±0.20	9.18	0.02
	150	3	6.24±0.63		
	300	3	6.31±0.69		
	Total	9	5.31±0.56		
Leaf Na ⁺	0	3	3.53±0.60	558.22	0.00
	150	3	65.75±1.59		
	300	3	78.80±2.41		
	Total	9	49.36±11.64		
Leaf K ⁺	0	3	2.58±0.09	6.26	0.03
	150	3	2.21±0.12		
	300	3	2.19±0.04		
	Total	9	2.32±0.08		
Leaf Ca ⁺⁺	0	3	1.16±0.06	5.20	0.05
	150	3	0.93±0.07		
	300	3	0.78±0.12		
	Total	9	0.96±0.07		

Plant parameters	Salt levels	n	Mean±S.E	F	Sig.
Leaf Mg ⁺⁺	0	3	0.27±0.01	13.68	0.01
	150	3	0.22±0.01		
	300	3	0.21±0.01		
	Total	9	0.23±0.01		
Leaf Cl ⁻	0	3	7.43±1.03 c	54.78	0.00
	150	3	45.25±2.96 b		
	300	3	68.14±6.45 a		
	Total	9	40.28±9.09		
Removal Na ⁺ (mmol pot ⁻¹)	0	3	0.57±0.13 c	70.05	0.00
	150	3	21.56±1.38 b		
	300	3	28.60±2.68 a		
	Total	9	16.91±4.30		
Removal Na ⁺ (kg ha ⁻¹)	0	3	8.10±1.86 c	69.90	0.00
	150	3	304.57±19.58 b		
	300	3	404.17±37.88 a		
	Total	9	238.94±60.74		
DNA tail length	0	3	29.00±2.89 a	0.58	0.59
	150	3	31.00±3.79 a		
	300	3	34.00±3.21 a		
	Total	9	31.331.81		
DNA damage	0	3	4.50±0.58 a	0.28	0.77
	150	3	4.60±0.67 a		
	300	3	5.13±0.70 a		
	Total	9	4.74±0.34		

Both proline and MDA contents of *P. harmala* increased at 150-300 mmol L⁻¹ NaCl stress conditions. At the highest NaCl level (300 mmol L⁻¹), proline and MDA contents were 3.3 and 2.5 times higher, respectively than those of leaves in the control group (Fig. 4A, 4B, Table 2).

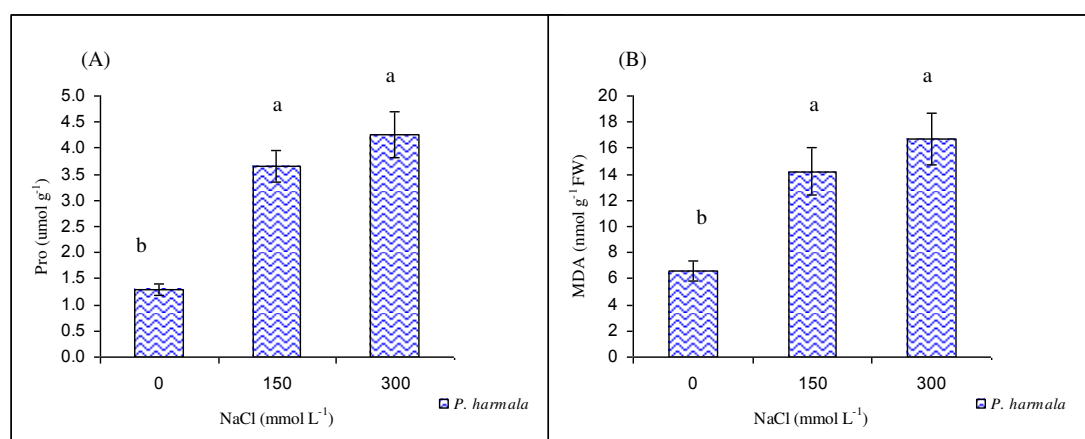


Figure 4. A) Proline (Pro); B) MDA of *P. harmala* plants at different NaCl concentrations. Bars indicate the means of threes replicates ± standard error. Bars with different letters indicate the significant differences from one another according to Duncan's Multiple Range Test at $P \leq 0.05$

CAT and POX enzymes showed also increasing trend as the concentration of NaCl increased. At 150- and 300 mmol L⁻¹ NaCl concentrations, both enzymes were remarkably expressed. At 300 mmol L⁻¹ NaCl, the expression of both enzymes were still high although slightly decreases were evident. However, this was not statistically significant (*Fig. 5A and 5B, Table 2*).

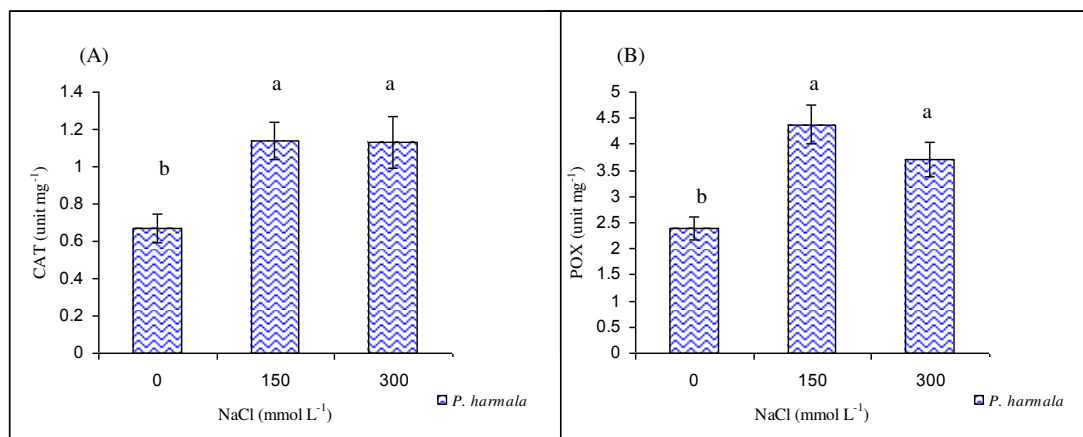


Figure 5. A) CAT; B) POX of *P. harmala* plants at different NaCl concentrations. Bars indicate the means of threes replicates ± standard error. Bars with different letters indicate the significant differences from one another according to Duncan's Multiple Range Test at $P \leq 0.05$

Along with the other enzymes and metabolites, level of oxidant molecules (H₂O₂) showed an increasing trend from 3.4 μmol g⁻¹ FW at control conditions to 6.3 μmol g⁻¹ FW at 300 mmol L⁻¹ NaCl conditions. The important issue here is that there was no significant difference between 150- and 300 mmol L⁻¹ NaCl conditions in that the difference between them in terms of H₂O₂ accumulation was negligible indicating that *P. harmala* was able to stabilize the toxic ions till 300 mmol L⁻¹ NaCl level after 150 mmol L⁻¹ NaCl concentration (*Fig. 6, Table 2*).

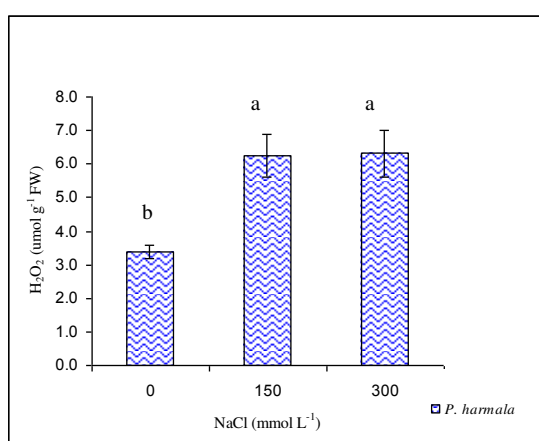


Figure 6. H₂O₂ of *P. harmala* plants at different NaCl concentrations. Bars indicate the means of threes replicates ± standard error. Bars with different letters indicate the significant differences from one another according to Duncan's Multiple Range Test at $P \leq 0.05$

Determination of ion contents of *P. harmala* under high NaCl stress

The accumulation of Na⁺ and Cl⁻ ions showed an increasing trend along with the decrease of K⁺, Ca⁺⁺ and Mg⁺⁺ ions in the leaves of *P. harmala* plants. In *P. harmala* leaves, Na⁺ ion contents increased 19 and 22 times at 150- and 300 mmol L⁻¹ NaCl conditions, respectively, when compared to those of control plants. K⁺, Ca⁺⁺ and Mg⁺⁺ ions contents were 1.2, 1.5 and 1.3 times were decreases, respectively than those of leaves in the control group. The plants also accumulated Cl⁻ ions 9 times higher under at 300 mmol L⁻¹ NaCl conditions than those of control plants (Fig. 7A-E, Table 2).

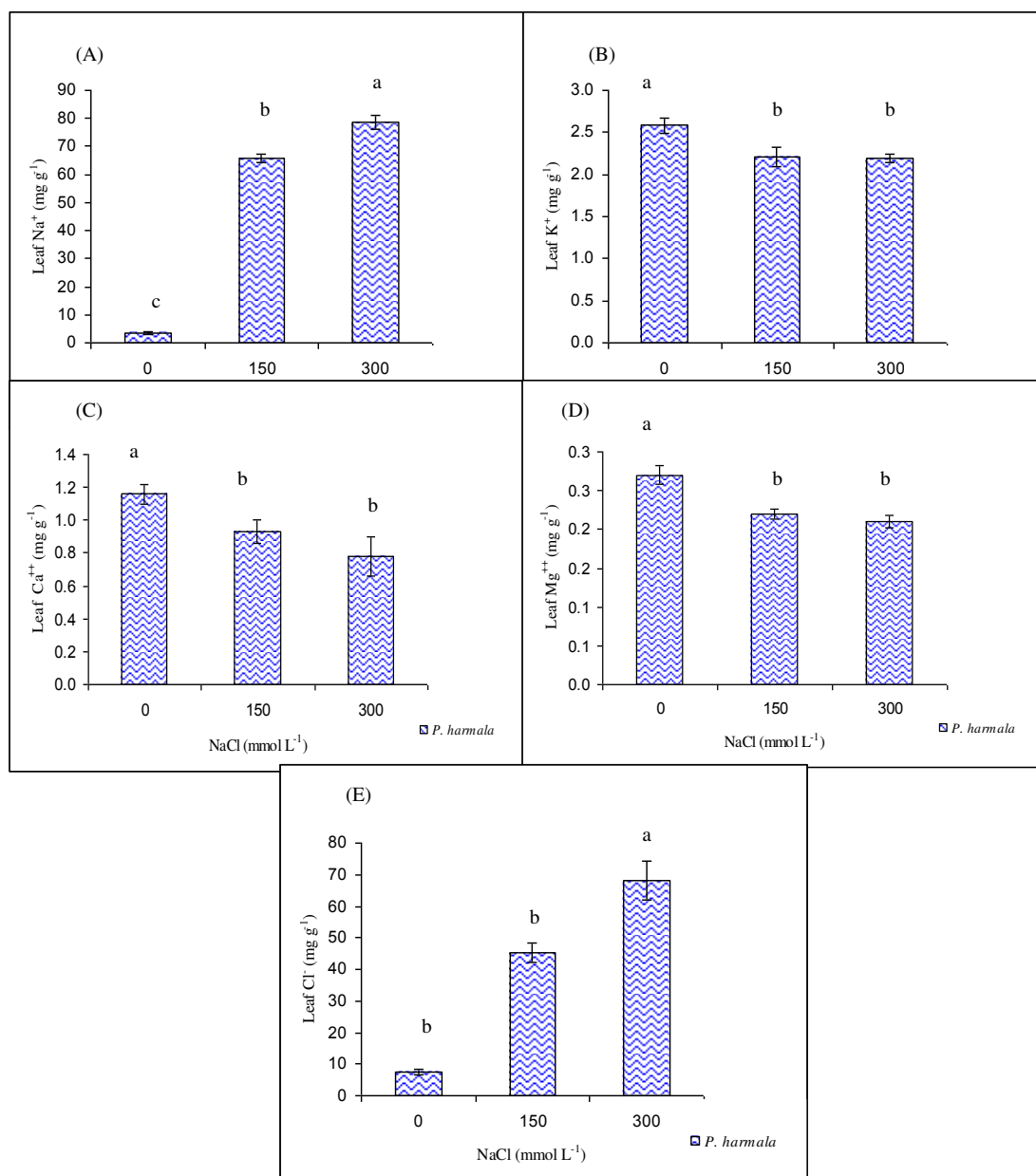


Figure 7. A) Na⁺; B) K⁺; C) Ca⁺⁺; D) Mg and E) Cl⁻ ions contents of *P. harmala* plants at different NaCl concentrations. Bars indicate the means of threes replicates ± standard error. Bars with different letters indicate the significant differences from one another according to Duncan's Multiple Range Test at P ≤ 0.05

Determination of sodium ion removal of *P. harmala* under high NaCl stress

P. harmala was determined to be quite effective in removing salt from the soils. It was capable of removing 0.6-, 21.6-, and 28.6 mmol pot⁻¹ Na⁺ ion, respectively at 0-, 150-, and 300 mmol L⁻¹ in NaCl conditions. With regard to the mass removal of ions, we estimated that *P. harmala* was capable of removing 404.2 kg ha⁻¹ at 300 mmol L⁻¹ NaCl conditions (Fig. 8A and 8B, Table 2).

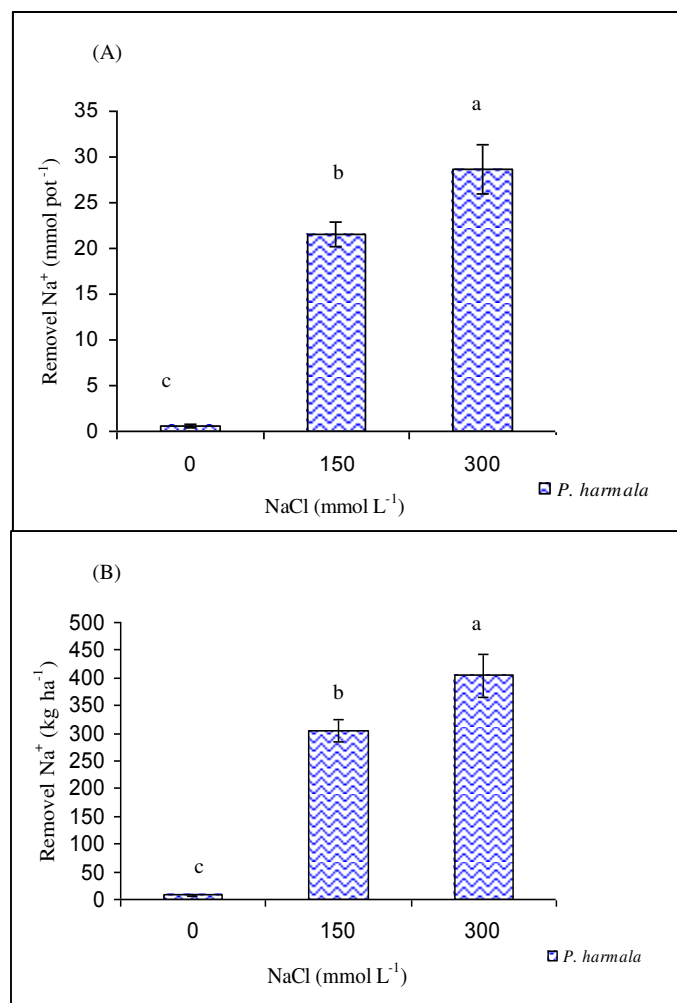


Figure 8. A) The removal of Na⁺ from pots; B) The adjusted removal capacity under field conditions. *P. harmala* plants at different NaCl concentrations. Bars indicate the means of three replicates ± standard error. Bars with different letters indicate the significant differences from one another according to Duncan's Multiple Range Test at P ≤ 0.05

Assessment of DNA damage caused by NaCl showed that *P. harmala* did not show any dose response to NaCl stress up to 300 mmol L⁻¹ NaCl level. DNA integrity measurement showed that DNA of the halophyte preserved its uniform shape and was not affected by the toxicity of NaCl as the other components of cell material. DNA tail length and the percentage of tail DNA did not differ from each other (Fig. 9A, 9B, Table 2).

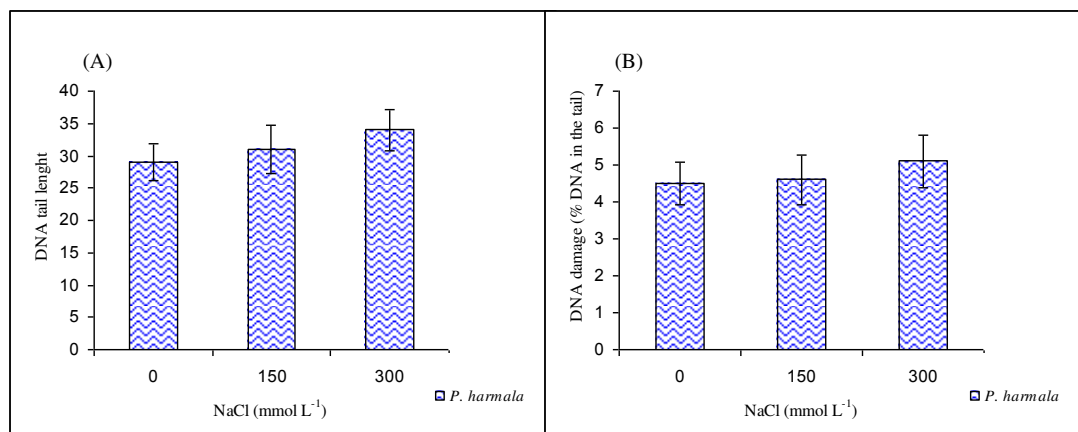


Figure 9. A) DNA tail length B) Percentage of DNA damage of *P. harmala* at different NaCl concentrations. Bars indicate the means of three replicates \pm standard error. Bars with different letters indicate the significant differences from one another according to Duncan's Multiple Range Test at $P \leq 0.05$

Discussion

Salinity is one of the most important abiotic stress factors reducing crop yields as well as their quality significantly (Okorogbona et al., 2015). Salinity tolerance of plants is achieved by a series of complex and diverse mechanisms; these involve physiological, biochemical and molecular adaptational traits. Halophyte plants, in general, exhibit high salt tolerance, allowing them to survive and thrive under extremely saline conditions (Meng and Sui, 2018). They can tolerate high levels of salt concentrations between from 200 and 1000 mmol L⁻¹ of NaCl (Flowers and Colmer, 2008). For example, the halophyte *Arthrocnemum macrostachyum* survives up to 1000 mmol L⁻¹ NaCl (Khan et al., 2005). Similarly, Debez et al. (2010) applied the *Batis maritima*, a promising halophyte for sand-dune stabilization and saline-soil reclamation, into saline areas. The plant tolerated high salinity stress up to two-fold of seawater concentration (1000 mmol L⁻¹ NaCl). Plant biomass production was maximal at 200 mmol L⁻¹ NaCl.

On the other hand, halophyte plant *Carpobrotus acinaciformis* grow rapidly at moderate salt concentrations and is able to survive at extreme saline conditions almost close to seawater salt concentrations (Karakas et al., 2019a). In this study, biochemical responses and salt removal capacity of *P. harmala* under moderate and high NaCl stress were assessed. Evaluation of *P. harmala* was made in terms of growth, chlorophyll (Chl-*a* and Chl-*b*), proline, malondialdehyde (MDA) contents along with the activities of, CAT and POX antioxidant enzymes and H₂O₂ changes as well as with the determination of mineral contents (Na⁺, K⁺, Ca⁺⁺, Mg⁺⁺, Cl⁻). In our findings, the growth of *P. harmala* under NaCl (150-300 mmol L⁻¹) conditions showed great performance when FW and DW of the plants were measured. Increases in salt concentrations of the soil positively correlated with the increases of FW and DW of the plant. Similar approaches were made by Suaire et al. (2016) who studied *Atriplex halimus* and *A. hortensis* exposed to a solution containing 2 g L⁻¹ of NaCl in a pot experiment for 60 days. The plants were able to accumulate >50 mg g⁻¹ of DW for Na⁺ ions within the aerial parts of the plants. They concluded that *Atriplex halimus* and *A. hortensis* had promising characteristics for phytodesalination of road runoff polluted by deicing salts.

Chl-*a* and chl-*b* contents significantly increased in *P. harmala* leaves with the high NaCl levels when compared to the control plants growing at no-salt conditions.

Our study showed that *P. harmala* significantly accumulated proline contents to adapt to saline conditions when compared to that of control group. The ability of halophytes to accumulate osmolytes such as proline, glycine betaine, sorbitol, choline-O-sulphate or sugar have been intensively demonstrated in various studies (Tipirdamaz et al., 2006; Arbona et al., 2010; Lugan et al., 2010; Slama et al., 2015). Many physiological measurements of different species emphasize an elevated proline level as a response to salt stress (Szabados and Savoure, 2010; Zhang et al., 2019). In these studies, researchers stated that accumulation of proline prevented the loss of water through evaporation via increasing osmotic pressure. By this way, tolerant plants could survive longer in harsh conditions. In the current experiment, MDA and H₂O₂ contents increased along with the increase of NaCl concentrations as a response to NaCl toxicity. However, increases in MDA and H₂O₂ contents were stabilized after 150 mmol L⁻¹ NaCl concentration. Accumulations of MDA and H₂O₂ are both considered toxic molecules to be determined under stress conditions. They are also positive responses to stress. Therefore, their increases under stress conditions are inevitable, however, the most important issue here is the stabilization of toxic level of molecules after some stages that characterize the plants as tolerant. In our case, this was succeeded after 150 mmol L⁻¹ NaCl conditions. This made *P. harmala* as a good candidate to be employed in saline-affected areas. For example, Amjad et al. (2015) observed an increase of MDA in leaves of *Chenopodium quinoa* under salt stress. MDA is the measure of damage to membranes and is sometimes regarded as the single most important characteristic to assess the destruction of membranes (Esfandiari et al., 2007). MDA not only directly damages the membranes, but also indirectly causes damage to cell by generating lipid derived radicals that aggravate the oxidative stress (Montillet et al., 2005; AbdElgawad et al., 2016).

Antioxidants play an important role in adapting plants to abiotic stress by detoxifying reactive oxygen species (ROS). Plants evolved different antioxidative mechanisms, among them several enzymatic defense systems are available. The plant defence system includes enzymatic and non-enzymatic antioxidants such as superoxide dismutase (SOD), POX, CAT, glutathione peroxidase (GPX) and ascorbate peroxidase (APX). They act in a sequential concept to scavenge the ROS (Cavalcanti et al., 2007; You and Chan, 2015). In the present study, increased enzyme activities (POX and CAT) played significant roles under NaCl conditions to detoxify and stabilize the toxic molecules. Similar results have recently been documented by Amjad et al. (2015) in *Chenopodium quinoa*, and by Podar et al. (2019) in the halophyte *Petrosimonia triandra* and by Karakas et al. (2019a) in the *Carpobrotus acinaciformis*.

Apart from the accumulation of antioxidant molecules and osmoprotectants to compensate the toxic effects of NaCl, halophyte plants have remarkably high capacity to accumulate toxic ions in their structures. They can accumulate salts in their various parts such as leaves, stems, roots, and they can force them (Na⁺ and Cl⁻) across the tonoplast with highly Na⁺/K⁺ selective protein transporters (Radyukina et al., 2007; Guo et al., 2019). This and similar other attributes led researchers to suggest that halophyte plants could be grown in salt-affected soils to remove significant amounts of Na⁺ and Cl⁻ ions through their aerial parts (Qadir et al., 2002; Karakas et al., 2017, 2019b). We noticed that, accumulation of Na⁺ and Cl⁻ ions were remarkably high as compared to the plants in the control group. Decreases in K⁺, Ca⁺⁺ and Mg⁺⁺ ions were also noticed in leaves, however, this decrease was stabilized after 150 mmol L⁻¹ NaCl condition. Similar

findings were also reported by other workers on *Bruguiera parviflora*, *Ceriops tagal*, *Halopyrum mocoronatum*, *Haloxylon recurvum*, *Suaeda fruticosa* various plants (Parida and Das, 2005; Pan et al., 2016).

We demonstrated that *P. harmala* is quite effective in removing salt from the soils. Similarly, Karakas et al. (2017) observed *Salsola soda* and *Portulaca oleracea* removing of salt under soil salinity. This study showed that planting saline soils with *P. harmala* in moderate and high salt conditions might be an effective phytoremediation technique. Since we noticed that *P. harmala* showed great performances up to 300 mmol L⁻¹ NaCl as it showed at 150 mmol L⁻¹ NaCl level. We should see the performances at much higher NaCl concentrations to desalinize heavily salinized soils. This would increase the characteristics of *P. harmala* if pesticide-polluted soils are to be remediated via the use of this plant. Similarly, Yucel et al. (2017) stated that *Salicornia europaea* removed 426 to 475 kg salt/ha from the saline area. They stated that *Salicornia* biomass also provided sufficient amounts of salt to the animals. Otherwise, the senesced litter-fall of *Salicornia* would contribute to accelerated secondary soil salinization. Availability of these species help us clean up soils characterized with moderate or high salinity. Easy germination and fast growth have been considered as one of the good properties since the fast vegetative growth and accumulation of toxic ions help removing great amount of salt ions from the soil. Management of these species could be one of the novel and holistic approaches for sustainable phytoremediation of saline-affected soils.

Since accumulation of toxic molecules such as H₂O₂ was stabilized after 150 mmol L⁻¹ NaCl conditions up to 300 mmol L⁻¹ NaCl conditions, the integrity of DNA was noticed to be preserved. It is very well known that high ROS including H₂O₂ can damage to DNA via breaking single or double strands (Sharma et al., 2012). At this case, plants may not be able to recover due to damaged or not functional DNA. In our case, DNA preserved its uniform shape up to 300 mmol L⁻¹ NaCl conditions. With this measurement system, we could also test and measure the capacity of any plants aimed for cleaning up the soils contaminated with salt, pesticides, heavy metals etc.

Conclusion

This study suggests that *P. harmala* is a salt-tolerant plant. The plant not only tolerates, but needs salt for optimal growth and physiological processes in its natural habitat. Its adaptation mechanisms include physiological, biochemical and molecular adaptation mechanisms. Chlorophyll contents, accumulation of osmolyte proline, lipid peroxidation, activation of an efficient antioxidative system are good sources for antioxidant mechanisms. Understanding of the mechanisms regarding salt adaptation of *P. harmala* could be of great importance, possibly leading to the extension of the arable land by exploiting the phytoremediation capability of this halophyte in the salt area.

In future studies, these characteristics should be well evaluated by measuring toxic components such as superoxide (O₂^{•-}) and hydroxyl (OH[•]) ions. The salt tolerance characteristics of *P. harmala* should also be evaluated by increasing NaCl salinity further above 300 mmol L⁻¹ NaCl conditions to see if much higher salinity is to be tolerated by stabilizing the toxic ion levels. Since Na⁺ and Cl⁻ ions are accumulated in *P. harmala* leaves, salt ions removed from the soil due to the uptake should be measured if further accumulation capacity is achieved.

Acknowledgments. Biochemical and molecular analyses were performed in the laboratory of Dr. Murat Dikilitas. I thank Dr. Murat Dikilitas for the biochemical and and molecular analyses.

REFERENCES

- [1] AbdElgawad, H., Zinta, G., Hegab, M. M., Pandey, R., Asard, H., Abuelsoud, W. (2016): High Salinity Induces Different Oxidative Stress and Antioxidant Responses in Maize Seedlings Organs. – *Frontiers in Plant Science* 7: 276.
- [2] Acosta-Motos, J. R., Ortuño, M. F., Bernal-Vicente, A., Diaz-Vivancos, P., Sanchez-Blanco, M. J., Hernandez, J. A. (2017): Plant Responses to Salt Stress: Adaptive Mechanisms. – *Agronomy* 7(1): 18.
- [3] Arnon, D. I. (1949): Copper enzymes in isolated chloroplasts, polyphenol oxidase in *Beta vulgaris* L. – *Plant Physiology* 24: 1-15.
- [4] Ashraf, M., Harris, P. J. C. (2013): Photosynthesis under stressful environments: An overview. – *Photosynthetica* 51: 163-190.
- [5] Bouyoucos, G. J. (1953): An improved type of soil hydrometer. – *Soil Science* 76: 377-378.
- [6] Carillo, P., Annunziata, M. G., Pontecorvo, G., Fuggi, A., Woodrow, P. (2011): Salinity stress and salt tolerance. – In: Shanker, A. K., Venkateswarlu, B. (eds.) *Abiotic Stress in Plants Mechanisms and Adaptations*. Rijeka, InTech.
- [7] Carillo, P., Cirillo, C., De Micco, V., Arena, C., De Pascale, S., Roupheal, Y. (2019): Morpho-anatomical, physiological and biochemical adaptive responses to saline water of *Bougainvillea spectabilis* Willd. trained to different canopy shapes. – *Agricultural Water Management* 212: 12-22.
- [8] Cheeseman, J. M. (2015): The evolution of halophytes, glycophytes and crops, and its implications for food security under saline conditions. – *New Phytologist* 206: 557-570.
- [9] Collins, A. R. (2004): The comet assay for DNA damage and repair. – *Molecular Biotechnology* 26(3): 249-261.
- [10] Debez, A., Saadaoui, D., Slama, I., Huchzermeyer, B., Abdelly, C. (2010): Responses of *Batis maritima* plants challenged with up to two-fold seawater NaCl salinity. – *Journal of plant nutrition and soil science* 173: 291-299.
- [11] Dikilitas, M. (2003): Effect of salinity & its interactions with *Verticillium albo-atrum* on the disease development in tomato (*Lycopersicon esculentum* Mill.) and lucerne (*Medicago sativa* & *M. media*) plants. – University of Wales, Swansea.
- [12] Frison, G., Favretto, D., Zancanaro, F., Fazzin, G., Ferrara, S. D. (2008): A case of beta-carboline alkaloid intoxication following ingestion of *Peganum harmala* seed extract. – *Forensic Science International* 179: 37-43.
- [13] Gichner, T., Žnidar, I., Száková, J. (2008): Evaluation of DNA damage and mutagenicity induced by lead in tobacco plants. – *Mutation Research* 652: 186-190.
- [14] Guo, J., Dong, X., Han, G., Wang, B. (2019): Salt-Enhanced Reproductive Development of *Suaeda salsa* L. Coincided with ion transporter gene upregulation in flowers and increased pollen K⁺ content. – *Frontiers in Plant Science* 10: 333. doi: 10.3389/fpls.2019.00333.
- [15] Gupta, B., Huang, B. (2014): Mechanism of salinity tolerance in plants: physiological, biochemical, and molecular characterization. – *International Journal Genomics* ID 701596: doi: 10.1155/2014/701596.
- [16] Hussain, K., Majeed, A., Nawaz, K., Khizar, H. B., Nisar, M. F. (2009): Effect of different levels of salinity on growth and ion contents of black seeds (*Nigella sativa* L.). – *Current Research Journal of Biological Sciences* 1: 135-138.
- [17] Isayenkov, S. V., Maathuis, F. J. M. (2019): Plant salinity stress: many unanswered questions remain. – *Frontiers in Plant Science* 10: 80.

- [18] Karakas, S. (2013): Development of tomato growing in soil differing in salt levels and effects of companion plants on same physiological parameters and soil remediation. – PhD, University of Harran, Sanliurfa, Turkey.
- [19] Karakas, S., Dikilitas, M., Tırdamaz, R. (2019a): Biochemical and molecular tolerance of *Carpobrotus acinaciformis* L. halophyte plants exposed to high level of NaCl stress. – Harran Journal of Agricultural and Food Science 23(1): 99-107.
- [20] Karakas, S., Dikilitas, M., Aslan, M., Güze, A. N. (2019b): Evaluation of biochemical and physiological responses of salsola spp at their natural habitats. – Harran Journal of Agricultural and Food Science 23(2): 226-233.
- [21] Khan, M. A., Ungar, I. A., Showalter, A. M. (2005): Salt stimulation and tolerance in an intertidal stem-succulent halophyte. – Journal of Plant Nutrition 28: 1365-1374.
- [22] Konca, K., Lankoff, A., Banasik, A., Lisowska, H., Kuszewski, T., Gozdz, S., Koza, Z., Wojcik, A. (2003): A cross-platform public domain PC image-analysis program for the comet assay. – Mutation Research 534: 15-20.
- [23] Munns, R., Tester, M. (2008): Mechanisms of salinity tolerance. – Annual Review of Plant Biology 59: 651-681.
- [24] Pan, Y. Q., Guo, H., Wang, S. M., Zhao, B., Zhang, J. L., Ma, Q., Yin, H. J., Bao, A. K. (2016): The photosynthesis, Na⁺/K⁺ homeostasis and osmotic adjustment of *Atriplex canescens* in response to salinity. – Frontiers in Plant Science 7: 848.
- [25] Pourrut, B., Pinelli, E., Celiz Mendiola, V., Silvestre, J., Douay, F. (2015): Recommendations for increasing alkaline comet assay reliability in plants. – Mutagenesis 30: 37-43.
- [26] Richards, L. A. (1954): Diagnosis and improvement of saline and alkali soils. – US Salinity Lab., US Department of Agriculture Handbook 60, California, USA.
- [27] Roupael, Y., Raimondi, G., Lucini, L., Carillo, P., Kyriacou, M. C., Colla, G., Cirillo, V., Pannico, A., El-Nakhel, C., De Pascale, S. (2018): Physiological and metabolic responses triggered by omeprazole improve tomato plant tolerance to NaCl stress. – Frontiers in Plant Science 9: 249.
- [28] Sergiev, I., Alexieva, V., Karanov, E. (1997): Effect of spermine, atrazine and combination between them on some endogenous protective systems and stress markers in plants. – Comptes Rendus Academie Bulgare Sciences 51: 121-124.
- [29] Sharma, P., Jha, A. B., Dubey, R. S., Pessarakli, M. (2012): Reactive oxygen species, oxidative damage, and antioxidative defense mechanism in plants under stressful conditions. – Hindawi Publishing Corporation Journal of Botany, ID 217037. doi:10.1155/2012/217037.
- [30] Shrivastava, P., Kumar, R. (2015): Soil salinity: A serious environmental issue and plant growth promoting bacteria as one of the tools for its alleviation. – Saudi Journal of Biological Sciences 22: 123-131.
- [31] Simpson, C. R., Franco, J. G., King, S. R., Volder, A. (2018): Intercropping Halophytes to Mitigate Salinity Stress in Watermelon. – Sustainability 10(3): 1-17.
- [32] Stuart, J. R., Tester, M., Gaxiola, R. A., Flowers, T. J. (2012): Plants of saline environments. – Access Science <http://www.accessscience.com>.
- [33] Suaire, R., Durickovic, I., Framont-Terrasse, L., Leblain, J. Y., De Rouck, A. C., Simonnot, M. O. (2016): Phytoextraction of Na⁺ and Cl⁻ by *Atriplex halimus* L. and *Atriplex hortensis* L.: A promising solution for remediation of road runoff contaminated with deicing salts. – Ecological Engineering 94: 182-189.
- [34] Wanntorp, L., Ronse De Craene, L. P. (2011): Flowers on the Tree of Life. – In: Gower, D. J. (ed.) The Systematics Association Special Volume Series. Cambridge University Press, UK.
- [35] You, J., Chan, Z. (2015): ROS regulation during abiotic stress responses in crop plants. – Frontiers in Plant Science 6: 1092.
- [36] Yucel, C., Farhan, M. J., Khairo, A. M., Ozer, G., Cetin, M., Ortas, I., Islam, K. R. (2017): Evaluating *Salicornia* as a potential forage crop to remediate high groundwater-

- table saline soil under continental climates. – International Journal of Plant and Soil Science 16(6): 1-10.
- [37] Zakharin, A. A., Panichkin, L. A. (2009): Glycophyte salt resistance. – Russian Journal of Plant Physiology 56: 94-103.
- [38] Zhang, X., Liu, L., Chen, B., Qin, Z., Xiao, Y., Zhang, Y., Yao, R., Liu, H., Yang, H. (2019): Progress in understanding the physiological and molecular responses of *Populus* to salt stress. – International Journal of Molecular Sciences 20(6): 1312.

SOIL MICROBIAL COMMUNITY CHANGE DURING NATURAL FOREST CONVERSION TO RUBBER PLANTATIONS

LING, Z.^{1,2} – SHI, Z. T.^{2*} – DONG, M. H.¹ – YANG, F.³ – SU, B.²

¹*Kunming University, Kunming, 650214 Yunnan, China*

²*College of Tourism and Geographic Sciences, Yunnan Normal University, 650500 Yunnan, China*

³*Institute of Water Conservancy and Hydro-Electric Power, Xi'an University of Technology, 710048 Xi'an, China*

**Corresponding author
e-mail: shizhengtao@163.com*

(Received 9th Dec 2019; accepted 6th May 2020)

Abstract. Extensive conversion of natural forest to monoculture rubber plantation in Xishuangbanna. It is the 'non-traditional' rubber plantation areas in southwest (SW) of China has resulted in the soil microbial community change. The aim of our study was to identify the impacts of conversion of natural forests into rubber plantations on soil microorganisms. Soil microbial community from 10 old years rubber plantation (10aRP), 20 old years rubber plantation (20aRP), 30 old years rubber plantation (30aRP), Lower hill seasonal rainforest (LRF) and tropical ravine rainforest (RRF) were analysed by Illumina MiSeq technology. The results showed that changes in soil physical and chemical properties were strongly correlated with available phosphorus (AP), total nitrogen (TN), available potassium (AK) and total potassium (TP) which were lower in natural forests than in rubber plantations. And the dominant phylum were *Acidobacteria* (44.67%), *Proteobacteria* (13.92%), *Chloroflexi* (13.13%), *Verrucomicrobia* (9.99%) and *Planctomycetes* (5.23%) in 45 soil microbial communities. Microbial community in rubber plantations were less abundant than in natural forests. In addition, TP, AK, TN and AN were the main environmental factors which affected soil microbial composition. The soil health of rubber plantations were impacted by soil bacterial community.

Keywords: *Hevea brasiliensis* plantation, land-use change, soil microorganism, biodiversity, 16S rRNA gene

Introduction

Due to demand rapid growing in the rubber market, more than 500,000 ha of rubber plantation (*Hevea brasiliensis*) has been planted into tropical forest in Southeast Asia including southwest of China for decades (Kumagai et al., 2015). About 40% of the rubber plantations have grown in the Xishuangbanna, Southwest China. Land use Changes cause negative influence of ecosystem services which associated with the conversion to natural rainforests on monoculture rubber plantations, including loss of biodiversity, reduction of carbon pools, increased soil degradation, soil erosion and reduced soil fertility (Ahrends et al., 2015; Warren-Thomas et al., 2015; Drescher et al., 2016).

Plant rhizosphere microorganisms play crucial role in soil regulation which controlled the decomposition of organic matter, nutritional cycling and energy metabolism of soil (Godin et al., 2019). Indeed, soil microbial communities were closely related to the vegetation types. It has been suggested that vegetation types change in land would have further impacts on diversity, composition and activity of soil microbial communities (Crowther et al., 2014; Lagerlöf et al., 2014). Whereas, the

microbial community of soil is the most sensitive indicator of soil quality and fertility which have greatly affected by the soil microbial community during the conversion of vegetation in land. Also, soil microbial community is a vital reflection of human disturbance and land use change. It can reflected the benefits of land use because of the close relationship with soil quality and fertility (Cardoso et al., 2013).

Furthermore, soil ecosystem service would be significant influenced by rubber plantations after conversion from natural forests because of the change of vegetation types, soil microbial community and human activities like exploring, cleaning and fertilizing. Some researchers have shown that the soil microbial biomass decreased with rubber tree-age and afforestation activities increase (Guo et al., 2015). Moreover, prokaryotic community was significantly influenced during the conversion from natural forests to rubber plantations (Krashevskia et al., 2015; Schneider et al., 2015). Although the result of soil microbial diversity and environmental factors have be known during those natural forests conversion (Docherty et al., 2015), the gradient change of soil microbial community structure of rubber plantation with different forest ages in not traditional rubber growing environments need further research (Allen et al., 2015).

Previous researches have carried on the scientific planting techniques in the “traditional” rubber areas (Kerfahi et al., 2016; Wang et al., 2017). However, the soil microbial communities and environmental factors were impacted after the conversion from natural forest in ‘non-traditional’ rubber plantation areas are lacking. Xishuangbanna, Southwest of China, is rubber plantations highland. It is a biodiversity hotspot because of the extreme dry and rainy seasons where a ‘non-traditional’ rubber plantation areas beyond 477 m asl. About 54.17% of natural forests were converted into rubber plantation from 1990 to 2014. Rubber plantations were planted over about 500 m to 1,300 m a wide range of altitudes (Wu et al., 2001).

We sampled in 10 years old rubber plantation (10aRP), 20 years old rubber plantation (20aRP), 30 years old rubber plantation (30aRP), lower hill seasonal rainforest (LRF) and tropical ravine rainforest (RRF) in Xishuangbanna. Our objectives were: (1) to investigate the influence of soil microbial community to the conversion from natural forests to rubber plantations; (2) to research on the difference of microbial community in different ages rubber plantation; (3) to find out the major environmental factors cause soil microbial community change. It is critical for the sustainable management and restoration of soil to study on how the soil microbial community change during the conversion.

Materials and methods

Study site and soil sampling

Our research was carried out in Mengla, Xishuangbanna, Yunnan province, southwest of China. All the chosen sites were at elevations between 600 and 800 m asl. Soil samples mainly collect the upper layer 0~20 cm (Schulz et al., 2019). Due to the highest microbial density and activity can be observed in the surface soil where accurately representation of the microbial community inhabit (Kerfahi, 2016).

Three sampling sites were selected for each same type of forest. The samples collected from each site consisted of 3 parallel samples. So there were 15 soil profiles and 45 groups of soil samples in total. Soil were sampled on April 10, 2015. The 30aRP were marked A-C, the 20aRP were marked D-F, the 10aRP were marked G-I, the RRF were marked J-L, the LRF were marked M-O (21°15'7.20"N-22°5'56.54"N,

101°14'25.52"E-101°42'36.07"E). The sample sites of soil samples in our study were listed in *Figure 1*.

All soil samples were filtered through a 2 mm mesh to remove root and plant materials. Then, each soil sample was classified into two groups. One group was air-dried at room temperature before physical and chemical analysis. The other part was placed in a freezer at -4 °C which was then transported to the laboratory for DNA extraction within several hours.

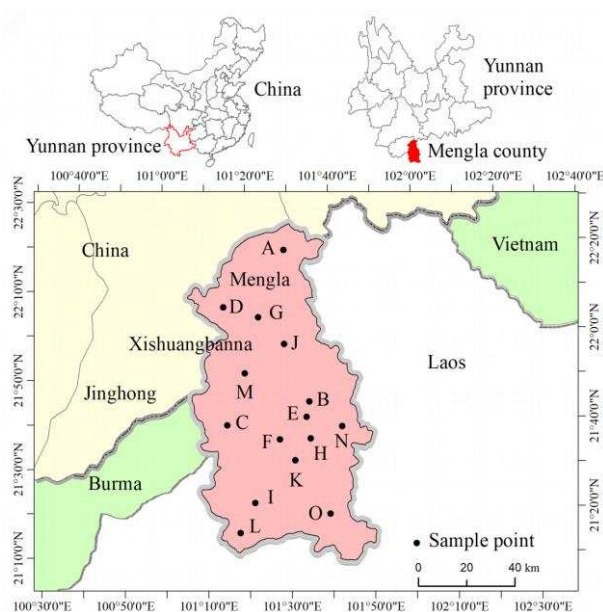


Figure 1. Map of study area located in Mengla, Xishuangbanna, China. There were 15 soil sites that A-C (30aRP), D-F (20aRP), G-I (10aRP), J-L (RRF), M-O (LRF)

Soil physical and chemical properties

Soil samples were sent to plateau environmental changes key laboratory of Yunnan for physical and chemical analysis. There are 8 indicators including pH, organic matter (OM), total potassium (TK), total nitrogen (TN), available potassium (AK), total phosphorus (TP), available phosphorus (AP), available nitrogen (AN), were determined. PH of soil was measured potentiometrically at a soil: water ratio of 1:2.5 in H₂O. OM was quantified by oxidation with a potassium dichromate solution in sulfuric acid (H₂SO₄-K₂Cr₂O₇). TK was determined by NaOH melting atomic absorption spectrophotometers; TN was determined by semi-micro-kjeldahl method. AK was determined by ammonium acetate extraction atomic absorption spectrophotometer; TP was determined by NaOH fused molybdenum-antimony anticolorimetric method. AP was determined by sodium bicarbonate extraction molybdenum blue colorimetric method; AN was determined by NaOH diffusion method (Bao, 2000).

DNA extraction and PCR amplification

The total DNA genome was extracted from 0.5 g of samples using the E.Z.N.A.®-Soil DNA Isolation Kit (Omega Bio-tek, Norcross, GA, U.S.). Monitoring the DNA concentration and purity on a 1% agarose gel and diluting the DNA was to 20 ng/mL with TE buffer.

Bacterial 16S rRNA genes in the V3-V4 region were exaggerated by using the bacterial primers 341F (5'-CCTACGGGRSGCAGCAG-3') and 806R (5'-GGACTACCAGGGTATCTAAT-3') with labelled barcodes sequence. All PCR reactions were performed in 30 μ L of solution using Kapa HotStart HiFi 2 \times ReadyMix DNA polymerase (Kapa Biosystems Ltd., London, UK), forward and reverse primers (0.2 mM), and approximately 10 ng of template DNA. First, the cycling conditions were denatured at 95 $^{\circ}$ C for 3 min and then 30 cycles were performed which were denatured at 95 $^{\circ}$ C for 30 s, annealed at 55 $^{\circ}$ C for 30 s and extended at 72 $^{\circ}$ C for 45 s. In the end, the sample was held at 72 $^{\circ}$ C for 5 min (Xu et al., 2016). For the convenience of qualitative and quantitative analysis on PCR products, fair volume of loading buffer (with SYBR green) and PCR solution were mixed before performing the electrophoresis detection on a 1% agarose gel. Samples that demonstrated a clear major of about 400-450 bp were applied to further experiments.

Illumina MiSeq sequencing

Sequence reads was carried out using a paired-end Illumine MiSeq sequencing method on an Illumine MiSeq device (Illumina Inc., San Diego, CA, USA) according to the manufacturer's instructions. Subsequently, reads from all samples were combined into a single dataset for processing with QIIME. All original datasets obtained in our research has been deposited to NCBI SRA repository and can be obtained by sequence number of PRJNA574017.

Diversity estimations

An open reference method of combination of de novo and reference based OTU identification was carried out in Qiime platform. RDP Classifier was using to determine taxonomic classification for each OTU of bacterial community at similarity level of 97%. On the basis of OTU results, a sample of alpha diversity was computed, which is the analysis of species diversity in a single sample, where ACE values, chao1, Shannon and the Simpson indices are included (Edgar, 2017).

Statistical analysis

Data for soil physical-chemical properties were conducted using the program SPSS 20.0 (SPSS Inc., Chicago, USA). Correlation analysis among all soil variables was performed. Duncan's test was used to compare the significant differences between land use types (30aRP, 20aRP, 10aRP, RRF and LRF) for each parameter. Data were tested for normal distribution and if needed log transformation was done in order not to violence the assumptions of normality and equal variances. A principal component analysis (PCA) was done to investigate differences in microbial community composition among land cover types.

Results

Soil physical and chemical properties

Land use change usually affected most soil physical and chemical parameters (Table 1). The pH of soil of different land cover types (30aRP, 20aRP, 10aRP, RRF and LRF) between 4.2 and 4.8. The content of OM was 0.35 ± 0.43 and AK was

113.54 ± 5.46 mg/kg in 20aRP. The OM and AK in 20aRP were significantly higher than others, While AK was 37.98 ± 4.61 mg/kg in RRF which was the lowest value of 5 sample sites. In LRF, TK and OM showed lowest value were 5.78 ± 0.67 g/kg and 0.03 ± 0.0012, respectively. It suggested the soil physical and chemical properties content increased with land use change and increased human disturbance.

Table 1. Physical and chemical properties at each sample sites. Values are means ± SD (n = 9)

Soil properties	30aRP	20aRP	10aRP	RRF	LRF
pH	4.48 ± 0.10a	4.72 ± 0.09a	4.20 ± 0.04a	4.80 ± 0.17a	4.70 ± 0.25a
OM (%)	0.15 ± 0.16a	0.35 ± 0.43a	0.04 ± 0.004b	0.05 ± 0.001b	0.03 ± 0.0012b
AN (mg/kg)	10.77 ± 0.49b	10.53 ± 1.80b	10.89 ± 1.32b	11.11 ± 0.64ab	13.10 ± 2.81a
TN (g/kg)	0.94 ± 0.035c	1.36 ± 0.089ab	1.26 ± 0.028b	1.39 ± 0.55ab	1.43 ± 0.39a
TP (g/kg)	0.11 ± 0.006a	0.12 ± 0.022a	0.13 ± 0.008a	0.12 ± 0.001a	0.11 ± 0.025a
AP (mg/k g)	2.38 ± 0.24c	3.91 ± 0.31b	4.85 ± 0.85a	4.36 ± 0.56ab	4.89 ± 2.47a
TK (g/kg)	7.16 ± 1.48b	13.94 ± 2.59a	11.54 ± 1.87ab	11.02 ± 0.61ab	5.78 ± 0.67c
AK (mg/kg)	50.78 ± 1.63bc	113.54 ± 5.46a	75.57 ± 3.54b	37.98 ± 4.61c	68.73 ± 6.61b

Different letters indicate significant differences between land cover types (P < 0.05). pH: pH, OM: organic matter, AN: available nitrogen, TN: total nitrogen, TP: total phosphorus, AP: available phosphor, TK: total potassium, AK: available potassium, 30aRP: 30 old years rubber plantation, 20aRP: 20 old years rubber plantation, 10aRP: 10 old years rubber plantation, RRF: tropical ravine rainforest), LRF: lower hill seasonal rainforest

The soil physical and chemical properties at each sampling site have significant differences except pH and TP. There were distinct differences in AP, TK and AK (P < 0.05). AP in LRF (a) and RRF (a) were significant differences between 30aRP (c). TK in LRF (c) differs from 30aRP (b), but the largest difference was between LRF (c) and 20aRP (a). AK was the largest difference in RRF (c) and 20aRP (a). Meanwhile, AK and TK were significant differences between soil samples of 30aRP, 20aRP and 10aRP.

Microbial community composition

Sequencing 45 soil samples using Miseq produced 1,738,755 high-quality tags. The endophytic bacteria with abundant diversity in 5 sample sites by the Alpha diversity estimation. As results shown in Table 2.

Table 2. Number OUTs and Alpha diversity of prokaryotic in soils

Sample ID	OTU number	Chao1	Ace	Shannon	Simpson
30aRP	1933	2139	2139	5.869	0.0083
20aRP	2040	2197	2197	5.946	0.0073
10aRP	1443	1625	1639	5.798	0.0087
RRF	1542	1726	1726	6.099	0.0067
LRF	1230	1511	1511	5.802	0.0083

The community richness index of Chao1 and Ace were from 1511 (LRF) to 2197 (20aRP). These can estimate the number of OTUs in the soil samples. The average number of OTUs ranging from 1230 (LRF) to 2040 (20aRP). The total number of OTUs

detected in different ages rubber plantations (97% sequence similarity) were much higher than in natural forests. The average of rubber plantations was 1850 and the natural forests was 1380. The average of Shannon index of rubber plantation was 5.871 and the natural forest was 5.924, respectively. The rubber plantation's was 0.053 lower than the natural forest. The Shannon index of RRF was 6.099 which was the highest value of 5 sample sites, and the lowest was 5.798 of 10aRP. On the contrary, the highest Simpson index was 0.0087 of RRF and the lowest was 0.0067 of 10aRP.

The whole sequences were categorized from phylum to genus. There were 42 different phyla, 42 classes or 48 orders were found by using the program RDP classifier Bayesian algorithm. 45 samples showed very different 16Sr RNA profiles at the phylum level (Fig. 2). About 17 different phylas occupy for 97.73% to 99.50% were common. The dominant phyla in each sample composed over 86% of the microbial community. There were *Acidobacteria* (44.67%), *Proteobacteria* (13.92%), *Chloroflexi* (13.13%), *Verrucomicrobia* (9.99%) and *Planctomycetes* (5.23%). *Acidobacteria* mainly contains *acidobacteraceae*.

Alphaproteobacteria was the main group of proteobacteria, while the rest were Myxococcales, Syntrophobacterales, Betaproteobacteria, Deltaproteobacteria.

Chloroflexi were mainly *Anaerolineae* (Fig. 2). As the hierarchical heat map shown in Figure 2 that the microbial community structure of RRF was different from other samples.

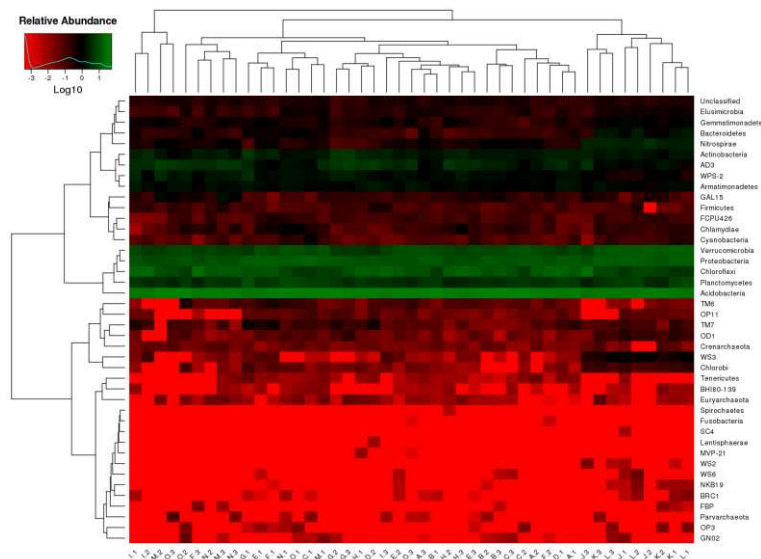


Figure 2. Soil microbial community distribution of the 42 Phylum among the 15 sample sites which marked A to O. The 30aRP were A-C, the 20aRP were D-F, the 10aRP were G-I, the RRF were J-L and the LRF were M-O, respectively. And 3 parallel samples collected from each sites like A1, A2, A3, so there were 45 soil samples in all. The relative values for bacterial family were inferred by color intensity with the legend indicated at the top left corner distribution

Differences in soil microbial community between natural forests and rubber plantations

In Figure 3 shown the relative abundances of different phylum in soil microbial community in 30aRP, 20aRP, 10aRP, RRF and LRF. Only a small amount of

Fusobacteria 0.0018% and *Lentisphaerae* 0.0084% was found in 20aRP. And a few of *Spirochaetes* 0.0043% was found in 10aRP. *Tenericutes* in RRF was 0.0127% which was less than that of other samples. Meanwhile, compared with other groups, the content of *Flavobacteriales* and *Cytophagales* were very low in 10aRP which only 0.0056% and 0.0074%, respectively.

Classify all sequences using the RDP Classifier at similarity level of 97%. It indicated that relative abundance of soil microbial communities in the RRF were significantly higher than in the rubber plantations. For example, *Verrucomicrobia*, *Nitrospirae*, *Bacteroidetes*, *Gemmatimonadetes* and *Elusimicrobia* were 3.74%, 1.42%, 0.62%, 0.31% and 0.18% higher than those in rubber plantations.

By difference analysis between each phylum microorganisms in the 5 sample sites. It was found that *Acidobacteria*, *Proteobacteria*, *Chloroflexi*, *Verrucomicrobia*, *Actinobacteria*, *WPS2*, *ADS3*, *Bacteroidetes*, *Gemmatimonadetes*, *Elusimicrobia*, *Nitrospirae*, *WS3* and *OD1* were extremely significant differences ($P < 0.01$). *WS25* was significant differences ($P < 0.05$).

Analyzing the differences between natural forests and rubber plantations, it was found that *Chloroflexi*, *Actinobacteria*, *Verrucomicrobia*, *Bacteroidetes*, *Gemmatimonadetes*, *Nitrospirae*, *WS3* and *OD1* were extremely significant differences ($P < 0.01$). *GAL15* and *OP112* were significant differences ($P < 0.05$).

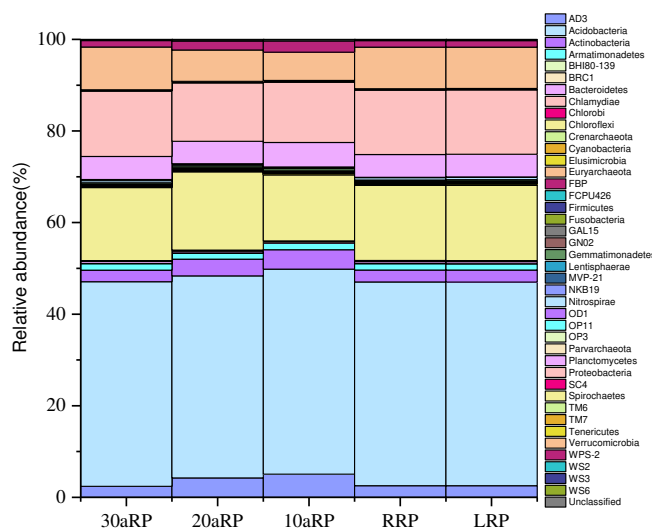


Figure 3. Abundances of different phylums in soil microbial community in the 5 different land cover types

As shown in *Figure 4a* and *b*, The LRF samples (purple points) on the PC1 axis were significant different from other samples by PCA. Compared with LRF (purple points), no significant difference between RRF (yellow points) and RP were found. Natural forests (red points) which were distributed to the left of the RP (blue points) were significant difference between them.

Correlation between microbial community structure and environmental factors

Environmental factors such as soil nutrient elements and organic matter have significant effects on soil microbial community (Docherty et al., 2015). The

environmental elements were influenced by the conversion from natural rainforests to rubber plantations. Thus it is critical to figure out the effects of environmental factors on soil microbial community during the conversion.

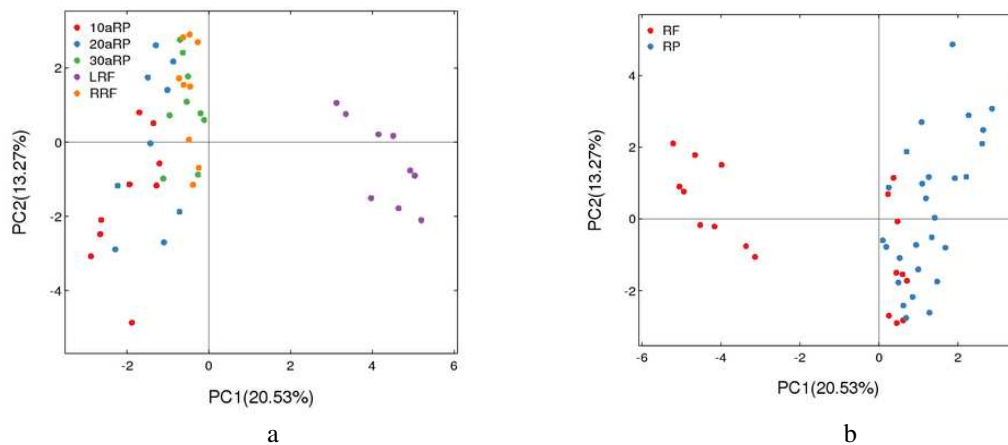


Figure 4. (a, b) Principal component analysis with similarity as instrumental variables was carried out with 45 soil samples from natural rainforests and rubber plantations

As results shown in Table 3. We can found *Chlamydiae* and *GAL15* were significantly correlated with AN. *Bacteroidetes*, *Gemmatimonadetes*, *Nitrospirae* and *Verrucomicrobia* were significantly correlated with TN. *Chloroflexi* was negatively significantly correlated with AK. While, *Proteobacteria* were negatively correlated with TK. *Planctomycetes* was negatively correlated with AK.

Discussion

The response of nature forest transformation to rubber tree plantations on soil microbial community

Illumina Mi Seq technology was used to figure out the reactions of soil microbial community in “Non-traditional” rubber plantation areas where with altitudes above 300 m asl and sharply sloping land. Alpha diversity estimation indicated microbial diversity richness in 5 sample sites shown in Table 2. The Shannon and Simposn index suggested that diversity of microbial community in rubber plantations was less abundant than natural forests. The diversity of microbial community of RRF was more abundant than LRF. And it showed 20aRP > 30aRP > 10aRP in rubber plantations. The 20aRP was the most abundant microbial community diversity of rubber plantations.

Prokaryotes in the soil were significant differences between natural forests and rubber plantations (Kerfahi et al., 2016; Schneider et al., 2015). Because the surface soil of rubber plantations were usually disturbed by human activities such as fertilizing and weeding. The living situation of soil microorganisms would be change by human activities to lead great influence of the quantity and structure of microbial community. Moreover, the leaf litter and soil nutrient cycle reduction lead to the diversity of native plants and the availability of nutrients decrease during the conversion of natural forests to monoculture rubber plantations (Kerfahi et al., 2016). Previous researchers also have proved that soil microorganisms change largely due to land use change. It caused many

negative ecological effects that the soil quality in the natural forests area were degraded (Guillaume et al., 2016), the decomposition rate of litter is slowed down, the degradability of organic matter was reduced and the total organic carbon, microbial biomass carbon and bioactive organic carbon were reduced (Kerfahi et al., 2016; Zhang et al., 2013).

Table 3. Pearson correlation coefficient analysis of soil microbial community structure and environmental factors in natural rainforests and rubber plantations

	Bacteroidetes	Chlamydiae	Chloroflexi	GAL15	Gemmatimonadetes	Nitrospirae	Planctomycetes	Proteobacteria	Verrucomicrobia
pH	0.59	0.488	-0.461	0.343	0.423	0.579	0.312	0.361	0.682
OM	-0.295	-0.206	0.522	-0.369	-0.352	-0.31	-0.811	-0.194	-0.193
AN	-0.318	.952*	-0.213	.965**	-0.123	-0.333	0.407	-0.497	-0.289
TN	.992**	-0.101	-0.461	-0.127	.892*	979**	0.51	0.648	.885*
TP	0.026	-0.423	0.793	-0.451	0.454	-0.049	-0.522	-0.481	-0.278
AP	0.08	0.379	0.243	0.424	0.588	0.008	0.245	-0.579	0.217
TK	-0.749	0.108	0.834	0.049	-0.379	-0.799	-0.725	-.911*	-0.828
AK	-0.222	-0.582	.906*	-0.665	0.028	-0.275	-.887*	-0.427	-0.38

**Significantly correlated at the 0.01 level. *Significantly correlated at the 0.05 level

Difference analysis of microbial community structure in rubber plantations of different ages

The Ace and Chao index of 5 different land use in our study were shown that 20aRP have the most community richness than others. Consistent with Kerfahi's recent research that the soil microbial ecosystem would be affected by land use change. During the natural forests converted into rubber plantations in Xishuangbanna, the differences of microbial community structure on the surface soil were affected by human activities. It suggested that the more the human disturb, the more the microbial community richness of rubber plantations have.

Compared with young rubber, mature rubber plantations have more litter decomposition (Puttaso et al., 2015). Since mature rubber plantations suffered more disturbance like harvesting, fertilizing and weeding. Those human activities possibly to lead negative influence on the nutrients in the soil. Thus the composition and structure of soil microbial community would be affected (Kang et al., 2019).

As we known, the 20RP was the most human disturbance sample site because of that large amount of fertilizer intake for rubber growth and latex harvest in the period (Lan et al., 2012). And LRF has less human disturbance than RRF. The rubber plantations basically have the similar community structure even they were different tree-ages. Furthermore, the 10RF and 20RF were more similar which consistent with the results of the intermicrobiome analysis.

Acidobacteria, *Proteobacteria*, *Chloroflexi*, *Verrucomicrobia* and *Planctomycetes* were the 5 microorganisms with high proportion of all sample sites. Others were significant differences except *Planctomycetes*.

Human activities affect soil microbial community structure. There were small amount of *Fusobacterium* and *Lentisphaerae* found in 20RF and a few of *Spirochaetes* were found in 10RF. Those microorganisms were proved from human or animal waste (Nie et al., 2017; Repass et al., 2018; Granja-Salcedo et al., 2017).

Correlation analysis of soil microorganisms and environmental factors

Consistent with correlation analysis results, The contents of TN and AN of soil in natural forests were higher than rubber plantations. The abundance of *Verrucomicrobia*, *Nitrospirae*, *Bacteroidetes*, *Gemmatimonadetes* and *Elusimicrobia* in natural forests were more richer than rubber plantation.

The physical and chemical properties of the soil have significantly changed during the conversion from natural forests to rubber plantations. The contents of AP, TN, AK and TK in soil have significant or very significant differences. Furthermore, there were also significant differences in soil physical and chemical properties between LRF, RRF and Rubber Plantations (10aRP, 20aRP, 30aRP). The differences in soil physicochemical properties would be increased with rubber tree growing.

The 30RF and RRF have the largest difference of soil physical and chemical properties by difference analysis. Meanwhile, the contents of AK, TK, TN, AP and AN in the soil were the main environmental factors which affect the difference of microbial community composition in 5 sample groups. The difference of microbial community composition was mainly affected by the physical and chemical properties of soil related to fertilize. Because it significantly changed the biogenic elements for the microorganisms growth and metabolism such as N, P, K and others which have significant effects on soil microorganisms (Krashevskaja et al., 2013; Kerekes et al., 2013).

Conclusion

In summary, the diversity of microbial community in rubber plantations were less abundant than in natural forests. Human activities actually affect soil microbial community structure. In addition, the difference of microbial community distribution was strongly affected by the physical and chemical properties of soil related to fertilize. Consequently, the reduced diversity in monoculture rubber plantations and the disturbance affected by the establishment of monoculture rubber plantations were all likely to negatively impact soil microbial community. Nowadays, the mixed rubber cultivations is establishing to reduce negative effects from the monoculture rubber plantations in Xishuangbanna. Further researches are obviously needed to evaluate the response of soil microbial community to land use change in different rubber agroforestry systems like *Hevea brasiliensis*-*Camellia sinensis* agroforestry systems, *Hevea brasiliensis*-*Coffea arabica* agroforestry systems (CAAs) and *Hevea brasiliensis*-*Theobroma cacao* agroforestry systems (TCAs).

Acknowledgements. We thank researchers in Institute of Microbial Engineering of Yunnan Normal University. The study financial supported by Universities Joint Fund of Yunnan Province (2017FH001-111) and Kunming University Program(YJL19004).

REFERENCES

- [1] Ahrends, A., Hollingsworth, P. M., Ziegler, A. D., Fox, J. M., Chen, H., Su, Y., Xu, J. (2015): Current trends of rubber plantation expansion may threaten biodiversity and livelihoods. – *Global Environmental Change* 34: 48-58. DOI: 10.1016/j.gloenvcha.2015.06.002.
- [2] Allen, K., Corre, M. D., Tjoa, A., Veldkamp, E. (2015): Soil nitrogen-cycling responses to conversion of lowland forests to oil palm and rubber plantations in Sumatra, Indonesia. – *PLOS ONE* 10(7): e0133325. DOI: 10.1371/journal.pone.0133325.
- [3] Bao, S. D. (2000): *Soil Agrochemical Analysis*. 3rd Ed. – China Agricultural Press, Beijing.
- [4] Cardoso, E. J. B. N., Vasconcellos, R. L. F., Bini, D., Miyauchi, M. Y. H., Santos, C. A. dos, Alves, P. R. L., Nogueira, M. A. (2013): Soil health: looking for suitable indicators. What should be considered to assess the effects of use and management on soil health? – *Scientia Agricola* 70(4): 274-289. DOI : 10.1590/S0103-90162013000400009.
- [5] Crowther, T. W., Maynard, D. S., Leff, J. W., Oldfield, E. E., McCulley, R. L., Fierer, N., Bradford, M. A. (2014): Predicting the responsiveness of soil biodiversity to deforestation: a cross-biome study. – *Global Change Biology* 20(9): 2983-2994. DOI: 10.1111/gcb.12565.
- [6] Docherty, K. M., Borton, H. M., Espinosa, N., Gebhardt, M., Gil-Loaiza, J., Gutknecht, J. L. M., Gallery, R. E. (2015): Key edaphic properties largely explain temporal and geographic variation in soil microbial communities across four biomes. – *PLoS ONE* 10(11): e0135352. DOI: 10.1371/journal.pone.0135352.
- [7] Drescher, J., Rembold, K., Allen, K., Beckschäfer, P., Buchori, D., Clough, Y., Scheu, S. (2016): Ecological and socio-economic functions across tropical land use systems after rainforest conversion. – *Philosophical Transactions of the Royal Society B: Biological Sciences* 371(1694): 20150275. DOI: 10.1098/rstb.2015.0275.
- [8] Edgar, R. C. 2017. Accuracy of microbial community diversity estimated by closed- and open-reference OTUs. – *Peer J* 5: e3889. DOI: 10.7717/peerj.3889.
- [9] Godin, A., Brooks, D., Grayston, S. J., Jones, M. D. (2019): Ectomycorrhizal and saprotrophic fungal communities vary across mm-scale soil microsites differing in phosphatase activity. – *Pedosphere* 29(3). DOI: 10.1016/S1002-0160(19)60808-8.
- [10] Granja-Salcedo, Y. T., Ramirez-Uscategui, R. A., Machado, E. G., Duarte Messana, J., Takeshi Kishi, L., Lino Dias, A. V., Berchielli, T. T. (2017): Studies on bacterial community composition are affected by the time and storage method of the rumen content. – *PLoS ONE* 12(4): e0176701. DOI: 10.1371/journal.pone.0176701.
- [11] Guillaume, T., Maranguit, D., Murtillaksono, K., Kuzyakov, Y. (2016): Sensitivity and resistance of soil fertility indicators to land-use changes: New concept and examples from conversion of Indonesian rainforest to plantations. – *Ecological Indicators* 67: 49-57. DOI: 10.1016/j.ecolind.2016.02.039.
- [12] Guo, H. C., Wang, W. B., Luo, X. H., Wu, X. P. (2015): Characteristics of rhizosphere and bulk soil microbial communities in rubber plantations in Hainan Island, China. – *Journal of Tropical Forest Science* 27(2): 202-212.
- [13] Kang, M. S., Hur, M., Park, S. J. (2019): Rhizocompartments and environmental factors affect microbial composition and variation in native plants. – *Journal of Microbiology* 57(7): 550-561. DOI: 10.1007/s12275-019-8646-1.
- [14] Kerekes, J., Kaspari, M., Stevenson, B., Nilsson, R. H., Hartmann, M., Amend, A., Bruns, T. D. (2013): Nutrient enrichment increased species richness of leaf litter fungal assemblages in a tropical forest. – *Molecular Ecology* 22(10): 2827-2838. DOI: 10.1111/mec.12259.
- [15] Kerfahi, D., Tripathi, B. M., Dong, K., Go, R., Adams, J. M. (2016): Rainforest conversion to rubber plantation may not result in lower soil diversity of bacteria, fungi, and nematodes. – *Microbial Ecology* 72(2): 359-371. DOI: 10.1007/s00248-016-0790-0.

- [16] Krashevskaya, V., Sandmann, D., Maraun, M., Scheu, S. (2013): Moderate changes in nutrient input alter tropical microbial and protist communities and belowground linkages. – *The ISME Journal* 8(5): 1126-1134. DOI: 10.1038/ismej.2013.209.
- [17] Krashevskaya, V., Klärner, B., Widyastuti, R., Maraun, M., Scheu, S. (2015): Impact of tropical lowland rainforest conversion into rubber and oil palm plantations on soil microbial communities. – *Biology and Fertility of Soils* 51(6): 697-705. DOI: 10.1007/s00374-015-1021-4.
- [18] Kumagai, T., Mudd, R. G., Giambelluca, T. W., Kobayashi, N., Miyazawa, Y., Lim, T. K., Kasemsap, P. (2015): How do rubber (*Hevea brasiliensis*) plantations behave under seasonal water stress in northeastern Thailand and central Cambodia? – *Agricultural and Forest Meteorology* 213: 10-22. DOI: 10.1016/j.agrformet.2015.06.011.
- [19] Lagerlöf, J., Adolfsson, L., Börjesson, G., Ehlers, K., Vinyoles, G. P., Sundh, I. (2014): Land-use intensification and agroforestry in the Kenyan highland: impacts on soil microbial community composition and functional capacity. – *Applied Soil Ecology* 82: 93-99. DOI: 10.1016/j.apsoil.2014.05.015.
- [20] Lan, G., Zhu, H., Cao, M. (2012): Tree species diversity of a 20-ha plot in a tropical seasonal rainforest in Xishuangbanna, Southwest China. – *Journal of Forest Research* 17(5): 432-439. DOI: 10.1007/s10310-011-0309-y.
- [21] Nie, Y., Zhou, Z., Guan, J., Xia, B., Luo, X., Yang, Y., Fu, Y., Sun, Q. (2017): Dynamic changes of yak (*Bos grunniens*) gut microbiota during growth revealed by PCR-DGGE and metagenomics. – *Asian Australasian Journal of Animal Sciences* 30(7): 957-966. DOI: 10.5713/ajas.16.0836.
- [22] Puttaso, P., Pnomkhum, P., Rungthong, R., Promkhambut, A., Kaewjampa, N., Lawongsa, P. (2015): Microbial biomass and activity under different ages of rubber tree plantations in Northeast Thailand. – *Khon Kaen Agric. J.* 43: 963-967.
- [23] Repass, J., Iorns, E., Denis, A., Williams, S. R., Perfito, N., Errington, T. M. (2018): Replication Study: *Fusobacterium nucleatum* infection is prevalent in human colorectal carcinoma. – *eLife* 7. DOI: 10.7554/eLife.25801.
- [24] Schneider, D., Engelhaupt, M., Allen, K., Kurniawan, S., Krashevskaya, V., Heinemann, M., Nacke, H., Wijayanti, M., Meryandini, A., Corre, M. D., Scheu, S., Daniel, R. (2015): Impact of lowland rainforest transformation on diversity and composition of soil prokaryotic communities in Sumatra (Indonesia). – *Front. Microbiol.* 6: 1339. DOI: 10.3389/fmicb.2015.01339.
- [25] Wang, J., Ren, C., Cheng, H., Zou, Y., Bughio, M. A., Li, Q. (2017): Conversion of rainforest into agroforestry and monoculture plantation in China: consequences for soil phosphorus forms and microbial community. – *Science of The Total Environment* 595: 769-778. DOI: 10.1016/j.scitotenv.2017.04.012.
- [26] Warren-Thomas, E., Dolman, P. M., Edwards, D. P. (2015): Increasing demand for natural rubber necessitates a robust sustainability initiative to mitigate impacts on tropical biodiversity. – *Conservation Letters* 8(4): 230-241. DOI: 10.1111/conl.12170.
- [27] Wu, Z. L., Liu, H. M., Liu, L. Y. (2001): Rubber cultivation and sustainable development in Xishuangbanna, China. – *International Journal of Sustainable Development & World Ecology* 8(4): 337-345. DOI: 10.1080/13504500109470091.
- [28] Xu, N., Tan, G., Wang, H., Gai, X. (2016): Effect of biochar additions to soil on nitrogen leaching, microbial biomass and bacterial community structure. – *European Journal of Soil Biology* 74: 1-8. DOI: 10.1016/j.ejsobi.2016.02.004.
- [29] Zhang, B., Wang, H., Yao, S., Bi, L. (2013): Litter quantity confers soil functional resilience through mediating soil biophysical habitat and microbial community structure on an eroded bare land restored with mono *Pinus massoniana*. – *Soil Biol. Biochem.* 57: 556-567.

CARBON STORAGE POTENTIAL OF NATURAL AND PLANTED MANGALS IN TRANG, THAILAND

CADIZ, P. L.^{1,2,3} – CALUMPONG, H. P.³ – SINUTOK, S.^{2,4} – CHOTIKARN, P.^{1,2,4*}

¹*Marine and Coastal Resources Institute, Prince of Songkla University, Hat Yai 90110, Thailand*

²*Coastal Oceanography and Climate Change Research Center, Prince of Songkla University, Hat Yai 90110, Thailand*

³*Silliman University Institute of Environmental and Marine Sciences, Dumaguete City 6200, Philippines*

⁴*Faculty of Environmental Management, Prince of Songkla University, Hat Yai 90110, Thailand*

**Corresponding author*

e-mail: ponlachart.c@psu.ac.th; phone: +66-74-282-335; fax: +66-74-212-782

(Received 10th Dec 2019; accepted 6th May 2020)

Abstract. This study aims to investigate the carbon storage potential for 25 year-old (planted) and >50 year-old (natural) mangrove stands and mangrove sediment, in three districts of Trang province, Thailand. The results show a lower carbon content in the aboveground biomass of 10-25-year-old (planted) stands than in the >50-year old (natural) stands. However, we found more organic carbon in sediments in planted sites than in natural sites, which could be partly due to the higher tree densities in the former. The derived organic carbon in particulate matter was lower in the planted forest than in the natural forest, which could be due to allochthonous inputs of organic matter from rivers and creeks, and to a higher number of species in the natural forests. This study demonstrated that the amount of carbon stored in mangroves increases with age, but the amount of carbon stored in mangrove soils could vary with mangrove density, sediment size, allochthonous inputs, and inundation. This study suggested that planted and natural mangrove forests can capture and store a substantial amount of carbon. Such information could motivate policymakers and local communities to conserve the last remaining mangrove forests, rehabilitate degraded ones, and replant abandoned fish and shrimp ponds.

Keywords: *carbon content, organic matter, carbon sink, reforested mangroves, mangrove ecosystem*

Introduction

Coastal ecosystems such as mangrove forests, saltmarshes, and seagrass meadows have a significant role in mitigating climate change impacts through carbon sequestration. McLeod et al. (2011), reported that fifty-five percent of the carbon can be sequestered in the vegetated coastal ecosystem (mangrove forest, seagrass beds, and salt marshes), because of their ability to store “blue C” in deep organic soils. “The blue C” refers to all the carbon captured from the ocean, including mangrove forests, seagrasses, meadows, and tidal saltmarshes (Thomas, 2014).

Mangroves are known as a diverse group of plants that grow in tropical to subtropical marine intertidal and estuarine areas (Tomlinson, 1986). The unique characteristics of the root systems of mangroves slow down the incoming tidal waters and allow organic and inorganic materials to settle on top of the sediment (Hutchings and Saenger, 1987) and thereby they mitigate siltation (Thampanya et al., 2006). These roots can also act as nursery grounds (Beaumont et al., 2014). The big trees act as buffer against waves (Horstman et al., 2012), and most importantly mangrove litter

is a source of nutrients (Boullion et al., 2008). However, these functions are often overlooked and mangroves are valued by humans for the goods they provide, such as charcoal and firewood, tannin, medicines, and as source of fishery products such as shellfish, crabs and shrimps (Aksornkoae, 1993). Mangroves are also often considered an “open access” resource for the local people. As such, mangroves remain among the most threatened ecosystems in the world, cut and cleared at an alarming rate (Valiela et al., 2001). The global estimates were as high as 15,642,673 (FAO, 2007) to 17,000,000 ha of mangroves in 5 countries of the world (Saenger et al., 1983) and trimmed down to 10,354,335 ha in 15 countries (Giri et al., 2011) during the 80’s to 90’s. The losses were rated at 1-2 percent per year by UNEP (2004), and particularly high in Asia due to massive aquaculture activities, urban settlements, and industrialization (Lewis, 2005; Primavera and Esteban, 2008; Romanach et al., 2018).

In Thailand, the mangrove area was recorded as 367,900 ha in 1961 (Aksornkoae, 1993; Havanond, 1997) and were reduced to 245,533 ha by 2015 (DMCR, 2015). Mangrove deterioration occurred especially during the 80’s when intensive shrimp farming and commercialization converted 5,700 ha of mangrove (Boromthanarat et al., 1991; Bantoon, 1994; Yee, 2010), causing major attention because some converted shrimp pond areas were left abandoned or unattended after the economic crises of the shrimp farming industry. The Government of Thailand conducted massive rehabilitation and conservation programs (Fast and Menasvita, 2003) backed-up with legislation and enforcement of laws and regulations on mangrove uses (Aksornkoae, 2012). The significant value of restoring mangrove areas was fully recognized after the Indian Ocean tsunami hit the Andaman areas of Thailand in 2004 (Barbier, 2008). Massive rehabilitation and reforestation spread out in various provinces, particularly in areas with land use change from shrimp farming activities. However, there was lack of monitoring whether these rehabilitation programs are ecologically sound and beneficial to restore degraded mangrove ecosystems, in particular with land use in shrimp farming. In Trang, land-use changes consisted by 2 percent of aquaculture land, by 47 percent of pararubber plantations, and by 17 percent of mangrove forest/evergreen forests and others classified as institutional land development, cities, paddy field, water bodies etc. (Land Use Development, 2013). Thus, this study is significant to Thailand’s marine resources, particularly mangroves that are still threatened by land-use changes.

Overall, increasing awareness of the carbon storage potential of mangrove ecosystems remains a prerequisite for alleviating climate change issues. This study addresses the community structure and carbon capture potential of mangrove with land-use changes from shrimp farming activities and natural stands of mangroves in Trang, Southern Thailand. Two aged group of mangrove forests, the 10-25-years old (YO) planted in mangrove areas with land-use change from shrimp farming activities and >50-YO natural stands, were measured and monitored in the study. The research findings provide information on the community structure of mangroves in Trang, Southern Thailand, and the carbon data obtained will serve as baseline information for future climate change impact studies. Overall this study helps recommend management strategies in promoting the functional role of mangrove as a source and sink of carbon for better management, protection, and conservation of mangrove forests in Southern Thailand.

Materials and Methods

Description of the Study Site

The study sites were located in Sikao (7.478961° N, 99.335952° E), Kantang (7.376096° N, 99.57253° E) and Palian (7.125833° N, 99.622948° E) districts of Trang, Southern Thailand (*Fig. 1*) where both 10-25-year old planted mangrove forest and >50-YO natural mangrove forest are found. In Trang, mangroves cover 249,331.25 ha of which 35,665.00 ha are designated as economic zone and 26,425.00 ha as preservation zone (Aksornkoae, 1993). Most of the mangroves in these districts are still pristine, except for some areas that have been excavated for shrimp farming 3-4 decades ago. These characteristics are common in these three districts: the areas have abandoned shrimp ponds, with some that have been reverted back into mangrove areas. The plantings of mangrove were mostly initiated by the Department of Marine and Coastal Resources (DMCR) and Thai Royal Department of Forestry (Havanond, 1997).

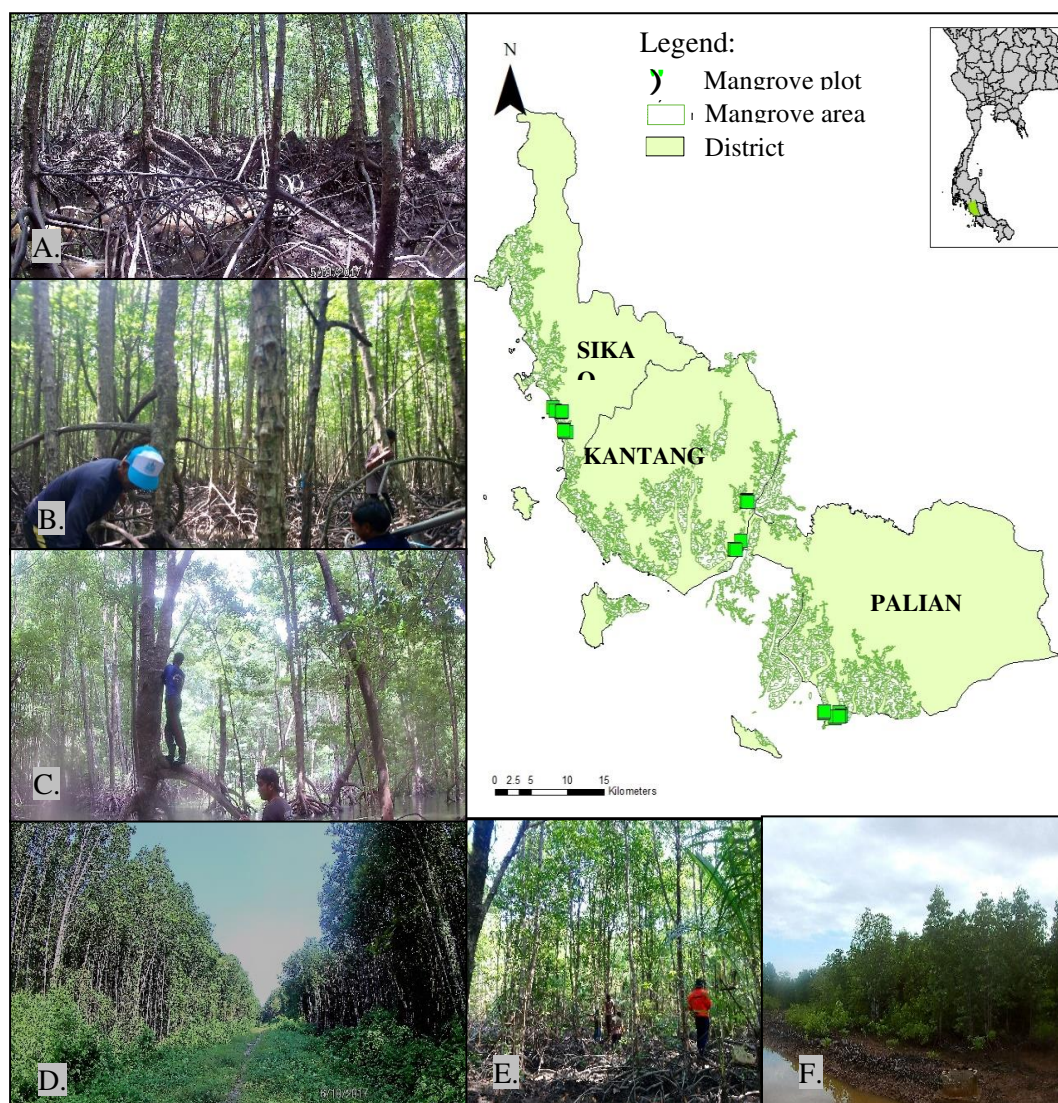


Figure 1. Map of the study sites showing the 3 districts, mangrove areas and permanent plots (green box) in Trang. A, D, and E are planted mangrove forest. B, C, and F are natural mangrove forest. Inset: Map of Thailand

There were ten permanent sampling plots (measuring 10x10 m) established in each district (*Fig. 1*). The sampling plots for the natural forest established in Sikao (SD) were located near a creek, bordered by Pakmeng Beach on the seaward side, while plots for the planted forest were located further southward. In Palian (PD), the plots were established along Palian estuary. The PD estuary is a junction between two big rivers of Klong Lak Khan and Khlong Rae (Horstman et al., 2013). In Kantang (KD), the plots were established inland, with an abandoned shrimp pond adjacent to the rubber plantation that has been replanted (*Fig. 1D*), while plots for the natural forest were located along the creeks and tributaries of KD River. The creeks and rivers receive water from adjacent shrimp pond areas and neighboring households. All plots are affected by the ebb and flow of the tides, except in SD where some of the plots established are inundated only during high tide due to large boulder crab mounds. The plots in PD were established near a concession area where most of the planted mangroves are cut for wood and construction materials (*Fig. 1F*).

Carbon in Aboveground Standing Biomass (CAGB)

To determine the age of a forest, secondary information was obtained from the Department of Marine and Coastal Resources (DMCR). The profile and vegetation structure, such as species composition, density, basal areas, and biomass were obtained (Cadiz and Chotikarn, 2018). Profiling of the community structure was only conducted once, in April 2017. The above-ground biomass estimates followed the allometric equations of Komiyana et al. (2008), using diameter at breast height (D), wood density (ρ) and with coefficient of determination (r^2) of 0.979 (*Eq.1*).

$$\text{Above ground biomass (kg)} = 0.251\rho D^{2.46} \quad (\text{Eq.1})$$

The AGB in kg was then converted to tonnes per hectare. The carbon content of standing biomass was obtained from tree biomass multiplied by 50 per cent, as shown below (Kauffman and Donato, 2012):

$$\text{C content of each tree (kgC)} = \text{tree biomass (kg)} \times \text{conversion factor (0.5)} \quad (\text{Eq.2})$$

Dry Bulk Density

The protocols for soil organic carbon (OC) were modified from Kaufman and Donato (2012), Schumacher (2012) and Hoyle (2013), where three parameters were considered to quantify soil carbon pool: 1. Soil depth, 2. Soil bulk density, and 3. Organic carbon concentration. In the determination of soil bulk density, the soil samples were taken in a known volume of 98.17 cm³ with a metal corer, oven dried at 60°C, and weighed. The bulk density was calculated as the ratio of the dry mass of soil sample to its volume:

$$\text{Dry bulk density (g cm}^{-3}\text{)} = \frac{\text{Mass of dry soil (g)}}{\text{Original volume sampled (cm}^{-3}\text{)}} \quad (\text{Eq.3})$$

$$\text{Soil mass}_{\text{at specified depth}} (\text{mg}) = \text{Bulk Density} (\text{mg m}^{-3}) \times 10,000 (\text{m}^2) \times \text{Depth} (\text{m}) \quad (\text{Eq.4})$$

$$\text{Soil C}_{\text{at specified depth}} (\text{mg}) = \frac{\text{Soil mass}_{\text{at specified depth}} (\text{mg}) \times \% \text{OC}_{\text{at specified depth}}}{100} \quad (\text{Eq.5})$$

Organic Carbon in Soil Sediments and Organic Matter: Field Sampling and Processing of Soil Samples

The fieldwork was carried out quarterly, in May, August, and November of 2017, and in February of 2018, for one year. August and November represent the wet season and May and February represent the dry season. Thirty permanent plots, measuring 10x10 m, were established and quarterly monitored in both 10-25-YO planted and >50-YO natural mangrove stands in the three districts.

Sediment cores were taken from a 100 m² plot in each district (n = 5) and extracted for organic carbon (OC-S). The sediments extracted for organic carbon were sampled from the depths of 0-15, 15-30, 30-50 and 50-100 cm. Sediment sampling was done using a locally manufactured stainless soil corer measuring 5 cm in diameter and 175 cm in length. The volume of the cored OC-S totaled 98.17 cm³. The soil samples collected quarterly were oven dried at 60°C to a constant weight that was recorded. In preparation for CHN Analysis using CN 628 (LECO Corporation), all the quarterly soil subsamples were cleared from any large particles and wood debris, homogenized, and brought to the Faculty of Science, Prince of Songkla University.

The organic carbon derived from particulate organic matter (OC-POM) in soil samples is classified as the organic component of the soil, which is humus formed by the decomposition of leaves and other plant materials. The OC-POM contents were determined from the Loss on Ignition (LOI). The coring of the sediments was performed three times in each plot (n = 3 per plot) and the soil cores were extracted for depths of 0-15 and 15-30 cm, making a total of 15 subsamples (n = 15) for each district. The volume of the soil core was constant at 294 cm³. Along with the soil classification, volumetric measurements were applied for further soil classification (Braley, 1992) as the soil was passed through a series of sieves, and the organic matter retained by the 1-2 mm mesh size was collected and air dried (Calumpong and Cadiz, 2012). After drying, the collected OM was put in an oven (Mettler UNB 500) at 60°C until constant weight. From the original weight of the OM/humus, a portion of dried OM or subsample was weighed into a crucible. The crucibles were placed in a muffle furnace (Digital Muffle Furnace FX-14) at 450-500°C for 4 to 5 hours. The organic matter content was calculated and converted to Mg C ha⁻¹ (Howard et al., 2014) as follows:

$$\% \text{OM} = \frac{\text{Mass of oven dried soil or humus (g)} - \text{ashed soil or humus (g)}}{\text{Mass of original volume sampled (g)}} \times 100 \quad (\text{Eq.6})$$

Physicochemical Parameters

Measurements of redox (Eh), pH, and temperature were done *in situ* using a handheld portable ORP and pH meter (WTW 3210). The probe was inserted into the soil at 0-2 cm depth. Three readings were taken during the day between 9:00 am to 3:00 pm within the sampling period. Rainfall data were obtained from the Meteorological Department, Trang.

Statistical Analyses

Multivariate analysis was used to determine significant differences in CAGB and OC-S and other related parameters, by site and by month. Two-way ANOVA was also used to determine significant differences in OC-S by mangrove age and by sampling month. Levene's test was applied in ANOVA for the equality of variances. When no significant differences were noted, the data were pooled by age and season and analyzed with a T-test. Post-hoc testing was performed to determine the variations by age (10-25-YO planted and >50-YO natural) and by season (wet and dry). Normality was tested with Shapiro–Wilk's test. Regression analysis was performed to find out the relationship between the production of OM and OC-POM, and DBD and OC-POM.

Results

Carbon Captured in Above Ground Biomass (CAGB)

The highest CAGB among all the sites was recorded in KD at 236.42 ± 35.17 t C ha⁻¹, followed by PD at 181.30 ± 23.25 t C ha⁻¹. The lowest was found in SD at 163.15 ± 27.36 t C ha⁻¹. Results on CAGB combined by the two ages (10-25-YO planted and >50-YO natural forests) in all sites showed that the 10-25-YO planted forest had lower CAGB (143.37 ± 19.12 t C ha⁻¹) than >50-YO natural forest (243.88 ± 22.22 t C ha⁻¹) ($p < 0.001$; Table 1).

Table 1. Mean values of the vegetation structure

Site/ Age	DE (stem ha ⁻¹)	BA (m ² ha ⁻¹)	Height (m)	Biomass (t ha ⁻¹)	CAGB (t C ha ⁻¹)	OC-S (Mg C ha ⁻¹)*	OM (%)
SD 10-25	1650.00 ±583.90	0.72 ±0.05	15.32 ±0.38	283.39 ±100.23	141.70 ±50.12	193.62 ±15.31	18.04 ±2.17
SD >50	1360 ±286.05	1.19 ±0.10	15.41 ±0.19	369.22 ±50.11	184.61 ±25.05	214.35 ±15.91	23.44 ±1.82
KD 10-25	6220.00 ±459.78	0.57 ±0.02	15.71 ±0.20	325.08 ±46.25	162.54 ±23.13	317.75 ±16.18	23.14 ±1.83
KD >50	616.00 ±131.76	2.47 ±0.25	16.27 ±0.35	620.60 ±95.99	310.30 ±47.99	257.98 ±13.04	19.52 ±1.61
PD 10-25	3667.78 ±1364.81	0.30 ±0.02	15.71 ±0.20	251.72 ±50.05	125.86 ±25.02	305.24 ±29.75	16.31 ±14.52
PD >50	560.71 ±103.55	1.19 ±0.13	15.87 ±0.19	473.48 ±32.84	236.74 ±16.42	293.58 ±13.91	44.39 ±14.52

DE-depth, BA-basal area and H-height (Source: Cadiz and Chotikarn, 2018) CAGB-carbon in above-ground biomass, OC-S-organic carbon in soil and OM-organic matter in 10-25-YO and >50-YO mangrove forests in Trang, Thailand. * 1 metric ton = 1 mega gram (Mg) or 1 000 000 grams. Data represents Mean ± S.E.

According to the species with the most biomass was indicated in *Rhizophora apiculata* Bl. in both of the 10-25-YO planted and >50-YO natural forests in KD at $464.25 \pm 130.16 \text{ t ha}^{-1}$ and $325.08 \pm 46.25 \text{ t ha}^{-1}$, respectively (Cadiz and Chotikarn, 2018). The higher biomass of these species also corresponds to the species of higher CAGB found in both 10-25 planted and >50-YO natural mangrove forests in the three sites as well ($p < 0.05$; Tables 1 and 2). The *R. apiculata* were consistently high in most of the sites, particularly in >50-YO natural forest in KD ($213.55 \pm 59.88 \text{ t C ha}^{-1}$). Among the species measured, the CAGB of *R. apiculata* were highest in all sites and between planted and natural sites (Fig. 2). For some species such as *Avicennia marina* (Forssk.) Vierh. and *Ceriops tagal* (Perr.) CB Rob, the CAGB located in PD >50-YO natural forest ranged from $1.50 \pm 1.50 \text{ t C ha}^{-1}$ to $45.10 \pm 22.41 \text{ t C ha}^{-1}$.

Table 2. ANOVA test to determine the significant effects of biomass in three different sites, age and sites vs. age at $p < 0.05$

Source	df	SS	F	p
Site	2	139614451.43	25.87	<0.001
Age	1	522219678.84	193.53	<0.001
Site vs. Age	2	180661336.55	33.47	<0.001

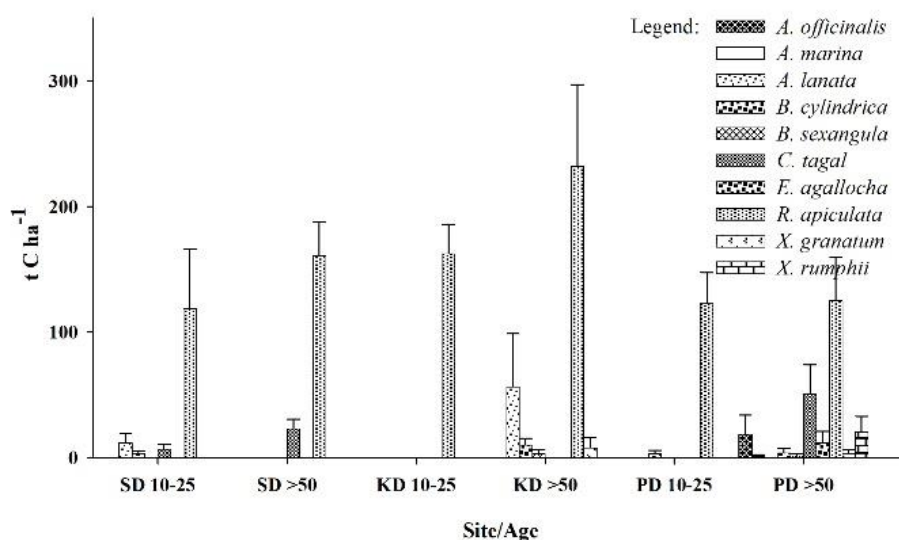


Figure 2. Carbon content (t C ha^{-1}) of the different species calculated from AGB

The Organic Carbon Stored Below Ground

Among the various sites, the organic carbon stored in the soil (OC-S) was significantly highest in PD at $299.41 \pm 15.60 \text{ Mg C ha}^{-1}$, followed by KD at $288.31 \pm 14.07 \text{ Mg C ha}^{-1}$. The least was observed in SD at $203.12 \pm 10.95 \text{ Mg C ha}^{-1}$. Comparing between planted and natural mangrove, the 10-25-YO planted forest showed higher OC-S ($272.49 \pm 14.55 \text{ Mg C ha}^{-1}$) than the >50-YO natural mangrove forest ($254.73 \pm 10.93 \text{ Mg C ha}^{-1}$; $p > 0.05$). A three-way ANOVA revealed no significant interaction among the sites, the months, and between planted and natural stands of mangroves ($p > 0.05$; Fig. 3). The 10-25-YO planted mangrove at KD and PD obtained

the OC-S values of $317.75 \pm 16.18 \text{ Mg C ha}^{-1}$ and $305.24 \pm 29.75 \text{ Mg C ha}^{-1}$, respectively (Fig. 3). Statistically significant variations only showed up in the mean quarterly OC-S in PD >50-YO natural forest, which was highest in August ($377.46 \pm 14.21 \text{ Mg C ha}^{-1}$), followed by PD 10-25-YO planted forest in November ($359.67 \pm 27.68 \text{ Mg C ha}^{-1}$). The SD 10-25-YO planted forest had the lowest OC-S at $171.10 \pm 22.87 \text{ Mg C ha}^{-1}$ in February (Fig. 3).

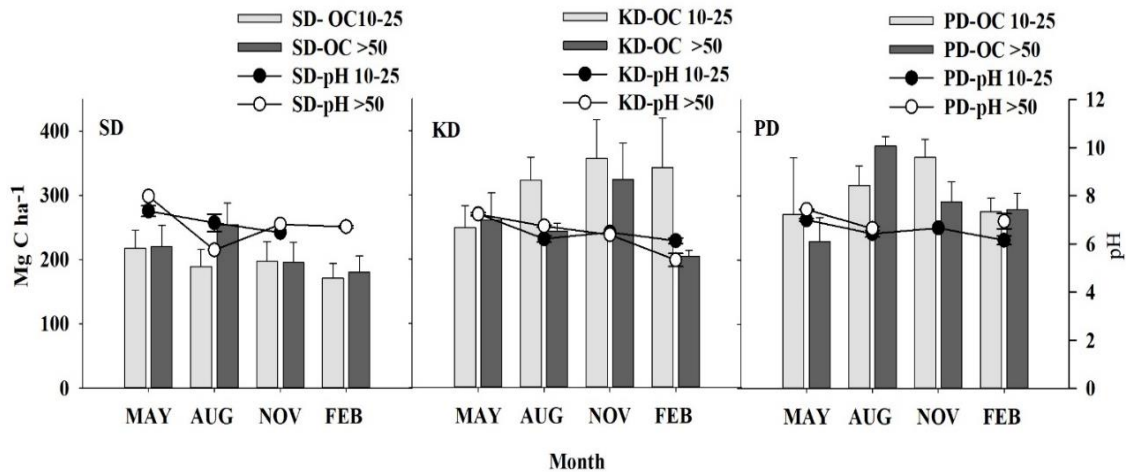


Figure 3. Organic Carbon stock from soil (OC-S) (Mg-C ha^{-1}) and pH at different sites in 10-25-YO planted and >50-YO natural mangrove forests. Error bars are for S.E.

Figures 4 and 5 show the overall mean OC-S for wet and dry seasons. The mean OC-S in wet season was significantly higher ($285.52 \pm 12.49 \text{ Mg C ha}^{-1}$) than in the dry season ($241.99 \pm 12.71 \text{ Mg C ha}^{-1}$; $p < 0.05$; Fig. 4).

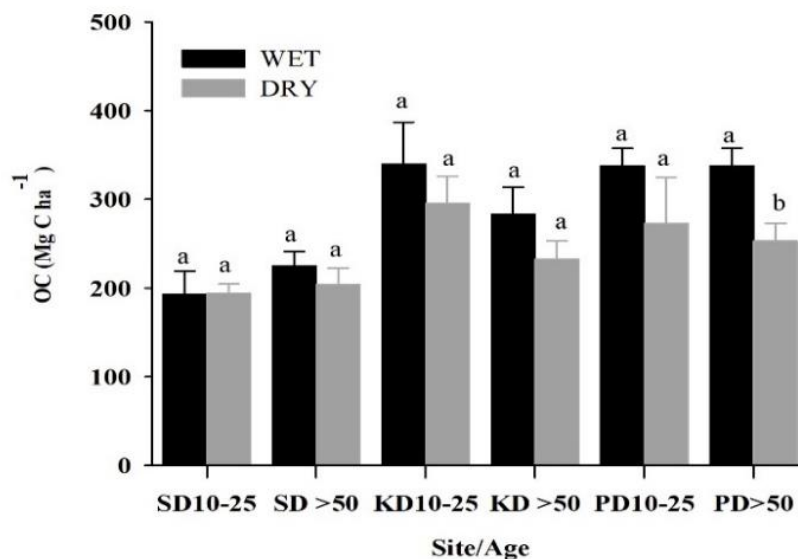


Figure 4. Overall mean OC-S (Mg C ha^{-1}) in the soil sediments between wet and dry seasons and 10-25-YO planted forest and >50-YO natural mangrove forests. Error bars are for S.E. 'a' on top of the error bar indicates $p < 0.05$ while b indicates $p > 0.05$ in the different sites; $n = 5$

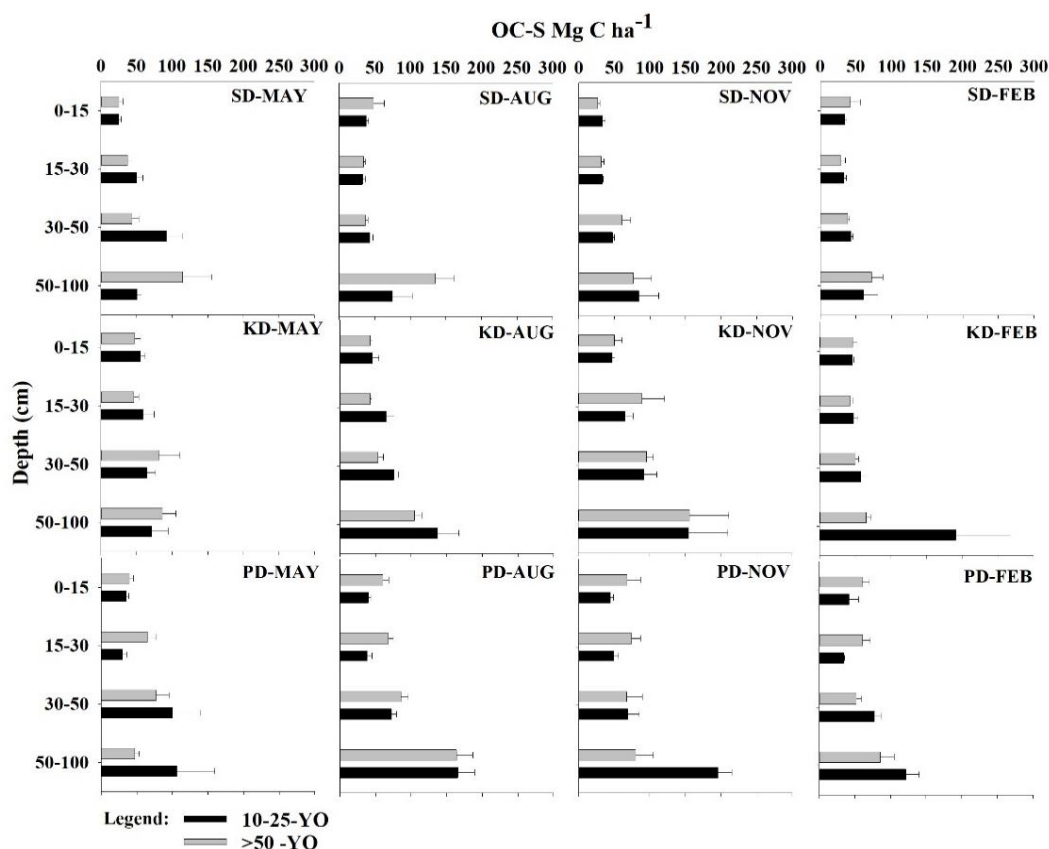


Figure 5. Organic carbon from soil (Mg C ha^{-1}) stored in various depths in 10-25-YO planted and >50-YO natural mangrove forests in Trang, Thailand, sampled in August 2017 to February 2018. The error bars are for S.E.

Figure 5 shows a summary of the mean quarterly OC-S and Figure 6 shows the OC-S in each site and at various depths. The OC-S content varied with depth (0-15, 15-30, 30-50 and 50-100 cm depths). A factorial ANOVA indicated significant differences between 10-25-YO planted and >50-YO natural forests in PD ($df=3.32$ and 5.96 ; $p<0.05$) and no significant differences were indicated in SD ($df=3.32$ and 2.30 , $p>0.05$) and KD ($df=3.32$ and 1.04 ; $p>0.05$) (Table 3). However, the overall trends across various depths in different sites showed higher OC-S at 50-100 cm depth in both 10-25-YO planted and >50-YO natural forest (Fig. 5). The values ranged from $27.19\pm 2.25 \text{ Mg C ha}^{-1}$ found in 0-15 cm depth in SD 10-25-YO planted forest to $161.17\pm 25.79 \text{ Mg C ha}^{-1}$ found in 50-100 cm depth in PD 10-25-YO planted forest (Fig. 5).

Dry Bulk Density

The trends in average Dry Bulk Density (DBD) of the sediments followed the same patterns as seen in OC-S. Overall DBD comparison between the two ages showed that 10-25-YO was higher ($2.57\pm 0.72 \text{ g cm}^{-3}$) and >50-YO forest was lower ($2.34\pm 0.17 \text{ g cm}^{-3}$) (Fig. 6B). In terms of the season, the results on DBD are similar to OC-S. It was higher during the wet season ($3.10\pm 0.11 \text{ mg cm}^{-3}$) than in the dry season ($2.04\pm 0.22 \text{ mg cm}^{-3}$) for both 10-25-YO planted and >50-YO natural (Fig. 6A).

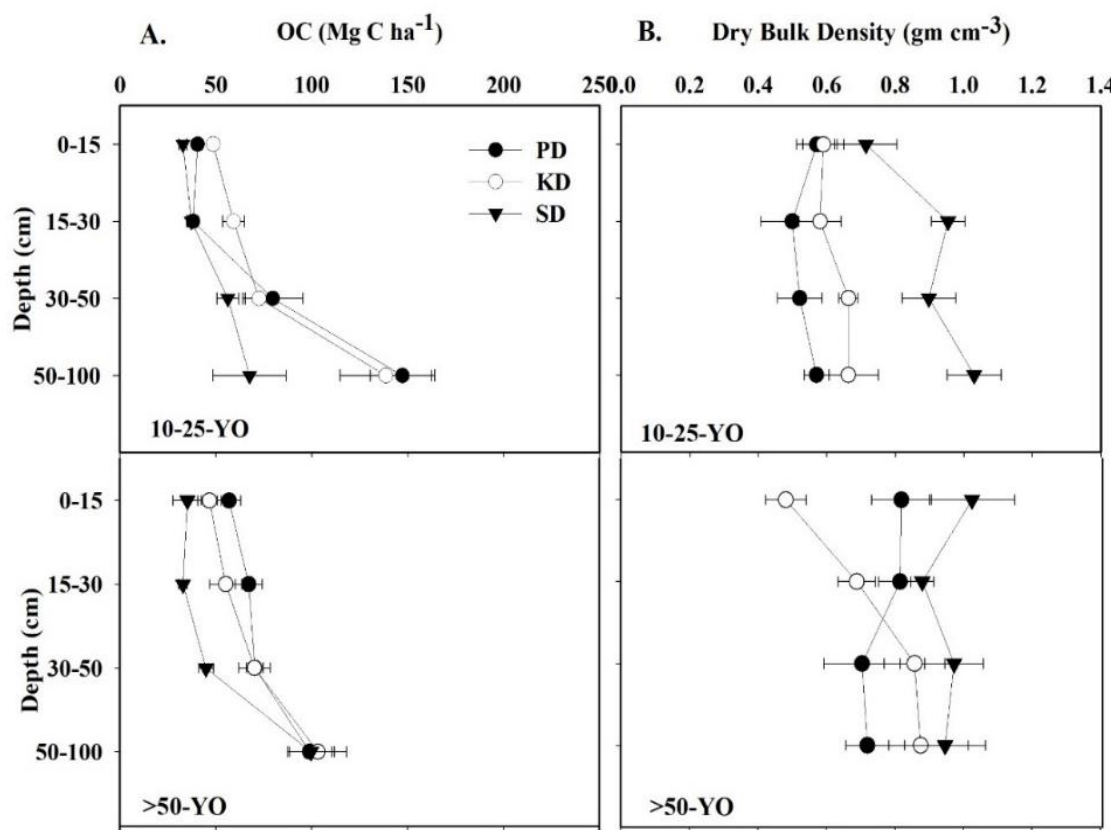


Figure 6. Mean OC-S (Mg C ha⁻¹; A) and Dry Bulk Density (g cm⁻³; B) at different depths of 10-25-YO planted and >50-YO natural mangrove forests in Trang, Thailand. Error bars are for S.E.

Table 3. The result of Two-Way ANOVA determining the effects on C of the following factors: Three different sites with 10-25-YO planted and >50-YO natural mangroves at four different depths (n=15)

Sources of Variation	Sites								
	SD			KD			PD		
	df	SS	p	df	SS	p	df	SS	p
Age	1	0.18	0.450	1	0.05	0.020	1	0.00	0.680
Depth	3	0.56	<0.001	3	0.60	<0.001	3	0.69	<0.001
Age vs. Depth	3	0.18	0.090	3	0.09	0.390	3	0.36	<0.001

Organic Carbon derived from Organic Particulate Matter (OC-POM)

The organic carbon derived from decayed materials in the mangroves was classified as humus/particulate organic matter (POM) in this study. The OC-POM compared between ages was higher in >50-YO natural forest (74.29±33.57 Mg C ha⁻¹) than in the 10-25-YO planted forest (52.27±9.45 Mg C ha⁻¹; t(25)=2.44; p<0.05; Table 1; Fig. 7A). The peak of OC-POM was in May for both 10-25-YO planted forest (37.42±5.43 Mg C ha⁻¹) and for >50-YO natural forests (35.01±10.76 Mg C ha⁻¹).

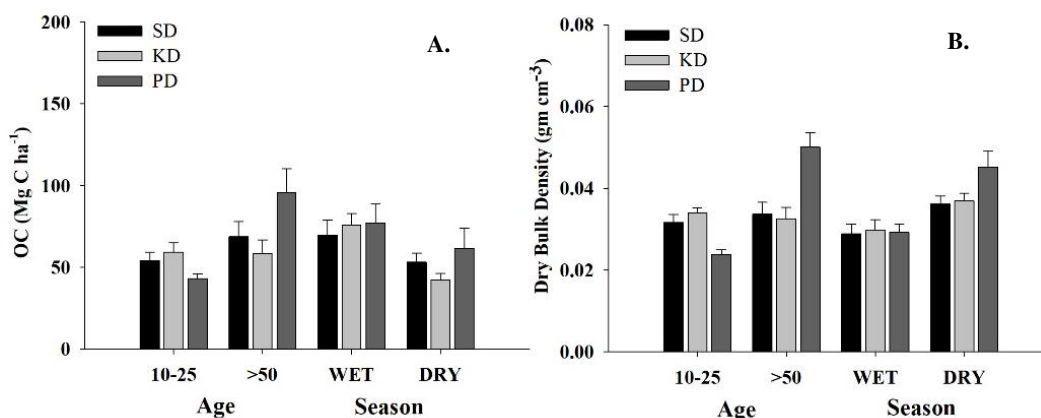


Figure 7. OC-POM in Mg C ha⁻¹ (A) and Dry bulk density in g cm⁻³ (B) from OM/humus in Trang districts. Error bars are for S.E.

During wet and dry seasons the OC-POM followed the same trend as OC-S, being higher in the wet season (74.15±5.48 Mg C ha⁻¹) than in the dry season (52.41±5.69 Mg C ha⁻¹; $p < 0.05$; Table 3; Fig. 7B).

Mean quarterly data of OC-POM varied significantly in >50-YO natural forests (Factorial ANOVA, $F(3,732.88) = 3.21$; $p < 0.05$); and in the three different sites (Factorial ANOVA, $F(14,1,750) = 3.21$; $p < 0.05$). The 10-25-YO followed the same pattern, (Factorial ANOVA, $F(3,1,824) = 3.21$; $p < 0.05$ and $F(14,86.44) = 1.68$; $p < 0.05$). OC-POM in the three sites were highest in August in PD 10-25-YO planted forest (59.23±27.72 Mg C ha⁻¹) and lowest also in PD 10-25-YO planted forest (8.07±0.85 Mg C ha⁻¹; Fig. 7A). The DBD followed the same pattern, with PD >50-YO natural forest being the highest at 1.97±0.22 g cm⁻³ (Fig. 7B).

In contrast to OC-S, the OC-POM showed variations in the 0-30 cm soil depth. Tested with linear regression, the mean quarterly POM (%) and OC-POM (Mg C ha⁻¹) appear to have no significant relationship ($p > 0.05$) and only have a weak correlation ($R^2 = 0.25$) (Fig. 8A). DBD and OC-POM were not correlated either ($p < 0.05$ and $R^2 = 0.26$) (Fig. 8B).

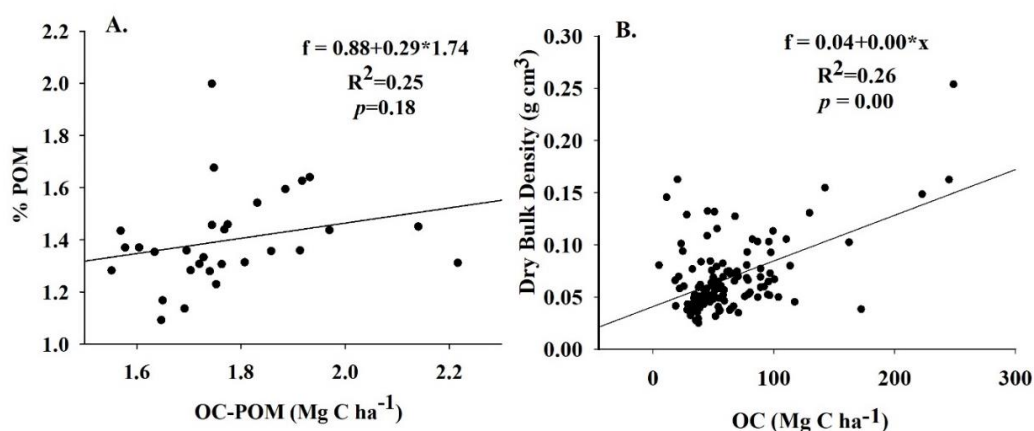


Figure 8. The log-transformed percent OM and OC (A), and DBD and OC (B). All values are derived from OM

Soil Characteristics

This study observed that silt/clay was the dominant soil type in both 10-25-YO and >50-YO mangrove forests in Trang (Fig. 9A-B). At depths of 0-15 and 15-30 cm, silt/clay dominated in the three sites and was followed by very fine sand and fine sand.

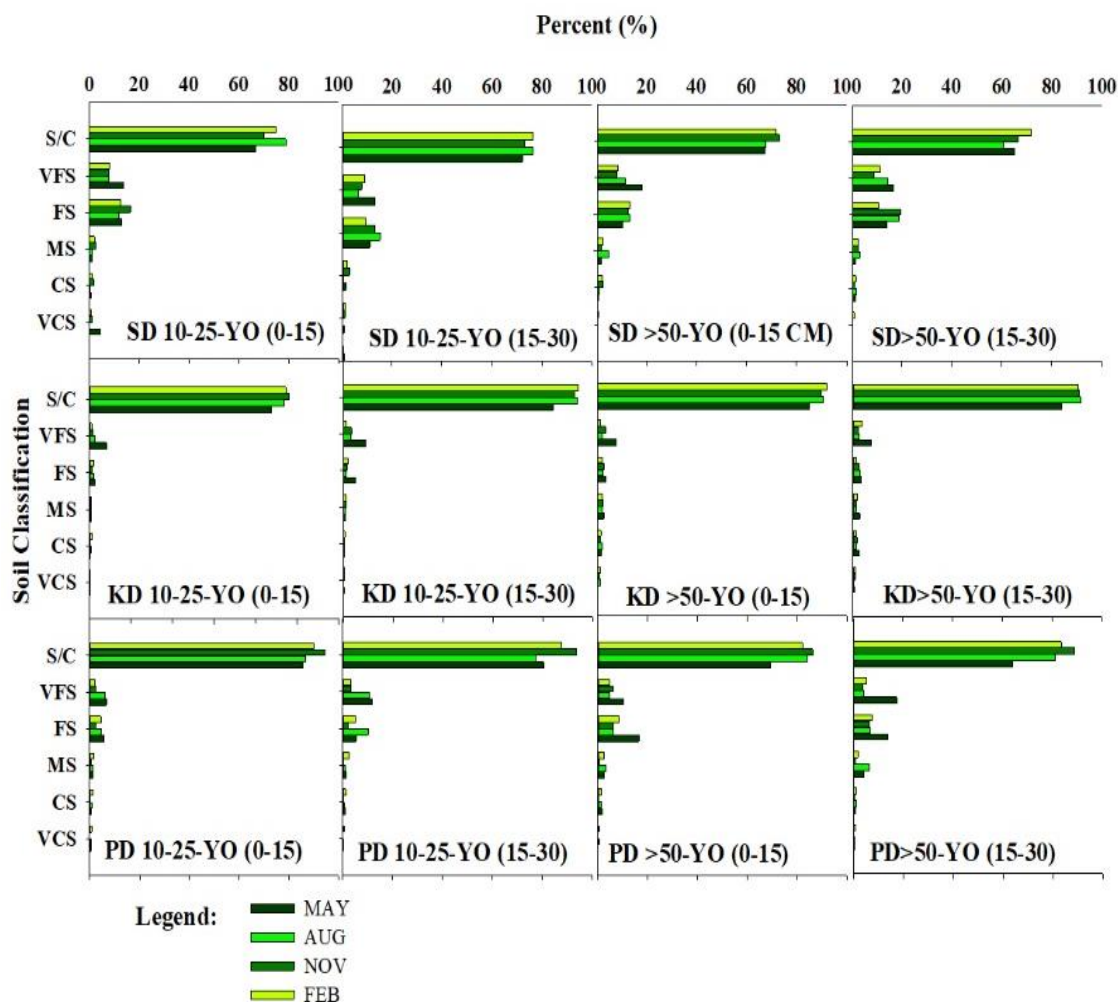


Figure 9. Dominant characteristics (%) of soil in Trang, Thailand. VCS-very coarse sand, CS-coarse sand, MS-medium sand, FS-fine sand, VFS-very fine sand and S/C-silt/clay

The Soil Properties

Figure 10 shows the soil temperature for the 10-25-YO planted and >50-YO natural mangrove forests. The mean soil temperature was $27.99 \pm 1.11^\circ\text{C}$ in >50-YO forest and 28.08 ± 0.55 in 10-25-YO forest. The mean value was higher in the wet season ($M = 28.08 \pm 0.14^\circ\text{C}$) than in the dry season ($M = 27.72 \pm 0.21^\circ\text{C}$); but this difference was not statistically significant ($p > 0.05$). The average daily rainfall during the sampling period was highest in August (14.90 ± 4.27 mm), followed by May (12.81 ± 3.65 mm) and November 2017 (12.81 ± 3.65 mm/day) (Figs. 10 and 11). February 2018 had the lowest rainfall (8.03 ± 2.55 mm).

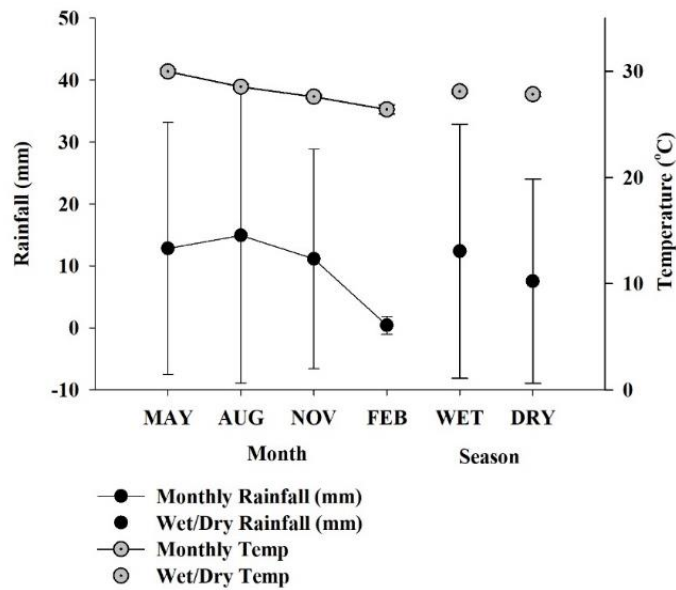


Figure 10. Mean daily rainfall data (mm) and temperature (°C) during the sampling periods (Source: Meteorological Department, Thailand)

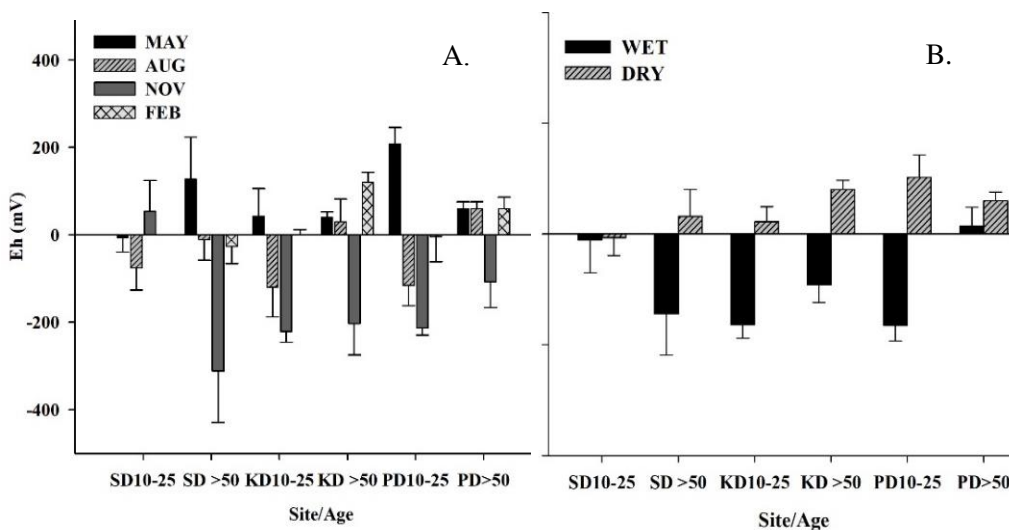


Figure 11. Eh (mV) quarterly (A) and during the wet and dry seasons (B), in Trang, Thailand

The pH of the soil had lower values in KD for both 10-25-YO planted (6.45 ± 0.07) and >50-YO natural forest (6.45 ± 0.04), while the highest pH (6.91 ± 0.09) was observed in PD for the >50-YO natural forest (Fig. 3). The results were higher in the wet season (6.77 ± 0.08) than in the dry season (6.59 ± 0.04 ; $p < 0.05$). Eh potential of the soil is characteristically anoxic ranging in -9.40 ± 36.36 mV in SD 10-25-YO planted and in -62.40 ± 19.00 mV in KD 10-25-YO planted forests (Fig. 11). The comparison between two seasons showed -93.62 ± 21.59 mV during the wet season with the most anoxic soil found in PD 10-25-YO planted forest (-163.72 ± 24.34 mV). Variation of Eh between the two seasons was statistically significant ($p < 0.05$; Fig. 11).

Discussion

Above and Below Ground Carbon, Dry Bulk Density and Organic Carbon from Particulate Organic Matter

This study investigated and monitored the organic carbon content in the 10-25-YO planted and >50-YO natural mangrove forests in the Southern part of Thailand. The findings showed that the variation of CAGB differed due to dense growth of *R. apiculata* in the 10-25-YO planted forest; while the >50-YO natural forests had mixed old stands of *Avicennia* spp., *Rhizophora*, *Bruguiera* spp, *Ceriops*, and *Xylocarpus* spp. (Fig. 2). The composition of 11 species in >50-YO natural forest gave taller plants and a wider range of sizes (i.e. diameter at breast height of trees) and densities (Fig. 2) compared to the 10-25-YO planted with only 3 species, and dominated by *R. apiculata*. In particular, the dense and mono-stand vegetation in KD 10-25-YO planted in unutilized shrimp pond area (Cadiz and Chotikarn, 2018) confirmed these species as the main contributors to CAGB (Figs. 1 and 2).

The estimates of CAGB at three sites show trends comparable to the estimates obtained by Komiyama et al. (2008), and Ong et al. (1995). Ranges of CAGB values around Asia were studied (Table 3), and Malaysia showed 116.79 t C ha⁻¹ (Chandra et al., 2011) and 305.46 t C ha⁻¹ for natural and 122.78 t C ha⁻¹ in degraded areas (Zhila et al., 2014). Putz and Chan (1986) reported 409 t C ha⁻¹ in 30-YO and Ong et al. (1995) reported 114 t C ha⁻¹ in a 20-year old dominantly *R. apiculata* in Matang Mangrove Reserve. The Philippines were in the range from 291.0 to 1578.6 t C ha⁻¹ (Abino et al., 2014) in natural areas and 282.64 t ha⁻¹ in 27-YO planted areas (Castillio and Bрева, 2012). The 10-years old *Rhizophora mucronata* Lamk. and *Bruguiera cylindrica* (L.) Blume planted in excavated shrimp pond areas in Khanom, Nakorn Sri Thammarat, Thailand, had 98.7 t C ha⁻¹ and 28.8 t C ha⁻¹ (Matsuie et al., 2012). It was also established in Ao Sawi, Thailand, that the above-ground biomass in old forest stands tends to have a higher capacity of carbon (about 27%) (Alongi et al., 2001); while this study had a similar trend of higher CAGB in >50-YO natural forest (243.88±22.24 t C ha⁻¹) than in the 10-25-YO planted forest (143.37±19.13 t C ha⁻¹; $p < 0.05$). This is caused by more species in the natural stands than in planted stands, highlighting that the species diversity affects the production of CAGB (MacKenzie et al., 2016).

Soil in mangroves is known as the largest source of organic carbon pool (Alongi et al., 2016), and carbon stored in the soil is the best indicator of productivity in the mangrove ecosystem (Boullion et al., 2008). The distribution and content of carbon stored in the soil are most likely dependent in geographic characteristics of the entire mangrove ecosystem, since all the established plots of the studied sites were directly connected with runoffs from tributaries of rivers, creeks/canals and adjacent shrimp ponds (Fig. 1) for ease and accessibility of sampling. However, we found that the similarities of OC-S content in both KD and PD have topographic influence as well. Unlike SD with lower OC-S because of the elevated topography characterized by the high boulders of crab mounds in both 10-25-YO planted and >50-YO natural mangrove forests (Fig. 1A-B). We observed that the large boulder crab mounds affect the consistency in coring the soil sediments. The crab mounds once covered the forest floor of the mangroves, and there is a high tendency to core the crab mounted areas instead of coring the forest floor; thus affecting the production of OC-S. These inconsistencies in sampling mangrove carbon affect the OC-S values obtained.

Between planted and natural stands of mangroves, this study observed that OC-S stored in the 10-25-YO planted ($272.49 \pm 19.16 \text{ Mg C ha}^{-1}$) is higher than in the >50-YO natural forest ($254.73 \pm 11.74 \text{ Mg C ha}^{-1}$). Categorically higher values of OC-S in the 10-25-YO planted forests were due to the higher density of trees (*Table 1*). This characteristic was observed in the 10-25-YO planted forest in KD with the highest OC-S of $317.75 \pm 16.18 \text{ Mg C ha}^{-1}$. The compacted soil in the pond perhaps has a tendency and high ability to hold and store sediments and organic matter for a certain period of time, facilitating growth of these 10-25-YO planted forests (*Fig. 1A, B and D*). Another contributing factor in OC-S production is the possibility of higher turn-over rate of defoliation from younger trees apart from dense cover (as closely planted in the shrimp pond areas).

However, the overall mean OC-S obtained in this study was below the global value of 749 Mg C ha^{-1} (Kauffman et al., 2018) but still comparable to observations in Singapore, Vietnam, Philippines, India, Africa, Palau and Micronesia and Brazil.

The temporal (dry and wet season) variations contributed to the variation of OC-S in the mangrove ecosystem. The higher OC-S during the wet season indicates that carbon buried in the soil favored by the right amount of rainfall and temperature (*Fig. 10*). Such that rainfall allows more water flow the movement (i.e., like density stratification and vertical circulation) (Mazda et al., 2007) which enhance the biotic activity of the mangrove soil and potentially contributing the OC-S production.

The overall trends in OC-S was to have more OC-S in deeper soil (50-100 cm depth) and this was particularly observed in the 10-25-YO planted forests in KD and PD (*Figs. 5 and 6*) where the OC-S increased with depth. Similar trend has been observed in the northeastern Brazilian mangroves (Kauffman et al., 2017) and Central-Western Region of Venezuela (Barreto et al., 2016). However, some studies have revealed the opposite trend with the concentration of carbon tending to decrease with depth (Ceron-Breton et al., 2014), because carbon also tends to be influenced by the rate of production of organic matter and not only the rate of decay (Alongi et al., 2016).

The derived OC-POM taken only at 0-30 cm depth is of primary concern in this study since rich POM is mostly found on surface of the forest floor. The result suggests no direct relationship between percent organic matter and OC-POM production (*Fig. 8A*). This indicates that OC-POM settled deeper while the OM settled more at the surface layer (0-30 cm depth) of the soil. The settled OM on soil surface allows more time to reach deeper prior to the integration of the OC-POM. The integration of organic matter in the forest floor and soil profile will only come after the integration and mineralization process (Salmo et al., 2013). While this increases the production of OM in the surface layer, there is also a presence of new litter (Punwong et al., 2018) and then this gradually decreases in the deeper part of the soil. This study indicates that the source of organic matter was mainly the shrimp ponds channeled through canals and rivers (*Figs. 1 and 2*). Hence, the topography at a site influenced the flows and transport of OM in the mangrove stands. Apart from the allochthonous material deposits in the mangrove ecosystem, the presence of different species, tidal range, topography, sediment chemistry, community structure, and substrate characteristics (Dittmar and Lara, 2001; Chaikaew and Chavanich, 2017) therefore affect the derived OC-POM.

Overall, the variation and range of OC in mangroves is affected by how sampling is done, along with plot size, precision, and accuracy of allometric models (Rodriguez et al., 2014), species diversity (MacKenzie et al., 2016), hydrogeomorphology, climate

and seasons (Ceron-Breton et al., 2014), while this study also considered soil depth induced variations in carbon measurements.

Soil Properties

The significance of soil characteristics such as soil type and composition are most influential in a mangrove ecosystem. The different mangrove species have different affinities to soil types (Calumpang and Cadiz, 1997) that influence the growth and survival of planted mangroves (Salmo et al., 2013). In this study, the results indicate that the soil type in most of the studied areas was muddy with typical silt/clay characteristics exhibited in the mangroves. As described regarding the study site, the deposition of fine particles that are carried with overflow from the big canals and rivers influenced stored carbon in mangroves. Since all the plots assessed were close to rivers, creeks or canals for ease and accessibility of working (*Figs. 1 and 2*), they had fine sand deposits and dense mangrove growth (Punwong et al., 2018), with silt/clay soil. Although the coring of the sediment for soil profile in this study was limited to 0-30 cm depth, the results suggest that silty/clay characteristics in both 10-25-YO planted and >50-YO natural forests tend to hold more carbon as one samples deeper (*Fig. 6A*). This characteristic contributes to the potential to retain organic carbon in the soil to influence DBD (Barreto et al., 2016; Phang et al., 2017). The soil profile in mangroves is generally dominated by silt/clay (*Fig. 9*) which is rich in organic clay and humus due to the biotic activity in the soil (Mazda et al., 2007). This is good for storing OC. This characteristic of soil is also found in Ao Nam Bor, Phuket, Thailand (Kristensen et al., 1995), following also the physical attributes in all the mangrove soils worldwide (Hossain and Nuruddin, 2016). However, the fact that mangroves exist in a wide range of soil types, even potentially within a single study area, contributes to large variability in reported soil C stocks.

Mangroves thrive well in tropical climate. The higher OC-S during wet season was enhanced by rainfall. In the process, the hydrological characteristics attributed by rainfall enhanced the biotic activity of the soil, thus influenced carbon stored in the mangrove soil. On May 2017 during the onset of rainy season, the second highest rainfall took place (*Fig. 8*), while February 2018 was the peak of the dry season, and rain occurred during sampling. However, the soil temperature averages over wet and dry seasons were considerably high, ranging within 24.76-30.02°C compared to 26.99-27.69°C in Phetchaburi (Jithaisong et al., 2012) or 25.8 to 28.9°C in Tungka Bay, Chumpon, Thailand (Matsui et al., 2015). Temperature and precipitation are known to influence the survival and growth of mangroves (Numbere and Camilo, 2017), as well as carbon densities.

Evidence of low pH and high redox was observed in KD during the wet season. The 10-25-YO planted area in KD located nearby a rubber plantation, and a former site with land-use change from shrimp farming activities. Perhaps this activity had left nutrients to influence Eh. Categorically, all sites for both stands had highly anoxic soil during the wet season (*Fig. 11A*). Anoxic soil causes faster decomposition of organic matter as revealed by the higher OC-POM during the wet season (*Fig. 7A*). What made Eh high in KD was that the planted mangroves were in an intact abandoned shrimp pond. The infiltration of rainfall in the pond took longer time, while allowing organic matter to settle in the pond. Further, the OC is highly correlated with pH and Eh because of its relation to transport in the mangrove ecosystem. Also the mobilities of phosphorus and magnesium depend on pH and Eh (Matsui et al., 2015). In addition, disturbing

mangrove areas triggered the formation of pyrite (a feature of mangrove sediments), which also influenced pH and Eh. This oxidation process occurs typically after a mangrove forest is cleared for aquaculture purposes, like shrimp ponds (Kristensen et al., 1995). Overall, however, neutral soil characteristics were observed in this study.

Conclusions

- 1) Based on this study, the knowledge gaps on the carbon storage potential of restored mangrove (mostly planted in abandoned shrimp ponds) and mangrove on natural stands were addressed. Sources and sinks of carbon in both types of stands were found in CAGB, OC-S and PO-POM, and their differences were influenced by the community structure and vegetation. The observed large variations in CAGB were likely due to the complexity of species; such as in >50-YO natural forests had 11 species while the 10-25-YO planted mangrove only had 3 species and was dominated by *R. apiculata*, in contrast to higher densities in planted stands than natural stands. Therefore, this study suggests that conservation of mangroves in natural stands remains the first and foremost source and sink of C.
- 2) While the soil samples cored in crab mounted areas such as in SD showed lower OC-S densities it is best to recommend that further study should be conducted at other sites with the same crab mounted characteristics. This is to ensure that a well-defined inventory approach in assessing ecosystem C stocks is necessary to better account for the heterogeneity in topographic characteristics.
- 3) This study also demonstrated that both stands of mangroves act as carbon sinks, and therefore planted stands are also carbon sinks similar to the natural stands, provided similar geomorphic and topographic characteristics. The significance of restored mangroves is that even relatively young stands of mangrove forest can sequester a substantial amount of carbon, stored either aboveground in biomass or below ground in the soil. These findings provide additional information for developing strategies for the management of carbon in relation to land-use change (Donato et al., 2012), particularly on reverted shrimp pond areas.
- 4) Furthermore, all restoration activities need to be well maintained and sustained by the local people, who should appreciate the indirect values of mangroves, specifically as carbon sinks. Since only little is known and no particular research has been done on the active involvement (i.e., experiences and motivations) of the local community towards blue carbon governance (Thomas et al., 2014), and for better management, trainings of the local people for blue carbon initiatives and governance should also be initiated.
- 5) Overall, this study showed the potential of natural as well as planted stands of mangrove in storing carbon in order to encourage and pursue local sectors of Trang, Thailand and policy makers in both local and national agencies to continue the efforts in mangrove restoration, particularly in areas abandoned from aquaculture activities.

Acknowledgments. This research was funded by the Graduate School, Prince of Songkla University (PSU) under the Thailand Education Hub for ASEAN Countries (TEH-AC) and in part from PADI Foundation. We gratefully acknowledge The Department of Marine and Coastal Resources, Trang for the logistics support and Pathompong Pramneecheote for his unselfish time all throughout the sampling; Mr. Jim Enright of Map Action Project (MAP, Asia), Trang for valuable assistance in choosing the study sites

and Pimchanok Buapet, Paramita Punwong and Bradly Walters for their invaluable comments and suggestions. Authors would like to thank to Seppo Karrila and Research and Development Office, PSU for English proof.

Conflict of Interests. The authors confirm that there is no conflict of interests in publishing this paper.

REFERENCES

- [1] Abino, A. C., Castillo, J. A., Lee, Y. J. (2014): Species Diversity, Biomass, And Carbon Stock Assessments Of A Natural Mangrove Forest In Palawan, Philippines. – *Pak. J. Bot.* 46(6): 1955-1962.
- [2] Aksornkoe, S. (1993): Ecology and Management of Mangroves. – IUCN, Bangkok, Thailand. Dyna Print Ltd., 392/9 2nd Siam Square, Soi 5, Bangkok, Thailand 2-35.
- [3] Aksornkoe, S. (2012): Mangroves... Coastal Treasure of Thailand. – *The Journal of the Royal Institute of Thailand* 1V: 73-75.
- [4] Alongi, D. M., Wattayakorn, G., Pfitzner, J., Tirende, F., Zagorskis, I., Brunskill, G. J., Davidson, A., Clough, B. G. (2001): Organic carbon accumulation and metabolic pathways in sediments of mangrove forests in southern Thailand. – *Marine Geology* 179(1-2): 85-103.
- [5] Alongi, D. M., Sasekumar, A., Chong, V. C., Pfitzner, J., Trott, L. A., Tirendi, F. (2004): Sediment accumulation and organic material flux in a managed mangrove ecosystem: estimates of land–ocean–atmosphere exchange in peninsular Malaysia. – *Marine Geology* 208: 383-402.
- [6] Alongi, D. M., Murdiyarso, D., Fourqurean, J. W., Kauffman, J. B., Hutahaean, A., Crooks, S., Lovelock, C. E., Howard, J., Herr, D., Fortes, M., Pidgeon, E., Wagey, T. (2016): Indonesia's blue carbon: a globally significant and vulnerable sink for seagrass and mangrove carbon. – *Wetlands Ecology* 24: 3-13. <https://doi.org/10.1007/s11273-015-9446-y>.
- [7] Bantoon, S. (1994): Using simulation modeling and remote sensing technique for an impact study of shrimp farms on mangrove area and aquatic animal production at Welu estuary, Klung district, Chantaburi Province. – Unpublished MSc thesis, Chulalongkorn University.
- [8] Barbier, E. B. (2008): In the wake of tsunami: Lessons learned from the household decision to replant mangroves in Thailand. – *Resource and Energy Economics* 30(2): 229-249. doi:10.1016/j.reseneeco.2007.08.002.
- [9] Barreto, M. B., Moaco, S. L., Diaz, R., Barreto-Pittol, E., Lopez, L., do Carmo Ruaro Peralba, M. (2016): Soil organic carbon of mangrove forests (*Rhizophora* and *Avicennia*) of the Venezuelan Caribbean coast. – *Organic Geochemistry* 100: 51-61.
- [10] Beaumont, N. J., Jones, L. M., Garbutt, A., Hansom, J. D., Toberman, M. (2014): The value of carbon sequestration and storage in coastal habitats. – *Estuarine, Coastal and Shelf Science* 137: 32-40. <http://dx.doi.org/10.1016/j.ecss.2013.11.022>.
- [11] Boromthanasat, S., Cobb, S., Lee, V. (1991): Coastal Management in Pak Phanang: A Historical Perspective of Resources and Issues. – Hat Yai, Thailand: Coastal Resources Institute, Prince of Songkla University.
- [12] Bouillon, S., Borges, A. V., Castañeda-Moya, E., Diele, K., Dittmar, T., Duke, N. C., Kristensen, E., Lee, S. Y., Marchand, C., Middelburg, J. J., Rivera-Monroy, V. H., Smith III, T. J., Twilley, R. R. (2008): Mangrove production and carbon sinks: A revision of global budget estimates. – *Global Biogeochemical Cycles* 22(2): 1-12.
- [13] Braley, R. D. (ed.) (1992): The Giant Clam: Hatchery and Nursery Culture Manual. – ACIAR Monograph 15: 144.
- [14] Cadiz, P., Chotikarn, P. (2018): Biomass Estimates and Species Diversity of Natural and Planted Mangroves in Trang, Thailand. – Proceedings of the 1st International Conference

- on Climate Change, Biodiversity, Food Security and Local Knowledge, 3-4 September 2018. Artha Wachana Christian University, Kupang, East Nusa Tenggara, Indonesia.
- [15] Calumpang, H. P., Cadiz, P. L. (1997): Mangrove Rehabilitation Efforts in Bais Bay. – *Silliman Journal* 37(3-4): 187-203.
- [16] Calumpang, H. P., Meñez, E. (1997): *Field Guide to the Common Mangroves, Seagrasses and Algae of the Philippines*. – Bookmark, Inc. Makati City, Philippines.
- [17] Calumpang, H. P., Cadiz, P. L. (2012): *Mangrove Rehabilitation in Ticao Island, Masbate, Philippines*. – SEARCA Agriculture and Development Discussion Paper Series: 2012-4(12).
- [18] Castillo, J. A., Breva, L. (2012): Carbon Stock of four Mangrove Reforestation/Plantation Stands in the Philippines. – In: Palis, H., Pasicolan, S., Villamor, C. (eds.) *Proceedings of the 1st ASEAN Congress on Mangrove Research and Development* (Century Park Hotel Manila, Philippines, December 3-7, 2012).
- [19] Cerón-Bretón, J. G., Cerón-Bretón, R. M., Guerra-Santos, J. J., Córdova-Quiroz, A. C. (2014): Estimation of Regional Carbon Storage Potential in Mangrove Soils on Carmen Island, Campeche, Mexico. – In: Morgado, C. R. V., Esteves, V. (eds.) *CO2 Sequestration and Valorization*. IntechOpen, DOI: 10.5772/57055. Available from: <https://www.intechopen.com/books/co2-sequestration-and-valorization/estimation-of-regional-carbon-storage-potential-in-mangrove-soils-on-carmen-island-campeche-mexico>
- [20] Chaikaew, P., Chavanich, S. (2017): Spatial Variability and Relationship of Mangrove Soil Organic Matter to Organic Carbon. – *Applied and Environmental Soil Science* 2017: 4010381. <https://doi.org/10.1155/2017/4010381>.
- [21] Chandra, I. A., Seca, G., Abu Hena, M. K. (2011): Aboveground Biomass Production of *Rhizophora apiculata* Blume in Sarawak Mangrove Forest. – *American Journal of Agricultural and Biological Sciences* 6(4): 469-474.
- [22] Department of Marine and Coastal Resource Research and Development (2015): *DMCR Annual Report*. – In: *Handbook of Thailand Marine Coastal Resources*. Ministry of Natural Resources and Environment. Printed by the Agricultural Cooperative Federation of Thailand., LTD. Bangkok. 249.
- [23] Dittmar, T., Lara, R. J. (2001): Driving Forces Behind Nutrient and Organic Matter Dynamics in a Mangrove Tidal Creek in North Brazil. – *Estuarine Coastal and Shelf Science* 52(2): 249-259.
- [24] Donato, D. C., Kauffman, J. B., MacKenzie, R. A., Ainsworth, A., Pflieger, A. Z. (2012): Whole-island carbon stocks in the tropical Pacific: Implications for mangrove conservation and upland restoration. – *Journal of Environmental Management* 97: 89-96.
- [25] FAO (2007): *The World's Mangroves 1980-2005*. – Electronic Publishing and Support Branch. Communication Division. FAO. Rome, Italy.
- [26] Fast, A. W., Menasvita, P. (2003): Mangrove Forest recovery in Thailand. – *World Aquaculture* 7: 6-9.
- [27] Giri, C., Ochieng, E., Tieszen, L. L., Zhu, Z., Singh, A., Loveland, T., Masek, J., Duke, N. (2011): Status and distribution of forests of the world using earth observation satellite data. – *Global Ecology and Biogeography* 20(1): 154-159.
- [28] Havanond, S. (1997): Mangrove Forest Conservation in Thailand. – *Biology Bulletin* 32(2): 97-102.
- [29] Horstman, E., Dohmen-Janssen, M., Narra, P., van den Berg, N.-J., Siemerink, M., Balke, T., Bouma, T., Hulscher, S. J. M. H. (2012): Wave Attenuation in Mangrove forests: field Data Obtained in Trang. – *Coastal Engineering* 2012.
- [30] Horstman, E., Dohmen-Janssen, C. M., Hulscher, S. J. M. H. (2013): Flow routing in mangrove forests: A field study in Trang province, Thailand. – *Continental Shelf Research* 71: 52-67.
- [31] Hossain, M. D., Nuruddin, A. A. (2016): Soil and Mangrove: A Review. – *Journal of Environmental Science and Technology* 9(2):198-207.

- [32] Howard, J., Hoyt, S., Isensee, K., Pidgeon, E., Telszewski, M. (eds.) (2014): Coastal Blue Carbon: Methods for assessing carbon stocks and emissions factors in mangroves, tidal salt marshes, and seagrass meadows. – Conservation International, Intergovernmental Oceanographic Commission of UNESCO, International Union for Conservation of Nature. Arlington, Virginia, USA.
- [33] Hoyle, F. (2013): Managing Soil Organic Matter: A practical guide. – Grains Research and Development Corporation (GRDC).
- [34] Hutchings, P., Saenger, P. (1987): The Ecology of Mangroves. – University of Queensland Press. Box 42, Sta. Lucia Queensland, Australia.
- [35] Jitthaisong, O., Dhanmanonda, P., Chunkao, K., Teejuntuk, S. (2012): Water Quality from Mangrove Forest: The King's Royally Initiated Laem Phak Bia Environmental Research and Development Project, Phetchaburi Province, Thailand. – Modern Applied Science 6(8).
- [36] Kauffman, J. B., Donato, D. C. (2012): Protocols for the measurement, monitoring and reporting structure, biomass and carbon stocks in mangrove forests. – CIFOR, Bogor, Indonesia, Working Paper 86.
- [37] Kauffman, J. B., Bhomia, R. K. (2017): Ecosystem carbon stocks of mangroves across broad environmental gradients in West-Central Africa: Global and regional comparisons. – PLOS ONE 12(11): e0187749. <https://doi.org/10.1371/journal.pone.0187749>.
- [38] Kauffman, J. B., Bernardino, A. F., Ferreira, T. O., Bolton, N. W., Gomes, L. E., Nobrega, G. N. (2018): Shrimp ponds lead to massive loss of soil carbon and greenhouse gas emissions in northeastern Brazilian mangroves. – Ecology and Evolution 8(2): 5530-5540.
- [39] Komiyama, A., Ong, J. E., Pongparn, S. (2008): Allometry, biomass, and productivity of mangrove forests: A review. – Aquatic Botany 89(2): 128-137.
- [40] Kristensen, E., Holmer, M., Banta, G. T., Jensen, M. H., Hansen, K. (1995): Carbon, nitrogen and sulfur Cycling in Sediments of the Ao Nam bor Mangrove forest, Phuket, Thailand: A Review. – Phuket Mar. Biol. Cet. Res. Bull. 60: 37-64.
- [41] Land Development Department. (2013): Land Use Map in Trang. – The Geoinformatics Research Center for Natural Resource and Environment. Prince of Songkhla University.
- [42] Lewis, R. R. (2005): Ecological Engineering for successful management and restoration of mangrove forests. – Ecological Engineering 24(4): 403-418.
- [43] MacKenzie, R. A., Foulk, P. B., Klump, J. V., Weckerly, K., Purbospito, J., Murdiyarso, D., Donato, D. C., Nam, V. N. (2016): Sedimentation and belowground carbon accumulation rates in mangrove forests that differ in diversity and land use: a tale of two mangroves. – Wetlands Ecology Management 24(2): 245-261.
- [44] Matsui, N., Morimune, K., Meepol, W., Chukwamdee, J. (2012): Ten Year Evaluation of Carbon Stock in Mangrove Plantation Reforested from an Abandoned Shrimp Pond. – Forests 3(2): 431-444. doi:10.3390/f3020431.
- [45] Matsui, N., Meepol, W., Chukwamdee, J. (2015): Soil Organic Carbon in Mangrove Ecosystems with Different Vegetation and Sedimentological Conditions. – Journal of Marine Science and Engineering 3(4): 1404-1424.
- [46] Mazda, Y., Wolanski, E., Ridd, P. V. (eds.) (2007): The Role of Physical Processes in Mangrove Environments: Manual for the preservation and utilization of mangrove ecosystems. – TERRAPUB. Sansei Jiyugaoka Haimu, 27-19 Okusawa 5-chrome, Setagaya-ku, Tokyo, Japan.
- [47] Mcleod, E., Chmura, G. L., Bouillon, S., Salm, R. V., Björk, M., Duarte, C. M., Lovelock, C. E., Schlesinger, W. H., Silliman, B. R. (2011): A blueprint for blue carbon: toward an improved understanding of the role of vegetated coastal habitats in sequestering CO₂. – Front Ecol Environ 9(10): 552-560.
- [48] Numbere, A. O., Camilo, G. R. (2017): Effect of Temperature and Precipitation on Global Mangrove Rhizophora Species Distribution. – American journal of Environmental Sciences 13(5): 342-350. DOI: 10.3844/ajessp.2017.

- [49] Ong, J. E., Khoon, G. W., Clough, B. F. (1995): Structure and Productivity of a 20-year old stand of *Rhizophora apiculata* Bl. Mangrove forest. – *Journal of Biogeography* 22(2-3): 417-424.
- [50] Phang, V. X. H., Chou, L. M., Friess, D. A. (2017): Ecosystem carbon stocks across a tropical intertidal habitat mosaic of mangrove forest, seagrass meadow, mudflat, and sandbar. – *Earth Surface Processes and Landforms* 40(10): 1387-1400. doi: 10.1002/esp.3745.61.
- [51] Primavera, J. H., Esteban, J. M. A. (2008): A review of mangrove rehabilitation in the Philippines: successes, failures and future prospects. – *Wetlands Ecology Management* 16: 345-358.
- [52] Punwong, P., Sritrairat, S., Selby, K., Marchant, R., Pumijumong, N., Traiperm, P. (2018): An 800 year record of mangrove dynamics and human activities in the upper Gulf of Thailand. – *Veget Hist Archeobot* 27: 535-549. DOI 10.1007/s00334-017-0651-x.
- [53] Putz, F. E., Chan, H. T. (1986): Tree Growth, Dynamics, and Productivity in a Mature Mangrove forest in Malaysia. – *Forest Ecology and Management* 17(2-3): 211-230.
- [54] Rodrigues, D. P., Hamacher, C., Estrada, G. C. D., Soares, M. L. G. (2014): Variability of carbon content in mangrove species: Effect of species, compartments, and tidal frequency. – *Aquatic Botany* 120(Part B): 346-351.
- [55] Romanach, S. S., DeAngeles, D. L., Koh, H. L., Li, Y., Teh, S. Y., Barizan, R. S. R., Zhai, L. (2018): Conservation and restoration of mangroves: Global status, perspectives, and prognosis. – *Ocean and Coastal Management* 154: 72-82.
- [56] Saenger, P., Hegerl, E. J., Davie, J. D. S. (eds.) (1983): *Global Status of Mangrove Ecosystem*. – International Union for Conservation of Nature and Natural Resources.
- [57] Salmo, S. G., Lovelock, C., Duke, N. C. (2013): Vegetation and soil characteristics as indicators of restoration trajectories in restored mangroves. – *Hydrobiologia* 720: 1-18.
- [58] Schumacher, B. A. (2012): *Methods for the Determination of Total Organic Carbon (TOC) in Soils and Sediments*. – The United States Environmental Protection Agency, Environmental Sciences Division National Exposure Research Laboratory. Ecological Risk Assessment Support Center Office of Research and Development US. Environmental Protection Agency.
- [59] Thampanya, U., Vermaat, J. E., Sinsakul, S., Panapitukkul, N. (2006): Coastal erosion and mangrove progradation of Southern Thailand. – *Estuarine, Coastal and Shelf Science* 68(1-2): 75-85.
- [60] Thomas, S. (2014): Blue carbon: Knowledge gaps, critical issues, and novel approaches. – *Ecological Economics* 107: 22-28.
- [61] Tomlinson, P. B. (1986): *The Botany of Mangroves*. – Cambridge University Press, UK.
- [62] UNEP (2004): *Mangroves in the South China Sea*. – UNEP/GEF/SCS Technical Publication.
- [63] Valiela, A., Bowen, J. L., York, J. K. (2001): Mangrove Forests: One of the World's Threatened Major Tropical Environments. – *Bioscience* 51(10): 807-815.
- [64] Yee, S. (2010): REDD and BLUE Carbon: Carbon Payments for Mangrove Conservation. – MAS Marine Biodiversity and Conservation Capstone Project, UC San Diego 24-27.
- [65] Zhila, H., Mahmood, H., Rozaina, M. Z. (2014): Biodiversity and biomass of a natural and degraded mangrove forest of Peninsular Malaysia. – *Environ Earth Science* 71: 4629-4635. DOI 10.1007/s12665-013-2853-6.

CONVERSION OF AMMONIUM POLYPHOSPHATE (APP) IN ACIDIC SOIL AND ITS EFFECT ON SOIL PHOSPHORUS AVAILABILITY

CHEN, Y. L.^{1#} – CHEN, X. J.^{1#} – ZHANG, C. L.¹ – TU, P. F.^{1,2} – DENG, L. S.^{1*}

¹*Department of Plant Nutrition, College of Resources and Environment, South China Agricultural University, 510642 Guangzhou, PR China*

²*Dongguan Yixiang Liquid Fertilizer Co., Ltd, 523125 Dongguan, PR China*

#These authors have contributed equally to this work

**Corresponding author
e-mail: lshdeng@scau.edu.cn*

(Received 10th Dec 2019; accepted 6th May 2020)

Abstract. To clarify the transformation of ammonium polyphosphate (APP) in acidic soil and its effect on soil phosphorus availability is prerequisite for the rational application of APP with different degrees of polymerization. The present study used industrial-grade monoammonium phosphate (MAP) as control, lateritic red soil and latosol were used as test soils, the soil culture experiments were conducted for 50 days. The effects of different fertilization treatments on soil availability and transformation of inorganic phosphorus forms in lateritic red soil and latosol were compared between three kinds of APP (APP1, APP2, APP3) with different degree of aggregation and APP3 with MAP (A3:M). Among them, APP1 (15-62-0) is ammonium polyphosphate mainly composed of low and middle polymer; APP2 (20-43-0) is ammonium polyphosphate mainly composed of middle and high polymer; and APP3 (13-70-0) is evenly distributed. The results showed that (1) in lateritic red soil, the effect of APP1 alone was the best, while in latosol, the effect of A3:M on improving soil available phosphorus content was remarkable; (2) the available phosphorus content in lateritic red soil under fertilizer treatment was much higher than that in latosol; (3) the content of inorganic phosphorus in the two soil types were O-P > Fe-P > Al-P > Ca-P.

Keywords: *slow release phosphate fertilizer, degree of polymerization composition, forms of phosphorus, transformation of inorganic phosphorus, soil culture, Olsen-P*

Introduction

As one of the essential nutrient elements in plant growth and development, phosphorus (P) is an important component of nucleic acids, nucleoproteins, phospholipids and adenine nucleoside triphosphate (ATP) while playing a vital role for plants. Numerous studies showed the significant effect of the application of P fertilizer on promoting crop growth and increasing yield. For example, an early study showed that the different P fertilizer affected the yield of herbage differently in the growing season (Sheil et al., 2016). The study of Rosen et al. (2014) revealed that appropriate phosphorus application is the key to optimizing tuber yield, solid content, nutritional quality and disease resistance of potato (*Solanum tuberosum* L.). Furthermore, Singh et al. (2014) demonstrated that phosphorus deficiency would reduce leaf area and thus affects the photosynthesis, which ultimately affects growth and development of soybean (*Glycine max* (Linn.) Merr.). Normally, phosphorus absorbed by plants is composed of organic phosphorus and inorganic phosphorus, mainly inorganic phosphorus. From inorganic phosphorus, orthophosphate is the main form of plant uptake; plants can also absorb pyrophosphate and metaphosphate, and quickly hydrolyze into orthophosphate,

which is used by plants. Orthophosphates absorbed by plants from the soil are mainly H_2PO_4^- and HPO_4^{2-} whilst PO_4^{3-} is not suitable for plants to absorb (de Oliveira Araújo et al., 2012).

The main forms of phosphorus in soil are inorganic phosphorus. Soil types, crop rhizosphere, crop cultivation methods, types and amounts of phosphorus fertilizer have different effects on soil phosphorus transformation (Giles et al., 2015). Moreover, pH, species of soil ions, aeration, temperature and water are also important factors affecting plant phosphorus uptake, among which pH is the most important one (Smith et al., 2011). In recent years, as a new type of phosphate fertilizer with high nutrient concentration, ammonium polyphosphate (APP) has gradually come into the public's view and is a compound with different degree of polymerization (n) (Yang et al., 2019). As a new type of phosphate fertilizer, agricultural ammonium polyphosphate has many advantages. For example, the solubility of short-chain ammonium polyphosphate is higher than that of ordinary phosphate fertilizer, which can increase the content of phosphorus in liquid fertilizer (Do Nascimento et al., 2018). The study of Summerhays et al. (2017) indicated polyphosphate is not directly absorbed by plants, but is gradually hydrolyzed into orthophosphate in soil and used by plants, so it is a slow-soluble and long-term phosphorus fertilizer.

Although short-chain ammonium polyphosphate has a series of advantages, its application effect is closely related to soil texture type, soil pH, soil ion composition, temperature and soil biological characteristics. At present, there are few reports on the transformation and availability of phosphorus forms of ammonium polyphosphate in highly acidic soils. Thus, different degree of polymerization (APP) was used to carry out soil culture experiments in present study in order to explore the effects of different degree of polymerization (APP) on the forms and availability of phosphorus in acidic soils.

Materials and methods

Test soil

Present study was conducted in College of resources and environment, South China Agricultural University, Guangzhou, Guangdong Province, China. The tested soil were latosol and lateritic red soil, and the physicochemical properties of the tested soil were shown in *Table 1*. Among them, pH was measured by pH meter (PHS-3G, INESA Scientific Instrument Co., Ltd, Shanghai). EC was measured by salinometer (SX-650, Shanghai San-Xin Instrument, Shanghai). Soil organic matter was measured by potassium dichromate-volumetric method (external heating method) (Shaw, 1959). Soil available phosphorus was extracted with $\text{NH}_4\text{F-HCl}$, and determined with ultraviolet visible spectrophotometer (UV-5100B, Shanghai Metash Instruments Co., Ltd, Shanghai) at $\lambda = 700$ nm by molybdenum antimony anti colorimetry (Lu, 1999). Soil available iron was extracted with DTPA solution and measured by atomic absorption spectrophotometer (SP-3530AA, Shanghai Chenqiao Biosciences Co., Ltd, Shanghai) (Lu, 1999). Soil exchangeable calcium was also measured by atomic absorption spectrophotometer (SP-3530AA, Shanghai Chenqiao Biosciences Co., Ltd, Shanghai) (Martin and Reeve, 1955).

It could be seen from *Table 1* that the acidity of latosol was stronger than that of lateritic red soil. The content of organic matter, available iron and exchangeable calcium in latosol was higher than that in lateritic red soil, but the content of available

phosphorus in both soil types were $1.6 \text{ mg}\cdot\text{kg}^{-1}$, less than $5.0 \text{ mg}\cdot\text{kg}^{-1}$, so they were all serious phosphorus deficient soils, which could eliminate the interference of phosphorus in the soil. It was found that the two kinds of soil can be rubbed into 3 mm thin strips after being fully moistened with water and evenly mixed, but they were easy to break when bending, so they were medium loam.

Table 1. The physicochemical properties of the tested soil

Soil type	pH	EC ($\mu\text{S}\cdot\text{cm}^{-1}$)	Organic matter ($\text{g}\cdot\text{kg}^{-1}$)	Available phosphorus ($\text{mg}\cdot\text{kg}^{-1}$)	Available iron ($\text{mg}\cdot\text{kg}^{-1}$)	Exchangeable calcium ($\text{mg}\cdot\text{kg}^{-1}$)
Lateritic red soil	$5.72 \pm 0.05\text{a}$	$200.0 \pm 0.02\text{a}$	$3.4 \pm 0.32\text{b}$	$1.6 \pm 0.18\text{a}$	$1.3 \pm 0.22\text{b}$	$644.0 \pm 28.6\text{b}$
Latosol	$4.98 \pm 0.03\text{b}$	$68.0 \pm 0.03\text{b}$	$13.6 \pm 0.58\text{a}$	$1.6 \pm 0.15\text{a}$	$7.0 \pm 0.40\text{a}$	$820.0 \pm 15.9\text{a}$

Test fertilizer

Taking industrial grade monoammonium phosphate (MAP) as control, solid APP was the test fertilizer, ammonium sulfate ($(\text{NH}_4)_2\text{SO}_4$, 21-0-0) was used to make up for the lack of nitrogen. Solid APP was provided by the College of chemical engineering of Sichuan University, which was called APP1, APP2 and APP3 for short. The main polymerization degree of APP1 (15-62-0) is middle low polymer (oligomer: middle polymer: high polymer = 73%: 27%: 0.2%); the main polymerization degree of APP2 (20-43-0) is middle high polymer (oligomer: middle polymer: high polymer = 4%: 76%: 20%); the polymerization degree of APP3 (13-70-0) is evenly distributed (oligomer: middle polymer: high polymer = 23%: 43%: 34%). (see Table 2 for the specific aggregation degree distribution of APP).

Table 2. Composition distribution of APP polymerized salt

Phosphate species	$\text{P}_2\text{O}_5\%$		
	APP1	APP2	APP3
Orthophosphate	9.79	0.49	4.95
Pyrophosphate	35.50	1.39	11.39
Tripolyphosphate	13.11	10.18	10.05
Tetrapolyphosphate	3.67	22.59	19.88
Pentapolyphosphate	0.09	6.34	7.27
Polyphosphate	0.05	2.64	16.80
Total phosphorus	43.76	43.50	60.00

In this experiment, orthophosphoric acid and pyrophosphoric acid were set as oligomer, tripolyphosphate and tetrachlorophosphoric acid as medium polymer, and pentamer or more as high polymer.

Experimental details

In this experiment, MAP, APP1, APP2, APP3, APP3: MAP (P_2O_5 mass ratio 2:1, A3:M in the following text) and CK (no phosphorus) were respectively set on the latosol and lateritic red soil. The phosphorus application amount was $\text{P}_2\text{O}_5:0.1 \text{ g}$ (equal

phosphorus and other nitrogen, and supplement the insufficient nitrogen with $(\text{NH}_4)_2\text{SO}_4$, as shown in *Table 3*). Take a 2 mm air dried soil sample and put it into a plastic cup (the cup height was 6.6 cm, the cup mouth diameter was 6.4 cm, and the cup bottom diameter was 4.0 cm). After fully mixing the said fertilizer with 100 g soil, spray the same amount of water evenly on the soil surface, and put it in a constant temperature and humidity incubator (LHS-250HC- I , Shanghai Bluepard Instruments Co., Ltd., Shanghai) with a temperature of 25 °C and a humidity of 80%. During this period, the soil moisture content was kept at 60-65% of the field water capacity by weighing method. Soil samples were taken at 5, 10, 15, 30, and 50 days of culture respectively, five times at a time. The samples were dried and screened for 2 mm. And then, the contents of Al-P, Fe-P, O-P, Ca-P and Olsen-P in soil were determined respectively.

Table 3. Fertilization amount of each fertilization treatment on two kinds of soil ($\text{g}\cdot 100\text{ g}^{-1}$ soil)

Treatments	APP	MAP	$(\text{NH}_4)_2\text{SO}_4$	Nitrogen from phosphate fertilizer
APP1	0.230	-	0.066	0.032
APP2	0.230	-	-	0.046
APP3	0.170	-	0.114	0.022
APP3:MAP (2:1)	0.111	0.023	0.138	0.017
MAP	-	0.160	0.124	0.020
CK	-	-	0.218	-

Grading determination of inorganic phosphorus forms in acid soil

The inorganic phosphorus in acid soil was classified into four grades: Al-P, Fe-P, O-P and Ca-P (Chang and Jackson, 1957). Refer to soil agrochemical analysis Soil agrochemical analysis (Lu, 1999), the inorganic phosphorus in acid soil was extracted by $1\text{ mol}\cdot\text{L}^{-1}\text{ NH}_4\text{Cl}$, $0.5\text{ mol}\cdot\text{L}^{-1}\text{ NH}_4\text{F}$, $0.1\text{ mol}\cdot\text{L}^{-1}\text{ NaOH}$, $0.3\text{ mol}\cdot\text{L}^{-1}\text{ Na}_3\text{C}_6\text{H}_5\text{O}_7\cdot 2\text{H}_2\text{O}$, $\text{Na}_2\text{S}_2\text{O}_4$ and $0.5\text{ mol}\cdot\text{L}^{-1}\text{ H}_2\text{SO}_4$, and determined with ultraviolet visible spectrophotometer (UV-5100B, Shanghai Metash Instruments Co., Ltd, Shanghai) at $\lambda = 700\text{ nm}$ by molybdenum antimony anti colorimetry.

Determination of available phosphorus in acid soil

Refer to soil agrochemical analysis (Lu, 1999), the content of available phosphorus in soil was extracted with $\text{NH}_4\text{F}\cdot\text{HCl}$, and determined with ultraviolet visible spectrophotometer (UV-5100B, Shanghai Metash Instruments Co., Ltd, Shanghai) at $\lambda = 700\text{ nm}$ by molybdenum antimony anti colorimetry.

Statistical analyses

This study was managed as a split block design. Data were analyzed using statistical software ‘Statistix 8.1’ (Analytical Software, Tallahassee, FL, USA) while differences among means were separated by using least significant difference (LSD) test at 5% probability level. ‘Sigma Plot 14.0’ was used for graphical representation.

Results

Available P content in soil

As shown in *Figure 1*, soil available P content was significantly affected by different phosphorus source treatments in different periods. For lateritic red soil, the highest available P content were recorded in APP1 in whole cultured time. There was no significant difference between MAP and APP3 at 15, 30 and 50 days after the fertilization while lower available P content was recorded in A3:M than MAP in whole cultured time. For latosol, the highest available P content was recorded in APP1 at both 5 and 10 days after fertilization whilst at 15, 30 and 50 days after fertilization the highest content was all recorded in A3:M. Both APP3 and A3:M had higher available P content than MAP at 15, 30 and 50 days after fertilization.

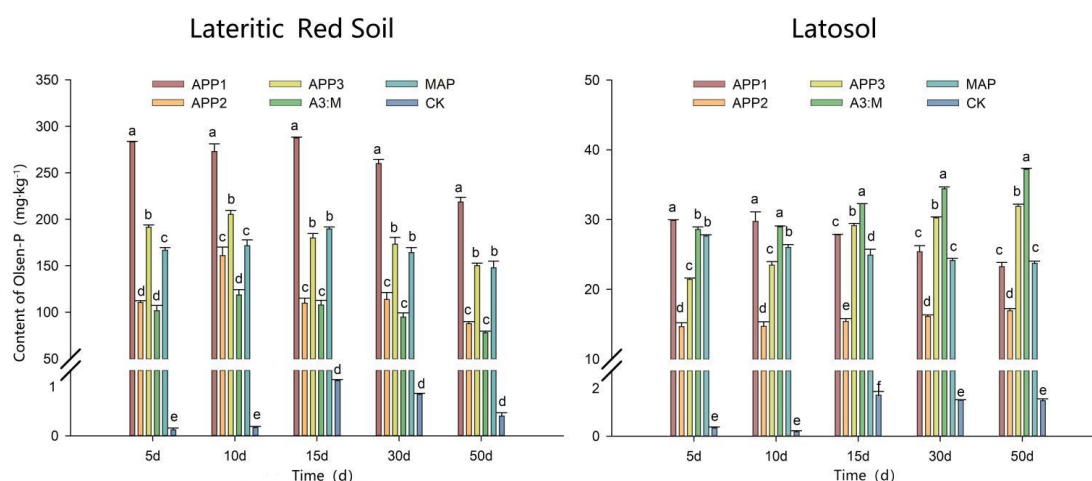


Figure 1. Effects of different treatments on soil availability of lateritic red soil and latosol. (Capped bars represent S. E. of three replicates. Means sharing a common letter do not differ significantly at ($P \leq 0.05$) according to least significant difference (LSD) test)

Al-P content in soil

As shown in *Figure 2*, different phosphorus source treatments can significantly affect the content of Al-P in soil at different stages. For lateritic red soil, the lower Al-P contents were recorded in APP2, APP3 and A3:M than MAP in whole cultured time. Moreover, there was no remarkable difference between MAP and APP1 and MAP at 15 and 30 days after fertilization. For latosol, there was no remarkable difference among APP1, APP3, A3:M and MAP in Al-P content while the lower content was recorded in APP2 than APP1, APP3, A3:M and MAP.

Fe-P content in soil

As shown in *Figure 3*, For lateritic red soil, higher Fe-P contents were recorded in APP1 and APP3 than MAP at 10, 15, 30 and 50 days after fertilization whilst the highest content was recorded in APP1 at 15, 30 and 50 days after the fertilization; For latosol, the highest Fe-P content was recorded in APP2 in whole cultured time while there was no remarkable difference between APP1 and MAP at 15, 30 and 50 days after the fertilization.

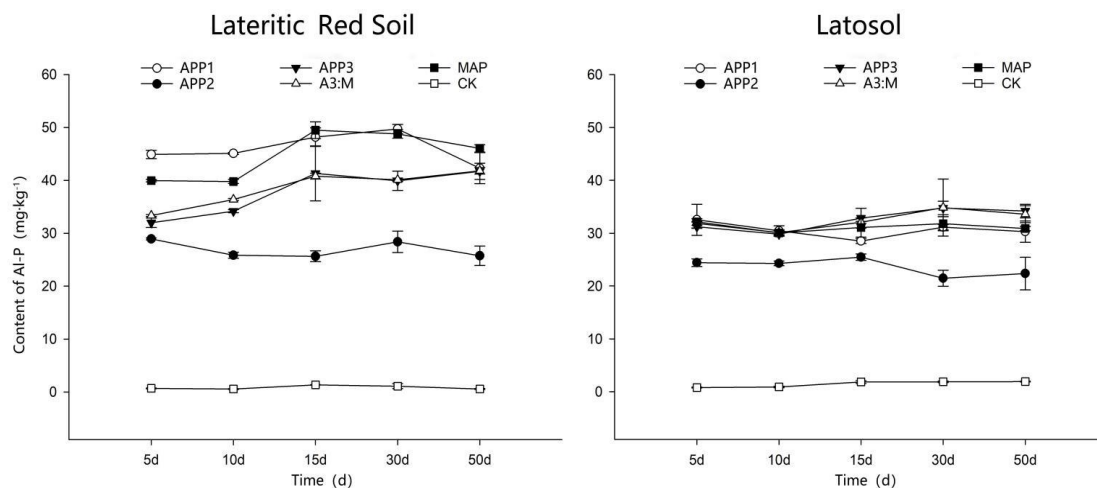


Figure 2. Dynamic changes of Al-P content in lateritic red soil and latosol under different phosphorus source treatments

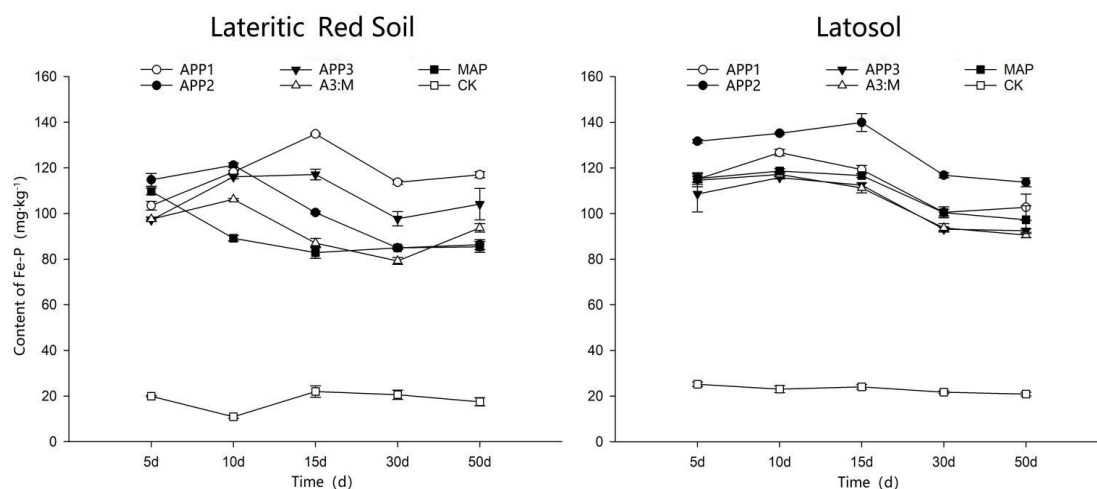


Figure 3. Dynamic changes of Fe-P content in lateritic red soil and latosol under different phosphorus source treatments

O-P content in soil

As shown in *Figure 4*, different phosphorus source treatments could significantly affect the content of O-P in soil. For lateritic red soil, the highest O-P content was recorded in APP2 in whole cultured time while there was no significant difference among APP1, APP3, A3:M and MAP in O-P content at 5, 15, 30 and 50 days after the fertilization; For latosol, the highest O-P content was also recorded in APP2 in whole cultured time while there was no significant difference among APP1, APP3, A3:M and MAP in O-P content at 15, 30 and 50 days after the fertilization.

Ca-P content in soil

As shown in *Figure 5*, no matter in latosol or in lateritic soil, no matter whether there was fertilization treatment or not, the Ca-P content of each treatment was low. For

lateritic red soil, the Ca-P content in the soil could be significantly increased at 5 and 10 days after fertilization, but at 15 and 30 days, the Ca-P content of each fertilization treatment was not significantly higher than that of CK treatment. In addition, the content of Ca-P fluctuated in the range of 3-9 mg·kg⁻¹. For latosol, the Ca-P content of fertilization treatment was significantly higher than that of CK treatment at 5 days, but with the extension of time, the Ca-P content of each treatment gradually stabilized in the range of 4-6 mg·kg⁻¹.

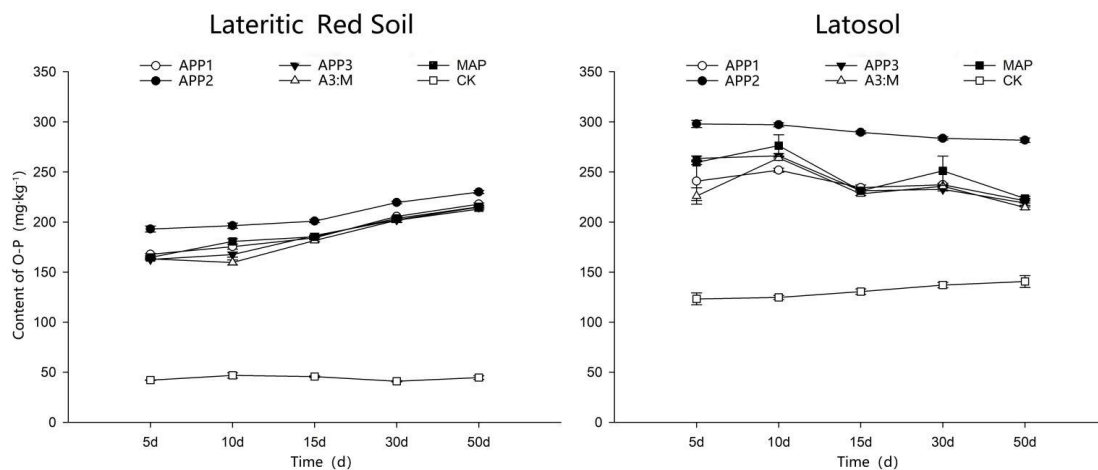


Figure 4. Dynamic changes of O-P content in lateritic red soil and latosol under different phosphorus source treatments

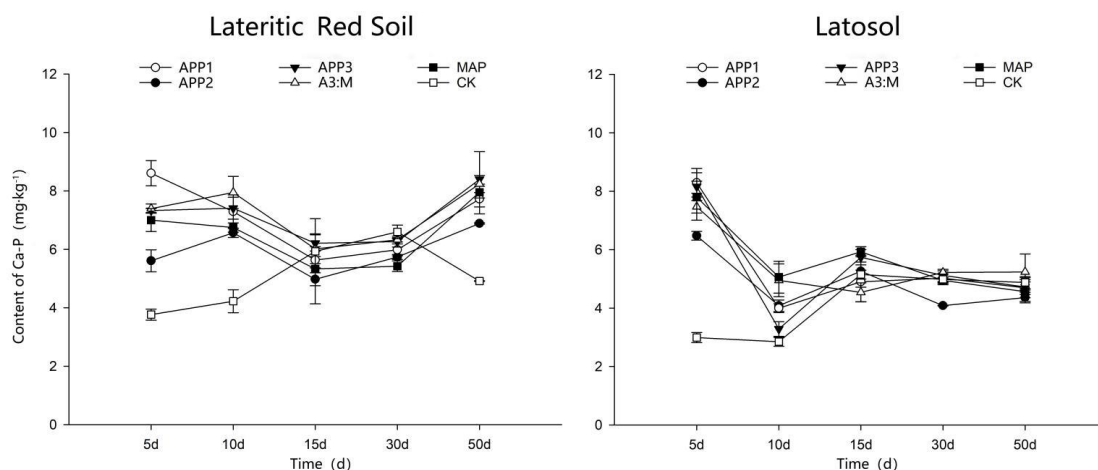


Figure 5. Dynamic changes of Ca-P content in lateritic red soil and latosol under different phosphorus source treatments

Discussion

The phosphorus content is an important index to determinate the soil fertility. Many studies have been conducted with the objective to improve soil phosphorus concentration. For example, the study of de Medeiros et al. (2019) found that application of green manure with rock phosphate was able to significantly increase soil phosphorus content. Present study revealed the effects of different degree of APP on the

forms and availability of phosphorus in acidic soils. As far as available P content in soil was concerned, different phosphorus fertilizer treatments had different effects on available phosphorus content in latosol and lateritic red soil. For example, lower available P content was recorded in A3:M than MAP in lateritic red soil whilst in latosol, the available P content in soil increased significantly due to A3:M compared to MAP. The differences between two soil types might be attributed to the P fixation ability of soil because P fixation ability of different soils varies greatly, which also significantly affects the change of available P content in soils (Netzer et al., 2019; Shen et al., 2019). The study of Gao et al. (2019) showed that the application of ammonium polyphosphate in calcareous soil could significantly improve the available P and reduce the transformation from unstable P to recalcitrant P. In this study, we have come to a new conclusion: it was difficult for ammonium polyphosphate to show slow-release property in lateritic red soil, while in latosol, only APP3 and A3:M which were evenly distributed showed slow-release property. The new conclusions might be due to the different soil pH, which was also proposed by Wang et al. (2019) in her study. Subbarao and Ellis (1975) study showed that APP hydrolysis rate was faster in acid soil, which was not conducive to the accumulation of soil available phosphorus. The study of Hong et al. (2018) showed that the effects of biochar, fly ash and lime on phosphorus availability in acidic soils vary greatly, which also proves the effect of pH on the availability of phosphorus in acid soil. Do Nascimento et al. (2018) demonstrated that the application of granular monoammonium phosphate as based fertilizers could significantly affected the P mobility and behavior in soils. Koch et al. (2018) showed that phosphorus is the limiting nutrient element in the soil, and improving the utilization efficiency of phosphorus will help to improve the yield of crops. The study of Kang et al. (2018) showed that the application of liquid fertilizer was helpful to the absorption of nutrients and the yield of strawberry. Therefore, it also showed that liquid phosphorus fertilizer was beneficial to the utilization efficiency of phosphorus. In our study, in order to improve the content of available phosphorus in soil, APP1 is the most suitable phosphorus fertilizer to be applied in lateritic red soil while the application of APP3 combined with MAP can promote the increase of available phosphorus content in latosol. In addition, in the process of agricultural planting, if APP liquid phosphate fertilizer is applied, the content of available phosphorus in soil and the utilization efficiency of phosphate fertilizer will be improved.

For the transformation of different phosphorus sources in two soils, whether latosol or lateritic red soil, the inorganic phosphorus content in the soil could be expressed by $O-P > Fe-P > Al-P > Ca-P$ after applying phosphorus fertilizer (*Table 4*). The results showed that the total phosphorus content of the two soils were basically the same, but the biggest difference was that the O-P content of latosol was significantly higher than that of lateritic red soil, which was the reason why the available phosphorus in latosol was significantly lower than that of lateritic red soil. Therefore, two hypotheses can be drawn. The first one is that the application of phosphorus fertilizer in latosol is easier to convert Olsen-P into O-P form, and the increase of O-P may inhibit the content of Al-P. Second, O-P in lateritic red soil was more easily transformed into Olsen-P and Al-P forms by fertilization. Cheng et al. (2019) showed that high load agricultural planting will lead to the transformation of Al-P, Fe-P and Ca-P into O-P. Therefore, how to prevent the transformation of available phosphorus into unusable invalid phosphorus (O-P) will be the key to improve the utilization efficiency of phosphate fertilizer and alleviate the shortage of phosphate fertilizer resources. Besides, it can also help to

improve the slow release of ammonium polyphosphate, so as to effectively reduce the times of fertilization to achieve the purpose of saving labor costs and ensuring the effect of fertilization.

Table 4. The content range of various forms of phosphorus in two soil types after fertilization treatment in 50 days

Soil type	Al-P (mg·kg ⁻¹)	Fe-P (mg·kg ⁻¹)	O-P (mg·kg ⁻¹)	Ca-P (mg·kg ⁻¹)	Olsen-P (mg·kg ⁻¹)
Lateritic red soil	25-50	80-140	150-230	3-9	100-300
Latosol	20-35	80-140	220-300	3-9	15-40

Conclusion

For lateritic red soil, the combination of APP3 and MAP could enhance the fixation of soil phosphorus and reduce the ability of improving soil available phosphorus, and the effect of APP1 alone was the best. For latosol, APP3 combined with MAP could significantly improve the release of soil available phosphorus, and had good slow-release performance. Although the early effect was good, the slow-release performance of APP1 was poor, as time goes on, the effective phosphorus of APP1 was fixed by the soil faster than the release rate of effective phosphorus. In addition, in the two soils, the soil available phosphorus content of APP2 were low, and there was no obvious trend to improve the soil available phosphorus, which indicates that APP with too few low polymer cannot provide enough phosphorus for plants in the early stage, and the released phosphorus in the middle and later stage is easy to be fixed by the soil, which is not conducive to the accumulation of soil available phosphorus. Therefore, the effect of APP on the content of soil available phosphorus and the application effect were not necessarily better than MAP. In addition, although the content of inorganic phosphorus in the two soils were O-P > Fe-P > Al-P > Ca-P, the content of O-P in latosol was significantly higher than that in lateritic red soil, which was the main reason that the content of Olsen-P in latosol was significantly lower than that in lateritic red soil. Therefore, it is necessary to study the transformation relationship and conditions between O-P and Olsen-P, which will greatly reduce the fixation of available phosphorus in soil and improve the utilization rate of phosphorus fertilizer.

Acknowledgements. This study was supported by National Science and technology support program in rural areas during the 12th Five Year Plan (2013BAD05B04F05) and National key R & D projects of the Ministry of science and technology (2016YFD0200404).

REFERENCES

- [1] Chang, S. C., Jackson, M. L. (1957): Fractionation of soil phosphorus. – Soil Science 84: 133-144.
- [2] Cheng, Z., Chen, Y., Gale, W. J., Zhang, F. (2019): inorganic phosphorus distribution in soil aggregates under different cropping patterns in Northwest China. – Journal of Soil Science and Plant Nutrition 19(1): 166-174.
- [3] de Medeiros, E. V., Silva, A. O., Duda, G. P., Santos, U. J. D., de Souza Junior, A. J. (2019): The combination of Arachis pintoi green manure and natural phosphate improves

- maize growth, soil microbial community structure and enzymatic activities. – *Plant & Soil*. DOI: 10.1007/s11104-018-3887-z.
- [4] de Oliveira Araújo, É., Ferreira Dos Santos, E., Queiroz De Oliveira, G., Camacho, M. A., Mugnol Dresch, D. (2012): Nutritional efficiency of cowpea varieties in the absorption of phosphorus. – *Agronomía Colombiana* 30: 419-424.
- [5] Do Nascimento, C. A. C., Pagliari, P. H., Faria, L. D. A., Vitti, G. C. (2018): Phosphorus mobility and behavior in soils treated with calcium, ammonium, and magnesium phosphates. – *Soil Science Society of America Journal* 82: 622-631.
- [6] Gao, Y., Wang, X., Shah, J. A., Chu, G. (2019): Polyphosphate fertilizers increased maize (*Zea mays*, L.) P, Fe, Zn, and Mn uptake by decreasing P fixation and mobilizing microelements in calcareous soil. – *Journal of Soils and Sediments* 20: 1-11.
- [7] Giles, C. D., Cade-Menun, B. J., Liu, C. W., Hill, J. E. (2015): The short-term transport and transformation of phosphorus species in a saturated soil following poultry manure amendment and leaching. – *Geoderma* 257: 134-141.
- [8] Hong, C., Su, Y., Lu, S. (2018): Phosphorus availability changes in acidic soils amended with biochar, fly ash, and lime determined by diffusive gradients in thin films (DGT) technique. – *Environmental Science and Pollution Research* 25: 30547-30556.
- [9] Kang, R., Niu, J., Chen, Z., Zhang, J. (2018): Effects of different water-soluble fertilizers on yield and quality of strawberry under integrated application of water and fertilizer. – *Asian Agricultural Research* 10: 63-65+70.
- [10] Koch, M., Kruse, J., Eichler-Löbermann, B., Zimmer, D., Siebers, N. (2018): Phosphorus stocks and speciation in soil profiles of a long-term fertilizer experiment: evidence from sequential fractionation, P K-edge XANES, and ³¹P NMR spectroscopy. – *Geofísica Internacional* 316: 115-126.
- [11] Lu, R. (1999): *Soil Agrochemical Analysis Method*. – China Agricultural Science and Technology Press, Beijing.
- [12] Martin, A. E., Reeve, R. (1955): A rapid manometric method for determining soil carbonate. – *Soil Science* 79: 187-198.
- [13] Netzer, F., Turnbull, T., Mult, S., Alfarraj, S., Albasher, G., Herschbach, C., Adams, M., Rennenberg, H. (2019): Mineral nutrition of sub-alpine Australian vegetation under nutrient deficiency depends on lifeform. – *Environmental and Experimental Botany* 160: 92-100.
- [14] Rosen, C. J., Kelling, K. A., Stark, J. C., Porter, G. A. (2014): Optimizing phosphorus fertilizer management in potato production. – *American Journal of Potato Research* 91: 145-160.
- [15] Shaw, K. (1959): Determination of organic carbon in soil and plant material. – *European Journal of Soil Science* 10: 316-326.
- [16] Sheil, T. S., Wall, D. P., Culleton, N., Murphy, J., Grant, J., Lalor, S. T. J. (2016): Long-term effects of phosphorus fertilizer on soil test phosphorus, phosphorus uptake and yield of perennial ryegrass. – *Journal of Agricultural Science* 154: 1068-1081.
- [17] Shen, Y., Duan, Y., McLaughlin, N., Huang, S., Guo, D., Xu, M. (2019): Phosphorus desorption from calcareous soils with different initial Olsen-P levels and relation to phosphate fractions. – *Journal of Soils and Sediments* 19: 2997-3007.
- [18] Singh, S. K., Reddy, V. R., Fleisher, D. H., Timlin, D. J. (2014): Growth, nutrient dynamics, and efficiency responses to carbon dioxide and phosphorus nutrition in soybean. – *Journal of Plant Interactions* 9: 838-849.
- [19] Smith, S. E., Jakobsen, I., Gronlund, M., Smith, F. A. (2011): Roles of arbuscular mycorrhizas in plant phosphorus nutrition: interactions between pathways of phosphorus uptake in arbuscular mycorrhizal roots have important implications for understanding and manipulating plant phosphorus acquisition. – *Plant Physiology* 156: 1050-1057.
- [20] Subbarao, Y. V., Ellis, R. (1975): Reaction products of polyphosphates and orthophosphates with soils and influence on uptake of phosphorus by plants. – *Soil Science Society of America Journal* 39: 1085.

- [21] Summerhays, J. S., Jolley, V. D., Hill, M. W., Hopkins, B. G. (2017): Enhanced phosphorus fertilizers (Carbond P (R) and Avail (R)) supplied to maize in hydroponics. – Journal of Plant Nutrition 40: 2889-2897.
- [22] Wang, X., Gao, Y., Hu, B., Chu, G. (2019): Comparison of the hydrolysis characteristics of three polyphosphates and their effects on soil P and micronutrient availability. – Soil Use and Management. <https://doi.org/10.1111/sum.12526>.
- [23] Yang, J., Kong, X., Xu, D., Xie, W., Wang, X. (2019): Evolution of the polydispersity of ammonium polyphosphate in a reactive extrusion process: polycondensation mechanism and kinetics. – Chemical Engineering Journal 359: 1453-1462.

APPENDIX



Appendix 1. Equipment

LITTER DECOMPOSITION AND SOIL NUTRIENTS PRINCE RUPPRECHT'S (*LARIX PRINCIPIS-RUPPRECHTII*) PLANTATIONS AREA IN SAIHANBA, NORTHERN CHINA

MUHAMMAD, B.¹ – ILAHI, T.² – ULLAH, S.¹ – WU, X.¹ – SIDDIQUE, M. A.² – KHAN, M. A.¹ – BADSHAH, M. T.¹ – JIA, Z.^{1*}

¹College of Forestry, Engineering Technology Research Center of *Pinus tabuliformis* of National Forestry and Grassland Administration, Beijing Forestry University University, No. 35 Qinghua East Road, Haidain District 100083, Beijing, China
(e-mails: yousafzaibil1992@yahoo.com. – B. Muhammad; sajfkhan@bjfu.edu.cn – S. Ullah; 1132466807@qq.com – X. Wu; asifkhanbaluch@yahoo.com – M. A. Khan; Badshahgi90@gmail.com – M. T. Badshah)

²School of Landscape Architecture, Beijing Forestry University, No. 35 Qinghua East Road, Haidain District 100083, Beijing, China
(e-mails: tajdar_2050@yahoo.com – T. Ilahi; muhammad_amir@bjfu.edu.cn – M. A. Siddique)

*Corresponding author
e-mail: jiazk@bjfu.edu.cn; phone: +86-106-233-7682

(Received 11th Dec 2019; accepted 6th May 2020)

Abstract. *Larix principis-rupprechtii* (Prince Rupprecht's larch) is a deciduous tree that grows well at high altitudes, sun light and low temperatures. *Larix principis-rupprechtii* produces a huge quantity of litter, but the rate of litter decomposition is slow compared to coniferous trees. Therefore, we tested different treatments with different concentrations such as External nitrogen (N) source concentrations (Control, 15 g·N· m⁻²· y⁻¹, 10 g·N·m⁻²·y⁻¹ and 5 g·N·m⁻²·y⁻¹), wood vinegar (WV) concentrations as control, 400, 600 and 800 dilutions, thinning intensities (TI) with control, 10%, 20% and 30%, Mix litter (ML) treatment using pure litter of *Larix principis-rupprechtii* and *Betula platyphylla* (white birch) with mixing ratios (PL, PB, 8L:2B, 5L:5B, 7L:3B and 6L:4B) for two consecutive years with six intervals. The results revealed that external WV application with concentration of 400 dilutions improved the litter decomposition (LD) and soil properties. Nitrogen (N) source concentration 10 g·N·m⁻²·y⁻¹ resulted in higher litter decomposition and soil Organic matter (OM) while soil nutrients increased with N concentration 15 g·N·m⁻²·y⁻¹. Mix litter treatment (6L:4B) and moderate thinning (20%) were found best as compared to other concentrations for increasing LD rate and soil properties. Thus, we concluded that the WV application (400 dilutions) was the best treatment followed by external N source (10 g·N·m⁻²·y⁻¹), ML treatment (6L: 4B) and TI (20%) respectively. Our results conclude that, the present study will help improve the litter decomposition, soil nutrients and soil organic matter under *Larix principis-rupprechtii*.

Keywords: litter decomposition, thinning intensity, wood vinegar (WV), nitrogen (N) source, mix-litter (ML)

Introduction

The *Larix principis-rupprechtii* plantation is mainly found in Northern China. It is the main timber forest in the region, which was planted on a large scale and the plantation area was continuously expanded since 1950. *Larix principis-rupprechtii* Mayr. is a deciduous tree that grows well under high light and low temperatures (Yuan et al., 2018). This species is mostly used for forestation in warm temperate regions of china, because of its fast growth high-quality wood, resistance to ruthless climate and high wind and improvement in soil conditions (Yuan et al., 2018). Previously, it has been reported that the rate of falling of litter and afterward decomposing play a vital role in nutrient cycling, primary productivity and maintain the soil fertility of forest ecosystem as it acts as input and output system of nutrients (Fioretto et al., 2003; Onyekwelu et al., 2006; Pandey et al., 2007). Forest are

providing huge quantity of ecosystem services and playing their vital role in carbon, water and nutrient cycling (Polyakova and Billor, 2007; Wang et al., 2017; Li et al., 2019; Farooqi et al., 2020a, b & c). Organic and inorganic elements for nutrient cycling are mainly provided by litter decomposition that controls nutrient return to the forest ecosystem. For a while the decomposition of litter is primarily influenced by the environmental conditions in which decay takes place, the process (slow/fast) of decaying is further dependent by the chemical quality of leaf litter, the nature and abundance of decomposing organisms present (Polyakova and Billor, 2007). The significant effect of external N availability on litter decay rate was noted by Hobbie (2000), Carreiro et al. (2000) and Hobbie and Vitousek (2000). Sinsabaugh et al. (2002) stated that external N availability significantly affects microbial decay by the degradation of polysaccharides and polyphenols. This hypothesis is supported by the study of Carreiro et al. (2000), Frey et al. (2004), Sinsabaugh et al. (2002) and Ullah et al. (2019). They stated that high N availability increases the activity of cellulolysis and considerably forcibly stop the activity of lignin-degrading enzymes. Another study by Matson et al. (2002) reported that nitrogen addition has an effect on processes and properties of large range of temperate forest ecosystem varying the nutrient cycling of the ecosystem and increasing the soil nutrients.

Silvicultural practices like thinning, tending and pruning have a significant effect on litter decomposition. These practices increase the light availability and air soil temperature resulting changes in nutrient mineralization rates (Kunhamu et al., 2009). Thinning results in changing the soil environment like moisture and temperature of the soil as well as the quality and quantity of litter and further affect the P bioavailability of soil (Hu et al., 2016). Kim et al. (2018) noted that microbial biomass increases as a result of thinning and is associated with C and N of soil. Moreover, this effect of thinning is directly related to thinning intensity.

Wood vinegar also is known as pyro ligneous acid, wood distillate or bio-oil is a water-soluble fraction of liquid produced as a result of organic materials pyrolysis. It can act as a biocide for microorganisms, pesticide, and fungicide and can also be used for improving soil nutrients, root and shoot growth as well microbial activity (Baimark and Niamsa, 2009; Steiner et al., 2008; Tiilikkala and Setälä, 2009; Velmurugan et al., 2009; Wei et al., 2009; Yatagai et al., 2002). Wood vinegar is commonly used in Japan for improving fertility of soil (Kadota and Niimi, 2004).

Mix litter is obtained by mixing different leaf litters which have a significant effect on leaf litter nutrients and the surrounding soil micro environment (Mao et al., 2015). Different studies have shown that chemical diversity of litter increase and physical spatial structure of leaf litter is changed as a result of mix litter decomposition, which in turn gives a more appropriate microhabitat and more nutrients to the decomposers which at the end leads to changes in biodiversity and population of the decomposer (Chapman et al., 2013; Liu et al., 2010). The decomposition of mix litter has the ability to change the activity of different types of soil enzymes (Li and Liu, 2013). In addition, due to the different substrate quality, controlling of nutrients and decomposition processes of leaf litter, like N and P, can transferred from nutrient-rich litter to nutrient-poor litter, as a result, the overall leaf litter mixture decomposition is affected (Hättenschwiler et al., 2005).

This present study was carried out to find the effect of different treatments on leaf litter decomposition of *Larix principis-rupprechtii*, soil nutrients and soil organic matter.

Materials and methods

Geographical site description

The present study was intended at Yinhe Forest Farm, the general site of Saihanba Mechanical Forest Farm, Chengde City, Hebei Province, China. Geographical location of sampling site with 42°02'~42° 36' N, 116° 51'~117° 39' E (Fig. 1), Elevation of 1650 ~ 1830 m. This area located in the semi-humid and semi-dry early region. So it belongs to the continental monsoon climate in the cold temperate zone. The annual average temperature is -1.5 °C. The annual average precipitation and evaporation rate of this area reported about ~ 530.9 mm and ~ 1388 mm respectively. The main tree species are *Larix principis-rupprechtii*, *Mongolia Scotch pine*, *Picea asperata* and *Betula platyphylla*. The area covered ~80.74% by forest.

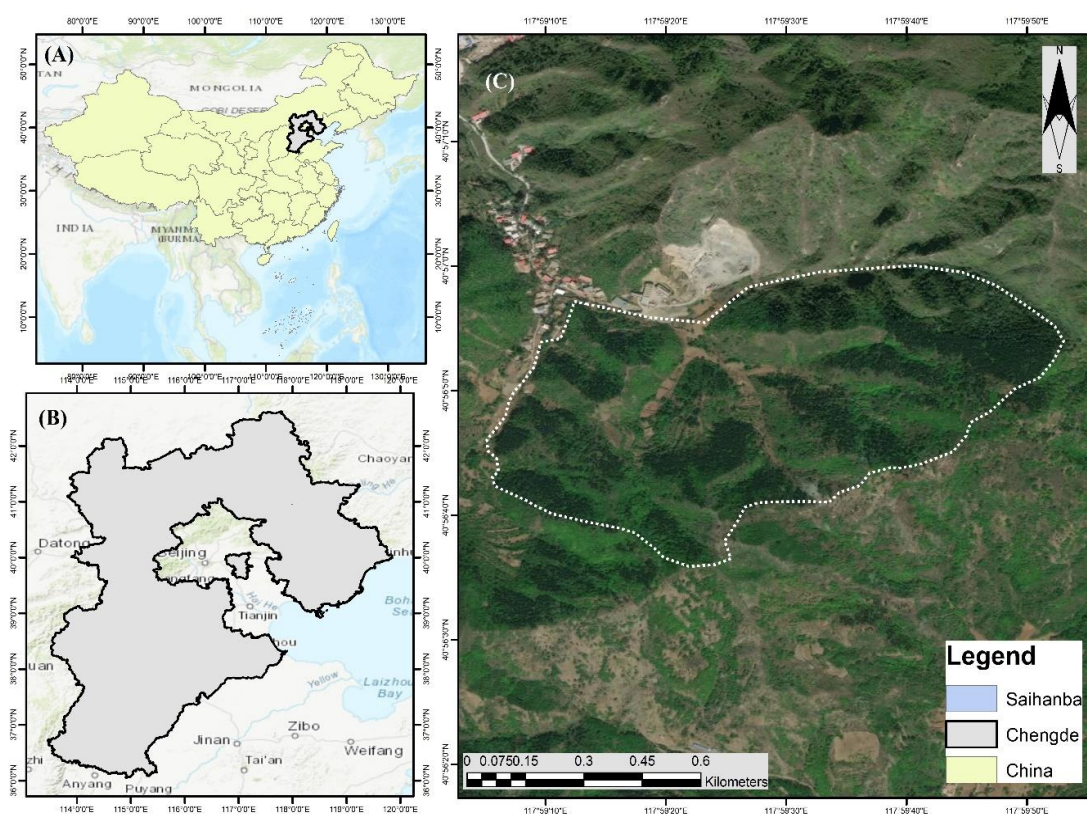


Figure 1. The study area of experiment

In this study, the 22-year-old *Larix principis* plantation in Saihanba area was selected to find the effect of four different treatments i.e. nitrogen, wood vinegar, thinning intensities and mixed litter (pure *Larix principis* (PL) and pure *Betula platyphylla* (PB) on litter decomposition rate and soil nutrients of *Larix principis*. The experiment of tending and thinning was laid under thinned forest, and the other three treatments (external nitrogen source, external application of wood oxalic liquor, mixed litter) were tested in the un-thinned forest. The treatments used in the study are in Table 1.

Three 20 m × 20 m repetitive plots were set up for each test treatment, and a total of 54 plots were set up for 18 treatments. The DBH and height of trees in the sample plot

were measured, and the information of landform, slope, soil condition, elevation and age class of the sample plot were recorded as shown in *Table 2*.

Table 1. Basic information of stands

External nitrogen application	External wood vinegar application	Thinning intensities	(PL) and (PB) ratio
Control (Ck)	Control (Ck)	Control (Ck)	Control Ck)
5 g.N.m ⁻² .y ⁻¹	400 Dilutions	15%	PL (pure <i>Larix principis</i>)
10 g.N.m ⁻² .y ⁻¹	600 Dilutions	20%	PB (pure <i>Betula platyphylla</i>)
15 g.N.m ⁻² .y ⁻¹	800 Dilutions	30%	5L: 5B, 6L: 4B, 7L: 3B, 8L: 2B

Table 2. Basic information of stands

Stand overview	Site factor			Age class	Thinning %	Average BH/cm	Average tree H/m	Density /hm ²
	Slope	Soil L	Altitude/m					
1	15	Thick	1620	Middle age 25a	CK	10.92	11.8	2475
2	15	Thick	1620	Middle age 25a	15%	11.97	12.3	2150
3	15	Thick	1620	Middle age 25a	20%	12.93	12.5	2075
4	15	Thick	1620	Middle age 25a	30%	13.02	12.6	1800

Litter collection

Fresh Litter was collected under the 22-year-old *Larix principis-rupprechtii* and birch forest in the experimental area at the end of April 2015. The litter was collected and dried at 80 °C in the oven until the weight becomes constant. The litter was weighed and ready for bagging. The dried litter was packed in mesh bags (20 cm × 10 cm, mesh diameter 1 mm) according to the corresponding treatment of each test (Wu et al., 2007). While bagging, the treatments of tending thinning, external wood oxalic liquor and external nitrogen source were all loaded with fresh larch litter, while the mixed litter treatment was packed with each other according to different proportions. Each bag of litter was 20 g ± 0.1 g. The bags were tagged according to the test requirements. Eighteen treatments totaled 1080 bags, including 360 bags for mixed litter treatment and 240 bags for each of the other three treatments. The number of bags in each plot was 60, 45 were used for sampling, and the remaining 15 were reserved. In May 2015, litter bags were buried in the experimental plots with different treatments. Original litter from the experimental surface layer was removed while burying to bags of litter so that the litter bags and the understory humus layer could contact each other more effectively (Liu, 2013; Che, 2014).

Preparation and application of treatments

Urea treatments were prepared according to the contents of CK (control), 5 g N·m⁻².y⁻¹, 10 g N·m⁻².y⁻¹, 15gN·m⁻².y⁻¹, dissolved in water and fill it in the agricultural sprayer, sprayed on the litter bag in the sample, once every two months. Spraying concentrated liquid of wood vinegar produced by Shijiazhuang Shunqian Carbon Industry Environmental Protection Technology Co., Ltd. The concentrated liquid of the wood vinegar (WV) solution was diluted as blank, diluted 400 times, diluted 600 times,

and diluted 800 times. In the sample plot, spray it evenly on the litter bag using the agricultural sprayer according to its corresponding treatment, and spray it once every two months. In thinning intensities (TI) treatment the litter bags are properly placed without any treatments and naturally decomposed. In mix litter treatment the bags were filled with mixed and pure litter of *Larix principis* (PL) and pure *Betula platyphylla* (PB), buried and decomposed naturally.

Sample collection

Litter bags were collected in the month of July- September 2015 and May, July and September, 2016. Five samples were collected, and three litter bags were randomly selected each time. The debris on the surface of litter bags must be removed before sampling, in order to ensure that other substances do not affect the measurement results. In the same period, 18 soil samples were sampled in May, July, September 2015 and May, July and September 2016. Typical sampling methods were used in each sample plot. Three sampling points were randomly set up beside the drop bag to remove weeds, such as pine needles, and the soil samples of 0-20 cm were collected by ring knife.

Analysis

Residual weight of litter

The residual weight of litter was determined by taking back the buried litter bag and weighing it to get fresh weight, then weighing it to get dry weight. The oven temperature was adjusted to 80 °C to be dried at constant temperature and then weighing it. Finally, fresh weight and dry weight were used to calculate litter weight residue rate (*Eq. 1*).

$$Y = X_t/X_0 \quad (\text{Eq.1})$$

where Y represents the residual ratio, X_t represents the initial amount; and X_0 represents the residual amount at the time. Furthermore, for finding the litter decomposition rate, residual rate was subtracted from actual weight of litter.

Nutrient contents and soil organic matter

The soil sample was crushed first, filtered by 60 mesh sieve, and then classified according to different particle diameters for the determination of nutrient content. The nutrient contents of different soils were determined. Soil total nitrogen and total phosphorus contents of the soil were determined by sulfuric acid-hydrogen peroxide digestion and then measured by AA3 continuous flow analyzer. While the total potassium content of the soil was determined using a flame photometer after desulfurization with sulfuric acid-hydrogen peroxide. Soil organic matter content was determined by using the potassium dichromate-sulfuric acid oxidation method.

Statistical analysis

The variance analysis was conducted through Statistics 8.1 software, and principle component analysis was used to compare all the data. In addition, the factor analysis

method is adopted for the comprehensive comparison of each indicator with each index and use SPSS 25 for results visualization.

Results

Effects of litter decomposition of Larix principis-rupprechtii L. and soil properties under external nitrogen application

External nitrogen improve litter decomposition rate and soil organic matter

The application of external nitrogen source improved the litter decomposition rate. The highest litter decomposition rate was observed in nitrogen concentration (10 g.N.m⁻².y⁻¹), while the least effect was noted in control as evident from *Table 3*. Which shows that external nitrogen source has the ability to increase the decomposition rate of litter.

Table 3. Effect of external nitrogen source on soil N, P, K (mg g⁻¹), litter decomposition (g) and organic matter content (mg g⁻¹)

Concentrations	External nitrogen treatment				
	N (mg g ⁻¹)	P (mg g ⁻¹)	K (mg g ⁻¹)	LD (g)	OMC (mg g ⁻¹)
Control	9.140C	1.675B	3.7598C	1.5493C	45.758C
5 g.N.m ⁻² .y ⁻¹	10.128B	1.8195A	4.502B	2.0081B	49.560B
10 g.N. m ⁻² .y ⁻¹	10.956A	1.5718C	4.8482A	2.5209A	53.567A
15 g·N·m ⁻² ·y ⁻¹	11.140A	1.4766D	5.1111A	1.9898B	48.896B

Means** with in column sharing same letters are statistically significant at p ≤ 0.05. LD in the table represents litter decomposition while organic matter content is denoted by OMC

Application of different concentrations of nitrogen significantly improved the soil organic matter from May 2015 to July 2016, while the highest effect was noted in from May to July 2016 and then started gradual decrease from July to September 2016. The highest effect was noted as a result of nitrogen application concentration 10 g.N.m⁻².y⁻¹ followed by 15 g.N.m⁻².y⁻¹ and 5 g.N.m⁻².y⁻¹ respectively. While the lowest effect was observed in control as shown in *Table 3*. The results were the same as the result of litter decomposition which shows that the more litter decompose the more it increases soil organic matter.

External nitrogen enhances litter and soil nutrients (N, P, K)

Results showed that nitrogen application (ammonium source) to litter significantly increased the soil total nitrogen. Litter treated with external nitrogen source 15 g.N.m⁻².y⁻¹ has resulted in higher soil total nitrogen followed by 10 g.N.m⁻².y⁻¹ and 5 g.N.m⁻².y⁻¹ respectively. The lowest soil nitrogen was distinguished in an untreated litter (*Table 3*). The total nitrogen content increased slowly; from July to September, but later it declined; from September 2015 to May of the next year then again it increased rapidly; from May to July 2016 and then started falling rapidly from July to September in 2016. The rapid increase in nitrogen content from May to July 2016 may be due to temperature rise and rain which resulted in increased microbial activity and soil water content, which resulted in higher soil nitrogen.

Soil phosphorus content was also significantly affected as a result of nitrogen application. Nitrogen source $5 \text{ g.N.m}^{-2}.\text{y}^{-1}$ was noted to have highest phosphorus content followed by control. Nitrogen concentration $15 \text{ g.N.m}^{-2}.\text{y}^{-1}$ has noted to have the least nitrogen content followed by nitrogen litter treated with $10 \text{ g.N.m}^{-2}.\text{y}^{-1}$. As evidence from results phosphorous has adverse effects as a result of nitrogen application. Data regarding nitrogen effect on soil total phosphorous is shown in *Table 3* and *Figure 2*.

Likewise, the increase was noted in soil total potassium as a result of nitrogen application to litter from May to July 2015 while from July 2015 to May 2016 there was a decrease in potassium content (*Table 3*.) it may be due to litter accumulation because soil potassium is being transferred. From May-September 2016, it was first rising and then falling, which was related to nutrient cycling of litter, temperature, and rainfall. In general nitrogen has direct effect on soil total potassium content.

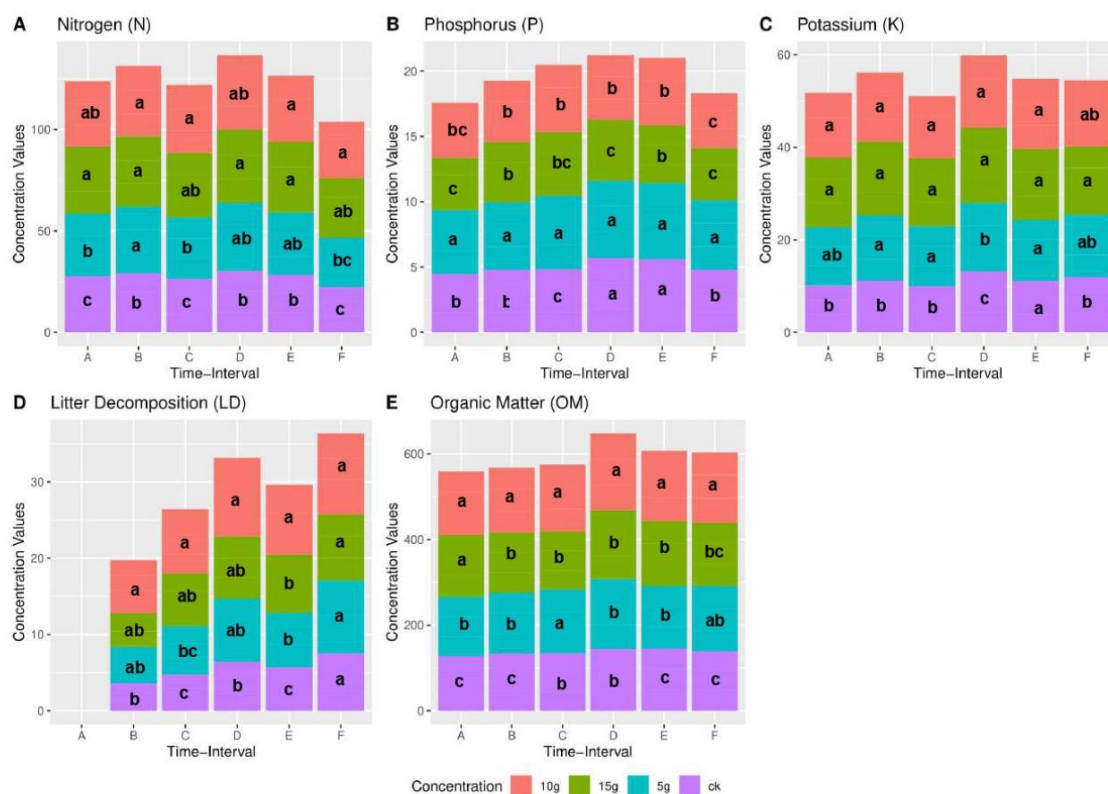


Figure 2. Effect of external nitrogen application (ammonia source) on litter decomposition and soil properties. A, B, C, D, E, and F in the figure shows different months for data collection for two consecutive years which are May 2015, July 2015 September

Effects of litter decomposition of *Larix principis-rupprechtii* L. and soil properties under external wood vinegar application

Wood vinegar have obvious effect on litter decomposition rate and soil organic matter

Wood vinegar application significantly increased the decomposition rate of the litter as compared to control. The maximum decomposition rate was noted in wood vinegar with 400 dilutions followed by 600 and 800 dilutions respectively. The lowest decomposition rate was noted in control as evidence from *Table 4*.

Data regarding soil organic content as shown in *Table 4* show that wood vinegar diluted 400 times has the highest effect on soil organic matter followed by 600 dilutions and 800 dilutions respectively. Soil organic matter was significantly improved by external wood vinegar application to the litter as compared to the control or untreated.

Wood vinegar not only effect litter but have significant effect on soil nutrients (N, P, K)

At the end of the experiment, the total nitrogen content of the soil from the largest to the smallest is diluted 400 times > 600 times diluted > CK > 800 times diluted as evident from *Table 4*. It can be seen that the total nitrogen content of the soil will be affected by the external application of wood vinegar. The best dilution factor is 400, with the decrease of the concentration of wood vinegar; the accumulation of nitrogen in the soil is no longer accelerated and is inhibited. Lower the concentration, the more significant the inhibition. From May to July 2015, the total nitrogen content of the soil gradually increased and from July to September and started decreasing from September 2015 to May of the next year, except for the dilution of 800 times, there has been a decrease; In the same year, the rapid increase in May-July, the reason for this change may be due to the snowmelt in the previous season and the increase in precipitation during the season, which shows in *Figure 3*.

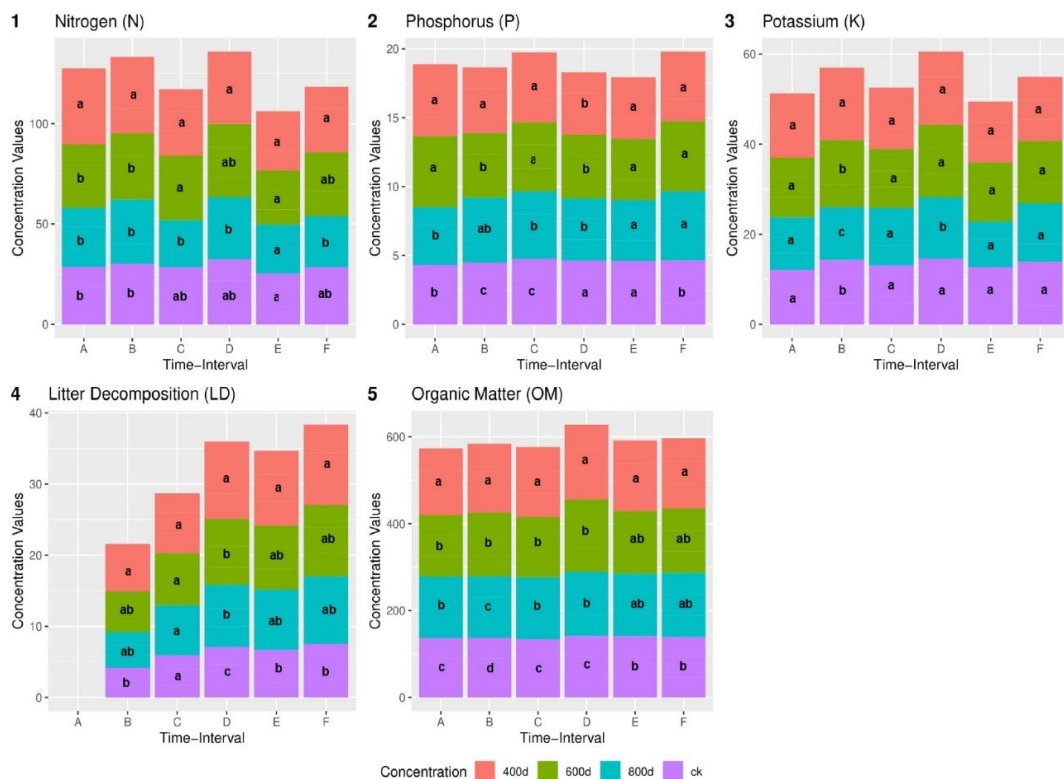


Figure 3. Effect of wood vinegar application on litter decomposition and soil properties. A, B, C, D, E, and F in the figure shows different months for data collection for two consecutive years which are May 2015, July 2015 September 2015, May 2016, July

The total phosphorus content of soil as a result of external wood vinegar was significantly increased as compared to control group. At the end of experiment, External

wood vinegar treatment with 400 dilutions has the highest phosphorus content followed by 600 times dilution and 1000 times dilution respectively. The control group has the lowest phosphorous content as shown in *Table 4* indicating that wood vinegar application increases the soil phosphorous content. Continuous rise in May-September 2015, followed by a slight decline from September 2015 to May 2016, the reasons may be related to temperature changes; it continued to rise from May to September 2016.

The effect of different wood vinegar concentrations on the soil total potassium content was significantly different, indicating that the external application of wood vinegar had a certain degree of influence on the total potassium content of the litter under *Larix principis-rupprechtii*. At the end of the experiment, the total potassium content in the soil was sorted as follows: dilution 400 times > dilution 600 times > CK > dilution 800 times (*Table 4*). The total potassium content of the soil increased from May to July 2015 and then decreased again in September; in 2016.

Table 4. Effect of wood vinegar on soil N, P, K (mg g^{-1}), litter decomposition (g) and organic matter content (mg g^{-1})

Concentrations	External Nitrogen treatment				
	N (mg g^{-1})	P (mg g^{-1})	K (mg g^{-1})	LD (g)	OMC (mg g^{-1})
CK	9.640C	1.5238B	4.4899B	1.7437C	46.099D
400d	11.491A	1.6161A	4.8753A	2.6559A	53.733A
600d	10.676B	1.6121A	4.6874AB	2.2963B	49.306B
800d	9.214C	1.5424B	4.0403C	2.1513B	48.086C

Means** with in column sharing same letters are statistically significant at $p \leq 0.05$. LD in the table represents litter decomposition while organic matter content is denoted by OMC

Effects of litter decomposition of *Larix principis-rupprechtii* L. and soil properties under different thinning intensities

Thinning intensities effect on Litter decomposition rate and soil organic matter

Thinning intensities shows the data regarding litter decomposition as a result of different thinning intensities (*Table 5*). It is evident from *Table 3* that decomposition rate was higher in control which were un-thinned trees followed by the trees which have thinning intensities of 30%. The least residues noted in 20% thinning intensities followed by 10%. This means that thinning intensities with 20% was the best treatment for litter decomposition.

Table 5. Effect of different thinning intensity on soil N, P, K (mg g^{-1}), litter decomposition (g) and organic matter content (mg g^{-1})

Concentrations	External nitrogen treatment				
	Nmg g^{-1})	P (mg g^{-1})	K (mg g^{-1})	LD (g)	OMC (mg g^{-1})
CK	8.607D	1.5303B	4.7330B	1.1298C	44.419D
10%	9.422C	1.5526AB	4.8864AB	1.7911B	48.321C
20%	10.459A	1.5562A	4.9750A	2.3944A	52.406A
30%	9.908B	1.5393AB	4.8459AB	2.1959A	50.990B

Means** with in column sharing same letters are statistically significant at $p \leq 0.05$. LD in the table represents litter decomposition while organic matter content is denoted by OMC

At the end of the experiment, the soil total organic content was significantly increased by thinning. The highest total organic content was noted as a result of 20% thinning followed by 30% and 10% respectively. The lowest organic content was noted as a result of un-thinned trees. The overall trend of soil organic matter content under the different thinning intensity of *Larix principis-rupprechtii* is influenced and changes with seasonal changes, which is as follows: from May to July 2015, the overall increase; from July to September 2015, except for the thinning intensity of 30%. The content of organic matter decreased in other tending thinning; from September 2015 to May of the next year, it increased rapidly from May to September of the following year, it slowly declined (Table 5 and Fig. 4).

Thinning intensities effect on soil nutrients (N, P, K)

Nitrogen content increased from May to September 2015 as a result of thinning intensities, and the increase was the fastest when the thinning intensity was 20% from September 2015 to May of the following year. It increased again in July 2016, but in up to September of the same year, it slowly declined. There were significant differences in soil total nitrogen content under the different thinning intensity of *Larix principis-rupprechtii* litter decomposition. The highest nitrogen content was noted as a result of thinning intensity 20% followed by 30% and 10% respectively as shown in Table 5. Lowest nitrogen content was noted as a result control or un-thinned trees which shows in Figure 4.

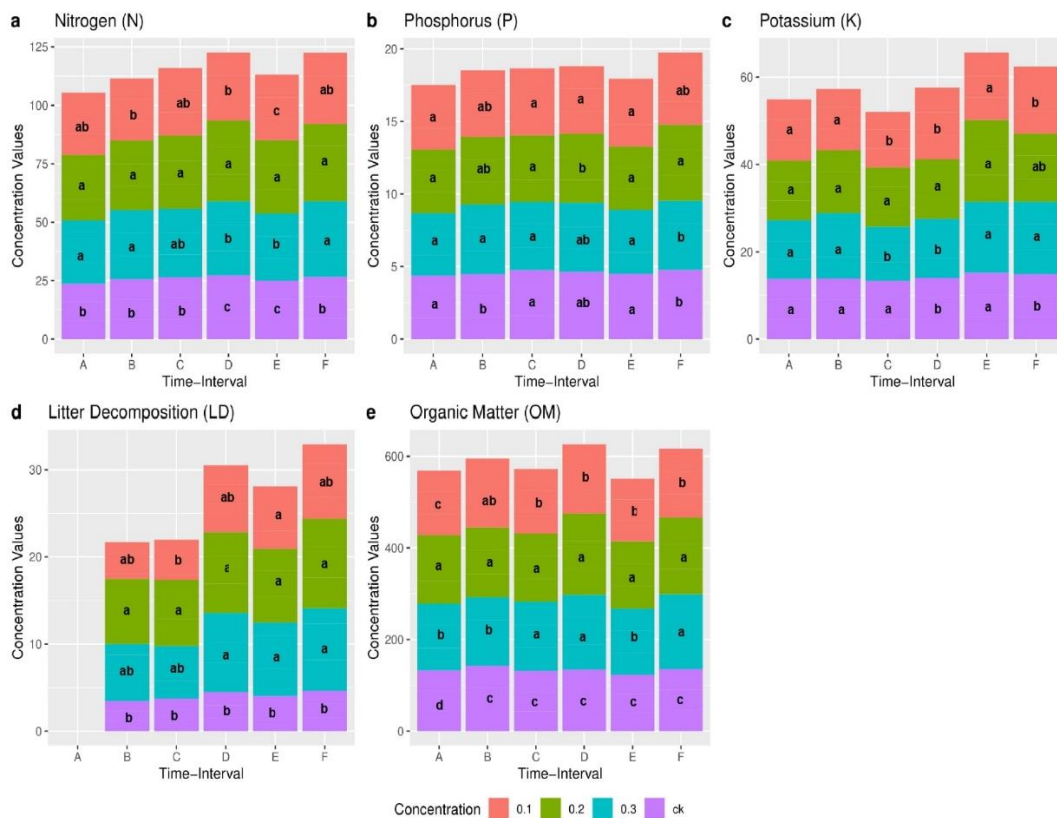


Figure 4. Effect of different Thinning intensities on litter decomposition and soil properties. A, B, C, D, E, and F in the figure shows different months for data collection for two consecutive years which are May 2015, July 2015 September 2015, May 2016

The total phosphorus content of soil with different thinning intensity showed a gradual increasing change. At the end of the experiment maximum soil total phosphorus content was noted in 20% thinning followed by 15% thinning and 30% thinning respectively. The lowest total phosphorous was noted in control (Table 5).

The total potassium content of the soil with different thinning intensity increased first and then decreased. When the thinning intensity is 20%, the soil potassium content in the forest increased rapidly from September 15 to June, which may be related to snow accumulation.

Effects of litter decomposition of Larix principis-rupprechtii L. and soil properties under different Mix litter ratios

Mix litter (pure Larix principis (PL) and pure Betula platyphylla (PB) effect on litter decomposition rate and soil organic matter

The decomposition rate of two pure litters was slower as compared to mixed litter ratios as evident from Table 6. All the mixed litter ratios showed to have best result than pure. The highest decomposition rate of litter was noted in 8L: 2B followed by 5L: 5B, 7L: 3B and 6L: 4B respectively. Check it which is best, mixed or pure or how much which one, draw fine conclusion.

Table 6. Effect of mix letter application on soil N, P, K (mg g^{-1}), litter decomposition (g) and organic matter content (mg g^{-1})

Concentrations	External nitrogen treatment				
	N (mg g^{-1})	P (mg g^{-1})	K (mg g^{-1})	LD (g)	OMC (mg g^{-1})
B	9.570C	1.5715D	4.7295B	0.0000F	44.262E
L	8.782D	1.5047E	4.6727B	2.5383E	46.215D
6L: 4B	10.571A	1.8534A	4.9832A	2.9574D	52.410A
7L: 3B	10.167B	1.7036B	4.7400B	3.5327C	50.250B
5L: 5B	9.885BC	1.6204C	4.7321B	3.8217B	48.230C
8L: 2B	9.673C	1.5751D	4.7408B	4.5406A	49.988B

Means** with in column sharing same letters are statistically significant at $p \leq 0.05$. LD in the table represents litter decomposition while organic matter content is denoted by OMC

The soil organic matter content of *Larix principis-rupprechtii* under different mixing ratios is increasing continuously, as shown in Table 3 At the end of experiment the maximum organic matter content was noted as 6L: 4B > 7L: 3B > 8L: 2B > 5L: 5B > PL > PB.

Mix litter of pure Larix principis (PL) and Betula platyphylla (PB) effect on soil nutrients (N, P, K)

The soil total nitrogen content of pure *Betula platyphylla* was higher than pure *Larix principis* (PL) because of the higher decomposition rate of pure *Betula platyphylla* (PB) than pure *Larix principis* (PL). Mix litter ratios had however more nitrogen contents noted than pure litter. At the end of the experiment the highest soil nitrogen observed in 6L: 4B followed by 7L: 3B, 5L: 5B and 8L: 2B respectively as evident from Table 6 and Figure 5.

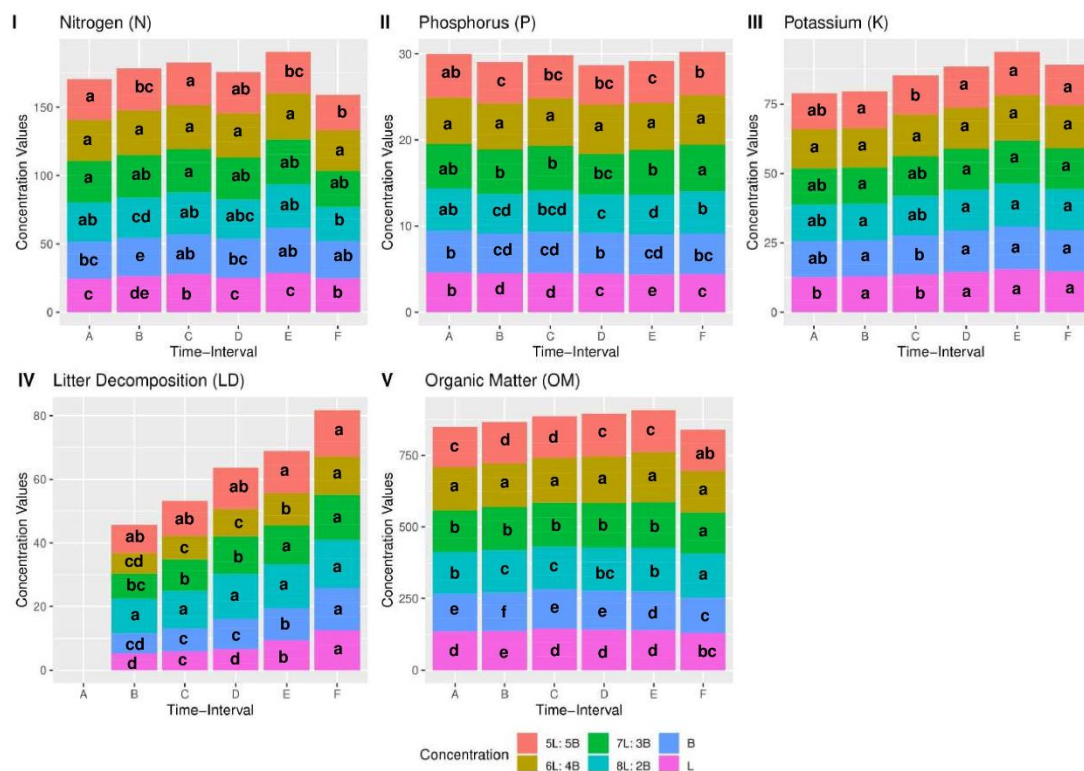


Figure 5. Effect of different mix litter application on litter decomposition and soil properties. A, B, C, D, E, and F in the figure shows different months for data collection for two consecutive years which are May 2015, July 2015 September 2015, May 20

The total phosphorus content of the soil under different mixed proportions of *Larix principis-rupprechtii* showed an increasing trend. By the end of the experiment, the total phosphorus content of the soil under mixed treatment was 6L: 4B > 5L: 5B > 7L: 3B > 8L: 2B (Table 6). 6L: 4B increased the total phosphorus in the soil most. Soil total potassium content was increased as a result of mix litter application but the change with in different mix litter application was non-significant as shown in Table 6 mix litter has no significant effect on soil total potassium.

Integrated score sorting for litter decomposition of *Larix principis-rupprechtii* L. and soil properties

The data regarding the best treatments for litter decomposition of *Larix principis-rupprechtii* L. and soil properties can be seen from the integrated score sorting of different treatments and total variance. External wood vinegar application (400 dilutions) stands first in the row followed by external nitrogen application ($10\text{g}\cdot\text{N}\cdot\text{m}^{-2}\cdot\text{y}^{-1}$), mixed litter (6L: 4B) and thinning (20%) respectively as shown in Table 7.

Principal component analysis

The evaluation of four treatment and to provide a comprehensive analysis, the principal component analysis was performed for whole treatment. The variance and variance cumulative rate of each component is shown in Table 8. SPSS extracted two

components along with their eigenvalues. The cumulative contribution of the three principal components is 95.819%

Table 7. The integrated score sorting of different treatments

Treatments	F1	F2	F3	Integrated score	Ranking
Wood vinegar application (400 d)	1.47151	-0.1744	-0.23293	0.627808	1
External nitrogen source (10g/m-2/y-1)	-0.38423	1.42391	-0.27359	0.126706	2
Mixed-litter (6L: 4B)	-0.3246	-0.34065	1.42429	0.083974	3
Thinning intensity (20%)	-0.76268	-0.90886	-0.91777	-0.83849	4

Table 8. Total variance explained and extraction method: principal component analysis

Components	Initial eigenvalues			Extraction sums of squared loadings			Rotation sums of squared loadings		
	Total	% of variance	Cumulative %	Total	% of variance	Cumulative %	Total	% of variance	Cumulative %
1	3.726	74.523	74.523	3.726	74.523	74.523	2.479	49.579	49.579
2	1.065	21.296	95.819	1.065	21.296	95.819	1.341	26.813	76.392
3	.209	4.181	100.000	.209	4.181	100.000	1.180	23.608	100.000
4	2.299E-16	4.597E-15	100.000						
5	3.772E-17	7.544E-16	100.000						

Discussion

Nitrogen source has an effect on litter decomposition at the early stages of decomposition which is later decreased due to higher lignin rate (Berg and Staaf, 1980). Litter decomposition has a vital role in nutrients cycling, transformation of materials and circulation of carbon and nitrogen in the ecosystem (Handa et al., 2014). Our study is in line with the study of Hobbie (2000) and Vestgarden (2001) who also noted the positive effect of nitrogen application on litter decomposition. This may be due to the fact that leaf litter having increased nitrogen is more favorable for both bacteria and fungi due to which it decomposes quickly (Aerts, 1997; Swift et al., 1979). N fertilization externally to litter increased the decomposition rate at two sites (Hobbie, 2005). An increase in soil organic content and soil nutrients may be due to higher decomposition rate of litter as a result of different treatments as described by Aerts (1997), Ahmad et al. (2018) and Swift et al. (1979) who stated that increase in litter decomposition results in higher soil organic matters and higher soil nutrients. Liu et al. (2013) stated that N application increases the soil nitrogen and N cycling which accelerates the decomposition rate of litter as a result soil nutrients and organic matter content is increased. Rapid decrease and increase in soil total nitrogen content in the study may be due to temperature rise and rain which resulted in increased microbial activity and soil water content which resulted in higher soil nitrogen. The two main processes which regulates the C cycling are plant litter decomposition and soil respiration.

Wood vinegar some concentrations were found to increase the activity of some enzymes (Koc et al., 2018). Wood vinegar is being commonly used in Japan for soil fertility and has significant effect on improving soil fertility (Kadota and Niimi, 2004). Jeong et al. (2015) stated that wood vinegar significantly improved the soil nutrients and soil chemical properties, therefore, the increased nutrients especially N increase can

be the reason for litter decomposition. Burnette (2010) stated that one of the most important uses of wood vinegar is improving soil quality. Our study is in line with the study of Jeong et al. (2015) who also noted that soil nutrients are improved as a result of wood vinegar application. We can conclude from the results that increased soil nutrients may be the reason for increased litter decomposition.

Thinning has been noted to have a positive effect on litter decomposition and forest productivity (Hoorens et al., 2010). It is reported (Hu et al., 2016) that thinning has an effect on leaf litter nutrients such as it increases the nitrogen content of the soil. Higher the soil N content results in more decomposition of litter (Pandey et al., 2007) also stated that thinning changes the overall canopy of the trees which results in change of microclimatic condition of the soil (i.e. uprising the temperature and moisture of the soil), These changes in soil conditions due to thinning results in higher decomposition of litter and nutrient cycling (Hoorens et al., 2010; Osono et al., 2003; Prescott, 2002; Ruano et al., 2013), however structural chemistry of litter can be affected as a result of high thinning intensities and increased biomass lead to lower tissue concentrations resulting in lower nutrients concentration which in turn lower the decomposition of leaf litter (Kunhamu et al., 2009). Nitrogen, phosphorous and lignin concentrations increase with the litter decomposition however potassium contents decrease regardless of thinning (Kunhamu et al., 2009). Our results are the same as Tian et al. (2019) who stated that higher P availability was reported in *Larix principis* as a result of moderate thinning.

Mix litter regularly increases the mass loss and had more nutrient concentration as compared to single litter, more soil nutrients mean less nutrient loss, mix litter can import nutrients from the surrounding litter and soil during decomposition (Gartner and Cardon, 2004). Mix litter has an increasing effect on decomposition in comparison to litter applied alone and have significant effect on nutrients content, abundant decomposers, and decomposition. During litter decomposition the microenvironment of mix litter decomposition is different from single litter decomposition environment (Chen et al., 2011; Liu et al., 2006). Mix litter significantly affects nutrient dynamics especially the P content (Chen et al., 2011). Mix litter results in more accurate litter decomposition and biogeochemical cycle (Li et al., 2016). The increase rate of litter decomposition may be due to the increase in soil nutrients especially N content which results in more litter decomposition and organic contents.

Conclusion

All the treatments improved leaf litter decomposition of *Larix principis* and enhanced the soil nutrients and soil organic contents. External wood vinegar application (400 dilutions), External nitrogen application ($10 \text{ g}\cdot\text{N}\cdot\text{m}^{-2}\cdot\text{y}^{-1}$), Mixed litter (6L: 4B) and Thinning (20%) are the best concentrations. While wood vinegar application with 400 dilutions is the best treatment for litter decomposition, increasing soil nutrients and soil organic contents followed by External nitrogen application ($10 \text{ g}\cdot\text{N}\cdot\text{m}^{-2}\cdot\text{y}^{-1}$), Mixed litter (6L:4B) and Thinning (20%) respectively. In future more combinations with various concentrations or other substance can be helpful to expand the area of litter decomposition of this species as well as other related species.

Acknowledgements. The authors would like to express their gratitude to all the contributed academic members for their constant support and sharing their skills. We are also thankful to the research team, Referees and Dr Adnan Ahmad and Dr Tauheed Ullah Marwat for guidance and timely suggestions.

Finally, we would also like to thank the funding agency “effects of spatial variability and biological factors on trunk respiration of *Larix principis-rupprechtii* and its internal mechanism” Grant No. (31870387) 2019.01-2022.12” to make this study successful.

Conflict of interests. The authors declare that they have no conflict of interests.

Data availability. The data [doc file, excel sheet] used to support the finding of this study are available from the corresponding author upon request.

REFERENCES

- [1] Aerts, R. (1997): Climate, leaf litter chemistry and leaf litter decomposition in terrestrial ecosystems. – *Oikos* 79: 439-449.
- [2] Ahmad, A., Liu, Q.-J., Nizami, S., Mannan, A., Saeed, S. (2018): Carbon emission from deforestation, forest degradation and wood harvest in the temperate region of Hindukush Himalaya, Pakistan between 1994 and 2016. – *Land Use Policy* 78: 781-790.
- [3] Baimark, Y., Niamsa, N. (2009): Study on wood vinegars for use as coagulating and antifungal agents on the production of natural rubber sheets. – *Biomass and Bioenergy* 33(6-7): 994-998.
- [4] Berg, B., Staaf, H. (1980): Decomposition rate and chemical changes of Scots pine needle litter. II. Influence of chemical composition. – *Ecological Bulletins* 32: 373-390.
- [5] Burnette, R. (2010): An introduction to wood vinegar. – ECHO Asia Regional Office. <http://c.ymcdn.com/sites/www.echocommunity.org> (accessed February 13, 2013).
- [6] Carreiro, M., Sinsabaugh, R., Repert, D., Parkhurst, D. (2000): Microbial enzyme shifts explain litter decay responses to simulated nitrogen deposition. – *Ecology* 81(9): 2359-2365.
- [7] Chapman, S. K., Newman, G. S., Hart, S. C., Schweitzer, J. A., Koch, G. W. (2013): Leaf litter mixtures alter microbial community development: mechanisms for non-additive effects in litter decomposition. – *PLoS One* 8(4): e62671.
- [8] Che, Y. (2014): Study on the Tending Technology of *Larix Principis-Rupprechtii* Plantation Forest in Saihanba. – Beijing Forestry University, Beijing.
- [9] Chen, J., Li, Y., Huang, J. (2011): Decomposition of mixed litter of four dominant species in an Inner Mongolia steppe. – *Chinese Journal of Plant Ecology* 35(1): 9-16.
- [10] Farooqi, T.J.A., Abbas, H., and Hussain, S. (2020a): The hydrological influence of forest harvesting intensity on streams: a global synthesis with implications for policy. – *Applied Ecology and Environmental Research*, ISSN 17850037 (*In press*).
- [11] Frootqi, T.J.A., Hayat, U., Roman, M., Abbas, H., Hussain, S. (2020b): Comparative study determining the impacts of broadleaved and Needle leaved forest harvesting on hydrology and water yield: State of knowledge and research outlook. -*International Journal of Biological sciences*. 16(2):231-240.
- [12] Farooqi, T.J.A., Li, X., Yu, Z., Liu, S., Sun, O.J. (2020c): Reconciliation of research on forest carbon sequestration and water conservation. -*Journal of Forestry Research*. pp.1-8.
- [13] Fioretto, A., Papa, S., Fuggi, A. (2003): Litter-fall and litter decomposition in a low Mediterranean shrubland. – *Biology and Fertility of Soils* 39(1): 37-44.
- [14] Frey, S. D., Knorr, M., Parrent, J. L., Simpson, R. T. (2004): Chronic nitrogen enrichment affects the structure and function of the soil microbial community in temperate hardwood and pine forests. – *Forest Ecology and Management* 196(1): 159-171.
- [15] Gartner, T. B., Cardon, Z. G. (2004): Decomposition dynamics in mixed-species leaf litter. – *Oikos* 104(2): 230-246.
- [16] Handa, I. T., Aerts, R., Berendse, F., Berg, M. P., Bruder, A., Butenschoen, O., Chauvet, E., Gessner, M. O., Jabiol, J., Makkonen, M. (2014): Consequences of biodiversity loss for litter decomposition across biomes. – *Nature* 509(7499): 218.

- [17] Hättenschwiler, S., Tiunov, A. V., Scheu, S. (2005): Biodiversity and litter decomposition in terrestrial ecosystems. – *Annu. Rev. Ecol. Evol. Syst.* 36: 191-218.
- [18] Hobbie, S. E. (2000): Interactions between litter lignin and soil nitrogen availability during leaf litter decomposition in a Hawaiian montane forest. – *Ecosystems* 3: 484-494.
- [19] Hobbie, S. E. (2005): Contrasting effects of substrate and fertilizer nitrogen on the early stages of litter decomposition. – *Ecosystems* 8(6): 644-656.
- [20] Hobbie, S. E., Vitousek, P. M. (2000): Nutrient limitation of decomposition in Hawaiian forests. – *Ecology* 81(7): 1867-1877.
- [21] Hoorens, B., Coomes, D., Aerts, R. (2010): Neighbour identity hardly affects litter-mixture effects on decomposition rates of New Zealand forest species. – *Oecologia* 162(2): 479-489.
- [22] Hu, B., Yang, B., Pang, X., Bao, W., Tian, G. (2016): Responses of soil phosphorus fractions to gap size in a reforested spruce forest. – *Geoderma* 279: 61-69.
- [23] Jeong, K. W., Kim, B. S., Ultra Jr, V. U., Lee, S. C. (2015): Effects of rhizosphere microorganisms and wood vinegar mixtures on rice growth and soil properties. – *Korean Journal of Crop Science* 60(3): 355-365.
- [24] Kadota, M., Niimi, Y. (2004): Effects of charcoal with pyroligneous acid and barnyard manure on bedding plants. – *Scientia Horticulturae* 101(3): 327-332.
- [25] Kim, S., Li, G., Han, S. H., Kim, H.-J., Kim, C., Lee, S.-T., Son, Y. (2018): Thinning affects microbial biomass without changing enzyme activity in the soil of *Pinus densiflora* Sieb. et Zucc. forests after 7 years. – *Annals of Forest Science* 75(1): 13.
- [26] Koc, I., Yardim, E. N., Akca, M. O., Namli, A. (2018): impact of pesticides and wood vinegar, used in wheat agro-ecosystems, on the soil enzyme activities. – *Fresenius Environmental Bulletin* 27(4): 2442-2448.
- [27] Kunhamu, T., Kumar, B., Viswanath, S. (2009): Does thinning affect litterfall, litter decomposition, and associated nutrient release in *Acacia mangium* stands of Kerala in peninsular India? – *Canadian Journal of Forest Research* 39(4): 792-801.
- [28] Li, X., Farooqi, T.J.A., Jiang, C, Liu., S. Sun., O.J. (2019): Spatiotemporal variations in productivity and water use efficiency across a temperate forest landscape of Northeast China. -*Forest Ecosystems*. 6(1): p.22.
- [29] Li, Q., Liu, Z. (2013): Effects of decomposed leaf litter mixtures from *Platycladus orientalis* and broadleaf tree species on soil properties. – *Scandinavian Journal of Forest Research* 28(7): 642-650.
- [30] Li, W., Yu, W., Bai, L., Liu, H., Yang, D. (2016): Effects of nitrogen addition on the mixed litter decomposition in *Stipa baicalensis* steppe in Inner Mongolia. – *American Journal of Plant Sciences* 7(03): 547.
- [31] Liu J. (2013): Effect of Tending Thinning and Pruning on Soil Quality of *Larix Principis-Rupprechtii* Plantation. – Beijing Forestry University, Beijing.
- [32] Liu, P., Huang, J., Han, X., Sun, O. J., Zhou, Z. (2006): Differential responses of litter decomposition to increased soil nutrients and water between two contrasting grassland plant species of Inner Mongolia, China. – *Applied Soil Ecology* 34(2-3): 266-275.
- [33] Liu, P., Huang, J., Sun, O. J., Han, X. (2010): Litter decomposition and nutrient release as affected by soil nitrogen availability and litter quality in a semiarid grassland ecosystem. – *Oecologia* 162(3): 771-780.
- [34] Liu, X., Zhang, Y., Han, W., Tang, A., Shen, J., Cui, Z., Vitousek, P., Erisman, J. W., Goulding, K., Christie, P. (2013): Enhanced nitrogen deposition over China. – *Nature* 494(7438): 459.
- [35] Mao, B., Yu, Z.-Y., Zeng, D.-H. (2015): Non-additive effects of species mixing on litter mass loss and chemical properties in a Mongolian pine plantation of Northeast China. – *Plant and Soil* 396(1-2): 339-351.
- [36] Matson, P., Lohse, K. A., Hall, S. J. (2002): The globalization of nitrogen deposition: consequences for terrestrial ecosystems. – *AMBIO: A Journal of the Human Environment* 31(2): 113-120.

- [37] Onyekwelu, J. C., Mosandl, R., Stimm, B. (2006): Productivity, site evaluation and state of nutrition of Gmelina arborea plantations in Oluwa and Omo forest reserves, Nigeria. – Forest Ecology and Management 229(1-3): 214-227.
- [38] Osono, T., Ono, Y., Takeda, H. (2003): Fungal ingrowth on forest floor and decomposing needle litter of Chamaecyparis obtusa in relation to resource availability and moisture condition. – Soil Biology and Biochemistry 35(11): 1423-1431.
- [39] Pandey, R., Sharma, G., Tripathi, S., Singh, A. (2007): Litterfall, litter decomposition and nutrient dynamics in a subtropical natural oak forest and managed plantation in northeastern India. – Forest Ecology and Management 240(1-3): 96-104.
- [40] Polyakova, O., Billor, N. (2007): Impact of deciduous tree species on litterfall quality, decomposition rates and nutrient circulation in pine stands. – Forest Ecology and Management 253(1-3): 11-18.
- [41] Prescott, C. E. (2002): The influence of the forest canopy on nutrient cycling. – Tree Physiology 22(15-16): 1193-1200.
- [42] Ruano, I., Rodríguez-García, E., Bravo, F. (2013): Effects of pre-commercial thinning on growth and reproduction in post-fire regeneration of Pinus halepensis Mill. – Annals of Forest Science 70(4): 357-366.
- [43] Sinsabaugh, R., Carreiro, M., Repert, D. (2002): Allocation of extracellular enzymatic activity in relation to litter composition, N deposition, and mass loss. – Biogeochemistry 60(1): 1-24.
- [44] Steiner, C., Das, K. C., Garcia, M., Förster, B., Zech, W. (2008): Charcoal and smoke extract stimulate the soil microbial community in a highly weathered xanthic Ferralsol. – Pedobiologia 51(5-6): 359-366.
- [45] Swift, M., Heal, O., Anderson, J. (1979): Decomposition in Terrestrial Ecosystems. – Blackwell Scientific, Oxford.
- [46] Tian, H., Cheng, X., Han, H., Jing, H., Liu, X., Li, Z. (2019): Seasonal variations and thinning effects on soil phosphorus fractions in Larix principis-rupprechtii Mayr. plantations. – Forests 10(2): 172.
- [47] Tiilikkala, K., Setälä, H. (2009): Birch tar oil-a new innovations as biological plant protection product. – NWBC-2009. The 2nd Nordic Wood Biorefinery Conference. Finlandia Hall, Helsinki, Finland, September 2-4, 2009.
- [48] Ullah, S., Muhammad, B., Amin, R., Abbas, H., Muneer, M. (2019): sensitivity of arbuscular mycorrhizal fungi in old-growth forests: direct effect on growth and soil carbon storage. – Applied Ecology and Environmental Research 17(6): 13749-13758.
- [49] Velmurugan, N., Chun, S., Han, S., Lee, Y. (2009): Characterization of chikusaku-eki and mokusaku-eki and its inhibitory effect on sapstaining fungal growth in laboratory scale. – International Journal of Environmental Science & Technology 6(1): 13-22.
- [50] Vestgarden, L. (2001): Carbon and nitrogen turnover in the early stage of Scots pine (Pinus sylvestris L.) needle litter decomposition: effects of internal and external nitrogen. – Soil Biology and Biochemistry 33(4-5): 465-474.
- [51] Wang, J., Zhang, D., Farooqi, T.J.A., Ma, L., Deng, Y. and Jia, Z. (2017): The olive (Olea europaea L.) industry in China: its status, opportunities and challenges. - Agroforestry Systems 93(2):395-417.
- [52] Wei, Q., Liu, G., Wei, X., Ma, X., Xu, D., Dong, R. (2009): Influence of wood vinegar as leaves fertilizer on yield and quality of celery. – Journal of China Agricultural University 14(1): 89-92.
- [53] Wu, H., Lu, X., Yang, Q. (2007): Problems and countermeasures of decomposition bag method in the study of wetland litter decomposition. – Journal of Northeast Forestry University 35(2): 82-85.
- [54] Yatagai, M., Nishimoto, M., Hori, K., Ohira, T., Shibata, A. (2002): Termiticidal activity of wood vinegar, its components and their homologues. – Journal of Wood Science 48(4): 338-342.

- [55] Yuan, J., Jose, S., Hu, Z., Pang, J., Hou, L., Zhang, S. (2018): Biometric and eddy covariance methods for examining the carbon balance of a *Larix principis-rupprechtii* forest in the Qinling Mountains, China. – *Forests* 9(2): 67.

STUDY OF MACROINVERTEBRATE FUNCTIONAL FEEDING GROUP ABUNDANCE IN TUANJIIE RESERVOIR OF NORTHEAST CHINA

CHEN, Q.^{1,2} – SUN, X.¹ – YU, H. X.^{1*}

¹*College of Wildlife and Protected Area, Northeast Forestry University, Harbin 150040, China*

²*Heilongjiang Forestry and Grassland Bureau, Harbin 150090, China*

**Corresponding author
e-mail: china.yhx@163.com*

(Received 12th Dec 2019; accepted 6th May 2020)

Abstract. In this study, the concept of functional feeding groups was used to classify macroinvertebrate community structure. A total of 55 genera or species were sampled in the Tuanjie Reservoir in China and identified into six functional feeding groups. The mean values of water transparency (SD), dissolved oxygen (DO), pH, water temperature (T), total phosphorus (TP), chemical oxygen demand (COD_{Mn}), dissolved copper (Cu²⁺), depth (D), electrical conductivity (EC), total nitrogen (TN) and dissolved iron (Fe³⁺) showed significant difference between sampling sites ($P < 0.05$), while ammonium nitrogen (NH₄⁺-N) and nitrate nitrogen (NO₃⁻-N) were not significantly different ($P > 0.05$). Macroinvertebrate samples were also different, we find that the highest abundance was observed in summer at all sampling sites except S5 which was documented in spring, while the lowest abundance recorded in autumn except for S1 (in spring). Pearson and redundancy analysis (RDA) results showed that T, NH₄⁺-N, Fe³⁺, DO and COD_{Mn} were the major factors influencing zooplankton functional groups in Tuanjie Reservoir.

Keywords: *macroinvertebrate, functional diversity, environmental factors, drinking water, correlation*

Introduction

Macroinvertebrates play an important role in the aquatic ecosystem, which is an important channel for nutrient recycling and energy flow to higher levels (Benke et al., 2010). Aquatic ecosystems are mostly affected by agricultural non-point source pollution which poses severe threats to macroinvertebrates (Shabani et al., 2019). The diversity of macroinvertebrates community structure can reflect the disturbance degree of long-term human activities aquatic ecosystem (Plafkin et al., 1989). Macroinvertebrates are widely used to monitor the damage of aquatic ecosystem. They are also an important part of aquatic food web and the basis of nutrient cycle and ecological balance of ecosystem (Liu et al., 2012; Mangadze et al., 2016; Hu et al., 2018). Benthic animals are the food source of aquatic animals such as fish and play an important role in fishery production. Therefore, the investigation of benthic animals in reservoirs has important reference value for understanding the nutritional status and water productivity of reservoirs. Benthic animals are the food source of aquatic animals such as fish and play an important role in fishery production. Therefore, the investigation of benthic animals in reservoirs has important reference value for understanding the nutritional status and water productivity of reservoirs (Chi et al., 2009).

Functional groups are classified based on physiological, morphological, life history or other biological characteristics associated with an ecosystem and with the behavior of species, and are aggregates of all species with similar functions in the community (An et

al., 2016). Because of the environmental and spatial scale changes caused by nature and human beings, aquatic organisms respond accordingly. Researchers classify the priority functional groups of species according to similar biological and ecological characteristics, and these characteristics are consistent with the gradient of the environment (Poff et al., 2006). Species characteristics of functional groups are more closely related to the environment, which can more directly reflect the ecological process of ecological environment affecting aquatic communities, and can understand the aquatic ecosystem and its biodiversity (An et al., 2017).

China is the country with the largest number of reservoirs in the world (Liu et al., 2012). In many provinces, reservoirs have become an important source of water supply (Han, 2010), and are considered as the last barrier for drinking water safety in China and even for human beings (Han et al., 2016). Although there are a large number of reservoirs in China, the importance of reservoirs is increasing day by day, but relative to lakes and rivers, the research on benthic zoology of reservoirs is still scarce and needs to be strengthened (Liu et al., 2012).

Tuanjie Reservoir was built in 1981 with the aim of supplying drinking water to the local village people. The main sources water of the reservoir is Muling River, which is the largest tributary of the Ussuri River on the left bank of the border between China and Russia. Recently, the ecological study of Tuanjie reservoir mainly focuses on plankton (Chen et al., 2019; Sun et al., 2019). In this study, the macroinvertebrate functional feeding groups (FFGs) were used to reveal the relationship between macroinvertebrate FFGs abundance and environmental factors in Tuanjie Reservoir. We aim to collect macroinvertebrate fauna, and explore the relationships between macroinvertebrate functional feeding groups and environmental factors in the Tuanjie Reservoir.

Materials and methods

Study area

Tuanjie Reservoir (130°8'-130°11'E, 44°01'-44°04'N) is located in the southeast of Heilongjiang Province Northeastern China (*Fig. 1*). The reservoir was built in 1981 in order to control floods, provide water for irrigation, fish farming, power generation and for aesthetic value. Tuanjie Reservoir has a surface area of 445 km², a capacity of 8.63×10⁷ m³ and it shaped like big “Y”. The region where the reservoir is located is influenced by temperate continental monsoon. The average annual evaporation and precipitation of the reservoir are 950 mm and 534 mm, respectively. The annual mean temperature is 1°C, which ranged between -44.1°C to 37.6°C. In winter, the surface water of the reservoir is covered by ice (Sun et al., 2019).

Environmental factors data sampling

We collected all samples three times from 5 sampling sites of Tuanjie Reservoir on 6th~13th May, 14th~21th July and 20th~27th September periods for spring, summer and autumn three seasons in 2015 (*Table 1*; *Fig. 1*). At each sampling site, water temperature (T), pH, electrical conductivity (EC), dissolved oxygen (DO) was measured in the field using a portable multi-probe (YSI 6600, YSI Inc.). Water transparency (SD) and depth (D) were measured using Secchi disk and longline method. Triplicate water samples for chemical analyses were collected at each sampling sites and put on

acid-washed plastic bottles, placed in ice box and transported to laboratory for analysis. The concentration of total nitrogen (TN), total phosphorus (TP), ammonium nitrogen ($\text{NH}_4^+\text{-N}$), nitrate nitrogen ($\text{NO}_3^-\text{-N}$), chemical oxygen demand (COD_{Mn}) and dissolved iron (Fe^{3+}) and dissolved copper (Cu^{2+}) were measured according to the standard methods for China (MEP, 2002).

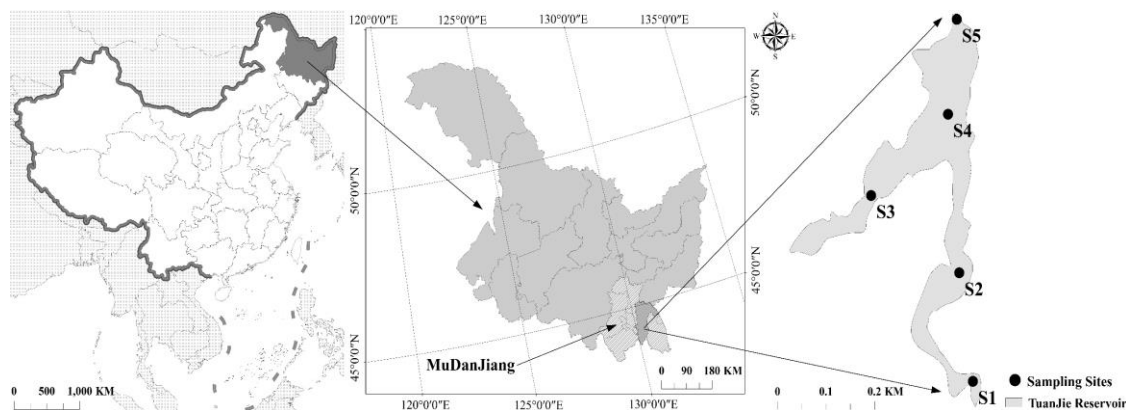


Figure 1. Map of sampling sites in Tuanjie Reservoir

Table 1. Five sampling sites coordinate in Tuanjie Reservoir in May (spring), July (summer) and September (autumn) in 2015

Sampling sites	Latitude	Longitude
S1	N44°01'48"	E130°11'24"
S2	N44°03'36"	E130°10'48"
S3	N44°03'00"	E130°09'36"
S4	N44°04'12"	E130°10'36"
S5	N44°04'48"	E130°10'48"

Macroinvertebrate FFGs data sampling

Three random subsamples were collected in comparable habitat at locations of 1 m^2 at each sampling site by using a Peterson mud bottom sampler (CN-150, $1/16 \text{ m}^2$). All macroinvertebrates samples were composited into a single sample, preserved in 75% ethanol and transported to the laboratory for identification. In the laboratory, all samples were sorted on white porcelain pans, identified, and counted with a light stereomicroscope. All individuals were identified to genera or species using appropriate identification guides (Morse et al., 1994; Epler, 2001). Taxa were divided into six functional feeding groups (FFGs) according to Cummins et al. (1974) and Duan et al. (2010): predators (PR), omnivores (OM), gatherers/collectors (GC), filterers/collectors (FC), scrapers (SC) and shredders (SH).

Data analysis

Statistical analyses were carried out using the SPSS 19.0 software. Variation and correlation of environmental factors and macroinvertebrate FFGs abundance in different sampling sites were analyzed by using One-way ANOVA. Relationship between macroinvertebrate FFGs abundance and environmental factors was done using CANOCO 4.5 software (Microcomputer Power, New York, USA). Before analysis, the

biological and abiotic data were transformed by $\log_{10}(x+1)$ to satisfy the normal distribution. We found that the detrended corresponding analysis (DCA) of the largest gradient length of the four axes was 0.648 (< 3). Therefore, linear ordination method of the redundancy analysis (RDA) was used to reveal the relationship. Monte Carlo simulations with 499 permutations were used to test the significance of the environmental factors in explaining the macroinvertebrate FFGs abundance in the RDA.

Results and discussion

Environmental factors data characteristics

The results of environmental factors mean values were shown in *Table 2* and *Table 3*. Many biotic and abiotic factors, such as sediment type, water depth, food, dissolved oxygen, etc., have an important impact on the distribution of benthos community in lakes and reservoirs (Ji et al., 2015). There are many factors affecting the community structure, density, biomass and biodiversity of macroinvertebrates, special some important physical and chemical factors change (Petridis and Sinis, 1993; Buss et al., 2002; Duran, 2006). The cold climate in the North determines that the impact of temperature on macroinvertebrates is higher than that in other areas (Wang et al., 2019). The mean values of SD, DO, pH, T, TP, COD_{Mn} and Cu^{2+} were extremely significant difference among sampling sites ($P < 0.01$). And the mean values of D, EC, TN and Fe^{3+} showed significantly difference among sampling sites ($P < 0.05$). While $\text{NH}_4^+\text{-N}$ and $\text{NO}_3^-\text{-N}$ were not difference among sampling sites ($P > 0.05$) (*Table 2*). Among sampling seasons, the mean values of D, EC, TN, $\text{NO}_3^-\text{-N}$ were not difference ($P > 0.05$), and Cu^{2+} showed significantly difference ($P < 0.05$). The other environmental factors were all extremely significant difference ($P < 0.01$) (*Table 3*).

Table 2. The values (mean \pm SE) of environmental factors among sampling sites in May (spring), July (summer) and September (autumn) in 2015

	S1	S2	S3	S4	S5	F	p
SD(m)	0.66 \pm 0.10	0.85 \pm 0.05	0.95 \pm 0.06	1.36 \pm 0.04	1.46 \pm 0.05	9.364	0.000**
D(m)	0.84 \pm 0.07	7.42 \pm 0.08	2.44 \pm 0.07	17.48 \pm 0.08	22.72 \pm 0.07	2.895	0.034*
EC(mS/cm)	0.31 \pm 0.03	0.08 \pm 0.01	0.15 \pm 0.01	0.10 \pm 0.01	0.08 \pm 0.01	2.633	0.048*
DO(mg/L)	9.10 \pm 0.21	8.27 \pm 0.09	8.90 \pm 0.21	9.00 \pm 0.26	8.33 \pm 0.07	5.016	0.002**
pH	7.69 \pm 0.09	7.65 \pm 0.04	7.71 \pm 0.06	8.06 \pm 0.02	7.44 \pm 0.05	10.994	0.000**
T($^{\circ}\text{C}$)	6.70 \pm 0.82	11.08 \pm 0.27	10.58 \pm 0.08	11.39 \pm 0.13	9.36 \pm 0.22	17.394	0.000**
TN(mg/L)	0.97 \pm 0.06	1.11 \pm 0.06	0.77 \pm 0.04	0.89 \pm 0.03	0.75 \pm 0.03	2.835	0.037*
TP(mg/L)	0.43 \pm 0.11	0.53 \pm 0.05	0.51 \pm 0.06	0.46 \pm 0.09	0.17 \pm 0.03	5.104	0.002**
$\text{NH}_4^+\text{-N}$ (mg/L)	0.18 \pm 0.02	0.18 \pm 0.03	0.16 \pm 0.03	0.14 \pm 0.03	0.19 \pm 0.01	1.807	0.147
$\text{NO}_3^-\text{-N}$ (mg/L)	0.47 \pm 0.07	0.47 \pm 0.12	0.43 \pm 0.20	0.33 \pm 0.12	0.43 \pm 0.09	0.382	0.820
COD_{Mn} (mg/L)	4.07 \pm 0.04	4.35 \pm 0.08	4.28 \pm 0.05	4.23 \pm 0.06	4.39 \pm 0.04	19.060	0.000**
Fe^{3+} (mg/L)	0.42 \pm 0.04	0.39 \pm 0.02	0.41 \pm 0.01	0.41 \pm 0.01	0.41 \pm 0.01	3.696	0.012*
Cu^{2+} (mg/L)	0.32 \pm 0.11	0.07 \pm 0.03	0.03 \pm 0.01	0.04 \pm 0.01	0.09 \pm 0.03	4.677	0.003**

Water transparency (SD), depth (D), electrical conductivity (EC), dissolved oxygen (DO), pH, water temperature (T), total nitrogen (TN), total phosphorus (TP), ammonium nitrogen ($\text{NH}_4^+\text{-N}$), nitrate nitrogen ($\text{NO}_3^-\text{-N}$), chemical oxygen demand (COD_{Mn}) and dissolved iron (Fe^{3+}) and dissolved copper (Cu^{2+}), F and p values from One-way ANOVA tested by post-hoc test using Tukey HSD ANOVA. * $p < 0.05$, ** $p < 0.01$

Table 3. The values (mean± SE) of environmental factors among sampling seasons in May (spring), July (summer) and September (autumn) in 2015

	May (Spring)	July (Summer)	September (Autumn)	F	p
SD(m)	0.69±0.06	0.96±0.1	1.06±0.09	4.974	0.012**
D(m)	8.07±1.97	10.77±2.57	10.18±2.28	0.387	0.681
EC(mS/cm)	0.08±0.02	0.14±0.02	0.14±0.02	0.369	0.694
DO(mg/L)	7.71±0.18	7.65±0.32	8.72±0.12	7.301	0.002**
pH	7.41±0.05	7.24±0.09	7.71±0.06	11.932	0.000**
T(°C)	17.47±0.59	23.35±0.3	9.82±0.48	204.801	0.000**
TN(mg/L)	1.09±0.1	0.94±0.07	0.9±0.04	1.921	0.159
TP(mg/L)	0.78±0.09	0.58±0.03	0.42±0.04	8.768	0.001**
NH ₄ ⁺ -N(mg/L)	0.21±0.02	0.3±0.03	0.17±0.01	10.984	0.000**
NO ₃ ⁻ -N(mg/L)	0.46±0.05	0.45±0.05	0.43±0.05	0.118	0.889
COD _{Mn} (mg/L)	4.48±0.04	3.86±0.09	4.26±0.04	25.529	0.000**
Fe ³⁺ (mg/L)	0.35±0.02	0.25±0.04	0.4±0.01	8.125	0.001**
Cu ²⁺ (mg/L)	0.23±0.03	0.17±0.02	0.11±0.04	4.556	0.016*

Water transparency (SD), depth (D), electrical conductivity (EC), dissolved oxygen (DO), pH, water temperature (T), total nitrogen (TN), total phosphorus (TP), ammonium nitrogen (NH₄⁺-N), nitrate nitrogen (NO₃⁻-N), chemical oxygen demand (COD_{Mn}) and dissolved iron (Fe³⁺) and dissolved copper (Cu²⁺), F and p values from One-way ANOVA tested by post-hoc test using Tukey HSD ANOVA. *p<0.05, **p<0.01

Macroinvertebrate data characteristics

During three sampling seasons, we totally collected 904 individuals and identified 11 orders, 23 family and 55 genera or species of macroinvertebrate belong to six FFGs from Tuanjie Reservoir (Table 4). Our findings agreed with the studies of Liu et al. (2019) and Shabani et al. (2019) who also observed the same six FFGs in the same province. According to Rosser and Pearson (2018), aquatic insects were the most abundant group in freshwater ecosystem, Chironomidae especially. Thus, we found that the abundance of *Chironomus kiiensisTokunaga* (11.62%) which was absolutely dominant species of macroinvertebrate community structure in Tuanjie Reservoir. The disturbance of Tubificid worms can significantly improve the nutrient level of the water body. These nutrients times of phytoplankton can promote the growth of phytoplankton (Jin et al., 2017), and phytoplankton is the opening bait of benthos. The dependence of benthos and phytoplankton cannot be separated from the change of nutrient concentration (Li et al., 2001; Cortes et al., 2010; Wang et al., 2019).

The highest macroinvertebrate abundance observed in summer at all sampling sites except S5 (in spring), while the lowest abundance presented in autumn except S1 (in spring) (Fig. 2). The temporal changes in macroinvertebrates functional feeding groups (FFGs) of three sampling seasons were shown in Table 5. We found that all macroinvertebrates FFGs top abundance presented in July (summer). Only group GC and total macroinvertebrates abundance showed extremely significant differences (P<0.01), and group FC presented significant differences (P<0.05) during sampling seasons. Both top abundance of group PR and SH showed at S4, group OM and FC observed at S2. Meanwhile, the top group GC abundance presented at S5, while group SC appeared at S1 (Fig. 3). In three seasons (spring, summer and autumn), the top abundance presented at S5, S2 and S1, respectively (Fig. 4). Both among sampling sites and seasons, FFGs of group GC accounted for most of the proportion (Fig. 5). Based on

the study of Zhang et al. (2012), the sediment of Danjiangkou reservoir is rich in organic matter, which is one of the important food sources for warworm and chironomid larvae (Li et al., 2018). We also found the similar results that relative abundance of group GC (including *Tubificidae* sp. and *Chironomidae* sp.) was higher than other groups (Fig. 5) (Benke, 1998; Chaloner et al., 2002).

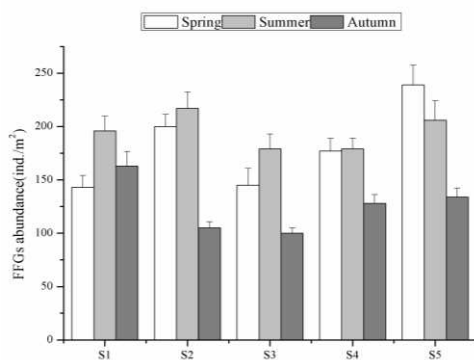


Figure 2. Seasonal variation of macroinvertebrate abundance (ind./m²) among sampling sites, error bars meaning standard error

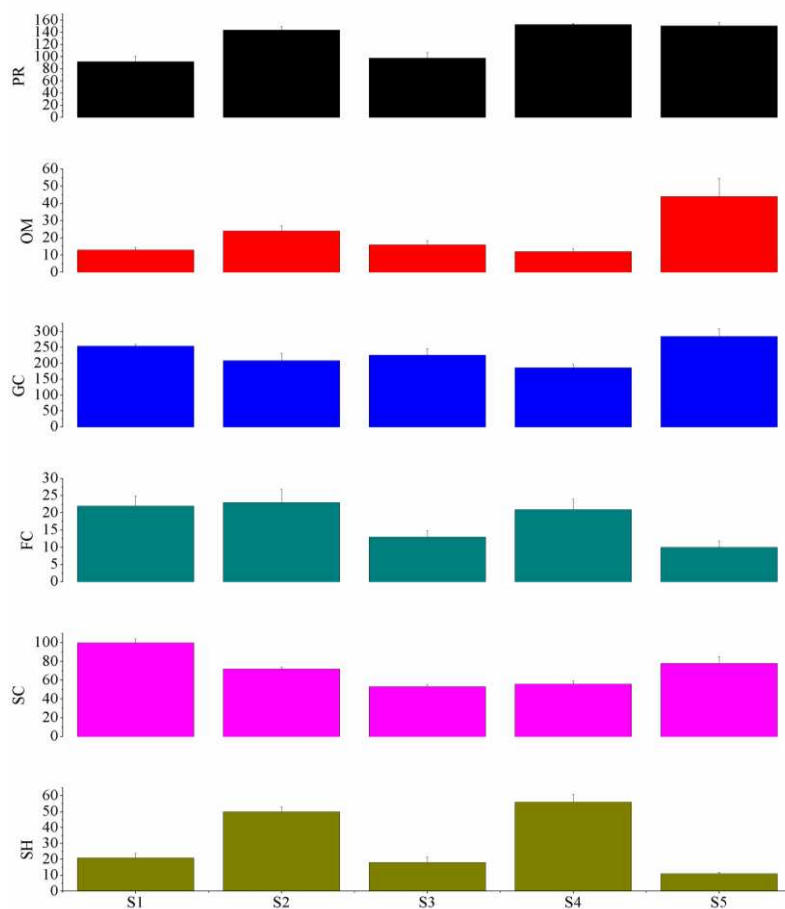


Figure 3. Macroinvertebrate abundance (ind./m²) among sampling sites. Predators (PR), omnivores (OM), gatherers/collectors (GC), filterers/collectors (FC), scrapers (SC) and shredders (SH)

Table 4. Macroinvertebrate community structure and abundance ratio in Tuanjie Reservoir in May (spring), July (summer) and September (autumn) in 2015

Order	Family	Genera or species	FFGs	Ratio
Hemiptera Diptera	Corixidae	<i>Corixa substriata</i>	PR	2.65%
	Chironomidae	<i>Diplocladius</i> sp.	GC	2.21%
		<i>Synorthocladius semivirens</i>	GC	1.66%
		<i>Thienemannia gracilis kiffer</i>	GC	3.43%
		<i>Chironomus kitiensisTokunaga</i>	GC	11.62%
		<i>Chironomus flaviplumus</i>	GC	7.96%
		<i>Dicrotendipes pelochloris</i>	GC	2.10%
		<i>Chironomus plumosus</i>	OM	1.33%
		<i>Cryptochironomus maculipennis</i>	PR	4.42%
		<i>Parachironomus arcnatus</i>	PR	2.43%
		<i>Eukiefferiella fittkau</i>	GC	1.44%
		<i>Polypedilum laetum</i>	SH	1.55%
		<i>Apsectrotanypus</i> sp.	PR	2.54%
		<i>Stictochironomus akizukii</i>	OM	5.09%
		<i>Stictochironomus maculipennis</i>	OM	0.33%
		<i>Paracladopelma undine</i>	GC	1.77%
		<i>Paracladopelma nigriflora</i>	GC	0.88%
		<i>Chironomus anthracinus</i>	GC	0.66%
		<i>Micropsectra chuzeprima</i>	GC	0.66%
		<i>Tanytarsus chinyensis</i>	FC	0.44%
		<i>Tanytarsus signatus</i>	FC	1.22%
Trichoptera	Hydropsychidae	<i>Hydropsyche</i> sp.	FC	0.66%
	Goeridae	<i>Goera ramosa</i>	SC	0.33%
		<i>Goera kyotonis</i>	SC	0.22%
	Rhyacophilidae	<i>Rhyacophila</i> sp.	PR	0.44%
	Limnephilidae	<i>Apatania</i> sp.	SC	1.44%
		<i>Glyphotaelius admorsus</i>	SH	2.54%
		<i>Stenophylax koizumii</i>	SH	0.66%
Ephemeroptera	Ephemeridae	<i>Ephemera shengmi</i>	GC	0.33%
		<i>Ephemera nigroptera</i>	GC	1.11%
	Heptageniidae	<i>Heptagenia</i> sp.	SC	0.22%
	Baetidae	<i>Baetis</i> sp.	GC	1.66%
	Ephemerellidae	<i>Ephemerella nigra</i>	GC	0.22%
		<i>Ephemerella fusongensis</i>	GC	1.11%
Plecoptera	Pelidae	<i>Cyamia</i> sp.	PR	0.22%
Odonata	Libellulidae	<i>Epiophcetia superstes</i>	PR	0.77%
	Libellulidae	<i>Hydrobasileus</i> sp.	PR	0.44%
	Gomphidae	<i>Anisogomphus</i> sp.	PR	0.33%
Coleoptera	Dytiscidae	<i>Cybister japonicus</i>	PR	1.66%
	Hydrophilidae	<i>Hydrophilus acuminatus</i>	PR	0.22%
Rhynchobdellida Tubificida	Glossiphoniidae	<i>Helobdella nuda</i>	PR	2.54%
	Tubificinae	<i>Limnodrilus hoffmeisteri</i>	GC	6.75%
		<i>Limnodrilus claparedeianus</i>	GC	3.76%
		<i>Branchiura sowerbyi</i>	GC	0.33%
	Naididae	<i>Nais variabilis</i>	GC	4.42%
		<i>Dero</i> sp.	GC	1.00%
Mesogastropoda	Viviparidae	<i>Bellamyia purrificata</i>	SC	1.88%
	Hydrobiidae	<i>Parafossarulus striatus</i>	SC	0.88%
Basommatophora	Lymnaeidae	<i>Radix auricularia</i>	SC	1.00%
		<i>Radix plicatula</i>	SC	0.77%
		<i>Radix swinhoei</i>	SC	1.44%
		<i>Radix ovata</i>	SC	1.00%
		<i>Radix lagotis</i>	SC	0.88%
		<i>Galba pervia</i>	SC	1.44%
		<i>Polypylis hemisphaerula</i>	SC	0.88%

Predators (PR), omnivores (OM), gatherers/collectors (GC), filterers/collectors (FC), scrapers (SC) and shredders (SH)

Table 5. The abundance (ind./m²) values (mean± SE) of macroinvertebrate FFGs among sampling seasons in May (spring), July (summer) and September (autumn) in 2015

	Spring	Summer	Autumn	F	p
PR	41.4±9.67	49.60±1.29	36.60±3.82	1.548	0.225
OM	12.20±5.85	4.40±1.91	5.20±1.83	0.768	0.470
GC	89.4±9.04 a	94.00±7.65 a	48.60±11.34 b	8.421	0.001**
FC	6.40±1.86	8.60±2.16	2.80±1.24	3.460	0.041*
SC	22.40±4.60	27.40±4.45	22.00±2.53	1.090	0.346
SH	9.00±4.92	11.40±3.06	10.80±3.06	0.223	0.801
Total	180.80±18.00 a	195.40±7.47 a	126.00±11.30 b	6.633	0.003**

Predators (PR), omnivores (OM), gatherers/collectors (GC), filterers/collectors (FC), scrapers (SC) and shredders (SH). F and p values from One-way ANOVA, a and b mean differences between the seasons were tested by post-hoc test using Tukey HSD ANOVA. *p<0.05, **p<0.01

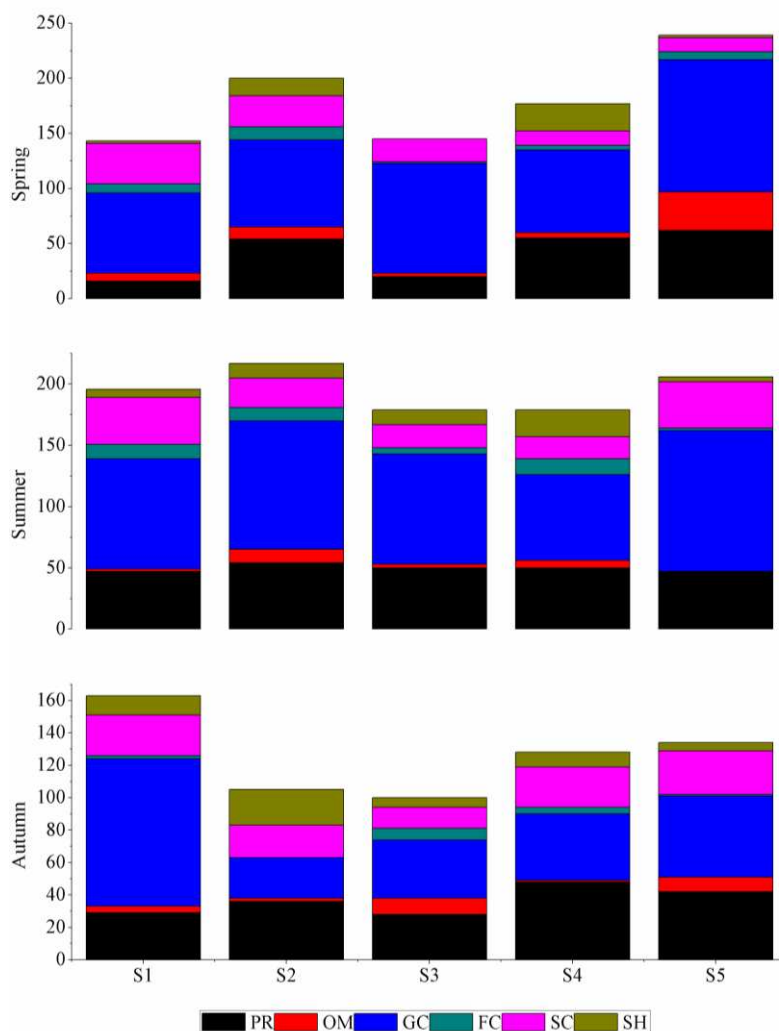


Figure 4. Macroinvertebrate FFGs abundance (ind./m²) of spring, summer and autumn among sampling sites. Predators (PR), omnivores (OM), gatherers/collectors (GC), filterers/collectors (FC), scrapers (SC) and shredders (SH)

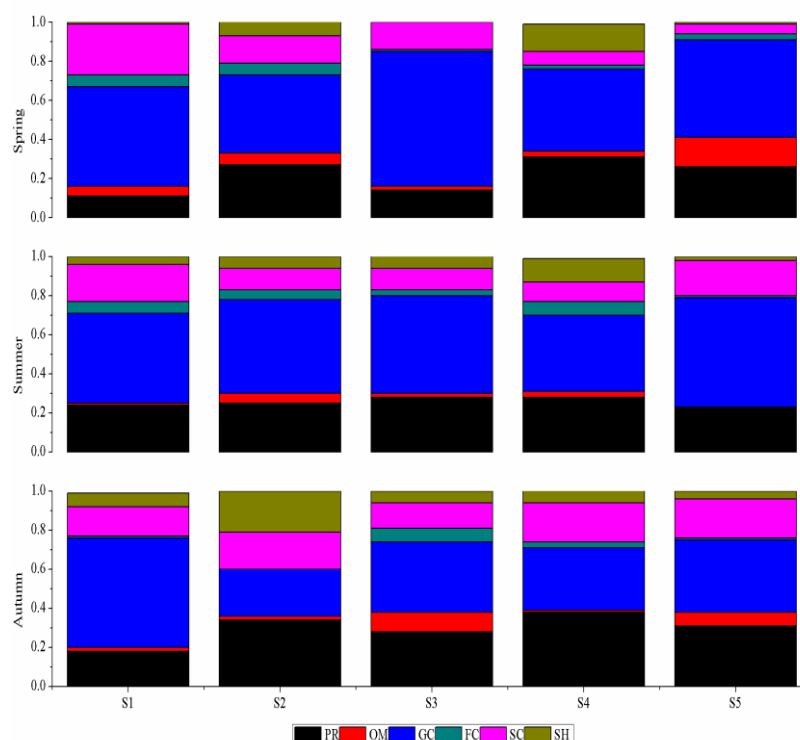


Figure 5. Macroinvertebrate FFGs relative abundance of spring, summer and autumn among sampling sites. Predators (PR), omnivores (OM), gatherers/collectors (GC), filterers/collectors (FC), scrapers (SC) and shredders (SH)

Correlation analysis between macroinvertebrate FFGs abundance and environmental factors

Correlation coefficient is significant if the correlation coefficient is low it did not suppose a close correlation between the studied variables (Pries et al., 2000; Sponseller et al., 2001; Richards et al., 2003; Barquín and Death, 2006). As shown in *Table 6*, group FC and SC were extremely positive correlated with T ($r=0.398$) and NO_3^- -N ($r=0.381$). Meanwhile, group PR and GC were both positively correlated with T ($r=0.372$, $r=0.377$), and group FC was both positively correlated with TN ($r=0.355$) and NH_4^+ -N ($r=0.305$). By contrast, group GC was both negatively correlated with DO ($r=-0.315$) and pH ($r=-0.299$).

Li et al. (2018) compared with the results of other reservoirs, it can be seen that the emergence of pollution resistant species, such as *Limnodrilus hoffmeisteri* and *Limnodrilus claparedianus*, can play an indicative role in reservoir water quality. With the increase of temperature, the release rate of NH_4^+ -N from the *Limnodrilus hoffmeisteri* (group GC) increased gradually (Gong et al., 2017). Meanwhile, the *Limnodrilus hoffmeisteri* has strong pollution resistance, can grow and reproduce normally in the low oxygen environment, and even survive for a short time in the low oxygen environment. It is often used as a symbol of organic pollution or eutrophication (Lee, 1970; Wildung et al., 1993; Batzer et al., 2004; Bonada et al., 2007).

Table 6. Pearson correlation analysis of between FFGs and environmental factors in May (spring), July (summer) and September (autumn) in 2015

	SD	D	DO	pH	T	TN	TP	NH ₄ ⁺ -N	NO ₃ ⁻ -N	COD _{Mn}	Fe ³⁺	Cu ²⁺
PR	0.093	0.169	0.029	-0.262	0.372*	0.003	0.026	0.079	-0.175	-0.024	-0.036	-0.165
OM	-0.008	0.097	0.196	-0.269	0.019	0.198	-0.096	-0.022	-0.042	0.185	0.171	-0.224
GC	-0.104	0.150	-0.315*	-0.299*	0.377*	0.263	0.166	0.217	-0.051	0.000	-0.140	-0.009
FC	-0.263	-0.131	-0.201	-0.148	0.398**	0.355*	0.047	0.305*	-0.015	0.100	-0.149	0.001
SC	0.189	0.090	-0.229	-0.060	0.084	-0.055	0.095	0.223	0.381**	-0.263	-0.122	0.035
SH	0.151	0.073	-0.185	0.138	-0.007	-0.224	0.037	-0.151	0.069	-0.133	-0.272	0.015

Water transparency (SD), depth (D), electrical conductivity (EC), dissolved oxygen (DO), pH, water temperature (T), total nitrogen (TN), total phosphorus (TP), ammonium nitrogen (NH₄⁺-N), nitrate nitrogen (NO₃⁻-N), chemical oxygen demand (COD_{Mn}) and dissolved iron (Fe³⁺) and dissolved copper (Cu²⁺), predators (PR), omnivores (OM), gatherers/collectors (GC), filterers/collectors (FC), scrapers (SC) and shredders (SH). *p<0.05, **p<0.01

There are many factors affecting the community structure, density, biomass and biodiversity of benthos (Shen et al., 2015; Rodrigues et al., 2019; Oremo et al., 2019; Ruaro et al., 2019; Santonja et al., 2020; Taylor et al., 2020). The summary of Monte Carlo test showed that the first canonical axis and all canonical axes were significant ($F=5.059$, $p=0.002$; $F=1.260$, $p=0.002$; 499 random permutations). The eigenvalues of the four axes were 0.140, 0.095, 0.055, 0.032, respectively (Table 7). The species-environment correlations for Axis 1 and Axis 2 were 0.674 and 0.753, respectively. The first two axes account for 23.6% of FFGs data relation (axis 1: 14.0%, axis 2: 9.6%) and 68.2% of FFGs-environment data (axis 1: 40.6%, axis 2: 27.6%). The Axis1 was mainly positively correlated with T, NH₄⁺-N and TN, and negatively correlated with pH, SD and D. TN content reflects the nutritional status of water body. A large number of studies showing that the input of nutrients leads to a higher TN, and the nutritional status of water body is closely related to the secondary productivity of benthos (Heino, 2005; Benke, 2010; Dolbeth et al., 2012; Hughes et al., 2012). The Axis 2 was positively correlated with T and NH₄⁺-N, and negatively correlated with Fe³⁺, DO and COD_{Mn}. Groups FC was mainly influenced by T and NH₄⁺-N, and group GC was influenced by EC. While group PR was mainly influenced by TN, and OM was influenced by COD_{Mn}. The main environmental factors were T, NH₄⁺-N, Fe³⁺, DO and COD_{Mn} in Tuanjie Reservoir (Fig. 6).

Table 7. RDA results of macroinvertebrate FFGs abundance in May (spring), July (summer) and September (autumn) in 2015

Axes	1	2	3	4
Eigenvalues	0.140	0.095	0.055	0.032
Species-environment correlations	0.674	0.753	0.716	0.366
Cumulative percentage variance of species data	14.0	23.6	29.0	32.2
of species-environment relation	40.6	68.2	84.0	93.2

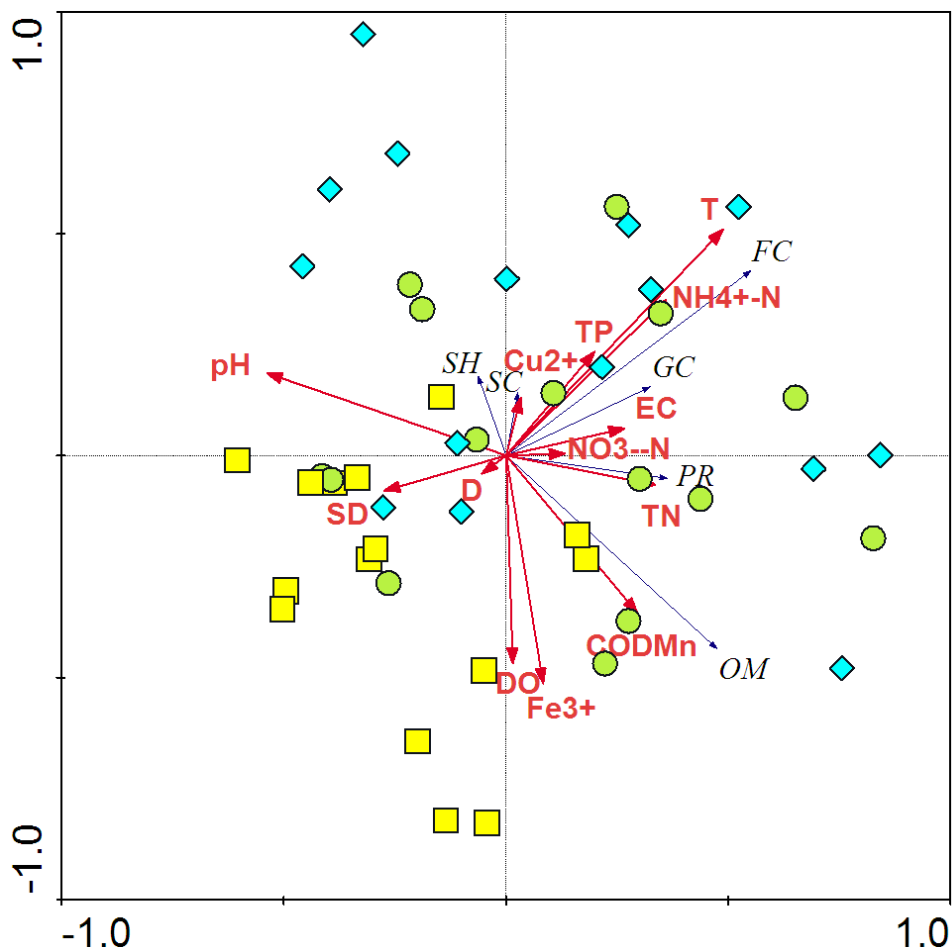


Figure 6. RDA biplot of macroinvertebrate FFGs and environmental factors. Green circle: Spring; Blue diamond: Summer; Yellow square: Autumn. Water transparency (SD), depth (D), electrical conductivity (EC), dissolved oxygen (DO), pH, water temperature (T), total nitrogen (TN), total phosphorus (TP), ammonium nitrogen ($\text{NH}_4^+\text{-N}$), nitrate nitrogen ($\text{NO}_3^-\text{-N}$), chemical oxygen demand (COD_{Mn}) and dissolved iron (Fe^{3+}) and dissolved copper (Cu^{2+}), predators (PR), omnivores (OM), gatherers/collectors (GC), filterers/collectors (FC), scrapers (SC) and shredders (SH)

Conclusion

During the study period, we totally collected 904 individuals and identified 11 orders, 23 family and 55 genera or species of macroinvertebrate belong to six FFGs (PR, OM, GC, FC, SC and SH) from study area. The mean values of SD, DO, pH, T, TP, COD_{Mn} and Cu^{2+} were extremely significant difference among sampling sites ($P < 0.01$). The main environmental factors were T, $\text{NH}_4^+\text{-N}$, Fe^{3+} , DO and COD_{Mn} in Tuanjie Reservoir. Our findings can provide strong recommendations for scientific basis for the biological resources protection and water quality operation and management of Tuanjie reservoir for future.

Acknowledgements. We sincerely acknowledge the National Key Research and Development Program of China (2016YFC0500406).

REFERENCES

- [1] An, R., Wang, F. Y., Yu, H. X., Ma, C. X. (2016): Characteristics and physical factors of phytoplankton functional groups in Small Xingkai Lake. – Res. Environ. Sci. 29(7): 985-994. (in Chinese with English abstract).
- [2] An, R., Wang, F. Y., Yu, H. X., Ma, C. X. (2017): Seasonal dynamics of zooplankton functional groups and their relationships with environmental factors in the sanhuanpao wetland reserve. – Acta Ecologica Sinica 37(6): 1851-1860. (in Chinese with English abstract).
- [3] Barquín, J., Death, R. G. (2006): Spatial patterns of macroinvertebrate diversity in new zealand springbrooks and rhithral streams. – J. of the Nor. Ameri. Benth. Soci. 25(4): 768-786.
- [4] Batzer, D. P., Palik, B. J., Buech, R. (2004): Relationships between environmental characteristics and macroinvertebrate communities in seasonal woodland ponds of minnesota. – J. of the Nor. Ameri. Benth. Soci. 23(1): 50-68.
- [5] Benke, A. C. (1998): Production dynamics of riverine chironomids: Extremely high biomass turnover rates of primary consumers. – Ecology 79(3): 899-910.
- [6] Benke, A. C. (2010): Secondary production as part of bioenergetic theory-contributions from freshwater benthic science. – River Res. Appl. 26: 36-44.
- [7] Bonada, N., Rieradevall, M., Prat, N. (2007): Macroinvertebrate community structure and biological traits related to flow permanence in a mediterranean river network. – Hydrobiologia 589: 91-106.
- [8] Buss, D. F., Baptista, D. F., Silveira, M. P., Nessimian, J. L., Dorvillé, L. F. M. (2002): Influence of water chemistry and environmental degradation on macroinvertebrate assemblages in a river basin in south-east Brazil. – Hydrobiologia 481: 125-136.
- [9] Chaloner, D., Wipfli, M. S., Caouette, J. P. (2002): Mass loss and macroinvertebrate colonization of pacific salmon carcasses in south-eastern Alaska streams. – Fresh. Bio. 47(2): 263-273.
- [10] Chen, J. X., Sun, X., Chai, Q. Y., Yu, H. X., Chai, F. Y., Yu, T., Chen, J. G. (2019): Phytoplankton community structure and water quality assessment in Tuanjie Reservoir. – J. Northeast Fore. Univ. 47(03): 85-88. (in Chinese with English abstract).
- [11] Chi, S. Y., Peng, J. H., Wan, C. Y., Zou, X., Li, M. (2009): Preliminary study on macrozoobenthos of Sandaohe Reservoir, Hubei Province. – J. Lake Sci. 21(5): 705-712. (in Chinese with English abstract).
- [12] Cortes, R. M. V., Ferreira, M. T., Oliveira, S. V., Oliveira, D. (2010): Macroinvertebrate community structure in a regulated river segment with different flow conditions. – River Res. App. 18(4): 367-382.
- [13] Cummins, K. W. (1974): Structure and function of stream ecosystems. – Bio Science 24: 631-641.
- [14] Dolbeth, M., Cusson, M., Sousa, R. (2012): Secondary production as a tool for better understanding of aquatic ecosystems. – Canad. J. of Fish. Aqu. Sci. 69: 1230-1253.
- [15] Duan, X. H., Wang, Z. Y., Xu, M. Z. (2010): Benthic macroinvertebrate and application in the assessment of stream ecology. – Tsinghua University Press, Beijing. (in Chinese).
- [16] Duran, M. (2006): Monitoring water quality using benthic macroinvertebrates and physiochemical parameters of Behzat stream in Turkey. – Pol. J. Environ. Stud. 15(5): 709-717.
- [17] Epler, J. H. (2001): Identification manual for the larval Chironomidae (Diptera) of North and South Carolina. – FEBS Letters 81(2).
- [18] Gong, Z. J., Liu, J. S., Li, Y., Cai, Y. J., Xue, Q. J., Xu, H. (2017): Potential excretion of $\text{NH}_4^+\text{-N}$ and $\text{PO}_4^{3-}\text{-P}$ by *Limnodrilus hoffmeisteri* Claparède in Lake Taihu. – J. Lake Sci. 29(2): 389-397. (in Chinese with English abstract).
- [19] Han, B. P. (2010): Reservoir ecology and limnology in China: A retrospective comment. – J. Lake Sci. 22(2): 151-160. (in Chinese with English abstract).

- [20] Han, B. P., Shi, Q. C., Chen, W. X. (2016): China's Ecology and Water Quality Management of Reservoir. – Beijing: Science Press. (in Chinese).
- [21] Heino, J. (2005): Functional biodiversity of macroinvertebrate assemblages along major ecological gradients of boreal headwater streams. – *Fresh. Bio.* 50(9): 1578-1587.
- [22] Hu, T., Wei, K. J., Zhang, G. R., Xu, L., Ma, X. F., Zhao, J. W., Liu, C., Wu, X. H. (2018): Macroinvertebrate communities and bioassessment of water quality in Miyun Reservoir, Beijing. – *J. Hydroecol.* 39(4): 79-88. (in Chinese with English abstract).
- [23] Hughes, R., Herlihy, A., Gerth, W., Pan, Y. D. (2012): Estimating vertebrate, benthic macroinvertebrate, and diatom taxa richness in raftable pacific northwest rivers for bioassessment purposes. – *Envir. Moni. Assess.* 184(5): 3185-3198.
- [24] Ji, L., Song, C., Cao, X., Zhou, Y., Deng, D. (2015): Spatial variation in nutrient excretion by macrozoobenthos in a Chinese large shallow lake (Lake Taihu). – *J. Freshw. Ecol.* 30(1): 169-180.
- [25] Jin, H., Gu, J., Cai, Y. J., He, H., Ning, X. Y., Shen, R. J., Yang, G. J., Li, K. Y. (2017): Inhibiting effect of benthic algae on the bioturbation of *Limnodrilus hoffmeisteri*. – *Acta Sci. Circum.* 37(6): 2055-2060. (in Chinese with English abstract).
- [26] Lee, G. F. (1970): Factors affecting the transfer of materials between water and sediments. – University of Wisconsin, Water Resources Center, Eutrophication Information Program.
- [27] Li, J., Herlihy, A., Gerth, W., Kaufmann, P., Gregory, S., Urquhart, S., Larsen, D. P. (2001): Variability in stream macroinvertebrate at multiple spatial scales. – *Fresh. Bio.* 46(1): 87-97.
- [28] Li, B., Zhang, M., Cai, Q. H. (2018): Spatial distribution of macrobenthic secondary production of Danjiangkou Reservoir. – *Asi. J. of Ecot.* 13(4): 22-29. (in Chinese with English abstract).
- [29] Li, Y. G., Hu, Q. J., Qu, J. Q., Zong, H. M., Wang, J., Zhang, Q. J. (2018): Community structure and spatial-temporal variation of zoobenthos in Miyun Reservoir, Beijing. – *J. Hydroecol.* 39(5): 32-38. (in Chinese with English abstract).
- [30] Liu, Q. G., Zha, Y. T., Chen, L. Q., Gu, Z. M., Jia, Y. Y., Hu, Z. J. (2012): Macrozoobenthos community structure and its indicative significance in water quality bio-assessment of Fenshuijiang Reservoir, Zhejiang Province of East China. – *Chin. J. Appl. Ecol.* 23(5): 1377-1384. (in Chinese with English abstract).
- [31] Liu, M. H., Meng, Y., Cao, J. J., Cui, X. B., Al, M. N. (2019): Functional traits of macroinvertebrates in Naolihe Wetland. – *J. Northeast Fore. Univ.* 47(01): 76-82. (in Chinese with English abstract).
- [32] Mangadze, T., Bere, T., Mwedzi, T. (2016): Choice of biota in stream assessment and monitoring programs in tropical streams: a comparison of diatoms, macroinvertebrates and fish. – *Ecol. Ind.* 63(4): 128-143.
- [33] MEP. (2002): China national environmental quality standards for surface water. – GB3838-2002 (in Chinese).
- [34] Morse, J. C., Yang, L. F., Tian, L. X. (1994): Aquatic insects of China useful for monitoring water quality. – Nanjing: Hohai University Press.
- [35] Oremo, J., Orata, F., Owino, J., Shivoga, W. (2019): Assessment of heavy metals in benthic macroinvertebrates, water and sediments in River Isiukhu, Kenya. – *Envir. Moni. Asse.* 191(11): 646-658.
- [36] Petridis, D., Sinis, A. (1993): Benthic macrofauna of Tavropos Reservoir (central Greece). – *Hydrobiologia* 262(1): 1-12.
- [37] Pires, A. M., Cowx, I. G., Coelho, M. M. (2000): Benthic macroinvertebrate communities of intermittent streams in the middle reaches of the guadiana basin (portugal). – *Hydrobiologia* 435(1): 167-175.
- [38] Plafkin, J. L., Barbour, M. T., Porter, K. D. (1989): Rapid bioassessment protocols for use in streams and rivers: benthic macroinvertebrates and fish. – Washington DC: US Environmental Protection Agency.

- [39] Poff, N. L., Olden, J. D., Vieira, N. K. M., Finn, D. S., Simmons, M. P., Kondratieff, B. C. (2006): Functional trait niches of North American lotic insects: traits-based ecological applications in light of phylogenetic relationships. – *The North Amer. Benth. Soci.* 25(4): 730-755.
- [40] Richards, C., Haro, R., Johnson, L., Host, G. (2003): Catchment and reach-scale properties as indicators of macroinvertebrate species traits. – *Fresh. Bio.* 37(1): 219-230.
- [41] Rodrigues, C., Guimaraes, L., Vieira, N. (2019): Combining biomarker and community approaches using benthic macroinvertebrates can improve the assessment of the ecological status of rivers. – *Hydrobiologia* 839: 1-24.
- [42] Rosser, Z. C., Pearson, R. G. (2018): Hydrology, hydraulics and scale influence macroinvertebrate responses to disturbance in tropical streams. – *J. Fresh. Ecol.* 33(1): 1-17.
- [43] Ruaro, R., Gubiani, É. A., Cunico, A. M., Higuti, J., Moretto, Y., Piana, P. A. (2019): Unified multimetric index for the evaluation of the biological condition of streams in southern Brazil based on fish and macroinvertebrate assemblages. – *Envir. Manag.* 64(5): 661-673.
- [44] Santonja, M., Rodríguez-Pérez, H., Le Bris, N., Piscart, C. (2020): Leaf nutrients and macroinvertebrates control litter mixing effects on decomposition in temperate streams. – *Ecosystems* 23: 400-416.
- [45] Shabani, I. E., Liu, M. H., Yu, H. X., Muhigwa, J., Geng, F. F. (2019): Benthic macroinvertebrate diversity and functional feeding groups in relation to physicochemical factors in Sanjiang plain wetlands, northeast China. – *Appl. Ecol. Environ. Res.* 17(2): 3387-3402.
- [46] Shen, H. Y., Cao, Z. H., Liu, J. W., Wang, W. H., Zhang, Y. (2015): Relationship between functional feeding groups of macroinvertebrates and environmental factors in Taizi River basin. – *China Envir. Sci.* 35(2): 579-590. (in Chinese with English abstract).
- [47] Sponseller, R. A., Benfield, E. F., Valett, H. M. (2001): Relationships between land use, spatial scale and stream macroinvertebrate communities. – *Fresh Bio.* 46(10): 1409-1424.
- [48] Sun, X., Chai, F. Y., Mwagona, P. C., Shabani, I. E., Hou, W. J., Li, X. Y., Yu, H. X. (2019): Seasonal variations of zooplankton functional groups and relationship with environmental factors in a eutrophic reservoir from cold region. – *Appl. Ecol. Environ. Res.* 17(4): 7727-7740.
- [49] Taylor, M. D., Fowler, A. M., Suthers, I. (2020): Insights into fish auditory structure–function relationships from morphological and behavioural ontogeny in a maturing sciaenid. – *Mari. Biol.* 167(2): 163-176.
- [50] Wang, H. B., Huang, X. L., Wu, J. S., Du, X., Wang, Q. S., Song, D., Huo, T. B. (2019): Effect of agricultural non-point source pollution on plankton and zoobenthos communities in a reservoir in Morin Dawa Daur Autonomous Banner. – *Chin. J. Fish.* 32(4): 55-62. (in Chinese with English abstract).
- [51] Wildung, R. E., Schmidt, R. L. (1993): Phosphorus release from lake sediments. – USA Environmental Protection Agency, Office of Research and Monitoring.
- [52] Zhang, M., Cai, Q. H., Xu, Y. H. (2012): Zonation and its influencing factors of a large subtropical reservoir (Danjiangkou Reservoir in central China), based on macroinvertebrates. – *Fres. Envir. Bull.* 22(6): 2095-2104.

SPATIOTEMPORAL DISTRIBUTION CHARACTERISTICS OF SOIL EROSION IN THE LOWER REACHES OF THE CHISHUI RIVER BASIN, CHINA

WANG, X.¹ – LI, S. D.^{1*} – LIU, H. H.¹ – LIU, Y. Y.^{1,2}

¹*College of Earth Sciences, Chengdu University of Technology, Chengdu 610059, China*

²*Earth and Environmental Department, University of West Florida, Pensacola 32514, USA*

**Corresponding author
e-mail: 2793213288@qq.com*

(Received 12th Dec 2019; accepted 6th May 2020)

Abstract. Soil erosion leads to a decrease in land productivity, and a series of ecological and environmental security problems. China is one of the most susceptible country to severe soil erosion in the world. The spatial-temporal differentiation of soil erosion is the precondition to understand the regional soil erosion, which reflects the spatial and temporal variation of soil erosion. This paper took the lower reaches of the Chishui River Basin as the research area and the 2000-2015 period as the time interval of the study. The article considers the impact factors in the revised General Soil Loss Equation (RUSLE), and comprehensively evaluates the spatial distribution of soil erosion sensitivity. According to national standards, the soil erosion in the basin can be divided into six grades. At the same time, the GIS software platform was used to analyze the changing trend of water and soil loss in the basin during the 15 years. The quantitative driving force analysis of soil and water loss in the study area was carried out by using a geo-detector. Soil erodibility factor is the main driving force for soil erosion.

Keywords: *RUSLE, change slope method, GIS, soil erosion, geo-detector*

Introduction

Soil erosion can destroy land resources (Ochoa et al., 2016), reduce land productivity (Rodrigo-Comino et al., 2016), increase riverbed (Gogichaishvili et al., 2014), silt rivers (Abidin et al., 2017), exacerbate floods (Osouli and Bahri, 2018) and droughts (Kosmowski, 2018). Soil erosion is posing an increasing threat to soil structure (Kosmas et al., 2000), sustainable agricultural development (Montgomery, 2007), Water quality (Khaledian et al., 2017) and the global environment (Cerdà et al., 2018). This became one of the most serious problems all over the world. China is one of the countries with the most serious soil erosion in the world. The area of soil erosion is as high as 3.56×10^6 km², accounting for 37% of the total land area. The annual loss of topsoil is more than 5 billion tons. The soil nutrient loss is equivalent to the annual fertilizer production in China (Sheng and Shi, 2001). Among them, the area of hydraulic erosion is 1.65×10^6 km², and the area of wind erosion is 1.91×10^6 km². Soil erosion is the greatest in Sichuan Province in China. The areas of water erosion and wind erosions are 11.442×10^4 km² and 0.6622×10^4 km², respectively (Wang and Wang, 2011).

Soil erosion is affected and restricted by many factors (Borrelli et al., 2017), some are natural factors such as climate, topography, soil, vegetation, etc., and the other part is human activity factors, such as land use, soil and water conservation measures, etc. Under the combined effect of both natural factors and human activities, soil erosion presents regional differentiation in spatial distribution, and agricultural soil erosion can

disrupt the global carbon cycle and affect sustainable development (Montgomery, 2007). Recently, soil erosion assessment has been included in the United Nations Environment Programme (UNEP) report on the sustainable potential of land resources (Panagos and Katsoyiannis, 2019). Therefore, it is important to study the regional differentiation characteristics of soil erosion to guide the prevention and control of regional soil erosion. In recent years, GIS and remote sensing technologies have developed rapidly, which provides strong technical support for relevant research on the ecological environment (Pham et al., 2018). The USLE (Universal Soil Loss Equation) has been officially promoted in the US Department of Agriculture Agricultural Handbook No. 282 in 1965. This model is usually used in loss research of the watersheds within the basin (Wischmeier, 1965) and under different evaluation units (Singh and Panda, 2017). GIS software is used to predict soil erosion (Abdulkareem et al., 2019), grade according to soil erosion intensity (Bera, 2017), and take effective control measures for key erosion areas (Uri, 2001; Fenta et al., 2016). Since the USLE model is an empirical model, it has been proved that it is not suitable for ridge cropping, contour farming, and strip-type farming measures for sediment deposition. Soil erosion research experts decided to use the latest research and computer technology (Mondal et al., 2018) to re-improve the USLE in different directions (Preetha and Al-Hamdan, 2019), the most widely used of which is RUSLE (The Revised Universal Soil Loss Equation) (Wijesundara et al., 2018; Mahala, 2018). Based on the GIS platform (Cunha et al., 2017), the RUSLE and SWAT models (Lakkad et al., 2018), SCS-CN method (Kayet et al., 2018), SEDD model (Fu et al., 2006) and other models are combined to effectively simulate the soil erosion process.

The Chishui River Basin is developed in southwestern China and it is a large tributary on the southern bank of the upper reaches of the Yangtze River. The Chishui River Basin is located in the transitional zone between the Yunnan-Guizhou Plateau and the Sichuan Basin. It is an important ecological barrier in the upper reaches of the Yangtze River and plays an important role in the ecological security construction of Sichuan Province (Wang et al., 2007). At the same time, the surface of the basin is undulating, with relatively large differences in height and complex geological structures. It is an ecologically sensitive and vulnerable area with an important ecological function. Besides, due to the long-term unreasonable development and utilization of hydropower, forestry, minerals, agriculture and animal husbandry, and other resources it has not only failed to fully exert its ecological barrier function but instead, it has become a prominent area for soil erosion problems, which has threatened the safety of Sichuan Province and the entire Yangtze River Basin. It is of great strategic significance to protect and construct the ecological environment of the basin. The quantitative evaluation of the trend of soil erosion before and after the implementation of the ecological engineering of the basin is aimed at grasping the impact of environmental engineering on soil erosion improvement, to provide a scientific basis for further planning and implementation of ecological engineering in the basin. The main objectives of this study are as follows: (1) The slope method based on the ecological environment vulnerability is combined with the RUSLE model for dynamic monitoring of long-term sequences; (2) Based on the regression status of soil erosion, the trend is predicted; (3) Geographic detector model is widely used in natural and social sciences. This paper uses it to explore the relative importance and interaction between the driving forces of factors affecting soil erosion in the long time series of the study area; (4) Accurate assessment of the temporal and spatial distribution of soil

erosion will contribute to the sustainable use of land resources. According to the research results, suggestions for prevention and treatment of future soil erosion in the Chishui River Basin are proposed.

Materials and methods

Study area

The study area is located between 105°08' E-106°28' E to 27°39' N-29°01' N, covers an area of 9796.13 km² (Fig. 1). It is located in the transitional zone between the southern margin of the Sichuan Basin and the Yunnan-Guizhou Plateau. The terrain is higher in the north and lowers in the south. The northern part of the area involves mostly valleys, low-lying hills and flat dams, which is a land flowing with tea, bamboo shoots and litchi. The southern part of study area is connected to the Yunnan-Guizhou Plateau and belongs to the northern foot of Ta-lou Mountains. The landform of this place is low mountain cut deeply by the river. The geological structure of the study area is complex, and the strata are dominated by various sedimentary rocks, so the mineral resources are rich and diverse. There are more than 20 proven minerals, such as coal, oil, natural gas, pyrite, iron, copper, gold, refractory clay, solvent dolomite, limestone for cement, kaolin, phosphorus, sand for glass, gypsum, marble, calcite, etc. (Cai et al., 2015). The climate type is humid subtropical climate, which shows its typical characteristics in Southern mountainous region. The average annual temperature is about 18.0 °C, the average temperature in the coldest month (January) is about 7 °C, the average temperature in the hottest month (July) is about 27 °C, the extreme maximum temperature can reach 40 °C, and the extreme minimum temperature is about minus 1 °C (Chen and Tong, 2012). However, due to the topography of the Sichuan basin, The Chishui River Basin is rich in rainfall, with annual rainfall of about 1000 mm, mainly concentrated in May-September, accounting for more than 75% of the total annual rainfall. The frost-free period in this area is longer than 300 days, so it is suitable for long growing periods of crops.

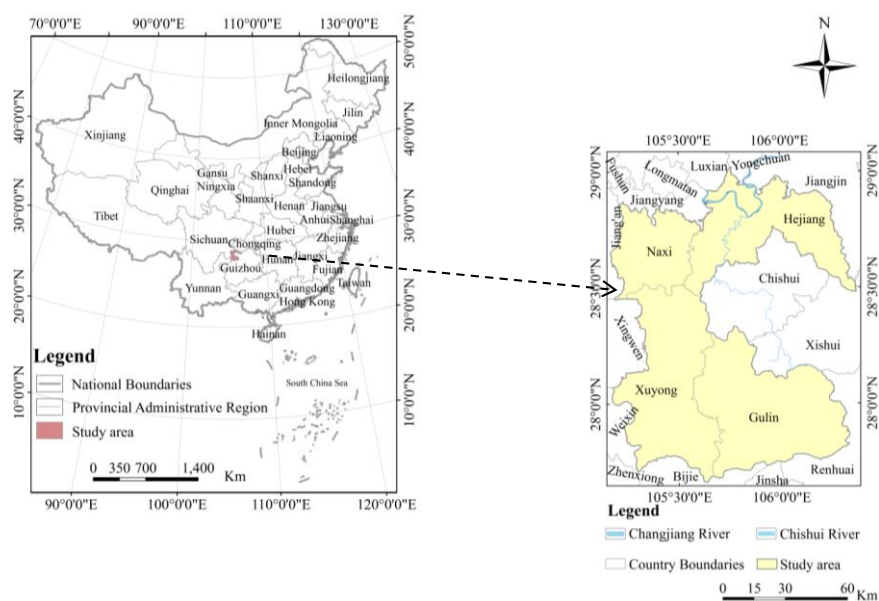


Figure 1. Location of the study area

Materials

Topographic factor (LS) (Alexakis et al., 2013). The terrain is one of the most basic elements of natural geography. It is also one of the important factors determining the intensity and type of soil erosion. Topographic factors such as slope direction, slope (Hickey et al., 1994), slope length (Kayet et al., 2018), and undulation degree directly affect the occurrence of soil erosion. Slope factor and slope length factor are important topographic factors that lead to soil erosion. It is difficult to cause a lot of soil erosion in areas with slow slopes, and it is more likely to occur in areas with steep slopes. For example, the soil erosion in the southwestern mountainous areas of China is serious, while the intensity of soil erosion is relatively low in some basins and plains. The slope factor quantitatively reflects the relationship between the slope and the amount of soil loss (Liu et al., 2000). The slope length refers to the projected length of the distance from a point along the direction of water flow to the end point under the action of gravity on the horizontal plane. Slope length factor is one of the important landforms that affects runoff from slopes, and it quantitatively reflects the relationship between slope length and soil loss. The LS factor is extracted from the 30 m spatial resolution digital elevation model (DEM) data provided by geospatial data cloud (<http://www.gscloud.cn>). Equation 1 is the slope formula:

$$S = \begin{cases} 10.8 \times \sin\theta + 0.036 & \theta < 5^\circ \\ 16.8 \times \sin\theta - 0.5 & 5^\circ \leq \theta < 10^\circ \\ 21.9 \times \sin\theta - 0.96 & \theta > 10^\circ \end{cases} \quad (\text{Eq.1})$$

Since the S in the formula is radian, so it is necessary to turn the angle unit into radian according to Equation 2:

$$L = (\lambda / 22.13)^m \quad (\text{Eq.2})$$

where λ is slope length, and m is slope length factor, the range of the value of m is shown as Equation 3:

$$m = \begin{cases} 0.2 & \theta < 1^\circ \\ 0.3 & 1^\circ < \theta \leq 3^\circ \\ 0.4 & 3^\circ < \theta \leq 5^\circ \\ 0.5 & \theta > 5^\circ \end{cases} \quad (\text{Eq.3})$$

Using the analysis function of ArcGIS 10.2 software, the distribution of L factor and S factor in the study area were obtained (Fig. 2).

Rainfall erosivity factor (R) (Schmid, 2012). Rainfall is a factor affecting soil erosion. During rainfall, the kinetic energy of the raindrops splashing on the soil particles, cause runoff and soil erosion. The value of rainfall erosivity factor is related to rainfall dynamics and intensity. Rainfall erosivity is a function of rain pattern, raindrop kinetic energy, rainfall, and rainfall intensity. It is the potential for soil erosion caused by precipitation (Efthimiou, 2018). By comparing the method of calculating rainfall erosivity by domestic and foreign scholars, we chose the most suitable formula for the

study area (Wu et al., 2001). Monthly and annual rainfall data from 2000-2015 meteorological stations in the study area were derived from the China Meteorological Data Network (<http://data.cma.cn/>). The annual rainfall erosivity of 4 periods was calculated using Equation 4, and the spatial interpolation (kriging interpolation method) was used to calculate the annual rainfall erosivity data. The annual rainfall erosivity map of the study area (Fig. 3) was obtained.

$$R = \left(\sum_{i=1}^{12} - 2.6389 + 0.3046P_i \right) \times 17.2 \quad (\text{Eq.4})$$

where P_i represents the average monthly rainfall over many years (mm).

Soil erodibility factor (K). Soil erosion is mainly affected by various physical and chemical characteristics of the soil itself, such as permeability, texture, structure, stability of aggregates, organic matter content, compactness, particle composition, properties of clay minerals, soil thickness and chemical composition. It is an indispensable parameter in the soil erosion model (RUSLE) (Torri et al., 1997). Soil erosion is the separation and transport of soil particles (Buttafuoco et al., 2012) caused by the combined action of hydraulic and wind forces (Rammahi and Khassaf, 2018). Data of 1:100 soil types in the watershed study area, including physical and chemical data from various soil types, are derived from China soil database. This paper selects the EPIC Equation 5 to calculate soil erodibility factors in the study area:

$$K_{EPIC} = \left\{ \begin{array}{l} 0.2 + 0.3 \exp\left[0.256SAN\left(1 - \frac{SIL}{100}\right)\right] \times \left(\frac{SIL}{CAL + SIL}\right)^{0.3} \\ \times \left[1 - \frac{0.25C}{C + \exp(3.72 - 2.95C)}\right] \times \left[1 - \frac{0.75SN1}{SN1 + \exp(-5.51 + 22.9SN1)}\right] \end{array} \right\} \quad (\text{Eq.5})$$

Among them, Equation 6 is used to calculate SN1:

$$SN1 = \frac{SAN}{100} \quad (\text{Eq.6})$$

where SAN represents gravel (0.05-2.0 mm) content (%); SIL (0.002-0.05 mm) is the content of powder (%); CLA (< 0.002 mm) is the clay content (%) in the soil; C is the percent organic matter. We perform a small operation on the K value obtained after the calculation and convert the U.S. unit into an international unit: $K \text{ (U.S. unit)} \times 0.1317 = K \text{ (international unit)}$. Since the soil properties in China are quite different from those in the United States, the revised EPIC Equation 7 is used to estimate the K value of soil erodibility in the study area:

$$K = -0.1383 + 0.051575K_{EPIC} \quad (\text{Eq.7})$$

where K is the corrected soil erodibility value and K_{EPIC} is the soil erodibility value estimated using the EPIC formula.

Soil erodibility also reflects the sensitivity of the soil itself to erosion by external forces. Under the same conditions, the greater the soil erodibility, the more easily the soil is eroded, and the less soil erodibility is, the less likely the soil is to be eroded. Through

the above formula, the K value of each soil type in the lower reaches of the Chishui River is calculated (Fig. 4). From the figure, we can see that the overall soil erodibility K value sensitivity is low, and the average sensitivity to the erosion process is low. Because of the good stability of soil particle size, there are no major changes in the period of the study. Therefore, only one stage data is needed for a comprehensive study.

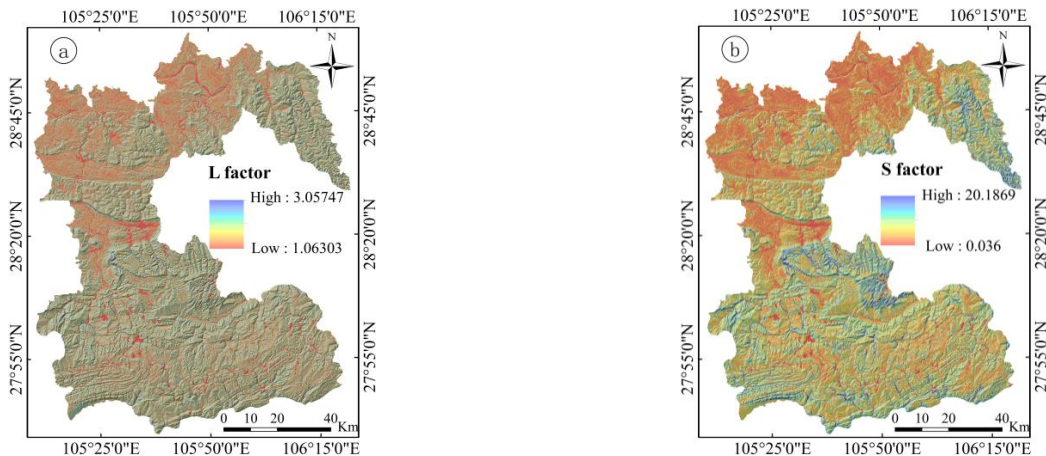


Figure 2. L, S factor in the study area

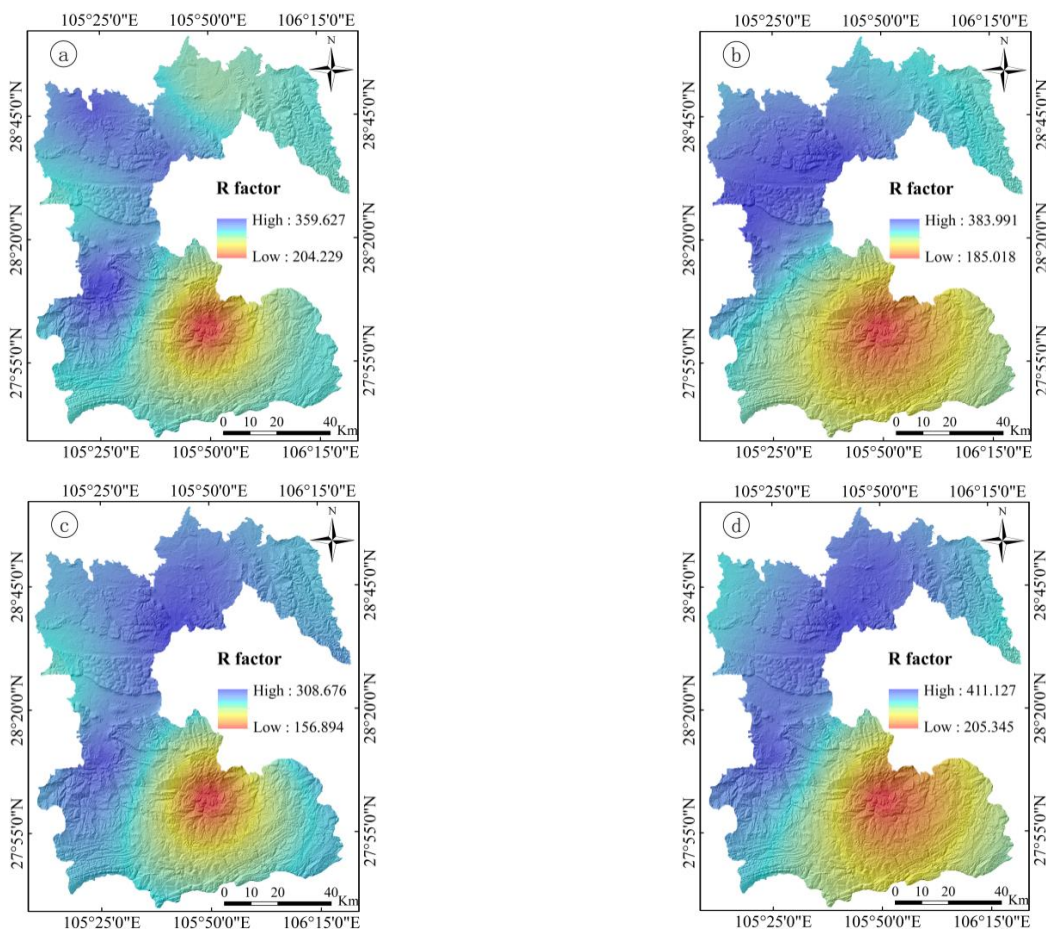


Figure 3. L, S factor in the study area. Spatial distribution of rainfall erosivity in 2000 (a), 2005 (b), 2010 (c), 2015 (d)

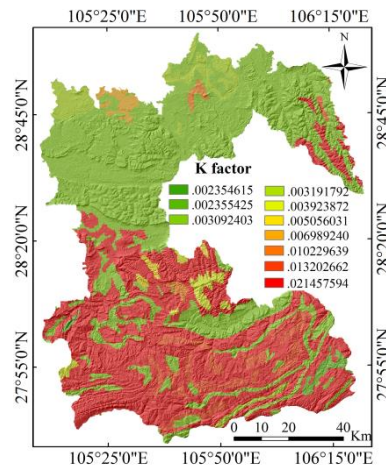


Figure 4. Spatial distribution of soil erosivity factor in the study area

Vegetation cover management factor (C). Vegetation coverage and management factors refer to the comprehensive effect of soil erosion on the change of vegetation coverage in natural conditions. We use the vegetation index conversion method to analyze the vegetation types and distribution characteristics in each pixel to establish the conversion relationship between the vegetation index and the vegetation coverage to obtain the vegetation coverage. At present, this method is relatively mature, and its advantage is that it is easy to operate and implement remote sensing monitoring of vegetation coverage on a regional scale. The MODIS data was obtained from the geospatial data cloud (<http://www.gscloud.cn>), and the data was processed by MVC maximum value synthesis. Finally, pixel bisection was used to extract NDVI data. Using *Equation 8* established (Cai, 2000) to calculate the C value of the study area:

$$C = \begin{cases} 1 & c = 0 \\ 0.6508 - 0.3634 \lg c & 0 < c < 78.3\% \\ 0 & c \geq 78.3\% \end{cases} \quad (\text{Eq.8})$$

where *C* is the vegetation cover and management factor, *c* is the vegetation coverage. When the *c* value is greater than or equal to 78.3%, the *C* value is equal to 0, indicating that no soil erosion has occurred on the ground surface. When the *c* value is equal to 0, the *C* value is equal to 1, indicating that the surface soil erosion is severe. In the range of 0 to 1, as the *C* value increases, the surface soil erosion becomes more severe. Using the ArcGIS Raster Calculator, the Distribution of Vegetation Coverage and Management Factors from 2000 to 2015 (*Fig. 5*).

Soil and water conservation practice factor (P) (Karydas et al., 2009). It is a quantitative indicator used to reflect the degree of influence of soil and water conservation measures on soil erosion. Specifically, it refers to the ratio of the amount of soil and water loss after the implementation of soil and water conservation measures to the amount of soil and water loss without any soil and water conservation measures for a certain soil and water loss area under the same conditions. The value ranges from 0 to 1. When the *P* value is 0, no soil erosion occurs in the study area. When the *P* value is 1, it indicates that no soil and water conservation measures have

been taken in the study area, and soil erosion is serious. The existing method of determining the P-value was mainly obtained through experience (Vaezi et al., 2017). This article obtained the land use (Anache et al., 2018) data of 4 years' spatial resolution of 30 m from the resources and environmental science data center of the Chinese Academy of Sciences (<http://www.resdc.cn>) and looked up the information of the predecessors (Kavian et al., 2015). We have consulted previous data and assigned a value of 1 to land use types such as forest land, shrubs, grasslands, and unused land that could be considered as not having any soil and water conservation measures. And land use types such as water bodies, towns and construction land, which did not cause soil erosion in principle, were assigned a value of 0, 0.1 for water and land, and 0.35 for dry land. Form all of this, we could get the distribution of soil and water conservation measures factors as shown in *Figure 6*.

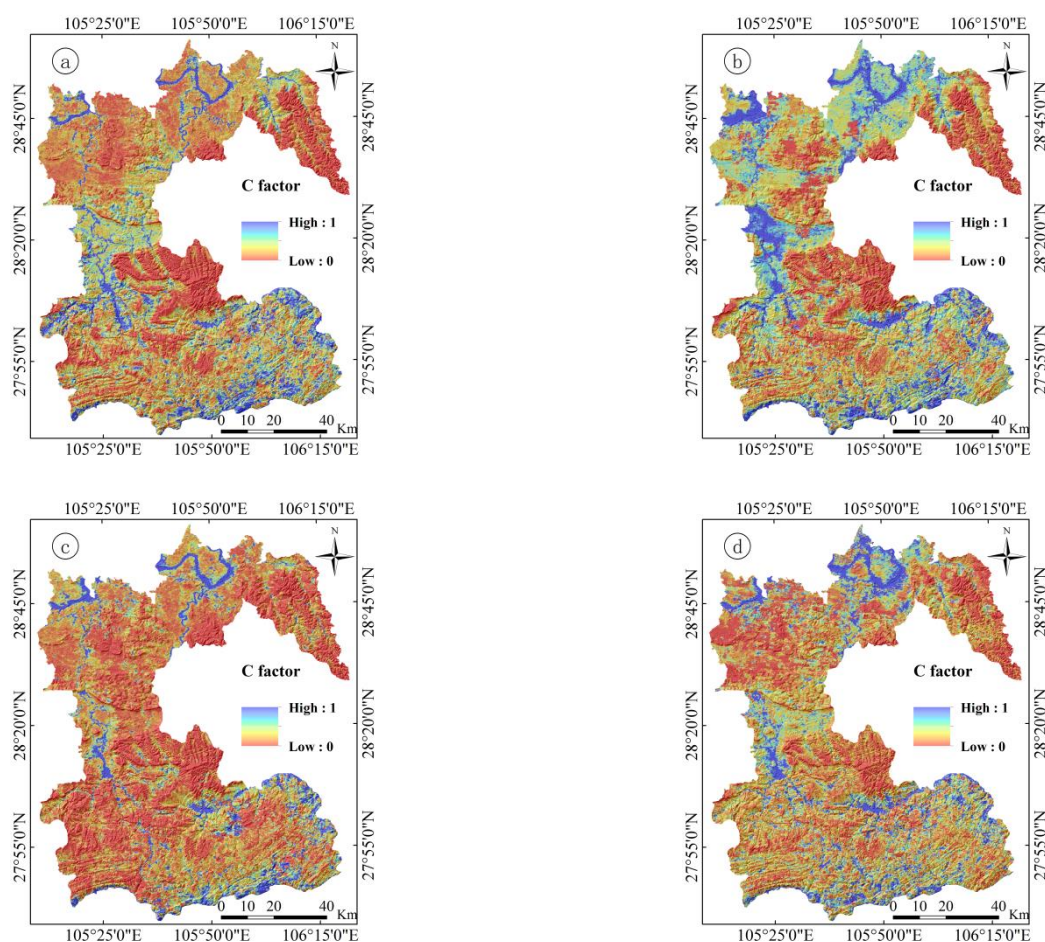


Figure 5. Spatial distribution of land cover and management factors in the study area in 2000 (a), 2005 (b), 2010 (c), 2015 (d)

Methods

RUSLE model

The concept of soil processes (Ostovari et al., 2017) was introduced base on the USLE equation (Leys et al., 2010). After correction, a more comprehensive soil erosion loss (RUSLE) *Equation 9* was obtained (Das et al., 2018).

$$A = R \times K \times L \times S \times C \times P \quad (\text{Eq.9})$$

where A is the annual soil erosion modulus ($t/(hm^2 \cdot a)$); R is the rainfall erosivity factor ($MJ \cdot mm/(hm^2 \cdot h \cdot a)$); K is soil erodibility factor ($t \cdot hm^2 \cdot h/(hm^2 \cdot MJ \cdot mm)$); L is slope length and slope factor; C is vegetation cover and management factor; P is soil and water conservation factor.

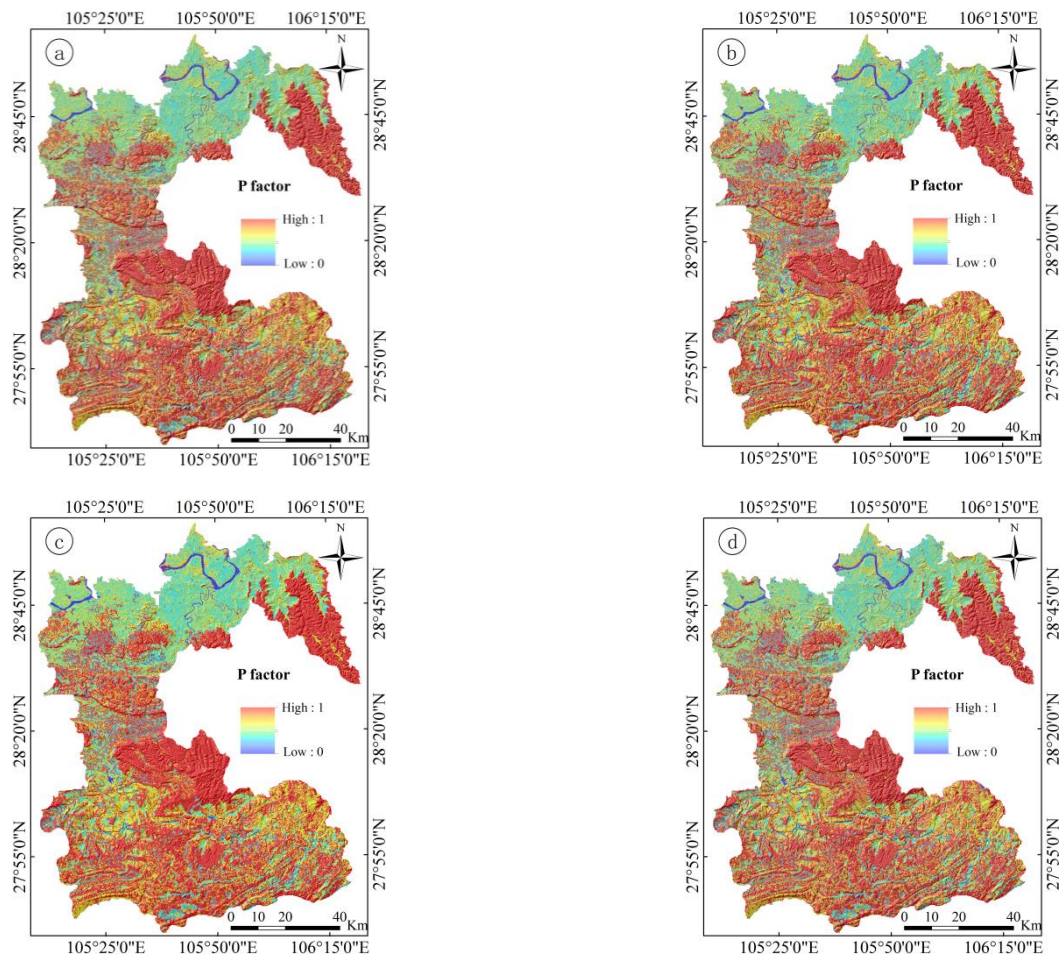


Figure 6. Spatial distribution of soil and water conservation in the study area from 2000 to 2015

Change slope method

The change slope method (Yang et al., 2018) is the regression analysis of a group of time-varying variables and predicts the trend of their change (Krellenberg and Welz, 2017). This method uses the least squares method to calculate the regression line between the annual soil erosion modulus sequence and time of all the pixels on the data set. The result is a slope image. It expresses the linearity of the annual soil erosion modulus represented by each pixel on the image. In China, it is widely used in ecological vulnerability research. This paper uses this method to simulate the inter-annual change of soil erosion, that is, to use the least-squares method to regression fit the annual soil erosion model values and time. Before the operation, the annual soil

erosion modulus is standardized between 0-1. It is convenient for the next comparison. Equation 10 of the variation slope method is shown as follows:

$$X = \frac{n \times \sum_{i=1}^n i \times A_i - \left(\sum_{i=1}^n A_i\right)}{n \times \sum_{i=1}^n i^2 - \left(\sum_{i=1}^n i^2\right)} \quad (\text{Eq.10})$$

where X is the change slope; n is the number of years Ai is the soil erosion modulus in a year i. The slope is positive, indicating that the soil erosion is increasing; the slope is negative, indicating that the soil erosion is decreasing. The significance test of the changing trend uses the F test (Eq. 11). The statistics are calculated as follows:

$$F = U \times \frac{n - 2}{Q} \quad (\text{Eq.11})$$

where $Q = \sum_{i=1}^n (y_i - \hat{y}_i)^2$ is the square root of error; $U = \sum_{i=1}^n (\hat{y}_i - \bar{y}_i)^2$ is regression square sum; y_i is the actual value of soil erosion modulus for the year I; \hat{y}_i is the regression value of soil erosion modulus in the year I; \bar{y}_i is the regression value of soil erosion modulus in the year i. According to the changing trend and significance level of soil erosion modulus A, the change trends were divided into three categories: significant increase ($X > 0, P < 0.05$), a significant decrease ($X < 0, P < 0.05$), and no significant change ($P \geq 0.05$).

Principles and applications of the geographical detector

The Geo-Detector is a new statistical method used by the Chinese Academy of Sciences (Wang and Xu, 2017), it investigates spatial differentiation and tries to explain potential drivers that affect its geographic phenomena. Compared with the traditional correlation analysis method, the geographic detector does not need too many assumptions, and avoids the defects of some methods in processing category traversal. It can be used to detect both numerical data and qualitative data. It can also effectively analyze the two quantitatively. The geographic detector does not need to consider the problem of collinearity of multiple variables, and it is more clear than the physical meaning of analysis of variance. It can also detect the real situation of the interaction of two variables, including non-linear enhancement, mutual independence, two-factor enhancement, and single-factor non-linear attenuation. The geography detector is mainly composed of four parts: “risk detector, factor detector, ecological detector, and interaction detector”. This paper uses the factor detector to detect and analyze the soil in the lower reaches of the Chishui River Basin from 2005 to 2015. Quantitative correlation was investigated between erosion and its driving factors.

Factor detector: detecting the efficiency of the evaluation index X that can explain the dependent variable Y, this can be quantified by index $Q_{D,H}$. The larger the value is,

the greater the contribution to soil erosion will be, and vice versa. The statistical model is shown in *Equation 12*:

$$Q_{D,H} = 1 - \frac{1}{n\sigma^2} \sum_{h=1}^L n_h^2 \sigma \quad (\text{Eq.12})$$

where D indicates the evaluation index, H indicates the amount of soil erosion, $Q_{D,H}$ indicates the explanatory power of the evaluation index factor on soil erosion, ranging from 0-1, n indicates the number of samples, L indicates the number of indicators, n_h indicates the h layer sample Quantity, n_h^2 represents the variance of the amount of soil erosion in the layer.

Results

Spatiotemporal analysis of soil erosion

In order to unify the investigation of soil and water loss and carry out soil and water conservation work, the Ministry of Water Resources of the People's Republic of China has formulated the classification of soil erosion applicable to the whole country. There are three types of soil erosion in the country: hydraulic erosion, wind erosion, and freeze-thaw erosion. The Chishui River Basin is located in the southern fringe of Sichuan Province and belongs to the southwestern earth and rock mountain area. It is dominated by hydraulic erosion. According to the "Classification Standard of Soil Erosion". We divided the soil erosion module in the lower reaches of the Chishui River Basin from 2000 to 2015 into six categories: micro, mild (500–2500 t/(km²·a)), moderate (2500–5000 t/(km²·a)), strong (5000–8000 t/(km²·a)), extremely strong (8000–15000 t/(km²·a)), and severe (> 15000 t/(km²·a)). The unit of soil erosion modulus calculated by RUSLE is t/(hm²·a), and the unit in the "Classification Standard of Soil Erosion" is t/(km²·a). So we need to multiply the RUSLE calculation result by 100 and then classify it. The study area was generally in a state of moderate erosion. The spatial distribution characteristics of soil erosion were obvious, showing a pattern of High South and low North (*Fig. 7*). The areas with slight or below soil erosion were mainly distributed in most areas of Naxi and Hejiang counties. The moderate and strong soil erosion areas were widely distributed in most areas of the southern part of the study area, and the very strong and strong soil erosion areas were concentrated in the intersection of Xuyong county and Gulin county.

By counting the different soil erosion grade areas, the number of soil erosion graded pixels in the lower reaches of the Chishui River Basin from 2000 to 2015 was obtained (*Fig. 8*). The results show that the overall improvement of soil erosion in the study area in 2015: a large number of areas with moderate erosion have been transformed into micro erosion and light erosion, which shows that the government has achieved preliminary results in land-based management. Grades above moderate erosion have increased slightly. By consulting the data, we can find that in 2015, there were many heavy rains in the lower reaches of the Chishui River Basin, and the daily rainfall of the station reached a maximum of 256.6 mm. Summer rainstorms are concentrated, with a short duration and high intensity, which provides erosive external forces for the occurrence of soil and water loss. Once the vegetation is destroyed, severe soil erosion occurs very easily. The soil developed in the strongly eroded area and the extremely strongly eroded area has good

water permeability, but the soil layer is shallow. Under the condition of loss of vegetation protection and heavy rainfall, soil erosion is prone to occur.

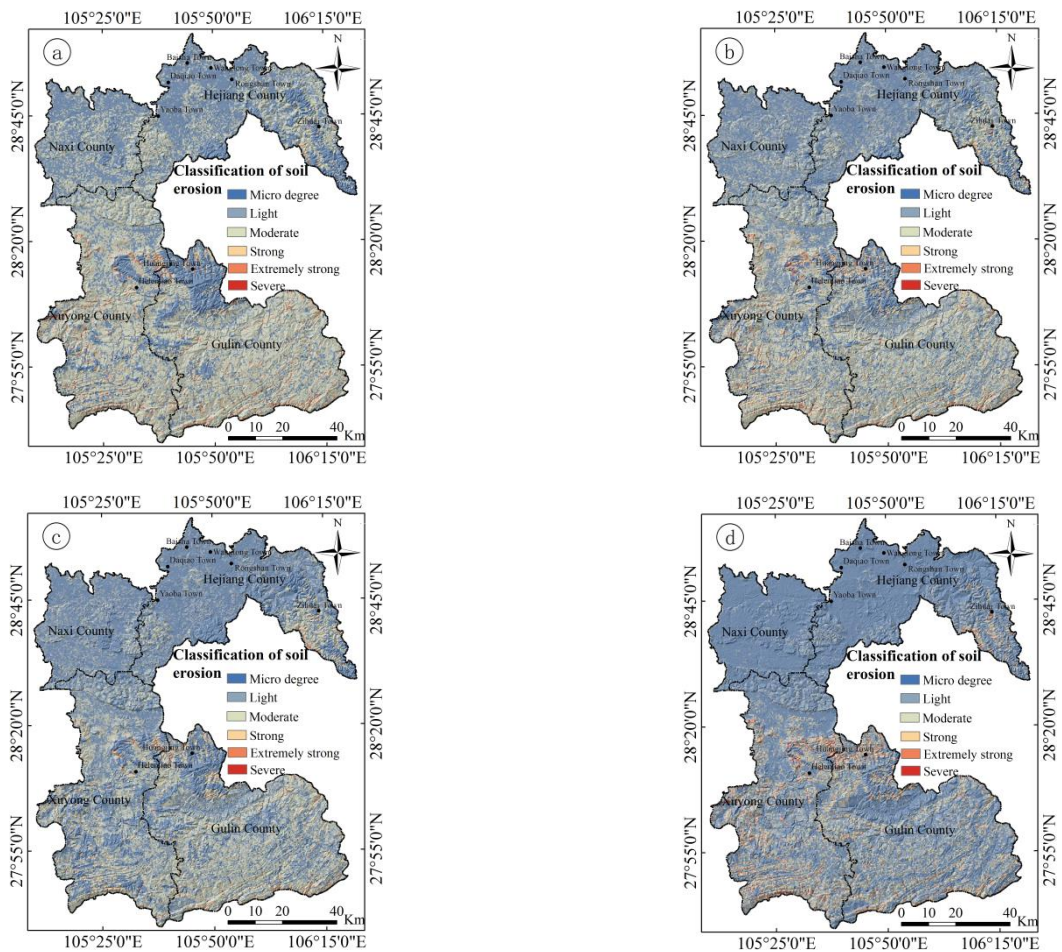


Figure 7. Spatial distribution of soil erosion in the lower reaches of the Chishui River Basin in 2000 (a), 2005 (b), 2010 (c), 2015 (d)

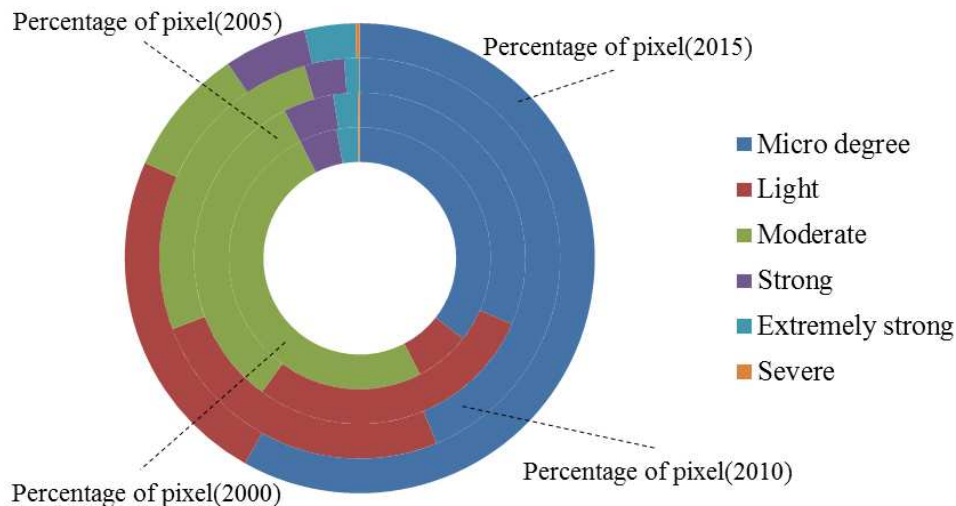


Figure 8. Statistics of grade pixel number of soil erosion in the lower reaches of the Chishui River Basin from 2000 to 2015

Trend analysis

Through the results of the soil erosion modulus (A) sequence fitting, we could find that from 2000 to 2015, the number of pixels with a changing slope greater than 0 was 14849, accounting for a region of 34.8% of the total area, and the soil erosion in these areas was increasing. The remaining 27824 pixels change slope was less than 0, which accounted for 65.2% of the total area (Fig. 9a). The results of F test (Fig. 9b) showed that the number of pixels with a significant increase in soil erosion was 2564 ($X > 0, P \leq 0.05$), accounting for 6.14% of the total number of pixels. The region is mainly concentrated in several villages and towns on the border between Xuyong and Gulin, such as Guihua Town, Helemiao Town, Dazhaimiao Town, Huangjing Town, etc., as well as Zihua Town, Tiantangba Town, and Fubao Town in Hejiang County. The number of pixels with a significant reduction in soil erosion was 12284 ($X < 0, P \leq 0.05$), accounting for 29.43% of the total number of pixels. This type was scattered all over the study area, most concentrated in the Daqiao town, Baisha Town, Wanglong Town, Rongshan town and Yaoba town in the northwest direction of Hejiang County.

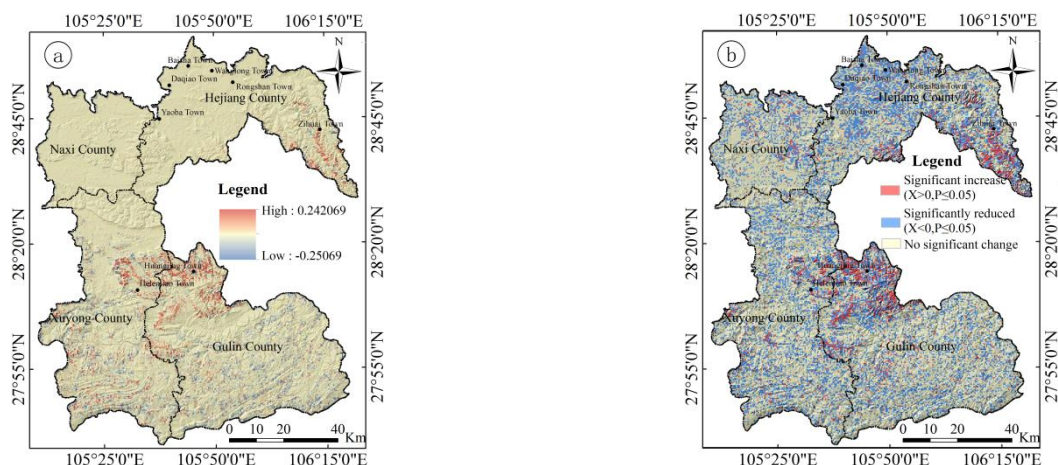


Figure 9. Variation trend of soil erosion (a) and significance test of the trend (b) in the lower reaches of the Chishui River Basin

Quantitative attribution of soil erosion based on Geographical Detector

From the results of the factor detector (Fig. 10) the main driving force factors' validity of the lower reaches of the Chishui River were compared from 2000 to 2015. From the time distribution of the mean value based on the main driving factors and the degree of soil erosion in the lower reaches of the Chishui River, it was concluded that there are significant driving factors and explanatory strengths: soil erodibility, the intensity of the fourth-stage soil erosion interpretation is greater than 0.15, and the other factors are not more than 0.1. Soil erodibility has the greatest quantitative interpretation of soil erosion in the lower reaches of the Chishui River Basin. Soil is the main target of erosion. Soil erodibility shows the greatest temporal similarity between soil erosion results in the lower reaches of the Chishui River Basin. Erodibility plays a leading role in soil erosion in the lower reaches of the Chishui River Basin. The more obvious the spatial distribution difference of the slope in the basin is, the more easily the rainwater will form a runoff and then cause water erosion. Therefore, the interpretation of soil erosion in the basin is followed by factors such as rainfall erosivity, slope, and soil and water conservation measures.

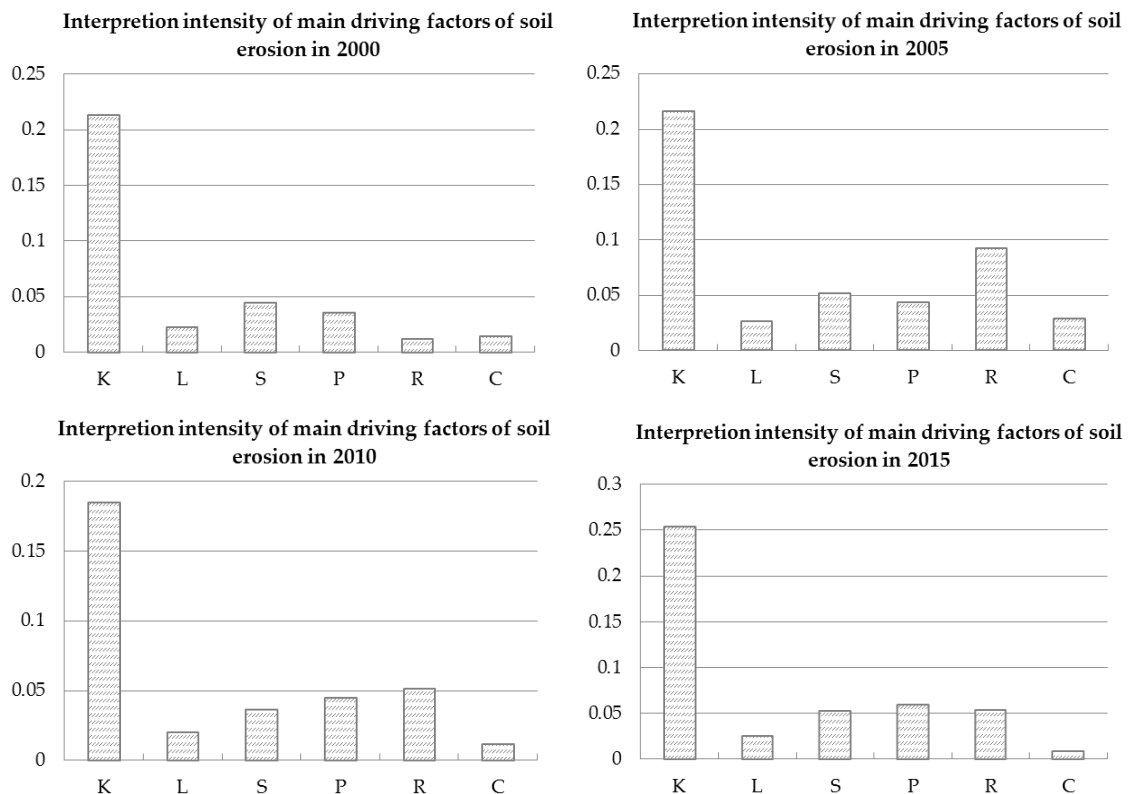


Figure 10. Interpretation intensity of main driving factors of soil erosion in the lower reaches of Chishui River Basin from 2000 to 2015 (K: Soil erodibility factor; L: Slope length factor; S: Slope factor; P: Soil and water conservation practice factor; R: Rainfall erosivity factor; C: Vegetation cover management factor)

Discussion

The Chishui river basin has always been an important waterway for shipping and transportation since ancient times. The state council attaches great importance to the protection of the basin and the rational utilization and development of regional water conservancy. In this paper, the commonly used trend change analysis method for the ecological environment is combined with the soil loss correction model (RUSLE). The selected model factors can reflect the impact of natural factors and human factors on soil and water loss. Due to the uncertainty of natural factors in different years within the study time interval, soil erosion in some regions is sometimes very bad. The changing trend of multi-period image soil erosion in the study area can be visualized by using the slope-changing method.

The assessment of soil erosion at watershed scales is vital for sustainable land use planning (Ostovari et al., 2017). According to Ganasri and Ramesh (2016), moderate erosion is mostly concentrated in the location of agricultural areas with gentle slope in the watershed study area. The early grade of soil erosion in the Chishui River Basin was mainly moderate. This was because the population growth in the study area at that time increased the development and utilization of agricultural and forestry resources, especially the demand for slope cropland. Irrational farming methods have a strong disturbance on the soil, which has changed and destroyed the soil structure and its erosion resistance. Due to the lack of vegetation cover and bare soil, wasteland is prone to soil and water loss under the influence of external forces such as precipitation

(Zerihun et al., 2018). The non-productive land in the study area is mostly residential land, highway land, etc., because the ground has hardened, the erosion modulus is very small.

From the relevant contents of the “Chishui River Cascade Hydropower Development” in “Report on the Key Points of the Comprehensive Utilization Plan of the Yangtze River Basin” in 1991, to the 2004 China Environment and Development International Cooperation Committee Basin Management Group set “Promoting Integrated River Basin Management and Rebuilding the River of Life in China”, About regarding the selection of the Chishui River Basin to carry out the pilot work of integrated river basin management, the formulation of the Regulations on the Management and Protection of the Chishui River Basin and the Comprehensive Planning of the Chishui River Basin, etc., were planned for the comprehensive blueprint of soil erosion in Sichuan in 2017. The Chishui River is a national-level key area for soil erosion and a series of ecological protection and construction projects such as “natural forest protection” and “returning farmland to forests” implemented by the Chinese government in the basin. The prevention and control of soil erosion in this area had a positive effect. Since the implementation of a series of beneficial ecological measures such as “returning farmland to forests” in the research area in 2000, the overall situation of soil and water loss has been greatly alleviated. However, during the whole research stage, there was still an increasing trend of soil and water loss in some areas, which was due to the increasing area of soil and water loss caused by current production activities. The Chishui river basin is rich in rainfall, especially in summer when the intensity of rainstorm is extremely high. The main soil types in this area are yellow soil and paddy soil with good water retention, which is beneficial to strengthen the fundamental construction of farmland. In the future, sloping farmland management should be given priority to, the management of existing forest land should be strengthened, and the key areas of population concentration should be controlled, to maintain the benign cycle of ecological environment in the study area.

Conclusion

This paper combines the trend change analysis method commonly used in the ecological environment research with the soil loss correction model (RUSLE). The selected model factors can reflect the intuitive influence of natural and man-made factors on soil erosion. During the study interval, uncertain changes in natural factors in different years resulted in changeable soil erosion status. The change slope method can directly show the trend of a multi-phase image change in the study area.

(1) Judging from the comprehensive evaluation of soil erosion sensitivity in the lower reaches of the Chishui River Basin, the early stage of soil erosion in the region is mainly dominated by moderate erosion, the areas of light and soil loss in the later period are gradually increasing, mainly distributed in some areas in the north. The area is a parallel fold extension zone in eastern Sichuan. It belongs to the southern margin of the hilly Middle Sichuan area. Most of them are agricultural areas, and their soil water retention is good, and their slopes are low. Moderate soil erosion areas are widely distributed in most of the mid-altitude areas of Xuyong County and Naxi County; The strong and extremely strong soil erosion areas are concentrated in the low-middle mountain areas in the south, including most of the areas in Xuyong County and Gulin County, and a small part of Hejiang County. The exposed strata are dominated by

limestone and mudstone, and the slope of the ground is large. Unutilized land and low-coverage grasslands are densely populated here.

(2) Cultivated land and forest land are still the most important types of land use in the basin study area. The terrain is broken, and the topography is steep. Besides, the rainfall in the Chishui River Basin is relatively rich, which leads to potential soil erosion in the region.

(3) The change slope method was used to study the trend of soil erosion in the study area during the period from 2000 to 2015. The area where soil erosion is significantly increased ($X > 0$, $P \leq 0.05$) accounts for 6.14% of the total area. The area where soil erosion is significantly decreased ($X < 0$, $P \leq 0.05$) accounts for 29.43% of the total area, and there was no significant change in the remaining areas. The results of the study fully demonstrate that long-term governance has achieved initial results.

(4) Geo-detectors were used to quantitatively analyze the strength of the main driving factors of the fourth-stage soil erosion results. Soil erodibility is the most explanatory factor among all driving factors. It played a leading role in the process of soil erosion in the lower reaches of the Chishui River Basin during the past 15 years.

(5) As a traditional method for observing soil erosion, the artificial field survey is time-consuming, labor-intensive, and requires a large amount of funds. It is only suitable for small areas. We combine RUSLE with Remote Sensing and Geographic Information Systems to achieve long-term soil erosion research in large areas. In the future, we plan to introduce landscape pattern, a landscape ecology research category, to study the distribution characteristics and evolution of soil erosion. From the perspective of landscape ecology, soil erosion is regarded as a spatial arrangement and combination of patch types with different erosion levels, which is the product of the merger of different soil erosion levels in space. The purpose of establishing the relationship between soil erosion and landscape pattern is to analyze the temporal and spatial characteristics of soil erosion in the study area from the perspective of landscape ecology, and use landscape pattern index to describe the characteristics of soil erosion types.

Acknowledgements. This research was funded by the National Natural Science Foundation of China (Grants No. 51609209) and the Education Department of Sichuan Province (Grants No. 18ZA0061).

REFERENCES

- [1] Abdulkareem, J. H., Pradhan, B., Sulaiman, W. N. A., Jamil, N. R. (2019): Prediction of spatial soil loss impacted by long-term land-use/land-cover change in a tropical watershed. – *Geoscience Frontiers* 10(2): 389-403.
- [2] Abidin, R. Z., Sulaiman, M. S., Yusoff, N. (2017): Erosion risk assessment: a case study of the Langat River bank in Malaysia. – *International Soil and Water Conservation Research* 5(1): 26-35.
- [3] Alexakis, D. D., Hadjimitsis, D. G., Agapiou, A. (2013): Integrated use of remote sensing, GIS and precipitation data for the assessment of soil erosion rate in the catchment area of “Yialias” in Cyprus. – *Atmospheric Research* 131: 108-124.
- [4] Anache, J. A. A., Flanagan, D. C., Srivastava, A., Wendland, E. C. (2018): Land use and climate change impacts on runoff and soil erosion at the hillslope scale in the Brazilian Cerrado. – *Science of The Total Environment* 622-623: 140-151.

- [5] Bera, A. (2017): Assessment of soil loss by universal soil loss equation (USLE) model using GIS techniques: a case study of Gumti River Basin, Tripura, India. – *Modeling Earth Systems and Environment* 3(1): 29.
- [6] Borrelli, P., Robinson, D. A., Fleischer, L. R., Lugato, E., Ballabio, C., Alewell, C., Meusburger, K., Modugno, S., Schütt, B., Ferro, V., Bagarello, V., Oost, K. V., Montanarella, L., Panagos, P. (2017): An assessment of the global impact of 21st century land use change on soil erosion. – *Nature Communications* 8(1): 2013.
- [7] Buttafuoco, G., Conforti, M., Aucelli, P. P. C., Robustelli, G., Scarciglia, F. (2012): Assessing spatial uncertainty in mapping soil erodibility factor using geostatistical stochastic simulation. – *Environmental Earth Sciences* 66(4): 1111-1125.
- [8] Cai, C. (2000): Study of applying USLE and geographical information system IDRISI to predict soil erosion in small watershed. – *Journal of Soil Water Conservation* 14(2): 19-24.
- [9] Cai, H., He, Z. W., An, Y. L., Zhang, C., Deng, H. (2015): Response relationship between land use and water quality in Chishui river basin based on RS and GIS. – *Resources & Environment in the Yangtze Basin* 24(2): 286-291.
- [10] Cerdà, A., Rodrigo-Comino, J., Novara, A., Brevik, E. C., Vaezi, A. R., Pulido, M., Giménez-Morera, A., Keesstra, S. D. (2018): Long-term impact of rainfed agricultural land abandonment on soil erosion in the Western Mediterranean basin. – *Progress in Physical Geography: Earth and Environment* 42(2): 202-219.
- [11] Chen, G. B., Tong, X. S. (2012): Temporal and spatial change of urban air quality in Luzhou from 2004 to 2009. – *Environmental Science & Technology* 35(6I): 217-220.
- [12] Cunha, E., Bacani, V., Panachuki, E. (2017): Modeling soil erosion using RUSLE and GIS in a watershed occupied by rural settlement in the Brazilian Cerrado. – *Natural Hazards* 85(2): 851-868.
- [13] Das, B., Paul, A., Bordoloi, R., Tripathi, O. P., Pandey, P. K. (2018): Soil erosion risk assessment of hilly terrain through integrated approach of RUSLE and geospatial technology: a case study of Tirap District, – Arunachal Pradesh. *Modeling Earth Systems and Environment* 4(1): 373-381.
- [14] Eftimiou, N. (2018): Evaluating the performance of different empirical rainfall erosivity (R) factor formulas using sediment yield measurements. – *Catena* 169: 195-208.
- [15] Fenta, A. A., Yasuda, H., Shimizu, K., Haregeweyn, N., Negussie, A. (2016): Dynamics of soil erosion as influenced by watershed management practices: a case study of the Agula watershed in the semi-arid highlands of northern Ethiopia. – *Environmental Management* 58(5): 1-17.
- [16] Fu, G., Chen, S., McCool, D. K. (2006): Modeling the impacts of no-till practice on soil erosion and sediment yield with RUSLE, SEDD, and ArcView GIS. – *Soil and Tillage Research* 85(1): 38-49.
- [17] Ganasri, B. P., Ramesh, H. (2016): Assessment of soil erosion by RUSLE model using remote sensing and GIS—a case study of Nethravathi Basin. – *Geosci Front* 7: 953-961.
- [18] Gogichaishvili, G. P., Kirvalidze, D. R., Gorjomeladze, O. L. (2014): Testing of the hydromechanical prediction model of soil erosion under the conditions of Georgia. – *Eurasian Soil Science* 47(9): 917-22.
- [19] Hickey, R., Smith, A., Jankowski, P. (1994): Slope length calculations from a DEM within ARC/INFO grid. – *Computers, Environment and Urban Systems* 18(5): 365-380.
- [20] Karydas, C. G., Sekuloska, T., Silleos, G. N. (2009): Quantification and site-specification of the support practice factor when mapping soil erosion risk associated with olive plantations in the Mediterranean island of Crete. – *Environmental Monitoring and Assessment* 149(1): 19-28.
- [21] Kavian, A., Sabet, S. H., Solaimani, K., Jafari, B. (2015): Simulating the effects of land use changes on soil erosion using RUSLE model. – *Geocarto International* 32(1): 97-111.

- [22] Kayet, N., Pathak, K., Chakrabarty, A., Sahoo, S. (2018): Evaluation of soil loss estimation using the RUSLE model and SCS-CN method in hillslope mining areas. – *International Soil and Water Conservation Research* 6(1): 31-42.
- [23] Khaledian, Y., Kiani, F., Ebrahimi, S., Brevik, E. C., Aitkenhead-Peterson, J. (2017): Assessment and monitoring of soil degradation during land use change using multivariate analysis. – *Land Degradation & Development* 28(1): 128-141.
- [24] Kosmas, C., Gerontidis, S., Marathianou, M. (2000): The effect of land use change on soils and vegetation over various lithological formations on Lesvos (Greece). – *Catena* 40(1): 51-68.
- [25] Kosmowski, F. (2018): Soil water management practices (terraces) helped to mitigate the 2015 drought in Ethiopia. – *Agricultural Water Management* 204: 11-16.
- [26] Krellenberg, K., Welz, J. (2017): Assessing urban vulnerability in the context of flood and heat hazard: pathways and challenges for indicator-based analysis. – *Social Indicators Research* 132(2): 709-731.
- [27] Lakkad, A. P., Patel, G. R., Sondarva, K. N., Shrivastava, P. K. (2018): Estimation of sediment delivery ratio at sub-watershed level using revised and modified USLE. – *Agricultural Science Digest* 38(1): 11-16.
- [28] Leys, A., Govers, G., Gillijns, K., Berckmoes, E., Takken, I. (2010): Scale effects on runoff and erosion losses from arable land under conservation and conventional tillage: the role of residue cover. – *Journal of Hydrology* 390(3): 143-154.
- [29] Liu, B. Y., Nearing, M., Shi, P. J., Jia, Z. W. (2000): Slope length effects on soil loss for steep slopes. – *Soil Science Society of America Journal* 64: 1759-1763.
- [30] Mahala, A. (2018): Soil erosion estimation using RUSLE and GIS techniques—a study of a plateau fringe region of tropical environment. – *Arabian Journal of Geosciences* 11(13): 335.
- [31] Mondal, A., Khare, D., Kundu, S. (2018): A comparative study of soil erosion modelling by MMF, USLE and RUSLE. – *Geocarto International* 33(1): 89-103.
- [32] Montgomery, D. R. (2007): Soil erosion and agricultural sustainability. – *Proceedings of the National Academy of Sciences* 104(33): 13268 LP-13272.
- [33] Ochoa, P. A., Fries, A., Mejía, D., Burneo, J. I., Ruíz-Sinoga, J. D., Cerdà, A. (2016): Effects of climate, land cover and topography on soil erosion risk in a semiarid basin of the Andes. – *CATENA* 140: 31-42.
- [34] Osouli, A., Bahri, P. S. (2018): Erosion rate prediction model for levee-floodwall overtopping applications in fine-grained soils. – *Geotechnical and Geological Engineering* 36(5): 2823-2838.
- [35] Ostovari, Y., Ghorbani-Dashtaki, S., Bahrami, H. A., Naderi, M., Dematte, J. A. M. (2017): Soil loss estimation using RUSLE model, GIS and remote sensing techniques: a case study from the Dembecha Watershed, Northwestern Ethiopia. – *Geoderma Regional* 11: 28-36.
- [36] Panagos, P., Katsoyiannis, A. (2019): Soil erosion modelling: the new challenges as the result of policy developments in Europe. – *Environmental Research* 172: 470-474.
- [37] Pham, T. G., Degener, J., Kappas, M. (2018): Integrated universal soil loss equation (USLE) and Geographical Information System (GIS) for soil erosion estimation in A Sap basin: Central Vietnam. – *International Soil and Water Conservation Research* 6(2): 99-110.
- [38] Preetha, P. P., Al-Hamdan, A. Z. (2019): Multi-level pedotransfer modification functions of the USLE-K factor for annual soil erodibility estimation of mixed landscapes. – *Modeling Earth Systems and Environment* 5(3): 767-779.
- [39] Rammahi, A. H. J. A., Khassaf, P. D. S. (2018): Estimation of soil erodibility factor in rusle equation for euphrates river watershed using GIS. – *International Journal of GEOMATE* 14: 164-169.

- [40] Rodrigo-Comino, J., Ruiz-Sinoga, J. D., Senciales-González, J. M., Guerra-Merchán, A., Seeger, M., Ries, J. B. (2016): High variability of soil erosion and hydrological processes in Mediterranean hillslope vineyards (Montes de Málaga, Spain). – *Catena* 145: 274-284.
- [41] Schmid, A. (2012): Spatial and temporal variability of rainfall erosivity factor for Switzerland. – *Hydrology & Earth System Sciences Discussions* 16: 167-177.
- [42] Sheng, H. Y., Shi, X. J. (2001): Geological background of soil and water erosion and water conservation problems. – *Soil and Water Conservation Science and Technology in Shanxi* 3: 15-17.
- [43] Singh, G., Panda, R. K. (2017): Grid-cell based assessment of soil erosion potential for identification of critical erosion prone areas using USLE, GIS and remote sensing: a case study in the Kapgari watershed, India. – *International Soil and Water Conservation Research* 5(3): 202-211.
- [44] Torri, D., Poesen, J., Borselli, L. (1997): Predictability and uncertainty of the soil erodibility factor using a global dataset. – *Catena* 46(4): 309-310.
- [45] Uri, N. D. (2001): A note on soil erosion and its environmental consequences in the United States. – *Water Air & Soil Pollution* 129(1-4): 181-197.
- [46] Vaezi, A. R., Zarrinabadi, E., Auerswald, K. (2017): Interaction of land use, slope gradient and rain sequence on runoff and soil loss from weakly aggregated semi-arid soils. – *Soil and Tillage Research* 172: 22-31.
- [47] Wang, J. F., Xu, C. D. (2017): Geodetector: principle and prospective. – *Acta Geographica Sinica* 72: 116-134.
- [48] Wang, Y., Wang, G. Q. (2011): A study of distribution regularity of soil erosion in Sichuan Province. – *Scientific & Technological Management of Land & Resources* 28(6): 50-55.
- [49] Wang, Z. S., Jiang, L. G., Huang, M. J., Zhang, C., Yu, X. B. (2007): Biodiversity status and its conservation strategy in the Chishui river basin. – *Resources & Environment in the Yangtze Basin* 16(2): 175-180.
- [50] Wijesundara, N. C., Abeysingha, N. S., Dissanayake, D. M. S. L. B. (2018): GIS-based soil loss estimation using RUSLE model: a case of Kirindi Oya river basin, Sri Lanka. – *Modeling Earth Systems and Environment* 4(1): 251-262.
- [51] Wischmeier, W. H. (1965): Predicting rainfall erosion losses from cropland east of the Rocky Mountain. – *Agriculture Handbook* 282: 47.
- [52] Wu, Y., Xie, Y., Zhang, W. B. (2001): Comparison of different methods for estimating average annual rainfall erosivity. – *Journal of Soil Water Conservation* 15(3): 31-34.
- [53] Yang, J., Guan, Y., Li, X. M., Xi, J. C. (2018): Urban fringe area ecological vulnerability space-time evolution research: the case of Ganjingzi District, Dalian. – *Acta Ecologica Sinica* 38(3): 388-405.
- [54] Zerihun, M., Mohammedyasin, M. S., Sewnet, D., Adem, A. A., Lakew, M. (2018): Assessment of soil erosion using RUSLE, GIS and remote sensing in NW Ethiopia. – *Geoderma Regional* 12: 83-90.

MITIGATION OF LOW TEMPERATURE STRESS BY POLYTHENE FOR QUALITY PRODUCTION OF GLADIOLUS (*Gladiolus hortulanus* L.) DURING WINTER

QAYYUM, M. M.^{1*} – HASSAN, I.¹ – ABBASI, N. A.¹ – KHALID, A.²

¹*Department of Horticulture, Pir Mehr Ali Shah Arid Agriculture University, Rawalpindi, Pakistan*

²*Department of Environmental Science, Pir Mehr Ali Shah Arid Agriculture University, Rawalpindi, Pakistan*

*Corresponding author
e-mail: mazhar.hort.aup@gmail.com

(Received 16th Dec 2019; accepted 20th Mar 2020)

Abstract. Temperature plays a crucial role in growth rate and development of a plant. Low temperature damages plant metabolic processes. The poly tunnel is used to mitigate low temperature stress for quality production of gladiolus. The Randomized complete block design with two factors factorial was used to carry this experiment. Protective field conditions enhanced temperature level that resulted in longer spike length, higher number of leaves per plant, more leaf area, maximum spike diameter, more number of florets per spike, larger diameter of flower, more fresh and dry weight, higher photosynthetic rate and less days to taken flowering, were obtained during November and December under poly tunnel conditions. Chlorophyll contents and transpiration rate significantly increased during early warmer months. Stomatal conductance not significantly changes. More antioxidant enzyme (POD and CAT) activity was recorded and less electrolyte leakage due to which vase life remained higher in November and December under protective planting conditions. Moreover, gladiolus cut flowers quality features were significantly improved in protective growing conditions in poly tunnel during January and February. Protective growing conditions mitigated low temperature stress in cold months and significantly enhanced yield as well as quality characteristics of gladiolus cut flowers.

Keywords: *antioxidant enzymes, protected cultivation, prolonged season, temperature stress, vase life*

Introduction

Gladiolus (*Gladiolus hortulanus* L.) among the cut flowers stands second in term of production and consumers' predilection. Gladiolus with imperial spikes is one of the most common and well-known cut flowers in the world that encompass striking, elegant and elusive florets (Saeed et al., 2013). It has virtuous keeping ability because its florets open in an order for extended period. It is often used in bouquets, bedding, landscape, flower arrangement etc. (Arora, 2007). It has occupied an area of 7,384.34 ha worldwide with a trade worth of US \$ 3,100 million. The Netherlands shares 48.5% and Germany 45.3% in world trade (Ahmad and Rab, 2020). Commercial gladiolus production not only generates good profits, but can also earn foreign exchange. The length of spike, florets count, intact flower quality, freshness of flower, and vase life are major market indices. Therefore, superfluous attention is given to quality of flower rather than its production (Bhande et al., 2015). A key factor to the aesthetic and marketable quality is the postharvest longevity of cut flowers (Saeed et al., 2013). Preharvest growth circumstances determine ultimate postharvest fate of flower. The gladiolus life cycle is divided in two phases. The first phase is vegetative growth and second is flower initiation and development. These phases are characterized by several processes, viz., cellular

division, differentiation, expansion and eventual petal senescence. Therefore, it is need for prodigious attention to enhance all the physiological and biochemical processes that occur during flower growth and development (Sood et al., 2006).

Plant growth and crop productivity is badly affected by low temperature stress that leads to considerable damages in production of crops (Jiang, 2011). The consequences of low temperature stress since temperatures cool enough to induce damages within tissues of plant. The level of tolerance to freezing ($<0^{\circ}\text{C}$) and chilling ($0\text{-}15^{\circ}\text{C}$) temperature ranges are specific to different plant species. The cold stress or low temperature stress includes chilling and freezing stress. The growth features of crop plants include rate of survival, water balance, transportation, cell division and development, and photosynthesis, all of them are affected by low temperature stress (Sanghera et al., 2011). Plant growth rate depends upon ranges of ambient temperature of the crop species. Therefore, every plant species have a precise level of least, extreme and optimal temperature range (Hatfield et al., 2011). Proper growth and development of gladiolus depend on abundant light, appropriate temperature and plenty of soil moisture. Gladiolus plants prefer a temperature regime between $12\text{-}20^{\circ}\text{C}$ (Khodorova and Boitel-Conti, 2013). The selected progenies of gladiolus are hardy to -6°C that is not within minimum range required in USDA Z3-4 (Anderson et al., 2012). The low temperature below 10°C causes an arrest in growth and development of the plant (Mayoli and Isutsa, 2012). The plant metabolic processes and development of whole plant, tissues, cells and even at sub-cellular levels are distraught by low temperatures. The morphology, anatomy, phenology and plant biochemistry at all levels of organization also may affected by temperature variation (Porter, 2005; Waraich et al., 2012). The leaf initiation, enlargement and flowering are totally temperature dependent. Also growth and development of plants primarily influence by air temperature of the growing environment (von Caemmerer and Evans, 2015). The stress induced by low temperature influenced the vegetative as well as reproductive stages in the plant's life cycle. The different characteristics like flower initiation, abscission, pollen sterility, pollen tube distortion, and ovule abortion during reproductive development inversely affected by low temperature stress that eventually reduced the production (Khodorova and Boitel-Conti, 2013).

There are various strategies which are being used to mitigate the detrimental effects of low temperature stress. The polythene tunnel cultivation is used as one approach to mitigate the damaging effects of low temperature that is most suitable for growing high value horticultural crops (Hanan, 2017). Polythene house is an enclosed structure protected with polyethylene sheet which might provide the promising environments intended for the better growth of the plants in numerous ways, viz., shield from hostile ecological circumstances, protection from heavy winds, pests, diseases and other antagonistic weather conditions (Cowan et al., 2014). Agro-meteorological indices and temperature sensitivity of gladiolus are directly affected in low temperature stressed circumstances, which is yet to be studied. In present research, an exertion was made to evaluate the morpho-physiological in relation to low temperature stress and mitigation of effects for quality cut flower production.

Materials and Methods

The study was carried out at Horticulture department research area in PMAS Arid Agriculture University, Rawalpindi, Pakistan (Latitude: $33^{\circ}38'51''$, Longitude: $73^{\circ}4'57.72''$), during 2013-2014 and 2014-2015. The corms of the gladiolus cultivar

"White Prosperity" were planted on monthly interval basis during months (November, December, January and February) in open field conditions to check the low temperature effects and in Poly tunnel conditions to evaluate the mitigation effects. Randomized complete block design (RCBD) with two factors factorial. The growing conditions were factor one and planting times were second factor. The corms were planted in sand bed for uniform germination and planted in research area when they reached up to 10-15 cm in height. The corms were transplanted at a row to row distance of 30 cm while distance of 20 cm was kept between two plants in a raised bed. The experiment was carried in a randomized complete block design replicated thrice. The five plants were randomly selected for each observation. Before the plantation of corms well rotten farm yard manure was mix in soil. The tunnel was covered with 0.6 mm thick polythene sheet and tunnel dimensions were 12 m long, 3 m wide and 2.5 m high. Data regarding temperature and relative humidity was noticed two times in a day for both in open field and inside polythene tunnel (*Figure 1*). Other cultural operations like irrigation, fertilization, weeding, and plant protection measures were alike for all treatments. The data was recorded separately for every month from date of sowing for following characteristics.

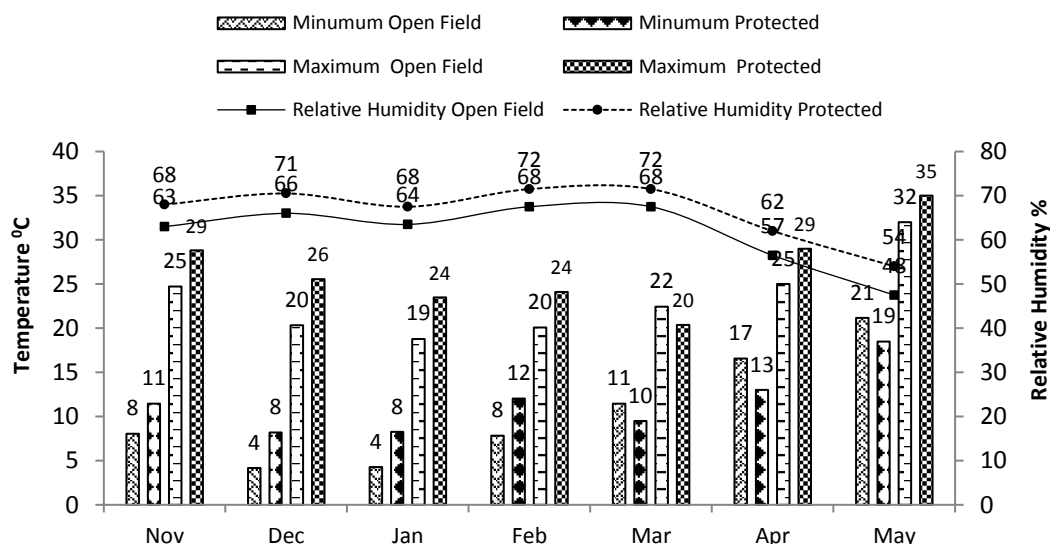


Figure 1. Average weather data during study period

Morphological and floral characteristics

Data on number of plant height (cm), leaves plant⁻¹, leaf area (cm²), number of days taken to flowering from date of sowing for each month, number of cormels plant⁻¹, corm diameter (cm), corm weight (g), spike length (cm), spike thickness (mm), number of florets spike⁻¹, flower diameter (cm) and fresh weight of spike were recorded at harvest stage.

Vase life parameters

There were three cut spikes placed in vase for vase life attributes in every replication. Percentage of florets opened, days to open florets, and vase life were recorded put in vase.

Bio-chemical attribute

Spade meter (SPAD 502 Konica Minolta, Japan) used for determining chlorophyll contents in plant leaves.

Physiological characteristics

Photosynthetic rate, transpiration rate and stomatal conductance were measured according to the method described by Long and Bernacchi (2003). LCA-4 ADC portable infrared gas analyzer (Analytical Development Company, Hoddesdon, England) was used between the hours of 12:00 and 15:00 at the prevailing solar radiation on flowering stage.

Relative water content

Relative water content (RWC) was determined according to the method given by Bars and Weatherley (1962). Leaves were excised and fresh weight (FW) was immediately recorded then leaves were soaked for 4 h in distilled water at room temperature and turgid weight (TW) was recorded. After drying for 24 h at 80°C, dry weight (DW) was recorded. The RWC was calculated as follows:

$$RWC (\%) = \frac{(FW - DW)}{(TW - DW)} \times 100 \quad (\text{Eq.1})$$

Electrolyte leakage (EL)

Electrolyte leakage was calculated using the procedure quoted by Singh et al. (2008) with minor modification. Five floral petal discs with a diameter of 10 mm from each treatment were put together in a test tube containing 10 mL of distilled water. Initially leakage of membrane was measured with a conductivity meter after incubation at 25°C for 180 min of that test tube. Before the final conductivity was measured, solution was boiled for 10 min in a water bath to release all the electrolytes.

The leakage of the membrane was measured as below:

$$EL(\%) = \frac{C1}{C2} \times 100 \quad (\text{Eq.2})$$

where, C1 is electrical conductivity of petals after 180 min incubation in room and C2 is final electrical conductivity of the solution.

Enzyme extracts preparation

Flowers were frozen in liquid nitrogen and one gram sample was carried from every replication. The sample was grinded in pre-cold mortar and pestle. The floral tissues were precipitated in 5 mL of 0.1 M KPO₄ buffer (pH 7.8) having 0.5% Triton and 0.2 g of PVPP. The prepared mixture was centrifuged for 30 min at 4°C at 27,000 x g (Abbasi et al., 1998).

Assessment of peroxidase

The activity of peroxidase (POD) was tested with minor changes according to the procedure described by Shaheen et al. (2015). The mixture of assay comprised of 1 mM H₂O₂, 0.1 mM guaiacol in 15 mM NaKPO₄ buffer (pH 6.0) and 200 µL basic extract of enzymes. The activity of POD was noted as a change in the optical density (OD) over a three min period at 470 nm and measured as unit g⁻¹ fresh weight.

Catalase assessment

The activity of catalase (CAT) was tested according to the procedure with slight changes used by Saeed et al. (2013). Two buffer solutions were used to start reaction, one holding 50 mM KPO₄ and second comprising of 12.5 mM H₂O₂ in 50 mM KPO₄ (pH 7.0). The 300 µL enzyme to each buffer added in 3 mL cuvettes for reaction was started, and OD was noted at 240 nm. The unit for catalase activity was unit g⁻¹ fresh weight.

Statistical analysis

The statistically analysis of data was carried out by ANOVA technique in Randomized complete block design (RCBD) with two factors factorial. The means were compared using Duncan's multiple ranges tested at 5% significance level.

Results

Morphological characteristics

Morphological parameters are presented in *Table 1*. Prominently highest values for plant height (136 cm) and leaf area (53.7 cm²) were in November under the poly tunnel conditions while in months of January (47.41 cm, 15.35 cm²) and February (46.23 cm, 15.04 cm²) in open filed conditions remained lowest. More number of leaves per plant (8.13), number of corms & cormels (34.31) and corm size (3.88 cm) was noticed in poly tunnel conditions and lower number leaf per plant (6.39), number of corms & cormels (26.8) and corm size (3.52 cm) was recorded in open field conditions. Also prominently early flowering was noted in poly tunnel (71.76 day) than open field (99.74 days) while prolonged flowering was in January (91.63) and February (87.99 days).

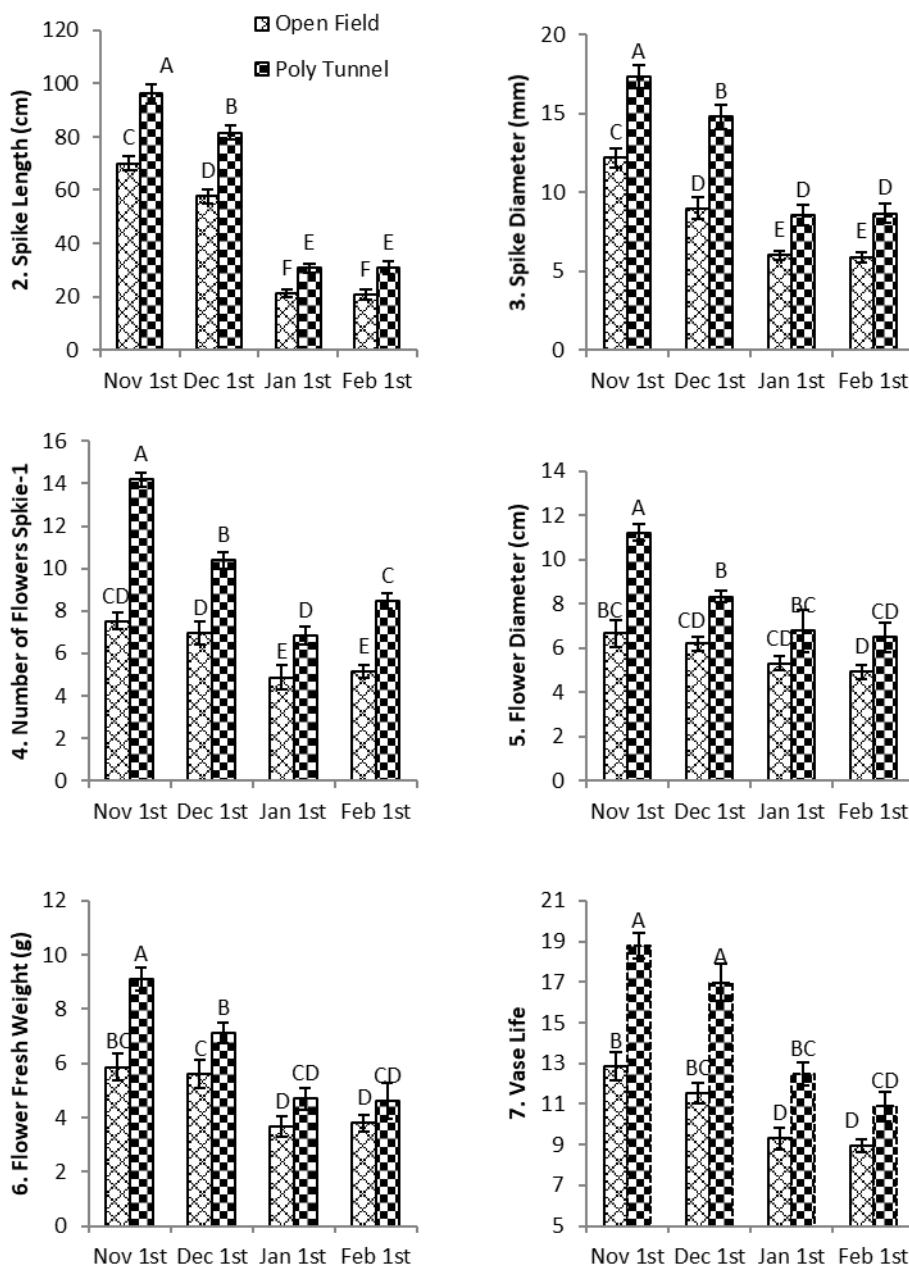
Floral and vase quality parameters

Floral characteristics were presented in *Figures 2-7*. The longest spikes were noticed in November (96.18 cm) under poly tunnel conditions and smallest in January (21.15 cm) and February (20.55 cm) in open field conditions. The thickest diameter of spike was noted under poly tunnel in November (12.19 mm) while thinnest in January (6 mm) and February (5.89 mm) in open field. The highest number of florets were recorded in November (14.18) under poly tunnel while lowest in January (4.87) and February (5.16) in open field. The flower diameter was more in November (11.22 cm) in protected conditions while least in January (5.3 cm), February (4.93 cm) in open field. The maximum fresh weight of flower spike was in November (9.11 g) under poly tunnel growing conditions and minimum in January (3.67 g), February (3.8 g) in open field. The longest vase life was recorded in November (18.78 days), December (16.99 days) in poly tunnel conditions while shortest in January (9.32 days) and February (8.96 days) in open filed environment. Percentage of florets opened and days to open florets were non-significant (data not shown).

Table 1. Effect of growing conditions and planting times on various morphological characteristics of gladiolus

Treatments		Plant Height (cm)	Number of Leaves Plant ⁻¹	Leaf Area (cm ²)	Days Taken to Flowering	No. of Corms & Cormels Plant ⁻¹	Corm's Diameter (cm)
Growing Conditions (GC)	Open Field	63.99 ± 4.51 ^B	6.39 ± 0.58 ^B	23.11 ± 1.65 ^B	99.74 ± 2.07 ^A	26.8 ± 2.24 ^B	3.52 ± 0.18 ^B
	Poly Tunnel	91.41 ± 4.29 ^A	8.13 ± 0.37 ^A	36.83 ± 2 ^A	71.76 ± 3.35 ^B	34.31 ± 1.75 ^A	3.88 ± 0.2 ^A
	P Value	<0.001	<0.001	<0.001	<0.001	<0.05	<0.001
	LSD	7.39	0.78	3.03	4.49	1.63	0.32
Date of Planting (DP)	Nov 1st	113.06 ± 4.75 ^A	11.11 ± 0.8 ^A	43.09 ± 1.89 ^A	80.49 ± 3.46 ^B	36.86 ± 2.12 ^A	4.2 ± 0.11 ^A
	Dec 1st	88.84 ± 4.72 ^B	9.19 ± 0.34 ^B	37.75 ± 2.06 ^B	82.89 ± 2.29 ^{AB}	35.17 ± 2.36 ^A	3.84 ± 0.29 ^{AB}
	Jan 1st	56.14 ± 3.26 ^C	4.44 ± 0.35 ^C	19.47 ± 1.43 ^C	91.63 ± 3.01 ^A	24.75 ± 1.49 ^B	3.38 ± 0.15 ^{BC}
	Feb 1st	52.76 ± 4.89 ^C	4.31 ± 0.42 ^C	19.56 ± 1.92 ^C	87.99 ± 2.09 ^{AB}	25.45 ± 2.01 ^B	3.49 ± 0.21 ^C
	P Value	<0.001	<0.001	<0.001	<0.001	<0.001	<0.001
	LSD	10.45	1.11	4.29	6.36	2.31	0.45
Interaction (GC X DP)	OF X Nov	89.75 ± 5.22 ^C	10.06 ± 0.96	32.47 ± 1.21 ^C	96.71 ± 2.5	32.19 ± 2.33	3.82 ± 0.11
	OF X Dec	72.58 ± 3.21 ^D	7.91 ± 0.34	29.57 ± 1.26 ^{CD}	97.69 ± 1.06	30.52 ± 2.56	3.71 ± 0.22
	OF X Jan	47.41 ± 2.92 ^E	3.84 ± 0.45	15.35 ± 1.8 ^E	103.08 ± 2.46	21.56 ± 1.67	3.27 ± 0.19
	OF X Feb	46.23 ± 6.68 ^E	3.76 ± 0.58	15.04 ± 2.32 ^E	101.49 ± 2.25	22.94 ± 2.39	3.27 ± 0.19
	PT X Nov	136.37 ± 4.27 ^A	12.16 ± 0.64	53.7 ± 2.57 ^A	64.27 ± 4.41	41.52 ± 1.91	4.37 ± 0.1
	PT X Dec	105.1 ± 6.22 ^B	10.46 ± 0.34	45.93 ± 2.85 ^B	68.09 ± 3.52	39.82 ± 2.15	3.96 ± 0.35
	PT X Jan	64.86 ± 3.59 ^D	5.03 ± 0.24	23.59 ± 1.05 ^D	80.18 ± 3.55	27.93 ± 1.3	3.49 ± 0.11
	PT X Feb	59.29 ± 3.09 ^{DE}	4.86 ± 0.25	24.08 ± 1.52 ^D	74.49 ± 1.93	27.97 ± 1.63	3.71 ± 0.22
	P Value	<0.05	>0.05	<0.01	>0.05	>0.05	>0.05
LSD	14.79	1.58	6.07	8.99	3.26	0.62	
CV	5.56	12.42	11.57	5.99	10.83	16.77	

Means sharing same letters are none significant and ± showed the standard error of three means of each replicates. Abbreviations: (DP = Date of planting, OF = Open Field, PT = Polythene Tunnel, P Value: shows the significance level, LSD = Least Significant Difference, CV = Coefficient of Variation)

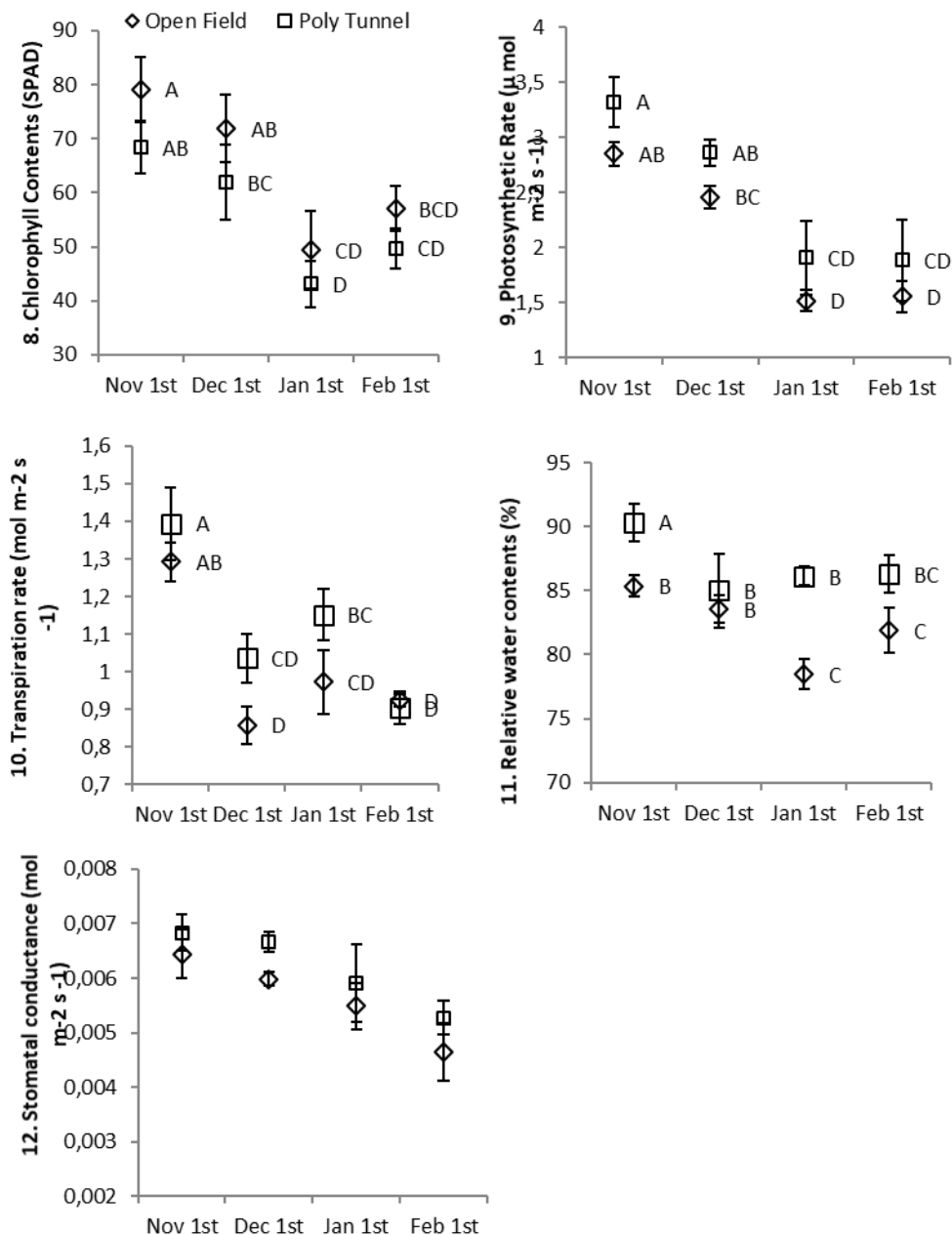


Figures 2-7. Effect of growing conditions and planting time on floral attributes (Bar shows standard error of means)

Bio-chemical and physiological characteristics

Bio-chemical and physiological characteristics are shown in *Figures 8-12*. The chlorophyll (SPAD) contents were highest in November (79.20, 68.45) and minimum in January (49.44, 43.15). Photosynthetic rate was more during November ($3.32 \text{ mol m}^{-2} \text{ s}^{-1}$, $2.85 \text{ mol m}^{-2} \text{ s}^{-1}$) in both conditions while minimum during January ($1.52 \text{ mol m}^{-2} \text{ s}^{-1}$) and February ($1.56 \text{ mol m}^{-2} \text{ s}^{-1}$) in open field conditions. The highest transpiration rate was noticed during November ($1.39 \text{ mol m}^{-2} \text{ s}^{-1}$, $1.29 \text{ mol m}^{-2} \text{ s}^{-1}$) while minimum during February ($0.9 \text{ mol m}^{-2} \text{ s}^{-1}$) in both conditions, respectively. The maximum relative water

contents were recorded in November (90.33%) under poly tunnel while lowest in January (78.44%) in open field. Stomatal conductance was more November (0.0064, 0.0068 mol m⁻² s⁻¹) and least in February (0.0046, 0.0053 mol m⁻² s⁻¹) in both conditions, respectively.

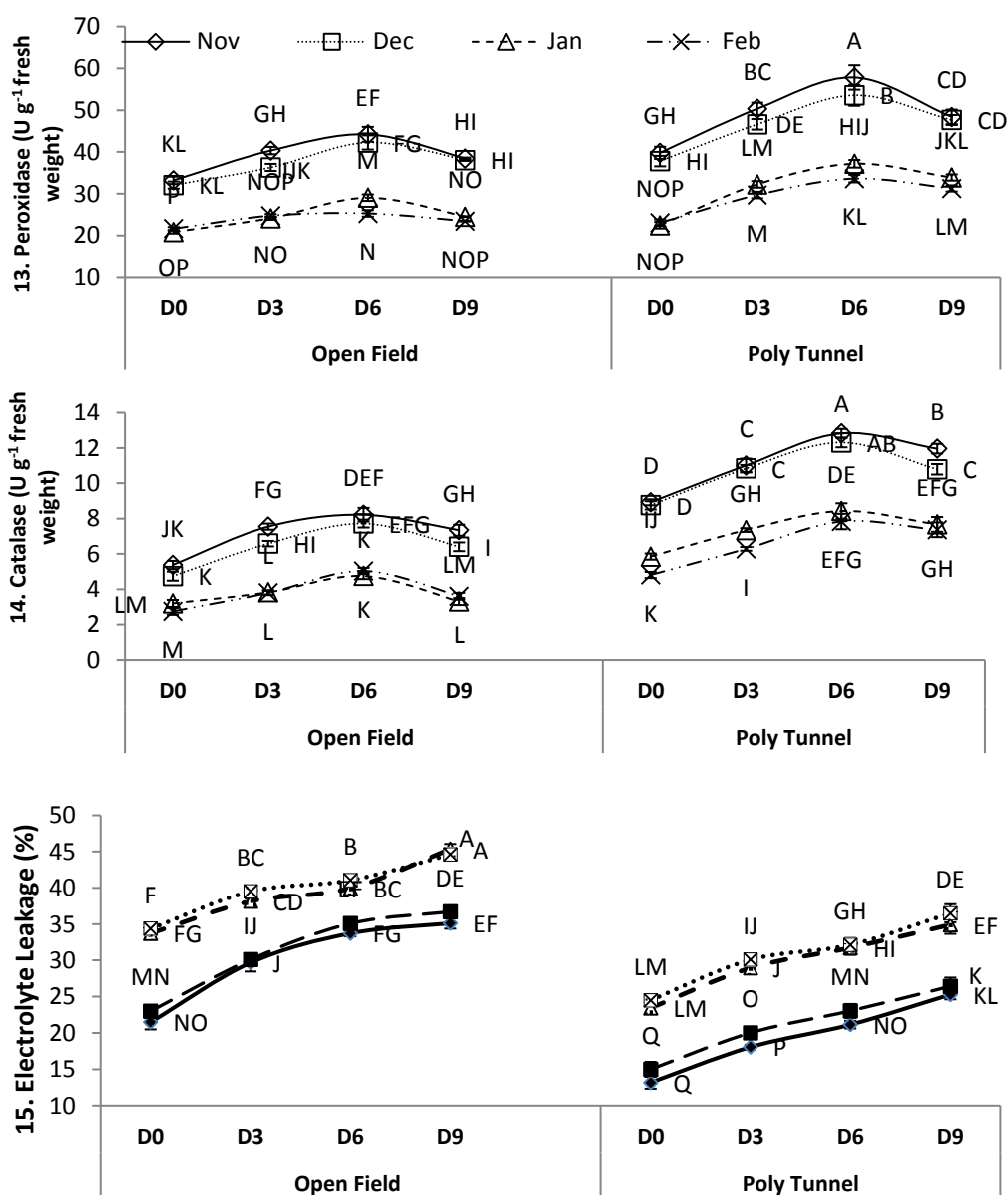


Figures 8-12. Effect of growing conditions and planting time on biochemical and physiological features (Bar shows standard error of means)

Antioxidant enzyme activity and membrane leakage

Antioxidant enzyme activities (POD & CAT) and electrolyte leakage are given in Figures 13-15. The maximum peroxidase activity in gladiolus cut flower were recorded

in gladiolus spikes grown in November (57.85 U g⁻¹ fresh weight) and December (53.60 U g⁻¹ fresh weight) under poly tunnel conditions at day 6 stage throughout the vase period while least during January (20.83 U g⁻¹ fresh weight) and February (21.62 U g⁻¹ fresh weight) at harvest day in open field conditions. The maximum catalase activity in gladiolus cut flower were recorded in gladiolus spikes grown under the polythene tunnel planting in the month of November (12.83 U g⁻¹ fresh weight) and December (12.31 U g⁻¹ fresh weight) at day 6 while the least during January (3.25 U g⁻¹ fresh weight) and February (2.75 U g⁻¹ fresh weight) at harvest day in open field condition. The maximum electrolyte leakage was recorded in gladiolus spikes grown under the open field in the month of January (45.36%), February (44.6%) while minimum in November (25.28%) and December (26.43%).



Figures 13-15. Effect of growing conditions and planting time on antioxidant activities (POD, CAT) and electrolyte leakage (Bar shows standard error of means)

Correlation of characteristics with temperature

Correlation of various studied characteristic with growing temperature is presented in Figure 16. The most of the correlation coefficient values (r) for morphological, physiological and antioxidant activities showed a stronger positive relation with average temperature in respective growing condition. The temperature ranges from 13-25°C. As temperature decrease the growth of the gladiolus also decreases. However, correlation coefficient values showed that days taken to flowering and days to open florets prolonged as temperature decreased. Also electrolyte leakage increased with the decreasing of temperature.

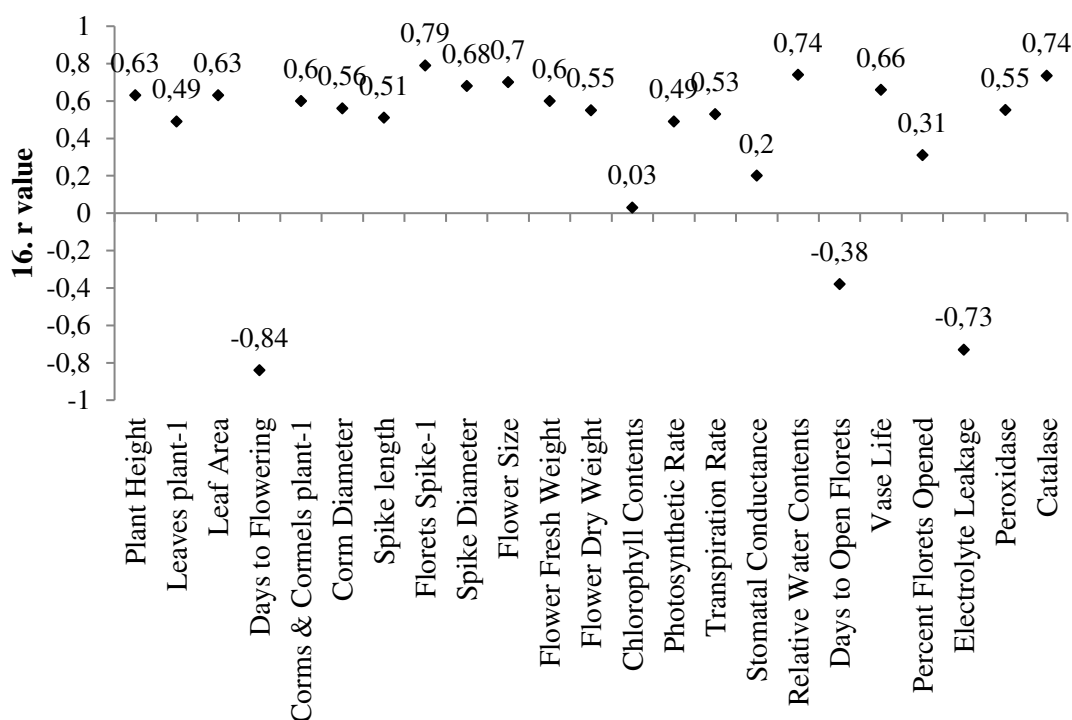


Figure 16. Correlation coefficient (r) with temperature of studied characteristics

Discussion

Morphological, floral and vase life attributes

Morphological, floral and vase life attributes significantly affected by temperature. The temperature is a principal feature influencing the plant growth rate and development. Optimum temperature enhanced the growth of plants positively (Khodorova and Boitel-Conti, 2013; Hatfield and Prueger, 2015). The growth of vegetative parts enhances as temperature increased to optimum level of the species (Paustian et al., 2004; Hatfield et al., 2011; Abbas et al., 2017). Temperature may influence the cell division and cell enlargement because all metabolic processes need a certain temperature and all enzymes functions at a specific temperature generally higher than freezing temperature. The polythene tunnel system enhances the temperature of the microclimate which favors the plants internal enzymes and photosynthates ultimately increasing leaf number per plant. As observed in gerbera cut flower produced under protected conditions (Soni and Godara, 2017). The temperature and relative humidity regulate the transpiration rate that involved

in nutrients and water uptake from root to leaves and thus higher rate of nutrients accumulation positively influenced the leaf size (Jezek et al., 2015). The cold temperature, by distressing the carbonic anhydrase activity lessens net photosynthesis in plants. Carbonic anhydrase is a restrictive enzyme for CO₂. The decrease fresh weight due to low temperature might be ascribed to the lower carbonic anhydrase activity or impaired protein synthesis that limited the growth (Franklin, 2009). Also, short days in later month with low temperature reduced the photosynthetic activity, due to which carbohydrate accumulation and the diameter of spikes ultimately reduced (Klein et al., 2007; Sacks and Kucharik, 2011). The temperature below freezing point during winter season reduces growth and energy storage of plants. Plants are prepared better to resist cold temperature when they are sheltered from severe circumstances (Ali et al., 2016). The low temperature during later months of January and February may reduce assimilates which can be insufficient to maintain flower meristem differentiation and cessation of cell division due to which carbohydrate accumulation reduced that eventually lower floral quality (Streck, 2004; Klein et al., 2007; Sacks and Kucharik, 2011). Low temperature damages several enzymes, their functional and structural component, such as alcohol dehydrogenase, phospholipase, carbonic anhydrase, alkaline phosphatase, RNA polymerase and carboxypeptidase which reduced fresh and dry weight (Mohanty et al., 2011). Alike results were reported on increased dry matter production in favorable temperature under protected production conditions in roses (Ahmad et al., 2011).

The application of protective polythene tunnel increased the inside temperature that promoted the translocation of photosynthates from the source to sink which favors growth attributes (Barthel et al., 2014; Schwab et al., 2015). Also the favorable temperature might enhance the carbohydrates and sugar translocation by formation of B-polyol complex (sugars alcohols binding with boric acid). Thus, enhanced its accumulation within plant, caused to form the more floral primordia in the shoot apical meristem resulted in higher number of florets per spike (Usha et al., 2002). The greater area of a leaf give assurance that higher chlorophyll contents will be present and leaf absorb more photosynthetically active radiations (PAR). Hence, both these aspects regulate higher rate of photosynthesis which enhanced accumulation of carbohydrates for growth and development (Sage and Kubien, 2007; Ahmad et al., 2011). The temperature up to favorable range with higher day length incriminate in the uptake and translocation of nutrients inside plant which leads to increase in underground parts production of plant (Joshi et al., 2011). Furthermore, higher area of leaves and more photosynthates in the particular month inside protected polythene tunnel treatment might be supportive in enhancing the corms and cormels number per plant and size of corms (Laishram et al., 2011; Mahesh and Moond, 2011).

The temperature inside the protected structure rose due to the blocking of infrared radiations (Lim et al., 2017). Temperature influence the time taken to flowering significantly. During early stages at which floret differentiation occur was most sensitive to temperatures and light intensities. Photoperiods and temperature influenced the time taken to flowering and flower development (Motomura et al., 2002; Sudhakar and Kumar, 2015). At warmer temperatures plants attain more carbohydrates for growth and development which ultimately helped plants to take lesser time to flowering (Shillo et al., 1981). Similar result of earlier maturity under protected structures in comparison to open field in tomato was reported by Parvej et al. (2010).

Senescence is the ultimate phase of flower life, which results in drooping of whole flower or the floral parts. The genetically controlled programmed known as senescence

in flower petals is directly triggered on the opening of floral bud. This process is not reversible in floral tissues (van Doorn and Woltering, 2004; Kumar et al., 2008). Overall growth of spikes is responsible for the opening of florets. Pre harvest growth designates the ultimate postharvest life of the flower spike (Gupta and Dubey, 2018). Vase life can be affected by transpiration, respiration, reactive oxygen species, and membrane leakage (Ezhilmathi et al., 2007). Preharvest morphological and physiological parameters at harvest were relevant to a considerable extent in vase life. Water uptake from the vase solution is attributed to better water balance, flower freshness and fresh weight and prevents the cut flower from early wilting (Ataï et al., 2015). The pre harvest accumulation of carbohydrates plays significant role in postharvest life of the cut flowers. These carbohydrates maintain osmotic potential within plants, which results in improved water uptake in cut spike. Thus better growth is maintained in pre harvest life and provides cut flowers with a better opportunity to perform in shelf life period (Da Silva, 2006). Healthier spike in respect to diameter, fresh weight, and floret size ensures the longer vase life (Slootweg et al., 1999). In the current studies the vase life was positively correlated with these morphological and physiological parameters.

Biochemical and physiological parameters

Chlorophyll contents were higher in plants those grown in earlier planting times when the temperature and long days having more light availability. More chlorophyll contents were notice in open field as compared to protected field conditions might be due to more availability of photo active radiations (Mohanty et al., 2006). These findings confirmed the findings of Ahmad and Usman (2013) and Qasim et al. (2008) who noticed more chlorophyll contents in open field production of rose. The relative water contents (RWC) might differ significantly with changing temperature in fast growing tissues, irrespective of the any growth stage. However, measurement of RWC remains very small because of limited potential for expansion of cells. Low cell metabolism rates in more mature and slow-growing leaves (Shinozaki et al., 2003; Kaplan et al., 2004).

The light-dependent photosynthetic reactions are not influenced by modifications in temperature. However, the photosynthetic light independent reactions are significantly affected by changes in temperature. There were various enzymes that catalysed these reactions. The rate of catalysis of these enzymes was increased as their temperatures attained at optimum levels. The rate starts to decline at low temperature, as enzymes became denatured (Schwender et al., 2004). The plant exposure to low temperature stress contributes to metabolism alterations in two ways. Formerly, because of increasing or decreasing the temperature, plants try to regulate the cellular metabolism. Secondly, structural changes, catalytic properties, enzyme functions and membrane metabolite transporters alter due to temperature stress. The enzymes that carry out photosynthesis do not work efficiently at low temperatures between 0 and 10, and this decreases the photosynthetic rate (Kubien et al., 2003; Fernie et al., 2005).

Temperature stress alone or in combination with CO₂ fluctuation alters the stomatal conductance in plants. Particularly in the leaf petiole reduction of both stomatal conductance and mesophyll conductance about 10-30% occurs only within 10 minutes of lower temperature. Likewise, major responses of stomatal conductance within 20-30 min took place due to variations in leaf temperature in plants acclimated together to low temperature (Gorton et al., 2003; Warren and Dreyer, 2006). The similar response of both mesophyll and stomatal variations in almost all environmental variables signifies that stomatal conductance co-regulated in order to availability of favorable temperature.

These findings favour the current study that in protected conditions and early month of plantations the temperature was favorable, due to which the stomatal conductance was better (Kerstiens, 2006; Morison and Lawson, 2007).

The temperature significantly affects the magnitude of the driving force to move water out of a plant instead of directly affecting stomata. The water holding capability of air rises abruptly as temperature rises. The warmer air can hold more water as compared to cooler air. Therefore, the driving force for transpiration rise in warmer air and reduced in the cooler air (Thakur et al., 2010; Mantri et al., 2012; Bala and Singh, 2013). The photosynthetic activity was good due to better stomatal conductance and transpiration which ultimately favors the growth and floral quality of gladiolus plants in protected conditions.

Antioxidant enzyme activity and membrane leakage attributes

The preeminent antioxidant enzymes (POD, CAT) activity was noticed in experiment during the early month November and December plantations. It might be characterized to strong activity antioxidative enzymes during favorable temperature conditions. However, during severe low temperature conditions in January and February, the antioxidant activities were remained lower in gladiolus cut flowers. Various toxic reactive oxygen species are generated due to stress. H_2O_2 is one the most abundantly produced radical, which in excess could harm the cell. The antioxidants enzymes peroxidase (POD) and catalase (CAT) are responsible for the biological removal of H_2O_2 from the cell (Mei and Song, 2008; Akhtar et al., 2010). These enzymes are produced in plant tissues according to their defence system during growth stages progression which specifies the defence mechanism in the shelf life of cut flower. The ROS is possibly generated due to low temperature stress (Hasegawa et al., 2000; Guo et al., 2016). The activities of antioxidative enzymes are reduced in extreme coldness beyond the plant's tolerant level or in chilling sensitive plants due to that ROS accumulated in greater extent (Solanke and Sharma, 2008; Chen and Arora, 2011). These higher amounts of ROS imposed the stress. The lipid, protein, carbohydrate and DNA damaged by this stress ultimately effecting physiological processes (Gill and Tuteja, 2010), thus causes cell death and adversely affect plants (Apel and Hirt, 2004). The excessive amount of H_2O_2 accumulation would be toxic to plants tissue in plant exposed to the abiotic stress (Zheng et al., 2009). It could be the reason that excess H_2O_2 imposed due to lower temperature stress resulted lower POD and CAT activity and short vase life in gladiolus cut flowers. Optimum temperature supply might be resulted in H_2O_2 release, thus enhanced POD and CAT level and extended vase life was noted (Nahar et al., 2009).

Electrolyte leakage was higher in plants grown in low temperature months at open field environment. The leakage of electrolyte in intact plant cells is a characteristic of stress response. This phenomenon is commonly used as a measure of plant stress tolerance (Bajji et al., 2004; Lee and Zhu, 2010). The membrane structure of tissues in plants was damaged under stress induced by low temperature. The intracellular leakage rate of electrolyte induced by cold stress reflected the amount of cell membrane damage. The plant response aptitude to cold stress is efficiently assessed indirectly by the relative conductance value. With the continuity of low temperature stress, the degree of damage was aggravated in cellular membrane (Liu et al., 2013). Increase in electrolyte leakage due to low temperature stress also observed in wheat (Chen et al., 2006), coffee seedlings (Azzarello et al., 2009) and tomato (Ghiasi and Razavi, 2013).

Conclusion

Gladiolus grown in two different growing environments revealed significant variations in morpho-physiological characteristics from November until February. Climate variables had a significant impact on growth and development of gladiolus. In early planting during November and December under polythene tunnel has positive effects on growth, production and floral characteristics of gladiolus cut flowers. The quality and vase life of cut flowers improved as biochemical characteristics, antioxidative enzymes activities enhanced and membrane remained stable. The application of polythene sheet during November and December months render the best results for improving growth and quality of gladiolus cut flowers. The polythene sheet significantly lower the stress imposed by low temperature. Moreover, mitigation with polythene sheet during January and February gives significant improvement in the growth and vase life attributes of gladiolus. However, lowest morpho-physiological indices of gladiolus were observed in January and February. Positive correlation of temperature was observed regarding growth and development of gladiolus. Such observations and previous literature findings indicate that more research is needed to measure the interactions between temperature and plant hardiness of gladiolus across germplasm within a species and between species to evaluate possible adaptation strategies to mitigate the negative effects of extreme temperature events.

Acknowledgements. The authors gratefully acknowledge the support of my beloved father “MUHAMMAD ABDUL QAYYUM AZIZ, Chief Engineer WAPDA Pakistan” for studies and throughout my career. The results presented here are part of PhD research of principal author. The authors acknowledge my Supervisor “Dr. Imran Hassan, Associate Professor” for providing the guidance and moral support. The authors also appreciate Plant Physiology & Central Laboratory, PMAS, Arid Agriculture University, Rawalpindi, Pakistan for provision of facilities and instruments.

REFERENCES

- [1] Abbas, Z. K., Saggi, S., Rehman, H., Al Thbiani, A., Ansari, A. A. (2017): Ecological variations and role of heat shock protein in *Artemisia judaica* L. in response to temperature regimes of Tabuk, Saudi Arabia. – *Saudi Journal of Biological Science* 24: 1268-1273.
- [2] Abbasi, N. A., Kushad, M. M., Endress, A. G. (1998): Active oxygen-scavenging enzymes activities in developing apple flowers and fruits. – *Scientia Horticulturae* 74: 183-194.
- [3] Ahmad, I., Khalid, M. S., Khan, M. A., Saleem, M. (2011): Morpho-physiological comparison of cut rose cultivars grown in two production systems. – *Pakistan Journal of Botany* 43: 2885-2890.
- [4] Ahmad, I., Usman, S. R. (2013): Humic acid and cultivar effects on growth, yield, vase life, and corm characteristics of gladiolus. – *Chilean Journal of Agricultural Research* 73: 339-344.
- [5] Ahmad, M., Rab, A. (2020): Calcium effects on post-harvest attributes and vase life of gladiolus using different methods of application. – *Pakistan Journal of Botany* 52(1): 167-179.
- [6] Akhtar, A., Abbasi, N. A., Hussain, A. (2010): Effect of calcium chloride treatments on quality characteristics of loquat fruit during storage. – *Pakistan Journal of Botany* 42: 181-188.
- [7] Ali, Z., Shabbir, M., Qadeer, A., Ahmad, H., Qasim, M., Aziz, O. (2016): Performance evaluation of *Gladiolus* varieties under diverse climatic conditions. – *Plant Gene & Trait* 7(4): 1-9.

- [8] Anderson, N. O., Frick, J., Younis, A., Currey, C. (2012): Heritability of cold tolerance (winter hardiness) in *Gladiolus* × *grandiflorus*. – In: Abdurakhmonov, I. Y. (ed.) *Plant Breeding*, InTech, chapter 13: 297-331.
- [9] Apel, K., Hirt, H. (2004): Reactive oxygen species: metabolism, oxidative stress, and signal transduction. – *Annual Review of Plant Biology* 55: 373-399.
- [10] Arora, J. S. (2007): *Introductory Ornamental Horticulture*. – Kalyani publishers, New Delhi, India: 61-67.
- [11] Ataii, D., Naderi, R., Khandan-Mirkohi, A. (2015): Delaying of postharvest senescence of *lisianthus* cut flowers by salicylic acid treatment. – *Journal of Ornamental Plants* 5: 67-74.
- [12] Azzarello, E., Mugnai, S., Pandolfi, C., Masi, E., Marone, E., Mancuso, S. (2009): Comparing image (fractal analysis) and electrochemical (impedance spectroscopy and electrolyte leakage) techniques for the assessment of the freezing tolerance in olive. – *Trees* 23: 159.
- [13] Bajji, M., Bertin, P., Lutts, S., Kinet, J. (2004): Evaluation of drought resistance-related traits in durum wheat somaclonal lines selected in vitro. – *Australian Journal of Experimental Agriculture* 44: 27-35.
- [14] Bala, M., Singh, K. (2013): Effect of different potting media for pot mum production in *chrysanthemum* grown under open and polyhouse conditions. – *Journal of Ornamental Horticulture* 16: 35-39.
- [15] Bars, H. D., Weatherley, P. E. (1962): A re-examination of relative turgidity technique for estimating water deficit in leaves. – *Australian Journal of Biological Science* 15: 413-428.
- [16] Barthel, M., Cieraad, E., Zakharova, A., Hunt, J. (2014): Sudden cold temperature delays plant carbon transport and shifts allocation from growth to respiratory demand. – *Biogeosciences* 11: 1425-1433.
- [17] Bhande, M. H., Neha, C., Sushma, L., Parinita, W. (2015): Effect of spacing and corm size on growth, yield and quality of *gladiolus*. – *Plant Archives* 15(1): 541-544.
- [18] Chen, Y., Zhang, M., Chen, T., Zhang, Y., An, L. (2006): The relationship between seasonal changes in anti-oxidative system and freezing tolerance in the leaves of evergreen woody plants of *Sabina*. – *South African Journal of Botany* 72: 272-279.
- [19] Chen, K., Arora, R. (2011): Dynamics of the antioxidant system during seed osmopriming, post-priming germination, and seedling establishment in *Spinach* (*Spinacia oleracea*). – *Plant Science* 180: 212-220.
- [20] Cowan, J. S., Miles, C. A., Andrews, P. K., Inglis, D. A. (2014): Biodegradable mulch performed comparably to polyethylene in high tunnel tomato (*Solanum lycopersicum* L.) production. – *Journal of the Science of Food and Agriculture* 94(9): 1854-1864.
- [21] Da Silva, J. A. T. (2006): Ornamental cut flowers: physiology in practice. – In: *Floriculture, Ornamental and Plant Biotechnology: Advances and Tropical Issues*, pp. 124-140.
- [22] Ezhilmathi, K., Singh, V., Arora, A., Sairam, R. (2007): Effect of 5-sulfosalicylic acid on antioxidant activity in relation to vase life of *Gladiolus* cut flowers. – *Plant Growth Regulation*: 51(2): 99-108.
- [23] Fernie, A. R., Geigenberger, P., Stitt, M. (2005): Flux an important, but neglected, component of functional genomics. – *Current Opinion on Plant Biology* 8: 174-182.
- [24] Franklin, K. A. (2009): Light and temperature signal crosstalk in plant development. – *Current Opinion on Plant Biology* 12: 63-68.
- [25] Ghiasi, N., Razavi, F. (2013): Impact of postharvest prohexadione calcium treatment on PAL activity in tomato fruit in response to chilling stress. – *Iranian Journal of Plant Physiology* 4(1): 865-871.
- [26] Gill, S. S., Tuteja, N. (2010): Reactive oxygen species and antioxidant machinery in abiotic stress tolerance in crop plants. – *Plant Physiology & Biology* 48: 909-930.
- [27] Gorton, H. L., Herbert, S. K., Vogelmann, T. C. (2003): Photoacoustic analysis indicates that chloroplast movement does not alter liquid-phase CO₂ diffusion in leaves of *Alocasia brisbanensis*. – *Plant Physiology* 132: 1529-1539.

- [28] Guo, W., Nazim, H., Liang, Z., Yang, D. (2016): Magnesium deficiency in plants: an urgent problem. – *The Crop Journal* 4: 83-91.
- [29] Gupta, J., Dubey, R. (2018): Factors Affecting Post-Harvest Life of Flower Crops. – *International Journal of Current Microbiology and Applied Sciences* 7: 548-557.
- [30] Hanan, J. J. (2017): Greenhouses: advanced technology for protected horticulture. – CRC press, p.684.
- [31] Hasegawa, P. M., Bressan, R. A., Zhu, J. K., Bohnert, H. J. (2000): Plant cellular and molecular responses to high salinity. – *Annual Review of Plant Biology* 51: 463-499.
- [32] Hatfield, J. L., Boote, K. J., Kimball, B. A., Ziska, L. H., Izaurralde, R. C., Ort, D., Wolfe, D. (2011): Climate impacts on agriculture: implications for crop production. – *Agronomy Journal* 103(2): 351-370.
- [33] Hatfield, J. L., Prueger, J. H. (2015): Temperature extremes: Effect on plant growth and development. – *Weather and Climate Extremes* 10: 4-10.
- [34] Jezek, M., Geilfus, C.-M., Bayer, A., Mühling, K. H. (2015): Photosynthetic capacity, nutrient status, and growth of maize (*Zea mays* L.) upon MgSO₄ leaf-application. – *Frontiers in Plant Science* 5: 781.
- [35] Jiang, X. B. (2011): Physiological and biochemical responses to low temperature stress in hybrid clones of *Populus ussuriensis* Kom. × *P. deltoides* Bartr. – *African Journal of Biotechnology* 10(82): 58-97.
- [36] Joshi, K., Gautam, D., Baral, D., Pun, U. (2011): Effect of corm size and varieties on corm/cormels production and vase life of gladiolus. – *Nepal Journal of Science and Technology* 12: 35-40.
- [37] Kaplan, F., Kopka, J., Haskell, D. W., Zhao, W., Schiller, K. C., Gatzke, N., Sung, D. Y., Guy, C. L. (2004): Exploring the temperature-stress metabolome of *Arabidopsis*. – *Plant Physiology* 136: 4159-4168.
- [38] Kerstiens, G. (2006): Water transport in plant cuticles: an update. – *Journal of Experimental Botany* 57: 2493-2499.
- [39] Khodorova, N. V., Boitel-Conti, M. (2013): The Role of Temperature in the Growth and Flowering of Geophytes. – *Plants (Basel)* 2(4): 699-711.
- [40] Klein, J. A., Harte, J., Zhao, X. Q. (2007): Experimental warming, not grazing, decreases rangeland quality on the Tibetan Plateau. – *Ecological Application* 17: 541-557.
- [41] Kubien, D. S., von Caemmerer, S., Furbank, R. T., Sage, R. F. (2003): C₄ photosynthesis at low temperature. A study using transgenic plants with reduced amounts of Rubisco. – *Plant Physiology* 132: 1577-1585.
- [42] Kumar, N., Srivastava, G. C., Dixit, K. (2008): Role of sucrose synthase and invertases during petal senescence in rose (*Rosa hybrida* L.). – *The Journal of Horticultural Science & Biotechnology* 83: 520-524.
- [43] Laishram, N., Singh, A., Hatibarua, P. (2011): Division of corms for increasing planting material of gladiolus: Cut corm segments of gladiolus increases number of propagules. – Lambert Academic Publishing, pp. 25-46.
- [44] Lee, B. H., Zhu, J. K. (2010): Phenotypic analysis of *Arabidopsis* mutants: electrolyte leakage after freezing stress. – *Cold Spring Harbor Protocols*: 49-70.
- [45] Lim, J. H., Choi, H. W., Ha, S. T., In, B. C. (2017): Greenhouse dehumidification extends postharvest longevity of cut roses in winter season. – *Korean Journal of Horticultural Science & Technology* 35: 737-746.
- [46] Liu, W., Yu, K., He, T., Li, F., Zhang, D., Liu, J. (2013): The low temperature induced physiological responses of *Avena nuda* L., a cold-tolerant plant species. – *The Scientific World Journal* 17(4): 113-119.
- [47] Long, S. P., Bernacchi, C. J. (2003): Gas exchange measurements, what can they tell us about the underlying limitation to photosynthesis procedures and sources of error. – *Journal of Experimental Botany* 54: 2393-2401.
- [48] Mahesh, C., Moond, S. A. K. (2011): Correlation studies in gladiolus. – *Research in Plant Biology* 1: 68-72.

- [49] Mantri, N., Patade, V., Penna, S., Ford, R., Pang, E. (2012): Abiotic stress responses in plants: present and future. – In: Ahmad, P., Prasad, M. N. V. (eds.) Abiotic stress responses in plants. Chapter 1: 1-19.
- [50] Mayoli, R. N., Isutsa, D. K. (2012): Relationships of light intensity and temperature with growth and development of preconditioned and shaded ranunculus plants under high altitude tropical conditions. – International Journal of Advanced Biological Research 2(1): 24-29.
- [51] Mei, Y., Song, S. (2008): Cross-tolerance is associated with temperature and salinity stress during germination of barley seeds. – Seed Science and Technology 36: 689-698.
- [52] Mohanty, S., Grimm, B., Tripathy, B. C. (2006): Light and dark modulation of chlorophyll biosynthetic genes in response to temperature. – Planta 224: 692-699.
- [53] Mohanty, C., Mohanty, A., Das, A., Kar, D. (2011): Comparative performance of some rose varieties under open and protected environment. – Asian Journal of Horticulture 6: 288-293.
- [54] Morison, J. I., Lawson, T. (2007): Does lateral gas diffusion in leaves matter? – Plant Cell & Environment 30: 1072-1085.
- [55] Motomura, S., Doi, M., Inamoto, K., Imanishi, H. (2002): Postharvest factors affecting the vase life of cut roses. – Journal of Japanese Society of Horticulture Science 71: 415.
- [56] Nahar, K., Biswas, J., Shamsuzzaman, A., Hasanuzzaman, M., Barman, H. (2009): Screening of indica rice (*Oryza sativa* L.) genotypes against low temperature stress. – Botany Research International 2: 295-303.
- [57] Parvej, M., Khan, M., Awal, M. (2010): Phenological development and production potentials of tomato under polyhouse climate. – Journal of Agriculture Science 5(1): 19-31.
- [58] Paustian, K., Babcock, B., Hatfield, J., Kling, C., Lal, R., McCarl, B., McLaughlin, S., Mosier, A., Post, W., Rice, C. (2004): Climate change and greenhouse gas mitigation: challenges and opportunities for agriculture. – CAST Task Force Report: 141.
- [59] Porter, J. R. (2005): Rising temperatures are likely to reduce crop yields. – Nature 436(7048): 174.
- [60] Qasim, M., Ahmad, I., Ahmad, T. (2008): Optimizing fertigation frequency for *Rosa hybrida* L. – Pakistan Journal of Botany 40: 533-545.
- [61] Sacks, W. J., Kucharik, C. J. (2011): Crop management and phenology trends in the US Corn Belt: Impacts on yields, evapotranspiration and energy balance. – Agricultural and Forest Meteorology 151: 882-894.
- [62] Saeed, T., Hassan, I., Jilani, G., Abbasi, N. A. (2013): Zinc augments the growth and floral attributes of gladiolus, and alleviates oxidative stress in cut flowers. – Scientia Horticulturae 164: 124-129.
- [63] Sage, R. F., Kubien, D. S. (2007): The temperature response of C3 and C4 photosynthesis. – Plant, Cell and Environment 30: 1086-1106.
- [64] Sanghera, G. S., Wani, S. H., Hussain, W., Singh, N. (2011): Engineering cold stress tolerance in crop plants. – Current Genomics 12(1): 30-43.
- [65] Schwab, N. T., Streck, N. A., Becker, C. C., Langner, J. A., Uhlmann, L. O., Ribeiro, B. S. M. R. (2015): A phenological scale for the development of Gladiolus. – Annual of Applied Biology 166: 496-507.
- [66] Schwender, J., Ohlrogge, J., Shachar-Hill, Y. (2004): Understanding flux in plant metabolic networks. – Current Opinion on Plant Biology 7: 309-317.
- [67] Shillo, R., Valis, G., Halevy, A. H. (1981): Promotion of flowering by photoperiodic lighting in winter-grown gladiolus planted at high densities. – Scientia Horticulturae 14: 367-375.
- [68] Shinozaki, K., Yamaguchi-Shinozaki, K., Seki, M. (2003): Regulatory network of gene expression in the drought and cold stress responses. – Current Opinion on Plant Biology 6: 410-417.

- [69] Singh, A., Kumar, J., Kumar, P. (2008): Effect of plant growth regulators and sucrose on postharvest physiology, membrane stability and vase life of cut spikes of gladiolus. – *Plant Growth Regulation* 55: 221-229.
- [70] Slootweg, G., Ten Hoope, M., De Gelder, A. (1999): Seasonal changes in vase life, transpiration and leaf drying of cut roses. – VII International Symposium on Postharvest Physiology of Ornamental Plants 543: 337-342.
- [71] Solanke, A. U., Sharma, A. K. (2008): Signal transduction during cold stress in plants. – *Physiology & Molecular Biology of Plants* 14: 69-79.
- [72] Soni, S. S., Godara, A. K. (2017): Evaluation of Gerbera Varieties for Growth and Floral Characters Grown Under Greenhouse Condition. – *Journal of Current Microbiology and Applied Sciences* 6: 2740-2745.
- [73] Sood, S., Vyas, D., Nagar, P. K. (2006): Physiological and biochemical studies during flower development in two rose species. – *Scientia Horticulturae* 108: 390-396.
- [74] Streck, N. A. (2004): A temperature response function for modeling leaf growth and development of the African violet (*Saintpaulia ionantha* Wendl.). – *Ciência Rural* 34: 55-62.
- [75] Sudhakar, M., Kumar, S. (2015): Studies on the influence of planting season and weather parameters on growth parameters of two different varieties of *G. grandiflorus* L. – *Asian Journal of Horticulture* 10: 36-40.
- [76] Thakur, P., Kumar, S., Malik, J. A., Berger, J. D., Nayyar, H. (2010): Cold stress effects on reproductive development in grain crops: an overview. – *Environmental & Experimental Botany* 67: 429-443.
- [77] Usha, B. T., Chandara Sekhar, R., Reddy, Y. (2002): Vase life studies of three gladiolus cultivars as influenced by dates of planting and iron sulphate sprays. – *The Journal of Research Angraui* 30: 40-43.
- [78] van Doorn, W. G., Woltering, E. J. (2004): Senescence and programmed cell death: substance or semantics? – *Journal of Experimental Botany* 55: 2147-2153.
- [79] von Caemmerer, S., Evans, J. R. (2015): Temperature responses of mesophyll conductance differ greatly between species. – *Plant, Cell & Environment* 38(4): 629-637.
- [80] Waraich, E. A., Ahmad, R., Halim, A., Aziz, T. (2012): Alleviation of temperature stress by nutrient management in crop plants. – *Journal of Soil Science and Plant Nutrition* 12(2): 221-244.
- [81] Warren, C., Dreyer, E. (2006): Temperature response of photosynthesis and internal conductance to CO₂: results from two independent approaches. – *Journal of Experimental Botany* 57: 3057-3067.
- [82] Zheng, Y. L., Feng, Y. L., Lei, Y. B., Yang, C. Y. (2009): Different photosynthetic responses to night chilling among twelve populations of *Jatropha curcas*. – *Photosynthetica* 47: 559-566.

LINKING SOIL BACTERIAL COMMUNITY AND CROP YIELD IN A WHEAT (*TRITICUM AESTIVUM* L.) - ALFALFA (*MEDICAGO SATIVA* L.) INTERCROPPING SYSTEM

LI, X.^{1,2,3} – ZHAO, Y. S.^{1*} – SUN, G. Y.^{2,4*} – JIN, W. W.² – SUN, M. L.⁵ – ZHANG, H. H.³ – XU, N.⁶
– CAI, D. J.⁷ – LI, D. M.⁸

¹*School of Forestry, Northeast Forestry University, Harbin, 150040, China*

²*College of Life Science, Northeast Forest University, Harbin, 150040, China*

³*College of Resources and Environment, Northeast Agricultural University, Harbin 150030,
China*

⁴*Key Laboratory of Saline-Alkali Vegetation Ecology Restoration, Ministry of Education,
Northeast Forestry University, Harbin, 150040, China*

⁵*Institute of Crop Breeding, Heilongjiang Academy of Agriculture Sciences, Harbin, 150040,
China*

⁶*Natural Resources and Ecology Institute, Heilongjiang Academy of Sciences, Harbin, 150040,
China*

⁷*Institute of Crops, Heilongjiang Academy of Land Reclamation and Agricultural Sciences,
Jiamusi, 154000, China*

⁸*Department of Product Distribution, Forestry Department of Heilongjiang Province, Harbin,
150040, China*

**Corresponding authors*

*e-mail/phone: zhaoy1957@163.com/+86-451-8219-1501; sungy@vip.sina.com/+86-451-
8219-1507*

(Received 18th Dec 2019; accepted 6th May 2020)

Abstract. Diverse intercropping has been utilized to improve crop productivity on agricultural fields. Beneficial plant rhizobacteria are associated with plant root surface and may increase yield. In the research, the bacterial communities in soils of monoculture and intercropping wheat and alfalfa (cv. Winter star) were studied using MiSeq sequencing of the 16S rDNA gene. Intercropping pattern improved wheat yield in the field. The dominant taxonomic groups in the rhizosphere soil were *Proteobacteria*, *Acidobacteria*, *Bacteroidetes*, *Actinobacteria*, *Planctomycetes*, *Chloroflexi* and *Nitrospirae* and these were present across 4 samples. Intercropping significantly affected the diversity and composition of bacterial communities compared to monoculture. The enrichment of bacterial communities such as the populations of *Rhizobiales*, *Burkholderiales*, *Pseudomonales* and *Bacillus* could be important factors contributing to yield increases in intercropping wheat. In addition, some populations, such as *Sphingomonadals* and *Xanthomonadales*, indicated contrary changes, their diversity declined in intercropping systems, meaning that these bacterial populations were affected by cropping patterns.

Keywords: *monoculture, intercropping, bacterial community composition, MiSeq, rhizosphere*

Introduction

Intercropping has been used for many years to grow two or more plants in the same area of land simultaneously (Vandermeer, 1992). Intercropping ecosystems have

demonstrated to be better than monoculture in terms of yields as a consequence of intercropping can make better use of one or more agricultural resources in time and space, through different rooting depths or over a year, to maximum the access to nutrients (Ma et al., 2017; Ren et al., 2017; Sylvain et al., 2018). Furthermore, the advantage of intercropping systems in yield is due to the interaction between intercropped species on the above- and below-ground (Du et al., 2011; Hauggaard-Nielsen et al., 2001). There are more reports about interspecies above-ground than below-ground interactions for interspecies interactions (Vandermeer, 1992; Willey, 1999). However, the effects of below-ground may be greater than above-ground species interactions for intercrop productivity (Hanming et al., 2012; Yue et al., 2014). There are compact relationships between yield advantage and water content, root morphologies nutrient uptake and root-associated microbes in intercropped soils (Choudhary et al., 2016; Zhou et al., 2011).

Intercropping of leguminous crops and cereals is one of the most practical intercropping techniques (Hesler and Kieckhefer, 2018) for improving crop yields and land use efficiency (Bhatti et al., 2006). Therefore, perennial alfalfa and annual wheat were selected to set up intercropping system in our study. In consequence, the root morphological and physiological characteristics of alfalfa and wheat are very different, and co-cultivation of both species can improve the absorption of water and nutrients by the root system (Skelton and Barrett, 2005). Leguminous plants could improve harsh environmental conditions or the available resources for other adjacent species by transferring of symbiotically fixed nitrogen (N) (Jensen, 1996a) and dissolving of inorganic phosphorus (P) fixed in soil (Yan et al., 1996). Furthermore, intercropping may increase soil microbial diversity, which usually has a positive effect on crop productivity (Xin et al., 2016). Free-living microorganisms strongly regulate plant productivity by mineralizing and competing nutrients that maintain plant productivity (Van Der Heijden et al., 2008).

Microorganisms are ubiquitous in the environment and play an essential role in the global biogeochemical cycles that sustain all life on Earth (Su et al., 2012; Zarraonaindia et al., 2013). It is well known that soil microbes carry out fundamental processes that contribute to nutrient acquisition (Li et al., 2016, 2020), nitrogen cycling (Li et al., 2017), carbon cycling (Schimel and Schaeffer, 2012) and soil formation (Rillig and Mummey, 2006). Soil microbes are crucial regulators of plant productivity (Van Der Heijden et al., 2008), and plant community composition considerably influences the community composition of rhizosphere microbes. The aboveground trophic interactions have indirect effects on soil biota by affecting the quantity and quality of resources that plants produce (Wardle et al., 2004). The roots of different plant species are in direct contact in intercropping ecosystem, and the root-associated communities of both plants species can therefore interact. The resulting microbial community composition is likely to be a mixture of the species-specific communities but may be dominated by the community composition of one plant species (Song et al., 2007). However, while it is widely recognized that microbes perform crucial roles in biogeochemical cycling, the impact of soil microbes on plant productivity is still poorly understood. Therefore, in order to better understand the changes of bacterial communities of monoculture versus intercropped plants in soils, 16S rDNA gene-based MiSeq sequencing approach was employed in wheat/alfalfa intercropping system, which may contribute to the greater yield in intercropping compared with sole cropping.

Materials and methods

Field plots

A field experiment was conducted at Heilongjiang Academy of Land Reclamation and Agricultural Sciences, Jiamusi city of Heilongjiang province, China (latitude, 46°46'N; longitude, 130°27'E) in 2014. The region has a typical temperate continental climate with an average annual temperature of -3.0~-1.5 °C and the mean temperature of 20 °C in July. The mean annual precipitation is 450~550 mm and nearly 59% of total rainfall is received by northwest monsoons from July-September. The active accumulated temperature (≥ 10 °C) is 2000~2800 °C per year, and a frost-free period of 115~130 days. The soil is classified as a meadow black soil. Soil samples contained organic of 3.9%, available nitrogen of 46.9 mg·kg⁻¹, available phosphorus of 145.5 mg·kg⁻¹, available potassium of 121.0 mg·kg⁻¹, pH of 6.7.

The experimental design was a plot divided into three blocks (three replicates), each block being further divided into three plots. Each plot was used for one of the following cropping systems: (1) wheat monoculture, (2) alfalfa monoculture, and (3) wheat intercropped with alfalfa. The experiment covered an area of 405.8 m². Each plot unit comprised 12 rows that were 5 m long and 0.66 m wide, each 39.6 m² in size. Plots and blocks were separated from each other by 1-meter walkways. For the intercropped treatment, two alfalfa rows were intercropped with two rows of wheat. The single cropping plots consisted of 12 rows of one plant species. Edges of each plot were sown with a mix of wheat and alfalfa to minimize edge effects but these plants were not included in the harvest.

The wheat (*Triticum aestivum* L. cv. Kenfeng No.1) and alfalfa (*Medicago sativa* L. cv. Winter star) were sown manually on 10 and 14 June 2014, respectively. Seedlings in each row were thinned after emergence to leave a density of 30 plants m⁻² for alfalfa and 600 plants for wheat. Prior to sowing, fertilizer in the form of (NH₄)₂HPO₄ (150 kg·hm⁻²) were applied and the soil was disked to a depth of 10 cm. A conventional herbicide treatment was applied.

The yield of wheat and alfalfa was investigated using the quadrat harvesting method, and was determined in August 2014. The plants were killed at 105 °C for 30 min and dried at 60 °C to a constant weight.

Soil samples were collected from three different sampling sites at the flowering stage on 26 July 2014. Non-rhizosphere soil were removed by shaking the root gently, Rhizosphere soils, adhering to the roots (Nazih et al., 2001), were placed into sterile petri plates. Three random sampling points were chosen for each sampling plot. Nine random single samples of rhizosphere soil were collected and thoroughly mixed in order to obtain a composite sample. The soil samples were sieved (2 mm) and stored at -80 °C until DNA extraction.

DNA extraction and PCR amplification 16S rRNA

The genome DNA was isolated using an Omega Bio-Tek E.Z.N.A. Soil DNA Extraction Kit (Omega Bio-Tek, Atlanta, GA, USA) according to the manufacturer's instructions. The equality of extracted DNA was examined following electrophoresis in a 1% agarose gels. The V4-V5 regions of the 16S rRNA gene were PCR amplified by using barcoded fusion primers 515F (5'-GTGCCAGCMGCCGCGG-3') and 907R (5'-CCGTCAATTCMTTTRAGTTT-3'). For each sample, three independent amplification reactions were performed. The reaction mixture (20 µL) contained 5 µM

of each primer, ~10 ng of template DNA, 5× FastPfu PCR buffer, 2.5 mM dNTPs and 2.5 U of FastPfu DNA Polymerase (MBI, Fermentas, USA). The amplification conditions were: 95 °C for 3 min and 7 cycles of denaturation at 95 °C at 30 s, annealing at 55 °C for 30 s, and extension at 72 °C for 45 s, followed by a final extension period at 72 °C for 10 min. During amplification, a negative control reaction (lacking template DNA) was included to check the experimental contamination. All reactions were performed in triplicate. The PCR products were detected by electrophoresis in a 2% agarose gel and purified using the AxyPrep DNA Gel Extraction Kit (Axygen Biosciences, Union City, CA, USA).

MiSeq sequencing and data analysis

The Illumina MiSeq PE250 was applied to perform barcoded V4-V5 amplicons by Shanghai Majorbio Bio-Pharm Biotechnology (Shanghai, China). Raw fastq files were demultiplexed and quality-filtered using QIIME (version 1.17). Sequences were clustered and assigned to operational taxonomic units (OTUs) at a 97% similarity level using UPARSE (version 7.1). To assess phylogenetic affiliations, taxonomic ranks were assigned to each sequence using Ribosomal Database Project (RDP). Compositional differences between libraries were determined using distance matrices and LIBSHUFF comparisons (Singleton et al., 2001). Alpha diversity (Ace, Chao 1, Simpson and Shannon) was calculated with QIIME (Version 1.7.0) and displayed with R software (Version 2.15.3). Venn diagrams of unique and OTUs (0.03 cut-off value) were drawn to highlight the similarities and shared sequences between the different analyzed samples. Principal Component Analysis (PCA) in genus level was performed using ggplot2 package in R software (Version 2.15.3). Hierarchical cluster (Heatmap) analyses were generated in MOTHUR using the gplots package of R software (Version 2.15.3).

Statistical analysis

We used SPSS for windows (version 19) to test for significance ($P < 0.05$) between treatments of relative abundances, Alpha diversity and richness of bacterial communities using Duncan post-hoc test at 95% confidence level. To determine the key factor(s) affecting microbial parameters, stepwise multiple regression analysis was applied using the probability criteria of $P < 0.05$ to accept and $P > 0.1$ to remove a variable from the analysis.

Results

Plant yields

The yield of wheat and alfalfa were measured in September 2014 (*Fig. 1*). The intercropping significantly increased wheat yield compared with monoculture ($P < 0.05$). The yield in the intercropped wheat was 39.65% higher than monoculture. However, intercropping systems slightly decreased the biomass of alfalfa and there was no significant difference between monoculture and intercropping treatments ($P > 0.05$).

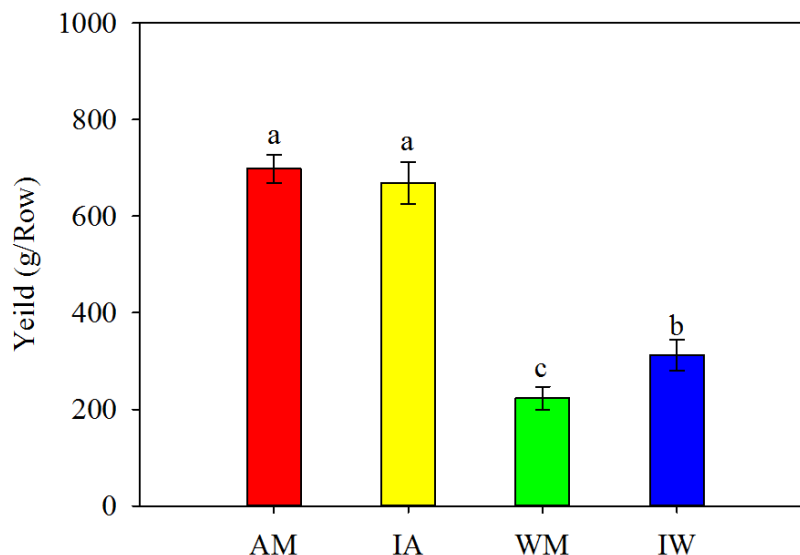


Figure 1. The yield of wheat and alfalfa. Alfalfa monoculture (AM), intercropping alfalfa (IA), wheat monoculture (WM), and intercropping wheat (IW). Bars with different letters indicate significant difference at $P < 0.05$. The significant differences between the means were determined using Duncan post-hoc test

Bacterial community analysis

A total of 148,259 paired-end ≥ 300 -bp reads were acquired from all 12 samples, with 31,242, 42,231, 39,239 and 35,547 high quality reads at the monoculture alfalfa, alfalfa intercropping, monoculture wheat, and wheat intercropping soils, respectively (Table A1 in the Appendix). The average read length was 396 bp. Based on 97% species similarity, 1,231, 1,188, 1,161 and 1,280 operational taxonomic units (OTUs) were obtained from monoculture alfalfa, alfalfa intercropping, monoculture wheat, and wheat intercropping soils, respectively.

Bacterial diversity and richness

To determine rarefaction curves and other measures of diversity, OTUs (operational taxonomic units) were identified at 3% genetic distance. Rarefaction curves indicated consistent differences in all 4 libraries (Fig. A1 in the Appendix). At 3% genetic distances, almost all rarefaction curves reached saturation, indicating that the surveying effort covered almost the full extent of taxonomic diversity at this genetic distance.

The comparison of mean Chao 1 richness estimates of alfalfa rhizosphere soils and wheat rhizosphere soils showed no differences at genetic distances of 3% (421 OTUs and 424 OTUs, respectively) (Table 1). Analysis of differences of cropping pattern by at genetic distances of 3% showed that the intercropping patterns varied in the predicted number of OTUs ($P > 0.05$). The uniform conclusion was seen using the Ace richness index (Table 1). Moreover, the comparison of the mean Shannon diversity index of 4 libraries revealed that the highest bacterial diversity at analyzed genetic distances was found in intercropping wheat and alfalfa soils, followed by monoculture wheat and alfalfa. The predicted richness and diversity in the intercropping rhizosphere soils exceeded that of the corresponding monoculture soils. Meanwhile, an influence of plant species on bacterial diversity was observed. Wheat soils demonstrated higher diversity

than corresponding alfalfa in different cropping patterns. Thus, both intercropping system and plant species impacted overall bacterial diversity and richness.

Table 1. The diversity index of 4 libraries. Means of three replicates \pm SE. Different letters following the mean values within each column indicates significant differences at $P < 0.05$

Sample	0.97			
	Ace	Chao 1	Shannon	Simpson
Monoculture alfalfa	406.0 \pm 12.83 a	403.3 \pm 14.61 a	4.81 \pm 0.029 a	0.0181 \pm 0.0008 b
Alfalfa intercropping	420.3 \pm 12.47 b	439.3 \pm 25.84 b	5.13 \pm 0.021b	0.0101 \pm 0.0003 a
Monoculture wheat	401.7 \pm 9.18 a	406.7 \pm 14.27 a	5.11 \pm 0.021 a	0.0104 \pm 0.0003 a
Wheat intercropping	449.3 \pm 10.34 b	441.7 \pm 9.18 b	5.27 \pm 0.025 b	0.0093 \pm 0.0004 a

Distribution of taxa and phylotypes across 4 liberates

The 49,394 classifiable sequences were affiliated with 9 bacterial phyla (Fig. A2). The groups accounted for 97.31% of all sequences, and a few sequences (< 1%) could not be shown. The dominant phyla were as follows: *Proteobacteria*, *Acidobacteria*, *Bacteroidetes*, *Actinobacteria*, *Planctomycetes*, *Chloroflexi*, and *Nitrospirae*, representing 42.60, 25.10, 8.93, 4.92, 4.73, 4.15 and 3.72%, respectively, of all sequences that were classified below the domain level. These dominant bacterial phyla were shared in all samples (Table 2). Other sequences belonged to *Firmicutes*, *Gemmatimonadetes* and unclassified bacteria, and they were invariably found in very low proportions (< 2%). *Proteobacteria* accounting for 42.60% was the most dominant among the 9 phyla in all samples, regardless of the different samples. *Acidobacteria* was the second largest phylum in all groups accounting for 25.10%. The other 7 phyla sequences accounting for 8.93-1.07% (Fig. A2).

Comparative analysis of the 4 libraries revealed a distinct distribution of the bacterial phyla (Table 2). On average, *Proteobacteria* and *Actinobacteria* showed a higher relative abundance in alfalfa rhizosphere soils than in wheat rhizosphere soils, whereas *Bacteroidetes* and *Chloroflexi* showed the opposite pattern. The phyla of *Actinobacteria*, *Acidobacteria*, *Proteobacteria*, *Bacteroidetes*, *Firmicutes*, *Bacteria_unclassified*, *Gemmatimonadetes* and *Nitrospirae* were found in variable proportions, depending on the use of monoculture or intercropping; Most of *Bacteroidetes*, *Bacteria_unclassified* and *Gemmatimonadetes* were found in alfalfa intercropping libraries ($P < 0.05$), whereas *Proteobacteria* and *Firmicutes* were present at higher percentages in monoculture alfalfa libraries ($P < 0.05$). Moreover, the relative abundances of *Actinobacteria* and *Firmicutes* in wheat intercropping were significantly higher than that of monoculture wheat ($P < 0.05$), whereas *Acidobacteria* and *Nitrospirae* were present at higher percentages in monoculture wheat libraries ($P < 0.05$).

Proteobacteria sequences

The dominant phyla across all 4 libraries were *Proteobacteria* representing 42.60%, which predominated in all 4 libraries and showed the greatest diversity. Four classes: α -*Proteobacteria*, β -*Proteobacteria*, δ -*Proteobacteria* and γ -*Proteobacteria*, were affiliated with the *Proteobacteria* phylum (Fig. 2). The β -*Proteobacteria* sequences were most abundant, representing 41.00% of the *Proteobacteria*. The α -*Proteobacteria*

and γ -*Proteobacteria* were relatively abundant, representing 25.36 and 27.65% of the *Proteobacteria*, respectively. The γ -*Proteobacteria* sequences representing 5.99% of the *Proteobacteria*.

Table 2. Relative abundance of the phylogenetic groups presents in the monoculture and intercropping soils. Note: a one factor (niche) ANOVA (Duncan post-hoc test) was applied on the relative distribution values and results are presented in the column entitled 'statistics'. ns: non-significant differences. The phylogenetic groups for which a significant or nearly significantly effect of the niche are presented. AM > IA means significantly more present in the AM soil than in IA soil. AM < IA means significantly more present in the IA soil than in AM soil. WM > IM means significantly more present in the WM soil than in IM soil. WM < IM means significantly more present in the IM soil than in WM soil

	Alfalfa monoculture			Intercropping alfalfa			Statistics	Wheat monoculture			Intercropping wheat			Statistics
	AM1	AM2	AM3	IA1	IA2	IA3		WM1	WM2	WM3	IW1	IW2	IW3	
Proteobacteria	51.02	50.13	47.05	37.64	42.94	40.98	AM>IA (P=0.0106)	42.02	46.19	39.60	43.20	44.23	41.98	ns
Acidobacteria	18.93	22.38	23.69	21.99	25.66	26.99	ns	23.23	24.87	27.21	16.90	15.86	21.20	WM>IW (P=0.0237)
Actinobacteria	8.99	6.69	6.99	8.94	9.12	10.47	ns	5.52	4.18	5.06	10.02	8.79	7.17	IW>WM (P=0.015)
Bacteroidetes	2.89	3.56	3.78	8.13	5.79	5.83	IA>AM (P=0.0179)	10.57	7.46	8.76	6.37	7.29	7.04	ns
Chloroflexi	2.96	3.43	3.47	4.76	3.02	3.35	ns	3.42	3.62	5.41	6.14	7.11	5.23	ns
Firmicutes	5.63	6.29	6.95	2.53	1.86	1.76	AM>IA (P=0.0007)	1.78	1.58	1.47	5.02	4.14	3.89	IW>WM (P=0.0015)
Nitrospirae	2.72	3.82	2.40	4.13	2.83	2.86	ns	4.00	3.55	3.62	2.03	2.18	3.01	WM>IW (P=0.0171)
Planctomycetes	3.02	2.04	2.90	4.64	3.39	2.73	ns	5.12	4.46	4.61	4.78	3.61	3.91	ns
Bacteria_unclassified	0.23	0.27	0.32	3.45	2.67	2.46	IA>AM (P=0.001)	2.01	1.52	1.38	2.11	2.46	1.92	ns
Gemmatimonadetes	1.60	1.01	1.02	2.48	1.94	1.85	IA>AM (P=0.0336)	1.41	1.51	1.69	1.39	1.42	1.82	ns
Others	2.01	0.38	1.43	1.31	0.78	0.72	ns	0.92	1.06	1.19	2.04	2.91	2.83	IW>WM (P=0.006)

The α -*Proteobacteria* were relatively abundant and diversity. 5 orders were identified as being related to α -*Proteobacteria* (Fig. 2A). The *Rhizobiales* was the most abundant order in 4 libraries, representing 63.47%. The relatively abundant orders affiliated to α -*Proteobacteria* were *Caulobacterales*, *Rhodospirillales*, *Richettsiales* and *Sphingomonadals*, representing 9.82, 11.42, 0.03 and 15.25%. Depending on the use of monoculture and intercropping, most of *Rhizobiales* and *Rhodospirillales* were found in intercropping alfalfa, whereas low abundance was found in intercropping wheat ($P < 0.05$). *Sphingomonadals* showed a contrary variation, presenting at higher abundances in intercropping wheat and lower abundances in intercropping alfalfa comparing with monoculture ($P < 0.05$), respectively. The comparison of relative abundances of *Caulobacterales* revealed no significant differences between intercropping and monoculture libraries ($P > 0.05$). 1 OTU was related to *Richettsiales* and identified in alfalfa monoculture libraries only.

The β -*Proteobacteria* were most abundant and diversity in 4 libraries. 8 orders were identified as being related to β -*Proteobacteria* (Fig. 2B). The *Burkholderiales* was the most abundant order in 4 libraries, representing 65.60%. The relatively abundant orders

affiliated to β -Proteobacteria were *Nitrosomonadales*, SC-I-84 and *Methylophilales*, representing 13.91, 13.78 and 1.77%. Depending on the use of monoculture and intercropping, most of *Burkholderiales* and *Methylophilales* were found in monoculture libraries (WM and AM) ($P < 0.05$), whereas *Betaproteobacteria_unclassified*, *Nitrosomonadales* and SC-I-84 were present at higher abundances in intercropping alfalfa compared with monoculture alfalfa ($P < 0.05$). The comparison of relative abundances of TRA3-2 revealed no significant differences between intercropping and monoculture libraries ($P > 0.05$). 95 and 2 OTUs were related to *Hydrogenophilales* and B1-7BS, respectively, while *Hydrogenophilales* appeared in intercropping wheat libraries only and B1-7BS in alfalfa monoculture and wheat monoculture libraries.

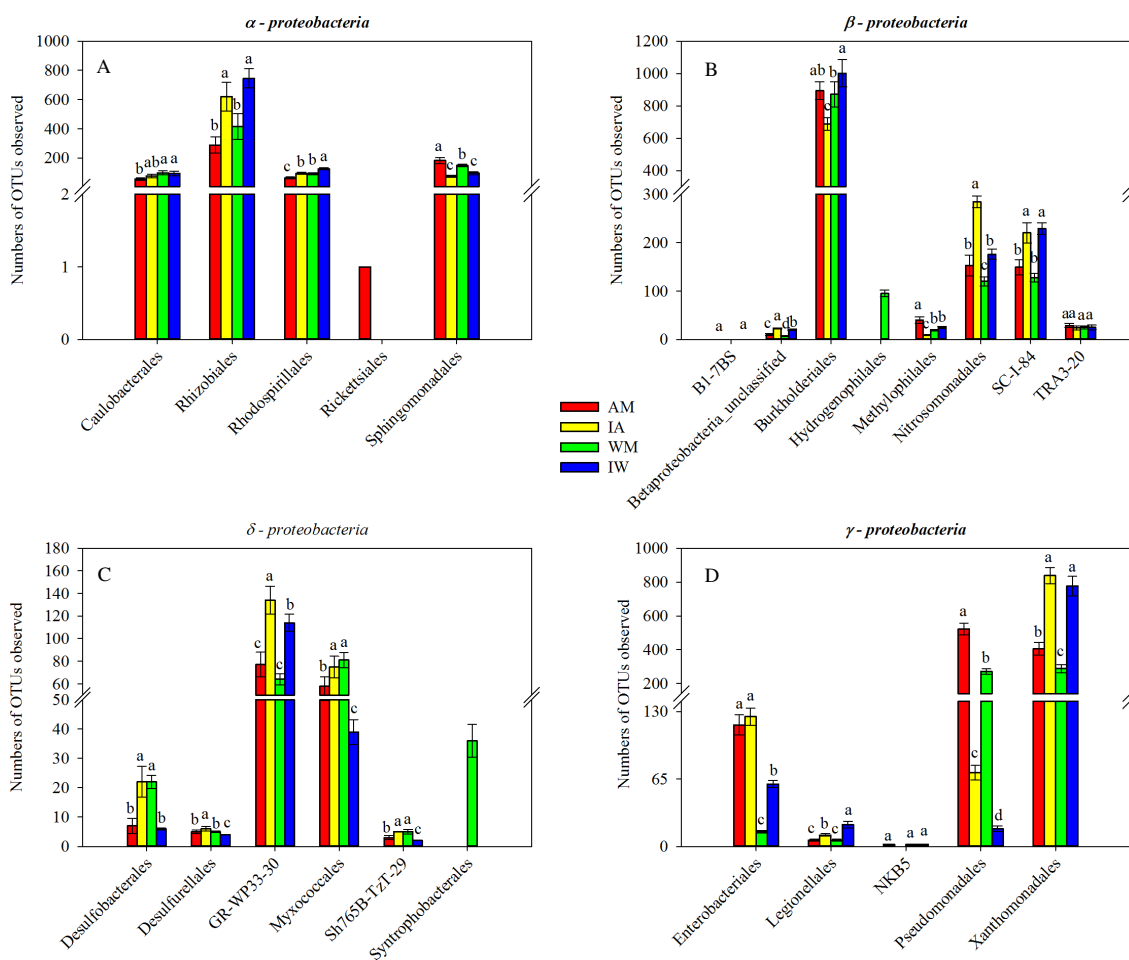


Figure 2. Numbers of OTUs of Proteobacteria orders in 4 libraries. The significant differences between the means were determined using Duncan post-hoc test

The δ -Proteobacteria were relatively abundant and diversity. 6 orders were identified as being related to δ -Proteobacteria (Fig. 2C). The GR-WP33-30 was the most abundant order in 4 libraries, representing 50.52%, with a relative abundance in intercropping alfalfa higher compared to corresponding monoculture alfalfa, whereas GR-WP33-30 was present at lower relative abundances in intercropping wheat. The relatively abundant orders affiliated to δ -Proteobacteria were *Desulfobacterales* and *Myxococcales*, representing 7.40 and 32.86%. Depending on the use of monoculture and

intercropping, most of *Desulfobacterales*, *Desulfurellales*, *Myxococcales* and *Sh765B-TzT-29* were found in intercropping alfalfa libraries ($P < 0.05$), whereas low abundance was found in intercropping wheat libraries ($P < 0.05$). 36 OTUs was related to *Syntrophobacterales* and identified in intercropping wheat libraries only.

The γ -*Proteobacteria* were relatively abundant and diversity. 5 orders were identified as being related to γ -*Proteobacteria* (Fig. 2D). The *Xanthomonadales* was the most abundant order in 5 libraries, representing 64.93%, with a relative abundance in intercropping alfalfa higher compared to corresponding monoculture alfalfa, whereas *Xanthomonadales* was present at lower relative abundances in intercropping wheat. The relatively abundant orders affiliated to γ -*Proteobacteria* were *Pseudomonadales*, *Enterobacterales*, *Legionellales* and NKB5 representing 24.77, 8.89, 1.24 and 0.17%. Depending on the use of monoculture and intercropping, most of *Pseudomonadales* were found in monoculture libraries ($P < 0.05$). The comparison of relative abundances of *Enterobacterales* and NKB5 revealed no significant differences between intercropping and monoculture alfalfa ($P > 0.05$), whereas *Enterobacterales* and *Legionellales* was present at higher abundances in intercropping wheat ($P < 0.05$). 6 OTUs was related to NKB5 and appeared in AM, IW, WM libraries, respectively.

***Acidobacteria* sequences**

25.10% of the total clones were affiliated with the *Acidobacteria* phylum. These sequences were affiliated with 10 orders of *Acidobacteriales*, Subgroup 3, 4, 5, 6, 7, 10, 11, 17, 25 and no rank *Acidobacteria* (Fig. 3). The Subgroup 6, 4 and 3 were the most abundant order in 4 libraries, representing 66.01, 18.93 and 6.95%, respectively. The relative abundances of Subgroup 3 and 6 in intercropping alfalfa were higher than monoculture alfalfa ($P < 0.05$). A similar trend was also found by comparison of intercropping and monoculture wheat. In addition, sequences affiliated to Subgroup 5, 7, 17 and 25 were relatively abundant order in 4 libraries. The comparison of relative abundances of Subgroup 5 revealed no significant differences between intercropping and monoculture libraries ($P > 0.05$). We observed higher relative abundances of Subgroup 7 in intercropping libraries compared to corresponding monoculture libraries ($P < 0.05$). Depending on the use of monoculture and intercropping, most of Subgroup 17 was found in intercropping alfalfa libraries, and high abundance of Subgroup 25 was found in intercropping wheat libraries ($P < 0.05$). The abundance of Subgroup 10, 11, *Acidobacteriales* and no rank *Acidobacteria* were low, representing 0.80, 0.19, 0.30 and 0.42%.

Sequences of other relatively abundant groups

The *Bacteroidetes* were relatively abundant and diversity, accounting for 8.93% of the analyzed OTUs. These OTUs were affiliated with 4 orders of *Cytophagales*, *Flavobacteriales*, *Sphingobacteriales* and *VadinHA17_norank* (Fig. 4). The relative abundances of *Cytophagales* in intercropping libraries were higher than monoculture, while *Flavobacteriales* and *Sphingobacteriales* in intercropping alfalfa were higher than monoculture. In addition, 80 OTUs was related to *VadinHA17_norank* and identified in IW libraries only.

The Actinobacteria had most abundant orders, affiliated with 11 orders of *Acidimicrobiales*, *Corynebacteriales*, *Frankiales*, *Gaiellales*, *Micrococcales*,

Micromonosporales, Propionibacteriales, Pseudonocardiales, Solirubrobacteriales, Streptomycetales and Actinobacteria_norank (Fig. 4). The relatively abundances of Acidimicrobiales, Frankiales, Gaiellales, Propionibacteriales and Solirubrobacteriales in intercropping libraries were higher than monoculture.

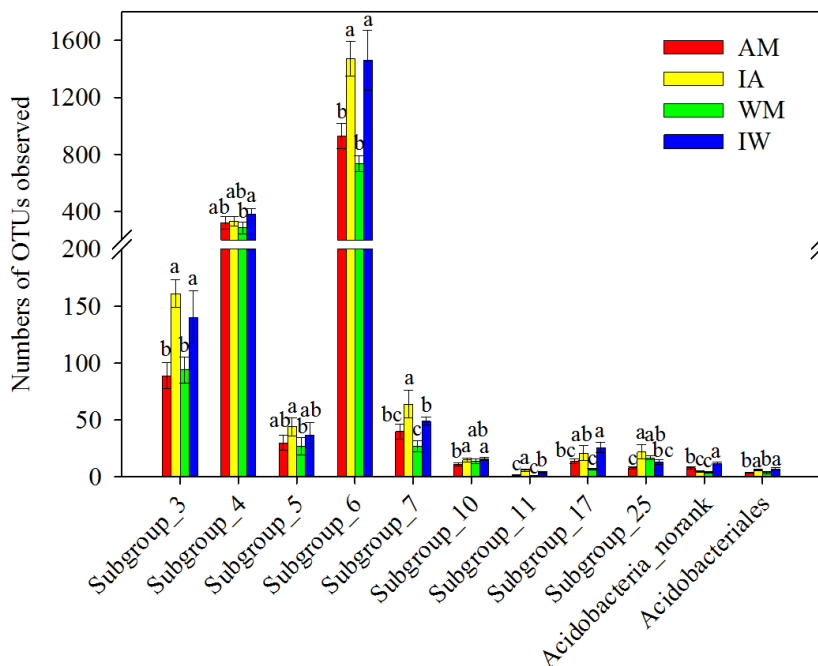


Figure 3. Numbers of OTUs of Acidobacteria orders in 4 libraries. The significant differences between the means were determined using Duncan post-hoc test

In addition, some orders affiliated to other phylum had significant differences between intercropping and monoculture libraries. Such as *Anaerolineales*, *Caldilineales*, *Clostridiales* (affiliated to *Chloroflexi*) and *Lactobacillales* (affiliated to *Fimicutes*) showed a higher relative abundance in intercropping libraries compared with monoculture libraries, regardless of plant species (Fig. 4). Whereas, depending on the use of monoculture and intercropping, *Bacillus* (affiliated to *Fimicutes*) was present at higher relatively abundances in intercropping alfalfa only.

Shared bacterial OTUs

Venn diagrams revealed that the sum of total observed OTUs in the four soil samples was 475 (Fig. 5), and 307 OTUs were shared all of the soil samples. Moreover, the distribution of sequences demonstrated once again that each plant rhizosphere had its own microbial population.

PCA analysis

This was supported by the principal component analysis (PCA) with the weighted Unifrac distance (Fig. 6). Overall, the two PCA axes explained 81.41% of the variation between the different communities. The PCA score plot revealed that intercropping patterns significantly change bacterial communities in wheat and alfalfa rhizosphere soils. The intercropping (IA and IW) soil microbiota clustered separately from the

microbiota of the monoculture (AM and WM) soils along principal components 1 (Fig. 6), suggesting that the application of intercropping pattern influenced the population structure of the soil bacteria.

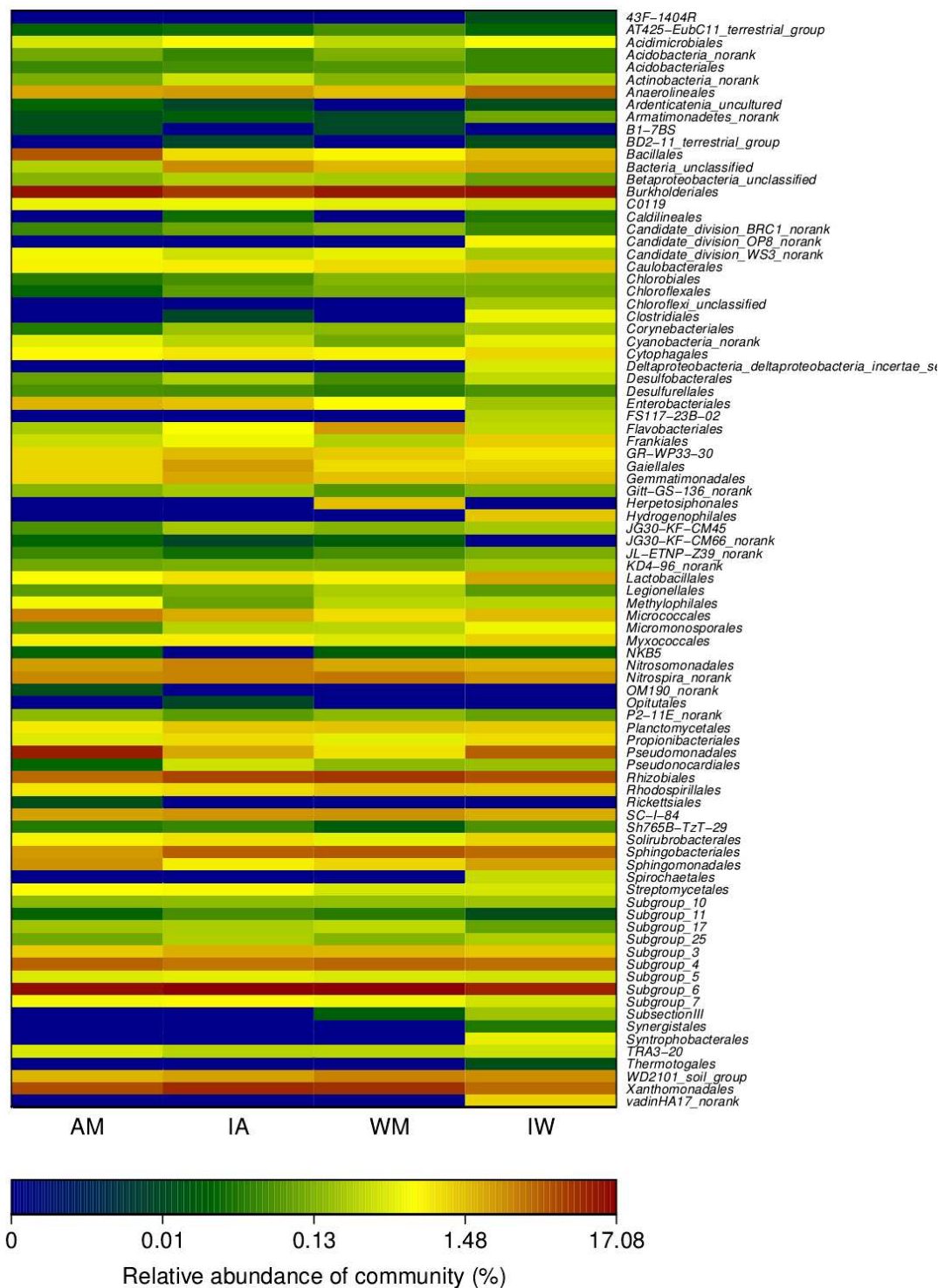


Figure 4. Hierarchical cluster analysis of predominant orders among the 4 libraries. The color intensity of scale indicates relative abundance of each OTU read. Relative abundance was defined as the number of sequences affiliated with that OTU divided by the total number of sequences per sample

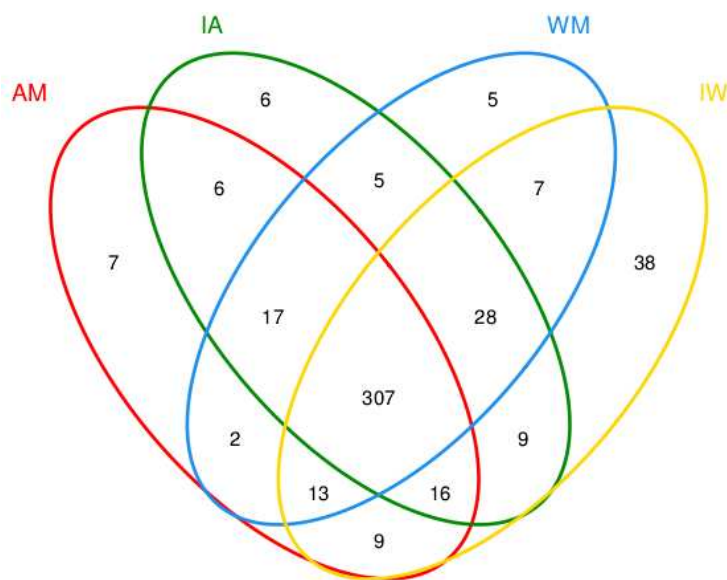


Figure 5. Venn diagram showing the shared bacterial OTUs (at a distance of 0.03) in 4 soil samples. Alfalfa monoculture (AM), intercropping alfalfa (IA), wheat monoculture (WM), and intercropping wheat (IW)

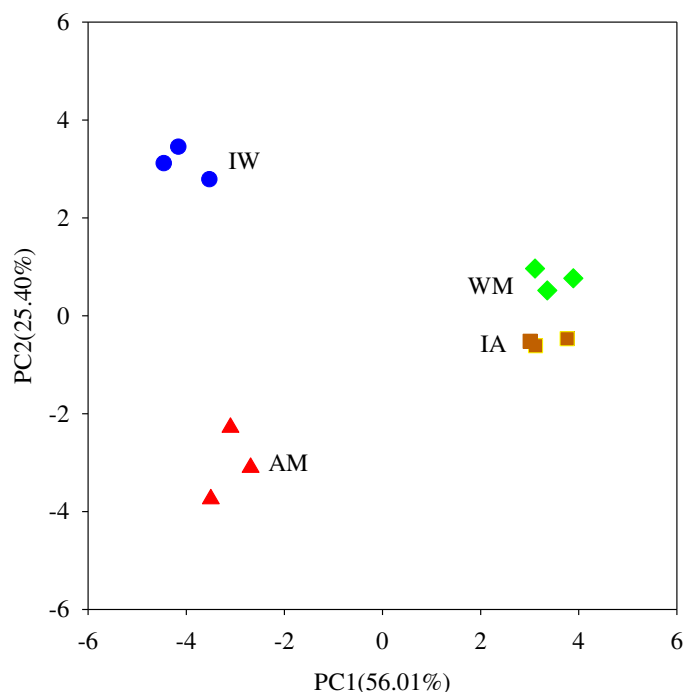


Figure 6. Principal component analysis (PCA) of bacterial communities from Alfalfa monoculture (AM), intercropping alfalfa (IA), wheat monoculture (WM), and intercropping wheat (IW) based on pyrosequencing of the 16S rDNA gene. PCA were generated using the presence of each OTU (at a distance level of 3%) found in each clone library. Principal components (PCs) 1 and 2 explained 56.01% and 25.40% of the variance, respectively

Discussion

In this study, 16S rDNA gene clone library analyses were undertaken to study soil bacterial communities in wheat-alfalfa intercropping systems. A single study refers to cereal-legume intercropping, dominantly focusing on soil cultivable microbial flora (Chai et al., 2004). But data on overall bacterial communities living in cereal and legume roots vicinity are still lacking. To our knowledge, this study is the first to report data concerning the uncultivable microbial flora surrounding wheat and alfalfa in monoculture and intercropping systems, respectively. It is known that a wide range of factors influences soil bacterial communities. Soil type, plant species and cropping patterns are the reasons that most affect the bacterial communities in soils (Igwe Vannette, 2019; Rui et al., 2015). Shannon diversity analyses revealed a richer bacterial community in intercropping soil than that of monoculture (*Table 1*). This observation may be supported by PCA result that demonstrates that soil bacterial communities obtained from monoculture and intercropping system were different, regardless of plant species (*Fig. 6*). The result demonstrated bacterial communities in rhizosphere soils were indeed affected by intercropping patterns. The presence of alfalfa plants contributed to attenuate eventual bacterial community variations occurring in intercropping wheat. Indeed, legume-based intercropping systems present a more heterogeneous vegetation cover, a patchier distribution of plant litter and rooting patterns that can affect soil properties and microbial communities (Lacombe et al., 2009; Reynolds et al., 2007). The result demonstrated bacterial communities in rhizosphere soils were indeed affected by intercropping patterns. Moreover, an influence of plant species on bacterial diversity was observed.

The high diversity of soil bacteria in intercropping and monoculture systems were shown based on the sequence analyses. For microbial analysis of soil, the dominant taxonomic groups were *Proteobacteria*, *Acidobacteria*, *Bacteroidetes*, *Actinobacteria*, *Planctomycetes*, *Chloroflexi*, and *Nitrospirae* (*Fig. A2*). These phyla have been described as common inhabitants of farmland soils (Li et al., 2016, 2020). The diversity of *Actinobacteria* and *Bacteroidetes* were relatively abundant in 4 libraries and present at higher percentages in intercropping libraries. Additionally, some phylum that were not abundant in these libraries, including *Gemmatimonadetes* and *Bacteria_unclassified*, showed higher percentages in intercropping alfalfa soils ($P < 0.05$), which indicated an important role of intercropping in shaping the soil microbial communities. Other phylotypes showed the opposite variation in monoculture and intercropping system. The diversity of *Acidobacteria* and *Nitrospirae* were relatively abundant in 4 libraries and present at higher percentages in monoculture wheat libraries ($P < 0.05$). In addition, *Firmicutes* showed higher percentages in monoculture alfalfa soils. There were another two different changes including bacterial populations absent or appeared only in monoculture libraries, whereas the phylotypes of *Syntrophobacterales* and *Hydrogenophilale* appeared only in intercropping libraries.

Most of previous studies have indicated that legume and cereal intercropping is profitable for increasing crop yield (Li et al., 2007). In our research, the yield data clearly demonstrates the superiority of the use of intercropping pattern (*Fig. 1*). This beneficial effect may be attributed to the maintenance and improvement of microbial activity and community composition (Fu et al., 2018). Two main mechanisms that soil microbes affect plant productivity can be distinguished: direct effects on plants by means of root-associated organisms that form mutualistic or pathogenic relationships with plants, and indirect effects by means of the action of free-living microbes that

change rates of nutrient supply and the partitioning of resources (Van Der Heijden et al., 2008). In our study, the complex changes of bacterial community diversity and abundant identified in monoculture and intercropping libraries raises one question. What relationship did the changing bacterial population and increasing of crop yield in intercropping pattern? Soil nutrition (eg. nitrogen, phosphorus and potassium or some other non-N nutrient that is limiting in a habitat) limits plant productivity (Chapin III, 1980), which showed plant-soil feedback processes are also dominating. Beneficial plant rhizobacteria are associated with the surfaces of plant roots and may increase plant yield via mechanisms that improved mineral nutrient uptake, disease suppression, or phytohormone production (Sameh and Youseif, 2018; Sood et al., 2018; Hokkanen and Lynch, 1995). Legumes and nonlegumes can “complement” each other in the use of N sources since both the legume and nonlegume utilize soil inorganic N sources, but nodule in leguminous plants can also fix atmospheric N₂ in symbiosis with *Rhizobiales* (Jensen, 1996a, b). Wheat intercropping libraries had more *Rhizobiales* than wheat monoculture libraries (Fig. 2). The amount of soil nitrogen-fixing bacteria in alfalfa intercropping soils increased mainly in the presence of wheat. Previous studies also confirm that N₂ fixation of legumes may be improved by intercropping when the no legume is a strong competitor for soil inorganic N (Giller et al., 1991; Karpenstein-Machan et al., 2000; Hauggaard-Nielsen et al., 2001).

The recent studies of overyielding in agriculture intercropping systems found a important mechanism underlying such facilitation is the ability of some crop species to chemically mobilize otherwise-unavailable forms of one or more limiting soil nutrients such as phosphorus (Li et al., 2014). Plant do not take up organic P directly, rather, organic P is first hydrolyzed by microbial or root-related phosphatases. Therefore, phosphate solubilizing bacteria have a important role in soils with low concentration of available phosphorus. Phosphate solubilizing bacteria were present in different proportions in monoculture and intercropping soils. *Burkholderiales* and *Pseudomonadales* were more abundance in intercropping soils than that monoculture soils. These bacteria can improve solubilization of fixed soil phosphorus and applied phosphates resulting in higher crop yields (Nautiyal, 1999). Moreover, *Actinobacteria* have a critical role in decomposition of soil organic materials, such as cellulose and chitin (Sykes et al., 1973). *Actinobacteria* of intercropping soils were higher than that of monoculture soils, which may be due to the presence of more organic matter used by plants in intercropping soils. Compared with monoculture, the number of organic acid in the roots exudates was increased in wheat/maize intercropping (Hao et al., 2003), which might affect some acid-sensitive microbes. *Acidobacteria* of intercropping alfalfa soils were higher than that of monoculture soils, which may be due to the presence of more organic matter used by plants in intercropping soils. *Acidobacteria* are capable of degradation of plant litter in soils (Eichorst et al., 2011), the presence of wheat debris in monoculture samples and alfalfa root exudates and litter in intercropping samples may have contributed to the observed differences.

Another route by which soil microbes affect plant productivity is disease suppression, as an example through the production of antifungal metabolites (Weller et al., 2002). Plants release enormous of chemicals through their roots, at a significant carbon cost, to combat pathogenic microorganisms and attract beneficial ones (Badri et al., 2009). The activity and effects of beneficial rhizosphere microorganisms on plant growth and health are well documented for bacteria like by *Pseudomonales* and *Burkholdera* (Badri et al., 2009). *Pseudomonales* and *Burkholderiales* were present at

higher relatively abundances in intercropping alfalfa and wheat, respectively. These bacteria protect several major agricultural crops against disease phenomenon that is likely to be also important in natural ecosystems (Van Der Heijden et al., 2008). Moreover, it is reported *Bacillus* also was major antagonists (Yuan et al., 2016), which can promote plant growth, protect against fungal pathogen attack (Asaka and Shoda, 1996), and play a role in the degradation of organic polymers in the soil (Emmert and Handelsman, 1999). Similar as *Pseudomonales*, *Bacillus* was present at higher relatively abundances in intercropping alfalfa. There are four main groups of plant pathogens, but only fungi and nematodes are major players in the soil (Hilbig and Allen, 2019). The structure and function of other plant pathogens also need further discovery. Consequently, the analyses of bacterial communities in our study can provided general information about the relationships between soil bacterial communities and intercropping patterns. Many of bacterial populations identified in 4 libraries showed significant differences between monoculture and intercropping systems, but only a few have been reported as being able to improve plant productivity and the functions of other populations also still await discovery.

Conclusion

Intercropping pattern improve crop productivity in the field. Our findings indicated that intercropping is a determinant in shaping bacterial community in soils. Intercropping led to variations in the plant-growth promoting rhizobacteria in the rhizosphere of wheat and alfalfa. The resulting microbial community is likely to be a mixture of the species-specific. The results provide a strong evidence for improving the microbial diversity of rhizosphere soil and the nutrients of rhizosphere soil in wheat/alfalfa intercropping, and provide a direction for further research on the role of specific microorganisms. The reason of the yield advantage of intercropping system caused by the change of crop rhizosphere microbial community structure needs further study.

Acknowledgements. The study was supported by the National Natural Science Foundation of China (41701289) and (C030301), China Postdoctoral Science Foundation (2018M640287).

REFERENCES

- [1] Asaka, O., Shoda, M. (1996): Biocontrol of *Rhizoctonia solani* damping-off of tomato with *Bacillus subtilis* RB14. – *Applied Environmental Microbiology* 62: 4081-4085.
- [2] Badri, D. V., Weir, T. L., Lelie, D. V. D., Vivanco, J. M. (2009): Rhizosphere chemical dialogues: plant–microbe interactions. – *Current Opinion Biotechnology* 20(6): 642-650.
- [3] Bhatti, I. H., Ahmad, R., Jabbar, A., Nazir, M., Mahmood, T. (2006): Competitive behaviour of component crops in different sesame-legume intercropping systems. – *International Journal of Agriculture and Biology (Pakistan)* 8(2): 165-167.
- [4] Chai, Q., Huang, P., Huang, G. (2004): Effect of intercropping on soil microbial and enzyme activity in the rhizosphere. – *Acta Prataculturae Sinica* 14: 105-110.
- [5] Chapin III, F. S. (1980): The mineral nutrition of wild plants. – *Annual Review of Ecology Systematics* 11(1): 233-260.

- [6] Choudhary, V. K., Kumar, P. S. (2016): Productivity, water use and energy profitability of staggered maize-legume intercropping in the eastern Himalayan region of India. – Proceedings of the National Academy of Sciences India 86(3): 547-557.
- [7] Du, W., He, X., Hu, Z., Zia, S., Muller, J. (2011): Effect of different irrigation technology on production of winter wheat. – Journal of drainage and irrigation machinery engineering 29(2): 170-174.
- [8] Eichorst, S. A., Kuske, C. R., Schmidt, T. M. (2011): Influence of plant polymers on the distribution and cultivation of bacteria in the phylum Acidobacteria. – Applied Environmental Microbiology 77(2): 586-596.
- [9] Emmert, E. A., Handelsman, J. (1999): Biocontrol of plant disease: a (Gram-) positive perspective. – Fems Microbiology Letters 171: 1-9.
- [10] Giller, K. E., Wilson, K. J. (1991): Nitrogen Fixation in Tropical Cropping Systems. – CAB Int., Wallingford.
- [11] Hanming, H., Lei, Y., Zhao, L. H., Han, W., Fan, L. M., Yong, X., Zhu, Y. Y., Li, C. Y. (2012): The temporal-spatial distribution of light intensity in maize and soybean intercropping systems. – Journal of Resources and Ecology 3(2): 169-173.
- [12] Hao, Y., Lao, X., Sun, W., Peng, S. (2003): Interaction of roots and rhizosphere in the wheat/maize intercropping system. – Rural Eco-Environment 19(4): 18-22.
- [13] Hauggaard-Nielsen, H., Ambus, P., Jensen, E. S. (2001): Interspecific competition, N use and interference with weeds in pea-barley intercropping. – Field Crops Research 70(2): 101-109.
- [14] Heijden, M. G. A. V. D., Bardgett, R. D., Straalen, N. M. V. (2008): The unseen majority: soil microbes as drivers of plant diversity and productivity in terrestrial ecosystems. – Ecology Letters 11(3): 296-310.
- [15] Hesler, L. S., Kieckhefer, R. W. (2018): Wheat stem maggot in spring wheat-alfalfa intercrops with different crop management intensities. – Great Lakes Entomologist 33(1): 33-39.
- [16] Hilbig, B. E., Allen, E. B. (2019): Fungal pathogens and arbuscular mycorrhizal fungi of abandoned agricultural fields: potential limits to restoration. – Invasive Plant Science and Management 12(3): 186-193.
- [17] Hokkanen, H., Lynch, J. (1995): Benefits and Risks of Introducing Biocontrol Agents. – Plant and Microbial Biotechnology Series, Cambridge University Press, Cambridge, UK.
- [18] Igwe, A. N., Vannette, R. L. (2019): Bacterial communities differ between plant species and soil type, and differentially influence seedling establishment on serpentine soils. – Plant & Soil 441: 423-437.
- [19] Jensen, E. (1996): Barley uptake of N deposited in the rhizosphere of associated field pea. – Soil Biology and Biochemistry 28(2): 159-168.
- [20] Jensen, E. S. (1996): Grain yield, symbiotic N₂ fixation and interspecific competition for inorganic N in pea-barley intercrops. – Plant & Soil 182: 25-38.
- [21] Karpenstein-Machan, M., Stuelpnagel, R. (2000): Biomass yield and nitrogen fixation of legumes monocropped and intercropped with rye and rotation effects on a subsequent maize crop. – Plant & Soil 218(1-2): 215-232.
- [22] Kowalchuk, G. A., Stephen, J. R. (2001): Ammonia-oxidizing bacteria: a model for molecular microbial ecology. – Annual Reviews in Microbiology 55: 485-529.
- [23] Lacombe, S., Bradley, R. L., Hamel, C., Beaulieu, C. (2009): Do tree-based intercropping systems increase the diversity and stability of soil microbial communities? – Agriculture, Ecosystems & Environment 131(1): 25-31.
- [24] Li, J., Huang, B., Wang, Q. X., Li, Y., Fang, W. S., Han, D. W., Yan, D. D., Guo, M. X., Cao, A. C. (2017): Effects of fumigation with metam-sodium on soil microbial biomass, respiration, nitrogen transformation, bacterial community diversity and genes encoding key enzymes involved in nitrogen cycling. – Science of the Total Environment 598(15): 1027-1036.

- [25] Li, L., Li, S. M., Sun, J. H., Zhou, L. L., Bao, X. G., Zhang, H. G., Zhang, F. S. (2007): Diversity enhances agricultural productivity via rhizosphere phosphorus facilitation on phosphorus-deficient soils. – Proceedings of the National Academy of Sciences 104(27): 11192-11196.
- [26] Li, L., Tilman, D., Lambers, H., Zhang, F. S. (2014): Plant diversity and overyielding: insights from belowground facilitation of intercropping in agriculture. – New Phytologist 203(1): 63-69.
- [27] Li, R., Liu, Y., Chu, G. X. (2015): Effects of different cropping patterns on soil enzyme activities and soil microbial community diversity in oasis farmland. – Chinese Journal of Applied Ecology 26(2): 490-496.
- [28] Li, X., Sun, M., Zhang, H., Xu, N., Sun, G. (2016): Use of mulberry-soybean intercropping in salt-alkali soil impacts the diversity of the soil bacterial community. – Microbial Biotechnology 9(3): 293-304.
- [29] Li, X., Zhang, H. H., Sun, M. L., Xu, N., Sun, G. Y., Zhao, M. C. (2020): Land use change from upland to paddy field in Mollisols drives soil aggregation and associated microbial communities. – Applied Soil Ecology 146: 103351.
- [30] Ma, X. L., Zhu, Q. L., Geng, C. X., Lu, Z. G., Long, G. Q., Tang, L. (2017): Contribution of nutrient uptake and utilization on yield advantage in maize and potato intercropping under different nitrogen application rates. The Journal of Applied Ecology 28(4): 1265.
- [31] Morris, R., Garrity, D. (1993): Resource capture and utilization in intercropping; non-nitrogen nutrients. – Field Crops Research 34: 319-334.
- [32] Nazih, N., Finlay-Moore, O., Hartel, P., Fuhrmann, J. (2001): Whole soil fatty acid methyl ester (FAME) profiles of early soybean rhizosphere as affected by temperature and matric water potential. – Soil Biology and Biochemistry 33(4): 693-696.
- [33] Ren, Y. Y., Wang, X. L., Zhang, S. Q., Palta, J. A., Chen, Y. L. (2017): Influence of spatial arrangement in maize-soybean intercropping on root growth and water use efficiency. – Plant & Soil 415(1-2): 131-144.
- [34] Reynolds, P. E., Simpson, J. A., Thevathasan, N. V., Gordon, A. M. (2007): Effects of tree competition on corn and soybean photosynthesis, growth, and yield in a temperate tree-based agroforestry intercropping system in southern Ontario, Canada. – Ecological Engineering 29: 362-371.
- [35] Rillig, M. C., Mummey, D. L. (2006): Mycorrhizas and soil structure. – New Phytologist 171: 41-53.
- [36] Schimel, J. P., Schaeffer, S. M. (2012): Microbial control over carbon cycling in soil. – Frontiers in Microbiology 3: 348.
- [37] Singleton, D. R., Furlong, M. A., Rathbun, S. L., Whitman, W. B. (2001): Quantitative comparisons of 16S rRNA gene sequence libraries from environmental samples. – Applied Environmental Microbiology 67(9): 4374-4376.
- [38] Skelton, L. E., Barrett, G. W. (2005): A comparison of conventional and alternative agroecosystems using alfalfa (*Medicago sativa*) and winter wheat (*Triticum aestivum*). – Renewable Agriculture and Food Systems 20(1): 38-47.
- [39] Song, Y., Zhang, F., Marschner, P., Fan, F., Gao, H., Bao, X., Sun, J., Li, L. (2007): Effect of intercropping on crop yield and chemical and microbiological properties in rhizosphere of wheat (*Triticum aestivum* L.), maize (*Zea mays* L.), and faba bean (*Vicia faba* L.). – Biology and Fertility of Soils 43(5): 565-574.
- [40] Sood, G., Kaushal, R., Chauhan, A., Gupta, S. (2018): Indigenous plant-growth-promoting rhizobacteria and chemical fertilisers: impact on wheat (*Triticum aestivum*) productivity and soil properties in North Western Himalayan region. – Crop & Pasture Science 69(5): 460-468.
- [41] Su, C., Lei, L., Duan, Y., Zhang, K. Q., Yang, J. (2012): Culture-independent methods for studying environmental microorganisms: methods, application, and perspective. – Applied Microbiology and Biotechnology 93(3): 993-1003.

- [42] Vandermeer, J. (1995): The ecological basis of alternative agriculture. – Annual Review of Ecology and Systematics 26(1): 201-224.
- [43] Vandermeer, J. H. (1992): The Ecology of Intercropping. – Cambridge University Press.
- [44] Vrignon-Brenas, S., Celette, F., Piquet, A., Corre, G., David, C. (2018): Intercropping strategies of white clover with organic wheat to improve the trade-off between wheat yield, protein content and the provision of ecological services by white clover. – Field Crops Research 224(1): 160-169.
- [45] Wang, Y., Yuan, Y. H., Liu, B., Zhang, Z. W., Yue, T. L. (2016): Biocontrol activity and patulin-removal effects of *Bacillus subtilis*, *Rhodobacter sphaeroides* and *Agrobacterium tumefaciens* against *Penicillium expansum*. – Journal of Applied Microbiology 121(5): 1384-1393.
- [46] Wardle, D. A., Bardgett, R. D., Klironomos, J. N., Setälä, H., Putten, V. D. W. H., Wall, D. H. (2004): Ecological linkages between aboveground and belowground biota. – Science 304(5677): 1629-1633.
- [47] Weller, D. M., Raaijmakers, J. M., Gardener, B. B. M., Thomashow, L. S. (2002): Microbial populations responsible for specific soil suppressiveness to plant pathogens 1. – Annual Review of Phytopathology 40: 309-348.
- [48] Willey, R. (1999): Intercropping - its importance and research needs. Part 1. Competition and yield advantages. – Field Crop Abstracts 32: 1-10.
- [49] Yan, F., Schubert, S., Mengel, K. (1996): Soil pH changes during legume growth and application of plant material. – Biology and Fertility of Soils 23(3): 236-242.
- [50] Youseif, S. H. (2018): Genetic diversity of plant growth promoting rhizobacteria and their effects on the growth of maize plants under greenhouse conditions. – Annals of Agricultural Sciences 63(1).
- [51] Yue, L., Charles, F., Pute, W., Xiao, L. C. (2014): Maize–soybean intercropping interactions above and below ground. – Crop Science 54(3): 914-920.
- [52] Zarraonaindia, I., Smith, D. P., Gilbert, J. A. (2013): Beyond the genome: community-level analysis of the microbial world. – Biology Philosophy 28(2): 261-282.
- [53] Zhi-dan, F. U., Zhou, L., Chen, P., Du, Q., Pang, T., Song, C., Wang, X. C., Liu, W. G., Yang, W. Y., Yong, T. W. (2019): Effects of maize-soybean relay intercropping on crop nutrient uptake and soil bacterial community. – Journal of Integrative Agriculture 18(9): 2006-2018.
- [54] Zhou, X., Yu, G., Wu, F. (2011): Effects of intercropping cucumber with onion or garlic on soil enzyme activities, microbial communities and cucumber yield. – European Journal of Soil Biology 47(5): 279-287.

APPENDIX

Table A1. Number of 16S rDNA gene sequences derived from 4 libraries

Sample	No. obtained sequences \geq 400 bp	Bases (bp)	Average length (bp)
Monoculture alfalfa	10405	4123641	396.31
Alfalfa intercropping	14044	5565166	396.27
Monoculture wheat	13043	5165858	396.06
Wheat intercropping	11902	4716160	396.25

Figure A1. Rarefaction curves indicating the observed number of OTUs at 3% genetic distances in 4 libraries. Alfalfa monoculture (AM), intercropping alfalfa (IA), wheat monoculture (WM), and intercropping wheat (IW)

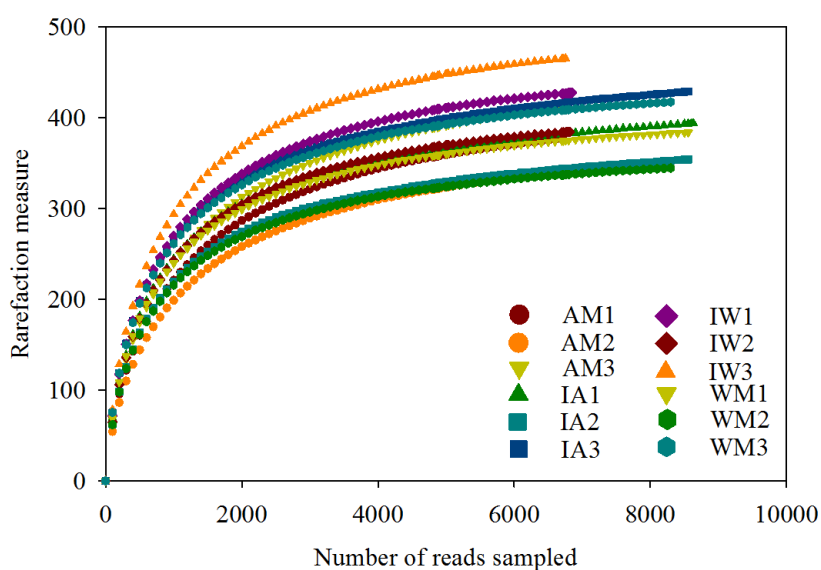
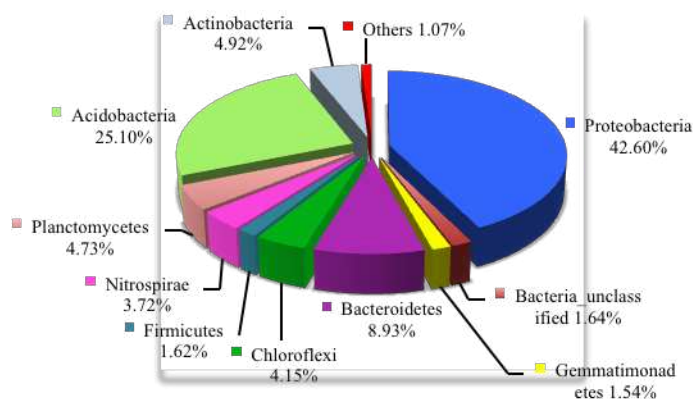


Figure A2. Composition of bacterial taxonomic groups



DIURNAL VARIATION IN THE RESPIRATION OF RECONSTRUCTED SOIL MASSES AND HYDROTHERMAL INFLUENCING FACTORS

LEI, N.^{1,2,3,4,5*} – SUN, Z. H.^{1,3,4,5} – WANG, H. Y.^{1,3,4,5} – DONG, Q. G.^{1,3,4,5}

¹*Shaanxi Provincial Land Engineering Construction Group Co., Ltd., Xi'an 710075, China*

²*Institute of Soil and Water Conservation, Northwest A&F University, Yangling Shaanxi 712100, China*

³*Institute of Land Engineering and Technology, Shaanxi Provincial Land Engineering Construction Group Co., Ltd., Xi'an 710075, China*

⁴*Key Laboratory of Degraded and Unused Land Consolidation Engineering, the Ministry of Natural Resources, Xi'an 710075, China*

⁵*Shaanxi Provincial Land Consolidation Engineering Technology Research Center, Xi'an 710075, China*

* *Corresponding author*

e-mail: linye2323@126.com; phone: +86-029-8862-5020

(Received 21st Dec 2019; accepted 6th May 2020)

Abstract. Diurnal variation characteristics in the respiration of four reconstructed soil masses in a barren gravel land were monitored using soil carbon flux measurement system. The results showed that (1) the variation had a single-peak curve, with the lowest value recorded at 6:00 or 20:00, and the highest value at 10:00, 12:00, or 14:00. The soil respiration values of the four reconstructed soil masses reached the maximum and minimum in August and January, respectively. (2) The variation can be explained by a single factor of soil temperature (i.e., index model), soil volumetric water content (i.e., quadratic model), or both factors (i.e., power-index model). However, the explanatory power was different, i.e., generally higher than 50.0% for the two-factor model, and the interpretation ability of temperature was significantly higher than that of water for the single-factor model. (3) The three-model fitting of the hydrothermal factors and reconstructed soil mass, with the added meteorite, showed that these factors had the lowest ability to explain the diurnal variations in soil respiration. In contrast, the quadratic curve model of the soil volume water content and reconstructed soil mass, with the added shale, had the highest ability to interpret the diurnal variation in soil respiration.

Keywords: *diurnal variation, soil respiration, hydrothermal factors, soil temperature, soil moisture*

Introduction

Soil respiration affects the acceleration of climate change due to its role in regulating the carbon cycle of various ecosystems. Therefore, soil respiration characteristics of different types of ecosystems (Lai et al., 2012; Yu et al., 2019), land use (Hu et al., 2018), regions (Goldberg et al., 2017; Li et al., 2018) and degraded land (Rey et al., 2010) have been studied. Research generally began with a minimum time scale study of diurnal changes in soil respiration. The study on the diurnal variation of soil respiration can provide supporting data for further understanding of the seasonal changes in soil respiration and its causative factors, as well as an accurate accounting of regional carbon emissions. Studies (Wang et al., 2007; Zhou et al., 2017) found that the temperature and moisture were the critical environmental factors for the diurnal

changes in the soil respiration. A significant correlation was found between soil respiration rate and atmospheric temperature or soil temperature at different depths. Generally, the relationship between both the parameters can be described statistically through approaches, such as linear and exponential functions (Meyer et al., 2018; Sun et al., 2019).

At present, land remediation has evolved from simple land levelling and supporting facilities construction to soil reconstruction in China. It aims to build high-quality cultivated land with high nutrient content and good soil structure through remediation. Huayin, Baoji and other places of Shaanxi, China, there are a large number of barren gravel lands. The existing projects have carried out soil masses reconstruction by adding different soil materials and improved materials. The reconstructed soil masses will become the main direction of land remediation in the future and an important means to supplement cultivated land resources. At the same time, the soil masses reconstruction changed the underlying surface conditions of the area, resulting in changes in the soil respiration of the newly formed soil masses, which in turn affected the regional climate, but at this stage, the study of respiration of reconstructed soil masses is still rare. In this study, four reconstructed soils added with meteorite, shale, sand and soft rock were selected as research objects. The typical day was selected every month, and soil carbon flux measurement system was used to observe soil respiration and its components. At the same time, hydrothermal factors were measured to find out the diurnal variation characteristics of respiration and hydrothermal influence factors of four reconstructed soils and their relationship. The study would provide a scientific reference and data support for the accurate assessment of regional CO₂ emissions and the development of reasonable CO₂ reduction measures.

Materials and methods

Overview of test plots

The test plot is located in Shangwang Village, Tangyu Town, Meixian County, Baoji City, Shaanxi Province (107°53'50"E, 34°8'33"N), and a demonstration area for the barren gravel land remediation project. The total area is 8.00 hm², and the newly added cultivated land is 6.80 hm². Four materials of soft rock, sand, shale, and meteorite were selected, crushed through a 10 mm sieve, disinfected, sterilized, and mixed with the constructed soil source to form a mixed layer (30 cm) of meteorite, shale, sand and meteorite, and soil. Lou soil, which was the local common soil type, was used for construction. Finally, four reconstituted soil masses were formed, i.e., gravel + meteorite + lou, gravel + shale + lou, gravel + sand + lou, and gravel + soft rock + lou soil types (hereinafter referred to as meteorite, shale, sand, and soft rock reconstituted soil masses) long-term positioning test. The dosage of meteorite, shale, sand, and soft rock was $1 \times 10^{-3} \text{ m}^3/\text{m}^2$. The dimensions of all test plots were $20 \times 30 \text{ m}^2$.

Test methods

From November 2017 to October 2018, all the soil respiration rings of four test plots were measured on the typical day each month. The measurement time per typical day was at 6:00, 8:00, 10:00, 12:00, 14:00, 16:00, 18:00, 20:00, and the time interval was 2 hours. Soil respiration measurements were performed using a soil carbon flux measurement system (LI-8100, LI-COR Biosciences, Lincoln, NE, USA) equipped

with a soil respiration chamber and equipped with an auxiliary sensor connected to the main unit. The sensor can be connected to up to 4 thermocouples (3 input voltages and 1 soil water content channel). When measuring soil respiration, the respiration chamber was placed on the buried soil respiration ring to ensure that the connection between the respiration ring and the soil respiration chamber was sealed, and the electronic temperature probe were connected to the sensor. Moreover, the time domain reflectometry probes were inserted vertically into the soil near each respiration ring to measure soil carbon flux, soil temperature at 5 cm, and water content at 10 cm. Each soil respiration ring was measured 3 times and the measurement time was 4 min.

Data analyses

One-way ANOVA was used to analyse differences in soil temperature, soil volumetric water, and soil respiration of the four reconstructed soils. All statistical tests were carried out using SPSS software (version 16.0; SPSS Inc., Chicago, IL, USA). Nonlinear regression was used to assess the relationship between soil respiration and hydrothermal influence factors of the four reconstructed soils, and Q_{10} was estimated. The relationship between soil respiration and soil temperature was fitted by an exponential model (Eq.1) and the relationship between soil respiration and water content was fitted by a quadratic curve model (Eq.2). Additionally, the relationship between soil respiration and both soil temperature and soil volumetric water content was fitted by a power-index model (Eq.3):

$$R_S = a e^{bT}, Q_{10} = e^{10b} \quad (\text{Eq.1})$$

$$R_S = a w^2 + b w + c \quad (\text{Eq.2})$$

$$R_S = a e^{bT} w^c \quad (\text{Eq.3})$$

where R_S is the soil respiration rate ($\mu\text{mol m}^{-2} \text{s}^{-1}$); T is the soil temperature ($^{\circ}\text{C}$); w is the soil volumetric water content (%); a , b , and c are the model parameters, and Q_{10} is the sensitivity coefficient of soil respiration, which refers to the change in entropy of soil respiration rate when the soil temperature rises by 10°C .

Results and analysis

Diurnal variation in the respiration of reconstructed soil masses

Diurnal variation in the respiration of four reconstructed soil masses showed a single-peak curve and the lowest value appeared at 6:00 or 20:00. In contrast, the highest value appeared at 10:00, 12:00, or 14:00 in the observed months. This result was mainly influenced by the material properties of reconstructed soil masses, which included meteorite, shale, sand, and soft rock. In the observed months, the diurnal variation in the respiration of four reconstructed soil masses with the addition of meteorite, shale, sand, and soft rock ranged from 0.37 to 3.42 $\mu\text{mol}\cdot\text{m}^{-2}\cdot\text{s}^{-1}$, 0.52 to 4.34 $\mu\text{mol}\cdot\text{m}^{-2}\cdot\text{s}^{-1}$, 0.71 to 4.62 $\mu\text{mol}\cdot\text{m}^{-2}\cdot\text{s}^{-1}$, and 0.55 to 4.03 $\mu\text{mol}\cdot\text{m}^{-2}\cdot\text{s}^{-1}$, respectively. The order of diurnal variation in the respiration of four reconstructed soil masses was as follows: sand > shale > soft rock > meteorite (Fig. 1).

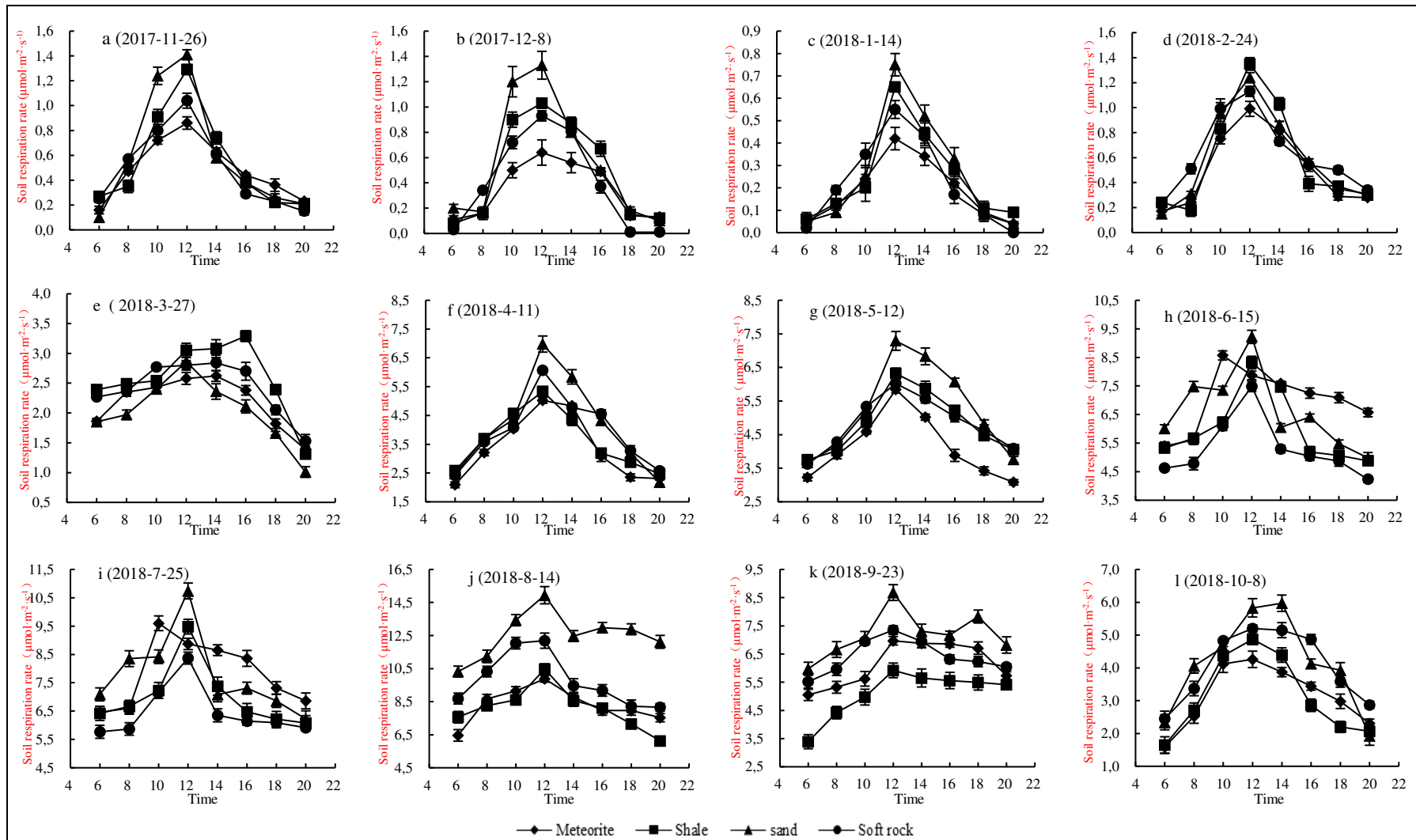


Figure 1. Diurnal variation in respiration, per month, of the four reconstructed soil masses

In November and December, the temperature was lower, soil microorganisms and crops were dormant, soil respiration rate in the four reconstructed soil masses was low, and the diurnal variation was insignificant. In November, the minimum soil respiration rate in the reconstructed soil masses, modified by adding meteorite, shale, sand, and soft rock, was $0.16 \mu\text{mol}\cdot\text{m}^{-2}\cdot\text{s}^{-1}$, $0.21 \mu\text{mol}\cdot\text{m}^{-2}\cdot\text{s}^{-1}$, $0.10 \mu\text{mol}\cdot\text{m}^{-2}\cdot\text{s}^{-1}$, and $0.15 \mu\text{mol}\cdot\text{m}^{-2}\cdot\text{s}^{-1}$, respectively. The maximum values for all reconstructed soil masses appeared at 12:00 (*Fig. 1a*). In December, the minimum soil respiration rate in reconstructed soil masses modified by adding meteorite, shale, sand, and soft rock was $0.11 \mu\text{mol}\cdot\text{m}^{-2}\cdot\text{s}^{-1}$, $0.08 \mu\text{mol}\cdot\text{m}^{-2}\cdot\text{s}^{-1}$, $0.1 \mu\text{mol}\cdot\text{m}^{-2}\cdot\text{s}^{-1}$, and $0 \mu\text{mol}\cdot\text{m}^{-2}\cdot\text{s}^{-1}$, respectively. The maximum values for all reconstructed soil masses appeared at 12:00 (*Fig. 1b*).

In January, the atmospheric temperature reached the minimum value of the year, and the physiological activities of crops and microorganisms stopped. Similarly, the respiration values of reconstructed soil masses reached the lowest during the observation period, and the diurnal variation was also the smallest. The minimum respiration rate in the reconstructed soil masses modified by adding meteorite, shale, sand, and soft rock was $0.04 \mu\text{mol}\cdot\text{m}^{-2}\cdot\text{s}^{-1}$, $0.06 \mu\text{mol}\cdot\text{m}^{-2}\cdot\text{s}^{-1}$, $0.04 \mu\text{mol}\cdot\text{m}^{-2}\cdot\text{s}^{-1}$, and $0 \mu\text{mol}\cdot\text{m}^{-2}\cdot\text{s}^{-1}$, respectively. The maximum values were all recorded at 12:00, and the daily variation ranges were $0.37 \mu\text{mol}\cdot\text{m}^{-2}\cdot\text{s}^{-1}$, $0.59 \mu\text{mol}\cdot\text{m}^{-2}\cdot\text{s}^{-1}$, $0.71 \mu\text{mol}\cdot\text{m}^{-2}\cdot\text{s}^{-1}$, and $0.55 \mu\text{mol}\cdot\text{m}^{-2}\cdot\text{s}^{-1}$, respectively (*Fig. 1c*).

In February, the temperature began to rise, crops and microorganisms began to recover, and soil respiration in the four reconstructed soil masses also began to rise. The minimum soil respiration in the reconstructed soil masses, modified by adding meteorite, shale, sand, and soft rock, was $0.17 \mu\text{mol}\cdot\text{m}^{-2}\cdot\text{s}^{-1}$, $0.24 \mu\text{mol}\cdot\text{m}^{-2}\cdot\text{s}^{-1}$, $0.15 \mu\text{mol}\cdot\text{m}^{-2}\cdot\text{s}^{-1}$, and $0.23 \mu\text{mol}\cdot\text{m}^{-2}\cdot\text{s}^{-1}$, respectively. The maximum values were all recorded at 12:00 (*Fig. 1d*).

In March, April, and May, soil respiration rate in the four reconstructed soil masses continued to increase. Specifically, the maximum soil respiration, in March, was $2.62 \mu\text{mol}\cdot\text{m}^{-2}\cdot\text{s}^{-1}$, $3.08 \mu\text{mol}\cdot\text{m}^{-2}\cdot\text{s}^{-1}$, $2.86 \mu\text{mol}\cdot\text{m}^{-2}\cdot\text{s}^{-1}$, and $2.84 \mu\text{mol}\cdot\text{m}^{-2}\cdot\text{s}^{-1}$, respectively. The minimum values were all recorded at 20:00 (*Fig. 1e*). In contrast, the maximum soil respiration in April was $5.02 \mu\text{mol}\cdot\text{m}^{-2}\cdot\text{s}^{-1}$, $5.33 \mu\text{mol}\cdot\text{m}^{-2}\cdot\text{s}^{-1}$, $6.98 \mu\text{mol}\cdot\text{m}^{-2}\cdot\text{s}^{-1}$, and $6.06 \mu\text{mol}\cdot\text{m}^{-2}\cdot\text{s}^{-1}$, respectively. The minimum values for all reconstructed soil masses were recorded at 12:00 (*Fig. 1f*). While, in May, the maximum soil respiration rate was $5.84 \mu\text{mol}\cdot\text{m}^{-2}\cdot\text{s}^{-1}$, $6.32 \mu\text{mol}\cdot\text{m}^{-2}\cdot\text{s}^{-1}$, $7.29 \mu\text{mol}\cdot\text{m}^{-2}\cdot\text{s}^{-1}$, and $6.02 \mu\text{mol}\cdot\text{m}^{-2}\cdot\text{s}^{-1}$, respectively, and the minimum values were recorded at 6:00 or 20:00 (*Fig. 1g*).

In June and July, the soil respiration rate in the four reconstructed soil masses continued to increase, and the minimum value for all soil masses appeared at 6:00 or 12:00. In June, the maximum soil respiration rate was $8.57 \mu\text{mol}\cdot\text{m}^{-2}\cdot\text{s}^{-1}$, $8.32 \mu\text{mol}\cdot\text{m}^{-2}\cdot\text{s}^{-1}$, $9.22 \mu\text{mol}\cdot\text{m}^{-2}\cdot\text{s}^{-1}$, and $7.48 \mu\text{mol}\cdot\text{m}^{-2}\cdot\text{s}^{-1}$ (*Fig. 1h*); In July, the maximum soil respiration rate in reconstructed soil masses was $9.60 \mu\text{mol}\cdot\text{m}^{-2}\cdot\text{s}^{-1}$, $9.48 \mu\text{mol}\cdot\text{m}^{-2}\cdot\text{s}^{-1}$, $10.74 \mu\text{mol}\cdot\text{m}^{-2}\cdot\text{s}^{-1}$, and $8.37 \mu\text{mol}\cdot\text{m}^{-2}\cdot\text{s}^{-1}$, with the addition of meteorite, shale, sand, and soft rock respectively (*Fig. 1i*).

At the peak of the crop season, i.e., in August, the atmospheric temperature was high, and the rainfall was abundant. The respiration values of reconstructed soil masses reached the maximum. This maximum was recorded at 12:00, while the minimum was recorded at 6:00 or 20:00. The maximum respiration rate in reconstructed soil masses was $9.88 \mu\text{mol}\cdot\text{m}^{-2}\cdot\text{s}^{-1}$, $10.47 \mu\text{mol}\cdot\text{m}^{-2}\cdot\text{s}^{-1}$, $14.94 \mu\text{mol}\cdot\text{m}^{-2}\cdot\text{s}^{-1}$, and $12.19 \mu\text{mol}\cdot\text{m}^{-2}\cdot\text{s}^{-1}$ for soil masses with the meteorite, shale, sand, and soft rock, respectively. The extent of

daily variation was $3.42 \mu\text{mol}\cdot\text{m}^{-2}\cdot\text{s}^{-1}$, $4.34 \mu\text{mol}\cdot\text{m}^{-2}\cdot\text{s}^{-1}$, $4.62 \mu\text{mol}\cdot\text{m}^{-2}\cdot\text{s}^{-1}$, and $4.03 \mu\text{mol}\cdot\text{m}^{-2}\cdot\text{s}^{-1}$, respectively (Fig. 1j).

In September and October, the soil respiration rate in the four reconstructed soil masses continued to decrease, and the maximum value for all soil masses was recorded at 12:00. Specifically, the minimum respiration rate of reconstructed soil masses in September was $5.05 \mu\text{mol}\cdot\text{m}^{-2}\cdot\text{s}^{-1}$, $3.39 \mu\text{mol}\cdot\text{m}^{-2}\cdot\text{s}^{-1}$, $5.98 \mu\text{mol}\cdot\text{m}^{-2}\cdot\text{s}^{-1}$, and $5.52 \mu\text{mol}\cdot\text{m}^{-2}\cdot\text{s}^{-1}$ for soil masses with the meteorite, shale, sand, and soft rock, respectively. The minimum values were recorded at 6:00 (Fig. 1k). In October, the minimum respiration rate of reconstructed soil masses was $1.59 \mu\text{mol}\cdot\text{m}^{-2}\cdot\text{s}^{-1}$, $1.65 \mu\text{mol}\cdot\text{m}^{-2}\cdot\text{s}^{-1}$, $1.93 \mu\text{mol}\cdot\text{m}^{-2}\cdot\text{s}^{-1}$, and $2.45 \mu\text{mol}\cdot\text{m}^{-2}\cdot\text{s}^{-1}$ for soil masses with the meteorite, shale, sand, and soft rock, and the minimum values appeared at 6:00 or 20:00 (Fig. 1l).

Hydrothermal factors influencing the diurnal variation in reconstructed soil masses

The diurnal variation in temperature in the four reconstructed soil masses showed a single-peak curve. The trend in the diurnal variation of temperature, in different months, in the four reconstructed soil masses was about the same. The maximum temperature was recorded at 10:00, 12:00, or 14:00. In contrast, the minimum temperature was recorded at 6:00 or 20:00. The temperature in the reconstructed soil masses with sand was the highest in each month, while the reconstructed soil masses with meteorite had the lowest temperature in each month. During the observation months, the maximum temperature range of the reconstructed soil masses, with the meteorite, shale, sand, and soft rock, was $1.77\text{--}29.94^\circ\text{C}$, $1.87\text{--}30.56^\circ\text{C}$, $2.01\text{--}32.34^\circ\text{C}$, and $1.84\text{--}32.36^\circ\text{C}$, respectively. In contrast, the minimum temperature range was $0.27\text{--}27.02^\circ\text{C}$, $0.41\text{--}27.72^\circ\text{C}$, $0.31\text{--}29.20^\circ\text{C}$, and $0.11\text{--}29.26^\circ\text{C}$, respectively. The maximum and minimum temperatures were recorded in August and January 2018, respectively.

On the other hand, the maximum range of volumetric water content in reconstructed soil masses, with the meteorite, shale, sand, and soft rock, was $4.2\text{--}26.0\%$, $3.2\text{--}26.3\%$, $4.1\text{--}26.9\%$, and $5.9\text{--}26.1\%$, respectively. While, the minimum range was $1.3\text{--}23.12\%$, $1.5\text{--}23.42\%$, $0.2\text{--}23.02\%$, and $0.6\text{--}23.56\%$, respectively. The differences in soil volumetric water content among the four reconstructed soil masses were not significant ($p < 0.05$). The maximum and minimum values occurred in June 2018 and November 2017, respectively.

Diurnal variation relationship between soil respiration and hydrothermal factors

Relationship between soil respiration and soil temperature

The exponential model can characterise the diurnal relationship between soil respiration and temperature of the four reconstructed soil masses. There was a significant positive exponential correlation between the soil respiration rate and soil temperature for the four reconstructed soil masses. The temperature of reconstructed soil mass, with the meteorite, shale, sand, and soft rock, can explain the diurnal variation of soil respiration by $41.0\%\text{--}96.0\%$, $53.0\%\text{--}98.0\%$, $76.0\%\text{--}98.0\%$, and $66.0\%\text{--}96.0\%$, respectively (Table 1). The temperature of reconstructed soil masses with sand and meteorite had the highest and lowest explanatory capability, respectively, for the diurnal variation in soil respiration.

Table 1. Relationship between soil respiration rate and temperature for reconstructed soil masses ($R_S=ae^{bT}$)

Date	meteorite			shale		sand		soft rock	
	a	b	R ²	a	R ²	a	R ²	a	R ²
11-26	0.0053	0.5971	0.85	0.0022	0.89	0.0018	0.84	0.0041	0.94
12-8	0.0113	0.6412	0.93	0.0009	0.98	0.0029	0.93	0.0053	0.8
1-14	0.1054	1.6142	0.41	0.1133	0.76	0.0704	0.86	0.0838	0.66
2-24	0.005	0.3788	0.92	0.0012	0.84	0.0001	0.86	0.0045	0.84
3-27	0.305	0.1296	0.49	0.2237	0.53	0.1651	0.87	0.2925	0.9
4-11	0.5737	0.1057	0.8	0.5862	0.96	0.4076	0.98	0.6669	0.87
5-12	0.4896	0.1032	0.81	0.2495	0.91	0.1836	0.94	0.5519	0.93
6-15	0.8877	0.0836	0.61	0.6772	0.95	0.4751	0.83	0.6433	0.74
7-25	1.07	0.0732	0.63	0.7522	0.51	0.6225	0.76	0.6557	0.67
8-14	1.4698	0.0674	0.6	1.3315	0.59	1.3642	0.97	1.5094	0.96
9-23	1.0979	0.0913	0.82	0.7797	0.59	0.7207	0.79	1.3289	0.6
10-8	0.6334	0.0903	0.96	0.5484	0.87	0.368	0.85	0.8892	0.81

Relationship between soil respiration and soil volumetric water content

The quadratic curve model can explain the diurnal relationship between soil respiration and soil volumetric water content for the four reconstructed soil masses. There was significant negative correlation between both soil respiration and soil volumetric water content; however, the explanatory power was significantly lower than the soil temperature. The volumetric water content of the reconstructed soil mass, with the meteorite, shale, sand, and soft rock, explained the diurnal variation in soil respiration by 23.0%–46.0%, 28.0%–53.0%, 26.0%–44.0%, and 24.0%–50.0%, respectively (Table 2). The volumetric water content of the reconstructed soil masses with shale and meteorite had the highest and lowest explanatory power, respectively, for diurnal variation in soil respiration.

Table 2. Relationship between soil respiration rate and volumetric water content for reconstructed soil masses ($R_S=aw^2+bw+c$)

Date	meteorite				shale		sand		soft rock	
	a	b	c	R ²	a	R ²	a	R ²	a	R ²
11-26	-0.0074	0.0563	-0.0002	0.23	-0.2907	0.41	-0.5006	0.26	-0.4018	0.37
12-8	-0.3027	0.0857	-0.0138	0.27	-1.2562	0.53	-0.6835	0.32	-0.1040	0.26
1-14	-0.2926	0.321	-0.0447	0.27	-2.4507	0.49	-2.4507	0.49	-0.6520	0.47
2-24	-1.0419	0.2341	-0.0171	0.46	-1.3107	0.34	-0.4457	0.38	-0.6641	0.46
3-27	-4.5251	1.5778	-0.0874	0.46	-1.4536	0.36	-1.7270	0.40	-3.2451	0.40
4-11	-7.2434	3.9182	-0.4361	0.43	-9.3423	0.37	-18.921	0.29	-11.501	0.38
5-12	-16.848	3.9518	-0.2945	0.46	-2.1421	0.40	-9.8838	0.44	-7.6091	0.44
6-15	-3.8989	1.0745	-0.0794	0.33	-5.1743	0.28	-4.0945	0.41	-6.4708	0.24
7-25	-8.4506	0.0718	-0.0391	0.37	-8.2741	0.42	-8.3395	0.29	-6.2462	0.40
8-14	-5.2308	0.6053	-0.0220	0.31	-8.5168	0.31	-13.644	0.29	-17.665	0.49
9-23	-5.1123	0.2868	-0.0130	0.38	-4.4172	0.53	-4.9809	0.37	-8.5975	0.45
10-8	-1.4618	0.7283	-0.0577	0.46	-5.5392	0.39	-0.8546	0.23	-3.4286	0.5

Relationship between soil respiration and temperature, volumetric water content

The power-exponential model was sufficient to characterise the diurnal relationship between soil respiration and temperature, volumetric water content, of the four reconstructed soil masses. The results showed significant positive correlation between the respiration and both factors. Temperature and volumetric water content of the reconstructed soil masses, with the meteorite, shale, sand, and soft rock, explained the daily variation in soil respiration by 56.0%–94.0%, 67.0%–53.0%, 83.0%–98.0%, and 56.0%–99.0%, respectively (Table 3). The two factors of temperature and volumetric water content for reconstructed soil masses with sand and meteorite had the highest and lowest explanatory capability, respectively, of the diurnal variation in soil respiration.

Table 3. Relationship between soil respiration rate and hydrothermal factors for reconstructed soil masses ($R_s = ae^{bT}w^c$)

Date	meteorite				shale		sand		soft rock	
	a	b	c	R ²	a	R ²	a	R ²	a	R ²
11-26	0.009	0.515	0.072	0.9	0.001	0.91	0.001	0.93	0.004	0.99
12-8	0.032	0.602	0.412	0.91	0.002	0.98	0.003	0.99	0.002	0.93
1-14	0.142	1.053	0.034	0.56	0.031	0.92	0.040	0.95	1.315	0.56
2-24	0.013	0.407	0.207	0.91	0.001	0.88	0.001	0.95	0.005	0.87
3-27	0.052	0.236	0.118	0.75	0.001	0.90	0.020	0.85	0.486	0.92
4-11	0.020	0.328	0.036	0.97	0.056	0.99	0.067	0.93	0.122	0.97
5-12	0.032	0.228	0.022	0.92	0.027	0.88	0.007	0.98	0.079	0.95
6-15	0.322	0.120	0.060	0.87	0.103	0.98	0.113	0.97	0.055	0.87
7-25	0.250	0.126	0.074	0.90	0.162	0.90	0.432	0.68	0.668	0.72
8-14	0.994	0.076	0.083	0.77	0.127	0.91	0.737	0.97	0.186	0.93
9-23	0.003	0.388	0.006	0.94	0.009	0.67	0.111	0.86	0.018	0.95
10-8	0.109	0.189	0.016	0.85	0.021	0.89	0.038	0.83	0.068	0.90

Discussion

Effects of different reconstructed materials on soil respiration

Sixty types of mineral materials have been studied locally and globally for improving soil quality, and a series of improved products have been formed, such as mineral fertilisers, growth agents, and nutrient carriers. The additive materials selected in this study were mineral materials, which have natural and unique crystal structures and good physical and chemical characteristics. They have the advantage of improving soil structure, improving soil water retention capacity, increasing soil fertility, adjusting soil pH, and repairing heavy metal pollution (Wen, 2014; Zhang et al., 2016; Sun et al., 2018). The addition of the improved materials changed the physical and chemical properties of the reconstructed soil masses and the ecological environment at the study area (Lin et al., 2016; Wang et al., 2018). This caused the changes in the gas and material cycle processes to affect the soil activity of plant root microorganisms (Keiluweit, 2015). Consequently, this has an effect on soil respiration in reconstructed soil masses.

Properties of different reconstructed materials may cause differences in soil respiration and soil respiration intensity, which was not conducive to environmental protection. The temperature in the reconstructed soil masses, with the addition of sand,

was the highest in each month. The temperature of the reconstructed soil masses with meteorite was the lowest in each month. The order of the diurnal variation in the respiration of the four reconstructed soil masses was as follows: sand > shale > soft rock > meteorite, respectively, over the observed months. This is mainly due to the difference in specific heat capacity. The meteorite has excellent water retention performance, and the sand heats up faster as it is closer to the air temperature. Once the sand and the ambient temperature are consistent, heat conduction will no longer occur. The meteorite takes a long time to heat up due to the large specific heat capacity; thus, the adjacent sand temperature decreases rapidly. Soft rock and shale with high clay content can be used as soil-forming materials. In contrast, meteorite can be used as modified material. Simultaneously, these three materials can increase soil water retention. The water occupied the soil gap, resulting in relatively low CO₂ content in the soil, and the soil respiration was low. Therefore, this was conducive to environmental protection. Meanwhile, sand, as a soil improvement material, can increase the CO₂ content in the soil and soil respiration intensity, thus leading to non-conductive conditions for environmental protection.

Relationship between respiration and hydrothermal factors of reconstructed soil masses

The diurnal changes in the soil respiration in the four reconstructed soil masses showed a single-peak curve, and the patterns of diurnal changes in respiration were similar for different months. This result is consistent with the study of Fu et al. (2019) and Shi et al. (2012a) conducted in the farmland of the Western Sichuan Plain and *Platycladus orientalis* forest on the Loess Plateau of the arid and semi-arid region, respectively. However, in Cui et al. (2016), the soil respiration patterns differed per month, and not all of them showed a single-peak curve. This finding may be caused by the differences in the study area, management measures (i.e., artificial), and soil-grown crops (Li, 2014b; Zhou, 2014). The maximum and minimum soil respiration values were recorded at 10:00 – 16:00 and 03:00 – 05:00 (Zhao et al., 2014), 12:00 – 16:00, and 6:00 (Shi et al., 2012b), 12:00 – 15:00, 2:00 – 6:00 (Fu et al., 2019). The test observation showed that the lowest value was recorded at 6:00 or 20:00, while the highest value was recorded at 10:00, 12:00, or 14:00. This finding indicates that the maximum and minimum values of the diurnal soil respiration changed after adding different materials. However, the results are consistent with previous studies. The soil respiration values of the four reconstructed soil masses reached the maximum and minimum in August and January, respectively. Moreover, the diurnal variation was the smallest in January. This finding is consistent with Tu et al. (2015). This variation was caused by the growth of vegetation and changes in seasonal climatic factors (Kuzyakov et al., 2010; Wang et al., 2015). In summer, the soil temperature and humidity conditions are high, the root system is enhanced, the soil microbial metabolism is strong, and the decomposition of organic matter is also enhanced (Fang et al., 2015; Yu et al., 2019). These conditions promote soil respiration.

Among the many factors affecting soil respiration rate, studies show that temperature is the most vital factor. Moreover, soil temperature can indirectly affect soil respiration by affecting plant roots and soil microbial activity (Fu et al., 2012, 2018). The lowest and highest value of the reconstructed soil masses appeared in January and August, respectively. This is because the soil temperature is the process of absorbing and releasing energy according to changes in the solar radiation and atmospheric

temperature. It is affected by solar radiation balance, soil heat balance, and soil temperature change with air temperature. Therefore, the temperature can also be a good indicator of soil respiration in different climates (Zhang et al., 2013). However, the maximum value in soil respiration sometimes lags, mainly because the soil temperature does not show high peak that is consistent with the air temperature but lags behind it (Qin and Shang-guan, 2012). The exponential model explained most of the variability in soil respiration rate (Zhang et al., 2013, 2014). This study found that the diurnal respiration in the four reconstructed soil masses was significantly positively correlated with soil temperature. The conclusions are, therefore, the same as previous studies.

Water is one of the necessary conditions for plant life. Soil texture and structure affect the water dynamics. Due to the different topographical conditions of the underlying surface, the soil texture, and the crop types, the depth and water absorption of the root system are also different, and there is also a vertical variation in the spatial distribution of soil moisture (Zhu et al., 2019). Under different surface conditions, the spatial variability of soil moisture distribution is vast. Even if the differences in underlying surface conditions were minimal, the unevenness of soil moisture distribution was widespread, and the soil moisture content had an apparent variability. This is consistent with the conclusion that the water volume in the reconstructed soil masses has a significant variation after adding different materials. The effect of soil volumetric water content on soil respiration is complicated. The conclusions by scholars in different regions, research periods, and ecosystems are often inconsistent (Ma et al., 2016; Ding et al., 2017). In addition to root growth and microbial activity, soil volumetric water content can also affect soil respiration rate by affecting soil CO₂ content and transmission process (Wang et al., 2007, 2014). The relationship between soil volumetric water content and soil respiration can be simulated by the logarithmic model, quadratic curve, and linear relationship (Geng et al., 2012). Soil volumetric water content and soil respiration were significantly negatively correlated (Tu et al., 2015; Duan et al., 2018). Some studies show that when soil moisture stress occurs, water can be a dominant factor affecting soil respiration (Kosugi et al., 2007; Wang et al., 2014). This study found that the quadratic curve can characterise the relationship between volumetric water content and soil respiration. However, the correlation coefficient and the effect on soil respiration were minimal.

Temperature and moisture are the critical environmental factors for the diurnal change of soil respiration. Generally, both soil temperature and soil humidity affect the soil respiration intensity. Therefore, the combination of the two can be used to characterise the diurnal change in soil respiration (Shi et al., 2012b; Li et al., 2014a). This study fitted the relationship between soil respiration and soil temperature using an exponential model. In contrast, the relationship between soil respiration and soil water content was fitted with a quadratic curve model; and, soil respiration and soil hydrothermal factors were simulated using a power-exponential model. However, the power-exponential model has an explanatory power of more than 56%, and its interpretation ability was much higher than that of the quadratic curve model. In most cases, the power-exponential model had higher explanatory power than the exponential model. Wang et al. (2006) studied soil respiration in six ecosystems in China's temperate forests. They found that the explanatory power of the two-factor model was usually higher than that of the single-factor model. Moreover, the explanatory power was generally higher than 50%. In another study, Tu et al. (2015) studied the soil respiration in *Platycladus orientalis* plantation in Xishan, Beijing. They obtained

power-exponential model that can better describe the response of soil respiration rate to soil hydrothermal factors, with an explanatory power of 86.8%. Previous studies achieved similar conclusions to the current study.

Conclusions

(1) The daily variation in the respiration of four reconstructed soil masses showed a single-peak curve, and the pattern of respiratory diurnal changes was basically the same. The lowest value appeared at 6:00 or 20:00 in the observed months, and the highest value appeared at 10:00, 12:00, or 14:00. The soil respiration values of the four reconstructed soil masses reached the maximum and minimum in August and January, respectively. The order of diurnal variation in the respiration of four reconstructed soil masses was as follows: sand > shale > soft rock > meteorite.

(2) The diurnal variation in the respiration of four reconstructed soil masses can be explained by a single factor of soil temperature (i.e., index model), soil volumetric water content (i.e., quadratic model), or both factors (i.e., power-index model). However, the explanatory power was different, i.e., generally higher than 50.0% for the two-factor model, and the interpretation ability of temperature was significantly higher than that of water for the single-factor model. The model involving both factors were the best to characterize the relationship between hydrothermal influence factors and respiration of four reconstructed soil masses.

(3) This study concludes that the respiration in the reconstructed soil masses was different according to the added materials; thus, the corresponding carbon emissions were also different. The reconstructed soil with meteorite was conducive to the protection of the ecological environment. In this context, the government should add materials that are conducive to environmental protection to reduce CO₂ emissions when implementing land remediation. When formulating regional ecological policies, CO₂ emissions in reconstructed soil masses should also be considered to ensure accurate regional measures.

(4) This study analysed the diurnal dynamics in respiration from the reconstructed soil masses and its relationship with hydrothermal factors. The relationship between microbes in the reconstructed soil masses and physicochemical properties with soil respiration should be studied in the future, as well as the main factors affecting soil respiration. The quality of reconstructed soil masses should be characterised more rapidly through dynamic monitoring of the soil respiration. Moreover, the influence of biological factors on soil respiration cannot be ignored. Therefore, the relationship between biological factors and soil respiration should be considered in future studies. Additionally, the carbon emissions from the reconstructed soil masses, as one of the regional carbon emission sources, should be quantified to support accurate regional emission reduction measures.

Acknowledgements. This study was supported by Shaanxi Provincial Land Engineering Construction Group, China, Project No. DJNY2019-20; Industry of Ministry of Water Resources Public Welfare Profession, China, Project No. 201501049.

REFERENCES

- [1] Cui, H., Zhang, Y. H. (2016): Diurnal and seasonal dynamic variation of soil respiration and its influencing factors of different fenced enclosure years in desert steppe. – *Environmental Science* 37: 331-339.
- [2] Ding, X. Y., Wang, Z. K., Yang, X., Du, S. S., Shen, Y. Y. (2017): Response of dry land soil respiration to conservation tillage practices during drying-wetting cycles. – *Scientia Agricultura Sinica* 50: 4759-4768.
- [3] Duan, B. X., Man, X. L., Song, H., Liu, J. L. (2018): Soil respiration and its component characteristics under different types of *Larix gmelinii* forests in the north of Daxing'an Mountains of northeastern China. – *Journal of Beijing Forestry University* 40: 40-50.
- [4] Fang, H. J., Cheng, S. L., Lin, E. D., Yu, G. R., Niu, S. L., Wang, Y. S., Xu, M. J., Dang, X. S., Li, L. S., Wang, L. (2015): Elevated atmospheric carbon dioxide concentration stimulates soil microbial activity and impacts water extractable organic carbon in an agricultural soil. – *Biogeochemistry* 122: 253-267.
- [5] Fu, G., Shen, Z. X., Zhang, X. Z., Zhou, Y. T. (2012): Response of soil microbial biomass to short-term experimental warming in alpine meadow on the Tibetan Plateau. – *Applied Ecology and Environmental Research* 61: 158-160.
- [6] Fu, G., Shen, Z. X., Zhang, X. Z. (2018): Increased precipitation has stronger effects on plant production of an alpine meadow than does experimental warming in the Northern Tibetan Plateau. – *Agricultural and Forest Meteorology* 249: 11-21.
- [7] Fu, Y., Wang, T., Yang, Z. P., Zhou, W., Liu, Q., Ren, W. J., Chen, Y. (2019): Annual soil respiration characteristics of different paddy-upland rotations in irrigation areas of the Western Sichuan Plain. – *Acta Ecologica Sinica* 39: 6701-6709.
- [8] Geng, Y., Wang, Y., Yang, K., Wang, S., Wang, H., Zeng, H., Baumann, F., Kuehn, P., Scholten, T., He, J. (2012): Soil respiration in Tibetan alpine grasslands: belowground biomass and soil moisture, but not soil temperature, best explain the large-scale patterns. – *Plos One* 7: e34968.
- [9] Goldberg, S. D., Zhao, Y., Harrison, R. D., Monkai, J., Li, Y., Chau, K., Xu, J. (2017): Soil respiration in sloping rubber plantations and tropical natural forests in Xishuangbanna, China. – *Agriculture, Ecosystems & Environment* 249: 237-246.
- [10] Hu, S. D., Li, Y. F., Chang, S. X., Li, Y. C., Yang, W. J., Fu, W. J., Liu, J., Jiang, P. K., Lin, Z. W. (2018): Soil autotrophic and heterotrophic respirations respond differently to land-use change and variations in environmental factors. – *Agricultural and Forest Meteorology* 250-251: 290-298.
- [11] Keiluweit, M., Bougoure, J. J., Nico, P. S., Pett-Ridge, J., Weber, P. K., Kleber, M. (2015): Mineral protection of soil carbon counteracted by root exudates. – *Nature Climate Change* 5: 588-595.
- [12] Kosugi, Y., Mitani, T., Itoh, M., Noguchi, S., Tani, M., Matsuo, N., Takanashi, S., Ohkubo, S., Nik, A. R. (2007): Spatial and temporal variation in soil respiration in a Southeast Asian tropical rainforest. – *Agricultural and Forest Meteorology* 147: 35-47.
- [13] Kuzyakov, Y., Gavrichkova, O. (2010): Time lag between photosynthesis and carbon dioxide efflux from soil: a review of mechanisms and controls. – *Global Change Biology* 16: 3386-3406.
- [14] Lai, L. M., Jiang, L. H., Wang, Y. J., Zheng, Y. R., Chen, X., Rimmington, G. M. (2012): Soil respiration in different agricultural and natural ecosystems in an arid region. – *Plos One* 7: e48011.
- [15] Li, H. S., Wang, J. S., Liu, X., Jiang, S. S., Zhang, C. Y., Zhao, X. H. (2014a): Effects and its sustained effect of simulated nitrogen deposition on soil respiration in *Pinus tabulaeformis* forests in the Taiyue Mountain, China. – *Acta Scientiae Circumstantiae* 34: 238-249.

- [16] Li, Q., Zhou, D. W., Jin, Y. H., Wang, M. L., Sun, Y. T., Li, G. D. (2014b): Effects of fencing on vegetation and soil restoration in a degraded alkaline grassland in northeast China. – *Journal of Arid Land* 6: 478-487.
- [17] Li, X. D., Guo, D., Zhang, C. P., Niu, D. C., Fu, H., Wan, C. G. (2018): Contribution of root respiration to total soil respiration in a semi-arid grassland on the Loess Plateau, China. – *Science of the Total Environment* 627: 1209-1217.
- [18] Lin, Y. L., Li, Y., Chen, Y. H., Fan, H., Wang, Y. N., Wang, J. J. (2016): Effects adding sand on soil physical and chemical property and corn yield in alkalized solonchak soil. – *Soil and fertilizer Science in China* 53: 119-123.
- [19] Ma, H. P., Guo, Q. Q., Li, J. R., Zhou, C. N. (2016): Soil Respiration and Its Affecting Factors Relative to Type of Forest in the Sygera Mountains of Southeast Tibetan Plateau. – *Acta Pedologica Sinica* 53: 253-260.
- [20] Meyer, N., Meyer, H., Welp, G., Amelunga, W. (2018): Soil respiration and its temperature sensitivity (Q_{10}): Rapid acquisition using mid-infrared spectroscopy. – *Geoderma* 323: 31-40.
- [21] Qi, J., Shang-guan, Z. P. (2012): Variation characteristics of soil respiration rate in *Ulms pumila* Robinia pseudociain different forest types of during the growing season. – *Journal of Northwest A & F University (Natural Science Edition)* 40: 91-98.
- [22] Rey, A., Raimundo, J., Oyonarte, C. (2010): Temporal and spatial variation in soil respiration in two semiarid steppe ecosystems with different degrees of land degradation. – *Geophysical Research Abstracts* 12: 2451.
- [23] Shi, W. Y., Zhang, J. G., Yan, M. J., Guan, J. H., Du, S. (2012a): Diurnal and seasonal dynamics of soil respiration in a *Platycladus orientalis* forest stand on the semiarid Loess Plateau, China. – *Journal of Earth Environment* 3: 1144-1148.
- [24] Shi, W. Y., Zhang, J. G., Yan, M. J., Norikazu, Y., Sheng, D. (2012b): Seasonal and diurnal dynamics of soil respiration fluxes in two typical forests on the semiarid Loess Plateau of China: temperature sensitivities of autotrophs and heterotrophs and analyses of integrated driving factors. – *Soil Biology & Bio-chemistry* 52: 99-107.
- [25] Sun, Z. H., Han, J. C. (2018): Effect of soft rock amendment on soil hydraulic parameters and crop performance in Mu Us sandy land, China. – *Field Crops Research* 222: 85-93.
- [26] Sun, S., Lei, H., Chang, S. X. (2019): Drought differentially affects autotrophic and heterotrophic soil respiration rates and their temperature sensitivity. – *Biology and Fertility of Soils* 55: 275-283.
- [27] Tu, Z. H., Pang, Z., Zhao, Y., Zheng, L. W., Yu, X. X., Chen, L. H. (2015): Soil respiration components and their controlling factors in a *Platycladus orientalis* plantation in west mountain area of Beijing. – *Acta Scientiae Circumstantiae* 35: 2948-2956.
- [28] Wang, C. K., Yang, J. Y., Zhang, Q. Z. (2006): Soil respiration in six temperate forests in China. – *Global Change Biology* 12: 2103-2114.
- [29] Wang, X. G., Zhu, B., Wang, Y. Q., Zheng, X. H. (2007): Soil respiration and its sensitivity to temperature under different land use conditions. – *Acta Ecologica Sinica* 27: 1960-1967.
- [30] Wang, B., Zha, T. S., Jia, X., Wu, B., Zhang, Y. Q., Qin, S. G. (2014): Soil moisture modifies the response of soil respiration to temperature in a desert shrub ecosystem. – *Biogeosciences* 11: 259-268.
- [31] Wang, B., Zha, T. S., Jia, X., Gong, J. N. (2015): Microtopographic variation in soil respiration and its controlling factors vary with plant phenophases in a desert-shrub ecosystem. – *Biogeosciences* 12: 5705-5714.
- [32] Wang, Z. G., Bing, Y. L., Song, Z. H., Zhang, J., Cai, Y., Gong, Y. L., Hu, J. J. (2018): Substrate compositions facilitate clay restoration of the simulation study in an opencast coal mine in the eastern steppe of China. – *Acta Ecologica Sinica* 38: 5865-5875.
- [33] Wen, J. (2014): Study on Remediation of Heavy Metal Contaminated Soil by Soft rock. – Master Thesis, College of Resources and Environment, Northwest A&F University and Shaanxi Province.

- [34] Yu, C. Q., Han, F. S., Fu, G. (2019): Effects of 7 years experimental warming on soil bacterial and fungal community structure in the Northern Tibet alpine meadow at three elevations. – *Science of total Environment* 655: 814-822.
- [35] Zhang, D. C., Cai, D. X., Dai, K., Feng, Z., Zhang, X., Wang, X. (2013): Soil respiration and its responses to soil moisture and temperature under different tillage systems in dryland maize fields. – *Acta Ecologica Sinica* 33: 1916-1925.
- [36] Zhang, Q., Lei, H. M., Yang, D. W. (2013): Seasonal variations in soil respiration, heterotrophic respiration and autotrophic respiration of a wheat and maize rotation cropland in the North China Plain. – *Agricultural and Forest Meteorology* 180: 34-43.
- [37] Zhang, C., Niu, D., Hall, S., Wen, H., Li, X., Fu, H., Wan, C., Elser, J. J. (2014): Effects of simulated nitrogen deposition on soil respiration components and their temperature sensitivities in a semiarid grassland. – *Soil Biology & Biochemistry* 75: 113-123.
- [38] Zhang, T. B., Zhan, X. Y., Kang, Y. H., Wan, S. Q., Feng, H. (2016): Amelioration of high saline-sodic wasteland of takyric solonetz by cropping lycium barbarum with drip irrigation and shallow sand-filled niches. – *Transactions of the Chinese Society for Agricultural Machinery* 47: 139-149.
- [39] Zhao, B. Y., Hong, M., Liang, C. Z., Bao, W. Y., Zhang, J. X. (2014): Effect of fertilization on soil respiration in the *Stipa breviflora* desert steppe of Inner Mongolia. – *Chinese Journal of Applied Ecology* 25: 687-694.
- [40] Zhou, X. B., Zhang, Y. M. (2014): Seasonal pattern of soil respiration and gradual changing effects of nitrogen addition in a soil of the Gurbantunggut Desert, northwestern China. – *Atmospheric Environment* 85: 187-194.
- [41] Zhou, W. P., Shen, W. J., Li, Y. E., Hui, D. F. (2017): Interactive effects of temperature and moisture on composition of the soil microbial community. – *European Journal of Soil Science* 68: 909-918.
- [42] Zhu, X., Shao, M., Liang, Y., Tian, Z. Y., Wang, W., Qu, L. (2019): Mesoscale spatial variability of soil-water content in an alpine meadow on the northern Tibetan Plateau. – *Hydrological Processes* 33: 2523-2534.

SPATIOTEMPORAL DYNAMICS AND INFLUENCING FACTORS OF SOIL EROSION IN THE DIANCHI LAKE BASIN, CHINA

PENG, S. Y. * – ZHAO, Z. X.

School of Tourism and Geography, Yunnan Normal University, Kunming 650500, China

**Corresponding author
e-mail: frankmei@126.com*

(Received 22nd Dec 2019; accepted 22nd May 2020)

Abstract. Mastering the spatiotemporal evolution tendency of soil erosion and its influencing factors is of great significance for optimizing regional soil and water conservation measures, ensuring sustainable development. This study calculated the soil erosion modulus and investigated the spatiotemporal dynamics of soil erosion intensity in the Dianchi Lake basin of China during the 1999-2014 period based on the revised universal soil loss equation (RUSLE) model and geographic information system (GIS) and remote sensing (RS) techniques. The results showed that the soil erosion in the Dianchi Lake basin has been improved in the past fifteen years, and the erosion area is shrinking continuously, but the unit erosion intensity is increasing, indicating that local area erosion is still serious. The analysis results show that soil erosion can easily occur of cultivated lands with slopes of 8-25° and a vegetation coverage in 0%-45% forestland. The area of intensity of soil erosion exhibited a decreasing trend, indicating a gradual improvement in the situation of soil erosion. However, the soil erosion phenomenon in cultivated land, forest land and bare land with a slope of 8-25° and a vegetation coverage of 45% or less is severely. This study provides a theoretical foundation and methodological reference for research on soil erosion and its influencing factors in similar highlands Lake basin.

Keywords: *soil erosion, RUSLE, geographic information system, spatial relationship, erosion factor, highland lakes*

Introduction

Soil erosion is a global environmental problem, which can cause issues such as land degradation, declines in soil fertility and quality, and deterioration of the ecological environment (Montgomery et al., 2007; Lal, 2003). During soil erosion, large amounts of slope sediment are scoured, transported, and deposited into rivers and lakes, resulting in sedimentation of these water bodies, weakening the flood discharge capacity of riverbeds and increasing the risk of flood disasters (Gao and Cao, 2011). Additionally, large amounts of soil nutrients such as nitrogen, phosphorus, and potassium are lost, resulting in land infertility, water eutrophication, and ecological imbalances, severely restricting the sustainable development of society, the economy, and environment (Hartanto et al., 2003; Pimentel et al., 1995). China has vast amounts of land and yet suffers from relatively severe soil erosion. According to the second national remote sensing survey of soil erosion, soil and water loss comprised 37.42% of China's total land area. In this scenario, the economic loss caused by soil and water loss can no longer be understated.

The traditional method of soil erosion survey is time-consuming and long-term, and it is almost impossible to determine the amount of soil erosion in the medium-scale basin. The Universal Soil Loss Equation (USLE) has been widely used in soil erosion related research because of its simple calculation method, low data volume and versatile results. The model is an empirical model which is derived from the inductive statistics of soil erosion and runoff observations from the US Department of Agriculture (USDA)

using more than 10,000 runoff plots (Wischmerie and Smith, 1965). However, due to the limitations of the USLE model, the US Department of Agriculture organized scientists to improve the model in 1985, and in 1992 a revised version of the Universal Soil Loss Equation (RUSLE) was issued (Fu et al., 2011; Kinnel et al., 2010). The RUSLE model involves a wide range of areas, considers multiple natural influence factors, and has a simple form and a straightforward calculation method (Angima et al., 2003). Therefore, the model has strong practicability and has been widely used in soil erosion evaluation by scholars, institutions and government departments at home and abroad. Since the 1980s, with the rapid development of spatial information technology, RS and GIS have been widely used in soil erosion assessment (Peng et al., 2018). RS is mainly used for the collection and extraction of soil erosion information. GIS is mainly used for the management and analysis of erosion data and the calculation of impact factors. The integration of RUSLE model with GIS and RS technology can quantitatively analyze the spatial and temporal changes of soil erosion in the basin and the relationship between soil erosion and impact factors (Zhu et al., 2015). Alexakis et al. (2013), Xin et al. (2009), Zha et al. (2015), Lin et al. (2011) evaluated the evolutionary trend of the temporal and spatial patterns of erosion areas by integrating of the RUSLE model with GIS. Slope, land use type, vegetation coverage and soil erodibility factors are important factors affecting soil erosion. Therefore, it is necessary to explore their relationship with soil erosion. Vijith et al. (2012), Kinnell et al. (2014, 2018) and Hu et al. (2018) compared the differences in soil erosion on different slopes based on soil erosion models. The study of land use and soil erosion focuses on the extent to which land cover types and their effects have an impact on soil erosion intensity (Li et al., 2014; Manojlovic et al., 2017; Mondal et al., 2015; Xiao et al., 2015; Zokaib and Naser, 2011). The increase in vegetation coverage can effectively slow down the occurrence of soil erosion. The research in this area mainly focuses on the relationship between the change of coverage and erosion, and the study of erosion under different coverage conditions of different rainfall (Jian et al., 2016; Yan et al., 2013; Yao et al., 2018; Zhou et al., 2006). Soil erodibility is an important indicator for assessing soil sensitivity to erosion and an important parameter for soil erosion prediction. Since this factor is closely related to the physical and chemical properties of the soil and the rainfall erosion intensity, many studies have focused on the determination of soil erodibility values under different rainfall conditions in different regions (Panagos et al., 2012; Saygin et al., 2017; Wang et al., 2013).

The Dianchi Lake basin is the most densely populated area in Yunnan Province of China, characterized by a high level of human activities and economic development. In recent years, rapid development and urbanization have resulted in the continuous deterioration of water quality in the Dianchi Lake basin, where soil erosion has emerged as a primary source of pollution. It is necessary to analyze the soil erosion trend in the lake basin from the perspective of spatial variation, and identify the significance of the effects of various factors on soil erosion. Such work can provide decision-making support for pollution prevention and control measures as well as sustainable urban development in the Dianchi Lake basin area.

Based on the above reasons, RUSLE model was selected and used in this study by integrating with GIS and RS to analyse the spatial variation of soil erosion and its influencing factors in the Dianchi Lake basin, China, over the 1999-2014 period. The objectives of this present were: (1) to reveal the spatiotemporal changes of soil erosion; (2) to find major influencing factors on soil erosion in the study area.

Materials and methods

Study sites

The Dianchi Lake basin is located in the middle of the Yunnan, China (*Fig. 1*). It is located in the watershed of the Yangtze River, the Pearl River and the Honghe River. The geographical coordinates are 24°28'-25°28'N, 102°30'-103°00'E. The drainage area is 2,920 km², the hilly area is relatively large, accounting for 69.5% of the total area; the plains and basins account for 20.2% of the total area; the Dianchi Lake water body accounts for 10.3%.

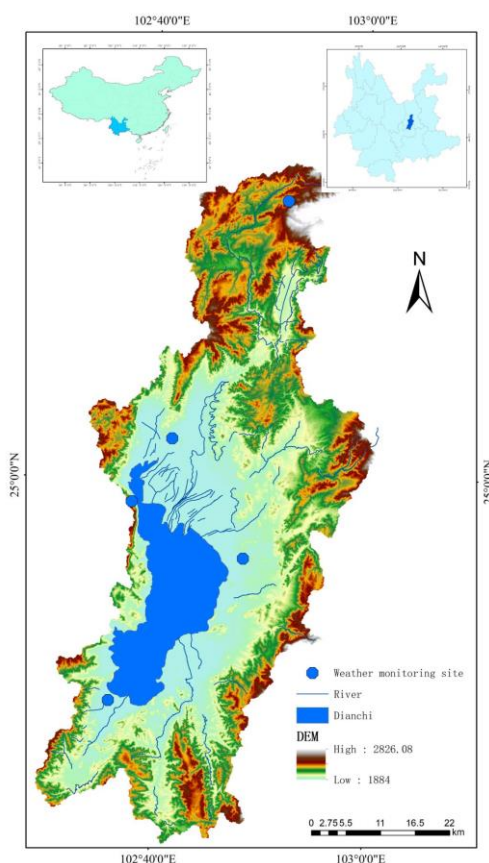


Figure 1. Location of Dianchi basin, Yunnan, China

Data source

The data used in this study include: (1) Daily rainfall data of five monitoring points (Kunming Station, Taihuashan Station, Jinning Station, Yuming Station, Chenggong Station) in Dianchi basin in 1999, 2005 and 2014; (2) Remote sensing image data includes: LandsatTM images on December 25, 1999, March 01, 2005, and November 25, 2014; (3) Digital elevation model (DEM) data in Dianchi basin with spatial resolution of 30 m; (4) Soil data, Dianchi basin 1:25 Million soil type data.

Soil erosion model

The RUSLE comprehensively reflects the effects of natural factors and human activities on soil erosion using five factors, namely rainfall erosivity factor, soil

erodibility factor, topographic factor, vegetation cover factor, and soil and water conservation practice factor. Among the factors, rainfall erosivity is a dynamic factor of soil erosion. The soil erodibility factor reflects the difficulty level of soil erosion caused by rainfall (Wang et al., 2018; Wen et al., 2013). Topographic factors affect the formation and development of surface vegetation thus controlling the movement state and direction of surface runoff (Wang et al., 2018). The vegetation cover factor as well as the soil and water conservation practice factor affect the distribution of surface vegetation and the level of human activities, thereby directly or indirectly affecting the occurrence and development of soil erosion (Miao et al., 2012). This model is expressed as follows:

$$A=R*K*LS*C*P \quad (\text{Eq.1})$$

where A is the annual average erosion modulus ($\text{t}\cdot\text{hm}^{-2}\cdot\text{a}^{-1}$); R is the rainfall erosivity factor ($\text{MJ}\cdot\text{mm}\cdot\text{hm}^{-2}\cdot\text{h}^{-1}\cdot\text{a}^{-1}$); K is the soil erodibility factor ($\text{t}\cdot\text{hm}^2\cdot\text{h}\cdot\text{hm}^{-2}\cdot\text{MJ}^{-1}\cdot\text{mm}^{-1}$); L is the slope length factor; S is the slope steepness factor; C is the vegetation coverage and management factor; P is the soil and water conservation measure factor. Among them, L , S , C , and P are all dimensionless.

Rainfall erosivity factor

The rainfall erosivity factor R refers to the potential ability of rainfall to cause soil erosion and is related to the intensity, duration, raindrop size, raindrop velocity, and amount of rainfall (Nyssen et al., 2005). Zhang et al. compared the results of rainfall erosivity from different types of representative rainfall data, indicating that the calculation of mean annual erosivity based on daily rainfall yielded the highest accuracy (Zhang and Jin, 2003). In the present study, the rainfall erosivity model was constructed based on daily rainfall data using the following equation:

$$M_i = \alpha \sum_{j=1}^k (D_j)^\beta \quad (\text{Eq.2})$$

$$\beta = 0.8363 + \frac{18.144}{P_{d12}} + \frac{24.455}{P_{y12}} \quad (\text{Eq.3})$$

$$\alpha = 21.586\beta^{-7.1891} \quad (\text{Eq.4})$$

In *Equation 2*, M_i is rainfall erosivity in the i -th half month ($\text{MJ}\cdot\text{mm}\cdot\text{hm}^{-2}\cdot\text{h}^{-1}\cdot\text{a}^{-1}$), K is the number of days in the i -th half month, D_j is the erosive daily rainfall on the j -th day in the i -th half month (daily rainfall ≥ 12 mm; otherwise $D_j = 0$), and α and β are two model parameters to be determined by *Equation 2*. In *Equation 3*, P_{d12} and P_{y12} are the daily and yearly averages of ≥ 12 mm daily rainfall, respectively. According to these equations, daily rainfall erosivity data at monitoring points in the Dianchi Lake basin were calculated for three study years, using the 1999, 2005, and 2014 data from five weather stations in the lake basin. The spatial distribution of rainfall erosivity across the lake basin was then calculated by spatial interpolation using the ArcGIS tool (*Fig. 2*).

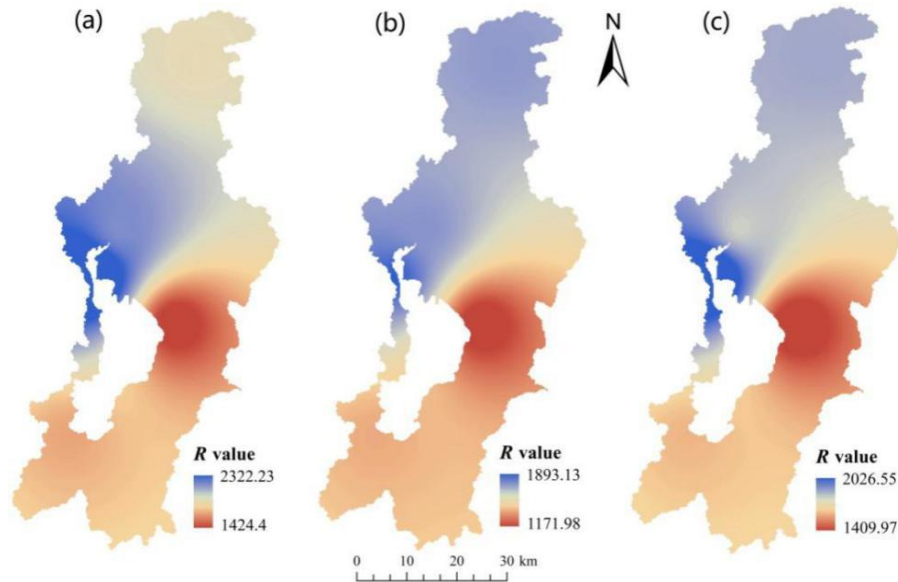


Figure 2. Rainfall erosivity distribution map of Dianchi Lake basin. (a) 1999, (b) 2005 and (c) 2014

Soil erodibility factor

In the present study, the soil erodibility factor K was calculated using the erosion productivity impact calculator (EPIC) of Wischmeier and Smith (1971), which is expressed as follows:

$$K_{EPIC} = 0.1317 \left\{ 0.2 + 0.3 \exp \left[-0.0256 SAD \left(1 - \frac{SIL}{100} \right) \right] \right\} \left[\frac{SIL}{CLA + SIL} \right]^{0.3} \left\{ 1.0 - \frac{0.25C}{C + \exp(3.72 - 2.95C)} \right\} \left\{ 1.0 - \frac{0.7(1 - SAD/100)}{(1 - SAD/100) + \exp(-5.51 + 22.9(1 - SAD/100))} \right\} \quad (\text{Eq.5})$$

where SAD , SIL , CLA , and C are the sand, silt, clay, and organic carbon contents, respectively (unit: %). The K values in the Dianchi Lake basin were calculated by querying the “Records of Yunnan Soil Species” in combination with the soil distribution map of Yunnan Province. The spatial distribution map of the K values was obtained using the ArcGIS (Fig. 3a).

Slope length and steepness factor

The slope length factor L and slope steepness factor S affect the formation and erosion level of surface runoff, reflect the topographic features, and play a relatively important role in soil erosion among topographic indicators. Thus, the slope length and steepness factor (LS) is an external factor that must be considered for soil erosion as it determines the accuracy and reliability of the soil erosion study. In this study, the LS factor was calculated using the equation proposed by Liu et al. (2000). The slope length factor L is calculated as follows:

$$L = (h / 22.13)^m \quad (\text{Eq.6})$$

where L is the slope length factor, h is the slope length value, and m is the slope length index. The value of m is as follows:

$$m = \begin{cases} 0.5 & \theta > 5^\circ \\ 0.4 & 3^\circ < \theta \leq 5^\circ \\ 0.3 & 1^\circ < \theta \leq 3^\circ \\ 0.2 & \theta \leq 1^\circ \end{cases} \quad (\text{Eq.7})$$

where θ is the slope value.

The S factor is the ratio of soil loss per unit area at any slope to that at the slope of a standard plot, provided all other conditions are identical. Slope is a relatively stable parameter. In this study, the slope steepness factor algorithm of McCool for gentle slopes was combined with the slope steepness factor equation of Liu et al. (Liu et al., 2000; Mccool et al., 1987). for steep slopes to calculate the S factor as follows:

$$\begin{cases} 10.8 \sin \theta + 0.03 & \theta < 5^\circ \\ 16.8 \sin \theta - 0.5 & 5^\circ \leq \theta < 10^\circ \\ 21.9 \sin \theta - 0.96 & \theta \geq 10^\circ \end{cases} \quad (\text{Eq.8})$$

The spatial distribution map of the LS factor (Fig. 3b) was obtained based on calculations using a combination of Equations 6-8.

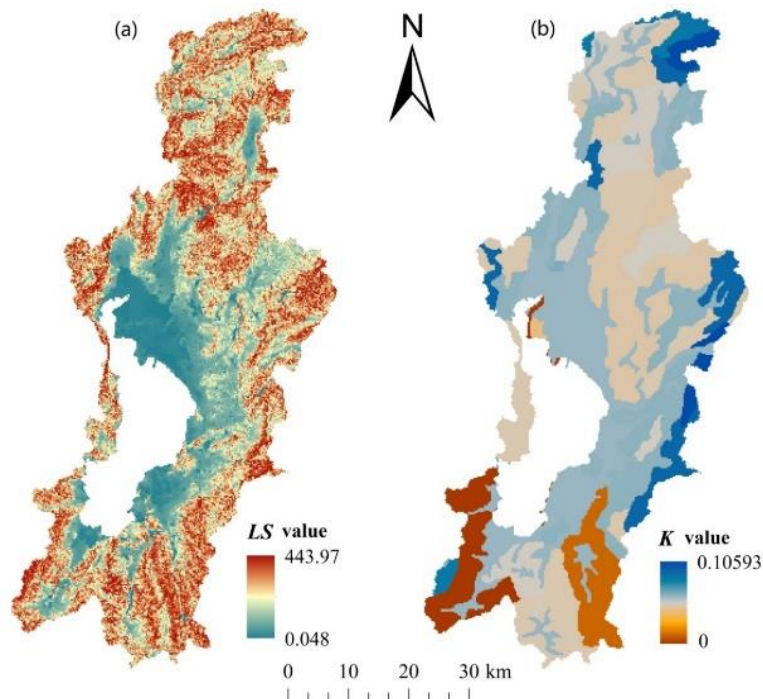


Figure 3. The distribution of slope length factor (LS) and soil erodibility factor (K) in Dianchi Lake basin. (a) LS and (b) K

Vegetation cover and management factor

In this study, the C factor in the Dianchi Lake basin was estimated using the calculation model established by Cai et al. (Chong, 2000):

$$\begin{cases} C = 1 & c < 0 \\ C = 0.6508 - 0.3436 \lg c & 0 < c < 78.3\% \\ C = 0 & c > 78.3\% \end{cases} \quad (\text{Eq.9})$$

where C is the vegetation cover and management factor and c is the vegetation coverage. First, the c value was extracted using remote sensing images. Then, the spatial distribution map of the C value (Fig. 4) was obtained through calculation using the ArcGIS software according to Equation 9.

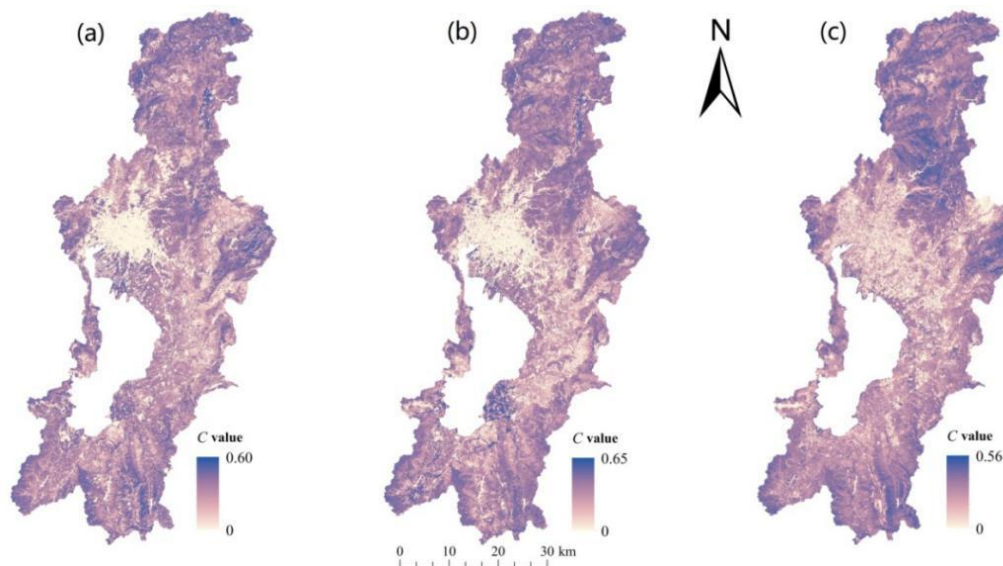


Figure 4. The distribution of vegetation coverage and management factors (C) in Dianchi Lake basin. (a) 1999, (b) 2005 and (c) 2014

Soil and water conservation practice factor

The soil and water conservation practice factor P is the proportion of the soil loss under specific practice in the corresponding soil loss under no conservation practice, ranging between 0 and 1 (Renard et al., 1997). P value of 0 indicates that soil and water conservation practices are well implemented in a region where erosion is unlikely to occur. P value of 1 indicates no implementation of any soil and water conservation practices. The conservation practices are generally of cultivation and engineering types. Common conservation practices include strip tillage and contour tillage, whereas engineering practices include building terraces, establishing drainage practices, and returning cropland to forests. According to existing studies, the P value was determined in the present study based on the land use situation and the soil and water conservation practices implemented in the lake basin area (Zhao et al., 2007). Specifically, the P value in the lake basin was obtained using a combination of land use/cover types and soil and water conservation practices implemented in the Dianchi Lake basin (Table 1).

Table 1. The P value of soil and water conservation measures factor in Dianchi basin

Land use/land cover	Water	Cropland	Forest land	Bare land	Construction land	Grass land
P value	0	0.59	1.0	1.0	0	1.0

Results

Spatial distribution of the influence factors

As can be seen from *Figure 2*, significant consistency can be witnessed in the spatial distribution of rainfall erosivity factor (R) during the studied period. The areas with the strongest and weakest rainfall erosions are located on the northwestern and eastern shores of Dianchi Lake, respectively. On the whole, rainfall erosion in the north of the basin is remarkably stronger than that in the south. According to *Figure 3a*, the slope length and steepness factor (LS) is distributed in a pattern that is low in the center and high in the surroundings. And in *Figure 3b*, the area with the largest soil erodibility factor (K) is located in the north and eastern edge of the basin; and the area with the lowest value is basically located in the south of the basin. Besides, the vegetation cover and management factor (C) is fluctuated between 0 and 0.65 (as shown in *Fig. 4*). The area with high values is mainly located at the higher elevation at the northern and southern ends of the basin, while the area with low values is at the main urban area of Kunming in the middle of the basin. And the scope of the low-value area has been continuously extended due to the massive increase in the impermeable surface with the acceleration of urbanization from 1999 to 2014.

Classification of soil erosion in the basin

The above-mentioned maps were subjected to overlay analysis using the ArcGIS grid calculator to obtain the soil erosion modulus in the study area for the three years of 1999, 2005, and 2014. The soil erosion intensity map of the lake basin (*Fig. 5*) was generated based on classification following the “Standard for Classification and Grading of Soil Erosion (SL90-2007)” enacted in 2007 by the Ministry of Water Resources of China.

Figure 5 shows that in all three stages, most of the study area is yellow with a small erosion modulus between 0 and 500 t/(km²·a), which belongs to a tiny erosion area according to the erosion standard enacted by the Ministry of Water Resources of China. Green areas representing an erosion modulus of 500-2,500 t/(km²·a) and purple representing an erosion modulus of 2,500-5,000 t/(km²·a) were prevalent in the remaining parts of the study area, denoting slight and moderate erosion areas, respectively. Only a small proportion of the study area is depicted in red, indicating severe erosion. With regard to spatial distribution, tiny erosion areas were primarily distributed in the main city district of Kunming in the northern basin and Jinning County in the southern basin. Slight and moderate erosion classes exhibited a staggered distribution in the northern, southern, and eastern basins, being especially concentrated in the northernmost and southernmost parts. Severe erosion was sporadically distributed in a very small proportion of the lake basin area.

Spatiotemporal dynamics of soil erosion

According to the statistic results of soil erosion in the lake basin (*Table 2*), tiny and slight erosion classes were prevalent in the Dianchi Lake basin. Areas of tiny and slight

erosion exhibited an increasing trend during the 1999-2014 period, increasing from 87.05% to 91.3% of the lake basin area. Areas of moderate and severe erosion amounted to a small proportion of the study area, decreasing from 12.95% to 8.72% over the 15-year period. Despite the small proportion of moderate and severe erosion areas and the declining trend over time, these two erosion classes contributed a large proportion to total soil erosion, with each contributing more than 42%. Considering the entire Dianchi Lake basin, soil erosion was markedly inhibited over the 15-year period and the erosion area decreased considerably, although prominent erosion persisted in local areas.

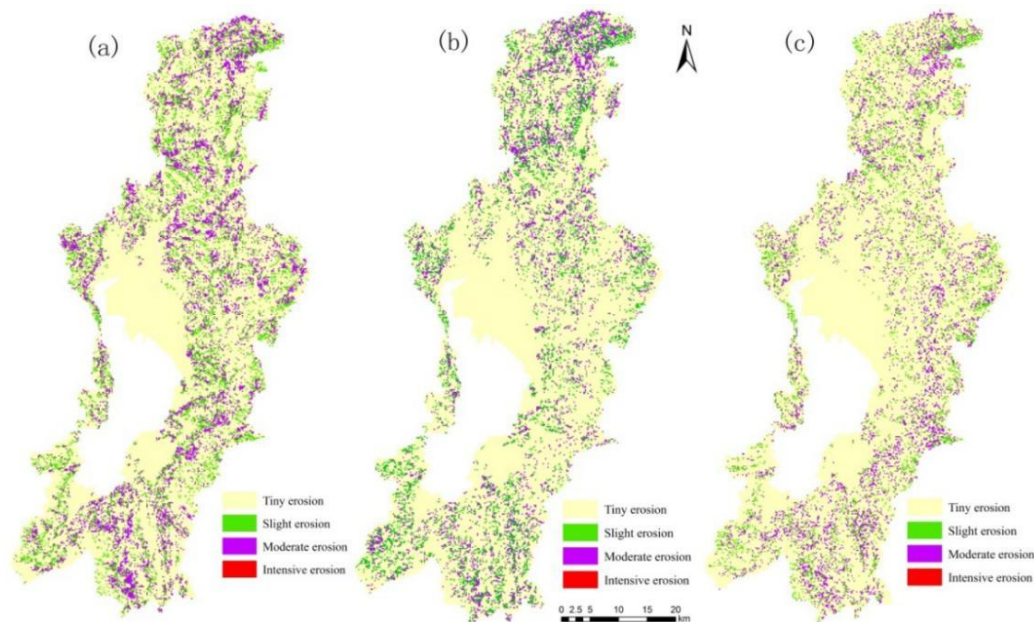


Figure 5. Spatial distribution of soil erosion intensity. (a) 1999, (b) 2005 and (c) 2014

Table 2. Soil erosion intensity statistics in Dianchi Lake basin

Erosion intensity	Mean erosion modulus ($t \cdot km^{-2} \cdot a^{-1}$)	1999			2005			2014		
		Erosion area (km^2)	Contribution rate (%)	Area ratio (%)	Erosion area (km^2)	Contribution rate (%)	Area ratio (%)	Erosion area (km^2)	Contribution rate (%)	Area ratio (%)
Tiny erosion	< 500	1853.82	28.32	72.31	2056.23	35.59	80.21	2111.21	35.00	82.37
Slight erosion	500~2500	378.07	21.14	14.74	281.14	21.64	10.97	228.77	17.26	8.91
Moderate erosion	2500~5000	331.72	50.52	12.94	226.29	42.77	8.82	223.68	47.74	8.72
Severe erosion	> 5000	0.05	0.02	0.01	0	0	0	0	0	0

Discussion

Soil erosion and slope

Soil erosion was highly related to the slope. Slope was extracted using the ArcGIS software based on DEM data in this study, divided into six classes according to the “Soil Erosion Classification and Grading Standard (SL90-2007)”. Maps of slope class and soil

loss were subjected to spatial overlap analysis to acquire the relationship between slope and soil loss during the three years 1999, 2005, and 2014 (Table 3). Concerning soil loss, areas with a slope of 8-25° accounted for more than 52%, the largest proportion, of the total soil loss in the basin. Theoretically, the higher the slope is, the stronger the rainfall erosion kinetic energy will be and the more serious the erosion will be (Liu et al., 1994; Wang, 1998; Berger et al., 2010; Zhao et al., 2015). However, this study found that soil loss presented a prominent decreasing trend when the slope is more than 25°. An overlay analysis of the erosion data of different slopes and high-resolution satellite remote sensing images revealed that areas with a slope greater than 25° had high vegetation coverage, with slope cropland in a small area and karst rock surface in local areas reducing the occurrence of soil erosion to a large extent. This phenomenon of weakening of erosion intensity with increasing slope due to changes in land cover has been verified by many scholars (Bochet et al., 2009; Zhou et al., 2014).

Table 3. Different slope and soil erosion statistics in Dianchi Lake basin

Slope (°)	1999			2005			2014		
	Area (km ²)	Soil erosion loss (10 ⁴ t·a ⁻¹)	Contribution rate (%)	Area (km ²)	Soil erosion loss (10 ⁴ t·a ⁻¹)	Contribution rate (%)	Area (km ²)	Soil erosion loss (10 ⁴ t·a ⁻¹)	Contribution rate (%)
0~5	761.71	24.18	17.96	766.15	13.39	13.09	767.92	10.76	11.14
5~8	217.04	15.88	11.79	213.23	9.83	9.61	214.66	9.3	9.63
8~15	494.15	35.03	26.01	486.7	24.63	24.08	488.23	24.44	25.31
15~25	586.28	34.63	25.71	590.87	29.75	29.08	592.93	28.69	29.71
25~35	354.91	18.06	13.41	345.59	17.44	17.05	347.39	16.65	17.24
> 35	143.08	6.89	5.12	154.63	7.25	7.09	146.04	6.74	6.98

Soil erosion and land use type

Land use is one of the most important factors affecting regional soil erosion. This factor affects soil erosion by altering vegetation cover on the land surface, physical and chemical soil properties, runoff characteristics, and regional climate conditions. Comparative analysis on the relationship between different land use types and the spatial differentiation of soil erosion intensity plays a crucial role in identifying more reasonable land use structures and adopting rational and effective soil and water conservation practices. Herein, the land use types in the Dianchi Lake basin were divided into five classes: cropland, forestland, bare land, construction land, and grassland. The soil erosion area, soil erosion modulus, and annual soil loss in relation to different land use types during the three years of 1999, 2005, and 2014 were acquired using the spatial overlay function of ArcGIS (Table 4). During the 15-year period (1999-2014), cropland area decreased rapidly, whereas construction land and bare land increased sharply; forestland and grassland areas did not change markedly. Total soil loss decreased rapidly by approximately 26.8%, from 134.44*10⁴ t·a⁻¹ in 1999 to 98.41*10⁴ t·km⁻²·a⁻¹ in 2014, indicating that cropland had a prominent effect on soil erosion in the Dianchi Lake basin. In terms of erosion intensity, the different land use types are ranked as bare land > cropland > forestland > grassland > construction land. Despite the small area of bare land, its mean erosion modulus was relatively high and exhibited rapid growth, increasing 11.9-fold over the 15 years from 1999 to 2014. The erosion contribution from bare land also increased from 0.6% to 9.1% over the study period, suggesting that bare land is a priority area that demands attention for the prevention and control of soil erosion in the lake basin area in the future. In particular,

the cropland area decreased prominently by 60%, from 843.47 km² in 1999 to 334.91 km² in 2014, and total soil erosion loss was reduced by 72%. Forestland area generally followed a decreasing trend but with a small magnitude of decrease, i.e., only a 7.14% decline over the 15-year period, whereas the soil loss decreased by 12.9%, indicating an improvement in soil erosion mitigation on forestland. Construction land increased rapidly from 1999 to 2014 by three-fold in both area and related soil loss. However, the erosion intensity was substantially low for construction land owing to the special underlying structure, making it a tiny erosion area. Although the erosion area of grassland increased by 1.3-fold, its soil loss increased by only 13%, and the soil loss per unit area exhibited a decreasing trend, suggesting an improvement in soil erosion mitigation for grassland areas.

Table 4. Different land use types and soil erosion statistics in Dianchi Lake basin

Land use type	1999			2005			2014		
	Erosion area (km ²)	Mean erosion modulus (t·km ⁻² ·a ⁻¹)	Erosion loss (10 ⁴ t·a ⁻¹)	Erosion area (km ²)	Mean erosion modulus (t·km ⁻² ·a ⁻¹)	Erosion loss (10 ⁴ t·a ⁻¹)	Erosion area (km ²)	Mean erosion modulus (t·km ⁻² ·a ⁻¹)	Erosion loss (10 ⁴ t·a ⁻¹)
Cropland	844.47	743.17	62.68	655.36	584.93	38.33	334.93	519.42	17.40
Forestland	1298.74	450.57	58.52	1263.15	394.96	49.89	1205.35	422.66	50.97
Bare land	7.51	1070.05	0.80	19.49	951.59	1.85	89.74	706.22	6.34
Construction land	225.64	178.87	4.03	421.55	156.61	6.60	680.9	183.26	12.48
Grassland	170.98	492.08	8.41	187.79	304.89	5.72	236.42	393.67	9.50

In summary, soil erosion under different land use is significantly different, and the contribution rate of different land use to soil erosion varies greatly. Among the land use types, the contribution rate of bare land is the largest (Cerdan et al., 2010; Guo et al., 2013). Labriere et al. (2015) found that soil erosion in the humid tropics is dramatically concentrated in bare land by analyzing more than 3,600 measurement data of soil erosion from 55 references covering 21 countries. Since the building land is isolated from the surface water infiltration into the soil, soil erosion will hardly occur after the construction (Yang, 2019).

Soil erosion and vegetation coverage

In this study, vegetation coverage is indicated by the normalized difference vegetation index (NDVI). NDVI values were calculated based on the remote sensing image data of the Dianchi Lake basin. The NDVI map was overlaid with the soil erosion map to obtain the relationship between vegetation coverage and soil erosion (Table 5). During the 1999-2014 period, soil erosion correlated with vegetation coverage levels in the lake basin that were between 0 and 45%. The largest erosion contribution occurred when vegetation coverage was between 15 and 30%, and the maximum contribution was 66.35% in 2014. Little erosion occurred when vegetation coverage was 45% or higher, and there was generally no erosion when vegetation coverage was 60% or higher, indicating that higher vegetation coverage exerted a more prominent inhibiting effect on soil erosion. Thus, vegetation is an important factor in protecting soil against erosion. This result is consistent with the research results of many scholars. Zheng (2006) found that once vegetation restoration, soil erosion was very low in the Loess Plateau, China. And once the vegetation destroyed, soil erosion

increased markedly. Hou (2014) further revealed that soil erosion was not only affected by vegetation coverage, but also affected by vegetation diversity in the same distribution pattern. The reasons why vegetation plays a significant role in inhibiting soil erosion are as follows: (1) vegetative shoots can satisfactorily reduce the effect of raindrop splash on soil, whereas litter can attenuate the erosion of soil by surface runoff; (2) vegetative roots play a role in retaining the soil, making it difficult to be scoured and transported (Zhang et al., 2014).

Table 5. Statistics of different vegetation coverage and soil erosion in Dianchi Lake basin

Vegetation coverage (%)	1999			2005			2014		
	Erosion area (km ²)	Mean erosion modulus (t·km ⁻² ·a ⁻¹)	Contribution rate (%)	Erosion area (km ²)	Mean erosion modulus (t·km ⁻² ·a ⁻¹)	Contribution rate (%)	Erosion area (km ²)	Mean erosion modulus (t·km ⁻² ·a ⁻¹)	Contribution rate (%)
0~15	869.78	524.60	33.9	876.44	258.87	22.1	619.26	179.61	11.48
15~30	1058.36	564.84	44.4	842.67	495.78	40.7	1401.30	458.10	66.35
30~45	563.93	454.63	19.0	663.76	458.94	29.7	528.29	398.16	21.74
45~60	68.94	517.78	2.7	162.01	441.45	7.0	12.16	340.85	0.43
60~75	0	0	0	16.13	290.63	0.5	0	0	0
> 75	0	0	0	0	0	0	0	0	0

Soil erosion and soil erodibility

The soil erodibility factor K, an intrinsic factor of soil erosion intensity, is the comprehensive expression of soil erosion resistance (Zhang et al., 2011). The relationship between soil erosion modulus and the K factor in the Dianchi Lake basin was obtained using overlay analysis (Fig. 6).

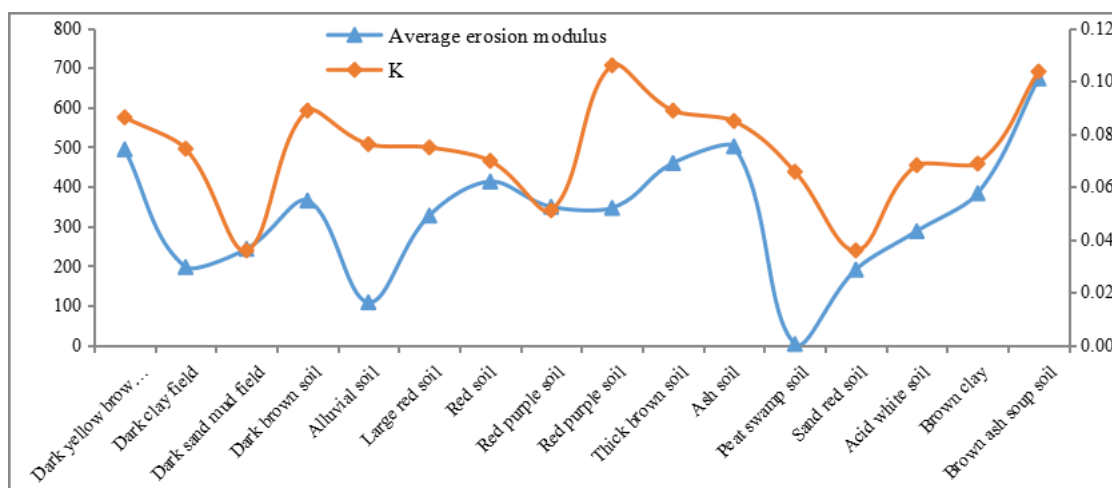


Figure 6. Soil erodibility factor and soil erosion statistics in Dianchi Lake basin

The soil erosion modulus corresponding to various soil types differed. The brownish soup soil had the largest erosion modulus of 672.9 t·(km⁻²·a⁻¹), which corresponded to a high K value of 0.10357 (t·hm²·h)/(MJ·mm·hm²), suggesting that this type of soil was prone to erosion. The peat swamp soil had the lowest K value of 0.03583(t·hm²·h)/(MJ·mm·hm²), whereas the corresponding soil erosion modulus was

not the lowest. According to the patterns observed in *Figure 6*, the K value and soil erosion typically exhibited inconsistent trends in most soil types, except for a few soil types that showed consistent trends, suggesting that the K factor had a low correlation with soil erosion and hence it is a secondary factor affecting erosion. Theoretically, under the same conditions of rainfall, land use and slope, soils with high erodibility are more susceptible to erosion than those with low erodibility (Panagos et al., 2012; Liu et al., 2020). However, the way of land use indirectly affects the physical and chemical characteristics of soil, which leads to a certain change in soil erodibility (Panagos et al., 2014). Therefore, it is difficult to form a consistent law between soil erosion and K factor in different regions due to differences in land use patterns (Raquel et al., 2007).

Conclusions

This study investigated the situation of soil erosion and its relationship with the influencing factors in the Dianchi Lake basin over a 15-year period. The RUSLE model was integrated with remote sensing and GIS, and the remote sensing images of 1999, 2005, and 2014 were used as data sources. The conclusions of the study are as follows:

(1) Analysis of the spatiotemporal dynamics of soil erosion revealed that tiny and slight classes of soil erosion were prevalent in the Dianchi Lake basin during the 15-year 1999-2014 period. The tiny erosion area increased over time and amounted to 82.37% of the lake basin area in 2014, whereas the area and soil loss of light and moderate erosion both decreased over time. As for severe erosion, the erosion contribution was 0 and thus negligible in both 2005 and 2014.

(2) Analysis of the relationship between slope and soil erosion revealed that erosion was primarily concentrated in areas with a slope in the range of 8-25°. The large areas with a slope of 0-5° were primarily comprised of urban areas, which contributed little to soil erosion and exhibited a decreasing trend in soil erosion over time. For areas with a slope greater than 25°, the soil loss gradually decreased as the slope increased.

(3) Both soil loss and erosion intensity varied significantly between various types of land use. In terms of soil loss, cropland and forestland ranked the highest, which accounted for a decreasing proportion of soil loss over the 15 years, with a maximum of 90% in 1999 and a minimum of 71% in 2014. Bare land, construction land, and grassland accounted for a considerably increasing proportion of soil loss, with a total erosion increase of 20% over the 15 years and the most rapid growth for bare land. As for erosion intensity, the five types of land use were ranked as bare land > cropland > forestland > grassland > construction land, exhibiting a decreasing trend over time.

(4) Considering the relationship between vegetation coverage and soil erosion, erosion was primarily concentrated in areas where the vegetation coverage was less than 45%. In particular, the most intense erosion occurred in areas with vegetation coverage of 15-30%, where the erosion contribution and erosion intensity were at their maximums. Little erosion occurred in areas with vegetation coverage of 45% or higher, and there was approximately no erosion in areas with vegetation coverage of 60% or higher. Given the prominent effect of vegetation on mitigating soil erosion, it is recommended that vegetation coverage be increased in the Dianchi Lake basin through various policies, including afforestation and returning cropland to forestland and grassland, to reduce the occurrence of erosion.

(5) The overlay analysis of the K factor and soil erosion modulus revealed considerable differences in their change trends, indicating that soil type had a limited effect on erosion.

In summary, the area and intensity of soil erosion exhibited a decreasing trend in the Dianchi Lake basin from 1999 to 2014, indicating a gradual improvement in the situation of soil erosion. There was considerable spatial differentiation in the effects of slope, land use type, vegetation coverage, and soil erodibility on soil erosion. The slope effect on soil erosion was primarily concentrated in the slope range of 8-25°, whereas in areas with a slope greater than 25° there was a gradually decreasing trend in erosion with increasing slopes. In terms of different types of land use, soil erosion primarily occurred on cropland and forestland. However, as the cropland area decreased rapidly over the 15-year period, its erosion contribution also dropped significantly. Bare land area, however, expanded rapidly and gradually became a major source of erosion because of its high erosion intensity. Areas with vegetation coverage of 15-30% suffered from the most intense erosion, whereas little erosion occurred in areas with vegetation coverage of 45% or higher.

Among the above factors, slope, soil erodibility and vegetation coverage were relatively stable, while land use factor was sensitive and had a greater impact on soil erosion. However, land use is significantly affected by human activities. So, further revealing the relationship between human activities factors, such as socio-economic characteristics and regional planning, etc., will help to understand the knowledge of soil erosion mechanism, which will be the focus of the next research.

Acknowledgements. This study was funded by the National Natural Science Foundation of China (No. 41971369, 41561086, 41661082, 41461038).

REFERENCES

- [1] Alexakis, D. D., Hadjimitsis, D. G., Agapiou, A. (2013): Integrated use of remote sensing, GIS and precipitation data for the assessment of soil erosion rate in the catchment area of “Yialias” in Cyprus. – *Atmospheric Research* 131: 108-124.
- [2] Angima, S. D., Stott, D. E., O’Neill, M. K., Ong, C. K., Weesies, G. A. (2003): Soil erosion prediction using RUSLE for central Kenyan highland conditions. – *Agriculture, Ecosystems & Environment* 97: 295-308.
- [3] Berger, C., Schulze, M., Rieke-Zapp, D., Schlunegger, F. (2010): Rill development and soil erosion: a laboratory study of slope and rainfall intensity. – *Earth Surface Processes & Landforms* 35(12): 1456-1467.
- [4] Bochet, E., Garcia-Fayos, P., Poesen, J. (2009): Topographic thresholds for plant colonization on semi-arid slopes. – *Earth Surface Processes & Landforms* 34(13): 1758-1771.
- [5] Cerdan, O., Govers, G., Le Bissonnais, Y., Van Oost, K., Poesen, J., Saby, N., Gobin, A., Vacca, A., Quinton, J., Auerswald, K., Klik, A., Kwaad, F. J. P. M., Raclot, D., Ionita, I., Rejman, J., Rousseva, S., Muxart, T., Roxo, M. J., Dostal, T. (2010): Rates and spatial variations of soil erosion in Europe: a study based on erosion plot data. – *Geomorphology* 122(1-2): 167-177.
- [6] Chong, C. (2000): Study of applying USLE and geographical information system IDRISI to predict soil erosion in small watershed. – *Journal of Soil and Water Conservation* 14: 19-24.

- [7] Fu, B., Yu, L., Lü, Y., He, C., Yuan, Z., Wu, B. (2011): Assessing the soil erosion control service of ecosystems change in the Loess Plateau of China. – *Ecological Complexity* 8: 284-293.
- [8] Gao, Y., Cao, S. (2011): A degradation threshold for irreversible loss of soil productivity: a long-term case study in China. – *Journal of Applied Ecology* 48: 1145-1154.
- [9] Guo, T. L., Wang, Q. J., Bai, W. J. (2013): Effect of land use on scouring flow hydraulics and transport of soil solute in erosion. – *Journal of Hydrologic Engineering* 23(1A): 215-222.
- [10] Hartanto, H., Prabhu, R., Widayat, A., Asdak, C. (2003): Factors affecting runoff and soil erosion: plot-level soil loss monitoring for assessing sustainability of forest management. – *Forest Ecology & Management* 180: 361-374.
- [11] Hou, J., Fu, B., Wang, S., Zhu, H. (2014): Comprehensive analysis of relationship between vegetation attributes and soil erosion on hillslopes in the Loess Plateau of China. – *Environmental Earth Sciences* 72(5): 1721-1731.
- [12] Hu, G., Song, H., Shi, X., Zhang, M., Liu, X., Zhang, X. (2018): Soil Erosion Characteristics Based on RUSLE in the Wohushan Reservoir Watershed. – *Scientia Geographica Sinica* 38: 610-617.
- [13] Jian, H., Wang, H., Fu, B., Zhu, L., Wang, Y., Li, Z. (2016): Effects of plant diversity on soil erosion for different vegetation patterns. – *Catena* 147: 632-637.
- [14] Kinnell, P. (2010): Event soil loss, runoff and the Universal Soil Loss Equation family of models: a review. – *Journal of Hydrology* 385: 384-397.
- [15] Kinnell, P. (2014): Applying the RUSLE and the USLE-M on hillslopes where runoff production during an erosion event is spatially variable. – *Journal of Hydrology* 519: 3328-3337.
- [16] Kinnell, P., Wang, J., Zheng, F. (2018): Comparison of the abilities of WEPP and the USLE-M to predict event soil loss on steep loessal slopes in China. – *Catena* 171: 99-106.
- [17] Labriere, N., Locatelli, B., Laumonier, Y., Freycon, V., Bernoux, M. (2015): Soil erosion in the humid tropics: a systematic quantitative review. – *Agriculture Ecosystems & Environment* 203: 127-139.
- [18] Lal, R. (2003): Soil erosion and the global carbon budget. – *Environment International* 29(4): 0-450.
- [19] Li, L., Wang, Y., Liu, C. (2014): Effects of land use changes on soil erosion in a fast developing area. – *International Journal of Environmental Science & Technology* 11: 1549-1562.
- [20] Lin, C., Zhou, S. L., Wu, S. H. (2011): Evolution of soil erosion degree in 30 years in Granite Hills, Southeastern of China - a case study of Changting County, Fujian. – *Scientia Geographica Sinica* 31: 1235-1241.
- [21] Liu, B. Y., Nearing, M. A., Risse, L. M. (1994): Slope gradient effects on soil loss for steep slopes. – *Transactions of the ASAE* 37(6): 1835-1840.
- [22] Liu, B. Y., Nearing, M. A., Shi, P. J., Jia, Z. W. (2000): Slope length effects on soil loss for steep slopes. – *Soil Science Society of America Journal* 64: 1759-1763.
- [23] Liu, M., Han, G., Li, X., Zhang, S., Zhou, W., Zhang, Q. (2020): Effects of soil properties on K factor in the granite and limestone regions of China. – *International Journal of Environmental Research and Public Health* 17(3): 801.
- [24] Manojlovic, S., Antic, M., Sibinovic, M., Dragicevic, S., Novkovic, I. (2017): Soil erosion response to demographic and land use changes in the Nišava River basin, Serbia. – *Fresenius Environ Bull* 26: 7547-7560.
- [25] Mccool, D. K., Brown, L. C., Foster, G. R., Mutchler, C. K., Meyer, L. D. (1987): Revised slope steepness factor for the universal soil loss equation. – *Transactions of the Asae* 30: 1387-1396.
- [26] Miao, C. Y., Yang, L., Chen, X. H., Gao, Y. (2012): The vegetation cover dynamics (1982–2006) in different erosion regions of the Yellow River Basin, China. – *Land Degradation & Development* 23: 62-71.

- [27] Mondal, A., Khare, D., Kundu, S., Meena, P. K., Mishra, P. K., Shukla, R. (2015): Impact of climate change on future soil erosion in different slope, land use, and soil-type conditions in a part of the Narmada River basin, India. – *Journal of Hydrologic Engineering* 20(6): C5014003.
- [28] Montgomery, D. R. (2007): Soil erosion and agricultural sustainability. – *Proceedings of the National Academy of Sciences* 104: 13268-13272.
- [29] Nyssen, J., Vandenreyken, H., Poesen, J., Moeyersons, J., Deckers, J., Haile, M. (2005): Rainfall erosivity and variability in the northern Ethiopian highlands. – *Journal of Hydrology* 311(1-4): 0-187.
- [30] Panagos, P., Meusburger, K., Alewell, C., Montanarella, L. (2012): Soil erodibility estimation using LUCAS point survey data of Europe. – *Environmental Modelling & Software* 30: 143-145.
- [31] Panagos, P., Meusburger, K., Ballabio, C., Borrelli, P., Alewell, C. (2014): Soil erodibility in Europe: a high-resolution dataset based on LUCAS. – *Science of the Total Environment* 479: 189-200.
- [32] Peng, S., Yang, K., Hong, L., Xu, Q., Huang, Y. (2018): Spatio-temporal evolution analysis of soil erosion based on USLE model in Dianchi Basin. – *Transactions of the Chinese Society of Agricultural Engineering* 34: 138-146 + 305.
- [33] Pimentel, D., Harvey, C., Resosudarmo, P., Sinclair, K., Kurz, D., Mcnair, M. (1995): Environmental and economic costs of soil erosion and conservation benefits. – *Science* 267: 1117-1123.
- [34] Raquel, P. R., Marques, M. J., Ramón, B. (2007): Spatial variability of the soil erodibility parameters and their relation with the soil map at subgroup level. – *Science of the Total Environment* 378(1-2): 166-173.
- [35] Renard, K. G., Foster, G. R., Weesies, G. A., McCool, D. K., Yoder, D. C. (1997): Predicting soil erosion by water: a guide to conservation planning with the Revised Universal Soil Loss Equation (RUSLE). – *Agriculture Handbook* 703: 1-367.
- [36] Saygin, S. D., Chi, H. H., Flanagan, D. C., Erpul, G. (2017): Process-based soil erodibility estimation for empirical water erosion models. – *Journal of Hydraulic Research* 56: 1-15.
- [37] Vijith, H., Rekha, V. B., Shiju, C., Rejith, P. G. (2012): An assessment of soil erosion probability and erosion rate in a tropical mountainous watershed using remote sensing and GIS. – *Arabian Journal of Geosciences* 5: 797-805.
- [38] Wang, B., Zheng, F., Roemkens, M. J. M., Darboux, F. (2013): Soil erodibility for water erosion: a perspective and Chinese experiences. – *Geomorphology* 187: 1-10.
- [39] Wang, G. P. (1998): Summary of rill erosion study. – *Soil and Water Conservation in China* 8: 23-26.
- [40] Wang, T. (2018): Quantitative analysis on influencing factors of soil erosion using RUSLE: a case study of the Luohe basin in Northern Shanxi Province. – *Environmental Science & Technology* 41: 170-177.
- [41] Wen, Y., Liu, X. N., Cheng, J. (2013): Assessment and feature analysis of soil erosion in mountainous area of Guangdong Province based on USLE. – *Bulletin of Soil & Water Conservation* 33: 112-118.
- [42] Wischmeier, W. H., Johnson, C., Cross, B. (1971): Soil erodibility nomograph for farmland and construction sites. – *Journal of Soil and Water Conservation* 26: 189-193.
- [43] Wischmeier, W. H., Smith, D. D. (1965): Predicting Rainfall Erosion Losses from Cropland East of the Rocky Mountains: Guide for Selection of Practices for Soil and Water Conservation. – In: *Agricultural Research Service (ed.) Agr Handbook*. No 282. US Dept. Agr., Washington DC.
- [44] Xiao, L., Yang, X., Chen, S., Cai, H. (2015): An assessment of erosivity distribution and its influence on the effectiveness of land use conversion for reducing soil erosion in Jiangxi, China. – *Catena* 125: 50-60.

- [45] Xin, Z., Xu, J., Yu, X. (2009): Temporal and spatial variability of sediment yield on the Loess Plateau in the past 50 years. – *Acta Ecologica Sinica* 29: 1129-1140.
- [46] Yan, Y., Xin, X., Xu, X., Wang, X., Yang, G., Yan, R., Chen, B. (2013): Quantitative effects of wind erosion on the soil texture and soil nutrients under different vegetation coverage in a semiarid steppe of northern China. – *Plant Soil* 369: 585-598.
- [47] Yang, M. (2019): The Impact of Urban building planning on soil and water loss in the peripheral eco-environment. – *Ekoloji* 28(107): 2521-2531.
- [48] Yao, J., Cheng, J., Zhou, Z., Sun, L., Zhang, H. (2018): Effects of herbaceous vegetation coverage and rainfall intensity on splash characteristics in northern China. – *Catena* 167: 411-421.
- [49] Zha, L., Deng, G., Gu, J. (2015): Dynamic changes of soil erosion in the Chaohu Watershed from 1992 to 2013. – *Acta Geographica Sinica* 70: 1708-1719.
- [50] Zhang, J., DeAngelis, D., Zhuang, J. (2011): Spatial Variability of Soil Erodibility (K Factor) at a Catchment Scale in Nanjing, China. – In: DeAngelis, D. L. et al. (eds.) *Theory and Practice of Soil Loss Control in Eastern China*. Springer, New York.
- [51] Zhang, W. B., Fu, J. S. (2003): Rainfall erosivity estimation under different rainfall amount. – *Resources Science* 7: 35-41.
- [52] Zhang, X., Yu, G. Q., Li, Z. B., Li, P. (2014): Experimental study on slope runoff, erosion and sediment under different vegetation types. – *Water Resources Management* 28(9): 2415-2433.
- [53] Zhao, L., Yuan, G. L., Zhang, Y., Bin, H. E., Liu, Z. H., Wang, Z. Y., Jing, L. I. (2007): The amount of soil erosion in Baoxiang watershed of Dianchi Lake based on GIS and USLE. – *Bulletin of Soil & Water Conservation* 3: 42-46.
- [54] Zhao, Q., Li, D., Zhuo, M., Guo, T., Liao, Y., Xie, Z. (2015): Effects of rainfall intensity and slope gradient on erosion characteristics of the red soil slope. – *Stochastic Environmental Research & Risk Assessment* 29(2): 609-621.
- [55] Zheng, F. L. (2006): Effect of vegetation changes on soil erosion on the Loess Plateau. – *Pedosphere* 16(4): 420-427.
- [56] Zhou, Q., Yang, S., Cai, M., Lu, Y., Zhao, H., Luo, Y. (2014): Soil erosion and its relationship with topographical factors in a mountainous watershed in the upper Mekong River in Yunnan Province, China. – *Fresenius Environmental Bulletin* 23(1A): 215-222.
- [57] Zhou, Z. C., Shang, Z. P., Zhao, D. (2006): Modeling vegetation coverage and soil erosion in the Loess Plateau Area of China. – *Ecological Modelling* 198: 263-268.
- [58] Zhu, M. (2015): Soil erosion assessment using USLE in the GIS environment: a case study in the Danjiangkou Reservoir Region, China. – *Environmental Earth Sciences* 73: 7899-7908.
- [59] Zokaib, S., Gh., N. (2011): Impacts of land uses on runoff and soil erosion a case study in Hilkot watershed Pakistan. – *International Journal of Sediment Research* 3: 92-101.

FERTILIZATION AND SOIL AERATION EFFECTS ON GRASSLAND PRIMARY PRODUCTIVITY AND SPECIES DIVERSITY IN A MEADOW STEPPE, NORTHERN CHINA

BAI, Y.^{1,2#} – LV, S.^{1#} – SCHELLENBERG, M. P.² – YAN, R.³ – ZHANG, R.^{1,2} – WIE, Z.^{1*}

¹*College of Grassland, Resources and Environment, Key Lab. of Grassland Resources of the Ministry of Education of China, Key Lab. of Forage Cultivation, Processing and High Efficient Utilization of the Ministry of Agriculture of China, Inner Mongolia Agricultural Univ., No. 29 Erdos Street, Hohhot, Inner Mongolia 010011, China*

²*Swift Current Research and Development Centre, Agriculture and Agri-Food Canada, 1 Airport Rd, Box 1030, Swift Current, Saskatchewan S9H 3X2, Canada*

³*Institute of Agricultural Resources and Regional Planning, Chinese Academy of Agricultural Sciences, Beijing 100081, China*

#These authors contributed equally to this study and share first authorship

**Corresponding author
e-mail: nmndwzj@163.com*

(Received 22nd Dec 2019; accepted 23rd Mar 2020)

Abstract. In the grassland ecosystem, soils are subjected to a range of stresses which may affect their physical and biological properties, as well as the plant community biomass. As biomass is affected by long-term soil properties, we sought to establish a direct link between biomass and resilience to fertilization and soil aeration. We evaluated biomass yield in grasslands managed across a gradient of nitrogen (N), phosphorus (P), and potassium (K) fertilizers at Hulunbuir in Inner Mongolia, China, from 2014 to 2017. Based on the estimates from the simulated optimization and optimal theoretical regression model, we recommend applying N (231.50–238.82 kg ha⁻¹), and P (187.25–218.75 kg ha⁻¹), and K (28.28–33.32 kg ha⁻¹) annually to maximize biomass in the non-aerated grassland. The positive effect of nitrogen and phosphorus on biomass was significantly higher than unfertilized treatment. The effects of aeration on biomass were less explicit. Simultaneously, we compared the Shannon-Wiener Index and Species richness for the suitable fertilizer levels. Shannon-Wiener diversity and Species richness became lower the longer the fertilization treatments lasted. Thus, nutrient resorption is resulting in a decrease in species diversity and richness, while it is an important strategy for increasing plant biomass.

Keywords: *nitrogen fertilizer, phosphorus fertilizer, potassium fertilizer, soil improvement, community biomass, species diversity*

Introduction

Temperate and semiarid grasslands comprise 80% of the land area on the Mongolian Plateau and environs, which includes Mongolia, and the province of Inner Mongolia, China (John et al., 2018). The increased degradation of Inner Mongolia steppe in recent years mainly occurred due to changes in the forms of land-use (Aguiar et al., 1996; Lambin and Meyfroidt, 2011). Long-term hay harvesting in Inner Mongolia Steppe through exportation of nutrients in the hay affects nutrient availability by decreasing soil K and N contents, and leading to significant changes in the above- and belowground components of the ecosystem (Bardgett et al., 1998; Kuzyakov et al., 1999; Olde Venterink et al., 2009). Fertilizers application is potentially key for the fast-growing species that typically establish in moderately fertile grasslands and during the early stages

of restoration (Yahdjian et al., 2011). However, there are striking discrepancies in the fertilizer effect on productivity, which is largely due to the great variation in fertilizer type and concentration, soil fertility, amount of rainfall, temperature variations, and management practices (Gough et al., 2000; Hofer et al., 2017; Zhou et al., 2018). It is known that fertilization often decreases soil pH and that subsequent soil acidification has negative effects on plant communities (Basso et al., 2016; Liu et al., 2017). Therefore, determining the appropriate fertilizer type and concentration is essential for the sustainable management of ecosystems with nutrient additions.

Productivity and plant diversity are important indicators of grassland structure and function. The primary productivity of grasslands is the capability of their plant communities to convert carbon dioxide and water into energy-rich organic material (Yu et al., 2015). Nitrogen (N), phosphorus (P), and potassium (K) are common nutrient elements constraining plant productivity in most grassland ecosystems. Their input often has multiple effects including changes in aboveground primary productivity, biodiversity, species composition, and ecosystem functioning (Bai et al., 2010; Li et al., 2010). Although the influence of N addition on grassland plant communities has been widely studied, it is still unclear whether observed patterns and underlying mechanisms are constant across biomes (Haque et al., 2009; Humbert et al., 2016; Long et al., 2016; Plassmann et al., 2009). The effects of N addition can alter plant community structure including plant productivity and plant diversity (Gough et al., 2000; Han et al., 2011; Plassmann et al., 2009). Some studies, however, have shown that the composition and proportion of the original plant community (i.e. grasses, forbs, legumes and sedges), can influence the direction and magnitude of the changes from N addition (Bai et al., 2010; Bassin et al., 2007; Tilman et al., 2001). Grasses are generally favoured by N addition, while legumes are not. Compared to nitrogen fertilizer, phosphorus fertilizer is beneficial to the growth of legumes. P is an essential macronutrient in plant nutrition and the second most important nutrient after N, 30–65% of which is present in organic forms (Harrison, 1983). Despite many soils containing a large amount of total P, only a small proportion is available for plant uptake. Moreover, plant yield response to P fertilization can vary greatly (George et al., 2011; Schulte and Herlihy, 2007). Organic P in soil plays an important role in determining the overall biological availability of P, and it is influenced by environment conditions, together with land use (Turner et al., 2003). Long-term N addition facilitates more P stored in organic forms, the prevalence of co-limitation by N and phosphorus (P) is increasingly recognized (Agren et al., 2012; Elser et al., 2007; Fay et al., 2015; Zhang and MacKenzie, 1997). K occurs in high concentrations in plant tissues and its uptake is correlated with that of other nutrients. N increases will potentially limit increases of other nutrients, such as P, K, or trace elements. Multiple-nutrient limitations of grassland productivity often occur in the form of co-limitation, while it is synergistic when the response to multiple nutrients is greater than the sum of the responses to each nutrient added individually. The collective effect of N, P and K on grassland productivity and plant diversity are the focus of our attention.

In general, the grassland systems are rather stable compared to arable systems. However, the soil may be compacted due to deterioration inappropriate management system and weather impacts and their interaction (wheel traffic, drought, winter damages, flooding, slurry application, under- or overgrazing) (Kayser et al., 2018). Moreover, the vegetation of grassland in our study is dominated by *Leymus chinensis* (Trin.) Tzvel. *Leymus chinensis* a perennial rhizomatous grass. Development of rhizomes results in the decreased aeration resulting in decreased yield of *Leymus*

chinensis over time. The intention of perforation on the soil is to bring grasslands back to the state of aeration which they once had (Franklin et al., 2006). Soil aeration may partially incorporate fertilizer applied to the soil, increase contact time between water, fertilizer, and soil to facilitate nutrient adsorption by the soil, and ideally even improve the swards by taking advantage of improvement in fertilization and soil aeration (Franklin et al., 2006). The objectives of this study were to: (1) determine the coupling effects of soil aeration and NPK fertilizer on aboveground net primary productivity, and (2) determine optimal options for improvement of grassland yield through the different combination of NPK fertilizer, and (3) compare the change trend of species richness and Shannon-Wiener Index of optimal fertilization levels in different years.

Materials and methods

Study sites and experimental design

The fertilization experiment was conducted near Hulunbuir Grassland Ecosystem National Field Observation Station, China (49.2313N, 120.0247E). The station, which was built in 1997 by the Chinese Academy of Agricultural Sciences, is located in the core area of Hulunbuir Meadow steppe. The average elevation of this area is 4320 m.a.s.l. The climate is continental semi-arid with a dry and cold winter and a rainy summer. The mean annual temperature is 0 °C. The annual precipitation ranges from about 250–350 mm, of which about half falls between June and August. The frost-free period is 85 to 155 days. The type of soil is Kastanozem (FAO). The vegetation is dominated by *Leymus chinensis* (Trin.) Tzvel., *Vicia amoena* (Fisch. ex DC.), *Thalictrum squarrosum* (Steph.), *Pulsatilla turczaninowii* (Kryl. et Serg.), *Stipa baicalensis* (Roshev.), and *Cleistogenes squarrosa* (Trin.) Keng, and accompanied by *Carex duriuscula* (C. A. Mey.), *Allium bidentatum* (Allium L.), and *Artemisia tanacetifolia* (Linn.). Prior to 2014, the grassland was irregularly grazed by cattle and the site was hayed once a year in autumn.

In order to prevent grazing, the fertilization experiment was started at a number of permanent plots within an enclosure in 2013, along with the haying regime. The plots had similar plant community composition and structure before fertilizer addition. Fourteen, 6 m × 10 m, plots were randomly placed on the two soil mechanical treatments perforated or non-perforated respectively with an average separation distance of about 2 m in May 2014 (Fig. 1). The soil perforated by using mechanical with 12 cm depth and 15 cm distance between two holes, and only use it once before the experiment started (Fig. 2). An L14 (3⁴) orthogonal test was chosen to test their effects on the biomass of plant community and *Leymus chinensis*. The orthogonal test is an effective measurement to assay the comprehensive effect of multiple factors, finding the dominant factors and the best combination of levels for them with the least experimental trials, enhancing the reproducibility of the experimental results (Montgomery, 1991). The L14 (3⁴) orthogonal test for the experiment was to reduce workload, while it could arrange fourteen treatments with three factors and their four levels each, and test the interactions between factors if they exist. The local soil nutrient survey results in 2013 (total N content in 0–30 cm soil was 2.86 g·kg⁻¹, the total P was 0.49 g·kg⁻¹ and the total K was 22.96 g·kg⁻¹) were used along with consideration of local traditional fertilization in selecting fourteen fertilizer treatments (T1 to T14) with N, P, and K, and four fertilization concentrations for each fertilizer by artificial fertilization (Table 1). We mixed the fertilizer in advance, and

spread fertilizer by artificial in late May. The perforated and non-perforated blocks with denoted as T1 (1) ~ T14 (1) and T1 (2) ~ T14 (2) respectively.

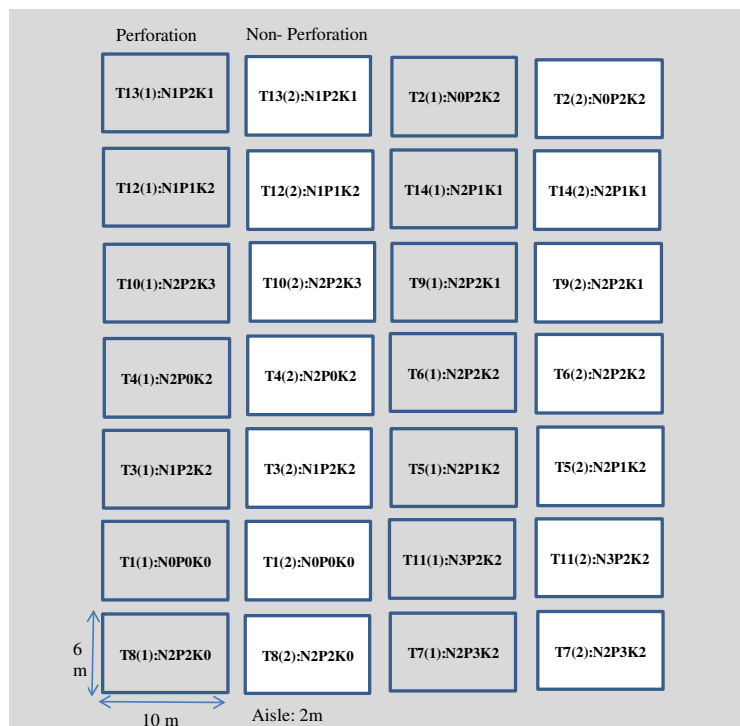


Figure 1. Map of the experimental site



Figure 2. The photo of soil perforation equipment and taking sample

Table 1. L14 (3^4) orthogonal test for the combinational effect trial and fertilization amounts of nitrogen (N), phosphorous (P) and potassium (K) applied

Plot number	Treatment	Factors			Fertilization amounts of N, P, K		
		N (X1)	P (X2)	K (X3)	CON ₂ H ₄ (kg ha ⁻¹)	CaP ₂ H ₄ O ₈ (kg ha ⁻¹)	K ₂ SO ₄ (kg ha ⁻¹)
T1	N0P0K0	0	0	0	0	0	0
T2	N0P2K2	0	2	2	0	350	57
T3	N1P2K2	1	2	2	91	350	57
T4	N2P0K2	2	0	2	183	0	57
T5	N2P1K2	2	1	2	183	175	57
T6	N2P2K2	2	2	2	183	350	57
T7	N2P3K2	2	3	2	183	525	57
T8	N2P2K0	2	2	0	183	350	0
T9	N2P2K1	2	2	1	183	350	28
T10	N2P2K3	2	2	3	183	350	85
T11	N3P2K2	3	2	2	274	350	57
T12	N1P1K2	1	1	2	91	175	57
T13	N1P2K1	1	2	1	91	350	28
T14	N2P1K1	2	1	1	183	175	28

The Urea (N \geq 46.4%), Calcium superphosphate (P₂O₅ \geq 16%), Potassium sulfate (K₂O \geq 51%) were applied for nitrogen fertilizer (N), phosphate fertilizer (P), and potassium fertilizer (K) respectively with artificial fertilization

Biomass sampling

Except for surface litter, the total biomass of all plants was harvested from 0.5 m \times 0.5 m squares in August of each year between 2014 and 2017 with three repetitions randomly selected in each plot. Different species were separately cut to the ground level using scissors in each square area. All species were separately weighed after drying at 65 °C for 24 h in the oven. The plant community biomass was the total of all plants biomass in each plot (Sala et al., 1988).

Species diversity

In each plot, we randomly selected three 0.25 m² quadrats for the investigation of plant diversity. Every August was chosen to test because of the peak number of plant species biomass at this time. The richness was measured using number of species per square area. The diversity index was calculated using the Shannon-Wiener diversity index (Shannon, 1949).

Statistical analysis

The analysis of mono-fertilizer

Based on the design and character of the orthogonal experiment, the effect of the nitrogen fertilizer gradient on biomass in the perforated plots was analyzed using the same fertilizer gradient of phosphate fertilizer and potassium fertilizer. Nitrogen fertilizer was used as follows T1 (N0P0K0), T2 (N0P2K2), T3 (N1P2K2), T6 (N2P2K2), and T11 (N3P2K2); phosphate fertilizer was used as follows T1 (N0P0K0),

T4 (N2P0K2), T5 (N2P1K2), T6 (N2P2K2), and T7 (N2P3K2); and potassium fertilizer was used as follows T1 (N0P0K0), T8 (N2P2K0), T9 (N2P2K1), T6 (N2P2K2), and T10 (N2P2K3). The method of non-perforated plots was the same. The average of no fertilizer (N0P0K0) and nitrogen-free fertilizer (N0P2K2) was used for the initial gradient of nitrogen fertilizer.

The analysis of double-fertilizer effect

The double-fertilizer effect of N and P was calculated using all the treatments which contained second gradient of K (T1~T7 and T11~T12), and nitrogen-free fertilizer (N0P2K2); the effect of N and K was calculated using all the treatments which contained second gradient of P (T1~T3, T6, T8~T11, and T13), and nitrogen-free fertilizer (N0P2K2); the effect of P and K was calculated using all the treatments which contained second gradient of N (T1, T4~T10, and T14), and nitrogen-free fertilizer (N0P2K2). The contour map with selected data above was drawn using SigmaPlot (Version 10.0).

Full information model and simulation optimization

The full information model is a comprehensive model, which contains to the linear effect, parabola effect, and interaction of independent variable. In our study, we use two full information to obtain the linear effect and parabola effect between the four years average biomass (Y) and nitrogen (X1), phosphorous (X2), and potassium (X3), as well as the interaction of dual-fertilizer. that specifies the relationship between a dependent biomass (Y) and nitrogen (X1), phosphorous (X2) and potassium (X3). Due to a field semi-control experiment with the fertilizer gradient, we believed the actual circumstances are reflected primarily by the regression model, and it was accepted that the liner positive correlation coefficient reached 75%.

According to the full information model ($P < 0.15$), the theoretical biomass was recalculated with the 0.2 step size and the code 0,1,2,3 for the mono-fertilizer gradient. The 4096 samples data were available in the perforated and non-perforated plots respectively and the highest one in each plot were taken as the standard. Any greater than the value in each plot was considered to be the optimal values for the biomass. The theoretical range of optimal fertilization amount and biomass were obtained by using recalculating the optimal values.

Optimal theoretical regression model

The average biomass of four years in the in perforated and non-perforated plots were overall analyzed, a new stepwise regression model was obtained, to identify the key factors on biomass. The probability of variable introduction and rejection were all set to 0.15. All above statistical analyses were carried out with SAS 9.0 (SAS Institute Inc., Cary NC, USA).

Results

Environmental conditions during the fertilization experiment

During fertilization, the monthly averages of growing-season air temperature from May to August were similar in 2014–2017, but there was a great difference in rainfall (Fig. 3). The average of rainfall in 2014 growing-season was 82.28 mm, 78%, 114%

and 108.03% higher than that in 2015, 2016 and 2017 respectively. Especially in June and July, the average of rainfall in 2014 was 3.58, 2.37 and 4.05 times more than that in 2015, 2016 and 2017.

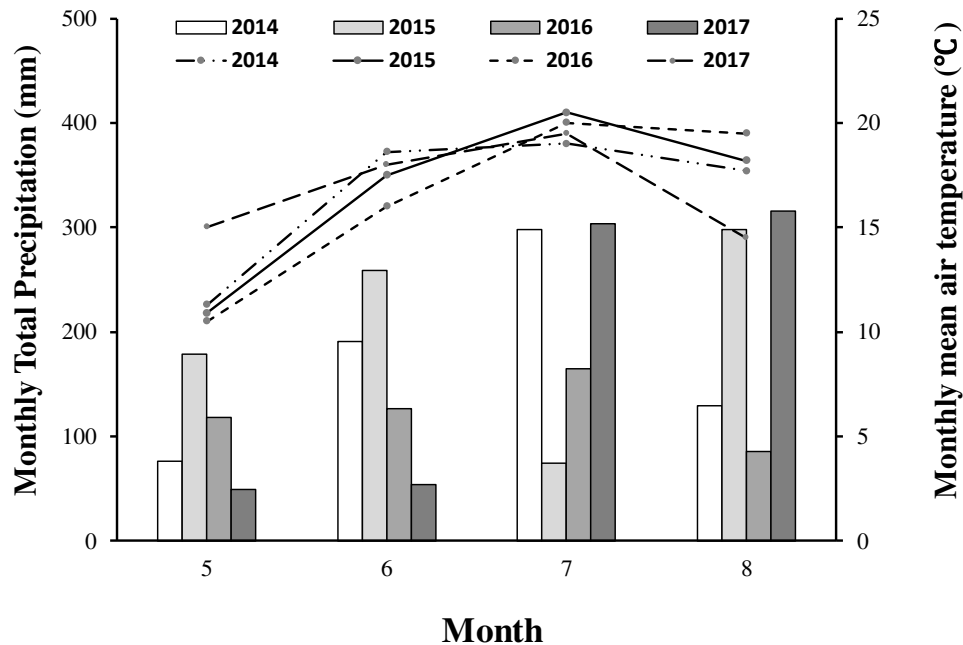


Figure 3. Monthly (May to August) mean air temperature (lines) and rainfall (bars) received during the study period in 2014-2017 at the experiment site near Hulunbuir Grassland Ecosystem National Field Observation Station

The effect of mono-nutrient

The plant community biomass showed a clear response to the single fertilizer application (Fig. 4). The biomass in the perforated plots initially declined slowly with an increase of P and K. Then beyond the second gradient, the biomass increased. The biomass improved continuously with an increase of N. Compared with perforated plots, the trend in non-perforated plots was completely opposite. The biomass increased with a slow decline of P and K, but beyond a certain concentration, the biomass of P and K actually decreased: excess application of P and K reduced the plant community biomass in the non-perforated plots.

The effect of binary fertilizer formulations

The effect of binary formulations of NP and NK played a positive role in the increase of biomass in the perforated or non-perforated plots (Fig. 5). The differences for phosphate and potassium fertilizers were more complex for the PK combination. Notably, there is an interaction between nitrogen and potassium in the perforated area. This phenomenon was more pronounced in the effect of double-fertilizer of PK in the perforated plots. In the non-perforated plots, the biomass increased with the increase of the phosphorus and potassium fertilizer gradient. When P = 2 and K = 1.5, the highest biomass was achieved. The effect of double-fertilizer on biomass in the perforated plots and non-perforated plots were almost the similar (the contour line density and variation range represent the influence degree).

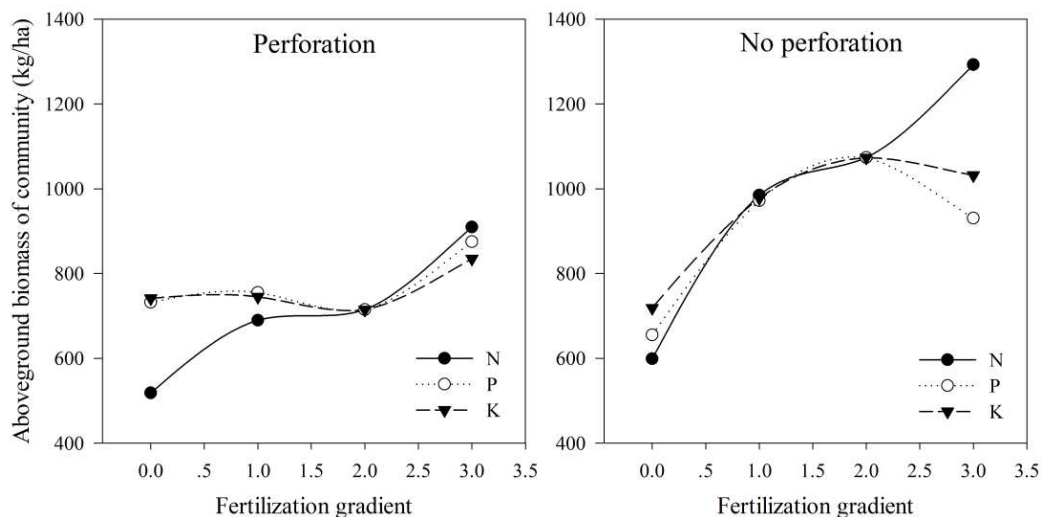


Figure 4. Mono-fertilizer effect on the plant community biomass from 2014 to 2017. The amount of each fertilizer were shown in Table 1

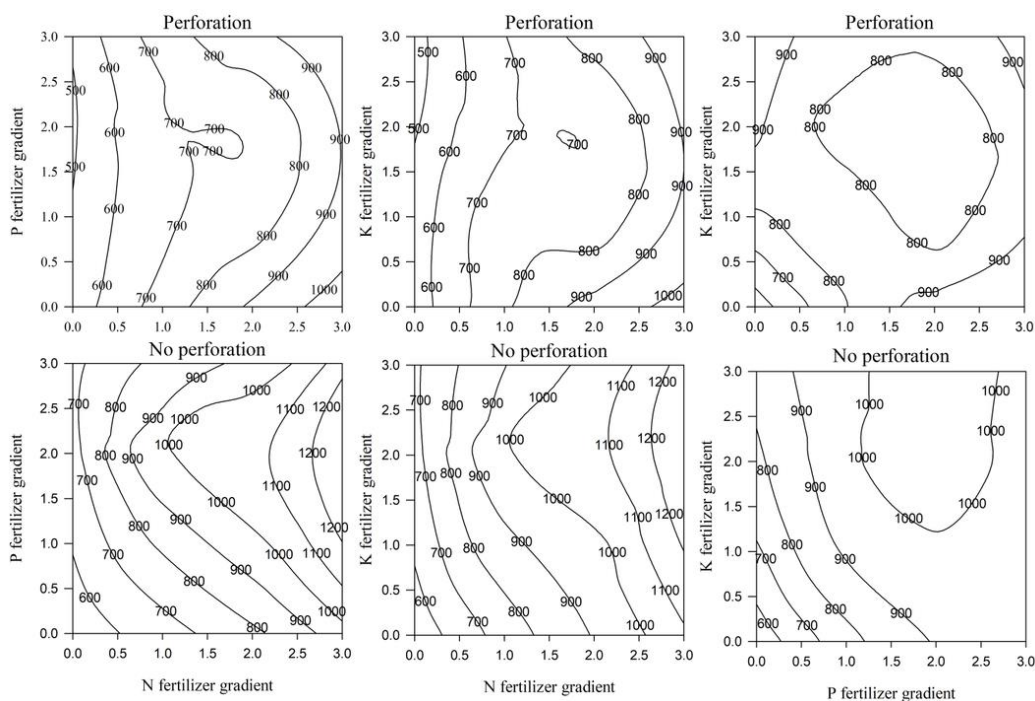


Figure 5. Binary fertilizer effect on the plant community biomass from 2014 to 2017

The effect of total-fertilizer

A significance test of the regression model showed that the probabilities were: $P = 0.07$ and $P = 0.02$ in perforated and non-perforated plots respectively (Table 2). The actual circumstances are reflected primarily by the regression model, with a liner positive correlation coefficient (R^2) between theoretical biomass (Y) and objective biomass (y) of 0.9160 and 0.9578 in perforated and non-perforated plots, respectively.

This is a highly significant fit between theoretical and objective biomass. The full information model met pre-set conditions for further analysis.

Table 2. Parameter test of full information model

Physical treatment	Index	DF	SS	R-square	F	P > F
Perforation	Linear	3	1861.85	0.7857	12.48	0.02
	Quadratic	3	192.08	0.0811	1.29	0.39
	Cross product	3	116.62	0.0492	0.78	0.56
	Total model	9	2170.56	0.9160	4.85	0.07
No perforation	Linear	3	3581.79	0.8284	26.18	0.00
	Quadratic	3	364.37	0.08431	2.66	0.18
	Cross product	3	195.19	0.0451	1.43	0.36
	Total model	9	4141.35	0.9578	10.09	0.02

The regression coefficient was analyzed by *t*-test, showing the mono-factor coefficient and reciprocal factors were not significant except X2*X2 in the non-perforated (Table 3). The *t*-test showed that the combined effects of nitrogen, phosphorous and potassium had non-significant regularity on biomass.

Table 3. Results of model parameter estimation and significance test

Physical treatment	Parameter	DF	Estimate	SE	T	Pr > t
Perforation	Intercept	1	55.85	7.02	7.96	0.00
	X1	1	23.31	14.18	1.64	0.18
	X2	1	-3.34	14.18	-0.24	0.83
	X3	1	-12.22	14.18	-0.86	0.44
	X1*X1	1	-1.35	2.83	-0.48	0.66
	X2*X1	1	-4.37	6.42	-0.68	0.53
	X2*X2	1	5.01	2.83	1.77	0.15
	X3*X1	1	0.67	6.42	0.1	0.92
	X3*X2	1	-2.45	6.42	-0.38	0.72
	X3*X3	1	4.14	2.83	1.46	0.22
No perforation	Intercept	1	52.63	6.72	7.83	0.00
	X1	1	-1.84	13.58	-0.14	0.90
	X2	1	30.81	13.58	2.27	0.09
	X3	1	5.34	13.58	0.39	0.71
	X1*X1	1	0.64	2.71	0.24	0.82
	X2*X1	1	2.7	6.14	0.44	0.68
	X2*X2	1	-8.76	2.71	-3.23	0.03
	X3*X1	1	6.76	6.14	1.1	0.33
	X3*X2	1	-1.81	6.14	-0.29	0.78
	X3*X3	1	-3.25	2.71	-1.2	0.30

The simulated optimization and optimal theoretical regression model

The highest biomass in the perforated plots was 93.48 kg ha⁻¹, while it was 129.25 kg ha⁻¹ in the non-perforated plots. The number of samples that were greater than the maximum value were 549 and 19 in perforated plots and non-perforated plots respectively. The recalculated sample data, the resulting coded value and its optimal fertilization amount and maximum biomass are shown in *Table 4*. The biomass variable amplitude in the perforated plots was 99.16–99.98 kg ha⁻¹ with the variation range N (231.50–238.82 kg ha⁻¹), P (187.25–218.75 kg ha⁻¹), and K (28.28–33.32 kg ha⁻¹), while the variable amplitude of biomass in the non-perforated plots was 130.31–131.21 kg ha⁻¹ with the variation range N (274.00–274.00 kg ha⁻¹), P (311.50–358.75 kg ha⁻¹), and K (75.37–81.03 kg ha⁻¹). Compared with the perforated plots, a higher theoretical biomass and fertilization amount could be obtained in the non-perforated plots.

Table 4. Perforation effect on statistical parameters of simulation optimization of optimal theoretical regression model

Physical treatment	Parameter	Nitrogen	Phosphorus	Potassium	Biomass
Perforation	Mean	2.57	1.16	1.1	99.57
	Standard error	0.02	0.05	0.05	0.21
	Coding interval (95%)	2.53~2.61	1.07~1.25	1.01~1.19	–
	Actual interval (95%)	231.50~238.82	187.25~218.75	28.28~33.32	99.16~99.98
No perforation	Mean	3	1.92	2.76	130.76
	Standard error	0	0.07	0.05	0.23
	Coding interval (95%)	3.00~3.00	1.78~2.05	2.66~2.86	–
	Actual interval (95%)	274.00~274.00	311.50~358.75	75.37~81.03	130.31~131.21

The optimal theoretical regression model

We used a gradual regression analysis for the full information model in the perforated- and non-perforated plots respectively and chose the coefficients that had significant effects on the biomass (*Table 5*). The effects of N were all significant in perforated and non-perforated plots ($P < 0.05$). The interaction between P and K was significant in the non-perforated area ($P < 0.05$, $R^2 = 0.12$), which was lower than the effect of nitrogen ($P < 0.05$, $R^2 = 0.6977$), and the combined effect reached 81.61%. The effects of nitrogen (N), dummy variables (B) and phosphate (P) on the biomass reached 57.71%, 18.50% and 2.03%, respectively.

The effects of optimal concentration of fertilizers on plant diversity

By optimal theoretical regression model, we got optimal fertilization level and analyzed the Richness and Shannon-Wiener diversity index with corresponding plots in 2014–2017 (*Fig. 6*). Our results showed that plant diversity responded differently to different years. As the fertilization period increased, whichever fertilizers and whether perforated or not, the values of the Shannon-Wiener index decreased. These changes were more evident in 2017, which was in the fourth year of fertilization. The Shannon-Wiener index decreased by 44.82–71.94% compared with 2014 in the perforated and non-perforated plots. The change for four years' species richness in the perforated plots

was regular, and it was shown decreased gradually every year. Although the change in the non-perforated plots was irregular, whichever fertilizer, decreased obviously in 2017 compare to 2014.

Table 5. The optimal theoretical regression model

Treatments of perforation	Variable entered	Estimate	Number Vars In	Partial R-Square	Model R-Square	C(p)	F	Pr>F	Model Pr>F
Total	Intercept	47.81					109.71	<.0001	<.0001
	X1	15.06	1	0.5771	0.5771	10.61	35.47	<.0001	
	B	14.73	2	0.1850	0.7620	-2.53	19.43	0.0002	
	X2	3.07	3	0.0203	0.7823	-2.19	2.23	0.1480	
Perforation	Intercept	54.60					188.46	<.0001	<.0001
	X1	13.82	1	0.7597	0.7597	1.45	37.94	<.0001	
No perforation	Intercept	56.75					109.24	<.0001	<.0001
	X1	16.62	1	0.6977	0.6977	18.66	27.70	0.0002	
	X2*X3	3.09	2	0.1184	0.8161	9.44	7.08	0.0222	

R-Square represents coefficient of determination. Variable B was dummy variable which combined the data of perforated- and non-perforated plots to perform a new regression analysis with fertilization

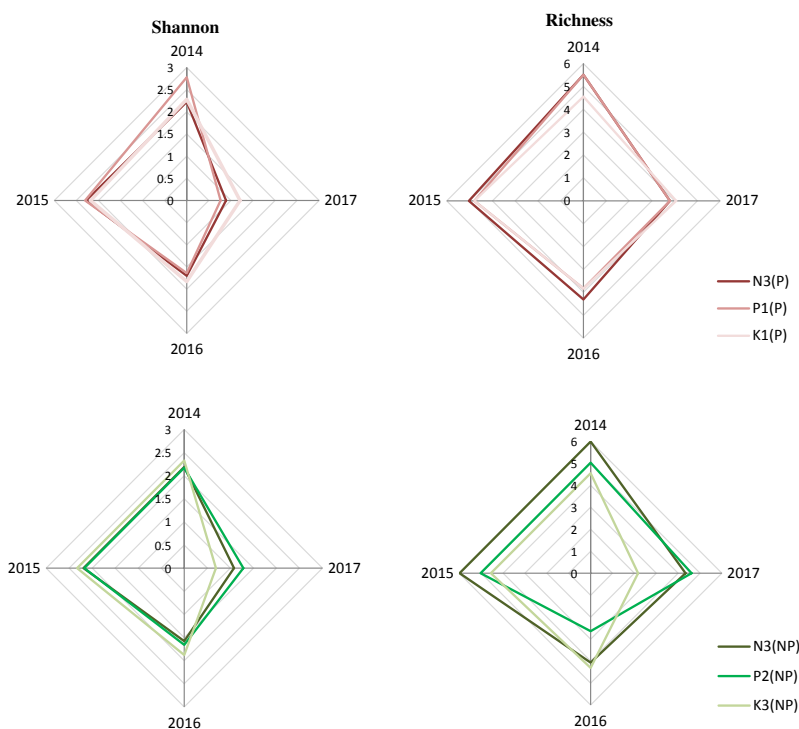


Figure 6. Radar charts showing Shannon-Wiener Index and Species richness, which were the suitable fertilizer level in Table 4. N, P and K represent nitrogen fertilizer, phosphate fertilizer and potash respectively. The letters 'P' and 'NP' in brackets represent the samples in the perforated and non-perforated plots

Discussion

The biomass responses to mono-fertilizer

The positive effect of N fertilizer on biomass yield in this study is consistent with other fertilization research on mixed-species grasslands (Boyer et al., 2012; Haque et

al., 2009; Lee et al., 2013). In our study, the significant effect of N existed in both perforated and non-perforated plots. The biomass consistently rising with increased N on Hulunbuir grassland was differed from other studies (Lee et al., 2013). This may have been due to a number of environmental changes beyond the control of this project such as annual rainfall and the perforated treatment. Many previous studies have observed these divergent effects of fertilizer addition are mediated by many factors which vary in time and space, including but not limited to fertilizer dosage, the traits of the species composing the community, soil moisture and climate (Heggenstaller et al., 2009; Kang et al., 2013; Ma et al., 2008). Irrespective of rainfall availability from 2014 to 2017, the biomass increased significantly as fertilizer concentration increased. This result is unexpected. Drought is usually the reason for the biomass of high-diversity communities having a strong reduction, or the reduction of species or plant functional groups that are sensitive to drought, such as legumes (Pfisterer and Schmid, 2002). Contrary to our hypothesis, average yield was lower from 2014 to 2017 in the perforated plots compared to the non-perforated plots-possibly due to the variation in the rate of the fertilizers or drought which affected the biomass response to fertilizer. However, it was not possible to identify the mechanism responsible for the changing response factors. In the perforated plots, P and K harvest were lower compared to the reported values in the non-perforated plots. Unlike N, P and K saturated at medium fertilization concentration in the non-perforated plots. However, there is a threshold grassland productivity response to fertilization (Kidd et al., 2017; Silvertown, 1980). This may also include a failure to detect beyond critical environmental thresholds. The inconsistencies are likely to exist due to the differences between the designs of grassland experiments, while the magnitude of fertilization effects may differ depending on the length of the experiment (Kidd et al., 2017).

The interaction of nitrogen, phosphorus and potassium fertilizer on biomass

Long-term grassland management practices of adding NPK, which could be considered a disturbance on above- and below-ground community compositions, intended to increase vegetation productivity affect the composition and diversity of the plant community (Cassman et al., 2016; Leff et al., 2015; Pickett et al., 1989). Nitrogen may enhance plant acquisition of P in a number of ways (Bobbink et al., 1998; Long et al., 2016; Lü et al., 2012; Pardo et al., 2007; Sardans and Peñuelas, 2012). For example, the effects of P on plant nutrition may be regulated by N addition due to the synergistic interaction between N and P in plant metabolism (Güsewell, 2004; Niklas et al., 2005). However, we did not find significant NP interaction in our study while the interaction effects of NK and PK were larger in the perforated plots. We supposed that (1) P and K addition alone would not achieve the effect of our experiment because Inner Mongolia grasslands are mainly N limited (Bai et al., 2010), and (2) the interaction of PK would be enhanced because of the positive effect of N addition on plant P and K uptake, and (3) compared to non-perforated plots, the plants in perforated plots may have benefited from improved nutrient uptake.

Effects of aeration

Most studies of grassland aeration have concentrated on forage production with mixed results. Aeration has been found to increase, decrease, or have no effect on forage production (Chapman et al., 2000; Taylor et al., 1983; Gordon et al., 2000; Malhi

et al., 2000). The perforated plots in our study seemed to need a slightly lower nutrients than the non-perforated plots but increased biomass was found in the non-perforated plots. We might ignore the plants that might have been killed as a result of the mechanical operation, resulting in the biomass in the perforated plots being lower. From an economic point of view, it is more conducive to increase profits by fertilizing only the native grassland without perforating. Studies have shown that the effect of aeration is likely to vary depending on soil hydrological properties and the features may be indicative as to when aeration may reduce runoff and P losses (Pierson et al., 2001). The lack of our hypothetical effect of aeration on biomass yield may have been caused by the loss of soil moisture from removal of vegetative thatch, as well as the differences in soil characteristics or by other environmental factors such as drought. The area in which this study was conducted was exposed to haying for decades prior to the present study. Thus, the improvement of soil compaction was the expected result may not have occurred because of the limitation of machinery, which would limit the response to aeration (Franklin et al., 2006). On the other hand, the effect of soil aeration appears to be greater than the fertilization effect in our study resulting in lower biomass in the perforated plots. This will be a consideration for future research.

Species richness and Shannon diversity response to fertilizers

Species richness, Shannon diversity and other dimensions commonly lead to enhanced productivity through the mechanism of complementarity (Hejman et al., 2007; Yahdjian et al., 2011). Species losses and declines in species richness per unit area are commonly induced by fertilizer addition. Shannon index decreased to a better extent with fertilization period increased (Bobbink et al., 2010; Kahmen et al., 2002). This is a good illustration of the theory that the longer the fertilization treatments lasted, the lower Shannon diversity became. It suggests that adding fertilizers has the tendency to decrease Shannon diversity, although other factors, such as the addition of NPK, can have interactive effects (Kahmen et al., 2002; Moog et al., 2002). Species richness was obviously negatively change to fertilizer period increased. There are several ecological mechanisms that can drive grassland plant community changes. First, it has been demonstrated that fertilization can negatively impact species richness, which diminishes trade-off opportunities that allow species coexistence (Levine and HilleRisLambers, 2009). Second, the stronger negative effects on plant species richness might be found when P and K were jointly added to N compared to N alone, it suggested nutrient colimitation fertilization can also increase belowground root competition and cause additional competitive exclusion among species (Dickson and Foster, 2011; Humbert et al., 2016).

Conclusion

In this study, we have shown the effect of grassland fertilization and soil aeration on plant community biomass in the semi-arid steppe, Northern China. Based on the estimates from the simulated optimization and optimal theoretical regression model, we recommend applying fertilizers with the variation range N (231.50–238.82 kg ha⁻¹), and P (187.25–218.75 kg ha⁻¹), and K (28.28–33.32 kg ha⁻¹), and annually to maximize biomass from the semi-arid grassland in Hulunbuir Inner Mongolia, China. Plant community biomass increases following N addition appear to be a universal pattern across grassland systems. Here, we further establish that effects on plant community

biomass are negatively and additively influenced by the dose of N applied and duration of application, as well as the lower Shannon diversity and Species richness became as the longer the fertilization treatments lasted. In our study, the effectiveness of soil aeration appears to be greater than the fertilization effect and it will be a consideration for future research. We therefore conclude that short-term studies are unlikely to possess the required timeframe to accurately predict long-term responses, requiring long-term experiments to explain the effectiveness of aeration on biomass of grassland community in Inner Mongolian Steppe. In future experiment, water control will be carried out the original design, to simulate the impact of different precipitation on the experimental results of this study.

Acknowledgements. This study was supported by National public welfare industry (agriculture) research project (No. 2013060), National Key Project (No. 2016YFC0500603), Inner Mongolia Key Lab of Grassland Management and Utilization, and Innovative Team of Grassland Resources from the Ministry of Education of China (IRT_17R59). We gratefully acknowledge the technical support of the staff of the Hulunbuir Grassland Ecosystem National Field Observation Station. Special thanks go to Jingzhong Dai and Jing Yao for support during the data collection and regular management of the experimental plots.

REFERENCES

- [1] Agren, G. I., Wetterstedt, J. A., Billberger, M. F. (2012): Nutrient limitation on terrestrial plant growth-modeling the interaction between nitrogen and phosphorus. – *New Phytol* 194: 953-960.
- [2] Aguiar, M. R., Paruelo, J. M., Sala, O. E., Lauenroth, W. K. (1996): Ecosystem responses to changes in plant functional type composition: an example from the Patagonian steppe. – *Journal of Vegetation Science* 7: 381-390.
- [3] Bai, Y., Wu, J., Clark, C. M., Naeem, S., Pan, Q., Huang, J. (2010): Tradeoffs and thresholds in the effects of nitrogen addition on biodiversity and ecosystem functioning: evidence from inner Mongolia Grasslands. – *Global Change Biology* 16: 358-372.
- [4] Bardgett, R. D., Wardle, D. A., Yeates, G. W. (1998): Linking above-ground and below-ground interactions: how plant responses to foliar herbivory influence soil organisms. – *Soil Biology and Biochemistry* 30: 1867-1878.
- [5] Bassin, S., Volk, M., Suter, M., Buchmann, N., Fuhrer, J. (2007): Nitrogen deposition but not ozone affects productivity and community composition of subalpine grassland after 3 yr of treatment. – *New Phytologist* 175: 523-534.
- [6] Basso, B., Dumont, B., Cammarano, D., Pezzuolo, A., Marinello, F., Sartori, L. (2016): Environmental and economic benefits of variable rate nitrogen fertilization in a nitrate vulnerable zone. – *Science of The Total Environment* 545-546: 227-235.
- [7] Bobbink, R., Hornung, M., Roelofs, J. G. M. (1998): The effects of air-borne nitrogen pollutants on species diversity in natural and semi-natural European vegetation. – *Journal of Ecology* 86: 717-738.
- [8] Bobbink, R., Hicks, K., Galloway, J., Spranger, T., Alkemade, R., Ashmore, M. (2010): Global assessment of nitrogen deposition effects on terrestrial plant diversity: a synthesis. – *Ecological Applications* 20: 30-59.
- [9] Boyer, C. N., Tyler, D. D., Roberts, R. K., English, B. C., Larson, J. A. (2012): Switchgrass yield response functions and profit-maximizing nitrogen rates on four landscapes in Tennessee. – *Agronomy Journal* 104: 1579-1588.
- [10] Cassman, N. A., Leite, M. F. A., Pan, Y., de Hollander, M., van Veen, J. A., Kuramae, E. E. (2016): Plant and soil fungal but not soil bacterial communities are linked in long-term fertilized grassland. – *Scientific Reports* 6: 23680.

- [11] Chapman, R., Singleton, P. L., Thom, E. R. (2000): Shallow mechanical loosening of a soil under dairy cattle grazing: effects on soil and pasture AU - Burgess, C. P. – *New Zealand Journal of Agricultural Research* 43: 279-290.
- [12] Dickson, T. L., Foster, B. L. (2011): Fertilization decreases plant biodiversity even when light is not limiting. – *Ecology Letters* 14: 380-388.
- [13] Elser, J. J., Bracken, M. E., Cleland, E. E., Gruner, D. S., Harpole, W. S., Hillebrand, H. (2007): Global analysis of nitrogen and phosphorus limitation of primary producers in freshwater, marine and terrestrial ecosystems. – *Ecology Letters* 10: 1135-1142.
- [14] Fay, P. A., Prober, S. M., Harpole, W. S., Knops, J. M. H., Bakker, J. D., Borer, E. T. (2015): Grassland productivity limited by multiple nutrients. – *Nature Plants* 1: 15080.
- [15] Franklin, D. H., Cabrera, M. L., Calvert, V. H. (2006): Fertilizer source and soil aeration effects on runoff volume and quality. – *Soil Science Society of America Journal* 70. DOI: 10.2136/sssaj2003.0114.
- [16] George, T. S., Fransson, A. M., Hammond, J. P., White, P. J. (2006): Phosphorus nutrition: rhizosphere processes, plant response and adaptations. – *Phosphorus in Action*: 245-271.
- [17] Gordon, R., Patterson, G., Harz, T., Rodd, V., MacLeod, J. (2000): Soil aeration for dairy manure spreading on forage: effects on ammonia volatilization and yield. – *Canadian Journal of Soil Science* 80: 319-326.
- [18] Gough, L., Osenberg, C. W., Gross, K. L., Collins, S. L. (2000): Fertilization effects on species density and primary productivity in herbaceous plant communities. – *Oikos* 89: 428-439.
- [19] Güsewell, S. (2004): N: P ratios in terrestrial plants: variation and functional significance. – *New Phytologist* 164: 243-266.
- [20] Han, L., Tsunekawa, A., Tsubo, M. (2011): Effect of frozen ground on dust outbreaks in spring on the eastern Mongolian Plateau. – *Geomorphology* 129: 412-416.
- [21] Haque, M., Epplin, F. M., Taliaferro, C. M. (2009): Nitrogen and harvest frequency effect on yield and cost for four perennial grasses. – *Agronomy Journal* 101: 1463-1469.
- [22] Harrison, A. F. (1983): Relationship between intensity of phosphatase activity and physico-chemical properties in woodland soils. – *Soil Biology and Biochemistry* 15: 93-99.
- [23] Heggenstaller, A. H., Moore, K. J., Liebman, M., Anex, R. P. (2009): Nitrogen influences biomass and nutrient partitioning by perennial, warm-season grasses. – *Agronomy Journal* 101: 1363-1371.
- [24] Hejcmán, M., KlauDISOVÁ, M., Schellberg, J., Honsová, D. (2007): The Rengen grassland experiment: plant species composition after 64 years of fertilizer application. – *Agriculture, Ecosystems and Environment* 122: 259-266.
- [25] Hofer, D., Suter, M., Buchmann, N., Lüscher, A. (2017): Nitrogen status of functionally different forage species explains resistance to severe drought and post-drought overcompensation. – *Agriculture, Ecosystems and Environment* 236: 312-322.
- [26] Humbert, J. Y., Dwyer, J. M., Andrey, A., Arlettaz, R. (2016): Impacts of nitrogen addition on plant biodiversity in mountain grasslands depend on dose, application duration and climate: a systematic review. – *Global Change Biology* 22: 110-120.
- [27] John, R., Chen, J., Giannico, V., Park, H., Xiao, J., Shirkey, G. (2018): Grassland canopy cover and aboveground biomass in Mongolia and Inner Mongolia: spatiotemporal estimates and controlling factors. – *Remote Sensing of Environment* 213: 34-48.
- [28] Kahmen, S., Poschlod, P., Schreiber, K. F. (2002): Conservation management of calcareous grasslands. Changes in plant species composition and response of functional traits during 25 years. – *Biological Conservation* 104: 319-328.
- [29] Kang, M., Dai, C., Ji, W., Jiang, Y., Yuan, Z., Chen, H. Y. H. (2013): Biomass and its allocation in relation to temperature, precipitation, and soil nutrients in Inner Mongolia grasslands, China. – *PLoS ONE* 8: e69561.

- [30] Kayser, M., Müller, J., Isselstein, J. (2018): Grassland renovation has important consequences for C and N cycling and losses. – *Food and Energy Security* 7: e00146.
- [31] Kidd, J., Manning, P., Simkin, J., Peacock, S., Stockdale, E. (2017): Impacts of 120 years of fertilizer addition on a temperate grassland ecosystem. – *PLoS ONE* 12: e0174632.
- [32] Kuzyakov, Y., Kretzschmar, A., Stahr, K. (1999): Contribution of *Lolium perenne* rhizodeposition to carbon turnover of pasture soil. – *Plant and Soil* 213: 127-136.
- [33] Lambin, E. F., Meyfroidt, P. (2011): Global land use change, economic globalization, and the looming land scarcity. – *Proceedings of the National Academy of Sciences* 108: 3465.
- [34] Lee, D. K., Aberle, E., Chen, C., Egenolf, J., Harmony, K., Kakani, G. (2013): Nitrogen and harvest management of Conservation Reserve Program (CRP) grassland for sustainable biomass feedstock production. – *GCB Bioenergy* 5: 6-15.
- [35] Leff, J. W., Jones, S. E., Prober, S. M., Barberán, A., Borer, E. T., Firm, J. L. (2015): Consistent responses of soil microbial communities to elevated nutrient inputs in grasslands across the globe. – *Proceedings of the National Academy of Sciences* 112: 10967-10972.
- [36] Levine, J. M., HilleRisLambers, J. (2009): The importance of niches for the maintenance of species diversity. – *Nature* 461: 254.
- [37] Li, L. J., Zeng, D. H., Yu, Z. Y., Fan, Z. P., Mao, R. (2010): Soil microbial properties under N and P additions in a semi-arid, sandy grassland. – *Biology and Fertility of Soils* 46: 653-658.
- [38] Liu, Y., Taxipulati, T., Gong, Y., Sui, X., Wang, X., Parent, S. É. (2017): N-P Fertilization inhibits growth of root hemiparasite *Pedicularis kansuensis* in natural grassland. – *Frontiers in Plant Science* 8.
- [39] Long, M., Wu, H. H., Smith, M. D., La Pierre, K. J., Lü, X. T., Zhang, H. Y. (2016): Nitrogen deposition promotes phosphorus uptake of plants in a semi-arid temperate grassland. – *Plant and Soil* 408: 475-484.
- [40] Lü, X. T., Kong, D. L., Pan, Q. M., Simmons, M. E., Han, X. G. (2012): Nitrogen and water availability interact to affect leaf stoichiometry in a semi-arid grassland. – *Oecologia* 168: 301-310.
- [41] Ma, W., Yang, Y., He, J., Zeng, H., Fang, J. (2008): Above- and belowground biomass in relation to environmental factors in temperate grasslands, Inner Mongolia. – *Science in China Series C: Life Sciences* 51: 263-270.
- [42] Malhi, S. S., Heier, K., Nielsen, K., Davies, W. E., Gill, K. S. (2000): Efficacy of pasture rejuvenation through mechanical aeration or N fertilization. – *Canadian Journal of Plant Science* 80: 813-815.
- [43] Montgomery, D. C., Mastrangelo, C. M. (1991): Some statistical process control methods for autocorrelated data. – *Journal of Quality Technology* 23(3): 179-193.
- [44] Moog, D., Poschlod, P., Kahmen, S., Schreiber, K. F. (2002): Comparison of species composition between different grassland management treatments after 25 years. – *Applied Vegetation Science* 5: 99-106.
- [45] Niklas, K. J., Owens, T., Reich, P. B., Cobb, E. D. (2005): Nitrogen/phosphorus leaf stoichiometry and the scaling of plant growth. – *Ecology Letters* 8: 636-642.
- [46] Olde Venterink, H., Kardel, I., Kotowski, W., Peeters, W., Wassen, M. J. (2009): Long-term effects of drainage and hay-removal on nutrient dynamics and limitation in the Biebrza mires, Poland. – *Biogeochemistry* 93: 235-252.
- [47] Pardo, L. H., McNulty, S. G., Boggs, J. L., Duke, S. (2007): Regional patterns in foliar ¹⁵N across a gradient of nitrogen deposition in the northeastern US. – *Environmental Pollution* 149: 293-302.
- [48] Pfisterer, A. B., Schmid, B. (2002): Diversity-dependent production can decrease the stability of ecosystem functioning. – *Nature* 416: 84.
- [49] Pickett, S. T. A., Kolasa, J., Armesto, J. J., Collins, S. L. (1989): The ecological concept of disturbance and its expression at various hierarchical levels. – *Oikos* 54: 129-136.

- [50] Pierson, S. T., Cabrera, M. L., Evanylo, G. K., Kuykendall, H. A., Hoveland, C. S., McCann, M. A. (2001): Phosphorus and ammonium concentrations in surface runoff from grasslands fertilized with broiler litter. – *Journal of Environmental Quality* 30: 1784-1789.
- [51] Plassmann, K., Edwards Jones, G., Jones, M. L. M. (2009): The effects of low levels of nitrogen deposition and grazing on dune grassland. – *Science of The Total Environment* 407: 1391-1404.
- [52] Sala, O. E., Biondini, M. E., Lauenroth, W. K. (1988): Bias in estimates of primary production: an analytical solution. – *Ecological Modelling* 44: 43-55.
- [53] Sardans, J., Peñuelas, J. (2012): The role of plants in the effects of global change on nutrient availability and stoichiometry in the plant-soil system. – *Plant Physiology* 160: 1741-1761.
- [54] Schulte, R. P. O., Herlihy, M. (2007): Quantifying responses to phosphorus in Irish grasslands: interactions of soil and fertilizer with yield and P concentration. – *European Journal of Agronomy* 26: 144-153.
- [55] Shannon, C. E., Weaver, W. (1949): *The Mathematical Theory of Communication*. – University of Illinois Press, Urbana, IL.
- [56] Silvertown, J. (1980): The dynamics of a grassland ecosystem: botanical equilibrium in the park grass experiment. – *Journal of Applied Ecology* 17: 491-504.
- [57] Taylor, E. W., McMurphy, W. E., McLaughlin, G. L. (1983): Equipment for aerating Bermudagrass pastures. – *Transactions of the ASAE* 26: 352-0353.
- [58] Tilman, D., Reich, P. B., Knops, J., Wedin, D., Mielke, T., Lehman, C. (2001): Diversity and productivity in a long-term grassland experiment. – *Science* 294: 843.
- [59] Turner, B. L., Chudek, J. A., Whitton, B. A., Baxter, R. (2003): Phosphorus composition of upland soils polluted by long-term atmospheric nitrogen deposition. – *Biogeochemistry* 65: 259-274.
- [60] Yahdjian, L., Gherardi, L., Sala, O. E. (2011): Nitrogen limitation in arid-sub humid ecosystems: a meta-analysis of fertilization studies. – *Journal of Arid Environments* 75: 675-680.
- [61] Yu, L., Song, X. L., Zhao, J. N., Wang, H., Bai, L., Yang, D. L. (2015): Responses of plant diversity and primary productivity to nutrient addition in a *Stipa baicalensis* grassland, China. – *Journal of Integrative Agriculture* 10(14): 2099-2108
- [62] Zhang, T. Q., MacKenzie, A. F. (1997): Changes of soil phosphorous fractions under long-term corn monoculture. – *Soil Science Society of America Journal* 61: 485-493.
- [63] Zhou, X., Bowker, M. A., Tao, Y., Wu, L., Zhang, Y. (2018): Chronic nitrogen addition induces a cascade of plant community responses with both seasonal and progressive dynamics. – *Science of The Total Environment* 626: 99-108.

PHYSIOLOGICAL RESPONSES OF ALFALFA SEEDLINGS TO FREEZE-THAW, NaCl AND Na₂SO₄ STRESS

BAO, G.^{1*} – QU, Y.¹ – YAN, B.² – BIAN, W.¹ – CHEN, W.¹ – LI, Y.¹ – CUI, X.³

¹*Key Laboratory of Groundwater Resources and Environment (Jilin University), Ministry of Education, Changchun 130012, China*

²*Environmental Monitoring Center Station of Jilin Province, Changchun 130011, China*

³*Jilin University School of Law, Jilin University, Changchun 130012, China*

**Corresponding author*

e-mail: baogz@jlu.edu.cn; fax: +86-0431-8850-2606

(Received 23rd Dec 2019; accepted 23rd Mar 2020)

Abstract. NaCl and Na₂SO₄, two common neutral salts, often cause salt stress in saline-alkaline grassland in Northeast China. The purpose of this experiment is to reveal the effects of the combined stress of these two neutral salts and the freeze-thaw cycles of spring and autumn on the physiological and ecological characteristics of alfalfa seedlings. By measuring the soluble protein, soluble sugar, proline, malondialdehyde (MDA) content, Peroxidase activity (POD) and Superoxide dismutase (SOD) activity of alfalfa seedlings treated with two types of salt solution (NaCl and Na₂SO₄) in a freeze-thaw cycle, the physiological and ecological responses of alfalfa seedlings under combined stress were investigated, and the differences in the stress of plant seedlings between the two salt solutions were compared. Stress damage mainly resulted from low temperature, penetration and ionic toxicity. A series of tolerance mechanisms were observed in the plants to cope with the stress. Under the compound stress, plant damage was exacerbated. The highlight of this study is that two different types of salinity had ion specificity for the toxic effects of alfalfa, and the toxic effects of Cl⁻ were the main factors, not Na⁺ or SO₄²⁻. Alfalfa exposed to SO₄²⁻ salt could cope with salt stress relatively better.

Keywords: *alfalfa, freeze-thaw, tolerance mechanisms, salinity, combined stress*

Introduction

The northern part of China is cold in winter, and pasture survives winter difficultly. In the spring and autumn, pastures are often affected by cold currents, and are subjected to freeze-thaw cycles, resulting in poor growth and low yield, which reduce the utilization value of pasture. Therefore, temperature is one of the important limiting factors for the use value of pasture (Stushnoff and Junttila, 1986). At the same time, soil salinization in Northeast China is serious, and salt is one of the main limiting factors for improving crop growth and productivity (Flowers, 2004; Kanmani et al., 2017). The main consequences of plant exposed to salt stress are water deficits and excess ions, leading to several morphological and physiological changes (Greenway and Munns, 2003; Türkan and Demiral, 2009). High concentrations of ions in the external solution may be absorbed at a high rate, which may result in excessive accumulation in plant tissues. These ions may affect the membrane's ability to selectively permeate and interfere with the absorption of other ions, thereby altering the amount of a series of elements in the tissue (Hu and Schmidhalter, 2005). Therefore, in the face of soil salinization, breeding salt-tolerant varieties and direct use of saline-alkali land are more cost-effective solutions for improving and utilizing saline-alkali land.

According to the survey, alfalfa (*Medicago sativa* L.) is one of the most common saline-alkali land forage in northeastern China and high latitudes. As a high-quality forage cultivated artificially, alfalfa has strong cold and salt resistance. It is a common plant for the improvement of saline-alkali land in Northeast China, and also a test material commonly used in the study of cold tolerance and salt-tolerance of plants. Alfalfa is sensitive to salt at seedling stage, and the seedlings have a consistent response to salt throughout the growth stage, and salt selection is most suitable at this stage (Al-Khatib et al., 1994, 1987).

At present, researches on the cold tolerance and salt tolerance of seedlings mainly focus on single factor stress conditions, such as salt tolerance physiology (Akandi et al., 2017), cold resistance and survival rate (Skinner and Bellinger, 2017), and drought resistance (Pompeiano et al., 2016), and those on the physiological laws of compound stress are rare. In the early spring and late autumn of the cold regions of Northeast China, freeze-thaw and salt stresses are the most common, and the salt types in the saline-alkaline grasslands in Northeast China are mainly alkaline salts, and some are neutral salts. The main components of neutral salts are sodium salts, including sodium chloride and sodium sulfate. Most studies on the salt tolerance of plant species are based on experiments where NaCl is the main salt, and the symptoms of injury are usually attributed to the toxicity of Na⁺ and Cl⁻. Relatively few studies (Nguyen et al., 2006; Renault et al., 2001; Rogers et al., 1998) focus on the effects of Na₂SO₄ on plant growth and physiology. Therefore, this study used Dongmu-1 alfalfa as the experimental object to study the changes of soluble protein, malondialdehyde (MDA), soluble sugar, proline content and SOD and POD activity in the alfalfa seedlings under the combined stress of freeze-thaw and salt (NaCl or Na₂SO₄). The physiological response mechanism of cold resistance and salt tolerance in alfalfa seedlings was revealed.

Materials and methods

Experimental materials

In this study, the indoor culture experiment method was adopted, and the test seedlings were Dongmu-1 alfalfa. The alfalfa seeds with uniform grain size and no pests were picked carefully, disinfected with 0.1% KMnO₄ for 10 min, rinsed with double distilled water, and then cultured in several culture dishes with a diameter of 100 mm. Two layers of filter paper were laid in each dish, and around 100 seeds were placed evenly place, immersed appropriate amount of water. The culture dishes were placed in a constant temperature incubator for growth and germination, and the light collection period was 12 h, with illumination time at 25 °C and non-lighting time at 15 °C. During the germination period, appropriate amount of water was added three times a day. When the third cotyledon grew, the plants with the same growth were selected for stress treatment.

Experimental methods

The treatment solvents selected were NaCl and Na₂SO₄, and according to the growth condition of the seedling, the concentration of each salt was 100 mmol/L. After the treatment, the plants were cultured for two days. The salt-treated experimental groups and the control group (CK) were divided into two groups respectively. One was subjected to freeze-thaw stress, and the other was cultured at room temperature. The

temperature of the freeze-thaw cycle was controlled by an ultra-low temperature alternating test chamber, and the temperature was set to 10 °C, 5 °C, 0 °C, -3 °C (Deng et al., 2005) have found that -3 °C is the lowest temperature for alfalfa seedlings to withstand low temperature), 0 °C, 5 °C and 10 °C, with an interval of two hours. Treated groups and control groups were sampled at each temperature. Three sets of parallel samples were taken from each group, and the relevant indicators were determined after sampling.

CK group is blank control group without salt solution and freeze-thaw cycle; FT group is only treated by a freeze-thaw cycle; FT + NaCl group is the one with NaCl solution and a freeze-thaw cycle; FT + Na₂SO₄ group is the one added Na₂SO₄ solution and subjected to a freeze-thaw cycle. T1-T7 correspond to 10 °C, 5 °C, 0 °C, -3 °C, 0 °C, 5 °C, 10 °C, respectively.

Samples were grinded to homogenate with 5 ml distilled water (5 ml of 10% trichloroacetic acid solution used for MDA and soluble sugar content, and 5 ml of 3% sulfosalicylic acid solution used for proline content instead) in a mortar. After centrifugation for 10 min (3000 r/min), the supernatant was picked for measurement (protein: G250-Coomassie brilliant blue method; MDA and soluble sugar: thiobarbituric acid method; proline: acid ninhydrin colorimetry). The SOD and POD activity was determined by SOD (superoxide dismutase) and POD (peroxidase) kits (Nanjing Jiancheng Bioengineering Institute), respectively.

Data analysis

The experimental data were graphed with Microsoft (Redmond, USA) Excel, and statistical analysis was performed with SPSS 16.0 statistical software (IBM SPSS Statistics, Chicago, USA) using single factor variance analysis (one-way analysis of variance) and multiple comparisons with least significant difference (LSD). The significance level was at 0.05, the experiments were repeated five times, and all of the results are presented as mean ± SE.

Results and discussion

Change in osmotic adjustment substance content

Soluble protein, soluble sugar, and proline are common osmotic adjustment substances in plants, and their levels can reflect the degree of stress on plants.

As can be seen from *Figure 1*, the three treatment groups exhibited substantially the same trend throughout the freeze-thaw cycle. At the initial stage of temperature decrease, the protein content increased slightly, mainly due to the small temperature stress, and the plant stress response rapidly regulated the metabolism and increased protein content. At the lowest temperature (-3 °C), the degree of stress reached the maximum and the protein content went up significantly, indicating that alfalfa seedlings were most sensitive at -3 °C. The low temperature caused plants to produce a stress-resistant reaction, and the related genes were overexpressed (Guy, 1990; Hannah et al., 2005; Hahn and Walbot, 1989; Seppänen et al., 1998), and cold-resistant proteins were synthesized, resulting in an increase in the total amount of protein. This is consistent with the conclusion of (Weiser, 1970) who proposed that low temperature could induce plant protein production. When the temperature gradually rose, the soluble protein content of the three treatment groups decreased (Bian et al., 2018). However, the

difference was that the FT group and the FT + Na₂SO₄ group decreased significantly, while the FT + NaCl group decreased slowly, indicating that as the temperature rose, the low temperature stress on the plants was gradually reduced, and the excess soluble proteins were catabolized progressively. The addition of salt could destroy plant cells, causing cells to rupture in high salinity solutions, which is an irreversible process. Cl⁻ had strong destructive power to cells, and even if the temperature rose, a large amount of soluble proteins could not be metabolized, while the destructive power of SO₄²⁻ was relatively weaker, and soluble proteins in FT + Na₂SO₄ group were partially metabolized.

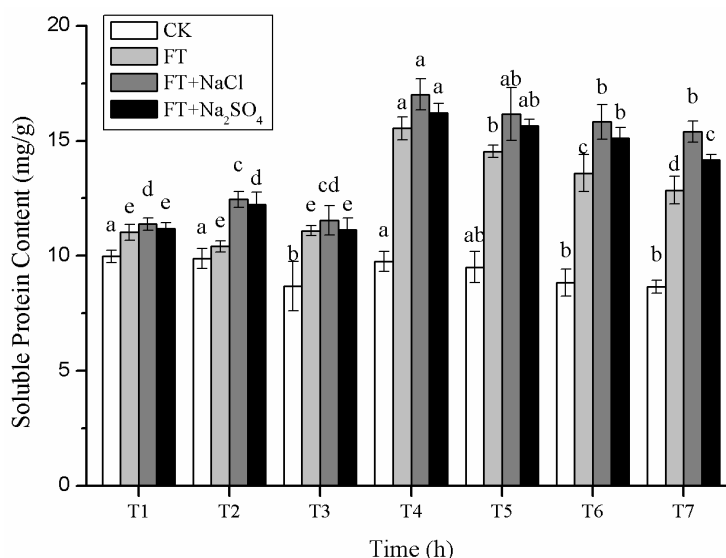


Figure 1. Effect of freezing-thawing cycle and two neutral salts on the content of soluble protein

Studies have shown that freeze-thaw cycles can change the accumulation of lipids and carbohydrates in plants (Skinner et al., 2014). A large amount of ions would be accumulated in the salt-treated plants and are sequestered in the vacuole, and non-absorbable compounds, such as sugar (Briens and Larher, 2010; Matoh and Matsushita, 2010) and leaf proline (Pagter et al., 2009), may act as compatible organic solutes to balance cytoplasmic osmotic pressure (James et al., 2002; Volkmar et al., 1998). As can be seen from *Figures 2* and *3*, as the temperature descended, the soluble sugar and proline contents gradually ascended, reaching the highest at the lowest temperature (-3 °C) (Bao et al., 2017). Cooling allowed the seedlings to actively accumulate soluble sugar and proline, maintain the osmotic potential inside and outside the cells, ensure the normal structure of the cell membrane, reduce the freezing point of the cells, increase the hydration of the cells, giving rise to enhancement of water retention capacity and avoidance of probiotic damage to dehydration at low temperature. The soluble sugar and proline contents decreased slightly as the temperature went up in the late stage of the experiment, but they were still high. There was almost no significant difference between the groups ($P > 0.05$). The cell thawing process was slow, and sustained low temperature damage resulted in accumulation of soluble sugar and proline used to reduce coercive damage in plants. Moreover, the changes of the index of each group were roughly as follows: FT + NaCl group > FT + Na₂SO₄ group > FT group > CK

group, indicating that compound stress was severer than single stress, and the increased osmotic adjustment substance was both used to maintain the osmotic potential of the cells and to resist the damage caused by low temperature. Therefore, the content of osmotic adjustment substances in the complex stress group was significantly higher than that in the freeze-thaw group. However, if the increase of osmotic adjustment substances was only related to the external environmental salt concentration, it was independent of the salinity type. It should have shown that the FT + Na₂SO₄ group had more osmotic adjustment substances, since Na₂SO₄ in the equimolar two salt solutions should contain a higher concentration of Na⁺. Therefore, the difference between the two salt-treated groups was caused by the difference between Cl⁻ and SO₄²⁻ ions, and the alfalfa seedlings were more sensitive to Cl⁻.

Changes in biofilm damage

MDA is a product of membrane lipid peroxidation in plant cells. Studies (Bailly et al., 1996; Greenway and Munns, 2003) have shown that degree of could be reflected in the content of MDA. It can be seen from *Figure 4* that there was no significant change in MDA content in the CK group ($P > 0.05$), and the MDA changes in the freeze-thaw group and the two compound stress groups were the same. With the decrease of temperature, the MDA content increased significantly, and the three groups all peaked at T4 (-3 °C), 18.30 $\mu\text{mol}\cdot\text{L}^{-1}$, 23.75 $\mu\text{mol}\cdot\text{L}^{-1}$, 21.55 $\mu\text{mol}\cdot\text{L}^{-1}$, respectively. Compared with T1, T2 and T3, there were significant differences ($P > 0.05$), indicating that the lower the temperature was, the higher the MDA content produced in the alfalfa seedlings. With the increase of temperature, the MDA content of the three treatment groups decreased slightly but remained high. There was almost no significant difference between the groups ($P > 0.05$). This may be due to the membrane lipid peroxidation caused by low temperature and resulted in the accumulation of MDA. The continuous low temperature caused the cells to thaw slowly, and although the temperature gradually went up, plants were still subjected to cold stress, showing a slight decline and followed a trend to be stable.

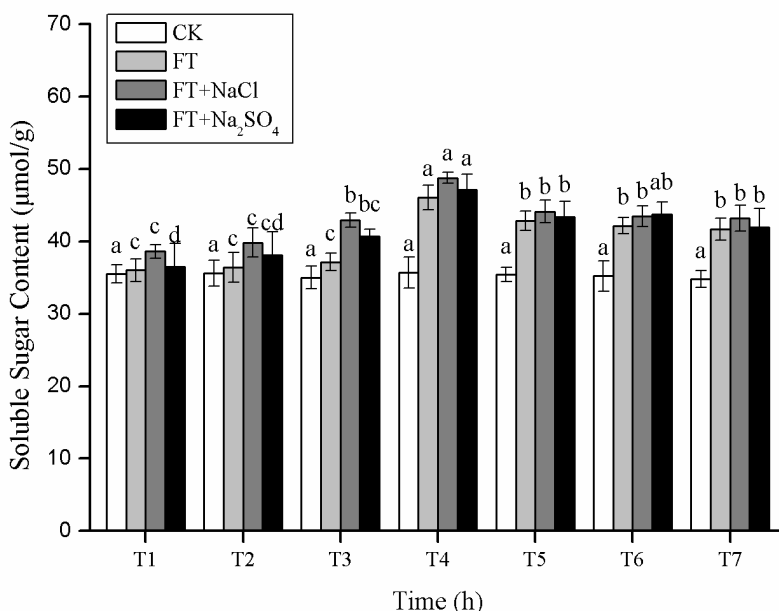


Figure 2. Effect of freezing-thawing cycle and two neutral salts on the content of soluble sugar

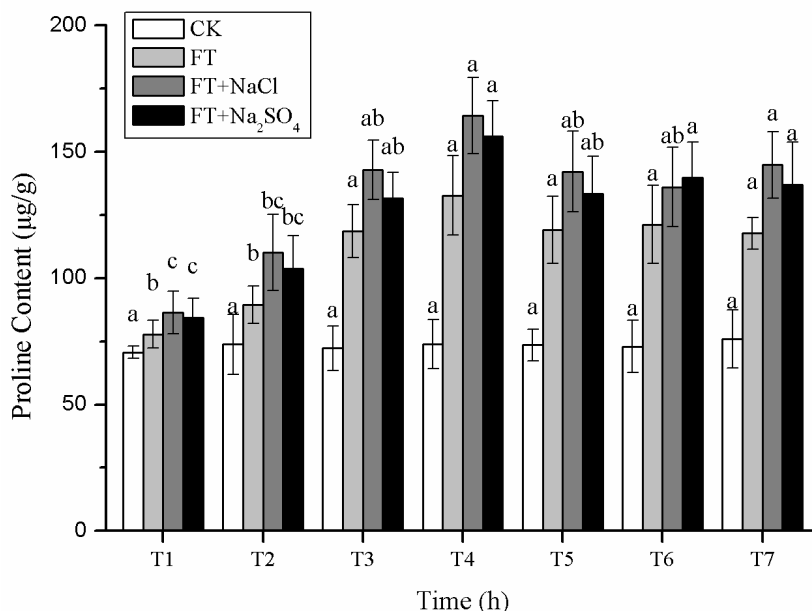


Figure 3. Effect of freezing-thawing cycle and two neutral salts on the content of proline

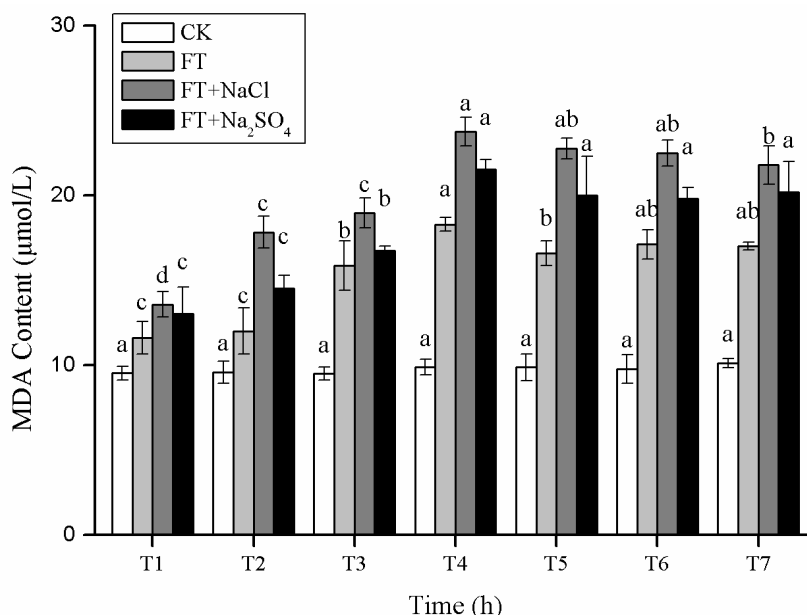


Figure 4. Effect of freezing-thawing cycle and two neutral salts on the content of MDA

In the longitudinal comparison, the MDA content of the three treatment groups was higher than that of the CK group, indicating that the alfalfa seedlings started to be subjected to cold stress at 10 °C. The combined stress of freeze-thaw and NaCl resulted in the highest MDA content in the seedlings, 4.28-13.84% more than that in the FT + Na₂SO₄ group, and the MDA content in the FT group was the lowest, indicating that the alfalfa seedlings were subjected to salt stress after the salt solution treatment. Research showed that plants responded to salinity in a two-stage response (Munns, 2005). The first stage was due to the osmotic pressure caused by the salt outside the

plants, and the second stage was due to the toxic effect of the salt, which exceeded the ability of the cells to divide the salt in the vacuole. Salinity exacerbated cell membrane lipid peroxidation and accumulated more MDA. Cl⁻ and SO₄²⁻ showed differences in plant stress, and the damage caused by Cl⁻ was stronger than by SO₄²⁻, probably because alfalfa had effective mechanisms to exclude Na and S and part Cl ions from leaves. The remaining not excluded Cl ions produced toxic effects, destroyed cell structure and inhibited plant growth. The decrease in growth may also be due to an increase in the metabolic cost of excluding, separating, or increasing the synthesis of the permeate, reducing the amount of organic compound available for growth (Lissner and Schierup, 1997; Mccree, 1986).

Changes in antioxidant enzyme activity

Salinity-induced increased antioxidant activity is associated with plant salt tolerance (Bose et al., 2014). It can be seen from *Figures 5 and 6* that the trend of SOD and POD activity in the treated groups was consistent, and the change rule was first raised and then maintained at a higher level during the whole freeze-thaw cycle. As the temperature decreased, the SOD activity gradually increased, and the maximum value appeared at T4 (-3 °C), then decreased slightly, but was still very high. POD activity increased first, and the maximum value appeared at T4 (-3 °C), then the decrease was not obvious, and there was no significant difference between the groups ($P > 0.05$). The activity of SOD and POD increased significantly with temperature, indicating that membrane lipid peroxidation occurred in plants under low temperature and salt stress, and a large amount of superoxide anion radicals were produced. ROS was rapidly produced in plants in the form of H₂O₂ and O₂⁻ (Zang et al., 2015). The production of ROS led to the activation of programmed cell death, and the cells underwent various stages of apoptosis, such as externalization of phosphatidylserine, DNA laddering, loss of plasma membrane integrity (Swapnil et al., 2017). The stress resistance of plants induced the activity of SOD and POD. SOD could convert superoxide anion into H₂O₂, whereas POD could decompose H₂O₂ and synergize with SOD to scavenge reactive oxygen species in order to reduce cell membrane damage. In the late stage of freeze-thaw cycle (temperature rose phase), the plants were exposed to sustained low temperature, SOD and POD activity was still high, mainly because the long-term cold environment caused the active oxygen free radicals to continue to accumulate, although the temperature was in the recovery phase, plants were still severely stressed. SOD is an important component of the active oxygen scavenging system in plants (Zhu et al., 2007). When plants responded to external environmental stress, POD and SOD acted synergistically to protect the body from external stress, and the activity changes of the two were significantly correlated (Qi et al., 2003).

The three treated groups showed the strongest POD and SOD activity in the FT + NaCl group, the second in the FT + Na₂SO₄ group, and the weakest in the FT group, indicating that compound stress could lead to increased cell membrane lipid peroxidation, and different types of salt solutions had different effects on plant cells. Compared with Na⁺ (Bhivare et al., 1988; Chavan and Karadge, 1980) and SO₄²⁻, plants were more sensitive to Cl⁻, which may give rise to enhancement of cell membrane lipid peroxidation, and ROS was produced enough to increase the antioxidant activity of plants. In addition, studies (Cameron and Pakrasi, 2010) have shown that sulfate in cells could promote the synthesis of glutathione, which had been shown to be critical for many processes in plants and promoted plant growth.

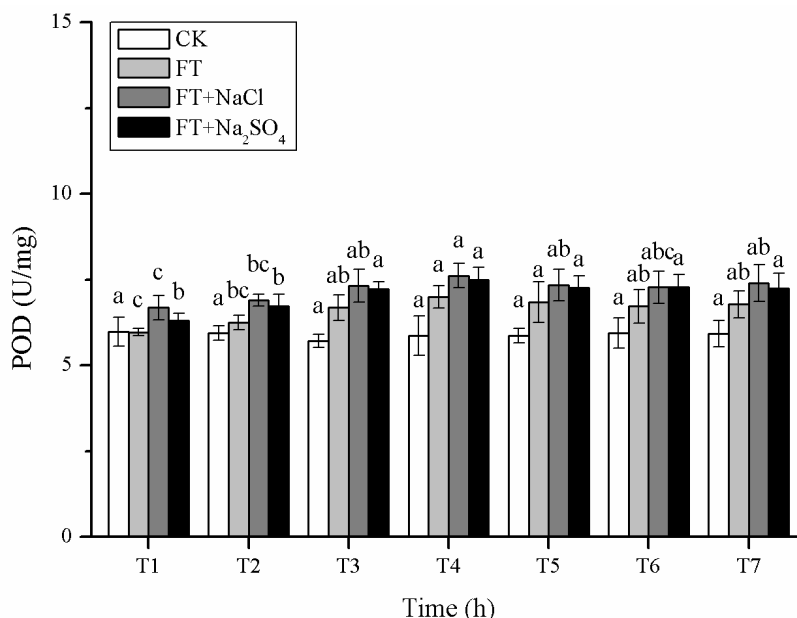


Figure 5. Effect of freezing-thawing cycle and two neutral salts on the content of POD

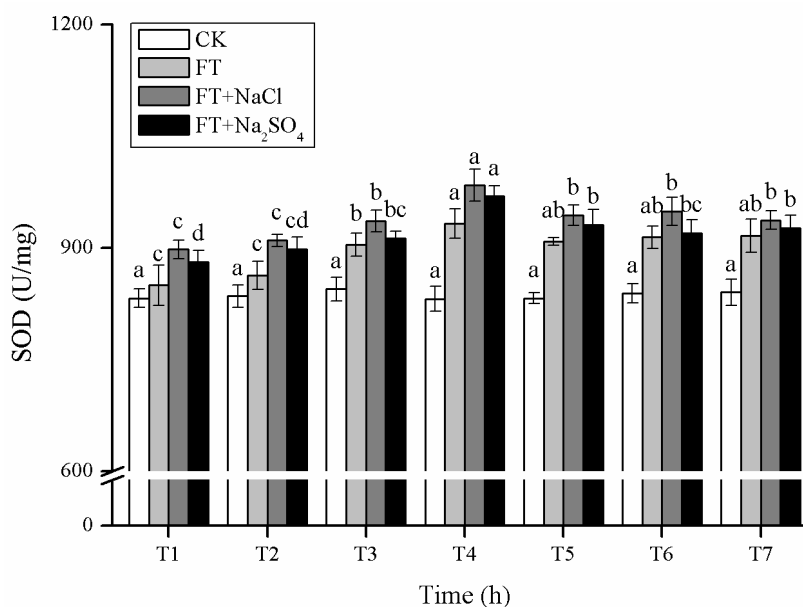


Figure 6. Effect of freezing-thawing cycle and two neutral salts on the content of SOD

Conclusion

Freeze-thaw cycles and salinity have a negative impact on the growth of alfalfa seedlings and have certain regularity, which could be proved by many related studies as well (Lissner and Schierup, 1997; Lissner et al., 1999; Matsushita and Match, 1991; Vasquez et al., 2006). Our research suggested that this might be due to temperature, penetration and ion specificity. Alfalfa showed certain tolerance to low temperature and salinity, which was characterized by overexpression of related genes to synthesize soluble protein, huge production of soluble sugar, proline and other solutes regulating

osmotic potential, the accumulation of MDA by cell membrane lipid peroxidation, and the enhancement of antioxidant enzyme activity to scavenge ROS. In a freeze-thaw cycle, each indicator and temperature had a certain degree of negative correlation. Compared with single freeze-thaw stress, compound stress had stronger ability to inhibit plant growth, mainly due to the penetration and toxicity of salt ions. For different types of salinity, the plant response was different, showing pronounced ion specificity. Equimolar NaCl was more stressful than Na₂SO₄ on alfalfa seedlings, and the stress was mainly from the toxic effect of Cl⁻ rather than Na⁺ or SO₄²⁻. This may be due to the fact that alfalfa was more sensitive to Cl⁻ and had Na⁺, SO₄²⁻ and partial Cl⁻ efflux mechanisms. Cl⁻ might affect a variety of important chemical actions in cells, and cells underwent normal metabolic activities, thereby inhibiting plant growth. It can provide a reference for scientific management of either farmland or lawn of alfalfa. However, whether the adaptation mechanisms of short-term stress were consistent with those of long-term one, it needs to be further investigated.

Acknowledgments. This work was supported by the [National Natural Science Foundation of China] under Grant [31772669].

Conflict of interests. The authors declare no conflict of interests.

REFERENCES

- [1] Akandi, Z. N., Pirdashti, H., Yaghoobian, Y., Omran, V. G. (2017): Response of quantitative and physiological parameters of stevia (*Stevia rebaudiana* Bertoni) medicinal plant to salinity stress under controlled conditions. – *Journal of Science and Technology of Greenhouse Culture* 8(1): 9-20.
- [2] Al-Khatib, M. M., McNeilly, T., Collins, J. C. (1994): Between and within cultivar variability in salt tolerance in lucerne (*Medicago sativa* L.). – *Genetic Resources and Crop Evolution* 41(3): 159-164.
- [3] Bailly, C., Benamar, A., Corbineau, F., Come, D. (1996): Changes in malondialdehyde content and in superoxide dismutase, catalase and glutathione reductase activities in sunflower seeds as related to deterioration during accelerated aging. – *Physiologia Plantarum* 97(1).
- [4] Bao, G. Z., Ao, Q., Li, Q. Q., Bao, Y. S., Zheng, Y., Feng, X. X., Ding, X. M. (2017): Physiological characteristics of *Medicago sativa* L. in response to acid deposition and freeze-thaw stress. – *Water Air and Soil Pollution* 228(9).
- [5] Bhivare, V. N., Nimbalkar, J. D., Chavan, P. D. (1988): Photosynthetic carbon metabolism in French bean leaves under saline conditions. – *Environmental & Experimental Botany* 28(2): 117-121.
- [6] Bian, W. J., Bao, G. Z., Qian, H. M., Song, Z. W., Qi, Z. M., Zhang, M. Y., Chen, W. W., Dong, W. Y. (2018): Physiological response characteristics in *Medicago sativa* under freeze-thaw and deicing salt stress. – *Water Air and Soil Pollution* 229(6).
- [7] Bose, J., Rodrigo-Moreno, A., Shabala, S. (2014): ROS homeostasis in halophytes in the context of salinity stress tolerance. – *Journal of Experimental Botany* 65(5): 1241-1257.
- [8] Briens, M., Larher, F. (2010): Osmoregulation in halophytic higher plants: a comparative study of soluble carbohydrates, polyols, betaines and free proline. – *Plant Cell & Environment* 5(4): 287-292.
- [9] Cameron, J. C., Pakrasi, H. B. (2010): Essential role of glutathione in acclimation to environmental and redox perturbations in the Cyanobacterium *Synechocystis* sp. PCC 6803. – *Plant Physiology* 154(4): 1672-1685.

- [10] Chavan, P. D., Karadge, B. A. (1980): Influence of sodium chloride and sodium sulfate salinities on photosynthetic carbon assimilation in peanut. – *Plant and Soil* 56(2): 201-207.
- [11] Deng, X., Qiao, D., Li, L., Yu, X., Zhang, N., Lei, G., Cao, Y. (2005): Effect of low temperature stress on physiological characteristics of alfalfa. – *Journal of Sichuan University (Natural Science Edition)*: 42(1): 190-194.
- [12] Flowers, T. J. (2004): Improving crop salt tolerance. – *Journal of Experimental Botany* 55(396): 307-319.
- [13] Greenway, H., Munns, R. (2003): Mechanisms of salt tolerance in nonhalophytes. – *Annual Review of Phytopathology* 31(4): 149-190.
- [14] Guy, C. L. (1990): Cold acclimation and freezing stress tolerance: role of protein metabolism. – *Annual Review of Plant Physiology and Plant Molecular Biology* 41: 187-223.
- [15] Hannah, M. A., Heyer, A. G., Hinch, D. K. (2005): A global survey of gene regulation during cold acclimation in *Arabidopsis thaliana*. – *Plos Genetics* 1(2): 179-196.
- [16] Hu, Y. C., Schmidhalter, U. (2005): Drought and salinity: a comparison of their effects on mineral nutrition of plants. – *Journal of Plant Nutrition and Soil Science* 168(4): 541-549.
- [17] James, R. A., Rivelli, A. R., Munns, R., von Caemmerer, S. (2002): Factors affecting CO₂ assimilation, leaf injury and growth in salt-stressed durum wheat. – *Functional Plant Biology* 29(12): 1393-1403.
- [18] Kanmani, E., Ravichandran, V., Sivakumar, R., Alagarwamy, S., Krishna Surendar, K., Parasuraman, B. (2017): Influence of plant growth regulators on physiological traits under salinity stress in contrasting rice varieties (*Oryza sativa* L.). – *International Journal of Current Microbiology and Applied Sciences* 6: 1654-1661.
- [19] Lissner, J., Schierup, H.-H. (1997): Effects of salinity on the growth of *Phragmites australis*. – *Aquatic Botany* 55(4).
- [20] Lissner, J., Schierup, H. H., Comin, F. A., Astorga, V. (1999): Effect of climate on the salt tolerance of two *Phragmites australis* populations. I. Growth, inorganic solutes, nitrogen relations and osmoregulation. – *Aquatic Botany* 64(3-4): 317-333.
- [21] Hahn, M., Walbot, V. (1989): Effects of cold-treatment on protein synthesis and mRNA levels in rice leaves. – *Plant Physiology* 91(3).
- [22] Matoh, T., Matsushita, N. (2010): Salt tolerance of the reed plant *Phragmites communis* [halophytes]. – *Physiologia Plantarum* 72(1): 8-14.
- [23] Matsushita, N., Matoh, T. (1991): Characterization of Na⁺ exclusion mechanisms of salt-tolerant reed plants in comparison with salt-sensitive rice plants. – *Physiologia Plantarum* 83(1): 170-176.
- [24] McCoy, T. J. (1987): Tissue culture evaluation of NaCl tolerance in *Medicago* species: cellular versus whole plant response. – *Plant Cell Reports* 6(1).
- [25] Mccree, K. J. (1986): Whole-plant carbon balance during osmotic adjustment to drought and salinity stress. – *Functional Plant Biology* 13(1): 33-43.
- [26] Munns, R. (2005): Genes and salt tolerance: bringing them together. – *New Phytologist* 167(3): 645-663.
- [27] Nguyen, H., Polanco, M. C., Zwiazek, J. J. (2006): Gas exchange and growth responses of ectomycorrhizal *Picea mariana*, *Picea glauca*, and *Pinus banksiana* seedlings to NaCl and Na₂SO₄. – *Plant Biology* 8(5): 646-652.
- [28] Pagter, M., Bragato, C., Malagoli, M., Brix, H. (2009): Osmotic and ionic effects of NaCl and Na₂SO₄ salinity on *Phragmites australis*. – *Aquatic Botany* 90(1): 43-51.
- [29] Pompeiano, A., Di Patrizio, E., Volterrani, M., Scartazza, A., Guglielminetti, L. (2016): Growth responses and physiological traits of seashore paspalum subjected to short-term salinity stress and recovery. – *Agricultural Water Management* 163: 57-65.
- [30] Qi, D., Li, X., Wang, L., Deng, X., Yang, Y., Liu, Y. (2003): Effects of simulated low temperature stress on the protective enzyme system of reactive oxygen species - a case

- study of *Podocarpus fleuryi* Hickel seedlings. – *Journal of Southwest University (Natural Science Edition)*: 25(5): 385-388.
- [31] Renault, S., Croser, C., Franklin, J. A., Zwiazek, J. J. (2001): Effects of NaCl and Na₂SO₄ on red-osier dogwood (*Cornus stolonifera* Michx) seedlings. – *Plant and Soil* 233(2): 261-268.
- [32] Rogers, M. E., Grieve, C. M., Shannon, M. C. (1998): The response of lucerne (*Medicago sativa* L.) to sodium sulphate and chloride salinity. – *Plant and Soil* 202(2): 271-280.
- [33] Seppänen, M. M., Majaharju, M., Somersalo, S., Pehu, E. (1998): Freezing tolerance, cold acclimation and oxidative stress in potato. Paraquat tolerance is related to acclimation but is a poor indicator of freezing tolerance. – *Physiologia Plantarum* 102(3).
- [34] Skinner, D. Z., Bellinger, S. B., Hansen, C. J., Kennedy, C. A. (2014): Carbohydrate and lipid dynamics in wheat crown tissue in response to mild freeze-thaw treatments. – *Crop Science* 54(4).
- [35] Skinner, D. Z., Bellinger, B. S. (2017): Freezing tolerance of winter wheat as influenced by extended growth at low temperatures and exposure to freeze-thaw cycles. – *Canadian Journal of Plant Science* 97(2): 250-256.
- [36] Stushnoff, C., Junttila, O. (1986): Seasonal development of cold stress resistance in several plant species at a coastal and a continental location in North Norway. – *Polar Biology* 5(3): 129-133.
- [37] Swapnil, P., Yadav, A. K., Srivastav, S., Sharma, N. K., Srikrishna, S., Rai, A. K. (2017): Biphasic ROS accumulation and programmed cell death in a cyanobacterium exposed to salinity (NaCl and Na₂SO₄). – *Algal Research* 23: 88-95.
- [38] Türkan, I., Demiral, T. (2009): Recent developments in understanding salinity tolerance. – *Environmental and Experimental Botany* 67(1).
- [39] Vasquez, E. A., Glenn, E. P., Guntenspergen, G. R., Brown, J. J., Nelson, S. G. (2006): Salt tolerance and osmotic adjustment of *Spartina alterniflora* (Poaceae) and the invasive M haplotype of *Phragmites australis* (Poaceae) along a salinity gradient. – *American Journal of Botany* 93(12): 1784-1790.
- [40] Volkmar, K. M., Hu, Y., Steppuhn, H. (1998): Physiological responses of plants to salinity: a review. – *Canadian Journal of Plant Science* 78(1): 19-27.
- [41] Weiser, C. J. (1970): Cold resistance and injury in woody plants. – *Science* 169(3952): 1269-1278.
- [42] Zang, D., Wang, C., Ji, X., Wang, Y. (2015): *Tamarix hispida* zinc finger protein ThZFP1 participates in salt and osmotic stress tolerance by increasing proline content and SOD and POD activities. – *Plant Science* 235: 111-121.
- [43] Zhu, H., Sun, W., Deng, B., Yan, N., Wu, J., Fan, H., Ye, J., Zeng, J., Liu, Y., Zhang, Y. (2007): Study on cold hardiness and its physiological and biochemical characteristics of winter turnip rape (*Brassica campestris*). – *Northwest Agricultural Journal* 16(4): 34-38.

THE RESPONSES OF NET ECOSYSTEM PRODUCTION TO CLIMATE CHANGE: A MODELLING STUDY TO IDENTIFY THE SINK AND SOURCE OF CARBON REGIONS AT THE PAN-EUROPEAN SCALE

SAKALLI, A.

*Department of Industrial Engineering, Faculty of Engineering and Natural Sciences, Iskenderun Technical University, Merkez Kampus, TR-31230 Iskenderun (Hatay), Turkey
(e-mail: abdulla.sakalli@iste.edu.tr; phone: +90-536-506-9191)*

(Received 25th Dec 2019; accepted 25th May 2020)

Abstract. Identifying sinks or sources of CO₂ in the terrestrial biosphere has become an important topic in the last decades. Net Ecosystem Production (NEP) is one of the most used parameters for the understanding and visualization of change in a sink or source of CO₂ under consideration of climate change, and transient CO₂ in modelling and in-situ studies. In this study, NEP was obtained by running the Community Land Model (CLM version 4.5) with 25 × 25 km high spatial resolution between 1971 and 2100. It was focused on analyzing the NEP for two periods (i.e. 1971-2000 as past period and 2071-2100 as future period). Within the study, the model was integrated with used bias corrected six climate parameters and transient CO₂ up to 2100. Validation of the model results showed a quite good correlation (ca. 77%) with observed NEP data. NEP will have an increase up to ca. 118% on an average, at pan-European scale in 2100. Although carbon accumulation in terrestrial biosphere will increase in most of the areas of the pan-European region, the accumulation will decrease in Eastern Europe. These results particularly highlight the spatial and temporal distribution of NEP, and also a significant increase of NEP in the terrestrial biosphere under climate change and transient CO₂ at pan-Europe scale.

Keywords: *ecosystem exchange, biogeochemistry, carbon uptake, dynamic modelling, earth system modelling, operational research, industrial engineering, Industry 4.0*

Introduction

Modelling studies are quite essential research activities for investigations related to changes in the sensitivities of climate, depending on biogeochemical processes in terrestrial biosphere. In the last century, the significance of anthropogenic greenhouse gas emission due to industrial development (from industry 1.0 to Industry 4.0) and climate change effects on carbon cycle in terrestrial biosphere has been increasing, and various researches have been conducted on it. In this topic, Net Ecosystem Production has high importance for clarifying the change in organic carbon storage capacity of terrestrial biosphere. The oldest known modern definition of NEP was published in the late 60s (Woodwell and Whitthaker, 1968). They defined the NEP as the difference between Gross Primary Production (GPP) and ecosystem respiration. NEP is defined as the import of organic carbon in or out of the ecosystems, i.e., increase or decrease of organic carbon via carbon storage in vegetation, sediments, and soils, or the carbon lost through land-use change, fire, respiration, and oxidation, regulate carbon budget between the atmosphere and terrestrial biosphere (Lovett et al., 2006; Hinojo-Hinojo et al., 2019). Ecosystems with $NEP > 0$ are considered as carbon sink ecosystems where carbon binding into the biomass or other organic and non-organic materials is greater than carbon emission (Esser et al., 2011). Also, ecosystems with $NEP < 0$ are considered as carbon source ecosystems where the carbon emission processes greater than carbon storage. A measure of Net Ecosystem Production is of great interest for

investigations to be made of carbon balance between atmosphere and terrestrial biosphere. There are various factors which can affect the NEP in different ecosystems in a timescale, from seconds to millennium (Randerson et al., 2002; Chen et al., 2019; Wong et al., 2020). GPP and ecosystem respiration can have an influence in a timescale from seconds to years, fire and leaching processes from year to decades, and soil formation and erosion from decades to millennium. Esser et al. (2011) also referred to the meaning of studying and analyzing the missing sink of carbon onto the Earth ecosystems during the last century. Their modelling experiments pointed to globally ~160 Pg C missing sink, and it is highly affected by the available nitrogen in terrestrial biosphere during long-term simulations. Climate variability, nitrogen deposition, and plant growth by elevated atmospheric CO₂ are often considered to be the main processes (i.e., in ecological terms, consequences for C fluxes), which have direct relationships with NEP in terrestrial biosphere (Jarvis, 1995; Campbell et al., 2004; Han et al., 2019). There are numerous methods to investigate the effects of atmospheric change on biogeochemical cycles, e.g., carbon exchange between atmosphere and terrestrial biosphere (Turner et al., 2007; Jiang et al., 2013; Liu et al., 2015; Seidensticker et al., 2019; Schulze et al., 2019). Erickson et al. (2013) aimed to measure both direct and indirect effects of elevated ambient CO₂ on NEP using an open top chamber method for eighteen years experiments. Under doubled atmospheric CO₂, the NEP had an increase of about 20-25% in study areas and biomes. NEP is highly depended on plant functional types in terrestrial ecosystem. For instance, needleleaf evergreen forests exchange about six times more carbon than broadleafed deciduous forest (Potter et al., 1993). Grasslands and cultivated crop lands have lower NEP than temperate forests in the northern hemisphere. In an in-situ study of temperate pine plantation, NEP showed a strong dependence on temperature, light regime, and water vapor pressure deficit (Arain and Restrepo-Coupe, 2005; Fernandez-Martinez et al., 2019). A modelling study about NEP under climate change on pan-European scale can indicate the regions of carbon sink or source, and the changes in the sink to source or vice versa. Although there are various studies about carbon sinks/sources by regions or biomes at a global scale, there is little information about carbon sinks/sources in pan-European biomes (Pan et al., 2011; Nabuurs et al., 2013; Fernandez-Martinez et al., 2019). Nabuurs et al. (2013) and Pittau et al. (2019) found valuable signs for saturation of carbon sink in European forests. They observed three types of warnings (i.e., decrease in stem diameter, increase in land-use change, and increase in natural disturbances), which features a decrease in the sink/source ratio in European forests. However, there are still open questions about the behavior of the source and sink of the carbon regions in pan-European forests under climate changes in the future.

In this study, the main aim is to investigate the alteration in potentiality of carbon sink or source of the pan-European forests under climate change of 2100.

Materials and methods

For an estimation of the net ecosystem production, the Community Land Model version 4.5 (Oleson et al., 2013) was established at a pan-European scale on 25 × 25 km grid resolution. The model was run with bias corrected climate data for 800 years, in accelerated mode, to get the main carbon pools of the terrestrial biosphere in a steady state. The methodology of accelerated mode and steady state run (spin-up) was published by Koven et al. (2013). After spinning up of the model, it was run with

required climate data from 1970 to 2100. Two 30 year-periods (1971-2000 and 2070-2100) were taken into account for an investigation of the change of the NEP in the past observed period (1971-2000) since we have bias corrected climate data for this time range and future projected period (2071-2100) at a pan-European scale. To force the model with required climate, six climate parameters (*Table 1*) from the CSC-REMO regional climate model (RCM), driven by MPI-ESM-LR-r1 General Circulation Model (GCM) were used for this modelling study. All climate parameters were bias corrected through a method by Jacob et al. (2013). The conditions of the Representative Concentration Pathway 4.5 (RCM 4.5) scenario are the most plausible conditions that we can reach it under climate change at the end of this century (Jacob et al., 2013). Therefore, we decided to use the RCM model, which was implemented under consideration with regards to the RCP4.5 scenario for prediction of the climate parameter from 2005 to 2100. The CLM model was forced with transient CO₂ for this modelling study. The transient data for CO₂ were obtained from IIASA RCP database (<http://tntcat.iiasa.ac.at/RcpDb>) from 1850 to 2100. The CO₂ data was historical data for the time range 1850-2004, and the projected data for RCP4.5 scenario was from 2005 to 2100.

Table 1. The used climate variable for atmospheric forcing of CLM4.5 model

Code	Variable name as daily mean value (unit)
tas	Surface temperature at 2 m (°C)
pr	Sum of precipitation (mm)
rlds	Surface downwelling longwave radiation ($\frac{W}{m^2}$)
rsds	Surface downwelling shortwave radiation ($\frac{W}{m^2}$)
huss	Near surface specific humidity ($\frac{kg}{kg}$)
sfcWind	Near surface wind speed ($\frac{m}{sn}$)

The CLM4.5 was configured with CLM4.5-CN (i.e., open carbon-nitrogen interaction, no fire, land-use from 2000, and no land-use) component set for enabling full carbon-nitrogen interaction in the model.

The NEP is defined as in *Equation 1* in the model.

$$NEP = GPP - (R_p + R_h + R_d) \quad (\text{Eq.1})$$

where GPP is gross primary production, R_p, R_h, R_d are respiration by plants, heterotrophs, and decomposers, respectively. For statistical analysis, SPSS statistic software (version 23) was used to define the multiple linear regressions between NEP and it used six climate parameters. For this statistical analysis, the average data of pan-European domain were extracted for the time between 1971 and 2100. A total of 130 data sample (1971-2100) for all six climate and NEP were used in the regression analysis.

To validate the results of the model for NEP, a collection of NEP observation data from the research article Arain and Restrepo-Coupe (2005) was used. In the data

collection, there was NEP data from 20 study sites, located in different climate zones on the Earth (*Fig. 1*). Eight locations, situated within the domain of the CLM4.5 in this study, were selected for the validation of the model. The observed NEP data were obtained in different time scales. Therefore, the results of the model were selected for the same time range and locations as the validation processes.

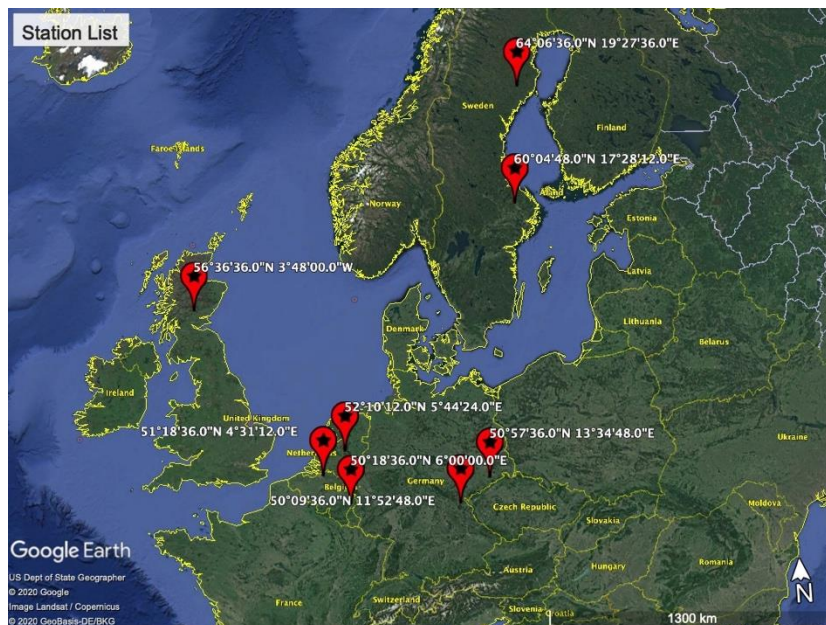


Figure 1. Station locations with the observed NEP data

For the correlation analysis, the index of agreement method was used (Willmott, 1981). The index of agreement method is a standardized measure of the degree of model prediction errors and varies from 0 to 1. The value of 1 indicates a very well agreement of the model results with the observation.

$$d = 1 - \frac{\sum_{i=1}^n (o_i - p_i)^2}{\sum_{i=1}^n (|p_i - \sigma| + |o_i - \sigma|)^2}, \quad 0 \leq d \leq 1 \quad (\text{Eq.2})$$

Results and discussion

Temporal progression of NEP from 1971 to 2100 is plotted in *Figure 2*. It is clearly seen that there is, on an average, an upward tendency in the change of NEP from being carbon source to carbon sink in pan-European regions (*Fig. 2*). In the figure, the trendline show that the NEP has, in average, an increase about $65 \frac{gC}{m^2 \cdot yr}$, which is equal to ca. 118% increase from 1971 to 2100. In the same figure, a remarkable point is that the inter-annual amplitude starts to considerably increase after 2050 up to 2100. The increase of CO₂ in the atmosphere, for different RCP scenarios, is shown in *Figure 3*. The atmospheric CO₂ concentration increases within the RCP4.5 emission scenario from 2000 up to 2080. According to the RCP4.5 scenario, the atmospheric CO₂ concentration has a rapid increase between 2030 and 2060, however, NEP mostly has minimal amplitude, and saturates at a CO₂ concentration between 450 and 550 ppm

during that time range (Fig. 2). That means, an increase in CO₂ expedites total ecosystem respiration more than carbon assimilation in terrestrial biosphere at a pan-European scale. These results match the results of the study about dynamic response of terrestrial biosphere under climate change (Cao and Woodward, 1998).

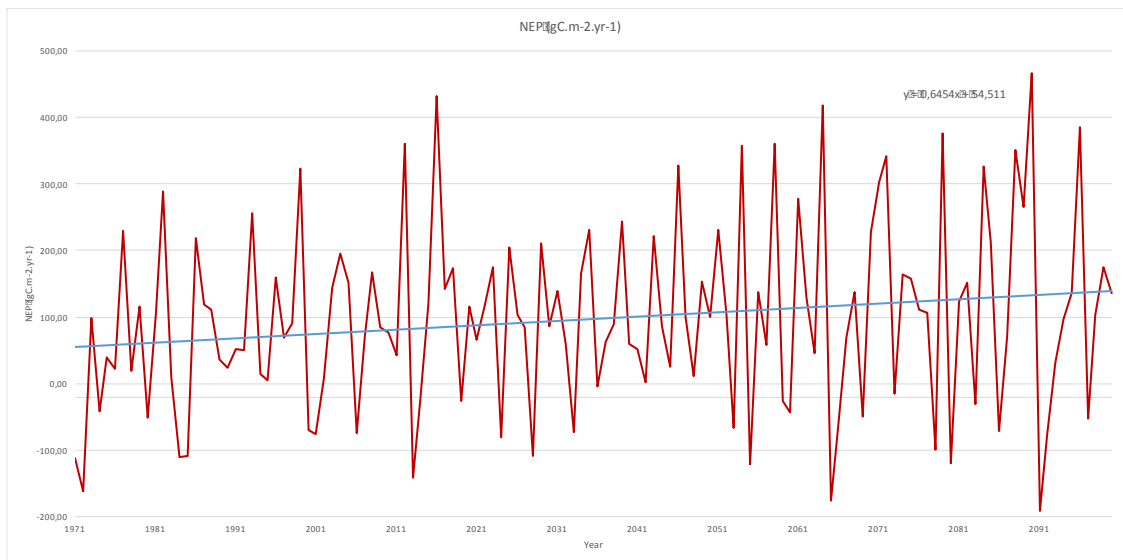


Figure 2. The pan-European average NEP change, which is predicted by CLM4.5 under consideration the RCP4.5 emission scenario from 1971 to 2100

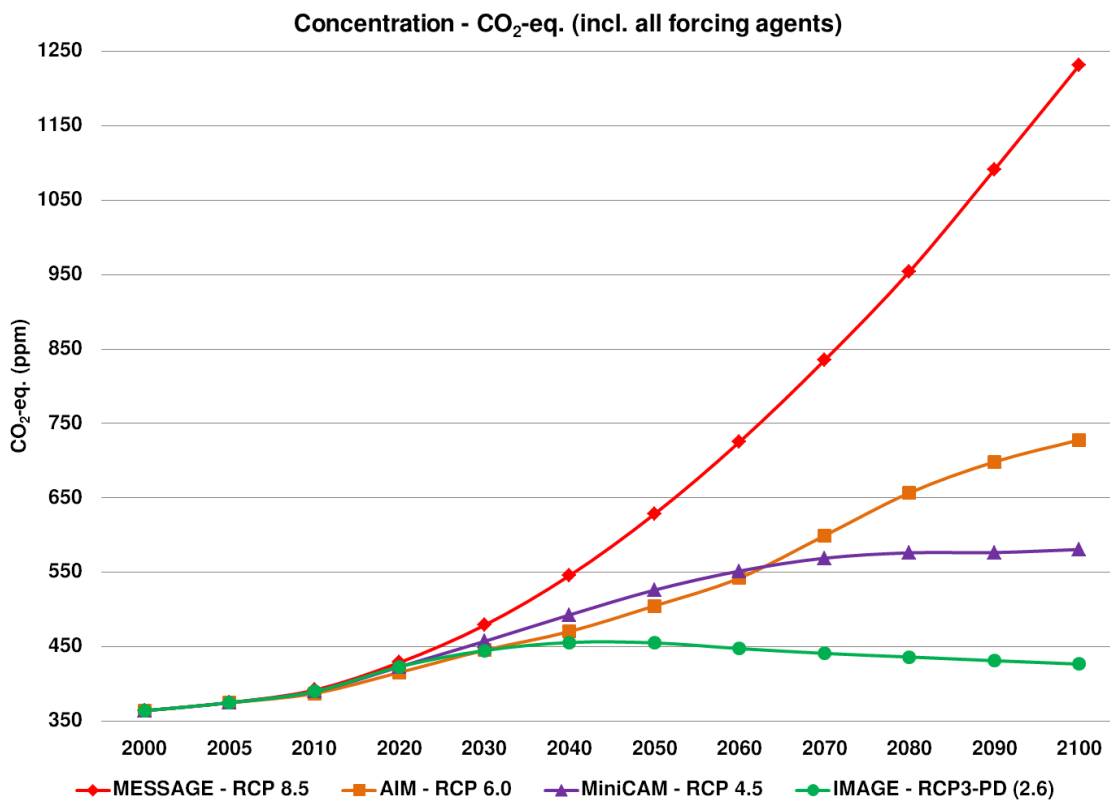


Figure 3. Atmospheric CO₂ concentration under different RCP scenarios from 2000 to 2100

The observed and predicted NEP data are presented with the coordinates of the study sites, the name of the climate zones, and the collection years in *Table 2*. The NEP results of the model were selected for the same locations of the validation data. In *Figure 4*, the correlation scatter plot was presented. The amount of the NEP from different study sites were illustrated with different shape and color. The figure shows that there is quite a good correlation ($R^2 = 0.77$) between observed and predicted NEP in the study sites and times. And also, all the points distributed evenly around the linear regression line. The correlation analysis by using the index of agreement (according to *Eq. 2*) method indicates also very good result ($d = 0.90$).

Table 2. The observed and predicted NEP in different climate zones

Latitude, longitude	Year	Climate zone	NEP Obs. ($\frac{gC}{m^2 \cdot yr}$)	NEP CLM4.5 ($\frac{gC}{m^2 \cdot yr}$)
51.31, 4.52	1997	Temperate	-76	80
	1998		-105	-35
	1999		-130	-185
	2000		-255	-330
	2001		9	40
50.31, 6.0	1997	Temperate	430	391
	1998		435	317
	1999		760	424
	2000		740	372
52.17, 5.74	1997	Temperate	323	448
	1998		338	261
	1999		230	184
	2000		344	151
60.08, 17.47	1995	Boreal	-90	-59
	1996		5	48
	1997		-80	-28
64.11, 19.46	1997	Boreal	173	112
	1998		-53	-17
56.61, -3.8	1997	Temperate	670	326
	1998		570	240
50.96, 13.58	1996	Temperate	330	430
	1997		480	376
	1998		540	273
	1999		628	565
	2000		648	316
50.16, 11.88	1997	Temperate	77	13
	1998		-9	-35
	1999		76	164

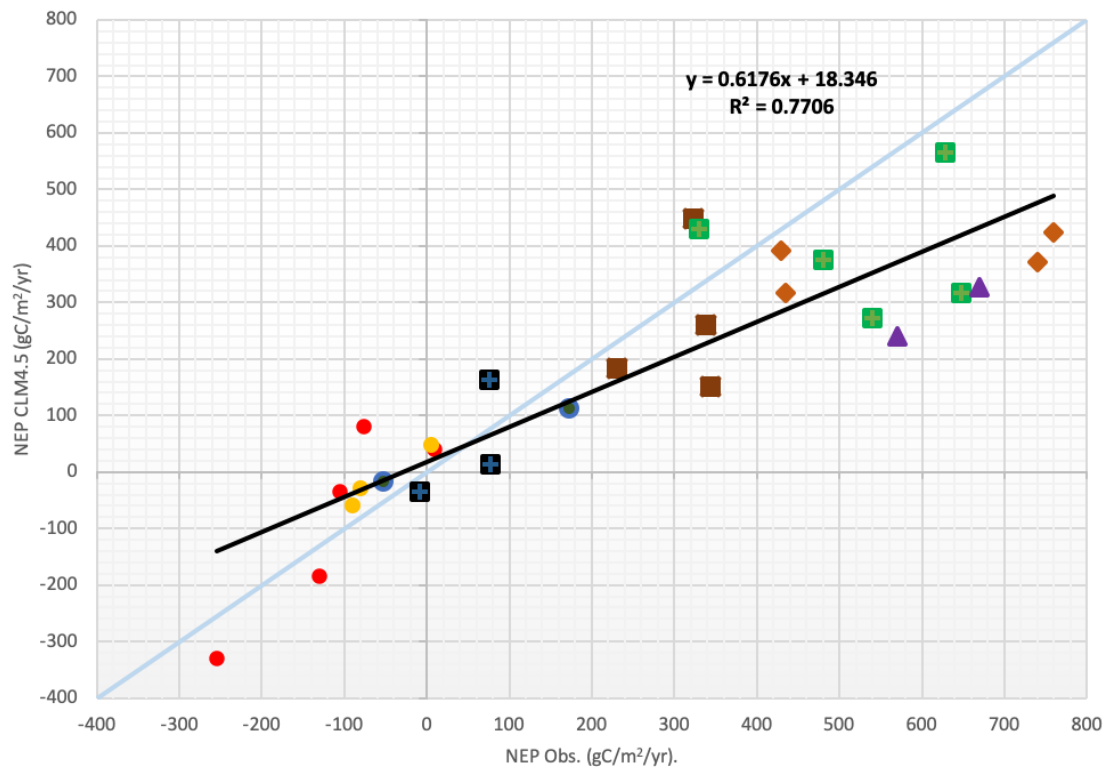


Figure 4. The correlation between observed and predicted NEP in eight study areas, which are located in different climate zones in Europe. The colors indicate each study site location

In this study it is also aimed to find out whether there is a correlation between used six climate variables, atmospheric CO₂ concentration and NEP. The multi regression analysis shows that there is no significant correlation between the climate variables and atmospheric CO₂ in pan-European scale. The considered six climate variable and atmospheric CO₂ concentration explains ca. 7% of variation in NEP of this study, from 1971 to 2100 (*Table 1*). The statistical analysis shows no direct correlation between any single climate variable, CO₂ and NEP (*Table 3*). In similar early studies, the correlation between NEP and climate variables (i.e., temperature and precipitation) was also analyzed in different biome types (Law et al., 2002; Luysaert et al., 2007). They published similar correlation results between the used climate variables and NEP (i.e., no correlation). On the other hand, Magnani et al. (2007) pointed out that the NEP is strongly related to nitrogen deposition, and not to the annual average temperature in both temperate and boreal forests. The inter-annual variability of NEP was well studied in different biome types (Nayak et al., 2015; Baldocchi et al., 2018; Yang et al., 2019). They concluded the study noting that NEP is highly dependent on biome types as well as on annual climatology across the country. Such results refer to study the effects of PFTs on NEP at a pan-European scale.

In *Figure 5*, the 30 years average of NEP on pan-European scale is shown. Most of the regions in pan-Europe are sink for carbon, however, some regions, especially in the central and southern Europe, are sources of carbon (*Fig. 5*). In the source regions, the vegetation types are mainly grasslands and cultivated croplands. Here, the total respiration (i.e., plant, heterotrophs, decomposer) is more dominant than the carbon uptake by GPP (according to the *Eq. 1*). As it is expected, the sink regions of carbon are

mainly in the eastern and southeastern parts of Europe, where the temperate deciduous broadleaved forests are the dominant biome types (Fig. 5). Luysaert et al. (2007) published the results of different measurements techniques for NEP in eight different biome types at a global scale. In their study, the highest NEP was found in temperate humid evergreen forests. The reason behind high NEP is the fact that biome is most probably due to high carbon storage capacity of the managed forests.

Table 3. Multi regression analysis between NEP and used seven variables

Model Summary				
Model	R	R Square	Adjusted R Square	Std. Error of the Estimate
1	.268 ^a	.072	.018	13,894254363

a. Predictors: (Constant), sfcWind (m s-1), pr, rlds (W m-2), rsds (W m-2), CO2 (ppm), huss (kg/kg), tas (K)

ANOVA						
Model		Sum of Squares	df	Mean Square	F	Sig.
1	Regression	1817,899	7	259,700	1,345	.235 ^b
	Residual	23552,137	122	193,050		
	Total	25370,036	129			

a. Dependent Variable: NEP (gC.m-2.yr-1)
b. Predictors: (Constant), sfcWind (m s-1), pr, rlds (W m-2), rsds (W m-2), CO2 (ppm), huss (kg/kg), tas (K)

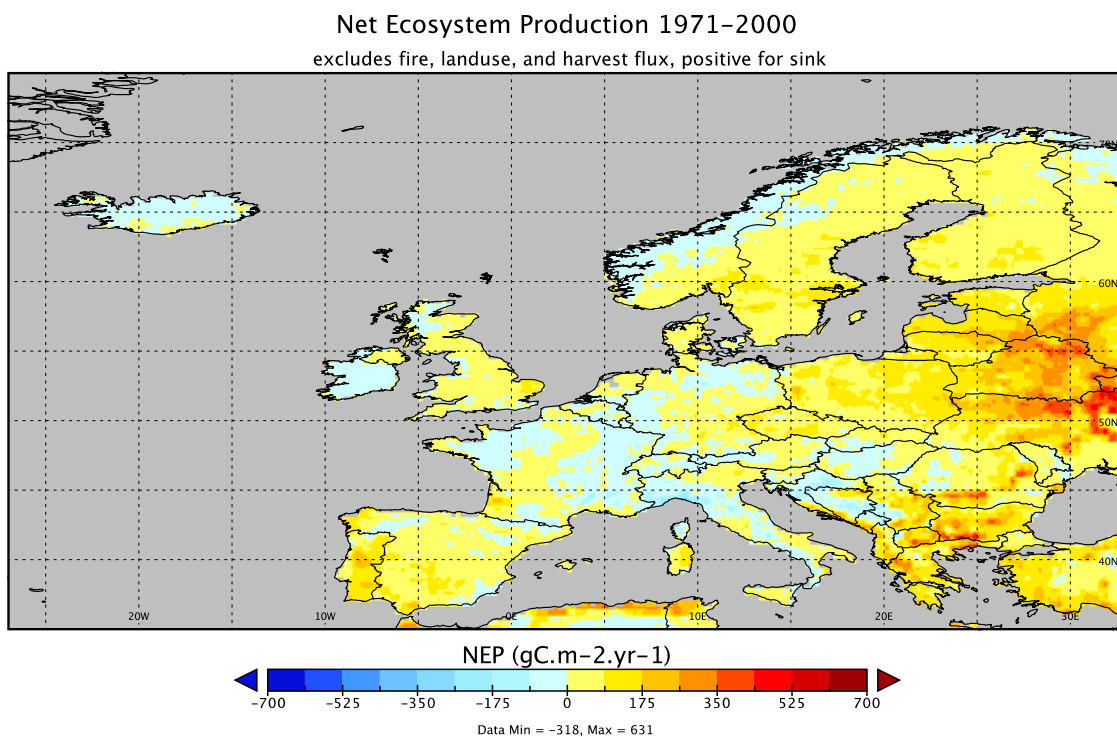


Figure 5. The 30 years (i.e. from 1971 to 2000) average of NEP at pan-European scale

After running the model with climate variables from the CSC-REMO regional climate model (RCM), driven by RCP4.5 emission scenario at a pan-European scale, transient from 2005 to 2100, the result of NEP for 30 years average (i.e. 2071-2100) is shown in Figure 6. In the future projected period, almost all regions and biomes in pan-

Europe are shown as sink for carbon (Fig. 6). Only a few regions (mountain regions in Norway, in the Alps, and some localities in Spain) are predicted as the source for carbon by the CLM4.5 model under consideration of the RCP4.5 emission scenario (Fig. 6). It is interesting to see that the highest NEP is predicted in the Balkan regions, where mostly temperate broadleaved deciduous forest are noted, and also southern Europe, which shows higher carbon capture capacity than the other regions in Europe during the future period (comparing Figs. 5 and 6). Those ecosystems show a wide carbon storage ability in the future.

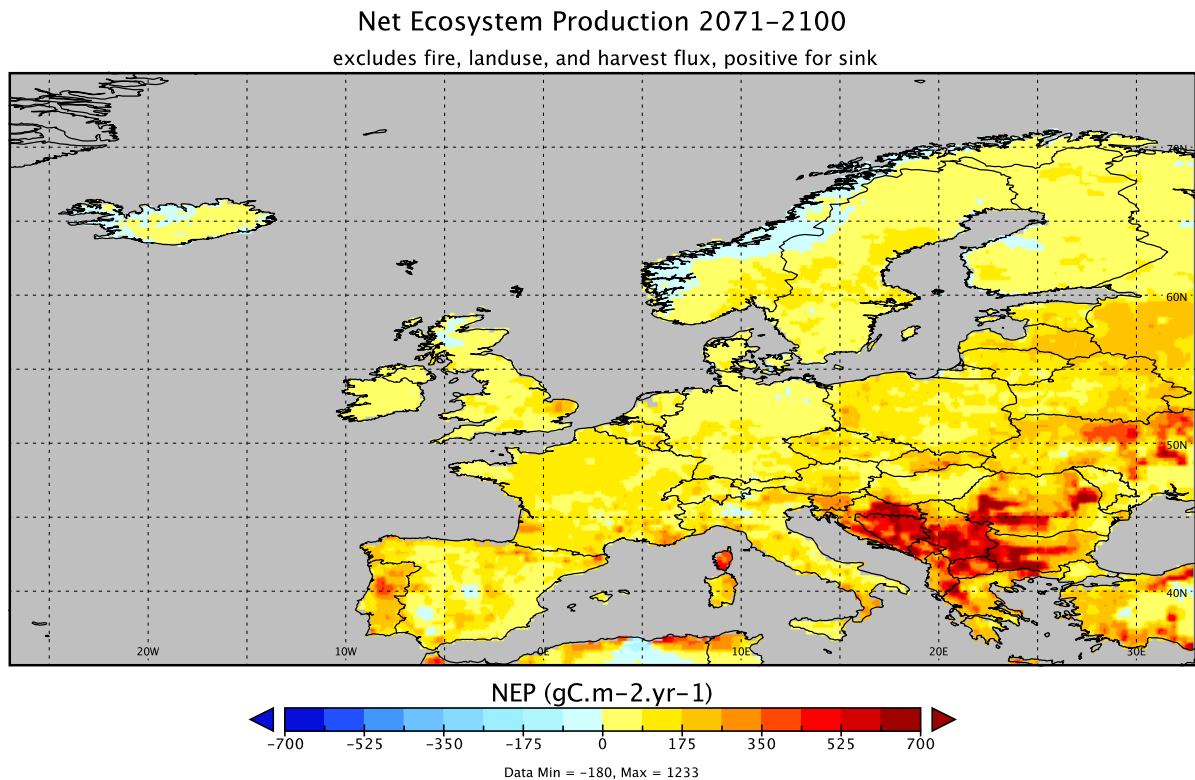


Figure 6. The 30 years (2071–2100) average of NEP at pan-European scale having regard to RCP4.5 emission scenario

The absolute change in NEP, that is, the difference between the past period (1971–2000) and future projected period (2071–2100) is shown at pan-European level in Figure 7. This remarkable result is the absolute change of NEP in Eastern and Southeastern Europe. Although most of the pan-European regions are predicted as sink regions for carbon in the future projected period, the analysis about absolute change in NEP shows that carbon storage capacity of eastern temperate broadleaved deciduous forests will decrease by about $30 \frac{gC}{m^2 \cdot yr}$ (~10%) in the future (Fig. 7). It seems that the ecosystem of this regions could be carbon-saturated under climate change and rising CO₂ at the end of the 21st century (Nabuurs et al., 2013; Dirnböck et al., 2020). Those forests currently have the highest carbon storage capacity at a pan-European level. In the past period, the forests in that regions had ca. $178 \frac{Pg}{yr}$ (1 Pg = 10¹² g) carbon storage capacity, however, in the future projected period, it decreases to ca. 166 Pg. It shows

that these forests will store ca. $12 \frac{Pg}{yr}$ less carbon than what it stores today. In the whole pan-European domain, the carbon storage capacity of the vegetated areas will increase under climate change at the end of the 21st century. While the carbon storage capacity of the vegetated regions of pan-European studied domain was, on an average, ca. $0.57 \frac{Gt}{yr}$ in the past period, it will increase up to $0.91 \frac{Gt}{yr}$ in the future period. That shows that the vegetated areas in pan-European domain will store ca. 37% more carbon at the end of the 21st century.

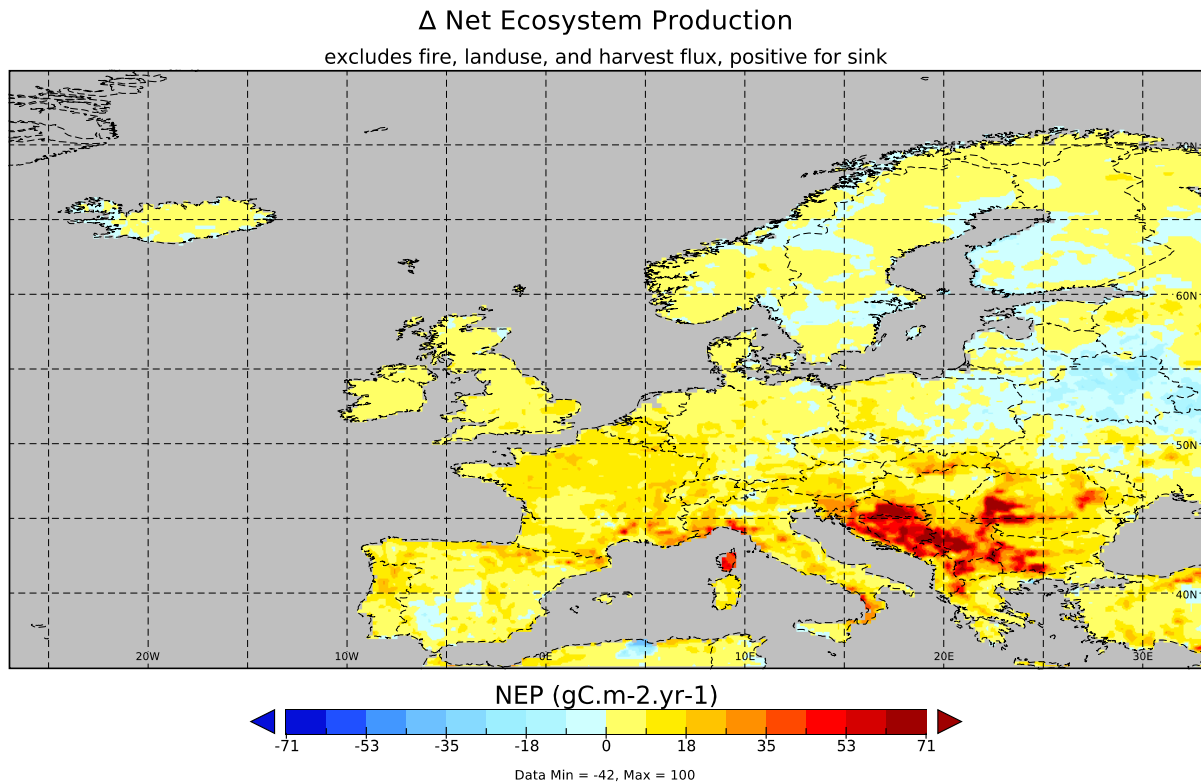


Figure 7. The relative difference between past and future predicted periods (i.e. 1971-2000 and 2071-2100)

Conclusion

In this study, the main aim was to find the information about the temporal and spatial change in carbon storage capacity of the vegetated areas at a pan-European scale. In general, the pan-European vegetated regions will be considered to be sink areas for carbon. Nearly 1 Gt C will be stored in the biomass of European vegetation under climate change, by considering the emission scenario RCP4.5 each year. Although the carbon storage capacity of pan-European vegetation will increase in most of the regions, the forests of Eastern Europe show a downward tendency for the accumulation of carbon in the ecosystem. In those regions, the ecosystem shows a trend to lose nearly 12 Pg C each year. Furthermore, multiple regression analysis shows no correlation between NEP and used seven variables. The results of this study point to the importance of the investigations of temporal and spatial change in carbon storage capacity of European forests. That will help the researcher to understand the action of forests for being carbon

source or sink under different climate change scenarios in the future. For the future studies, we are planning to collect more observation data and run the model at global scale to define the carbon sink and source locations.

Acknowledgements. The research has received funding from the scientific and technological research council of Turkey (TUBITAK agreement nr: 2017O394).

REFERENCES

- [1] Arain, M. A., Restrepo-Coupe, N. (2005): Net ecosystem production in a temperate pine plantation in southeastern Canada. – *Agricultural and Forest Meteorology* 128: 223-241.
- [2] Baldocchi, D., Chu, H., Reichstein, M. (2018): Inter-annual variability of net and gross ecosystem carbon fluxes: a review. – *Agricultural and Forest Meteorology* 249: 520-533.
- [3] Campbell, J. L., Sun, O. J., Law, B. E. (2004): Disturbance and net ecosystem production across three climatically distinct forest landscapes. – *Global Biogeochemical Cycles* 18 GB4017: 1-11.
- [4] Cao, M., Ian Woodward, F. (1998): Dynamic responses of terrestrial ecosystem carbon cycling to global climate change. – *Nature* 393: 249-252.
- [5] Chen, Z., Yu, G., Wang, Q. (2020): Effects of climate and forest age on the ecosystem carbon exchange of afforestation. – *Journal of Forestry Research* 31: 365-374.
- [6] Dirnböck, T., Grote, R., Klatt, S., Kobler, J., Schindlbacher, A., Seidl, R., Thom, D., Kiese, R. (2020): Substantial understory contribution to the C sink of a European temperate mountain forest landscape. – *Landscape Ecology* 35: 483-499.
- [7] Erickson, J. E., Peresta, G., Montovan, K. J., Drake, B. G. (2013): Direct and indirect effects of elevated atmospheric CO₂ on net ecosystem production in a Chesapeake Bay tidal wetland. – *Global Change Biology* 19: 3368-3378.
- [8] Esser, G., Kattge, J., Sakalli, A. (2011): Feedback of carbon nitrogen cycles enhances carbon sequestration in the terrestrial biosphere. – *Global Change Biology* 17(2): 819-842.
- [9] Fernandez-Martinez, M., Sardans, J., Chevallier, F., Ciais, P., Obersteiner, M., Vicca, S., Canadell, J. G., Bastos, A., Friedlingstein, P., Stich, S., Piao, S. L., Janssens, I. A., Penuelas, J. (2019): Global trends in carbon sink and their relationship with CO₂ and temperature. – *Nature Climate Change* 9: 73-79.
- [10] IIASA (2014): International Institute for Applied System Analysis. RCP database version 2.0.5. – <http://tntcat.iiasa.ac.at/RcpDb> (accessed 15 June 2014).
- [11] Jacob, D., Petersen, J., Eggert, B., Alias, A., Christensen, O. B., Bouwer, L. M., Braun, A., Colette, A., Deque, M., Georgievski, G., Georgopoulou, E., Gobiet, A., Menut, L., Nikulin, G., Haensler, A., Hempelmann, N., Jones, C. et al. (2013): EURO-CORDEX: new high-resolution climate change projections for European impact research. – *Regional Environmental Change* 14(2): 563-578.
- [12] Jarvis, P. G. (1995): The role of temperate trees and forests in CO₂ fixation. – *Vegetatio* 121(1): 157-174.
- [13] Jiang, Z., Lian, Y., Qin, X. (2013): Carbon cycle in the epikarst systems and its ecological effects in South China. – *Environmental Earth Sciences* 68: 151-158.
- [14] Han, P., Lin, X., Zhang, W., Wang, G., Wang, Y. (2019): Projected changes of alpine grassland carbon dynamics in response to climate change and elevated CO₂ concentrations under Representative Concentration Pathways (RCP) scenarios. – *PLoS ONE* 14(7): e0215261.
- [15] Hinojo-Hinojo, C., Castellanos, A. E., Huxman, T., Rodriguez, J. C., Vargas, R., Romo-Leon, J. R., Biederman, J. A. (2019): Native shrubland and managed buffelgrass savanna

- in drylands: Implications for ecosystem carbon and water fluxes. – *Agricultural and Forest Meteorology* 268: 269-278.
- [16] Koven, C. D., Riley, W. J., Subin, Z. M., Tang, J. Y., Torn, M. S., Collins, W. D., Bonan, G. B., Lawrence, D. M., Swenson, S. C. (2013): The effect of vertically resolved soil biogeochemistry and alternate soil C and N models on C dynamics of CLM4. – *Biogeosciences* 10: 7109-7131.
- [17] Law, B. E., Flage, E., Gu, L., Baldocchi, D. D., Bakwin, P., Berbigier, P., Davis, K., Dolman, A. J., Falk, M., Fuentes, J. D., Goldstein, A., Granier, A., Grelle, A., Hollinger, D., Janssens, I. A., Jarvis, P., Jensen, N. O., Katul, G., Mahli, Y., Matteucci, G., Meyers, T., Monson, R., Munger, W., Oechel, W., Olson, R., Pilegaard, K., Paw U. K. T., Thorgeirsson, H., Valentini, R., Verma, S., Vesala, T., Wilson, K., Wofsy, S. (2002): Environmental controls over carbon dioxide and water vapor exchange of terrestrial vegetation. – *Agricultural and Forest Meteorology* 113: 97-120.
- [18] Liu, J., Feng, W., Zhang, Y-Q., Jia, X., Wu, B., Qin, S., Fa, K., Lai, Z. (2015): Abiotic CO₂ exchange between soil and atmosphere and its response to temperature. – *Environmental Earth Sciences* 73: 2463-2471.
- [19] Lovett, G. M., Cole, J. J., Pace, M. L. (2006): Is net ecosystem production equal to ecosystem carbon accumulation? – *Ecosystems* 9: 152-155.
- [20] Luysaert, S., Inglima, I., Jung, M., Richardson, A. D., Reichstein, M., Papale, D., Piao, S. L., Schulze, E. D., Wingate, L., Matteucci, G., Aragao, L., Aubinet, M., Beer, C., Bernhofer, C., Black, K. G., Bonal, D., Bonnefond, J. M., Chambers, J., Ciais, P., Cook, B., Davis, K. J., Dolman, A. J., Gielen, B., Goulden, M., Grace, J., Granier, A., Grelle, A., Griffis, T., Grünwald, T., Guidolotti, G. et al. (2007): CO₂ balance of boreal, temperate, and tropical forests derived from a global database. – *Global Change Biology* 13: 2509-2537.
- [21] Magnani, F., Mencuccini, M., Borghetti, M., Berbigier, P., Berninger, F., Delzon, S., Grelle, A., Hari, P., Jarvis, P. G., Kolari, P., Kowalski, A. S., Lankreijer, H., Law, B. E., Lindroth, A., Loustau, D., Manca, G., Moncrieff, J. B., Rayment, M., Tedeschi, V., Valentini, R., Grace, J. (2007): The human footprint in the carbon cycle of temperate and boreal forests. – *Nature* 447: 848-850.
- [22] Nabuurs, G.-J., Lindner, M., Verkerk, P. J., Gunia, K., Deda, P., Michalak, R., Grassi, G. (2013): First signs of carbon sink saturation in European forest biomass. – *Nature Climate Change* 3: 792-796.
- [23] Nayak, R. K., Patel, N. R., Dadhwal, V. K. (2015): Spatio-temporal variability of net ecosystem productivity over India and its relationships to climatic variables. – *Environmental Earth Sciences* 74: 1743-1753.
- [24] Oleson, K., Lawrence, D., Bonan, G., Drewniak, B., Huang, M., Koven, C., Levis, S., Li, F., Riley, W., Subin, Z., Swenson, S., Thornton, P., Bozbiyik, A., Fisher, R., Heald, C., Kluzek, E., Lamarque, J-F., Lawrence, P., Leung, L., Yang, Z-L. (2013): Technical description of version 4.5 of the Community Land Model (CLM). – NCAR Technical Note NCAR/TN-503+STR, National Center for Atmospheric Research, Boulder, CO.
- [25] Pan, Y., Birdsey, R. A., Fang, J., Houghton, R., Kauppi, P. E., Kurz, W. A., Phillips, O. L., Shvidenko, A., Lewis, S. L., Canadell, J. G., Ciais, P., Jackson, R. B., Pacala, S. W., McGuire, A. D., Piao, S., Rautiainen, A., Sitch, S., Hayes, D. (2011): A large and persistent carbon sink in the world's forests. – *Science* 333: 988-992.
- [26] Pittau, F., Lumia, G., Heeren, N., Iannaccone, G., Habert, G. (2019): Retrofit as a carbon sink: the carbon storage potentials of the EU housing stock. – *Journal of Cleaner Production* 214: 365-376.
- [27] Potter, C. S., Randerson, J. T., Field, C. B., Matson, P. A., Vitousek, P. M., Mooney, H. A., Klooster, S. A. (1993): Terrestrial ecosystem production: a process model based on global satellite and surface data. – *Global Biogeochemical Cycles* 7(4): 811-841.

- [28] Randerson, J. T., Chapin, F. S., Harden, J. W., Neff, J. C., Harmon, M. E. (2002): Net ecosystem production: a comprehensive measure of net carbon accumulation by ecosystems. – *Ecological Applications* 12(4): 937-947.
- [29] Seidensticker, L. E., Najjar, R. G., Herrmann, M., Boyer, J. N., Briceno, H. O., Kemp, W. M., Tomaso, D. J. (2019): Seasonal and interannual variability in net ecosystem production of a subtropical coastal lagoon inferred from monthly oxygen surveys. – *Estuaries and Coasts* 42: 455-469.
- [30] Schulze, E-D., Beck, E., Buchmann, N., Clements, S., Müller-Hohenstein, K., Scherer-Lorenzen, M. (2019): Biogeochemical fluxes in terrestrial ecosystems. – *Plant Ecology* 16: 529-577.
- [31] Turner, D. P., Ritts, W. D., Law, B. E., Cohen, W. B., Yang, Z., Hudiburg, T., Campbell, J. L., Duane, M. (2007): Scaling net ecosystem production and net biome production over a heterogeneous region in the western United States. – *Biogeosciences* 4: 597-612.
- [32] Wong, G. X., Hirata, R., Hirano, T., Kiew, F., Aeries, E. B., Musin, K. K., Waili, J. W., Lo, K. S., Melling, L. (2020): How do land use practices affect methane emissions from tropical peat ecosystems? – *Agricultural and Forest Meteorology* 282-283: 107869.
- [33] Woodwell, G. M., Whittaker, R. H. (1968): Primary production in terrestrial ecosystems. – *Am Zoologist* 8: 19-30.
- [34] Yang, F., Zhang, Q., Zhou, J., Yue, P., Wang, R., Wang, S. (2019): East Asian summer monsoon substantially affects the inter-annual variation of carbon dioxide exchange in semi-arid grassland ecosystem in Loess Plateau. – *Agriculture, Ecosystems & Environment* 272: 218-229.

GROWTH AND FLOWERING OF ENDEMIC WILD LIBYAN GEOPHYTE, *CYCLAMEN ROHLFSIANUM* ASCHER, WITH A HIGH ORNAMENTAL VALUE

KHALAFALLA, M. M.¹ – MENESY, F.¹ – MAGOUZ, M. R.² – HAMED, E. B.^{3*}

¹Hort. Dept., Fac. Agric., Kafrelsheikh Univ., Kafrelsheikh 33516, Egypt

²Hort. Res. Inst., Agric. Res. Center, Giza, Egypt

³Hort. Dept., Fac. Agric., Al-Bieda Univ., El Bieda, Libya

*Corresponding author

e-mail: Eman.B.A.Hamed@gmail.com

(Received 31st Dec 2019; accepted 6th May 2020)

Abstract. Seeds of *Cyclamen rohlfsianum* showed high germination percentage ($88 \pm 4\%$), followed by a rapid development of the fat hypocotyl during 29-35 days of growth and the lastly, one leafy cotyledon emerged from the seed coat. In the present study we measured the annual increments of leaves and tuber size in seedlings of the common geophyte ornamental perennial endemic Libyan, *C. rohlfsianum*, predicted by shrubs in their native habitat, over 6-year growing period. The results showed that the tuber fresh weight and diameter varied with the age of the plants, depending on the leaf number and area. These slowly increased for the first 3 years, then at a more rapid rate for the following 2 years with the highest reached at 6 years. Flowering did not occur until number of leaves and total leaf area were at least 3 and 49 cm², respectively. The vegetative tuber size of 6.15 g fresh weight and 2.8 cm diameter, (4-year-old plants) were probably large enough to produce, in the next year (5th year of growing period), three or more flowers (3.5 ± 0.9) and thereafter, more than three leaves emerged (3.76) whereas, $79 \pm 3.5\%$ of plants flowered. However, flowering tuber size sharply increased to 21.27 g and 5.49 cm, respectively for 6-year-old plants, which were associated with increases in flowering percentage ($98 \pm 7\%$), number of flowers (4.3 ± 0.4) and total leaf area (111.78 cm²).

Keywords: germination, seedling growth, flowering tuber size, hysteroanthous, floral trunks

Introduction

The genus *Cyclamen* L. (Myrsinaceae formerly Primulaceae) consists of 22 species (Grey-Wilson, 2002), which are distributed in and near the Mediterranean region and western Asia. It is an attractive plant with potential as a commercial flowering pot plant and garden plants (Dole and Wilkins, 2005). Although cyclamens are dicotyledonae, the embryo consists of only a single cotyledon (pseudomonocotyledonae) (Le Nard and De Hertogh, 1993a).

Cyclamen is classified either according to the flowering periods or by their growth cycle. Flowering periods vary with the species, but can be divided into two groups: autumn flowering (*C. africanum*, *C. cilicicum*, *C. graecum*, *C. cyprium*, *C. hederifolium*, and *C. rohlfsianum*) and spring flowering (*C. balearicum*, *C. orbiculatum*, *C. persicum*, *C. pseudibericum*, and *C. repandum*). The growth cycle classification is based on the appearance of the flowers and leaves. Group 1, the synanthous growth, in which flowering occurs after the appearance of leaves, e.g., *C. persicum*. In group 2, the hysteroanthous growth, in which flowering occurs before leaf emergence, e.g., *C. rohlfsianum*, *C. cilicicum*.

A tetraploid *Cyclamen rohlfsianum* (Sibusawa and Ogawa, 1997; Grey-Wilson, 2002) is endemic to Al-Jabal Al-Akhdar and locally known as “Racuf” (El-Darier and El-Mogaspi, 2009). It is one of the most beautiful ornamental perennial geophytes in Libya. Such tetraploid cyclamen ($2n = 4x = 96$) offers useful opportunities to produce new varieties from which can be improve this crop.

Environmental conditions, especially temperature, control annual development and florogenesis in geophytes (Le Nard and De Hertogh, 1993b). Autumn flowering *Cyclamen* of the Mediterranean region are adapted to warm environmental conditions (tender plants). Therefore, tubers flowering in September-November before leaf emergence, when soil temperature decreases. Thereafter, leaves grow and accumulate metabolic reserves throughout the wet and cool season (autumn to spring), until the dormancy period, which begins in late spring. Hence, during summer the flowers initiation and differentiation occur in the mature tubers (Rees, 1992; Le Nard and De Hertogh, 1993b).

Extensive studies have been conducted for elucidation of the growth habit, flowering and production of commercially important *C. persicum* (Sundberg, 1981a, b, 1982; Karlsson and Werner, 2001; Takamura, 2007; Oh et al., 2008) while, little is known for most other species in this genus (Affre and Thomson, 1999; Muftuoglu et al., 2009; Seyring et al., 2009; Lazarevic and Lazarevic, 2010; Jalali et al., 2012; Curuk et al., 2015, 2016; Mammadov et al., 2016). In addition, no precise information is available for wild tuber of *C. rohlfsianum* (Grey-Wilson, 2002).

In natural conditions, observations reported that *C. rohlfsianum* is grown in well-drained soil and prefers shady locations (shade of sheltering rocks or bushes). Leaves are rounded to kidney-shaped, (usually hearted in young plants), sometimes toothed or broadly triangular lobed, deep green, to 12cm diameter, patterned pale grey or silvery green patterns above, and purplish red below (Fig. 1). The leaves have long, brownish-purple petioles arising from the crown (12-25 cm).



Figure 1. The leaves broadly triangular lobes, toothed margin, deep green above with pale grey blotch marks. Right: note leaf emergence after flowering, sometimes one or two flowers appearing with the mature leaves. Left: not the new fruit capsule, drawn down to the soil surface by the coiling of the pedicel

The pink flowers of 2.5-3.5 cm long (Fig. 2), are solitary on leafless scapes (pedicels) 6-13 cm in height, each have five reflexed petals, sometimes twisted, whose bases constitute a short tube, with deep maroon mouth ‘eye’ and projecting anthers (1.0-

1.5 cm). The fruit is a capsule, drawn down to the soil surface by the coiling of the pedicel to release the rip dark brown and dry seeds (*Fig. 3*).



Figure 2. The mature tuber, nodding flowers arise from several growing points (right) in September-November before leaf emergence, note pink flowers, with deep maroon mouths and the stamen cone with long style protruding from the mouth of the corolla (left)



Figure 3. The tuber grows among rocks and beneath bushes in the wild, it has a depression in the top and roots produced from sides and the center of the base, note the ten flowers appearing from one growth point of 6-year-old tuber (right). The fruit capsule on tightly coiled pedicel at the top of floral trunk (left)

The tuber is generally large and corky fleshy and continue to enlarge laterally every year. The size of mature tubers can reach more than 30 cm in diameter. It is more or less globose in form, often regular and becomes very irregular by time and consists of several swollen legs joined together by narrower ‘necks’ of tissue. Young tubers generally have a single growing point on the upper surface (those producing flowers and

leaves), but as they age the growing point divides and may eventually end up well separated and confined on the upper surface of the tubers. Some mature tubers produced slender woody necks (these are called floral trunks) by elongation of the growing points, which have the flowers and leaves at the tip (Figs. 3 and 4); though it is often associated with plants that grow in rather rocky soils, especially in woodland or on screes. It happens also, when the growing points become widely spaced and the tubers become increasingly irregular, especially when they become squeezed between rocks. Roots are produced at the base and lower sides of the tuber (Widmer, 1992; Le Nard and De Hertogh, 1993a; Grey-Wilson, 2002).

The growth of geophytes is generally considered to be quite slow and usually need to reach a certain size before they can be used for flowering pot plant production (Le Nard and De Hertogh, 1993b). Therefore, during six consecutive years, this study initiated to determine the period from sowing to flowering tuber of *Cyclamen rohlfsianum* under the native habitat.



Figure 4. *Cyclamen rohlfsianum* self-sown, Al-Jabal Al-Akhdar, East of Libya, where it is a common wild plant (note three seedlings)

Materials and methods

The present research was conducted at the laboratory of Department of Horticultural, Faculty of Agriculture, Omar Al-Moukhtar University, Al-Bieda for the laboratory experiments, but the field experiments were carried out in private farm at Al-Bieda located at Al-Jabal Al-Akhdar region, Libya (30°33'N latitude and 20°25'E longitude at an altitude 590 m above the mean sea level). Mean monthly temperature, and rainfall at the study site for 6 years (2014-2019) were recorded daily at the Shahat meteorological station (Fig. 5).

Germination and seedling growth

Seeds of *C. rohlfsianum* used in the present study were collected between March and April 2013, before the leaves begin to be yellow, separated and stored at 4 °C until sown in early September. They were washed three times with a tap water and sown into plastic trays with 200 of 3 × 3 cm cells filled with a mixture of vermiculite and peat (1:1 by volume). The trays were placed at a private nursery greenhouse and covered with

black polyethylene sheet until commencement of germination, where the minimum temperature was maintained at 15 °C.

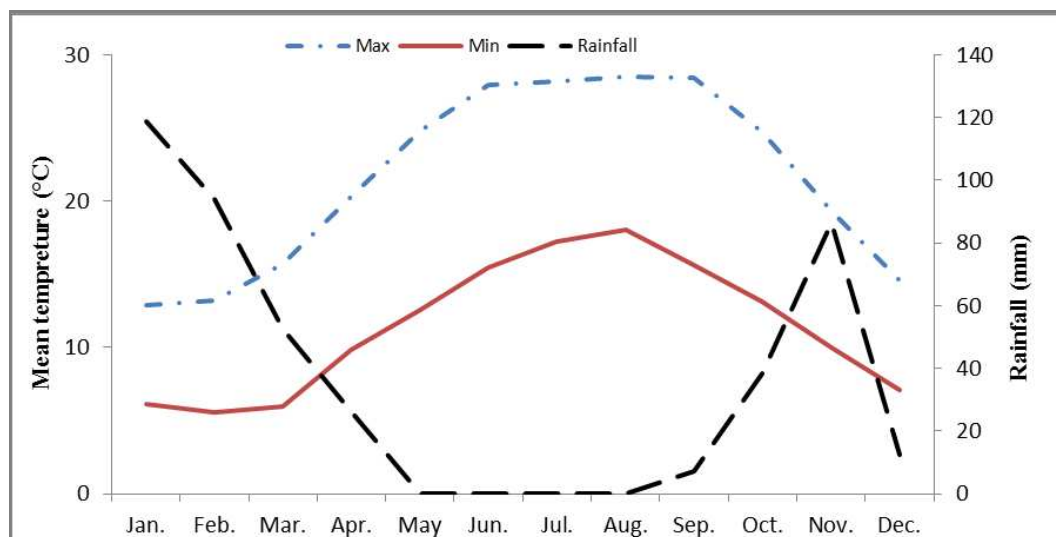


Figure 5. Monthly rainfall and air temperature. Air temperature represents the average daily maxima (Max) or daily minima (Min) during the study period (2014-2019)

The seed germination criterion was noticed as visible protrusion on the surface of soil at least 0.5 cm of the expanded hypocotyl of seedling. Germination was noted periodically every week from the date of sowing and continued till the germination ceased with final germination percentages recorded by using three replicates, each replicate contained 2 trays.

For studying the characteristics of seed germination during imbibition period, seeds were germinated in 9 cm petri dishes on moistened filter paper placed in dark place at room temperature of 22 ± 2 °C. Three replicates of 25 seeds per dish were used. Number of days from sowing to commencement of germination during imbibition period (emergence of the radicle), elongation of the hypocotyl, initial development of the primary root, protrusion the cotyledon blade and germination period were recorded.

Data for germination and seedling growth were expressed as mean \pm standard deviation for 18 measurements in each replicate.

Field studies

To determine the period from seed germination to flowering tuber *Cyclamen rohlfsianum* under field conditions, 65-day-old seedlings were transplanted from trays to their native habitat protected by shrubs (*Pistacia lentiscus* and *Juniperus phoenicia*). The seedlings were planted in fine tilth soil (well-drained, dark reddish brown and friable clay soils) at a depth of 1.5 to 2 cm in the three growing beds of 1.5×3 m, approximately 0.5 m apart between beds. The spacing and density used were 15 cm between seedlings with 10 seedlings in a single row, respectively. Light intensity in the planes of plants beneath bushes averaged about 47 klx, during most of the growing season (measured with a light meter, ST-85 Auto-range illuminance meter, Beijing, China). In addition to natural rainfall, (between October and April; Fig. 5), plants were irrigated in October-November and March-April once every 10 days.

Soil samples were collected at random from the site, air-dried, crushed and analyzed for chemical properties according to Jackson (1967) (0.25% total N, 10.96 ppm available P, 17.21 ppm available K, 4.79% calcium carbonate and 6.48% organic matter). The pH and electrical conductivity of the soil solution prepared by diluting the soil with water (1:1, v/v) were measured using digital pH and EC meters (7.8 and 0.75 mS/cm, respectively). Seedlings were monthly fertilized once with 200 g/bed kristalon (19N:19P:19K) beginning from the second year from October till April.

During six consecutive years, vegetative parameters were recorded in early March when leaves were still green (length of leaf petioles (cm) and total leaf area (cm²) and number). The total leaf area was measured with, CI-202 laser area meter, made in USA. Sixty tubers (two rows for each bed) were harvested in mid-May, after leaf yellowing. The medium was washed off roots and the expanded hypocotyl (stem tuber) then fresh weight (g) and diameter (cm) of tuber were determined.

After 5 years from sowing, when flowering occurred in September-November, percentage of flowering, number of flowers per plant and length of flower pedicels (cm) (at first reflexed petal) were recorded.

The experiment was arranged in randomized complete block design, as included 6 years each consisted of 20 plants and replicated three times. Data were analyzed using analysis of variance and means were compared according to Duncan's multiple range test at 0.05 level (Snedecor and Cochran, 1980).

Results

Germination and seedling growth

Seeds of *C. rohlfsianum* showed high percentage of germination. Although at 26 days (imbibition period) germination was $37 \pm 3\%$, (radicle emergence) thereafter, becomes increasingly evident until maximum germination, of $88 \pm 4\%$, was reached after approximately 32 days from sowing (total germination period).

After seeds germinate, the radicle extended within 26-32 days from seeding and a definite swelling on the hypocotyl became apparent during 29-35 days. The great increase in length during this period resulted from a rapid elongation of the hypocotyl and the initial development of the primary root. The hypocotyl was several times larger in diameter (3.2 ± 0.3 mm) than the radicle. The primary root at this age was well developed and was 2.5 ± 0.5 cm long with one or more lateral roots (*Fig. 6*).

At 9 days (after the hypocotyls were apparent) the one leafy cotyledon showed rapid elongation and remained tightly coiled in seed coat. Thereafter, at 13 days, the cotyledons had uncoiled and rapid increase in length to maximum elongation of 2.6 ± 0.4 cm, during 5 days.

Field studies: leaf and tuber development and flowering

Changes in leaf number and total leaf area of plants (planted under the nurse shrubs in the field) were monitored over a 6-year growing period to flowering.

Number of leaves on plant (*Fig. 7*) was assumed to be constant during the first 3 years of growth (1.16-2.0 leaves), whereas 4, 5 and 6-year-old ones have three or more leaves and reached a maximal (4.21) at six year-old plants, which was significantly the largest over the past 5 years.



Figure 6. Germination and seedling of *Cyclamen rohlfsianum*. a: The radicle extended with 26 days after the seeds were moistened, b: A short, fat hypocotyl (tiny tuber) became apparent during 29 days (note the cotyledon still tightly coiled in the seed coat), c: The initial development of the primary roots, 30 days after sowing, d: The cotyledon remain tightly coiled in the seed coat and rapid increased in length to approximately 3-fold that of the hypocotyl, e: A seedling in which the only one leafy cotyledon has just expanded after 42 days, f: A 6-month-old seedling that has one leafy cotyledon and one true leaf (note cotyledon closely resembles the heart-shaped true leaf), tiny tuber and primary root, g: A 1-year-old plant with new leaf emergence in autumn

Total leaf area and petiole length were significantly gradually increased during the 6-year growing period, and reached a maximal (111.78 cm² and 13.33 cm, respectively) for 6-year-old plants (Fig. 7).

The tuber fresh weight and diameter significantly varied with age of the plants, depending on number of leaves and total leaf area. However, there were nonsignificant differences in both tuber fresh weight and diameter between the 2- and 3-year-old plants. At the end of 4th year growing period, tuber fresh weight and diameter were significantly higher than the first 3 years of growing period and progressively increased as the growing period became longer, whereas they were 10.97 g and 3.88 cm at 5-year-old plants and 21.27 g and 5.49 cm, respectively at 6-year-old plants (Fig. 8).

The increase in tuber fresh weight and diameter were affected more by total leaf area than by leaf number (Fig. 7). The increase in total leaf area from 25.88 cm² for a 3-year-old plants to 49.00 cm² for 4-year-old ones increased the tuber fresh weight and

diameter by 2.87 and 1.43-fold respectively, then sharply increased, with a further increase in total leaf area to 74.68 and 111.78 cm² in five and 6-year-old plants, respectively, (by about 5.13, 1.98-fold and 9.94, 2.80-fold, respectively).

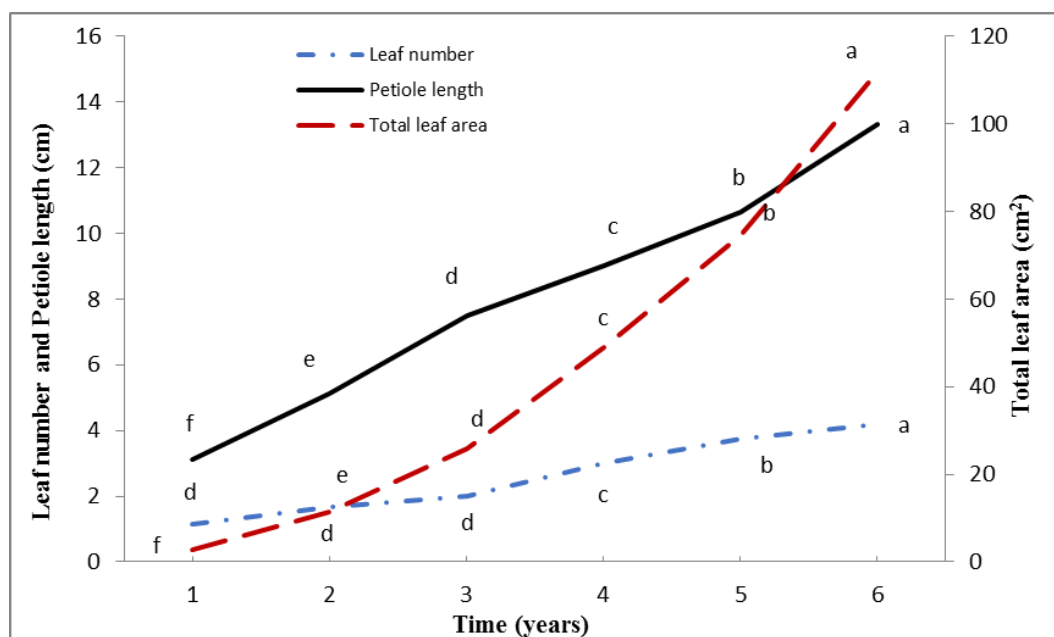


Figure 7. Annual increments of leaf number, total leaf area (cm²) and petiole length (cm) in the seedling of *C. rohlfsianum* during 6 years, in the Al-Bieda, East of Libya. Means with different letters above points are significantly different, according to Duncan's multiple range test, $P = 0.05$

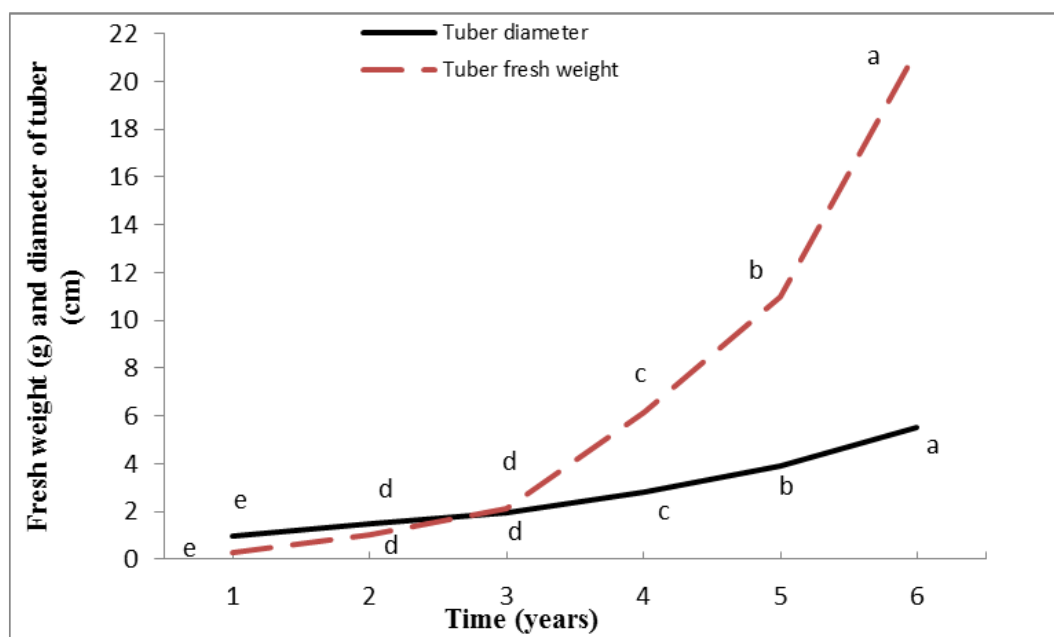


Figure 8. Annual increments of tuber fresh weight (g) and diameter (cm) in the seedling of *Cyclamen rohlfsianum* during 6 years, in the Al-Bieda, East of Libya. Means with different letters above points are significantly different, according to Duncan's multiple range test, $P = 0.05$

Following 4 years of vegetative growth, flowering began in the next growing season at early October, and $79 \pm 3.5\%$ of plants flowered, with only 2.5 ± 0.9 flowers per plant. At 6-year-old plants, flowering began in late September and increased to $98 \pm 7\%$, with 4.2 ± 0.4 flowers per plant. Similarly, length of petioles increased from 5.5 ± 0.6 cm to 7.5 ± 1.0 cm, respectively (Table 1).

A fruit capsule had 15 ± 4 seeds. Seed fresh weight was 15.5 ± 5 mg. The fruit capsule (0.87 ± 0.5 g) color was green in November and changed to dark brown in late January.

Table 1. Percentage of flowering, time of flowering, number of flowers per plant and length of pedicel during six consecutive years from sowing to flowering tuber size of *Cyclamen rohlfsianum*

Time (years)	Percentage of flowering (%)	Time of flowering	Number of flowers/plant	Length of pedicel (cm)
First to fourth	-	-	-	-
Fifth	79 ± 3.5	2-5 October	3.5 ± 0.9	5.5 ± 0.6
Sixth	98 ± 7.0	21-25 September	4.3 ± 0.5	7.5 ± 1.0

Data expressed as mean \pm standard deviation (n = 54)

Discussion

The vegetative propagation method of cyclamen by division or splitting of the tuber is difficult. Therefore, cyclamen is usually propagated by seeds (Fig. 5). Seed germination at 15 °C and darkness are suitable for the optimum germination in many cyclamens (Neveur et al., 1986; Corbineau et al., 1989).

The pattern of *C. rohlfsianum* germination was fairly consistent with those of *C. persicum*, which was first described by Anderson and Widmer (1975) and Widmer (1992). They reported that, at 5 days old the primary root penetrates the soil, at 28 days old the fat hypocotyls are evident (tiny tubers), and at the last, cotyledon is emerged from the seed coat. However, the germination percentage was 90% or more but 80 to 85% was more common. Although, in the current study (Fig. 6), the germination percentage ($88 \pm 4\%$) was similar to that of *C. persicum*, there was a few days slower, in imbibition period and total germination period, than *C. persicum*.

Continued growth of the underground tuber, storage of food, and the production of the flower bud are dependent upon photosynthesis. Hence, plant at an earlier age of growth would be less able to sufficient accumulate reserves for increase in size of the tuber. Consequently, the photosynthetic area per plant has an important influence on accumulating reserves for increasing size of the tubers, which are properly large enough to produce flowers in the next year.

In this study, the tuber size (fresh weight and diameter) varied with age of plants, depending on number of leaves and leaf area. However, the time to produce flowers was based on tuber size. Hence, plant at an earlier age of growth would be less able to accumulate sufficient metabolites reserves for increasing size of the tuber. For example, number of leaves, total leaf area and tuber fresh weight were 1.16, 2.85 cm² and 0.29 g for 1-year-old plants, reached up to about 3.0, 49.0 cm² and 6.15 g for 4-year-old plants (tuber flowering size for next growing season), up to 3.76, 74.68 cm² and 10.97 g for 5-year-old plants, and then sharply increased to 4.21, 111.78 cm² and 21.27 g, respectively for 6-year-old plants. However, the percentage of flowering, number of

flowers and length of pedicle for 5-year-old plants ($79 \pm 3.5\%$, 3.5 ± 0.9 and 5.5 ± 0.6 cm, respectively) were lower than did 6-year-old plants ($98 \pm 7\%$, 4.3 ± 0.4 and 7.5 ± 1.0 cm), which had a higher leaf number, leaf area and tuber size.

In some geophytes, the development of leaves is closely correlated with the initiation of flowers. A specific leaf number may be required before flower buds are initiated. In tulip, a flowering bulb produces three to five leaves, while a nonflowering bulb produces one leaf only. In the case of Dutch Iris, a vegetative plant can produce only one up to three leaves and, therefore, a knowledge of minimum leaf numbers for each species is vital information (Le Nard and De Hertogh, 1993b). Moreover, it is assumed that increasing in tuber size could be related to the increase in leaf number and area. Furthermore, the leaf number counted and total leaf area were related to initiation of flowers (Figs. 7 and 8).

The critical geophyte size can vary with the geophytic organ, genus, species, cultivar and the environmental conditions. However, above the critical size, flower production and quality often increase with size (Le Nard and De Hertogh, 2002). Therefore, tuber size is the major, and easily measured, factor that determining the capacity to flower. Moreover, the location of tuber is an important factor affecting the morphological traits of wild cyclamen by controlling the tuber size (Curuk, 2017).

These results are in agreement with those of Grey-Wilson (2002). He found that the high polyploidy species such as *C. rohlfsianum* ($2n = 4x = 96$) are the slowest to reach flowering size from seed. It also requires about 4 to 5 years of vegetative growth to produce a flowering plant from a seedling. On the other hand, the seed propagated commercially important *C. persicum* and its cultivars, produced today, are expected to flower within 6-7 months from sowing (Widmer, 1992; Karlsson and Werner, 2001). Therefore, further researches are required to accelerate seedling development to maturity.

Conclusion

As a result, it is recommended for the grower to use the tuber size, which had at least three leaves, more than 3 cm diameter, or 6.15 g fresh weigh before planting to predict flowering in next growing season (5-year period). However, further increase in the tuber size is associated with increases in all the growth and flowering variables. It is obvious that further researches are needed to elucidate the influence of temperature, light and mineral elements on production of *C. rohlfsianum*, in order to reduce the time needed for tubers to reach flowering size when produced by growers, under protected cultivation.

REFERENCES

- [1] Affre, L., Thomson, J. D. (1999): Variation in self-fertility, inbreeding depression and levels of inbreeding in four *Cyclamen* species. – J. Evolutionary Bio. 12(1): 113-122.
- [2] Anderson, R. G., Widmer, R. E. (1975): Improving vigor expression of cyclamen seed germination with surface disinfestations and gibberellin treatment. – J. Amer. Soc. Hort. Sci. 100: 597-601.
- [3] Corbineau, F., Neveur, N., Côme, D. (1989): Seed germination and seedling development in *Cyclamen persicum*. – Annals of Botany 63: 87-96.

- [4] Curuk, P. (2017): Impact of tuber location on morphological characteristics of cyclamen. – Pak. J. Bot. 49(1): 317-324.
- [5] Curuk, P., Sogut, Z., Bozdogan, E., İzgu, T., Sevindik, B., Tagipour, E. M., Teixeira da Silva, J. A., Serce, S., Aka Kacar, Y., Yalcin Mendi, Y. (2015): Morphological characterization of *Cyclamen* sp. grown naturally in Turkey: Part I. – South Afr. J. Bot. 100: 7-15.
- [6] Curuk, P., Sogut, Z., Izgu, T., Sevindik, B., Tagipur, E. M., Teixeira da Silva, J. A., Serce, S., Solmaz, I., Kacar, Y. A., Mendi, N. Y. Y. (2016): Morphological characterization of *Cyclamen* sp. grown naturally in Turkey: Part II. – Acta Sci. Pol. Hortorum Cultus 15(5): 205-224.
- [7] Dole, J. M., Wilkins, H. F. (2005): Floriculture: Principles and Species. 2nd Ed. – Pearson Education, Upper Saddle River, NJ, pp. 414-420.
- [8] El-Darier, S. M., El-Mogaspi, F. M. (2009): Ethnobotany and relative importance of some endemic plant species at El-Jabal El-Akhdar Region (Libya). – World J. Agric. Sci. 5(3): 353-360.
- [9] Grey-Wilson, C. (2002): Cyclamen. – Timber Press, Portland.
- [10] Jackson, M. L. (1967): Soil Chemical Analysis. – Prentice-Hall of India, New Delhi.
- [11] Jalali, N., Naderi, R., Shahi-Gharahlar, A., Teixeira da Silva, J. A. (2012): Tissue culture of *Cyclamen* spp. – Sci. Horticult. 137: 11-19.
- [12] Karlsson, M., Werner, J. (2001): temperature affects leaf unfolding rate and flowering of cyclamen. – HortScience 36(3): 292-294.
- [13] Lazarević, J., Lazarević, S. (2010): Possibilities for production and application of native *Cyclamen neapolitanum* in landscape architecture and horticulture. – Biol. Nyss. 1(1-2): 105-109.
- [14] Le Nard, M., De Hertogh, A. A. (1993a): General Chapter on Spring Flowering Bulbs. – In: De Hertogh, A. A., Le Nard, M. (eds.) The Physiology of Flower Bulbs. Elsevier, Amsterdam, pp. 750-740.
- [15] Le Nard, M., De Hertogh, A. A. (1993b): Bulb Growth and Development and Flowering. – In: De Hertogh, A. A., Le Nard, M. (eds.) The Physiology of Flower Bulbs. Elsevier, Amsterdam, pp. 29-44.
- [16] Le Nard, M., De Hertogh, A. A. (2002): Research needs for flower bulbs (geophytes). – Acta Hort. 570: 113-120.
- [17] Mammadov, R., Dusen, O., Ozay, C. (2016): Autoecological characteristics of *Cyclamen mirabile* Hildebr. (Primulaceae) - an endemic species of Turkey. – J. Res. Ecology 4(1): 1-9.
- [18] Muftuoglu, N. M., Altay, H., Sungur, A., Erken, K., Turkmen, C. (2009): Effects of different N, P, and K applications on the mineral contents of tuber and leaves of *Cyclamen hederifolium* plants. – Biol. Div. Conserv. 2(1): 21-26.
- [19] Neveur, N., Corbineau, F., Côme, D. (1986): Some characteristics of *Cyclamen persicum* L. seed germination. – J. Hort. Sci. 61: 379-387.
- [20] Oh, W., Rhie, Y., Park, J. H., Runkle, E. S., Kim, K. S. (2008): Flowering of cyclamen is accelerated by an increase in temperature, photoperiod, and daily light integral. – J. Hort. Sci. & Bio. 83(5): 559-562.
- [21] Rees, A. R. (1992): Ornamental Bulbs, Corms and Tubers. – CAB International, Wallingford.
- [22] Seyring, M., Ewald, A., Mueller, A., Haensch, K. (2009): Screening for propagation suitability in vitro of different *Cyclamen* species. – Elec. J. Bio. 12(4): 1-10.
- [23] Sibusawa, N., Ogawa, K. (1997): Production of interspecific hybrids between *Cyclamen persicum* Mill. and *C. rohlfsianum* Aschers. or *C. persicum* and *C. libanoticum* Hirdebr. – Bull. Tokyo Agr. Exp. Stn. 27: 9-15.
- [24] Snedecor, G. M., Cochran, W. G. (1980): Statistical Methods. 7th Ed. – Iowa State Univ. Press, Ames.

- [25] Sundberg, M. D. (1981a): Apical events prior to floral evocation in *Cyclamen persicum* “F-1 Rosemunde” (Primulaceae). – Bot. Gaz. 142: 27-35.
- [26] Sundberg, M. D. (1981b): The development of leaves and axillary flowers along the primary shoot axis of *Cyclamen persicum* “F-1 Rosemunde” (Primulaceae). – Bot. Gaz. 142: 214-221.
- [27] Sundberg, M. D. (1982): Leaf initiation in *Cyclamen persicum* (Primulaceae). – Can. J. Bot. 60(11): 2231-2234.
- [28] Takamura, T. (2007): Cyclamen. *Cyclamen Persicum* Mill. – In: Anderson, N. O. (ed.) Flower Breeding and Genetics Issues, Challenges and Opportunities. Springer, The Netherlands, pp. 459-478.
- [29] Widmer, R. E. (1992): Cyclamen. – In: Larson, R. A. (ed.) Introduction to Floriculture. 2nd Ed. Academic Press, Cambridge, MA, pp.385-407.

MORPHOTYPOLOGICAL ANALYSIS OF STARCH GRANULES THROUGH DISCRIMINANT METHOD AND ITS APPLICATION IN PLANT ARCHEOLOGICAL SAMPLES

WAN, Z. W.¹ – LIN, S. P.¹ – JU, M.¹ – LING, C. H.² – JIA, Y. L.^{1,3} – JIANG, M. X.¹ – LIAO, F. Q.^{1*}

¹*Key Laboratory of Poyang Lake Wetland and Watershed Research Ministry of Education, School of Geography and Environment, Jiangxi Normal University, Nanchang 330022, China*

²*State Key Laboratory of Lake Science and Environment, Nanjing Institute of Geography and Limnology, Chinese Academy of Sciences, Nanjing 210008, China*

³*Shandong Provincial Key Laboratory of Water and Soil Conservation and Environmental Protection, Linyi University, Linyi 276000, China*

*Corresponding author
e-mail: liaofuqiang@jxnu.edu.cn

(Received 8th Jan 2020; accepted 6th May 2020)

Abstract. Starch granule analysis effectively recovers microbotanical residues of starchy plants from archaeological contexts. Morphometric analysis is a common method to identify starch granules. However, this technique is time-consuming and inaccurate. Morphotypological differences in plants may also cause inconsistent results during microscopic observations. To address this problem, we evaluated the morphotypological features of three types of starch granules, specifically those found in wheat, millet, and yam, through light microscopy. Moreover, we used morphotypological analysis and discriminant analysis by ImageJ and SPSS software to perform computer-assisted analysis on the data set of geometric characteristics of the three types of starch granules, as well as the starch granule fossils from the Xianrendong and Diaotonghuan archaeological sites. Results are detailed and comparable to the light microscopy findings. The improved method with ImageJ and SPSS software required less time by direct measurement with a light microscopy and enhanced the accuracy of starch granule identification with the reduction of subjectivity. Therefore, the combination of ImageJ and SPSS software is a promising technique for the morphotypological analysis and identification of starch granules in archaeological starch granule analysis.

Keywords: *archaeobotany, ancient recipes, neolithic revolution, geometric characteristic, microfossils, residue analysis*

Introduction

The origin of agriculture and crop domestication in the Neolithic worldwide is becoming increasingly important in many disciplines (Diamond, 2002; Balter, 2007; Gremillion et al., 2014; Herzog et al., 2018; Mickleburgh et al., 2019; Li et al., 2020). Rice, millet, wheat, barley, and other types of mainstay crops have played very important roles in the early periods of human society around 12,000 years ago (Weber and Fuller, 2008; Lu et al., 2009; Jones et al., 2011). All these important crops comprise of up to 90% starch (Torrence and Barton, 2006; Ciofalo et al., 2019; Zhu et al., 2020). However, considering that conservation conditions are poor in the archaeological context, few crop relics are found during excavation, which are difficult to identify (Moore, 1998). Thus, information on crop utilization and domestication remains limited, thereby impeding the reconstruction of crop domestication and origin of agriculture. To solve this problem, a novel method called starch granule analysis was developed, which was performed by identifying ancient starch fossils retrieved from

archaeological contexts and comparing them with a modern plant starch morphology database.

Starch is a common component of higher plants (BeMiller and Whistler, 2009; Xu et al., 2019; Zhu et al., 2020). This molecule is mainly found in parenchymal cells in the form of semi-crystalline granules with birefringence characteristics, which are manifested through Maltese crosses under polarized light microscopy. Starch granules from various plants exhibit different structures and diagnostic features, which are controlled by genetic and environmental diversity (Torrence and Barton, 2006; Mercader, 2009; Yang et al., 2012). The morphotypological differences of starch granules are essential for the identification of vegetal residues, particularly food and plant remains from archaeological contexts. Starch granules have been considered an important factor to interpret ancient plant information because such granules can survive on the surface of archaeological tools, dental calculus, cultural deposits, and other contexts for up to more than 50,000 years (Torrence and Barton, 2006; Barton and Torrence, 2015). Furthermore, starch granule analysis has provided novel insights into paleoethnobotany and agricultural archaeology (Piperno et al., 2009). Thus, identification of ancient starch granules has become a primary approach to investigate agriculture origins, plant utilization by ancient people (Wan et al., 2012a), and paleoenvironment reconstruction (Lentfer et al., 2002; Vojtekova et al., 2019).

For instance, some plant residues are occasionally found during excavation with serious damage, which cannot be identified by traditional methods. Consequently, Ugent et al. (1981) first employed this new method to retrieve starch granule fossils from eight archaeological sites in central and southern Peru and confirmed that the plant relics belong to sweet potato (*Ipomoea batatas*) dating from 1,000 AD to 1,500 AD. Ugent et al. (1987) also used this method to demonstrate that aboriginal peoples who lived in Chile utilized potato (*Solanum tuberosum*) as early as 13,000 BP before the beginning of the Neolithic agricultural revolution. If starch granule analysis was not used to identify ancient plant relics, plant species can only be confirmed using incomplete plant fragments.

As a result, reconstruction of ancient plant utilization requires accurate identification of ancient starch granules (Piperno et al., 2004; Torrence and Barton, 2006). However, traditional methods to identify such granules mainly rely on morphometric analysis by comparing the starch granules retrieved from archaeological contexts with modern starch granule reference data in terms of properties such as shape, size, hilum position, surface ornament, and other anatomical features (Coster and Field, 2015; Farley et al., 2018). All these variants are recorded by directly observing plant specimens through microscopy, and identification almost entirely depends on personal judgment, which is also a laborious procedure. Nevertheless, few studies on the comprehensive geometric characteristics of these starch granules have been conducted with computer-assisted methods (Wu and Wang, 2011). Consequently, the data recorded by various individuals or at different instances by the same person may result in diverse outcomes because of the lack of consistent recording standards. Thus, scientists often require much time to confirm the sources of starch granules and precisely identify such sources.

According to previous studies, some of the common types of Triticeae seeds, such as wheat and barley, are composed of starch granules with bimodal size feature, that is, this type of starch can be either large or small (Yang and Perry, 2013). Morphotypological changes in Triticeae maturation significantly influence the accuracy of identification. These changes also require further research and elucidation (Wu et al.,

2014). Therefore, we aimed to evaluate the morphotypological changes in different stages of wheat maturity through light microscopy. Our previous studies indicated that the usual starch type can be divided into three geometric categories, namely, polygonal (as in millet), round (as in wheat), or oval (as in yam) (Wan et al., 2011a). Accordingly, we evaluated the morphotypological features of modern millet and yam.

We used ImageJ software for computer-assisted analysis of the geometric characteristics of starch granules. The outcomes were then used to identify ancient starch granules retrieved from Xianrendong and Diaotonghuan sites in China dating from the late Paleolithic to the early Neolithic period (Wan et al., 2012b). The proposed method required less time and exhibited greater efficiency than previous methods. Our experimental results confirmed that starch granules from wheat are characterized by different types of granules at different stages and determined the geometric features of three modern crops common in China. Photomicrographs of starch granules from millet, wheat, and yam were obtained through light microscopy and analyzed using ImageJ and SPSS software. Comparison of the ancient starch granules with modern samples by using computer-assisted analysis reduced the subjectivity of starch granule identification. Furthermore, the proposed method enhanced the efficiency and accuracy of measurement.

Materials and methods

Materials

Wheat (*Triticum aestivum*) was planted in Xichuan County, Henan, China and then collected in the late stage of wheat maturity. Six batches of wheat seeds were collected on May 5, 8, 11, 15, 20, and 26, 2014 and correspondingly labeled as W1 to W6. W6 was composed of fully mature wheat seeds. There are 5 grains of wheat in each batch.

Millet (*Setaria italica*) and yam (*Dioscorea opposita*) consist of one type of starch granule each. Thus, in this study, only the mature samples were collected. Millet samples were obtained from Chaoyang County, Liaoning, China in the autumn of 2017, and yam samples were obtained from Nanchang County, Jiangxi, China in the winter of 2018. The millet sample used in the experiment was 5 grains, and the yam sample was 3 g.

Ancient starch granule samples were retrieved from the Xianrendong and Diaotonghuan sites located in eastern Jiangxi, China dating to 20,000 ~ 12,000 cal. a BP. Two agricultural tools were examined in our previous study, and more than 200 starch granule fossils were retrieved from residues on the surface of these tools. Based on direct identification under microscopy, these ancient starch granules might have come mainly from species within Poideae, Paniceae, and unidentified underground tubers.

Methods

Modern observation of starch granules

Plant starch granules were observed using modern sample methods as previously researches (Piperno et al., 2004; Perry et al., 2007). Briefly, a small amount of sample was placed in a 15 mL disposable plastic test tube. Afterward, 5 mL of ultrapure water was added, and the sample was soaked for more than 12 h. The sample was then ground using a glass rod until it was completely broken. The solution was stirred using a rod.

Subsequently, 200 μL of the starch suspension was drawn and transferred to a glass slide. A drop of a solution containing 50% glycerol and 50% water was applied. The specimen was covered with a cover slip.

The slides were viewed under a Nikon ECLIPSE 50iPOL microscopy at 400 \times magnification. The photomicrographs of the starch granules were obtained using a digital camera. The size of each granule was recorded using a scale under the microscopy.

Morphotypological analysis

ImageJ is an image processing software developed by the National Institutes of Health (USA). This software can be used in biological studies to analyze geometric characteristics, such as length, angle, area, major axis, minor axis, perimeter, roundness, Feret's diameter, best-fitting ellipse, and centroid coordinates (Schneider et al., 2012). In this study, ImageJ 1.48 (download at <http://rsbweb.nih.gov/ij/index.html>) was employed to analyze the images of starch granules. The *Straight Line* and *Set Scale* tools were used to ensure that the images were set at the desired scale. The image was then changed to 8-bit grayscale. The images were converted to binary images through binarization by using the *Make Binary* tool. Geometric characteristics were obtained by selecting *Analyze Particles* under the *Analyze* menu bar.

Since most starch granules are irregularly shaped, it is difficult to describe their size in terms of diameter. Therefore, the Feret's diameter is used for measurement. Feret's diameter is the size of an object measured in a certain direction (Isobe et al., 2013; Drazic et al., 2016). Generally speaking, the measurement method is defined as the distance between two parallel planes. These two parallel planes need to jam the object and be perpendicular to the specified direction.

Comparison with ancient starch granules

To test the effectiveness of identification criteria obtained from ImageJ software analysis, ancient starch granules retrieved from the Xianrendong and Diaotonghuan sites, Jiangxi, China were selected as test samples (Wan et al., 2012b). The images of ancient starch granules were preliminarily identified as Pooideae, Paniceae, and unidentified underground tubers and then measured using ImageJ. Consequently, a series of geometric characteristics was obtained and used as identification criteria for precise species-level identification. The overall experiment and method were conceived and completed in 2019.

Results

Morphotypological analysis of wheat starch

Six slides corresponding to W1 to W6 were observed through microscopy. A representative image from each sample is shown in *Figure 1*. Based on the measurement analysis results (*Figure 2*), the size of the wheat starch granule gradually increased from 3.23 μm to 22.48 μm during maturity. The starch granules can be divided into two groups, namely, large group ($>10 \mu\text{m}$) and small group ($<10 \mu\text{m}$). The percentage of starch granules belonging to the large group exhibited an increasing trend from W1 to W6 (*Table 1*).

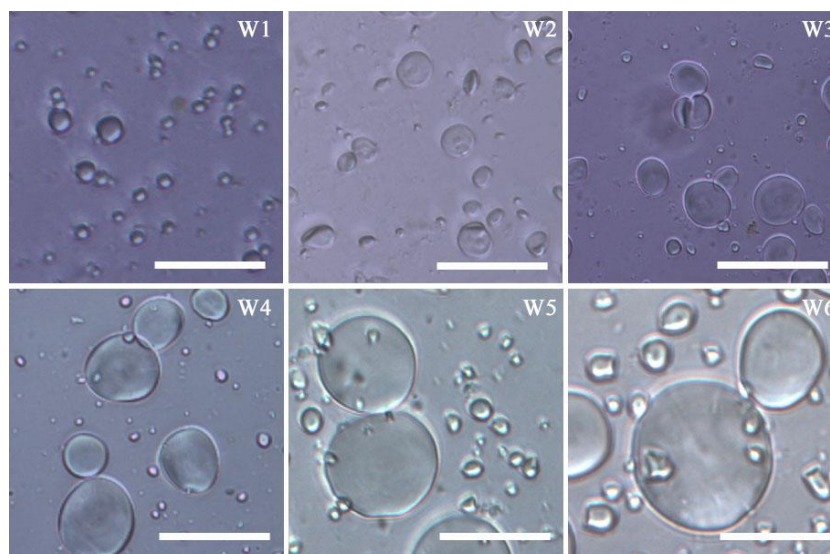


Figure 1. Wheat starch granules from different stages (W1 to W6). Scale bar = 20 μm

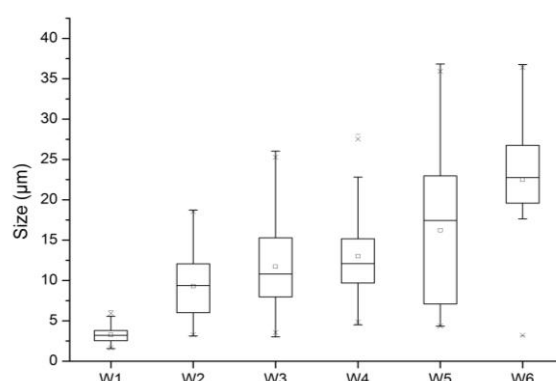


Figure 2. Box-whisker plot of the starch granule size from W1 to W6

Table 1. Percentages of large group ($>10 \mu\text{m}$) and small group ($<10 \mu\text{m}$) from W1 to W6

Group	W1	W2	W3	W4	W5	W6
Big group	0	45	57	72	64	91
Small group	100	55	43	28	36	9

Morphotypological analysis of millet and yam starch

Millet contains polygon starch granules showing centric and closed hila, as well as indemonstrable lamellae (Figure 3A). Some granules exhibited fissures across the hila under light microscopy. Millet starch granules showed wrinkled surfaces and coarse edges, which may have been caused by contact with the other starch granule. The mean size of millet starch granule was 9.47 μm , which was almost 70% smaller than 15 μm .

Yam is composed of singular starch granules that are oval and exhibiting eccentric hila (Figure 3B), and the mean size is 30.89 μm . Almost 80% of the granules measured within 26.13 μm to 36.76 μm in size. The lamellae of yam starch granule were evident under light microscopy.

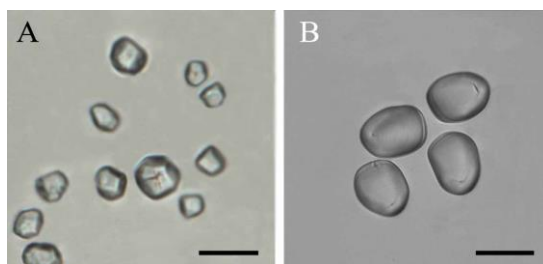


Figure 3. (A) Starch granule from millet (*Setaria italica*), Scale bar = 10 μm . (B) Starch granule from yam (*Dioscorea opposita*), Scale bar = 30 μm

Morphotypological analysis in ImageJ

For wheat, each image at different stages was processed using ImageJ software. W4 was considered as representative of the results obtained in each stage because this sample was obtained in the middle stage (*Figure 4A*). W4 picture was selected as a sample to show how to use ImageJ software for analysis. W4 image was changed to 8-bit grayscale such that only white and black pixels were present. As a result, this image was easily converted to a binary image. In the binary image, the starch granule appeared as a solid black region, and the other components appeared white (*Figure 4B*). These steps were accomplished through computer-assisted analysis, which was more efficient than the manual process. In the final step (*Figure 4C*), the software was used to extract the outline of each granule and determine the centroid area. In *Figure 4D*, the centroid area appears as a small point.

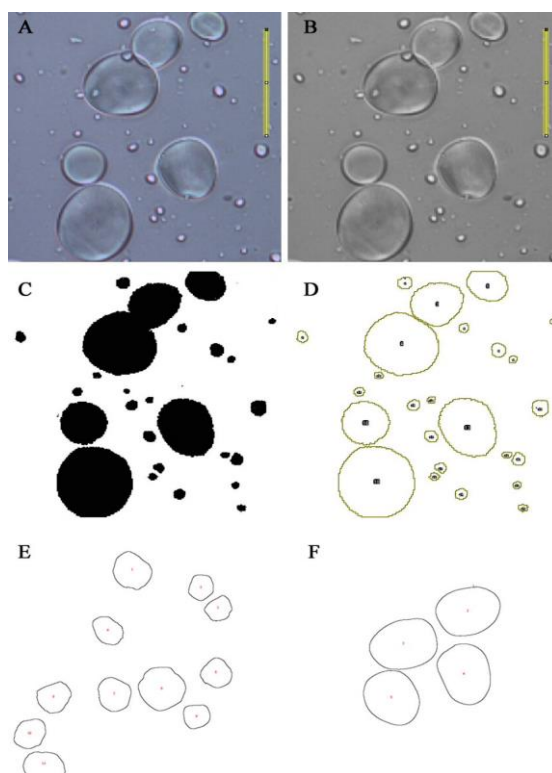


Figure 4. ImageJ analysis of microscopy image. (A) Setting the scale; (B) Converting the image to 8-bit grayscale; (C) Converting to a binary image; (D) Extracting the outline of wheat starch granule; (E) Outline of millet starch granule; (F) Outline of yam starch granule

Using the same procedure, the starch granule images of millet (*Figure 3A*) and yam (*Figure 3B*) can also be processed, and the results are shown in *Figures 4E and 4F*.

Geometric characteristics

The geometric characteristics were simultaneously determined when the outline of each starch granule was obtained. The results of each variant are listed in *Table 2*. Given that the size of each wheat granule ranged from 3.23 μm to 22.48 μm , particles smaller than 3.23 μm were not considered starch granules and may have been impurities from the slide preparation. The geometric characteristics of millet and yam starch granules were also analyzed (*Table 2*).

Table 2. Geometric characteristics of starch granules

No.	Area	Perimeter	Major axis	Minor axis	Feret's diameter	Roundness
1	58.90	30.4652	9.8877	7.5845	10.1213	0.767
2	7.90	10.9113	3.3929	2.9646	3.662	0.874
3	103.96	41.1647	12.3914	10.6821	12.9468	0.862
4	211.28	57.9286	17.455	15.4117	17.6822	0.883
5	9.32	11.9841	3.6261	3.2725	3.8949	0.902
6	154.5	51.9203	15.628	12.5874	16.2413	0.805
7	12.55	14.4326	4.147	3.8531	4.4944	0.929
8	94.87	40.0049	11.082	10.8999	11.6726	0.984
9	7.00	10.277	3.3057	2.6962	3.6125	0.816
10	259.54	63.7831	18.4037	17.9559	19.0547	0.976
11	26.962	19.856	6.307	5.443	6.579	0.863
12	12.52	13.379	4.311	3.697	4.36	0.858
13	12.245	13.514	4.273	3.648	4.486	0.854
14	16.077	15.438	5.254	3.896	5.361	0.742
15	17.106	15.879	4.763	4.573	5.02	0.96
16	38.823	23.471	7.135	6.928	7.419	0.971
17	21.978	17.829	5.681	4.926	5.792	0.867
18	19.586	17.094	5.357	4.655	5.51	0.869
19	13.064	13.607	4.178	3.981	4.446	0.953
20	18.355	16.306	5.363	4.358	5.535	0.813
21	22.491	18.59	6.558	4.367	6.534	0.666
22	528.044	87.251	29.137	23.075	29.11	0.792
23	580.795	91.363	30.92	23.916	30.562	0.774
24	535.515	88.595	30.118	22.639	30.146	0.752
25	507.801	85.375	27.734	23.312	27.958	0.841

Note: Nos.1~10 represents wheat starch granules; Nos.11~21 represents millet starch granules; Nos.22~25 represents yam starch granules

Archaeological application

To demonstrate the effectiveness of morphotypological analysis and identification by ImageJ software, different starch granule fossil residues (*Figures 5A ~ C*) were retrieved from Xianrendong and Diaotonghuan sites, which are important early human

archaeological sites in Jiangxi, China dating from 20,000 ~ 12,000 cal. a BP. These archaeological starch granule images were analyzed using ImageJ software, and a series of geometric characteristics was obtained and compared with the modern plant data, thereby facilitating rapid identification of the species of these starch fossils with enhanced accuracy. The final images processed using ImageJ software are shown in *Figures 5D ~ F*, and the geometric characteristics of each archaeological starch granule fossil were also obtained (*Table 3*).

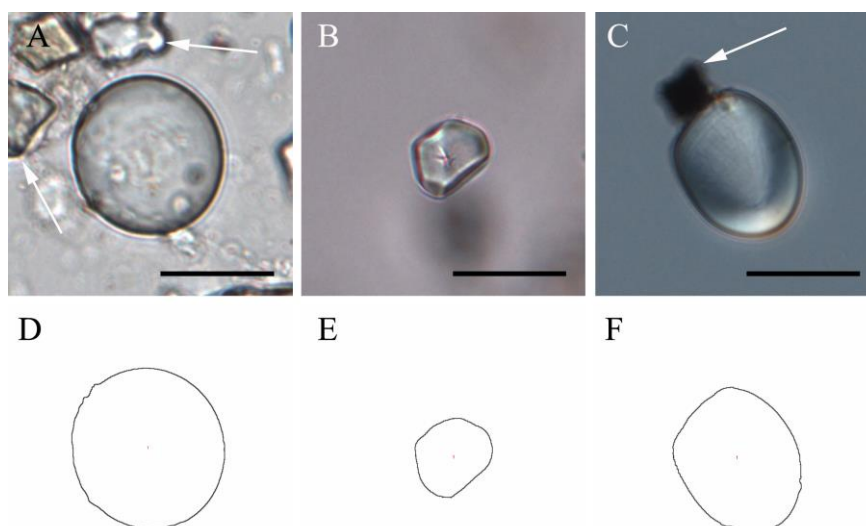


Figure 5. Archaeological starch granule retrieved from tools found in the Xianrendong and Diaotonghuan sites. The white arrowhead highlights impurities that are very common in archaeological sample. (A~C) Images obtained under a light microscope; (D~F) Images processed using ImageJ software. Scale bar = 20 μ m

Table 3. Geometric characteristics of archaeological starch granules from Xianrendong and Diaotonghuan sites

No.	Area	Perimeter	Major axis	Minor axis	Feret's diameter	Roundness
1(Fig.5A)	598.448	92.519	28.528	26.709	29.013	0.936
2(Fig.5B)	161.891	48.568	15.668	13.156	15.763	0.84
3(Fig.5C)	378.761	74.071	24.228	19.905	24.703	0.822

The geometric characteristics of the three types of starch granules in wheat, millet, yam, and the ancient starch granule fossils were calculated by ImageJ software, and sufficient variants became available for construction of a discriminant formula by SPSS 20 software. The analysis results are shown in *Figure 6*, indicating that all scatter points have been clustered into three groups corresponding to wheat, millet, and yam starch granules. The ancient starch granules can thus be automatically allocated to their corresponding groups. Ancient starch granules in *Figure 5A* are classified as wheat, those in *Figure 5B* are classified as millet, and those in *Figure 5C* are classified as yam.

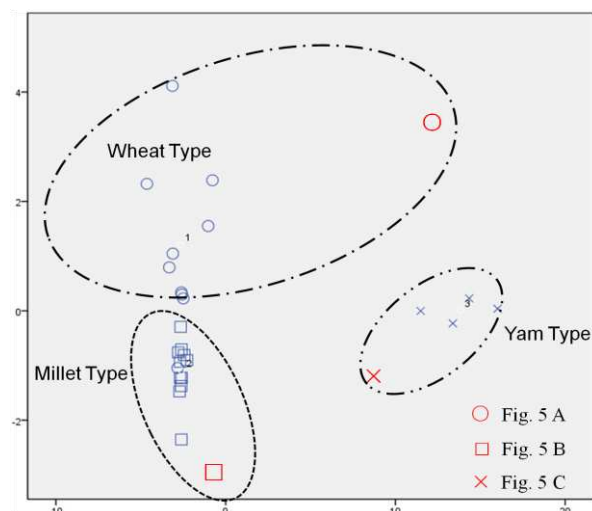


Figure 6. SPSS discriminant scatter plot of the three types of starch granules. The red dot indicates ancient starch granule fossils retrieved from Xianrendong and Diaotonghuan archaeological sites

Discussion

China is an important agricultural origin center and a domestication center for crops. Many crops such as millet, rice, barley, barley, etc. have played an important role in the agricultural development of Chinese history. Recently, Li et al. (2020) studied the changes of starch grains of four crops such as rice (*Oryza sativa* L.), foxtail millet (*Setaria italica*), Job's tears (*Coix lacryma-jobi* L.) and barley (*Hordeum vulgare* L.) after different milling methods, and explained that the treatment methods have different effects on starch grains. Zupancich et al. (2019) used 3D modeling and spatial analysis to reveal the function of grinding stones. And Owen et al. (2019) used ancient starch analysis on grinding stones to discuss plant utilization. All these indicate that there is an urgent need for a fast and stable starch granule identification method and process (Peng et al. 2019).

Although some physical means and chemical analysis reagents are used in the extraction of starch granules from archeological samples, such as ultrasound, hydrochloric acid, etc., related studies (Cuthrell and Murch, 2016; Yang, 2017) have shown that these means have a smaller effect on the shape of starch granules at lower intensity. Research and analysis of related foods and starch granules show that the changes in morphology and physicochemical properties of starch granules during processing are mainly caused by heating (Henry et al., 2009; Barton and Torrence, 2015). Considering that starch granule analysis experiments are carried out at normal temperature, the properties and morphology of starch granules are generally not affected by changes in identification.

Three other aspects of starch identification have to be addressed. First, the results of this study confirmed that wheat starch granule size gradually increases with wheat seed growth. The mean size of the six samples increased from 3.23 μm to 22.48 μm ; this value is similar to that obtained in our previous study in northern China (Wan et al., 2011b). We also confirmed that wheat starch can be divided into two groups of granules: the large group and the small group (Piperno et al., 2004). This grouping is an important identification criterion in research related to archaeobotany and ancient diet

reconstruction (Piperno et al., 2004; Yang and Perry, 2013; Calo et al., 2019; Kendal et al., 2019).

The second problem is related to the data set of geometric characteristics of the three types of starch granules. Only the major axis of each granule was recorded in previous studies because appropriate tools to accurately describe the shape of starch granules were lacking (Wan et al., 2012a). This process is thus inaccurate and time-consuming. In the present study, ImageJ software was used to process the images obtained using a digital camera during light microscopy. The results showed that a series of geometric characteristics, including the area, perimeter, major axis, minor axis, Feret's diameter, and roundness, can be simultaneously obtained. The number of obtained variants corresponds to the accuracy of the identification. Hence, we can identify a starch granule from archaeological contexts based on the multivariate criteria without relying solely on the major axis data. Feret's diameter is different from the major axis (*Table 2*); in particular, the former is greater than the latter because Feret's diameter represents the distance between the two parallel planes orienting the object perpendicular to a particular direction. However, this variant was not included in previously described identification criteria because Feret's diameter is difficult to measure through microscopy. Using ImageJ software, we can measure Feret's diameter and consider this variant as a criterion to enhance the accuracy of measurement.

The roundness and centroid of the granules were also obtained (*Table 2* and *Figure 4D*); similar to Feret's diameter, these variants can be used as important criteria in future studies. Considering that starch granules, which may also appear as oval granules, are not as round as wheat granules, we cannot easily determine the centroid of the starch granules under a microscopy. Thus, the centroid of granules should be determined to identify other plant species. Similarly, roundness is difficult to determine. Starch granules are usually depicted as round or oval because of the lack of some specific parameters. We found that the roundness of wheat, millet, and yam are distinguishable (*Table 2* and *Figure 6*). The area, perimeter, and other parameters can also be simultaneously determined using ImageJ software. This software can be applied to obtain the above parameters automatically and efficiently, as well as to reduce subjective errors when these parameters are observed by different people (Collins, 2007; Tavarone et al., 2019).

The third aspect is that identification of starch granules requires extensive previous experience, necessitating an automated identification method to ensure that the starch granule fossil retrieved from an archaeological site is classified correctly according to the type of starch granules observed. Hence, we tested three starch granule fossils obtained from the investigated archaeological sites. We then used SPSS 20 software to process the data of geometric characteristics of each starch granule, as well as discriminant analysis to construct a discriminate formula that can correctly classify the ancient samples according to the type of starch granule. The discriminant scatter plot in *Figure 6* shows that this method is viable. The ancient starch granules in *Figures 5A~C* were successfully classified as wheat-type, millet-type, and yam-type. This new method was more efficient than the method described in our previous study.

Nevertheless, the entire process cannot be completely replaced with ImageJ. Hence, we cannot simply rely on the parameters obtained by this software to verify the species from which starch granules are derived. However, by using computer-assisted technology, we can rapidly obtain results and consider additional parameters, which can therefore allow accurate identification.

Conclusion

In this study, starch granules were observed from samples of wheat seeds prior to maturity. Millet and yam samples were also processed. The mean size of wheat starch granules gradually increased with wheat seed growth. The wheat starch granules can be divided into large and small groups. This bimodal feature was considered as an identification criterion in traditional starch granule identification practices. Through ImageJ and SPSS software, data sets of geometric characteristics of wheat, millet, and yam starch granules were automated, reducing subjectivity in identification. To improve the efficiency in processing a large number of images obtained using a digital camera and a light microscope, as well as to obtain parameters objectively and automatically, we proposed the use of ImageJ and SPSS rather than traditional methods for morphotypological analysis. The processing results of ImageJ and SPSS are detailed and comparable to those directly obtained through light microscopy. Finally, the experiment on three ancient starch granules from archaeological sites successfully showed that discriminant analysis correctly classified them into existing groups, facilitating automated identification. Therefore, the combination of ImageJ and SPSS software is a promising technique for the morphotypological analysis of starch granules, which can facilitate automated identification of starch granule fossils in the future.

There are still some recommendations for future studies. (1) For the small round starch granules often extracted from archeological sites, it is likely that they are a smaller group of starch granules of wheat plants. In the future, detailed geometric morphological analysis can be performed on this part of starch granules, and a discriminant equation can be constructed for automatic identification, which can improve the accuracy of plant starch granule identification at archeological sites. (2) This article only tentatively analyzes the relevant starch granules of common crops in China. In the future, different regions can analyze the crops in their region and expand the scope of ancient recipe research. (3) The geometric morphological indicators of starch granules need to be strengthened. In the next step, more mathematical processing methods, such as Fourier transform and wavelet analysis, can be introduced to increase the use of existing data and improve the accuracy of discriminant analysis.

Acknowledgements. This study was supported by National Natural Science Foundation of China (41761045) and Open fund of Shandong Provincial Key Laboratory of Water and Soil Conservation and Environmental Protection (STKF201909). Thanks to the anonymous reviewers for their constructive comments, which greatly improved the quality of this article.

Conflict of Interests. The authors declare no conflict of interests.

REFERENCES

- [1] Balter, M. (2007): Seeking agriculture's ancient roots. – *Science* 316(5833): 1830-1835.
- [2] Barton, H., Torrence, R. (2015): Cooking up recipes for ancient starch: assessing current methodologies and looking to the future. – *Journal of Archaeological Science* 56(1): 194-201.
- [3] BeMiller, J. N., Whistler, R. L. (2009): *Starch: chemistry and technology*. – Academic Press, Burlington.
- [4] Calo, C. M., Rizzutto, M. A., Watling, J., Furquim, L., Shock, M. P., Andrello, A. C., Appoloni, C. R., Freitas, F. O., Kistler, L., Zimpel, C. A., Hermenegildo, T., Neves, E.

- G., Pugliese, F. A. (2019): Study of plant remains from a fluvial shellmound (Monte Castelo, RO, Brazil) using the X-ray MicroCT imaging technique. – *Journal of Archaeological Science: Reports* 26: 101902.
- [5] Ciofalo, A. J., Sinelli, P., Hofman, C. (2019): Late Precolonial Culinary Practices: Starch Analysis on Griddles from the Northern Caribbean. – *Journal of Archaeological Method and Theory* 26(4): 1632-1664.
- [6] Collins, T. J. (2007): ImageJ for microscopy. – *Biotechniques* 43(1): 25-30.
- [7] Coster, A. C., Field, J. H. (2015): What starch grain is that? A geometric morphometric approach to determining plant species origin. – *Journal of Archaeological Science* 58(1): 9-25.
- [8] Cuthrell, R. Q., Murch, L. V. (2016): Archaeological laboratory extraction procedures and starch degradation: Effects of sonication, deflocculation, and hydrochloric acid on starch granule morphology. – *Journal of Archaeological Science: Reports* 9(1): 695-704.
- [9] Diamond, J. (2002): Evolution, consequences and future of plant and animal domestication. – *Nature* 418(6898): 700-707.
- [10] Drazic, S., Sladoje, N., Lindblad, J. (2016): Estimation of Feret's diameter from pixel coverage representation of a shape. – *Pattern Recognition Letters* 80(1): 37-45.
- [11] Farley, G., Schneider, L., Clark, G., Haberle, S. G. (2018): A Late Holocene palaeoenvironmental reconstruction of Ulong Island, Palau, from starch grain, charcoal, and geochemistry analyses. – *Journal of Archaeological Science: Reports* 22: 248-256.
- [12] Gremillion, K. J., Barton, L., Piperno, D. R. (2014): Particularism and the retreat from theory in the archaeology of agricultural origins. – *Proceedings of the national academy of sciences of the United States of America* 111(17): 6171-6177.
- [13] Henry, A. G., Hudson, H. F., Piperno, D. R. (2009): Changes in starch grain morphologies from cooking. – *Journal of Archaeological Science* 36(3): 915-922.
- [14] Herzog, N. M., Louderback, L. A., Pavlik, B. M. (2018): Effects of cultivation on tuber and starch granule morphometrics of *Solanum jamesii* and implications for interpretation of the archaeological record. – *Journal of Archaeological Science* 98(1): 1-6.
- [15] Isobe, A., Akaji, M., Kurokawa, S. (2013): Proposal of New Polishing Mechanism Based on Feret's Diameter of Contact Area between Polishing Pad and Wafer. – *Japanese Journal of Applied Physics* 52(12): 6503.
- [16] Jones, M., Hunt, H., Lightfoot, E., Lister, D., Liu, X., Motuzaite-Matuzeviciute, G. (2011): Food globalization in prehistory. – *World Archaeology* 43(4): 665-675.
- [17] Kendal, E., Karaman, M., Tekdal, S., Dogan, S. (2019): Analysis of Promising Barley (*Hordeum vulgare* L.) Lines Performance by Ammi and Gge Biplot in Multiple Traits and Environment. – *Applied Ecology and Environmental Research* 17(2): 5219-5233.
- [18] Lentfer, C., Therin, M., Torrence, R. (2002): Starch Grains and Environmental Reconstruction: a Modern Test Case from West New Britain, Papua New Guinea. – *Journal of Archaeological Science* 29(7): 687-698.
- [19] Li, W., Pagán-Jiménez, J. R., Tsoraki, C., Yao, L., Van Gijn, A. (2020): Influence of grinding on the preservation of starch grains from rice. – *Archaeometry* 62(1): 157-171.
- [20] Lu, H. Y., Zhang, J. P., Liu, K.-B., Wu, N. Q., Li, Y. M., Zhou, K. S., Ye, M. L., Zhang, T. Y., Zhang, H. J., Yang, X. Y., Shen, L. C., Xu, D. K., Li, Q. (2009): Earliest domestication of common millet (*Panicum miliaceum*) in East Asia extended to 10,000 years ago. – *Proceedings of the national academy of sciences of the United States of America* 106(18): 7367-7372.
- [21] Mercader, J. (2009): Mozambican grass seed consumption during the Middle Stone Age. – *Science* 326(5960): 1680-1683.
- [22] Mickleburgh, H. L., Laffoon, J. E., Pagán-Jiménez, J. R., Mol, A. A. A., Walters, S., Beier, Z. J. M., Hofman, C. L. (2019): Precolonial/early colonial human burials from the site of White Marl, Jamaica: New findings from recent rescue excavations. – *International Journal of Osteoarchaeology* 29(1): 155-161.

- [23] Moore, P. D. (1998): Plant domestication: Getting to the roots of tubers. – *Nature* 395(6700): 330-331.
- [24] Owen, T., Field, J., Luu, S., Kokatha Aboriginal People, Stephenson, B., Coster, A. C. F. (2019): Ancient starch analysis of grinding stones from Kokatha Country, South Australia. – *Journal of Archaeological Science: Reports* 23(1): 178-188.
- [25] Peng, H., Xu, C., Yuan, Y., Zha, L., Chen, H., Guan, L., Kang, L.-P., Yang, J., Wang, Y., Cao, L., Cheng, J., Huang, L. (2019): The earliest excipient products of Traditional Chinese Medicine: Identification and analysis of samples from wooden lacquer box unearthed from Haihunhou tomb in the Western Han Dynasty. – *Chinese Science Bulletin* 64(9): 935-947.
- [26] Perry, L., Dickau, R., Zarrillo, S., Holst, I., Pearsall, D. M., Piperno, D. R., Berman, M. J., Cooke, R. G., Rademaker, K., Ranere, A. J., Raymond, J. S., Sandweiss, D. H., Scaramelli, F., Tarble, K., Zeidler, J. A. (2007): Starch fossils and the domestication and dispersal of chili peppers (*Capsicum* spp. L.) in the Americas. – *Science* 315(5814): 986-988.
- [27] Piperno, D. R., Weiss, E., Holst, I., Nadel, D. (2004): Processing of wild cereal grains in the Upper Palaeolithic revealed by starch grain analysis. – *Nature* 430: 670-673.
- [28] Piperno, D. R., Ranere, A. J., Holst, I., Iriarte, J., Dickau, R. (2009): Starch grain and phytolith evidence for early ninth millennium BP maize from the Central Balsas River Valley, Mexico. – *Proceedings of the national academy of sciences of the United States of America* 106(13): 5019-5024.
- [29] Schneider, C. A., Rasband, W. S., Eliceiri, K. W. (2012): NIH Image to ImageJ: 25 years of image analysis. – *Nature methods* 9(7): 671-675.
- [30] Tavarone, A., de Los Milagros Colobig, M., Fabra, M. (2019): Late Holocene plant use in lowland central Argentina: Microfossil evidence from dental calculus. – *Journal of Archaeological Science: Reports* 26: 101895.
- [31] Torrence, R., Barton, H. (2006): *Ancient starch research*. – Left Coast Press, Walnut Creek.
- [32] Ugent, D., Pozorski, S., Pozorski, T. (1981): Prehistoric remains of the sweet potato from the Casma valley of Peru. – *Phytologia* 49(5): 401-415.
- [33] Ugent, D., Dillehay, T., Ramirez, C. (1987): Potato remains from a Late Pleistocene settlement in southcentral Chile. – *Economic Botany* 41(1): 17-27.
- [34] Vojteková, J., Vojtek, M., Tirpáková, A., Vlkolinská, I. (2019): Spatial Analysis of Pottery Presence at the Former Pobedim Hillfort (an Archeological Site in Slovakia). – *Sustainability* 11(23): 6873.
- [35] Wan, Z., Yang, X., Ge, Q., Jiang, M. (2011a): Morphological characteristics of starch grains of root and tuber plants in South China. – *Quaternary Sciences* 31(4): 736-745.
- [36] Wan, Z., Yang, X., Ma, Z. (2011b): Morphological Change of Starch Grain Based on Simulated Experiment and its Significance of Agricultural Archaeology. – *Agricultural Science and Technology* 12(11): 1621-1624.
- [37] Wan, Z., Yang, X., Ge, Q., Fan, C., Zhou, G., Jiang, M. (2012a): Starch grain analysis reveals Late Neolithic plant utilization in the middle reaches of the Ganjiang River. – *Science China Earth Sciences* 55(12): 2084-2090.
- [38] Wan, Z., Ma, Z., Yang, X., Zhang, C., Zhou, G., Fan, C., Ge, Q. (2012b): Starch residues from shell tools from sites of Xianrendong and Diaotonghuan and its implications for paleoclimate. – *Quaternary sciences* 32(2): 256-263.
- [39] Weber, S., Fuller, D. Q. (2008): Millets and their role in early agriculture. – *Pragdhara* 18(1): 69-90.
- [40] Wu, Y., Wang, C. (2011): EDF phytolith analysis from Heying site, southeast China, Shang-Zhou dynasties. – *Microscopy research and technique* 74(11): 1062-1068.
- [41] Wu, Y., Yang, Y., Xiao, T., Gu, Z., Hill, D. V., Wang, C. (2014): Characterization of silica distribution in rice husk using Synchrotron Radiation μ CT and its implications for archaeological interpretation. – *Microscopy research and technique* 77(10): 785-789.

- [42] Xu, L., Ma, X., Zhang, B., Zhang, Q., Zhao, P. (2019): Multi-analytical Studies of the Lime Mortars from the Yanxi Hall in the Yangxin Palace of the Palace Museum (Beijing). – *Archaeometry* 61(2): 309-326.
- [43] Yang, X., Zhang, J., Perry, L., Ma, Z., Wan, Z., Li, M., Diao, X., Lu, H. (2012): From the modern to the archaeological: starch grains from millets and their wild relatives in China. – *Journal of Archaeological Science* 39(2): 247-254.
- [44] Yang, X., Perry, L. (2013): Identification of ancient starch grains from the tribe Triticeae in the North China Plain. – *Journal of Archaeological Science* 40(8): 3170-3177.
- [45] Yang, X. (2017): Ancient Starch Research in China: Progress and Problems. – *Quaternary Sciences* 37(1): 196-210.
- [46] Zhu, Z., Yu, C., Luo, W., Miao, Y., Lu, Z., Liu, L., Yang, J. (2020): Accurate identification of the pastry contained in a ceramic pot excavated from Jurou Li's grave from the Jin dynasty (1115-1234 CE) in Xi'an, Shaanxi, China. – *Archaeometry* 62(1): 130-140.
- [47] Zupancich, A., Mutri, G., Caricola, I., Carra, M. L., Radini, A., Cristiani, E. (2019): The application of 3D modeling and spatial analysis in the study of groundstones used in wild plants processing. – *Archaeological and Anthropological Sciences* 11(9): 4801-4827.

INFLUENCE OF DIVERSE CLIMATIC AND SOIL CONDITIONS ON THE PHYSIOLOGICAL AND BIOCHEMICAL ATTRIBUTES AND ANTIOXIDANT ACTIVITIES OF WILD MILK THISTLE (*SILYBUM MARIANUM* L. GAERT.)

JAVERIA, M. – HUSSAIN, K.*

Department of Botany, University of Gujrat, Gujrat, Pakistan

**Corresponding author*

e-mail: khalid.hussain@uog.edu.pk

(Received 13th Jan 2020; accepted 6th May 2020)

Abstract. Wild Milk thistle (*Silybum marianum* L. Gaert.) plants were collected from ten different locations of Punjab, Pakistan during the years 2018 and 2019. These locations have variations for soil characteristics and climatic conditions. Significant variations were noted in all the parameters from location to location as well as year to year. Antioxidant activities i.e. catalases (CAT), peroxidase dismutase (POD) and superoxide dismutase (SOD) changed significantly under fluctuating climatic conditions. Changes in antioxidant activities altered the defense mechanism of milk thistle and caused better balance in plant metabolism to survive. Ionic concentrations (NPK) in stem, leaves and roots also changed significantly. Location Dina showed the best results for physiological, antioxidant activities and ionic contents among all the locations. The soil of Dina location was sandy loam with 0.65 dS/m EC, 0.65% organic matter and 47% soil saturation. Location Dina had a maximum temperature of 25 °C, average temperature of 21 °C and high amounts of rainfall (838 mm) with 84% humidity. It was concluded that milk thistle required an optimum soil and climatic conditions similar to location Dina for its best growth and metabolism. These physiological and biochemical indicators can be used to evaluate the milk thistle response towards diverse climatic conditions.

Keywords: *temperature, plant growth, ion contents, silymarin, rainfall*

Introduction

Silybum marianum (L.) Gaert. generally called as milk thistle that is a yearly/biennial plant belongs to Asteraceae family, Mediterranean territory native and now growing as well as cultivated throughout the world (Bijak, 2017; Abenavoli et al., 2018). Purpose for the cultivation of this plant is to produced silymarin contents (Alemardan et al., 2013), while the other use of this plant is generation of bioenergy as well as oil from seeds and entire plant biomass (Cui et al., 2015; Dominguez et al., 2017). Silymarin complex typically comprises 36.3% of silybin, 15.7% silychristin, 5.9% of silydianin, and 5.1% of isosilybin that is a liver tonic (Sersen et al., 2006).

Studies related to milk thistle revealed that the growth and crop yield strictly depend upon climatic and environmental conditions and optimum crop cultivation should, therefore, be in accordance with rainfall and temperature regime (Karkanis et al., 2011). The environmental factors effect on seed maturation and agronomic quality of Milk thistle. Accelerated aging of seeds is different between various plant species and inside one seed clone but it induced by several days of exposure to high temperature and high humidity (Wong et al., 1986). Faster aging likewise brought about enhanced peroxidation of lipid, diminished antioxidant levels and also decreased action of a few chemicals associated with peroxides and free radicals scavenging (Bailly et al., 1998; Carlsson et al., 2003).

Distinctive medicinal species of plant indicated a well-marked variation in dynamic ingredients during various seasons; these have been generally credited to variation in different ecological factors, for example, temperature and rainfall (Ghimire et al., 2006; Kumar et al., 2007; Ahmad et al., 2008, 2009). Impacts of regular changes on biological systems are impinging hugely and progress in climate conditions, temperature variety, patterns of rainfall and corresponding mechanisms are related to natural changes (Root et al., 2003). Analysts opine that synthetic constituent and perseverance of medicinal plants are influenced significantly by climatic changes. Regularly plants under pressure conditions can gather increasingly secondary metabolites because of growth inhibition and fixed carbon diversion in the biosynthesis of phenolics and glycosidic mixes rather than photosynthesis (Gairola et al., 2010).

Contingent on natural variations, photosynthesis vary among species and decline relentlessly with enhancement of leaf age (Herath and Ormrod, 1979). Numerous studies have exhibited that ascent in temperature upgraded the production of secondary metabolites (Litvak et al., 2002), in spite of the fact that others believe that these metabolites declined (Snow et al., 2003). Tholl et al. (2006) also described that increment in temperature just increase the flowing of synthetic production in most plants and the impacts of high temperature are still getting attention (Wahid et al., 2007). Activities of enzymes (CAT, POD and SOD) are a significant index to foretell the plant responses to the changing environments (Sen and Mukherji, 2009). In plants, antioxidants activities may act like a defense line for many troublesome conditions. (Lohrmann et al., 2004). In plants specialized mechanisms for antioxidant defense contains many types of enzymes, for example enlistment of glutathione reductase, POD, CAT, SOD (Keles and Oncel, 2002). Research results show that the yield of milk thistle fruit (Andrzejewska and Sadowska, 2008) is determined by various agro-technological factors, including NPK fertilization.

In the light of above-mentioned literature, the main objectives of this study was to find out the effects of various agro climatic conditions on physio-chemical attributes of milk thistle and to determine the optimum soil and climatic conditions required for its better growth and metabolism.

Materials and methods

Wild Milk thistle (*Silybum marianum* L.) plants were collected from ten different locations of Punjab, Pakistan (Jalalpur Jattan, Gujrat, Kharian, Sarai Alamgir, Mandi Bauhudin, Dina, Sohawa, Gujar Khan, Rawalpindi and Islamabad) during the years of 2018 and 2019 as described in *Figure A1* in the *Appendix*. Five plant samples were collected randomly from each location between 9:00 am to 2:00 pm. Samples were collected from the away of road side that have no influence of automobile and industries pollutants. The meteorological data of these locations were noted with the help of Pakistan Meteorological Department (PMD), Pakistan. Soil samples were also collected from these locations for the study of soil characteristics with the help of Punjab Agriculture Soil Testing Labs, Pakistan. Photosynthetic pigments like chlorophyll *a*, *b* and total chlorophyll and carotenoid contents were measured using the method given by Arnon (1949). Gas exchange parameters such as photosynthetic rate, stomatal conductance, transpiration rate and sub stomatal CO₂ concentration were measured from fully expanded young leaves using LCA-4 ADC portable infrared gas analyzer (Analytical Development Company, Hoddeson, England. Model C1-340) along with

climatic factors described in *Table 1*. All the measurements were taken between 10:00 am - 02:00 pm as described by Khalid et al. (2017). The adjustments/specifications of IRGA were: leaf surface area 11.35 cm², temperature of leaf chamber (Tch) varied from 29.2 to 37.5 °C, ambient CO₂ concentration (Cref) 349.12 μmol mol⁻¹, ambient temperature ranged from 31-36 °C, leaf chamber volume gas flow rate (v) 397 ml min⁻¹, water vapor pressure in chamber ranged from 6-9.0 m bar, molar flow of air per unit leaf area (Us) 401.06 mol m⁻² s⁻¹, ambient pressure (P) 99.95 KPa, PAR (Q leaf) at leaf surface was up to 1515 μmolm⁻².

Table 1. Means of 2018 and 2019 Meteorological data of various locations

Locations	Average rainfall (mm)	Average temperature (°C)	Minimum average temperature (°C)	Maximum average temperature (°C)	Humidity (%)
L1(Jalalpur Jattan)	802	20	4	23.9	49
L2(Gujrat)	706	18	4	19.0	76
L3(Kharian)	809	18	4	23.7	78
L4(Sarai Alamgir)	726	18	4	17.7	77
L5(Mandi Bauhudin)	576	10	4	23.9	74
L6(Dina)	838	21	4	25.5	84
L7(Sohawa)	779	13	4	22.9	75
L8(Gujar Khan)	747	18	9	22.5	75
L9(Rawalpindi)	941	15	2.5	17.0	67
L10(Islamabad)	809	17	3.6	23.0	60

Whole plant water use efficiency (WUE) were measured from a mature and intact fully expanded upper leaves by following formula (Guo et al., 2006; Bacon, 2009):

$$\text{WUE (g/L)} = (\text{dry weight of final biomass} - \text{dry weight of initial biomass}) / \text{total water consumed} / \text{rainfall}$$

Estimation of CAT, POD and SOD activities were determined by the procedure of Chance and Maehly (1955). Determination of nitrogen contents according to Kjeldhal procedure as described by Bremner (1965) method and Phosphorous contents was measured with the help of Jackson (1962) method. Contents of potassium were detected with the help of Wolf method (1982).

Data were analyzed statistically using analysis of variance (ANOVA) technique using Ministate-C software. Data were presented as mean ± SE of five replicates and subjected to one-way analysis of variance (ANOVA) and mean separation was done at $P \leq 0.05$ by using Tukey's test (Silverman, 2018).

Results

There were following results from these experiments:

Meteorological characteristics

Mean data related to meteorology of two years is given in *Table 1*. Data was collected for those months (October, November, December, January, February, March and April) in which milk thistle completed its life cycle. Data was complied with the help Pakistan Meteorological Department (PMD) from ten different locations which

were under considerations. All the locations had varied rainfall, average, minimum and maximum temperature and humidity. Maximum rainfall (838 mm) was noted in location Dina and minimum (576 mm) rainfall was noted in Mandi Bauhudin. Maximum average temperature (21 °C) was in location Dina and minimum in location Sohawa (13 °C). In Location Dina maximum temperature was noted upto 25.5 °C. Location Dina had also maximum humidity (84%).

Soil properties

Physiochemical soil properties were studied of all the locations from which wild plants of milk thistle were collected (*Table 2*). There were clay loamy soils in all the locations except Rawalpindi and Islamabad. Soil collected from location Dina was best due to low EC, normal pH, high organic matter, nitrogen and potassium contents. There was high soil saturation % in location Dina that was 46 while other locations had up to 40% soil saturation percentage.

Table 2. Physiochemical properties of the soil collected from various locations

Soil characteristics	Soil texture	EC (dS/m)	pH	Organic matter (%)	N (mg/kg)	P (mg/kg)	K (mg/kg)	Saturation %age
L1(Jalalpur Jattan)	Clay loam	0.98	7.1	0.45	0.44	3	112	40
L2(Gujrat)	Clay loam	0.88	7.6	0.77	0.88	5	102	40
L3(Kharian)	Clay loam	0.88	7.3	0.69	0.31	5	104	40
L4(Saraialamgeer)	Clay loam	0.75	7.5	0.66	0.22	5	98	40
L5(Mandi Bauhudin)	Clay loam	0.74	7.0	0.57	0.16	5	98	38
L6(Dina)	Clay loam	0.65	7.2	0.85	0.87	5	100	46
L7(Sohawa)	Clay loam	0.75	7.1	0.62	0.12	7	98	42
L8(Gujarkhan)	Clay loam	0.85	7.2	0.50	0.32	3	102	40
L9(Rawalpindi)	Sandy clay loam	1.07	7.6	0.55	0.74	6	98	42
L10(Islamabad)	Sandy clay loam	1.02	7.5	0.57	0.76	3	114	40

Photosynthetic pigments

Results from analysis of variance (ANOVA) indicated that the effect of different climatic conditions on chlorophyll a, b, total chlorophyll and carotenoids contents were highly significant among different locations, years and their interaction in milk thistle collected from various locations (*Table 3*). *Figure 1A-D* showed that maximum amount of chlorophyll a, b total and carotenoids contents were recorded at L6 (Dina) in 2019 and minimum contents at L8 (Gujar Khan) in 2018. Location Dina was also best for soil and climatic conditions. Overall, there were high contents of photosynthetic pigments in the plants collected 2019 as compared to 2018.

Photosynthetic rate

Data revealed that maximum rate of photosynthesis was measured in the plants collected from L6 (Dina) during 2019 (*Fig. 1E*). ANOVA related to photosynthetic rate was highly significant for locations, years and its interaction (*Table 3*). Photosynthetic rate was significantly varied under different locations by the influence of ecological conditions. There was low photosynthetic rate during the year 2018 that might be due to changes in climatic conditions observed in both the years.

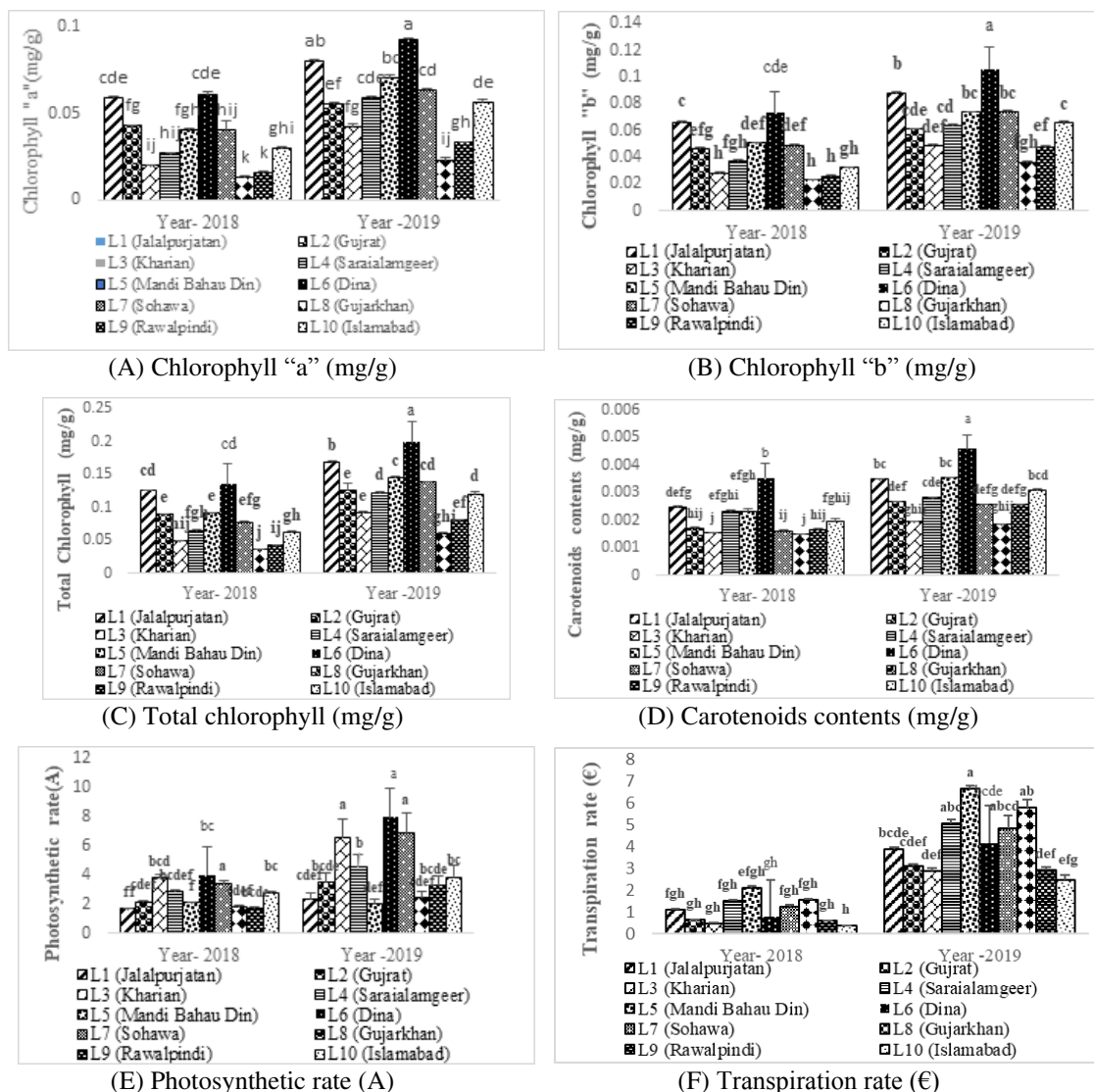


Figure 1. Influence of climatic conditions on photosynthetic and physiological attributes of milk thistle (*Silybum marianum*) at various ecological locations

Transpiration rate

Table 3 demonstrated that the impact of environmental factors on transpiration rate of milk thistle was highly significant among all the location. Variations among years and its interaction were also highly significant. High transpiration rate of milk thistle was noted in 2019 as compared to 2018 (Fig. 1E). Highest transpiration rate was noted in 2019 at Location-5 (Mandi Bahaudin) and minimum at Location-10 (Islamabad) in 2018. Results also indicated that effect of factors on transpiration rate was highly observed at Location-5 (Mandi Bahaudin) during 2018 as well as in 2019. High temperature resulted high rate of transpiration in milk thistle.

Stomatal conductance

Effect of various ecological factors (temperature, soil and rain fall) had significant results stomatal conductance. Variations between years were significant while,

interaction between locations and years was non-significant results (Table 3). Maximum stomatal conductance was observed in 2018 and minimum in 2019 (Fig. 2A). Data narrated that high stomatal conductance was noted at L8 (Gujar Khan) in 2018 and low conductance was in 2019 at L2 (Gujrat). During 2018, there was less variations in the data related to stomatal conductance. These changes were due to variations in climatic conditions in the both the years.

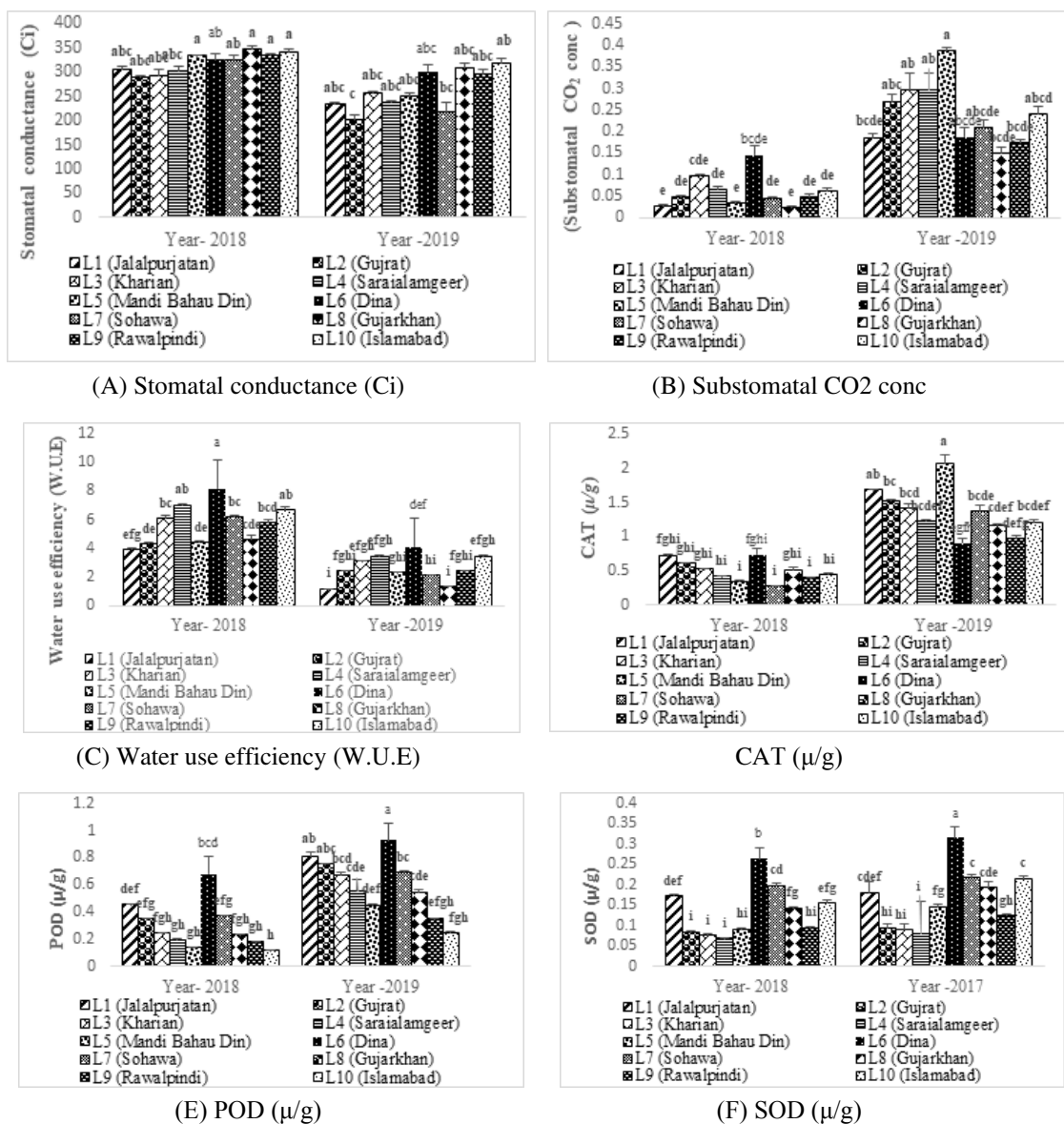


Figure 2. Influence of climatic conditions on physiological attributes and antioxidant activities of milk thistle (*Silybum marianum*) at various ecological locations

Substomatal CO₂ concentrations

Results present in Table 3 indicated that effect of different environmental conditions was significant on concentration of substomatal CO₂. Response of years and its interaction with locations was also highly significant. Concentration of substomatal CO₂

was high during 2019 as compared to 2018 (*Fig. 2B*). *Figure 2B* illustrated that high concentration of substomatal CO₂ was detected in 2019 at L5 (Mandi Bahaudin) and low values were noted in 2018 at L8 (Gujar Khan).

Water use efficiency (WUE)

Effect of climatic conditions was highly significant on whole water use efficiency of milk thistle (*Table 3*). High water use efficiency was noted at L6 (Dina) in 2018 and low water use efficiency was noted in 2019 at L1 (Jalalpur Jattan) due to climatic temperature and rainfall variations among locations and years (*Fig. 2C*). Water use efficiency was high during 2018 as compared to 2019. Location-6 (Dina) showed highest values on water use efficiency in both years as it has much varied climatic conditions from other location.

Catalase activity (CAT)

Effect of ecological factors on CAT was highly significant. Year response was also highly significant with its interaction (*Table 4*). Results from *Figure 2D* narrated that best antioxidant activities of CAT were noted at L5 (Mandi Bahaudin) in 2019 and low activity was in 2018 at L7 (Sohawa). Results also indicated that highest Catalase activities were observed in 2019 at all locations. CAT activities can be good indicators to show the environmental variation.

Peroxidase activity (POD)

Table 4 demonstrated that impact of various ecological factors was highly significant for POD activities with yearly and their interaction. *Figure 2E* indicated that high POD activities were obtained at Location-6 (Dina) in 2019 and minimum in 2018 at L10 (Islamabad). POD activities were high during at Dina during both the years 2018 and 2019. It was also clear from the results that in 2019 highest POD activities were obtained in comparison with 2018.

Superoxide-dismutase activity (SOD)

ANOVA results showed that SOD activities were highly significant in milk thistle under varied climatic conditions (*Table 4*). *Figure 2F* indicated that maximum activities of SOD were observed at L6 (Dina) in 2019 and Minimum activities was detected at L4 (Sarai Alamgir) in 2018. Results also revealed that the effect of factors on superoxide-dismutase activities was highly detected in all location of 2019 as compare to 2018. Changes in SOD was due to variations in climatic conditions.

Nitrogen (N) contents (mg/g)

Means square from ANOVA (*Table 5*) showed effect of ecological factors on nitrogen contents in root, stem, leaves and seeds were highly significant. Results indicated that effect of temperature, rain fall, soil and pH on nitrogen contents was highly significant among different variation and years. While the interaction between location and years showed non-significant results. *Figure 3A* showed that maximum contents of nitrogen were noted in stem part and minimum contents of nitrogen was noted in seeds at both 2018 and 2019. However, L6 (Dina) showed highest contents of nitrogen on all plants part at both the years.

Table 3. Means squares (MS) from the Analysis of variance (ANOVA) for photosynthetic and physiological attributes of milk thistle (*Silybum marianum*) collected from various ecological locations

Source	df	MS of chlorophyll a	MS of chlorophyll b	MS of total chlorophyll	MS of total carotenoids	MS of photosynthetic rate	MS of transpiration rate	MS of stomatal conductance	MS of substomatal CO ₂ conc.	MS of water use efficiency (W.U.E)
Location	9	0.03422***	0.003419***	0.013743***	0.000005***	29.4768***	9.599***	8406***	0.016912**	12.535***
Year	1	0.013512***	0.013366***	0.048146***	0.000018***	30.008***	248.252***	81693***	0.808201***	244.844***
Location × year	9	0.000238***	0.000107**	0.001104***	0.000001*	4.5499***	1.810**	2155 ns	0.016710**	1.326**
Error	80	0.000033	0.000042	0.000065	0.000002	0.6175	0.803	2375	0.007338	0.552
Total	99	0.049095	0.048460	0.187002	0.000073	385.65	415.20	366761	1.6979	413.73

Table 4. Means squares (MS) from the analysis of variance (ANOVA) for antioxidant activities of milk thistle (*Silybum marianum*) collected from various ecological locations

Source	df	MS of catalase activity (CAT)	MS of peroxidase activity (POD)	MS of superoxide-dismutase activity (SOD)
Location	9	0.3210***	0.35089***	0.046313***
Year	1	18.0889***	2.33356***	0.023525***
Location × year	9	0.4030***	0.02295**	0.001117***
Error	80	0.0468	0.01031	0.000272
Total	99	28.345	6.5234	0.47212

Table 5. Means squares (MS) from the analysis of variance (ANOVA) for ion concentrations in milk thistle (*Silybum marianum*) collected from various ecological locations

Source	df	MS of N-contents in root	MS of N-contents in stem	MS of N-contents in leaves	MS of N-contents in seeds	MS of K-contents in root	MS of K-contents in stem	MS of K-contents in leaves	MS of K-contents in seeds	MS of P-contents in root	MS of P-contents in stem	MS of P-contents in leaves	MS of P contents in seeds
Location	9	77.480***	75.969***	91.247***	53.470***	94.388***	82.112***	108.027***	94.804***	0.0026530***	0.016790***	0.002950***	0.000515***
Year	1	137.124***	85.748***	427.662***	165.894***	90.250***	327.610***	33.640***	17.640***	0.001600***	0.027275***	0.005127***	0.001190***
Location × year	9	0.932ns	1.824ns	2.310ns	1.546ns	2.406ns	2.032ns	2.262ns	1.440ns	0.000083ns	0.000772ns	0.000012ns	0.000010ns
Error	80	2.322	2.032	4.072	1.536	3.150	2.770	2.795	2.100	0.000222	0.000633	0.000025	0.000014
Total	99	185.74	948.44	1595.46	783.95	1213.39	136.51	1249.84	1051.84	0.226950	0.048253	0.33789	0.007005

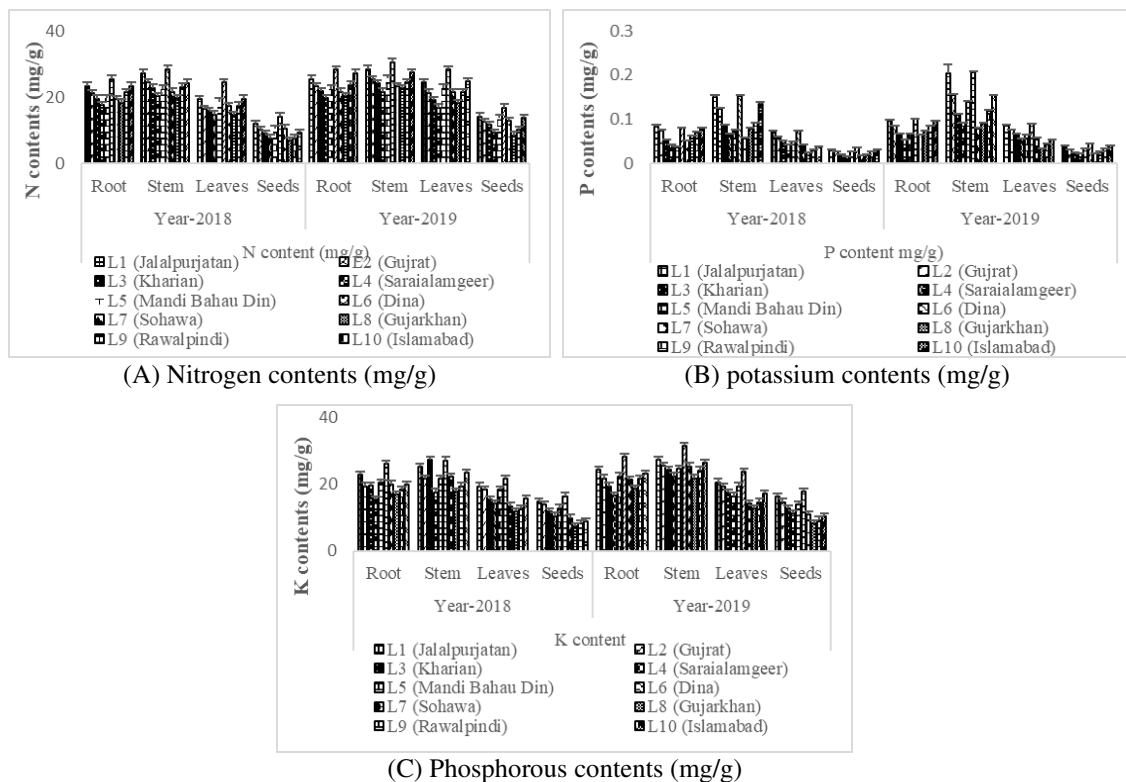


Figure 3. Influence of climatic conditions on ions concentrations of milk thistle (*Silybum marianum*) at various ecological locations

Potassium (K) contents (mg/g)

Maximum potassium contents were noted in stem and minimum in seeds during both the years (Fig. 3B). ANOVA results showed that Location Dina showed maximum potassium contents on various parts of the plant (Table 5). Diverse climate (temperature, rain fall and soil) had highly significant results on different locations as well as years for K contents. While the interaction between years and location showed non-significant results. It was observed that maximum K contents were measured during 2019 from all locations as compared to 2018.

Phosphorous (P) contents (mg/g)

Table 3 showed the impacts of environmental factors on phosphorous contents on root, stem, leaves and seeds. There were highly significant among different locations and years. However, its interaction was non-significant (Table 5). Figure 3C showed that maximum phosphorous contents were present in stem and seeds during 2018 and 2019. Maximum phosphorous contents were measured in Location-1 (Jalalpur Jattan) and Location-6 (Dina) during both the years (2018 and 2019).

Discussion

It is observed that changes occurring in the environment create negative effects on milk thistle. These effects create an impression on the physiology of this plant and change it in various respects. Researches carried out to notice such type of changes have

shown reductions in chlorophyll pigment in numerous plants as *Eucalyptus citriodora*, *Mangifera indica*, *Shorea robusta*, *Tectona grandis* (Joshi and Sawami, 2007), *Duranta repens* (Raina and Bala, 2011), *Prosopis juliflora* (Seyyednejad and Koochak, 2013) and *Artemisia maritima* (Laghari et al., 2015) as a result of the effects of environmental changes. It is, therefore, argued that a decrease within the pigment contents that results from the impact of various factors in the environment creates a degradation of pigments and destruction of plastid in cells (Satija et al., 2009). Swaisgood et al. (2018) also reported in earlier study that variations in the environment cause a decrease in photosynthetic pigments of plants.

The photosynthetic machinery of plants is sensitive to temperature especially biosynthesis of chlorophyll, activity of enzyme Rubisco, PS- II and net rate of photosynthesis are the main targets of heat damage in plants (Sinsawat et al., 2004). Heat stress damage the process of photosynthesis in plants which lead to photo-inhibition. As a result reduced electron acceptors accumulates and reactive oxygen species form (hydrogen peroxide) hence cause oxidative damage (Cui et al., 2006). Heat stress causes the accumulation ROS in excess amount at cellular level leading to lipid peroxidation and damage nucleic acid, proteins and especially photosynthetic pigments (Wang et al., 2014). Due to climatic conditions related to temperature stress, 15-20% of maize production has been lost throughout the world (Chen et al., 2012). The C4 plants like maize are more adapted to temperature stress but net rate of photosynthesis drops down when temperature of leaves of this plant increases up to 38°C (Crafts-Brandner and Salvucci, 2002; Coskun, 2011).

Due to global warming, air vapor pressure deficit of leaves will increase (Kirschbaum, 2000; Way et al., 2013). So the rate of transpiration may also increase in high temperature (Rawson et al., 1977; Kirschbaum, 2004). However, plants may close their stomata to cope with high temperature so that water loss may be prevented in arid ecosystem (Larcher, 2003). After that the rate of transpiration can decrease under warming climate. Previous studies showed that under supplemental precipitation, the rate of transpiration in plants was also high (Wullschleger and Hanson, 2006; Patrick et al., 2007). According to Starck et al. (1993) stomatal conductance decrease in tomato when temperature increases. Von Caemmerer and Farquhar (1981) reported that net changes in the rate of CO₂ show fluctuations in both conductance of stomata and capacity of mesophyll cells for the process of photosynthesis. According to Camejo et al. (2006), reduced CO₂ assimilation was seen in heat shocked Amalia plants could be due to decreased stomatal conductance, but fluorescence emission of chlorophyll in the genotype of Amalia was also altered because of heat shock, showing to modifications in mesophyll content of leaf.

High temperature (above 33°C) cause oxidative stress that degrade the proteins and enzyme activity which in turns damage the cell membrane (Bavita et al., 2012). The rate of respiration in plants increase in high temperature that enhance antioxidant response to accumulation of reactive oxygen species (ROS) in mitochondria. According to Dizengremel (2001), increased NADH synthesis enhance SOD formation under high rate of respiration. Respiration rate and SOD-manganese enzyme activity increase due to heat stress in *Nicotiana plumbagifolia* (Bowler et al., 1992). Alterations in evapotranspiration and ambient temperature were highly significant among environmental fluctuations. Osmotic strain over the leaves and induction enzymatic antioxidants caused by these fluctuations are well reported in abiotic stresses such as heat stress (Wahid et al., 2007), cold stress (Wu et al., 1999; McKersie et al., 1999),

high light intensity (Gupta et al., 1993) and drought stress (Farooq et al., 2009). Various other studies have reported that different conditions of agriculture can influence concentration of bioactive compounds like silymarin in milk thistle. Hammouda et al. (1993) reported that individual silymarin constituents and silymarin levels were influenced by levels of nitrogen and moisture availability. In the plants grown at 60% field capacity, highest level of silymarin (63.1% Silymarin in ethyl acetate extract) was observed. At this water level, the levels of silybin, silychristin and isosilybin were also highest.

Conclusion and recommendations

It was concluded that milk thistle plants were flourishing best at location Dina that had an optimum soil characteristics i.e. Sandy loam, 0.65 dS/m EC, 0.65% organic matter and 47% soil saturation) and climatic conditions (a maximum temperature of 25 °C, average temperature of 21 °C and high amounts of rainfall (838 mm) with 84% humidity). So, it is proposed that such categories of soil and climatic conditions are best for the cultivation of milk thistle at commercial scale. These physiological and biochemical indicators can be used to evaluate the milk thistle response towards diverse climatic conditions.

It is recommended to grow the milk thistle at an average temperature of 25 °C, rainfall amount 838 mm and humidity 84%. Further studies are required to evaluate its active constituents at varied climatic conditions for quality medicines.

REFERENCES

- [1] Abenavoli, L., Izzo, A. A., Milic, N., Cicala, C., Santini, A., Capasso, R. (2018): Milk thistle (*Silybum marianum*): a concise overview on its chemistry, pharmacological, and nutraceutical uses in liver diseases. – *Phytotherapy Research* 32: 2202-2213.
- [2] Ahmad, I., Hussain, M., Ahmad, M. S. A., Ashraf, M. Y., Ahmad, R., Ali, A. (2008): Spatio-temporal variations in physiochemical attributes of *Adiantum capillus-veneris* from Soone Valley of salt range (Pakistan). – *Pakistan Journal of Botany* 40: 1387-1398.
- [3] Ahmad, I., Ahmad, M. S. A., Hussain, M., Hameed, M., Ashraf, M. Y., Koukab, M. Y. (2009): Spatio-temporal effects on species classification of medicinal plants in Soone Valley of Pakistan. – *International Journal of Agriculture and Biology* 11: 64-68.
- [4] Alemardan, A., Karkanis, A., Salehi, R. (2013): Breeding objectives and selection criteria for milk thistle (*Silybum marianum* (L.) Gaertn.) improvement. – *Notulae Botanicae Horti Agrobotanici Cluj-Napoca* 41: 340-347.
- [5] Andrzejewska, J., Sadowska, K. (2008): Effect of cultivation conditions on the variability and interrelation of yield and raw material quality in milk thistle (*Silybum marianum* (L.) Gaertn.). – *Acta Scientiarum Polonorum Agricultura* 7(3): 3-7.
- [6] Arnon, D. I. (1949): Copper enzymes in isolated chloroplasts. Polyphenoloxidase in *Beta vulgaris*. – *Plant Physiology* 24: 1.
- [7] Bailly, M., Condeelis, J. S., Segall, J. E. (1998): Chemoattractant-induced lamellipod extension. – *Microscopy Research and Technique* 43: 433-443.
- [8] Bavita, A., Shashi, B., Navtej, S. B. (2012): Nitric oxide alleviates oxidative damage induced by high temperature stress in wheat. – *Indian Journal of Experimental Biology* 50(5): 372-380.
- [9] Bacon, M. (Ed.) (2009): *Water Use Efficiency in Plant Biology*. – John Wiley & Sons, New York.

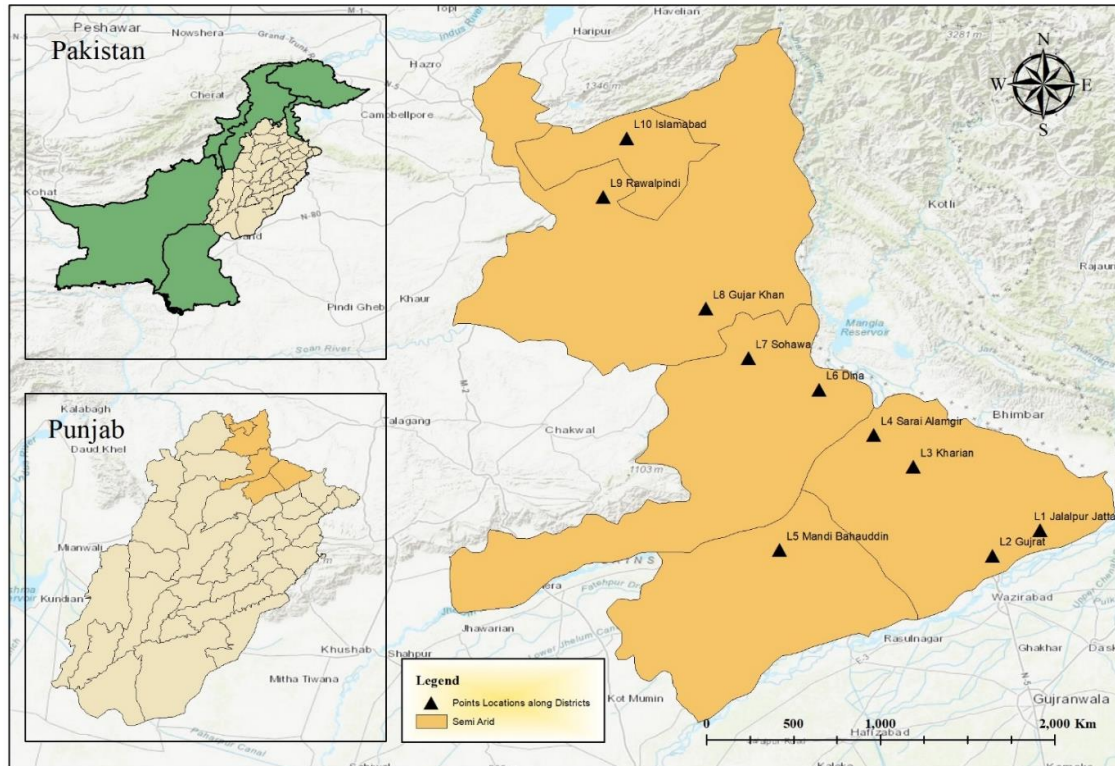
- [10] Bijak, M. (2017): Silybin, a major bioactive component of milk thistle (*Silybum marianum* L. Gaert.). – Chemistry, Bioavailability & Metabolism Molecules 22: 1942.
- [11] Bowler, C., Montagu, M. V., Inze, D. (1992): Superoxide dismutase and stress tolerance. – Annual Review of Plant Biology 43: 83-116.
- [12] Bremner, J. M. (1965): Total Nitrogen. – In: Black, C. A. (ed.) Methods of Soil Analysis. Part 2: Chemical and Microbial Properties. Number 9 in Series Agronomy. American Society of Agronomy, Inc. Publisher, Madison, WI, pp. 1049-1178.
- [13] Camejo, D., Ana, J., Juan, J. A., Walfredo, T., Juana, M. G., Francisca, S. (2006): Changes in photosynthetic parameters and antioxidant activities following heat-shock treatment in tomato plants. – Functional Plant Biology 33: 177-187.
- [14] Carlsson, G. E., Moller, A., Blomstrand, C., Ueda, T., Mizushige, K., Yukiiri, K., Yang, C. C. (2003): European stroke initiative recommendations for stroke management - update 2003. – Cerebrovascular Diseases 16: 311-337.
- [15] Chance, M., Maehly, A. C. (1955): Assay of catalases and peroxidases. – Methods in Enzymology 2: 764-817.
- [16] Chen, W. E. N. R. O. N. G., Cen, W., Chen, L., Di, L., Li, Y.-Q., Guo, W. (2012): Differential sensitivity of four highbush blueberry (*Vaccinium corymbosum* L.) cultivars to heat stress. – Pakistan Journal of Botany 44: 853-860.
- [17] Coskun, Y., Coskun, A., Demirel, U., Ozden, M. (2011): Physiological response of maize (*Zea mays* L.) to high temperature stress. – Australian Journal of Crop Science 5: 966.
- [18] Crafts-Brandner, S. J., Salvucci, M. E. (2002): Sensitivity of photosynthesis in a C4 plant, maize, to heat stress. – Plant Physiology 129: 1773-1780.
- [19] Cui, L., Li, J., Fan, Y., Xu, S., Zhang, Z. (2006): High temperature effects on photosynthesis, PSII functionality and antioxidant activity of two *Festuca arundinacea* cultivars with different heat susceptibility. – Botanical Studies 47: 61-69.
- [20] Cui, L. L., Kerkela, E., Bakreen, A., Nitzsche, F., Andrzejewska, A., Nowakowski, A., Jolkkonen, J. (2015): The cerebral embolism evoked by intra-arterial delivery of allogeneic bone marrow mesenchymal stem cells in rats is related to cell dose and infusion velocity. – Stem Cell Research and Therapy 6: 11.
- [21] Dizengremel, P. (2001): Effects of ozone on the carbon metabolism of forest trees. – Plant Physiology & Biochemistry 39: 729-742.
- [22] Dominguez, M. T., Montiel-Rozas, M. M., Madejon, P., Diaz, M. J., Madejon, E. (2017): The potential of native species as bioenergy crops on trace-element contaminated Mediterranean lands. – Science of the Total Environment 590: 29-39.
- [23] Farooq, M., Wahid, A., Kobayashi, N., Fujita, D. B. S. M. A., Basra, S. M. A. (2009): Plant Drought Stress: Effects, Mechanisms and Management. – In: Lichtfouse, E. et al. (eds.) Sustainable Agriculture. Springer, Dordrecht, pp. 153-188.
- [24] Gairola, S., Shariff, N. M., Bhatt, A. (2010): Influence of climate change on production of secondary chemicals in high altitude medicinal plants: issues needs immediate attention. – Journal of Medicinal Plants Research 4: 1825-1829.
- [25] Ghimire, S. K., Mckey, D., Aumeeruddy-Thomas, Y. (2006): Himalayan medicinal plant diversity in an ecologically complex high altitude anthropogenic landscape, Dolpo, Nepal. – Environmental Conservation 33: 128-140.
- [26] Giannopolitis, C. N., Ries, S. K. (1977): Superoxide dismutases: I. Occurrence in higher plants. – Plant Physiology 59: 309-314.
- [27] Guo, S. W., Zhou, Yi., Song, N., Shen, Q. (2006): Some physiological processes related to water use efficiency of higher plants. – Agricultural Sciences in China 5: 403-411.
- [28] Gupta, A. S., Heinen, J. L., Holaday, A. S., Burke, J. J., Allen, R. D. (1993): Increased resistance to oxidative stress in transgenic plants that overexpress chloroplastic Cu/Zn

- superoxide dismutase. – Proceedings of the National Academy of Sciences 90: 1629-1633.
- [29] Hammouda, F. M., Ismail, S. I., Hassan, N. M., Zaki, A. K., Kamel, A., Rimpler, H. (1993): Evaluation of the silymarin content in *Silybum marianum* (L.) Gaertn. Cultivated under different agricultural conditions. – Phytotherapy Research 7: 90-91.
- [30] Herath, H. M. W., Ormrod, D. P. (1979): Effects of temperature and photoperiod on winged beans (*Psophocarpus tetragonolobus* L. DC). – Annals of Botany 43: 729-736.
- [31] Jackson, M. L. (1962): Soil Chemical Analysis. – Constable and Co. Ltd., London.
- [32] Joshi, P. C., Swami, A. (2007): Physiological responses of some tree species under roadside automobile pollution stress around city of Haridwar, India. – The Environmentalist 27: 365-374.
- [33] Karkanis, A., Bilalis, D., Efthimiadou, A. (2011): Cultivation of milk thistle (*Silybum marianum* L. Gaertn.), a medicinal weed. – Industrial Crops and Products 34: 825-830.
- [34] Keleş, Y., Oncel, I. (2002): Response of antioxidative defence system to temperature and water stress combinations in wheat seedlings. – Plant Science 163: 783-790.
- [35] Khalid, N., Mumtaz, H., Mansoor, H., Rashid, A. (2017): Physiological, biochemical and defense system response of parthenium hysterophorus to vehicular exhaust pollution. – Pakistan Journal of Botany 49: 67-75.
- [36] Kirschbaum, M. U. (2000): Forest growth and species distribution in a changing climate. – Tree Physiology 20: 309-322.
- [37] Kirschbaum, M. U. F. (2004): Direct and indirect climate change effects on photosynthesis and transpiration. – Plant Biology 6: 242-253.
- [38] Kumar, A., Kaul, M. K., Bhan, M. K., Khanna, P. K., Suri, K. A. (2007): Morphological and chemical variation in 25 collections of the Indian medicinal plant, *Withania somnifera* (L.) Dunal (Solanaceae). – Genetic Resources & Crop Evolution 54: 655-660.
- [39] Laghari, M., Mirjat, M. S., Hu, Z., Fazal, S., Xiao, B., Hu, M., Guo, D. (2015): Effects of biochar application rate on sandy desert soil properties and sorghum growth. – Catena 135: 313-320.
- [40] Larcher, W. (2003): Ecophysiology and Stress Physiology of Functional Groups. – In: Larcher, W. (ed.) Physiological Plant Ecology. Springer Science & Business Media, Berlin.
- [41] Litvak, M. E., Constable, J. V., Monson, R. K. (2002): Supply and demand processes as controls over needle monoterpene synthesis and concentration in Douglas fir (*Pseudotsuga menziesii* (Mirb.)). – Oecologia 132: 382-391.
- [42] Lohrmann, N. L., Logan, B. A., Johnson, A. S. (2004): Seasonal acclimatization of antioxidants and photosynthesis in *Chondrus crispus* and *Mastocarpus stellatus*, two co-occurring red algae with differing stress tolerances. – The Biological Bulletin 207: 225-232.
- [43] McKersie, B. D., Bowley, S. R., Jones, K. S. (1999): Winter survival of transgenic alfalfa overexpressing superoxide dismutase. – Plant Physiology 119: 839-848.
- [44] Patrick, L., Cable, J., Potts, D., Ignace, D., Barron-Gafford, G., Griffith, A., Zak, J. (2007): Effects of an increase in summer precipitation on leaf, soil, and ecosystem fluxes of CO₂ and H₂O in a sotol grassland in Big Bend National Park, Texas. – Oecologia 151: 704-718.
- [45] Raina, A. K., Bala, C. (2011): Effect of vehicular pollution on *Duranta repens* L. in Jammu City. – Journal of Applied and Natural 3: 211-218.
- [46] Rawson, H. M., Begg, J. E., Woodward, R. G. (1977): The effect of atmospheric humidity on photosynthesis, transpiration and water use efficiency of leaves of several plant species. – Planta 134: 5-10.
- [47] Root, T. L., Price, J. T., Hall, K. R., Schneider, S. H., Rosenzweig, C., Pounds, J. A. (2003): Fingerprints of global warming on wild animals and plants. – Nature 421: 57.

- [48] Satija, N. K., Singh, V. K., Verma, Y. K., Gupta, P., Sharma, S., Afrin, F. (2009): Mesenchymal stem cell-based therapy: a new paradigm in regenerative medicine. – *Journal of Cellular and Molecular Medicine* 13: 4385-4402.
- [49] Sen, S., Mukherji, S. (2000): Season-induced alterations in levels of antioxidants and polygalacturonase activity in tomato (*Lycopersicon esculentum* Mill.) fruit. – *Journal of Environment and Pollution* 7: 303-308.
- [50] Sersen, F., Vencel, T., Annus, J. (2006): Silymarin and its components scavenge phenylglyoxylic ketyl radicals. – *Fitoterapia* 77: 525-529.
- [51] Seyyedneiad, S. M., Koochak, H. (2013): Some morphological and biochemical responses due to industrial air pollution in *Prosopis juliflora* (Swartz) DC plant. – *African Journal of Agricultural Research* 8: 1968-1974.
- [52] Silverman, B. W. (2018): *Density Estimation for Statistics and Data Analysis*. – CRC Press, Taylor & Francis Group, Routledge.
- [53] Sinsawat, V., Leipner, J., Stamp, P., Fracheboud, Y. (2004): Effect of heat stress on the photosynthetic apparatus in maize (*Zea mays* L.) grown at control or high temperature. – *Environmental and Experimental Botany* 52: 123-129.
- [54] Snow, M. D., Bard, R. R., Olszyk, D. M., Minster, L. M., Hager, A. N., Tingey, D. T. (2003): Monoterpene levels in needles of Douglas fir exposed to elevated CO₂ and temperature. – *Physiologia Plantarum* 117: 352-358.
- [55] Starck, Z., Wazynska, Z., Kucewicz, O. (1993): Comparative effects of heat stress on photosynthesis and chloroplast ultrastructure in tomato plants with source-sink modulated by growth regulators. – *Acta Physiologiae Plantarum* 15: 125-133.
- [56] Swaisgood, R. R., Wang, D., Wei, F. (2018): Panda downlisted but not out of the woods. – *Conservation Letters* 11: 12355.
- [57] Tholl, D., Boland, W., Hansel, A., Loreto, F., Rose, U. S., Schnitzler, J. P. (2006): Practical approaches to plant volatile analysis. – *The Plant Journal* 45: 540-560.
- [58] Von Caemmerer, S. V., Farquhar, G. D. (1981): Some relationships between the biochemistry of photosynthesis and the gas exchange of leaves. – *Planta* 153: 376-387.
- [59] Wahid, A., Gelani, S., Ashraf, M., Foolad, M. R. (2007): Heat tolerance in plants: an overview. – *Environmental & Experimental Botany* 61: 199-223.
- [60] Wang, C., Wen, D., Sun, A., Han, X., Zhang, J., Wang, Z., Yin, Y. (2014): Differential activity and expression of antioxidant enzymes and alteration in osmolyte accumulation under high temperature stress in wheat seedlings. – *Journal of Cereal Science* 60: 653-659.
- [61] Way, D. A., Domec, J. C., Jackson, R. B. (2013): Elevated growth temperatures alter hydraulic characteristics in trembling aspen (*Populus tremuloides*) seedlings: implications for tree drought tolerance. – *Plant, Cell & Environment* 36: 103-115.
- [62] Wolf, B. (1982): A comprehensive system of leaf analyses and its use for diagnosing crop nutrient status. – *Communications in Soil Science and Plant Analysis* 13: 1035-1059.
- [63] Wong, E. H., Kemp, J. A., Priestley, T., Knight, A. R., Woodruff, G. N., Iversen, L. L. (1986): The anticonvulsant MK-801 is a potent N-methyl-D-aspartate antagonist. – *Proceedings of the National Academy of Sciences* 83: 7104-7108.
- [64] Wu, G., Wilen, R. W., Robertson, A. J., Gusta, L. V. (1999): Isolation, chromosomal localization, and differential expression of mitochondrial manganese superoxide dismutase and chloroplastic copper/zinc superoxide dismutase genes in wheat. – *Plant Physiology* 120: 513-520.
- [65] Wullschleger, S. D., Hanson, P. J. (2006): Sensitivity of canopy transpiration to altered precipitation in an upland oak forest: evidence from a long-term field manipulation study. – *Global Change Biology* 12: 97-109.

APPENDIX

Figure A1. Map showing the different locations where study was conducted



A COMPARISON OF SEVERAL COMMON MATHEMATICAL INDICES FOR MEASURING FUNCTIONAL DIVERSITY IN FOREST COMMUNITIES IN THE WULINGSHAN NATURE RESERVE, NORTH CHINA

SONG, N. Q.¹ – ZHANG, Y. L.² – ZHANG, J. T.^{2*}

¹*School of Chinese Materia Medica, Beijing University of Chinese Medicine, Beijing 102488, China*

²*Key Laboratory of Biodiversity Science and Ecological Engineering, Ministry of Education; College of Life Sciences, Beijing Normal University, Beijing 100875, China*

**Corresponding author*

e-mail: Zhangjt@bnu.edu.cn; phone: +86-10-5880-3093; fax: +86-10-5880-7721

(Received 23rd Jan 2020; accepted 22nd May 2020)

Abstract. Functional diversity and its change mechanisms are important for forest conservation. Change patterns of functional diversity in forest communities along altitudinal and disturbance gradients in the Wulingshan Nature Reserve were analyzed using several common indices. Forty-one 20 m × 20 m plots of forest communities were established along the altitudinal gradient. Plant species, functional traits and environmental variables were measured and recorded. Six functional diversity indices, Functional Attribute Diversity (FAD), Modified Functional Attribute Diversity (MFAD), Functional diversity based on dendrogram (FDp and FDc), Functional evenness (FEve) and Functional divergence (FDiv), were employed to quantify functional diversity. The results showed a great change in functional diversity of the forest communities in the Wulingshan Reserve. Functional diversity was significantly correlated with altitude and disturbance gradients. A non-linear “humped” change pattern along the altitudinal gradient and a non-linear or near linear decrease pattern along the disturbance intensity gradient were identified. Elevation and disturbance were the key factors influencing functional diversity. Functional diversity was closely related to species diversity in forests. The six common indices used were all effective and complementary to each other in functional diversity analysis in forests. MFAD, FEve and FDiv should be preferred in practice.

Keywords: *environmental gradient, disturbance intensity, functional diversity index, functional traits, forest conservation*

Introduction

Biodiversity and its conservation are two among the hottest topics in ecological studies (Austrheim, 2002). Species diversity, the measure of diversity in a community, is frequently studied in community ecology. Species diversity takes into consideration species richness and evenness, i.e. the total number of different species and the variation of abundance in individuals per species in a community (Perronne et al., 2014). However, the variation of species functions or in other words, functional diversity, has been poorly studied (Laliberte and Legendre, 2010). Functional diversity refers to the variation of species functions in a community (Petchey and Gaston, 2002; Zhang et al., 2015a). Plant species functions can be reflected by the type, change amplitude and stability of plant functional traits in a community (Villéger et al., 2008). Functional diversity is an important driver of ecological processes in a community (Zhang et al., 2014) and has become a key concept in ecology in recent years (Spasojevic et al., 2014; Rossi et al., 2020).

The variation of functional diversity and its mechanism is the bases for forest conservation and have become attractive to forest ecologists and conservators (Muhumuza and Byarugaba, 2009; Pavoine and Bonsall, 2011). Nature reserves in the mountains are significant in forest conservation and ecological protection since most nature forests are distributed in mountainous regions with limited area in countries like China (Cui et al., 2008; Zhang et al., 2015a). Variation patterns of species diversity along altitudinal gradient have been studied frequently (e.g. Austrheim, 2002; Zhang et al., 2013; Perronne et al., 2014; Bricca et al., 2019) and most of them found a “humped” distribution pattern showing the maximum species diversity near the middle of the gradient (Austrheim, 2002; Otypkova et al., 2011; Zhang et al., 2014). However, functional diversity and its change patterns along environmental gradients have not been sufficiently studied (Albert et al., 2012; Zhang et al., 2015b).

The Wulingshan reserve is a famous eco-tourism destination for citizens in Beijing and Hebei Province (Xiang and Zhang, 2009). Forests are significant in the local economy and development and should be conserved effectively in this reserve. Some researches on eco-tourism resources and evaluation (Zhang et al., 2003), plant resources and floristic characteristics (He et al., 1992; Duan, 2009), the vertical distribution of forest communities (Liu and Xi, 1997), vegetation landscape patterns (Bai et al., 2006), and so on have been conducted in this Reserve. However, the variation of functional diversity associated with the major environmental gradients has not been examined. This study aimed to analyze the interdependencies of functional diversity, environmental variables and disturbance in forest communities, to compare the effectiveness of several common functional diversity indices, and to test the hypothesis that functional diversity peaks at an intermediate altitude and medium disturbance in forests in the Wulingshan Nature Reserve.

Materials and methods

Study area

The Wulingshan Nature Reserve, located at 117°17'- 117°35'E, 40°29'- 40°36'N, is in the Miyun County of Beijing and Xinglong County in Hebei Province (*Fig. 1*). The reserve was established to protect the typical forest ecosystems and the northern limit of distribution of the rhesus macaque in 1984. It covers an area of 14,337 ha (Liu and Xi, 1997). Its highest peak, 2116 m ASL, is in the northern part of Xinglong County. Its climate is deeply affected by the warm temperate southeastern monsoon. The annual mean temperature is 7.6 °C; the mean monthly temperature of July is 17.7 °C, whereas the mean monthly temperature of January is -15.6 °C. The annual mean precipitation varies from 600 mm (northern slope) to 720 mm (southern slope). The main soil types include cinnamon soil in the lower area, brown forest soil in typical forest area and mountain meadow soil over the forest line of this mountain. The vegetation includes secondary forests with some plantations from 700 to 1900 m ASL and mountain meadows and scrublands above 1900 m ASL.

Data collection

Based on a general survey, 16 sampling points separated by 60-80 m in altitude were set up along the altitudinal gradient in forest area between 700 and 1900 m ASL in the Wulingshan Reserve. Two to four plots (20 m × 20 m) around each sampling point were

established randomly. The cover, height, individual abundance and diameter at breast height (DBH) for tree species and the height and cover for shrubs and herbs were measured and recorded for each plot. Tree height was measured using a height-meter (Haguang CGQ-1, 0-77 m) and shrub and herb height using a tape ruler. DBH was measured using a caliper (Argus PiCUS Calliper, 0-150 cm). A total of 172 plant species were recorded in 41 plots.

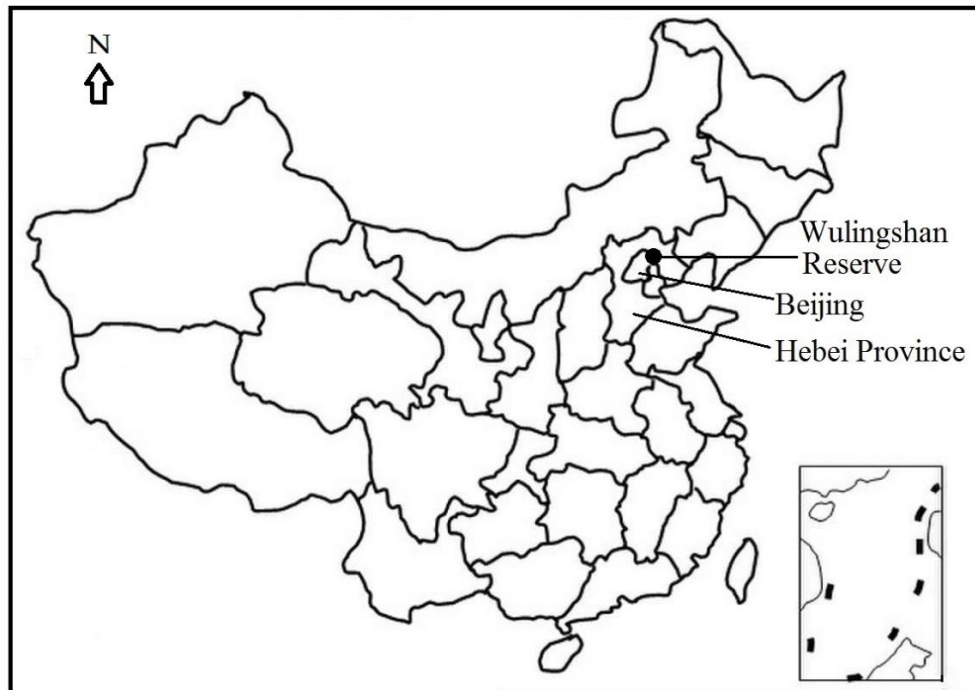


Figure 1. Geographical location of the study area, the Wulingshan Nature Reserve, China

Twelve plant functional traits were selected to reflect species functions in the plant community (*Table 1*). Photosynthesis pathway, pollination manner, seed dispersal, life-form, root system and nitrogen-fixing type were identified from local flora. Leaf form, leaf hair, plant height, flowering date and period, and fruit maturity date were investigated in the field. Functional diversity indices were calculated using a data matrix of plant species by functional traits for each plot. There were 41 data matrices for 41 plots in total.

Five environmental variables, altitude, slope, aspect, soil depth and litter thickness, were measured and recorded for each plot. The elevation was measured using a GPS, the slope and aspect were measured using a compass meter, the soil depth was measured using a soil depth instrument and the litter thickness was measured using a ruler directly (Zhang et al., 2015a). The elevation, slope, litter thickness and soil depth were measured values, while the slope aspect was transformed to 1-8 values: 1 (337.6°-22.5°), 2 (22.6°-67.5°), 3 (292.6°-337.5°), 4 (67.6°-112.5°), 5 (247.6°-292.5°), 6 (112.6°-157.5°), 7 (202.6°-247.5°), and 8 (157.6°-202.5°). The greater the value, the more sunlight is available.

The disturbance intensity from human activity (mainly tourism activity) was evaluated as scores of 1-5 based on tourist density, trampling extent on understory plants, distance from traveling pathway, number of pieces of garbage, and ratio of

human accompanying plant species in a plot: 1 (non-obvious disturbance), 2 (weak disturbance), 3 (medium disturbance), 4 (heavy disturbance) and 5 (very heavy disturbance) (Zhang et al., 2013).

Table 1. Plant functional traits and their values in forest communities in the Wulingshan Nature Reserve, North China

Functional trait type	Data type	Functional traits and values
Photosynthesis pathway	Attribute value	1 Crassulacean pathway, 2 C3 pathway, 3 between C3 and C4 pathway, 4 C4 pathway
Nitrogen-fixing	Attribute value	0 No nitrogen-fixing, 1 Elaeagnaceae nitrogen-fixing, 2 Leguminosae nitrogen-fixing, 3 mycorrhiza nitrogen-fixing
Seed dispersal	Attribute value	1 Automatic spreading, 2 gravity spreading, 3 wind spreading, 4 animals spreading, 5 non-flowering plant
Pollination method	Attribute value	1 Anemophilous, 2 entomophilous, 3 self-pollinated
Life-form	Attribute value	1 Tree, 2 shrubs, 3 woody vine, 4 perennial herb, 5 annual herb
Leaf form	Attribute value	1 Coniferous, 2 Broad leaf, 3 non leaf
Leaf hairs	Attribute value	0 No hair, 1 hairs on top surface, 2 hairs on back surface, 3 hairs on both sides
Root system	Duality value	1 Taproot system, 2 Fibre system
Plant height	Quantitative value	Measured value in m
Flowering date	Quantitative value	Beginning month of flowering
Flowering period	Quantitative value	Flowering months
Fruit maturity date	Quantitative value	Beginning month of fruit mature

Data analysis

Functional diversity indices

Six common functional diversity indices were used to calculate functional diversity in forest communities:

Functional attribute diversity (FAD)

FAD is a measure of species dispersion in trait space and refers to the sum of the pairwise species functional distances (Walker et al., 1999):

$$FAD = \sum_{i,j} d_{ij} \quad (\text{Eq.1})$$

where d_{ij} is the functional distance between species i and j in functional trait space. S is the number of species in a plot.

Modified functional attribute diversity (MFAD)

For MFAD, the functional unit was defined by combining the species with the same values in all the traits into one unit. The number of species will be reduced from S to M ($M \leq S$) (Casanoves et al., 2011).

$$MFAD = \frac{\sum_{i,j}^M d_{ij}}{M} \quad (\text{Eq.2})$$

where d_{ij} is the distance between functional units i and j , and M is the number of functional units.

Functional diversity based on dendrogram (FDp and FDc)

Functional diversity based on a dendrogram refers to the sum of branch length of the dendrogram produced by a clustering method based on the data matrix of S species \times N traits in a plot. FDp is plot based functional diversity index and FDc is community based index (Petchey and Gaston, 2006).

Functional divergence (FDiv)

Functional divergence is related to how abundance is distributed within the volume of functional traits space.

$$FDiv = \frac{\sum_{i=1}^S w_i (dG_i - \overline{dG}) + \overline{dG}}{\sum_{i=1}^S w_i |dG_i - \overline{dG}| + \overline{dG}} \quad (\text{Eq.3})$$

dG_i is the functional distance from species i to the gravity center of species that form the vertices of the convex hull, and \overline{dG} is the mean distance of the S species to the gravity center, and w_i is the relative abundance of species i .

Functional evenness (FEve)

FEve measures the regularity of spacing between species in the functional trait space and the evenness of the distribution of the species abundance. The minimum spanning tree (MST) was used to transform a multidimensional space to a distribution on a single axis. This index measures both the sum of branch lengths in the MST and the evenness of species abundance (Villéger et al., 2008). The index:

$$FEve = \frac{\sum_{b=1}^{S-1} \min(PEW_b, \frac{1}{S-1}) - \frac{1}{S-1}}{1 - \frac{1}{S-1}} \quad (\text{Eq.4})$$

where: $PEW_b = \frac{EW_b}{\sum_{b=1}^{S-1} EW_b}$, $EW_b = \frac{d_{ij}}{w_i + w_j}$.

There are $S-1$ branches in the MST of S species and each of the b branch length is divided by the sum of the abundance of the species linked. EW_b is the weighted evenness, d_{ij} is the Euclidean distance between species i and j , those involved in the

branch b , and w_i and w_j are the relative abundance of these species. It is useful to compute the partial weighted evenness dividing by the sum of the across the branches.

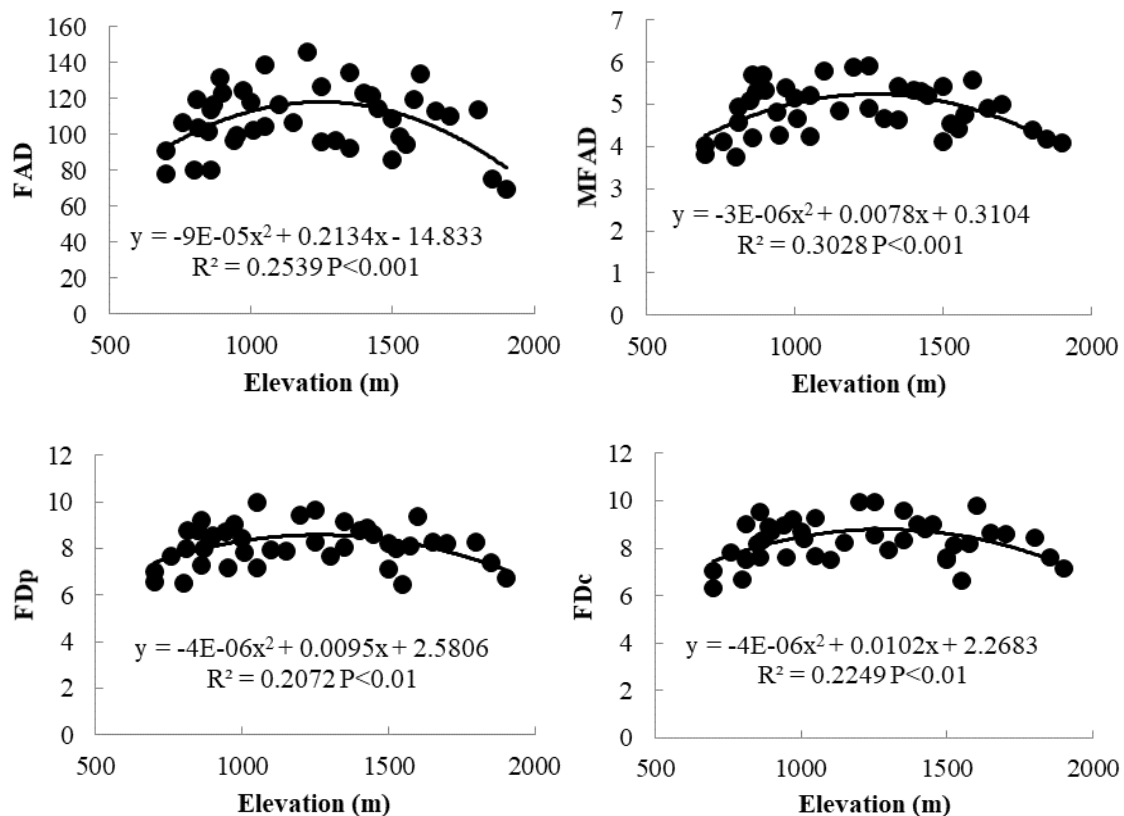
Species diversity

Three species diversity indices, species number (as a richness index) $D=S$, Shannon-Wiener index $H' = -\sum P_i \ln P_i$, Pielou evenness index $E = H' / \ln(S)$, were used to measure species diversity in a community. Where P_i is the relative abundance of species i , $P_i = N_i / N$, N_i the abundance of species i , N the sum of abundance for all species in a plot, S the species number present in a plot.

Spearman correlation and regression were used to analyse the relationships of functional diversity, species diversity and environmental variables.

Results

Plant functional diversity demonstrated by the six indices showed great variations in forest communities in the Wulingshan Nature Reserve. FAD varied between 69.76 and 145.62 with a mean 107.99 and a standard deviation 18.10, MFAD between 3.81 and 5.92 with a mean 4.87 and a standard deviation 0.59, FDP between 6.44 and 9.97 with a mean 8.13 and a standard deviation 0.88, FDC between 6.33 and 9.95 with a mean 8.31 and a standard deviation 0.90, FEve between 0.68 and 0.88 with a mean 0.79 and a standard deviation 0.05, and FDiv between 0.69 and 0.90 with a mean 0.81 and a standard deviation 0.05 (Fig. 2).



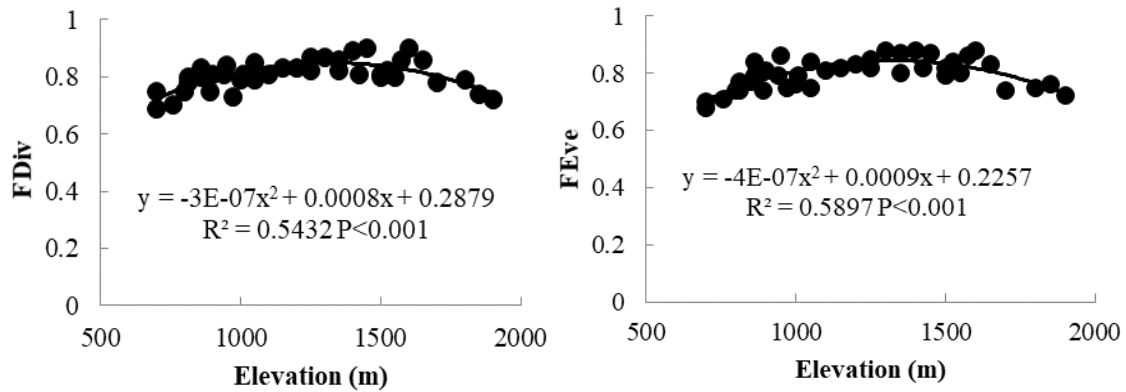


Figure 2. Variation of functional diversity in forest communities along the altitudinal gradient in the Wulingshan Nature Reserve, North China

Functional diversity indices were significantly correlated with an altitudinal gradient (Fig. 2) and with a disturbance intensity gradient (Fig. 3) in the Wulingshan Nature Reserve. All six indices showed similar variation pattern with altitudinal and disturbance gradients. Functional diversity showed a non-linear “humped” change pattern along the altitudinal gradient, i.e. it increased with elevation firstly, and reached its maximum between 1300 and 1400 m, and then decreased gradually (Fig. 2). Functional diversity showed a non-linear or near linear decrease pattern along the disturbance intensity gradient, i.e. it was gradually decreased with the maximum value at the lowest disturbance community and the minimum value under the heaviest disturbance (Fig. 3).

In addition to altitude and disturbance, litter thickness was also significant in affecting spatial variation of functional diversity in the Wulingshan Reserve (Table 2). The litter thickness played a special role in two functional diversity indices, FEve and FDiv. However, the soil depth, slope, and aspect were not significant in influencing functional diversity change in this reserve (Table 2). Different indices showed different significance for their relationships with functional diversity, but the positive or negative feature of the relationships was clear. Elevation, soil depth and litter thickness showed positive correlations, and disturbance and aspect negative correlations with the functional diversity indices (Table 2).

Table 2. Spearman correlation coefficients between functional diversity and environmental variables in the Wulingshan Nature Reserve, North China

Environmental variables	FAD	MFAD	FDp	FDc	FEve	FDiv
Elevation	0.053	0.084	0.077	0.109	0.374*	0.321*
Slope	0.232	0.222	0.133	0.013	-0.226	-0.188
Aspect	-0.175	-0.170	-0.189	-0.276	0.004	-0.040
Litter thickness	0.199	0.212	0.178	0.197	0.440**	0.414**
Soil depth	0.137	0.103	0.156	0.152	0.297	0.268
Disturbance intensity	-0.342*	-0.414**	-0.368*	-0.367*	-0.747***	-0.739***

Functional diversity was significantly correlated with species diversity (Table 3). The Shannon-Wiener index was most significantly correlated with all the functional

diversity indices, species richness significantly correlated with all functional indices except FDP and FDiv, and species evenness significantly correlated with all functional indices except FDP and FD, in the Wulingshan Reserve (Table 3). Functional diversity indices were positively related to species richness, diversity and evenness, i.e. functional diversity increased with species diversity increase.

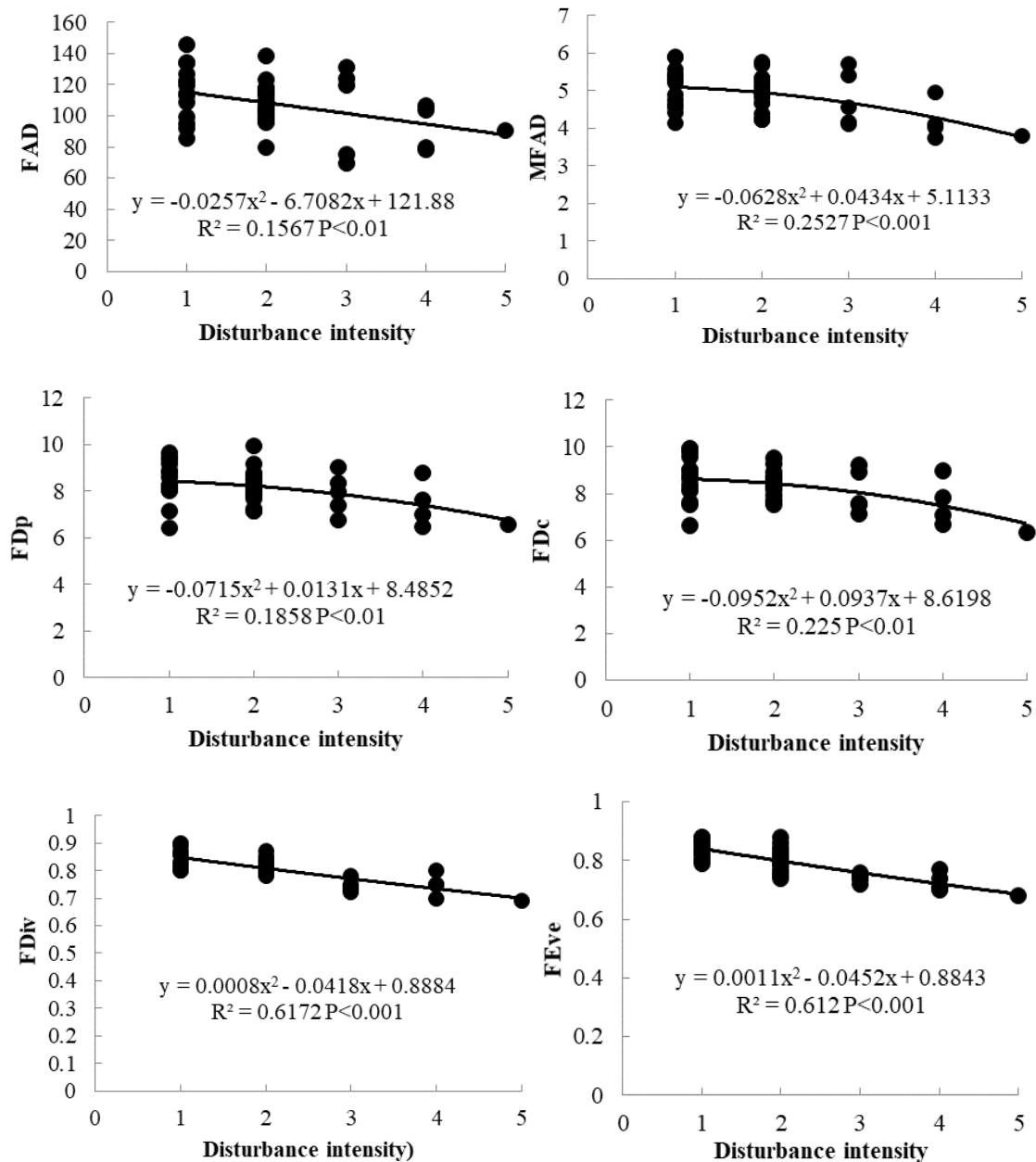


Figure 3. Change of functional diversity in forest communities along the disturbance intensity gradient in the Wulingshan Nature Reserve, North China

The six functional diversity indices were significantly correlated with each other and hence provided similar results (Table 4). Among them, MFAD, FEve and FDiv provided better correlations with elevation and disturbance.

Table 3. Spearman correlation coefficients between functional diversity and species diversity in the Wulingshan Nature Reserve, North China

Species diversity	FAD	MFAD	FDp	FDc	FEve	FDiv
Species richness	0.338*	0.374*	0.278	0.350*	0.330*	0.277
Shannon-Weiner index	0.509***	0.483**	0.317*	0.367*	0.433**	0.406**
Species evenness	0.369*	0.339*	0.184	0.208	0.442**	0.392*

Table 4. Spearman correlation coefficients between functional diversity indices in the Wulingshan Nature Reserve, North China

	FAD	MFAD	FDp	FDc	FEve	FDiv
FAD	1.000					
MFAD	0.815***	1.000				
FDp	0.775***	0.826***	1.000			
FDc	0.724***	0.743***	0.921***	1.000		
FEve	0.320*	0.405**	0.322*	0.400**	1.000	
FDiv	0.341*	0.441**	0.390*	0.444**	0.948***	1.000

Discussion

Functional diversity can be used as an indicator of ecosystem functioning and can demonstrate the relationships of species function, composition, structure and environmental factors (de Bello et al., 2006; Spasojevic et al., 2014). The six functional diversity indices all showed a great change of functional diversity in forest communities in the Wulingshan Nature Reserve, which suggested that forest communities varied in species function, composition, diversity, structure and inner environment (Zhang et al., 2013; Rossi et al., 2020). Eight forest formations were identified from 700 to 1900 m in this reserve (Liu and Xi, 1997; Zhang et al., 2014). These vegetation formations were as follows from lower to upper hills, Form. *Pinus tabulaeformis*, Form. *Juglans mandshurica*, Form. *Betula platyphylla*, Form. *Quercus mongolica*, Form. *Betula dahurica* + *Populus davidiana* + *Betula platyphylla*, Form. *Populus davidiana*, Form. *Tilia mandschurica* + *Tilia mongolica*. Form. *Larix principis-rupprechtii* (Cui et al., 2008; Zhang et al., 2014). The variation of functional diversity successfully reflected the change of forest communities along the altitudinal gradient, which suggests that each community has special functional composition and diversity (Zhang et al., 2014), which was also proved by other studies (e.g. Perronne et al., 2014; Zhang et al., 2013, 2015a).

The variation of functional diversity is usually related to changes in environmental gradients (Zhang et al., 2015b; Bricca et al., 2019). All the six indices were significantly correlated with altitudinal and disturbance gradients in the Wulingshan Nature Reserve, which suggested that elevation and disturbance were key factors influencing functional diversity in this reserve (de Bello et al., 2006; Fayiah et al., 2019). This was identical with the conclusion that altitude and disturbance were most important factors affecting forest structure, diversity and distribution in this reserve (Liu and Xi, 1997; Cui et al., 2008). All the six functional diversity indices showed the same variation pattern, non-linear “humped” change, along the altitudinal gradient, i.e. it increased firstly, and reached its maximum between 1300 and 1400 m, and then decreased with elevation

increase (Zhang et al., 2013; Boehnke et al., 2014). This change pattern of functional diversity is consistent with the most commonly observed pattern that the maximum diversity to be appeared at intermediate altitude (Austrheim, 2002; Villéger et al., 2008). Altitudinal gradient represents a comprehensive gradient of heat and moisture in mountains, i.e. the change of heat and moisture with elevation will influence the change pattern of functional diversity (Zhang et al., 2013; Perronne et al., 2014). All the six indices showed the same pattern, non-linear or near linear decrease pattern, along the disturbance intensity gradient in the Wulingshan Nature Reserve. The maximum functional diversity appeared at the lowest disturbance and the minimum functional diversity was under the heaviest disturbance (Zhang et al., 2014). This pattern of functional diversity is not consistent with the hypothesis that the maximum diversity to be appeared at medium disturbance (Spasojevic et al., 2014). Disturbance from tourist activities such as trampling, damaging plant, rubbish etc. can affect functional diversity directly, and it can also influence functional diversity indirectly by changing environmental features such as soil physical characteristics (Duivenvoorden and Cuello, 2012).

Besides elevation and disturbance, soil litter thickness was significantly affecting functional diversity in the Wulingshan Nature Reserve, which was supported by some other studies (Duivenvoorden and Cuello, 2012; Zhang et al., 2014). Litter thickness affects soil water and soil nutrients which further affect functional diversity (Otypkova et al., 2011). Soil depth, slope, and aspect was not significant in influencing functional diversity change in this reserve. Former studies showed that forest vegetation was significantly correlated with slope, aspect and soil depth in this reserve (Liu and Xi, 1997; Cui et al., 2008), which suggests that the formation and maintain of functional diversity in community is different from that of vegetation and species diversity (Zhang et al., 2013) and needs special attentions in conservation (Boehnke et al., 2014).

Functional diversity was significantly correlated with species diversity in the Wulingshan Reserve, which is consistent with many other studies (Ricotta and Moretti, 2008; de Bello et al., 2009). Functional diversity and species diversity were interrelated with each other, but they were different and could not be replaced with each other (Butterfield and Suding, 2013; Zhang et al., 2015a).

The six common indices used for measuring functional diversity were all effective in quantifying functional diversity and its variation in forest communities in the Wulingshan Nature Reserve. These indices were significantly correlated with each other since they all based on the functional distances between species in functional trait space with some theoretically differences (Casanoves et al., 2011; Song and Zhang, 2013). MFAD, FEve and FDiv performed better in describing the relationships of functional diversity with elevation and disturbance, and should be firstly used in research practice.

Conclusions

Functional diversity showed a great change in forest communities in the Wulingshan Nature Reserve, China. Elevation and disturbance were most important factors influencing functional diversity in forest communities. Functional diversity showed a non-linear “humped” change pattern along the altitudinal gradient and a non-linear or near linear decrease pattern along the disturbance intensity gradient. Functional diversity was significantly correlated with species diversity in forests in this reserve. The interactions between functional diversity, species diversity and phylogenetic

diversity should be further studied in the forest communities. Among the six common indices used, MFAD, FEve and FDiv should be recommended in practice in future study.

Acknowledgements. This study was financially supported by the Young Teachers Found of Beijing University of Chinese Medicine (Grant No. 2018-JYB-JS) and the National Natural Science Foundation of China (No. 31170494).

REFERENCES

- [1] Albert, C. H., de Bello, F., Boulangeat, I., Pellet, G., Lavorel, S., Thuiller, W. (2012): On the importance of intraspecific variability for the quantification of functional diversity. – *Oikos* 121: 116-126.
- [2] Austrheim, G. (2002): Plant diversity patterns in semi-natural grasslands along an elevational gradient in southern Norway. – *Plant Ecology* 161(2): 193-205.
- [3] Bai, S., Lu, G., Gu, J., Zhang, S., Zheng, H., Wang, X. (2006): Studies on species and landscape pattern diversities of Wuling Mountain. – *Journal of Agricultural University of Hebei* (2): 1-4.
- [4] Boehnke, M., Kroeber, W., Welk, E., Bruehlheide, H. (2014): Maintenance of constant functional diversity during secondary succession of a subtropical forest in China. – *Journal of Vegetation Science* 25: 897-911.
- [5] Bricca, A., Conti, L., Tardella, M. F., Catorci, A., Iocchi, M., Theurillat, J. P., Cutini, M. (2019): Community assembly processes along a sub-Mediterranean elevation gradient: analyzing the interdependence of trait community weighted mean and functional diversity. – *Plant Ecology* 220: 1139-1151. DOI: 10.1007/s11258-019-00985-2.
- [6] Butterfield, B. J., Suding, K. N. (2013): Single-trait functional indices outperform multi-trait indices in linking environmental gradients and ecosystem services in a complex landscape. – *Journal of Ecology* 101: 9-17.
- [7] Casanoves, F., Pla, L., Di Rienzo, J., Diaz, S. (2011): Diversity: a software package for the integrated analysis of functional diversity. – *Methods in Ecology Evolution* 2: 233-237.
- [8] Cui, G. F., Xing, S. H., Zhao, B. (2008): Conservation of Mountain Plants and Vegetation in Beijing. – China Forestry Press, Beijing (in Chinese).
- [9] de Bello, F., Lepš, J., Sebastia, M. T. (2006): Variations in species and functional plant diversity along climatic and grazing gradients. – *Ecography* 29: 801-810.
- [10] de Bello, F., Thuiller, W., Lepš, J., Choler, P., Clement, J., Macek, P., Sebastia, M.-T., Lavorel, S. (2009): Partitioning of functional diversity reveals the scale and extent of trait convergence and divergence. – *Journal of Vegetation Sciences* 20: 475-486.
- [11] Duan, D. (2009): Study on the diversity of wild plants resources in Wuling Mountain and their garden application evaluation. – *Journal of Anhui Agricultural Sciences* (11): 8-10.
- [12] Duivenvoorden, J. F., Cuello, N. L. (2012): Functional trait state diversity of Andean forests in Venezuela changes with altitude. – *Journal of Vegetation Sciences* 23: 1105-1113.
- [13] Fayiah, M., Dong, S. K., Li, Y., Xu, Y. D., Gao, X. X., Li, S., Shen, H., Xiao, J. N., Yang, Y. F., Wessell, K. (2019): The relationships between plant diversity, plant cover, plant biomass and soil fertility vary with grassland type on Qinghai-Tibetan Plateau. – *Agriculture Ecosystems and Environment* 286. DOI: 10.1016/j.agee.2019.106659.
- [14] He, S. Y., Xing, Q. H., Yin, Z. T. (1992): Flora of Beijing. – Beijing Press, Beijing (in Chinese).
- [15] Laliberte, E., Legendre, P. (2010): A distance-based framework for measuring functional diversity from multiple traits. – *Ecology* 91: 299-305.

- [16] Liu, J., Xi, W. (1997): The main vegetation types and vertical distribution laws in Wulingshan Mountains. – *Journal of Capital Normal University* 18(1): 95-103.
- [17] Muhumuza, M., Byarugaba, D. (2009): Impact of land use on the ecology of uncultivated plant species in the Rwenzori mountain range, mid western Uganda. – *African Journal of Ecology* 47: 614-621.
- [18] Otypkova, Z., Chytry, M., Tichy, L., Pechanec, V., Jongepier, J. W., Hajek, O. (2011): Floristic diversity patterns in the White Carpathians Biosphere Reserve, Czech Republic. – *Biologia* 66: 266-274.
- [19] Pavoine, S., Bonsall, M. B. (2011): Measuring biodiversity to explain community assembly: a unified approach. – *Biological Reviews* 86: 792-812.
- [20] Perronne, R., Mauchamp, L., Mouly, A., Gillet, F. (2014): Contrasted taxonomic, phylogenetic and functional diversity patterns in semi-natural permanent grasslands along an altitudinal gradient. – *Plant Ecology and Evolution* 147: 165-175.
- [21] Petchey, O., Gaston, K. (2002): Functional diversity (FD), species richness and community composition. – *Ecology Letters* 5(3): 402-411.
- [22] Petchey, O., Gaston, K. (2006): Functional diversity: back to basics and looking forward. – *Ecology Letters* 9(6): 741-758.
- [23] Ricotta, C., Moretti, M. (2008): Quantifying functional diversity with graph-theoretical measures: advantages and pitfalls. – *Community Ecology* 9(1): 11-16.
- [24] Rossi, C., Kneubuler, M., Schutz, M., Schaepman, M. E., Haller, R. M., Risch, A. C. (2020): From local to regional: functional diversity in differently managed alpine grassland. – *Remote Sensing of Environment* 236. DOI: 10.1016/j.rse.2019.111415.
- [25] Song, N. Q., Zhang, J.-T. (2013): An index for measuring functional diversity in plant communities based on neural network theory. – *Journal of Applied Mathematics* Article ID 320905.
- [26] Spasojevic, M. J., Copeland, S., Suding, K. N. (2014): Using functional diversity patterns to explore metacommunity dynamics: a framework for understanding local and regional influences on community structure. – *Ecography* 37: 939-949.
- [27] Villéger, S., Mason, N. W. H., Moullot, D. (2008): New multidimensional functional diversity indices for a multifaceted framework in functional ecology. – *Ecology* 89: 2290-2301.
- [28] Walker, B. H., Kinzig, A., Langridge, J. L. (1999): Plant attribute diversity, resilience, and ecosystem function: the nature and significance of dominant and minor species. – *Ecosystems* 2: 95-113.
- [29] Xiang, C. L., Zhang, J.-T. (2009): Changes in species diversity and contributing factors in subalpine meadows in Dongling Mountain. – *Journal of Beijing Normal University (Natural Science)* 45(3): 275-278.
- [30] Zhang, J.-T., Xu, B., Li, M. (2013): Vegetation patterns and species diversity along elevational and disturbance gradients in the Baihua Mountain Reserve, Beijing, China. – *Mountain Research and Development* 33(2): 170-178.
- [31] Zhang, J.-T., Li, M., Nie, E. B. (2014): Pattern of functional diversity along an altitudinal gradient in the Baihua Mountain Reserve of Beijing, China. – *Brazilian Journal of Botany* 37: 37-45.
- [32] Zhang, J.-T., Xiao, J., Li, L. F. (2015a): Variation of plant functional diversity along a disturbance gradient in mountain meadows of the Donglingshan Reserve, Beijing, China. – *Russian Journal of Ecology* 46(2): 157-166.
- [33] Zhang, J.-T., Zhang, B., Qian, Z. Y. (2015b): Functional diversity of *Cercidiphyllum japonicum* communities in the Shennongjia Reserve, central China. – *Journal of Forestry Research* 26(1): 171-177.
- [34] Zhang, W. M., Qin, A. C., Feng, X. Q., Li, D. Y., Huang, D. Z. (2003): Evaluation of tourist resources in Wulingshan Reserve. – *Hebei Research of Forest and Fruit* 18(2): 184-189 (in Chinese).

CALCULATION AND VALIDATION OF ACTUAL EVAPOTRANSPIRATION FROM SATELLITE DERIVED INDICES WITH OBSERVED DATA IN DELINEATED AGRO-CLIMATIC ZONES OF PUNJAB USING REMOTE SENSING AND GIS TECHNIQUES

AMIN, M.^{1*} – KHAN, M. R.¹ – BAIG, M. H. A.¹ – BAIG, I. A.² – IMRAN, M.¹ – HANIF, M.³

¹*Institute of Geo-Information & Earth Observation, PMAS Arid Agriculture University, Rawalpindi, Pakistan*

²*Department of Agribusiness and Applied Economics, Muhammad Nawaz Sharif University of Agriculture, Multan, Pakistan*

³*Department of Mathematics and Statistics, PMAS Arid Agriculture University, Rawalpindi, Pakistan*

**Corresponding author
e-mail: m.amin@uaar.edu.pk*

(Received 24th May 2019; accepted 15th Nov 2019)

Abstract. Water is the major restrictive constraint for agricultural growth and production. Agro-climate zones refer to the areas with homogenous agro-potential characteristics. The objective of this study is to delineate the agro-climate zones of Punjab, Pakistan and to calculate Actual evapotranspiration (ET^a) from actual and satellite data. Potential evapotranspiration (ET⁰) was calculated by using climatic normal of 25 years (1990-2015). On the basis of Potential evapotranspiration (ET⁰) and Moisture Index, study area was delineated into seven agro-climatic zones. Secondly, ET^a was investigated by adopting a fraction of Normalized difference vegetation index. Landsat 8 data for the year (2016) was used to determine pixel-based vegetation coefficients. Actual ET maps were prepared to analyze spatial variation of ET^a in all zones. Actual ET was determined in mm/day. Daily ET^a values in the months of Jan, Feb, Mar, Apr, May, Jun, Jul, Aug, Sep, Oct and Dec were 1.0, 1.71, 2.70, 3.5, 4.41, 5.01, 5.2, 4.5, 4.37, 3.01, 2.0 and 1.4 mm respectively. Finally, it was observed that there is a strong relation between both results calculated from satellite data and climatic data of selected crops, i.e. wheat, rice, cotton, sugarcane and maize R² = 0.96, 0.94, 0.90, 0.98 and 0.95 respectively. Above results shown that satellite data are widely useful with ground validation for sustainable crop production as well as for policy makers with respect to water conservation.

Keywords: *agro-climate zones, potential evapotranspiration, moisture index, fraction of vegetation, actual evapotranspiration*

Introduction

Water resources in Pakistan are not sufficient for the proper growth and production of crops. Agriculture is the core of Pakistan's economy; giving about 21-25% share in Gross Domestic Product (GDP) and serving to about 45-50% labor force of Pakistan (Bhatti et al., 2009). Pakistan covers about 79.61 million ha, out of which 22 million ha are under cultivation and 75-80% area is under irrigation while rest of area is rain fed (Iqbal and Ahmad, 2005). About 75-80% geographical area receives only 250 to 500 mm rainfall annually, contributing to the arid and semi-arid environment in Pakistan (Baig et al., 2013). Our main objective and primitive need is to calculate ET^a of major crops under available agro-climate and water conditions. The studied rabi

crops are Wheat, Tomato and kharif crops are Rice, Cotton, Sugarcane, Maize and Citrus Good quality water is the major restrictive constraint for agricultural growth and production (Doorenbos and Kassam, 1979).

Agro-climatic zone is a land unit defined in terms of major climate and growing periods, which is climatically suitable for certain, range of crops and cultivators (Aggarwal, 1993). It requires climatic parameters, i.e. temperature, rainfall, humidity, sunshine hours, wind speed, crop calendar, cropping patterns and land-use information to delineate agro-climatic zones. In Pakistan rainfall mostly occurs in summer due to monsoon winds originating from Indian Ocean especially its north-eastern part. Winter rainfall depends upon western depressions (Ahmad et al., 2015). Pakistan has classified in six Agro-climate zones on the basis of climate and Moisture Index (Chaudhry and Rasul, 2004).

Actual evapotranspiration is the amount of water that is actually removed from a surface through the process of evaporation and transpiration when soil moisture/water source is limited (McKenney and Rosenberg, 1993). Crop evapotranspiration (ET^c) was estimated by using remote sensing techniques (Singh et al., 2013). Simplified surface energy balance approach was tested to estimate daily Actual evapotranspiration by using Landsat-5 TM data (cropping season, 2007) and ground truth data from Lysimeters (Gowda et al., 2008)

Wheat yield forecasting is analyzed in Punjab province by using satellite data of Landsat 5 TM and MODIS (Dempewolf et al., 2014). Water use for crops was estimated by using simple but robust SSEBop model in United States (Senay et al., 2013). To analyze the impact of land use changes NDVI, ET^0 , and temperature fraction approach was used with the help of satellite data (Carlson and Arthur, 2000). Vegetation index (VI) based crop coefficients and ET^0 calculated from Penman Monteith method was used to calculate actual evapotranspiration of some selected crops by using time series data of Moderate Resolution Imaging Spectroradiometer (MODIS) sensor on Terra satellite (Glenn et al., 2011). Surface energy balance approach was attempted to estimate actual ET from Landsat 5 satellite images and validating it with ground truth data of Oklahoma Mesonet stations to use it for urban area (Liu et al., 2010). Landsat 8 images were used for evaluation of comparison between a remote sensed based reference ET fraction (ET_{rf}) and Mapping EvapoTranspiration at high Resolution with Internalized Calibration (METRIC) model to estimate crop ET coefficients in Idaho, USA. They used 12 images (2000 year) of Landsat to derive NDVI based ET_{rf} (Rafn et al., 2008).

Materials and methods

The present study was investigated in Punjab, Pakistan lies between 31.17° N latitude and 72.70° E longitude. It covers an area of about 79,284 mi² area and it covers about 26% land area of country. According to the world's temperature zones Pakistan lies in Sub-tropical zone except some northern mountain areas having moderate climate. Overall it falls in arid and semi-arid type of climate. Air temperature varies from -2°C to 45°C , can reach 51°C in summer. Maximum annual temperature ranges between 28°C and 32°C and minimum annual temperature varies between 15°C and 19°C in Punjab. Rainy season in Punjab starts from July and runs till September.

Rainfall occurs in summer due to monsoon winds and in winter due to western depressions. Average annual rainfall varies from 270 to 1400 mm. Humidity fluctuates

from 53 to 64%. Punjab is thickly populated province with an estimated population of about 110.012 million and Lahore is the metropolitan city with the population of 11.1 million according to the census of 2017.

Data requirements

To accomplish the objectives of the research, climate data from 1990-2015 of 22 weather stations installed in all over Punjab was collected from Pakistan Meteorological Department as shown in *Figure 1*. The climatic parameters are maximum and minimum temperature, relative humidity, wind speed, sunshine hours and rainfall. Kc values were taken from available literature by (Allen et al., 1998). The Advanced Space borne Thermal Emission and Reflection Radiometer, Global digital elevation model (ASTER GDEM) with spatial resolution of 30 meters was used in the study to show elevation in different parts of Punjab.

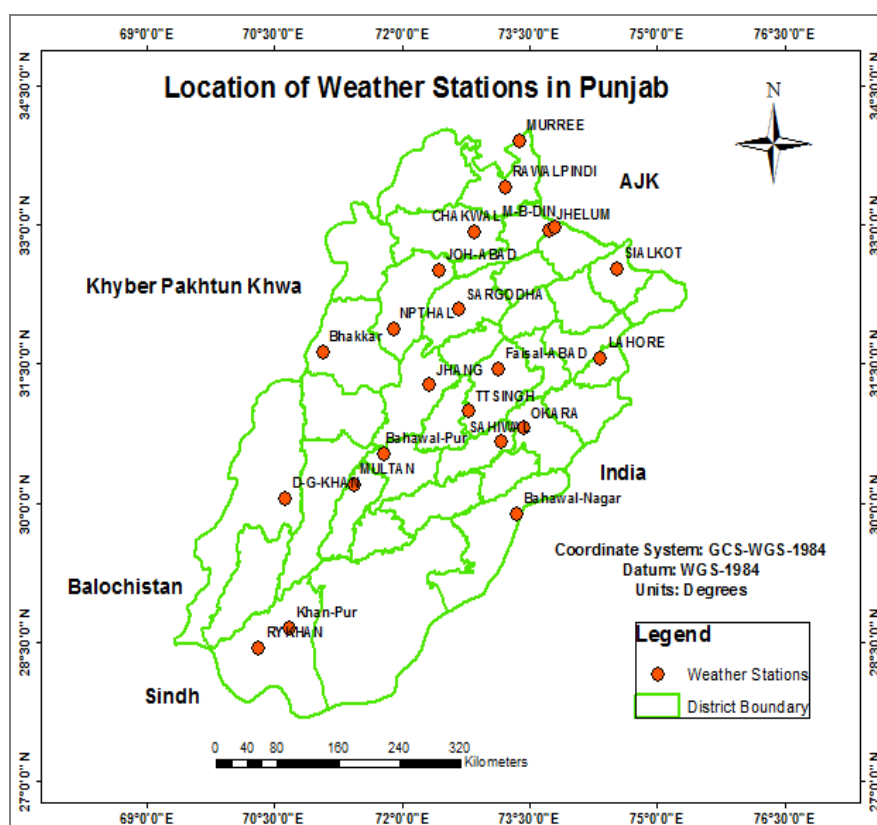


Figure 1. Map showing location of weather stations in Punjab

Satellite data for deriving fraction of vegetation

Landsat 8 satellite data with less than 10% cloud cover, were browsed and downloaded for the year 2016 (Rabi-Kharif season), from USGS Earth Explorer website. One limitation was unavailability of images for the month of August, so image for the month of July was used to calculate NDVI fraction. Some images were not fit to the study due to some errors. So, 176 images were selected and utilized in the study. Whole Punjab covers almost 16 images to make one scene/image assuming to be one date image for one date. *Figure 2* shows the methodology flow chart of the study.

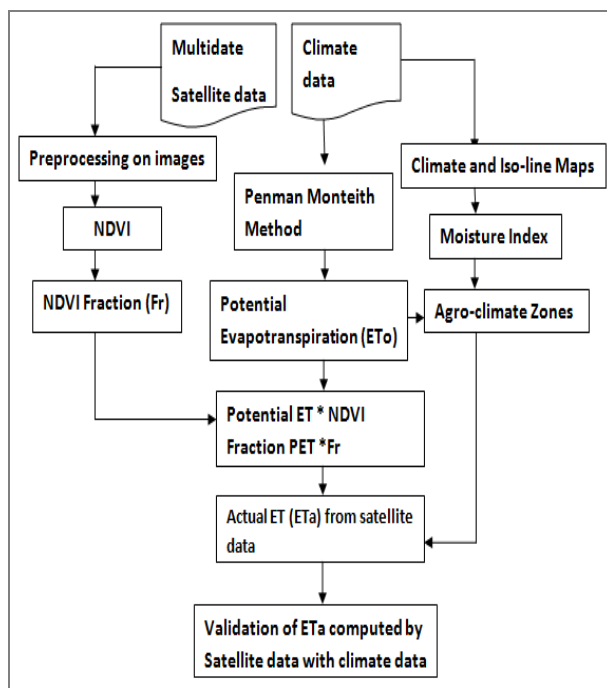


Figure 2. Research methodology flow chart

Potential evapotranspiration (PET)

Modified Penman Monteith equation was used to estimate ET^0 by using climatic variables of maximum and minimum temperature, humidity, sunshine hours and wind speed. Additionally, elevation data of weather stations was also used during calculation ET^0 , mathematical equation for ET^0 is given below:

$$ET_o = \frac{0.408\Delta(R_n - G) + \gamma \frac{900}{T + 273} u_2 (e_s - e_a)}{\Delta + \gamma(1 + 0.34u_2)} \quad (\text{Eq.1})$$

Thornthwaite moisture index (TMI)

Thornthwaite Moisture Index (TMI) is a dimensionless index varying from -100 to +100 (Karunaratne et al., 2016). This index was firstly used by (Thornthwaite, 1948). The revised moisture index of Thornthwaite and Marthur (1955) was calculated with the combination of annual potential evapotranspiration and annual rainfall data.

$$TMI = [P - ET^0 / ET^0] \times 100 \quad (\text{Eq.2})$$

where: TMI = moisture index, P = precipitation, ET^0 = potential evapotranspiration. It is an indicator of available soil moisture and water need in any region.

NDVI fraction (Fr)

Vegetation fraction is an indicator for the percentage of vegetation cover (Kharrou et al., 2011) Following formula was used by Gillies et al. (1997) to calculate fraction of vegetation cover (Fr/Fov) as an indicator of vegetation coefficient in a pixel.

$$Fr = \left(\frac{NDVI - NDVI_s}{NDVI_v - NDVI_s} \right)^2 \quad (\text{Eq.3})$$

where: Fr = fractional vegetation cover, NDVI = NDVI value of image. NDVI_s = NDVI value of bare soil, NDVI_v = NDVI value of vegetation.

Once the interpolation was done, actual evapotranspiration was estimated by using outputs of potential evapotranspiration (ET⁰) and fraction of vegetation (presuming more ET in intense vegetation) with the help of Raster calculations in GIS environment. Equation for calculating Actual ET is given below:

$$\text{Actual ET} = ET^0 \times Fr \quad (\text{Eq.4})$$

where: Actual ET = actual evapotranspiration, ET⁰ = potential evapotranspiration, Fr = fractional vegetation cover.

Results and discussion

Firstly, potential evapotranspiration (ET⁰) of all weather stations was calculated through Penman Monteith method by using CROPWAT 8.0 software. The maps of all climatic variables, minimum-maximum temperature, humidity, sunshine, wind speed, rainfall and ET⁰ were prepared in Arc GIS 10.3 While executing interpolation, ninety percent of the values were used whereas remaining ten percent were used as validation data set. The predicted values for the corresponding validation data set were obtained by overlay function in ArcGIS and scatter plots were made to check the accuracy of the interpolation results for validation purpose as shown in *Figure 3*. There is strong relation of both datasets as R² is about 0.99.

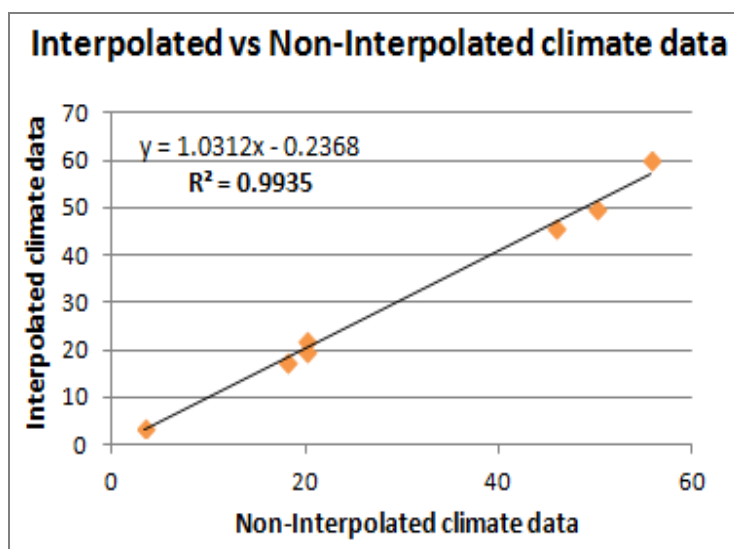


Figure 3. Regression analysis of interpolated vs non-interpolated data

The results of climatic variable shown that temperature of Punjab province increasing trend from upper area (Rawalpindi District) to lower area (D. G Khan and Rajanpur District), Maximum humidity was observed in upper part of Punjab (Murree,

Rawalpindi and Attock) and minimum humidity was observed in those areas of Punjab where temperature is too high. Maximum sunshine hours were observed in district Rajanpur (8.37) and the minimum sunshine hour in Rawalpindi district (6.71). The maximum wind speed was observed in Muzaffargarh (2.08 m/s) and the minimum wind speed was observed in Toba-Tek Singh (0.31 m/s). Rainfall variability of Punjab was observed in gradually increasing trend from south to north due to topography of the area as well as severity of monsoon season as shown in *Figure 4*. About 1000 to 1500 mm rainfall mapped in upper districts (Rawalpindi, Attock, Jhelum and Chakwal, Sialkot and Gujrat) of Punjab. Lower or southern part of the Punjab have received very low amount of rainfall due to aridity, about 50 to 351 mm rainfall mapped in Rajanpur and D. G. Khan, Bahawalnagar districts.

Figure 5a showed very low average daily ET^0 in upper part of Punjab (Rawalpindi, Attock, Sialkot and Gujrat) while high ET^0 was mapped in lower parts of Punjab Bahawalnagar, Rajanpur, Rahim Yar Khan and D. G. Khan districts ranged from 3.0 mm to 3.19 mm/day.

Agro-climate zones of Punjab based on climatic parameters

Contour map of elevation, Iso-line maps of climatic variables were generated in GIS environment. Agro-climatic zones were delineated on the basis of Iso-line/Isopleth maps of climatic parameters.

Moisture index was calculated by using *Equation 2*. As shown in *Table 1*, negative values indicate arid climate comprising less precipitation, which cannot fulfill the water need of crops while positive values define moisture and water supply. With the combination of ET^0 average annual rainfall maps and Moisture index seven moisture zones were created comprising homogenous characteristics of ET^0 . Rainfall and moisture supply. In *Figure 5b*. Agro-climate zone map based on moisture index was prepared in GIS environment by using TMI equation with the help of ET^0 and rainfall data. In Zone A with high soil moisture content and Zone B with adequate moisture supply are favorable for crops grown under rain fed conditions.

Table 1. Scaling of moisture index

Climate type	Moisture index	Zone symbol
Hyper-arid	-92.2 to -76.1	Hyper arid
Arid	-76.0 to -63.3	Arid
Semi-arid	-63.2 to -48.1	Semi-arid
Dry sub-humid	-48.0 to -1.0	Dry sub-humid
Moist sub-humid	1.0 to 20.0	Moist sub-humid
Humid	20.1 to 100	Humid
Very humid	> 100	Very humid

Zone C1 and C2 having moderate soil moisture, Rabi crops can be grown with slight irrigations but kharif crops require more water for irrigation, as C2 zone is best for Rice cultivation. The agro-climatic zone map of the study area is shown in *Figure 6*.

In zone D, E crops need water for irrigation during their development stages. These zones consist on arid and semi-arid type of climate with 250-500 mm annual rainfall.

Zone H shows hyper-arid climate, Cotton and Wheat are major crops grown here, require supplement irrigations for their proper nourishment, growth and yield. The results revealed that these agro-climate zones are different from the zones presented by Chaudhry and Rasul (2004) due to the change in climate. They classified Pakistan into six agro-climate zones in 2004. At that time climatic conditions were different from recent. Recent study presents seven agro-climatic zones with different homogenous potentials and constraints.

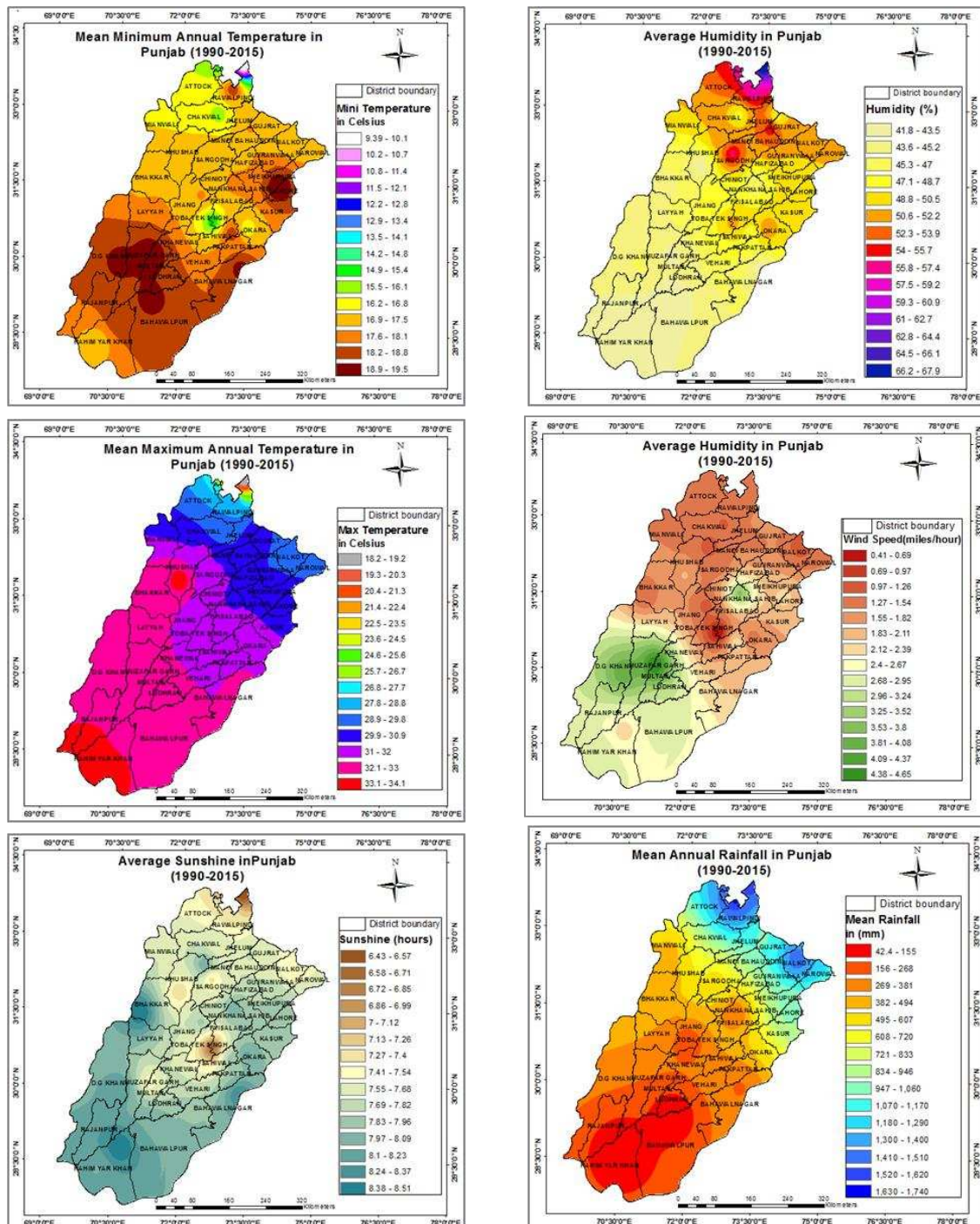


Figure 4. Maps showing mean minimum, maximum temperature (°C), humidity (%), sunshine (hours), wind speed (mph) and mean annual rainfall (mm)

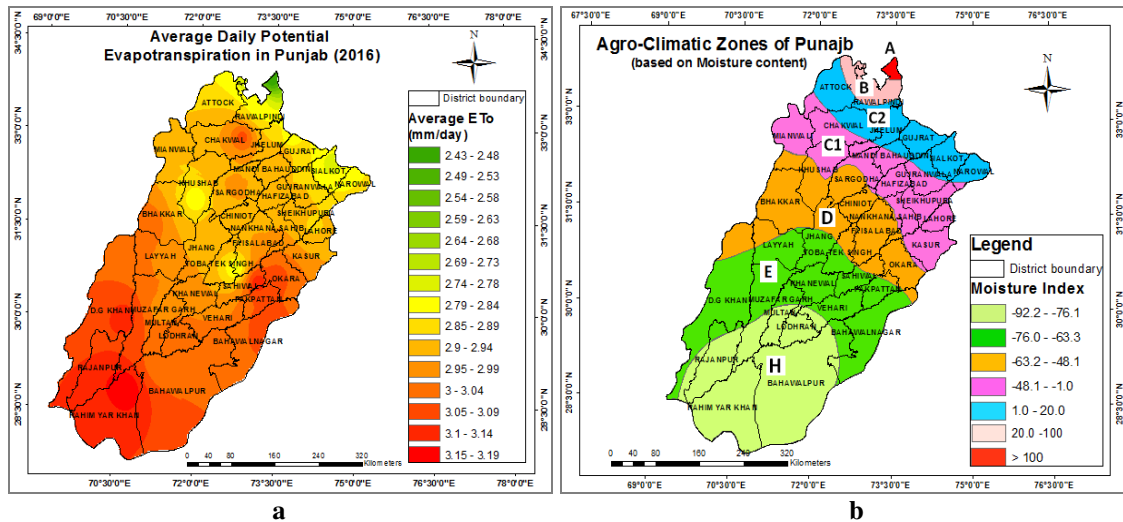


Figure 5. (a) Map showing average daily ET^0 (mm) in Punjab. (b) Map showing moisture index

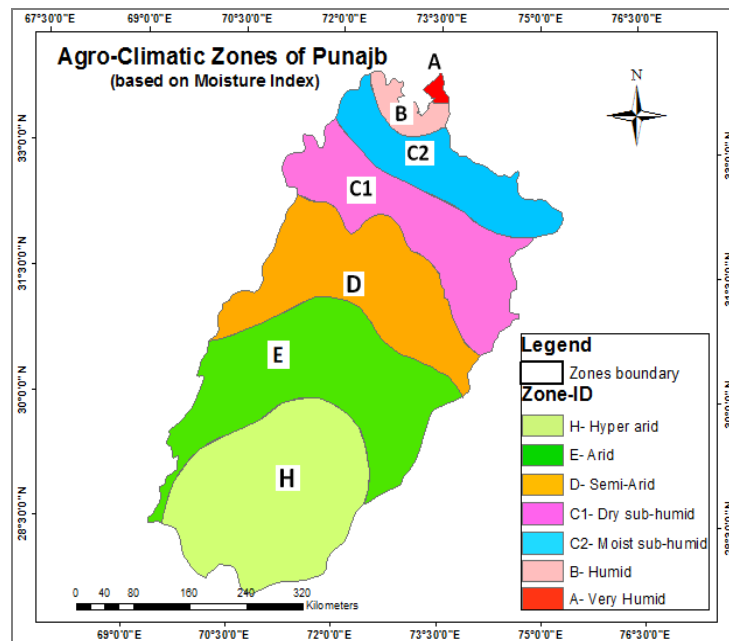


Figure 6. Map showing agro-climatic zones of Punjab

Unsupervised classification of NDVI images

Crop maps were presented in Figure 7 show most concentrated wheat grown areas are Lahore, Hafizabad, Faisalabad, Gujranwala, Multan and Rawalpindi. It is a widely grown food crop in Pakistan. North-eastern districts, like Sialkot, Narowal, Gujranwala, Hafizabad, Lahore shown highly spatial concentration of rice.

Major Sugarcane growing districts are Sargodha, Lahore, Faisalabad, Toba-Tek Singh and Jhang. Spatial cluster of Cotton is observed in southern Punjab in the districts of Multan, Khanewal, Bahawalnagar, D. G. Khan, Lodhran and Rajanpur. Major maize growing areas are in Gujranwala, Lahore, Hafizabad, Sargodha, Chiniot and Faisalabad districts.

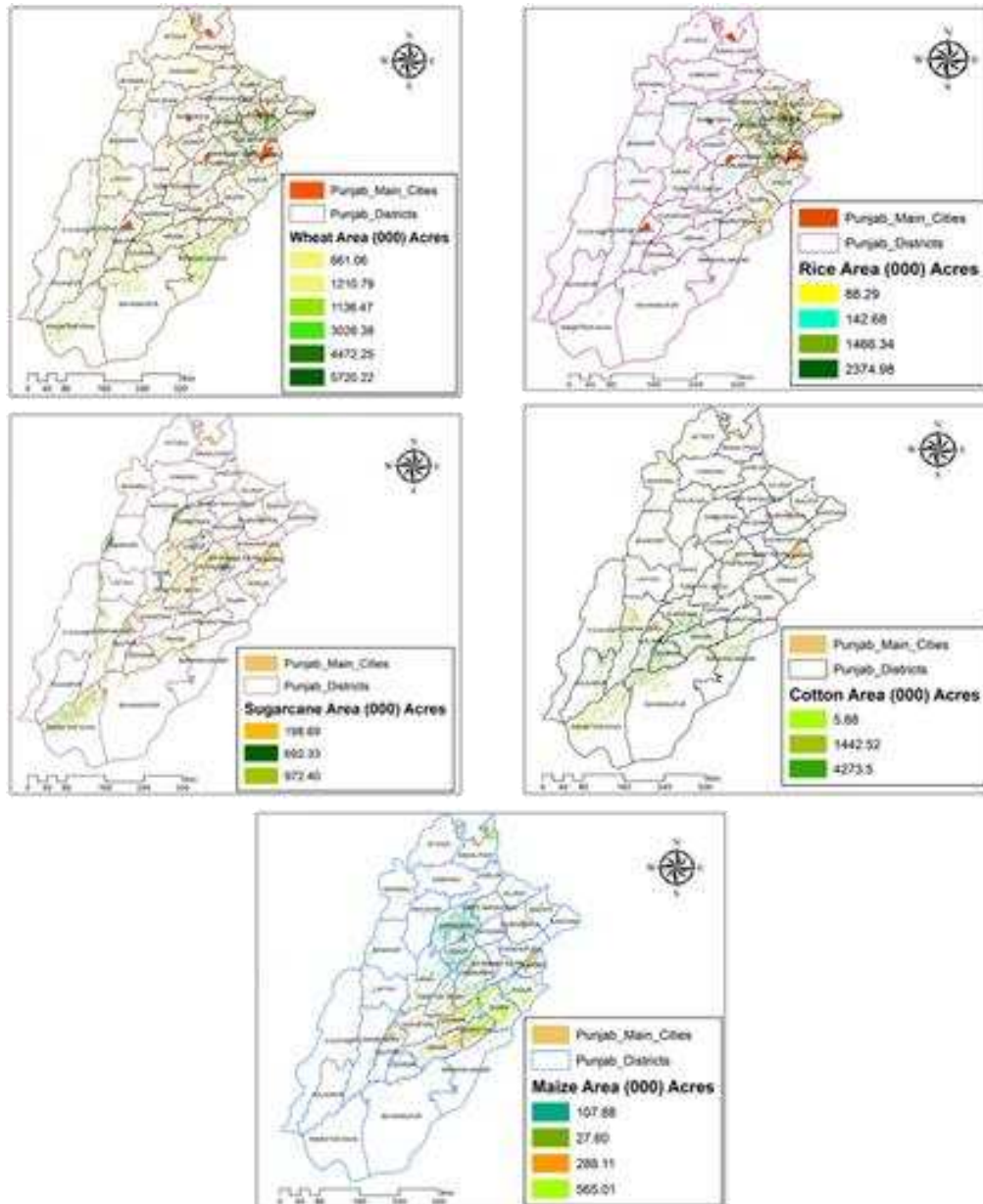


Figure 7. Rabi and kharif crop maps prepared from NDVI classified images

NDVI fraction calculated by satellite images

NDVI fraction was calculated from NDVI output images and Fr maps were prepared by using Equation 4 in GIS environment. Further, these Fr values were identified for each crop with respect to crop calendar and validated with classified pixels for crops.

ET⁰ calculated by climatic data

ET⁰ was calculated by using the Equation 1 with the help of climate data. High ET⁰ was observed in the months of March, April and May, June, July, August and September for all selected crops. The estimated ET⁰ results show potential evapotranspiration is high due to hot temperature, long sunshine hours in these months.

Also wind speed higher in middle and lower part of the study area as compared to upper part. For less ET^0 in upper part low temperature is also one reason.

ETa calculated by satellite image

ET^0 maps were generated by using Spline interpolation method within its areal extent of Punjab. By using Equation 4 in raster calculator (ET^0 maps* Fr maps) ET^a maps were produced in Arc GIS 10.3 software. In Figures 8 and 9, PET and ET^a of wheat, rice, cotton, sugarcane and maize crop are shown for 01/Jan, 27/Feb, 30/Mar, 16/Apr, 24/May, 16/June, 20/July, 20/Aug, 15/Sep, 15/Oct, 16/Nov, 27/Dec at satellite overpass time (10:00 AM). Also figure Figure 10 shows month wise relation in all agro climatic zones of ET^0 and ET^a .

Wheat can be grown in upper districts of Punjab under rainfed conditions. High ET^a was observed in the months of May, June, July, August and September for kharif crops in southern districts of Punjab. Also, high ET^a was observed in month of March, April and may for rabi crops. For sugarcane ET^a was high from month of May to September due annual crop season.

Water demand increases in June and July, because June serves as the hottest month of the year. Overall ET^a in the months of November and December is low due to low temperature and less sunshine hours. Month wise crop seasonal actual evapotranspiration for wheat, rice, cotton, sugarcane and maize is 333.6, 758.4, 654, 1019.7 and 1172.4 mm, respectively (Tables 2 and 3).

Table 2. Daily ET^a (mm) of all selected crops by using satellite data

Crops	Daily ETa of all selected crops (mm/day) by using satellite data											
	Jan 01	Feb 27	Mar 30	Apr 16	May 24	Jun 15	Jul 20	Aug 20	Sep 15	Oct 15	Nov 16	Dec 27
Wheat	0.82	1.37	2.72	2.70	2.05						0.68	0.78
Rice					3.57	4.88	4.80	4.45	4.37	2.04	1.17	
Cotton					1.74	3.85	5.29	4.41	4.30	1.59	0.62	
Sugarcane	0.57	0.91	1.80	2.69	4.04	4.83	5.27	4.58	4.32	2.66	1.56	0.76
Maize							0.66	2.86	4.08	1.77	0.99	

Table 3. Month wise crop Seasonal ET^a (mm) of all selected crops by using satellite data

Crops	Daily ETa of all selected crops (mm/month) by using satellite data												
	Jan	Feb	Mar	Apr	May	Jun	Jul	Aug	Sep	Oct	Nov	Dec	Annual ETa (mm)
Wheat	24.6	41.1	81.6	81	61.5						20.4	23.4	333.6
Rice					107.1	146.4	144	133.5	131.1	61.2	35.1		758.4
Cotton					52.2	115.5	158.7	132.3	129	47.7	18.6		654
Sugarcane	17.1	27.3	54	80.7	121.2	144.9	158.1	137.4	129.6	79.8	46.8	22.8	1019.7
Maize							19.8	85.8	122.4	53.4	891		1172.4

Validation of ETa computed by both datasets

The validation of actual ET at pixel basis is a major issue, so that ET^a from climate data is also used for comparison. Results showed actual evapotranspiration calculated from satellite data; provide accurate results with minor deviation from satellite data. ET^a

values computed from satellite data were validated with ET_a computed from climate data by a statistical analysis in MS Excel software. Coefficient values of wheat, rice, cotton, sugarcane, maize are $R^2 = 0.96, 0.94, 0.90, 0.98, 0.95$ respectively (Fig. 11). These coefficient values show strong relationship of ET^a estimated from both data sets.

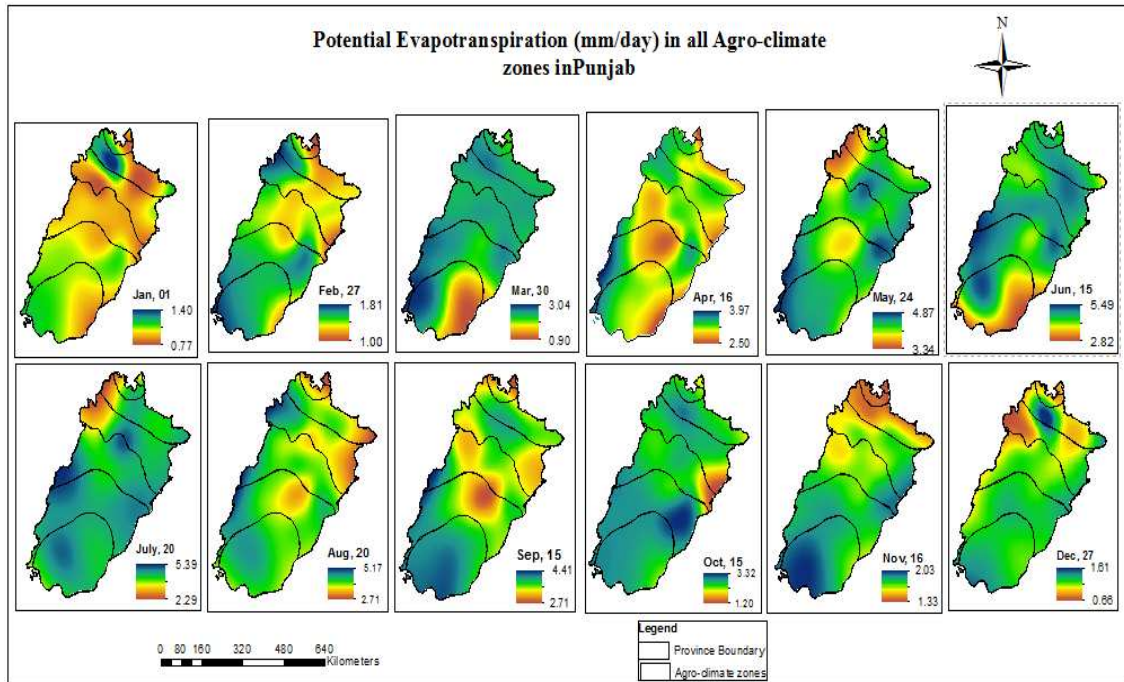


Figure 8. Daily ET^0 maps for all the months

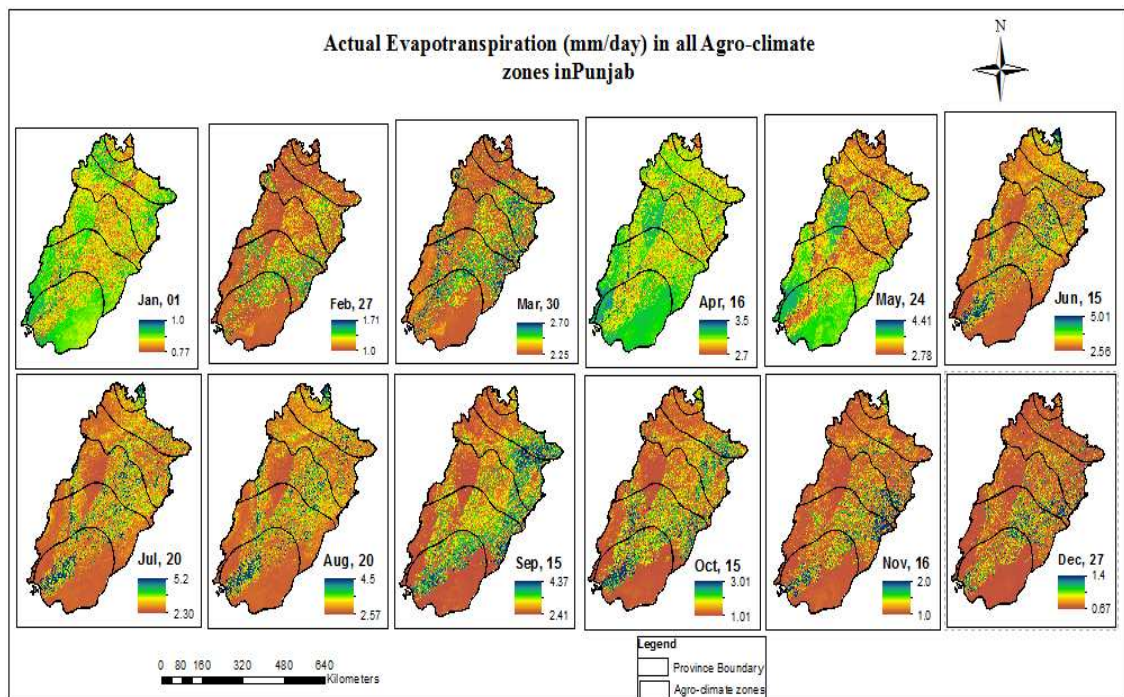


Figure 9. Daily ET^a maps for all the months

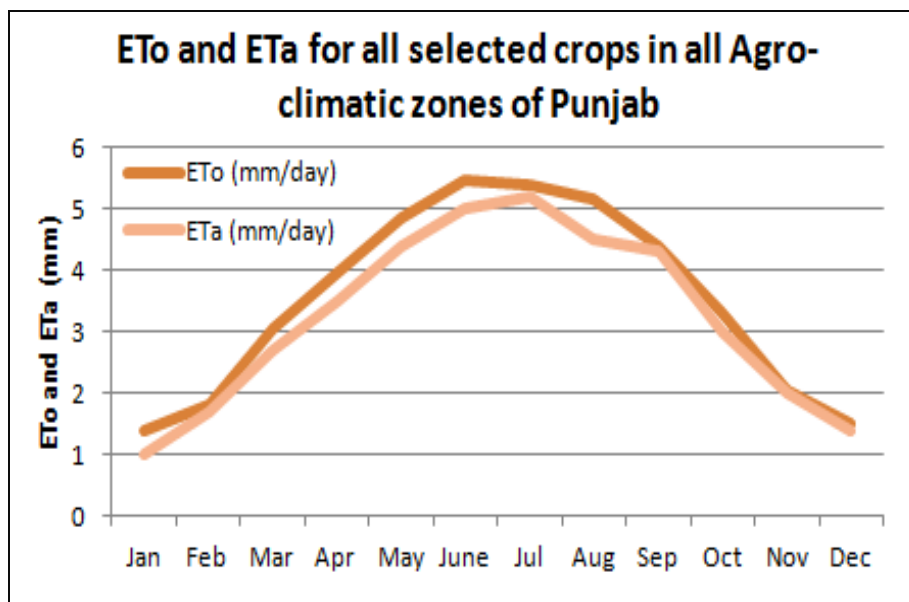


Figure 10. Month wise comparison of ET^0 and ET^a

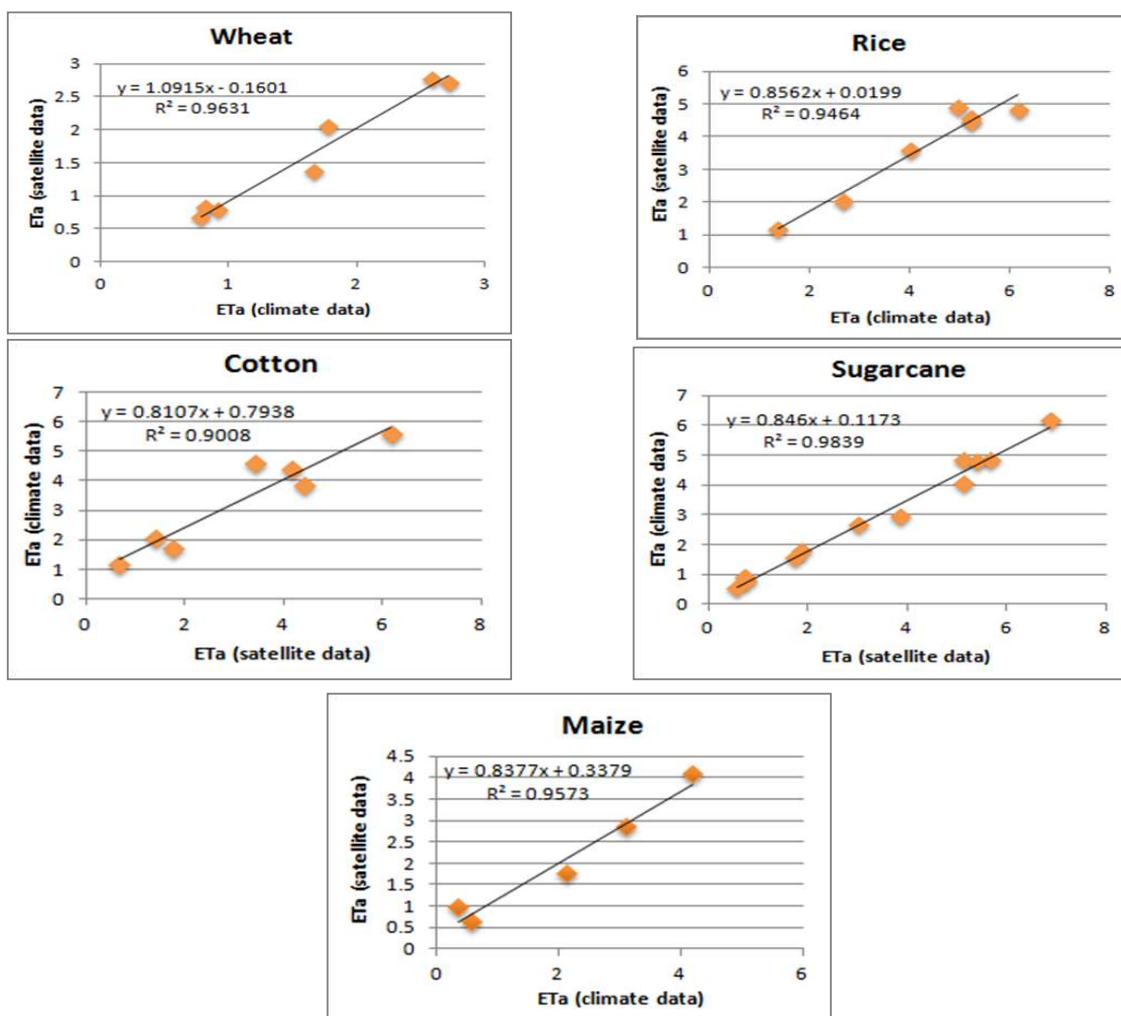


Figure 11. Statistical relationship of ET^a computed from both datasets

Conclusion

The research findings show NDVI fraction approach gives the best result with minimum degree of variation of spatial distribution of ET^a over large area. It serves as best method to apply at regional level in Pakistan when dealing with multi-date satellite data. Wheat, and Maize can be grown under rainfall conditions with minimum irrigations but Rice, Cotton and Sugarcane, require supplement irrigations throughout their growth. More water is required in zone I, II and III (southern zones) in the months of May, June, July, August and September as compared to other zones. Strong positive coefficient values show Remote sensing based ET^a can provide helpful and in time need of water for crops. Such type of studies should be made in other provinces of Pakistan for better use of water resources and sustainable agriculture.

Acknowledgements. Thanks to research collaborators and for institutional support of "Institute of Geo-Information & Earth Observation, PMAS Arid Agriculture University Rawalpindi".

REFERENCES

- [1] Aggarwal, P. (1993): Agro-Ecological Zoning Using Crop Growth Simulation Models: Characterization of Wheat Environments of India. – In: Penning de Vries, F. et al. (eds.) Systems Approaches for Agricultural Development. Springer, Dordrecht, pp. 97-109.
- [2] Ahmad, A., Ashfaq, M., Rasul, G., Wajid, S. A., Khaliq, T., Rasul, F., ... Ahmad Baig, I. (2015): Impact of Climate Change on the Rice–Wheat Cropping System of Pakistan. – In: Rosenzweig, C., Hillel, D. (eds.) Handbook of Climate Change and Agroecosystems: The Agricultural Model Intercomparison and Improvement Project Integrated Crop and Economic Assessments, Part 2. World Scientific, Singapore, pp. 219-258.
- [3] Allen, R., Pereira, L., Raes, D., Smith, M. (1998): Guidelines for Computing Crop Water Requirements. FAO Irrigation and Drainage Paper 56. – FAO-Food and Agriculture Organisation of the United Nations, Rome. <http://www.fao.org/docrep>.
- [4] Baig, M. B., Shahid, S. A., Straquadine, G. S. (2013): Making rainfed agriculture sustainable through environmental friendly technologies in Pakistan: a review. – International Soil and Water Conservation Research 1(2): 36-52.
- [5] Bhatti, A. M., Suttinon, P., Nasu, S. (2009): Agriculture water demand management in Pakistan: a review and perspective. – Society for Social Management Systems 9(172): 1-7.
- [6] Carlson, T. N., Arthur, S. T. (2000): The impact of land use – land cover changes due to urbanization on surface microclimate and hydrology: a satellite perspective. – Global and Planetary Change 25(1-2): 49-65.
- [7] Chaudhry, Q., Rasul, G. (2004): Agroclimatic classification of Pakistan. – Science Vision 9(3-4): 59-66.
- [8] Dempewolf, J., Adusei, B., Becker-Reshef, I., Hansen, M., Potapov, P., Khan, A., Barker, B. (2014): Wheat yield forecasting for Punjab Province from vegetation index time series and historic crop statistics. – Remote Sensing 6(10): 9653-9675.
- [9] Doorenbos, J., and Kassam, A. (1979): Yield Response to Water. – FAO Irrigation and Drainage Paper 33. FAO, Rome.
- [10] Gillies, R., Kustas, W., Humes, K. (1997): A verification of the ‘triangle’ method for obtaining surface soil water content and energy fluxes from remote measurements of the Normalized Difference Vegetation Index (NDVI) and surface e. – International Journal of Remote Sensing 18(15): 3145-3166.

- [11] Glenn, E. P., Neale, C. M., Hunsaker, D. J., Nagler, P. L. (2011): Vegetation index-based crop coefficients to estimate evapotranspiration by remote sensing in agricultural and natural ecosystems. – *Hydrological Processes* 25(26): 4050-4062.
- [12] Gowda, P. H., Senay, G. B., Colaizzi, P. D., Howell, T. A. (2008): Simplified surface energy balance (SSEB) approach for estimating actual ET: an evaluation with lysimeter data. – Paper presented at the 2008 Providence, Rhode Island, June 29–July 2, 2008.
- [13] Iqbal, M., Ahmad, M. (2005): Science & Technology Based Agriculture Vision of Pakistan and Prospects of Growth. – Paper presented at the Proceedings of the 20th Annual General Meeting Pakistan Society of Development Economics, Islamabad. Pakistan Institute of Development Economic (PIDE), Islamabad, Pakistan.
- [14] Karunarathne, A., Gad, E., Disfani, M., Sivanerupan, S., Wilson, J. (2016): Review of calculation procedures of Thornthwaite Moisture Index and its impact on footing design. – *Australian Geomechanics* 51(1): 85-95.
- [15] Kharrou, M. H., Er-Raki, S., Chehbouni, A., Duchemin, B., Simonneaux, V., LePage, M., ... Jarlan, L. (2011): Water use efficiency and yield of winter wheat under different irrigation regimes in a semi-arid region. – *Agricultural Sciences in China* 2(3): 273-282.
- [16] Liu, W., Hong, Y., Khan, S. I., Huang, M., Vieux, B., Caliskan, S., Grout, T. (2010): Actual evapotranspiration estimation for different land use and land cover in urban regions using Landsat 5 data. – *Journal of Applied Remote Sensing* 4(1): 041873.
- [17] McKenney, M. S., Rosenberg, N. J. (1993): Sensitivity of some potential evapotranspiration estimation methods to climate change. – *Agricultural and Forest Meteorology* 64(1-2): 81-110.
- [18] Rafn, E. B., Contor, B., Ames, D. P. (2008): Evaluation of a method for estimating irrigated crop-evapotranspiration coefficients from remotely sensed data in Idaho. – *Journal of Irrigation and Drainage Engineering* 134(6): 722-729.
- [19] Senay, G. B., Bohms, S., Singh, R. K., Gowda, P. H., Velpuri, N. M., Alemu, H., Verdin, J. P. (2013): Operational evapotranspiration mapping using remote sensing and weather datasets: a new parameterization for the SSEB approach. – *JAWRA Journal of the American Water Resources Association* 49(3): 577-591.
- [20] Singh, S., Dutta, S., Dharaiya, N. (2013): Estimation of crop evapotranspiration of cotton using remote sensing technique. – *Int. J. Environ. Eng. Manag.* 4: 523-528.
- [21] Thornthwaite, C. W. (1948): An approach toward a rational classification of climate. – *Geographical Review* 38(1): 55-94.

NITRATE SOURCE DISTRIBUTION IN RIVERS, ESTUARIES AND GROUNDWATER USING A DUAL ISOTOPE APPROACH AND A BAYESIAN ISOTOPE MIXING MODEL

XUE, D. – LI, J. – WANG, Y. – WANG, J. – WANG, Z.*

Tianjin Key Laboratory of Water Resources and Environment, Tianjin Normal University, Tianjin 300387, China

Tianjin Key Laboratory of Environmental Change and Ecological Restoration, School of Geographic and Environmental Sciences, Tianjin Normal University, Tianjin 300387, China

**Corresponding author*

e-mail: wangzhongliang@vip.skleg.cn; phone/fax: +86-222-3766-6256

(Received 15th Jul 2019; accepted 25th Nov 2019)

Abstract. Identification and quantification of nitrate (NO_3^-) sources in rivers, estuaries and shallow groundwater (SG) may help implementation in the water quality control measures. In this study, a dual isotope approach ($\delta^{15}\text{N}$ - and $\delta^{18}\text{O}$ - NO_3^-) and Bayesian isotope mixing model (SIAR) have applied to estimate the proportional contributions of NO_3^- from precipitation (NP), NO_3^- fertilizer (NF), ammonia nitrogen (NH_4^+) from fertilizer and rain (NF&R), soil N (Soil), and manure and sewage (M&S) for six rivers, two estuaries and SG in a coastal municipality in northern China. The combination of “M&S” (17-56%), “Soil” (21-37%), and “NF&R” (14-25%) contributions occupied more than 60% in total, and were considered as the dominant NO_3^- sources for the rivers and estuaries. The mean proportions of “NF” ranged from 6 to 20% and “NP” ranged from 2 to 11%, respectively. For SG, the mean proportions of “M&S” (27%), “Soil” (22%), and “NF&R” (21%) occupied about 70% in total, while the residual two NO_3^- sources occupied about 19% for “NF” and 11% for “NP”. We suggest that this approach can be easily modified determine NO_3^- sources and help to develop better N management practices in other environments where NO_3^- is a major N contributor.

Keywords: $\delta^{15}\text{N}$ - NO_3^- , $\delta^{18}\text{O}$ - NO_3^- , sources identification, SIAR, N contribution

Introduction

NO_3^- contamination in aquatic systems has become a serious environmental problem throughout the world. With the increasing population, extensive agricultural activities and rapid development of urbanization, the high NO_3^- levels of water impose a serious threat to drinking water and promote eutrophication, hypoxia, loss of biodiversity and habitat destruction both in riverine and coastal ecosystems (Galloway et al., 2003; Li et al., 2013; Umezawa et al., 2008; Villnäs et al., 2013). Monitoring NO_3^- concentrations alone cannot fully assess the sources and distribution of NO_3^- inputs in aquatic systems, which are the key factors in protecting water quality and reducing NO_3^- loadings.

Since NO_3^- from different sources (fertilizer, manure, human sewage, soil N and atmospheric deposition) have distinct isotopic compositions, it is possible to identify these different sources using N ($\delta^{15}\text{N}$) and O ($\delta^{18}\text{O}$) isotopic values (Xue et al., 2012; Wankel et al., 2015). Pardo et al. (2004) successfully used a dual isotope approach ($\delta^{15}\text{N}$ - and $\delta^{18}\text{O}$ - NO_3^-) to identify atmospheric deposition and microbial nitrification as the two main sources of NO_3^- in stream water at two forested watersheds. Chang et al. (2002) found that $\delta^{15}\text{N}$ and $\delta^{18}\text{O}$ values of NO_3^- indicated manure as the predominant source when discharge and NO_3^- concentrations were low (winter), and soil-derived NO_3^- as the predominant source when discharge and NO_3^- concentrations were high

(spring-summer) in Mississippi River Basin. For the second tributary Pearl River in southern China, Chen et al. (2009) and Jin et al. (2017) pointed out that the N and O isotopic values fell in the range of nitrification of reduced fertilizer N in soil zones. Li et al. (2010) found that the $\delta^{15}\text{N}$ - and $\delta^{18}\text{O}$ - NO_3^- values of the Yangtze River indicating a main source from urban sewage effluent.

In addition, to reduce NO_3^- loadings in aquatic systems, it is quite meaningful to quantify the contributions of different NO_3^- sources. Some researchers, Deutsch et al. (2006) and Yang et al. (2018) also applied $\delta^{15}\text{N}$ - and $\delta^{18}\text{O}$ - NO_3^- to quantify NO_3^- source distribution in water via a mass balance mixing model (Semmens et al., 2013). However, this method is limited to (1) temporal and spatial variability in $\delta^{15}\text{N}$ - and $\delta^{18}\text{O}$ - NO_3^- ; (2) isotope fractionation by denitrification; and (3) number of sources > number of isotopes + 1 (Moore et al., 2008; Xue et al., 2009). A mixing model for stable isotope analysis called SIAR (stable isotope analysis in R) under a Bayesian framework has been developed to solve source distribution problems (Parnell et al., 2010). The disadvantages of a mass balance mixing model mentioned above are overcome. Xue et al. (2012) successfully applied SIAR to estimate NO_3^- source distribution of surface waters of Flanders in Belgium. Thereafter, SIAR was also applied to evaluate contributions of NO_3^- sources in underground water (Gaouzi et al., 2013; Chen et al., 2015), rivers (Ding et al., 2014) and reservoir (Yang et al., 2013), respectively.

Tianjin is an important coastal municipality located in the Bohai Bay in northern China. An investigation of surface waters of Tianjin (Wang et al., 2009) reported that NO_3^- concentrations could highly reach up to 10.3 mg L^{-1} in rivers, and about 8.1% of agricultural drainages that NO_3^- concentrations were over 15 mg L^{-1} . Wang et al. (2011) concluded that NO_3^- was the dominant Dissolved inorganic nitrogen (DIN) species in coastal water of Tianjin, with water quality deteriorating. Thus, it is essential to specify predominant NO_3^- sources and assess potential NO_3^- source distribution, which is of great significance to control water contamination and protect coastal ecological system. The aim of this study is to: (1) apply a dual isotope bi-plot approach ($\delta^{15}\text{N}$ - and $\delta^{18}\text{O}$ - NO_3^-) combining with physicochemical properties to identify NO_3^- sources; and (2) apply the SIAR model to estimate the contributions of potential NO_3^- sources in rivers, estuaries and shallow groundwater (SG) in Tianjin.

Material and methods

Study area

The investigated rivers, estuaries and SG are located in Tianjin, a coastal municipality in northern China (*Fig. 1*). The study region is mainly influenced by a warm temperate semi-humid monsoon climate with an average annual temperature of 11.4 - $12.9 \text{ }^\circ\text{C}$, and the annual precipitation of 520 - 660 mm (Yue et al., 2010; Wang et al., 2014). The geological structure is complex, and mostly covered by Cenozoic sediments. The terrain is dominated by plains and depressions, with low mountains and hills in the north, and the altitude gradually decreases from north to south. The highest and lowest altitude are 1052 m and 3.5 m in the north and southeast, respectively. The total area of Tianjin is 11919.7 km^2 and the coastline is about 153.0 km (Wang et al., 2013).

The six rivers distributed from north to south are Jiyun River (JY River), Chaobaixin River (CB River), Haihe River (HH River), Dagu sewage River (DG River), Duliujian River (DL River), and Ziyaxin River (ZY River), respectively. The properties of the river are shown in *Table 1*. The northern rivers, the JY River and the CB River flowing

through a rural area and are characterized by 144 km and 81 km in length, 300 m and 700 m in width, 7 m and 5-7 m in depth, and a watershed area of 2416 km² and 1387 km², respectively (Starks et al., 2014; Chen et al., 2000). Precipitation is the main water supply of the JY River so that the runoff seasonally changed. There is an important livestock breeding base in the watershed area of the CB River. Upper reaches are the main water supply of CB River. The rivers of HH and DG flow through the urban and industrial area in the middle of the municipality. The DG River is characterized by 71 km in length, 54-120 m in width, and a watershed area of 1000 km², which is an important river channel that holds industrial wastewater and domestic sewage (Guo et al., 2009). The HH River is characterized by 72 km in length, 100 m in width, 3-5 m in depth, and a watershed area of 2066 km², and water mainly come from the precipitation and upper reaches (Liu et al., 2010). The HH River is separated by a floodgate into two parts: the upstream of the HH River (HHup) flow through the center of the municipality, while the downstream of the HH River (HHdw) flow through the industrial area. The southern rivers DL and ZY flow through the agricultural and industrial area. The DL River is characterized by 70 km in length, and 400 m in width (Lai et al., 2001), where the upper reaches is the main water supply of DL River. The ZY River is characterized by 29 km in length and 100-300 m in width (Ding et al., 2016), and water mainly come from the precipitation and upper reaches. One of the studied estuaries is the confluence of the JY and the CB River (CJ Estuary) in north, and the design flow is 4640 m³/s (Dong et al., 2007). The other is the estuary of the HH River (HH Estuary) in middle, and the design flow is 800 m³/s (Dong et al., 2007).

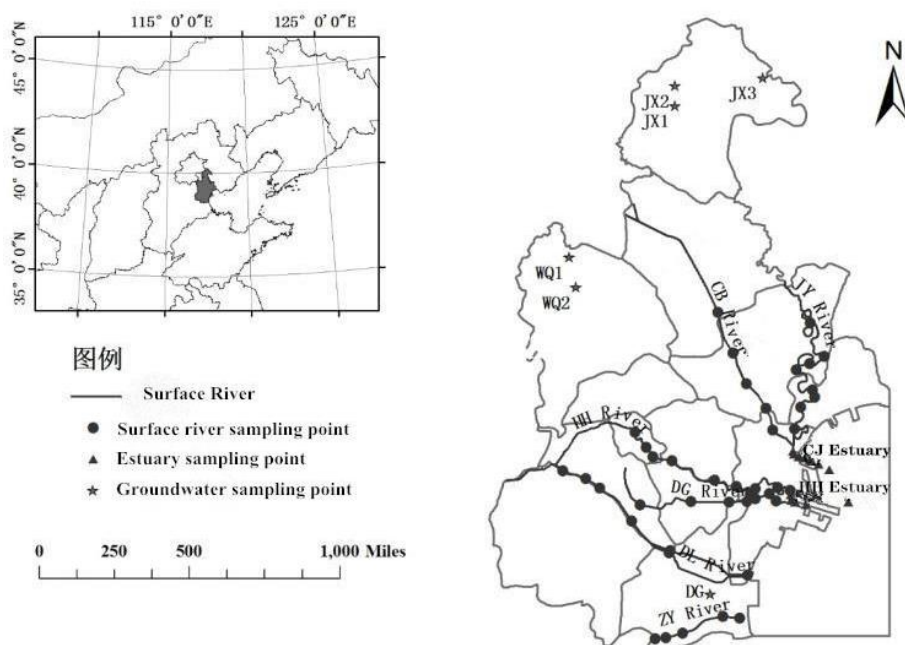


Figure 1. Sampling locations for six rivers, two estuaries and groundwater. JY, CB, HH, DG, DL and ZY River are the abbreviations of the Jiyun River, the Chaobaixin River, the Haihe River, the Dagang sewage River, the Duliujian River and the Ziyaxin River, respectively. CJ, HH are the abbreviations of the CJ Estuary (co-estuary of the JY and the CB River) and Haihe Estuary, respectively. DG, JX and WQ are the abbreviations of Dagang, Jixian and Wuqing, which are all located in the rural areas of Tianjin. Number represent different sampling locations and -May and -Nov represent samples were collected in mid-May and mid-November during dry and wet periods, respectively

Table 1. Properties of the rivers and the corresponding estuaries

Location	Longitude	Latitude	Length (km)	Width (m)	Depth (m)	Drainage area (km ²)	Design flow (m ³ /s)
JY River	117.83732 °E	39.34846 °N	144	300	7	2416	–
CB River	117.38531 °E	39.60658 °N	81	700	5~7	1387	–
CJ Estuary	117.48532 °E	39.03454 °N	–	–	–	–	4640
HH River	117.19165 °E	39.14954 °N	72	100	3~5	2066	–
HH Estuary	117.46202 °E	38.57143 °N	–	–	–	–	800
DG River	117.21497 °E	38.95831 °N	71	54~120	–	1000	–
DL River	116.94644 °E	39.04793 °N	70	400	–	–	–
ZY River	117.25816 °E	38.60085 °N	29	100~300	–	–	–

The water table of SG in the study area displays different spatial distribution: it is about 10 to 50 m in the northern piedmont plain, 30 to 80 m in the middle plain and 2 to 3 m in the southern littoral plain. Particularly, in recent 20 years, the SG table is steady in northwest and eastern plain of Tianjin, while it goes down yearly in the coastal areas (Wang et al., 2014). Most rivers in this study are artificial, where groundwater cannot compensate because of the relatively low groundwater table level. The flood seasons occurred in July and August, while from May to June and September to next February were dry seasons.

Sampling and analysis

Samples were collected along the rivers and estuaries in November 2012 and SG samples were sampled in mid-May 2014 and mid-November 2014, during dry and wet periods, respectively. Water samples were taken on a bridge using a bucket serially from upstream downwards for the rivers and on a ship for estuarine water. The bucket was put into the river/estuary water until it reached ~0.5 m below the surface to sample water. SG is extracted by pumping pump and collected after the water flow is stable (about 5 min). Then, the water samples were stored frozen in 1 L high-density polyethylene (HDPE) bottles for determination of physico-chemical properties and $\delta^{15}\text{N}$ - and $\delta^{18}\text{O}$ - NO_3^- . Salinity, pH and dissolved oxygen (DO) were determined in situ by a portable water quality probe (Thermo Orion, USA). Water samples were filtered through 0.45 μm membrane filters and stored at 4 °C until analysis. NO_3^- , nitrite (NO_2^-) and NH_4^+ concentrations were analyzed on a continuous flow analyzer (Auto Analyzer 3, Seal, Germany). Chloride (Cl^-) was determined by ion chromatography (ICS–2100, Dionex, USA). The $\delta^{15}\text{N}$ - and $\delta^{18}\text{O}$ - NO_3^- values were determined by “Bacterial denitrification method” (Mcilvin et al., 2011; Templer et al., 2011; Xue et al., 2010) in the UC Davis Stable Isotope Facility of California University.

Stable isotope data of ^{15}N and ^{18}O are expressed in delta (δ) units in per mill (‰) relative to their respective international standards: atmospheric air (AIR) and Vienna standard mean ocean water 2 (VSMOW 2):

$$\delta_{\text{sample}} (\text{‰}) = \left(\frac{R_{\text{sample}}}{R_{\text{standard}}} - 1 \right) * 1000 \quad (\text{Eq.1})$$

where R_{sample} and R_{standard} refer to the $^{15}\text{N}/^{14}\text{N}$ or $^{18}\text{O}/^{16}\text{O}$ ratio of the sample and standard for $\delta^{15}\text{N}$ and $\delta^{18}\text{O}$, respectively. The calibration standards are the nitrate salts USGS 32, USGS 34, and USGS 35, supplied by NIST (National Institute of Standards and Technology, Gaithersburg, MD).

Source distribution mixing model (SIAR)

The contribution proportions of NO_3^- sources to surface water samples were quantified using the SIAR model (Parnell et al., 2010) as follows:

$$\begin{aligned} X_{ij} &= \sum_{k=1}^K p_k (s_{jk} + c_{jk}) + \varepsilon_{ij} \\ s_{jk} &\sim N(\mu_{jk}, \omega_{jk}^2) \\ c_{jk} &\sim N(\lambda_{jk}, \tau_{jk}^2) \\ \varepsilon_{ij} &\sim N(0, \sigma_j^2) \end{aligned} \quad (\text{Eq.2})$$

where X_{ij} is the observed isotope value j of the sample i ($i = 1, 2, 3, \dots, N$ and $j = 1, 2, 3, \dots, J$); s_{jk} is the source value k on isotope j ($k = 1, 2, 3, \dots, K$) and normally distributed with mean μ_{jk} and variance ω_{jk}^2 ; c_{jk} is the fractionation factor for isotope j on source k and normally distributed with mean λ_{jk} and variance τ_{jk}^2 ; ε_{ij} is the residual error which describes additional variation between sample measurements, and it is normally distributed with mean 0 and variance σ_j^2 ; p_k is the proportion of source k estimated by SIAR.

The fractionation factor, c_{jk} is relevant to denitrification. This process can result in an exponential increase of $\delta^{15}\text{N}$ - and $\delta^{18}\text{O}$ - NO_3^- as NO_3^- concentration decreases. An enrichment of ^{15}N relative to ^{18}O by a factor between 0.8 and 2.0 gives evidence for denitrification (Aravena and Robertson., 2010; Fukada et al., 2003; Xue et al., 2009). The enrichment factors (ε) of denitrification can be calculated via the relation between the isotopic values and the logarithm of residual NO_3^- and are expected to fall into the range from -40‰ to -5‰ for $\varepsilon^{15}\text{N}$ and from -18‰ to -8‰ for $\varepsilon^{18}\text{O}$ (Hubner, 1986; Bottcher et al., 1990; Smith et al., 1991; Mengis et al., 1999; Fukada et al., 2003; Sebiló et al., 2003; Knöller et al., 2011).

Statistical analysis

In this study, the principle coordinate analysis (PCoA) has been applied to evaluate the data sets of physicochemical properties of the six rivers and the corresponding estuaries and shallow groundwater samples.

Results and discussion

Physicochemical properties of the rivers and the corresponding estuaries

The physicochemical properties and isotopic values of the water samples were shown in *Table 2*. The mean pH of the rivers and their corresponding estuaries changed from 7.4 to 8.4, and the mean DO concentrations ranged from 4.1 to 11.2 mg L⁻¹. The mean salinity of the middle rivers (2.5-3.2) except the HHup (0.7) was higher than the northern (0.5-0.7) and southern rivers (1.9-2.5). The municipality had been suffering multiple seawater intrusion and regression, which results in the salinization of the rivers and soil (Wang, 2004).

Table 2. *Physicochemical properties and isotopic composition of NO₃⁻ for the rivers and the corresponding estuaries*

Location	pH	DO	Salinity	Cl ⁻	NO ₃ ⁻	NH ₄ ⁺	NO ₂ ⁻	δ ¹⁵ N- NO ₃ ⁻	δ ¹⁸ O- NO ₃ ⁻
				mg L ⁻¹				‰	
CB River	7.9	8.9	0.5	117.0	7.4	6.0	1.8	13.7	4.0
	8.6	10.5	0.5	138.5	8.3	3.0	0.5	14.0	4.8
	8.5	9.1	0.5	161.4	9.8	6.8	0.6	13.9	3.9
	8.5	9.9	0.5	180.6	10.6	2.6	0.5	12.2	4.3
	8.6	10.4	0.6	184.0	10.6	6.6	0.4	13.7	4.8
	8.2	10.0	0.6	195.0	9.4	3.8	0.3	14.1	5.6
Mean ± SD	8.4 ± 0.3	9.8 ± 0.7	0.5 ± 0.1	162.8 ± 30.0	9.4 ± 1.3	4.8 ± 1.9	0.7 ± 0.6	13.6 ± 0.7	4.6 ± 0.6
JY River	8.1	7.2	0.6	171.4	2.5	1.3	0.3	6.5	0.9
	8.2	8.7	0.7	194.9	2.6	1.2	0.3	6.3	2.0
	8.2	7.5	0.7	206.4	2.7	1.0	0.2	6.4	1.4
	8.4	9.3	0.7	215.6	2.9	0.9	0.2	5.8	0.8
	8.4	9.3	0.8	233.7	4.7	0.2	0.3	5.3	1.3
	8.4	9.7	0.8	251.1	4.8	0.5	0.2	5.3	1.1
	8.5	9.9	0.8	254.3	5.2	0.2	0.1	4.4	2.8
	8.5	9.9	0.8	254.5	5.1	0.6	0.1	4.4	5.3
Mean ± SD	8.3 ± 0.2	8.9 ± 1.1	0.7 ± 0.1	222.7 ± 30.8	3.8 ± 1.2	0.7 ± 0.4	0.2 ± 0.1	5.6 ± 0.8	2.0 ± 1.5
CJ Estuary	8.2	10.6	2.0	7028.2	9.5	5.9	0.2	13.6	5.9
	8.2	11.4	2.5	4973.9	7.4	5.5	0.2	15.0	6.1
	8.3	11.5	2.7	1201.1	6.8	5.1	0.4	14.7	6.4
	8.3	11.1	4.2	1216.8	8.1	5.2	0.3	13.6	6.4
	8.3	11.4	9.0	509.6	2.3	3.3	0.4	11.9	6.2
	8.3	11.3	13.7	2172.8	1.5	2.2	0.3	9.3	6.7
	8.3	11.3	13.7	2172.8	1.5	2.2	0.3	9.3	6.7
	8.2	11.2	20.0	9831.6	0.4	0.8	0.2	7.1	6.9
Mean ± SD	8.3 ± 0.1	11.2 ± 0.3	7.7 ± 6.9	3847.7 ± 3537.1	5.1 ± 3.6	4.0 ± 1.9	0.3 ± 0.1	12.2 ± 3.0	6.4 ± 0.3
HHup River	7.5	2.7	0.7	207.2	13.6	4.0	0.8	-0.2	-0.5
	7.7	4.0	0.7	184.6	9.0	6.0	0.8	0.5	0.2
	7.7	4.8	0.7	219.1	8.3	5.6	0.9	0.6	0.2
	7.9	5.0	0.8	275.8	6.5	5.9	1.0	1.1	0.5
Mean ± SD	7.7 ± 0.2	4.1 ± 1.0	0.7 ± 0.1	221.7 ± 38.8	9.4 ± 3.0	5.4 ± 0.9	0.9 ± 0.1	0.5 ± 0.5	0.1 ± 0.4
HHdw River	8.1	8.2	1.0	408.2	5.9	2.8	1.0	4.5	0.6
	8.4	10.4	2.3	1441.5	5.6	2.2	0.3	4.6	1.1
	8.5	10.5	2.4	1696.6	5.8	2.3	0.5	4.3	1.3
	8.3	10.4	3.7	1983.0	5.5	2.3	0.4	3.9	1.2
	8.3	9.9	4.6	2673.9	3.9	2.8	0.7	8.4	1.5
	8.2	9.4	4.9	3486.6	4.3	2.7	0.7	7.4	1.4
Mean ± SD	8.3 ± 0.1	9.8 ± 0.9	3.2 ± 1.5	1948.3 ± 1057.0	5.2 ± 0.8	2.5 ± 0.3	0.6 ± 0.3	5.5 ± 1.9	1.2 ± 0.3

HH Estuary	8.1	10.7	18.6	10225.6	1.6	1.6	0.3	8.0	5.4
	8.1	10.7	20.6	10519.7	1.1	1.4	0.3	7.9	5.6
	8.2	10.7	21.3	12202.2	0.9	1.4	0.3	8.1	5.7
	8.2	10.7	24.1	13270.0	0.4	1.2	0.3	8.3	5.8
Mean ± SD	8.2 ± 0.1	10.7 ± 0.0	21.2 ± 2.3	11554.4 ± 1437.5	1.0 ± 0.5	1.4 ± 0.2	0.3 ± 0.0	8.1 ± 0.2	5.6 ± 0.2
DG River	8.1	9.1	1.8	707.9	6.0	2.5	0.7	7.2	3.0
	7.0	5.7	1.7	699.8	5.3	14.5	0.4	8.4	2.9
	7.2	3.8	2.3	1050.9	0.2	16.7	0.0	11.6	5.1
	7.1	5.5	3.0	1397.3	3.9	14.2	0.6	7.7	0.5
7.8	8.7	3.6	1804.1	6.9	10.6	0.5	6.2	1.5	
Mean ± SD	7.4 ± 0.5	6.6 ± 2.3	2.5 ± 0.8	1132.0 ± 473.1	4.4 ± 2.6	11.7 ± 5.6	0.4 ± 0.3	8.2 ± 2.0	2.6 ± 1.7
DL River	8.2	10.8	1.8	723.7	9.6	2.7	0.4	4.0	2.5
	7.7	7.7	1.8	731.3	12.5	10.4	0.9	6.8	3.6
	7.7	8.3	2.0	791.4	11.2	9.0	1.0	6.5	7.2
	8.3	10.9	2.5	1043.5	12.5	1.2	0.3	4.3	2.5
	8.2	11.3	2.4	1105.3	11.1	0.1	0.1	4.2	3.0
8.2	11.1	2.9	1410.1	11.2	2.0	0.0	6.4	7.7	
Mean ± SD	8.1 ± 0.3	10.0 ± 1.6	2.2 ± 0.4	967.6 ± 270.9	11.4 ± 1.1	4.2 ± 4.3	0.5 ± 0.4	5.4 ± 1.3	4.4 ± 2.4
ZY River	7.3	9.1	1.8	736.7	5.5	34.3	2.2	8.2	7.7
	7.5	10.1	1.8	697.9	5.4	51.9	2.1	7.9	8.2
	7.3	9.1	1.7	701.4	4.9	52.4	1.9	8.7	9.2
	7.4	9.4	1.9	839.8	4.4	55.7	2.0	8.9	8.9
	7.4	9.3	2.1	929.3	2.4	61.2	1.8	14.1	13.4
Mean ± SD	7.4 ± 0.1	9.4 ± 0.4	1.9 ± 0.2	781.0 ± 100.8	4.5 ± 1.3	51.1 ± 10.1	2.0 ± 0.2	9.6 ± 2.6	9.5 ± 2.3

The mean Cl^- concentrations were relatively high, varying from 162.8 to 1948.3 mg L^{-1} for the rivers and from 3847.7 to 11554.4 mg L^{-1} for the estuaries. Both the salinization and anthropogenic activities, such as sewage and livestock effluent can cause relatively high Cl^- concentrations in the rivers (Yao et al., 2007). The relatively higher mean NO_3^- concentrations appeared in the rivers of DL (11.4 mg L^{-1}), CB (9.4 mg L^{-1}) and the HHup (9.4 mg L^{-1}); the relatively lower mean NO_3^- concentrations appeared in the rivers of JY (3.8 mg L^{-1}). The mean NO_3^- concentrations of the estuaries were 5.1 mg L^{-1} for the CJ Estuary and 1.0 mg L^{-1} for the HH Estuary. The mean NH_4^+ concentrations varied largely from 0.7 to 51.1 mg L^{-1} . The highest mean NH_4^+ concentration appeared in the ZY River because of intensive industry along the upstream of the river and large volume discharge of low treatment rate of sewage (He and Huang, 2013).

The mean NO_2^- concentrations of the rivers and their corresponding estuaries changed from 0.2 to 2.0 mg L^{-1} . The isotopic composition of NO_3^- varied spatially among the rivers and the corresponding estuaries (Table 2). The mean $\delta^{15}\text{N}-\text{NO}_3^-$ values varied from 0.5 to 13.6‰ and the mean $\delta^{18}\text{O}-\text{NO}_3^-$ values varied from 0.1 to 9.5‰. The relatively large isotopic range potentially indicates that the rivers and estuaries were influenced by complex NO_3^- sources.

The PCoA results revealed that the rivers and the corresponding estuaries were divided into three parts (Fig. 2). The rivers of CB, JY and HHup with low salinity located in the north of Tianjin were grouped together, while the rivers of HHdw, DG, DL and ZY with high salinity were grouped together. The residual two estuaries (CJ and HH) were grouped together with highest salinity.

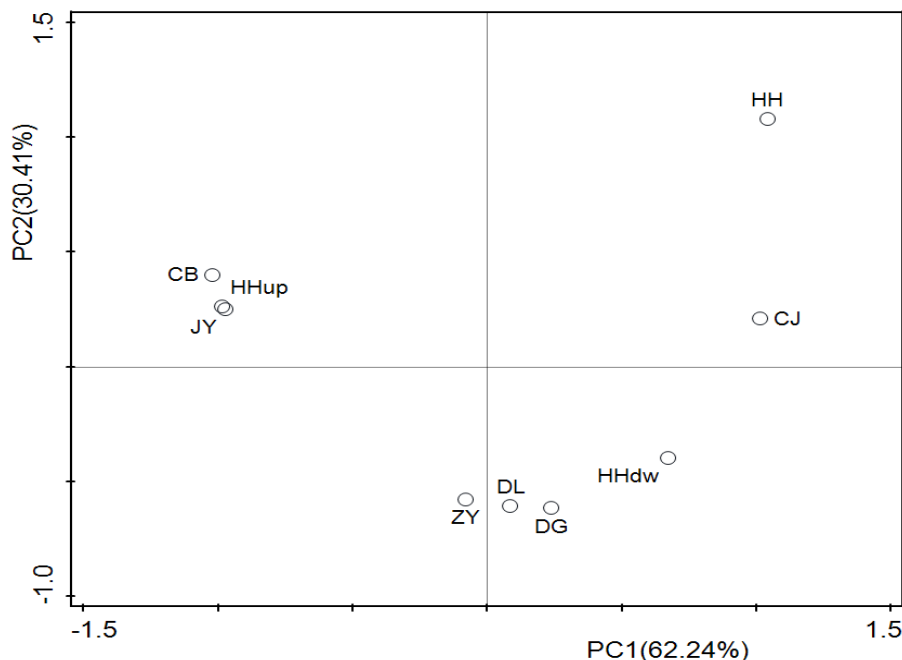


Figure 2. Principle coordinate analysis for physicochemical properties of the six Rivers and the corresponding Estuaries. CB, JY, HHup, HHdw, DL, ZY and DG River are the abbreviations of the Chaobaixin River, the Jiyun River, the upstream of the Haihe River, the downstream of the Haihe River, the Duliujian River, the Ziyaxin River and the Dagu sewage River, respectively. CJ, HH are the abbreviations of the CJ Estuary (co-estuary of the JY and the CB River) and Haihe Estuary, respectively

Physicochemical properties of the SG

The physicochemical properties and isotopic values of the SG were shown in Table 3. The average pH of SG in May and November was 7.1 and 7.4, with a range between 6.6 to 7.8 and 6.9 to 8.2, respectively. The mean DO was 4.6 mg L⁻¹ and 5.9 mg L⁻¹, and varied from 1.9 to 7.9 mg L⁻¹ and 1.7 to 8.4 mg L⁻¹, respectively. The average salinity and its variations ranged between 0.4 to 3.2 with a mean value of 1.1 in May and between 0.4 to 3.3 with a mean value of 1.2 in November, respectively.

The mean Cl⁻ concentrations in SG were higher in May (1085.2 mg L⁻¹) than that in November (420.1 mg L⁻¹), with a maximum Cl⁻ concentration achieved as high as 2704.3 mg L⁻¹. The average concentration of NO₃⁻ in May was 117.5 mg L⁻¹ lower than that of 159.8 mg L⁻¹ in November. The variation was in a large range, from 0.3 to 221.9 mg L⁻¹ and 6.7 to 360.3 mg L⁻¹ in May and November, respectively.

The average concentrations of NO₂⁻ in November and May were 0.06 mg L⁻¹ and 0.06 mg L⁻¹, with a range from 0.01 to 0.15 mg L⁻¹ and 0.01 to 0.21 mg L⁻¹, respectively. The average concentration of NH₄⁺ was 0.3 mg L⁻¹ and 0.2 mg L⁻¹ in May and November, with variations ranging from 0 to 0.9 mg L⁻¹ and 0 to 1.0 mg L⁻¹, respectively. The δ¹⁵N-NO₃⁻ values varied from +10.2 to +45.9‰ and +2.9 to +38.2‰ in May and November, with a mean δ¹⁵N-NO₃⁻ value of +22.5‰ and +13.5‰, respectively. The average value of δ¹⁸O-NO₃⁻ was relatively close in May (+9.9‰) and November (+10.8‰), ranging from -7.9 to +28.4‰ and +2.2 to +22.6‰.

The PCoA results revealed that groundwater sampling points of Jixian, Wuqing and Dagang were grouped into three parts (Fig. 3) based on their spatial locations.

Table 3. Physicochemical properties and isotopic composition of NO_3^- for the shallow groundwater

Season	Sampling point	pH	Salinity	DO	Cl ⁻	NO ₃ ⁻	NO ₂ ⁻	NH ₄ ⁺	$\delta^{15}\text{N} - \text{NO}_3^-$	$\delta^{18}\text{O} - \text{NO}_3^-$
			(ppt)	mg/L						‰
May	JX1	6.6	0.5	7.9	640.6	238.0	0.04	0.0	19.6	7.5
	JX2	6.9	0.5	7.3	40.0	221.9	0.03	0.0	10.4	0.9
	JX3	6.6	0.4	4.4	551.0	128.1	0.02	0.0	10.2	-7.9
	WQ1	7.5	1.2	2.6	1291.6	0.3	0.01	0.9	31.0	28.4
	WQ2	7.2	0.9	1.9	1283.5	59.8	0.04	0.8	17.6	8.7
	DG	7.8	3.2	3.5	2704.3	56.9	0.21	0.0	45.9	21.9
	Mean ± S D	7.1 ± 0.4	1.1 ± 0.9	4.6 ± 2.3	1085.2 ± 844.5	117.5 ± 87.8	0.06 ± 0.07	0.3 ± 0.4	22.5 ± 12.6	9.9 ± 12.2
November	JX1	7.1	0.6	8.4	64.4	276.1	0.02	0.0	10.7	5.4
	JX2	7.2	0.6	7.7	62.0	360.3	0.03	0.0	3.2	7.1
	JX3	6.9	0.4	3.4	44.3	186.9	0.01	0.0	2.9	2.2
	WQ1	7.5	1.1	7.3	424.8	6.7	0.14	1.0	15.5	17.0
	WQ2	7.3	1.1	1.7	272.2	74.1	0.15	0.2	10.5	10.6
	DG	8.2	3.3	6.8	1652.7	54.7	0.03	0.1	38.2	22.6
	Mean ± S D	7.4 ± 0.4	1.2 ± 0.9	5.9 ± 2.5	420.1 ± 568.2	159.8 ± 126.7	0.06 ± 0.06	0.2 ± 0.3	13.5 ± 11.9	10.8 ± 7.0

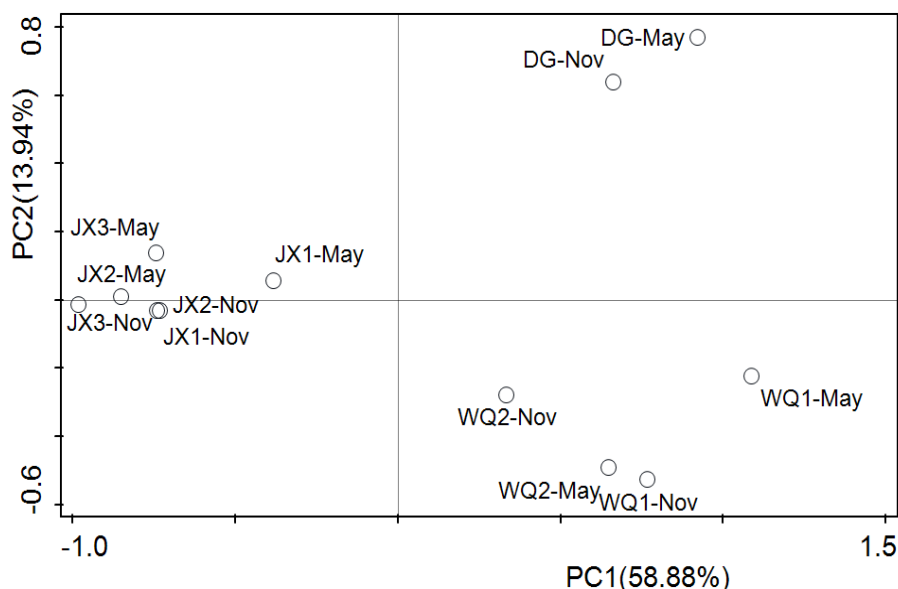


Figure 3. Principle coordination analysis for physicochemical properties of the shallow groundwater. DG, JX and WQ are the abbreviations of Dagang, Jixian and Wuqing, which are all located in the outskirts of Tianjin. Number represent different sampling locations and -May and -Nov represent samples were sampled in mid-May and mid-November, during dry and wet periods, respectively

Potential NO_3^- source identification for the rivers and the corresponding estuaries

A classical dual isotope bi-plot approach ($\delta^{15}\text{N}-\text{NO}_3^-$ vs. $\delta^{18}\text{O}-\text{NO}_3^-$) was applied to identify the potential dominant NO_3^- sources in different rivers and the corresponding estuaries (Fig. 4). It is clear that the predominant NO_3^- sources are “Soil” and/or “M&S” for the HH River, the CB River, the JY River, the CJ and the HH Estuary. The isotopic

signatures of the DL River were mainly concentrated in the “Soil” source box, indicating NO_3^- derived from soil organic, N. The $\delta^{15}\text{N}$ - and $\delta^{18}\text{O}$ - NO_3^- values of the DG River and the ZY River were distributed in the source box of “M&S”. In general, more than half of the sampling locations were mainly influenced by “manure” and/or sewage, but it is difficult to specify whether the predominant NO_3^- source is from only one or both two sources based on the bi-plot.

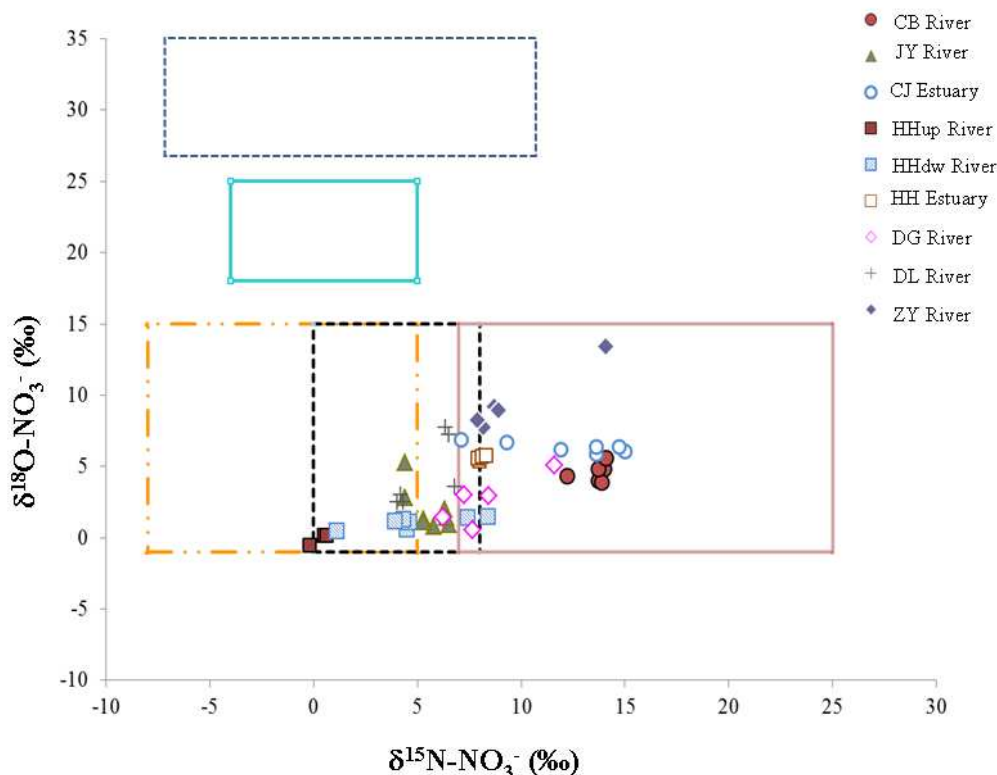


Figure 4. The $\delta^{15}\text{N}$ - and $\delta^{18}\text{O}$ - NO_3^- of the rivers and the corresponding estuaries. CB, JY, HHup, HHdw, DL, ZY and DG River are the abbreviations of the Chaobaixin River, the Jiyun River, the upstream of the Haihe River, the downstream of the Haihe River, the Duliujian River, the Ziyaxin River and the Dagu sewage River, respectively. CJ, HH are the abbreviations of the CJ Estuary (co-estuary of the JY and the CB River) and Haihe Estuary, respectively. Ranges of the isotopic composition for five potential NO_3^- sources are adapted from Kendall et al. (2007) and Xue et al. (2009) and indicated by boxes: NO_3^- in precipitation (NP), NO_3^- fertilizer (NF), NH_4^+ in fertilizer and rain (NF&R), soil N (Soil) and manure and sewage (M&S). To provide a wider and clear range of $\delta^{18}\text{O}$ - NO_3^- values, the upper limit of NP reaches 35‰

Cl^- is a useful indicator for contamination source tracking. High levels of Cl^- have been detected in sewage and livestock effluent (Yao et al., 2007). Thus, a plot of $\delta^{15}\text{N}$ - NO_3^- vs. $\text{NO}_3^-/\text{Cl}^-$ molar ratio might reveal further detailed information for source identification (Fig. 5). As shown in Figure 5, in the “M&S” source box, the majority of the rivers and estuaries were potentially influenced by four sources: (a) extremely low $\text{NO}_3^-/\text{Cl}^-$ molar ratio and relatively low $\delta^{15}\text{N}$ - NO_3^- values (mainly appeared in the HH Estuary, box A in Fig. 5); (b) relatively low $\text{NO}_3^-/\text{Cl}^-$ molar ratio and high $\delta^{15}\text{N}$ - NO_3^- values (mainly appeared in the CJ Estuary, box B in Fig. 5); (c) high $\text{NO}_3^-/\text{Cl}^-$ molar ratio and high $\delta^{15}\text{N}$ - NO_3^- values (mainly appeared in the CB River, box C in Fig. 5);

and (d) relatively low $\text{NO}_3^-/\text{Cl}^-$ molar ratio and relatively low $\delta^{15}\text{N}-\text{NO}_3^-$ values (mainly appeared in the ZY River, box D in Fig. 5). Since the HH River discharge was limited due to the floodgate at the end, the HH Estuary (box A) and the highest salinity sampling location of the CJ Estuary might be regarded as the coast end-member. The last two sampling locations of the HH River were obvious to be influenced by seawater from the HH Estuary not sewage. There are mooring ships in the vicinity of the CJ Estuary all year around, domestic sewage is the main NO_3^- source in this estuary. Thus, the CJ Estuary (box B) can be considered as domestic sewage end-member. Along with point-source contamination was diluted by estuarine water, the residual sampling locations of the CJ Estuary were close to the HH Estuary end-member (box A). The CB River (box C) was considered as the manure end-member, as this watershed plays the role of important livestock breeding base for the municipality (Shao et al., 2010). Furthermore, the $\delta^{15}\text{N}-\text{NO}_3^-$ values were enriched and varied around 14‰, indicating anthropogenic NO_3^- derived from manure (Kendall et al., 2007; Xue et al., 2009). The ZY River (box D) was considered as the industrial sewage end-member, as industry was intensively distributed along the upstream of the river and low treatment rate of sewage was largely discharged into the river. The data distribution of the DG River is quite scattered, possibly resulting from multiple NO_3^- source inputs.

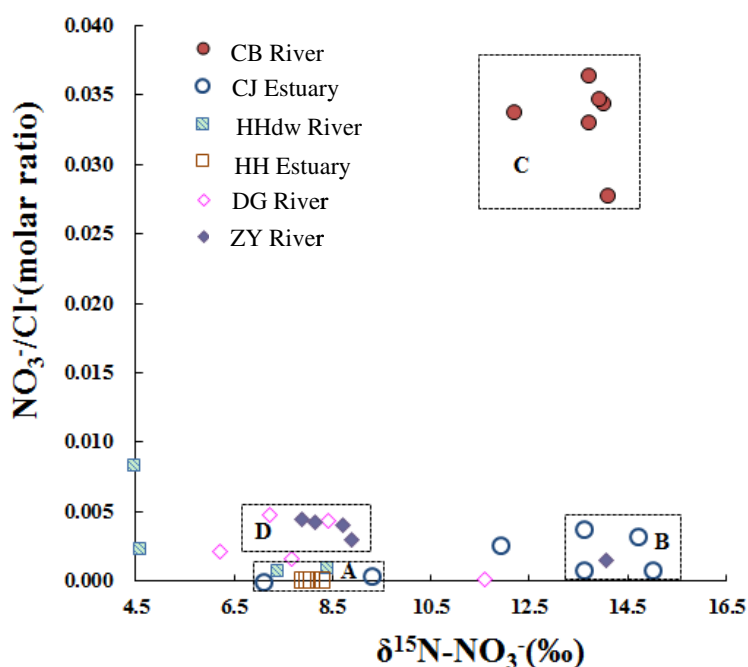


Figure 5. The $\text{NO}_3^-/\text{Cl}^-$ molar ratio versus the nitrogen isotope of NO_3^- in the rivers and the corresponding estuaries. Boxes A, B, C, and D represent different end-members. CB, HHdw, ZY and DG River are the abbreviations of the Chaobaixin River, the downstream of the Haihe River, the Ziyaxin River and the Dagu sewage River, respectively. CJ, HH are the abbreviations of the CJ Estuary (co-estuary of the JY and the CB River) and Haihe Estuary, respectively

Wide ranges of the $\delta^{15}\text{N}$ - and $\delta^{18}\text{O}-\text{NO}_3^-$ values of the rivers and corresponding estuaries showed that surface waters in Tianjin are mainly influenced by multiple NO_3^- sources, but dominated by one or two. To get more specific information, a more quantitative technique based on isotopic mixing model has been applied.

Potential NO_3^- source identification for the SG

As shown in *Figure 6*, the values of $\delta^{15}\text{N}$ - and $\delta^{18}\text{O}$ - NO_3^- seasonally varied in a wide range and increased from north to south (along the direction of groundwater flow), resulting in a linear positive correlation of 0.82 and 0.53, which indicated that significant denitrification occurred in SG (Xue et al., 2009; Aravena and Robertson, 2010; Fukada et al., 2003; Mengis et al., 2005). In the northern part of SG, the lower $\delta^{15}\text{N}$ - and $\delta^{18}\text{O}$ - NO_3^- values were mainly located in the “M&S” source box in May and in the “NF&R” and “Soil” in November.

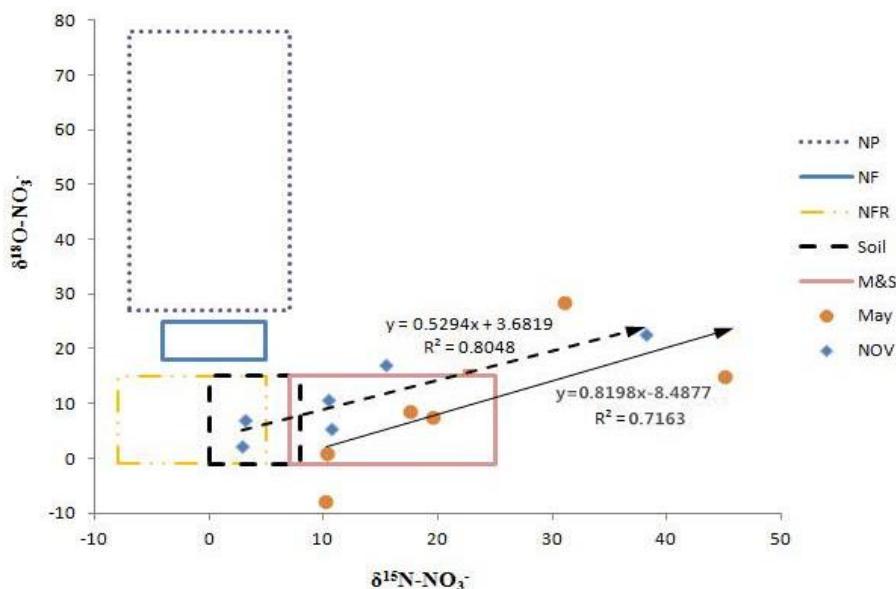


Figure 6. The $\delta^{15}\text{N}$ - and $\delta^{18}\text{O}$ - NO_3^- of the shallow ground. Orange dots and blue diamonds represent the distribution area of the $\delta^{15}\text{N}$ - NO_3^- and $\delta^{18}\text{O}$ - NO_3^- during May and November, respectively. NP, NF, NF&R, Soil, M&S are the abbreviations of NO_3^- in precipitation, NO_3^- fertilizer, NH_4^+ in fertilizer and rain, soil N and manure and sewage, respectively

Potential NO_3^- source contributions estimated from the rivers and the corresponding estuaries by SIAR

The SIAR mixing model was applied to estimate proportional contributions of five potential NO_3^- sources (NP, NF, NF&R, Soil and M&S). The observed linear relationship between the $\delta^{15}\text{N}$ - and $\delta^{18}\text{O}$ - NO_3^- values of the rivers and the corresponding estuaries indicated that no obvious denitrification occurred. The mean oxygen concentrations of all surface waters were above 4.1 mg L^{-1} , which is not ideal for denitrification (Piña-Ochoa et al., 2006). Thus, we assumed parameter $c_{jk} = 0$ in *Equation 2*.

The SIAR mixing model outputs revealed a high variability in contributions of the five potential NO_3^- sources to the rivers and the corresponding estuaries as shown in *Figure 7*. The overall mean contributions of each NO_3^- source to the study area are as follows: “M&S” contributed 35%, “Soil” contributed 27%, “NF&R” contributed 20%, “NF” contributed 12%, and “NP” contributed 6% (dash line in *Fig. 7*). The combination of “M&S” and “Soil” contributions occupied more than 60% in total, which are considered as the dominant NO_3^- sources for the rivers and the corresponding estuaries.

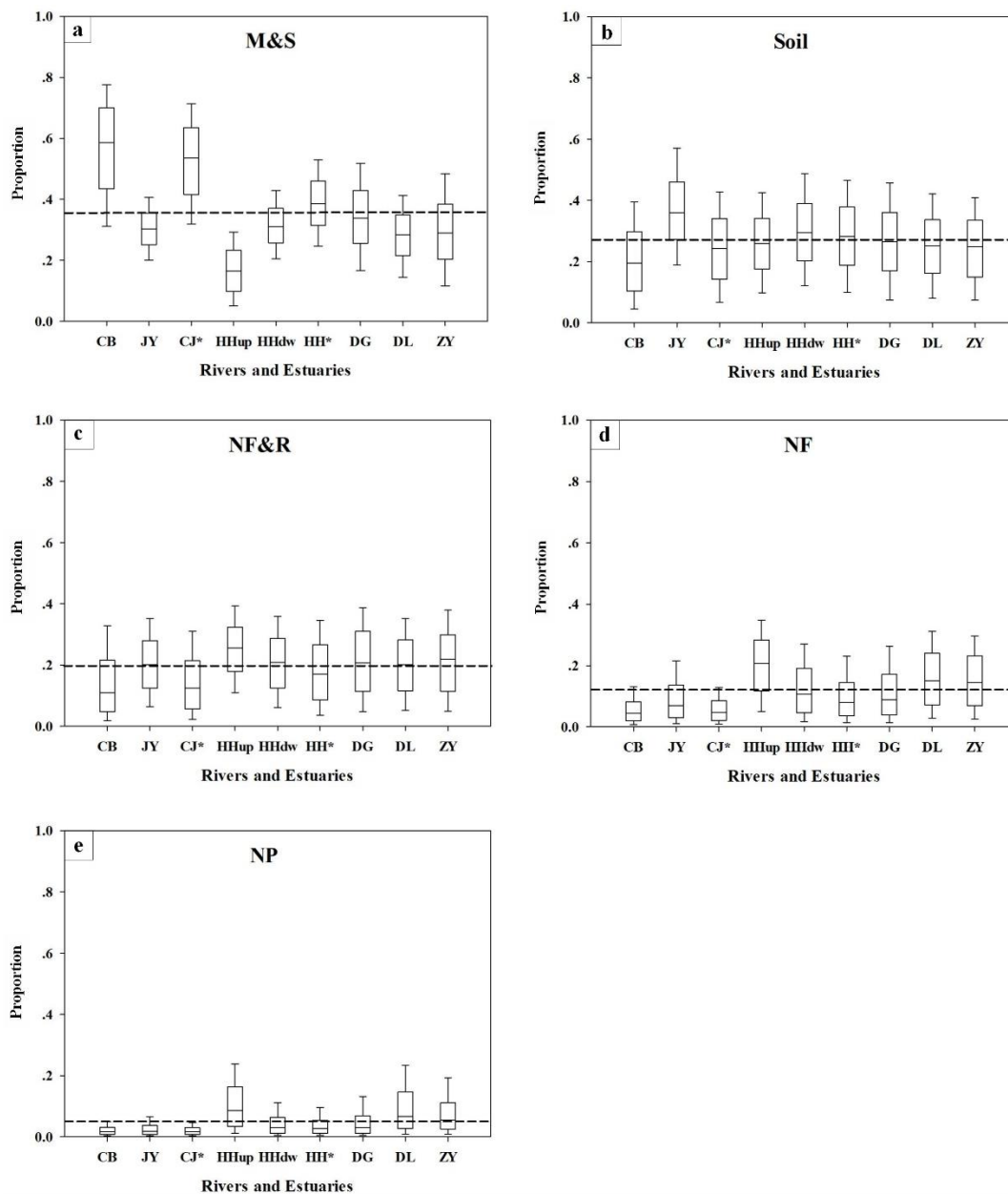


Figure 7. Contribution proportions of NO_3^- sources to the rivers and the corresponding estuaries estimated by SIAR. The dash line in each graph represents the overall mean proportional contribution of the corresponding NO_3^- source. CJ* represents the CJ Estuary, HH* represents the HH Estuary. NP, NF, NF&R, Soil, M&S are the abbreviations of NO_3^- in precipitation, NO_3^- fertilizer, NH_4^+ in fertilizer and rain, soil N and manure and sewage, respectively

The highest contribution source, the “M&S” demonstrated a wide range of proportional contributions for most of the rivers and estuaries, with mean proportions from 17 to 56%. In general, the “M&S” contributed more for the northern rivers and estuary than the rivers and estuary in the middle and southern area. Relatively high mean proportional contributions were observed for the CB River and the CJ Estuary, up to 56% and 52%, respectively. The reason could be that the watershed of the CB River

is the base of livestock breeding for the municipality. Thus, manure showed significant effect on NO_3^- of the river. Furthermore, the CJ Estuary is not only influenced by the CB River, but also greatly influenced by sewage because of the mooring ships in the vicinity of the estuary. For the middle and southern rivers of the municipality, the mean contributions of the “M&S” fluctuated in a narrow range between 28 and 39%, excluding the HHup (17%).

The source of “Soil” is another important potential source of NO_3^- for the rivers and the estuaries, which contributed with the mean proportions ranging from 21 to 37%. In addition, “Soil” is the highest contributing NO_3^- source to the rivers of JY and HHup, occupying 37% and 26% contribution, respectively. This finding revealed that the dominant NO_3^- source of the two rivers mainly originated from nitration of nitrogenous organic matter mineralization.

The mean contributions of the residual three NO_3^- sources occupied about 40% in total, and the mean contribution from high to low are as follows “NF&R” (14–25%) > “NF” (6–20%) > “NP” (2–11%). It has been observed that the contribution pattern of the three NO_3^- sources is quite similar for the rivers and estuaries, indicating spatial consistency of the source distribution.

Although the SIAR model overcome the questions, e.g. multiple NO_3^- sources, isotopic fractionation and spatial variability of $\delta^{15}\text{N}$ - and $\delta^{18}\text{O}$ - NO_3^- values, the limitation of the SIAR model cannot be neglected. The relatively wide ranges of $\delta^{15}\text{N}$ - and $\delta^{18}\text{O}$ - NO_3^- values of the five potential NO_3^- sources resulted in the contribution ranges estimated by SIAR are wide as well. Furthermore, the isotopic composition of NO_3^- in part of the samples appeared in the overlapping area of different NO_3^- source boxes, in which even small variations in isotopic values of NO_3^- might result in large changes in source distribution. To improve the SIAR outputs, it is essential to narrow the isotopic ranges of the potential NO_3^- sources.

Potential NO_3^- source contributions estimated from the SG by SIAR

According to the output of the SIAR mixed model, the NO_3^- contribution proportions of the potential NO_3^- sources to the SG in Tianjin demonstrated seasonal similarity (Fig. 8): “M&S” > “Soil” > “NF&R” > “NF” > “NP”.

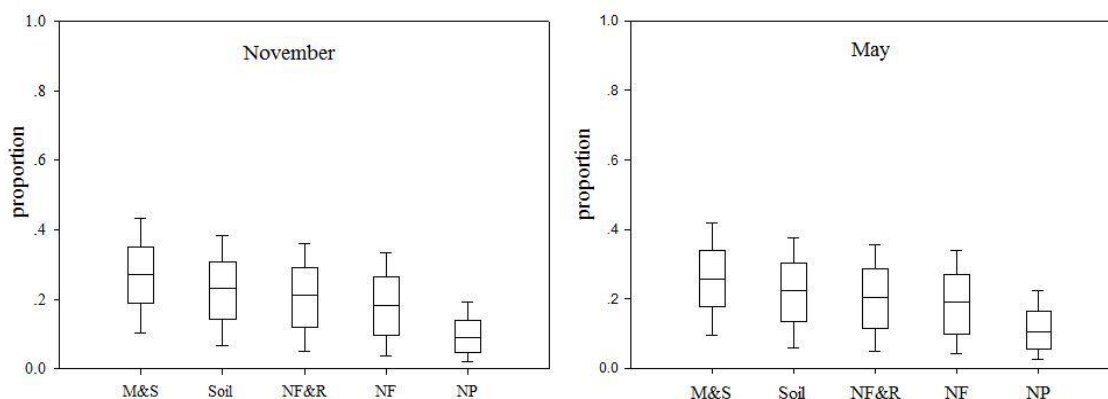


Figure 8. Contribution proportions of NO_3^- sources in May and November to the shallow groundwater estimated by SIAR. NP, NF, NF&R, Soil, M&S are the abbreviations of NO_3^- in precipitation, NO_3^- fertilizer, NH_4^+ in fertilizer and rain, soil N and manure and sewage, respectively

In November and May, “M&S” contributed an average proportion of 27.4% and 26.2%, respectively; “Soil” averagely contributed about 23.0% and 21.0%, respectively; “NF&R” mean contribution was 21.0% and 20.7%, respectively; “NF” mean contribution was 18.6% and 19.2%, respectively, and “NP” was 10.0% and 11.6%, respectively. Compared with rivers and estuaries, there was small difference in the contribution proportions among NO_3^- sources. The mean contribution proportions of “M&S”, “Soil” and “NF&R” occupied about 70% in total. The residual 30% contribution originated from “NF” and “NP”. Although atmospheric precipitation is an important water supply for SG, it is not the main NO_3^- source in this research area.

Conclusion

Extensive agricultural activity, increasing population and rapid development of urbanization resulted in high NO_3^- levels in the rivers, the corresponding estuaries and the shallow groundwater in the coastal municipality of Tianjin in China. Identification and quantification of different NO_3^- sources are imperative to control water quality in this area. By combining dual isotope data of NO_3^- ($\delta^{15}\text{N}-\text{NO}_3^-$ and $\delta^{18}\text{O}-\text{NO}_3^-$) with a Bayesian isotope mixing model (SIAR), we estimated the contribution of five potential NO_3^- sources for the rivers, estuaries and the SG. Despite of some uncertainties, SIAR performed reasonably well in estimating the contributions of potential NO_3^- sources. Future research required to improve the SIAR outputs by using original source material, which might provide more narrow ranges of the isotopic composition of NO_3^- sources. In addition, NO_3^- source apportionment should consider temporal variations. In general, the finding from this research may help to develop better nitrogen management practices in other environments where NO_3^- is a major N contributor.

Acknowledgements. We gratefully acknowledge Linzhen Guo and Mengfan Yang for soil sampling. This work was financially supported by the Ministry of Science and Technology of the People’s Republic of China (2018YFD0800400), the National Natural Science Foundation of China (41973017), the Natural Science Foundation of Tianjin (19JCZDJC40700).

REFERENCES

- [1] Aravena, R., Robertson, W. D. (2010): Use of multiple isotope tracers to evaluate denitrification in ground water: study of nitrite from a large-flux septic system plume. – *Groundwater* 36(6): 975-982.
- [2] Chang, C. C. Y., Kendall, C., Silva, S. R., Battaglin, W. A., Campbell, D. H. (2002): Nitrate stable isotopes: tools for determining nitrate sources among different land uses in the Mississippi River Basin. – *Canadian Journal of Fisheries and Aquatic Sciences* 59: 1874-1885.
- [3] Chen, D. J. Z., Macquarrie, K. T. B. (2015): Correlation of $\delta^{15}\text{N}$ and $\delta^{18}\text{O}$ in NO_3^- during denitrification in groundwater. – *Journal of Environmental Engineering and Science* 4(3): 221-226.
- [4] Chen, F., Jia, G. D., Chen, J. (2009): Nitrate sources and watershed denitrification inferred from nitrate dual isotopes in the Beijiang River, south China. – *Biogeochemistry* 94: 163-174.
- [5] Chen, L., Li, J., Guo, X., Fu, B. (2000): Temporal and spatial characteristics of surface water quality in Jiyun River. – *Chinese Journal of Environmental Science* 21: 61-64 (in Chinese with English abstract).

- [6] Deutsch, B., Mewes, M., Liskow, I., Voss, M. (2006): Quantification of diffuse nitrate inputs into a small river system using stable isotopes of oxygen and nitrogen in nitrate. – *Organic Geochemistry* 37: 1333-1342.
- [7] Ding, J., Li, B., Gao, R., He, L., Liu, H., Dai, X., Yu, Y. (2014): Identifying diffused nitrate sources in a stream in an agricultural field using a dual isotopic approach. – *Science of the Total Environment* 484: 10-18.
- [8] Ding, Y., Rong, N., Shan, B. (2016): Impact of extreme oxygen consumption by pollutants on macroinvertebrate assemblages in plain rivers of the Ziya River basin, North China. – *Environmental Science & Pollution Research* 23(14): 14147-14156.
- [9] Dong, L., Bai, H., Xu, J. (2007): Comprehensive ecological environment evaluation of estuaries in Tianjin. – *Binhai New Area Plan* 7: 1-3 (in Chinese with English abstract).
- [10] Frey, C., Hietanen, S., Jürgens, K., Labrenz, M., Voss, M. (2014): N and O isotope fractionation in nitrate during chemolithoautotrophic denitrification by *Sulfurimonas gotlandica*. – *Environmental Science & Technology* 48(22): 13229-37.
- [11] Fukada, T., Hiscock, K. M., Dennis, P. F., Grischek, T. (2003): A dual isotope approach to identify denitrification in ground water at a river bank infiltration site. – *Water Research* 37: 3070-3078.
- [12] Galloway, J. N., Aber, J. D., Erisman, J. W., Seitzinger, S. P., Howarth, R. W., Cowling, E. B., Cosby, B. J. (2003): The Nitrogen Cascade. – *Bioscience* 53: 341-356.
- [13] Gaouzi, F. J. E., Sebilo, M., Ribstein, P., Plagnes, V., Boeckx, P., Xue, D., Derenne, S., Zakeossian, M. (2013): Using $\delta^{15}\text{N}$ and $\delta^{18}\text{O}$ values to identify sources of nitrate in karstic springs in the Paris basin (France). – *Applied Geochemistry* 35: 230-43.
- [14] Guo, P., Wang, C. (2009): The investigation and evaluation of sewage draining outlets along the Dagu Sewage River in Tianjin, China. – *The Monograph of Academic Annual Conference of Chinese Environmental Sciences Association in 2009* 4: 203-210 (in Chinese with English abstract).
- [15] He, X., Huang, B. (2013): Analysis of the water quality of Haihe River system and pollution control measures. – *Safety and Environmental Engineering* 20: 28-32 (in Chinese with English abstract).
- [16] Hobbie, E. A., Ouimette, A. P. (2009): Controls of nitrogen isotope patterns in soil profiles. – *Biogeochemistry* 95(2/3): 355-371.
- [17] Jin, Z. F., Gong, J. L., Shi, Y. L., Jin, M. T., Li, F. L. (2017): Nitrate source identification and nitrification-denitrification at the sediment-water interface. – *Huanjing Kexue* 38(4): 1423-1430.
- [18] Knöller, K., Vogt, C., Haupt, M., Feisthauer, S., Richnow, H. (2011): Experimental investigation of nitrogen and oxygen isotope fractionation in nitrate and nitrite during denitrification. – *Biogeochemistry* 103(1/3): 371-384.
- [19] Kendall, C., Elliott, E. M., Wankel, S. D. (2007): Tracing Anthropogenic Inputs of Nitrogen to Ecosystems. – In: Michener, R., Lajtha, K. (eds.) *Stable Isotopes in Ecology and Environmental Science*. Blackwell, Maiden, pp. 375-449.
- [20] Lai, X., Guo, F., Liu, J., Shi, B., Chen, S. (2001): *Tianjin Dictionary*. – Tianjin Academy of Social Sciences Press, Tianjin (in Chinese).
- [21] Li, R., Liu, S., Zhang, G., Ren, J., Jing, Z. (2013): Biogeochemistry of nutrients in an estuary affected by human activities: the Wanquan River estuary, eastern Hainan Island, China. – *Continental Shelf Research* 57(1): 18-31.
- [22] Li, S. L., Liu, C. Q., Li, J., Liu, X., Chetelat, B., Wang, B. et al. (2010): Assessment of the sources of nitrate in the Changjiang River, China using a nitrogen and oxygen isotopic approach. – *Environmental Science & Technology* 44(5): 1573-1578.
- [23] Liu, X., Li, G., Liu, Z., Guo, W., Gao, N. (2010): Water pollution characteristics and assessment of lower reaches in Haihe River basin. – *Procedia Environmental Sciences* 2(6): 199-206.
- [24] Mcilvin, M. R., Casciotti, K. L. (2011): Technical updates to the bacterial method for nitrate isotopic analyses. – *Analytical Chemistry* 83(5): 1850-1856.

- [25] Mengis, M., Schiff, S. L., Harris, M., English, M. C., Aravena, R., Elgood, R. J. et al. (2005): Multiple geochemical and isotopic approaches for assessing ground water NO_3^- elimination in a riparian zone. – *Groundwater* 37(3): 448-457.
- [26] Moore, J. W., Semmens, B. X. (2008): Incorporating uncertainty and prior information into stable isotope mixing models. – *Ecology Letters* 11: 470-480.
- [27] Pardo, L. H., Kendall, C., Pett-Ridge, J., Chang, C. C. Y. (2004): Evaluating the source of streamwater nitrate using $\delta^{15}\text{N}$ and $\delta^{18}\text{O}$ in nitrate in two watersheds in New Hampshire, USA. – *Hydrological Processes* 18: 2699-2712.
- [28] Parnell, A. C., Inger, R., Bearhop, S., Jackson, A. L. (2010): Source partitioning using stable isotopes: coping with too much variation. – *PLoS One* 5(3): e9672.
- [29] Piña-Ochoa, E., Álvarez-Cobelas, M. (2006): Denitrification in aquatic environments: a cross-system analysis. – *Biogeochemistry* 81: 111-130.
- [30] Sebilo, M., Billen, G., Grably, M., Mariotti, A. (2003): Isotopic composition of nitrate-nitrogen as a marker of riparian and benthic denitrification at the scale of the whole Seine River system. – *Biogeochemistry* 63: 35-51.
- [31] Semmens, B., Ward, E., Parnell, A., Phillips, D., Bearhop, S., Inger, R., et al. (2013): Statistical basis and outputs of stable isotope mixing models: comment on Fry (2013). – *Marine Ecology Progress Series* 490: 285-289.
- [32] Shao, X., Deng, X., Yuan, X., Jiang, W. (2010): Identification of potential sensitive areas of non-point source pollution in downstream watershed of Chaobaixin River. – *Environmental Science Survey* 29: 37-41 (in Chinese with English abstract).
- [33] Starks, P. J., Fiebrich, C. A., Grimsley, D. L., Garbrecht, J. D., Steiner, J. L., Guzman, J. A., et al. (2014): Upper Washita River experimental watersheds: meteorologic and soil climate measurement networks. – *Journal of Environmental Quality* 43(4): 1239.
- [34] Templer, P. H., Weathers, K. C. (2011): Use of mixed ion exchange resin and the denitrifier method to determine isotopic values of nitrate in atmospheric deposition and canopy throughfall. – *Atmospheric Environment* 45(11): 2017-2020.
- [35] Torrentó, C., Urmeneta, J., Otero, N., Soler, A., Viñas, M., Cama, J. (2011): Enhanced denitrification in groundwater and sediments from a nitrate-contaminated aquifer after addition of pyrite. – *Chemical Geology* 287(1): 90-101.
- [36] Umezawa, Y., Hosono, T., Onodera, S., Siringan, F., Buapeng, S., Delinom, R., Yoshimizu, C., Tayasu, I., Nagata, T., Taniguchi, M. (2008): Sources of nitrate and ammonium contamination in groundwater under developing Asian megacities. – *Science of the Total Environment* 404: 361-376.
- [37] Villnäs, A., Norkko, J., Hietanen, S., Josefson, A., Lukkari, K., Norkko, A. (2013): The role of recurrent disturbances for ecosystem multifunctionality. – *Ecology* 94: 2275-2287.
- [38] Wang, H., Jia, Y. W., Yang, G. Y., Zhou, Z. H., Chou, Y. Q., Niu, C. W., Peng, H. (2013): Comprehensive simulation of binary water cycle and its associated process in Haihe River Basin. – *Science Bulletin* 58(12): 1064-1077.
- [39] Wang, K., Wang, W., Li, Q., Yu, M., Li, P. (2014): Characteristics of changes of groundwater buried depth and influencing factors in Tianjin plain area over past 21 years. – *Water Resources Protection* 30(3): 45-49 (in Chinese with English abstract).
- [40] Wang, L. (2004): A discussion on the deep fresh water salinization in the plain region of Tianjin City. – *Geological Survey and Research* 27: 169-176 (in Chinese with English abstract).
- [41] Wang, X., Yang, H., Sun, J., Wang, W. (2011): Distribution of nutrients and eutrophication assessment in Tianjin coastal area. – *Marine Sciences* 35: 56-61 (in Chinese with English abstract).
- [42] Wang, Z., Gao, X., Li, M., Pan, J., Yu, C. (2009): Investigation and spatial distribution on nitrate contamination in water of Tianjin. – *Journal of Agro-Environment Science* 28(3): 592-596 (in Chinese with English abstract).
- [43] Wankel, S. D., Kendall, C., Paytan, A. (2015): Using nitrate dual isotopic composition ($\delta^{15}\text{N}$ and $\delta^{18}\text{O}$) as a tool for exploring sources and cycling of nitrate in an estuarine

- system: Elkhorn Slough, California. – *Journal of Geophysical Research Biogeosciences* 114(G1): 315-327.
- [44] Xue, D., Botte, J., Baets, B. D., Accoe, F., Nestler, A., Taylor, P., Van, Cleemput, O., Berglund, M., Boeckx, P. (2009): Present limitations and future prospects of stable isotope methods for nitrate source identification in surface- and groundwater. – *Water Research* 43: 1159-1179.
- [45] Xue, D., Baets, B. D., Vermeulen, J., Botte, J., Cleemput, O. V., Boeckx, P. (2010): Error assessment of nitrogen and oxygen isotope ratios of nitrate as determined via the bacterial denitrification method. – *Rapid Communications in Mass Spectrometry* 24: 1979-1984.
- [46] Xue, D., Baets, B. D., Cleempu, O. V., Hennessy, C., Berglund, M., Boeckx, P. (2012): Use of a Bayesian isotope mixing model to estimate proportional contributions of multiple nitrate sources in surface water. – *Environmental Pollution* 161: 43-49.
- [47] Yang, B., Hui, W., Jiang, Y., Fang, D., He, X., Lai, X. (2018): Combing $\delta^{15}\text{N}$ and $\delta^{18}\text{O}$ to identify the distribution and the potential sources of nitrate in human-impacted watersheds, Shandong, China. – *RSC Advances* 8(41): 23199-23205.
- [48] Yang, L., Han, J., Xue, J., Zeng, L., Shi, J., Wu, L., Jiang, Y. (2013): Nitrate source apportionment in a subtropical watershed using Bayesian model. – *Science of the Total Environment* 463-464: 340-347.
- [49] Yao, L., Li, G., Tu, S., Gavin, S., He, Z. (2007): Salinity of animal manure and potential risk of secondary soil salinization through successive manure application. – *Science of the Total Environment* 383: 106-114.
- [50] Yue, F., Liu, X., Li, J., Zhu, Z., Wang, Z. (2010): Using nitrogen isotopic approach to identify nitrate sources in waters of Tianjin, China. – *Bulletin of Environmental Contamination and Toxicology* 85: 562-56.

IMPACTS OF SPARTINA ALTERNIFLORA EXPANSION ON LANDSCAPE PATTERN AND HABITAT QUALITY: A CASE STUDY IN YANCHENG COASTAL WETLAND, CHINA

ZHANG, H.-B.* – LIU, Y.-Q. – XU, Y. – HAN, S. – WANG, J.

School of Urban and Planning, Yancheng Teachers University, Yancheng 224007, China
(e-mails: liuyuqing02102123@163.com – Y. Q. Liu; xeniayy@hotmail.com – Y. Xu;
hanshuang412@163.com – S. Han; wangjisyctu@163.com – J. Wang)

*Corresponding author

e-mail: yctuzhanghb@163.com; phone: +86-133-7526-7876

(Received 24th Dec 2019; accepted 22nd May 2020)

Abstract. Yancheng National Nature Reserve (YNNR) in Jiangsu province is the largest wintering habitat for red-crowned cranes (*Grus japonensis*) in the world. However, the *Spartina alterniflora* (*S. alterniflora*) expansion had caused a series of ecological problems. In the paper, by using ETM + images as data source, GIS technology and the InVEST model were used to analyze the influence of *S. alterniflora* expansion on the landscape pattern and habitat quality through scenario simulation. We found that: from 2000 to 2020, under the current conditions, the percentage of landscape (PLAND) of *S. alterniflora* marsh would increase from 17.525% to 51.522%, which would result in a risk of extinction for the *Suaeda salsa* (*S. salsa*) marsh; the habitat quality index (Q) would be decreased from 0.8183 to 0.7074. Under the condition of removing *S. alterniflora*, the PLAND of *S. salsa* marsh would be restored to 43.8317%, and the Q would be increased to 0.9463. Under the condition of controlling *S. alterniflora* expansion, the PLAND of *S. alterniflora* marsh would be decreased to 8.678%, the PLAND of *S. salsa* marsh would be restored to 43.8653%, and the Q would be increased to 0.9198. The results would be beneficial to the management of the YNNR.

Keywords: scenario simulation, habitat protection, species invasion, InVEST, the YNNR

Introduction

The Yancheng coastal wetland is located in the middle of the Jiangsu coast. It is one of the most typical and representative distribution areas of muddy coastal wetlands integrating tidal flats, tides, rivers, salt marshes, *Phragmites australis* (*P. australis*) marshes, and *Spartina alterniflora* (*S. alterniflora*) marshes in China and in the world. It is the first world natural heritage site in Jiangsu province, the first natural heritage site of a coastal wetland in China, and the second such site in the world. Yancheng Coastal Wetland has basically maintained its natural ecological structure and function (Liu et al., 2003) with the Yancheng National Nature Reserve (YNNR) and Jiangsu Dafeng Elk National Nature Reserve. There are 17 species listed in the International Union for Conservation of Nature (IUCN) red list of species. It is an irreplaceable natural habitat that provides protection for rare and endangered migratory birds and has global value.

S. alterniflora is a perennial herb that is native to the west coast of the Atlantic and the Gulf of Mexico. It plays an important role in protecting coastal wetlands from wave erosion because of its rapid spread and great ability to promote silt deposition (Ayres et al., 2002). Therefore, *S. alterniflora* was successfully introduced in Yancheng coastal wetlands in the 1980s. In the 1990s, a large community was formed and rapidly expanded, and the species has become the dominant vegetation in the YNNR. The invasion of *S. alterniflora* has caused significant changes to the native ecosystems, including alteration of habitat structures, the extinction of native species, and altered

ecosystem productivity (Vitousek et al., 1996; Pimentel et al., 2000; Neira et al., 2006; Liao et al., 2008; Wang et al., 2008). Invaders can have spatially variable effects on the ecosystem structure and function through their exploitation of different patches as they advance across landscapes (Sharp et al., 2019). The expansion of *S. alterniflora* has reduced the living space of other intertidal organisms and caused negative ecological effects (Liu et al., 2009). Cranes and other rare species primarily forage in *P. australis* marshes and *S. salsa* marshes in Yancheng Coastal Wetland (Wang et al., 2019). The landward expansion has led to the loss and fragmentation of *S. salsa* marshes, which is used as a wintering habitat for cranes.

The impact of the invasion of *S. alterniflora* on the coastal wetlands has become an important research topic in recent years (Liu et al., 2007; Schindler et al., 2013; Ayres et al., 2004). However, most studies focus on the population scale. *S. alterniflora* competes with native plants, and the habitat fragmentation of *P. australis* communities has led to the forced miniaturization of *Paradoxornis heudei*, which depends on these habitats (Dong et al., 2010). The invasion of *S. alterniflora* has resulted in the gradual shrinking of the habitat areas of *S. salsa*. This has led to significant changes in the spatial distribution pattern of the nesting sites of *Saunders's gull* during the breeding period, which has had a significant impact on the population (Liu et al., 2009). The invasion has also led to a large reduction of suitable wetland areas for red-crowned cranes to live and feed, which has had a certain impact on the dynamic distribution of their wintering population (Liu et al., 2016; Wang et al., 2019).

The mentioned study clarified the influence of *S. alterniflora* expansion on population dynamics, which could provide a scientific basis for the protection of specific population. With the extensive application of remote sensing technology, studies have been widely carried out on the impact of *S. alterniflora* expansion on the landscape pattern (Zhang et al., 2013; Wang et al., 2014; Fang et al., 2014). In this context, the InVEST model was used to analyze the impact of *S. alterniflora* expansion on habitat quality at the landscape scale. We examined how much the expansion could extend in the study area in the future and what it could look like. From the perspective of sustainable development of nature reserves, we also examined the possible trends of landscape change and habitat quality development of nature reserves in the future, which would provide reference for the sustainable construction and management of the research area.

Material and methods

Study area

The YNNR is located at 32°20' N - 34°37' N and 119°29' E - 121°16' E (Fig. 1a). It covers 4.533×10^5 hm², and the length of the coastline is 582 km. The YNNR is located in a transition zone between a subtropical zone and a warm temperate zone. It was established in 1983 and upgraded to a national nature reserve in 1992. It is an important member of the World Biosphere Reserve, the Northeast Asia Crane Network, and the East Asia-Australia Wader Migration network and has been added to the list of Wetlands of International Importance.

The core zone of the YNNR has a total area of 1.92×10^4 hm² and reaches the Xinyang River in the north, the Doulong River in the south, the seawall road in the west, and the edge of mudflats in the east (Fig. 1b). It is a typical tidal muddy wetland. The core area of the YNNR is divided into north and south areas by Zhonglugang Road. In the north, a project was carried out for the artificial restoration of *P. australis*

marshes in an area that covers about 0.52×10^4 hm². The southern part is weakly affected by human activities, and the evolution of the landscape pattern is mainly affected by natural factors such as climate, topography, hydrology, soil, and vegetation. It has become a typical area with natural conditions and covers about 1.11×10^4 hm². The southwest is an aquaculture pond with an area of 0.29×10^4 hm². In this study, the area of natural conditions was selected as the study area (Fig. 1c), in which the development of *S. alterniflora* is typical and well preserved.

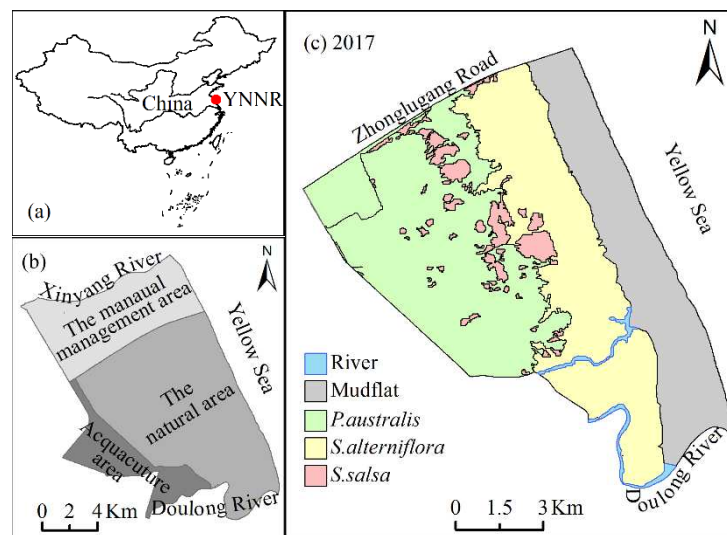


Figure 1. The location and scope of the study area. (a) The Yancheng National Nature Reserve (YNNR) is located in the central east coast of China. (b) The scope of the core zone of the YNNR. (c) Landscape classification of the study area in 2017

Data source and landscape type

The ETM + remote sensing images in May 4, 2000, May 21, 2006 and September 24, 2011 were used as data sources. The ETM + remote sensing image includes seven multispectral images and one panchromatic image, and the former has a resolution of 30 m while the latter has a resolution of 15 m. In ENVI 5.0, on the basis of atmospheric correction and geometric correction, the methods of the unsupervised classification and the decision tree classification were used to interpret the remote sensing images. In ArcGIS 10.0, the landscape type maps were completed, as shown in Figure 2. A coastal wetland is a complex natural complex between the land and sea with various types of ecosystems. The landscape in the core area of the YNNR is divided into three categories: natural wetland, artificial wetland and non-wetland. The division is based on the landscape characteristics of the study area and the definition of the Convention on Wetlands of International Importance as a Waterfowl Habitat. The natural wetland includes five types: *P. australis* marsh, *S. salsa* marsh, *S. alterniflora* marsh, mudflats, and rivers. The artificial wetland are aquaculture ponds, and the non-wetland area are dams.

Landscape pattern analysis

To analyze landscape pattern change, FRAGSTATS 4.2 was developed by the United States Department of Agriculture (USDA). Six landscape indices describe the characteristics of the landscape structure composition and spatial configuration of the

Percentage of Landscape (PLAND), the Fractal Dimension Index (FRAC), Shannon's Diversity Index (SHDI), Landscape Dominance Index (LDI), Landscape Evenness Index (SHEI), and Aggregation Index (AI). The landscape transfer matrix can also help to explain how the composition and types of landscape change. It can also comprehensively and concretely describe the structural characteristics of the landscape and the changes of quantity and direction between landscape types.

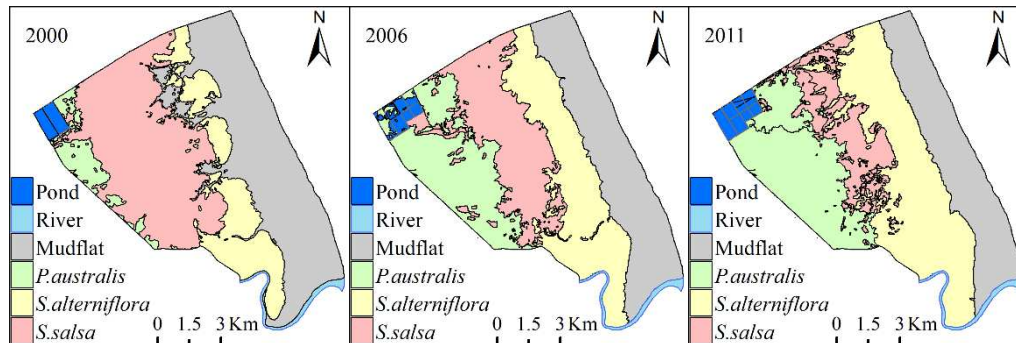


Figure 2. Landscape type maps in 2000, 2006 and 2011

Landscape change scenario simulation

A mechanism model (V 1.0) was developed for the landscape pattern of Yancheng coastal wetland based on the soil moisture and salinity processes (Software copyright: No.01678102, 2017). The model was designed by using the platforms ArcGIS 10.0 and MATLAB 2008. It can dynamically display the regional landscape changes and explain their mechanisms from the perspective of ecological processes (Zhang et al., 2014)

The system is composed of four parts. First, the main program reveals the relationship between landscape pattern change and ecological process. The second is that time function requires continuous changes in time and can realize the landscape simulation of any time (unlimited time interval) in the study area. The third part is visual expression, and the fourth part is used to call commands.

The model includes the threshold parameters of soil moisture and salinity of different types of landscapes and their annual change parameters, which are driven by different factors (Zhang, 2018). In this study, the soil moisture and salt parameters were adjusted based on the landscape types and soil moisture and salinity in 2011 to simulate the landscape pattern changes in 2020 under different scenarios. The change of the landscape pattern was simulated under three scenarios: the current situation (Scenario A), *S. alterniflora* would continue to expand in accordance with the present natural conditions and without any interference. Removal of *Spartina alterniflora* (Scenario B), *S. alterniflora* would be removed completely through certain artificial measures. Ecological restoration (Scenario C), *S. salsa* marsh would be restored and the expansion of *S. alterniflora* to *S. salsa* marsh would be controlled by techniques.

In the study, we used the images of 2017 to verify, and the overall accuracy of the simulation was 82.03%. The Kappa coefficient value was 0.72. When the Kappa coefficient was greater than 0.7, the consistency between the simulation result and the real value was considered to be quite satisfactory (Monserud and Leemans, 1992; Landis and Kochm,1997).

Habitat quality assessment

The Integrated Valuation of Ecosystem Services and Trade-offs (InVEST) model were developed by Stanford University, The Nature Conservancy (TNC), and World Wide Fund for Nature or World Wildlife Fund (WWF) to simulate the change of quality and value of ecosystem processes under different land cover scenarios. The biodiversity module in the InVEST model can assess changes in habitat quality in different times. In the model, habitat quality is generally affected by threat factors, habitat suitability, and ecological protection policies. Relevant parameters are shown in *Tables 1* and *2*.

Table 1. Attribute table of ecological threat factors

Threat factors	Maximum impact distance (km)	Weight	Linear correlation of regression
Aquaculture pond	1	0.6	0
River	3	0.4	1
Road	5	0.8	1
<i>S. alterniflora</i>	3	0.8	0

Table 2. Habitat suitability and sensitivity to threat factors of different landscape types

Landscape types	Habitat suitability	Aquaculture pond	River	Road	<i>S. alterniflora</i>
Aquaculture pond	0.5	0	0.5	0	0.5
River	0.5	0.5	0	0.8	0.5
Mudflat	0.8	0.5	0.3	0.3	0.8
Road	0	0	0	0	0
<i>P. australis</i>	1	0.3	0.6	0.6	0.5
<i>S. alterniflora</i>	0.5	0.5	0.5	0.7	0
<i>S. salsa</i>	1	0.5	0.8	0.5	0.8

The threat factors and habitat suitability are based on whether they are beneficial to the health of habitats of rare species, such as red-crowned cranes. The InVEST model can use either a linear or an exponential model depending on the particular relationship between the distance-decay rate of a threat and the maximum effective distance to a threat. The habitat quality index was calculated as follows (Sharp et al., 2017):

$$D_{xj} = \sum_{r=1}^R \sum_{y=1}^{y_r} \left(\frac{w_r}{\sum_{r=1}^R w_r} \right) r_y i_{rxy} \beta_x s_{jr} \quad (\text{Eq.1})$$

In this equation, D_{xj} is the habitat degradation index, which characterizes the degree of habitat degradation. R is the number of threat factors, y_r is the number of grid cells on the threat factor layer, w_r is the weight value of the threat factor, r_y is the number of raster unit threat factors in the layer, i_{rxy} represents the influence degree of threat factor r in grid y on habitat grid x , β_x is the degree of protection, and s_{jr} is the sensitivity of the threat factor, which refers to the degree of change of different landscape types under the influence of threat factors with a range of 0 to 1.

$$Q_{xj} = H_j \left(1 - \frac{D_{xj}^2}{D_{xj}^2 + k^2} \right) \quad (\text{Eq.2})$$

In this equation, Q_{xj} is the habitat quality index, H_j is the habitat suitability, which refers to the suitability of different landscape types for reproduction, habitat and activities of organisms, ranging from 0 to 1. D_{xj} is the degree of habitat degradation, and k is the half-saturation coefficient, which is set to 15 (half of the grid resolution). z is generally set to 2.5.

Results

Landscape pattern changes

The landscape change in Yancheng Coastal Wetland is the result of human activities and natural conditions. Human activities mainly include building dams and roads, artificial breeding, and the introduction of exotic species. The natural conditions include hydrogeomorphic processes, vegetation processes, and soil processes. Natural conditions are a basic driving force for the change of coastal wetland landscapes. Human activities change the natural conditions of coastal wetlands, resulting in the change of the landscape.

The landscape structure of the study area in the YNNR is dominated by *P. australis* marsh, *S. salsa* marsh, *S. alterniflora* marsh, and mudflats (Fig. 2). The change of the landscape structure showed that the areas of *P. australis* marsh and *S. alterniflora* marsh were expanding constantly, and the area of the *S. salsa* marsh was obviously decreasing. From 2000 to 2011, the PLAND of the *P. australis* marsh increased from 5.042% to 23.601%, that of the *S. alterniflora* marsh increased from 17.525% to 34.466%, and that of the *S. salsa* marsh decreased from 36.910% to 14.414%.

In 2000, 2006, and 2011, the FRAC was 1.046, 1.038, and 1.035, respectively. The continuous decline of the FRAC indicated that the landscape patches in the study area had a trend of regular development. The AI in 2000, 2006, and 2011 was 95.453, 95.553, and 95.244 respectively, showing a slow trend of first rising and then falling with weak change overall. This indicated that the landscape changes in the study area were generally subject to less artificial interference and followed the laws of natural development with a high degree of aggregation among different landscape types. From 2000 to 2011, the SHDI first increased and then decreased. In contrast, the LDI first decreased and then increased. From 2000 to 2006, the proportion of different landscape types developed towards a relatively balanced situation, and the LDI declined due to the expansion of *P. australis* and *S. alterniflora* and the decrease of *S. salsa* marsh. From 2006 to 2011, the *S. salsa* marsh continued to decrease with the continuous expansion of *P. australis* and *S. alterniflora*, the proportion of different landscape types began to develop imbalance again, and LDI increased.

The expansion rate of the *S. alterniflora* marsh was first slow and then became faster. From 2000 to 2006, the annual expansion rate was 163.167 hm²/a, which was significantly lower than the rate of 182.364 hm²/a from 2006 to 2011. The variation trend of the FRAC and AI of the *S. alterniflora* marsh was not obvious from 2000 to 2011. The FRAC values in 2000, 2006, and 2011 were 1.031, 1.049, and 1.030, respectively, which indicated that the shape of the *S. alterniflora* marsh changed little in the natural state. The AI in 2000, 2006, and 2011 was 89.712, 94.605, and 94.336, respectively. The spatial aggregation of the *S. alterniflora* marsh showed consistent characteristics with the overall landscape.

Habitat quality changes

From 2000 to 2011, the habitat quality in the study area showed an overall degradation trend (Fig. 3). The habitat quality index (Q) decreased from 0.8183 to 0.7569 (a decrease of 7.5034%). From 2000 to 2006, the Q decreased from 0.8183 to 0.7924 with an average annual decrease of 0.0043. From 2006 to 2011, the Q decreased to 0.7569 with an average annual decrease of 0.0071. Habitat quality declined more rapidly in the latter period than in the previous period. The decrease of habitat quality was closely related to the expansion speed of the *S. alterniflora* marsh.

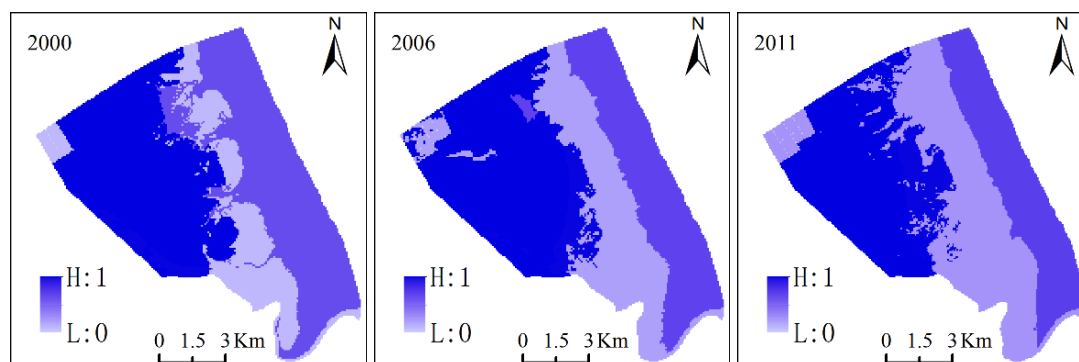


Figure 3. Habitat quality maps in 2000, 2006 and 2011

According to the classification method of equal intervals, the Q of the study area was divided into four intervals of 0–0.25, 0.25–0.5, 0.5–0.75, and 0.75–1, which indicate poor, general, good, and excellent habitat quality, respectively. As shown in Table 3, the overall habitat quality of the study area was relatively high and was rated as excellent in most areas, followed by general grades and poor grades with no distribution of good grades.

Table 3. Habitat quality classification statistics from 2006 to 2011

Grading ranges	2000		2006		2011	
	Area ($\times 10^2 \text{hm}^2$)	Percentage (%)	Area ($\times 10^2 \text{hm}^2$)	Percentage (%)	Area ($\times 10^2 \text{hm}^2$)	Percentage (%)
0-0.25	0.070	0.064	0.114	0.104	0.200	0.182
0.25-0.50	22.208	20.189	32.448	29.498	42.026	38.205
0.50-0.75	0	0	0	0	0	0
0.75-1.00	87.722	79.747	77.438	70.398	64.774	61.613

There was a trend of polarization in habitat quality in the study area. The changes of the proportion of the space area of the three grades were compared. The areas with excellent habitat quality showed a continuous decline, and the proportion of such areas dropped from 79.747% in 2000 to 61.613% in 2011 (a decrease of 22.739%). The areas with general and poor habitat quality increased. The proportion of areas with poor habitat quality increased from 0.064% in 2000 to 0.182% in 2011 (nearly double). Areas of general habitat quality increased from 20.189% in 2000 to 38.205% in 2011 (an increase of 89.237%).

Discussion

Factors affecting the S. alterniflora expansion

Due to very strict environmental protection policies, human activities in the research area are weak, so the expansion of *S. alterniflora* is mainly driven by natural factors such as climate, hydrological dynamics, geomorphic processes, and vegetation. The main factors are coastal geomorphic processes and the change of plant-cover types. The process of landscape change is continuous and stable. The spatial gradient changes of geomorphic processes and hydrological processes result in the landscape of the study area having a parallel belt pattern extending from north to south and changing from land to sea (Zhang et al., 2013).

The climate in the Yancheng coastal area is basically similar to the east coast of the United States, and the broad intertidal zone is very suitable for the growth of *S. alterniflora* (Callaway et al., 1999; Liu et al., 2004). The coast of the study area is also a typical muddy coast. Under the action of tides and tideways, the average high-water line keeps advancing towards the sea. The subtidal zone and lower intertidal zone are flat, and a tidal creek has developed (Zhang et al., 2006). The fast silting and the wide and gentle beach surface provide a good sedimentary environment for the development of *S. alterniflora*. The tidal amphidromic system of the South Yellow Sea and the tidal advancing system of the East China Sea meet at the Yancheng coast, which makes it difficult for the seeds of *S. alterniflora* to drift with the tides, and they fall on the beach to germinate (Liu et al., 2004).

The geomorphic processes affect the hydrological processes and then affect the physical and chemical properties of the soil, especially the moisture and salinity. Soil is an important driving force of landscape change and has a direct impact on the development and succession of vegetation. A comparison was conducted using elevation data from land to sea in 2002 and 2011 in the study area (Fig. 4) (Hou et al., 2003). The elevation changes from 2002 to 2011 showed an increasing trend overall, and the increasing degree of elevation gradually increased from *P. australis* marsh and *S. salsa* marsh, to *S. alterniflora* marsh. In 2002, the elevation gradually decreased from the land to the sea, but in 2011, the strong ability of *S. alterniflora* to collect silt led to the elevation being significantly increased in *S. alterniflora* marsh. As a result, the elevation of the study area had a “U” shape (Hou et al., 2013).

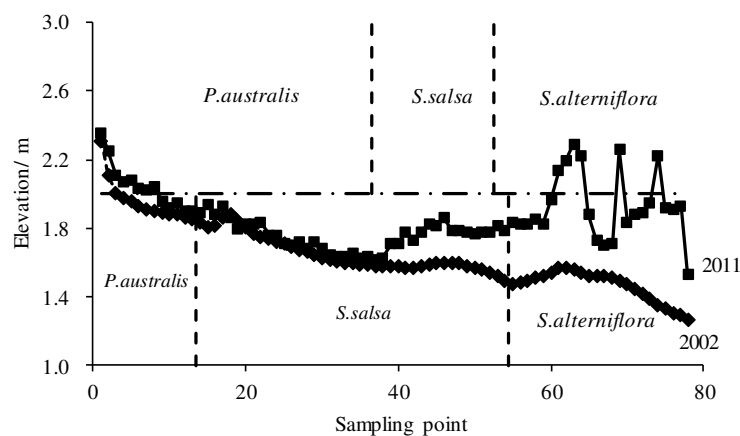


Figure 4. Elevation changes from 2002 to 2011

Furthermore, the response of vegetation to hydrology and geomorphology promotes the expansion of *S. alterniflora*. *S. alterniflora* marshes are distributed in the upper of intertidal zone from the upper edge to the average high-tide level and to the lower edge to the average tide level. The frequency of tidal invasion is between 20% and 80%. The geomorphic processes provide a vast space and environmental conditions for the development of *S. alterniflora* (Zhang et al., 2004), forming an evolution pattern of a mudflat-*S. alterniflora* marsh. The native pioneer plant is *S. salsa*, which spreads and expands through seeds. Because of its short plants, a higher frequency of tidal invasion results in smaller plants and fewer branches, which seriously affect the expansion of *S. salsa* to the sea. Its niche cannot reach the tidal flat when the frequency of tidal invasion is more than 20%. Therefore, the expansion ability of *S. salsa* to the sea is far less than that of *S. alterniflora*, and it cannot match the expansion speed of the beach surface in a rapidly silted beach (Zhang et al., 2004; Hou et al., 2013).

As the elevation of the *S. alterniflora* marsh increased, a sharp decrease in the frequency of tides passed through it to reach the *S. salsa* marsh. This restricted the water and salinity conditions needed for the development of the *S. salsa* marsh and promoted the expansion of the *S. alterniflora* marsh to the lower edge of the *S. salsa* marsh. *S. alterniflora* has strong resistance to silting, wind, and waves, and it can grow in most areas of the intertidal zone (Yuan, et al., 2009). Therefore, the expansion of *S. alterniflora* is the fastest, leading to a change of the coastal wetland pioneer community from *S. salsa* to *S. alterniflora*.

S. alterniflora also has two ways of reproduction: sexual and asexual. Sexual reproduction has certain advantages in adapting to different environments. The genetic composition of progeny produced by asexual reproduction is always the same as that of the mother. However, *S. salsa* mainly depends on seed propagation and expansion. The plant is short and has a disadvantageous position in interspecific competition. Therefore, at the upper edge of the *S. alterniflora* marsh, the species can rapidly occupy the growth space when in competition with *S. salsa*, as well as absorb and utilize resources. Thus, it occupies more favorable habitat and forms the new evolution pattern of *S. salsa* marsh - *S. alterniflora* marsh in the study area.

***S. alterniflora* expansion affecting on landscape patterns**

The spatial distribution, expansion characteristics, and pattern changes of *S. alterniflora* have a significant impact on the coastal wetland landscape. These factors change the composition of the landscape structure, the diversity, and the heterogeneity characteristics (Zhang et al., 2018). Diverse mechanisms of *S. alterniflora*, such as marginal expansion, external isolation expansion, and tidal creek expansion, have a profound impact on the landscape pattern changes (Wang et al., 2018). The introduction of *S. alterniflora* was successful, and the pioneer community and the dominant population in the coastal wetland gradually changed to *S. alterniflora*. The expansion of *S. alterniflora* changed the landscape succession sequence of the coastal wetland: the succession sequence of mudflat to *S. alterniflora* marsh appeared in the coastal wetland since the introduction of *S. alterniflora*, the succession sequence of mudflat to *S. salsa* marsh gradually disappeared after the formation of the ecotone between *S. alterniflora* and *S. salsa*, and the succession sequence of *S. salsa* marsh to *S. alterniflora* marsh appeared. From land to sea, the landscape spatial pattern changed from “*P. australis* marsh – *S. salsa* marsh – *S. alterniflora* marsh – mudflat” to “*P. australis* marsh – *S. alterniflora* marsh – mudflat.”

The landscape transfer matrix (Fig. 5) showed that from 2000 to 2006, in the source composition of *S. alterniflora* marsh, mudflats accounted for 34.331%, and *S. salsa* marsh accounted for 2.483%. From 2006 to 2011, the mudflat accounted for 10.591%, and *S. salsa* marsh accounted for 14.503%. Comparing the two periods, *S. alterniflora* dominated the expansion towards the sea in the earlier period, while in the later period, *S. alterniflora* expanded to both the ocean and the land. The expansion to the land is greater than the expansion to the sea. From 2000 to 2006, the average width of the *S. alterniflora* marsh increased by 767.393 m, and it pushed forward to the sea about 965 m. From 2006 to 2011, *S. alterniflora* marsh expanded toward both the sea and the land. It expanded about 325 m to the sea and 445 m to the land, and the average width increased by 771.410 m (Fig. 6).

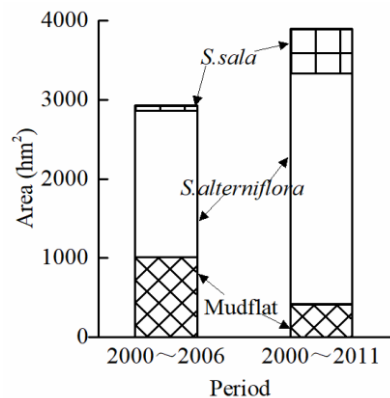


Figure 5. Landscape composition transformed into *S. alterniflora*

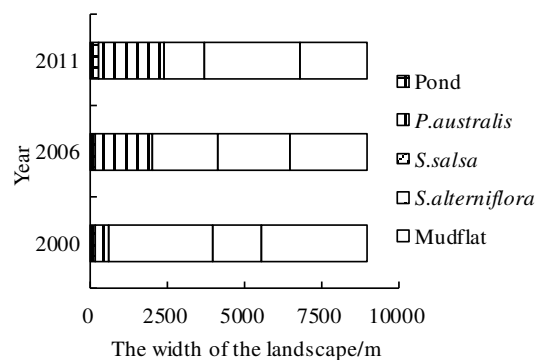


Figure 6. Landscape pattern change of the study area

According to the current development mode (Scenario A), by 2020, the PLAND of *S. alterniflora* marsh would increase to 51.522%, and the expansion rate would reach 210.357 hm²/a, while the PLAND of *S. salsa* marsh would decrease to 2.999% under two-way compression. In terms of the spatial pattern (Fig. 7), the *S. alterniflora* marsh would basically connect with the *P. australis* marsh, and the competition between the *P. australis* population and the *S. alterniflora* population for spatial resources would be the most intense in the middle tide wetland. Even in the local area of high-tide beaches, the *S. alterniflora* population could form small-scale patches and spread to the *P. australis* population (Pan et al., 2012).

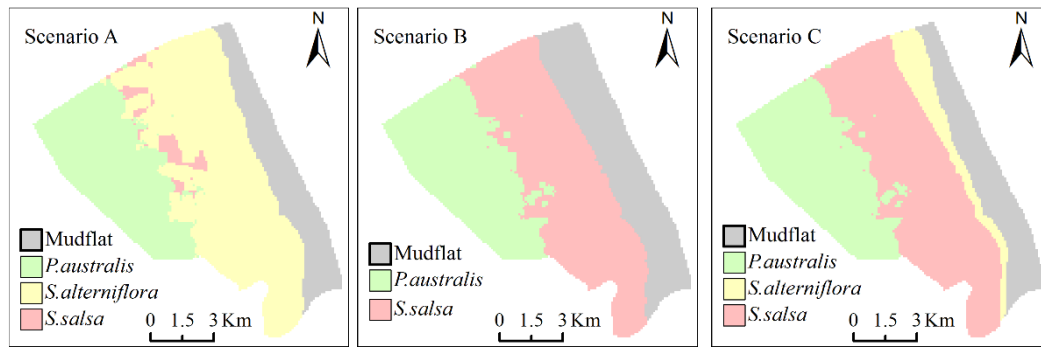


Figure 7. Simulation results of landscape pattern in different scenarios

The expansion of *S. alterniflora* gradually formed a single plant community, which reduced the biodiversity of bird habitat and the number of suitable habitats (Wang et al., 2019). Furthermore, the structure of bird community tended to be simplified (Guntenspergen et al., 2006). The native species of *S. salsa* played an important role in the process of overwintering and reproduction for birds. Thus, it is necessary to take measures for the protection and restoration of the *S. salsa* marsh and to delay the expansion of *S. alterniflora* (Zhang et al., 2017). Scenario B examined the removal of *S. alterniflora*. By 2020, the PLAND of *S. salsa* marsh would be recovered to 43.832%, and *S. alterniflora* marsh would disappear (Fig. 7). In Scenario C, a certain scale of *S. alterniflora* would be reserved to protect the coast, and it would no longer expand to the direction of *S. salsa* marsh. Moreover, artificial measures would be taken to restore the evolution sequence from mudflat to *S. salsa* marsh. The results showed that by 2020, the PLAND of *S. salsa* marsh would be recovered to 43.865%, and the PLAND of *S. alterniflora* marsh would be controlled to 8.678% (Fig. 7). The landscape pattern index of the three models were compared, and the following results were obtained (Fig. 8): SHDI, scenario C > scenario A > scenario B; the difference of the FRAC was small, scenario A > scenario C > scenario B; SHEI, scenario B > scenario C > scenario A; AI: scenario B (98.0113) > scenario C (97.4472) > scenario A (97.0993).

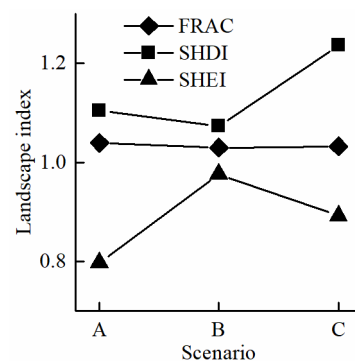


Figure 8. Landscape index scenario simulation results

S. alterniflora expansion affecting habitat quality

The expansion of *S. alterniflora* changed the vegetation structure, geomorphic pattern, and hydrological processes in the study area, as well as the service function of

the ecosystem. The benthos of *S. alterniflora* is rich, and the height of the vegetation on the surface is often more than 1.5 m. But the vegetation coverage of *S. alterniflora* is up to 90-100%, and there is no other vegetation among the plants after two or more years of growth. Consequently, *S. alterniflora* marsh is unsuitable for the habitat and reproduction of birds (Deng et al., 2009).

Furthermore, the blocking of *S. alterniflora* from the tide inhibited the growth of *S. salsa* (Shen et al., 2003) and had adverse effects on the birds that depend on the propagation and habitat of the *S. salsa* community, such as *Saunders's gull*, *Sternahirundo*, *S. albifrons*, and *Trigatotanus*. The results showed that with the expansion of *S. alterniflora*, the Q values of the study area showed a significant decline. Based on the remote sensing image analysis of YNNR from 1983 to 2017, it was found that the Q was negatively related to the expansion of *S. alterniflora*. Faster expansion of *S. alterniflora* correlated with a faster decline of habitat quality. In scenario A, *S. alterniflora* would continue to expand, and the Q would decrease to 0.7074. In scenario B, *S. alterniflora* would be removed, and the Q would increase to 0.9463. In scenario C, *S. alterniflora* would be controlled to a certain scale, and the Q would increase to 0.9198 (Figs. 9 and 10).

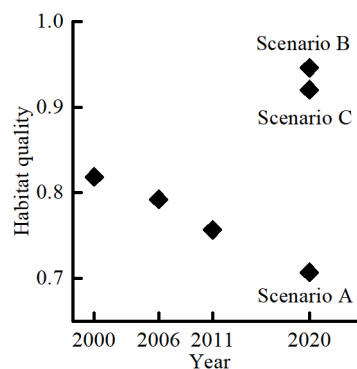


Figure 9. The value changes of habitat quality

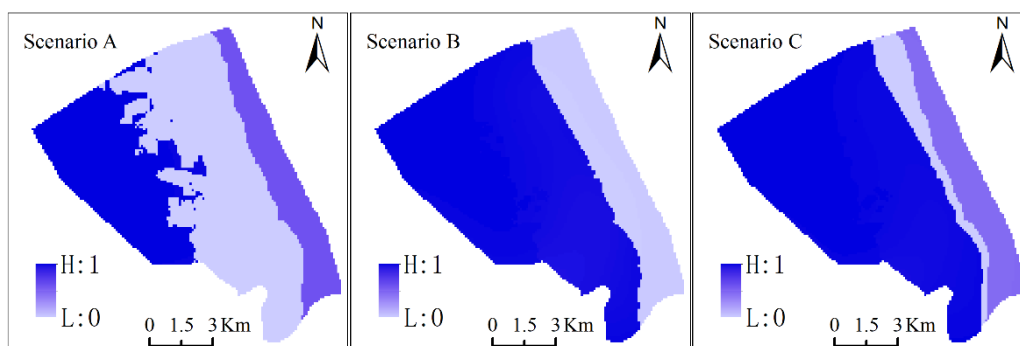


Figure 10. Simulation results of habitat quality in different scenarios

Based on the results, rich landscape diversity should be maintained along with the stability of the coast, and the wetland habitat quality should be improved. Scenario C would be a relatively ideal model for three reasons. First, it would help to retain a certain scale of *S. alterniflora* marsh, prevent erosion from tidal water on the coast, and

promote the deposition of the beach surface, although further study is needed to determine the appropriate scale of *S. alterniflora*. Secondly, it would protect the local species *S. salsa* and improve the suitability of habitat areas for rare species such as the red crowned crane. Thirdly, it would maintain the landscape diversity; the SHDI of scenario C was the highest and reached 1.236.

Ecological engineering measures, physical engineering measures, and biological measures could be effective means to control the expansion of *S. alterniflora* based on maintaining the integrity and continuity of the coastal ecosystem. In addition, some research has shown that the changes in habitats caused by inventors could limit the inventors over time because the acquisition of habitat changes created certain habitat properties that exceeded the optimal range for inventors (Tang et al., 2012).

Conclusions

This study quantitatively evaluated the effects of the expansion of *S. alterniflora* on the landscape pattern and habitat quality in the YNNR. The results showed that the rapid expansion led to a sharp reduction of the local species of *S. salsa*, which has posed a serious threat to the biodiversity. The landscape pattern gradually changed from “*P. australis* marsh – *S. salsa* marsh – *S. alterniflora* marsh – mudflat” to “*P. australis* marsh – *S. alterniflora* marsh – mudflat.” It affected the living environment of species that use the *S. salsa* community as a habitat and breeding ground. With the expansion of *S. alterniflora*, the habitat quality decreased significantly. Controlling the expansion of *S. alterniflora* and restoring the *S. salsa* marsh would be an ideal choice for the sustainable development of the YNNR. In the future, it will be an important task for the YNNR to control the *S. alterniflora* expansion and restore the *S. salsa* marsh. On one hand, we need to study the suitable scale of *S. alterniflora* in order to play its ecological function. On the other hand, we need to explore the approach of utilization for *S. alterniflora* and give full play to the comprehensive benefits.

Acknowledgements. This research was supported by National Natural Science Foundation of China (No.41771199, No.41501567), Basic Research Project of Jiangsu Province, China (No. BK20171277), Natural science research projects of colleges and universities in Jiang Province (No.18KJD170001) and Qing Lan Project in Jiangsu University of China.

REFERENCES

- [1] Ayres, D. R., Strong, D. R. (2002): The spartina invasion of San Francisco Bay. – Aquatic Nuisance Species Digest 4: 38-40.
- [2] Ayres, R. D., Smith, D. L., Zaremba, K., Klohr, S., Strong, D. R. (2004): Spread of exotic cordgrasses and hybrids (*Spartina* sp.) in the tidal marshes of San Francisco Bay, California, USA. – Biological Invasions 6: 221-231.
- [3] Callaway, J. C., Josselyn, M. N. (1999): The introduction and spread of smooth cordgrass (*Spartina-alterniflora*) in south San Francisco Bay. – Estuaries 15: 218-226.
- [4] Deng, Z. F., Deng, Z. W., An, S. Q., Wang, Z. S., Liu, Y. H., Ouyang, Y., Zhou, C. F., Zhi, Y. B., Li, H. L. (2009): Habitat choice and seed–seedling conflict of *Spartina alterniflora* on the coast of China. – Hydrobiologia 630: 287-297.
- [5] Dong, B., Song, G. X., Xie, Y. M., Xie, Y. M., Pei, E. L., Wang, T. H. (2010): Research on the habitat-selection of Reed Parrotbill (*Paradoxornis heudei*) during the winter in Chongming Dongtan, Shanghai. – Acta Ecologica Sinica 30: 4351-4358.

- [6] Fang, R. J., Shen, Y. M., Wu, D. L. (2014): Landscape pattern change in different sedimentary coastal areas of Yancheng, Jiangsu. – Chinese Journal of Ecology 4: 1096-1103.
- [7] Guntenspergen, G. R., Nordby, J. C. (2006): The impact of invasive plants on tidal-marsh vertebrate species, common reed (*Phragmites australis*) and smooth cordgrass (*Spartina alterniflora*) as case studies. – Terrestrial Vertebrates of Tidal Marshes Evolution Ecology & Conservation 32: 229-237.
- [8] Hou, M. H., Liu, H. Y., Zhang, H. B., Wang, C., Tan, Q. M. (2013): Influences of topographic features on the distribution and evolution of landscape in the coastal wetland of Yancheng. – Acta Ecologica Sinica 33: 3765-3773.
- [9] Landis, J. R., Koch, G. G. (1997): The measurement of observer agreement for categorical data. – Biometrics 33: 159-174.
- [10] Liao, C. Z., Luo, Y. Q., Jiang, L. F., Zhou, X. H., Wu, X. W., Chen, J. K., Li, B. (2007): Invasion of *Spartina alterniflora* enhanced ecosystem carbon and nitrogen stocks in the Yangtze estuary, China. – Ecosystems 10: 1351-1361.
- [11] Liu, C. Y., Zhang, S. Q., Jiang, H. X., Wang, H. (2009): Spatiotemporal dynamics and landscape pattern of alien species *Spartina alterniflora* in Yancheng coastal wetlands of Jiangsu Province. – Chinese Journal of Applied Ecology 20: 901-908.
- [12] Liu, D. W., Zhang, Y. L., Sun, Y., Lu, S. C., Cheng, H., Mu, S. J., Lu, C. H. (2016): Population dynamics and habitat selection of overwintering Red-Crowned Crane in coastal wetland of Yancheng, Jiangsu Province. – Journal of Ecology and Rural Environment 32: 473-477.
- [13] Liu, J. E., Zhou, H. X., Qin, P., Zhou, J. (2007): Effects of *Spartina alterniflora* salt marshes on organic carbon acquisition in intertidal zones of Jiangsu Province, China. – Ecological Engineering 30: 240-249.
- [14] Liu, Q. S., Li, Y. F., Zhu, X. D. (2003): Characteristics of coastal wetland ecosystem and their healthy design, a case study from Yancheng Nature Reserve, Jiangsu Province, China. – Acta Oceanologica Sinica 25: 43-148.
- [15] Liu, Y. X., Li, M. C., Zhang, R. S. (2004): Approach on the dynamic change and influence factors of *S. alterniflora* Loisel salt-marsh along the coast of the Jiangsu Province. – Wetland Science 2: 116-121.
- [16] Monserud, R. A., Leemans, R. (1992): Comparing global vegetation maps with the Kappa statistic. – Ecological Modelling 62: 275-293.
- [17] Neira, C., Grosholz, E. D., Levin, L. A., Blake, R. (2006): Mechanisms generating modification of benthos following tidal flat invasion by a *Spartina* hybrid. – Ecological Applications 16: 1391-1404.
- [18] Pan, Y., Li, D. Z., Yuan, Y., Xu, J., Gao, J. J., Lu, Y. Y. (2012): Distribution pattern of *Phragmites australis* and *Spartina alterniflora* populations in Chongming Dongtan wetland and its correlation with habitat. – Journal of Plant Resources and Environment 21: 1-9.
- [19] Pimentel, D., Lach, L., Zuniga, R., Morrison, D. (2000): Environmental and economic costs of nonindigenous species in the United States. – Bioscience 50: 53-65.
- [20] Schindler, S., von Wehrden, H., Poirazidis, K., Wrbka, T., Kati, V. (2013): Multiscale performance of landscape metrics as indicators of species richness of plants, insects and vertebrates. – Ecological Indicators 31: 41-48.
- [21] Sharp, R., Chaplin-Kramer, R., Wood, S., Guerry, A., Tallis, H., Ricketts, T. (2017): InVEST 3.2.0 User's Guide, Integrated Valuation of Environmental Services and Tradeoffs. – The Natural Capital Project, Stanford.
- [22] Sharp, S. J., Angelini, S. (2019): The role of landscape composition and disturbance type in mediating salt marsh resilience to feral hog invasion. – Biological Invasions 21: 2857-2869.
- [23] Shen, Y. M., Zhang, R. S., Wang, Y. H. (2003): The tidal creek character in salt marsh of *Spartina alterniflora* Loisel on strong tide coast. – Geographical Research 22: 520-527.

- [24] Tang., L., Yang, G. C., Wang, C. H., Zhao, B., Li, Bo. (2012): A plant invader declines through its modification to habitats. A case study of a 16-year chronosequence of *Spartina alterniflora* invasion in a salt marsh. – *Ecological Engineering* 49: 181-185.
- [25] Vitousek, P. M., D'antonio, C. M., Loope, L. L., Marcel, R., Westbrooks, R. (1996): Introduced species, a significant component of human-caused global change. – *New Zealand Journal of Ecology* 21: 1-16.
- [26] Wang, C., Liu, H. Y. (2014): The impact of *spartina alterniflora* expansion on vegetation landscapes in the Yancheng tidal flat wetland. – *Resources Science* 36: 2413-2422.
- [27] Wang, J., Liu, H. Y., Li, Y. F., Liu, L., Xie, F. F. (2018): Recognition of spatial expansion patterns of invasive *Spartina alterniflora* and simulation of the resulting landscape changes. – *Acta Ecologica Sinica* 38: 5413-5422.
- [28] Wang, J., Liu, H. Y., Li, Y. F., Liu, L., Xie, F. F., Lou, C. R., Zhang, H. B. (2019): Effects of *Spartina alterniflora* invasion on quality of the red-crowned crane (*Grus japonensis*) wintering habitat. – *Environmental Science and Pollution Research* 26: 21546-21555.
- [29] Wang, J. Q., Zhang, X. D., Nie, M., Fu, C. Z., Chen, J. K., Li, B. (2008): Exotic *Spartina alterniflora* provides compatible habitats for native estuarine crab *Sesarma dehaani* in the Yangtze River estuary. – *Ecological Engineering* 34: 57-64.
- [30] Yuan, H. W., Li, S. Z., Zheng, H. Z., Fang, Z. Y. (2009): Evaluation of the influences of foreign *S. alterniflora* on ecosystem of Chinese coastal wetland and its countermeasures. – *Marine Science Bulletin* 28: 122-128.
- [31] Zhang., H. B. (2018): *Landscape Pattern Change and Ecological Process Response in Yancheng Coastal Wetland*. – Science Press, Beijing.
- [32] Zhang, H. B., Liu, H. Y., Hou, M. H. (2013): Spatiotemporal characteristics of *Spartina alterniflora* marsh change in the coastal wetlands of Yancheng caused by natural processes and human activities. – *Acta Ecologica Sinica* 33: 4767-4775.
- [33] Zhang., H. B., Liu., H. Y., Hou., M. H., Li., Y. F. (2014): Building model based on processes and simulating landscape change in the coastal wetlands-A case study of the core area in Yanchegn Natural Reaerve. – *Journal of Natural Resources* 29: 1105-1115.
- [34] Zhang, J. C., He, D. J., You, W. B., Deng, X. P., Zhang, F. Y., Liu, J. C. (2018): Invasion impact of *Spartina alterniflora* on the landscape of coastal wetland in Xiapu County. – *Journal of Forest and Environment* 38: 302-308.
- [35] Zhang, R. S., Shen, Y. M., Lu, L. Y., Yan, G. S., Wang, Y. H., Li, J. L., Zhang, Z. L. (2004): Formation of *S. alterniflora* salt marshes on the coast of Jiangsu Province, China. – *Ecological Engineering* 23: 95-105.
- [36] Zhang, X. Q., Wang, G. X., Wang, Y. H., Wang, Z. L. (2006): The changes of erosion or progradation of tidal flat and retreat or extension of wetland vegetation of the Yancheng coast, Jiangsu. – *Marine Sciences* 30: 35-39.
- [37] Zhang., Y., Sun, Y., Lu, C. H., Zhang, Y. L., Lu, S. C. (2017): Pattern of wintering bird community in three habitats after invasion of *Spartina alterniflora* in Yancheng National Nature Reserve. – *Wetland Science* 15: 433-440.

EXPRESSION AND BIOINFORMATIC ANALYSIS OF THE ROP FAMILY GENE *TaRAC* IN WHEAT (*TRITICUM AESTIVUM* L.)

JIANG, Y. M. – YANG, J. W. – LIU, L. L. – LI, W. C. – ZHANG, B. Z. – YIN, J. – LI, L. *

National Engineering Research Center for Wheat, State Key Laboratory of Wheat and Maize Crop Science, Collaborative Innovation Center of Henan Grain Crop, Henan Agricultural University, Zhengzhou 450002, China

*Corresponding author

e-mail: nercw@126.com; phone: +86-135-9259-7894

(Received 27th Jan 2020; accepted 22nd May 2020)

Abstract. The Ras related C3 botulinum toxin substrate (RAC) play a key role in dealing with abiotic stresses in plants. The full-length open reading frame of a *TaRAC* was firstly cloned from wheat. Bioinformatic analysis and expression profile analysis of the *TaRAC* gene were carried out. The results indicated that the full-length open reading frame of *TaRAC* was 594bp which encoded 197 amino acid residues. The genomic *TaRAC* gene had no introns. The protein encoded by the *TaRAC* gene consisted of a small GTPase Rho family domain profile. Blast and phylogenetic analysis showed that the protein encoded by *TaRAC* shared the identity with *RAC* from corn (*Zea mays* L.). The result of qRT-PCR showed that expression of *TaRAC* gene was significantly tissue-specific. The result of qRT-PCR showed that *TaRAC* in the seeds was significantly higher than the expression of gene expression after soaking germination. The sensitivity of this gene to abscisic acid (ABA) significantly increased. *TaRAC* gene may play an important role in seed dormancy during germination, which could be used to improve the preharvest sprouting (PHS) resistance of wheat.

Keywords: wheat, preharvest sprouting, seed dormancy, abscisic acid, tissue-specific

Introduction

Preharvest sprouting (PHS) in wheat (*Triticum aestivum* L.) is the germination of grains in the ears when long range rainfall or damp conditions prior to harvest occur (Li et al., 2019c). Small GTP binding proteins have a class of GTP binding proteins with molecular weight of 20-40 KD, including five families of Ras, Ran, Rab, Rho and Arf, which are involved in the regulation of eukaryotic cell proliferation, signal transduction and material transport (Takai et al., 2001; Kahn et al., 1992; Christensen et al., 2004). At present, more than 100 small GTP binding proteins have been found in eukaryotes, forming a huge superfamily.

There are many members in Rho subfamily. A group of small GTP binding proteins related to Rho subfamily were isolated by sequencing *Arabidopsis* genome. These proteins are evolutionarily independent and unique to plants. Because of their highest similarity with Ras related C3 botulinum toxin substrate (RAC) protein in animals, they are called RAC (Rho related GTPase from plant) or Rop protein family. The small GTP binding proteins of the Rop family have many functions, including the regulation of plant cell polarity, cell growth, morphological development, cytokinesis, hormone signaling, plant pathogen interaction, stress response and so on (Berken and Wittinghofer, 2008).

Several reports have suggested a function of RAC/ROPs as direct or indirect modulators of plant gene expression (Poraty-Gavra et al., 2013; Scheler et al., 2016). RHO GTPases were considered as transcriptional regulators because their downstream factors strongly affect gene expression and chromatin structure (Rajakyla and

Vartiainen, 2014; Yu and Brown, 2015). It was found that a subset of plant Rac/Rop GTPases functions in mediating the auxin signal to downstream responsive genes basing on the tobacco overexpressing Rac/Rop GTPase, NtRac1 (Tao et al., 2002). Barley susceptibility factor RACB modulates transcript levels of signaling protein genes in compatible interaction with *Blumeria graminis* F. sp. *hordei* (Schnepf et al., 2018).

Transgenic crops can be used as powerful supplements to traditional breeding methods to meet the world's demand for high-quality food, and help combat malnutrition by improving yield, nutritional quality and resistance to various biological and abiotic stresses (Kamthan et al., 2016). *RsRHA2b* improves dormancy and preharvest sprouting tolerance in transgenic wheat (Bornman et al., 2019). Exogenous *RsRHA2b* gene promoted the expression of *YTH2456* (Li et al., 2019a). *TaRHA2b* interacts with *TaRAC* and other proteins (Li et al., 2019b). Blast analysis of the *YTH2456* show the sequence (AK251632.1) in barley and the *RAC* gene sequence (GU452718.1) in Wheat.

In order to make full use of the Rop family gene to improve the resistance to PHS in wheat, a Rop gene *TaRAC* was cloned from wheat by RT-PCR amplification. Bioinformatic analysis and expression profile analysis of the *TaRAC* gene with the treatment of different abscisic acid (ABA) concentration were carried out. The research could provide some reference for studying the mechanism of *TaRAC* gene in wheat dormancy, which may be used as an excellent gene resource to improve PHS resistance.

Materials and methods

Materials and ABA treatment

The wheat variety “Zhengmai 9023” was tested. The elite Chinese bread wheat cultivar Zhengmai 9023, a hexaploid wheat cultivar with weak resistance to PHS, which is widely cultivated in Henan Province.

Extraction of total DNA and RNA and synthesis of cDNA first strand

DNA was extracted from wheat germ with MiniBEST Plant Genomic DNA Extraction Kit. Trizol reagent was used to extract the total RNA from wheat germ. The extracted RNA was tested for quality and purity and then stored in a refrigerator at -80 °C for reserve. PrimeScript™ RT reagent Kit (Perfect Real Time) was used to synthesize cDNA from total RNA. All operations are performed according to the instructions of the kits. The cDNA was stored at -80 °C for later use.

Cloning of *TaRAC* gene

According to the amino acid sequence of the *RAC* gene sequence (GU452718.1) in Wheat, specific Primer5.0 software was used to design the primers for the experiment (Table 1), and target gene prediction and in vitro splicing were conducted. The wheat cDNA was used as template for PCR amplification. PCR reaction system 20 µL: 10x PCR Buffer 2.0 µL, 2.5 mM dNTPs 1.6 µL, 10 pM upstream and downstream primers each 0.8 µL, Taq enzyme (5 U/µL) 0.3 µL, cDNA template 1.0 µL, ddH₂O complement 20 µL. Reaction conditions: 94 °C pre degeneration 3 min; 94 °C modified 30 s, 50 °C annealing 40 s, 72 °C for 1 min, 30 cycle; 72 °C extension time for 10 min.

The primer pairs P1 and P2 were designed according to the sequence of wheat *TaRAC* gene. The target sequence was obtained by RT-PCR amplification with primers

P1 and P2. The PCR products were recovered and connected with the pGEMT vector, and the recombinant plasmid transformed into *E. coli* DH5 α competent cells, and the positive clones were screened and sent to BGI (HuaDa Biotechnology co., ltd., China) for sequencing.

Table 1. Primers sequences of the experiment

Primers name	Primer sequence (from 5' sequence-3' sequence)
P1	ATGAGCGCTTCTCGGTTTCAT
P2	TTACAAAAAGGTGGATCCTT
P3	GTTCCAATCTATGAGGGATACACGC
P4	GTTCCAATCTATGAGGGATACACGC
P5	CAGGTGGTCCGGCCGAGGTCGAT
P6	CCAGGCACACGATGCACGTCGCCG

Biological information analysis of *TaRAC* gene

A comprehensive bioinformatics analysis was conducted using tools including the NCBI (<https://www.ncbi.nlm.nih.gov/>), Swiss-Prot databases (<https://prosite.expasy.org/>), DNAMAN and MEGA 7.0. Based on cDNA sequence, using NCBI site ORF Finder (<https://www.ncbi.nlm.nih.gov/orffinder/>) speculation *TaRAC* open reading frame. The consistency of *TaRAC* homologous genes with other species was analyzed using DNAMAN, and the evolution tree was constructed with the software MEGA 7.0.

***TaRAC* gene expression analysis**

The root, stem, leaf, cob, lemma and endosperm from 25 d flowering wheat plants were taken. RNA was extracted, and reverse transcription was conducted to synthesize the first strand of cDNA. And PCR amplification was conducted with the first strand of cDNA as template. PCR reaction system 20 μ L: 10x PCR Buffer 2.0 μ L, 2.5 mM dNTPs 1.6 μ L, 10 pM upstream and downstream primers each 0.8 μ L, Taq enzyme (5 U/ μ L) 0.3 μ L, cDNA template 1.0 μ L, ddH₂O complement 20 μ L. Reaction conditions: 94 $^{\circ}$ C for 3 min, 94 $^{\circ}$ C for 30 s, 54 $^{\circ}$ C for 30 s, 72 $^{\circ}$ C for 40 s, a total of 28 cycle, 72 $^{\circ}$ C extension time for 10 min, electrophoresis detection of PCR products.

The *Actin* gene products amplified by wheat *Actin* gene specific primers were taken as internal reference. The primers of *Actin* gene used in PCR reaction were P3 and P4 (Table 1). And the primers of *TaRAC* gene were P5 and P6 (Table 1). According to the PCR reaction mixture system, PCR amplification conditions as follows: 94 $^{\circ}$ C 3 min, 94 $^{\circ}$ C for 30 s, 54 $^{\circ}$ C for 30 s, 72 $^{\circ}$ C for 35 s, a total of 28 cycle. 72 $^{\circ}$ C for 10 min, RT-PCR product after 1.0% agarose electrophoresis detecting camera, preservation. The experiment was repeated for three times.

Wheat seeds (n = 150) with full and equal size after disinfection were soaked with ABA solution of 0.5 μ M (Li et al., 2019c), treatment without ABA was set for control, and samples were taken at different time (Table 2). RNA of dry seeds without soaking was extracted at the same time. PrimeScriptTM RT reagent Kit (Perfect Real Time) was used to synthesize cDNA from total RNA. The cDNA was numbered and stored at -80 $^{\circ}$ C for later use.

Fluorescence quantitative PCR was used to analyze the *TaRAC* gene expression under ABA treatment with the primers P5 and P6 and internal reference *Actin* gene primers P3 and P4 (Table 1). According to the relative quantitative method to calculate: The relative expression of gene (Rel.Exp) = $2^{-\Delta\Delta Ct}$, among them $-\Delta\Delta Ct = \text{Calibrator } \Delta Ct - \Delta Ct$ (the unknown sample), ΔCt (unknown sample) = (Ct) internal gene - (Ct) target gene, Calibrator $\Delta Ct =$ (Ct) reference sample internal gene - (Ct) reference sample target gene. The reaction system of fluorescence quantitative PCR was 20 μL : SYBR Premix Ex TaqTM II, 10 μL , PCR Forward Primer (10 μM) 0.8 μL , PCR Reverse Primer (10 μM) 0.8 μL , ROX Reference Dye II (50x), cDNA template 2 μL , ddH₂O up to 20 μL .

Table 2. Sampling time of the experiments with the treatment of 0.5 μM ABA

Group number	Sampling time (h)
1	0
2	1
3	2
4	4
5	8
6	12

Statistical analysis

The GraphPad Prism 8 was used for statistical analysis and drawing. For comparing results of different treatments, Variance analysis is followed by a post-hoc test in order to determine pairwise differences. Differences were considered significant for $P < 0.05$.

Results

Sequence analysis of gDNA and cDNA of *TaRAC* gene

It shows that the ORF region of *TaRAC* is 594 bp in length (Fig. 1). The obtained plasmid pGEM-T-*TaRAC* was sequenced. The results of sequences are listed in Figure 2. The sequencing results were matched with the accession number GU452718.1 after blast on NCBI, encoding 197 amino acid residues in an open reading frame with molecular weight of 21.662 kD and isoelectric point of 9.26. The obtained pGEM-T-*TaRAC* plasmids from cDNA and gDNA were sequenced and the results showed that there was no intron in the *TaRAC* gene in Figure 3.

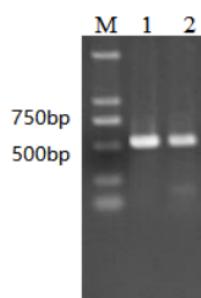


Figure 1. Sequence of the *TaRAC* gene. M, marker. 1 and 2, the target *TaRAC* fragment


```

1      ATGAGCGCTT CTCGGTTCAT CAAGTGCCTG ACGGTGGGGG ACGGTGCCGT CGGCAAGACT
61     TGCCCTCTCA TCTCCTACAC ATCCAACACC TTCCCACCG ACTATGTCCC AACAGTCTTC
121    GACAACTTCA GCGCTAACGT TGTGGTTGAC GGGAGCACCG TCAACCTCGG ATTATGGGAT
181    ACTGCAGGAC AAGAGGACTA TAATAGACTA CGCCACTGA GCTACCAGAG TGCCGATGTC
241    TTCCTGCTCG CCTTTTCTCT TATCAGCAAA GCAAGCTACG AGAATGTAC TAAGAAGTGG
301    ATCCCTGAGC TACGGCACTA TGCTCCTGGT GTGCCATAA TTCTTGTGCG GACAAAAGCTT
361    GATCTGCGGG ATGACCAGCA GTTTTTGCTG GATCACCTG GGGCTGTTCC TATTTCCACC
421    GCTCAGGGTG AAGAGCTGAA GAAGGTAATT GGC GCGACGG CCTACATCGA GTGCAGCTCA
481    AAAACACAGC AGAACATCAA GGGGGGGTTT GATGGGGGAA TCAAGGGGTT TCTCCACCTT
541    CCAAACCAGA AGCGGAAGAA GAGGAAGTCG CAAAAGGAT CCACCTTTT GTAA

```

Figure 2. The *TaRAC* fragment amplified by PCR

TaRac1-cDNA.txt	ATGAGCGCATCTCGGTTTCATCAAGTGCCTGACGGTGGGGGACGGCGCCGT	50
TaRac1-gDNA.txt	ATGAGCGCATCTCGGTTTCATCAAGTGCCTGACGGTGGGGGACGGCGCCGT	50
Consensus	atgagcgcatctcggtttcatacaagtgctgacggtgggggacggcgccgt	
TaRac1-cDNA.txt	GGGAAAGACATGCCTCCTCATCTCATACACATCCAACACCTTCCCCACAG	100
TaRac1-gDNA.txt	GGGAAAGACATGCCTCCTCATCTCATACACATCCAACACCTTCCCCACAG	100
Consensus	gggaaagacatgcctcctcatctcatacacatccaacaccttccccacag	
TaRac1-cDNA.txt	ACTATGTCCCAACAGTTTTCGACAACCTCAGCGCTAACGTCGTGGTTGAC	150
TaRac1-gDNA.txt	ACTATGTCCCAACAGTTTTCGACAACCTCAGCGCTAACGTCGTGGTTGAC	150
Consensus	actatgtcccaacagttttcgacaacttcagcgctaa cgtcgtggttgac	
TaRac1-cDNA.txt	GGCAGCACCGTCAACCTCGGATTATGGGATACTGCAGGACAAGAAGACTA	200
TaRac1-gDNA.txt	GGCAGCACCGTCAACCTCGGATTATGGGATACTGCAGGACAAGAAGACTA	200
Consensus	ggcagcacctgcaacctcggattatgggatactgcaggacaagaagacta	
TaRac1-cDNA.txt	TAATCGACTACGCCACTAAGCTACCGTGGTGCCTGATGTCCTTCTGCTCG	250
TaRac1-gDNA.txt	TAATCGACTACGCCACTAAGCTACCGTGGTGCCTGATGTCCTTCTGCTCG	250
Consensus	taatcgactacgccactaagctaccgtggtgccgatgtccttctgctcg	
TaRac1-cDNA.txt	CCTTTTCTCTCATCAGCAAAGCAAGCTACGAGAATGTACTAAGAAGTGG	300
TaRac1-gDNA.txt	CCTTTTCTCTCATCAGCAAAGCAAGCTACGAGAATGTACTAAGAAGTGG	300
Consensus	ccttttctctcatcagcaaagcaagctacgagaatgtactaagaagtgg	
TaRac1-cDNA.txt	ATTCCAGAGTTACGGCACTATGCTCCTGGCGTGCCCATAAITCTTGTGG	350
TaRac1-gDNA.txt	ATTCCAGAGTTACGGCACTATGCTCCTGGCGTGCCCATAAITCTTGTGG	350
Consensus	attccagagttacggcactatgctcctggcgtgccccataattctgtgg	
TaRac1-cDNA.txt	AACAAAGCTTGATCTGCGGGATGACAAGCAGTTTTTTGTGGATCACCCCTG	400
TaRac1-gDNA.txt	AACAAAGCTTGATCTGCGGGATGACAAGCAGTTTTTTGTGGATCACCCCTG	400
Consensus	aacaaagcttgatctgcgggatgacaagcagttttttgtggatcacccctg	
TaRac1-cDNA.txt	GCGCGGTTCTTATTTCCACTGCTCAGGGTGAAGAGCTGAAGAAGGTGATT	450
TaRac1-gDNA.txt	GCGCGGTTCTTATTTCCACTGCTCAGGGTGAAGAGCTGAAGAAGGTGATT	450
Consensus	gcgcggttcttattttccactgctcagggatgaagagctgaagaaggtgatt	
TaRac1-cDNA.txt	GGCGCGACTGCCTACATCGAGTGCAGCTCAAAAACACAGCAGAACATCAA	500
TaRac1-gDNA.txt	GGCGCGACTGCCTACATCGAGTGCAGCTCAAAAACACAGCAGAACATCAA	500
Consensus	ggcgcgactgcctacatcgagtgcagctcaaaaacacagcagaacatcaa	
TaRac1-cDNA.txt	GGCGGTGTTTGATGCGGCGATCAAGGTGGTCTCCAGCCTCCGAAGCAGA	550
TaRac1-gDNA.txt	GGCGGTGTTTGATGCGGCGATCAAGGTGGTCTCCAGCCTCCGAAGCAGA	550
Consensus	ggcggtgtttgatgcgcgatcaaggtggctccagcctccgaagcaga	
TaRac1-cDNA.txt	AGCGGAAGAAGGAAGTACAGAAAGGATGCAGCATCTTGTAA	594
TaRac1-gDNA.txt	AGCGGAAGAAGGAAGTACAGAAAGGATGCAGCATCTTGTAA	594
Consensus	agcggaagaaggaagtacagaaaggatgcagcatcttgtaa	

Figure 3. Comparative analysis between gDNA and cDNA sequences of *TaRAC*

TaRAC encoding amino acid sequence alignment and phylogenetic tree

After functional domain analysis of the encoded amino acids, it was found that there was a small GTPase Rho family profile, as shown in *Figures 4* and *5*. It contains a small

GTPase Rho family domain. It is a polypeptide formed by 1-177 amino acids and belongs to an alkaline protein. *TaRAC* shared the identity with *RAC* from the corn.

Expression analysis of the *TaRAC* gene

The relative expression of *TaRAC* gene in different tissues (*Fig. 6*) showed that the specific expression bands of *TaRAC* gene could also be detected in the root, stem, leaf, cob, lemma and endosperm samples of wheat. The highest expression bands were found in leaves, cob, lemma and endosperm, and the signal intensity was significantly higher than that in roots and stems, which indicated that the transcriptional expression of *TaRAC* gene had strong tissue specificity.

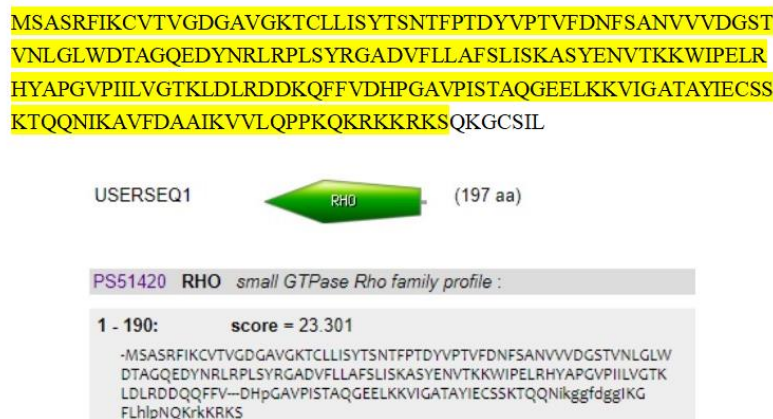


Figure 4. Domain analysis of amino acids encoded by *TaRAC* gene. The yellow part of amino acid corresponds to the green part of the functional domain

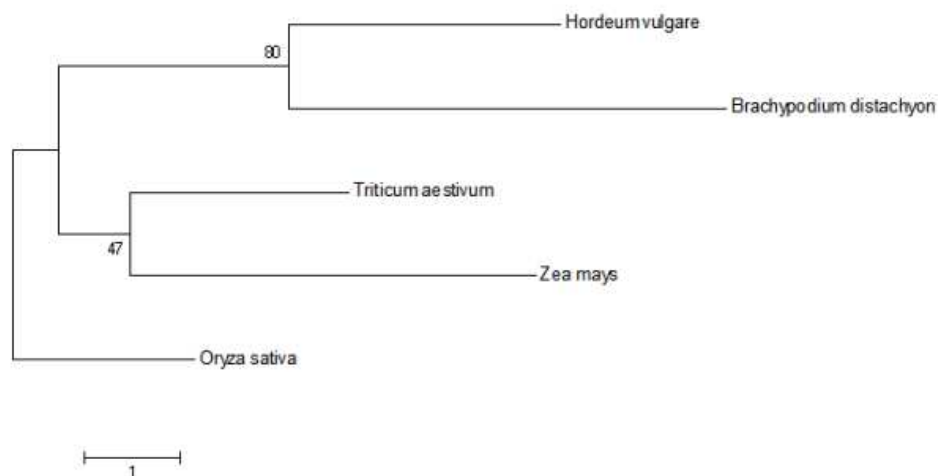


Figure 5. A phylogenetic tree of homology sequence with the *TaRAC* gene (with the software MEGA7.0). GU452718.1, *Triticum aestivum*, *rac*-type small GTP-binding protein mRNA; AK251632.1, *Hordeum vulgare*; XM_003570698.4, *Brachypodium distachyon*, *rac*-like GTP-binding protein 5 mRNA; EU968843.1, *Zea mays* clone 324497, *rac*-like GTP-binding protein 5 mRNA; AF218381.1, *Oryza sativa*, subsp. *japonica* small GTP binding protein *RACP* (*RAC*) mRNA

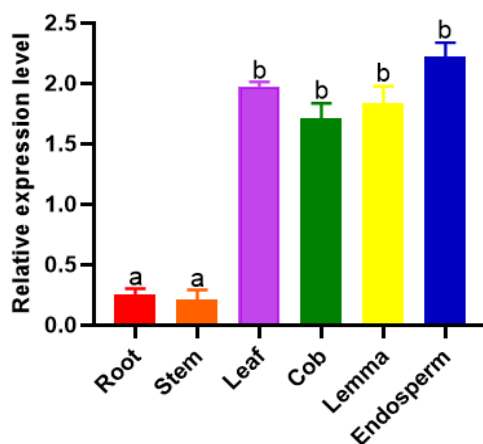


Figure 6. Expression analysis of *TaRAC* gene in different tissues of wheat. The letters 'a' to 'b' indicate statistically significant differences $P < 0.05$ (Tukey's least significantly difference test). Data are expressed as mean values standard errors from three replicates and error bars represent standard errors

***TaRAC* gene expression is sensitive to exogenous ABA treatment**

Different concentrations of ABA were used to treat wheat seedlings at two-leaf stage. Real-time fluorescence quantitative PCR (RT-PCR) amplification was performed with primers to analyze the response of *TaRAC* gene to ABA in early germination seedlings. Quantitative fluorescence assay (Fig. 7) showed that under 5 mol/L ABA treatment, the expression of *TaRAC* gene peaked at 8 h, and the response was obvious. The results showed that *TaRAC* gene was sensitive to the change of ABA concentration. Within a certain ABA concentration range, the response time of *TaRAC* gene would be shortened, but when beyond a specific ABA concentration range, the response of *TaRAC* gene was passivated.

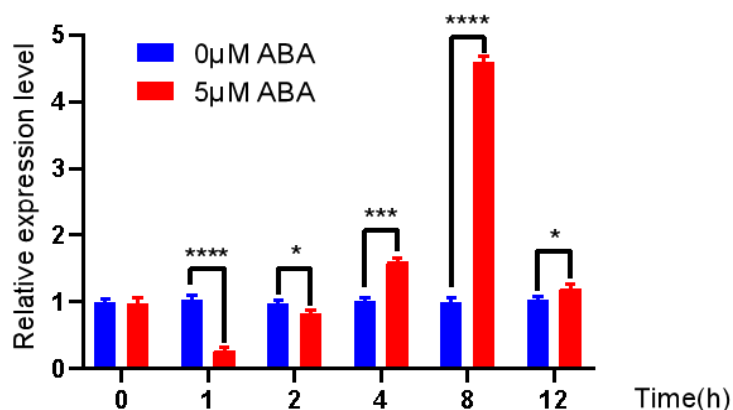


Figure 7. Relative expression levels of *TaRAC* gene at different times with 0 μM and 5 μM ABA treatment. The symbol '*' indicates statistically differences $P < 0.05$, the symbol '**' indicates statistically differences $P < 0.01$; the symbol '***' indicates statistically differences $P < 0.001$; the symbol '****' indicates statistically differences $P < 0.0001$ (Turkey's least significantly difference test). Data are expressed as mean values standard errors from three replicates and error bars represent standard errors

Discussion

Plant RAC/ROP proteins are involved in a series of important biological processes, such as plant polar growth, hormone signal transduction, plant disease resistance and abiotic stress resistance, by regulating the assembly of cytoskeleton actin, the production of reactive oxygen species and the change of Ca^{2+} concentration in cells (Zheng and Yang, 2000; Li et al., 2001). *RAC1* was cloned from pea for the first time and found to be related to the growth of pea pollen tube (Yang and Watson, 1993). RAC protein was involved in the polar growth of pollen tube and root hair cells (Ye et al., 2003; Lee and Yang, 2008; Hwang et al., 2010).

The expression of *TaRAC* in different tissues of wheat was detected by qRT-PCR. The results showed that the gene had different abundances in different tissues of wheat, with certain tissue specificity, and the highest expression in leaves, cob, lemma and endosperm.

RAC/ROP protein was also involved in plant hormone signal transduction. For example, auxin related genes were also induced in tobacco and corresponding active mutants that overexpress *NTRac1* (Morel et al., 2004). Exogenous ABA can inhibit the expression of *AtRop10* in *Arabidopsis*, while the deletion mutant of this gene is more sensitive to ABA (Zheng et al., 2002). RAC/ROP protein was also involved in the response of plants to abiotic stress, and the salt resistance of *Arabidopsis* plants overexpressing tobacco *NtRop1* was improved (Cao et al., 2010). *Arabidopsis AtRop6* and *AtRop11* enhanced drought resistance of plants through stomatal closure regulated by ABA (Lemichez and E., 2001; Zheng et al., 2002).

Plant RAC/ROP protein genes are involved in many plant stress responses. *TaRAC* can promote ABA induced responses, such as seed germination, root elongation, stomatal closure, and ABA can also play a negative role in regulating *TaRAC*. In the present study, the *TaRAC* gene of wheat was cloned, and its molecular structure, tissue expression specificity and expression under ABA treatment were analyzed. It is suggested that the gene may be involved in wheat development, especially in response to abiotic stress, which provides a theoretical basis for further study of the role of *TaRAC* protein in plant resistance to spike germination.

ABA signaling pathway is closely related to plant stress resistance. In the present study, exogenous ABA promoted the expression of *TaRAC* gene. It is suggested that the increase of *TaRAC* gene expression may promote the cascade amplification of ABA signal transduction and improve plant resistance.

The expression profile of *TaRAC* gene with the treatment of different ABA concentration showed that *TaRAC* gene was highly expressed in seedlings. The results indicated that the function of *RAC* gene in plants is related with ABA signal transduction pathway. The results showed that *TaRAC* gene may be an excellent genetic resource to improve PHS resistance.

Rac GTPases play an important role in the regulation of secondary metabolism in plant cells and that overexpression of the gene(s) may be capable of enhancing the production of natural products accumulated in higher plant cells (Asano et al., 2013). The expression profile of *TaRAC* gene and the main functional domain of the protein encoded by a gene were analyzed to reveal that the gene may be involved in the regulation of wheat resistance to PHS. More work is needed for using *TaRAC* gene to improve dormancy and PHS tolerance in wheat.

Conclusion

The full-length ORF of the *TaRAC* gene was cloned from wheat. The full-length ORF of *TaRAC* encoded 197 amino acid residues, which was consisted of a small GTPase Rho family profile. The genomic *TaRAC* gene had no introns. *TaRAC* shared the identity with *RAC* from the corn. The expression of *TaRAC* gene was significantly tissue-specific. The expression of *TaRAC* in the seeds was significantly higher than the expression of gene expression after soaking germination. The sensitivity of the *TaRAC* gene to ABA was significantly increased. In the next step, we will use transgenic wheat lines to further clarify the function, subcellular localization of *TaRAC* gene and its role in ABA mediated signal transduction pathway, providing effective candidate genes for wheat resistance to PHS and stress breeding.

Acknowledgements. This work was supported by the National key R & D Projects (2017YFD0301101).

Conflict of interests. The authors state no conflict of interest.

REFERENCES

- [1] Asano, K., Lee, J., Yamamura, Y., Kurosaki, F. (2013): Enhanced accumulation of atropine in *Atropa belladonna* transformed by *Rac* GTPase gene isolated from *Scoparia dulcis*. – *Transgenic Research* 22: 1249-1255.
- [2] Berken, A., Wittinghofer, A. (2008): Structure and function of Rho-type molecular switches in plants. – *Plant Physiology and Biochemistry* 46: 380-393.
- [3] Bornman, J. F., Barnes, P., Robson, T. M., Robinson, S. A., Jansen, M. a. K., Ballare, C. L., Flint, S. D. (2019): Linkages between stratospheric ozone, UV radiation and climate change and their implications for terrestrial ecosystems. – *Photochemical and Photobiological Sciences* 18: 681-716.
- [4] Cao, Y. R., Zhigang, L. I., Tao, C., Zhang, Z. G., Zhang, J. S., Chen, S. Y. (2010): Overexpression of a tobacco small G protein gene *NtRop1* causes salt sensitivity and hydrogen peroxide production in transgenic plants. – *Phytochemical Analysis* 13: 189-194.
- [5] Christensen, T., Vejlpkova, Z., Sharma, Y., Arthur, K., Spatafora, J., Albright, C., Meeley, R., Duvick, J., Quatrano, R., Fowler, J. (2004): Conserved subgroups and developmental regulation in the monocot *rop* gene family. – *Plant Physiology* 133: 1791-1808.
- [6] Hwang, J., Wu, G., Yan, A., Lee, Y., Grierson, C. S., Yang, Z. (2010): Pollen-tube tip growth requires a balance of lateral propagation and global inhibition of Rho-family GTPase activity. – *Journal of Cell Science* 123: 340-350.
- [7] Kahn, R., Der, C., Bokoch, G. (1992): The RAS superfamily of GTP-binding proteins: guidelines on nomenclature. – *FASEB Journal* 6: 2512-2513.
- [8] Kamthan, A., Chaudhuri, A., Kamthan, M., Datta, A. (2016): Genetically modified (GM) crops: milestones and new advances in crop improvement. – *Theoretical and Applied Genetics* 129: 1639-1655.
- [9] Lee, Y. J., Yang, Z. (2008): Tip growth: signaling in the apical dome. – *Current Opinion in Plant Biology* 11: 662-671.
- [10] Lemichez, E. (2001): Inactivation of *AtRac1* by abscisic acid is essential for stomatal closure. – *Genes & Development* 15: 1808-1816.
- [11] Li, D., Lyu, G., Jiang, Y., Niu, H., Wang, X., Jun, Y. (2019a): Effects of exogenous *RsRHA2b* gene on key enzyme activities and expression of related genes in grain filling

- stage of wheat (*Triticum aestivum* L.). – Applied Ecology and Environmental Research 17: 15073-15086.
- [12] Li, D., Lyu, G., Jiang, Y., Niu, H., Wang, X., Jun, Y. (2019b): Interaction network of TaRHA2b of wheat (*Triticum aestivum* L.) based on high-throughput yeast two-hybrid screening. – Applied Ecology and Environmental Research 17: 13105-13124.
- [13] Li, D., Lyu, G., Lyu, J., Niu, H., Wang, X., Jun, Y. (2019c): Cloning and characterization of a wheat RING finger gene *TaRHA2b* whose expression is up-regulated by ABA treatment. – Applied Ecology and Environmental Research 17: 7495-7510.
- [14] Li, H., Shen, J., Zheng, Z., Lin, Y., Yang, Z. (2001): The Rop GTPase switch controls multiple developmental processes in *Arabidopsis*. – Plant Physiology 126: 670-684.
- [15] Morel, J., Fromentin, J., Blein, J., Simonplais, F., Elmayan, T. (2004): Rac regulation of NtrbohD, the oxidase responsible for the oxidative burst in elicited tobacco cell. – Plant Journal 37: 282-293.
- [16] Poraty-Gavra, L., Zimmermann, P., Haigis, S., Bednarek, P., Hazak, O., Stelmakh, O. R., Sadot, E., Schulze-Lefert, P., Gruissem, W., Yalovsky, S. (2013): The Arabidopsis Rho of plants GTPase AtROP6 functions in developmental and pathogen response pathways. – Plant Physiology 161: 1172-1188.
- [17] Rajakylä, E. K., Vartiainen, M. K. (2014): Rho, nuclear actin, and actin-binding proteins in the regulation of transcription and gene expression. – Small GTPases 5: 1-14.
- [18] Scheler, B., Schnepf, V., Galgenmüller, C., Ranf, S., Huckelhoven, R. (2016): Barley disease susceptibility factor RACB acts in epidermal cell polarity and positioning of the nucleus. – Journal of Experimental Botany 67: 3263-3275.
- [19] Schnepf, V., Vlot, A. C., Kugler, K. G., Huckelhoven, R. (2018): Barley susceptibility factor RACB modulates transcript levels of signalling protein genes in compatible interaction with *Blumeria graminis* f. sp. *hordei*. – Molecular Plant Pathology 19: 393-404.
- [20] Takai, Y., Sasaki, T., Matozaki, T. (2001): Small GTP-binding proteins. – Physiological Reviews 81: 153-208.
- [21] Tao, L., Cheung, A. Y., Wu, H. (2002): Plant Rac-like GTPases are activated by auxin and mediate auxin-responsive gene expression. – The Plant Cell 14: 2745-2760.
- [22] Yang, Z., Watson, J. C. (1993): Molecular cloning and characterization of Rho, a Ras-related small GTP - binding protein from the garden pea. – Proceedings of the National Academy of Sciences of the United States of America 90: 8732-8736.
- [23] Ye, J., Huang, M., Wu, N. (2003): Fertility analysis of the Arabidopsis transformed with antisense rice osRACD gene. – Progress in Natural Science 13: 424-428.
- [24] Yu, O. M., Brown, J. H. (2015): G Protein-coupled receptor and RhoA-stimulated transcriptional responses: links to inflammation, differentiation, and cell proliferation. – Molecular Pharmacology 88: 171-180.
- [25] Zheng, Z. L., Yang, Z. (2000): The ROP GTPase: an emerging signaling switch in plants. – Plant Molecular Biology 44: 1-9.
- [26] Zheng, Z. L., Nafisi, M., Tam, A., Li, H., Crowell, D. N., Chary, S. N., Schroeder, J. I., Shen, J., Yang, Z. (2002): Plasma membrane-associated ROP10 small GTPase is a specific negative regulator of abscisic acid responses in Arabidopsis. – Plant Cell 14: 2787-2797.

RANDOMLY DIRECTED AND LIGHT WINDS EXACERBATE THE EMERGENCE OF LARGE-SCALE CYANOBACTERIAL BLOOM AREAS IN LAKE TAIHU, CHINA

XU, D.¹ – CHEN, H.^{2,3*}

¹*College of Water Conservancy and Hydropower Engineering, Hohai University, No. 1 Xikang Road, Nanjing 210098, China*

²*School of Materials Engineering (School of Environmental Engineering), Changzhou Institute of Industry Technology, Changzhou 213164, China*

³*College of Environment, Hohai University, No. 1 Xikang Road, Nanjing 210098, China*

**Corresponding author
e-mail: huaiminchen@163.com*

(Received 31st Jan 2020; accepted 22nd May 2020)

Abstract. The global warming, decline in wind speed and extreme rainfall have been documented to promote the expansion of bloom area. However, few studies focus on the effect of wind direction on bloom area. The monthly data between May and September from 2011 to 2018 were collected to analyze the relationship between environmental factors and bloom area. Pearson correlation analysis indicated that bloom area was negatively correlated with monthly proportion of consecutive unidirectional wind days (P_{CUWD}) but positively correlated with chlorophyll a (Chl-a). During the whole studied period, wind speeds were lower than 3.1 m/s and Chl-a concentrations were higher than 20 $\mu\text{g/L}$ in all months. In this case, the sufficient *Microcystis* biomass could aggregate into large-scale bloom area only by vertical floating. This could explain why no significant relationship between wind speed and bloom area was found in our study. Except for August, wind speed declined each month which promoted the increase of total phosphorus (TP) and Chl-a concentrations. The low value of P_{CUWD} insufficiently transported cyanobacterial patches from other zones to accumulate with the existing cyanobacterial patches in the downwind area of the lake into dense and small-scale surface scum. In May and June, the decreased P_{CUWD} was conducive to maintain a large-scale bloom area.

Keywords: *climate change, environmental factors, wind direction, vertical aggregation, horizontal transportation*

Introduction

The excessive releases of nitrogen and phosphorus have accelerated eutrophication in lakes and reservoirs, which has induced frequent occurrence of cyanobacterial blooms (Xiao et al., 2018). Cyanobacterial blooms may initiate a chain of serious environmental and ecological events, resulting in blockage of drinking-water supply systems, reduction of water clarity and production of unpleasant odors, etc. (Qin et al., 2010; Zhang et al., 2011). Moreover, some species of cyanobacteria would produce a variety of potent toxins and pose severe risks to human health (Funari and Testai, 2008). Bloom area is one of the common indicators used in water resource management to rank the alert levels of cyanobacterial blooms (Li et al., 2016). In 2017, a large-scale bloom area of 1403 km² occurred in Lake Taihu, which has attracted much attention. However, our knowledge on the formation of large-scale bloom areas is still limited.

Sufficient cyanobacterial biomass is a prerequisite for the formation of cyanobacteria bloom (Reynolds, 2006). Many previous studies have revealed that nutrients play a

leading role in rapid cyanobacterial growth and domination in freshwater ecosystem (Hecky and Kilham, 1988). In addition, climate change is expected to affect the cyanobacterial development throughout their entire annual cycle in both direct and indirect ways (Jeppesen et al., 2014). The warming trend of air temperature affects cyanobacterial biomass by prolonging the duration of the growing season globally (O'Reilly et al., 2015). The change of rainfall intensity and frequency also affects cyanobacterial biomass due to a large amount of nutrients input into water bodies by flushing (Michalak et al., 2013; Reichwaldt and Ghadouani, 2012).

Wind-induced turbulence directly determines the formation and disappearance of cyanobacterial blooms (Wu et al., 2013; Zhu et al., 2014b). Numerous field studies have reported that cyanobacterial blooms in lakes and reservoirs disappear when wind speeds exceeding the critical value, namely 3-4 m/s (Cao et al., 2006; Ma et al., 2015; Moreno-Ostos et al., 2008). When the wind speeds drop below the critical value, cyanobacteria would overcome the weak mixing and float up to the surface to form the blooms. In recent years, there are reported studies showing the global warming could cause the decline of wind speeds (Deng et al., 2018; McVicar et al., 2012). Meanwhile, the decrease of wind speeds could promote the annual mean bloom area in lakes as confirmed by other scholars (Deng et al., 2018; Wu et al., 2015).

Aforementioned researches mainly focused on the effects of climate-induced temperature and precipitation changes on the growth of cyanobacterial biomass, and the decreases of wind speeds on the expansion of bloom areas. In addition to wind speed, wind direction is also an important indicator of wind field. Present studies regarding wind direction are mainly focused on how does it affect the horizontal distributions of cyanobacterial blooms in lakes (Cyr, 2017; Deng et al., 2016). These studies only indicated that cyanobacterial blooms tend to occur in downwind areas of lakes (George and Edwards, 1976). Little attention has been paid to the effect of wind direction on bloom areas.

The cyanobacterial biomass in summer and autumn is much higher than that in spring and winter, which is conducive to the emergence of larger-scale and more serious cyanobacterial blooms (Deng et al., 2014; Shi et al., 2019). The mature blooming stage is usually from May to September in Lake Taihu, when the temperature reaches the optimum temperature for the growth of *Microcystis* (Feng et al., 2018). Elucidation of the responses of bloom area to environmental changes during this period can improve our understanding for better controlling water blooms. In this study, we collected a 8-year data series between May and September from Lake Taihu to examine: (1) temporal variations in the meteorological data, nutrient factors and cyanobacterial biomass, (2) the primary factors affecting cyanobacterial bloom area, and (3) the effect of wind direction on large-scale bloom area.

Materials and methods

Study area

Lake Taihu is a large shallow freshwater lake, which is situated in the southeastern part of Yangtze River Delta in China (30°55'40"–31°32'58" N; 119°52'32"–120°36'10" E). The lake is 68.5 km long from north to south and 34 km wide from east to west with a surface area of 2338 km² (Han et al., 2015; Havens et al., 2016). Its average depth is 1.9 m with a maximum depth of 2.6 m. The water quality of Lake Taihu has been seriously affected by eutrophication and surficial cyanobacterial blooms

due to the large amount of pollutants input from industry, agriculture and tourism activities over the past 3 decades (Li et al., 2014; Wang et al., 2016). It is well-known that Lake Taihu was subjected to a severe cyanobacterial bloom in May 2007, depriving more than 2 million people of drinking water for several days.

Data collection

Meteorological data between May and September from 2011 to 2018 were obtained from Wuxi weather station of National Meteorological Information Center (<http://data.cma.cn>). The monthly meteorological data were calculated from the daily records of air temperature (T_{air}), precipitation (P) and wind speed (WS).

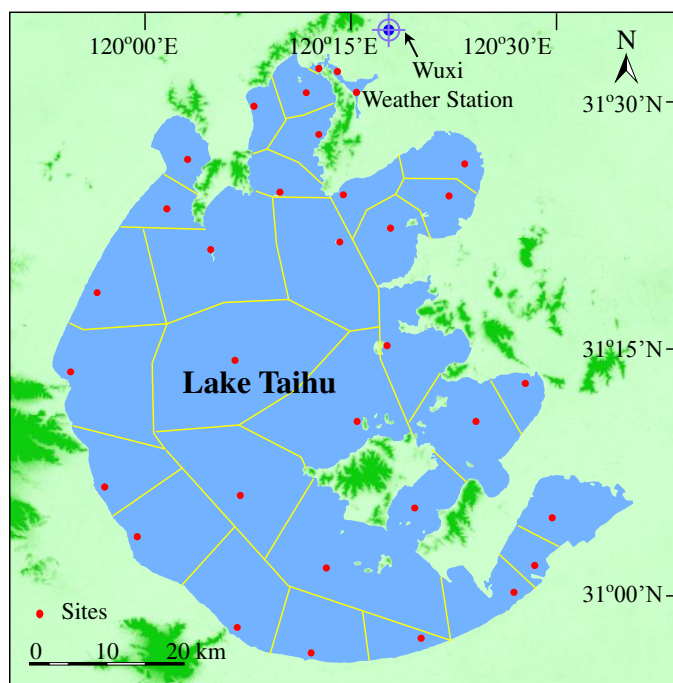


Figure 1. Location of sampling sites and Wuxi weather station in Lake Taihu

Consecutive unidirectional winds days (*CUWD*) indicates a continuous period that the difference between the maximum and minimum wind direction is less than 45° , which is calculated as follows (Eq. 1):

$$CUWD = \text{Count}(x_i : x_j) \text{ If } \text{Max}(x_i : x_j) - \text{Min}(x_i : x_j) \leq 45^\circ \text{ and } j - i \geq 3 \quad (\text{Eq.1})$$

where x_i and x_j are the values of wind direction at day i and j , respectively. In order to measure the length of *CUWD* in a month, the following formula (Eq. 2) is given to calculate the monthly proportion of *CUWD* (P_{CUWD}):

$$P_{CUWD} = \frac{\sum (CUWD_k - 2)}{T} \quad k = 1, 2, \dots, n \quad (\text{Eq.2})$$

where T is the total days in each month.

Monthly total nitrogen (TN), total phosphorus (TP), and chlorophyll a (Chl-a) concentration from 33 sampling sites of Lake Taihu were collected from Taihu Basin Authority of Ministry of Water Resources (<http://www.tba.gov.cn/>) between May and September from 2011 to 2018. The entire lake was divided into 33 sections based on sampling sites using the Tyson polygon method (*Fig. 1*). Then, a weight factor was calculated as the area of each polygon relative to the total area of the lake for each sampling site. Finally, the summation of concentration multiplied with weight factor in each site was defined as monthly concentration of entire lake, in order to address spatial heterogeneity.

Bloom areas were derived from remote sensing images from May to September during 2011-2018, which were obtained from the Lake-Watershed Science Data Center, National Earth System Science Data Sharing Infrastructure, National Science & Technology Infrastructure of China (<http://lake.geodata.cn>). Monthly bloom area is calculated by the average of 5 images selected at 5-day intervals each month. If there was cloudy or rainy weather on that day, the photos before or after a day were used.

Data analysis

Principal components analysis (PCA) were carried out to identify the the role of the various environmental factors contributing to the bloom area. The principal components (PCs) were extracted for eigenvalues that were > 1 . The Kaiser-Meyer-Olkin (KMO) and Bartlett's test were introduced to evaluate the validity of PCA, and a > 0.5 of KMO and significant Bartlett's test were requisite before the PCA. The relationships of monthly bloom areas with environmental factors were analyzed by Pearson correlation coefficient. All statistical analysis were performed by SPSS 19.0 software (IBM, Armonk, NY, USA).

Results

Monthly variations in meteorological data

The temporal variations of meteorological factors in the Lake Taihu from 2011 to 2018 are presented in *Figure 2*. During the whole studied period, monthly air temperature between May and September was higher than 20 °C with a maximum value in July. The changing trend of air temperature from 2011 to 2018 was not obvious. Most of the heaviest precipitation was concentrated in June, and the maximal monthly precipitation of 2015 and 2016 were 711 mm and 607 mm, respectively. The increasing trend for precipitation emerged in September from 2011 to 2018.

Wind speeds declined in May, June, July and September from 2011 to 2018 (*Fig. 2c*). And monthly wind speed was below 3.1 m/s during the whole studied period. The P_{CUWD} exhibited a decline trend in May and June from 2011 to 2018 (*Fig. 2d*). The maximum P_{CUWD} concentrated in summer. Especially, the P_{CUWD} were above 48% in August 2016 and July 2017.

Monthly variations in nutrient, Chl-a and bloom area

TN showed a decreasing trend in May and June from 2011 to 2018 (*Fig. 3a*). The peak values of TP mainly appeared in August, which varied from 0.062 to 0.144 mg/L. TP showed increasing trends in May and July. On the whole, TP raised from 2011 to 2018 (*Fig. 3b*).

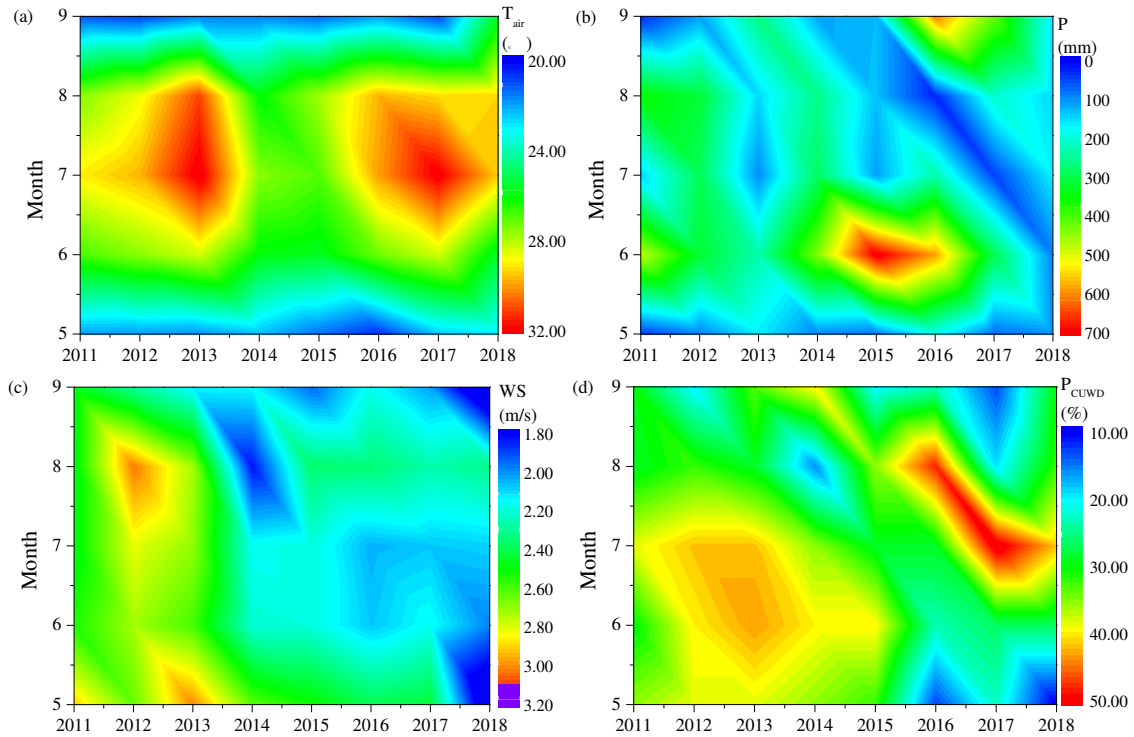


Figure 2. The temporal variations of (a) air temperature (T_{air}), (b) precipitation (P), (c) wind speed (WS) and (d) the month proportion of consecutive unidirectional winds days (P_{CUWD}) between May and September from 2011 to 2018

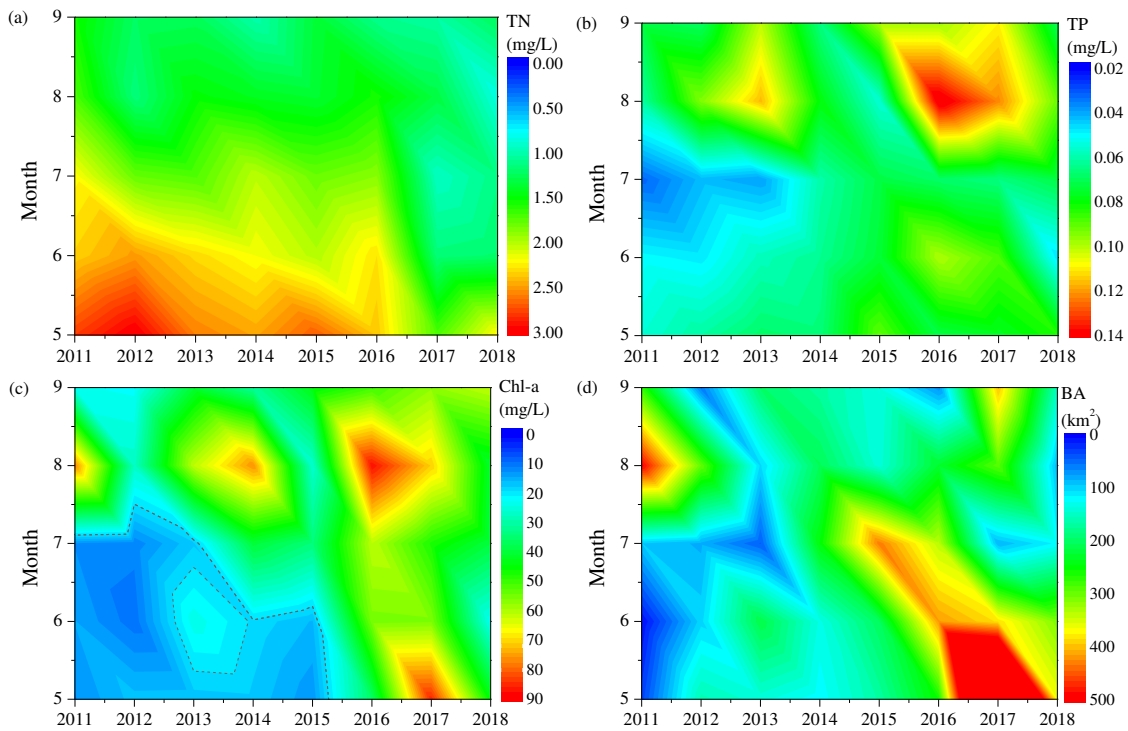


Figure 3. The temporal variations of (a) total nitrogen (TN), (b) total phosphorus (TP), (c) chlorophyll a ($Chl-a$) and (d) bloom area (BA) between May and September from 2011 to 2018

Generally, the Chl-a concentration reached the maximum in August. In some cases, the Chl-a concentration reached 20 µg/L, which was necessary for the formation of water bloom ahead of time, such as in May and June of 2016 and May 2017 with the highest Chl-a concentration reaching 86.2 µg/L (*Fig. 3c*). The increasing trends of Chl-a concentrations were found in May, July and September from 2011 to 2018. Unlike the temporal distribution of Chl-a concentration, the maximum bloom area is more random in temporal distribution. This means the bloom area may not reach the largest area when Chl-a concentration is the highest value (*Fig. 3c, d*). The bloom area showed increasing trends in May and June and decreasing trends in Aug and September during the studied period.

Principle component analysis

The results of KMO and significant Bartlett's test were 0.574 and 0.000, respectively, which demonstrated the validity of PCA approach. The PCA results showed (*Table 1*) that three eigenvalues were higher than one and the three components explained 72.201% of the total variance of the selected environmental parameters. PC1, PC2, and PC3 contributed 37.223%, 20.383% and 14.595% to the total variance, respectively. PCA 1 was mainly positively related to wind speed, P_{CUWD} , and TN, and negatively related to TP and Chl-a. PC2 and PC3 were mainly correlated with air temperature and precipitation, respectively.

Relationship between bloom area and environmental factors

As shown in *Table 2*, the Chl-a concentration was significantly negatively correlated with wind speed ($P < 0.01$), P_{CUWD} ($P < 0.05$) and TN ($P < 0.01$) and positively correlated with TP ($P < 0.01$). There was no significant correlation between Chl-a concentration and air temperature. P_{CUWD} and Chl-a concentration were the significant negative ($P < 0.01$) and positive ($P < 0.01$) factors affecting bloom area, respectively.

Discussion

Previous studies have confirmed that the formation of a surface water bloom is determined by two preconditions, i.e. sufficient biomass of buoyant cyanobacteria and weak hydrodynamics (Paerl and Otten, 2013; Reynolds, 2006). Wu et al. (2015) found that the decline of wind speed had significantly promoted the extension of bloom area from 2000 to 2011. However, our results showed that the monthly bloom area between May to September from 2011 to 2018 was positively correlated with Chl-a concentration ($P < 0.01$), but not with wind speed (*Table 2*). *Microcystis*, one of cyanobacteria species, is the dominant algae with biovolume accounting for > 95% from May to September in Lake Taihu (Chen et al., 2003; Otten and Paerl, 2011). Hence, Chl-a concentration was often used to represent *Microcystis* biomass in the previous field researches (Ding et al., 2012; Wu et al., 2013; Zhu et al., 2014a). Qin et al. (2015) defined Chl-a concentration above 20 µg/L as the visible surface cyanobacterial bloom in Taihu Lake. Our results indicated that most of Chl-a concentrations were higher than 20 µg/L between May and September during the studied period (*Fig. 3c*). Such a large amount of *Microcystis* float up and aggregate on water surface, which is enough to meet the biomass for the bloom formation. Cao et al. (2006) reported that the critical wind speed for bloom formation in Lake Taihu is 3.1 m/s. Wu et al. (2015) determined that

the annual mean wind speed noticeably declined from 2000 to 2011 and ranged from 3.10 to 3.68 m/s. Although wind speed in our study decreased in May, June and July, the wind speeds of all months during the whole studied period were below the 3.1 m/s (Fig. 2c). According to the above results, we can infer that no matter what the wind speed changes from 2011 to 2018, *Microcystis* in our studied months can overcome the wind-induced turbulence and rise to the water surface to form a bloom. Therefore, the correlation between wind speed and bloom area is not significant between May and September from 2011 to 2018.

Table 1. Total variance explained by the principle components during the bloom between May to September from 2011 to 2018 and the component matrix of different variables

	PC1	PC2	PC3
Air temperature	0.124	0.910	0.018
Precipitation	-0.116	0.127	0.955
Wind speed	0.713	0.071	-0.193
P_{CUWD}	0.663	0.561	-0.089
Total nitrogen	0.643	-0.456	0.050
Total phosphorus	-0.725	0.051	-0.160
Chlorophyll a	-0.830	0.229	-0.190
Eigenvalues	2.606	1.427	1.022
% of Variance	37.223	20.383	14.595
Cumulative %	37.223	57.606	72.201

P_{CUWD} : monthly proportion of consecutive unidirectional winds days

Table 2. Pearson correlation coefficients between the monthly bloom area and environmental factors

	T _{air}	P	WS	P_{CUWD}	TN	TP	Chl-a	BA
T _{air}	1							
P	0.091	1						
WS	0.133	-0.120	1					
P_{CUWD}	0.442**	-0.071	0.429**	1				
TN	-0.208	-0.042	0.434**	0.164	1			
TP	-0.084	0.063	-0.227	-0.355*	-0.353*	1		
Chl-a	0.128	-0.009	-0.466**	-0.401*	-0.456**	0.630**	1	
BA	-0.094	0.019	-0.213	-0.448**	-0.078	0.228	0.571**	1

T_{air}: air temperature; P: precipitation; WS: wind speed; P_{CUWD} : monthly proportion of consecutive unidirectional winds days; TN: total nitrogen; TP: total phosphorus; Chl-a: chlorophyll a; BA: bloom area. **P < 0.01; *P < 0.05

Interestingly, wind direction, another important indicator of wind speed, significantly affects the bloom area in this study. Our results illustrated a negative relationship between the bloom area and P_{CUWD} (P < 0.05, Table 2). In order to better understand the influence of wind direction on bloom area, two typical months were selected, i.e. August 2016 and May 2017. The two months showed a big difference in bloom areas but very similar conditions of wind speeds and Chl-a concentrations. Specifically, the

monthly bloom area was 231 km² in Aug 2016 and 917 km² in May 2017, the monthly mean wind speed was 2.35 m/s in Aug 2016 and 2.44 m/s in May 2017, and the Chl-a concentration was 88.1 µg/L in Aug 2016 and 86.2 µg/L in May 2017 (Fig. 3).

The structures of the lake currents are determined by in-out flows and wind. However, the horizontal migration of *Microcystis* is mainly induced by the surface current since *Microcystis* mainly concentrated on the water surface. Wu et al. (2018) indicated that surface current of Lake Taihu was driven by wind, and its entrainment could transfer energy further toward the lake bottom with increasing wind speed. In-out flows mainly contribute to lake currents when wind speed is 0 m/s, but the multiyear mean incidence of 0 m/s in Lake Taihu is only 2.1% (Wu et al., 2013). Thus, impacts of in-out flows on water bloom in Lake Taihu was negligible. The wind field over Lake Taihu is composed of lake-land wind and East Asian monsoon (Wu et al., 2018). The hourly wind speed and direction are shown in Figure 4. Our results showed that wind speed had a diurnal periodic fluctuation, which was typically driven by the lake-land wind. However, the wind direction was generally more stable and did not appear obvious opposite situations between day and night. Lee et al. (2014) also indicated that lake-land breeze circulations were less prevalent in the Taihu lake basin than in lake basins in northern latitudes. Therefore, the calculated daily wind direction did not mask the information of hourly wind direction to some extent in this study.

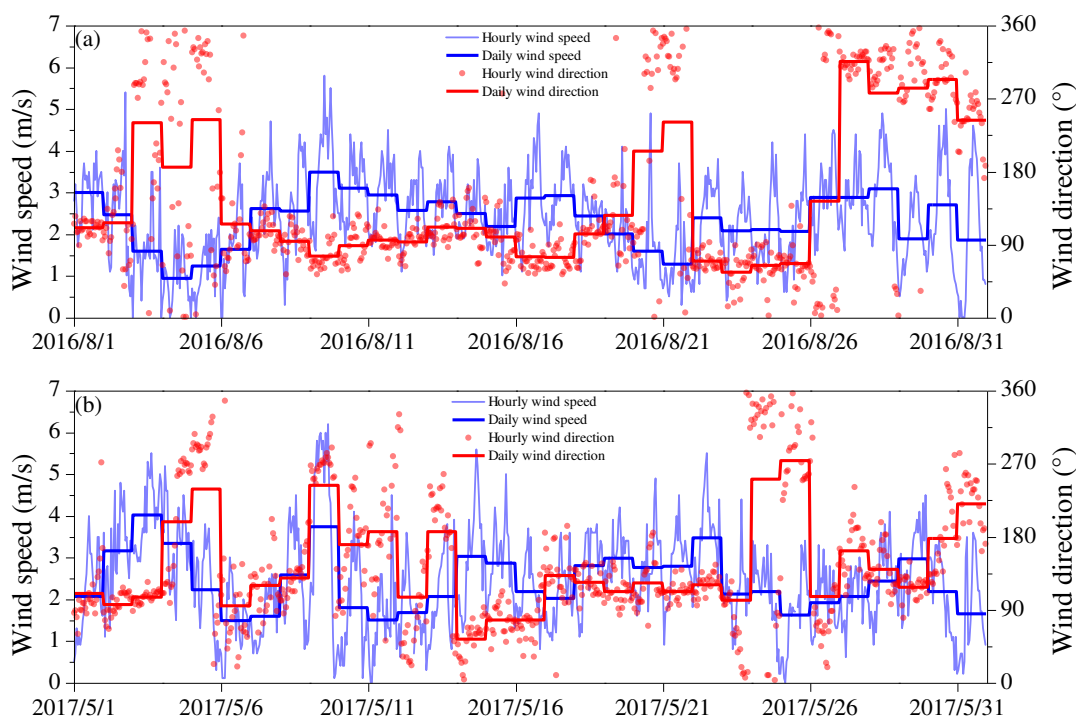


Figure 4. The hourly and daily wind speed and direction in (a) August 2016 and (b) May 2017

The proportion of hourly wind speed lower than 3.1 m/s was 75.5% in August 2016 and 73.1% in May 2017 (Fig. 4). The low wind conditions in two months are favorable for the *Microcystis* to float on water surface. Moreover, the Chl-a concentration was both higher than 20 µg/L in the two months. These means the current *Microcystis* biomass can form water blooms only by vertical migration without horizontal drift

under low wind speed (3.1 m/s) (Cao et al., 2006; Qin et al., 2015). In previous field studies, it was observed that *Microcystis* patches were horizontally transported to downwind zone by wind-driven current under critical wind speed during summer (Bai et al., 2005; Deng et al., 2016; Moreno-Ostos et al., 2009). Meanwhile, positively buoyant *Microcystis* can resist downwelling to accumulate large biomass on the water surface of downwind end of the lake (Cyr, 2017). As shown in *Figure 5*, the bloom area was 625 km² on 5th August, but reduced to 236 km² on 15th August, and then continued to shrink to 62 km² 25th August under the influence of consecutive east winds in 2016. The maximum value of *CUWD* (consecutive unidirectional winds days) in August 2016 was 14 days (*Fig. 4*). Compared with 2017, the bloom covered an area of 1309 km² on 6th May and maintained 1209 km² on 16th May under the effect of widely fluctuating wind directions. Then, after 7 days of unidirectional winds and 2 days of west wind, the bloom area was reduced to 649 km² on 26th May 2017, mostly accumulated in the eastern lake area (*Fig. 5*). The maximum value of *CUWD* in May 2017 was only 7 days (*Fig. 4*). Wu et al. (2010) found that, under the south wind, the Chl-a continuously increased in Meliang Bay and decreased in open water of Lake Taihu. We can infer from above that, under the effect of consecutive unidirectional winds, newly transported *Microcystis* patches from other zones will inevitably converge with the existing cyanobacterial patches in the downwind area of lake to form dense surface scum, resulting in the reduction of bloom area. Hence, the significantly different of bloom area in August 2016 and May 2017 was mainly affected by different wind direction variation patterns. The longer consecutive unidirectional winds days resulted in substantial reduction of bloom area, whereas unstable wind direction was beneficial to the stability of the bloom area.

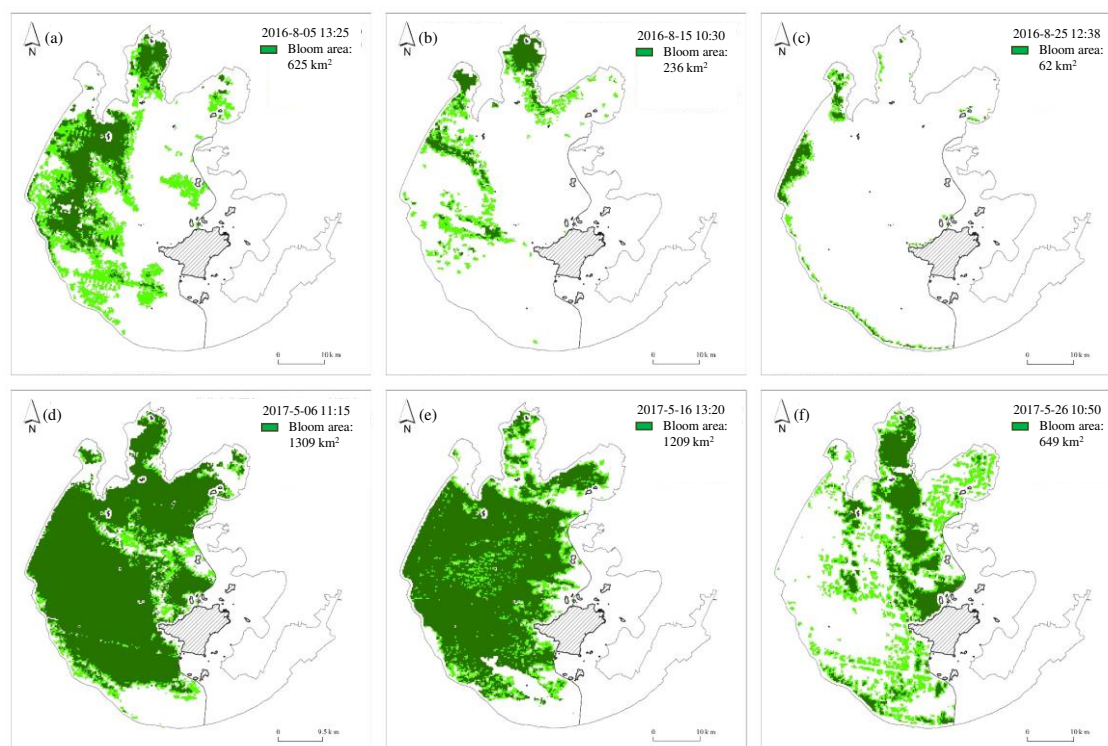


Figure 5. Bloom distribution Taihu on 3 days in (a, b and c) August 2016 and (d, e and f) May 2017, respectively

After the 2007 water crisis in Wuxi, a series of comprehensive measures were conducted to control eutrophication and cyanobacterial bloom in Lake Taihu. The concentration of TN was effectively controlled and showed a noticeable decline in May and June, while the concentration of TP obviously rose in May and July from 2011 to 2018 (Fig. 3a and b). Heavy precipitation above 600 mm both occurred in June 2015 and 2016 (Fig. 2b), and subsequent floods brought a large amount of nutrients input into Lake Taihu. As the floods receded, most phosphorous was gradually deposited into the sediment as particulate form while most nitrogen was discharged away Lake Taihu in dissolved form (Gouze et al., 2008; Zhu et al., 2018). Although decreased wind speed leads to reduce sediment resuspension, *Microcystis* easily float on water surface to obtain sufficient light for growth. The high aggregation of *Microcystis* on water surface, in turn, may promote phosphorus release from the sediment due to the low dissolved oxygen conditions near the bottom (Deng et al., 2018; Tang et al., 2015). These processes were indirectly supported by the positive relationship between Chl-a and TP ($P < 0.01$) and the negative relationship between Chl-a and wind speed ($P < 0.01$, Table 2). Some climate prediction studies suggested that the increase of air temperature and precipitation and decline of wind speed will continue in the Lake Taihu Basin in the future (IPCC, 2013; O'Reilly et al., 2015; Sun and Ding, 2010; Xu and Liu, 2012). Our result also showed the P_{CUWD} decreased in May and June. Correspondingly, the bloom area showed an obvious increasing trend in May and June from 2011 to 2018. However, in July and August, the wind direction is steady and not conducive to the large-scale cyanobacterial bloom (Fig. 2d and 4d; Table 1). Since the wind speed will continue to decrease in the Lake Taihu Basin in the future according to IPCC reports (IPCC, 2013), the lake-land wind with opposite wind directions between day and night will possibly dominate in the wind field in Lake Taihu. Thus, the future wind direction of Lake Taihu will become more unstable, which would be more conducive to the emergence of large-scale cyanobacterial bloom in future. The large-scale cyanobacterial bloom would prevent the light penetration to inhibit the growth of green algae and diatoms below the water surface, thus reducing the phytoplankton biodiversity and aggravating eutrophication in lakes (Janatian et al., 2019; Shi et al., 2018; Xiao et al., 2018).

Conclusion

The obviously declined wind speeds between May and September, except for August, promoted the increases of TP and Chl-a concentrations from 2011 to 2018. During the whole studied period, the wind speeds were below the critical value for bloom formation and enough *Microcystis* biomass could aggregate into large-scale bloom area only by vertical floating. The decrease of wind speed has limited effects on the bloom areas. Randomly directed winds were conducive to maintain large-scale bloom area in May and June, while unidirectional winds could lead to shrink the bloom area in July and August. As the wind speed decreases in the future, the wind direction of Lake Taihu will become more unstable due to the influence of the lake-land wind. Future studies need to consider the impact of lake-land wind on the formation of large-scale cyanobacterial bloom in Lake Taihu.

Acknowledgements. Acknowledgement for the data support from Lake-Watershed Science Data Center, National Earth System Science Data Sharing Infrastructure, National Science & Technology Infrastructure of China (<http://lake.geodata.cn>).

REFERENCES

- [1] Bai, X., Hu, W., Hu, Z., Li, X. (2005): Importation of wind-driven drift of mat-like algae bloom into Meiliang Bay of Taihu Lake in 2004 summer. – *Huanjing Kexue* 26(6): 57-60.
- [2] Cao, H., Kong, F., Luo, L., Shi, X., Yang, Z., Zhang, X., Tao, Y. (2006): Effects of wind and wind-induced waves on vertical phytoplankton distribution and surface blooms of *Microcystis aeruginosa* in Lake Taihu. – *Journal of Freshwater Ecology* 21(2): 231-238.
- [3] Chen, Y., Qin, B., Teubner, K., Dokulil, M. T. (2003): Long-term dynamics of phytoplankton assemblages: *Microcystis*-domination in Lake Taihu, a large shallow lake in China. – *Journal of Plankton Research* 25(4): 445-453.
- [4] Cyr, H. (2017): Winds and the distribution of nearshore phytoplankton in a stratified lake. – *Water Res* 122: 114-127.
- [5] Deng, J., Qin, B., Paerl, H. W., Zhang, Y., Ma, J., Chen, Y. (2014): Earlier and warmer springs increase cyanobacterial (*Microcystis* spp.) blooms in subtropical Lake Taihu, China. – *Freshwater Biology* 59(5): 1076-1085.
- [6] Deng, J., Chen, F., Liu, X., Peng, J., Hu, W. (2016): Horizontal migration of algal patches associated with cyanobacterial blooms in an eutrophic shallow lake. – *Ecological Engineering* 87: 185-193.
- [7] Deng, J. M., Paerl, H. W., Qin, B. Q., Zhang, Y. L., Zhu, G. W., Jeppesen, E., Cai, Y. J., Xu, H. (2018): Climatically-modulated decline in wind speed may strongly affect eutrophication in shallow lakes. – *Science of the Total Environment* 645: 1361-1370.
- [8] Ding, Y., Qin, B., Zhu, G., Wu, T., Wang, Y., Luo, L. (2012): Effects of typhoon Morakot on a large shallow lake ecosystem, Lake Taihu, China. – *Ecohydrology* 5(6): 798-807.
- [9] Feng, T., Wang, C., Wang, P., Qian, J., Wang, X. (2018): How physiological and physical processes contribute to the phenology of cyanobacterial blooms in large shallow lakes: a new Euler-Lagrangian coupled model. – *Water Res* 140: 34-43.
- [10] Funari, E., Testai, E. (2008): Human health risk assessment related to cyanotoxins exposure. – *Critical Reviews in Toxicology* 38(2): 97-125.
- [11] George, D., Edwards, R. (1976): The effect of wind on the distribution of chlorophyll a and crustacean plankton in a shallow eutrophic reservoir. – *Journal of Applied Ecology* 667-690.
- [12] Gouze, E., Raimbault, P., Garcia, N., Bernard, G., Picon, P. (2008): Nutrient and suspended matter discharge by tributaries into the Berre Lagoon (France): the contribution of flood events to the matter budget. – *Comptes Rendus Geoscience* 340(4): 233-244.
- [13] Han, T., Zhang, H., Hu, W., Deng, J., Li, Q., Zhu, G. (2015): Research on self-purification capacity of Lake Taihu. – *Environmental Science and Pollution Research* 22(11): 8201-8215.
- [14] Havens, K., Paerl, H., Phlips, E., Zhu, M., Beaver, J., Srifa, A. (2016): Extreme weather events and climate variability provide a lens to how shallow lakes may respond to climate change. – *Water* 8(6).
- [15] Hecky, R., Kilham, P. (1988): Nutrient limitation of phytoplankton in freshwater and marine environments: a review of recent evidence on the effects of enrichment 1. – *Limnology and Oceanography* 33(4part2): 796-822.
- [16] IPCC (2013): Climate Change 2013. The Physical Science Basis. – In: Stocker, T. F., Qin, D., Plattner, G.-K., Tignor, M., Allen, S. K., Boschung, J., Nauels, A., Xia, Y., Bex, V., Midgley, P. M. (eds.) Working Group 464 I Contribution to the Fifth Assessment Report of the Intergovernmental Panel on Climate Change. Cambridge University Press, Cambridge, UK and New York.

- [17] Janatian, N., Olli, K., Cremona, F., Laas, A., Nõges, P. (2019): Atmospheric stilling offsets the benefits from reduced nutrient loading in a large shallow lake. – *Limnology and Oceanography*. <https://doi.org/10.1002/lno.11342>.
- [18] Jeppesen, E., Meerhoff, M., Davidson, T. A., Trolle, D., Sondergaard, M., Lauridsen, T. L., Beklioglu, M., Brucet, S., Volta, P., Gonzalez-Bergonzoni, I., Nielsen, A. (2014): Climate change impacts on lakes: an integrated ecological perspective based on a multi-faceted approach, with special focus on shallow lakes. – *Journal of Limnology* 73: 88-111.
- [19] Lee, X., Liu, S. D., Xiao, W., Wang, W., Gao, Z. Q., Cao, C., Hu, C., Hu, Z. H., Shen, S. H., Wang, Y. W., Wen, X. F., Xiao, Q. T., Xu, J. P., Yang, J. B., Zhang, M. (2014): The Taihu Eddy flux network an observational program on energy, water, and greenhouse gas fluxes of a large freshwater lake. – *Bulletin of the American Meteorological Society* 95(10): 1583-1594.
- [20] Li, M., Zhu, W., Dai, X., Xiao, M., Appiah-Sefah, G., Nkrumah, P. N. (2014): Size-dependent growth of *Microcystis* colonies in a shallow, hypertrophic lake: use of the RNA-to-total organic carbon ratio. – *Aquatic Ecology* 48(2): 207-217.
- [21] Li, Q., Hu, W., Zhai, S. (2016): Integrative indicator for assessing the alert levels of algal bloom in lakes: Lake Taihu as a case study. – *Environmental Management* 57(1): 237-250.
- [22] Ma, X., Wang, Y., Feng, S., Wang, S. (2015): Vertical migration patterns of different phytoplankton species during a summer bloom in Dianchi Lake, China. – *Environmental Earth Sciences* 74(5): 3805-3814.
- [23] McVicar, T. R., Roderick, M. L., Donohue, R. J., Li, L. T., Van Niel, T. G., Thomas, A., Grieser, J., Jhajharia, D., Himri, Y., Mahowald, N. M., Mescherskaya, A. V., Kruger, A. C., Rehman, S., Dinpashoh, Y. (2012): Global review and synthesis of trends in observed terrestrial near-surface wind speeds: implications for evaporation. – *Journal of Hydrology* 416: 182-205.
- [24] Michalak, A. M., Anderson, E. J., Beletsky, D., Boland, S., Bosch, N. S., Bridgeman, T. B., Chaffin, J. D., Cho, K., Confesor, R., Daloglu, I., DePinto, J. V., Evans, M. A., Fahnenstiel, G. L., He, L., Ho, J. C., Jenkins, L., Johengen, T. H., Kuo, K. C., LaPorte, E., Liu, X., McWilliams, M. R., Moore, M. R., Posselt, D. J., Richards, R. P., Scavia, D., Steiner, A. L., Verhamme, E., Wright, D. M., Zagorski, M. A. (2013): Record-setting algal bloom in Lake Erie caused by agricultural and meteorological trends consistent with expected future conditions. – *Proceedings of the National Academy of Sciences* 110(16): 6448-6452.
- [25] Moreno-Ostos, E., Cruz-Pizarro, L., Basanta, A., George, D. G. (2008): The influence of wind-induced mixing on the vertical distribution of buoyant and sinking phytoplankton species. – *Aquatic Ecology* 43(2): 271-284.
- [26] Moreno-Ostos, E., Cruz-Pizarro, L., Basanta, A., George, D. G. (2009): Spatial heterogeneity of cyanobacteria and diatoms in a thermally stratified canyon-shaped reservoir. – *International Review of Hydrobiology* 94(3): 245-257.
- [27] O'Reilly, C. M., Sharma, S., Gray, D. K., Hampton, S. E., Read, J. S., Rowley, R. J., Schneider, P., Lenters, J. D., McIntyre, P. B., Kraemer, B. M., Weyhenmeyer, G. A., Straile, D., Dong, B., Adrian, R., Allan, M. G., Anneville, O., Arvola, L., Austin, J., Bailey, J. L., Baron, J. S., Brookes, J. D., de Eyto, E., Dokulil, M. T., Hamilton, D. P., Havens, K., Hetherington, A. L., Higgins, S. N., Hook, S., Izmet'eva, L. R., Joehnk, K. D., Kangur, K., Kasprzak, P., Kumagai, M., Kuusisto, E., Leshkevich, G., Livingstone, D. M., MacIntyre, S., May, L., Melack, J. M., Mueller-Navarra, D. C., Naumenko, M., Noges, P., Noges, T., North, R. P., Plisnier, P.-D., Rigosi, A., Rimmer, A., Rogora, M., Rudstam, L. G., Rusak, J. A., Salmaso, N., Samal, N. R., Schindler, D. E., Schladow, S. G., Schmid, M., Schmidt, S. R., Silow, E., Soylu, M. E., Teubner, K., Verburg, P., Voutilainen, A., Watkinson, A., Williamson, C. E., Zhang, G. (2015b): Rapid and highly

- variable warming of lake surface waters around the globe. – *Geophysical Research Letters* 42(24): 10773-10781.
- [28] Otten, T. G., Paerl, H. W. (2011): Phylogenetic inference of colony isolates comprising seasonal *Microcystis* blooms in Lake Taihu, China. – *Microb Ecol* 62(4): 907-918.
- [29] Paerl, H. W., Otten, T. G. (2013): Harmful cyanobacterial blooms: causes, consequences, and controls. – *Microb Ecol* 65(4): 995-1010.
- [30] Qin, B., Zhu, G., Gao, G., Zhang, Y., Li, W., Paerl, H. W., Carmichael, W. W. (2010): A drinking water crisis in Lake Taihu, China: linkage to climatic variability and lake management. – *Environmental Management* 45(1): 105-112.
- [31] Qin, B., Li, W., Zhu, G., Zhang, Y., Wu, T., Gao, G. (2015): Cyanobacterial bloom management through integrated monitoring and forecasting in large shallow eutrophic Lake Taihu (China). – *Journal of Hazardous Materials* 287: 356-363.
- [32] Reichwaldt, E. S., Ghadouani, A. (2012): Effects of rainfall patterns on toxic cyanobacterial blooms in a changing climate: between simplistic scenarios and complex dynamics. – *Water Res* 46(5): 1372-1393.
- [33] Reynolds, C. S. (2006): *The Ecology of Phytoplankton*. – Cambridge University Press, Cambridge.
- [34] Shi, K., Zhang, Y., Zhu, G., Qin, B., Pan, D. (2018): Deteriorating water clarity in shallow waters: evidence from long term MODIS and in-situ observations. – *International Journal of Applied Earth Observation and Geoinformation* 68: 287-297.
- [35] Shi, K., Zhang, Y., Zhang, Y., Li, N., Qin, B., Zhu, G., Zhou, Y. (2019): Phenology of phytoplankton blooms in a trophic lake observed from long-term MODIS data. – *Environmental Science & Technology* 53(5): 2324-2331.
- [36] Sun, Y., Ding, Y. (2010): A projection of future changes in summer precipitation and monsoon in East Asia. – *Science China Earth Sciences* 53(2): 284-300.
- [37] Tang, C., Li, Y., Jiang, P., Yu, Z., Acharya, K. (2015): A coupled modeling approach to predict water quality in Lake Taihu, China: linkage to climate change projections. – *Journal of Freshwater Ecology* 30(1): 59-73.
- [38] Wang, H., Zhang, Z., Liang, D., du, H., Pang, Y., Hu, K., Wang, J. (2016): Separation of wind's influence on harmful cyanobacterial blooms. – *Water Res* 98: 280-292.
- [39] Wu, T., Qin, B., Zhu, G., Luo, L., Ding, Y., Bian, G. (2013): Dynamics of cyanobacterial bloom formation during short-term hydrodynamic fluctuation in a large shallow, eutrophic, and wind-exposed Lake Taihu, China. – *Environmental Science and Pollution Research* 20(12): 8546-8556.
- [40] Wu, T., Qin, B., Brookes, J. D., Shi, K., Zhu, G., Zhu, M., Yan, W., Wang, Z. (2015): The influence of changes in wind patterns on the areal extension of surface cyanobacterial blooms in a large shallow lake in China. – *Science of The Total Environment* 518-519: 24-30.
- [41] Wu, T. F., Qin, B. Q., Ding, W. H., Zhu, G. W., Zhang, Y. L., Gao, G., Xu, H., Li, W., Dong, B. L., Luo, L. C. (2018): Field observation of different wind-induced basin-scale current field dynamics in a large, polymictic, eutrophic lake. – *Journal of Geophysical Research-Oceans* 123(9): 6945-6961.
- [42] Wu, X., Kong, F., Chen, Y., Qian, X., Zhang, L., Yu, Y., Zhang, M., Xing, P. (2010): Horizontal distribution and transport processes of bloom-forming *Microcystis* in a large shallow lake (Taihu, China). – *Limnologica - Ecology and Management of Inland Waters* 40(1): 8-15.
- [43] Xiao, M., Li, M., Reynolds, C. S. (2018): Colony formation in the cyanobacterium *Microcystis*. – *Biological Reviews* 93(3): 1399-1420.
- [44] Xu, Z., Liu, L. (2012): Detection of climate change and projection of future climate change scenarios in Taihu Lake Basin. – *Advances in Science and Technology of Water Resources* 32(1): 1-7.

- [45] Zhang, X., Chen, C., Lin, P., Hou, A., Niu, Z., Wang, J. (2011): Emergency drinking water treatment during source water pollution accidents in China: origin analysis, framework and technologies. – *Environmental Science & Technology* 45(1): 161-167.
- [46] Zhu, M., Paerl, H. W., Zhu, G., Wu, T., Li, W., Shi, K., Zhao, L., Zhang, Y., Qin, B., Caruso, A. M. (2014a): The role of tropical cyclones in stimulating cyanobacterial (*Microcystis* spp.) blooms in hypertrophic Lake Taihu, China. – *Harmful Algae* 39: 310-321.
- [47] Zhu, W., Li, M., Luo, Y., Dai, X., Guo, L., Xiao, M., Huang, J., Tan, X. (2014b): Vertical distribution of *Microcystis* colony size in Lake Taihu: its role in algal blooms. – *Journal of Great Lakes Research* 40(4): 949-955.
- [48] Zhu, W., Tan, Y., Wang, R., Feng, G., Chen, H., Liu, Y., Li, M. (2018): The trend of water quality variation and analysis in typical area of Lake Taihu, 2010-2017. – *Journal of Lake Sciences* 30(2): 296-305.

INTEGRATED MANAGEMENT OF ROOT-KNOT NEMATODE (*MELOIDOGYNE* SPP.) IN CUCUMBER (*CUCUMIS SATIVUS* L.) AND ITS EFFECT ON NEMATODE POPULATION DENSITY, PLANT GROWTH AND YIELD IN SULAIMANI GOVERNORATE, KURDISTAN, IRAQ

ISMAEL, J. H. S.¹ – MAHMOOD, A. A.²

¹*Department of Horticulture, College of Agricultural Engineering Sciences, University of Sulaimani, 46001 Sulaimani, Kurdistan Region, Iraq*

²*Ministry of Agriculture and Water Resources, DAR/Sulaimani, Kurdistan Region, Iraq*

**Corresponding author
e-mail: jalal.ismael@univsul.edu.iq*

(Received 1st Feb 2020; accepted 25th May 2020)

Abstract. Samples of cucumber plants (*Cucumis sativus* L.) were collected from different locations of Bakrajo/Sulaimani governorate, Kurdistan region, Iraq. The collected plants were by stunting and yellowing while the roots with obvious root-knots. For nematode identification two methods were used for nematode identification, Perennial Patterns and PCR, with species-specific primers, showing that there were two species; *Meloidogyne incognita* (Kofoid & White) Chitwood, and *M. javanica* (Treub) Chitwood. An experiment was designed, different methods have been used for controlling RKN, The results showed that after application of the above treatments whether alone or in combination, the minimum numbers of juvenile 2 (J2) were as well as in Nemakey, Humic acid and Chitosan combination treatment to be (66.33) recorded the maximum number after 30 days of application. Plant receiving combined treatments (Nemakey, Humic acid and Chitosan) significantly reduced the number of total nematode population at ($p \leq 0.05$) in comparison to controls. The minimum number of gall formation on the cucumber root system and galling index with the highest percentage of gall decreasing (23.76, 3.1 and 77.00%) were revealed in case of combined treatments (Nemakey, Humic acid and Chitosan). A significant decrease ($p \leq 0.05$) of disease severity percentage was recorded under Humic acid and Chitosan treatment (66%). The combination (Nemakey, Humic acid and Chitosan) also recorded vigorous growth and high yield. This paper is first scientific report about diagnosing and controlling the cucumber root-knot nematode in the region.

Keywords: *Meloidogyne, species-specific primers, PCR, Nemakey, Chitosan, Besto humic, Rugby*

Introduction

Cucumber (*Cucumis sativus* L.) is an economic crop considered as one of the most popular vegetables which ranked the fourth most important vegetable after tomato, cabbage and onion in the world, and belongs to the Cucurbitaceae family (Tatlioglu, 1993; Wehner and Maynard, 2003; Weng and Sun, 2011). It contributes in human health and it has an important role in antioxidant, metabolism processes. It contains lariciresinol, pinosresinol and secoisolariciresinol – 3 lignans which have a strong history of research in connection in reducing risks of several types of cancer including colon, breast, prostate cancer, uterine and ovarian cancers (Maheshwari et al., 2014).

In Iraq, cucumber is an important economical crop to the farmers and is widely cultivated in Summer depending on irrigation throughout the year (Soppe and Saleh, 2012). Estimates cultivated area with cucumber in Sulaimani governorate under protected cultivation is 602 ha.

Plastic house are often used to obtain the highest production per unit area, which attains the most practical method of achieving the objectives of protected agriculture and is considered cropping technique where the environmental condition surrounding the plant is controlled partially/fully as plant need during their period of growth which target get maximum yield and resource saving (Nair and Barche, 2014).

Cucumber in plastic houses is attacked by many diseases that are caused by bacteria, fungi, viruses, and nematodes. But nematodes are the most important and causes yield loses (Agrios, 2005). Plant Parasitic Nematodes (PPNs) contribute limited production of vegetables, estimated annual losses caused by (PPN) more than US\$100 billion worldwide (Bird et al., 2008).

Most of the (PPN) that attack the roots of plants are Root-Knot Nematode (RKN). The most economically important genus which obligates plant roots is the genus *Meloidogyne* distributed worldwide. This genus includes 98 described species (Moens et al., 2009; Jones et al., 2013), and infect more than 2000 to 3000 species including almost all cultivated plants; including vegetables, fruit trees, oil crops, fiber crops, grains crops and leguminous crops. The most well-known species for genus *Meloidogyne* include *Meloidogyne incognita* *M. incognita* (Kofoid & White) Chitwood, *M. javanica* (Treub,) Chitwood, *M. arenaria* (Neal), Chitwood and *M. hapla* Chitwood were of outstanding economic importance because they were responsible for at least 90% of all damage caused by root-knot nematodes (Castagnone-Sereno, 2002; Agrios, 2005).

The symptoms of infected plants by (RKN) appear in both aboveground and underground, aboveground shows poor growth, fewer and small pale green leaves that tend to wilt in warm weather, the quality and production always reduced result of fewer of blossoms and fruits. The underground symptoms appear by information galls on the roots which are two to several times as larger in diameter as the healthy root that impact of absorbing and translocating water and dissolved nutrients to the plants. The nematodes parasitize roots cause injuries, which facilitate entry by other soil-borne pathogens (Agrios, 2005).

Management of (RKN) is often difficult and requires multiple and intensive efforts because they live in the soil and complete their life cycle inter plant tissues (endo-parasitic nature). At the same time, they have wide host ranges, short generation times, and high reproductive rates, however, discourage uses nematicides because they are highly toxic and contribute risk to human and animal health. In additional, they have negative influences on the environment (Abawi and Widmer, 2000; Trudgill and Blok, 2001; Hildalgo-Diaz and Kerry, 2008). Depending on single process to manage (RKN) is not often gives satisfactory results. Thus, a combination of management various techniques (Mesiha, 2019), generally provide acceptable management of (RKNs) and at the same time economic and eco-friendly method e.g. bioagent methods (Dong et al., 2012; Huang, et al., 2016), it is necessary promote techniques that aimed at integrated management to minimize their populations below the economic threshold level (Mitkowski and Abawi, 2003).

Although spread and distribution information of Root-Knot Nematode (RKN) species in Kurdistan especially in Sulaimani area is very little, yet, little work has been done to manage this disease. This work comes into request of the general directorate of Sulaimani Agricultural and Water Resources Office.

Therefore, this study is aimed to identify and diagnose of the nematode(s) *Meloidogyne* species based on morphological characteristics and molecular method which cause root-knot diseases of cucumber plant and its management by using different modern methods.

Materials and methods

Identification and diagnosis of root-knot nematode (RKN)

For identification of the isolated RKNs two different methods were used: morphological characteristics (*Perineal Patterns*) according to (Hartman and Sasser, 1985). Three to four perineal patterns from a single population positioned on the slide with outer side uppermost and a glass cover slide applied (Taylor and Netscher, 1974; Taylor and Sasser, 1978; Eisenback and Hunt, 2009). The second method was *molecular marker*; species-specific primers have been prepared by (Sinacion, Bioscience Co. Iran), for identifying species of *Meloidogyne* as shown in *Table 1*. The extraction of DNA for *Meloidogyne* spp. and DNA amplification have been conducted at the Graduate Studies Laboratory- Animal Science Department – College of Agricultural Sciences, Sulaimani University.

Table 1. Species-specific primers used for Meloidogyne identification

1	2	3	4	5	6	7	8
Primer name	OD (1000 µm)	MW	nmol	Water/tube (µl)	TM	Seq. (5' __ 3')	mer
AS1F	7	6029	38.31	383.15	55.9	CTCTGCCCAATGAGCTGTCC	20
AS1R	7	5410	42.70	426.99	50.3	CTCTGCCCTCACATTAGG	18
AS2F	7	5939	38.90	388.95	53.2	TAGGCAGTAGGTTGTCTGGG	19
AS2R	7	6412	36.03	360.26	52.4	CAGATATCTCTGCATTGGTGC	21
AS3F	6	6188	32.00	319.97	51.8	GGGATGTGTAATGCTCCTG	20
AS3R	7	5917	39.04	390.40	55.9	CCCGCTACACCCCTCAACTTC	20
AS4F	7	6117	37.76	377.57	55.9	GTGAGGATTCAGCTCCCCAG	20
AS4R	7	6968	33.15	331.52	57.1	ACGAGGAACATACTTCTCCGTC	23
AS5F	7	6663	34.67	346.69	53	CCTTAATGTCAACACTAGAGCC	22
AS5R	7	6110	37.81	378.07	49.7	GGCCTTAACCGACAATTAGA	20
AS6F	7	6198	37.27	372.70	55.9	GGTGCGCGATTGAACTGAGC	20
AS6R	7	7008	32.96	329.62	57.1	CAGGCCCTTCAGTGGAACCTATAC	23
AS7F	7	6102	37.86	378.56	53.8	ACGCTAGAATTCGACCCTGG	20
AS7R	7	6136	37.65	376.47	55.9	GGTACCAGAAGCAGCCATGC	20

Molecular method

In this study, species-specific primers have been prepared by (Sinacion, Bioscience Co. Iran), for identifying species of *Meloidogyne* as shown in *Table 1*. The extraction of DNA for *Meloidogyne* spp. and DNA amplification have been conducted at the Graduate Studies Laboratory- Animal Science Department – College of Agricultural Sciences, Sulaimani University.

DNA extraction

DNA of J2s and adult males isolated from soil were extracted by extraction-tray model (Thomas, 1958; Whitehead and Hemming, 1965). The females have been

isolated from root tissue with sharp needle under stereo microscope. Therefore, J2s, males and female were collected with enough water in a tube that obtained by using standard technique (1.5 ml tube), the tube was put in a centrifuge (226R Refrigerated Universal Microcentrifuge, Labnet International Inc.) in 10000 rpm for 3 min in order to precipitate nematodes down to the bottom of the tube, then excess water was removed from the upper part. An amount of 25 mg from the precipitated nematodes was transferred to a slide and 20 μ L of ethanol was added, waited till dry then the precipitate nematodes were powdered by sharp needle under stereo microscope (ST-39 Series, Motic Co, United Kingdom). DNA of RKN was extracted utilizing AccuPrep® Genomic DNA Extraction Kit from (BIONEER) which involved isolation of DNA from mammalian tissue.

Polymerase chain reactions (PCR) amplification

Different primers were used for DNA amplification. The polymerase chain reactions (PCR) were carried out using the extracted RKN DNA as a template. *Table 2* shows preparing different PCR reaction tube volume (25 μ L and 50 μ L) using the following ingredients.

The DNA samples were amplified using primers for two common species in separate PCR reactions. All PCR reactions were carried out in MUTIGENE OptiMAX machine, Labnet International Inc. (PCR Thermal Cycler). Similar PCR programs were used to identify *Meloidogyne* spp. (Powers and Harris, 1993; Zijlstra et al., 2000; Meng et al., 2004; Adam et al., 2007). The program has been changed and different annealing temperatures have been used for amplifying the DNA of the species according to the previous studies.

Table 2. Different ingredients amount used to complete (25 μ L and 50 μ L) of the PCR reaction tube volume

Ingredients	Amount	Unit	Details
Master Mix	7.5, 12.5 and 25	μ L	Including of dATP, dCTP, dGTP, dTTP, Taq DNA polymerase and PCR buffer
Sterilized distilled water	4.5, 7.5, 12.5 and 22	μ L	
Forward primer	1	μ L	
Reverse primer	1	μ L	
DNA extraction	3, 6 and 1	μ L	

Gel electrophoresis

The gel used for electrophoresis (2.5%) was prepared by weighing out 2.5 g of agarose powder and dissolving in 100 ml of 1X TBE buffer (100 ml of 10X TBE was diluted in 900 ml of distilled water). The buffer was heated for 1 min in a microwave oven to dissolve the agarose powder and allowed to cool slightly (55 °C) before adding 6 μ L ethidium bromide. The mixture was poured into the electrophoresis chamber and allowed to cool. Combs with 16 and 13 teeth per row, were placed in the liquid agarose to make 16 and 13 μ L wells. Once the gel had solidified, the electrophoresis chamber was filled with sufficient 1X TBE buffer to cover the gel. Once the gel set, the combs were gently removed to avoid damaging the wells. The wells were loaded with 10 μ L of

the PCR products mixed well with 3 μ L of 6X loading buffer and 6 μ L of DNA ladder was loaded into the left and right corner wells. The electrophoresis was run at 90-95 V and 65 A for 90 min to allow the separation of the fragments. The gel was placed in a UV transilluminator (Enduro™ GDS Touch, Labnet International Inc.). The gel pictures were digitally recorded and named with the sample number. DNA ladder (100-3000 bp) was used to approximate the size of the fragments. The size of bands on the gel was compared to the expected band size of *Meloidogyne* spp.

Plastic house experiment

Site study

The experiment was conducted in the plastic house during July- December 2015 in Bakrajo 2 km far from the College of Agricultural Sciences, Sulamani University. The plastic house is located on a latitude of 35° 32' 03.2" N and longitude 45° 21' 15.7" E. GPS map (76CS, Garmin Co, Taiwan) had been used for this purpose.

Site description and experimental design

This study was conducted in the plastic house during 25th July to 5th December 2015. The total area of the plastic house 450 m² (9 × 50 m). This experiment was carried out by using the Randomized Complete Block Design (RCBD) with three replicates, each replicate consisted of nine plots (experiment units) distributed to three rows, the area of each plot = 2.7 m² (0.85 m × 3.2 m), the distance between plots was 1 m within one replicate, while 2 m was used between replicates, four pathways extend parallel to an along plastic house, the width of each pathway was 0.70 m. The soil of the plastic house was naturally infected by RKN (*Meloidogyne* spp) and soil samples (1 kg) have been taken randomly prior the applying of the treatments for the chemical and physical analysis at the soil department laboratory/Sulaimani Agricultural Research Center. For watering the plants, dripping system was used. Another one kg of soil sample/plot was taken before and after applying treatments within three periods (10, 20 and 30 days of applying the treatments (100 g of soil was taken for each experimental unit (plot)). For preparing seedling of cucumber cv. Naseem F1, seeds were sown in a special place near the plastic house. After 10 days, the seedlings reached to appropriate length (2-3 leaves stage) were transplanted to the permanent place in the plastic house, all needed agricultural processes have been conducted for all plots and treatments.

The physical and chemical properties of the greenhouse soil

Physical and chemical soil analysis of the greenhouse soil prior treatments was conducted at the Sulaimani Applied Agricultural Research Center-Department of Soil and Water Resource/GDAWR, Ministry of Agriculture and Water Resources, KRG, Iraq (Table 3).

Table 3. Some physical and chemical properties of the greenhouse soil before applying the treatments

Soil texture	EC dsm ⁻¹	PH	Total N %	Available P (ppm)	Exch. K ⁺ ppm	Exch. Na ⁺ meq/L	Soluble Ca ²⁺ meq/L	Soluble Mg ²⁺ meq/L	Cl ⁻ meq/L	% O.M	% CaCO ₃	HCO ₃	CO ₃ ⁼
Clay loam	0.18	7.5	0.11	9.25	333.100	74.93	1.8	0.7	0.2	1.3	20	1.9	0

The treatments

In the plastic house, different chemicals and organic substrates were used alone and in combinations as follows:

1. Nemakey 1.5 ml/m² (The soil sprayed thrice, 10 days interval was between the spraying 12-8-2015, 22-8-2015 and 1-9-2015, respectively).
2. Besto Humic (Humic acid 15%) 1.5 ml/m² (the soil sprayed thrice, 10 days interval was between the spraying 12-8-2015, 22-8-2015 and 1-9-2015, respectively).
3. Chitosan (2%) 1 g/500 ml water (C₆H₁₂O₄)n Assay 98% (The foliar sprayed twice, 10 days interval was between the spraying 26-8-2015 and 6-9-2015, respectively).
4. Nemakey 1.5 ml/m² + Besto Humic (Humic acid 15%) 1.5 ml/m².
5. Nemakey 1.5 ml/m² + Chitosan (2%) 1 g/500 ml water.
6. Besto Humic (Humic acid 15%) 1.5 ml/m² + Chitosan (2%) 1 g/500 ml water.
7. Nemakey 1.5 ml/m² + Besto Humic (Humic acid 15%) 1.5 ml/m² + Chitosan (2%) 1 g/500 ml water.
8. Rugby® 100 ME 1.6 ml/m² chemical nematicide (positive control) (reference treatment) (The soil sprayed thrice, 10 days interval was between the spraying 12-8-2015, 22-8-2015 and 1-9-, respectively).

The manufacturers of the chemical as in *Table 4* (all the chemicals were purchased from the local market).

RKN population density

One kg soil at the depth of 20-30 cm was collected from each plot and treatment, and mixed thoroughly, 100 g of this soil was taken at 12-8-2015 in order to calculate the no. of nematodes (J2) after applying the treatments, the process repeated for 10, 20 and 30 days. In order to isolate nematodes from the subsample soil (100 g) modified extraction-tray method was used according to (Thomas, 1958; Whitehead and Hemming, 1965), which the soil was placed on a double layer of paper towel (kitchen paper) supported by a metal buckle and placed over the extraction tray. Water was gently added to the tray until the soil was completely wet and then left for 48 h so that the nematodes would be washed down. counting dish digital hand counter and light stereo microscope (ST-39 Series, Motic Co. United Kingdom) 4× magnifications have been used to calculate the nematodes (Atamian et al., 2012; Bonuke, 2013).

Reproduction factor (Rf)

The purpose of Reproduction factor (Rf) was to evaluate the effect of the different treatments on the population densities of the nematodes, if the recorded number was at least more than one, this means that the treatment had bad effect on the decreasing of the nematode population, while if the number was less than one, this means an excellent effect of the treatment was produced on the nematode densities. For calculating Rf the following equation was used (Timper et al., 2006; Lima et al., 2009).

$$\text{Reproduction factor (Rf)} = \frac{\text{Final population of the nematodes (Pf)}}{\text{Initial population (Pi)}} \quad (\text{Eq.1})$$

Table 4. The organic and chemical substrates were used in plastic house experiment

No.	Trade name	Active ingredient	Manufacturer
1.	Nemakey	Organic	Merkez Anadolu Kimya Sanayi Co., Turkey
2.	Besto humic	Humic acid (15%)	Organik Tarim Market Co., Turkey
3.	Chitosan (98%)	N- acetyl- glucosamine*	Xi'an Lyphar Biotechnology Co., Ltd., China
4.	Rugby® 100 ME	Cadosaphos	FMC corporation, Agricultural Products Group, Philadelphia, Pennsylvania, USA

Root galling index (RGI)

120 days after transplanting cucumber plant cv. Naseem F1 to permanent place, the plants were carefully uprooted from the soil in each plot and washed in running tap water to remove the adhering soil particles. After that the galls were removed from the root systems in each plant in order to calculate the number of the galls. From each plot 10 plants have been taken. For root gall index evaluating standard scale has been used as described by Taylor and Sasser (1978) shown in *Table 5*, for calculating disease severity and gall index the equations below has been used according to Zewain (2014), the percentage of gall decreasing also has been calculated equations (Kesba and Al-Shalaby, 2008).

$$\text{Disease severity (\%)} = \frac{\Sigma (\text{No.of galled plants} \times \text{its galling degree})}{\text{Total galled plant no.} \times \text{highest galling degree}} \times 100 \quad (\text{Eq.2})$$

$$\text{Gall index} = \frac{\Sigma (\text{No.of galled plants} \times \text{its galling degree})}{\text{Total galled plant}} \quad (\text{Eq.3})$$

$$\text{Gall reduction (\%)} = \frac{(\text{Control 2}) - \text{Treatment}}{(\text{Control 2})} \times 100 \quad (\text{Eq.4})$$

Table 5. Standard scale of Root-knot index

Root-knot index	Number of galls/root system
0	0
1	1-2
2	3-10
3	11-30
4	31-100
5	> 100

Plant growth and yield parameters

For calculating each parameter 10 plants have been used from each experimental unit (plot), for vegetative system; plant height (cm), stem diameter (cm), no. of nodes/plant, no. of leaves/plant, fresh weight (gm/plant), % of dry weight of vegetative parts and leaf area (cm²) have been measured. For root system; root length (cm), at the end of the seasons, the root system was extracted manually for the representative plants, then main root length (cm) was measured from the crown zone to its farthest point using the metric tape, and fresh and dry root weights (gm/plant) have been calculated. Leaf chlorophyll (9 leaves of each 10 plants randomly selected) (Romero et al., 2012), Leaf chlorophyll

intensity (SPAD unit) (Konica-Minolta, Osaka, Japan) (Coste et al., 2010), and leaf NPK content also calculated. For yield parameters; no. of aborted flowers/plant, no. of setting flowers/plant, fresh weight of fruits (gm/kg), diameter and length of fruits and moisture content, vegetative ratio (w/w), and finally the % of increased yield has been calculated for each treatment. The followings are the formula of the measured and calculated growth and yield parameters.

$$\text{Dry vegetative parts weight (\%)} = \frac{\text{Dry weight (g)}}{\text{Fresh weight}} \times 100 \quad (\text{Van De Sande - Bakhuyzen, 1928}) \quad (\text{Eq.5})$$

$$\text{Fruit moisture content (\%)} = \frac{\text{Fresh fruit weight} - \text{Dry fruit weight}}{\text{Fresh fruit weight}} \times 100 \quad (\text{FAO, 2013}) \quad (\text{Eq.6})$$

$$\text{Vegetative/fruit ratio (w/w) (\%)} = \frac{\text{Fresh plant weight (vegetative part)}}{\text{Total harvested fruit (total yield)}} \times 100 \quad (\text{Eq.7})$$

$$\text{Percentage of increased yield (\%)} = \frac{\text{Yield (weight) of a treatment} - \text{Yield (weight) of control}}{\text{Yield (weight) of control}} \times 100 \quad (\text{Hasabo and Noweer, 2005}) \quad (\text{Eq.8})$$

Statistical analysis

Randomized Complete Block Design (RCBD) was used in this study, the treatments repeated thrice (three replicates) (Crotty et al., 2009; Machado et al., 2014), the data were analyzed using XLSTAT program version 7.5 (XLSTAT, 2004). For the comparisons between means, Least Significant Difference (LSD) at the probability level of 5% was used (Williams and Abdi, 2010; Chapuis-Lardy et al., 2015).

Results

Identification and descriptions of isolated Root-Knot Nematodes (RKNs)

One of the most important purposes of this study was to identify and put light on RKN *Meloidogyne* species present in the galls of the infected cucumber cv. Naseem F1 roots which was grown in the plastic house Bakrajo region. During isolation process the females of RKN from infected cucumber roots under stereo microscope, two species have been recorded *Meloidogyne incognita* and *Meloidogyne javanica* (Fig. 1A, B, C). The mature females of *M. incognita* under stereo microscope have a spherical shaped body, short projecting neck and white color (Fig. 1A, B).

Morphological characteristics (perineal patterns)

The perineal patterns observed under light microscope (Fig. 2A) very closely resembled to the descriptions of *M. incognita* which typically high with square-like dorsal arch. Lateral field weakly demarcated by breaks and forked striae. Striae were distinct and wavy. Dorsal striae smooth, closely placed wavy to zigzag that appear the dorsal and ventral striae are interrupted and forked at the lateral line.

Molecular identification

Accurate identification of RKN was obtained using molecular characteristics. Specific primers of *M. incognita* and *M. javanica* were used to amplify DNA fragment for all sample tested including J2s, males and females of *Meloidogyne* obtained from

plastic house. The extracted DNA was visualized using Agarose gel and then the concentration of DNA was tested by Nanodrop 2000C device.

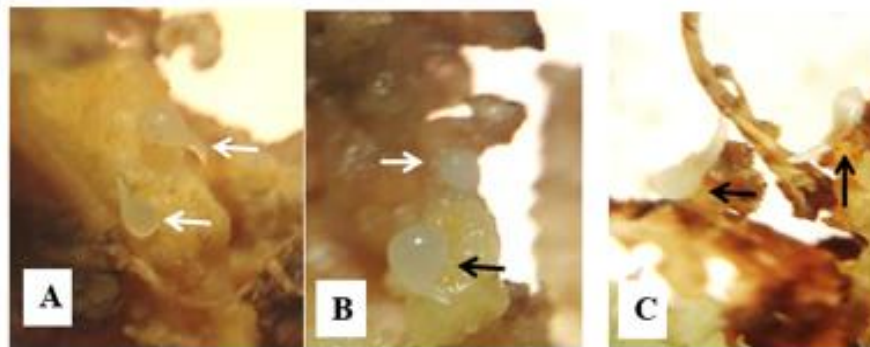


Figure 1. Stereo microscope photograph of female *M. incognita* (A), (B) and female of *M. javanica* (C) from infected cucumber root tissue (galls)

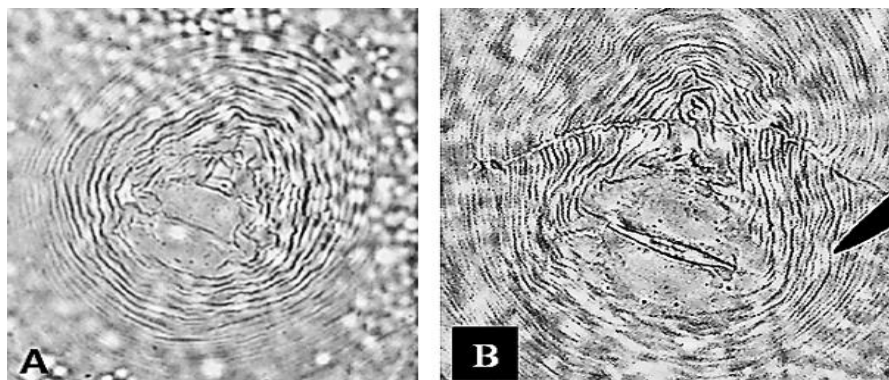


Figure 2. Perineal pattern of (A) *M. ingonita* and (B) *M. javanica* under light stereomicroscope (Binocular Digital Compound Microscope (X400))

The procedure of DNA amplification has been performed six times and all pair primers were set up according to the annealing temperature for first and second times that mentioned by the manufacture company (Sinacion, Bioscience Co. Iran). The DNA samples were run again with all seven primers. They were set up according to the denaturation and annealing temperature conducted by previous studies. The ingredients amount of PCR reaction tube volume (25 μ L and 50 μ L) has been changed in every time.

Significant result of DNA amplification was able to be obtained using annealing temperature of 49 $^{\circ}$ C and 50 μ L of the PCR reaction volume. Master mix, sterilized distilled water, forward primer, reverse primer and DNA extraction were 25, 22, 1, 1 and 1 μ L in size respectively when tested on agarose gel (Figs. 3A, B and 4A, B).

The fail in obtaining positive result for both species using, AS2F AS2R, AS4F AS4R, AS5F AS5R primers might be refer to the specificity of these two races of nematodes used in the current study, being different from those used for other investigations. The occurrence of genetic mutation and the variation due to mating system in the species might made the primers to misplacing the flanked region of target fragment on the species DNA.

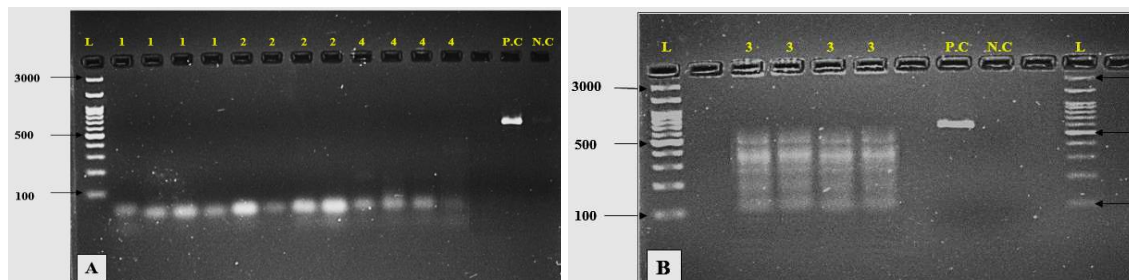


Figure 3. PCR products. (A) Extracts DNA amplified using species-specific primers name of primer 1 = AS1, 2 = AS2, 4 = AS4 (1200 bp, 1350 bp, and 955 bp) respectively for *M. incognita*, L = DNA ladder (100-3000 bp). P.C = Positive control, N.C = Negative control. (B) Extracts DNA amplified using species-specific primers 3 = AS3F AS3R (399 bp), for *M. incognita*. L = DNA ladder (100-3000 bp). P.C = Positive control, N.C = Negative control

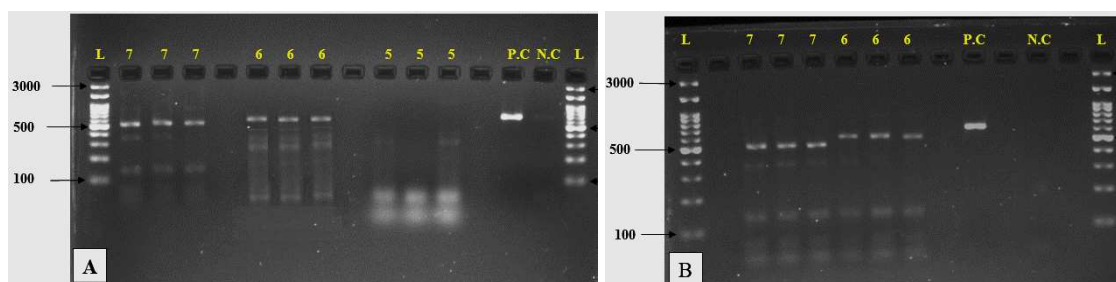


Figure 4. PCR products. (A) Extracts DNA amplified using species-specific primers name of primer 7 = AS7, 6 = AS6, 5 = AS5 (517 bp, 670 bp and 1650 bp) respectively for *M. javanica*, L = DNA ladder (100 bp-3000 bp), P.C = Positive control, N.C = Negative control. (B) Extracts DNA amplified using species-specific primers 7 = AS7, 6 = AS6 respectively for *M. javanica*, L = DNA ladder (100 bp-3000 bp), P.C = Positive control, N.C = Negative control

Nematode population density

Population densities of root-knot nematode (Juveniles 2) in the soil before and after treatment application

In the plastic house experiment, different treatments have been used in order to investigate their influence on controlling the population densities and numbers of juveniles 2 before applying the treatments and after 10, 20 and 30 days. *Table 6* shows that at ($p \leq 0.05$) the minimum numbers of juveniles 2 (J2s) were in using (Nemakey, Humic acid and Chitosan) which was (66.33), while maximum number of nematodes observed control (1 + 2). There were significant differences among the treatments ($P \leq 0.05$) with the control 2. On the other hand, there were no significant differences among the treatments and control after 10 and 20 days (*Table 6*).

The present results show an approach to control *M. incognita* and *M. javanica* in cucumber plant using modern methods and more active for controlling *Meloidogyne* which are safer than nematicides. These results should be considered during designing an integrated pest management program for RKN or other nematode pathogens in cucumber and other crops.

Table 6. Effect of different treatments for controlling root-knot nematode (*Meloidogyne* spp.) on population densities (Juveniles 2)

Treatment sets	Population densities (Juveniles 2) / 100 g soil			
	One day before applying treatments (Pi)	After 10 days of application	After 20 days of application	After 30 days of application (Pf)
Nemakey	163.00 a	234.33 ab	192.33 a	151.66 c
Besto Humic	152.00 a	321.66 ab	222.00 a	140.00 cd
Chitosan	123.66 a	296.00 ab	310.33 a	301.66 b
Nemakey + Besto Humic	180.66 a	312.66 ab	348.00 a	125.33 cd
Nemakey + Chitosan	208.66 a	264.33 ab	330.00 a	133.00 cd
Besto Humic + Chitosan	141.66 a	235.33 ab	447.00 a	120.66 cd
Nemakey + Besto Humic + Chitosan	133.33 a	227.66 ab	508.00 a	66.33 d
Rugby® 100 ME (Control 1)	148.33 a	150.00 b	197.00 a	363.33 b
Water (Control 2)	159.66 a	592.66 a	503.66 a	587.33 a
LSD (P ≤ 0.05)	101.75 u	403.02 u	464.49 u	80.87 u

Data followed by the same letter in each column are not significantly different according to (LSD) test

Reproduction factor (Rf)

Data in *Figure 5* illustrate the impact of Nemakey, Humic acid and Chitosan alone or in combination comparing to Rugby® 100 ME as (Control 1) and spray water only as (control 2) on reducing *Meloidogyne incognita* and *Meloidogyne javanica* which infected cucumber plant (cv. Naseem F1) under plastic house condition. Results revealed that reproduction factor (Rf) was adversely affected by treatments whether alone or in combination. It has been considered the best significant treatment was the three combinations (Nemakey + Best Humic (Humic acid 15%) + Chitosan), the Rf value was less than one, although the others (Nemakey, Humic acid 15%), (Nemakey + Chitosan 2%), and (Humic acid 15% + Chitosan 2%) treatments gave the same result, that mean the efficacy of the treatments in reducing the population density of root-knot nematodes (Juveniles 2).

Root gall index (RGI)

Data presented in *Table 7* show the influence of various treatments Nemakey, Humic acid and Chitosan whether alone or in combination in comparison to with controls (1 + 2) against RKN which infected cucumber crop (cv. Naseem F1) under plastic house condition.

Results indicated that all treatments obviously were reducing the number of gall index, disease severity percentage and percentage of gall decreasing (reduction). Among the treatments, combined treatments (Nemakey + Humic acid + Chitosan) recorded (23.76) of reducing the gall formation on the root system of the cucumber crop and achieved higher significant ($p \leq 0.05$) with the highest percentage of gall decreasing (77.00%) and found to be the most effective, since it reduced the number of galls more than those of the other treatment, followed by (Nemakey + Chitosan) (39.40 galls/plant, 61.86% reduction) and (Humic acid + Chitosan) (39.90 galls/plant, 61.38% reduction) as compared with controls (69.46, 103.33, 32.77% reduction) respectively. Minimum galling index (3.1) was recorded when the cucumber plant was treated with combined of (Nemakey, Humic acid and Chitosan) followed by (Humic acid and chitosan) (3.3) and (Nemakey and Humic acid) (3.6) as compared to controls (4.1 and 4.5) respectively.

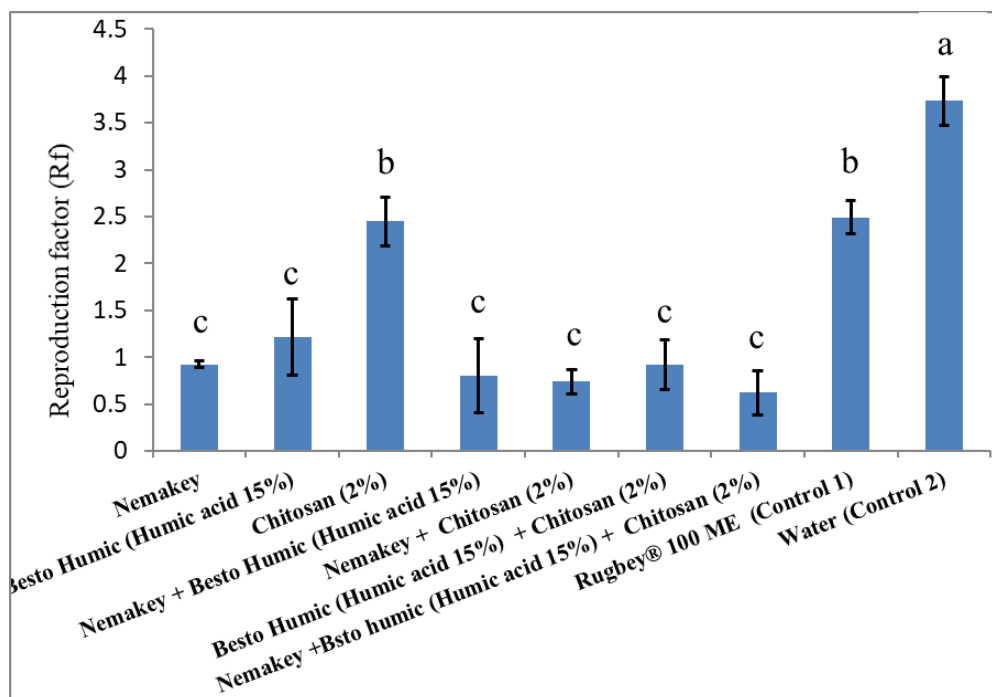


Figure 5. Effect of different methods of controlling on reproduction factor (Rf) after 30 days of calculating the no. of the nematodes (juveniles 2). The bars refer to the standard errors (SE) at ($P \leq 0.05$)

Table 7. Effect of different treatments for controlling root-knot nematode (*Meloidogyne* spp.) on number of galls in the roots of cucumber (cv. Naseem F1)

Treatment sets	Means of number of the galls		Gall index	Disease severity %	% of gall decreasing
	Average 0.05	Average 0.01			
Nemakey	50.29 bc	50.29 bc	3.70	74.00	51.33
Besto Humic	50.86 bc	50.86 bc	3.90	97.50	50.77
Chitosan	54.23 bc	54.23 bc	3.90	78.00	47.51
Nemakey + Besto Humic	40.40 cd	40.40 bc	3.60	90.00	60.90
Nemakey + Chitosan	39.40 cd	39.40 bc	3.70	93.00	61.86
Besto Humic + Chitosan	39.90 cd	39.90 bc	3.30	66.00	61.38
Nemakey + Besto Humic + Chitosan	23.76 d	23.76 c	3.10	77.50	77.00
Rugby® 100 ME (Control 1)	69.46 b	69.46 ab	4.10	82.00	32.77
Water (Control 2)	103.33 a	103.33 a	4.50	90.00	–
LSD ($P \leq 0.05$)	25.83	35.58			

Data are means of three replicates. Data followed by the same letter in each column are not significantly different according to (LSD) test

Disease severity as shown in *Table 7* appeared that lowest disease severity percentage was recorded by (Humic acid and Chitosan) which achieved higher significant ($p \leq 0.05$) effect followed by Chitosan and (Nemakey, Humic acid and Chitosan) compared to controls.

Plant growth characters

Vegetative system

The combination treatments Nemakey, Humic acid and Chitosan significantly ($P \leq 0.05$) affected against RKN (*M. incognita* and *M. javanica*) infection as compared to controls treatment. The reduction in growth parameters was indirectly proportional with the number of root-galls, so all screened treatments obviously improved plant growth parameters with various degrees (Table 8). Among tested treatments, plant receiving combined treatments (Nemakey, Humic acid and Chitosan) improved significantly in plant height and stem diameter with percentage of the dry weight of the vegetable parts amounted to 2.97 cm, 8.46 cm and 11.67% respectively which exceeded all other treatments as compared to control 2 (1.61 cm, 6.17 cm, and 28.07%). On the other hand, it was also observed that there were significant differences among the treatments ($p \leq 0.05$) with control 2, while with Rugby® 100 ME (Conventional chemical control) or (Reference treatment), they were relatively had least effect. However, there were no significant differences among the treatments (with themselves).

Table 8. Effect of different treatments for controlling root-knot nematode (*Meloidogyne* spp.) on some plant growth parameters (vegetative parts) of cucumber (cv. Naseem F1)

Treatment sets	Plant height (cm)	Stem diameter (cm)	No. of nodes. plant ⁻¹	No. of leaves. plant ⁻¹	Fresh plant weight (vegetable parts) g plant ⁻¹	Leaf area. plant ⁻¹ (cm ²)	% of the dry weight of the vegetative parts
Nemakey	2.40 bc	7.68 bc	40.66 de	26.66 b	293.30 cde	250.68 ab	20.87
Besto Humic (Humic acid)	2.38 c	7.86 b	39.66 e	26.66 b	271.66 de	241.13 abc	20.91
Chitosan	2.35 c	7.14 c	39.33 e	26.66 b	274.90 de	215.07 cd	16.10
Nemakey + Besto Humic (Humic acid)	2.63 b	7.84 b	48.66 b	40.00 a	424.90 ab	261.52 ab	13.96
Nemakey + Chitosan	2.46 bc	7.67 bc	42.66 cd	40.00 a	339.43 bcd	231.68 bcd	17.03
Besto Humic (Humic acid) + Chitosan	2.52 bc	7.76 b	44.66 c	39.66 a	386.33 abc	239.30 abc	14.67
Nemakey + Besto Humic (Humic acid) + Chitosan	2.97 a	8.46 a	50.33 ab	42.33 a	480.20 a	266.99 a	11.67
Rugby® 100 ME (Control 1)	2.07 d	7.47 bc	34.33 f	26.66 b	229.96 e	231.12 bcd	24.05
Water (Control 2)	1.61 e	6.17 d	27.66 g	21.00 b	201.30 e	196.63 d	28.07
LSD ($P \leq 0.05$)	0.24 u	0.56 u	2.17 u	7.91 u	96.75 u	35.09 u	–

Data are means of three replicates. Data followed by the same letter in each column are not significantly different according to (LSD) test

Results in Table 8 show that other parameters of cucumber plant growth i.e. no. of nodes/plant and plant weight (vegetative parts) / plant (g) were significantly affected by applying these combined treatments (Nemakey, Humic acid and Chitosan) and (Nemakey and Humic acid) when compared to controls. On the other hand, there was less effect of the treatments on the no. of leaves. plant⁻¹ if compared to the controls (1 + 2).

Root system

There was a significant ($P \leq 0.05$) difference between the root length (cm), fresh root weight (g) and dried root weight (g) of the cucumber plants treated with different treatments of Nemakey, Humic acid, Chitosan and controls as shown in Table 9.

All the treatments were significantly ($P \leq 0.05$) different on the basis of root length. Maximum root length (32.08, 31.74 and 31.70 cm) was recorded in the plants treated with combined (Nemakey, Humic acid and Chitosan), (Nemakey and Humic acid) and

(Nemakey and Chitosan) respectively, as compared to controls. Minimum root length (25.38 cm) was recorded in untreated control plants (control 2). It can also be noticed that (Nemakey + Humic acid and Chitosan), (Humic acid and Chitosan) and (Nemakey and Humic acid) were significantly showed reasonable improved fresh root weight and ranked the most active one among the other treatments for increasing fresh root weight of cucumber plant with 34.86, 30.60 and 30.76 g, respectively as compared to control 2, which was recorded 24.46 g. In the meanwhile, plants receiving combined treatments (Nemakey, Humic acid and Chitosan) and (Humic acid and Chitosan) gave significantly better dried root weight than all other treatments, followed by (Nemakey and, Humic acid) as compared to control.

Table 9. Effect of different treatments for controlling root-knot nematode (*Meloidogyne* spp.) on some plant growth (root parts) of cucumber (cv. Naseem F1)

Treatment sets	Root length (cm)	Fresh root weight (g)	Dried root weight (g)
Nemakey	30.24 abc	29.13 b	11.31 d
Besto Humic (Humic acid)	29.86 abc	29.03 b	12.91 cd
Chitosan	27.19 bcd	28.70 bc	11.76 d
Nemakey + Besto Humic (Humic acid)	31.74 a	30.76 ab	14.23 bc
Nemakey + Chitosan	31.70 a	29.43 b	11.81 d
Besto Humic (Humic acid) + Chitosan	31.58 ab	30.60 ab	15.07 ab
Nemakey + Besto Humic (Humic acid) + Chitosan	32.08 a	34.86 a	16.46 a
Rugby® 100 ME (Conventional chemical control) (Control 1)	27.10 cd	27.50 bc	8.22 e
Water (Control 2)	25.38 d	24.46 c	6.06 f
LSD ($P \leq 0.05$)	4.42	4.29	1.72

Data are means of three replicates. Data followed by the same letter in each column are not significantly different according to (LSD) test

Leaf chlorophyll and NPK content

Data as shown in *Table 10* summarize the description of the leaf chlorophyll intensity, the percentage of the Nitrogen (N), Phosphor (P) and potassium (K) content in the cucumber leaves as influenced by *M. incognita* and *M. javanica* infection and effect of applying Nemakey, Humic acid and Chitosan whether alone or in combination in comparison to Rugby® 100 ME (Conventional chemical control) (Reference treatment) or (control 1) and spray water only (control 2) in the greenhouse conditions.

Obviously, results in *Table 11* show that two of them significantly ($P \leq 0.05$) achieved high percentage increase the values of the leaf chlorophyll intensity and percentage of the Nitrogen (N) content in the leaf per (1 g) of dry weight under study. Among tested treatments, the combined treatments (Nemakey, Humic acid and Chitosan), (Nemakey and Humic acid) and (Humic acid and Chitosan) were superior in values of leaf chlorophyll (38.19, 35.35 and 35.10) respectively as compared to controls (28.77 and 24.79), whereas the combined treatments (Nemakey, Humic acid and Chitosan) and (Nemakey and Humic acid) ranked the first increase in percentage values of Nitrogen (N) content in the leaf per (1 g) of dry weight which were 4.86 and 4.83% respectively as compared to control 2 (4.56%). In addition, it is appeared that there were no significant differences among the treatments and controls on percentage of the

Phosphor (P) and Potassium (K) content in the leaves (Table 8), and chlorosis of the leaves (pale green tended to yellowing).

Table 10. Effect of different treatments for controlling root-knot nematode (*Meloidogyne* spp.) on some plant content of cucumber (cv. Naseem F1)

Treatment sets	Leaf chlorophyll intensity (SPAD unit)	% of the nitrogen (N) content in the leaf dry weight	% of the phosphor (P) content in the leaf dry weight	% of the potassium (K) content in the leaf dry weight
Nemakey	31.58 cd	4.66 abc	0.36 a	3.08 a
Besto Humic (Humic acid)	31.54 cd	4.60 bcd	0.35 a	3.23 a
Chitosan	31.50 cd	4.40 d	0.32 a	3.22 a
Nemakey + Besto Humic (Humic acid)	35.35 ab	4.83 ab	0.31 a	3.43 a
Nemakey + Chitosan	33.64 bc	4.66 abc	0.36 a	3.46 a
Besto Humic (Humic acid) + Chitosan	35.10 ab	4.70 abc	0.35 a	3.22 a
Nemakey + Besto Humic (Humic acid) + Chitosan	38.19 a	4.86 a	0.36 a	3.23 a
Rugby® 100 ME (Control 1)	28.77 d	4.73 abc	0.35 a	3.24 a
Water (Control 2)	24.79 e	4.56 cd	0.32 a	3.14 a
LSD ($P \leq 0.05$)	3.33 u	0.25 u	0.07 u	0.51 u

Data are means of three replicates. Data followed by the same letter in each column are not significantly different according to (LSD) test

Table 11. Effect of different treatments for controlling root-knot nematode (*Meloidogyne* spp.) of cucumber (cv. Naseem F1) on floral growth

Treatment sets	No. of flowers. plant ⁻¹	No. of aborted flowers. plant ⁻¹	No. of fruit. plant ⁻¹	Fresh weight of fruit. plant ⁻¹ (g)	Diameter of fruits (cm)	Length of fruits (cm)	Fruit moisture content (%)	Vegetative/fruit ratio (W/W)
Nemakey	41.00 cd	48.93 ab	33.00 cd	85.76 ab	2.77 a	13.70 ab	97.59 a	29.91
Besto Humic (Humic acid)	44.00 ab	50.50 a	34.66 bcd	86.70 ab	2.79 a	13.27 bc	97.52 a	32.44
Chitosan	41.00 cd	47.66 ab	31.66 d	84.75 ab	2.68 a	13.12 bc	97.63 a	32.05
Nemakey + Besto Humic (Humic acid)	44.66 a	46.06 ab	36.66 ab	92.05 a	2.78 a	14.31 a	97.41 a	21.71
Nemakey + Chitosan	43.00 abc	44.80 ab	36.33 abc	88.81 ab	2.69 a	13.39 b	97.69 a	27.91
Besto Humic (Humic acid) + Chitosan	42.00 bcd	46.13 ab	36.66 ab	89.27 ab	2.76 a	13.51 ab	97.66 a	23.20
Nemakey + Besto Humic (Humic acid) + Chitosan	43.66 ab	42.96 b	38.66 a	92.70 a	2.75 a	14.30 a	97.47 a	19.36
Rugby® 100 ME (Control 1)	39.66 de	51.23 a	27.00 e	84.77 ab	2.66 a	13.52 ab	97.49 a	36.51
Water (Control 2)	38.00 e	51.00 a	24.00 e	80.74 b	1.70 b	12.50 c	96.15 b	44.08
LSD ($P \leq 0.05$)	2.49 u	7.21 u	3.53 u	10.67 u	0.14 u	0.85 u	0.64 u	–

Data are means of three replicates. Data followed by the same letter in each column are not significantly different according to (LSD) test

Plant yield parameters

Floral growth

Data in Table 9 elicit the impact of Nemakey, Humic acid and Chitosan in comparison with Rugby® 100 ME (Conventional chemical control)(control 1) and water spray (control 2) on RKN, *M. incognita* and *M. javanica* infection and the consequent effect on plant yield parameters of cucumber plant under plastic house conditions. The highest and significant ($P \leq 0.05$) number of flowers per plant was recorded (44.66) when plant received the combined treatments (Nemakey and Humic acid) as compared to controls (39.66 and 38.00) respectively. Meanwhile, combined

treatments (Nemakey, Humic acid and Chitosan) significantly were the highest effective on reduction number of aborted flowers per plant and increasing number of fruit. plant⁻¹ which recorded (42.96 and 38.66) respectively as compared to controls. In addition, the fresh weight of fruit (g) per plant and length of fruits (cm) in (Nemakey and Humic acid) and (Nemakey, Humic acid, Chitosan) combined treatments recorded significantly higher than those recorded in the other treatments as compared to controls. Whereas no significant differences were found in diameter of fruits (cm) and percentage of fruit moisture content among the treatments with themselves but at the same time there were significant effects among those treatments in comparison to control 2. In addition, the vegetative / Fruit ratio (W/W) was influenced by treatment with (Nemakey, Humic acid and Chitosan) that produced significantly result with least value than the other treatments and recorded (19.36), followed by (Nemakey, Humic acid) and (Humic acid and Chitosan) were (21.71 and 23.20) respectively as compared to control 1.

Yield growth

Table 12 shows the effect of each of Nemakey, Humic acid and Chitosan alone or in combination on early yield, total yield and percentage of yield increasing of cucumber plant which influence by infection of RKN *M. incognita* and *M. javanica* under plastic house condition. In spite of no significant differences were found among treatments with controls in early yield, but among the three combined treatments, one of them recorded the highest value as compared to controls. Meanwhile, the higher and significant marketable total yields and percentage of yield increasing obtained in combination treatments (Nemakey, Humic acid and Chitosan) and (Nemakey, Humic acid) which recorded (6.36 and 6.29%) and (167.22 and 164.28%), respectively as compared to controls (4.19 and 2.38%).

Table 12. Effect of different treatments for controlling root-knot nematode (*Meloidogyne* spp.) of cucumber (cv. Naseem F1) on yield

Treatment sets	Early yield (kg. plant ⁻¹)	Total yield (kg. plant ⁻¹)	% of yield increasing
Nemakey	0.70 ab	4.76 bc	100.00
Besto Humic (Humic acid)	0.72 ab	4.87 abc	104.62
Chitosan	0.87 ab	4.48 c	88.23
Nemakey + Besto Humic (Humic acid)	1.00 ab	6.29 ab	164.28
Nemakey + Chitosan	0.99 ab	4.96 abc	108.40
Besto Humic (Humic acid) + Chitosan	1.09 ab	5.38 abc	126.05
Nemakey + Besto Humic (Humic acid) + Chitosan	1.27 a	6.36 a	167.22
Rugby® 100 ME (Control 1)	0.89 ab	4.19 c	76.05
Water (Control 2)	0.42 b	2.38 d	–
LSD (P ≤ 0.05)	0.79 u	1.52 u	–

Data are means of three replicates. Data followed by the same letter in each column are not significantly different according to (LSD) test

Discussion

Depending on the morphological characteristic (perineal patterns), it has been revealed that there were two species of root-knot nematodes, described and recorded as *Meloidogyne incognita* and *M. javanica* (Whitehead, 1968; Esser et al., 1976). The two species usually accompanied with many vegetable and non-vegetable plant, previous

studies showed the same results (Taylor and Sasser, 1978; Moens et al., 2009). On the other hand, these two species were found in a mixed population as mentioned by (Marahatta et al., 2012; Kayani et al., 2013). when explained perineal pattern of *M. incognita*. Whereas, the perineal patterns for *M. javanica* was typical with a rounded to flattened dorsal arch and conspicuous lateral lines that clearly separated the dorsal and ventral regions of the patterns (Fig. 2A, B). Same notation observed by Eisenback et al. (1985), Sen and Chatterjee (2007), Bohra (2011) For confirmation of the diagnosing and identification of the nematodes molecular markers have been used, by applying specific- species primers. The concentration and purity of DNA extraction for 25 mg of J2s, males and females of *M. incognita* and *M. javanica* were 69.4 ng/ μ L and 2.52 purity respectively when measured by using NanoDrop 2000C device. Different programs and annealing temperature were followed to amplify the specific DNA position of both species (*Meloidogyne incognita* and *Meloidogyne javanica*. The procedure of DNA amplification has been performed six times and all pair primers were set up according to the annealing temperature for first and second times that mentioned by the manufacture company (Sinacion, Bioscience Co. Iran). Our result was agreed with the outcome of other researchers) according to Zijlstra et al. (2000), Dong et al. (2001), Devran et al. (2009), Mwesige (2013), Toumi et al. (2014), Chanmalee (2014), Zhuran et al. (2014), Temple et al. (2015), Kemei et al. (2015), Ye et al. (2015), Agenbag (2016) and Aydinli and Mennan (2016) who used these species-specific primers for diagnosing both species of *Meloidogyne* by molecular characteristics.

In the plastic house experiment, different treatments have been used in order to investigate their influence on controlling the population densities and numbers of juveniles 2 before applying the treatments and after 10, 20 and 30 days. The present results show an approach to control *M. incognita* and *M. javanica* in cucumber plant using modern methods and more active for controlling *Meloidogyne* which are safer than nematicides. These results should be considered during designing an integrated pest management program for RKN or other nematode pathogens in cucumber and other crops.

The reduction of RKNs population in combination (Nemakey, humic acid and Chitosan) could be attributed to Nemakey extracts compounds (marigold, sesame, thyme, etc.), this extract contains Allelopathic compounds such as alpha-terthienyl which produced by plants as secondary metabolites that have significant effects on the activity of nematodes and were thought to be toxins and act as nematicidal action affected on reducing population densities. These finding completely agreed with the previous studies when they used these extracts in their researches (Visser and Vythftingam, 1959; Tsay et al., 2004; Ibrahim et al., 2006; Kong et al., 2007; Krueger et al., 2007; Elbadri and Yassin, 2010; Hooks et al., 2010). The effect of Nemakey was appeared after 30 days of application, this time agreed with the manufacturer product (Nemakey) who mentioned the effecting time of Nemakey is between 25-35 days. On the other hand, Humic acid also reduced nematode population due to improving the nutrient availability and impact on other important chemical, biological, and physical properties of soils, this conclusion in agreement with (Khaled and Fawy, 2011; Fahramand et al., 2014). It was also observed that the efficiency of Humic acid increased when it applied in combination, these outcomes were in comport with those investigation of (Saravanapriya and Subramanian, 2007; Gondal et al., 2014; El-Sherif et al., 2015). At the same time Chitosan also played its role during increasing cytosolic Ca^{2+} , activation of MAP-kinases, oxidative burst, callus apposition, increase in pathogen-

related proteins (PRP), phenolic acid synthesis, phytoalexin accumulation, hypersensitive response (HR) proteinase inhibitors and lignin synthesis subsequently enhance the defense of the cucumber plant to RKN infections and decreasing nematode population densities (Hadwiger, 2013; Malerba and Cerana, 2016). Results revealed that reproduction factor (Rf) was adversely affected by treatments whether alone or in combination. Plants which received combined treatments (Nemakey, Humic acid and Chitosan) and (Nemakey and Chitosan) significantly ($p \leq 0.05$) dominated other treatments in reducing number of total nematode population (pf) as compared to controls. It is worthy to observe that Nemakey's compound as a nematicide ranked first in diminishing nematode final population with Humic acid and Chitosan which they have the important role for the decreasing nematode population in the soil as shown in *Table 6* subsequently it has role of reducing the (Rf) value. This conclusion is approved by many previous studies when they used Humic acid or Chitosan whether alone or in a combination with other treatments (Elmiligy and Norton, 1973; Kesba and Al-Shalaby, 2008; Khalil and Badawy, 2012; Dina et al., 2013; El-Sayed and Mahdy, 2015; El-Sherif et al., 2015; Mota and dos Santos, 2016).

As the organic fertilizer and nematicide, Nemakey has been newly manufactured by the Turkish Merkez Anadolu Kimya Sanayi Company. In fact, during reconsideration the references, it could not be found any researches in this field whether applied it alone or in combination to control RKN, so we could not compare our results with the results of previous studies, but depend on its compounds (marigold, sesame, thyme, organic acid oils, free natural amino acids) we could compare our results with the results of other researchers who they used these components in their researches.

All the treatments had significantly reduced the root galls, gall index, disease severity and percentage of gall decrease as compared to controls, a great variability was observed in nematode development and reproduction. Good efficacy of Nemakey, Humic acid and plant protector Chitosan found to be the most effective in reducing the root galls, gall index and disease severity and percentage of gall decreasing endorsing the plant growth parameters. Chitosan show good effect in reducing RKN due to developed systemic acquired resistance (SAR) in cucumber plants. This result agrees with Hadwiger (2013), Malerba and Cerana (2016) and Mota and dos Santos (2016). Nemakey affected on RKN due to its potential killing nematodes at all of its stages of life. Nemakey destroys nematode eggs and creates an unfriendly environment in the soil, which complicate reproduction and proliferation of plant parasitic nematodes in addition to its activity as a bio-stimulant product to promote the production of main and secondary roots (<http://www.merkezanadolu.com.tr/nemakey-e0f>), the present results in agreement with other studies (Husain et al., 1984; Swamy et al., 1995; Krueger et al., 2007; Abd-Elgawad and Omer, 1995; Ibrahim et al., 2006; Natarajan et al., 2006). Humic acid has role in reducing number of galls. The present results were in agreement with the findings that reported by Kesba and Al-Shalaby (2008) and Saravanapriya and Subramanian (2005). It was observed that the chemical nematicide Rugby® 100 ME had lower effect on reducing number of galls, this outcome came to an agreement with another study (Safdar et al., 2013).

In the present study, effect of the essential oils and extract Nemakey's compounds which are mixture of different compound made more than one mechanism of action exist. Some of the recently proposed hypotheses concerning mechanisms of action of essential oils include denaturation of proteins, inhibition of enzyme action, and interference with electron flow in the respiratory chain, or with ADP phosphorylation

(Abd-Elgawad and Omer, 1995). On the other hand, Humic acid has been reported to improve root development and plant growth (Adani et al., 1998). This finding is in agreement with earlier observations made by many scientists who confirmed that Nemakey's compound enhanced the growth parameters of tomato plant (Natarajan et al., 2006).

Using Humic acid through soil might be more helpful in enhancing the plant growth under RKN infection (Gondal et al., 2014), so applied Humic acid stimulation cucumber plant growth parameters through increasing cell division, as well as optimizing uptake of nutrients and water (El-Sherif et al., 2015) as compared to controls due to their effect on the reducing by its influences on the nematode infecundity (nematode population) subsequently decreasing the root galls as compared to controls.

The present results were in agreement with the findings that reported by Kesba and El-Beltagi (2012) in grape rootstocks, Gondal et al. (2014) in potato plant and Dina et al. (2013) improved plant growth parameters of sugar-beet against nematode infection. On the other hand Chitosan was very effective against the RKN under plastic house conditions (Malerba and Cerana, 2016) so it has been used in this experiment as a powerful elicitor than a direct antimicrobial or toxic agent, therefore it had important role to increase plant parameter due to promote elicitation and signaling to systemic acquired resistance (SAR) subsequently protective mechanisms activation in plant tissues inhibited the growth of RKN (Dörnenburg and Knorr, 1997; Heil, 1999; Neto et al., 2005; Strange, 2006; Choudhary et al., 2007; Badawy and Rabea, 2011; Zargar et al., 2015), these results in agreement with the results of others researcher who used chitosan in their studies (Zinov'eva et al., 1999; Kloepper et al., 2004; Khalil and Badawy, 2012; El-Sayed and Mahdy, 2015).

There was a correlation between root growth parameters and nematode infestations, Kankam and Adomako (2014) also pointed to the same fact. The present study showed that Nemakey compounds, Humic acid and Chitosan compounds enhanced the cucumber root growth to a different extent over the controls. This finding is in agreement with earlier observations made by many scientists who confirmed that Nemakey's compound, Humic acid and Chitosan in a combination stimulated the development of the growth in root system (Radwan et al., 2012); Dina et al., 2013; Gondal, et al., 2014; Khalil and Badawy, 2012; El-Sayed and Mahdy, 2015).

It is appeared that there were no significant differences among the treatments and controls on percentage of the Phosphor (P) and Potassium (K) content in the leaves, chlorosis (pale green tended to yellowing) this result also mentioned by Olsen (2011), Karssen and Moens (2006) and Mitkowski and Abawi (2003). In fact, leaves chlorosis not only caused by the low availability of mineral nutrient in soil but also to the impaired translocation of nutrients in plants infested by RKN that is able to damage and to block the vascular system of host plants similar results were obtained by Ogaraku (2007) on cowpea plants, therefore leaf chlorophyll intensity in cucumber plants was influenced by the higher and lower level of RKN as reported by Amin and Abd El-Wanis (2014). The leaf chlorophyll and Nitrogen (N) content have the important role for increasing process of photosynthesis and increasing crop yield, the present results were in agreement with the findings that reported by Hao and Papadopoulos (1999) and Yang et al. (2009) who recorded the same result in cucumber plant.

A positive correlation has noticed between treatments and cucumber floral parameters, therefore all screened treatments whether alone or in combination obviously improved plant floral growth due to effect on inhibition nematodes population directly

or indirectly (*Tables 8 and 9*) and improved crop yield quality and quantity during increasing vegetative growth of cucumber, subsequently increasing number of flowers and decreasing number of aborted flowers per plant, this finding is in agreement with Polthanee and Yamazaki (1996), Elbadri and Yassin (2010), Arncon et al. (2006), Shafeek et al. (2016) and Malerba and Cerana (2016).

The early and total yield reductions were often directly related to the RKN levels in the soil table (4.2) and the environmental stresses imposed upon the plant during crop growth. In general, the more presence of root-knot suggests a potentially serious problem, so at very high levels the RKN significantly affect plant health especially the roots function; stabilization of the plant, ability of the absorption and root secretions (the healthy plant root usually secretes various compounds involved phenolic compounds, complex saturas, simple saturas and growth hormones) therefore it indirectly influence on significantly marketable yield as reported also by Noling (1999). So, treating cucumber plant with Nemakey, Humic acid and Chitosan improve total yield and percentage of yield increasing, as mentioned by many researchers in their studies (Arancon et al., 2006 on pepper plant; Saravanapriya and Subramanian, 2007; Amin and Abd El-Wanis, 2014; Shafeek et al., 2016).

Conclusion

It is concluded from the results that based on the morphological and molecular characteristics in the current study, two species of *Meloidogyne* RKN were diagnosed as; *Meloidogyne incognita* (Kofoid & White) Chitwood, and *M. javanica* (Treub) Chitwood which are common in green or plastic houses at Bakrajo district. The combination of treatments (Nemakey, Humic acid and Chitosan) gave the best results in the majority of studied parameters followed by (Nemakey and Humic acid) and (Humic acid, Chitosan) which gave better results after the three combined treatment for controlling RKN. From this study revealed that these improved the health of cucumber plants and increased the nitrogen content in the leaves (*Tables 3 and 10*). More studies need to be conducted to obtain detail surveying and investigation about other species which might be accompanied with vegetable crops especially cucumber. We recommend using other methods like biological control as a complementary of integrated disease management (IDM). It was recommended studying some botanical nematicide like garlic, rosemary and mints.

REFERENCES

- [1] Abawi, G. S., Widmer, T. L. (2000): Impact of soil health management practices on soilborne pathogens, nematodes and root diseases of vegetable crops. – *Applied Soil Ecology* 15: 37-47.
- [2] Abd-Elgawad, M. M., Omer, E. A. (1995): Effect of essential oils of some medicinal plants on phytonematodes. – *Anzeiger für Schädlingskunde, Pflanzenschutz, Umweltschutz* 68: 82-84.
- [3] Adam, M., Phillips, M., Blok, V. (2007): Molecular diagnostic key for identification of single juveniles of seven common and economically important species of root-knot nematode (*Meloidogyne* Spp.). – *Plant Pathology* 56: 190-197.
- [4] Adani, F., Genevini, P., Zaccheo, P., Zocchi, G. (1998): The effect of commercial humic acid on tomato plant growth and mineral nutrition. – *Journal of Plant Nutrition* 21: 561-575.

- [5] Agenbag, M. (2016): Identification and reproduction potential of South African *Meloidogyne* species. – Magister Scientiae, Environmental Sciences, Potchefstroom Campus of the North-West University.
- [6] Agrios, G. N. (2005): Plant Pathology. Fifth Ed. – Elsevier Academic Press, New York.
- [7] Amin, A. W., Abd El-Wanis, M. (2014): Protecting cucumber against root-knot nematode, *Meloidogyne Incognita* using grafting onto resistant cucurbit rootstocks and interplanted *Tagetes* Spp. as an alternative to Cadusafos nematicide under protected plastic house conditions. – Middle East Journal of Agriculture Research 3: 167-175.
- [8] Arancon, N. Q., Edwards, C. A., Lee, S., Byrne, R. (2006): Effects of humic acids from vermicomposts on plant growth. – European Journal of Soil Biology 42: 65-69.
- [9] Atamian, H. S., Roberts, P. A., Kaloshian, I. (2012): High and low throughput screens with root-knot nematodes *Meloidogyne* spp.– Journal of Visualized Experiments 61: 1-5.
- [10] Aydinli, G., Mennan, S. (2016): Identification of root-knot nematodes (*Meloidogyne* spp.) from greenhouses in the Middle Black Sea region of Turkey. – Turkish Journal of Zoology 40: 675-685.
- [11] Badawy, M. E. I., Rabea, E. I. (2011): A biopolymer chitosan and its derivatives as promising antimicrobial agents against plant pathogens and their applications in crop protection. – International Journal of Carbohydrate Chemistry 2011(Special issue): 1-29.
- [12] Bird, D. M., Opperman, C. H., Williamson, V. M. (2008): Plant Infection by Root-Knot Nematode. – In: Berg, R. H., Taylor, C. G. (eds.) Cell Biology of Plant Nematode Parasitism. Plant Cell Monographs. Springer Science & Business Media, Berlin Heidelberg, pp. 1-13.
- [13] Bohra, P. (2011): Pictorial Handbook on Plant and Soil Nematodes of Rajasthan. – Zoological Survey of India, Kolkata.
- [14] Bonuke, N. S. (2013): Incidence, prevalence and management of root-knot nematodes (*Meloidogyne* spp.) on selected indigenous leafy vegetables in Kisii and Trans-Mara Counties, Kenya. – Master of Science, Plant Pathology, Kenyatta University, Kenya.
- [15] Castagnone-Sereno, P. (2002): Genetic variability in parthenogenetic root-knot nematodes, *Meloidogyne* spp., and their ability to overcome plant resistance genes. – Nematology 4: 605-608.
- [16] Chanmalee, T. (2014): Variation of root-knot nematode infecting chili in Thailand. – Master of Science, Agricultural Biotechnology, Kasetsart University, Thailand.
- [17] Chapuis-Lardy, L., Diakhaté, S., Djigal, D., Ba, A. O., Dick, R. P., Sembéne, P. M., Masse, D. (2015): Potential of Sahelian native shrub materials to suppress the spiral nematode *Helicotylenchus dihystera*. – Journal of Nematology 47: 214-217.
- [18] Choudhary, D. K., Prakash, A., Johri, B. N. (2007): Induced systemic resistance (ISR) in plants: mechanism of action. – Indian Journal of Microbiology 47: 289-297.
- [19] Coste, S., Baraloto, C., Leroy, C., Marcon, É., Renaud, A., Richardson, A. D., Roggy, J.-C., Schimann, H., Uddling, J., Hérault, B. (2010): Assessing foliar chlorophyll contents with the SPAD-502 Chlorophyll meter: a calibration test with thirteen tree species of tropical rainforest in French Guiana. – Annals of Forest Science 67: 607-607.
- [20] Crotty, F., Adl, S. M., Clegg, C. D., Blackshaw, R. P., Murray, P. J. (2009): Investigating soil food webs - tracking the translocation of C-13 and N-15 through microbial interactions within the soil. – Journal of Nematology 41: 321-322.
- [21] Devran, Z., Söğüt, M. A. (2009): Distribution and identification of root-knot nematodes from Turkey. – Journal of Nematology 41: 128-133.
- [22] Dina, S. S. I., Nour El-Deen, A. H., Khalil, A. E., Fatma, A. M. M (2013): Induction of systemic resistance in sugar-beet infected with *Meloidogyne incognita* by humic acid, hydrogen peroxide, thiamine and two amino acids. – Egypt J. Agro-nematol 12: 22-41.
- [23] Dong, K., Dean, R. A., Fortnum, B. A., Lewis, S. A. (2001): Development of PCR primers to identify species of root-knot nematodes: *Meloidogyne arenaria*, *M. hapla*, *M. incognita* and *M. javanica*. – Nematopica 31: 271-280.

- [24] Dong, L., Huang, C., Huang, L., Li, X., Zuo, Y. (2012): Screening plants resistant against *Meloidogyne incognita* and integrated management of plant resources for nematode control. – *Crop Protection* 33: 34-39.
- [25] Dörnenburg, H., Knorr, D. (1997): Evaluation of elicitor-and high-pressure-induced enzymatic browning utilizing potato (*Solanum tuberosum*) suspension cultures as a model system for plant tissues. – *Journal of Agricultural and Food Chemistry* 45: 4173-4177.
- [26] Eisenback, J., Sasser, J., Carter, C. (1985): Diagnostic Characters Useful in the Identification of the Four Most Common Species of Root-Knot Nematodes (*Meloidogyne* Spp.). – In: Sasser J. N. et al. (eds.) *An Advanced Treatise on Meloidogyne*. Vol. 1. North Carolina State University, Raleigh, NC, pp. 95-112.
- [27] Eisenback, J. D., Hunt, D. J. (2009): General Morphology. – In: Perry, R. N., Moens, M., Starr, J. L. (eds.) *Root-Knot Nematodes*. CABI, London, pp. 18-54.
- [28] Elbadri, G. A., Yassin, A. M. (2010): Sesame's Protective Role in Crop Nematode Control. – In: Bedigian, D. (ed.) *Sesame: The Genus Sesamum*. CRC Press, Boca Raton, pp. 211-218.
- [29] Elmiligy, I. A., Norton, D. C. (1973): Survival and reproduction of some nematodes as affected by muck and organic acids. – *Journal of Nematology* 5: 50-54.
- [30] El-Sayed, S., Mahdy, M. (2015): Effect of chitosan on root-knot nematode, *Meloidogyne javanica* on tomato plants. – *International Journal of ChemTech Research* 7: 1985-1992.
- [31] El-Sherif, A. G., Gad, S. B., Khalil, A. M., Mohamedy, R. H. E. (2015): Impact of four organic acids on *Meloidogyne Incognita* infecting tomato plants under greenhouse conditions. – *Global Journal of Biology, Agriculture & Health Sciences* 2: 94-100.
- [32] Esser, R. P., Perry, V. G., Taylor, A. L. (1976): A diagnostic compendium of the genus *Meloidogyne* (Nematoda: Heteroderidae). – *Proceedings of the Helminthological Society of Washington* 43: 138-150.
- [33] Fahramand, M., Moradi, H., Noori, M., Sobhkhizi, A., Adibian, M., Abdollahi, S., Rigi, K. (2014): Influence of humic acid on increase yield of plants and soil properties. – *International Journal of Farming and Allied Sciences* 3: 339-341.
- [34] FAO (2013): *Dried Fruit*. – Food & Agriculture Organization of the United Nation, Rome.
- [35] Gondal, A. S., Javed, N., Khan, S. A., Shahid, M. (2014): Use of nutritional supplements for the management of root-knot nematode (*Meloidogyne incognita*) infecting potato. – *Journal of Nematology*: 46: 13-160 (abstract).
- [36] Hadwiger, L. A. (2013): Multiple effects of chitosan on plant systems: solid science or hype. – *Plant Science* 208: 42-49.
- [37] Hao, X., Papadopoulos, A. P. (1999): Effects of supplemental lighting and cover materials on growth, photosynthesis, biomass partitioning, early yield and quality of greenhouse cucumber. – *Scientia Horticulturae* 80: 1-18.
- [38] Hartman, K. M., Sasser, J. N. (1985): Identification of *Meloidogyne* Species on the Basis of Differential Host Test and Perineal-Pattern Morphology. – In: Sasser, J. N. et al. (eds.) *An Advanced Treatise on Meloidogyne*. Vol. 1. Biology and Control. North Carolina State University Graphics, Raleigh, NC, pp. 69-77.
- [39] Hasabo, S. A., Noweer, E. M. A. (2005): Management of root-knot nematode *Meloidogyne Incognita* on eggplant with some plant extracts. – *Egyptian Journal of Phytopathology* 33: 65-72.
- [40] Heil, M. (1999): Systemic acquired resistance: available information and open ecological questions. – *Journal of Ecology* 87: 341-346.
- [41] Hildalgo-Diaz, L., Kerry, B. R. (2008): Integration of Biological Control with Other Methods of Nematode Management. – In: Ciancio, A., Mukerji, K. G. (eds.) *Integrated Management and Biocontrol of Vegetable and Grain Crops Nematodes*. Springer, Dordrecht, pp. 29-49.
- [42] Hooks, C. R. R., Wang, K.-H., Ploeg, A., McSorley, R. (2010): Using marigold (*Tagetes* spp.) as a cover crop to protect crops from plant-parasitic nematodes. – *Applied Soil Ecology* 46: 307-320.

- [43] Huang, W.; Cui, J.; Liu, S.; Kong, L.; Wu, Q.; Peng, H.; He, W.; Sun, J., Peng, D. (2016): Testing various biocontrol agents against the root-knot nematode (*Meloidogyne incognita*) in cucumber plants identifies a combination of *Syncephalastrum racemosum* and *Paecilomyces lilacinus* as being most effective. – *Biological Control* 92: 31-37.
- [44] Husain, S. I., Kumar, R., Khan, T. A., Titov, A. (1984): Effect of root -dip treatment of egg plant seedlings with plant extracts, nematicides, oil-cake extracts and anthelmintic drugs on plant growth and root -knot development. – *Pak. J. Nematol* 2: 79-83.
- [45] Ibrahim, S. K., Traboulsi, A. F., El-Haj, S. (2006): Effect of essential oils and plant extracts on hatching, migration and mortality of *Meloidogyne incognita*. – *Phytopathologia Mediterranea* 45: 238-246.
- [46] Jones, J. T., Haegeman, A., Danchin, E. G. J., Gaur, H. S., Helder, J., Jones, M. G. K., Kikuchi, T., Manzanilla-López, R., Palomares-Rius, J. E., Wesemael, W. M. L. (2013): Top 10 plant-parasitic nematodes in molecular plant pathology. – *Molecular Plant Pathology* 14: 946-961.
- [47] Kankam, F., Adomako, J. (2014): Influence of inoculum levels of root knot nematodes (*Meloidogyne* Spp.) on tomato (*Solanum lycopersicum* L.). – *Asian Journal of Agriculture and Food Science* 2: 171-178.
- [48] Karssen, G., Moens, M. (2006): Root-Knot Nematodes. – In: Perry, R. N., Moens, M. (eds.) *Plant Nematology*. CABI, London, pp. 59-90.
- [49] Kayani, M. Z., Mukhtar, T., Hussain, M. A., Ul-Haque, M. I. (2013): Infestation assessment of root-knot nematodes (*Meloidogyne* spp.) associated with cucumber in the Pothowar Region of Pakistan. – *Crop Protection* 47: 49-54.
- [50] Kemei, L., Yanqiu, D., Xuesong, C. B. (2015): Occurrence and identification of root-knot nematode on greenhouse vegetables in Xinjiang. – *Plant Protection* 41: 191-194.
- [51] Kesba, H. H., Al-Shalaby, M. E. M. (2008): Survival and reproduction of *Meloidogyne incognita* on tomato as affected by humic acid. – *Nematology* 10: 243-249.
- [52] Kesba, H. H., El-Beltagi, H. S. (2012): Biochemical changes in grape rootstocks resulted from humic acid treatments in relation to nematode infection. – *Asian Pacific Journal of Tropical Biomedicine* 2: 287-293.
- [53] Khaled, H., Fawy, H. A. (2011): Effect of different levels of humic acids on the nutrient content, plant growth, and soil properties under conditions of salinity. – *Soil and Water Research* 6: 21-29.
- [54] Khalil, M. S., Badawy, M. E. L. (2012): Nematicidal activity of a biopolymer chitosan at different molecular weights against root-knot nematode, *Meloidogyne incognita*. – *Plant Protection Science* 48(4): 170-178.
- [55] Klopper, J. W., Reddy, M. S., Rodríguez-Kabana, R., Kenney, D. S., Kokalis-Burelle, N., Martinez-Ochoa, N., Vavrina, C. S. (2004): Application for Rhizobacteria in transplant production and yield enhancement. – *Acta Horticulturae* 631: 217-230.
- [56] Kong, J.-O. K., Park, I.-K., Choi, K.-S., Shin, S.-C., Ahn, Y.-J. (2007): Nematicidal and propagation activities of thyme red and white oil compounds toward *Bursaphelenchus xylophilus* (Nematoda: Parasitaphelenchidae). – *Journal of Nematology* 39: 237-242.
- [57] Krueger, R., Dover, K. E., McSorley, R., Wang, K. H. (2007): Marigolds (*Tagetes* spp.) for Nematode Management. – ENY-056 (NG045). Entomology and Nematology Department, Florida Cooperative Extension Service, Institute of Food and Agricultural Sciences, University of Florida, Gainesville, FL.
- [58] Lima, E. A., Mattos, J. K., Moita, A. W., Carneiro, R. G., Carneiro, R. M. D. G. (2009): Host status of different crops for *Meloidogyne ethiopica* control. – *Tropical Plant Pathology* 34: 152-157.
- [59] Machado, A. C. Z., Mattei, D., Silva, S. A., Dorigo, O. F., Ito, D. S. (2014): Host status of green manures to four species of root-knot nematodes in Brazil. – *Journal of Nematology* 46: 197-197.

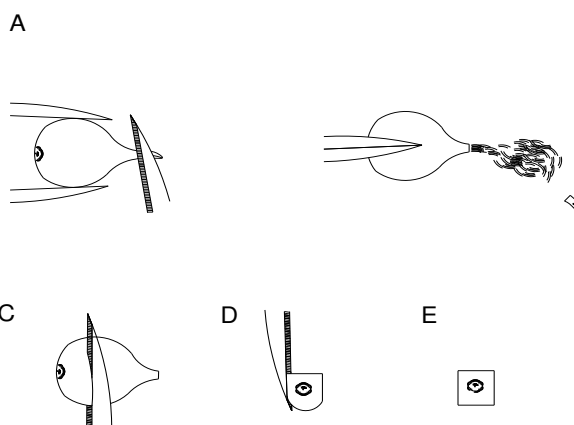
- [60] Maheshwari, R. K., Mohan, L., Malhotra, J., Updhuay, B., Rani, B. (2014): Invigorating efficacy of *Cucumis sativus* for healthcare & radiance. – International Journal of Chemistry and Pharmaceutical Sciences 2: 737-744.
- [61] Malerba, M., Cerana, R. (2016): Chitosan effects on plant systems. – International Journal of Molecular Sciences 17: 1-15.
- [62] Marahatta, S. P., Wang, K.-H., Sipes, B. S., Hooks, C. R. R. (2012): Effects of *Tagetes patula* on active and inactive stages of root-knot nematodes. – Journal of Nematology 44: 26-30.
- [63] Meng, Q., Long, H., Xu, J. (2004): PCR assays for rapid and sensitive identification of three major root-knot nematodes, *Meloidogyne incognita*, *M. javanica* and *M. Arenaria*. – Acta Phytopathologica Sinica 34: 204-210.
- [64] Mesiha, F. K. (2019): Management of root rot and root knot nematode disease complex of pepper. – PhD Dissertation. Department of Plant Pathology, Faculty of Agriculture, University of Zagazig, Egypt.
- [65] Mitkowski, N. A., Abawi, G. S. (2003): Root-knot nematodes. – The Plant Health Instructor 917: 1-12.
- [66] Moens, M., Perry, R. N., Starr, J. L. (2009): *Meloidogyne* Species - A Diverse Group of Novel and Important Plant Parasites. – In: Perry, R. N., Moens, M., Starr, J. L. (eds.) Root-Knot Nematodes. CABI, London.
- [67] Mota, L. C. B., dos Santos, M. A. (2016): Chitin and chitosan on *Meloidogyne javanica* management and on chitinase activity in tomato plants. – Tropical Plant Pathology 41: 84-90.
- [68] Mwesige, R. (2013): Identification and pathogenicity of root-knot nematodes from tomatoes grown in Kyenjojo and Masaka Districts in Uganda. – Master of Nematology, Department of Biology, Faculty of Science, University of Gent, Gent.
- [69] Natarajan, N., Cork, A., Boomathi, N., Pandi, R., Velavan, S., Dhakshnamoorthy, G. (2006): Cold aqueous extracts of african marigold, *tagetes erecta* for control tomato root knot nematode, *Meloidogyne incognita*. – Crop Protection 25: 1210-1213.
- [70] Neto, C. G. T., Dantas, T. N. C., Fonseca, J. L. C., Pereira, M. R. (2005): Permeability studies in chitosan membranes. Effects of crosslinking and poly (ethylene oxide) addition. – Carbohydrate Research 340: 2630-2636.
- [71] Noling, J. W. (1999): Nematode Management in Cucurbits (Cucumber, Melons, Squash). – University of Florida Cooperative Extension Service, Institute of Food and Agriculture Sciences, EDIS, Gainesville, FL.
- [72] Ogaraku, A. O. (2007): The effect of animal manures on susceptibility of cowpea var. Moussa local to infection by root-knot nematode; *Meloidogyne javanica* Treub. – Pakistan Journal of Biological Sciences 10: 2980-2983.
- [73] Olsen, M. W. (2011): Root-Knot Nematode. – The University of Arizona Cooperative Extension, Tuscon, AZ.
- [74] Polthanee, A., Yamazaki, K. (1996): Effect of marigold (*Tagetes patula* L.) on parasitic nematodes of rice in Northeast Thailand. – Khon Kaen Agriculture Journal (Thailand) 24: 105-107.
- [75] Powers, T. O., Harris, T. S. (1993): A polymerase chain reaction method for identification of five major *Meloidogyne* species. – Journal of Nematology 25: 1-6.
- [76] Powers, T. O., Mullin, P. G., Harris, T. S., Sutton, L. A., Higgins, R. S. (2005): Incorporating molecular identification of *Meloidogyne* spp. into a large-scale regional nematode survey. – Journal of Nematology 37: 226-235.
- [77] Radwan, M. A., Farrag, S. A. A., Abu-Elamayem, M. M., Ahmed, N. S. (2012): Extraction, characterization, and nematicidal activity of chitin and chitosan derived from shrimp shell wastes. – Biology and Fertility of Soils 48: 463-468.
- [78] Romero, P., Dodd, I. C., Martinez-Cutillas, A. (2012): Contrasting physiological effects of partial root zone drying in field-grown grapevine (*Vitis vinifera* L. Cv. Monastrell) according to total soil water availability. – Journal of Experimental Botany 63: 4071-4083.

- [79] Safdar, A., Mahdi, M. M., McKenry, M. V. (2013): Organic amendments for management of root knot nematode of tunnel crops. – *Journal of Nematology* 45: 279-280 (abstract).
- [80] Saravanapriya, B., Subramanian, S. (2005): Effect of humic acid against *Meloidogyne incognita* on tomato. – *Annals of Plant Protection Sciences* 13: 441-444.
- [81] Saravanapriya, B., Subramanian, S. (2007): Management of *Meloidogyne incognita* on tomato with humic acid and bioinoculants. – *Annals of Plant Protection Sciences* 15: 195-197.
- [82] Sen, D., and Chatterjee, A. (2007): Phytophagous Nematodes (Order Tylenchida, Suborder Tylenchina). – In: *Zoological Survey of India (ed.) Fauna of Mizoram*. Zoological Survey of India, Kolkata.
- [83] Shafeek, M. R., Helmy, Y. L., Omar, N. M. (2016): Effect of spraying or ground drench from humic acid on growth, total output and fruits nutritional values of cucumber (*Cucumis sativus* L.) grown under plastic house conditions. – *International Journal of Pharm, Tech, Research* 9: 52-57.
- [84] Soppe, R., Saleh, R. O. (2012): Report B2.1 Historical agricultural production data in Iraq. – <http://icarda.org/iraq-salinity-project/teaser> 8: 1-25.
- [85] Strange, R. N. (2006): *Introduction to Plant Pathology*. – John Wiley & Sons, London.
- [86] Swamy, S. D., Reddy, P. P., Jegowda, D. N., Swamy, B. C. (1995): Management of *Meloidogyne incognita* in tomato nursery by growing trap/antagonistic crops in rotation. – *Current Nematology* 6: 9-12.
- [87] Tatlioglu, T. (1993): Cucumber (*Cucumis Sativus* L. – In: Kalloo, G., Bergh, B. O. (eds.) *Genetic Improvement of Vegetable Crops*. 7th Ed. Pergamon Press Ltd, Oxford, UK.
- [88] Taylor, D. P., Netscher, C. (1974): An improved technique for preparing perineal patterns of *Meloidogyne* spp. – *Nematologica* 20: 268-269.
- [89] Taylor, A., Sasser, J. (1978): *Biology, Identification and Control of Root-Knot Nematodes*, North Carolina State University Graphics. – International Meloidogyne Project, USA.
- [90] Temple, V., Mowbray, D., Rai, P. P., Gideon, O., Kaluwin, C., Watmelik, J. (eds.) (2015): *Promoting Responsible Sustainable Development Through Science & Technology, the PNG Way*. – School of Natural and Physical Sciences, and School of Medicine and Health Sciences, University of Papua New Guinea, pp 1-18.
- [91] Thomas, H. A. (1958): On *Criconeimoides xenoplax* raski, with special reference to its biology under laboratory conditions. – *Proceedings of the Helminthological Society of Washington* 26: 55-59.
- [92] Timper, P., Davis, R. F., Tillman, P. G. (2006): Reproduction of *Meloidogyne incognita* on winter cover crops used in cotton production. – *Journal of Nematology* 38: 83-89.
- [93] Toumi, F., Waeyenberge, L., Yousef, R., Khalil, H., Al-Assas, K., Moens, M. (2014): Distribution of the root-knot nematode *Meloidogyne* spp., in tomato greenhouses at Lattakia and Tartus Province in Syria. – *Pakistan Journal of Nematology* 32: 163-172.
- [94] Trudgill, D. L., Blok, V. C. (2001): Apomictic, polyphagous root-knot nematodes: exceptionally successful and damaging biotrophic root pathogens. – *Annual Review of Phytopathology* 39: 53-77.
- [95] Tsay, T. T., Wu, S. T., Lin, Y. Y. (2004): Evaluation of asteraceae plants for control of *Meloidogyne incognita*. – *Journal of Nematology* 36: 36-41.
- [96] Van De Sande-Bakhuyzen, H. L. (1928): Studies upon wheat grown under constant conditions II. – *Plant Physiology* 3: 7.
- [97] Visser, T., Vythftingam, M. K. (1959): The effect of marigolds and some other crops on the *Pratylenchus* and *Meloidogyne* populations in tea soil. – *Tea Quarterly* 30: 30-38.
- [98] Wehner, T. C., Maynard, D. N. (2003): Cucurbitaceae (Vine Crops). – ELS. <https://doi.org/10.1038/npg.els.0003723>.
- [99] Weng, Y., Sun, Z. (2011): Major Cucurbit Crops. – In: Cseke, L. J., Kirakosyan, A., Kaufman, P. B., Westfall, M. V. (eds.) *Handbook of Molecular and Cellular Methods in Biology and Medicine*. CRC Press, Boca Raton, pp. 1-16.

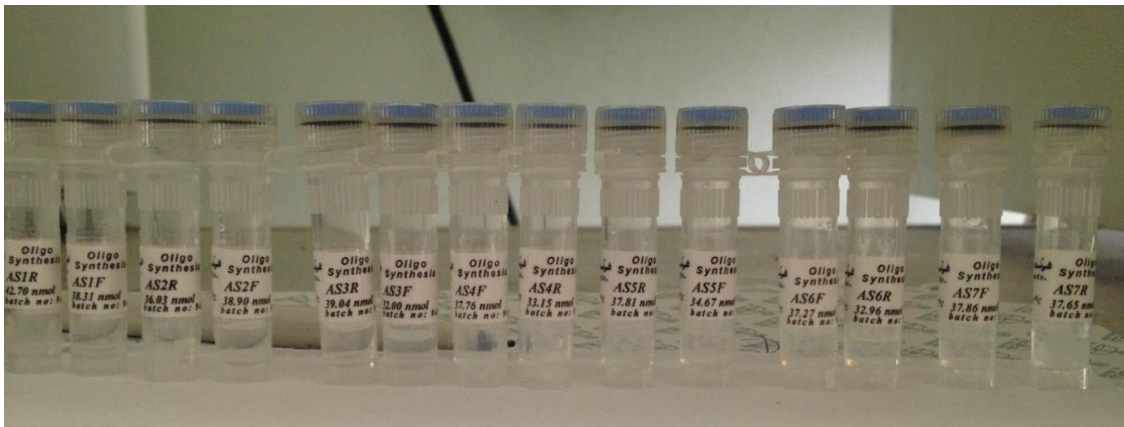
- [100] Whitehead, A. G. (1968): Taxonomy of *Meloidogyne* (Nematodea: Heteroderidae) with descriptions of four new species. – The Transactions of the Zoological Society of London 31: 263-401.
- [101] Whitehead, A. G., Hemming, J. R. (1965): A comparison of some quantitative methods of extracting small vermiform nematodes from soil. – Annals of Applied Biology 55: 25-38.
- [102] Williams, L. J., Abdi, H. (2010): Fisher's Least Significant Difference (LSD) Test. – In: Salkind, N. (ed.) Encyclopedia of Research Design. Sage, Thousand Oaks, CA, pp. 1-5.
- [103] XLSTAT Institute (2004): Statistical Analysis System Procedures Guide, Version 7.5. – SAS Institute, Cary, NC.
- [104] Yang, X., Wang, X., Wei, M., Hikosaka, S., Goto, E. (2009): Changes in growth and photosynthetic capacity of cucumber seedlings in response to nitrate stress. – Brazilian Journal of Plant Physiology 21: 309-317.
- [105] Ye, W., Zeng, Y., Kerns, J. (2015): Molecular characterization and diagnosis of root-knot nematodes (*Meloidogyne* spp.) from turfgrasses in North Carolina, USA. – PLoS ONE 10: 1-16.
- [106] Zargar, V., Asghari, M., Dashti, A. (2015): A Review on chitin and chitosan polymers: structure, chemistry, solubility, derivatives, and applications. – Chem. Bio. Eng. Reviews 2: 204-226.
- [107] Zewain, Q. k. (2014): Evaluation of some chemical nematicides and organic formulations in management of root knot nematode *Meloidogyne* spp. on eggplant. – Tikrit University for Agricultural Sciences. 3: 8-14.
- [108] Zhuran, Q., Tianhong, L., Ning, W., Xuan, W., Hairun, Z., Hongmei, L. (2014): Occurrence and species identification of nematode parasites of vegetables and horticultural plant seedlings in export plantations. – Journal of Nanjing Agricultural University 37: 93-100.
- [109] Zijlstra, C., Donkers-Venne, D. T., Fargette, M. (2000): Identification of *Meloidogyne incognita*, *M. javanica* and *M. arenaria* using sequence characterized amplified region (SCAR)-based PCR assays. – Nematology 2: 847-885.
- [110] Zinoveva, S. V., Vasyukova, N. I., Ilinskaya, L. I., Varlamov, V. P., Ozeretskovskaya, O. L., Sonin, M. D. (1999): Effect of chitosan on interactions in a plant-parasitic nematode system. – Doklady Biological Sciences 367: 400-402.

APPENDICES

Appendix 1. How to cut perineal patterns. A, B: excised female with neck region removed and body contents gently expelled; C: posterior body with perineal pattern removed; D: trimming surplus cuticle around perineal pattern; E: trimmed perineal pattern ready for mounting



Appendix 2. Species specific primers prepared by Sinacion, Bioscience Co. Iran



Appendix 3. MULTIGENE OptiMAX machine (PCR Thermal Cycler)



Appendix 4. PCR programs

	Step 1	Step 2	Step 3	Step4	Step5	Step 6
	Initial denaturation	Denaturation	Annealing temp. °C	Extension	Final extension	Hold
Temp.	94.0 and 95.0	94.0 and 95.0	49.0-64.0	72.0	72.0	4.00
Time	8:00	30-60 s	1:00	2.00	7:00	∞
	← Repeated for 35 cycles →					

Appendix 5. Programs and different annealing temperatures were used for amplifying the DNA of the species

Species	Primers	Fragment bp	Denaturation temperature °C	Annealing temperature °C	References
<i>M. incognita</i>	AS1F AS1R	1200	94 and 95	49, 50, 54 and 55	Sinacion, Bioscience Co. Iran; Zijlstra et al., 2000; Mwesige, 2013; Toumi et al., 2014; Temple et al., 2015; Agenbag, 2016
	AS2F AS2R	1350	94 and 95	49, 50, 54 and 55	Sinacion, Bioscience Co. Iran; Dong et al., 2001; Toumi et al., 2014; Temple et al., 2015
	AS3F AS3R	399	94 and 95	49, 50, 55, 60 and 64	Sinacion, Bioscience Co. Iran; Devran et al., 2009; Toumi et al., 2014; Ye et al., 2015; Agenbag, 2016
	AS4F AS4R	955	94 and 95	49, 50, 55, 60, 61, 62 and 63	Sinacion, Bioscience Co. Iran; Devran et al., 2009; Toumi et al., 2014; Chanmalee, 2014; Zhuran et al., 2014; Kemei et al., 2015; Agenbag, 2016
<i>M. javanica</i>	AS5F AS5R	1650	94 and 95	49, 50, 52 and 55	Sinacion, Bioscience Co. Iran; Dong et al., 2001; Devran et al., 2009; Toumi et al., 2014
	AS6F AS6R	670	94 and 95	49, 50, 55, 60, 63 and 64	Sinacion, Bioscience Co. Iran; Zijlstra et al., 2000; Devran et al., 2009; Toumi et al., 2014; Chanmalee, 2014; Aydinli and Mennan, 2016
	AS7F AS7R	517	94 and 95	49, 50, 55, 61 and 62	Sinacion, Bioscience Co. Iran; Zhuran et al., 2014; Toumi et al., 2014; Kemei et al., 2015

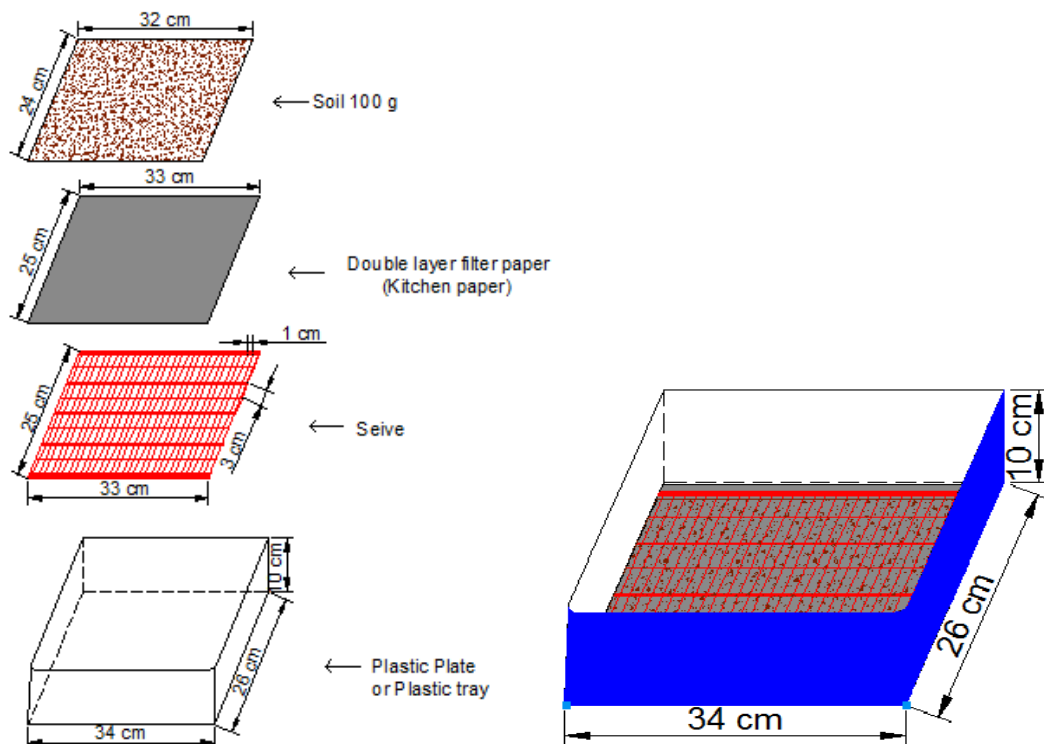
Appendix 6. Electrophoresis chamber (power supply and the tray)



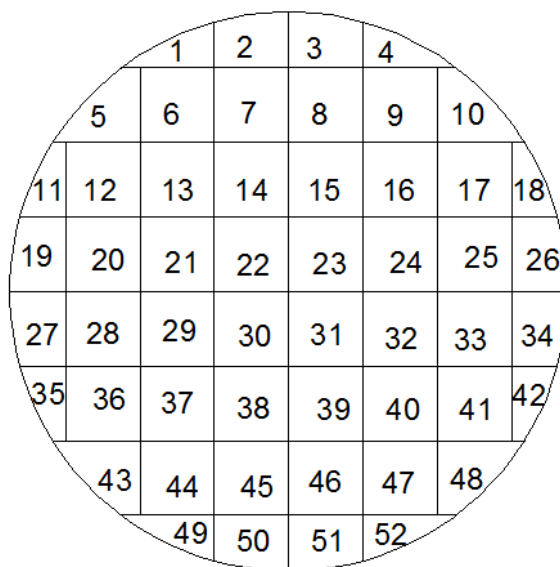
Appendix 7. UV transilluminator



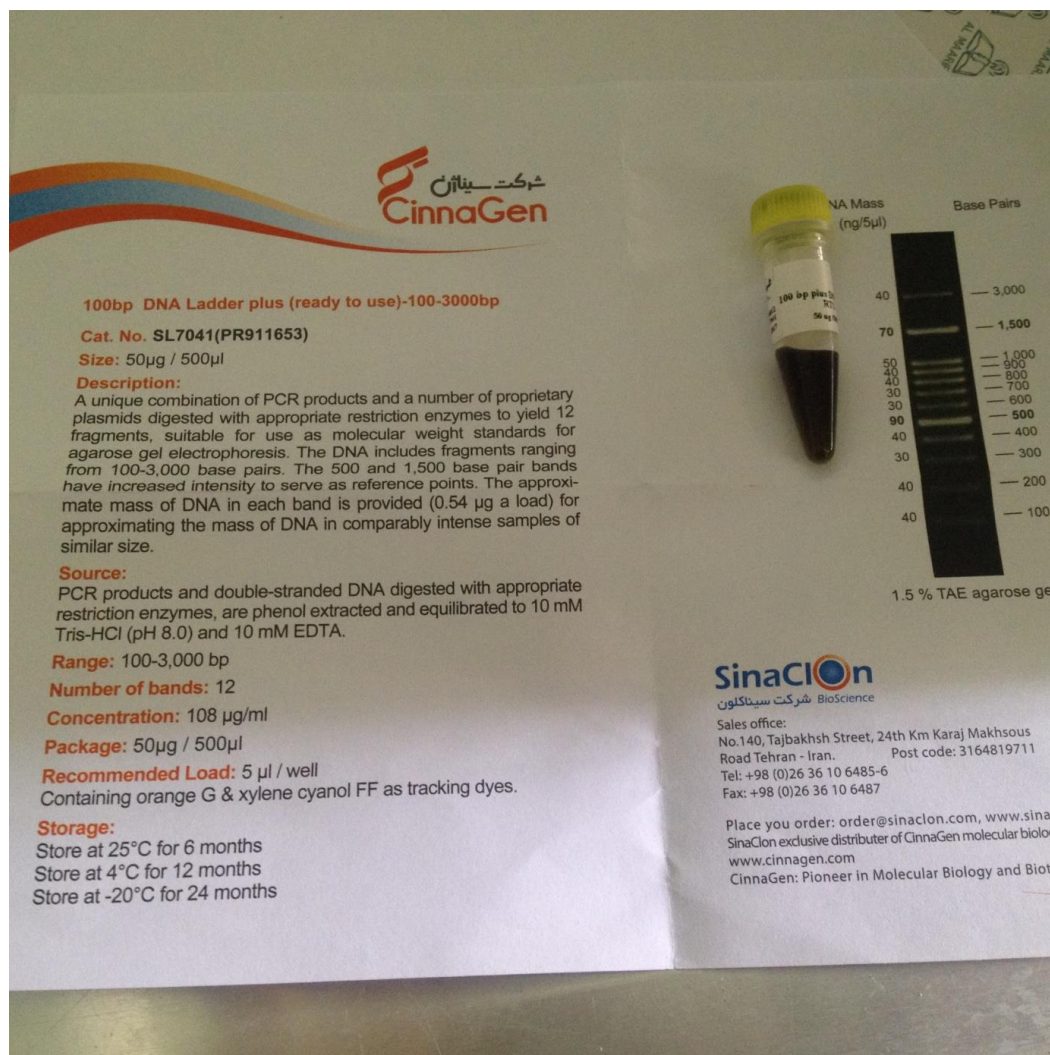
Appendix 8. Extraction-tray models for isolating the nematodes (Juveniles 2) (original)



Appendix 9. Counting dish designed for calculating the nematodes (Juveniles 2) (original)



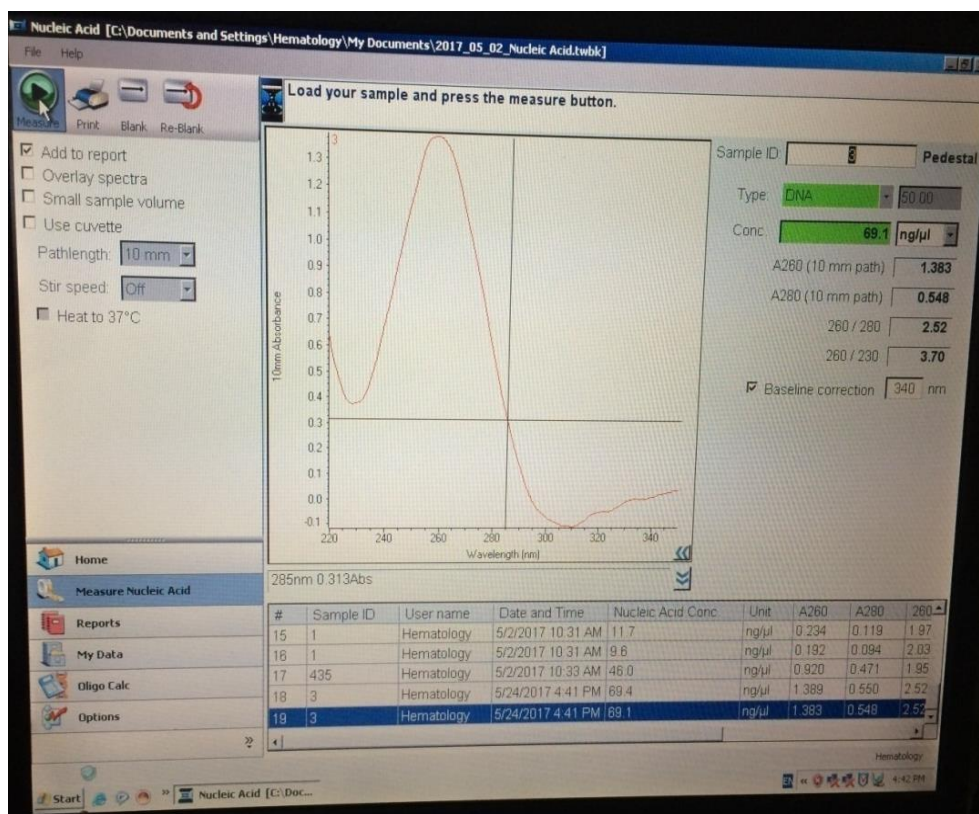
Appendix 10. The tube of ladder and its information paper by Sinacion company-Iran



Appendix II. (A) The device of thermo Scientific Nanodrop 2000C. (B) The concentration and purity diagram of *Meloidogyne* spp. DNA extraction as tested by Nanodrop 2000C device



A



B

Appendix 12. Analysis of variance including degree of freedom (df) and mean squares of replication, treatments and error for Population densities (Juveniles 2) / 100 g soil and number of galls

Characters	Replications	Treatments	Error
	(d.f = 2)	(d.f = 8)	(d.f = 16)
	Mean square	Mean square	Mean square
One day before of applying treatments (Pi)	13980.778	1979.500NS	3455.944
After 10 days of application	51674.704	46246.315 NS	54210.204
After 20 days of application	126899.593	46380.759 NS	72008.676
After 30 days of application (Pf)	3831.148	83707.037**	2182. 773
Number of the galls ($P \leq 0.05$)	771.797	1569.273**	222.680
Number of the galls ($P \leq 0.01$)	771.797	1569.273*	222.680

* indicates significant difference at $P \leq 0.05$, ** indicates high significant difference at $P \leq 0.05$ and Ns indicates non-significant difference

Appendix 13. Analysis of variance including degree of freedom (df) and mean squares of replication, treatments and error for some plant growth parameters (vegetative parts) of cucumber (cv. Naseem F1)

Characters	Replications	Treatments	Error
	(d.f = 2)	(d.f = 8)	(d.f = 16)
	Mean square	Mean square	Mean square
Plant height (cm)	0.138	0.420**	0.020
Stem diameter (cm)	0.658	1.186**	0.108
No. of nodes. plant ⁻¹	21.333	164.833**	1.583
No. of leaves. plant ⁻¹	11.704	198.009NS	20.912
Fresh plant weight (vegetable parts) g. plant ⁻¹	10901.248	25751.528*	3124.286
Leaf area. plant ⁻¹ (cm ²)	3402.690	1456.129*	411.055

* indicates significant difference at $P \leq 0.05$, ** indicates high significant difference at $P \leq 0.05$ and Ns indicates non-significant difference

Appendix 14. Analysis of variance including degree of freedom (df) and mean squares of replication, treatments and error for some plant growth (root parts) of cucumber (cv. Naseem F1)

Characters	Replications	Treatments	Error
	(d.f = 2)	(d.f = 8)	(d.f = 16)
	Mean square	Mean square	Mean square
Root length (cm)	11.576	18.532*	6.530
Fresh root weight (g)	78.390	23.188*	6.146
Dried root weight (g)	13.863	31.973**	0.988

* indicates significant difference at $P \leq 0.05$, ** indicates high significant difference at $P \leq 0.05$ and Ns indicates non-significant difference

Appendix 15. Analysis of variance including degree of freedom (df) and mean squares of replication, treatments and error for some plant content of cucumber (cv. Naseem F1)

Characters	Replications	Treatments	Error
	(d.f = 2)	(d.f = 8)	(d.f = 16)
	Mean square	Mean square	Mean square
Intensity of leaf chlorophyll (SPAD unit)	18.498	46.605**	3.707
% of the Nitrogen (N) content in the leaf dry weight	0.034	0.060*	0.022
% of the Phosphor (P) content in the leaf dry weight	0.011	0.001 NS	0.002
% of the Potassium (K) content in the leaf dry weight	0.097	0.046NS	0.087

* indicates significant difference at $P \leq 0.05$, ** indicates high significant difference at $P \leq 0.05$ and Ns indicates non-significant difference

Appendix 16. Analysis of variance including degree of freedom (df) and mean squares of replication, treatments and error for floral growth

Characters	Replications	Treatments	Error
	(d.f = 2)	(d.f = 8)	(d.f = 16)
	Mean square	Mean square	Mean square
No. of flowers. plant ⁻¹	132.333	14.333*	2.083
No. of aborted flowers. plant ⁻¹	330.581	25.753 NS	17.356
No. of fruit. plant ⁻¹	179.593	71.759*	4.176
Fresh weight of fruit. plant ⁻¹ (g)	179.505	43.718 NS	38.041
Diameter of fruits. plant ⁻¹ (cm)	0.032	0.365 NS	0.007
Length of fruits (cm)	0.955	0.979 NS	0.243
Fruit moisture content (%)	0.593	0.690NS	0.141

* indicates significant difference at $P \leq 0.05$, ** indicates high significant difference at $P \leq 0.05$ and Ns indicates non-significant difference

Appendix 17. Analysis of variance including degree of freedom (df) and mean squares of replication, treatments and error for yield

Characters	Replications	Treatments	Error
	(d.f = 2)	(d.f = 8)	(d.f = 16)
	Mean square	Mean square	Mean square
Early yield (kg. plant ⁻¹)	0.019	0.182 NS	0.211
Total yield (kg. plant ⁻¹)	4.972	4.234*	0.781

* indicates significant difference at $P \leq 0.05$, ** indicates high significant difference at $P \leq 0.05$ and Ns indicates non-significant difference

EFFECT OF DIFFERENT MICROBIAL AGENTS ON CORN STALK COMPOSTING

CHANG, H. Y.^{1,2} – LU, S. F.^{1,2} – HUANG, Z. Y.^{1,2} – LIU, Y. X.^{1,2} – WANG, T. Y.^{1,2} – WANG, C. Y.^{1,2*} –
LIU, S. X.^{1,2*}

¹*College of Resources and Environmental, Jilin Agricultural University, Xincheng Street
No.2888, Changchun 130118, People's Republic of China*

²*Key Laboratory of Soil Resources Sustainable Utilization for Jilin Province Commodity Grain
Bases, Changchun 130118, Jilin Province, China*

**Corresponding authors*

e-mail: wangchengyu2001@163.com; phone: +86-1894-6690-848;

e-mail: liushuxia69@163.com; phone: +86-1554-3133-987

(Received 4th Feb 2020; accepted 6th May 2020)

Abstract. This study explored the effects of different microbial agents on corn stalk composting to enable the development of agents suitable for composting corn stalks in cold regions of northern China. Four different microbial treatment groups were established: CK (straw), L (straw + 1% low-temperature bacteria), M (straw + 1% normal-temperature bacteria), LM (straw + 0.5% low-temperature bacteria + 0.5% normal-temperature bacteria), and tests were repeated 3 times for each group. The results show that the temperature of the heap reached 50°C on the second day of the L and LM treatments and reached 50°C on the sixth day of M. CK did not reach 50°C during the entire composting cycle. During the composting process, the seed germination index, the degradation rate of total nitrogen, the total potassium, the total phosphorus, the cellulose, and the hemicellulose degradation rates increased; In contrast, the water content, conductivity, organic carbon and C/N showed a downward trend. The humic acid and fulvic acid contents in each treatment showed a downward trend, while the humic acid and HA/FA increased compared to CK. The conclusion of this experiment provides a theoretical basis for achieving the rapid degradation of straw in the cold regions of northern China.

Keywords: *low-temperature bacteria, corn straw, compost, maturity, North China*

Introduction

Corn stalk is a rich natural organic resource and can be used as a fertilizer source in agricultural production (Wang, 2018). At present, the world's straw resources are substantial and widely distributed, but the utilization rate is not high (Mulumba et al., 2008; Lou et al., 2011). Straw returning is one of the main ways to utilize straw resources. It is beneficial to the renewal of soil humus, the maintenance of soil organic matter balance and the improvement of soil quality and can contribute to fertility, protect the environment, increase the crop yield and is an important measure for promoting the sustainable development of agriculture (Hachicha et al., 2012; Hu et al., 2016). However, due to the influence of climate in the cold regions of northern China, the slow decomposition of straw after being returned to the field affects the planting and the cropping of the next year's crops. Further, this slow decomposition also allows some pests to survive in the soil for a long time, which can cause serious damage to crop growth (Gong et al., 2018). Therefore, accelerating the decomposition of straw is important. The application of microbial agents is an effective measure for achieving the rapid degradation of straw (Gao et al., 2014). Microbial agents can effectively break down straw into a large number of elements such as the nitrogen, phosphorus and

potassium required by crops and trace elements such as calcium, magnesium, manganese and molybdenum, which can improve the physical and chemical properties of soil, improve soil organic matter, enhance soil aeration, protect fertilizer and water retention function, and stimulate crop growth and development (Zhou et al., 2018). Additionally, composting is an effective way to quickly dispose of livestock manure and agricultural waste. The heat generated during composting can kill viruses and weed seeds while decomposing the organic matter into stable humic substances that can be used as organic fertilizers (Yan et al., 2018). Therefore, this study conducted a simple composting test on straw by adding low-temperature bacteria, normal-temperature bacteria and low-temperature and normal-temperature mixed bacteria to study the dynamic changes occurring in the various maturity indexes during the composting process, thus providing feasible management methods for straw wastes in northern areas.

Materials and Methods

Composting materials and devices

The corn stalks were collected in the experimental field of Jilin Agricultural University and pulverized to approximately 5 cm with a pulverizer. The basic properties are shown in *Table 1*. The low-temperature bacterial agent is composed of low-temperature bacteria preserved in the laboratory, including 14 (Yellow bacillus), 49 (Chain mildew genera) and NX5 (Section coli); the normal-temperature bacterium is Y2 (Short-wave pseudomonas); and the effective viable number of bacteria is $\geq 10^8$ cfu/g.

Table 1. Basic properties of corn straw

Organic carbon (g·kg ⁻¹)	Total nitrogen (g·kg ⁻¹)	Total phosphorus (g·kg ⁻¹)	Total potassium (g·kg ⁻¹)	Moisture content (%)
512.27	8.42	0.67	8.31	9.85

Composting device

A soil trough with dimensions of 80×50×40 was excavated on the outdoor test site, and a layer of plastic cloth was placed on the bottom to prevent water from penetrating the ground. The pulverized straw was covered with plastic cloth to prevent water loss and reduce the effects of rainy day.

Compost design

Four treatments were established: CK (straw), L (straw + 1% low-temperature bacteria), M (straw + 1% normal-temperature bacteria), LM (straw + 0.5% low-temperature bacteria + 0.5% normal-temperature bacteria), and each treatment had 3 replications. Each treatment received 15 kg of corn stover, 1% of the microbial agent, and added groundwater to adjust the straw water content to approximately 65%, with the C/N being adjusted with urea to approximately 25. The mixture was uniformly mixed and placed in the composting device, where it was piled into a small hill shape so that the straw was approximately 20 cm higher than the composting device. The experiment was conducted at the outdoor breeding ground of Jilin Agricultural University. Composting began on April 20, 2019, and the piles were piled up and sampled every 5 days. The composting time lasted for 40 days.

Sample collection

The heaps were piled up and sampled every 5 days. The samples from the upper, middle and lower parts were collected and mixed thoroughly. Then, approximately 200 g of the composting material was placed in two Ziploc bags: one for water content, pH and conductivity (EC); one for the seed germination index (GI) and other indicators; and the third one for natural air drying for organic carbon, total nitrogen, total phosphorus, total potassium, cellulose degradation rate, hemicellulose degradation rate and humus content.

Determination methods

Determination of temperature

The temperature was measured at the center of the pile at 8:30 am and 16:30 pm every day, and the average of the two measured temperatures was taken as the stack temperature of the day; the ambient temperature was also measured.

Determination of water content

Samples were taken, and 10.00 g of each were dried to a constant weight at 105°C.

Extraction

Extracts were obtained by using a water: fresh sample ratio of 10:1 mL/g on a shaker for 2 h; the mixture was then filtered, and the filtrate served as the extract for the determination of the pH, conductivity (EC) and seed germination index.

The pH was measured by using a pH meter, and the conductivity (EC) was measured with a TM-03 waterproof conductivity meter.

Determination of the seed germination index (GI)

An appropriately sized filter paper was placed in a high-temperature sterilization dish with a diameter of 90 mm. Ten soybean seeds were evenly spaced on the paper, and 10 mL of the extract was added to the culture dish. Treated water was used as a blank control. The dish was placed in a constant temperature incubator at 25°C and cultured in the dark for 48 h to determine the seed germination rate and root length. The seed germination index (GI) = (sample germination rate × sample root length) / (control germination rate × control root length) × 100%.

The determination of organic carbon, total nitrogen, total phosphorus and total potassium was carried out according to the method for determining organic fertilizer-related indicators following the national standard (Cao et al., 2014).

Cellulose and hemicellulose degradation rates were determined by the Van Soest (Wang et al., 2016) washing method.

Determination of the components of the humus

The extraction of the components of the humus is based on the humus composition modification method (Dou et al., 2007). The carbon contents of the extracted humus, humic acid (HA) and fulvic acid (FA) were determined by external heating while using potassium dichromate.

The data processing

Excel 2016 and SPSS 24.0 were used for data collation and statistical analysis.

Results

Stack temperature

As can be seen from *Fig. 1*, the ambient temperature varies from 11.0°C to 27.5°C during the composting period, and the ambient temperature in the early composting period is less than 25°C. On the first day of composting, the ambient temperature was 21.5°C, and the temperatures of the treated CK, L, M, and LM stacks were 21.7°C, 20.7°C, 22.0°C, and 21.6°C, respectively. After treatment, the temperature of L and LM increases rapidly, reaching 50°C or more on the next day and staying above 50°C for 10 days. The maximum temperature of the treatment M was 60.6°C, and the maximum temperature of LM was 61.8°C, with a temperature of more than 60°C being maintained for 3 days. The treatment M reached 50°C on the sixth day, where it stayed for 6 days. The CK, which lacked the added microbial agent, did not reach 50°C during the entire composting process. After the high-temperature period, the temperature of the reactor began to decrease. After 20 days, the temperature of each treatment reactor was basically maintained at approximately 30°C. The heap temperature, except for that of CK, was maintained at 55°C for more than 3 days or at 50°C for more than 5-7 days, which is sufficient to kill harmful substances.

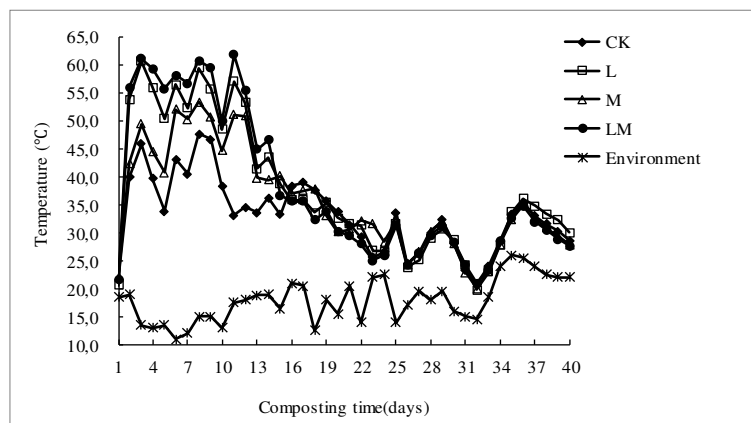


Figure 1. Change of compost temperature during composting

Water content of the heap

As shown in *Fig. 2*, the water content of the pile gradually decreased with the composting time. The water content when composting was initiated was approximately 65%. At 5 days, the water content of each treatment was significantly reduced. The water contents of CK, L, M and LM decreased by 7.51%, 10.44%, 9.11% and 11.39%, respectively. During the entire composting cycle, the moisture content of LM was the largest, CK was the smallest, and the treatment L and M were between the two. At the end of composting, the water contents of CK, L, M and LM were 43.51%, 38.19%, 39.21% and 36.35%, respectively, and these values were 22.03%, 26.77%, 25.79% and 28.92% lower than the initial values.

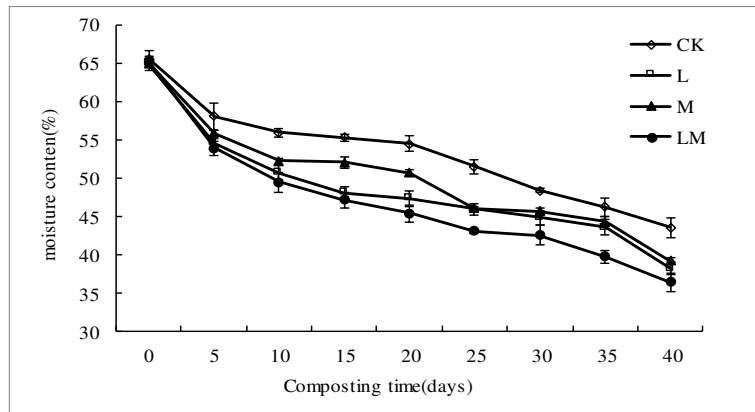


Figure 2. Change in moisture content during composting (The error bars displayed in the figure is the positive and negative deviation of the standard deviation of data in different sampling days for each treatment)

pH and conductivity (EC)

As shown in Fig. 3, the pH values of the CK, L, M, and LM treatments before composting were 7.54, 7.61, 7.61, and 7.59, respectively. The pH of the treated LM increased rapidly, reaching a maximum of 8.42 on the 10th day, whereas the pH of the treated L, M and CK peaked on days 15, 20 and 20, respectively, with values of 8.61, 8.50 and 8.36. Afterward, the pH of each treatment decreased to a different extent. At the end of composting, the pH values of the CK, L, M and LM treatments were 8.16, 8.33, 8.35 and 8.11, respectively.

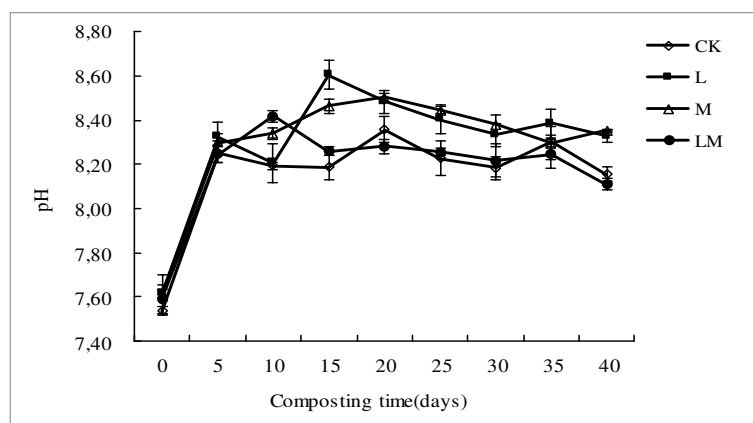


Figure 3. Changes in pH during composting (The error bars displayed in the figure is the positive and negative deviation of the standard deviation of data in different sampling days for each treatment)

As shown in Fig. 4, with the change in composting time, the conductivity of each treatment shows a general trend of decreasing first and then slowly increasing before stabilizing. At 60 days, the conductivity of the LM treatment was the smallest, CK was the highest, and L and M were between the two. Over the entire composting period, the conductivity change between treatments was not particularly significant but was less than 3000 $\mu\text{s}/\text{cm}$.

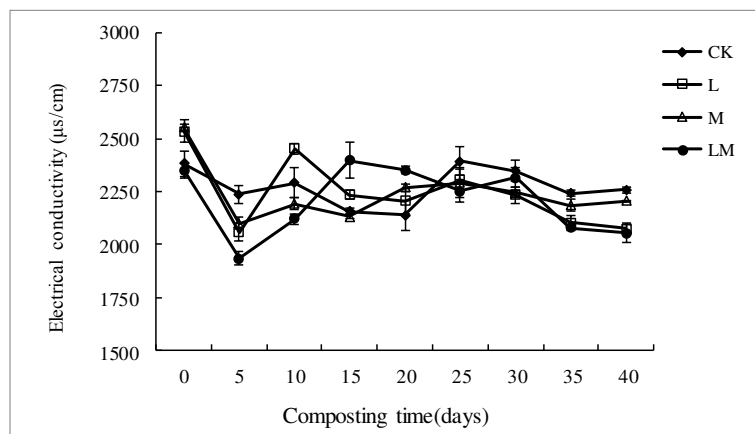


Figure 4. Changes in electrical conductivity during composting (The error bars displayed in the figure is the positive and negative deviation of the standard deviation of data in different sampling days for each treatment)

Seed Germination Index (GI)

As shown in Fig. 5, the seed germination index gradually increases with the composting time, but on the fifth day, the seed germination index of each treatment is reduced, which may be due to the generation of harmful substances in the heap. After the fifth day, the seed germination index of each treatment increased significantly, with that of the LM treatment increasing most obviously, CK increasing the least, and L and M increasing with values between the two. On the 15th day of treatment, for LM, the seed germination index reached 80%. For L and M, it reached 80% on the 20th day, and for CK, it reached 80% on the 25th day. At the end of composting, the germination index of the L, M and LM seeds treated with added microbial agents was 100%, and for CK, it was 95.27%, which indicated that the compost had reached maturity. This result may be obtained because the corn stalk itself contains less toxicity, and composting can increase the nutrients of the heap, thus providing sufficient seed germination and nutrients.

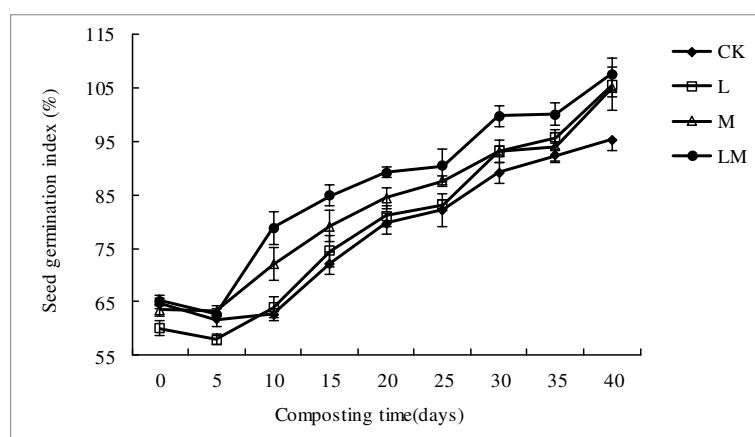


Figure 5. Changes in the seed germination index during the composting process (The error bars displayed in the figure is the positive and negative deviation of the standard deviation of data in different sampling days for each treatment)

Total nitrogen, organic carbon and C/N

As shown in Fig. 6, during the composting process, the total nitrogen content generally increased, and the total nitrogen following the addition of the microbial agent was significantly higher than that of CK. The initial total nitrogen was approximately 2%. At the end of composting, the total nitrogen contents of L, M and LM were 2.35%, 2.38% and 2.56%, respectively, and were 0.14%, 0.17% and 0.35% higher than that of CK. The microbial agent had a significant increasing effect on the total nitrogen during composting. On the 10th day, a decline occurred that was probably due to the high microbial activity at this stage, which led to an increase in temperature and, as a result, a large release of NH_3 , thus decreasing the nitrogen content; then the nitrogen content gradually increased gradually, probably due to composting. With the maturation of the organic matter, the decomposition of the minerals and the organic carbon content continued to decline, thus promoting the enrichment of total nitrogen (Li et al., 2015).

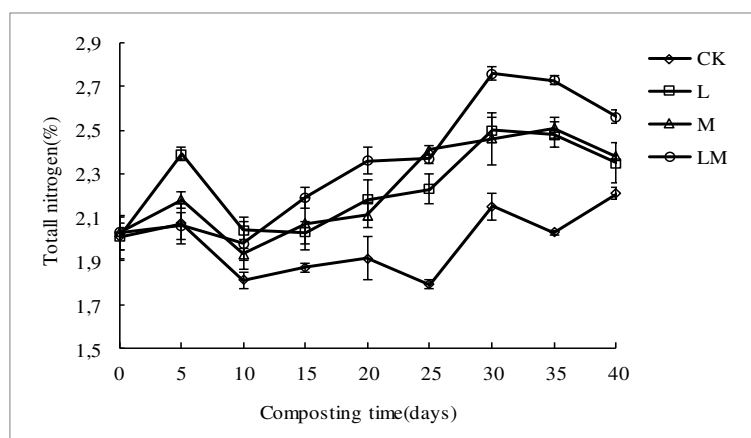


Figure 6. Changes in total nitrogen during the composting process (The error bars displayed in the figure is the positive and negative deviation of the standard deviation of data in different sampling days for each treatment)

As shown in Fig. 7, the organic carbon content is approximately 52% at the beginning of composting and then decreases with the increase in composting time. The LM treatment showed a rapid decrease in the organic carbon content, whereas the CK showed a slow decrease, with L and M falling in between the two. In the first 20 days, the decline in the organic carbon in each treatment was greater, but this decline slowed and basically stabilized after 20 days. This pattern may be due to the strong energy consumption of the microorganisms in the early composting period, which caused the loss of carbon sources. At the end of composting, the organic carbon contents of CK, L, M and LM were 33.67%, 31.95%, 32.77% and 29.88%, respectively. The organic carbon content of the LM treatment was significantly ($p < 0.05$) lower than in the other treatments.

The initial C/N range of composting is 25-30 (Zhang et al., 2015). As shown in Fig. 8, the C/N values of CK, L, M and LM at the initial composting are 26.24, 26.13, 25.78 and 25.98, respectively, which is especially suitable for microbial survival. However, as the composting test progressed, the C/N of each treatment gradually decreased and finally stabilized. This pattern occurred because the microorganisms in the composting process need to consume a large amount of carbon sources to gradually

reduce the organic carbon, whereas the relative content of the total nitrogen is increased, which means the C/N is lowered. At the end of composting, the C/N of the CK, L, M, and LM treatments decreased to 15.24, 13.60, 13.77 and 11.67, respectively, with all being lower than 20.

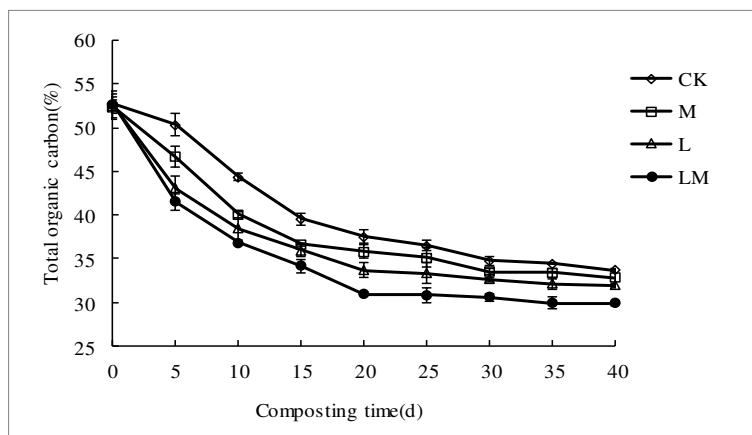


Figure 7. Changes in organic carbon during the composting (The error bars displayed in the figure is the positive and negative deviation of the standard deviation of data in different sampling days for each treatment)

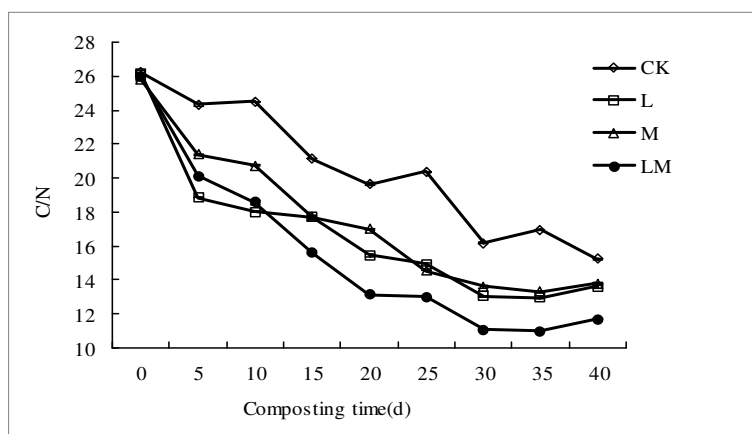


Figure 8. Changes of C/N during composting

Total potassium and total phosphorus

As shown in Fig. 9, the total potassium content of each treatment showed an increasing trend at the beginning of composting, and after 20 days, different trends began to appear. Treatments L and M reached the highest values at the end of composting with values of 15.18 g/kg and 14.94 g/kg, respectively, whereas the highest values for LM and CK appeared on days 35 and 30 with values of 14.27 g/kg and 14.41 g/kg. For the entire composting process, the total potassium content of the added microbial agents was higher than that of CK, indicating that the addition of microbial agents can promote the increase in the total potassium content.

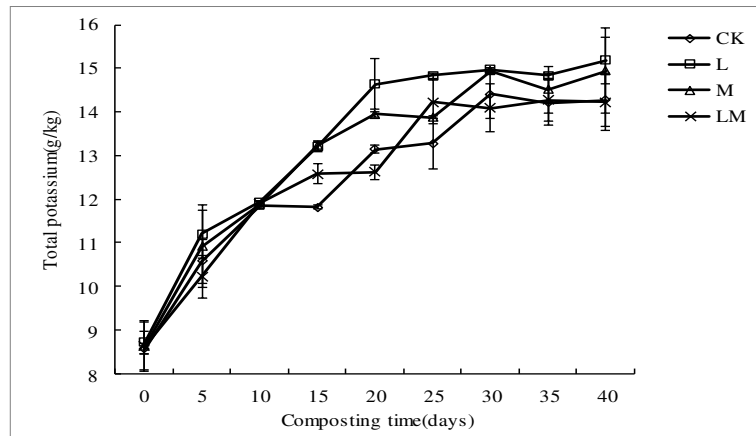


Figure 9. Change in the total potassium during the composting process (The error bars displayed in the figure is the positive and negative deviation of the standard deviation of data in different sampling days for each treatment)

As shown in Fig. 10, the total phosphorus content of each treatment gradually increased with the increase in the composting time. At 40 days of composting, the total phosphorus contents of CK, L, M and LM were 1.81 g/kg, 1.88 g/kg, 1.92 g/kg and 2.11 g/kg, respectively. In contrast, the composting increased by 1.41 times, 1.37 times, 1.37 times and 1.81 times, respectively. The total phosphorus content observed over the entire composting process was as follows: LM>M>L>CK. As indicated, the low-temperature and normal-temperature mixed bacterial treatment had the best effect.

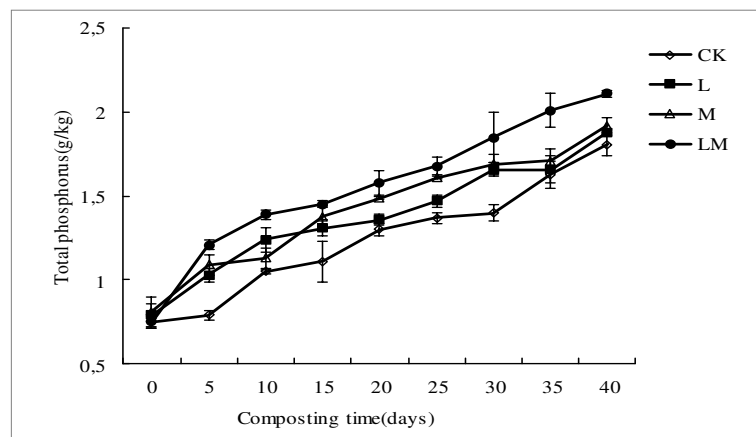


Figure 10. Change in the total phosphorus during the composting process (The error bars displayed in the figure is the positive and negative deviation of the standard deviation of data in different sampling days for each treatment)

Degradation rate of cellulose and hemicellulose

The main components of corn stalks include cellulose, hemicellulose, and lignin, which are difficult to decompose under natural conditions, and microorganisms provide the best means of degradation. As shown in Fig. 11, in the composting process, hemicellulose is decomposed by continuous consumption due to the vigorous activity of the microorganisms, so the degradation rate of the hemicellulose is continuously

increased. However, the degradation rate of hemicellulose treated with added bacteria was significantly higher than that of CK, and the degradation rate of LM was always the greatest, with L and M being in between the two. At the end of composting, the hemicellulose degradation rates of CK, L, M and LM were 25.65%, 31.22%, 33.33% and 37.52%, respectively, indicating that the addition of microbial treatment can significantly reduce the hemicellulose content, especially when inoculated at low or optimal temperatures.

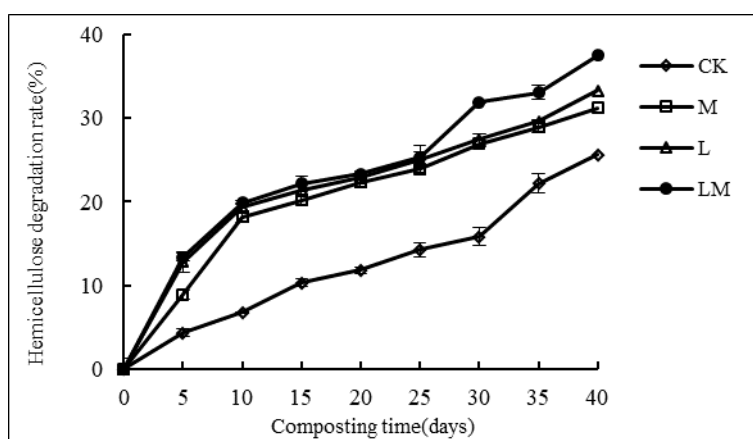


Figure 11. Changes in the degradation rate of the hemicellulose during the composting process (The error bars displayed in the figure is the positive and negative deviation of the standard deviation of data in different sampling days for each treatment)

The rate of degradation of cellulose was somewhat slower than that of the hemicellulose. As shown in Fig. 12, the cellulose degradation rates of CK, L, M and LM were 4.15%, 5.21%, 6.81% and 6.87%, respectively, at 5 days of composting, and they were 23.05%, 25.18%, 28.71% and 32.15%, respectively, at 40 days. The degradation rate of cellulose treated with added bacteria was significantly higher than that of CK. The degradation rate of cellulose in the whole composting process was as follows: LM>L>M>CK, which was consistent with the trend for changes in the hemicellulose degradation rate and indicates that the addition of microbial agents could promote the decomposition of cellulose and hemicellulose.

Changes in humus composition

As shown in Table 2, the humus, fulvic acid, humic acid and HA/FA were basically the same as before composting, and the difference was not significant ($p < 0.05$); when composted for 60 days, humus and fulvic acid showed a downward trend, whereas the humic acid and HA/FA showed an increasing trend. The humic and fulvic acids of CK (72.55 and 37.06) and M (79.82 and 16.74) were significantly higher ($p < 0.05$) than those of L (53.04 and 12.21) and LM (63.31 and 12.90); compared with CK, in the treatments with added bacteria, the humic acid content of the treatments showed a significant increase ($p < 0.05$). The order of HA/FA for the treatments was LM>M>L>CK, and the humus quality of the added bacteria was better than that of CK. The humus contents of L and LM were lower, probably because the temperature of the heap was higher than that of M and CK during the composting process. Such an

increase in temperature may lead to the more rapid decomposition rate of organic materials and to a lesser degree of humification.

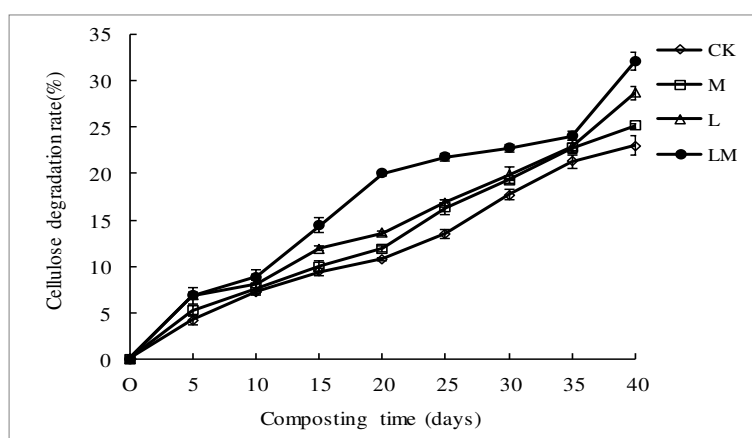


Figure 12. The change in the cellulose degradation rate during composting process (The error bars displayed in the figure is the positive and negative deviation of the standard deviation of data in different sampling days for each treatment)

Table 2. Changes in humus composition at the beginning and end of composting

Time (d)	Treatment	Humus (g/kg)	Fulvic acid (g/kg)	Humic acid (g/kg)	HA/FA
0	CK	90.99±0.10a	61.44±0.92a	29.55±1.91a	0.48±0.04a
	L	92.40±1.45a	63.29±0.83a	29.11±1.81a	0.46±0.03a
	M	92.49±0.41a	61.38±2.64a	31.11±3.03a	0.49±0.07a
	LM	91.30±5.51a	63.81±3.52a	27.50±2.02a	0.43±0.01a
40	CK	72.55±0.68a	37.06±0.42a	35.49±1.09d	0.96±0.04c
	L	53.04±2.55c	12.21±0.16c	40.83±2.42c	3.34±0.16b
	M	79.82±6.70a	16.74±0.68b	63.08±6.06a	3.64±0.32a
	LM	63.31±2.82b	12.90±0.76c	50.41±2.08b	3.91±0.09a

The data in the table were $\bar{x} \pm SD$, different lowercase letters in the same column indicated significant difference ($P < 0.05$)

Discussion

Composting is one of the means by which agricultural waste can be effectively utilized (Chen et al., 2015), and microbes play a leading role in the whole process of composting; thus, the addition of exogenous microorganisms is beneficial to accelerate the composting process (Wang et al., 2005). Composting studies on livestock manure, agricultural waste, and sludge have shown that the addition of microbial agents can increase the rate of decomposition and demonstrate the feasibility of adding exogenous agents (Lu et al., 2010; Gou et al., 2017). In this study, different microbial inoculants were added to the simple compost of corn stover, and the results showed that the temperature progression of the added bacteria treatment was accelerated, the high temperature period was prolonged, the seed germination index, total nitrogen, total potassium, total phosphorus, cellulose degradation rate, hemicellulose degradation rate, humic acid and HA/FA increased; however, the water content, conductivity, organic

carbon, C/N, humus and fulvic acid decreased, shortening the maturity time and increasing the maturity effect.

Temperature is an important indicator of composting, which can reflect the degradation of organic components and affect the composting effect (Luo et al., 2013): the higher the temperature is, the more likely the death of any pathogens (González et al., 2015). In this study, the temperature of the corn stalk heap reached 50°C, whereas in other studies that only used straw and cow dung or pig manure and other mixed composting, the temperatures reached 50°C or more. During the entire composting process in a study on fresh pig manure and wheat straw compost, the temperature did not reach 60°C (Ma et al., 2018). The current study shows that the addition of microbial agents can increase the temperature of the heap and quickly start and prolong the high temperature period, especially as observed with the LM treatment; these results are consistent with the results of Gou et al. (2017). An increase in temperature causes the water to evaporate, which affects the water content of the heap. Most studies have shown that, at the end of composting, the water content of the heap is less than 30% (Feng et al., 2013; Li et al., 2014), and at the end of the composting, the water content of each treatment is greater than 30%, which may occur because part of the heap is buried in the soil and all of the heap is covered with a plastic sheet with a small vent, thus resulting in undisturbed water dispersion.

The increase in pH is due to the decomposition of proteins and amino acids during composting to produce ammonia, which increases the pH (Jiang et al., 2015). The pH reduction is due to the formation and nitrification of low molecular weight fats (Zorpas et al., 2008). The final pH of the test is less than 9, which meets the compost maturity standard (Debertoldi et al., 1983). Conductivity (EC) is an important indicator for use when measuring the compostability of materials. The conductivity of each treatment at the end of composting was less than 2500 µs/cm, so it meets the requirements of compost maturity (Sheng et al., 2017) and will not affect the normal growth of plants. Some studies have suggested that when GI>50%, compost is basically harmless to plant growth and development and reaches basic maturity, whereas when GI>80%, compost can be considered fully decomposed (Zucconi et al., 1981). In all the treatments in this study, the seed germination index was more than 50% during the whole period of composting. This result may be obtained because the corn stalk itself contains less toxicity, and composting can increase the nutrients of the heap, thus providing sufficient seed germination and nutrients.

Composting can increase the total nitrogen, total potassium and total phosphorus content of organic matter, especially the addition of microbial agents, which is consistent with the results of Jia et al. (2011) and Gou et al. (2017). The reduction in the organic carbon in corn stalks is caused by the respiration of microorganisms, which causes the carbon source in the straw to be released in the form of CO₂. The greater the number of microorganisms, the stronger the activity is and the greater the consumption of the carbon sources; thus, the organic carbon decreases more rapidly (Yang et al., 2013), C/N is an important indicator to measure the degree of compost maturity. Generally, when C/N is 15-20, the compost has reached the maturity standard (Shi, 2010). At the end of composting, the C/N of each treatment was less than 20, so the decomposing effect was achieved. In comparison, the C/N ratio reported by Wei et al. (2007) and for other domestic waste composts is 12.95 at 63 days, but most of the research on compost has reported a C/N greater than 15 (Lao et al., 2015), which may be related to the initial adjustment of the C/N ratio during composting.

The addition of microbial compost is beneficial to the degradation of cellulose and hemicellulose, which is consistent with the results of Gou et al. (2015). This may be because, after the addition of the microbial agent, the enzyme produced can hydrolyze the cellulose and hemicellulose in the straw, thereby destroying the complex structure of the lignocellulose and promoting the rapid degradation of the straw. The composition, content and quality of humus in the compost can be used as important parameters for compost quality and maturity (Bremanis et al., 2013). The compost in this study showed a downward trend in the humus and fulvic acid, whereas the humic acid and HA/FA showed an increasing trend, which is consistent with the results of Chen et al. (2007) and Liu et al. (2018). Thus indicating that compost is beneficial to the transformation of organic matter to humus and to its stabilization.

Conclusion

The results of this study show that, compared with CK, the treatments receiving the added microbial agents showed the rapid initiation of a high temperature period that was prolonged and showed beneficial changes in the seed germination index, total nitrogen, total potassium, total phosphorus, cellulose degradation rate, and hemicellulose degradation rate. The carbon content of HA and the HA/FA showed an increasing trend, whereas the water content, conductivity, organic carbon, C/N, humus and eucalyptus carbon content of the heap showed a downward trend with the addition of the low-temperature bacteria + normal-temperature bacteria. The LM treatment showed the best effect, not only shortening the maturity cycle but also increasing the compost quality, which provides a theoretical basis for straw composting in areas with low temperatures.

Implications for conservation

This study explored the effects of different microbial agents on corn stalk composting to enable the development of microbial agents suitable for composting corn stalks in cold regions of northern China. Microbial agents can effectively breakdown straw into a large number of elements such as the nitrogen, phosphorus and potassium required by crops and trace elements such as calcium, magnesium, manganese and molybdenum, which can improve the physical and chemical properties of the soil, improve the soil organic matter, enhance soil aeration, protect fertilizer and water retention function, and stimulate crop growth and development. Additionally, composting is an effective way to quickly dispose of livestock manure and agricultural waste. The heat generated during composting process can break down organic matter into stable humus, which can be used as organic fertilizer. Therefore, this study conducted a simple composting test on straw by adding low-temperature bacteria, normal-temperature bacteria and low-temperature and normal-temperature mixed bacteria to study the dynamic changes occurring in the various maturity indexes during the composting process, thus providing feasible utilization measures for straw wastes in northern areas.

The results of this study show that, compared with CK, the treatments receiving the added microbial agents showed the rapid initiation of a high temperature period that was prolonged and showed beneficial changes in the seed germination index, total nitrogen, total potassium, total phosphorus, cellulose degradation rate, and hemicellulose degradation rate. The carbon content of HA and the HA/FA showed an increasing trend, whereas the water content, conductivity, organic carbon, C/N, humus and eucalyptus

carbon content of the heap showed a downward trend with the addition of the low-temperature bacteria + normal-temperature bacteria. The LM treatment showed the best effect, not only shortening the maturity cycle but also increasing the compost quality, which provides a theoretical basis for straw composting in areas with low temperatures.

Acknowledgements. We thank Yanan Li from Jilin University for her help in technical, and we are grateful to Yangsheng Wu, Yan Du, Jinxiu Li, Rong Cui, Xinyu Zhang and Qiuping Feng for their help with sample extraction. Moreover, we thank two anonymous reviewers for their comments on an earlier draft of this manuscript.

Author Contributions. Hongyan Chang, Shuifeng Lu, Ziyuan Huang, Yuxin Liu, Tianye Wang, Chengyu Wang and Shuxia Liu conceived the study. Hongyan Chang, Shuifeng Lu, Ziyuan Huang and Yuxin Liu performed the experiments. Hongyan Chang, Shuifeng Lu, Chengyu Wang and Tianye Wang wrote the manuscript. All authors reviewed the manuscript and agree with its contents.

Data Availability. The data used in this study is available from the corresponding author upon request.

Declaration of Conflicting Interests. The author(s) declared no potential conflicts of interest with respect to the research, authorship, and/or publication of this article.

Funding. The author(s) disclosed receipt of the following financial support for the research, authorship, and/or publication of this article: This work is a contribution of the Jilin Province Science and Technology Development Plan (20160307006NY), National Key Research and Development Programme (2017YFD0300405-4), Natural Science Foundation of Jilin Province, China (20170101077JC).

Ethical approval. This article does not contain any studies with human participants or animals performed by any of the authors. The article is an original paper, is not under consideration by another journal, and has not been published previously. All authors read and approved the final manuscript.

REFERENCES

- [1] Bremanis, G., Klavinš, M., Purmalis, O., Ziemelis, R., Malecka, S. (2013): Peat humic substances and earthworm biohumus extracts for agricultural applications. – Proceedings of the Latvian Academy of Sciences 67(3): 236-241.
- [2] Cao, X. Y., Li, J. P., Yan, W. D. (2014): Distribution characteristics and coupling relationship of soil organic carbon and nitrogen, phosphorus and potassium in Chinese fir forests of different age groups. – The soil and water conservation 45(5): 1137-1143.
- [3] Chen, G. Y., Wang, D. H., Wu, Y., Li, J. F., Liu, C. H., Xiang, Q. B. (2007): Dynamic changes of organic matter during defoliation composting. – Journal of South China Agricultural University 28(2): 1-4.
- [4] Chen, M., Xu, P., Zeng, G. M., Yang, C. P., Huang, D. L., Zhang, J. H. (2015): Bioremediation of soils contaminated with polycyclic aromatic hydrocarbons, petroleum, pesticides, chlorophenols and heavy metals by composting: Applications, microbes and future research needs. – Biotechnology Advances 33(6): 745-755.
- [5] Debertoldi, M., Vallini, G., Pera, K. A. (1983): The biology of composting: A review. – Waste Management & Research 1(1): 157-176.
- [6] Dou, S., Yu, S. Q., Zhang, J. J. (2007): Effect of CO₂ Concentration on Soil Humus Formation during Decomposition of Corn Stalk. – Journal of Soil Science 44(3): 458-466.
- [7] Feng, Z., Li, J., Zhang, G. B., Li, W. L., Jia, H. Y., Liu, Z. F., Yu, J. H. (2013): Effect of different microbial agents on aerobic composting of corn stover. – Chinese vegetables 1(6x): 82-87.

- [8] Gao, Y. H., Gou, C. L., Wang, Y. Q., Wang, W., Zhao, H. X., Lou, Y. J. (2014): Study on the Effect of Low Temperature Compound Bacteria on Cow Manure Composting Fermentation. – *Journal of Environmental Science* 34(12): 3166-3170.
- [9] Gong, J. J., Hu, H. X., Zhu, C. X., Tang, M. M., Xia, X. (2018): A Summary of the Effects of Straw Returning on Farmland Ecological Environment. – *Jiangsu Agricultural Science* 46(23): 44-48.
- [10] González, I., Robledo-Mahón, T., Silva-Castro, G. A., Rodríguez-Calvo, A., Gutiérrez, M. C., Martín, M. Á., Chica, A. F., Calvo, C. (2015): Evolution of the composting process with semi-permeable film technology at industrial scale. – *Journal of Cleaner Production* 115: 245-254.
- [11] Gou, C. L., Wang, Y. Q., Wang, W., Zhao, H. X., Lou, Y. J., Gao, Y. H. (2015): Screening and Identification of Low Temperature Cellulose Degrading Fungi from Two Changbai Mountain Areas and Optimization of Its Enzyme Production Conditions. – *Journal of Sun Yat-sen University (Natural Science Edition)* 54(5): 115-121.
- [12] Gou, C., Wang, Y., Zhang, X., Lou, Y., Gao, Y. (2017): Inoculation with a psychrotrophic-thermophilic complex microbial agent accelerates onset and promotes maturity of dairy manure-rice straw composting under cold climate conditions. – *Bioresource Technology* 243: 339-346.
- [13] Hachicha, R., Rekik, O., Hachicha, S., Ferchichi, M., Woodward, S., Moncef, N., Cegarra, J., Mechichi, T. (2012): Co-composting of spent coffee ground with olive mill wastewater sludge and poultry manure and effect of *Trametes versicolor* inoculation on the compost maturity. – *Chemosphere* 88(6): 677-682.
- [14] Hu, C., Chen, Y. F., Qiao, Y., Liu, D. H., Zhang, S. T., Li, S. L. (2016): Improvement effect of straw returning with decomposing agent on low-yield yellow muddy field. – *Journal of Plant Nutrition and Fertilizer* 22(1): 59-66.
- [15] Jia, C. J., Zhang, Y. X., Du, W. C., Wang, D. G., Shi, T., Li, Y. K., Niu, Z. Y. (2011): Effect of microbial inoculation on the composting effect of pig manure. – *Journal of Animal Ecology* 32(5): 73-76.
- [16] Jiang, J. S., Liu, X. L., Huang, Y. M., Huang, H. (2015): Inoculation with nitrogen turnover bacterial agent appropriately increasing nitrogen and promoting maturity in pig manure composting. – *Waste Management* 39: 78-85.
- [17] Lao, D. K., Zhang, L. L., Li, Y. B., Du, Y., Han, H., Li, J. (2015): Effects of microbial straw decomposing agents with different inoculum on composting effect of vegetable by-products. – *Journal of Environmental Engineering* 9(6): 2979-2985.
- [18] Li, J., Yu, J. H., Feng, Z., Jie, J. M., Jie, X., Jiang, L., Zhang, J. (2014): Effect of different microbial agents on aerobic composting of cow manure. – *Arid area resources and environment* 28(2): 109-113.
- [19] Li, Y., Li, W. (2015): Nitrogen transformations and losses during composting of sewage sludge with acidified sawdust in a laboratory reactor. – *Waste Manage Res* 33(2): 139-145.
- [20] Liu, Y. Y., Xu, Z., Chen, Z. J., Tang, L. (2018): Effect of exogenous phosphorus phosphogypsum on carbon content and humus quality of compost. – *Journal of Agricultural Environmental Science* 37(11): 2483-2490.
- [21] Lou, Y., Xu, M., Wang, W., Sun, X., Zhao, K. (2011): Return rate of straw residue affects soil organic c sequestration by chemical fertilization. – *Soil and Tillage Research* 113(1): 70-73.
- [22] Lu, B. L., Wang, W. L., Li, J., Ma, Z. M. (2010): Effect of adding wheat straw on the composting process of pig manure at high temperature compost. – *Journal of Environmental Engineering* 4(4): 926-930.
- [23] Luo, Y. M., Xu, D. G., Li, G. X. (2013): Effect of superphosphate as additive on nitrogen and carbon losses during pig manure composting. – *Applied Mechanics and Materials* 295-298: 1675-1679.

- [24] Ma, S. S., Sun, X. X., Fang, C., He, X. Q., Han, L. J., Huang, G. Q. (2018): Exploring the mechanisms of decreased methane during pig manure and wheat straw aerobic composting covered with a semi-permeable membrane. – *Waste Management* 78: 393-400.
- [25] Mulumba, L. N., Lal, R. (2008): Mulching effects on selected soil physical properties. – *Soil & Tillage Research* 98(1): 106-111.
- [26] Sheng, D. C., Ao, J. H., Zhou, W. L., Chen, D. W., Huang, Y., Huang, Z. R., Li, Q. W., Jiang, Y. (2017): Effect of Different Organic Materials Ratio on High Temperature Composting of Corn Stover. – *Guangdong Agricultural Science* 44(11): 86-91.
- [27] Shi, C. C. (2010): Study on co-metabolism degradation and kinetics of organic pollutants. – *Chemical engineering and equipment* 7: 164-167.
- [28] Wang, W. P., Wang, K. Y., Xue, Z. Y., Zhu, F. X. (2005): Effect of different microbial agents on ammonia volatilization in pig manure compost. – *Journal of Applied Ecology* 4: 693-697.
- [29] Wang, C. F., Ma, S. C., Huang, Y., Liu, L. Y., Fan, H., Deng, Y. (2016): Degradation of rice straw complex strains and microbial community structure succession. – *Journal of microbiology* 12.
- [30] Wang, X. L. (2018): Analysis of the role of organic fertilizer in agricultural production. – *Rural economy and technology* 442(14): 43.
- [31] Wei, Z. M., Wang, S. P., Xi, B. D., Zhao, Y., He, L. S., Jiang, Y. H., Liu, H. L. (2007): Changes of humus and organic nitrogen components during composting of domestic waste. – *Journal of Environmental Science* 27(2): 235-240.
- [32] Yan, X., Hou, M. Y., Li, B. Q., Wang, S., Liang, Y. C. (2018): Effects of Microbial Fermentation Bacteria, Biomass Carbon and Mushroom Slag on Sludge Composting. – *Environmental science research* 31(01): 136-142.
- [33] Yang, X. Y., Lin, X. W., Dou, S. (2013): Effects of Different Oxygen Conditions on the Humus of Corn Straw in Soil. – *Journal of Northeast Forestry University* 41(1): 106-108.
- [34] Zhang, L., Ma, H., Zhang, H., Xun, L., Chen, G., Wang, L. (2015): *Thermomyces lanuginosus* is the dominant fungus in maize straw composts. – *Bioresource Technology* 197: 266-275.
- [35] Zhou, Y., Zhu, N. W., Liu, B. W., Zhang, T. P. (2018): Analysis on the effect of microbial agent compounding and strengthening aerobic composting of kitchen waste. – *Journal of Environmental Engineering* 12(01): 294-303.
- [36] Zorpas, A. A., Loizidou, M. (2008): Sawdust and natural zeolite as a bulking agent for improving quality of a composting product from anaerobically stabilized sewage sludge. – *Bioresour Technol* 99(16): 7545-7552.
- [37] Zucconi, F., Forte, M., Monac, A. (1981): Evaluating toxicity of immature compost. – *Biocycle* 22(2): 54-57.

A GENERIC AGROHYDROLOGICAL MODEL WITH READILY AVAILABLE PARAMETERS FOR WATER MANAGEMENT IN CROP PRODUCTION

WU, F. Q. – LI, P. – WU, G. F. – ZHANG, K. F.*

*Ningbo Institute of Technology, Zhejiang University, Ningbo 315100, China
(phone: +86-574-8813-0254; fax: +86-574-8813-0283)*

*Corresponding author
e-mail: kfzhang@nit.zju.edu.cn

(Received 6th Feb 2020; accepted 6th May 2020)

Abstract. Agrohydrological models have increasingly become more and more powerful tools for precise agricultural water management. Although there are numerical models available, many of them are either oversimplified leading to unreliable results, or too complex and difficult to use. In this study, an agrohydrological model, which strikes a balance between the accuracy, complexity and generality, was first proposed by integrating a newly developed module for computing crop evapotranspiration using the dual crop coefficient approach by FAO56 into the widely employed HYDRUS-1D model. The proposed model was then validated and rigorously assessed against data from the field experiments of winter wheat grown in two contrasting soils. Results showed that the proposed model made good predictions for soil water content in various layers over the growing period. Also, it was revealed that the water initially contained in the subsoil accounted for about half of the total evapotranspired amount. The simulated proportions of root water uptake from each quarter of rooting depth coincided well with those from the previous studies under the condition of crops grown free from water stress. This indicates that the devised easy-to-use model had the potential to be utilised in studying soil-crop water relations.

Keywords: *HYDRUS-1D, soil-crop system, soil water dynamics, evapotranspiration, agricultural water management*

Introduction

Agriculture is the biggest water consumer in the world. It consumes about 70% world's accessible fresh water, and 60% of the applied water is wasted (Clay, 2004). It is, therefore, crucially important to manage precisely agricultural water use to save the world's most precious resource. With advances in soil and plant sciences and computer technology, more and more agrohydrological models, which accounts for the key processes governing the water cycle in the soil-crop system, have been developed, and are now playing an important role in agricultural water management (see reviews by Bastiaanssen et al. (2007) and more recently by Siad et al. (2019)).

In agrohydrological models, the algorithms of cascade type are often used for modeling soil water movement due to its simplicity (Burns, 1974; Arnold et al., 1993; Brisson et al., 1998; Droogers et al., 2001; Greenwood, 2001; Zhang et al., 2007, 2020; Renaud et al., 2008; Steduto et al., 2009; Rahn et al., 2010; Strati et al., 2018). Such models assume that downwards water flow only occurs when soil water content in a layer exceeds its field capacity and upwards flow is not allowed. The models use few parameters such as water content at saturation and field capacity and employ simple numerical algorithms. However, the determination of the flow coefficient in these models has proven problematic as it varies with time step, soil texture and other soil physical properties (Yang et al., 2009). As a result the flow coefficient often requires to be calibrated using a trial-and-error approach in advance.

On the other hand, the numerical models using Richards' equation for soil water movement are more accurate, but more complex in predicting water dynamics in the soil-crop system. Enormous efforts have been made in developing agrohydrological models using the basic theory for soil water movement. Although great progress has been achieved (Bastiaanssen et al., 2007), the developed models use many parameters which are difficult to obtain, especially in the aspect of plant (Keating et al., 2003; Stöckle et al., 2003; Rahil and Antonopoulos, 2007). Dozens of parameters and complex algorithms describing crop physiology are normally involved in such as the EPIC models by Williams et al. (1993) and the DSSAT models by Jones et al. (2003). The models of this kind are often used in basic research or for specific crops, but are difficult to be applied universally and practically, resulting in low uptake of such models in crop production in agriculture (Bastiaanssen et al., 2007). Further, a review on agrohydrological models by Cannavo et al. (2008) revealed that a majority of models only dealt with a single crop.

Although numerous agrohydrological models have been proposed during the last decades, the importance of coupling hydrological and crop models for water use in crop management has been stressed in the recent review by Siad et al. (2019). A large body of literature show that such models have been further developed and widely applied for research and practical purposes. Bao et al. (2017) compared CSM-CERES-Maize and EPIC models for maize production, while Dokoohaki et al. (2016) developed a new version of CSM-CERES-Maize model by coupling SWAP and DSSAT package. Tribouillois et al. (2018) used AqYield model for predicting water balance of wheat and crop rotations. Autovino et al. (2018) employed Hydrus-2D model to study soil and plant water status dynamics in olive orchards under different irrigation systems.

It is clear from the above that agrohydrological models have become powerful tools for agricultural water management. In spite of great efforts directed in developing agrohydrological models, there is still a clear need to devise models which strike the right balance between models' accuracy, complexity and generality. This is especially true for models to be used for the practical purpose where parameter values for sophisticated models are often unavailable.

In this study we aimed to develop and validate an agrohydrological model which uses the basic theory for soil water movement and relatively easily available parameters for crops. Since the HYDRUS-1D model (Šimunek et al., 2005) was well validated and widely used for simulating water movement and solute transport in agricultural soils (Shelia et al., 2017; Wang et al., 2017), it was chosen to form the framework of the agrohydrological model proposed in the study. The model was devised by combining the HYDRUS-1D model with a newly developed module for estimating potential evapotranspiration based on the dual crop coefficient approach by FAO56 (Allen et al., 1998) which could be used over a wide range of crops with readily available parameter values. Upon the completion of the model, the performance of the model was objectively evaluated against a widely used and commonly available dataset from the field experiments on winter wheat grown in two contrasting soils.

Materials and methods

Model description and evaluation

Model description

The simulations in this study were carried out by using the HYDRUS-1D model integrated with the module for estimating potential crop transpiration and soil evaporation. As mentioned the above, HYDRUS-1D is a universal model simulating water movement and solute transport in porous media. Due to its nature of generality and well validated, the model has widely been applied successfully in a wide range of field. However, the model cannot be directly employed to simulate the dynamic process of water cycle in the soil-crop system during growth due to its inability of estimating evapotranspiration. In order to overcome the problem, we first developed a module for computing potential crop transpiration and soil evaporation based on the dual crop coefficient approach by the FAO56 (Allen et al., 1998), and then incorporated it into the HYDRUA-1D model. In the following we highlight the theory of developing such a module, while the detailed description of the HYDRUS-1D model can be seen elsewhere (Šimunek et al., 2005).

The potential crop transpiration and soil evaporation were calculated according to the dual crop efficient approach and estimated evapotranspiration by FAO56 (Allen et al., 1998). Both crop coefficients are dependent on crop species and its growth stages. Such an approach, simple though, has well validated over a wide range of crops under conditions of various climates and soils, and was employed by our previous studies (Yang et al., 2009; Zhang et al., 2009, 2010, 2020).

Daily potential evapotranspiration (*Equation 1*) is calculated by the Penman-Monteith equation (Allen et al., 1998):

$$ET_0 = \frac{0.408\delta(R_n - G) + 900\gamma/(T + 273)u_2(e_s - e_a)}{\delta + \gamma(1 + 0.34u_2)} \quad (\text{Eq.1})$$

where R_n ($\text{MJ m}^{-2} \text{d}^{-1}$) is the net radiation at the crop surface, G ($\text{MJ m}^{-2} \text{d}^{-1}$) is the soil heat flux density, u_2 (m s^{-1}) is the 24 h average, wind speed at 2 m height, e_s (kPa) is the saturation vapor pressure, e_a (kPa) is the actual vapor pressure, δ ($\text{kPa } ^\circ\text{C}^{-1}$) is the slope of the vapor pressure curve, γ ($\text{kPa } ^\circ\text{C}^{-1}$) is the psychrometric constant.

The calculated potential evapotranspiration ET_0 is partitioned into crop evaporation and soil evaporation using (Allen et al., 1998) (*Equations 2 and 3*):

$$ET_c = T_{pot} + E_{pot} = (K_{cb} + K_e)ET_0 \quad (\text{Eq.2})$$

in which:

$$K_e = \min(K_{c_{max}} - K_{cb}, fK_{c_{max}}) \quad (\text{Eq.3})$$

where T_{pot} and E_{pot} are the potential transpiration and evaporation, respectively, K_{cb} and K_e are the basal crop coefficient for transpiration and the evaporation coefficient, respectively, $K_{c_{max}}$ is the maximum evapotranspiration coefficient, and f is the soil fraction not covered by plants and exposed to evaporation.

K_{cb} increases with time at the crop development stage in a linear manner, and reaches its maximum and is stabilized in the middle growth stage when the ground is fully covered before it decreases with time towards crop maturity. K_e , however, changes in the opposite direction as K_{cb} . For the different crops, the values of both K_{cb} and K_e together with the definition of crop growth stages are given in Allen et al. (1998).

Figure 1 illustrates the calculation procedures in the agrohydrological outlined the above.

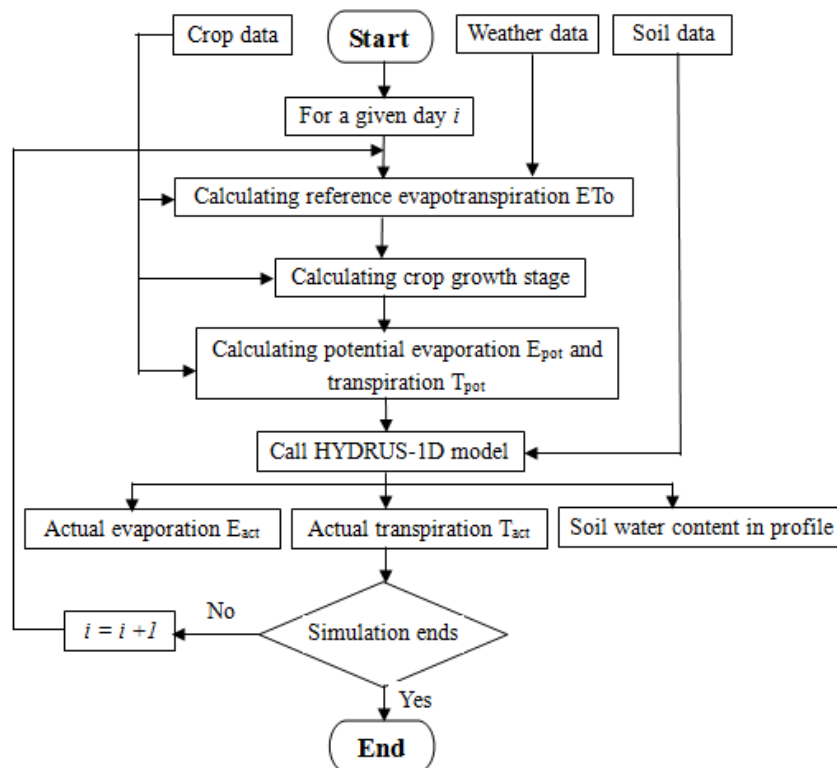


Figure 1. Flow chart of the proposed agrohydrological model for water dynamics

The biggest advantage of employing the dual crop coefficient approach by FAO56 (Allen et al., 1998) for estimating soil evaporation and crop transpiration was its generality. It could be applied with readily available parameter values for various crops. This approach was well validated and accepted worldwide and was successfully adopted in numerous agrohydrological models for calculating evapotranspiration (Zhang et al., 2010; Rahn et al., 2010).

Model parameters

Only few parameters are needed for running the model. Basically they are composed of three different types: soil data, crop data and weather data. The van Genuchten soil hydraulic properties (van Genuchten, 1980) describing the relations between soil water content, soil hydraulic conductivity and soil water potential in different soil layers are required. For the crop data they are the crop species, the dates of crop sowing/planting and harvest, the durations of various crop growth stages (initial, development, middle and late) and their corresponding values of dual crop coefficients K_{cb} and K_e according to

FAO56 (Allen et al., 1998). The weather data include daily solar radiation, maximum and minimum air temperature, relative humidity, air speed and rainfall. The model can be run with the values of the above parameter together with soil boundary conditions and initial water content distribution in the soil profile.

Model evaluation

The model performance was assessed using the commonly adopted statistical indices of the Nash–Sutcliffe model efficiency coefficient (NSE) (Nash and Sutcliffe, 1970) (Equation 4), the root of the mean squared errors (RMSE) (Equation 5) and the mean error (ME) (Equation 6). Such an approach for assessing hydrological models was widely applied (Bohne and Salzmann, 2002; Yang et al., 2009; Zhang et al., 2020).

$$NSE = 1 - \frac{\sum_{i=1}^N (Y - Y')^2}{\sum_{i=1}^N (Y - \bar{Y}')^2} \quad (\text{Eq.4})$$

$$RMSE = \sqrt{\frac{1}{N} \sum_{i=1}^N (Y - Y')^2} \quad (\text{Eq.5})$$

$$ME = \frac{1}{N} \sum_{i=1}^N (Y - Y') \quad (\text{Eq.6})$$

where Y and Y' are the simulated and measured values, respectively, N is the total number of measurements, and \bar{Y}' is the average of the measured values.

Experiments

The data from field experiments on winter wheat conducted at the Institute for Soil Fertility Research, The Netherlands from 1983 to 1984 (Groot and Verberne, 1991) was used to validate the model outlined the above. The measured dataset was comprehensive, and has been used extensively in previous studies to test agrohydrological models (De Willigen, 1991; Yang et al., 2009). A brief description of the experiments is given below, while the detailed description of the experiments can be found elsewhere (Groot and Verberne, 1991).

The experiments were conducted on two sites with contrasting soils: the Bouwing experiment (silty clay loam) and the PAGV experiment (silty loam) for the purpose of investigating the effects of both nitrogen and water on wheat growth. The crop was planted on 27 October, 1983, and harvested on 21 August, 1984. The total growth duration was 299 days. The durations of initial, development, middle and late growth stages were 37 days, 175 days, 50 days and 37 days, respectively. The soil physical properties in the 0–40 and 40–100 cm in the Bouwing farm, and in the 0–25, 25–40 and 40–100 cm in the PAGV farm were measured for determining soil hydraulic properties. The gravimetric soil water content in the layers of 0–20, 20–40, 40–60, 60–80 and 80–100 cm were measured from soil cores taken in eight replicates at intervals of three weeks on 14 Feb., i.e. Day of Year 45 (DOY 45), 13 Mar. (DOY 73), 03 Apr. (DOY 94), 24 Apr. (DOY

115), 08 May (DOY 129), 28 May (DOY 149), 19 Jun. (DOY 171), 03 Jul. (DOY 185), 17 Jul. (DOY 199), and 07 Aug. (DOY 220) in 1984 in each experiment. Also, the development of root growth was measured in the experiments, and the maximum rooting depth of 100 cm at harvest was measured. The measured weather variables included daily radiation, air temperature, relative humidity and rainfall. The measurements, taken at the Wageningen meteorological station located at a distance of 7 km from the Bouwing experiment and the Swifterbant meteorological station located at a distance of 15 km from the PAGV experiment, covered the entire crop growth period (Groot and Verberne, 1991).

Preparation of model run

Model parameterization

The model operated with a daily time step, with the data from soil, crop and weather as model inputs.

Soil data included the parameters describing the relationships of soil water content and hydraulic conductivity with soil water pressure head. The measurements for such relationships were carried out in the experiments (Groot and Verberne, 1991), but the measured parameters were not related in the way proposed by van Genuchten (1980). Since the model only used van Genuchten soil hydraulic parameters, the fitting procedure was implemented based on the measured layered datasets and the commonly available RETC software (van Genuchten, 1991). The fitted van Genuchten soil hydraulic properties for the various layers in both experiments are shown in *Table 1* (after Yang et al., 2009).

Table 1. Fitted van Genuchten soil hydraulic parameter values using the RETC software (after Yang et al., 2009)

	0–40 cm	40–100 cm	0–25 cm	25–40 cm	40–100 cm
θ_s (cm ³ cm ⁻³)	0.51	0.49	0.42	0.50	0.53
θ_r (cm ³ cm ⁻³)	0.00	0.00	0.04	0.06	0.06
α	0.0266	0.0046	0.0162	0.0096	0.0098
n	1.1841	1.1835	1.299	1.3460	1.3193
K_s (cm d ⁻¹)	40.0	2.0	160.0	33.0	200.0

Crop data used in the model were the dates of crop sowing and harvest, and the durations of various crop growth stages and their associated dual coefficients for soil evaporation and crop transpiration. The durations of the initial, development, middle and late crop growth stages was calculated according to the proportionalities over the entire growth period given in the FAO56 (Allen et al., 1998) for the studied crop. Also, the corresponding values of crop coefficients were taken from the FAO56. Thus, on any day during growth, the crop growth stage and the coefficients for evaporation and transpiration could be determined, given the reference evapotranspiration ET_0 (Equation 1) was known.

Weather data together with the geographical properties of the experimental plots were used for computing ET_0 . The weather data included daily air temperature, relative humidity, solar radiation, wind speed and rainfall. These items were all measured and used directly in the model run.

Computational domain and boundary conditions

In both experiments, the calculated soil depth was 120 cm, 20 cm longer than the measured maximum rooting depth. The lower boundary in the Bouwing experiment was set as free drainage as there were layers of gravel at that depth, while in the PAGV experiment the lower boundary was specified as soil in saturation based on the experimental observations of the groundwater table (Groot and Verberne, 1991). These boundary conditions were identical as those used in the study by Yang et al. (2009). The date of the first measurements was used as the starting point, while the measured values of soil water content along the profile to the 120 cm depth were used as the initial conditions in the simulations.

Results and discussion

Overall assessment of the model performance

The statistical analyses between the simulated and measured values of soil water content at different depths collected during growth reveal that the model performed satisfactorily in simulating water dynamics for the studied cases (Table 2). The calculated values of *RMSE* and *ME*, both less than $0.05 \text{ cm}^3 \text{ cm}^{-3}$, are all small, and the *NSE* values are relatively high. While the model over- and under-predicted slightly for the Bouwing and PAGV experiments (Table 2), respectively, no noticeable mean error was found in the overall comparison between simulation and measurement. This is also reflected in Figure 2 where the best fitted line is virtually overlapped the 1:1 line. Judged from Table 2 and Figure 2, it is reasonable to conclude that the simulated values of soil water content in various layers at various time intervals are in good agreement with the measurements, indicating the model is able to make good predictions.

Table 2. Statistical indices between the simulated and measured values of soil water content

	RMSE ($\text{cm}^3 \text{ cm}^{-3}$)	ME ($\text{cm}^3 \text{ cm}^{-3}$)	NSE (-)
Bouwing experiment	0.033	-0.012	0.586
PAGV experiment	0.043	0.010	0.550
Both experiments	0.038	-0.001	0.634

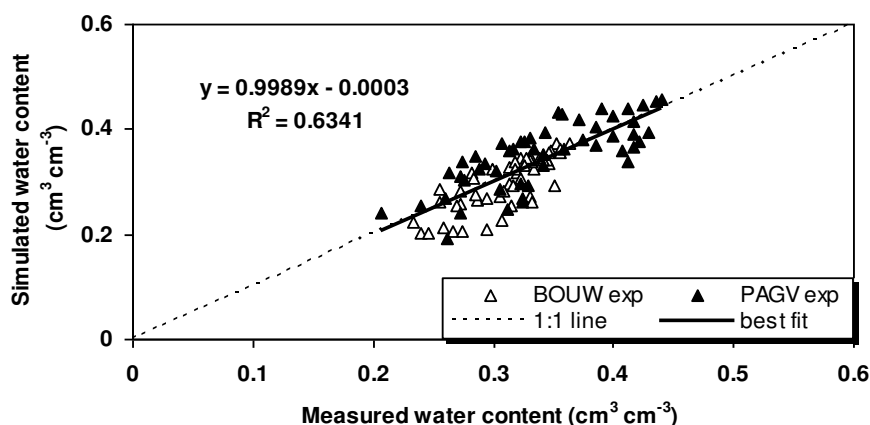


Figure 2. Comparison of soil water content between simulation and measurement in both experiments

Comparison of soil water content between simulation and measurement

Detailed comparisons of soil water content over the entire simulation period in the different layers for both experiments are carried out, and *Figure 3* shows some of such comparisons as an example. Except for the layers of 20-40 cm where the noticeable discrepancies occur between simulation and measurement, all the other simulated values of soil water content agreed well with the measured values. Also it reveals that only in the top soil layer did the changes in soil water content correlate highly with rainfall, suggesting that the effect of rainfall mainly limited in the 20 cm depth. The discrepancies in the 20-40 cm layer might be due to the fact that this is the region where the boundary lies to separate the topsoil from the subsoil, and thus is difficult to determine soil hydraulic properties with accuracy (Yang et al., 2009). Overall *Figure 3* confirms the results from statistical analyses shown previously that the model is capable of reproducing the results from the experiment.

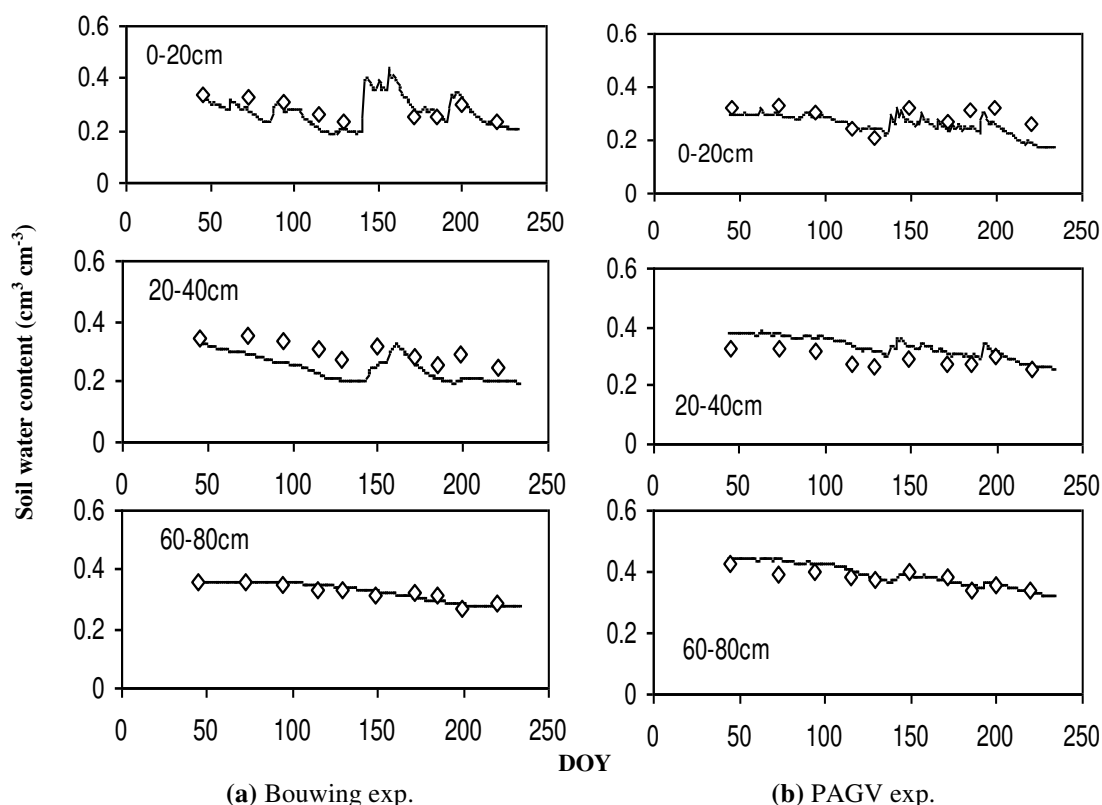
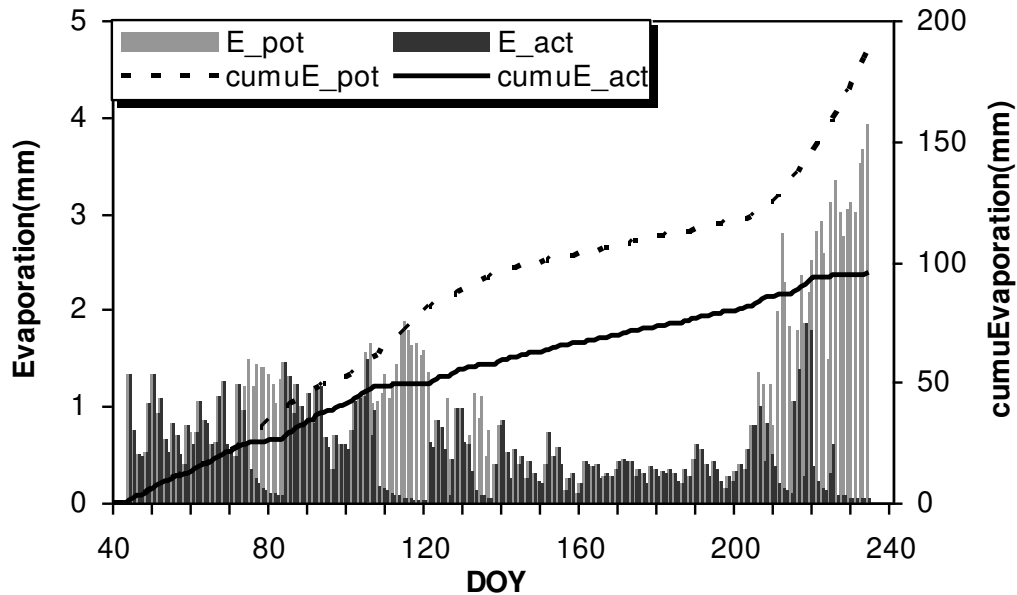


Figure 3. Comparison between the measured and simulated volumetric soil water content at different soil layers in the Bouwing experiment (a) and in the PAGV experiment (b)

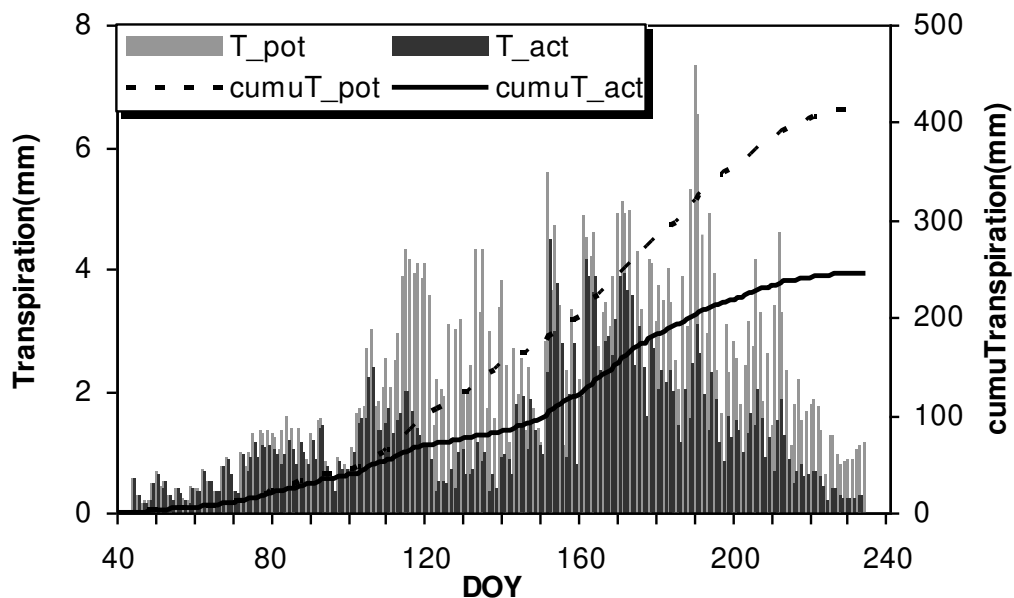
Simulated soil evaporation and crop transpiration

Soil evaporation and crop transpiration for the experiments were simulated and plotted in *Figures 4* and *5*. Clearly both the potential soil evaporation and crop transpiration estimated by the FAO56 were not met in the Bouwing experiment (*Figure 4*). During the periods of DOY 73-83, DOY 106-121 and after DOY 211, the simulated soil evaporation values were less than the potential ones. As for the crop transpiration, there were two periods of DOY 103-143 and DOY 180-234 when the simulated values were greatly

smaller than the potential ones (*Figure 4b*). However, the situation in the PAGV experiment was rather opposite. *Figure 5* demonstrates that only in a very small period towards the harvest when the simulated values of soil evaporation and crop transpiration did not achieve the potential values, the demanded crop evapotranspiration for the maximum growth was met, suggesting that the crop was not stressed induced by water deficit.



(a)



(b)

Figure 4. Simulated daily and cumulative potential and actual evaporation (a) and transpiration (b) in the Bouwing experiment

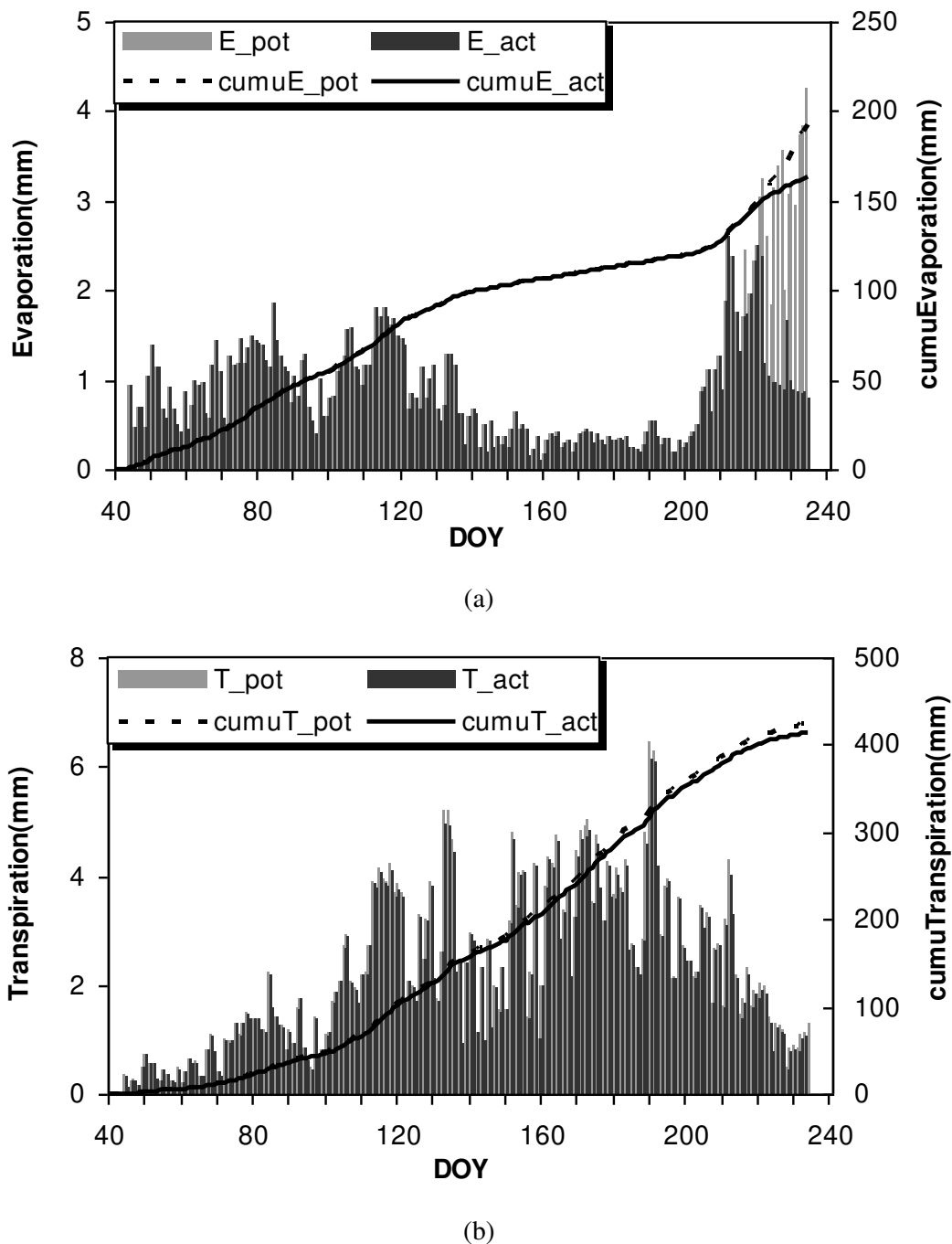


Figure 5. Simulated daily and cumulative potential and actual evaporation (a) and transpiration (b) in the PAGV experiment

Water uptake from different portions of the rooting depth

It is important to know the contribution of soil water in various part of the root zone to meet the crop demand for growth. Greenwood et al. (2010) argued that the subsoil could make a great contribution in meeting crop demand for water, while Molz and Remson (1970) and Kumar et al. (2013) estimated that each quarter of the rooting depth from the surface accounted for about 40%, 30%, 20% and 10% of the total water uptake.

In the studied experiments the amounts of water uptake from different soil layers were calculated (*Figure 6*). During the first 50 days of the simulation period, the daily water uptake was small and mainly occurred in the top 20 cm layer due to the infancy of the crop. With the increase in time, roots gradually penetrated to the deeper soil and water uptake occurred in a wider region. 53.4% and 44.9% of total water uptake were from the top 20 cm soil layer in the Bouwing and PAGV experiments, respectively. Since only a small amount of rainfall water reached the soil below 20 cm depth (*Figure 3*), it supports the argument by Greenwood et al. (2010) that water initially contained in the subsoil played an important role in meeting the crop demand for water. In the studied cases, approximately a half of the total transpired water was from the subsoil. Also, calculations show that in the Bouwing experiment, the proportions of the total water uptake from each quarter of the rooting depth were 48.3%, 25.3%, 16.9% and 9.5%, respectively, while the corresponding values were 40.4%, 32.3%, 19.8% and 7.4% in the PAGV experiment. The simulated proportions in the PAGV experiment are in good agreement with the previous studies (Molz and Remson, 1970; Kumar et al., 2013). However, for the crop grown under the condition of water deficit such proportions of water uptake from the root zone might not be held, as shown in the Bouwing experiment.

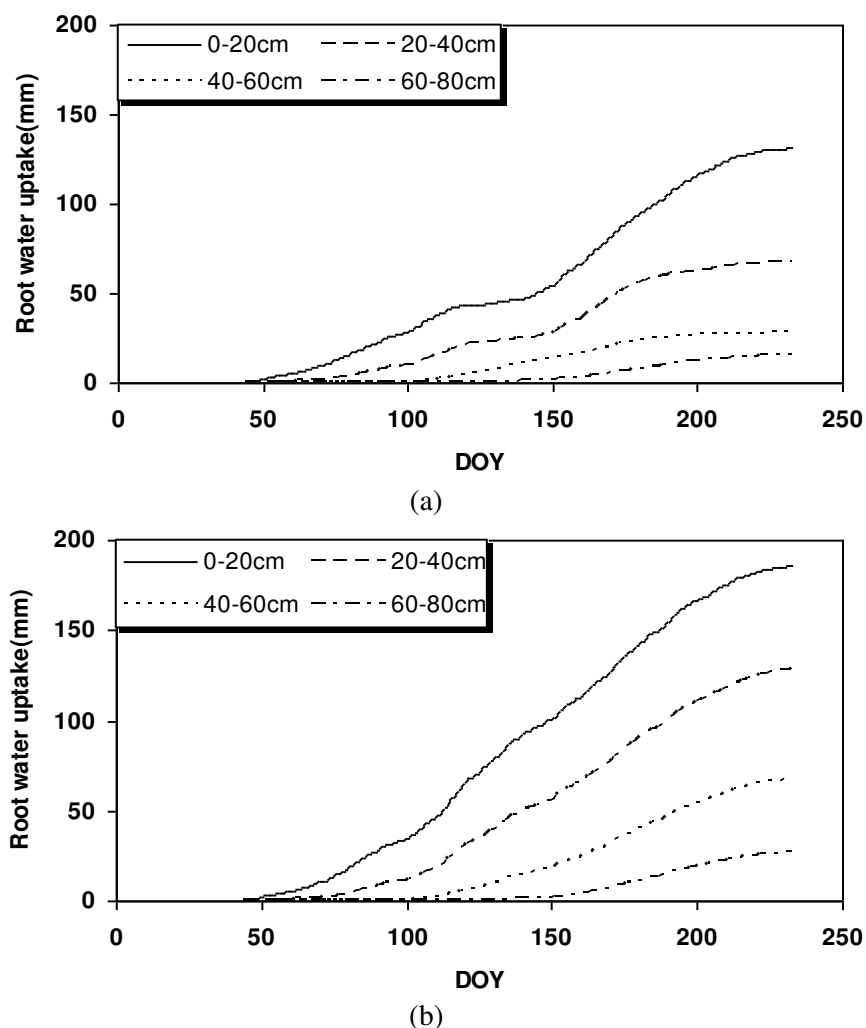


Figure 6. Simulated cumulative root water uptake in different soil layers in the Bouwing experiment (a) and in the PAGV experiment (b)

Possible use of the proposed model

As discussed the above, the proposed model performed well in predicting soil water dynamics in the soil-crop system for the studied cases. The model has the advantage of using easily available parameters, compared with most existing models which are more mechanistic, but are problematic in parameter determination. It is, therefore, that the model presented in this study has the potential to be applied more widely for the practical purpose.

Once it is validated extensively, it could be employed to study soil-crop water relations at the field scale or to form the core for devising model-based decision support systems for water management in a wide range of crop production. Also the model could be used for irrigation scheduling based on the predicted soil water status. Since soil water dynamics is an indispensable process in predicting soil nutrients availability, the model could further widen its application for crop nutrients management by extending its functions for simulating solute transport in soil and coupling it with crop models.

Conclusions

In this study an agrohydrological model was devised by integrating a module for estimating potential soil evaporation and crop transpiration into the HYDRUS-1D model. The model was easy to operate and could be applied universally with readily available parameters. Rigorous validation of the model revealed that the model was able to predict temporal and spatial soil water content in the soil-crop system. In the studied cases, the model produced fairly good predictions of soil water content during the growth of winter wheat in two contrasting soils and under different soil water regimes. The simulated results were not only in good agreement with the measurements, but also were supported by the findings from previous studies. This suggests that the development of the model was successful, and the proposed model could potentially be used in studying soil-crop water relations and in precise water use in agriculture.

Future work includes further validating the model against measured data on more crops and coupling the model with crop models for water and nutrients management. Efforts should also be made to investigate the effects of the uncertainty of model parameters on the predicted results of the model.

Acknowledgements. The authors wish to acknowledge the financial support from National Natural Science Foundation of China (51379187), National Natural Science Foundation of Zhejiang Province (LY17E090001), and Ningbo Science and Technology Bureau, China (2016C10057) for this study.

REFERENCES

- [1] Allen, R. G., Pereira, L. S., Raes, D., Smith, M. (1998): Crop Evapotranspiration-Guidelines for Computing Crop Water Requirements. – FAO, Irrigation and Drainage Paper No. 56. United Nations Food and Agriculture Organization, Rome, Italy.
- [2] Arnold, J. G., Allen, P. M., Bernhardt, G. T. (1993): A comprehensive surface-ground water flow model. – *Journal of Hydrology* 142: 47-69.
- [3] Autovino, D., Rallob, G., Provenzano, G. (2018): Predicting soil and plant water status dynamic in olive orchards under different irrigation systems with Hydrus-2D: Model performance and scenario analysis. – *Agricultural Water Management* 203: 225-235.

- [4] Bao, Y., Hoogenboom, G., McClendon, R., Vellidis, G. (2017): A comparison of the performance of the CSM-CERES-Maize and EPIC models using maize variety trial data. – *Agricultural Systems* 150: 109-119.
- [5] Bastiaanssen, W. G. M., Allen, R. G., Droogers, P., D’Urso, G., Steduto, P. (2007): Twentyfive years modeling irrigated and drained soils: state of the art. – *Agricultural Water Management* 92: 111-125.
- [6] Bohne, K., Salzman, W. (2002): Inverse simulation of non-steady-state evaporation using nonequilibrium water retention data: a case study. – *Geoderma* 110: 49-62.
- [7] Brisson, N., Mary, B., Ripoche, D., Jeuffroy, M. H., Ruget, F., Nicoulaud, B., Gate, P., Devienne-Barret, F., Antonioletti, R., Durr, C., Richard, G., Beaudoin, N., Recous, S., Tayot, X., Plenet, D., Cellier, P., Machet, J.-M., Meynard, J. M., Delécolle, R. (1998): STICS: a generic model for the simulation of crops and their water nitrogen balances. I. Theory and parameterization applied to wheat and corn. – *Agronomie* 18: 311-346.
- [8] Burns, I. G. (1974): A model for predicting the redistribution of salts applied to fallow soils after excess rainfall or evaporation. – *Journal of Soil Science* 25: 165-178.
- [9] Cannavo, P., Recous, S., Parnaudeau, V., Reau, R. (2008): Modelling N dynamics to assess environmental impacts of cropped soils. – *Advances in Agronomy* 97: 131-174.
- [10] Clay, J. (2004): *World Agriculture and the Environment: A Commodity-by-Commodity Guide to Impacts and Practices*. – Washington, DC: Island Press.
- [11] De Willigen, P. (1991): Nitrogen turnover in the soil–crop system; comparison of fourteen simulation models. – *Fertilizer Research* 27: 141-149.
- [12] Dokoochaki, H., Gheysari, M., Mousavi, S. F., Zand-Parsa, S., Miguez, F. E., Archontoulis, S. V., Hoogenboom, G. (2016): Coupling and testing a new soil water module in DSSAT CERES-Maize model for maize production under semi-arid condition. – *Agricultural Water Management* 163: 90-99.
- [13] Droogers, P., Tobari, M., Akbari, M., Pazira, E. (2001): Field-scale modeling to explore salinity problems in irrigated agriculture. – *Irrigation and Drainage* 50: 77-90.
- [14] Greenwood, D. J. (2001): Modelling N-response of field vegetable crops grown under diverse conditions with N_ABLE: a review. – *Journal of Plant Nutrition* 24: 1799-1815.
- [15] Greenwood, D. J., Zhang, K., Hilton, H., Thompson, A. (2010): Opportunities for improving irrigation efficiency with quantitative models, soil water sensors and wireless technology. – *Journal of Agricultural Science* 148: 1-16.
- [16] Groot, J. J. R., Verberne, E. L. J. (1991): Response of wheat to nitrogen fertilization, a data set to validate simulation models for nitrogen dynamics in crop and soil. – *Fertilizer Research* 27: 349-383.
- [17] Jones, J. W., Hoogenboom, G., Porter, C. H., Boote, K. J., Batchelor, W. D., Hunt, L. A., Wilkens, P. W., Singh, U., Gijsman, A. J., Ritchie, J. T. (2003): The DSSAT cropping system model. – *European Journal of Agronomy* 18: 235-265.
- [18] Keating, B. A., Carberry, P. S., Hammer, G. L., Probert, M. E., Robertson, M. J. (2003): An overview of APSIM, a model designed for farming systems simulation. – *European Journal of Agronomy* 18: 235-266.
- [19] Kumar, R., Jat, M. K., Shankar, V. (2013): Evaluation of modeling of water ecohydrologic dynamics in soil-root system. – *Ecological Modelling* 269: 51-60.
- [20] Molz, F. J., Remson, L. (1970): Extraction term models of water soil moisture use by transpiring plants. – *Water Resources Research* 6(5): 1346-1356.
- [21] Nash, J. E., Sutcliffe, J. V. (1970): River flow forecasting through conceptual models part 1—a discussion of principles. – *Journal of Hydrology* 10: 282-290.
- [22] Rahil, M. H., Antonopoulos, V. Z. (2007): Simulating soil water flow and nitrogen dynamics in a sunflower field irrigated with reclaimed wastewater. – *Agricultural Water Management* 92: 142-150.
- [23] Rahn, C. R., Zhang, K., Lillywhite, R., Ramos, C., Doltra, J., de Paz, J. M., Riley, H., Fink, M., Nendel, C., Thorup-Kristensen, K., Pedersen, A., Piro, F., Venezia, A., Firth, C., Schmutz, U., Rayns, F., Strohmeyer, K. (2010): EU-Rotate_N - a decision support system

- to predict environment and economic consequences of the management of nitrogen fertilizer in crop rotations. – *European Journal of Horticultural Science* 75(1): 20-32.
- [24] Renaud, F. G., Bellamy, P. H., Brown, C. D. (2008): Simulation pesticides in ditches to assess ecological risk (SPIDER): I. Model description. – *The Science of Total Environment* 394: 112-123.
- [25] Shelia, V., Šimuněk, J., Boote, K., Hoogenboom, G. (2017): Coupled the DSSAT and hydrus-1D for soil water dynamics simulation in the soil-plant-atmosphere system. – ASA, CSSA and SSSA International Annual Meetings 2016.
- [26] Siad, S. M., Iacobellis, V., Zdruli, P., Gioia, A., Stavi, I., Hoogenboom, G. (2019): A review of coupled hydrologic and crop growth models. – *Agricultural Water Management* 224: 105746.
- [27] Šimuněk, J., van Genuchten, M. Th., Šejna, M. (2005): The HYDRUS-1D software package for simulating the movement of water, heat, and multiple solutes in variably saturated media. – University of California-Riverside, Research Report 3: 1-240.
- [28] Steduto, P., Hsiao, T. C., Raes, D., Fereres, E. (2009): Aquacrop-the fao crop model to simulate yield response to water: I. Concepts and underlying principles. – *Agronomy Journal* 101: 426-437.
- [29] Stöckle, C. O., Donatelli, M., Nelson, R. (2003): CropSyst, a cropping systems simulation model. – *European Journal of Agronomy* 18: 289-308.
- [30] Strati, V., Albéri, M., Anconelli, S., Baldoncini, M., Bittelli, M., Bottardi, C., Chiarelli, E., Fabbri, B., Guidi, V., Raptis, K. G. C., Solimando, D., Tomei, F., Villani, G., Mantovani, F. (2018): Modelling Soil Water Content in a Tomato Field: Proximal Gamma Ray Spectroscopy and Soil–Crop System Models. – *Agriculture* 8: 60. doi:10.3390/agriculture8040060.
- [31] Tribouillois, H., Constantin, J., Willaume, M., Brut, A., Ceschia, E., Tallec, T., Beaudoin, N., Therond, O. (2018): Predicting water balance of wheat and crop rotations with a simple model: AqYield. – *Agricultural and Forest Meteorology* 262: 412-422.
- [32] van Genuchten, M. Th. (1980): A closed-form equation for predicting the hydraulic conductivity of unsaturated soils. – *Soil Science Society of America Journal* 44: 892-898.
- [33] van Genuchten, M. Th., Leij, F. J., Yates, S. R. (1991): The RETC code for quantifying the hydraulic functions of unsaturated soils. – Robert S. Kerr Environmental Research Laboratory, US Environmental Protection Agency, Oklahoma, USA.
- [34] Wang, X., Liu, G., Yang, J., Huang, G., Yao, R. (2017): Evaluating the effects of irrigation water salinity on water movement, crop yield and water use efficiency by means of a coupled hydrologic/crop growth model. – *Agricultural Water Management* 185: 13-26.
- [35] Williams, J. R., Jones, C. A., Dyke, P. T. (1993): The Epic model. – In: Sharpley, A. N., Williams, J. R. (eds.) *Epic–Erosion Productivity Impact Calculator*. 1. Model documentation. U S Department of Agriculture Technical Bulletin No 1768. USDA: Washington DC.
- [36] Yang, D., Zhang, T., Zhang, K., Greenwood, D. J., Hammond, J., White, P. J. (2009): An easily implemented agro-hydrological procedure with dynamic root simulation for water transfer in the crop-soil system: validation and application. – *Journal of Hydrology* 370: 177-190.
- [37] Zhang, K., Greenwood, D. J., White, P. J., Burns, I. G. (2007): A dynamic model for the combined effects of N, P and K fertilizers on yield and mineral composition: description and experimental test. – *Plant and Soil* 298: 81-98.
- [38] Zhang, K., Yang, D., Greenwood, D. J., Rahn, C. R., Thorup-Kristensen, K. (2009): Development and critical evaluation of a generic 2-D agro-hydrological model (SMCR_N) for the responses of crop yield and nitrogen composition to nitrogen fertilizer. – *Agriculture Ecosystems and Environment* 132: 160-172.
- [39] Zhang, K., Greenwood, D. J., Spracklen, W. P., Rahn, C. R., Hammond, J. P., White, P. J., Burns, I. G. (2010): A universal agro-hydrological model for water and nitrogen cycles in

- the soil-crop system SMCR_N: Critical update and further validation. – *Agricultural Water Management* 97: 1411-1422.
- [40] Zhang, K., Li, C., Hu, Z., Huang, S., Chen, J., Ma, X. (2020): Simulations of water cycle in the soil-crop system: model improvement and validation. – *Applied Ecology and Environmental Research* 18: 2163-2177.

WEEDS AND THEIR ECOLOGICAL INDICATOR VALUES IN A LONG-TERM EXPERIMENT

NIKOLIĆ, LJ. – ŠEREMEŠIĆ, S. – LJEVNAIĆ-MAŠIĆ, B. – LATKOVIĆ, D. – KONSTANTINOVIĆ, B.*

*Faculty of Agriculture, University of Novi Sad, Trg Dositeja Obradovića 8, Novi Sad, Serbia
(phone: +381-21-485-3500; fax: +381-21-459-761)*

**Corresponding author*

e-mail: bojank@polj.uns.ac.rs; phone: +381-21-485-3315; fax: +381-21-450-616

(Received 12th Feb 2020; accepted 22nd May 2020)

Abstract. The floristic composition and weed infestation in wheat and maize crops were studied in a long-term field experiment in Serbia. A total of 35 weed species were identified, out of which 12 were common for both crops. The greatest floristic diversity (20 species) was found under wheat crops in unfertilized two-year rotation, while the lowest diversity (5 species) was determined in maize crops in monoculture and fertilized four-year rotation. The highest weed infestation was observed in wheat monoculture (490.47 ind/m²) and maize monoculture (111.98 ind/m²), while the lowest level of weed infestation (17.31 ind/m²) was observed in maize crops under intensive two-year rotation. Significant differences were found in the number of weed species and in the level of weed infestation between wheat and maize, as well as in the level of weed infestation in monoculture compared to other treatments of crop rotation for both crops. Ecological analysis indicated that the type of crop rotation and the species of crops have impact on the ecological characteristics of the studied area, which is reflected in different floristic composition and differences in the abundance of certain weeds.

Keywords: *wheat, maize, ecological indices, crop rotation*

Introduction

Agricultural production is facing a number of problems related to weed emergence in crops. Although intensive agricultural production offers effective combinations of chemical inputs used for weed control (Kim et al., 2002), it is necessary to make efforts at both local and global levels to reduce their use for the sake of preserving natural resources and ensuring food safety. Due to the exceptional plasticity and excellent adaptation of weeds to different anthropogenic influences, weed management and control produce best results when carried out continuously and adequately (Avola et al., 2008; Tyr, 2016). Apart from the usual cropping practices and application of chemicals, which have unfavourable impacts on human health and the environment, one of the most important preventive measures used for weed reduction is crop rotation, which is environmentally acceptable (Barberi et al., 1997; Suarez et al., 2001; Derksen et al., 2002; Nikolić et al., 2012, 2018; Wozniak and Soroka, 2015). Considering the long-term effects, cultivation of crops in crop rotation also leads to reduction of seed reserves in the soil, resulting in a lower level of weed infestation in a succeeding crop (Teasdale et al., 2004; Koocheki et al., 2009). Over a longer period of time, properly implemented crop rotation can have positive environmental effects on preservation of weed flora biodiversity, since crops are typical habitats for certain segetal weeds which are increasingly endangered due to intensive cropping practices (Hulina, 2005).

A particularly suitable method for determining the impact of crop rotation on weed infestation is a long-term experiment. The study presented in this paper was thus carried out in a long-term experiment with different crop rotation treatments, some of which

were established 70 years ago. However, estimating the contribution of crop rotation to yield realization is difficult given the fact that weed control includes a number of different preventive and direct measures. As the effect of crop rotation is reflected in the cumulative effect on weed infestation, it is very important to follow the succession of the weed synusia, which is a topic scarcely studied in the literature. In addition, by determining weed communities specific for certain species, it is possible to select appropriate cropping practices to increase the anthropogenic pressure on these weeds and reduce their abundance.

Therefore, the aim of this paper was to analyse the weed flora, the level of weed infestation and the role of weeds as bioindicators in wheat and maize crops grown in different treatments of long-term crop rotation and fertilization. The obtained results can be used as a good basis for monitoring biodiversity of weeds and their role as bioindicators, as well as for determining the most favourable treatment of crop rotation for reducing weed infestation in wheat and maize crops.

Materials and methods

The floristic survey presented in this paper examined weeds in wheat (2010 year) and maize (2011 year) crops in long-term trials “Plodoredi” on the experimental field Rimski Šančevi (Serbia) of the Institute of Field and Vegetable Crops in Novi Sad (45.19°N, 19.50°E). Crop rotation was arranged as a single crop rotation in which all crops were grown each year according to the experimental design, and plots were divided into three subplots (90 × 30 m) representing the repetitions. Winter wheat and maize were continuously grown from the beginning of the trial (1946/47), whereas soybean was introduced in 1969/70. The total area of the experimental field was 6.5 ha.

The trials were set on chernozem soil, which belongs to automorphic soil types, class A-C (humus-accumulative soil, the subtype chernozem on loess and loess-like sediments, the carbonate chernozem variety, medium-depth) (Škorić, 1985). This type of soil is characterised by slightly alkaline reaction with higher calcium content. It is rich in phosphorus and potassium, while the content of organic matter is lower than 3% as a result of intensive farming (*Table 1*).

Table 1. Basic chemical soil properties on the experimental field (mean values ± SD)

Year	pH		CaCO ₃ %	Organic matter %	Total N %	Al-P ₂ O ₅ mg/100 g	Al-K ₂ O mg/100 g
	in KCl	in H ₂ O					
2009/11	7.52 ± 0.10	8.1 ± 0.12	5.64 ± 4.23	2.7 ± 0.38	0.2 ± 0.02	65.93 ± 61.50	37.56 ± 12.98

The long-term climate (1970–2009) at the investigated site (Rimski Šančevi experimental station) is continental, with an average annual precipitation of 617 mm and average annual temperature of 11.3 °C (HMZS, 2020). The climate is considered favorable for production of major crops: winter wheat, maize, soybean, sunflower etc. Compared with the long-term climate records, an increase in yearly average temperature and precipitation was observed. In the investigated period, both years were higher in average yearly temperatures, but 2009/10 was lower in precipitation and 2010/11 had above average precipitation compared to long-term average. The temperatures during the growing period, as well as for individual months, were very similar during

investigated period. However, the timing and quantity of precipitation significantly differed, as 2009/10 had significantly higher precipitation than 2010/11, particularly in July (Fig. 1).

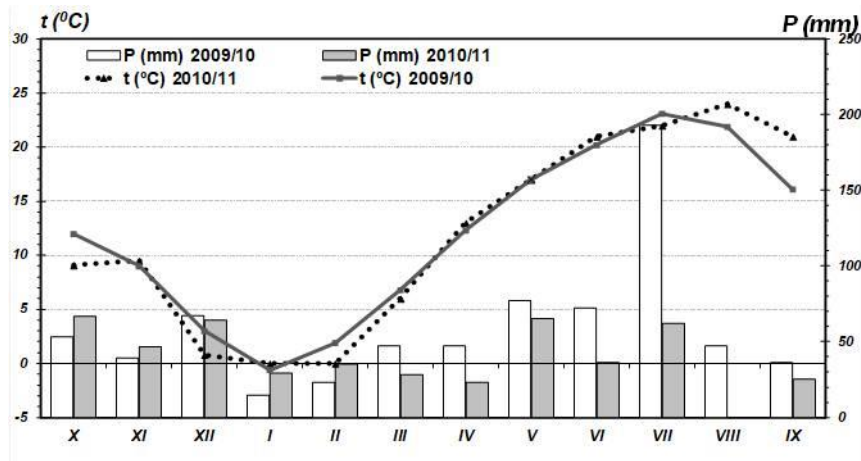


Figure 1. Medium monthly temperatures and precipitations in two production years (2009/10 and 2010/11)

The weed flora was investigated in the following experimental treatments: extensive (unfertilized) two-year rotation (maize-winter wheat) – E2 and extensive (unfertilized) three-year rotation (maize-soyabean-winter wheat) – E3, established in 1946/47, intensive (fertilized) two-year rotation (maize-winter wheat) – I2, intensive (fertilized) three-year rotation (maize-soyabean-winter wheat) – I3 with the application of organic and mineral fertilizers, established in 1969/70, three-year rotation with the application of organic fertilizers – (maize-soyabean-winter wheat) – IS3 (intensive three-year rotation), intensive four-year rotation with the application of organic and mineral fertilizers (maize-winter wheat-soyabean-sunflower) – I4, established in 1969/70, and monoculture of winter wheat – MoW and maize – MoM with the application of organic and mineral fertilizers, established in 1969/70. During the investigated period winter wheat variety Simonida was grown and maize hybrid NS640 created at the Institute of Field and Vegetable Crops Novi Sad. In the long-term experiment, sowing density was adjusted to 450 viable seeds per m² for winter wheat that is 240 kg ha⁻¹ seeds. For maize, recommended density was 23 × 70 cm that is approximately 60.000 plants per hectare.

In the fertilized treatments, nitrogen mineral fertilizers were applied every year in the amount of 100 kg/ha for wheat and sunflower, and 120 kg/ha for maize. The amount of applied P and K depended on agrochemical analyses performed every year. Soyabean crops were not directly treated with fertilizers, but with microbiological fertilizer Nitragin.

The herbicide used for controlling the emergence of sorghum (*Sorghum halepense* (L.) Pers.) is glyphosate applied every year in July after wheat harvest. Also, herbicides 2.4D and iodosulfuron-methyl-sodium + amidosulfuron were introduced in 2000 for weed control in winter wheat.

Weed control in maize was based on S-metolachlor (960 g/l) dose of 1.4 l/ha and 375 g/l S-Metolachlor + 125 g/l Terbutylazine + 37.5 g/l Mesotrione dose of 3.5-4 l/h.

During the vegetation season, *Sorghum* and other narrow-leaved weeds were controlled by applying Nicosulfuron or Rimsulfuron 50-60 g/ha. During the vegetation season of maize, inter-row cultivation was carried out two times at 3-5 leaf stage and 5-7 leaf stage.

Determination and nomenclature of weed species was done according to Josifović (1986) and Tutin et al. (1980). Life forms are given according to Ujvárosi (1973). Counting of the plants, on randomly chosen area of 1 m², in all treatments of experiment was done three times during the vegetation period, in relation to the phenological development of winter wheat (BBCH 30, BBCH 53, BBCH 85) and maize (BBCH 11, BBCH 55, BBCH 89) according to decimal BBCH (Biologische Bundesanstalt, Bundessortenamt und Chemische Industrie) scale, with three repetitions.

Bioindicator values (ecological indices) for the main ecological factors (climate indicators: temperature – T, continentality – K and light – L; soil indicators: moisture – F, reaction – R, nutrients – N, humus – H and aeration – D) were analyzed based on the values given by Landolt (2010). Plant species were characterised by a specific value of the ecological index which determines the ecological optimum for a particular species compared with some habitat traits. Values of the ecological indices are expressed on the scale from 1 to 5, where 1 stands for minimum requirements and 5 for maximum requirements. For gaining the better insight in the ecological conditions based on bioindicator values, abundance of present weed species was taken into account. Hence, values of ecological indices for every weed species were multiplied by the average number of individuals of that species in the given variant of the experiment. Obtained values were added together and divided by the average weed density of all of the weed species in the analysed variant of the experiment, thence, the average value of every ecological index on all of the variants of the experiment was acquired.

The difference in the number of weed species between different treatments of crop rotation and crops were determined using t-test. The differences in the number of ind/m² of different weed species and differences in weed infestation of different crop rotation were determined using ANOVA and Duncan test, respectively. The relationship between ecological indices and treatments was examined using Cluster and Correspondent analyses. All statistical analyses were performed using STATISTICA 13.2 software (Dell™ Statistica™ 13.2 University License).

Results

Weed composition

During the two-year study of weed flora in wheat and maize crops in long-term crop rotations at the experimental field Rimski Šančevi, a total of 35 weed species were identified (Table 2). The study showed that, out of this total number of weeds, 33 weed species were identified in the first year in wheat crops, including 32 weed species from the class of dicotyledon (Magnoliopsida) and only one species (*Sorghum halepense*) from the class of monocotyledon (Liliopsida). In the second year, only 14 species were recorded in maize crops, including 13 species from the class of dicotyledons and (the same as in wheat crops) only one species (*Sorghum halepense*) from the monocotyledon class. During the two studied years, 12 weed species were identified in both wheat and maize, and there were 21 differential species in wheat crops, while the species *Amaranthus retroflexus* and *Xanthium italicum* were found only in maize. Although

there were not any species recorded in all treatments of crop rotation during the two-year period, *Sorghum halepense* stood out as the most frequent species as it was identified in 11 (79%) crop rotation treatments. It is important to note that the studied weed flora included seven species (*Amaranthus retroflexus*, *Ambrosia artemisiifolia*, *Datura stramonium*, *Helianthus tuberosus*, *Oxalis stricta*, *Sorghum halepense* and *Xanthium italicum*) from the category of invasive plants (DAISIE, 2008; Lazarević et al., 2012).

In both studied years, the biological spectrum (Fig. 2) was characterized by therophyte (T) and geophyte (G) life forms. The analysis showed that therophytes predominated (82.85%; 29 species), while the most abundant were T4 therophytes (42.86%; 15 species), i.e. annual plants that germinate in spring and mature at the end of summer, and T2 therophytes (22.86%; 8 species), i.e. annual plants that germinate in autumn and early spring, and mature at the beginning of summer. Perennial plants, geophytes, were less abundant (17.14%; 6 species). In the first studied year, the biological spectrum in wheat crops showed almost identical life form distribution, absolutely dominated by therophytes (81.83%; 27 species), with T4 (39.39%, 13 species) and T2 therophytes (24.24%; 8 species) being most abundant, while geophytes accounted for only 18.2% (6 species) of the identified life forms. In the second studied year, the biological spectrum of weed flora in maize crops also had very similar life form distribution, with dominance of therophytes (71.42%; 10 species), including 50% of T4 therophytes, and a higher percentage of geophytes (28.28%, 4 species) (Fig. 2).

The highest number of weed species (20) was recorded in wheat crops grown in unfertilized two-year rotation, 15 species were found in wheat cultivated in two-year rotation and 14 species in wheat grown in monoculture (Fig. 3). Considering the differences in the average number of weed species between different wheat treatments (t-test), statistically highly significant and statistically significant differences were found between the abovementioned unfertilized two-year rotation, two-year rotation and monoculture of wheat compared to other crop rotation treatments (Table 3). The lowest floristic diversity was found in maize crops grown in monoculture and four-year rotation, where only 5 weed species were recorded. Considering the differences in the average number of weed species between individual maize treatments (t-test), statistically significant differences were found only between monoculture and two-year and three-year rotation with the application of organic fertilizers, and between two-year and three-year rotation with the application of organic fertilizers and four-year rotation (Table 3). In the second year, the number of weed species in maize was significantly reduced, with the highest reduction of 70% recorded in unfertilized two-year rotation, monoculture (64%), followed by two-year rotation (64%), four-year rotation (44%) and unfertilized three-year rotation (42%). Slightly smaller differences in the number of weed species were determined between wheat and maize grown in three-year rotation and three-year rotation with the application of organic fertilizers (30% and 28%, respectively). Statistical data analysis showed that the differences in the number of weed species found in wheat and maize crops are statistically highly significant (Table 4).

Weed infestation

Considering the level of weed infestation (Fig. 4), the highest values were determined in the treatments of monoculture in wheat crops, where the average number

of ind/m² was 490.47, and maize crops, where the level of weed infestation was 111.98 ind/m². These values were the highest recorded values for wheat and maize considering all treatments of crop rotation. Although the highest level of weed infestation was recorded in monoculture for both crops, it should be noted that maize cultivated in monoculture showed 75% lower level of weed infestation compared to wheat. High levels of weed infestation were recorded also in wheat crops grown in the treatment of unfertilized three-year rotation (198.61 ind/m²), two-year rotation (186.03 ind/m²), unfertilized two-year rotation (124.57 ind/m²) and three-year rotation with the application of organic fertilizer (101.15 ind/m²). The lowest values of weed infestation in wheat crops were determined in the treatments of three-year rotation (39.93 ind/m²) and four-year rotation (52.83 ind/m²). Weed infestation in maize, with the exception of monoculture, was at a significantly lower level and was around 36 ind/m² in the treatments of unfertilized two-year rotation, unfertilized three-year rotation, and four-year rotation, while the lowest weed infestation was recorded in the treatment of intensive two-year rotation (17.31 ind/m²) and three-year rotation with the application of organic fertilizer (20.86 ind/m²). It is also interesting to point out that the level of weed infestation in maize is considerably lower compared to the same treatments of crop rotation in wheat: by 91% in two-year rotation, 82% in unfertilized three-year rotation, 79% in three-year rotation with the application of organic fertilizer, 70% in unfertilized two-year rotation, 48% in three -field rotation and by 32% in four-year rotation.

Statistical analysis indicated statistically significant difference between the overall weed infestation found in wheat (all treatments) and weed infestation in maize crops (all treatments) (*Table 4*).

Statistical analysis (*Table 5*), of the level of weed infestation in different crops in different treatments of the experiment in the first year in wheat indicated statistically highly significant difference between weed infestation in wheat monoculture and all other crop rotation treatments. In the second year, statistically significant difference was determined in maize crops also only for weed infestation in maize monoculture compared to other crop rotation treatments.

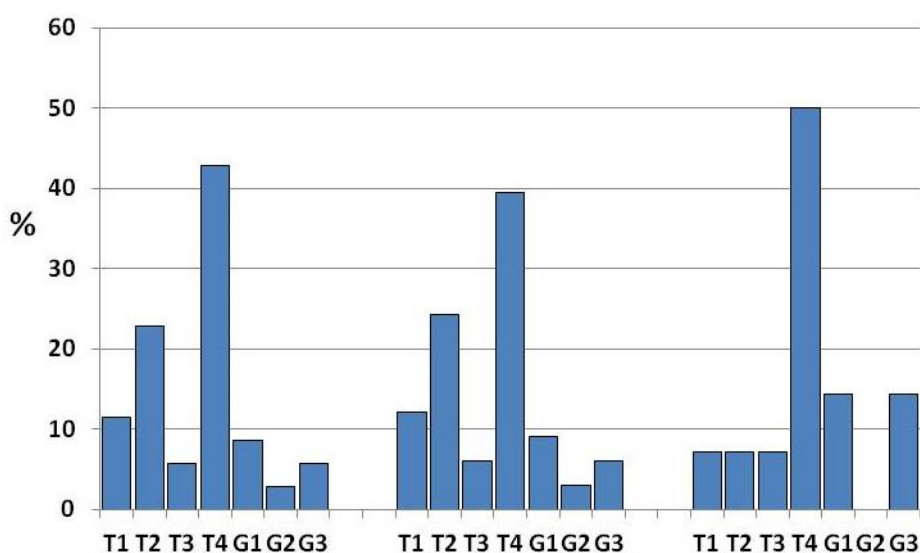


Figure 2. Biological spectrum of weed flora (2010 and 2011)

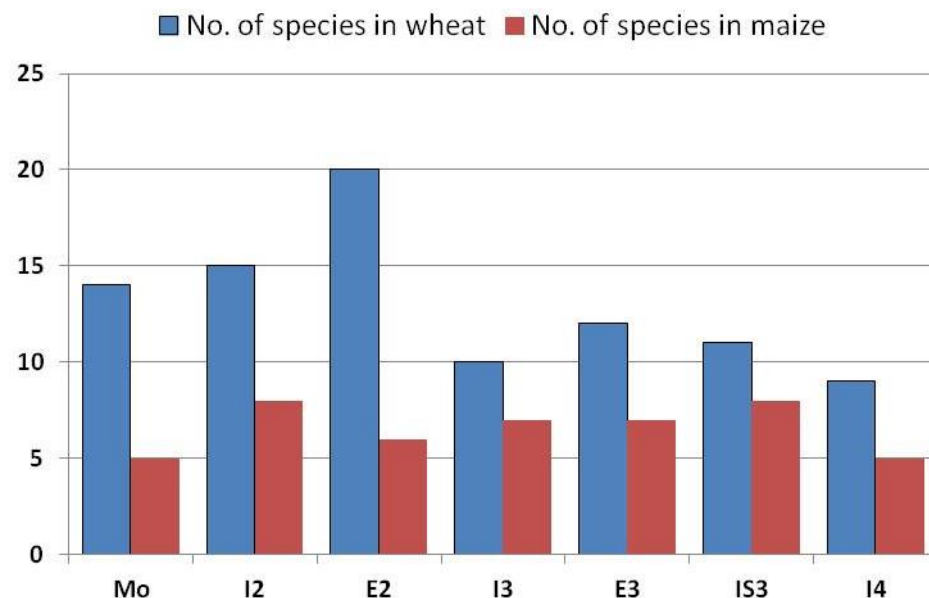


Figure 3. Number of weed species in wheat (2010) and maize (2011) in different crop rotations

Table 2. Review of weeds with the average number of individuals per square meter in wheat (2010) and maize (2011) in different variants of the experiment

Plant species	Life form	Mo		I2		E2		I3		E3		IS3		I4	
		W	M	W	M	W	M	W	M	W	M	W	M	W	M
1. <i>Adonis aestivalis</i> L.	T2	0.44												0.44	
2. <i>Amaranthus retroflexus</i> L.	T4				4.44				2.66						6.22
3. <i>Ambrosia artemisiifolia</i> L.	T4				5.33	29.55	1.78	1.78	77.77	4	2.66	0.89			
4. <i>Anagallis arvensis</i> L.	T4					0.44									
5. <i>Anagallis femina</i> Mill.	T4				0.44	0.44									0.89
6. <i>Bilderdykia convolvulus</i> (L.) Dum.	T4	59.11		25.66		2.22		5.33		2.22		15		6.21	
7. <i>Capsella bursa-pastoris</i> (L.) Medik.	T1	31.11		0.44		0.44						1.77			

8. <i>Centaurea cyanus</i> L.	T2	1.77		0.88												
9. <i>Chenopodium album</i> L.	T4	0.44	0.44		0.89	0.44		4.88			0.89	10.21	0.44	9.33		
10. <i>Chenopodium hybridum</i> L.	T4	0.44		1.33				1.77	0.89			3.1	0.44	0.44		
11. <i>Cirsium arvense</i> (L.) Scop.	G3		1.33			2.22	0.44		1.78				0.89			
12. <i>Consolida regalis</i> S.F. Gray.	T2	110.64		45.77	0.44	3.10		15.99		0.44		11.55		8.44		
13. <i>Convolvulus arvensis</i> L.	G3		4		1.78			2.66	0.44	1.33		0.89	2.21		1.77	
14. <i>Datura stramonium</i> L.	T4													2.66		
15. <i>Euphorbia helioscopia</i> L.	T4					11.55					12.44					
16. <i>Fumaria officinalis</i> L.	T3			0.44												
17. <i>Galeopsis tetrahit</i> L.	T4	0.11		0.44												
18. <i>Galium aparine</i> L.	T2	13.77		17.33		4										
19. <i>Helianthus tuberosus</i> L.	G2							4.88				3.11				
20. <i>Lamium amplexicaule</i> L.	T1	0.44		1.33								2.66	0.44			
21. <i>Lathyrus tuberosus</i> L.	G1			1.33		1.33	1.78			1.77	1.78					
22. <i>Lithospermum arvense</i> (L.) Vahl.	T2	0.88		0.88								0.44				
23. <i>Medicago lupulina</i> L.	T4					1.33										
24. <i>Oxalis stricta</i> L.	G1					7.1										
25. <i>Papaver rhoeas</i> L.	T2	14.88		1.33												
26. <i>Polygonum aviculare</i> L.	T4					2.66					5.33			0.88		
27. <i>Ranunculus arvensis</i> L.	T2					0.44										
28. <i>Sinapis arvensis</i> L.	T3	0.44				44				72.44	2.22	9.77				
29. <i>Solanum nigrum</i> L.	T4			0.88		1.77		0.44		1.33	0.44					
30. <i>Sorghum halepense</i> (L.) Pers.	G1		103.55		3.55	10.22	29.77	3.55	4.89	7.55	26.22		9.33	0.44	12	
31. <i>Stachys annua</i> L.	T4									1.33						
32. <i>Stellaria media</i> (L.) Vill.	T1					0.88				15.55						
33. <i>Veronica hederifolia</i> L.	T1	256		87.55		0.44		1.77		0.44		40.88		23.99		
34. <i>Viola arvensis</i> Murr.	T2			0.44												
35. <i>Xanthium italicum</i> L.	T4		2.66		0.44		0.44		8				6.22		15.11	
Total of plant species		14	5	15	8	20	6	10	7	12	7	11	8	9	5	
Average no. of individuals/m² (weed density)		490.47	111.98	186.03	17.31	124.57	36.87	39.93	21.33	198.61	36.44	101.15	20.86	52.83	35.99	

W – wheat; M-maize; Mo - monoculture; I2 – intensive (fertilized) two-year rotation; E2 - extensive (unfertilized) two-year rotation; E3 - extensive (unfertilized) three-year rotation; IS3 - three-year rotation with the application of organic fertilizers; I4 - intensive four-year rotation with the application of organic and mineral fertilizers; T – therophyte; G – geophyte

Table 3. Significance of the differences in the number of weed species between different treatments of crops rotations and crops (t-test)

Crop rotation	I2	E2	I3	E3	IS3	I4
Wheat						
Mo		0.001**	0.008**		0.021*	0.017*
I2		0.003**	0.003**	0.021*	0.008**	0.009**
E2			0.000**	0.000**	0.000**	0.001**
Maize						
Mo	0.021*				0.021*	
I2						0.021*
IS3						0.021*

** p < 0.01, * p < 0.05

Table 4. Significance of differences between the examined parameters

Examined parameters	df	t-value	p
No. of weed species in wheat / No. of weed species in maize	12	4.30364	0.00**
Average no. of ind/m ² in wheat / Average no. of ind/m ² in maize	12	2.19914	0.04*

** p < 0.01, * p < 0.05

Table 5. Significance of differences in weed infestation (ind m⁻²) in different treatments of crop rotation (ANOVA, Duncan test)

Crop rotation	I2	E2	I3	E3	IS3	I4
Wheat						
Mo	0.002**	0.003**	0.000**	0.002**	0.000**	0.000**
Maize						
Mo	0.013*	0.027*	0.015*	0.034*	0.016*	0.039*
Two-year period						
Mo	0.002**	0.001**	0.000**	0.006**	0.000**	0.000**

**p < 0.01, *p < 0.05

Significance of the difference in the number of individuals in certain weed species was analysed using ANOVA and Duncan's test, indicating statistically highly significant differences in the number of ind/m² for *Consolida regalis* (Fig. 5, species 12) and *Veronica hederifolia* (Fig. 5, species 33), which had the greatest influence on weed infestation in wheat crops compared to other weed species, and the species *Sorghum halepense* (Fig. 5, species 30), whose number of ind/m² in maize crops was also statistically highly significant compared to other identified species. In addition, based on the number of ind/m², the species *Ambrosia artemisiifolia*, *Bilderdykia convolvulus* and *Sinapis arvensis* (Fig. 5, species 3, 6 and 28, respectively) also had statistically significant influence on weed infestation in wheat.

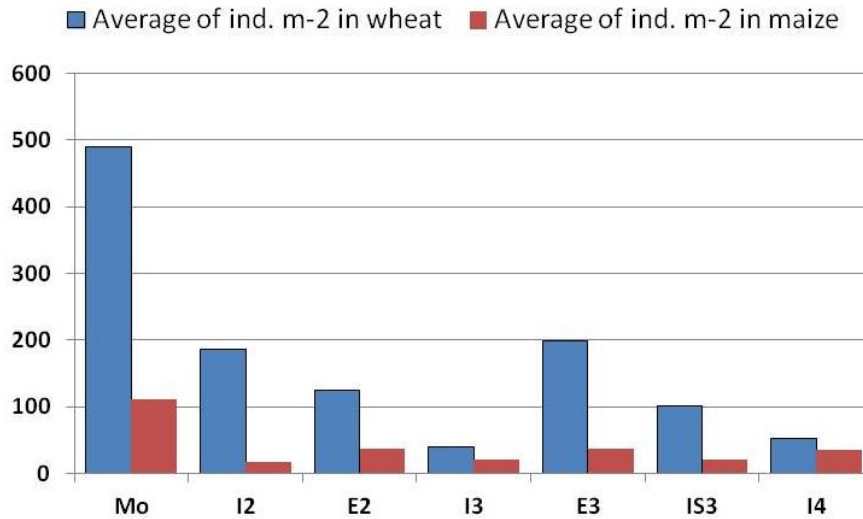


Figure 4. Average weed infestation in wheat (2010) and maize (2011) in different crop rotations

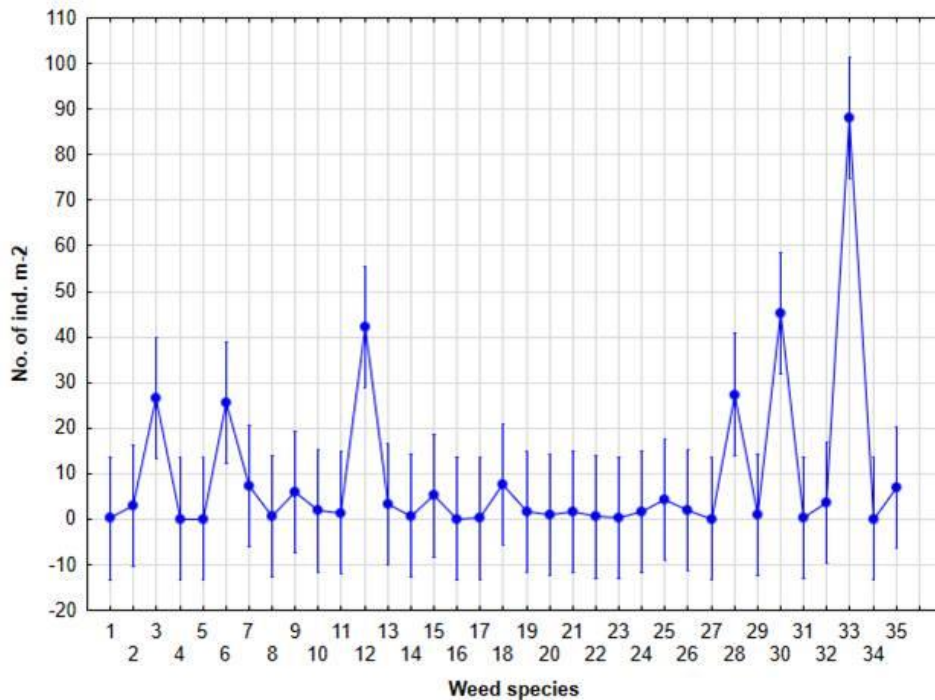


Figure 5. Significance of differences in the number of individuals per square meter (2010 and 2011) of different weed species (ANOVA)

Weeds as bioindicators

Apart from determining the basic meteorological and chemical properties of the soil in the studied area (Table 1; Fig. 1), indirect ecological analysis was also carried out based on the ecological indicator values of the identified weed species.

In all crop rotation treatments, the average values of climate indicators were favourable: the value of the ecological index for temperature suggested favourable temperature conditions ($T_{\bar{x}} = 4.4$), and the value of the ecological index for light

showed favourable light regime ($L_{\bar{x}} = 3.76$), which is in line with the mean value of the continentality index which indicated subcontinental conditions ($K_{\bar{x}} = 2.73$). Soil indicators suggested relatively favourable moisture content of the substrate in the studied crop rotation treatments ($F_{\bar{x}} = 2.48$), slightly acidic to neutral values of the chemical reaction of the substrate ($R_{\bar{x}} = 3.54$), fertile soil ($N_{\bar{x}} = 3.99$), with medium content of humus ($H_{\bar{x}} = 3$) and well aerated ($D_{\bar{x}} = 2.84$) (Table 6). However, certain differences, although not statistically significant (t-test), related to ecological conditions (expressed by bioindicator values) were found between different crop rotation treatments. Thus, four clusters were distinguished: first included fertilized wheat crop rotations, second included maize treatments in monoculture and unfertilized treatments, third cluster included fertilized maize treatments, and fourth cluster was formed of unfertilized wheat treatments (Fig. 6). Correspondent analysis also showed that some groups and types of treatments differ in relation to certain ecological indicators (Fig. 7). Specifically, clustering of fertilized wheat treatments was more intensively influenced by the moisture content in the substrate (F) and partly by continentality (K), while the nutrient content (N) affected clustering of fertilized maize treatments. Clustering of maize monoculture and unfertilized treatments was influenced by brightness (L) and substrate reaction (R), while aeration (D) and humus content (H) influenced clustering of unfertilized wheat treatments.

Discussion

Studying agrophytocenoses and their floristic composition is an important component in global biodiversity monitoring, as agroecosystems are characterised by strong anthropogenic influence and constant intensification of agricultural production (Nowak and Nowak, 2013). This study indicated significant differences in the composition of weeds in wheat and maize crops. In addition to 12 species common to both crops, as many as 21 species were recorded only in wheat, while the species *Amaranthus retroflexus* and *Xanthium italicum* were recorded only in maize (Table 2). The species which stood out in terms of the abundance in both crops was *Sorghum halepense*, which was found in 79% of the experimental treatments. These floristic differences were most likely a result of specific ecological conditions related to the species of crops, their rotation treatment and application of different cropping practices, as was noted also by Hosseini et al. (2014) and Campiglia et al. (2018). Since it is known that crop rotation reduces floristic diversity (Moss et al., 2004; Randy, 2005; Nikolić et al., 2018), this study also included analysis of weed flora in individual treatments of crop rotation. Statistical data analysis showed that the differences in the number of weed species found in wheat and maize crops are statistically highly significant (Table 4), indicating that crop rotation and crop species influence the structure of weed flora (Koocheki et al., 2009; Nikolić et al., 2018).

It is important to note that, according to DAISIE database (www.europe-aliens.org) and Lazarević et al. (2012), there were seven invasive alien species in the weed flora of the studied area (*Amaranthus retroflexus*, *Ambrosia artemisiifolia*, *Datura stramonium*, *Helianthus tuberosus*, *Oxalis stricta*, *Sorghum halepense* and *Xanthium italicum*). Due to their capability to highly successfully reproduce and spread to new areas, they are undesirable and their dynamics should be closely monitored (Richardson et al., 2000; Pyšek et al., 2004), as their spreading can have negative ecological, economic and health impacts.

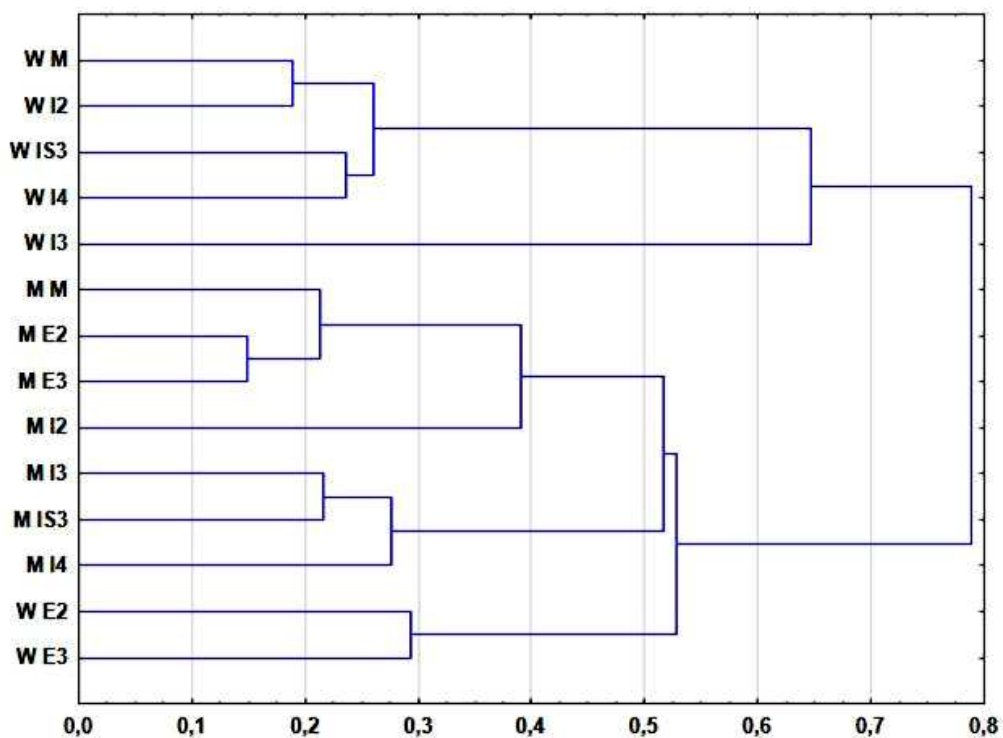


Figure 6. Dendrogram of different treatments of crop rotation based on ecological indices

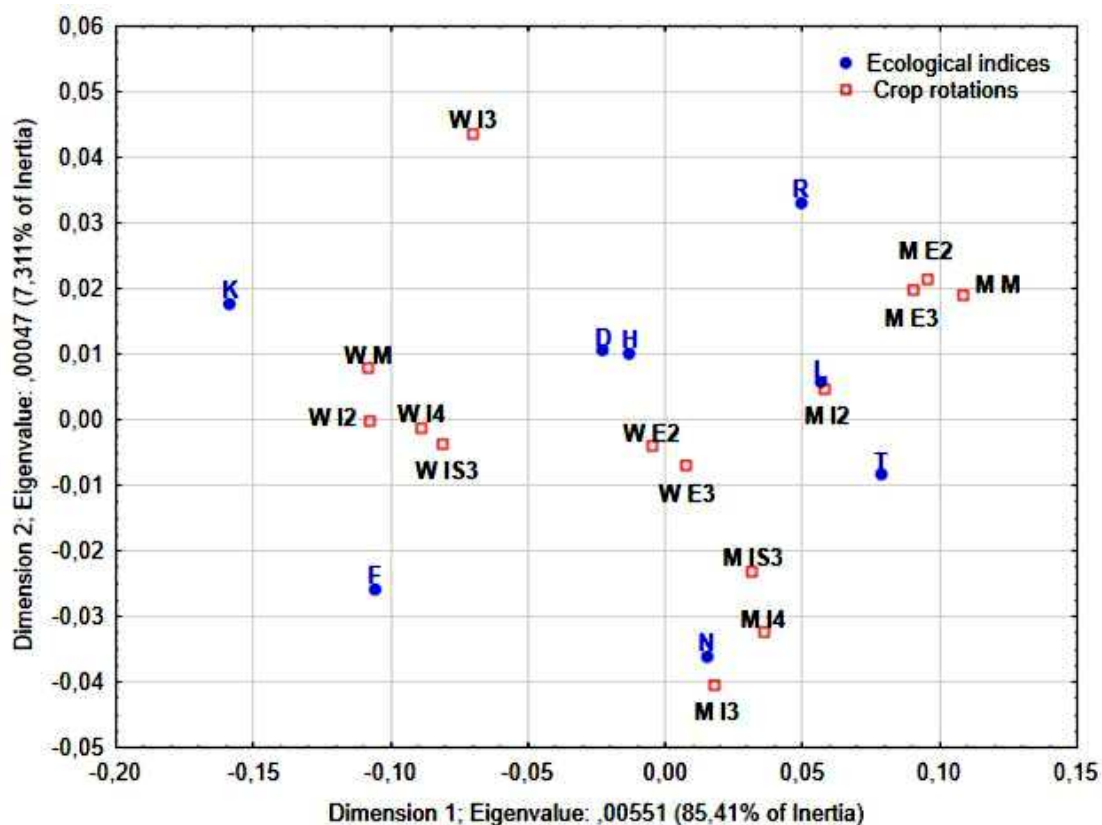


Figure 7. Biplot of different treatments of crop rotation and ecological indices

Table 6. Average values of ecological indices in different variants of the experiment

Ecological index	Mo		I2		E2		I3		E3		IS3		I4		Wheat	Maize	\bar{x}
	W	M	W	M	W	M	W	M	W	M	W	M	W	M			
T	3.8	4.94	3.88	4.6	4.22	4.89	4	4.73	4.32	4.82	4.02	4.76	3.83	4.84	4.01	4.8	4.4
K	3.26	2.11	3.28	2.38	2.65	2.26	3.34	2.67	2.56	2.24	3.15	2.66	3.1	2.57	3.05	2.41	2.73
L	3.22	3.98	3.19	3.97	3.85	3.99	3.83	3.92	3.92	4	3.45	3.96	3.38	4	3.55	3.97	3.76
F	2.73	2.05	2.78	2.22	2.64	2.06	2.58	2.59	2.56	2.09	2.72	2.43	2.68	2.53	2.67	2.28	2.48
R	3.26	3.96	3.28	3.62	3.6	3.93	3.56	3.46	3.49	3.87	3.25	3.57	3.18	3.58	3.37	3.71	3.54
N	3.77	3.99	3.82	3.97	3.98	3.96	3.6	4.38	3.99	3.95	3.88	4.3	3.83	4.4	3.84	4.14	3.99
H	3	3	3	3	2.99	3	3	3	3	3	3	3	3	3	3	3	3
D	2.94	2.9	2.79	2.79	2.76	2.74	2.73	2.71	2.97	2.85	2.94	2.7	3	2.9	2.88	2.8	2.84

T – temperature; K – continentality; L - light; F – moisture; R – reaction; N – nutrients; H – humus; D – aeration. Mo - monoculture; I2 – intensive (fertilized) two-year rotation; E2 - extensive (unfertilized) two-year rotation; E3 - extensive (unfertilized) three-year rotation; IS3 - three-year rotation with the application of organic fertilizers; I4 - intensive four-year rotation with the application of organic and mineral fertilizers

The biological spectrum was absolutely dominated by therophytes, which accounted for 82.85% and 71.42% of the analyzed flora in wheat and maize, respectively (Fig. 2). McIntyre et al. (1995) also found that therophyte life form dominated in arable agricultural land. Such life form distribution is common for weed flora under the strong influence of cropping practices (Kovačević et al., 2008).

Considering weed infestation in different treatments in the studied two-year period (in both wheat and maize), the highest average values were recorded in wheat monoculture (490.47 ind/m²) and maize monoculture (111.98 ind/m²) (Table 2; Fig. 4), statistically highly significant difference was found also only between monoculture and other crop rotation treatments (Table 5), which is in line with the findings of other authors who reported that crop rotation and soil cultivation result in reduction of weed density and biomass (Demjanova et al., 2009). The weed species which, due to their abundance, had the greatest influence on weed infestation were *Consolida regalis* and *Veronica hederifolia* in wheat, and *Sorghum halepense* in maize, which was statistically significant in relation to other weed species.

Since the composition of weed flora depends on the ecological characteristics of the environment and the intensity of anthropogenic influence (Šilc, 2010; Jarić et al., 2015), different weed species can be found in different crop rotation treatments, so some treatments differ considerably in relation to their floristic composition. However, our results indicate that higher floristic diversity is not proportional to the level of weed infestation in crops (Table 2).

Knowing that each plant species has certain requirements regarding the ecological characteristics of the habitat, which are expressed by ecological indices (bioindicator values), it is possible to make ecological assessment of the habitat characteristics and the site class. It should be noted that the assessment takes into consideration the average abundance for each weed species, so that the obtained values of the analysed ecological indices represent a reliable indicator of ecological conditions in studied crop rotation treatments.

Therefore, the obtained results are in line with the findings of Šilc (2010) and Jarić et al. (2015) who stress that the composition of weed flora depends on ecological characteristics of the environment and intensity of anthropogenic influence. Although the average ecological indicator values for the main environmental factors pointed to favorable light regime, pH, nutrient content and soil aeration in all experimental

treatments, there were some differences in ecological conditions, as was indicated by clustering of certain experimental treatments in four clusters (*Fig. 6*). It can be concluded that both the type of crop rotation, application of fertilizers and the species of crops had impact on ecological conditions of the studied experimental treatments, which resulted in their clustering and differentiation, expressed by the ecological indicator values of the weed species.

Studying weed flora in long-term crop rotations clearly showed that the structure of weed flora and the level of weed infestation depend on the applied cropping practices and crop rotation treatment. The experiment thus showed that the highest reduction of weed infestation in both crops was achieved in intensive (fertilized) three-year and four-year rotations (*Fig. 4*), which is in line with results of previous studies (Smit and Gross, 2007; Milošev et al., 2014; Nikolić et al., 2018).

Conclusion

The obtained results on weed flora and weed infestation in this research are based on a long-term crop rotation experiment with some of the experimental treatments formed more than seven decades ago. The specific scientific contribution of this paper is that the habitat is characterized on the basis of the ecological indicator values of the determined weed species, and it is possible to identify specific crop rotation treatments in which a certain ecological characteristic has significant effect on weed infestation.

Considering the findings of this research and the results from literature (Smith and Gross, 2007; Koocheki et al., 2009), it can be concluded that the long-term effects of crop rotation are positive since this agricultural practice does not lead to increased weed abundance or development of weed communities that could be difficult to control. Crop rotation is justified also from the aspect of environmental protection, as it contributes to reduced application of chemicals, which is in line with generally accepted views on the preservation, sustainability and balanced use of agricultural land (Liebeman and Dyck, 1993; Milošev et al., 2014; Nikolić et al., 2018).

In the future research, the soil seed bank for these long-term experiments could be analysed. Thus, the prediction of the weed growth would be enabled which could ensure additional reduction and selection of the applied herbicides with the adequate crop rotation.

Acknowledgements. We are grateful to the Institute of Field and Vegetable Crops in Novi Sad for allowing us to work in their fields “Plodoredi”.

REFERENCES

- [1] Avola, G., Tuttobene, R., Gresta, F., Abbate, V. (2008): Weed control strategies for grain legumes. – *Agronomy for Sustainable Development* 28: 389-395.
- [2] Barberi, P., Silvestri, N., Bonari, E. (1997): Weed communities of winter wheat as influenced by input level and rotation. – *Weed Research* 37: 301-313.
- [3] Campiglia, E., Radicetti, E., Mancinelli, R. (2018): Floristic composition and species diversity of weed community after 10 years of different cropping systems and soil tillage in a Mediterranean environment. – *Weed Research* 58: 273-283.
- [4] Delivering Alien Invasive Species Inventories for Europe (DAISIE) (2018): www.europe-aliens.org. – Accessed on 15 December 2018.

- [5] Demjanova, E., Macak, M., Đalović, I., Majernik, F., Tyr, Š., Smatana, J. (2009): Effects of tillage systems and crop rotation on weed density, weed composition and weed biomass in maize. – *Agronomy Research* 7: 785-792.
- [6] Derksen, A. D., Andersen, L. R., Blackshaw, E. R., Maxwell, B. (2002): Weed dynamics and management strategies for cropping systems in the Northern Great Plains. – *Agronomy Journal* 94: 174-185.
- [7] HMZS (2020): Republic Hydrometeorological Service of Serbia. – www.hidmet.gov.rs (accessed on 09.04.2020).
- [8] Hosseini, P., Karimi, H., Babaei, S., Mashhadi, H. R., Oveisi, M. (2014): Weed seed bank as affected by crop rotation and disturbance. – *Crop Protection* 64: 1-6.
- [9] Jarić, V. S., Karadžić, D. B.; Vrbničanin, P. S., Mitrović, M. M., Kostić, A. O., Pavlović, Ž. P. (2015): Floristic and phytocoenological research of segetal plant communities in cultivated areas of southern Srem. – *Archives of Biological Sciences* 67: 591-609.
- [10] Josifović, M. (ed.) (1986): *Flora Republike Srbije*. – Serbian Academy of Sciences and Arts, Beograd.
- [11] Kim, D. S., Brain, P., Marshall, E. J. P., Caseley, J. C. (2002): Modelling herbicide dose and weed density effects on crop: weed competition. – *Weed Research* 42: 1-13.
- [12] Koocheki, A., Nassiri, M., Alimoradi, L., Ghorbani, R. (2009): Effect of cropping systems and crop rotations on weeds. – *Agronomy for Sustainable Development* 29: 401-408.
- [13] Kovačević, D., Dolijanović, Ž., Oljača, S., Jovanović, Ž. (2008): The Effect of Crop Rotation on Weed Control. – *Acta Herbologica* 17: 23-38.
- [14] Landolt, E. (ed.) (2010): *Flora Indicativa. Ecological Indicator Values and Biological Attributes of the Flora of Switzerland and the Alps*. – Haupt Verlag, Bern-Stuttgart-Wien.
- [15] Lazarević, P., Stojanović, V., Jelić, I., Perić, R., Krsteski, B., Ažić, R., Sekulić, N., Branković, S., Sekulić, G., Bjedov, V. (2012): Preliminarni spisak invazivnih vrsta u republici Srbiji sa opštim merama kontrole i suzbijanja kao potpora budućim zakonskim aktima. – *Protection Nature* 62: 5-31.
- [16] McIntyre, S., Lavorel, S., Tremont, R. M. (1995): Plant life-history attributes: their relationship to disturbance response in herbaceous vegetation. – *Journal of Ecology* 83: 31-44.
- [17] Milošev, D., Šeremešić, S., Đalović, I., Pejić, B., Ćirić, V. (2014): Assessing the agroecosystem performance in a long-term winter wheat cropping. – *Contemporary Agriculture* 63: 494-500.
- [18] Moss, R. S., Storkey, J., Cussans, W. J., Perryman, A. M. S., Hewitt, V. M. (2004): Symposium The Broadbalk long-term experiment at Rothamsted: what has it told us about weeds? – *Weed Science* 52: 864-873.
- [19] Nikolić, Lj., Milošev, D., Šeremešić, S., Đalović, I., Vuga Janjatov, V. (2012): Diversity of weed flora in wheat depending on crop rotation and fertilisation. – *Bulgarian Journal of Agricultural Science* 18: 608-615.
- [20] Nikolić, Lj., Šeremešić, S., Milošev, D., Đalović, I., Latković, D. (2018): Weed infestation and biodiversity of winter wheat under the effect of long-term crop rotation. – *Applied Ecology and Environmental Research* 16: 1413-1426.
- [21] Nowak, S., Nowak, A. S. (2013): Weed communities of root crops in the Pamir Alai Mts, Tajikistan (Middle Asia). – *Acta Societatis Botanicorum Poloniae* 82: 135-146.
- [22] Pyšek, P., Richardson, M. D., Rejmánek, M., Webstwer, L. G., Willianson, M., Kirschner, J. (2004): Alien plants in checklists and floras: towards better communication between taxonomists and ecologists. – *Taxon* 53: 131-143.
- [23] Randy, L. A. (2005): A multy-tactic approach to manage weed population dynamics in crop rotations. – *Agronomy Journal* 97: 1579-1583.
- [24] Richardson, M. D., Pyšek, P., Rejmanek, M., Barbour, G. M., Panetta, F. D., West, J. C. (2000): Naturalization and invasion of alien plants: concepts and definitions. – *Diversity and Distribution* 6: 93-107.

- [25] Smith, R. G., Gross, L. K. (2007): Assembly of weed communities along a crop diversity gradient. – *Journal of Applied Ecology* 44: 1046-1056.
- [26] Suarez, A. S., De La Fuente, B. E., Ghersa, M. C., Leon, J. C. R. (2001): Weed community as an indicator of summer crop yield and site quality. – *Agronomy Journal* 93: 524-530.
- [27] Šilc, U. (2010): Synanthropic vegetation: pattern of various disturbances on life history traits. – *Acta Botanica Croatica* 69: 215-227.
- [28] Škorić, A., Filipovski, G., Ćirić, M. (1985): Klasifikacija zemljišta Jugoslavije. – Academy of Sciences and Arts Bosnia and Herzegovina, Sarajevo.
- [29] Teasdale, R. J., Mangum, W. R., Radhakrishnan, J., Cavigelli, A. M. (2004): Weed seedbank dynamics in three organic farming crop rotations. – *Agronomy Journal* 96: 1429-1435.
- [30] Tutin, G., Heywood, V. H., Burges, N. A., Valentine, D. H., Walters, S. M., Webb, D. A. (eds.) (1980): *Flora Europea*, 1-5. – University Press, Cambridge, UK.
- [31] Týr, Š. (2016): Actual weed infestation and sustainable farming systems in winter wheat. – *Research Journal of Agricultural Science* 48: 211-216.
- [32] Ujvárosi, M. (1973): *Gyomnövények*. – Mezőgazdasági Kiadó, Budapest.
- [33] Woźniak, A., Soroka, M. (2015): Structure of weed communities occurring in crop rotation and monoculture of cereals. – *International Journal of Plant Production* 9: 487-506.

EFFECTS OF RIVER BANK SOIL PHYSICAL AND CHEMICAL FACTORS ON *POPULUS PRUINOSA* SCHRENK CLONAL GROWTH

GAI, Z.[#] – LI, X.[#] – ZHAI, J. – CHEN, X. – LI, Z.*

College of Plant Sciences, Tarim University, Alar 843300, China

*Key Laboratory of Biological Resource Protection and Utilization of Tarim Basin, Xinjiang
Production and Construction Group, Alar 843300, China*

Desert Poplar Research Center of Tarim University, Alar 843300, China

[#]These authors contributed equally to this study.

**Corresponding author*

e-mail: lizhijun0202@126.com; phone: +86-997-468-1202

(Received 13th Feb 2020; accepted 22nd May 2020)

Abstract. In this study, soil physical and chemical factor changes before and after flooding and the effects of such changes on the clonal regeneration of *Populus pruinosa* Schrenk were investigated. The results show that soil moisture content and field water capacity had the greatest direct effect on the clonal growth of *P. pruinosa* before flood overtopping. Soil porosity had the greatest direct effect after flood overtopping. Soil organic matter content and alkaline nitrogen had the greatest direct effect on the clonal growth of *P. pruinosa* before flood overtopping. Available phosphorus and available potassium had the greatest direct effect after flood overtopping. The flooded woodland was conducive to clonal growth of *P. pruinosa*, but flood overtopping for too long led to increased soil bulk density, decreased porosity, and increased soil salinity, all of which hindered clonal growth. We suggest the implementation of flood diversion measures in flooding woods to ensure normal post-flooding clonal growth. Meanwhile, water retained in the soil after flooding would also be available to promote clonal growth the following spring. These may be of great significance for increasing the benefits of seasonal flooding in this arid area.

Keywords: *clonal ramets, soil nutrient, flood overtopping, desert riparian, population regeneration*

Introduction

Clonal plants exhibit a clonal growth habit. Such plants colonise reproductive organs, including buds, by tillering or by propagation from the branches of maternal ramets to produce vegetative propagated plants (propagules). Propagules develop into potentially independent offsprings (clonal ramets) that are connected to maternal ramets and eventually form a group of interconnected clonal plants (Alpert, 1996). Under natural conditions, clonal plants produce clonal ramets with potentially independent survival abilities that can undergo widespread horizontal and vertical vegetative growth that characterises the clonal growth observed in fields (Silvertown, 1984). Therefore, individual ramets of clonal plants morphologically and physiologically develop and increase their territories through clonal growth. Ultimately, clonal growth allows a genetically identical group of cloned plants to occupy a considerable habitat area while concurrently increasing the number of plant populations engaging in interspecies competition (Zhang and Wang, 2005).

In arid and semi-arid areas, soil moisture is the dominant ecological factor affecting plant growth. Plants respond to soil water conditions through phenotypic plasticity. For clonal plants, the response is reflected not only by their clonal growth characteristics but

also in their clonal morphological characteristics (such as the distribution pattern of individual ramets and individual morphological changes), which are closely related to the ecological adaptations and resource acquisition of plant populations (Luo and Dong, 2002). Previous studies have shown that clonal plants have strong phenotypic plasticity under various soil conditions whereby clonal plant growth and morphology may exhibit strong phenotypic diversity. Moreover, the mechanisms, degree, and trends of phenotypic plasticity may vary among different plants (He et al., 2007). For the number of ramets, some studies have shown that with increased available soil moisture, the number of clonal ramets of *Hippophae rhamnoides* Linnaeus and *Leymus secalinus* (Georgi) Tzvelev significantly increased (He et al., 2007; Ren, 1999). Moreover, the height and biomass of the population have been observed to increase with high soil moisture (He et al., 2007).

The heterogeneous distribution of soil nutrients also affects the changes in growth characteristics of clone plants. Such changes further influence the spatial distribution patterns and clonal plasticity of the plant components of an entire clonal plant or even of an entire plant population. The size of clonal plants has been demonstrated to change in response to changing soil nutrient availability, as reflected by the biomass of both a population and its components, including the average basal diameter, average plant height, and allocation of aboveground biomass (Bai et al., 2019; Heng, 2002; Pan et al., 2005; Yue et al., 2002). In a high-quality habitat (low salt, high light, and high nutrient levels), *Scirpus olneyi* rhizome ramets have been shown to spread clearly into a population of many densely distributed short-rhizome clonal ramets. Conversely, in a low-quality habitat (high salt, low light, and low nutrient levels) many sparsely distributed clonal ramets have been shown to emerge (Ikegami et al., 2007). Roilola et al. (2006) reported similar results for *Fragaria vesca* and proposed that more ramets were distributed in high-quality patches within a heterogeneous habitat. In a different study, *Vallisneria spiralis* L. was also reported to exhibit more growth in a heterogeneous habitat, as reflected by longer leaves and larger sizes observed in patches with higher nutrient levels (Hodge, 2004).

Populus pruinosa and the related species *Populus euphratica* are members of the *Salicaceae* family. *P. pruinosa* achieves reproduction and regeneration by the development of adventitious buds on underground horizontal lateral roots, which develop into clonal ramets to maintain the desert riparian forest population (Li et al., 2012; Zheng et al., 2016a). Previous researches showed that the density of clonal ramets of *P. euphratica* was markedly influenced by light and soil conditions (water and nutrients) (Wu et al., 2008). Soil structure was also observed to play a decisive role in the emergence of clonal ramets, which were observed only after buds on the lateral root penetrated a certain thickness of the soil layer. Consequently, if the soil structure is too tight, it is difficult for a bud to form a ramet. Therefore, loose soil facilitates the formation of clonal ramets (Zhang et al., 2007). Meanwhile, one study demonstrated that a 15% soil water content was the optimum moisture content for *P. euphratica* root germination (Jing et al., 2013), in agreement with a study of *P. pruinosa* woodland forest far from a river, where clonal growth was observed only in the presence of 15% soil moisture content or higher (Zheng et al., 2016b). A later study showed that with increased soil moisture content, the numbers of adventitious buds and unearthed and earthed ramets significantly increased, indicating that soil moisture was an important factor affecting the growth of poplar clones (Zheng et al., 2016a). In addition, the number of adventitious buds, underground ramets and unearthed ramets in the forest was significantly lower than that in the forest edge, in the

forest edge, the number of adventitious buds was close related to the content of soil organic matter, alkali nitrogen and available potassium, and there was also a significant correlation between the underground ramets and the content of soil alkali nitrogen and available phosphorus, indicating that soil fertility also was an important factor affecting the growth of poplar clones (Zheng et al., 2019).

Although flood overtopping causes changes in *P. pruinosa* forest soil physical and chemical factors, it is still unclear how such soil physical and chemical factor changes affect clonal growth of *P. pruinosa* throughout the growing season. These effects must all be understood to determine the impact that flooding has on the clonal growth of *P. pruinosa* with specific regard to clonal reproduction and regeneration. The goals of this study are to (1) reveal the dynamic variation in the numbers of adventitious buds, unearthed/earthed clonal ramets, and growth rates of ramets of *P. pruinosa* before and after flooding; (2) uncover the dynamic changes in both physical and chemical soil factors before and after flooding; and (3) clarify the relationship between clonal growth dynamics of *P. pruinosa* and dynamic changes in soil physical and chemical factors to assess the impact of flooding on riparian forest *P. pruinosa* clonal reproduction and regeneration. The results of this study should provide a theoretical basis for effectively utilizing flood overflow to promote clone reproduction and regeneration of *P. pruinosa*.

Materials and methods

The study was conducted in a natural woodland of *P. pruinosa* on the Tarim River in Xinjiang in northwest China, located at 80°50'E, 40°29'N. A few accompanying herbaceous or shrub plants, such as *Tamarix chinensis* Lour., *Glycyrrhiza uralensis* Fisch, *Phragmites australis* (Cav.) Trin. Ex Steud., and *Aeluropus sinensis*, also commonly grow in these woodlands. Annual river floods are known to expand into the woodland near river banks when flood overtopping occurs. For example, woodland was flooded during the flood overtopping that occurred from July 25 to August 18 of 2014 and again from July 26 to August 21 of 2015.

Three sample plots were studied in parallel, each 30 m×30 m in size and located within a vertical height of 200 m above the river. All plots were fenced to protect them from sheep grazing (Fig. 1). Clone growth indexes were surveyed, and soil samples were collected every 20 days from April early August in both 2014 and 2015; From the beginning of August to the end of September, the investigation was conducted once a month due to the difficulty caused by surface water after flooding; The survey was conducted on 20 days from the end of September to the end of October.

In each survey, 10 clonal ramets were randomly dug up from each sample plot. For each unearthed ramet, the horizontal lateral root on either side was identified as either the proximal end root (the clonal ramet root portion closer to the mother plant) or the distal end root (the clonal ramet root portion further from the mother plant). Both ends encompassed a total root length span of 2.5 m symmetrically spanning both sides of the clonal ramet. The point on a lateral root at which the clonal ramet emerged, defined as the middle of the lateral root, was defined as the middle of the 50-cm central root segment. Horizontal lateral roots were then divided into four segments, two 50-cm segments adjacent to the proximal end of the central root segment and two 50-cm segments adjacent to the distal end of the central root segment. Thus, five segments were selected along each root over a total length of 2.5 m (defined as the unit length). The depth of each root segment was measured to

determine its soil profile. Surveys of the numbers of adventitious buds and unearthed/earthed clonal ramets along each unit length of horizontal lateral root were conducted. At the same time, the number of ramets in each cluster, ramet height, and ramet basal diameter of all ramets in each plot were also measured.

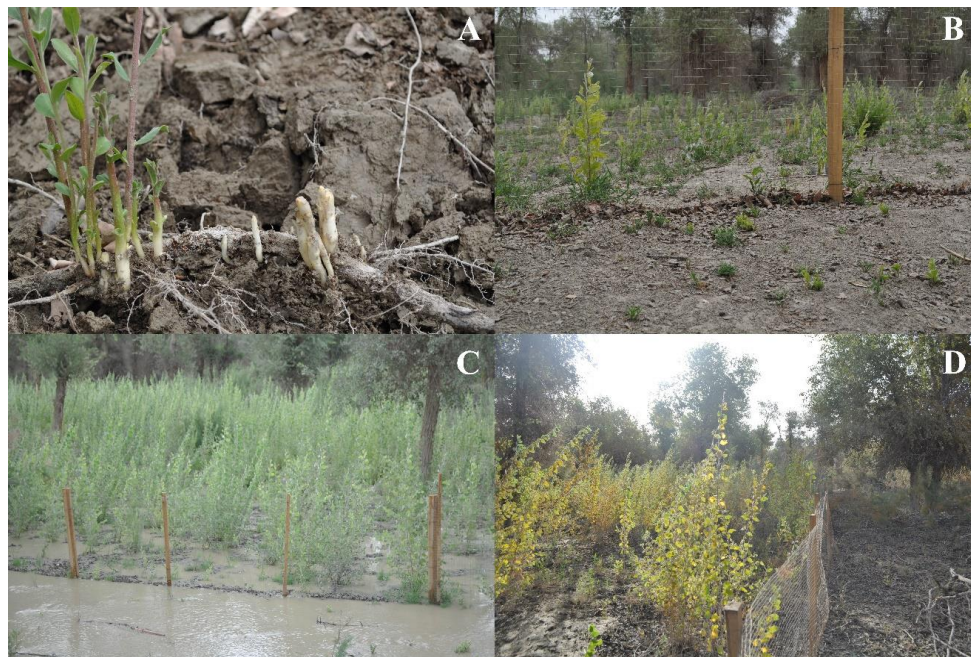


Figure 1. Growth of clone plants of *P. pruinosa* before and after flood overtopping. (A) clonal plants of *P. pruinosa*, (B) the experimental sites of clone plants of *P. pruinosa*, (C) woodland was flooded during the flood overtopping and (D) the growth of clone plants after flood overtopping

Collection and analyses of soil samples were performed to determine soil physical and chemical characteristics. Each survey was performed at the time of digging to assay each unit length of horizontal lateral root. Soil samples were also excavated at the point of emergence of each clonal ramet to construct a soil profile within a square area of 1 m × 1 m around the ramet emergence point. Within this sampling area, soil samples at 20 cm, 40 cm, and 60 cm depths were collected and analysed.

Soil moisture was determined using a previously reported oven-drying method, soil bulk density, porosity, and field capacity were determined using samples collected using a cutting ring (ring knife) and analysed in the laboratory (Zhao, 2015). Soil pH was measured using the potentiometric method. Soil total salt was measured using the gravimetric extraction method, whereby soil samples were mixed with water in a known ratio and mixed by oscillation for a specific period of time, followed by extraction of soluble salt from the liquor by filtration. The filtrate was tested in liquid form to determine soil water-soluble salts and other chemical characteristics. Soil organic matter content was determined using a potassium dichromate-based method in combination with a heating method (Wei et al., 2015). Alkaline nitrogen was determined using the alkaline hydrolysis diffusion method (Wei et al., 2015). Available phosphorus was determined using the sodium bicarbonate method (Ren et al., 2015), and available potassium was determined using the ammonium acetate-flame photometer method (Ren et al., 2015).

The computational formulas are as follows:

$$\text{Soil moisture content} = \frac{\text{mass of aluminium box and soil sample before baking} - \text{mass of aluminium box and soil after baking}}{\text{mass of aluminium box and soil sample after baking} - \text{mass of empty aluminium box}} \times 100\% \quad (\text{Eq.1})$$

$$\text{Soil bulk density} = \frac{\text{dry soil mass in ring knife}}{\text{ring knife volume}} \quad (\text{Eq.2})$$

$$\text{Soil porosity} = \frac{1 - \text{soil bulk density}}{2.65} \times 100\% \quad (\text{Eq.3})$$

$$\text{Field capacity} = \frac{\text{wet soil weight} - \text{dry soil weight}}{\text{dry soil weight}} \times 100\% \quad (\text{Eq.4})$$

Data analysis

The data was entered into an Excel table, and the average value of each factor was calculated using the size of the average drawing. A one-way ANOVA was conducted on the variance in clonal growth and soil physical and chemical factors (at level of $\alpha = 0.05$). Path analysis used by SPSS 15.0 was applied to calculate the effect of soil physical and chemical factors on the growth of clones.

Results

Dynamic variation patterns of *Populus pruinosa* clonal growth

In 2014 and 2015, the Tarim River flood overtopped the riparian forest on July 25 and July 28, respectively. Using the late July flood overtopping date as the reference time node, clonal growth characteristics at the forest edge both before and after flood overtopping were determined. The result shows that the number of adventitious buds and earthed clonal ramets from late April to early June increased gradually (*Fig. 2A*) and the numbers of them from late June to late October decreased gradually (*Fig. 2B* and *Table A1* in the *Appendix*). The number of unearthed clonal ramets exhibited gradually decreasing trends before and after flood overtopping in both years, there was a significant difference in the number of unearthed clonal ramets in late April and late October—the total numbers before flood overtopping was higher than that after flood overtopping (*Fig. 2C*). The growth rate of ramets height from late April to late June increased gradually and that from early August to late October decreased gradually (*Fig. 2D*). The growth rate of ramets height was significantly different among the four time points (4/27, 6/29, 8/5, 10/21). The growth rate of clonal ramets basal diameter from late April to late June increased gradually and that from middle July to late October decreased gradually (*Fig. 2E*). The number of per cluster ramet from late April to late June increased gradually and that from early August to late October decreased gradually (*Fig. 2F*). It was also significantly different among the four time points (4/27, 6/29, 8/5, 10/21).

Overall, the period from late April to late June before flood overtopping is a period of fast *P. pruinosa* clonal growth, the number of adventitious buds, earthed clonal ramets and per cluster ramet in July were significantly decreased, which may be related to the significant reduction of soil moisture content from late June to late July (*Fig. 3A*). In different years, the trends of clone reproductions of *P. pruinosa* is consistent, but the clone growth of the same period is different.

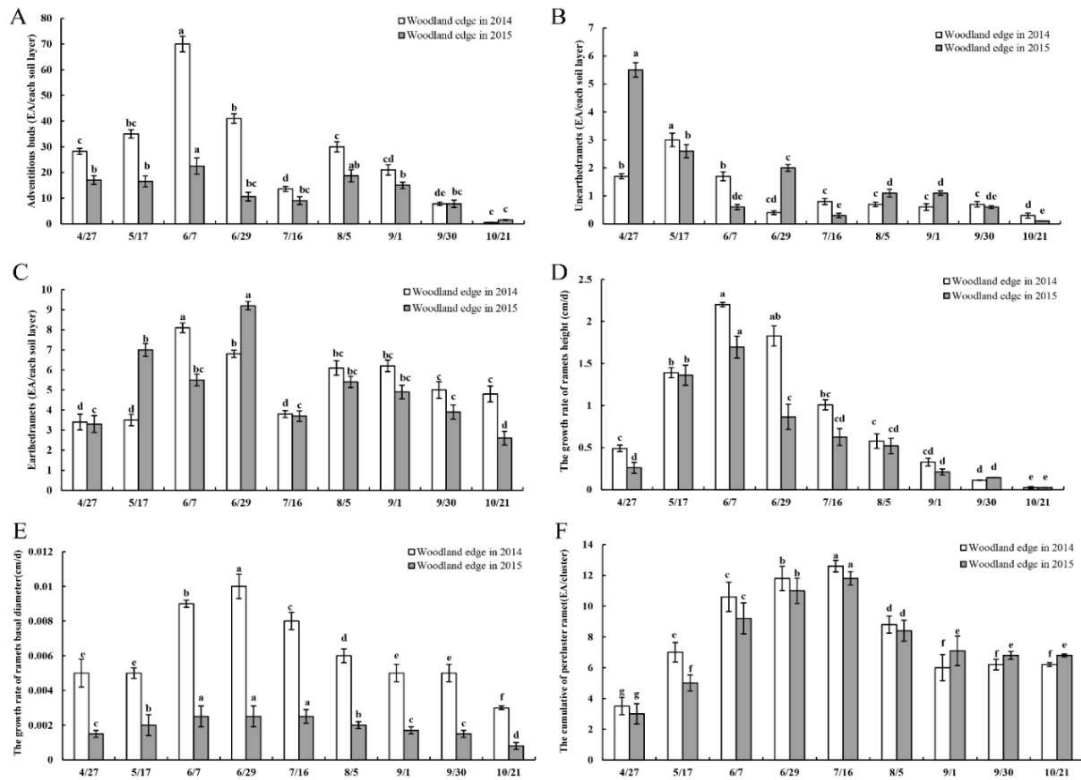


Figure 2. Dynamic variation in *P. pruinosa* clonal growth before and after flood overtopping. (A) The number of adventitious buds, (B) the number of unearthed clonal ramets, (C) the number of adventitious buds and earthed clonal ramets, (D) the growth rate of ramets height, (E) the growth rate of ramets basal diameter and (F) the cumulative of per cluster ramet

Dynamic variation patterns of soil physical factors

The results showed that the change trends of soil moisture content, field capacity, soil bulk density and soil porosity were almost consistent in 2014 and 2015 (Fig. 3; Table A2). The soil moisture content significantly increased in August after flood overtopping and then later declined gradually to reach minimum values by late October each year, but the soil moisture content was higher after the flood than before (Fig. 3A). Field capacity values all exhibited an a very gradual decreasing trend from April to mid-July (just before flood overtopping), and the field capacity in August significantly increased above July levels, and then remain consistent (2015) or decreased gradually (2014) (Fig. 3B). The soil bulk density and soil porosity in August after flood overtopping exhibited the gradually increasing and decreasing trends, respectively (Fig. 3C and 3D). The results showed that the change trends of soil moisture content, field capacity, soil bulk density and soil porosity were inconsistent before and after flood overtopping.

Dynamic variation patterns of soil chemical factors

The results showed that the change trends of soil organic matter, alkaline nitrogen, available phosphorus, available potassium, total salt content and pH values were almost consistent in 2014 and 2015 (Fig. 4; Table A3). The contents of soil organic matter (Fig. 4A). and the alkaline nitrogen (Fig. 4B). from late April to middle July before

flood overtopping exhibited the trends of increasing first and then decreasing, and the contents of them from late August to late October after flood overtopping decreased gradually.

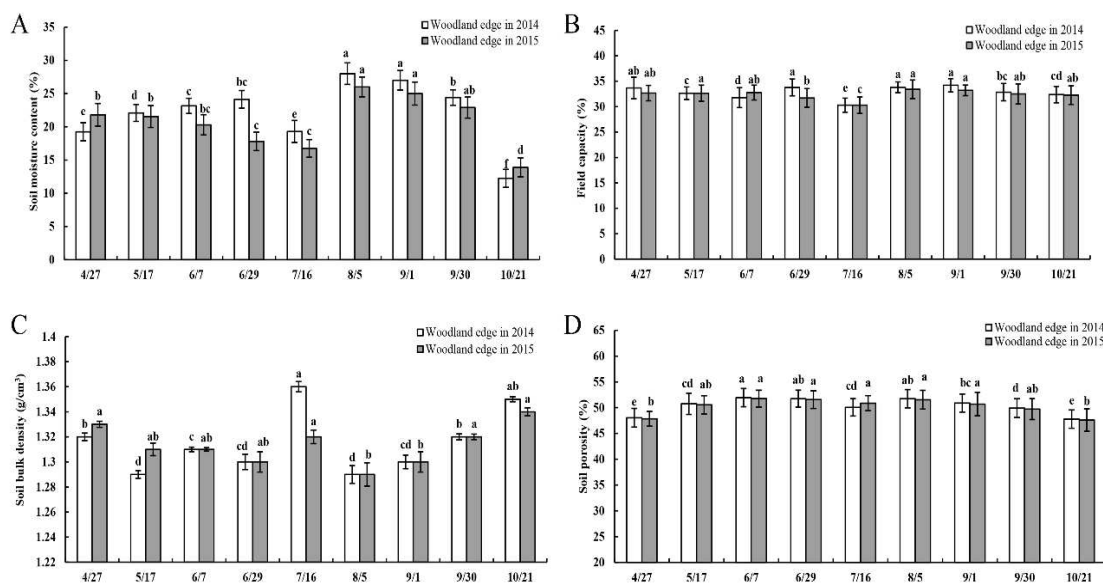


Figure 3. The dynamic change in soil physical factors before and after flood overtopping. (A) Soil moisture content (Eq. 1), (B) field capacity (Eq. 4), (C) soil bulk density (Eq. 2) and (D) soil porosity (Eq. 3)

The content of soil available phosphorus from late April to middle July before flood overtopping exhibited the trends of increasing first and then decreasing, the content of soil available phosphorus decreased to its lowest value in August and it from late August to late October after flood overtopping increased gradually (Fig. 4C). The content of soil available potassium remained at its highest level for the entire growing season from late April to late June and then significantly decreased in the middle of July, it from late August to late October after flood overtopping increased gradually (Fig. 4D). The content of total salt (Fig. 4E) and pH values (Fig. 4F) from late April to middle July before flood overtopping exhibited gradually the trends of decrease and the content of them from late August to late October after flood overtopping showed gradually the trends of increase, the significant difference were observed among the four time points (4/27, 7/16, 8/5, 10/21). The results showed that the change trends of soil organic matter, alkaline nitrogen, available phosphorus, available potassium, total salt content and pH values were inconsistent before and after flood overtopping.

Relationship between clonal growth and soil physical factors

The result showed that after flood overtopping, the number of adventitious buds exhibited a highly significant negative correlation with soil bulk density but significant and positive correlations with soil porosity and field capacity. The number of unearthed clonal ramets exhibited highly significant positive correlations with both soil moisture content and field capacity. The number of earthed clonal ramets exhibited a significant positive correlation with soil porosity. while the clonal ramet height growth rate

exhibited highly significant positive and negative correlations with field capacity and soil bulk density, respectively (*Table A4*). The results showed that the changes of the numbers of adventitious buds, numbers of clonal ramets and the clonal ramet height growth rate were correlated with the changes of soil moisture content, soil bulk density, soil porosity, and field capacity before and after flooding overflow, the same soil physical factors before and after flood exerted different effects on the clone growth.

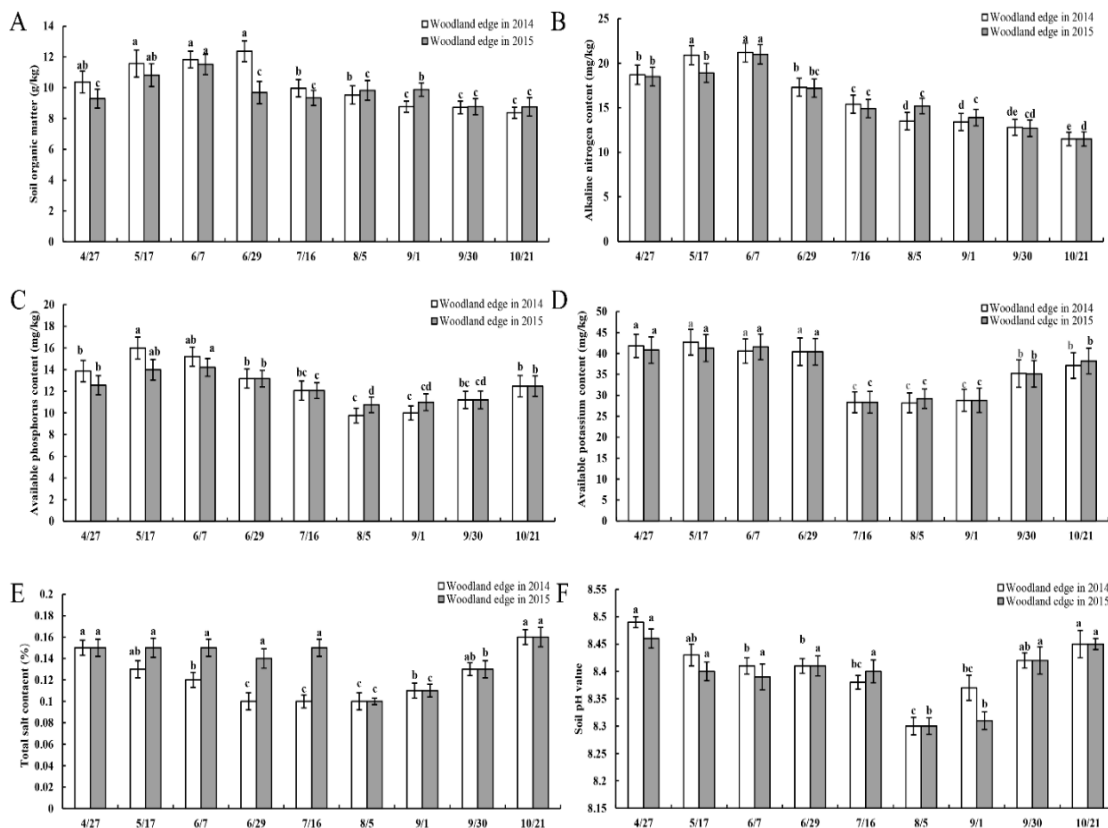


Figure 4. The dynamic change in soil chemistry factors before and after flood overtopping. (A) The content of soil organic matter, (B) the content of the alkaline nitrogen, (C) the content of soil available phosphorus, (D) the content of soil available potassium, (E) the content of total salt and (F) the content of pH values

Relationship between clonal growth and soil chemical factors

The correlation analysis results showed that the clone ramet height rate of increase before flood overtopping had a significant positive correlation with soil organic matter but a highly significant negative correlation with pH value. After flood overtopping, the number of adventitious buds had a significant positive correlation with both soil organic matter content and alkaline nitrogen but highly significant negative correlations with available phosphorus, available potassium, total salt and pH value. Meanwhile, the number of unearthed clonal ramets had a significant positive correlation with alkaline nitrogen, while the number of earthed clonal ramets had a highly significant negative correlation with available potassium. The rate of increase in ramet height had a significant negative correlation with total salt (*Table A5*), The results indicated that the

changes of the numbers of adventitious buds, numbers of clonal ramets and the clonal ramet height growth rate were correlated with soil organic matter, alkaline nitrogen, available phosphorus, available potassium, total salt and pH value, the same soil chemical factors before and after flood had varying effects on the clone growth.

Path analysis of soil physical factors on the clonal growth of *Populus pruinosa*

On the basis of correlation analysis, further path analysis shows that before flood overtopping (from April to July), soil moisture content and field capacity were the main physical factors affecting the numbers of adventitious buds, numbers of unearthed or earthed clonal ramets, numbers of ramets per cluster, ramet height growth rate and basal growth rate; After flood overtopping (from August to October), soil porosity was the main physical factor affecting the numbers of adventitious buds, numbers of unearthed or earthed clonal ramets, numbers of ramets per cluster, ramet height growth rate (Table 1). These implied that soil moisture content and field water capacity were the main factors affecting the clonal growth of *P. pruinosa* before flood overtopping, and soil porosity was the main factors affecting the clonal growth of *P. pruinosa* after flooding overtopping.

Path analysis of soil chemical factors on the clonal growth of *Populus pruinosa*

Path analysis shows that before flooding overtopping, soil organic matter content and alkaline nitrogen were the main chemical factors affecting the numbers of adventitious buds, numbers of unearthed or earthed clonal ramets, numbers of ramets per cluster, ramet height growth rate and basal growth rate. After flood overtopping, available phosphorus and available potassium were the main chemical factors affecting the numbers of adventitious buds, numbers of unearthed or earthed clonal ramets, numbers of ramets per cluster, ramet height growth rate (Table 2). These implied that soil organic matter content and alkaline nitrogen were the main factors affecting the clonal growth of *P. pruinosa* before flood overtopping, and available phosphorus and available potassium were the main factors affecting the clonal growth of *P. pruinosa* after flood overtopping.

Discussion

Among soil physical factors, soil water is the main ecological factor influencing the growth and reproduction of plants. Plants adapt to the availability of water resources mainly through plant plasticity. When the availability of soil water is high, clonal plants grow to a high density, reach a large size, and exhibit strong clonal growth capacity that leads to a predictably large number of clonal offspring, high ramet fitness, and a low death risk (He, 2007). Several studies have demonstrated that the clonal growth of *P. pruinosa* was conducted only in the presence of 15% soil moisture content or higher, the number of adventitious buds and the number of earthed clonal ramets had significant positive correlation with soil moisture content (Zheng et al., 2016b). Our study revealed that before flood overtopping (from April to June), the rapid increase in the number of adventitious buds and the number of clonal ramets of *P. pruinosa* is the most vigorous stage of clone reproductions in a year, which is related to the biological characteristics and the gradual increase in temperature and surface temperature (Zheng et al., 2016a), path analysis showed that soil moisture content and field capacity were the main soil

physical factors affecting the clonal growth of *P. pruinosa*. The soil moisture content in each period of this stages was over 15%, and the field capacity remained above 30%, which satisfied the water requirement of the clone growth of *P. pruinosa* at this stage. Remarkable, In the middle of July, the soil moisture content was the lowest before the flood overflows, the number of adventitious buds, the number of clonal ramets clones and the number of ramets per cluster were also significantly reduced, indicating that they were very sensitive to the change of soil moisture.

Our analysis also revealed that the high level of soil moisture content from April to June was related to the flood overtopping occurred in the previous year. Despite the significant decrease in soil water content in October after flood overtopping, field capacity exhibited no significant decline and remained constant through April of the next year. This result suggests that a high soil effective moisture content resulted from an increase in the underground water level and persistence of abundant water in the soil after flood overtopping. Therefore, water retained in the soil after flooding before the previous autumn replenished soil moisture for the following spring by storage of water through winter freezing. Subsequent spring thawing then released water to support the clonal growth of *P. pruinosa* from April to May. On the other hand, as the ground temperature and air temperature increased gradually from April to June, surface evaporation increased gradually, which promoted soil moisture to move from deeper layers to the 0-40-cm soil layer, gradually increasing both soil moisture content and field capacity during the spring phase. The significance of this process is that it also leads to the migration of soil organic matter, alkaline nitrogen, available phosphorus, and available potassium to improve habitat quality. The improved habit in turn is more conducive to supporting increased numbers of adventitious buds and greater clone ramet growth. This shows that the flooding of forestland last year has an important effect on the clonal reproduction of *P. pruinosa* from April to June next year. From August to October after flood overtopping, the number of adventitious buds, the number of clonal ramets of *P. pruinosa* and the growth rate of clone ramets were obviously decreased, these changes were related to the gradual decrease of land surface temperature and air temperature at this stage (Zheng et al., 2016a). Our results showed that the change was significantly affected by the change of soil physical factors during the same period. The soil physical factors of forestland have larger changes compare with before the flood overtopping, the soil moisture content ranged from 25% to below 15%, with gradual decreases in both field capacity and soil porosity and gradual increases in soil bulk density, they were positive or negative correlation with the number of adventitious buds, the number of unearthed/earthed clonal ramets and the growth rate of clone ramets, path analysis showed that soil porosity was the main factors affecting the clonal growth of *P. pruinosa* after flooding overtopping. Analysis suggested that after the forestland was flooded in late July, the forestland was in the state of water accumulation from August to September due to the large amount of overflowed flood, it will cause increased soil bulk density lead to the soil structure to tighten and soil porosity to decrease, both of which are disadvantageous to the adventitious bud formation of clonal ramets. This finding is consistent with the conclusion reached by Zhang et al. (2007) and Jing et al. (2013), suggesting that the high soil moisture content will lead to the increase of soil compactness, and the resistance to the growth of tiller buds of *P. euphratica* was larger, which is not conducive to the formation of clonal seedling of *P. euphratica*. The results suggested that the excessive and long flood. overtopping in forestland has certain inhibitory effect on the clonal growth of *P. pruinosa*.

Table 1. The path analysis of clonal growth indexes and soil physical factors in 2014 and 2015

		Woodland edge in 2014				Woodland edge in 2015			
		Direct effect				Direct effect			
Index	Month	Soil moisture content	Soil bulk density	Field capacity	Soil porosity	Soil moisture content	Soil bulk density	Field capacity	Soil porosity
Unearthed ramets	4~7	-1.561	-1.1232	0.4175	1.5158	-0.4503	0.2314	0.8492	-0.7132
	8~10	0.5934	0.0247	-0.2705	-0.1487	0.8303	-0.4438	1.0506	-1.262
Earthed ramets	4~7	2.8241	1.5284	-0.7358	-2.389	-0.488	-0.4247	0.751	0.053
	8~10	-0.6716	-0.6854	0.6595	0.3647	0.0162	-0.2727	0.1661	0.4518
Adventitious buds	4~7	0.8731	0.0294	-0.0386	-0.1624	-1.0779	-1.0745	2.2182	-0.0876
	8~10	-0.7317	-1.2084	0.0433	1.6095	-0.5762	-1.1502	0.0867	1.5251
Ramets per cluster	4~7	1.6353	1.1283	-0.9465	-1.0542	-0.1372	-0.134	-0.3361	0.7112
	8~10	-0.8042	-0.2821	-0.7034	1.8477	-1.8749	-0.3819	-2.1129	4.0415
Clone ramet height	4~7	1.1674	0.2274	-0.5493	-0.1167	-0.4713	-0.9913	0.9105	0.771
	8~10	-1.0058	-1.3499	0.1188	1.731	-0.788	-1.2896	0.243	1.5408
Basal diameter	4~7	3.1189	1.9932	-0.8364	-2.6403	-1.8356	-0.4446	1.9794	-0.3363
	8~10	0.8534	0.3348	0.1005	-0.2712	1.0988	0.3711	0.4042	-0.7973

Table 2. The path analysis of clonal growth indexes and soil chemical factors in 2014 and 2015

		Woodland edge in 2014						Woodland edge in 2015					
		Direct effect						Direct effect					
Index	Month	Alkaline nitrogen	Available phosphorus	Available potassium	Total salt content	pH value	Soil organic matter	Alkaline nitrogen	Available phosphorus	Available potassium	Total salt content	pH value	Soil organic matter
Unearthed ramets	4~7	0.3934	-0.0143	-1.0423	0.922	-0.2988	0.5959	19.7537	38.4471	-22.9292	0.0289	-4.4559	-38.5662
	8~10	1.1028	-0.7677	0.5053	1.2211	-0.7739	0.1307	-1.4196	-3.461	5.5317	0.0932	-2.0523	4.8764
Earthed ramets	4~7	1.4751	-1.6677	-0.1188	-0.123	0.0577	0.6388	-15.7853	-28.7587	18.2588	0.2381	3.2797	29.0582
	8~10	-0.421	1.3944	-1.0881	-1.149	0.401	-0.1493	8.6738	19.7736	-36.8747	-0.5142	12.8065	-30.0733
Adventitious buds	4~7	2.3372	-1.9114	-0.687	0.3751	0.081	1.007	-22.0788	-45.2123	27.2463	-0.234	5.6132	44.8165
	8~10	0.3139	0.2457	-0.7341	0.1799	-0.2237	0.482	-1.3648	-5.0562	9.6097	-0.0434	-3.5602	7.953
Ramets per cluster	4~7	0.6993	-0.4714	-0.5894	-0.4281	0.2355	0.345	-21.7366	-42.7332	25.2295	-0.5997	5.7702	42.771
	8~10	-0.5239	-0.3354	0.0726	-0.086	0.3523	0.6321	-16.3575	-39.7764	74.907	0.2628	-25.3393	60.7634
Clone ramet height	4~7	0.8933	-0.4259	-1.7771	0.7254	-0.2895	1.819	-26.1817	-50.621	30.7549	-0.3377	6.3253	51.0733
	8~10	-0.5476	-0.1118	-0.6908	-0.3661	0.2714	0.4392	4.4945	8.39	-15.0579	-0.0371	4.6477	-12.1749
Basal diameter	4~7	1.0998	-1.4355	-0.2117	-0.1761	0.3083	0.6802	-26.2869	-52.24	31.3363	-0.7127	7.1231	51.6999
	8~10	-1.1161	-2.7277	1.3629	-0.5975	1.3412	-0.1433	-3.8594	-8.8175	14.7609	-0.1122	-4.2438	12.3232

Flooding also contributes to the heterogeneous distribution of soil nutrients, including that of belowground building blocks that affect the development of plant root systems and clonal organs and alter growth characteristics. Such factors further influence the spatial distribution pattern and clonal plasticity of the building blocks of the plant, the entire clonal plant, and even the entire population. For example, clonal plant size can change with changing soil nutrient availability, which would alter the biomass of both the population and its building blocks as measured by the average basal diameter, average plant height, and allocation of above ground biomass (Pan et al., 2005; Yue et al., 2002). As a specific example, with an increase in soil nitrogen content, the number of *Phyllostachys praecox* clonal population ramets, plant height, and base diameter were observed to clearly increase (Yue et al., 2002). However, with a decline in soil nutrient content, underground biomass as a proportion of total biomass was observed to increase (Shang, 2000; Yue et al., 2002), while the increase of the alkaline nitrogen and available potassium content in soil were observed to effectively promote increased numbers of adventitious buds (Zheng et al., 2016b, 2019).

Our study revealed that before flood overtopping (from April to June), the rapid increase in the number of adventitious buds and the number of clonal ramets of *P. pruinosa* were positive or negative correlation with the increase of soil organic matter, alkaline nitrogen, and available phosphorus, total salt remained below 0.2%, and the decrease of pH value. Path analysis showed that soil organic matter content and alkaline nitrogen were the main factors affecting the clonal growth of *P. pruinosa*. At this stage, with gradually increasing ground temperature and air temperature, sufficient soil moisture content, gradual increased contents of soil organic matter, alkaline nitrogen and available phosphorus, elevated habitat nutrient quality to a higher level favoured an increase in the number of adventitious buds and clonal ramets, ramet height, and base diameter growth. From August to October after flood overtopping, the gradual decrease in the number of adventitious buds and the number of clonal ramets of *P. pruinosa* have closely relation with the gradual decrease of soil organic matter and alkaline nitrogen, the gradual increase of available phosphorus, available potassium and total salt. Among the six soil chemical factors, the content of available phosphorus and available potassium in soil were the main factors affecting the clonal growth of *P. pruinosa* in this stage. Obviously, the increased content of available phosphorus and available potassium in the forestland after the flood overtopping had certain inhibitory effect on the increase in the number of adventitious buds and clonal ramets, ramet height, and base diameter growth in this stage. Previous studies have noted that flood overtopping changes soil nutrients by bringing in topsoil partially composed of organic matter while inducing leaching and flushing that reduce the levels of organic matter within the 0-40 cm deep soil layer. Therefore, organic matter content after flood overtopping exhibited characteristics opposite to those observed before overtopping with a gradual reduction in the effects observed with increased soil depth (Zhou et al., 2010). We speculate that many factors contribute to the significant reductions of organic matter and alkaline nitrogen observed after flood overtopping. The reductions may result from nutrient consumption during the clonal growth process. However, these reductions may instead be due to leaching and flushing after flood overtopping. Both types of processes lead to the reduction of organic matter and alkaline nitrogen within the 0-60 cm soil depth layer, with a gradual decrease in organic matter and alkaline nitrogen and a gradual increase in available phosphorus, available potassium, total salt, and pH. Regardless of mechanism, such changes contribute to observed decreases in the

numbers of adventitious buds, earthed/unearthed clonal ramets, ramets per cluster, and rate of increase in clonal ramet height.

Conclusion

This study showed that flooded woodland was conducive to clonal growth of *P. pruinosa*, but flood overtopping for too long led to increase soil bulk density, decrease soil porosity, decrease of soil organic matter and alkaline nitrogen content, and increased of soil salinity and PH value, all of which hindered clonal growth. Therefore, the future work should focus on the relationship between clone growth and flood overflow, the research will need to confirm flood volume and duration for ensuring normal post-flooding clonal growth in the current year. At the same time, water retained in the soil after flooding does not affect the clonal growth during the following spring from April to May. The scheme can guide forestland managers how to realize the natural regeneration of *P. pruinosa* forest scientifically by using the methods of artificial drainage and flood diversion for irrigation after forestland flood overtopping, these may be of great significance for exploiting the effective utilization of seasonal flooding in this arid area to promote the clonal reproduction of natural woodland plants.

Acknowledgements. This work was financially supported by the National Natural Sciences Foundation of China (U1803231, 31260072), Innovative team Building Plan for key areas of Xinjiang Production and Construction Corps (2018CB003).

REFERENCES

- [1] Alpert, P. (1996): Nutrient sharing in natural clonal fragments of *Fragaria chiloensis*. – *Journal of Ecology* 84: 395-406.
- [2] Bai, W., Hou, X., Wu, Z., Ren, W., Zhao, Q. (2019): Advances in studies on morphological plasticity of *Leymus chinensis* rhizome. – *Pratacultural Science* 36(3): 821-834.
- [3] He, B., Li, G. Q., Gao, H. Y., Chen, W. H., Li, G., Qiao, W. L., Jb, N. (2007): A comparison study on the clonal growth of *Hippophae rhamnoides* L. subsp. *Sinensis* at different soil moisture condition. – *Journal of Yunnan University* 29: 101-107.
- [4] Hodge, A. (2004): The plastic plant: root responses to heterogeneous supplies of nutrients. – *New Phytol* 162: 9-24.
- [5] Ikegami, M., Whigham, D. F., Werger, M. J. A. (2007): Responses of rhizome length and ramet production to resource availability in the clonal sedge *Scirpus olneyi* A. Gray. – *Plant Ecology* 189: 247-259.
- [6] Jing, J., Xia, Y. (2013): Impacts of soil type, water content and salinity on the root sucker occurrence mechanism of *Populus euphratica*. – *Journal of Northeast Forestry University* 41: 42-46.
- [7] Li, Z. J., Jiao, P. P., Zhou, Z. L., Li, Q., Jq, L. (2012): Morphological and anatomical features of root sucker propagation of *Populus pruinosa*. – *Chinese Bulletin of Botany* 47(2): 133-140. DOI: 10.3724/SP.J.1259.2012.00133.
- [8] Luo, X. G., Dong, M. (2002): Architectural plasticity in response to soil moisture in the stoloniferous herb, *Duchesnea indica*. – *Acta Botanica Sinica* 44: 97-100.

- [9] Pan, Q., Bai, Y., Han, X., Yang, J. (2005): Effects of nitrogen additions on a *Leymus chinensis* population in typical steppe of Inner Mongolia. – *Acta Phytoecologica Sinica* 29: 311-317.
- [10] Ren, A. (1999): Effect of drought stress on clonal growth of *Pennisetum centrasianicum* and *Leymus Secalinus*. – *Journal of Desert Research* 19: 30-34.
- [11] Ren, M., Wei, C., Pei, Z. (2015): Influences of different vegetation types on soil parameters in degraded sandy lands of Songnen Plain. – *Bulletin of Botanical Research* 35: 765-771.
- [12] Roiloa, S. R., Retuerto, R. (2006): Small-scale heterogeneity in soil quality influences photosynthetic efficiency and habitat selection in a clonal plant. – *Annals of Botany* 98: 1043-1052.
- [13] Shang, B.-Q., Du, G.-Z., Liu, Z.-H. (2000): Clonal growth of *Ligularia virgaurea*: morphological responses to nutritional variation. – *Acta Phytoecologica Sinica* 24: 46-51.
- [14] Silvertown, J. W. (1984): Introduction to plant population ecology. – *Vegetatio* 56: 86-86.
- [15] Wei, C., Shen, G., Pei, Z. (2015): Effects of different plants cultivation on soil physical-chemical properties and fine root growth in saline-alkaline soil in Songnen Plain, Northeastern China. – *Bulletin of Botanical Research* 35(5): 759-764.
- [16] Wu, F. P., Li, J. Q., Li, J. W., Cheng, C. L., Wang, X. H. (2008): The characteristics of root suckers of *Populus euphratica* Oliv. in three habitats of Ejina oasis. – *Acta Ecologica Sinica* 28: 4703-4709.
- [17] Yue, C., Wang, K., He, Q., Weng, F. (2002): Comparative research on clonal growth of *Phyllostachys praecox* in different conditions of soil nitrogen content. – *Journal of Bamboo Research* 21: 38-45.
- [18] Zhang, D. Y., H. L. W. (2005): Preliminary study on the growth pattern of several clonal plants in desert zones of Xinjiang. – *Arid Zone Research* 22: 219-224.
- [19] Zhang, H., Li, J., Li, J., Zhang, Y., Sun I, Wu, P., Zhao, J. (2007): The reproductive phenological rhythm characteristics of *Populus euphratica* Oliv. Population in The Ejina Oasis of Inner Mongolia. – *Journal of Inner Mongolia Agricultural University* 28: 66-72.
- [20] Zhao, Z. (2015): The growth of *Populus Pruinosa* clonal dynamics and its influencing factors. – Master Thesis, Tarim University, Alar.
- [21] Zheng, Y., Jiao, P., Zhao, Z., Li, Z. (2016a): Clonal growth of *Populus Pruinosa* Schrenk and its role in the regeneration of riparian forests. – *Ecological Engineering* 94: 380-392.
- [22] Zheng, Y., Zhang, X., Liang, J., Li, Z., Han, Z. (2016b): Clonal growth characteristics of the endangered species *Populus euphratica* Oliv and *Populus pruinosa* Schrenk. – *Acta Ecologica Sinica* 36: 1331—1341.
- [23] Zheng, Y., Zhai, J., Chen, J., Han, Z., Jiao, P., Li, Z. (2019): Seasonal variations of clonal propagation characteristics of *Populus pruinosa* Schrenk, organ nutrient and soil fertility, and their coupling associations in the forest and forest edges. – *Bulletin of Botanical Research* 39(3): 347-357.
- [24] Zhou, B., Yang, H.-M., Hu, S.-J., Xiong, H.-G. (2010): Effect of river-flooding on soil physical-chemical properties and vegetation. – *Arid Land Geography* 33: 130-136.

APPENDIX

Table A1. Dynamic variation on the clonal growth of *P. pruinosa*

Month	Adventitious bud		Unearthed ramets		Earthed ramets		Clone ramets height		Basal diameter		Ramets per cluster	
	Woodland edge in 2014	Woodland edge in 2015	Woodland edge in 2014	Woodland edge in 2015	Woodland edge in 2014	Woodland edge in 2015	Woodland edge in 2014	Woodland edge in 2015	Woodland edge in 2014	Woodland edge in 2015	Woodland edge in 2014	Woodland edge in 2015
4/27	28.2±1.16c	17±1.67b	1.7±0.09b	5.5±0.256a	3.4±0.39d	3.3±0.42c	0.490±0.04c	0.260±0.07d	0.005±0.0008e	0.0015±0.0002c	3.5±0.56g	3±0.66g
5/17	35±1.59bc	16.5±2.12b	3±0.24a	2.6±0.235b	3.5±0.28d	7±0.32b	1.390±0.06b	1.360±0.12b	0.005±0.0003e	0.0020±0.0006b	7±0.64e	5±0.52f
6/7	70±3.02a	22.5±3.15a	1.7±0.16b	0.6±0.09de	8.1±0.24a	5.5±0.29bc	2.20±0.003a	1.695±0.13a	0.009±0.0002b	0.0025±0.0006a	10.6±0.95c	9.2±1.01c
6/29	41±1.87b	10.6±1.68bc	0.4±0.07cd	2±0.12c	6.8±0.18b	9.2±0.21a	1.827±0.12ab	0.865±0.15c	0.010±0.0007a	0.0025±0.0006a	11.8±0.79b	11±0.82b
7/16	13.6±0.98d	9±1.52bc	0.8±0.11c	0.3±0.08e	3.8±0.17d	3.7±0.26c	1.008±0.06bc	0.625±0.1cd	0.008±0.0005c	0.0025±0.0004a	12.6±0.38a	11.8±0.44a
8/5	30±1.96c	18.7±2.36ab	0.7±0.08c	1.1±0.14d	6.1±0.36bc	5.4±0.28bc	0.577±0.009c	0.520±0.09cd	0.006±0.0004d	0.0020±0.0002b	8.8±0.55d	8.4±0.68d
9/1	21±2.03cd	15±1.23b	0.6±0.12c	1.1±0.08d	6.2±0.29bc	4.9±0.34bc	0.328±0.045cd	0.217±0.04d	0.005±0.0005e	0.0017±0.0002c	6±0.85f	7.1±0.96e
9/30	7.8±0.68de	7.8±1.42bc	0.7±0.01c	0.6±0.05de	5.0±0.42c	3.9±0.35c	0.113±0.002d	0.143±0.001d	0.005±0.0005e	0.0015±0.0002c	6.2±0.34f	6.8±0.26e
10/21	0.5±0.13e	1.5±0.14c	0.3±0.09d	0.1±0.009e	4.8±0.39c	2.6±0.34d	0.025±0.012e	0.025±0.003e	0.003±0.0001f	0.0008±0.0002d	6.2±0.12f	6.8±0.09e

Table A2. The dynamic change in soil physical factors

Month	Soil moisture content		Field capacity		Soil bulk density		Soil porosity	
	Woodland edge in 2014	Woodland edge in 2015	Woodland edge in 2014	Woodland edge in 2015	Woodland edge in 2014	Woodland edge in 2015	Woodland edge in 2014	Woodland edge in 2015
4/27	19.25±1.362 e	21.8±1.71 b	33.67±2.12 ab	32.67±1.52 ab	1.32±0.0 3 b	1.33±0.0024 a	48.04±1.81 e	47.84±1.43 b
5/17	22.09±1.275 d	21.55±1.65 b	32.64±1.23 c	32.64±1.59 a	1.29±0.0031 d	1.31±0.005 ab	50.74±2.05 cd	50.54±1.78 ab
6/7	23.15±1.143 c	20.3±1.52 bc	31.77±1.96 d	32.77±1.46 ab	1.31±0.0018 c	1.31±0.0014 ab	51.94±1.77 a	51.75±1.63 a
6/29	24.13±1.33 bc	17.81±1.39 c	33.78±1.65 a	31.71±1.84 b	1.3±0.0061 cd	1.30±0.0081 ab	51.74±1.65 ab	51.55±1.71 a
7/16	19.3±1.65 e	16.75±1.33 c	30.28±1.39 e	30.28±1.62 c	1.36±0.0041 a	1.32±0.0054 a	50.06±1.68 cd	50.87±1.465 a
8/5	28±1.621 a	26±1.49 a	33.81±1.06 a	33.42±1.82 a	1.29±0.0071 d	1.29±0.0093 b	51.73±1.78 ab	51.54±1.82 a
9/1	27±1.47 a	25±1.73 a	34.2±1.31 a	33.20±1.04 a	1.3±0.0054 cd	1.30±0.0081 b	50.89±1.75 bc	50.70±2.278 a
9/30	24.4±1.16 b	22.9±1.59 ab	32.85±1.703 bc	32.49±1.98 ab	1.32±0.0024 b	1.32±0.0022 a	49.91±1.82d	49.72±2.03 ab
10/21	12.24±1.35 f	13.9±1.42 d	32.37±1.61 cd	32.27±1.83 ab	1.35±0.002 ab	1.34±0.0032 a	47.78±1.77 e	47.59±2.172 b

Table A3. The dynamic change in soil chemistry factors

Month	Soil organic matter		Alkaline nitrogen		Available phosphorus		Available potassium		Total salt content		pH value	
	Woodland edge in 2014	Woodland edge in 2015	Woodland edge in 2014	Woodland edge in 2015	Woodland edge in 2014	Woodland edge in 2015	Woodland edge in 2014	Woodland edge in 2015	Woodland edge in 2014	Woodland edge in 2015	Woodland edge in 2014	Woodland edge in 2015
4/27	10.37±0.71ab	9.29±0.61c	18.7±1.08b	18.5±1.06b	13.86±0.98b	12.56±0.89b	41.8±2.78a	40.8±3.16a	0.15±0.007a	0.15±0.008a	8.49±0.01a	8.46±0.018a
5/17	11.57±0.88a	10.82±0.74ab	20.9±1.07a	18.9±1.06b	15.99±1.01a	13.98±0.95ab	42.67±3.06a	41.27±3.21a	0.13±0.008ab	0.15±0.009a	8.43±0.02ab	8.4±0.017a
6/7	11.83±0.54a	11.51±0.66a	21.2±1.06a	21±1.08a	15.2±0.88ab	14.2±0.82a	40.56±2.91a	41.56±3.06a	0.12±0.007b	0.15±0.008a	8.41±0.015b	8.39±0.024a
6/29	12.37±0.68a	9.69±0.72c	17.3±1.01b	17.2±1.02bc	13.17±0.88b	13.17±0.76b	40.4±3.29a	40.4±3.17a	0.1±0.008c	0.14±0.009a	8.41±0.013b	8.41±0.018a
7/16	9.97±0.56b	9.34±0.49c	15.4±1.02c	14.9±1.03c	12.06±0.89bc	12.06±0.73c	28.33±2.50c	28.33±2.58c	0.1±0.006c	0.15±0.008a	8.38±0.01bc	8.4±0.021a
8/5	9.53±0.59b	9.83±0.64c	13.5±0.98d	15.2±0.87c	9.76±0.68c	10.75±0.72d	28.2±2.37c	29.2±2.29c	0.1±0.008c	0.10±0.003c	8.3±0.016c	8.3±0.015b
9/1	8.77±0.36c	9.88±0.44b	13.4±0.96d	13.9±0.92c	9.99±0.65c	10.99±0.78cd	28.8±2.65c	28.8±2.90c	0.11±0.007b	0.11±0.006c	8.37±0.023bc	8.31±0.016b
9/30	8.72±0.41c	8.77±0.52c	12.8±0.89de	12.7±0.93cd	11.2±0.79bc	11.2±0.82cd	35.2±3.29b	35.12±3.17b	0.13±0.006ab	0.13±0.008b	8.42±0.014ab	8.42±0.025a
10/21	8.37±0.36c	8.76±0.6c	11.5±0.75e	11.5±0.81d	12.47±0.99b	12.47±0.94b	37.1±3.07b	38.2±3.05b	0.16±0.007a	0.16±0.009a	8.45±0.025a	8.45±0.01a

Table A4. The correlation analysis between clonal growth indexes and soil physical factors

Index	Month	Woodland edge in 2014				Woodland edge in 2015			
		Soil moisture content	Soil bulk density	Soil porosity	Field capacity	Soil moisture content	Soil bulk density	Soil porosity	Field capacity
Numbers of adventitious bud	4-7	0.57	0.06	-0.8	0.71	0.58	0.37	0.36	0.89*
	8-10	0.85	-0.96**	0.89*	0.95*	0.92*	-0.99**	0.98**	0.98**
Numbers of unearthed ramets	4-7	-0.40	-0.32	-0.49	-0.23	0.51	0.81	-0.97**	0.14
	8-10	0.96**	-0.86	0.67	0.89*	0.96*	-0.98**	0.97**	0.95*
Numbers of earthed ramets	4-7	0.76	0.05	-0.43	0.79	-0.80	-0.94*	0.75	-0.79
	8-10	0.68	-0.83	0.95*	0.79	0.96*	-0.99**	0.99**	0.96**
Numbers of ramets per cluster	4-7	0.98**	-0.39	-0.27	0.95*	-0.90*	-0.88*	0.90*	-0.63
	8-10	0.47	-0.63	0.40	0.65	0.60	0.80	0.76	0.83
Clone ramets height	4-7	0.92*	-0.41	-0.59	0.98**	-0.10	-0.59	0.81	0.24
	8-10	0.77	-0.91*	0.81	0.90*	0.80	-0.92*	0.90*	0.90*
Basal diameter	4-7	0.71	0.06	0.19	0.59	-0.77	-0.90*	0.98**	-0.45
	8-10	0.20	-0.46	0.46	0.44	0.97**	-0.97**	0.99**	0.90*

*P <0.05, **P<0.01

DETERMINATION IN THE PHENOLOGICAL DIFFERENCE LEVELS OF SEEDLINGS OF SOME WALNUT GENOTYPES (*JUGLANS REGIA* L.)

BÜKÜCÜ, Ş. B.^{1*} – ÖZCAN, A.² – SÜTYEMEZ, M.³ – YILDIRIM, E.³

¹*Department of Plant and Animal Production, Silifke Taşucu Vocational School, Selçuk University, 33900 Silifke Taşucu, Mersin, Turkey*

²*Afsin Vocational School, University of Kahramanmaraş Sutcu Imam, 46500 Afsin, Kahramanmaraş, Turkey*

³*Department of Horticulture, Faculty of Agriculture, University of Sütçü İmam, 46040 Onikisubat, Kahramanmaraş, Turkey*

*Corresponding author

e-mail: burakbukucu@gmail.com, phone: +90-553-638-4276

(Received 26th Feb 2020; accepted 25th May 2020)

Abstract. Walnut is a tree adversely affected by late spring and early autumn frosts. Therefore, it is one of the main goals to obtain late leafing and early defoliation genotypes in breeding studies on walnuts. The aim of this research is to determine the levels of phenological differences in walnut genotypes derived from the open-pollinated seeds of Bilecik, Chandler, Franquette, Howard, Kaman 1, Maraş 12, Pedro, Sütyemez 1 and Gimar (Gimnut). In this study, the bud burst, leafing, leaf yellowing and defoliation dates of seventy-five genotypes obtained from nine different walnut cultivars and their parents were determined. Cluster and PCA analyses were performed on a total of 684 genotypes to determine genetic diversity based on phenological markers. As a result of cluster analysis, all genotypes including their parents were clustered in three major groups. PCA analysis also confirmed the presence of genetic diversity-based phenological markers in our walnut seedling collection with PC1 50.226%, PC2 36.635%, PC3 12.413% and PC4 0.726% of the total variation. Pearson Correlation Coefficient among our walnut collection showed that there were very significant associations with budburst and leafing date ($r = 0.97$). As a result, we determined a wide variation in our walnut seedling collection, and these findings are potentially useful for future breeding studies in terms of late leafing and early defoliation.

Keywords: cluster analyses, PCA, breeding, budburst, leafing, defoliation

Introduction

Walnut is among the widely cultivated nuts in the world due to its nutrient contains. English or Persian walnut (*Juglans regia* L.) is one of the 20 species of the genus *Juglans*, which belongs to the *Juglandaceae* family (Şen, 2011). *J. regia* L. is long-lived, deciduous, monoecious and heterodichogamous. Walnut tree domestication is thought to be carried out in Central Asia, and today it is distributed and grown commercially over a wide geographical range, including West-Central Asia, southern Europe, North and South America, Australia and New Zealand (Gunn et al., 2010).

Walnut is the most cultivated nuts in the world. Due to the important nutrients it contains, the demand for this species of fruit is increasing every day. Therefore, scientific studies and production fields of this fruit are increasing every day. Genetic and morphological markers have become indispensable parts of plant breeding studies. To date, genetic diversity studies have been carried out with molecular or morphological markers on various fruit species including walnut under different

ecological conditions (Hernández-Delgado et al., 2007; Hong et al., 2008; Ferreira et al., 2010; Torres-Calzada et al., 2013; Rana et al., 2015; Kabiri et al., 2018; Sütyemez et al., 2018). Although morphological characters are often stated to hinder a clear character distinction among genotypes due to environmental impacts (Wang et al., 2015), they are indispensable and essential for breeding studies. That is, morphological markers have an important role in the selection and classification of the promising genotypes in plant breeding studies. Flowering-related traits, growing habits, yield and fruit quality are very important parameters for walnut breeding. Late leafing and early defoliation also are important breeding characteristics in walnuts, especially to avoid late spring and early autumn frosts.

The objective of this study was to determine the levels of genetic differences in walnut genotypes obtained by open-pollination of 9 different cultivars (Bilecik, Chandler, Franquette, Howard, Kaman 1, Maraş 12, Pedro, Sütyemez 1 and Gimar) by using some important phenological markers. Results obtained from this characterization would provide useful information and contribute to future walnut breeding programs.

Materials and methods

Materials

This study was carried out in the vegetation period of 2017 and 2018 and, the data of these 2 consecutive years were used in the data analysis. In the study, nine important walnut genotypes including Bilecik, Chandler, Franquette, Howard, Kaman 1, Maraş 12, Pedro, Sütyemez 1, Gimar in Nuts Application and Research Center (SEKAMER), Kahramanmaraş, Turkey and 75 seedlings obtained from their open-pollinated seeds were used as material. According to the parents, the healthy seedlings were given codes between 1 and 75. The codes given to genotypes according to their parents are presented in *Table 1*. Bilecik, Kaman 1, Maras 12 and Sütyemez 1 walnut cultivars originated from Turkey and are grown considerably commercially in Turkey. Among these walnut cultivars, Maraş-12 has a cluster-bearing habit and Sütyemez-1 has very large nuts (Sütyemez, 2016; Sütyemez et al., 2019). Howard, Pedro and Chandler are walnut cultivars of USA origin. These cultivars have good nut quality and fruitfulness. Franquette is of French origin and its late leafing is an important trait of this cultivar (Ramos, 1997). In order to determine the genetic diversity, four phenological features were identified on a total of 684 seedlings including their parents, which are very important for breeding.

Table 1. Descriptive statistics for phenological traits in our walnut collection

Parent	Seedling code
Bilecik	BI1-75
Chandler	CH1-75
Franquette	FR1-75
Gimar	GI1-75
Howard	HO1-75
Kaman1	KA1-75
Maraş12	MA1-75
Pedro	PE1-75
Sutyemez1	SU1-75

Methods

Phenological traits

In the study, phenological traits such as budburst, leafing, leaf yellowing, and defoliation dates were examined to determine the levels of genetic difference. The walnut accessions were characterized based on the Descriptor for Walnut (IPGRI, 1994) and Sütyemez (1998). List of traits and their definitions are presented in *Table 2*.

Table 2. Definitions used in the determination of phenological traits. (Source: IPGRI, 1994; Sütyemez, 1998)

Traits	Description
Date of budburst	When over 50% of terminal buds have enlarged and the bud scales have split exposing the green of the leaves inside
Leafing date	Date when 50% of terminal buds have enlarged and the bud scales have split exposing the green leaves
Leaf yellowing date	The date when more than 50% of the green leaves on the plant turn yellow
Defoliation date	When all the leaves of the plant fall

Data analysis

The observation of phenotypic data as dates was recorded as the number of days from January 1st for statistical analyses. The data were analyzed statistically with descriptive statistics, cluster analyses, Principal Component Analyses (PCA) and correlation by using the JMP13 Statistical Package Program for genetic diversity based on phenological traits. Phenological pair-wise distances of the walnut genotypes were clustered using Ward's method (Anderberg, 1973).

Results and discussion

Phenological traits are very significant during the domestication and introduction of fruit species (Khadivi-Khub et al., 2015). We determined a very large phenological diversity in our walnut accessions. Genotypes were found to have quite different characteristics in terms of phenological traits. The highest coefficient of variation belonged to budburst (CV = 12.49%), while the lowest CV was given by leaf yellowing (1.86%) (*Table 3*). The summary findings of budburst, leafing, leaf yellowing and defoliation dates of genotypes are presented in *Table 3*. Khadivi-Khub et al. (2015) reported that CV for leafing date was 77.78% on 540 walnut tree accessions selected in Neiriz region, Iran.

Table 3. Descriptive statistics for phenological traits in our walnut collection

Traits	Unit	Min.	Max.	Mean	SD	CV (%)
Budburst	Day	64	134	86.84	10.84	12.49
Leafing	Day	74	140	95.76	10.37	10.83
Leaf-yellowing	Day	290	342	309.78	5.77	1.86
Defoliation	Day	306	363	333.20	7.39	2.22

SD standard deviation, CV coefficient of variation = (SD / mean) × 100

Late spring and early autumn frosts cause significant economic losses in walnut. The yield is significantly reduced due to spring frosts, especially in early leafing and flowering genotypes. Therefore, late leafing is an ideal character in walnut to escape the spring frost injury as shown by other walnut cultivars such as Chico, Serr, Ashley and Sunland (Khadivi et al., 2019). Early defoliation date is important for the ecological region with a short vegetation period. Because late spring frosts, as well as autumn frosts, can cause significant losses in walnut. In this study, it was aimed to determine the new genotypes having both of these important traits and to determine the relationships between them. The date of leafing ranged from 16 March to 21 May for all walnut genotypes. The date of defoliation was between 3 November and 30 December. Among all genotypes, the earliest budburst and leafing was observed in SU72 and the latest in FR70. Franquette is known as one of the most late-leafing walnut cultivars in the world. Among the walnut genotypes obtained, it is important that a large proportion of the latest leafing twenty genotypes were obtained from the seeds of the Franquette cultivar. Furthermore, as a result of the observations made about the defoliation date, it was determined that the earliest defoliation genotype was FR 72 and the latest was FR66. Hassankhah et al. (2017) reported that the budburst dates of 6 different walnut genotypes ranged from 16 March to 2 April. In a study conducted by Bükücü and Sütyemez (2016), it was reported that the defoliation dates for 8 important walnut genotypes changed between 8-29 November. Akca et al. (2018) reported that the dates of defoliation ranged from 17 November to 4 December in 12 different walnut genotypes.

Pearson Correlation Coefficient was used to determine the associations between the phenological traits. We determined a very significant correlation between budburst and leafing dates ($r = 0.970$). In addition, a significant positive correlation was found between leaf yellowing and defoliation date ($r = 0.482$). In addition, we found positive relationships between leafing and defoliation dates ($r = 0.050$). However, since this value was quite low, the not strong association was detected between them. Amiri et al. (2010) found similar relationships associated with these two traits ($r = 0.298$). Significant correlations between leafing date and some horticultural traits were determined on walnut by other researchers (Ebrahimi et al., 2015; Khadivi-Khub et al., 2015; Abedi and Parvaneh, 2016). However, studies investigating the relationships with the dates of the defoliation remains are limited (Amiri et al., 2010). Correlations of phenological traits are presented in *Figure 1*.

Multivariate Analysis can summarize the variability of a complex dataset and present it in a most interpretable form, such as principal components (Ribeiro et al., 2013). In other words, the aim of PCA is to determine the main factors and effective parameters to discriminate among accessions (Khadivi-Khub, 2015). Therefore, PCA analysis was carried out to make an overall view of the differences in our walnut accession. PCA showed that the first component (PC1) for phenological traits explained 50.226% of the total variance. The second component (PC2) represented a total variance of 36.635%, while the third (PC3) and fourth (PC4) components explained 12.413% and 0.726% of the total variance, respectively. The bi-plot segregated the walnut genotypes into groups based partially on their parents (*Table 4; Fig. 2*). Although PCA analysis has been performed on many horticultural traits in walnut, the findings of this phenological traits studied have remained limited (Cosmulescu and Trandafir, 2011; Ercisli et al., 2012; Pop et al., 2013; Bou Abdallah et al., 2016; Arab et al., 2019).

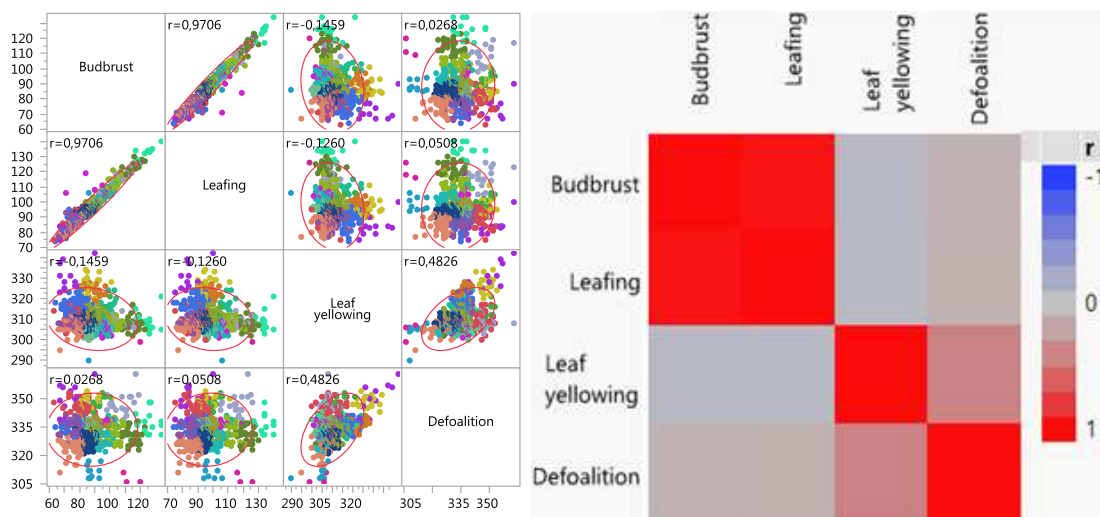


Figure 1. Scatterplot matrix and heatmap of correlations of phenological traits

Table 4. Eigenvectors of the principal components (PC) for the studied walnut accessions

Phenological traits	PC1	PC2	PC3	PC4
Budburst	0.69**	0.11	0.09	0.70**
Leafing	0.69**	0.14	0.18	-0.71**
Leaf-yellowing	-0.21	0.67**	0.71**	0.01
Defoliation	-0.05	0.72**	-0.69**	0.01
% of variance	50.226	36.635	12.413	0.726
Cumulative variance	50.226	86.861	99.274	100

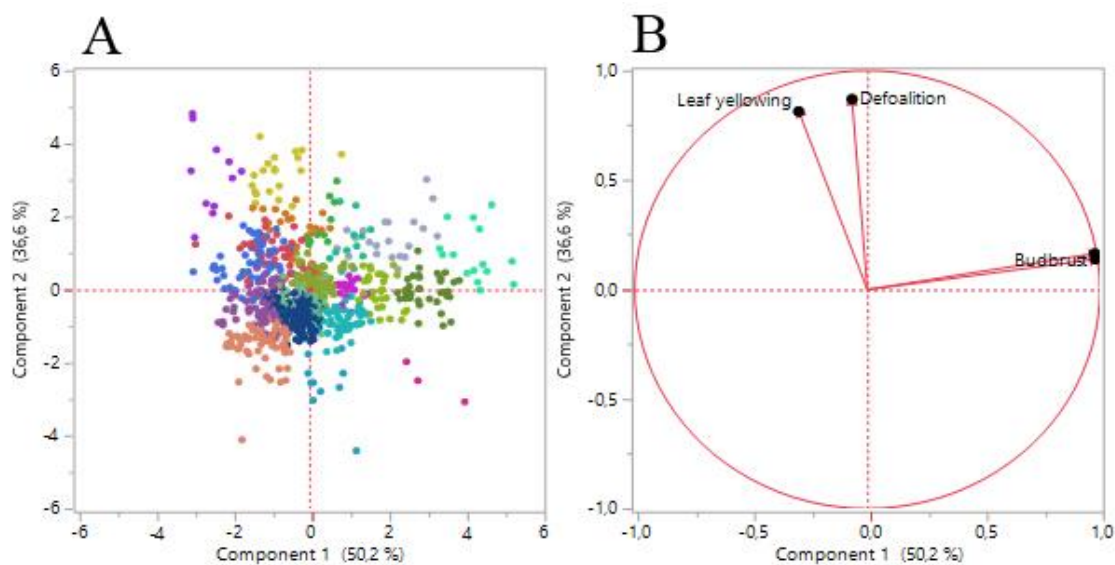


Figure 2. (A) Scatter plot for the first two principal components for the studied walnut accessions based on phenological traits. (B) Principal component analysis biplot of phenological traits of 684 walnut genotypes

Cluster analysis of the 684 genotypes including seedling and their parents on the basis of four phenological traits was performed to estimate the relationships between the walnut genotypes in a dendrogram (Fig. 3). Based on this analysis, walnut accessions were classified into mainly three cluster groups. Genotypes obtained from the seeds of Bilecik and Kaman-1 cultivars, which were early leafing and deciduous compared to other genotypes examined, were generally included in Cluster 1. In Cluster 3, it has been determined that genotypes were generally derived from seeds of late-leaved cultivars such as Franquette, Chandler, and Pedro cluster together. Other genotypes examined in the study were found to be in Cluster 3 (Fig. 3). The results of the cluster analysis partially confirmed the results of PCA on the genotypes (Fig. 2). These findings show that although walnut has heterozygote, it has dominant genes especially in terms of traits like leafing and defoliation dates. Morphological traits have been used effectively in detecting genetic variation on walnut in various studies (Arzani et al., 2008; Ebrahimi et al., 2010, 2011; Ghasemi et al., 2012; Norouzi et al., 2013; Hussain et al., 2016; Cosmulescu and Stefanescu, 2018; Rezaei et al., 2018).

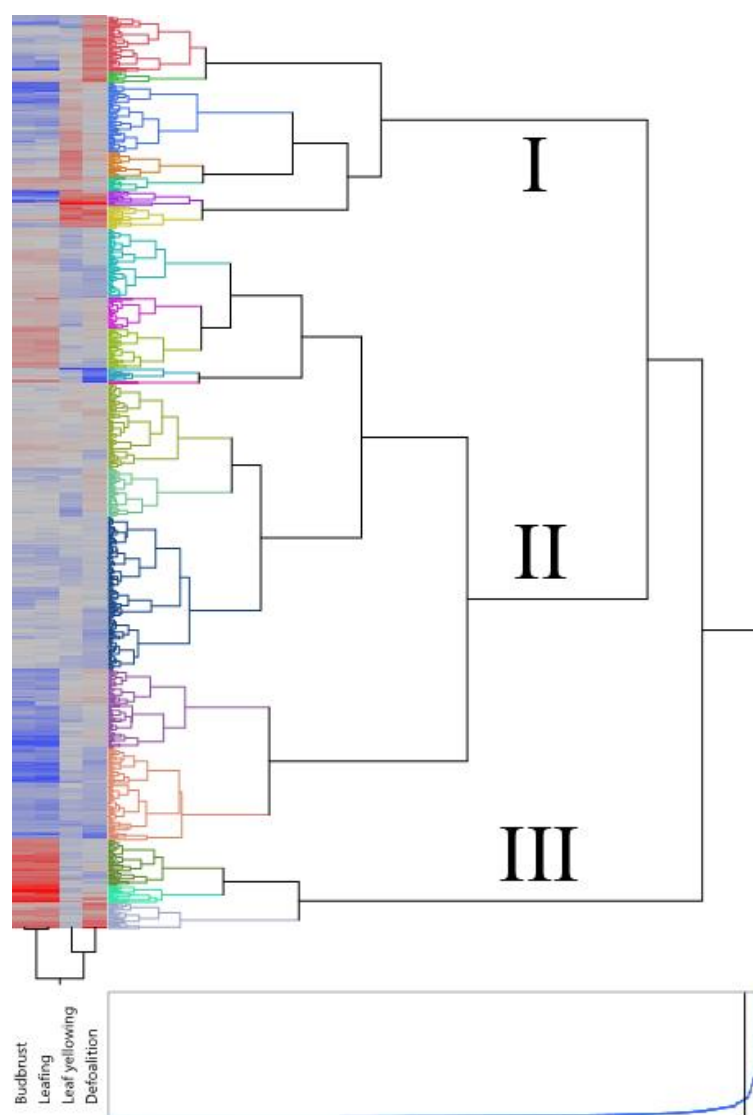


Figure 3. Phenotypic clustering of 684 walnut genotypes based on Ward's phenological pairwise distance and phenological heat map

Conclusions

Walnut seedlings constitute the infrastructure of breeding programs both in terms of production and plant resources. Genotypes obtained from seeds in fruit species such as walnut are very important sources in terms of biodiversity. Walnut has a long juvenile period therefore breeding programs require a long time. Breeding programs carried out in the young periods of walnut contribute to shortening this period and reaching the early goal. Thus, identification of phenotypic differences provides an insight for future breeding studies. The results from the present study clearly showed that morphological markers are able to partially differentiate seedling obtained from open pollinated walnut cultivars seed. Based on our results, morphological markers should be used to describe genetic diversity and relationships among seedling walnut genotypes. Moreover, the findings provide an important source of information in the selection of walnut genotypes with new superior properties in the future.

REFERENCES

- [1] Abedi, B., Parvaneh, T. (2016): Study of correlations between horticultural traits and variables affecting kernel percentage of walnut (*Juglans regia* L.). – Journal of Nuts 7(1): 35-44. DOI: 10.22034/JON.2016.522951.
- [2] Amiri, R., Vahdati, K., Mohsenipoor, S., Mozaffari, M. R., Leslie, C. (2010): Correlations between some horticultural traits in walnut. – HortScience 45(11): 1690-1694. DOI: 10.21273/HORTSCI.45.11.1690.
- [3] Anderberg, M. R. (1973): Cluster Analysis for Applications. – Academic Press, New York, pp. 2-18.
- [4] Arab, M. M., Marrano, A., Abdollahi-Arpanahi, R., Leslie, C. A., Askari, H., Neale, D. B., Vahdati, K. (2019): Genome-wide patterns of population structure and association mapping of nut-related traits in Persian walnut populations from Iran using the Axiom *J. regia* 700K SNP array. – Scientific Reports 9(1): 6376. DOI: 10.1038/s41598-019-42940-1.
- [5] Arzani, K., Mansouri-Ardakan, H., Vezvaei, A., Roozban, M. R. (2008): Morphological variation among Persian walnut (*Juglans regia*) genotypes from central Iran. – New Zealand Journal of Crop and Horticultural Science 36(3): 159-168. DOI: 10.1080/01140670809510232.
- [6] Bou Abdallah, I., Baatour, O., Mechrgui, K., Herchi, W., Albouchi, A., Chalghoum, A., Boukhchina, S. (2016): Essential oil composition of walnut tree (*Juglans regia* L.) leaves from Tunisia. – Journal of Essential Oil Research 28(6): 545-550. DOI: 10.1080/10412905.2016.1166157.
- [7] Bükücü, Ş. B., Sütyemez, M. (2016): The determination of the chilling requirements of some walnut (*Juglans regia* L.) cultivars and types. – Turkish Journal of Agricultural and Natural Science 3(4): 305-310.
- [8] Cosmulescu, S., Stefanescu, D. (2018): Morphological variation among Persian walnut (*Juglans regia*) genotypes within the population and depending on climatic year. – Scientia Horticulturae 242: 20-24. DOI: 10.1016/j.scienta.2018.07.018.
- [9] Cosmulescu, S., Trandafir, I. (2011): Variation of phenols content in walnut (*Juglans regia* L.). – South Western Journal of Horticulture, Biology and Environment 2(1): 25-33.
- [10] Ebrahimi, A., Fatahi, M. M., Zamani, Z. A., Vahdati, K. (2010): An investigation on genetic diversity of 608 Persian walnut accessions for screening of some genotypes of superior traits. – Iranian Journal of Horticultural Sciences 40(4): 83-94.

- [11] Ebrahimi, A., Fatahi, R., Zamani, Z. (2011): Analysis of genetic diversity among some Persian walnut genotypes (*Juglans regia* L.) using morphological traits and SSRs markers. – *Scientia Horticulturae* 130(1): 146-151. DOI: 10.1016/j.scienta.2011.06.028.
- [12] Ebrahimi, A., Khadivi-Khub, A., Nosrati, Z., Karimi, R. (2015): Identification of superior walnut (*Juglans regia*) genotypes with late leafing and high kernel quality in Iran. – *Scientia Horticulturae* 193: 195-201. DOI: 10.1016/j.scienta.2015.06.049.
- [13] Ercisli, S., Sayinci, B., Kara, M., Yildiz, C., Ozturk, I. (2012): Determination of size and shape features of walnut (*Juglans regia* L.) cultivars using image processing. – *Scientia Horticulturae* 133: 47-55. DOI: 10.1016/j.scienta.2011.10.014.
- [14] Ferreira, J. J., Garcia-González, C., Tous, J., Rovira, M. (2010): Genetic diversity revealed by morphological traits and ISSR markers in hazelnut germplasm from northern Spain. – *Plant Breeding* 129(4): 435-441. DOI: 10.1111/j.1439-0523.2009.01702.x.
- [15] Ghasemi, M., Arzani, K., Hassani, D. (2012): Evaluation and identification of walnut (*Juglans regia* L.) genotypes in Markazi province of Iran. – *Crop Breeding Journal* 2(2): 119-124. DOI: 10.22092/cbj.2012.100429.
- [16] Gunn, B. F., Aradhya, M., Salick, J. M., Miller, A. J., Yongping, Y., Lin, L., Xian, H. (2010): Genetic variation in walnuts (*Juglans regia* and *J. sigillata*; *Juglandaceae*): species distinctions, human impacts, and the conservation of agrobiodiversity in Yunnan, China. – *American Journal of Botany* 97(4): 660-671. DOI: 10.3732/ajb.0900114.
- [17] Hassankhah, A., Vahdati, K., Rahemi, M., Hassani, D., Sarikhani Khorami, S. (2017): Persian Walnut phenology: effect of chilling and heat requirements on budbreak and flowering date. – *International Journal of Horticultural Science and Technology* 4(2): 259-271. DOI: 10.22059/IJHST.2018.260944.249.
- [18] Hernández-Delgado, S., Padilla-Ramírez, J. S., Nava-Cedillo, A., Mayek-Pérez, N. (2007): Morphological and genetic diversity of Mexican guava germplasm. – *Plant Genetic Resources* 5(3): 131-141. DOI: 10.1017/S1479262107827055.
- [19] Hong, S. K., Kim, W. G., Yun, H. K., Choi, K. J. (2008): Morphological variations, genetic diversity and pathogenicity of *Colletotrichum* species causing grape ripe rot in Korea. – *The Plant Pathology Journal* 24(3): 269-278. DOI: 10.5423/PPJ.2008.24.3.269.
- [20] Hussain, I., Sulatan, A., Shinwari, Z. K., Raza, G., Ahmed, K. (2016): Genetic diversity based on morphological traits in walnut (*Juglans regia* L.) landraces from Karakoram Region-I. – *Pak. J. Bot.* 48(2): 653-659.
- [21] IPGRI (1994): Descriptors for Walnut (*Juglans* spp.). – International Plant Genetic Resources Institute, Rome.
- [22] Kabiri, G., Bouda, S., Elhansali, M., Haddioui, A. (2018): Morphological and pomological variability analysis of walnut (*Juglans regia* L.) genetic resources from the middle and high Atlas of Morocco. – *Atlas Journal of Biology* 2018: 575-582. DOI: 10.5147/ajb.v0i0.179.
- [23] Khadivi-Khub, A., Ebrahimi, A., Sheibani, F., Esmaeili, A. (2015): Phenological and pomological characterization of Persian walnut to select promising trees. – *Euphytica* 205(2): 557-567. DOI: 10.1007/s10681-015-1429-9.
- [24] Khadivi, A., Montazeran, A., Yadegari, P. (2019): Superior spring frost resistant walnut (*Juglans regia* L.) genotypes identified among mature seedling origin trees. – *Scientia Horticulturae* 253: 147-153. DOI: 10.1016/j.scienta.2019.04.041.
- [25] Norouzi, R., Heidari, S., Asgari-Sarcheshmeh, M. A., Shahi-Garahlar, A. (2013): Estimation of phenotypical and morphological differentiation among some selected Persian walnut (*Juglans regia* L.) accessions. – *Intl. J. Agron. Plant Prod.* 4(9): 2438-2445.
- [26] Pop, I. F., Vicol, A. C., Botu, M., Raica, P. A., Vahdati, K., Pamfil, D. (2013): Relationships of walnut cultivars in a germplasm collection: comparative analysis of phenotypic and molecular data. – *Scientia Horticulturae* 153: 124-135. DOI: 10.1016/j.scienta.2013.02.013.

- [27] Ramos, D. E. (ed.) (1997): Walnut Production Manual (Vol. 3373). – UCANR Publications Oakland.
- [28] Rana, J. C., Chahota, R. K., Sharma, V., Rana, M., Verma, N., Verma, B., Sharma, T. R. (2015): Genetic diversity and structure of Pyrus accessions of Indian Himalayan region based on morphological and SSR markers. – Tree Genetics & Genomes 11(1): 821. DOI: 10.1007/s11295-014-0821-2.
- [29] Rezaei, Z., Khadivi, A., ValizadehKaji, B., Abbasifar, A. (2018): The selection of superior walnut (*Juglans regia* L.) genotypes as revealed by morphological characterization. – Euphytica 214(4): 69. DOI 10.1007/s10681-018-2153-z.
- [30] Ribeiro, A. B., Bonafé, E. G., Silva, B. C., Montanher, P. F., Santos Júnior, O. O., Boeing, J. S., Visentainer, J. V. (2013): Antioxidant capacity, total phenolic content, fatty acids and correlation by principal component analysis of exotic and native fruits from Brazil. – Journal of the Brazilian Chemical Society 24(5): 797-804. DOI: 10.5935/0103-5053.20130105.
- [31] Şen, S. M. (2011): Ceviz yetiştiriciliği, besin değeri, folklorü. 4th Ed. – ÜÇM Yayıncılık, Ankara.
- [32] Sütyemez, M. (1998): Researches on walnut selection and fertilization biology of selected types in Kahramanmaraş region. (Kahramanmaraş bölgesinde ceviz seleksiyonu ve seçilmiş bazı tiplerin dölllenme biyolojileri üzerine araştırmalar). – PhD Thesis. Çukurova University Institute of Natural and Applied Sciences.
- [33] Sütyemez, M. (2016): New Walnut Cultivars: Maras 18, Sütyemez 1, and Kaman 1. – HortScience 51(10): 1301-1303. DOI: 10.21273/HORTSCI10972-16.
- [34] Sütyemez, M., Özcan, A., Bükücü, Ş. B. (2018): Walnut cultivars through cross-breeding: ‘DİRİLİŞ’ and ‘15 TEMMUZ’. – The American Pomological Society 72(3): 173-180.
- [35] Sütyemez, M., Bükücü, Ş. B., Özcan, A. (2019): Maraş 12: A walnut cultivar with cluster-bearing habit. – HortScience 54(8): 1437-1438. DOI: 10.21273/HORTSCI14226-19.
- [36] Torres-Calzada, C., Tapia-Tussell, R., Higuera-Ciapara, I., Perez-Brito, D. (2013): Morphological, pathological and genetic diversity of Colletotrichum species responsible for anthracnose in papaya (*Carica papaya* L.). – European Journal of Plant Pathology 135(1): 67-79. DOI: 10.1007/s10658-012-0065-7.
- [37] Wang, H., Wu, W., Pan, G., Pei, D. (2015): Analysis of genetic diversity and relationships among 86 Persian walnut (*Juglans regia* L.) genotypes in Tibet using morphological traits and SSR markers. – The Journal of Horticultural Science and Biotechnology 90(5): 563-570. DOI: 10.1080/14620316.2015.11668715.